Virchows Arch (2011) 459:1–10
DOI 10.1007/s00428-011-1097-7

ORIGINAL ARTICLE

Comparison of hormonal receptor and HER-2 status between breast primary tumours and relapsing tumours: clinical implications of progesterone receptor loss

Giuseppe Bogina · Laura Bortesi · Marcella Marconi · Marco Venturini · Gianluigi Lunardi · Francesca Coati · Alberto Massocco · Erminia Manfrin · Cristina Pegoraro · Giuseppe Zamboni

Received: 31 March 2011 / Revised: 20 May 2011 / Accepted: 23 May 2011 / Published online: 4 June 2011
© The Author(s) 2011. This article is published with open access at Springerlink.com

Abstract Differences in hormone receptor and HER-2 status between primary tumour and corresponding relapse could have a substantial impact on clinical management of patients. The aim of this study was to evaluate change in expression of hormone receptors and HER-2 status between primary tumour and corresponding local recurrence or distant metastasis. We analysed 140 primary tumours and related recurrent or metastatic samples. Hormone receptors status was evaluated by immunohistochemistry, while HER-2 status by immunohistochemistry and silver in situ hybridisation. A change in HER-2 was rare; 3.7% of cases by immunohistochemistry and only 0.7% by silver in situ hybridisation analysis. A change in estrogen and progesterone receptors was seen in 6.4% and 21.4% of cases, respectively. Estrogen receptor change was not affected by adjuvant therapy, whereas progesterone receptor was influenced by adjuvant chemotherapy associated to hormone therapy (P=0.0005). A change in progesterone receptor was more frequent in distant metastases than in local recurrences (P=0.03). In the setting of estrogen receptor positive tumours, patients with progesterone receptor loss in local recurrence had a statistically significant lower median metastasis free survival compared to others patients; progesterone receptor positive, 112 months; progesterone receptor negative, 24 months (P=0.005). A change between primary tumour and corresponding relapse is frequent for progesterone receptor, infrequent for estrogen receptor and rare for HER-2. In cases with changes in HER-2, it is worthwhile reassessing HER-2 status with both immunohistochemistry and in situ hybridisation analysis. Progesterone receptor loss seems to be influenced by therapy and to correlate with a worse prognosis.

Keywords Breast carcinoma · HER-2 · Hormone receptor · Metastasis

G. Bogina · L. Bortesi · M. Marconi · G. Zamboni
Department of Pathology, Sacro Cuore Hospital of Negrar, Verona, Italy

M. Venturini · G. Lunardi · F. Coati
Department of Oncology, Sacro Cuore Hospital of Negrar, Verona, Italy

A. Massocco
Department of Surgery, Sacro Cuore Hospital of Negrar, Verona, Italy

E. Manfrin
Department of Pathology, University of Verona, Verona, Italy

C. Pegoraro
Department of Oncology, Montecchio, Vicenza, Italy

G. Bogina (✉)
Istituto di Anatomia Patologica, Ospedale Sacro Cuore, Via Don A Sempreboni 5, Negrar, 37024 Verona, Italy
e-mail: giuseppe.bogina@sacrocuore.it

Introduction

Hormone receptor and HER-2 status are the most important predictive markers in breast cancer. Their assessment is generally performed on resected primary tumour (PT) in order to select patients eligible for hormone and HER-2 directed therapies [1–7]. Most of the tumours that do respond initially to targeted therapies will gain acquired resistance [8]. Differences in hormone receptor and HER-2 status between PT and corresponding relapse could help to

explain this acquired resistance and have a substantial impact on clinical management of these patients. Nevertheless, the results reported in different studies, concerning expression of biomarkers in PT and corresponding metastasis, are not homogeneous (Table 1) [1–30]. There are many hypotheses that could explain biomarkers change between PT and corresponding metastasis: clonal selection for hormone receptor and HER-2 during tumour progression due to intratumoral heterogeneity and/or to selective pressure from therapy; independent evolution of an early stem cell clone in both sites, instead of a linear progression from the PT to metastasis; false shifts related to detection and evaluation including tissue processing, reagent variability, type of test and scoring interpretation [1, 2, 8, 14, 18, 22, 26, 31]. The aim of this study was to compare the expression of estrogen receptor (ER), progesterone receptor (PR) and HER-2 status between PT and corresponding local recurrence (LR) or distant metastasis (DM) to evaluate whether therapy can modify this status and whether biomarkers change can affect prognosis.

Materials and methods

For this study, we considered all consecutive breast cancer DM and LR diagnosed at the Institute of Pathology of Sacro Cuore Hospital, Negrar, Verona between January 1998 and December 2009. There were 198 patients with histological samples of breast LR or DM. For 140 of these patients, the corresponding PT samples were retrieved from the files of the Institute of Pathology. For the remaining 58 cases, corresponding PT samples were not available. Cases

Table 1 Literature review of ER, PR and HER-2 discordance between primary tumours and corresponding metastatic sites

	Cases	Metastatic sites	Type of analysis	ER (%)	PR (%)	HER-2 (%)
Andersen 1988 [10]	143	ALM/DM	Biomarkers reassessment	10		
Li 1994 [17]	83	LR/DM	Biomarkers reassessment	29	44	
Van Agthoven 1995 [28]	26	ALM	Biomarkers reassessment	0		
Johnston 1995 [8]	34	LR	Biomarkers reassessment	23	26	
Kuukasjarvi 1996 [16]	50	LR	Biomarkers reassessment	24	24	
Shimizu 2000 [24]	21	LR/DM	Biomarkers reassessment	25	30	0
Zheng 2001 [30]	52	ALM	Biomarkers reassessment	6		
Tanner 2001 [6]	45	LR/DM	Biomarkers reassessment			0
Simon 2001 [25]	125	ALM	Biomarkers reassessment			3
Gancberg 2002 [1]	100	DM	Biomarkers reassessment			6
Vincent-Salomon 2002 [29]	44	DM	Biomarkers reassessment			4
Edgerton 2003 [13]	113	LR/DM	Biomarkers reassessment			20
Iguchi 2003 [15]	87	ALM	Biomarkers reassessment	24		
Carlsson 2004 [12]	47	ALM	Biomarkers reassessment			0
Regitnig 2004 [21]	31	DM	Biomarkers reassessment			10
Gong 2005 [2]	60	ALM/LR/DM	Biomarkers reassessment			3
Zidan 2005 [7]	58	LR/DM	Biomarkers reassessment			14
Lower 2005 [20]	200	LR/DM	Reports review	30	39	
Tapia 2007 [26]	105	DM	Biomarkers reassessment			3
Guarneri 2008 [3]	75	LR/DM	Reports review	22	36	16
Gomez-Fernandez 2008 [14]	278	LR/DM	Biomarkers reassessment	3		
Santinelli 2008 [22]	119	ALM/LR/DM	Biomarkers reassessment			14
Broom 2009 [11]	100	DM	Reports review	18	37	5
Simmons 2009 [5]	29	DM	Biomarkers reassessment	12	28	8
Liedtke 2009 [18]	211	LR/DM	Reports review	18	40	14
Idirisinghe 2010 [4]	117	LR/DM	Biomarkers reassessment	16	38	5
Sari 2010 [23]	78	LR/DM	Biomarkers reassessment	36	54	15
Thompson 2010 [27]	137	LR/DM	Biomarkers reassessment	10	25	3
Amir 2010 [9]	271	LR/DM	Biomarkers reassessment	13	34	5
Locatelli 2010 [19]	255	DM (liver)	Reports review	14	48	14

ALM axillary lymph node metastases, *LR* local recurrences, *DM* distant metastases, *ER* estrogen receptor, *PR* progesterone receptor

with in situ, multifocal or bilateral breast PT were excluded. In cases with multiple LR or DM, we considered samples obtained from the first (chronologically) detected LR or DM site. For each PT, the following information was obtained from pathology reports: patient age, histological type, tumour size, grading, ER, PR and HER-2 status.

Data regarding adjuvant therapy and follow-up were retrieved from the files of the department of oncology. Tissue samples were fixed in 10% buffered formalin for 20–24 h before processing and embedding. Hormone receptors status was evaluated by immunohistochemistry (IHC), while HER-2 status by IHC and silver in situ hybridisation (SISH). All samples were reassessed with the same validated staining techniques to reduce inter-laboratory variability and reviewed by a single dedicate breast pathologist (G.B.) to decrease inter-observer variability. These results were compared to the original report; this comparison was possible in 280 samples for ER and PR and in 82 samples for HER-2 because, in our institute, it has been evaluated routinely since 2005.

A high loss rate of PR in LR and DM has been previously reported (Table 1). On this way, we examined whether this finding could have any clinical impact, evaluating metastasis free survival (MFS), defined as elapsed months since LR to first DM, in the subset of patients with ER positive PT and LR, but with different PR status. ER negative tumours were excluded because there were no ER negative/PR positive tumours, and then the choice of therapy was not influenced by PR status. Patients with DM prior or synchronous to LR were excluded, because patient's management was determined by the presence of DM, regardless of LR features.

Immunohistochemistry

IHC to detect hormone receptors was performed with the CONFIRM® anti-ER clone SP1, rabbit monoclonal primary antibody and CONFIRM® anti-PR clone 1E2 (VMS, Tucson AZ, USA) using an automated BenchMark XT staining system (VMS, Tucson AZ, USA) with a reduced CC1 (pH 8.2 for 30 min) unmasking protocol. Sections were incubated at 37°C for 20 min and then developed with the UltraView Universal Dab Detection Kit. According to the ASCO/CAP guidelines, we defined as positive tumours with ER/PR ≥1% [32]; we considered as shifted those cases that changed from ≥1% to <1% and vice versa.

HER-2 was performed using the primary antibody PATHWAY® anti-HER2/neu clone 4B5 (VMS, Tucson AZ, USA) in the automated BenchMark XT staining system (VMS, Tucson, AZ, USA) using a reduced (pH 8.2 for 30 min) CC1-unmasking protocol. Sections were incubated at 37°C for 16 min and developed with the UltraView Universal Dab Detection Kit.

According to ASCO/CAP guidelines, HER-2 expression was scored as 0 (no staining or weak/moderate, incomplete/complete staining in ≤10% of cells), 1+ (weak and incomplete staining in >10% of cells), 2+ (weak/moderate complete staining in >10% of cells or strong, complete staining in ≤30% of cells) and 3+ (strong, complete staining in >30% of cells) [33].

In addition, we detected Ki-67 (CONFIRM® anti-Ki-67 clone 30–9, rabbit monoclonal primary antibody) and E-cadherin (clone 36, mouse monoclonal primary antibody) in all cases using an automated BenchMark XT staining system (VMS, Tucson, AZ, USA) with a reduced CC1 (pH 8.2 for 30 min) unmasking protocol. Sections were incubated at 37°C for 20 min and then developed with the UltraView Universal Dab Detection Kit.

Silver in situ hybridisation

SISH was performed in BenchMarK XT staining system (VMS, Tucson AZ, USA) according to the manufacturer's instructions. Testing for the HER-2 gene and chromosome 17 was performed on sequential sections. Briefly, formalin-fixed, paraffin-embedded tissues were cut in 4.5 μm thick sections, put on polarized slides, dried overnight at 40°C and placed in the automated staining system (one slide for each probe). The principal steps were heat pre-treatment with citrate buffer pH 6 at 90°C, enzymatic digestion with protease at 37°C for 8 min, probe dispensation, denaturation at 95°C for 8 min, hybridisation at 52/54°C for 3 h, stringent washes, indirect detection and counterstaining with haematoxylin. Slides were progressively dehydrated with increasing alcohol concentrations, cleared in xylene and mounted. HER-2 3-in-1 xenograft control slides were used as reaction and quality controls. The number of signal deposits was counted in 20 tumour nuclei in two distinct areas, in the slide reactive for HER-2 and in the same areas in the slide reactive for chromosome 17. The HER-2/chromosome 17 ratio was calculated and scored according to ASCO/CAP guidelines: ratio <1.8, HER-2 gene not amplified; ratio >2.2, HER-2 gene amplified; ratio between 1.8 and 2.2, uncertain [33].

Discordant HER-2 status was considered when there was a shift from 0, 1+, 2+ (SISH non-amplified) IHC to 2+ (SISH amplified) or 3+ IHC and vice versa. In case of discordance between IHC and SISH, the HER-2 was defined according to the SISH status. In our routine work up for breast cancer, the discordance rate between IHC and SISH to HER-2 determination is 2.8%.

Statistical analysis

Agreement for ER, PR and HER-2 between PT and corresponding relapses was expressed by discordance

percentage. Significant changes in one direction (positive or negative) of ER, PR and HER-2 between PT and corresponding metastases were calculated using the McNemar's test. Comparisons of percentages between groups were performed using the chi-square or Fisher's exact test. The MFS in the group of patients considered was described by the Kaplan–Meier method and compared with the use of the log-rank test. A two-sided *P* value of 0.05 was considered a statistically significant difference.

A multivariable Cox proportional hazard regression model was used to evaluate the independent prognostic relevance of the following factors for MFS: PT pathological size (T1 vs T2–T4); pathological node status (negative vs positive ≤3 vs positive >3); PT histological grade (grade 1–2 vs grade 3), PT Ki-i67 level (examined as continuous variable); PT/LR HER-2 status (negative vs positive); PT/LR ER positive proportion (examined as continuous variable); LR free survival (≤1 year vs 1–5 years vs >5 years); PR status (PR positive in PT and LR vs PR positive PT and negative LR vs PR negative in PT and LR). Stata/IC for Windows version 11.1 was used for all analyses.

Results

Pathological results

We analysed 140 PT and their corresponding relapses (90 LR and 50 DM). Clinical and pathological features of the PT are shown in Table 2. The mean interval of LR was 55 months (range, 5–232 months); sites of LR were: breast (21), chest wall (44), axilla (23) and homolateral clavicular nodes (two). All samples of LR were surgical specimens. Forty-six DM were metachronous and four synchronous. The mean interval of metachronous DM was 73.6 months (range, 6–216 months). The sites of metachronous DM were: liver (five), lung (nine), pleura (two), bone (ten), skin (three), ovary (three), peritoneum (one), stomach (five), duodenum (three), thyroid (one), cervix (one) and node (three). The sites of synchronous DM were: colon (one), bone (one), node (one) and brain (one). Twenty-seven samples of DM were surgical samples, whereas 23 were bioptic specimens.

The results regarding ER, PR and HER-2 status in PT and corresponding metastatic sites are shown in Table 3. ER and PR status was available for all 140 paired samples, whereas HER-2 status for 136 paired samples, since four cases were not evaluable due to unreliable tissue processing. In these cases, the chromosome 17 marker could not be identified by SISH analysis. We found ten cases with significant changes between the original report and the reassessed IHC staining. In five cases, there was a different ER value, while in the remaining cases differences in PR were seen, all in the PT.

Table 2 Clinical and pathologic features of 140 primary breast tumours

	Primary tumours
Age (years)	
Mean	61.7
Range	34–93
Size (cm)	
Mean	2.6
Range	0.5–9.5
Histologic type	
Ductal	101
Lobular	32
Others	7
Grading	
G1	24
G2	63
G3	53
ER status	
Positive	111
Negative	29
PR status	
Positive	91
Negative	49
HER-2 status	
Positive	18
Negative	118
Non-informative	4
Therapy	
None	43
CT	25
HT	24
CT and HT	36
Not available	12

ER estrogen receptor, *PR* progesterone receptor, *CT* chemotherapy, *HT* hormone therapy

A discrepancy in ER was present in nine (6.4%) of paired samples, eight (7.2%) lost and one (3.4%) gained ER (P=0.04). In four (three loss and one gain) of these nine paired samples, there was a similar discrepancy in PR, while in the other five cases with ER loss, PR was negative in both PT and relapse.

A change in PR status was present in 30 (21.4%) of paired samples; 25 (27.5%) lost and five (10.2%) gained PR (P=0.0003). The change rate between PR and ER was statistically significant (P=0.0004).

Comparison between LR and DM showed a difference not statistically significant with regards to the rate of

Table 3 Change of ER, PR and HER-2 in different metastatic sites

	ER			PR			HER-2		
	Change	Pos–neg	Neg–pos	Change	Pos–neg	Neg–pos	Change	Pos–neg	Neg–pos
LR	5/90 (5.5%)	5/70 (7.1%)	0/20	14/90 (15.5%)	11/58 (18.9%)	3/32 (9.3%)	1/88 (1.1%)	0/11	1/77 (1.3%)
DM	4/50 (8%)	3/41 (7.3%)	1/9 (11.1%)	16/50 (32%)	14/33 (42.4%)	2/17 (11.8%)	0/48	0/7	0/41
Total	9/140 (6.4%)	8/111 (7.2%)	1/29 (3.4%)	30/140 (21.4%)	25/91 (27.5%)	5/49 (10.2%)	1/136 (0.7%)	0/18	1/118 (0.8%)

LR local recurrences, *DM* distant metastases, *ER* estrogen receptor, *PR* progesterone receptor

change in ER (P=0.72), while it showed a trend towards a statistical significance for change in PR, more frequent in DM than in LR (P=0.03). This trend was maintained even in the group of untreated patients (P=0.02).

HER-2 change was present in 5 of 136 paired samples (3.7%) using IHC and in only one paired samples after SISH (0.7%). In four of these IHC–HER-2-shifted paired samples, there was discordance between IHC and SISH; one sample was IHC positive and SISH negative, whereas three were IHC negative and SISH positive. Analysis of the our case with HER-2 shift showed a PT negative to IHC and not amplified to SISH, while the axillary recurrence, developed 96 months after mastectomy and axillary lymph node dissection, showed IHC positivity and SISH amplification. The comparison of the two tumours demonstrated a shift from primary ductal type carcinoma (E-cadherin positivity) to lobular type carcinoma (E-cadherin negativity) (Fig. 1). In no other case, there was a change in histologic type and E-cadherin expression between PT and corresponding relapse.

The relationship between hormone receptor status and therapy is shown in Table 4. Thirty-six patients were treated with chemotherapy associated with hormone therapy, 25 were treated with chemotherapy only and 24 were treated with hormone therapy only. Forty-three patients received no adjuvant therapy. In this latter group, we included the four patients with synchronous DM, considering that hormone receptor status could not be affected by therapy. Only five patients were treated with trastuzumab (two with LR and three with DM). There was no clinical information in 12 patients. There were not statistically significant differences in ER change among the four groups of patients, whereas there was a statistically significant PR loss in patients treated with chemotherapy and hormone therapy (P=0.0005). There were no significant associations between histological type (ductal vs lobular), grading (G1–G2 vs G3), Ki-67(low < median value, 14% vs high ≥ median value, 14) and hormone receptors shift (data not shown).

Clinical results

The analysis of MFS in the subset of patients with ER positive PT and LR, but with different PR status was possible in 56 patients: 20 patients with ER negative PT, five patients with ER negative LR and nine patients with DM prior or synchronous to LR were excluded. Out of 56 patients evaluated, there was only one patient with PR negative PT and positive LR. This single patient was excluded from analysis. Therefore, we overall analysed MFS in 55 patients.

Kaplan–Meier MFS curves (Fig. 2) showed a significant difference in MFS among groups of patients with ER positive local recurrence but different PR status: primary tumour and local recurrence both PR positive (group A, 40 patients); primary tumour and local recurrence both PR negative (group B, seven patients) and primary tumour PR positive and local recurrence PR negative (group C, eight patients). Group C patients had significantly worse MFS (median 24.1 months) compared with group A patients (median 111.8 months) (log-rank=0.005). Multivariate analysis showed that PR status in LR was independently associated with MFS and that PR loss in LR (group C) was also strongly associated with poor outcome: hazard ratio, 8.9 (95% CI, 2.3–34.5) (P=0.002).

Discussion

The development of target therapy has changed the prognosis of patients both in adjuvant and metastatic setting [34–38]. Although therapy targets metastases, the hormone receptors and HER-2 status are almost always evaluated on PT [1–3, 5–7]. Thus, it is crucial to determine whether there is concordant biomarkers expression between PT and corresponding metastasis, since the data available from literature show very discordant results about this issue (Table 1) [1–30]. In almost all previous reports, the adopted threshold of positivity for hormone receptors is ≥10% of neoplastic cells [3–5, 10, 14–16, 18, 28, 30], while for HER-2 is >10% of neoplastic cells with intense continuous membrane staining for IHC [1, 3, 7, 13, 22, 25] or ratio >2 for in situ hybridisation [1–3, 13, 21, 26]. The recent ASCO/CAP guidelines considered receptor positive for a tumour with a minimum of 1% of positive tumour cells [32] and HER-2 positive for a tumour with an intense

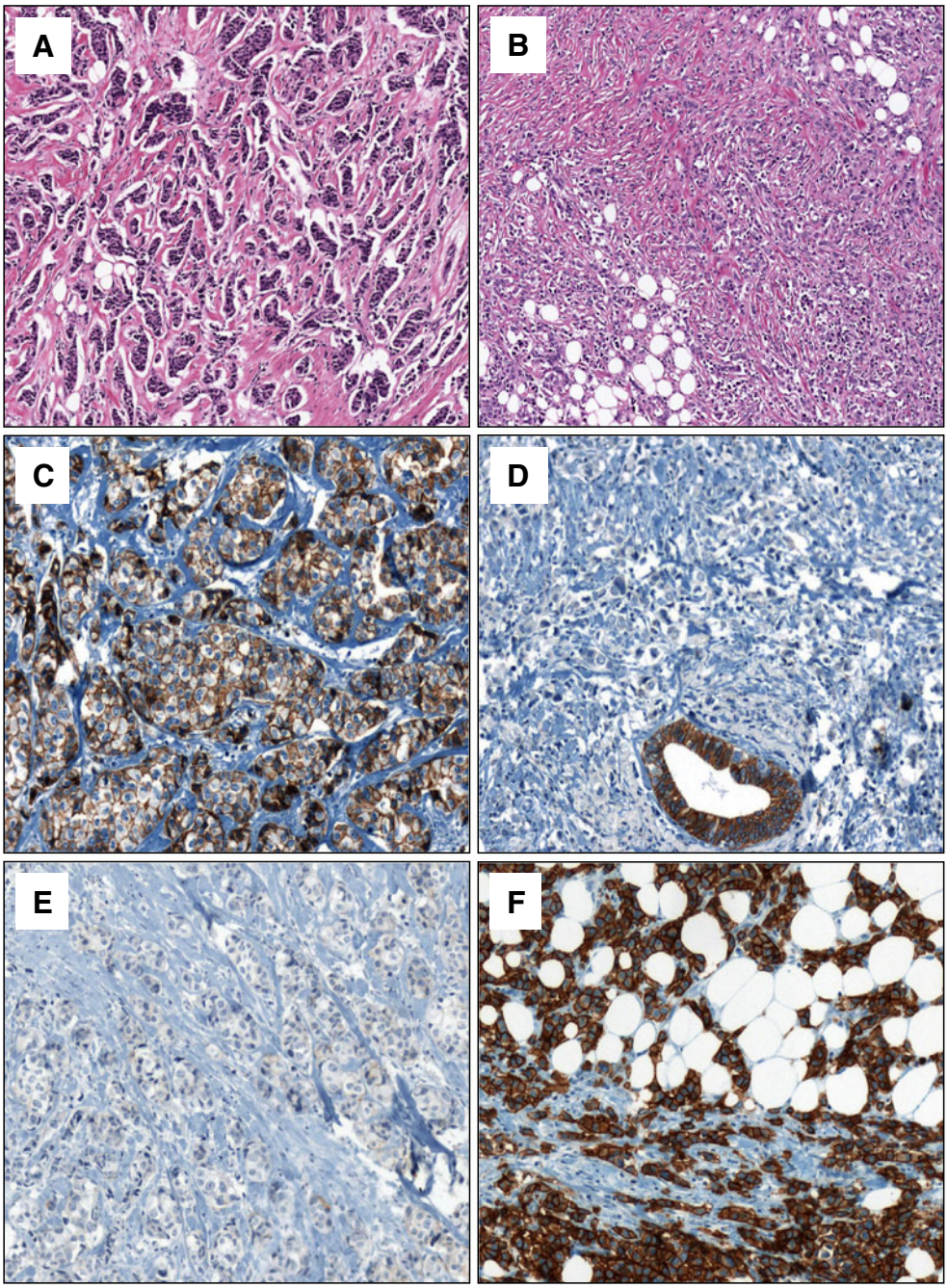

Fig. 1 Different morphology (H&E) between ductal like primary tumour (**a**) and lobular like local recurrence (**b**). Immunohistochemistry showed different staining for E-cadherin and HER-2 between the primary tumour (**c**, **e**) and the recurrence (**d**, **f**)

Table 4 Correlation between changes in ER, PR and therapy

	ER			PR		
	Change	Pos–neg	Neg–pos	Change	Pos–neg	Neg–pos
CT	0/25	0/10	0/15	2/25 (8%)	0/8	2/17 (11.7%)
HT	1/24 (4.1%)	1/24 (4.1%)	0/0	6/24 (25%)	4/18 (22.2%)	2/6 (33%)
CT and HT	2/36 (5.5%)	2/34 (5.9%)	0/2	12/36 (33.3%)	12/29 (41.4%)	0/7
None	6/43 (13.9%)	5/31 (16.1%)	1/12 (8.3%)	6/43 (13.9%)	5/26 (19.2%)	1/17 (5.9%)

ER estrogen receptor, *PR* progesterone receptor, *CT* chemotherapy, *HT* hormone therapy

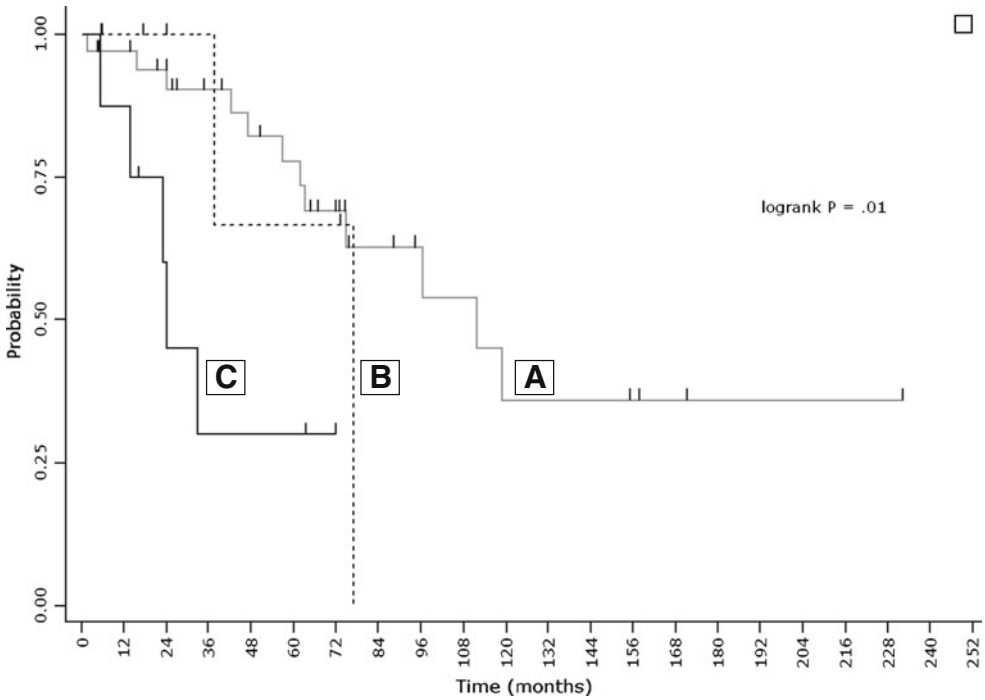

Fig. 2 Kaplan–Meier estimate of metastasis free survival according to PT/LR receptor status. Groups (*A*, *B*, C) are defined in Clinical results

continuous staining in >30% of neoplastic cells in IHC and/or a ratio >2.2 in situ hybridisation [33]. In this work, we have adopted the positivity threshold proposed by the ASCO/CAP guidelines. We reassessed ER, PR and HER-2 status in PT and corresponding metastasis in 140 paired samples including 90 LR and 50 DM.

We found a significant change for hormone receptors between the original report and the reassessed IHC staining in 3.6% of samples, all in the PT. In these tumour samples, the original report was done before 2000. Amir et al. reported a change in 5.8%, 11.5% and 8.7% after reassessment for ER, PR and HER-2, respectively [9]. This discrepancy might be due to differences in analytic factors such as use of manual or automated methods, tests reagents and type of antigen retrieval.

The rate of change in ER staining was 6.1%. Overall, there was a trend towards a statistical significance for ER loss (P=0.04). ER change was not affected by therapy. In agreement with Shimizu et al. [24], in the majority of our cases with ER change, there was a corresponding change in PR status. This is likely due to fact that PR is regulated by ER [39].

A change in PR status was seen in 21.4% of cases, significantly more frequently than ER change (P<0.0001). These data are in agreement with the majority of previous publications [4, 8, 9, 11, 17–20, 23, 24, 27]. Overall, a PR positive PT with a negative relapse was the most frequent event (P=0.0003).

Overall, we had six cases in which the PT was negative for hormone receptors (one ER and five PR), but the corresponding relapse was positive. This event has been reported by other authors [4, 9, 11, 15, 17, 19, 20, 23, 27]. False negative assessment in PT cannot be excluded; however, our cases showed hormone receptors positive control in normal breast tissue associated with the PT, ruling out the possibility that technical factors, including poor fixation, influenced the different receptors status. While the loss of hormone receptors, during metastasis process, might be related with clonal selection or tumour dedifferentiation, these mechanisms could not explain hormone receptors gain. Molecular analyses showed the presence of different clones of cells having different genetic profile in the same tumour; metastasis might be established by one of these clones. The parallel progression model posits parallel, independent evolution of metastasis arising from early disseminated tumour cells clone rather than a linear progression of primary tumour to metastasis [40].

HER-2 change was present in 3.7% of paired samples using IHC and in only 0.7% after SISH analysis. In four of these five IHC–HER-2-shifted paired samples, there was discordance between IHC and SISH. In discordant cases, the reassessment of HER-2 status on PT and relapse with both techniques is warranted. The analysis of the case with HER-2 shift showed an HER-2 negative PT to IHC and SISH and a HER-2 positive axillary recurrence to IHC and SISH. The comparison of the two tumours demonstrated a shift from primary ductal type carcinoma (E-cadherin positivity) to lobular type carcinoma (E-cadherin negativity) (Fig. 2). Although Wu et al. reported a similar case of E-cadherin positive primary ductal carcinoma with corresponding multiple metastases characterized by lobular morphology and E-cadherin loss

expression [41], a second tumour arising from residual mammary parenchyma rather than a real recurrence can be supposed. Indeed, there are no reliable morphologic or clinical criteria to distinguish LR from secondary tumour. Clinically, controlateral cancer is generally considered to represent independent tumour, in ipsilateral disease, tumour having a longer mean time to recurrence or occurring in different quadrant from the initial tumour is also regarded as new primary tumour. Finally, concerning pathological features, the presence of in situ carcinoma, different histological type or better differentiation of second tumour may help in identifying independent tumours [42]. Research using genomic analyses may replace these criteria [43].

Changes in PR status were more frequent in DM than LR (P=0.003) and this trend was maintained in patients not undergoing any therapy (P=0.002). Most of previous papers, investigating the difference in hormone receptor status between DM and LR, have shown a similar rate of discordance between DM and LR [17, 20, 23, 27], while Idirisinghe et al. demonstrated a higher rate of discordance for both ER and PR in DM [4]. A higher rate of HER-2 shift in DM in comparison to LR has been reported by several authors [2, 4, 21, 22, 26]. Since LR was made up exclusively of surgical specimens and nearly half of DM of bioptic specimens, one possible reason for this difference might be related to the size of the samples analysed. The discordance rate of hormone receptors and HER-2 between core biopsy and corresponding surgical specimen in breast cancer varies from 1% [44] to 18.7% [45] for hormone receptors and from 1.2% [46] to 13.5% [44] for HER-2. However, in our cases of DM, there was no statistically significant difference in ER and PR change between bioptic (n=23) and surgical (n=27) specimens (P=0.61 and P=0.55, respectively). Thus, it is likely that the greater degree of biomarkers change in DM compared with either LR likely reflects the complex biologic process to establish growth in a new site. The basic steps of metastasis include the progression of the PT towards dispersion of cancer cells through the blood vessels. Circulating cancer cells could infiltrate distant organs and, in the new microenvironment, might proceed towards overt metastasis [47].

Regarding therapeutic implications, since there were no ER negative/PR positive tumour samples, there was a theoretical change in clinical management in 7.3% of patients corresponding to nine cases with ER change and to case with HER-2 change. Amir et al. [9], Locatelli et al. [19] and Thompson et al. [27] reported a therapeutic change of management in 15.1%, 12.1% and 17.5%, respectively. Simmons et al. [5] demonstrated a significant change in patient management in 6 of 29 cases (20%). However, in that prospective study, the diagnosis of suspicious "metastatic" biopsy was a benign lesion in three cases and lymphoma in one case. Consequently, in only 2 of 25 cases (8%) was there a change in management due to a genuine change in biomarker status.

Concerning the relation between hormone receptor change and therapy, we showed that ER change was not affected by therapy (P=0.7), whereas a significant change was observed only for PR loss in patients who underwent chemotherapy and hormone therapy (P<0.0005). Li et al. demonstrated a lack of influence of hormone therapy and chemotherapy on ER and PR status [17], while Idirisinghe et al. showed a correlation between ER and PR loss and hormone therapy [4]. Sequential breast cancer biopsies have shown that ER levels are reduced slightly with intervening endocrine therapy, while PR levels decrease more dramatically with up to half of tumours completely losing PR expression when resistance develops [48].

Few studies have shown a shorter survival among women with ER negative metastatic and locally recurrent tumours, regardless of the primary tumour ER status [4, 20], while whether and how the loss of PR affects the clinical course of ER positive/PR negative metastatic tumours remains to be clarified [48]. The study of Brankovic-Magic et al., based on reports review of 23 breast cancer and corresponding metastases, suggests that PR loss in metastasis may be an important marker in predicting response failure to endocrine therapy in metastatic disease [49].

In our study, the analysis of patients with ER positive PT and LR showed that the MFS was significantly worse in patients with a PR positive PT and negative LR than in those with both PR positive PT and LR (log-rank=0.01) (Fig. 2). Noteworthy, all the eight patients with ER positive PT and LR who lost PR in LR had received therapy after LR diagnosis: six had hormone therapy, one had chemotherapy and one hormone therapy associated to chemotherapy. The very short median MFS time (24 months) observed in this group of patients seems to indicate that hormone therapy, received by seven out of eight PR-shifted patients, may be not enough to treat this disease. A more aggressive approach by combining extensive local therapy with chemotherapy and hormone therapy is probably required. Nevertheless, our data clearly indicate that PR-shifted patients have a poor prognosis and should be accurately followed-up after their LR.

In summary, in the present study, a change between PT and corresponding metastasis was frequent for PR and less frequent for ER, whereas it was very rare for HER-2. In cases with HER-2 shift, reassessment of HER-2 status on PT and corresponding relapse with both techniques (IHC and in situ hybridisation) is warranted. Changes in biomarkers may occur sporadically, preferably in DM compared to LR, although the loss of PR appears to be affected by chemotherapy associated to hormone therapy. In

patients with ER positive PT and LR, PR loss in LR correlates with a more aggressive behaviour of the tumour.

Acknowledgements The authors thank Patrick Moore for the English revision of the manuscript.

Conflicts of interest The authors declare that they have no conflicts of interest.

Open Access This article is distributed under the terms of the Creative Commons Attribution Noncommercial License which permits any noncommercial use, distribution, and reproduction in any medium, provided the original author(s) and source are credited.

References

1. Gancberg D, Di Leo A, Cardoso F, Rouas G, Pedrocchi M, Paesmans M, Verhest A, Bernard-Marty C, Piccart MJ, Larsimont D (2002) Comparison of HER-2 status between primary breast cancer and corresponding distant metastatic sites. Ann Oncol 13 (7):1036–1043
2. Gong Y, Booser DJ, Sneige N (2005) Comparison of HER-2 status determined by fluorescence in situ hybridization in primary and metastatic breast carcinoma. Cancer 103(9):1763–1769
3. Guarneri V, Giovannelli S, Ficarra G, Bettelli S, Maiorana A, Piacentini F, Barbieri E, Dieci MV, D'Amico R, Jovic G, Conte P (2008) Comparison of HER-2 and hormone receptor expression in primary breast cancers and asynchronous paired metastases: impact on patient management. Oncologist 13 (8):838–844
4. Idirisinghe PK, Thike AA, Cheok PY, Tse GM, Lui PC, Fook-Chong S, Wong NS, Tan PH (2010) Hormone receptor and c-ERBB2 status in distant metastatic and locally recurrent breast cancer. Pathologic correlations and clinical significance. Am J Clin Pathol 133(3):416–429
5. Simmons C, Miller N, Geddie W, Gianfelice D, Oldfield M, Dranitsaris G, Clemons MJ (2009) Does confirmatory tumor biopsy alter the management of breast cancer patients with distant metastases? Ann Oncol 20(9):1499–1504
6. Tanner M, Jarvinen P, Isola J (2001) Amplification of HER-2/neu and topoisomerase IIalpha in primary and metastatic breast cancer. Cancer Res 61(14):5345–5348
7. Zidan J, Dashkovsky I, Stayerman C, Basher W, Cozacov C, Hadary A (2005) Comparison of HER-2 overexpression in primary breast cancer and metastatic sites and its effect on biological targeting therapy of metastatic disease. Br J Cancer 93(5):552–556
8. Johnston SR, Saccani-Jotti G, Smith IE, Salter J, Newby J, Coppen M, Ebbs SR, Dowsett M (1995) Changes in estrogen receptor, progesterone receptor, and pS2 expression in tamoxifen-resistant human breast cancer. Cancer Res 55(15):3331–3338
9. Amir R, Clemons M, Freedman OC, Miller N, Coleman RE, Purdie C, Jordan L, Quinlan P, Thompson AM (2010) Tissue confirmation of disease recurrence in patients with breast cancer: pooled analysis of two large prospective studies. J Clin Oncol 28:15s
10. Andersen J, Poulsen HS (1988) Relationship between estrogen receptor status in the primary tumor and its regional and distant metastases. An immunohistochemical study in human breast cancer. Acta Oncol 27(6A):761–765
11. Broom RJ, Tang PA, Simmons C, Bordeleau L, Mulligan AM, O'Malley FP, Miller N, Andrulis IL, Brenner DM, Clemons MJ (2009) Changes in estrogen receptor, progesterone receptor and Her-2/neu status with time: discordance rates between primary and metastatic breast cancer. Anticancer Res 29 (5):1557–1562
12. Carlsson J, Nordgren H, Sjostrom J, Wester K, Villman K, Bengtsson NO, Ostenstad B, Lundqvist H, Blomqvist C (2004) HER2 expression in breast cancer primary tumours and corresponding metastases. Original data and literature review. Br J Cancer 90(12):2344–2348
13. Edgerton SM, Moore D 2nd, Merkel D, Thor AD (2003) erbB-2 (HER-2) and breast cancer progression. Appl Immunohistochem Mol Morphol 11(3):214–221
14. Gomez-Fernandez C, Daneshbod Y, Nassiri M, Milikowski C, Alvarez C, Nadji M (2008) Immunohistochemically determined estrogen receptor phenotype remains stable in recurrent and metastatic breast cancer. Am J Clin Pathol 130(6):879–882
15. Iguchi C, Nio Y, Itakura M (2003) Heterogeneic expression of estrogen receptor between the primary tumor and the corresponding involved lymph nodes in patients with node-positive breast cancer and its implications in patient outcome. J Surg Oncol 83(2):85–93
16. Kuukasjarvi T, Kononen J, Helin H, Holli K, Isola J (1996) Loss of estrogen receptor in recurrent breast cancer is associated with poor response to endocrine therapy. J Clin Oncol 14(9):2584–2589
17. Li BD, Byskosh A, Molteni A, Duda RB (1994) Estrogen and progesterone receptor concordance between primary and recurrent breast cancer. J Surg Oncol 57(2):71–77
18. Liedtke C, Broglio K, Moulder S, Hsu L, Kau SW, Symmans WF, Albarracin C, Meric-Bernstam F, Woodward W, Theriault RL, Kiesel L, Hortobagyi GN, Pusztai L, Gonzalez-Angulo AM (2009) Prognostic impact of discordance between triple-receptor measurements in primary and recurrent breast cancer. Ann Oncol 20(12):1953–1958
19. Locatelli MA, Curigliano G, Fumagalli L, Bagnardi V, Aurilio G, Della Vigna P, Monfardini L, Giudici S, Viale G, Goldhirsch A (2010) Should liver metastases of breast cancer be biopsied to improve treatment choice? J Clin Oncol 28:18s
20. Lower EE, Glass EL, Bradley DA, Blau R, Heffelfinger S (2005) Impact of metastatic estrogen receptor and progesterone receptor status on survival. Breast Cancer Res Treat 90(1):65–70
21. Regitnig P, Schippinger W, Lindbauer M, Samonigg H, Lax SF (2004) Change of HER-2/neu status in a subset of distant metastases from breast carcinomas. J Pathol 203(4):918–926
22. Santinelli A, Pisa E, Stramazzotti D, Fabris G (2008) HER-2 status discrepancy between primary breast cancer and metastatic sites. Impact on target therapy. Int J Cancer 122(5):999–1004
23. Sari E, Guler G, Hayran M, Gullu I, Altundag K, Ozisik Y (2010) Comparative study of the immunohistochemical detection of hormone receptor status and HER-2 expression in primary and paired recurrent/metastatic lesions of patients with breast cancer. Med Oncol 28(1):57–63
24. Shimizu C, Fukutomi T, Tsuda H, Akashi-Tanaka S, Watanabe T, Nanasawa T, Sugihara K (2000) c-erbB-2 protein overexpression and p53 immunoreaction in primary and recurrent breast cancer tissues. J Surg Oncol 73(1):17–20
25. Simon R, Nocito A, Hubscher T, Bucher C, Torhorst J, Schraml P, Bubendorf L, Mihatsch MM, Moch H, Wilber K, Schotzau A, Kononen J, Sauter G (2001) Patterns of her-2/neu amplification and overexpression in primary and metastatic breast cancer. J Natl Cancer Inst 93(15):1141–1146
26. Tapia C, Savic S, Wagner U, Schonegg R, Novotny H, Grilli B, Herzog M, Barascud AD, Zlobec I, Cathomas G, Terracciano L, Feichter G, Bubendorf L (2007) HER2 gene status in primary breast cancers and matched distant metastases. Breast Cancer Res 9(3):R31

27. Thompson AM, Jordan LB, Quinlan P, Anderson E, Skene A, Dewar JA, Purdie CA (2010) Prospective comparison of switches in biomarker status between primary and recurrent breast cancer: the Breast Recurrence in Tissues Study (BRITS). Breast Cancer Res 12(6):R92
28. van Agthoven T, Timmermans M, Dorssers LC, Henzen-Logmans SC (1995) Expression of estrogen, progesterone and epidermal growth factor receptors in primary and metastatic breast cancer. Int J Cancer 63(6):790–793
29. Vincent-Salomon A, Jouve M, Genin P, Freneaux P, Sigal-Zafrani B, Caly M, Beuzeboc P, Pouillart P, Sastre-Garau X (2002) HER2 status in patients with breast carcinoma is not modified selectively by preoperative chemotherapy and is stable during the metastatic process. Cancer 94(8):2169–2173
30. Zheng WQ, Lu J, Zheng JM, Hu FX, Ni CR (2001) Variation of ER status between primary and metastatic breast cancer and relationship to p53 expression*. Steroids 66(12):905–910
31. Carney WP, Leitzel K, Ali S, Neumann R, Lipton A (2007) HER-2/neu diagnostics in breast cancer. Breast Cancer Res 9(3):207
32. Hammond ME, Hayes DF, Dowsett M, Allred DC, Hagerty KL, Badve S, Fitzgibbons PL, Francis G, Goldstein NS, Hayes M, Hicks DG, Lester S, Love R, Mangu PB, McShane L, Miller K, Osborne CK, Paik S, Perlmutter J, Rhodes A, Sasano H, Schwartz JN, Sweep FC, Taube S, Torlakovic EE, Valenstein P, Viale G, Visscher D, Wheeler T, Williams RB, Wittliff JL, Wolff AC (2010) American Society of Clinical Oncology/College Of American Pathologists guideline recommendations for immunohistochemical testing of estrogen and progesterone receptors in breast cancer. J Clin Oncol 28(16):2784–2795
33. Wolff AC, Hammond ME, Schwartz JN, Hagerty KL, Allred DC, Cote RJ, Dowsett M, Fitzgibbons PL, Hanna WM, Langer A, McShane LM, Paik S, Pegram MD, Perez EA, Press MF, Rhodes A, Sturgeon C, Taube SE, Tubbs R, Vance GH, van de Vijver M, Wheeler TM, Hayes DF (2007) American Society of Clinical Oncology/College of American Pathologists guideline recommendations for human epidermal growth factor receptor 2 testing in breast cancer. J Clin Oncol 25(1):118–145
34. Arpino G, Weiss H, Lee AV, Schiff R, De Placido S, Osborne CK, Elledge RM (2005) Estrogen receptor-positive, progesterone receptor-negative breast cancer: association with growth factor receptor expression and tamoxifen resistance. J Natl Cancer Inst 97(17):1254–1261
35. Piccart-Gebhart MJ, Procter M, Leyland-Jones B, Goldhirsch A, Untch M, Smith I, Gianni L, Baselga J, Bell R, Jackisch C, Cameron D, Dowsett M, Barrios CH, Steger G, Huang CS, Andersson M, Inbar M, Lichinitser M, Lang I, Nitz U, Iwata H, Thomssen C, Lohrisch C, Suter TM, Ruschoff J, Suto T, Greatorex V, Ward C, Straehle C, McFadden E, Dolci MS, Gelber RD (2005) Trastuzumab after adjuvant chemotherapy in HER2-positive breast cancer. N Engl J Med 353(16):1659–1672
36. Pritchard KI, Shepherd LE, O'Malley FP, Andrulis IL, Tu D, Bramwell VH, Levine MN (2006) HER2 and responsiveness of breast cancer to adjuvant chemotherapy. N Engl J Med 354 (20):2103–2111
37. Romond EH, Perez EA, Bryant J, Suman VJ, Geyer CE Jr, Davidson NE, Tan-Chiu E, Martino S, Paik S, Kaufman PA, Swain SM, Pisansky TM, Fehrenbacher L, Kutteh LA, Vogel VG, Visscher DW, Yothers G, Jenkins RB, Brown AM, Dakhil SR, Mamounas EP, Lingle WL, Klein PM, Ingle JN, Wolmark N (2005) Trastuzumab plus adjuvant chemotherapy for operable HER2-positive breast cancer. N Engl J Med 353 (16):1673–1684
38. Slamon DJ, Leyland-Jones B, Shak S, Fuchs H, Paton V, Bajamonde A, Fleming T, Eiermann W, Wolter J, Pegram M, Baselga J, Norton L (2001) Use of chemotherapy plus a monoclonal antibody against HER2 for metastatic breast cancer that overexpresses HER2. N Engl J Med 344(11):783–792
39. Kim HJ, Cui X, Hilsenbeck SG, Lee AV (2006) Progesterone receptor loss correlates with human epidermal growth factor receptor 2 overexpression in estrogen receptor-positive breast cancer. Clin Cancer Res 12(3 Pt 2):1013s–1018s
40. Arslan C, Sari E, Aksoy S, Altundag K (2011) Variation in hormone receptor and HER-2 status between primary and metastatic breast cancer: review of the literature. Expert Opin Ther Targets 15(1):21–30
41. Wu JM, Fackler MJ, Halushka MK, Molavi DW, Taylor ME, Teo WW, Griffin C, Fetting J, Davidson NE, De Marzo AM, Hicks JL, Chitale D, Ladanyi M, Sukumar S, Argani P (2008) Heterogeneity of breast cancer metastases: comparison of therapeutic target expression and promoter methylation between primary tumors and their multifocal metastases. Clin Cancer Res 14(7):1938–1946
42. Schlechter BL, Yang Q, Larson PS, Golubeva A, Blanchard RA, de las Morenas A, Rosenberg CL (2004) Quantitative DNA fingerprinting may distinguish new primary breast cancer from disease recurrence. J Clin Oncol 22(10):1830–1838
43. Brown M, Bauer K, Pare M (2010) Tumor marker phenotype concordance in second primary breast cancer, California, 1999–2004. Breast Cancer Res Treat 120(1):217–227
44. Park SY, Kim KS, Lee TG, Park SS, Kim SM, Han W, Noh DY, Kim SW (2009) The accuracy of preoperative core biopsy in determining histologic grade, hormone receptors, and human epidermal growth factor receptor 2 status in invasive breast cancer. Am J Surg 197(2):266–269
45. Tamaki K, Sasano H, Ishida T, Miyashita M, Takeda M, Amari M, Tamaki N, Ohuchi N (2010) Comparison of core needle biopsy (CNB) and surgical specimens for accurate preoperative evaluation of ER, PgR and HER2 status of breast cancer patients. Cancer Sci 101(4):1051–1058
46. Arnedos M, Nerurkar A, Osin P, A'Hern R, Smith IE, Dowsett M (2009) Discordance between core needle biopsy (CNB) and excisional biopsy (EB) for estrogen receptor (ER), progesterone receptor (PgR) and HER2 status in early breast cancer (EBC). Ann Oncol 20(12):1948–1952
47. Nguyen DX, Bos PD, Massague J (2009) Metastasis: from dissemination to organ-specific colonization. Nat Rev Cancer 9 (4):274–284
48. Cui X, Schiff R, Arpino G, Osborne CK, Lee AV (2005) Biology of progesterone receptor loss in breast cancer and its implications for endocrine therapy. J Clin Oncol 23(30):7721–7735
49. Brankovic-Magic M, Jankovic R, Neskovic-Konstantinovic Z, Nikolic-Vukosavljevic D (2002) Progesterone receptor status of breast cancer metastases. J Cancer Res Clin Oncol 128(1):55–60

Virchows Arch (2011) 459:11–20
DOI 10.1007/s00428-011-1061-6

ORIGINAL ARTICLE

Relationship between placental morphology and histological findings in an unselected population near term

Sangeeta Pathak · Neil J. Sebire · Liz Hook · Gerald Hackett · Edile Murdoch · Flora Jessop · Christoph Lees

Received: 11 January 2011 / Revised: 14 February 2011 / Accepted: 16 February 2011 / Published online: 12 April 2011
© Springer-Verlag 2011

Abstract Whilst individual histological features are well described, there are no universally agreed criteria as to what constitutes a clinically significant histological lesion of the placenta in an uncomplicated pregnancy, nor has the presence of such histological findings been systematically related to quantitative morphological characteristics of the placenta (such as placental shape, cord insertion and cord coiling). This study aims to explore this relationship and further to describe the incidence of predefined categories of histological lesions of the placenta in an unselected obstetric population recruited prior to delivery. The study is based upon the placental examination of 1,156 women with singleton pregnancies recruited prospectively in a single unit. Placentas were analysed where deliveries occurred between 34–43 weeks. The incidence of normal histological findings and specific histological categories, such as ascending genital tract infection, chronic placental underperfusion, intervillous thrombus and villitis of unknown aetiology, were noted. The relationship between placental morphological indices: coiling index, cord centrality index (distance of cord insertion on the chorionic plate from the centre) and eccentricity (shape of the placenta) and histological lesions was investigated. There were no significant differences between cord centrality and eccentricity between placentas with and without histological lesions except an association between hypercoiling of the umbilical cord and intervillous thrombosis and villitis of unknown aetiology ($p=0.024$ and $p=0.009$, respectively). The macroscopic morphological features of the placenta cannot predict the presence or absence of the histological placental lesions, nor are these lesions in general associated with differences in cord centrality, placental eccentricity or cord coiling.

Keywords Digital imaging · Cord centrality · Eccentricity · Coiling index · Villitis · Chorioamnionitis · Ascending genital tract infection · Infarction · Thrombosis

S. Pathak · G. Hackett · C. Lees (✉)
Division of Fetal-Maternal Medicine,
Rosie Maternity-Addenbrooke's Hospital,
Cambridge University Hospitals NHS Foundation Trust,
Hills Road,
Cambridge CB2 2QQ, UK
e-mail: christoph.lees@addenbrookes.nhs.uk

N. J. Sebire
Histopathology Department, Great Ormond Street Hospital,
London WC1N 3JH, UK

L. Hook · F. Jessop
Department of Pathology, Addenbrooke's Hospital,
Cambridge University Hospitals NHS Foundation Trust,
Hills Road,
Cambridge CB2 2QQ, UK

E. Murdoch
Neonatal Unit, Rosie Maternity-Addenbrooke's Hospital,
Cambridge University Hospitals NHS Foundation Trust,
Hills Road,
Cambridge CB2 2QQ, UK

Introduction

Despite many studies defining histological lesions of the placenta, the clinical significance of many of these lesions remains uncertain in many cases, particularly if occurring in uncomplicated pregnancies [1]. Guidelines suggest the submission of the placenta for histopathological examination in cases with specific maternal, fetal and neonatal indications [2, 3], and a range of placental histological lesions are well described in relation to high-risk groups identified by their adverse pregnancy outcomes [4, 5]. However, there is little data regarding the association between such placental histological lesions and placental

morphological characteristics such as shape, umbilical cord insertion site and cord coiling, and most studies are retrospective, reporting on clinically indicated examinations, whilst not examining those with normal outcomes. Hypercoiling of the umbilical cord has been reported in association with histologically proven thrombosis [6, 7], but limited data exist allowing the comparison of other placental features (umbilical cord coiling and measurements describing both umbilical cord insertion and placental shape) with other specific histological lesions. Studies have reported either a small number of cases in a preselected population, or have not provided quantitative data [8–10].

The aim of this study is to describe the relationship between morphological parameters of the placenta in an unselected reference population [10, 11] and the frequency of the most common categories of placental histological lesion, as identified according to generally accepted predefined standard descriptions [12].

Methods

This was a prospective study performed in a large maternity and neonatal unit offering care and delivery for 'low risk' pregnancies and those requiring tertiary services. The study was approved by the Cambridgeshire ethical committee (ref. no. 07/Q0106/51), and a written consent was obtained from the women taking part in the study. No attempt was made at selection by any maternal characteristics. Over a 13-month period, 2007–2008, women were approached in antenatal clinics and at other contacts before delivery with a written invitation for study inclusion.

Of 1,159 women with singleton pregnancy recruited for the study, 1,153 women were included who delivered at 34–43 weeks gestation.

Details of the methods are described elsewhere [10] and are abbreviated here. The placentas were examined grossly by the midwife as per the departmental protocols and placed in a double bagged and labelled within 20 min of delivery, which was kept in a dry, clean 1–2 l plastic container with an airtight lid and in a fridge with the temperature maintained at 4–6°C. The cord was then excised from the point of insertion into the chorionic plate; blood was drained from the placenta, and adherent blood clots were removed from the maternal surface of the placenta. All extraplacental membranes were trimmed from the chorionic plate, and the placenta was weighed on a fixed electronic scale.

We performed both manual and digital measurements. Digital measurements were performed using software image J following standard photography using a common protocol and scale for calibration [11]. Digital indices derived were cord centrality index and eccentricity. The umbilical cord coiling index was calculated using manual measurements only. Details of how these indices were calculated, are described previously [10, 11], but are outlined below:

The cord coiling index was calculated using an established method by dividing the number of coils by the length of the umbilical cord in centimetre [13]. The cord 'centrality-index' (CI) is the term used in this study to define how close or far the point of umbilical cord insertion is from the centre of the placenta. The greater the CI, the more peripheral the umbilical cord insertion is with 0 representing an absolutely central insertion and 1 representing a completely marginal insertion. The eccentricity index signifies the shape of the placenta, in other words, how deviant from circular it is, and is calculated as the ratio of the distance between the foci and the length of the major axis of the placenta. This varies from 0 to 1, with 0 representing a completely circular shape.

The placenta was examined, and blocks were obtained from membranes, umbilical cord and the full thickness of the placental parenchyma according to standard diagnostic protocols [1]. Three standard blocks were taken from the umbilical cord: maternal end, fetal end and from the centre of the cord. Three full-thickness central and one peripheral parenchymal blocks were taken. One block was taken 'en-face' from the maternal surface. Additional blocks were taken from any macroscopic abnormality. Histological examination of haematoxylin and eosin-stained sections was performed by two specialist paediatric pathologists (NJS/FAJ), who were completely blind to all clinical information, including gestational age at delivery and pregnancy outcome/course, the cases being identified by study number only. Histological lesions present were classified according to previously agreed criteria (Table 1). Pathological lesions were determined as 'present' or 'absent', not by their severity. In cases where there was presence of more than one histological lesion, each lesion was counted separately.

Specific histological subtypes predefined in this study included normal histology, ascending genital tract infection, chronic placental underperfusion, intervillous thrombus (IVT) and villitis of unknown aetiology (VUE), fetal thrombotic vasculopathy, massive perivillous fibrin deposition, features of pre-eclampsia, chronic histiocytic intervillositis, chorangiosis, chorangioma and abruption.

Statistical analysis

Statistical analysis was performed using SPSS software, version 15 (Statistical Package for Social Sciences software, Windows, version 15; Chicago IL, USA). Descriptive statistics of manual and digital measurements are presented.

Table 1 Diagnostic criteria for predefined histological categories

Diagnosis	Diagnostic criteria
Ascending genital tract infection	Any combination of: neutrophils in the fetal membranes, accumulating at the choriodecidual junction or umbilical cord
Chronic placental underperfusion	Small, hypovascular chorionic villi with increased syncytial knots, placental infarction >1 cm (non-peripheral) and/or atherosis
Intervillous thrombus	Localised, nodular and circumscribed old or recent thrombi within the intervillous space
Villitis of unknown aetiology	Morphologically increased chronic inflammatory cells affecting groups of chorionic villi in the absence of known clinical or histological aetiological factor/organisms (such as the TORCH group, enterovirus, varicella, syphilis, syphilitic spirochetosis, and other bacterial and protozoal infections)
Fetal thrombotic vasculopathy	Lesions of the placenta due to occlusion of the chorionic or major fetal villous stem artery by a thrombus, causing avascular distal villi
Chorangiosis	10 or more villi with 10 or more capillaries/villous cross section in 10 or lower power microscopic fields
Maternal pre-eclampsia	Included cases with fully developed atherosis only
Massive perivillous fibrin deposition	Significant deposition of perivillous fibrin involving more than 50% of the villous parenchyma
Chorangioma	A well-circumscribed, nodular lesion composed of vascular channels, stromal cells and surrounded by trophoblast
Chronic histiocytic intervillositis	Marked mononuclear histiocytic inflammatory cell infiltrate with associated fibrin deposition in the intervillous space without associated villitis or chorioamnionitis
Acute abruption	The presence of significant retroplacental haematoma or haemorrhage or clot with features of compression of the overlying parenchyma

The normality of each distribution was assessed for cord coiling, centrality and eccentricity indices for reference population, ascending genital tract infection, chronic placental underperfusion, intervillous thrombus and villitis of unknown aetiology groups, by analysing the spread of the distribution in each frequency histogram.

Descriptive statistics for the cord coiling, cord centrality and eccentricity indices in the reference population, ascending genital tract infection, chronic placental underperfusion, intervillous thrombus and villitis of unknown aetiology groups were performed. As the variables coiling index, cord centrality index and eccentricity showed an approximation to normal distributions, a parametric test (*t* test) was performed to compare the means of affected with non-affected cases. A p value of <0.05 was considered significant.

Results

Table 2 describes the maternal, neonatal, manual and digital placental characteristics. The defining criteria of the outcome groups (pre-eclampsia, pregnancy-induced hypertension, gestational diabetes and small for gestational age<10th centile) are defined elsewhere [10]. Of the 1,153 cases, histological examination data were available in 1,122 cases. Some placentas showed more than one histological lesion, and each placental lesion was counted separately.

Of 1,122 placentas from singleton pregnancies, the mean gestational age at delivery was 39.5 (34–43) weeks, and 72.3% ($n=809$) of cases showed no histological abnormalities. Three hundred thirty-eight placentas showed one or more histological lesion (Table 3). Histological subtypes for which analyses are presented were: ascending genital tract infection, chronic placental underperfusion, IVT and VUE. Fetal thrombotic vasculopathy ($n=11$), massive perivillous fibrin deposition ($n=5$), features of pre-eclampsia ($n=7$), chronic histiocytic intervillousitis ($n=3$), chorioangiosis ($n=9$), chorangioma ($n=4$) and abruption ($n=1$) occurred too infrequently to allow statistical analysis.

Digital measurements (cord centrality and eccentricity indices) were available for 887 placentas. Manual measurements (coiling index) were performed on 1,137 cases, as in 16 cases either the umbilical cord was missing or was too short to measure.

Table 4 describes the comparative morphological indices coiling index, centrality index and eccentricity in the reference population and in different histological lesion groups versus non-affected cases in each category.

Coiling index The difference between cases with normal histology (802) and those with abnormal histology ($n=308$) was significant ($p=0.02$), with relative hypercoiling. The mean coiling indices of those with ascending genital tract infection and chronic placental underperfusion were no different whilst cases with intervillous thrombus and villitis of unknown aetiology showed relative hypercoiling (greater coiling index) compared to non-affected cases ($p=0.024$ and $p=0.009$, respectively).

Table 2 Baseline maternal demographic and outcome data

	Number	
Maternal characteristics		
Maternal age (SD)	1,153	30.9 (5.73)
% Nulliparity (*n*)	1,148	48 (551)
% Smokers (*n*)	1,150	9.2 (106)
% Caucasians (*n*)	1,143	91.4 (1,045)
% Pre-eclampsia (*n*)	1,153	2.3 (27)
% Pregnancy-induced hypertension (*n*)	1,153	2.6 (30)
% Gestational diabetes (*n*)	1,153	4 (46)
% Small for gestational age (<10th percentile) (*n*)	1,153	9.3 (107)
Mean gestation age at delivery (SD)	1,153	39.5 (1.39)
% Emergency C/section	1,153	11.4 (131)
Neonatal characteristics		
Birth weight	1,153	3,488.7 (495)
% Males (*n*)	1,153	53.5 (617)
% Admissions to neonatal unit (*n*)	1,153	5.7 (66)
Manual measurements of placenta and cord		
Cord length (cm)	1,146	41.7 (14.27)
Cord coils	1,140	8.52 (4.89)
Placenta weight in grams (SD)	1,145	483.4 (99.77)
Digital measurements		
Placenta long axis (cm)	887	19.0 (2.46)
Placenta short axis (cm)	887	15.9 (1.87)
Distance of cord insertion from centre (cm)	887	3.35 (1.92)
Placenta circumference (cm)	887	54.8 (5.7)

Cord centrality index There was no significant difference in the cord centrality index between any of the groups of histological lesions in comparison to normal histology cases.

Eccentricity There was no difference in eccentricity between any of the groups of histological lesions in comparison to normal histology cases.

Table 3 Incidence of predefined common histological lesions in the study population

N=1,122[a]	
Pathology	% (*n*)
Normal histology	72.1 (809)
Ascending genital tract infection	11 (123)
Chronic placental underperfusion	7.2 (81)
Intervillous thrombus	4.7 (53)
Villitis of unknown aetiology	3.7 (42)
Other predefined histological groups	3.6 (40)

[a] Total number is>*n* (>100%), as some placentas had more than one histological lesion, and each histological lesion has been counted separately

The frequency histograms of the coiling index, centrality index and eccentricity for all pathological variables including the reference population are shown in Figs. 1, 2 and 3. The frequency histograms for coiling index, centrality index and eccentricity for all histological groups showed a normal distribution.

Discussion

The findings of this study have described the pattern of common histological lesions seen in a completely unselected population on singleton pregnancies delivered at or near term, as identified by specialist placental pathologists who were completely blinded to all clinical information to minimise interpretive bias; reported lesions were based on predefined criteria. The findings demonstrate that there is no relationship between placental shape or umbilical cord insertion position and histological features, for the most commonly encountered histological groups. There is, however, a statistically significant association between hypercoiling of the umbilical cord and placentas demonstrating VUE or IVT. Comparison of these data with other studies is difficult since most are based on selected populations and non-blinding of pathologists to the clinical information.

Table 4 Morphological indices per histological lesion group

	Coiling index (SD)	*p* value (comparison with non-affected cases)	Centrality index (SD)	*p* value (comparison with non-affected cases)	Eccentricity (SD)	*p* value (comparison with non-affected cases)
Reference population	0.20 (0.10) (*n*=1,137)	N/A	0.36 (0.21) (*n*=887)	N/A	0.49 (0.18) (*n*=887)	N/A
Normal histology	0.20 (0.10) (*n*=802)	N/A	0.36 (0.21) (*n*=614)	N/A	0.48 (0.18) (*n*=614)	N/A
Ascending genital tract infection	0.20 (0.09) (*n*=122)	0.45	0.37 (0.23) (*n*=98)	0.64	0.52 (0.17) (*n*=98)	0.07
Chronic placental underperfusion	0.21 (0.11) (*n*=80)	0.31	0.32 (0.21) (*n*=68)	0.10	0.48 (0.19) (*n*=68)	0.76
IVT	0.23 (0.10) (*n*=53)	0.02	0.34 (0.20) (*n*=33)	0.52	0.54 (0.16) (*n*=33)	0.07
VUE	0.24 (0.10) (*n*=39)	0.009	0.35 (0.23) (*n*=33)	0.75	0.47 (0.15) (*n*=33)	0.59

With few exceptions, there has been little attempt at objectively defining placental morphological indices in relation to histological features. Secondly, there is little or no consensus amongst clinicians and pathologists as to the relationship between perinatal outcome with certain placental histological features, specific placental histological features with placental morphology and placental morphology with perinatal outcome, especially in low-risk groups, in whom placentas are not routinely examined. There remain considerable discrepancies in the diagnosis of placental disease, and it is common for general surgical pathologists not to recognise placental lesions that may have clinical relevance [14, 15].

A recent literature has highlighted the methodological difficulties in deriving and reproducing umbilical cord coiling index [16]. However, the abnormal coiling of the cord has been reported in association with adverse perinatal outcomes such as preterm delivery, fetal death, low Apgar score and IUGR [17–19]. Abnormal cord coiling is also described in relation to certain histopathological findings including thrombosis of chorionic plate vessels, umbilical venous thrombosis and umbilical cord stenosis [6]. We report a significant, but small, difference in the cord coiling index in cases of abnormal histology notably with IVT and VUE showing relative hypercoiling. The clinical significance of this finding remains uncertain, but it is difficult to postulate a plausible mechanism whereby both of these apparently unrelated histological features are causally related to cord coiling.

Hypercoiling has previously been associated with adverse pregnancy and neonatal outcomes. It has been suggested that abnormal cord coiling is a chronic state established in early gestation with effects on fetal well-being [6]. Intervillous thrombus appears to be usually incidental but can occasionally have detrimental effects on the fetus, if there is either large or multiple thrombi, in association with significant feto–maternal haemorrhage. Villitis of unknown aetiology is one of the more commonly found placental lesions and has been reported in association with recurrent reproductive failure [20–23], perinatal asphyxia [24] and adverse fetal neurological outcomes [25]. However, there are no previous data suggesting an association of VUE and abnormal cord coiling and its significance; if any, it is uncertain.

Central and eccentric cord insertions account for more than 90% of cord insertions and have no clinical importance. Marginal and velamentous cord insertions are theoretically more susceptible to vessel rupture [26] and have been described in association with an increased incidence of miscarriage, fetal growth restriction, preterm delivery, fetal hypoxia, intra-uterine and neonatal death though there remains no consensus on whether these outcomes are truly associated [27–31]. The classification of the umbilical cord insertion has been qualitative/descriptive in most studies and hence may carry subjective error particularly in cases of adverse perinatal outcome, where small numbers of cases have been described. Umbilical cord insertion has been variously defined as how far the insertion point is located from the centre of the placenta or how close is the umbilical cord insertion from the chorionic plate margin [9]. The distance of the umbilical cord insertion from the centre has been proposed as a useful clinical marker of placental insufficiency [32, 33].

We have proposed that the distance of the umbilical cord insertion from the centre (or from the chorionic plate margin) is quantified in order to obtain reproducible results [10, 11]. In this study, the measurement to describe the relationship of the cord insertion with the centre of the placenta is defined as cord centrality index. We found no

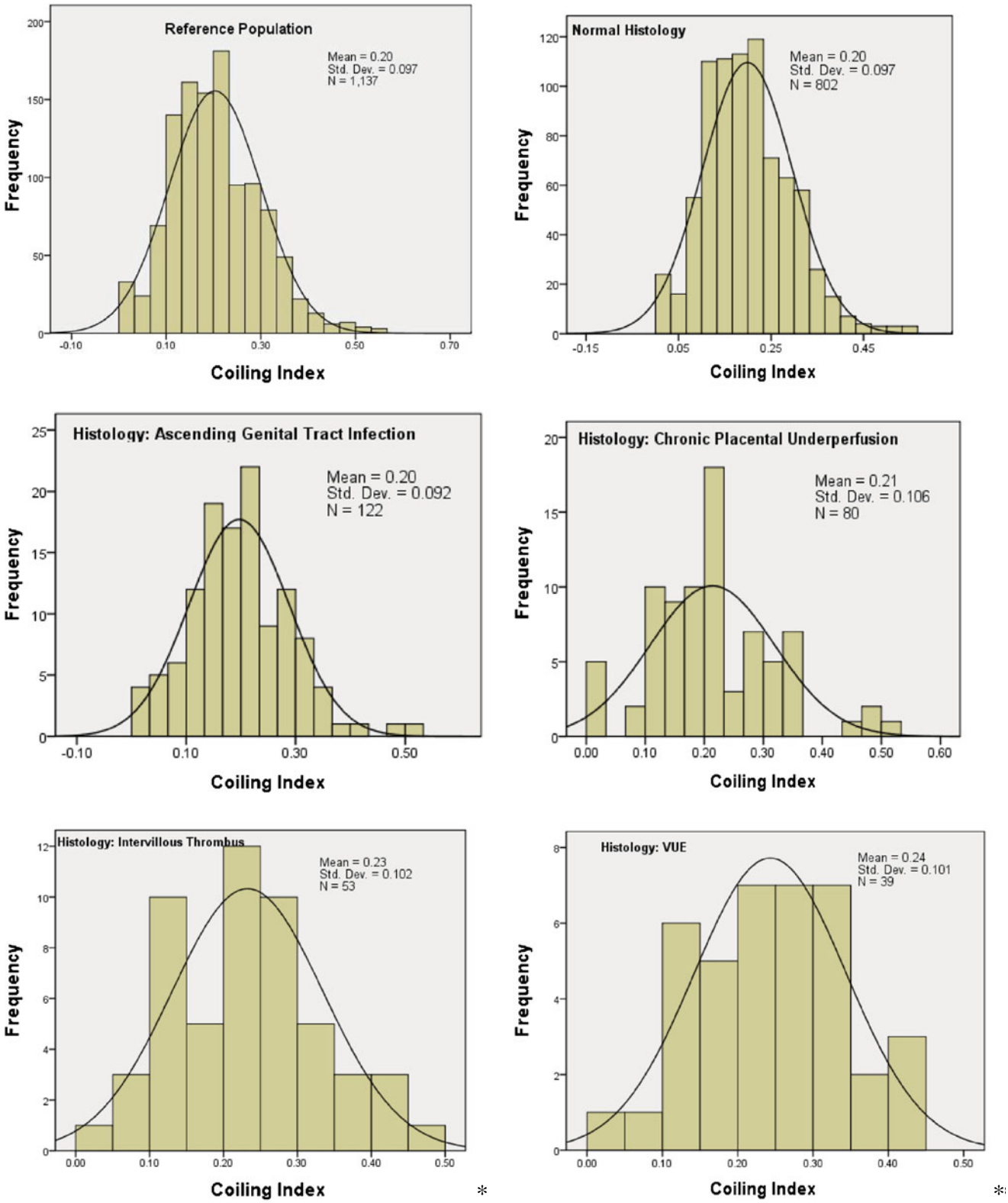

*Significant difference of coiling index as compared to non-affected cases.

Fig. 1 Frequency histograms for coiling index for all pathological variables

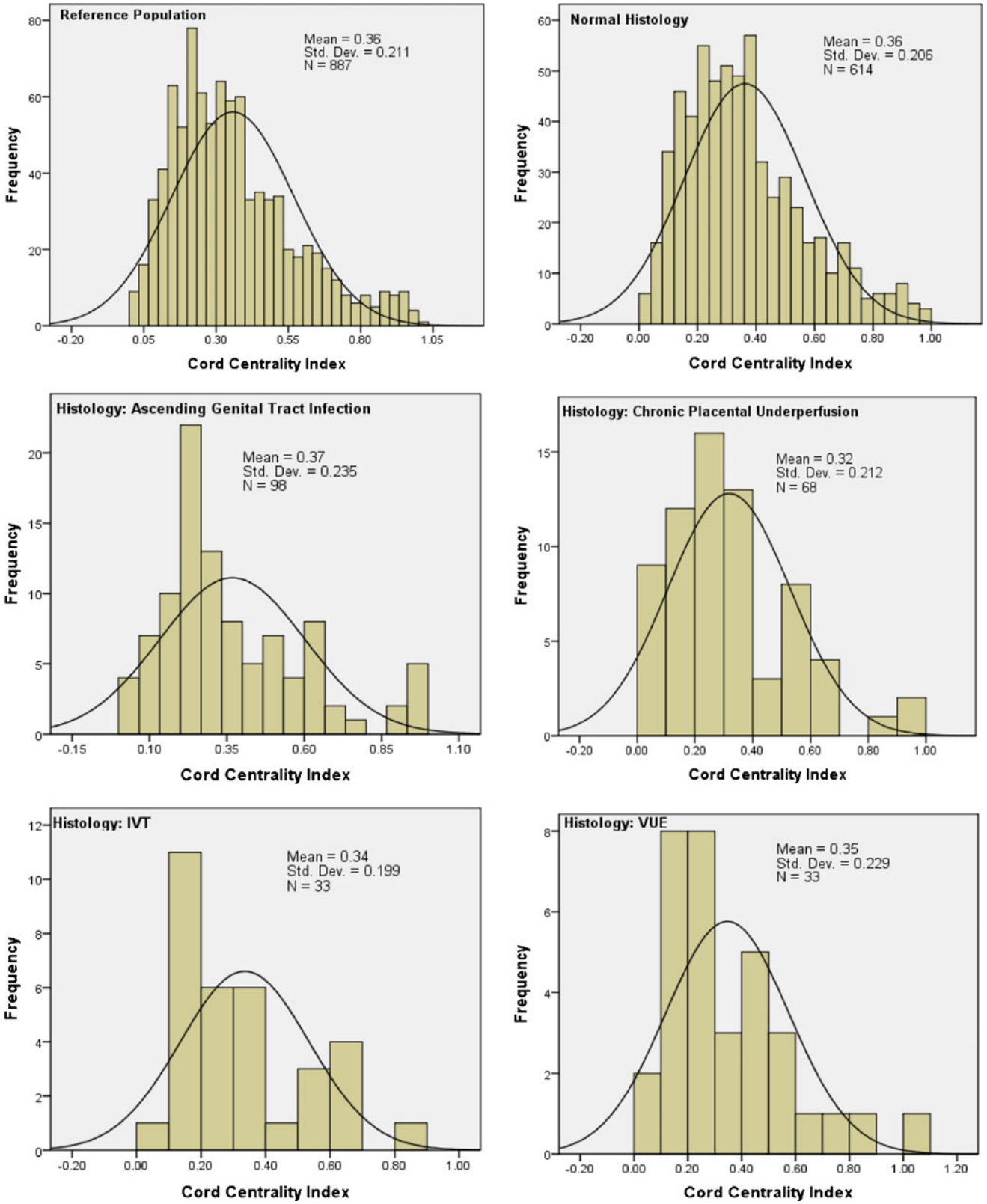

Fig. 2 Frequency histograms for cord centrality index for all pathological variables

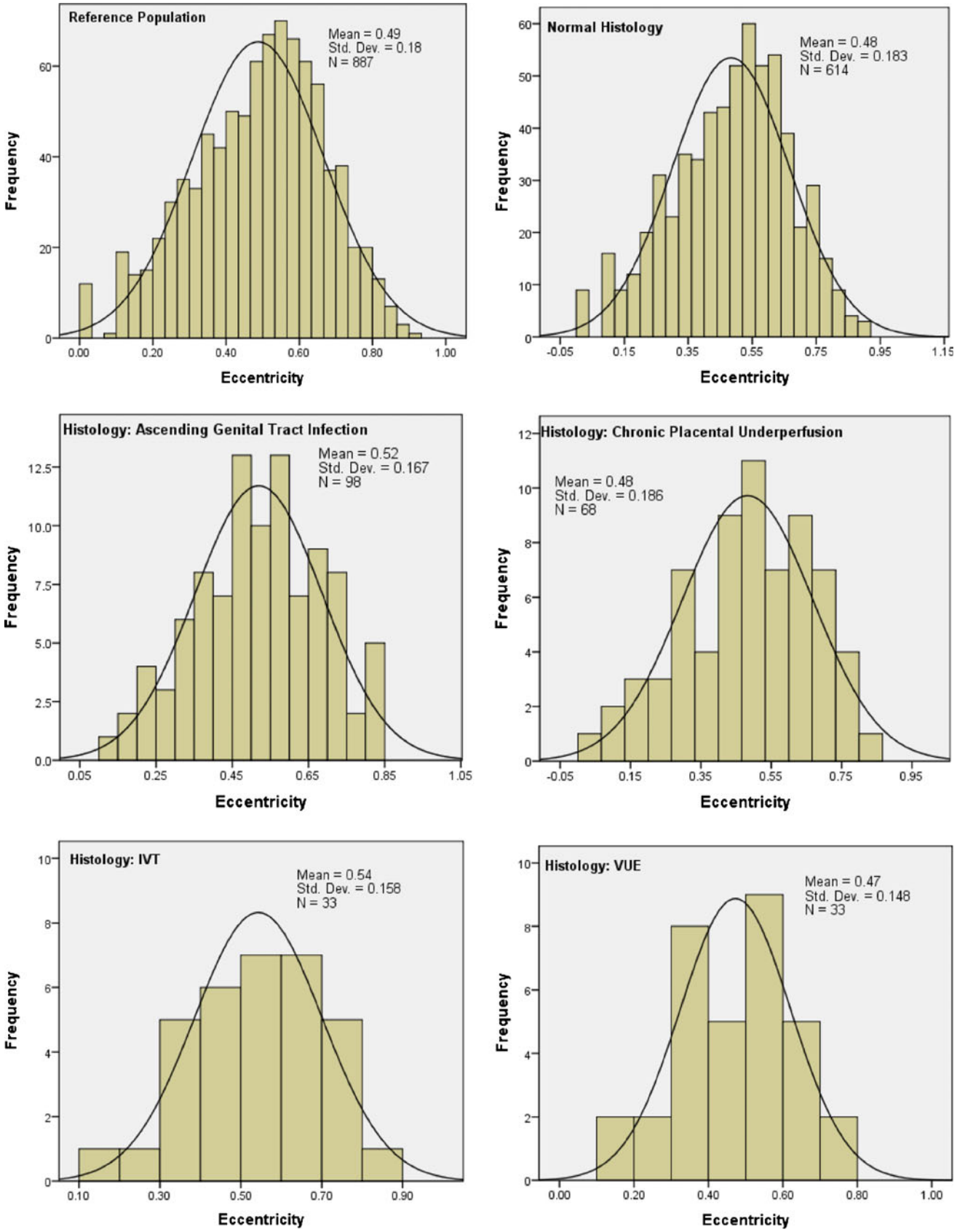

Fig. 3 Frequency histograms for placental eccentricity for all pathological variables

differences in cord centrality index between groups and therefore conclude that cord centrality has no significant association with these histological lesions [10].

It has been postulated that placental shape has an association with perinatal outcome; 'abnormal' shapes have been reported with placental abruption, preterm delivery, oligohydramnios and even fetal death [34, 35]. The shape of the placenta may closely mirror the pattern of chorionic vascular growth; studies modelling the placenta vascular tree have suggested that irregular shapes of placenta are common and associated with low birth weight [8]. The placental shape (defined in our study as the eccentricity index—its 'ovalness' or 'roundness'), showed no relationship with histological findings.

The major strengths of this study are that women were recruited prospectively from an unselected singleton population, and that histological examination was performed by specialist pathologists who were blinded to all clinical details and outcome of the pregnancy, minimising bias. The indices derived allow comparison of a continuous variable, namely a distribution, rather than relying on the qualitative descriptors of cord coiling, cord insertion and placental shape. This allows a much more powerful analysis than has hitherto been described—that of comparing distributions.

A potential weakness is that a relationship between morphology and histological group may exist where we find no significance due to the modest number of cases in the abnormal histology groups, though the numbers in these groups that we report generally exceed those of previous studies. Furthermore, in common with other authors, we are unable to advance a biologically plausible explanation for the association between hypercoiling of the cord and IVT.

To our knowledge, the effect of and/or association between specific histological lesions and the morphological characteristics of the placenta has not been described in an unselected population, using quantitative measurements and strict histological criteria combined with blinded histological review. We report that certain common histological lesions show a statistical association with umbilical cord coiling, but most histological abnormalities are completely unrelated to placental macroscopic features such as shape, (eccentricity index) or cord insertion point (centrality index). Macroscopic abnormalities of placental shape and cord insertion do not, therefore, predict the presence or absence of histological features and would appear to be of limited clinical significance in this population.

Acknowledgement SP's salary was in part funded through Cambridge Fetal Care and Pathology costs through a grant from Addenbrooke's Charitable Trust.

Conflict of interest We declare that we have no conflict of interest.

References

1. Fox H, Sebire NJ (2007) Pathology of the placenta. W.B. Saunders, London
2. Hargitai B, Marton T, Cox PM (2004) Best practice no 178. Examination of the human placenta. J Clin Pathol 57:785–792
3. Langston C, Kaplan C, Macpherson T, Manci E, Peevy K, Clark B, Murtagh C, Cox S, Glenn G (1997) Practice guideline for examination of the placenta: developed by the Placental Pathology Practice Guideline Development Task Force of the College of American Pathologists. Arch Pathol Lab Med 121:449–476
4. Roberts DJ, Post MD (2008) The placenta in pre-eclampsia and intrauterine growth restriction. J Clin Pathol 61:1254–1260
5. Redline RW (2008) Placental pathology: a systematic approach with clinical correlations. Placenta 29(Suppl A):S86–S91
6. Machin GA, Ackerman J, Gilbert-Barness E (2000) Abnormal umbilical cord coiling is associated with adverse perinatal outcomes. Pediatr Dev Pathol 3:462–471
7. De Laat MW, Van Alderen ED, Franx A, Visser GH, Bots ML, Nikkels PG (2007) The umbilical coiling index in complicated pregnancy. Eur J Obstet Gynecol Reprod Biol 130:66–72
8. Yampolsky M, Salafia CM, Shlakhter O, Haas D, Eucker B, Thorp J (2008) Modeling the variability of shapes of a human placenta. Placenta 29:790–797
9. Coall DA, Charles AK, Salafia CM (2009) Gross placental structure in a low-risk population of singleton, term, first-born infants. Pediatr Dev Pathol 12:200–210
10. Pathak S, Hook E, Hackett G, Murdoch E, Sebire NJ, Jessop F, Lees C (2010) Cord coiling, umbilical cord insertion and placental shape in an unselected cohort delivering at term: relationship with common obstetric outcomes. Placenta 31:963–968
11. Pathak S, Jessop F, Hook L, Sebire NJ, Lees CC (2010) Placental weight, digitally derived placental dimensions at term and their relationship to birth weight. J Matern Fetal Neonatal Med 23:1176–1182
12. Kraus FT, Redline RW, Gersell DJ, Nelson DM, Dicke JM (2004) Placental pathology. American Registry of Pathology, Washington, DC
13. Strong TH Jr, Jarles DL, Vega JS, Feldman DB (1994) The umbilical coiling index. Am J Obstet Gynecol 170:29–32
14. Khong TY, Gordijn SJ (2003) Quality of placental pathology reports. Pediatr Dev Pathol 6:54–58
15. Sun CC, Revell VO, Belli AJ, Viscardi RM (2002) Discrepancy in pathologic diagnosis of placental lesions. Arch Pathol Lab Med 126:706–709
16. Khong TY (2010) Evidence-based pathology: umbilical cord coiling. Pathology 42:618–622
17. Sebire NJ (2007) Pathophysiological significance of abnormal umbilical cord coiling index. Ultrasound Obstet Gynecol 30:804–806
18. De Laat MW, Franx A, Nikkels PG, Visser GH (2006) Prenatal ultrasonographic prediction of the umbilical coiling index at birth and adverse pregnancy outcome. Ultrasound Obstet Gynecol 28:704–709
19. Strong TH Jr, Finberg HJ, Mattox JH (1994) Antepartum diagnosis of noncoiled umbilical cords. Am J Obstet Gynecol 170:1729–1731, Discussion, 1731–3
20. Becroft DM, Thompson JM, Mitchell EA (2005) Placental villitis of unknown origin: epidemiologic associations. Am J Obstet Gynecol 192:264–271
21. Russell P, Atkinson K, Krishnan L (1980) Recurrent reproductive failure due to severe placental villitis of unknown etiology. J Reprod Med 24:93–98

22. Redline RW, Patterson P (1994) Patterns of placental injury. Correlations with gestational age, placental weight, and clinical diagnoses. Arch Pathol Lab Med 118:698–701
23. Oliveira LH, Xavier CC, Lana AM (2002) Changes in placental morphology of small for gestational age newborns. J Pediatr (Rio J) 78:397–402
24. Salafia CM, Minior VK, Lopez-Zeno JA, Whittington SS, Pezzullo JC, Vintzileos AM (1995) Relationship between placental histologic features and umbilical cord blood gases in preterm gestations. Am J Obstet Gynecol 173:1058–1064
25. Redline RW, O'riordan MA (2000) Placental lesions associated with cerebral palsy and neurologic impairment following term birth. Arch Pathol Lab Med 124:1785–1791
26. Heifetz SA (1996) The umbilical cord: obstetrically important lesions. Clin Obstet Gynecol 39:571–587
27. Brody S, Frenkel DA (1953) Marginal insertion of the cord and premature labor. Am J Obstet Gynecol 65:1305–1312
28. Hathout H (1964) The vascular pattern and mode of insertion of the umbilical cord in abortion material. J Obstet Gynaecol Br Commonw 71:963–964
29. Monie IW (1965) Velamentous insertion of the cord in early pregnancy. Am J Obstet Gynecol 93:276–281
30. Heinonen S, Ryynanen M, Kirkinen P, Saarikoski S (1996) Velamentous umbilical cord insertion may be suspected from maternal serum alpha-fetoprotein and hCG. Br J Obstet Gynaecol 103:209–213
31. Uyanwah-Akpom P, Fox H (1977) The clinical significance of marginal and velamentous insertion of the cord. Br J Obstet Gynaecol 84:941–943
32. Viero S, Chaddha V, Alkazaleh F, Simchen MJ, Malik A, Kelly E, Windrim R, Kingdom JC (2004) Prognostic value of placental ultrasound in pregnancies complicated by absent end-diastolic flow velocity in the umbilical arteries. Placenta 25:735–741
33. Whittle W, Chaddha V, Wyatt P, Huppertz B, Kingdom J (2006) Ultrasound detection of placental insufficiency in women with 'unexplained' abnormal maternal serum screening results. Clin Genet 69:97–104
34. Costa SL, Proctor L, Dodd JM, Toal M, Okun N, Johnson JA, Windrim R, Kingdom JC (2008) Screening for placental insufficiency in high-risk pregnancies: is earlier better? Placenta 29:1034–1040
35. Suzuki S (2008) Clinical significance of pregnancies with circumvallate placenta. J Obstet Gynaecol Res 34:51–54

Virchows Arch (2011) 459:21–29
DOI 10.1007/s00428-011-1082-1

ORIGINAL ARTICLE

The cadherin switch in ovarian high-grade serous carcinoma is associated with disease progression

Livia Quattrocchi · Andrew R. Green · Stewart Martin · Lindy Durrant · Suha Deen

Received: 3 January 2011 / Revised: 7 March 2011 / Accepted: 4 April 2011 / Published online: 21 April 2011
© Springer-Verlag 2011

Abstract Ovarian high-grade serous carcinoma (HGSC) often has a poor prognosis because of late presentation, lack of sensitivity and specificity of screening modalities and the development of chemoresistance. New targeted therapy is required if survival in these cases is to improve. The profile of E-, P- and N-cadherins in ovarian cancer and its association with survival remain poorly understood. Reduced expression of E-cadherin in prostate cancer associated with increase in the expression of N- and P-cadherins is described as cadherin switch. We hypothesised that there is a switch in the expression of cadherins that regulates the behaviour of HGSC and possibly its outcome. To identify the stages of the cadherin switch in HGSC, we studied the immunoexpression of E-, P- and N-cadherins in a cohort of 177 cases of HGSC. High expression of P-cadherin was associated with poor patient survival and was significantly higher in stage 2 disease when compared with stage 1 and stage 3 disease (P=0.033). In contrast, loss of E-cadherin was observed in stage 3 HGSC when compared with other stages (P=0.050). E-, P- and N- cadherin expressions were significantly associated with disease outcome when assessed individually and in various combinations with an interesting profile. Our results indicate that the cadherin switch alters through progression of HGSC. The profile of combined cadherin expressions in association with survival raises expectations in targeted therapy.

Keywords Ovary · Cadherin · Cancer · Metastasis

L. Quattrocchi · S. Deen (✉)
Department of Histopathology,
Nottingham University Hospitals NHS Trust,
Queen's Medical Centre Campus,
Nottingham NG7 2UH, UK
e-mail: sdeen@doctors.org.uk

A. R. Green
Division of Clinical Pathology,
School of Molecular Medical Sciences,
University of Nottingham,
Nottingham NG5 1 PB, UK

S. Martin · L. Durrant
Division of Clinical Oncology,
School of Molecular Medical Sciences,
University of Nottingham, City Hospital Campus,
Nottingham NG5 1 PB, UK

Introduction

Ovarian high-grade serous carcinoma (HGSC) has a very poor 5-year survival rate of 30% because of its late presentation with tumour spread in the peritoneal cavity and resistance to chemotherapy [1]. Currently, there are no diagnostic methods to stratify patients according to their prognosis or response to therapy. Tumour spread and metastasis are complex processes that depend on active interaction between tumour cells and the tumour microenvironment.

In carcinogenesis, E-cadherin appears to play a key role in suppressing invasion and metastasis and is considered to be a late tumour suppressor [2]. It acts by maintaining intercellular adhesion amongst well-differentiated malignant cells [3]. It is suggested that cells showing reduced expression of E-cadherin undergo anoikis (cell death caused by disruption of cell–cell adhesion) [4]. Reduced expression of E-cadherin in poor prognostic prostate cancer with associated increased expression of N-cadherin has been described as cadherin switch [5]. Recent evidence suggests that a gain of expression of N-cadherin is associated with increased invasive potential in carcinomas of the breast, prostate and pancreas [5–8]. For example, over expression

of N-cadherin in E-cadherin-expressing breast cancer cells caused an increase in their invasive and metastatic potential [6], despite the vital role of E-cadherin in suppression of invasion and metastasis [2–4, 9]. There is conflicting evidence regarding the role of P-cadherin in carcinogenesis with increased P-cadherin expression associated with poor survival in breast and ovarian cancer [10–12] or with better survival [13].

Compared with E-cadherin, much less is understood about the role of N-cadherin in the metastasis of ovarian cancer. To date, no significant relationship between N-cadherin expression and ovarian cancer progression has been established [4]. A substantial increase in P-cadherin is seen in ovarian tumours indicates that P-cadherin may play a role in carcinogenesis and/or progression [10]. However, no previous studies have been performed on the role of this adhesion molecule in relation to overall survival or recurrence of ovarian tumours. Compared with stage 1 ovarian cancer, it has been reported that stage 2 disease showed upregulation of P-cadherin together with reduced E-cadherin expression [10]. Furthermore, there are relatively few studies to date on the cadherin switch in ovarian cancer with extremely scanty literature to explain the dysregulation of the repertoire of cadherins in metastatic foci.

In this study, we hypothesised that there is a switch in the expression of cadherins that regulates the behaviour of tumour cells in HGSC and possibly the disease outcome. To elucidate the cadherin profile expression in HGSC, 177 cases of HGSC were studied and immunostained with E-, P- and N-cadherins with further identification of distinct stages of the cadherin switch correlating with overall and progression-free survival.

Materials and methods

Patient cohort and clinicopathological variables

Archival paraffin-embedded tissue blocks from 177 patients, age range 36–86 (mean, 60) years, with HGSC dating back to January 1, 1991 to December 31, 2007 were used. All patients were treated with surgery in an attempt to achieve optimal debulking (where residual tumour was less than 2 cm) at Nottingham University Hospitals. Surgery included total abdominal hysterectomy with bilateral salpingo-oophorectomy and omentectomy or unilateral or bilateral oophorectomy with or without omentectomy with 52% optimal debulking. Chemotherapy was used when indicated as per local protocol. The reporting of this study adheres to the RECIST guidelines [14]. Information on disease FIGO (The International Federation of Gynecology and Obstetric) stage and presence (less or more than 2 cm) or absence of residual disease after surgery, date of recurrence and tumour-related death was collected (Table 1). Disease-specific survival was calculated from the date of surgery to August 2009 when any remaining survivors were censored.

Overall survival and progression-free survival

Overall survival data were available for 167 patients with a median of 29 months. Throughout the period of follow-up, 58% of patients had died at the time of conducting this study with an overall survival between 1 and 189 months. For the purpose of statistical assessment, the most recent case included had a follow-up of 36 months, and therefore the survival calculation was limited to 36 months survival for all patients for consistent assessment. Post-operative deaths were excluded. Data for progression-free survival was also calculated for 36 months and defined from the date of commencing chemotherapy or surgical treatment depending which one was the first treatment approach until the date when recurrence was confirmed clinically. The database was audited to ensure validity; there were no major discrepancies with >97% of data available.

All cases were subsequently reviewed by a specialist gynaecological pathologist (SD) to ensure accuracy of histologic type and grade. To build tissue microarray blocks, for each of the 177 patients, three tumour samples from different parts of the ovarian tumour mass were used to compensate for tumour heterogeneity.

Tissue microarray construction

All resection specimens were routinely fixed in 10% buffered formalin overnight and embedded in paraffin wax. The tissue microarrays (TMAs) were constructed first as outlined by Kononen et al. [15] from the original

Table 1 Patient and tumour characteristics

	Frequency (%)
FIGO stage	
I	28 (17)
II	19 (12)
III	99 (60)
IV	18 (11)
Macroscopic residual disease	
Absent	49 (37)
Less than 2 cm	19 (15)
More than 2 cm	62 (48)
Adjuvant therapy	
No	10 (8)
Yes	116 (92)

formalin-fixed paraffin-embedded blocks after selecting the areas of interest on the matching slide stained with haematoxylin and eosin. Four-micrometre sections of the TMA block were cut not more than 2 weeks before staining and placed on glass slides (Surgipath Ltd, Xtra adhesive) prior to immunohistochemistry bearing in mind that it has been demonstrates that many proteins retain their antigenicity for more than 60 years [16, 17].

Immunohistochemisty

The Dako REAL™ EnVision™ kit (Dako Ltd, Denmark) was used for immunohistochemical staining which was performed manually. Optimization of the staining was done on ovarian cancer whole-section mounts representing older and more recent cases and using a range of incubation times. The TMA sections were incubated at 60°C for 10 min to ensure firm adherence of the section to the slide. Sections were deparaffinized by immersing in two sequential xylene baths for 5 min each and rehydrated by immersing in three sequential 100% alcohol baths for 20 s each. Slides were washed in running tap water and incubated for 5 min with Peroxidase Block (DAKO Ltd) to block endogenous peroxidase activity. To retrieve antigenicity, sections were microwaved (1,000 W) in pH 6.0 citrate buffer for 20 min. Slides were immediately flooded with running tap water to stop the retrieval process, rinsed with Tris-buffered saline (TBS) pH 7.6. To reduce nonspecific adsorption of antibodies to tissue, the slides were incubated for 5 min with normal swine serum (diluted 1/5 in TBS). Sections were incubated with the primary antibody (Dako mouse anti-E-cadherin clone NCH-38 with 1:25 dilution, Invitrogen mouse anti-N-cadherin clone 3B9 with 1:25 dilution, Novocastra mouse anti-P-cadherin clone NCL-P-Cad with 1:10 dilution) at room temperature for 30 min under optimised conditions. After washing with TBS, sections were incubated for 30 min with EnVision A solution. The sections were rinsed with TBS and incubated for 6 min with freshly prepared EnVision C solution. After rinsing with TBS, sections were counterstained with fresh haematoxylin (DAKO Ltd) for 6 min, rinsed with tap water, dehydrated in three sequential 100% alcohol baths for 20 s each, and cleared in two sequential xylene baths, before mounting the slides. Positive control tissues for each antibody, selected according to the manufacturer's instructions (appendix used for E-cadherin, pancreatic tissue for N-cadherin and breast tissue for P-cadherin), were also stained.

Evaluation of the staining

High-resolution digital images at ×20 magnification of the immunohistochemically stained TMA were obtained (Nanozoomer, Hamamatsu Photonics) and assessed. Individual cores were assessed using H-scoring [18], where only staining of the invasive malignant cells within the tissue cores was considered. The H-score value ranged from 0 to 300, calculated as the sum of the products of percentage of positive cells multiplied by staining intensity graded from 1+ to 3+. The predominant subcellular localization was determined: cytoplasmic expression for N- and P-cadherins, membranous immunoreactivity for E-cadherin.

For each TMA, three copies were analysed. The validity of this technique has been repeatedly enforced by publication and especially in ovarian tumours where analysis of immunohistochemical markers in a two cores from each case provided sufficient information to represent similar results to those from whole sections [19]. An average of the three H-score figures was calculated. A tumour was not scored if fewer than 100 tumour cells were present in a core. All cores were assessed by two of the authors (SD, LQ) independently, both of whom were blinded to the clinical and pathologic variables of the case. When there was non-concordance in assessment, cases were discussed using a double-headed microscope, and a consensus was reached. Determination of the optimal cutoff points for the markers, based on overall survival, was assessed using X-tile Bioinformatics Software, version 3.6.1, 2003–2005 (Yale University, USA) [20]. The X-tile Bioinformatics Software derives an optimised cutoff by choosing the value that best correlates with survival data.

Statistical analysis

The statistical software package SPSS Version 16, (SPSS Inc., Chicago, IL, USA) was used to analyse the possible correlation between cadherin expression and clinicopathological parameters, using Pearson's χ^2 test. Survival analysis comparing protein expression and overall survival was calculated using the Kaplan–Meier method, and the statistical significance of the difference between the survival curves of evaluated groups was assessed using the logrank test. Multivariate analysis was performed using Cox regression. In all cases, a P value of <0.05 indicated statistical significance.

Results

This study illustrated the profile of cadherin switch in HGSC with a significantly reduced expression of E-cadherin between FIGO stage 2 and 3 and significantly increased expression of P-cadherin between FIGO stage

1 and 2. Tumours with two out of three cadherins showing poor prognostic expression had the worst disease outcome when compared with those with only one out of three cadherins showing poor prognostic expression.

E-Cadherin

Assessment of the TMA cores showed that E-cadherin staining was predominant within the cell membrane (Fig. 1) with no cytoplasmic or nuclear staining. There was no staining of the inflammatory cells, stromal cells or endothelial cells. A total of 165 cases were available for assessment. A total of three cases (2%) showed complete lack of staining, with the remaining 98% showing a range of staining with H-score ranging from 5 to 290 (mean, 110; median, 98; Fig. 1). Using the X-tile software, an H-score of 30 was used as a cutoff point between low (18 cases, 11%) and high (144 cases, 89%) intensity of E-cadherin expression.

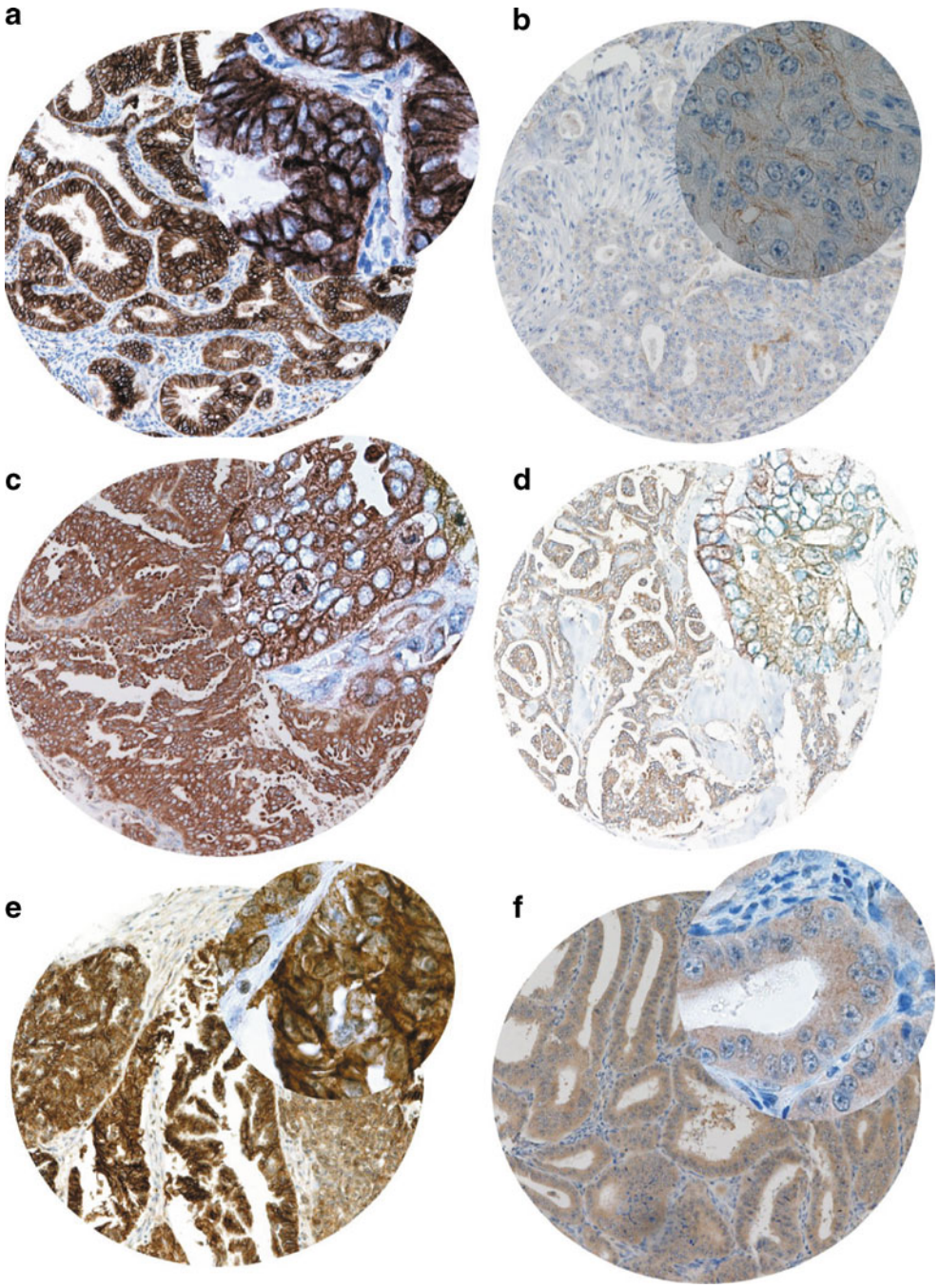

Fig. 1 Immunohistochemical analysis of cadherins. Cores from HGSC showing high (**a**) and low (**b**) expression of E-cadherin staining. Cores from HGSC showing high (**c**) and low (**d**) expression of P-cadherin staining. Cores from HGSC showing high (**e**) and low (**f**) expression of N-cadherin staining. ×50 magnification, *inset* ×200

Expression of E-cadherin in relation to overall survival and progression-free survival

The expression of E-cadherin was significantly positively correlated with overall survival (log rank 6.983, $P=0.008$) and progression-free survival of 36 months (logrank 19.675, $P=0.000$ (Fig. 2) with high expression predicting an improved overall survival (mean=19 and 27 months for low and high intensity, respectively) and progression-free survival (9 and 23 months for low and high intensity, respectively; Fig. 2a).

P-Cadherin

P-Cadherin staining was predominantly within the cytoplasm without significant nuclear staining. Plasma cells, neutrophils and macrophages were also stained positively. In addition, endothelial cells lining small vascular spaces

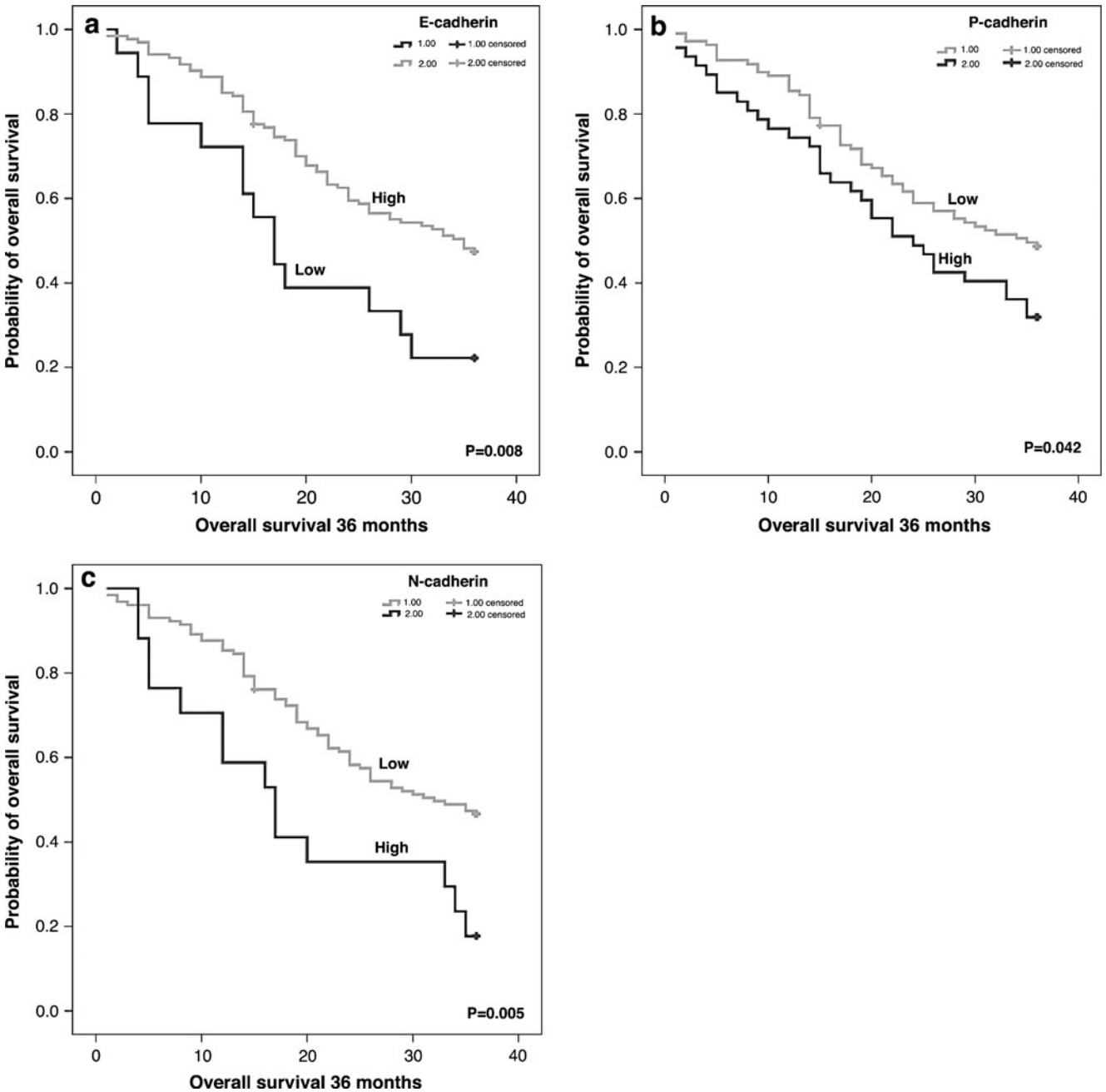

Fig. 2 Kaplan–Meier overall survival for patients with HGSC for E- (**a**), P-(**b**) and N-(**c**) cadherins

showed cytoplasmic staining. A total of 167 cores were available for scoring. All cores were positive with H-score values ranging from 35 to 280 (mean, 167; median, 168; Fig. 1). Using X-tile software, the expression was categorised as low and high expression with 200 as a cutoff point for the H-score data (121 cases (72%) in the low expression group and 46 cases (28%) in the high expression group).

Expression of P-cadherin in relation to overall survival and progression-free survival

Negative correlation between P-cadherin expression and 36-month overall survival was significant (logrank 4.146, P=0.042) with a mean of 26 and 23 months for low and high expression, respectively. Conversely, there was no significant association between P-cadherin expression and 36-month progression-free survival (Fig. 2b).

N-Cadherin

Staining of N-cadherin was predominantly within the cytoplasm with no significant nuclear staining. Plasma cells, macrophage and some stromal and endothelial cells also stained positively. One hundred fifty-eight cases were available for scoring. Two cases (1%) were negative, showing complete lack of staining, leaving 156 cases positive (99%) with H-score ranging from 10 to 250 (mean 115, median 114; Fig. 1). Using X-tile software, the expression was categorised as low and high intensity using an H-score of 190 as a cutoff point (90% of cases in the low expression group and 10% of cases in the high expression group).

Expression of N-cadherin in relation to overall survival and progression-free survival

A significant inverse correlation between N-cadherin expression and 36-month overall survival (logrank 7.784, P=0.005) with 26 and 19 months for the low and high expression groups, respectively, was observed. Moreover, there was a significant negative association between high expression of N-cadherin and progression-free survival (logrank 6.696, P=0.010) with 22 and 13 months for the low and high expression groups (Fig. 2c).

Using multivariate analysis, despite the fact that cadherins were significantly associated with overall survival, these univariate associations were not strong enough to compete with stage and residual disease, the two main independent prognostic factors.

Correlation of E-, P- and N-cadherins

Using the Spearman correlation test, there was a significant positive correlation between high P-cadherin and N-cadherin expression with low correlation coefficient (correlation coefficient 0.173, P=0.029) and a negative correlation between high E-cadherin and low N-cadherin expression with low correlation coefficient (−0.251, P=0.001).

Defining the point of switching of adhesion molecules expression: the cadherin switch

Using the χ^2 test, and unlike P-cadherin, there was a significant association between E- and N-cadherins and tumour stage (P=0.050, χ^2=7.816 and P=0.038, χ^2=8.428 respectively; Fig. 3).

To identify possible points in the switch of cadherin expression in different stages of the disease, the expression of individual cadherins was compared in the transition between stage 1 and 2 and between stage 2 and 3 tumours.

Unlike E- and N-cadherins, there was a significantly higher expression of P-cadherin in stage 2 compared with stage 1 tumours (P=0.033, χ^2=4.528) with 15% of stage 1 tumours (4/26) showing high expression of P-cadherin and 44% of stage 2 tumours (8/18) showing high expression.

Comparing stage 2 and 3 disease, E-cadherin showed a significantly reduced expression in stage 3 (P=0.050, χ^2= 3.855) compared with stage 2 disease with 18% of cases showing low expression (16/88) whereas none of the cases in stage 2 showed low expression. High expression of N-cadherin was seen in 14 cases of stage 3 disease (14%), whereas none of the cases in stage 2 disease showed high expression of N-cadherin. However, the difference was not statistically significant (Pvalue=0.08). On the other hand, there was no significant change in the expression of P=

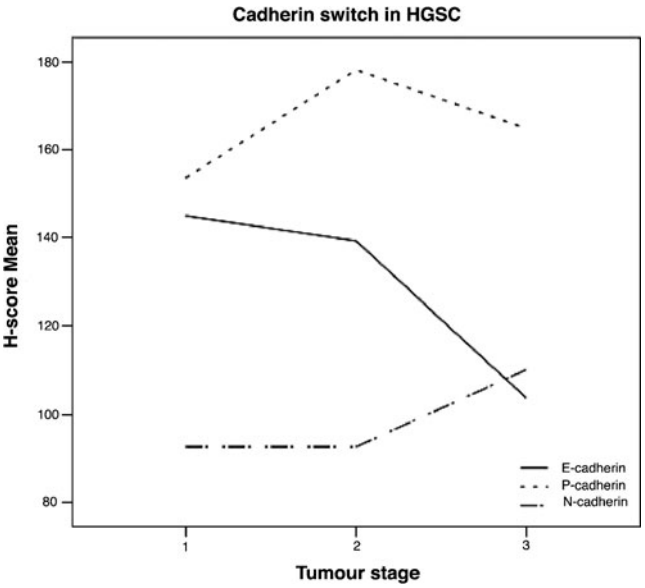

Fig. 3 Comparison of H-score of E-, P- and N-cadherins in the process of cadherin switch

cadherin between stage 2 and 3 disease groups. No significant change in E-, P- or N-cadherins expression between stage 3 and 4 disease was observed.

Combined expressions of E-, P- and N-cadherins

Cases were categorised in the eight possible combinations according to high and low expressions of the three markers. This generated eight categories; high E-, high P-, high N-cadherins (HHH; n=6, 4%), high E-, high P-, low N-cadherins (HHL; n=36, 23%), high E-, low P-, high N-cadherins (HLH; n=9, 6%), high E-, low P-, low N-cadherins (HLL; n=86, 56%), low E-, high P-, low N-cadherins (LHL) (n=3, 2%), low E-, low P-, high N-cadherins (LLH; n=5, 3%), low E-, low P-, low N-cadherins (LLL; n=9, 6%), and high E-, low P-, low N-cadherins (HLL; n=0).

The survival data illustrated earlier showed that poor disease outcome was associated with any of the following poor prognostic cadherin expressions: low expression of E-cadherin, high expression of P- or N-cadherins.

Analysing the combined categories with overall and progression-free survival data (Table 2) illustrated that cases with two out of three cadherins showing poor prognostic expressions had the shortest overall survival and earlier disease recurrence, whereas tumours that had only one out of three cadherins showing poor prognostic expression had a better disease outcome. Indeed those with three cadherins showing good prognostic expressions had the best disease outcome. A significant association was observed between the categories of various combinations of cadherins and overall survival (logrank 17.893, P=0.007) and with progression-free survival (logrank 20.048, P=0.003). No significant association with FIGO stage was identified.

It became apparent that further re-categorising of the groups was required to explore re-categorising the combined expression into three groups including: group A, two out of three cadherins showed poor prognostic expression (LHL, LLH and HHH), no cases showed LHH; group B, only one out of three cadherins showed poor prognostic expression (HHL, HLH and LLL) and group C, three cadherins showed good prognostic marker expression (HLL; Table 3).

A significant association between the three groups and overall and progression-free survival was observed (logrank 17.248 Pvalue=0.000 and logrank 14.913, P value=0.001, respectively) with group A showing a mean overall survival of 17 months and progression-free survival of 8 months and group B showing a mean overall survival of 23 months and progression-free survival of 21 months and group C showing a mean overall survival of 29 months and progression-free survival of 23 months (Fig. 4).

Neither the first set nor the second set of categories was associated with FIGO stage or showed significant correlation with survival when the assessment was extended to multivariate analysis.

Discussion

There has been increasing interest in adhesion molecules and their role in tumour spread and response to therapy. In tumour progression, the presence of E-cadherin plays a key role in suppressing invasion and metastasis [9] by main-

Table 2 Combined expression of E-, P- and N-cadherins in association with FIGO stage and overall and progression-free survival data

Categories of combined cadherin expressions (n, %)	FIGO stage				Mean overall survival (months)	Mean progression-free survival (months)
	1 (n=28)	2 (n=19)	3 (n=99)	4 (n=18)		
HHH (6, 4)	0	0	3	1	19	12
HHL (36, 23)	4	7	16	6	23	23
HLH (9,6)	0	0	7	0	22	20
HLL (86,56)	19	9	45	9	29	23
LHL (3,2)	0	0	2	1	17	6
LLH (5,3)	0	0	4	0	15	6
LLL (9,6)	1	0	7	0	22	14
P value	0.253				0.007	0.003

None of the cases showed LHH

HHH high E-, high P-, high N-cadherin; *HHL* high E-, high P-, low N-cadherin; *HLH* high E-, low P-, high N-cadherin; *HLL* high E-, low P-, low N-cadherin; *LHL* low E-, high P-, low N-cadherin; *LLH* low E-, low P-, high N-cadherin, *LLL* low E-, low P-, low N-cadherin

Table 3 Combined expression re-categorised into three groups: two poor prognostic marker expressions, one poor prognostic marker expression and none of the poor marker expression

Re-categorised combined cadherin expressions	Mean overall survival (months)	Mean progression-free survival (months)
Group A (n=14) (HHH, LHL, LLH)[a]	17	8
Group B (n=54) (HHL, HLH, LLL)	23	21
Group C (n=86) (HLL)	29	23
P value	0.000	0.001

Correlations with overall and progression-free survival is presented

[a] None of the cases showed LHH

taining intercellular adhesion amongst well-differentiated malignant cells [2, 4, 5], and thus, it is the hallmark of differentiated ovarian cancer [9].

The aim of the study was to define the stepwise changes in cadherin expression defined as cadherin switch and its prognostic significance in HGSC. This study provides a novel description of the cadherin profile in HGSC with the sequence of dysregulation of the cadherins. A significant increase in P-cadherin expression at stage 2 followed by a significant downregulation of E-cadherin at stage 3 has been identified. Tumours with two out of three cadherins showing poor prognostic expression had the worst disease outcome when compared to those with only one out of three cadherins showing poor prognostic expression.

The current study demonstrates that switching between different types of adhesion molecules appears to occur at different steps. In the spreading ovarian cancer, it is possible that adhesion molecular change starts initially with over expression of P-cadherin at stage 2 compared with stage 1 ovarian cancer. This is in agreement with the study by Patel et al. [10] who also reported a concomitant reduction in E-cadherin expression in ovarian tumours at stage 2, whereas in the current study, in line with other reports [21–23], a significant decrease in expression of E-cadherin was identified at stage 3 disease albeit of a P value of 0.050. The latter is marginally significant, and the number of cases in stage 1 and stage 2 disease was small. Therefore, future study on a larger number of cases seems to be a logical next step to verify the pattern of switch.

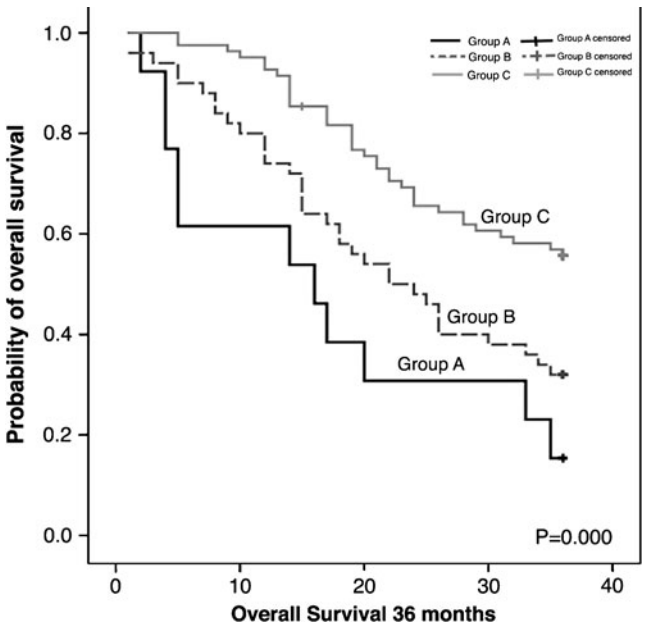

Fig. 4 Combined expressions of cadherins in association with overall survival data

High expression of N-cadherin, a marker of mesenchymal phenotype and enabling cell motility and invasion [4, 6], is seen in pancreatic, primary and metastatic carcinoma [7]. Furthermore, a study by Islam et al. [24] found that there was an inverse relationship between E- and N- cadherins expression in squamous cell carcinoma, as did two other studies investigating adhesion molecules in prostate cancer progression [5, 8], supporting the theory of adhesion molecule switching. Similarly, we demonstrated inverse correlation between the expressions of E- and N-cadherins in HGSC albeit with a low correlation coefficient. In agreement with previous studies [5–8], it has been demonstrated that there is a significant positive association between high N-cadherin expression and poor overall survival.

Considering the interesting cadherin switch profile observed in this study, categorising cases according to the combined expression of cadherins was explored. Eight categories were identified and appeared to show significant association with disease outcome. The pattern of expression in these groups lent itself into further re-categorization which again proved to show a significant association with disease outcome. The analysis illustrated that cases with two out of three cadherins showing poor prognostic expressions had the worst disease outcome in contrast to tumours showing only one out of three cadherins showing

poor prognostic expression. Indeed, cases with none of the poor prognostic cadherin expression had the best disease outcome. In fact, none of the cases that showed two poor prognostic cadherin expressions was in either stage 1 or 2 disease. Interestingly, none of the cases showed the worse prognostic combinations of cadherins of low E-cadherin and high P-and N-cadherins.

The presence of dual or single poor prognostic cadherin expression or, indeed, the absence of it suggests that assessing the cadherin profile in HGSC may be a significant addition to targeted therapy.

In summary, this study provides a novel description of the cadherin switch profile in HGSC with the sequence of dysregulation of the cadherins. A significant increase in P-cadherin expression at stage 2, followed by a significant downregulation of E-cadherin at stage 3 has been identified the current study. The combined expression of cadherins showed that tumours with two poor prognostic cadherin expressions had the worse disease outcome. This pattern presents a proposal to explore the cadherin profile when considering targeted therapy in HGSC.

Conflict of interest The authors declare that they have no conflict of interest.

References

1. Duncan TJ, Rolland P, Deen S, Scott IV, Liu DT, Spendlove I et al (2007) Loss of IFN gamma receptor is an independent prognostic factor in ovarian cancer. Clin Cancer Res 13:4139–4145
2. Elloul S, Silins I, Tropé CG, Benshushan A, Davidson B, Reich R (2006) Expression of E-cadherin transcriptional regulators in ovarian carcinoma. Virchows Arch 449:520–528
3. Jeschke U, Mylonas I, Kuhn C, Shabani N, Kunert-Keil C, Schindlbeck C, Gerber B, Friese K (2007) Expression of E-cadherin in human ductal breast cancer carcinoma in situ, invasive carcinomas, their lymph node metastases, their distant metastases, carcinomas with recurrence and in recurrence. Anticancer Res 27(4A):1969–1974
4. Hudson LG, Zeineldin R, Stack MS (2008) Phenotypic plasticity of neoplastic ovarian epithelium: unique cadherin profiles in tumor progression. Clin Exp Metastasis 25:643–655
5. Tomita K, van Bokhoven A, van Leenders GJ et al (2000) Cadherin switching in human prostate cancer progression. Cancer Res 60:3650–3654
6. Hazan RB, Phillips GR, Qiao RF, Norton L, Aaronson SA (2000) Exogenous expression of N-cadherin in breast cancer cells induces cell migration, invasion, and metastasis. J Cell Biol 148:779–790 [Erratum appears in J Cell Biol 2000;149:following 236]
7. Nakajima S, Doi R, Toyoda E et al (2004) N-cadherin expression and epithelial–mesenchymal transition in pancreatic carcinoma. Clin Cancer Res 10(12 Pt 1):4125–4133
8. Bussemakers MJG, Van Bokhoven A, Tomita K, Jansen CFJ, Schalken JA (2000) Complex cadherin expression in human prostate cancer cells. Int J Cancer 85:446–450
9. Wu C, Cipollone J, Maines-Bandiera S et al (2008) The morphogenic function of E-cadherin-mediated adherens junctions in epithelial ovarian carcinoma formation and progression. Differentiation 76:193–205
10. Patel IS, Madan P, Getsios S, Bertrand MA, MacCalman CD (2003) Cadherin switching in ovarian cancer progression. Int J Cancer 106:172–177
11. Paredes J, Albergaria A, Oliveira JT, Jerónimo C, Milanezi F, Schmitt FC (2005) P-cadherin over expression is an indicator of clinical outcome in invasive breast carcinomas and is associated with CDH3 promoter hypomethylation. Clin Cancer Res 11:5869–5877
12. Peralta Soler A, Knudsen KA, Salazar H, Han AC, Keshgegian AA (1999) P-cadherin expression in breast carcinoma indicates poor survival. Cancer 86:1263–1272
13. Sarrió D, Palacios J, Hergueta-Redondo M, Gómez-López G, Cano A, Moreno-Bueno G (2009) Functional characterization of E- and P-cadherin in invasive breast cancer cells. BMC Cancer 9:74
14. Eisenhauer EA, Therasse P, Bagaerts J, Schwartz LH, Sargent D, Ford R et al (2009) New response evaluation criteria in solid tumors: revised RECIST guideline (version 1.1). Eur J Cancer 45:228–247
15. Kononen J, Bubendorf L, Kallioniemi A et al (1998) Tissue microarrays for high-throughput molecular profiling of tumor specimens. Nat Med 4:844–847
16. Camp RL, Charette LA, Rimm DL (2000) Validation of tissue microarray technology in breast carcinoma. Lab Invest 80 (12):1943–1949
17. Shibata D, Fu YS, Gupta JW, Shah KV, Martin J, Arnheim N (1988) Analysis of DNA sequences in forty-year-old paraffin-embedded thin-tissue sections: a bridge between molecular biology and classical histology. Can Res 48:4564–4566
18. McCarty KS Jr, Miller LS, Cox EB, Konrath J, McCarty KS Sr (1985) Estrogen receptor analyses. Correlation of biochemical and immunohistochemical methods using monoclonal antireceptor antibodies. Arch Pathol Lab Med 109:716–721
19. Daniel G, Rosen XH, Deavers MT et al (2004) Validation of tissue microarray technology in ovarian carcinoma. Mod Pathol 17:790–797
20. Camp RL, Dolled-Filhart M, Rimm DL (2004) X-tile: a new bio-informatics tool for biomarker assessment and outcome-based cut-point optimization. Clin Cancer Res 10:7252–7259
21. Faleiro-Rodrigues C, MacEdo-Pinto I, Pereira D, Ferreira VM, Lopes CS (2004) Association of E-cadherin and beta-catenin immunoexpression with clinicopathologic features in primary ovarian carcinomas. Hum Pathol 35:663–669
22. Kuwabara Y, Yamada T, Yamazaki K et al (2008) Establishment of an ovarian metastasis model and possible involvement of E-cadherin down-regulation in the metastasis. Cancer Sci 99:1933–1939
23. Sundfeldt K, Piontkewitz Y, Ivarsson K et al (1997) E-cadherin expression in human epithelial ovarian cancer and normal ovary. Int J Cancer 74:275–280
24. Islam S, Carey TE, Wolf GT, Wheelock MJ, Johnson KR (1996) Expression of N-cadherin by human squamous carcinoma cells induces a scattered fibroblastic phenotype with disrupted cell-cell adhesion. J Cell Biol 135(6 Pt 1):1643–1654

Virchows Arch (2011) 459:31–39
DOI 10.1007/s00428-011-1096-8

ORIGINAL ARTICLE

Bmi-1, c-myc, and Snail expression in primary breast cancers and their metastases—elevated Bmi-1 expression in late breast cancer relapses

Kristiina Joensuu · Jaana Hagström · Marjut Leidenius · Caj Haglund · Leif C Andersson · Hannu Sariola · Päivi Heikkilä

Received: 14 February 2011 / Revised: 13 May 2011 / Accepted: 22 May 2011 / Published online: 3 June 2011
© Springer-Verlag 2011

Abstract Breast cancer is known for its propensity to recur decades after treatment. The biology behind the phenomenon of tumor dormancy is still poorly understood. Bmi-1, c-myc, and Snail are transcription factors that have prognostic roles in several malignancies. In order to reveal whether any of these markers has impact on late relapses, we used immunohistochemistry to study the expression of Bmi-1, c-myc, Snail, and estrogen receptor in 73 primary breast cancers and in their metastatic relapses detected within 2 years, or 5 or 10 years after primary surgery. The expression of Bmi-1 was higher in the metastases than in their corresponding primary tumors in both early and late relapses. The highest expression of Bmi-1 was seen in the very late relapsing tumors (first tumor relapse after 10 years). Previously, Bmi-1 has been reported to function as a marker of tumor stem cells in breast cancer. Our results indicate that metastases, when compared to primary tumors, arise from tumor cells that have retained stem cell properties. We also analyzed the relationship between the expression of these markers and clinical parameters. A significant association between the expression of Bmi-1 and estrogen receptor was found. Nuclear expression of c-myc in primary tumors correlated with an increased risk for axillary lymph node metastasis.

Keywords Breast cancer · Immunohistochemistry · Tumor dormancy

K. Joensuu (✉) · J. Hagström · C. Haglund · L. C. Andersson · P. Heikkilä
Department of Pathology, Haartman Institute,
University of Helsinki,
P.O. Box 21, 00014 Helsinki, Finland
e-mail: kristiina.joensuu@helsinki.fi

J. Hagström · P. Heikkilä
Department of Pathology, HUSLAB,
Helsinki University Central Hospital,
00290 Helsinki, Finland

M. Leidenius · C. Haglund
Department of Surgery, Helsinki University Central Hospital,
00290 Helsinki, Finland

H. Sariola
Department of Developmental Biology, Institute of Biomedicum,
University of Helsinki,
00014 Helsinki, Finland

Introduction

B cell-specific Moloney murine leukemia virus integration site 1 (Bmi-1), which was first identified by retroviral insertional mutagenesis and as a collaborating oncogene by retroviral insertional mutagenesis in Eμ-myc transgenic mice [1, 2], was assessed. Bmi-1 belongs to the mammalian polycomb group proteins which form multimeric complexes that regulate gene activity at the chromatin level [3]. Bmi-1 contributes to cell cycle regulation by acting as a transcriptional repressor of the INK4a/ARF (=human p19ARF) locus [4]. Kim et al. [5] demonstrated overexpression of Bmi-1 transcripts and protein in breast cancer and found high expression to correlate with axillary lymph node metastases. They suggested that cell cycle deregulation by Bmi-1 might play a role in the progression of breast cancer and lymph node metastasis. Al-Hajj et al. described the existence of a cancer stem cell population in human breast cancers [6]. These cancer stem cells displayed increased expression of Bmi-1 [7]. Overexpression of Bmi-1 correlates with a poor prognosis in non-keratinizing type of nasopharyngeal carcinoma and hepatocellular carci-

noma [8, 9] as well as in neural tumors, such as oligodendrogliomas and medulloblastomas [10, 11]. A correlation has also been reported with higher tumor stage in non-small cell lung cancer [12]. In squamous cell carcinoma of the tongue, the absence of Bmi-1 protein in the tumor cells was associated with a higher risk of recurrence [13].

Bishop and co-workers discovered c-myc in the late 1970s [14, 15]. C-myc is a DNA-binding, nuclear transcription factor involved in the regulation of the cell cycle [16], programmed cell death, and tumorigenesis [17, 18]. C-myc was first detected in Burkitt's lymphoma, but has later been connected with many other cancers, including breast and colon cancer, neuroblastoma, osteosarcoma, and melanoma [19]. Given the plethora of biological roles played by MYC gene products and the lack of reliable antibodies needed for immunohistochemical analysis, the clinical relevance of the overexpression of c-myc protein in breast cancer is not well known [20, 21]. On the other hand, MYC gene amplification has been associated with high histological grade, the presence of lymph node metastasis, a lack of progesterone receptor, and poor survival in breast cancer [21, 22]. Bmi-1 influences c-myc activity and vice versa, and both these oncogenes are able to immortalize certain cells [23–25].

Snail is a zinc-finger transcription factor essential for epithelial-mesenchymal transition (EMT). It downregulates the expression of cell adhesion and basement membrane proteins, most importantly cadherins [26]. Snail increases migration and invasion in various physiological and pathological conditions [26–28]. The involvement of Snail in tumor progression is supported by the expression of Snail in carcinoma cell lines having invasive and metastatic properties [27, 29, 30] in dedifferentiated breast cancer and hepatocellular carcinoma [31, 32]. Snail is required for tumor growth and lymph node metastasis of heterotransplanted human breast carcinoma MDA-MB-231 cells [33].

According to previous investigations, Bmi-1, c-myc, and Snail are stem cell-related proteins. On this basis, we investigated their association to late relapse of breast cancer by analyzing the expression of these proteins in both early and late relapsing tumors.

Materials and methods

Patients and tumors

Paraffin-embedded tissue blocks were obtained from 73 primary breast cancers and their metastatic lesions from the archives of the Department of Pathology, Helsinki University Hospital, as described previously [34]. Patients, from whom histological samples were available from both the primary tumor and metastases, were included in the study. The patients had undergone breast cancer surgery in 1974–2006. The cases were divided into three groups: Group 1 (n=19), tumors with metastatic recurrence within 2 years after primary surgery; Group 2 (n=33), tumors with metastatic recurrence in 5–10 years; and Group 3 (n=21), tumors with metastatic recurrence after more than 10 years (range, >10–23). The histological tumor type and grade were assigned according to the criteria of Elston and Ellis [35]. The clinicopathological characteristics of the patients and their cancers are summarized in Table 1. The Ethics Committee of the

Table 1 Clinicopathological parameters of the 73 breast cancer patients and the tissue site of metastastatic recurrence of their tumors

	Group 1 (n=19)	Group 2 (n=33)	Group 3 (n=21)
Age at surgery of primary tumor			
<50 years	10	14	13
≥50 years	9	19	8
Surgery			
Mastectomy	18	22	13
Partly mammary resection	1	11	8
Axillary lymph node evacuation	18	33	21
No axillary evacuation	1[a]		
Tumor size			
≥20 mm	4	19	13
<20 mm	15	14	8
Lymph node			
Negative	3	20	11
Positive	16	13	10
Grade			
1	0	5	3
2	8	19	14
3	11	9	4
Histological type			
Ductal	16	27	12
Lobular	3	5	9
Mucinous	0	1	0
Tissue site of metastasis			
Skin	5	8	11
Soft tissue	6	11	6
Subcutaneous tissue	0	5	2
Lung	0	4	0
Lymph node	1	0	0
Liver	5	1	0
Brain	2	2	0
Bone	0	1	1
Ovary	0	1	0
Stomach	0	0	1

In group 1, metastatic recurrences were detected within 2 years; in group 2, from 5 to 10 years; and in group 3, after 10 years

[a] No axillary lymph node evacuation was done in this case because the sentinel node was negative

Helsinki University Central Hospital approved the study protocol.

Immunohistochemistry

Four-micrometer-thick sections were deparaffinized in xylene and rehydrated through a graded alcohol series. The slides for Bmi-1, c-myc, and Snail immunolabeling were then pretreated in a PT module (LabVision UK Ltd, UK) in Tris–HCl buffer (pH 8.5) for 20 min at 98°C and with 0.3% Dako REAL Peroxidase-Blocking Solution for 5 min to block endogenous peroxidase. Immunostaining was done by incubating each antibody for 1 hour, followed by 30-min incubation with Dako REAL EnVision/HRP secondary antibodies. The antibody clones, their dilutions, and the manufacturers are presented in Table 2. Bound antibodies were finally visualized by Dako REAL DAB + Chromogen reaction for 10 min. The slides were washed between each step with PBS 0.04%–Tween20. For ER, PR, Ki67, and HER2, antigen retrieval was done by microwaving in 10 mM citric acid monohydrate for 1×5 min at 900 W and for 3×5 min at 600 W. Endogenous peroxidase activity was blocked by treatment with 0.5% H2O2. The slides were incubated overnight in a refrigerator at +4°C with appropriate dilutions of the primary antibodies. The same procedure was used for negative controls, except that the incubation overnight took place in PBS diluent without antibody. The reaction was visualized by the Elite ABC Kit (Vectastain, Vector Laboratories, Burlingame, CA, USA) for ER and Ki67. PR and HER2 staining was performed using the Envision kit (Dako, Copenhagen, Denmark). The result was quantified as the proportion of positively stained tumor cells (range, 0–100%) for Bmi-1, c-myc, Snail, ER, PR, and Ki67. In Bmi-1, Snail, ER, PR, and Ki67, the staining was nuclear. Both nuclear and cytoplasmic stainings of c-myc were evaluated. The invasive front (frontal) and central areas of the tumors were scored separately for Snail. The immunohistochemistry (IHC) of HER2 expression was scored based on the intensity and percentage of positive cells, giving a score of 0 to 3+ [36]. Tumors giving a score of 2+ or 3+ were recorded positive. The 2+ and 3+ IHC HER2 positive cases were validated by chromogenic in situ hybridization (data not shown). We evaluated the entire tumor area in one representative section from the primary tumor and metastasis. The results were scored independently by two experienced pathologists (KJ and JH). When there was a discrepancy between evaluations, a consensus was made.

Statistical methods

All statistical analyses were performed using SPSS 13.0 for Windows (SPSS Inc., Chicago, IL, USA). The differences between the staining of primary tumors and their corresponding metastases were analyzed by the paired samples *t* test. Kruskal–Wallis and Mann–Whitney *U* tests were used for comparing the groups. For analyzing the relationship between protein expression of Bmi-1, c-myc, ER, Snail and the clinical parameters and also for compairing the Bmi-1, c-myc, and Snail with PR, HER2, and Ki67 expression, the categorical Pearson's Chi-square test was used. As a cutoff point for positivity for Bmi-1 [5], c-myc [37, 38], ER, and PR, the frequency of 10% positive tumor cells was used. For Snail, the tumors were divided into high- and low-expressing groups, using 80% proportion of positively stained cells as a cutoff point [13]. Tumors were considered Ki67 positive, if ≥14% of the tumor cells showed positive nuclei [39]. Probability values of $p<0.05$ were considered statistically significant, except in the Mann–Whitney *U* test, where $p<0.0167$ (=<0.05/3) was used.

Results

Bmi-1

The expression of Bmi-1 in the groups is shown in Table 3. The metastases in groups 1 and 3 showed significantly more Bmi-1 (Fig. 1a, b) positivity than their corresponding primary tumors ($p=0.004$ in group 1 and $p=0.019$ in group 3, Table 3). The mean expression of Bmi-1 in the primary tumors did not differ between the three groups. In the metastases, there was significantly more Bmi-1 positivity in

Table 2 List of the antibodies, the laboratories manufacturing them, and the dilution used in immunohistochemical staining

Antigen	Antibody	Laboratory	Dilution
Bmi-1	Mouse monoclonal clone ab14389	Abcam, Cambridge, UK	1:400
c-myc	Mouse monoclonal clone 9E10	Santa Cruz, UK	1:400
Snail	Polyclonal rabbit clone ab17732	Abcam, UK,	1:2,000
ER alfa	Mouse monoclonal clone 6F11	Novocastra, Newcastle, UK	1:50
PR alfa	Mouse monoclonal clone PgR636	Daco Cytomation, Denmark	1:100
HER2	Mouse monoclonal clone CB11	Novocastra, United Kingdom	1:700
Ki67	Mouse monoclonal clone MIB-1	Daco Cytomation Denmark	1:75

Table 3 Differences in the mean proportion of positively stained tumor cells (percent; range, 0–100%) between the primary tumors and their corresponding metastases

	Bmi-1 Primary	Bmi-1 Metastases	*P* value
Group 1 (n=19)	30.1 (27.3)	53.9 (28.4)	0.004
Group 2 (n=33)	32.0 (35.7)	37.0 (33.4)	0.466
Group 3 (n=21)	41.9 (36.9)	64.9 (25.1))	0.019[a]
	c-myc nuclear Primary	c-myc nuclear Metastases	
Group 1 (n=19)	11.5 (17.9)	4.7 (9.9)	0.168
Group 2 (n=33)	2.3 (4.1)	8.6 (13.9)	0.013[a]
Group 3 (n=21)	16.0 (28.0)	18.9 (31.6)	0.783
	c-myc cytoplasmic Primary	c-myc cytoplasmic Metastases	
Group 1 (n=19)	17.9 (25.8)	12.4 (22.1)	0.306
Group 2 (n=33)	10.6 (20.9)	25.0 (31.6)	0.033[a]
Group 3 (n=21)	6.8 (15.9)	7.6 (19.9)	0.897
	Snail frontal Primary	Snail frontal Metastases	
Group 1 (n=19)	88.7 (17.5)	93.3 (8.2)	0.280
Group 2 (n=33)	85.5 (23.7)	88.5 (21.5)	0.497
Group 3 (n=21)	88.1 (21.7)	92.1 (10.5)	0.479
	Snail central Primary	Snail central Metastases	
Group 1 (n=19)	85.7 (14.0)	90.3 (10.7)	0.246
Group 2 (n=33)	77.0 (30.2)	78.5 (26.3)	0.801
Group 3 (n=21)	79.0 (30.5)	91.3 (10.8)	0.120

Values are shown as percent mean (SD). Paired samples t test was used. Group 1 represents tumors with metastases within 2 years. In group 2, metastases were detected at 5–10 years, and in group 3, after 10 years

[a] Significant

group 3 than in group 2 (p=0.007; Table 4; Kruskal–Wallis test and p=0.003; Table 5; Mann–Whitney U test).

Nuclear c-myc

The nuclear expression of c-myc in the tumor groups is shown in Table 3. In group 2, there was significantly more nuclear c-myc positivity in the metastases than in the corresponding primary tumors (p=0.013; Table 3). There were no statistical differences in the nuclear expression of c-myc between the three groups (Table 4).

Cytoplasmic c-myc

The cytoplasmic expression of c-myc in the groups is shown in Table 3. There was significantly more expression of cytoplasmic c-myc (Fig. 1c and d) in the metastases of group 2 than in the corresponding primary tumors (p=0.033; Table 3). The expression of cytoplasmic c-myc did not differ significantly between the three groups (Table 4).

Snail

Sometimes there was greater expression of Snail in frontal than in central areas of the tumor (Fig. 1e, f). Frontal and central Snail expression in the groups is shown in Table 3. The expression did not differ significantly between the primary tumors and their metastases in any of the three groups (Table 3). There was no statistical difference in Snail expression between the three groups (Table 4).

The relationship between Bmi-1, c-myc, Snail, ER protein, and clinical parameters

The significant results are shown in Table 6. For the analysis, the tumors were divided into positive and negative groups for Bmi-1, c-myc, and ER. For Snail, the tumors were divided into groups with high expression (≥80%) and low expression (<80%). These relations were evaluated in all primary tumors as one group (n=73) and in all metastases as another group (n=73). We also compared the protein expression of the primary tumors with axillary lymph node status. Comparisons were also made between tumor size, histological grade, type of tumor, and age of the patients (data not shown), but no positive correlation was seen.

Forty-eight (65%) of the primary cancers and 62 (84%) of their metastases were Bmi-1-positive. Bmi-1 positivity was associated with ER positivity in both the primary tumors and the metastases (p=0.012 in primary tumors and p=0.005 in metastases; Table 6). Bmi-1 positivity was associated significantly with high frontal and central Snail

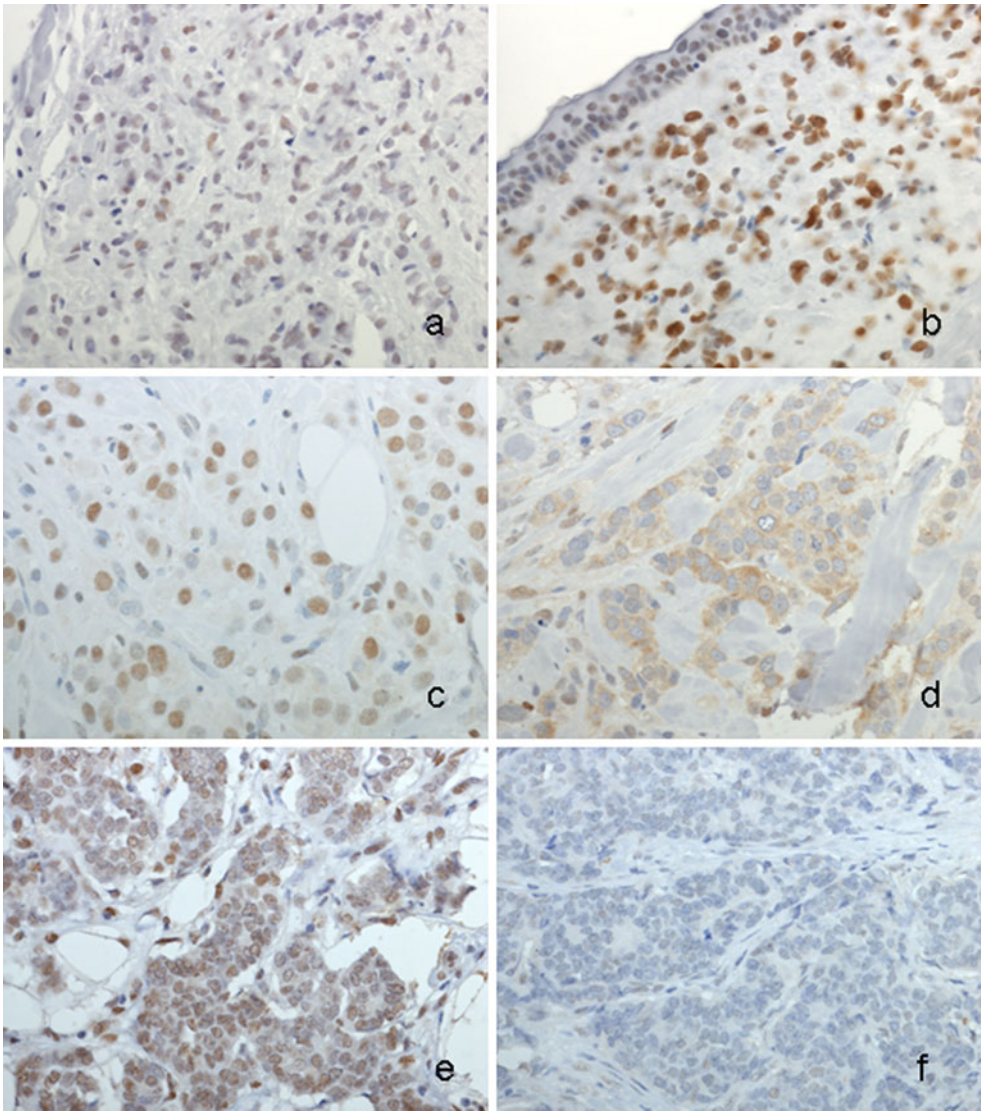

Fig. 1 Examples of immunohistochemical stainings of primary and metastatic breast cancers. Bmi-1 in a primary (**a**) and a metastatic (**b**) cancer. Nuclear c-myc in a primary (**c**) and cytoplasmic c-myc in a metastatic (**d**) tumor. Frontal (**e**) and central (**f**) Snail in a primary tumor

expression in the metastases (frontal Snail, $p=0.0001$, central Snail, $p=0.009$; Table 6). Bmi-1 expression was not associated with any of the analyzed clinical parameters.

There were 15 (20%) nuclear c-myc-positive tumors among the primary cancers and 19 (26%) in their corresponding metastases. Nuclear c-myc expression was not associated with the expression of the other proteins. Nuclear c-myc positivity of primary tumors was significantly associated with axillary node positivity of the patients ($p=0.021$; Table 6).

Positivity for cytoplasmic c-myc was seen in 27 (37%) of the primary tumors and in 29 (39%) of the corresponding metastases. No association with clinical parameters was obtained. Cytoplasmic c-myc was associated with high frontal and central Snail in primary tumors ($p=0.002$ and $p=0.011$, respectively; Table 6).

Sixty (81%) of the primary tumors and 67 (91%) of their metastases expressed high frontal Snail. However, high frontal Snail expression (Fig.1) was not associated with any clinical parameters. High frontal Snail expression was associated significantly with Bmi-1 positivity in the metastases ($p=0.0001$; Table 6), as mentioned above.

A high expression of central Snail was seen in 52 (70%) of the primary tumors and in 60 (81%) of the metastases. High central expression of Snail was not associated with any clinical parameters. High central Snail was associated with Bmi-1 in metastases ($p=0.009$; Table 6), as mentioned above.

The relationship between Bmi-1, c-myc, Snail and PR, HER2 and Ki67

In primary tumors, there was a significant association between nuclear c-myc positivity and HER2 positivity ($p=0.017$; Table 6). In metastases, there was no correlation between the expression of these antigens.

In conclusion, the expression of Bmi-1 was highest in metastases of the late (>10 years) relapsing tumor group. In all tumor groups, metastases expressed more Bmi-1 than

Table 4 Differences in the mean proportions of positively stained tumor cells between the three groups of 73 breast cancers, in primary tumors and in their metastases

Staining	Group	*n*	Mean rank	*P* value
Bmi-1				
Primary	1	19	37	
	2	33	38.8	
	3	21	41.8	0.397
Metastases	1	19	39.7	
	2	33	28.9	
	3	21	47.2	0.007[a]
c-mycnuclear				
Primary	1	19	44.2	
	2	33	31.3	
	3	21	39.4	0.071
Metastases	1	19	34.1	
	2	33	37.9	
	3	21	38.3	0.761
c-myc cytoplasmic				
Primary	1	19	43.3	
	2	33	35.9	
	3	21	32.9	0.219
Metastases	1	19	36.5	
	2	33	41.6	
	3	21	30.1	0.113
Snail frontal				
Primary	1	19	36.8	
	2	33	36.9	
	3	21	37.4	0.994
Metastases	1	19	37.3	
	2	33	37.2	
	3	21	36.4	0.986
Snail central				
Primary	1	19	36.8	
	2	33	36.1	
	3	21	38.5	0.919
Metastases	1	19	40.0	
	2	33	31.3	
	3	21	43.2	0.091

Kruskal–Wallis test was used. Group 1 represents tumors with metastases within 2 years. In group 2, metastases were detected at 5–10 years, and in group 3, after 10 years

[a] Significant

did the primary tumors. Bmi-1 positivity correlated with ER positivity in both primary tumors and metastases. Nuclear expression of c-myc in the primary tumors was associated with a positive lymph node status of the patients. There was a tendency of higher, both nuclear and cytoplasmic, c-myc expression in the metastases of the late relapsing tumors than in their primary counterparts. In primary tumors, nuclear c-myc positivity correlated with HER2 positivity.

Table 5 Bmi-1 immunostaining in breast cancer metastases compared between groups using Mann–Whitney *U* test

Bmi-1	*U*	*Z*	*P*
Group 1 vs. group 2	215.0	−1.880	0.060
Group 2 vs. group 3	178.0	−2.996	0.003[a]
Group 1 vs. group 3	153.0	−1.266	0.206

The Mann–Whitney *U* test was applied if Kruskal–Wallis test showed a significant difference between the three groups (Table 4)

[a] In metastases between groups 2 and 3, the difference was significant, i.e., <0.0167 (<0.05/3)

Discussion

In this study, we describe the expression of polycomb protein and oncogene Bmi-1, proto-oncogene c-myc, and transcription factor Snail in a series of 73 primary breast cancers and their corresponding metastases, from which 19 were early relapsing tumors and 54 late relapsing cancers (33 after 5 years and 21 after 10 years). Immunoexpression levels are compared between the primary tumors and their metastases, as well as between early and late relapsing tumors, and also with clinical parameters, in order to analyze their putative role in breast cancer progression.

A higher level of Bmi-1 expression has been reported during progression from in situ ductal breast carcinoma to invasive carcinoma linking Bmi-1 expression to malignant behavior [40]. In our study, we found metastases of breast cancer to express more Bmi-1 than the corresponding primary tumors. On the other hand, no such difference in Bmi-1 expression was detected in a melanoma study [41]. However, these tumors differ quite much since breast cancer is epithelial in origin whereas melanoma originates from melanocytes. We also found the highest level of Bmi-1 expression in the metastases of the very late relapsing tumors, suggesting that Bmi-1 is a marker of tumor cell dormancy [42].

The prognostic correlation studies of Bmi-1expression in breast cancer are contradictory, and association with both a poor as well as a favorable prognosis has been suggested [43]. We did not find Bmi-1 expression to correlate with lymph node metastasis or time of relapse. In our study, however, Bmi-1 positivity correlated significantly with ER expression both in the primary tumors and the metastases. Contrary to our findings, Feng et al. found a positive correlation between lymph node status and Bmi-1 expression, but no association between Bmi-1 and ER [43]. The differences between these results may be explained by the

Table 6 Relationship between Bmi-1, nuclear c-myc, cytoplasmic c-myc, ER protein expression, and axillary lymph node status in 73 primary breast cancers and their metastases

Primary tumors			
	Bmi-1	Bmi-1	*P* value
	Negative (row %)	Positive (row %)	
ER negative	19 (46)	22 (54)	
ER positive	6 (19)	26 (81)	0.014
	Nuclear c-myc	Nuclear c-myc	
	Negative (row %)	Positive (row %)	
Node negative	31 (91)	3 (9)	
Node positive	27 (69)	12 (31)	0.021
	Nuclear c-myc	Nuclear c-myc	
	Negative (row %)	Positive (row %)	
HER2 negative	48 (88%)	8 (14%)	
HER2 positive	8 (57%)	6 (43%)	0.017
	Cytoplasmic c-myc	Cytoplasmic c-myc	
	Negative (row %)	Positive (row %)	
Snail frontal low	13 (100)	0	
Snail frontal high	33 (55)	27 (45)	0.002
Snail central low	18 (86)	3 (14)	
Snail central high	28 (54)	24 (46)	0.011
Metastases			
	Bmi-1	Bmi-1	*P* value
	Negative (row %)	Positive (row %)	
Snail frontal low	4 (67)	2 (33)	
Snail frontal high	7 (10)	60 (90)	0.0001
Snail central low	5 (39)	8 (62)	
Snail central high	11 (18)	49 (82)	0.009
ER negative	10 (26)	28 (74)	
ER positive	1 (3)	34 (97)	0.005

Categorical Pearson's Chi-square test was used

scoring method of positive cells. Feng et al. analyzed four randomly selected fields, while we evaluated the whole tumor area. In line with our results, Choi et al. [44] showed a favorable prognostic impact of Bmi-1 expression in breast cancer, but only in ER-positive patients, by evaluating the whole tumor area, the same way as we did.

Pavelic et al. [37] found heterogeneity in c-myc expression within individual tumors and substantial differences in the level of expression among different tumors. Andrechek et al. used a mouse model to study mammary carcinogenesis and found substantial heterogeneity in Myc-induced tumors, in terms of different gene expression and histological phenotypes [45]. We also found a different expression of c-myc between tumors, while we found a tendency of higher expression of both nuclear and cytoplasmic c-myc in the metastases of the late relapsing tumors than in their primary counterparts, suggesting that c-myc may be connected to tumor dormancy as well.

The significance of the different subcellular sites of c-myc staining, either nuclear, cytoplasmic or both, has not yet been clarified [37]. We speculate that active c-myc is located in the nucleus, where the transcription factors can operate. In our study, nuclear c-myc expression correlated significantly with axillary lymph node positivity. In agreement with our results, Rodriguez-Pinilla et al. found MYC amplification to be an independent predictor of lymph node metastasis [20]. On the contrary, some breast cancer studies have not found any correlation between c-myc expression and axillary lymph node status [46, 47]. The controversy may be due to the differences in the scoring methods. Locker et al. [48] did not find a correlation between axillary lymph node metastases and c-myc in their flow cytometric assay, but they reported that high levels of c-myc expression were found frequently in well-differentiated tumors.

No significant variability in Snail expression levels neither in the primary tumors nor in their metastases and no correlation to clinical parameters were found in our material. Contrary to our results, however, Snail expression has been shown to correlate inversely with the differentiation grade of breast tumors [31]. Come et al. analyzed the levels of Snail, Slug, and E-cadherin RNA expression and protein localization in large numbers of transformed cell lines and breast carcinomas, and they suggested that there is a link between Snail, Slug, and lymph node metastasis in

mammary carcinomas. They detected a positive correlation between Snail expression and lymph node invasion by PCR [49]. We were unable to corroborate this association by immunohistochemistry. Instead, we found an association between high Snail expression and Bmi-1 in the metastases. This finding could be explained by a link between Snail and Bmi-1 function via E-cadherin. Bmi-1 expression has been shown to downregulate tumor suppressors, such as p16INK4a p14ARF, and cell adhesion molecules, such as E-cadherin [50]. Snail is essential for the EMT by down-regulating the expression of cell adhesion and basement membrane proteins, most importantly cadherins [26].

In conclusion, we found higher Bmi-1 expression in breast cancer metastases than in primary tumors. The highest Bmi-1 expression was seen in the very late metastazing tumor group. These results suggest that small populations of Bmi-1-positive cells in the primary tumor survive long dormancy after primary therapy and retain their capacity for late relapsing. Our results also show an association of nuclear c-myc expression in primary tumors with axillary lymph node positivity, indicating nuclear c-myc expression to correlate with an increased risk for axillary lymph node metastasis.

Acknowledgments We thank Eija Heiliö, Päivi Peltokangas, and Tuire Koski for excellent technical assistance, Antti Nevanlinna for assistance with the statistics, and Doctor Aaron S. Mansfield for proofreading this manuscript. This work was supported by the Helsinki University Central Hospital Research Foundation, the Finnish Cancer Foundation, The Sigrid Juselius Foundation, and the Finnish Breast Cancer Group.

Conflict of interest There is no conflict of interest.

References

1. van Lohuizen M, Verbeek S, Scheijen B, Wientjens E, van der Gulden H, Berns A (1991) Identification of cooperating oncogenes in Eμ-myc transgenic mice by provirus tagging. Cell 65 (5):737–752
2. Haupt Y, Alexander WS, Barri G, Klinken SP, Adams JM (1991) Novel zinc finger gene implicated as myc collaborator by retrovirally accelerated lymphomagenesis in Eμ-myc transgenic mice. Cell 65(5):753–763
3. Satijn DP, Hamer KM, den Blaauwen J, Otte AP (2001) The polycomb group protein EED interacts with YY1 and both proteins induce neural tissue in Xenopus embryos. Mol Cell Biol 21(4):1360–1369
4. Jacobs JJ, Scheijen B, Voncken JW, Kieboom K, Berns A, van Lohuizen M (1999) Bmi-1 collaborates with c-Myc in tumorigenesis by inhibiting c-Myc-induced apoptosis via INK4a/ARF. Genes Dev 13(20):2678–2690
5. Kim JH, Yoon SY, Jeong SH, Kim SY, Moon SK, Joo JH, Lee Y, Choe IS, Kim JW (2004) Overexpression of Bmi-1 oncoprotein correlates with axillary lymph node metastases in invasive ductal breast cancer. Breast 13(5):383–388
6. Al-Hajj M, Wicha MS, Benito-Hernandez A, Morrison SJ, Clarke MF (2006) Prospective identification of tumorigenic breast cancer cells. Proc Natl Acad Sci U S A 100(7):3983–3988
7. Liu S, Dontu G, Mantle ID, Patel S, Ahn NS, Jackson KW, Suri P, Wicha MS (2006) Hedgehog signalling and Bmi-1 regulate self-renewal of normal and malignant human mammary stem cells. Cancer Res 66(12):6063–6071
8. Song LB, Zeng MS, Liao WT, Zhang L, Mo HY, Liu WL, Shao JY, Wu QL, Li MZ, Xia YF, Fu LW, Huang WL, Dimri GP, Band V, Zeng YX (2006) Bmi-1 is a novel molecular marker of nasopharyngeal carcinoma progression and immortalizes primary human nasopharyngeal epithelial cells. Cancer Res 66(12):6225–6232
9. Wang H, Pan K, Zhang HK, Weng DS, Zhou J, Li JJ, Huang W, Song HF, Chen MS, Xia J (2008) Increased polycomb-group oncogene Bmi-1 expression correlates with poor prognosis in hepatocellular carcinoma. J Cancer Res Clin Oncol 134(5):535–541
10. Häyry V, Tynninen O, Haapasalo HK, Wölfer J, Paulus W, Hasselblatt M, Sariola H, Paetau A, Sarna S, Niemelä M, Wartiovaara K, Nupponen NN (2008) Stem cell protein Bmi-1 is an independent marker for poor prognosis in oligodendroglial tumors. Neuropathol Appl Neurobiol 34(5):555–563
11. Leung C, Lingbeek M, Shakhova O, Liu J, Tanger E, Saremaslani P, van Lohuizen M, Marino S (2004) Bmi1 is essential for cerebellar development and is overexpressed in human medulloblastomas. Nature 428(6980):337–341
12. Vrzalikova K, Skarda J, Ehrmann J, Murray PG, Fridman E, Kopolovic J, Knizetova P, Hajduch M, Klein J, Kolek V, Radova L, Kolar Z (2008) Prognostic value of Bmi-1 oncoprotein in NSCLC patients: a tissue microarray study. J Cancer Res Clin Oncol 134(9):1037–1042
13. Häyry V, Mäkinen LK, Atula T, Sariola H, Mäkitie A, Leivo I, Keski-Säntti H, Lundin J, Haglund C, Hagström J (2010) Bmi-1 expression predicts prognosis in squamous cell carcinoma of the tongue. Br J Cancer 102(5):892–897
14. Bishop JM (1982) Retroviruses and cancer genes. Adv Cancer Res 37:1–32
15. Vennstrom B, Sheiness D, Zabielski J, Bishop JM (1982) Isolation and characterization of c-myc, a cellular homolog of the oncogene (v-myc) of avian myelocytomatosis virus strain 29. J Virol 42 (3):773–779
16. Rabbits PH, Watson JV, Lamond A, Forster A, Stinson MA, Evan G, Fischer W, Atherton E, Sheppard R, Rabbitts TH (1985) Metabolism of c-myc gene products: c-myc mRNA and protein expression in the cell cycle. EMBO J 4(8):2009–2015
17. Harrington EA, Bennett MR, Fanidi A, Evan GI (1994) c-Myc-induced apoptosis in fibroblasts is inhibited by specific cytokines. EMBO J 13(14):3286–3295
18. Amundadottir LT, Johnson MD, Merlino G, Smith GH, Dickson RB (1995) Synergistic interaction of transforming growth factor alfa and c-myc in mouse mammary and salivary gland tumorigenesis. Cell Growth Differ 6(6):737–748
19. Pelengaris S, Khan M, Evan G (2002) c-MYC: more than just a matter of life and death. Nat Rev Cancer 2(10):764–776
20. Rodriguez-Pinilla SM, Jones RL, Lambros MB, Arriola E, Savage K, James M, Pinder SE, Reis-Filho JS (2007) MYC amplification in breast cancer: a chromogenic in situ hybridisation study. J Clin Pathol 60(9):1017–1023
21. Liao DJ, Dickson RB (2000) c-Myc in breast cancer. Endocr Relat Cancer 7(3):143–164
22. Deming SL, Nass SJ, Dickson RB, Trock BJ (2000) C-myc amplification in breast cancer: a meta-analysis of its occurrence and prognostic relevance. Br J Cancer 83(12):1688–1695
23. van Lohuizen M, Frasch M, Wientjens E, Berns A (1991) Sequence similarity between the mammalian *bmi-1* proto-oncogene and *Drosophila* regulatory genes *Psc* and *Su(z)2*. Nature 353(6342):353–355
24. Haupt Y, Bath ML, Harris AW, Adams JM (1993) Bmi-1 transgene induces lymphomas and collaborates with myc in tumorigenesis. Oncogene 8(11):3161–3164

25. Levy LS, Lobelle-Rich PA, Overbaugh J (1993) Flvi-2, a target of retroviral insertional mutagenesis in feline thymic lymphosarcomas, encodes bmi-1. Oncogene 8(7):1833–1838
26. Batlle E, Sancho E, Francí C, Domínguez D, Monfar M, Baulida J, García De Herreros A (2000) The transcription factor Snail is a repressor of E-cadherin gene expression in epithelial tumor cells. Nat Cell Biol 2(2):84–89
27. Cano A, Pérez-Moreno MA, Rodrigo I, Locascio A, Blanco MJ, del Barrio MG, Portillo F, Nieto MA (2000) The transcription factor Snail controls epithelial-mesenchymal transitions by repressing E-cadherin expression. Nat Cell Biol 2(2):76–83
28. Peinado H, Olmeda D, Cano A (2007) Snail, Zeb and bHLH factors in tumor progression: an alliance against the epithelial phenotype? Nat Rev Cancer 7(6):415–428
29. Cheng CW, Wu PE, Yu JC, Huang CS, Yue CT, Wu CW, Shen CY (2001) Mechanisms of inactivation of E-cadherin in breast carcinoma: modification of the two-hit hypothesis of tumor suppressor gene. Oncogene 20(29):3814–3823
30. Poser I, Domínguez D, de Herreros AG, Varnai A, Buettner R, Bosserhoff AK (2001) Loss of E-cadherin expression in melanoma cells involves up-regulation of the transcriptional repressor Snail. J Biol Chem 276(27):24661–24666
31. Blanco MJ, Moreno-Bueno G, Sarrio D, Locascio A, Cano A, Palacios J, Nieto MA (2002) Correlation of Snail expression with histological grade and lymph node status in breast carcinomas. Oncogene 21(20):3241–3246
32. Sugimachi K, Tanaka S, Kameyama T, Taguchi K, Aishima S, Shimada M, Sugimachi K, Tsuneyoshi M (2003) Transcriptional repressor Snail and progression of human hepatocellular carcinoma. Clin Cancer Res 9(7):2657–2664
33. Olmeda D, Moreno-Bueno G, Flores JM, Fabra A, Portillo F, Cano A (2007) SNAI1 is required for tumor growth and lymph node metastasis of human breast carcinoma MDA-MB-231 cells. Cancer Res 67(24):11721–11731
34. Joensuu K, Heikkilä P, Andersson LC (2008) Tumor dormancy: elevated expression of stanniocalcins in late relapsing breast cancer. Cancer Lett 265(1):76–83
35. Elston CW, Ellis IO (1991) Pathological prognostic factors in breast cancer. I. The value of histological grade in breast cancer: experience from a large study with long-term follow-up. Histopathology 19(5):403–410
36. Wolff AC, Hammond ME, Schwarts JN, Hagerty KL, Allred DC, Cote RJ, Dowsett M, Fitzgibbons PL, Hanna WM, Langer A, McShane LM, Paik S, Pegram MD, Perez EA, Press MF, Rhodes A, Sturgeon C, Taube SE, Tubbs R, Vance GH, van de Vijver M, Wheeler TM, Hayes DF (2007) American Society of Clinical Oncology/College of American Pathologists guideline recommendations for human epidermal grwth factor receptor 2 testing in breast cancer. Arch Pathol Lab Med 131(1):18–43
37. Pavelic ZP, Pavelic K, Carter CP, Pavelic L (1992) Heterogeneity of c-myc expression in histologically similar infiltrating ductal carcinomas of the breast. J Cancer Res Clin Oncol 118 (1):16–22
38. Pertschuk LP, Tobin EH, Tanapat P et al (1980) Histochemical analyses of steroid hormone receptors in breast and prostatic carcinoma. J Histochem Cytochem 28(8):799–810
39. Cheang MC, Chia SK, Voduc D, Gao D, Leung S, Snider J, Watson M, Davies S, Bernard PS, Parker JS, Perou CM, Ellis MJ, Nielsen TO (2009) Ki67 index, HER2 status, and prognosis of patients with luminal B breast cancer. J Natl Cancer Inst 101 (10):736–750
40. Raaphorst FM, Meijer CJ, Fieret E, Blokzijl T, Mommers E, Buerger H, Packeisen J, Sewalt RA, Otte AP, van Diest PJ (2003) Poorly differentiated breast carcinoma is associated with increased expression of the human polycomb group EZH2 gene. Neoplasia 5(6):481–488
41. Mihic-Probst D, Kuster A, Kilgus S, Bode-Lesniewska B, Ingold-Heppner B, Leung C, Storz M, Seifert B, Marino S, Schraml P, Dummer R, Moch H (2007) Consistent expression of the stem cell renewal factor BMI-1 in primary and metastatic melanoma. Int J Cancer 121(8):1764–1770
42. Aguirre-Ghiso JA (2007) Models, mechanisms and clinical evidence for cancer dormancy. Nat Rev Cancer 7(11):834–846
43. Feng Y, Song LB, Guo BH, Liao WT, Li MZ, Liu WL, Zeng MS, Zhang L (2007) Expression and significance of Bmi-1 in breast cancer. Chin J of Cancer 26(2):154–157
44. Choi YJ, Choi YL, Cho EY, Shin YK, Sung KW, Hwang YK, Lee SJ, Kong G, Lee JE, Kim JS, Kim JH, Yang JH, Nam SJ (2009) Expression of Bmi-1 protein in tumor tissues is associated with favourable prognosis in breast cancer patients. Breast Cancer Res Treat 113(1):83–93
45. Andrechek ER, Cardiff RD, Chang JT, Gatza ML, Acharya CR, Potti A, Nevins JR (2009) Genetic heterogeneity of Myc-induced mammary tumors reflecting diverse phenotypes including metastatic potential. Proc Natl Acad Sci U S A 106(38):6387–16392
46. Spandidos DA, Yiagnisis M, Papadimitriou K, Field JK (1989) Ras, c-myc and c-erB-2 oncoproteins in human breast cancer. Anticancer Res 9(5):1385–1393
47. Pavelic ZP, Pavelic L, Lower EE, Gapany M, Gapany S, Barker EA, Preisler HD (1992) c-myc, c-erB-2, and Ki-67 expression in normal breast tissue and in invasive and non-invasive breast carcinoma. Cancer Res 52(9):2597–2602
48. Locker AP, Dowle CS, Ellis IO, Elston CW, Blamey RW, Sikora K, Evan G, Robins RA (1989) c-myc oncogene product expression and prognosis in operable breast cancer. Br J Cancer 60(5):669–672
49. Côme C, Magnino F, Bibeau F, De Santa BP, Becker KF, Theillet C, Savagner P (2006) Snail and slug play distinct roles during breast carcinoma progression. Clin Cancer Res 12(18):5395–5402
50. Song LB, Li J, Liao WT, Feng Y, Yu CP, Hu LJ, Kong QL, Xu LH, Zhang X, Liu WL, Li MZ, Zhang L, Kang TB, Fu LW, Huang WL, Xia YF, Tsao SW, Li M, Band V, Band H, Shi QH, Zeng YX, Zeng MS (2009) The polycomb group protein Bmi-1 represses the tumor suppressor PTEN and induces epithelial-mesenchymal transition in human nasopharyngeal epithelial cells. J Clin Invest 119(12):3626–3636

Virchows Arch (2011) 459:41–46
DOI 10.1007/s00428-011-1081-2

ORIGINAL ARTICLE

Podoplanin expression in adamantinoma of long bones and osteofibrous dysplasia

Takeshi G. Kashima · Arunthati Dongre · Adrienne M. Flanagan · Pancras C. W. Hogendoorn · Richard Taylor · Nicholas A. Athanasou

Received: 20 December 2010 / Revised: 8 March 2011 / Accepted: 3 April 2011 / Published online: 16 April 2011
© Springer-Verlag 2011

Abstract Adamantinoma of long bones (ALB) and osteofibrous dysplasia (OFD) are rare osteolytic bone tumours that principally arise in the tibia. Both ALB and OFD contain epithelial and stromal elements, as well as areas of fibro-osseous proliferation. We assessed expression of podoplanin, a glycoprotein found in osteocytes, in OFD and ALB as well as in fibrous dysplasia and metastatic cancer. Forty-two cases of ALB and OFD, 20 cases of fibrous dysplasia and 20 cases of metastatic carcinoma to bone were stained by immunohistochemistry for expression of podoplanin, epithelial (cytokeratin, epithelial membrane antigen) and vascular (CD34, LYVE-1) markers. Podoplanin was expressed in epithelial cells and tumour glands in ALB as well as in scattered intertrabecular stromal cells in both ALB and OFD. Podoplanin was not expressed by intertrabecular stromal cells in fibrous dysplasia or in metastatic adenocarcinoma. Podoplanin was expressed by osteocytes but not osteoblasts of woven and lamellar bone trabeculae in ALB, OFD, fibrous dysplasia and skeletal metastases. The finding of a common osteocyte marker in OFD/ALB stromal cells is in keeping with a close histogenetic relationship between OFD and ALB; this may reflect the prominence of fibro-osseous proliferation in these tumours. The expression of podoplanin in an osteolytic tumour of the tibia may be useful as a diagnostic discriminant in distinguishing OFD from fibrous dysplasia and ALB from metastatic adenocarcinoma.

Keywords Podoplanin · Osteofibrous dysplasia · Adamantinoma of long bone · Fibrous dysplasia · Bone tumour · Metastasis

T. G. Kashima · A. Dongre · R. Taylor · N. A. Athanasou (✉)
Nuffield Department of Orthopaedics,
Rheumatology and Musculoskeletal Science,
University of Oxford, Nuffield Orthopaedic Centre,
Oxford OX3 7LD, UK
e-mail: nick.athanasou@ndorms.ox.ac.uk

A. M. Flanagan
Histopathology Department,
Royal National Orthopaedic Hospital,
London, UK

P. C. W. Hogendoorn
Department of Pathology, Leiden University Medical Center,
Leiden, The Netherlands

Introduction

Adamantinoma of long bones (ALB) and osteofibrous dysplasia (OFD) are rare osteolytic primary bone tumours of uncertain origin that principally arise in the tibia but less commonly can involve the fibula and other bones [1–3]. Both ALB and OFD contain areas of fibrous and fibro-osseous proliferation. Intertrabecular stromal cells in OFD frequently express the epithelial markers, cytokeratin and epithelial membrane antigen (EMA) [4–6], a feature that distinguishes OFD from fibrous dysplasia, which OFD resembles morphologically. ALB is characterised histologically by the presence of a more prominent epithelial component and is divided into two major categories: classic and differentiated [1, 2]. Classic ALB typically presents in patients older than 20 years, is often a larger tumour and contains a well-defined epithelial element. Differentiated (OFD-like) ALB arises at a younger age, is usually confined to the cortex and contains a significant OFD-like component [7]. The skeleton is a common site of metastasis; classic ALB is a rare primary

bone tumour and needs to be distinguished from involvement of the tibia by metastatic carcinoma.

Podoplanin, a transmembrane glycoprotein originally identified on the surface of podocytes in renal glomeruli [8], is expressed by a number of cell types in human tissues, including lymphatic endothelial cells, squamous epithelium, lung alveolar cells, rat osteocytes and osteoblasts [9–11]. Podoplanin has also been reported in a number of neoplasms including angiosarcoma [9], germ cell tumours [12], primary squamous cell carcinomas [12, 13], bone and cartilage-forming tumours [14] and tumours of the central nervous system [15]. It has been noted in a number of biphasic tumours that contain epithelial and mesenchymal elements, such as synovial sarcoma [16], mesothelioma [17, 18] and ameloblastoma (adamantinoma) of the jaw [19].

In this study, our aim has been to determine the expression of podoplanin in ALB and OFD, both tumours which have an epithelial and stromal cell component and contain a prominent fibro-osseous component. We have analysed the relationship between podoplanin expression by intertrabecular fibroblast-like stromal cells in ALB and OFD and bone-forming cells (osteoblasts/osteocytes) in these lesions. We have also examined whether the epithelial component in ALB expresses podoplanin and investigated whether podoplanin expression can be used to assist in the differential diagnosis of ALB from metastatic carcinoma and OFD from fibrous dysplasia.

Materials and methods

Tumour samples

Twenty cases of OFD (M:F=13:7; average age 13, range 5 to 43) and twenty-two cases of ALB (M:F=15:7; average age 24, range 8 to 62), including 14 cases of classic ALB and eight cases of differentiated ALB were retrieved from the files of the Histopathology Departments of RNOH Stanmore, LUMC Leiden and NOC Oxford. All cases of ALB were monofocal. The cases of ALB and OFD were independently diagnosed histologically by at least two specialist bone histopathologists from the above centres. In addition, 20 cases of metastatic carcinoma involving the bone (five squamous cell carcinomas and fifteen adenocarcinomas) and 20 cases of monostotic fibrous dysplasia were analysed in this study. Informed patient consent and/or local ethical approval was obtained for samples to be used in this study.

Immunohistochemistry

Five micrometer sections of formalin-fixed paraffin-embedded tissue was cut and stained by an indirect immunoperoxidase technique (chemMate Envision, Dako, UK) with the monoclonal antibodies shown in Table 1 directed against human podoplanin, vimentin, pan-cytokeratin, epithelial membrane antigen, LYVE1 and CD34. Sections of normal skin and lymph node were employed as positive control. Staining was quantitatively determined as weak or strong relative to the positive control. The negative controls consisted of sections stained without the primary antibodies.

Results

All ALB and OFD cases involved the tibia and showed typical radiological features of an eccentric, lytic and sclerotic lesion of variable size that predominantly involved the anterolateral cortex. Histologically, most ALB cases were classic in type and showed variable morphology; most had basaloid or tubular areas. A focal squamoid pattern was seen in four cases. Immunohistochemistry showed cytokeratin and EMA expression in the epithelial component of ALB and in a variable number of stromal cells in both ALB and OFD. Both epithelial and stromal cell components reacted for vimentin in ALB, and all stromal cells stained uniformly for vimentin in OFD. CD34 was only expressed in blood vessel endothelial cells; there was no expression of the lymphatic endothelial cell marker LYVE-1.

Podoplanin expression in ALB and OFD

Podoplanin expression was noted in the epithelial component of all cases of ALB; both tumour glands and clumps of tumour cells strongly expressed podoplanin (Fig. 1a). Podoplanin expression was also noted in fibroblast-like stromal cells in all cases of ALB. Intertrabecular fibroblastic stromal cells in OFD also strongly expressed podoplanin (Figs. 1b and 2). Osteoblasts lining the woven bone trabeculae were negative for podoplanin, but podoplanin was expressed by osteocytes (Figs. 1b and 2a). In some cases of ALB and OFD, numerous podoplanin-expressing stromal cells were seen in fibrous tissue around newly formed bone trabeculae (Figs. 1 and 2, Table 2) .

Table 1 Monoclonal antibodies used in this study

Antigen	Antibody	Source
Podoplanin	D2-40	Signet
Vimentin	V9	Dako
Pan-cytokeratin	AE1/AE3	Dako
EMA	E29	Dako
Lyve-1	Anti-LYVE-1	Dr. D. Jackson, IMM Oxford
CD34	Q Bend 10	Dako

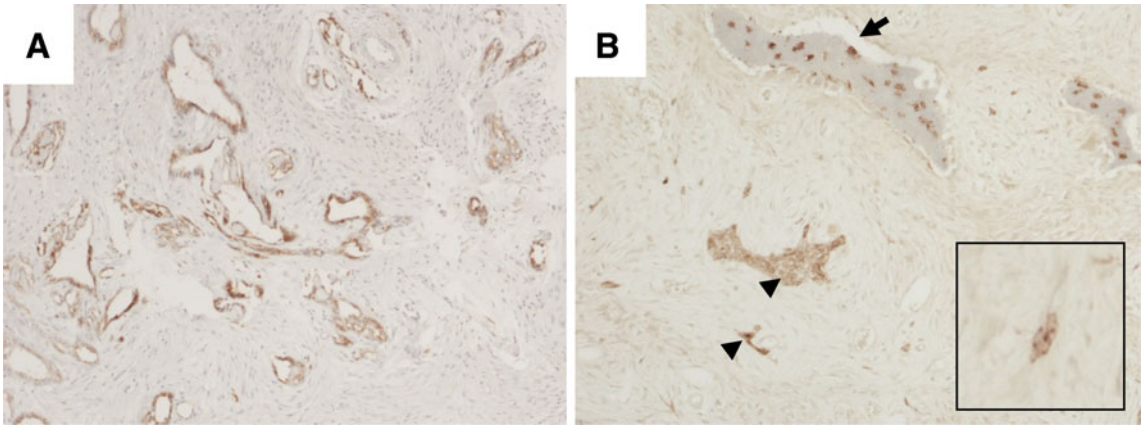

Fig. 1 Podoplanin expression in ALB. Indirect immunoperoxidase staining of ALB for podoplanin showing expression in: (**a**) tumour glands, (**b**) scattered intertrabecular stromal cells (*inset*) and osteocytes in neighbouring, newly formed bone. *Arrows* and *arrowheads* indicate osteocytes and epithelial component, respectively

Podoplanin expression in fibrous dysplasia and metastatic carcinoma

Osteocytes in the irregularly shaped spicules of woven bone formed in fibrous dysplasia strongly expressed podoplanin (Fig. 3). No evidence of podoplanin expression by stromal cells was seen in intertrabecular cellular fibrous tissue. Both stromal fibroblastic cells and osteocytes strongly expressed vimentin but showed no expression of cytokeratin or EMA. There was no expression of LYVE-1 in ALB or OFD and CD34 expression was confined to blood vessel endothelial cells.

Twenty metastatic carcinomas to bone (including six adenocarcinomas that had metastasised to the tibia) were analysed for expression of podoplanin. Podoplanin was not expressed by tumour cells in any of the 15 metastatic adenocarcinomas analysed in this study (Fig. 4a, b). Three cases of metastatic squamous cell carcinoma did not express podoplanin; diffuse podoplanin expression by tumour cells (but not stromal cells) was noted in two cases of well-differentiated metastatic squamous cell carcinoma (Fig. 4c, d). In all cases of fibrous dysplasia and metastatic carcinoma, osteocytes but not osteoblasts in uninvolved cortical and cancellous bone also showed podoplanin expression (Figs. 3, 4 and 5).

Discussion

The clinical, radiological, histological and cytogenetic similarities that exist between OFD and ALB suggest that these two primary bone tumours may be related [1–3, 20, 21]. In this study, we have found that intertrabecular stromal cells in both OFD and ALB express podoplanin, an osteocyte marker, and that the epithelial component of ALB also expresses podoplanin. Podoplanin expression in osteocytes and stromal cells in ALB and OFD is in keeping with the frequent finding of extensive new bone formation in these tumours. Co-expression of podoplanin and epithelial markers in ALB and OFD is also in keeping with the

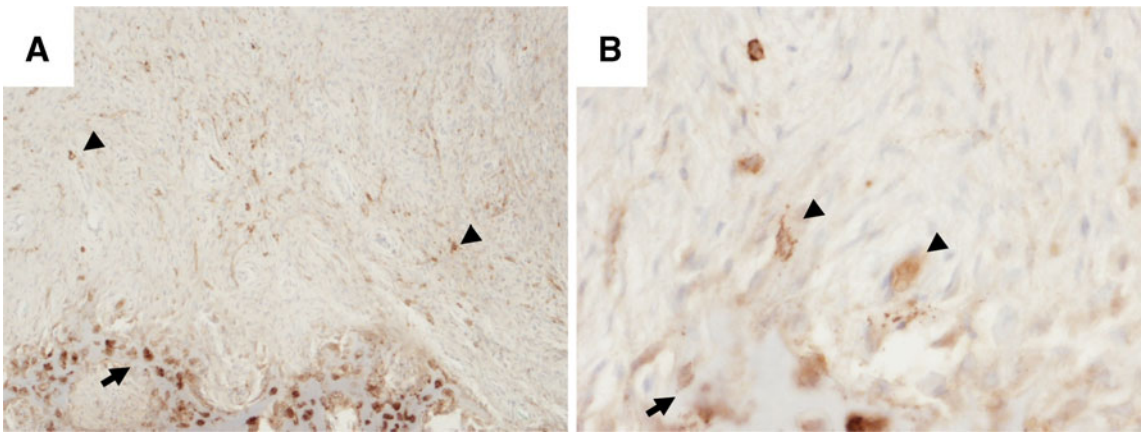

Fig. 2 Podoplanin expression in OFD. Indirect immunoperoxidase staining of OFD for podoplanin (**a**, low-power view and **b**, high-power view) showing expression in intertrabecular stromal cells (*arrowheads*) and in osteocytes of woven bone (*arrow*)

Table 2 Podoplanin expression in bone lesions of ALB, OFD, FD and metastatic carcinoma

	Intertrabecular stromal cells	Epithelial tumour cells	Osteoblasts	Osteocytes
Adamantinoma (ALB)	+	+	−	+
Osteofibrous dysplasia (OFD)	+	–[a]	−	+
Fibrous dysplasia (FD)	−	–[a]	−	+
Metastatic adenocarcinoma	−	−	−	+
Metastatic squamous cell carcinoma	−	+ (40%) − (60%)	−	+

[a] Not applicable

hypothesis that the epithelial component of ALB is derived from a common mesenchymal precursor, suggesting that OFD, differentiated ALB and classic ALB may represent a continuum of lesions.

The term "ossifying fibroma" was originally used to describe OFD in order to distinguish it from fibrous dysplasia [22]. Absence of podoplanin expression in intertrabecular stromal cells in fibrous dysplasia, in contrast to OFD, suggests that these two lesions are not identical and that OFD does not represent a form of "intracortical fibrous dysplasia", another term that has been used in the past to describe OFD [23]. Although woven bone formation characteristically occurs in both OFD and fibrous dysplasia, the latter is distinguished morphologically from that of OFD by the fact that the bone trabeculae are often thick, interconnected and lined by plump osteoblasts. This difference in podoplanin expression between fibrous dysplasia and OFD is mirrored by the differences between fibrous dysplasia and other bone-forming tumours in the expression of osteocalcin and other bone-related proteins [24].

The pathogenesis of OFD and ALB is not known, but it has been proposed that OFD represents a regressed form of ALB rather than its precursor and that the epithelial elements in ALB may result from implantation of soft tissue epithelial cell nests in cortical bone, or from mesenchymal–epithelial transformation. [7, 25–28]. Podoplanin is expressed in normal epithelial cells but overexpression by squamous and breast cancer epithelial cells has been associated with increased cell spreading, migration and invasive behaviour [29, 30]; this has been linked to modulation of the actin cytoskeleton. We noted that an increase in podoplanin expression was seen in stromal cells as well as epithelial cells lining tumour glands in ALB, a locally aggressive, potentially metastatic tumour.

OFD and ALB have been shown to differentially express markers of osteoblast differentiation, such as osteocalcin, osteonectin and osteopontin [30, 31]. We have recently shown that podoplanin expression is upregulated in transformed osteoblasts and that this expression is modulated by TGFβ1 and c-Fos. (Kunita et al., unpublished observation). Podoplanin expression is locally regulated by several growth factors, such as TGFβ and FGF, as well as by transcription factors including c-Fos [32], and it has been noted that FGF2, TGFβ and c-Fos expression is increased in OFD [25, 33, 34]. Podoplanin is expressed by osteocytes and other cells of the osteoblast lineage [11]. Podoplanin

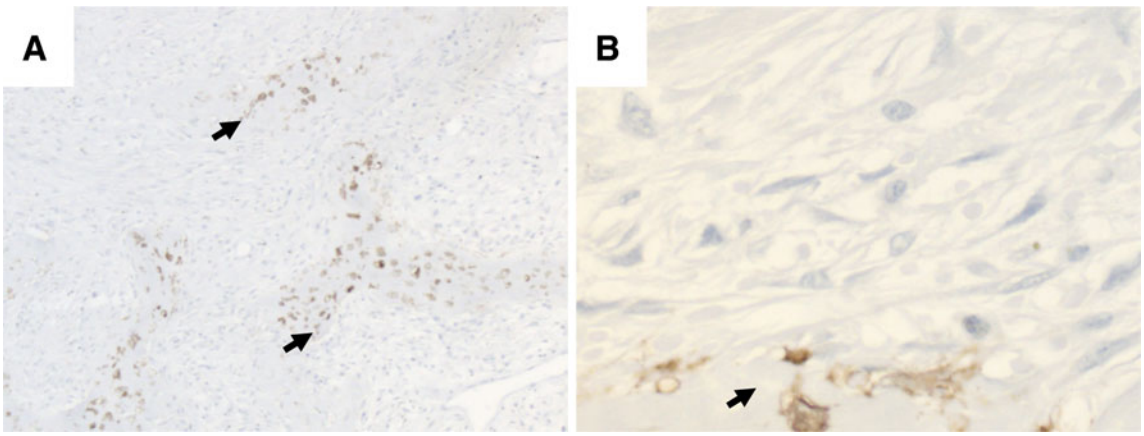

Fig. 3 Podoplanin expression in fibrous dysplasia. Indirect immunoperoxidase staining of fibrous dysplasia for podoplanin (**a**, low-power view and **b**, high-power view), showing the absence of podoplanin expression in the stromal fibroblastic cells and podoplanin expression in osteocytes

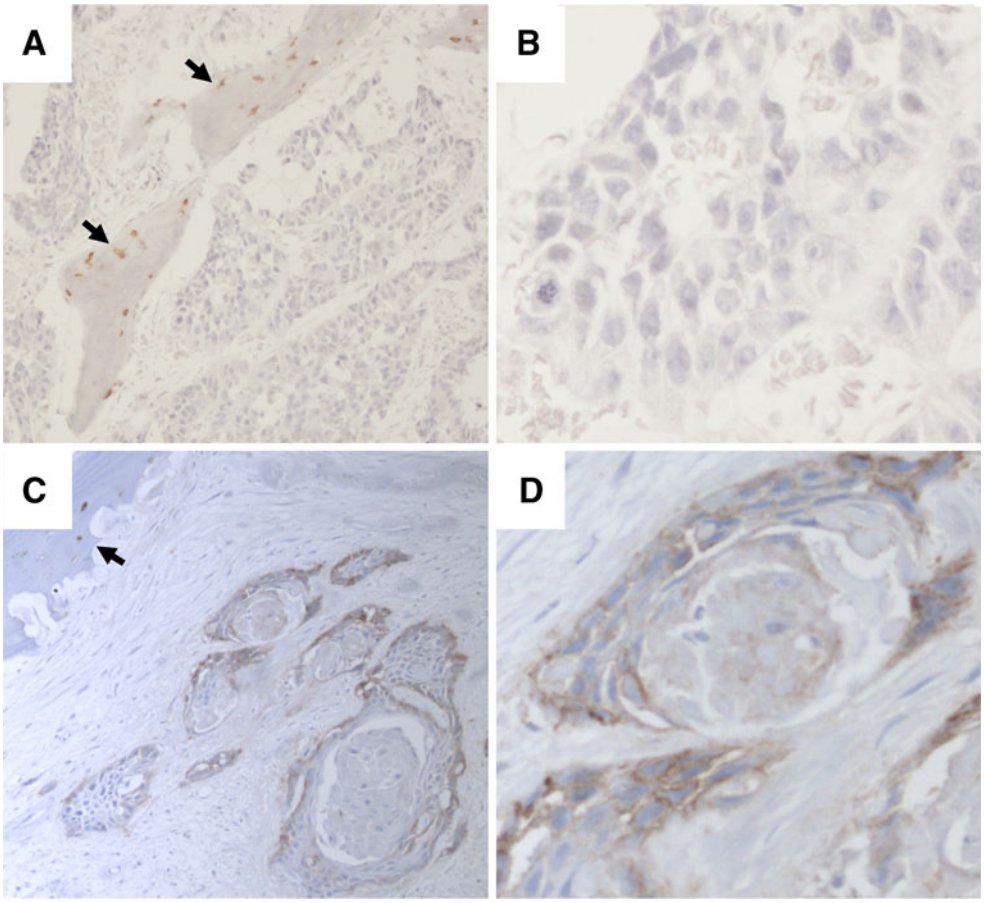

Fig. 4 Podoplanin expression in metastatic carcinoma. Indirect immunoperoxidase staining of metastatic carcinomas to bone for podoplanin showing: Low-power (**a**) and high-power (**b**) views of metastatic adenocarcinoma showing the absence of podoplanin expression by tumor cells; and low-power (**c**) and high-power (**d**) views of metastatic well-differentiated squamous cell carcinoma showing podoplanin expression by tumour cells (*arrowheads*). *Arrows* indicate podoplanin expression by osteocytes in (**a**) and (**c**)

expression by intertrabecular stromal cells in OFD and ALB is in keeping with the partly sclerotic nature of these tumours where there is formation of woven bone trabeculae which merge with overlying cortical bone.

In this study, we noted that podoplanin was not expressed by spindle-shaped fibroblastic cells in the cellular fibrous component of fibrous dysplasia or by tumour cells in most metastatic carcinomas. These findings provide a means of distinguishing fibrous dysplasia from OFD and ALB from metastatic carcinoma immunohistochemically. Podoplanin expression by intertrabecular fibroblastic stromal cells was a feature of OFD in our study and was not seen in fibrous dysplasia, indicating that its presence points to a diagnosis of OFD and its absence to one of fibrous dysplasia. The main differential diagnosis of ALB is a metastatic carcinoma involving the tibia. Podoplanin was strongly expressed in the epithelial component of all ALBs. It was, however, not expressed in metastatic adenocarcinomas and detected in only two (of five) metastatic squamous cell carcinomas analysed in this study. Podoplanin expression should thus provide a useful marker to distinguish ALB, in particular the tubular and basaloid subtypes of this tumour, from metastatic adenocarcinoma. Podoplanin expression has been noted in primary squamous cell carcinomas [12, 13], and our findings show that the expression of podoplanin is retained in metastatic squamous cell carcinomas in bone; some caution should thus be employed in using podoplanin expression to distinguish an ALB that has a significant squamoid component from metastatic squamous cell carcinoma.

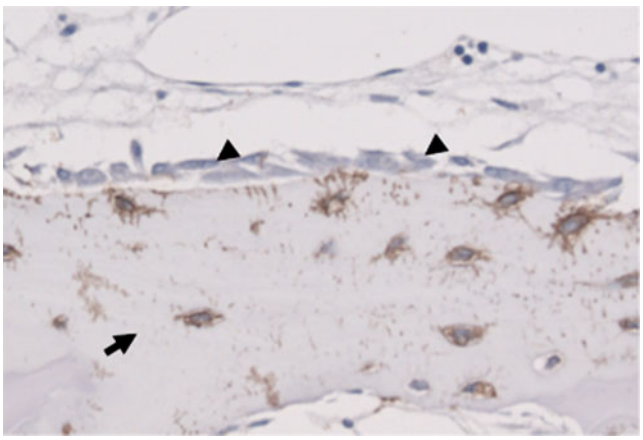

Fig. 5 Podoplanin expression in normal bone. Indirect immunoperoxidase staining of normal bone for podoplanin showing expression in osteocytes (*arrow*) but not osteoblasts (*arrowheads*)

Acknowledgements The authors would like to thank Chris Lowe for typing the manuscript. This study was carried out by the EuroBoNet consortium, a Network of Excellence funded by the European Union.

Conflicts of interest We declare that we have no conflicts of interest.

References

1. Hogendoorn PCW, Hashimoto H (2002) Adamantinoma. In: Fletcher C, Unni K, Mertens F (eds) Pathology and genetics of tumours of soft tissue and bone. IARC, Lyon, pp 332–334
2. Unni KK, Inwards YI, Bridge AN, Kindblom LG, Wold EW (2005) Tumors of the bones and joints AFIP atlas of tumor pathology. AFIP, pp. 281–298
3. Vigorita VJ, Whelman B, Hogendoorn PCW (2002) Osteofibrous dysplasia. In: Fletcher C, Unni K, Mertens F (eds) Pathology and genetics of tumours of soft tissue and bone. IARC, Lyon, pp 332–334
4. Benassi MS, Campanacci L, Gamberi G, Ferrari C, Picci P, Sangiorgi L, Campanacci M (1994) Cytokeratin expression and distribution in adamantinoma of the long bones and osteofibrous dysplasia of tibia and fibula. An immunohistochemical study correlated to histogenesis. Histopathology 25:71–76
5. Hazelbag HM, Fleuren GJ, Van den Broek LJCM, Taminiau AHM, Hogendoorn PCW (1993) Adamantinoma of the long bones: keratin subclass immunoreactivity pattern with reference to its histogenesis. Am J Surg Pathol 17:1225–1233
6. Ishida T, Iijima T, Kikuchi F, Kitagawa T, Tanida T, Imamura T, Machinami R (1992) A clinicopathological and immunohistochemical study of osteofibrous dysplasia, differentiated adamantinoma, and adamantinoma of long bones. Skeletal Radiol 21:493–502
7. Hazelbag HM, Taminiau AHM, Fleuren GJ, Hogendoorn PCW (1994) Adamantinoma of the long bones. A clinicopathological study of thirty-two patients with emphasis on histological subtype, precursor lesion, and biological behavior. J Bone Joint Surg Am 76:1482–1499
8. Breiteneder-Geleff S, Matsui K, Soleiman A, Meraner P, Poczewski H, Kalt R, Schaffner G, Kerjaschki D (1997) Podoplanin, novel 43-kd membrane protein of glomerular epithelial cells, is down-regulated in puromycin nephrosis. Am J Pathol 151:1141–1152
9. Breiteneder-Geleff S, Soleiman A, Kowalski H, Horvat R, Amann G, Kriehuber E, Diem K, Weninger W, Tschachler E, Alitalo K, Kerjaschki D (1999) Angiosarcomas express mixed endothelial phenotypes of blood and lymphatic capillaries: podoplanin as a specific marker for lymphatic endothelium. Am J Pathol 154:385–394
10. Rishi AK, Joyce-Brady M, Fisher J, Dobbs LG, Floros J, VanderSpek J, Brody JS, Williams MC (1995) Cloning, characterization, and development expression of a rat lung alveolar type I cell gene in embryonic endodermal and neural derivatives. Dev Biol 167:294–306
11. Wetterwald A, Hoffstetter W, Cecchini MG, Lanske B, Wagner C, Fleisch H, Atkinson M (1996) Characterization and cloning of the E11 antigen, a marker expressed by rat osteoblasts and osteocytes. Bone 18:125–132
12. Schacht V, Dadras SS, Johnson LA, Jackson DG, Hong YK, Detmar M (2005) Up-regulation of the lymphatic marker podoplanin, a mucin-type transmembrane glycoprotein, in human squamous cell carcinomas and germ cell tumors. Am J Pathol 166:913–921
13. Shimada Y, Ishii G, Nagai K, Atsumi N, Fujii S, Yamada A, Yamane Y, Hishida T, Nishimura M, Yoshida J, Ikeda N, Ochiai A (2009) Expression of podoplanin, CD44, and p63 in squamous cell carcinoma of the lung. Cancer Sci 100:2054–2059
14. Ariizumi T, Ogose A, Kawashima H, Hotta T, Li GD, Xu YJ, Umezu H, Sugai M, Endo N (2010) Expression of podoplanin in human bone and bone tumors: new marker of osteogenic and chondrogenic bone tumors. Pathol Int 60:193–202
15. Shibahara J, Kashima T, Kikuchi Y, Kunita A, Fukayama M (2006) Podoplanin is expressed in subsets of tumors of the central nervous system. Virchows Arch 448:493–499
16. Edwards JR, Williams K, Kindblom LG, Meis-Kindblom JM, Hogendoorn PCW, Hughes D, Forsyth RG, Jackson D, Athanasou NA (2008) Lymphatics and bone. Hum Pathol 39(1):49–55
17. Kalof AN, Cooper K (2009) D2–40 immunohistochemistry–so far! Adv Anat Pathol 16:62–64
18. Kimura N, Kimura I (2005) Podoplanin as a marker for mesothelioma. Pathol Int 55:83–86
19. Gonzalez-Alva P, Tanaka A, Oku Y, Miyazaki Y, Okamoto E, Fujinami M, Yoshida N, Kikuchi K, Ide F, Sakashita H, Kusama K (2010) Enhanced expression of podoplanin in ameloblastomas. J Oral Pathol Med 39:103–109
20. Czerniak B, Rojas-Corona RR, Dorfman HD (1989) Morphologic diversity of long bone adamantinoma. The concept of differentiated (regressing) adamantinoma and its relationship to osteofibrous dysplasia. Cancer 64:2319–2334
21. Springfield DS, Rosenberg AE, Mankin HJ, Mindell ER (1994) Relationship between osteofibrous dysplasia and adamantionma. Clin Orthop Relat Res 309:234–244
22. Kempson RL (1966) Ossifying fibroma of the long bones. A light and electron microscopic study. Arch Pathol 82:218–233
23. Campbell CJ, Hawk T (1982) A variant of fibrous dysplasia (osteofibrous dysplasia). J Bone Joint Surg Am 64:231–236
24. Hopyan S, Gokgoz N, Bell RS, Andrulis IL, Alman BA, Wunder JS (1999) Expression of osteocalcin and its transcriptional regulators core-binding factor alpha 1 and MSX2 in osteoid-forming tumours. J Orthop Res 17:633–638
25. Bovee JVMG, van den Broek LJCM, de Boer WI, Hogendoorn PCW (1998) Expression of growth factors and their receptors in adamantinoma of long bones and the implication for its histogenesis. J Pathol 184:24–30
26. Hazelbag HM, Van den Broek LJCM, Fleuren GJ, Taminiau AHM, Hogendoorn PCW (1997) Distribution of extracellular matrix components in adamantinoma of long bones suggests fibrous-to-epithelial transformation. Hum Pathol 28:183–188
27. Lichtenstein L (1997) Dermal inclusion tumours in bone (so-called adamantinoma of limb bones). In: Lichtenstein L (ed) Bone Tumours. C.V. Mosby Co., St. Louis, pp 355–362
28. Povysil C, Matejovsky Z (1981) Ultrastructure of adamantinoma of long bones. Virchows Arch A Pathol Anat Histol 393:233–244
29. Wicki A, Christofori G (2007) The potential role of podoplanin in tumour invasion. Br J Cancer 96:1–5
30. Wicki A, Lehembre F, Wick N, Hantusch B, Kerjaschki D, Christofori G (2006) Tumor invasion in the absence of epithelial-mesenchymal transition: podoplanin-mediated remodeling of the actin cytoskeleton. Cancer Cell 9:261–272
31. Maki M, Athanasou N (2004) Osteofibrous dysplasia and adamantinoma: correlation of proto-oncogene product and matrix protein expression. Hum Pathol 35:69–74
32. Durchdewald M, Guinea-Viniegra J, Haag D, Riehl A, Lichter P, Hahn M, Wagner EF, Angel P, Hess J (2008) Podoplanin is a novel fos target gene in skin carcinogenesis. Cancer Res 68:6877–6883
33. Maki M, Saitoh K, Kaneko Y, Fukayama M, Morohoshi T (2000) Expression of cytokeratin 1, 5, 14, 19 and transforming growth factors-beta1, beta2, beta3 in osteofibrous dysplasia and adamantinoma: a possible association of transforming growth factor-beta with basal cell phenotype promotion. Pathol Int 50:801–807
34. Sakamoto A, Oda Y, Iwamoto Y, Tsuneyoshi M (2007) Frequent immunoexpression of TGF-beta1, FGF-2 and BMP-2 in fibroblast-like cells in osteofibrous dysplasia. Oncol Rep 17:531–535

Virchows Arch (2011) 459:47–53
DOI 10.1007/s00428-010-1032-3

ORIGINAL ARTICLE

Absence of nucleolar parafibromin immunoreactivity in subsets of parathyroid malignant tumours

C. Christofer Juhlin · Felix Haglund · Takao Obara · Andrew Arnold · Catharina Larsson · Anders Höög

Received: 1 November 2010 / Revised: 13 December 2010 / Accepted: 20 December 2010 / Published online: 8 January 2011
© Springer-Verlag 2011

Abstract Hyperparathyroidism 2 (*HRPT2*) gene mutations underlie hereditary and sporadic forms of primary hyperparathyroidism (PHPT), and the encoded product parafibromin has been established as a marker for facilitating parathyroid tumour classification. *HRPT2* mutations and reduced nuclear expression of parafibromin are readily observed in parathyroid carcinomas but rarely in benign tumours, thereby aiding the identification of malignant PHPT. Recently, parafibromin has been shown to localize to the nucleolar compartment, and nucleolar parafibromin exhibits tumour-suppressive properties in vitro. In this study, nucleolar parafibromin immunoreactivity was assessed by high-power magnification microscopy in 82 parathyroid tumours previously analysed for nuclear parafibromin, including 23 carcinomas, 16 atypical adenomas, and 43 adenomas. Absent nucleolar expression was evident in three carcinomas and in one atypical adenoma, which also showed expression of nuclear parafibromin in all or subsets of the tumour cells. All three carcinomas carried *HRPT2*-inactivating mutations predicted to abolish the three nucleolar localization signals of parafibromin. The demonstrated absence of nucleolar parafibromin in three carcinomas with *HRPT2* mutations suggests that parafibromin exhibits nucleolar tumour suppressor properties also in vivo, and disruption of nucleolar localization might propel parathyroid tumorigenesis independent of nuclear parafibromin expression. The loss of nucleolar staining in the presence of nuclear parafibromin suggests that parafibromin immunoreactivity should also be assessed in the nucleoli, as the sensitivity for the detection of malignant and atypical PHPT is increased compared to scoring of nuclear parafibromin alone.

Keywords Parafibromin · *HRPT2* · *CDC73* · Primary hyperparathyroidism · Parathyroid · Carcinoma · Nucleolus

Electronic supplementary material The online version of this article (doi:10.1007/s00428-010-1032-3) contains supplementary material, which is available to authorized users.

C. C. Juhlin (✉) · F. Haglund · C. Larsson
Department of Molecular Medicine and Surgery,
Karolinska University Hospital Solna,
SE-171 76, Stockholm, Sweden
e-mail: christofer.juhlin@ki.se

C. C. Juhlin · A. Höög
Department of Oncology-Pathology,
Karolinska University Hospital Solna,
SE-171 76, Stockholm, Sweden

C. C. Juhlin · F. Haglund · C. Larsson
Center for Molecular Medicine CMM, Karolinska Institutet,
Karolinska University Hospital Solna,
SE-171 76, Stockholm, Sweden

T. Obara
Department of Endocrine Surgery,
Tokyo Women's Medical College,
8-1 Kawada-Cho, Shinjuku-Ku,
Tokyo 162-8666, Japan

A. Arnold
Center for Molecular Medicine and the Division of Endocrinology and Metabolism, University of Connecticut School of Medicine,
Farmington, CT 06030-3101, USA

Introduction

Germline mutations in the hyperparathyroidism 2 (*HRPT2,* also known as *CDC73*) tumour suppressor gene cause the hyperparathyroidism-jaw tumour syndrome (HPT-JT), an autosomal dominant form of primary hyperparathyroidism (PHPT) in which the afflicted members often present with malignant parathyroid tumours [1]. Somatic *HRPT2* mutations are also commonly found in sporadic parathyroid carcinomas [2, 3] and subsets of atypical adenomas [4, 5], but are rarely observed in adenomas [1].

Parathyroid carcinoma is the unusual but potentially lethal variant of PHPT. The diagnosis is made upon identification of malignant behaviour at postsurgical histopathological examination; however, histopathology alone confers reduced sensitivity and specificity for its proper recognition [6, 7]. As a consequence of the frequent findings of *HRPT2* mutations in this PHPT subtype, immunohistochemical analyses of the encoded parafibromin protein have been suggested as a diagnostic instrument, as parafibromin expression has been found to be reduced or absent in the majority of parathyroid carcinomas and in subsets of atypical adenomas, but retained in the majority of benign tumours [4, 5, 8, 9]. Current studies agree that presence of nuclear parafibromin staining strongly suggests a benign tumour, whereas negative or reduced levels of nuclear parafibromin expression suggest parathyroid carcinoma or HPT-JT-associated disease, more rarely atypical parathyroid adenoma and very seldom adenoma. Nevertheless, parafibromin immunohistochemistry lacks the sensitivity to properly identify all cases of malignant PHPT, and adjunct markers have since been sought for facilitating the identification [10–12].

Hahn and Marsh reported that parafibromin has three distinct nucleolar localization signals (NoLS) at amino acid residues 76–92 (NoLS 1), 192–194 (NoLS 2), and 393–409 (NoLS 3) in addition to its known nuclear localization (NLS) signal at 125–139 [13]. The authors demonstrated NoLS-dependent nucleolar localization of parafibromin, which could imply one or more nucleolar function in addition to the known nuclear roles. Mutational inactivation of any of the three NoLS sequences, particularly NoLS 1 and/or 3, led to a reduction in cells exhibiting parafibromin nucleolar localization, and the combined inactivation of NoLS 1–3 led to a complete abolishment of nucleolar localization [13]. Interestingly, each NoLS sequence was also shown to mediate nuclear import of parafibromin to some extent, whereas the NLS sequence at 125–139 was unable to confer nucleolar import of parafibromin [13]. These observations would suggest that a hypothetical *HRPT2* mutation afflicting one or several of the NoLS regions would obstruct nucleolar localization of parafibromin, whereas the nuclear import could be retained primarily by the NLS, or aided by any of the NoLS sequences.

Recently, an *HRPT2* missense mutation (L95P) located just downstream of NoLS 1 was identified in a kindred with the HPT-JT syndrome, and shown to be deficient in nucleolar localization of parafibromin in vitro [14]. The L95P mutant also inhibited wild-type parafibromin, leading to cell cycle progression and augmented cell survival, findings that would suggest that parafibromin exerts important tumour-suppressive properties in the nucleolus in vitro.

We have previously investigated a large tumour material for parafibromin immunoreactivity [5, 15]. Given the proposed roles for nucleolar parafibromin, we here applied high-power magnification to analyse whether the previously stained parathyroid carcinomas exhibited lack of nucleolar parafibromin staining as an additional marker for parathyroid malignancy.

Materials and methods

Tissue samples

The tumour material consisted of 23 parathyroid carcinomas (T1–T23, previously referred to as unequivocal), 16 atypical adenomas (T24–T39, of which some were previously referred to as equivocal carcinomas), and 43 sporadic adenomas used as controls (T40–T82) (Supplemental Table A). The clinical details and nuclear parafibromin scoring results have been previously reported for all cases including T1–22, 24–34, 40–64 [5] and T23, 35–39, 65–82 [15]. Cases T1, 2, 6, 20, 21, and 24 have been previously screened for *HRPT2* gene mutations by sequencing [5] (Supplemental Table A). Sample classifications were according to the World Health Organization system, in which carcinomas displayed vascular, perineural, and/or local tissue invasion and/or distant metastases. Atypical adenomas are tumours with an unknown malignant potential which demonstrate one or several atypical features not present in regular adenomas, such as marked nuclear atypia, fibrous bands, trabecular growth, and/or an elevated mitosis count. HeLa and COS cells transfected with the wild-type *HRPT2* sequence [5] as well as normal parathyroid rim present on tumour tissue slides were evaluated as positive controls for nucleolar expression of parafibromin.

Immunohistochemical scoring procedures

Parafibromin nucleolar expression was independently evaluated and scored using a Leica DM 2000 microscope and a high-power magnification objective (×63) (Leica, Microsystems GmbH, Wetzlar, Germany). The ×20 and ×40 objectives previously used for assessment of nuclear parafibromin [5, 15] were found to be suboptimal for analysing parafibromin staining of the nucleolar compartment; in our experience the ×63 objective was required to fully distinguish nucleolar from nuclear staining. Negative nucleolar staining was defined as an absence of staining reaction in the nucleolar compartment in the vast majority of tumour cells in the presence of nuclear parafibromin expression. All cases examined had been stained using 2H1 (Santa Cruz Biotechnology, Santa Cruz, CA, USA), a monoclonal antibody targeting aa 87–100 of parafibromin [5, 15]. For confirmation , carcinomas T1–22 and atypical adenomas T24–34 were further assessed for nucleolar

parafibromin at ×63 magnification for the three polyclonal parafibromin antibodies: TNYV (targeting aa 39–58), BL648 (Bethyl Laboratories, Montgomery, TX, USA) (targeting an unknown sequence within aa 250–300), and APVF (targeting aa 509–531) reported in [5].

Results

A total of 82 parathyroid tumours were investigated for nucleolar parafibromin immunoreactivity in high magnification, and the results are exemplified by photomicrographs in Figs. 1 and 2 and detailed in Supplemental Table A. Three cases of parathyroid carcinomas (T1, T6, T21) and one atypical adenoma (T31) displayed lack of nucleolar staining of parafibromin in the presence of nuclear parafibromin expression in all or subsets of the tumour cells (Fig. 1). By contrast, all 43 adenomas displayed strong nucleolar and nuclear expression in the vast majority of cells analysed (Fig. 2a). Similarly, strong nuclear and nucleolar expression were observed in normal parathyroid rim and *HRPT2*-transfected COS and HeLa cells (Fig. 2b–d). Cases T1 and T31 displayed positive nuclear parafibromin expression and absent nucleolar expression, whereas cases T6 and T21 displayed partial loss of nuclear parafibromin (patterned mixture of positive and negative nuclei) with absent nucleolar parafibromin. Absent nucleolar staining was also observed in the carcinoma (T5) that was entirely negative for nuclear parafibromin. In the remaining carcinomas and atypical adenomas the nucleolar and nuclear parafibromin-staining pattern were corresponding. Hence, these cases showed either positive nuclear and nucleolar expression in the vast majority of tumour cells, or nuclear and nucleolar expression in a subset of tumour cells only (Supplemental Table A). To verify the observations with the 2H1 parafibromin antibody, three different parafibromin antibodies were similarly evaluated in high-power magnification for 33 carcinomas and atypical adenomas. Analogous results were obtained using four different antibodies directed at four diverse epitopes of parafibromin, supporting that full-length parafibromin is absent from the nucleoli in cases T1, T6, T21, and T31 (Fig. 1). Positive nucleolar signals were completely abolished in either peptide competition assays with the 2H1-immunizing peptide or by omitting the primary antibody, suggesting that the positive nucleolar signals obtained were specific for parafibromin.

The known *HRPT2* mutational status of the cases studied are presented in Table 1. All three carcinomas with absent nucleolar immunoreactivity displayed one or two somatic *HRPT2* mutations. Case T1 harbour a 226C>T substitution in exon 2, rendering a truncated parafibromin protein at residue 76, corresponding to the first amino acid of NoLS 1. Case T6 presents with two somatic mutations, 70G>T in exon 1, and 746delT in exon 8, leading to truncations at amino acid residue 24 and 256, respectively, whereas case T21 displays a 23TGCG>GTG mutation in exon 1, leading to a stop at amino acid residue 20 (Table 1). Hence, each carcinoma carried at least one mutation that was predicted to lead to premature protein truncation and disruption of the three NoLS sequences of parafibromin.

Our previous study identified loss or partial loss of nuclear parafibromin in the majority of parathyroid carcinomas (15/22; 68%) and approximately half of the atypical adenomas (5/11; 45%) examined [5]. If absence of nucleolar staining was added as an additional criterion to reduce nuclear parafibromin expression, the sensitivity would reach 17/23 (74%) for the carcinomas and 8/16 (50%) for the atypical adenomas, whereas the specificity would remain at 100% since no parathyroid adenoma displayed this pattern. Regarding the sensitivity for *HRPT2* mutations, reduced expression of nuclear parafibromin was evident in 3/6 (50%) cases with established *HRPT2* mutations, whereas reduced nuclear and/or nucleolar parafibromin immunoreactivity was observed in 4/6 (67%) of the cases with known *HRPT2* mutations.

Discussion

The nucleolar compartment is a non-membrane bound region of the nucleus in which ribosomal RNA is transcribed. Several tumour suppressor proteins have been endowed with nucleolar localization signals, such as the p14ARF tumour suppressor protein, which inhibits the nucleolar B23 protein to induce cell death, and the JmjC-domain-containing histone demethylase 1B protein (JHDM1B) that repress transcription of rRNA genes and is downregulated in aggressive brain tumours [16, 17]. Cell cycle progression is often linked to upregulation of nucleolar function and increased nucleolar size, and evidence is emerging that the nucleolar compartment is important to the proliferating cell and that nucleolar processes are tightly regulated by various tumour suppressor proteins [18]. Our finding of absent nucleolar parafibromin immunoreactivity in three carcinomas and one atypical adenoma with various levels of nuclear parafibromin suggests that parafibromin might display nucleolar tumour suppressor properties also in vivo.

Cases T1, T6, and T21 all presented with one or several somatic *HRPT2* mutations [5]. Given the scattered positions of NoLS 1–3 in parafibromin, all mutations are believed to afflict one or several of the known NoLS sequences. The mutation in case T1 is predicted to lead to a premature truncation at amino acid 76, the first residue of NoLS 1. Case T6 has two somatic mutations resulting in protein truncations that will delete NoLS 1–3 in first allele and

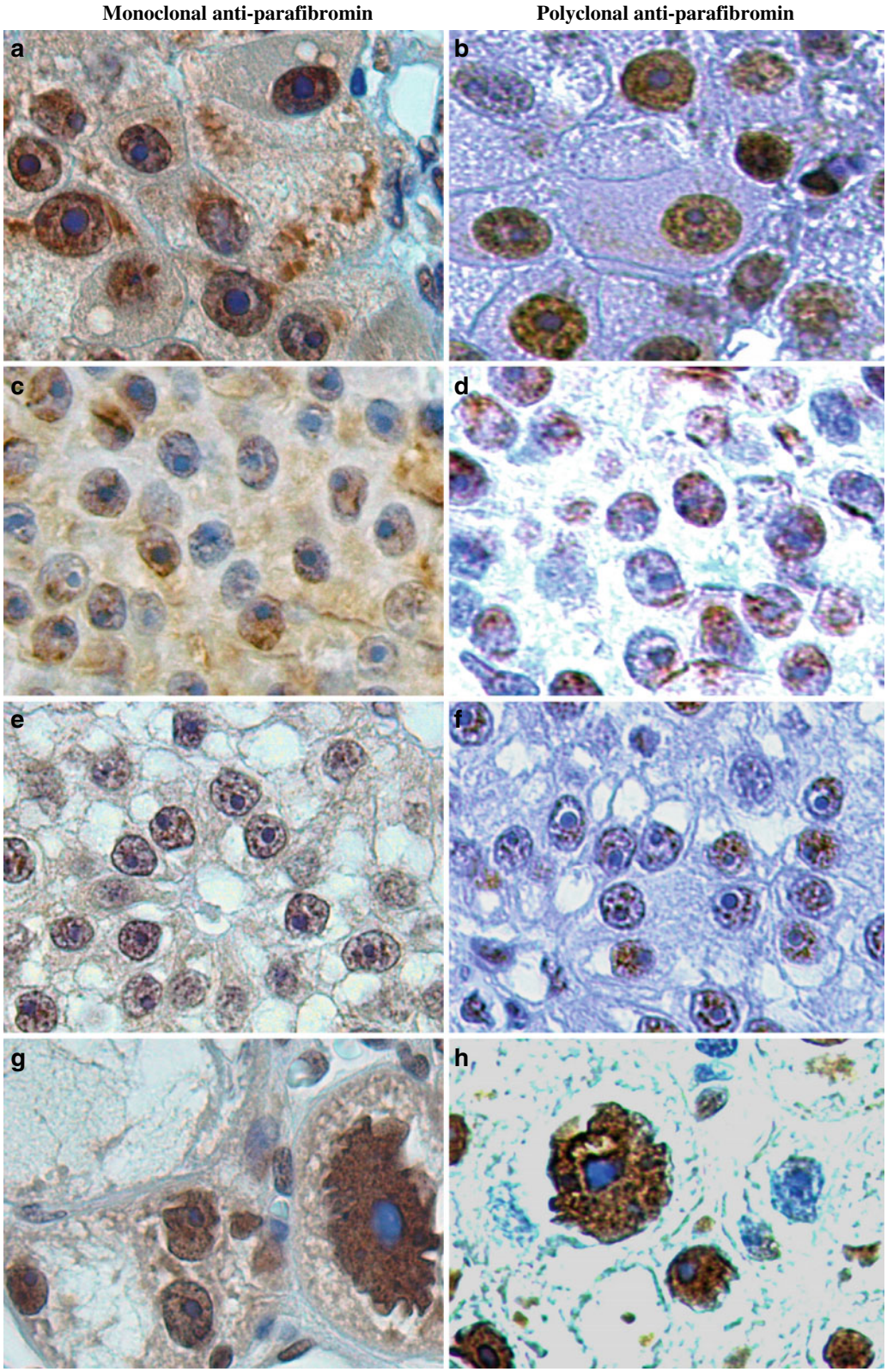

Fig. 1 Photomicrographs demonstrating absence of nucleolar parafibromin immunoreactivity in parathyroid carcinoma cases T1 (**a**, **b**), T21 (**c**, **d**), and T6 (**e**, **f**), and atypical adenoma T30 (**g**, **h**). All four cases invariably displayed negative nucleolar immunoreactivity for the different parafibromin antibodies employed. For each case, the monoclonal antibody 2H1 is shown to the *left*, and one polyclonal antibody is illustrated to the *right*. T1 is exemplified by parafibromin staining with the BL648 antibody (**b**), T21 by the APVF antibody (**d**), T6 by the APVF antibody (**f**), and T30 by the TNYV antibody (**h**). All photomicrographs were taken using a ×63 objective

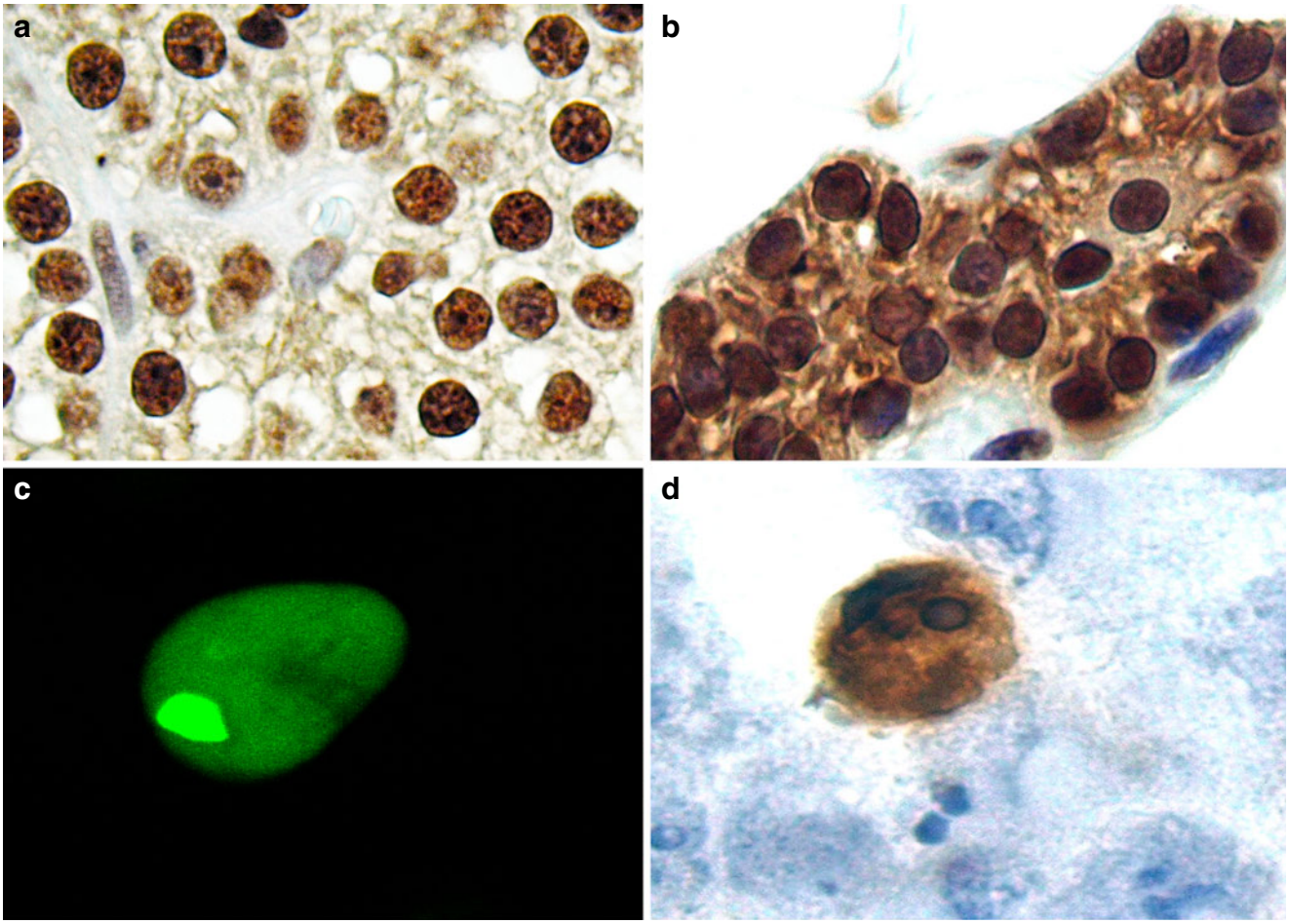

Fig. 2 Photomicrographs showing nucleolar and nuclear parafibromin expression in a parathyroid adenoma (**a**) and in normal parathyroid rim (**b**) using the 2H1 antibody and a ×63 objective. For comparison, nucleolar and nuclear parafibromin expression is shown after transfection with a *HRPT2* construct with mGFP tagging to COS cells (**c**) and to HeLa cells after immunohistochemistry with the 2H1 antibody (**d**) as described in [5]

Table 1 Parafibromin immunoreactivity in cases with defined *HRPT2* mutations

Case no	Nucleolar parafibromin	Nuclear parafibromin (% positive tumour cells)	*HRPT2* mutation	Predicted effects	Afflicted signals	
					NLS[1]	NoLS[2]
Parathyroid carcinomas						
T1	Absent in all tumour cells	Positive (100%)	Ex 2: 226C>T	Stop at aa 76	Yes	1, 2, 3
T2	Positive in nuclear positive cells	Partial loss (74%)	Ex 7: 664C>T	Stop aa 222	No	3
T6	Absent in all tumour cells	Partial loss (55%)	Ex 1: 70G>T	Stop at aa 24	Yes	1, 2, 3
			+ Ex 8: 746delT	+ at aa 256	No	3
T20	Positive in nuclear positive cells	Positive (100%)	Ex 1: 82del4	Stop at aa 35	Yes	1, 2, 3
			+ Ex 8: 732delT	+ at aa 256	No	3
T21	Absent in all tumour cells	Partial loss (73%)	Ex 1: 23TGCG>GTG	Stop at aa 20	Yes	1, 2, 3
Atypical adenoma						
T24	Positive in all tumour cells	Positive (100%)	Ex 1: c127insC	Stop at aa 65	Yes	1, 2, 3

NLS[1] nuclear localization signal at aa 125–139, *NLS* [2] nucleolar localization signals at aa 76–92 (NoLS 1), 192–194 (NoLS 2), and 393–409 (NoLS 3)

NoLS 3 in the second allele. The retained NLS in allele 2 could in theory allow parafibromin to enter the nuclear compartment, which is consistent with the finding of nuclear immunoreactivity, albeit nucleolar absence of parafibromin for this case. Finally, case T21 displays a somatic mutation that yields a premature stop at amino acid residue 20, thereby probably abolishing all three NoLS sequences altogether from this transcript. The status of the remaining allele in cases T1 and T21 is unknown, although the positive nuclear signals obtained when using four different parafibromin antibodies would suggest that full-length parafibromin or splicing variants of the protein are retained in the nuclear compartment. One should also bear in mind that recent in vitro studies suggest that mutant parafibromin unable to reach the nucleolar compartment overrides the antiproliferative effects of wild-type parafibromin and could act in a dominant negative manner, supporting the notion that nucleolar-deficient and nuclear wild-type parafibromin could coexist, but still augment proliferation [14].

Two of the cases with negative nucleolar staining (T1 and T6) display clinical evidence of malignant behaviour, as case T1 is parathyroid tissue derived from a lung metastasis and case T6 derives from the primary tumour with medical history of recurrent disease and lung metastases. This fact demonstrates that absent nucleolar parafibromin is not found only in parathyroid tumours with fulfilled histopathological criteria of malignancy, but also in cases with clinical evidence of malignant behaviour. Given the fact that the current histopathological criteria display reduced sensitivity and specificity for the detection of parathyroid malignancy, the findings of absent nucleolar parafibromin in cases with clinically overt and manifest malignant disease argue in favour of a nucleolar tumour suppressor function which may be associated to malignant potential.

Subsets of malignant parathyroid tumours probably fail to be recognized by parafibromin immunohistochemistry [4, 5, 8, 9], partly because *HRPT2* mutations are believed to be present in the majority, but not all, cases of parathyroid carcinoma, and partly because not all *HRPT2* gene mutations are detected by aberrant nuclear parafibromin immunoreactivity [5]. Our results indicate that the addition of nucleolar staining as a criterion when assessing parafibromin immunoreactivity increased both sensitivity for the detection of parathyroid carcinoma as well as *HRPT2* gene mutations, suggesting that this assessment could be of value to parathyroid tumour classification. Negative nucleolar staining in the presence of nuclear parafibromin might indicate an *HRPT2* mutation interfering with one or several NoLS sequences of parafibromin, and *HRPT2* mutations in turn point to parathyroid malignancy.

To summarize, this is the first report of absent parafibromin nucleolar immunoreactivity in a fraction of parathyroid carcinomas endowed with various quantities of nuclear expression and associated to inactivating *HRPT2* mutations predicted to disrupt one or several NoLS sequences. The findings imply that parafibromin exerts nucleolar tumour-suppressive properties also in vivo, and support the addition of nucleolar evaluation in parafibromin immunohistochemistry.

Acknowledgements The authors wish to thank Ingo Leibiger and Barbara Leibiger for proficient help in acquiring images from previous live cell imaging experiments. The study was financially supported by the Swedish Cancer Society, the Swedish Research Council, the Cancer Society in Stockholm, the Gustav V Jubilee Foundation, the Göran Gustafsson Foundation for Research on Natural Sciences and Medicine, the Stockholm County Council and Karolinska Institutet.

Conflict of interest statement We declare that we have no conflict of interest.

References

1. Carpten JD, Robbins CM, Villablanca A et al (2002) HRPT2, encoding parafibromin, is mutated in hyperparathyroidism-jaw tumor syndrome. Nat Genet 32:676–680
2. Howell VM, Haven CJ, Kahnoski K et al (2003) HRPT2 mutations are associated with malignancy in sporadic parathyroid tumours. J Med Genet 40:657–663
3. Shattuck TM, Välimäki S, Obara T et al (2003) Somatic and germ-line mutations of the HRPT2 gene in sporadic parathyroid carcinoma. N Engl J Med 349:1722–1729
4. Tan MH, Morrison C, Wang P et al (2004) Loss of parafibromin immunoreactivity is a distinguishing feature of parathyroid carcinoma. Clin Cancer Res 10:6629–6637
5. Juhlin CC, Villablanca A, Sandelin K et al (2007) Parafibromin immunoreactivity: its use as an additional diagnostic marker for parathyroid tumor classification. Endocr Relat Cancer 14:501–512
6. Sandelin K, Tullgren O, Farnebo LO (1994) Clinical course of metastatic parathyroid cancer. World J Surg 18:594–598, discussion 599
7. Ippolito G, Palazzo FF, Sebag F et al (2007) Intraoperative diagnosis and treatment of parathyroid cancer and atypical parathyroid adenoma. Br J Surg 94:566–570
8. Gill AJ, Clarkson A, Gimm O et al (2006) Loss of nuclear expression of parafibromin distinguishes parathyroid carcinomas and hyperparathyroidism-jaw tumor (HPT-JT) syndrome-related adenomas from sporadic parathyroid adenomas and hyperplasias. Am J Surg Pathol 30:1140–1149
9. Juhlin C, Larsson C, Yakoleva T et al (2006) Loss of parafibromin expression in a subset of parathyroid adenomas. Endocr Relat Cancer 13:509–523
10. Fernandez-Ranvier GG, Khanafshar E, Tacha D et al (2009) Defining a molecular phenotype for benign and malignant parathyroid tumors. Cancer 115:334–344
11. Howell VM, Gill A, Clarkson A et al (2009) Accuracy of combined protein gene product 9.5 and parafibromin markers for immunohistochemical diagnosis of parathyroid carcinoma. J Clin Endocrinol Metab 94:434–441

12. Juhlin CC, Haglund F, Villablanca A et al (2009) Loss of expression for the Wnt pathway components adenomatous polyposis coli and glycogen synthase kinase 3-beta in parathyroid carcinomas. Int J Oncol 34:481–492
13. Hahn MA, Marsh DJ (2007) Nucleolar localization of parafibromin is mediated by three nucleolar localization signals. FEBS Lett 581:5070–5074
14. Panicker LM, Zhang JH, Dagur PK et al (2010) Defective nucleolar localization and dominant interfering properties of a parafibromin L95P missense mutant causing the hyperparathyroidism-jaw tumor syndrome. Endocr Relat Cancer 17:513–524
15. Juhlin CC, Nilsson IL, Johansson K et al (2010) Parafibromin and APC as screening markers for malignant potential in atypical parathyroid adenomas. Endocr Pathol 21:166–177
16. Itahana K, Bhat KP, Jin A et al (2003) Tumor suppressor ARF degrades B23, a nucleolar protein involved in ribosome biogenesis and cell proliferation. Mol Cell 12:1151–1164
17. Frescas D, Guardavaccaro D, Bassermann F et al (2007) JHDM1B/FBXL10 is a nucleolar protein that represses transcription of ribosomal RNA genes. Nature 450:309–313
18. Montanaro L, Treré D, Derenzini M (2008) Nucleolus, ribosomes, and cancer. Am J Pathol 173:301–310

Virchows Arch (2011) 459:55–63
DOI 10.1007/s00428-011-1080-3

ORIGINAL ARTICLE

Differential clinicopathological features in microsatellite instability-positive colorectal cancers depending on CIMP status

Jeong Mo Bae · Mi Jung Kim · Jung Ho Kim · Jae Moon Koh · Nam-Yun Cho · Tae-You Kim · Gyeong Hoon Kang

Received: 7 December 2010 / Revised: 28 February 2011 / Accepted: 3 April 2011 / Published online: 15 April 2011
© Springer-Verlag 2011

Abstract Microsatellite instability-positive (MSI+) colorectal cancers (CRCs) are divided into CpG island methylator phenotype-positive (CIMP+) and CpG island methylator phenotype-negative (CIMP−) tumors. The repertoire of inactivated genes in CIMP+/MSI+ CRCs overlaps with but is likely to differ from that of CIMP−/MSI+ CRCs. Because epigenotypic differences are likely to be manifested as phenotypic differences, CIMP+/MSI+ CRCs are expected to differ from CIMP−/MSI+ CRCs in some clinicopathological features. This study aimed to characterize both common and different features between the two subtypes. A total of 72 MSI+ CRCs were analyzed for their methylation status in eight CIMP panel markers using MethyLight assay. CIMP+/MSI+ and CIMP−/MSI+ CRCs were compared regarding clinicopathologic features and mutation in *KRAS*/*BRAF*. An independent set of MSI+ CRCs (n=97) was analyzed for their relationship of CIMP+ status with clinical outcome. Eighteen cases (25%) were CIMP+, and this CIMP+ subtype was highly correlated with older age (P<0.001). Polypoid gross appearance without ulceration was observed only in CIMP−/MSI+ CRCs (18.5%, P=0.057). CIMP+/MSI+ CRCs were closely associated with poor differentiation, medullary appearance, signet ring cell appearance, and acinar-form appearance, whereas the CIMP−/MSI+ subtype was closely associated with intraglandular eosinophilic mucin and stratified nuclei (all P values <0.05). Patients with CIMP+/MSI+ CRCs showed worse overall survival than patients with CIMP−/MSI+ CRCs. Our results demonstrate heterogeneity in the clinicopathological features of MSI+ CRCs depending on CIMP status. The observation that CIMP+ and CIMP− subtypes showed different clinical behaviors may provide a clue for establishing subtype-specific therapeutic strategies for these two subtypes.

Keywords Colon cancer · CpG island · DNA methylation · Microsatellite instability · Prognosis

Jeong Mo Bae and Mi Jung Kim equally contributed to this work.

J. M. Bae · J. H. Kim · J. M. Koh · G. H. Kang (✉)
Department of Pathology,
Seoul National University College of Medicine,
28 Yongon-dong, Chongno-gu,
Seoul 110-744, South Korea
e-mail: ghkang@snu.ac.kr

M. J. Kim
Department of Diagnostic Pathology, Asan Medical Center,
Seoul, South Korea

N.-Y. Cho · G. H. Kang
Laboratory of Epigenetics,
Cancer Research Institute and 2nd Stage Brain Korea,
Seoul National University College of Medicine,
Seoul, South Korea

T.-Y. Kim
Department of Internal Medicine,
Seoul National University College of Medicine,
Seoul, South Korea

Colorectal cancer (CRC) is one of the most common malignancies worldwide and has shown a gradual increase in its annual incidence in Eastern Asia [1]. CRC is a heterogeneous disease in terms of its molecular carcinogenesis [2–4]. Two molecular pathways to colorectal carcinogenesis are well known and include the chromosomal instability pathway and the mutator (microsatellite instability, MSI) pathway. Another molecular pathway, the epigenetic instability or CpG island methylator phenotype (CIMP), was first described by Issa's group [5, 6] and is characterized by widespread hypermethylation of promoter

CpG island loci, which results in the inactivation of tumor suppressor genes or tumor-related genes [6, 7]. CIMP+ CRCs (often referred to as CIMP-high CRCs) are a subset of CRCs that occur through the epigenetic instability pathway. CRCs could be subdivided into MSI− carcinomas and MSI+ carcinomas (often referred to as MSI-high or MSI-H): MSI− carcinomas represent chromosomal instability carcinomas and approximately 60% of CIMP+ carcinomas, whereas MSI+ carcinomas represent approximately 40% of sporadic CIMP+ carcinomas and hereditary carcinomas (Lynch syndrome) arising via the mutator pathway [4].

MSI+ CRCs occur through two different mechanisms, namely mutations in genes for mismatch repair enzymes and promoter CpG island hypermethylation of *MLH1*; the former accounts for hereditary MSI+ CRCs (Lynch syndrome), and the latter accounts for sporadic MSI+ CRCs [8–10]. *MLH1* hypermethylation is not an isolated event and is usually accompanied by concordant hypermethylation in the promoter CpG island loci of multiple genes, an essential feature of CIMP+ CRCs [11]. Although MSI+ CRCs with genetic changes in mismatch repair genes (CIMP−/MSI+ CRCs) and CIMP-associated MSI+ CRCs (CIMP+/MSI+ CRCs) share common alterations at numerous microsatellite loci, a considerable difference probably exists in gene expression profiles between them because CIMP+/MSI+ CRCs harbor CpG island hypermethylation of multiple genes [12]. Thus, it is highly plausible that epigenotypic differences between these two subtypes may be reflected in their phenotypic differences. Of the known clinicopathological features of MSI+ CRCs [13, 14], including synchronous or metachronous CRC occurrence, preponderance toward the proximal colon, more frequent exophytic or polypoid growth, more frequent poor differentiation, more frequent extracellular mucin production, and a higher number of tumor-infiltrating lymphocytes (TIL), it is not known which are shared or different between CIMP−/MSI+ and CIMP+/MSI+ CRCs. A few studies [15–18] have addressed this issue; specifically Ogino et al. [17] and Dahlin et al. [16] addressed the differences in clinicopathological and molecular findings between CIMP−/MSI+ and CIMP+/MSI+ CRCs in the Western population. Moreover, Ward et al. [19] and Barault et al. [20] reported no differences in clinical outcomes between CIMP−/MSI+ and CIMP+/MSI+ CRC patients.

Here, we analyzed 72 MSI+ CRCs for their CIMP status with MethyLight analysis and then compared the known clinicopathological or molecular features between CIMP+ and CIMP− subtypes. We found clinicopathological differences between these two subtypes, and in particular, we noted that the CIMP+ subtype showed a significantly worse clinical outcome than the CIMP− subtype, which was confirmed in an independent set of MSI+ CRCs (n=97).

Materials and methods

Of a consecutive series of 989 patients who underwent curative surgery for CRCs in Seoul National University Hospital, Seoul, South Korea from 2004 to 2006, 78 MSI+ cases (7.9%) were identified. Six cases of MSI+ CRCs were excluded from the study because the patients received preoperative radiation or because paraffin tissue blocks were unavailable. Formalin-fixed, paraffin-embedded tissues were obtained from 72 MSI+ CRCs. Another independent set of MSI+ CRCs (n=97) was recruited from the surgical files of the Department of Diagnostic Pathology, Asan Medical Center, Seoul, South Korea in order to validate the significant association of CIMP status with survival of MSI+ CRCs. These patients received curative surgery for CRCs at Asan Medical Center from 2004 to 2006. The study was approved by the Institutional Review Board.

Histologic assessment

Through microscopic examination of representative sections of tumors (n=72), two pathologists (GHK and MJK) evaluated the following parameters without knowledge of the CIMP status of the specimen: tumor differentiation, Crohn's-like lymphoid reaction, peritumoral lymphocytic reaction, eosinophilic intraluminal (intraglandular) mucin, pseudostratified or stratified nuclei, serrated luminal appearance, signet ring cell, acinar-form appearance, and villous or papillary appearance (Fig. 1). These histopathologic parameters were chosen because they were frequently investigated in CIMP+ or MSI+ CRCs by several researchers [2, 17, 21–23]. We adopted the defining criteria for many of these parameters from the study of Ogino et al. [17] except for intraluminal eosinophilic mucin, stratified nuclei, serrated luminal appearance, signet ring cell appearance, acinar-form appearance, and villous appearance. Intraluminal eosinophilic mucin was defined as the presence of eosinophilic mucin filling the glandular or cystic spaces of the tumor glands. The presence or absence of serrated luminal appearance, signet ring cell, acinar-form appearance, and villous appearance was evaluated, regardless of whether each parameter was the major component. Serrated luminal appearance was recognized by the presence of glandular serration. Acinar-form appearance was defined by cellular areas with scanty fibrous stroma, indistinct glandular lumina, and polarized outside arrangement of nuclei and inside abundant cytoplasm (Fig. 1).

DNA isolation and determination of MSI

After microscopic examination of hematoxylin-and-eosin-stained tissue slides, we used blades to microdissect tumor areas in which tumor cells comprised more than 50% of the

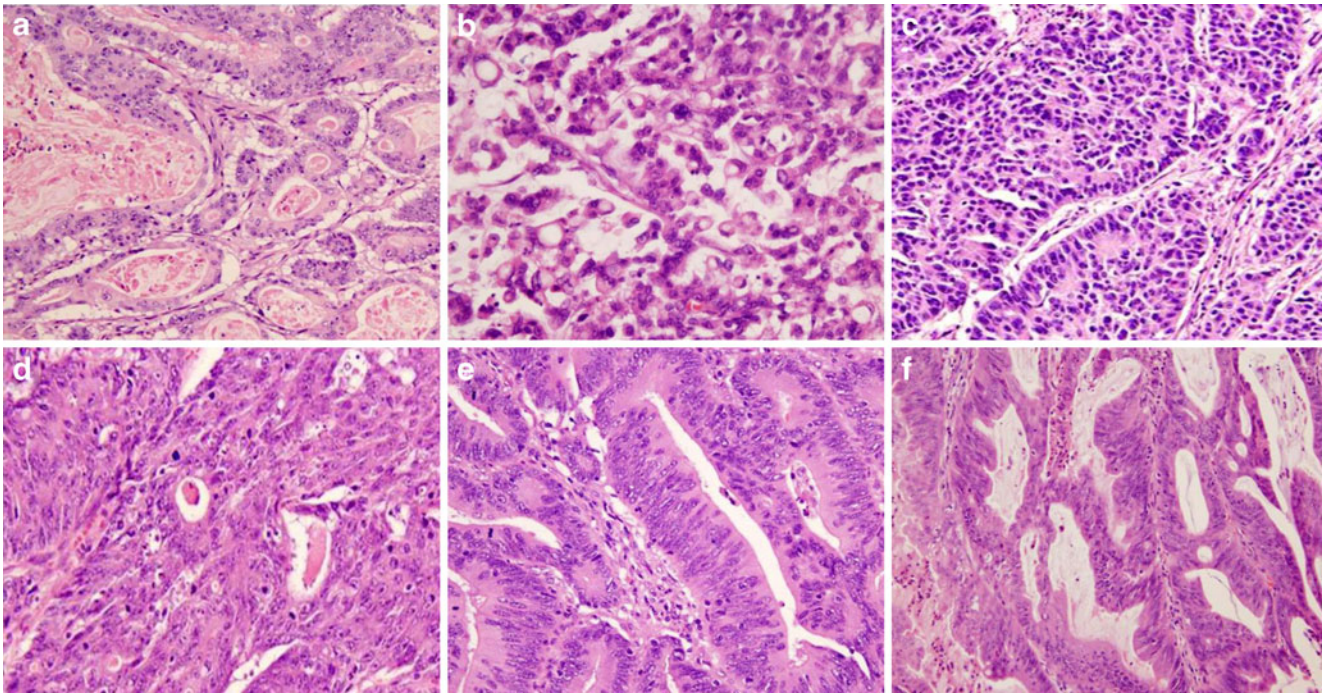

Fig. 1 Histopathological features of colorectal carcinomas. **a** Intraglandular eosinophilic mucin (original magnification, ×100). **b** Signet ring cell appearance (original magnification, ×400). **c** Acinar-form appearance (original magnification, ×200). **d** Poorly differentiated adenocarcinoma with a medullary (sheet-like) growth pattern (original magnification, ×200). **e** Moderately differentiated adenocarcinoma with stratified nuclei (original magnification, ×200). **f** Moderately differentiated adenocarcinoma with a serrated appearance (original magnification, ×200)

cells and paired normal mucosal tissue areas in which no tumor cells were found. Dissected tissue samples were collected into 1.5-mL microtubes containing 50 μL tissue lysis buffer (0.5% Tween 20 (Sigma, St. Louis, MO), 100 mM of Tris HCl buffer (pH 7.6), 1 mM of EDTA, and 20 μg of proteinase K (Sigma)). Samples were incubated at 55°C overnight. Proteinase K was then inactivated by incubating at 95°C for 10 min, and the extracted DNA was stored at −20°C until use. MSI was assessed at the following loci: *BAT25*, *BAT26*, *D2S123*, *D5S346*, and *D17S250*. Samples were classified as MSI+ when at least 40% of loci showed MSI.

Analysis of *KRAS*/*BRAF* mutations

KRAS codons 12 and 13 and *BRAF* codon 600 were assessed by PCR and sequence analysis as described [24, 25].

CIMP determination

DNA was bisulfite modified with the EZ DNA methylation kit (Zymo Research, Orange, CA, USA). In our previous study [15], we used four different CIMP marker panels to determine CIMP positivity and compared these differently defined CIMP+ CRCs for their associations with known clinicopathological features of CIMP+ CRCs. As a result, we found that an eight-marker panel with a cutoff value of five was optimal for MethyLight-based determination of CIMP. Thus, we used the eight-marker panel (*CACNA1G*, *CDKN2A* (*p16*), *CRABP1*, *IGF2*, *MLH1*, *NEUROG1*, *RUNX3*, and *SOCS1*) and determined CIMP status in 169 MSI+ CRCs. Methylation was quantified with MethyLight, a methylation-specific, probe-based, real-time PCR technique. DNA methylation at each methylation marker was reported as a percent of methylated reference (PMR). PMR = $100 \times [(\text{methylated reaction/ALU})_{\text{sample}}/(\text{methylated reaction/ALU})_{\text{M.}SssI\text{-reference}}]$. We considered a CpG island locus methylated when an exponential amplification curve was present and the PMR value was >4.

Immunohistochemistry

Core tissue biopsies (2 mm in diameter) were taken from individual paraffin-embedded adenocarcinomas and were arranged in a new recipient paraffin block (tissue array block) with a trephine apparatus (Superbiochips Laboratories, Seoul, South Korea). Using a microtome, tissue array blocks were cut into 4-μm-thick slices for immunohistochemical staining of tumor cell nuclei with commercially

available monoclonal anti-MSH2 (Oncogene Science, Cambridge, MA, USA) or monoclonal anti-hMLH1 (PharMingen, San Diego, CA, USA) [26]. Nuclear expression was classified as present or absent relative to staining of non-neoplastic cell nuclei, which provided a positive internal control for each slide.

Assessment of tumor-infiltrating lymphocytes

One pathologist (JHK) who was blinded to the CIMP status of individual cases counted lymphocytes infiltrating tumor glands. Cytotoxic T lymphocytes that reacted positively to anti-CD8 (mouse, DAKO) were quantified. Under a light microscope at ×400 magnification, five visual fields were randomly selected, and the number of positive cells was counted to determine the number of lymphocytes infiltrating tumor glands. The mean TIL/high-power field for each tumor was then calculated by dividing the total number of TIL by 5.

Statistics

For statistical analysis, the chi-square test (or Fisher's exact test for categories with an n value of <10) was performed on categorical data, and the two-tailed Student's t test was used to evaluate the significance of the differences between two means. Survival was measured from the date of resection of CRC to the date of death or the last clinical follow-up time (before 31 May 2009 for the first set of CRC patients and before 31 May 2010 for the second set of CRC patients). The average follow-up time (from surgery to death or the last follow-up) was 38 months (range, 1–63 months) and 53 months (range, 4–73 months) for the first and the second sets of CRC cases, respectively. Overall survival rates were assessed with the Kaplan–Meier log-rank test, and multivariate analysis was performed with Cox proportional hazards regression models in a backward manner to determine association between survival and CIMP, adjusting for variables that may be significant prognostic factors from univariate analysis. All statistical analyses were conducted with the SPSS program (version 15.0, Chicago, IL, USA). All P values were two sided, and statistical significance was set at $P<0.05$.

Results

Pathological and molecular differences between CIMP+ and CIMP− microsatellite-unstable CRCs

Using the MethyLight assay, we found that 25% of the 72 MSI+ CRCs were CIMP+. We then compared these two subtypes of MSI+ CRCs for their association with known clinicopathological features of MSI+ CRCs. Compared with CIMP−/MSI+ CRCs, CIMP+/MSI+ CRCs were closely associated with older age at onset, poor differentiation, frequent medullary (sheet-like) appearance, frequent acinar-form appearance, frequent signet ring cell appearance, and frequent *BRAF* mutation ($P<0.05$ for all six, Tables 1 and 2). A marginal association of CIMP+/MSI+ CRCs with higher numbers of tumor-infiltrating lymphocytes was identified ($P=0.059$). *BRAF* mutations were never found in CIMP−/MSI+ CRCs. Polypoid tumors without ulceration and eosinophilic intraluminal mucin were found only in CIMP−/MSI+ CRCs (18.2% and 18.5%, respectively). No differences were found in the proportion of female patients, occurrence rate of multiple CRCs, frequency of proximal colon location, frequency of mucinous carcinoma, degree of peritumoral lymphocytic infiltration, frequency of papillary appearance, frequency of serrated luminal appearance, *KRAS* mutation rate, or cancer stage. MLH1 loss was significantly frequent in CIMP+/MSI+ CRCs, whereas MSH2 loss was exclusively found in CIMP−/MSI+ CRCs (Table 1).

Survival analysis

To identify whether a difference existed in the survival of patients with CIMP+ vs. CIMP− MSI+ CRCs, we performed Kaplan–Meier analysis with a log-rank test. CIMP+/MSI+ CRCs ($n=18$) showed a worse clinical outcome than CIMP−/MSI+ CRCs ($n=54$; $P=0.019$; Fig. 2a). To validate a close association of CIMP+ status with worse survival in MSI+ CRCs, we performed Kaplan–Meier survival analysis in a second independent MSI+ CRC set ($n=97$) from another hospital. Stage distribution of CIMP+ and CIMP− tumors in a validation set was summarized in supplementary Table. Independent set also showed a worse clinical outcome in CIMP+/MSI+ CRCs ($n=36$) compared with CIMP−/MSI+ CRCs ($n=61$; $P<0.001$; Fig. 2b). To determine whether CIMP is an independent prognostic factor, we conducted multivariate survival analysis in a combined set of 72+ 97 MSI+ CRCs. Table 3 summarizes the prognostic significance of clinicopathologic and molecular factors determined by univariate analysis. Age, *BRAF* mutation, CIMP status, differentiation, Crohn's-like lymphoid reaction, peritumoral lymphocytic reaction, and AJCC cancer staging were significant factors, whereas postoperative chemotherapy (received or not) was a marginally significant factor. These factors were entered into a multivariate analysis to identify independent predictors of overall survival. Multivariate analysis using the Cox proportional hazards model revealed that CIMP status was an independent prognostic factor affecting overall survival of MSI+ CRC patients (Table 3).

Table 1 Comparison of clinicopathological and molecular features between CIMP− and CIMP+ microsatellite-unstable colorectal cancers

		Case no.	CIMP− (n=54)	CIMP+ (n=18)	P value
Age (year) ± SD		72	52.3±10.75	71.6±8.38	<0.001
Gender	Male	43	32 (59.3%)	11 (61.1%)	1.000
	Female	29	22 (40.7%)	7 (38.9%)	
Gross type	Polypoid	10	10 (18.5%)	0	0.057
	Ulcerative	62	44 (81.5%)	18 (100%)	
Location	Right	48	33 (61.1%)	15 (83.3%)	0.147
	Left	24	21 (38.9%)	3 (16.7%)	
Multiplicity	Single	60	43 (79.6%)	17 (94.4%)	0.272
	Multiple	12	11 (20.4%)	1 (5.6%)	
AJCC stage	Stage I, II	45	37 (68.5%)	8 (44.4%)	0.171
	Stage III	25	16 (29.6%)	9 (50.0%)	
	Stage IV	2	1 (1.9%)	1 (5.6%)	
KRAS	Wild type	55	39 (81.3%)	16 (88.9%)	0.713
	Mutant	11	9 (18.8%)	2 (11.1%)	
BRAF	Wild type	68	54 (100%)	14 (77.8%)	0.002
	Mutant	4	0	4 (22.2%)	
Loss of MLH1 expression	Loss	46	31 (60.8%)	15 (83.3%)	0.144
	No loss	23	20 (39.2%)	3 (16.7%)	
Loss of MSH2 expression	Loss	23	20 (39.2%)	3 (16.7%)	0.144
	No loss	46	31 (60.8%)	15 (83.3%)	
Tumor-infiltrating lymphocytes ±		72	32.5±30.7/HPF	52.7±37.3/HPF	0.059

In cases with two or more synchronous cancers, only the largest was assessed

CIMP CpG island methylator phenotype, *AJCC* American Joint Committee on Cancer

Discussion

MSI+ CRCs are well known for their peculiar clinicopathological features. In previous studies attempting to characterize molecular subtypes determined by the combinatory status of MSI and CIMP, MSI+ subtypes (regardless of CIMP status) tended to show a preponderance toward proximal colon location, poor differentiation, lower cancer stage, lower *KRAS* mutation frequency, and better prognosis when compared with the CIMP−/MSI− subtype, which comprises 60–80% of CRCs [2, 4, 15, 17, 27–29]. However, as revealed in our current study, MSI+ CRCs showed

Table 2 Comparison of histological features between CIMP− and CIMP+ microsatellite-unstable colorectal cancers

		Case no.	CIMP−	CIMP+	P value
Differentiation	Differentiated	61	51 (94.4%)	10 (55.6%)	<0.001
	Poorly differentiated	11	3 (5.6%)	8 (44.4%)	
Extracellular interstitial mucin pool	Absent	31	25 (46.3%)	6 (33.3%)	0.336
	Mild or marked	41	29 (53.7%)	12 (66.7%)	
Intraglandular eosinophilic mucin	Absent	57	39 (72.2%)	18 (100%)	0.015
	Present	15	15 (27.8%)	0	
Crohn's-like lymphoid reaction	Absent	16	10 (18.5%)	6 (33.3%)	0.205
	Mild or marked	56	44 (81.5%)	12 (66.7%)	
Peritumoral lymphocytic reaction	Absent	12	9 (16.7%)	3 (16.7%)	1.000
	Mild or marked	60	45 (83.3%)	15 (83.3%)	
Papillary appearance	Absent	65	49 (90.7%)	16 (88.9%)	1.000
	Present	7	5 (9.3%)	2 (11.1%)	
Stratified nuclei	Absent	19	7 (13.0%)	12 (66.7%)	<0.001
	Present	53	47 (87.0%)	6 (33.3%)	
Medullary appearance	Absent	40	35 (64.8%)	5 (27.8%)	0.006
	Present	32	19 (35.2%)	13 (72.2%)	
Serrated appearance	Absent	61	48 (88.7%)	13 (72.2%)	0.128
	Present	11	13 (21.3%)	5 (27.8%)	
Acinar-form appearance	Absent	51	43 (79.6%)	8 (44.4%)	0.004
	Present	21	11 (20.4%)	10 (55.6%)	
Signet ring cell appearance	Absent	65	52 (96.3%)	13 (72.2%)	0.009
	Present	7	2 (3.7%)	5 (27.8%)	

CIMP CpG island methylator phenotype

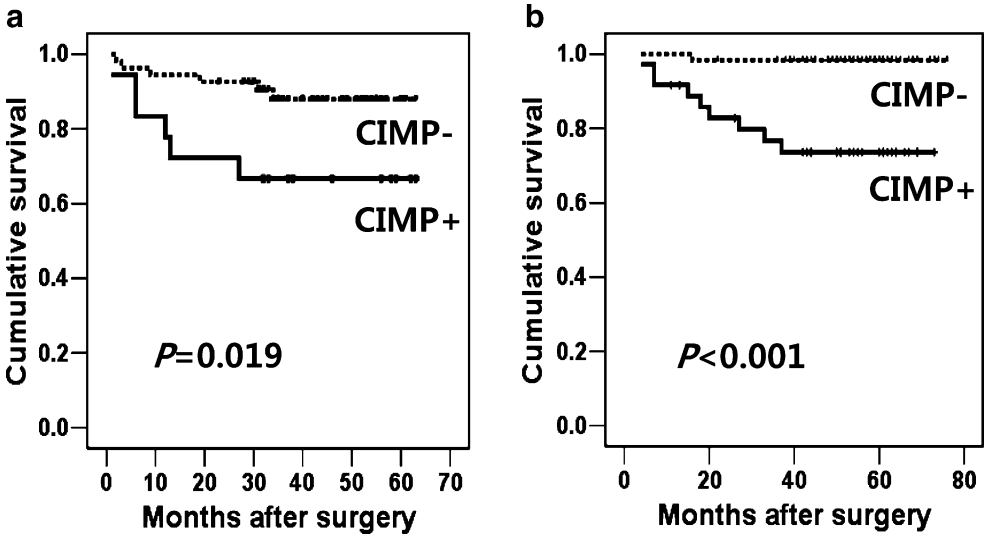

Fig. 2 Kaplan–Meier survival analysis with log-rank test. **a** Survival analysis was performed for patients with CIMP+/MSI+ (n=18) and CIMP−/MSI+ colorectal cancers (n=54). **b** Survival analysis in an independent set of MSI+ CRCs composed of 36 CIMP+ tumors and 61CIMP− tumors

Table 3 Univariate and multivariate survival analysis in a combined set of MSI+ colorectal carcinomas (n=169)

Parameters	n	Univariate analysis		Multivariate analysis	
		Mean survival time (months; 95% confidence interval)	P value	Hazard ratio (95% confidence interval)	P value
CIMP			<0.001		0.033
Negative	115	72 (70–75)		Reference	
Positive	54	56 (49–64)		2.807 (1.084–7.266)	
Age			0.008		0.972
55 years or less	91	73 (70–76)		–	
56 years or more	98	65 (60–69)		–	
BRAF			0.011		0.138
Wild	153	69 (66–72)		–	
Mutant	16	49 (35–62)		–	
AJCC staging			<0.001		<0.001
Stage I, II	115	73 (70–75)		Reference	
Stage III	47	61 (53–68)		3.217 (1.198–8.641)	0.020
Stage IV	7	30 (9–51)		20.721 (5.280–81.318)	<0.001
Differentiation			<0.001		0.033
Differentiated	122	70 (67–73)		Reference	
Poorly differentiated	47	58 (50–66)		2.697 (1.086–6.699)	
Crohn's-like lymphoid reaction			<0.001		0.003
Absent	25	43 (34–53)		Reference	
Mild or marked	144	71 (68–73)		0.236 (0.092–0.608)	
Peritumoral lymphocytic reaction			0.048		0.200
Absent	24	50 (40–59)		–	
Mild or marked	145	69 (66–72)		–	
Tumor-infiltrating lymphocytes[a]			0.347		
<7/HPF	28	59 (50–67)			
≥7/HPF	141	68 (65–72)			
Chemotherapy			0.086		0.012
Not treated	76	64 (59–68)		Reference	
Treated	93	71 (68–75)		0.234 (0.075–0.724)	

MSI microsatellite instability; *CIMP* CpG island methylator phenotype; *AJCC* American Joint Committee on Cancer; *HPF* high power field (x400)

[a] Tumor infiltrating lymphocytes were graded into <7 and ≥7/HPF

heterogeneous clinicopathological findings depending on CIMP status, which is consistent with the study of Ogino et al. [17] who reported marked tumor infiltrating lymphocytes, tumor necrosis, tumor cell sheeting (medullary appearance), and poor differentiation significantly more often in CIMP+/MSI+ tumors compared with CIMP−/MSI+ tumors. In addition, our current study shows that CIMP+/MSI+ tumors were more frequently associated with signet ring cell appearance and acinar-form appearance than CIMP−/MSI+ tumors. In contrast, CIMP−/MSI+ tumors showed more frequent intraglandular eosinophilic mucin and stratified nuclear appearance than CIMP+/MSI+ tumors. Although the difference was of marginal significance, polypoid gross appearance without ulceration was observed only in CIMP−/MSI+ tumors, and right-side location was more frequent in CIMP+ tumors than in CIMP− tumors. These phenotypic differences between CIMP+ and CIMP− microsatellite-unstable tumors reflect not only a difference in gene expression profiles between them but also a difference in the morphological multistep progression pathways. Hereditary MSI+ CRCs are known to develop through tubular adenomas with or without villosity [30], whereas CIMP+/MSI+ CRCs are generally thought to arise on a background of sessile serrated adenoma [10, 31, 32]. However, it needs to be pointed out that although there were statistical differences in some of the histological features, there is great overlap between categories, and some of the features are more or less common in the MSI cases regardless of CIMP status (for example, signet ring appearance shows a significant difference; yet, it is a feature which is absent in a vast majority of both CIMP− and CIMP+ carcinomas (3.7% and 27%, respectively)); hence, these features are of much clinical or diagnostic significance.

In our current study, CIMP+ tumors displayed significantly worse clinical outcomes than those of CIMP− tumors regardless of the center where curative surgery and/or postoperative chemotherapy were performed. To the best of our knowledge, our current study is the first to demonstrate a difference in clinical outcomes between CIMP+ and CIMP− microsatellite-unstable CRCs. Through multivariate analysis incorporating prognostic factors, including cancer stage, differentiation grade, CIMP status, and *BRAF* mutation, which were all found to be statistically significant by univariate analysis, we found that CIMP status was an independent prognostic factor.

Several studies have compared clinical outcomes between CIMP−/MSI+ and CIMP+/MSI+ tumors; they did not find any significant difference. Specifically, the study of Ward et al. [19] demonstrated that patients with MSI+ tumors had better disease-specific survival than patients with MSI− tumors and that increasing levels of tumor methylation were not related to outcome for the MSI+ tumors. In the study of Barault et al., no difference was observed between the different CIMP groups within the MSI-H cancers. Their findings were contrasted by ours and the possible causes for such differences might be related to the differences of CIMP marker panels and methylation analysis methodology. Both the studies of Ward et al. and Barault et al. [20] determined CIMP status using methylation-specific PCR-based five- or six-marker panel (*p16*, *MLH1*, *MINT1*, *MINT2*, and *MINT31* and p16, *MLH1*, *MINT1*, *MINT2*, *MINT12*, and *MINT31*, respectively). Although MSP is a very sensitive study, it is unreliable in detection of low-level methylation and could give false-positive data by detecting very infrequent methylation at few CpG sites. In our previous study [15] in which we analyzed clinical outcomes in four molecular subtypes according to combined CIMP and MSI statuses, no difference was noted between CIMP+/MSI+ and CIMP−/MSI+. However, the previous study analyzed a small number of MSI+ CRCs (n=43, 31 CIMP− and 12 CIMP+) and no difference in clinical outcomes between MSI+/CIMP+ and MSI+/CIMP− might be attributed to the limited number of the analyzed MSI+ cases.

The heterogeneity of the two MSI+ subtypes regarding prognosis may provide a clue to explain the controversial prognostic value of MSI in patients with CRC; some studies showed significantly better clinical outcomes in MSI+ CRCs than in MSI− CRCs, whereas other studies showed no survival differences between them [33]. These controversial results were usually seen in small-scale studies [33], which are vulnerable to variability in the ratio of CIMP+ to CIMP− tumors among MSI+ CRCs: based upon the findings of the present study, it is expected that better clinical outcomes will be found in MSI+ CRCs compared with MSI− CRCs when more CIMP−/MSI+ tumors are included in the studies. It is also possible that CIMP+/MSI+ CRCs and CIMP−/MSI+ CRCs may respond differently to cytotoxic chemotherapeutic agents. CIMP+ CRCs have been reported to respond to 5-Fluorouracil (5-FU)-based regimens [34], but MSI+ CRCs have been demonstrated to show inconsistent responses to 5-FU-based therapy [35–38]. CIMP status in MSI+ CRCs is likely to influence the response of MSI+ CRCs to 5-FU and may explain the discordant published results pertaining to the predictive value of MSI status. Little is known about whether MSI+ CRCs may respond differently to the combined regimens of FOLFOX (Folinic acid-Fluorouracil-Oxaliplatin) and FOLFIRI (Folinic acid-Fluorouracil-Irrinotecan) depending on CIMP status. A recent study has demonstrated that MSI+ CRCs might benefit from irrinotecan-based therapy (IFL, bolus Irrinotecan, Fluorouracil, and Leucovorin), but this study did not analyze the effect of CIMP status in the response of MSI+ CRCs to irrinotecan-based therapy [39]. Randomized clinical trials are necessary to determine whether irrinotecan-based therapy is effective against CIMP+/MSI+ CRCs.

In our current study, the frequency of MSI+ tumors was 7.9% in a consecutive series of CRCs (n=989) and 6.9% in an independent consecutive series (n=1,406), which were lower than that of CRCs in a Western population (13–15%) [11, 33, 40–43]. Because the proportion of hereditary MSI+ CRCs may be similar in Western and Eastern CRCs (approximately 3% of CRCs [44, 45]), sporadic MSI+ CRCs that are believed to be mainly due to CIMP-associated silencing and minor somatic mutations of the mismatch repair gene *MLH1* may explain the large difference in the proportion of MSI+ CRCs between Western and Eastern CRCs. Consistent with this idea, the proportion of CIMP+ tumors among MSI+ CRCs was 32% (54 in 169) in our series, which is much lower than the proportion of CIMP+ tumors in MSI+ CRCs in the Western population: It has been estimated that 55–80% of MSI+ tumors in nonselected CRC series are CIMP+, depending on the criteria used to define CIMP+ tumors [11, 27, 29, 46, 47]. The lower proportion of CIMP+ tumors in our MSI+ CRC cases was a consistent finding regardless of the CIMP panel markers and methods of methylation analysis [15, 24, 25]. Currently, no satisfactory answer can be provided for this discrepancy, but ethnic and environmental differences, especially diet differences, may explain the discrepancy. Many studies have demonstrated close associations between nutrition and DNA methylation changes in human cancers of the colon and other tissue types [48–52].

Although the eight-marker CIMP panel allows for the three-tiered classification of CIMP-0, CIMP-L, and CIMP-H (or CIMP+), we did not further classify CIMP− tumors into CIMP-0 and CIMP-L tumors. The reason for choosing two-tiered classification was because the eight-marker CIMP panel was specific for CIMP+ (or CIMP-high) tumors but not ideal for identification of CIMP-L. Most of the panel markers were found to be selective for CIMP+ tumors but do not discriminate CIMP-L from CIMP-0 tumors [53].

In conclusion, our results clearly demonstrate differences in clinicopathological features between CIMP+/MSI+ and CIMP−/MSI+ CRCs, suggesting that epigenotypic differences are manifested as phenotypic differences. The differences in clinical outcomes between these two subtypes may reflect the difference in the underlying causes leading to MSI, which may be implicated in the differential responses to cytotoxic chemotherapeutic agents. Further study is necessary to determine whether CIMP status is a determining factor in the response of MSI+ CRCs to cytotoxic chemotherapeutic regimens.

Grant information The study was supported by a grant from the Korea Healthcare Technology R&D Project, Ministry for Health, Welfare and Family Affairs, Republic of Korea (A091081).

Disclosure The authors declare that they have no conflict of interest.

References

1. Sung JJ, Lau JY, Goh KL, Leung WK (2005) Increasing incidence of colorectal cancer in Asia: implications for screening. Lancet Oncol 6:871–876
2. Jass JR (2007) Classification of colorectal cancer based on correlation of clinical, morphological and molecular features. Histopathology 50:113–130
3. Samowitz WS (2008) Genetic and epigenetic changes in colon cancer. Exp Mol Pathol 85:64–67
4. Snover DC (2011) Update on the serrated pathway to colorectal carcinoma. Hum Pathol 42:1–10
5. Toyota M, Ahuja N, Ohe-Toyota M et al (1999) CpG island methylator phenotype in colorectal cancer. Proc Natl Acad Sci USA 96:8681–8686
6. Toyota M, Ohe-Toyota M, Ahuja N, Issa JP (2000) Distinct genetic profiles in colorectal tumors with or without the CpG island methylator phenotype. Proc Natl Acad Sci USA 97:710–715
7. Issa JP (2004) CpG island methylator phenotype in cancer. Nat Rev Cancer 4:988–993
8. Kane MF, Loda M, Gaida GM et al (1997) Methylation of the hMLH1 promoter correlates with lack of expression of hMLH1 in sporadic colon tumors and mismatch repair-defective human tumor cell lines. Cancer Res 57:808–811
9. Cunningham JM, Christensen ER, Tester DJ et al (1998) Hypermethylation of the hMLH1 promoter in colon cancer with microsatellite instability. Cancer Res 58:3455–3460
10. Goldstein NS (2006) Small colonic microsatellite unstable adenocarcinomas and high-grade epithelial dysplasias in sessile serrated adenoma polypectomy specimens: a study of eight cases. Am J Clin Pathol 125:132–145
11. Boland CR, Goel A (2010) Microsatellite instability in colorectal cancer. Gastroenterology 138(2073–2087):e2073
12. Watanabe T, Kobunai T, Toda E et al (2006) Distal colorectal cancers with microsatellite instability (MSI) display distinct gene expression profiles that are different from proximal MSI cancers. Cancer Res 66:9804–9808
13. Jenkins MA, Hayashi S, O'Shea AM et al (2007) Pathology features in Bethesda guidelines predict colorectal cancer microsatellite instability: a population-based study. Gastroenterology 133:48–56
14. Young J, Simms LA, Biden KG et al (2001) Features of colorectal cancers with high-level microsatellite instability occurring in familial and sporadic settings: parallel pathways of tumorigenesis. Am J Pathol 159:2107–2116
15. Kim JH, Shin SH, Kwon HJ, Cho NY, Kang GH (2009) Prognostic implications of CpG island hypermethylator phenotype in colorectal cancers. Virchows Arch 455:485–494
16. Dahlin AM, Palmqvist R, Henriksson ML et al (2010) The role of the CpG island methylator phenotype in colorectal cancer prognosis depends on microsatellite instability screening status. Clin Cancer Res 16:1845–1855
17. Ogino S, Odze RD, Kawasaki T et al (2006) Correlation of pathologic features with CpG island methylator phenotype (CIMP) by quantitative DNA methylation analysis in colorectal carcinoma. Am J Surg Pathol 30:1175–1183
18. Jass JR, Walsh MD, Barker M et al (2002) Distinction between familial and sporadic forms of colorectal cancer showing DNA microsatellite instability. Eur J Cancer 38:858–866
19. Ward RL, Cheong K, Ku SL et al (2003) Adverse prognostic effect of methylation in colorectal cancer is reversed by microsatellite instability. J Clin Oncol 21:3729–3736

20. Barault L, Charon-Barra C, Jooste V et al (2008) Hypermethylator phenotype in sporadic colon cancer: study on a population-based series of 582 cases. Cancer Res 68:8541–8546
21. Halvarsson B, Anderson H, Domanska K, Lindmark G, Nilbert M (2008) Clinicopathologic factors identify sporadic mismatch repair-defective colon cancers. Am J Clin Pathol 129:238–244
22. Chirieac LR, Shen L, Catalano PJ, Issa JP, Hamilton SR (2005) Phenotype of microsatellite-stable colorectal carcinomas with CpG island methylation. Am J Surg Pathol 29:429–436
23. Greenson JK, Bonner JD, Ben-Yzhak O et al (2003) Phenotype of microsatellite unstable colorectal carcinomas: well-differentiated and focally mucinous tumors and the absence of dirty necrosis correlate with microsatellite instability. Am J Surg Pathol 27:563–570
24. Lee S, Cho NY, Choi M et al (2008) Clinicopathological features of CpG island methylator phenotype-positive colorectal cancer and its adverse prognosis in relation to KRAS/BRAF mutation. Pathol Int 58:104–113
25. Lee S, Cho NY, Yoo EJ, Kim JH, Kang GH (2008) CpG island methylator phenotype in colorectal cancers: comparison of the new and classic CpG island methylator phenotype marker panels. Arch Pathol Lab Med 132:1657–1665
26. Lee HS, Choi SI, Lee HK et al (2002) Distinct clinical features and outcomes of gastric cancers with microsatellite instability. Mod Pathol 15:632–640
27. Ogino S, Goel A (2008) Molecular classification and correlates in colorectal cancer. J Mol Diagn 10:13–27
28. Sanchez JA, Krumroy L, Plummer S et al (2009) Genetic and epigenetic classifications define clinical phenotypes and determine patient outcomes in colorectal cancer. Br J Surg 96:1196–1204
29. Hawkins N, Norrie M, Cheong K et al (2002) CpG island methylation in sporadic colorectal cancers and its relationship to microsatellite instability. Gastroenterology 122:1376–1387
30. Pino MS, Mino-Kenudson M, Wildemore BM et al (2009) Deficient DNA mismatch repair is common in Lynch syndrome-associated colorectal adenomas. J Mol Diagn 11:238–247
31. Goldstein NS, Bhanot P, Odish E, Hunter S (2003) Hyperplastic-like colon polyps that preceded microsatellite-unstable adenocarcinomas. Am J Clin Pathol 119:778–796
32. Noffsinger AE (2009) Serrated polyps and colorectal cancer: new pathway to malignancy. Annu Rev Pathol 4:343–364
33. Popat S, Hubner R, Houlston RS (2005) Systematic review of microsatellite instability and colorectal cancer prognosis. J Clin Oncol 23:609–618
34. Iacopetta B, Kawakami K, Watanabe T (2008) Predicting clinical outcome of 5-fluorouracil-based chemotherapy for colon cancer patients: is the CpG island methylator phenotype the 5-fluorouracil-responsive subgroup? Int J Clin Oncol 13:498–503
35. Liang JT, Huang KC, Lai HS et al (2002) High-frequency microsatellite instability predicts better chemosensitivity to high-dose 5-fluorouracil plus leucovorin chemotherapy for stage IV sporadic colorectal cancer after palliative bowel resection. Int J Cancer 101:519–525
36. Ribic CM, Sargent DJ, Moore MJ et al (2003) Tumor microsatellite-instability status as a predictor of benefit from fluorouracil-based adjuvant chemotherapy for colon cancer. N Engl J Med 349:247–257
37. Carethers JM, Smith EJ, Behling CA et al (2004) Use of 5-fluorouracil and survival in patients with microsatellite-unstable colorectal cancer. Gastroenterology 126:394–401
38. Benatti P, Gafa R, Barana D et al (2005) Microsatellite instability and colorectal cancer prognosis. Clin Cancer Res 11:8332–8340
39. Bertagnolli MM, Niedzwiecki D, Compton CC et al (2009) Microsatellite instability predicts improved response to adjuvant therapy with irinotecan, fluorouracil, and leucovorin in stage III colon cancer: cancer and leukemia group B protocol 89803. J Clin Oncol 27:1814–1821
40. Nosho K, Irahara N, Shima K et al (2008) Comprehensive biostatistical analysis of CpG island methylator phenotype in colorectal cancer using a large population-based sample. PLoS ONE 3:e3698
41. Ward R, Meagher A, Tomlinson I et al (2001) Microsatellite instability and the clinicopathological features of sporadic colorectal cancer. Gut 48:821–829
42. Samowitz WS, Curtin K, Ma KN et al (2001) Microsatellite instability in sporadic colon cancer is associated with an improved prognosis at the population level. Cancer Epidemiol Biomark Prev 10:917–923
43. Samowitz WS, Holden JA, Curtin K et al (2001) Inverse relationship between microsatellite instability and K-ras and p53 gene alterations in colon cancer. Am J Pathol 158:1517–1524
44. Zhang YZ, Sheng JQ, Li SR, Zhang H (2005) Clinical phenotype and prevalence of hereditary nonpolyposis colorectal cancer syndrome in Chinese population. World J Gastroenterol 11:1481–1488
45. Hampel H, Frankel WL, Martin E et al (2008) Feasibility of screening for Lynch syndrome among patients with colorectal cancer. J Clin Oncol 26:5783–5788
46. van Rijnsoever M, Grieu F, Elsaleh H, Joseph D, Iacopetta B (2002) Characterisation of colorectal cancers showing hyper-methylation at multiple CpG islands. Gut 51:797–802
47. Poynter JN, Siegmund KD, Weisenberger DJ et al (2008) Molecular characterization of MSI-H colorectal cancer by MLHI promoter methylation, immunohistochemistry, and mismatch repair germline mutation screening. Cancer Epidemiol Biomark Prev 17:3208–3215
48. Nystrom M, Mutanen M (2009) Diet and epigenetics in colon cancer. World J Gastroenterol 15:257–263
49. Christensen BC, Kelsey KT, Zheng S et al (2010) Breast cancer DNA methylation profiles are associated with tumor size and alcohol and folate intake. PLoS Genet 6:e1001043
50. Schernhammer ES, Giovannucci E, Kawasaki T et al (2010) Dietary folate, alcohol and B vitamins in relation to LINE-1 hypomethylation in colon cancer. Gut 59:794–799
51. Curtin K, Slattery ML, Ulrich CM et al (2007) Genetic polymorphisms in one-carbon metabolism: associations with CpG island methylator phenotype (CIMP) in colon cancer and the modifying effects of diet. Carcinogenesis 28:1672–1679
52. Diergaarde B, Braam H, van Muijen GN et al (2003) Dietary factors and microsatellite instability in sporadic colon carcinomas. Cancer Epidemiol Biomark Prev 12:1130–1136
53. Kaneda A, Yagi K (2011) Two groups of DNA methylation markers to classify colorectal cancer into three epigenotypes. Cancer Sci 102:18–24

Virchows Arch (2011) 459:65–71
DOI 10.1007/s00428-011-1088-8

ORIGINAL ARTICLE

Immunohistochemical study of stromal and vascular components of tonsillar polyps: high endothelial venules as participants of the polyp's lymphoid tissue

Icléia Barreto · Ana Flávia Costa · Marília Trierveiler Martins · Cristiane Furuse · Vera Cavalcanti de Araújo · Albina Altemani

Received: 16 March 2011 / Revised: 25 April 2011 / Accepted: 26 April 2011 / Published online: 12 May 2011
© Springer-Verlag 2011

Abstract Tonsillar polyps are nonneoplastic lesions usually composed of variable amounts of lymphoid and vascular and connective tissues. All of them are generally assumed to be hamartomatous proliferations, but the profile of vascular and connective components has yet to be explored. The vascular system of the tonsils is complex and includes highly specialized structures (i.e., high endothelial venules (HEVs)) involved in lymphocyte homing into lymphoid tissues. In 14 tonsillar polyps and 26 control tonsils, an immunohistochemical study was performed using CD34 (blood vessels and HEVs), MECA-79 (HEVs), D2-40 (lymphatic vessels), Ki-67, collagens I and III, fibronectin, and tenascin-C. The polyps showed increased total lymphatic area, whereas the number of blood vessels and lymphatics and the blood vascular area did not differ significantly from those of control tonsils. Rare Ki-67+ endothelial cells were found. In the polyps, we detected, possibly for the first time, HEVs amid lymphoid tissue, and that the amount of the latter correlated positively with HEV density. The polyps also presented lesser amounts of fibronectin and collagens I and III than in normal tonsils, which were distributed in a disorganized fashion. Tenascin-C expression was uncommon in the polyps and control tonsils. Tonsillar polyps are composed of disorganized connective tissue and lymphatic channels which can be considered hamartomatous proliferations. However, the lymphoid component is possibly reactive due to its relationship with the HEVs. The highly differentiated phenotype of the HEVs and their complex biology are not in agreement with what would be expected for a component of hamartomatous nature.

Keywords Tonsillar polyps · Immunohistochemistry · Stromal component · High endothelial venules

I. Barreto · A. F. Costa · A. Altemani (✉)
Department of Pathology, Medical Science Faculty,
University of Campinas (UNICAMP),
Rua Tessália Vieira de Camargo 126,
13084-971, Campinas, São Paulo, Brazil
e-mail: aaltemani@uol.com.br

M. T. Martins
Department of Oral Pathology, School of Dentistry,
University of São Paulo (USP),
São Paulo, Brazil

C. Furuse · V. C. de Araújo
Department of Oral Pathology,
São Leopoldo Mandic Institute and Research Center,
Campinas, Brazil

Introduction

Tonsillar polyps are uncommon nonneoplastic lesions which may clinically be mistaken for malignant neoplasms [1]. They are composed of variable amounts of different tissues, and in the literature, these lesions have been variously referred to as lymphoid, lymphangiomatous, lymphangiectatic fibrous, or only fibrous polyps [1–4]. Recently, we have shown that lymphoid polyps are clinically comparable to the reported ones with nonlymphoid tissue predominance, i.e., those composed mainly of connective tissue and/or dilated lymphatic vessels [3]. Both types are unilateral and affect mainly young individuals. Apparently, they are not preceded by a predisposing factor and are successfully treated by complete excision.

Regarding the pathogenesis of tonsillar polyps, two hypotheses have been proposed: (a) hamartomatous overgrowth of tonsillar tissues (the most accepted origin) and

(b) chronic inflammatory hyperplasia resulting in irreversible obstruction of the lymphatic vessels and lymphangiectasia [1–3, 5, 6]. However, to date, both hypotheses have been based either on histological observations only or on immunohistochemical findings, in which the vascular component of the polyps was not fully explored. The vascular system of the tonsils is complex and includes highly specialized structures involved in lymphocyte homing into lymphoid tissues, such as the high endothelial venules (HEV) [7, 8]. Therefore, whether the immunoprofile of the vascular component of the tonsillar polyps presents a parallel with that of the tonsils is a question yet to be verified. Furthermore, although connective tissue is a prominent component of the tonsillar polyps, no data are available on its composition. The connective tissue is comprised of a large number of elements with varying structural and cell regulatory functions [9]. Some are ubiquitously distributed whereas others, such as tenascin and myofibroblasts, are mainly associated with tissue remodeling [10–12]. Remodeling of the extracellular matrix would be worth investigating due to its potential involvement in the formation of tonsillar polyps.

In order to broaden our understanding of the pathogenesis of tonsillar polyps, in a series of lesions containing variable amounts of different tissues, we: (a) performed a morphometric study of the vascular component using antibodies specific for blood and lymphatic vessels and (b) verified the location and abundance of a set of molecules of the extracellular matrix. In addition, we compared the findings with those in control tonsils (without polyps) and, in six cases, we studied the polyp along with the parent tonsil.

Material and methods

The present study was approved by the Committee of Ethics of the University of Campinas, Brazil and was performed in 14 tonsillar polyps and 26 palatine tonsils removed for nonneoplastic reasons (control tonsils). The cases, which were diagnosed between 1983 and 2008, were retrieved from the files of the Department of Pathology of the University of Campinas. Demographic and clinical information were collected from review of the patients' medical records. The group of tonsillar polyps included nine men and five women with average age of 29 (9–53 years) and average size of the lesion, 1.5 cm (range, 0.6 to 4.0 cm), and all were described as polypoid masses arising from the surface of the tonsil. The control tonsils were from patients between 08 and 55 years of age (mean, 25.3 years). All polyps were reviewed by two pathologists (AA and IB) using 5-μm sections obtained from formalin-fixed paraffin-embedded samples and routinely stained with hematoxylin–eosin.

Immunohistochemistry

One paraffin block from each case was chosen for the immunohistochemical study. The following antibodies (Table 1) were used: CD34 for blood vessels and HEVs [13, 14], MECA-79 for HEVs [15], D2-40 for lymphatic vessels [16], Ki-67 for proliferating endothelial cells, α-smooth muscle actin (α-SMA) for myofibroblasts [17], and collagens I and III, fibronectin, and tenascin-C for proteins of the extracellular matrix.

Single staining for CD34, MECA-79, D2-40, α-SMA, collagens I and III, fibronectin, and tenascin-C was carried out using the EnVision System (DAKO, Denmark). Briefly, 5-μm sections from each paraffin block were deparaffinized and hydrated, and endogenous peroxidase activity was quenched by immersion of the slides in 3% hydrogen peroxide. The antigen retrieval (AR) for CD34 was achieved by boiling them in a steamer immersed in citrate buffer (pH 6.0), and for D2-40 and MECA-79, AR was performed using Tris–EDTA (pH 9.0). For collagens I and III, fibronectin, and tenascin-C, AR was performed using 0.4% pepsin for 30 min. For α-SMA, AR was not done. Subsequently, for all antibodies, the sections were incubated overnight at 4°C with the primary antibody and afterwards with the EnVision polymer horseradish peroxidase and Envision+(code K1491, DAKO, SA, Denmark) for 1 h at 37°C. Sections were stained for 5 min at 37°C

Table 1 Details of the antibodies used for immunohistochemistry

Specificity	Clone	Isotype	Dilution	Source	Buffer
CD34	QBEnd	IgG1	1:50	DAKO	Citrate
MECA-79	MECA-79	IgM	1:100	Santa Cruz	Tris–EDTA
D2-40	D2-40	IgG1	1:200	DAKO	Tris–EDTA
Ki-67	MIB-1	IgG1	1:150	DAKO	Tris–EDTA
α-SMA	1A4	IgG2	1:100	DAKO	None
Collagen I	Polyclonal	IgG	1:75	Biogenesis	Pepsin
Collagen III	4B11.1	IgG1	1:300	Chemicon	Pepsin
Tenascin-C	T2H5	IgG1	1:300	NeoMarkers	Pepsin
Fibronectin	Polyclonal	IgG	1:1,700	DAKO	Pepsin

DAKO Dako Corporation Glostrup, Dinamarca; *Santa Cruz* Santa Cruz Biotechnology, USA; *Biogenesis* Biogenesis, Poole, UK; *Chemicon* Chemicon, Millipore Corporate, USA; *NeoMarkers* NeoMarkers, Thermo Scientific, USA

with 3.3′-diaminobenzidine tetrahydrochloride (DAB) and counterstained with hematoxylin. Negative controls were run by omitting primary antibodies.

Double-labeling immunohistochemical staining (EnVision doublestain, code K1395, Dakopatts S/A, Denmark) was performed for Ki67/D2-40. Briefly, anti-Ki67 was applied after antigen retrieval using Tris–EDTA buffer (pH 8.9) and incubated overnight at 4°C; detection was achieved using the EnVision polymer HRP and DAB to visualize the binding of the first antibody. The sections were then incubated with a second antibody against D2-40 at 4°C overnight. EnVision polymer linked to alkaline phosphatase and fast red as a substrate chromogen system were used to complete the second immunostaining.

Microvessel density and microvessel area assessments for CD34 and for D2-40

The most vascularized areas at low-power magnification (hot spots) within each polyp and control tonsil (interfollicular lymphoid tissue) were chosen for quantitative analysis. In the hot spot areas, three digital images per case were obtained using a CCD camera adapted to an Olympus CX30 microscope (×40 objective, 0.44 mm field diameter) and analyzed with Image Lab analysis software (version 2.4), which allows manual segmentation of target areas (vessels). Microvessel density (MVD) for CD34 as well as for D2-40 was considered the mean number of microvessels. Microvessel area (MVA) was the area occupied by microvessels per unit area of the polyp or of the interfollicular lymphoid tissue of the control tonsil, i.e., that corresponded to one field using the ×40 objective—0.152 mm². Lymphatic endothelial proliferation was assessed by counting the number of Ki-67 positive lymphatic endothelial cells per lymphatic vessel.

Statistical analysis

Kruskal–Wallis test and Mann–Whitney *U* test were used for comparison of the variables between the different groups as appropriate. Data were presented as mean+SD, and the results with $p<0.05$ were considered significant. All the statistical procedures were performed using the statistical analysis performed with SPSS software for Windows, version 12.0 (SPSS® Inc. Illinois, USA).

Results

The tonsillar polyps were classified according to the amount of the lymphoid component, less than or more than 80% of the lesion, in nonlymphoid and lymphoid types, respectively [3]. Both types of polyps were covered by squamous epithelium and contained varying amounts of connective tissue and vessels (Fig. 1). In the nonlymphoid polyps, the few lymphoid nodules were usually located in the periphery of the lesion, and some of them contained small germinal centers. Adipose tissue was found only in this type of polyp (usually in small quantity). The lymphoid polyps showed frequent follicles with germinal centers of variable size, short crypts lined by lymphoepithelium, and small amount of connective tissue and vessels, which were located in the central portion of the lesion.

Vascular component

Table 2 shows MVD and MVA for CD34 and D2-40 in the tonsillar polyps and control tonsils. In lymphoid and nonlymphoid polyps, the number of blood vessels and lymphatics and the blood vascular area did not differ significantly from those of control tonsils, whereas the lymphatic vascular area was significantly increased. In only one case (a nonlymphoid polyp), dual immunohistochemistry using D2-40 and the cell proliferation marker Ki-67 revealed the existence of rare proliferating lymphatic endothelial cells (i.e., very few lymphatic vessels showed rare Ki-67+ endothelial cells).

In the control tonsils, MECA-79-positive vessels with morphological appearance of HEVs were numerous and

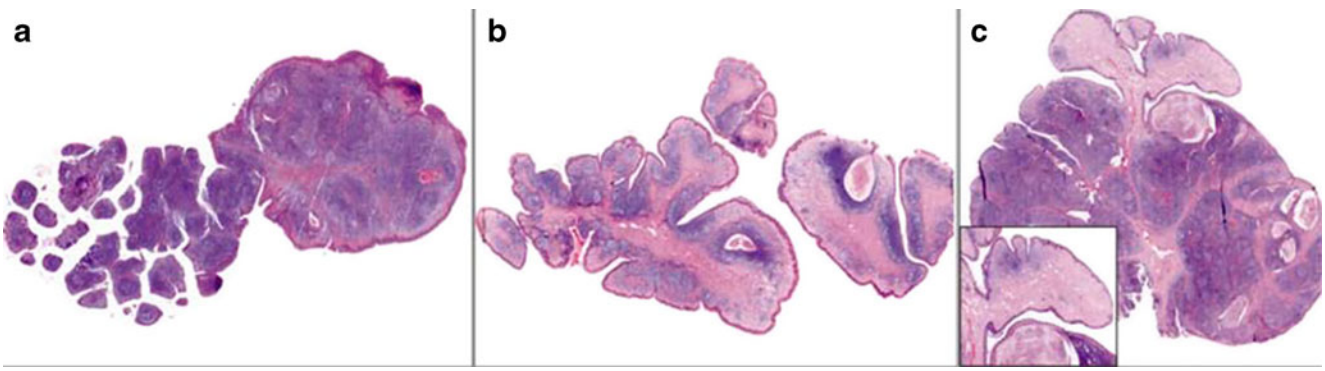

Fig. 1 Lymphoid (**a**) and nonlymphoid (**b**, **c**) polyps. Note the nonlymphoid polyp along with the parent tonsil (**c**) (hematoxylin & eosin, original magnification ×5, ×3, and ×3, respectively)

Table 2 MVD and MVA in tonsillar polyps and control tonsils

Group	MVD (mean±SD)		MVA (mean±SD)	
	CD34	D2-40	CD34	D2-40
Lymphoid polyps	8.38±3.54	5.24±1.25	4.70±2.12	7.65±4.19*
Nonlymphoid polyps	6.10±2.92	3.71±0.37	9.22±8.55	11.6±9.19**
Control tonsils (lymphoid area)	10.15±5.07	5.17±2.44	6.75±6.02	3.03±1.76
p (Kruskal–Wallis test)	*p*=0.083	*p*=0.057	*p*=0.554	*p*=0.001

*p=0.002, Mann–Whitney test;
**p=0.004, Mann–Whitney test

located in interfollicular and lymphoepithelial areas (Fig. 2a). In the tonsillar polyps, HEVs were always related to the lymphoid tissue. They were frequent and unevenly distributed in the lymphoid polyps (Fig. 2b). In contrast, in the nonlymphoid ones, HEVs were less numerous and restricted to the lymphoid nodules (Fig. 2c).

Expressions of fibronectin, collagens I and III, and tenascin

Fibronectin: in the control tonsils, this protein was found in large amount in the connective tissue of the septa and capsule (Fig. 3a) and in the vascular walls, particularly in the blood vessels, including capillaries and HEVs. In the septa and capsule, fibronectin fibrils were arranged in an organized fashion, i.e., in bundles. Some small foci were also found underneath the epithelium covering the tonsillar surface or crypts. In these two regions, the foci were encountered mainly in areas with loss of the lymphoepithelium pattern. In the polyps, small or no quantity of fibronectin was found (Fig. 3b, c). The fibronectin fibrils were arranged in a disorganized fashion in all lesions, and this alteration was more evident in the nonlymphoid polyps.

Tenascin: only discrete foci of this protein were found in the control tonsils as well as in the polyps. Tenascin-positive foci were usually located underneath the squamous epithelium that covered the polyps or underneath the altered crypt epithelium, i.e., without the lymphoepithelial characteristics (Fig. 3d–f). In some cases, the reticular fibers of the lymphoid tissue of the tonsils expressed tenascin in small areas.

Collagens I and III: these proteins were found in larger amounts in the control tonsils (Fig. 4a, d) than in the polyps (Fig. 4b, c, e, f) and presented patterns of distribution and organization similar to that of fibronectin. In the control tonsils, collagen I and III fibers were arranged in bundles in the septa and capsule, whereas in the polyps, small or no quantity of these proteins was found.

Myofibroblasts: few α-SMA-positive cells were found in the septa of the control tonsils and in the connective tissue of the polyps.

Discussion

The tonsils are lymphoepithelial organs capable of a variety of complex immunological functions which are initiated in specialized compartments, namely crypt epithelium (lymphoepithelium), lymphoid follicles, and extrafollicular region [7]. In the blood vascular system of the tonsils, HEVs are the structures that control lymphocyte recruitment from the blood [7]. A cascade of adhesive interactions between circulating lymphocytes and the specialized endothelial cells

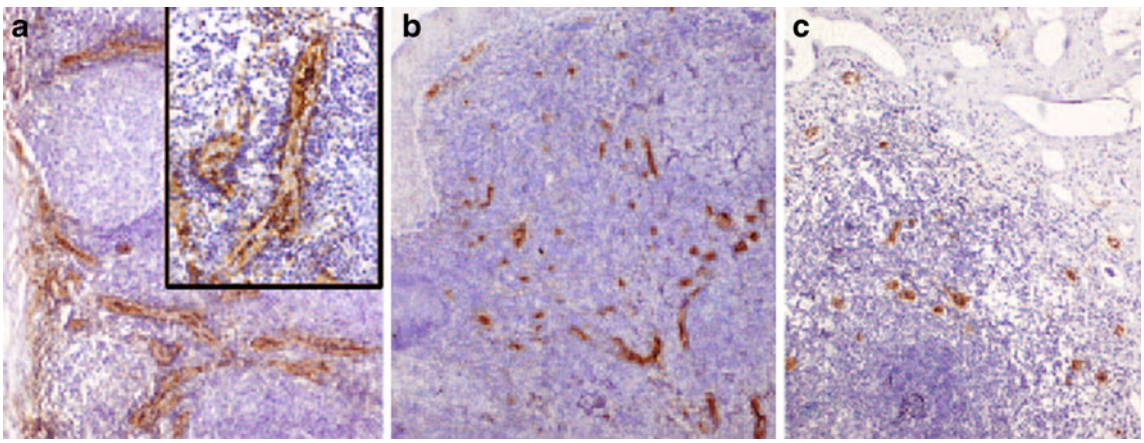

Fig. 2 MECA-79-positive HEVs amid lymphoid tissue in control tonsil (**a**, see above detail of the HEV) and lymphoid (**b**) and nonlymphoid (**c**) polyps (immunohistochemistry, original magnification **a**, **b**, and **c** ×100, detail ×400). In nonlymphoid polyp, MECA-79-positive HEVs are present only in the lymphoid nodule

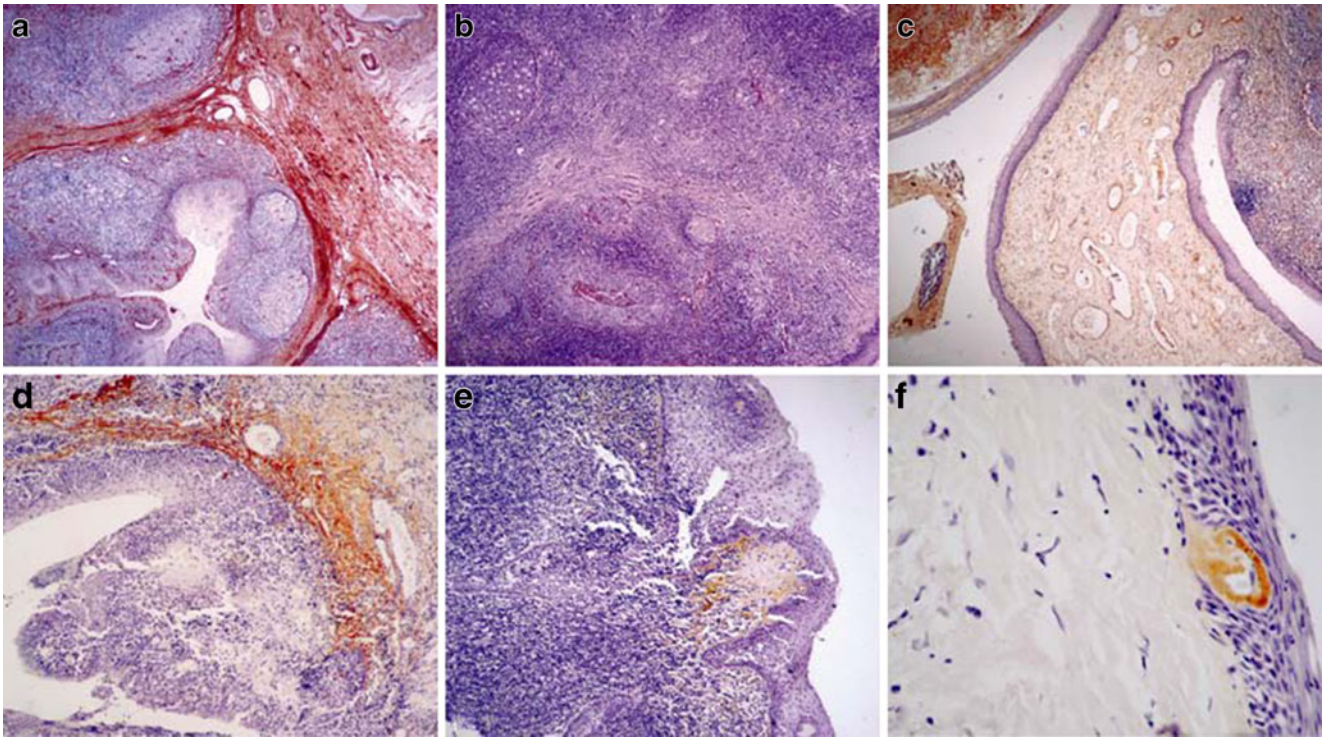

Fig. 3 Expressions of fibronectin (**a**–**c**) and tenascin-C (**d**–**f**) in tonsils (**a**, **d**) and lymphoid (**b**, **e**) and nonlymphoid polyps (**c**, **f**). Small or no quantity of these proteins is seen in the polyps. In these lesions, fibronectin can be observed mainly in the vascular walls (immunohistochemistry, original magnification **a**–**e** ×100, **f** ×400)

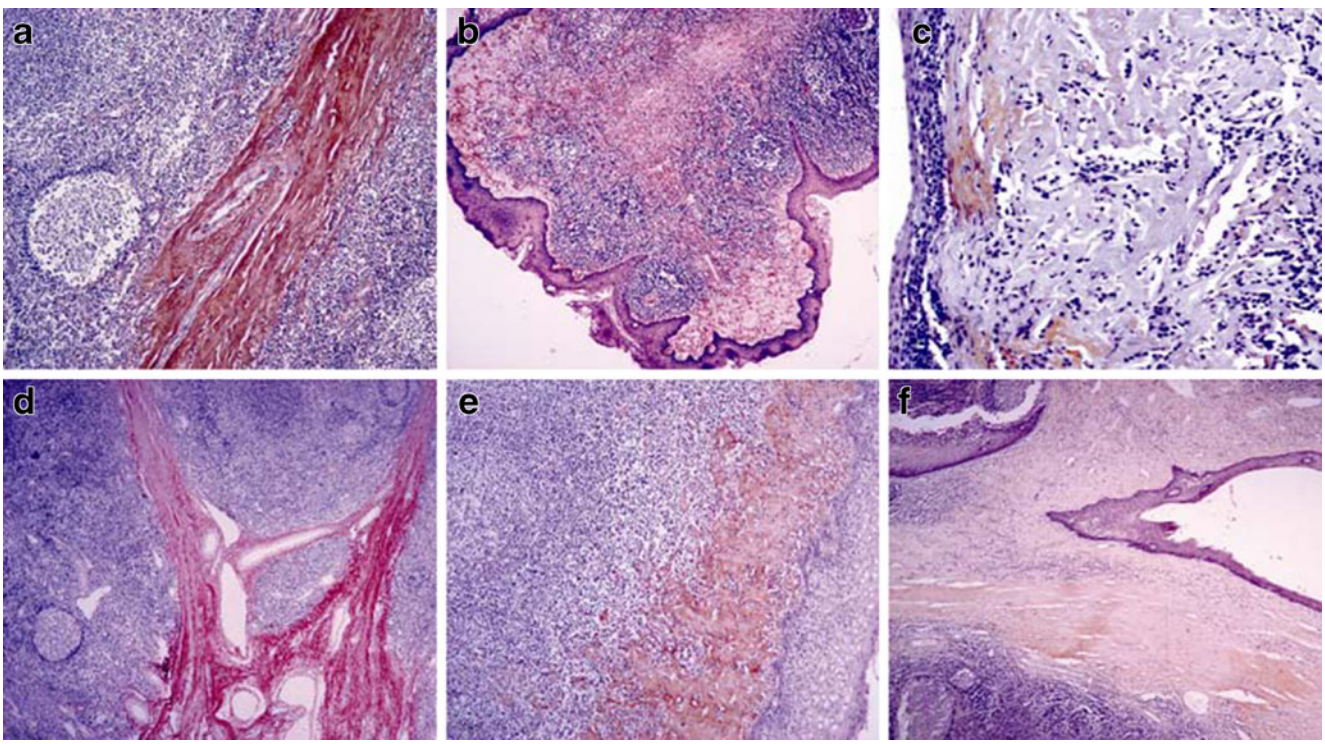

Fig. 4 Expressions of collagens I (**a**–**c**) and III (**d**–**f**) in tonsils (**a**, **d**) and lymphoid (**b**, **e**) and nonlymphoid polyps (**c**, **f**). Small or no quantity of these proteins is seen in the polyps (immunohistochemistry, original magnification **a**, **b**, **d** ×100; **e** and **f** ×200; **c** ×400)

of the HEVs mediate lymphocyte homing in both interfollicular and lymphoepithelial areas [8] There are few HEV-specific markers, and MECA-79 (that indicates the presence of L-selectin ligand) has been considered as the best one [15]. Regarding the lymphatic system, in contrast to lymph nodes which depend on antigenic delivery through afferent lymphatics, the tonsils possess only efferent lymphatics [7, 8].

In the current series, we showed that, regardless of the morphological appearance of the tonsillar polyps, lymphatic vascular area (but not the number of lymph vessels) was increased in the majority of lesions when compared with control tonsils. Therefore, tonsillar lymphangiectatic polyp can be considered as the most adequate term for these lesions, even for those referred to as lymphoid polyps. Furthermore, our results suggest that the lymphoid tissue of the polyps is possibly reactive due to its relationship with the HEVs, which seem to have their functions preserved and, consequently, supporting the lymphocyte recruitment into the lesion.

It is believed that postcapillary venules differentiate from primitive capillaries in response to steady, slow blood flow and low pressure, and that the local environment plays a critical role to maintain all of the specialized features of the HEVs [18, 19]. A great body of evidence suggests that cytokines produced locally, extracellular matrix proteins surrounding the high endothelial cells, and interdigitating dendritic cells are involved in the induction and maintenance of the specialized HEV phenotype [15] .By definition, hamartomas are disorganized proliferations of tissues indigenous to the area in which they arise [20]. Therefore, the highly differentiated phenotype of the HEVs and their complex biology are not in agreement with what would be expected for a component of hamartomatous nature. Furthermore, our previous findings in lymphoid polyps, showing that the lymphoid component of the polyps maintains an architectural pattern and cellular composition similar to those of the palatine tonsil [3], reinforce our current assumption that this tissue probably only comes with the lesion.

The dilated appearance of the lymphatic channels along with the fact that tonsils possess only efferent lymph vessels led us to verify if inflammatory hyperplasia with obstruction of lymphatic channels could be a contributing factor for the polyp formation [5]. Nevertheless, no evidence of lymphatic obstruction was found in the polyps or in the tonsils removed along with the lesion, even after serial sectioning of the tissue specimens. In addition, myofibroblasts and tenascin-C were not detected in significant quantities as it would be expected of a tissue that had undergone remodeling associated to inflammatory hyperplasia [12, 21]. The small foci of tenascin-C expression found in the polyps as well as in the tonsils were located in areas in which some degree of tissue remodeling due to traumatism (underneath the squamous epithelium which covers the polyps) or ordinary infection of the tonsils (underneath the damaged crypt epithelium) is expected. Taken together, these findings suggest that the dilated channels in the tonsillar polyps are results of disorganized overgrowth of lymphatic vessels rather than consequence of a chronic obstruction to the lymphatic flow.

In the current study, we also compared the expression of proteins of the extracellular matrix between tonsillar polyps and palatine tonsils. Collagens I and III and fibronectin participate in tissue architecture and are ubiquitously distributed [9]. In terms of function, the deposition of extracellular matrix fibronectin fibrils is important in regulating the organization and maintenance of types I and III collagen fibrils [22]. In the tonsils, we found deposition of these three proteins in large amounts and arranged in an organized fashion in the tonsillar septa and capsule. In the tonsillar polyps, fibronectin and collagens I and III presented a disorganized pattern of distribution, reinforcing the hamartomatous nature of this component. Furthermore, despite the fact that in the literature some tonsillar polyps have been termed fibrous polyps [23, 24], in our series, the expression of fibrillar proteins in the polyps, such as collagens I and III and fibronectin, was markedly low. This finding was observed even in the lesions composed predominantly of connective tissue or in those that formed a continuum with the tonsillar septum. Taking our results into consideration, they suggest that the connective tissue of the polyps presents modifications of the extracellular matrix regarding organization as well as composition. The extracellular matrix is an important substrate for tissue morphogenesis, imparting instructive signals for cell proliferation, migration, and differentiation [9, 22, 25]. Therefore, it would be reasonable to hypothesize that alteration of the extracellular matrix may be an important event in the pathogenesis of the tonsillar polyps.

In conclusion, the tonsillar polyps are lymphangiectatic lesions where the lymphoid tissue is reactive and closely associated with the hamartomatous proliferation of the connective tissue and lymphatic channels.

Acknowledgment This work was funded by FAPESP (Fundação de Amparo à Pesquisa do Estado de São Paulo)—grant numbers 04/13759-6 and 10/51571-0.

Conflict of interest The authors declare that they have no conflict of interest.

References

1. Kardon DE, Wenig BM, Heffner DK, Thompson LD (2000) Tonsillar lymphangiomatous polyps: a clinicopathologic series of 26 cases. Mod Pathol 13:1128–1133

2. Pilch BZ (2007) The nasopharynx and Waldeyer's ring. In: Pilch BZ (ed) Head and neck surgical pathology. Lippincott Williams & Wilkins, Philadelphia, pp 159–194
3. Barreto I, Juliano P, Chagas C, Altemani A (2007) Lymphoid polyps of the palatine tonsil. Int J Surg Pathol 15:155–159
4. Wenig BM (2008) Oral cavity, nasopharynx and oropharynx. In: Wenig BM, Heffess CS (eds) Atlas of head and neck pathology, 2nd edn. Saunders Elsevier Press, China, pp 163–401
5. Hiraide F, Inouye T, Tanaka E (1985) Lymphangiectatic fibrous polyp of the palatine tonsil: a report of three cases. J Laryngol Otol 99:403–409
6. Heffner DK (1987) Pathology of the tonsils and adenoids. Otolaryngol Head Neck Surg 20(2):279–286
7. Perry M, Whyte A (1998) Immunology of the tonsils. Immunol Today 19:414–421
8. Van Kempen MJP, Rijkers GT, Van Cauwenberge PB (2000) The immune response in adenoids and tonsils. Int Arch Allergy Immunolol 122:8–19
9. Mutsaers SE, Bishop JE, McGrouther G, Laurent GJ (1997) Mechanisms of tissue repair: from wound healing to fibrosis. Int J Biochem Biol 29:5–17
10. Chiquet-Ehrismann R, Chiquet M (2003) Tenascins: regulation and putative functions during pathological stress. J Pathol 200:488–499
11. Midwood KS, Williams LV, Schwarzbauer JE (2004) Tissue repair and dynamics of the extracellular matrix. Int J Biochem Cell Biol 36:1031–1037
12. Desmoulière A, Chaponnier C, Gabbiani G (2005) Tissue repair, contraction, and the myofibroblast. Wound Repair Regen 13(1):7–12
13. Perry ME, Brown KA, von Gaudecker B (1992) Ultrastructural identification and distribution of the adhesion molecules ICAM-1 and LFA-1 in the vascular and extravascular compartments of the human palatine tonsil. Cell Tissue Res 268:317–326
14. Fox SB, Harris AL (2004) Histological quantitation of tumour angiogenesis. APMIS 112:413–430
15. Girard JP, Springer TA (1995) High endothelial venules (HEVs): specialized endothelium for lymphocyte migration. Immunol Today 16:449–457
16. Evangelou E, Kyzas PA, Trikalinos TA (2005) Comparison of the diagnostic accuracy of lymphatic endothelium markers: Bayesian approach. Mod Pathol 18:1490–1497
17. Tomasek JJ, Gabbiani G, Hinz B, Chapponnier C, Brown RA (2002) Myofibroblasts and mechano-regulation of connective tissue remodeling. Nat Rev Mol Cell Biol 3:349–363
18. Thurston G, Baluk P, McDonald DM (2000) Determinants of endothelial cell phenotype in venules. Microcirculation 7:67–80
19. Lacorre DA, Baekkevold ES, Garrido I, Brandtzaeg P, Haraldsen G, Amalric F, Girard JP (2004) Plasticity of endothelial cells: rapid dedifferentiation of freshly isolated high endothelial venule endothelial cells outside the lymphoid tissue microenvironment. Blood 103:4164–4172
20. Stricker TP, Kumar V (2010) Neoplasia. In: Kumar V, Abbas AK, Fausto N, Aster J, SL Robbins, RS Cotran (eds) Pathologic basis of disease, 8th professional edition. Saunders Elsevier, Philadelphia, pp 259–330
21. Chiquet-Ehrismann R (2004) Tenascins. Int J Biochem Cell Biol 36:986–990
22. Sottile J, Hocking DC (2002) Fibronectin polymerization regulates the composition and stability of extracellular matrix fibrils and cell-matrix adhesions. Mol Biol Cell 13:3546–3559
23. Nayak DR, Murthy PS, Gopalakrishna RK, Padhee A (1993) Fibroma of the tonsil. J Indian Med Assoc 91:108
24. Sah SP, Bahadur KC, Rani S (2000) Lymphangiectatic fibrolipomatous polyp of the palatine tonsil. Indian J Pathol Microbiol 43:449–451
25. Jones FS, Jones PL (2000) The tenascin family of ECM glycoproteins: structure, function, and regulation during embryonic development and tissue remodeling. Dev Dyn 218:235–259

Virchows Arch (2011) 459:73–80
DOI 10.1007/s00428-011-1092-z

ORIGINAL ARTICLE

Claudin-18 in biliary neoplasms. Its significance in the classification of intrahepatic cholangiocarcinoma

Aya Shinozaki · Junji Shibahara · Naohiro Noda · Mariko Tanaka · Taku Aoki · Norihiro Kokudo · Masashi Fukayama

Received: 21 March 2011 / Revised: 8 May 2011 / Accepted: 12 May 2011 / Published online: 24 May 2011
© Springer-Verlag 2011

Abstract Claudin-18 (CLDN18), a tight junction protein specific to stomach and lung, is aberrantly expressed in preinvasive and invasive neoplasms of the pancreas. To investigate the significance of CLDN18 expression in biliary neoplasms, immunohistochemical analysis was performed. CLDN18 expression was frequently observed in the epithelial cells of extrahepatic bile duct carcinomas (90%, n=99), intrahepatic intraductal papillary neoplasms of the bile duct (IPNBs, 100%, n=11), and extrahepatic IPNBs (89%, n=9), while it was less frequent in intrahepatic cholangiocarcinomas (ICCs, 43%, n=83). Interestingly, CLDN18 expression was also frequently observed in precancerous lesions such as biliary intraepithelial neoplasias (78%, n=18). Among ICCs, CLDN18-positive cases showed higher frequencies of periductal infiltrative growth, perineural invasion, and lymph node metastasis. Multivariable analysis demonstrated that positive CLDN18 expression was an independent risk factor for lymph node metastasis in ICCs. Furthermore, CLDN18 expression was associated with poor overall survival by univariable analysis, as well as lymph node metastasis. These results suggest that CLDN18 may play an important role in biliary carcinogenesis, and especially in ICCs, it is associated with aggressive behavior and serves as a useful marker for the classification of ICC.

Keywords Claudin-18 · Intrahepatic cholangiocarcinoma · Intraductal papillary neoplasm of the bile duct · Extrahepatic bile duct carcinoma · Biliary intraepithelial neoplasia

A. Shinozaki (✉) · J. Shibahara · N. Noda · M. Tanaka · M. Fukayama (✉)
Department of Pathology, Graduate School of Medicine,
The University of Tokyo,
7-3-1 Hongo, Bunkyo-ku,
Tokyo 113-0033, Japan
e-mail: ashinozaki-tky@umin.ac.jp

M. Fukayama
e-mail: mfukayama-tky@umin.ac.jp

T. Aoki · N. Kokudo
Hepato-Biliary-Pancreatic Surgery Division,
Department of Surgery, Graduate School of Medicine,
The University of Tokyo,
Tokyo, Japan

Introduction

Intrahepatic cholangiocarcinoma (ICC) and extrahepatic bile duct carcinoma (EBDC) develop through a multistep process of carcinogenesis and share common histologic features. Accumulating evidence suggests that these invasive carcinomas are preceded by two distinct precancerous lesions: biliary intraepithelial neoplasia (BilIN), a dysplastic epithelium with flat or low-papillary growth, and intraductal papillary neoplasm of the bile duct (IPNB), which is characterized by papillary growth of the tumor within the bile duct on gross examination and microscopic papillary proliferation of the dysplastic epithelium. These two precursor lesions correspond to well-known non-invasive lesions of the pancreas, namely, pancreatic intraepithelial neoplasia (PanIN) and intraductal papillary mucinous neoplasm (IPMN). Previous studies have revealed close similarities between precancerous lesions or invasive carcinomas of the bile duct and their pancreatic counterparts [1–3].

Among these neoplasms of bile duct origin, ICC is quite heterogeneous in its clinical features, biological behavior, and histologic differentiation. ICC has been traditionally classified into two types, hilar type and peripheral type. In the recent review of Nakanuma et al., ICC is classified into four types according to its location, gross and microscopic growth

pattern, and the degree of differentiation of the tumor cells [4]. The classification well reflects the differences between tumors originated from large bile ducts and those from small bile ducts. In some cases, however, it is difficult to clearly determine their origins only from morphological aspect, and some diagnostic markers are necessary. Furthermore, the associations between morphological subtypes and biological behavior of the tumors also remain to be clarified.

Claudins (CLDNs) constitute a family of proteins with 27 members in humans and are essential for the formation of tight junctions and the maintenance of polarity in epithelial and endothelial cells [5, 6]. The expression pattern of each CLDN gene determines the epithelial phenotype of normal tissues and is frequently altered under neoplastic conditions [7]. Previous studies have investigated CLDN expression pattern in tumors of biliary tract and pancreas [8–11]. Among several CLDNs investigated, CLDN 4 is frequently upregulated in intrahepatic and extrahepatic bile duct carcinomas, and serves as a useful marker that differentiates ICC from hepatocellular carcinoma. CLDN4 expression is also frequently observed in ductal adenocarcinoma of the pancreas, although it is negative in endocrine tumors. In our preliminary assessment, we found that CLDNs 3, 4, and 7 were pervasive in various kinds of carcinomas of digestive system, while CLDN 18 expression was relatively rare in these cancers (unpublished data). CLDN18 is known to be specifically expressed in the stomach and lung [7, 12]. In a previous study, we demonstrated that CLDN18 expression is present in the fetal stomach at the ninth gestational week and is maintained throughout the entire developmental process, whereas it is diminished in intestinal metaplasia and gastric carcinoma [13]. Other studies have also shown that CLDN18 is a key molecule that determines the gastric epithelial phenotype [12, 14]. Interestingly, CLDN18 is aberrantly expressed in PanIN, IPMN, and invasive pancreatic cancer and is considered to play an important role in pancreatic carcinogenesis [15, 16]. However, no previous study has investigated CLDN18 expression in biliary neoplasms.

In the present study, we examined the expression of CLDN18 in various types of intrahepatic and extrahepatic biliary neoplasms to elucidate its significance in biliary carcinogenesis. We also investigated the association between CLDN18 expression and clinicopathologic parameters in ICCs to clarify the impact of CLDN18 on tumor aggressiveness and prognosis.

Materials and methods

Case selection

The present study included 83 ICCs, 11 intrahepatic IPNBs, 99 EBDCs, nine extrahepatic IPNBs, and 18 BilINs. The records for these cases were retrieved from the pathology archives of the University of Tokyo Hospital. All aspects of the study were approved by the University of Tokyo Ethics Committee. Pathology reports and tissue slides were reviewed along with medical charts when necessary. Recurrent cases and cases with neoadjuvant treatment that significantly affected tumor morphology were excluded.

The intrahepatic tumors (ICCs and intrahepatic IPNBs) were consecutive cases from 1995 to 2009. We retrieved records for 83 ICCs of the non-papillary type with or without periductal infiltrative growth. The intrahepatic IPNBs included six carcinomas with invasion, three carcinomas in situ, and two adenomas.

The EBDCs were consecutive cases from 1998 to 2007, including hilar bile duct carcinomas (Klatskin tumors).

The extrahepatic IPNB cases included in the present study met the following criteria: (1) tumors with grossly discernible intraductal papillary growth and (2) papillary lesions with low-grade (adenomatous) components at least focally on microscopic examination. The second criterion was essential because EBDCs frequently exhibit intraductal papillary growth macroscopically. Nine cases met these criteria, including six carcinomas with invasion, one carcinoma in situ, and two adenomas.

Biliary intraepithelial neoplasias, including BilIN-2 and BilIN-3 cases, were retrieved from the surgical materials of three kinds of biliary diseases—hepatolithiasis, primary sclerosing cholangitis, and extrahepatic biliary dilatation—which occasionally develop into biliary neoplasms [17]. Two pathologists independently reviewed the specimens, followed by discussion to resolve an interobserver disagreement. We did not included BilIN-1 lesions in the present study because of the difficulty in differentiating them from reactive or hyperplastic lesions.

To form a control group, we also investigated areas of normal mucosa and inflammatory mucosa in the above specimens.

Immunohistochemistry

To investigate CLDN18 expression in biliary neoplasms, we carried out immunohistochemical analysis using a polyclonal antibody against CLDN18 (1:1,000 dilution; Zymed, San Francisco, CA, USA). Four-micrometer-thick, paraffin-embedded tissue sections from the representative area of each case were used for the analysis. Immunohistochemical staining was performed using the Ventana BenchMark automated immunostainer (Tucson, AZ, USA) according to the peroxidase-labeled streptavidin–biotin method and visualized with 3, 3-diaminobenzidine.

We semiquantitatively assessed high-intensity membrane staining, but not cytoplasmic or weak membrane staining. CLDN18 expression was scored according to the propor-

tion of positively stained cells: 0 (negative), <1%; 1+, 1–25%; 2+, 25–50%; and 3+, 50–100%.

Statistics

Associations between clinicopathologic parameters and CLDN18 expression were analyzed using Fisher's exact test, the Mann–Whitney *U* test, and logistic regression model. Survival analysis was performed using Kaplan–Meier method, followed by log-rank test and Breslow–Gehan–Wilcoxon test. A Cox proportional hazards model was used to investigate the significance of several clinicopathologic parameters on overall survival time. Differences were considered statistically significant at $p < 0.05$.

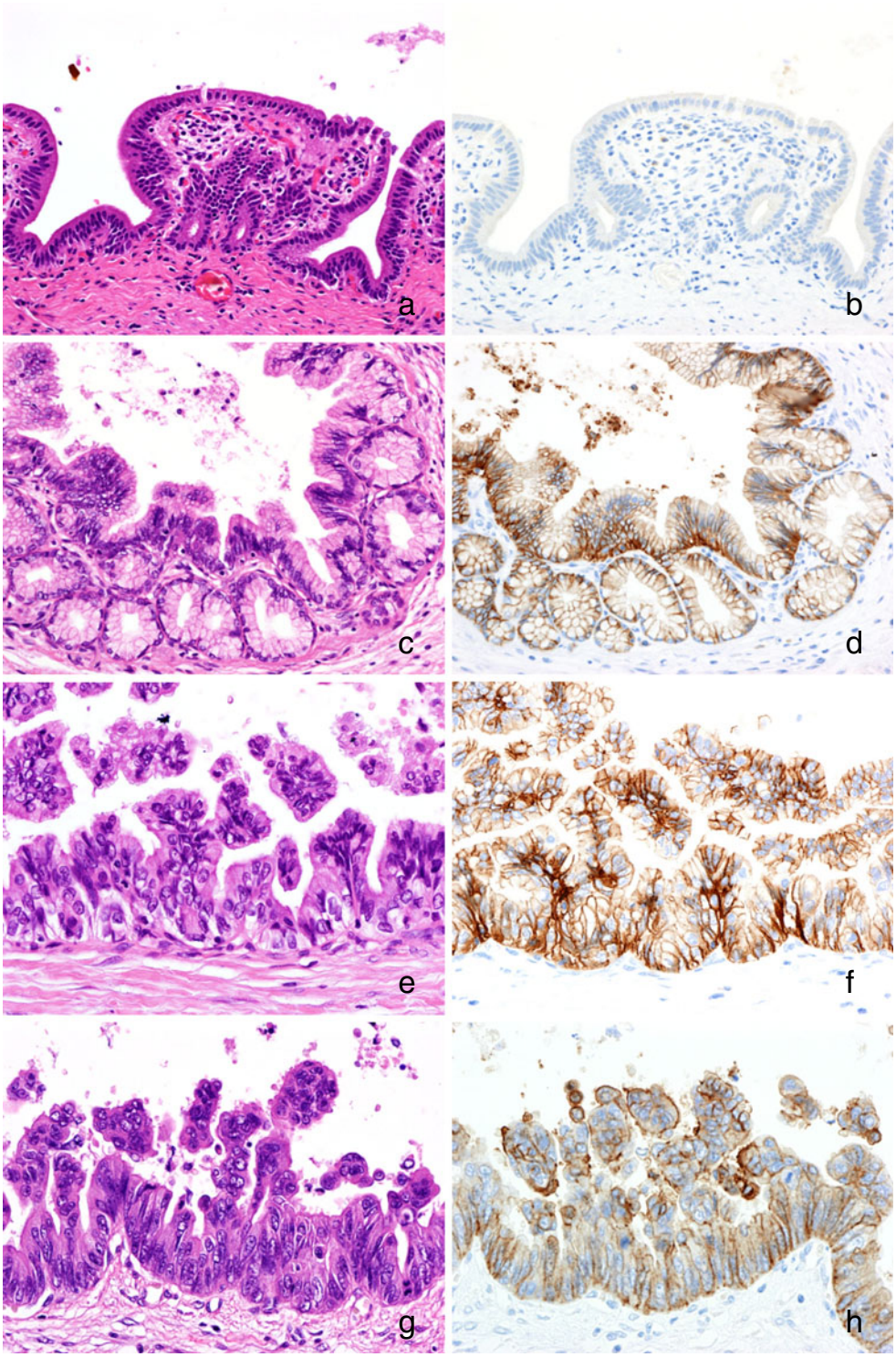

Fig. 1 CLDN18 expression in non-neoplastic biliary mucosa and biliary dysplasia. Normal biliary epithelium was negative for CLDN18 expression (**a**, **b**). Metaplastic epithelium showed positive staining for CLDN18 (**c**, **d**). Biliary intraepithelial neoplasia, BilIN-2 (**d**, **e**), and BilIN-3 (**g**, **h**) were positive for CLDN18

Results

CLDN18 expression in non-neoplastic biliary tract and liver

Normal intrahepatic and extrahepatic biliary epithelia of any size and peribiliary gland epithelia were negative for CLDN18 (Fig. 1a, b). Inflammatory mucosa occasionally showed CLDN18 expression on the basolateral membrane, especially in the presence of reactive, hyperplastic, and metaplastic changes (Fig. 1c, d), while reactive ductules in the portal or periportal area were negative for CLDN18. Neither hepatocytes nor vascular endothelial cells were positive for CLDN18.

CLDN18 expression in biliary neoplasms

The frequency of CLDN18 expression in biliary neoplasm is summarized in Table 1. In contrast with the lack of CLDN18 expression in normal biliary epithelium, BilINs and neoplastic lesions frequently showed CLDN18 expression (Figs. 1e–h and 2). Of the 18 BilINs, 14 (78%) showed positive CLDN18 expression, including nine out of 12 BilIN-2 cases (75%) and five out of six BilIN-3 cases (83%). CLDN18 expression was usually heterogeneous, even in the positive cases, and lesion morphology was not associated with expression status.

Among the biliary neoplasms examined, ICCs showed CLDN18 expression least frequently (36/83, 43%) as compared with intrahepatic IPNBs (11/11, 100%), EBDCs (89/99, 90%), and extrahepatic IPNBs (8/9, 89%). These differences were statistically significant (p=0.0005, p< 0.0001, and p=0.0125, respectively, Fisher's exact test).

Table 1 CLDN18 expression status in non-neoplastic condition and neoplastic lesions of the biliary tract

	CLDN18 positive rate	Expression score			
		3+	2+	1+	0 (negative)
Biliary dysplasia	14/18 (78%)	8	3	3	4
BilIN-2	9/12 (75%)	4	2	3	3
BilIN-3	5/6 (83%)	4	1	0	1
Intrahepatic biliary neoplasms					
ICC	36/83 (43%)	15	4	17	47
Intrahepatic IPNB	11/11 (100%)	9	0	2	0
Extrahepatic biliary neoplasms					
EBDC	89/99 (90%)	31	15	43	10
Extrahepatic IPNB	8/9 (89%)	5	1	2	1

BilIN biliary intraepithelial neoplasia, *ICC* intrahepatic cholangiocarcinoma, *IPNB* intraductal papillary neoplasm of the bile duct, *EBDC* extrahepatic bile duct carcinoma

No statistically significant difference in CLDN18 expression was observed between intrahepatic and extrahepatic IPNBs (p=0.2207, Mann–Whitney U test).

CLDN18 expression in ICCs

There were 36 cases (43%) of ICCs that showed positive staining for CLDN18 primarily on the basolateral membrane of the tumor cells. To investigate the impact of CLDN18 expression on the biological behavior of ICCs, the clinicopathologic features of CLDN18-positive and CLDN18-negative cases were compared (Table 2). On gross examination, CLDN18-positive cases were often associated with a hilar location and periductal infiltrative growth (p=0.005 and 0.0058, respectively, as compared with CLDN18-negative cases, Fisher's exact test). Microscopically, prominent intraductal growth was observed more frequently in CLDN18-positive cases (p<0.0001, Fisher's exact test). One third of the CLDN18-positive cases were associated with epithelial dysplasia of the adjacent bile ducts, whereas only two of 47 CLDN18-negative cases had co-existing dysplasia (p= 0.0007, Fisher's exact test). Notably, perineural invasion and lymph node metastases were observed more frequently in CLDN18-positive cases (p=0.0155 and 0.0098, respectively, Fisher's exact test). Results of the logistic regression model demonstrated that positive CLDN18 expression [odds ratio 5.888, 95% CI (confidence interval) 1.116–31.069, p= 0.0367], intrahepatic metastasis (odds ratio 10.024, 95% CI 1.583–63.458, p=0.0144), and perineural invasion (odds ratio 6.860, 95% CI 1.156–40.706, p=0.0340) were associated with an increase in the risk of lymph node metastasis.

The results of survival analyses were shown in Fig. 3. There was no significant difference in disease-free survival (p=0.1664) or overall survival (p=0.0686) between CLDN18-positive cases and negative cases by log-rank test. However, Breslow–Gehan–Wilcoxon test, which weighted earlier differences higher than later differences, demonstrated that CLDN18-positive cases were associated with poorer overall survival than CLDN18-negative cases, suggesting that disease-related death occurred earlier in CLDN18-positive cases. Furthermore, 3-year survival rate was significantly lower in CLDN18-positive cases (6/15, 28.6%) than CLDN18-negative cases (19/31, 61.3%) (p= 0.0026, Fisher's exact test). Additionally, three other parameters were associated with poor overall survival: intrahepatic metastasis, perineural invasion, and lymph node metastasis. Cox proportional hazards analysis revealed that lymph node metastasis was the only one factor that significantly affected on overall survival (relative risk 3.042, 95% CI 1.235–7.497, p=0.0156,), while CLDN18 expression, intrahepatic metastasis, perineural invasion, age, sex, and tumor size did not have significant impact on overall survival.

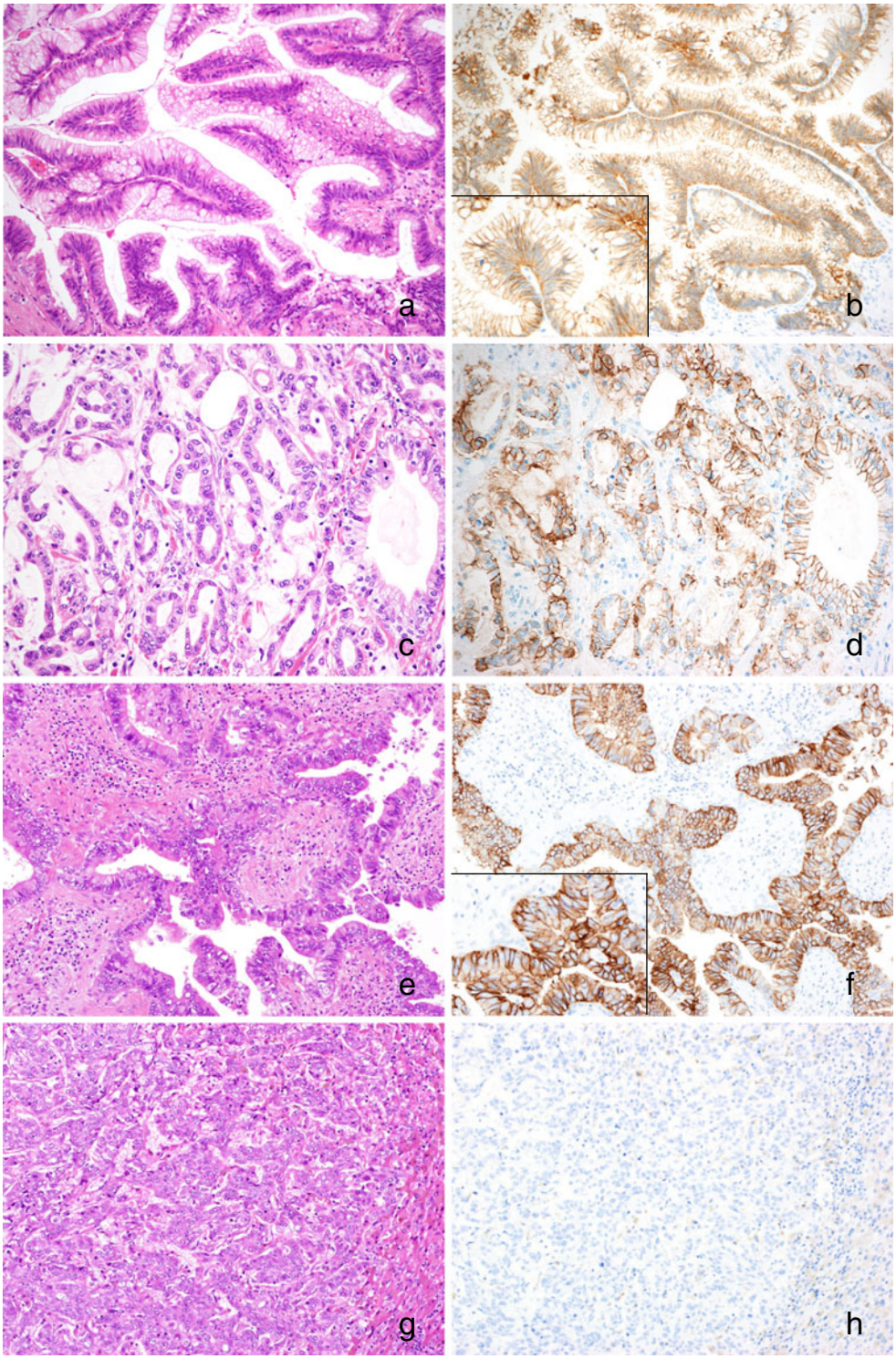

Fig. 2 CLDN18 expression in biliary neoplasms. CLDN18 expression was observed in intraductal papillary neoplasm of the bile duct (**a**, **b**) and extrahepatic bile duct carcinoma (**c**, **d**). Intrahepatic cholangiocarcinoma showing positive CLDN18 expression (**e**, **f**) and negative CLDN18 expression (**g**, **h**)

Discussion

The present study is the first to demonstrate a high frequency of CLDN18 expression in various kinds of biliary neoplasms, in contrast with the absence of CLDN18 expression in the normal bile duct epithelium. Immunohistochemical analysis revealed that more than 80% of the intrahepatic IPNB, EBDC, and extrahepatic IPNB cases examined showed CLDN18 expression, although CLDN18 expression was generally less frequent in ICCs. Interestingly, frequent CLDN18 expression was demonstrated in two precancerous lesions, BilINs, and non-invasive IPNBs. In addition, CLDN18-positive ICCs were associated with prominent intraductal component and co-existing dysplasia,

Table 2 Associations between CLDN18 expression and clinicopathologic features of ICCs

	CLDN18-positive ICCs (n=36)	CLDN18-negative ICCs (n=47)	p value
Age (≥65 years/<65 years)	22/14	20/27	0.1222
Sex (M/F)	19/17	26/21	0.8281
Hepatitis C virus infection (positive/negative)	9/27	15/32	0.6263
Hepatitis B virus infection (positive/negative)	5/31	10/37	0.5661
Tumor size (≥4 cm/<4 cm)	23/13	31/16	>0.9999
Location (hilar/peripheral (indeterminate))	16/14 (6)	7/29 (11)	0.005*
Periductal infiltrative growth[a] (present/absent)	16/20	7/40	0.0058*
Prominent intraductal component[b] (present/absent)	15/21	2/45	<0.0001*
Co-existing dysplasia (present/absent)	12/24	2/45	0.0007*
Vascular invasion (present/absent)	36/0	45/2	0.5028
Perineural invasion (present/absent)	23/13	17/30	0.0155*
Intrahepatic metastasis (present/absent)	7/29	9/38	>0.9999
Lymph node metastasis (present/absent)	12/24	4/43	0.0098*

ICC intrahepatic cholangiocarcinoma

*p value <0.05 was considered statistically significant, Fisher's exact test

[a] Gross finding

[b] Microscopic finding

suggesting that these ICCs may have been preceded by precancerous lesions. Similar findings have been reported in pancreatic neoplasms. CLDN18 is expressed frequently in PanINs and well-differentiated ductal adenocarcinoma [15]. Other pancreatic precursor lesions, namely, IPMNs and mucinous cystic tumors, also exhibit high CLDN18 expression (Tanaka M. et al. submitted). In the study, we investigated CLDN18 expression in pancreatic carcinomas both in vivo and in vitro using immunohistochemistry and reverse transcription–polymerase chain reaction (RT–PCR) of mRNA, and demonstrated that CLDN18 was upregulated by phorbol 12-myristate 13-acetate (PMA), an activator of protein kinase C (PKC)-associated signal pathway in pancreatic cell lines. These results suggest that activation of PKC pathway may be involved in the upregulation of CLDN18 in the early stage of pancreatic carcinogenesis, and the similar mechanism may be associated with biliary carcinogenesis. It is problematic that inflammatory mucosa in some of the cases, especially those with metaplastic changes, also showed focal CLDN18 expression. Whether these were true precursor lesions or not remains to be investigated in the future studies.

In contrast with the frequent CLDN18 expression in these biliary neoplasms, ICC showed less frequent CLDN18 expression. It is thought that two distinct types of ICCs exist, one originates from the large bile duct, and the other arises from the periphery, and that they differ not only in their clinicopathologic characteristics but also in their carcinogenic processes. The former may be essentially identical to EHBD in terms of their morphology and carcinogenic process, whereas the typical form of the latter is "bile ductular carcinoma," proposed by Kozaka et al., which morphologically resembles reactive bile ductules [18]. Recently, Aishima et al. subclassified ICCs into a hilar type and a peripheral type according to the tumor location and histology, and revealed that hilar type ICCs had an aggressive clinical course [19]. Although this classification nicely highlights two distinct ICC types, some problems still remain. In our review of ICCs, some tumors with hilar type histology arose in a peripheral location, while ICCs with peripheral type histology were located at the hilar portion. Furthermore, this classification excludes tumors larger than 5 cm, making it impossible to classify large tumors. With these limitations, morphological assessment seems to be insufficient for differentiating the two categories of ICCs.

The present study provides a novel classification of ICCs based on CLDN18 expression. Immunohistochemically, 43% of the ICCs examined were positive for CLDN18 expression. Many of the CLDN18-positive ICCs were hilar type tumors, whereas some were located in peripheral regions, indicating that the epithelial phenotype of the tumor is not determined by its location. This classification also enabled us to differentiate large tumors. Thus, CLDN18 expression is a useful diagnostic marker to differentiate two distinct types of ICCs with different origins.

Notably, CLDN18-positive ICCs were associated with tumor aggressiveness, i.e., periductal infiltrative growth, perineural invasion, and lymph node metastasis. Multivariable analysis also showed that CLDN18 expression was an independent risk factor for lymph node metastasis. Furthermore, CLDN18 expression was associated with decreased 3-year survival rate and poor overall survival. Although CLDN18 expression is not an independent risk factor for poor survival in Cox proportional hazards model, CLDN18 expression is important because it is closely associated with lymph node metastasis which is a crucial prognostic factor. These results suggest that CLDN18 expression status is essential for the appropriate management of the patient.

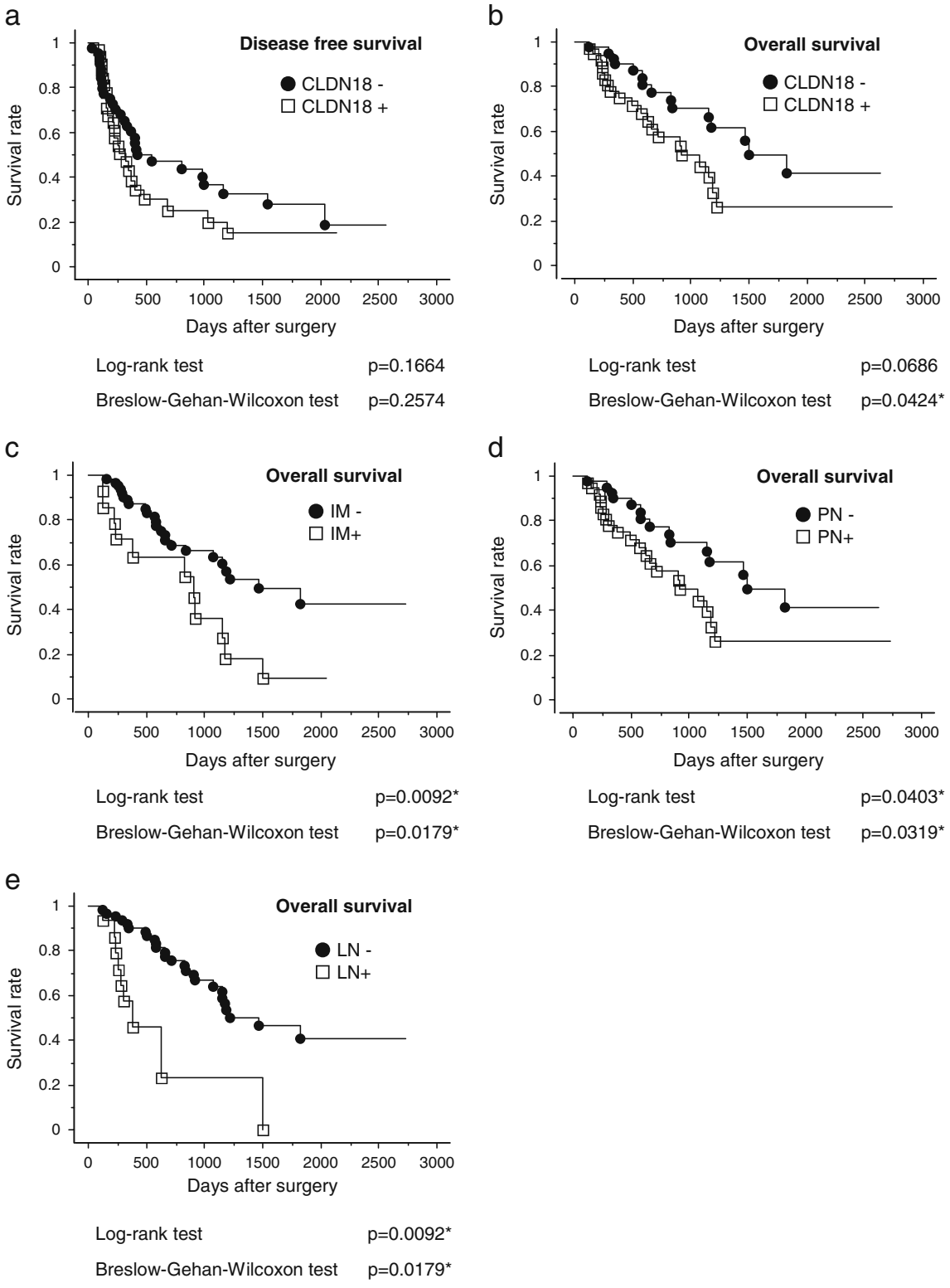

Fig. 3 Survival analysis of intrahepatic cholangiocarcinoma. **a** Disease-free survival of CLDN18 +/− cases. **b** Overall survival of CLDN18 +/− cases. **c** Overall survival of intrahepatic metastasis (*IM*) +/− cases. **d** Overall survival of perineural invasion (*PN*) +/− cases. **e** Overall survival of lymph node metastasis (LN) +/− cases. **p* <0.05 was considered statistically significant

In summary, we observed frequent CLDN18 expression in various kinds of biliary neoplasms, including precancerous lesions. Our results show that CLDN18 might be associated with invasiveness in intrahepatic bile duct epithelium, and serves as a useful marker for the classification of ICC.

Disclosure statement The authors declare that they have no conflict of interest.

References

1. Nakanuma Y (2010) A novel approach to biliary tract pathology based on similarities to pancreatic counterparts: is the biliary tract an incomplete pancreas? Pathol Int 60(6):419–429
2. Kim GE, Bae HI, Park HU, Kuan SF, Crawley SC, Ho JJ, Kim YS (2002) Aberrant expression of MUC5AC and MUC6 gastric mucins and sialyl Tn antigen in intraepithelial neoplasms of the pancreas. Gastroenterology 123(4):1052–1060
3. Aishima S, Kuroda Y, Nishihara Y, Taguchi K, Taketomi A, Maehara Y, Tsuneyoshi M (2006) Gastric mucin phenotype defines tumour progression and prognosis of intrahepatic cholangiocarcinoma: gastric foveolar type is associated with aggressive tumour behaviour. Histopathology 49(1):35–44
4. Nakanuma Y, Sato Y, Harada K, Sasaki M, Xu J, Ikeda H (2010) Pathological classification of intrahepatic cholangiocarcinoma based on a new concept. World J Hepatol 2(12):419–427
5. Mineta K, Yamamoto Y, Yamazaki Y, Tanaka H, Tada Y, Saito K, Tamura A, Igarashi M, Endo T, Takeuchi K, Tsukita S (2011) Predicted expansion of the claudin multigene family. FEBS Lett 585(4):606–612
6. Tsukita S, Furuse M (2000) Pores in the wall: claudins constitute tight junction strands containing aqueous pores. J Cell Biol 149(1):13–16
7. Hewitt KJ, Agarwal R, Morin PJ (2006) The claudin gene family: expression in normal and neoplastic tissues. BMC Cancer 6:186
8. Comper F, Antonello D, Beghelli S, Gobbo S, Montagna L, Pederzoli P, Chilosi M, Scarpa A (2009) Expression pattern of claudins 5 and 7 distinguishes solid-pseudopapillary from pancreatoblastoma, acinar cell and endocrine tumors of the pancreas. Am J Surg Pathol 33(5):768–774
9. Nemeth Z, Szasz AM, Tatrai P, Nemeth J, Gyorffy H, Somoracz A, Szijarto A, Kupcsulik P, Kiss A, Schaff Z (2009) Claudin-1, -2, -3, -4, -7, -8, and -10 protein expression in biliary tract cancers. J Histochem Cytochem 57(2):113–121
10. Lodi C, Szabo E, Holczbauer A, Batmunkh E, Szijarto A, Kupcsulik P, Kovalszky I, Paku S, Illyes G, Kiss A, Schaff Z (2006) Claudin-4 differentiates biliary tract cancers from hepatocellular carcinomas. Mod Pathol 19(3):460–469
11. Borka K, Kaliszky P, Szabo E, Lotz G, Kupcsulik P, Schaff Z, Kiss A (2007) Claudin expression in pancreatic endocrine tumors as compared with ductal adenocarcinomas. Virchows Arch 450 (5):549–557
12. Sanada Y, Oue N, Mitani Y, Yoshida K, Nakayama H, Yasui W (2006) Down-regulation of the claudin-18 gene, identified through serial analysis of gene expression data analysis, in gastric cancer with an intestinal phenotype. J Pathol 208(5):633–642
13. Shinozaki A, Ushiku T, Morikawa T, Hino R, Sakatani T, Uozaki H, Fukayama M (2009) Epstein–Barr virus-associated gastric carcinoma: a distinct carcinoma of gastric phenotype by claudin expression profiling. J Histochem Cytochem 57(8):775–785
14. Sentani K, Oue N, Tashiro T, Sakamoto N, Nishisaka T, Fukuhara T, Taniyama K, Matsuura H, Arihiro K, Ochiai A, Yasui W (2008) Immunohistochemical staining of Reg IV and claudin-18 is useful in the diagnosis of gastrointestinal signet ring cell carcinoma. Am J Surg Pathol 32(8):1182–1189
15. Karanjawala ZE, Illei PB, Ashfaq R, Infante JR, Murphy K, Pandey A, Schulick R, Winter J, Sharma R, Maitra A, Goggins M, Hruban RH (2008) New markers of pancreatic cancer identified through differential gene expression analyses: claudin 18 and annexin A8. Am J Surg Pathol 32(2):188–196
16. Sanada Y, Hirose Y, Osada S, Tanaka Y, Takahashi T, Yamaguchi K, Yoshida K (2010) Immunohistochemical study of claudin 18 involvement in intestinal differentiation during the progression of intraductal papillary mucinous neoplasm. Anticancer Res 30 (7):2995–3003
17. Zen Y, Adsay NV, Bardadin K, Colombari R, Ferrell L, Haga H, Hong SM, Hytiroglou P, Kloppel G, Lauwers GY, van Leeuwen DJ, Notohara K, Oshima K, Quaglia A, Sasaki M, Sessa F, Suriawinata A, Tsui W, Atomi Y, Nakanuma Y (2007) Biliary intraepithelial neoplasia: an international interobserver agreement study and proposal for diagnostic criteria. Mod Pathol 20(6):701–709
18. Kozaka K, Sasaki M, Fujii T, Harada K, Zen Y, Sato Y, Sawada S, Minato H, Matsui O, Nakanuma Y (2007) A subgroup of intrahepatic cholangiocarcinoma with an infiltrating replacement growth pattern and a resemblance to reactive proliferating bile ductules: 'bile ductular carcinoma'. Histopathology 51(3):390–400
19. Aishima S, Kuroda Y, Nishihara Y, Iguchi T, Taguchi K, Taketomi A, Maehara Y, Tsuneyoshi M (2007) Proposal of progression model for intrahepatic cholangiocarcinoma: clinicopathologic differences between hilar type and peripheral type. Am J Surg Pathol 31(7):1059–1067

Virchows Arch (2011) 459:81–89
DOI 10.1007/s00428-011-1091-0

ORIGINAL ARTICLE

Histochemical localization of caldesmon isoforms in colon adenocarcinoma and lymph node metastases

Christoph Köhler

Received: 8 February 2011 / Revised: 15 April 2011 / Accepted: 10 May 2011 / Published online: 29 May 2011
© Springer-Verlag 2011

Abstract Alternative splicing of the caldesmon gene results in high (*h*-caldesmon) and low (*l*-caldesmon) molecular weight isoforms of the cytoskeleton-associated protein caldesmon. *h*-Caldesmon is predominantly expressed not only in smooth-muscle cells but also in pericryptal fibroblasts in colon. *l*-Caldesmon is widely expressed and localized in podosomes/invadopodia. Studies with transformed and cancer cell lines suggest that a reduction in *l*-caldesmon facilitates podosome/invadopodia formation and metastasis. We investigated caldesmon isoforms in colon adenocarcinoma and their lymph node metastases using immunohistochemistry. Caldesmon immunoreactivity of colon adenocarcinoma primary tumors and lymph node metastases was very similar. *l*-Caldesmon immunoreactivity of cancer epithelial cells in primary tumors and lymph node metastases varied ranging from reduced to stronger as compared to immunoreactivity of normal areas. The variation did not show a consistent relation to the tumor center or invasive margin. While *h*-caldesmon immunoreactivity of pericryptal fibroblasts and blood vessels in the stroma of primary tumors and lymph node metastases was markedly reduced, cancer-associated fibroblasts and blood vessels in the stroma were strongly immunoreactive for *l*-caldesmon. Our results show a differential behavior of *h*- and *l*-caldesmon isoforms in epithelium and stroma of colon adenocarcinoma and lymph node metastases.

Keywords Colon adenocarcinoma · Stroma · Myofibroblasts

C. Köhler (✉)
Institute II of Anatomy, Medical Faculty, University of Cologne,
Kerpener Str. 62,
50924 Cologne, Germany
e-mail: c.koehler@uni-koeln.de

Introduction

Metastasis to regional lymph nodes is among the factors that most strongly predict outcome following surgical resection of colorectal cancer [1]. Important steps of the metastatic cascade are detachment from the bulk tumor, destruction of the basal membrane, motility, and migration [2, 3].

Podosomes are dynamic adhesion structures typically found in motile cells like macrophages and osteoclasts. They have a similar molecular composition as invadopodia in transformed and cancer cells. Invadopodia allow cancer cells to cross the basement membrane and invade adjacent tissues [4, 5]. Caldesmon, a cytoskeleton-associated protein, is localized in podosomes [6–8]. Caldesmon overexpression supresses podosome/invadopodia formation, extracellular matrix degradation, and invasion in several cancer cell lines, while caldesmon depletion facilitates it [9]. Caldesmon is upregulated by the tumor suppressor p53 [10] and inhibits the initial stage of podosome formation by competing with the Arp2/3 complex for actin binding as shown in Rous sarcoma virus-transformed fibroblasts [7]. Thus, the observed reduction in caldesmon in several transformed and cancer cell lines, including human colon adenocarcinoma-derived HCA-7 cells, may contribute to the cells ability to form invadopodia, degrade the extracellular matrix, and invade tissues [9, 11–14].

Alternative splicing results in high (*h*-caldesmon, 120–150 kD) and low (*l*-caldesmon, 70–80 kD) molecular weight isoforms of caldesmon that differ by the insertion of a central "spacer" region in *h*-caldesmon [15, 16]. *h*-Caldesmon is mainly expressed in differentiated smooth-muscle cells (smcs) where it is thought to regulate contraction and also in a few other cell types like pericryptal fibroblasts (PCFs) in colon [17, 18]. *l*-Caldesmon is thought to be ubiquitously

distributed in non-muscle tissues [19] influencing organization and stabilization of the microfilament network [20, 21]. Four *l*-caldesmon isoforms are known: WI-38 I *l*-caldesmon, WI-38 II *l*-caldesmon, and HeLa I and II *l*-caldesmons, the latter are characterized by a shorter N-terminus [22–24].

In contrast to many in vitro studies with transformed and cancer cell lines, expression of caldesmon in metastases has not been analyzed in tissue sections. We have studied the behavior of caldesmon isoforms in colon adenocarcinoma and lymph node metastases using three different, commercially available antibodies against caldesmon.

Materials and methods

Clinicopathological data

Formalin-fixed, paraffin-embedded tissue blocks from surgical resections of 15 colon adenocarcinomas, nine with lymph node metastases, were retrieved from the archives of the Institute for Pathology, University Hospital of Cologne, Germany. Hematoxylin and eosin-stained slides from primary tumors and lymph nodes were reviewed. Two blocks from each primary tumor were selected for further sectioning. Lymph nodes were sectioned if they contained metastases. Forty-two lymph nodes with metastases were immunostained for caldesmon. Most sections were not counter-stained; unstained structures were visualized using phase contrast. The normal pattern of immunoreactivity was evaluated in tumor-free areas from the same sections. The data of the patients and the tumor–node–metastasis classification of the tumors are listed in Table 1.

Antibodies

Three different antibodies against caldesmon were used for immunohistochemistry. An affinity-isolated rabbit polyclonal antibody produced by immunization against a sequence that is present in human *l*- and *h*-caldesmon (HPA017330, Sigma-Aldrich, Taufkirchen, Germany; see http://www.proteinatlas.org, HPA017330 for additional information) was used diluted 1:2,000. A human *l*-caldesmon mouse monoclonal antibody (clone 8/L-caldesmon, catalog no. 610660, BD Transduction Laboratories, Heidelberg, Germany) was used diluted 1:50. This antibody was raised against a fragment of human *l*-caldesmon corresponding to amino acids 251–395, a sequence both present in *l*- and *h*-caldesmon. Clone 8/L-Caldesmon is not absolutely specific for *l*-caldesmon but recognizes *h*-caldesmon in Western blots of mouse uterus that has a high content of *h*-caldesmon [25]. A mouse monoclonal antibody to human uterus smooth muscle extract (clone h-CD catalog no. C 4562, Sigma-Aldrich), specific for human *h*-caldesmon, was used diluted 1:400. Alpha smooth muscle actin (α-SMA) was stained with clone 1A4 (DAKO, Hamburg, Germany) diluted 1:100.

Immunohistochemistry

Five-micrometer-thick sections were cut, and immunohistochemistry was performed using the avidin–biotin peroxidase method. Paraffin sections were deparaffinized in xylene, rehydrated and pretreated by boiling three times for 5 min in citrate buffer (pH 6.0) in a microwave oven. Endogenous peroxidase activity was inhibited by incubating the sections in

Table 1 Clinicopathological characteristics of patients

Age	Gender	Tumor		Number of lymph nodes with metastases examined
72	m	Colon adenocarcinoma	pT1 N0 MX G2	–
59	m	Colon adenocarcinoma	pT2 N0 MX G1	–
75	f	Sigma adenocarcinoma	pT2 N0 MX G2	–
75	f	Colon adenocarcinoma	pT3 N0 MX G2	–
71	m	Colon adenocarcinoma	pT3 N0 MX G2	–
66	m	Colorectal adenocarcinoma	pT3 N0 MX G2	–
69	m	Colon adenocarcinoma	pT2 N1 MX G2	2
68	m	Colon adenocarcinoma	pT3 N1 MX G2	2
61	f	Colon adenocarcinoma, solid growth	pT3 N1 MX G3	1
39	m	Colon adenocarcinoma;	pT3 N2 M1 G2	6
67	m	Colon adenocarcinoma	pT3 N2 M1 Hep G2	6
79	f	Colorectal adenocarcinoma,	pT3 N2 MX G2	7
60	f	Colon adenocarcinoma, solid growth	pT3 N2 MX G3	5
58	m	Colon adenocarcinoma;	pT4 N2 M1 Lym G2-3	9
72	m	Colon adenocarcinoma	pT4 N2 MX G2	4

0.03% H_2O_2 in Tris-buffered saline (TBS) (pH 7.6) for 30 min. After washing in TBS three times for 5 min and blocking of unspecific binding sites with 20% FBS+1% BSA for 45 min, primary antibodies, diluted in TBS containing 3% nonfat dry milk, were applied, and the sections were incubated over night at 4°C. After another three washes in TBS, sections were incubated with the appropriate biotinylated secondary antibody for 30 min at room temperature (RT) (anti-rabbit IgG, Dianova, Hamburg, Germany, 1:400; anti-mouse IgG, Dianova, 1:250). Sections were again washed and incubated with an avidin-biotinylated horseradish peroxidase complex (ABC Elite kit, Linaris, Wertheim-Bettingen, Germany) for another 30 min at RT. Peroxidase activity was visualized by incubating the sections in a chromogen-solution containing 3,3′-diaminobenzidine intensified by the inclusion of 0.6% ammonium nickel sulphate (Fluka, Buchs, Switzerland) and 0.05% imidazol (Fluka) what resulted in a deep blue-gray reaction product or 3,3′-diaminobenzidine alone what resulted in a brown reaction product.

Double staining

Immunofluorescence double staining was performed with primary antibodies consecutively applied over night at 4°C. Incubation with the first primary antibody (clone 1A4 against α-SMA) was followed by incubation with biotinylated anti mouse IgG (Dianova, Hamburg, Germany 1:250) for 30 min at RT and then by Alexa Fluor 488-conjugated streptavidin (MoBiTec, Göttingen, Germany, 1:200) for another 30 min at RT. The second primary antibody (HPA017330) was detected with Alexa Fluor 546-conjugated anti-rabbit IgG (MoBiTec, 1:400).

Digital imaging

Sections stained for light microscopy were examined with a BX40-microscope (Olympus, Hamburg, Germany) equipped with phase contrast and a ColorView II digital camera (Olympus Soft Imaging Solutions, Münster, Germany). Confocal laser scanning microscopy was performed with a LSM510 confocal microscope (Zeiss, Jena, Germany).

Results

Immunoreactivity of caldesmon isoforms in normal colon

In the normal colon, smcs in the muscularis propria, muscularis mucosae, and in the wall of blood vessels were immunoreactive with antibody HPA017330, clone 8/L-caldesmon, and clone h-CD. Consistent with a previous report, clone h-CD, which is specific for *h*-caldesmon, stained colorectal PCFs located adjacent to epithelial cells, but no other cells in the lamina propria [18] (Fig. 1c). In contrast, antibodies HPA017330 and clone 8/L-caldesmon, which also recognize *l*-caldesmon, stained additional cells in the lamina propria that often had a spindle-shaped morphology and small blood vessels (Fig. 1a, b). Epithelial cells were not labeled with clone h-CD and clone 8/L-caldesmon, but displayed immunoreactivity of the apical region with antibody HPA017330 (Fig. 1a).

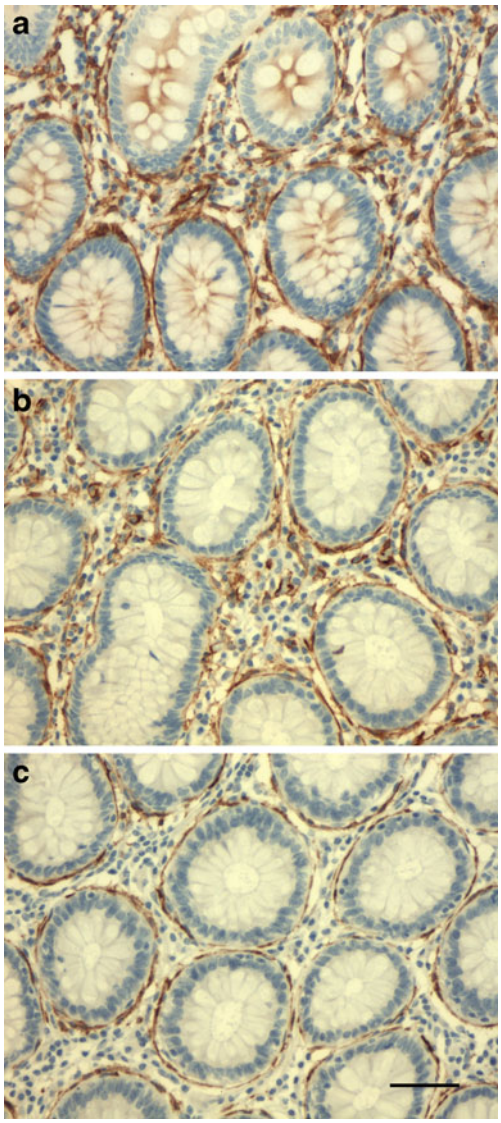

Fig. 1 Expression of caldesmon isoforms in the mucosa of normal colon. Five-micrometer-thick, paraffin serial sections of colon crypts and lamina propria from a normal appearing area, 3,3′-diaminobenzidine stain with hematoxylin counterstain. The polyclonal antibody HPA017330 (**a**) stains the apical region of enterocytes, pericryptal fibroblasts adjacent to the epithelium, small blood vessels, and additional, often spindle-shaped cells in the lamina propria. Clone 8/L-caldesmon (**b**) produces the same pattern, but immunoreactivity of enterocytes is absent. *h*-Caldesmon specifically detected with clone h-CD (**c**) is only expressed in pericryptal fibroblasts. *Scale bar* **a**–**c** 50 μm

h-Caldesmon immunoreactivity of primary tumors and lymph node metastases

In colon adenocarcinomas, the regular pattern of *h*-caldesmon-positive PCFs around epithelial cells has disappeared, except for one well-differentiated (G1) tumor where it was partly conserved. Large areas of the stroma were devoid of *h*-caldesmon immunoreactivity. Remaining *h*-caldesmon immunoreactivity of some spindle-shaped cells located adjacent to cancer epithelial cells was observed in 12 of 15 primary tumors examined (Fig. 2e, f). Single or groups of *h*-caldesmon-positive cells located in the stroma further apart from epithelial cells were present in 14 of 15 primary tumors examined. These *h*-caldesmon-positive cells likely represent smcs and PCFs. The number of immunoreactive blood vessels in tumors was lower than in normal areas and immunoreactivity of blood vessels in tumors appeared reduced if compared to normal areas. The cancer epithelium did not stain for *h*-caldesmon.

In normal appearing regions of lymph nodes, staining for *h*-caldesmon was confined to smcs as previously reported for rat and mouse lymph nodes [26]. Lymph node metastases displayed only little *h*-caldesmon immunoreactivity of the stroma (Fig. 3e, f). If present, *h*-caldesmon immunoreactivity showed the same pattern as observed in primary tumors.

l-Caldesmon immunoreactivity of primary tumors and lymph node metastases

Similar to normal epithelial cells, the apical region of primary tumor epithelial cells was only immunoreactive with antibody HPA017330 (Fig. 2b). The extent of this immunoreactivity varied between different regions of primary tumors ranging from markedly reduced to increased if compared to normal areas, but did not show a consistent relation to the tumor center or invasive margin. As in primary tumors, antibody HPA017330 variably stained epithelial cells in metastases

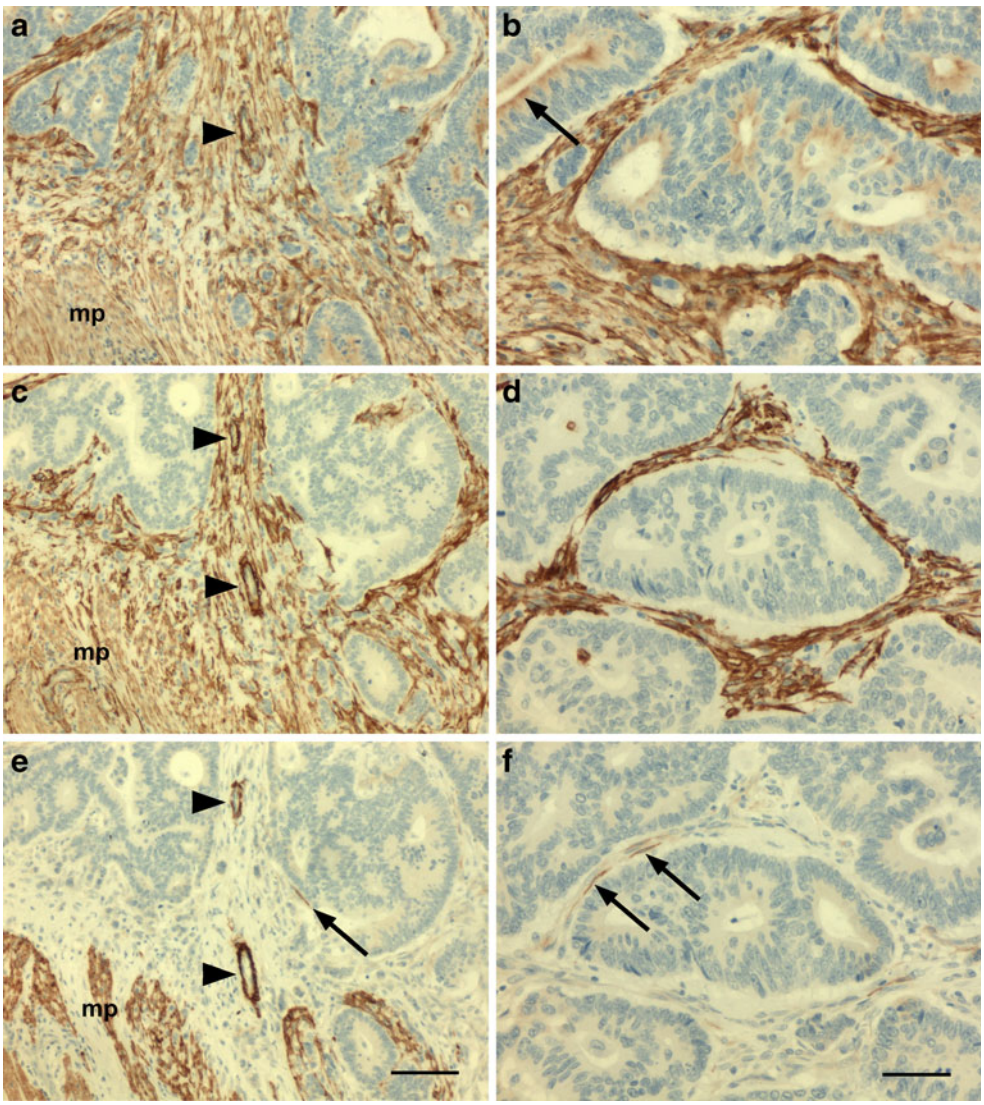

Fig. 2 Expression of caldesmon isoforms in colon adenocarcinoma primary tumors. 5-μm thick, paraffin serial sections of the tumorfront at the muscularis propria (**a**, **c**, **e**) and an area in the center of the same tumor (**b**, **d**, **f**). 3,3′-Diaminobenzidine stain with hematoxylin counterstain; **a**, **b** HPA017330, **c**, **d** clone 8/L-caldesmon, **e**, **f** clone h-CD. A blood vessel (*arrowheads* in **a**, **c**, **e**) and the muscularis propria (*mp*) are stained by all three antibodies. **a**, **c** Strong staining of the stroma is evident if the antibody recognizes *l*-caldesmon. **e** There is only little *h*-caldesmon immunoreactivity of the stroma (*arrow* points to a single positive cell in the position of a pericryptal fibroblast). **b**, **d** The antibodies that recognize *l*-caldesmon stain elongated cells in the stroma strongly; antibody HPA017330 also stains the apical region of some tumor epithelial cells (*arrow*). **f** The stroma is *h*-caldesmon-negative, except for a few cells. The *arrows* point to positive cells in the position of pericryptal fibroblasts. *Scale bar* **a**, **c**, **e** 100 μm, **b**, **d**, **f** 50 μm

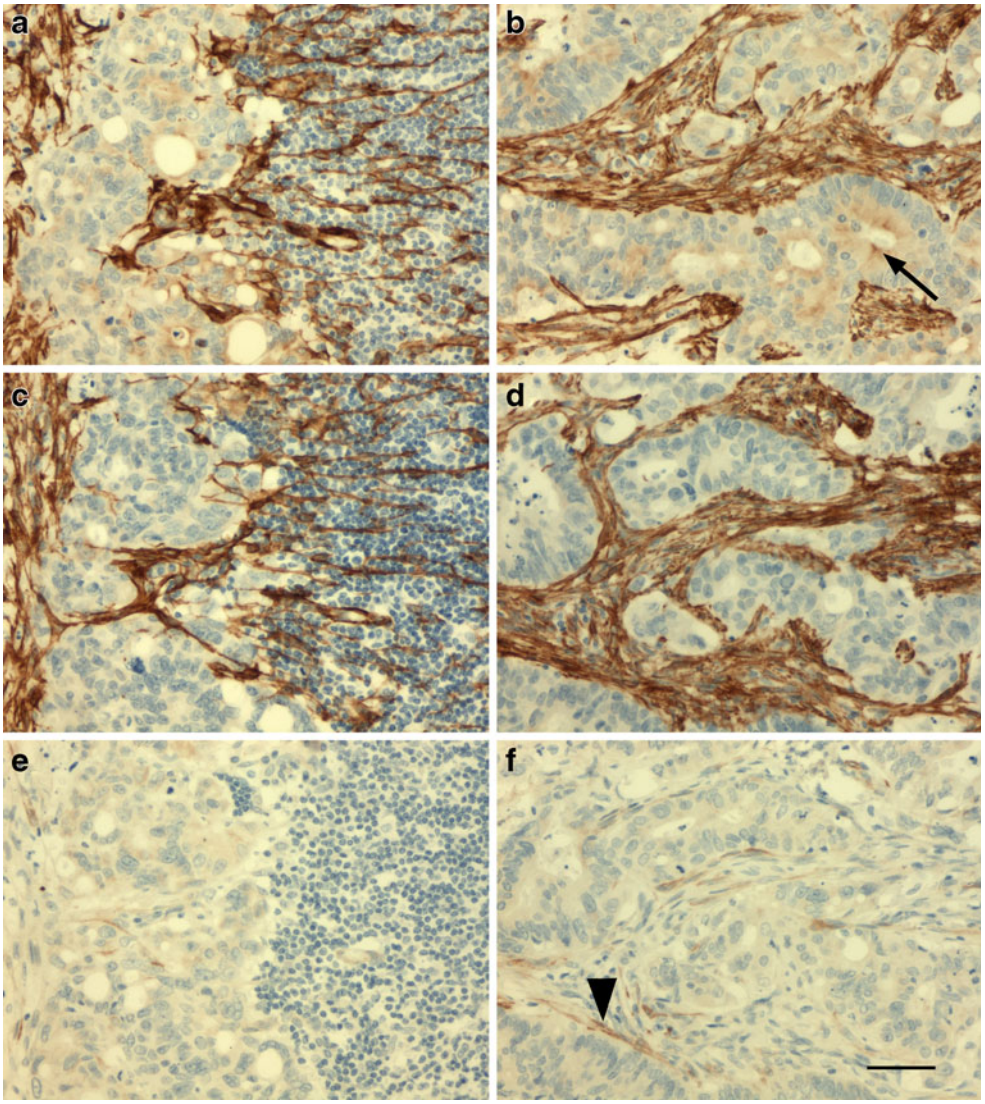

Fig. 3 Expression of caldesmon isoforms in lymph node metastases of colon adenocarcinoma. 5-μm thick, paraffin serial sections of a lymph node metastasis from the tumor shown in Fig. 2. **a**, **c**, **e** The *left halves* of the images show the margin of the metastasis; the *right halves* show lymphocytes and *l*-caldesmon-positive reticular cells. **b**, **d**, **f** Inner region of the metastasis. 3,3′-Diaminobenzidine stain with hematoxylin counterstain; **a**, **b** antibody HPA017330, **c**, **d** clone 8/L-caldesmon, **e**, **f** clone h-CD. **a**, **c** As in the primary tumor, elongated stromal cells are strongly *l*-caldesmon-positive (**a**–**d**), but there is little *h*-caldesmon immunoreactivity (**e**, **f**). The strongly *l*-caldesmon-positive stromal cells seem to be continuous with the lymph node reticulum (**a**, **c**). The *arrow* in **b** points to some staining of epithelial cells with antibody HPA017330, the *arrowhead* in **f** points to a *h*-caldesmon-positive cell adjacent to epithelial cells. *Scale bar* **a**–**f** 50 μm

(Figs. 3b, 4e, and 5b). Staining of the apical region of tumor epithelial cells was absent from the two primary tumors that displayed solid growth and from their metastases.

Large, elongated cells representing cancer associated fibroblasts (CAFs) and blood vessels were stained with antibody HPA017330 and clone 8/L-caldesmon in all primary tumors and in lymph node metastases if stromal cells were present (Figs. 2a–d and 3a–d). In normal lymph nodes, reticular cells, follicular dendritic cells, and smcs were stained with antibody HPA017330 and clone 8/L-caldesmon. The strong caldesmon immunoreactivity of CAFs in the stroma of lymph node metastases contrasted with the fine reticular meshwork of normal areas rendering the stroma discernable from the normal lymph node reticulum (Figs. 3a, c and 4b, e). Presumably, all CAFs in the stroma of primary tumors and metastases were stained. Since few cells in the stroma of primary tumors and metastases were stained for *h*-caldesmon, it indicates that most caldesmon immunoreactive cells in the stroma express the *l*-caldesmon isoform.

The morphological appearance and pattern of *l*-caldesmon immunoreactivity varied between different primary tumors, but was similar between primary tumor and its local metastases. Most obviously, the pattern of the stroma and *l*-caldesmon immunoreactivity of tumors with solid growth was different from the pattern of tumors with tubular growth (Fig. 4a–d).

Groups of tumor cells in vessels and distant metastases in preaortic lymph nodes (Fig. 4e, f) and liver displayed the same pattern of immunoreactivity of caldesmon isoforms as primary tumors and metastases in local lymph nodes.

Double staining

Based on morphology, elongated caldesmon single-positive cells in the stroma of primary tumors were identified as CAFs. Primary tumors double stained for caldesmon and α-SMA showed co-location in blood vessels and in most elongated caldesmon-positive cells in the stroma, suggesting that these

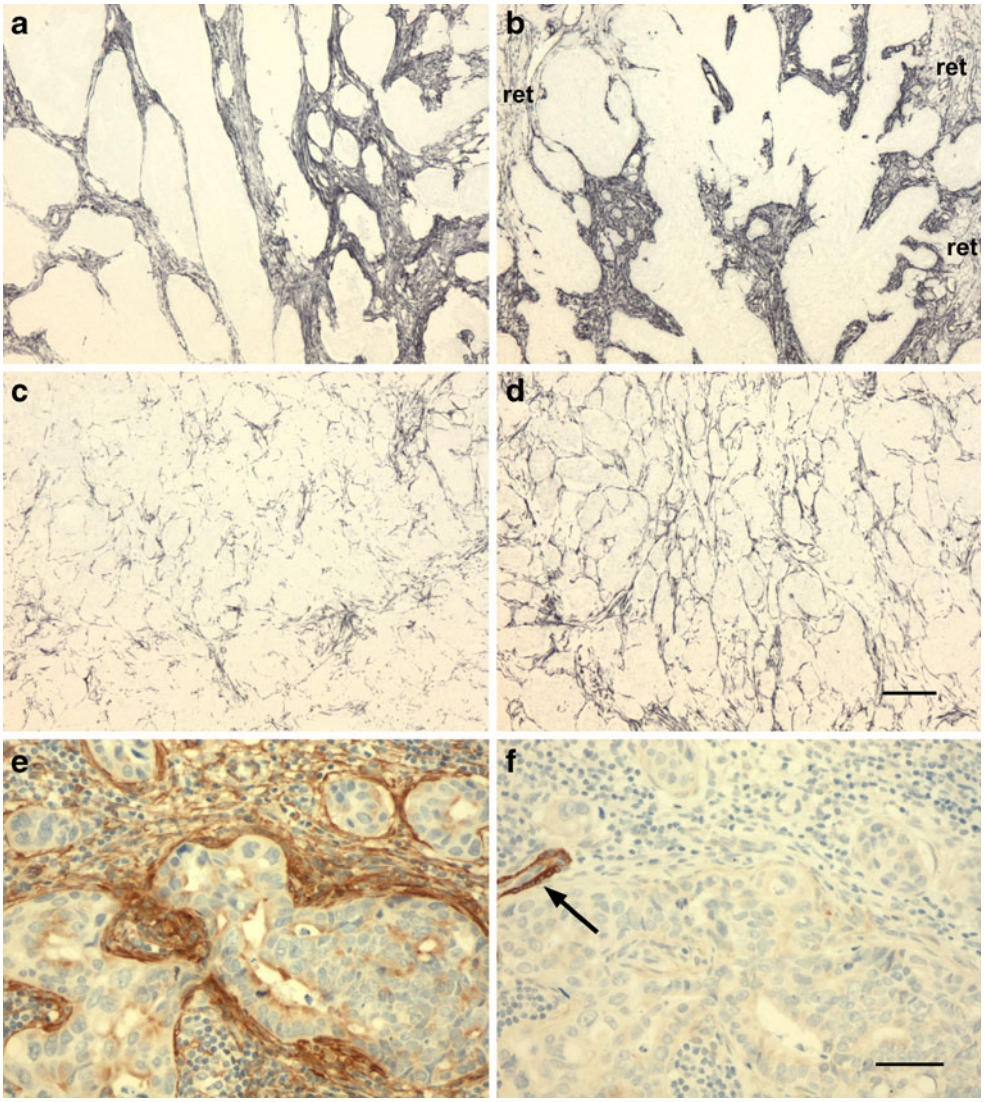

Fig. 4 Patterns of *l*-caldesmon-positive stroma in primary tumors and lymph node metastases. **a**–**d** 5-μm thick, paraffin serial sections of primary tumors and lymph node metastases, 3,3′-diaminobenzidine stain with nickel-enhancement, no counterstain. **a**, **b** Characteristic pattern of the stroma of primary tumors with tubular growth (**a**) and their lymph node metastases (**b**) stained with clone 8/L-caldesmon. The metastasis is flanked by reticular tissue (*ret*). **c**, **d** Characteristic pattern of the stroma of the two primary tumors with solid growth (**c**) and their lymph node metastases (**d**) stained with clone 8/L-caldesmon. Epithelial cells and lumina in **a**–**d** appear as unstained areas. **e**, **f** Five-micrometer thick, paraffin serial sections of a lymph node metastasis in a preaortic lymph node. 3,3′-Diaminobenzidine stain with hematoxylin counterstain; **e** antibody HPA017330, **f** clone h-CD. The distant metastasis shows the same pattern of expression of caldesmon isoforms as local metastases and primary tumors. The *arrow* points to an *h*-caldesmon-positive blood vessel. Some weak and diffuse staining of epithelial cells in **f** is not considered to be specific. *Scale bar* **a**–**d** 200 μm, **e**, **f** 50 μm

cells are CAFs with myofibroblast differentiation. This was observed in all primary tumors examined except for the well-differentiated (G1) adenocarcinoma, where α-SMA-positive cells in the stroma were comparably few.

In normal appearing areas of lymph nodes, caldesmon and α-SMA were co-located in blood vessels and reticular cells in the deep cortex and medulla. In the stroma of lymph node metastases, blood vessels and most elongated caldesmon-positive cells also expressed α-SMA (Fig. 5a–f).

Discussion

Our examination of tissue sections of colon adenocarcinoma and their lymph node metastases showed a very similar pattern of caldesmon immunoreactivity in primary tumors and metastases, but revealed a differential behavior of caldesmon isoforms in different tumor-associated cell types.

In the normal colon, *h*-caldesmon is expressed by smcs and PCFs. PCFs are thought to drive epithelial differentiation, produce components of the basement membrane, and secrete paracrine factors [27, 28]. α-SMA and HHF-35 immunoreactive PCFs decrease along the adenoma–carcinoma sequence [27, 29, 30]. More immunoreactive PCFs were found in well-differentiated adenocarcinoma than in moderately differentiated adenocarcinoma [29]. *h*-caldesmon immunoreactivity of PCFs behaves like these other markers of smc-like differentiation. Since expression of *h*-caldesmon is downregulated in dedifferentiated smcs [17, 31], reduced *h*-caldesmon immunoreactivity of PCFs in primary tumors and metastases could indicate the dedifferentiation of these cells. However, an electron microscopic study reported the absence of the PCF layer in the "transitional" mucosa adjacent to large bowel carcinoma [32].

Similar to our findings in colon adenocarcinoma, reduced expression of *h*-caldesmon has also been reported for vascular smcs in malignant melanoma. It was inversely

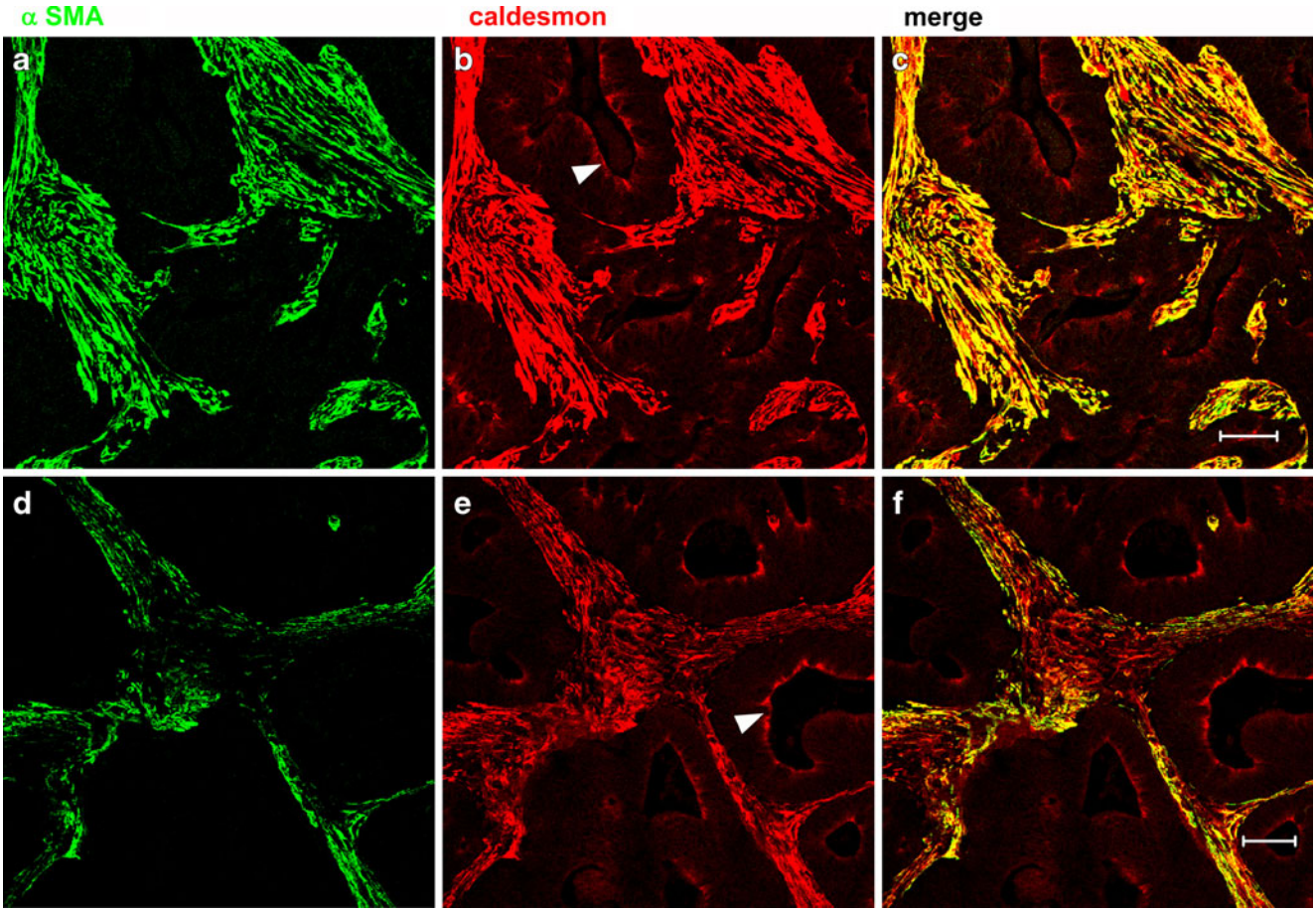

Fig. 5 Representative patterns of co-location of α-SMA and caldesmon detected with antibody HPA017330 in lymph node metastases. Confocal microscopy analysis at 0.5 μm optical thickness of lymph node metastases. **a**–**c** Almost complete co-location of caldesmon and α-SMA. **d**–**f** Caldesmon immunoreactivity exceeds α-SMA immunoreactivity. *Arrowheads* in **b**, **e** point to apical staining of epithelial cells. *Scale bar* **a**–**c** 50 μm, **d**–**f** 50 μm

correlated with the frequency of metastases and positively correlated with survival rate, possibly due to a higher fragility of *h*-caldesmon negative vessels [33].

In contrast to α-SMA, *h*-caldesmon is not expressed by myofibroblasts [18]. Therefore, *h*-caldesmon has been used as smooth-muscle differentiation marker in many histopathological studies (e.g. [34–39]). Given the specificity of clone h-CD for *h*-caldesmon [17], these studies did not provide information about the *l*-caldesmon isoform. However, expression of *l*-caldesmon in tumor vasculature, especially in glioma, has been reported [23, 24]. Our results show that myofibroblasts also strongly express the *l*-caldesmon isoform.

Of the antibodies recognizing *l*-caldesmon isoforms, only the polyclonal antibody HPA017330 labeled epithelial cells. It should be noted that antibody HPA017330 recognizes additional bands in Western blot of U-251 MG glioma cells (http://www.proteinatlas.org, [40]). However, caldesmon immunoreactivity of the apical region of colon enterocytes is in line with results from rat and mouse enterocytes where it is thought to represent caldesmon located in the terminal web underneath the brush border [41, 42]. The variation in caldesmon immmunoreactivity of cancer epithelial cells did not allow a conclusion about reduction in *l*-caldesmon in metastasizing epithelial cells from colon adenocarcinoma.

In contrast, our results show strong expression of the *l*-caldesmon isoform in the stroma of primary tumors and metastases with both antibody HPA017330 and clone 8/L-caldesmon. The great number and size of strongly *l*-caldesmon-immunoreactive fibroblasts in the stroma are in line with quantitative data [43] and suggests an at least proportional increase in *l*-caldesmon in proliferated CAFs. Others observed an increased number of caldesmon-immunoreactive cells in the stroma of colon adenocarcinoma that were also positive for vimentin- and other microfilament-associated proteins like filamin, gelsolin, and talin [44].

In lymph nodes that normally contain only a small and restricted connective tissue component, the stroma of metastases is thought to be derived from fibroblasts and pericytes

that accompanied metastasizing epithelial cells or from local fibroblasts in the capsule and septa [45]. Epithelial–mesenchymal transition of metastatic epithelial cells and a contribution from bone marrow-derived mesenchymal stem cells may also occur [3, 46]. Results from this study suggest that lymph node reticulum cells may also contribute.

Antibody HPA017330 and clone 8/L-caldesmon recognize sequences that are common to all caldesmon isoforms and therefore do not differentiate between the widely expressed WI-38 II *l*-caldesmon isoform, HeLa *l*-caldesmon isoforms, or the WI-38 I *l*-caldesmon isoform. An antibody specific to HeLa *l*-caldesmon, which recognized the N-terminal 18 residues, only stained some co-opted vessels in colon adenocarcinoma, although there was considerable immunostaining of other kinds of tumors [24]. Vessels in normal colon were not stained. The WI-38 I *l*-caldesmon isoform has so far only been demonstrated in WI-38 cells and in gliomas [22, 23]. Since *l*-caldesmon is expressed in normal fibroblasts [13] and because proliferating CAFs are regarded activated, rather than derived from transformed cells [47, 48], it may be the normal WI-38 II *l*-caldesmon isoform that is upregulated in CAFs.

In summary, immunoreactivity of caldesmon isoforms in colon adenocarcinoma primary tumors and lymph node metastases was very similar. *l*-Caldesmon immunoreactivity of cancer epithelial cells varied in primary tumors and lymph node metastases not allowing a conclusion about reduction in *l*-caldesmon in metastasizing epithelial cells from colon adenocarcinoma. While *h*-caldesmon immunoreactivity of blood vessels and PCFs in the stroma of primary tumors and lymph node metastases was reduced, blood vessels and CAFs in the stroma were strongly immunoreactive for *l*-caldesmon.

Acknowledgments The author thanks Professor H. P. Dienes for providing examined surgical specimens from the archives of the Institute for Pathology for this study. The excellent technical assistance of Mrs. M. Dinekov is gratefully acknowledged.

Conflict of interest statement The author declares that he has no conflict of interest.

References

1. Compton CC, Fielding LP, Burgart LJ, Conley B, Cooper HS, Hamilton SR, Hammond ME, Henson DE, Hutter RV, Nagle RB, Nielsen ML, Sargent DJ, Taylor CR, Welton M, Willett C (1999) Prognostic factors in colorectal cancer. College of American Pathologists Consensus Statement 1999. Arch Pathol Lab Med 124:979–994
2. Wittekind C, Neid M (2005) Cancer invasion and metastasis. Oncology 69(Suppl 1):14–16
3. Geiger TR, Peeper DS (2009) Metastasis mechanisms. Biochim Biophys Acta 1796:293–308
4. Weaver AM (2006) Invadopodia: specialized cell structures for cancer invasion. Clin Exp Metastasis 23:97–105
5. Yamaguchi H, Pixley F, Condeelis J (2006) Invadopodia and podosomes in tumor invasion. Eur J Cell Biol 85:213–218
6. Tanaka J, Watanabe T, Nakamura N, Sobue K (1993) Morphological and biochemical analyses of contractile proteins (actin, myosin, caldesmon and tropomyosin) in normal and transformed cells. J Cell Sci 104:595–606
7. Morita T, Mayanagi T, Yoshio T, Sobue K (2007) Changes in the balance between caldesmon regulated by p21-activated kinases and the Arp2/3 complex govern podosome formation. J Biol Chem 282:8454–8463
8. Zheng PP, van der Weiden M, Kros JM (2007) Hela l-CaD is implicated in the migration of endothelial cells/endothelial progenitor cells in human neoplasms. Cell Adh Migr 1:84–91
9. Yoshio T, Morita T, Kimura Y, Tsujii M, Hayashi N, Sobue K (2007) Caldesmon suppresses cancer cell invasion by regulating podosome/invadopodium formation. FEBS Lett 581:3777–3782
10. Mukhopadhyay UK, Eves R, Jia L, Mooney P, Mak AS (2009) p53 suppresses Src-induced podosome and rosette formation and cellular invasiveness through the upregulation of caldesmon. Mol Cell Biol 29:3088–3098
11. Owada MK, Hakura A, Iida K, Yahara I, Sobue K, Kakiuchi S (1984) Occurrence of caldesmon (a calmodulin-binding protein) in cultured cells: comparison of normal and transformed cells. Proc Natl Acad Sci USA 81:3133–3137
12. Lin JJ, Lin JL, Davis-Nanthakumar EJ, Lourim D (1988) Monoclonal antibodies against caldesmon, a Ca++/calmodulin- and actin-binding protein of smooth muscle and nonmuscle cells. Hybridoma 7:273–288
13. Novy RE, Lin JL, Lin JJ (1991) Characterization of cDNA clones encoding a human fibroblast caldesmon isoform and analysis of caldesmon expression in normal and transformed cells. J Biol Chem 266:16917–16924
14. Ross DT, Scherf U, Eisen MB, Perou CM, Rees C, Spellman P, Iyer V, Jeffrey SS, Van de Rijn M, Waltham M, Pergamenschikov A, Lee JC, Lashkari D, Shalon D, Myers TG, Weinstein JN, Botstein D, Brown PO (2000) Systematic variation in gene expression patterns in human cancer cell lines. Nat Genet 24:227–235
15. Sobue K, Sellers JR (1991) Caldesmon, a novel regulatory protein in smooth muscle and nonmuscle actomyosin systems. J Biol Chem 266:12115–12118
16. Huber PA (1997) Caldesmon. Int J Biochem Cell Biol 29:1047–1051
17. Frid MG, Shekhonin BV, Koteliansky VE, Glukhova MA (1992) Phenotypic changes of human smooth muscle cells during development: late expression of heavy caldesmon and calponin. Dev Biol 153:185–193
18. Nakayama H, Miyazaki E, Enzan H (1999) Differential expression of high molecular weight caldesmon in colorectal pericryptal fibroblasts and tumour stroma. J Clin Pathol 52:785–786
19. Sobue K, Fukumoto K (2010) Caldesmon, an actin-linked regulatory protein, comes across glucocorticoids. Cell Adh Migr 4:1–5
20. Dabrowska R, Kulikova N, Gagola M (2004) Nonmuscle caldesmon: its distribution and involvement in various cellular processes. Protoplasma 224:1–13
21. Kordowska J, Hetrick T, Adam LP, Wang CL (2006) Phosphorylated l-caldesmon is involved in disassembly of actin stress fibers and postmitotic spreading. Exp Cell Res 312:95–110
22. Payne AM, Yue P, Pritchard K, Marston SB (1995) Caldesmon mRNA splicing and isoform expression in mammalian smooth-muscle and non-muscle tissues. Biochem J 305:445–450
23. Zheng PP, Sieuwerts AM, Luider TM, van der Weiden M, Sillevis-Smitt PA, Kros JM (2004) Differential expression of

splicing variants of the human caldesmon gene (CALD1) in glioma neovascularization versus normal brain microvasculature. Am J Pathol 164:2217–2228
24. Zheng PP, van der Weiden M, Kros JM (2005) Differential expression of Hela-type caldesmon in tumour neovascularization: a new marker of angiogenic endothelial cells. J Pathol 205:408–414
25. Köhler CN (2011) Histochemical localization of caldesmon in the CNS and Ganglia of the mouse. J Histochem Cytochem 59:504–517
26. Köhler CN (2010) The actin-binding protein caldesmon is in spleen and lymph nodes predominately expressed by smooth muscle cells, reticular cells, and follicular dendritic cells. J Histochem Cytochem 58:183–193
27. Higaki S, Tada M, Nishiaki M, Mitani M, Yanai H, Okita K (1999) Immunohistological study to determine the presence of pericryptal myofibroblasts and basement membrane in colorectal epithelial tumors. J Gastroenterol 34:215–220
28. Powell DW, Adegboyega PA, Di Mari JF, Mifflin RC (2005) Epithelial cells and their neighbors I. Role of intestinal myofibroblasts in development, repair, and cancer. Am J Physiol Gastrointest Liver Physiol 289:G2–G7
29. Yao T, Tsuneyoshi M (1993) Significance of pericryptal fibroblasts in colorectal epithelial tumors: a special reference to the histologic features and growth patterns. Hum Pathol 24:525–533
30. Li A, Hasui K, Yonezawa S, Tanaka S, Sato E (1999) Immunohistochemical analysis of pericryptal fibroblast sheath and proliferating epithelial cells in human colorectal adenomas and carcinomas with adenoma components. Pathol Int 49:426–434
31. Ueki N, Sobue K, Kanda K, Hada T, Higashino K (1987) Expression of high and low molecular weight caldesmons during phenotypic modulation of smooth muscle cells. Proc Natl Acad Sci USA 84:9049–9053
32. Balázs M, Kovács A (1982) The 'transitional' mucosa adjacent to large bowel carcinoma-electron microscopic features and myofibroblast reaction. Histopathology 6:617–629
33. Koganehira Y, Takeoka M, Ehara T, Sasaki K, Murata H, Saida T, Taniguchi S (2003) Reduced expression of actin-binding proteins, h-caldesmon and calponin h1, in the vascular smooth muscle inside melanoma lesions: an adverse prognostic factor for malignant melanoma. Br J Dermatol 148:971–980
34. Miettinen MM, Sarlomo-Rikala M, Kovatich AJ, Lasota J (1999) Calponin and h-caldesmon in soft tissue tumors: consistent h-caldesmon immunoreactivity in gastrointestinal stromal tumors indicates traits of smooth muscle differentiation. Mod Pathol 12:756–762
35. Ceballos KM, Nielsen GP, Selig MK, O'Connell JX (2000) Is anti-h-caldesmon useful for distinguishing smooth muscle and myofibroblastic tumors? An immunohistochemical study. Am J Clin Pathol 114:746–753
36. Visée S, Soltner C, Rialland X, Machet MC, Loussouarn D, Milinkevitch S, Pasco-Papon A, Mercier P, Rousselet MC (2005) Supratentorial primitive neuroectodermal tumours of the brain: multidirectional differentiation does not influence prognosis. A clinicopathological report of 18 patients. Histopathology 46:403–412
37. Perez-Montiel MD, Plaza JA, Dominguez-Malagon H, Suster S (2006) Differential expression of smooth muscle myosin, smooth muscle actin, h-caldesmon, and calponin in the diagnosis of myofibroblastic and smooth muscle lesions of skin and soft tissue. Am J Dermatopathol 28:105–111
38. Qiu X, Montgomery E, Sun B (2008) Inflammatory myofibroblastic tumor and low-grade myofibroblastic sarcoma: a comparative study of clinicopathologic features and further observations on the immunohistochemical profile of myofibroblasts. Hum Pathol 39:846–856
39. Council L, Hameed O (2009) Differential expression of immunohistochemical markers in bladder smooth muscle and myofibroblasts, and the potential utility of desmin, smoothelin, and vimentin in staging of bladder carcinoma. Mod Pathol 22:639–650
40. Uhlén M, Björling E, Agaton C, Szigyarto CA, Amini B, Andersen E et al (2005) A human protein atlas for normal and cancer tissues based on antibody proteomics. Mol Cell Proteomics 4:1920–1932
41. Ishimura K, Fujita H, Ban T, Matsuda H, Sobue K, Kakiuchi S (1984) Immunocytochemical demonstration of caldesmon (a calmodulin-binding, F-actin-interacting protein) in smooth muscle fibers and absorptive epithelial cells in the small intestine of the rat. Cell Tissue Res 235:207–209
42. Bretscher A, Lynch W (1985) Identification and localization of immunoreactive forms of caldesmon in smooth and nonmuscle cells: a comparison with the distributions of tropomyosin and alpha-actinin. J Cell Biol 100:1656–1663
43. Ohtani H, Sasano N (1983) Stromal cell changes in human colorectal adenomas and carcinomas. An ultrastructural study of fibroblasts, myofibroblasts, and smooth muscle cells. Virchows Arch A Pathol Anat Histopathol 401:209–222
44. Porter RM, Holme TC, Newman EL, Hopwood D, Wilkinson JM, Cuschieri A (1993) Monoclonal antibodies to cytoskeletal proteins: an immunohistochemical investigation of human colon cancer. J Pathol 170:435–440
45. Sivridis E, Giatromanolaki A, Koukourakis MI (2004) "Stromatogenesis" and tumor progression. Int J Surg Pathol 12:1–9
46. Alison MR, Lovell MJ, Direkze NC, Wright NA, Poulsom R (2006) Stem cell plasticity and tumour formation. Eur J Cancer 42:1247–1256
47. Giatromanolaki A, Sivridis E, Koukourakis MI (2007) The pathology of tumor stromatogenesis. Cancer Biol Ther 6:639–645
48. Kalluri R, Zeisberg M (2006) Fibroblasts in cancer. Nat Rev Cancer 6:392–401

Virchows Arch (2011) 459:91–97
DOI 10.1007/s00428-011-1095-9

ORIGINAL ARTICLE

Alpha-methylacyl-CoA racemase (AMACR) expression in epithelial ovarian cancer

Aurelia Noske · Anne-Katrin Zimmermann · Rosmarie Caduff · Zsuzsanna Varga · Daniel Fink · Holger Moch · Glen Kristiansen

Received: 28 March 2011 / Revised: 17 May 2011 / Accepted: 19 May 2011 / Published online: 4 June 2011
© Springer-Verlag 2011

Abstract Alpha-methylacyl-CoA racemase (AMACR) is involved in the cellular metabolism of fatty acids. It is a prognostic factor in prostate and colorectal cancer. So far, little is known about its expression and prognostic role in ovarian cancer. We investigated the expression of AMACR in a total of 420 ovarian tumors (388 carcinomas, 32 borderline tumors) by immunohistochemistry on tissue microarrays of two independent patient cohorts. In both cohorts, cytoplasmic AMACR expression was identified in 11.8% (16/136) and 5.4% (13/239), respectively, of the ovarian carcinomas. In contrast, borderline tumors did not show any AMACR expression. AMACR expression was significantly associated with histological subtype, FIGO stage, and grade in one cohort and low estrogen receptor levels in the other cohort. In univariate analysis, AMACR expression was significantly associated with poor overall survival (log rank, $p=0.006$) and an independent prognostic factor in a multivariate analysis (HR 3.3; CI 1.3–7.9; $p=0.008$) but could not be verified in the second cohort. Unlike in other tumor entities, AMACR expression does not seem to have an unequivocal prognostic impact in ovarian cancer. The prevalence may limit the value of AMACR for the differential diagnosis between metastatic colorectal carcinomas and primary ovarian carcinomas, whereas the association with estrogen receptor expression deserves further studies.

Keywords Epithelial ovarian cancer · Ovarian borderline tumors · Alpha-methylacyl-CoA racemase (AMACR, p504S) · Prognosis

A. Noske · A.-K. Zimmermann · R. Caduff · Z. Varga · H. Moch
Institute of Surgical Pathology, University Hospital Zurich,
Schmelzbergstr.12,
CH-8091 Zurich, Switzerland

D. Fink
Department of Obstetrics and Gynecology,
University Hospital Zurich,
Zurich, Switzerland

G. Kristiansen (✉)
Institute of Surgical Pathology, University Hospital Bonn,
Sigmund-Freud-Str. 25,
Bonn 53127, Germany
e-mail: glen.kristiansen@ukb.uni-bonn.de

Introduction

Ovarian cancer is associated with the highest mortality among gynecologic malignancies, which is due to the primary diagnosis in an advanced tumor stage as well as the resistance to conventional chemotherapeutic approaches. Therefore, it is a necessity to identify molecular targets for diagnosis, estimation of clinical course, prediction of therapy response, and novel therapies of patient prognosis.

Epidemiologic studies have shown that dietary products enhance the risk of hormone-related cancer. The consumption of high-fat meat may also increase the risk of ovarian cancer [1, 2]. Alpha-methylacyl-CoA racemase (AMACR), a peroxisomal and mitochondrial enzyme, plays a central role in metabolic pathways and is involved in the beta oxidation of branched-chain fatty acids (including phytanic and pristanic acid) and bile acid synthesis [3]. High intake of branched-chain fatty acids in dairy and beef products may result in an overproduction of AMACR protein and increase the risk of prostate cancer [4, 5]. AMACR was previously identified by cDNA microarray analysis as overexpressed in cancer and intraepithelial neoplasia of the prostate [6]. Meanwhile it is an established diagnostic biomarker for prostatic cancer in the practice of surgical pathologists in difficult needle core biopsies [7, 8]. Recent reports have

shown that AMACR is not restricted to prostate tissues but widely expressed in several cancer types and precursor lesions [9, 10]. Varying levels of AMACR expression have been suggested as prognostic markers in several cancer types including prostate and colon cancer [11, 12].

So far, there are only few studies on AMACR expression in ovarian cancer. The investigated ovarian tumor groups were relatively small, and the findings have not been correlated with clinical features and course of disease. Reported prevalence of AMACR protein expression ranges from 0% to 60% [9, 13, 14]. It is currently unclear whether AMACR expression has also a clinical significance in ovarian tumors. To get more insights on the potential prognostic significance of immunohistochemical quantification of AMACR expression in ovarian cancer, we utilized tissue microarrays (TMA) from two independent ovarian cancer patient cohorts, including 388 carcinoma samples. To our knowledge, we compared for the first time AMACR expression data with clinicopathological factors and patient outcome.

Patients and methods

Study cases and tissue microarray construction

Two different tissue microarrays were used for this study. The first TMA was constructed from 168 ovarian tumors, consisting of 136 primary epithelial ovarian carcinomas, 31 borderline tumors (19 serous, 11 mucinous, and 1 endometrioid), and 1 benign Brenner tumor, as well as 6 samples of the fallopian tube. Patients were surgically treated at the University Hospital Zurich (Switzerland) between 1995 and 2005. Clinical and pathological characteristics were taken from the clinical database and pathology records. Tissue samples were fixed in 4% neutral buffered formaldehyde and embedded in paraffin. Routine hematoxylin and eosin sections were performed for histopathological evaluation. The stage of tumors was assessed according to the International Federation of Gynecology and Obstetrics (FIGO) staging system. The tumor grade and histological subtype were defined according to the WHO classification 2003. All tumors were reviewed by one gynecologic pathologist (RC). The median patient age at the time of surgery was 60 years, ranging from 20 to 87 years. The median follow-up time of the surviving patients was 59 months. Data on adjuvant chemotherapy were known for all patients. In the majority (68.5%), a platinum-based combination therapy was administered.

Representative tumor areas were marked on the HE-stained slides. Two 0.6-mm tissue cores were then punched from each case, and transferred into a TMA format as described [15]. The second TMA has been manufactured at the University Hospital Basel and consists of 268 ovarian carcinomas as described before [16–18]. Undifferentiated carcinomas (n=16) were excluded from the study. The distribution of patient age (median 60.8 years) and median follow-up time of the surviving patients of 56 months was similar to the other cohort. However, data on adjuvant therapy were not available. The clinicopathological characteristics of the ovarian carcinomas from each TMA are summarized in Tables 1 and 2. The study was approved by the Cantonal Ethics Committee of Zurich (StV 27–2009).

Immunohistochemistry

The TMA blocks were freshly cut and mounted on superfrost slides (Menzel Gläser, Braunschweig, Germany). Briefly, slides were pretreated with CC1 mild (TRIS buffer with slightly increased pH) for 30 min and incubated with a rabbit monoclonal AMACR antibody (Biologo, Kronshagen, Germany; clone 13H4) which was diluted 1:200 in Ventana dilution buffer. After incubation for 1 h at room temperature, the staining was further conducted with the Ventana Benchmark automated system (Ventana Medical Systems, Tucson, AZ, USA) using Ventana reagents as well as UltraVIEW™

Table 1 Characteristics of 136 invasive ovarian carcinomas (Zurich cohort)

Characteristics	Cases, n (%)
AMACR expression	
Positive	16 (11.8)
Negative	120 (88.2)
Histological type	
Serous	66 (48.5)
Clear cell	24 (17.6)
Endometrioid	31 (22.8)
Mucinous	15 (11)
FIGO stage (n=131)	
I	33 (25.2)
II	10 (7.6)
III	50 (38.2)
IV	38 (29)
Tumor grade	
1	22 (16.2)
2	58 (42.6)
3	56 (41.2)
Residual disease (n=90)	
<1 cm	26 (28.9)
1–2 cm	27 (30)
>2 cm	37 (41.1)
Estrogen receptor expression (n=135)	
Low	38 (29)
High	97 (72)

Table 2 Characteristics of 252 invasive ovarian carcinomas (Basel cohort)

Characteristics	Cases, *n* (%)
AMACR expression (*n*=239)	
Positive	13 (5.4)
Negative	226 (94.6)
Histological type	
Serous	120 (47.6)
Clear cell	24 (9.5)
Endometrioid	68 (27)
Mucinous	40 (15.9)
FIGO stage (*n*=192)	
I	50 (26)
II	22 (11.5)
III	110 (57.3)
IV	10 (5.2)
Tumor grade (*n*=247)	
1	86 (34.8)
2	87 (35.2)
3	74 (30)
Residual disease (*n*=103)	
<2 cm	73 (70.9)
>2 cm	30 (29.1)
Estrogen receptor expression (*n*=220)	
Low	117 (53.2%)
High	103 (46.8%)

DAB detection kit. The expression analysis was performed by two pathologists (AKZ and AN). The expression was evaluated according to the percentage of positive cells and the intensity of staining. The percentage of positive cells was scored as: 0 (0%), 1 (<10%), 2 (11–50%), 3 (51–80%), and 4 (>80%). The staining intensity was scored as: 0 (negative), 1 (weak), 2 (moderate), and 3 (strong). For the immunoreactive score, the percentage of positive cells and staining intensity was multiplied, resulting in a value between 0 and 12. Negative controls were performed by replacement of the primary antibody by non-reactive rabbit IgG (DAKO). For positive controls, sections from prostatic cancer and benign prostatic glands were used. In addition, both TMAs were incubated with an antibody to detect the estrogen receptor (ER) expression (Ventana medical systems, clone SP1). Carcinomas were considered positive for ER expression (high levels) when at least 10% nuclear positivity of the tumor cells was seen.

Statistical analysis

The median value of the immunoreactive score of AMACR expression was used as cutoff point to dichotomize the carcinomas into "negative" (no expression) and "positive" (any expression). The statistical significance of the association between AMACR expression and clinicopathological parameters was assessed by chi-square test for trends. The probability of overall survival as a function of time was determined by the Kaplan–Meier method. For survival analysis only the patients with ovarian carcinomas were included. Differences in survival curves were compared by the log rank test. Multivariate survival analysis was performed using the Cox model of proportional hazards. Generally, p values smaller than 0.05 were considered as significant. For the statistical evaluation the SPSS software Version 18.0 (SPSS Inc., Chicago, IL, USA) was used.

Results

AMACR expression in ovarian carcinomas

Immunohistochemical AMACR analysis was successful in all samples of the "Zurich cohort" and in 233 of 239 cases of the "Basel cohort" due to the lack of tumor tissue in some TMA spots. In both cohorts, we observed a cytoplasmic granular expression pattern of AMACR in ovarian carcinomas. The fraction of AMACR positive cases was 11.8% (16/136) in one cohort and 5.4% (13/239) in the other cohort. In contrast, borderline tumors and epithelium of the fallopian tube did not show any expression. Representative images are shown in Fig. 1a–d.

For the "Zurich cohort," we found that AMACR expression was significantly associated with low estrogen receptor levels (chi-square test for trends, p=0.001) but not with other clinicopathological factors like FIGO stage, histological subtype, grading, intraoperative residual disease, and patient age. For the "Basel cohort," AMACR expression was significantly related to the endometrioid and clear cell histological subtype (chi-square test for trends, p=0.017), early FIGO stage (chi-square test for trends, p=0.037), and better differentiated carcinomas (chi-square test for trends, p=0.037) but not to the estrogen receptor expression (p=0.29)

Association of AMACR with overall survival

To investigate an association of AMACR expression with overall survival of ovarian cancer patients, we performed uni- and multivariate survival analyses including only invasive carcinomas. Follow-up data of the "Zurich cohort" was known in 134 cases. We found that established prognostic factors for ovarian cancer as listed in Table 3 reached significant prognostic impact on univariate logistic regression analysis. In Kaplan–Meier analysis (log rank, p=0.006) and univariate logistic regression analysis (p=0.007, HR 2.6 CI 1.3–5.1), AMACR expression was significantly associated with poor overall survival (Fig. 2, Table 3). In multivariate COX regression analysis adjusted

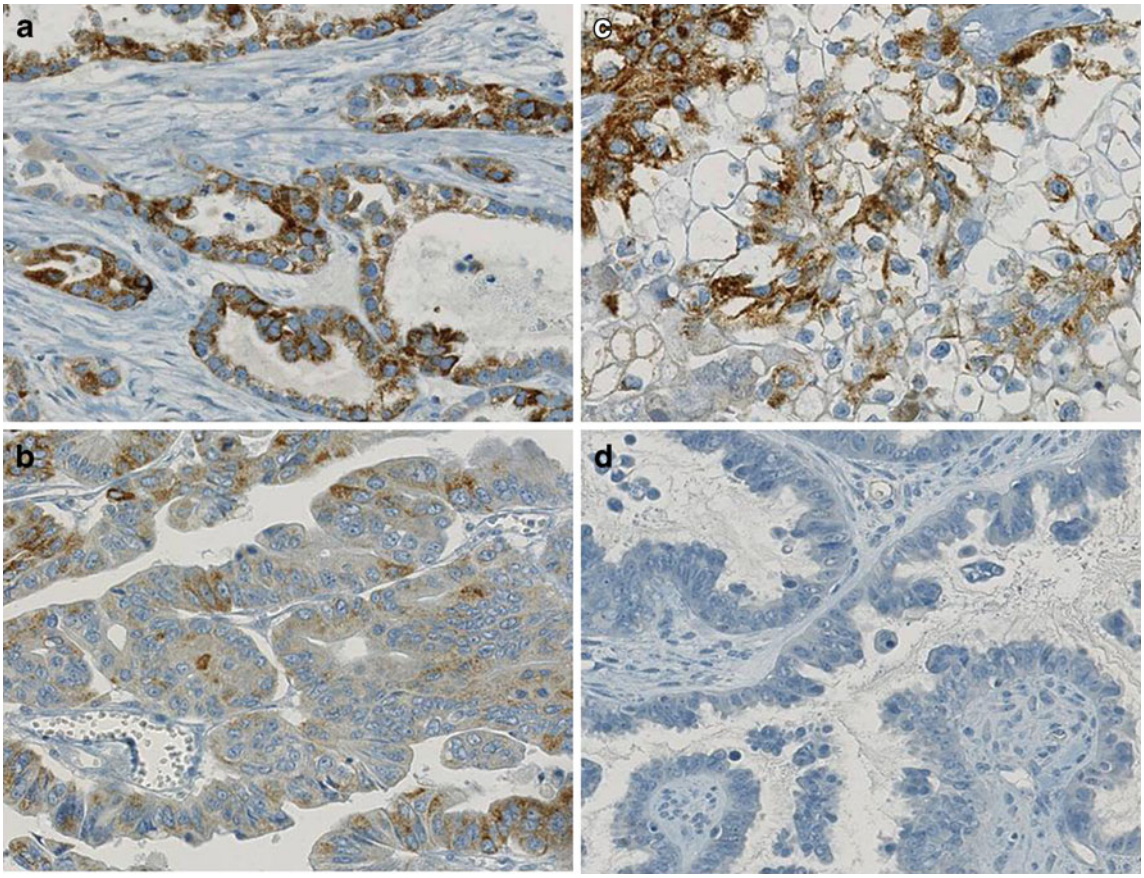

Fig. 1 Immunohistochemical staining of AMACR. **a**, **b** Examples of cytoplasmic expression in serous carcinomas (×200). **c** Cytoplasmic expression in a clear cell carcinoma (×200). **d** No staining in a serous borderline tumor (×200)

for other prognostic factors, AMACR expression reached independent prognostic information (Table 4).

Follow-up data of the "Basel cohort" was known in 136 cases. We observed that FIGO stage (p=0.0005, HR 2.13 CI 1.58–2.89), grading (p=0.028, HR 1.37 CI 1.03–1.81), and intraoperative residual tumor (p=0.036, HR 1.80 CI 1.04–3.14) had also significant prognostic impact on overall survival in univariate logistic regression analysis. However, AMACR expression (p=0.2, HR 0.046 CI 0.00–5.32) and the histological subtype (p=0.138, HR 0.85 CI 0.69–1.05) did not reach prognostic significance.

Discussion

In this study, we observed an expression of AMACR in 11.8% and 5.4%, respectively, of the primary ovarian carcinomas, but not in borderline tumors. A prognostic relevance of AMACR expression was identified in one ovarian cancer patient cohort but could not be verified in a second independent patient cohort.

AMACR is widely expressed in several cancer types. Increased AMACR protein expression levels were found in prostate, colorectal, breast, lung, and upper urothelial tract

Table 3 Univariate logistic regression analysis: factors predicting overall survival

Characteristic	*n*	HR (CI 95%)	*p* value
AMACR (positive vs. negative)	134	2.6 (1.29–5.08)	0.007
Age	134	1.0 (1.02–1.06)	0.0001
Histological subtypes	134	0.9 (1.73–1.12)	0.39
Tumor grade (1 vs. 2 vs. 3)	134	1.6 (1.13–2.32)	0.009
FIGO stage (I vs. II vs. III vs. IV)	129	2.0 (1.56–2.66)	0.0001
Residual disease (<1 vs. <2 vs. >2 cm)	89	1.9 (1.35–2.70)	0.0001
Chemotherapy (yes vs. no)	134	1.0 (0.83–1.11)	0.64
Estrogen receptor (low vs. high)	133	1.0 (0.60–1.77)	0.91

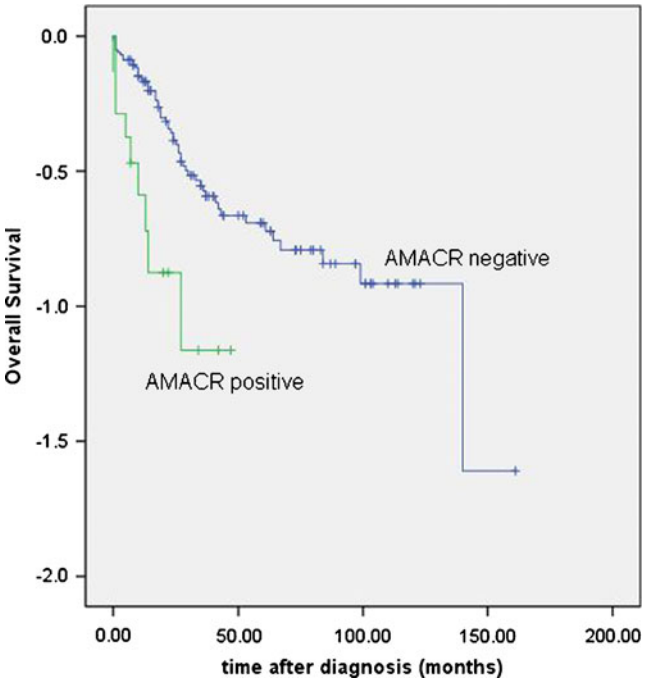

Fig. 2 Univariate survival analysis. In Kaplan–Meier analysis, positive AMACR expression is associated with poor overall survival (p=0.006)

carcinomas, lymphoma, and melanoma [8, 9, 13, 19]. There are only few reports on AMACR expression in ovarian carcinomas and no studies on the prognostic impact. Zhou et al. observed AMACR protein expression in up to 60% of ovarian carcinomas [13]. In contrast, Jiang et al. found AMACR expression in only 7% of 27 carcinomas, and two other studies did not detect any expression in 26 and 23 ovarian carcinomas [9, 14, 20]. The authors assume that different antibodies may be responsible for these variable results. Our study was conducted with the rabbit monoclonal antibody clone 13H4, which was also used by Jiang et al. [9]. Consistent with the results of Jiang et al., we found an expression of AMACR about 10%. This prevalence may limit the value of AMACR as a tool for the differential diagnosis between metastatic colorectal carcinomas and primary ovarian cancer, as suggested by Logani et al. [20]. Logani and colleagues recently reported that diffuse expression of CDX2, beta-catenin, and AMACR in a tumor in the ovary is diagnostic of metastasis from a colorectal primary. However, they analyzed only 23 primary ovarian carcinomas and all were AMACR negative, whereas 32% of metastatic colorectal carcinomas showed AMACR expression.

To our knowledge, the prognostic value of AMACR in ovarian cancer has not yet been investigated. Therefore, the main purpose of this study was to determine whether different levels of AMACR expression might be associated with overall survival and clinicopathological features. Our data do not provide strong evidence for a clinically useful prognostic value of AMACR expression in ovarian cancer. Although there was a statistically significant association between high AMACR expression levels and poor overall survival in one patient cohort, this finding could not be confirmed in a second independent cohort. Both patient cohorts were treated in similar time spans but there were differences in the distribution of FIGO stage, grade, residual tumor after surgery, and probably also in treatment modalities. Such discrepancies between different patient cohorts are frequently observed for prognostic biomarkers, especially if a biomarker is expressed only in a small subgroup of cases. Therefore, it is strongly recommended to confirm the prognostic value of a biomarker at least in two independent patient cohorts to prevent the over interpretation of findings obtained in single studies.

Further, we observed an association between AMACR expression and FIGO stage, grading, as well as histological subtype in one cohort which could not be verified in a second cohort. Relationships between AMACR and clinicopathological factors and survival were also reported for other cancer types. AMACR expression was also related to better tumor differentiation in prostate cancer [21]. Rubin et al. demonstrated a significant increase in the risk of cancer-specific death for prostatic carcinomas with decreased AMACR [12]. In colorectal cancer, decreased AMACR staining was also significantly associated with adverse clinical and pathological features (e.g., high-grade cancer, lymphatic vascular invasion, and worse survival) has been reported [11]. This is in contrast to upper urothelial cancer, where strong AMACR expression was associated with high-stage and high-grade tumors [19]. Similarly, high-

Table 4 Multivariate logistic regression analysis

Characteristic	n	HR (CI 95%)	p value
AMACR (positive vs. negative)	134	3.3 (1.37–7.99)	0.008
Age	134	1.0 (1.00–1.05)	0.016
Histological subtypes	134	0.9 (0.76–1.19)	0.7
Tumor grade (1 vs. 2 vs. 3)	134	1.4 (0.84–2.23)	0.2
FIGO stage (I vs. II vs. III vs. IV)	129	1.2 (0.76–1.72)	0.5
Residual disease (<1 vs. <2 vs. >2 cm)	89	1.8 (1.16–2.85)	0.009

grade invasive breast carcinomas were also associated with high AMACR protein expression levels [22].

So far, the role of AMACR in cancer biology is unclear. The mitochondrial and peroxisomal located enzyme is involved in the metabolic pathway of dietary branched-chain fatty acids (phytanic acid). In our analysis, we observed a relationship between high AMACR expression and low estrogen receptor levels in one patient cohort but could not be verified in the second cohort. We found high expression levels of the estrogen receptor in 46.8% and 72%, respectively, which is in line with the reported range of 25–86% in ovarian carcinomas as reviewed in Issa et al. [23]. To our knowledge, a linkage between AMACR and the estrogen receptor has not yet been reported. The association might indicate that the role of fatty acid metabolism, which is so far only poorly understood in tumor biology, may differ in dependence of estrogenic signaling, since we found AMACR particularly prevalent in ER-negative cases. However, no association between AMACR and estrogen receptor status was found in breast cancer [22]. Interestingly, a relationship between AMACR and androgen receptor expression was recently described in prostate cancer. Inhibition of AMACR expression using AMACR siRNA induced an increase of androgen receptor expression [24]. The authors concluded that AMACR inhibition may be a new strategy for treatment of patients with hormone-refractory prostate cancer. Possibly, the hormone-dependent regulation of AMACR induction explains also the different prognostic values of AMACR found in other tumor entities as discussed above.

Finally, obesity might be a risk factor in human cancer types with frequent AMACR overexpression, such as prostate and colorectal cancer. In prostate cancer, the consumption of fatty acids (phytanic and pristanic acids) of dairy and red meat products results in an overproduction of AMACR protein and may increase the risk for prostate cancer development [4, 5]. Given the relationship between obesity and increased ovarian cancer risk [25], it is tempting to speculate that AMACR expression is also regulated by high-fat diet and/or disturbed hormone synthesis in ovarian cancer patients. Relationships between diet and hormone levels in ovarian cancer have been reported [26].

In summary, our data suggest a role of AMACR in a subset of epithelial ovarian carcinomas. The prognostic value remains controversial, and the possible link to the estrogen receptor expression has to be evaluated in further studies.

Acknowledgments We thank Silvia Behnke and Martina Storz for the excellent technical assistance.

Conflict of interest statement The authors declare that they have no conflict of interest.

References

1. Schulz M, Lahmann PH, Riboli E, Boeing H (2004) Dietary determinants of epithelial ovarian cancer: a review of the epidemiologic literature. Nutr Cancer 50:120–140
2. Kolahdooz F, Ibiebele TI, van der Pols JC, Webb PM (2009) Dietary patterns and ovarian cancer risk. Am J Clin Nutr 89:297–304
3. Amery L, Fransen M, De Nys K, Mannaerts GP, Van Veldhoven PP (2000) Mitochondrial and peroxisomal targeting of 2-methylacyl-CoA racemase in humans. J Lipid Res 41:1752–1759
4. Xu J, Thornburg T, Turner AR, Vitolins M, Case D, Shadle J, Hinson L, Sun J, Liu W, Chang B, Adams TS, Zheng SL, Torti FM (2005) Serum levels of phytanic acid are associated with prostate cancer risk. Prostate 63:209–214
5. Mobley JA, Leav I, Zielie P, Wotkowitz C, Evans J, Lam YW, L'Esperance BS, Jiang Z, Ho SM (2003) Branched fatty acids in dairy and beef products markedly enhance alpha-methylacyl-CoA racemase expression in prostate cancer cells in vitro. Cancer Epidemiol Biomarkers Prev 12:775–783
6. Xu J, Stolk JA, Zhang X, Silva SJ, Houghton RL, Matsumura M, Vedvick TS, Leslie KB, Badaro R, Reed SG (2000) Identification of differentially expressed genes in human prostate cancer using subtraction and microarray. Cancer Res 60:1677–1682
7. Jiang Z, Wu CL, Woda BA, Dresser K, Xu J, Fanger GR, Yang XJ (2002) P504s/alpha-methylacyl-CoA racemase: a useful marker for diagnosis of small foci of prostatic carcinoma on needle biopsy. Am J Surg Pathol 26:1169–1174
8. Kristiansen G, Fritzsche FR, Wassermann K, Jager C, Tolls A, Lein M, Stephan C, Jung K, Pilarsky C, Dietel M, Moch H (2008) Golph2 protein expression as a novel tissue biomarker for prostate cancer: implications for tissue-based diagnostics. Br J Cancer 99:939–948
9. Jiang Z, Fanger GR, Woda BA, Banner BF, Algate P, Dresser K, Xu J, Chu PG (2003) Expression of alpha-methylacyl-CoA racemase (p504s) in various malignant neoplasms and normal tissues: a study of 761 cases. Hum Pathol 34:792–796
10. Gunia S, May M, Scholmann K, Storkel S, Hoschke B, Koch S, Dietel M, Kristiansen G (2008) Expression of alpha-methylacyl-CoA racemase correlates with histopathologic grading in noninvasive bladder cancer. Virchows Arch 453:165–170
11. Lin A, Weiser MR, Klimstra DS, Paty PB, Tang LH, Al-Ahmadie H, Hoo Park S, Guillem JG, Temple L, Wong WD, Gerald WL, Shia J (2007) Differential expression of alpha-methylacyl-coenzyme A racemase in colorectal carcinoma bears clinical and pathologic significance. Hum Pathol 38:850–856
12. Rubin MA, Bismar TA, Andren O, Mucci L, Kim R, Shen R, Ghosh D, Wei JT, Chinnaiyan AM, Adami HO, Kantoff PW, Johansson JE (2005) Decreased alpha-methylacyl CoA racemase expression in localized prostate cancer is associated with an increased rate of biochemical recurrence and cancer-specific death. Cancer Epidemiol Biomarkers Prev 14:1424–1432
13. Zhou M, Chinnaiyan AM, Kleer CG, Lucas PC, Rubin MA (2002) Alpha-methylacyl-CoA racemase: a novel tumor marker over-expressed in several human cancers and their precursor lesions. Am J Surg Pathol 26:926–931
14. Nassar A, Amin MB, Sexton DG, Cohen C (2005) Utility of alpha-methylacyl coenzyme A racemase (p504s antibody) as a diagnostic immunohistochemical marker for cancer. Appl Immunohistochem Mol Morphol 13:252–255
15. Mirlacher M, Simon R (2010) Recipient block TMA technique. Methods Mol Biol 664:37–44
16. Moch H, Schraml P, Bubendorf L, Mirlacher M, Kononen J, Gasser T, Mihatsch MJ, Kallioniemi OP, Sauter G (1999) High-throughput tissue microarray analysis to evaluate genes uncovered

by cDNA microarray screening in renal cell carcinoma. Am J Pathol 154:981–986
17. Kononen J, Bubendorf L, Kallioniemi A, Barlund M, Schraml P, Leighton S, Torhorst J, Mihatsch MJ, Sauter G, Kallioniemi OP (1998) Tissue microarrays for high-throughput molecular profiling of tumor specimens. Nat Med 4:844–847
18. Schraml P, Schwerdtfeger G, Burkhalter F, Raggi A, Schmidt D, Ruffalo T, King W, Wilber K, Mihatsch MJ, Moch H (2003) Combined array comparative genomic hybridization and tissue microarray analysis suggest PAK1 at 11q13.5-q14 as a critical oncogene target in ovarian carcinoma. Am J Pathol 163:985–992
19. Langner C, Rupar G, Leibl S, Hutterer G, Chromecki T, Hoefler G, Rehak P, Zigeuner R (2006) Alpha-methylacyl-CoA racemase (AMACR/p504s) protein expression in urothelial carcinoma of the upper urinary tract correlates with tumour progression. Virchows Arch 448:325–330
20. Logani S, Oliva E, Arnell PM, Amin MB, Young RH (2005) Use of novel immunohistochemical markers expressed in colonic adenocarcinoma to distinguish primary ovarian tumors from metastatic colorectal carcinoma. Mod Pathol 18:19–25
21. Kuefer R, Varambally S, Zhou M, Lucas PC, Loeffler M, Wolter H, Mattfeldt T, Hautmann RE, Gschwend JE, Barrette TR, Dunn RL, Chinnaiyan AM, Rubin MA (2002) Alpha-methylacyl-CoA racemase: expression levels of this novel cancer biomarker depend on tumor differentiation. Am J Pathol 161:841–848
22. Witkiewicz AK, Varambally S, Shen R, Mehra R, Sabel MS, Ghosh D, Chinnaiyan AM, Rubin MA, Kleer CG (2005) Alpha-methylacyl-CoA racemase protein expression is associated with the degree of differentiation in breast cancer using quantitative image analysis. Cancer Epidemiol Biomarkers Prev 14:1418–1423
23. Issa RM, Lebeau A, Grob T, Holst F, Moch H, Terracciano L, Choschzick M, Sauter G, Simon R (2009) Estrogen receptor gene amplification occurs rarely in ovarian cancer. Mod Pathol 22:191–196
24. Takahara K, Azuma H, Sakamoto T, Kiyama S, Inamoto T, Ibuki N, Nishida T, Nomi H, Ubai T, Segawa N, Katsuoka Y (2009) Conversion of prostate cancer from hormone independency to dependency due to AMACR inhibition: involvement of increased AR expression and decreased IGF1 expression. Anticancer Res 29:2497–2505
25. McLemore MR, Miaskowski C, Aouizerat BE, Chen LM, Dodd MJ (2009) Epidemiological and genetic factors associated with ovarian cancer. Cancer Nurs 32:281–288, quiz 289–290
26. McCann SE, Freudenheim JL, Marshall JR, Graham S (2003) Risk of human ovarian cancer is related to dietary intake of selected nutrients, phytochemicals and food groups. J Nutr 133:1937–1942

Virchows Arch (2011) 459:99–108
DOI 10.1007/s00428-011-1100-3

ORIGINAL ARTICLE

Afferent arteriolopathy and glomerular collapse but not segmental sclerosis induce tubular atrophy in old spontaneously hypertensive rats

Sabine Leh · Michael Hultström · Christian Rosenberger · Bjarne M. Iversen

Received: 6 March 2011 / Revised: 10 May 2011 / Accepted: 26 May 2011 / Published online: 10 June 2011
© The Author(s) 2011. This article is published with open access at Springerlink.com

Abstract In chronic renal disease, the temporal and spatial relationship between vascular, glomerular and tubular changes is still unclear. Hypertension, an important cause of chronic renal failure, leads to afferent arteriolopathy, segmental glomerulosclerosis and tubular atrophy in the juxtamedullary cortex. We investigated the pathological changes of hypertensive renal disease in aged spontaneously hypertensive rats using a large number of serial sections, where we traced and analyzed afferent arteriole, glomerulus and proximal tubule of single nephrons. Our major finding was that both afferent arteriolopathy and glomerular capillary collapse were linked to tubular atrophy. Only nephrons with glomerular collapse (n=13) showed tubules with reduced diameter indicating atrophy [21.66±2.56 μm vs. tubules in normotensive Wistar Kyoto rats (WKY) 38.56±0.56 μm, p<0.05], as well as afferent arteriolar wall hypertrophy (diameter 32.74±4.72 μm vs. afferent arterioles in WKY 19.24±0.98 μm, p<0.05). Nephrons with segmental sclerosis (n=10) did not show tubular atrophy and tubular diameters were unchanged (35.60±1.43 μm). Afferent arteriolar diameter negatively correlated with glomerular capillary volume fraction (r=−0.36) and proximal tubular diameter (r=−0.46) implying reduced glomerular and tubular flow. In line with this, chronically damaged tubules showed reduced staining for the ciliary protein inversin indicating changed ciliary signalling due to reduced urinary flow. This is the first morphological study on hypertensive renal disease making correlations between vascular, glomerular and tubular components of individual nephron units. Our data suggest that afferent arteriolopathy leads to glomerular collapse and reduced urinary flow with subsequent tubular atrophy.

Keywords Spontaneously hypertensive rats · Serial sections · Focal and segmental glomerulosclerosis · Glomerular collapse · Tubular atrophy · Inversin

S. Leh · M. Hultström · B. M. Iversen
Renal Research Group, Institute of Medicine,
University of Bergen,
Bergen, Norway

S. Leh · M. Hultström · B. M. Iversen
Department of Medicine, Haukeland University Hospital,
Bergen, Norway

S. Leh (✉)
Department of Pathology, Haukeland University Hospital,
5021 Bergen, Norway
e-mail: sabine.leh@helse-bergen.no

M. Hultström
Department of Medical Cell Biology, Uppsala University,
Uppsala, Sweden

C. Rosenberger
Department of Nephrology,
Charité,
Berlin, Germany

Introduction

Hypertension is a common cause of end-stage renal disease [1] and greater insight into the pathogenesis of renal hypertensive disease is of major importance. When the kidney is chronically exposed to elevated blood pressure, morphologic changes initially develop in the juxtamedullary cortex, where the pressure gradient along the afferent arterioles is greatest [2, 3]. Arterioles develop hypertrophy, glomeruli exhibit segmental sclerosis and there is focal tubular atrophy and interstitial fibrosis. The long-term prognosis is adverse [4]. Progress of chronic renal failure, indicated by serum creatinine, is strongly correlated with

the extent of tubular atrophy and interstitial fibrosis [5, 6]. The pathogenesis of tubular atrophy in hypertensive renal disease is not well known.

One of the prevailing theories is that tubular atrophy is directly linked to segmental glomerulosclerosis and two main hypotheses have been put forward in order to explain the mechanism involved. Firstly, misdirected filtration from an area with glomerular segmental sclerosis might spread into the paraglomerular space along the Bowman's capsule to the tubular outlet and downstream at the outside of the proximal tubule causing tubular degeneration and atrophy [7]. Alternatively, segmental glomerulosclerosis might reduce blood flow to the postglomerular peritubular capillaries leading to local interstitial hypoxia and subsequently tubular atrophy [8]. In misdirected filtration, tubular atrophy would originate in the glomerulotubular junction and extend downstream the nephron but would remain confined to its parent nephron. In postglomerular ischemia—as efferent arterioles not only supply their parent nephron [9]—tubular atrophy would initially be segmental and involve more than one nephron including nephrons with normal glomeruli.

Spontaneously hypertensive rats (SHR) develop chronic hypertension at young age. Proteinuria and a decline in glomerular filtration rate develop in relatively high age and the morphological pattern of renal damage in old animals is similar to that described for human decompensated nephrosclerosis [10, 11]. Changes in vascular function and morphology precede renal damage in this model indicating that this might be an early step and important mechanism in the pathogenesis of glomerulosclerosis and tubular atrophy [10, 12–14].

It is important to recognize that although vascular, glomerular and tubular pathology likely are related to each other, so far, no study has attempted to correlate changes between these components of individual nephrons in hypertensive renal disease. In the present study, our goal was to fill this gap with the help of large numbers of serial sections from SHR kidneys with hypertensive damage. We demonstrate that, despite current belief, focal and segmental glomerulosclerosis is not associated with tubular atrophy. Instead, tubular atrophy correlates well with glomerular collapse and arteriolopathy, suggesting a causal relationship.

Methods

Tissue

Paraffin-embedded kidney tissue from a previous study of 60-week-old SHR (n=7) and normotensive Wistar Kyoto (WKY) rats (n=3) was used [11]. Rats were anesthetized with pentobarbital (120 mg/kg). The kidneys were perfused with ice-cold PBS by cannulating the distal abdominal aorta, ligating the aorta proximal to the renal arteries and opening the renal vein. The study was performed in accordance with and under the approval of the Norwegian State Board for Biological Experiments with Living Animals at the University of Bergen, Bergen, Norway.

Two millimetre thick transversal slices of the kidney were fixed with 4% buffered formaldehyde by immersion. Smaller pieces with an edge length of about 2 mm including the cortex in its entire thickness were processed according to standard procedures and embedded in paraffin. Consecutive sections with 5 μm thickness were cut without precooling the paraffin blocks and stained with periodic acid Schiff.

Glomeruli were chosen and both, glomeruli, their afferent arteriole and the proximal tubule were followed through series of sections. Images were taken from every section. The ×20 objective was used resulting in images 479.6 by 479.6 μm with a resolution of 0.2482 μm/pixel. The structures of interest were identified and marked in each image and could easily be followed from afferent arteriole through the glomerulus and down the proximal tubule which was studied through minimum 8 and maximum 189 sections (mean 52 sections).

Groups

In order to investigate the distribution of tubular atrophy and to get an idea about the relationship between tubular atrophy and glomerular changes, two cortical areas from one SHR with focal tubular atrophy were initially chosen. All glomeruli visible in these areas and their proximal tubules were investigated through the series of sections assessing qualitative changes. For this part of the study, 40±12 serial sections/nephron including 24±5 glomerular sections/nephron and 41±27 tubular sections/nephron were investigated.

Based on the results of this study, nephrons from sections of all rats were chosen for morphometry and divided into groups according to these criteria: (a) all nephrons were localized in the juxtamedullary cortex and (b) only nephrons allowing the investigation of complete glomeruli with enough adjacent sections to assess changes in proximal tubules and afferent arterioles were chosen. Four groups with a total of 33 nephrons were investigated. Nephrons with normal glomeruli were randomly selected for the control groups of WKY (n=5) and SHR (n=5). The third group called "SHR segmental sclerosis" included all nephrons with segmental glomerular sclerosis. This resulted in ten nephrons. The fourth group called "SHR capillary collapse" consisted of 13 randomly selected nephrons from SHR with glomerular capillary collapse. Table 1 displays an overview about rats and nephrons and Fig. 1 shows typical

Table 1 Systolic blood pressure, numbers of nephrons investigated and morphological findings in the studied Wistar Kyoto rats and spontaneously hypertensive rats

Rat	Strain	Blood pressure systolic	Number of nephrons investigated	Normal	Segmental sclerosis	Capillary collapse
1	WKY	135	1	1		
2	WKY	135	2	2		
3	WKY	135	2	2		
4	SHR	235	4		2	2
5	SHR	205	2	2		
6	SHR	245	6	1	2	3
7	SHR	245	1			1
8	SHR	185	7		5	2
9	SHR	205	2			2
10	SHR	205	6	2	1	3

SHR spontaneously hypertensive rats, *WKY* Wistar Kyoto rats

glomeruli from the four groups. For this part of the study, 41±12 serial sections/nephron were carried out. The serial sections included 13±8 sections from arterioles/nephron, 26±4 glomerular sections/nephron and 52±40 tubular sections/nephron. Qualitative pathological findings were recorded and supplied by quantitative morphometric measurements of arteriolar, glomerular and tubular parameters.

Definitions of qualitative findings

Segmental glomerulosclerosis—segmental increase of extracellular matrix and capillary lumen obliteration with adherence to Bowman's capsule

Glomerular collapse—retracted capillary convolute

Bowman's capsule thickening—thickening and multilayering of the capsular basement membrane

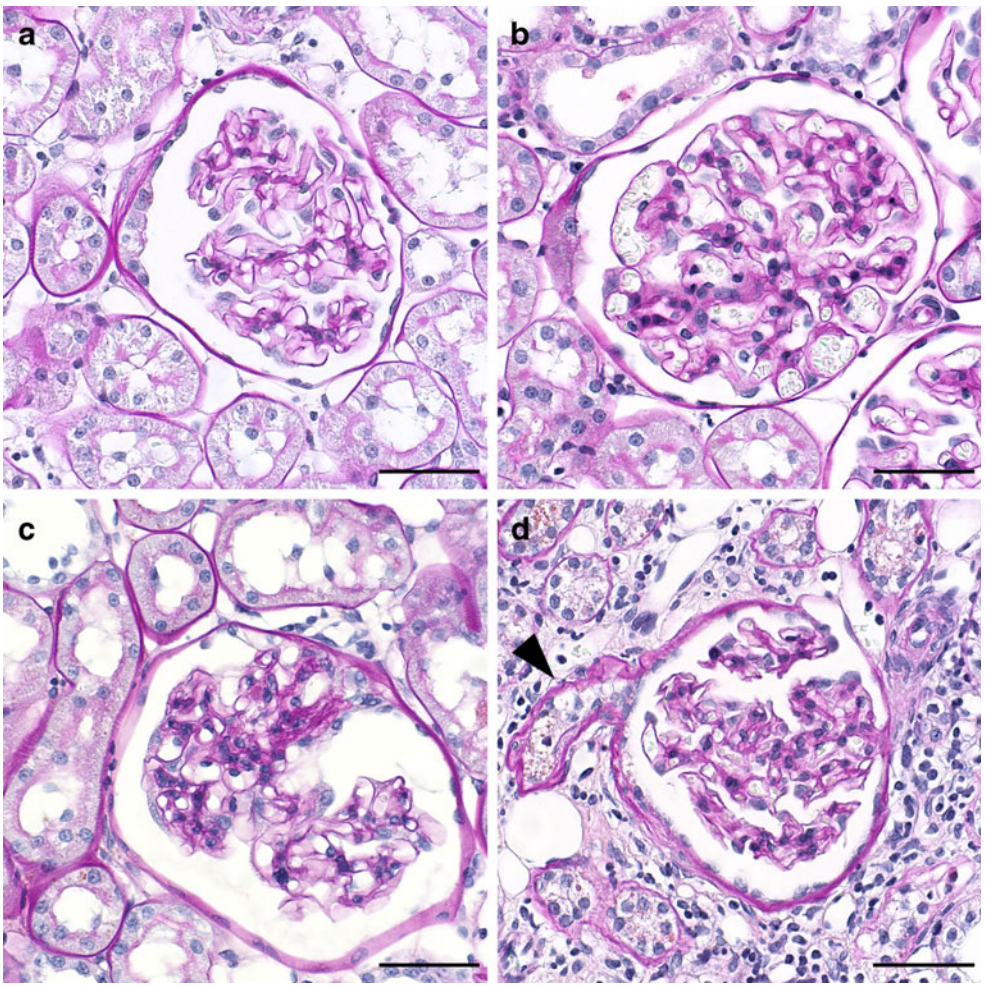

Fig. 1 Representative glomeruli from the four groups. **a** Normal glomerulus from WKY rat with segmental thickening and lamellation of Bowman's capsule. **b** Normal glomerulus from SHR. **c** Glomerulus with segmental sclerosis from SHR. **d** Glomerulus from SHR with collapsed capillary convolute and thickened and lamellated Bowman's capsule. The outlet of the atrophic proximal tubule is also seen (*arrowhead*). (All images *scale bar* 50 μm, PAS stain)

Tubular atrophy—tubules with reduced diameter, flattened epithelium and thickened basement membrane.

Morphometry

The diameter of an afferent arteriole in an elliptic profile was defined as the short axis from one outer media border to the other, in a longitudinal profile as a straight line perpendicular to the longitudinal axis from one outer media border to the other. The media thickness was measured along the diameter axis from the inner to the outer media border. This resulted in two measurements. The definitive value of the media thickness was the mean value. Measurements were done in 5-μm distances along the course of the arteriole. The number of arteriolar diameter measurements was 27±15/nephron.

The glomerular tuft volume was estimated by the Cavalieri method [15]. A point grid with a point distance of 20 μm was used and all points hitting the glomerular tuft were counted. The glomerular tuft volume was calculated by the equation:

$$\text{Glomerular tuft volume} = n \times A \times t$$

where n is the number of points hitting the glomerular tuft, A the area per point and t the section thickness. The volume of segmental sclerosis and the glomerular capillary volume were measured in the same session according to the calculation of glomerular tuft volume. For estimation of the volume of segmental sclerosis points hitting areas with obliterated capillaries, increased extracellular matrix and adherences with Bowman's capsule were counted. For the estimation of the glomerular capillary volume, points hitting capillary lumens were counted. All glomerular sections (26±4 per nephron) were used for these measurements.

The tubular diameter was defined as the length of the shortest possible straight line that passes through the centre of a symmetrically sectioned tubule. The diameter did not include the basement membrane. The tubule cell height was measured along the diameter axis from the base and to the apical surface of a tubule cell [16] not including the brush border. The mean of the resulting two measurements was calculated. Asymmetrically sectioned tubules were excluded from the measurement. In each nephron, 25±16 tubular diameter measurements were carried out. Point counting was done in ImageJ and distance measurements were performed in Cell^D.

Immunohistochemistry and immunofluorescence

Stainings were performed on formalin-fixed, paraffin-embedded sections. The following antibodies were used: hypoxia inducible factor 1 alpha (HIF-1 alpha, monoclonal, mouse, NB100-105, Novus Biologicals, Littleton), prolyl hydroxylase 2 (rabbit polyclonal, Novus Biologicals, Littleton), vimentin (monoclonal, mouse, M0725, DakoCytomation, Glostrup), inversin (polyclonal, rabbit, 10585-1-AP, Proteintech group, Chicago) and acetylated alpha tubulin (monoclonal, mouse, Clone 6-11B-1, Sigma, Saint Louis). Antibody binding was detected by enzyme- and antibody-marked polymer (DAKO EnVision, K4011 for polyclonal rabbit antibodies, K4007 for mouse antibodies, DakoCytomation, Glostrup) or a catalyzed signal amplification system (DakoCytomation, Glostrup). The positive controls for HIF-1 alpha were kidneys from rats kept in a hypoxic chamber [17]. For immunofluorescence multilabelling, AlexaFluor conjugated secondary anti-mouse and anti-rabbit antibodies were used (AlexaFluor 555 and AlexaFluor 647, 1:200, Molecular Probes, Invitrogen). Nuclei were stained with DAPI (P36935, Molecular Probes, Invitrogen). The stained sections were visualized by a Zeiss LSM 510 META confocal scanning microscope.

Statistics

Values are expressed as mean±standard error of mean. One-way ANOVA with a priori contrasts was used to compare mean values. For correlation analysis, Spearman's rho correlation coefficient was used. Calculations were carried out in SPSS 14.0. A $p<0.05$ was considered significant.

Results

Tubular atrophy is restricted to its own nephron and related to glomerular collapse

In order to assess the distribution of tubular atrophy within and between nephrons and to get an idea about relationships between tubular and glomerular changes, two areas with focal tubular atrophy in one SHR were chosen and all glomeruli visible in these two areas were followed through serial sections including their proximal tubules. These resulted in 28 nephrons, 1,117 images and 40±12 images/nephron.

All nephrons with glomerular or tubular damage were localized in the juxtamedullary cortex. Atrophy of proximal tubules was present in four nephrons and all parent glomeruli showed capillary collapse. The collapsed capillary tufts did not display clues to segmental sclerosis. Two nephrons with segmental glomerulosclerosis showed normal proximal tubules. One glomerulus showed both mesangial and endocapillary hypercellularity. The associated tubule was acutely damaged with flattened epithelium and detached epithelial cells in the tubular lumen.

The remaining 21 nephrons showed normal glomeruli and proximal tubules. We did not observe segmental tubular

atrophy neither in normal nephrons nor in diseased nephrons.

Arteriolopathy is most pronounced in nephrons with glomerular collapse and tubular atrophy

Since tubular atrophy was found to be associated with glomerular collapse in one SHR, we next confirmed this observation in seven SHR by quantitative measurements. To obtain this, nephrons from the juxtamedullary cortex of SHR with glomerular collapse or segmental sclerosis were compared to nephrons with normal glomeruli from WKY and SHR (Table 2). Only nephrons with glomerular collapse showed proximal tubular atrophy indicated by significantly reduced diameter and epithelial cell height. In contrast, tubular parameters were not different between normal WKY nephrons, SHR nephrons with normal glomeruli and SHR nephrons with segmental sclerosis. This pattern was repeated regarding arteriolar wall hypertrophy; only nephrons with collapsed glomeruli showed significant increased arteriolar diameter and media thickness. Representative changes in a nephron with glomerular collapse are illustrated in Fig. 2.

Segmental glomerulosclerosis is not associated with tubular atrophy

Tubular atrophy was not present in nephrons with segmental sclerosis, since neither tubular diameter nor tubular epithelial cell height were reduced (Table 2, Fig. 3). In line with this, we did not find evidence for the postulated links from segmental glomerulosclerosis to tubular atrophy [7, 8].

First, a positive signal for HIF-1 alpha as an indicator of hypoxia was not detected in the cortex or in the medulla of both SHR and WKY, whereas the positive control showed a strong reaction. To exclude that the negativity of HIF-1 alpha was the result of an upregulation of its target gene PHD-2, an immunohistochemical stain for prolyl hydroxylase 2 was carried out. Prolyl hydroxylase 2 was positive in single distal tubules mainly in the medulla; however, areas in the cortex with damaged tubules did not show positivity (results not shown).

Second, thickened Bowman's capsule, one feature of misdirected filtration, was indeed present in five of ten nephrons with segmental sclerosis, but also in three of five nephrons from WKY control rats and in 10 of 13 nephrons with glomerular collapse. Therefore, this finding does not support the presence of misdirected filtration.

Hypoperfusion and reduced urine flow are the mechanisms behind tubular atrophy

Tubular diameter significantly correlated with glomerular capillary volume fraction and both parameters negatively correlated with afferent arteriolar diameter (Table 3). Obviously, increased afferent arteriolar diameter and media thickness correlated with the progression of renal disease and the data suggest reduced arteriolar blood flow and subsequent glomerular hypoperfusion as well as reduced urine flow as mechanisms behind tubular atrophy. We used immunohistochemistry for inversin, a ciliary protein constitutively expressed in tubular epithelial cells exposed to flow [18], to support this assumption. While normal proximal tubules in the SHR and WKY kidneys showed nuclear positivity for inversin, inversin expression was lost in vimentin positive damaged tubules in SHR (Fig. 4). This result was confirmed by immunofluorescence (Fig. 5).

Table 2 Morphometric findings in nephrons with normal glomeruli from WKY and SHR, glomeruli with segmental sclerosis in SHR and glomeruli with ischemic collapse in SHR

	WKY	SHR	SHR	SHR
	Normal	Normal	Segmental sclerosis	Capillary collapse
Number of nephrons	5	5	10	13
Afferent arteriole				
Diameter (μm)	19.24±0.98	25.49±1.46	25.01±2.61	32.74±4.72[c]
Media thickness (μm)	5.77±0.39	7.54±0.53	7.61±1.01	10.75±1.70[c]
Glomerulus				
Volumes (10^6 μm^3)				
Tuft	0.91±0.06	0.90±0.06	1.24±0.15[a]	0.73±0.10[b]
Capillaries	0.22±0.03	0.22±0.04	0.22±0.06	0.07±0.02[a, b]
Segmental sclerosis			0.10±0.02	
Volume fractions (%)				
Capillaries	23.20±2.51	24.37±3.46	15.75±2.07[a]	8.20±1.02[a, b]
Segmental sclerosis			8.90±1.68	
Proximal tubule				
Diameter (μm)	38.56±0.56	36.29±1.76	35.60±1.43	21.66±2.56[a, b]
Epithelial cell height (μm)	11.42±0.54	10.05±0.92	9.29±0.64	6.04±0.54[a, b]

SHR spontaneously hypertensive rats, *WKY* Wistar Kyoto rats

[a] $p<0.05$ vs. WKY normal and SHR normal

[b] $p<0.05$ vs. SHR segmental sclerosis

[c] $p<0.05$ vs. WKY normal

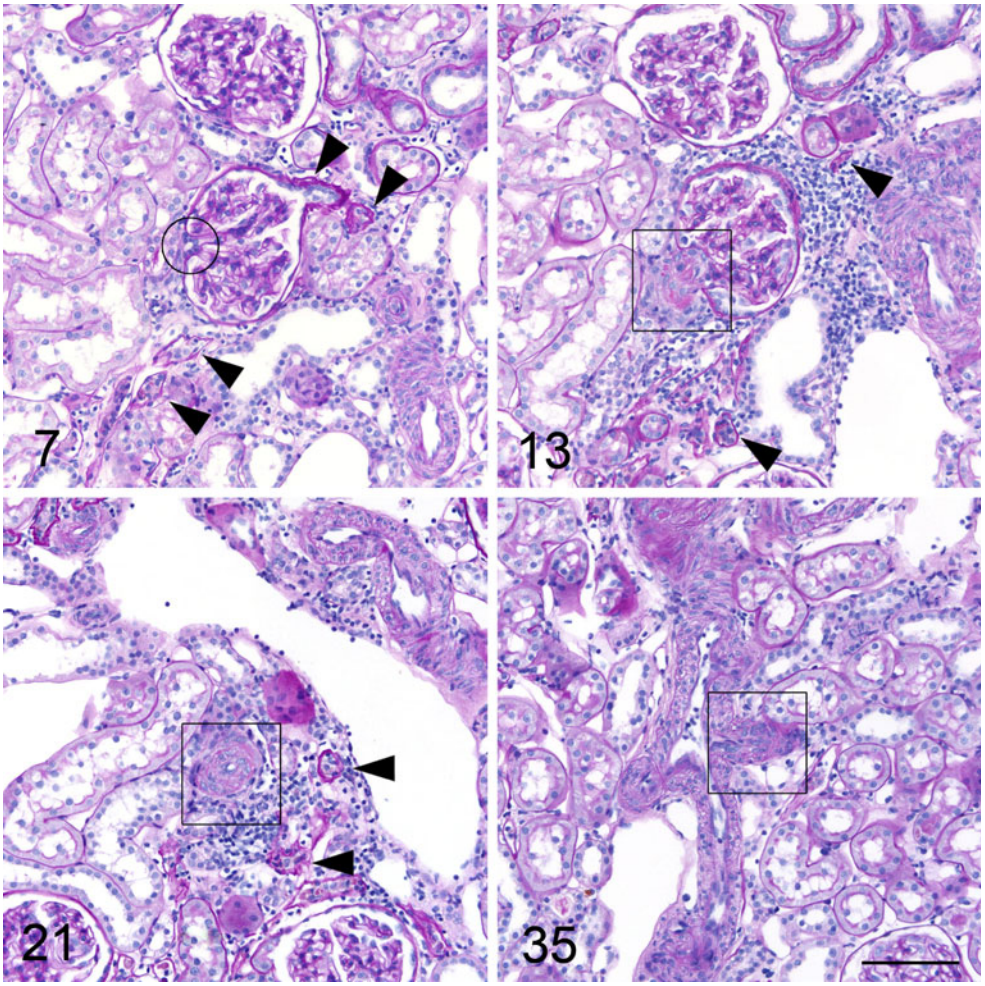

Fig. 2 Example from serial sections of a nephron with glomerular capillary collapse in a SHR. *Numbers* indicate the consecutive numbers of the serial sections beginning with the number 1 for the first section of the glomerulus. *Arrowheads* point to related proximal tubules. *Rectangles* indicate afferent arteriole, the *circle* efferent arteriole. The glomerulus shows focally thickened Bowman's capsule, there are no signs of segmental sclerosis in the collapsed tuft. The proximal tubule is atrophic with reduced diameter and thickened basement membrane. The tubular neck area is seen in *image 7*. The wall of the afferent arteriole is hypertrophic. *Image 35* shows the outlet of the afferent arteriole from the interlobular artery. (All images PAS stain, *scale bar* 100 μm)

Normal proximal tubules showed nuclear and cytoplasmic positivity in the apical part of the cell below the brush border. In atrophic tubules, inversin positivity was lost while cilia were still present.

Discussion

The new finding emerging from the present paper is that tubular atrophy in the juxtamedullary cortex of SHR is closely associated with glomerular collapse and not with segmental sclerosis. Glomerular collapse was correlated with arteriolar hypertrophy and indicated glomerular hypoperfusion. The reduced flow through the proximal tubular system seemed to induce tubular atrophy as tubular diameters were significantly reduced. These findings were unexpected and indicate that tubular flow is of major importance in preserving normal tubular cell function. Neither misdirected filtration from an area of segmental sclerosis nor postglomerular hypoperfusion of the peritubular capillaries seemed to be involved in tubular atrophy in old SHR.

The focal nature of tubular atrophy in the studied histological sections was due to the degradation of whole nephrons as no segmental tubular atrophy was observed by analyzing all nephrons in a given area. This finding is in accordance with other investigations [7] and argues against hypoxia of the postglomerular capillary bed as a cause of tubular atrophy. "The hypoxia hypothesis" proposes that blood flow and oxygen supply to the peritubular postglomerular capillaries are reduced due to obliteration of the glomerular capillaries [8]. As efferent arterioles in the middle and inner cortex of the kidney supply not only their parent nephron [19], one would expect zonal atrophy involving several adjacent nephrons and tubular atrophy initially would be segmental. In line with this view, we could not detect the oxygen sensor and transcription factor HIF-1 alpha as well as increased expression of one of its target gene products, the enzyme prolyl hydroxlase. These findings indicate that hypoxia does not play a role in tubular atrophy in SHR.

In the present study, we have shown that tubular atrophy always involved single nephrons indicating a causative process directly related to the affected nephron. Since all diseased nephrons showed some kind of glomerular

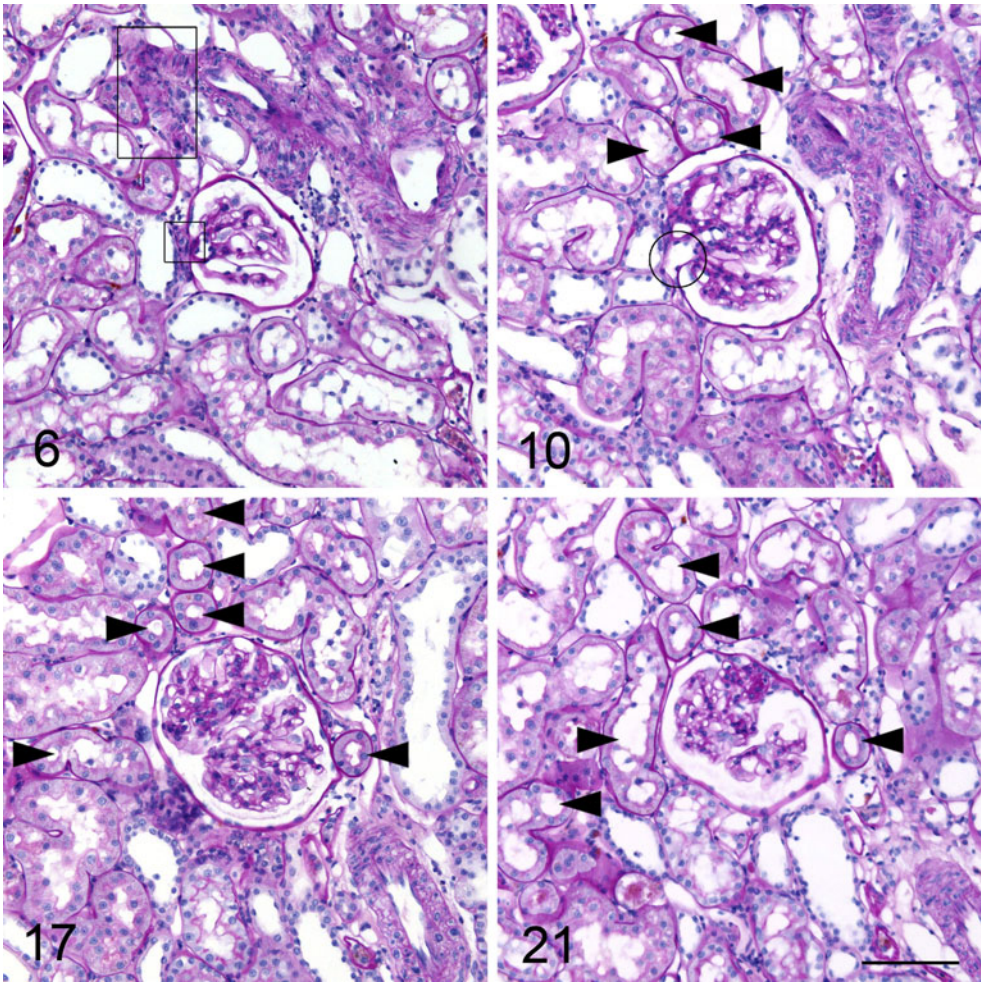

Fig. 3 Example from serial sections of a nephron with a glomerulus with segmental sclerosis in a SHR. *Numbers* indicate the consecutive numbers of the serial sections beginning with the number 1 for the first section of the glomerulus. *Arrowheads* point to related proximal tubules. *Rectangles* indicate afferent arteriole, the *circle* efferent arteriole. *Image 21* shows segmental sclerosis of the glomerular tuft. Proximal tubules are normal. The afferent arteriole is not hypertrophied. The outlet area of the afferent arteriole from the interlobular artery is seen in *image 6* (*large rectangle*). (All images PAS stain, *scale bar* 100 μm)

damage and no nephron with a normal glomerulus showed an atrophic tubule, it is more likely that the atrophy-causing process is localized to the glomerulus.

Segmental glomerulosclerosis has been causatively linked to tubular atrophy and a proposed mechanism is misdirected filtration through bare areas of capillary walls towards the interstitium and along the Bowman's capsule towards the proximal tubule [20]. Evidence for this mechanism was found in different rat models of focal and segmental glomerulosclerosis with or without hypertension [7, 21, 22]. Misdirected filtration is described as an expansion of the parietal basement membrane [23]. In the present study, five out of ten glomeruli with segmental sclerosis showed such changes. However, identical changes were also found in most nephrons with glomerular collapse and even in some normal nephrons from WKY rats. From the present data, it cannot be concluded that the finding of a thickened Bowman's capsule supports misdirected filtration.

Most important is the finding that nephrons with segmental sclerosis did not show reduced tubular diameter or reduced epithelial cell height as signs of tubular atrophy. Therefore, in this phase of hypertensive kidney disease, segmental glomerulosclerosis could not be the cause of tubular atrophy. It is conceivable, since segmental lesions were rather small in our study and some progression seems to occur up to 90 weeks of age (unpublished observation,

Table 3 Correlations between proximal tubular diameters, glomerular morphology and afferent arteriolar diameters

Correlation coefficient		
Proximal tubule diameter (μm) with		
Glomerulus	Tuft volume (μm^3)	0.63**
	Capillary volume (μm^3)	0.68**
	Capillary volume fraction (%)	0.70**
	Segmental sclerosis volume fraction (%)	−0.13
Afferent arteriole	Diameter (μm)	−0.46**
Glomerulus capillary volume fraction (%) with		
Afferent arteriole	Diameter (μm)	−0.36*

*$p<0.05$, **$p<0.01$

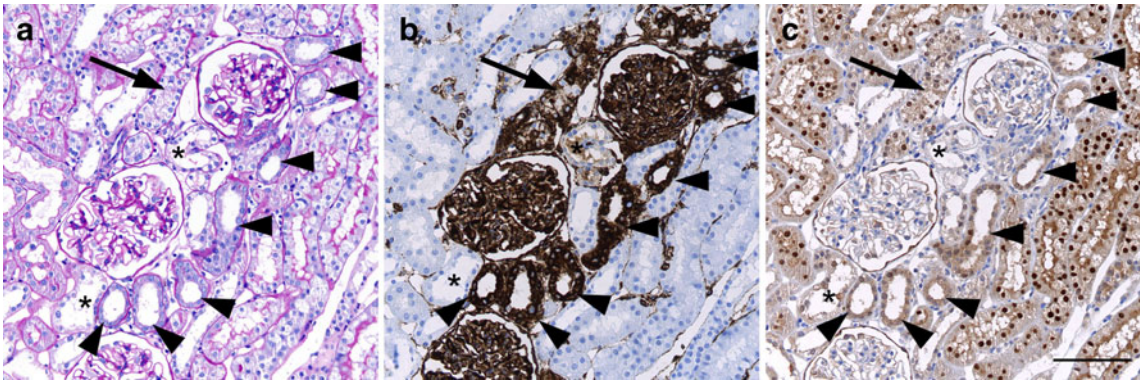

Fig. 4 Consecutive sections of an area with tubular damage in the inner cortex of a SHR. Chronically damaged tubules are indicated by *arrowheads*, an acutely damaged tubule by an *arrow* and some distal tubules by an *asterisk*. *Scale bar* 100 μm. **a** Conventional histology (PAS). Chronically damaged tubules show slightly thickened basement membrane and flattened epithelium. The acutely damaged tubule shows swollen epithelium and loss of brush border. Immunohistochemistry for vimentin (**b**) and inversin (**c**). Acutely and chronically damaged tubules are positive for vimentin, preserved tubules are negative. Normal proximal tubules show nuclear positivity for inversin, distal tubules are negative. Inversin expression is lost in damaged tubules

Bjarne M. Iversen) that the development of segmental sclerosis has not gone far enough to cause tubular atrophy.

Tubular atrophy was observed in nephrons with glomerular collapse and the collapsed glomerular tufts did not show any clues of segmental sclerosis. Glomerular collapse was quantified by the volume fraction of patent capillary lumina to the tuft volume. In collapsed glomeruli, this fraction was reduced. We suppose that these glomeruli have

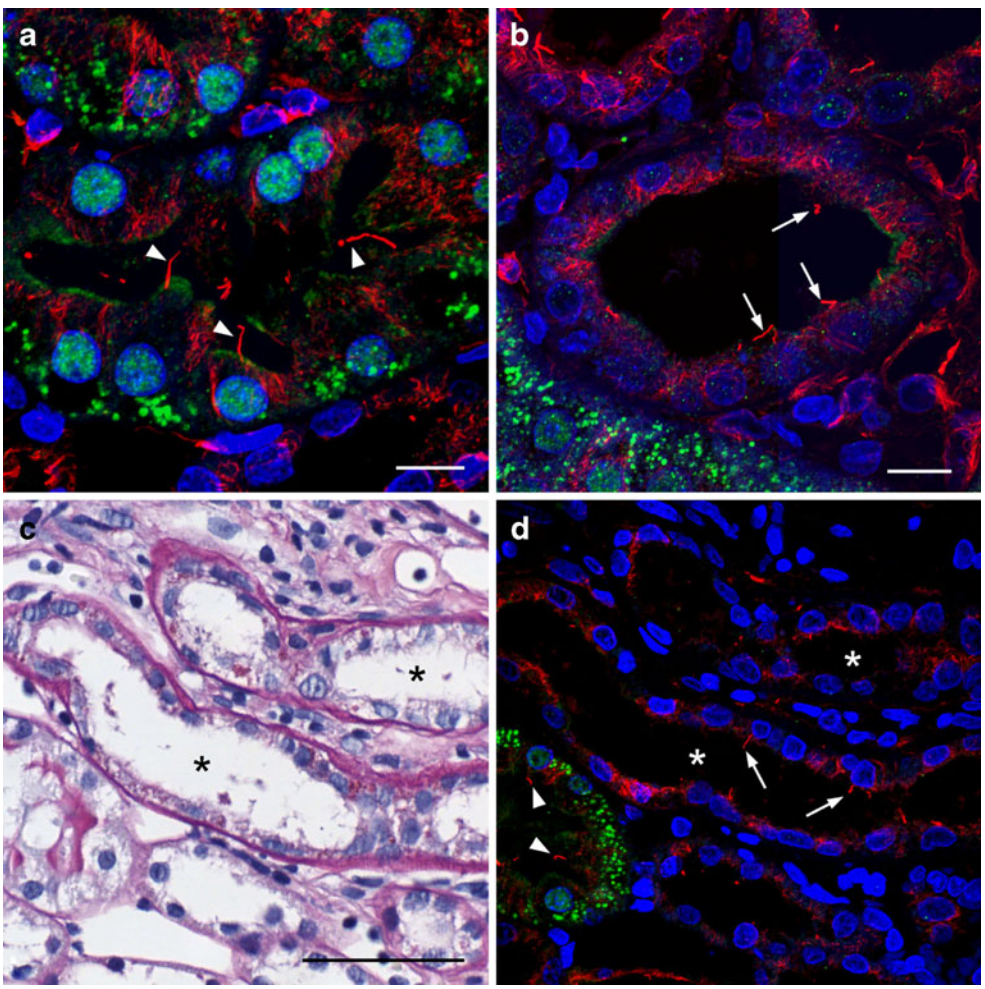

Fig. 5 Inversin expression and cilia in normal and atrophic proximal tubules in SHR. Inversin *green* acetylated alpha-tubulin indicating cilia *red*, nuclei *blue*. **a** normal proximal tubule with multiple cilia (*arrowheads*) and nuclear and cytoplasmic positivity for inversin. **b** Chronically damaged proximal tubule with minor rests of apical cytoplasmic positivity for inversin. Nuclear positivity is completely lost. Cilia (*arrows*) are still present. **c** (PAS) and **d** show consecutive sections of two atrophic tubules (*asterisk*). Cilia are present both in normal (*arrowheads*) and atrophic tubules (*arrows*). Complete loss of inversin positivity is seen in the atrophic tubules. (*Scale bars* **a**, **b** 10 μm; **c**, **d** 50 μm)

a lower perfusion pressure and a reduced filtration rate [24]. As the capillary volume fraction was strongly correlated with tubular diameter and tubular atrophy, this finding suggests that tubular atrophy develops as a consequence of reduced tubular flow.

It has been demonstrated that locking of proximal tubular lumens is followed by tubular atrophy due to a reduced flow [25]. We suggest that the loss of inversin positivity in damaged tubules in this study serves as a sign of reduced tubular flow. The cystoprotein inversin is involved in multiple signalling processes dependent of mechanosensation by tubular cilia. Ciliary bending by urine flow induces an increase in inversin positivity [18]. We have shown that cilia are still present in degenerating tubules. Minimal or no inversin positivity in these tubules is thus likely caused by the reduced bending of cilia due to the reduced flow.

The concept of tubular atrophy due to reduced tubular flow might not only apply to nephrons with collapsed glomeruli but might be the mechanism behind tubular atrophy in models with obstruction of the tubular outlet by crescents such as it has been shown in anti-Thy-1 nephritis [21] and murine anti-glomerular basement membrane glomerulonephritis [26].

The importance of glomerular collapse to the development of tubular atrophy in the juxtamedullary cortex in hypertensive kidney disease has not been recognized although there are a number of observations that are consistent with this theory. In a biopsy study of primary focal and segmental glomerulosclerosis, a subgroup of hypertensive patients showed ischemic glomeruli [27] and tubular atrophy was found to be associated with these ischemic glomeruli in nine out of nine glomeruli.

Further support of our study comes from an experiment in five-sixths renal ablation. In this rat model, which was studied 10 and 25 weeks after subtotal renal ablation, not all glomeruli connected to atrophic tubules showed segmental sclerosis, but these glomeruli were smaller than the glomeruli connected to normal tubules [28], indicating some degree of collapse. In puromycin nephrosis, a subset of glomeruli was small and collapsed and connected to atrophic tubules 10 weeks after induction [29]. Together, these and our findings provide a strong argument for glomerular collapse as a cause of tubular atrophy. However, this does not explain the pathogenesis of glomerular collapse.

Hypertrophy and remodelling of the muscular wall of afferent arterioles are known phenomena in rodent hypertension [30]. Afferent arterioles in the juxtamedullary cortex are exposed to a higher pressure than the afferent arterioles in the outer cortex because intraarterial pressure drops along the course of the interlobular artery [31]. This higher pressure causes a more rapid development of kidney damage and is a major argument for the importance of perfusion pressure in the development of hypertensive kidney damage. In the present study, nephrons with collapsed glomeruli in the juxtamedullary cortex showed increased media thickness of the afferent arterioles, and the outer arteriolar diameter was negatively correlated with both glomerular capillary volume fraction and tubular diameter. This relationship suggests that afferent arteriolar hypertrophy may decrease glomerular perfusion and induce glomerular collapse. This finding is supported by the lack of hyperperfusion damage in these glomeruli.

In conclusion, tubular atrophy in old SHR is probably the result of reduced tubular flow due to arteriolar hypertrophy and subsequent glomerular hypoperfusion and glomerular collapse. Our findings do not support the idea of a direct causal connection between segmental sclerosis and tubular atrophy either by misdirected filtration or hypoxia in the postglomerular capillary bed.

Acknowledgements We wish to thank Bendik Nordanger, Aud Strømme, Tina Dahl and Edith Fick for excellent technical assistance. The study was supported by a PhD fellowship from Helse Vest (Western Norway Regional Health Authority).

Disclosure The authors declare that they have no conflict of interests.

Open Access This article is distributed under the terms of the Creative Commons Attribution Noncommercial License which permits any noncommercial use, distribution, and reproduction in any medium, provided the original author(s) and source are credited.

References

1. U.S. Renal Data System, USRDS (2009) Annual Data Report: atlas of end-stage renal disease in the United States, National Institutes of Health, National Institute of Diabetes and Digestive and Kidney Diseases, Bethesda, MD
2. Bohle A, Wehrmann M, Greschniok A, Junghans R (1998) Renal morphology in essential hypertension: analysis of 1177 unselected cases. Kidney Int Suppl 67:S205–S206
3. Ito S, Nagasawa T, Abe M, Mori T (2009) Strain vessel hypothesis: a viewpoint for linkage of albuminuria and cerebro-cardiovascular risk. Hypertens Res 32:115–121
4. Wehrmann M, Bohle A (1998) The long-term prognosis of benign nephrosclerosis accompanied by focal glomerulosclerosis and renal cortical interstitial fibrosis, designated so-called decompensated benign nephrosclerosis by Fahr, Bohle and Ratscheck. Pathol Res Pract 194:571–576
5. Risdon RA, Sloper JC, De Wardener HE (1968) Relationship between renal function and histological changes found in renal-biopsy specimens from patients with persistent glomerular nephritis. Lancet 2:363–366
6. Schainuck LI, Striker GE, Cutler RE, Benditt EP (1970) Structural-functional correlations in renal disease. II. The correlations. Hum Pathol 1:631–641
7. Kriz W, Hartmann I, Hosser H, Hahnel B, Kranzlin B, Provoost A, Gretz N (2001) Tracer studies in the rat demonstrate misdirected

filtration and peritubular filtrate spreading in nephrons with segmental glomerulosclerosis. J Am Soc Nephrol 12:496–506
8. Fine LG, Bandyopadhay D, Norman JT (2000) Is there a common mechanism for the progression of different types of renal diseases other than proteinuria? Towards the unifying theme of chronic hypoxia. Kidney Int Suppl 75:S22–S26
9. Kriz W, Barrett JM, Peter S (1976) The renal vasculature: anatomical-functional aspects. Int Rev Physiol 11:1–21
10. Iversen BM, Amann K, Kvam FI, Wang X, Ofstad J (1998) Increased glomerular capillary pressure and size mediate glomerulosclerosis in SHR juxtamedullary cortex. Am J Physiol 274: F365–F373
11. Hultstrom M, Leh S, Skogstrand T, Iversen BM (2008) Upregulation of tissue inhibitor of metalloproteases-1 (TIMP-1) and procollagen-N-peptidase in hypertension-induced renal damage. Nephrol Dial Transplant 23:896–903
12. Roald AB, Ofstad J, Iversen BM (2002) Attenuated buffering of renal perfusion pressure variation in juxtamedullary cortex in SHR. Am J Physiol Renal Physiol 282:F506–F511
13. Kimura K, Nanba S, Tojo A, Hirata Y, Matsuoka H, Sugimoto T (1989) Variations in arterioles in spontaneously hypertensive rats. Morphometric analysis of afferent and efferent arterioles. Virchows Arch A Pathol Anat Histopathol 415:565–569
14. Skov K, Mulvany MJ (2004) Structure of renal afferent arterioles in the pathogenesis of hypertension. Acta Physiol Scand 181:397–405
15. Howard CV, Reed MG (1998) Unbiased stereology. Springer, New York
16. Rangan GK, Wang Y, Tay YC, Harris DC (1999) Inhibition of nuclear factor-kappaB activation reduces cortical tubulointerstitial injury in proteinuric rats. Kidney Int 56:118–134
17. Rosenberger C, Mandriota S, Jurgensen JS, Wiesener MS, Horstrup JH, Frei U, Ratcliffe PJ, Maxwell PH, Bachmann S, Eckardt KU (2002) Expression of hypoxia-inducible factor-1alpha and -2alpha in hypoxic and ischemic rat kidneys. J Am Soc Nephrol 13:1721–1732
18. Simons M, Gloy J, Ganner A, Bullerkotte A, Bashkurov M, Kronig C, Schermer B, Benzing T, Cabello OA, Jenny A, Mlodzik M, Polok B, Driever W, Obara T, Walz G (2005) Inversin, the gene product mutated in nephronophthisis type II, functions as a molecular switch between Wnt signaling pathways. Nat Genet 37:537–543
19. Beeuwkes R III (1980) The vascular organization of the kidney. Annu Rev Physiol 42:531–542
20. Kriz W, LeHir M (2005) Pathways to nephron loss starting from glomerular diseases—insights from animal models. Kidney Int 67:404–419
21. Kriz W, Hahnel B, Hosser H, Ostendorf T, Gaertner S, Kranzlin B, Gretz N, Shimizu F, Floege J (2003) Pathways to recovery and loss of nephrons in anti-Thy-1 nephritis. J Am Soc Nephrol 14:1904–1926
22. Javaid B, Olson JL, Meyer TW (2001) Glomerular injury and tubular loss in adriamycin nephrosis. J Am Soc Nephrol 12:1391–1400
23. Kriz W, Hosser H, Hahnel B, Simons JL, Provoost AP (1998) Development of vascular pole-associated glomerulosclerosis in the Fawn-hooded rat. J Am Soc Nephrol 9:381–396
24. Feld LG, Zamlauski-Tucker MJ, Springate JE, Van Liew JB (1995) Single nephron hemodynamics in spontaneously hypertensive rats. Proc Soc Exp Biol Med 209:185–189
25. Evan AP, Tanner GA (1986) Proximal tubule morphology after single nephron obstruction in the rat kidney. Kidney Int 30:818–827
26. Le Hir M, Besse-Eschmann V (2003) A novel mechanism of nephron loss in a murine model of crescentic glomerulonephritis. Kidney Int 63:591–599
27. Bonsib SM (1999) Focal-segmental glomerulosclerosis. The relationship between tubular atrophy and segmental sclerosis. Am J Clin Pathol 111:343–348
28. Gandhi M, Olson JL, Meyer TW (1998) Contribution of tubular injury to loss of remnant kidney function. Kidney Int 54:1157–1165
29. Rasch R, Nyengaard JR, Marcussen N, Meyer TW (2002) Renal structural abnormalities following recovery from acute puromycin nephrosis. Kidney Int 62:496–506
30. Wang PX, Sanders PW (2005) Mechanism of hypertensive nephropathy in the Dahl/Rapp rat: a primary disorder of vascular smooth muscle. Am J Physiol Renal Physiol 288:F236–F242
31. Heyeraas KJ, Aukland K (1987) Interlobular arterial resistance: influence of renal arterial pressure and angiotensin II. Kidney Int 31:1291–1298

Virchows Arch (2011) 459:109–113
DOI 10.1007/s00428-011-1101-2

ORIGINAL ARTICLE

p63 expression in adamantinoma

Brendan C. Dickson · Yair Gortzak · Robert S. Bell · Peter C. Ferguson · David J. C. Howarth · Jay S. Wunder · Rita A. Kandel

Received: 3 April 2011 / Revised: 23 May 2011 / Accepted: 29 May 2011 / Published online: 15 June 2011
© Springer-Verlag 2011

Abstract Adamantinoma is a rare primary bone neoplasm with epithelial differentiation that is frequently associated with a concomitant fibrous component. Clinical, cytogenetic and histomorphologic overlap has previously been described with osteofibrous dysplasia, thereby suggesting a relationship between these two lesions. We performed a retrospective review of our archives to characterize the clinical and pathologic aspects of adamantinoma and osteofibrous dysplasia diagnosed at our institution, and to compare the expression patterns of p63 and keratin. Nine cases of adamantinoma (six classical, three osteofibrous dysplasia-like) and 11 cases of osteofibrous dysplasia were identified. The epithelial component in adamantinoma was found to stain for p63. Rare cells expressing p63 were also identified in eight cases of osteofibrous dysplasia. Expression of p63 was not identified in any of the five cases of fibrous dysplasia controls. The presence of staining for p63, albeit rare, in osteofibrous dysplasia supports the notion of a possible relationship between osteofibrous dysplasia and adamantinoma. Furthermore, our results suggest that, in some situations, p63 may be useful in helping differentiate metastatic carcinoma from adamantinoma.

Keywords Adamantinoma · Osteofibrous dysplasia · Fibrous dysplasia · p63 · Pathogenesis

B. C. Dickson · D. J. C. Howarth · R. A. Kandel
Department of Pathology and Laboratory Medicine,
Mount Sinai Hospital, University of Toronto,
Toronto, ON, Canada

Y. Gortzak
The National Unit of Orthopedic Oncology,
Tel Aviv Sourasky Medical Center,
Tel Aviv, Israel

R. S. Bell · P. C. Ferguson · J. S. Wunder
University Musculoskeletal Oncology Unit,
Mount Sinai Hospital, University of Toronto,
Toronto, ON, Canada

B. C. Dickson (✉)
Department of Pathology and Laboratory Medicine,
Mount Sinai Hospital,
600 University Ave, Suite 6.500.12(1/2),
Toronto, ON, Canada M5G 1X5
e-mail: bdickson@mtsinai.on.ca

Introduction

Adamantinoma is an uncommon primary bone neoplasm that frequently exhibits a biphasic pattern of epithelial differentiation with a concomitant fibro-osseous component [1, 2]. These tumours most commonly occur in the tibia and tend to predominate during the second to fourth decades without an obvious sex predilection; tumours may, however, show a broader range in age and anatomic distribution [1, 3–7]. The epithelial component can assume basaloid, spindle cell, squamoid and tubular patterns that frequently occur together in the same tumour [2, 4]. The fibrous component may be inconspicuous or constitute the majority of the neoplasm; indeed, prior to modern descriptions of osteofibrous dysplasia [8], and its recognized association with adamantinoma [4, 9], early investigators likened such lesions to fibrous dysplasia [2, 10]. Very rarely, adamantinoma may undergo dedifferentiation with sarcomatoid transformation [11, 12].

The histogenesis of adamantinoma has long been a source of controversy. The application of electron microscopy [13, 14] and immunohistochemistry [4, 9, 15, 16] confirms initial reports of an epithelial derivation; nevertheless, the pathogenesis and cell of origin are yet to be characterized. A homologue of the p53 tumour suppressor

gene, p63, is a protein with complex and incompletely understood contributions to epithelial differentiation and bone development [17]. The purpose of this study was to characterize the expression of p63 in adamantinoma and osteofibrous dysplasia to interrogate the pathogenetic and diagnostic relevance of this marker.

Materials and methods

Following institutional Research Ethics Board approval, the pathology and clinical archives of Mount Sinai Hospital (Toronto, ON, Canada) were retrospectively reviewed for cases with the diagnosis of adamantinoma and osteofibrous dysplasia (1990–2010). Each case was re-reviewed and classified as adamantinoma, osteofibrous dysplasia-like adamantinoma and osteofibrous dysplasia using established criteria. Adamantinoma was defined by the presence of a primary epithelial neoplasm of bone and subclassified based into basaloid, spindle, squamous and tubular patterns of differentiation [1, 2, 18]. Osteofibrous dysplasia was defined as a bland hypocellular spindle cell proliferation containing interspersed bone spicules with osteoblastic rimming and a 'zonal' architecture [19, 20]. A predominance of osteofibrous tissue with only rare groups of epithelial cells denoted osteofibrous dysplasia-like variant of adamantinoma [1, 4, 18]. Five cases of fibrous dysplasia served as controls. The clinical records were further reviewed to determine patient outcome.

Immunohistochemical stains were performed using a formalin-fixed paraffin-embedded tissue. Sections, 5 μm, were subjected to microwave pretreatment (10 mM citrate buffer, pH 6.0 for 15 min) and incubated with p63 (A4A, LabVision Corp, Freemont, CA, USA; 1:1,000, 60 min at room temperature) or pancytokeratin (5D3&LP4, Vector Laboratories, Burlingame, CA USA; 1:150, 30 min at room temperature). Visualization was accomplished by sequential incubation with a secondary antibody (1:200; Vector Laboratories, Burlington, Canada), avidin–biotin peroxidase complex and 3,30-diaminobenzidine (Sigma-Aldrich, St Louis, MO, USA). The sections were counterstained with haematoxylin. Normal skin was used as the control tissue; positive staining was observed in the epidermis (p63 [nuclear] and keratin [cytoplasmic]), whereas the dermal fibroblasts and vasculature were negative for staining. In addition, in each case, a negative control slide was run without a primary antibody.

Results

Following histopathologic review, 9 cases of adamantinoma (six classical, three osteofibrous dysplasia-like) and 11 cases of osteofibrous dysplasia were identified. The clinical findings are summarized in Table 1. All tumours were monostotic. None of the patients received adjuvant chemotherapy or radiation therapy. Follow-up ranged from 8–172 months post-surgery.

In adamantinoma, the epithelial component in all cases was found to diffusely express p63 and keratin (Fig. 1). p63 expression was evenly distributed amongst the cell nuclei. Rarely, this was accompanied by a very pale cytoplasmic blush. Keratin expression was evenly distributed in a cytoplasmic distribution. The fibrous component contained only rare scattered positivity for both keratin and p63 in staining patterns analogous to that previously described.

In osteofibrous dysplasia, immunohistochemistry for keratin highlighted the presence of rare scattered positivity (≤1%) amongst individual and small clusters of epithelial cells in seven cases (63.6%; Fig. 2). Subjectively smaller numbers of p63 positive cells (≤1%) were seen in 8 of the 11 cases of osteofibrous dysplasia (72.7%). The keratin and/or p63-positive cells appeared to be randomly interspersed amongst the spindle cells and were not closely associated with either the vasculature or bone trabeculae.

Table 1 Summary of clinical details for each patient

Age	Sex	Location	Treatment	Outcome
Adamantinoma				
39	F	Tibia, D	Amputation, BKA	ANED
36	M	Tibia, D	Amputation, BKA	ANED
18	F	Tibia, D	Allograft	ANED
22	F	Tibia, P	Allograft	AWED
39	M	Tibia, P	Allograft	ANED
72	M	Tibia, D	Amputation, BKA	ANED
39	M	Tibia, M	Allograft	ANED
64	M	Tibia, M	Allograft	ANED
19	F	Tibia, D	Allograft	ANED
Osteofibrous dysplasia				
37	F	Tibia, P	Curettage	ANED
29	F	Femur, D	Allograft and autograft	ANED
20	M	Tibia, P	NA	ANED
19	F	Tibia, P	NA	ANED
25	M	Tibia, M	Allograft and autograft	ANED
17	M	Tibia, NS	En bloc resection	LTF
22	M	Tibia, P	Allograft	ANED
15	F	Tibia, P	NA	ANED
25	F	Tibia, P	Allograft	ANED
21	F	Tibia, NS	NA	LTF
41	F	Tibia, P	Allograft	ANED

D distal, *P* proximal, *M* mid, *NS* not specified, *BKA* below knee amputation, *NA* not applicable–no surgery following biopsy, *ANED* alive with no evidence of disease, *AWED* alive with evidence of disease, *LTF* lost to follow-up

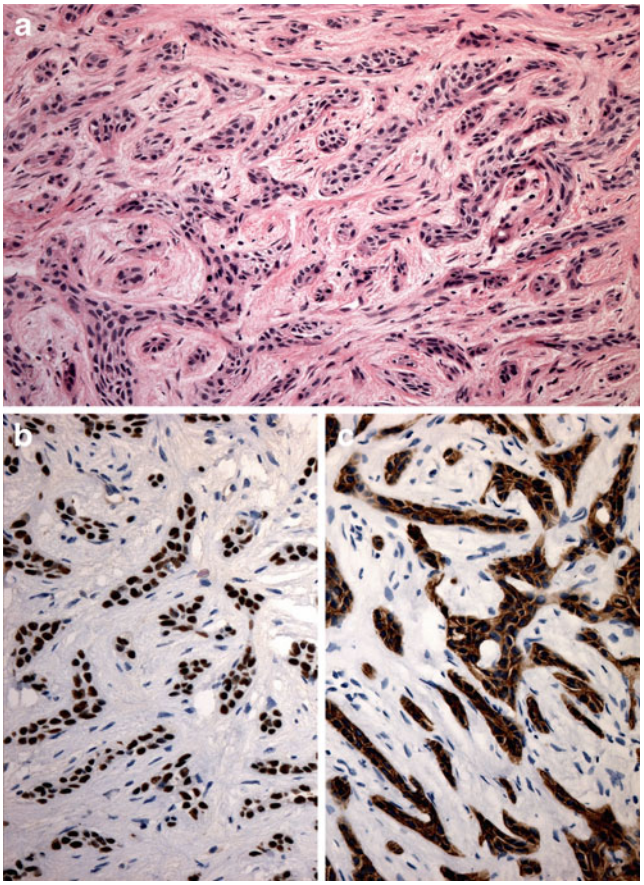

Fig. 1 **a** Classic adamantinoma (haematoxylin and eosin) showing immunoreactivity for **b** p63 and **c** pankeratin

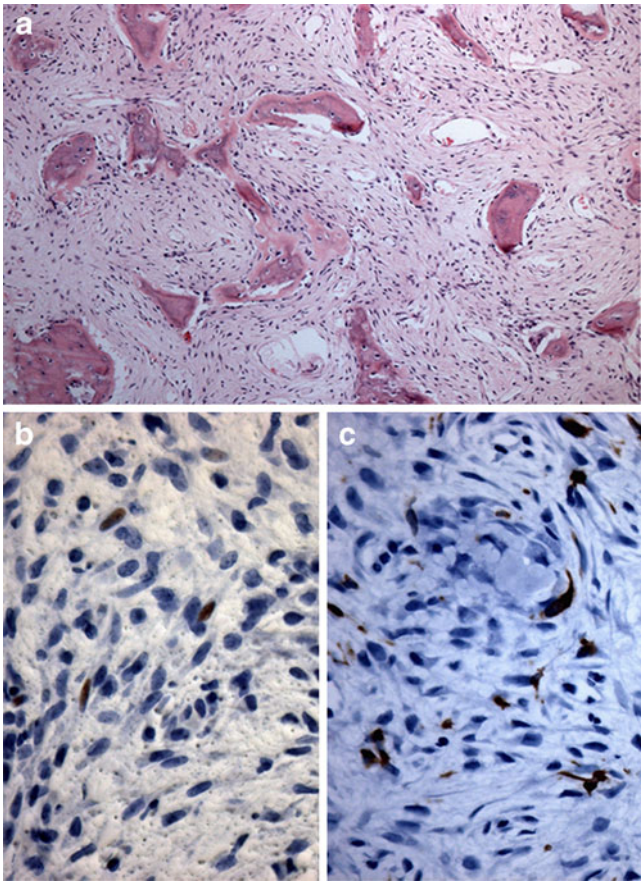

Fig. 2 **a** Osteofibrous dysplasia (haematoxylin and eosin) showing rare immunoreactivity for **b** p63 and **c** pankeratin

None of the five cases of fibrous dysplasia contained discernable keratin or p63 expression (not shown).

Discussion

We identified p63 expression in the epithelial cell component of adamantinoma. Staining, albeit extremely rare, was also observed in many cases of osteofibrous dysplasia. The target of staining in both lesions appears to be similar to that which is highlighted by keratin. Our observations therefore lend additional support to the notion that osteofibrous dysplasia falls on a histopathologic continuum with adamantinoma. Further, in some circumstances, p63 may represent a useful biomarker for the diagnosis of adamantinoma.

Campanacci proposed the term osteofibrous dysplasia to describe a group of lesions that, while sharing some morphologic similarity, remain distinct from fibrous dysplasia in terms of the age and site of involvement, and radiographic findings [8, 20, 21]. These are self-limited lesions that were initially thought to be reactive in nature, although the demonstration of clonality suggests a neoplastic basis. [22, 23] Adamantinoma is a biphasic neoplasm with a spectrum of epithelial and mesenchymal differentiation [1, 2, 24, 25]. The epithelial component has been proposed to originate from a foetal rest [26], or implantation or 'thwarted repair' following trauma [27]; more recent evidence indicates it may have a mesenchymal origin [28, 29]. This is generally believed to represent the malignant component of tumours [30]. The fibrous component, on the other hand, has been suggested to represent a secondary phenomena, perhaps resulting from tumefactive compromise of nutrient vessels [31] or a reactive/reparative response to the presence of adamantinoma [4, 32, 33]. Morphologic overlap with osteofibrous dysplasia [3, 10, 31, 34], hence the term osteofibrous dysplasia-like adamantinoma, has additionally led to the proposal that osteofibrous dysplasia represents a precursor to adamantinoma [18, 28, 33, 35]. This suggestion is supported by immunohistochemical [4, 9, 14, 16, 25, 36, 37] and cytogenetic similarities [22, 23, 33].

In our series, similar to previous reports, all of the cases of adamantinoma, and all but one of osteofibrous dysplasia, were located in the tibia on presentation. We had slightly more males than females in both the osteofibrous dysplasia

and adamantinoma groups. Patients with osteofibrous dysplasia were generally younger than those with adamantinoma. Differing somewhat from the literature, however, is the average age of patients which was higher amongst our study population for adamantinoma and particularly osteofibrous dysplasia. This is not an unexpected observation because patients were encountered in an adult tertiary care centre, and this study did not capture a paediatric population.

Using immunohistochemistry, we identified p63 expression in the epithelial component of adamantinoma and amongst rare scattered cells in the fibrous component of both osteofibrous dysplasia-like adamantinoma and osteofibrous dysplasia. This observation is potentially of diagnostic and pathogenetic relevance. In view of the restricted pattern of p63 expression amongst many epithelial tumours, the presence or absence of p63 staining is of potential diagnostic value when evaluating the possibility of metastatic carcinoma in bone, notably the tibia. Given that all of the cases we tested expressed p63, the absence of staining in a tumour would argue against a diagnosis of adamantinoma. Squamous cell carcinoma and urothelial carcinoma are known to commonly express p63; exclusion of these entities from the differential diagnosis can be readily accomplished based on tumour morphology, patient demographics and/or clinical–radiologic evaluation. p63 expression can also be seen in thymic carcinoma, some salivary gland tumours and a small number of other tumours which very uncommonly metastasize to bone. It is possible that the presence of rare p63 expression in an osteofibrous background may favour a diagnosis of osteofibrous dysplasia-like adamantinoma over osteofibrous dysplasia; nevertheless, the limited distribution of staining renders p63 less useful in this setting, as one might expect with a histopathologic continuum.

p63 is a p53 homolog and remains to be fully characterized. It contains two promotors and with alternative splicing yields six distinct isoforms [38], leading to a complex array of biologic functions [39]. Mutation of p63 in humans is associated with, amongst other things, abnormalities in craniofacial and limb development and maldevelopment of epithelium [38, 40–42]. Expression normally occurs amongst populations with a basal/myoepithelial phenotype, and it is commonly expressed in areas such as the bladder, breast, cervix, cornea, prostate and skin where it has been proposed to contribute to epithelial proliferation, differentiation and maintenance of basal stem cell populations [43–47]. In vitro studies suggest marrow-derived mesenchymal stem cells may, in certain circumstances, have the capability to differentiate into epidermal-like cells based on the detection of keratin and p63 expression [48]. The presence of p63 staining in osteofibrous dysplasia and adamantinoma is intriguing. This may be concomitant with epithelial-type differentiation; alternatively, it is conceivable this may reflect underlying basal stem cell properties. Interestingly, a basal keratin phenotype has previously been described in both osteofibrous dysplasia-like adamantinoma and classic adamantinoma [25]. Additional studies are necessary to further characterize the relationship between osteofibrous dysplasia and adamantinoma and the underlying pathogenesis of these tumours.

Acknowledgements The authors are grateful for the technical assistance of Ms. Patricia Wegrynowski and Mr. Anthony Wing. In addition, Mr. Anthony Griffin provided invaluable assistance in reviewing the clinical records.

This research was presented at the 2010 Meeting of the US and Canadian Academy of Pathology (Washington, DC, USA).

Conflict of interest The authors declare that they have no conflict of interest.

References

1. Hogendoorn PCW, Hashimoto H (2002) Adamantinoma. In: Fletcher CDM, Unni KK, Mertens F (eds) Pathology & Genetics: Tumours of Soft Tissue and Bone. IARC Press, Lyon, pp 332–334
2. Weiss SW, Dorfman HD (1977) Adamantinoma of long bone. An analysis of nine new cases with emphasis on metastasizing lesions and fibrous dysplasia-like changes. Hum Pathol 8:141–153
3. Unni KK, Dahlin DC, Beabout JW, Ivins JC (1974) Adamantinomas of long bones. Cancer 34:1796–1805
4. Czerniak B, Rojas-Corona RR, Dorfman HD (1989) Morphologic diversity of long bone adamantinoma. The concept of differentiated (regressing) adamantinoma and its relationship to osteofibrous dysplasia. Cancer 64:2319–2334
5. Keeney GL, Unni KK, Beabout JW, Pritchard DJ (1989) Adamantinoma of long bones. A clinicopathologic study of 85 cases. Cancer 64:730–737
6. Mills SE, Rosai J (1985) Adamantinoma of the pretibial soft tissue. Clinicopathologic features, differential diagnosis, and possible relationship to intraosseous disease. Am J Clin Pathol 83:108–114
7. Bambirra EA, Nogueira AM, Miranda D (1983) Adamantinoma of the soft tissue of the leg. Arch Pathol Lab Med 107:500–501
8. Campanacci M, Laus M (1981) Osteofibrous dysplasia of the tibia and fibula. J Bone Joint Surg Am 63:367–375
9. Benassi MS, Campanacci L, Gamberi G, Ferrari C, Picci P, Sangiorgi L, Campanacci M (1994) Cytokeratin expression and distribution in adamantinoma of the long bones and osteofibrous dysplasia of tibia and fibula. An immunohistochemical study correlated to histogenesis. Histopathology 25:71–76
10. Cohen DM, Dahlin DC, Pugh DG (1962) Fibrous dysplasia associated with adamantinoma of the long bones. Cancer 15:515–521
11. Hazelbag HM, Laforga JB, Roels HJ, Hogendoorn PC (2003) Dedifferentiated adamantinoma with revertant mesenchymal phenotype. Am J Surg Pathol 27:1530–1537
12. Izquierdo FM, Ramos LR, Sanchez-Herraez S, Hernandez T, de Alava E, Hazelbag HM (2010) Dedifferentiated classic adamantinoma of the tibia: a report of a case with eventual complete revertant mesenchymal phenotype. Am J Surg Pathol 34:1388–1392

13. Rosai J (1969) Adamantinoma of the tibia. Electron microscopic evidence of its epithelial origin. Am J Clin Pathol 51:786–792
14. Knapp RH, Wick MR, Scheithauer BW, Unni KK (1982) Adamantinoma of bone. An electron microscopic and immunohistochemical study. Virchows Arch A Pathol Anat Histopathol 398:75–86
15. Mori H, Yamamoto S, Hiramatsu K, Miura T, Moon NF (1984) Adamantinoma of the tibia. Ultrastructural and immunohistochemic study with reference to histogenesis Clin Orthop Relat Res 190:299–310
16. Ishida T, Iijima T, Kikuchi F, Kitagawa T, Tanida T, Imamura T, Machinami R (1992) A clinicopathological and immunohistochemical study of osteofibrous dysplasia, differentiated adamantinoma, and adamantinoma of long bones. Skeletal Radiol 21:493–502
17. Bertoni F, Campanacci M (1976) Ewing's sarcoma of the soft tissues? Case report. Ital J Orthop Traumatol 2:413–416
18. Hazelbag HM, Taminiau AH, Fleuren GJ, Hogendoorn PC (1994) Adamantinoma of the long bones. A clinicopathological study of thirty-two patients with emphasis on histological subtype, precursor lesion, and biological behavior. J Bone Joint Surg Am 76:1482–1499
19. Kumamoto H, Ohki K, Ooya K (2005) Expression of p63 and p73 in ameloblastomas. J Oral Pathol Med 34:220–226
20. Campanacci M (1976) Osteofibrous dysplasia of long bones a new clinical entity. Ital J Orthop Traumatol 2:221–237
21. Campanacci M, Giunti A, Bertoni F, Laus M, Gitelis S (1981) Adamantinoma of the long bones. The experience at the Istituto Ortopedico Rizzoli. Am J Surg Pathol 5:533–542
22. Bridge JA, Dembinski A, DeBoer J, Travis J, Neff JR (1994) Clonal chromosomal abnormalities in osteofibrous dysplasia. Implications for histopathogenesis and its relationship with adamantinoma. Cancer 73:1746–1752
23. Hazelbag HM, Wessels JW, Mollevangers P, van den Berg E, Molenaar WM, Hogendoorn PC (1997) Cytogenetic analysis of adamantinoma of long bones: further indications for a common histogenesis with osteofibrous dysplasia. Cancer Genet Cytogenet 97:5–11
24. Rosai J, Pinkus GS (1982) Immunohistochemical demonstration of epithelial differentiation in adamantinoma of the tibia. Am J Surg Pathol 6:427–434
25. Hazelbag HM, Fleuren GJ, vd Broek LJ, Taminiau AH, Hogendoorn PC (1993) Adamantinoma of the long bones: keratin subclass immunoreactivity pattern with reference to its histogenesis. Am J Surg Pathol 17:1225–1233
26. Fischer B (1913) Über ein primäres adamantinoma der tibia. Frankf Z Pathol 12:422–441
27. Ryrie BJ (1932) Adamantinoma of the tibia: aetiology and pathogenesis. Br Med J 2:1000–1003
28. Hazelbag, HM (1996) On the histogenesis of adamantinoma of long bones. Ph.D. Thesis, University of Leiden, Leiden
29. Hazelbag HM, Van den Broek LJ, Fleuren GJ, Taminiau AH, Hogendoorn PC (1997) Distribution of extracellular matrix components in adamantinoma of long bones suggests fibrous-to-epithelial transformation. Hum Pathol 28:183–188
30. Bovee JV, van den Broek LJ, de Boer WI, Hogendoorn PC (1998) Expression of growth factors and their receptors in adamantinoma of long bones and the implication for its histogenesis. J Pathol 184:24–30
31. Baker PL, Dockerty MB, Coventry MB (1954) Adamantinoma (so-called) of the long bones; review of the literature and report of three new cases. J Bone Joint Surg Am 36-A:704–720
32. Ueda Y, Blasius S, Edel G, Wuisman P, Bocker W, Roessner A (1992) Osteofibrous dysplasia of long bones—a reactive process to adamantinomatous tissue. J Cancer Res Clin Oncol 118:152–156
33. Gleason BC, Liegl-Atzwanger B, Kozakewich HP, Connolly S, Gebhardt MC, Fletcher JA, Perez-Atayde AR (2008) Osteofibrous dysplasia and adamantinoma in children and adolescents: a clinicopathologic reappraisal. Am J Surg Pathol 32:363–376
34. Dockerty MB, Meyerding HW (1942) Adamantinoma of the tibia: report of two new cases. J Am Med Assoc 119:932–937
35. Springfield DS, Rosenberg AE, Mankin HJ, Mindell ER (1994) Relationship between osteofibrous dysplasia and adamantinoma. Clin Orthop Relat Res 309:234–244
36. Kashima, TG Dongre, A Flanagan, AM Hogendoorn, PC Taylor, R Athanasou NA (2011) Podoplanin expression in adamantinoma of long bones and osteofibrous dysplasia. Virchows Arch. doi:10.1007/s00428-011-1081-2
37. Sweet DE, Vinh TN, Devaney K (1992) Cortical osteofibrous dysplasia of long bone and its relationship to adamantinoma. A clinicopathologic study of 30 cases. Am J Surg Pathol 16:282–290
38. Yang A, McKeon F (2000) P63 and P73: P53 mimics, menaces and more. Nat Rev Mol Cell Biol 1:199–207
39. Dotsch V, Bernassola F, Coutandin D, Candi E, Melino G (2010) p63 and p73, the ancestors of p53. Cold Spring Harb Perspect Biol 2:a004887
40. Yang A, Schweitzer R, Sun D, Kaghad M, Walker N, Bronson RT, Tabin C, Sharpe A, Caput D, Crum C, McKeon F (1999) p63 is essential for regenerative proliferation in limb, craniofacial and epithelial development. Nature 398:714–718
41. van Bokhoven H, Hamel BC, Bamshad M, Sangiorgi E, Gurrieri F, Duijf PH, Vanmolkot KR, van Beusekom E, van Beersum SE, Celli J, Merkx GF, Tenconi R, Fryns JP, Verloes A, Newbury-Ecob RA, Raas-Rotschild A, Majewski F, Beemer FA, Janecke A, Chitayat D, Crisponi G, Kayserili H, Yates JR, Neri G, Brunner HG (2001) p63 Gene mutations in eec syndrome, limb-mammary syndrome, and isolated split hand-split foot malformation suggest a genotype–phenotype correlation. Am J Hum Genet 69:481–492
42. Mills AA, Zheng B, Wang XJ, Vogel H, Roop DR, Bradley A (1999) p63 is a p53 homologue required for limb and epidermal morphogenesis. Nature 398:708–713
43. Pellegrini G, Dellambra E, Golisano O, Martinelli E, Fantozzi I, Bondanza S, Ponzin D, McKeon F, De Luca M (2001) p63 identifies keratinocyte stem cells. Proc Natl Acad Sci U S A 98:3156–3161
44. Brunner HG, Hamel BC, Bokhoven Hv H (2002) P63 gene mutations and human developmental syndromes. Am J Med Genet 112:284–290
45. Reis-Filho JS, Schmitt FC (2002) Taking advantage of basic research: p63 is a reliable myoepithelial and stem cell marker. Adv Anat Pathol 9:280–289
46. Blanpain C, Fuchs E (2007) p63: revving up epithelial stem-cell potential. Nat Cell Biol 9:731–733
47. Senoo M, Pinto F, Crum CP, McKeon F (2007) p63 Is essential for the proliferative potential of stem cells in stratified epithelia. Cell 129:523–536
48. Chun-mao H, Su-yi W, Ping-ping L, Hang-hui C (2007) Human bone marrow-derived mesenchymal stem cells differentiate into epidermal-like cells in vitro. Differentiation 75:292–298

Virchows Arch (2011) 459:115–116
DOI 10.1007/s00428-011-1089-7

LETTER TO THE EDITOR

Vanishing prostate cancer on radical prostatectomy (RP) in the PSA era: incidence and follow-up data from a cohort of 1,060 patients between 1998 and 2010

Vikas Mehta · Swati Mehrotra · Robert C. Flanigan · Eva M. Wojcik · Girish Venkataraman

Received: 18 February 2011 / Revised: 26 April 2011 / Accepted: 5 May 2011 / Published online: 17 May 2011
© Springer-Verlag 2011

Sir:

There have been a few studies investigating the incidence and prognostic relevance of the "vanishing cancer" phenomenon in the radical prostatectomy specimen (RP), in particular, in the last decade [1, 2]. We undertook this study to determine incidence and prevalence of "vanishing prostatic adenocarcinoma" at our institution and to correlate the outcome of these patients with histopathology findings. We searched our institutional database and identified a total of 18 patients with no residual cancer out of 1,060 radical prostatectomies performed between 1998 and 2010. Four patients were excluded from the analysis due to preoperative hormonal therapy (three cases) and immunotherapy (one case). In the remaining 14 cases, clinical data including age and PSA levels with biopsy data (highest Gleason score, highest percentage of carcinoma, number of biopsy sites, number of positive biopsy sites, use of immunohistochemistry, and number of previous biopsies) and RP data (number of examined slides, highest Gleason score, percentage of carcinoma, and presence of high-grade prostatic intraepithelial neoplasia) were extracted. In all 14 cases, the radical prostatectomy specimens were submitted entirely. The incidence of the vanishing cancer phenomenon was 1.3% in our series (14/1,060 RPs). Among the 14 RPs studied, residual cancer was not identified in 11 patients despite careful and extensive sampling. Three cases showed microscopic foci of cancer involving less than 0.5% of the tissue. The mean age of the patients was 59.09 (44–75). The total number of biopsy sites ranged from 2 to 14 with a mean of 7. The mean PSA was 5.8 units (3.6–9.0). The Gleason score in the biopsy ranged from 4 to 8, with a mean of 6 (12 patients with GS 6, and one each with GS 4 and GS 8). The mean number of positive biopsy sites was 1.33 (range, 1–4). The number of biopsy sites ranged from 2 to 14 with a mean of 5.89. The mean number of examined slides was 39.55 (11–63). In the RP, six cases showed residual high-grade prostatic intraepithelial neoplasia, and two showed atrophy. The follow-up ranged from 8–144 months (mean=64 months, median=64, and SD=38.4). All patients are currently alive with no cancer recurrence, and the serum PSA concentration remains at <0.2 ng/mL.

The reported incidence of "vanishing cancer" in different studies has ranged from 0.2% to up to 4% with a notable decreasing trend reported between the early 1980s and the early 1990s [3, 4]. A recent study evaluated 31 cases with no residual cancer using polymerase chain reaction (PCR)-based microsatellite markers and concluded that most cases of "vanishing cancer" in RP specimens reflect a chance sampling of a minute cancer and not a switch in specimens. However, this poses a medico-legal problem and should be probed. Recently, PCR-based microsatellite marker analysis has become the gold standard [2] to evaluate patient identity. Some

V. Mehta (✉) · S. Mehrotra · E. M. Wojcik · G. Venkataraman
Department of Pathology, Loyola University Medical Center,
Room 2233, Building 110, 2160 South First Avenue,
Maywood, IL 60153, USA
e-mail: vmehta@lumc.edu

R. C. Flanigan
Department of Urology, Loyola University Medical Center,
Maywood, IL, USA

authors suggest a protocol in cases of no residual cancer in radical prostatectomy specimens which includes re-reviewing the biopsy, use of immunostains, additional levels, and ultimately flipping the blocks [4, 5].

Based on our cohort of patients, we tend to see this entity in patients with well-differentiated adenocarcinoma on the biopsy although a definite statistical association cannot be gleaned due to the low frequency of the outcome analyzed. The prognosis in this cohort of patients is excellent. Our series does not show apparent clinical significance to microscopic foci of cancer that remains undetected after extensive pathological sampling of the radical prostatectomy tissue. Nevertheless, a close clinical follow-up is necessary.

References

1. Bostwick DG, Bostwick KC (2004) 'Vanishing' prostate cancer in radical prostatectomy specimens: incidence and long-term follow-up in 38 cases. BJU Int 94:57–58
2. Cao D, Hafez M, Berg K, Murphy K, Epstein JI (2005) Little or no residual prostate cancer at radical prostatectomy: vanishing cancer or switched specimen? A microsatellite analysis of specimen identity. Am J Surg Pathol 29:467–473
3. Bostwick DG (1997) Evaluating prostate needle biopsy: therapeutic and prognostic importance. CA Cancer J Clin 47:297–319
4. Mazzucchelli R, Barbisan F, Tagliabracci A et al (2007) Search for residual prostate cancer on pT0 radical prostatectomy after positive biopsy. Virchows Arch 450(4):371–378
5. Loeb S, Schaeffer EM, Epstein JI (2005) The vanishing prostate cancer phenomenon. Urology 76:605–607

Virchows Arch (2011) 459:117–118
DOI 10.1007/s00428-011-1098-6

LETTER TO THE EDITOR

Mammary analogue secretory carcinoma: a new twist to the diagnostic dilemma of zymogen granule poor acinic cell carcinoma

Christopher Griffith · Raja Seethala · Simion I. Chiosea

Received: 14 April 2011 / Revised: 16 May 2011 / Accepted: 22 May 2011 / Published online: 3 June 2011
© Springer-Verlag 2011

Dear Editor,

The prior report of our consultative experience with 205 salivary gland tumors reviewed over one academic year (2007–2008) featured zymogen granule poor acinic cell carcinoma (ACC) as a recurring problematic theme [1]. Recently, Skalova et al. described 16 cases of a new tumor entity—mammary analogue secretory carcinoma (MASC) of salivary glands, characterized by the *ETV6-NTRK3* translocation and morphologic features resembling ACC [2]. Prompted by the report of Skalova et al., we have subsequently reexamined our cases for histologic features suggesting MASC.

Of the ten cases previously reported by us as ACC and available for rereview, five showed a predominance of intercalated duct-type cells (Fig. 1a, b) and only scant zymogen granules (as was seen on periodic acid Schiff with diastase, PASD). All five cases were strongly positive for S100 by immunohistochemistry. Three showed a papillary cystic growth pattern, and two showed a mixed microcystic and follicular growth pattern. These five cases were examined by fluorescence in situ hybridization (FISH) using break-apart *ETV6* probe (Abbot Molecular, Des Plains, IL). The presence of an *ETV6* translocation was identified in four cases (Fig. 1c), and in the remaining one case, in situ hybridization failed.

Table 1 shows some of the clinicopathologic features of the four *ETV6* translocation-positive tumors. As previously reported, there was a wide age range in affected patients, from 15 to 72 years of age. The 15-year-old male is the youngest reported patient with MASC. While three tumors arose in the parotid, we report only the second MASC to arise in the upper lip.

Based on our own findings and the report by Skalova et al., salivary gland tumors with a predominance of intercalated duct-type cells, rudimentary serous acinar differentiation (i.e., scant PASD resistant granules), and strong S100 positivity are best designated as MASC. FISH studies for *ETV6* translocation are helpful in confirming the diagnosis. We feel that our report on reclassification of these four cases from ACC to MASC is necessary to set the record straight and to "bridge" the newly described entity of MASC to a well-recognized diagnostic problem with ACC.

C. Griffith · R. Seethala · S. I. Chiosea (✉)
Department of Pathology,
University of Pittsburgh Medical Center,
200 Lothrop St, PUH A616.2,
Pittsburgh, PA 15213, USA
e-mail: chioseasi@upmc.edu

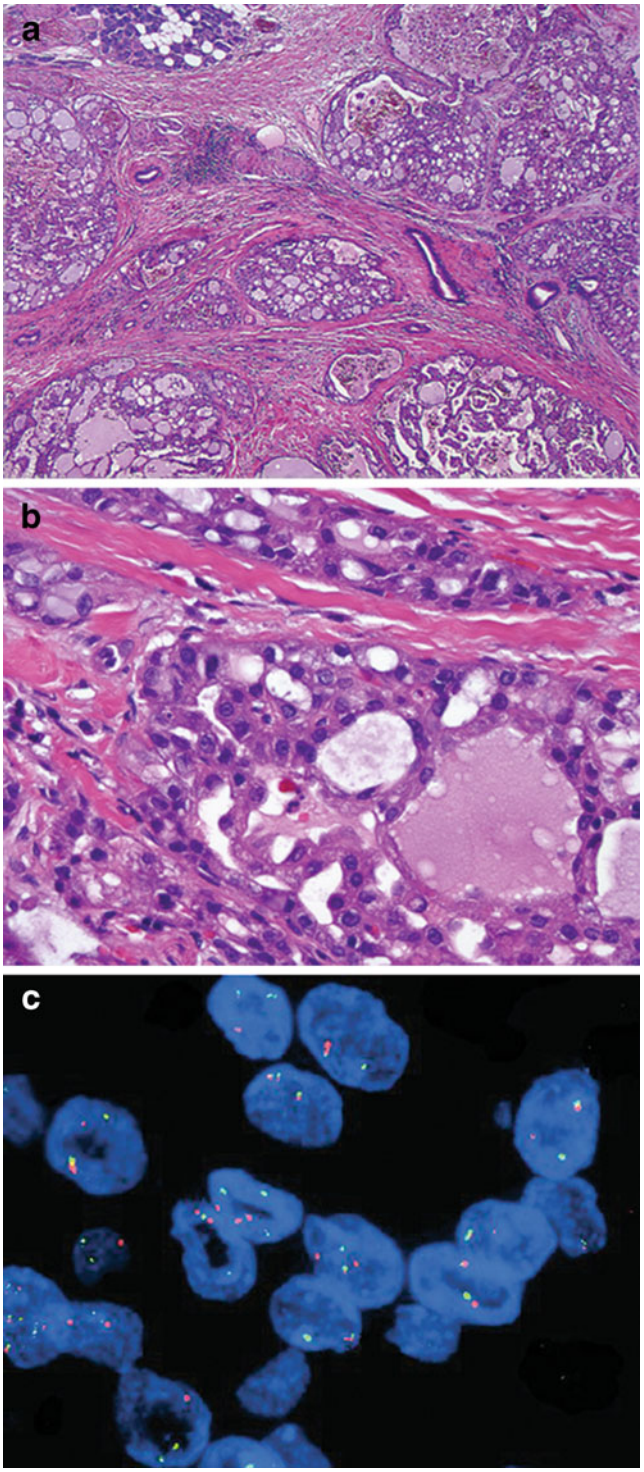

Fig. 1 **a** Mammary analogue secretory carcinoma involving parotid gland (residual parotid tissue in the upper left corner), characterized by lobular growth with fibrous septa and microcystic architecture, H&E, ×100. **b** Colloid-like bubbly secretions in glands/microfollicles formed by intercalated duct-type cells; note the absence of basophilic zymogen granules, H&E, ×400. **c** Fluorescence in situ hybridization with *ETV6* (12p13) break-apart probe. Nuclei with split *red* and *green signals* indicate *ETV6* break. Chromosomes with normal *ETV6* gene show *yellow signal* (overlapping green and red)

Table 1 Clinicopathologic features of patients with mammary analogue secretory carcinoma

Age/sex	Location	Size (cm)	Stage	Diagnosis rendered by submitting pathologist
50/M	Parotid	1.5	T1N0	MEC
72/M	Parotid	2.0	T1N0	Oncocytoma vs. ACC
48/F	Parotid	2.0	T1NX	MEC vs. ACC
15/M	Upper lip	1	T1NX	Neoplasm, NOS

M man, *F* female, *MEC* mucoepidermoid carcinoma, *ACC* acinic cell carcinoma, *NOS* not otherwise specified

References

1. Chiosea SI, Peel R, Barnes EL et al (2009) Salivary type tumors seen in consultation. Virchows Arch 454:457–466
2. Skalova A, Vanecek T, Sima R et al (2010) Mammary analogue secretory carcinoma of salivary glands, containing the ETV6-NTRK3 fusion gene: a hitherto undescribed salivary gland tumor entity. Am J Surg Pathol 34:599–608

Virchows Arch (2011) 459:119–120
DOI 10.1007/s00428-011-1093-y

LETTER TO THE EDITOR

In response—A modified staining protocol for Smoothelin immunostaining

Ranjani Chakravarthy · Khalid Ahmed · Salma Abbasi · Andrew Cotterill · Nazia Parveen

Received: 12 May 2011 / Accepted: 17 May 2011 / Published online: 3 June 2011
© Springer-Verlag 2011

Dear Editor,

In response to the article by Lindh et al. [1] in which they have discussed the utility of Smoothelin and have concluded that Smoothelin should be used cautiously, we would like to share our experience on the usefulness of Smoothelin staining. We performed a study assessing the utility of Smoothelin immunostaining in distinguishing muscularis mucosa (MM) from muscularis propria (MP) in 103 urinary bladder specimens, including 90 TURBTS and 13 cystectomies (results yet to be published).

Immunohistochemical staining was performed using the Dako Autostainer Plus platform (Dako, Glostrup, Denmark) in order to validate the anti-Smoothelin primary antibody (clone R4A; Menarini Diagnostics, Wokingham, UK) for purposes of our study. Heat-induced epitope retrieval (HIER) was performed using the Dako PT link (Dako). Sections were incubated in the appropriate antigen retrieval buffer for 20 min at 97°C and were then allowed to cool to 65°C before transferring to distilled water. Two antigen retrieval buffers were used to establish the optimal HIER protocol. These HIER buffers were as follows:

(a) High pH (9.5) Target Retrieval Solution (Dako)
(b) Low pH (6.0) Target Retrieval Solution (Dako)

Enzyme antigen retrieval was attempted using Proteinase K (Dako) at room temperature. Sections were incubated in Proteinase K solution for 6 min prior to immunohistochemical staining.

Optimal antibody titre was established using double dilutions, using 1:50 as an initial reference point. Intense staining of MP was noted with high pH HIER (pH 9.5), suboptimal staining with low pH HIER (pH 6.0) and absent staining using enzyme antigen retrieval methods (proteinase K). High pH HIER, however, also resulted in moderate to intense staining of MM. We overcame these issues by using high pH HIER and by titrating the dilution of antibody to 1:500 [2]. Immunoreactivity for MM and MP was then assessed semi-quantitatively. MM showed no staining with Smoothelin in 45 cases (43%), weak staining in 52 (51%) and moderate staining in 6 cases (6%). MP showed weak staining in two cases (2%); immunostaining was, however, negative in MM in both cases. Moderate staining was observed in MP in 22 (21%) cases and strong staining in 79 cases (77%). In all the cases, MP exhibited a greater intensity of staining than the MM included in the sections.

In conclusion, we faced similar difficulties, as the authors, in establishing a robust staining protocol for Smoothelin immunostaining. However, by modifying our staining protocol, we overcame the problem of double staining and achieved optimal staining. Our results show that Smoothelin can be a useful adjunct in distinguishing MM from MP in TURBT specimens, in concordance with several other studies [3–5].

R. Chakravarthy (✉) · K. Ahmed · S. Abbasi · A. Cotterill · N. Parveen
The Royal Oldham Hospital, Pennine Acute NHS Trust, Rochdale Road,
Oldham OL1 2JH, UK
e-mail: cpranjani@yahoo.com

References

1. Lindh C, Nilsson R et al. (2011) Detection of smoothelin expression in the urinary bladder is strongly dependent on pretreatment conditions: a critical analysis with possible consequences for cancer staging. Virchows Arch. doi:10.1007/s00428-011-1076-z

2. Khayyata S, Dudas M, Rohan SM et al (2009) Distribution of smoothelin expression in the musculature of the genitourinary tract. Mod Pathol 22:175A
3. Miyamoto H, Sharma RB et al (2010) Pitfalls in the use of smoothelin to identify muscularis propria invasion by urothelial carcinoma. Am J Surg Pathol 34(3):418–422
4. Council L, Hameed O (2009) Differential expression of immunohistochemical markers in bladder smooth muscle and myofibroblasts, and the potential utility of desmin, smoothelin, and vimentin in staging of bladder carcinoma. Mod Pathol 22 (5):639–650
5. Paner GP, Shen SS et al (2009) Diagnostic utility of antibody to smoothelin in the distinction of muscularis propria from muscularis mucosae of the urinary bladder: a potential ancillary tool in the pathologic staging of invasive urothelial carcinoma. Am J Surg Pathol 33(1):91–98

Virchows Arch (2011) 459:121–127
DOI 10.1007/s00428-011-1115-9

ORIGINAL ARTICLE

Liver histology as predictor of outcome in patients with acute-on-chronic liver failure (ACLF)

Archana Rastogi · Ashish Kumar · Puja Sakhuja · Chhagan Bihari · Ranjana Gondal · Syed Hissar · Hitendra Garg · Shiv Kumar Sarin

Received: 20 March 2011 / Revised: 20 June 2011 / Accepted: 22 June 2011 / Published online: 9 July 2011
© Springer-Verlag 2011

Abstract There is paucity of literature on liver histological spectrum of acute-on-chronic liver failure (ACLF). The aims of this study are to (a) to characterize the liver histological features in ACLF, (b) to correlate histological parameters with prognosis, and (c) to investigate whether etiology influences prognosis. We retrospectively studied liver biopsies of patients with ACLF. The histological findings were correlated with the clinical outcome. Fifty cases (median age, 39 years [10–69 years]; M/F, 3:1) were included. Etiology of acute insult was viral or alcohol in majority of the cases. Twenty-five patients survived (good outcome, 50%) and 25 died (poor outcome, 50%). On a univariate analysis, the outcome correlated with fibrosis, ballooning, eosinophilic degeneration, ductular proliferation, pericellular fibrosis, Mallory's hyaline, foci of confluent necrosis and/or bridging necrosis (CN/BN), cholestasis, apoptosis (present), and parenchyma left. However, on a multivariate analysis, only fibrosis, ballooning, ductular proliferation, apoptosis, and parenchyma left were found to be independently associated with outcome. Two distinct patterns of liver histology were observed: pattern I, observed in cases with poor outcome, showing marked ductular proliferation, coarse inspissated ductular bile plugs, eosinophilic degeneration of hepatocytes, foci of CN/BN, higher apoptosis, pericellular fibrosis, Mallory's hyaline, and higher stage of fibrosis. Pattern II is seen in cases with good outcome, show prominent hepatocyte ballooning with lesser parenchymal involvement by fibrosis and necrosis. Histological features of liver biopsy are: extent of fibrosis, ballooning, ductular proliferation, apoptosis, and lesser degree of parenchymal replacement by fibrosis or necrosis which correlates with the outcome in patients with ACLF. Two distinct patterns of liver histology are seen which help in prognostication.

Keywords Liver · Biopsy · Acute · Chronic · Liver failure · Histopathology

A. Rastogi (✉) · C. Bihari
Department of Pathology,
Institute of Liver and Biliary Sciences (ILBS),
D-1, Vasant Kunj,
New Delhi 110 070, India
e-mail: drarchanarastogi@gmail.com

A. Kumar · H. Garg · S. K. Sarin
Department of Hepatology,
Institute of Liver and Biliary Sciences (ILBS),
New Delhi, India

A. Kumar
e-mail: ashishk10@yahoo.com

P. Sakhuja · R. Gondal
Department of Pathology, G B Pant Hospital,
New Delhi, India

S. Hissar · S. K. Sarin
Department of Gastroenterology, G B Pant Hospital,
New Delhi, India

A. Kumar · S. K. Sarin
Special Centre for Molecular Medicine,
Jawaharlal Nehru University (JNU),
New Delhi, India

Introduction

Liver failure can develop either as acute liver failure in the absence of any preexisting liver disease, as chronic decompensation of an end-stage liver disease (ESLD), or as an acute deterioration of known or unknown chronic liver disease—the acute-on-chronic liver failure (ACLF).

ACLF constitutes an illness where two insults to the liver are operating simultaneously: one acute and other chronic.

There is limited data on the entity of ACLF. The Asian Pacific Association for the Study of the Liver (APASL) has defined ACLF as acute hepatic insult manifesting as jaundice and coagulopathy, complicated within 4 weeks by ascites, and/or encephalopathy in a patient with previously diagnosed or undiagnosed chronic liver disease [1]. Presentation, course, and outcome of these patients are different from patients of acute liver failure (ALF) and from ESLD. ACLF is potentially reversible, more so with the emergence of newer liver support strategies, hence it has become necessary to distinguish these entities.

Early and accurate diagnosis and prognosis of patients with ACLF is of critical importance for optimum management. There is paucity of literature highlighting the liver histological spectrum of ACLF. The role of liver biopsy as an outcome predictor in ACLF is not clear and has not been highlighted so far. We undertook this study with the following aims: (a) to characterize the liver histological features in ACLF, (b) to investigate whether histological parameters can determine the prognosis and differentiate end-stage fibrotic liver disease from ACLF, and (c) to investigate whether etiology influences histology–prognosis relationship.

Patients and methods

Patients

A retrospective study was conducted in which we evaluated liver biopsies of 50 patients with clinical diagnosis of ACLF that were received in the department of pathology. These cases were included in the study based on the APASL criteria of ACLF [1] and availability of an adequate liver biopsy (≥1 cm in length). Patients with HCC or portal vein thrombosis or cardiovascular comorbidities were excluded from the study.

Methods

Demographic, clinical findings, and outcome were recorded from the hospital medical records. The main clinical outcome measures were survival (good outcome) versus death (poor outcome).

Histology

Formalin-fixed paraffin-embedded transjugular liver biopsies were retrospectively reviewed by three histopathologists (AR, PS, RG) blinded to individual patient's etiological details, clinical findings, and to the eventual outcome. Almost perfect concordance was found amongst them for most of the parameters and minor discrepancies encountered were resolved by reviewing the cases together on multilateral microscope. Serial sections of liver biopsies stained with hematoxylin and eosin (H&E), Masson's Trichrome, and Shikata's orcein were examined in all the cases. Reticulin stain for reticulin fibers and Fouchet's stain for bile were also done in most of the cases.

The degree of hepatic inflammation and fibrosis were graded using Ishak's score [2]. Histological activity index (HAI) ≥6 and fibrosis score ≥3 were considered significant for the present study.

Following histological features were also assessed and semiquantitatively graded for each of the 50 biopsies of ACLF patients available for analysis: hepatocyte ballooning, eosinophilic degeneration of hepatocytes, rosette formation by hepatocytes, pericellular fibrosis, ductular proliferation, cholangiolitis, apoptosis, and Mallory's hyaline. Hepatocytes were said to be undergoing eosinophilic degeneration when the cytoplasm showed hypereosinophilia. These histological features were visually estimated on a scale of 0 to 3 (0, absent; 1, occasional to mild; 2, moderate; 3, marked). A score of 2–3 was considered positive for analysis.

Cholestasis is a common feature of acute hepatocellular injury. Ductular cholestasis is a more advanced form of cholestasis, and usually develops in a background of cellular and canalicular cholestasis. It is often seen in systemic conditions, extensive hepatocellular necrosis, and chronic liver disease in terminal stages. Cholestasis was defined as type 1 when fine granular intrahepatocytic and canalicular bile was seen; type 2 when in addition to type 1, coarse inspissated canalicular and few ductular bile plugs were seen; and type 3 when in addition to type 2, prominent ductular bile plugs along with the cellular cholestasis was seen. Type 2 and 3 were taken together for correlation.

For parenchyma left (percentage) a cutoff of 50% was considered significant (fraction of total surface area of the biopsy that is not occupied by parenchymal necrosis or fibrosis). Fatty change involving ≥30% of the liver biopsy parenchyma was considered significant for the present study.

Foci of confluent necrosis and/or bridging necrosis (CN/BN) were visualized on H&E-stained sections and confirmed by orcein and reticulin stain. Bridging necrosis is confluent necrosis that bridges terminal hepatic venules to portal tracts. When hepatocytes are damaged and undergo necrosis, the reticulin fibers surrounding them collapse in the empty space left behind. Reticulin crowding is seen in areas of focal hepatocyte loss and reticulin collapse in large areas of necrosis. Orcein stains elastic fibers and helps distinguish areas of bridging necrosis from bridging fibrosis and in assessment of periportal fibrosis in severely inflamed portal areas. Foci CN/BN were visually estimated on a scale

of 0 to 3 (0, absent; 1, occasional to mild; 2, moderate; 3, marked). A score of 2–3 was considered significant.

All the histological parameters were correlated with the outcome. Presence of histological features was also compared amongst the major etiological groups—group I, acute viral hepatitis (AVH) superimposed on chronic liver disease (CLD) of any etiology; group II, reactivation of chronic hepatitis B (CHB); and group III, alcoholic hepatitis on underlying chronic alcoholic liver disease (ALD).

Statistical analysis

All results were expressed as mean (±SD), median (range), or number (%). Comparisons between the two groups (good outcome versus poor outcome) were carried out by Student's *t* test for parametric data, Mann–Whitney *U* test for nonparametric data, and Fischer's exact test for categorical data. Differences were considered significant at p value of <0.05. Statistical analyses were performed with the SPSS 15.0 statistical package (SPSS Inc., Chicago, IL).

Results

Demographic characteristics

A total of 50 cases were included in this study. The median age of the patients was 39 years (range, 10–69 years). There were 36 males and 14 females (M/F ratio, 2.6:1).

Etiology of acute insult and chronic liver disease

Chronic liver disease was due to hepatitis B virus (n=32) and alcohol (n=10) in most of the cases. Possible etiology of acute decompensation was viral (n=37) or alcoholic (n=7) in majority of the cases. Major etiologic groups were reactivation of chronic hepatitis B (n=20), acute alcoholic hepatitis superimposed on alcoholic liver disease (n=7), and acute hepatitis of any etiology superimposed on chronic liver disease of different etiology (n=23) (Table 1).

Outcome of patients

An equal number of patients had good (n=25, 50%) and poor (n=25, 50%) outcome. All deaths occurred during the same admission. The median time (from hospital admission) to death was 15 days (range, 2 to 102).

Demographic and biochemical characteristics in patients with good and poor outcome

The median age was similar in patients with good and poor outcome. Mean serum bilirubin and albumin levels were 22.0±9.5 mg/dl and 3.0±0.7 g/dl, respectively. Serum bilirubin levels (mean±SD) for the groups with good and poor outcome were 19.7±8.8 and 24.1±9.8 mg/dl, respectively (p<0.05). Serum albumin levels (mean±SD) for the groups with good and poor outcome were 3.3±0.8 and 2.7 ±0.6 g/dl, respectively (p<0.05).

Table 1 Etiological classification of ACLF patients (n=50)

Etiology of chronic liver disease	Etiology of acute insult	
Hepatitis B (n=32)	Reactivation of hepatitis B	(n=20)
	Acute viral hepatitis	(n=10)
	Sepsis	(n=2)
Alcohol (n=10)	Acute alcoholic hepatitis	(n=7)
	Acute viral hepatitis	(n=3)
Cryptogenic (n=6)	Acute viral hepatitis	(n=2)
	Unknown	(n=4)
Hepatitis C (n=1)	Acute viral hepatitis	(n=1)
NASH (n=1)	Acute viral hepatitis	(n=1)

NASH non-alcoholic steatohepatitis

Histological characteristics of ACLF

Mean core tissue length of liver biopsy specimens was 1.2 cm. All cases showed features of acute and chronic hepatitis in variable combinations. Features of acute injury such as ballooning degeneration of hepatocytes, cellular, and/or ductular cholestasis, ductular proliferation with variable degree of parenchymal necrosis/collapse along with the features of chronic liver disease as periportal fibrous extensions, bridging fibrosis or cirrhosis, pericellular fibrosis and interface activity, were seen in all the biopsies.

Correlation of liver histology with outcome in ACLF

Table 2 summarizes histological characteristics in both the outcome groups. On a univariate analysis, the following factors were found to be associated with poor outcome: fibrosis (stage, ≥3); ballooning inversely correlates with poor outcome (score, 2–3); eosinophilic degeneration (score, 2–3); ductular proliferation (score, 2–3); pericellular fibrosis (score, 2–3); Mallory's hyaline (score, 2–3); foci of CN/BN (score, 2–3); cholestasis (types, 2–3); apoptosis (present); and parenchyma left (> 50%) inversely correlates with poor outcome. However, on a multivariate analysis (Table 3) fibrosis, ductular proliferation, and apoptosis independately correlate with poor outcome; whereas ballooning and parenchyma left correlate inversely with poor outcome.

Table 2 Univariate analysis of correlation of liver histology with outcome in patients of ACLF

Liver histology variable	Good outcome (n=25)	Poor outcome (n=25)	P value
HAI (index≥6)	17 (68%)	19 (76%)	0.754
Fibrosis (stage≥3)	14 (56%)	25 (100%)	<0.001
Ballooning (score, 2–3)	22 (88%)	6 (24%)	<0.001
Eosinophilic degeneration (score, 2–3)	0 (0%)	15 (60%)	<0.001
Rosettes (score, 2–3)	10 (40%)	8 (32%)	0.769
Ductular proliferation (score, 2–3)	4 (16%)	22 (88%)	<0.001
Pericellular fibrosis (score, 2–3)	0 (0%)	18 (72%)	<0.001
Cholangiolitis (score, 2–3)	4 (16%)	9 (36%)	0.196
Mallory's hyaline (score, 2–3)	0 (0%)	6 (24%)	0.022
Foci of CN/BN (score, 2–3)	0 (0%)	9 (36%)	0.002
Cholestasis (types, 2–3)	13 (52%)	24 (96%)	0.001
Apoptosis (present)	17 (68%)	24 (96%)	0.023
Parenchyma left (≥50%)	24 (96%)	12 (48%)	<0.001
Fatty change (≥30%)	0 (0%)	2 (8%)	0.490

Correlation of histological characteristics amongst the major etiologic groups

Based on etiology, the patients were categorized into the following three groups: group I, AVH superimposed on CLD of any etiology (n=23); group II, reactivation of CHB (n=20); and group III, alcoholic hepatitis on underlying chronic ALD (n=7). The presence of all the histological parameters were assessed in the three major etiologic groups to confirm that such histologic patterns and their prognostic value were not related to any specific etiology. Most of the 14 histological parameters did not show any association with the etiologic groups, except that Mallory's hyaline and pericellular fibrosis which were significantly more common in group III than group I or II. Similarly, HAI was more marked in group I than III (Table 4).

Histological patterns

Two distinct patterns of liver histology were observed. Pattern I was observed in cases with poor outcome, and biopsy showed marked ductular proliferation, coarse inspissated ductular bile plugs, eosinophilic degeneration of hepatocytes, foci of confluent necrosis/bridging necrosis, higher apoptosis, pericellular fibrosis, Mallory's hyaline, and higher stage of fibrosis. Pattern II was seen in cases with good outcome, show prominent hepatocyte ballooning with lesser parenchymal involvement by fibrosis and necrosis (Figs. 1 and 2).

Table 3 Results of multivariate analysis of liver histology parameters found independently associated with poor outcome in patients of ACLF

Variable	Log likelihood	P value
Fibrosis (stage, ≥3)	−76.203	<0.01
Ballooning (score, 2–3)	−44.127	<0.01
Ductular proliferation (score, 2–3)	−7.625	0.041
Apoptosis (present)	−9.011	0.008
Parenchyma left (≥50%)	−18.399	<0.01

Discussion

This is a study of the liver histology of 50 cases of ACLF, first to the best of our knowledge, in which 14 liver histological features and their role as outcome predictor were studied. Liver histology revealed features of acute injury and chronic liver diseases with/without necrosis, in varying combinations and variable degrees of severity. Two distinct histological patterns were observed. Eosinophilic degeneration of hepatocytes, ductular cholestasis, advanced fibrosis, ductular proliferation, increased apoptosis, foci of confluent necrosis/bridging necrosis, pericellular fibrosis, and Mallory's hyaline emerged as predictors of poor outcome, whereas ballooning degeneration of hepatocytes and lesser degree of parenchymal involvement by fibrosis or necrosis were indicators of good outcome, on a univariate analysis. The multivariate analysis showed fibrosis, ductular proliferation, and apoptosis to be independently associated with poor outcome and ballooning degeneration and parenchymal (left) with good outcome in patients with ACLF. These features were also compared amongst the main etiological groups (AVH superimposed on CHB, HBV reactivation, and exacerbation of ALD). Of the 14 histological features, pericellular fibrosis and Mallory's hyaline showed etiologic association and were significantly more commonly seen in the alcoholic group. HAI was more marked in group I than III. These findings need validation by studies in larger disease groups.

Table 4 Correlation of liver histology with major etiologic groups

Liver histology variable	*P* value: group 1 vs 2	*P* value: group 1 vs 3	*P* value: group 2 vs 3
HAI (index≥6)	0.148	0.033	0.391
Fibrosis (stage≥3)	0.728	0.304	0.155
Ballooning (score, 2–3)	0.365	0.392	1.000
Eosinophilic degeneration (score, 2–3)	0.728	0.153	0.365
Rosettes (score, 2–3)	1.000	1.000	1.000
Ductular proliferation (score, 2–3)	1.000	0.104	0.091
Pericellular fibrosis (score, 2–3)	1.000	0.009	0.024
Cholangiolitis (score, 2–3)	0.501	1.000	0.633
Mallory's hyaline (score, 2–3)	0.491	0.016	0.002
Foci of CN/BN (score, 2–3)	1.000	0.603	0.580
Cholestasis (types 2–3)	0.497	1.000	0.633
Apoptosis (present)	1.000	1.000	1.000
Parenchyma left (≥50%)	0.473	0.060	0.365
Fatty change (≥30%)	0.491	1.000	1.000

Group I, AVH superimposed on CLD of any etiology (n=23); group II, reactivation of CHB (n=20); and group III, alcoholic hepatitis on underlying chronic ALD (n=7)

ACLF is a serious condition with varied acute and chronic underlying etiologies and high mortality. This term was first used in 1995 to describe a condition where two insults to the liver are operating simultaneously, an acute event occurring on an underlying chronic liver disease [3]. However, this entity of acute-on-chronic liver failure still remains poorly defined.

With the emergence of newer liver support strategies and encouraging results reported in patients with ACLF, it has become essential to define this entity, its pathophysiology, and the prognosis determinants [4].

The APASL's definition of ACLF is "Acute hepatic insult manifesting as jaundice and coagulopathy, complicated within 4 weeks by ascites and/or encephalopathy in a patient with previously diagnosed or undiagnosed chronic liver disease" [1].

Whether the prognosis of the patient depends on the degree of acute insult or chronic insult or the combination of the two is still not well defined. It is essential to separate ACLF from ALF and CLD as presentation, course, and outcome differ from them.

There is scarcity of histological data on ACLF. The role of liver biopsy in diagnosing underlying chronic liver disease and its prognostic significance are not clear and have not been studied so far.

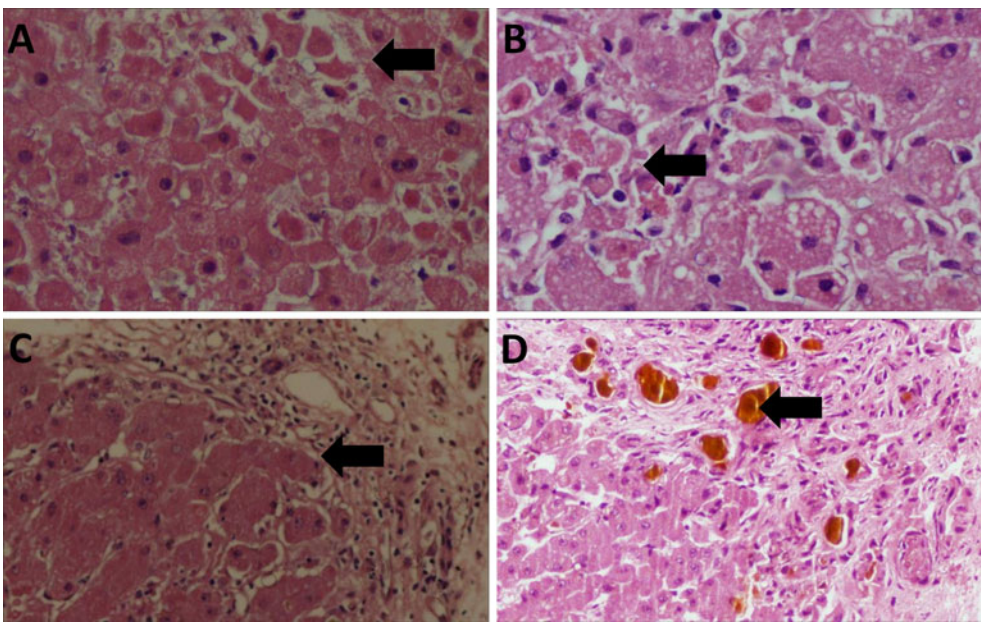

Fig. 1 Photomicrograph of liver histology showing pattern I of ACLF in a case of reactivation of HBV with cirrhosis. **a** Confluent necrosis in low power. **b** Confluent necrosis in high power. **c** Eosinophilic degeneration. **d** Prominent ductular bile plugs

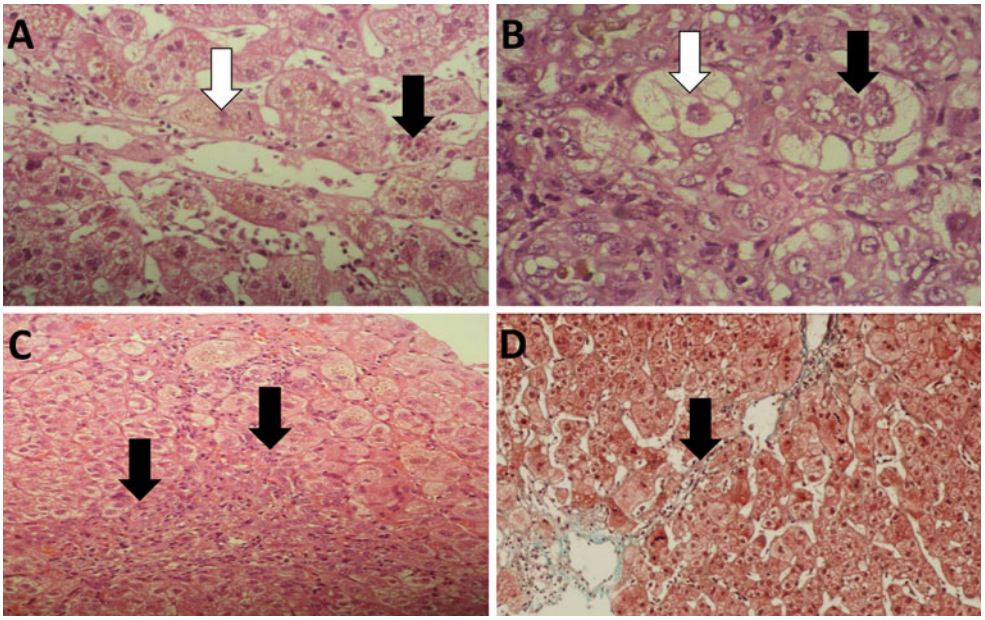

Fig. 2 Photomicrograph of liver histology showing pattern II of ACLF in a case of HEV infection superimposed on chronic HBV. **a** Cellular cholestasis and apoptosis. **b** Ballooning degeneration and giant cell transformation of hepatocytes. **c** Interface activity. **d** Bridging fibrous septa

In the present study, liver biopsies in all the cases revealed features of both acute and chronic hepatitis with variable severity. Liver histology comprised of hepatocyte ballooning and eosinophilic degeneration of hepatocytes, rosette formation by hepatocytes, apoptosis (councilman bodies), fatty change, cholestasis (hepatocyte, canalicular, bile ductular, and ducts), lobular inflammation, portal inflammation, Mallory's hyaline, percentage of parenchyma left (not involved by necrosis/fibrosis), foci of CN/BN with portal/periportal fibrosis, ductular proliferation, pericellular fibrosis, and cholangiolitis [5, 6].

Previous studies in patients with liver failure have shown that liver biopsy can be very helpful particularly in prognostication by determining the extent of necrosis, liver damage, and fibrosis. It can help in differentiating acute liver failure from acute-on-chronic liver failure by confirming chronic liver disease [7–10].

Liver biopsy can also provide clues to the underlying etiology if the diagnosis remains elusive after extensive initial evaluation as is recommended in AASLD position paper on acute liver failure which states that liver biopsy may be appropriate to attempt to identify a specific etiology that might influence treatment strategy—malignant infiltration, autoimmune hepatitis, certain viral infections, Wilson disease, drug-induced injury [11].

Although terminology used in various studies differ, the importance of liver histology in predicting outcome is well emphasized particularly of parenchymal necrosis, fibrosis, ductular cholestasis, and hepatocyte changes. These findings are similar to our study in which all these parameters were studied in a large group of ACLF patients.

Distinct histological patterns identified in our patients have not been previously reported in literature; however, some of the individual parameters were found to be quite convincing and consistent with the observations of other studies in a small number of patients [8].

Boyer and Klatskin [7], in their study of 170 patients, had emphasized the importance of liver biopsy in assessing prognosis during the acute phase of viral hepatitis by assessing presence of bridging necrosis (subacute hepatic necrosis). One hundred eighteen of their patients who had a benign clinical course revealed only spotty necrosis in liver biopsy, whereas in 50 patients (subacute hepatic necrosis group), outcome was poor (19% died and 37% developed cirrhosis), and their diagnosis in most of the cases depended on liver biopsy.

Nayak et al. [8], in their study of 42 patients of subacute hepatic failure, reported presence of bridging necrosis, ductular cholestasis, and nonreactive/eosinophilic change in hepatocytes to be more common in fatal group. Nonreactive change in hepatocytes appeared to be directly related to mortality in subacute hepatic failure. Twenty-two out of 23 patients in the group with poor outcome and one out of 19 in patients with good outcome showed nonreactive change in liver biopsy. Ductular cholestasis alone or along with cellular cholestasis was much more common in fatal cases (19/21 vs 8/19, respectively). Bridging necrosis was also more common in the fatal group, and it was more extensive and wide, 22/23 (96%) vs 14/19 (74%), respectively.

Tandon et al. [12] have shown, in their study of 33 patients of subacute hepatic failure, submassive and bridging necrosis as the main liver histological findings.

We also found similar correlation of histology with prognosis in our study. Eosinophilic degeneration of hepatocytes (<0.001), ductular cholestasis (<0.001), advanced fibrosis (<0.001), ductular proliferation (<0.001), foci of confluent necrosis/bridging necrosis (0.002), apoptosis (0.001), pericellular fibrosis (<0.001), Mallory's hyaline (0.022) emerged as predictors of poor outcome, whereas ballooning degeneration of hepatocytes (<0.001) and lesser degree of parenchymal replacement by fibrosis or necrosis (<0.001) were indicators of good outcome on univariate analysis. Multivariate analysis showed fibrosis, ductular proliferation, and apoptosis to be independently associated with poor outcome and ballooning degeneration and parenchyma left with good outcome in patients with ACLF. Scotto et al. have also shown that early liver biopsy during acute liver failure allows a good estimation of remaining functional hepatocyte volume and prognosis [13].

None of the previous studies have discussed the influence of etiology on the role of histological features as outcome predictors. In our study, we have assessed all the features in three main etiologic groups, and pericellular fibrosis and Mallory's hyaline were significantly more common in the alcoholic group. HAI was more marked in group I than III.

Liver biopsy provides useful prognostic information by determining the extent of necrosis, liver damage, and fibrosis. Two distinct patterns of liver histology are seen in ACLF, and a classification based on histopathology can help in management and prognostication. Extensive necrosis, advanced fibrosis, ductular cholestasis, and proliferation, pericellular fibrosis, increased apoptosis along with eosinophilic degeneration of hepatocytes were predictors of poor outcome in ACLF. The impact of the histological parameters and of the etiology on prognosis needs validation by studies on larger groups of patients, postmortem biopsies, and explant data. Biopsy in ACLF should be need-based/individualized.

Conflict of interest statement We declare that we have no conflict of interest.

References

1. Sarin SK, Kumar A, Almeida J et al (2009) Acute on chronic liver failure (ACLF): consensus recommendations of the Asia Pacific Association for the Study of the Liver (APASL). Hepatol Int 3:269–282
2. Ishak K, Baptista A, Bianchi L et al (1995) Histological grading and staging of chronic hepatitis. J Hepatol 22:696–699
3. Ohnishi H, Sugihara J, Moriwaki H, Muto Y (1995) Acute-on-chronic liver failure. Ryoikibetsu Shokogun Shirizu 7:217–219
4. Bauer M, Winning J, Kortgen A (2005) Liver failure. Curr Opin Anaesthesiol 18:111–116
5. Suriawinata AA, Thung SN (2006) Acute and chronic hepatitis. Semin Diagn Pathol 23:132–148
6. Burt AD, Portmann BC, Ferrell LD (2007) MacSween's pathology of the liver, 5th edn. Churchill Livingstone, Edinburgh
7. Boyer JL, Klatskin G (1970) Pattern of necrosis in acute viral hepatitis. Prognostic value of bridging (subacute hepatic necrosis). N Engl J Med 283:1063–1071
8. Nayak NC, Dutta Gupta S, Tandon A, Dasarathy S, Acharya SK (1993) Pathology of sub-acute hepatic failure. Indian J Gastroenterol 12(suppl 3):11–14
9. Liu Q, Liu Z, Wang Q, Wang Q, Shi X, Dao W (2007) Characteristics of acute and sub-acute liver failure in China: nomination, classification and interval. J Gastroenterol Hepatol 22:2101–2106
10. Donaldson BW, Gopinath R, Wanless IR et al (1993) The role of transjugular liver biopsy in fulminant liver failure: relation to other prognostic indicators. Hepatology 18:1370–1376
11. Polson J, Lee WM (2005) AASLD position paper: the management of acute liver failure. Hepatology 41:1179–1197
12. Tandon BN, Joshi YK, Krishnamurthy L, Tandon HD (1982) Subacute hepatic failure: is it a distinct entity? J Clin Gastroenterol 4:343–346
13. Scoto J, Opolon P, Itipvi J, Vergoz D, Thomas M, Caroli J (1973) Liver biopsy and prognosis in acute liver failure. Gut 14:927–933

Virchows Arch (2011) 459:129–139
DOI 10.1007/s00428-011-1103-0

ORIGINAL ARTICLE

Clinical significance of histone deacetylases 1, 2, 3, and 7: HDAC2 is an independent predictor of survival in HCC

Karl Quint · Abbas Agaimy · Pietro Di Fazio · Roberta Montalbano · Claudia Steindorf · Rudolf Jung · Claus Hellerbrand · Arndt Hartmann · Helmut Sitter · Daniel Neureiter · Matthias Ocker

Received: 28 February 2011 / Revised: 4 May 2011 / Accepted: 30 May 2011 / Published online: 29 June 2011
© Springer-Verlag 2011

Abstract Histone deacetylases (HDAC) are responsible for the transcriptional control of genes through chromatin remodeling and control tumor suppressor genes. In several tumors, their expression has been linked to clinicopathological factors and patient survival. This study investigates HDACs 1, 2, 3, and 7 expressions in hepatocellular carcinoma (HCC) and their correlation with clinical data and patient survival. Tissue microarrays of 170 surgically resected primary HCCs and adjacent uninvolved tissue were evaluated immunohistochemically for the expression of HDACs 1, 2, 3, 7, and Ki-67 and were analyzed with respect to clinicopathological data and patient survival. HDACs 1, 2, 3, and Ki-67 were expressed significantly higher in cancer cells compared to normal tissue (HDAC1: $p=0.034$, HDACs 2 and 3 and Ki-67: $p<0.001$), while HDAC7 expression did not differ between HCC and non-cancerous liver tissue. In tumor tissue HDACs 1–3 expression levels showed high concordance with each other, Ki-67 and tumor grade ($p<0.001$). High HDAC2 expression was associated with poor survival in low-grade and early-stage tumors ($p<0.05$). The expression of the HDACs 1, 2, and 3 (but not HDAC7) isoenzymes correlates with clinicopathological factors, and HDAC2 expression has an impact on patient survival.

Keywords Correlation analysis · Expression analysis · Hepatocellular carcinoma · Histone deacetylases · Overall survival · Tissue microarray

Electronic supplementary material The online version of this article (doi:10.1007/s00428-011-1103-0) contains supplementary material, which is available to authorized users.

K. Quint · P. Di Fazio · R. Montalbano · H. Sitter · M. Ocker (✉)
Institute for Surgical Research, Philipps University Marburg, Baldingerstrasse,
35033 Marburg, Germany
e-mail: matthias.ocker@staff.uni-marburg.de

K. Quint · C. Steindorf · M. Ocker
Department of Medicine 1, University Hospital Erlangen, Erlangen, Germany

A. Agaimy · R. Jung · A. Hartmann
Department of Pathology, University Hospital Erlangen, Erlangen, Germany

R. Jung
Department of Pathology, University Hospital Regensburg, Regensburg, Germany

C. Hellerbrand
Department of Internal Medicine I, University Hospital Regensburg, Regensburg, Germany

D. Neureiter
Institute of Pathology, Paracelsus Private Medical University, Salzburg, Austria

Introduction

Hepatocellular carcinoma (HCC) belongs to the most common tumor diseases worldwide, and its incidence is increasing in industrial nations [1, 2]. The causes for HCC are diverse and include chronic viral hepatitis, heavy alcohol use, or metabolic diseases such as hemochromatosis. The diversity of the pathophysiological processes that results from these different etiological factors makes HCC a heterogeneous tumor [3]. Curative therapies, such as liver resection and transplantation, are possible in only 15% of patients, but recurrence rates are high. Those not eligible for

surgical intervention benefit from locoregional therapies, such as transarterial chemoembolization and radiofrequency ablation, but these therapies, too, are limited by high recurrence rates. Although several new chemotherapeutic approaches targeting different oncogenic signaling pathways have been introduced into HCC therapy, only the multikinase inhibitor sorafenib showed a beneficial clinical response and improved overall survival of patients [4, 5]. Yet, additional new therapies are urgently needed as many patients experience dose-limiting toxicity and tumor progression.

Recently, epigenetic regulation of gene transcription, e.g., by DNA methylation or histone acetylation, has been shown to be a promising new therapeutic target in oncology [6]. Specifically in tumor cells, inhibition of histone deacetylases (HDACs) leads to cell cycle inhibition, e.g., by upregulation of $p21^{cip1/waf1}$ and various pro-apoptotic effects that are also mediated by non-nuclear signalling of HDAC inhibitors [6–8]. Our own previous data also show that inhibition of HDACs sensitizes HCC cell lines to various chemotherapeutics and therefore provide a rationale for further clinical investigation as a potential therapeutic target in HCC [9, 10].

Different patterns of HDAC overexpression have been shown for various human cancers [11] and these results indicate that HDACs have a prognostic value in renal cell carcinomas [12], tumors of the gastrointestinal tract [13, 14], and prostate cancer [15]. In HCC, out of 18 known HDAC isoforms (HDACs 1–11 and Sirtuins 1–7), only one isoform (HDAC1) has been analyzed in 47 human tumor samples from Asian HCCs and the results indicate a role in patient outcome [16]. We here examined the expression of class I HDACs (1, 2, and 3) and class II HDAC7 in a cohort of 170 European HCC patients along with corresponding uninvolved normal hepatic tissue to correlate their relationship with clinicopathological factors and the impact on patient survival. Specifically with respect to HDAC inhibitor therapy, HDAC expression, determined prior to HDAC inhibitor therapy, could help predict early and overall therapeutic response before treatment initiation [3, 17–19].

Materials and methods

Patients and tissue samples

Archived HCC tumor samples, corresponding adjacent non-tumorous hepatic tissue and clinical data were obtained from 170 patients who underwent curative surgical resection at the Department of Surgery, University Hospital Erlangen, Germany, and at the Department of Surgery, University Hospital, Regensburg, Germany, between 2001 and 2007. Laboratory and clinical data were retrieved from the hospitals' case files, laboratory information systems, and tumor registers. Detailed patient data is presented in Table 1. This study was covered by ethical votes of the medical faculties of the Universities of Regensburg and Erlangen–Nuremberg [20, 21].

Tissue microarray and immunohistochemical staining

The surgical specimens were obtained during routine hepatectomy, fixed in formalin and embedded in paraffin. For each patient, one tumor sample and one sample from adjacent normal tissue uninvolved by the tumor were used in the array. The punches were transferred onto a new paraffin block, forming the tissue microarrays as described previously [20, 21]. Two to three-micrometer slices of these were cut, deparaffinized in xylene, and rehydrated in descending dilutions of ethanol. The following antibody

Table 1 Patient characteristics

			N (percent of total)
Patients	*n*=170	Male	145 (85.3%)
		Female	24 (14.7%)
Age	61.7±11.2 years	Male	63.0±10.4 years
		Female	55.4±12.4 years
pT		1	67 (39.4%)
		2	49 (28.8%)
		3a	47 (27.6%)
		3b	4 (2.4%)
		4	3 (1.8%)
pN		N0	85.7%
		N1	14.3%
pM		M0	91.4%
		M1	8.6%
Tumor grade		G1	13.1%
		G2	59.8%
		G3	27.1%
Child-Pugh classification		No cirrhosis	16.7%
		A	48.4%
		B	27.8%
		C	7.1%
CLIP score		0	75.6%
		1	16.7%
		2	6.4%
		3	1.3%
Etiology	Viral		20%
	Alcohol		35.3%
	Viral and alcohol		2.9%
	Cholangitis		1.8%
	Cryptogenic		9.4%
	No information available		30.6%

labeling was achieved using EnVision+Dual Link System HRP (K4061, Dako GmbH, Hamburg, Germany). Antigen retrieval was done using 1 mM Tris-EDTA buffer in a pressure cooker at 120°C for 5 min. Endogenous peroxidases were blocked by incubating the slices for 5 min with blocking solution (S2023, Dako), followed by 5 min of washing. Primary antibodies were applied for 30 min at room temperature at the given dilutions (using antibody diluent, S2022, Dako): anti-HDAC1 (ready-to-use dilution, ab15316, Abcam plc, Cambridge, UK), anti-HDAC2 (1:500, ab12169, Abcam), anti-HDAC3 (1:500, 612635, BD Biosciences, Heidelberg, Germany), anti-HDAC7 (1:100, ab53101, Abcam), and anti-Ki-67/MIB-1 (1:50, F7268, Dako). Following 5 min of washing, labeled polymer-HRP (goat-anti-rabbit or goat-anti-mouse secondary antibodies linked with horseradish peroxidase, Dako) was applied for 30 min at room temperature. Positive antibody binding was stained using DAB+(K3467, Dako) for 10 min; the nuclei were counterstained using Mayers's hematoxylin (S3309, Dako) for 1 min. Positive controls were run in parallel. In addition, HDAC stainings for random tumors were performed on traditional slides to ensure homogenous distribution of HDAC expression throughout the tumor.

Interpretation of immunohistochemical staining

The sections were investigated by two investigators (AA and KQ), who were blinded to the patient characteristics and outcome. Evaluation of the staining was done in four high-power fields for each case. HDAC expression was evaluated using a semi-quantitative composite categorical score for immunohistochemical intensity and extent (immunoreactivity score, IRS). Intensity of staining (score 0–3: 0, negative; 1, weak; 2, moderate; 3 strong) as well as percentage of cells stained (score 0–3: 0, 0%; 1, 1–25%; 2, 25–50%; 3, >50%) were evaluated separately for each case. The IRS was calculated by adding the intensity and frequency scores, resulting in values ranging from 0 to 6. Inflammatory cells which stained positive were not counted. Ki-67 was quantified by counting the number of positive nuclei per 100 cells in a representative tumor area and scored as follows: 0, negative; 1, 1–5%; 2, 6–10%; 3, 11–20%; 4, 21–30%; 5, 31–40%; and 6, 41–100%. Tumor grade scoring was G1: well-differentiated (WHO grade 1), G2: moderately differentiated (WHO grade 2), and G3: poorly and undifferentiated (WHO grades 3 and 4). Interobserver variability was determined by the κ value (κ=0.946).

Statistical analysis

Statistical analysis was performed using SPSS 17 (SPSS Inc., Chicago, IL, USA). Values for albumin, aspartate transaminase (AST/GOT), alanine transaminase (ALT/GPT), total bilirubin, thromboplastin time (Quick), gamma glutamyl transpeptidase (gamma-GT), lactate dehydrogenase (LDH), cholineesterase (CHE), alpha-1-fetoprotein (AFP), volume of resected tissue, resection weight, and the diameter of the largest tumor were provided as continuous variables, while the categorical variables were defined as follows (as provided by the tumor register database)—carcinoembryonic antigen (CEA): normal (<5 ng/ml), intermediate (5–10 ng/ml), high (>10 ng/ml), carbohydrate antigen 19–9 (CA19–9): normal (<40 IE/ml), intermediate (40–50 IE/ml), high (>50 IE/ml), invasion of lymphatic vessels (yes, no), intrahepatic (yes, no), or extrahepatic blood vessels (no, microscopic, macroscopic), cirrhosis at the time of surgery (yes, no), hepatic steatosis (none: <5% of hepatocytes, slight: 5–33%, strong: >34%, which corresponds with the Brunt steatosis grades 0, 1, and 2/3) [22] and were provided as such by the tumor registers.

Because of the lack of any natural grouping tendencies within the HDAC immunoreactivity scores, patients were stratified into low and high HDAC expression groups based on the median expression levels of each isoenzyme.

Univariate analyses between different subgroups were computed using the Mann–Whitney *U* test (continuous and categorical data) as well as with Pearson's χ^2 test (nominal data). Correlation of continuous variables was analyzed with Spearman's rank-order correlation. Univariate analysis of variance (ANOVA) was used to test for differences between the Child-Pugh groups (using least significant difference test and the Bonferroni's post hoc test to adjust for multiple comparisons). Univariate survival analysis was performed using the Kaplan–Meier method comparing the survival curves with the log-rank test. For multivariate survival analysis, the Cox proportional hazards model was used. All tests were performed two tailed. *P* values of less than 0.05 were considered statistically significant.

Results

The clinicopathological data of the patients are summarized in Tables 1, 2, and 3. Histological samples were available from 170 HCC patients along with corresponding normal hepatic tissue for each patient. Mean age at diagnosis was 61.7±11.2 years with 85.3% male and 14.7% female patients. According to the seventh edition of the TNM classification [23], stage distribution of the primary tumors was 37.2%, 28.8%, 27.6%, 2.4%, and 1.8% for pT1, pT2, pT3a, pT3b, and pT4, respectively. Nodal status was negative (pN0) in 85.7% of patients and positive (pN1) in 14.3%. All HCC were curatively resected (R0). Additionally, most cases (91.4%) lacked distant metastases (M0). Distribution of tumor grades was 13.1%, 59.8%, and 27.1% for G1, G2 and G3, respectively. Of all patients, 48.4% were

Table 2 Laboratory parameters

	Cases with data available	Mean±SD
Albumin (g/l)	99	38.54±7.27
GOT (U/l)	48	61.06±59.01
GPT (U/l)	46	58.87±55.75
Total bilirubin (mg/dl)	114	1.15±1.1
Thromboplastin time (quick,%)	43	85.3±16.84
Gamma-GT (U/l)	43	234.65±412.17
LDH (U/l)	31	223.32±65.59
CHE (U/l)	37	4,306.32±2,015.9
AFP (ng/ml)	124	8,379.87±56,168.74
Volume of resected tissue (cm^3)	82	1,562.33±1,702.29
Resection weight (g)	64	635.63±626.8
Diameter of largest tumor (mm)	143	31.26±36.78

classified as Child A, 27.8% Child B, and 7.1% Child C, while 16.7% did not show cirrhosis at the time of diagnosis. Within the Child-Pugh classification groups, there were no significant differences in the distribution of tumor grade and pT stage (ANOVA, $p>0.1$). Because of the retrospective nature of this study, which spans two centers, not all clinical data were available for all patients. Table 2 indicates mean values along with the number of cases with available data for each value.

Table 3 Additional laboratory and pathologic parameters

	Cases with data available	Category	*N* (percent of total)
CEA	42	Normal	38 (90.5%)
		Intermed	2 (4.8%)
		High	2 (4.8%)
CA19-9	39	Normal	29 (74.4%)
		Intermed	4 (10.3%)
		High	6 (15.4%)
Intrahepatic vessel invasion	78	Yes	14 (17.9%)
		No	64 (82.1%)
Extrahepatic vessel invasion	83	No	67 (80.7%)
		Microscopic	10 (12.0%)
		Macroscopic	6 (7.2%)
Invasion of lymphatic vessels	83	Yes	4 (4.8%)
		No	79 (95.2%)
Number of tumors	134	1	113 (84.3%)
		2	16 (11.9%)
		≥3	5 (3.7%)
Steatosis	52	None	28 (53.8%)
		Slight	7 (13.5%)
		Strong	17 (32.7%)
Cirrhosis	143	Yes	100 (69.9%)
		No	43 (30.1%)

Table 3 summarizes additional categorized pathologic and laboratory findings that were used in the statistical analysis.

Expression pattern of HDACs 1–3 and 7 isoenzymes in HCC and adjacent normal hepatic tissue

In general, all HDAC class I isoenzymes were expressed both in the majority of tumor samples and in the adjacent uninvolved hepatic tissue. Negative status (IRS=0) for the HDACs 1, 2, or 3 isoenzymes in tumor tissue was observed in 15, 9, and 1 cases, respectively (8.8%, 5.3%, and 0.6%), vs. 23, 11, and 12 cases in the corresponding normal hepatic tissue (13.5%, 6.5%, and 7.1%). Complete negative staining for HDACs 1–3 (IRS=0 for all three isoenzymes simultaneously) was observed in three cases (1.8%) within normal hepatic tissue and in no case of the tumors. If present, inflammatory cells were also positive for HDACs 1–3 and were not included in the analysis.

HDACs 1–3 were expressed in the nuclei of cancer cells and in the nuclei of corresponding normal hepatocytes. There was no cytoplasmic expression in either tumor or cancer cells for HDACs 1 and 2, while HDAC3 was occasionally observed as granular cytoplasmic staining. All three isoenzymes exhibited higher IRS in cancer cells compared to uninvolved normal hepatocytes: median HDAC1 IRS in normal uninvolved hepatocytes was 3 (quartiles 2–5) vs. 4 (quartiles 2–5) (Mann–Whitney *U* test, $p=0.034$) in tumor tissue, median HDAC2 IRS 4 (quartiles 3–5) vs. 5 (quartiles 4–6) ($p<0.001$), median HDAC3 IRS 4 (quartiles 3–5) vs. 5 (quartiles 5–6) ($p<0.001$), and median Ki-67 IRS 1 (quartiles 1–1) vs. 1 (quartiles 1–2) ($p<0.001$).

HDAC-positive cancer cells were homogenously distributed throughout the tumor section, as exemplified on traditional slides (Online resource 1). Figure 1 shows representative examples of HDAC and Ki-67 expression from the TMA in normal hepatocytes as well as in grades 1, 2, and 3 tumors. In some cases, we observed differential HDAC expression within the same tumor, in what appeared to be a more malignant progressive cell clone and which corresponded to higher-grade tumor cells (Fig. 1c).

HDAC7 expression was generally lower compared to HDACs 1–3 and stained positive in endothelial cells within tumors and within endothelial cells of uninvolved hepatic tissue, without showing a clear preference for any subcellular compartment (Fig. 1b). Median IRS in endothelial cells within normal hepatic tissue and in tumor endothelium was 2 (quartiles 1–2), without showing any significant differences in expression ($p=0.579$). Weak expression in tumor cells or normal hepatocytes was observed occasionally. Complete negative staining (IRS=0) for HDAC7 was observed in 56 samples (32.9%) in endothelia of normal hepatic tissue and in 60 tumor samples (35.3%).

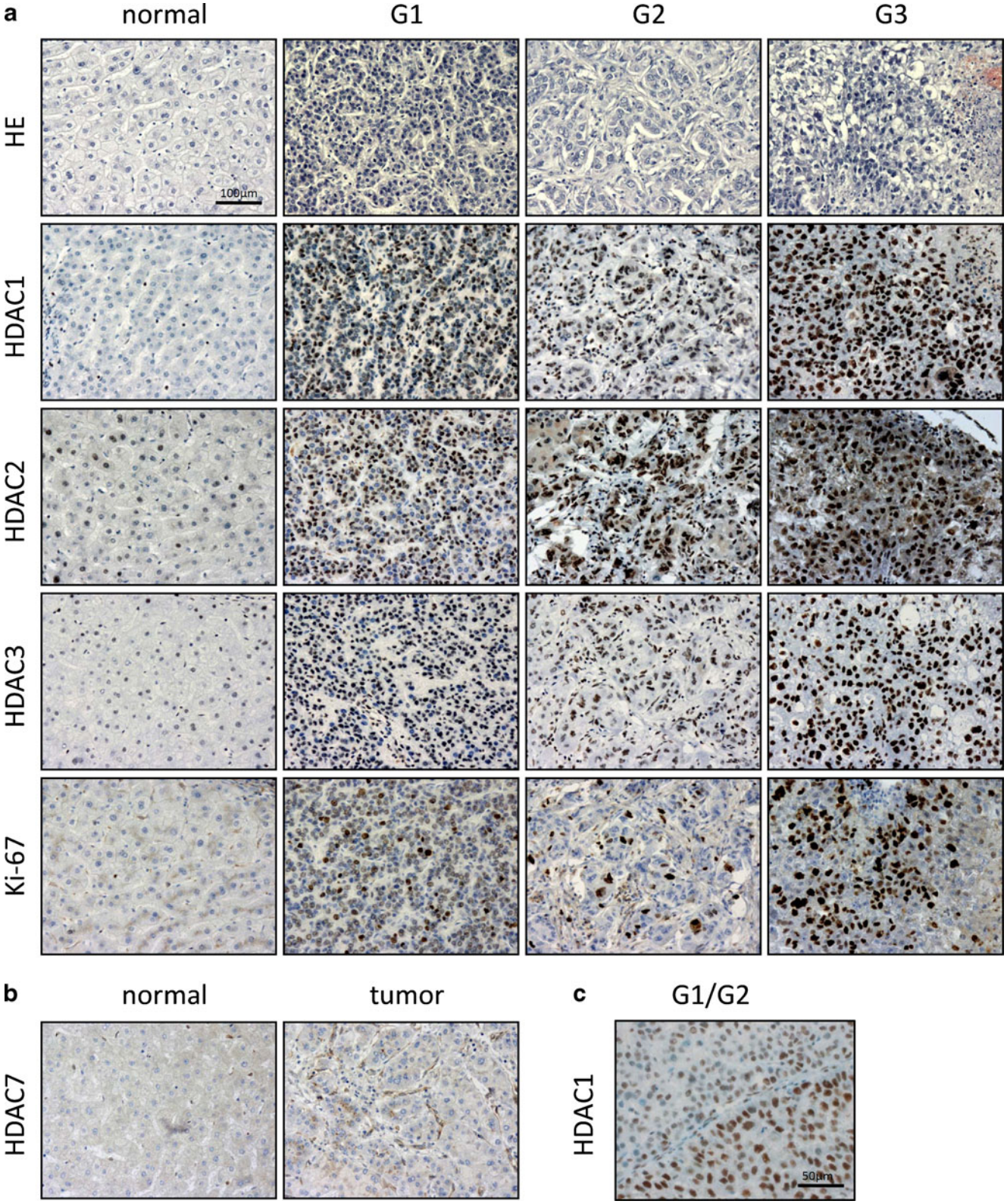

Fig. 1 Representative photomicrographs of HDAC isoenzymes and Ki-67 immunohistochemistry in uninvolved liver tissue and HCCs of different histological grades. **a** Expression of class I HDACs 1, 2, and 3 and of Ki-67. **b** Expression of HDAC7 in normal and HCC tissue. **c** Differential expression of HDAC1 within the same tumor showing higher expression in a G2 subclone than in juxtaposed G1 differentiated tumor areas. Magnification is ×200 for **a** and **b** and ×400 for **c**

As described previously in other solid tumors, expression levels of HDAC isoforms show concordance among themselves [12, 14, 24], with tumor proliferation and tumor dedifferentiation. Using Spearman's correlation coefficient, we compared tumor HDAC immunoreactivity scores between the isoenzymes, with Ki-67 and tumor grades (Table 4). Tumor IRS of HDACs 1–3 correlated significantly with each other and with Ki-67 expression ($p<0.001$). HDACs 1–3 expression in uninvolved and tumor tissue also correlated with each other, showing an overall lower correlation coefficient of maximal $r=0.332$. The expression of HDACs 1–3 and Ki-67 correlated significantly with tumor grade ($p<0.001$). HDAC7 expression did not correlate with any parameter.

Relationship between HDAC isoenzyme expression and clinicopathological factors

In order to assess the relationship between HDAC expression and other clinicopathological parameters, we divided the patients in two groups based on median tumoral HDAC expression of each isoenzyme independently (low vs. high expression, HDAC1 IRS≤4 vs. >4; HDACs 2 and 3 ≤5 vs. >5).

Figure 2 shows the relationship of HDAC expression with pathological parameters which are used to describe the aggressiveness and progression of the tumors and with the clinically prognostic Child-Pugh status. High HDAC expression was associated with tumor dedifferentiation for all three isoenzymes ($p<0.05$, χ^2 test), as indicated by a higher number of G3 and a lower number of G1 tumors in the high HDAC expression groups. High HDACs 1 and 2 isoenzyme expression were associated with pT status, indicated by an increased number of pT3 tumors in the high HDAC2 expression group (HDAC1 $p<0.05$, χ^2 test). Interestingly, we observed an inverse relationship between HDAC isoenzyme expression and Child-Pugh score: high HDAC2 expression was significantly associated with an increased number of child A cases (HDAC2 $p<0.05$, χ^2 test).

Table 4 Correlation analysis showing the Spearman's correlation coefficients (r) for immunoreactivity scores of HDAC isoenzyme and Ki-67 expression and tumor grades

	HDAC2	HDAC3	Ki-67	Grade
HDAC1	0.636	0.530	0.591	0.468
HDAC2		0.544	0.534	0.389
HDAC3			0.515	0.489
Ki-67				0.513

All values were significant at $p<0.001$. HDAC7 did not show a correlation with any other parameter

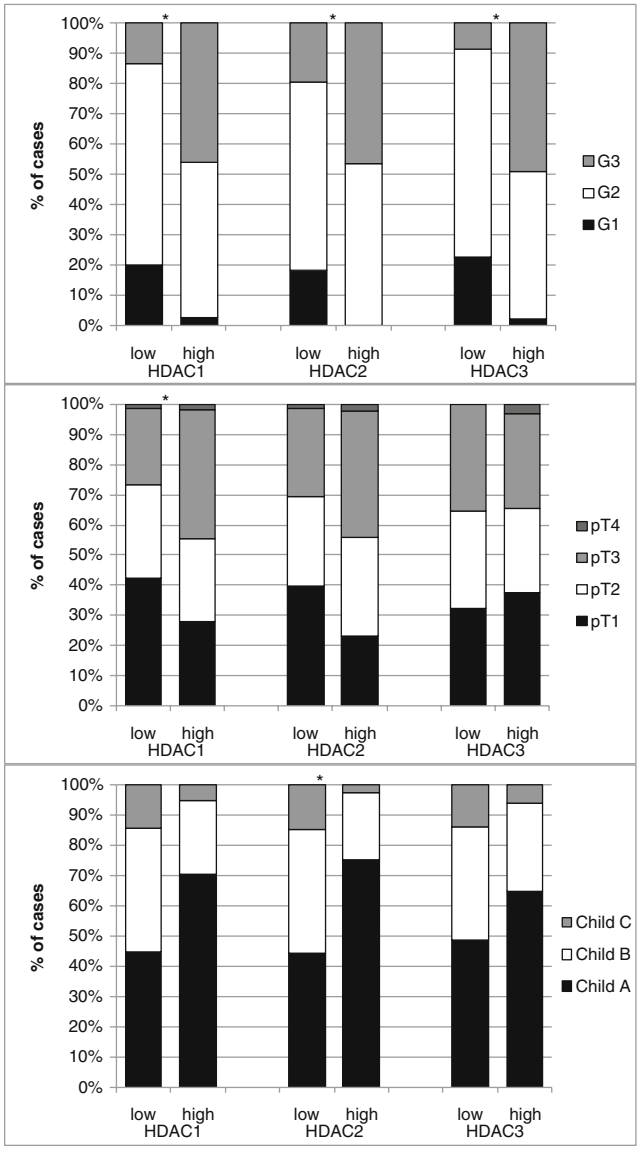

Fig. 2 Tumor differentiation, ungrouped pT, and Child-Pugh status in dependence on HDAC isoform expression levels. Grouped HDAC expression correlates positively with tumor dedifferentiation for all isoenzymes. Significant correlation is also observed for HDAC1 expression with pT status and for HDAC2 with the Child-Pugh classification. *Asterisks* indicate a significance level of $p<0.05$ (χ^2 test)

We further compared the low and high HDAC expression groups with various clinical and pathological data. As illustrated in Table 5, low and high HDAC1 expression groups differed significantly with respect to the volume/weight of the resected tissue, Ki-67 score, tumor grade, steatosis of the hepatocytes, distribution of the patients within the Child-Pugh subgroups, and intrahepatic blood vessel invasion. Low and high HDAC2 expression differed significantly in the AFP levels, volume of the resected tissue, Ki-67 score, tumor grade, and patient distribution in the Child-Pugh scoring. Low and high HDAC3 expression

Table 5 Analysis of continuous and grouped clinicopathological parameters in low and high HDAC expression groups

	Expression level	HDAC1			HDAC2			HDAC3		
		No.	Mean±SD	*p* value	No.	Mean±SD	*p* value	No.	Mean±SD	*p* value
AFP (ng/ml)	Low	51	12,181.55±82,692.61	0.216	68	9,413.23±71,712.22	**<0.001**	55	11,170.3±79,650.45	0.216[a]
	High	47	5,622.72±27,275.57		36	6,838.88±30,665.69		50	54,38.71±26,438.81	
Volume of resected tissue (3rd root of volume, mm)	Low	35	115.8±108.89	**0.002**	41	110.68±108.43	**0.035**	24	106.17±101.06	0.468[a]
	High	23	92.11±100.34		18	92.95±98.43		36	107.38±110.59	
Resection weight (g)	Low	26	700.38±459.74	**0.004**	32	552.81±421.81	0.051	19	536.95±416.73	0.397[a]
	High	18	276.72±311.85		13	311.69±321.84		27	495.93±479.55	
Ki-67 (score)	Low	75	1.13±1.09	**<0.001**	91	1.35±1.52	**<0.001**	74	1.08±0.96	**<0.001[b]**
	High	55	2.93±2.32		46	2.96±2.11		65	2.78±2.24	
Tumor grade (n in groups norm./G1/G2/G3)	Low	62	2/12/40/8	**0.001**	77	1/14/47/15	**0.008**	60	2/13/40/5	**<0.001[b]**
	High	40	1/1/20/18		31	1/0/16/14		50	1/1/24/24	
pT category (pT1/pT2/pT3/pT4)	Low	71	30/22/18/1	0.194	88	35/26/26/1	0.267	68	22/22/24/0	0.435[b]
	High	54	15/15/23/1		43	10/14/18/1		64	24/18/20/2	
Steatosis (none, slight, strong)	Low	25	19/0/6	**0.001**	28	17/2/9	0.222	15	9/0/6	0.219[b]
	High	16	4/5/7		14	5/3/6		28	14/5/9	
Child-Pugh classification (A, B/C)	Low	49	22/27	**0.028**	54	24/30	**0.005**	43	21/22	0.144[b]
	High	37	26/11		36	27/9		48	31/17	
Intrahepatic vessel invasion (no/yes)	Low	33	32/1	**0.048**	39	37/2	0.110	22	0/22	0.059[b]
	High	21	17/4		16	13/3		34	29/5	

The number of cases (*n*) with available retrospective data is given for each parameter. Statistically significant results are printed in *bold*. HDAC low and high groups were divided at the mean HDAC expression in the tumor tissue for each isoenzyme (HDAC1 low IRS≤4, high IRS>4; HDAC2 low IRS≤5, high IRS>5; HDAC3 low IRS≤5, high IRS>5)

[a] Statistical analysis used the Mann–Whitney *U* test

[b] Statistical analysis used the χ^2 -test

differed with respect to tumor grade and Ki-67 expression levels. No differences were found for the low and high HDAC7 groups.

Survival analysis

Using the Kaplan–Meier survival method, we analyzed overall survival after curative surgery in dependence on the HDAC expression status of each of the enzymes and on Ki-67 expression status (Fig. 3). Therefore, the consecutive statistical analysis was performed only for the M0 patient group (91.4% of patients), and then stratified for the pT1/pT2 vs. pT3/pT4 and G1 vs. G2/G3 subgroups.

Patient survival in the whole M0 group was influenced by the HDAC2 expression status: Median survival in the low HDAC2 expression group (IRS≤4) was 32.0 months (standard error 9.4, 95% CI 13.5–50.5) vs. 20.0 months (3.9, 12.3–27.7) in the high HDAC2 expression group (IRS>4, p=0.018, Fig. 3b). HDACs 1 and 3 expression status did not influence survival (Fig. 3a and c) in the whole M0 group.

As expected, patients in the pT1/pT2 group survived longer compared to the pT3/pT4 patients (p=0.038, not shown). In the pT1/2 subgroup, median survival in the low HDAC2 expression group was 47.0 months (15.4, 16.8–77.2) vs. 23.2 months (5.8, 11.9–34.5) in the high HDAC2 expression group (p=0.014, Fig. 3e). In pT3/4 patients, median survival in the low HDAC2 expression group was 32.0 months (11.8, 8.9–55.1) vs. 17.6 months (2.9, 11.9–23.4) in the high HDAC2 expression group (p=0.519, Fig. 3f).

In the low-grade subgroup, median survival in the low HDAC2 expression group was 22.0 months (16.4, 0–54.2) vs. 9.0 months (5.4, 0–19.7) in the high HDAC2 expression group (p=0.015) (Fig. 3d). In the high-grade subgroup, median survival in the low HDAC2 expression group was 40.0 months (11.8, 16.9–63.1) vs. 17.6 months (4.6, 8.6–26.7) in the high HDAC2 expression group (p=0.105,

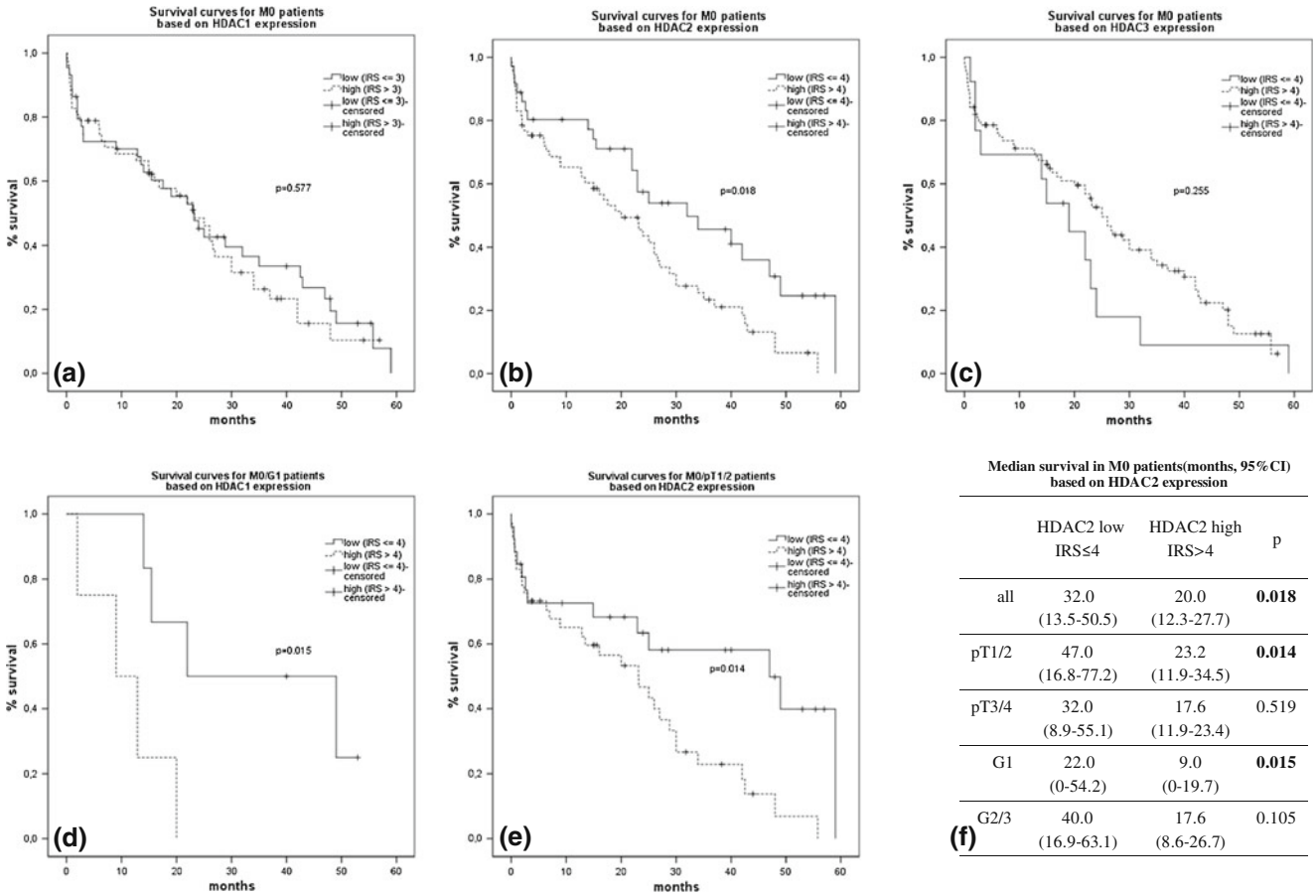

Median survival in M0 patients(months, 95% CI) based on HDAC2 expression

	HDAC2 low IRS≤4	HDAC2 high IRS>4	p
all	32.0 (13.5-50.5)	20.0 (12.3-27.7)	**0.018**
pT1/2	47.0 (16.8-77.2)	23.2 (11.9-34.5)	**0.014**
pT3/4	32.0 (8.9-55.1)	17.6 (11.9-23.4)	0.519
G1	22.0 (0-54.2)	9.0 (0-19.7)	**0.015**
G2/3	40.0 (16.9-63.1)	17.6 (8.6-26.7)	0.105

(f)

Fig. 3 Comparative overall survival in dependence on HDAC expression levels in tumor tissue. Shown are survival data for HDAC1 (**a**), HDAC2 (**b**), and HDAC3 (**c**) in unstratified patients, for HDAC2 stratified for low-tumor grade (G1, **d**) and early-tumor stage (pT1/pT2, **e**), and the survival times in months along with the 95% confidence intervals (**f**). Significance levels were computed using the log-rank test. The low and high HDAC expression groups were divided at IRS 3 for HDAC1 and IRS 4 for HDACs 2 and 3, which corresponds to the mean expression in uninvolved hepatic tissue

Fig. 3f). There was no significant difference in survival between the G1 vs. G2/G3 patients ($p=0.996$), most probably because of the low number of G1 patients compared to the G2/G3 patients (Table 1).

In multivariate analysis with the inclusion of age, tumor grade, pT category, Ki-67 expression, HDACs 1–3 expression as well as HDACs 1–3 expression groups (low, high), HDAC2 retained its independent statistical significance ($p=0.001$, HR 5.5, 95% CI 2.0–14.9)

Discussion

In this study, we show that class I HDACs, i.e., HDACs 1–3, are expressed significantly higher in HCC than in the normal liver and correlate with tumor dedifferentiation and proliferative activity of the tumor cells. In addition to an impact on clinicopathological factors such as resection weight, AFP levels and an association with the Child-Pugh score, we found that patient survival was negatively affected by high HDAC2 expression levels, especially in the pT1/pT2 subgroup of HCC.

Nuclear expression of class I HDAC isoenzymes is a common feature, shared by most carcinomas analyzed for this marker, including colon, gastric, renal prostate and pancreatic cancers, and endometrioid carcinoma [12, 14, 15, 24, 25]. In addition, there are other common factors shared by the HDAC expression studies performed so far: the first one is the positive correlation of HDAC expression with histological grade, which was reported for prostate [15], renal cell [12], colorectal [14], pancreatic [26] and gastric cancer [14], while this was not observed in some tumors like breast cancer [27]. Second, a correlation between HDAC expression with the respective pT categories was shown in renal cell [12], colorectal [14] and gastric [14], but not in prostate cancer [15]. The third common feature is the correlation of HDACs with one another, which was reported for ovarian and endometrial carcinomas [24], renal cell [12], and colorectal cancer [14], suggesting common regulatory mechanisms. In our study, we found a correlation with grading and with the proliferation marker Ki-67. There was also concordance among class I HDAC expression, but interestingly no correlation with pT categories. In the only study investigating HDAC expression in HCC, Rikimaru et al. reported a poorer differentiation which is associated with high HDAC1 expression [16]. Our results are in accordance with these data, and we additionally report a correlation of HDAC2 and HDAC3 (but not HDAC7) with tumor dedifferentiation in HCC. In the same study, a higher incidence of cancer cell invasion into the portal vein in the high HDAC1 expression group is reported. Concordantly, our data show a correlation between high HDAC1 expression and intrahepatic vessel invasion.

The observed HDAC7 expression pattern in our samples is in line with a study in pancreatic adenocarcinomas [13] showing a cytoplasmic and nuclear staining, which has been described for class II HDACs (HDACs 4, 5, 7, and 9), as these enzymes exhibit nucleocytoplasmic shuttling [6]. Although in this study HDAC7 was associated with pancreatic adenocarcinoma, we could not establish a similar role for HDAC7 in our samples: no statistically different expression between normal and tumor tissue as well as no correlation with either proliferation or any of the other three HDAC isoenzymes was found. This is a novel finding, as the expression of HDAC7 has so far not been investigated in HCC and here we show that it does not seem to play a role in this malignancy. A study investigating the effects of siRNA-mediated knockdown of various HDACs on Hela cancer cell proliferation showed no effect with regard to HDAC7, in contrast to HDACs 1 and 3, a finding which is in line with our data [28]. While most studies agree on the common factors of HDAC expression in tumors, there is diverse data regarding their association with clinicopathological and laboratory data. Our data show an increased percentage of cases with Child A cirrhosis in the high HDACs 1–3 expression groups, reaching significance for HDAC2. While a variety of speculations about this finding are possible, we mainly attribute it to the patient selection bias: Patients in our cohort were selected for curative surgery, most of them (48%) represent Child A cirrhosis and, along with this, a less advanced disease stage. On the other hand, the finding that in our patients, hepatic steatosis occurs more often in the high HDAC1 expression group, suggests a possible regulation of the individual isoenzymes under certain conditions, and possibly also changes in HDAC expression levels prior to tumor initiation.

In previous studies, HDAC expression showed varying correlations with overall survival and tumor stage [12, 14, 15, 27]. This indicates that while the expression of HDACs 1–3 correlates with cellular proliferation and histological grade in many investigated tumors, it does not necessarily translate into other prognostically relevant factors. However, in our patient group, the histopathological correlations with tumor grade and proliferation translate into clinical outcome with regard to HDAC2, for which high expression is associated with poor outcome, both in the general patient population, comparing all cases (HDAC low vs. high expression) as well as in low-grade (G1) and early-tumor stage (pT1/2) patients. This finding corroborates a previous result from prostate cancer patients, where HDAC2 was associated with PSA relapse-free survival [15]. In the first study of HDAC1 expression in HCC, it was shown by Rikimaru et al. that low HDAC1 expression is linked to better overall survival [16]. In comparison to our patient collective, those results were obtained in a smaller cohort of Asian HCC patients who develop HCC on the basis of

chronic viral hepatitis in the majority of cases, while in our cohort only 20% of the patients had a virus-related disease. These differences in etiology could also explain our findings that HDAC2, but not HDAC1 or HDAC3, were prognostic markers in our cases, in contrast to the results reported from Asia. Interestingly, patients with G2/3 tumors showed a better (although not significant) overall survival both in the low (p=0.819) and high (p=0.112) HDAC expression groups compared to G1 tumors. In our cohort, patients with G1 tumor grades are rare compared to patients with G2/G3 (Table 1), and this result might be explained by a disproportionately small G1 group. In contrast, the pT1/2 and pT3/4 groups are more balanced and the results are concordant with what was expected.

Although we show a direct influence of HDAC expression on survival, these findings have to be carefully interpreted, since our retrospective data acquisition did not appreciate the importance of second-line therapies, which themselves could crucially influence survival and thus demand further investigations to evaluate and to compare HDAC expression patterns in resected primary, resected recurrent, or differentially treated HCCs. However, in our cohort, this would lead to small-sized groups and possible selection bias, prompting us to omit such stratification, as done by Rikimaru et al. [16], since we wanted to investigate the expression pattern of HDACs isoenzymes in primary HCC as well as the impact on overall survival.

While most HDAC studies so far have focused on expression analyses in various tissues and tumor entities, very few studies have addressed the specific roles of the HDAC isoenzymes. In endometrial carcinoma, HDAC2, but not HDAC1, was found to be associated with increased proliferation and poor prognosis. HDAC inhibition decreased proliferation and increased apoptosis in vitro, most likely through HDAC2 interaction [29]. In oesophageal adenocarcinomas, HDAC2, but not HDAC1, was associated with tumor dedifferentiation [30]. The role of HDAC2 is further emphasized through a study in which specific knockdown of HDAC2 had the strongest impact on cell viability [14]. These and further studies in endometrial stromal sarcoma cells [31] and in colon and cervical cancers [32] indicate a specific involvement of the HDAC2 isoenzyme in the context of tumor differentiation, proliferation, and impact on survival. However, the exact mechanisms of the isoenzymes and their distinct functions remain elusive.

Considering the fact that several clinical trials are currently ongoing with different pharmacologic inhibitors of HDAC activity (e.g., NCT00823290 indexed at http://clinicaltrials.gov), studies are urgently warranted to provide novel biomarkers for monitoring treatment response and for sensible patient stratification [19]. Based on our data, the most important factor to analyze in subsequent studies is the susceptibility of HDAC expressing tumors to HDACi treatment and the benefit on survival in this patient group, a claim that is based on the fact that class I HDACs (HDACs 1–3) are highly expressed in HCCs, are associated with clinicopathological factors and correlate with patient survival.

Acknowledgments The authors thank Dr. Peter Rexin and Susanne Lingelbach for their help in this study. This study is supported by a Research Grant of the University Medical Center Giessen and Marburg (UKGM).

Conflict of interest The authors declare that they have no conflict of interest.

References

1. Bosch FX, Ribes J, Cleries R, Diaz M (2005) Epidemiology of hepatocellular carcinoma. Clin Liver Dis 9(2):191–211
2. Llovet JM, Burroughs A, Bruix J (2003) Hepatocellular carcinoma. Lancet 362(9399):1907–1917
3. Okamoto K, Neureiter D, Ocker M (2009) Biomarkers for novel targeted therapies of hepatocellular carcinoma. Histol Histopathol 24(4):493–502
4. Greten TF, Korangy F, Manns MP, Malek NP (2009) Molecular therapy for the treatment of hepatocellular carcinoma. Br J Canc 100(1):19–23
5. Finn RS (2010) Development of molecularly targeted therapies in hepatocellular carcinoma: where do we go now? Clin Canc Res 16 (2):390–397
6. Ocker M, Schneider-Stock R (2007) Histone deacetylase inhibitors: signalling towards p21cip1/waf1. Int J Biochem Cell Biol 39 (7–8):1367–1374
7. Ocker M (2010) Deacetylase inhibitors-focus on non-histone targets and effects. World J Biol Chem 1(5):55–61
8. Di Fazio P, Schneider-Stock R, Neureiter D, Okamoto K, Wissniowski T, Gahr S, Quint K, Meissnitzer M, Alinger B, Montalbano R, Sass G, Hohenstein B, Hahn EG, Ocker M (2010) The pan-deacetylase inhibitor panobinostat inhibits growth of hepatocellular carcinoma models by alternative pathways of apoptosis. Cell Oncol 32(4):285–300
9. Gahr S, Peter G, Wissniowski TT, Hahn EG, Herold C, Ocker M (2008) The histone-deacetylase inhibitor MS-275 and the CDK-inhibitor CYC-202 promote anti-tumor effects in hepatoma cell lines. Oncol Rep 20(5):1249–1256
10. Ocker M, Alajati A, Ganslmayer M, Zopf S, Luders M, Neureiter D, Hahn EG, Schuppan D, Herold C (2005) The histone-deacetylase inhibitor SAHA potentiates proapoptotic effects of 5-fluorouracil and irinotecan in hepatoma cells. J Canc Res Clin Oncol 131(6):385–394
11. Weichert W (2009) HDAC expression and clinical prognosis in human malignancies. Canc Lett 280(2):168–176
12. Fritzsche FR, Weichert W, Roske A, Gekeler V, Beckers T, Stephan C, Jung K, Scholman K, Denkert C, Dietel M, Kristiansen G (2008) Class I histone deacetylases 1, 2 and 3 are highly expressed in renal cell cancer. BMC Canc 8:381
13. Ouaissi M, Sielezneff I, Silvestre R, Sastre B, Bernard JP, Lafontaine JS, Payan MJ, Dahan L, Pirro N, Seitz JF, Mas E, Lombardo D, Ouaissi A (2008) High histone deacetylase 7 (HDAC7) expression is significantly associated with adenocarcinomas of the pancreas. Ann Surg Oncol 15(8):2318–2328

14. Weichert W, Roske A, Gekeler V, Beckers T, Ebert MP, Pross M, Dietel M, Denkert C, Rocken C (2008) Association of patterns of class I histone deacetylase expression with patient prognosis in gastric cancer: a retrospective analysis. Lancet Oncol 9(2): 139–148
15. Weichert W, Roske A, Niesporek S, Noske A, Buckendahl AC, Dietel M, Gekeler V, Boehm M, Beckers T, Denkert C (2008) Class I histone deacetylase expression has independent prognostic impact in human colorectal cancer: specific role of class I histone deacetylases in vitro and in vivo. Clin Canc Res 14(6):1669–1677
16. Rikimaru T, Taketomi A, Yamashita Y, Shirabe K, Hamatsu T, Shimada M, Maehara Y (2007) Clinical significance of histone deacetylase 1 expression in patients with hepatocellular carcinoma. Oncology 72(1–2):69–74
17. Lesko LJ, Atkinson AJ Jr (2001) Use of biomarkers and surrogate endpoints in drug development and regulatory decision making: criteria, validation, strategies. Annu Rev Pharmacol Toxicol 41:347–366
18. Bakhtiar R (2008) Biomarkers in drug discovery and development. J Pharmacol Toxicol Meth 57(2):85–91
19. Llovet JM, Di Bisceglie AM, Bruix J, Kramer BS, Lencioni R, Zhu AX, Sherman M, Schwartz M, Lotze M, Talwalkar J, Gores GJ (2008) Design and endpoints of clinical trials in hepatocellular carcinoma. J Natl Canc Inst 100(10):698–711
20. Amann T, Maegdefrau U, Hartmann A, Agaimy A, Marienhagen J, Weiss TS, Stoeltzing O, Warnecke C, Scholmerich J, Oefner PJ, Kreutz M, Bosserhoff AK, Hellerbrand C (2009) GLUT1 expression is increased in hepatocellular carcinoma and promotes tumorigenesis. Am J Pathol 174(4):1544–1552
21. Hellerbrand C, Amann T, Schlegel J, Wild P, Bataille F, Spruss T, Hartmann A, Bosserhoff AK (2008) The novel gene MIA2 acts as a tumour suppressor in hepatocellular carcinoma. Gut 57(2):243–251
22. Tannapfel A, Denk H, Dienes HP, Langner C, Schirmacher P, Trauner M, Flott-Rahmel B (2010) Histopathological diagnose of non-alcoholic and alcoholic fatty liver disease. Z Gastroenterol 48 (4):486–498
23. Sobin LH, Gospodarowicz MK, Wittekind C (2009) TNM Classification of Malignant Tumours. Wiley-Blackwell
24. Weichert W, Denkert C, Noske A, Darb-Esfahani S, Dietel M, Kalloger SE, Huntsman DG, Kobel M (2008) Expression of class I histone deacetylases indicates poor prognosis in endometrioid subtypes of ovarian and endometrial carcinomas. Neoplasia 10 (9):1021–1027
25. Miyake K, Yoshizumi T, Imura S, Sugimoto K, Batmunkh E, Kanemura H, Morine Y, Shimada M (2008) Expression of hypoxia-inducible factor-1alpha, histone deacetylase 1, and metastasis-associated protein 1 in pancreatic carcinoma: correlation with poor prognosis with possible regulation. Pancreas 36(3): e1–e9
26. Lehmann A, Denkert C, Budczies J, Buckendahl AC, Darb-Esfahani S, Noske A, Muller BM, Bahra M, Neuhaus P, Dietel M, Kristiansen G, Weichert W (2009) High class I HDAC activity and expression are associated with RelA/p65 activation in pancreatic cancer in vitro and in vivo. BMC Canc 9:395
27. Krusche CA, Wulfing P, Kersting C, Vloet A, Bocker W, Kiesel L, Beier HM, Alfer J (2005) Histone deacetylase-1 and −3 protein expression in human breast cancer: a tissue microarray analysis. Breast Canc Res Treat 90(1):15–23
28. Glaser KB, Li J, Staver MJ, Wei RQ, Albert DH, Davidsen SK (2003) Role of class I and class II histone deacetylases in carcinoma cells using siRNA. Biochem Biophys Res Commun 310(2):529–536
29. Fakhry H, Miyamoto T, Kashima H, Suzuki A, Ke H, Konishi I, Shiozawa T (2010) Immunohistochemical detection of histone deacetylases in endometrial carcinoma: involvement of histone deacetylase 2 in the proliferation of endometrial carcinoma cells. Hum Pathol 41(6):848–858
30. Langer R, Mutze K, Becker K, Feith M, Ott K, Hofler H, Keller G (2010) Expression of class I histone deacetylases (HDAC1 and HDAC2) in oesophageal adenocarcinomas: an immunohistochemical study. J Clin Pathol 63:994–998
31. Hrzenjak A, Moinfar F, Kremser ML, Strohmeier B, Staber PB, Zatloukal K, Denk H (2006) Valproate inhibition of histone deacetylase 2 affects differentiation and decreases proliferation of endometrial stromal sarcoma cells. Mol Canc Ther 5(9): 2203–2210
32. Huang BH, Laban M, Leung CH, Lee L, Lee CK, Salto-Tellez M, Raju GC, Hooi SC (2005) Inhibition of histone deacetylase 2 increases apoptosis and p21Cip1/WAF1 expression, independent of histone deacetylase 1. Cell Death Differ 12(4):395–404

Virchows Arch (2011) 459:141–146
DOI 10.1007/s00428-011-1099-5

ORIGINAL ARTICLE

OATP 1B1/1B3 expression in hepatocellular carcinomas treated with orthotopic liver transplantation

Francesco Vasuri · Rita Golfieri · Michelangelo Fiorentino · Elisa Capizzi · Matteo Renzulli · Antonio D. Pinna · Walter F. Grigioni · Antonia D'Errico-Grigioni

Received: 18 April 2011 / Revised: 16 May 2011 / Accepted: 23 May 2011 / Published online: 21 June 2011
© Springer-Verlag 2011

Abstract The organic anion transporter peptides (OATP) 1B1 and 1B3 are hepatocytic-specific transporters determinant for the uptake of the contrast media Gd-EOB-DTPA during magnetic resonance, but variably lost in hepatocellular carcinoma (HCC). Here, we studied a series of HCCs from livers that underwent liver transplantation (OLT) and correlated the expression of OATP 1B1/1B3 with HCC morphological features and the expression of the biliary-type keratins K7 and K19, the latter previously correlated with a worse prognosis after OLT. Seventy-five HCCs from 69 OLT patients were evaluated by histology and immunohistochemistry with monoclonal antibodies against OATP 1B1/1B3, K7, and K19. Histopathological and immunohistochemical features were therefore compared to recipient follow-up data. Thirty-four (45%) HCCs were completely OATP−, and 18 (24%) showed positivity for K7 and/or K19. We observed a significant inverse correlation between OATP and K7/19 expression ($P<0.001$): all OATP+ cases were K7/19−, while all K7+ and/or K19+ cases were OATP−. Sixteen cases were negative for all antibodies. No correlation was found between histopathological features and immunohistochemistry. Twenty-five recipients experienced HCC recurrence, and ten died from neoplastic recurrence. Neither OATP nor keratin expressions were correlated with HCC recurrence, while OATP negativity significantly correlated with HCC-related death after recurrence ($P=0.036$). In conclusion, HCCs show a progressive loss in OATP immunoreactivity that correlates with the gain of a biliary phenotype. Although further studies are required to define these findings better, our results support the idea that OATP could be used together with K7/19 to identify a phenotypical "spectrum" in HCC progression.

Keywords Keratin 19 · Keratin 7 · Gd-EOB-DTPA · Organic anion transporter peptide · Hepatocellular carcinoma · Cholangiocellular carcinoma

F. Vasuri · M. Fiorentino · E. Capizzi · W. F. Grigioni · A. D'Errico-Grigioni (✉)
Pathology Unit, "F. Addarii" Institute of Oncology and Pathology, S. Orsola-Malpighi Hospital,
Viale Ercolani 4/2,
40138 Bologna, Italy
e-mail: derrico@aosp.bo.it

R. Golfieri · M. Renzulli
Radiology Unit, S. Orsola-Malpighi Hospital, Bologna University, Bologna, Italy

A. D. Pinna
Unit of General and Transplantation Surgery, S. Orsola-Malpighi Hospital, Bologna University, Bologna, Italy

Introduction

The prognosis for patients with symptomatic hepatocellular carcinoma (HCC) is very poor, and an improvement in survival is correlated with early diagnosis and early treatment by surgical resection, local treatment, or orthotopic liver transplantation (OLT) [1, 2]. Early diagnosis of HCC is performed by several imaging techniques, among which magnetic resonance imaging (MRI) with 3D gadolinium-enhanced dynamic sequences seems to be the most sensitive, particularly in the identification of early HCCs [3–5].

The organic anion transporter peptides OATP 1B1 (OATP2, SLC21A6) and OATP 1B3 (OATP8, SLC21A8) are liver-specific molecules, located on the basolateral (i.e., sinusoidal) face of hepatocytes. They are transporters of cholephilic organic anions, thus playing an important role in the first step of bile formation [6–10]. OATP is determinant for the uptake of the MRI contrast media Gd-EOB-DTPA [11–13], and it is typically described as inhibited

in malignant liver lesions, which show hypointensity in the hepatobiliary (HB) phase [11]. A recent study suggested that OATP expression induced Gd-EOB-DTPA retention in the HB phase better than tumor differentiation or bile production [12]. Nevertheless, OATP expression in HCC is highly variable, with a percentage of negative cases ranging from at least 20% to 55% according to different series [6, 12, 14]. Furthermore, in a previous gene analysis study, underexpression of OATP 1B1 mRNA was found in 55% of the HCCs examined [15]. The real meaning of this loss in OATP expression is not completely clarified, depending both on HCC loss of differentiation and paracrine factors (e.g., serum cytokines, among which hepatocyte nuclear factor 3β, interleukin-1β, interleukin-6, and tumor necrosis factor-α) that were described to modulate the expression of OATP and other canalicular transporters in HCC [16–18].

Currently, few efforts have been made to find other phenotypical differences among HCCs, to establish better a prognostic behavior. Although a mature hepatocyte classically does not express the biliary-type keratin 7 (K7) and keratin 19 (K19), immunoreactivity for these antibodies was described in up to 30% of HCCs [17–19], despite the absence of biliary morphology [19–23]. Furthermore, some authors described a minor recurrence time and a poorer prognosis in the subset of HCCs expressing K19 [20, 21].

The aim of this study was to correlate the immunohistochemical expression of OATP 1B1/1B3 with the morphological and phenotypical features of a series of HCCs in cirrhotic livers that underwent OLT.

Materials and methods

Patients and histopathology

Informed consent at the moment of surgery was obtained from all patients for the use of surgical specimens. We retrospectively evaluated 69 patients who underwent OLT for genotype 1b HCV hepatic cirrhosis complicated by HCC (57 males and 12 females; mean age at surgery, 56.77±9.66 years; range, 36–82). Sixty-four patients had a single tumor, while five patients showed up to three tumors less than 3 cm in diameter, according to Milan criteria [24]. None of them received pre-OLT local therapy or neoadjuvant chemotherapy. A total of 75 HCCs were finally collected. Histopathological features evaluated for each tumor included: tumor grade according to Edmondson–Steiner [25], neoplastic vascular invasion (present or absent), pattern of growth (expansive or infiltrative), prevalent histological architecture (trabecular, acinar, or solid), tumor size, and tumor stage according to the tumor, node, metastasis (TNM) staging system. In all cases, histology at hematoxylin–eosin confirmed the absence of any area of morphological biliary differentiation.

Fifty-eight (84%) patients were followed over time, and occurrence and timing of HCC recurrences, as well as cancer-related deceases, were recorded. In 11 (16%) cases, follow-up data were not available, primarily because some recipients were followed in different Italian regions after transplantation, making very difficult the collection of adequate post-OLT data.

We also included five normal liver specimens, seven combined hepatocellular–cholangiocellular carcinomas (CHC), and three pure cholangiocellular carcinomas (CC) as controls for immunohistochemistry (IHC) reactions and for comparison of the results obtained. Primary biliary malignancies were graded according to the WHO.

Immunohistochemistry

Three-micrometer-thick sections were cut from formalin-fixed, paraffin-embedded specimens, mounted on positively charged slides (SuperFrost Plus, Menzel, Braunschweig, Germany), and baked overnight at 37°C. Keratin 7 and 19 IHC stainings were performed with prediluted monoclonal antibodies (Cytokeratin7 CONFIRM, clone SP52, and Cytokeratin19, clone A53-B/A2.26; Ventana Medical Systems, Tucson, AZ, USA) in the BenchMark XT automated stainer (Ventana) using the Ultraview DAB Detection kit (Ventana). Immunostaining for the human organic anion transporters OATP 1B1 (OATP2, SLC21A6) and OATP 1B3 (OATP8, SLC21A8) was performed manually as previously described [6] with a dilution of 1:100 of the original concentration of primary antibody (clone mMDQ, PROGEN Biotechnik, Heidelberg, Germany) which detects both SLC21A6 (OATP 1B1) and SLC21A8 (OAPT1B3). Negative controls were performed by omitting the primary antibodies. The percentage of positive cells was semi-quantitatively assessed, and the presence of scattered positive cells (<5%) was considered as negative.

Statistical analysis

Data are reported as means ± standard deviations and ranges. The Spearman test, the Mann–Whitney test, and the Kaplan–Meier log rank analysis for survival were applied when appropriate. Data analysis was performed using SPSS for Windows (version 17.0). A two-tailed *P* value less than 0.05 was used to define statistical significance.

Results

Histology

The 75 HCCs were graded as: Edmondson–Steiner grade 1 in 3 (4%) cases, grade 2 in 13 (17%), grade 3 in 53 (71%), and grade 4 in 6 (8%). Neoplastic vascular invasion was

Table 1 Biliary-type keratin expression and follow-up data of OATP-positive and OATP-negative hepatocellular carcinomas (sig.: statistical significance)

	OATP+	OATP−	Sig.
K7/K19-positive HCC (n=18)	0 (0%)	18 (100%)	P<0.001[a]
HCC Recurrence (n=25)	11 (44%)	14 (56%)	P=0.310[a]
HCC-related decease (n=10)	2 (20%)	8 (80%)	P=0.036[b]

[a] Mann–Whitney test

[b] Kaplan–Meier log rank analysis

detected in 54 (72%) cases. The pattern of growth was pushing in 15 (20%) cases, infiltrative in 43 (57%), and mixed pushing and infiltrative in 17 (23%). Most HCCs showed generally a mixed architecture, with a prevalent trabecular pattern in 28 (37%) cases, a prevalent solid pattern in 25 (33%), and a prevalent acinar pattern in 22 (30%). Tumor size ranged from 0.5 to 5 cm (mean, 2.48± 1.29 cm); the five patients with multiple lesions showed HCCs <3 cm in diameter. According to the TNM staging system, 15 (22%) patients had stage I HCCs, 44 (64%) had stage II, 7 (10%) had stage III (involvement of major vascular structures and/or extrahepatic spread), and 3 (4%) had stage IV (lymph node or distant metastasis detected during OLT).

Liver tissue surrounding HCCs showed a complete cirrhosis in all cases, with mild inflammatory activity in 49 patients and moderate activity in 20. Biliary duct proliferation of variable degree was observed in most cases.

Immunohistochemistry

On IHC grounds, 18 out of 75 HCCs (24%) showed positivity (more than 5% of positive cells) for at least one of the two biliary cytokeratins: in particular, five cases were K19+ and K7−, seven cases were K7+ and K19−, and six cases showed double positivity. A total of 41 (55%) HCCs showed OATP expression at the perisinusoidal membrane level, with a percentage of positive neoplastic hepatocytes ranging from 30% to 80% (mean, 57.14±23.99%), and with different expression patterns, ranging from diffuse to patchy. Thirty-four (45%) HCCs were completely negative or showed only a few scattered cells positive for OATP (less

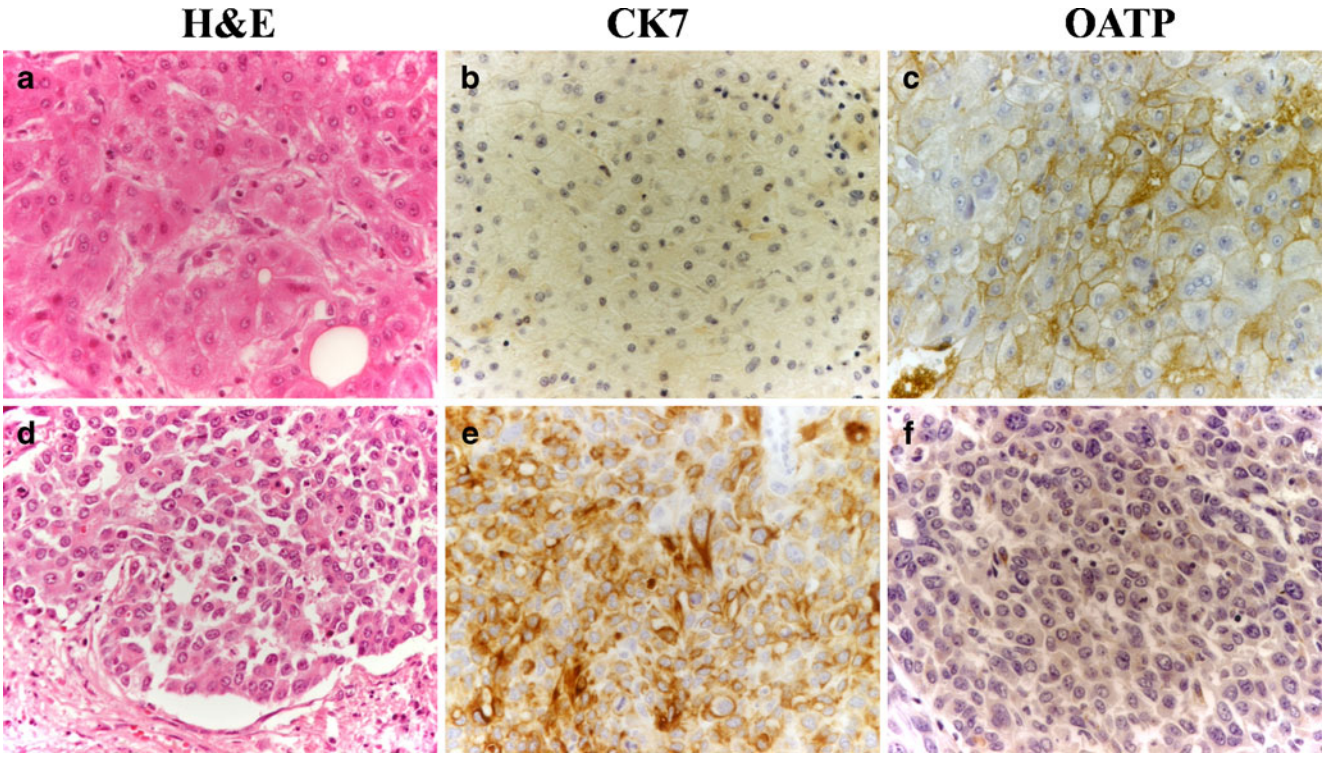

Fig. 1 Two cases of HCC without morphological features of biliary differentiation (**a**, **d**) and with opposite immunohistochemical profiles. The *upper* HCC is completely negative for K7 (**b**) and shows a diffuse membrane positivity for OATP (**c**). Conversely, the *lower* HCC is strongly positive for K7 (**e**) and completely negative for OATP (**f**)

Table 2 Differences in histopathological features between the 58 followed recipients with and without HCC recurrence (sig.: statistical significance)

[a] Mann–Whitney test

	Recurrence (n=25)	No recurrence (n=33)	Sig.[a]
Mean tumor size (mm)	35.9±17.8	25.4±13.6	P=0.017
Vascular invasion	22 (88%)	17 (51%)	P=0.017
Infiltrative growth pattern	20 (80%)	14 (42%)	P=0.019
Edmondson's grade 3 or 4	24 (96%)	23 (70%)	P=0.008

than 5% of neoplastic hepatocytes). Cirrhotic tissue adjacent to HCC showed a patchy or diffuse positivity for OATP in cytoplasms and along the perisinusoidal membrane, sometimes diffuse in the regenerative nodules and sometimes more pronounced in periseptal hepatocytes. Normal liver tissue showed a constant positivity, with an increasing gradient from periportal to centrilobular hepatocytes, as previously reported [6].

As expected, the three CC in our series showed a strong immunoreactivity for K7 and K19 and a total negativity for OATP. All the seven CHC cases resulted OATP−, both in biliary and hepatocellular areas, with variable positivity for K7 and K19.

Correlation among variables

No statistically significant correlation between K7/19 and OATP expression and the collected histopathological features was found (data not shown). Of note, a strong inverse correlation was found between OATP and biliary keratin expression (P<0.001, Spearman test; see also Table 1). In particular, all the 41 OATP+ HCCs were negative for biliary keratins, and conversely, all the 18 HCCs expressing K7 and/or K19 were invariably OATP− (see Fig. 1). Finally, 16 cases were negative for both OATP and K7/19.

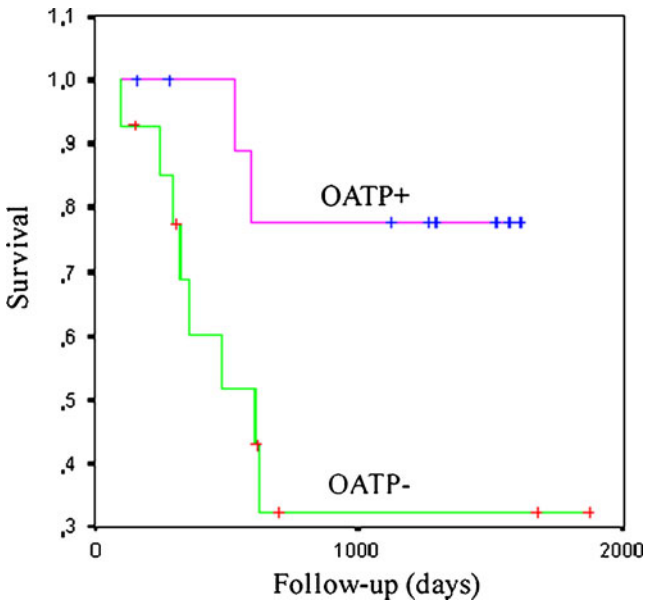

Fig. 2 Kaplan–Meier curve of survival of the patients with HCC recurrence after OLT, divided according to the OATP expression of the primary tumor. At 2 years after OLT, 80% of the patients with OATP+ HCC are alive, versus 30% of the patients with OATP− HCC. This difference in recipient survival is statistically significant at P=0.036 level

Follow-up and recipient survival

Fifty-eight recipients were followed over time, with a mean follow-up time of 852±522.75 days (range, 40–1,876) and a median follow-up time of 985 days after OLT. Twenty-five (43%) patients experienced HCC recurrence, with a mean recurrence time of 299±214 days (range, 29–978) and a median recurrence time of 283 days. HCC recurrence was directly correlated to Edmondson's grade (P=0.008), vascular invasion (P=0.017), infiltrative growth pattern (P=0.019), tumor size (P=0.017, see also Table 2), and TNM stage (P=0.008), while no correlation with OATP, K7 or K19 expression, and tumor recurrence was found (P=0.310, P=0.243, and P=0.124, respectively, Mann–Whitney test). The presence of multiple tumors (all within the Milan criteria) was not correlated with HCC recurrence (P=0.423).

Ten recipients died of neoplastic recurrence after a mean of 417±176 days (range, 102–622): eight had an OATP− HCC at the time of OLT, representing 23.5% of the OATP-negative group, while two had OATP+ HCC, which represents 5% of the OATP+ group. Interestingly, the loss of OATP correlated with HCC-related death after recurrence (P=0.036, Kaplan–Meier log rank analysis; see Fig. 2 and Table 1). Conversely, survival after recurrence was not significantly related to K7 and/or K19 positivity (P=0.856 and P=0.159, respectively), nor to the presence of multiple HCC (P=0.221) and the collected histopathological tumor features (data not shown).

Chemotherapy (CHT) was performed after systemic HCC recurrence (i.e., extrahepatic localization of recurrent HCC) in nine out of 25 cases, with capecitabine or gemcitabine: five of these recipients had OATP-negative HCC, and three (60% of this group) died of HCC recurrence; four had OATP-positive HCC, with no recorded HCC-related deaths. Among the remaining 16 recipients who did not receive CHT, nine had OATP-negative HCC, among which five (56% of this group) died of neoplastic recurrence, and seven had OATP-positive HCC, with two

(28%) HCC-related deaths. No changes in survival rates were therefore found in CHT recipients, both in OATP-negative HCCs and OATP-positive HCCs (data not shown).

Discussion

In this paper, we describe the immunoreactivity for OATP in a series of HCCs treated with OLT, and we compare it to tumor histopathological features and biliary-type keratin expression. The OATP isoforms 1B1 and 1B3 are hepatocyte specific, while biliocytes and biliary malignancies are invariably negative (as confirmed also by our data) [6]. In the last few decades, several studies have made it possible to identify a morphological spectrum in primitive carcinomas of the liver, from HCC to CC [19–23, 26]. The morphological features of HCC and CC are quite dissimilar and well recognizable. However, tumors with morphological features of HCC can show phenotypical aspects both of hepatocytic and biliary lineages. Among these aspects, the immunoreactivity for K7 and K19 in neoplastic hepatocytes has been used as criteria to identify this spectrum in HCC progression. In particular, according to some authors, the phenotypical expression of K19 implies a major risk of a faster recurrence and an overall worse prognosis [20, 21]. In this study, we analyzed 75 primary hepatic tumors, in the absence of any morphological biliary features. Positivity for K7 and/or K19 was found in 24% of HCCs, very close to the 29% originally found by Wu et al. [19]. Interestingly, OATP was always negative in this group, while it was conversely expressed by the majority (71%) of the K7/19-negative HCCs. An inverse correlation therefore exists between the OATP expression in the basolateral hepatocytic membrane and the acquisition of a biliary "phenotype" by the same hepatocytes. Although the meaning of this correlation is not clear, since OATP and keratins are molecules with different functions and intracellular localization, our findings seem to support once more the existence of a morphological spectrum in liver malignancies. HCCs evaluated in this study showed a hepatocellular morphology, and the biliary-type keratin expression could develop from a dedifferentiation process or could represent a "stem/progenitor cell immunophenotype" as recently defined [27].

Besides the totally OATP-negative HCCs, all tumors in our series showed a variable loss in OATP expression—in comparison with the surrounding cirrhotic tissue—with a mean percentage of positive hepatocytes of 57%. This is particularly important also because OATP expression in HCC is strongly correlated to HB-phase intensity during MRI [12, 14, 28]. In this paper, we describe for the first time the strong correlation between OATP negativity and the expression of at least one biliary-type keratin. Furthermore, we found a significantly higher HCC-related death rate among the recipients with recurrence of OATP-negative HCC. This more aggressive behavior seems to be related more to the loss of OATP than to the expression of biliary keratins, at least in our series. A possible mechanism explaining why recurrence-related death rate changes with OATP, while recurrence rate does not, could be related to a different response to the medical treatment after HCC recurrence. In our series, just the 36% of recipients with HCC recurrence received CHT, but the survival rates in OATP-negative HCCs were similar independently from CHT. The presence or absence of the transmembrane carriers could play a pivotal role in the pharmacokinetics of chemotherapy drugs [7], but other factors can probably explain the worst prognosis observed in the OATP-negative HCCs after recurrence. It is noteworthy that in our series, no clear correlation between biliary keratins and HCC recurrence was found, unlike other authors [20, 21]: other perspective studies are certainly required in order to find the real prognostic value of these markers, especially in a very challenging setting such as the transplanted (and immunosuppressed) patients.

In conclusion, HCCs show a progressive loss in OATP immunoreactivity; this loss correlates well with the gain of a biliary phenotype by the neoplastic hepatocytes, and finally, OATP expression is totally lost in CHC and CC cases. These observations may justify the progressive hypointensity of many HCCs at MRI.

In our series of HCCs treated with OLT, the expression of OATP and K7/19 did not correlate with neoplastic recurrence, but OATP negativity alone correlated with a worse prognosis after recurrence (P=0.036). Other studies are required to define these conclusions better, particularly with patients with HCCs treated with OLT.

Conflict of interest statement We declare that we have no conflict of interest.

References

1. Mazzaferro V, Llovet JM, Miceli R, Bhoori S, Schiavo M, Mariani L, Camerini T, Roayaie S, Schwartz ME, Grazi GL et al (2009) Predicting survival after liver transplantation in patients with hepatocellular carcinoma beyond the Milan criteria: a retrospective, exploratory analysis. Lancet Oncol 10:35–43
2. Xu LB, Wang J, Liu C, Pang HW, Chen YJ, Ou QJ, Chen JS (2010) Staging systems for predicting survival of patients with hepatocellular carcinoma after surgery. World J Gastroenterol 16:5257–5262
3. Hayashi M, Matsui O, Ueda K, Kawamori Y, Gabata T, Kadoya M (2002) Progression to hypervascular hepatocellular carcinoma: correlation with intranodular blood supply evaluated with CT during intrarterial injection of contrast material. Radiology 225:143–149

4. Hayashi M, Matsui O, Ueda K, Kawamori Y, Kadoya M, Yoshikawa J, Gabata T, Takashima T, Nonomura A, Nakanuma J (1999) Correlation between the blood supply and grade of malignancy of hepatocellular nodules associated with liver cirrhosis: evaluation by CT during intraarterial injection of contrast medium. AJR Am J Roentgenol 172:969–976
5. Leoni S, Piscaglia F, Golfieri R, Camaggi V, Vidili G, Pini P, Bolondi L (2010) The impact of vascular and non vascular findings on the non invasive diagnosis of small hepatocellular carcinoma based on EASL and AASLD criteria. Am J Gastroenterol 105:599–609
6. Cui Y, König J, Nies AT, Pfannschmidt M, Hergt M, Franke WW, Alt W, Moll R, Keppler D (2003) Detection of the human organic anion transporters SLC21A6 (OATP2) and SLC21A8 (OATP8) in liver and hepatocellular carcinoma. Lab Invest 83:527–538
7. Kalliokoski A, Niemi M (2009) Impact of OATP transporters on pharmacokinetics. Br J Pharmacol 158:693–705
8. Oswald M, Kullak-Ublick GA, Paumgartner G, Beuers U (2001) Expression of hepatic transporters OATP-C and MRP2 in primary sclerosing cholangitis. Liver 21:247–253
9. Kojima H, Nies AT, König J, Hagmann W, Spring H, Uemura M, Fukui H, Keppler D (2003) Changes in the expression and localization of hepatocellular transporters and radixin in primary biliary cirrhosis. J Hepatol 39:693–702
10. Dumont M, Jacquemin E, D'Hont C, Descout C, Cresteil D, Haouzi D, Desrochers M, Stieger B, Hadchouel M, Erlinger S (1997) Expression of the liver Na + −independent organic anion transporting polypeptide (oatp-1) in rats with bile duct ligation. J Hepatol 27:1051–1056
11. Reimer P, Rummeny EJ, Shamsi K, Balzer T, Daldrup HE, Tombach B, Hesse T, Berns T, Peters PE (1996) Phase II clinical evaluation of Gd-EOB-DTPA: dose, safety aspects, and pulse sequence. Radiology 199:177–183
12. Narita M, Hatano E, Arizono S, Miyagawa-Hayashino A, Isoda H, Kitamura K, Taura K, Yasuchika K, Nitta T, Ikai I, Uemoto S (2009) Expression of OATP1B3 determines uptake of Gd-EOB-DTPA in hepatocellular carcinoma. J Gastroenterol 44:793–798
13. Hamm B, Staks T, Mühler A, Bollow M, Taupitz M, Frenzel T, Wolf KJ, Weinmann HJ, Lange L (1995) Phase I clinical evaluation of Gd-EOB-DTPA as a hepatobiliary MR contrast agent: safety, pharmacokinetics, and MR imaging. Radiology 195:785–792
14. Tsuboyama T, Onishi H, Kim T, Akita H, Hori M, Tatsumi M, Nakamoto A, Nagano H, Matsuura N, Wakasa K, Tomoda K (2010) Hepatocellular carcinoma: hepatocyte-selective enhancement at gadoxetic acid-enhanced MR imaging–correlation with expression of sinusoidal and canalicular transporters and bile accumulation. Radiology 255:824–833
15. Kinoshita M, Miyata M (2002) Underexpression of mRNA in human hepatocellular carcinoma focusing on eight loci. Hepatology 36:433–438
16. Vee ML, Lecureur V, Stieger B, Fardel O (2009) Regulation of drug transporter expression in human hepatocytes exposed to the proinflammatory cytokines tumor necrosis factor-alpha or interleukin-6. Drug Metab Dispos 37:685–693
17. Vee ML, Gripon P, Stieger B, Fardel O (2008) Down-regulation of organic anion transporter expression in human hepatocytes exposed to the proinflammatory cytokine interleukin 1beta. Drug Metab Dispos 36:217–222
18. Vavricka SR, Jung D, Fried M, Grützner U, Meier PJ, Kullak-Ublick GA (2004) The human organic anion transporting polypeptide 8 (SLCO1B3) gene is transcriptionally repressed by hepatocyte nuclear factor 3beta in hepatocellular carcinoma. J Hepatol 40:212–218
19. Wu PC, Fang JW, Lau VK, Lai CL, Lo CK, Lau JY (1996) Classification of hepatocellular carcinoma according to hepatocellular and biliary differentiation markers. Clinical and biological implications. Am J Pathol 149:1167–1175
20. Durnez A, Verslype C, Nevens F, Fevery J, Aerts R, Pirenne J, Lesaffre E, Libbrecht L, Desmet V, Roskams T (2006) The clinicopathological and prognostic relevance of cytokeratin 7 and 19 expression in hepatocellular carcinoma. A possible progenitor cell origin. Histopathology 49:138–151
21. Uenishi T, Kubo S, Yamamoto T, Shuto T, Ogawa M, Tanaka H, Tanaka S, Kaneda K, Hirohashi K (2003) Cytokeratin 19 expression in hepatocellular carcinoma predicts early postoperative recurrence. Cancer Sci 94:851–857
22. D'Errico A, Baccarini P, Fiorentino M, Ceccarelli C, Bonazzi C, Ponzetto A, Scoazec JY, Mancini AM, Grigioni WF (1996) Histogenesis of primary liver carcinomas: strengths and weaknesses of cytokeratin profile and albumin mRNA detection. Hum Pathol 27:599–604
23. Zhang F, Chen XP, Zhang W, Dong HH, Xiang S, Zhang WG, Zhang BX (2008) Combined hepatocellular cholangiocarcinoma originating from hepatic progenitor cells: immunohistochemical and double-fluorescence immunostaining evidence. Histopathology 52:224–232
24. Mazzaferro V, Regalia E, Doci R, Andreola S, Pulvirenti A, Bozzetti F, Montalto F, Ammatuna M, Morabito A, Gennari L (1996) Liver transplantation for the treatment of small hepatocellular carcinomas in patients with cirrhosis. N Engl J Med 334:693–699
25. Edmondson HA, Steiner PE (1954) Primary carcinoma of the liver: a study of 100 cases among 48,900 necropsies. Cancer 7:462–503
26. Goodman ZD, Ishak KG, Langloss JM, Sesterhenn IA, Rabin L (1985) Combined hepatocellular-cholangiocarcinoma. A histologic and immunohistochemical study. Cancer 55:124–135
27. Roncalli M, Park YN, Di Tommaso L (2010) Histopathological classification of hepatocellular carcinoma. Dig Liver Dis 42S: S228–S234
28. Kudo M (2010) Will Gd-EOB-MRI change the diagnostic algorithm in hepatocellular carcinoma? Oncology 78(Suppl 1):87–93

Virchows Arch (2011) 459:147–154
DOI 10.1007/s00428-011-1118-6

ORIGINAL ARTICLE

Hormonally defined pancreatic and duodenal neuroendocrine tumors differ in their transcription factor signatures: expression of ISL1, PDX1, NGN3, and CDX2

Gratiana Hermann · Björn Konukiewitz · Anja Schmitt · Aurel Perren · Günter Klöppel

Received: 22 February 2011 / Revised: 15 April 2011 / Accepted: 20 April 2011 / Published online: 8 July 2011
© Springer-Verlag 2011

Abstract We recently identified the transcription factor (TF) islet 1 gene product (ISL1) as a marker for well-differentiated pancreatic neuroendocrine tumors (P-NETs). In order to better understand the expression of the four TFs, ISL1, pancreatico-duodenal homeobox 1 gene product (PDX1), neurogenin 3 gene product (NGN3), and CDX-2 homeobox gene product (CDX2), that mainly govern the development and differentiation of the pancreas and duodenum, we studied their expression in hormonally defined P-NETs and duodenal (D-) NETs. Thirty-six P-NETs and 14 D-NETs were immunostained with antibodies against the four pancreatic hormones, gastrin, serotonin, calcitonin, ISL1, PDX1, NGN3, and CDX2. The TF expression pattern of each case was correlated with the tumor's hormonal profile. Insulin-positive NETs expressed only ISL1 (10/10) and PDX1 (9/10). Glucagon-positive tumors expressed ISL1 (7/7) and were almost negative for the other TFs. Gastrin-positive NETs, whether of duodenal or pancreatic origin, frequently expressed PDX1 (17/18), ISL1 (14/18), and NGN3 (14/18). CDX2 was mainly found in the gastrin-positive P-NETs (5/8) and rarely in the D-NETs (1/10). Somatostatin-positive NETs, whether duodenal or pancreatic in origin, expressed ISL1 (9/9), PDX1 (3/9), and NGN3 (3/9). The remaining tumors showed labeling for ISL1 in addition to NGN3. There was no association between a particular TF pattern and NET features such as grade, size, location, presence of metastases, and functional activity. We conclude from our data that there is a correlation between TF expression patterns and certain hormonally defined P-NET and D-NET types, suggesting that most of the tumor types originate from embryologically determined precursor cells. The observed TF signatures do not allow us to distinguish P-NETs from D-NETs.

Keywords Neuroendocrine tumors · Pancreas · Duodenum · Insulinoma · Glucagonoma · Gastrinoma · Transcription factors · ISL1 · PDX1 · NGN3 · CDX2

Abbreviations

ISL1	Islet 1 gene product
PDX1	Pancreatico-duodenal homeobox 1 gene product
NGN3	Neurogenin 3 gene product
CDX2	CDX-2 homeobox gene product

Introduction

Transcription factors (TFs) that play a crucial role in the early development of endocrine cells in the intestine and the pancreas are CDX-2 homeobox gene product (CDX2), pancreatico-duodenal homeobox 1 gene product (PDX1), islet 1 gene product (ISL1), and neurogenin 3 gene product

G. Hermann
Department of Pathology, Assaf Harofeh Medical Center and Sackler Faculty of Medicine, Tel Aviv University, Tel Aviv, Israel

G. Hermann · B. Konukiewitz · G. Klöppel (✉)
Department of Pathology, Technical University of München, Ismaningerstr. 22,
81675 München, Germany
e-mail: guenter.kloeppel@alumni.uni-kiel.de

A. Schmitt · A. Perren
Department of Pathology, University of Bern, Bern, Switzerland

G. Klöppel
Department of Pathology, University of Kiel, Kiel, Germany

(NGN3). CDX2 governs the differentiation of the intestinal cells into enterocytes, Paneth cells, goblet cells, and endocrine cells. In adult life, it is expressed in terminally differentiated intestinal cells [1]. In endocrine cells, nuclear CDX2 immunoreactivity was found in all serotonin-producing cells, in about 10% of gastrin-producing cells, in about 30% of gastric inhibitory peptide cells, and in a few motilin-positive cells of the normal intestinal mucosa, while other gastrointestinal endocrine cell types were CDX2 negative [1–3]. PDX1 directs the development of both the exocrine and the endocrine pancreas [4, 5]. During adult life, PDX1 is expressed in islet cells, especially insulin cells, and some centro-acinar and ductal cells [6]. NGN3 is a transcription factor that is responsible for endocrine differentiation of intestinal progenitor cells, temporarily directs the development of the four endocrine cell lineages in the pancreas, and is expressed in somatostatin and gastrin cells of the duodenum [5, 7–9]. ISL1 is a transcription factor that binds to an islet beta cell-specific enhancer element in the insulin gene. In adult life, it is expressed in all pancreatic endocrine cell types [10–12].

Because neoplasms in general and neuroendocrine tumors in particular recapitulate embryological–cellular differentiation, it is of interest to analyze the expression of TFs in NETs, first in order to trace the cell lineage of these tumors back to their origin [13], and second to study the association between the expression of TFs and the biology of the neoplasms. So far, most investigations focused on the expression of CDX2 and found that this TF is a hallmark of neoplasms derived from the intestine, including NETs [1, 2, 14]. Almost all NETs of the ileum and appendix (ileal and appendiceal carcinoids) were found to be CDX2 positive [1], while only a minority of pancreatic and other extraintestinal NETs showed CDX2 expression [1]. ISL1 expression, on the other hand, characterized pancreatic NETs and their metastases [15]. PDX1 was found to be expressed in almost 40% of pancreatic endocrine neoplasms [6]. In another study, PDX1 labeled pancreatic but not duodenal gastrinomas [16]. As for NGN3, data on its expression were reported in individual hormonally defined pancreatic NETs, which often showed combined nuclear–cytoplasmic staining [17].

Pancreatic and duodenal NETs are very much interrelated. Gastrin- and somatostatin-producing NETs may occur in both sites. Moreover, both groups of NETs show conspicuous heterogeneity in terms of clinical syndromes and biology, as defined by the hormonal cell type that composes the neoplasm [18]. The origin of these hormonally characterized neoplasms may be a common stem cell that is capable of giving rise to all the different hormone-producing cells encountered. Alternatively, the tumor originates from preprogrammed cells that give rise to cells committed to a certain cell lineage.

The objective of this study was to analyze the expression of ISL1, PDX1, NGN3, and CDX2 in hormonally defined pancreatic and duodenal NETs in order to find out whether these four key TFs yield signatures that characterize certain tumor entities and indicate a pancreatic or duodenal origin of the tumors. To this end, we examined a series of well-differentiated pancreatic and duodenal NETs producing either insulin, glucagon, somatostatin, pancreatic polypeptide, gastrin, or calcitonin as the predominant hormone. These NETs included tumors with and without a hormonal syndrome and with either benign or malignant behavior. The results revealed that hormonally defined NETs of the pancreas and duodenum may display distinct TF signatures.

Material and methods

A total of 50 resected NETs of the duodenum and pancreas that had been collected between 1984 and 2009 were retrieved from the consultation archives of the Departments of Pathology of the Technical University München and the University of Kiel (Germany). A number of these tumor cases were included in previous studies investigating different aspects of duodenal and pancreatic NET biology. The resection procedures included tumor excision, enucleation, duodenectomy, Whipple operations, and left partial pancreatectomy. The tumor series comprised 50 primary NETs, 14 from the duodenum (bulb, second part, some of them periampullary, and one from the distal part), and 36 from the pancreas.

The tumors were classified according to recent WHO criteria for endocrine tumors [19]. All NETs were well differentiated and therefore designated as G1 (54%) or G2 (46%) NETs, regardless of whether they showed evidence of malignant behavior or not. They were grouped on the basis of their predominant (more than 60–80%) immunohistochemical hormone expression and hormonal syndrome. Classified according to the previous WHO classification [20, 21], there were 13 well-differentiated endocrine tumors and 37 well-differentiated endocrine carcinomas.

The following tumor groups were defined: ten insulin-producing P-NETs (all insulinomas); seven glucagon-producing P-NETs (four glucagonomas and three nonfunctioning tumors); ten nonfunctioning somatostatin-producing NETs (five of pancreatic and five of duodenal origin); three nonfunctioning polypeptide-producing P-NETs; 18 gastrin-producing NETs (including five gastrinomas, five nonfunctioning tumors of duodenal origin, and eight gastrinomas of pancreatic origin), one nonfunctioning calcitonin-expressing P-NET, and two nonfunctioning P-NETs without significant hormone expression.

All tissue blocks were formalin fixed and paraffin embedded. Appropriate hematoxylin and eosin-stained sections, most of which contained tumor tissue next to normal parenchyma, were examined. Immunostaining was performed on 3-μm-thick sections. They were immunostained for synaptophysin (polyclonal antibody, DakoCytomation, Glostrup, Denmark, 1:50), chromogranin A (monoclonal antibody, Ventana medical systems, Tucson, AZ, USA, 1:2), insulin (monoclonal antibody, Biogenex, San Ramon, CA, USA, 1:40), glucagon (polyclonal antibody, Biogenex, 1:60), somatostatin (polyclonal antibody, DakoCytomation, 1:200), pancreatic polypeptide (PP, polyclonal antibody, DakoCytomation, 1:5000), gastrin (polyclonal, Paesel, Frankfurt, Germany, 1:3000), PDX1 (1:200, clone 267712, R&D Systems, Wiesbaden, Germany), ISL1 (rat 1:100, C-terminal portion, Developmental Studies Hybridoma Bank, Univ. of Iowa, Iowa City, USA), NGN3 (neurogenin 3, 1:500, Developmental Studies Hybridoma Bank, University of Iowa), and CDX2 (1:20, clone AMT28, Novocastra Laboratories Ltd, Newcastle, UK). MIB1 staining was performed using a mouse monoclonal antibody (M0722, DAKO, Hamburg, Germany 1:100). Immunostaining was carried out using the avidin–biotin peroxidase complex method. All immunohistochemical staining was performed after high temperature antigen retrieval (125°C for 1 min) using Dako Pascal Microprocessor/heat-induced epitope retrieval procedures at pH 6.7. Endogenous peroxidase blocking was performed for 15 min before application of the primary antibody. Positive internal controls included normal duodenal mucosa for CDX2, normal pancreas for ISL1 and PDX1, and isolated endocrine cells of the duodenal and submucosal and intrapancreatic nerve fibers for NGN3. Negative controls consisted in omitting the primary antibody and replacing it with normal rabbit serum at an equivalent concentration. Positive staining for the TFs was visualized as a dark brown reaction localized to the nucleus. It was considered strong if it had the same intensity as the internal control, weak if it was barely visible without a cytoplasmic stain, and moderate if it was weaker than that of the internal control tissue but still well recognizable. Negative immunostaining was recorded if only a few isolated cells were weakly or moderately positive (<5%). Positive immunostaining was recorded and scored as 1 if 5–10% of the cells were positive; 2 if 10–50% of the cells were positive, and 3 if more than 50% of the cells were positive. In cases with strong nuclear positivity, the percentage of stained cells always exceeded 5%. The results for Mib1 were given as percentage of positive tumor cells.

Results

The study included 50 NETs of the pancreas (36/50, 71%) and the duodenum (14/50, 29%), whose detailed clinicopathological data are listed in Table 1. There were 24 female (48%) and 26 male patients (52%) with ages ranging from 17 to 88 years. The size of the tumors ranged from 0.6 to 14 cm. A hormonal syndrome was observed in 54% of the cases. Seventy-two percent of the pancreatic NETs and 70% of the duodenal NETs were classified as tumors associated with malignant behavior.

All NETs stained for synaptophysin and chromogranin A. Table 2 summarizes the immunohistochemical findings for the seven hormones and the four TFs tested. Immunostaining for the hormones revealed a monohormonal pattern (i.e., a significant expression of only one hormone) in 9/10 insulin-positive NETs, in 6/7 glucagon-positive NETs, in

Table 1 Clinicopathologic features of pancreatic and duodenal neuroendocrine tumors (NETs)

NET type[a]	No.	Age (mean, years)	Sex (m/f)	Site	Size (mean, cm)	Hormonal syndrome[b]	WHO		Grade		Met[c]
							wdet	wdec	1	2	
INS expressing	10	51.4	6/4	Pancreas	1.9	10/10	6/10	4/10	8/10	2/10	1/10
GLU expressing	7	57.4	3/4	Pancreas	6.2	4/7	1/7	6/7	2/7	5/7	5/7
SOM expressing	5	46	1/4	Pancreas	6.4	0/5	1/5	4/5	3/5	2/5	1/5
	4	58.5	3/1	Duodenum	3.8	0/4	0/4	4/4	1/4	3/4	2/4
PP expressing	3	57.7	0/3	Pancreas	6.4	0/3	1/3	2/3	0/3	3/3	1/3
CAL/non-expressing	3	65	1/2	Pancreas	6	0/3	0/3	3/3	0/3	3/3	0/3
GAS expressing	8	53	5/3	Pancreas	4.9	8/8	0/8	8/8	5/8	3/8	5/8
	10	71	7/3	Duodenum	1.4	5/10	4/10	6/10	8/10	2/10	3/10

INS insulin, *GLU* glucagon, *SOM* somatostatin, *PP* pancreatic polypeptide, *CAL* calcitonin, *GAS* gastrin, *wdet* well-differentiated endocrine tumors, *wdec* well-differentiated endocrine carcinomas, *NETs* neuroendocrine tumors, *MET* metastases, *m* male, *f* female

[a] Predominant hormone expression

[b] Hypoglycemic hyperinsulinism, glucagonoma syndrome or Zollinger-Ellison-syndrome

[c] Metastases, lymph node and/or liver

Table 2 Expression of the transcription factors PDX1, ISL1, NGN3, and CDX2 in pancreatic and duodenal NETs

NET type[a]	Site	Transcription factors				Other hormone expression
		PDX1	ISL1	NGN3	CDX2	
INS expressing	Pancreas	9/10 (1/0/8)[b]	10/10 (2/0/8)	0/10	0/10	SOM1/10
GLU expressing	Pancreas	1/7 (1/0/0)	7/7 (1/0/6)	0/7	1/7 (0/1/0)	PP 1/7
SOM expressing	Pancreas	1/5 (0/0/1)	5/5 (0/1/4)	2/5 (1/0/1)	0/5	PP 1/5
	Duodenum	2/4 (0/0/2)	4/4 (0/0/4)	1/4 (0/1/0)	0/4	0/4
PP expressing	Pancreas	0/3	3/3 (0/0/3)	1/3 (0/1/0)	0/3	0/3
CAL/non-expressing	Pancreas	0/3	3/3 (0/0/3)	1/3 (0/0/1)	0/3	GLU 1/3
GAS expressing	Pancreas	7/8 (3/3/1)	4/8 (1/2/1)	5/8 (2/2/1)	5/8 (2/2/1)	PP 2/8
	Duodenum	10/10 (2/0/8)	10/10 (1/1/8)	9/10 (2/2/5)	1/10 (0/0/3)	SERO 1/10

INS insulin, *GLU* glucagon, *SOM* somatostatin, *PP* pancreatic polypeptide, *CAL* calcitonin, *GAS* gastrin, *SERO* serotonin, *NET* neuroendocrine tumor, *ISL1* islet 1 gene product, *PDX1* pancreatico-duodenal homeobox 1 gene product, *NGN3* neurogenin 3 gene product, *CDX2* CDX-2 homeobox gene product

[a] Predominant hormone expression

[b] No. of cases with 5–10%, 10–50%, or >50% positive cells

5/6 PP- and calcitonin-positive NETs, in 5/18 gastrin-positive NETs, and in 8/9 somatostatin-positive NETs.

TF patterns by tumor type

All insulin-positive NETs expressed ISL1 and 9/10 expressed PDX1 (Table 2 and Fig. 1). In contrast, none of the insulin-positive NETs stained for CDX2 or NGN3. All glucagon-positive tumors expressed ISL1 (Fig. 2). In addition, there was weak staining for PDX1 and CDX2 in two different glucagon-positive NETs. The PP-positive tumors, the calcitonin-positive tumor and the non-expressing P-NETs all labeled for ISL1 and 2/6 additionally for NGN3, while they were negative for PDX1 and CDX2. Gastrin-positive NETs, whether of duodenal or pancreatic origin, frequently expressed PDX1 (17/18), ISL1 (14/18), and NGN3 (14/18) (Fig. 3). CDX2 was mainly found in the gastrin-positive P-NETs (5/8) and rarely in the D-NETs (1/10). All somatostatin-positive NETs, whether duodenal or pancreatic in origin, expressed ISL1, and 3/9 expressed PDX1. NGN3 was also expressed by 3/9 (Fig. 2).

TF expression frequency

ISL1 was expressed in all NETs of this series, except for four gastrin-positive P-NETs (92%). PDX1 was predominantly found in insulin- and gastrin-positive NETs (26/28, 92%). In addition to PDX1 and ISL1, NGN3 was commonly expressed in gastrin-positive P-NETs and D-NETs (14/18, 77%), while it was rarely found in other NETs (6/32, 2%). CDX2 was only found in five P-NETs (one glucagon and four gastrin positive) and one D-NET (6/50, 12%).

TF expression and biological features

The biological NET features such as location, grade, size, presence of metastases, and functional activity did not correlate with any particular TF pattern (Table 3).

Discussion

The expression of TFs has successfully been used to identify the site of origin of neoplasms. CDX2, for instance, serves as a marker for intestinal type carcinomas, including NETs of the ileum and the appendix [1, 2], while ISL1 was found to label predominantly P-NETs [15]. This study, which is restricted to the expression of ISL1, PDX1, NGN3, and CDX2 and based on a functionally well defined, though rather small, number of NETs from the pancreas and duodenum, revealed that the expression patterns of the tested TFs show a relationship to hormonally defined P- and D-NET types such as insulinomas, glucagonomas, gastrinomas, and others. The four TFs failed, however, to distinguish whether gastrin- or somatostatin-positive NETs were of duodenal or pancreatic origin.

Insulin-producing tumors form a rather homogeneous group among the P-NETs [22]. The majority of them are smaller than 2 cm, behave benignly after resection, are monohormonal (i.e., rarely contain other endocrine cells than insulin cells), occur in the pancreas and are functionally active so that they are all termed insulinomas. In our study, which included insulinomas considered to be benign or malignant, all expressed the TFs ISL1 and PDX1. This expression pattern closely reflects the expression of these

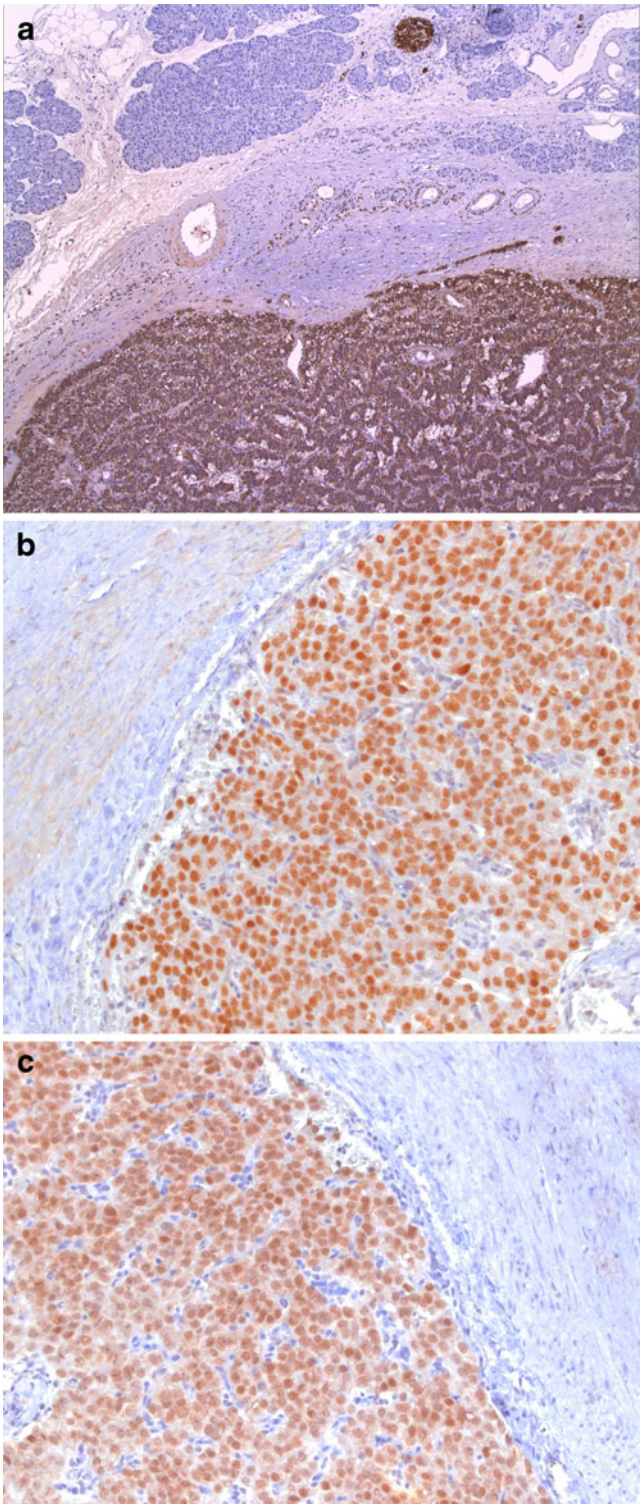

Fig. 1 Pancreatic well-differentiated tumor (insulinoma): immunostaining for insulin (**a**), ISL1(**b**), and PDX1 (**c**)

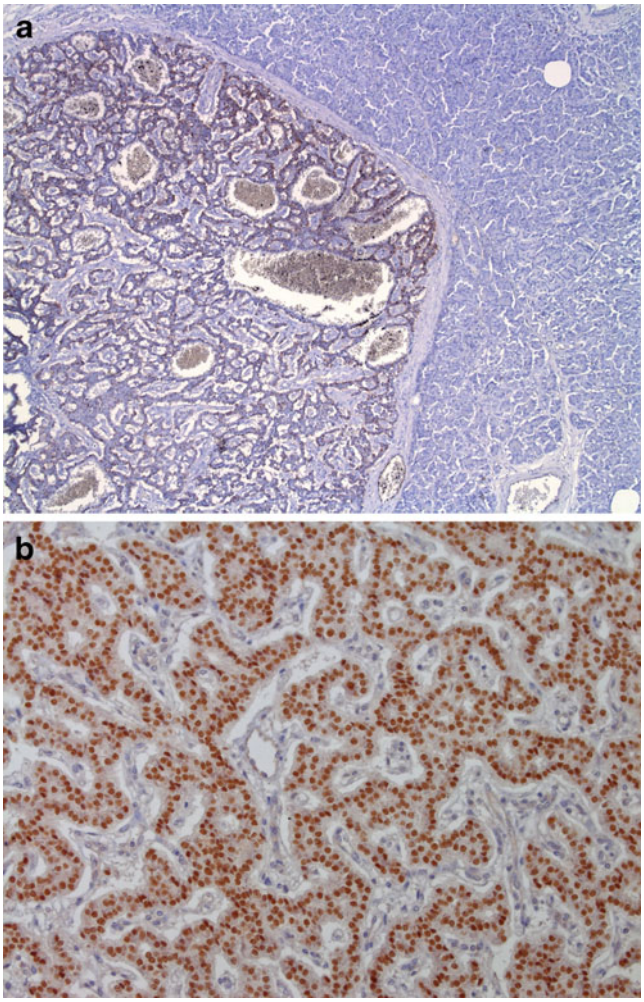

Fig. 2 Pancreatic well-differentiated tumor (glucagon producing): immunostaining for glucagon (**a**) and ISL1(**b**)

TFs in the normal pancreas, where ISL1 is exclusively and PDX1 predominantly expressed in the nuclei of islet cells. In the case of PDX1, the islet cell labeling resides in the nuclei of the beta cells, while ISL1 occurs in all islet cell types. The strong expression of ISL1 and PDX1 in insulinomas combined with a complete absence of NGN3 and CDX2 was not observed in any of the other P-NETs or D-NETs tested. It is thus highly characteristic for this specific type of P-NET.

NETs positive for glucagon may be functionally active, in which case they are called glucagonoma, or inactive and are then termed glucagon-producing tumor [19, 21, 23]. They occur predominantly in the pancreas and are frequently malignant when sporadic and larger than 2 cm. When associated with MEN1, they are benign and often cystic [24]. Here, we found that all glucagon-positive tumors, regardless of their biological features, strongly expressed ISL1 and were (with two exceptions) almost completely negative for the other three TFs tested. This TF signature is, like that of the insulinomas, unique among the various types of P-NET and D-NET in our series. It reflects the fact that the mature glucagon cell in the pancreas is solely ISL1-positive and does not express either PDX1,

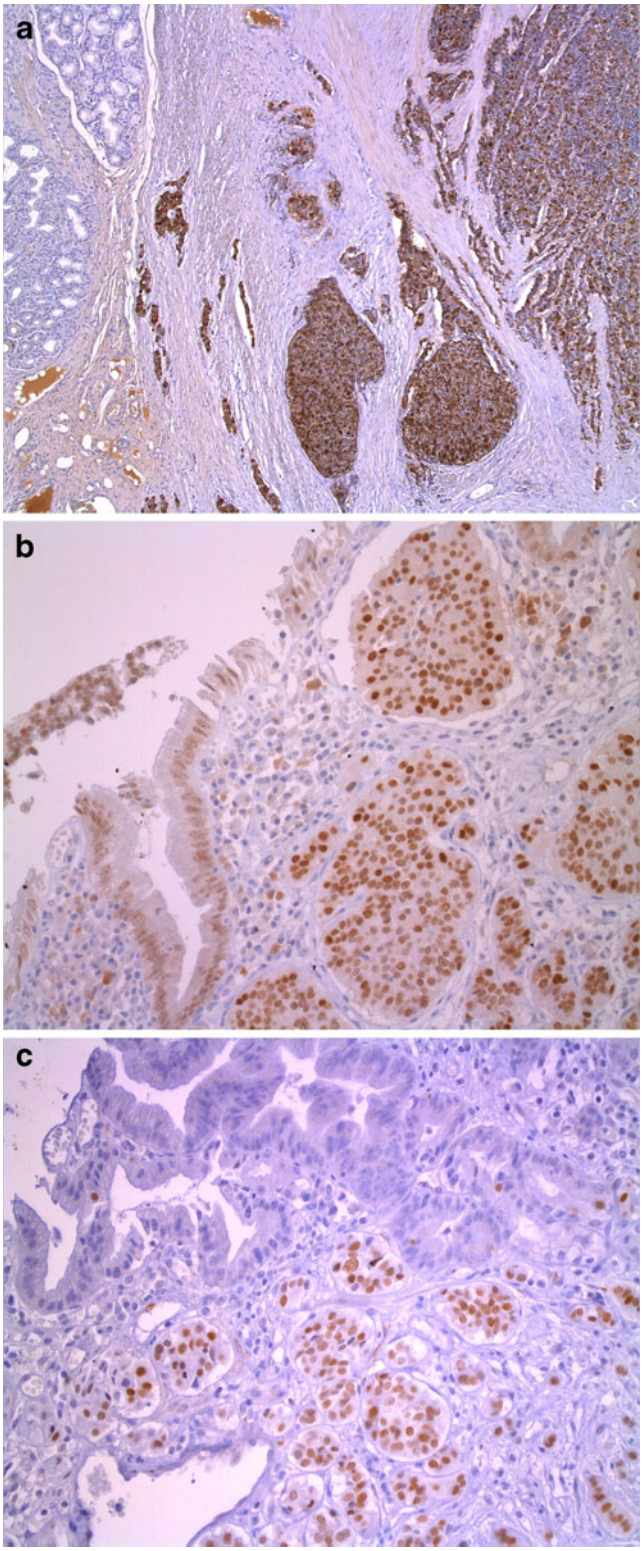

Fig. 3 Duodenal well-differentiated neuroendocrine tumor (gastrinoma): immunostaining for gastrin (**a**), PDX1 (**b**), and NGN3 (**c**)

NGN3, or CDX2. The neoplastic glucagon cell therefore appears to preserve the cell type specific features of the nonneoplastic cell lineage from which it might derive and thereby distinguishes itself from other cell lineages giving rise to P-NETs.

The remaining P-NET types, including PP- and calcitonin-producing and hormonally non-expressing tumors, show more complex TF expression patterns than insulinomas and glucagonomas. They all label for ISL1 and, in addition, variably for PDX1 and/or NGN3. Though the informative value of the TF patterns in this group is limited by the small number of tumors tested, it might indicate, on the one hand, that the cell lineages giving rise to these tumors differ from those associated with insulinomas and glucagonomas. On the other hand, it might suggest that ISL1, PDX1, and NGN3 may collaborate in the cell lineages forming these P-NETs.

A special group of tumors in our series is the one that includes NET types occurring in both the pancreas and the duodenum. These are the gastrin-producing and the somatostatin-producing NETs. While the former tumors included functionally active NETs, i.e., gastrinomas, and nonfunctioning gastrin-producing tumors (all of duodenal origin), the latter tumors were all nonfunctioning. Somatostatin-producing NETs, whether duodenal or pancreatic in origin, showed a TF pattern that was characterized by the expression of ISL1 together with occasional positivity for PDX1 and NGN3 in the absence of CDX2. Gastrin-producing NETs, whether functioning or not, whether of duodenal or pancreatic origin, presented in most cases with a "full house" TF signature consisting of the expression of ISL1, PDX1, NGN3, and CDX2.

Although the distinction between the expression patterns of the hormonally defined P-NETs and D-NETs in our series was not completely "black and white", they showed distinct differences that suggest an origin from different cell lineages. This is most obvious for the insulinomas and glucagonomas. However, it is also recognizable in other tumor entities tested. For instance, in the case of the gastrin-positive NETs it may be speculated that the gastrin-positive P-NETs and D-NETs originate from two different cell lineages. While the gastrin-positive P-NETs may be related to a cell lineage with intestinal features, since they commonly expressed the intestinal transcription factor CDX2 in addition to ISL1, PDX1, and NGN3, the gastrin-positive D-NETs almost entirely lacked CDX2 expression and may therefore have a cell origin distinct from that of their pancreatic counterparts. How the gastrin-producing tumors in the pancreas keep contact with the intestine is not known, but it is interesting to note that the pancreatic gastrinomas preferably occur in the head region of the gland, close to the duodenum. In the case of the somatostatin-producing NETs, the cell of origin appears to be pancreatic rather than intestinal in nature, as their TF signature lacks the intestinal marker CDX2. In this context, it is of interest that the duodenal somatostatin-producing

Table 3 Expression of the transcription factors PDX1, ISL1, NGN3, and CDX2 in pancreatic and duodenal NETs correlated with clinicopathologic features

NET type	Site	F/NF	Behavior	Transcription factors			
				PDX1	ISL1	NGN3	CDX2
INS expressing	Pancreas	F 10/10	ben 9/10	5/6	5/6	0/6	0/6
			mal 1/10	4/4	4/4	0/4	0/4
GLU expressing	Pancreas	F 4/7	mal 4/4	0/4	4/4	0/4	0/4
		NF 3/7	ben 1/3	0/1	1/1	0/1	0/1
			mal 2/3	1/2	2/2	0/2	1/2
SOM expressing	Pancreas	NF 5/5	ben 4/5	1/4	4/4	2/4	0/4
			mal 1/5	0/1	1/1	0/1	0/1
	Duodenum	NF 4/4	ben 2/4	1/2	2/2	1/2	0/2
			mal 2/4	1/2	2/2	0/2	0/2
PP expressing	Pancreas	NF 3/3	ben 2/3	0/2	2/2	1/2	0/2
			mal 1/3	0/1	1/1	0/1	0/1
CAL/non-expressing	Pancreas	NF 3/3	ben 2/3	0/2	2/2	1/2	0/2
			mal 1/2	0/1	1/1	0/1	0/1
GAS expressing	Pancreas	F 8/8	ben 2/8	2/2	1/2	2/2	2/2
			mal 6/8	4/6	3/6	2/6	3/6
	Duodenum	F 5/10	ben 2/5	2/2	2/2	1/2	0/2
			mal 3/5	3/3	3/3	3/3	1/3
		NF 5/10	ben 5/5	5/5	5/5	5/5	0/5

INS insulin, *GLU* glucagon, *SOM* somatostatin, *PP* pancreatic polypeptide, *CAL* calcitonin, *GAS* gastrin, *NET* neuroendocrine tumor, *ISL1* islet 1 gene product, *PDX1* pancreatico-duodenal homeobox 1 gene product, *NGN3* neurogenin 3 gene product, *CDX2* CDX-2 homeobox gene product

tumors are known for their preferential location in the ampullary region, an area that is intimately connected with the pancreas.

While we were able to relate some TF signatures to hormonally defined P-NET and D-NET entities, it was not possible to clearly distinguish between duodenal and pancreatic NETs. This observation was somewhat unexpected, since in our previous study on the expression of ISL1 in gastroenteropancreatic NETs, it appeared that this TF was virtually specific to P-NETs. However, already in this study we noticed that two of the four D-NETs tested were positive for ISL1 and these two tumors were gastrinomas [15]. A similar result was reported by La Rosa et al. [1]). ISL1 is therefore a marker that, in addition to P-NETs, also labels most D-NETs, particularly if they produce gastrin. Conversely, the expression of CDX2 is not restricted to D-NETs, as representatives of intestinal tumors, but may also occur in P-NETs, particularly if they belong to the gastrinoma group. These findings imply that predicting that the pancreas or the duodenum as the site of origin of a liver metastasis of a gastrin-positive NET is not possible on the basis of their positivity for ISL1 or CDX2.

A comparison of the expression of the four TFs in individual tumors belonging to the various entities reveals differences in extent and intensity in about 20% of the cases. The explanation for these differences might lie in technical criteria, since the quality of the TF staining is sensitive to factors related to tissue preservation, antigen retrieval, and antibody source. Another explanation for the inhomogeneous TF findings in some tumors within a group is tumor heterogeneity. Although the NETs in our series were mostly monohormonal, implying that they predominantly expressed only one hormone out of the seven hormones that were regularly tested, a significant expression of more than one hormone was recognized in about 15% of the cases. As multihormonality may be an indication that the tumor originated from different cell lineages, it may also explain the fact that the TF expression was never completely homogeneous in the examined tumor entities, although we were not able to correlate a multihormonal tumor with a particular TF signature. Another explanation for an "aberrant" TF expression pattern could be the plasticity of neoplastic cells enabling them to go through various phenotypical changes. These considerations are also valid for the interpretations of findings reported in other studies on TFs in P-NETs and D-NETs, which vary to some extent from those in our investigations [16, 17].

In summary, the signatures of the four TFs, ISL1, PDX1, NGN3, and CDX2, recognize hormonally defined NET entities of the pancreas and duodenum and may contribute to their identification as special D-NETs or P-NETs. The TF signatures point to an origin from embryologically determined and hormonally committed precursor cells of the various cell lineages from which the tumors may derive. The TF signatures do not allow a distinction between P-NETs and D-NETs.

Conflict of interest We declare that we have no conflict of interest.

References

1. La Rosa S, Rigoli E, Uccella S, Chiaravalli AM, Capella C (2004) CDX2 as a marker of intestinal EC-cells and related well-differentiated endocrine tumors. Virchows Arch 445:248–254
2. Barbareschi M, Roldo C, Zamboni G, Capelli P, Cavazza A, Macri E, Cangi MG, Chilosi M, Doglioni C (2004) CDX-2 homeobox gene product expression in neuroendocrine tumors: its role as a marker of intestinal neuroendocrine tumors. Am J Surg Pathol 28:1169–1176
3. Srivastava A, Hornick JL (2009) Immunohistochemical staining for CDX-2, PDX-1, NESP-55, and TTF-1 can help distinguish gastrointestinal carcinoid tumors from pancreatic endocrine and pulmonary carcinoid tumors. Am J Surg Pathol 33:626–632
4. Habener JF, Kemp DM, Thomas MK (2005) Minireview: transcriptional regulation in pancreatic development. Endocrinology 146:1025–1034
5. Schonhoff SE, Giel-Moloney M, Leiter AB (2004) Minireview: development and differentiation of gut endocrine cells. Endocrinology 145:2639–2644
6. Park JY, Hong SM, Klimstra DS, Goggins MG, Maitra A, Hruban RH (2011) Pdx1 expression in pancreatic precursor lesions and neoplasms. Appl Immunohistochem Mol Morphol (in press)
7. Cano DA, Hebrok M, Zenker M (2007) Pancreatic development and disease. Gastroenterology 132:745–762
8. Bernardo AS, Hay CW, Docherty K (2008) Pancreatic transcription factors and their role in the birth, life and survival of the pancreatic beta cell. Mol Cell Endocrinol 294:1–9
9. Rukstalis JM, Habener JF (2009) Neurogenin3: a master regulator of pancreatic islet differentiation and regeneration. Islets 1:177–184
10. Ahlgren U, Pfaff SL, Jessell TM, Edlund T, Edlund H (1997) Independent requirement for ISL1 in formation of pancreatic mesenchyme and islet cells. Nature 385:257–260
11. Jensen J (2004) Gene regulatory factors in pancreatic development. Dev Dyn 229:176–200
12. Karlsson O, Thor S, Norberg T, Ohlsson H, Edlund T (1990) Insulin gene enhancer binding protein Isl-1 is a member of a novel class of proteins containing both a homeo- and a Cys-His domain. Nature 344:879–882
13. Abate-Shen C (2002) Deregulated homeobox gene expression in cancer: cause or consequence? Nat Rev Cancer 2:777–785
14. Moskaluk CA, Zhang H, Powell SM, Cerilli LA, Hampton GM, Frierson HF Jr (2003) Cdx2 protein expression in normal and malignant human tissues: an immunohistochemical survey using tissue microarrays. Mod Pathol 16:913–919
15. Schmitt AM, Riniker F, Anlauf M, Schmid S, Soltermann A, Moch H, Heitz PU, Klöppel G, Komminoth P, Perren A (2008) Islet 1 (Isl1) expression is a reliable marker for pancreatic endocrine tumors and their metastases. Am J Surg Pathol 32:420–425
16. Fendrich V, Ramerth R, Waldmann J, Maschuw K, Langer P, Bartsch DK, Slater EP, Ramaswamy A, Rothmund M (2009) Sonic hedgehog and pancreatic-duodenal homeobox 1 expression distinguish between duodenal and pancreatic gastrinomas. Endocr Relat Cancer 16:613–622
17. Lejonklou MH, Edfeldt K, Johansson TA, Stalberg P, Skogseid B (2009) Neurogenin 3 and neurogenic differentiation 1 are retained in the cytoplasm of multiple endocrine neoplasia type 1 islet and pancreatic endocrine tumor cells. Pancreas 38:259–266
18. Klöppel G, Rindi G, Anlauf M, Perren A, Komminoth P (2007) Site-specific biology and pathology of gastroenteropancreatic neuroendocrine tumors. Virchows Arch 451(Suppl 1):S9–S27
19. Rindi G, Klöppel G (2010) WHO classification of tumours of the digestive system. IARC, Lyon
20. Solcia E, Sobin LH, Klöppel G (2000) WHO classification of tumours of the digestive system. IARC, Lyon
21. Heitz PU, Komminoth P, Perren A (2004) WHO classification of tumours of the endocrine pancreas. IARC, Lyon
22. de Herder WW, Niederle B, Scoazec JY, Pauwels S, Klöppel G, Falconi M, Kwekkeboom DJ, Öberg K, Eriksson B, Wiedenmann B, Rindi G, O'Toole D, Ferone D, all other Frascati Consensus Conference participants (2006) Well-differentiated pancreatic tumor/carcinoma: insulinoma. Neuroendocrinology 84:183–188
23. Ruttman E, Klöppel G, Bommer G, Kiehn M, Heitz PU (1980) Pancreatic glucagonoma with and without syndrome. Immunocytochemical study of 5 tumour cases and review of the literature. Virchows Arch A Pathol Anat 388:51–67
24. Konukiewitz B, Enosawa T, Kloppel G (2011) Glucagon expression in cystic pancreatic neuroendocrine neoplasms: an immunohistochemical analysis. Virchows Arch 458:47–53

Virchows Arch (2011) 459:155–160
DOI 10.1007/s00428-011-1094-x

ORIGINAL ARTICLE

Mutation analysis of *KRAS* prior to targeted therapy in colorectal cancer: development and evaluation of quality by a European external quality assessment scheme

Elisabeth Dequeker · Marjolijn J. L. Ligtenberg · Sara Vander Borght · Johan H. J. M. van Krieken

Received: 16 March 2011 / Revised: 21 April 2011 / Accepted: 18 May 2011 / Published online: 24 June 2011
© Springer-Verlag 2011

Abstract In Europe, the use of anti-EGFR monoclonal antibodies is restricted to Kirsten RAS (*KRAS*) wild-type colorectal tumors. Information on the *KRAS* status of the patients tumor is thus key for clinical practice; however, there is little guidance or definition on which *KRAS* mutations to assess and how to assess them. To ensure the consistency and the quality of *KRAS* test results in Europe, an interlaboratory control network needs to be set up. This pilot study aimed to identify the variables that need to be assessed in a quality control scheme and to provide a first assessment in a selected set of laboratories. Fourteen different tumor cases were circulated between 13 laboratories by a central laboratory acting as the referent for the mutation status determination. This study illustrated that of 13 experienced laboratories that perform *KRAS* testing only ten correctly identified the *KRAS* in all 14 cases that were circulated. There was no harmonization in DNA isolation and *KRAS* mutation detection method between the laboratories. These results indicate that future standardization is needed in *KRAS* mutation detection methodology. An expansion of the European Society of Pathology *KRAS* program could identify areas of difficulty in *KRAS* testing and provide the basis for harmonization.

Keywords Colorectal cancer · External quality assessment scheme · *KRAS* · Proficiency testing · Quality assurance

E. Dequeker (✉)
Centre for Human Genetics, Biomedical Quality Assurance Research Unit, University Hospitals KULeuven,
KULeuven, Herestraat 49, box 602, 3000 Leuven, Belgium
e-mail: els.dequeker@med.kuleuven.be

M. J. L. Ligtenberg · J. H. J. M. van Krieken
Department of Pathology,
Radboud University Nijmegen Medical Centre,
Nijmegen, The Netherlands

S. Vander Borght
Department of Pathology, University Hospitals KULeuven,
Leuven, Belgium

Introduction

Cetuximab and Panitumumab, two anti-EGFR monoclonal antibodies, have been approved in several countries for the treatment of CRC. However, these therapies are only effective in a subset of patients [1]. It has been clearly shown that in patients with CRC, anti-EGFR treatment is only effective in those patients that have a wild-type Kirsten RAS (*KRAS*) gene [2]. The recommended use of EGFR therapy was amended both by EMEA and FDA but with different approaches. Whereas FDA issued a recommendation for a single assay detecting seven mutations on codon 12 and 13, EMEA changed the approval for these drugs in wild-type populations only without further indications which mutations have to be tested and how. Consequently, there is no standard methodology, and the laboratories often test for different mutation panels.

Point mutations in codons 12 and 13 of the *KRAS* oncogene can be detected in approximately 30% to 40% of all patients with CRC [3]. Although a group of different methods is available for *KRAS* genotyping, there is no uniformity about the use of one test and the definition of required mutations in the analysis. Offering tests as a way to decide on treatment must comply with rigorous quality control procedures in order to ensure consistency and accuracy of results. The evidence for the necessity to improve quality in molecular diagnostics was demonstrated for genetic testing in cystic fibrosis in 2000 [4]. This study

showed that less than half of the laboratories that participate yearly to an external quality assessment scheme (EQA) correctly identify genotypes in each of the three trials. Thirty-nine percent made a mistake only once, while 2% of labs consistently failed in each trial. After 5 years of repeated testing, a clear improvement was demonstrated [5]. Since this initial report, additional external quality assessment schemes have been developed for many other diseases [6, 7].

A harmonization of testing methods and procedures is critical for accurate and reliable *KRAS* mutation testing in clinical practice [1]. In previous reports, a proposal was done for a European quality assurance program to help ensure accuracy and proficiency in *KRAS* mutation testing [1]. This paper presents the findings of a first phase of the development of a European EQA scheme for *KRAS* testing in collaboration with the European Society of Pathology (ESP). The first EQA round focused on the development of a European ESP EQA scheme for *KRAS* (selection, validation, preparation, and sending of the slides), the selection of regional laboratories to evaluate the assessment of the amount of tumor cells by pathologists, the reliability of the detection of *KRAS* mutations (the molecular analysis) in formalin-fixed paraffin-embedded colorectal cancer tissue, and the necessity to estimate the need for further improvement in the quality assurance of *KRAS* testing.

Materials and methods

Participants

This phase of the external quality assessment scheme was organized in collaboration with the ESP and in close collaboration with existing national *KRAS* EQA programs (Table 1). In total, 13 laboratories from 13 different European countries (Austria, Belgium, Denmark, France, Germany, Greece, Italy, Portugal, Spain, Sweden, The Netherlands, Turkey, and UK) were invited and agreed to participate in the trial. An identification number was assigned to each of the participating laboratories before the start of the scheme to protect the identity of the participants.

Twelve of these laboratories frequently perform *KRAS* mutation testing for diagnostic purposes and one laboratory performs analyses for research purposes only; all these laboratories are early adaptors of this new test in their country. The number of tests performed in these laboratories ranges from 50 to 3,000 tests/year anno 2008.

Set-up of the external quality assessment scheme

Paraffin-embedded material from 14 invasive colorectal carcinomas with known *KRAS* mutational status was collected. The series of cases consisted of six wild-type and eight mutated samples (c.34G>A p.Gly12Ser, c.34G>C p.Gly12Arg, c.35G>A p.Gly12Asp (3×), c.35G>T p.Gly12Val, c.38G>A p.Gly13Asp (2×)). All cases had initially been tested in one of the participating laboratories and were subsequently blindly analyzed in the coordination center (Leuven) and reference laboratory (Nijmegen). From these blocks, 14 samples were selected and six serial unstained 4-μm sections were sent to all participating laboratories on the same day by courier. To exclude differences due to differences in tumor depth, it was analyzed that if a mistake was made, the laboratories that received the sections before or after these sections made the same mistake. A final slide was stained with H&E and evaluated for the presence and amount of tumor cells in the reference laboratory. No clinical information of the patients from whom the 14 samples were derived was provided. The slides were labeled with a specimen ID and section number. Due to the damage of some of the slides during shipment, a second set of slides of the same specimens was cut from the same blocks and sent to seven of the laboratories. The last set of sections was again tested by the reference laboratory

Table 1 Existing national *KRAS* EQA programs

Country	Organized since	No. participating laboratories	Nature of material	Kind of assessment
France	2009	45	DNA	Genotype
Germany	2008	2008: 74	Unstained slides	Genotype/Histological
		2009: 85	Unstained slides	Genotype/Histological
Sweden	2008	2008 (a): 6	DNA	Genotype/Histological
		2008 (b): 9	Unstained slides	Genotype/Histological
		2009: 7	Unstained slides	Genotype/Histological
United Kingdom	2009	19	Unstained slides	Genotype
The Netherlands	2008 (for NSCLC)	2008: 10	2008: DNA, unstained slides	Genotype/Histological
		2009: 12	2009: DNA, unstained slide of a tissue micro-array (TMA)	Genotype/Histological

to analyze the impact of the depth in tumor. The laboratories were asked to use their routine protocol for HE staining, slide evaluation, DNA isolation, and molecular testing and to return the datasheet with results to the European scheme organizer within 14 days after arrival of the samples.

Mutation nomenclature

The mutation nomenclature complies with the guidelines from the Human Genome Variation Society (www.hgvs.org). These state that nucleotide number 1 should correspond to the A of the ATG translation initiation site. The description of all variants is preceded by a letter indicating the type of reference sequence used; "c." relates to a coding DNA sequence and "p." to a protein sequence.

Data analysis

A panel of quality assessors, among whom the scheme organizer and the chair of the working QA group, evaluated the submitted results and raw data. The results of the pilot ESP *KRAS* EQA scheme were discussed with the participants on a separate meeting. These final results were made available anonymously among the participants, but each participating laboratory received individual feedback.

Results

Differences in methodology

No requirement was made concerning the used testing method (for DNA extraction or mutation analysis) and the spectrum of mutations analyzed. In total, six different DNA extraction methods were used; seven of the 13 labs (54%) used the commercial Qiagen extraction kit (Table 2). From the beginning, the participants were informed that if a laboratory that does not test a particular mutation and typed it as "wild type," it would not be assigned as "incorrect" (Table 3). For the mutation detection method, no harmonization could be recognized. The most frequent methods used in this pilot group were the TheraScreen DxS kit and dideoxysequencing (both 38%).

Mutations

All participating laboratories reported the results in time. Out of 13 laboratories (77%), ten correctly identified the *KRAS* mutation status in all 14 samples. Three laboratories were not able to identify all 14 samples correctly. In total, eight false-negative results and one false-positive result were reported (Table 4). Laboratories that had incorrect calls had one to four mistakes. The mistakes were at random, i.e., that no sample was called wrongly by more than three laboratories.

Evaluation of the tumor content and the genotype

Estimates were made of the percentage of viable tumor cells present in the sections (Table 5). This is a subjective procedure, which depends both on the region selected for microdissection and the assessment of ratio between tumor and normal nucleated cells. The differences in some cases were however quite large, varying from 20% to 90%. There was no consistent pattern in the estimations by the different labs.

Discussion

The detection of a *KRAS* mutation in a colorectal cancer specimen is nowadays important for patients eligible for

Table 2 Mutations tested by the participating laboratories

	Laboratory	1	2	3	4	5	6	7	8	9	10	11	12	13
DNA extraction methods	phenol/chloroform	✓												
	Qiagen extraction			✓	✓		✓	✓	✓			✓		✓
	ProtK lysate		✓										✓	
	Invisorb® kit					✓								
	Nucleospin® Tissue kit									✓				
	MagNa Pure LC										✓			
KRAS mutation detection methods	KRAS genotyping kit (Taq)	✓												
	TheraScreen® DxS				✓	✓		✓			✓			✓
	HRM								✓					
	Dideoxysequencing		✓					✓	✓	✓			✓	
	Pyrosequencing			✓								✓		
	Enriched PCR RFLP						✓							

Table 3 Used DNA extraction methods and methods for mutation detection

	Laboratory	1	2	3	4	5	6	7	8	9	10	11	12	13
Mutation	p.Gly12Ala	✓	✓	✓	✓	✓	ND	✓	✓	✓	✓	✓	✓	✓
	p.Gly12Cys	✓	✓	✓	✓	✓	ND	✓	✓	✓	✓	✓	✓	✓
	p.Gly12Asp	✓	✓	✓	✓	✓	ND	✓	✓	✓	✓	✓	✓	✓
	p.Gly12Arg	✓	✓	✓	✓	✓	ND	✓	✓	✓	✓	✓	✓	✓
	p.Gly12Ser	✓	✓	✓	✓	✓	ND	✓	✓	✓	✓	✓	✓	✓
	p.Gly12Val	✓	✓	✓	✓	✓	ND	✓	✓	✓	✓	✓	✓	✓
	p.Gly13Cys		✓				ND	✓	✓	✓		✓	✓	
	p.Gly13Asp	✓	✓	✓	✓	✓	ND	✓	✓	✓	✓	✓	✓	✓
				✓	laboratory can detect mutation									
				ND	No data available									

treatment with an EGFR targeting drug. Like for any other clinical test, quality assurance is also important for *KRAS* testing, but to date there is limited experience. The Quality Assurance (QAu) program of the European Society of Pathology (www.esp-pathology.org) started this initiative, partly driven by the experience of poor reliability of HER2 testing [1]. The aim of this QAu program is to ensure optimal accuracy and proficiency in *KRAS* mutation testing across all countries or institutions in the European Union. Our results, using standard samples, with ample tumor cells in the specimen reveals that only ten out of 13 laboratories labeled all 14 cases correctly, the other labs made one to four mistakes. These results indicate that QAu programs are needed indeed. It has to be taken into account that the laboratories involved in this test were selected based on their prominent position in the field and sufficient experience. Since the testing will be spread to many less experienced laboratories, the QAu system becomes even more important.

The results from this study provide information both on currently used mutation detection methods in diagnostic laboratories and on the technical quality of the analysis in these laboratories. Given the limited number of laboratories participating in the pilot scheme, it is clear that at present a wide variety of different DNA extraction methods and mutation analysis methods is being used in European diagnostic laboratories. The most popular DNA extraction method for paraffin slides was the commercial Qiagen extraction kit (54%). The most frequent mutation detection methods used in this pilot group were the TheraScreen DxS kit and the dideoxysequencing method (both 38%). There was no methodology that outperformed others, but the numbers are too small to give an advice on which test method is the most robust. After several rounds of EQA, the data will become larger, and it may well be that such an advice can be given in the future. At present, only a limited number of countries (see Table 1) have recently set up a national ESP *KRAS* EQA program. The design of the national schemes varied in the kind of samples ((un)stained paraffin slides, extracted DNA) and in the method of assessment (histological analysis in combination with genotyping or only genotyping).

Table 4 Genotyping results

Sample	% of labs typed correctly	Kind of error
KRAS09.1 wild type	92%	1 lab found mutation c.35G > A p.Gly12Asp
KRAS09.2 c.35G>A p.Gly12Asp	100%	
KRAS09.3 c.38G>A p.Gly13Asp	100%	
KRAS09.4 wild type	100%	
KRAS09.5 wild type	100%	
KRAS09.6 wild type	100%	
KRAS09.7 wild type	100%	
KRAS09.8 wild type	100%	
KRAS09.9 c.35G>A p.Gly12Asp	100%	
KRAS09.10 c.35G>T p.Gly12Val	92%	1 lab did not find a mutation
KRAS09.11 c.38G>A p.Gly13Asp	92%	1 lab did not find a mutation
KRAS09.12 c.35G>A p.Gly12Asp	100%	
KRAS09.13 c.34G>C p.Gly12Arg	84%	2 labs did not find a mutation
KRAS09.14 c.34G>A p.Gly12Ser	77%	3 labs did not find a mutation

Table 5 Estimated percentage of tumor cells in the samples after assessment by microscopic analysis (H&E staining)

Sample	Laboratory identification number												
	1	2	3	4	5	6	7	8	9	10	11	12	13
KRAS09.1	50	70	ND	50	90	50	40	33	ND	50	ND	60	50
KRAS09.2	70	80	ND	60	90	70	65	36	ND	80	ND	90	60
KRAS09.3	80	70	ND	70	90	80	75	63	ND	75	ND	95	80
KRAS09.4	30	40	ND	50	82	60	60	35	ND	50	ND	95	40
KRAS09.5	70	60	ND	70	82	62	60	48	ND	80	ND	95	70
KRAS09.6	60	70	ND	50	82	60	35	48	ND	75	ND	95	50
KRAS09.7	70	80	ND	60	95	80	75	32	ND	85	ND	95	75
KRAS09.8	40	50	ND	70	90	40	45	48	ND	50	ND	60	7
KRAS09.9	80	80	ND	50	62	72	60	25	ND	75	ND	90	80
KRAS09.10	10	80	ND	40	18	35	30	9	ND	85	ND	90	20
KRAS09.11	20	40	ND	70	82	60	60	40	ND	33	ND	40	70
KRAS09.12	70	70	ND	50	90	80	50	40	ND	75	ND	80	70
KRAS09.13	50	50	ND	30	37	75	15	40	ND	50	ND	90	50
KRAS09.14	10	40	ND	20	37	20	20	2	ND	20	ND	10	20

The columns in the table represent the different participating laboratories. The individual results for each of the 14 samples are shown per row

For the organization of the European ESP *KRAS* EQA, two groups were assigned by the ESP QAu group, the Department of Pathology of the Radboud University Nijmegen and the Biomedical Quality Assurance Research unit of the University of Leuven. Both groups are supplementing each other, as the group of Nijmegen has a lot of experience in setting up and performing molecular pathology tests and the group of the university in Leuven is one of the leading groups in doing longitudinal research of quality assurance in molecular testing.

As instructed by the pilot ESP *KRAS* EQA scheme, the laboratories used their routine protocol for H&E staining, slide evaluation, DNA isolation, and molecular testing. All labs returned the datasheet with results to the European scheme organizer within 14 days after receiving the samples. In the opinion of the centers involved, a turnaround time of ten working days is acceptable, although a faster process is desirable.

The first phase of the EQA scheme evaluated the practical analysis of the *KRAS* test including the evaluation of the percentage of tumor cells in the sample and the correct identification of the mutations. The laboratories were asked to estimate the percentage of tumor cells in their microdissected area, an important issue that determines the reliability, especially with respect to the sensitivity, of the test. The differences in some cases are however so large that it is obvious that more standardization in estimating tumor cell percentages and optimization of microdissection is required. Therefore, a web-based system using digitized slides will be set up to improve this part of the process.

Obtaining sufficient patient material for running a European wide *KRAS* external quality assessment scheme was a big challenge. To have sufficient tissue sections from the same tissue block with an almost similar amount of tumor cells is not easy. It would therefore be desirable to work with standardized control samples. In one of the next QA rounds such an approach will be piloted, using artificial tissue samples made from cell lines.

We conclude that an external quality assessment scheme is needed for several reasons. An EQA organized by an independent body provides the laboratories with the possibility to evaluate their performance and to compare it with that of other (European) laboratories. If genotyping errors are found in the EQA trial, the laboratories can identify the source of their mistake(s) and eliminate them.

Diagnostic laboratories should improve the validation of their technical procedures to avoid errors at every stage of the procedure. Therefore, we recommend that all diagnostic laboratories would regularly participate in external quality assessment schemes.

To make this possible, we have decided to set up a general ESP *KRAS* EQA scheme in Europe. This scheme is organized by the ESP together with regional scheme organizers who take care of the preparation and distribution of the samples in a subscheme in collaboration with the coordination center. After a turnaround time of 14 days, the results from all participating laboratories will be evaluated in collaboration with all the scheme organizers of these countries. This allows us to reach standards for *KRAS* testing and reporting in Europe. All laboratories can participate in the ESP *KRAS* EQA scheme. The aim is to reach universal high quality standards for *KRAS* testing and reporting.

Acknowledgments This work was performed in collaboration with the European Society of Pathology. We would like to thank the *KRAS* Quality Assurance workgroup of ESP (alphabetically by name): Edsjo Anders (Sweden), E Dequeker (Belgium), K de Stricker (Denmark), A Ensari, G Hoefler (Austria), A Jung (Germany), A Kotsinas (Greece), M Ligtenberg (The Netherlands), F Lopez-Rios (Spain), JC Machado (Portugal), M Marichal (Belgium), C Mazzanti (Italy), TP Hansen (Denmark), S Richman (United Kingdom), E Rouleau (France), S Tejpar (Belgium), and JHJM van Krieken (The Netherlands). The authors thank the participating laboratories in this pilot scheme; Prof. G Hofler and Prof. A Kotsina for providing tissue blocks for this scheme; Prof. G De Hertogh for evaluating the tissue blocks; Prof. dr P Vandenbergh for the molecular analysis; the technicians from the departments of pathology in Leuven and Nijmegen for the preparation of the slides and the validation of the samples; W De Kelver, B Biesmans, and K Cox for the assistance in the evaluation of the results; and E Bellon for the administrative support.

Conflict of interest The authors have declared no conflicts of interest.

Funding The work was supported by a grant of AMGEN.

References

1. van Krieken JH, Jung A, Kirchner T et al (2008) *KRAS* mutation testing for predicting response to anti-EGFR therapy for colorectal carcinoma: proposal for a European quality assurance program. Virchows Arch 453:417–431
2. Van Krieken H, Tol J (2009) Setting future standards for *KRAS* testing in colorectal cancer. Pharmacogenomics 10(1):1–3
3. Monzon FA, Ogino S, Hammond ME et al (2009) The role of *KRAS* mutation testing in the management of patients with metastatic colorectal cancer. Arch Pathol Lab Med 133(10):1600–1606
4. Dequeker E, Cassiman JJ (2000) Genetic testing and quality control in diagnostic laboratories. Nat Genet 25(3):259–260
5. Dequeker E, Ramsden S, Grody WW et al (2001) Quality control in molecular genetic testing. Nat Rev Genet 2(9):717–723
6. Seneca S, Morris MA, Patton S et al (2008) Experience and outcome of 3 years of a European EQA scheme for genetic testing of the spinocerebellar ataxias. Eur J Hum Genet 16:913–920
7. Touitou I, Rittore C, Philibert L et al (2009) An international external quality assessment for molecular diagnosis of hereditary recurrent fevers: a 3-year scheme demonstrates the need for improvement. Eur J Hum Genet 17(7):890–896

Virchows Arch (2011) 459:161–166
DOI 10.1007/s00428-011-1111-0

ORIGINAL ARTICLE

Expression of Krűppel-like factor 5 in gastric cancer and its clinical correlation in Taiwan

Maw-Soan Soon · Li-Sung Hsu · Chih-Jung Chen · Pei-Yi Chu · Jia-Hung Liou · Shu-Hui Lin · Jeng-Dong Hsu · Kun-Tu Yeh

Received: 28 December 2010 / Revised: 25 May 2011 / Accepted: 17 June 2011 / Published online: 6 July 2011
© Springer-Verlag 2011

Abstract Krűppel-like factors (KLFs), highly conserved zinc-finger proteins, play either anti- or pro-proliferation roles in different human cancers through regulating a wide range of genes' expression. Here, we investigated the expression of KLF5 in gastric cancers and its correlation with clinicopathological parameters and overall survival rates. In this study, KLF5 expression was measured by an immunohistochemical micro-array assay of tissue taken from 76 surgical specimens. Higher KLF5 expression was significantly associated with lower tumor grade ($P<0.001$). Nuclear staining of the KLF5 expression was significantly associated with a higher tumor grade ($P=0.000$), higher clinical stage ($P=0.019$), lymph node status ($P=0.016$), and 2-year survival ($P=0.017$). Patients with nuclear staining of KLF5 had a significantly lower disease-free survival rate compared to patients with negative nuclear staining, as defined by a log-rank test ($P=0.041$). Our results revealed that KLF5 may play an oncogenetic role in gastric carcinogenesis.

Keywords Krűppel-like factors · Gastric adenocarcinoma · Immunohistochemical stain · Prognosis

Maw-Soan Soon and Li-Sung Hsu contribute equally to this research as the first authors.

Electronic supplementary material The online version of this article (doi:10.1007/s00428-011-1111-0) contains supplementary material, which is available to authorized users.

M.-S. Soon
Department of Gastroenterology, Changhua Christian Hospital, Changhua, Taiwan

L.-S. Hsu
Institute of Biochemistry and Biotechnology, Chung Shan Medical University, Taichung, Taiwan

L.-S. Hsu
Clinical Laboratory, Chung Shan Medical University Hospital, Taichung 402, Taiwan

C.-J. Chen
Institute of Medicine, Chung Shan Medical University, Taichuang, Taiwan

C.-J. Chen
Institute of Medical and Molecular Toxicology, Chung Shan Medical University, Taichuang, Taiwan

C.-J. Chen
Department of Surgical Pathology, Changhua Christian Hospital, Changhua, Taiwan

C.-J. Chen
Department of Medical Technology, Jen-Teh Junior College of Medicine, Nursing and Management, Miaoli, Taiwan

P.-Y. Chu · J.-H. Liou · S.-H. Lin · K.-T. Yeh (✉)
Department of Pathology, Changhua Christian Hospital, 135, Nan-Hsiao Street, Changhua, Taiwan
e-mail: 10159@cch.org.tw

P.-Y. Chu
Department of Veterinary Medicine, National Taiwan University, Taipei, Taiwan

J.-D. Hsu · K.-T. Yeh
Department of Pathology, School of Medicine, Chung Shan Medical University, Taichung, Taiwan

K.-T. Yeh
Institute of Clinical Medicine, Kaohsiung Medical University, Kaohsiung, Taiwan

Introduction

Intestinal-enriched Krűppel-like factor (IKLF or KLF5) belongs to the KLF family of proteins containing zinc-finger motif that regulates a broad range of cellular processes. KLF5 is widely distributed in many human tissues including the colon, small intestine, and breast [1, 2].

It is well-accepted that KLF5 plays a positive role in cell proliferation [3]. First, KLF5 is abundantly expressed in the proliferating crypt cells, and the deletion of one KLF5 allele results in shorter crypts and villi [4, 5]. Furthermore, KLF5 is expressed in the proliferating cells of skin and activated vascular smooth cells [6, 7]. NIH3T3 cells transfected with KLF5 have been shown to increase proliferation and serum-independent growth [5]. KLF5 facilitates normal intestinal epithelial cell growth as well as increased colony formation and cyclin D expression [8]. The high expression of KLF5 is associated with shorter survival duration in breast cancer [9], and the silencing of KLF5 expression blocks lysophosphatidic acid-stimulated proliferation of SW480 and HCT116 colon cancer cells [10]. KLF5 is also involved in androgen-mediated CXCR4 expression, which, in turn, triggers the migration of prostate cancer cells [11]. However, in contrast, KLF5 has been shown to be downregulated in colon cancer cell lines [8]. In gastric cancer, the survival time of patients with higher levels of KLF5 was shown to be longer than that of patients with low levels of KLF5 [12]. The overexpression of KLF5 inhibits the colony formation ability of the T-47D breast cancer cell line and reduces the proliferation of TE2 esophageal cancer cells [1, 13].

Gastric adenocarcinoma is one of the leading causes of cancer-related deaths in Taiwan. In this study, we sought to determine the expression pattern and clinical relationship of KLF5 in gastric cancer in Taiwan.

Materials and methods

Sample collection

From 1999 to 2008, 76 formalin-fixed and paraffin-embedded gastric cancer specimens were obtained from patients who underwent surgical resection at the Department of Surgery, Changhua Christian Hospital, and tissue blocks were obtained from the Department of Pathology, Chung Shan Medical University Hospital. The stages and grades were classified according to the TNM and World Health Organization classification systems. All samples were arranged in tissue array blocks. The histopathological and clinical data were obtained from the cancer registry of Changhua Christian Hospital and the Department of Pathology, Chung Shan Medical University Hospital. Disease-free survival was measured as the time interval between the surgical operation and either the date of death or the end of follow-up. This research was approved by the internal review board of Chung Shan Medical University Hospital.

Tissue microarrays (TMAs)

A tissue core section (2 μm in diameter) from cancer and non-cancer tissues in each paraffin block was longitudinally cut and arranged into new paraffin blocks using a fine steel needle to generate TMAs. A 4-μm section was stained with hematoxylin and eosin to confirm the presence of morphologically representative areas of the original cancers.

Analyses of KLFs expression by immunohistochemistry

The immunohistochemical analysis was performed using the streptavidin peroxidase protocol. Briefly, 4-μm sections containing paraffin-embedded cancer tissue and paired non-cancerous tissue sections were deparaffinized. After blocking with 3% H_2O_2, the sections were rehydrated and the antigen was retrieved by heating at 100°C for 20 min in 10 mM citrate buffer (pH 6.0). After incubation with anti-KLF5 antibody [1:70 dilution, rabbit polyclonal (sc-22797), Santa Cruz Biotechnology Inc., Santa Cruz, CA, USA] for 20 min at room temperature, slides were incubated with a horseradish peroxidase/Fab polymer conjugate for an additional 30 min, followed by thorough washing three times with PBS. The color was developed using 3,3'-diamino-benzidine tetrahydrochloride as a chromogen and counterstained with hematoxylin. Appropriate positive and negative controls were also included in the immunohistochemical staining. After staining, slides were scored by two pathologists (KT Yeh and PY Chu). Paraffin-embedded and fresh frozen sections of normal colonic epithelium of a homogeneous immunophenotype for the studied antigens were included as positive controls. Negative controls had the primary antibody omitted and replaced by PBS. The intensity of cytoplasmic and nuclear staining of KLF proteins was scored semiquantitatively using scores according to the percentage of positive cells in individual lesions: 0–10% KLF protein staining was defined as negative (−) and greater than 10% KLF protein staining was defined as positive (+) as previously described [14]. The staining intensity of the cytoplasm was scored ranging from 0 to 4 as previous report [14]. The intensity was classified as either weak (<2) or strong (≧2).

Statistical analysis

Statistical analysis was performed using SPSS software (SPSS, Inc.). The correlation between the expression levels of KLF proteins with different clinicopathological parameters was measured by a Chi-square test with a Fisher extract test.

The disease-free survival rate was estimated by a Kaplan-Meier plot and log-rank test. Multivariate analysis with a Cox proportional hazard regression model was used to evaluate the prognostic significance of clinical variables. A P value <0.05 was considered to be statistically significant.

Results

Patient characteristics

A total of 76 patients, including 51 men and 25 women, were enrolled in this retrospective study. Table 1 shows KLF5 expression and patients' clinicopathological parameters. The median age was 55 years (range, 31–88). There were 12 patients at WHO stage I, 23 at stage II, 22 at stage III, and 19 stage IV tumors. Seven tumors were well-differentiated, 27 were moderately differentiated, and 42 were poorly differentiated. Disease-free survival time ranged from 0.1 to 7.9 years, with a mean survival time of 3.5 years and a median survival time of 3.8 years. Adjuvant therapy was performed according to individual considerations, performance status, patient compliance, and clinicopathological parameters.

Correlation of nuclear KLF5 expression with the clinicopathological parameters of gastric cancer

It has been shown that KLF5 is involved in human tumorigenesis [15]. In this study, we performed immunohistochemical (IHC) staining of KLF5 in 76 gastric cancer sections to determine the expression level and clinical correlation of the KLF5 protein in gastric cancer patients. The protein expression level of KLF5 was semiquantified by IHC staining. For KLF5, a weak expression level was found in 50.1% (39 out of 76) of the patient sections. Both cytoplasmic and nuclear localization of KLF5 were observed in 40.7% (31 out of 76) gastric cancer patients (Fig. 1). The correlation between the expression level of KLF5 and clinical parameters is summarized in Table 1. A significantly reduced KLF5 expression level was associated with high tumor grade (P=0.011 and P=0.001; Table 1). In addition, we also determined whether the nuclear localization of KLF5 in gastric cancer was correlated with any clinical outcome. Positive nuclear staining of KLF5 was associated with a higher histological grade (P=0.000), lymph node metastasis (P=0.016), and poorer 2-year survival (P=0.017; Table 2).

Table 1 Clinicopathological characteristics of patients and cytoplasmic staining of KLF5 protein

	KLF5 expression level		
	<2 n=39	≧2 n=37	P value
Gender			
Female	13	12	1.000
Male	26	25	
Grade			
Well/moderate	10	24	<0.001*
Poor	29	13	
Stage			
I/II	20	15	0.368
III/IV	19	22	
Lymph node metastasis			
No	16	11	0.345
Yes	23	26	
Survival			
≤2 years	16	13	0.642
>2 years	23	24	

*P<0.001

Nuclear expression of KLF5 and patient survival

As a transcription factor, it has been speculated that KLF performs its biological function within the nucleus. It has been determined very recently that the nuclear localization of KLF4 is an independent factor in a poor prognosis in breast cancer [15]. Thus, we evaluated the relationship between nuclear expression of KLF5 and disease-free survival. A Kaplan-Meier analysis indicated a significantly shorter disease-free survival in patients with high nuclear KLF5 expression (P=0.041) (Fig 2).

Loss of nuclear localization of KLF5, grade, stage, and lymphoid node metastasis was associated with poor prognosis in univariate analysis (Supplementary Table 1). In the multivariate analysis that included the variable of KLF5 expression, histological grade, tumor stage, lymph node status, and T status, nuclear KLF5 was not found to be an independent prognostic factor. Yet, pathological grade was an independent prognostic factor (P=0.020; hazard ratio, 2.7; 95% confidence interval, 1.16 to 6.21; Table 3).

Discussion

KLFs, a group of zinc-finger transcription factors, can bind to CG-rich sequences and function as both transcriptional activators and repressors [16]. Through the regulation of downstream gene expression, KLFs have been shown to play an essential role in a broad range of cellular functions [16]. However, the role of KLF in tumorigenesis still remains controversial. In this study, we have demonstrated an association between the expression level of KLF 5 and clinical parameters of gastric cancers.

KLF5 functions as a positive regulator for cell proliferation and tumor formation. KLF5 has been shown to be involved in

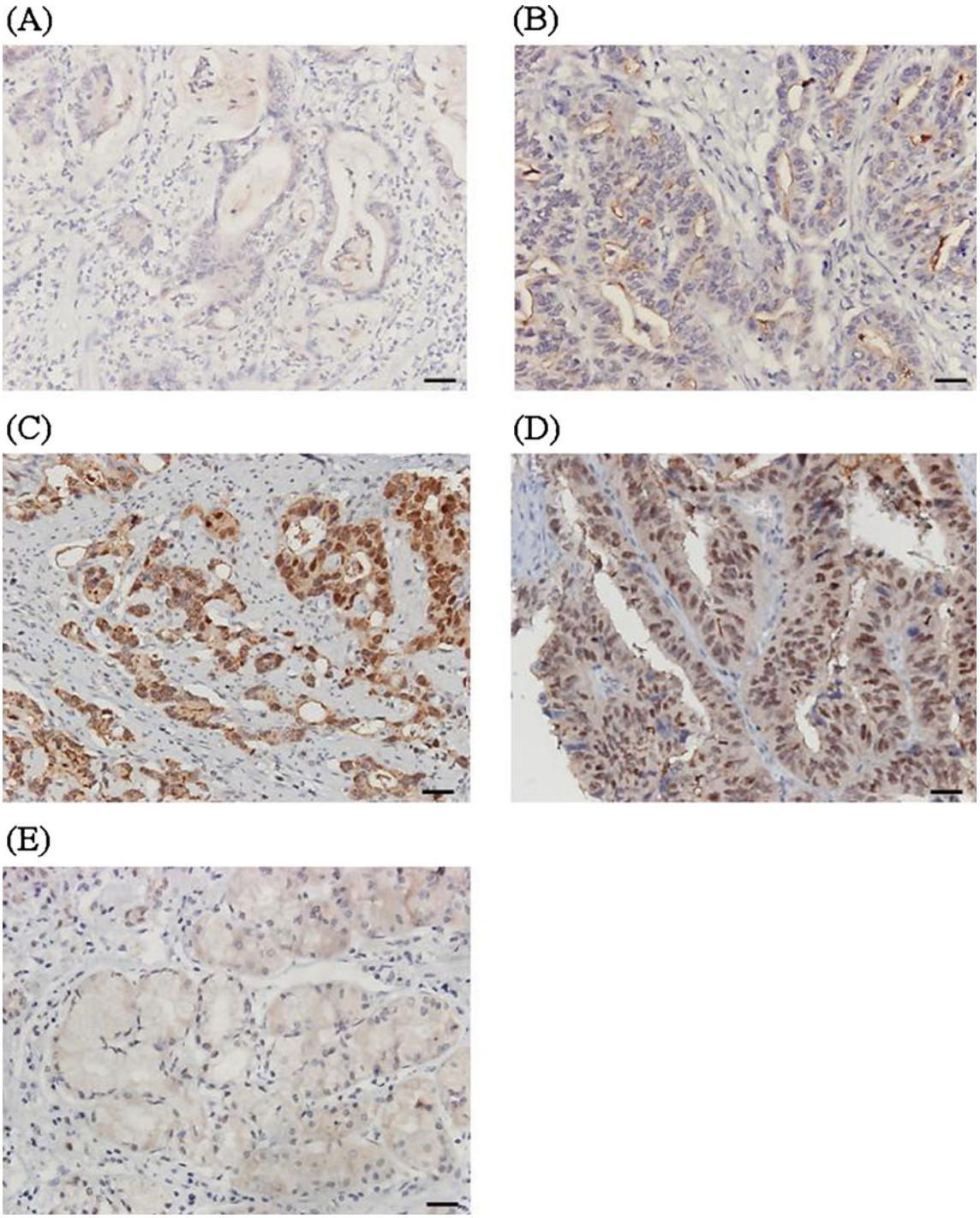

Fig. 1 Immunohistochemical staining for the expression of KLF5 in gastric carcinoma. The staining patterns of KLF5 were predominantly cytoplasmic (**a**) and (**b**) mixed cytoplasmic and nuclear (**c**), predominantly nuclear (**d**). **a**, **b** Weak staining. **c**, **d** Strong staining. Weakly cytoplasmic and no nuclear staining of KLF5 was found in non-tumor part of gastric samples (**e**). *Scale bar* denotes 100 μm

oncogenic Ras-mediated cell transformation [17, 18], and ectopically expressed KLF5 triggers proliferation and tumorigenesis in TSU-Pr-1 human bladder cells [19]. KLF5 also interacts with p53, which in turn elevates survivin expression and may contribute to the pathogenesis and chemoresistance of cancer [20]. In this study, positive nuclear expression of KLF5 was correlated with tumor grade, lymph node metastasis, and poorer 2-year survival. A greater nuclear staining of KLF5 was inversely correlated with disease-free survival time, as analyzed by a Kaplan-Meier analysis. Consistent with our observation, Tong and co-workers have shown that breast cancer patients with stronger KLF5

Table 2 Clinicopathological characteristics of patients and nuclear staining of KLF5 protein

		KLF5 nuclear stain		
		No n=45	Yes n=31	P value
Gender	Female	13	12	0.458
	Male	32	19	
Grade	Well/moderate	28	6	0.000**
	Poor	17	25	
Stage	I/II	26	9	0.019*
	III/IV	19	22	
Lymph node metastasis	No	21	6	0.016*
	Yes	24	25	
Survival	≤2 years	12	17	0.017*
	>2 years	33	14	

*P<0.05, **P<0.01

Table 3 Multivariate analysis of the nuclear staining for KLF5 and the prognostic variables

Variable	Hazard ratio	95% CI	P value
KLF5 nuclear stain			
No	1.0	0.60 to 2.50	0.573
Yes	1.2		
Grade			
Well/moderate	1.0	1.16 to 6.21	0.020*
Poor	2.7		
Stage			
I/II	1.0	0.43 to 3.49	0.697
III/IV	1.2		
Lymph node metastasis			
No	1.0	0.93 to 9.79	0.067
Yes	3.0		

*P<0.05

expression had a shorter disease-free survival time and overall survival rate [9]. Moreover, KLF5 promotes matrix metalloproteinase-9 (MMP-9) expression in a chondrogenic cell line [21]. It has been reported that a significant correlation was obtained between MMP-9 expression levels and lymph node involvement in gastric cancer [22]. Whether KLF5 also stimulates MMP-9 expression and subsequently enhances lymph node metastasis in gastric cancer is now under investigation. Conversely, reduced KLF5 expression through hemizygous deletion has been frequently observed in breast cancer and prostate cancer [1, 23]. The overexpression of KLF5 decreases colony formation efficiency in T-47D breast cancer cells [1]. Similarly, restoration of KLF5 in human prostate cancer cell lines diminishes cell proliferation [23]. Very recently, discrepant results from Kwak et al. revealed that significantly decreased KLF5 expression was found in gastric tumors with a higher stage, larger size, and lymph node metastases [12]. These authors also demonstrated that gastric patients with positive KLF5 expression have longer overall survivals, although this finding did not reach statistical significance [12]. These authors also demonstrated that KLF5 was strongly expressed in the nucleus of normal gastric samples. On the other hand, our results revealed weakly cytoplasmic but no nuclear localization in adjacent non-tumor region of gastric samples. Moreover, the detection rate was higher in our study compared to previous reports. The controversial role of KLF5 in tumorigenesis was also found in breast cancer. Chen et al. indicated that decreased KLF5 resulted from chromosome deletion was found in 43% of breast cancer cell lines [1]. These authors suggested that KLF5 may function as tumor suppressor gene in breast cancer [1]. In contrast, higher KLF5 expression was

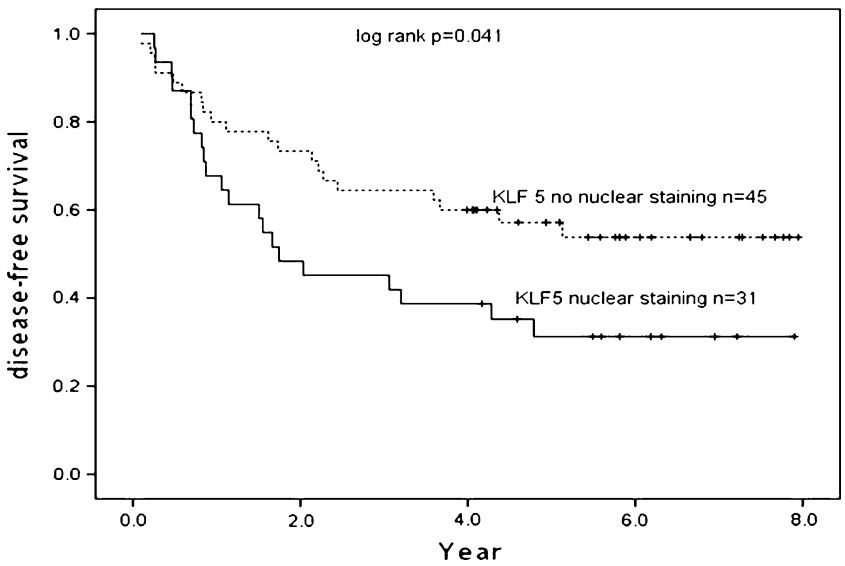

Fig. 2 A Kaplan-Meier survival curve for the 76 gastric cancer patients with nuclear expression of KLF5 protein. Patients with nuclear staining for KLF5 had a significantly lower disease-free survival rate compared to patients with negative nuclear staining, as defined by a log-rank test (P=0.041)

associated with shorter disease-free and overall survival time in breast cancer patients in Austria [9]. More recently, it has been shown that WWP1, an E3 ubiquitin ligase, can target KLF5 for proteolysis. WWP1 was overexpressed in a subset of prostate and breast cancer cell lines [24]. These conflicting observations between our results and those of Kwak et al. may derive from the geographical variation which contributed different degradation system for KLF5. In addition, nuclear KLF5 was correlated with tumor grade; nonetheless, total KLF5 expression was inversely associated with tumor grade. One possible reason was that distinct subcellular localization led to different biological function of KLF5. In the nuclear region, KLF5 can bind to specific DNA element and regulate downstream genes' expression, whereas KLF5 may subject to degradation by proteosome system in the cytoplasmic region. Collectedly, our results suggested that KLF5 may be involved in gastric carcinogenesis in Taiwan.

Our results reveal that positive nuclear localization of KLF5 is correlated with a higher tumor grade and proximal metastases. Patients with nuclear KLF5 demonstrated a decreased survival rate. In conclusion, our results indicate that KLF5 may play an important role in the carcinogenesis of gastric cancers.

Acknowledgment This work was supported by grant 99-CCH-IRP-09 from Changhua Christian Hospital and grants from National Science Council (NSC-94-2311-B-040-002 and NSC-93-2311-B-040-009), Taiwan.

Conflict of interest We declare that we did not have conflict of interest.

References

1. Chen C, Bhalala HV, Qiao H, Dong JT (2002) A possible tumor suppressor role of the KLF5 transcription factor in human breast cancer. Oncogene 21:6567–6572
2. Shi H, Zhang Z, Wang X, Liu S, Teng CT (1999) Isolation and characterization of a gene encoding human Kruppel-like factor 5 (IKLF): binding to the CAAT/GT box of the mouse lactoferrin gene promoter. Nucleic Acids Res 27:4807–4815
3. Ghaleb AM, Nandan MO, Chanchevalap S, Dalton WB, Hisamuddin IM, Yang VW (2005) Kruppel-like factors 4 and 5: the yin and yang regulators of cellular proliferation. Cell Res 15:92–96
4. Conkright MD, Wani MA, Anderson KP, Lingrel JB (1999) A gene encoding an intestinal-enriched member of the Kruppel-like factor family expressed in intestinal epithelial cells. Nucleic Acids Res 27:1263–1270
5. Sun R, Chen X, Yang VW (2001) Intestinal-enriched Kruppel-like factor (Kruppel-like factor 5) is a positive regulator of cellular proliferation. J Biol Chem 276:6897–6900
6. Nagai R, Shindo T, Manabe I, Suzuki T, Kurabayashi M (2003) KLF5/BTEB2, a Kruppel-like zinc-finger type transcription factor, mediates both smooth muscle cell activation and cardiac hypertrophy. Adv Exp Med Biol 538:57–65, discussion 66
7. Ohnishi S, Laub F, Matsumoto N, Asaka M, Ramirez F, Yoshida T, Terada M (2000) Developmental expression of the mouse gene coding for the Kruppel-like transcription factor KLF5. Dev Dyn 217:421–429
8. Bateman NW, Tan D, Pestell RG, Black JD, Black AR (2004) Intestinal tumor progression is associated with altered function of KLF5. J Biol Chem 279:12093–12101
9. Tong D, Czerwenka K, Heinze G, Ryffel M, Schuster E, Witt A, Leodolter S, Zeillinger R (2006) Expression of KLF5 is a prognostic factor for disease-free survival and overall survival in patients with breast cancer. Clin Cancer Res 12:2442–2448
10. Zhang H, Bialkowska A, Rusovici R, Chanchevalap S, Shim H, Katz JP, Yang VW, Yun CC (2007) Lysophosphatidic acid facilitates proliferation of colon cancer cells via induction of Kruppel-like factor 5. J Biol Chem 282:15541–15549
11. Frigo DE, Sherk AB, Wittmann BM, Norris JD, Wang Q, Joseph JD, Toner AP, Brown M, McDonnell DP (2009) Induction of Kruppel-like factor 5 expression by androgens results in increased CXCR4-dependent migration of prostate cancer cells in vitro. Mol Endocrinol 23:1385–1396
12. Kwak MK, Lee HJ, Hur K, Park do J, Lee HS, Kim WH, Lee KU, Choe KJ, Guilford P, Yang HK (2008) Expression of Kruppel-like factor 5 in human gastric carcinomas. J Cancer Res Clin Oncol 134:163–167
13. Yang Y, Goldstein BG, Chao HH, Katz JP (2005) KLF4 and KLF5 regulate proliferation, apoptosis and invasion in esophageal cancer cells. Cancer Biol Ther 4:1216–1221
14. Pandya AY, Talley LI, Frost AR, Fitzgerald TJ, Trivedi V, Chakravarthy M, Chhieng DC, Grizzle WE, Engler JA, Krontiras H, Bland KI, LoBuglio AF, Lobo-Ruppert SM, Ruppert JM (2004) Nuclear localization of KLF4 is associated with an aggressive phenotype in early-stage breast cancer. Clin Cancer Res 10:2709–2719
15. Bieker JJ (2001) Kruppel-like factors: three fingers in many pies. J Biol Chem 276:34355–34358
16. Pearson R, Fleetwood J, Eaton S, Crossley M, Bao S (2008) Kruppel-like transcription factors: a functional family. Int J Biochem Cell Biol 40:1996–2001
17. Nandan MO, McConnell BB, Ghaleb AM, Bialkowska AB, Sheng H, Shao J, Babbin BA, Robine S, Yang VW (2008) Kruppel-like factor 5 mediates cellular transformation during oncogenic KRAS-induced intestinal tumorigenesis. Gastroenterology 134:120–130
18. Nandan MO, Yoon HS, Zhao W, Ouko LA, Chanchevalap S, Yang VW (2004) Kruppel-like factor 5 mediates the transforming activity of oncogenic H-Ras. Oncogene 23:3404–3413
19. Chen C, Benjamin MS, Sun X, Otto KB, Guo P, Dong XY, Bao Y, Zhou Z, Cheng X, Simons JW, Dong JT (2006) KLF5 promotes cell proliferation and tumorigenesis through gene regulation and the TSU-Pr1 human bladder cancer cell line. Int J Cancer 118:1346–1355
20. Zhu N, Gu L, Findley HW, Chen C, Dong JT, Yang L, Zhou M (2006) KLF5 interacts with p53 in regulating survivin expression in acute lymphoblastic leukemia. J Biol Chem 281:14711–14718
21. Shinoda Y, Ogata N, Higashikawa A, Manabe I, Shindo T, Yamada T, Kugimiya F, Ikeda T, Kawamura N, Kawasaki Y, Tsushima K, Takeda N, Nagai R, Hoshi K, Nakamura K, Chung UI, Kawaguchi H (2008) Kruppel-like factor 5 causes cartilage degradation through transactivation of matrix metalloproteinase 9. J Biol Chem 283:24682–24689
22. Tang Y, Zhu J, Chen L, Chen L, Zhang S, Lin J (2008) Associations of matrix metalloproteinase-9 protein polymorphisms with lymph node metastasis but not invasion of gastric cancer. Clin Cancer Res 14:2870–2877
23. Chen C, Bhalala HV, Vessella RL, Dong JT (2003) KLF5 is frequently deleted and down-regulated but rarely mutated in prostate cancer. Prostate 55:81–88
24. Chen C, Sun X, Guo P, Dong XY, Sethi P, Cheng X, Zhou J, Ling J, Simons JW, Lingrel JB, Dong JT (2005) Human Kruppel-like factor 5 is a target of the E3 ubiquitin ligase WWP1 for proteolysis in epithelial cells. J Biol Chem 280:41553–41561

Virchows Arch (2011) 459:167–173
DOI 10.1007/s00428-011-1107-9

ORIGINAL ARTICLE

Genetic markers of oral malignant melanoma analysed by fluorescence in situ hybridisation (FISH)

Chiara Baldovini · Anna L. Tosi · Enrico Di Oto · Camilla Reggiani · Susanna Cappia · Christine M. Betts · Carmine Gallo · Lisa Ricchieri · Roberto Cocchi · Maria P. Foschini

Received: 28 April 2011 / Revised: 25 May 2011 / Accepted: 9 June 2011 / Published online: 29 June 2011
© Springer-Verlag 2011

Abstract Oral malignant melanoma (OMM) is a rare condition, and our knowledge about morphological and genetic modifications is scanty and incomplete. The aim of this study is to report morphological and fluorescent in situ hybridisation (FISH) data obtained in four cases of OMM. FISH results were also compared with those of cutaneous malignant melanoma (CMM, three cases), desmoplastic cutaneous melanoma (DMM, four cases) and spindle cells cutaneous melanoma (SCCM, one case). All the OMM cases showed a combined radial and vertical growth pattern, with the invasive component characterised by malignant spindle cells intermingled among collagen bundles. Two cases of OMM resulted positively stained with p16, in contrast with frequent loss of immunoreactivity in CMM. Three OMM were suitable for FISH analysis: 9p21 locus was deleted in 1/3, 1p36 resulted deleted 3/3, while EGFR gene showed a relative deletion. Similar genetic alterations were found in DMM and SCMM, but not in CMM. Ultrastructural findings further enhanced differences between OMM and CMM; OMM displayed, mature-staged melanosomes only within in situ component. In conclusion, OMM presents a morphological and genetic profile similar to DMM; and SCCM, however, displays some differences from CMM.

Keywords Melanoma · Oral cavity · Desmoplastic melanoma · Spindle cell melanoma · 9p21 · EGFR

C. Baldovini · A. L. Tosi · E. Di Oto · C. Gallo · L. Ricchieri · M. P. Foschini
Department of hematology and Oncology "L. and A. Seragnoli", Secyion of Anatomic Pathology at Bellaria Hospital, University of Bologna, Bologna, Italy

C. Reggiani
Operative Unit of Dermatology, Bellaria Hospital, Bologna, Italy

C. M. Betts
Department of Experimental Pathology, University of Bologna, Bologna, Italy

S. Cappia
Division of Pathology, San Luigi Hospital, Orbassano, Torino, Italy

R. Cocchi
Operative Unit of Maxillo-Facial Surgery, Bellaria Hospital, Bologna, Italy

M. P. Foschini (✉)
Section of Anatomic Pathology "M. Malpighi", Department of Haematology and Oncology "L. and A. Seragnoli", Bellaria Hospital, University of Bologna, Via Altura, 3, 40139 Bologna, Italy
e-mail: mariapia.foschini@unibo.it

Introduction

Malignant melanoma very occasionally arises in the oral cavity (OMM). Its incidence ranges from 0.2% to 8% of all malignant melanomas [1]. Due to its rarity, knowledge about development and behaviour of OMM is still scanty and incomplete. Usually, OMM is considered similar to cutaneous malignant melanoma (CMM); however, Kato et al. in 1987 [2] underlined the significant differences in clinical, histological features and natural history between OMM and CMM. The 1995 Western Society of Teachers of Oral Pathology Banff Workshop [3] recommended that oral melanoma should be classified separately from CMM.

Reasons to consider OMM a distinct entity from CMM have appeared in recent literature. Risk factors,

aetiology and precursors of disease have not yet been identified for OMM, while they are well known for CMM. Furthermore, it is generally agreed that OMM has a poorer prognosis compared to CMM. This is probably related to the site and delayed diagnosis. In addition, the biological behaviour of OMM may not be the same as CMM due to different genetic mechanisms of malignant transformation.

Several genetic alterations including 9p21, 1p36 deletions and EGFR amplification have been described in the literature as characteristic of CMM [4–6]. On the contrary, data on genetic alterations in OMM are still scanty.

Therefore, the purpose of the present work was to study a series of OMM applying morphologic and fluorescence in situ hybridisation (FISH) techniques and to compare the results with those described in CMM in order to better understand similarities and differences between the two entities.

Materials and methods

Four cases of OMM were retrieved from files of the Anatomic Pathology Section at Bellaria Hospital of the Department of Haematology and Oncology, University of Bologna, Italy. All slides were reviewed. The diagnosis of OMM was confirmed based on the currently available criteria (WHO). Patients' stage was reclassified according to the 2010 American Joint Committee on Cancer melanoma TNM staging system [7]. Clinical data from patients' medical records included age, sex, clinical examination, diagnostic imaging, surgical procedure and follow-up. Tissues had been fixed in 10% formalin and embedded in paraffin. Serial sections were cut from selected paraffin blocks.

Immunohistochemistry Immunostaining was performed in 3 μm thick sections serially cut from the selected blocks and stained by a routine immunohistochemical method using the Ventana system, employing the following prediluted antibodies: MART-1, HMB45, S-100, p16, EGFR and smooth muscle actin (SMA; Ventana, Benchmark, Tucson, AZ, USA).

All cases were studied with FISH as follows:

Standard 4 μm sections of formalin fixed and paraffin embedded tissue were used. Sections were incubated at 56°C for 2 h in dry-oven, deparaffinised by washing in three 15-min steps using Bioclear (natural terpene-based clearing agent, Bio-Optica, Milano, Italy), dehydrated in two 5-min steps in Dehyol absolute (alcoholic mixture made up of ethanol, Bio-Optica, Milano, Italy) and air-dried at RT. After incubation in 2× saline sodium citrate buffer (2×SSC; pH 7.0) at 75°C for 14 min, sections were digested with proteinase K (0.25 mg/ml in 2×SSC; pH 7.0) at 45°C for 14 min, rinsed in 2×SSC (pH 7.0) at room temperature for 5 min, and dehydrated using a series of increasing concentration of ethanol (70%, 85% and 100%) for 2 min each. The Vysis LSI 1p36/LSI 1q25 and LSI EGFR SpectrumOrange/CEP 7 SpectrumGreen Probe and the Vysis LSI p16(9p21)/CEP9 Dual Color Probe (Abbott/Vysis, Des Plaines, Illinois) were applied following the manufacturer's instructions onto the selected area based on the presence of tumour foci on each slide, and the hybridisation area was covered with a coverslip and sealed with rubber cement. The slides were incubated at 75°C for 10 min for co-denaturation of chromosomal and probe DNA and then at 37°C for 20–24 h to allow hybridisation to occur. Post-hybridisation washes were performed in NP40 0.5%/2×SSC (pH 7.0–7.5) at 75°C for 2 min and in 2×SSC for 2 min at room temperature. The samples were then dehydrated in ethanol as above, then 4′,6′-diamidino-2-phenylindole suspended in Antifade diluents 1 μg/7 ml (KREATECH Diagnostics, Amsterdam, The Netherlands) was applied for chromatin counterstaining. FISH analysis was performed using an Olympus BX61 Epifluorescence Microscope (Olympus, Melville, New York), for each case, at least 60 tumour nuclei were counted, and the copy numbers of 1p36/1q25 and EGFR/CEP7, respectively, were recorded for each nucleus. Cut-off values for designation of deletion were applied following previously described recommendations for 1p [8] and for EGFR/CEP7 [9, 10].

For comparison, the same FISH tests were performed on three cases of cutaneous melanoma (CMM) mainly composed of epithelioid cells, on one case of spindle cells cutaneous melanoma (SCCM) and on three cases of desmoplastic cutaneous melanoma (DCM).

Electron microscopy (EM) was performed as follows in OMM cases 1, 3 and 4 (in case 2, EM had been performed and reported previously by Farnedi et al. [11]). Small blocks were micro-dissected from paraffin embedded samples and then routinely dewaxed by overnight immersion in xylol and rehydrated to phosphate buffer through a graduated diluted alcohol series. Fragments were then re-fixed in phosphate-buffered glutaraldehyde and post-fixed in OsO4, dehydrated in alcohol and propylene oxide and embedded in Epon 812. Thin sections were stained with uranyl acetate and Reynold's lead citrate and observed in a Philips CM 10 TEM.

Results

Clinical history

Case 1 A 57-year-old man first presented with tooth decay in the left mandible. One year later, a swelling on the

gingival fornix was found during clinical examination. The diagnosis of OMM was assessed on incisional biopsy. The lesion was surgically removed. A few months later, the lesion recurred and was surgically resected. One year later, a second local recurrence, measuring 3.8 cm, appeared. The patient underwent to wide surgical resection. Further follow-up is lacking after discharge.

Case 2 This case was the subject of a previous report [11]. A 69-year-old woman presented with a slightly raised and irregular brownish lesion localised on the border between hard and soft palate, measuring 1.7×1 cm. After the histologic diagnosis of OMM performed on incisional biopsy, a radical surgical excision of the maxillary bone was performed. The patient died of unrelated causes (myocardial infarction) 4 months later, with no evidence of recurrence or metastasis.

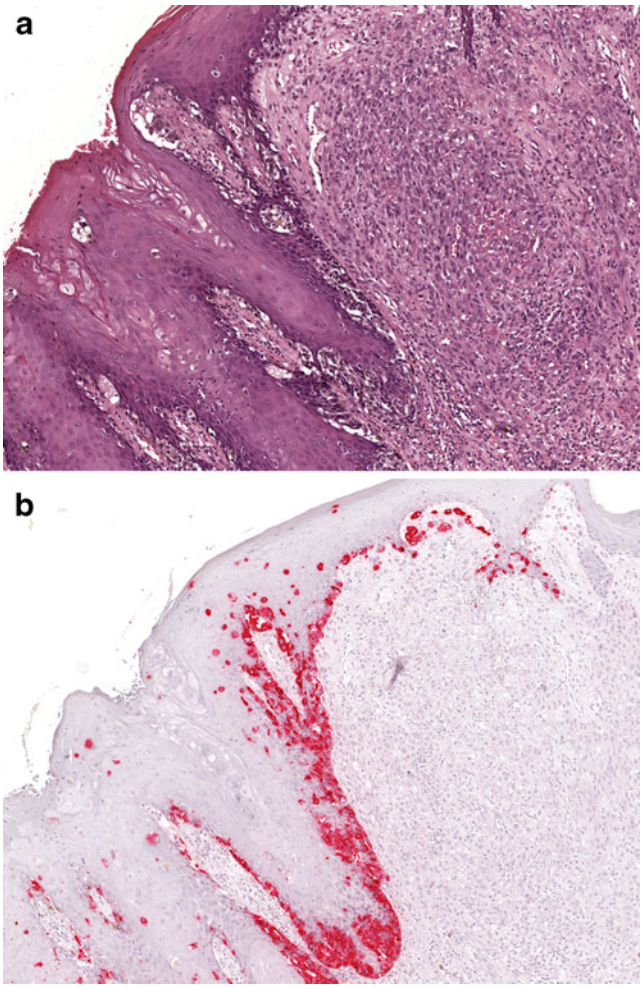

Fig. 1 **a** Case 3. At histology (H&E), it shows a combined pattern of radial and vertical growth; the invasive component is characterised by malignant spindle-shaped cells. **b** Case 3. MART-1 positivity is limited to the superficial, radially growing, component of the tumour

Case 3 A 29-year-old man presented with a painless pigmented lesion incidentally observed during a clinical routine examination. Within 1 month, the lesion grew considerably. On clinical examination, the lesion had irregular borders, involved both the hard and soft palate and measured 0.7×1 cm. Following diagnosis of OMM, performed on incisional biopsy, the patient underwent radical surgical resection followed by reconstruction of the whole palate. One year later, two lateral cervical lymph nodes revealed metastatic involvement. Lymph node removal was followed by chemotherapy. At the latest follow-up, 3 years after the initial diagnosis, the patient is disease free.

Case 4 A 80-year-old man presented with protruding pigmented lesion of the right mandibular gingiva measuring 3.8×2.7 cm, which had been present from 4 months. Radical surgical excision was performed. At the time of diagnosis, two sub-mandibular lymph nodes presented metastatic involvement. One year later, the patient presented local recurrence of disease and metastatic involvement of lateral cervical lymph nodes, lung and liver.

All four cases underwent dermatological examination to exclude CMM.

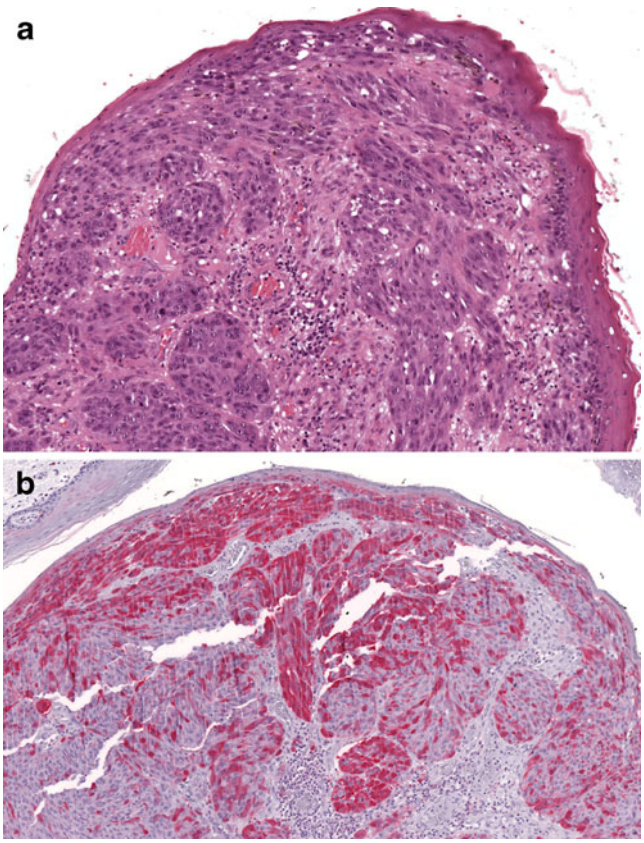

Fig. 2 **a** Case 4. On H&E, it is mainly composed of spindle cells intermingled with collagen bundles. **b** Case 4. p16 is strongly positive

Table 1 Immunohistochemical results

	p16	MART-1	AML	HMB-45	S-100	EGFR
Case no. 1	++	+	–	+F	+F	–
Case no. 2	–	+S	+D	–	+S	–
Case no. 3	–	+S	–	+S	+S	–
Case no. 4	+S	+S	+D	–	+	–

S means in the superficial epithelioid component. D means in the deep spindle cell component. F means focal distribution

Histopathological features

Histopathology All the cases presented similar histological features, therefore they will be described together. A combined pattern of radial and vertical growth was present in all cases: atypical melanocytes with epithelioid appearance were limited to the radial growing component and to the more superficial part of the tumour. The invasive component was characterised by malignant spindle-shaped cells, mostly amelanotic, intermingled among collagen bundles. Collagen bundles were more evident in case 4. Most cells were elongated, showing pleomorphic and hyperchromatic nuclei, prominent eosinophilic nucleoli and numerous atypical mitotic figures (Figs. 1 and 2).

Immunohistochemistry MART-1 and S-100 protein were positive in all the cases, although staining was stronger in the superficial, radially growing, part of the tumour (Table 1). HMB45, p16 and SMA each focally stained two cases; positivity was limited to the superficial component of the tumours. No case stained positively for EGFR.

FISH findings Case 2 was excluded as it resulted unsuitable for FISH analysis (Table 2) (Fig. 3).

9p21 Only one of the three OMM cases showed 9p21 deletion, while the other two cases appeared wild type. The case of SCCM and the three cases of CMM all showed 9p21 deletion.

1p36 No 1p36 deletion was observed in the three cases of OMM, or in the cases of SCCM and desmoplastic cutaneous melanoma (DMM). All three cases of CMM were deleted in the 1p36 locus.

EGFR (7p12) The three cases of OMM showed polysomy of chromosome 7 [9]. In the same cases, the ratio between EGFR gene and centromeric probe signals was <0.80 (relative deletion) [10]. The case of SCCM and the three

Table 2 FISH results

	1p36	9p21	Egfr
OMM case 1	undeleted	undeleted	deleted
OMM case 2	*nd	*nd	*nd
OMM case 3	undeleted	undeleted	deleted
OMM case 4	undeleted	deleted	deleted
SCCM	undeleted	deleted	deleted
CMM	deleted	deleted	undeleted
CMM	deleted	deleted	undeleted
CMM	deleted	deleted	undeleted
DCM	undeleted	*nd	deleted
DCM	undeleted	*nd	deleted
DCM	undeleted	*nd	deleted

**nd* not done

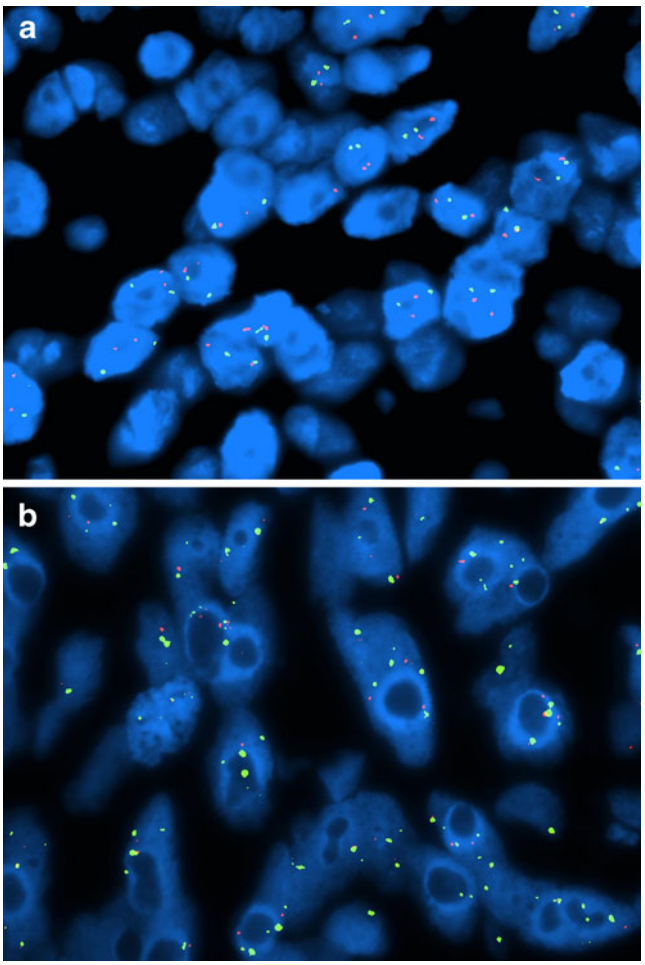

Fig. 3 **a** Case 4. FISH analysis for 1p36 shows a diploid pattern. **b** Case 4. EGFR: neoplastic nuclei show polysomy of chromosome 7 (*green signal*), while the EGFR locus specific (*red signal*) is not present in all the supernumerary chromosomes (relative deletion)

cases of DMM had the same FISH profile. On the contrary, the three cases of CMM showed chromosome 7 polysomy and an EGFR gene amplification.

EM findings Figure 4 melanoma cells were polygonal or spindle in shape, and fusiform melanocytes were mostly present in the invasive and deepest part of the tumour. Nuclei were round or elongated and nucleoli were well evident. Within the cytoplasm variably shaped melanosomes were observed mostly being ovoid. Melanosomes appeared smaller and less numerous compared to those of CMM. In addition, their numbers decreased in the deeper invasive component of the neoplasm.

Intermediate filaments were often visible within the cytoplasm, together with mitochondria, rough endoplasmic reticulum, Golgi complexes and ribosomes.

Discussion

The four cases of OMM showed a morphologic and genetic profile, detected by FISH analysis, similar to SCCM and DMM, while different from CMM. Deletion in 9p21 locus is a frequent finding in CMM [12–15]. On the contrary, FISH analysis of 9p21 locus in the present OMM cases revealed deletion in only 1/3 cases. Moreover, OMM case 2 which had been previously studied by cytogenetic analysis [11] showed chromosome 9 trisomy, in contrast to the frequent finding of chromosome 9 monosomy in CMM [16].

The data obtained here are consistent with the results of Chang et al., who established a new cell line from a melanoma of the palatal mucosa, and did not find deletion of the p16 gene (9p21) in the primary tumour [17].

Further genetic similarities between OMM and DMM and SCCM were evidenced by studying the locus-specific probes 1p36 and EGFR. All the four cases of OMM, one case of SCCM and three cases of DMM resulted wild type for 1p36, while 1p36 deletion was observed in all the three cases of CMM. This finding is consistent with previously reported data showing that deletion of 1p36 is a frequent finding in CMMs [5, 6], while it has not been described in OMM and in DMM.

Moreover, the OMM, DMM and SCCM cases shared the same peculiar EGFR profile: neoplastic nuclei showed a higher number of chromosome 7 (polysomy of chromosome 7), although the EGFR locus specific was not present in all the supernumerary chromosomes (relative deletion).

On the contrary, CMM cases resulted undeleted, showing chromosome 7 polysomy, with all the supernumerary chromosomes presenting the EGFR locus specific gene (EGFR amplification). Differences between OMM and CMM also became evident analysing the histological and immunohistochemical features and the clinical behaviour.

At histology, the present OMM cases presented an invasive component characterised by fascicles of spindle cells intermingled with collagen bundles. The OMM invasive component stained positively with SMA in two cases and showed a focal reactivity with S-100 in two cases, while HMB-45 and MART-1 staining was almost negative. These features are closer to those found in the desmoplastic variant of cutaneous malignant melanoma (DMM). On immunohistochemistry, DMM is frequently

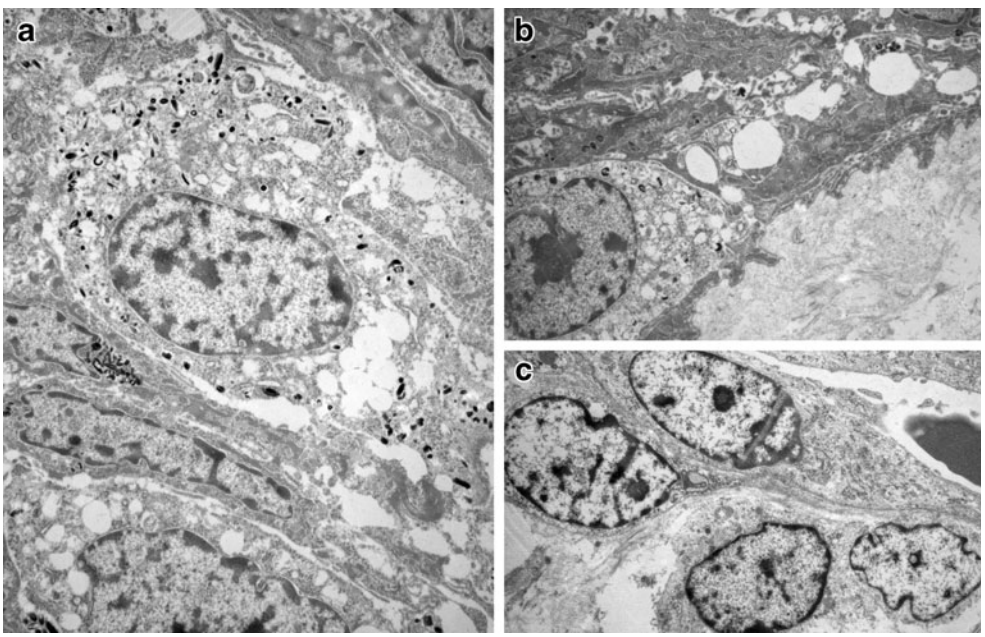

Fig. 4 At ultrastructure, case 3 shows melanosomes in the neoplastic cells (melanosomes diminish towards the invasive component). **a** In situ component. **b**, **c** Invasive components

more positive for S-100 protein, while positivity for HMB-45 and Melan-A is not a constant feature [18, 19]. In addition, DMM can present SMA positivity [18].

A further peculiar finding on the OMM immunohistochemical profile was the p16 protein expression. It is well-known that CMM frequently loose p16 immunoreactivity during malignant transformation. Indeed in metastatic CMM, immunohistochemical reactivity is only present in about 28% [15]. Furthermore, a decreased p16 immunostaining is useful in the differential diagnosis between benign Spitz nevi and CMM [20]. The same is not true in cases of OMM. In the present OMM series 2/4 cases resulted negative with p16. This finding is consistent with data reported by Tanaka et al. who found that 6/13 cases of OMM resulted negative with p16 staining [21]. These differences in p16 immunoreactivity could be explained by the different genetic profile regarding the 9p2.1 locus.

OMM also differed from CMM at the ultrastructural level. OMM displayed only a very small number of mature-staged melanosomes in the deeper component; moreover, the rare melanosomes present seemed to be smaller compared with those described in CMM.

The genetic and morphological variations between OMM and CMM detected in the present study might explain their different clinical behaviour. Compared to CMM, OMM shows a tendency to become thicker in a shorter period of time [22]. Indeed cases 1, 3 and 4 grew to become large lesions in a relatively short period of time ranging from 1 to 12 months.

Consistently, all the OMM cases here showed a thickness >1.5 mm at presentation. Deep tissue invasion and greater thickness at presentation is a common feature in cases of DMM. In the series of DMM reported by Kay et al., the mean thickness at presentation was 1.6 cm, and 28 cases studied presented at Clark level 5 [18].

Desmoplastic features in OMM have been originally described in 1979 by Batsakis et al. [23]. Since then, several desmoplastic OMM has been the subject of case reports [24–28]; therefore, it is difficult to understand its real incidence. In the present series, even if small, all the cases were predominantly composed of spindle cells intermingled with collagen bundles, indicating that probably these features are not so rare in OMM.

To summarise, the data presented highlight the genetic differences between OMM and CMM. The genetic profile, morphological features and clinical behaviour of OMM seem to show similarities with SCCM and DMM.

Acknowledgements This work was financed by grants from the Ministry of the University and Research (Fund ex 40% "Fundamental Oriented Research") and Regione Emilia Romagna (Funds: Region-University Research Program 2007–2009, Project Oncology). ALT is supported with Vanini-Cavagnino grants from the Centro Interdipartimentale di Ricerca sul Cancro "G.Prodi".

Conflict of interest statement None declared

References

1. Aguas SC, Quarracino MC, Lence AN, Lanfranchi-Tizeira HE (2009) Primary melanoma of the oral cavity: ten cases and review of 177 cases from literature. Med Oral Patol Oral Cir Bucal 14(6): E265–E271
2. Kato T, Takematsu H, Tomita Y, Takahashi M, Abe R (1987) Malignant melanoma of mucous membranes. A clinicopathologic study of 13 cases in Japanese patients. Arch Dermatol 123 (2):216–220
3. Barker BF, Carpenter WM, Daniels TE, Kahn MA, Leider AS, Lozada-Nur F, Lynch DP, Melrose R, Merrell P, Morton T, Peters E, Regezi JA, Richards SD, Rick GM, Rohrer MD, Slater L, Stewart JC, Tomich CE, Vickers RA, Wood NK, Young SK (1997) Oral mucosal melanomas: the WESTOP Banff workshop proceedings. Western Society of Teachers of Oral Pathology. Oral Surg Oral Med Oral Pathol Oral Radiol Endod 83(6):672–679
4. Rákosy Z, Vízkeleti L, Ecsedi S, Vokó Z, Bégány A, Barok M, Krekk Z, Gallai M, Szentirmay Z, Adány R, Balázs M (2007) EGFR gene copy number alterations in primary cutaneous malignant melanomas are associated with poor prognosis. Int J Cancer 121(8):1729–1737, 15
5. Poetsch M, Dittberner T, Woenckhaus C (2003) Microsatellite analysis at 1p36.3 in malignant melanoma of the skin: fine mapping in search of a possible tumour suppressor gene region. Melanoma Res 13(1):29–33
6. Hussein MR, Roggero E, Tuthill RJ, Wood GS, Sudilovsky O (2003) Identification of novel deletion Loci at 1p36 and 9p22-21 in melanocytic dysplastic nevi and cutaneous malignant melanomas. Arch Dermatol 139(6):816–817
7. American Joint Committee on Cancer (2010) Cancer Staging Manual, 7th edn. Springer Pub, London
8. Smith JS, Perry A, Borell TJ, Lee HK, O'Fallon J, Hosek SM, Kimmel D, Yates A, Burger PC, Scheithauer BW, Jenkins RB (2000) Alterations of chromosome arms 1p and 19q as predictors of survival in oligodendrogliomas, astrocytomas, and mixed oligoastrocytomas. J Clin Oncol 18:636–645
9. Cappuzzo F, Hirsch FR, Rossi E, Bartolini S, Ceresoli GL, Bemis L, Haney J, Witta S, Danenberg K, Domenichini I, Ludovini V, Magrini E, Gregorc V, Doglioni C, Sidoni A, Tonato M, Franklin WA, Crino L, Bunn PA Jr, Varella-Garcia M (2005) Epidermal growth factor receptor gene and protein and gefitinib sensitivity in non-small-cell lung cancer. J Natl Cancer Inst 97(9):643–655
10. Sauer T, Guren MG, Noren T, Dueland S (2005) Demonstration of EGFR gene copy loss in colorectal carcinomas by fluorescence in situ hybridization (FISH): a surrogate marker for sensitivity to specific anti-EGFR therapy? Histopathology 47:560–564
11. Farnedi A, Magrini E, Betts CM, Cocchi R, Pession A, Foschini MP (2005) Cytogenetic analysis of oral malignant melanoma. Oral Surg Oral Med Oral Pathol Oral Radiol Endod 99(6):655–656
12. Kamb A, Shattuck-Eidens D, Eeles R, Liu Q, Gruis NA, Ding W, Hussey C, Tran T, Miki Y, Weaver-Feldhaus J, McClure M, Aitken JF, Anderson DE, Bergman W, Frants R, Goldgar DE, Green A, MacLennan R, Martin NG, Meyer LJ, Youl P, Zone JJ, Skolnick MH, Cannon-Albright LA (1994) Analysis of the p16 gene (CDKN2) as a candidate for the chromosome 9p melanoma susceptibility locus. Nat Genet 8(1):23–26
13. Nobori T, Miura K, Wu DJ, Lois A, Takabayashi K, Carson DA (1994) Deletions of the cyclin-dependent kinase-4 inhibitor gene in multiple human cancers. Nature 368(6473):753–756, 21
14. Talve L, Sauroja I, Collan Y, Punnonen K, Ekfors T (1997) Loss of expression of the p16INK4/CDKN2 gene in cutaneous malignant

melanoma correlates with tumor cell proliferation and invasive stage. Int J Cancer 74(3):255–259, 20
15. Reed JA, Loganzo F Jr, Shea CR, Walker GJ, Flores JF, Glendening JM, Bogdany JK, Shiel MJ, Haluska FG, Fountain JW, Albino AP (1995) Loss of expression of the p16/cyclin-dependent kinase inhibitor 2 tumor suppressor gene in melanocytic lesions correlates with invasive stage of tumor progression. Cancer Res 55(13):2713–2718, 1
16. Isshiki K, Seng BA, Elder DE, Guerry D, Linnenbach AJ (1994) Chromosome 9 deletion in sporadic and familial melanomas in vivo. Oncogene 9(6):1649–1653
17. Chang KW, Lin SC, Chao SY, Kwan PC, Chiu CP, Wong YK (2001) Establishment and characterization of an oral melanoma cell line (ME). Oral Oncol 37(3):301–307
18. Kay PA, Pinheiro AD, Lohse CM, Pankratz VS, Olsen KD, Lewis JE, Nascimento AG (2004) Desmoplastic melanoma of the head and neck: histopathologic and immunohistochemical study of 28 cases. Int J Surg Pathol 12(1):17–24
19. Kucher C, Zhang PJ, Pasha T, Elenitsas R, Wu H, Ming ME, Elder DE, Xu X (2004) Expression of Melan-A and Ki-67 in desmoplastic melanoma and desmoplastic nevi. Am J Dermatopathol 26 (6):452–457
20. George E, Polissar NL, Wick M (2010) Immunohistochemical evaluation of p16INK4A, E-cadherin, and cyclin D1 expression in melanoma and Spitz tumors. Am J Clin Pathol 133(3):370–379
21. Tanaka N, Odajima T, Mimura M, Ogi K, Dehari H, Kimijima Y, Kohama G (2001) Expression of Rb, pRb2/p130, p53, and p16 proteins in malignant melanoma of oral mucosa. Oral Oncol 37 (3):308–314
22. Hicks MJ, Flaitz CM (2000) Oral mucosal melanoma: epidemiology and pathobiology. Oral Oncol 36(2):152–169
23. Batsakis JC, Bauer R, Regezi JA, Campbell T (1979) Desmoplastic melanoma of the maxillary alveolus. J Oral Surg 37 (2):107–109
24. Dallera P, Bertoni F, Marchetti C, Bacchini P (1982) Atypical melanocytic hyperplasia concomitant with malignant desmoplastic melanoma of the oral cavity. Minerva Stomatol 31(2):153–164
25. Kurihara K, Sanada E, Yasuda S, Yamasaki H (1992) Desmoplastic malignant melanoma of the gingiva. Oral Surg Oral Med Oral Pathol 74(2):201–205
26. Ueta E, Miki T, Osaki T, Iwata J, Sonobe H (1996) Desmoplastic malignant melanoma of the gingiva: case report and review of the literature. Eur J Cancer B Oral Oncol 32B(6):423–427
27. Kilpatrick SE, White WL, Browne JD (1996) Desmoplastic malignant melanoma of the oral mucosa. An underret diagn pitfall Cancer 78(3):383–389
28. Kavanagh BD, Campbell RL, Patterson JW, O'Neill RL, Cardinale RM, Kaugars GE (2000) Desmoplastic malignant melanoma of the palatal alveolar mucosa: sustained disease-free survival after surgery and postoperative radiotherapy. Oral Surg Oral Med Oral Pathol Oral Radiol Endod 89(4):465–470

Virchows Arch (2011) 459:175–182
DOI 10.1007/s00428-011-1106-x

ORIGINAL ARTICLE

Interactive digital slides with heat maps: a novel method to improve the reproducibility of Gleason grading

Lars Egevad · Ferran Algaba · Daniel M. Berney · Liliane Boccon-Gibod · Eva Compérat · Andrew J. Evans · Rainer Grobholz · Glen Kristiansen · Cord Langner · Gina Lockwood · Antonio Lopez-Beltran · Rodolfo Montironi · Pedro Oliveira · Matthias Schwenkglenks · Ben Vainer · Murali Varma · Vincent Verger · Philippe Camparo

Received: 23 March 2011 / Revised: 12 May 2011 / Accepted: 9 June 2011 / Published online: 23 June 2011
© Springer-Verlag 2011

Abstract Our aims were to analyze reporting of Gleason pattern (GP) 3 and 4 prostate cancer with the ISUP 2005 Gleason grading and to collect consensus cases for standardization. We scanned 25 prostate biopsy cores diagnosed as Gleason score (GS) 6–7. Fifteen genitourinary pathologists graded the digital slides and circled GP 4 and 5 in a slide viewer. Grading difficulty was scored as 1–3. GP 4 components were classified as type 1 (cribriform), 2 (fused), or 3 (poorly formed glands). A GS of 5–6, 7 (3+4), 7 (4+3), and 8–9 was given in 29%, 41%, 19%, and 10% (mean GS 6.84, range 6.44–7.36). In 15 cases, at least 67% of observers agreed on GS groups (consensus cases). Mean interobserver weighted kappa for GS groups was 0.43. Mean difficulty scores in consensus and non-consensus

L. Egevad (✉)
Department of Oncology-Pathology, Karolinska Institutet,
Radiumhemmet P1:02 Karolinska University Hospital,
171 76 Stockholm, Sweden
e-mail: lars.egevad@ki.se

F. Algaba
Fundacio Puigvert-University Autonomous,
Barcelona, Spain

D. M. Berney
Institute of Cancer, St Bartholomew's Hospital,
Queen Mary, University of London, London, UK

L. Boccon-Gibod
Hopital Armand Trousseau, Paris, France

E. Compérat
Hopital La Pitié-Salpetrière, Paris, France

A. J. Evans
University of Toronto, Toronto, Canada

R. Grobholz
Kantonsspital Aarau, Aarau, Switzerland

G. Kristiansen
University Hospital Zurich, Zurich, Switzerland

C. Langner
Medical University of Graz, Graz, Austria

G. Lockwood
Canadian Partnership Against Cancer,
Toronto, Canada

A. Lopez-Beltran
Cordoba University Medical School,
Cordoba, Spain

R. Montironi
Polytechnic University of the Marche Region,
Ancona, Italy

P. Oliveira
Hospital da Luz, Lisbon, Portugal

M. Schwenkglenks
University of Basel, Basel, Switzerland

B. Vainer
Rigshospitalet, Copenhagen, Denmark

M. Varma
University Hospital of Wales, Cardiff, UK

V. Verger
CCITI, Dijon, France

P. Camparo
Hopital Foch, Paris, France

cases were 1.44 and 1.66 (p=0.003). Pattern 4 types 1, 2, and 3 were seen in 28%, 86%, and 67% of GP 4. All three coexisted in 16% (11% and 23% in consensus and non-consensus cases, p=0.03). Average estimated and calculated %GP 4/5 were 29% and 16%. After individual review, the experts met to analyze diagnostic difficulties. Areas of GP 4 and 5 were displayed as heat maps, which were helpful for identifying contentious areas. A key problem was to agree on minimal criteria for small foci of GP 4. In summary, the detection threshold for GP 4 in NBX needs to be better defined. This set of consensus cases may be useful for standardization.

Keywords Prostate cancer· Biopsy· Gleason grading · Digital pathology· Reproducibility· Consensus

Introduction

In 2005 the International Society of Urological Pathology (ISUP) organized a consensus conference on Gleason grading of prostate cancer [1]. Since its inception in the 1960s, the Gleason grading has undergone a gradual transition in its practical application. The purpose of the meeting was to reach a consensus as to how the grading system should be used in needle biopsy (NBX) and radical prostatectomy (RP) specimens. The conference addressed issues in the interpretation of morphological patterns and how to summarize and report grade information.

It is not clear how the ISUP revision of Gleason grading has affected the pathology community. Multiple studies were performed on grading reproducibility in the years prior to the ISUP consensus conference [2–6], but it is unknown how reproducible the modified Gleason grading is among experts in urological pathology. There is also a need to set a standard among general pathologists in application of the new guidelines.

In previous reproducibility studies on prostate cancer grading, the observers assigned Gleason scores, but to our knowledge, no attempts were made to analyze which areas the grading decisions were based upon. In this study, 15 experts in urological pathology were asked to circle areas of Gleason patterns (GP) 4 and 5. This enabled an analysis of how grading decisions are made and identification of controversies and agreements that are not reflected by the Gleason scores (GS) alone. The aims were both to assess reproducibility and to better define the critical transition between GP 3 and 4. Interpretation difficulties were analyzed. Our purpose was not only to study areas of disagreement but also to collect consensus cases for standardization of grading. By publication of such cases, it is possible to minimize the interobserver variation among pathologists.

Materials and methods

A total of 220 prostate NBX cases were reported at the Karolinska University Hospital, Stockholm, Sweden, in January and February 2008, 99 of them as prostate cancer. A set of NBX cores diagnosed as GS 6–7 prostate cancer was selected. Only GS 6 cases that were borderline to GS 7 were included, i.e., cases in which a GS 7 or higher theoretically might be diagnosed. One representative core was chosen from each of 30 biopsy sets, recut and stained with hematoxylin and eosin. The slides were reviewed by one of the authors (LE). Cases with technical artifacts were omitted. and 27 slides were scanned in a digital slide scanner (CCITI, Dijon, France). Among them two were excluded because of unsatisfactory image quality, leaving 25 digital slides for analysis.

Fifteen experts in urological pathology from 11 countries were invited to participate: Austria (1), Canada (1), Denmark (1), France (3), Germany (1), Italy (1), Portugal (1), Spain (2), Sweden (1), Switzerland (1), and the United Kingdom (2). The experts were asked to assign primary and secondary Gleason grades to the digital slides and a GS was automatically generated. Grading difficulty was scored as 1–3. Score 1 meant that in the expert's opinion only one GS was possible, score 2 that another GS was considered but the pathologist was convinced that the selected GS was the best choice, and score 3 meant that the observer was uncertain if the selected GS was the best score and another score would also be acceptable. GP 4 components were classified as type 1 (cribriform), 2 (fused), or 3 (poorly formed glands, Fig. 1a–c). Each expert circled areas of GP 4 and 5 in the slide viewer and were asked to estimate percentage of GP 4 and 5. These percentages were also calculated from the circled areas. In the image analyzer, the circled areas were layered on top of each other to obtain a summation area, similar to a heat map showing the frequency with which a certain GP was assigned within the biopsy core (Fig. 1d–f). The darker the color, the more often a GP had been assigned. Green was used for GP 4 and yellow for GP 5. GP 3 was not marked on the digital slides.

After individual review, 11 of the experts met in Paris in October 2009 to analyze diagnostic difficulties and agree on a set of consensus cases (LBG, PC, EC, DB, LE, RG, GK, CL, PO, BV, and MV). The grades were analyzed by individual Gleason scores and by GS categories 5–6, 3+4=7, 4+3=7, 8, and 9.

Statistical analysis

Unpaired Student's t test was used for comparison of means and chi-square test for comparison of proportions. A p value less than 0.05 was considered significant. Unweighted and weighted kappa statistics was used to measure interobserver reproducibility.

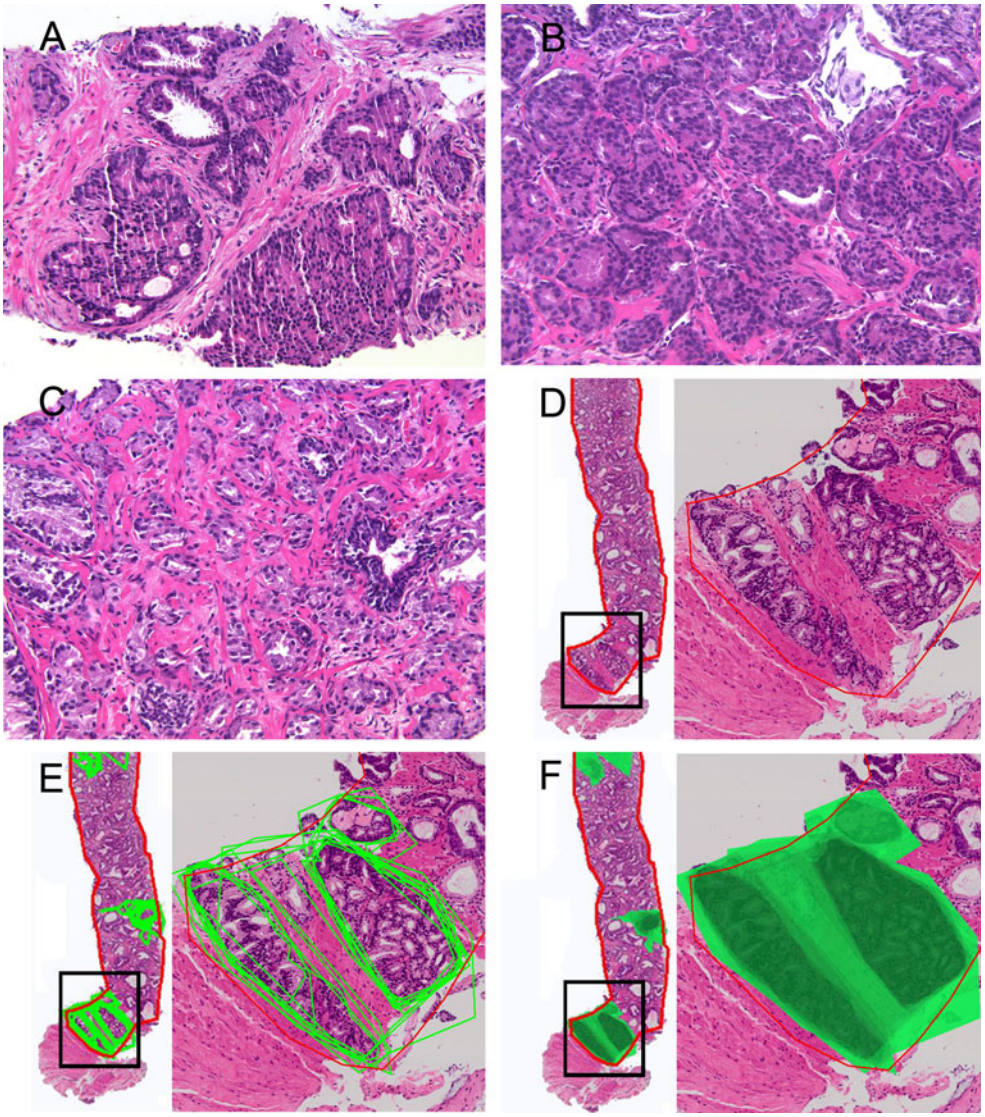

Fig. 1 **a** GP 4 of cribriform type (type 1). **b** GP 4 of fusion type (type 2). **c** GP 4 with incomplete glands (type 3). ×20 lens magnification in **a**–**c**. **d** Needle biopsy with cancer encircled by *red line*. Overview to the *left*, medium slide viewer magnification to the *right*. **e** Areas of GP 4 marked with *green lines* by individual observers. **f** Marked areas were added on top of each other to produce a heat map showing the frequency with which a certain GP was assigned within the biopsy core. The darker the green, the more often a GP 4 was assigned

Results

The original GS distribution was 6 (10, 40%), 3+4=7 (11, 44%), and 4+3=7 (4, 16%), respectively (mean 6.6). The 15 experts assigned a GS of 5 (4, 1%), 6 (106, 28%), 3+4=7 (154, 41%), 4+3=7 (72, 19%), 8 (24, 6%), and 9 (15, 4%), respectively (mean 6.84, range 6.44–7.36). The observers reported a GS of 5 in 0–12%, 6 in 0–52%, 7 in 44–100%, 8 in 0–24%, and 9 in 0–16%.

The unweighted kappas of presence of GP 4 and 5 were 0.54 and 0.81, respectively. The weighted kappas of Gleason scores 5–9 and of the GS categories 5–6, 3+4=7, 4+3=7, 8, and 9 were 0.35 and 0.43, respectively.

An average of 74% of the experts agreed on the most commonly assigned GS (5, 6, 7, 8, or 9) with a range of 47–93% in the 25 cases. A 100% concordance was not reached for any of the cases either for the Gleason scores or the GS categories. A concordance of at least 80% was obtained in 12 cases for Gleason scores and in six cases for the GS categories. A concordance of at least 67% was obtained in 19 cases for Gleason scores. In 15 cases there was a concordance of at least 67% for the GS categories 5–6, 3+4=7, 4+3=7, 8, and 9 and these were designated as consensus cases. Their Gleason scores were 6, 3+4=7, and 4+3=7 in six, seven, and two cases, respectively (Table 1). A concordance of 33–60% was reached for GS categories in 10 cases, which were designated as non-consensus cases (Table 2). In one of these cases, the spread of GS was from 6 to 9 and in two other cases from 6 to 8.

Difficulty scores were reported by 13 of the 15 observers. A difficulty score of 1, 2, or 3 was assigned in 58%, 32%, and 10%, respectively (Table 3). The average reported difficulty score was 1.53 (range 1.20–1.88 among 13 observers). Eight observers had a median difficulty score of 1 and 5 had a median score of 2. In the 15 consensus cases, the average difficulty score was 1.44 as compared to

Table 1 Fifteen consensus cases with at least 67% agreement for Gleason score categories

Gleason score categories						
Case	5–6	7 (3+4)	7 (4+3)	8	9	Agreement (%)
1	**12**	3	0	0	0	80
2	0	**10**	2	3	0	67
4	2	**10**	3	0	0	67
6	2	**11**	1	0	1	73
10	**13**	2	0	0	0	87
12	1	**11**	1	2	0	73
14	0	1	**13**	0	1	87
15	1	**10**	3	1	0	67
16	0	**13**	1	1	0	87
17	**11**	3	1	0	0	73
18	**10**	4	1	0	0	67
19	**11**	4	0	0	0	73
21	1	0	**11**	3	0	73
22	1	**14**	0	0	0	93
23	**12**	3	0	0	0	80

Number of votes for most commonly assigned grade shown in bold

1.66 in the 10 non-consensus cases (p=0.003). Among consensus cases a difficulty score of 1, 2, or 3 was assigned in 65%, 27%, and 8%, respectively. Among non-consensus cases a difficulty score of 1, 2, or 3 was assigned in 48%, 38%, and 14%, respectively. When biopsies were assigned a difficulty score 3, 53% (18 of 34) were non-consensus cases compared to 33% (62 of 188) when a score 1 was assigned (p=0.026).

Thirteen observers categorized the GP 4 according to type. GP 4 type 1 (cribriform), 2 (fused), or 3 (poorly formed glands) were seen in 20%, 61%, and 47%, respectively (Table 4). A GP 4 was reported in 70% (228 of 325). When a GP 4 was reported, types 1, 2, and 3 were seen in 28%, 86%, and 67%. When a GP 4 was reported, all three patterns, two patterns, and one pattern were seen in 16%, 50%, and 34%, respectively (Table 5). All three patterns were seen in 11% of the consensus cases and 23% of the non-consensus cases (p=0.03). Per case, 1.88, 6.88, and 2.56 observers assigned a GP type of 1, 2, and 3, respectively. A GP 5 was assigned by at least one observer in seven cases (by one to eight observers).

Regions were marked by 14 of 15 observers. The precision of marking the areas was highly variable. The mean percentage of GP 4 cancer was 28% when estimated subjectively and 16% when calculated by the image analyzer. The mean percentage of GP 5 was 0.5% as estimated and 0.1% as calculated.

Areas of GP 4 and 5 were displayed as heat maps with overlaying regions. The maps were helpful for identifying contentious areas. A key problem was to agree on minimal criteria for small foci of GP 4 (Fig. 2). In an open discussion, areas were identified where the majority had overlooked a minute component of cancer that might be interpreted as high-grade carcinoma. These included occasional solid strands (Fig. 2a, b) or fusion patterns (Fig. 2c, d) in GS 3+3=6, which could be considered tangential sections of GP 3 cancer glands. In other cases, such structures were too abundant to be overlooked (Fig. 2e, f), leading to a consensus grading of GS 3+4=7.

Discussion

Over the past decades, there has been a gradual change of the practice of Gleason grading, causing considerable grade shift upwards [7]. The recent ISUP revision of the Gleason grading system has contributed to this upgrading. Helpap et al. showed that the number of NBX cases diagnosed as GS 6 decreased from 48% to 22% when adopting the ISUP modification of Gleason grading, while the number of GS 7 cases increased from 26% to 68% [8]. In a recent study by Delahunt et al. on patients with locally advanced prostate cancer, the number of cases diagnosed as GS 6 decreased from 11% to 5% when going from conventional to ISUP modified GS [9].

Reasons for upgrading include both changed pattern interpretation and new recommendations for how to report the GS on NBX specimens. The ISUP guidelines proposed that GP 1 should be avoided "with extremely rare exception," that GS 2+2=4 should rarely be diagnosed on NBX, and that most cribriform cancers should be diagnosed as GP 4 rather than 3 [1]. Furthermore, cancers with incomplete, poorly formed glands were now included in GP

Table 2 Ten non-consensus cases with agreement for Gleason score categories in less than 67%

Gleason score categories						
Case	5–6	7 (3+4)	7 (4+3)	8	9	Agreement (%)
3	**8**	7	0	0	0	53
5	2	**5**	3	2	3	33
7	0	6	**8**	1	0	53
8	0	6	**8**	1	0	53
9	2	**9**	1	3	0	60
11	0	2	**8**	3	2	53
13	**8**	7	0	0	0	53
20	6	**7**	2	0	0	47
24	0	0	4	3	**8**	53
25	**7**	6	1	1	0	47

Number of votes for most commonly assigned grade shown in bold

Table 3 Difficulty scores in 15 consensus and 10 non-consensus cases

	Difficulty scores					
	1	2	3	Total	Mean	*p* value
Consensus	65% (126)	27% (53)	8% (16)	195	1.44	0.003
Non-consensus	48% (62)	38% (50)	14% (18)	130	1.66	
Total	58% (188)	32% (103)	10% (34)	325		

Score 1, only one GS was possible; score 2, another GS was considered but the pathologist was convinced that the selected GS was the best choice; and score 3, uncertain if the selected GS was the best score

4. Some of these rules for pattern interpretation were implemented by many experts already before the ISUP revision. Perhaps more important, there was previously a widespread tradition to overlook small foci of higher grade or to diagnose them as tertiary pattern of higher grade, but not include them in the GS. Prior to the ISUP consensus meeting, a GP of higher grade was generally included only if more than 5% of all cancer is present [10]. One of the key recommendations of the ISUP meeting was that even minute foci of higher grade should be included in the GS on NBX specimens, regardless of the extent though it was added that they should be identified at "low to medium power." This possible equivocation has probably meant that pathologists may have different detection thresholds for small high-grade components and there is a need to standardize this interpretation. In retrospect, this part of the ISUP revision of Gleason grading can be questioned. The consequences have evidently been a substantial upgrading in some institutions. There is now considerable uncertainty among pathologists where to place the threshold for recognition of minute high-grade components. There is also a concern among urologists how a GS 7 cancer on needle biopsy should now be treated. It would have been very helpful if the ISUP consensus meeting 2005 had presented more precise practical guidelines regarding GP 4 detection with, e.g., ample illustrations. The best that can be done in the current situation is that experts attempt to agree on a standardized interpretation of the GP 3 to 4 transition. As a first step, we aim to use the microphotograph material from this study to set up a web-based image library that is made accessible for European pathologists.

The weighted kappa of Gleason scores in the present study was lower than reported in many previous studies on interobserver reproducibility of Gleason grading [2, 3, 5, 6]. However, the results are not comparable as the biopsy cores of the present study were selected to include borderline cases between GS 6 and 7. The unweighted kappas of presence of GP 4 and particularly of GP 5 were far better. The latter may be an overestimation as the cases were primarily selected to lack a GP 5 component. There are indeed multiple pitfalls with the use of kappa statistics. How study cases are selected is of critical importance. The safest method to avoid selection bias is to use a consecutive series. Unfortunately, it is not feasible to make such a study on a consecutive series that is sufficiently large to include difficult and interesting cases. More commonly, there is an accumulation of cases that experts consider unequivocal so the golden standard of the study cannot be criticized. By contrast, in the present study, we have selected cases with borderline morphology. The easiest cases of GS 6 were excluded and only GS 6 cases where it was thought that someone might diagnose a GS 7 were included. We have also refrained from inclusion of classical GS 9–10 cases, which would also most likely give a high-grading reproducibility. Thus, it is not surprising that the kappa statistics in our study were comparatively low and they should rather be used for comparisons within the study.

We here used digitized slides that were read in a slide viewer. It has been shown that the diagnostic accuracy using digital slides is similar to conventional glass slides [11]. It would not have been possible to circulate glass slides to 15 experts in 11 countries within a reasonable time

Table 4 Gleason pattern 4 types in consensus and non-consensus cases

	Type of Gleason pattern 4				
	1	2	3	Total	*p* value
Consensus	24% (31)	81% (106)	67% (88)	131	0.38
Non-consensus	35% (34)	94% (91)	66% (64)	97	
Total	28% (65)	86% (197)	67% (152)	228	

GP4 type 1, cribriform glands; type 2, fused glands; and type 3, poorly formed glands. Percentages of cases with a GP 4 reported

Table 5 Number of Gleason pattern 4 types in consensus and non-consensus cases

	Number of Gleason pattern 4 types				
	1	2	3	Total	*p* value
Consensus	39% (51)	50% (66)	11% (14)	131	0.03
Non-consensus	28% (27)	50% (48)	23% (22)	97	
Total	34% (78)	50% (114)	16% (36)	228	

Percentages of cases with a GP 4 reported

frame. The other advantage with digital slide is that they allow marking of regions of interest. To our knowledge this is the first attempt to identify the areas that Gleason grading decisions are based upon. The advantage of the heat map system is that it enables an analysis of which patterns are controversial and which are easier to grade. After an independent assessment of grades a majority of the group met in Paris to discuss controversies and analyze why there was disagreement in some cases. In the discussion the heat maps could be removed from the digital slides to show the detailed histological morphology. While doing this we compared morphological features with lists of individual grading results. It was sometimes evident that disagreement was caused by an occasional outlier, while in other cases, the participants were split into more equal groups of different standpoints. Certain patterns seemed to be more difficult than others, such as incomplete glands where the detection threshold was critical for accurate grading.

We found that there is not only a variability in how Gleason scores are assigned but also in terms of what

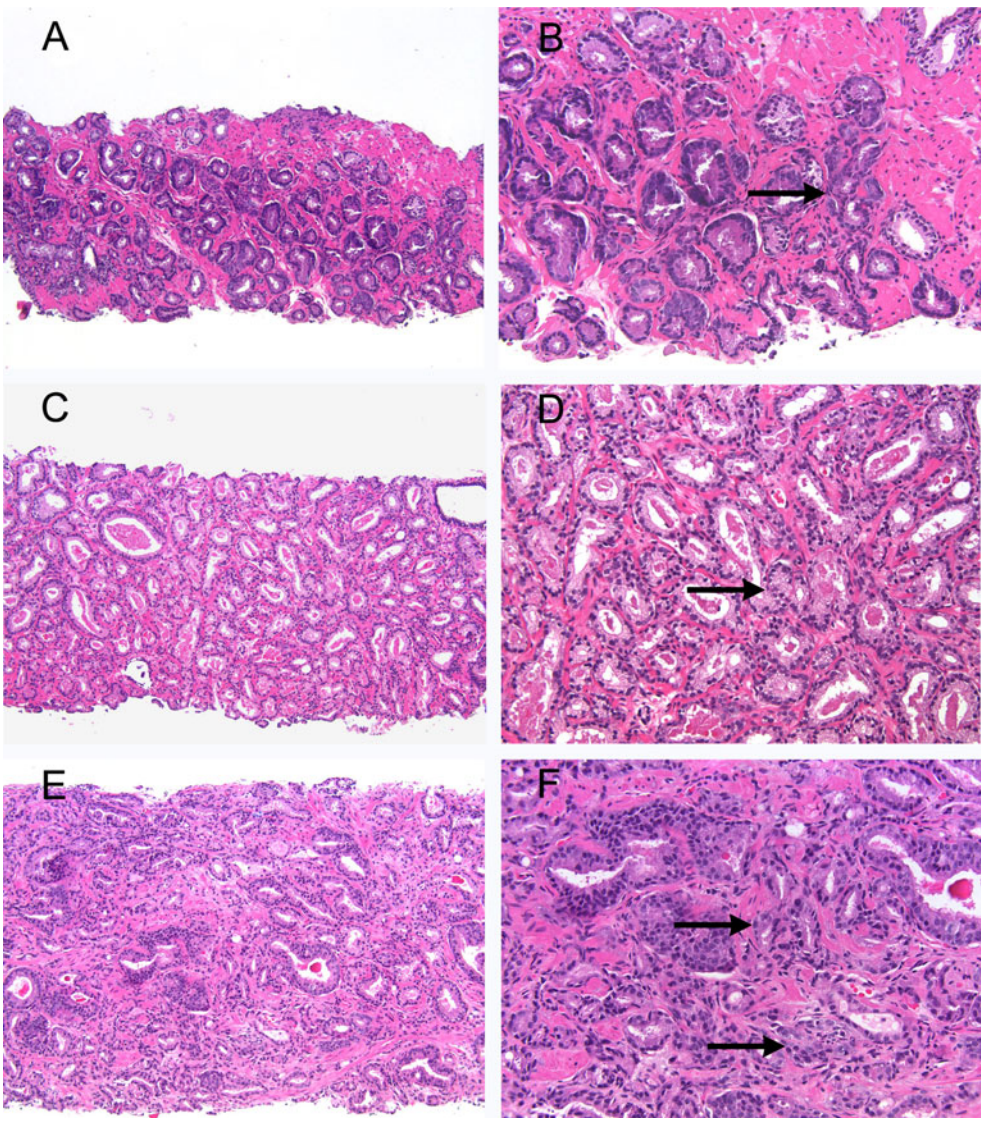

Fig. 2 **a** Consensus case of GS 3+3=6, ×10 lens magnification. **b** The same consensus case of GS 3+3=6. Most glands are circumscribed and well defined. *Arrow* indicates a few epithelial strands that can be overlooked, as they possibly represent tangential cuts. To be ignored such structures must be only occasional finding, ×20 lens magnification. **c** Consensus case of GS 3+3=6, ×10 lens magnification. **d** The same consensus case of GS 3+3=6. *Arrow* indicates a few seemingly fused glands. When only occasional merged glandular structures are found, they should not be interpreted as a fusion pattern, as they possibly represent tangential cuts; ×20 lens magnification. **e** Consensus case of GS 3+4=7, ×10 lens magnification. **f** The same consensus case of GS 3+4=7. Some glands are circumscribed and well defined. However, *arrow* indicates poorly formed glands that are too abundant to be and dispersed throughout the visual field to be overlooked. The 2005 ISUP consensus meeting decided to include such poorly formed or incomplete glands in GP 4; ×20 lens magnification

precise areas decisions are based on. When minute foci of higher grade should be included in the GS on NBX specimens, regardless of the extent, it is necessary to define a detection threshold in order to avoid the degeneration of Gleason grading into a three-tiered grading system running from GS 7 to 9. In the open discussion, such examples were found to include possible tangential cuts of complete or incomplete glandular structures.

Fusion pattern was found to be the most common GP 4 type, while cribriform cancer, i.e., one of the classical variants of GP 4, was least common. A novel feature of the ISUP revision is that poorly formed or incomplete glands are included in GP 4, which is in line with the general concept of GP 4 as cancer that attempts to form glands, yet falls short of forming complete, circumscribed glands. Poorly formed glands were seen in 47% of GP 4, making it the next most common type of GP 4 after the fusion pattern. All three patterns were seen in 16% of GP 4 cases, more commonly in non-consensus cases than in consensus cases, indicating that the presence of a heterogeneous GP 4 component adds to the grading difficulty.

The purpose of the study was primarily to define the transition between Gleason patterns 3 and 4, and the cases were selected accordingly. Yet a GP 5 was assigned by at least one observer in seven cases (by one to eight observers). In a study by Egevad et al., a questionnaire was distributed to 91 genitourinary pathologists in countries around the world [12]. Rare individual cells, strands, or nests identified only at less than ×40 lens magnification were considered sufficient to diagnose GP 5 on needle biopsy by 17% of pathologists, whereas 83% required clusters of such structures seen at lower than ×40 magnification. The GP 5 identified by occasional observers in some cases proved to be minute components rather than cohesive areas and should be overlooked according to the vast majority of observers.

Interestingly, cases with higher self-rated grading difficulty had lower reproducibility. A difficulty score of 1, 2, or 3 was assigned in 58%, 32%, and 10%, respectively, which means that as many as 42% of assessments were accompanied with a certain degree of doubt as to the correct grade. It is on the other hand surprising that in 42% of non-consensus cases, the experts gave a difficulty score of 1, i.e., they were absolutely certain that their grade was the correct one. Thus, there is a discrepancy between our self-confidence and the performance as a group. These results have to be interpreted with some caution as a research study differs from routine pathology work. A limited number of cases are reviewed, and the participants are usually devoted to the task. A certain fear to deviate from the midstream of the group may add to the motivation. Thus, study participants are more likely to report a high self-rated grading difficulty in cases where they fail to reach consensus, while in a busy routine practice, mistakes may also be done in cases that are felt to be easy.

Percent high-grade cancer (percentage of Gleason pattern 4 or 5, %GP 4/5) has been suggested as a prognostic factor for prostate cancer [13–16]. The Gleason grading system was originally a nine-tiered system, but only some of the grades are actually commonly used. Therefore, %GP 4/5 may help to separate cases in the mid-range of the Gleason scores. A "sliding scale" grading system similar to nomograms has attractions over a stochastic grading system, which can fall prey to the problems exemplified by this study. The present study is to our knowledge the first time that a comparison has been done between subjective and objective assessment of %GP 4/5. Interestingly, the subjectively estimated area was almost twice as large as the objective measurement. This may be explained by some inherent difficulties in the assessment of proportions of GPs. Prostate cancer specimens contain a mixture of malignant and benign glands and also of epithelial and stromal components. When there are multiple GPs present, e.g., GP 3 and 4, they are often mixed. The assessment of areas occupied by a certain GP is thus not quite straightforward. It may vary between individuals how much of non-cancerous elements within the tumor we include or subtract. The higher percentages by subjective assessment may indicate that the human eye tends to overlook presence of e.g., occasional GP 3 glands within a GP 4 or the presence of benign glands within the tumor. When we are asked to document our assessment by outlining a high-grade component digitally, it seems to make us more aware of such non-high-grade components. On the other hand, the subjective estimation of %GP 4/5 has been shown to be at least as reproducible as that of the GS. In an interobserver reproducibility study, four observers had a mean weighted kappa for biopsy GS and %GP 4/5 of 0.48–0.55 (overall mean 0.51) and 0.52–0.68 (overall mean 0.60), respectively [17]. However, it was found that we subjectively overestimated %GP 4/5 as compared to computerized calculation of the percentage. A difficulty in the assessment of percentages of Gleason patterns is that malignant glands are often mixed with stroma and benign glands and it is difficult to know how much of intervening tissues should be subtracted.

The clinical performance of GS as predictor of outcome is evidently most important when determining the optimal definition of grade. Billis et al. showed that both conventional and modified GS on NBX predicted outcome after RP [18]. A lower p value was obtained with the modified GS and the authors concluded that the conventional grading was outperformed. However, the Kaplan–Meier curves for GS 6 and 7 were almost identical with modified grading and the separation seems to be between GS 7 vs. 8 or higher. Delahunt et al. recently questioned the performance of the modified GS as predictor of disease progression [9]. Further studies are

needed and it is important that those studies clearly define how the GS was obtained. A major disadvantage of the ISUP 2005 revision of the Gleason grading system was that it did not include any validation studies comparing the revised and the conventional versions of this grading system.

Perhaps the most useful part of this study was the identification of a set of 15 cases in which there was a 67% consensus among experts in terms of GS categories. This set of cases may serve as a library for standardization among general pathologists. For this purpose, we intend to use the European Network of Uropathology (ENUP), an international network of communication recently organized by the Uropathology Working Group of the European Society of Pathology [19]. The purpose of ENUP is to establish a channel for distribution of information about urological pathology such as guidelines, consensus documents, meetings, and courses, to organize research collaborations and to set up mechanisms for survey studies. ENUP has recruited a total of 374 individual members from 338 pathology laboratories in 15 west European countries. Email is used for all communication, and studies are carried out through interactive websites. Our intention is to invite the ENUP members to use the same set of cases as in the expert study for a larger reproducibility study and then give feedback as to how experts agreed on the same cases. Thereby, it will be possible to use a library of digital slides for standardization of histopathological grading.

In summary, there is still a considerable disagreement among experts on borderline GS 6–7 cases, using the ISUP revision of the Gleason grading of prostate cancer. A major source of disagreement is that the detection threshold for minimal foci of GP 4 in NBX needs to be better defined. Yet, we were able to identify a set of consensus cases that are likely to be useful for standardization of Gleason grading.

Acknowledgment Source of support: DMB is supported by Orchid.

Conflict of interest statement We declare that we have no conflict of interest.

References

1. Epstein JI, Allsbrook WC Jr, Amin MB, Egevad LL (2005) The 2005 International Society of Urological Pathology (ISUP) consensus conference on gleason grading of prostatic carcinoma. Am J Surg Pathol 29:1228–1242
2. Allsbrook WC Jr, Mangold KA, Johnson MH, Lane RB, Lane CG, Amin MB, Bostwick DG, Humphrey PA, Jones EC, Reuter VE, Sakr W, Sesterhenn IA, Troncoso P, Wheeler TM, Epstein JI (2001) Interobserver reproducibility of Gleason grading of prostatic carcinoma: urologic pathologists. Hum Pathol 32:74–80
3. Allsbrook WC Jr, Mangold KA, Johnson MH, Lane RB, Lane CG, Epstein JI (2001) Interobserver reproducibility of Gleason grading of prostatic carcinoma: general pathologist. Hum Pathol 32:81–88
4. Carlson GD, Calvanese CB, Kahane H, Epstein JI (1998) Accuracy of biopsy Gleason scores from a large uropathology laboratory: use of a diagnostic protocol to minimize observer variability. Urology 51:525–529
5. Egevad L (2001) Reproducibility of Gleason grading of prostate cancer can be improved by the use of reference images. Urology 57:291–295
6. Lessells AM, Burnett RA, Howatson SR, Lang S, Lee FD, McLaren KM, Nairn ER, Ogston SA, Robertson AJ, Simpson JG, Smith GD, Tavadia HB, Walker F (1997) Observer variability in the histopathological reporting of needle biopsy specimens of the prostate. Hum Pathol 28:646–649
7. Berney DM, Fisher G, Kattan MW, Oliver RT, Moller H, Fearn P, Eastham J, Scardino P, Cuzick J, Reuter VE, Foster CS (2007) Major shifts in the treatment and prognosis of prostate cancer due to changes in pathological diagnosis and grading. BJU Int 100:1240–1244
8. Helpap B, Egevad L (2006) The significance of modified Gleason grading of prostatic carcinoma in biopsy and radical prostatectomy specimens. Virchows Arch 449:622–627
9. Delahunt B, Lamb DS, Srigley JR, Murray JD, Wilcox C, Samaratunga H, Atkinson C, Spry NA, Joseph D, Denham JW (2010) Gleason scoring: a comparison of classical and modified (International Society of Urological Pathology) criteria using nadir PSA as a clinical end point. Pathology 42:339–343
10. Deshmukh N, Foster CS (1998) Grading prostate cancer. In: Foster CS, Bostwick DG (eds) Pathology of the prostate. Saunders, Philadelphia, pp 191–227
11. Koch LH, Lampros JN, Delong LK, Chen SC, Woosley JT, Hood AF (2009) Randomized comparison of virtual microscopy and traditional glass microscopy in diagnostic accuracy among dermatology and pathology residents. Hum Pathol 40:662–667
12. Egevad L, Allsbrook WC Jr, Epstein JI (2005) Current practice of Gleason grading among genitourinary pathologists. Hum Pathol 36:5–9
13. Egevad L, Granfors T, Karlberg L, Bergh A, Stattin P (2002) Percent Gleason grade 4/5 as prognostic factor in prostate cancer diagnosed at transurethral resection. J Urol 168:509–513
14. Stamey TA, McNeal JE, Yemoto CM, Sigal BM, Johnstone IM (1999) Biological determinants of cancer progression in men with prostate cancer. JAMA 281:1395–1400
15. Stamey TA, Yemoto CM, McNeal JE, Sigal BM, Johnstone IM (2000) Prostate cancer is highly predictable: a prognostic equation based on all morphological variables in radical prostatectomy specimens. J Urol 163:1155–1160
16. Vis AN, Roemeling S, Kranse R, Schroder FH, van der Kwast TH (2007) Should we replace the Gleason score with the amount of high-grade prostate cancer? Eur Urol 51:931–939
17. Glaessgen A, Hamberg H, Pihl CG, Sundelin B, Nilsson B, Egevad L (2003) Interobserver reproducibility of percent Gleason grade 4/5 in prostate biopsies. J Urol 171:664–667
18. Billis A, Guimaraes MS, Freitas LL, Meirelles L, Magna LA, Ferreira U (2008) The impact of the 2005 international society of urological pathology consensus conference on standard Gleason grading of prostatic carcinoma in needle biopsies. J Urol 180:548–552, discussion 552–543
19. Egevad L, Algaba F, Berney DM, Boccon-Gibod L, Griffiths DF, Lopez-Beltran A, Mikuz G, Varma M, Montironi R (2009) The European Network of Uropathology: a novel mechanism for communication between pathologists. Anal Quant Cytol Histol 31:90–95

Virchows Arch (2011) 459:183–191
DOI 10.1007/s00428-011-1110-1

ORIGINAL ARTICLE

Intratumoral lymphocyte density in serous ovarian carcinoma is superior to ERCC1 expression for predicting response to platinum-based therapy

Hans Bösmüller · Sophie Haitchi-Petnehazy · Gerald Webersinke · Renate Marschon · Franz Roithmeier · Wolfgang Stummvoll · Tanja Fehm · Margit Klier-Richter · Irina Bonzheim · Annette Staebler · Falko Fend

Received: 2 May 2011 / Revised: 14 June 2011 / Accepted: 15 June 2011 / Published online: 29 June 2011
© Springer-Verlag 2011

Abstract Intratumoral immune cells and ERCC1 expression are likely to play a role in the response of ovarian carcinoma to chemotherapy, but their impact on therapy outcome is still unclear. Therefore, 41 cases of optimally resected high grade serous ovarian carcinomas were examined retrospectively for stromal and intraepithelial lymphocyte populations and *ERCC1* status in relation to response to platinum-based therapy. Based on RECIST criteria, 27 patients were classified as responsive and 14 as therapy resistant, respectively. Using immunohistochemistry for CD3, CD8, CD4, TIA1, MUM1 and FOX P3 on representative tumor sections, we quantitatively evaluated the intratumoral density of lymphocyte subpopulations. In addition, *ERCC1* protein and mRNA expression were determined by immunohistochemistry using the Steffensen score and quantitative RT-PCR, respectively. Furthermore, *ERCC1* SNP's C8092A and codon 118 were analysed. Response to chemotherapy was significantly associated with higher numbers of stromal CD3+ (mean 21.33 lymphocytes/HPF versus 8.21 lymphocytes/HPF, $p=0.002$) and CD8+ lymphocytes (mean 9.22 lymphocytes/HPF versus 4.57 lymphocytes/HPF, $p=0.013$). Counts of intraepithelial CD3+ and CD8+ lymphocytes, stromal and intraepithelial FOXP3+ and TIA1+ cells, CD4+ lymphocytes, and MUM1+ plasma cells did not reach statistical significance. Neither ERCC1 protein expression ($p=0.232$) nor SNPs codon 118 and C8092A of the *ERCC1* gene ($p=0.269$ and $p=0.543$) showed an association with therapy response. The same was true for *ERCC1* mRNA levels ($p=0.896$), probably due to intratumoral lymphocyte contamination. In conclusion, the density of CD3+ and CD8+ T-cells in tumor stroma proved to be a significant predictor for response to platinum-based therapy, whereas examination of *ERCC1* failed to identify therapy-responsive patients.

Keywords Serous ovarian adenocarcinoma · *ERCC1* immunohistochemistry · *ERCC1* mRNA expression · *ERCC1* SNP · Intraepithelial lymphocytes · Stromal lymphocytes

Abbreviations

ERCC1	Excision repair cross-complementing rodent repair deficiency complementation group 1
HPF	High power field
IHC	Immunohistochemistry
IL	Intraepithelial lymphocytes

H. Bösmüller (✉) · S. Haitchi-Petnehazy
Department of Pathology,
Krankenhaus Barmherzige Schwestern Linz,
Seilerstätte 4,
4020 Linz, Austria
e-mail: hans-christian.boesmueller@bhs.at

G. Webersinke · R. Marschon
Laboratory of Molecular Biology,
Krankenhaus Barmherzige Schwestern Linz,
Linz, Austria

F. Roithmeier · W. Stummvoll
Department of Gynecology,
Krankenhaus Barmherzige Schwestern Linz,
Linz, Austria

T. Fehm
Department of Gynecology, University of Tübingen,
Tübingen, Germany

H. Bösmüller · M. Klier-Richter · I. Bonzheim · A. Staebler · F. Fend
Department of Pathology, University of Tübingen,
Tübingen, Germany

NSCLC	Non-small cell lung cancer
OS	Overall survival
PFS	Progression-free survival
SL	Stromal lymphocytes
SNP	Single nucleotide polymorphism
SOC	Serous ovarian cancer
TBP	TATA box-binding protein

Introduction

Platinum-based chemotherapy is the standard of care for ovarian carcinoma of tumor stages FIGO Ic to FIGO IV. Major side effects such as myelotoxicity are observed in about 20% of patients, and approximately 20% of serous ovarian carcinomas show primary resistance to Platinum-containing regimes. Therefore, there is particular interest in finding markers predictive of chemotherapy response. However, currently proposed biomarkers still lack predictive power in order to be used for pretherapeutic decision making. In recent years, both intra- and peritumoral immune cell infiltration and expression of proteins involved in the cellular response to chemotherapeutic agents have come into focus as potential predictors of chemotherapy response.

Among the specific markers investigated for their predictive value, the significance of *ERCC1* (Excision repair cross-complementing rodent repair deficiency group 1) in ovarian carcinoma has received significant attention, analogous to non-small cell lung cancer [1–9]. Strongly positive ERCC1 immunohistochemistry (IHC) and a high level of *ERCC1* mRNA are regarded as an indication for efficient repair of tumor DNA damaged by cytostatic agents, resulting in therapy resistance [10, 11]. A weak expression on mRNA or protein level is thought to indicate a higher likelihood of response to platinum-based chemotherapy [12–14]. In addition, the variant form of the single nucleotide polymorphism (SNP) of the *ERCC1* gene in codon 118 was found to be associated with a worse outcome in ovarian carcinoma [15, 16].

In recent years and with refined techniques, the density and composition of the intratumoral lymphocyte population have been found to be of prognostic relevance in a wide variety of neoplasms. In ovarian carcinoma, most studies so far have investigated their impact on overall and disease-free survival, mainly pointing out the importance of intraepithelial CD8+ lymphocytes [17–24]. The correlation between tumor-associated lymphocytes and chemotherapy response has been the subject of only a very limited number of studies [25, 26].

Given the in part contradictory results concerning the role of ERCC1 and the scarcity of data concerning the impact of intratumoral lymphocytes on therapy response, the present study of 41 cases of high grade serous ovarian carcinomas uniformly treated by platinum-based chemotherapy aims at elucidating the potential of ERCC1 immunohistochemistry, mRNA expression and the codon 118 polymorphism on one hand, and intratumoral lymphocyte content on the other hand as predictive markers for ovarian carcinoma chemotherapy.

Material and methods

Patients

Forty-one women aged 40 to 79 years with high grade serous ovarian carcinoma (SOC) were included in the present study. All patients had undergone optimal surgical resection (no visible residual tumor) under standardized conditions, including hysterectomy, bilateral adnexectomy, omentectomy, debulking procedures, peritoneal biopsies, and peritoneal lavage for cytologic examination. Thirty-two patients had undergone pelvine as well as paraaortal lymphadenectomy. Nine patients without evidence for retroperitoneal involvement had not received lymphadenectomy based on preoperative risk evaluation. Patients with lymph node metastasis, extraperitoneal metastasis or visible residual tumor were not included in the study. Pathologically, 36 patients were diagnosed with SOC pT 3c, two with pT 2c and five with pT 1c exhibiting tumor masses in both ovaries and positive peritoneal fluid, but without fallopian tube infiltration.

Standardized Carboplatin-Taxane chemotherapy was administered every three weeks for six cycles in all patients. Platinum resistance was defined as a relapse during or within 6 months after the end of six cycles of chemotherapy, proven by CT and/or PET-CT. Cancer Antigen 12-5 (CA 12.5) was used as an additional parameter of recurrence. Platinum sensitivity was defined by a progression-free interval for at least 12 months after the end of six cycles of chemotherapy. No second look surgery or tumor sampling in cases of recurrence was done. By means of these criteria, 14 tumors were classified as platinum-resistant and 27 as platinum-sensitive. Patients with partial platinum resistance, defined by recurrences within 6 up to 12 months after the end of six cycles of chemotherapy were not included in the study.

Eleven patients aged 36 to 54 years with serous borderline tumors, including two of micropapillary type, were recruited as a control group. Eight patients had a single lesion, three women showed involvement of both ovaries, including the two micropapillary tumors. The surgery performed was identical to the procedure described above, but patients did neither undergo lymphadenectomy nor chemotherapy.

Immunohistochemisty and molecular analyses

All cases were reviewed by an experienced gynecopathologist (A.S.), and appropriate formalin-fixed and paraffin-embedded tumor blocks were selected. Matched, but tumor-free fallopian tubes or uninvolved ovarian stroma served as control tissues for IHC, mRNA quantitation was calibrated with selected fallopian tube tissue.

The following primary antibodies were used for immunohistochemistry: ERCC1 (1:50, monoclonal 8F1, DCS Innovative Diagnostics, Hamburg, Germany), CD3/pan-T-cell (1:100, rat monoclonal SP7, DCS), CD4/T-helper cells (1:100, rat monoclonal SP35; Cytomed Baden-Baden, Germany), CD8/cytotoxic T-cells (1:200, mouse monoclonal C8/144B, DAKO, Glostrup, Denmark), MUM1/plasma cells (1:200 MUM1p, DAKO), TIA1/cytotoxic T-cells (1:200, mouse monoclonal GMP12, Cytomed), FOX-P3/regulatory T-cells (1:150, mouse monoclonal, mA22509, ABCAM, MA USA). The tissue sections were pre-treated with EDTA-buffer solution (pH 8.6) at 95° for 36 min (ERCC1, CD3, CD8), 64 min (MUM1, TIA-1) and 76 min (CD4). The antibodies were incubated at 37° for 32 min (ERCC1, CD3, CD8, MUM1, TIA-1) and 42° for 40 min, immunohistochemical staining was based on the avidin–biotin method. One representative paraffin section was used per case and antibody.

For the semiquantitative evaluation of ERCC1 staining, we used the Steffensen score [15]. Based on the staining intensity of the control tissue, the intensity of ERCC1 expression in the tumor tissue was graded from 0 to 3, with 0 as negative staining, grade 1 as weaker, grade 2 as equal and grade 3 stronger than control tissue. The score was obtained by multiplying this grade with a factor determined by the percentage of positive tumor cells (0–10% / 0.1; 10–50% / 0.5; 50–100% / 1). Scores>1 were considered positive.

The quantification of lymphocytes was carried by counting the average number of cells per high power field (HPF=400×) reviewing a total of ten HPF, additionally we documented the maximum range for each subset. To control for observation bias, we statistically evaluated both average and maximum counts for each category. The lymphocyte subsets of the tumor stroma were quantified at the invasive tumor front in the stains for CD3, CD8, CD4, TIA 1, MUM1 and FOXP3. In a second step, intraepithelial lymphocytes were counted.

mRNA and DNA for *ERCC1* quantitation and SNP analysis, respectively, were extracted after macrodissection of hematoxylin–eosin stained slides. The extraction of total RNA from paraffin-embedded tumor tissue was performed as described by Specht et al. [27]. Five hundred nanogram of RNA was transcribed with Superscript II (Invitrogen, Carlsbad, CA) according to the manufacturer. Quantitative PCR was performed on a LightCycler 480 (Roche Diagnostics, Mannheim, Germany) using previously published intron-spanning primers and probes for the quantification of *ERCC1* and *TATA* box-binding protein (TBP), which served as a reference gene [12]. To calculate the real-time PCR results we used the ΔΔCt-method, normalising ERCC1 against TBP in the first step (ΔCt). In the second step, these data were calibrated to the ratio of the mean value of the control tissue (ΔΔCt), defining mRNA of fallopian tubes as 100%. A relative expression of 140% and higher was considered as high expression in the tumor.

Genomic DNA of tumor tissue and control tissue was isolated by the use of Maxwell® 16 FFPE Custom Kit (Promega, WI, USA) after denaturation with proteinase K. The SNPs for Codon 118 (rs11615) and C8092A (rs3212986) were analysed with TaqMan SNP genotyping assays (Applied Biosystems, CA, USA), according to the recommendations of the manufacturer [6]. Allelic discrimination was performed on a 7900HT Fast real-time PCR System using SDS 2.2.2 Software Version (Applied Biosystems).

Statistical analysis was performed using SSPS statistical software (Microsoft, CA, USA). Univariate analyses were carried out using the Chi-Squared statistic. *P* values less than 0.05 were considered significant.

Results

ERCC1 protein and mRNA expression and SNP analysis

Immunohistochemical staining of control slides of corresponding ovarian stroma and fallopian tubes for ERCC1 always showed intense staining. The carcinoma was negative for ERCC1 in six patients (15%), and positive in 35 patients (85%) (Figs. 1 and 2). All tumors with positive IHC had a homogenous distribution. According to Steffensen [15] only one of six negative cases had a score 0, the remaining five ranged between 0.1 and 0.8. All six ERCC1 negative tumors showed platinum responsiveness, all resistant tumors had a positive immunostaining result. ERCC1 was positive in all 11 serous borderline tumors (see Table 1).

For the evaluation of *ERCC1* mRNA, the *ERCC1/TBP* mRNA ratio of normal fallopian tube tissue was set at 100%. For tumor tissue, a ratio 140% or more was considered to represent high expression. In summary, 24 patients (59%) showed low to normal levels, 17 patients (41%) high *ERCC1* mRNA levels. There was no correlation between ERCC1 mRNA expression and chemotherapy response, as 16 (60%) of 27 chemosensitive and six (42%) of 14 resistant tumors had low to normal mRNA levels (range 62–139%), whereas high mRNA levels (range

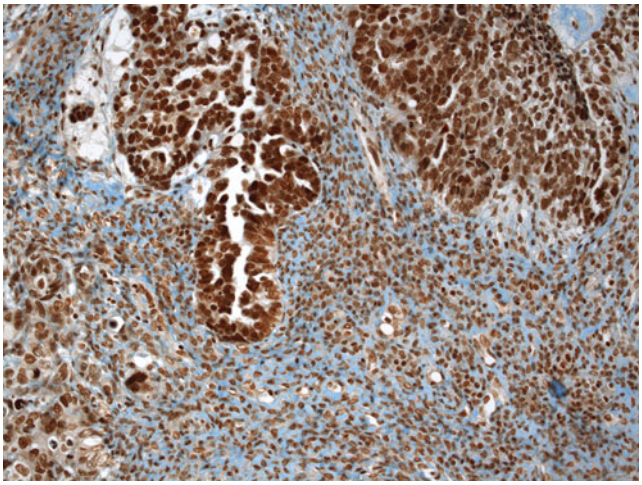

Fig. 1 Strongly positive nuclear staining for ERCC1 in a case of serous ovarian carcinoma. Note the weaker positivity of adjacent stromal cells. Immunoperoxidase ×200

140–192%) were encountered in 11 (40%) responsive and eight (58%) unresponsive carcinomas (p=0.896). There was a poor correlation between ERCC1 protein expression by immunohistochemistry and *ERCC1* mRNA levels.

The 11 serous borderline tumors exhibited *ERCC1* expression levels comparable to the control tissue. None of the cases showed high *ERCC1* expression.

The analysis of *ERCC1* single nucleotide polymorphisms (SNP) of codon 118 (Asn118Asn) and C8092A showed allele distributions similar to published data, but failed to show a significant association with therapy response. Details are shown in Table 1.

Table 1 Correlation of chemotherapy response with *ERCC1* protein and mRNA expression and ERCC1 SNPs at Codon 118 and C8092A

	Responder	Non-responder	p value
ERCC1 immunostaining			
Negative	6	0	0.232
Positive	21	14	
ERCC1 mRNA level			
Low	16	8	0.896
High	11	6	
ERCC1 SNP codon 118			
T/T	11	3	0.269
T/C	9	5	
C/C	7	6	
ERCC1 SNP C8092A			
C/C	17	5	0.543
C/A	9	7	
A/A	1	2	

Distribution of lymphocyte subsets

In order to identify a potential predictive impact of tumor infiltrating lymphocytes with special reference to their precise localization, lymphocyte counts were performed separately for intraepithelial and stromal subsets for each antibody, except for CD4+ lymphocytes and MUM1+ plasma cells, which were only detected in stromal areas (Figs. 3 and 4). Based on the distribution of each subset, we defined three categories of high (H), medium (M) and low (L) lymphocyte density. Due to the relative rarity and the irregular distribution, we did not define frequency categories for MUM1 and FOXP3 stains, which usually revealed very low numbers of positive cells.

Stromal CD3 lymphocytes showed the highest density and a significant association with therapy response, with a mean value of 21.33 lymphocytes/HPF (median 18/HPF) for chemosensitive versus 8.21/HPF (median 6/HPF) for chemoresistant tumors (p=0.002) (Fig. 5). The same

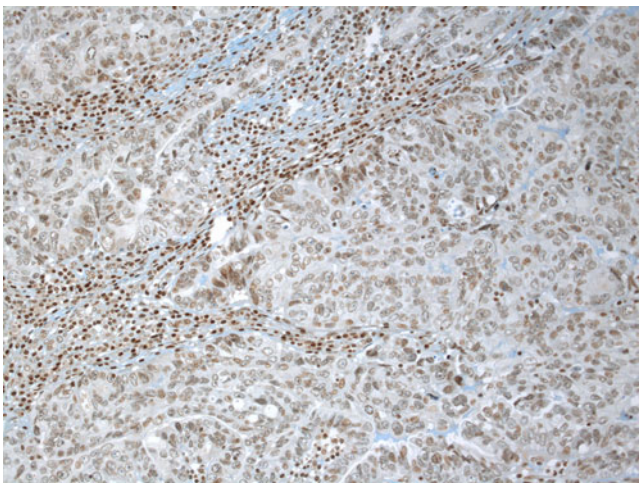

Fig. 2 Ovarian carcinoma with weak ERCC1 expression in tumor cells, but retained reactivity in stromal cells. Immunoperoxidase ×200

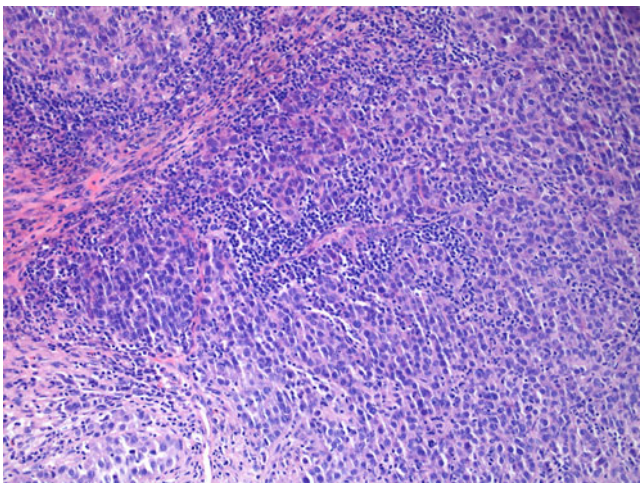

Fig. 3 Serous ovarian carcinoma with dense lymphocyte infiltrates. H&E ×200

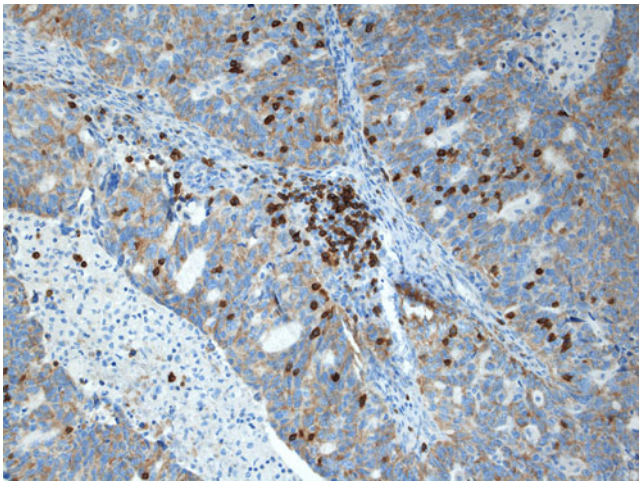

Fig. 4 The CD3 immunostain highlights the stromal and intraepithelial distribution of T-cells. Immunoperoxidase ×200

correlation was found for stromal CD8 positive lymphocytes, with a mean of 9.22/HPF (median 8/HPF) in the chemosensitive subset versus 4.57/HPF (median 4/HPF) for non-responders (p=0.013). The statistical significance for these two markers was retained when the maximum lymphocyte count per HPF, rather than the average count was used for calculation (Table 2). The other lymphocyte subset counts failed to show statistical significance, which in part was probably due to low overall numbers of cells expressing these antigens (Table 2).

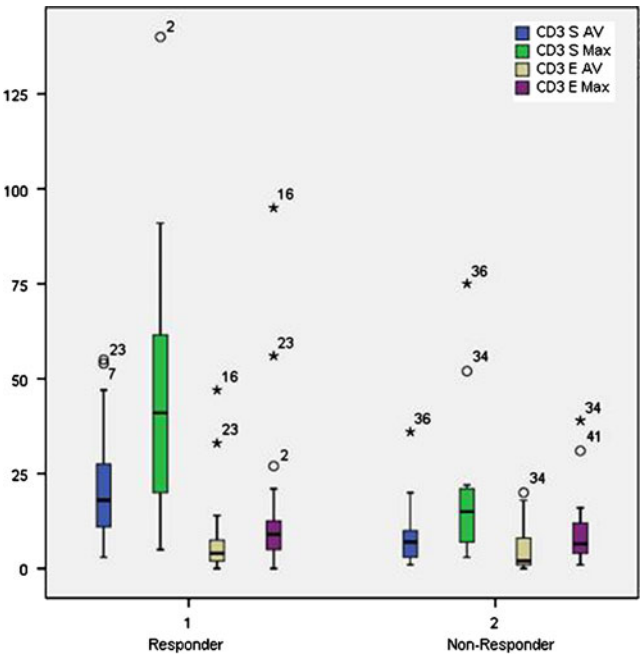

Fig. 5 Box plots for the sensitive subset and the resistant subset for selected lymphocyte populations (*blue*: mean CD3+ stromal cells, *green*: maximum stromal CD3 count, *grey*: mean epithelial CD3 count, *purple*: maximum epithelial CD3 count). The *numbers* indicate individual outlier cases

Grouping together cases with low to medium versus high lymphocyte scores, we assessed the predictive value of the different lymphocyte subsets. A high stromal CD3+ lymphocyte count showed a positive predictive value (PPV) of 0.91 for chemotherapy response. The same was true for high CD8+ stromal lymphocyte counts with a PPV of 0.82. The negative predictive value was lower in both subsets, indicating better prediction for platinum sensitivity than resistance (Table 3). Again, the other markers failed to show statistical significance.

The serous borderline tumors used as controls had low lymphocyte counts in general. Of note, we did not find any differences for stromal and intraepithelial lymphocytes in the stains for CD3 and CD8. (0–5 cells/HPF). CD4, MUM1 and TIA1A-positive cells were sparse, FOXP3+ lymphocytes were virtually absent.

Discussion

In order to avoid ineffective and potentially toxic chemotherapy in women with advanced ovarian carcinoma, there is increasing interest in reliable predictive markers for platinum responsiveness. The intention of the present study was to compare the predictive values of *ERCC1* expression both on mRNA and protein levels, the influence of ERCC1 SNPs and the density of intratumoral lymphocytes in a very homogenously treated patient collective of serous ovarian carcinoma. The study demonstrates that a high density of stromal T-cells is predictive of response to platinum-based chemotherapy, whereas *ERCC1* expression and ERCC1 allelotypes failed to identify patients who would benefit from this therapy.

ERCC1 is a key enzyme in the nucleotide excision repair pathway of platinum-damaged cells [11, 13, 14] and therefore has been the subject of many studies using different approaches, including immunohistochemistry, mRNA quantification and SNP analyses from peripheral blood cells or tissue. The group studied most extensively for the impact of ERCC1 so far were patients with non-small cell lung cancer (NSCLC), though the studies differed substantially with regard to selection criteria such as adjuvant therapy versus palliative treatment or progressive disease [1–3]. The different methods used, mostly IHC and RT-PCR, and the heterogeneous patient collectives do not always allow comparison of results. The same heterogeneity also applies to *ERCC1* studies of ovarian carcinoma. An association between low *ERCC1* expression both by RT-PCR, as well as by immunohistochemistry and improved overall survival (OS) has been described for patients with progressive disease [11, 14, 28] whereas Steffensen found a better response to platinum-based chemotherapy for patients negative by IHC, but no

Table 2 Lymphocyte subset counts in responders versus non-responders

	Responder (27) mean (range)	Non-responder (14) mean (range)	*p* value average (maximum)
CD3 S/HPF	21.33 (3–55)	8.21 (0–36)	0.002 (0.005)
CD8 S/HPF	9.22 (0–25)	4.57 (0–16)	0.013 (0.009)
FOXP3 E/HPF	0.65 (0–3)	0.92 (0–3)	0.162 (0.642)
TIA1 S/HPF	2.51 (0–9)	1.71 (0–9)	0.352 (0.153)
CD4/HPF	2.22 (0–17)	0.71 (0–6)	0.362 (0.449)
CD3 E/HPF	7.18 (0–47)	4.64 (0–20)	0.377 (0.544)
CD8 E/HPF	3.88 (0–17)	3.42 (0–9)	0.512 (0.456)
MUM1/HPF	9.48 (0–67)	10.78 (0–50)	0.719 (0.778)
FOXP3 S/HPF	0.95 (0–5)	1.35 (0–6)	0.812 (0.653)
TIA1 E/HPF	1.40 (0–7)	1.42 (0–5)	0.942 (0.889)

E: intraepithelial cells; S: cells in tumor stroma

Average: *p* value for the average lymphocyte count/HPF; maximum: *p* value for the HPF with the highest lymphocyte count

influence on OS [8, 15]. Further investigations concentrated on mRNA (RT-PCR) and SNP analyses, pointing out a correlation between platinum sensitivity on one side and low mRNA levels and T/T and C/T alleles in codon 118 on the other side, respectively. Similarly, a relation was found between poor response and positive ERCC1 IHC and C/C variant in codon 118 [5, 7, 15, 16]. Krivak identified the polymorphism *C8092A* of ERCC1 as an independent marker for progression-free survival (PFS) [6], but failed to find clinical relevance for OS [6, 29]. Our results reflect this lack of a clear-cut predictive value of ERCC1 immunohistochemistry, mRNA expression levels and SNPs codon 118 and C8092A. The main limitation of immunohistochemistry lies in the poor reproducibility and the difficulties in quantification of immunostaining results despite the use of the standard antibody clone 8F1.

Table 3 Correlation of chemotherapy response with density of tumour infiltrating lymphocyte subsets

	Responder	Non-responder		Responder	Non-responder
CD3 S/HPF			TIA1 S/HPF		
≥11 (high)	**21**	**2**	≥3	10	3
6–10 (medium)	*2*	*5*	2	3	2
0–5 (low)	*4*	*7*	0–1	14	9
	PPV=0.91	NPV=0.61			
CD3 E/HPF			TIA1 E/HPF		
≥4 (high)	**16**	**5**	≥3	5	5
2–3 (medium)	*5*	*4*	2	2	0
0–1 (low)	*6*	*5*	0–1	20	9
	PPV=0.76	NPV=0.45			
CD8 S/HPF			FOXP3 S/HPF		
≥6 (high)	**19**	**4**	≥2	8	5
3–5 (medium)	*4*	*6*			
0–2 (low)	*4*	*4*	0–1	19	9
	PPV=0.82	NPV=0.55			
CD8 E/HPF			FOXP3 E/HPF		
≥4 (high)	**9**	**5**	≥2	8	5
2–3 (medium)	*9*	*1*			
0–1 (low)	*9*	*8*	0–1	19	9
	PPV=0.64	NPV=0.33			
CD4/HPF			MUM1/HPF		
≥4	5	0	≥7	8	4
1–3	7	5			
0	15	9	0–6	18	10

E: intraepithelial cells; S: cells in tumor stroma

HPF: counts per high power field. For calculating the correlation between lymphocyte subsets and therapy response, the high density group (bold) was compared with the combined low and medium density groups (italics)

(*PPV* positive predictive value; responder high density versus sum of responder and non-responder high, *NPV* negative predictive value, non-responder M + L versus sum of responder and non-responder M + L)

Although absent or reduced staining seems to be an indication for therapy response also in our study, immunopositivity is nevertheless found in a significant fraction of responders, making ERCC1 staining unsuited for therapy planning. It needs to be demonstrated whether automated image analysis of ERCC1 immunostaining will produce better results [8, 30].

The SNP C8092A showed identical allele distributions to already published data, but did not correlate with platinum responsiveness in our series (p=0.543) [6] (Table 1).

Results for the SNP in codon 118 showed a trend towards discrimination of chemoresistant and chemosensitive tumors, but failed to reach statistical significance in our small collective. Larger studies are needed to decide whether SNP in codon 118 may form part of a marker panel for predicting response to platinum-based therapy.

The lack of a predictive value of *ERCC1* mRNA levels may seem surprising at first. Most studies on *ERCC1* mRNA quantification relied on RT-PCR of frozen tissue, and it could be argued that technical factors play a role [10, 11]. However, we have previously shown the high reliability of mRNA quantification on formalin-fixed, paraffin-embedded and manually dissected tissue, using the protocol initially published by Specht et al, and employing intron-spanning primers to avoid DNA contamination [27, 31]. When comparing our *ERCC1* expression data with the lymphocyte counts, we observed a notable correlation between stromal CD3 counts and mRNA levels in the chemosensitive subset (p=0.009), indicating that a high number of contaminating lymphocytes correlates with higher *ERCC1* levels and thus possibly obscures any correlation between low ERCC1 expression in tumor cells and chemoresponse. All 13 tumors with less than 18 lymphocytes/HPF had only low *ERCC1* mRNA levels, whereas seven tumors with more than 26 lymphocytes/HPF revealed only high levels.

The dataset for the resistant subset was not as consistent, but four tumors with few lymphocytes showed markedly elevated levels, indicating that increased *ERCC1* mRNA levels indeed derived from the neoplastic population. In conclusion, these results throw doubt on the practical value of *ERCC1* mRNA quantification in ovarian carcinoma tissue without correction for lymphocyte density.

Tumor-associated lymphocytes are a common feature of serous ovarian cancer and have been investigated in many studies concerning their potential prognostic or predictive impact. Most published data have shown an improved overall survival for cases with increased intratumoral/intraepithelial CD8+ lymphocytes, [17–19, 21, 24], a finding which is also supported by the results of our study. The phenotype and function of this T-cell subset and its interactions with other lymphocyte subpopulations still remain unclear, but the microenvironment is thought to play a major role [32]. CD4+ intraepithelial lymphocytes and regulatory T-cells (FOXP3+) are supposed to counterbalance the beneficial effect of a high CD8+ T-cell density. Only high CD8/CD4 and CD8/Treg ratios were associated with better prognosis [20].

Reports about the correlation between intratumoral CD3+ lymphocytes and overall survival are inconsistent. Whereas Sato and Clarke failed to find a correlation between OS and intraepithelial lymphocytes [18, 20], Milne and Tomsova demonstrated intraepithelial lymphocytes to be relevant for survival, when stromal and intraepithelial lymphocytes were evaluated separately [33, 34]. In a recent study Al-Attar et al. counted intraepithelial and stromal lymphocytes in ovarian cancer and calculated a ratio, emphasising that high numbers of intraepithelial CD3+ lymphocytes correlated with longer survival. High numbers of stromal CD3+ lymphocytes and a low intraepithelial/stromal ratio predicted worse prognosis [35].

These survival data have to be discerned from data correlating lymphocyte counts with response to chemotherapy, which has been investigated only in a handful of studies. Stumpf et al. pointed out the predictive value of intraepithelial CD8+ lymphocytes, whereas Raspollini et al. observed a correlation between response and tumor infiltrating CD3+ lymphocytes [25, 26].

A recurrent problem in comparing studies on lymphocyte densities in ovarian cancer is the lack of a stringent terminology. Not all investigators make a clear distinction between stromal and intraepithelial lymphocyte populations. In particular, the term “intraepithelial” is misguiding in some publications, since it is used as a generic term for tumor infiltrating lymphocytes.

In our study, intratumoral lymphocytes were differentiated based on their location and phenotype. Whereas intraepithelial CD3+ and CD8+ lymphocytes (IL) were seen throughout the tumor, stromal lymphocytes (SL) were increased at the invasion front. These distribution patterns could not be identified for TIA1 and FOXP3-positive cells, probably due to their low numbers. CD4+ lymphocytes and plasma cells were strictly restricted to the tumor stroma.

The number, function and relevance of FOXP3+ T-cells in ovarian cancer are still a matter of controversy. The presence of FOXP3+ T-cells was initially thought to be a feature of advanced serous ovarian cancer and unfavourable prognosis, but recent studies found the reverse [36, 37]. In our hands, the low numbers of FOXP3+ cells probably played a role in the lack of statistical significance with the approach used in this study.

Conclusions

In conclusion, only the density of stromal CD3+ and CD8+ lymphocytes proved to be significantly associated with

response to platinum-based chemotherapy in our study. Quantification of ERCC1 *mRNA* is probably influenced by the amount of intratumoral lymphocytes and therefore does not faithfully reflect the ERCC1 levels in tumor cells, resulting in poor response prediction. Larger prospective studies will be required to confirm these findings.

Conflict of interests The authors declare that they have no competing interests.

References

1. Jeong SH, Jung JH, Han JH, Kim JH, Choi YW, Lee HW, Kang SY, Hwang YH, Ahn Ms, Choi JH OHYT, Chun M, Kang S, Park KJ, Hwang SC, Sheen SS (2009) Expression of Bcl-2 predicts outcome in locally advanced non-small cell lung cancer patients treated with cisplatin-based concurrent chemoradiotherapy. Lung Cancer 65:377–382
2. Olaussen KA, Dunant A, Fouret P, Brambilla E, André F, Haddad V, Taranchon E, Filipits M, Pirker R, Popper HH, Stahel R, Sabatier L, Pignon JP, Tursz T, Le Chevalier T, Soria JC, Bio Investigators IALT (2006) DNA repair by ERCC1 in non-small lung cancer and cisplatin-based adjuvant chemotherapy. N Engl J Med 355:983–991
3. Vilmar A, Sorensen JB (2009) Excision repair cross-complementation group 1 (ERCC1) in platinum-based treatmend of non-small cell lung cancer with spezial emphasis on carboplatin: a review of current literature. Lung Cancer 64:131–139
4. Darcy KM, Tian C, Reed E (2007) A Gynecologic Oncology Group study of platinum-DNA adducts and excision repair cross-complementation group 1 expression in optimal, stage III epithelial ovarian cancer treated with platinum-taxane chemotherapy. Cancer Res 67:4474–4481
5. Kang S, Ju W, Kim JW, Park NH, Song YS, Kim SC, Park SY, Kang SB, Lee HP (2006) Association between excision repair cross-complementation group 1 polymorphism and clinical outcome of platinum-based chemotherapy in patients with epithelial ovarian cancer. Exp Mol Med 38:320–324
6. Krivak TC, Darcy KM, Tian C, Armstrong D, Baysal BE, Gallion H, Ambrosone CB, DeLoia JA, Gynecologic Oncology Group Phase III Trial (2008) Relationship between ERCC1 polymorphisms, disease progression, and survival in the Gynecologic Oncology Group Phase III Trial of intraperitoneal versus intravenous cisplatin and paclitaxel for stage III epithelial ovarian cancer. J Clin Oncol 26:3598–3606
7. Smith S, Su D, Rigault de la Longrais IA, Schwartz P, Puopolo M, Rutherford TJ, Mor G, Yu H, Katsaros D (2007) ERCC1 genotype and phenotype in epithelial ovarian cancer identify patients likely to benefit from paclitaxel treatment in addition to platinum-based therapy. J Clin Oncol 25:5172–5179
8. Steffensen KD, Waldstrom M, Jakobson A (2009) The relationship of platinum resistance and ERCC1 protein expression in epithelial ovarian cancer. Int J Gynecol Cancer 19:820–825
9. Altaha R, Liang X, Yu JJ, Reed E (2004) Excision repair cross complementing-group. Gene expression and platinum resistance. Int J Mol Med 14:959–970
10. Dabholkar M, Vionnet J, Bostick-Bruton F, Yu JJ, Reed E (1994) Messenger RNA levels of XPAC and ERCC1 in ovarian cancer tissue correlate with response to platinum-based chemotherapy. J Clin Invest 94:703–708
11. Weberpals J, Garbuio K, O'Brian A, Clark-Knowles K, Doucette S, Antoniuk O, Goss G, Dimitroulakos J (2009) The DNA repair proteins BRCA1 and ERCC1 as predictive markers in sporadic ovarian cancer. Int J Cancer 124:806–815
12. Bellmunt J, Paz-Ares L, Cuello M, Cecere FL, Albiol S, Guillem V, Gallardo E, Carles J, Mendez P, de la Cruz JJ, Taron M, Rosell R, Baselga J (2007) Gene expression of ERCC1 as a novel prognostic marker in advanced bladder cancer patients receiving cisplatin-based chemotherapy. Ann Oncol 18:522–528
13. Selvakumaran M, Pisarcik DA, Bao R, Yeung AT, Hamilton TC (2003) Enhanced cisplatin cytotoxicity by disturbing the nucleotide excision repair pathway in ovarian cancer cell lines. Cancer Res 63:1311–1316
14. Weberpals JI, Clark-Knowles KV, Vanderhyden BC (2008) Sporadic epithelial ovarian cancer Clinical relevance of BRCA1 inhibition in the DNA damage and repair pathway. J Clin Oncol 26:3259–3267
15. Steffensen KD, Waldstrom M, Jeppesen U, Brandslund I, Jakobson A (2008) Prediction of response to chemotherapy by ERCC1 immunohistochemistry and ERCC1 polymorphism in ovarian cancer. Int J Gynecol Cancer 18:702–710
16. Yu JJ, Lee KB, Mu C, Li Q, Abernathy TV, Bostick-Bruton F, Reed E (2000) Comparison of two ovarian carcinoma cell lines (A2780/CP70 an MCAS) that are equally resistant to platinum, but differ at codon 118 of the ERCC1 gene. Int J Oncol 16:555–560
17. Adams SF, Levine DA, Cadungog MG, Hammond R, Facciabene A, Olvera N, Rubin SC, Boyd J, Gimotty PA, Coukos G (2009) Intraepithelial T cells and tumor proliferation: impact on the benefit from surgical cytoreduction in advanced serous ovarian cancer. Cancer 115:2891–2902
18. Clarke B, Tinker AV, Lee CH, Subramanian S, van de Rijn M, Turbin D, Kalloger S, Han G, Ceballos K, Cadungog MG, Huntsman DG, Coukos G, Gilks CB (2009) Intraepithelial T cells and prognosis in ovarian carcinoma: novel associations with stage, tumor type, and BRCA1 loss. Mod Pathol 22:393–402
19. Kondratiev S, Sabo E, Yakirevich E, Lavie O, Resnick MB (2004) Intratumoral CD8+ T lymphocytes as a prognostic factor of survival in endometrial carcinoma. Clin Cancer Res 10:4450–4456
20. Sato E, Olson SH, Ahn J, Bundy B, Nishikawa H, Qian F, Jungbluth AA, Frosina D, Gnjatic S, Ambrosone C, Kepner J, Odunsi T, Ritter G, Lele S, Chen YT, Ohtani H, Old LJ, Odunsi K (2005) Intraepithelial CD8+ tumor-infiltrating lymphocytes and a high CD8+/regulatory T cell ratio are associated with favorable prognosis in ovarian cancer. Proc Natl Acad Sci USA 102:18538–18543
21. Tel-A H, Alla AE, Laban MA, Fahmy RM (2004) Immunophenotyping of tumor-infiltrating mononuclear cells in ovarian carcinoma. Pathol Oncol Res 10:80–84
22. Thompson MS, Mok SC (2009) Immunopathogenesis of ovarian cancer. Minerva Med 100:357–370
23. Webb JR, Wick DA, Nielsen JS, Tran E, Milne K, McMurtrie E, Nelson BH (2010) Profound elevation of CD8+ T cells expressing the intraepithelial lymphocyte marker CD103 (alphaE/beta7 Integrin) in high-grade serous ovarian cancer. Gynecol Oncol 118:228–236
24. Yang T, Wall EM, Milne K, Theiss P, Watson P, Nelson BH (2007) CD8+ T cells induce complete regression of advanced ovarian cancers by an interleukin (IL)-2/IL-15 dependent mechanism. Clin Cancer Res 13:7172–7180
25. Raspollini MR, Castiglione F, Rossi Degl'innocenti D, Amunni G, Villanucci A, Garbini F, Baroni G, Taddei GL (2005) Tumour-infiltrating gamma/delta T-lymphocytes are correlated with a brief disease-free interval in advanced ovarian serous carcinoma. Ann Oncol 16:590–596

26. Stumpf M, Hasenburg A, Riener MO, Jütting U, Wang C, Shen Y, Orlowska-Volk M, Fisch P, Wang Z, Gitsch G, Werner M, Lassmann S (2009) Intraepithelial CD8-positive T lymphocytes predict survival for patients with serous stage III ovarian carcinomas: relevance of clonal selection of T lymphocytes. Br J Cancer 101:1513–1521
27. Specht K, Kremer M, Müller U, Dirnhofer S, Rosemann M, Höfler H, Quintanilla-Martinez L, Fend F (2002) Identification of cyclin D1 mRNA overexpression in B-cell neoplasias by real-time reverse transcription-PCR of microdissected paraffin sections. Clin Cancer Res 8:2902–2911
28. Scheil-Bertram S, Tylus-Schaaf P, du Bois A, Harter P, Oppitz M, Ewald-Riegler N, Fisseler-Eckhoff A (2010) Excision repair cross-complementation group 1 protein overexpression as a predictor of poor survival for high-grade serous ovarian adenocarcinoma. Gynecol Oncol 119:325–331
29. Krivak TC, Darcy KM, Tian C, Bookman M, Gallion H, Ambrosone CB, Deloia JA (2011) Single nucleotide polypmorphisms in ERCC1 are associated with disease progression, and survival in patients with advanced stage ovarian and primary peritoneal carcinoma; A Gynecologic Oncology Group Study. Gynecol Oncol 122:121–126
30. Bhagwat NR, Roginskaya VY, Acquafondata MB, Dhir R, Wood RD, Niedernhofer LJ (2009) Immunodetection of DNA repair endonuclease ERCC1-XPF in human tissue. Cancer Res 69:6831–6838
31. Specht K, Haralambieva E, Bink K, Kremer M, Mandl-Weber S, Koch I, Tomer R, Hofler H, Schuuring E, Kluin PM, Fend F, Quintanilla-Martinez L (2004) Different mechanisms of cyclin D1 overexpression in multiple myeloma revealed by fluorescence in situ hybridization and quantitative analysis of mRNA levels. Blood 104:1120–1126
32. Martinet L, Poupot R, Mirshahi P, Rafii A, Fournié JJ, Mirshahi M, Poupot M (2010) Hospicells derived from ovarian cancers stroma inhibit T-cell immune responses. Int J Cancer 126:2143–2152
33. Tomsová M, Melichar B, Sedláková I, Steiner I (2008) Prognostic significance of CD3+ tumor-infiltrating lymphocytes in ovarian carcinoma. Gynecol Oncol 108:415–420
34. Milne K, Köbel M, Kalloger SE, Barnes RO, Gao D, Gilks CB, Watson PH, Nelson BH (2009) Systematic analysis of immune infiltrates in high-grade serous ovarian cancer reveals CD20, FoxP3 and TIA-1 as positive prognostic factors. PLoS One 4: e6412
35. Al-Attar A, Shehata M, Durrant L, Moseley P, Deen S, Chan S (2010) T cell density and location can influence the prognosis of ovarian cancer. Pathol Oncol Res 16:361–370
36. Barnett JC, Bean SM, Whitaker RS, Kondoh E, Baba T, Fujii S, Marks JR, Dressman HK, Murphy SK, Berchuck A (2010) Ovarian cancer tumor infiltrating T-regulatory (Treg) cells are associated with a metastatic phenotype. Gynecol Oncol 116:556–562
37. Wolf D, Wolf AM, Rumpold H, Fiegl H, Zeimet AG, Muller-Holzner E, Deibl M, Gastl G, Gunsilius E, Marth C (2005) The expression of the regulatory T cell-specific forkhead box transcription factor FoxP3 is associated with poor prognosis in ovarian cancer. Clin Cancer Res 11:8326–8331

Virchows Arch (2011) 459:193–200
DOI 10.1007/s00428-011-1105-y

ORIGINAL ARTICLE

Overexpression of carbonic anhydrase IX (CAIX) is an independent unfavorable prognostic marker in endometrioid ovarian cancer

Matthias Choschzick · Egbert Oosterwijk · Volkmar Müller · Linn Woelber · Ronald Simon · Holger Moch · Pierre Tennstedt

Received: 3 March 2011 / Revised: 3 June 2011 / Accepted: 5 June 2011 / Published online: 21 June 2011
© Springer-Verlag 2011

Abstract Carbonic anhydrase IX (CAIX) is a strictly membranous expressed metalloenzyme involved in cell adhesion, pH homeostasis, and cancer progression. This study was designed to assess the role of CAIX in primary ovarian cancer. Two hundred five well-characterized primary ovarian carcinomas were analyzed on a tissue microarray. CAIX expression was determined by immunohistochemistry using a four-step scoring system. Moderate and strong membranous CAIX expression was found in 37 out of 205 (18%) of all assessable ovarian cancer specimens. High levels of CAIX expression were related to mucinous and endometrioid phenotype of ovarian carcinomas ($p<0.05$). There was no association between CAIX overexpression and tumor stage, grading, and mitotic count of ovarian carcinomas ($p>0.05$). In univariate Cox regression analysis, advanced tumor stage ($p<0.01$), high tumor grade ($p=0.017$), high mitotic count ($p=0.025$), and high CAIX expression levels ($p=0.031$) were correlated to shorter overall patient survival. High pT stage ($p=0.036$) and CAIX overexpression were connected to poor clinical outcome in endometrioid ovarian carcinomas. Multivariate Cox regression hazard analysis comprising tumor stage, tumor grade, mitotic count, and CAIX expression revealed pT2/3 stage and CAIX overexpression (scores 2 and 3) as independent prognostic markers in ovarian cancer ($p<0.01$, each) as well as in the subgroup of endometrioid carcinomas ($p<0.05$, each). In conclusion, CAIX is overexpressed in a substantial proportion of mucinous and endometrioid ovarian carcinomas and connected to poor patient outcome. Our data support the potential therapeutic benefit of newly developed targeting antibodies in advanced ovarian cancer.

Keywords Carbonic anhydrase · Ovarian cancer · Prognosis

M. Choschzick (✉) · R. Simon
Institute of Pathology,
University Medical Centre Hamburg-Eppendorf,
Martinistr. 52,
20246 Hamburg, Germany
e-mail: mchoschz@uke.uni-hamburg.de

E. Oosterwijk
Department of Urology,
Radboud University Nijmegen Medical Centre,
Nijmegen, the Netherlands

V. Müller · L. Woelber
Department of Gynecology,
University Medical Centre Hamburg-Eppendorf,
Hamburg, Germany

H. Moch
Institute of Surgical Pathology, University Hospital Zürich,
Zürich, Switzerland

P. Tennstedt
Martini-Clinic, Prostate Cancer Center,
University Medical Centre Hamburg-Eppendorf,
Hamburg, Germany

Introduction

Carbonic anhydrase IX (CAIX) is a transmembrane zinc metalloenzyme which was first detected in the HeLA cancer cell line [1]. The enzyme catalyzes the reversible hydration of CO_2 to HCO_3^- and plays a pivotal role in tissue pH homeostasis. Apart from its role in the regulation of pH, CAIX has a function in cell adhesion and is important for the growth and survival of tumor cells under normoxia and hypoxia [2, 3]. CAIX expression is strongly induced by hypoxia through stabilization of the transcription factor HIF-1α [4]. In non-neoplastic tissues, CAIX shows a very limited

expression pattern. Low levels of CAIX have been reported to be immunohistochemical detectable in mesothelial cells, gland epithelium of the stomach, biliary tract, and small intestine as well as the choroid plexus [5]. In contrast to its sparse expression in normal tissues, CAIX is overexpressed in a wide variety of malignant cell lines and tumors. High levels of CAIX were found to be associated with unfavorable patient outcome in breast carcinomas, bladder cancer, advanced cervical carcinomas, and lung cancer [6–9].

Ovarian cancer is the seventh most common malignant tumor of females in Germany with approximately 10,000 new cases per year [10]. Despite standardized therapeutic procedures, the overall prognosis is poor with a 5-year survival rate of approximately 43%. Only little is known about the role of CAIX in the development of ovarian carcinomas. Recently, Hynninen et al. reported wide expression of CAIX in different types of ovarian tumors [11]. The authors describe a tendency to shortened overall survival in tumors with strong CAIX expression, but the result failed to reach statistical significance.

In order to gain more insight into the potential role of CAIX expression in prognosis of ovarian cancer, a tissue microarray containing 297 tumor samples with clinical follow-up data was surveyed for CAIX expression. Our data suggest that CAIX overexpression may be linked to poor outcome in ovarian cancer patients, which has potential therapeutic implications.

Material and methods

Ovarian cancer tissue microarray

A total of 297 formalin-fixed (buffered neutral aqueous 4% solution), paraffin-embedded ovarian carcinomas were available from the Institute of Pathology, Basel University Clinics, the Institute of Clinical Pathology in Basel, and the Triemli Hospital in Zurich. The Ethics Committee of the Basel University Clinics approved the use of these specimens and the data in this research. Raw survival data were either obtained from the cancer registry of Basel or collected from the patients' attending physicians. The mean follow-up time was 42 months (range 1–210). Postoperative management was conducted in different institutions, and uninterrupted surveillance of patients was not possible at all. Complete follow-up information was available in 169 out of 297 (56.9%) tumor patients. The pathologic stage, tumor grading, and histological tumor type were obtained from the primary pathology reports. The slides from all tumors were reviewed by one pathologist (H.M.) to define the histological grade and the histological tumor type. Determination of the mitotic index was performed by counting of mitotic figures in a grid of 10 high-power fields (HPF). The most proliferative active area of large tumor sections was used for this analysis.

Tissue microarray (TMA) construction was as described previously [12]. Briefly, tissue cylinders with a diameter of 1.3 mm were punched from representative non-necrotic tumor areas of a "donor" tissue block using a homemade semiautomatic robotic precision instrument and brought into two different recipient paraffin blocks each containing 153 and 144 individual samples, respectively.

Immunohistochemistry

Four micrometer sections of the multitumor TMA blocks were transferred to an adhesive-coated slide system (Instrumedics, Hackensack, NJ, USA). For immunohistochemical detection of CAIX, we used a non-commercial mouse monoclonal anti-CAIX antibody (clone M75, kindly

Table 1 Relationship between CAIX expression and clinicopathological characteristics of ovarian cancer

		On array (*n*)	Analyzable (*n*)	Carbonic anhydrase IX		*p* value
				Scores 0 and 1 (%)	Scores 2 and 3 (%)	
All samples		297	205	168 (82.0)	37 (18.0)	–
Histologic tumor type	Serous	128	88	76 (86.4)	12 (13.6)	<0.05[b]
	Mucinous	38	22	12 (54.5)	10 (45.5)	
	Endometrioid	67	47	34 (72.3)	13 (27.7)	
	Others[a]	64	47	45 (95.7)	2 (4.3)	
Tumor stage	pT1	58	41	31 (75.6)	10 (24.4)	>0.05
	pT2	36	23	18 (78.3)	5 (21.7)	
	pT3	99	72	62 (86.1)	10 (13.9)	
Grading	G1	81	50	39 (78.0)	11 (22.0)	>0.05
	G2	91	64	50 (78.1)	14 (21.9)	
	G3	91	68	57 (83.8)	11 (16.2)	

[a] Twenty-four clear cell carcinomas, 15 malignant mixed Mullerian tumors, four transitional cell carcinomas, and 21 non-specified

[b] Mucinous/endometrioid vs. serous/others

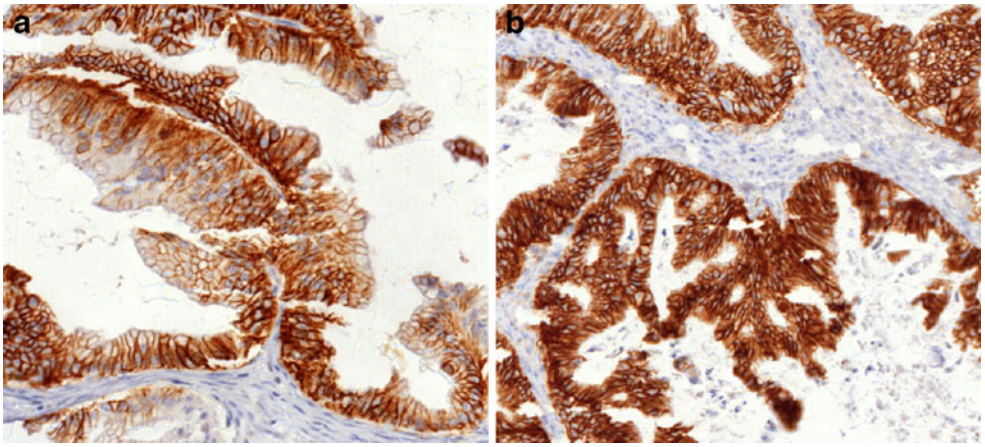

Fig. 1 Example of diffuse strong membranous CAIX expression in a mucinous (**a**) and an endometrioid (**b**) ovarian carcinoma (×40)

provided by E Oosterwijk, Department of Urology, University Medical Center Nijmegen, the Netherlands) at a dilution of 1:1,000. Slides were de-waxed in xylene, rehydrated through a graded ethanol series, and washed in Tris buffer saline. Endogenous peroxidase was blocked by incubation for 10 min in 3% hydrogen peroxide in methanol. Antigen retrieval was performed in 0.01 mol/l sodium citrate buffer, pH 6, for 25 min at 98°C in a microwave oven. The reactions were detected using the DAB detection kit (DAKO).

CAIX expression level was determined by using a four-step scoring system. In brief, the CAIX staining intensity and the fraction of stained tumor cells were recorded for each tissue spot. Only a membranous staining pattern was considered positive. The staining intensity was estimated in a four-step scale (none, weak, moderate, strong). The final staining pattern was scored according to the following criteria: negative=score 0 (no staining or membrane staining <10% of tumor cells), weak=score 1 (partial membrane staining or weak complete membrane staining >10% of tumor cells), moderate=score 2 (weak to moderate complete membrane staining >10% of tumor cells), and strong=score 3 (strong and complete membrane staining in >10% of tumor cells).

Statistics

Pearson's chi-squared test and Student's *t* test were used to study the relationship between CAIX and clinicopathological parameters. The survival effect of CAIX was assessed by Kaplan–Meier curves and log-rank tests. A Cox proportional hazards model was used to identify independent factors associated with overall survival. $p<0.05$ was considered significant. The end point of overall survival was death after 10 years and is designated as "event" in this study. Analysis was performed using R statistical software package for Windows (version 2.7.2, R Foundation for Statistical Computing).

Results

CAIX immunohistochemistry

A total of 205 cancerous samples were informative for the determination of CAIX expression. CAIX was detectable in 54 out of 205 (26.3%) of all interpretable specimens. Thirty-seven (18%) samples exhibited a moderate or strong staining result (Table 1). Figure 1a, b shows representative examples of mucinous and endometrioid ovarian cancers with strong diffuse CAIX overexpression. CAIX protein expression was always membranous. Weak cytoplasmic signals occurred occasionally in cases with low CAIX expression (scores 0 and 1). Tumor-associated stromal cells, as well as inflammatory cells, stained negative for CAIX.

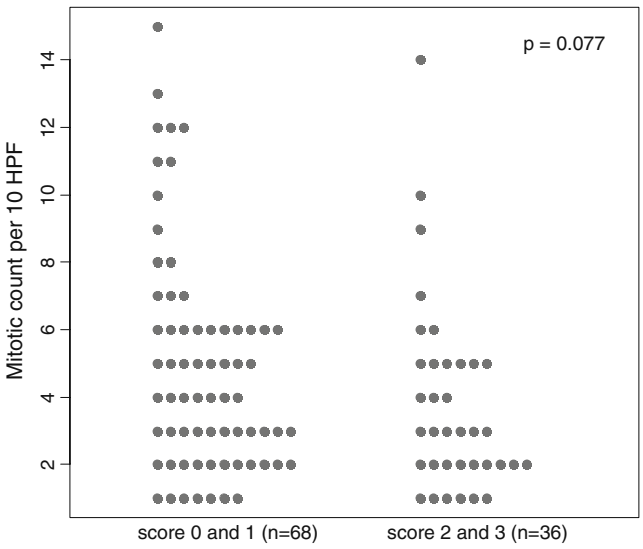

Fig. 2 Relationship between CAIX expression and mitotic index of ovarian carcinomas: There was no statistical association between CAIX expression levels and mitotic count per 10 HPF (*t* test, two-sided)

CAIX expression and clinicopathological parameters

Table 1 summarizes the association of CAIX expression in ovarian carcinomas to clinicopathological parameters. CAIX overexpression in ovarian carcinomas was strongly associated with the histological tumor type. Endometrioid and mucinous ovarian carcinomas exhibited more frequently high CAIX expression levels than serous carcinomas (27.7% and 45.5%, respectively vs. 13.6%; $p<0.05$). Transitional cell carcinomas, clear cell carcinomas, and not otherwise specified carcinomas always stained immunohistochemically negative or weakly positive for CAIX. Only two cases of malignant Mullerian mixed tumors (epithelial component) stained strongly positive in CAIX IHC. There was no association between CAIX expression and tumor grade as well as tumor stage of ovarian carcinomas ($p>0.05$). Furthermore, no relation of CAIX level and mitotic count of ovarian carcinomas could be found ($p=0.077$, Fig. 2).

CAIX expression and patient survival

After a median follow-up time of 42 months, 106 events (62.7%) in 169 patients with survival data were reported. Tumor stage, tumor grading, and mitotic count per 10 HPF were strongly related to patient overall survival in univariate Cox regression analysis (Table 2). The clinical outcome in pT1 and G1 carcinomas was significantly better than in pT2/pT3 or G2/G3 tumors. No differences in patient survival were found between pT2 and pT3 nor between G2 and G3 carcinomas. According to these results, high proliferation activity (mitotic index >3) significantly worsens the prognosis of ovarian cancers. Tumors with high CAIX expression levels were also associated with shorter overall survival ($p=0.03$, Fig. 3a). The subtype of ovarian carcinoma was not related to survival.

Next we analyzed the impact of CAIX expression on overall patient survival in different histopathological ovarian cancer subtypes. Clinicopathological details are reported in Table 3. Distribution of tumor stage and grading were similar as described elsewhere [13]. CAIX overexpression in endometrioid carcinomas was strongly associated to lower survival rates in univariate analysis ($p=0.0023$, Table 2 and Fig. 3b). Grading and mitotic index >3 showed no relation to survival in this subgroup. The p values for tumor stage were just over the significance level, probably because too small sample sizes. However, an association between tumor stage and overall survival in endometrioid cancers was demonstrable if pT2 and pT3 factors are put together (pT1 vs. pT2+pT3, $p=0.036$). The

Table 2 Cox univariate regression analysis of overall survival in ovarian cancer

	All tumors			Endometrioid carcinomas		
	HR	CI 95%	p value	HR	CI 95%	p value
Tumor type						
Serous vs. mucinous	1.13	0.56–2.21	0.75	–	–	–
Serous vs. endometrioid	0.72	0.45–1.17	0.18	–	–	–
Serous vs. others	1.00	0.61–1.66	0.99	–	–	–
Mucinous vs. endometrioid	0.67	0.32–1.39	0.28	–	–	–
Mucinous vs. others	0.94	0.44–1.98	0.87	–	–	–
Endometrioid vs. others	1.36	0.78–2.38	0.28	–	–	–
Tumor stage						
pT1 vs. pT2	4.14	1.71–10.1	0.0017	3.94	0.98–15.8	0.053
pT1 vs. pT3	6.11	2.73–13.7	<0.001	3.74	0.97–14.5	0.056
pT2 vs. pT3	1.46	0.83–2.56	0.18	0.94	0.32–2.82	0.92
Grading						
G1 vs. G2	1.37	0.79–2.39	0.27	1.78	0.68–4.66	0.24
G1 vs. G3	1.90	1.12–3.21	0.02	2.11	0.67–6.61	0.20
G2 vs. G3	1.40	0.86–2.27	0.17	1.20	0.46–3.11	0.70
Mitotic index						
≤3	1	–	–	1	–	–
>3	1.61	1.06–2.45	0.025	1.48	0.69–3.19	0.31
CAIX						
Score 0 and score 1	1	–	–	1	–	–
Score 2 and score 3	1.92	1.06–3.45	0.031	4.6	1.72–12.3	0.0023

HR hazard ratio, *CI* confidence interval

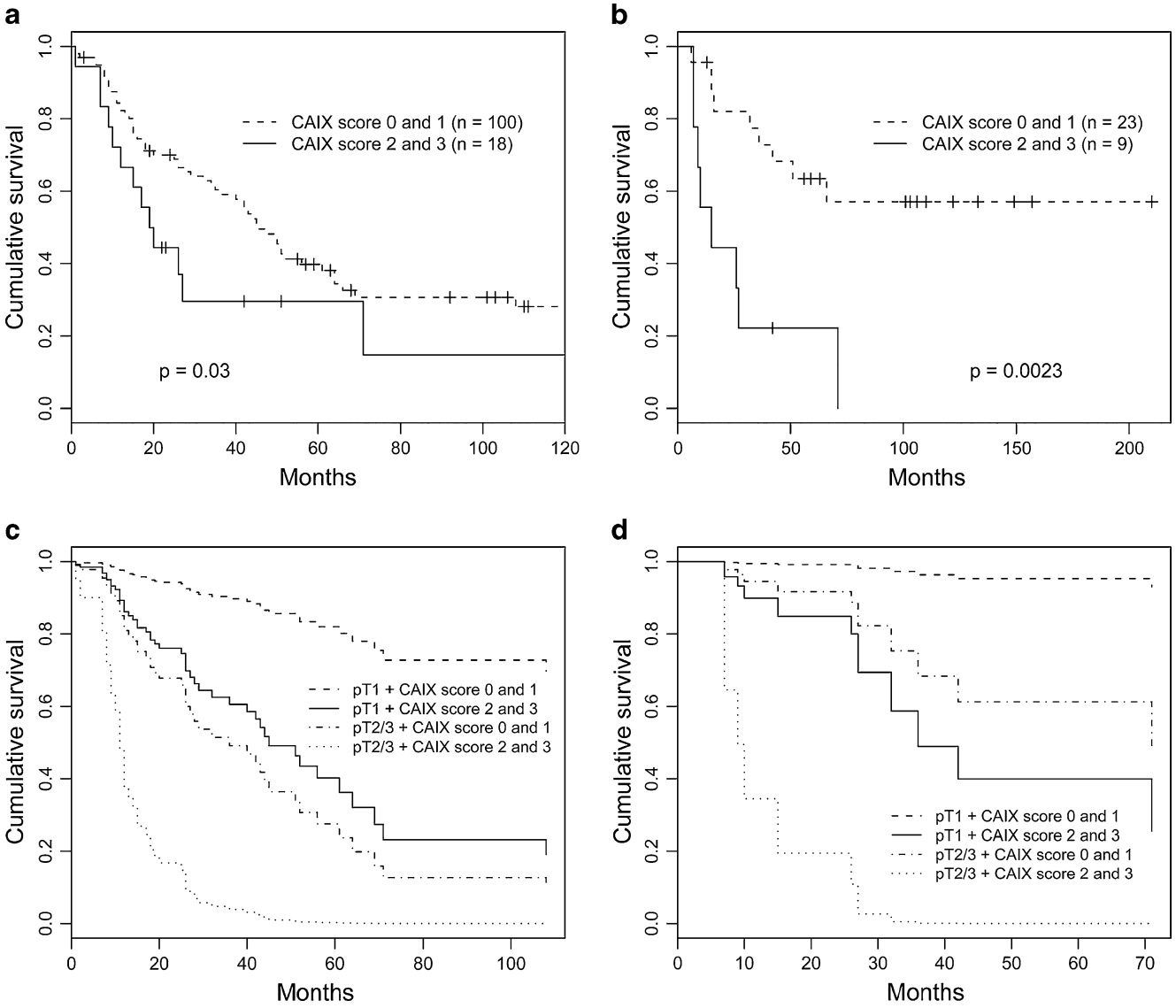

Fig. 3 Prognostic relevance of CAIX expression in ovarian carcinomas: **a** Kaplan–Meier survival curve of 118 ovarian cancer patients with and without CAIX overexpression. **b** Overall patient survival in 32 patients with endometrioid carcinomas in dependence from CAIX expression. **c** Expected survival times in 75 ovarian cancer patients in tumor stages pT1 and pT2/3 with and without CAIX overexpression according the multivariate Cox regression model in Table 3. **d** Expected survival time of patients with endometrioid carcinomas according the Cox regression model in Table 3

number of events in serous and mucinous carcinomas as well as in the "others" group was not sufficient for further statistical analysis.

Multivariate analysis of overall survival data included in the univariate analysis established prognostic markers: tumor stage, grading, mitotic index, and CAIX expression level (Table 4). This analysis revealed an independent adverse prognostic value of high pT category and high CAIX expression in the whole cohort as well as in endometrioid carcinomas. Hazard ratios for overall survival were 6.37 and 4.68 in all ovarian carcinomas and 9.97 and 18.68 in endometrioid carcinomas for these both parameters. In this statistical model, ovarian cancer patients with tumors in pT1 stage with and without CAIX overexpression have an expected 5-year survival rate of 36.2% vs. 80.2% and in the higher tumor stages pT2/3 of <10% and 23.7%, respectively (Fig. 3c). The results in endometrioid cancers are similar (Fig. 3d). Remarkably, the prognosis in pT1 tumors with CAIX overexpression seems to be worse than in advanced tumors without CAIX overexpression.

Discussion

Overexpression of CAIX is an important feature of ovarian cancer. In the present study, 18% of ovarian carcinomas

Table 3 Clinicopathological features and survival data of histopathologic subtypes of ovarian carcinomas, which were analyzable for CAIX expression

		Histologic tumor type			
		Serous (%)	Mucinous (%)	Endometrioid (%)	Others[a] (%)
All samples		88	22	47	47
Tumor stage	pT1	11 (16.7)	6 (54.5)	12 (41.4)	12 (35.3)
	pT2	12 (18.2)	1 (9.1)	4 (13.8)	9 (26.5)
	pT3	43 (65.2)	4 (36.4)	13 (44.8)	13 (38.2)
Grading	G1	9 (10.3)	16 (72.7)	15 (31.9)	9 (36.0)
	G2	26 (29.9)	5 (22.7)	25 (53.2)	8 (32.0)
	G3	52 (59.8)	1 (4.5)	7 (14.9)	8 (32.0)
Mitotic index	≤3	36 (41.4)	19 (86.4)	30 (63.8)	17 (68.0)
	>3	51 (58.6)	3 (13.6)	17 (36.2)	8 (32.0)
Survival data		51	8	32	27
No. of events	CAIX score 0+1	29	4	9	15
No. of events	CAIX score 2+3	2	3	8	1

[a] Eighteen clear cell carcinomas, 11 malignant mixed Mullerian tumors, three transitional cell carcinomas, and 15 non-specified

showed a moderate or strong membranous CAIX expression. Numerous studies have previously demonstrated that TMAs are reliable tools for immunohistochemical examination of protein expression [14, 15]. As demonstrated in comparative experiments, analysis of a single high-density tissue microarray section is representative for the whole tumor and may even be superior to large section data for some biomarkers [16]. These data have clearly shown that TMA analysis uncover the important biological information about protein expression patterns in tumors. Taken together, the results of the present study suggest that CAIX is frequently expressed, albeit at variable levels, in ovarian cancer. Hynninen et al. described remarkably high CAIX expression in mucinous ovarian tumors [11]. This finding is in line with the elevated CAIX expression levels in endometrioid and mucinous ovarian tumors found in our examination. The percentage of CAIX-positive tumors in the present analysis was somewhat lower than described by Hynninen et al. [11]. Differences in sample size may explain this inconsistency.

Serous ovarian carcinomas expressed less frequently high CAIX levels than mucinous or endometrioid carcinomas in our examination. The clinicopathological features of different ovarian cancer subtypes in the present study are similar as found in large epidemiological studies [13]. Thus, the data of our study are representative for the range of ovarian cancer, and systematic selection bias is unlikely responsible for the observed variations. The subtypes of ovarian carcinomas follow quite different molecular pathways. Abrogation of the p53 pathway plays the central role in serous carcinomas whereas in mucinous and endometrioid tumors activating mutations of *KRAS* and inactivation of the Wnt/beta-catenin and the PI3K/PTEN pathways are crucial

Table 4 Cox multivariate regression analysis of overall survival in ovarian cancer including significant parameters in univariate analysis

	No. of patients	No. of events	All tumors			No. of patients	No. of events	Endometrioid carcinomas		
			HR	CI 95%	*p* value			HR	CI 95%	*p* value
Tumor stage										
pT1	19	6	1			9	3	1		
pT2 and pT3	56	30	6.37	2.54–16.03	<0.001	12	8	9.97	1.66–60	0.012
Grading										
G1 and G2	45	26	1			–	–	–	–	–
G3	30	20	1.37	0.65–2.87	0.41	–	–	–	–	–
Mitotic index										
≤3	45	30	1			–	–	–	–	–
>3	30	16	0.68	0.32–1.46	0.33	–	–	–	–	–
CAIX										
Score 0 and score 1	61	35	1			13	4	1		
Score 2 and score 3	14	11	4.68	2.15–10.22	0.0001	8	7	18.68	3.26–107	0.001

[17]. Tissue hypoxia is the main regulator for CAIX expression in tumors as shown in numerous earlier studies [18]. However, cell culture experiments showed that CAIX could also be up-regulated by high cell density via the phosphatidylinositol-3-kinase pathway and by the mitogen-activated protein kinase pathway during both normoxia and hypoxia [19, 20]. Loss of PTEN leads to constitutive activation of the PI3K pathway via diminished dephosphorylation of membrane lipids and therefore recruitment and activation of AKT to the cell membrane [21]. Thus, CAIX expression in malignant tumors may also be more pathway-driven without significant correlation to tumor hypoxia. Furthermore, amplification of PI3K seems to be frequently involved in the development of ovarian cancer [22]. The preferential CAIX overexpression in endometrioid ovarian carcinomas suggest that such molecular mechanisms, rather than simple tissue hypoxia, may also be involved in the regulation of CAIX expression in ovarian cancer. However, mucinous and other ovarian carcinomas frequently contain areas of tumor necrosis and/or large mucous filled cysts. Therefore, hypoxia-induced CAIX overexpression may be an important mechanism in ovarian cancer too.

We detected no relationship between CAIX expression and tumor stage, grading or mitotic count of ovarian carcinomas. Furthermore, Hynninen et al. detected high CAIX levels in ovarian borderline tumors [11]. These data suggest that CAIX expression in ovarian cancer is mainly independent from tumor stage and can already be observed in early stages of tumor development. CAIX overexpression may be an indicator for an unfavorable clinical course in ovarian carcinomas at least in some histopathological subtypes. The poor prognosis of pT1 endometrioid carcinomas with CAIX overexpression found in the current study strongly point in this direction. Besides the cell-associated membranous form of CAIX, there is a soluble isoform that is released by proteolytic cleavage and can be detected in the serum [23]. Serum CAIX has been shown to serve as a promising marker for therapy monitoring and prediction of prognosis in patients with cancer of the kidney [23]. The ubiquitous CAIX expression throughout the different tumor stages raises the possibility that CAIX measurement in serum could be a useful diagnostic marker in ovarian carcinomas, too.

In the present study, CAIX overexpression has been proved as strong negative prognostic marker in ovarian carcinomas. This result is in line with the prognostic relevance of CAIX expression in other tumor entities. Furthermore, this finding underlines the important role of CAIX in the development of the malignant phenotype of ovarian tumors. The exclusive expression of CAIX in cancerous tissues makes the enzyme a suitable target for therapeutic interventions. Currently developed CAIX-targeting antibodies (G250) achieved anti-tumor activity in mouse xenograft tumor models and phase II clinical trials [24, 25]. In renal cell cancer, overexpression of CAIX is common and the possible role of CAIX-targeting antibodies (WX-G250, Rencarex®) is currently being evaluated in phase III adjuvant immunotherapy as well as radiotherapy trials [26, 27].

In summary, our results show that CAIX is expressed in ovarian cancers at variable levels and the expression is related to tumor phenotype and poor prognosis. These data support the concept that CAIX may represent a suitable therapeutic as well as diagnostic target in human cancer as suggested in cell line and animal experiments.

Conflict of interest statement We declare that we have no conflict of interest.

References

1. Zavada J, Zavadova Z, Pastorekova S et al (1993) Expression of MaTu-MN protein in human tumor cultures and in clinical specimens. Int J Cancer 54:268–274
2. Potter C, Harris AL (2004) Hypoxia inducible carbonic anhydrase IX, marker of tumour hypoxia, survival pathway and therapy target. Cell Cycle 3:164–167
3. Robertson N, Potter C, Harris AL (2004) Role of carbonic anhydrase IX in human tumor cell growth, survival, and invasion. Cancer Res 64:6160–6165
4. Kaluz S, Kaluzova M, Liao SY et al (2009) Transcriptional control of the tumor- and hypoxia-marker carbonic anhydrase 9: a one transcription factor (HIF-1) show? Biochim Biophys Acta 1795:162–172
5. Ivanov S, Liao SY, Ivanova A et al (2001) Expression of hypoxia-inducible cell-surface transmembrane carbonic anhydrases in human cancer. Am J Pathol 158:905–919
6. Hussain SA, Ganesan R, Reynolds G et al (2007) Hypoxia-regulated carbonic anhydrase IX expression is associated with poor survival in patients with invasive breast cancer. Br J Cancer 96:104–109
7. Klatte T, Seligson DB, Rao JY et al (2009) Carbonic anhydrase IX in bladder cancer: a diagnostic, prognostic, and therapeutic molecular marker. Cancer 115:1448–1458
8. Loncaster JA, Harris AL, Davidson SE et al (2001) Carbonic anhydrase (CA IX) expression, a potential new intrinsic marker of hypoxia: correlations with tumor oxygen measurements and prognosis in locally advanced carcinoma of the cervix. Cancer Res 61:6394–6399
9. Swinson DE, Jones JL, Richardson D et al (2003) Carbonic anhydrase IX expression, a novel surrogate marker of tumor hypoxia, is associated with a poor prognosis in non-small-cell lung cancer. J Clin Oncol 21:473–482
10. Pfisterer J, du Bois A (2007) [Therapeutic standards for ovarian cancer]. Pathologe 28:222–228
11. Hynninen P, Vaskivuo L, Saarnio J et al (2006) Expression of transmembrane carbonic anhydrases IX and XII in ovarian tumours. Histopathology 49:594–602
12. Simon R, Mirlacher M, Sauter G (2004) Tissue microarrays. Biotechniques 36:98–105
13. Partridge EE, Phillips JL, Menck HR (1996) The National Cancer Data Base report on ovarian cancer treatment in United States hospitals. Cancer 78:2236–2246

14. Bubendorf L, Nocito A, Moch H et al (2001) Tissue microarray (TMA) technology: miniaturized pathology archives for high-throughput in situ studies. J Pathol 195:72–79
15. Ruiz C, Seibt S, Al Kuraya K et al (2006) Tissue microarrays for comparing molecular features with proliferation activity in breast cancer. Int J Cancer 118:2190–2194
16. Torhorst J, Bucher C, Kononen J et al (2001) Tissue microarrays for rapid linking of molecular changes to clinical endpoints. Am J Pathol 159:2249–2256
17. Kurman RJ, Shih Ie M (2008) Pathogenesis of ovarian cancer: lessons from morphology and molecular biology and their clinical implications. Int J Gynecol Pathol 27:151–160
18. Ruan K, Song G, Ouyang G (2009) Role of hypoxia in the hallmarks of human cancer. J Cell Biochem 107:1053–1062
19. Kaluz S, Kaluzova M, Chrastina A et al (2002) Lowered oxygen tension induces expression of the hypoxia marker MN/carbonic anhydrase IX in the absence of hypoxia-inducible factor 1 alpha stabilization: a role for phosphatidylinositol 3′-kinase. Cancer Res 62:4469–4477
20. Kopacek J, Barathova M, Dequiedt F et al (2005) MAPK pathway contributes to density- and hypoxia-induced expression of the tumor-associated carbonic anhydrase IX. Biochim Biophys Acta 1729:41–49
21. Cantley LC, Neel BG (1999) New insights into tumor suppression: PTEN suppresses tumor formation by restraining the phosphoinositide 3-kinase/AKT pathway. Proc Natl Acad Sci U S A 96:4240–4245
22. Shayesteh L, Lu Y, Kuo WL et al (1999) PIK3CA is implicated as an oncogene in ovarian cancer. Nat Genet 21:99–102
23. Zavada J, Zavadova Z, Zat'ovicova M et al (2003) Soluble form of carbonic anhydrase IX (CA IX) in the serum and urine of renal carcinoma patients. Br J Cancer 89:1067–1071
24. Mulders P, Bleumer I, Debruyne F et al (2004) Specific monoclonal antibody-based immunotherapy by targeting the RCC-associated antigen carbonic anhydrase-IX(G250/MN). Urologe A 43(Suppl 3):S146–S147
25. Bauer S, Oosterwijk-Wakka JC, Adrian N et al (2009) Targeted therapy of renal cell carcinoma: synergistic activity of cG250-TNF and IFNg. Int J Cancer 125:115–123
26. Stillebroer AB, Mulders PF, Boerman OC et al (2010) Carbonic anhydrase IX in renal cell carcinoma: implications for prognosis, diagnosis, and therapy. Eur Urol 58:75–83
27. Wilex: Phase III ARISER Study (Adjuvant RENCAREX®Immuno-therapy Phase III trial to Study Efficacy in non-metastatic RCC). http://www.wilex.de/R&D/RENCAREX_PhaseIII.htm

Virchows Arch (2011) 459:201–211
DOI 10.1007/s00428-011-1079-9

ORIGINAL ARTICLE

DNA methylation profile during multistage progression of pulmonary adenocarcinomas

Jin-Haeng Chung · Hyun Ju Lee · Baek-hui Kim · Nam-Yun Cho · Gyeong Hoon Kang

Received: 12 January 2011 / Revised: 28 March 2011 / Accepted: 31 March 2011 / Published online: 15 April 2011
© Springer-Verlag 2011

Abstract Multiple genetic and epigenetic alterations are known to be involved in the carcinogenesis of peripheral pulmonary adenocarcinoma (ADC). However, epigenetic abnormalities have not been extensively investigated in the following multistage progression sequence: atypical adenomatous hyperplasia (AAH) to adenocarcinoma in situ (AIS), to invasive ADC. To determine the potential role of promoter methylation during ADC development of the lung, we examined methylation status in 20 normal, 20 AAH, 30 AIS, and 60 ADC lung tissues and compared methylation status among the lesions. The MethyLight assay was used to determine the methylation status of 18 CpG island loci, which were hypermethylated in ADC compared to noncancerous lung tissues. The mean number of methylated CpG island loci was significantly higher in ADC than in AAH and AIS, ($p < 0.003$ between ADC and AAH, $p < 0.005$ between ADC and AIS). Aberrant methylation of *HOXA1*, *TMEFF2*, and *RARB* was frequently observed in preinvasive lesions, including AAH and AIS. Furthermore, methylation of *PENK*, *BCL2*, *RUNX3*, *DLEC1*, *MT1G*, *GRIN2B*, *CDH13*, *CCND2*, and *HOXA10* was significantly more frequent in invasive ADC than AAH or AIS. Our results indicate that epigenetic alterations are involved in the multistep progression of pulmonary ADC development, and aberrant CpG island methylation accumulates during multistep carcinogenesis. In addition, aberrant methylation of *HOXA1*, *TMEFF2*, and *RARB* occurred in preinvasive lesions, which indicates that epigenetic alterations of these genes are involved in the early stages of pulmonary ADC development. In contrast, hypermethylation of *PENK*, *BCL2*, *RUNX3*, *DLEC1*, *MT1G*, *GRIN2B*, *CDH13*, *CCND2*, and *HOXA10* was more frequent in invasive ADC than in preinvasive lesions, which indicates that methylation of these genes occurs later during tumor invasion in the AAH–AIS–ADC sequence.

Keywords Lung cancer · AIS · Adenocarcinoma · CpG island · DNA methylation

J.-H. Chung · H. J. Lee
Department of Pathology,
Seoul National University Bundang Hospital,
Seongnam, Gyeonggi-do, South Korea

J.-H. Chung · H. J. Lee · N.-Y. Cho · G. H. Kang
Department of Pathology,
Seoul National University College of Medicine,
Seoul, South Korea

B.-h. Kim
Department of Pathology, Korea University Guro Hospital,
Seoul, South Korea

N.-Y. Cho · G. H. Kang
Laboratory of Epigenetics, Cancer Research Institute,
Seoul National University College of Medicine,
Seoul, South Korea

G. H. Kang (✉)
Department of Pathology, Seoul National University
College of Medicine and Cancer Research Institute,
Seoul National University Hospital,
28 Yongon-dong, Chongno-gu,
Seoul 110–744, South Korea
e-mail: ghkang@snu.ac.kr

Introduction

The development of peripheral lung cancer, including atypical adenomatous hyperplasia (AAH), has been hypothesized to progress from a precursor lesion of adenocarcinoma (ADC), to adenocarcinoma in situ (AIS; formerly bronchioloalveolar carcinoma (BAC)), to invasive ADC with features of lepidic

growth pattern [1, 2]. This model is supported by the frequent coexistence of characteristics of non-invasive lepidic growth pattern at the periphery of invasive ADC and the morphological similarity between AAH and BAC [1–3]. The development of peripheral pulmonary ADC involves multiple genetic alterations [3]. Mutations of *epidermal growth factor receptor (EGFR)* or *K-ras* genes have been detected in preinvasive lesions such as AAH, AIS (formerly BAC), and ADC [2, 4–12]. Somatic mutations and increased expression of *p53* were detected in advanced ADC [13]. While genetic alterations have been extensively studied in the multistep carcinogenesis model in the peripheral airway, epigenetic abnormalities have not been identified [2, 3, 6, 7, 9, 10, 14, 15].

The aberrant CpG island hypermethylation of various tumor suppressor genes (TSGs) is an important mechanism in human cancer development [16–20]. CpG islands are DNA segments at least 0.5 kb in size that are rich in G:C and often located in the promoter or 5′-exon sequences of genes. About 50% of human gene promoters are located in CpG islands which are protected from methylation in normal cells, with the exception of those on the inactive X chromosome. Hypermethylation of CpG islands in the promoter regions is an important mechanism of gene silencing for TSGs [21]. In fact, various tissue types of human cancers involve CpG island hypermethylation in some gene promoters, although there are variations in the prevalence of CpG island hypermethylation between tumor types [22, 23]. Aberrant DNA methylation of multiple cancer-related genes has been widely identified in non-small cell lung carcinoma [24–27]. However, most of these studies have focused on aberrant methylation in advanced cancer tissues.

There are few hypermethylated genes in the development of small ADC sequence [14, 15]. Shu et al. suggested that the aberrant CpG island methylation of *ACIN1* is one of the earliest events in lung ADC development [14]. Kubo et al. identified that hypermethylation of $p16^{INK4a}$, *CDH13*, and *RASSF1A* was related to the acquirement of invasiveness in small peripheral ADC [15].

In this study, we selected 18 genes that were frequently methylated in ADC. These genes are involved in different carcinogenic pathways such as development and differentiation (*HOXA1*, *HOXA10*, *RUNX3*, *RARRES1*, *GATA3*, *RARB*, and *CRABP1*), cell cycle regulation (*CCND2*), growth factor (*TMEFF2*), apoptosis (*BCL2* and *PENK*), signal transduction and tumor suppression (*SFRP5*, *GRIN2B*, *DLEC1*, and *SEZ6L*), invasion and metastasis (*CDH13* and *ITGA4*) and DNA repair or protection (*RARB* and *MT1G*; Table 1). We determined the methylation pattern of these genes in normal lung tissues, AAH, AIS, and ADC harboring peripheral lepidic growth pattern to characterize this epigenetic event in neoplastic processes of the lung. This series included the full spectrum of sequential development, which provided better subjects for investigating the early molecular events of pulmonary ADC.

Materials and methods

Prescreening test

We did a MethyLight analysis of 61 CpG island loci on a total of 40 lung tissue samples, including ADC (n=20) and noncancerous lung tissues (n=20), and determined percentage of methylated reference (PMR) values for each sample and CpG island locus (Fig. 1). Nineteen CpG island loci were significantly methylated in lung ADC samples at levels higher than those of noncancerous lung tissues (P<0.05, Mann–Whitney test): *BCL2*, *CDH13*, *CRABP1*, *HOXA1*, *PENK*, *RARB*, *SEZ6L*, *TMEFF2*, *CCND2*, *MT1G*, *GRIN2B*, *ITGA4*, *RUNX3*, *DLEC1*, *HOXA10*, *SFRP5*, *GATA3*, *CYP27B1*, and *RARRES1* (in descending order of statistical significance). When we calculated DNA methylation frequencies for each CpG island locus (PMR>4) for lung ADC and noncancerous lung tissues, ADC tissues showed hypermethylation at 18 CpG island loci at frequencies higher than those of noncancerous lung tissues (P<0.05, Fisher's exact test). These 18 CpG island loci were also included in those 19 CpG island loci showing significantly higher methylation levels in ADC than in noncancerous lung tissues. But *CYP27B1* was found to be not significantly methylated at a frequency higher than that of noncancerous lung tissues (p=0.605, Fisher's exact test). Eighteen CpG island loci except for *CYP27B1* were considered cancer-specific CpG island loci because they were hypermethylated in ADC at levels and frequencies significantly higher than the respective ones of noncancerous lung tissues.

Patients and tissue samples

A total of 130 formalin-fixed paraffin-embedded archival tissues from 108 patients with peripheral neoplastic lesions were collected from the Department of Pathology, Seoul National University Bundang Hospital, Korea, between June 2003 and April 2009. The histologic diagnoses of the 130 tissue samples were normal lung tissues (n=20), AAH (n=20), AIS (n=30), and invasive ADC with lepidic growth pattern (n=60). Of these, eight patients had synchronous multiple lesions. These patients had undergone curative surgical treatment (wedge resection, n=21; lobectomy, n=85; and segmentectomy, n=2). None of these patients were treated with preoperative neoadjuvant chemotherapy or radiation therapy. Clinicopathological characteristics including patient

Table 1 MethyLight primers and probes of the 18 genes

Genes	Full name	Chromosomal position	Primer and probe sequences	Size (bp)	AT (°C)
HOXA1	Homeobox A1	7p15.3	F: TTGTTTATTAGGAAGCGGTCGTC R: TCGAACCATAAAATTACAACTTTCCA Pr: 6FAM-TCGTACGCGATCAACGCCAAC AATTA-TAMRA	83	59
TMEFF2	Transmembrane protein with EGF-like and two follistatin-like domains 2	2q32.3	F: CGACGAGGAGGTGTAAGGATG R: CAACGCCTAACGAACGAACC Pr: 6FAM-TATAACTTCCGCGACCGCCTC CTCCT-TAMRA	73	59
RARB	Retinoic acid receptor, beta	3p24	F: TTTATGCGAGTTGTTTGAGGATTG R: CGAATCCTACCCCGACGATAC Pr: 6FAM-CTCGAATCGCTCGCGTTCTC GACAT-TAMRA	86	59
PENK	Proenkephalin	8q23-q24	F: GGTTAATTATAAAGTGGTTTTAGTA GTCGTTAAG R: CAACGTCTCTACGAAATCACGAAC Pr: 6FAM-AACGCCTACCTCGCCGTCC CG-TAMRA	99	59
BCL2	B-cell CLL/lymphoma 2	18q21.33; 18q21.3	F: TCGTATTTCGGGATTCGGTC R: AACTAAACGCAAACCCCGC Pr: 6FAM-ACGACGCCGAAAACAACCGA AATCTACA-TAMRA	84	59
RUNX3	Runt-related transcription factor 3	1p36	F: CGTTCGATGGTGGACGTGT R: GACGAACAACGTCTTATTACAACGC Pr: 6FAM-CGCACGAACTCGCCTACGTAA TCCG-TAMRA	117	59
DLEC1	Deleted in lung and esophageal cancer 1	3p21.3	F: TCGTTGCGTATTTAAGATATTTCGTATT R: CGTAACGCTCATTCTCGCTACC Pr: 6FAM-TAATCAAACTTACGCTCACTTCG TCGCCG-TAMRA	130	59
MT1G	Metallothionein 1 G	16q13	F: CGTTTAAGGGATTTTGTATTTGGTTTAT R: CCGCTAAATCCGCACCG Pr: 6FAM-CGCGATCCCGACCTAAACTATA CGCA-TAMRA	77	59
GRIN2B	Glutamate receptor, ionotropic, N-methyl D-aspartate 2B	12p12	F: GTCGGATTTACGCGTCGAGT R: CTACCGCCGCGCTAAAATAC Pr: 6FAM-ACGCACGAAACTTCACCTACA ACGTATCG-TAMRA	83	59
GATA3	GATA binding protein 3	10p15	F: TGTATCGGGACGGAATCGTT R: ACGCGCGCTCTAACCCTT Pr: 6FAM-AAATATAACCGCGACTCCTACCA ATTCATTCG-TAMRA	80	59
CDH13	Cadherin 13, H-cadherin (heart)	16q23.3	F: AATTTCGTTCGTTTTGTGCGT R: CTACCCGTACCGAACGATCC Pr: 6FAM-AACGCAAAACGCGCCC GACA-TAMRA	103	59
RARRES1	Retinoic acid receptor responder (tazarotene induced) 1	3q25.32	F: GGCGAGTCGGATCGGAA R: CGCAAACTCCTACAACAAACGA Pr: 6FAM-CGCGCGACGCTTCACTTCT TCAA-TAMRA	65	59
SFRP5	Secreted frizzled-related protein 5	10q24.1	F: GCGTTTGTAGTTTATCGTGTGGTAGA R: GAACCGCTACACGACCGCT Pr: 6FAM-CGCCGCAATACCTTAACATCC CTACCG-TAMRA	93	59
CCND2	Cyclin D2	12p13	F: GGAGGGTCGGCGAGGAT R: TCCTTTCCCCGAAAACATAAAA Pr: 6FAM-CACGCTCGATCCTTCGC CCG-TAMRA	64	59

Table 1 (continued)

Genes	Full name	Chromosomal position	Primer and probe sequences	Size (bp)	AT (°C)
CRABP1	Cellular retinoic acid binding protein 1	15q24	F: TCGAAATTTTCGTTGTTGCGT R: TATCCGTACCTACCGCCGC Pr: 6FAM-ACCATACCCAACTTCGCCGA CACCTAA-TAMRA	82	59
SEZ6L	Seizure related 6 homolog (mouse)-like	22q12.1	F: GCGTTAGTAGGGAGAGAAAACGTTC R: ATACCAACCGCCTCCTCTAACC Pr: 6FAM-CCGTCGACCCTACAAAATTT AACGCCA-TAMRA	103	59
HOXA10	Homeobox A10	7p15.2	F: ATCGGAAGTGCGTTATTTCGTG R: TTCCGTCTCTCGACTCGAAACT Pr: 6FAM-CTCCGACCCAACCTAAA CGCGCA-TAMRA	76	59
ITGA4	Integrin, alpha 4 (antigen CD49D, alpha 4 subunit of VLA-4 receptor)	2q31.3	F: TGCGGAGGCGTAGGGTC R: CAACCGAAATTCCCCAACG Pr: 6FAM-CCTACAACCGCGCGTAAACAA AAACG-TAMRA	71	59

AT annealing temperature, *F* forward primer, *R* reverse primer, *Pr* probe

age, sex, smoking status, and tumor size were obtained from medical records. This study was approved by the Institutional Review Board of Seoul National University Bundang Hospital (B-1001-091-301) and the patient's consent for inclusion in this study was waived.

Histologic examination of tissue specimens

All sections of the tumors and suspicious lesions were submitted for microscopic examination. Histopathologic diagnoses of preinvasive and invasive ADC were based on the multidisciplinary classification of lung adenocarcinoma [28]. The new classification recommends discontinuing the use of the term "BAC" and introduced AIS (one of the lesions formerly known as BAC in the many studies) that is a localized small (≤3 cm) ADC with growth restricted to neoplastic cells along preexisting alveolar structures (lepidic growth), lacking stromal, vascular, or pleural invasion, and AAH was considered to be a precursor lesion. The ADC samples were obtained from definite invasive tumor portions of surgical specimens. The representative examples of pathological findings are shown in Fig. 2. Two pulmonary pathologists reviewed all of the surgical specimens (J.H.C & H.J.L).

DNA extraction and bisulfite modification

Five serial sections (8 μm thick) from each paraffin block sample were stained with hematoxylin and eosin. Through light microscopic examination, we marked tumor areas where neoplastic cells occupied more than 80% of the area, and we manually dissected and placed the tissue samples in microtubes. Dissected tissue samples were subjected to tissue lysis using proteinase K lysis buffer. Bisulfite modification of the digested tissue samples (18 μl) was performed using the EZ DNA methylation kit (Zymo Research Co., Orange, CA, USA) according to the manufacturer's protocol [29].

DNA methylation analysis

DNA methylation analyses were performed using the MethyLight assay as previously described [30]. Based on our preliminary study, we selected 18 promoter CpG island loci that were frequently methylated in ADC compared to normal lung tissues. The gene names, locations, oligonucleotide primer sequences, probe sequences, and PCR conditions (annealing temperature and product size) are summarized in Table 1. A 30-μl PCR mixture contained 0.2 mM deoxyribonucleotide triphosphates, 0.3 μM forward and reverse primers, 0.05 μM probe, 3.5 mM $MgCl_2$, 0.05% gelatin, 0.01% Tween-20, 1× PCR buffer, and 0.5 U of AmpliTaq Gold polymerase. The PCR conditions were as follows: initial denaturation at 95°C for 10 min followed by 50 cycles of 95°C for 15 s and 60°C for 1 min. The *ALU* repeats were used as an internal reference to normalize input DNA and to generate a standard curve. Bisulfite-modified placental genomic DNA treated with M.SssI was used as a reference sample for complete methylation to determine the percentage of fully methylated alleles (PMR) at a particular locus. The PMR value was calculated by dividing the *GENE/ALU* ratio of a sample by the *GENE/ALU* ratio of the M.SssI-treated human genomic DNA sample and multiplying by 100 [29]. The methylation status of each sample was determined as positive when PMR>4, a cutoff value based on validated data [31].

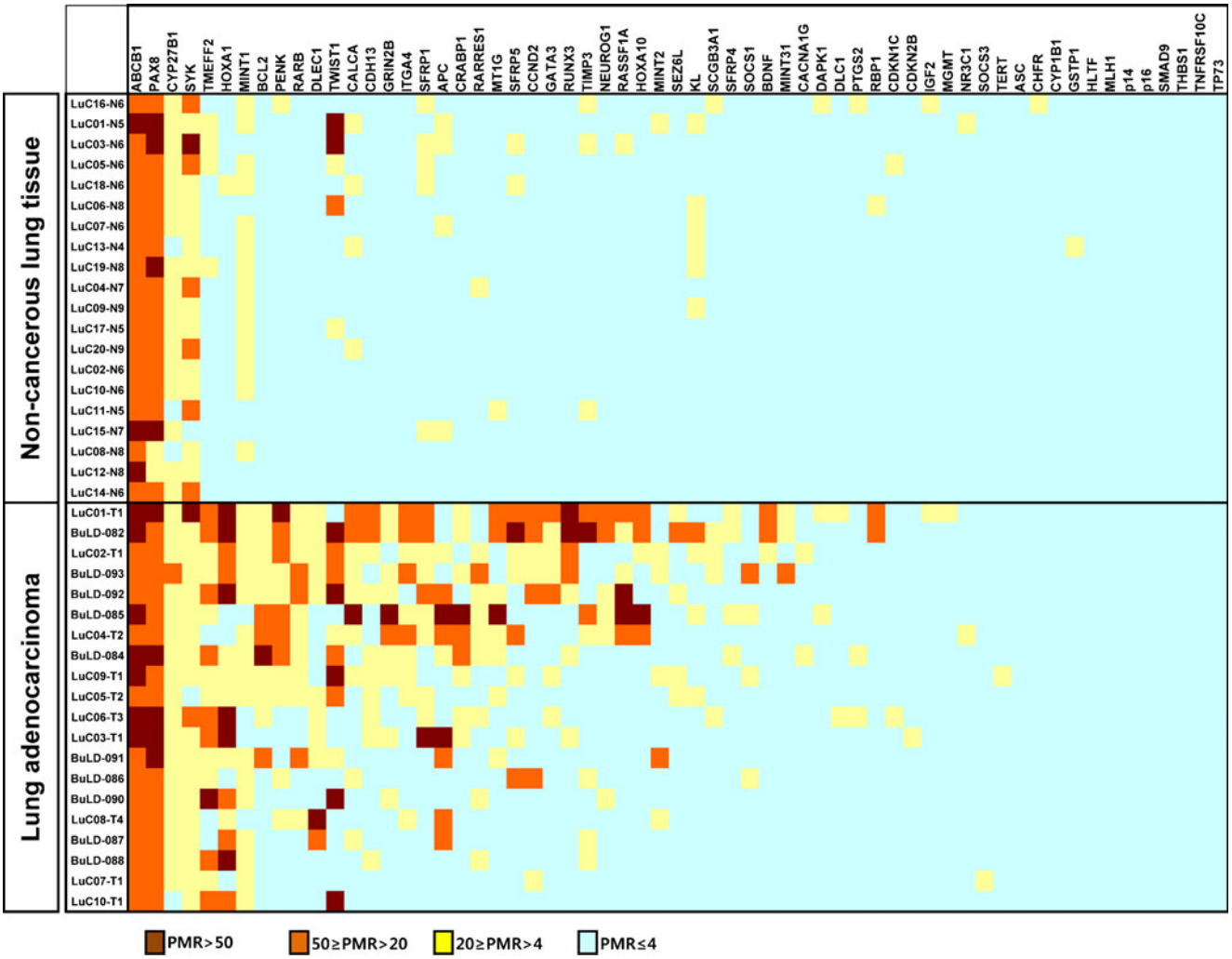

Fig. 1 Prescreening map of gene methylation of 61 CpG island loci in noncancerous lung tissues (n=20) and adenocarcinoma (ADC, n=20). The *box colors* represent the degrees of allele methylation (PMR≥50 (*brown*), 20≤PMR<50 (*orange*), 4≤PMR<20 (*yellow*), and PMR<4 (*blue*)). PMR, percentage of methylated reference

Statistical analysis

All of the statistical analyses were conducted using SPSS software version 15.0 (SPSS, Inc., Chicago, IL, USA). Pearson's chi-squared test, Mann–Whitney test and one-way analysis of variance were used to evaluate the significance of the differences between two and three groups, respectively. A $p<0.05$ was considered statistically significant.

Results

Patients and samples characteristics

Some clinical characteristics of the group studied are shown in Table 2. The patients (48 men and 60 women) were aged 34–85 years (median age=59.2 years) at surgery. All cases of AIS (former BAC) in this series were non-mucinous, and all cases of invasive ADC harbored lepidic growth pattern. Of the AAH cases, four were concurrent with ADC, and two cases included incidental findings of hamartoma (n=1) or tuberculosis (n=1). The AAH nodules ranged between 1.5 and 9 mm in diameter, and the average size was 5.9 mm.

Of the AAH nodules, some cases measured more than 5 mm in diameter; however, the lesions showed a discontinuous lining of cells with small nuclei and minimal cytologic atypia, which were short of those accepted as AIS [28]. Of the AIS nodules, five cases were obtained from the lung harboring ADC. The maximum diameter of these AIS nodules ranged between 5 and 21 mm, with an average size of 11.0 mm. The size of all nodules (AAH, AIS, and ADC) ranged between 1.5 and 60 mm, with an average size of 18.2 mm. The patients included 33 current and former (<10 years) smokers and 75 non-smokers. The patients with ADC were older than the patients with AAH or AIS (p=0.034), and the tumor size of ADC was larger than AAH or AIS ($p<0.001$).

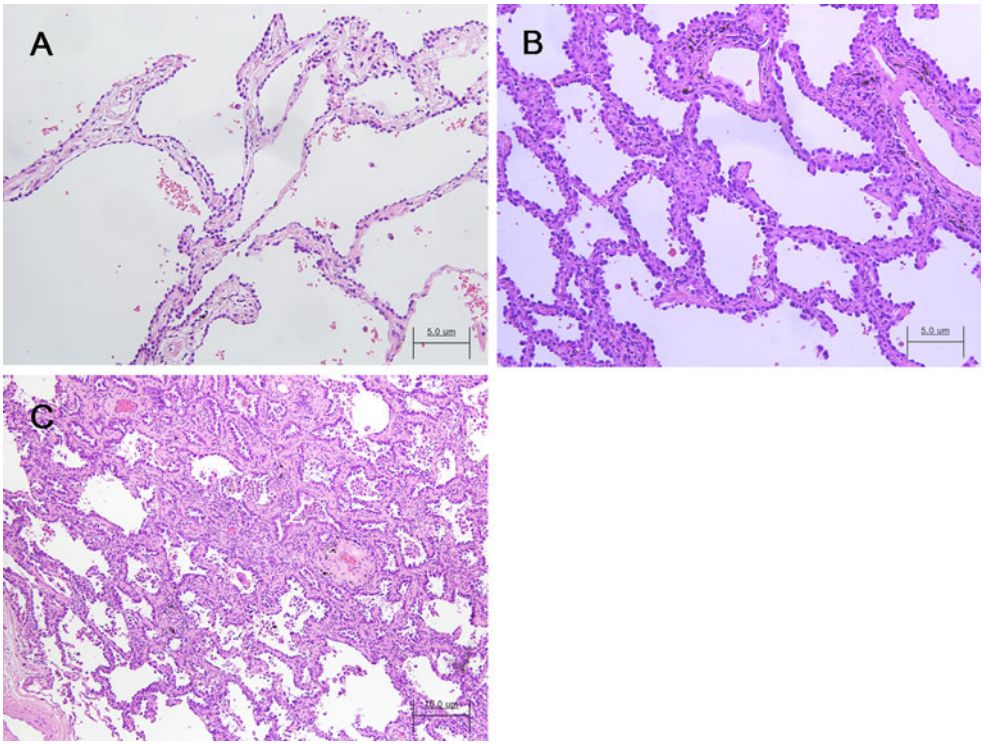

Fig. 2 Representative histologic features of lesions. **a** Atypical adenomatous hyperplasia (AAH) consists of slightly atypical pneumocytes that are cuboidal and show gaps between the cells along preexisting alveolar walls (original magnification ×200), **b** adenocarcinoma in situ (AIS) shows growth of neoplastic cells proliferating along the slightly thickened but preserved alveolar walls, namely lepidic pattern (original magnification x 200), and **c** invasive adenocarcinoma (ADC) with lepidic growth pattern (original magnification ×100)

Methylation profiles of 18 CpG island loci in normal lungs, AAH, AIS, and ADC

Methylation of more than one CpG island locus was observed in 6 (30%) of the 20 normal lung tissues, 15 (75.0%) of the 20 AAH, 27 (90.0%) of the 30 AIS, 59 (98.3%) of the 60 ADC. Detailed results of PMR values for the methylation of 18 genes in normal lung tissues, AAH, AIS, and ADC samples were calculated using MethyLight data, as shown in Fig. 3. The genes tested were less methylated in normal lung tissues. The mean number of methylated CpG island loci was significantly higher in ADC than in AAH and AIS ($p=0.003$ between ADC and AAH, $p=0.005$ between ADC and AIS, Pearson chi-squared test, Fig. 4). The profiles show an accumulation of DNA methylation from AAH to ADC.

Differential methylation patterns in the AAH–AIS–ADC sequence

Based on the methylation PMR values or frequency of these 18 genes, two different classes of genes were recognizable according to their methylation patterns during multistep carcinogenesis: (1) genes methylated in non-invasive stage (AAH and AIS); *HOXA1* (PMR=5.0 in AAH and PMR=7.7 in AIS), *TMEFF2* (PMR=6.7 in AAH and PMR=8.6 in AIS), and *RARB* (PMR=4.9 in AAH and PMR=8.3 in AIS; Fig. 5): and (2) genes more frequently methylated in the invasive stage (ADC) than the non-invasive stage; *PENK* (PMR=10.1 in ADC, $p<0.001$), *BCL2* (PMR=7.5 in ADC, $p<0.001$), *RUNX3* (PMR=8.5 in ADC, $p=0.002$), *DLEC1* (PMR=4.2 in ADC, $p=0.007$), *MT1G* (PMR=5.7 in ADC, $p=0.001$), *GRIN2B* (PMR=5.1 in ADC, $p=0.003$), *CDH13* (PMR=4.9 in ADC, $p=0.006$), *CCND2* (PMR=4.3 in ADC, $p=0.012$), and *HOXA10* (PMR=5.4 in ADC, $p=0.016$; Pearson chi-squared test; Fig. 6).

Methylation patterns in ADC

Six genes demonstrated a methylation frequency exceeding 30%: *HOXA1* (85%), *TMEFF2* (72%), *RARB* (48%), *PENK* (43%), *BCL2* (42%) and *RUNX3* (40%). Of these six genes, *HOXA1* and *TMEFF2* were also methylated in AIS at frequencies higher than 50%. Aberrant methylation of *CRABP1*, *SEZ6L*, *HOXA10*, and *ITGA4* was relatively low (<20%). *DLEC1*, *MT1G*, *CCND2*, and *HOXA10* were not methylated in AAH, and *GRIN2B*, *CDH13*, *HOXA10*, and *ITGA4* were not methylated in AIS. The methylation frequencies of *RARRES1* and *ITGA4* were similar in ADCs and AAHs. Based on PMR methylation values, hypermethylation (PMR>4) was not detected in four genes (*SFRP5*, *CRABP1*, *SEZ6L*, and *ITGA4*).

Discussion

Aberrant DNA methylation in human cancer cells is characterized by the hypermethylation of gene-associated

Table 2 Clinical Features of AAH, AIS, and ADC

	AAH (n=20)	AIS (n=30)	ADC (n=60)	Total (n=110)	P value[a]
Age (yr)					
Average	51.2	58.6	62.3	59.2	0.034
Range	36–77	34–75	39–85	34–85	
Sex					
Males	4	18	27	48	0.086
Females	16	12	33	60	
Size (mm)					
Average	5.9	11.0	26.1	18.2	<0.001
Range	1.5–9	5–21	11–60	1.5–60	
Smoking					
No	16	21	39	75	0.462
Yes	4	9	21	33	
Stage					
Tx	20			20	
Tis		30		30	
T1aN0			27	27	
T1aN1			3	3	
T1bN0			16	16	
T1bN1			2	2	
T2aN0			7	7	
T2aN1			4	4	
T2bN1			1	1	
CT findings					
pGGO	20	22		42	<0.001
mGGO		8	60	68	

[a] P value between groups

AAH atypical adenomatous hyperplasia, *AIS* adenocarcinoma in situ, *ADC* adenocarcinoma, *pGGO* pure ground-glass opacity, *mGGO* mixed ground-glass opacity

CpG islands, which are found in virtually all types of human cancer and methylation itself is a secondary event related to tumor progression [21]. By aberrant promoter hypermethylation, transcription of the promoter regions of tumor suppressor genes is repressed leading to gene silencing. Subsets of CpG island loci are hypermethylated in premalignant or in situ neoplastic lesions, including extrahepatic biliary intraepithelial neoplasia [32], colon adenomas [33], gastric adenomas [34], pancreatic intraepithelial neoplasia [35], and prostatic intraepithelial neoplasia [36], although the methylation frequencies or methylation levels at each locus are generally lower in premalignant lesions than in their malignant counterparts.

In the present study, we prescreened the methylation status of 61 promoter CpG island loci and found that 18 CpG island loci were frequently hypermethylated in ADC. Subsequently, we analyzed the methylation pattern of the 18 CpG island loci in another set of 130 lung tissue samples (20 normal lung tissues, 20 AAH, 30 AIS, and 60 ADC-T1a, 2 cm or less, n=30; more than 2 cm, n=30). We observed differential epigenetic changes during the development of peripheral lung ADC. Our major findings were as follows: (1) aberrant methylation of *HOXA1*, *TMEFF2* and *RARB* occurred in non-invasive stages (AAH and AIS), which represented the early stages of pulmonary ADC development; and (2) aberrant methylation of *PENK*, *BCL2*, *RUNX3*, *DLEC1*, *MT1G*, *GRIN2B*, *CDH13*, *CCND2*, and *HOXA10* was more closely associated with the invasive stage (ADC) than the non-invasive stage. These findings suggest that promoter CpG island hypermethylation occurs at an early stage of multistep pulmonary ADC development and accumulates to the progression of ADC.

Regarding the relationship between methylation and peripheral lung ADC development, Kubo et al. reported that aberrant methylation of *CDH13* was significantly more frequent in invasive tumors (Noguchi type C tumors) than in non-invasive tumors (Noguchi type A or B tumors) using a methylation-specific PCR (MSP) assay [15, 37]. They also found that the frequencies of *RARB* aberrant hypermethylation were relatively high in non-invasive tumors (Noguchi type A or B tumors) compared to the other genes. In this study, we expanded the number of genes to investigate epigenetic alterations in the multistep carcinogenesis of lung ADC with lepidic growth pattern and used the MethyLight assay, which sensitively detected DNA methylation in a small amount of template DNA. The methylation frequencies of *CDH13* and *RARB* in our study and Kubo's study were concordant despite the different methodology.

Several investigators have attempted to develop molecular markers to detect pulmonary ADC [14, 38]. DNA methylation markers may be useful because of their chemical stability and because they are relatively easy to detect. Shu et al. observed hypermethylation of the *ACIN1* gene in some non-tumorous regions of ADC as well as in early stage lung ADC [14]. They suggested that methylation of *ACIN1* is one of the earliest events in lung ADC development and suggested that it may be possible to identify individuals with a high risk of developing lung ADC [14]. To date, however, few sensitive and specific molecular markers for pulmonary ADC have been identified. In this study, *HOXA1*, *TMEFF2* and *RARB* were hypermethylated (PMR>4) in preinvasive lesions (AAH and AIS) compared to normal lung tissue samples. Thus, *HOXA1*, *TMEFF2* and *RARB* methylation may be promising for use as a tumor biomarker for the early detection of pulmonary ADC. A detailed clinicopathologic correlative study using sputum or serum is warranted to validate this finding.

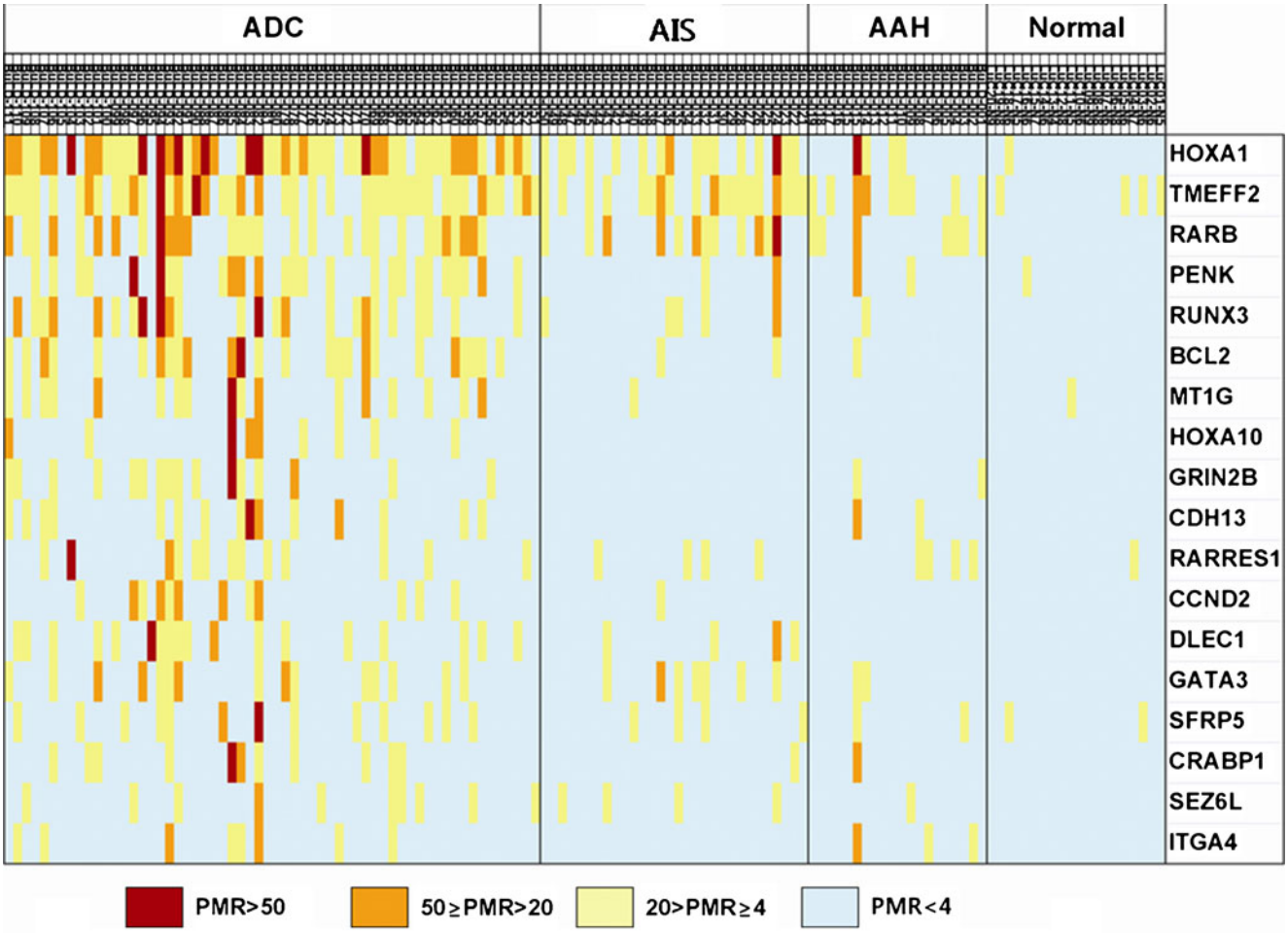

Fig. 3 Methylation map of 18 CpG island loci in normal lung tissue (n=20), atypical adenomatous hyperplasia (AAH, n=20), adenocarcinoma in situ (AIS, n=30) and invasive adenocarcinoma (ADC, n=60). The *box colors* represent the degrees of allele methylation (PMR≥50 (*brown*), 20≤PMR<50 (*orange*), 4≤PMR<20 (*yellow*), and PMR<4 (*blue*)). PMR, percentage of methylated reference

There were some limitations to this study. First, we could not analyze survival data because the follow-up period was too short to determine 5-year survival rates, and the number of ADC cases was too small. Second, it is still necessary to study these 18 CpG island loci with regard to the function and mechanism of each gene in multistep

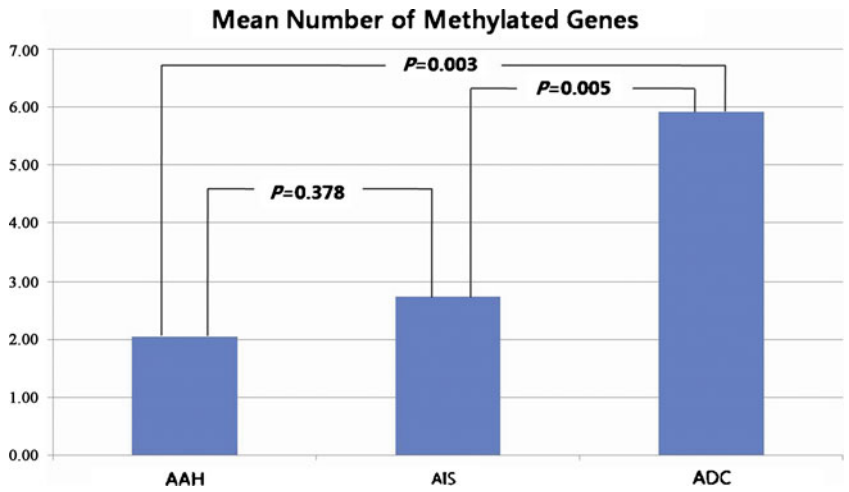

Fig. 4 Comparison of mean numbers of methylated genes of the 18 CpG island loci in atypical adenomatous hyperplasia (AAH, n=20), adenocarcinoma in situ (AIS, n=30) and invasive adenocarcinoma (ADC, n=60) tissue samples. The significance (p) after Pearson chi-squared test analysis is shown

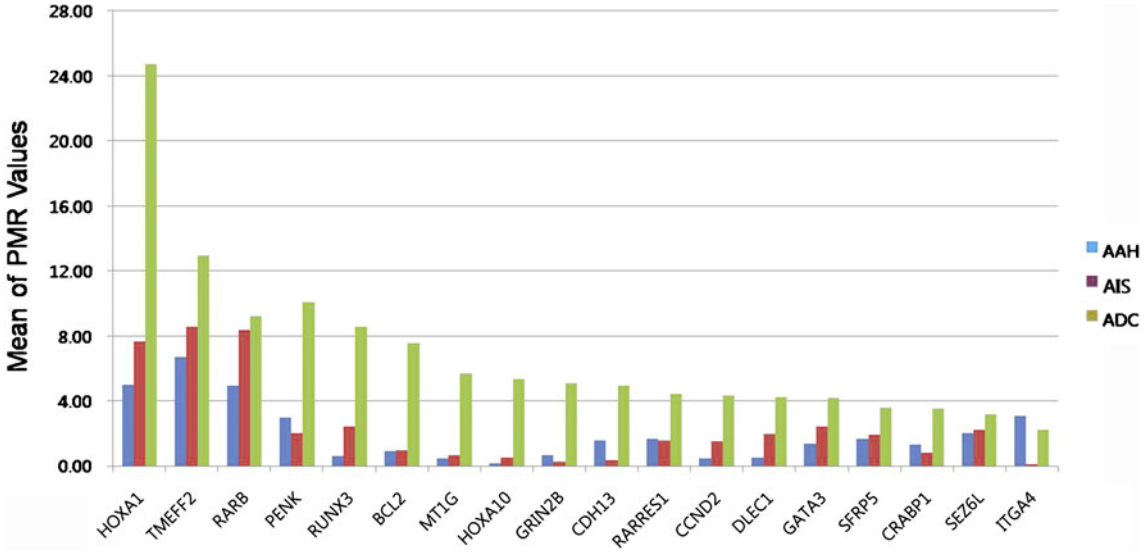

Fig. 5 Comparison of the methylation levels (mean PMR values) of 18 CpG island loci among atypical adenomatous hyperplasia (AAH, $n=20$), adenocarcinoma in situ (AIS, $n=30$) and invasive adenocarcinoma (ADC, $n=60$) tissue samples. The 3 CpG island loci on the left of the *X* axis (from *HOXA1* to *RARB*) showed significantly higher methylation levels in AAH and AIS

peripheral lung carcinogenesis. Despite these limitations, this was a relatively large-scale study that examined 18 CpG island loci in a series of 130 normal, AAH, AIS, and ADC lung tissue samples.

In conclusion, epigenetic alterations are involved in the progression of multistep pulmonary ADC development, and aberrant CpG island methylation accumulates during multistep carcinogenesis. In addition, our results suggested that methylation of *HOXA1*, *TMEFF2* and *RARB* is involved in the early stages of tumor initiation. In contrast, hypermethylation of *PENK*, *BCL2*, *RUNX3*, *DLEC1*, *MT1G*, *GRIN2B*, *CDH13*, *CCND2*, and *HOXA10* was more frequently found in invasive ADC than non-invasive lesions, which suggests that methylation of these genes is a late event in the AAH–AIS–ADC tumor invasion sequence.

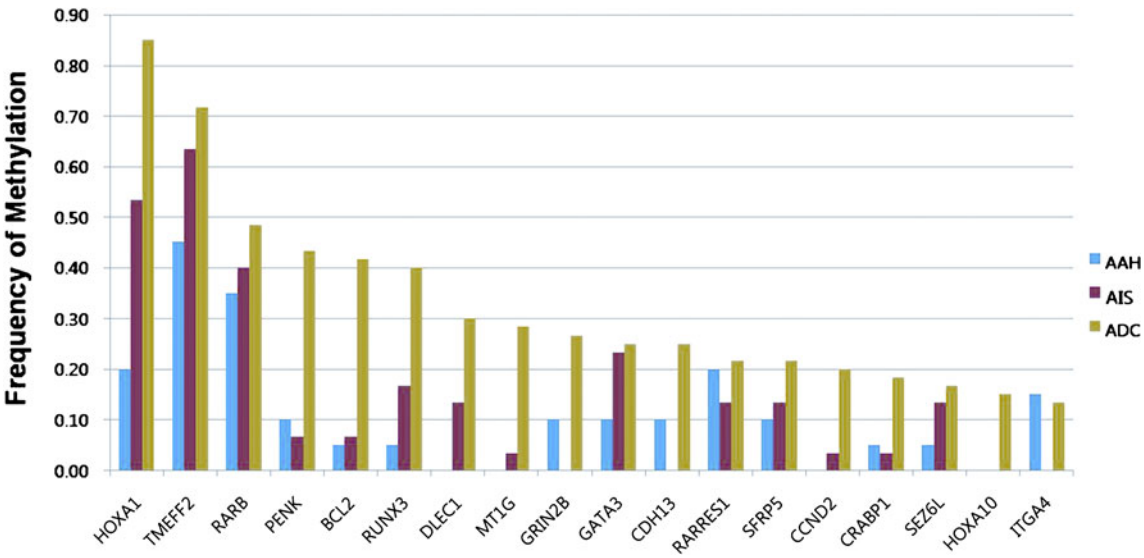

Fig. 6 Comparison of the methylation frequency of 18 CpG island loci among atypical adenomatous hyperplasia (AAH, $n=20$), adenocarcinoma in situ (AIS, $n=30$) and invasive adenocarcinoma (ADC, $n=60$) tissue samples. *PENK* ($p<0.001$), *BCL2* ($p<0.001$), *RUNX3* ($p=0.002$), *DLEC1* ($p=0.007$), *MT1G* ($p=0.001$), *GRIN2B* ($p=0.003$), *CDH13* ($p=0.006$), *CCND2* ($p=0.012$), and *HOXA10* ($p=0.016$) showed significantly higher methylation levels in ADC samples than those in AAH and AIS samples (Pearson chi-squared test)

Acknowledgments This study was supported by the 21C Frontier Functional Human Genome Project, Ministry of Science & Technology in Korea (FG09-11-02; to GHK), by a grant from the National R&D Program for Cancer Control, Ministry of Health & Welfare, Republic of Korea (0720540; to GHK), by a grant no 03-2009-002 from the SNUBH Research Fund (to JHC) and by a grant from Korea Healthcare technology R&D project, Ministry of Health and Welfare, Republic of Korea (A084578; to JHC)

Conflict of interest statement We declare that we have no conflicts of interest.

References

1. Mori M, Rao SK, Popper HH, Cagle PT, Fraire AE (2001) Atypical adenomatous hyperplasia of the lung: a probable forerunner in the development of adenocarcinoma of the lung. Mod Pathol 14:72–84
2. Soh J, Toyooka S, Ichihara S, Asano H, Kobayashi N, Suehisa H, Otani H, Yamamoto H, Ichimura K, Kiura K, Gazdar AF, Date H (2008) Sequential molecular changes during multistage pathogenesis of small peripheral adenocarcinomas of the lung. J Thorac Oncol 3:340–347
3. Lantuejoul S, Salameire D, Salon C, Brambilla E (2009) Pulmonary preneoplasia–sequential molecular carcinogenetic events. Histopathology 54:43–54
4. Yoo SB, Chung JH, Lee HJ, Lee CT, Jheon S, Sung SW (2010) Epidermal growth factor receptor mutation and p53 overexpression during the multistage progression of small adenocarcinoma of the lung. J Thorac Oncol 5:964–969
5. Sugio K, Kishimoto Y, Virmani AK, Hung JY, Gazdar AF (1994) K-ras mutations are a relatively late event in the pathogenesis of lung carcinomas. Cancer Res 54:5811–5815
6. Yoshida Y, Shibata T, Kokubu A, Tsuta K, Matsuno Y, Kanai Y, Asamura H, Tsuchiya R, Hirohashi S (2005) Mutations of the epidermal growth factor receptor gene in atypical adenomatous hyperplasia and bronchioloalveolar carcinoma of the lung. Lung Cancer 50:1–8
7. Sakamoto H, Shimizu J, Horio Y, Ueda R, Takahashi T, Mitsudomi T, Yatabe Y (2007) Disproportionate representation of KRAS gene mutation in atypical adenomatous hyperplasia, but even distribution of EGFR gene mutation from preinvasive to invasive adenocarcinomas. J Pathol 212:287–294
8. Sakuma Y, Matsukuma S, Yoshihara M, Nakamura Y, Noda K, Nakayama H, Kameda Y, Tsuchiya E, Miyagi Y (2007) Distinctive evaluation of nonmucinous and mucinous subtypes of bronchioloalveolar carcinomas in EGFR and K-ras gene-mutation analyses for Japanese lung adenocarcinomas: confirmation of the correlations with histologic subtypes and gene mutations. Am J Clin Pathol 128:100–108
9. Ikeda K, Nomori H, Ohba Y, Shibata H, Mori T, Honda Y, Iyama K, Kobayashi T (2008) Epidermal growth factor receptor mutations in multicentric lung adenocarcinomas and atypical adenomatous hyperplasias. J Thorac Oncol 3:467–471
10. Sartori G, Cavazza A, Bertolini F, Longo L, Marchioni A, Costantini M, Barbieri F, Migaldi M, Rossi G (2008) A subset of lung adenocarcinomas and atypical adenomatous hyperplasia-associated foci are genotypically related: an EGFR, HER2, and K-ras mutational analysis. Am J Clin Pathol 129:202–210
11. Chung JH, Choe G, Jheon S, Sung SW, Kim TJ, Lee KW, Lee JH, Lee CT (2009) Epidermal growth factor receptor mutation and pathologic-radiologic correlation between multiple lung nodules with ground-glass opacity differentiates multicentric origin from intrapulmonary spread. J Thorac Oncol 4:1490–1495
12. Horiike A, Kimura H, Nishio K, Ohyanagi F, Satoh Y, Okumura S, Ishikawa Y, Nakagawa K, Horai T, Nishio M (2007) Detection of epidermal growth factor receptor mutation in transbronchial needle aspirates of non-small cell lung cancer. Chest 131:1628–1634
13. Sekido Y, Fong KM, Minna JD (2003) Molecular genetics of lung cancer. Annu Rev Med 54:73–87
14. Shu Y, Iijima T, Sun W, Kano J, Ishiyama T, Okubo C, Anami Y, Tanaka R, Fukai S, Noguchi M (2006) The ACIN1 gene is hypermethylated in early stage lung adenocarcinoma. J Thorac Oncol 1:160–167
15. Kubo T, Yamamoto H, Ichimura K, Jida M, Hayashi T, Otani H, Tsukuda K, Sano Y, Kiura K, Toyooka S (2009) DNA methylation in small lung adenocarcinoma with bronchioloalveolar carcinoma components. Lung Cancer 65:328–332
16. Isaacs WB, Bova GS, Morton RA, Bussemakers MJ, Brooks JD, Ewing CM (1994) Molecular biology of prostate cancer. Semin Oncol 21:514–521
17. Baylin SB, Herman JG (2000) DNA hypermethylation in tumorigenesis: epigenetics joins genetics. Trends Genet 16:168–174
18. Lee S, Lee HJ, Kim JH, Lee HS, Jang JJ, Kang GH (2003) Aberrant CpG island hypermethylation along multistep hepatocarcinogenesis. Am J Pathol 163:1371–1378
19. Hake SB, Xiao A, Allis CD (2004) Linking the epigenetic 'language' of covalent histone modifications to cancer. Br J Cancer 90:761–769
20. Cho NY, Kim JH, Moon KC, Kang GH (2009) Genomic hypomethylation and CpG island hypermethylation in prostatic intraepithelial neoplasm. Virchows Arch 454:17–23
21. Jones PA, Baylin SB (2002) The fundamental role of epigenetic events in cancer. Nat Rev Genet 3:415–428
22. Costello JF, Fruhwald MC, Smiraglia DJ, Rush LJ, Robertson GP, Gao X, Wright FA, Feramisco JD, Peltomaki P, Lang JC, Schuller DE, Yu L, Bloomfield CD, Caligiuri MA, Yates A, Nishikawa R, Su Huang H, Petrelli NJ, Zhang X, O'Dorisio MS, Held WA, Cavenee WK, Plass C (2000) Aberrant CpG-island methylation has non-random and tumour-type-specific patterns. Nat Genet 24:132–138
23. Esteller M, Corn PG, Baylin SB, Herman JG (2001) A gene hypermethylation profile of human cancer. Cancer Res 61:3225–3229
24. Tsou JA, Hagen JA, Carpenter CL, Laird-Offringa IA (2002) DNA methylation analysis: a powerful new tool for lung cancer diagnosis. Oncogene 21:5450–5461
25. Belinsky SA (2004) Gene-promoter hypermethylation as a biomarker in lung cancer. Nat Rev Cancer 4:707–717
26. Tsou JA, Shen LY, Siegmund KD, Long TI, Laird PW, Seneviratne CK, Koss MN, Pass HI, Hagen JA, Laird-Offringa IA (2005) Distinct DNA methylation profiles in malignant mesothelioma, lung adenocarcinoma, and non-tumor lung. Lung Cancer 47:193–204
27. Shames DS, Girard L, Gao B et al (2006) A genome-wide screen for promoter methylation in lung cancer identifies novel methylation markers for multiple malignancies. PLoS Med 3:e486
28. Travis WD, Brambilla E, Noguchi M et al (2011) International Association for the Study of Lung Cancer/American Thoracic Society/European Respiratory Society International Multidisciplinary Classification of Lung Adenocarcinoma. J Thorac Oncol 6:244–285
29. Weisenberger DJ, Campan M, Long TI, Kim M, Woods C, Fiala E, Ehrlich M, Laird PW (2005) Analysis of repetitive element DNA methylation by MethyLight. Nucleic Acids Res 33:6823–6836
30. Kang GH, Lee S, Cho NY, Gandamihardja T, Long TI, Weisenberger DJ, Campan M, Laird PW (2008) DNA methylation

profiles of gastric carcinoma characterized by quantitative DNA methylation analysis. Lab Invest 88:161–170
31. Ogino S, Kawasaki T, Brahmandam M, Cantor M, Kirkner GJ, Spiegelman D, Makrigiorgos GM, Weisenberger DJ, Laird PW, Loda M, Fuchs CS (2006) Precision and performance characteristics of bisulfite conversion and real-time PCR (MethyLight) for quantitative DNA methylation analysis. J Mol Diagn 8:209–217
32. Kim BH, Cho NY, Shin SH, Kwon HJ, Jang JJ, Kang GH (2009) CpG island hypermethylation and repetitive DNA hypomethylation in premalignant lesion of extrahepatic cholangiocarcinoma. Virchows Arch 455:343–351
33. Lee S, Hwang KS, Lee HJ, Kim JS, Kang GH (2004) Aberrant CpG island hypermethylation of multiple genes in colorectal neoplasia. Lab Invest 84:884–893
34. Kang GH, Lee S, Kim JS, Jung HY (2003) Profile of aberrant CpG island methylation along the multistep pathway of gastric carcinogenesis. Lab Invest 83:635–641
35. Sato N, Fukushima N, Hruban RH, Goggins M (2008) CpG island methylation profile of pancreatic intraepithelial neoplasia. Mod Pathol 21:238–244
36. Yamanaka M, Watanabe M, Yamada Y, Takagi A, Murata T, Takahashi H, Suzuki H, Ito H, Tsukino H, Katoh T, Sugimura Y, Shiraishi T (2003) Altered methylation of multiple genes in carcinogenesis of the prostate. Int J Cancer 106:382–387
37. Noguchi M, Morikawa A, Kawasaki M, Matsuno Y, Yamada T, Hirohashi S, Kondo H, Shimosato Y (1995) Small adenocarcinoma of the lung. Histologic characteristics and prognosis. Cancer 75:2844–2852
38. Lee HJ, Choe G, Jheon S, Sung SW, Lee CT, Chung JH (2010) CD24, a novel cancer biomarker, predicting disease-free survival of non-small cell lung carcinomas: a retrospective study of prognostic factor analysis from the viewpoint of forthcoming (seventh) new TNM classification. J Thorac Oncol 5:649–657

Virchows Arch (2011) 459:213–219
DOI 10.1007/s00428-011-1116-8

ORIGINAL ARTICLE

Growth patterns of lung metastases from sarcomas

Stefan Welter · Florian Grabellus · Sebastian Bauer · Kurt Werner Schmid · Georgios Stamatis · Martin Tötsch

Received: 11 April 2011 / Revised: 6 June 2011 / Accepted: 22 June 2011 / Published online: 6 July 2011
© Springer-Verlag 2011

Abstract Complete resection of pulmonary metastases from sarcomas is an established method of treatment. While resection margins are well described for primary sarcoma lesions, minimal knowledge is available about margins and factors influencing local tumour control in the lung. The objective of the present study was to describe intrapulmonary patterns of growth for sarcoma metastases as a basis for planning resections. From January 2006 to January 2009, we retrospectively analysed 261 resected pulmonary sarcoma metastases from 52 patients. All metastases were reviewed for histological characteristics and resection margins. Metastases characterised by a solid, well-defined tumour mass were found in 127 of 261 metastases (48.7%). Interstitial spread (39.8%), vascular infiltration (20.7%), satellite nodules (16.1%) and lymphangitic spread (10.7%) were identified as aggressive histological growth characteristics. Forty-five of 52 patients (86.5%) had metastases with a mitotic index of 10 or more per 10 HPF, underlining their high-grade malignant potential. The following characteristics of aggressive intrapulmonary growth were highly correlated with each other: interstitial growth and lymphangitic spread ($p=0.002$), interstitial growth and vascular infiltration ($p<0.001$), vascular infiltration and satellite nodules ($p=0.009$), interstitial growth and pleural invasion ($p=0.004$); by contrast, the presence of a fibrous pseudocapsule (17.2%) was not associated with aggressive growth patterns. Almost half of all pulmonary sarcoma metastases could be identified with aggressive patterns of local growth, and only 17.2% are surrounded by a pseudocapsule which might allow safe resection margins.

Keywords Metastasectomy · Sarcoma metastasis · Growth patterns · Mitotic index · Safety margins

S. Welter (✉) · G. Stamatis
Department of Thoracic Surgery, Ruhrlandklinik Essen,
Tüschener Weg 40,
45239 Essen, Germany
e-mail: stefan.welter@ruhrlandklinik.uk-essen.de

G. Stamatis
e-mail: georgios.stamatis@ruhrlandklinik.uk-essen.de

F. Grabellus · K. W. Schmid · M. Tötsch
Institute of Pathology and Neuropathology,
University Duisburg-Essen,
Hufelandstr. 55,
45122 Essen, Germany

F. Grabellus
e-mail: florian.grabellus@uk-essen.de

K. W. Schmid
e-mail: kw.schmid@uk-essen.de

M. Tötsch
e-mail: martintoetsch@klinikum-graz.at

S. Bauer
West German Cancer Center, Department of Medical Oncology,
University Duisburg-Essen,
Hufelandstr. 55,
45122 Essen, Germany
e-mail: sebastian.bauer@uni-due.de

Present Address:
M. Tötsch
Institute of Cytology, University Hospital of Graz,
Graz, Austria

Introduction

Sarcoma is a rare malignancy, most often arising in the extremities. Additionally, it can develop in almost every mesenchymal tissue. The histopathological growth patterns of the periphery of primary musculoskeletal sarcomas have

been well described [1]. The primary tumour mass is surrounded by a pseudocapsule and a reactive zone. Satellite micronodules, although rare, may be found within these zones in almost every sarcoma subtype; hence, they are considered an integral part of the malignant lesion. The surgical implication for a curative resection is a wide intracompartmental or a radical compartment resection for high-grade sarcomas [2]. Thus, even in the presence of micronodules around the surface of the sarcoma, the whole tumour is surrounded by solid tissue, which provides a certain barrier from uncontrolled local growth, which is different in lung tissue.

To our knowledge, there is only one description of sarcoma metastasis growth in the lung, focused on the subtype "liposarcoma" [3]. The knowledge about growth patterns, however, is the basis for surgeons to plan safety margins during resection. This question is of particular interest in the lung because lung tissue offers a wide range of possibilities for tumour cell dissemination due to the lung's sponge-like architecture with alveolar spaces, interlobular septae and its rich network of capillaries. The possible ways of tumour cell dissemination raise the question whether the four types of resections—intralesional, marginal, wide and radical—described by Enneking [1] for primary sarcomas and their influence on local recurrence can be simply transferred to pulmonary distant recurrences of sarcomas as well. Thus, to answer this question, our intention was to perform a systematic analysis of all resected pulmonary sarcoma metastases at the tumour to lung tissue transition from all our patients and describe the intrapulmonary growth patterns.

Materials and methods

We retrospectively analysed all patients who were completely resected for histologically proven pulmonary metastases derived from sarcomas. Our clinical review board waived the need for patient consent based on the anonymous data interpretation and the fact that no further manipulation of tumour tissue was performed. Altogether, 52 patients who were operated on in our department from January 2006 to January 2009 were retrospectively included in this study. All metastasectomies were performed through an anterolateral muscle-sparing thoracotomy to allow for a systematic palpation of the whole lung. All lung resections were performed due to the surgeon's discretion as wedge resection or segmentectomy. All medical records were reviewed for biographic data, date of resection and the number of metastases.

Histology All histological specimens were reexamined together with two pathologists who are especially qualified in sarcoma and lung pathology (FG^2, MT^2). Immunohistochemistry was used to confirm the sarcoma subtype based on the current World Health Organization classification of tumours for soft tissue and bone sarcomas [4]. For each metastasis, up to three haematoxylin–eosin-stained slices were reexamined to assess for pseudocapsule, pleural penetration, invasion of greater blood vessels or lymphangitic spread, interstitial spread, tumour satellites, signs of regression, resection margins and exceptional features (Table 1). At least one resected metastasis per operation was further evaluated for the degree of tumour necrosis and the number of mitoses per 10 high-power fields (HPFs) as well.

Statistical analysis The data were analysed using SPSS 15 for Windows (SPSS Inc., Chicago, IL). The pathological growth factors were correlated to each other with the Chi-squared test and, if adequate, with the Fisher's exact test. A probability value of 0.05 or less was considered significant.

Results

Patient characteristics The patients' characteristics are listed in detail in Table 2. Twenty-three women and 29 men had a median age of 55.8 years (19.1–80.3 years). The site of the primary tumour was the uterus in 8 patients, the extremities in 25 patients and the trunk in 19 patients. The most common histology was leiomyosarcomas in 17, synovial sarcomas in 8, bone sarcomas in 7, sarcoma not otherwise specified (NOS) in 13, followed by 13 other sarcomas with 10 different histological subtypes. Altogether, 261 metastases had been removed in 89 operations including 15 repeated thoracotomies. The subgroup with leiomyosarcomas had the highest number of metastases with a median of 6, followed by the subgroup with synovial sarcoma having a median of 4.5 metastases. All other histological subgroups had a median of 2 metastases or less. Thirty-four patients (65.4%) faced tumour recurrence at any site in the course of their disease. Altogether, 261 metastases were histologically reviewed (512 slides) and described as mentioned above. Concerning repeated thoracotomies, 11 metastases were local recurrences and all of higher grade (G2 or G3), 8 of them had been incompletely resected at the microscopic level and 3 of them had been declared to be completely resected before. Their predominant growth patterns had been pleural penetration in four, vascular infiltration in three and interstitial growth in two lesions. Four histologies of former metastases at the recurrence sites were not available.

Histological features Pulmonary metastases from sarcomas showed variable growth patterns. Some were sharply

Table 1 Description of histopathological criteria

Fibrous pseudocapsule	Compression and fibrosis of alveolar tissue around the tumour, which is not penetrated
Pleural penetration	Infiltration and destruction of all visceral pleural layers by the tumour
Infiltration of blood vessels	Complete destruction of the wall of a large blood vessel with complete or partial obstruction of the lumen
Lymphangitic spread	Complete or partial destruction of a lymph vessel or obstruction of the lumen seen on haematoxylin–eosin or immunohistochemical staining when available
Interstitial spread	Diffuse growth in the alveolar wall between alveolar air spaces
Tumour satellites	Tumour islands with no direct contact with the main metastases that were not spread via the lymphatics
Resection margins	
R0	Resected metastasis is surrounded by at least a complete layer of normal alveoli
R1	Resected metastasis is not covered by lung or pleural tissue
Special features	Exceptional features were described from case to case
Degree of tumour necrosis	0=no, 1=1–50%, 2=more than 50%
Number of mitoses	1=1–9, 2=10–19, 3=20 or more per 10 high-power fields

bordered with a pseudocapsule and were well defined in the lung (Fig. 1a). Another subset was well demarcated in the lung but showed broad penetration of the visceral pleura, some even presenting a surface elevated over the visceral pleura (Fig. 1b). Some of them revealed an obvious growth along anatomic structures like blood vessels or bronchi, going far beyond the edge of the metastasis (Fig. 1c). Others grew into alveolar septae and spread like fingers into the surrounding tissue, subsequently described as interstitial spread (Fig. 1c). At least one other subset was found with satellite nodules (Fig. 1d) or diffuse growth with lymphangitic and/or haemangiomatous spread. In particular, the combination of the latter growth patterns appeared extremely aggressive.

Examining all 261 metastases, pseudocapsules were found in 45 (17.2%), visceral pleural penetration occurred in 67 (25.7%), greater blood vessels were infiltrated in 54 (20.7%), lymphangitic spread occurred in 28 (10.7%), interstitial spread occurred in 104 (39.8%), satellite nodules were present in 42 (16.1%), signs of regression were found in 80 (30.7%) and incomplete resection margins were found in 63 (24.1%) of all metastases (Table 3).

Table 2 Patients' characteristic

Males/females		29/23	
Age (years)		Median, 55.8; mean, 52.7; range, 19.1–80.3	
DFI (months)		Median, 33.6; mean, 51.6; range, 0–248	
Site of primary tumour		Uterus, 8; extremities, 25; trunk, 19	
Grading of the primary tumour		G1=5, G2=8, G3=21, not available=18	
Metastases	Number, 261	median, 3; mean, 5.0; range, 1–29	
	Diameter (mm)	median, 25.0; mean, 34.9; range, 4.0–115	
Cases	Histology	Metastases	Largest diameter (mm)
		n (range)	Median (range)
1	Angiosarcoma	3	25
3	Chondrosarcoma	11 (1–9)	25 (17–96)
1	Ewing's sarcoma	1	65
5	Fibrosarcoma	13 (1–6)	25 (4–70)
1	Clear cell sarcoma	12	13
17	Leiomyosarcoma	134 (1–29)	22 (6–115)
2	Liposarcoma	3 (1–2)	38.5 (32–45)
2	MPNST	6 (1–5)	67.5 (35–100)
1	Myogenic sarcoma	1	15
4	Osteosarcoma	9 (1–6)	52 (33–85)
7	Sarcoma (NOS)	13 (1–4)	17 (9–80)
8	Synovial sarcoma	55 (1–16)	22 (6–61)

MPNST malignant peripheral nerve sheath tumour

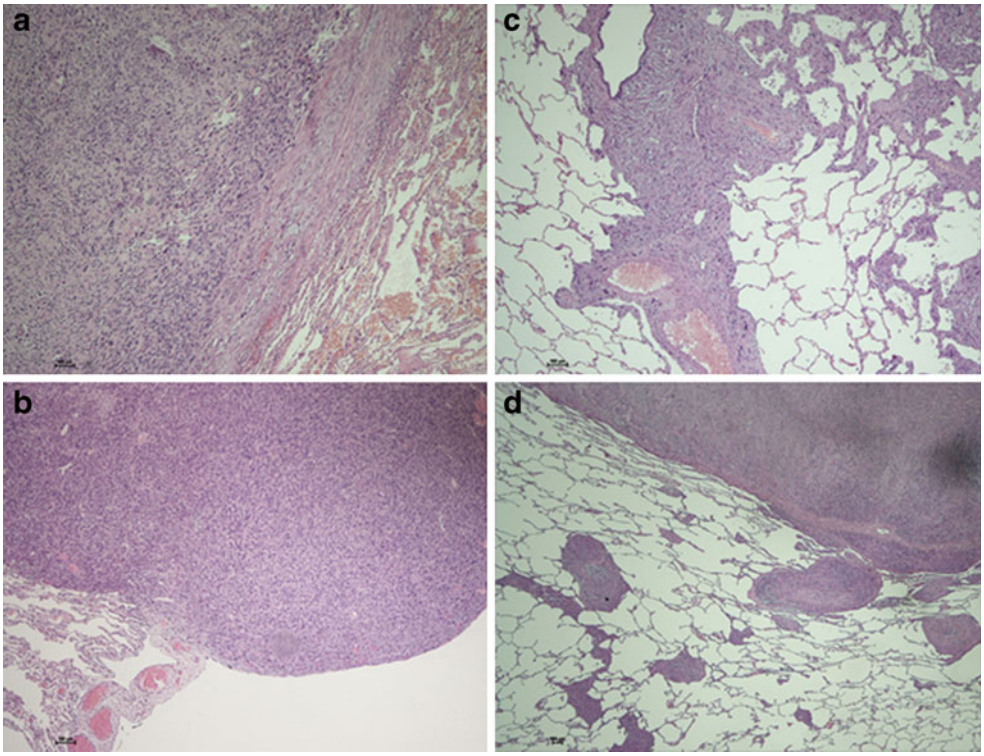

Fig. 1 **a**–**d** Pictures of the different histological growth patterns. **a** H&E-stained leiomyosarcoma with a pseudocapsule. Magnification, ×10; **b** H&E-stained leiomyosarcoma growing over the visceral pleural surface. Magnification, ×4; **c** H&E-stained sarcoma (NOS) demonstrating interstitial growth and growth along bronchial and vascular structures. Magnification, ×4; **d** H&E-stained leiomyosarcoma with satellite nodules around the metastasis. Magnification, ×4

None of the characteristics of aggressiveness (vascular infiltration, interstitial spread and satellite nodules) were found in 127 (48.7%) metastases, whereas the combined presence of all these characteristics was only found in 18 (6.9%) metastases. Referred to the 52 patients, the predominant patterns of growth were interstitial spread (49.1%), vascular infiltration (43.4%), satellite nodules (35.8%), signs of regression (35.8%), pleural penetration (34.0%) and presence of a pseudocapsule (20.8%). A mitotic index of 1, 2 and 3 was found in 22.6%, 30.2% and 45.3% of the patients. The subgroup of metastases with pseudocapsules contained 10/11 (82%) chondrosarcomas, 1/1 Ewing`s sarcoma, 15/134 (11%) leiomyosarcomas, 3/3 liposarcomas, 3/13 (23%) fibrosarcomas, 1/6 MPNST (16.6%), 2/13 (15%) sarcomas (NOS) and 12/55 (22%) synovial sarcomas. We found three exceptional features: one tumour nodule was surrounded by many lymph vessels, the latter ones were completely obstructed with tumour-mimicking satellite nodes, one lesion was a bronchus surrounded by a small layer of sarcoma tissue and one lesion from a proven synovial sarcoma showed pronounced calcification. Looking at the distribution of histopathological features of 17 chondrosarcoma metastases from three patients, we found 15 metastases with a pseudocapsule, and all had no pleural infiltration, no vascular infiltration, no lymphangitic nor interstitial spread. Only one metastasis had a single satellite nodule which might be considered as another metastasis. All of these 11 metastases had a mitotic index of <10/10 HPF which corresponds to a low-grade lesion (G1). The corresponding primaries had been of low grade as well (G1).

Table 3 Pathological features of 261 metastases from 52 patients

Criteria	Metastases	(%)	Patients	(%)
Pseudocapsule	45	(17.2)	11	(21.2)
Pleural penetration	67	(25.7)	18	(34.6)
Vascular infiltration	54	(20.7)	23	(44.2)
Lymphangitic spread	28	(10.7)	8	(15.4)
Interstitial spread	104	(39.8)	26	(50.0)
Resection margins				
R0	194	(74.3)	36	(69.2)
R1	63	(24.1)	16	(30.8)
Tumour satellites	42	(16.1)	19	(36.5)
Tumour regression	80	(30.7)	20	(38.5)
Necrosis (0/<50%/>50%)	26 (50)/20 (38.5)/6 (11.5)			
Mitoses per HPF (0–9/10–19/more)	12 (23.1)/16 (30.8)/24 (46.1)			
Grading (metastasis) (G1/G2/G3)	7 (13.5)/20 (38.4)/25 (48.1)			

Analysing all patients who had more than two metastases, only one of them had histological uniform metastases (chondrosarcoma), indicating that different lung metastases show different growth patterns within the same patient or some growth patterns are related to tumour doubling time respectively tumour progress. From 261 lesions, 63 (24.1%) metastases had been incompletely resected at the microscopic level. An increased risk for incomplete resection was found in association with pleural invasion (p=0.03),

metastasis diameter >35 mm (p=0.02) and interstitial growth (p=0.06). All other features of aggressive growth were not found associated and in similar frequency in those metastases resected R0 and those metastases resected R1.

Interactions of histopathological factors mentioned in Table 1 were calculated based on the Chi-squared test (Table 4). The most important finding was that the presence of a pseudocapsule was not associated with indicators of malignancy such as satellite nodules (p=0.01), higher mitotic index (>10 per 10 HPFs; p=0.01), higher degree of necrosis (p=0.05), lymphangitic spread (p=0.03), interstitial growth (p=0.008) or with vascular infiltration (p=0.03) and, therefore, can be interpreted as proof of a rather benign and clearly confined lesion. The other features regarded as characteristic for aggressive intrapulmonary growth were highly associated with each other, including lymphangitic spread and satellite nodules (p=0.002), interstitial growth and lymphangitic spread (p=0.002), interstitial growth and vascular infiltration (p<0.001), interstitial growth and pleural invasion (p=0.004) as well as vascular infiltration and satellite nodules (p=0.009). All of these associations were statistically significant, which suggests an interrelation of all signs of aggressive local growth in the lung.

The overall mean survival after resection of the primary was 188 months (median, 271 months; 95% confidence interval (CI), 143–233) with a 5-year survival rate of 63.6%. The overall mean post-metastasectomy survival was 94 months (95% CI, 73–114), and the corresponding 5-year survival was 57.5%. With only 20 events until January 2010 in 52 cases, a median survival could not be calculated. A higher mitotic index (≥10/10 HPF) of the metastasis (p=0.04) and the presence of tumour recurrence at any site after metastasectomy (p<0.001) were risk factors for death. Age over 55 years (p=0.06), soft tissue primary sarcoma (p=0.08), high-grade (G2 or G3) metastases (p=0.08), the presence of necrosis (p=0.07), a metastasis ≥35 mm (p=0.07) and incomplete resection (R1; p=0.07) showed a tendency for reduced survival, whereas lymphangitic spread, interstitial growth, vascular infiltration and pleural infiltration did not reach significance.

Table 4 Associations among pathological factors (Chi-square test)

Growth pattern 1	Growth pattern 2	Significance
Pseudocapsule	No satellite nodules	p=0.01
Pseudocapsule	No lymphangitic spread	p=0.031
Pseudocapsule	No interstitial growth	p=0.008
Pseudocapsule	No vascular invasion	p=0.03
No pseudocapsule	>19 mitoses/10 HPF	p=0.01
Incomplete resection (R1)	Metastasis >35 mm	p=0.02
Pleural infiltration	Incomplete resection (R1)	p=0.03
Interstitial growth	Incomplete resection (R1)	p=0.06
Metastasis >35 mm	Interstitial growth	p=0.04
Interstitial growth	Lymphangitic spread	p=0.002
Interstitial growth	Satellite nodules	p=0.01
Vascular infiltration	Interstitial growth	p<0.000
Vascular infiltration	Satellite nodules	p=0.009
Pleural infiltration	Lymphangitic spread	p=0.02
Pleural infiltration	Interstitial growth	p=0.004
Lymphangitic spread	Satellite nodules	p=0.002
Lymphangitic spread	Vascular infiltration	p=0.001
Tumour regression	Diameter >35 mm	p=0.004

Discussion

Isolated lung metastases will develop in about 20% of patients with extremity soft tissue sarcoma during the course of their disease [5]. Resection of lung metastases from soft tissue sarcoma is considered to be potentially beneficial and is associated with a reported 5-year survival rate of 25–38% [6–8]. The single most important factor that determines the outcome in these patients is complete resection of the metastases [9]. In our daily practice, we found that despite macroscopically complete metastasectomy, early local tumour recurrence in the lung occurs in some patients. Because local recurrence at the resection site may be prevented by tumour-free resection margins, it is of great importance that we improve our knowledge of histological growth patterns. Therefore, our retrospective study was conducted to describe intrapulmonary patterns of metastatic growth for different sarcoma subtypes as a first step to find risk factors for local intrapulmonary tumour recurrence.

To our knowledge, there is only one description of growth patterns of pulmonary sarcoma metastases and their prognostic influence: Nicolas et al. [3] published a series of 24 cases with liposarcoma metastases. They found well-circumscribed metastatic lesions from myxoid liposarcomas compared to the irregular tumour periphery in metastatic pleomorphic liposarcoma due to invading tumours, dispersed single cells or tight clusters. They also reported metastases from dedifferentiated liposarcomas with histological features of undifferentiated pleomorphic sarcomas, rhabdomyosarcomas as well as osteosarcomas. The authors observed a correlation between aggressive histological patterns in the lung and an impaired clinical course of the disease.

In our study, pleural invasion (p=0.03), metastasis diameter >35 mm (p=0.02) and interstitial growth (p=0.06) were associated with an increased risk for incomplete resection which again is a well-known cause for local

recurrence. To our knowledge, this study offers the first description of intrapulmonary patterns of growth of various types of sarcoma metastases with details on frequency. Sarcomas that had spread into the lung were rarely found to have a pseudocapsule (only 17.5% of all metastases). This is completely different from the growth patterns of their soft tissue or bone primaries, which usually have a pseudocapsule and a reactive zone as characteristic features [1].

Primary sarcomas Looking at the description of primary soft tissue sarcoma growth patterns and their implications for surgical procedures, there are many powerful retrospective and prospective series published since the 1960s. The growth of sarcoma primaries is characterised by the tumour mass, a pseudocapsule and a reactive zone [2]. Fingers of neoplastic skip lesions or satellite nodules, especially in high-grade sarcomas, are common within the pseudocapsule and less common in the reactive zone and lead to a higher rate of local recurrence if they are not resected with adequate margins [1, 10, 11]. The rate of local primary recurrence differed in patients with wide margins between low-grade (0%) and high-grade (30%) sarcomas in a further series from Enneking in 1981 [2]. Because the tumour typically respects anatomical barriers, such as synovia, periosteum or fascia, a radical resection (of limb sarcomas) can be achieved by a compartment resection, avoiding amputation. Billingsley et al. [9] found that the incidence of pulmonary metastases correlates with the incidence of high-grade lesions within different histological sarcoma subtypes. Thus, the grading of the sarcoma may play a major role in local tumour control, frequency of metastatic spread and survival according to Coindre [12, 13].

The grading of soft tissue sarcomas based on the Fédération Nationale des Centres de Lutte Contre le Cancer (FNCLCC) system [14] include tumour differentiation, mitotic index and tumour necrosis, and it was exclusively developed for untreated primary tumours. So, the interesting question of whether metastases are more or less aggressive than the primary tumour unfortunately cannot be easily answered with grading. In our study, we examined the mitotic index and the amount of tumour necrosis in the metastases, as described by Guillou et al. [14].

Metastases In our study, we demonstrated some parallels between the growth patterns of primary sarcomas and lung metastases. Tumour satellites (16.1%), vascular infiltration (20.7%) and interstitial growth (39.8%) which is comparable to tumour fingers in soft tissues could be found in the lung as well as in primary sarcomas. However, pseudocapsules were infrequent (17.2%), and no reactive zone consisting of compressed degraded, inflamed or haemorrhaged tissue around the tumour could be demonstrated. This absence may be due to the sponge-like architecture of the lung, which provides no solid structure resisting tumour growth and thus may be the most important difference between primary growth in soft tissue and bone and metastatic growth in the lung. Some sarcoma metastases preferentially grow along anatomic structures like blood vessels and bronchi. This feature is difficult to quantify but could be demonstrated in several specimens (Fig. 1c). Interstitial growth and satellite nodules around the metastases, as demonstrated in this study, result in ill-defined margins, which could explain the higher risk for incomplete resection (24.1%) in sarcoma metastases and may lead to local recurrence. Pulmonary metastases from chondrosarcoma presented with an 88% rate of pseudocapsules and therefore might be the only sarcoma subtype where a marginal resection is justified.

In our study, 40 of 52 patients had a mitotic index of 10 or more per 10 HPFs in their metastases, which, in conjunction with the amount of necrosis and the tumour differentiation score of the primary tumour, classified them as high-grade sarcomas due to the FNCLCC system for soft tissue primaries [14]. Therefore, we can support the assumption of Pisters [15] that most lung metastases are of high grade. Two of five patients with low-grade primaries had high-grade secondaries in the lung. This phenomenon of high-grade local or distant tumour recurrence in patients with low-grade primaries was already described in 46 patients by the group of Canter [16]. Low-grade secondaries following a high-grade primary fibrosarcoma was identified only once in our series. A marginal change of the grading (G2 to G3) was found in five and G3 to G2 in eight patients from the primary sarcoma to the secondaries. In this study, we found lymphangitic spread in 10.7% of all metastases, affecting 15.4% of patients. This rather high number contrasts the rare event of lymphatic involvement in primary sarcomas but can be affirmed by a series from Pfannschmidt et al. [17], who found a 23.4% involvement of intrathoracic lymph nodes during resection of pulmonary sarcoma metastases.

Risk for intrapulmonary tumour recurrence As we demonstrated, microscopically incomplete resection is a major risk factor for local recurrence. Eight of 11 local recurrences, which were found during repeated resections, had been reported to be incompletely resected before.

In our study, we found tumour recurrence at any site in 16 out of 18 patients in case the largest metastasis had a diameter of >35 mm, which confirms the findings of Weiser et al. [18].

Evaluating the follow-up reports, we were unable to differentiate local intrapulmonary recurrence from newly evolved metastases in those patients who did not come for a repeated resection. Therefore, we cannot provide a local recurrence rate. But we could demonstrate that aggressive

patterns of tumour growth like lymphangitic spread, vascular infiltration, tumour satellite nodules and may be tumour growth along vascular or bronchial structures, which we observed in our study (Fig. 1c), raised the risk of microscopically incomplete resection.

To identify those metastases with a pseudocapsule and/or those without patterns of aggressive local growth, which suggests a low risk for incomplete resection and the need for only a marginal resection, further scientific efforts are necessary to correlate imaging with growth patterns. Once metastases with aggressive local growth can be identified preoperatively, wide resection is necessary but cannot specifically be given in millimetres because growth along preexisting structures is unforeseeable. In those cases, anatomical resections might be a logical consequence.

Study limitations The limitations of this study are its retrospective design of a single centre and the relatively small number of cases. However, the number of reviewed metastases is high and, to our knowledge, this is the first description of metastatic growth patterns in the lung from different sarcoma subtypes. Nevertheless, prospective studies are necessary to correlate preoperative imaging with histological patterns of growth.

Conclusion

Sarcoma metastases in the lung typically present high-grade malignancies, and half of them are ill defined by aggressive patterns of local spread like interstitial growth, tumour satellites, vascular infiltration, lymphangitic spread and growth along vascular and bronchial structures. Fibrous pseudocapsules are rare, and reactive zones are completely absent. However, chondrosarcoma metastases seem to present pseudocapsules frequently (90%) and therefore might be resected marginally instead of taking wide resection margins.

Conflict of interest statement We declare that we have no conflict of interest.

References

1. Enneking WF, Spanier SS, Goodman MA (1980) A system for the surgical staging of musculoskeletal sarcoma. Clin Orthop Relat Res 153:106–120
2. Enneking WF, Spanier SS, Malawer MM (1981) The effect of the anatomic setting on the results of surgical procedures for soft parts sarcoma of the thigh. Cancer 47:1005–1022
3. Nicolas M, Moran CA, Suster S (2005) Pulmonary metastasis from liposarcoma. A clinicopathologic and immunohistochemical study of 24 cases. Am J Clin Pathol 123:265–275
4. Fletcher C, Unni K, Mertens F (eds) (2002) Pathology & genetics. Tumours of soft tissue and bone. IARC Press, Lyon
5. Gadd MA, Casper ES, Woodruff JM, McCormack PM, Brennan MF (1993) Development and treatment of pulmonary metastases in adult patients with extremity soft tissue sarcoma. Ann Surg 218:705–712
6. Pastorino U, Buyse M, Friedel G, Ginsberg RJ, Girard P, Goldstraw P, Johnston M, McCormack P, Pass H, Putnam JB (1997) Long-term results of lung metastasectomy: prognostic analyses based on 5206 cases. J Thorac Cardiovasc Surg 113:37–49
7. Rehders A, Hosch SB, Scheunemann P, Stoecklein NH, Knoefel WT, Peiper M (2007) Benefit of surgical treatment of lung metastasis in soft tissue sarcoma. Arch Surg 142:70–75
8. van Geel AN, Pastorino U, Jauch KW, Judson IR, van CF, Buesa JM, Nielsen OS, Boudinet A, Tursz T, Schmitz PI (1996) Surgical treatment of lung metastases: TheEuropean Organization for Research and Treatment of Cancer-Soft Tissue and Bone Sarcoma Group Study of 255 patients. Cancer 77:675–682
9. Billingsley KG, Burt ME, Jara E, Ginsberg RJ, Woodruff JM, Leung DH, Brennan MF (1999) Pulmonary metastases from soft tissue sarcoma: analysis of patterns of diseases and postmetastasis survival. Ann Surg 229:602–610
10. Sampo M, Tarkkanen M, Huuhtanen R, Tukiainen E, Bohling T, Blomqvist C (2008) Impact of the smallest surgical margin on local control in soft tissue sarcoma. Br J Surg 95:237–243
11. Gerrand CH, Wunder JS, Kandel RA, O'Sullivan B, Catton CN, Bell RS, Griffin AM, Davis AM (2001) Classification of positive margins after resection of soft-tissue sarcoma of the limb predicts the risk of local recurrence. J Bone Joint Surg Br 83:1149–1155
12. Coindre JM (2006) Grading of soft tissue sarcomas: review and update. Arch Pathol Lab Med 130:1448–1453
13. Coindre JM, Terrier P, Guillou L, Le Doussal V, Collin F, Ranchere D, Sastre X, Vilain MO, Bonichon F, N'Guyen BB (2001) Predictive value of grade for metastasis development in the main histologic types of adult soft tissue sarcomas: a study of 1240 patients from the French Federation of Cancer Centers Sarcoma Group. Cancer 91:1914–1926
14. Guillou L, Coindre JM, Bonichon F, Nguyen BB, Terrier P, Collin F, Vilain MO, Mandard AM, Le Doussal V, Leroux A, Jacquemier J, Duplay H, Sastre-Garau X, Costa J (1997) Comparative study of the National Cancer Institute and French Federation of Cancer Centers Sarcoma Group grading systems in a population of 410 adult patients with soft tissue sarcoma. J Clin Oncol 15:350–362
15. Pisters PW, Leung DH, Woodruff J, Shi W, Brennan MF (1996) Analysis of prognostic factors in 1,041 patients with localized soft tissue sarcomas of the extremities. J Clin Oncol 14:1679–1689
16. Canter RJ, Qin LX, Ferrone CR, Maki RG, Singer S, Brennan MF (2008) Why do patients with low-grade soft tissue sarcoma die? Ann Surg Oncol 15:3550–3560
17. Pfannschmidt J, Klode J, Muley T, Dienemann H, Hoffmann H (2006) Nodal involvement at the time of pulmonary metastasectomy: experiences in 245 patients. Ann Thorac Surg 81:448–454
18. Weiser MR, Downey RJ, Leung DH, Brennan MF (2000) Repeat resection of pulmonary metastases in patients with soft-tissue sarcoma. J Am Coll Surg 191:184–190

Virchows Arch (2011) 459:221–226
DOI 10.1007/s00428-011-1117-7

ORIGINAL ARTICLE

Chromosomal imbalances in carcinoma showing thymus-like elements (CASTLE)

Lothar Veits · Gunhild Mechtersheimer · Christina Steger · Jens Freitag · Gregor Mikuz · Kurt W. Schmid · Walter Hofmann · Peter Schirmacher · Arndt Hartmann · Ralf J. Rieker

Received: 16 May 2011 / Revised: 24 June 2011 / Accepted: 26 June 2011 / Published online: 7 July 2011
© Springer-Verlag 2011

Abstract Carcinoma showing thymus-like elements (CASTLE) is a rare neoplasm of the thyroid gland resembling lymphoepithelioma-like and squamous cell carcinoma of the thymus and is thought to arise from ectopic thymic tissue within the thyroid gland or rudimentary branchial pouches along the thymic line. Using comparative genomic hybridization (CGH), chromosomal imbalances have been detected in several types of thymomas and thymic carcinomas. To evaluate whether there are hints of an underlying sequence in the pathogenesis of CASTLE analogue to those found in thymomas and thymic carcinomas, we evaluated four of these rare neoplasms for chromosomal imbalances using CGH. The most frequent gains were seen on chromosomal arm 1q (3/4), and losses were most frequently detected on 6p (4/4), 6q (3/4) and 16q (3/4). These CGH data show that CASTLE is characterized by chromosomal imbalances similar to those found in thymomas and thymic carcinomas and indicate a similar sequence in tumour development.

Keywords CASTLE · Carcinoma showing thymus-like elements · Chromosomal imbalances · CGH

Lothar Veits and Gunhild Mechtersheimer contributed equally to this publication.

L. Veits (✉) · C. Steger · G. Mikuz
Institute of Pathology, Medical University of Innsbruck,
Muellerstrasse 44,
6020 Innsbruck, Austria
e-mail: Lothar.Veits@i-med.ac.at

G. Mechtersheimer · P. Schirmacher · R. J. Rieker
Institute of Pathology, University Hospital Heidelberg,
INF 220/221,
69120 Heidelberg, Germany

J. Freitag
Moselstraße 1,
73529 Oberbettringen, Germany

K. W. Schmid
Institute of Pathology and Neuropathology,
University Hospital Essen,
Hufelandstraße 55,
45122 Essen, Germany

W. Hofmann
Institute of Pathology, Klinikum Memmingen,
Bismarckstraße 23,
87700 Memmingen, Germany

A. Hartmann · R. J. Rieker
Institute of Pathology, University Hospital Erlangen,
Krankenhausstr. 12,
91054 Erlangen, Germany

Introduction

Carcinoma showing thymus-like elements (CASTLE) is a rare tumour of the thyroid gland first described by Miyauchi et al. [1] in 1985 as "intrathyroidal epithelial thymoma". The tumours are thought to arise from ectopic thymic tissue within the thyroid gland or rudimentary branchial pouches along the thymic line, exhibit analogy to foetal or mature thymus and were first named CASTLE by Chan and Rosai [2]. CASTLE belong to a group of ectopic tumours of thymic differentiation: ectopic hamartomatous thymoma, ectopic cervical thymoma, spindle epithelial tumours with thymus-like differentiation and CASTLE. Although CASTLE shows some tendency for squamous differentiation, it is considered to represent an independent entity and has newly been adopted by the recent WHO classification [3].

Using comparative genomic hybridization (CGH) and loss of heterozygosity (LOH) chromosomal imbalances have been detected in several types of thymomas and thymic carcinomas [4–8]. These results indicate that there might be an underlying sequence in the pathogenesis of some thymomas and that early events are gains on chromosomal arm 1q followed by losses on chromosome 6q and on other chromosomal regions (e.g. 17p and 16q) [9]. Especially aggressive epithelial tumours with numerous chromosomal imbalances, e.g. type B3-thymoma, as well as thymic carcinomas show changes in these regions [10]. For this study, we collected four cases of the rare entity of CASTLE by contacting reference pathologists and 20 institutes of pathology in Germany and Austria, to investigate possible chromosomal imbalances using CGH. Our analysis shows that castle tumours have chromosomal imbalances similar to those found in thymomas and thymic carcinomas.

Materials and methods

Tissue

Tissue samples were obtained from semi-, subtotal or total thyroidectomy. Diagnosis of CASTLE was confirmed by histological criteria according to the WHO classification [3] and by immunohistochemical stains with antibodies against CD5, CD117, thyroglobulin, calcitonin, TTF-1 and CK5/6. All samples were fixed in 4% neutral buffered formaldehyde and paraffin embedded via routine procedures.

Clinical data

Clinical data are summarized in Table 1. In this study, we investigated the tumour tissue of four patients, two males and two females, with a median age of 61.75 years, ranging from 59 to 68 years. In one case, local recurrence developed after 2 months. Three patients received post-operational radiation therapy, and one patient underwent radiochemotherapy.

Comparative genomic hybridization

Paraffin-embedded tumour DNA was isolated from three to four representative 20-μm tissue sections using proteinase K digestion (2 mg/ml in 50 mM Tris–HCl, 1 mM EDTA, 0.5% Tween 20) followed by ethanol precipitation. Control DNA was isolated from paraffin-embedded placenta tissue. Tumour DNA was labelled using Biotin-16-dUTP (Roche, Mannheim, Germany) and control DNA was labelled using digoxigenin-11-dUTP (Roche) using nick translation according to the manufacturer's instructions. Approximately 1 mg of biotin-labelled tumour DNA, 1 mg of digoxigenin-labelled control DNA and 50 mg Cot-1-DNA (Gibco/BRL, Gaithersburg, MD, USA) were denatured at 75°C for 6 min followed by pre-annealing at 37°C for 30 min. Hybridization was performed at 37°C for 24–48 h in a humid chamber. Afterwards, several post-hybridization washes and detection of hybridized DNA by fluorescein and rhodamine were performed. The results were analysed by using an epifluorescence microscope (Zeiss, Wetzlar, Germany) and the ISIS CGH software package (Metasystems, Altlußheim, Germany). Grey level images of 10–15 metaphase spreads were recorded separately for each fluorochrome, and the ratio of fluorescein isothiocyanate/tetramethyl rhodamine isothiocyanate fluorescence intensities along each individual chromosome was calculated and averaged. Chromosomal imbalances were detected on the basis of ratio profiles deviating from the balanced value of 1.0 with the values of 1.25 and 0.75 as diagnostic cut-off levels for over- and underrepresentation of chromosomal material. These thresholds have been thoroughly tested in numerous studies and provide a robust diagnostic criterion [10]. Because CGH has been reported to yield false positive results in critical chromosomal regions, i.e. pericentromeric subregions 1q11–q12, 9q11–q12 and 16q11.1–11.2, chromosome subregion 1p32–pter as well as chromosomes 19 and Y [11, 12], these regions were excluded from the analysis (Fig. 1).

Immunohistochemistry

For immunohistochemistry, 5-μm sections on poly-L-lysine-coated slides were used after drying in an oven, followed by dewaxing and peroxidase blocking with 1% H_2O_2. The specificity of immunostaining was tested by replacing primary antisera with normal rabbit serum. No additional pretreatment procedure for antigen retrieval was done. The immunoreactions were performed with the following primary monoclonal antibodies: anti-CD5 (monoclonal mouse IgG; Novocastra, Leica Microsystems, Wetzlar, Germany; 1:25), anti-CK 5/6 (monoclonal mouse IgG, M7237; Dako Cytomation, Glostrup, Denmark; 1:50) and anti-TTF-1 (monoclonal mouse, IgG, SPT24; Menarini, Florence, Italy; 1:100). Further, the primary polyclonal antibodies against CD117 (polyclonal rabbit, A4502; Dako Cytomation; 1:50), against thyroglobulin (polyclonal rabbit, A0251; Dako Cytomation; 1:80,000) and against calcitonin (polyclonal rabbit, A0576; Dako Cytomation; 1:40,00) were used. After washing steps, signal detection was performed (EnVision+ system-HRP, AEC, Dako Hamburg, Germany; 1:200) followed by counterstaining in hemalaun. The presence of clearly visible dark brown precipitation was considered as immunoreaction, evaluated by a score for staining intensity (0— no staining, 1—weak, 2—moderate, 3—strong reaction intensity).

Table 1 Patient characteristics and tumour progression

No.	Gender	Age	Stage	Therapy	Progression
1	Female	68	pT4, N1b (18/21), MX, R0	Total thyroidectomy, left central neck dissection, resection of the left recurrent laryngeal nerve and the left internal jugular vein, chemotherapy, radiation (50 Gy) After recurrence: tumourectomy, bilateral neck dissection, transsternal lymphadenectomy	Local recurrence after 2 months
2	Female	59	pT2, N0 (0/7), MX	Hemithyroidectomy right, then resection of residual thyroid, microdissection of the central cervical compartment, radiation of the thyroid bed (59,4 Gy)	No recurrence (time of observation 15 months)
3	Female	60	pT3, N1 (1/19), MX	En bloc resection with the right lobe, neurolysis of the right N. laryngeus recurrens, neck dissection right, supraclavicular cervical lateral dissection, radiation (50 Gy)	No recurrence (time of observation: 17 months)
4	Male	60	pT4a, N1 (1/5), M0, R0	Total thyroidectomy, neck dissection, radiation of the neck region (50 Gy)	No recurrence (time of observation 22 months)

No. case number, *Stage* TNM classification

Statistics

Since only four cases were evaluated and therefore a statistical analysis is not reasonable, the results of the immunohistochemical and chromosomal investigations are presented in a descriptive way.

Results

Histological findings and immunohistochemistry

By histology, the resected specimens showed solid tumour islands of variable size surrounded by fibrous septae resulting in a lobulated appearance. Especially the peripheral tumour tissue was infiltrated by small lymphocytes. Scattered blood vessels were found, surrounded by fibrous cuffs. Overall, all four tumours showed very similar histomorphological features, but in case 4, a predominant lobulation subdivided by broad septae was evident (see Fig. 2d), whereas in the cases 1–3 here and there, a dense lymphocytic infiltrate could be found between solid tumour islands, which were separated by delicate septae, in which several small arteries were visible (see Fig. 2a–c).

Tumour cells were varying in shape: Irregular cells as well as spindle-shaped and epithelioid cells were observed. Occasionally, squamoid or spindle-shaped epithelial cells with whorls resembling Hassall's corpuscles were seen. The cytoplasm of the tumour cells was pale.

There was a moderate expression of CD5 in the cases 1, 2 and 4 and a strong staining reaction in case 3. For CD117, the epithelial component in the cases 1, 2 and 4 showed a weak to moderate positivity, and only in case 3 a strong signal could be detected. CK 5/6 showed a weak reaction in case 1, and all other samples expressed a moderate (cases 2 and 3) or strong signal (case 4). All cases were negative for calcitonin, thyroglobulin and TTF-1 (see Table 2). A

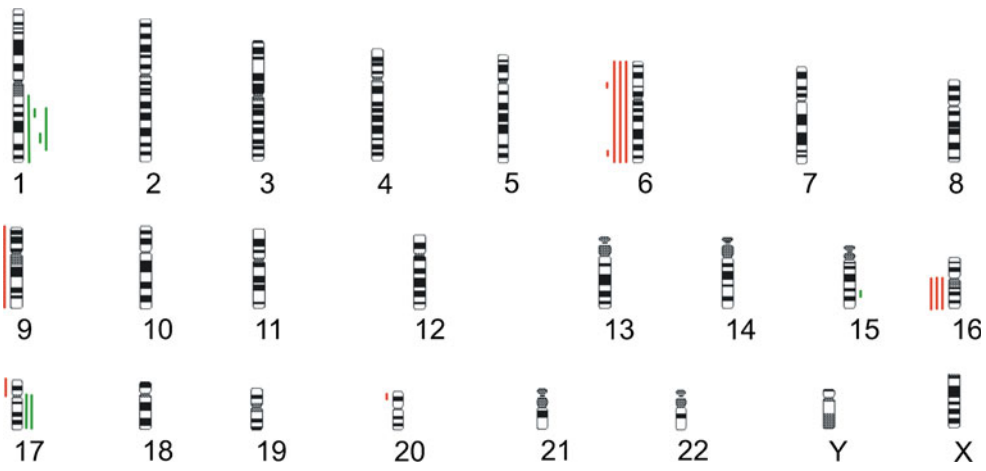

Fig. 1 Summary of chromosomal imbalances. The *lines on the right side of chromosome ideograms* indicate gains (*green*); the *lines on the left side* correspond to losses (*red*) of chromosomal material. Pericentromeric subregions 1q11–q12, 9q11–q12 and 16q11.1–11.2, chromosome subregion 1p32–pter as well as chromosomes 19 and Y were excluded from analysis (see "Materials and methods")

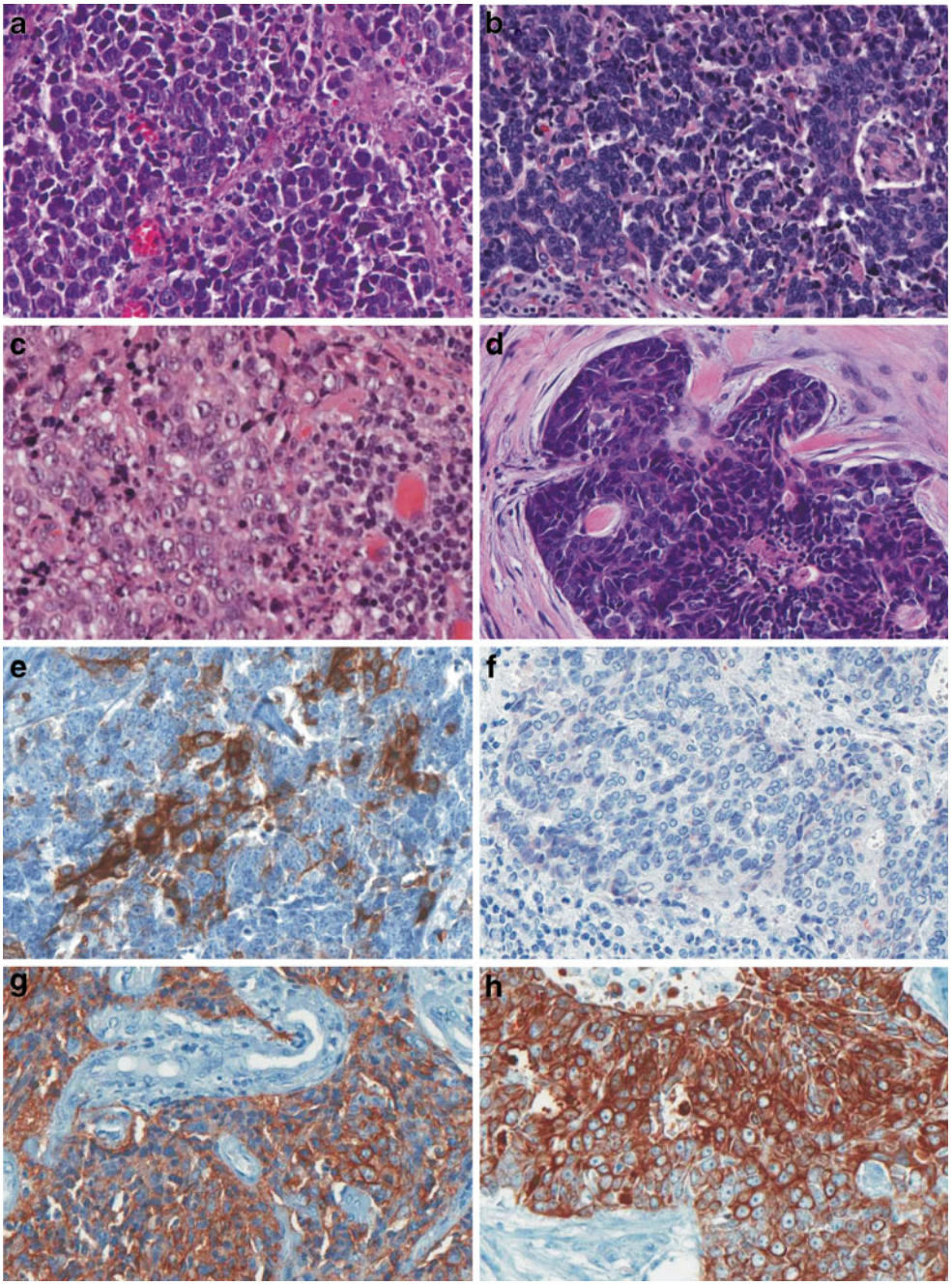

Fig. 2 HE and immunohistochemical stainings. **a** HE case 1, **b** HE case 2, **c** HE case 3, **d** HE case 4, **e** CD5 case 1, **f** TTF-1 case 2, **g** CD117 case 3, **h** CK5/6 case 4

representative example of the immunohistochemical stainings for CD5, CD117 and CK5/6 in the cases 1, 3 and 4 as well as the negative staining result for TTF-1 in case 2 can be seen in Fig. 2e–h. Overall, the histological findings and the immunophenotype expression pattern confirmed the diagnosis of CASTLE.

Chromosomal imbalances

DNA hybridization revealed gains and losses of chromosomal material in three cases, and in one case, only losses were detectable (see Table 3 and Fig. 1). In three out of four cases, gains were found on chromosomal arm 1q, affecting the whole arm in one case and subregions in two cases. Gains of the entire chromosomal arm 17q were found in two cases, and in a subregion of chromosomal arm 15q in one case. In all four cases, losses on chromosome 6 were observed, in three cases affecting the entire chromosome and in one case comprising subregions. Furthermore, losses of the whole chromosomal arm 16q were detected in three cases. Losses on chromosomes 9, 17 and 20 were each found in one tumour.

Table 2 Immunohistochemical expression pattern

No.	CD5	CD117	CK5/6
1	2	1	1
2	2	1	2
3	3	3	2
4	2	2	3

No. case number; *0* no staining, *1* weak, *2* moderate, *3* strong reaction intensity

Discussion

In this study, we investigated four cases of CASTLE for chromosomal imbalances using CGH. The most frequent gains were seen on chromosome 1q (3/4). Losses were most frequently detected on 6p (4/4), 6q (3/4) and 16q (3/4), regions in which chromosomal imbalances were also reported for classical thymomas and thymic carcinomas [4–9].

In contrast, a completely different genetic profile is found in thyroid carcinoma. Although no or few chromosomal changes are seen in early stages of papillary thyroid carcinoma, gains on chromosomal arms 1q and 5p as well as losses on 9q appear in advanced stages of this type of thyroid carcinoma [11]. Changes that are similar to those found in follicular carcinomas show gains on chromosome 5 and 19 and loss of 8p in early tumour stages and gains on 1q, 5, 7, 12q and 17q as well as losses on 13q and 22q in advanced tumours [12]. It is assumed that there is a sequence in carcinogenesis of thyroid carcinomas leading from well-differentiated carcinomas to anaplastic carcinomas. Gains on 8q23 and 19q and losses on 22q are seen as early events, followed by gains on 1p34–p36, 6p21, 9q34, 17q25 and 20q and losses on 1p11–p31, 2q32–q33, 4q11–q13, 6q21 and 13q21–q31. As an end point in the transformation into anaplastic carcinoma, gains on 3p13–p14 and 11q13 and losses on 5q11–q13 are supposed [13–16].

Table 3 Chromosomal gains and losses

No	Gains	Losses
1	1q, 17q	6p, 6q, 9p, 9q, 16q
2	1q24, 1q32–34, 15q24–ter, 17q	6p, 6q, 20p12–ter
3		6p21.1–ter, 6q25–ter, 16q, 17p
4	1q24–41	6p, 6q, 16q

No. case number

In the same way, there are hints for an underlying sequence in carcinogenesis for some thymic carcinomas and some thymomas since there are several reports regarding combined subtypes of thymic tumours as, e.g. type B2/B3 thymomas or combined type B3 thymomas/thymic carcinomas [17]. Furthermore, cluster analysis of genomic imbalances detected by CGH as well as oncogenetic tree models indicate that such a molecular sequence may exist for some of these tumours [5, 9]. However, some other mechanisms such as, e.g. microsatellite instability and certain mutations (e.g. KIT) may also play a role in the carcinogenesis of these rare tumours [7, 18]. Gains on chromosomal arm 1q as well as losses on 6q and 6p are considered to be early events in the tumourigenesis of thymomas. This is confirmed by LOH studies, which indicate that there is a loss on 6q25 in almost every thymoma subtype including early tumour stages [4, 7]. Especially the chromosomal subregions 6q25.2–q25.3, in which several tumour suppressor genes involved in the pathogenesis of thymomas are located, seem to be affected, making it interesting for further investigation [5, 6, 8]. In our study, we found gains on chromosomal arm 1q in three cases and losses on chromosome 6 in all four cases as well, indicating similar genetic changes in the tumourigenesis of CASTLE to those detected in thymic carcinomas and thymomas. Losses on 16q and 17p occur with increasing malignancy in thymomas and thymic carcinomas [4–7, 19]. Particularly in invasive carcinomas losses on 17p can be found including the subregion encoding for the tumour suppressor gene TP53 [4, 6, 7]. Losses on chromosomal arm 16q, in which several tumour suppressor genes such as CDH1, CTCF and WWOX are located, seem to occur later in carcinogenesis. Inoue et al. observed a LOH on 16p in two out of three thymic carcinomas [4]. In this study, we also found losses on 16q in two cases and on 17p in one case. All three cases have in common that an advanced tumour stage is on hand (pT3 in case 3, pT4/pT4a in cases 1 and 4) and that the tumours have already metastasized in regional lymph nodes (pN1 in cases 3 and 4, pN1b in case 1). The only pT2 tumour in our group showed no losses on 16q or 17p.

In conclusion, our study shows that CASTLE displays chromosomal imbalances, which are similar to those found in thymomas and thymic carcinomas, indicating an analogue mechanism of tumourigenesis.

Acknowledgements Special thanks to Prof. Klaus Kaserer (Labor Kaserer and Salzer OG, Labor Kaserer and Salzer OG Vienna, Austria; klaus.kaserer@meduniwien.ac.at) and Prof. Sören Schröder (Lademannbogen Laboratories, Institute of Pathology, Hamburg, Germany; schroeder@labor-lademannbogen.de) for providing paraffin-embedded material.

Conflict of interest The authors declare that they have no conflict of interest.

References

1. Miyauchi A, Kuma K, Matsuzuka F, Matsubayashi S, Kobayashi A, Tamai H et al (1985) Intrathyroidal epithelial thymoma: an entity distinct from squamous cell carcinoma of the thyroid. World J Surg 9:128–135
2. Chan JK, Rosai J (1991) Tumors of the neck showing thymic or related branchial pouch differentiation: a unifying concept. Hum Pathol 22:349–367
3. Cheuk W, Chan JKC, Dorfmann DM et al (2004) Spindle cell tumour with thymus-like differentiation. In: DeLellis RA, Lloyd RV, Heitz PU, Eng C (eds) World Health Organization classification of tumours. Tumours of endocrine organs. IARC, Lyon, pp 96–97
4. Inoue M, Starostik P, Zettl A, Ströbel P, Schwarz S, Scaravilli F et al (2003) Correlating genetic aberrations with World Health Organization-defined histology and stage across the spectrum of thymomas. Cancer Res 63:3708–3715
5. Penzel R, Hoegel J, Schmitz W, Blaeker H, Morresi-Hauf A, Aulmann S et al (2003) Clusters of chromosomal imbalances in thymic epithelial tumours are associated with the WHO classification and the staging system according to Masaoka. Int J Cancer 105:494–498
6. Zettl A, Ströbel P, Wagner K, Katzenberger T, Ott G, Rosenwald A et al (2000) Recurrent genetic aberrations in thymoma and carcinoma. Am J Pathol 157:257–266
7. Zhou R, Zettl A, Ströbel P, Wagner K, Müller-Hermelink HK, Zhang S et al (2000) Thymic epithelial tumors can develop along two different pathogenetic pathways. Am J Pathol 159:1853–1860
8. Inoue M, Marx A, Zettl A, Ströbel P, Müller-Hermelink HK, Starostik P (2002) Chromosome 6 suffers frequent and multiple aberrations in thymoma. Am J Pathol 161:1507–1513
9. Rieker RJ, Penzel R, Aulmann S, Blaeker H, Morresi-Hauf A, Hecker E et al (2005) Oncogenetic tree models based on cytogenetic data: new insights into the development of epithelial tumors of the thymus. Cancer Genet Cytogenet 158:75–80
10. Ströbel P, Marx A, Zettl A, Müller-Hermelink HK (2005) Thymoma and thymic carcinoma: an update of the WHO classification 2004. Surg Today 35:805–811
11. Kjellmann P, Lagercrantz S, Höög A, Wallin G, Larsson C, Zedenius J (2001) Gain of 1q and loss of 9q21.3–q32 are associated with less favorable prognosis in papillary thyroid carcinoma. Genes Chromosomes Cancer 32(1):43–49
12. Castro P, Eknaes M, Teixeira MR, Danielsen HE, Soares P, Lothe RA, Sobrinho-Simoes M (2005) Adenomas and follicular carcinomas of the thyroid display two major patterns of chromosomal changes. J Pathol 206(3):305–311
13. Wreesmann VB, Ghossein RA, Patel SG, Harris CP, Schnaser EA, Shaha AR, Tuttle RM, Shah JP, Rao PH, Singh B (2002) Genome-wide appraisal of thyroid cancer progression. Am J Pathol 161 (5):1549–1556
14. Roque L, Rodrigues R, Pinto A, Moura-Nunes V, Soares J (2003) Chromosome imbalances in thyroid follicular neoplasms: a comparison between follicular adenomas and carcinomas. Genes Chromosomes Cancer 36(3):292–302
15. Wilkens L, Benten D, Tchinda J, Brabant G, Pötter E, Dralle H, Von Wasielewski R (2000) Aberrations of chromosomes 5 and 8 as recurrent cytogenetic events in anaplastic carcinoma of the thyroid as detected by fluorescence in situ hybridisation and comparative genomic hybridisation. Virchows Arch 436:312–318
16. Rodrigues RF, Roque L, Rosa-Santos J, Cid O, Soares J (2004) Chromosomal inbalances associated with anaplastic transformation of follicular thyroid carcinomas. Br J Cancer 90 (2):492–496
17. Verghese ET, den Bakker MA, Campbell A et al (2008) Interobserver variation in the classification of thymic tumours—a multicentre study using the WHO classification system. Histopathology 53:218–223
18. Girard N, Shen R, Guo T, Zakowski MF, Heguy A, Riely GJ, Huang J, Lau C, Lash AE, Ladanyi M, Viale A, Antonescu CR, Travis WD, Rusch VW, Kris MG, Pao W (2009) Comprehensive genomic analysis reveals clinically relevant molecular distinctions between thymic carcinomas and thymomas. Clin Cancer Res 15 (22):6790–9799
19. Marx A, Rieker RJ, Toker A, Länger F, Ströbel P (2011) Thymic carcinoma: is it a separate entity? From molecular to clinical evidence. Thorac Surg Clin 21(1):25–31

Virchows Arch (2011) 459:227–234
DOI 10.1007/s00428-011-1090-1

ORIGINAL ARTICLE

Tyrosine phosphatase SHP-1 is expressed higher in multisystem than in single-system Langerhans cell histiocytosis by immunohistochemistry

Ichiro Murakami · Takashi Oka · Satoshi Kuwamoto · Masako Kato · Kazuhiko Hayashi · Jean Gogusev · Toshihiko Imamura · Akira Morimoto · Shinsaku Imashuku · Tadashi Yoshino

Received: 12 April 2011 / Revised: 6 May 2011 / Accepted: 7 May 2011 / Published online: 22 May 2011
© Springer-Verlag 2011

Abstract Langerhans cell histiocytosis (LCH) is a proliferative disorder of Langerhans cell (LC)-like CD1a-positive cell (LCH cell) with unknown causes. LCH consists of two subtypes: single-system LCH (LCH-SS) with favorable prognosis and multisystem LCH (LCH-MS) with poor prognosis. LCH has been indicated as a neoplastic disorder from monoclonal characteristics of LCH cells. This study aimed to investigate an expression of tyrosine phosphatase SHP-1 in LCH, since its expression levels were variously reported in many tumors, overexpression in ovarian cancers (a candidate oncoprotein), and downregulation by methylation in gastric cancers, prostate cancers, malignant lymphomas, and leukemias (a putative tumor suppressor). By immunohistochemistry (IHC), the SHP-1 expression in LCs and LCH cells was compared in LCH (two subtypes: LCH-SS=21, LCH-MS=12), dermatopathic lymphadenopathy (DLA) (n=9) and normal epidermal LCs (n=3) near LCH lesion. IHC results were analyzed semiquantitatively using a Photoshop software. The mean intensity score (IS) of DLA, LCH-SS, LCH-MS, and LCs were 47, 100, 139, and 167 (in arbitrary unit), respectively. The IS had significant differences among LCH-SS, LCH-MS, and DLA ($p<0.01$). SHP-1 is expressed significantly higher in LCH-MS than in LCH-SS. SHP-1 can be a progression marker of LCH. SHP-1 is also useful for differential diagnosis between LCH in lymph nodes and DLA.

Keywords Langerhans cell histiocytosis · Tyrosine–protein phosphatase nonreceptor type 6 (PTPN6, SHP-1) · Immunohistochemistry · Photoshop-assisted image analysis · Staining intensity

Abbreviations

B-ALL	B lymphoblastic leukemia
CMYK	Cyan/magenta/yellow/key
IF	Immunofluorescence
IHC	Immunohistochemistry
IS	Intensity score
ISs	Intensity scores
LC	Langerhans cell
LCH	Langerhans cell histiocytosis
LCH cell	Langerhans cell-like CD1a-positive cell

I. Murakami (✉) · S. Kuwamoto · M. Kato · K. Hayashi
Faculty of Medicine, Division of Molecular Pathology,
Tottori University,
86 Nishi-cho Yonago-shi,
Tottori 683–0834, Japan
e-mail: ichiro.murakami.09@gmail.com

T. Oka · T. Yoshino
Department of Pathology,
Okayama University Graduate School of Medicine,
Dentistry and Pharmaceutical Sciences,
Okayama, Japan

J. Gogusev
Inserm U90 and U507, Hôpital Necker-Enfants-Malades,
Paris, France

T. Imamura
Department of Pediatrics,
Kyoto Prefectural University of Medicine,
Kyoto, Japan

A. Morimoto
Department of Pediatrics,
Jichi Medical University School of Medicine,
Shimotsuke, Japan

S. Imashuku
Division of Pediatrics and Hematology, Takasago-seibu Hospital,
Takasago, Japan

LCH-MS	Multisystem LCH
LCH-SS	Single-system LCH
LCS	LC sarcoma
meV	Viable motheaten mice
MHC	Major histocompatibility complex
PTPN6	Tyrosine–protein phosphatase nonreceptor type 6
SHP-1	Src homology region 2 domain-containing phosphatase 1
SHPS-1	Substrate of SHP-1
T-ALL	T lymphoblastic leukemia

Introduction

Langerhans cells (LCs) are specialized immature dendritic cells (DCs) in the skin. When LCs encounter exogenous antigens, they capture and process them to generate major histocompatibility complex (MHC)/peptide complexes on their surface. LCs migrate from epidermis to draining lymphoid tissues in order to initiate and present the MHC/peptide complexes to the T cells. During this migration, LCs mature, and the expressions of their cell-surface molecules are changed [1, 2]. Langerhans cell histiocytosis (LCH) is a proliferative disorder of Langerhans cell (LC)-like CD1a-positive cell (LCH cell) with unknown causes. Patients with LCH develop as two clinical subtypes: single-system LCH (LCH-SS) and multisystem LCH (LCH-MS).

LCH tissues are known to have monoclonal characteristics of LCH cells by the *human androgen receptor* gene assay [3, 4]. LCH cells of two LCH patients suffering from T lymphoblastic leukemia (T-ALL) have T cell receptor rearrangement of the same cell origin as T-ALL cells [5]. In addition, LC sarcoma (LCS) cells in a patient who suffered from B lymphoblastic leukemia (B-ALL) were found to have identical immunoglobulin heavy chain rearrangements in both LCS cells and B-ALL cells [6]. Signal transduction pathways, such as the IL-17A-dependent pathway, have been reported to have abnormalities in LCH cells [7, 8]. More recently, *BRAF* mutation (V600E) was reported in 57% of LCH cases [9].

These accumulated data indicate that LCH is a neoplastic disease with abnormalities of signal transduction pathways. Tyrosine–protein phosphatase nonreceptor type 6 (PTPN6, src homology region 2 domain-containing phosphatase 1 (SHP-1), Hep, HepH, HPTP1C, SH-PTP1, HCP) is known to be one of nonmembranous type phosphatases and plays an important role in many signal transduction pathways especially in hematopoietic neoplasms. Downregulation of SHP-1 was widely reported in lymphomas and leukemias at a high rate by our group and other groups [10, 11], while SHP-1 was overexpressed in epithelial tumors such as ovarian cancers [12, 13]. In cases of downregulation, epigenetic mechanisms such as methylation have been proposed, and loss of SHP-1 function in cytokine signaling has been shown to have a relationship with neoplastic mechanisms. In contrast, affected signaling events of overexpressed SHP-1 were not known in ovarian cancers [13], although some epithelial cell lines such as 293 cells and Hela cells, SHP-1 acts positively for stimulation such as epidermal growth factor [14, 15].

LCH cells in LCH-MS are known to have an immature character of LC compared with LCH-SS [16], and one of the substrates of SHP-1, termed as SHPS-1, was reported to regulate the induction of murine LCs into maturation [17]. However, to date, little is known about the role of SHP-1 in both LCs and LCH cells in humans. Such paucity of data has driven us to analyze SHP-1 in human LCs and LCH tissues. We hypothesized that downregulation of SHP-1 might have a role in the pathogenesis of LCH because LC is one myeloid-derived dendritic cell. The objective of the present study was to clarify the relationship of the expression levels of SHP-1 between tissues from patients with LCH-SS and LCH-MS and other control tissues, the dermatopathic lymphadenopathy (DLA) as a control of mature LC, and the epidermal LC as a control of immature LC, using the immunohistochemical method.

Materials and methods

Patients, samples, and clinical data

The study was approved by the Institutional Review Board of Okayama University Graduate School of Medicine, Dentistry and Pharmaceutical Sciences, Okayama, Japan. Tissues of LCH were obtained from patients registered with the Japan LCH Study Group (JLSG) between 2002 and 2009. Tissues of DLA and normal skin tissues contained in the dermal tumors (such as dermatofibroma) were from patients who visited Okayama University Hospital between 2002 and 2009. Histological sections and immunohistochemistry (IHC) such as the CD1a of all the specimens were reviewed by pathologists to confirm the diagnosis. Information on patients including laboratory data at onset of disease was obtained from the JLSG registration center and the medical records of patients at Okayama University Hospital. The clinical data are as follows: hemoglobin, platelet, white blood cell, lymphocyte, total protein, albumin, total bilirubin, lactate dehydrogenase, glutamic–oxaloacetic transaminase (aspartate aminotransferase), glutamic pyruvic transaminase (alanine transaminase), C-reactive protein, erythrocyte sedimentation rate, and soluble interleukin-2 receptor.

Antibodies for immunofluorescence and immunohistochemistry

Rabbit polyclonal antibody directed against SHP-1 (SH-PTP1 (C-19): sc-287, Santa Cruz Biotechnology, Inc., CA, USA) was used at 1:1,600 dilution. Anti-CD1a antibody (monoclonal mouse anti-human CD1a antibody (IgG1, kappa), O10, Dako Japan, Kyoto, Japan) was used at 1:100 dilution.

Immunofluorescence

Tissue samples were fixed in 10% neutral-buffered formalin and embedded in paraffin. Sections were deparaffinized in xylene and rehydrated in a graded ethanol series. Antigen retrieval was performed by heating slides in 0.01 M citrate-buffered solution, pH 6.0, in a pressure cooker at 98°C for 15 min. The slides were incubated for 1 h in 5% skim milk, then primary antibodies were applied against both SHP-1 and CD1a, and the slides were maintained for 3 h at 37°C. After washing first antibodies, second antibodies, Alexa Fluor® 555 goat anti-mouse IgG (H+L) and Alexa Fluor® 488 goat anti-rabbit IgG (H+L) (Molecular Probes, Inc., Eugene, OR, USA) were applied for 1 h at room temperature. Images were captured and analyzed using Image Gauge version 3.3 (Fujifilm Corporation, Tokyo, Japan).

Immunohistochemistry

For IHC, treatment of tissue samples is the same as described in immunofluorescence (IF). For blocking endogenous peroxidase activity, hydrogen peroxide was used. Antigen retrieval and incubation were the same as described. Next, 1 h of incubation of secondary antibody at room temperature and staining were performed using the DAKO EnVision+system (Dako Japan, Kyoto, Japan) and 3,3′-diaminobenzidine as a chromogen. The slides were counterstained with hematoxylin. As appropriate, positive controls and negative controls, normal lymph nodes, and skin samples, respectively, were used throughout. An isotype control was not performed.

Digital image capture

Digital images for photomicroscopy of the best-stained area of the sections as representative of the overall immunostaining were acquired with the Olympus DP71 microscope digital camera (Olympus, Tokyo, Japan). All images were obtained using a ×40 objective of the Olympus BX51 microscope. The software used was the Olympus DP2-BSW. For the entire study, the camera was manipulated with manual controls with its auto mode turned off and used to adjust the image intensity, which was kept at an identical level during the entire study. Conditions were as follows: manual exposure, 720 μs; ISO 1600; tagged image format, 4,140×3,096 pixel shift. Files were saved in uncompressed TIFF format so that their sizes were fixed to 36.7 MB.

Quantification of immunohistochemical chromogen

The determination of immunostaining intensity was assisted by the use of Adobe Photoshop, version 5.0 J (Adobe Systems Incorporated, Japan office, Shinagawa, Tokyo, Japan) as described by Lehr et al. [18]. Using the magic wand tool in the select menu of Photoshop, the cursor was placed on SHP-1-positive cytoplasm. The tolerance level of the magic wand tool was adjusted so that the entire positive cytoplasm was selected automatically. This selection was confirmed by checking both the selected figure and its inverted figure, which was made using the inverse tool. A yellow optical density plot of the selected area was generated using the histogram tool in the image menu as described by Pham et al. [19]. The mean staining intensity was calculated as follows: intensity score (IS)=255−mean of brightness of yellow channel score on a cyan/magenta/yellow/key color model (in arbitrary unit, AU). Immunohistochemical data as IS (AU) of LC, DLA, LCH-SS, and LCH-MS were plotted using the SPSS software (version 15.0 J, SPSS Japan Inc., Tokyo, Japan).

Necrosis and mitotic index in LCH specimens

In LCH specimens, we also determined necrosis (+ or −) and mitotic index (mitotic number/10 high-power field using an Olympus BX50 microscope with SWH10X-H/26.5 eyepieces), compared between LCH-SS and LCH-MS subtypes.

Statistical analysis

Analyses were performed using the SPSS software or Microsoft Office Excel 2003 (Microsoft Corporation, Tokyo, Japan). Comparisons of immunohistochemical data of SHP-1 between LCH and DLA, between LCH-MS and LCH-SS, were performed using Wilcoxon's signed-rank test. Immunohistochemical data of SHP-1 and histological data such as necrosis were compared using Wilcoxon's signed-rank test. The correlation of SHP-1 data, mitotic index, and clinical data were determined using regression analyses. Comparisons of the LCH subtypes and histological data such as necrosis or mitotic index were performed using Fisher's exact test or Wilcoxon's signed-rank test. Differences between values were considered statistically significant at $p<0.01$ or $p<0.05$.

Results

Characteristics of patients

The characteristics of patients are summarized in Table 1. The numbers of patients were 21 patients with LCH-SS, 12 patients with LCH-MS, and nine patients with DLA. The median ages of the LCH-SS patients were 6 years 6 months old (range, 0–71 years old). The median ages of the LCH-MS patients were 1 year 6 months old (range, 0–62 years old). The median age of DLA patients was 78 years old (range, 72–87 years old). The male to female ratio of LCH-SS was 16:5. The male to female ratio of LCH-MS was 6:6. The male to female ratio of DLA was 6:3. Epidermal LCs were analyzed from three dermal LCH.

IF: identification of SHP-1-and CD1a-double positive cells

We first demonstrated that CD1a-positive LCs [20] in normal epidermis were proven to express SHP-1 by double staining. Spinous cells showed weak positivity and granular cells showed strong positivity (Fig. 1a).

Quantification of IHC of SHP-1 in epidermal LC, DLA, and LCH

LCs in the epidermis expressed SHP-1, and spinous cells showed weak positivity and granular cells showed just a little strong positivity (Fig. 1b). LCs in DLA and LCH cells in LCH showed negative to high expression of SHP-1 as shown in Fig. 1c–f. Immunohistochemical data as ISs (AU)

Table 1 Clinical characteristics of LCH patients and SHP-1 intensity score

Patient number	Age	Sex	Subtype	Biopsy site	Necrosis	MI	IS
1000114	2 years 3 months	M	SS	Bone	+	0	68
1000115	1 year 1 month	M	SS	Bone	−	0	63
1000179	58 years	F	SS	LN	−	15	96
1000202	71 years	M	SS	Skin	−	12	78
1000219	2 years 11 months	M	SS	Bone	+	4	114
1000222	5 years 1 month	F	SS	Bone	−	1	118
1000227	1 years 5 months	M	SS	Bone	−	0	103
1000267	4 years 2 months	M	SS	Bone	−	0	97
1000275	6 years 6 months	M	SS	Bone	−	2	140
13001	11 years	F	SS	Bone	+	0	126
130011	65 years	M	SS	Orbit	+	2	112
130012	29 years	M	SS	Lung	−	0	100
130015	32 years	M	SS	LN	−	9	62
130016	61 years	M	SS	Lung	+	2	105
130017	2 years 5 months	M	SS	Bone	−	23	60
13002	39 years	M	SS	Lung	−	0	58
13003	7 years	M	SS	Bone	+	3	93
13005	0 month	M	SS	Bone	+	1	111
13006	4 years	F	SS	Bone	+	4	158
13007	4 years	F	SS	Bone	+	0	131
13008	7 years	M	SS	Bone	+	0	97
1000159	2 years	F	MS	Bone	−	0	108
1000178	1 month	F	MS	Liver	−	1	97
1000185	10 months	M	MS	LN	+	6	85
1000201	5 months	M	MS	Bone	+	1	128
1000216	1 year 1 month	F	MS	LN	+	20	179
1000230	4 months	F	MS	Skin	+	20	179
1000234	4 year 2 months	F	MS	Bone	−	0	161
1000249	62 years	M	MS	Skin	−	17	176
1000273	7 years 8 months	M	MS	Bone	−	1	94
1000277	0 month	M	MS	Skin	−	4	180
130014	7 years	M	MS	Skin, LN	+	1	128
13009	8 years	F	MS	Bone	+	4	150

MI mitotic index, *M* male, *F* female, *LN* lymph node

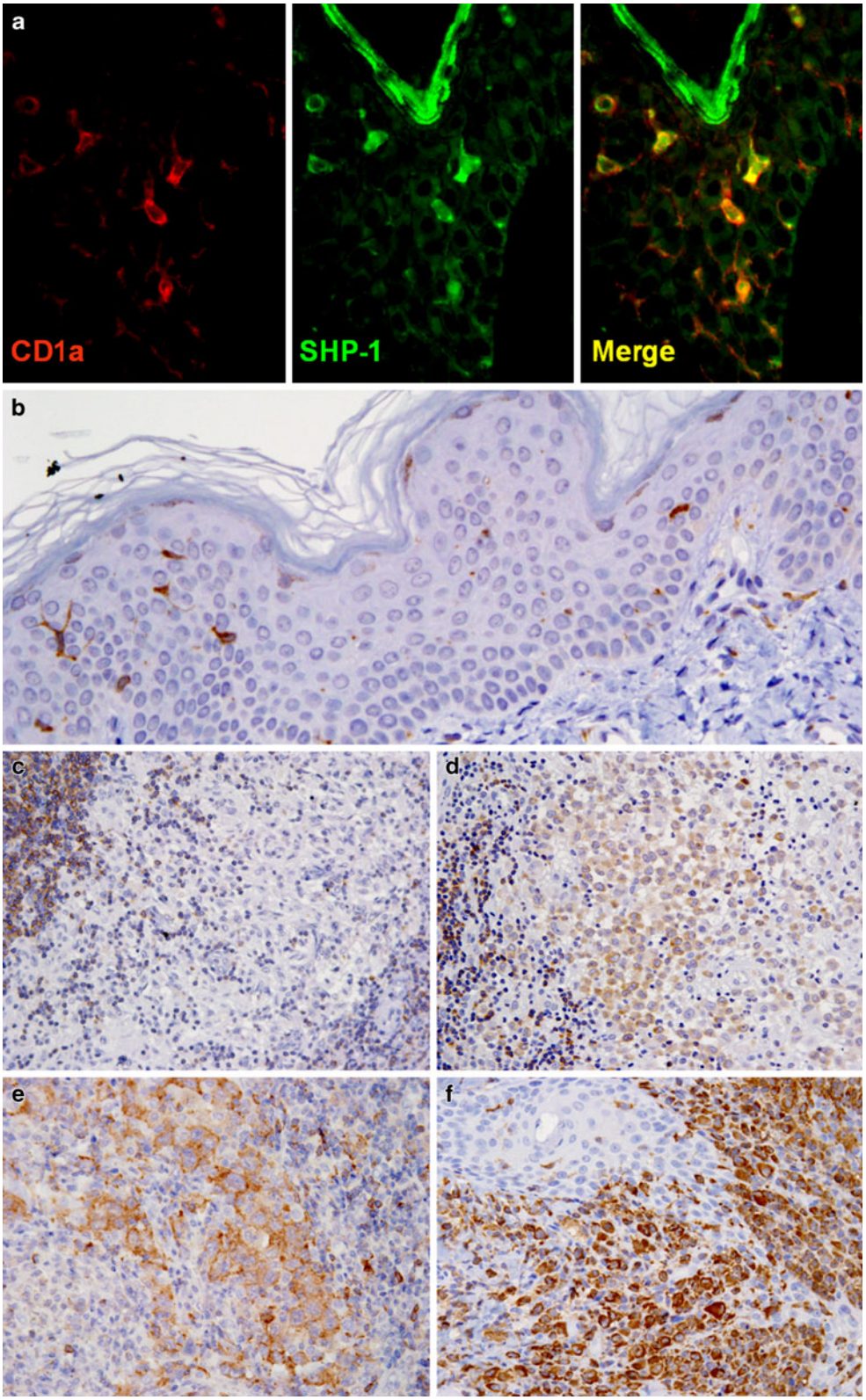

Fig. 1 **a** Detection of CD1a and SHP-1 in skin (epidermis) by IF is shown from a 55-year-old female abdominal skin. Left, CD1a positive LCs. Middle, IF of SHP-1 revealed the strong immunoreactivity in LCs and granular cells, and weak positivity in spinous cells. Right, merge of left and middle images. **b** Detection of SHP-1 protein expression by IHC in normal skin of baby with LCH-MS (1000277). LCs (IS=164 AU) and granular cells in epidermis showed positivity for SHP-1. Spinous cells in epidermis showed vague positivity. **c–f** Detection of SHP-1 protein in the tissues from DLA and LCH by IHC. **c** LCs (IS=45 AU) in DLA of 87-year-old male (150034678). Lymphocytes showed positivity. **d** Bone lesion (IS=93 AU) of LCH-SS (13003). **e** Lung lesion (IS=105 AU) of LCH-SS (130016). **f** Skin lesion (IS=179 AU) of LCH-MS (1000230)

of epidermal LC, DLA, LCH-SS, and LCH-MS were plotted respectively, as shown in Fig. 2, using the SPSS software. As shown, ISs of SHP-1 ranged from 42 (negative) to 180 (strong staining) in the cytoplasm of LCs/LCH cells of DLA and LCH. On the other hand, ISs of SHP-1 expressed in the cytoplasm of LCs in normal epidermis of dermal LCH cases were 164 (patient 1000277), 165 (patient 1000249), and 173 (patient

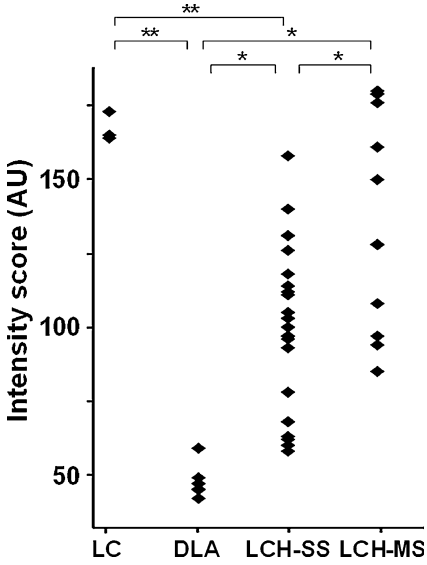

Fig. 2 Dot plots of IS of LCs in the normal epidermis of LCH patients, proliferating cells in DLA, LCH-SS, and LCH-MS. The *x*-axis shows LC, DLA, LCH-SS, and LCH-MS. An *asterisk* means $p<0.01$. A *double asterisk* means $p<0.05$

1000230). The mean IS of DLA, LCH-SS, LCH-MS, and epidermal LC were 47, 100, 139, and 167 AU. A significant difference of SHP-1 reactivity was observed between DLA and LCH-SS ($p<0.01$), DLA and LCH-MS ($p<0.01$), and LCH-SS and LCH-MS ($p<0.01$). Also, a significant difference of SHP-1 reactivity was observed between epidermal LC and DLA ($p<0.05$) and epidermal LC and LCH-SS ($p<0.05$). Between epidermal LC and LCH-MS, there was no significant difference. In skin samples, the dermis as negative control did not give background staining.

Correlation of LCH subtypes with necrosis/mitotic index

LCH subtypes did not have a relationship with the rates of necrosis (Fisher's exact test) or mitotic index (Wilcoxon's signed-rank test) in LCH tissues.

Correlation of SHP-1 expression with necrosis/mitotic index and various clinical variables in LCH

The expression levels of SHP-1 did not correlate with the rates of necrosis (Wilcoxon's signed-rank test) or mitotic index in LCH tissues (regression analyses), nor with any clinical variables (regression analyses).

Discussion

LCs are specialized immature DCs in the skin. Ramachandran et al. showed that SHP-1 was an important inhibitor of mice DC signaling, targeting multiple activation pathways [21]. Accumulated data showed that SHP-1 exerted either putative oncogenic or tumor suppressive functions, depending on the cellular context. Considering the fact that no data of SHP-1 in human LCs were available in the past, our data could be the first in human LCs

The aim of our study was to determine whether SHP-1 expression was related to LCH. Our hypothesis was that SHP-1 was negative or showed low expression in LCH, as in other hematopoietic cell neoplasms such as malignant lymphoma or leukemia. The results of SHP-1 expression analysis showed the opposite of this hypothesis. Higher SHP-1 expression was correlated with worse LCH subtype and thus with worse prognosis (LCH-MS).

Our study had five novel findings: (1) LCs in the epidermis were highlighted compared with spinous cells in the epidermis, except for granular cells, using highly diluted anti-SHP-1 polyclonal antibody (1,600:1). At a dilution of 1,600:1 of anti-SHP-1 antibody, LCs in epidermis (not LCH cells that were in the dermis) of patients 1000249, 1000277, and 1000230 were strongly positive and the epidermis showed faint positivity in IHC and IF, as shown in Fig. 1a, b. Differences of sensitivity between IF and IHC were thought to cause faint positivity of granular cells as well as spinous cells in IHC of Fig. 1b compared with IF of Fig. 1a. (2) Semiquantitative analyses could be performed among LCH cells using highly diluted anti-SHP-1 antibody (1,600:1). (3) LCH cells in LCH-MS did not show a significant difference in SHP-1 intensity compared with LCs in the epidermis. (4) SHP-1 intensity of LCH cells in LCH-SS was weaker in IHC compared with that of LCH-MS (Fig. 1d–f). (5) Proliferating nonneoplastic LC of DLA showed negative or very weak reaction of SHP-1 in IHC (Fig. 1c).

Based on the formerly described data about cell volume of LCs [22], LCH cell diameters [23], and LCH cell nucleus diameters [24], LCH cell cytoplasm volumes are thought to reach 8.7 times those of epidermal LCs. The cell size differences between LCH cells and epidermal LCs and calculation of SHP-1 staining intensity in AU indicate difficulty to compare total volumes of SHP-1 between LCH cells and epidermal LCs.

From the pathological point of view, LCH-SS was described to have more necrotic tissues compared with LCH-MS by Bank et al. [25]; however, our data of almost all Japanese patients were different from those of Bank et al., and we could not confirm this. SHP-1 expression correlates with neither mitotic index in LCH tissue nor any other clinical data at onset of disease.

Low or negative expression of SHP-1 in LCs in DLA is compatible with the theory that SHP-1 negatively regulates LCs migration to lymph nodes from epidermis [17]. Thus, our SHP-1 data could be compatible with data by Geissman

et al. that LCH cells of self-healing or isolated cutaneous LCH (LCH-SS) have a more mature phenotype (with low expression of SHP-1) than those in disseminated disease (LCH-MS) [16]. SHP-1 is also useful for the differential diagnosis between LCH in lymph nodes and DLA. Organs which LCH involves are various. A lymph node may be a presenting and only site of LCH. LCH involves only skin and lymph nodes [23]. Those cases without characteristic features such as increased eosinophil levels give a diagnostic problem at the point of differential diagnosis with DLA containing proliferating LCs in lymph nodes [26].

Motheaten mice or viable motheaten mice (meV) lacks the SHP-1 expression [27]. meV shows normal LC numbers in the epidermis at birth, but the numbers decrease along with mouse maturation [28, 29]. SHP-1 might be necessary to maintain the LC number in the epidermis by maintaining immaturity of the mouse skin. Data on such mice LCs and human LCs in DLA may suggest that SHP-1 in the skin (keratinocytes) and/or SHP-1 in LCs themselves play a role in maintaining the immaturity of LCs.

Very recently, *BRAF* mutation was described in LCH including LCH-SS cases involving the lungs [9]. *BRAF* mutation is also related with many cancers [30]. Such data point out the neoplastic possibility of LCH as well as a clonal association between LCH and a lymphoblastic leukemia [5, 6]. It is an important question whether LCH-SS involving the lungs is neoplastic or nonneoplastic. Our data about SHP-1 expression of two cases LCH-SS involving the lungs looks same as in other LCH-SS cases, but two cases are not enough to talk about the role of SHP-1 expression in this differential diagnosis statistically. SHP-1 exists in some signaling pathways relating to BRAF [31, 32]. Thus, it is an important question whether SHP-1 relates or not with BRAF or mitogen-activated protein/extracellular signal-regulated kinase pathways in LCH. We are currently analyzing roles or functions of SHP-1 using transfectants derived from a cell line with LC character.

In conclusion, SHP-1 expressions were negative, low and high among DLA (nine patients), LCH-SS (21 patients), and LCH-MS (12 patients), respectively, with a significant difference. This difference can be used to provide insight into LCH and differential diagnosis among DLA, LCH-SS, and LCH-MS, especially between LCH in LNs and DLA.

Acknowledgments This work was partly supported by a grant from Hamazaki Cancer Fund. We thank Dr. Daiichiro Hasegawa (Hyogo Children's Hospital), Dr. Chihiro Shimazaki (Kyoto Prefectural University of Medicine), Dr. Nobuyo Yoshida (Kagoshima University Graduate School of Medicine and Dental Sciences), Dr. Teruhisa Koyama (NHO Okayama Medical Center), Dr. Sanae Kawakami (Ehime University School of Medicine), Dr. Takashi Kanazawa (Gunma University School of Medicine), Dr. Toshinori Hori (Aichi Medical University), Dr. Takashi Sato (Hiroshima University), Dr. Yoshiyuki Kosaka (Hyogo Children's Hospital), Dr. Chihaya Imai (Niigata University), Dr. Banryoku Higuchi (Nara Medical University), Dr. Keigo Hamahata (Japanese Wakayama Red Cross Medical Center), Dr. Yutaka Kobayshi (Kyoto Second Red Cross Hospital), Dr. Ritsuo Nishiuchi (Kochi Medical Center), Dr. Yasuo Horikoshi (Shizuoka Prefectural Children's Hospital), Dr. Yoshihiko Hoshida (Sumitomo Hospital), Dr. Kunimitsu Kawahara (Osaka Prefectural Medical Center for Respiratory and Allergic Diseases), Dr. Ichiro Yamadori (NHO Okayama Medical Center), Dr. Nobuya Ohara (Okayama Red Cross Hospital), Dr. Yasushi Horie (Tottori University Hospital), Dr. Francis Jaubert (Hôpital Necker-Enfants-Malades), Dr. Takehiro Tanaka, Dr. Koichi Ichimura, and Dr. Hiroyuki Yanai (Okayama University Hospital) for providing clinical information and specimens and Dr. Kenji Yokota (Okayama University Graduate School of Health Sciences) and the Central Research Laboratory, Okayama University Medical School for the help with the microscopes and software.

Conflict of interest We declare that we have no conflict of interest.

References

1. Aiba S, Katz S (1990) Phenotypic and functional characteristics of in vivo activated Langerhans cells. J Immunol 145:2791–2796
2. Fukunaga A, Nagai H, Yu X et al (2006) Src homology 2 domain-containing protein tyrosine phosphatase substrate 1 regulates the induction of Langerhans cell maturation. Eur J Immunol 36:3216–3226
3. Willman CL, Busquet L, Griffith BB et al (1994) Langerhans'-cell histiocytosis (histiocytosis X): a clonal proliferative disease. N Engl J Med 331:154–160
4. Yu RC, Chu C, Buluwela L, Chu AC (1994) Clonal proliferation of Langerhans cells in Langerhans cell histiocytosis. Lancet 343:767–768
5. Feldman AL, Berthold F, Arceci RJ et al (2005) Clonal relationship between precursor T-lymphoblastic leukaemia/lymphoma and Langerhans-cell histiocytosis. Lancet Oncol 6:435–437
6. Magni M, Di Nicola M, Carlo-Stella C et al (2002) Identical rearrangement of immunoglobulin heavy chain gene in neoplastic Langerhans cells and B-lymphocytes: evidence for a common precursor. Leuk Res 26:1131–1133
7. Coury F, Annels N, Rivollier A et al (2008) Langerhans cell histiocytosis reveals a new IL-17A-dependent pathway of dendritic cell fusion. Nat Med 14:81–87
8. Allen CE, McClain KL (2009) Interleukin-17A is not expressed by CD207(+) cells in Langerhans cell histiocytosis lesions. Nat Med 15:483–484
9. Badalian-Very G, Vergilio JA, Degar BA et al (2010) Recurrent BRAF mutations in Langerhans cell histiocytosis. Blood 116:1919–1923
10. Zhang Q, Raghunath PN, Vonderheid E, Odum N, Wasik MA (2000) Lack of phosphotyrosine phosphatase SHP-1 expression in malignant T-cell lymphoma cells results from methylation of the SHP-1 promoter. Am J Pathol 157:1137–1146
11. Oka T, Yoshino T, Hayashi K et al (2001) Reduction of hematopoietic cell specific tyrosine phosphatase SHP-1 gene expression in natural killer cell lymphoma and various types of lymphomas/leukemias: combination analysis with cDNA expression array and tissue microarray. Am J Pathol 159:1495–1505
12. Mok SC, Kwok TT, Berkowitz RS, Barrett AJ, Tsui FW (1995) Overexpression of the protein tyrosine phosphatase, non-receptor type 6 (PTPN6), in human epithelial ovarian cancer. Gynecol Oncol 57:299–303
13. Julien SG, Dubé N, Hardy S, Tremblay ML (2011) Inside the human cancer tyrosine phosphatome. Nat Rev Cancer 11:35–49

14. Su L, Zhao Z, Bouchard P et al (1996) Positive effect of overexpressed protein-tyrosine phosphatase PTP1C on mitogen-activated signaling in 293 cells. J Biol Chem 271:10385–10390
15. You M, Zhao Z (1997) Positive effects of SH2 domain-containing tyrosine phosphatase SHP-1 on epidermal growth factor- and interferon-gamma-stimulated activation of STAT transcription factors in HeLa cells. J Biol Chem 272:23376–23381
16. Geissmann F, Lepelletier Y, Fraitag S et al (2001) Differentiation of Langerhans cells in Langerhans cell histiocytosis. Blood 97:1241–1248
17. Fukunaga A, Nagai H, Noguchi T et al (2004) Src homology 2 domain-containing protein tyrosine phosphatase substrate 1 regulates the migration of Langerhans cells from the epidermis to draining lymph nodes. J Immunol 172:4091–4099
18. Lehr HA, Mankoff DA, Corwin D, Santeusanio G, Gown AM (1997) Application of Photoshop-based image analysis to quantification of hormone receptor expression in breast cancer. J Histochem Cytochem 45:1559–1565
19. Pham NA, Morrison A, Schwock J et al (2007) Quantitative image analysis of immunohistochemical stains using a CMYK color model. Diagn Pathol. doi:10.1186/1746-1596-2-8
20. Emile JF, Wechsler J, Brousse N et al (1995) Langerhans' cell histiocytosis. Definitive diagnosis with the use of monoclonal antibody O10 on routinely paraffin-embedded samples. Am J Surg Pathol 19:636–641
21. Ramachandran IR, Song W, Lapteva N et al (2011) The phosphatase SRC homology region 2 domain-containing phosphatase-1 is an intrinsic central regulator of dendritic cell function. J Immunol 186:3934–3945
22. Yu RC, Abrams DC, Alaibac M, Chu AC (1994) Morphological and quantitative analyses of normal epidermal Langerhans cells using confocal scanning laser microscopy. Br J Dermatol 131:843–848
23. Jaffe R (2005) The diagnostic histopathology of Langerhans cell histiocytosis. In: Weitzman S, Egeler M (eds) Histiocytic disorders of children and adults. Cambridge University Press, Cambridge, pp 14–39
24. Jaffe R, Weiss LM, Facchetti F (2008) Tumours derived from Langerhans cells. In: Swerdlow SH, Campo E, Harris NL et al (eds) WHO classification of tumors of haematopoietic and lymphoid tissues, 4th edn. IARC, Lyon, pp 358–360
25. Bank MI, Rengtved P, Carstensen H, Petersen BL (2003) Langerhans cell histiocytosis: an evaluation of histopathological parameters, demonstration of proliferation by Ki-67 and mitotic bodies. APMIS 111:300–308
26. Shamoto M, Osada A, Shinzato M, Kaneko C, Shimizu M (1995) A comparative study on Langerhans cells in lymph nodes with dermatopathic lymphadenopathy and histiocytosis X cells. Adv Exp Med Biol 378:139–141
27. Shultz LD, Schweitzer PA, Rajan TV et al (1993) Mutations at the murine motheaten locus are within the hematopoietic cell protein-tyrosine phosphatase (Hcph) gene. Cell 73:1445–1454
28. Nakayama K, Takahashi K, Shultz LD, Miyakawa K, Tomita K (1997) Abnormal development and differentiation of macrophages and dendritic cells in viable motheaten mutant mice deficient in haematopoietic cell phosphatase. Int J Exp Pathol 78:245–257
29. Sprecher E, Becker Y, Kraal G, Hall E, Shultz LD (1990) Effect of genetically determined immunodeficiency on epidermal dendritic cell populations in C57BL/6 J mice. Arch Dermatol Res 282:188–193
30. Wellbrock C, Karasarides M, Marais R (2004) The RAF proteins take centre stage. Nat Rev Mol Cell Biol 5:875–885
31. Lahlou H, Saint-Laurent N, Estève JP et al (2003) sst2 Somatostatin receptor inhibits cell proliferation through Ras-, Rap1-, and B-Raf-dependent ERK2 activation. J Biol Chem 278:39356–39371
32. Reth M, Brummer T (2004) Feedback regulation of lymphocyte signalling. Nat Rev Immunol 4:269–277

Virchows Arch (2011) 459:235–238
DOI 10.1007/s00428-011-1108-8

CASE REPORT

Mediastinal fetal rhabdomyoma in nevoid basal cell carcinoma syndrome: a case report and review of the literature

Shaomin Yang · Chuan Zhao · Yan Zhang · Songlin Liao

Received: 17 March 2011 / Revised: 9 June 2011 / Accepted: 13 June 2011 / Published online: 28 June 2011
© Springer-Verlag 2011

Introduction

Fetal rhabdomyoma (FR) usually occurs in the soft tissue or mucosa in the head and neck region of young children. These tumors are divided into classic (myxoid) and intermediate (cellular, juvenile) subtypes. The intermediate subtype was first described by Di Sant'Agnese and Knowles in 1980 [1]. This tumor is much less frequently encountered than the classic subtype and has never been reported in the mediastinum. Nevoid basal cell carcinoma syndrome (NBS) is an autosomal dominant disorder characterized by the premature appearance of basal cell carcinoma, keratocysts of the jaw, abnormalities in the skeletal, ocular, and nervous systems, and various other types of neoplasms [2]. Here, we present the first report of a patient with intermediate FR located in the posterior mediastinum and associated NBS.

Case presentation

Clinical history

This 17-year-old male was admitted to a hospital with multiple bilateral cysts of the jaw. He also showed polydactylia of his hands. Prior to the surgical excision of these jaw cysts, a routine chest radiograph showed a mass in the left posterior–inferior mediastinum and a bifid deformity of the fourth rib. Physical examination was otherwise noncontributory, and the patient had no other past medical problems. Pathological examination showed that the cysts of the jaw were keratocysts. No other family member had keratocysts or other findings like those of this patient.

Computed tomography confirmed the presence of a 9×5×5-cm mass with a focal contrast enhancement in the lower posterior mediastinum. Upper gastroenterography showed that the lower part of the esophagus was dislocated with no sign of mucous destruction or evidence of tumor invasion.

Operative findings

Operative excision of the mediastinal mass was carried out 6 months after the removal of the patient's jaw cysts. The mass was located in the lower posterior mediastinum and was adherent to the lower lobe of the left lung. One side of the mass was also closely associated with the esophagus and one aspect of the tumor was peeled from the muscle layer of the esophagus, but the esophageal mucosa was not affected. The mass was completely excised.

Material and methods

The resected tumor was fixed in buffered formalin and routinely embedded for histological evaluation. Immunohistochemical stains were performed on 4-μm paraffin sections, using primary antibodies against smooth muscle actin (SMA), desmin, myoglobin, HHF35, CD117, CD34, S-100, Ki-67, and keratin (AE1/AE3). All antibodies were purchased from DakoCytomation. After incubation with primary antibody,

S. Yang (✉) · Y. Zhang · S. Liao
Department of Pathology,
Peking University Health Science Center,
Beijing 100191, China
e-mail: yangshaomin@bjmu.edu.cn

C. Zhao
Department of Pathology,
The First Affiliated Hospital of Kunming Medical College,
Kunming, Yunnan 650032, China

sections were treated with polymer HRP-conjugated secondary antibodies (DakoCytomation, Inc.) and colorized with diaminobenzidene–hydrogen peroxide substrate (DakoCytomation, Inc). The nuclei were lightly counterstained with hematoxylin.

Results

Pathologic findings

The mass was nodular and measured 9×8.5×5 cm. Its cut surface was gray white and predominantly solid with a whorled pattern and focal hemorrhagic cystic areas. Histologically, the tumor was well encapsulated by a thick fibrous capsule. Although adhesion of this capsule to the adjacent lung and esophagus was observed, there was no evidence of invasion into the normal tissues (Fig. 1). The mass was composed primarily of spindle cells arranged in compact bundles and fascicles, with moderate cytoplasm, oval or spindle vesicular nuclei, and small nucleoli. Scattered among the spindle cells were large cells showing rhabdomyoblastic features, with abundant bright eosinophilic cytoplasm and shape varying from round to oval, polygonal, or band shape (Fig. 2). Intracytoplasmic cross striations were found in some rhabdomyoblastic cells under high magnification (Fig. 3). The myxoid matrix was sparse. No mitotic figures, nuclear pleomorphism, or necrosis was seen.

Immunohistochemical staining for HHF35 was diffused and strongly positive in almost all cells (Fig. 4a). Smooth muscle actin was expressed in the spindle cells (Fig. 4b). Desmin and myoglobin were positive in rhabdomyoblasts (Fig. 4c, d). Stains for myogenin, AE1/AE3, S-100, CD117, and CD34 were negative. Ki-67 staining showed no significant proliferating cell population.

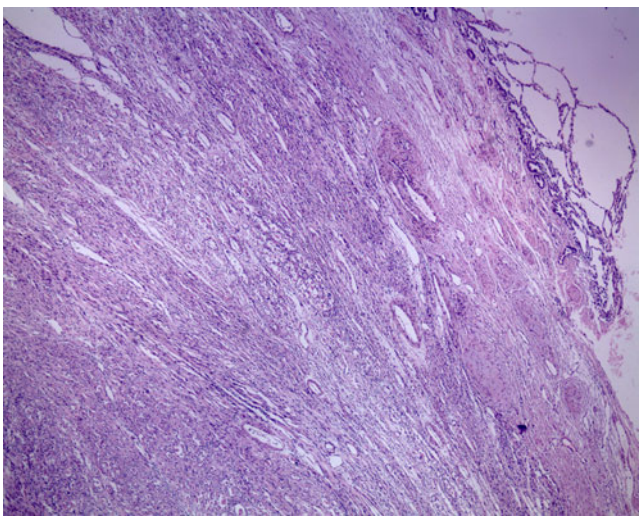

Fig. 1 The tumor was well circumscribed. One side of the tumor was adherent to but did not invade into lung tissue. H&E ×40

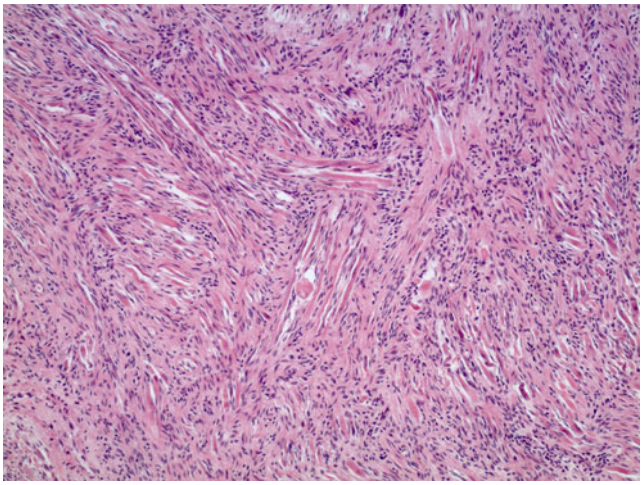

Fig. 2 The tumor was composed chiefly of spindle cells, arranged in a compact fascicular pattern. There were large cells with skeletal muscle differentiation scattered among these spindle cells. H&E ×100

Follow-up

The patient was followed up with no further treatment. Over a 24-month period of follow-up to the present, he remains asymptomatic, with no evidence of recurrence or progression.

Discussion

Extracardiac rhabdomyomas are uncommon benign neoplasms with striated muscle differentiation. Based on histology and location, they can be divided into three groups: fetal, adult, and genital. FR most commonly (70–90%) occurs in the head and neck region in the vicinity of the upper aerodigestive tract. A few cases have also been identified in other anatomic sites, such as the lower extremity [3], abdominal wall [4], mediastinum [5–7],

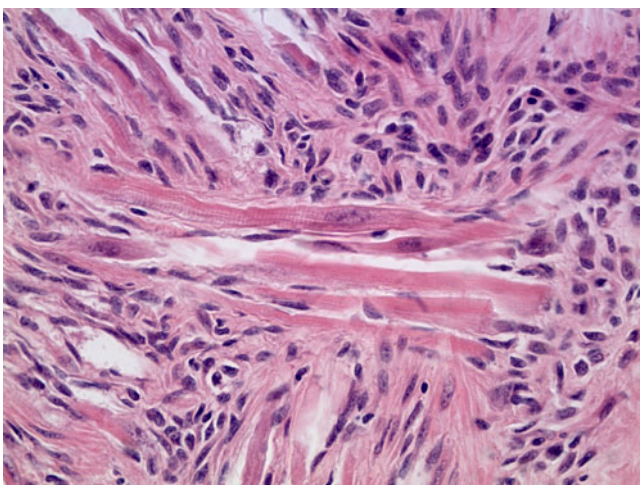

Fig. 3 Rhabdomyoblastic differentiation was confirmed by the presence of cross striations. H&E ×400

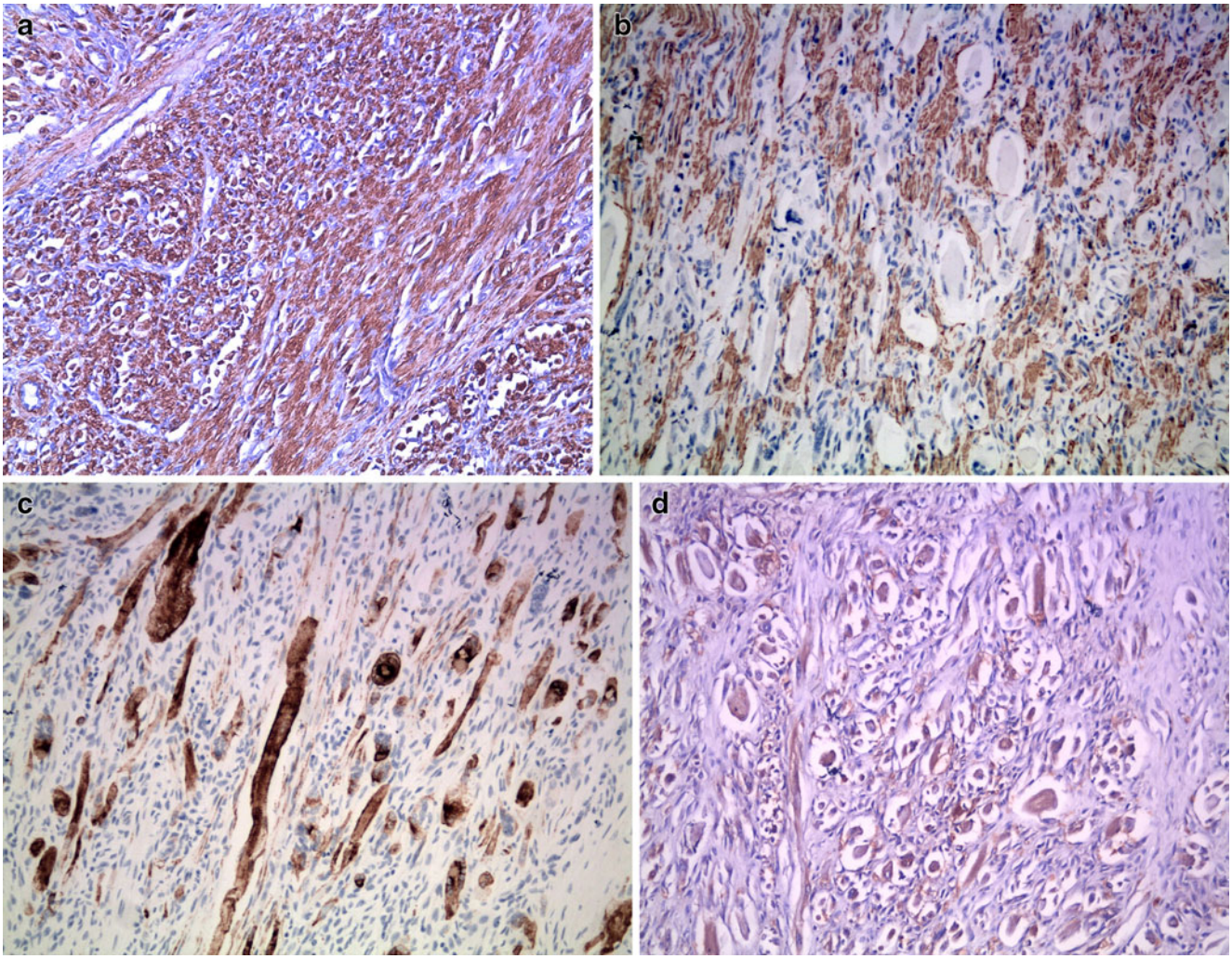

Fig. 4 Immunohistochemical results on tumor cells. H&E ×200. **a** Strong HHF35 staining was found in both spindle cells and differentiating skeletal muscle cells. **b** SMA expression in spindle cells. **c** Desmin expression in differentiating skeletal muscle cells. **d** Myoglobin expression in differentiating skeletal muscle cells

retroperitoneum [5], and so on. Histologically, FR can be further divided into classic (myoxid) and intermediate (cellular, juvenile) subtypes. The classic FR is composed of abundant myxoid stroma, primitive "undifferentiated" mesenchymal cells, and immature striated cells, which are similar to the 6~10-week stage of muscle development. The intermediate FR was first described in 1980 [1] as the "cellular" type and showed a high degree of cellularity, predominance of spindle cells, and more advanced and extensive skeletal muscle maturation than fetal rhabdomyoma. This subtype was therefore also referred to as the "juvenile" type [8]. Myxoid matrix is scare or absent in this subtype, and intermediate FR is therefore more likely to be misinterpreted as some other type of benign or malignant spindled cell tumor especially when arising in deep locations.

Based on the morphology, the case we present here is consistent with intermediate FR, but the occurrence of this tumor in the posterior mediastinum is unusual. This is the first reported case of intermediate type FR presenting in the mediastinum, although classic FRs [5] in the posterior mediastinum and adult rhabdomyomas in both the anterior and posterior mediastinum [6, 7] have been reported.

It is of great importance to correctly diagnose intermediate FR particularly in deep locations such as this tumor to avoid misinterpretation as a malignancy, especially rhabdomyosarcoma. The lack of nuclear dysplasia, mitoses, and necrosis and the noninfiltrative growth pattern are the key features in the diagnosis of benign rhabdomyoma. In addition, benign and malignant Triton tumors also must be excluded. Triton tumors show both neural and skeletal muscle differentiation. There was no S-100 positivity in the present tumor, excluding a diagnosis of Triton tumor.

The immunophenotypes reported for intermediate FR are not consistent in the literature. Chennagiri showed desmin

+/SMA− expression in their cases [3]. In our case, the spindle cells expressed SMA, and the cells showing features of developing skeletal muscle expressed desmin, raising the possibility that these tumor cells represent a spectrum of muscle cell differentiation.

Although there was no family history of NBS in the current case, the multiple keratocysts in the jaw, deformity of the rib, and polydactyly clearly demonstrate that this is an NBS patient. NBS showed autosomal dominant inheritance and was initially described in 1960 by Gorlin and Goltz [2]. The classic features they described included basal cell carcinoma, odontogenic keratocysts, and bifid ribs. Since that time, various deformities and neoplasms have been recognized as associated with this syndrome. Together with the current case presented here, there have been seven reported cases of FR in NBS patients, and all have been FR of either classic or intermediate type. However, to date, no adult rhabdomyoma or rhabdomyosarcoma has been found in association with NBS [5, 9–14]. This suggests that when a tumor with definitive evidence of skeletal muscle differentiation appears in NBS, it is likely to be a benign FR. Secondly, in FRs occurring in the context of NBS, only two of the seven have been located in the head and neck region [9, 14], which is notably different from FR without NBS.

In summary, the present case underscores the importance of making the correct histological diagnosis for this rare lesion, particularly when it is found in deeper locations. Failure to recognize this tumor may lead to unnecessarily aggressive treatment. The complete removal of the mass seems to be an effective and adequate treatment for this tumor.

Acknowledgment We gratefully acknowledge the assistance of Dr. Michael A. McNutt in editing this manuscript.

Conflict of interest The authors declare that they have no potential conflicts of interest which would warrant disclosure.

References

1. Di Sant'Agnese PA, Knowles DN (1980) Extracardiac rhabdomyoma: a clinicopathologic study and review of the literature. Cancer 46:780–789
2. Gorlin RJ, Goltz RW (1960) Multiple nevoid basal-cell epithelioma, jaw cysts and bifid rib. A syndrome. N Engl J Med 262:908–912
3. Premalata CS, Kumar RV, Saleem KM, Fathima LJ, Das K (2009) Fetal rhabdomyoma of the lower extremity. Pediatr Blood Cancer 52:881–883
4. Konrad EA, Meister P, Hubner G (1982) Extracardiac rhabdomyoma: report of different types with light microscopic and ultrastructural studies. Cancer 49:898–907
5. DiSanto S, Abt AB, Boal DK, Krummel TM (1992) Fetal rhabdomyoma and nevoid basal cell carcinoma syndrome. Pediatr Pathol 12:441–447
6. Miller R, Kurtz SM, Powers JM (1978) Mediastinal rhabdomyoma. Cancer 42:1983–1988
7. Kuschill-Dziurda J, Mastalerz L, Grzanka P, Nizankowska-Mogilnicka E (2009) Rhabdomyoma as a tumor of the posterior mediastinum. Pol Arch Med Wewn 119:599–602
8. Kapadia SB, Meis JM, Frisman DM, Ellis GL, Heffner DK (1993) Fetal rhabdomyoma of the head and neck: a clinicopathologic and immunophenotypic study of 24 cases. Hum Pathol 24:754–765
9. Watson J, Depasquale K, Ghaderi M, Zwillenberg S (2004) Nevoid basal cell carcinoma syndrome and fetal rhabdomyoma: a case study. Ear Nose Throat J 83:716–718
10. Shanley S, Ratcliffe J, Hockey A, Haan E, Oley C, Ravine D, Martin N, Wicking C, Chenevix-Trench G (1994) Nevoid basal cell carcinoma syndrome: review of 118 affected individuals. Am J Med Genet 50:282–290
11. Hardisson D, Jimenez-Heffernan JA, Nistal M, Picazo ML, Tovar JA, Contreras F (1996) Neural variant of fetal rhabdomyoma and naevoid basal cell carcinoma syndrome. Histopathology 29:247–252
12. Schweisguth O, Gerard-Marchant R, Lemerle J (1968) Basal cell nevus syndrome. Association with congenital rhabdomyosarcoma. Arch Fr Pediatr 25:1083–1093
13. Dahl I, Angervall L, Save-Soderbergh J (1976) Foetal rhabdomyoma. Case report of a patient with two tumours. Acta Pathol Microbiol Scand A 84:107–112
14. Klijanienko J, Caillaud JM, Micheau C, Flamant F, Schwaab G, Avril MF, Ponzio-Prion A (1988) Basal-cell nevomatosis associated with multifocal fetal rhabdomyoma. A case. Presse Med 17:2247–2250

Virchows Arch (2011) 459:239–243
DOI 10.1007/s00428-011-1109-7

CASE REPORT

Primary malignant tumour of the lung with neuroendocrine and melanoma differentiation

Emanuela Pilozzi · Claudio Cacchi · Arianna Di Napoli · Benedetto Pini · Enrico Duranti · Antonio D'Andrilli · Luigi Ruco

Received: 12 April 2011 / Revised: 6 June 2011 / Accepted: 13 June 2011 / Published online: 7 July 2011
© Springer-Verlag 2011

Introduction

Melanocytic differentiation has been described in rare cases of melanin-containing neuroendocrine tumours of the lung [1–5], thyroid [6] and thymus [7]. In some of the cases, neuroendocrine granules and melanosomes were lying free in the cytoplasm of tumour cells, thus indicating true co-expression of melanocytic and neuroendocrine differentiation. On the other hand, neuroendocrine differentiation, consisting in the presence of neuroendocrine granules at ultrastructural level and of intense immunostaining for chromogranin-A and synaptophysin, was described in three cases of cutaneous and mucosal malignant melanomas [8]. Divergent differentiation towards unrelated embryological tissue has been reported in malignant melanoma [9]. So far, cases of neuroendocrine carcinoma with associated melanomatous component in the lung have not been described. There is growing evidence that tumour development may derive from neoplastic transformation of adult stem cells [10]. In a recent publication, it was reported that in the human skin there is a SOX2-positive stem cell capable of differentiation along the neuroendocrine or melanocytic lines [11]. In the present report, we describe the first case of a malignant neoplasm of the lung showing unambiguous differentiation towards neuroendocrine carcinoma and malignant melanoma.

E. Pilozzi (✉) · C. Cacchi · A. Di Napoli · B. Pini · E. Duranti · L. Ruco
Department of Clinical and Molecular Medicine, Ospedale Sant'Andrea, Università di Roma "La Sapienza",
Via di Grottarossa 1035-1039,
00189 Rome, Italy
e-mail: emanuela.pilozzi@uniroma1.it

A. D'Andrilli
Thoracic Surgery Unit, Ospedale Sant'Andrea,
Università di Roma "La Sapienza",
Rome, Italy

Clinical history

An asymptomatic 62-year-old woman was referred to thoracic surgery for the presence of a central nodule in the lower lobe of the left lung, incidentally discovered. Its aspect in CT scan was consistent with a diagnosis of carcinoid (Fig. 1a). The lesion was excised with an intervention of wedge resection. The patient received no further treatment and is alive and well with no evidence of malignant tumour 1 year after the intervention.

Materials and methods

Immunohistochemistry

Tissue specimens were formalin-fixed and paraffin-embedded. Tissue sections were immunostained with monoclonal antibodies against S-100 protein (1:300, Biocare Medical), HMB45 (1:50, Dako), cytokeratin AE1/AE3 (1:50, Dako), CD56 (NCAM) (1:200, NeoMarkers), TTF-1 (1:100, Biocare Medical), chromogranin-A (1:200, Dako), synaptophysin (1:20, Dako), MART-1 (1:50, Dako), SOX2 (1:50, Spring Bioscience) and muscle-specific actin (1:200, Dako). The histochemical reaction of Masson–Fontana for melanin was performed (Bio-Optica, Milan, Italy).

For double staining, sections were treated with biotin block after the development of the first reaction (Dako biotin blocking system, Dakopatts, Denmark). The sections were then incubated with an optimal dilution of the second primary antibody for 1 h. The reaction product was

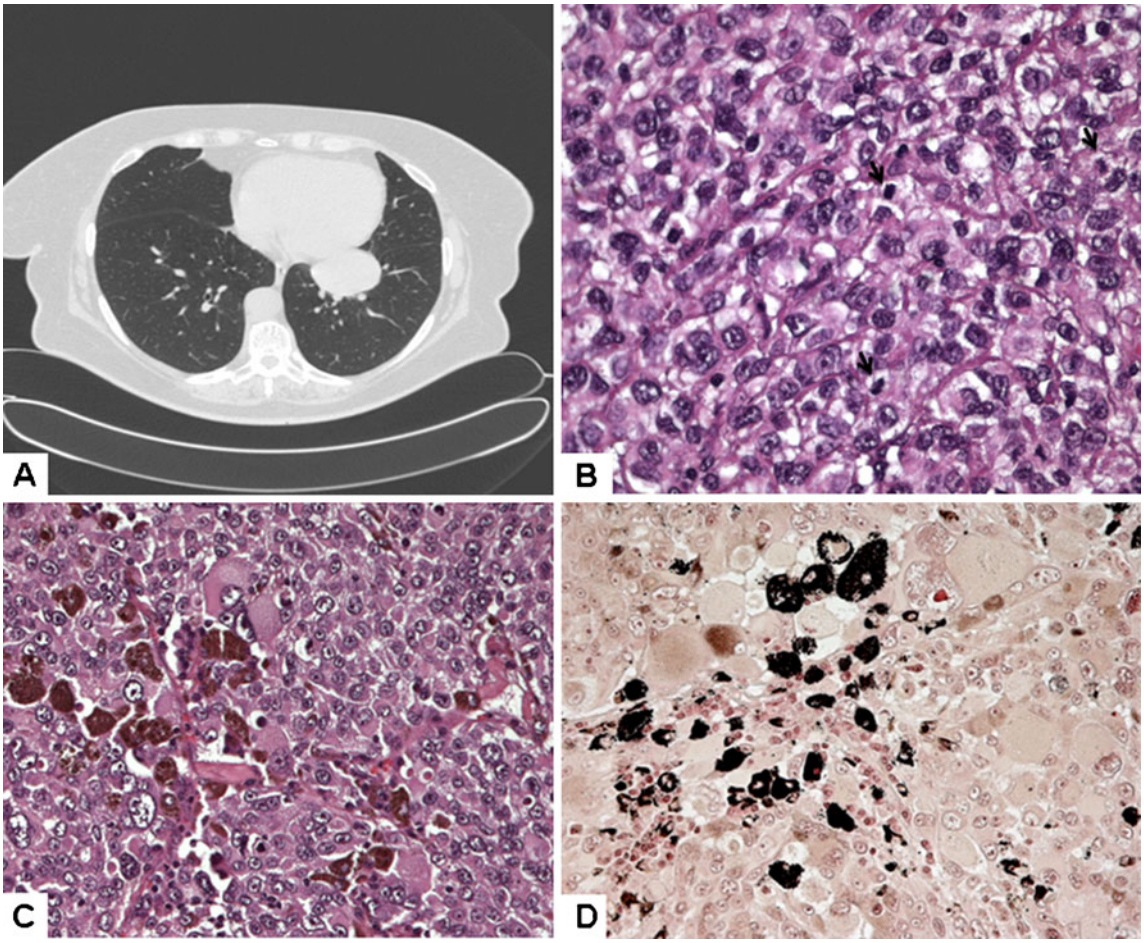

Fig. 1 **a** CT scan showing a well-defined parenchymal nodule. **b** Histology of the large neuroendocrine carcinoma component. *Arrows* indicate mitosis (H & E, ×400). **c** Histology of the melanoma component with melanin pigmentation (H & E, ×200). **d** Masson–Fontana positive staining (*black*) in melanoma cells (×200)

developed using anti-mouse anti-rabbit biotinylated immunoglobulins followed by streptavidin–alkaline phosphatase complex (Dako LSAB2 system alkaline phosphatase, Dakopatts, Denmark). Each incubation step lasted 10 min with multiple 5-min washes between each step. The sections were finally incubated with Fast-Red Substrate System for 20 min (Dako, Dakopatts, Denmark).

PCR amplification and direct sequencing of BRAF and C-KIT

Mutations of BRAF and C-KIT were investigated in the lung neoplasm. DNA was extracted from five sections 7 μm thick of a paraffin block in which the melanomatous part was largely represented. DNA was amplified for the segment of BRAF gene containing codon 600 and for exons 9 and 11 of the C-KIT gene. PCR products were directly sequenced using the FS Ready Reaction Dye Terminator Sequencing Kit, according to the instructions of the manufacturer, and analysed on an automated sequencer (ABI 3100, Applied Biosystems, Foster City, CA, USA).

Results

The gross appearance of the lesion was that of a 5×4×2.5 intraparenchymal tumour with well-defined margins, greyish colour and focal necrosis. Histologically, the tumour was made of two intimately admixed neoplastic components which were reminiscent of a large cell neuroendocrine carcinoma and of a malignant melanoma (Fig. 1b–d). The neuroendocrine component showed mainly a solid pattern of growth and was made of large cells with a small central nucleolus and with a mitotic rate of 70/10 HPF in the areas of highest mitotic density; tumour cells were positive for TTF-1, chromogranin-A, synaptophysin and CD56 (NCAM); showed focal reactivity for S-100 protein (10–20%) and cytokeratin (10% dot-like); and were negative for HMB45 and MART-1 (Fig. 2a–c). The melanoma compo-

nent was made of large, polymorphic cells, with a prominent nucleolus and with a brown pigmentation consistent with melanin that stains black with Masson–Fontana (Fig. 1d). The tumour cells were positive for HMB45, MART-1 and S-100 protein and were negative for TTF-1, synaptophysin, CD56 (NCAM) and cytokeratin (Fig. 2d); mitotic activity was 30/10 HPF. Double immunostaining for TTF-1 and HMB45 highlighted the presence of an intimate admixture of TTF-1+ neuroendocrine cells and of HMB45+ melanoma-like cells, but failed to show double immunostained cells (Fig. 3). Immunostaining for SOX2, a transcription factor expressed by stem cell capable of differentiation along neuroendocrine or melanocytic lines, was negative. DNA analysis did not show BRAF and C-KIT mutations.

The possibility of a tumour-to-tumour metastasis (i.e. melanoma metastasis to pulmonary neuroendocrine carcinoma) was ruled out by the clinical history of the patient who had no previous diagnosis of malignant tumour, nor she reported to have received previous interventions for excision of cutaneous or mucosal lesions; furthermore, post-intervention physical examination failed to show any cutaneous or mucosal lesion suspicious for malignant melanoma.

Discussion

We describe here a case of a malignant neoplasm of the lung with dual divergent differentiation towards neuroendocrine carcinoma and malignant melanoma. The neuroendocrine component of the lung tumour was unequivocal and was indicative of a diagnosis of large cell neuroendocrine carcinoma. In fact, tumour cells were TTF-1+, large, nucleolated, with little nuclear atypia and with high mitotic activity; neuroendocrine differentiation was supported by paranuclear dots of cytokeratin and by the expression of neuroendocrine markers, synaptophysin, chromogranin-A and CD56 (NCAM). The melanocytic component was also unequivocal; tumour cells exhibited an epithelioid morphology, were often atypical, contained melanin and were immunostained for S-100 protein, MART-1 and HMB45.

It seems reasonable to postulate that our case is related to previous descriptions of melanin pigmentation in rare cases

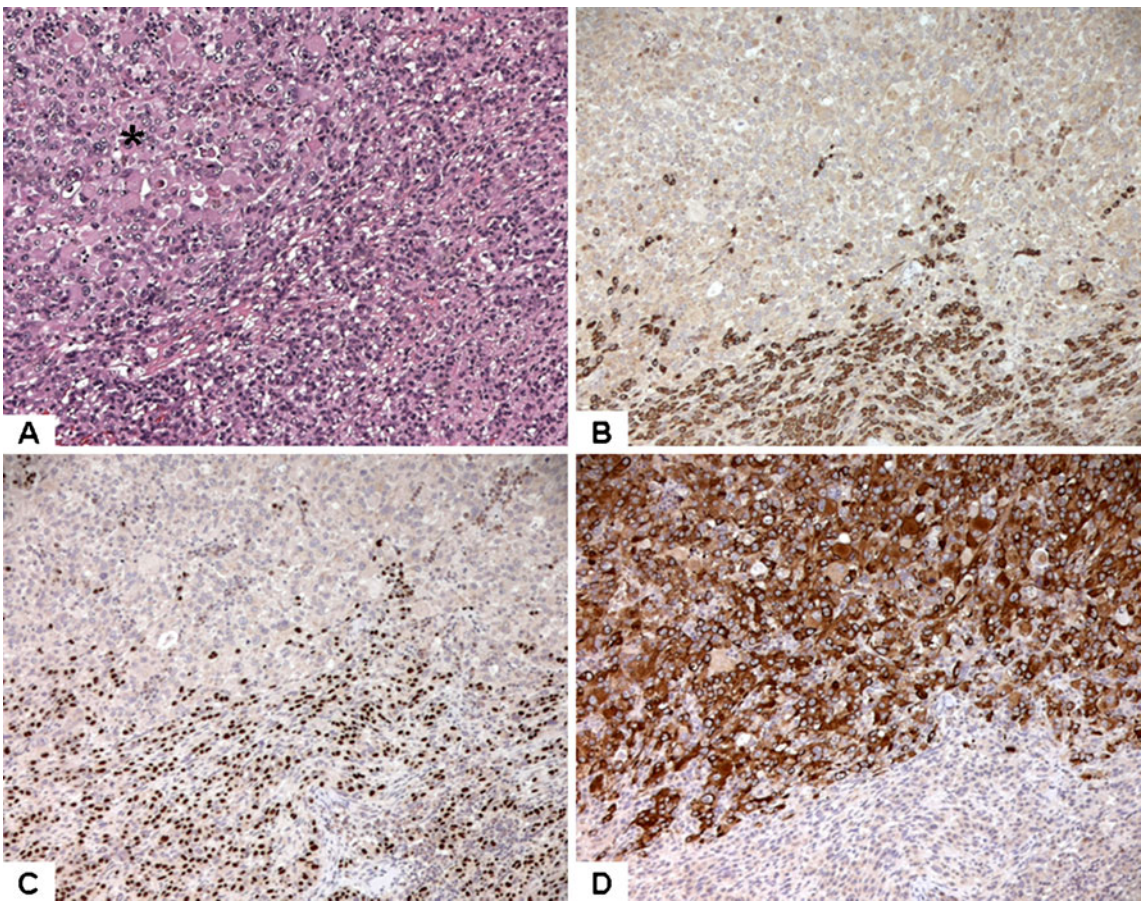

Fig. 2 **a** Neuroendocrine (*bottom*) and melanoma (*upper*) components were intimately admixed (H & E, ×100). Neuroendocrine tumour cells stain intensively for chromogranin-A (**b**) and TTF-1 (**c**) (ABC peroxidase counterstained with hematoxylin, ×100). **d** Melanoma cells stain intensively for HMB45 (ABC peroxidase counterstained with hematoxylin, ×100)

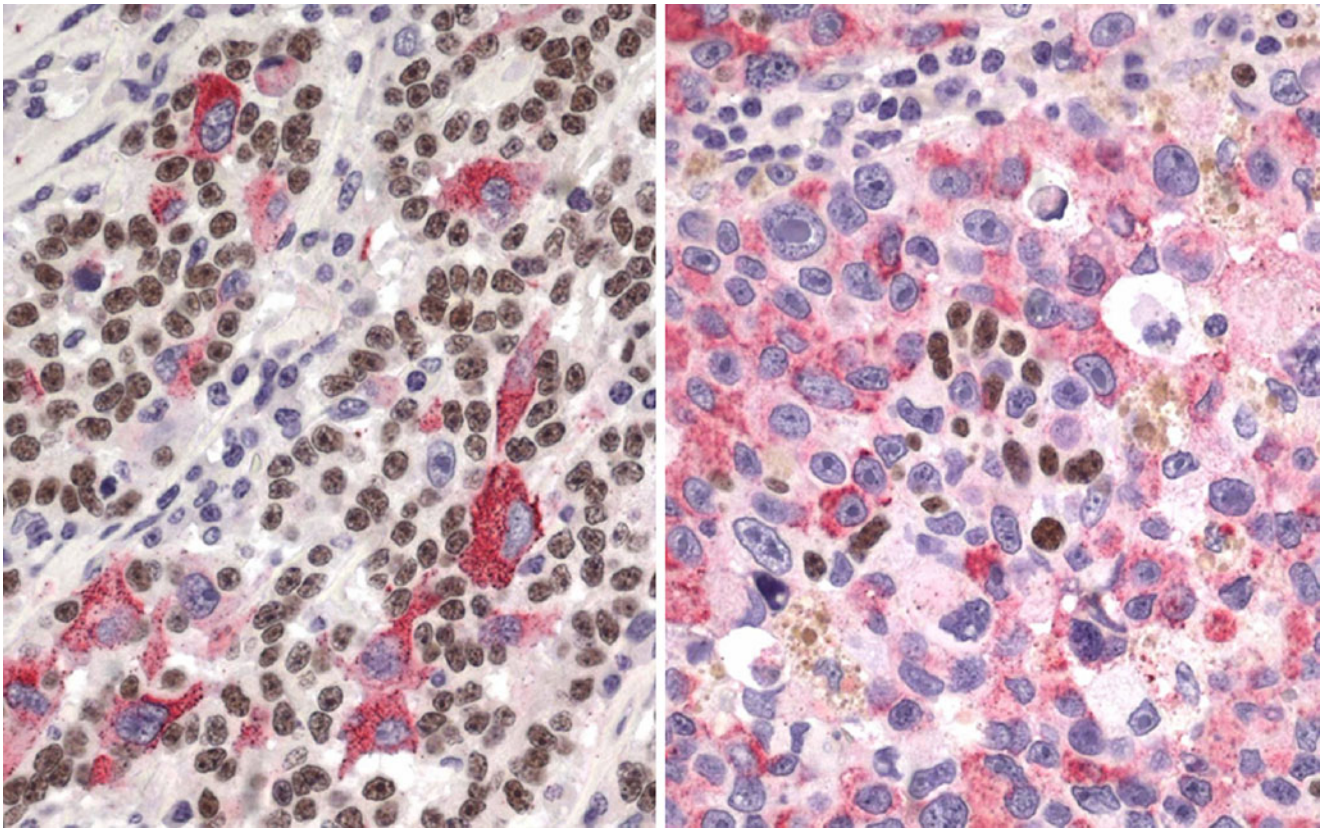

Fig. 3 Double immunostaining for TTF-1 and HMB45. TTF-1+ neuroendocrine cells and HMB45+ melanoma cells were intimately admixed. In some areas (*left panel*), few HMB45+ cells with melanoma morphology were surrounded by numerous TTF-1+ neuroendocrine cells; in other areas (*right panel*), nests of TTF-1 neuroendocrine cells were surrounded by numerous HMB45+ melanoma cells. No double stained cell was observed (ABC peroxidase TTF-1 (*brown*) and alkaline phosphatase HMB45 (*red*) counterstained with hematoxylin, ×200)

of typical and atypical carcinoids of the lung [1–5]; in one of these studies, electron microscopy revealed that pigmented tumour cells contained both neurosecretory granules and melanosomes, thus indicating a true melanocytic–neuroendocrine differentiation [3].

The cell of origin of this tumour is a matter of speculation. Although neuroendocrine and melanocytic cells have different embryological origin, it may be possible that a neoplasm with both aspects may derive from a single precursor irrespective of the different embryological origin. In fact, bronchopulmonary neuroendocrine tumours were derived from the pulmonary neuroendocrine cell system which is generally accepted to be of endodermal origin [12, 13], whereas normal melanocytes derived from the neural crest cells are supposed to be of ectodermal origin [14]. This apparent discrepancy might be overcome by the recent description of a SOX2-positive embryonic stem cell in the human skin, which is capable of divergent differentiation towards neuroendocrine and melanocytic cells [11]. Neoplastic transformation of this stem cell might be responsible for the few cases of malignant melanoma with neuroendocrine differentiation described in the skin [8]. Furthermore, a similar stem cell might be present in the epithelium of other organs, perhaps bronchus, where it might be responsible for the development of mixed tumours with divergent melanocytic and neuroendocrine differentiation; unfortunately, we have not been able to demonstrate SOX2 expression in tumour cells of our case using immunohistochemistry.

Another possibility to be taken into consideration is that our case might be related to a recently described case of clear-cell sugar tumour of the lung with melanin pigmentation [15]. In our case, however, the neoplastic melanoma cells showed HMB45 and MART-1 positivity indicating a true melanoma differentiation; moreover, neoplastic cells were not stained for muscle-specific actin.

It is known that a neoplasm may metastasize to another neoplasm. This infrequent case is defined as tumour-to-tumour metastasis [16]. Very few cases of malignant melanoma metastatic to other neoplasms (meningioma, renal cell carcinoma and neurocytoma) have been reported [17]. In our case, this possibility seemed very unlikely since

the patient had no previous diagnosis of malignant melanoma, and 1 year after this intervention, she had no evidence of any other malignancy. Moreover, double staining showed that endocrine and melanoma cells were intimately admixed rather than sharply separated.

KIT and BRAF mutations have been described in about 40% and 3% of mucosal melanomas, respectively, suggesting a different molecular pathogenesis for these tumours [18, 19]. In this regard, our findings were not informative since it showed a wild-type sequence of the two genes in both tumour components.

Finally, the histogenesis of primary malignant melanomas of the lung remains a controversial issue [20]. Melanocytes are not present in the epithelium of the normal bronchus. Thus, to provide a possible explanation for the origin of these tumours, it was suggested that they were derived from the malignant transformation of abnormally migrated melanoblasts. So far, there is no evidence supporting this hypothesis and the possibility of a stem cell origin capable of melanocytic differentiation opens a new scenario for understanding the histogenesis of these tumours.

Acknowledgement This work was supported by a grant from "Fondazione Eleonora Lorillard Spencer Cenci".

Conflict of interest statement We declare that we do not have conflict of interest.

References

1. Barbareschi M, Frigo B, Mosca L et al (1990) Bronchial carcinoids with S-100 positive sustentacular cells. A comparative study with gastrointestinal carcinoids, pheochromocytomas and paragangliomas. Pathol Res Pract 186:212–222
2. Cebelin MS (1980) Melanocytic bronchial carcinoid tumour. Cancer 46:1843–1848
3. Gal AA, Koss MN, Hochholzer L et al (1993) Pigmented pulmonary carcinoid tumour. An immunohistochemical and ultrastructural study. Arch Pathol Lab Med 117:832–836
4. Goel A, Addis BJ (2007) Pigmented atypical carcinoid of the lung. Histopathology 51:263–265
5. Iihara K, Yamaguchi K, Fujioka Y et al (1994) Pigmented neuroendocrine tumor of the lung, showing neuromelanin. Pathol Int 44:309–316
6. Marcus JN, Dise CA, LiVolsi VA (1982) Melanin production in a medullary thyroid carcinoma. Cancer 49:2518–2526
7. Klemm KM, Moran CA, Suster S (1999) Pigmented thymic carcinoids: a clinicopathological and immunohistochemical study of two cases. Mod Pathol 12:946–948
8. Eyden B, Pandit D, Banerjee SS (2005) Malignant melanoma with neuroendocrine differentiation: clinical, histological, immunohistochemical and ultrastructural features. Histopathology 47:402–409
9. Banerjee SS, Eyden B (2008) Divergent differentiation in malignant melanomas: a review. Histopathology 52:119–129
10. Eramo A, Lotti F, Sette G et al (2008) Identification and expansion of the tumorigenic lung cancer stem cell population. Cell Death Differ 15:504–514
11. Laga AC, Lai CY, Zhan Q et al (2010) Expression of the embryonic stem cell transcription factor SOX2 in human skin: relevance to melanocyte and merkel cell biology. Am J Pathol 176:903–913
12. Gustaffson BI, Kidd M, Chan A et al (2008) Bronchopulmonary neuroendocrine tumors. Cancer 133:5–21
13. Ito T, Nogawa H, Udaka N et al (1997) Developmental of pulmonary neuroendocrine cells of fetal hamster in explant culture. Lab Investig 77:449–457
14. Le Douarin NM, Calloni G, Dupin E (2008) The stem cells of neural crest. Cell Cycle 7:1013–1019
15. Yan B, Yau EX, Petersson F (2011) Clear cell "sugar" tumour of the lung with malignant histological features and melanin pigmentation—the first reported case. Histopathology 58:477–500
16. Petraki C, Vaslamatzis M, Argyrakos T (2003) Tumor to tumor metastasis: report of two cases and review of the literature. Int J Surg Pathol 11:127–135
17. Brown HM, McCutcheon IE, Leeds NE (2003) Melanoma metastatic to central neurocytoma: a novel case of tumor-to-tumor metastasis. J Neuro Oncol 61:209–214
18. Curtin JA, Fridlyand J, Kageshita T (2005) Distinct sets of genetic alterations in melanoma. N Engl J Med 353:2135–2147
19. Curtin JA, Busam K, Pinkel D (2006) Somatic activation of KIT in distinctive subtypes of melanoma. J Clin Oncol 24:4340–4346
20. Wilson RW, Moran C (1997) Primary melanoma of the lung: a clinicopathologic and immunohistochemical study of eight cases. Am J Surg Pathol 21:1196–1202

Virchows Arch (2011) 459:245–246
DOI 10.1007/s00428-011-1068-z

LETTER TO THE EDITOR

Localized giant inflammatory polyp of the colon in a patient without inflammatory bowel disease

Eva-Maria Wolf · Christa Strasser · Karel Geboes · Ekkehard Spuller · Michael Vieth · Cord Langner

Received: 24 February 2011 / Accepted: 3 March 2011 / Published online: 12 April 2011
© Springer-Verlag 2011

Dear Editor,

Gastrointestinal polyps are classified as neoplastic polyps, such as adenoma or polypoid adenocarcinoma, and non-neoplastic polyps of which inflammatory polyps may be regarded as a distinct entity [1]. Within the colon, inflammatory polyps have mainly been described to occur against a background of inflammatory bowel disease (IBD). Rarely, these lesions lead to stenosis, thereby mimicking a malignant tumor [2, 3]. But inflammatory polyps may also be observed in patients without history of IBD [4].

An asymptomatic 45-year-old male underwent routine colonoscopy because of a family history of colorectal cancer. There was no history of IBD. During colonoscopy, an irregular polypoid mass was detected at the hepatic flexure. Repeated biopsies showed chronic inflammation without evidence of malignancy. Prompted by the patient's positive family history and the suspicious endoscopic appearance of the lesion, a right-sided hemicolectomy was performed.

On gross inspection, an irregular villous polyp, measuring 4 cm in largest diameter was found. The lesion showed circumferential growth and extended with small polyps of gradually decreasing size into the neighboring normal mucosa (Fig. 1a).

Histological examination revealed irregular villous-like projections of the mucosa (Fig. 1b). The crypt architecture was markedly distorted, and the lamina propria contained a dense mixed inflammatory infiltrate. Crypt abscesses as well as hyperplastic lymphoid follicles were frequently observed, while epithelial dysplasia was lacking (Fig. 1c). One slide showed a circumscribed superficial ulcer which was bordered by unspecific granulation tissue. The non-polypoid mucosa of the resection specimen was entirely normal, without signs of inflammation, particularly IBD. Finally, a diagnosis of "localized giant inflammatory polyp" was made.

Localized giant pseudopolyps were first described in 1968 [5]. These lesions are almost invariably associated with IBD [2, 3]. Our case, however, clearly demonstrates that these lesions may also occur in patients without history of IBD. Moreover, the flat mucosa of the resection specimen was entirely normal, lacking signs of chronic inflammation. There is only a single report in the literature illustrating a case similar to ours. Tan et al. [4] reported upon a 64-year-old male without history of IBD who

E.-M. Wolf · C. Strasser · E. Spuller · C. Langner (✉)
Institute of Pathology, Medical University of Graz,
Auenbruggerplatz 25,
8036 Graz, Austria
e-mail: cord.langner@medunigraz.at

K. Geboes
Institute of Pathology, University Hospital KU Leuven,
Leuven, Belgium

M. Vieth
Institute of Pathology, Klinikum Bayreuth,
Bayreuth, Germany

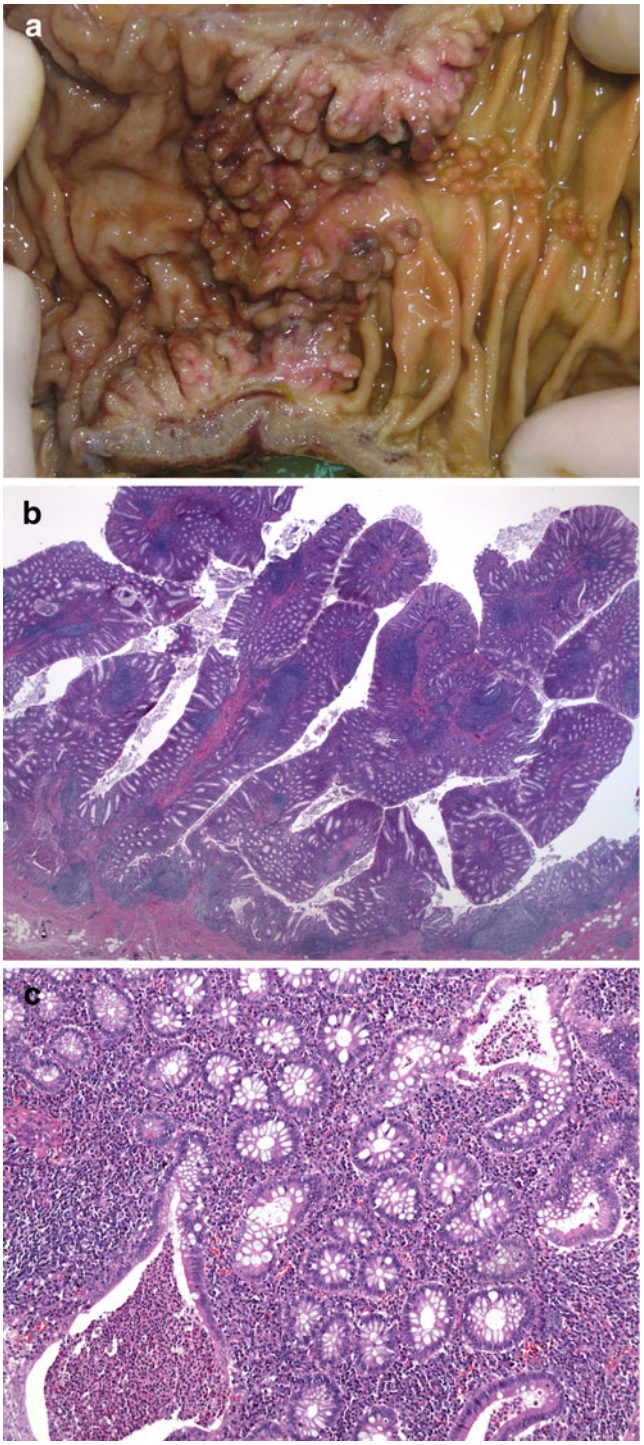

Fig. 1 Localized giant polyp of the colon, measuring 4 cm in largest diameter (**a**). Histology shows irregular villous-like projections of the mucosa; note the hyperplastic lymphoid follicles (**b**). On high magnification, crypt abscesses and crypt distortion as well as a mixed inflammatory infiltrate within the lamina propria are present (**c**)

presented with a huge polyp within the sigmoid colon, measuring 7 cm in largest diameter. Histological examination showed a villous-like mass with chronic inflammation, lacking evidence of neoplastic transformation.

The etiology of the giant pseudopolyps remains unclear in both cases. Overall, inflammatory polyps are believed to arise secondarily to ulceration and repair [1]. While Tan et al. [4] did not refer to possible etiologic factors, our patient denied previous gastrointestinal infections as well as the use of drugs known to cause side effects within the gastrointestinal tract, such as NSAIDs.

Both cases illustrate that IBD-like chronic inflammation with crypt abscesses and distortion may occur in patients without IBD. Moreover, pathologists should know that these changes may encounter in a localized fashion, forming a large tumor-like mass, thereby ultimately mimicking malignancy.

In conclusion, localized giant inflammatory polyps of the colon represent a distinct entity. They may very rarely occur in patients lacking a history of IBD which may cause serious diagnostic problems, especially if malignancy is suspected.

References

1. Watne AL (1997) Colon polyps. J Surg Oncol 66:207–214
2. Goldenberg B, Mori K, Friedman IH, Shinya H, Buchwald RP (1980) Fused inflammatory polyps simulating carcinoma in ulcerative colitis. Am J Gastroenterol 73:441–444
3. Munchar J, Rahman HA, Zawawi MM (2001) Localized giant pseudopolyposis in ulcerative colitis. Eur J Gastroenterol Hepatol 13:1385–1387
4. Tan KH, Meijer S, Donner R (1987) Giant localized pseudopolyp of the colon without colonic inflammatory disease—case report. Neth J Surg 39:95–97
5. Hinrichs HR, Goldman H (1968) Localized giant pseudopolyps of the colon. JAMA 205:248–249

Virchows Arch (2011) 459:247–254
DOI 10.1007/s00428-011-1122-x

REVIEW AND PERSPECTIVE

What skeletons tell us. The story of human paleopathology

Donald J. Ortner

Received: 17 June 2011 / Revised: 4 July 2011 / Accepted: 4 July 2011 / Published online: 21 July 2011
© Springer-Verlag (outside the USA) 2011

Abstract Human skeletal paleopathology provides important insight regarding the antiquity of some diseases and their distribution in past human groups. The history of human skeletal paleopathology extends back more than 150 years. Rudolf Virchow published reports on the subject, and research on paleopathology has provided critical data on important topics such as the origin of syphilis. With the development of powerful new research tools, human paleopathology will continue to be a source of data on the development of disease and its effect on human biological and cultural development.

Keywords Paleopathology · Skeletal disease · Ancient health

Introduction

Paleopathology is the study of disease that affected living organisms in the past. The major focus of this study has been human remains, but the discipline has its roots in the study of abnormalities encountered in non-human remains. One of the earliest reports of disease was written by a German naturalist and clergyman, Johann Friedrich Esper (1732–1781). Esper published a description of what he thought was an osteosarcoma in the femur of a cave bear [1]. A French zoologist, Georges Cuvier (1769–1821), described abnormalities in fossil animal remains [2]. Abnormalities in archaeological human remains that were identified and published in the nineteenth century were largely limited to basic descriptions and, where possible, diagnosis of the disorders. However, in the latter part of the century, the study of paleopathology became an important source of data in broader issues such as the debate regarding the antiquity and origin of syphilis. An example of this is a publication by Joseph Jones, M.D. (1833–1896) of a case of probable syphilis in a pre-Columbian archaeological burial [3]. Jones was an American physician, surgeon, and professor of medicine who also was interested in archaeology [4]. He served as a surgeon in the Confederate Army during the American Civil War. Given Jones' scholarly rigor, it seems likely that his diagnosis of syphilis was based on the earlier research by Rudolf Virchow, M.D. (1821–1902), the father of modern pathology who was also an anthropologist. Virchow had provided careful descriptions of the lesions of the skull that he associated with syphilis [5]. In a later publication, he highlighted Jones' case of syphilis in an archaeological burial [6].

Although there are other nineteenth-century isolated publications on ancient disease, the research and publications of Sir Marc Armand Ruffer, M.D. (1859–1917), largely on Egyptian mummies, mark the beginning of serious scientific interest in paleopathology. Ruffer received his medical training in England and was the first director of the British Institute of Preventive Medicine, which later became the Lister Institute. While conducting research on diphtheria at the Institute, he contracted the disease and was sufficiently disabled that he resigned his post and moved to Egypt to recover [7]. While in Egypt, he initiated his

D. J. Ortner (✉)
Department of Anthropology,
National Museum of Natural History, Smithsonian Institution,
Washington, DC 20560, USA
e-mail: ortner@si.edu

D. J. Ortner
Department of Archaeological Sciences,
The University of Bradford,
Bradford, West Yorkshire BD7 1DP, UK

research on mummy tissues and developed a solution to rehydrate the tissue.

One of his collaborators was Roy L. Moodie (1880–1934) who was trained and worked as an anatomist and paleontologist. Among his many research endeavors, he did considerable research on mummies making significant use of radiology [8] to obtain data while minimizing damage. Moodie's research illustrates very well the multidisciplinary collaboration that has characterized research in paleopathology throughout its history. This collaboration involved physicians, paleontologists, medical historians, and biological (physical) anthropologists, in which each specialist utilizes his or her area of expertise to clarify the diagnosis of abnormalities found in archaeological human remains and determine their significance.

Today, research in paleopathology draws on data from the analysis of several sources. Research on human mummy remains [9] continues to provide details unavailable from any other source, including evidence of tuberculosis in the New World about 1,000 years ago [10]. A major emphasis in current research on paleopathology is on the analysis of disorders in the skeleton [e.g., 11], but other sources of data include coprolites as well as ancient art and medical texts. Research methods include anatomical and radiological research, analysis of ancient biomolecules including pathogen ancient DNA (aDNA) and proteins, as well as stable isotopes [e.g., 12–14]. The major emphasis in this paper is on the evidence and significance of disorders found in archaeological human skeletal remains. The focus will be on a few representative infectious diseases that illustrate the data and conclusions that can be obtained from the careful analysis of archaeological human burials.

Skeletal mycobacterial pathology

Leprosy

The two major and closely related mycobacterial disorders, leprosy and tuberculosis, illustrate both the potential and the limitations of human skeletal paleopathology. In leprosy and tuberculosis, most people exposed to the pathogen remain asymptomatic throughout their lives. The earliest evidence of leprosy is from a description in an Indian medical text dated to about 600 B.C. [15]. Patients with leprosy range from mild symptoms and limited morbidity (tuberculoid leprosy) to severe manifestations with severe morbidity (lepromatous leprosy) including skeletal involvement. Variation in the immune response to the pathogen is the major factor in determining both acquisition of leprosy and its severity once the disease develops [16]. Although skeletal manifestations can occur in tuberculoid leprosy, skeletal involvement is much less common and less severe than in lepromatous leprosy. In interpreting the significance of skeletal evidence of leprosy, and other skeletal disorders, in an archaeological human skeletal sample, the researcher must remember that skeletal evidence of the disease usually represents only a fraction of those individuals who had the disease but do not exhibit skeletal abnormalities.

The skeletal features of lepromatous leprosy are well known and in typical cases provide pathognomonic evidence for the presence of the disease. The abnormalities that occur in the skull have been described by a Danish physician, V. Møller-Christensen (1903–1988), who conducted research on Danish archaeological human remains from cemeteries, dated to the medieval period, for patients with leprosy [17, 18]. These features, which he called *facies leprosa*, include enlargement and rounding of the margins of piriform aperture, and destructive remodeling of the anterior nasal spine and that portion of the maxilla associated with the premaxilla (Figs. 1 and 2). The orbital roof may develop porous bone on the underlying cortex. This presumably is associated with chronic inflammation of the eye, which occurs in some cases of leprosy and can lead to blindness in severely affected patients. The skull vault is not usually involved.

The early stages of facial abnormalities are characterized by active destruction of the affected sites. Because of the chronic nature of leprosy, most patients survive well past this initial stage of bone destruction. However, one of the burials from the medieval site of the Hospital of St. James and St. Mary Magdalene (ca. 1120–1650 A.D.) in Chichester, England [19] provides insight regarding the early stages of bone involvement of the face. The hospital provided care for patients with leprosy, although, particularly with the decline in the prevalence of leprosy in later years, patients with other disorders were admitted. The skeleton is from a young man about 18 years of age at the time he died. The bone surface of the nasal passage, the margin of the piriform aperture, and the external maxilla surrounding the aperture have a dense distribution of pits created by action of osteoclasts (Fig. 3).

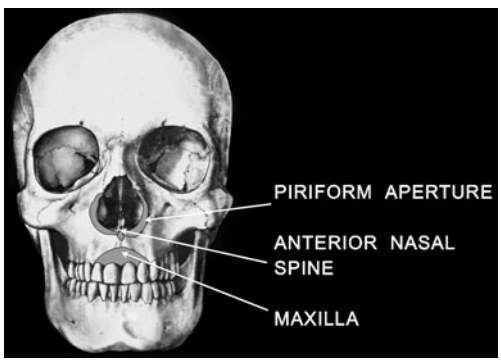

Fig. 1 Areas of the face that can be affected in typical cases of lepromatous leprosy

Fig. 2 Left lateral anterior view of an archaeological skull from the cemetery of the Hospital of St. James and St. Mary Magdalene, Chichester, England, dated between 1118 and 1700 A.D. Burial no. C-34 includes the fragmentary facial bones of an adult male. Note the rounded margins of the piriform aperture, the absence of the anterior nasal spine, and the destructive remodeling of the anterior maxilla, which has exposed the dental roots of the central incisors

Leprosy also affects the postcranial skeleton including destructive remodeling apparent in the metacarpals and metatarsals, as well as the phalanges of both the hands and feet (Figs. 4 and 5). In living patients, one of the complications, particularly apparent in the hands, is severe flexion contractures of the phalanges. This results in pressure erosion of the associated volar surfaces.

Postcranial skeletal changes, particularly of the lower extremity, may be complicated by the development of secondary infections, predominantly of the foot. This commonly leads to chronic infection with an inflammatory response that can extend well beyond the primary focus of infection and stimulate reactive bone formation on the diaphysis of the tibia and fibula. This expression of complications associated with leprosy is often unilateral, indicating the local nature of the infectious process.

Fig. 3 Early stages of destructive remodeling in the maxilla of a burial from the cemetery of the Hospital of St. James and St. Mary Magdalene, Chichester, England, dated between 1118 and 1700 A.D. Burial no. C-187 is the skeleton of a male about 18 years of age at the time of death. Note the pitted surface of the compact bone

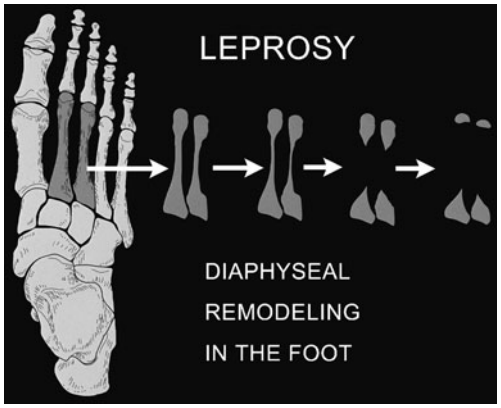

Fig. 4 Drawing of the stages in destructive remodeling of the diaphysis of the metatarsal bones of the foot that occurs in some patients with lepromatous leprosy

Tuberculosis

Mycobacterium tuberculosis and *Mycobacterium bovis* are the two organisms most commonly associated with human tuberculosis. The antiquity of tuberculosis and the relationship between this disease and animal intermediate hosts continue to be a source of controversy. There is reasonably convincing evidence from archaeological burials that the disorder occurs by the end of the Neolithic period (ca. 5000–4000 B.C.) [11, 20, 21]. The traditional hypothesis is that tuberculosis was acquired from cattle after they were domesticated during the Holocene period (ca. 6000 B.C.). However, DNA research on the human and bovid strains of

Fig. 5 Superior view of the destructive remodeling of the right foot from Burial no. C-62, the skeleton of an adult male from the cemetery of the Hospital of St. James and St. Mary Magdalene, Chichester, England

the disorder indicates that the bovid variety is a more recent development [22].

Tuberculosis rarely affects the skeleton. When the skeleton is affected, the lower spine is the site of involvement in about 50% of cases. Spinal tuberculosis tends to be unifocal, although involvement of more than one vertebra is common. This is helpful in distinguishing between this type of tuberculosis and other pathological conditions that result in destructive lesions of the spine such as brucellosis and echinococcosis. The second most common site for skeletal tuberculosis is the hip.

Throughout much of recent human history, the age of onset for tuberculosis was usually in childhood ([11] p. 229). The initial acute stage of skeletal tuberculosis is highly destructive. In the spine, the vertebral bodies are the typical site; the vertebral arch is very rarely involved. Destruction of the bodies results in varying degrees of kyphosis depending on how many vertebral bodies are involved. Reparative bone formation may be limited but can result in fusion of affected bones.

Tuberculosis of the hip can result in significant disability. Distinguishing between joint destruction caused by tuberculosis and septic arthritis from other infectious pathogens is not certain. An example of hip joint destruction that could have been caused by tuberculosis occurs in the historic period of Alaska that began about 1750 A.D. The skeleton is from a young adult female about 20 years of age (NMNH 345394) from an archaeological site in that state [11] (Fig. 6). Both the femoral head and the acetabulum exhibit severe destruction and subsequent remodeling. The shallowness of the remaining acetabulum and a wide depression in the superior margin indicate chronic subluxation. This would have resulted in shortened length of the left leg.

Comparison of the normal right and the abnormal left femur shows greatly reduced shaft diameter, although the length of the left femur is only slightly shorter than the right. There has been compensatory growth in length of the left tibia, which would have reduced the difference in total leg length. The young age at death and the remodeling that has occurred in the left acetabulum and femoral head, as well as the compensatory growth of the left tibia, suggest an age of onset during the later stages of growth and development. The interesting feature of this case is the disproportionate size in the length of the abnormal femur relative to the diameter of the diaphysis combined with the compensatory growth in the length of the tibia. Clearly, endochondral growth is virtually normal in the femur but abnormally enhanced with the tibia. However, intramembranous development is not normal. A possible explanation is failure of intramembranous growth due to a lack of biomechanical stimulation following destruction of the hip joint. Although the destruction apparent in this case could be an example of septic arthritis caused by pathogens other than tuberculosis, the widespread presence of tuberculosis among Native Alaskans particularly during the historic period raises the probability that this was the cause in this case.

Fig. 6 Possible tuberculosis of the hip with disrupted development of the affected femur in an adult female skeleton. The burial is from a historic site in the Yukon region of Alaska, USA, NMNH no. 345394

Skeletal treponematosis

As noted earlier, the skeletal manifestations of syphilis, which are predominantly associated with the tertiary stage of the disorder, were carefully described by Rudolf Virchow [5]. The description included a careful anatomical analysis that identified both the type and distribution of abnormalities within the skeleton. Virchow defined *caries sicca* as a characteristic lesion of syphilis (see below for details). He also noted the strong association between syphilis and reactive bone formation containing snail track grooves most commonly apparent in the lower extremity.

More recently, C.J. Hackett (1905–1995) did a detailed survey of many of the medically documented cases of syphilis found in European anatomical museums [23]. Hackett was born in Australia where he received his early education and his first medical degree. He refined Virchow's definition of caries sicca and demonstrated the sequence of bone changes associated with this lesion. The sequence begins with a more or less circular cluster, 1 to 2 cm in diameter, of fine holes in the outer table of the skull vault. The holes coalesce forming a depressed lesion which, in the later stages of the lesion development, heals creating a concave compact bone surface. Reactive bone formation takes place at the margins of the central focus giving rise to the characteristic crater–like lesion that is virtually pathognomonic for treponematosis.

Hackett had done a classic study of yaws and the clinical and skeletal changes associated with this syndrome of treponematosis based on his experience as a physician with patients in Uganda [24]. His publications have been the basis of much of the subsequent research on the three syndromes of treponematosis that affect the skeleton, but he emphasized that differentiating between the skeletal manifestations of the

three syndromes was difficult if not impossible and diagnosis would depend on the geographical location of the burial.

A major question that remains unresolved is the significance of the clinical differences that exist among the three syndromes of treponematosis that affect the skeleton (syphilis, bejel, and yaws), particularly between syphilis and the two non-venereal disorders, bejel and yaws. Do these differences reflect different diseases caused by different pathogenic organisms as Hackett argued or, as Hudson (1890–1992), an American physician and professor, argued [25], are they simply different manifestations of the same disease caused by different factors such as age of onset and variation in the immune response of different patients and groups of patients? The remarkable range of clinical and radiological manifestations apparent in patients with leprosy highlights the importance of the immune response and the considerable variability in the effect of the disease on organs, including the skeleton, associated with some disorders.

The origin of syphilis is probably one of the oldest controversies in medical history and paleopathology and very much linked to the question of how far back this syndrome extends in both the Old and New World. The venereal mode of transmission of syphilis, and the social approbation associated with it, has provided a social context in which careful evaluation of the evidence has been greatly influenced by opinion rather than data resulting from rigorous research. The traditional view is that syphilis was brought to the Old World by ship's crews returning from the Columbian voyages of discovery in the late fifteenth century. Until recently, much of the archaeological skeletal evidence of treponematosis before 1500 A.D. was in archaeological skeletons from the New World [26].

The presence of congenital treponematosis in archaeological human remains has been used as an argument for syphilis being present in a human population. A congenital variant is possible for any of the three syndromes of treponematosis that cause skeletal disease. However, transmission across the placental barrier tends to be associated with the initial stage of the disease. Since the non-venereal syndromes are usually acquired in childhood, congenital bejel or yaws rarely occurs since these diseases are usually past the initial acute stage when pregnancy occurs. Because of this, the probabilities favor a diagnosis of syphilis when a case of congenital treponematosis is encountered in archaeological skeletal sample.

A case of probable congenital treponematosis has been reported from a pre-Columbian site in Virginia, USA [11]. The site is dated between 1400 and 1500 A.D. The skeletal remains are from a child about 6 years of age at the time of death (NMNH 379177). The central incisors have deep hypoplastic defects in the crowns indicative of a congenital disorder sufficiently severe to disrupt dental development (Fig. 7). These defects resulted in portions of the dental crowns of the mandibular central incisors breaking off at the defect.

In the skull, reactive woven bone is apparent surrounding the piriform aperture. Woven reactive bone has greatly increased the diameter of both tibias and also occurs on the right fifth metacarpal. It may have occurred on other bones of the hands and feet, but most were not recovered at the time of excavation. The type and distribution of abnormalities in this burial are almost certainly attributable to congenital treponematosis, and the probability favors congenital syphilis.

A remarkable case of probable syphilis in an adult was excavated from a medieval friary site discovered during construction of the new magistrate's court in Hull, England. The friary is dated between 1317 and 1539 A.D. In 1537 A.D., Henry VIII established the Church of England and began the systematic destruction of Catholic monasteries, so the end date of occupation of the site is certain. The burial (HMC 1216) is that of a male about 35 years of age. The skeletal manifestations are multifocal and exhibit a range of development from recently formed abnormalities to compact bone lesions associated with the late stage in the development of the lesion.

The frontal bone exhibits the classic features of caries sicca with an early stage characterized by a roughly circular cluster of fine holes (Fig. 8, white arrow) to lesions that are well developed with a slight depression in the central portion of the lesion and a slightly raised compact bone margin (Fig. 8, black arrow). In the hard palate, there is a destructive lesion approximately 1 cm in diameter that penetrates through the bone. Abnormal bone-forming lesions occur throughout the skeleton including the bodies of the cervical vertebrae, the anterior diaphysis of the clavicles, and the long bones of the extremities. These bone-forming lesions consist of woven bone, compact

Fig. 7 Enamel hypoplasia of the incisors in a child, approximately 6 years of age, indicative of a disorder during uterine life. Note that part of the crown of the two lower central incisors has broken off at the location of the hypoplastic line. The distribution of abnormal conditions in this skeleton is almost certainly caused by congenital treponematosis. The case is from a site in Virginia, USA, probably dated before 1400 A.D., NMNH 379177

Fig. 8 A case of probable treponematosis from a medieval site (1317–1539 A.D.) in Hull, UK, Catalog no. HMC 1216. The burial is the skeleton of a 35-year-old male. Note the early stage of caries sicca formation in the frontal bone with a roughly circular cluster of fine holes (*white arrow*). Late stage caries sicca (*black arrow*) is located very close to the early stage lesion

bone, and combinations of woven and compact bone. Some woven bone lesions have a central depression, presumably the location of a granuloma in life, surrounded by reactive woven bone formation. The abnormalities of the skull are virtually pathognomonic for treponematosis, and this is supported by the distribution of reactive bone formation on the clavicles and most of the long bones. Although a non-venereal syndrome of treponematosis is a possibility, the geographic location of the burial in England, well away from the modern age geographic distribution of yaws and bejel, makes syphilis more probable. The archaeological dating of this burial in the medieval period certainly raises the possibility of a pre-Columbian case of syphilis, but the overlap with the post-Columbian range of dates leaves room for doubt. The presence of syphilis in the Old World before 1500 A.D. remains a very contentious issue, although there is more convincing evidence of the disease occurring well before the voyages of Columbus from the early medieval phase of a medieval site in London [27].

A recent publication by Cole and Waldron [28] of a case of probable syphilis in an adult male skeleton from an Anglo-Saxon site (sixth century A.D.) in England provides almost certain evidence of the presence of syphilis in Europe long before Columbus. The rich grave contents indicate the high social status of the individual. The cultural artifacts are unequivocally dated to the Anglo-Saxon period. The type and distribution of bone lesions, including bilateral involvement of the clavicles, are unlikely to be associated with any other disorder.

Echinococcosis

Another infectious disease that can cause destructive skeletal lesions is echinococcosis caused by the larval stage of a tapeworm in the genus *Echinococcus*. The most

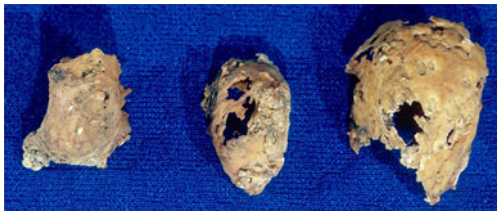

Fig. 9 Mineralized hydatid cysts from an adult burial (NMNH 374623, now reburied) from an archaeological site in Jones Point, Alaska, USA, dated between 1 and 1000 A.D.

common expression of the disease in humans is cystic echinococcosis caused by *Echinococcus granulosus*. The parasite can stimulate destructive lesions of bone. In soft

Fig. 10 Bone-forming lesions in the right tibia of an adult male stimulated by chronic infection associated with an overlying skin ulcer. The large lesion with the well-defined margin underlies the location of the skin ulcer. The bone is from an ossuary at the Juhle Site, Maryland, USA, NMNH 384299 dated between 1200 and 1650 A.D.

tissue, part of the host response to these organisms is to encapsulate cystic clusters of the parasite in connective tissue, which can then mineralize. It is rare that these mineralized cysts are noticed during excavation of archaeological burials, but an interesting example of this manifestation of the disease occurs in association with a skeleton from a prehistoric archaeological site in Alaska, USA (Fig. 9).

Periostosis

Periostosis of the long bones, particularly the bones of the lower leg, is probably the most common expression of skeletal disorder encountered in human archaeological skeletons. The typical appearance is a thin plaque of woven bone on the diaphysis of a long bone, often the medial surface of the tibia. It is unlikely that these lesions would be apparent in a plain-film radiograph of a patient and are probably not encountered clinically nearly as often as they occur in archaeological burials.

The development of abnormal bone lesions associated with periostosis can be caused by several skeletal disorders including trauma, infection, and cancer. In many cases of this disorder, it is not possible to determine the cause without additional evidence of disease in other areas of the skeleton. An exception to this is the bony response to chronic skin ulcer overlying bone. By far, the most common site for the skeletal expression of skin ulcer is the medial portion of the tibial diaphysis [29].

An example of this disorder occurs on the right tibia (NMNH 384299) from an ossuary excavated in Maryland, USA (Fig. 10). The chronic nature of skin ulcer in this case is apparent in the reactive bone formation with a well-defined margin and the porous surface of the large lesion. Inferior to the main lesion is a smaller area of reactive bone formation that has enlarged the cross-sectional size of the distal tibia. The organism causing the ulcer cannot be determined on the basis of anatomical evidence, although staphylococcal bacteria are high on the list of diagnostic options.

Conclusions

For at least one and a half centuries, analysis of skeletal disorders in archaeological human remains has provided both time depth and the geographical range of some diseases that confronted our ancestors. This research was based on observations resulting from careful analysis of anatomical and clinical dimensions of disorders that affect the skeleton. Unfortunately, the number of diseases that affect the skeleton is a very small fraction of the total number of disorders that affect humans, and differential diagnosis is often challenging and may not be possible. Ongoing research in orthopedic pathology and skeletal radiology, as well as recent clinical experience with human skeletal disorders, continues to clarify the skeletal manifestations of those diseases that affect the skeleton. In paleopathology, the potential exists for contributing to a greater understanding of the skeletal manifestations of disease since data on lesions not resolved by radiology and the distribution of lesions within a skeleton in multifocal disorders is possible.

With the emergence of evolution as a significant factor in our understanding of human host and infectious pathogen coevolution [e.g., 30–32], the time depth provided by human paleopathology is an additional source of data in achieving greater understanding of this relationship [11, 33]. Ensuring that this source of data is useful will depend on continuing and enhanced collaboration between the biological anthropologists studying human remains and medical specialists with the expertise to place the data from research on ancient remains in the context of modern medicine, particularly orthopedic pathology and skeletal radiology.

Acknowledgements Enrique Gerszten, a pathologist in the Department of Pathology, Medical College of Virginia, and well known for his work on the paleopathology of mummies, provided helpful suggestions on the content of this paper. I appreciate both his friendship and the continuing contribution he makes to the study of ancient disease. I also appreciate the assistance of Ms. Marcia Bakry in preparing the illustrations and Ms. Janet Beck for her editorial advice. Both work in the Department of Anthropology, National Museum of Natural History, Smithsonian Institution.

Conflict of interest statement I declare that I have no conflict of interest.

References

1. Esper J (1774) Ausführliche Nachricht von Neuentdeckten Zoolithen, Unbekannter Vierfüssiger Thiere, und denen sie Enthaltenden, so wie Verschiedenen Andern Denkwürdigen Grüften der Obergebürgischen Lande des Marggrafthums Bayreuth. Nürnberg
2. Cuvier G (1820) Recherches sur les Ossemens Fossiles, vol 4. G. Dufour & E. d'Ocagne, Paris
3. Jones J (1876) Explorations of the aboriginal remains of Tennessee. Smithsonian contributions to knowledge, vol 259. Smithsonian Institution, Washington, pp 1–17
4. Breeden JO (1975) Joseph Jones, M.D. Scientist of the Old South. University Press of Kentucky, Lexington
5. Virchow R (1858) Über die Natur der Constitutionell-syphilitischen Affectionen. Virchows Arch Pathol Anat Physiol Klin Med 15(217–236):243–253
6. Virchow R (1898) Knochen aus Alten Gräbern von Tennessee. Verh Berl Ges Anthrop 30:342–344
7. Sandison AT (1967) Sir Marc Armand Ruffer (1859–1917) pioneer of palaeopathology. Med Hist 11:150–156

8. Moodie RL (1931) Rentgenologic studies of Egyptian and Peruvian mummies. Anthropological memoirs, vol 3. Field Museum of Natural History, Chicago
9. Aufderheide AC (2003) The scientific study of mummies. Cambridge University Press, Cambridge
10. Salo WL, Aufderheide AC, Buikstra J, Holcomb TA (1994) Identification of *Mycobacterium tuberculosis* DNA in a pre-Columbian mummy. Proc Natl Acad Sci U S A 91:2091–2094
11. Ortner DJ (2003) Identification of pathological conditions in human skeletal remains, 2nd edn. Academic, Amsterdam
12. Katzenberg MA, Lovell NC (1999) Stable isotope variation in pathological bone. Int J Osteoarch 9:316–324
13. Katzenberg MA (2008) Stable isotope analysis: a tool for studying past diet, demography, and life history. In: Katzenberg MA, Saunders SR (eds) Biological anthropology of the human skeleton, 2nd edn. Wiley-Liss, Hoboken, pp 413–441
14. Kolman CJ, Centurion-Lara A, Lukehart SA, Owsley DW, Tuross N (1999) Identification of *Treponema pallidum* subspecies *pallidum* in a 200-year-old skeletal sample. J Infect Dis 180:2060–2063
15. Roberts C, Manchester K (2005) The archaeology of disease, 3rd edn. Sutton, Phoenix Mill
16. Jopling W (1978) Handbook of leprosy, 2nd edn. Heinemann, London
17. Møller-Christensen V (1961) Bone changes in leprosy. Munksgaard, Copenhagen
18. Møller-Christensen V (1978) Leprosy changes of the skull. Odense University Press, Odense
19. Magilton J, Lee F, Boylston A (2008) Lepers outside the gate. Chichester excavations 10, CBA Research Report 158. Council for British Archaeology, York
20. Aufderheide AC, Rodríguez-Martín C (1998) The Cambridge encyclopedia of human paleopathology. Cambridge University Press, Cambridge
21. Buikstra J (1999) Paleoepidemiology of tuberculosis in the Americas. In: Pálfi G, Dutour O, Deák J, Hutás (eds) Tuberculosis past and present. Golden Book, Szeged, Hungary, pp 479–494
22. Broach R, Gordon SV, Marmiesse M, Brodin P, Buchrieser C, Kiglmeier K, Garnier T, Gutierrez C, Hewinson G, Kremer K, Parsons LM, Pym AS, Samper S, van Soolingen D, Cole ST (2002) A new evolutionary scenario for the *Mycobacterium tuberculosis* complex. Proc Natl Acad Sci USA 99:3684–3689
23. Hackett C (1976) Diagnostic criteria of syphilis, yaws and treponarid (treponematoses) and of some other diseases in dry bones (for use in osteo-archaeology). In: Sitzungsberichte der Heidelberger Akademie der Wissenschaften Mathematisch-naturwissenschaftliche Klasse, Abhandlung 4. Springer-Verlag, Berlin
24. Hackett C (1947) The bone lesions of yaws in Uganda. Thesis. University of London, London
25. Hudson E (1968) Christopher Columbus and the history of syphilis. Acta Trop 25:1–16
26. Baker BJ, Armelagos GJ (1988) The origins and antiquity of syphilis. Curr Anthropol 29:721–723
27. Connell B, Gray Jones A, Redfern RC, Walker D (2011) Spitalfields: a bioarchaeological study of health and disease from a medieval London cemetery. Archaeological excavations at Spitalfields Market 1991–2007, vol 3. MoLA Monograph, London (in press)
28. Cole G, Waldron T (2011) Apple Down 152: a putative case of syphilis from sixth century AD Anglo-Saxon England. Am J Phys Anthropol 144:72–79
29. Boel LWT, Ortner DJ (2011) Skeletal manifestations of skin ulcer in the lower leg. Int J Osteoarch. doi:10.1002/oa.1248
30. Ewald P (1994) Evolution of infectious disease. Oxford University Press, Oxford
31. Ewald P (2000) Plague time. How stealth infections cause cancers, heart disease, and other deadly ailments. The Free, New York
32. Sterns SC, Koella JC (2008) Evolution in health and disease. Oxford University Press, Oxford
33. Ortner DJ, Schutkowski H (2008) Ecology, culture and disease in past human populations. In: Schutkowski H (ed) Between biology and culture. Cambridge University Press, Cambridge, pp 105–128

Virchows Arch (2011) 459:255–263
DOI 10.1007/s00428-011-1135-5

ORIGINAL ARTICLE

Overexpression of Frat1 correlates with malignant phenotype and advanced stage in human non-small cell lung cancer

Yong Zhang · Juan-Han Yu · Xu-Yong Lin · Yuan Miao · Yang Han · Chui-Feng Fan · Xin-Jun Dong · Shun-Dong Dai · En-Hua Wang

Received: 22 April 2011 / Revised: 13 July 2011 / Accepted: 23 July 2011 / Published online: 5 August 2011
© Springer-Verlag 2011

Abstract Frat1 has been reported to be overexpressed in several human malignant tumors, including esophageal squamous, cervical, breast, and ovarian carcinoma, but the role of Frat1 in lung cancer is unknown. Our purpose is to investigate the expression of Frat1 and its correlation with clinicopathologic features and prognosis in lung cancer patients. Immunohistochemistry was performed on 137 cases of non-small cell lung cancer (NSCLC), including 78 cases with clinical follow-up, and Western blot and reverse transcription-polymerase chain reaction (RT-PCR) assays were performed to detect the protein and mRNA expression levels in 30 NSCLC and autologous matched normal tissues. In addition, lung cancer cell line A549 was transfected with Frat1-siRNA plasmids and Matrigel invasive assay was carried out to study the function of Frat1 in cancer cell invasiveness. The results showed that Frat1 was expressed in 85 (62.04%) cases of NSCLC by immunohistochemistry, while all 30 specimens of normal lung tissues were negative. Western blot and RT-PCR results for Frat1 mRNA were in agreement with immunohistochemical findings. Of interest, the expression of Frat1 was strongly correlated with tumor differentiation, TNM stage, and lymph node metastasis ($P<0.05$). The Kaplan–Meier survival analysis demonstrated that the cases with Frat1 expression had significantly shorter survival than those without Frat1 ($P<0.001$). In addition, down-regulation of Frat1 expression reduced the invasive ability in the A549 cell line, further supporting the idea that Frat1 may play a crucial role in carcinogenesis, tumor invasiveness and dissemination in human lung cancer.

Keywords Frat1 · Oncogene · Non-small cell lung carcinoma · Prognosis · Wnt pathway

Abbreviations

Frat1	Frequently rearranged in advanced T-cell lymphomas 1
NSCLC	Non-small cell lung cancer
SCC	Squamous cell carcinoma
PBS	Phosphate-buffered saline
PVDF	Polyvinylidene fluoride
GBP	GSK3-binding protein
Frz	Frizzled protein
Dvl	Dishevelled protein

Introduction

For the past a few decades, the mortality and morbidity of lung cancer have been steadily increasing worldwide. Although combined therapeutic modalities (surgical resection, chemotherapy and radiotherapy) have been established, the prognosis for lung cancer patients continues to be poor with a low rate of long term survival. The emergence of targeted therapies has brought a more promising prognosis for lung cancer patients. In order to identify useful biomarkers and explore novel therapeutic targets for lung cancer, further characterization of its pathogenesis becomes an important task.

Y. Zhang · J.-H. Yu · X.-Y. Lin · Y. Miao · Y. Han · C.-F. Fan · X.-J. Dong · S.-D. Dai · E.-H. Wang (✉)
Department of Pathology, the First Affiliated Hospital and College of Basic Medical Sciences, China Medical University, Shenyang 110001, China
e-mail: wangeh@hotmail.com

Y. Zhang · J.-H. Yu · X.-Y. Lin · Y. Miao · Y. Han · C.-F. Fan · X.-J. Dong · S.-D. Dai · E.-H. Wang
Institute of pathology and pathophysiology, China Medical University, Shenyang 110001, China

Frat1, a member of the Frat (Frequently rearranged in advanced T-cell lymphomas) family, has been considered to be an activator in the Wnt signal transduction pathway [1, 2] and has been noted to be overexpressed in human esophageal squamous cell carcinomas [3] and ovarian cancers[4]. The expression of Frat1 is considered to be crucial for the maintenance of the malignant cellular phenotype. Recently, Frat1 has been shown to be expressed in human gliomas [5] and astrocytomas, [6], and its expression was associated with an aggressive phenotype. This data indicates Frat1 may function as an oncogene in human malignant tumors. However, the expression status of Frat1 in lung cancer and its role in the biological behavior of lung cancer are still unknown.

In the present study, we examined both mRNA and protein expression patterns and the prognostic significance of Frat1 in human NSCLC. Moreover, the effects of Frat1 expression on cancer cell invasiveness were also investigated in the A549 lung cancer cell line by using Frat1-siRNA.

Materials and methods

Patients and tissue samples

In total, 137 tissue samples diagnosed with NSCLC between 1998 and 2005 were analyzed in this study. Of these, 78 cases had clinical records of postoperative follow-up in the First Affiliated Hospital of China Medical University. None of the patients had received radiotherapy or chemotherapy before surgical resection of the lung cancer, and all the patients were treated with routine chemotherapy after the operation. Patients included 89 males and 48 females. The age ranged from 33 to76 years with a median of 58 years. The histologic types of tumors included squamous cell carcinoma (SCC) in 63 cases and adenocarcinoma in 74 cases. Histological grades of these tumors included well differentiated carcinoma in 30, moderately differentiated carcinoma in 74, and poorly differentiated carcinoma in 33 cases. All the patients were staged according to the TNM stage revised by the International Union Against Cancer (UICC) in 2010, which included stage I in 34, stage II in 37, stage III in 61, and stage IV in five cases. Of 137 cases in total, 59 patients had lymph node metastases when the patients were initially staged. All specimens were reviewed independently by three pathologists, and the diagnoses of NSCLC were confirmed according to the criteria for the classification of lung cancer by the World Health Organization (WHO). 30 cases of tumor and paired autologous non-tumor portions (with >5 cm distance from the margin of primary tumors) were quickly frozen in liquid nitrogen and were preserved at −70°C for protein and mRNA analysis. The study was conducted according to the regulations of the institutional review boards at China Medical University. Informed consent was obtained from all the enrolled patients prior to surgery.

Immunohistochemical analysis

All the resected specimens were fixed with 10% neutral-buffered formalin and were embedded in paraffin blocks. Tissue blocks were sectioned with a 4-μm-thick sequential cut and after dewaxing in xylene and rehydrating stepwise in alcohol, sections were boiled in citrate buffer (pH 6.0) for 105 s within an autoclave. Endogenous peroxidase was blocked by using 3% hydrogen peroxide in phosphate-buffered saline (PBS) for 20 min. The samples were washed three times with PBS and incubated for 30 min at room temperature with a protein blocking solution. Sections were then incubated with primary antibodies overnight at 4°C. Specifically, goat anti-human Frat1 polyclonal antibody (1:50) (Santa Cruz Biotechnology, Santa Cruz, CA, USA) was used at concentration of 4 μg/ml. This was followed by incubation with biotinylated secondary antibodies (Maixin Biotechnology, Fuzhou, China). The peroxidase reaction was then developed with 3,3′-diaminobenzidine tetrahydrochloride (MaiXin Biotechnology, Fuzhou, China). Counterstaining was carried out lightly with hematoxylin, and the sections were dehydrated in alcohol before mounting. For a negative control, PBS was used in place of the primary antibodies.

All of the stained sections were evaluated independently by three pathologists without knowledge of the patients' clinical status. The sections were examined at low magnification (×100) to identify the areas where anti-Frat1 was homogeneously stained. Totally, 400 tumor cells were counted at high magnification (×400) in each case, and the percentage of positively staining cells was calculated. The proportion of cells exhibiting Frat1 expression was categorized as follows: 0=less than 25%; 1=26%–50%; 2=51%–75%; 3=more than 75%. The staining intensity was categorized by relative intensity as follows: 0=negative; 1=weak; 2=intermediate; 3=strong staining. The proportion and intensity scores were then multiplied to have a total score index. Per statistical analysis, scores less than 2 were considered negative, while scores of 2 or more were considered positive.

Western blot analysis

Total protein from tissue samples and cell lines were extracted in lysis buffer and quantified using the Bradford method. Then, 50 μg protein from each specimen was loaded on and separated by SDS-PAGE (12%). After transferring to a polyvinylidene fluoride (PVDF) membrane

(Millipore, Billerica, MA, USA), the membranes were incubated overnight at 4°C with goat anti-human Frat1 polyclonal antibody (1:200) (Santa Cruz Biotechnology, USA). After incubation with peroxidase-coupled antigoat IgG (Santa Cruz Biotechnology) at 37°C for 2 h, bound proteins were visualized using ECL (Thermo Fisher Scientific Inc, Fremont, CA, USA) and detected using BioI-maging Systems (UVP Inc., Upland, CA, USA). The relative amount of Frat1 protein was calculated in reference to β-actin as a loading control. The experiment was repeated three times.

RT-PCR analysis

Total RNA from tissue samples and cell lines were isolated using the TRIzol reagent (Invitrogen). cDNA was prepared using the RNA PCR Kit (AMV) Version 3.0 (TaKaRa Bio Inc., Dalian, Liaoning, China), according to the manufacturer's instructions. The sequences of the primer sets for the human Frat1 cDNA were: forward primer, 5′-GCCCTGTCTAAAGTGTATTTTCAG-3′, and reverse primer, 5′-CGCTTGAGTAGGACTGCAGAG-3′. Polymerase chain reaction (PCR) conditions, including the linear amplification range, the annealing temperatures and the numbers of the PCR cycles were essentially the same as a published reference for quantitative amplification of human Frat1 transcripts. The PCR products were electrophoresed in a 1.5% agarose gel containing 0.1 μg/μl ethidium bromide and then visualized and analyzed using the BioImaging System (UVP, Upland, CA, USA). A grayscale intensity value was determined for each target band and normalized to the product amplified from β-actin transcripts to provide a numeric value for the transcriptional level of Frat1 in individual tissue sample or cell line. Each experiment was repeated three times.

Cell culture, siRNA interference, and Matrigel invasive assay

A549 cell line was purchased from American Type Culture Collection (Manassas, VA, USA). The cells were cultured in Dulbecco's modified Eagle's medium (Invitrogen, Carlsbad, CA, USA) containing 10% fetal calf serum (Invitrogen), 100 IU/ml penicillin (Sigma, St. Louis, MO, USA), and 100 μg/ml streptomycin (Sigma). Cells were grown on sterilized culture dishes and were passaged every 2 days with 0.25% trypsin treatment (Invitrogen).

On-Target Plus SMART pool siRNA for Frat1 (sc-105373-SH) and On-Target Plus siControl (sc-37007) were purchased from Dharmacon. For transfections, cells were seeded in a 6-well plate 24 h before the experiment. The cells were transfected with Frat1-siRNA or other control plasmids using the Dharma FECT 1 (0.20 μl/well; Thermo Fisher Scientific) according to the manufacturer's protocol.

The cells' invasive abilities were examined using a 6-well Transwell with 8-μm pore polycarbonate membrane inserts (Corning Inc., Corning, NY, USA) according to the manufacturer's protocol. To the upper surface of the membranes, 100 μl Matrigel (1:4 dilution) was applied. After solidification of the Matrigel, 100 μl of the cell suspension (5×10^5 cells/ml) was loaded into the upper chamber, while the medium supplemented with 10% FBS was added to the lower chamber as a chemoattractant. After incubation for 48 h, the filters were fixed with cold methanol, and the non-invading cells on the upper surface were removed by scrubbing with a cotton swab. The filters were then subjected to hematoxylin staining. Cells that appeared on the lower surface of the filter were counted in five random 200× fields using an inverted microscope (Olympus 1×51; Olympus America Inc., Melville, NY, USA). The experiments were performed in triplicate and were repeated three times independently.

Statistical analysis

SPSS version 14.0 for Windows was used for all analyses. Pearson's χ^2 test was used to examine possible correlations between Frat1 expression and clinicopathologic factors. Student's *t*-test was used to compare the data from densitometry of Western blots and reverse transcription-PCR (RT-PCR) between the categorized groups. The Kaplan–Meier survival analysis was carried out to assess the probability of patients' survival, measuring from the time when the diagnosis of NSCLC was made with subsequent surgical resection until death from any cause in individual patients. The differences in the survival of subgroups of patients were compared using Mantel's log-rank test. A multivariate analysis was performed using the Cox regression model to study the effects of different variables on survival. *P* value less than 0.05 was designated to be statistically significant to establish a difference between or among the categorized groups.

Results

Expression patterns of Frat1 in normal lung tissues and NSCLC tissues

Of 30 non-neoplastic lung tissue specimens, none (0%) showed expression of Frat1 either in the normal alveolar or bronchial epithelial cells (Fig. 1). These tissue specimens were thereby designated as negative for Frat1 expression. In contrast, of 137 cases of NSCLC, 85 (62%) demonstrated cytoplasmic expression of Frat1 ($P<0.001$ in comparison

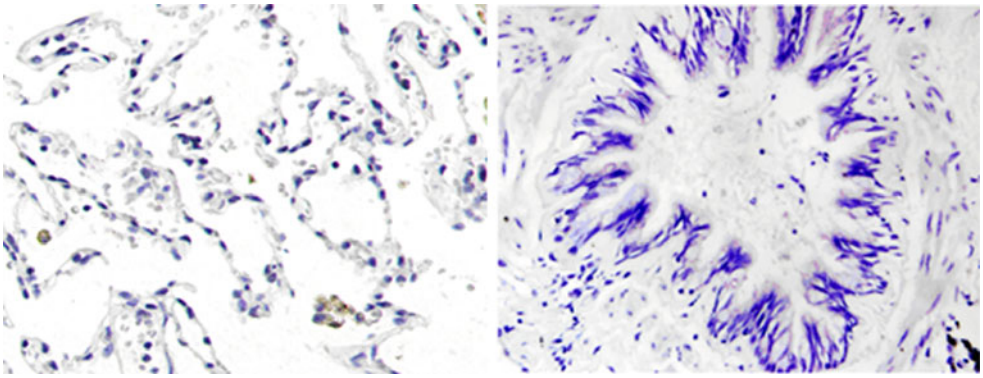

Fig. 1 Immunohistochemical analysis of Frat1 in normal lung tissues. Note a negative reactivity of Frat1 in the normal alveolar and bronchial epithelial cells. ×200

with the group of normal lung tissues) (Table 1). Of note, six of them also showed nuclear expression in addition to their cytoplasmic reactivity. There was no membrane reactivity observed in the cancer tissues.

Expression of Frat1 in NSCLC tissues was correlated with the patients' clinicopathologic features

The expressions of Frat1 in the categorized groups stratified by their clinicopathologic features in the patients with NSCLC are summarized in Table 1. The expression of Frat1 appeared to be increased with histological grade. The positive rate was 46.7% (14/30) in the well differentiated, 63.5% (47/74) in moderately differentiated and 77.4% (24/33) in poorly differentiated lung cancer tissues. There was a statistically significant difference among the histological grades (P=0.035) (Fig. 2). With regard to nodal status, 68% (66/97) of the cases with lymph node metastasis showed expression of Frat1 in contrast to 47.5% (19/40) of the cases without lymph node metastasis (P=0.024). Of 97 cases with lymph node metastasis, 59 had data of paired primary and metastatic tissues, which were analyzed and summarized in Table 2. Of these, the positive rate of Frat1 expression in the metastases was 83.1% (49/59), which is significantly higher than that in the paired primary lesions (64.4%; 38/59) (P=0.015). Notably, the intensity of immunostaining was apparently stronger in the metastases than in the matched primary lesions (Fig. 3). Interestingly, 19 (90.5%) out of 21 cases with negative staining of the primary lesions showed Frat1 expression in the metastases, whereas, eight (21.1%) of 38 cases with a positive staining of the primary cancer tissues demonstrated loss of expression in the metastases. In addition, the positive rate of Frat1 expression in the primary cancer tissues was higher in stages III+IV (73.5% [50/68]) than in stages I+II (50.7% [35/69]) (P=0.006). While it seemed that female patients tended to have a higher expression of Frat1 in their NSCLC tissues than male patients, the difference was not statistically significant. An increase in case number might improve the statistical power for detection of a difference between genders. There were no significant correlations between Frat1 expression and age or histological types (squamous versus adenocarcinoma).

We used Western blot and RT-PCR to test the expression of Frat1 at protein and transcript levels in 30 NSCLC tissues and in their autologous matched normal lung tissues. Expression of Frat1 was undetectable in the matched normal lung tissues but was significantly increased in the lung cancer tissues (Fig. 4). Furthermore, the level of Frat1 expression in the lung cancer tissues seemed to be inversely correlated with the degree of neoplastic differentiation, with well differentiated tumors showing the lowest expression. At the expression level by RT-PCR, the transcripts of Frat1 were zero in normal lung tissues, 0.405±0.03 in well differentiated adenocarcinoma, 0.687±0.04 in moderately

Table 1 Distribution of Frat1 status in NSCLC according to clinicopathological characteristics

Characteristics	Frat 1			
	Negative	Positive	Percentage	*P*
Gender				
Male	39	50	43.8	0.054
Female	13	35	72.9	
Age (years)				
≤57	29	40	58.0	0.380
>57	23	45	66.2	
Histology				
Squamous cell carcinoma	30	33	52.4	0.320
Adenocarcinoma	22	52	60.3	
Differentiation				
Well	16	14	46.7	0.035
Moderate	27	47	63.5	
Poor	9	24	77.4	
Nodal status				
No	21	19	47.5	0.024
Yes	31	66	68.0	
TNM stage				
I+II	34	35	50.7	0.006
III+IV	18	50	73.5	

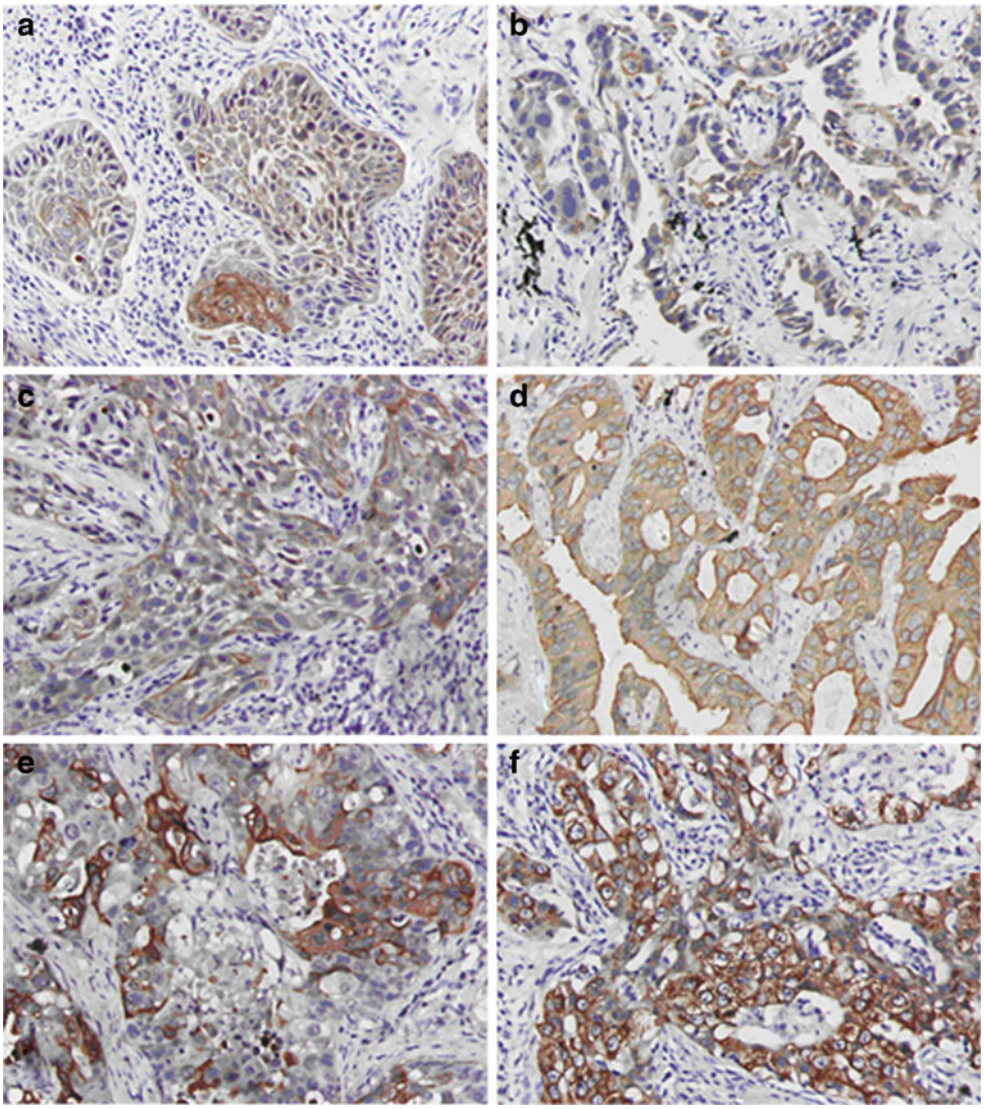

Fig. 2 Various levels of Frat1 expression correlate with tumor differentiation in lung squamous cell carcinoma (**a**, **c**, **e**) and lung adenocarcinoma (**b**, **d**, **f**). Note the expression of cytoplasmic Frat1 in moderately differentiated lung cancer (**c** and **d**) is higher than well differentiated (**a** and **b**) and lower than poorly differentiated lung cancer (**e** and **f**). **a**–**f** anti-Frat1 stain, ×400

differentiated adenocarcinoma, and 0.988±0.06 in poorly differentiated adenocarcinoma. Correspondingly, the Frat1 protein by Western blot analysis normalized to β-actin was 0 in normal lung tissues, 0.622±0.09 in well differentiated adenocarcinoma, 1.873±0.06 in moderately differentiated adenocarcinoma, and 2.623±0.09 in poorly differentiated adenocarcinoma. The results were in agreement with those obtained by immunohistochemical analysis.

Table 2 Frat1 expression in primary lesion and metastatic lesion

		Metastatic lesion		
		Negative	Positive	*P*
Primary lesion	Negative	2	19	0.015
	Positive	8	30	

The correlation between the expression of Frat1 and prognosis

Kaplan–Meier survival analyses demonstrated a median overall survival of 37.72 months (range, 3–112 months). When stratified by expression status of Frat1 in cancer tissues, the group with Frat1 expression showed significantly worse overall survival than the one without Frat1 expression (47.289±5.579 versus 70.176±7.528 months, P=0.037) (Fig. 5). However, multivariate Cox proportional hazard model analysis, which considers other variables, including gender, age, histology, differentiation, lymph node metastasis, and TNM stage, besides Frat1 expression, demonstrated that TNM stage was the sole independent prognostic predictor of overall survival, while the other factors, including the Frat1 expression, were not (Table 3).

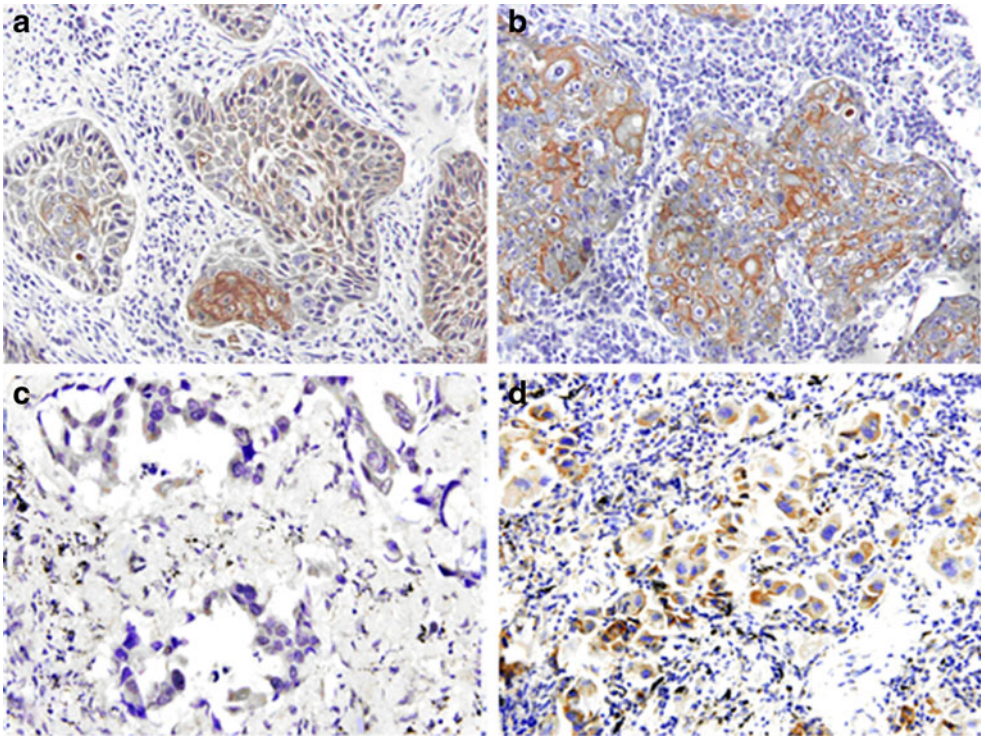

Fig. 3 Immunohistochemical analysis on primary lung cancer tissues and metastatic lymph nodes. Note that the expression of Frat1 in lymph node metastases (**b** and **d**) is higher than that in primary lesions (**a** and **c**). **a**, **b** Lung squamous cell carcinoma; **c**, **d** lung adenocarcinoma. **a**–**d** Anti-Frat1 stain, ×400

Interference of Frat1 expression can inhibit invasive ability of A549 cell line

We transfected an empty plasmid, scrambled siRNA and siRNA-Frat1 plasmids respectively into A549 cells, and enumerated invading cells at 6, 12 and 18 h after interference. The results showed that cell migration across the polycarbonate membrane was not observed in any group at 6-h point. It could be seen at 12-h point in all the groups, but the number of migrating cells across the membrane, indicating cell invasiveness, was varied among the three experimental groups, with the group of Frat1-siRNA showing significantly fewer invading cells than either of the other two control groups. The difference was statistically more significant at the 18-h point (84.55±10.78 versus 114.32±9.65, $P<0.05$ at 12-h point; and 133.18±17.06 versus 396.09±39.75, $P<0.001$ at 18-h point) (Fig. 6).

Discussion

The expression of Frat1 has been implicated in a limited number of human cancer tissues, including esophageal carcinoma, cervical carcinoma, breast carcinoma, ovarian carcinoma, and astrocytoma [3–6]. However, the expression status of Frat1 and its correlation with clinical and pathological factors have not been characterized in lung

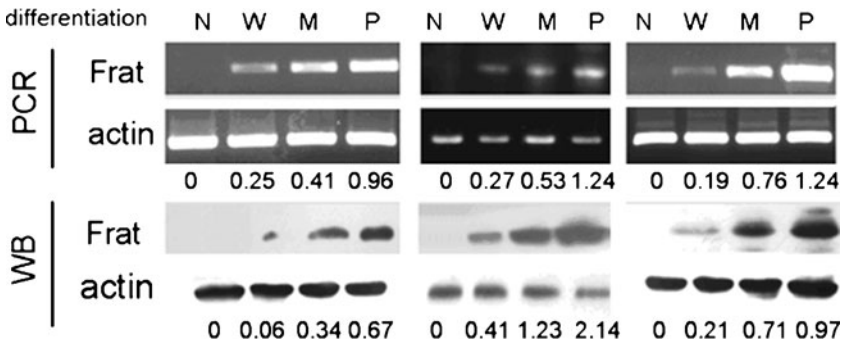

Fig. 4 Detection of Frat1 transcripts and protein in normal and lung cancer tissues by RT-PCR and Western blot analysis. Note the expression of Frat1 mRNA and protein in poorly differentiated lung adenocarcinoma was higher than that in either well or moderately differentiated lung adenocarcinoma. *N* Normal lung tissue, *W* well differentiated adenocarcinoma, *M* moderate differentiated adenocarcinoma, *P* poorly differentiated adenocarcinoma

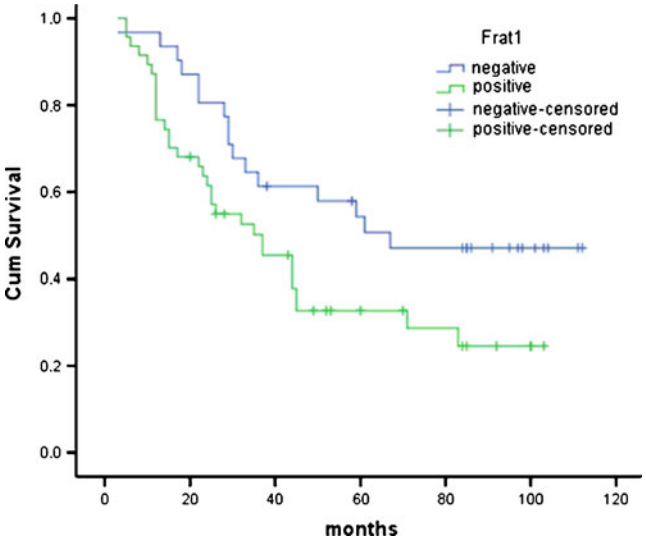

Fig. 5 Kaplan–Meier survival analysis of NSCLC patients, stratified by their status of Frat1 expression. Note the patients with cytoplasmic expression of Frat1 in tumor tissues correlates significantly with inferior survival in comparison with those without cytoplasmic Frat1

cancers. In this study, we demonstrated that the level of Frat1 expression in lung cancer tissues is significantly higher than that in normal lung tissues at both protein and transcript levels. In addition, there was a strong correlation between overexpression of Frat1 and advanced TNM stage. Expression levels of Frat1 were also correlated directly with nodal metastases and inversely with tumor differentiation (poorly differentiated tumors tended to have higher levels of Frat1 expression). Of more importance, overexpression of Frat1 was correlated with the poor overall survival in our lung cancer patients; however, its role in predicting clinical outcome might be confounded by its correlation with TNM staging. Not unexpectedly, down-regulation of Frat1 in lung cancer cells by using Frat1-siRNA resulted in inhibition of cancer cell invasion.

Frat was initially thought to be proto-oncogene of T-cell lymphomas [7, 8]. Previous studies showed that the human Frat family is composed of Frat1 and Frat2 [9]. The genes of these two Frat family members are intronless and localized to the same portion of chromosome 10q24.1 separated by only a 10.7 kb intervening sequence [10]. Recent studies have shown that Frat1 mRNA was undetectable in human normal lung tissues [4, 9]. Conversely, Frat1 was expressed in various cancer cell lines, including esophageal cancer cell lines TE2, TE3 and TE4, a cervical cancer cell line SKG-IIIa, and breast cancer cell lines MCF-7 and T-47D [10]. Moreover, expression of Frat1 was found in 47% of ovarian adenocarcinomas by in situ hybridization probes for Frat1 mRNA [4]. Frat1 protein expression, examined by immunohistochemistry and western blot analysis, was found to be much higher in human esophageal squamous cell carcinoma [3], gliomas [5] and human astrocytoma [6] compared to the autologous matched normal tissues. These data suggest that Frat1 may function as an oncoprotein in human malignancies in a more universal fashion. To address this issue, we examined Frat1 mRNA levels in 30 NSCLC tissues and their matched normal lung tissues by RT-PCR, and further tested Frat1 protein in 137 tumors by immunohistochemistry. We found that Frat1 expression was significantly higher in neoplastic than in non-neoplastic tissues at both mRNA and protein levels, which was in agreement with previous studies [3–6]. In addition, we demonstrated that expression of Frat1 was significantly correlated with tumor differentiation, lymph node metastasis and TNM stage in lung cancer patients, which was consistent with what was observed by Guo et al. [6] regarding correlation of Frat1 expression with proliferative index (PI) and pathologic grade in human astrocytoma. Importantly, our results for the first time showed that the expression of Frat1 was correlated with a poor overall survival in NSCLC patients. Because of the strong correlation of Frat1 expression with lymph node metastases and TNM stages, we thought that Frat1 might play a crucial role in lung cancer cell invasion. Thereby, we performed Trans-well cell migration assays and the result showed that Frat1 knockdown by transfection of Frat1-siRNA blocked

Table 3 Clinicopathological factors and Frat1 expression for overall survival in Cox regression analysis and independent predictor of overall survival in Cox regression analysis

Factors regression	Regression coefficient	Wald's χ^2 test	*P*
A. Clinicopathological factors and Frat1 expression for overall survival in Cox regression analysis			
Gender	0.044	0.580	0.446
Age	−0.015	0.492	0.483
Differentiation	0.032	0.081	0.776
TNM classification	0.005	6.020	0.014
Lymph node metastasis	0.015	4.244	0.039
Histological type	0.070	0.357	0.550
Frat1	−0.279	0.637	0.425
B. Independent predictor of overall survival in Cox regression analysis			
TNM classification	0.005	5.480	0.019

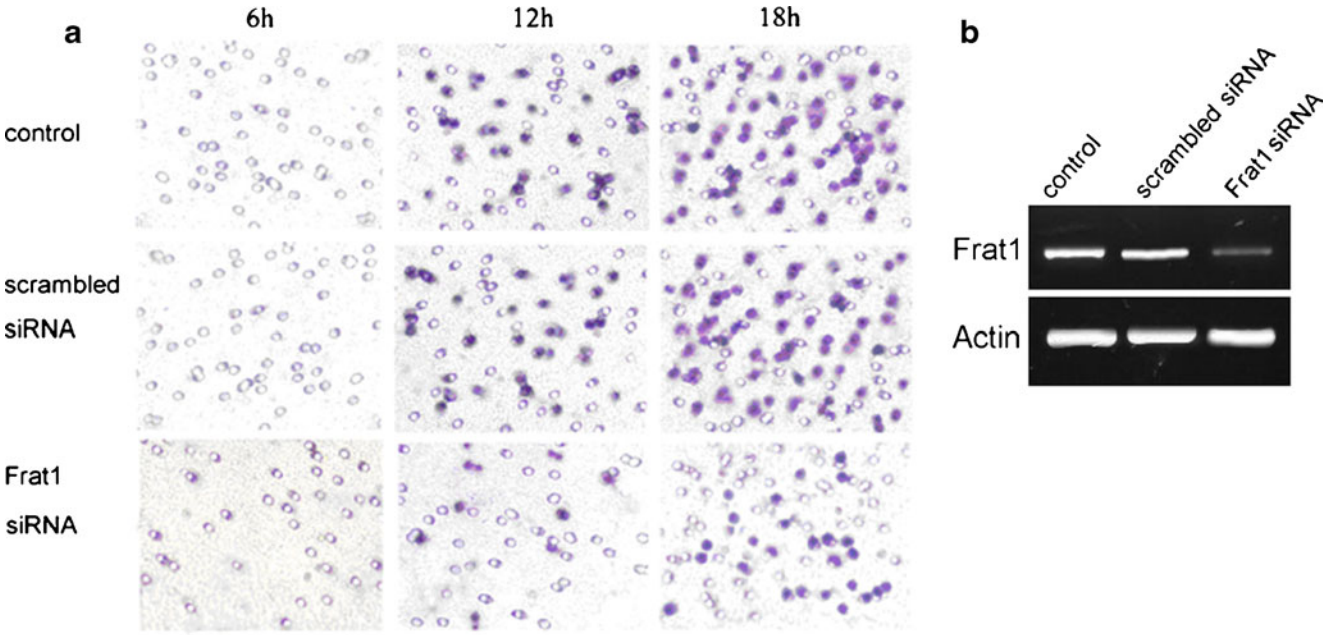

Fig. 6 Effect of Frat1 on cancer cell invasiveness. **a** Matrigel invasive assays. Note markedly decreased cell migration in the group transfected with Frat1-siRNA at 12- and 18-h time points in comparison to the two control groups. **b** RT-PCR for Frat1 transcripts. Note the markedly decreased Frat1 mRNA in the group transfected with Frat1-siRNA in comparison to the two control groups

cancer cell invasion in A549 cells. This result from an in vitro assay highly suggests that endogenous Frat1 may be involved in regulation of cell invasiveness in lung cancer. Taken together, the findings suggest that Frat1 might be up-regulated in NSCLC tissues resulting in lung cancer progression. Given the corresponding increase in both transcripts and protein in this study, the up-regulation of Frat1 expression seems to be at a transcriptional level in NSCLC.

Previous studies have provided evidence that up-regulation of Frat1 leads to carcinogenesis via the Wnt signal pathway in gastric cancer cell lines[10]. The exact role Frat1 plays in the canonical Wnt signal transduction pathway has been unknown until GBP, its homologous protein in *Xenopus* [11], was isolated from the GSK-3β complex [12–15]. When the Wnt signaling pathway is activated by binding of the Wnt ligand to the Frizzled (Frz) receptor, introcytoplasmic Dvl (Dishevelled) protein and Frat are activated in sequence [16–19]. Frat1 seems to be a positive regulator of the Wnt signaling pathway by relieving β-catenin from its multiprotein complex and thus stabilizing it [13, 20]. The accumulation of this key factor of the Wnt pathway in the cytoplasm facilitates its nuclear translocation and subsequent activation of Wnt/β-catenin target genes, such as c-*myc* and cyclin D1 [21, 22]. However, van Amerongen et al. [23–25] recently reported that the Frats are reminiscent of the dual function of Dvl in the Wnt/β-catenin and Frizzled/PCP pathways and suggested that Frat may also function to bridge the canonical and non-canonical Wnt pathways. The Wnt pathway is a complex system of cell signal transduction, and the exact role Frats plays in the pathway in governing carcinogenesis is largely unknown. Therefore, future studies focusing on the Wnt pathway in carcinogenesis, particularly on the function of Frats in lung cancer, may be warranted.

In summary, we demonstrated the overexpression of Frat1 at the mRNA and protein level in NSCLC, and the levels of its expression were strongly correlated with a malignant phenotype and clinical outcome. Correspondingly, down-regulation of Frat1 in the A549 lung cancer cell line significantly reduced its invasiveness. The findings suggest that Frat1 may play a crucial role in promoting lung cancer progression and tumor dissemination. However, the detailed mechanism underlying the overexpression of Frat1 in NSCLC and its exact role in the Wnt signal pathway remain to be further investigated. We hope that with further elucidation of the Wnt signaling pathway and its role in carcinogenesis, tumor invasiveness and dissemination, particularly in the development of lung cancer, Frat1 and/or other mediators in the Wnt pathway may serve not only as valuable biomarkers to predict clinical outcome in lung cancer patients, but also as therapeutic targets for specific pharmacologic or antibody-based therapeutic agents to circumvent the side effects of conventional chemotherapy currently used, and ultimately, improve the survival and quality of life for lung cancer patients.

Acknowledgements The authors thank Dr. Maggie Stoecker and Dr. Endi Wang, Department of Pathology, Duke University Medical Center, for their critical review and extensive editing of this revised manuscript. The study was supported by National Natural Scientific Foundation (grants 30870977 and 81071905 to Enhua Wang).

Conflict of interest The authors declare that they have no competing financial interests. No part of this article has been published or submitted elsewhere, and there are no financial or other relationships that might lead to a conflict of interest. The manuscript has been read and approved by all authors.

References

1. Culbert AA, Brown MJ, Frame S (2001) GSK-3inhibition by adenoviral Frat1 over-expression is neuroprotective and induces Tau dephosphorylation and beta-Catenin stabilisation without elevation of glycogensynthase activity. FEBS Lett 507(3):288–294
2. Hagen T, Cross DA, Culbert AA (2006) Frat1, a substrate-specific regulator of glycogen synthase kinase-3 activity, is a cellular substrate of protein kinase A. J Biol Chem 281(46):35021–35029
3. Wang Y, Liu S, Zhu H (2008) Frat1 over-expression leads to aberrant activation of beta-Catenin/TCF pathway in esophageal squamous cell carcinoma. Int J Cancer 123(3):561–568
4. Wang Y, Hewitt SM, Liu S (2006) Tissue microarray analysis of human Frat1 expression and its correlation with the subcellular localisation of beta-Catenin in ovarian tumours. Br J Cancer 13;94 (5):686–691
5. Guo G, Mao X, Wang P, Liu B (2010) The expression profile of Frat1 in human gliomas. Brain Res 1320:152–158
6. Guo G, Liu B, Zhong C (2009) Frat1 expression and its correlation with pathologic grade, proliferation, and apoptosis in human astrocytomas. Med Oncol 2009 Dec 30 [Epub ahead of print]
7. Jonkers J, Korswagen HC, Acton D (1997) Activation of a novel proto-oncogene, Frat1, contributes to progression of mouse T-cell lymphomas. EMBO J 16(3):441–450
8. Jonkers J, Weening JJ, van der Valk M (1999) Overexpressionof Frat1 in transgenic mice leads to glomerulosclerosis and nephrotic syndrome, and provides direct evidence for the involvement of Frat1 in lymphomaprogression. Oncogene 18(44):5982–5990
9. Freemantle SJ, Portland HB, Ewings K (2002) Characterization and tissue-specific expression of human GSK-3-binding proteins Frat1 and FRAT2. Gene 291(1–2):17–27
10. Saitoh T, Katoh M (2001) Frat1 and FRAT2, clustered in human chromosome 10q24.1 region, are up-regulated in gastric cancer. Int J Oncol 19:311–315
11. Salic A, Lee E, Mayer L (2000) Control of beta-Catenin stability: reconstitution of the cytoplasmic steps of the wnt pathway in *Xenopus* egg extracts. Mol Cell 5(3):523–532
12. Franca-Koh J, Yeo M, Fraser E (2002) The regulation of glycogen synthase kinase-3 nuclear export by Frat/GBP. J Biol Chem 277 (46):43844–43848
13. Hino S, Michiue T, Asashima M (2003) Casein kinase I epsilon enhances the binding of Dvl-1 to Frat-1 and is essential for Wnt-3a-induced accumulation of beta-Catenin. J Biol Chem 278(16):14066–14073
14. Webster MT, Rozycka M, Sara E (2000) Sequence variants of the axin gene in breast, colon, and other cancers: an analysis of mutations that interfere with GSK3 binding. Genes Chromosomes Cancer 28(4):443–453
15. Dajani R, Fraser E, Roe SM (2003) Structural basis for recruitment of glycogen synthase kinase 3beta to the axin-APC scaffold complex. EMBO J 22:494–501
16. Hay E, Faucheu C, Suc-Royer I (2005) Interaction between LRP5 and Frat1 mediates the activation of the Wnt canonical pathway. J Biol Chem 280(14):13616–13623
17. Ruiz S, Segrelles C, Santos M (2004) Functional link between retinoblastoma family of proteins and the Wnt signaling pathway in mouse epidermis. Dev Dyn 230(3):410–418
18. Fraser E, Young N, Dajani R (2002) Identification of the Axin and Frat binding region of glycogen synthase kinase-3. J Biol Chem 277(3):2176–2185, Epub 2001 Nov 13
19. Okino K, Nagai H, Hatta M (2003) Up-regulation and overproduction of DVL-1, the human counterpart of the Drosophila dishevelled gene, in cervical squamous cell carcinoma. Oncol Rep 10:1219–1223
20. Li L, Yuan H, Weaver CD (1999) Axin and Frat1 interact with dvl and GSK, bridging Dvl to GSK in Wnt-mediated regulation of LEF-1. EMBO J 18(15):4233–4240
21. Clements WM, Wang J, Sarnaik A (2002) beta-Catenin mutation is a frequent cause of Wnt pathway activation in gastric cancer. Cancer Res 62:3503–3506
22. Lim SC, Lee MS (2002) Significance of E-cadherin/beta-Catenin complex and cyclin D1 in breast cancer. Oncol Rep 9:915–928
23. Van Amerongen R, Berns A (2005) Re-evaluating the role of Frat in Wnt-signal transduction. Cell Cycle 4(8):1065–1072
24. Van Amerongen R, Nawijn MC, Lambooij JP (2010) Frat oncoproteins act at the crossroad of canonical and noncanonical Wnt-signaling pathways. Oncogene 29(1):93–104
25. Van Amerongen R, Nawijn M, Franca-Koh J (2005) Frat is dispensable for canonical Wnt signaling in mammals. Genes Dev 19(4):425–430

Virchows Arch (2011) 459:265–276
DOI 10.1007/s00428-011-1133-7

ORIGINAL ARTICLE

The preeminence of growth pattern and invasiveness and the limited influence of *BRAF* and *RAS* mutations in the occurrence of papillary thyroid carcinoma lymph node metastases

Catarina Eloy · Joana Santos · Paula Soares · Manuel Sobrinho-Simões

Received: 7 June 2011 / Revised: 12 July 2011 / Accepted: 12 July 2011 / Published online: 28 July 2011
© Springer-Verlag 2011

Abstract Prognostic factors indicative of papillary thyroid carcinoma (PTC) aggressive behaviour remain incompletely established partially due to the different composition of the series on record regarding the relative proportion of classic PTC (CPTC) and follicular variant PTC (FVPTC) subtypes. Several clinico-morphological features of PTC, together with the occurrence of *BRAF* mutations, are still not fully accepted as markers of aggressiveness. In the present clinico-pathological study of a series of 75 CPTC and FVPTC cases, we evaluated the relative contribution of the morphological features of the tumours and their *BRAF* and *N-RAS* status for the occurrence of nodal metastases. The morphological features most closely related to the occurrence of nodal metastases were extra-thyroid extension and poorly circumscribed growth pattern, in both CPTC and FVPTC. Additional features significantly associated to nodal metastases were multicentricity in the CPTC and vascular invasion in the FVPTC group. *BRAF* V600E mutation was detected in 29% of tumours, 41% of CPTC and 16% of FVPTC; *N-RAS* Q61R mutation was detected in 6% of tumours, 3% of CPTC and 10% of FVPTC. *BRAF* mutation was significantly more frequent in the CPTC group and in females, and it was detected only in patients older than 20 years, suggesting a late tumourigenic effect in the development of PTC. *BRAF* mutation was not significantly associated to any of the other studied features related to aggressiveness or nodal metastases. These results highlight the importance of infiltrative growth pattern and invasiveness over the presence of *BRAF* mutation in classic and follicular variant PTC for the development of nodal metastases.

Keywords Papillary thyroid carcinoma · *BRAF* · RAS · Staging · Prognosis

C. Eloy · M. Sobrinho-Simões
Pathology Department, Hospital de São João,
Oporto, Portugal

C. Eloy · P. Soares · M. Sobrinho-Simões
Pathology Department, Medical Faculty, University of Porto,
Oporto, Portugal

C. Eloy · J. Santos · P. Soares · M. Sobrinho-Simões
Institute of Molecular Pathology and Immunology
of the University of Porto (IPATIMUP),
Oporto, Portugal

C. Eloy
Dentistry Faculty, University of Porto,
Oporto, Portugal

C. Eloy (✉)
Anatomic Pathology, Hospital de São João,
Alameda Professor Hernani Monteiro,
4200-451 Oporto, Portugal
e-mail: catarinaeloy@hotmail.com

Introduction

Papillary thyroid carcinoma (PTC) is the most frequent malignant endocrine neoplasia encompassing 16 variants in the last WHO classification [1]. If one excludes the incidentally found papillary microcarcinomas, the classic PTC (CPTC) and the follicular variant of PTC (FVPTC) are the most frequently diagnosed variants. CPTC and FVPTC present distinct cytoarchitectural features [1], molecular alterations [2–4] and biological behaviour [2,

5, 6]. The majority of CPTC and FVPTC cases evolve favourably, and the patients have a 10-year survival up to 98% [1, 7]; the outcome is particularly favourable in patients with encapsulated tumours [8–10]. Despite the (very) good prognosis, PTCs may give rise to recurrences and/or metastases, sometimes many years after diagnosis [11].

There are several clinical and/or morphological features of PTC that have been frequently, though not always, associated to a less favourable prognosis, namely advanced age at time of diagnosis [6, 11, 12], male gender [11], tumour size above 1 cm [6, 13], extra-thyroid extension [6, 12, 14, 15], multicentricity [6], absence of total encapsulation [6, 8, 9, 14], vascular invasion [6] and distant metastases [6, 12]. The presence of lymph node metastases is not fully accepted as a prognostic factor, and it is not associated to an increased mortality rate despite being determinant for the type of surgical approach and radioactive iodine therapy [6, 12].

Part of the controversies on the prognostic value of the above-mentioned features reflects the variable composition of the different series. This holds particularly true regarding the relative proportion of CPTC and FVPTC in general and of the encapsulated subtype of FVPTC in particular [8, 16]. The variable percentages of CPTC and FVPTC in the different series also contribute to explain the variation of the prevalence of *BRAF* mutations from 7% to 83% [3, 4, 12, 14, 16–26] and that of *RAS* mutations from 0 to 43% [3, 4, 18, 24, 26–29].

BRAF is a critical effector of the canonic mitogen-activated protein kinase (MAPK) pathway having the V600E as its most frequent mutation; this mutation is present in 40–54% of CPTC [16, 17, 21, 23, 25] and in 7–29% of FVPTC [3, 16, 21, 23, 25, 26]. *BRAF* mutations have been associated to the classic PTC phenotype [16, 21, 23], advanced age at time of diagnosis [12, 16, 23], male gender [22], tumour size above 1 cm [25], extra-thyroid extension [23, 30, 31], absence of total encapsulation [3, 30], vascular invasion [12], lymph node metastases [14, 19, 30], distant metastases [20], recurrence [30] and higher tumour stages [12, 20].

RAS is an oncogene that also plays a role in the canonic MAPK pathway and is mutated in 0–23% of CPTC [4, 26–28] and in 25–43% of FVPTC [3, 4, 26, 27]. *RAS* mutations have been associated to large tumour size [26], encapsulation [3, 27, 31], vascular invasion [27], extra-thyroid extension [31], poorly differentiated areas [27] and low rate of lymph node metastases [27, 31]. *BRAF* and *RAS* mutations appear to be alternative events in PTC [18].

In the present clinico-pathological study of a series of 75 CPTC and FVPTC cases, we evaluate the relative contribution of the morphological features of the tumours (namely growth pattern and invasiveness) and their *BRAF* and *N-RAS* status for the occurrence of lymph node metastases.

Materials and methods

Tumour samples

A series of 75 PTC cases was retrieved from the Cancer Registry of the Pathology Department of Hospital São João: 42 CPTC and 33 FVPTC. Both CPTC and FVPTC groups included cases with lymph node metastases (+M), together or not with distant metastases, and cases without metastases and long-term follow-up (−M). The PTC−M subgroup included all the CPTC and FVPTC cases with at least 10 years of follow-up, available stored material representative of the tumour and imagiological and/or cytological data confirmative of the absence of metastases in the lymph nodes, lungs and bones. The PTC+M subgroup included more recent cases of CPTC and FVPTC with available material representative of the tumour and its lymph node metastases present at the time of surgery or developed during follow-up. Three cases disclosed, together with lymph node metastases, lung metastases detected in image studies (cases 36 and 37 of CPTC+M subgroup and case 33 of FVPTC+M subgroup). Both in cases with and without lymph node metastases, there were tumours larger than 1 cm and small tumours with 1 cm or less in diameter that were classified according to their growth pattern as CPTC or FVPTC. None of the patients of the PTC+M subgroup died from the disease (this information has limited value due to the short follow-up of most of the cases).

All samples had been fixed in formalin and included in paraffin. Clinical data were collected from the reports and clinical files; H&E slides were retrieved from the archives and reviewed independently by two pathologists (CE and MSS), and the tumours were classified using the WHO criteria [1]. Cases with doubtful PTC features were excluded. Well-circumscribed tumours were those with expansive pattern of growth without capsule or limited by a capsule with no or minimal invasion, and poorly circumscribed tumours were those with infiltrative pattern of growth or with a widely invaded capsule. Vascular invasion was considered to be present whenever at least one image of unequivocal venous vessel invasion was observed. Extra-thyroid extension was considered to be present when macroscopic extra-thyroid extension was observed. Under the designation of multicentricity, all multifocal lesions, regardless of representing multicentric tumours or intra-thyroidal disseminated carcinomas, were included. The presence of oncocytic cells was considered whenever they accounted for more than 10% of the tumour cells. Clinical and morphological features of the major tumour of each case were registered in an informatic supported database.

Mutation screening

Genomic DNA was extracted from 10-μm sections of 65 tumours: 34 CPTC and 31 FVPTC (the remaining cases have insufficient available material). Slides were microscopically examined, marked and dissected under microscopic observation. The obtained material was deparaffinized in xylene, washed in ethanol and rehydrated. DNA extraction was performed using the Genomic DNA Purification Kit (Gentra Systems, Inc., Minneapolis, MN) according to the manufacturer's instructions. Sequences of *BRAF* (exon 15) and *N-RAS* (exon 2) genes were amplified using primer pairs listed in Table 1, using a programmable thermocycler (MyCycler, Bio-Rad, USA). The PCR mixture (25 μl) contained 2.5 μl ×10 PCR buffer, 0.8 mM dNTPs (Fermentas), 0.07 μg each primer, 0.1–0.2 μg genomic DNA, 0.5 U Taq DNA Polymerase (Go Taq Flexi DNA Polymerase, Promega Corporation) and 2.5 mM magnesium chloride (Promega Corporation). After 10 min of initial denaturation, the PCR mixtures were subjected to 35 cycles of denaturation for 30 s at 95°C, annealing according to the amplicon and extension for 45 (*BRAF*) and 40 s (N-*RAS*) at 72°C. A final extension period of 10 min at 72°C was performed. PCR products were submitted to electrophoresis in agarose gel and purified by enzymatic treatment. Purified samples were sequenced on both strands as follows: 3 μl purified PCR product was added to 7 μl sequencing reaction containing 3.4 μl Sequencing Buffer (Applied Biosystems, Forester City, CA), 30 ng primer and 0.6 μl Big Dye Terminator (Applied Biosystems). Sequencing was performed in an ABI Prism 3100 Genetic Analyser (Applied Biosystems). Mutated samples were re-extracted, re-amplified and re-sequenced to confirm the result.

Statistical analysis

The results are expressed as absolute values, percentages and/or mean ± standard deviation. The χ^2 test with Yates correction and Student's *t* test (unpaired) were used in the statistic analysis. Two values were considered significantly different whenever $p<0.05$.

Results

Tables 2 and 3 summarize the clinical, morphological and molecular features of the 42 CPTC cases and those of the 33 FVPTC cases, respectively. CPTC and FVPTC cases had similar clinical and morphological features except different frequencies of poorly circumscribed tumours (83.3% of CPTC and 54.5% of FVPTC, $p=0.010$) and vascular invasion (28.6% of CPTC and 57.6% of FVPTC, $p=0.018$) (Tables 4 and 5).

CPTC

The 42 CPTC cases were 23 CPTC−M (54.8%) with a mean follow-up time of 19.9±2.5 years and 19 CPTC+M (45.2%) with a mean follow-up time of 5.5±3.2 years. The CPTC−M cases included 20 females (87.0%) with a mean age of 41.5±15.7 years and 3 males (13.0%) with a mean age of 49.3±21.4 years. The patients with CPTC−M underwent partial thyroidectomy (lobectomy or lobectomy plus isthmectomy) in 60.9% of cases and total thyroidectomy in 34.8% of cases; in 4.3% of the cases, the precise extension of the surgery was not known. The CPTC+M cases included 15 females (78.9%) with a mean age of 38.1±19.1 years and 4 males (21.1%) with a mean age of 22.3±14.0 years. The patients with CPTC+M underwent total thyroidectomy with or without lymph node dissection in 73.7% and 26.3% of cases, respectively.

CPTC−M tumours presented less often poorly circumscribed growth pattern (69.6% of CPTC−M and 100.0% of CPTC+M, $p=0.010$), extra-thyroid extension (13.0% of CPTC−M and 47.4% of CPTC+M, $p=0.020$) and multicentricity (26.1% of CPTC−M and 63.2% of CPTC+M, $p=0.028$) than CPTC+M (Table 4).

CPTC−M and CPTC+M cases were not significantly different concerning gender, age, size, presence of capsule or capsular invasion, vascular invasion (Table 4) and not also concerning necrosis (21.7% and 21.1%, respectively), intra-tumoural inflammation (60.9% and 63.2%, respectively), oncocytic cells (43.5% and 26.3%, respectively) and mitotic index (0.70 and 0.53 mitoses/10 HPF, respectively). The lymphocyte-rich stroma was detected only in two CPTC−M tumours (Table 2). In the adjacent thyroid

Table 1 Primers and PCR conditions

Gene	Exon	Primer sequence	Length (bp)	PCR annealing temperature (°C)	PCR annealing time (seconds)
BRAF	15	F:TCATAATGCTTGCTCTGATAGGA R: GGCCAAAAATTTAATCAGTGGA	224	58	40
N-RAS	2	F: GATTCTTACAGAAAACAAGT R: CCTTCGCCTGTCCTCATGTATT	119	57	35

Table 2 Clinical, morphological and molecular features of the CPTC cases

N	Gender	Age (years)	Follow-up (years)	Tumour size (cm)	Capsule	Capsular invasion	Growth pattern	Multicentricity	EE	Vascular invasion	Necrosis	Mitotic index[a]	Oncocytic cells	Stroma type	II	Thyroiditis[b]	BFP	Surgery type	At the time of diagnosis		*BRAF*	*N-RAS*	LNM
																			pTNM	Stage			
1	M	58	17	0.8	+	+	P	−	−	−	−	1	−	C	−	f	−	PT	T1aN0M0	I	ND	ND	−
2	F	66	19	1.5	+	+	W	−	−	−	−	1	−	C	+	−	NG	T	T1bN0M0	I	ND	ND	−
3	F	31	21	3.5	+	+	P	+	−	−	+	0	−	Pc	−	−	FA	PT	T2N0M0	I	−	−	−
4	F	59	21	0.6	+	+	P	+	−	−	+	1	+	−	−	−	NG	PT	T1aN0M0	I	−	−	−
5	F	37	21	1.0	+	−	W	+	−	−	−	1	+	L	+	f	−	T	T1aN0M0	I	ND	ND	−
6	F	35	18	0.3	+	+	P	−	−	−	−	0	−	Pc	−	−	NG	PT	T1aN0M0	I	ND	ND	−
7	F	40	18	1.5	−	NA	P	−	−	−	−	0	+	L	+	+	−	T	T1bN0M0	I	V600E	−	−
8	F	38	18	0.5	−	NA	P	−	−	−	−	0	−	C	−	−	NG	PT	T1aN0M0	I	ND	ND	−
9	M	25	20	1.2	−	NA	P	−	−	+	+	0	−	C	−	−	−	PT	T1bN0M0	I	−	−	−
10	F	30	21	0.6	−	NA	P	+	−	−	−	2	+	C	+	f	−	PT	T1aN0M0	I	V600E	−	−
11	F	40	20	2.2	−	NA	W	−	−	−	−	0	+	−	+	f	−	T	T2N0M0	I	−	−	−
12	F	50	20	3.0	+	+	W	−	−	−	+	0	−	C	+	f	−	PT	T2N0M0	II	V600E	−	−
13	F	25	17	2.1	+	+	W	−	−	−	+	0	−	Pc	+	−	−	T	T2N0M0	I	V600E	−	−
14	F	45	22	4.5	+	−	W	+	−	−	−	1	+	−	−	−	−	PT	T3N0M0	III	V600E	Q61R	−
15	F	23	24	2.5	−	NA	P	−	−	−	−	1	−	Pc	+	−	NG	ND	T2N0M0	I	−	−	−
16	M	65	24	2.3	−	NA	P	−	−	−	−	0	−	C	+	f	−	PT	T2N0M0	II	−	−	−
17	F	21	19	2.0	−	NA	P	−	−	+	−	3	−	C	+	f	−	PT	T1bN0M0	I	V600E	−	−
18	F	79	23	2.8	+	+	P	−	+	−	−	0	−	C	+	f	−	PT	T3N0M0	III	−	−	−
19	F	65	16	3.5	−	NA	P	−	+	−	−	1	+	Pc	+	f	NG	T	T3N0M0	III	V600E	−	−
20	F	28	24	2.5	−	NA	P	−	−	+	−	2	+	C	−	−	−	T	T2N0M0	I	−	−	−
21	F	28	20	2.0	−	NA	P	−	−	+	−	1	−	C	−	−	−	PT	T1bN0M0	I	V600E	−	−
22	F	43	18	1.5	+	+	W	+	−	+	−	0	+	C	+	−	−	PT	T1bN0M0	I	−	−	−
23	F	47	16	4.5	−	NA	P	−	+	+	−	1	+	Pc	+	f	−	T	T3N0M0	III	V600E	−	−
24	F	28	5	0.9	+	+	P	−	−	−	−	0	+	−	−	−	−	T	T1aN1M0	I	V600E	−	+
25	F	21	6	1.2	+	+	P	−	−	−	+	0	+	C	+	+	NG	TL	T1bN1M0	I	−	−	+
26	F	22	14	1.9	−	NA	P	+	−	−	−	1	−	−	−	−	−	TL	T1bN1M0	I	−	−	+
27	F	30	3	1.3	+	+	P	−	+	+	−	0	−	Pc	+	+	−	TL	T3N1M0	I	−	−	+
28	F	56	3	0.7	−	NA	P	+	−	−	−	0	−	−	+	−	NG	TL	T1aN1M0	III	−	−	+
29	F	18	3	1.5	−	NA	P	+	+	+	−	1	−	C	+	f	−	T	T3N1M0	I	−	−	+
30	M	22	4	1.1	−	NA	P	+	−	−	−	1	−	Pc	−	+	−	TL	T1bN1M0	I	−	−	+
31	F	22	6	0.8	−	NA	P	−	−	−	+	0	−	C	+	−	−	TL	T1aN1M0	I	ND	ND	+
32	F	56	3	0.8	−	NA	P	+	−	−	−	0	−	Pc	−	−	−	TL	T1aN1M0	III	ND	ND	+
33	M	42	5	1.6	−	NA	P	+	+	−	+	0	+	Pc	+	f	−	TL	T3N1M0	I	−	−	+
34	F	38	7	3.0	+	+	P	+	−	+	−	1	−	Pc	+	+	−	T	T2N1M0	I	V600E	−	+
35	F	35	5	1.7	+	+	P	−	−	+	−	0	−	C	+	f	−	TL	T1bN1M0	I	V600E	−	+
36	M	11	9	6.0	−	NA	P	+	+	+	−	0	−	C	+	f	−	TL	T4aN1M0	II	−	−	+[c]
37	F	56	4	2.4	−	NA	P	−	+	−	−	1	+	C	+	−	−	TL	T3N1M0	IVC	−	−	+[c]
38	F	83	1	7.5	−	NA	P	−	+	−	+	1	+	−	+	−	−	T	T4aN1M0	IVA	V600E	−	+
39	F	18	4	3.6	−	NA	P	+	−	+	−	0	−	C	−	−	−	TL	T2N1M0	I	−	−	+
40	M	14	4	2.5	−	NA	P	+	+	−	−	1	−	Pc	−	F	−	TL	T3N1M0	I	−	−	+

Table 2 (continued)

N	Gender	Age (years)	Follow-up (years)	Tumour size (cm)	Capsule	Capsular invasion	Growth pattern	Multicentricity	EE	Vascular invasion	Necrosis	Mitotic index[a]	Oncocytic cells	Stroma type	II	Thyroiditis[b]	BFP	Surgery type	At the time of diagnosis		*BRAF*	*N-RAS*	LNM
																			pTNM	Stage			
41	F	32	9	1.1	–	NA	P	–	+	–	–	1	–	C	–	F	NG	T	T3N1M0	I	V600E	–	+
42	F	56	10	7.5	–	NA	P	+	+	–	–	2	–	C	+	F	–	TL	T3N1M0	III	ND	ND	+

N number, *M* male, *F* female, + presence, – absence, *W* well circumscribed, *P* poorly circumscribed, *EE* extra-thyroid extension, *C* cellular, *Pc* poorly cellular, *L* lymphocyte rich, *II* intra-tumoural inflammation, *f* focal, *BFP* benign follicular pathology in the adjacent thyroid tissue, *NG* nodular goitre, *FA* follicular adenoma, *ND* not determined, *NA* not applicable, *LNM* lymph node metastases, *PT* partial thyroidectomy, *T* total thyroidectomy, *TL* total thyroidectomy with lymph node dissection

[a] Number of mitoses per 10 high power fields (×400)

[b] Thyroiditis was considered + whenever Hashimoto thyroiditis features were present

[c] Cases with concurrent distant metastases

parenchyma, there were no significantly different frequencies of focal or diffuse Hashimoto type thyroiditis in CPTC−M and CPTC+M cases (47.8% and 57.9%, respectively), nor of benign follicular pathology (30.4% and 15.8%, respectively) (Table 4).

FVPTC

The 33 FVPTC cases were 25 FVPTC−M (75.8%) with a mean follow-up time of 17.7±3.7 years and 8 FVPTC+M (24.2%) with a mean follow-up time of 6.9±4.1 years. The FVPTC−M cases included 22 females (88.0%) with a mean age of 41.7±12.2 years and 3 males (12.0%) with a mean age of 47.0±13.1 years. The patients with FVPTC−M underwent partial thyroidectomy (lobectomy or lobectomy plus isthmectomy) in 60.0% of cases or total thyroidectomy in 40.0% of cases. The FVPTC+M cases included five females (62.5%) with a mean age of 42.2±13.5 years and three males (37.5%) with a mean age of 47.0±22.7 years. The patients with FVPTC+M underwent total thyroidectomy with or without lymph node dissection in 75.0% and 25.0% of cases, respectively.

FVPTC−M tumours were significantly less often poorly circumscribed than FVPTC+M (40.0% of FVPTC−M and 100.0% of FVPTC+M, $p=0.004$), presented significantly less often extra-thyroid extension (0.0% of FVPTC−M and 50.0% of FVPTC+M, $p=0.002$) and vascular invasion (44.0% of FVPTC−M and 100.0% of FVPTC+M, $p=0.010$).

FVPTC−M and FVPTC+M displayed different mean mitotic indexes (0.28 and 1.25 mitoses/10 HPF, respectively; $p=0.031$). FVPTC−M cases presented significantly more often (56.0%) benign follicular pathology in the adjacent thyroid parenchyma than FVPTC+M tumours (12.5%) ($p=0.046$). In the subgroup of tumours with 1 cm or less, all the FVPTC−M had associated benign follicular pathology (8 out of 8), while none of the FVPTC+M had associated benign follicular pathology (0 out of 2). A similar difference was observed in the subgroup of tumours larger than 1 cm (14 out of 25 and 1 out of 8, respectively) ($p=0.022$).

FVPTC−M and FVPTC+M were not significantly different concerning gender, age, presence of capsule or capsular invasion, multicentricity (Table 4), nor necrosis (8.0% and 0.0%, respectively), intra-tumoural inflammation (32.0% and 62.5%, respectively), presence of oncocytic cells (36.0% and 0.0%, respectively), focal or diffuse Hashimoto type thyroiditis (36.0% and 25.0%, respectively) and stroma types (Table 4).

PTC+M versus PTC−M

Table 4 summarizes the differences between the 27 PTC+M and the 48 PTC−M. PTC+M cases presented more often a

Table 3 Clinical, morphological and molecular features of the FVPTC cases

N	Gender	Age (years)	Follow-up (years)	Tumour size (cm)	Capsule	Capsular invasion	Growth pattern	Multicentricity	EE	Vascular invasion	Necrosis	Mitotic index[a]	Oncocytic cells	Stroma type	I I	Thyroiditis[b]	BFP	Surgery type	At the time of diagnosis		*BRAF*	*N-RAS*	LNM
																			pTNM	Stage			
1	F	32	22	2.0	+	+	W	−	−	+	−	2	+	Pc	+	f	−	PT	T1bN0M0	I	−	−	−
2	F	26	21	1.8	−	NA	P	+	−	+	−	0	−	Pc	−	−	−	PT	T1bN0M0	I	V6ooE	−	−
3	F	59	19	0.5	+	−	W	−	−	−	+	0	+	−	+	−	NG	T	T1aN0M0	I	−	−	−
4	F	51	18	1.4	+	−	W	−	−	−	−	0	+	C	+	−	NG	T	T1bN0M0	I	−	−	−
5	F	36	18	0.5	−	NA	P	−	−	−	−	0	−	C	+	−	NG	PT	T1aN0M0	I	V6ooE	−	−
6	F	39	15	1.0	−	NA	W	+	−	−	−	1	−	−	−	−	NG	PT	T1aN0M0	I	−	Q61R	−
7	F	48	13	0.6	+	−	W	−	−	−	−	0	−	Pc	−	+	NG	PT	T1aN0M0	I	−	−	−
8	F	33	20	0.2	−	NA	P	−	−	−	−	0	−	C	+	+	FA	T	T1aN0M0	I	−	−	−
9	F	30	15	0.5	−	NA	W	−	−	−	−	0	−	−	−	−	NG	PT	T1aN0M0	I	−	−	−
10	F	21	21	0.6	−	NA	P	−	−	−	−	0	−	−	−	f	NG	T	T1aN0M0	I	−	−	−
11	F	37	18	0.3	−	NA	P	−	−	+	−	0	−	Pc	−	−	NG	PT	T1aN0M0	I	−	−	−
12	F	28	21	2.8	−	NA	W	+	−	+	−	0	−	Pc	−	−	−	T	T2N0M0	I	−	−	−
13	F	34	20	3.5	+	−	W	−	−	−	−	0	−	Pc	−	f	−	PT	T2N0M0	I	−	−	−
14	M	61	22	4.0	+	+	W	−	−	+	−	0	−	−	−	−	−	T	T2N0M0	II	V6ooE	−	−
15	M	35	20	3.5	+	+	W	−	−	+	−	0	−	−	−	−	−	PT	T2N0M0	I	−	Q61R	−
16	F	50	20	2.5	+	+	W	−	−	−	−	1	−	−	−	−	−	PT	T2N0M0	II	−	−	−
17	F	47	23	3.0	−	NA	P	−	−	−	−	0	+	−	−	−	−	PT	T2N0M0	II	−	Q61R	−
18	F	49	14	3.0	+	+	W	+	−	+	−	0	−	−	−	f	NG	T	T2N0M0	II	−	−	−
19	F	35	21	1.7	−	NA	P	+	−	+	−	1	−	Pc	+	f	NG	PT	T1bN0M0	I	ND	ND	−
20	F	32	13	4.7	−	NA	P	+	−	+	−	0	+	−	−	−	−	T	T3N0M0	I	−	−	−
21	F	52	13	2.5	+	+	W	+	−	−	−	1	−	Pc	−	−	NG	T	T2N0M0	II	−	−	−
22	F	66	13	2.5	+	+	W	+	−	−	+	0	+	Pc	−	f	−	PT	T2N0M0	II	−	−	−
23	F	58	13	1.5	−	NA	P	+	−	+	−	1	+	C	+	−	NG	PT	T1bN0M0	I	V6ooE	−	−
24	F	54	10	1.8	−	NA	P	+	−	+	−	0	+	Pc	+	f	NG	PT	T1bN0M0	I	−	−	−
25	M	45	20	4.0	+	+	W	−	−	−	−	0	+	−	−	−	−	T	T2N0M0	II	−	−	−
26	M	57	3	9.5	+	+	P	−	+	+	−	6	−	−	−	−	−	TL	T3N0M0	III	−	−	+
27	F	56	3	0.8	+	+	P	+	−	+	−	0	−	Pc	+	−	−	TL	T1aN1M0	III	−	−	+
28	M	21	4	2.5	−	NA	P	−	+	+	−	1	−	C	+	−	−	TL	T4aN1M0	I	−	−	+
29	F	20	14	1.0	−	NA	P	+	−	+	−	1	−	−	+	+	−	TL	T1aN1M0	I	ND	ND	+
30	F	49	4	2.2	+	+	P	−	−	+	−	1	−	−	−	−	−	T	T2N1M0	III	−	−	+
31	F	43	10	4.0	−	NA	P	+	+	+	−	1	−	−	+	f	−	TL	T4aN1M0	I	−	−	+
32	F	43	10	1.5	−	NA	P	+	+	+	−	0	−	C	+	−	−	TL	T3N1M0	I	V6ooE	−	+
33	M	63	7	1.8	+	+	P	−	−	+	−	0	−	−	−	−	FA	T	T1bN0M0	I	−	−	+[c]

N number, *M* male, *F* female, + presence, − absence, *W* well circumscribed, *P* poorly circumscribed, *EE* extra-thyroid extension, *C* cellular, *Pc* poorly cellular, *L* lymphocyte rich, *II* intra-tumoural inflammation, *f* focal, *BFP* benign follicular pathology in the adjacent thyroid tissue, *NG* nodular goitre, *FA* follicular adenoma, *ND* not determined, *NA* not applicable, *LNM* lymph node metastases, *PT* partial thyroidectomy, *T* total thyroidectomy, *TL* total thyroidectomy with lymph node dissection

[a] Number of mitoses per 10 high power fields (×400)

[b] Thyroiditis was considered + whenever Hashimoto thyroiditis features were present

[c] Cases with concurrent distant metastases

Table 4 Comparison of clinical and morphological features of CPTC and FVPTC cases with and without lymph node metastases (LNM)

PTC variant	Features	With LNM	Without LNM	*p* value
CPTC	Gender (female/male)	15:4	20:3	>0.1
	Age, years (mean ± SD)	34.7±19.0	42.5±16.2	
	Tumour size of tumours >1, cm (mean ± SD)	2.9±2.3	2.5±1.0	
	Tumour size of tumours ≤1, cm (mean ± SD)	0.8±0.1	0.6±0.2	
	Capsule (absence/total)	0.74	0.52	
	Capsule invasion (presence/total)	1.00	0.82	
	Vascular invasion (presence/total)	0.32	0.26	
	Multicentricity (presence/total)	0.63	0.26	<0.05
	Growth pattern (poorly circumscribed/total)	1.00	0.70	
	Extra-thyroid extension (presence/total)	0.47	0.13	
FVPTC	Gender (female/male)	5:3	22:3	>0.1
	Age, years (mean ± SD)	44.0±16.1	42.3±12.1	
	Tumour size of tumours >1, cm (mean ± SD)	3.6±3.0	2.7±1.0	
	Capsule (absence/total)	0.50	0.52	
	Capsule invasion (presence/total)	1.00	0.67	
	Multicentricity (presence/total)	0.50	0.40	
	Tumour size of tumours ≤1, cm (mean ± SD)	0.9±0.1	0.5±0.2	0.1–0.05
	Vascular invasion (presence/total)	1.00	0.44	<0.05
	Growth pattern (poorly circumscribed/total)	1.00	0.40	
	Extra-thyroid extension (presence/total)	0.50	0.00	
CPTC + FVPTC	Gender (female/male)	20:7	42:6	>0.1
	Age, years (mean ± SD)	37.5±18.4	42.4±14.1	
	Tumour size of tumours >1, cm (mean ± SD)	3.1±2.4	2.6±1.0	
	Capsule (absence/total)	0.67	0.52	
	Capsule invasion (presence/total)	1.00	0.74	
	Vascular invasion (presence/total)	0.52	0.35	
	Multicentricity (presence/total)	0.59	0.33	0.1–0.05
	Tumour size of tumours ≤1, cm (mean ± SD)	0.8±0.1	0.6±0.2	<0.05
	Growth pattern (poorly circumscribed/total)	1.00	0.54	
	Extra-thyroid extension (presence/total)	0.48	0.06	

poorly circumscribed growth pattern ($p<0.0001$), extra-thyroid extension ($p<0.0001$) and larger size of the tumours in the group with 1 cm or less ($p=0.019$) than PTC−M tumours. PTC+M tumours tended to be more often multicentric than PTC−M tumours ($p=0.051$).

When comparing poorly circumscribed CPTC+M and CPTC−M tumours, the former were more often multicentric than the latter (57.9% and 18.8%, respectively; $p=0.036$) (Table 6). Similarly, poorly circumscribed FVPTC+M tumours displayed more often extra-thyroid extension than FVPTC−M (50.0% and 0.00%, respectively; $p=0.023$) (Table 6).

Mutational analysis: BRAF and N-RAS

Overall, the *BRAF* V600E mutation occurred in 19 out of 65 PTC cases (29.2%), and the *N-RAS* Q61R mutation occurred in 4 out of 65 PTC tumours (6.2%). The frequency of *BRAF* mutation in the CPTC group was significantly higher than in the FVPTC group (41.2% and 16.1%, respectively) ($p=0.032$), and occurred in 13 out of 42 PTC−M tumours (31.0%) and in 6 out of 23 PTC+M tumours (26.1%). The *N-RAS* mutation occurred only in PTC−M tumours (Tables 2 and 3).

In the CPTC group, 9 out of 18 CPTC−M (50.0%) and 5 out of 16 CPTC+M (31.3%) displayed *BRAF* mutation. The presence of *BRAF* mutation in CPTC was significantly associated to female gender ($p=0.031$) (14 females and 0 males) (Table 5). *N-RAS* mutation was detected in 1 out of 34 CPTC tumours (2.9%); it was a Q61R mutation in a well-circumscribed encapsulated CPTC−M tumour (1 out of 18–5.6%).

In the FVPTC group, the *BRAF* V600E mutation was detected in four FVPTC−M (16.7%) and one FVPTC+M (14.3%). *N-RAS* Q61R mutation was detected in 3 out of 31 cases (9.7%); all of such cases were FVPTC−M tumours (3 out of 24–12.5%).

Table 5 Comparison of molecular features of CPTC and FVPTC cases

PTC variant	Features	*BRAF* wild type	*BRAF* V600E	*p* value
CPTC	Gender (female/male)	14:6	14:0	0.031
	Age, years (mean ± SD)	35.2±19.0	40.5±16.9	0.41
	Tumour size, cm (mean ± SD)	2.2±1.2	2.7±1.9	0.294
	Number of tumours (>1 cm/total)	0.90	0.86	>0.999
	Capsule (absence/total)	0.70	0.57	0.487
	Capsule invasion (presence/total)	1.00	0.83	>0.999
	Growth pattern (poorly circumscribed/total)	0.90	0.79	0.627
	Multicentricity (presence/total)	0.55	0.29	0.079
	Extra-thyroid extension (presence/total)	0.35	0.29	>0.999
	Vascular invasion (presence/total)	0.35	0.33	>0.999
	Lymph node metastases (presence/total)	0.55	0.36	0.315
	pT (T3 + T4/total)	0.35	0.36	>0.999
	Stage III + IV/total	0.15	0.29	0.410
FVPTC	Gender (female/male)	21:5	4:1	>0.999
	Age, years (mean ± SD)	43.5±12.5	44.8±14.8	0.837
	Tumour size, cm (mean ± SD)	2.4±1.9	1.9±1.3	0.576
	Number of tumours (>1 cm/total)	0.62	0.80	>0.999
	Capsule (absence/total)	0.73	0.94	0.172
	Capsule invasion (presence/total)	0.73	1.00	>0.999
	Growth pattern (poorly circumscribed/total)	0.46	0.80	0.333
	Multicentricity (presence/total)	0.35	0.60	0.350
	Extra-thyroid extension (presence/total)	0.23	0.20	>0.999
	Vascular invasion (presence/total)	0.50	0.80	0.345
	Lymph node metastases (presence/total)	0.23	0.20	>0.999
	pT (T3 + T4/total)	0.15	0.20	>0.999
	Stage III + IV/total	0.12	0.00	>0.999
CPTC + FVPTC	Gender (female/male)	35:11	18:1	0.093
	Age, years (mean ± SD)	39.9±16.0	41.6±16.1	0.689
	Tumour size, cm (mean ± SD)	2.3±1.6	2.5±1.7	0.647
	Number of tumours (>1 cm/total)	0.80	0.84	0.740
	Capsule (absence/total)	0.54	0.63	0.589
	Capsule invasion (presence/total)	0.81	0.86	>0.999
	Growth pattern (poorly circumscribed/total)	0.65	0.79	0.379
	Multicentricity (presence/total)	0.43	0.32	0.418
	Extra-thyroid extension (presence/total)	0.33	0.32	>0.999
	Vascular invasion (presence/total)	0.43	0.47	0.791
	Lymph node metastases (presence/total)	0.37	0.32	0.780
	pT (T3 + T4/total)	0.24	0.32	0.547
	Stage III + IV/total	0.13	0.21	0.461

The presence of *BRAF* and *N-RAS* mutation was not significantly associated to any other clinical or morphological feature (Tables 2, 3, 5 and 6).

Discussion and conclusions

Prognostic factors indicative of PTC metastatic capacity or aggressive behaviour still remain incompletely established. The same holds true regarding the prognostic value of *BRAF* V600E mutation per se, as well as the association between *BRAF* mutation and some pathological features with clinical significance [3, 12, 14, 16, 19–23, 25, 30, 31].

In the present study, we found that, both in CPTC and in FVPTC, extra-thyroid extension and poorly circumscribed growth pattern, rather than *BRAF* V600E mutation, were the pathological features most closely associated to lymph node metastases. In fact, all the PTCs metastatic to the lymph nodes were poorly circumscribed, whereas all well-circumscribed tumours were non-metastatic to the lymph nodes.

In the CPTC group, multicentricity was significantly associated to lymph node metastases, particularly in the

Table 6 Comparison of clinical and morphological features of poorly circumscribed CPTC and FVPTC cases with and without lymph node metastases (LNM)

PTC variant	Features	With LNM	Without LNM	*p* value
CPTC	Multicentricity (presence/total)	0.58	0.19	0.036
	Extra-thyroid extension (presence/total)	0.47	0.19	0.152
	Vascular invasion (presence/total)	0.32	0.31	>0.999
	BRAF V600E mutation	0.31	0.46	0.466
	N-RAS mutation	0.00	0.00	>0.999
FVPTC	Multicentricity (presence/total)	0.50	0.50	>0.999
	Extra-thyroid extension (presence/total)	0.50	0.00	0.023
	Vascular invasion (presence/total)	1.00	0.67	0.206
	BRAF V600E mutation	0.14	0.33	0.585
	N-RAS mutation	0.00	0.11	>0.999

subgroup of poorly circumscribed tumours. In the poorly circumscribed tumours of the FVPTC group, extra-thyroid extension was the most important feature associated to lymph node metastases. In FVPTC cases, vascular invasion and mitotic index were also significantly associated to lymph node metastases, although the latter may reflect the existence of a single case with six mitoses/ten HPF.

FVPTC tumours measuring 1 cm or less and arising in a gland with benign pathology other than thyroiditis were less often associated to lymph node metastases than solitary FVPTC. This difference probably reflects our biased sample of small tumours that was composed by incidentally found PTCs in patients operated on for benign pathology (nodular goitre or follicular adenoma). In our series, this difference was also observed in tumours larger than 1 cm. The low frequency of lymph node metastases from PTC arising together with concurrent benign pathology other than thyroiditis has not been reported before to the best of our knowledge and needs confirmation in larger series.

Our results support the assumption that encapsulated, non-angioinvasive FVPTCs carry an excellent prognosis even when the patients underwent partial thyroidectomy [4, 5, 8–10, 32, 33].

In our series, *BRAF* V600E mutation was less frequently detected than in most series on record [3, 4, 12, 14, 16–26]. It was significantly more frequent in CPTC than in FVPTC cases, an observation consistent with the results of Trovisco et al. [16], as well as those of many other series [21, 23].

BRAF V600E mutated CPTCs were significantly more often found in females than in males, in contrast with the previously observed higher frequency in males [22], or similar frequency in both genders [8, 9, 16, 21].

Although the mean age of PTC patients with and without the *BRAF* V600E mutation was not significantly different in CPTC and FVPTC groups, we did not find a single patient younger than 20 years with a mutated *BRAF* tumour, thus confirming that *BRAF* mutation is rarely present in PTCs of young patients [12, 16, 23]. In most series, *BRAF* mutated PTCs tend to occur in older patients than PTCs without the *BRAF* mutation and to be rarely found in children or young adults [12, 16]. The inverse holds true for RET/PTC rearrangements which are frequently detected in PTC occurring in children and adolescents [34, 35].

At variance with RET/PTC rearrangements that can be detected in cases of nodular goitres/follicular adenomas and Hashimoto thyroiditis displaying large, clear and irregular nuclei [36], *BRAF* mutations have not been detected in benign lesions of the thyroid [37] except in exceedingly rare cases [16, 18]. The reason for the absence of *BRAF* V600E mutation in benign lesions and in PTCs of children and adolescents remains unknown. It is tempting to speculate that *BRAF* mutation per se may induce senescence in thyroid cells as it has been observed in benign melanocytic lesions [38, 39]. Following this hypothesis, the tumourigenic effect of *BRAF* mutation would only be seen whenever the mutation is accompanied by synergic mutations and/or epigenetic changes in other pathways [39, 40]. We are advancing that the *BRAF* mutation may be tumourigenic for the human thyroid only in relatively late stages of PTC development (in normal thyroid and in early neoplastic stages, the mutation might induce a senescent phenotype). The results recently published by Franco et al. [41] in a mouse model support the hypothesis that the aforementioned synergies may be obtained in early stages via a TSH effect. Franco et al. [41] demonstrated that *BRAF* tumourigenic early effect can be mediated by cooperation with the thyrotrophin receptor signalling pathway [41]. In vitro and in vivo studies are necessary to test the aforementioned hypotheses that are also important from a prognostic standpoint (see below).

At variance with the results reported by others, we did not observe in our series a significant association between *BRAF* mutation and poor circumscription [3, 30], tumour size above 1 cm [25], extra-thyroid extension [23, 30, 31], vascular invasion [12] and lymph node metastases [14, 19, 30]. None of the three patients of our series with distant metastases had a *BRAF* mutated tumour in contrast with the results of Namba et al. [20].

In our series, the *N-RAS* mutation was detected in 6% of the tumours, a prevalence that lies within the interval of previously reported data in other PTC series [3, 4, 18, 24, 26–29]. We found no significant association of *N-RAS* Q61R mutation with any clinical or morphological feature, but these negative results may reflect the low number of mutated cases in our series. In one case (case 14 of the

CPTC group), there was coexistence of *BRAF* and *N-RAS* mutation demonstrating that, although rarely, *BRAF* and *RAS* mutations can coexist in the same tumour [18]. It remains to be verified if the two mutations coexist in the same cells or correspond to distinct clones, as demonstrated in melanomas [42].

In our series, there is not a significant association between the presence of *BRAF* mutation and lymph node metastases. This result fits with those of some studies on record [16, 17, 21] and contradict others [12, 14, 30]. *BRAF* mutation was strongly associated to the CPTC group, whose cases were more often poorly circumscribed than FVPTC cases. Within each group, no additional significant associations to other morphological features related to aggressiveness were found.

The detection of the V600E mutation in fine needle aspiration biopsy (FNAB) specimens is a powerful adjunct for the diagnosis of PTC and has increased the specificity of PTC cytological diagnosis to almost 100% [30, 43, 44], but unfortunately, the sensitivity of such detection remains low due to the high percentage of non *BRAF* mutated PTCs [15, 45, 46].

The practical value of the *BRAF* V600E detection for therapeutic purposes in metastatic follicular cell-derived carcinomas with sodium–iodine symporter and thyroid peroxidase down regulation not responding to radioactive iodine is also very promising [44, 46–49].

The preoperative prognostic value of such detection in PTC remains controversial [14, 43, 47]. The most important argument against such value stems from the relatively high percentage of papillary microcarcinomas that have an excellent prognosis [13, 14, 47] even if some of them tend to be locally infiltrative and carry a high rate of lymph node metastases [14, 15, 43, 50].

Basolo et al. [15] have shown that in small PTCs, there is a significant association between the presence of *BRAF* mutation and tumour invasiveness and nodal metastization [15]. These findings are very important from a pathological standpoint and support the oncobiological role attributed to activating *BRAF* mutations in cell lines [51] and animal models [41]. The issue of tumour invasiveness is crucial in most CPTCs which tend to be poorly circumscribed and in the infiltrative (poorly circumscribed) subtype of FVPTC [52]; both tend to give rise frequently to lymph node metastases even when the primary tumours are very small [50]. It remains to be clarified how *BRAF* mutation increases tumour cell invasiveness.

The data on *BRAF* mutated cell lines and experimental models, as well as the observational data on PTC on record, do not prove that *BRAF* mutation per se is a major prognostic factor in human PTC. Larger series, with long-term follow-up combining a thorough clinical and morphological evaluation with the detection of *BRAF* V600E and using multivariate analyses, are necessary to clarify the independent prognostic significance of the mutation. Similar studies are also needed to find a way of combining the clinico-imaging features of a given tumour with the FNAB detection of the *BRAF* V600E for deciding the best surgical approach [47].

Acknowledgements This work was partially supported by the grant Prof. Edward Limbert SPEND/GENZYME–Year 2007. Part of the data reported in this study were obtained in the project "Identificação de factores prognósticos e de selecção terapêutica em carcinomas diferenciados da tireoide", which is supported by Fundação Calouste Gulbenkian. IPATIMUP is an Associate Laboratory of the Portuguese Ministry of Science, Technology and Higher Education and is partly supported by the Fundação para a Ciência e Tecnologia.

Conflict of interest The authors declare no conflict of interest.

References

1. DeLellis RA, Lloyd RV, Heitz PU, Eng C (2004) World Health Organization classification of tumors of endocrine organs. IARC, Lyon
2. Sobrinho-Simões M, Preto A, Rocha AS, Castro P, Máximo V, Fonseca E, Soares P (2005) Molecular pathology of well-differentiated thyroid carcinomas. Virchows Arch 447:787–793
3. Rivera M, Ricarte-Filho J, Knauf J, Shaha A, Tuttle RM, Fagin JA, Ghossein RA (2010) Molecular genotyping of papillary thyroid carcinoma follicular variant according to its histologic subtypes (encapsulated vs infiltrative) reveals distinct BRAF and RAS mutation patterns. Mod Pathol 23:1191–1200
4. Di Cristofaro J, Marcy M, Vasko V, Sebag F, Fakhry N, Wynford-Thomas D, De Micco C (2006) Molecular genetic study comparing follicular variant versus classic papillary thyroid carcinomas: association of N-RAS mutation in codon 61 with follicular variant. Hum Pathol 37:824–830
5. Liu J, Singh B, Tallini G, Carlson DL, Katabi N, Shaha A, Tuttle RM, Ghossein RA (2006) Follicular variant of papillary thyroid carcinoma: a clinicopathologic study of a problematic entity. Cancer 107:1255–1264
6. Carcangiu ML, Zampi G, Pupi A, Castagnoli A, Rosai J (1985) Papillary carcinoma of the thyroid. A clinicopathologic study of 241 cases treated at the University of Florence, Italy. Cancer 55:805–828
7. Gilliland FD, Hunt WC, Morris DM, Key CR (1997) Prognostic factors for thyroid carcinoma. A population-based study of 15,698 cases from surveillance, epidemiology and end results (SEER) program 1973–1991. Cancer 79:564–573
8. Piana S, Frasoldati A, Di Felice E, Gardini G, Tallini G, Rosai J (2010) Encapsulated well-differentiated follicular-patterned thyroid carcinomas do not play a significant role in the fatality rates from thyroid carcinoma. Am J Surg Pathol 34:868–872
9. Sobrinho-Simões M, Eloy C, Vinagre J, Soares P (2010) Molecular pathology of thyroid tumors: diagnostic and prognostic relevance. Int J Surg Pathol 18:209S–212S
10. van Heerden JA, Hay ID, Goellner JR, Salomao D, Ebersold JR, Bergstralh EJ, Grant CS (1992) Follicular thyroid carcinoma with capsular invasion alone: a nonthreatening malignancy. Surgery 112:1130–1136
11. Tubiana M, Schlumberger M, Rougier P, Laplanche A, Benhamou E, Gardet P, Caillou B, Travagli JP, Parmentier C (1985) Long-term results and prognostic factors in patients with differentiated thyroid carcinoma. Cancer 55:794–804

12. Elisei R, Ugolini C, Viola D, Lupi C, Biagini A, Giannini R, Romei C, Miccoli P, Pinchera A, Basolo F (2008) BRAF(V600E) mutation and outcome of patients with papillary thyroid carcinoma: a 15-year median follow-up study. J Clin Endocrinol Metab 93:3943–3949
13. Rosai J, LiVolsi VA, Sobrinho-Simões M, Williams ED (2003) Renaming papillary microcarcinoma of the thyroid gland: the Porto proposal. Int J Surg Pathol 11:249–251
14. Niemeier LA, Kuffner HA, Carty S, Stewart AF, Nikiforov YE (2010) A combined molecular-pathological score to predict aggressiveness of thyroid papillary microcarcinoma. Mod Pathol. Abst 578, p. 131A
15. Basolo F, Torregrossa L, Giannini R, Miccoli M, Lupi C, Sensi E, Berti P, Elisei R, Vitti P, Baggiani A, Miccoli P (2010) Correlation between the BRAF V600E mutation and tumor invasiveness in papillary thyroid carcinomas smaller than 20 millimeters: analysis of 1060 cases. J Clin Endocrinol Metab 95:4197–4205
16. Trovisco V, Soares P, Preto A, de Castro IV, Lima J, Castro P, Máximo V, Botelho T, Moreira S, Meireles AM, Magalhães J, Abrosimov A, Cameselle-Teijeiro J, Sobrinho-Simões M (2005) Type and prevalence of BRAF mutations are closely associated with papillary thyroid carcinoma histotype and patients' age but not with tumour aggressiveness. Virchows Arch 446:589–595
17. Trovisco V, Couto JP, Cameselle-Teijeiro J, de Castro IV, Fonseca E, Soares P, Sobrinho-Simões M (2008) Acquisition of BRAF gene mutations is not a requirement for nodal metastasis of papillary thyroid carcinoma. Clin Endocrinol (Oxf) 69:683–685
18. Soares P, Trovisco V, Rocha AS, Lima J, Castro P, Preto A, Máximo V, Botelho T, Seruca R, Sobrinho-Simões M (2003) BRAF mutations and RET/PTC rearrangements are alternative events in the etiopathogenesis of PTC. Oncogene 22:4578–4580
19. Kim KH, Kang DW, Kim SH, Seong IO, Kang DY (2004) Mutations of the BRAF gene in papillary thyroid carcinoma in a Korean population. Yonsei Med J 45:818–821
20. Namba H, Nakashima M, Hayashi T, Hayashida N, Maeda S, Rogounovitch TI, Ohtsuru A, Saenko VA, Kanematsu T, Yamashita S (2003) Clinical implication of hot spot BRAF mutation, V599E, in papillary thyroid cancers. J Clin Endocrinol Metab 88:4393–4397
21. Puxeddu E, Moretti S, Elisei R, Romei C, Pascucci R, Martinelli M, Marino C, Avenia N, Rossi ED, Fadda G, Cavaliere A, Ribacchi R, Falorni A, Pontecorvi A, Pacini F, Pinchera A, Santeusanio F (2004) BRAF(V599E) mutation is the leading genetic event in adult sporadic papillary thyroid carcinomas. J Clin Endocrinol Metab 89:2414–2420
22. Xu X, Quiros RM, Gattuso P, Ain KB, Prinz RA (2003) High prevalence of BRAF gene mutation in papillary thyroid carcinomas and thyroid tumor cell lines. Cancer Res 63:4561–4567
23. Nikiforova MN, Kimura ET, Gandhi M, Biddinger PW, Knauf JA, Basolo F, Zhu Z, Giannini R, Salvatore G, Fusco A, Santoro M, Fagin JA, Nikiforov YE (2003) BRAF mutations in thyroid tumors are restricted to papillary carcinomas and anaplastic or poorly differentiated carcinomas arising from papillary carcinomas. J Clin Endocrinol Metab 88:5399–5404
24. Trovisco V, Soares P, Preto A, Castro P, Máximo V, Sobrinho-Simões M (2007) Molecular genetics of papillary thyroid carcinoma—great expectations… Arq Bras. Endocrinol Metab 51:643–653
25. Ito Y, Yoshida H, Maruo R, Morita S, Takano T, Hirokawa M, Yabuta T, Fukushima M, Inoue H, Tomoda C, Kihara M, Uruno T, Higashiyama T, Takamura Y, Miya A, Kobayashi K, Matsuzuka F, Miyauchi A (2009) BRAF mutation in papillary thyroid carcinoma in a Japanese population: its lack of correlation with high-risk clinicopathological features and disease-free survival of patients. Endocr J 56:89–97
26. Castro P, Rebocho AP, Soares RJ, Magalhães J, Roque L, Trovisco V, Vieira de Castro I, Cardoso de Oliveira M, Fonseca E, Soares P, Sobrinho-Simões M (2006) PAX8-PPARg rearrangement is frequently detected in the follicular variant of papillary thyroid carcinoma. J Clin Endocrinol Metab 91:213–220
27. Zhu Z, Gandhi M, Nikiforova MN, Fischer AH, Nikiforov YE (2003) Molecular profile and clinical-pathologic features of the follicular variant of papillary thyroid carcinoma. An unusual high prevalence of RAS mutations. Am J Clin Pathol 120:71–77
28. Karga H, Lee JK, Vickery AL Jr, Thor A, Gaz RD, Jameson JL (1991) RAS oncogene mutations in benign and malignant thyroid neoplasms. J Clin Endocrinol Metab 73:832–836
29. Shi YF, Zou MJ, Schmidt H, Juhasz F, Stensky V, Robb D, Farid NR (1991) High rates of RAS codon 61 mutation in thyroid tumors in an iodine deficient area. Cancer Res 51:2690–2693
30. Xing M, Clarck D, Guan H, Ji M, Dackiw A, Carson KA, Kim M, Tufaro A, Ladenson P, Zeiger M, Tufano R (2009) BRAF mutation testing of thyroid fine-needle aspiration biopsy specimens for preoperative risk stratification in papillary thyroid cancer. J Clin Oncol 27:2977–2982
31. Rivera M, Ricarte-Filho J, Tuttle RM, Ganly I, Shaha A, Knauf J, Fagin J, Ghossein R (2010) Molecular, morphologic, and outcome analysis of thyroid carcinomas according to degree of extrathyroid extension. Thyroid 20:1085–1093
32. Sobrinho-Simões M, Eloy C, Lobo C, Magalhães J, Amaro T (2011) Follicular thyroid carcinoma. Mod Pathol 24:S10–S18
33. Widder S, Guggisberg K, Khalil M, Pasieka JL (2008) A pathologic re-review of follicular thyroid neoplasms: the impact of changing the threshold for the diagnosis of the follicular variant of papillary thyroid carcinoma. Surgery 144:80–85
34. Fugazzola L, Pilotti S, Pinchera A, Vorontsova TV, Mondellini P, Bongarzone I, Greco A, Astakahova L, Butti MG, Demidchik EP, Pacini F, Pierotti MA (1995) Oncogenic rearrangements of the RET proto-oncogene in papillary thyroid carcinomas from children exposed to Chernobyl nuclear accident. Cancer Res 55:5617–5620
35. Nikiforov YE, Rowland JM, Bove KE, Monforte-Munoz H, Fagin JA (1997) Distinct pattern of ret oncogene rearrangements in morphological variants of radiation-induced and sporadic thyroid papillary carcinomas in children. Cancer Res 57:1690–1694
36. Rhoden KJ, Unger K, Salvatore G, Yilmaz Y, Vovk V, Chiappetta G, Qumsiyeh MB, Rothstein JL, Fusco A, Santoro M, Zitzelsberger H, Tallini G (2006) RET/Papillary thyroid cancer rearrangement in nonneoplastic thyrocytes: follicular cells of Hashimoto's thyroiditis share low-level recombination events with a subset of papillary carcinoma. J Clin Endocrinol Metab 91:2414–23
37. Xing M, Vasko V, Tallini G, Larin A, Wu G, Udelsman R, Ringel MD, Ladenson PW, Sidransky D (2004) BRAF T1796A transversion mutation in various thyroid neoplasms. J Clin Endocrinol Metab 89:1365–8
38. Dhomen N, Reis-Filho JS, da Rocha Dias S, Hayward R, Savage K, Delmas V, Larue L, Pritchard C, Marais R (2009) Oncogenic Braf induces melanocyte senescence and melanoma in mice. Cancer Cell 15:294–303
39. Dankort D, Curley DP, Cartlidge RA, Nelson B, Karnezis AN, Damsky WE Jr, You MJ, DePinho RA, McMahon M, Bosenberg M (2009) Braf(V600E) cooperates with Pten loss to induce metastatic melanoma. Nat Genet 41:544–52
40. Knauf JA, Sartor MA, Medvedovic M, Lundsmith E, Ryder M, Salzano M, Nikiforov YE, Giordano TJ, Ghossein RA, Fagin JA (2011) Progression of BRAF-induced thyroid cancer is associated with epithelial-mesenchymal transition requiring concomitant MAP kinase and TGFβ signaling. Oncogene. doi:10.1038/onc.2011.44
41. Franco AT, Malaguarnera R, Refetoff S, Liao XH, Lundsmith E, Kimura S, Pritchard C, Marais R, Davies TF, Weinstein LS, Chen M, Rosen N, Ghossein R, Knauf JA, Fagin JA (2011) Thyrotrophin receptor signaling dependence of BRAF-induced thyroid tumor initiation in mice. Proc Natl Acad Sci USA 108:1615–1620

42. Sensi M, Nicolini G, Petti C, Bersani I, Lozupone F, Molla A, Vegetti C, Nonaka D, Mortarini R, Parmiani G, Fais S, Anichini A (2006) Mutually exclusive NRASQ61R and BRAFV600E mutations at the single-cell level in the same human melanoma. Oncogene 25:3357–3364
43. Soares P, Sobrinho-Simões M (2009) Is BRAF mutation screening useful for preoperative risk stratification in papillary thyroid cancer? Future Oncol 5:1225–1229
44. Kim SK, Hwang TS, Yoo YB, Han HS, Kim DL, Song KH, Lim SD, Kim WS, Paik NS (2011) Surgical results of thyroid nodules according to a management guideline based on the BRAF(V600E) mutation status. J Clin Endocrinol Metab 96:658–664
45. Tang KT, Lee CH (2010) BRAF mutation in papillary thyroid carcinoma: pathologic role and clinical implications. J Chin Med Assoc 73:113–128
46. Melck AL, Yip L, Carty SE (2010) The utility of BRAF testing in the management of papillary thyroid cancer. Oncologist 15:1285–1293
47. Soares P, Sobrinho-Simões M (2011) Small papillary thyroid cancers—is BRAF of prognostic value? Nat Rev Endocrinol 7:9–10
48. Couto JP, Prazeres H, Castro P, Lima J, Máximo V, Soares P, Sobrinho-Simões M (2009) How molecular pathology is changing and will change the therapeutics of patients with follicular cell-derived thyroid cancer? J Clin Pathol 62:414–421
49. Gupta-Abramson V, Troxel AB, Nellore A, Puttaswamy K, Redlinger M, Ransone K, Mandel SJ, Flaherty KT, Loevner LA, O'Dwyer PJ, Brose MS (2008) Phase II trial of sorafenib in advanced thyroid cancer. J Clin Oncol 26:4714–4719
50. Wada N, Duh QY, Sugino K, Iwasaki H, Kameyama K, Mimura T, Ito K, Takami H, Takanashi Y (2003) Lymph node metastasis from 259 papillary thyroid microcarcinomas: frequency, pattern of occurrence and recurrence, and optimal strategy for neck dissection. Ann Surg 237:399–407
51. Mitsutake N, Knauf JA, Mitsutake S, Mesa C Jr, Zhang L, Fagin JA (2005) Conditional BRAFV600E expression induces DNA synthesis, apoptosis, dedifferentiation, and chromosomal instability in thyroid PCCL3 cells. Cancer Res 65:2465–2473
52. Castro P, Fonseca E, Magalhaes J, Sobrinho-Simoes M (2002) Follicular, papillary, and "hybrid" carcinomas of the thyroid. Endocr Pathol 13:313–320

Virchows Arch (2011) 459:277–281
DOI 10.1007/s00428-011-1130-x

ORIGINAL ARTICLE

The incidence of lymphocytic thyroid infiltration and Hashimoto's thyroiditis increased in patients operated for benign goiter over a 31-year period

Johannes Ott · Moritz Meusel · Andrea Schultheis · Regina Promberger · Shannon Joan Pallikunnel · Nikolaus Neuhold · Michael Hermann

Received: 16 April 2011 / Revised: 11 July 2011 / Accepted: 11 July 2011 / Published online: 24 July 2011
© Springer-Verlag 2011

Abstract The incidence of Hashimoto's thyroiditis (HT) seems to have increased over the last several decades. Since there is a lack of recent studies in the literature that evaluate this phenomenon on a histological basis, we aimed to assess the incidence of lymphocytic thyroid infiltration (LTI) in our large surgical patient collective over a 31-year period. In our study, a total of 1,050 patients who had undergone uni- or bilateral thyroid surgery for benign goiter were included (150 patients in each group, during 1979 to 2009). The stored histological sections of the removed thyroid specimens were re-analyzed, including routine grading of LTI severity on a scale of 0–4, according to Williams and Doniach. Positive correlations were seen for the incidences of LTI grading (0–4) (r=0.077, p=0.013) and HT (r=0.044, p=0.078) over the years. Furthermore, when comparing the years 1979–1989 and 1994–2009, i.e., before and after the second iodine prophylaxis had been introduced in Austria, a higher incidence of HT was found for the later years (2 out of 450, 0.4%, vs. 6 out of 600, 1.0%, respectively; p<0.0001). In conclusion, the data demonstrate that the incidence of LTI and HT has increased substantially over the last 31 years.

Keywords Autoimmune thyroiditis · Hashimoto's thyroiditis · Histology · Lymphocytic infiltration · Epidemiology

J. Ott · M. Meusel · R. Promberger · S. J. Pallikunnel · M. Hermann
Department of Surgery, Kaiserin Elisabeth Spital,
Huglgasse 1-3,
1150 Vienna, Austria

J. Ott (✉)
Department of Gynecologic Endocrinology and Reproductive Medicine, Medical University Vienna,
Waehringer Guertel 18-20,
1090 Vienna, Austria
e-mail: johannes.ott@meduniwien.ac.at

A. Schultheis · N. Neuhold
Department of Pathology and Microbiology,
Kaiserin Elisabeth Spital,
Huglgasse 1-3,
1150 Vienna, Austria

R. Promberger
Department of Surgery, Medical University of Vienna,
Waehringer Guertel 18-20,
1090 Vienna, Austria

Introduction

Hashimoto's thyroiditis, a chronic autoimmune thyroiditis, is a common disease and is the most prevalent cause of subclinical or overt hypothyroidism in areas with sufficient iodine intake [1]. Thus, it has a high clinical impact. The disease is characterized by lymphocytic infiltration of the thyroid gland and presence of oncocytic changes in the follicular thyroid epithelium [2]. This finding is associated with the presence of anti-thyroid peroxidase antibodies and thyroglobulin antibodies, which are generally used as serological markers of the disease [3].

After initial studies indicating that the incidence of Hashimoto's thyroiditis had been increasing over the last few decades [4, 5], Benvenga and Trimarchi demonstrated, in their recent retrospective analysis of approximately 23,000 subjects, that Hashimoto's thyroiditis, as diagnosed by laboratory and clinical findings as well as by ultrasound, had increased in Southern Italy over a 31-year period. Moreover, these authors found changes concerning various

characteristics of Hashimoto's thyroiditis, including: affected patients had become younger, the incidence in males had increased, and serum thyroid auto-antibodies had become less frequently positive [6]. Likewise, a recent study found a significant increase in the year-to-year frequency of cytologically diagnosed Hashimoto's thyroiditis over a time period of three decades [7].

However, to our knowledge, no study has been published in the last four decades that focused on alterations of the incidence of Hashimoto's thyroiditis, as evaluated by histological examinations. Thus, we aimed to assess the incidence of lymphocytic thyroid infiltration in our large surgical patient collective over a 31-year period.

Materials and methods

The primary objective was to evaluate whether the incidences of lymphocytic infiltration of the thyroid and/or of Hashimoto's thyroiditis, as evaluated by histology, had increased in patients with benign goiter over the past 31 years. Although Hashimoto's thyroiditis is known to be frequently associated with thyroid cancer, we decided to exclude patients with thyroid malignancies, since thyroid inflammation has been suggested to possibly represent a reaction of the body's immune system to the cancer [8]. Hence, it is unclear whether the pathophysiologic mechanisms of the development of Hashimoto's thyroiditis are similar in patients with and without thyroid cancer.

Starting with 1979, all patient characteristics, including the diagnostic findings as well as clinical and histological diagnoses for every patient, were entered by physicians into a computerized documentation system (MediCare ChirDok™ system from Micom, Wiener Neustadt, Austria). The data were stored in codified form; a built-in subroutine detects incompatible entry errors. Entries were independently double-checked by physicians. The system allows for data retrieval and evaluation by user-defined algorithms and thus supports the efficient analysis of large data sets. Based on this documentation system, a total of 1,050 patients who had undergone uni- or bilateral thyroid surgery for benign goiter were included in the study. Each 5 years, from 1979 to 2005 (e.g., 1979, 1984, 1989, 1994, 1999, 2004, and 2009), the first 150 patients of the alphabetically arranged lists were included. Due to the alphabetic order, a random distribution over the 1-year periods was achieved.

The stored histological sections of the removed thyroid specimens of these patients were re-analyzed as follows. The whole thyroid parenchyma was histologically examined. This comprised routine grading of thyroid inflammation severity, graded on a scale of 0–4 according to Williams and Doniach [2]. Hashimoto's thyroiditis was defined as a lymphocytic infiltration of grade 3 or 4 with destruction of follicular cells with the presence of oncocytic changes in the follicular thyroid epithelium [9, 10]. Scoring was performed by two independent investigators, namely AS and NN. In all patients, sufficient material had been excised to enable histological evaluation.

Variables are described by frequencies and mean ± standard deviation. Statistical analysis was performed using ANOVA analysis, the chi-square test, and Spearman's rank correlation. Differences were considered statistically significant if $p<0.05$. Statistical analysis was performed with SPSS 15.0.1 for Windows (SPSS Inc., 1989–2006).

Results

Patients were 51.1±13.4 years of age at the time of thyroid surgery (826 women, 50.9±13.4 years of age, and 224 men, 52.2±13.4 years of age). Lymphocytic infiltration of grades 0, 1, 2, 3, and 4 was found in 731 (69.6%), 203 (19.3%), 84 (8.0%), 25 (2.4%), and 7 (0.7%) cases, respectively. Histological signs of Hashimoto's thyroiditis were present in 8 out of 1,050 (0.8%) cases.

For further details on patient characteristics and results, see Table 1. When analyzing the incidence of thyroiditis grade (0–4) over the years, a positive correlation was seen with Spearman's rank test ($r=0.077$, $p=0.013$), indicating a significant rise over the past few decades. For Hashimoto's thyroiditis, a trend to an increasing incidence ($r=0.044$, $p=0.078$) was observed. All of the patients in whom thyroiditis of grades 3 and 4 as well as Hashimoto's thyroiditis were found were females.

In addition, we compared the incidence of Hashimoto's thyroiditis between the years 1979–1989 and 1994–2009, i.e., before and after the second iodine prophylaxis had been introduced in Austria, and found no significant difference (2 out of 450, 0.4%, vs. 6 out of 600, 1.0%, respectively; $p<0.0001$). When comparing these groups with regard to the presence of any kind of lymphocytic infiltration (grades 1–4), a higher incidence was found in the thyroid specimens of patients who had been operated on after introduction of the second iodine prophylaxis (197 out of 600, 32.8%, vs. 122 out of 450, 27.1%; $p=0.046$).

Discussion

In this retrospective study on 1,050 thyroid specimens of patients operated on for benign goiter, an overall incidence of Hashimoto's thyroiditis of 0.8% was found. The literature reports a somewhat higher incidence (of up to 6.6%) of thyroiditis caused by lymphocytic infiltration in histopathological studies [2, 11]. Most important, increasing incidences of both lymphocytic infiltration of the thyroid

Table 1 Patient characteristics and incidence of lymphocytic thyroid inflammation by year of surgery

		1979	1984	1989	1994	1999	2004	2009	*p* value
Sex	F (*n*, %)	123 (82.0)	130 (86.7)	125 (83.3)	122 (81.3)	107 (71.3)	115 (76.7)	104 (69.3)	0.001
	M (*n*, %)	27 (18.0)	20 (13.3)	25 (16.7)	28 (18.7)	43 (28.7)	35 (23.3)	46 (30.7)	
Age (years)		49.2±15.8	48.3±12.3	49.1±12.3	52.3±14.1	52.2±12.6	50.7±13.2	52.2±11.6	0.104
Grading	0 (*n*, %)	106 (70.7)	110 (73.3)	112 (74.7)	105 (70.0)	109 (72.7)	95 (63.3)	94 (62.7)	0.013
	1 (*n*, %)	30 (20.0)	28 (18.7)	21 (14.0)	29 (19.3)	28 (18.7)	34 (22.7)	33 (22.0)	
	2 (*n*, %)	13 (8.7)	9 (6.0)	12 (8.0)	10 (6.7)	9 (6.0)	13 (8.7)	18 (12.0)	
	3 (*n*, %)	1 (0.7)	3 (2.0)	4 (2.7)	4 (2.7)	4 (2.7)	7 (4.7)	2 (1.3)	
	4 (*n*, %)	0	0	1 (0.7)	2 (1.3)	0	1 (0.7)	3 (2.0)	
HT (*n*, %)		0	1 (0.7)	1 (0.7)	1 (0.7)	1 (0.7)	2 (1.3)	2 (1.3)	0.078

Each group consists of 150 patients

F females, *M* males, *HT* Hashimoto's thyroiditis

gland and Hashimoto's thyroiditis were found. This finding is in accordance with the results published by Benvenga and Trimarchi [6]. The authors reported that the absolute number of patients presenting with Hashimoto's thyroiditis, diagnosed based on various combinations of clinical, laboratory, and instrumental findings, increased in a linear fashion from 1975 to 2005. Accordingly, Hashimoto's thyroiditis accounted for 5% of the total number of thyroid diseases observed at their institution in new thyropathic patients admitted in 1975, and had increased about eightfold to a rate of 42% in 2005. Lower rates of Hashimoto's thyroiditis were found in our study. However, its incidence in removed thyroid specimens had also increased by trend from 0% in 1979 to 1.3% in 2004 as did the incidence of high-grade lymphocytic infiltration, i.e., grades 3 and 4 (an eightfold increase from 0.7% in 1979 to 5.3% in 2004). Likewise, a recent study focusing on the year-by-year frequency of cytologically diagnosed Hashimoto's thyroiditis also found a significant upward temporal trend over a time period of about three decades [7].

The exact reasons for this increase remain open for speculation. In general, autoimmune diseases, including those of the thyroid, result from two main factors, namely genetics and environment [12, 13]. Several environmental factors have been associated with an increased risk for Hashimoto's thyroiditis: (a) intrauterine exposure to enterovirus [14] and other microorganisms, including retroviruses, hepatitis C virus, human T lymphotropic virus-1, and many more [13, 15, 16]; (b) so-called "endocrine disrupters," such as industrial chemicals and heavy metals [13, 17]; and (c) nuclear radiation [18–20]. Notably, the considerably more marked increases in the incidences of both Hashimoto's thyroiditis and high-grade thyroid inflammation in our data set were seen somewhere between 1984 and 1989, which might be due to the nuclear accident in Chernobyl in April 1986. And, last but not least, (d) iodine prophylaxis, as achieved by iodination of salt, has been implicated as a possible factor in inducing or precipitating thyroid autoimmunity [21, 22]. This is based on both animal as well as observational studies, despite the fact that the results of observational studies are conflicting. As reviewed by Papanastasiou et al., epidemiological studies suggest that autoimmune thyroiditis is more common in areas with adequate iodine intake rather than in iodine-deficient areas. Moreover, after an iodine prophylaxis program in the USA, an increasing incidence of Hashimoto's thyroiditis was observed [21]. This is in accordance with older histopathological studies demonstrating an increase in lymphocytic infiltration in cases of thyroidectomy in the 1960s, compared to the 1920s, before iodine administration [23, 24]. In the present study, a twofold increase in the incidence of Hashimoto's thyroiditis, which was not statistically significant, is likely due to the small absolute number of Hashimoto

cases, and a slight increase of about 5% in the incidence of lymphocytic infiltration was found when the years before and after the introduction of the second iodine prophylaxis in Austria were compared. In the course of this second iodine prophylaxis, salt iodination was increased from 10 to 20 mg of potassium iodide per kilogram of salt in 1990. Due to this intervention, iodine deficiency is believed to be controlled in Austria, in contrast to many other countries all over Europe [25, 26]. Our data are in accordance with the published evidence, suggesting that the rise in the incidence of thyroiditis after the introduction of the iodine prophylaxes was also true for Austria [25]. However, the data presented in our study show a less dramatic increase in the incidence of lymphocytic thyroid infiltration and Hashimoto's thyroiditis.

The pathophysiologic mechanisms by which iodine might induce autoimmune reactions in the thyroid gland are poorly understood. Three hypotheses have been suggested: (a) an increased immunogenicity of a highly iodinated thyroglobulin, (b) a toxic effect of iodine on thyroid cells, and (c) a direct stimulation of immune and immunity-related cells by iodine [21]. However, independent of the responsible mechanisms, the increase in the incidence of Hashimoto's thyroiditis over the past few decades is of clinical relevance. In areas with sufficient iodine intake, Hashimoto's thyroiditis is the most prevalent cause of subclinical or overt hypothyroidism, which is associated with a large number of clinical manifestations, such as fatigue, weight gain, cold intolerance, constipation, depression, osteoporosis, anemia, early miscarriage, irregularities of the menstrual cycle, and many more [1, 3, 5]. Moreover, it is also of interest for the thyroid surgeon, since patients suffering from Hashimoto's thyroiditis often reveal thyroid glands that are diffusedly enlarged, irregular, firm, and more adherent to the adjacent structures. These factors may increase the risk for postoperative complications, namely hypoparathyroidism and recurrent laryngeal nerve injury [12]. It has also been reported that patients with Hashimoto's thyroiditis are at a higher risk for associated thyroid cancers [27, 28].

In addition to this increase in the incidence of Hashimoto's thyroiditis, Benvenga and Trimarchi also demonstrated a change in its presentation. Age at presentation has decreased, as has the female-to-male ratio, with more males being affected now; moreover, they observed a drop in the incidence of overt hypothyroidism [6]. Such observations have not been made in our data set: All of the patients for whom histological examination revealed Hashimoto's thyroiditis were females. Moreover, there was no trend toward a lower female-to-male ratio in patients with lymphocytic infiltration of grades 1–4. This may be due to the selected patient collective; only patients who were operated on for benign goiter were included.

One might consider it a study limitation that significant differences were found for the female-to-male ratio between the analyzed years. However, while the incidence of Hashimoto's thyroiditis increased with all affected patients being female, the female-to-male ratio decreased. This might have led only to a lower incidence of Hashimoto's thyroiditis in the late years. Thus, we consider our finding of a rising incidence of Hashimoto's thyroiditis valid. However, our study includes histological findings only and does not provide clinical data. We consider this a study limitation.

In conclusion, our data demonstrate that the incidence of lymphocytic infiltration of the thyroid gland and of Hashimoto's thyroiditis has increased about eightfold over the last 31 years. The nuclear accident in Chernobyl and the second iodine prophylaxis may have contributed to this effect.

Conflict of interest statement We declare that we have no conflict of interest.

References

1. Hayashi N, Tamaki N, Konishi J, Yonekura Y, Senda M, Kasagi K, Yamamoto K, Iida Y, Misaki T, Endo K (1986) Sonography of Hashimoto's thyroiditis. J Clin Ultrasound 14:123–126
2. Williams ED, Doniach I (1962) The post-mortem incidence of focal thyroiditis. J Pathol Bacteriol 83:255–264
3. Sinclair D (2006) Clinical and laboratory aspects of thyroid autoantibodies. Ann Clin Biochem 43:173–183
4. Pinchera A, Fenzi GF, Bartalena L, Chiovato L, Marcocci C (1980) Thyroiditis. In: de Visscher M (ed) The thyroid gland. Raven, New York, pp 413–441
5. Hueston WJ (2001) Treatment of hypothyroidism. Am Fam Physician 64:1717–1724
6. Benvenga S, Trimarchi F (2008) Changed presentation of Hashimoto's thyroiditis in North-Eastern Sicily and Calabria (Southern Italy) based on a 31-year experience. Thyroid 18:429–441
7. Rizzo M, Rossi RT, Bonaffini O, Scisca C, Altavilla G, Calbo L, Rosanò A, Sindoni A, Trimarchi F, Benvenga S (2010) Increased annual frequency of Hashimoto's thyroiditis between years 1988 and 2007 at a cytological unit of Sicily. Ann Endocrinol (Paris) 71:525–534
8. Cunha LL, Ferreira RC, Marcello MA, Vassallo J, Ward LS (2011) Clinical and pathological implications of concurrent autoimmune thyroid disorders and papillary thyroid cancer. J Thyroid Res 2011:387062
9. Biddinger PW (2009) Chronic thyroiditis. In: Biddinger PW, Thompson LDR, Nikiforov YE (eds) Diagnostic pathology and molecular genetics of the thyroid. Lippincott Williams & Wilkins, Baltimore, pp 45–59
10. Ravinsky E, Safneck JR (1988) Differentiation of Hashimoto's thyroiditis from thyroid neoplasms in fine needle aspirates. Acta Cytol 32:854–861
11. Fleischmann A, Hardmeier T (1999) Die autoptisch normale Schilddrüse: ein relativ seltener Befund. Schweiz Med Wochenschr 129:873–882

12. Hadj-Kacem H, Rebuffat S, Mnif-Féki M, Belguith-Maalej S, Ayadi H, Péraldi-Roux S (2009) Autoimmune thyroid diseases: genetic susceptibility of thyroid-specific genes and thyroid autoantigens contributions. Int J Immunogenet 36:85–96
13. Guarneri F, Benvenga S (2007) Environmental factors and genetic background that interact to cause autoimmune thyroid disease. Curr Opin Endocrinol Diabetes Obes 14:398–409
14. Svensson J, Lindberg B, Jonsson B, Ericsson UB, Olofsson P, Hyoty H, Ivarsson SA (2004) Intrauterine exposure to maternal enterovirus infection as a risk factor for development of autoimmune thyroiditis during childhood and adolescence. Thyroid 14:367–370
15. Chatzipanagiotu S, Legakis JN, Boufidou F, Petroyianni V, Nicolau C (2001) Prevalence of *Yersinia*-plasmid encoded outer protein (Yop) class-specific antibodies in patients with Hashimoto's thyroiditis. Clin Microbiol Infect 7:138–143
16. Tomer Y, Villanueva R (2004) Infection and autoimmune thyroid diseases. In: Rose NR, Schonfeld Y (eds) Infections and autoimmunity. Elsevier, Amsterdam, pp 517–532
17. Brucker-Davis F (1998) Effects of environmental synthetic chemicals on thyroid function. Thyroid 8:827–856
18. Tronko MD, Brenner AV, Olijnyk VA, Robbins J, Epstein OV, McConnell RJ, Bogdanova TI, Fink DJ, Likhtarev IA, Lubin JH, Markov VV, Bouville AC, Terekhova GM, Zablotska LB, Shpak VM, Brill AB, Tereshchenko VP, Masnyk IJ, Ron E, Hatch M, Howe GR (2006) Autoimmune thyroiditis and exposure to iodine 131 in the Ukrainian cohort study of thyroid cancer and other thyroid diseases after the Chornobyl accident: results from the first screening cycle (1998–2000). J Clin Endocrinol Metab 91:4344–4351
19. Lyon JL, Alder SC, Stone MB, Scholl A, Reading JC, Holubkov R, Sheng X, White GL Jr, Hegmann KT, Anspaugh L, Hoffman FO, Simon SL, Thomas B, Carroll R, Meikle AW (2006) Thyroid disease associated with exposure to the Nevada nuclear weapons test site radiation: a reevaluation based on corrected dosimetry and examination data. Epidemiology 17:604–614
20. Eheman CR, Garbe P, Tuttle RM (2003) Autoimmune thyroid disease associated with environmental thyroidal irradiation. Thyroid 13:453–464
21. Papanastasiou L, Vatalas IA, Koutras DA, Mastorakos G (2007) Thyroid autoimmunity in the current iodine environment. Thyroid 17:729–739
22. Harach HR, Ceballos GA (2008) Thyroid cancer, thyroiditis and dietary iodine: a review based on the Salta, Argentina model. Endocr Pathol 19:209–220
23. McConahey WM, Keating FR, Beahrs OH, Woolner LB (1962) On the increasing occurrence of Hashimoto's thyroiditis. J Clin Endocrinol Metab 22:542–544
24. Weaver DK, Nishiyama RH, Burton WD, Batsakis JG (1966) Surgical thyroid disease. A survey before and after iodine prophylaxis. Arch Surg 92:796–801
25. Lind P, Kumnig G, Heinisch M, Igerc I, Mikosch P, Gallowitsch HJ, Kresnik E, Gomez I, Unterweger O, Aigner H (2002) Iodine supplementation in Austria: methods and results. Thyroid 12:903–907
26. de Benoist B, Andersson M, Takkouche B, Egli I (2003) Prevalence of iodine deficiency worldwide. Lancet 362:1859–1860
27. Shih ML, Lee JA, Hsieh CB, Yu JC, Liu HD, Kebebew E, Clark OH, Duh QY (2008) Thyroidectomy for Hashimoto's thyroiditis: complications and associated cancers. Thyroid 18:729–734
28. Clark OH, Greenspan FS, Dunphy JE (1980) Hashimoto's thyroiditis and thyroid cancer: indications for operation. Am J Surg 140:65–71

Virchows Arch (2011) 459:283–289
DOI 10.1007/s00428-011-1132-8

ORIGINAL ARTICLE

Quality assessment of HER2 testing by monitoring of positivity rates

Harald Choritz · Guntram Büsche · Hans Kreipe · On behalf of the Study Group HER2 Monitor

Received: 17 May 2011 / Revised: 25 June 2011 / Accepted: 11 July 2011 / Published online: 2 August 2011
© The Author(s) 2011. This article is published with open access at Springerlink.com

Abstract Interlaboratory variation in human epidermal growth factor receptor 2 (HER2) testing provides a challenge for targeted therapy in breast and gastric cancer. Assessment of positivity rates among laboratories could help monitor their performance and define reference values for positivity rates to be expected in a geographic region. Pathologists regularly determined the number of HER2-positive cases (HER2 3+, HER2 2+/amplified or amplified) in their laboratory, and figures were continuously entered into a central website. The overall positivity rate of each participant was calculated and compared with the average rates of all other institutes (n=42). A total of 18,081 test results on breast cancer and 982 on gastric cancer were entered into the system. Positivity rates for HER2 in breast cancer ranged from 7.6% to 31.6%. Statistically, the results from six institutions qualified as outliers (p<0.000005). From the remaining institutions encompassing 10,916 assessments, the mean proportion of positive cases was 16.7±3.2% (99% confidence interval 16.6–16.8). The results from six institutions were in between the 95% and 99.5% confidence intervals. For gastric cancer, there was one outlier and the mean positivity rate was 23.2±5.7%. The proportion of HER2-positive breast cancer cases is considerably lower than could have been expected from published studies. By assessing the positivity rates and comparing them with that of all breast or gastric cancers in a given population, pathologists will be alerted to a potential systematic error in their laboratory assay, causative for over- or underestimation of cancer cases suited for anti-HER2 therapy.

H. Choritz · G. Büsche · H. Kreipe (✉)
Institute of Pathology, Medizinische Hochschule Hannover,
Carl Neuberg Str. 1,
30625 Hannover, Germany
e-mail: kreipe.hans@mh-hannover.de

Keywords HER2 · Breast cancer · Gastric cancer · Quality assurance · Predictive pathology

Introduction

Targeted therapy against human epidermal growth factor receptor 2 (HER2)-overexpressing tumours provides a major breakthrough in cancer therapy [1]. The identification of cancer patients who are suited for anti-HER2 therapy depends on the analysis of cancer tissue by immunohistochemistry (IH) or in situ hybridisation (ISH), which usually is performed by pathology departments. Central retesting within the framework of therapy trials has revealed considerable interlaboratory variation [2–4]. Testing inaccuracy was identified as a major issue with either assay, IH and ISH [5]. Proficiency testing by round robin tests was launched in several countries as a potential remedy [6–10]. Although useful and indispensable, proficiency testing surveys render only an incomplete and ephemeral assessment of testing performance and do not necessarily reflect the lasting reliability. Furthermore, they rely on artificial systems such as tissue microarrays or cell lines [9, 10]. Usually, they do not cover the whole process and omit decisive steps such as tissue fixation and processing [11].

From regular proficiency tests, it became obvious that inaccurate results were not haphazardly distributed but followed a systematic trait [7, 8]. Participating pathologists who were unsuccessful in most instances failed either because of systematic false-positive or false-negative staining [8]. In a central review of 1,459 cases from Germany in an international therapy trial and tested locally as HER2 3+, only 1,167 could be confirmed by central testing (80%) (results not published). The 1,459 cases were derived from 116 different centres, from which a small number (6%) were responsible for 23% of discrepant cases

with an average discordance rate of 50% (unpublished data). These observations led us to the conclusion that surveillance of positivity rates in HER2 testing may help identify laboratories with insufficient testing assays and a high yield of false-positive or negative results. Consequently, pathologists were offered the opportunity to compare their positivity rates with those of others in Germany, Austria and Switzerland. Because German guidelines require that every case of invasive breast cancer is tested for HER2, there are more than 40,000 HER2 tests of breast cancer in Germany per year [12]. From published results, it is difficult to calculate the proportion of positive cases to be expected when optimal testing circumstances are present. Initial studies suggested overexpression in as many as 30% of cases [13]. Larger series recently revealed lower positivity rates with either ISH or IH ranging from 18% to 22.7% [14, 15]. Therefore, a second aim of the study was to obtain an estimate of the positivity rate which has to be expected among a population of breast and gastric cancers in central Europe.

Material and methods

In 2010, all pathology departments in Germany, Austria and Switzerland were offered the opportunity by the German Society of Pathology and the Association of German Pathologists to enter their positivity rates for HER2 testing on breast and gastric cancer into a central web page. Institutes willing to participate received an access code to guarantee confidentiality. The individual figures could be entered on a weekly or monthly basis. The figures which were entered comprised the number of cases being HER2 0; HER2 1+; HER2 2+; HER2 2+; and amplified in ISH, HER2 3+. For those laboratories which only perform ISH, the numbers for cases not amplified or amplified or falling into the equivocal grey zone [5] were entered.

The average positivity rates of all other institutes corrected for the number of cases entered into the survey were compared to the individual result. A system of traffic lights was indicated to institutes whether they lay outside the 95% confidence interval (yellow) or the 99.5% confidence interval (red).

Statistics

Differences between institutions were analysed by using the χ^2 test. Before determining the rate of HER2-positive cases, the data were checked for outliers. The data from every institution were compared to the pooled data from the other institutions, and the data from those institutions differing highly significantly from the other institutions ($p<0.0005$) were excluded in a stepwise manner. The exclusion procedure was stopped when none of the remaining institutions differed highly significantly ($p<0.0005$) from the pooled data of the other laboratories that had not been excluded. Institutions excluded by this procedure were regarded as outliers and therefore not taken into consideration when determining the rate of HER2-positive cases.

On the basis of the rate of HER2-positive cases determined by the results from the laboratories not excluded as outliers, 95% and 99.5% confidence intervals were calculated for the number of HER2-positive cases applying the binomial distribution for $n\leq500$ and approximating the binomial distribution by the normal distribution for $n>500$.

Results

Within 1 year, 42 institutes of pathology (9 in academic institutions, 17 in community hospitals and 16 in private praxis) entered the results of their HER2 testing in breast cancer into the system. Test results on 18,081 breast cancers were communicated. The average number of cases per institute was 430.5 ranging from 4 to 2,733 cases. Seven institutes entered results of fewer than 50 cases of breast cancer. With regard to gastric cancer, 3 institutions communicated more than 50 assessments during the period under study. Positivity rates for HER2 in breast cancer ranged from 7.6% to 31.6%. The average positivity rate of all 42 institutes corrected for the number of cases was 14.61±4.55%. In order to exclude regional differences, the data were screened for potential association with postal codes, which turned out not to be the case (data not shown). Statistically, the results from six institutions were considered to be outliers ($p<0.000005$). Therefore, the results of these institutes were not included when the expected rate of HER2-positive cases per institute and the number of assays were determined. Of the remaining 10,916 assessments, the mean proportion of positive cases was 16.7% (99% confidence interval 16.6–16.8). Six institutions were outside of the 99.5% confidence interval (Fig. 1). The number of HER2 assessments performed by the institutes outside the 99.5% confidence interval ranged from 189 to 3,287 cases. There were two institutes outside the 99.5% confidence interval which had entered more than 2,500 cases. Two institutes assessed HER2 exclusively by in situ hybridisation and did not rely on immunohistochemistry. One of these institutions had performed 491 assessments and proved to be outside the 99.5% confidence interval with 8.35% unequivocally amplified cases.

Of the remaining 36 participating institutes, 6 institutions were in between the 95% and 99.5% confidence interval ($p<0.0005$) (Fig. 1). All of these institutions had commu-

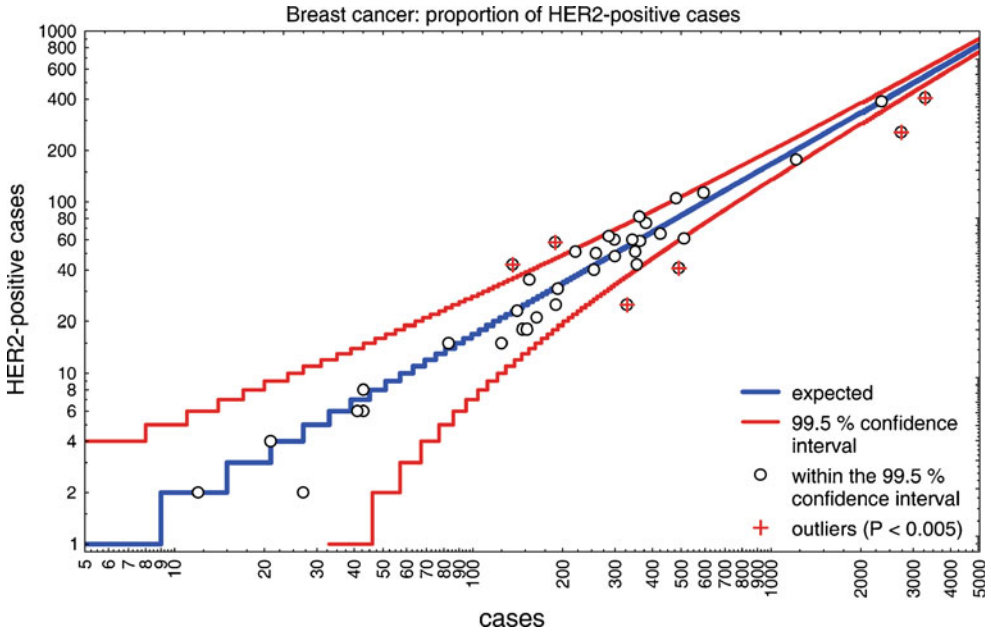

Fig. 1 The number of HER2-positive breast cancer cases (HER2 3+, HER2 2+/amplified, amplified) per institute of pathology in relation to the number of cases investigated was plotted on a logarithmic scale. The 99.5% confidence interval is indicated by *red lines*. In institutions with a low number of assessments, the confidence interval is broader. The expected rate calculated from the mean value of 36 institutions within the 99.5% confidence interval is demonstrated by a *blue line*. There are six institutions outside the 99.5% confidence interval (indicated by *red crosses*). Four of these potentially underestimate HER2 and two have a higher positivity rate than could have been expected. Institutes with a positivity rate within the 99.5% confidence interval are represented by *white circles*

nicated between 153 and 567 HER2 assays in breast cancer cases. No correlation to the type of institute (academic, community hospital or private praxis) could be observed.

The proportion of cases tested immunohistochemically as HER2 2+ ranged from 0% to 60.1% of all assessments (mean 16.5±15.5%). With regard to the 36 reference institutes within the 99.5% confidence interval, the mean percentage of HER2 2+ cases was 18.7±14.0% (Table 1). Of the HER2 cases which were further analysed by in situ hybridisation, 17.9±17.0% were amplified (range 0.0–75.0%) (Table 1). Two of the six institutes outside the 99.5% confidence interval rendered a HER2 2+ assessment on 2.8% and 7.6% of cases, respectively. Institutes, which had lower numbers of HER2-positive cases, also revealed a low percentage of 2+ assessments. There was a highly significant correlation between low HER2 positivity rates and low proportion of cases within the 2+ category ($p<0.000005$).

With regard to gastric cancer, 15 institutes of pathology took part and entered 982 results of their assays. The average positivity rate was 24.11±7.35%. After correction for one outlier, the mean positivity rate was 23.2±5.7% (Table 1). Because the number of cases per institute was rather small, there was a broad range of positivity rates which fell into the 99.5% confidence interval (Fig. 2). Of the 15 participating institutes, only one institute was outside the 99.5% confidence interval and none further outside the 95% interval (Fig. 2). The percentage of cases tested as HER2 2+ was 28.7±12.7% (range 0.0–71.4%). Of these, 30.5±12.1% were amplified by in situ hybridisation (range 0–52.2%) (Table 1).

Discussion

HER2 testing provides the prototype of a new field in pathology, which has been termed predictive pathology. The results of clinical trials demonstrated a significant benefit of HER2-targeted therapy for early and late stages of breast cancer [1, 16] as well as recently also for gastric cancer [17]. Interlaboratory variation in HER2 testing became obvious from trials with central re-testing [3, 4]. Although regular participation in proficiency testing significantly improved the performance of individual institutes [8], there are doubts that the current quality assurance methods are sufficient to reduce testing variation. In order to improve the reliability of testing, several efforts have been undertaken. Guideline recommendations have been published which set standards for thresholds between positive and negative HER2 test results and define algorithms [5, 18]. Furthermore, regular and predominantly tissue microarray-based proficiency tests are organised in Europe and USA [6, 9, 10].

Table 1 HER2 positivity rates in breast and gastric cancer

	Breast cancer	Gastric cancer
Number of HER2 assay results	18,081	982
Participating institutes of pathology	42	15
Average HER2 assay number per institute±standard deviation	430±705	65±118
Mean HER2 positivity rate[a]±standard deviation	16.7±3.2%	23.2±5.7%
Range[a]	11.8–23.1%	17.6–28.1%
Outliers	6 (14.3%)	1 (6.7%)
HER2 2+ (mean rate[a]±standard deviation)	18.7±14.0%	28.7±12.7%
Range[a]	0.0–54.0%	13.9–54.6%
HER2 gene amplification rate among HER2 2+ cases	17.9±17.0%	30.5±12.1%
Range[a]	0.0–75.0%	8.3–52.2%

[a] Institutes with outlying positivity rates were not included in the calculation of the mean value and range; institutes with ≤20 gastric cancer cases and <35 breast cancer cases were merged and considered as a single group

Proficiency tests take place once or twice a year and do not reflect the permanent accuracy of HER2 assessment in routine practice. An auxiliary instrument to compensate for this limitation and to assure quality of HER2 testing is presented here. By monitoring positivity rates in HER2 testing, institutes of pathology were identified, which lay outside the 99.5% confidence interval of expected results. The exact frequency of HER2-overexpressing or amplified cancers was not known and had to be determined in order to define a reference value. The positivity rates reported in the literature range from 18% to 30% [13–15]. On the basis of 10,916 assessments in 36 institutes of pathology, a mean positivity rate of 16.7% was determined (Table 1). Because HER2 testing is performed on every breast cancer in Germany, there is no selection bias in this study as might be the case in therapy trials. Six institutes were outside of the 99.5% confidence interval (Fig. 1). These outliers were informed that a systematic error in the methodology of HER2 assessment in their laboratory might cause over- or underestimation of HER2 in cancer. Of the six institutes

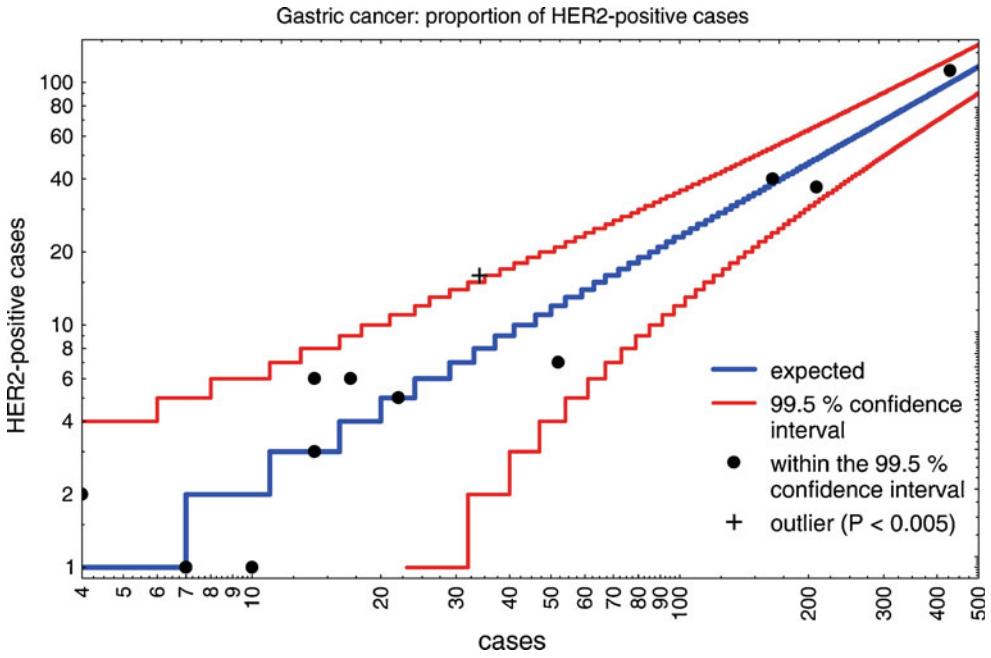

Fig. 2 The number of HER2-positive gastric cancer cases (HER2 3+, HER2 2+/amplified) per institute of pathology in relation to the number of cases investigated was plotted on a logarithmic scale. The 99.5% confidence interval is indicated by *red lines*. In institutions with a low number of assessments, the confidence interval is broader. The expected rate calculated from the mean value of 14 institutions within the 99.5% confidence interval is demonstrated by a *blue line*. There is one institution outside the 99.5% confidence interval (indicated by a *black cross*). Institutes with a positivity rate within the 99.5% confidence interval are represented by *black points*. The confidence interval might narrow over time when more assessments are available for consideration

which were outside the 99.5% confidence interval, five had participated in round robin tests on HER2 assessment offered in Germany. Three of the institutes with low positivity rates had received the information that the sensitivity of their detection method might be too low in at least one of the annual quality assurance trials. Interestingly, a high frequency of assessments did not protect from potential systematic errors. Two institutes which revealed positivity rates outside the 99.5% confidence interval had entered more than 2,500 cases (Fig. 1). It remains to be determined by further studies whether the traffic light system is efficient in improving HER2 assessments in underperforming institutes.

Diversity of positivity rates was highest when the HER2 2+ category was considered (Table 1). This finding indicates that the HER2 2+ category might be limited by subjectivity and poor reproducibility [19] (Fig. 3). In a recent meta-analysis on 17 studies encompassing 8,410 patients, the mean proportion of the HER2 2+ category was 23.2% with a broad range from 2.0% to 87.5% [20]. Only a slight enrichment for amplified cases was found (26.5% vs. 21.1%) [20]. When compared with ISH results in this study, there was no significant enrichment of amplified cases in the HER2 2+ group (Table 1).

Institutes which rely completely on ISH instead of IH to assess HER2 positivity were too few to allow for comparison (Fig. 3). Whether ISH or IH is more reliable and reproducible is a matter of debate [19]. In this study, one of the two institutes which exclusively performed ISH was outside the 99.5% confidence interval.

In order to keep the entering of data into the HER2 monitor as simple as possible and not to reduce the compliance of participants, no detailed information on methods or composition of cases was requested from the participants. It cannot be excluded that an abnormal proportion of low-grade cancers or other specific conditions may be responsible for an aberrant positivity rate. Therefore, a positivity rate outside the 99.5% confidence interval does not necessarily imply that the HER2 assessment method in use is inadequate. Such a finding should, however, urge pathologists to consider this possibility. The primary aim of monitoring HER2 positivity rates is to alert institutes of pathology to potential systematic errors which require further measures to assure quality of testing. As a consequence of abnormal positivity rates, tests in use could be validated or participation in proficiency tests could take place with higher frequency. Only if methodological problems have been excluded should secondary influences such as abnormal composition of the set of samples in which HER2 has been assessed be taken into consideration. Two institutes with a high number of tests and a low positivity rate outside the 99.5% confidence interval also documented extremely low HER2 2+ rates. Unlike the 3+ category, the 2+ category is not related to histological grade. Therefore, it appears highly unlikely that in these two institutes, which together performed more than 6,000 HER2 assessments in breast cancer, a selection bias towards grade 1 and 2 cases might be responsible for the low total positivity rate.

Most therapy trials on targeted HER2 therapy require central retesting of samples which were locally assessed as HER2 positive. As a consequence, central retesting in trials alerts pathologists to false-positive but not to false-negative assessments. This inherent tendency might explain why there are twice as many institutes which potentially underestimate HER2 positivity than institutes with potential overestimation (n=4; 99.5% confidence interval). Thus, without eliminating outliers, the mean rate of HER2-

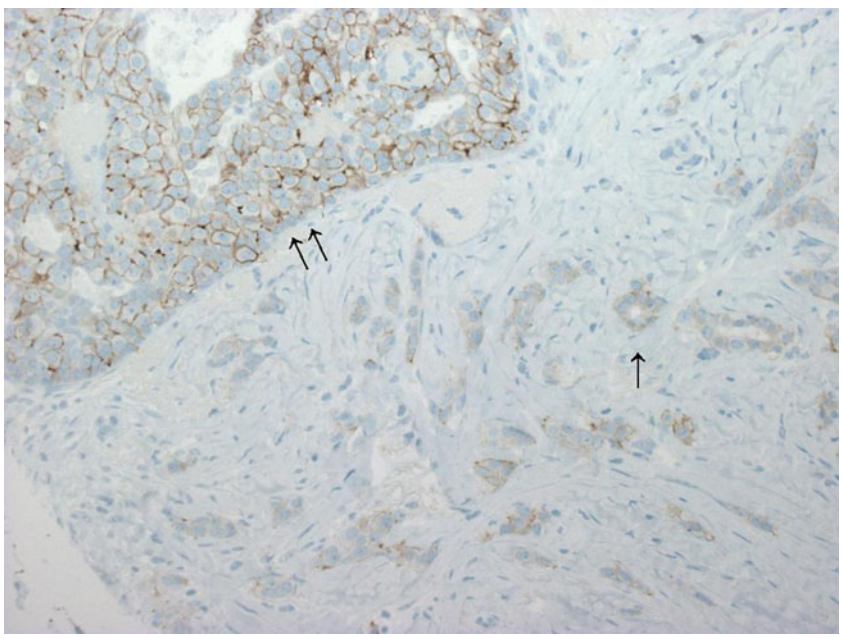

Fig. 3 A high degree of variability between institutes was observed with regard to the HER2 2+ category. In particular, the differentiation between HER2 2+ and HER2 1+ might be handled differently. This case illustrates the borderline between the 2+ category (intraductal carcinoma, *double arrow*) and the 1+ category (invasive carcinoma, *single arrow*) (immunohistochemistry with 4B5 anti-HER2 monoclonal antibody, ×200)

positive cases was lower (14.61±4.55% in 18,221 breast cancers). An almost identical rate was found by questionnaires on 4,940 breast cancer samples in Sweden [21] and slightly higher in Australia (17.1%, 6,512 cases) [22]. In contrast to the HER2 monitor presented here, in both studies, outliers had not been eliminated from the calculation of the expected positivity rate.

There are several measures which institutes of pathology can take to assure quality of HER2 testing. Besides on-slide controls [23], participation in proficiency tests and adherence to guidelines [5–10, 18, 24], a further instrument is proposed here. Monitoring of positivity rates and comparison with an expected value will help identify potential errors in HER2 assessment, which lead to systematic over- or underestimation of HER2 in cancer.

Acknowledgements We gratefully acknowledge the support by the German Cancer Society.

Conflicts of interest None.

Open Access This article is distributed under the terms of the Creative Commons Attribution Noncommercial License which permits any noncommercial use, distribution, and reproduction in any medium, provided the original author(s) and source are credited.

References

1. Piccart-Gebhart MJ, Procter M, Leyland-Jones B et al (2005) Trastuzumab after adjuvant chemotherapy in HER2-positive breast cancer. N Engl J Med 353:1659–1672
2. Paik S, Bryant J, Tan-Chiu E, Romond E, Hiller W et al (2002) Real-world performance of HER2 testing—National Surgical Adjuvant Breast and Bowel Project experience. J Natl Cancer Inst 94:852–854
3. Perez EA, Suman VJ, Davidson NE et al (2006) HER2 testing by local, central, and reference laboratories in specimens from the North Central Cancer Treatment Group N9831 intergroup adjuvant trial. J Clin Oncol 24:3032–3038
4. Roche PC, Suman VJ, Jenkins RB et al (2002) Concordance between local and central laboratory HER2 testing in the breast intergroup trial N9831. J Natl Cancer Inst 94:855–857
5. Wolff AC, Hammond ME, Schwartz JN et al (2007) American Society of Clinical Oncology/College of American Pathologists guideline recommendations for human epidermal growth factor receptor 2 testing in breast cancer. J Clin Oncol 25:118–145
6. Rhodes A, Jasani B, Anderson E et al (2002) Evaluation of HER-2/neu immunohistochemical assay sensitivity and scoring on formalin-fixed and paraffin-processed cell lines and breast tumors: a comparative study involving results from laboratories in 21 countries. Am J Clin Pathol 118:408–417
7. Rüdiger T, Höfler H, Kreipe HH et al (2002) Quality assurance in immunohistochemistry: results of an interlaboratory trial involving 172 pathologists. Am J Surg Pathol 26:873–882
8. von Wasielewski R, Hasselmann S, Rüschoff J et al (2008) Proficiency testing of immunohistochemical biomarker assays in breast cancer. Virchows Arch 453:537–543
9. von Wasielewski R, Mengel M, Wiese B et al (2002) Tissue array technology for testing interlaboratory and interobserver reproducibility of immunohistochemical estrogen receptor analysis in a large multicenter trial. Am J Clin Pathol 118:675–682
10. Fitzgibbons PL, Murphy DA, Dorfman DM et al (2006) Interlaboratory comparison of immunohistochemical testing for HER2: results of the 2004 and 2005 College of American Pathologists HER2 Immunohistochemistry Tissue Microarray Survey. Arch Pathol Lab Med 130:1440–1445
11. Tong LC, Nelson N, Tsourigiannis J et al (2011) The effect of prolonged fixation on the immunohistochemical evaluation of estrogen receptor, progesterone receptor, and HER2 expression in invasive breast cancer: a prospective study. Am J Surg Pathol 35:545–552
12. Wöckel A, Kreienberg R (2008) First revision of the German S3 guideline 'diagnosis, therapy, and follow-up of breast cancer'. Breast Care (Basel) 3:82–86
13. Slamon DJ, Clark GM, Wong SG et al (1987) Human breast cancer: correlation of relapse and survival with amplification of the HER-2/neu oncogene. Science 235:177–182
14. Yaziji H, Goldstein LC, Barry TS et al (2004) HER-2 testing in breast cancer using parallel tissue-based methods. JAMA 291: 1972–1977
15. Owens MA, Horten BC, Da Silva MM (2004) HER2 amplification ratios by fluorescence in situ hybridization and correlation with immunohistochemistry in a cohort of 6556 breast cancer tissues. Clin Breast Cancer 5:63–69
16. Dinh P, de Azambuja E, Piccart-Gebhart MJ (2007) Trastuzumab for early breast cancer: current status and future directions. Clin Adv Hematol Oncol 5:707–717
17. Bang YJ, Van Cutsem E, Feyereislova A et al (2010) Trastuzumab in combination with chemotherapy versus chemotherapy alone for treatment of HER2-positive advanced gastric or gastro-oesophageal junction cancer (ToGA): a phase 3, open-label, randomised controlled trial. Lancet 376:687–697
18. Rüschoff J, Dietel M, Baretton G et al (2010) HER2 diagnostics in gastric cancer-guideline validation and development of standardized immunohistochemical testing. Virchows Arch 457:299–307
19. Sauter G, Lee J, Bartlett JM (2009) Guidelines for human epidermal growth factor receptor 2 testing: biologic and methodologic considerations. J Clin Oncol 27:1323–1333
20. Dendukuri N, Khetani K, McIsaac M et al (2007) Testing for HER2-positive breast cancer: a systematic review and cost-effectiveness analysis. CMAJ 176:1429–1434
21. Rydén L, Haglund M, Bendahl PO et al (2009) Reproducibility of human epidermal growth factor receptor 2 analysis in primary breast cancer: a national survey performed at pathology departments in Sweden. Acta Oncol 48:860–866
22. Francis GD, Dimech M, Giles L et al (2007) Frequency and reliability of oestrogen receptor, progesterone receptor and HER2 in breast carcinoma determined by immunohistochemistry in Australasia: results of the RCPA Quality Assurance Program. J Clin Pathol 60:1277–1283
23. Mengel M, Hebel K, Kreipe H et al (2005) Standardized on-slide control for quality assurance in the immunohistochemical assessment of therapeutic target molecules in breast cancer. Breast J 11:34–40
24. von Wasielewski R, Krusche CA, Rüschoff J et al (2008) Implementation of external quality assurance trials for immunohistochemically determined breast cancer biomarkers in Germany. Breast Care (Basel) 3:128–133

The following institutes contributed data to the HER2 Monitor: Aarau (Kantonsspital, Prof. Grobholz); Aurich (Dres. Woziwodzki, Stachetzki, Tuma); Berlin (Vivantes Am Urban, Dr. Abraham); Bremen (Dr. Jäkel); Brandenburg (Dr. Pauli); Bremerhaven (Prof. Heine, Dr. Schmoll, PD Dr. Back); Bochum (Ruhr-Universität Bergmannsheil, Prof. Tannapfel); Bocholt (Dr. Gupta); Borstel (Forschungsinstitut, Dr. Lang); Dessau (Dr. Hege); Dortmund (Dres. Dykgers, Langwieder, Rees); Dresden (Universitätsklinikum Carl Gustav Carus, Dr. Friedrich), (Dres. Holotiuk, Zuber, Kellermann); Dresden-Friedrichstadt (Prof. Haroske); Duisburg (Prof. Gerharz); Düsseldorf (Universitätsklinikum, Prof. Gabbert); Grevenbroich (Dres. Hagen, Shadouh, Schmitz); Halberstadt (Dr. Erbstößer); Hannover (Medizinische Hochschule, Dr. Liessem); Kassel (Prof. Rüschoff); Kiel (Dres Rabenhorst, Janssen); Königs Wusterhausen (F. Zels); Leipzig (Dr. Wiechmann); Linz/Austria (Dr. Gruber); Lübeck (Universitätsklinikum, Dr. Wohlschläger); Ludwigshafen (Dr. Spiethoff); Lüneburg (Dr. Ahrens); Magdeburg (Dr. Hellwig); München (Universitätsklinik LMU, PD Dr. Mayer); Münster (PD Dr. Kasper); Neunkirchen (Dr. Hübschen); Neuwied (Dr. Bonse); Oberhausen (Dr. Kind); Regensburg (Universitätsklinikum, Dr. Ruemmele); Remscheid (Dr. Christians); Rendsburg (Dr. Grezella); Schüttorf (B. Arens); Schwerin (Dr. Hinze); Singen (Prof. Fellbaum); Spaichingen (Prof. Fischbach, Dres. Kleinschmidt, Wellens); Starnberg (PD Dr. Nagel); Troisdorf (Dres. Feldmann, Gerlach, Prof. Vogel, Weidhase); Tübingen (Universitätsklinik, Dr. Schittenhelm); Wesel (Dres. Berger, Fietze, Linke); Winterthur (Kantonsspital, Dr. Erdin); Wuppertal (Dr. Vogel); and Zwickau (Dr. Remmler).

Virchows Arch (2011) 459:291–297
DOI 10.1007/s00428-011-1125-7

ORIGINAL ARTICLE

Matrix metalloproteinase-11 overexpressed in lobular carcinoma cells of the breast promotes anoikis resistance

Tamotsu Takeuchi · Yoshihiro Adachi · Tomoko Nagayama · Mutsuo Furihata

Received: 3 June 2011 / Revised: 28 June 2011 / Accepted: 5 July 2011 / Published online: 20 July 2011
© Springer-Verlag 2011

Abstract The purpose of the present study was to examine the pathobiological properties of a matrix metalloproteinase, MMP-11 (also known as stromelysin-3), in the carcinogenesis of lobular carcinoma of the breast. Immunohistochemical staining demonstrated immunoreactivity with specific antibody to MMP-11 in 16 of 30 lobular carcinoma cells, but not in the non-cancerous terminal duct lobular unit. In positive cases, both noninvasive and invasive cancer cells exhibited immunoreactivity with anti-MMP-11 antibody; however, the staining patterns in noninvasive and invasive foci were distinct. In the noninvasive foci, immunoreactivity was observed in the cytoplasm beneath the plasma membrane, whereas immunoreactivity was found in all of the cytoplasm of infiltrating lobular carcinoma cells. Enforced expression of MMP-11 in the cultured lobular carcinoma MDA-MB-330 cells did not affect cell growth or Matrigel invasion activity. By contrast, overexpression of MMP-11 significantly increased resistance to anoikis, a programmed cell death triggered by a lack of proper cell matrix interaction, as evidenced by decrease in annexin V-positive cells and apoptotic DNA ladders. The present findings indicate that MMP-11 is overexpressed in many lobular carcinoma cells and that it may play a role in lobular carcinogenesis through increasing resistance to anoikis.

Keywords Lobular carcinoma of the beast · Anoikis · Apoptosis · Matrix metalloproteinase · MMP-11 · Stromelysin-3

T. Takeuchi (✉) · Y. Adachi · M. Furihata
Department of Pathology, Kochi Medical School,
Nankoku 783-8505, Japan
e-mail: takeutit@kochi-u.ac.jp

T. Nagayama
JST Innovation Satellite Kochi Practical Application Research,
Tosayamada,
Kōchi, Japan

Present Address:
Y. Adachi
Division of Signaling in Cancer and Immunology,
Institute for Genetic Medicine, Hokkaido University,
Sapporo, Japan

Present Address:
T. Nagayama
Department of Dermatology, Kochi Medical School,
Nankoku, Japan

Introduction

Invasive lobular carcinoma is the second most common type of invasive breast cancer and is known to have clinicopathological features different from those of the most common invasive ductal carcinoma including higher rate of estrogen receptor positivity, less frequent HER-2 expression, high incidence of bilaterality, and multiple metastases [10]. Histologically, invasive lobular carcinoma often lacks the desmoplastic stromal reaction and exhibits a loosely dispersed single-cell pattern of growth [18]. It is believed that these clinicopathological and histological properties are due to molecular specifications including the lack of E-cadherin expression in invasive lobular carcinomas [9, 26].

Matrix metalloproteinases (MMPs), 25 of which have been identified, play critical roles in promoting cancer development through many carcinogenic processes including the remodeling of the cancer microenvironment [15]. MMP-11 (also known as stromelysin-3) was originally identified as highly expressed in the stromal cells of invasive breast cancer compared to that of fibroadenoma

as determined by subtractive hybridization [5]. Subsequent studies revealed that MMP-11 is overexpressed in cancer stromal fibroblastic cells in many human carcinomas [4, 13]. Interestingly, MMP-11 expression by the fibroblastic cells surrounding cancer cells appears to promote tumorigenesis in paracrine fashion [11].

MMP-11 has unique biochemical properties. First, it is intracytoplasmically processed to be secreted as an active enzyme, whereas most MMPs are secreted as inactive zymogens [16]. Second, human MMP-11 does not readily cleave most other MMP substrates, such as laminin, fibronectin, and elastin. By contrast, MMP-11 induces the dedifferentiation of adipocytes and desmoplastic reaction surrounding the cancer stroma via cleavage of native collagen VI [3, 12]. These unique properties suggest that MMP-11 may have distinct pathological roles in various types of carcinogenesis.

Notably, recent advances have suggested that MMP-11 could be a good target candidate for cancer immunotherapy [17]. In this context, it is important to elucidate which tumor cells and/or cancer stromal cells express MMP-11. The expression status of MMP-11 in lobular carcinoma cells of the breast still remains unclear. Early studies reported that MMP-11 expression was never found in lobular cancer cells, using indirect immunoperoxidase and/or in situ hybridization [1, 25]. By contrast, Nakopoulou et al. found that tumor cells in 11 of 31 cases of invasive lobular carcinoma expressed MMP-11 using avidin–biotin complex (ABC) immunohistochemical staining [14]. Recently, Del Casar et al. also reported that MMP-11 was expressed in tumor cells of invasive lobular carcinoma cells using the labeled polymer and enhanced polymer systems [6].

To address the status of expression and pathobiological properties of MMP-11 in lobular cancer cells, we immunohistochemically examined the expression of MMP-11 in archival lobular cancer tissue specimens with invasive foci, noninvasive foci, and non-cancerous terminal duct lobular units. We preliminarily evaluated several commercially available antibodies to MMP-11 with combinations of various immunostaining procedures, i.e., indirect immunoperoxidase staining, ABC staining, polymerized reporter enzyme staining system, and tyramide-based signal intensification method. We determined the staining procedures needed to obtain intense-specific staining and verified the specificity by preadsorption of antibody with recombinant MMP-11.

Here, we show that MMP-11 was overexpressed in many lobular carcinoma cells, not only in invasive foci but also in in situ foci. Subsequently, we found that enforced expression of MMP-11 decreased the apoptosis of human lobular carcinoma MDA-MB-330 cells cultured under anchor-independent conditions. The present findings indicate that MMP-11 is expressed in many lobular carcinoma cells in both in situ and invasion foci and may rescue cancer cells from anoikis.

Materials and methods

Tissue specimens, antibody, and immunohistochemical staining

Archival pathological tissue specimens were obtained from 30 patients with invasive lobular carcinoma of the breast. All tissue specimens were surgically obtained, fixed in 10% buffered formalin, and paraffin-embedded. Fixation was begun within 30 min after surgical removal to avoid over fixation (>48 h).

The murine monoclonal antibody clone SL 3.05 was purchased from Thermo Fisher Scientific Inc. (Fremont, CA, USA). To verify the specificity of the antibody, it was preadsorbed with the lysates of MMP-11-expressing Cos7 cells or non-expressing Cos7 cells. For this procedure, Cos7 cells were transiently transfected with an expression vector containing human MMP-11 complementary DNA (cDNA), the preparation of which is described below, or an empty vector using diethylaminoethyl-dextran as described previously, and the transfected cells were harvested after 48 h. MMP-11 expression was confirmed by Western immunoblotting (Fig. 1a). For preadsorption, the antibody was incubated overnight with the cell lysates. The murine monoclonal antibody to E-cadherin was purchased from Dako (Glostrup, Denmark). Normal mouse IgG was prepared as previously reported.

The procedures used for immunohistochemical staining were previously described in detail [22]. Briefly, deparaffinized sections were autoclaved for 15 min with 10 mM of citrate buffer (pH 6.0). Next, the slides were incubated for 30 min in normal goat serum. The tissues were then immunostained with primary antibody using the ImmPRESS™ polymerized reporter enzyme staining system (Vector Laboratories, Inc., Burlingame, CA, USA). The procedures were performed according to the manufacturer's protocol.

Cell culture, plasmid, and transfection

A human lobular carcinoma of the breast cell line, MDA-MB-330 [7], was obtained from the American Type Culture Collection (ATCC, Manassas, VA, USA). Cos7 cell was maintained in our laboratory. Cells were cultured in Dulbecco's modified Eagle's medium (DMEM) (Gibco Life Technologies, Grand Island, NY, USA), containing 10% heat-inactivated fetal bovine serum (FBS) and 50 μg/ml gentamycin (Gibco Life Technologies).

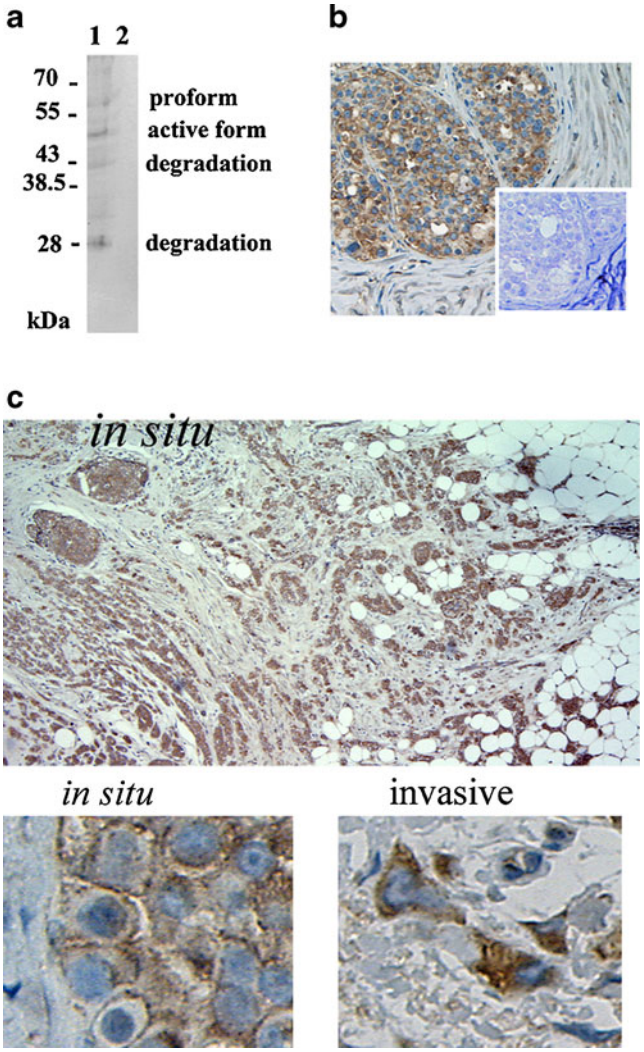

Fig. 1 **a** Western immunoblotting showed that the anti-MMP-11 antibody used in the present study specifically detected the MMP-11 molecules corresponding to the published molecular weight, including proform (~60 kDa), active form (~50 kDa), and degradation products (~35 kDa, ~28 kDa). The expression vector harboring human MMP-11 cDNA or the empty vector alone was transfected into Cos7 cells. After 48 h, the cells were harvested, lysated, and used for Western immunoblotting (*lane 1*, expression vector containing MMP-11 cDNA; *lane 2*, empty vector alone). **b** Immunoreactivity with the anti-MMP-11 antibody was found in the non-infiltrating lobular carcinoma cells. *Inset* shows immunostaining using the preadsorbed antibody with MMP-11-expressing cell lysates. **c** Immunoreactivity with anti-MMP-11 antibody was found in the cytoplasm of the infiltrating lobular carcinoma cells in the fibrous stroma and at invasion site to fat. Note the staining in noninvasive foci (indicated as in situ)

The procedure used to obtain stable transfectant cells was described previously [7]. Briefly, the human entire coding region of *MMP-11* cDNA, which was amplified from placenta messenger RNAs (mRNAs) by reverse transcriptase-polymerase chain reaction (RT-PCR) with sense 5′-GCCGCCATGGCTCCGGCCGCCTGGCTCCGC-3′ (the forward primer introduced an underlined strong Kozak sequence on the 5′-side untranslated region instead of the original 5′-GGGCGG-3′ sequence) and antisense 5′-TCA GAGGAAAGTGTTGGCAGGCTCGGCAC-3′ primers were cloned to the pTargeT mammalian expression vector (Promega, Madison, WI, USA). After verification by sequencing, the vector was designated pTargetT-MMP-11.

Preliminary RT-PCR assay showed that MDA-MB-330 cell did not express detectable levels of *MMP-11* mRNA. MDA-MB-330 cells were transfected with Cla1-cut pTargetT-MMP-11 or empty vector using DOTAP transfection reagent (Boehringer Mannheim GmbH, Mannheim, Germany) in accordance with the manufacturer's protocol. Three permanent MMP-11-expressing clones and control vector-transfected cell clones were established after G418 (Gibco Life Technologies) selection.

Reverse transcriptase-polymerase chain reaction (RT-PCR) and Western immunoblotting

RT-PCR was performed as previously described [21]. Briefly, total cellular RNA was prepared from cell lysates using RNA-zol B (Biotex Laboratory, Houston, TX, USA). cDNA synthesis from total RNA and subsequent PCR were performed using an RNA LA (long and accurate) PCR kit (Takara Bio, Ohtsu, Japan). The procedure was performed according to the manufacturer's protocol. The primer sets used in this study were sense 5′-GAGCAGGTGCGGCA GACGA-3′ and antisense 5′-CGAAAGGTGTAGAAGGCG GACA-3′ for MMP-11 (PCR product 345 bp), and sense 5′-ACCACAGTCCATGCCATCAC-3′ and antisense 5′-TCCACCACCCTGTTGCTGTA-3′ for glyceraldehyde-3-phosphate dehydrogenase (GAPDH) (PCR product 451 bp). The PCR-amplified products were electrophoretically separated on a 2% agarose gel.

Western immunoblotting was carried out according to the modified method of Towbin et al. [23], as previously reported [20]. Briefly, equal amounts of proteins were electrophoresed in sodium dodecyl sulfate polyacrylamide gel electrophoresis gels and electroblotted onto a polyvinylidine difluoride membrane (Millipore Corp., Bedford, MA, USA). After blocking with bovine serum albumin, membranes were incubated with antibodies. To confirm equal protein loading, the membranes were also incubated with anti-actin β antibody (Sigma Life Science, St. Louis, MO, USA). A Western immunoblotting detection kit (Promega, Madison, WI, USA) was used for detection of immunoreactivity.

Cell proliferation and Matrigel invasion assay

Cell proliferation was evaluated by counting the number of viable cells as previously described [22]. Briefly, 1×10^4 cells were cultured on standard 35-mm tissue culture dishes

(BD Biosciences, San Jose, CA, USA) in triplicate. Culture supernatants were replaced with fresh medium every 3 days. After 1 and 2 weeks, live cells were counted.

Matrigel invasion activity was evaluated using 24-well BD BioCoat Matrigel Invasion Chamber Plates (BD Biosciences) according to the manufacturer's protocol. The procedure was described in detail previously [19]. Briefly, 1×10^4 cells were placed in the upper compartment of an invasion chamber. After 72 h of incubation with DMEM containing 10% (lower chamber) or 0% (upper chamber) FBS, the cells on the lower surface of the filter were counted.

These assays were carried out in triplicate. Statistical analysis was performed by Student's t test for unpaired observation. Findings of $P<0.05$ were considered significant.

Anoikis assay and detection of apoptosis

Cells were grown in 75-cm^2 tissue culture flasks. For cultures in suspension, cells were detached from the tissue culture flasks using 0.25% trypsin. Once detached, cells were cultured in DMEM containing 10% FBS on a six-well plate (1×10^6/well) coated with Ultra-Low Attachment Surface, which prevents cell attachment (Corning Life Sciences, Teterboro, NJ, USA). After 72 h in suspension, cells were collected.

The number of cells undergoing apoptosis was quantified with the annexin V Fluos Apoptosis detection kit (Roche Molecular Biochemicals, Mannheim, Germany) following the manufacturer's instructions. Briefly, 1×10^4 cells in different culture conditions were harvested, washed, resuspended in binding buffer, mixed with annexin V-FITC and PI, and analyzed by flow cytometry (Becton Dickinson, Mountain View, CA, USA). Annexin V-positive and PI-negative cells were considered to be in the early apoptotic phase, and those with positive staining for both annexin V and PI were deemed to undergo late apoptosis.

Cellular fragmented DNA was extracted using Apoladder Ex (Takara Bio) according to the manufacturer's instructions. The DNA was resuspended and electrophoresed in a 2% agarose gel at 50 V for 3 h. DNA was visualized by ethidium bromide staining and photographed under UV light.

Results

MMP-11 was overexpressed in cancer cells of many lobular carcinomas of the breast

In the present study, we obtained satisfactory staining with SL 3.05 antibody to MMP-11 using the ImmPRESS™ polymerized reporter enzyme staining system. In this study, we focused on MMP-11 expression in cancer cells. The representative results of immunohistochemical staining are shown in Fig. 1. Positive staining for MMP-11 was observed in 16 of 30 lobular carcinoma tissue specimens. MMP-11 immunoreactivity was uniformly observed in most lobular cancer cells in 12 of 16 cases. Notably, intense MMP-11 immunoreactivity was also observed at the cancer invasion fronts. We observed staining in more than 80% and 50% of lobular cancer cells in cases 1 and 3, respectively. We also considered these four cases as MMP-11 positive.

In positive cases, both invasive and noninvasive cancer cells exhibited immunoreactivity with anti-MMP-11 antibody; however, the staining patterns in invasive and in noninvasive foci were distinct. In the infiltrating lobular carcinoma cells, immunoreactivity was found in all cytoplasm, whereas immunoreactivity was observed in the cytoplasm beneath the plasma membrane of many noninvasive cancer cells. By contrast, we did not find any significant immunoreactivity in non-cancerous mammary glands.

Preadsorption of the antibody with lysates of MMP-11-expressing Cos7 cells eliminated immunoreactivity; however, similar elimination of immunoreactivity was not observed in the case of non-expressing Cos7 cells. This finding verified the specificity of the present immunostaining procedure. The control murine IgGs exhibited no significant immunoreactivity. No significant staining was observed following staining with the anti-E-cadherin antibody, thereby supporting the diagnosis of lobular carcinoma. The enforced expression of MMP-11 decreased the apoptosis sensitizing activity of cultured lobular carcinoma cells without affecting cell growth or Matrigel invasion activity.

Immunohistochemical staining indicated that MMP-11 was overexpressed in many lobular carcinoma cells. We next examined whether MMP-11 expression affected the proliferation of lobular carcinoma cells. MDA-MB-330 was from a patient with lobular carcinoma of the breast. Our preliminary RT-PCR demonstrated that MDA-MB-330 did not express MMP-11. Three independent MMP-11-expressing MDA-MB-330 clones and control non-expressing clones were established after G418 selection (Fig. 2a). As demonstrated in Fig. 2b, exogenous expression of MMP-11 did not significantly affect the proliferation of MDA-MB-330-cultured lobular carcinoma cells (Fig. 2b).

Next, we examined the invasion of cultured cells using Matrigel invasion assay. MMP-11 expression resulted in no significant alteration of the invasion activity of MDA-MB-330 cells (Fig. 2c).

Finally, we examined whether MMP-11 expression affects the sensitivity of anoikis, anchorage-dependent

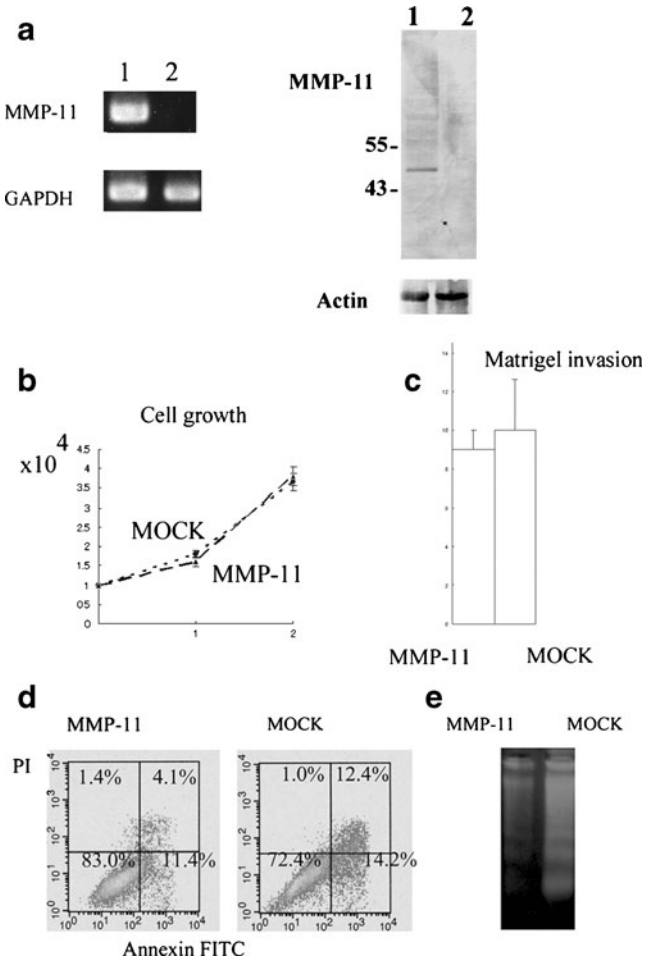

Fig. 2 **a** Representative data of RT-PCR (*left*) and immunoblotting (*right*). Exogenously MMP-11-expressing and control non-MMP-11 expressing MDA-MB-330 cell clones were established by transfection with expression vector, which contained full-length *MMP-11* cDNA, or empty vector (*lane 1* and *2*, respectively). Note the active MMP-11 form (~50 kDa) in MMP-11-expressing MDA-MB-330 cell. A representative result from three independent assays using different transfectant clones is shown. **b** Exogenous MMP-11 expression did not affect cell growth. MDA-MB-330 cells were cultured on 35-mm tissue culture dishes in triplicate. MDA-MB-330 is known to grow very slowly (doubling time 240 to 480 h). Culture supernatants were replaced with fresh medium every 3 days. After 1 and 2 weeks, live cells were counted. Any significant differences of cell growth were found between MMP-11-expressing and control MDA-MB-330 cells, indicated as MMP-11 and MOCK, respectively. Data are expressed as mean±SD. **c** Exogenous MMP-11 expression did not affect the Matrigel invasion activity; 1×10^4 cells were placed in the upper compartment of an invasion chamber. After 72 h of incubation with DMEM containing 10% (lower chamber) or 0% (upper chamber) FBS, the cells on the lower surface of the filter were counted. Data are expressed as mean±SD. **d** MMP-11 expression decreased the sensitivity of anoikis, anchorage-dependent programmed cell death, of MDA-MB-330 cells. Annexin V binding assay showed that overexpression of MMP-11 significantly eliminated the apoptosis of MDA-MP-330 cells in anchorage-independent culture condition. **e** Note the apoptotic DNA ladders in control MDA-MB-330 cells but to a lesser extent in MMP-11-expressing MDA-MB-330 cells under anchorage-independent culture conditions. **b**–**e** These assays were repeated three times using different clones, and consistent results were obtained as shown in the figure

programmed cell death, of MDA-MB-330 cells. Annexin V binding assay showed that overexpression of MMP-11 significantly eliminated the apoptosis of MDA-MP-330 cells in anchorage-independent culture conditions (Fig. 2d). As shown in Fig. 2e, we found apoptotic DNA ladders in control MDA-MB-330 cells but to a lesser extent in MMP-11-expressing MDA-MB-330 cells under anchorage-independent culture conditions. These results indicated that the expression of MMP-11 did not affect cell growth or Matrigel invasion activity, but did significantly increased anoikis resistance.

Discussion

Many previous studies of MMP-11 expression emphasized MMP-11 expression in cancer stromal cells. We also immunostained several invasive ductal carcinoma tissue specimens with anti-MMP-11 antibody in parallel (data not shown). We observed MMP-11 expression in both stromal and cancer cells in several invasive ductal carcinoma tissue specimens, which was consistent with the findings reported by Nakopoulou et al. [14]. During routine practical examinations, pathologists generally detect less stromal remodeling in invasive lobular carcinoma than in ductal carcinomas. Accordingly, recent advances in molecular biology suggest that MMP-11 may not physiologically degrade or target as many stromal molecules as classical MMPs do. Therefore, an investigation of the expression of MMP-11 in lobular cancer cells may support the idea that MMP-11 expression plays a role in carcinogenesis through molecular events other than degradation of the stromal matrix.

The present findings of immunohistochemical staining focused on MMP-11 expression in cancer cells and revealed that MMP-11 was overexpressed in many lobular carcinoma cells of the breast, in both noninvasive and invasive foci. Notably, gene profile expression data also indicate that the MMP-11 gene was overexpressed in three of five laser-captured lobular carcinoma cells [24].

We observed MMP-11 immunoreactivity in the stromal cells of invasive lobular carcinoma to a lesser extent; however, staining was limited to less than approximately 5% of fibroblastic stromal cells. Notably, overexpression of MMP-11 increased resistance to detachment-induced apoptosis, anoikis, in cultured MDA-MB-330 cells.

We detected no significant effects of MMP-11 expression on Matrigel invasion activity. Matrigel comprises laminin, collagen IV, heparin sulfate proteoglycan, entactin, and nidogen, all components of basement membranes. By contrast, MMP-11 is reported to cleave the adipocyte-related collagen VI, but not to target other major stromal components such as laminin, a major component of

Matrigel. Therefore, the present findings did not exclude the possibility that MMP-11 facilitates cancer cell invasion through the degradation of a component of stroma in vivo. In fact, the present immunohistochemical staining findings demonstrated that lobular cancer cells strongly expressed MMP-11 at cancer invasion fronts. Because MMP-11 also protected the lobular cancer cells from anoikis, we think that MMP-11 may lead to the progression of lobular carcinoma of the breast via pleiotropic pathobiological properties.

We cannot definitely explain the reason for the different MMP-11 staining patterns between in situ and invasive lobular carcinoma. MMP-11 is processed to its enzymatically active form by the Golgi-associated proteinase, furin, prior to secretion [16]. Thus, previous reports describe MMP-11 immunoreactivity in the entire cytoplasm in stromal and cancer cells [14]. Notably, Amano et al. observed that MMP-11 can bind to the laminin receptor precursor [2]. The human laminin receptor acts as both a component of the cytoplasmic 40S ribosomal subunit to mediate translation and as a cell surface receptor. It is likely that the MMP-11 immunoreactivity observed in noninvasive lobular carcinoma cells may be related to the cell surface laminin receptor.

The precise molecular mechanisms by which MMP-11 promote anoikis resistance are currently unknown. A recent study demonstrated that MMP-11 increased the resistance to apoptosis in human breast ductal carcinoma cells under 3D culture conditions through activating the p42/p44 MAPK and AKT pathways [8]. However, we found no significant differences in active phosphorylated status of p42/p44 MAPK or AKT molecules examined by immunoblotting (data not shown). Further studies are presently being performed to unravel the molecular mechanisms responsible for MMP-11-induced anoikis resistance.

Acknowledgements This work was supported by grants from the Ministry of Education of Japan (KAKEN 17590270), the Head of Kochi Medical School Hospital's Discretionary Grant, and the Medical Research Fund of Kochi Medical School.

Conflict of interest We declare that we have no conflict of interest.

References

1. Ahmad A, Hanby A, Dublin E, Poulsom R, Smith P, Barnes D, Rubens R, Anglard P, Hart I (1998) Stromelysin 3: an independent prognostic factor for relapse-free survival in node-positive breast cancer and demonstration of novel breast carcinoma cell expression. Am J Pathol 152:721–728
2. Amano T, Kwak O, Fu L, Marshak A, Shi YB (2000) The matrix metalloproteinase stromelysin-3 cleaves laminin receptor at two distinct sites between the transmembrane domain and laminin binding sequence within the extracellular domain. Cell Res 15:150–159
3. Andarawewa KL, Motrescu ER, Chenard MP, Gansmuller A, Stoll I, Tomasetto C, Rio MC (2005) Stromelysin-3 is a potent negative regulator of adipogenesis participating to cancer cell–adipocyte interaction/crosstalk at the tumor invasive front. Cancer Res 65:10862–10871
4. Anderson IC, Sugarbaker DJ, Ganju RK, Tsarwhas DG, Richards WG, Sunday M, Kobzik L, Shipp MA (1995) Stromelysin-3 is overexpressed by stromal elements in primary non-small cell lung cancers and regulated by retinoic acid in pulmonary fibroblasts. Cancer Res 55:4120–4126
5. Basset P, Bellocq JP, Wolf C, Stoll I, Hutin P, Limacher JM, Podhajcer OL, Chenard MP, Rio MC, Chambon P (1990) A novel metalloproteinase gene specifically expressed in stromal cells of breast carcinomas. Nature 348:699–704
6. Del Casar JM, González-Reyes S, González LO, González JM, Junquera S, Bongera M, García MF, Andicoechea A, Serra C, Vizoso FJ (2010) Expression of metalloproteases and their inhibitors in different histological types of breast cancer. J Cancer Res Clin Oncol 136:811–819
7. Engel LW, Young NA (1978) Human breast carcinoma cells in continuous culture: a review. Cancer Res 38:4327–4339
8. Fromigué O, Louis K, Wu E, Belhacène N, Loubat A, Shipp M, Auberger P, Mari B (2003) Active stromelysin-3 (MMP-11) increases MCF-7 survival in three-dimensional Matrigel culture via activation of p42/p44 MAP-kinase. Int J Cancer 106:355–363
9. Korkola JE, DeVries S, Fridlyand J, Hwang ES, Estep AL, Chen YY, Chew KL, Dairkee SH, Jensen RM, Waldman FM (2003) Differentiation of lobular versus ductal breast carcinomas by expression microarray analysis. Cancer Res 63:7167–7175
10. Lee JH, Park S, Park HS, Park BW (2010) Clinicopathological features of infiltrating lobular carcinomas comparing with infiltrating ductal carcinomas: a case control study. World J Surg Oncol 8:34
11. Masson R, Lefebvre O, Noël A, Fahime ME, Chenard MP, Wendling C, Kebers F, LeMeur M, Dierich A, Foidart JM, Basset P, Rio MC (1998) In vivo evidence that the stromelysin-3 metalloproteinase contributes in a paracrine manner to epithelial cell malignancy. J Cell Biol 140:1535–1541
12. Motrescu ER, Blaise S, Etique N, Messaddeq N, Chenard MP, Stoll I, Tomasetto C, Rio MC (2008) Matrix metalloproteinase-11/stromelysin-3 exhibits collagenolytic function against collagen VI under normal and malignant conditions. Oncogene 27:6347–6355
13. Muller D, Wolf C, Abecassis J, Millon R, Engelmann A, Bronner G, Rouyer N, Rio MC, Eber M, Methlin G, Chambon P, Basset P (1993) Increased stromelysin 3 gene expression is associated with increased local invasiveness in head and neck squamous cell carcinomas. Cancer Res 53:165–169
14. Nakopoulou L, Panayotopoulou EG, Giannopoulou I, Alexandrou P, Katsarou S, Athanassiadou P, Keramopoulos A (2002) Stromelysin-3 protein expression in invasive breast cancer: relation to proliferation, cell survival and patients' outcome. Mod Pathol 15:1154–1161
15. Nelson AR, Fingleton B, Rothenberg ML, Matrisian LM (2000) Matrix metalloproteinases: biologic activity and clinical implications. J Clin Oncol 18:1135–1149
16. Pei D, Weiss SJ (1995) Furin-dependent intracellular activation of the human stromelysin-3 zymogen. Nature 375:244–247
17. Peruzzi D, Mori F, Conforti A, Lazzaro D, De Rinaldis E, Ciliberto G, La Monica N, Aurisicchio L (2009) MMP11: a novel target antigen for cancer immunotherapy. Clin Cancer Res 15:4104–4113
18. Silverstein MJ, Lewinsky BS, Waisman JR, Gierson ED, Colburn WJ, Senofsky GM, Gamagami P (1994) Infiltrating lobular carcinoma. Is it different from infiltrating duct carcinoma? Cancer 73:1673–1677

19. Takeuchi T, Adachi Y, Nagayama T, Furihata M (2011) Nedd4L modulates the transcription of metalloproteinase-1 and -13 genes to increase the invasive activity of gallbladder cancer. Int J Exp Pathol 92:79–86
20. Takeuchi T, Adachi Y, Ohtsuki Y (2005) Skeletrophin, a novel ubiquitin ligase to the intracellular region of Jagged-2, is aberrantly expressed in multiple myeloma. Am J Pathol 166:1817–1826
21. Takeuchi T, Adachi Y, Sonobe H, Furihata M, Ohtsuki Y (2006) A ubiquitin ligase, skeletrophin, is a negative regulator of melanoma invasion. Oncogene 25:7059–7069
22. Takeuchi T, Misaki A, Liang SB, Tachibana A, Hayashi N, Sonobe H, Ohtsuki Y (2000) Expression of T-cadherin (CDH13, H-Cadherin) in human brain and its characteristics as a negative growth regulator of epidermal growth factor in neuroblastoma cells. J Neurochem 74:1489–1497
23. Towbin H, Staehelin T, Gordon J (1997) Electrophoretic transfer of proteins from polyacrylamide gels to nitrocellulose sheets: procedure and some applications. Proc Natl Acad Sci USA 76:4350–4354
24. Turashvili G, Bouchal J, Baumforth K, Wei W, Dziechciarkova M, Ehrmann J, Klein J, Fridman E, Skarda J, Srovnal J, Hajduch M, Murray P, Kolar Z (2007) Novel markers for differentiation of lobular and ductal invasive breast carcinomas by laser microdissection and microarray analysis. BMC Cancer 7:55
25. Wolf C, Rouyer N, Lutz Y, Adida C, Loriot M, Bellocq JP, Chambon P, Basset P (1993) Stromelysin 3 belongs to a subgroup of proteinases expressed in breast carcinoma fibroblastic cells and possibly implicated in tumor progression. Proc Natl Acad Sci (USA) 90:1843–1847
26. Zhao H, Langerød A, Ji Y, Nowels KW, Nesland JM, Tibshirani R, Bukholm IK, Kåresen R, Botstein D, Børresen-Dale AL, Jeffrey SS (2004) Different gene expression patterns in invasive lobular and ductal carcinomas of the breast. Mol Biol Cell 15:2523–2536

Virchows Arch (2011) 459:299–306
DOI 10.1007/s00428-011-1127-5

ORIGINAL ARTICLE

Usefulness of a break-apart FISH assay in the diagnosis of Xp11.2 translocation renal cell carcinoma

Soo Hee Kim · Yoomi Choi · Hae Yeon Jeong · Kyoungbun Lee · Ji Youn Chae · Kyung Chul Moon

Received: 23 February 2011 / Revised: 7 April 2011 / Accepted: 8 April 2011 / Published online: 20 July 2011
© Springer-Verlag 2011

Abstract Xp11.2 translocation renal cell carcinoma (RCC) is a rare subtype of RCC predominantly reported in young patients. It results from gene fusions between the transcription factor E3 (TFE3) gene, which is located on chromosome Xp11.2, and various fusion partners. Recently, a dual color, break-apart fluorescence in situ hybridization (FISH) assay to detect Xp11.2 translocation was reported. We performed this study to evaluate the usefulness of the FISH assay in the diagnosis of Xp11.2 translocation RCC using a commercially available TFE3 break-apart probe. We immunohistochemically analyzed TFE3 nuclear expression in 809 cases of RCCs using 14 tissue microarray blocks and selected nine cases those showed moderate to strong positive nuclear immunoreactivity for TFE3. The extent of TFE3 nuclear expression was variable. The TFE3 FISH assay was performed in these 9 selected cases and 44 negative control cases. Only four out of nine selected cases showed the TFE3 break-apart signal. TFE3 FISH-positive cases mainly showed diffuse and strong TFE3 immunopositivity, but one case revealed focal and moderate TFE3 staining. On the contrary, TFE3 FISH-negative cases mainly revealed focal and moderate TFE3 immunoreactivity, however, one FISH-negative case revealed diffuse and strong TFE3 nuclear immunopositivity. All negative control cases revealed normal TFE3 FISH results. Our results reveal that TFE3 immunohistochemistry can show false-positive results, and that the TFE3 break-apart FISH assay is a useful complementary method for confirming the diagnosis of Xp11.2 translocation RCC.

Keywords Fluorescence in situ hybridization · TFE3 · Xp11.2 translocation · Renal cell carcinoma

S. H. Kim · Y. Choi · H. Y. Jeong · K. Lee · J. Y. Chae · K. C. Moon (✉)
Department of Pathology and Kidney Research Institute, Medical Research Center, Seoul National University College of Medicine, 28 Chongno-gu Yongon-dong, Seoul 110-799, South Korea
e-mail: blue7270@snu.ac.kr

K. C. Moon
Kidney Research Institute, Medical Research Center, Seoul National University College of Medicine, Seoul, South Korea

Introduction

Xp11.2 translocation renal cell carcinoma (RCC) is a rare subtype of RCC that frequently affects children and adolescents [1, 2], and it is categorized as a separate entity in the 2004 World Health Organization classification of tumors of the urinary system [3]. This type of RCC results from gene fusions between the transcription factor E3 (*TFE3*) gene located on chromosome Xp11.2 and various fusion partners [4, 5]. Most common gene fusions are ASPL–TFE3 and PRCC–TFE3, resulting from the translocations t(X;17)(p11.2;q25.3) [6] and t(X;1)(p11.2;q21.2) [7].

Xp11.2 translocation RCCs account for 20% to 75% of pediatric RCC cases [8] and about 1.5% of RCC in adults [9]. Common initial presentations of Xp11.2 translocation RCC are hematuria, abdominal pain, and incidental mass [9–13]. The most characteristic microscopic feature of Xp11.2 translocation RCC is papillary architecture composed of cells with voluminous, clear or eosinophilic cytoplasms, and psammoma bodies [5]. Xp11.2 translocation RCCs with PRCC–TFE3 gene fusions frequently show a more nested, compact architecture with less abundant cytoplasm [14]. In addition, some cases show unusual morphology mimicking other types of RCC such as clear cell RCC [11], collecting duct carcinoma, mucinous tubular

and spindle cell carcinoma, sarcomatoid carcinoma [15], or multilocular cystic RCC [16].

Although the microscopic features of Xp11.2 translocation RCC are rather specific, confirmative diagnosis of this distinctive subtype of RCC needs further development, including cytogenetic studies. An immunohistochemical assay for TFE3 is a useful method for the diagnosis of Xp11.2 translocation RCC. Strong nuclear immunoreactivity for the TFE3 proved to be highly specific and highly sensitive for Xp11.2 translocation RCC [17]. Moreover, cathepsin-K is another possible immunohistochemical marker for TFE3 and TFEB translocation RCC [18].

Recently, Zhong et al. reported that a dual color, break-apart fluorescence in situ hybridization (FISH) assay is an effective adjunctive method to detect Xp11.2 translocation RCC [13]. We performed this study to evaluate the usefulness of the FISH assay in the diagnosis of Xp11.2 translocation RCC using TFE3 break-apart probes.

Materials and methods

Patients and tissue samples

A total of 809 patients who had undergone radical or partial nephrectomy for the treatment of RCC between 1995 and 2005 at the Seoul National University Hospital were included in the initial screening immunohistochemistry for TFE3 using 14 tissue microarray blocks. Among these 809 patients, only two were pediatric patients. Nine out of 809 cases showed moderate to strong positive nuclear immunoreactivity for TFE3, and the remaining studies were performed on these nine selected cases. All study samples were obtained from formalin-fixed paraffin-embedded tissue blocks. All hematoxylin and eosin (H&E)-stained slides were independently reviewed by two pathologists (K.C.M and S.H.K). Clinical data were obtained from a medical record review. All study protocols were performed according to ethical guidelines of the "World Medical Association Declaration of Helsinki—Ethical Principles for Medical Research Involving Human Subjects". This study was approved by the Institutional Review Board of Seoul National University Hospital (H-0910-035-296).

Tissue microarray

Tissue microarray blocks from 809 RCC cases were used in the initial screening of TFE3 immunohistochemistry, and nine cases showing moderate to strong nuclear TFE3 staining were selected. Another tissue microarray block was made from these nine cases. The hematoxylin–eosin slides were reviewed and one or two representative formalin-fixed, paraffin-embedded (FFPE) archival blocks were selected in each case. Three tumor cores and one normal core were obtained from each case. Core tissue biopsies (2 mm in diameter) were taken from the individual FFPE blocks (donor blocks) and arranged in recipient paraffin blocks (tissue array blocks) using a trephine apparatus (Superbiochips Laboratories, Seoul, South Korea).

TFE3 immunohistochemistry and assessment of staining

Immunohistochemical staining for the detection of TFE3 was performed on each tumor block and a tissue microarray block from nine selected cases using a goat polyclonal antibody for TFE3 (Santa Cruz, CA). Four-micrometer-thick sections were obtained. Heat-induced antigen retrieval was performed in EnVision FLEX Target Retrieval Solution, High PH (Dako, Glostrup, Denmark) in a PT link pretreatment module (Dako) for 30 min. Immunostaining was performed on an autostainer Link48 (Dako) using a peroxidase-blocking system. Primary antibody was incubated for 30 min at room temperature (dilution 1:500). The slides were counterstained with hematoxylin.

We analyzed the intensity and extent of the immunostained slides. The immunostaining results were analyzed semi-qualitatively. The staining intensity was graded as negative, weak, moderate, or strong, and the extent was graded by the percentage of positive cells as 0, 1+, 2+, and 3+, corresponding to less than 10%, between 10% and 25%, between 25% and 50%, and greater than 50% of tumor cells showing positivity, respectively.

Fluorescence in situ hybridization analysis

Two-micrometer-thick sections from the tissue microarray block were deparaffinized, dehydrated, immersed in 0.2 N HCl, boiled in a microwave in citrate buffer (pH 6.0), and incubated in 1 M NaSCN for 35 min at 80°C. Sections were then immersed in pepsin solution, and the tissues were fixed in 10% neutral-buffered formalin. Dual-probe hybridization was performed using the TFE3 (Xp11) break probe set (Poseidon, KREATECH Diagnostics, Amsterdam, Netherlands). The probe mixture was applied to the slides, which were then incubated in a humidified atmosphere with Hybrite™ (Vysis) at 73°C for 5 min to denature the probe and target DNA simultaneously. It was subsequently incubated at 37°C for 19 h for hybridization. The slides were then immersed in 0.4× saline–sodium citrate (SSC)/0.3% NP-40 for 2 min at room temperature, followed by 2× SSC/0.1% NP-40 for 5 min at 73°C. The nuclei were counterstained with 4,6-diamidino-2-phenylindole (DAPI) and anti-fade compound (*p*-phenylenediamine). After hybridization, all slides were maintained at −20°C in the dark. FISH signals for each locus-specific FISH probe were assessed under an Olympus BX51TRF microscope (Olympus, Japan) equipped with a triple-pass filter

Table 1 Summary of clinicopathologic characteristics of the nine cases of renal cell carcinoma showing TFE3 immunopositivity

Case no.	Age	Sex	Clinical presentation	Location	Tumor size (cm)	Initial classification	Stage (pTNM)	Operation	Follow-up time (years)	Outcome
1	45	M	Incidental renal mass	Left	5.0	Clear cell	T1bN0M0	RN	8.3	PD
2	46	M	Incidental renal mass	Right	3.5	Multilocular cystic	T1aN0M0	RN	9.2	FOD
3	40	M	Incidental renal mass	Left	4.5	Mixed papillary and clear cell	T1bN0M0	RN	8.9	FOD
4	7	M	Gross hematuria	Right	7.0	Granular cell	T3aN2M0	RN	1.4	DOD
5	43	M	Incidental renal mass	Left	3.0	Papillary	T1aN0M0	RN	9.9	FOD
6	54	M	Incidental renal mass	Left	3.5	Clear cell	T1aN0M0	RN	4.2	DUD
7	46	M	Abdominal mass palpation	Right	9.0	Papillary	T3bN1M1	RN	0.8	DOD
8	40	M	Incidental renal mass	Right	6.5	Clear cell	T3aN0M1	RN	3.5	PD
9	28	M	Gross hematuria	Right	2.2	Xp11.2 translocation	T1aN0M0	RN	4.0	FOD

M male, *RN* radical nephrectomy, *PN* partial nephrectomy, *FOD* free of disease, *DOD* died of disease, *DUD* died of causes unrelated to disease, *PD* progressive disease

(DAPI/Green/Orange; Vysis). The entire area of the tissue microarray core was evaluated in each case, and as many non-overlapping nuclei as possible were assessed by two pathologists (K.C.M and S.H.K). The interpretation of intact and split signals was based on the generally accepted guidelines recommended by other commercially available break-apart FISH assays using this method. We considered a break-apart signal when the distance between red and green signals was more than one signal diameter. Cells without the rearrangement had one or two sets of red and green fusion signals depending on patient sex. The FISH-positive cases were decided when greater than 10% of the tumor nuclei had break-apart signals.

Negative control cases

To evaluate the possibility of false-negative TFE3 immunostaining, we performed TFE3 FISH analysis on 44 non-Xp11.2 translocation RCC cases. This group consisted of 30 clear cell RCCs, 7 chromophobe RCCs, 5 papillary RCCs, and 2 collecting duct carcinomas. These cases were included in one of the tissue microarray blocks for the initial screening immunohistochemistry for TFE3, and none of them showed positive TFE3 immunoreactivity at initial screening TFE3 immunohistochemistry.

Results

Patient characteristics

Among the total 809 RCC patients, nine male patients (1.1%) showing moderate to strong positive TFE3 nuclear staining were included in this study. Their ages at diagnosis ranged from 7 to 54 years (mean age, 38.8; median age, 43). Only one

Table 2 TFE3 immunohistochemistry and break-apart FISH results for the nine cases of renal cell carcinoma showing TFE3 immunopositivity

Case no.	TFE3 immunohistochemistry		TFE3 break-apart FISH
	Intensity	Extent	
1	Strong	3+	Positive
2	Strong	3+	Positive
3	Moderate	2+	Positive
4	Strong	3+	Positive
5	Moderate	3+	Negative
6	Strong	3+	Negative
7	Moderate	1+	Negative
8	Moderate	1+	Negative
9	Moderate	2+	Negative

FISH fluorescence in situ hybridization, *1+* 10–25% positive cells, *2+* 25–50% positive cells, *3+* >50% positive cells

pediatric case was included (case 4). The most common initial clinical presentation was incidental mass (n=6). Other initial findings included gross hematuria (n=2) and abdominal mass palpation (n=1). All cases were not related to syndromatic or hereditary disease (e.g., von Hippel–Lindau syndrome) or previous chemotherapy history. The clinicopathologic characteristics of the cases are summarized in Table 1.

TFE3 immunohistochemistry and fluorescence in situ hybridization

The TFE3 immunohistochemical staining and TFE3 break-apart FISH assay results are provided in Table 2. All nine cases showed moderate to strong nuclear immunopositivity for TFE3 to variable extents. However, among these nine

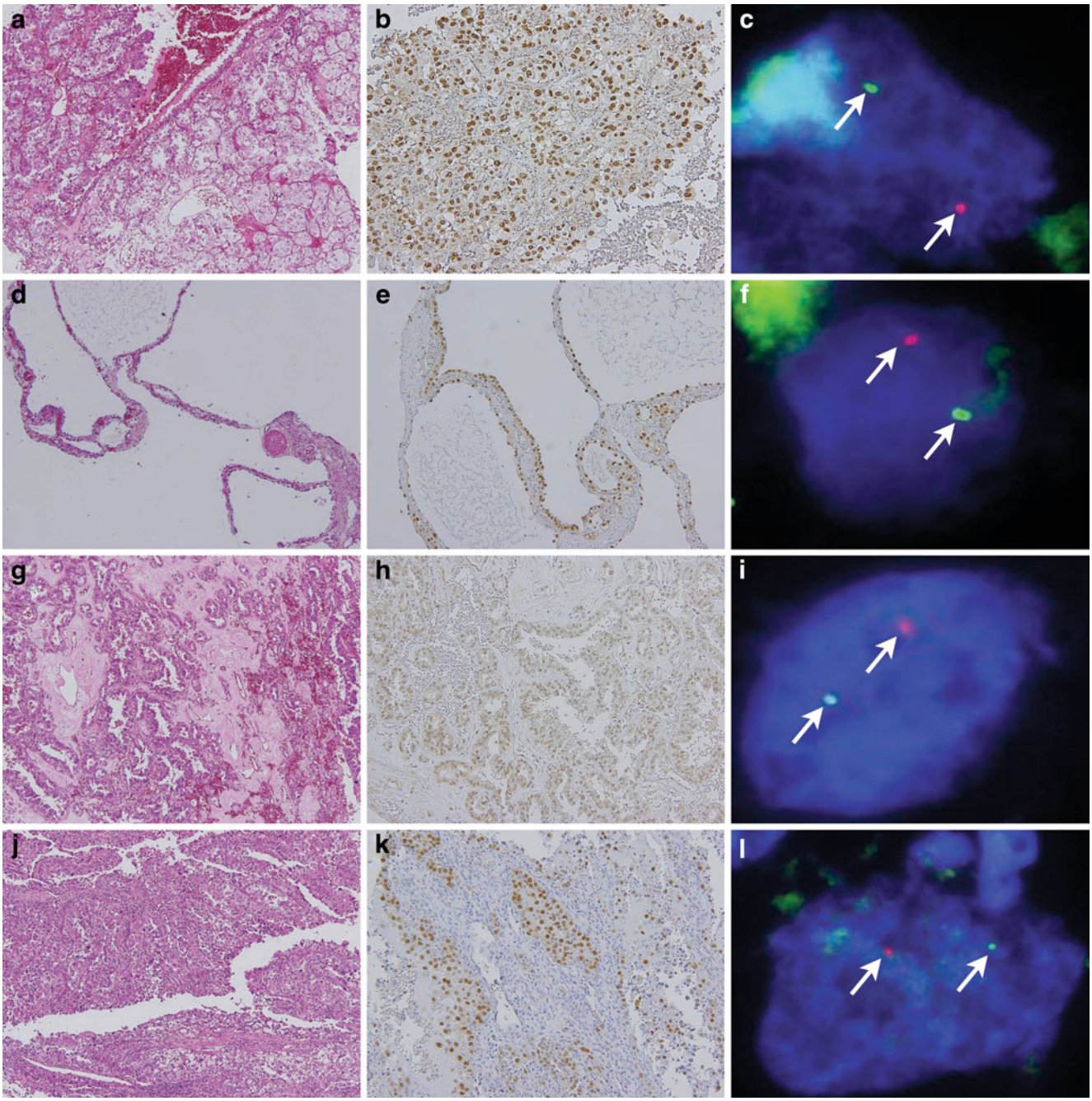

Fig. 1 Histologic features, TFE3 immunohistochemistry, and TFE3 FISH results of TFE3 FISH-positive cases [case 1 (**a**, **b**, **c**), case 2 (**d**, **e**, **f**), case 3 (**g**, **h**, **i**), case 4 (**i**, **k**, **l**)]. TFE3 FISH-positive cases showed variable histologic features (**a**, **d**, **g**, **j**) (H&E, ×100) and moderate to strong TFE3 nuclear staining (**b**, **e**, **h**, **k**) (×200). TFE3 FISH analysis showed split green and red signals (*arrows*) (**c**, **f**, **i**, **l**) (×1,000). Case 2 revealed typical histologic features of multilocular cystic RCC (**d**) with strong TFE3 nuclear immunoreactivity (**e**) and positive FISH result (**f**). Case 3 revealed moderate TFE3 nuclear immunoreactivity (**h**) with positive FISH result (**i**)

cases, only four (cases 1 to 4) showed TFE3 break-apart signals in the FISH assay (Fig. 1). Three TFE3 FISH-positive cases showed diffuse and strong TFE3 immunopositivity, but one case revealed focal and moderate TFE3 immunostaining (case 3, Fig. 1h). On the contrary, one TFE3 FISH-negative case revealed diffuse and strong TFE3 immunopositivity (case 6, Fig. 2b). Other TFE3 FISH-negative cases showed focal or moderate TFE3 immunopositivity (case 7, Fig. 2e). Nonneoplastic renal parenchyma and 44 non-Xp11.2 translocation RCC cases for negative control revealed normal TFE3 FISH patterns (Fig. 2g, h, i).

Pathologic findings

The initial subtype classifications of RCC of the study cases were variable (Table 1). Upon microscopic examination, the study cases had various morphologic patterns (Fig. 1 and Table 3). TFE3 FISH-positive tumors had alveolar, papillary, cystic, tubular, or solid patterns. One case showed features of typical multilocular cystic clear cell RCC (case 2, Fig. 1d). The tumor cells were medium to large in size with granular eosinophilic to clear cytoplasms.

TFE3 FISH-negative cases also showed variable morphologic patterns (Table 3). Two cases had areas showing typical clear cell RCC patterns (Fig. 2a), and three cases mainly showed papillary architecture with eosinophilic to clear cytoplasms (Fig. 2d).

Discussion

Xp11.2 translocation RCCs harbor a translocation involving the *TFE3* gene located on chromosome Xp11.2 [4, 5].

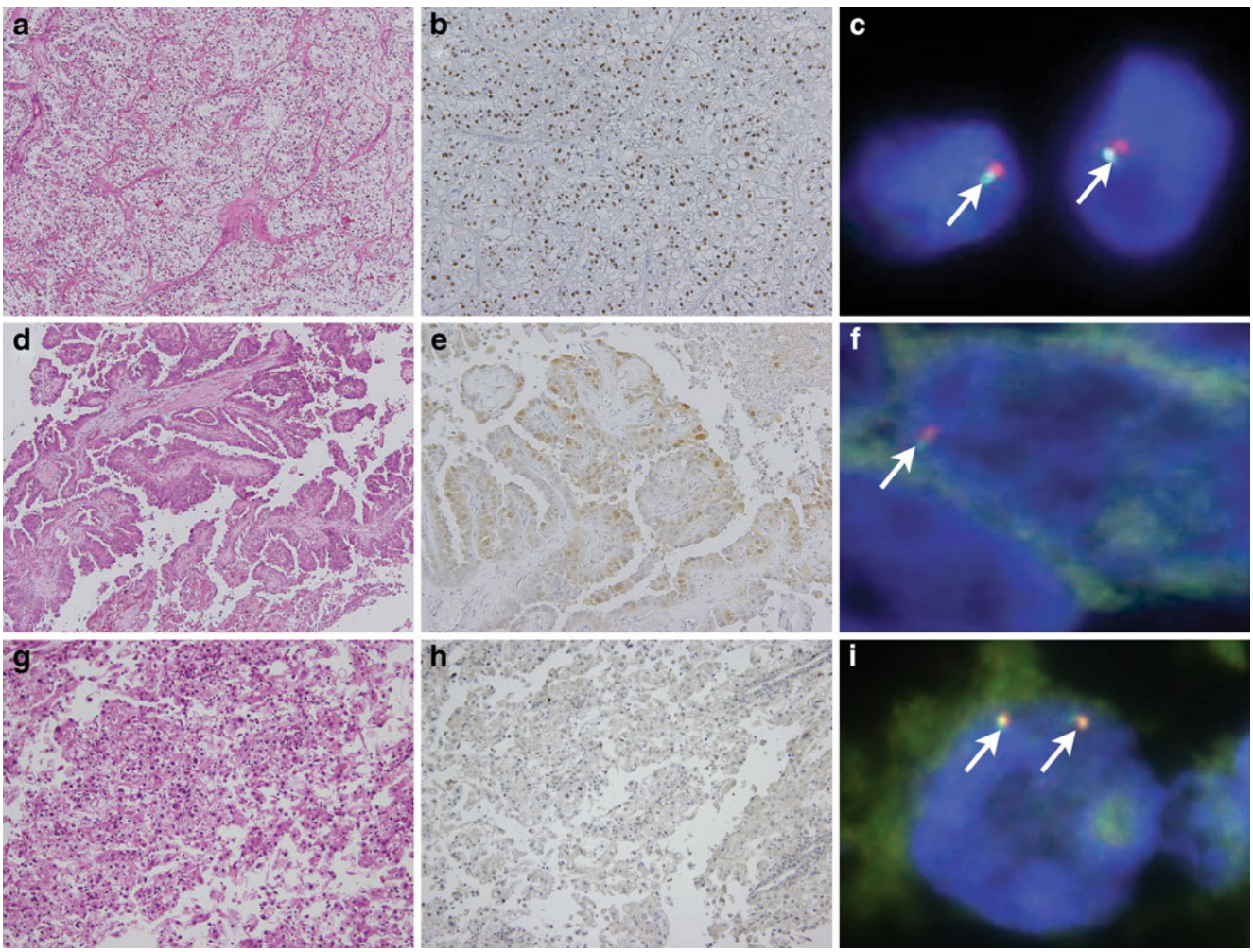

Fig. 2 Histologic features (**a**, **d**, **g**), TFE3 immunohistochemistry (**b**, **e**, **h**), and TFE3 FISH results (**c**, **f**, **i**) of TFE3 FISH-negative cases [case 6 (**a**, **b**, **c**), case 7 (**d**, **e**, **f**)] and one negative control case (**g**, **h**, **i**). These cases revealed clear cell (**a**) or papillary patterns (**d**) (H&E, ×100) and strong or moderate TFE3 nuclear staining (**b**, **e**) (×200). TFE3 FISH analysis showed a fused green and red signal (*arrows*) (**c**, **f**) (×1,000). One negative control clear cell RCC case (**g**) (H&E, ×200) showed negative TFE3 immunohistochemistry (**h**) (×200) and normal TFE3 FISH signals (*arrows*) (**i**) (×1,000)

Table 3 Microscopic features for the nine cases of renal cell carcinoma showing TFE3 immunopositivity

	Case no.								
FISH result	1 Pos	2 Pos	3 Pos	4 Pos	5 Neg	6 Neg	7 Neg	8 Neg	9 Neg
Microscopic features									
Solid pattern	A	A	P	P	A	A	N	P	A
Tubular pattern	A	A	P	A	P	A	A	P	A
Alveolar pattern	P	A	A	P	A	P	A	P	A
Papillary pattern	P	A	A	A	P	P	P	A	P
Cystic change	P	P	A	A	P	P	A	P	P
Psammoma bodies	A	A	P	A	A	P	A	A	A
Abundant cytoplasm	P	A	A	P	A	A	P	A	P
Clear cytoplasm	A	P	A	P	A	P	A	P	A
Eosinophilic cytoplasm	P	A	P	P	P	A	P	P	P
Foamy cytoplasm	A	A	P	A	A	A	A	P	P
Hyaline bodies	P	A	A	A	A	A	A	A	A
Fuhrman nuclear grade	3	2	2	3	3	2	3	3	3

FISH fluorescence in situ hybridization, *Pos* positive, *Neg* negative, *A* absent, *P* present

Although this tumor was initially known as RCC in pediatric patients, adult cases have been continuously reported [9, 10, 15, 19–23]. Furthermore, unusual morphologies mimicking other RCC subtypes have been found in some Xp11.2 translocation RCCs [11, 15, 16]. These clinical and morphologic variations suggest caution when diagnosing RCC. In particular, Xp11.2 translocation RCC should be included in the differential diagnosis of adult RCC, even those with morphologies that suggest other RCC subtypes such as clear cell, collecting duct, sarcomatoid, or multilocular cystic RCC. Therefore, additional ancillary tests are required to diagnose Xp11.2 translocation RCC. For verifying the translocation of TFE3 gene, molecular analysis methods such as karyotype analyses or reverse-transcriptase polymerase chain reaction can be applied. However, these methods are not easy to apply in routine laboratory work.

The FISH assay is widely used for the confirmative diagnosis of some soft tissue tumors with gene translocations, such as Ewing sarcoma and synovial sarcoma [24]. Although the FISH assay with break-apart probes cannot detect each partner of the specific translocation, this method is a convenient and conclusive tool for showing the presence or absence of a certain gene translocation. It can also be easily applied to paraffin-embedded tissue. Zhong et al. developed a dual color, break-apart FISH assay to identify the gene translocation harboring the *TFE3* gene, and it can be used to detect Xp11.2 translocation RCC and alveolar soft sarcoma [13].

In this study, we compared the results from TFE3 break-apart FISH to the results from TFE3 immunohistochemistry, and only four cases out of nine TFE3 immunoreactive cases showed positive FISH results. There were some discrepancies between the results from TFE3 immunohistochemistry and those from the FISH assay. Among four FISH-positive cases, three showed diffuse and strong TFE3 immunoreactivity, and four out of five FISH-negative cases revealed focal and/or moderate TFE3 immunoreactivity. If we apply the strict criteria for TFE3 immunohistochemistry, i.e., only diffuse and strong immunoreactivity is considered as positive TFE3 immunostaining, these seven cases showed concordant results between FISH and immunohistochemistry. However, one FISH-positive case (case 3) showed focal and moderate TFE3 immunoreactivity, and one FISH-negative case (case 6) revealed diffuse and strong TFE3 immunoreactivity. These two cases revealed the confusing results between TFE3 immunohistochemistry and TFE3 break-apart FISH.

The immunohistochemical staining for TFE3 has been known as a relatively accurate and convenient method for the diagnosis of Xp11.2 translocation RCC. However, its nuclear expression cannot directly indicate the translocation of the *TFE3* gene. Furthermore, some problems may exist in TFE3 immunohistochemistry. Scoring the intensity of immunoreactivity can be inevitably subjective. Argani and colleagues scored TFE3 nuclear immunoreactivity from 0 to 3+, and they defined 2+ or 3+ as positive [17]. However, a study that performed TFE3 immunohistochemistry with 31 adult translocation carcinomas reported that negative TFE3 immunoreactivity was noted in two Xp11.2 translocation RCCs with cytogenetically proven translocations, and an additional three Xp11.2 translocation RCCs showed very focal (10%) TFE3 immunostaining [10]. Some other studies have shown weak or equivocal TFE3 immunoreactivity in a few cases of RCCs with or without proven translocation [12, 25]. In our study, there were some

discrepancies between TFE3 immunohistochemistry and FISH. And in some cases, it was difficult to determine TFE3 positivity.

Some other factors can confuse the TFE3 immunohistochemical results. First, the possibility of false-positive or false-negative staining can be present in routine immunohistochemistry. Second, the fixation status of tumor can affect the immunostaining result. Third, the methods of immunohistochemistry also can affect the results. Argani et al. reported the different sensitivity and specificity in TFE3 immunohistochemistry between the manual overnight incubation and the automated, 30-min incubation methods [26]. They suspected that the automated detection system was more sensitive and less specific. We used the automated method in this study. We thought that the confusing results between TFE3 immunohistochemistry and FISH in this study may have been due to these factors. Thus, immunohistochemical staining for TFE3 may not be sufficient for a confirmative diagnosis of TFE3 translocation RCCs.

In terms of immunostaining method, the manual staining with overnight incubation appears more accurate than the automated staining [26]. But, nowadays, many routine diagnostic pathology laboratories use automated immunostainers, so it is not appropriate to apply manual method only for TFE3 immunostaining in routine laboratory work. In the present study, we revealed that TFE3 immunohistochemistry using automated immunostainers could show a false-positive result, and we could not find any case showing false-negative TFE3 immunoreactivity among 44 negative control cases. So, TFE3 immunohistochemistry using automated immunostainers is a sensitive but less specific method in the diagnosis of Xp11.2 translocation RCCs.

In summary, our study revealed that four cases were positive using the TFE3 break-apart FISH assay in a sample of nine cases showing moderate to strong nuclear TFE3 immunoreactivity. This result revealed that additional methods for determining the *TFE3* gene translocation may be mandatory for a more accurate diagnosis of Xp11.2 translocation RCC besides the TFE3 immunohistochemistry. Additionally, the TFE3 break-apart FISH assay is a relatively rapid and convenient method that can demonstrate the translocation, and it can be easily applied to a paraffin-embedded tissue. Therefore, in the diagnosis of Xp11.2 translocation RCC, we propose the TFE3 break-apart FISH assay as a supplementary tool for an accurate diagnosis after TFE3 immunohistochemistry.

Acknowledgments This study was supported by a grant of the Korea Health 21 R&D Project, Ministry of Health & Welfare, Republic of Korea (A080239).

Conflict of interest statement We declare that we have no conflict of interest.

References

1. Argani P, Antonescu CR, Illei PB, Lui MY, Timmons CF, Newbury R, Reuter VE, Garvin AJ, Perez-Atayde AR, Fletcher JA, Beckwith JB, Bridge JA, Ladanyi M (2001) Primary renal neoplasms with the ASPL-TFE3 gene fusion of alveolar soft part sarcoma: a distinctive tumor entity previously included among renal cell carcinomas of children and adolescents. Am J Pathol 159(1):179–192
2. Argani P, Ladanyi M (2005) Translocation carcinomas of the kidney. Clin Lab Med 25(2):363–378
3. Eble JN, Sauter G, Ebstein JI, Sesterhenn IA (eds) (2004) WHO classification of tumors. Pathology and genetics of tumors of the genitourinary and male genital organs. IARC Press, Lyon
4. Armah HB, Parwani AV (2010) Xp11.2 translocation renal cell carcinoma. Arch Pathol Lab Med 134(1):124–129
5. Argani P, Ladanyi M (2003) Distinctive neoplasms characterised by specific chromosomal translocations comprise a significant proportion of paediatric renal cell carcinomas. Pathology 35(6):492–498
6. Heimann P, El Housni H, Ogur G, Weterman MA, Petty EM, Vassart G (2001) Fusion of a novel gene, RCC17, to the TFE3 gene in t(X;17)(p11.2;q25.3)-bearing papillary renal cell carcinomas. Cancer Res 61(10):4130–4135
7. Shipley JM, Birdsall S, Clark J, Crew J, Gill S, Linehan M, Gnarra J, Fisher S, Craig IW, Cooper CS (1995) Mapping the X chromosome breakpoint in two papillary renal cell carcinoma cell lines with a t(X;1)(p11.2;q21.2) and the first report of a female case. Cytogenet Cell Genet 71(3):280–284
8. Ross H, Argani P (2010) Xp11 translocation renal cell carcinoma. Pathology 42(4):369–373
9. Komai Y, Fujiwara M, Fujii Y, Mukai H, Yonese J, Kawakami S, Yamamoto S, Migita T, Ishikawa Y, Kurata M, Nakamura T, Fukui I (2009) Adult Xp11 translocation renal cell carcinoma diagnosed by cytogenetics and immunohistochemistry. Clin Cancer Res 15 (4):1170–117
10. Camparo P, Vasiliu V, Molinie V, Couturier J, Dykema KJ, Petillo D, Furge KA, Comperat EM, Lae M, Bouvier R, Boccon-Gibod L, Denoux Y, Ferlicot S, Forest E, Fromont G, Hintzy MC, Laghouati M, Sibony M, Tucker ML, Weber N, Teh BT, Vieillefond A (2008) Renal translocation carcinomas: clinicopathologic, immunohistochemical, and gene expression profiling analysis of 31 cases with a review of the literature. Am J Surg Pathol 32(5):656–670
11. Wu A, Kunju LP, Cheng L, Shah RB (2008) Renal cell carcinoma in children and young adults: analysis of clinicopathological, immunohistochemical and molecular characteristics with an emphasis on the spectrum of Xp11.2 translocation-associated and unusual clear cell subtypes. Histopathology 53(5):533–544
12. Ramphal R, Pappo A, Zielenska M, Grant R, Ngan BY (2006) Pediatric renal cell carcinoma: clinical, pathologic, and molecular abnormalities associated with the members of the mit transcription factor family. Am J Clin Pathol 126(3):349–364
13. Zhong M, De Angelo P, Osborne L, Keane-Tarchichi M, Goldfischer M, Edelmann L, Yang Y, Linehan WM, Merino MJ, Aisner S, Hameed M (2010) Dual-color, break-apart FISH assay on paraffin-embedded tissues as an adjunct to diagnosis of Xp11 translocation renal cell carcinoma and alveolar soft part sarcoma. Am J Surg Pathol 34(6):757–766
14. Argani P, Antonescu CR, Couturier J, Fournet JC, Sciot R, Debiec-Rychter M, Hutchinson B, Reuter VE, Boccon-Gibod L, Timmons C, Hafez N, Ladanyi M (2002) PRCC-TFE3 renal carcinomas: morphologic, immunohistochemical, ultrastructural, and molecular analysis of an entity associated with the t(X;1)(p11.2;q21). Am J Surg Pathol 26(12):1553–1566
15. Argani P, Olgac S, Tickoo SK, Goldfischer M, Moch H, Chan DY, Eble JN, Bonsib SM, Jimeno M, Lloreta J, Billis A, Hicks J, De

Marzo AM, Reuter VE, Ladanyi M (2007) Xp11 translocation renal cell carcinoma in adults: expanded clinical, pathologic, and genetic spectrum. Am J Surg Pathol 31(8):1149–1160
16. Suzigan S, Drut R, Faria P, Argani P, De Marzo AM, Barbosa RN, Mello Denadai ER, Martins-Filho J, Martucci RC, Bauab T Jr (2007) Xp11 translocation carcinoma of the kidney presenting with multilocular cystic renal cell carcinoma-like features. Int J Surg Pathol 15(2):199–203
17. Argani P, Lal P, Hutchinson B, Lui MY, Reuter VE, Ladanyi M (2003) Aberrant nuclear immunoreactivity for TFE3 in neoplasms with TFE3 gene fusions: a sensitive and specific immunohistochemical assay. Am J Surg Pathol 27(6):750–761
18. Martignoni G, Pea M, Gobbo S, Brunelli M, Bonetti F, Segala D, Pan CC, Netto G, Doglioni C, Hes O, Argani P, Chilosi M (2009) Cathepsin-K immunoreactivity distinguishes MiTF/TFE family renal translocation carcinomas from other renal carcinomas. Mod Pathol 22(8):1016–1022
19. Armah HB, Parwani AV (2008) Renal cell carcinoma in a 33-year-old male with an unusual morphology and an aggressive clinical course: possible Xp11.2 translocation. Pathology 40(3):306–308
20. Armah HB, Parwani AV, Surti U, Bastacky SI (2009) Xp11.2 translocation renal cell carcinoma occurring during pregnancy with a novel translocation involving chromosome 19: a case report with review of the literature. Diagn Pathol 4:15
21. Kuroda N, Tamura M, Tanaka Y, Hes O, Michal M, Inoue K, Ohara M, Mizuno K, Lee GH (2009) Adult-onset renal cell carcinoma associated with Xp11.2 translocations/TFE3 gene fusion with smooth muscle stroma and abnormal vessels. Pathol Int 59(7):486–491
22. LaGrange CA, Lele SM, Strup SE (2007) Renal cell carcinoma associated with TFE3 gene fusion in an elderly woman. Urology 70(3):590 e511–592
23. Meyer PN, Clark JI, Flanigan RC, Picken MM (2007) Xp11.2 translocation renal cell carcinoma with very aggressive course in five adults. Am J Clin Pathol 128(1):70–79
24. Tanas MR, Goldblum JR (2009) Fluorescence in situ hybridization in the diagnosis of soft tissue neoplasms: a review. Adv Anat Pathol 16(6):383–391
25. Geller JI, Argani P, Adeniran A, Hampton E, De Marzo A, Hicks J, Collins MH (2008) Translocation renal cell carcinoma: lack of negative impact due to lymph node spread. Cancer 112(7):1607–1616
26. Argani P, Aulmann S, Illei PB, Netto GJ, Ro J, Cho HY, Dogan S, Ladanyi M, Martignoni G, Goldblum JR, Weiss SW (2010) A distinctive subset of PEComas harbors TFE3 gene fusions. Am J Surg Pathol 34(10):1395–1406

Virchows Arch (2011) 459:307–313
DOI 10.1007/s00428-011-1124-8

ORIGINAL ARTICLE

Alterations of ubiquitylation and sumoylation in conventional renal cell carcinomas after the Chernobyl accident: a comparison with Spanish cases

Luisa Morell-Quadreny · Alina Romanenko · Jose Antonio Lopez-Guerrero · Silvia Calabuig · Alexander Vozianov · Antonio Llombart-Bosch

Received: 20 April 2011 / Revised: 7 June 2011 / Accepted: 4 July 2011 / Published online: 23 July 2011
© Springer-Verlag 2011

Abstract We determined whether ubiquitylation and sumoylation processes are involved in conventional renal cell carcinogenesis associated with chronic, long-term, persistent low doses of ionizing radiation (IR) in patients living for more than 20 years in cesium-137 (^{137}Cs)-contaminated areas after the Chernobyl accident in Ukraine. To this end, we assessed the immunohistochemical expression of ubiquitin (Ub), SUMO1, SUMO E2 conjugating enzyme Ubc9, and the cell cycle regulators p53, mdm2, and p14^{ARF} in 38 conventional renal cell carcinomas from Ukrainian patients with different degrees of radiation exposure after the Chernobyl accident. As control cases, 18 conventional renal carcinoma (cRCC) tissues from a Spanish cohort were analyzed. No significant differences between the Ukrainian and Spanish groups were found regarding Ub overexpression, although being higher in the Ukrainian cases. Furthermore, this expression was inversely associated with SUMO1 and Ubc9, with no correlation with tumor nuclear grade. There was also a direct relationship between Ubc9 and inflammatory response. These findings do not allow us to consider the immunohistochemical expression of ubiquitylation and sumoylation as valuable markers for discriminating the effects of long-term, low-dose IR exposure in cRCC carcinogenesis.

Keywords Conventional renal cell carcinoma · Ionizing radiation · Ubiquitin · SUMO1 · Ubc9 · p53 · mdm2 · p14^{ARF}

Alina Romanenko is a visiting professor at the Department of Pathology, Medical School of Valencia University (grant for temporary stay for invited professors number UV-ESTPC-07-393, Valencia University, Spain).

L. Morell-Quadreny · S. Calabuig · A. Llombart-Bosch (✉)
Department of Pathology, Medical School of Valencia University,
Avda. Blasco Ibáñez 17,
46010 Valencia, Spain
e-mail: antonio.llombart@uv.es

A. Romanenko
Department of Pathology, Institute of Urology,
Academy of Medical Sciences of Ukraine,
9a, Yu. Kotzubinsky Street,
04053 Kiev, Ukraine

J. A. Lopez-Guerrero
Laboratory of Molecular Biology,
Fundación Instituto Valenciano de Oncología,
C/ Prof. Beltrán Bàguena, 8-11,
46009 Valencia, Spain

A. Vozianov
Department of Urology, Institute of Urology,
Academy of Medical Sciences of Ukraine,
9a, Yu. Kotzubinsky Street,
04053 Kiev, Ukraine

Introduction

Recent studies have shown that during the period subsequent to the nuclear Chernobyl accident (April 1986), an increase in morbidity (4.7 to 9.8 per 100,000 of the total population), aggressiveness, and proliferative activity of renal cell carcinomas (RCCs) from Ukrainian patients is recognized [1, 2]. Studies on the development of "radiation sclerosing proliferative atypical nephropathy" in peritumoral kidney tissue then followed and demonstrated a correlation with the duration of radiation exposure [3]. In addition, the influence of chronic, regular, and sustained low-dose ionizing radiation (IR) on RCCs was demonstrated in the population living in cesium-137 (^{137}Cs)-contaminated areas of Ukraine, which constitutes most of the exposed Ukrainian population [2].

The latest evidence suggests that the ubiquitin (Ub)–proteasome system may play a critical role in responses to IR, controlling a variety of fundamental cellular processes such as regulation of cell cycle progression, division, development and differentiation, apoptosis, cell trafficking, and modulation of the immune and inflammatory responses [4, 5], as well as DNA repair [6]. A major pathway for protein degradation is initiated by the addition of multiple 76-amino acid Ub monomers via a three-step process of Ub activation and substrate recognition. Polyubiquitylation targets proteins for recognition and processing by the 26S proteasome, a cylindrical organelle that recognizes ubiquitinated proteins, degrades proteins, and recycles Ub [7].

In addition to Ub, other related Ub-like proteins have been previously described. One of these molecules referred to as small Ub-related modifier 1 (SUMO1) and its homolog can be conjugated to a large number of cellular proteins that involve an enzymatic cascade that resembles ubiquitylation. However, sumoylation appears to regulate protein/protein interactions and intracellular location, and protects some modified targets from Ub-dependent degradation rather than leading to protein degradation. Sumoylation is achieved by the sequential action of several enzymes in which the SUMO E2 conjugating enzyme Ubc9 transfers SUMO from the E1 to the target. In this process, Ubc9 not only forms a triester bond with SUMO but also interacts with SUMO non-covalently [8]. Moreover, SUMO also plays a key role in genome maintenance as a response to genotoxic damage following ionizing radiation [9].

The critical roles played by Ub-mediated protein turnover in cell cycle regulation make this process a possible target for oncogenic alterations. A classic example of a target for Ub and SUMO regulation is the p53 tumor suppressor protein that plays an important role in the regulation of a variety of cellular processes through the p53/mdm2/$p14^{ARF}$ pathway involved in cell cycle control and apoptosis and known to be deregulated in many tumor types [10, 11]. Degradation of p53 hinders its role in apoptosis regulation. Mdm2 is well known as one of the p53 target genes that participate in cell cycle control and apoptosis induction and have recently been shown to mediate several p53 ubiquitylation processes [12]. Furthermore, the $p14^{ARF}$ tumor suppressor protein triggers sumoylation of many cellular proteins, including mdm2, with which $p14^{ARF}$ physically interacts in vivo, occurring equally well in cells expressing or lacking functional p53 [13].

Since ubiquitylation and sumoylation are intimately involved in major cellular biological processes and many effects of IR involve changes in protein stability, it is reasonable to study the chronic effects of long-term, low-dose IR exposure on these molecular processes in cRCC carcinogenesis.

Materials and methods

Case selection

Paraffin-embedded specimens of tumor and peritumoral tissue from 56 patients (35 men and 21 women; male/female ratio, 1.5:1) were selected for the present study. Eighteen patients with primary conventional (clear cell) renal carcinomas (cRCCs) who underwent surgery between 2005 and 2007 in the University Clinical Hospital of Valencia (Spain) represented control group 1, in comparison with 38 analogue patients with cRCCs who underwent surgery between 2005 and 2007 in the Institute of Urology, Academy of Medical Sciences of Ukraine in Kiev (Ukraine). The Ukrainian patients were placed into group 2 (13 patients from "clean" areas, with no indicated radio-contamination) and group 3 (25 patients from radio-contaminated areas, including the city of Kiev). These patients resided in the same geographical areas during the pre- and post-Chernobyl accident periods. All specimens were re-evaluated with regard to pT stage, grade, and histological subtype by two pathologists (L.M.Q. and A.R.). The pT stage was adjusted according to the International Union Against Cancer (UICC) TNM system [12, 13]. Histological nuclear grading was determined according to the method of Fuhrman et al. [14, 15]. Inflammatory response was considered "moderate–intense" when peritumoral and/or intratumoral lymphoid infiltrate were seen in a low-power field, and "low" when verifying the inflammation in a high-power field. Moreover, the presence and percentage of sarcomatoid changes as well as necrotic areas were also evaluated.

Immunohistochemistry

Diverse tissue microarrays (TMA) including the most representative areas of the cases were utilized for the immunohistochemical (IHC) study (Beecher Instr. Inc., Sun Prairie, WI, USA). Two different TMAs were constructed containing cRCCs, from groups 1 to 3, as well as normal kidney for the histological control. Due to the known histologic heterogeneity of cRCCs, at least two cores of tissue, 1.5 mm in diameter, were obtained from different areas within each tumor and arrayed in a recipient paraffin TMA block. Initial sections were stained with hematoxylin–eosin (H&E) to verify the histopathological findings. Sections (3-μm) from TMA blocks were mounted on ChemMate capillary gap microscope slides (DakoCytomation, Denmark) for IHC analysis. The slides were baked overnight in an oven at 56°C. Then, all the sections were deparaffinized in xylene for 20 min, rehydrated through a graded ethanol series, and washed with phosphate-buffered saline. Antigen retrieval was achieved by 2-min heat treatment in autoclave at

1.5 atm and using citrate buffer pH 6.5 (10 mM/L sodium citrate buffer, Dako, Denmark). Endogenous peroxidase activity was blocked with 1.5% hydrogen peroxide in methanol for 10 min. IHC staining was carried out on these sections using the primary antibodies against Ub (rabbit polyclonal, 1:2,000), DakoCytomation; SUMO1 (D-11, 1:20), Santa Cruz Technology; Ubc9 (goat polyclonal, 1:500), Santa Cruz Technology; p53 (DO7, 1:50), DakoCytomation; mdm2 (1B10, 1:20), Novocastra; and $p14^{ARF}$ (polyclonal, 1:50), Neomarkers. Immunodetection was performed with the LSAB visualization system (Dako) using 3.3′-diaminobenzidine chromogen as substrate. As controls, known positive tissue sections were used, and for negative controls, exposure to the primary antibody was omitted. The IHC analysis was performed independently by at least two pathologists in a blind fashion, without knowledge of the patient group.

The IHC score was evaluated according to the extent and intensity of staining and their distribution patterns. Intensity of immunostaining was scored using the following criteria: 0, no detectable staining; 1, low; 2, moderate; and 3, strong staining. The extent of staining was scored as 0, no detectable staining; 1, low (less than 10% scattered stained cells); 2, moderate (more than 10% but less than 50% stained cells); and 3, strong homogenous staining (more than 50% stained cells). The final scoring was determined as the product of intensity and extent.

Statistical analysis

Patient age and tumor size had a quantitative connotation, whereas the other variables (clinical, histological, and immunohistological) were qualitative. Statistical analysis was performed in order to determine whether pathological and IHC data were related to each other, as well as to the different group of patients. We applied a chi-square test for statistical analysis between qualitative variables. ANOVA and mean difference tests were used to assess the relationships between qualitative and quantitative variables. All analyses were made using the SPSS v.14.0 software package.

Results

Histopathology

Epidemiological and pathological features are summarized in Table 1.

Comparative analysis between groups showed that the frequency of high-grade cRCCs was higher in patients from radio-contaminated areas of Ukraine. In 15 (41%) of 38 Ukrainian cRCCs, sarcomatoid changes were detected compared with 3 (16%) of 18 Spanish analogue tumors. Predominantly, a low degree of inflammation was observed

Table 1 Patient epidemiological and pathological features

	Group 1	Group 2	Group 3	Significance
Males	12	7	16	ns
Females	6	6	9	
Mean age (range)	63 (29–81)	56 (40–69)	55 (35–76)	ns
Contamination level in soil (Ci/km^2)[a]	NC	NC	0.5–30	
Mean size (range)	5.27 cm (3–12)	4.30 cm (3–12)	7.12 cm (2–16)	$F=5.507$; $p<0.01$
Tumor stage				
pT1a	8	8	6	ns
pT1b	7	4	11	
pT2	3	1	6	
pT3	–	–	2	
Grade				
1	4	6	4	$\chi^2=17.26$; $p<0.01$
2	7	1	8	
3	5	4	7	
4	2	2	6	
Sarcomatoid changes	3 (16%)	6 (46%)	9 (36%)	ns
Inflammatory changes	17 (94%)	6 (46%)	9 (36%)	$\chi^2=20.92$; $p<0.001$
Necrosis	3 (16%)	2 (15%)	14 (56%)	$\chi^2=11.89$; $p=0.064$; ns

NC non-contaminated area

[a] Contamination data are from Raes et al. [22]

in 15 Ukrainian tumors, and only three tumors from group 2 patients showed moderate inflammatory infiltration, in contrast to eight tumors from group 1.

Immunohistochemistry

IHC data are summarized in Table 2 and illustrated in Fig. 1.

In most cases, normal kidney control had strong nuclear and less cytoplasmic staining, for Ub. Moreover, low–moderate cytoplasmic Ubc9 immunostaining was seen in all peritumoral kidney samples, but only 25% showed positive for SUMO1.

The majority (80%) of group 3 cRCCs showed >50% of tumor cells stained for Ub, compared with 66% of Spanish group 1 cRCCs and 76% of group 2, but without demonstrating significant differences between groups (Fig. 1a).

In contrast, SUMO1-positive tumor cells showed low intensity with predominance of cytoplasmic granular staining in 33%, 15%, and 16% of cRCCs from groups 1, 2, and 3, respectively, with significant differences between Ukrainian and Spanish groups. The expression pattern (extent and intensity) of Ubc9 was similar to that observed for SUMO1 in groups 1, 2, and 3, but significant differences were not seen.

Generally, mdm2 protein expression was detected with the same levels of expression in all groups (Fig. 1c). Moreover, $p14^{ARF}$ overexpression showed the highest score of stained cells in groups 2 and 3 cRCCs which, in all cases with scores 6–9, were scored 9 compared with group 1 which, of 18 cases included in scores 6–9, ten were scored 6 and eight were scored 9. No relationships were seen between IHC and pathological features, except for p53 staining that was associated to high-grade tumors and also

Table 2 Immunohistochemical results in relation to groups and tumor grade

	Groups			Significance	Tumor grade			Significance
	1	2	3		1	2	3+4	
p53								
Negative	12	10	15	ns	13	13	11	$\chi^2=17.84$; $p<0.05$
Score <3	6	3	9		1	3	14	
Score 3–5	–	–	–		–	–	–	
Score 6–9	–	–	1		–	–	1	
Mdm2								
Negative	3	4	7	ns	3	5	6	ns
Score <3	5	2	6		1	4	8	
Score 3–5	3	2	3		3	1	4	
Score 6–9	7	5	9		7	6	8	
$p14^{ARF}$								
Negative	–	–	–	ns	–	–	–	ns
Score <3	–	–	–		–	–	–	
Score 3–5	–	–	1		–	–	1	
Score 6–9	18	13	24		14	16	25	
Ubiquitin								
Negative	–	–	–	ns	–	–	–	ns
Score <3	1	2	–		–	2	1	
Score 3–5	5	1	5		4	3	4	
Score 6–9	12	10	20		10	11	21	
SUMO1								
Negative	12	11	21	$\chi^2=13.02$; $p<0.05$	13	12	19	ns
Score <3	6	2	4		1	4	7	
Score 3–5	–	–	–		–	–	–	
Score 6–9	–	–	–		–	–	–	
Ubc9								
Negative	3	4	11	$\chi^2=17.01$; $p=0.07$; ns	3	7	8	ns
Score <3	10	7	9		8	6	12	
Score 3–5	4	1	1		2	1	3	
Score 6–9	1	1	4		1	2	3	

for Ubc9 that showed a significant relationship with inflammation (χ^2=21.49; p<0.05).

Discussion

In the current study, analysis of several molecular components related to ubiquitylation and sumoylation processes in cRCCs revealed higher levels of Ub nuclear overexpression associated with downregulation of SUMO1 and Ubc9 proteins in the samples from Ukrainian cRCCs than analogue Spanish tumors.

Recent evidence suggests that the Ub/proteasome system may play a critical role in rapid and late responses to IR with radiation-induced impairment (through free radical damage) of proteasome function that results in the inhibition of proteolysis [16]. Because continuous radiation exposure can induce a strong cellular proliferative response in vitro [17], evaluating human response levels after chronic long-term, low-dose IR (more than 20 years after the Chernobyl accident) is warranted. The chronic oxidative stress induced by long-term, low-dose IR exposure might possibly enhance von Hippel Lindau (VHL) tumor suppressor gene inactivation, which in turn blocks Ub-mediated proteolysis, resulting in hypoxia-inducible factor 1 alpha (HIF-1α) stabilization, and translocates to the nuclei where it dimerizes with HIF-1β to form transcriptionally active HIF [18]. Detailed biochemical, structural, and functional analyses of pVHL identified its essential role as a part of a multiprotein E3 Ub ligase that targets specific proteins for destruction via the Ub–proteasome system [19, 20]. Thus, we considered it interesting to investigate if inactivation of VHL gene, which occurs in greater than 60% of sporadic cRCCs, is related with levels of Ub-related proteins as well as with cRCCs of patients from radio-contaminated areas from Ukraine.

Our results indicate that the highest levels of Ub-staining occurred in group 3 cRCCs, but were near group 2 and without significant differences between groups. In contrast, SUMO1 and Ubc9 staining was higher in the Spanish than in the Ukrainian groups, but with significant differences only in SUMO1 expression. Moreover, the significant relationship between SUMO1 and inflammatory peritumoral response has been reported previously in colon and prostate cancer, and although little information is available regarding a role of sumoylation in the immune system, it has been reported that Ubc9 modulates the activity of some transcription factors that regulate inflammatory response. On the other hand, a recent report has demonstrated that the IHC status and level of Uc9 is tissue specific and,

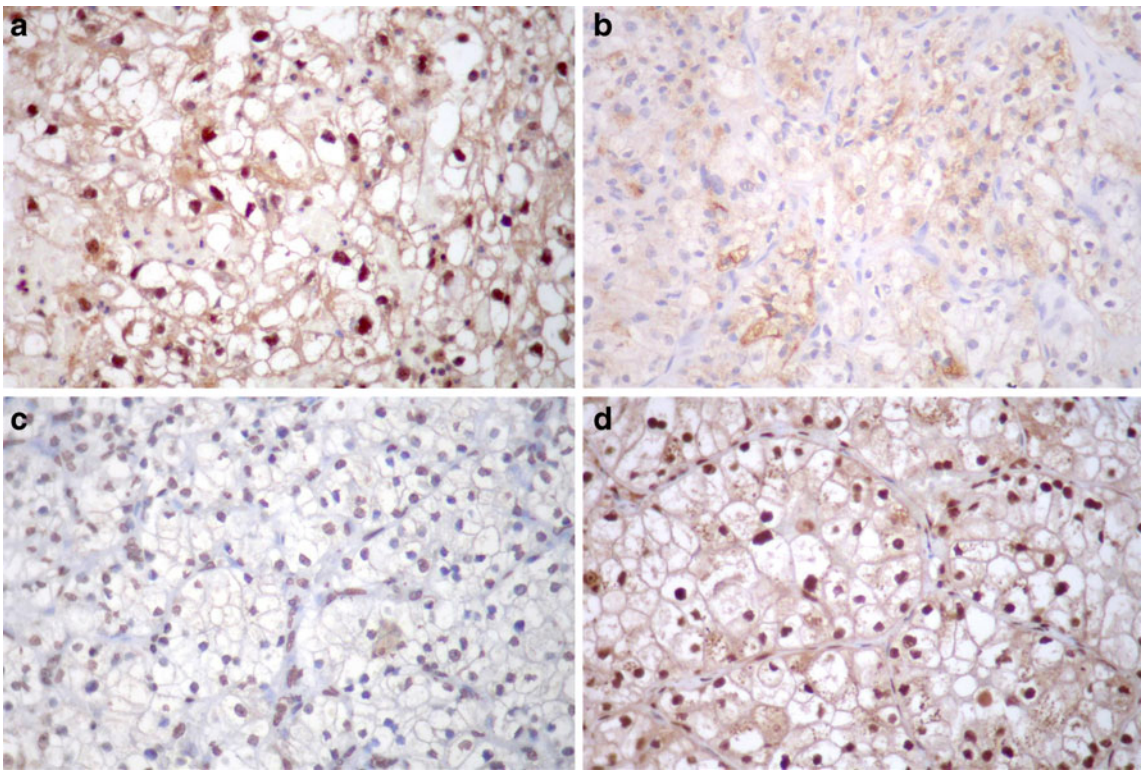

Fig. 1 Immunohistochemical findings for conventional renal cell carcinomas and peritumoral tissue from radio-contaminated areas. **a** cRCC ubiquitin expression. **b** cRCC Ubc9 expression. **c** cRCC mdm2 expression. **d** cRCC $p14^{ARF}$ expression

depending on the type, there is either a direct or an inverse correlation with tumor grade and/or histopathologic features [21]. In the future, similar reports will be necessary for correct evaluation of the IHC paraffin sections in relation to tissue and tumor type.

Recently, we described $p14^{ARF}$ promoter hypermethylation in 25% of a small series of Ukrainian cRCCs from contaminated areas [22] and showed that promoter hypermethylation of $p14^{ARF}$ is not necessarily related to RCCs with p53 mutations. Our present study shows a high percentage (40%) of p53-positive tumor cells in Ukrainian group 3 cRCCs, as well as Spanish group cases (30%), although with low levels of expression. Moreover, only p53 showed direct relation with high-grade tumors. In contrast with previous results in bladder lesions of patients from Ukrainian contaminated areas [23], our data cannot support that long-term, low-dose IR stimulates signal transduction $p14^{ARF}$/p53 pathway in clear cell renal carcinogenesis nor Ub overexpression. However, $p14^{ARF}$ overexpression with higher score was related to cases of Ukrainian cRCCs. In this respect, it would be interesting to determine if $p14^{ARF}$ expression is increased after exposure to either radiation or genotoxic drugs and if it contributes to the DNA response that eliminates damaged cells from the proliferative pool [24]. On the other hand, although some ARF mutations and methylations led to negative immunoreactivity, missense mutations produced nuclear positive overstaining in pancreatic adenocarcinomas [25]. Thus, the presence of positive staining does not necessarily indicate the presence of normal $p14^{ARF}$.

There is evidence of a link between ARF and the proteasome, since human and mouse ARF accumulate following treatment with proteasome inhibitors, suggesting that ARF degradation depends, at least in part, on the proteasome [26]. Thus, we propose that the $p14^{ARF}$ action mechanism may involve the covalent modifications of its binding partners with SUMO1 protein. Reactive oxygen species (ROS) at low concentrations are known to result in a rapid disappearance of most SUMO conjugates, including Ubc9, and thus ROS are key regulators of the sumoylation–desumoylation equilibrium [27].

In particular, we hypothesize that altered $p14^{ARF}$ loses its coordinate functions and cannot interact with the SUMO1 and Ubc9 proteins resulting in unwarranted cell growth and proliferation.

All these data suggest that ubiquitylation and sumoylation processes could be targets of long-term, low-dose IR exposure, probably leading to unscheduled protein degradation, but IHC analysis cannot provide any insight into basic molecular mechanisms of clear cell renal carcinogenesis associated to long-term, low-dose radiation exposure.

Acknowledgements This work was supported by a grant from the Conselleria Sanitat Comunitat Valenciana, Spain, ref. no. 909/2007. The authors are grateful to Alejo Sempere and Laura Martínez for their technical assistance.

Conflicts of interest We declare that we have no conflicts of interest.

References

1. Saydackova NA, Starceva LM, Kravchuk NC (2007) The state of urologic assistance for the population in Ukraine. Annual Report. Ministry of Health in Ukraine, Kiev, pp 146–153
2. Romanenko A, Morell-Quadreny L, Nepomnyaschy V, Vozianov A, Llombart-Bosch A (2000) Pathology and proliferative activity of renal-cell carcinomas (RCCs) and renal oncocytomas in patients with different radiation exposure after the Chernobyl accident in Ukraine. Int J Cancer 87:880–883
3. Romanenko A, Morell-Quadreny L, Nepomnyaschy V, Vozianov A, Llombart-Bosch A (2001) Radiation sclerosing proliferative atypical nephropathy of peritumoral tissue of renal-cell carcinomas after the Chernobyl accident in Ukraine. Virchows Arch 438:146–153
4. Glickman MH, Ciechanover A (2002) The ubiquitin-proteasome proteolytic pathway: distribution for the sake of construction. Physiol Rev 82:373–389
5. McBride WH, Iwamoto KS, Syljuasen R, Pervan M, Pajonk F (2003) The role of the ubiquitin/proteasome system in cellular responses to radiation. Oncogene 22:5755–5763
6. Huang TT, D'Andrea AD (2006) Regulation of DNA repair by ubiquitination. Nat Rev 7:323–337
7. Mani A, Gelmann EP (2005) The ubiquitin-proteasome pathway and its role in cancer. Clin Oncol 23:4776–4789
8. Knipscheer P, van Dijk WJ, Olsen JV, Mann M, Sixma TK (2007) Noncovalent interaction between Ubc9 and SUMO promotes SUMO chain formation. EMBO J 26:2797–2807
9. Bartek J, Hodny Z (2010) SUMO boosts the DNA damage response barrier against cancer. Cancer Cell 17:9–11
10. El-Deiry WS (2007) Targeting mutant p53 shows promise for sunscreens and skin cancer. J Clin Invest 117:3658–3660
11. Guo LL, Gao P, Wu YG, Jian WC, Hao CY, Li H, Lin XY (2007) Alteration of cyclin D1 in Chinese patients with breast carcinoma and its correlation with Ki-67, pRb, and p53. Arch Med Res 38:846–852
12. Saito A, Hayashi T, Okuno S, Nishi T, Chan PH (2005) Modulation of p53 degradation via MDM2-mediated ubiquitin-proteasome system during reperfusion after stroke: role of oxidative stress. J Cereb Blood Flow Metab 25:267–280
13. Tago K, Chiocca S, Sherr CJ (2005) Sumoylation induced by the ARF tumor suppressor: a p53-independent function. Proc Natl Acad Sci U S A 102:7689–7694
14. Eble JN, Sauter G, Epstein JI, Sesterhenn IA (eds) (2004) Pathology and genetics of tumours of the urinary system and male genetic organs. World Health Organization classification of tumours. IARC, Lyon
15. Fuhrman SA, Lesky LC, Limas C (1982) Prognosis significance of morphologic parameters in renal cell carcinoma. Am J Surg Pathol 6:655–663
16. Pajonk F, McBride WH (2001) Ionizing radiation affects 26 s proteasome function and associated molecular responses, even at low doses. Radioer Oncol 59:203–212
17. Contessa JN, Reardon DB, Todd D, Dent P, Mikkelsen RB, Valerie K (1999) The inducible expression of dominant-negative epidermal growth factor receptor—CD533 results in radiosensitiza-

tion of human mammary carcinoma cells. Clin Cancer Res 5:405–415
18. Haase VH (2006) The VHL/HIF oxygen-sensing pathway and its relevance to kidney disease. Kidney Int 69:1302–1307
19. Seliger B, Fedorushchenko A, Brenner W, Ackermann A, Atkins D, Hanash S, Lichtenfels R (2007) Ubiquitin COOH-terminal hydrolase 1: a biomarker of renal cell carcinoma associated with enhanced tumor cell proliferation and migration. Clin Cancer Res 13:27–37
20. Corn PG (2007) Role of the ubiquitin proteasome system in renal cell carcinoma. BMC Biochem 8(Suppl 5):S4
21. Moschos SJ, Jukic DM, Athanassiou C, Bhargava R, Dacic S, Wang X, Kuan S-F, Fayewicz SL, Galambos C, Acquafondata M, Dhir R, Becker D (2010) Expression analysis of Ubc9, the single small ubiquitin-like modifier (SUMO) E2 conjugating enzyme, in normal and malignant tissues. Human Pathol 41:1286–1298
22. Raes F, De Cort M, Graziani G (1991) Multi-fractal nature of radioactivity deposition on soil after the Chernobyl accident. Health Phys 61:271–274
23. Romanenko AM, Kinoshita A, Wanibuchi H, Wei M, Zaparin WK, Vinnichenko WI, Vozianov AF, Fukushima S (2006) Involvement of ubiquitination and sumoylation in bladder lesions induced by persistent long-term low dose ionizing radiation in humans. J Urol 175:739–743
24. Ozenne P, Eymin B, Brambilla E, Gazzeri S (2010) The ARF tumor suppressor: structure, functions and status in cancer. In J Cancer 127:2239–2247
25. Geradts J, Wilentz RE, Roberts H (2001) Immunohistochemical detection of the alternate INK4a-encoded tumor suppressor protein p14ARF in archival human cancers and cell lines using commercial antibodies: correlation with p16INKa expression. Mod Pathol 14(11):1162–1168
26. Pollice A, Vivo M, La Mantia G (2008) The promiscuity of ARF interactions with the proteasome. FEBS Lett 582:3257–3262
27. Bossis G, Melchior F (2006) Regulation of SUMOylation by reversible oxidation of SUMO conjugating enzymes. Mol Cell 21:349–357

Virchows Arch (2011) 459:315–319
DOI 10.1007/s00428-011-1104-z

ORIGINAL ARTICLE

Immunohistochemical localization of autophagosomal membrane-associated protein LC3 in granular cell tumor and schwannoma

Masayuki Shintaku

Received: 16 March 2011 / Revised: 26 April 2011 / Accepted: 30 May 2011 / Published online: 15 June 2011
© The Author(s) 2011. This article is published with open access at Springerlink.com

Abstract Granular cell tumor (GCT) is a neoplasm derived from Schwann cell or (in cases arising in the neurohypophysis) pituicyte and is characterized by abundant cytoplasm filled with numerous eosinophilic granules, which have been considered autophagolysosomes on the basis of their ultrastructure. To confirm that the formation of these granules is related to an autophagy phenomenon, 12 cases of GCT (including two cases of GCT of the neurohypophysis) were studied immunohistochemically using an antibody against LC3 (microtubule-associated protein 1 light chain 3, a specific marker of autophagy). All cases of GCT showed granular immunoreactivity for LC3 in the cytoplasm of tumor cells, indicating that the formation of intracytoplasmic granules in GCT is closely related to an autophagy phenomenon. For elucidation of the relationship between GCT and schwannoma, 20 cases of schwannoma were similarly studied using the anti-LC3 antibody. In eight of 20 cases, a small number of tumor cells showed granular immunoreactivity for LC3, suggesting an increased autophagic activity in some schwannomas and further reinforcing the close relationship between GCT and schwannoma.

Keywords Granular cell tumor · Schwannoma · Autophagy · Immunohistochemistry · LC3

M. Shintaku (✉)
Department of Pathology, Osaka Red Cross Hospital,
Tennoji,
Osaka 543-8555, Japan
e-mail: masa-s@sings.jp

Introduction

Granular cell tumor (GCT) is a neoplasm with distinctive histopathological and ultrastructural characteristics. It commonly arises in the skin and subcutaneous tissue, various visceral organs, especially the breast and upper aerodigestive tracts, and in the neurohypophysis [1]. Regarding the histogenesis of GCT, cases of GCT arising in the skin, subcutaneous tissue, and visceral organs are widely believed to originate from Schwann cells [2–7]. The histogenesis of GCT in the neurohypophysis remains controversial, but derivation from pituicyte has been proposed [8, 9]. Regardless of their localization or origin, the histopathology of GCT is quite uniform. It consists of a proliferation of large polyhedral cells with abundant cytoplasm which is loaded with numerous eosinophilic granules. Although these granules have been considered autophagosomes or autophagolysosomes based on their ultrastructural features [2, 3, 10], their exact nature and the process of their formation remain to be elucidated. It is also unknown why a large number of these granules are formed specifically in GCT.

In recent years, various genes and proteins related to autophagy (autophagocytosis) have been identified, and it has become possible to investigate the autophagy phenomenon by immunohistochemical methods, employing antibodies against these autophagy-related proteins [11, 12]. We investigated cases of GCT immunohistochemically employing an antibody that was raised against microtubule-associated protein 1 light chain 3 (LC3) [11]. This protein is considered to be specifically localized to the membranes of autophagosomes, and immunohistochemical studies employing this antibody have demonstrated its usefulness in the elucidation of the autophagy phenomenon [11, 12].

To clarify further the histogenetic relationship between GCT and schwannoma, we also examined cases of schwannoma for LC3 immunoreactivity.

Materials and methods

The surgical pathology files at Osaka Red Cross Hospital during the recent 6 years were searched for cases of GCT. Ten consecutive cases of GCT were retrieved for the study, and in all of these cases, the tumors exhibited a typical histopathological appearance of GCT. The clinicopathological features of individual cases are presented in Table 1. These consisted of four cases from the skin or subcutaneous tissue, five cases from the digestive tract, and one case from the trachea. Two GCTs of the neurohypophysis which were found incidentally at autopsies were also examined similarly. Twenty cases of schwannoma, which are listed in Table 2, were also retrieved from the surgical pathology files. These comprised 10 cases in which the tumors arose in the skin or subcutaneous tissue and another 10 cases in which the tumors arose in the cranial nerves or spinal nerve roots. Only tumors demonstrating histopathological features that were typical of conventional schwannoma were used for the study, and questionable or problematic cases were excluded. All tumors examined in this study had been fixed in 10% neutral buffered formalin and embedded in paraffin.

Immunohistochemical study was performed on paraffin sections using the Envision Plus detection system (Dako, Glostrup, Denmark), and polyclonal or monoclonal primary antibodies against the following substances were employed: LC3 (polyclonal; Medical & Biological Laboratories, Nagoya, Japan; 1:1,000), CD68 (clone KP1, Dako; 1:100), and S-100 protein (clone ER-PR8, Dako; 1:500). Two GCTs of the neurohypophysis were also examined for the expression of glial fibrillary acidic protein (GFAP, polyclonal; Dako; 1:100). Heat-induced epitope retrieval using a hot bath was performed before applying immunostains for LC3, CD68, and S-100 protein.

Table 1 Clinicopathological findings and results of LC3 immunohistochemistry in granular cell tumors

Case	Age/gender	Site/diameter (mm)	LC3
1	54/F	abdomen/40	+
2	76/F	face/18	+
3	60/M	inguinal region/20	+
4	35/F	chest wall/10	+
5	56/F	cecum/7	+
6	35/F	stomach/10	+
7	66/M	esophagus/5	+
8	41/M	esophagus/5	+
9	42/M	esophagus/5	+
10	13/F	trachea/15	+
11	74/M	neurohypophysis/1	+
12	59/F	neurohypophysis/4	+

Results

A summary of the results of immunohistochemical study is presented in Tables 1 and 2. In all cases of GCT, tumors consisted of an alveolar, trabecular, or diffuse proliferation of large polyhedral cells that had abundant cytoplasm loaded with numerous eosinophilic granules of variable sizes (Fig. 1a). These granules were strongly or weakly positive for periodic acid-Schiff reaction. The cytoplasm of tumor cells exhibited intense, coarsely or finely granular immunoreactivity for LC3 in all cases (Fig. 1b). The cytoplasm was similarly immunoreactive for CD68 and S-100 protein. Two GCTs of the neurohypophysis (Fig. 2a) also showed granular immunoreactivity of the cytoplasm for LC3 (Fig. 2b). Both tumors were also immunoreactive for CD68 and S-100 protein, but only one of the two tumors exhibited focal immunoreactivity for GFAP.

In 8 of 20 schwannomas examined, a small number of large polyhedral cells loaded with eosinophilic granules ("granular cells") were scattered within the tumors (Fig. 3a). These cells were easily overlooked or often difficult to distinguish from reactive macrophages on hematoxylin–eosin sections, but they showed intense granular immunoreactivity and stood out clearly on sections immunostained for LC3 (Fig. 3b). These LC3-immunoreactive cells within schwannoma were also immunoreactive for CD68 and S-100 protein on serial sections. However, immunohistochemistry for these two markers was not useful for the detection of "granular cells," because almost all tumor cells were immunoreactive for S-100 protein, and CD68 was intensely immunoreactive in reactive macrophages within the tumors. Most schwannomas contained both Antoni A and B areas in variable proportions within a given tumor, and the distribution of "granular cells" tended to be more prevalent in Antoni A area than in Antoni B area.

Discussion

Abundant intracytoplasmic granules that accumulate in tumor cells of GCT have been considered autophagosomes or autophagolysosomes on the basis of their ultrastructural features [2, 3, 10]. However, as pointed out by some investigators [13], the electron microscopic identification of intracytoplasmic inclusions as autophagy-related structures

Table 2 Clinicopathological findings and results of LC3 immunohistochemistry in schwannomas

Case	Age/gender	Site/diameter (mm)	Antoni A & B	Granular cells	LC3
1	51/F	shoulder/25	A=B	+	+
2	48/F	retroperitoneum/38	A>B	−	−
3	92/F	orbit/25	A>B	+	+
4	46/F	hand/13	A>B	−	−
5	29/F	forearm/17	A>B	−	−
6	58/M	forearm/29	A<B	−	−
7	36/M	finger/9	A<B	−	−
8	61/M	knee/13	A>B	−	−
9	60/F	thigh/40	A>B	−	−
10	52/F	upper arm/15	A>B	+	+
11	64/M	cauda equina/4	A	+	+
12	42/M	thoracic root/18	A<B	−	−
13	62/F	lumbar root/18	A>B	+	+
14	23/F	acoustic nerve/15	A>B	−	−
15	76/M	acoustic nerve/12	A	+	+
16	75/F	acoustic nerve/20	A<B	−	−
17	71/F	cauda equina/10	A	+	+
18	33/F	acoustic nerve/19	A	+	+
19	75/M	lumbar root/23	A>B	−	−
20	58/F	acoustic nerve/27	A	−	−

is occasionally not straightforward, and some structures unrelated to autophagy can be misinterpreted as autophagosomes. It is also unknown why autophagolysosomes are accumulated in a large amount specifically in tumor cells of GCT. Some intrinsic metabolic abnormalities within tumor cells of GCT probably result in focal cytoplasmic degradation and an accumulation of numerous autophagolysosomes.

Monoclonal antibodies against CD68 molecules, such as KP1 and PGM-1, have been employed as a marker for lysosome or phagolysosome [14–16], and several investigators demonstrated the immunoreactivity of GCT for these antibodies [14–16], which was also confirmed in our present study. We further applied an anti-LC3 antibody for the investigation of GCT and demonstrated that all GCTs examined showed immunoreactivity for LC3. LC3 is a protein located on the inner and outer membranes of autophagosomes [11, 12], and the findings of our study provide additional evidence for the autophagosomal origin of intracytoplasmic granules in tumor cells of GCT. Although the specificity of LC3 as a marker for autophagosome at the light microscopic level leaves some room for reservation because LC3 has been shown to be incorporated into protein aggregates independent of autophagy [12], the immunohistochemical reactivity of GCT for LC3 can be reasonably interpreted as representing an autophagy phenomenon in the light of their well-known ultrastructural features [2, 3, 10].

Concerning the histogenesis of GCT, the Schwann cell origin has been widely accepted in recent years [2–7]. The immunoreactivity of GCT for S-100 protein has been well known [5–7], and a recent study concerning many cases of peripheral nerve sheath tumors arising in the gastrointestinal tract demonstrated the immunoreactivity for CD56,

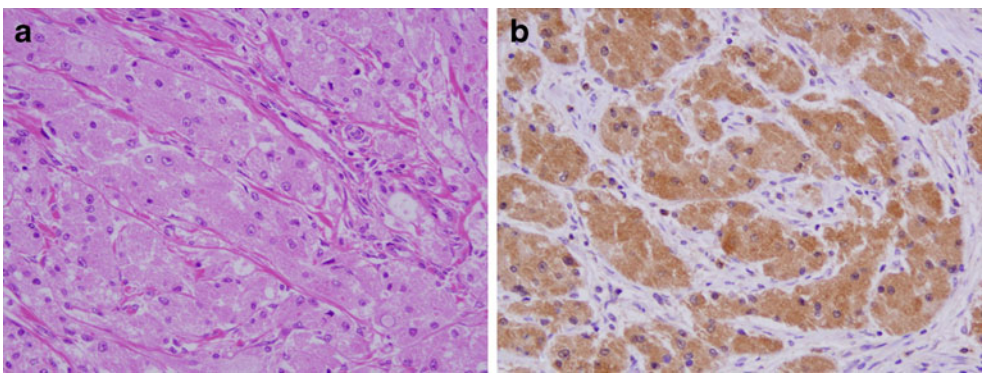

Fig. 1 **a** A subcutaneous GCT. Large polyhedral cells having abundant cytoplasm loaded with numerous eosinophilic granules proliferated diffusely (hematoxylin–eosin stain). **b** The intracytoplasmic granules in GCT showed an immunoreactivity for LC3 (immunoperoxidase method)

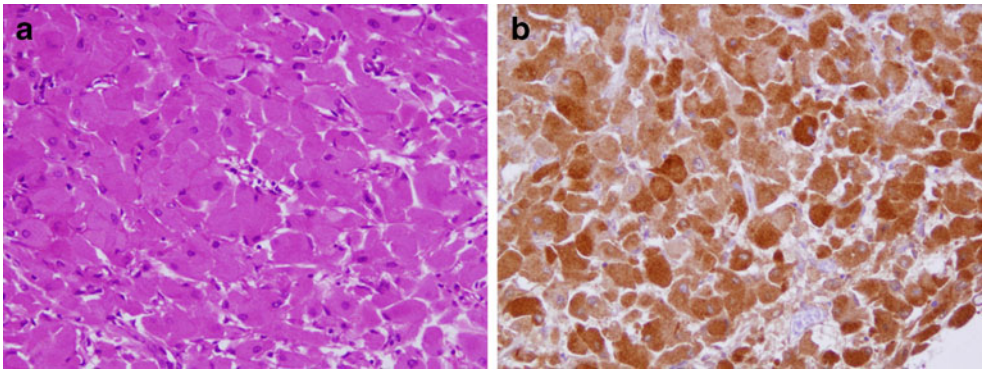

Fig. 2 **a** A GCT of the neurohypophysis. Large polyhedral cells having abundant granular cytoplasm formed a small nodule (hematoxylin–eosin stain). **b** The intracytoplasmic granules showed an immunoreactivity for LC3 (immunoperoxidase method)

calretinin, and α-inhibin (as additional markers of Schwann cell differentiation) in GCT [7]. Immunohistochemical studies employing antibodies against various proteinaceous components of the myelin sheath have shown that intracytoplasmic granules in GCT contain degradation products of the myelin sheath, thus emphasizing further the close relationship between Schwann cell and GCT [6]. However, the relationship between GCT and ordinary schwannoma remains unclear. In an ultrastructural study of schwannoma, Sian and Ryan reported the occurrence of many cells containing intracytoplasmic osmiophilic granules in the Antoni B area and pointed out the similarity of these granules to those found in GCT [17]. A few cases of schwannoma have been reported in which scattered or aggregated "granular cells" were found [4, 18]. In the present study, we examined schwannoma for the presence of LC3-immunoreactive granules in the cytoplasm. In 8 of 20 schwannoma cases, a small number of tumor cells showed cytoplasmic swelling, and the swollen cytoplasm contained numerous granules that were immunoreactive for LC3. This finding probably corresponds to the immunoreactivity for CD68 of autophagosomes in Schwann cells in cases of degeneration of nerve fibers and also in schwannoma and neurofibroma [15, 16]. The immunohistochemistry for LC3 is superior to that for CD68 in detection of "granular cells" within schwannoma, because, while not only "granular cells" but also reactive macrophages showed immunoreactivity for CD68, only the former was highlighted by immunohistochemistry for LC3. The presence of "granular cells" immunoreactive for LC3 indicates increased autophagic activity in some cases of schwannoma and further reinforces the close relationship between GCT and schwannoma.

Some neoplasms other than schwannoma, for example smooth muscle tumors [19], astrocytoma [20], glioblastoma [21], oligodendroglioma [22], and anaplastic medulloblastoma [23], are known to rarely exhibit a "granular cell change" of the cytoplasm. Mentzel et al. studied the "granular cell change" in smooth muscle tumors but found that the change was not related topographically to areas showing degenerative features such as necrosis, hemorrhage, hyalinization, or myxoid change [19]. Although it remains to be clarified whether these tumors also show immunoreactivities for proteins specific to the autophagy-related processes, this finding has something in common with findings we obtained in schwannoma, that is, the occurrence of "granular cells" was not always associated with degenerative changes represented by the Antoni B area in schwannoma. The role of autophagy is diverse and includes the adaptation to nutrient starvation by producing amino acids and the constitutive removal or turnover of cytosolic proteins and redundant or damaged organelles [11, 12, 24]. Autophagy phenomenon therefore does not necessarily indicate degenerative changes of the cells, but it is a dynamic adaptive response to sublethal stress [24].

In conclusion, we demonstrated immunoreactivity for LC3, an autophagy-specific marker, in tumor cells in all

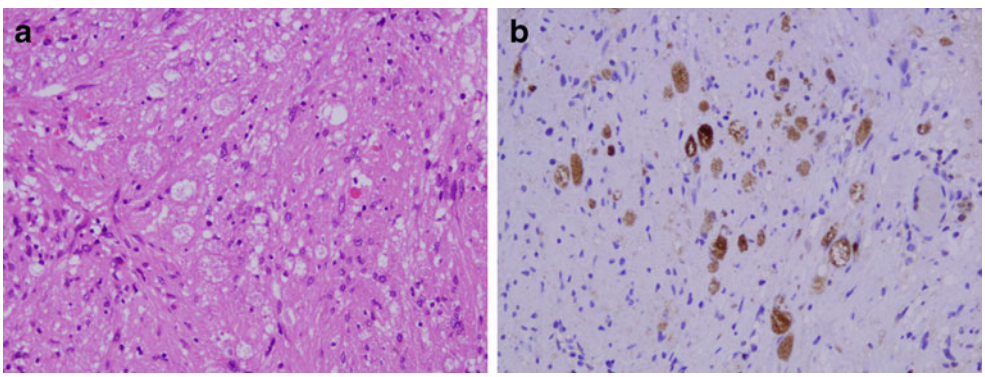

Fig. 3 **a** A subcutaneous schwannoma. A small number of large polyhedral cells with swollen cytoplasm filled with numerous, eosinophilic fine granules ("granular cells") were scattered within the tumor (hematoxylin–eosin stain). **b** The intracytoplasmic granules in these "granular cells" were immunoreactive for LC3 (immunoperoxidase method)

cases of GCT. Eight of 20 cases of schwannoma contained LC3-immunoreactive "granular cells." These results indicate that intracytoplasmic granules in tumor cells of GCT are actually autophagosomes or autophagolysosomes and the activity of autophagy is increased in some cases of schwannoma, supporting a close histogenetic relationship between GCT and schwannoma.

Acknowledgment We are grateful to Ms. Tomoko Honda for her skillful technical assistance in performing the immunohistochemical studies.

Conflict of interest statement We declare that we have no conflict of interest.

Open Access This article is distributed under the terms of the Creative Commons Attribution Noncommercial License which permits any noncommercial use, distribution, and reproduction in any medium, provided the original author(s) and source are credited.

References

1. Lack EE, Worsham GF, Callihan MD, Crawford BE, Klappenbach S, Rowden G, Chun B (1980) Granular cell tumor. A clinicopathologic study of 110 patients. J Surg Oncol 13:301–316
2. Fisher ER, Wechsler H (1962) Granular cell myoblastoma—a misnomer. Electron microscopic and histochemical evidence concerning its Schwann cell derivation and nature (granular cell schwannoma). Cancer 15:936–954
3. Sobel HJ, Marquet E, Avrin E, Schwarz R (1971) Granular cell myoblastoma. An electron microscopic and cytochemical study illustrating the genesis of granules and aging of myoblastoma cells. Am J Pathol 65:59–78
4. Sobel HJ, Marquet E, Schwarz R (1973) Is schwannoma related to granular cell myoblastoma? Arch Pathol 95:396–401
5. Nakazato Y, Ishizeki J, Takahashi K, Yamaguchi H (1982) Immunohistochemical localization of S-100 protein in granular cell myoblastoma. Cancer 49:1624–1628
6. Mukai M (1983) Immunohistochemical localization of S-100 protein and peripheral nerve myelin proteins (P2 protein, P0 protein) in granular cell tumors. Am J Pathol 112:139–146
7. Agaimy A, Märkl B, Kitz J, Wünsch PH, Arnholdt H, Füzesi L, Hartmann A, Chetty R (2010) Peripheral nerve sheath tumors of the gastrointestinal tract. A multicenter study of 58 patients including NF1-associated gastric schwannoma and unusual morphologic variants. Virchows Arch 456:411–422
8. Takei Y, Seyama S, Pearl GS, Tindall GT (1980) Ultrastructural study of the human neurohypophysis. II. Cellular elements of neural parenchyma, the pituicytes. Cell Tissue Res 205:273–287
9. Fuller GN, Wesseling P (2007) Granular cell tumour of the neurohypophysis. In: Louis DN, Ohgaki H, Wiestler OD, Cavenee WK (eds) WHO classification of tumors of the central nervous system, 4th edn. IARC, Lyon, pp 241–242
10. Ghadially FN (1988) Lysosomes in granular cell tumours. Ultrastructural pathology of the cell and matrix, 3rd edn. Butterworths, London, pp 684–689
11. Kabeya Y, Mizushima N, Ueno T, Yamamoto A, Kirisako T, Noda T, Kominami E, Ohsumi Y, Yoshimori T (2000) LC3, a mammalian homologue of yeast Apg8p, is localized in autophagosome membranes after processing. EMBO J 19:5720–5728
12. Kuma A, Matsui M, Mizushima N (2007) LC3, an autophagosome marker, can be incorporated into protein aggregates independent of autophagy. Caution in the interpretation of LC3 localization. Autophagy 3:323–328
13. Eskelinen EL (2008) To be or not to be? Examples of incorrect identification of autophagic compartments in conventional transmission electron microscopy of mammalian cells. Autophagy 4:257–260
14. Tsang WYW, Chan JKC (1992) KP1 (CD68) staining of granular cell neoplasms. Is KP1 a marker for lysosomes rather than the histiocytic lineage? Histopathology 21:84–86
15. Kaiserling E, Xiao JC, Ruck P, Horny HP (1993) Aberrant expression of macrophage-associated antigens (CD68 and Ki-M1P) by Schwann cells in reactive and neoplastic neural tissue. Light- and electron-microscopic findings. Mod Pathol 6:463–468
16. Kurtin PJ, Bonin DM (1994) Immunohistochemical demonstration of the lysosome-associated glycoprotein CD68 (KP-1) in granular cell tumors and schwannomas. Hum Pathol 25:1172–1178
17. Sian CS, Ryan SF (1981) The ultrastructure of neurilemoma with emphasis on Antoni B tissue. Hum Pathol 12:145–160
18. Carpenter PM, Grafe MR, Varki NM (1992) Granular cells in a cellular neurilemmoma. Arch Path Lab Med 116:1083–1085
19. Mentzel T, Wadden C, Fletcher CDM (1994) Granular cell change in smooth muscle tumours of skin and soft tissue. Histopathology 24:223–231
20. Brat DJ, Scheithauer BW, Medina-Flores R, Rosenblum MK, Burger PC (2002) Infiltrative astrocytomas with granular cell features (granular cell astrocytomas). A study of histopathologic features, grading, and outcome. Am J Surg Pathol 26:750–757
21. Kornfeld M (1986) Granular cell glioblastoma. A malignant granular cell neoplasm of astrocytic origin. J Neuropathol Exp Neurol 45:447–462
22. Takei Y, Mirra SS, Miles ML (1976) Eosinophilic granular cells in oligodendrogliomas. An ultrastructural study. Cancer 38:1968–1976
23. Rodriguez FJ, Scheithauer BW (2007) Anaplastic medulloblastoma with granular cell change. Acta Neuropathol 113:95–99
24. Hotchkiss RS, Strasser A, McDunn JE, Swanson PE (2009) Cell death. New Engl J Med 361:1570–1583

Virchows Arch (2011) 459:321–330
DOI 10.1007/s00428-011-1114-x

ORIGINAL ARTICLE

Peritubular capillary basement membrane changes in chronic renal allograft rejection

Comparison of light microscopic and ultrastructural observations

Bela Ivanyi · Eva Kemeny · Peter Rago · Norbert Lazar · Krisztina Boda · Zita Morvay · Pal Szenohradszky · Edit Szederkenyi

Received: 20 March 2011 / Revised: 18 June 2011 / Accepted: 21 June 2011 / Published online: 1 July 2011
© Springer-Verlag 2011

Abstract Marked peritubular capillary basement membrane (PTCBM) multilayering, the ultrastructural feature of chronic antibody-mediated rejection (ABMR) of kidney allografts, was found to correspond histologically to PTCs with thickened BMs; such PTCs have been suggested as a novel histological marker of chronic rejection. We investigated whether scoring of PTCBM thickening can substitute the ultrastructural search for PTCBM multilayering. The thickening was graded in PAS- and Jones-stained sections in 110 biopsies from recipients with a late dysfunction, all examined ultrastructurally for transplant capillaropathy (≥3 PTCs with ≥5 BM layers). Grade 0 indicated no thickening. Grade 1 and grade 2 were assigned when the PTCBMs were as thick as or thicker than those of the non-atrophic tubules, and duplication/chain-like lamination of the PTCBM was noted in ≤3 or ≥4 high-power fields, respectively. The series was enrolled in subgroups of those with and those without histopathological lesions of chronic rejection. Fifty-six biopsies displayed lesions of chronic ABMR. Transplant capillaropathy was demonstrated in 40 biopsies. Grade 2 thickening furnished a substantial interobserver concordance rate (κ=0.803) and correlated with the transplant capillaropathy. Jones staining performed somewhat better in scoring than PAS staining. Grade 2 thickening was verified in 35 biopsies involving chronic ABMR, and in one control biopsy (sensitivity 61.4%, specificity 0.98). Grade 1 thickening was not suggestive of chronic ABMR at all. In conclusion, grade 2 thickening can be regarded as the histopathological lesion of chronic ABMR; however, electron microscopy remains the gold standard in the assessment of PTCBM changes.

Keywords Chronic antibody-mediated rejection · Electron microscopy · Histology · Kidney allograft · Peritubular capillary

B. Ivanyi (✉) · E. Kemeny · P. Rago
Department of Pathology, University of Szeged,
Allomas u. 2,
6720 Szeged, Hungary
e-mail: ivanyi@patho.szote.u-szeged.hu

N. Lazar
Transplantation and Surgical Clinic, Semmelweis University,
Budapest, Hungary

K. Boda
Department of Medical Informatics, University of Szeged,
Szeged, Hungary

Z. Morvay
Department of Radiology, University of Szeged,
Szeged, Hungary

P. Szenohradszky · E. Szederkenyi
Renal Transplantation Unit of the Surgical Clinic,
University of Szeged,
Szeged, Hungary

Introduction

The most common cause of a late dysfunction of a kidney allograft is chronic rejection, mediated in the overwhelming majority of cases in the modern era of immunosuppression by alloantibodies. The biopsy diagnosis of chronic antibody-mediated rejection (ABMR) is based on the presence of an allograft dysfunction, the serological demonstration of donor-specific alloantibodies, and the morphologic confirmation of an alloantibody-induced tissue injury. The latter requires (a) a light microscopic assessment of interstitial fibrosis and tubular atrophy (IF/

TA) and/or glomerular double contours (transplant glomerulopathy) and/or arterial intimal fibrosis (transplant arteriopathy), (b) an immunohistochemical evaluation of the peritubular capillaries (PTCs) for complement 4d (C4d) deposition, and (c) an ultrastructural reading of the PTCs for "marked" circumferential basement membrane (BM) multilayering [1]. The role of peritubular capillary basement membrane (PTCBM) analysis in the establishment of the diagnosis of chronic ABMR, however, is not precisely known because not all laboratories sample kidney allograft biopsy tissue routinely for electron microscopy, the ultrastructural investigation is not carried out if the light microscopic lesions and the immunostaining for C4d are conclusive, and concise information as to how to read the multilayering of PTCBMs, and a clear cut-off for multilayering are not to be found in the consensus papers [1, 2].

While IF/TA, transplant glomerulopathy, and transplant arteriopathy can be adequately assessed in histologic sections, the light microscopic features of PTCBM multilayering have not yet been well characterized, probably because the PTCBMs are much thinner (mean thickness: 88 nm, range 46–123 [3]) than the glomerular BMs, and the magnification of the light microscope imposes a limit on the correct evaluation of the former structures. Ultrastructural measurements have revealed a robust increase in the width of the multilayered PTCBM in cases involving chronic rejection (the term chronic ABMR would be applied nowadays), up to >500 nm [4, 5], and a degree of thickening which amply exceeds the width of glomerular BMs should somehow be manifested histologically. Mauiyyedi et al. [6] reported PTCs in cases with chronic ABMR which appeared to have thickened and duplicated BMs on periodic acid-Schiff (PAS) staining, and the authors interpreted these lesions as the light microscopic manifestation of alloantibody-induced multilayering of the PTCBMs. In 2007, the electron microscopically measured thicknesses of PTCBMs were graded semiquantitatively on a 0–2+ scale in PAS-stained histologic sections of a series of biopsies involving or not involving chronic rejection (23 cases and 25 cases, respectively). A correlation was observed between the ultrastructural data and the histologic scores, and the thickening of the PTCBMs characterized the group of chronic rejection. The width of the BMs of non-atrophic proximal tubules served as reference structure in the assessment of the actual grade of PTCBM thickening [5]. The authors suggested that thickened PTCBMs might serve as a novel diagnostic marker of chronic rejection. Although that paper offered a promising approach for translation of the ultrastructural phenomenon of laminated PTCBMs to the level of histology, the sample size was too small to be conclusive as concerns whether the histologic scoring of PTCBM thickening can really substitute the electron microscopic evaluation of PTCBM multilayering. This work set out to clarify this important aspect of the daily diagnostic work.

A series of 110 biopsies, obtained from recipients with a late allograft dysfunction, were enrolled into two subgroups: those with the histopathological lesions of chronic ABMR, and those without them. All were examined electronmicroscopically for the presence of PTCBM multilayering, and histologically for the thickening of PTCBMs. Both lesions were graded according to established criteria. The analyses of interobserver agreement and correlations among histopathological parameters were carried out on the basis of the scoring of PTCBM thickening in PAS-stained sections, which allowed comparison of the results with those in the study of Aita et al. [5]. The PTCBM thickening was also graded in methenamine silver-stained sections, however, since Jones staining might perform better than PAS staining in the evaluation of subtle BM alterations. As the results will show, the group involving chronic ABMR was characterized histologically by pronounced thickening with duplication/chain-like lamination of the PTCBMs. The grading of PTCBM thickening in Jones-stained sections provided somewhat better parameters than the grading in PAS-stained sections. However, the ultrastructural evaluation of PTCBMs was found to be superior to light microscopy in the assessment of PTCBM changes.

Materials and methods

In our pathology department, renal transplant biopsies are routinely evaluated through the light microscopy of tissue sections prepared after fixation in 10% formalin and subsequently embedded in paraffin, and through immunofluorescence on frozen sections with commercially available antibodies to C4d, C3, HLA-DR, IgG, IgA and IgM; and tissue sampling is performed for optional electron microscopy. For light microscopy, serial sections cut at a thickness of 3 μm with a rotation microtome are stained with hematoxylin and eosin, PAS, trichrome, methenamine silver and elastin. The procedure of fixation and embedding is automated and is carried out according to standard histolaboratory protocols. In addition, all kidney allografts are subjected to needle core biopsies during implantation to document imported vascular lesions.

Study material

From the renal allograft biopsy material collected between 2001 and 2010, 110 biopsies that met two inclusion criteria were selected from recipients with a late allograft dysfunction: (1) the recipients had been immunosuppressed with a combination of steroids, calcineurin inhibitor and mycophenolate mofetil, and (2) the specimens were adequate for

morphological evaluation: the histological slides contained at least eight glomeruli and one interlobular artery; a portion of the cortex with at least four glomeruli could be investigated via immunofluorescence; and at least one glomerulus and at least ten periglomerular PTCs could be analyzed by electron microscopy. All recipients had received a deceased donor kidney matched for HLA and blood group antigens; both donors and recipients were adult Caucasians. The presence of panel reactive antibodies [PRAs] at the time of implantation, the highest PRA score while on the waiting list, and the number of HLA mismatches will be referred to in the Results. The biopsies were performed a median of 40 months (range 6–192) after transplantation. The median serum creatinine level at the time of the biopsy was 316 μmol/l (range 89–1,700). Serological testing for de novo donor-specific alloantibodies with a sensitive solid-phase assay such as the use of Luminex flow beads was not available in Hungary during the selection period. The series included nine patients with a clinical diagnosis of diabetes. Four patients had pretransplant diabetes of type 2 and received their allograft because of biopsy-proven diabetic nephropathy. The others had new-onset diabetes after transplantation, diagnosed according to accepted guidelines [7]. Four of the nine patients displayed 3+ proteinuria, detected by dipstick, which was accompanied by glucosuria in three patients. The biopsy procedure was carried out a median of 49 months after transplantation (range 17–156).

Study groups

Chronic rejection-positive group

The cases were classified as involving lesions of chronic ABMR if IF/TA and/or transplant arteriopathy and/or transplant glomerulopathy and/or transplant capillaropathy were observed [1].

(i) Transplant arteriopathy was indicated by new-onset fibrous intimal thickening.
(ii) Transplant glomerulopathy was defined if double contours were seen histologically in >10% of the capillary loops [8], or if thickening of the capillary wall was noted electron microscopically in at least three loops in consequence of expansion of the subendothelial space by abnormal BM material, with the formation of a new layer(s) of subendothelial basal lamina along the entire capillary circumference. The ultrastructural assessment was carried out in glomeruli not affected by segmental scarring or hyperfiltration [9].
(iii) The circumferential multilayering of PTCBMs was counted in the narrow peritubular interstitium, as described previously [10]. The multilayering was categorized as mild, moderate or severe if the PTCs displayed 2–4, 5–6 (Fig. 1) or ≥7 BM layers. The threshold for alloantibody-mediated chronic PTCBM lamination, termed transplant capillaropathy [10, 11], was the demonstration of ≥3 PTC profiles with moderate multilayering or one profile with severe multilayering.

The results of C4d staining are presented in the "Results" section, summarized as diffuse, focal or minimal.

Chronic active T-cell-mediated rejection was assigned if mononuclear cells were observed in intimal fibrosis [1]. Acute T-cell-mediated rejection was diagnosed if a Banff type IA or IB lesion was noted, or if changes suspicious of acute T-cell-mediated rejection and HLA-DR expression in the cytoplasm of tubular epithelial cells [12] were recorded in at least four tubular profiles.

Chronic rejection-free group (controls)

These were negative for the above-mentioned lesions of chronic rejection.

Semiquantitative evaluation of the severity of PTCBM thickening

The PTCBMs were revised by the first author in the archived PAS-stained and methenamine silver-stained histological slides in 15 biopsies with transplant glomerulopathy, and in ten protocol biopsies of allografts with a normal function. Three patterns were encountered: no change; focal thickening with or without duplication; and circumferential thickening with or without duplication/chain-like lamination. The experience gained led to the grades of thickening being defined as outlined in Table 1 (Figs. 2, 3, 4 and 5). PTCs complete with endothelial cell nuclei were assessed at an objective lens magnification of 40×. The sampling area, chosen randomly and marked in pencil, consisted of the tubulointerstitial space around eight non-obsolescent glomeruli. The tubules were regarded as non-atrophic if their segment-specific features could be identified. To explore potential differences in the degree of PTC thickening in different section planes, the PTCs were evaluated in the first and the sixteenth section plane of the index biopsies with transplant glomerulopathy, without noteworthy disagreement. The pilot study of the first author was then followed with a thorough learning phase of scoring by the participant pathologists (E.K., P.R., L.N. and B.I.). Finally, the biopsies were reviewed independently, blind to the clinical or morphological data, and the grade of thickening was determined. Cases which received different scores were re-evaluated and the final score was obtained by consensus.

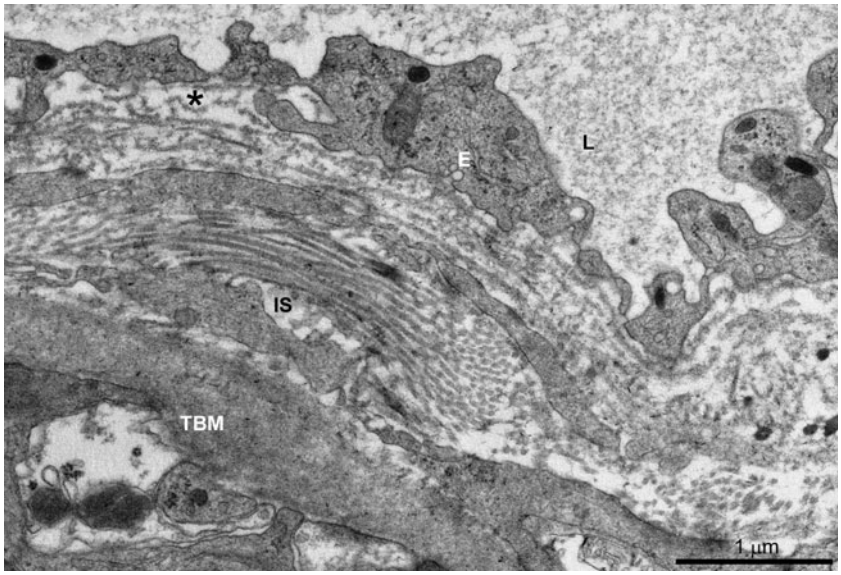

Fig. 1 Moderate multilayering (five to six layers; *asterisk*) and splitting of the peritubular capillary basement membrane. *E* endothelium, *L* capillary lumen, *IS* the narrow peritubular interstititum, *TBM* tubular basement membrane. ×10,000

Interobserver agreement and other statistics

The estimates and tests of agreement among the multiple observers were performed by calculating kappa (κ) for multiple observers per subject [13], using the%MAGREE macro of the SAS system for Windows version 9.1.3. κ values ranging from 0 to 0.20, from 0.21 to 0.40, from 0.41 to 0.60, from 0.61 to 0.80, or from 0.81 upward indicate poor, fair, moderate, substantial and almost perfect concordance, respectively. The distributions of the grades of thickening in cases involving chronic rejection vs. those without chronic rejection were analyzed with the χ^2 test ($p<0.001$). In the chronic rejection group, the two-tailed Pearson correlation, Kendall's tau and Spearman's rho were used to test the relationships between the grades of thickening, the grades of multilayering, the markers of chronic rejection, the C4d positivity of the PTCs, the presence of acute TCMR, and the Banff grades of interstitial infiltrates, tubulitis, interstitial fibrosis and tubular atrophy. Correlations were accepted as significant at a level of $p<0.01$. The extents of IF/TA, expressed in terms of the corresponding Banff scores, and the serological parameters were examined with the Student *t*-test ($p<0.05$). The calculations were carried with the SPSS software program.

Results

General features of the study groups

Fifty-seven biopsies involved chronic rejection. Lesions in various combinations indicating chronic ABMR were observed in 56 biopsies (Table 2). Transplant glomerulopathy was recorded in 46 biopsies, transplant capillaropathy in 40 biopsies, and transplant arteriopathy in 26 biopsies. Transplant glomerulopathy was identified by electron microscopy on five occasions. A total of 25 biopsies were C4d-positive (diffuse or focal or minimal in 16, six and three biopsies, respectively). Chronic active TCMR coincided in nine biopsies, and acute TCMR in 36 biopsies. Chronic rejection was frequently accompanied by non-alloimmune injuries. Calcineurin inhibitor toxicity was recorded on 22 occasions, manifested by peripheral nodular hyalinosis in the afferent arterioles and/or occasional isometric vacuolization of the tubules. Immune complex glomerular disease (membranous nephropathy or mesangial proliferative glomerulonephritis) or acute pyelonephritis or acute tubular necrosis was observed in four, four and six biopsies, respectively. The means of the Banff scores for IF/TA were 2.17±0.8 and 2.11±0.7 SD, respectively.

Table 1 Histological grades of PTCBM thickening

Grade 0	No change (Fig. 2).
Grade 1	Several PTCs have BMs that are as thick as or thicker than those of the nonatrophic tubules; PTC profiles with thickened BM displaying duplication/chain-like lamination may be visible in up to three high-power visual fields.
Grade 2	The majority of PTCs have thickened BMs; duplication/chain-like lamination is present in four or more high-power fields (Figs. 3, 4 and 5).

PTCBM peritubular capillary basement membrane

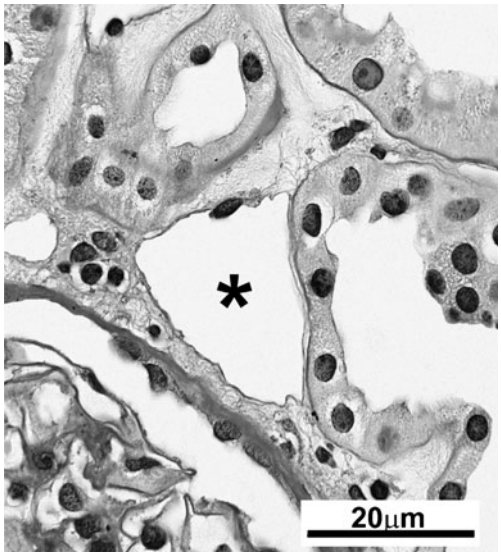

Fig. 2 Normally functioning renal allograft. The basement membrane of the peritubular capillary profile (*asterisk*) is thinner than that of the adjacent tubular profiles. PAS, ×630

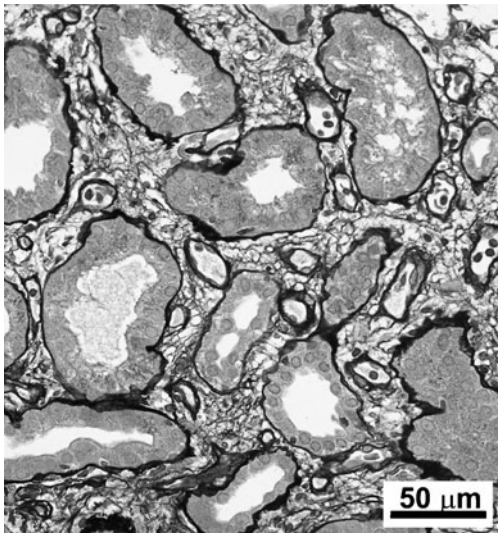

Fig. 4 Peritubular capillaropathy in chronic antibody-mediated rejection. The basement membranes of capillary profiles are as thick or thicker than those of the tubules and display duplication. Jones, ×400

Fifty-three biopsies were negative for the lesions of chronic rejection. This group comprised 23 cases of calcineurin inhibitor toxicity, 24 cases of acute TCMR, five cases of acute ABMR, four cases of acute pyelonephritis, three cases of IF/TA with no evidence of any specific etiology, three cases of mesangial proliferative glomerulonephritis, one case of de novo focal-segmental glomerulosclerosis, and one case of recurrent κ-light-chain nephropathy. These conditions occurred either alone or in various combinations. Calcineurin inhibitor toxicity was manifested as hyaline arteriolopathy and/or occasional vacuolar tubulopathy. The extents of IF/TA (2.14± 0.7 and 2.09±0.7 SD, respectively) did not differ significantly from those in the chronic rejection group.

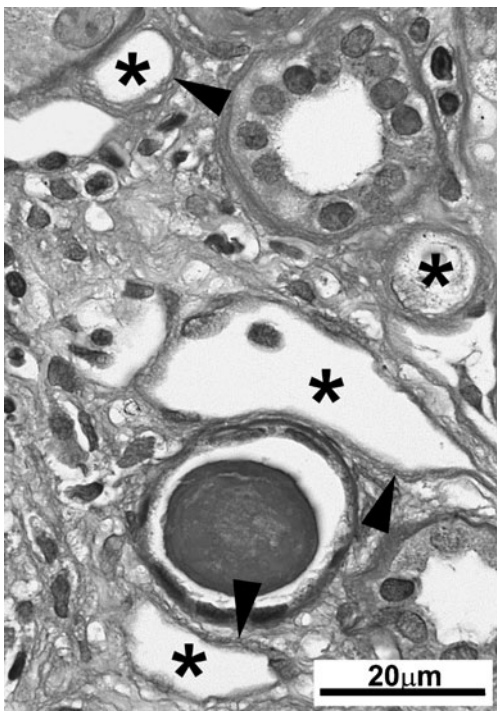

Fig. 3 Peritubular capillaropathy in chronic antibody-mediated rejection. The capillary profiles (*asterisks*) have thicker basement membranes than those of the tubular profiles shown in Fig. 2. The chain-like change in the peritubular capillary basement membrane is indicated by *arrowheads*. PAS, ×1000

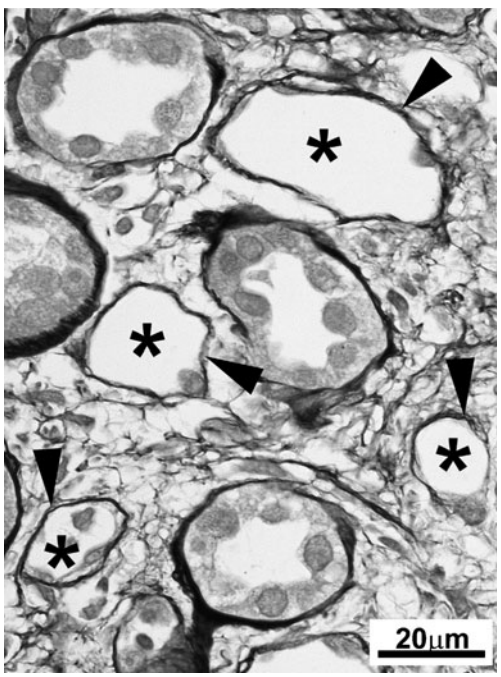

Fig. 5 Duplication and chain-like lamination of the basement membrane (*arrowheads*) of peritubular capillary profiles (*asterisks*). Jones, ×1,000

Table 2 Combinations of histopathological lesions of chronic ABMR

	C4d-negative: 31 biopsies (55%)	C4d-positive: 25 biopsies (45%)
TxA and TxG and TxC	7	8
TxA_m and TxG and TxC	2	3
TxA and TxG	3	2
TxA and TxC	2	1
TxA	2	1
TxA_m and TxG	0	3
TxA_m and TxC	0	1
TxG and TxC	8	4
TxG	4	2
TxC	3	0

C4d-positivity comprised diffuse, focal or minimal staining patterns

ABMR antibody-mediated rejection, *C4d* complement 4d, *TxA* transplant arteriopathy, TxA_m mononuclears in arterial intimal fibrosis, indicating coinciding chronic T-cell-mediated rejection, *TxC* transplant capillaropathy, *TxG* transplant glomerulopathy

As regards the serological parameters, the PRAs at the time of implantation significantly characterized the group of chronic rejection ($p=0.03$), whereas the highest PRAs while on the waiting list, and the number of mismatches did not differ significantly in the group of chronic rejection vs. the controls ($p=0.07$ and $p=0.46$, respectively).

PTCBM multilayering on electron microscopy

The distribution of the grades is presented in Table 3. In cases with chronic ABMR, transplant capillaropathy displaying profiles with severe multilayering was observed in 32 biopsies, and profiles with only moderate multilayering in eight biopsies. In the chronic rejection-free group, seven biopsies exhibited one profile or two profiles with moderate multilayering, and histologically acute TCMR, acute borderline rejection, and calcineurin inhibitor toxicity were observed in these cases in various combinations, accompanied by posttransplantation diabetes in a recipient with acute TCMR and calcineurin inhibitor toxicity.

PTCBM thickening on light microscopy

The panel of pathologists scored grade 2 thickening with substantial concordance ($\kappa=0.803$), and acceptable κ values were obtained with grade 1 thickening and no obvious change (0.584 and 0.486, respectively). The overall κ value was 0.652; every κ was significant at a level $p<0.0001$. The grades of thickening correlated significantly with the grades of multilayering (correlation coefficient: 0.633), transplant capillaropathy (0.579), transplant glomerulopathy (0.480), tubular atrophy (0.441), interstitial fibrosis (0.440) and C4d positivity (0.301). The grades of multilayering correlated significantly with transplant capillaropathy (0.824), transplant glomerulopathy (0.544), C4d positivity (0.374), interstitial fibrosis (0.298), acute TCMR (0.275) and tubular atrophy (0.265). The tubular HLA-DR expression correlated significantly with tubulitis (0.592).

The distribution of the grades is presented in Table 3. In the group involving chronic ABMR, the scoring in Jones-stained sections demonstrated grade 2 thickening in 35 biopsies, and grade 1 thickening in 21 biopsies. Transplant capillaropathy was observed in 30 and in ten of these cases, respectively. The scoring in PAS-stained sections was as follows: grade 2 thickening in 33 biopsies (transplant capillaropathy present in 28 of these cases), and grade 1 thickening in 23 biopsies (transplant capillaropathy in 12 of these cases). In the biopsy involving chronic active T-cell-mediated rejection, grade 1 thickening was scored in both stainings; a mild degree of PTCBM multilayering was observed ultrastructurally.

Table 3 Distributions of the ultrastructural and histological grades of PTCBM changes

Electron microscopy: PTCBM multilayering				
	None	Mild	Moderate	Severe
Chronic rejection	0	11	13	33
Chronic rejection-free	26	20	7	0

Light microscopy: PTCBM thickening						
	Grade 0		Grade 1		Grade 2	
	PAS	Jones	PAS	Jones	PAS	Jones
Chronic rejection	0	0	24	22	33	35
Chronic rejection-free	20	28	29	23	4	1

The numbers represent the numbers of cases displaying the lesion with the given staining technique

PTCBM peritubular capillary basement membrane, *Jones* methenamine silver staining of Jones, *PAS* periodic acid-Schiff staining

In the chronic rejection-free group, grade 2 thickening was scored in four cases, as detailed below. Grade 2 was recorded in both stainings in one biopsy with severe IF/TA and T-cell-mediated Banff IB rejection; electron microscopy revealed a single PTC profile with a moderate degree of multilayering. Clinically, posttransplant diabetes was diagnosed. Grade 2 thickening was assigned in the PAS-stained sections, and grade 1 in the Jones-stained sections in one biopsy of moderate IF/TA and ongoing acute pyelonephritis, and in one biopsy of severe IF/TA and acute T-cell-mediated Banff IB rejection and sclerosing immune complex-glomerulonephritis. Electron microscopy demonstrated a mild degree of PTCBM multilayering in both samples. In one biopsy with IF/TA, acute T-cell-mediated Banff IB rejection and foci of acute pyelonephritis, grade 2 thickening was scored in the PAS staining, and score 0 in the Jones staining; the ultrastructural evaluation revealed PTC profiles without any change in their BMs. As shown in Table 3, fewer biopsies with grade 1 thickening and more biopsies with grade 0 were recorded among the Jones-stained sections than among the PAS-stained sections.

PTCBMs in diabetic recipients

To diagnose diabetic nephropathy in an allograft, four features should be present simultaneously: hyalinization of the arterioles, mesangial expansion caused by increased matrix material, ultrastructurally observed diffuse thickening of the glomerular BMs, and pseudolinear IgG staining along the glomerular, tubular and Bowman's capsule BMs, seen on immunofluorescence microscopy [14]. None of the cases met these criteria. The lesions of chronic ABMR were observed in four biopsies (pretransplant diabetes 1, and posttransplant diabetes 3). Grade 2 thickening was scored in both stainings in two biopsies; and grade 1 thickening in the other two biopsies. Electron microscopy revealed transplant capillaropathy in one biopsy with grade 2 thickening, the other three biopsies exhibited moderate or mild BM multilayering. Chronic calcineurin inhibitor toxicity was diagnosed in five biopsies (pretransplant diabetes 3, and posttransplant diabetes 2). The PTCBM scores were similar in both stainings. Accordingly, grade 2 was assigned in that biopsy which was detailed first in the chronic rejection-free group. Grade 1 and grade 0 were each scored twice in the remaining biopsies; the ultrastructural evaluation revealed PTCBMs without reduplication or multilayering.

Discussion

The aim of our study was to examine whether light microscopic scoring of PTCBM thickening can substitute electron microscopy in transplant biopsies. The assessment of thickening and the methodological details differed from those applied by Aita et al. [5], shown in Table 4. We relied on the presence of the duplication or chain-like lamination of PTCBMs when the grades were defined, because this seemed most likely to correspond to the electron microscopically visible multilayering (and splitting) of the PTCBMs. With the use of high magnification and gentle variation of the actual focus, the lamination could be recognized unambiguously in 2- to 3-μm-thin sections. Efferent arteriolar cross-sections or tubular profiles with a thinned or detached epithelial layer occasionally mimicked PTCs with a thickened BM. To avoid misinterpretation, structures were recorded as PTCs only if the endothelial nuclei were present in the section plane and/or luminal erythrocytes or inflammatory cells clearly indicated that the evaluated structure was a PTC profile. Since the PTCs follow the convolutions of the proximal and distal tubules, relatively few profiles complete with endothelial nuclei appear perpendicular to the axis in section planes. This was the reason why a cut-off of three visual fields was applied to differentiate grade 1 thickening from grade 2. Although the interobserver agreement of the reading of grade 2 thickening concorded well in both studies (κ=0.803 vs. 0.89 in the Aita et al. study), there was much poorer agreement as concerns grade 1 thickening or no obvious change (κ for grade 1=0.584 vs. 0.1, and for grade 0= 0.486 vs. 0.09, respectively). For some reason, duplication or chain-like lamination was not included in the definition

Table 4 Scoring[a] of PTCBM thickening by Aita et al. [5]

ptcbm0	The ptcbm is normal/not thickened.
ptcbm1	Moderate thickening of the basement membrane. The circumference of the PTC is clearly recognizable.
ptcbm2	Severe thickening of the basement membrane, which is as thick or thicker than the basement membrane of the proximal tubule without atrophy.

PTCBM peritubular capillary basement membrane

[a] The score should be judged at the most severely affected lesion. A higher score should not be applied if only one or two thickened PTCs are present throughout the whole specimen. At least ten moderately or severely thickened PTCs in five fields of view at 200× magnification are desirable to apply ptcbm1 or ptcbm2, respectively

of the grades by Aita et al. [5], and this, together with the lower magnification with which they worked, might explain the poor concordance in the reading of grades 1 and 0 in their study.

The statistical analysis in the present study demonstrated significant correlations between the ultrastructural grades of PTCBM multilayering, the presence of transplant capillaropathy, transplant glomerulopathy, C4d positivity, and IF/TA. Since the grades of PTCBM thickening correlated with these variables, but not with transplant arteriopathy, the obtained results justified the assumption in earlier publications [5, 6] that chronic alloantibody-mediated PTC injury is manifested histologically in the thickening of PTCBMs. However, the comparison of the distribution of the grades of thickening in chronic ABMR vs. the controls (see Table 3) revealed that grade 1 thickening was not suggestive of chronic ABMR at all. Grade 2 thickening, on the other hand, appeared to be a marker of alloantibody-mediated chronic PTC injury, reflecting an advanced phase of PTCBM lamination, because the occurrences of grade 2 thickening and severe PTCBM multilayering were almost identical. Thirty-five cases with grade 2 thickening were identified in the Jones staining, and 33 in the PAS staining. In the controls, the Jones staining led to only one false positive case, whereas four false-positive cases were observed on PAS staining. Thus, the evaluation of Jones staining was found to be superior to that of PAS-staining in the verification of grade 2 thickening in terms of sensitivity and specificity. The calculated validity parameters of grade 2 thickening assessed in Jones-stained sections yielded a sensitivity of 61.4%, a specificity of 0.98, a false-negative rate of 38.6%, a false-positive rate of 1.8%, and positive and predictive values of 97.2% and 70.2%, respectively. In conclusion, the pronounced thickening with duplication or chain-like lamination of PTCBMs can be regarded as the histological manifestation of peritubular capillaropathy in chronic ABMR. Our experience may serve as reference for those who have no electron microscopic facility in the evaluation of renal transplant biopsies.

As concerns the value of the ultrastructural evaluation of PTCBM multilayering in establishing the diagnosis of chronic ABMR, our experience and the literature data now allow the conclusion of a reliable cut-off for BM lamination, which was liberally defined as “marked” in the consensus paper [1]. Methodologically, the reading of lamination should be carried out along the narrow peritubular interstitium, where the number of BM layers is consistently the lowest. Regele et al. [15] observed five layers or more in PTCs with C4d-positivity, and 16 of 18 cases with PTCBM multilayering also demonstrated transplant glomerulopathy. In the study by Sis et al. [16], the phenotypes of transplant glomerulopathy were investigated. In 91% of the biopsies with transplant glomerulopathy, multilayering of the PTCBMs was noted, and the median number of layers was 5±2.2. These values are in the range that we have used in our daily work since 2000. However, we rely on the verification of at least three periglomerular PTC profiles with five to six layers to be regarded as involving alloantibody-induced smouldering damage to the PTCs, because the PTCs may occasionally display a moderate degree of multilayering in chronic tubulointerstitial nephritis, thrombotic microangiopathy or reflux nephropathy [10]. In the study by Einecke et al. [17], the cut-off of a single PTC profile with >5 BM layers was applied. Both cut-offs guarantee a highly specific and sensitive ultrastructural lesion of chronic ABMR. The strength of assessing PTCBM multilayering over PTCBM thickening is the distinction of multilayering induced by chronic ABMR from occasional multilayering induced by non-alloimmune injuries, and the verification of early cases, in which the process of lamination has not yet resulted in seven or more layers.

In accord with the current shift in trend toward the ABR pathway, the overwhelming majority of our cases (53/57; 93%) displayed capillary lesions of alloantibody-mediated tissue injury in various combinations; and the statistics demonstrated significant correlations between these variables. The strongest correlation was noted between transplant capillaropathy and transplant glomerulopathy, probably because C4d positivity (diffuse, focal and minimal staining patterns were lumped together) was observed in only 45% of biopsies displaying lesions of chronic ABMR. The low occurrence of C4d positivity has two, mutually not exclusive, explanations. Either a significant number of the cases involving chronic ABMR were in fact C4d-negative, as reported in recent studies [17–19], or the negativity reflected the cessation of antibody production prior to the biopsy procedure. Since sensitive detection system, such as color-coded bead-based fluorometric assay to demonstrate donor-specific HLA class I/II antibodies and non-HLA directed antibodies was not available in our serology laboratory in the period when the majority of the biopsies were performed, we could not match the histopathological lesions of chronic ABMR and the corresponding titers of donor-specific alloantibodies in the presented series. We acknowledge, therefore, the possibility that several cases of transplant glomerulopathy with serologically confirmed alloantibodies might be C4d-negative, and we regard this as the reason why a considerable proportion of the cases of ABMR in our series were not captured by C4d staining. In the light of the potential false-negativity of C4d staining, the ultrastructural evaluation of BM changes in the glomerular capillaries and PTCs is of particular importance. Rejection pathology has an intrinsic focal nature. Accordingly, in the present series transplant glomerulopathy without transplant capillaropathy was detected in 14

biopsies and, conversely, transplant capillaropathy without transplant glomerulopathy was recorded in seven biopsies (data extracted from Table 2). Electron microscopy identified early transplant glomerulopathy on five occasions, and the cumulative occurrence of transplant capillaropathy and transplant glomerulopathy amounted to 93% (53/57). Thus, the incorporation of electron microscopy in the evaluation of the entire capillary bed of the allograft provides a sensitive tool with which to recognize chronic antibody-mediated tissue injury. Wavamunno et al. [20] reported similar experience with protocol biopsies.

Long-standing diabetes induces thickening of the glomerular and tubular BMs and also the PTCBMs [3]. In our series, the duration of the diabetic milieu did not influence the ultrastructural evaluation of the BM lamination, presumably because the thickening of the PTCBM in diabetes and the lamination of the PTCBM in chronic ABMR are pathogenetically different processes. Since none of our recipients fulfilled the criteria of post-transplant diabetic nephropathy, however, we could not obtain ultrastructural evidence from biopsies displaying both diabetic thickening of the PTCBM and chronic ABR-induced BM lamination. This topic awaits future collaborative studies.

In summary, the result of our study offers two messages. The first is for those who report kidney allograft biopsies on the basis of light microscopic staining and C4d immunostaining, i.e., the majority of nephropathologists at present. We suggest the routine search for grade 2 thickening during biopsy reading, because the lesion proved to have a substantial interobserver concordance rate, with a higher sensitivity than that of transplant arteriopathy (51.8% vs. 45.6%). The search does not require an excessive workload from those who regularly score peritubular capillaritis, as proposed recently by the Banff' 07 scheme [2]. The second message is our answer to the question of whether the histological evaluation of PTCBMs can adequately substitute an ultrastructural search for transplant capillaropathy. We recall that ten biopsies (17% of the chronic ABMR series) displayed only grade 1 thickening on light microscopy, whereas electron microscopy verified the presence of transplant capillaropathy in these biopsies. Furthermore, since the sensitivity of transplant capillaropathy unambiguously exceeded that of grade 2 thickening (70.1% vs. 61.4%), electron microscopy remains the gold standard in the identification of PTCBM changes. The recommended ultrastructural cut-off is the demonstration of at least three periglomerular PTC profiles with at least five layers or a single profile with six layers, counted along the narrow peritubular interstitium. The electron microscopic examination of the PTCBMs may be of particular value for the establishment of a diagnosis of chronic ABMR in biopsies with negative C4d staining, a recently described common phenotype.

Acknowledgement This study was supported in part by a grant to B.I. (TÁMOP-4.2.1/B-09/1/KONV-2010-0005, Budapest, Hungary). The authors appreciate the highly constructive comments of Reviewer 2.

Conflict of interest The authors declare that they have no conflict of interest.

References

1. Solez K, Colvin RB, Racusen LC et al (2007) Banff'05 meeting report: differential diagnosis of chronic allograft injury and elimination of chronic allograft nephropathy ('CAN'). Am J Transplant 7:518–552
2. Solez K, Colvin RB, Racusen LC et al (2008) Banff 07 Classification of renal allograft pathology: updates and future directions. Am J Transplant 8:753–760
3. Hvala A, Ferluga D, Rott T, Kobenter T (2005) Peritubular capillary changes in Alport syndrome, diabetic glomerulopathy, Balkan endemic nephropathy and hemorrhagic fever with renal syndrome. Ultrastruct Pathol 29:451–459
4. Hvala A, Ferluga D, Rott T, Kobenter T, Koselj-Kajtna M, Kaplan-Pavlovcic S, Bren A (2001) Interstitial capillary in normal and in transplanted kidneys: an ultrastructural study. Ultrastruct Pathol 25:295–299
5. Aita K, Yamaguchi Y, Horita S, Ohno M, Tanabe K, Fuchinoue S, Teraoka S, Toma H, Nagata M (2007) Thickening of the peritubular capillary basement membrane is a useful diagnostic marker of chronic rejection in renal allografts. Am J Transplant 7:923–929
6. Mauiyyedi S, Della Pelle P, Saidman S, Collins AB, Pascual M, Tolkoff-Rubin NE, Williams WW, Cosimi AB, Schneeberger EE, Colvin RB (2001) Chronic humoral rejection: identification of antibody-mediated chronic renal allograft rejection by C4d deposits in peritubular capillaries. J Am Soc Nephrol 12:574–582
7. Wilkinson A, Davidson J, Dotta F et al (2005) Guidelines for the treatment and management of new-onset diabetes after transplantation. Clin Transplant 9:291–298
8. Racusen LC, Solez K, Colvin RB et al (1999) The Banff 97 working classification of renal allograft pathology. Kidney Int 55:713–723
9. Ivanyi B, Kemeny E, Szederkenyi E, Marofka F, Szenohradszky P (2001) The value of electron microscopy in the diagnosis of chronic renal allograft rejection. Mod Pathol 14:1200–1208
10. Ivanyi B, Fahmy H, Brown H, Szenohradszky P, Halloran PF, Solez K (2000) Peritubular capillaries in chronic renal allograft rejection: a quantitative ultrastructural study. Hum Pathol 31:1129–1138
11. Ivanyi B (2003) Transplant capillaropathy and transplant glomerulopathy: ultrastructural markers of chronic renal allograft rejection. Nephrol Dial Transplant 18:655–660
12. Nickeleit V, Zeiler M, Gudat F, Thiel G, Mihatsch MJ (1998) Histological characteristics of interstitial renal allograft rejection. Kidney Blood Press Res 21:230–232
13. Fleiss JL (2003) Statistical methods for rates and proportions, 3rd edn. Wiley, New York
14. Bhalla V, Nast CC, Stollenwerk N, Tran S, Barba L, Kamil ES, Danovitch G, Adler SG (2003) Recurrent and de novo diabetic nephropathy in renal allografts. Transplantation 75:66–71
15. Regele H, Böhmig GA, Habicht A, Gollowitzer D, Schillinger M, Rockenschaub S, Watschinger B, Kerjaschki D (2002) Capillary deposition of complement split product C4d in renal allografts is associated with basement membrane injury in peritubular and glomerular capillaries: a contribution of humoral immunity to chronic allograft rejection. J Am Soc Nephrol 13:2371–2380

16. Sis B, Campbell PM, Mueller T, Hunter C, Cockfield SM, Cruz J, Meng C, Wishart D, Solez K, Halloran PF (2007) Transplant glomerulopathy, late antibody-mediated rejection and the ABCD tetrad in kidney allograft biopsies for cause. Am J Transplant 7:1743–1752
17. Einecke G, Sis B, Reeve J, Mengel M, Campbell PM, Hidalgo LG, Kaplan B, Halloran PF (2009) Antibody-mediated microcirculation injury is the major cause of late kidney transplant failure. Am J Transplant 9:2520–2531
18. Sis B, Jhangri GS, Bunnag S, Allanach B, Kaplan B, Halloran PF (2009) Endothelial gene expression in kidney transplants with alloantibody indicates antibody-mediated damage despite lack of C4d staining. Am J Transplant 9:2312–2323
19. Sis B, Halloran PF (2010) Endothelial transcripts uncover a previously unknown phenotype: C4d-negative antibody-mediated rejection. Curr Opin Organ Transplant 15:42–48
20. Wavamunno MD, O'Conell PJ, Vitalone M, Fung CL-S, Allen RDM, Chapman JR, Nankivell BJ (2007) Transplant glomerulopathy: ultrastructural abnormalities occur early in longitudinal analysis of protocol biopsies. Am J Transplant 7:2757–2768

Virchows Arch (2011) 459:331–338
DOI 10.1007/s00428-011-1102-1

ORIGINAL ARTICLE

Aberrant expression of the polarity complex atypical PKC and non-muscle myosin IIA in active and inactive inflammatory bowel disease

Flavia A. Wald · Radia Forteza · Runa Diwadkar-Watkins · Anastasia Mashukova · Robert Duncan · Maria T. Abreu · Pedro J. Salas

Received: 15 April 2011 / Revised: 19 May 2011 / Accepted: 28 May 2011 / Published online: 12 June 2011
© The Author(s) 2011. This article is published with open access at Springerlink.com

Abstract Epithelial barrier function is contingent on appropriate polarization of key protein components. Work in intestinal epithelial cell cultures and animal models of bowel inflammation suggested that atypical PKC (aPKC), the kinase component of the Par3–Par6 polarity complex, is downregulated by pro-inflammatory signaling. Data from other laboratories showed the participation of myosin light chain kinase in intestinal inflammation, but there is paucity of evidence for assembly of its major target, non-muscle myosin II, in inflammatory bowel disease (IBD). In addition, we showed before that non-muscle myosin IIA (nmMyoIIA) is upregulated in intestinal inflammation in mice and TNFα-treated Caco-2 cells. Thus far, it is unknown if a similar phenomena occur in patients with IBD. Moreover, it is unclear whether aPKC downregulation is directly correlated with local mucosal inflammation or occurs in uninvolved areas. Frozen sections from colonoscopy material were stained for immunofluorescence with extensively validated specific antibodies against phosphorylated aPKC turn motif (active form) and nmMyoIIA. Inflammation was scored for the local area from where the material was obtained. We found a significant negative correlation between the expression of active aPKC and local inflammation, and a significant increase in the apical expression of nmMyoIIA in surface colon epithelia in inflamed areas, but not in non-inflamed mucosa even in the same patients. Changes in aPKC and nmMyoIIA expression are likely to participate in the pathogenesis of epithelial barrier function in response to local pro-inflammatory signals. These results provide a rationale for pursuing mechanistic studies on the regulation of these proteins.

Keywords PKCι · PKCζ · Epithelial polarity · Crohn's disease · Ulcerative colitis · Non-muscle myosin IIA

Abbreviations

aPKC	Atypical PKC, comprises PKCι and PKCζ isoforms
MLCK	Myosin light chain kinase—phosphorylates the regulatory light chain of myosin II and promotes myosin II assembly and function
nmMyoIIA	Non-muscle myosin IIA—the heavy chains of this isoform are the products of the MYH9 gene
Par	Partition-defective mutants
ROI	Region of interest
TNF-α	Tumor necrosis factor alpha

Maria T. Abreu and Pedro J. Salas contributed equally.

Funding sources Funding source is from NIDDK, R01-087359.

F. A. Wald · R. Forteza · A. Mashukova · P. J. Salas (✉)
Department Cell Biology and Anatomy, University of Miami, Miller School of Medicine,
R-124, P.O. Box 016960, Miami, FL 33101, USA
e-mail: psalas@miami.edu

R. Diwadkar-Watkins
Department of Pediatrics, University of Miami, Miller School of Medicine,
Miami, FL, USA

R. Duncan
Department of Epidemiology and Public Health, University of Miami, Miller School of Medicine,
Miami, FL, USA

M. T. Abreu
Department of Medicine, University of Miami, Miller School of Medicine,
Miami, FL, USA

Introduction

The polarity complex is an evolutionarily conserved set of proteins involved in the development of cell polarity and the establishment of tight junctions in epithelia [1]. It comprises atypical protein kinase C (aPKC, PKCζ and PKCι/λ isoforms), as well as the orthologs of *Caenorhabditis elegans* PARtition-defective mutant proteins [2] Par3 and Par6 [3]. The polarity complex regulates the formation and positioning of tight junctions in *Drosophila* [4] and vertebrate epithelia [5–7]. Like other PKC isoforms, aPKC is activated by PDK1-dependent phosphorylation in the activation loop (T403 in PKCι, T410 in PKCζ) followed by autophosphorylation of the turn motif (T555 PKCι, T563 PKCζ). A phosphorylated turn motif is, therefore, a bona fide reporter of aPKC active conformation [8].

Mutations in the polarity complex-associated protein Crumbs are responsible for human retinal dystrophy (OMIM 600105) [9], and components of the polarity complex seem to participate in cancer [10], but other involvement of the polarity complex in human disease has not been reported so far. Because inflammatory bowel disease (IBD) pathogenesis includes opening of tight junctions with increased paracellular permeability in intestinal epithelia [11], we sought to identify changes in the aPKC–Par complex during inflammation. We found that aPKC and Par3 are downregulated in human intestinal cells in tissue culture in response to TNF-α stimulation under conditions that do not induce apoptosis. Likewise, aPKC was sharply downregulated in mouse intestinal epithelia in DSS-induced colitis [12]. The molecular mechanism underlying the aPKC downregulation was found to be entirely posttranslational and mediated by inhibition and downregulation of Hsp/Hsc70 chaperones. These are known to maintain steady-state aPKC levels by rescue from proteasomal degradation [13]. Other groups have reported downregulation of Hsp70 chaperones in intestinal inflammation as well [14]. Altogether, these data lead us to hypothesize that aPKC may be also downregulated in IBD patients.

It is broadly accepted that pro-inflammatory signaling results in activation of the long (225 kDa) isoform of myosin light chain kinase (MLCK) in the intestinal epithelium [15]. In fact, overexpression of MLCK was observed in IBD patients [16]. MLCK activity is known to induce non-muscle myosin II assembly in non-muscle cells, enhancing the assembly of stress fibers and other cortical acto-myosin structures [17, 18]. Accordingly, the implication for MLCK activation is that non-muscle myosin II assembly is a final effector of pro-inflammatory signaling on the epithelium resulting in either contractile mechanical tension applied on the tight junctions or endocytic removal of tight junction components [19]. From the three non-muscle myosin II isoforms (nmMyoIIA, nmMyoIIB, and nmMyoIIC heavy chains products of MYH9, MYH10, and MYH14, respectively), only nmMyoIIA is associated to tight junction function [20]. Coincidentally, we found that shRNA-mediated aPKC knockdown in intestinal cells results in apical upregulation of nmMyoIIA, but not IIB or IIC that mimics TNFα stimulation. Likewise, inflammation in a mouse model also resulted in specific upregulation of nmMyoIIA in the apical region of colonocytes [12]. In summary, our current hypothesis is that, in addition to MLCK activation, inflammatory cytokines induce post-translational downregulation of aPKC, which can also result in upregulation of nmMyoIIA. This work was undertaken to test if these predictions are true in patients with IBD.

Materials and methods

Bioethical considerations

Biopsies were obtained from patients with IBD, who provided consent under a University of Miami IBD-approved protocol for research. Patient identity was known only to the physician practicing the intervention and not revealed to the research team that handled codified specimens. Whenever possible, biopsies were taken from inflamed and uninflamed areas of the colon and terminal ileum in Crohn's disease (CD) and ulcerative colitis (UC) patients. Data on colonoscopic severity of inflammation were recorded at the time of endoscopy.

Tissue processing

The composition of the patient cohort is shown in Table 1. Biopsies were obtained by colonoscopy and immediately processed for standard pathology procedures. A small fraction of the tissues obtained in the colonoscopy was fixed in 10% trichloroacetic acid for 10 min, a procedure known to specifically preserve phospho-epitopes [21]. We have demonstrated that this fixation is appropriate for the preservation of the phosphorylated turn motif of aPKC (pT555 PKCι and pT563 PKCζ) [13]. It also preserves the antigenicity of human nmMyoIIA for the antibodies utilized in this study [12]. The tissues were then transferred to phosphate-buffered saline and frozen in OCT in isopentane at melting temperature. Frozen blocks were sectioned and processed within 3 months. Frozen sections were processed for immunofluorescence with any of the following antibodies: polyclonal anti-pT555/pT563 aPKC (Abcam, hereafter referred to as pT555) and polyclonal anti-nmMyosin IIA (isoform specific, Covance), both raised in rabbit, and the appropriate CY3-coupled affinity-purified secondary antibody raised in donkey (Jackson Laboratories). For

Table 1 Patient sample composition and scoring

	Ulcerative colitis		Crohn's disease	
	Scores 1–3	Score 0	Scores 1–3	Score 0
Total number of patients	10	5	13	3
Male	2	3	5	2
Female	8	2	8	1
		Percent of patients	Expected random proportion (%)	
Fully consistent scores (0 or 3)		54.8	25	
Mismatching score component for 1 or 2 score values:				
Macroscopic		19.3	25	
Pathology report		6.4	25	
Infiltration in the same sample		19.3	25	

colocalization, the same antibodies were used following a published protocol for differential identification of two primary antibodies raised in the same species [22]. Briefly, one of the primary antibodies (anti-nmMyoIIa) was mixed with an approximately equimolecular concentration of Dylight 488-conjugated affinity-purified Fab fragments of anti-rabbit IgG raised in goat (Jackson Laboratories). Then the excess of fluorescent antibody was removed on rabbit IgG covalently bound to Sepharose 4B. The samples were first incubated with the other primary antibody (anti-pT555 aPKC), then with a CY3-labeled anti-rabbit antibody, then with non-immune rabbit IgG, and, finally, with the mixture described above. All sections were counterstained with DAPI. The sections were mounted in buffered 10% polyvinyl alcohol supplemented with 1% propyl gallate (anti-fading agent), and imaged within 48 h. The antibodies used in the study were all from the same batch, aliquoted at the beginning of the procedures. Independent aliquots were kept frozen and used for each group of tissues (normally two to four) processed at the same time.

Image acquisition and processing

Image acquisition was performed blindly in a Leica SP5 confocal microscope using a ×63 oil-immersion 1.3 numerical aperture objective. Confocal acquisition parameters were determined at the beginning of the study and the same parameters (e.g., gains, slit aperture, laser intensity) used for all the images. Confocal optical sections were 0.6 μm thick. Importantly, image acquisition was performed blindly by block number without information of the inflammation score. Field selection was performed using the DAPI channel to identify epithelial structures, without checking the red channel (for pT555 or nmMyoIIA signal). All the cells showing apical and basal domains in every image were used for quantification (i.e., oblique sections were excluded). The cells per sample ranged 6–42.

Measurement of specific signals was performed also blindly from inflammation status by another individual. In all cases regions of interest (ROI) were selected following preestablished rules as follows. For pT555-aPKC signal, small ROIs at the apical edge of the cells (determined by the end of slim background signal) were compared with ROIs randomly localized in the subapical cytoplasm of the same cell. For each cell the average pixel intensity (red channel) was determined in a pair of ROIs and the cytoplasmic signal ("background") was subtracted from the apical signal. For nmMyoIIA signals, the procedure was similar but one of the ROIs was located at the always positive basal side of the epithelial cells, so that the average basal signal was subtracted from the average apical signal. For each image, ROI pairs were measured in all visible epithelial cells with identifiable apical/cytoplasmic or apical/basal regions. Only a few patients were excluded from the study. Exclusion criteria were as follows: (1) lack of antibody reactivity in a certain aliquot, with the impossibility of re-sectioning the same block due to block aging or lack of additional tissue, or (2) missing histopathological or endoscopy report data to calculate a score.

Inflammation scores

Scores were calculated assigning each block a 0 or 1 value for each one of the following criteria: (1) physician colonoscopy image evaluation of the area, tissue presenting any sign of macroscopic active inflammation was assigned a 1; (2) histopathological report of the biopsied tissue: any microscopic sign of active inflammation was assigned a 1; and (3) infiltration of the section analyzed, as judged by separation between crypts and density of lymphocytes. Only the latter was known to the individuals analyzing the images. The full score was assembled in separate spreadsheets after the immunofluorescence pixel values in the images were measured.

Statistical procedures

The SAS statistical software was used for all statistical computations and analyses. The data were first assessed for normality using SAS PROC UNIVARIATE. There was no evidence for non-normality of the data so standard normal theory statistical procedures were followed. Means and standard errors were calculated using PROC MEANS. Difference between clinical score groups was compared in a one-way analysis of variance using PROC GLM followed by comparisons to the group with clinical score equal to zero as the control using Dunnett's test. The same procedure was used for comparing aPKC expression among different intestine sites with the exception that pairwise Student *t* tests were used following the ANOVA. Correlations were analyzed using PROC CORR. Significant differences were tested at alpha=0.05.

Results

Patient population and scoring

Patients were consented among adult individuals diagnosed with either CD or UC, many of them currently under standard specific treatment of IBD, and undergoing colonoscopy as part of their diagnosis and follow-up (Table 1). Only 8.3% of the patients were smokers. Samples were taken in parallel and processed for hematoxylin and eosin stain for standard pathology report, and for the procedures reported here. To evaluate local inflammation in the mucosa at the point where the sample was taken, we used three independent observations: a macroscopic assessment by the endoscopist, the pathology report of a parallel sample, and the degree of lamina propria infiltration within the sample used for immunofluorescence. Importantly, all three parameters were fully consistent (scores 0 or 3) in 55% of the samples (Table 1), well above of the proportion expected by random coincidence. Furthermore, in cases where one of the parameters was different from the other two (scores 1 and 2), the histopathology was the mismatching component of the score only in 6% of the the cases, indicating strong agreement of this component of the score with at least one of the other components (Table 1). In 12 patients of the cohort, we had samples obtained from different regions, normally inflamed and uninflamed. Accordingly, the scores matched only in two of these patients, and were different by two or three in seven of the patients. These differences in the scores in samples taken from the same patient at the same time indicate that the inflammation score is representative of the local status of the mucosa and not an overall indicator of disease. This was further highlighted by the fact that the scores were independent of the treatment (Table 2). For this reason, although some patients were enrolled in the study with quiescent disease ("controls"), we preferred to compare samples according to their score, with score 0 being considered hereafter as controls.

Validation of the antibodies

The antibodies used in this study were validated by immunoblot using SDS extracts of Caco-2 human intestinal epithelial cells. The anti-pT555 PKCι was validated as a phospho-epitope antibody by treatment of the blots with either calf intestinal alkaline phosphatase or lambda protein phosphatase, both of which abrogated antibody recognition of the specific band. Likewise, the anti-nmMyoIIA was validated by immunoblot using Caco-2 cell SDS extracts. The 220-kDa band recognized by the antibody was strongly downregulated by specific anti-nmMyoIIA shRNA (not shown). The same batch of antibody, appropriately aliquoted, was used throughout the study.

aPKC pT555 signal decreases with inflammation

We first sought to assess the expression of aPKC in its active conformation in IBD patients. In samples from patients with score 0, pT555 aPKC signal appeared like apical "puncta" in most confocal images (Fig. 1, arrows). It also showed belt-like images around the apical region in tangential sections (not shown). Finally, it was indistinguishable from published images in mouse colon using the same antibody and fixation [12]. The apical aPKC belts have been shown to colocalize with tight junction markers [23]. In patients with scores 1–2, increasing proportions of epithelial cells either showed faint aPKC pT555 signal or no signal at all. In samples graded 3, there was no signal in most of the cells (Fig. 1). To quantify these changes, small

Table 2 Patient treatment and scoring

	Scores 1–3	Score 0
Immune modifiers	4	1
TNF-α inhibitors	3	1
Immune modifiers and TNF-α inhibitors	2	0
Other treatment	9	3
Patients under treatment/total patients with the same score (%)	78	63

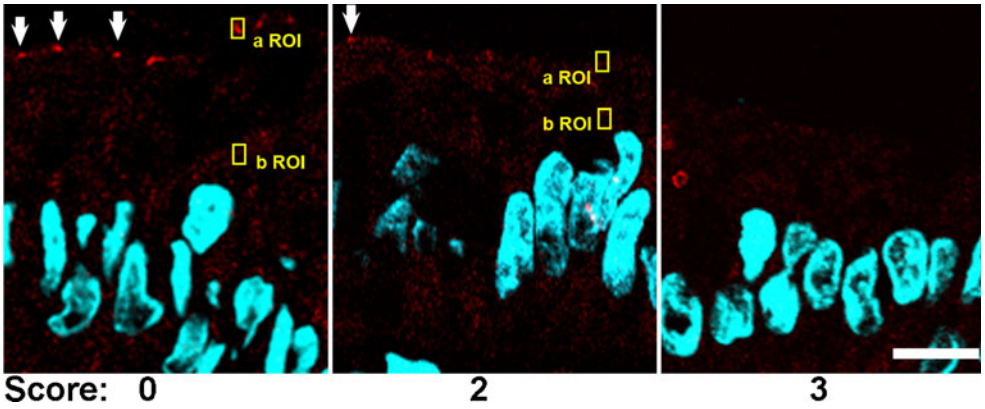

Fig. 1 Representative confocal immunofluorescence images of pT555 aPKC signal (*red channel*). The *arrows* point at positive pT555 aPKC signal in the apical domain. *Yellow boxes* are examples of typical apical (*a ROI*) and background (*b ROI*) regions of interest used for quantification of the signal (Figs. 2 and 3). DAPI (*blue channel*) was used to counter-stain DNA. *Bar*, 10 μm

ROI were sampled around the apical puncta when observable, or randomly on the apical border of the cytoplasm when the puncta could not be distinguished. Similar ROI were sampled on the supranuclear cytoplasm to quantify non-tight junctional signal. Because this signal is identical to background, these cytoplasmic samples were termed background signal (b ROI, typical examples in Fig. 1). The difference of the average pixel values from several randomly selected cells was averaged per patient and is shown in Fig. 2. Samples with score 0 showed all positive values, while the differences in samples with score 3 distributed around a null or slightly negative value, indicating lack of apical aPKC pT555 signal in the presence of inflammation. When the pT555 values were compared, there was a statistically significant difference among the four inflammation score groups ($F_{3,\ 28}$=12.81, p<0.0001). Each of the higher inflammation score groups (1–3) had significantly lower pT555 change values than did the group with inflammation score of zero (t=2.49, p<0.05). We could not detect any difference between CD or UC patients. To determine if there is a natural difference in the distribution of aPKC signal, we plotted the values from score 0 samples obtained from the terminal ileum (not used in the rest of the study), right, transverse, and left colon. No significant differences were found among the different regions reached by endoscopy (Fig. 3).

Apical localization of nmMyoIIA increases with inflammation

In parallel sections from the same samples, we studied the distribution of nmMyoIIA. In score 0 samples, this protein distributed to the basolateral domain with faint or no apical

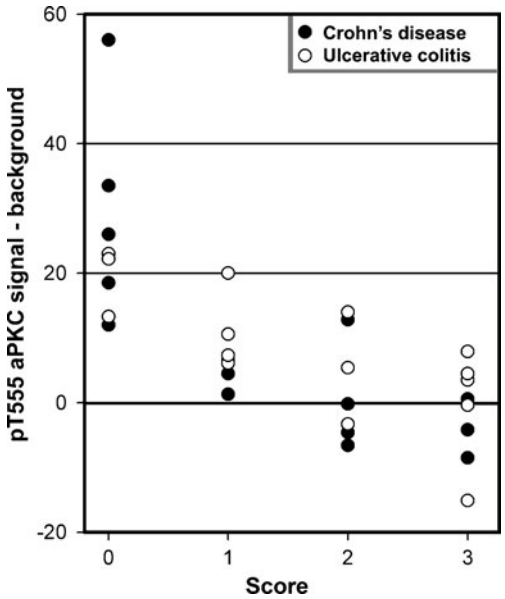

Fig. 2 pT555 aPKC signal quantified in IBD patients. Average pixel intensities in one a ROI and one b ROI per cell were measured in several (6–42) randomly selected cells per sample. The average of the differences a ROI–b ROI for each sample was plotted against the inflammation score. Differences among all score groups were statistically significant (p<0.0001)

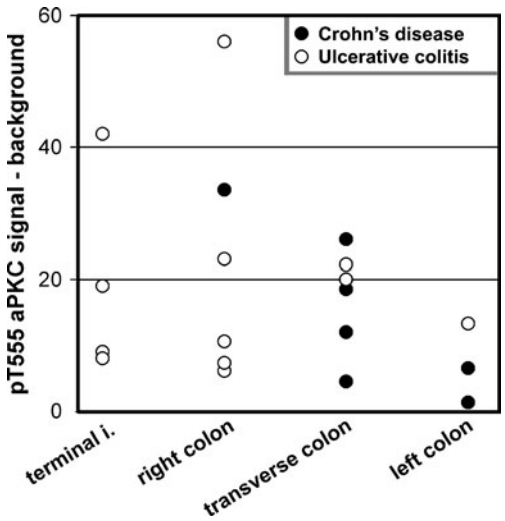

Fig. 3 Distribution of values of pT555 aPKC signal in terminal ileum (*terminal i.*), right colon, transverse colon, and left colon. Data are shown as in Fig. 2, but only from samples with score 0. In this case, samples obtained from the same patient (in 12 cases) were included. There were no statistically significant differences among the values for the different sites

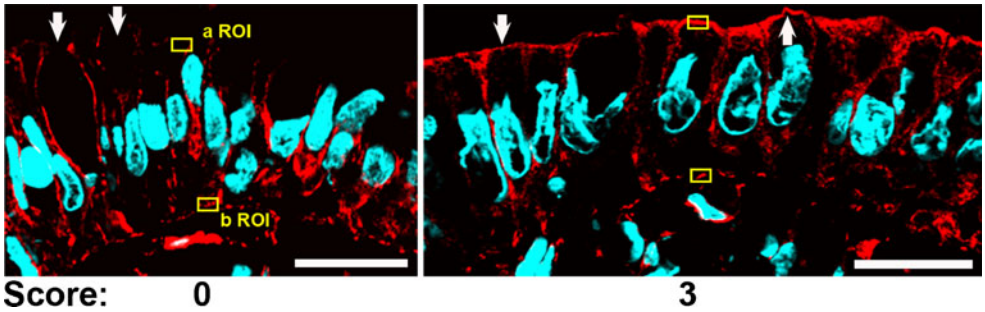

Fig. 4 Representative confocal immunofluorescence images of nmMyoIIA signal (*red channel*). The *arrows* point at typical nmMyoIIA signal in the apical domain. *Yellow boxes* are examples of typical apical (*a ROI*) and basal (*b ROI*) regions of interest used for quantification of the signal (Fig. 5). DAPI (*blue channel*) was used to counterstain DNA. *Bar*, 20 μm

signal. In these samples, only sporadically, some cells showed apical signal. The proportion of cells with apical signal increased with the score, and most of the cells showed a robust apical nmMyoIIA signal in score 3 samples (Fig. 4, arrows). Like in the case of aPKC, we quantified pixel values in ROI on the apical domain (a ROI) or on the basal domain (b ROI). Unlike for aPKC, the latter do not represent background, but rather a positive signal relatively constant in all cases (typical examples shown in Fig. 4). The pixel values were quantified like in Fig. 3 and the differences are shown in Fig. 5. The group with an inflammation score of 3 had significantly higher nmMyoIIA values than did the group with a 0 inflammation score (t=2.57, p<0.05).

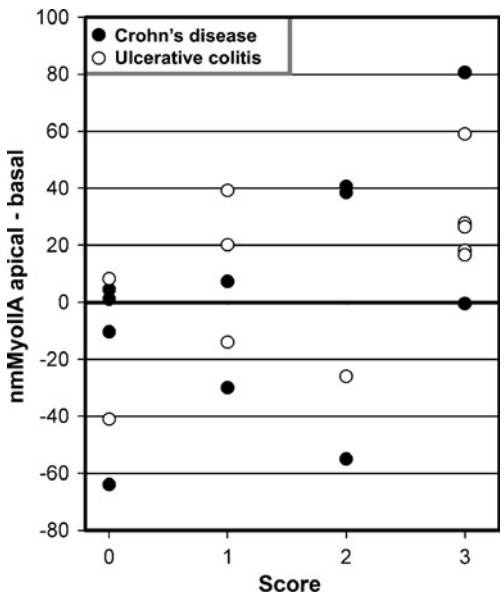

Fig. 5 nmMyoIIA signal quantified in IBD patients. Average pixel intensities in one a ROI and one b ROI per cell were measured in several randomly selected cells per patient. The average of the differences for each patient was plotted against the inflammation score. There was a statistically significant difference (p<0.05) between the score 0 and 3 groups

Correlation between apical expression of nmMyoIIA and pT555 aPKC signal

The correlation between both variables was studied on a cell-by-cell basis. We took advantage of the fact that samples with scores 1–2 often showed mixed populations of cells with and without pT555 expression (e.g., Fig. 1, score 2) and also variable levels of apical nmMyoIIA expression. Additional sections from samples scored 1–2 were double stained for both signals. In Fig. 6, the full image of the epithelium showing the nmMyoIIA signal (green) and DAPI is shown in the bottom panel. The top panel shows only the apical border of the same cells in the red channel (pT555 signal). Some cells were positive for pT555 (arrows). The apical layer of nmMyoII was missing or discontinuous in those cells. Conversely, cells with a robust apical layer of nmMyoIIA (arrows in the green image) displayed little or no pT555 signal. Images from 8 different patients were quantified for both signals as described for Figs. 2 and 5. The values for individual cells were plotted and showed a strong negative correlation (F=34.6130, p<0.0001; Fig. 7).

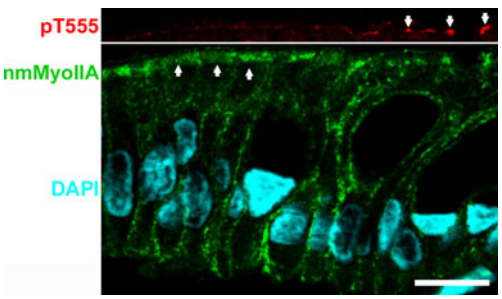

Fig. 6 Immunofluorescence colocalization of pT555 aPKC and nmMyoIIA in samples with intermediate inflammation scores. Section of colon surface epithelium of a sample with score 2. Top panel represents the apical border of the same field as the bottom panel and is aligned. *Bar*, 10 μm

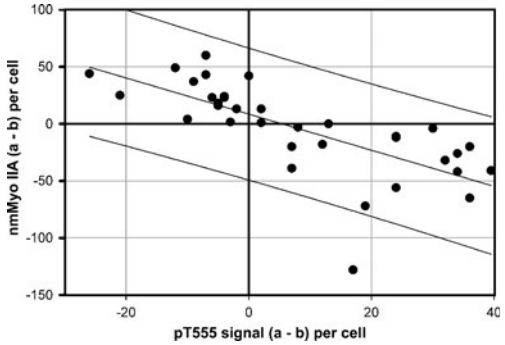

Fig. 7 Cell-by-cell correlation between nmMyoIIA and pT555 aPKC signals in samples with intermediate (1–2) inflammation scores. The signals were measured as described in Figs. 2 and 5 for each individual cell (represented by *one dot* in the plot). Cells from eight different images from different samples were measured. *Lines* represent the best linear regression (*central*) and the 95% prediction band

Discussion

We conclude that in IBD patients, steady-state levels of aPKC in the active conformation decrease with inflammation while apical expression of nmMyoIIA increases with inflammation, and that there is a negative correlation between both signals. While these observations cannot be used to draw cause–effect conclusions, they are very consistent with published mechanistic observations in human intestinal epithelial cells in culture, showing similar variations in both proteins in response to non-apoptotic TNF-α stimulation. More importantly, shRNA-mediated knockdown of aPKC alone was shown to induce accumulation of apical nmMyoIIA [12], raising the possibility that the observations in the human biopsies reported here may be representative of a causal relationship. It is of note that the basolateral distribution of nmMyoIIA observed here is consistent with localization of nmMyoIIA to stress fibers [24], to the basal domain of MDCK cells [25], and to human colon epithelium [26]. It is also consistent with our previous observation of a constant basal nmMyoIIA signal with variable apical localization depending on inflammatory status in tissue culture intestinal cells and murine colon [12]. We conclude that the inflammatory stimulation modulates mostly the apical expression of nmMyoIIA, with little or no detectable changes in the basal domain distribution of this protein.

In regards to nmMyoIIa regulation, inflammation has been shown to result in upregulation of MLCK, specifically in the apical domain, in human IBD samples [16], which, predictably, would result in increased apical non-muscle myosin II polymerization. The aPKC and MLCK pathways are, thus, potentially complementary and synergistic. Because MLCK upregulation occurs at earlier times than aPKC downregulation in tissue culture cells subjected to pro-inflammatory signaling [27], it is also possible that MLCK upregulation may represent an acute response that is later enhanced by aPKC downregulation. The relationship between these two pathways, though, remains unknown. At this time we cannot rule out the possibility that aPKC downregulation may be a downstream consequence of MLCK upregulation.

Both aPKC and nmMyoIIA are involved in epithelial barrier permeability, an important pathophysiologic factor of IBD: (1) aPKC participates in the organization of tight junctions [23, 28]; (2) downregulation of aPKC results in a substantial decrease in transepithelial electrical resistance and an increase in nonionic fluorescent marker permeability [12]; and (3) nmMyosin II is necessary for tight junction disassembly [19]. Therefore, the changes reported here are likely to participate in the barrier function failure associated with IBD. Further mechanistic studies of the aPKC pathway in epithelial inflammatory response are necessary, as it may present novel therapeutic options. For example, a rescue of Hsp70 chaperoning activity, inhibited during inflammation [12], may prevent or ameliorate aPKC downregulation. Therefore, assessing the relative importance of this pathway as compared to other known pathways, such as MLCK, seems to be a reasonable future direction.

Acknowledgments The authors are grateful to Mrs. Yolanda Figueroa-Menendez for the excellent technical assistance. This study is funded by grant NIDDK R01-DK076652 to PJS. Flavia A. Wald was a recipient of a Career Development Award from the Crohn's and Colitis Foundation of America.

Conflict of interest statement We declare that we have no conflict of interest.

Open Access This article is distributed under the terms of the Creative Commons Attribution Noncommercial License which permits any noncommercial use, distribution, and reproduction in any medium, provided the original author(s) and source are credited.

References

1. Suzuki A, Ohno S (2006) The PAR–aPKC system: lessons in polarity. J Cell Sci 119:979–987
2. Guo S, Kemphues KJ (1996) Molecular genetics of asymmetric cleavage in the early *Caenorhabditis elegans* embryo. Curr Opin Genet Dev 6:408–415
3. Macara IG (2004) Parsing the polarity code. Nat Rev Mol Cell Biol 5:220–231
4. Tanentzapf G, Tepass U (2003) Interactions between the crumbs, lethal giant larvae and bazooka pathways in epithelial polarization. Nat Cell Biol 5:46–52
5. Hurd TW, Gao L, Roh MH et al (2003) Direct interaction of two polarity complexes implicated in epithelial tight junction assembly. Nat Cell Biol 5:137–142
6. Anderson JM, Van Itallie CM, Fanning AS (2004) Setting up a selective barrier at the apical junction complex. Curr Opin Cell Biol 16:140–145

7. Mertens AE, Rygiel TP, Olivo C et al (2005) The Rac activator Tiam1 controls tight junction biogenesis in keratinocytes through binding to and activation of the Par polarity complex. J Cell Biol 170:1029–1037
8. Gould CM, Newton AC (2008) The life and death of protein kinase C. Curr Drug Targets 9:614–625
9. Bulgakova NA, Knust E (2009) The Crumbs complex: from epithelial-cell polarity to retinal degeneration. J Cell Sci 122:2587–2596
10. Rothenberg SM, Mohapatra G, Rivera MN et al (2010) A genome-wide screen for microdeletions reveals disruption of polarity complex genes in diverse human cancers. Cancer Res 70:2158–2164
11. Laukoetter MG, Nava P, Nusrat A (2008) Role of the intestinal barrier in inflammatory bowel disease. World J Gastroenterol 14:401–407
12. Mashukova A, Wald FA, Salas PJ (2011) Tumor necrosis factor alpha and inflammation disrupt the polarity complex in intestinal epithelial cells by a posttranslational mechanism. Mol Cell Biol 31:756–765
13. Mashukova A, Oriolo AS, Wald FA et al (2009) Rescue of atypical protein kinase C in epithelia by the cytoskeleton and Hsp70 family chaperones. J Cell Sci 122:2491–2503
14. Ciancio MJ, Chang EB (2008) Do heat shock proteins play any role in gut inflammation? Inflamm Bowel Dis 14(Suppl 2):S102–S103
15. Marchiando AM, Graham WV, Turner JR (2010) Epithelial barriers in homeostasis and disease. Annu Rev Pathol 5:119–144
16. Blair SA, Kane SV, Clayburgh DR et al (2006) Epithelial myosin light chain kinase expression and activity are upregulated in inflammatory bowel disease. Lab Invest 86:191–201
17. Totsukawa G, Yamakita Y, Yamashiro S et al (2000) Distinct roles of ROCK (Rho-kinase) and MLCK in spatial regulation of MLC phosphorylation for assembly of stress fibers and focal adhesions in 3T3 fibroblasts. J Cell Biol 150:797–806
18. Matsumura F, Totsukawa G, Yamakita Y et al (2001) Role of myosin light chain phosphorylation in the regulation of cytokinesis. Cell Struct Funct 26(6):639–644
19. Ivanov AI, Parkos CA, Nusrat A (2010) Cytoskeletal regulation of epithelial barrier function during inflammation. Am J Pathol 177:512–524
20. Ivanov AI, Bachar M, Babbin BA et al (2007) A unique role for nonmuscle myosin heavy chain IIA in regulation of epithelial apical junctions. PLoS One 2:e658
21. Hayashi K, Yonemura S, Matsui T et al (1999) Immunofluorescence detection of ezrin/radixin/moesin (ERM) proteins with their carboxyl-terminal threonine phosphorylated in cultured cells and tissues. J Cell Sci 112:1149–1158
22. Wald FA, Oriolo AS, Mashukova A et al (2008) Atypical protein kinase C (iota) activates ezrin in the apical domain of intestinal epithelial cells. J Cell Sci 121:644–654
23. Suzuki A, Yamanaka T, Hirose T et al (2001) Atypical protein kinase C is involved in the evolutionarily conserved par protein complex and plays a critical role in establishing epithelia-specific junctional structures. J Cell Biol 152:1183–1196
24. Even-Ram S, Doyle AD, Conti MA et al (2007) Myosin IIA regulates cell motility and actomyosin–microtubule crosstalk. Nature Cell Biol 9:299–309
25. Watanabe T, Hosoya H, Yonemura S (2007) Regulation of myosin II dynamics by phosphorylation and dephosphorylation of its light chain in epithelial cells. Mol Biol Cell 18:605–616
26. Babbin BA, Koch S, Bachar M et al (2009) Non-muscle myosin IIA differentially regulates intestinal epithelial cell restitution and matrix invasion. Am J Pathol 174:436–448
27. Wang F, Graham WV, Wang Y et al (2005) Interferon-gamma and tumor necrosis factor-alpha synergize to induce intestinal epithelial barrier dysfunction by up-regulating myosin light chain kinase expression. Am J Pathol 166:409–419
28. Suzuki A, Ishiyama C, Hashiba K et al (2002) aPKC kinase activity is required for the asymmetric differentiation of the premature junctional complex during epithelial cell polarization. J Cell Sci 115:3565–3573

Virchows Arch (2011) 459:339–346
DOI 10.1007/s00428-011-1129-3

ORIGINAL ARTICLE

Lysozyme-rich mucus metaplasia in duodenal crypts supersedes Paneth cells in celiac disease

Carlos A. Rubio

Received: 16 March 2011 / Revised: 20 April 2011 / Accepted: 20 April 2011 / Published online: 18 July 2011
© Springer-Verlag 2011

Abstract Lysozyme is as an innate enzyme with potent antibacterial properties found in Paneth cells in normal duodenal crypts. Since celiac disease concurs with an abnormal duodenal microbiota we explored the expression of lysozyme in this disease. Fifty-three duodenal biopsies were stained with anti-lysozyme: 15 had normal duodenal mucosa (NDM), 7 chronic active duodenitis (CAD), 3 borderline (BL), 17 subtotal villous atrophy (SVA) and 11 total villous atrophy (TVA). NDM showed lysozyme-positive Paneth cells arranged in "Indian file" in 93.3%. In contrast, lysozyme-positive mucus metaplasia in crypts (LPMMC) replacing Paneth cells was found in 71.5% in CAD, in 96.4% in SVA/TVA, and in 2 cases with B. In 19.3% cases with BL/SVA/TVA, LPMMC replaced all Paneth cells in all crypts in entire sections. In crypts and villi, lysozyme-positive goblet cells (LPGC) were found in 92.8%. Changes were more frequent in the duodenal bulb than in *pars descendens*. In normal duodenal mucosa, absorptive enterocytes and goblet cells migrate from stem cells upwards, while Paneth cells migrate downwards, towards the base of the crypts. In celiac disease stem cells seem to have been re-programmed, as the normal production of Paneth cells in the crypts was replaced by lysozyme-producing mucus cells. LPMMC and LPGC in celiac disease might mirror an antimicrobial adaptation of stem cells to signals generated by pathogenic duodenal bacteria. The molecular mechanism(s) behind the abrogation of Paneth cells in duodenal crypts and its substitution by LPMMC in celiac disease remains to be elucidated.

Keywords Celiac disease · Crypts · Panneth cells · Mucus metaplasia

C. A. Rubio
Department of Pathology, Karolinska Institute and University Hospital,
Stockholm, Sweden

C. A. Rubio (✉)
Gastrointestinal and Liver Pathology Research Laboratory,
Department of Pathology, Karolinska Institute and University Hospital,
Building P1/03/057,
17176 Stockholm, Sweden
e-mail: Carlos.Rubio@ki.se

Introduction

The normal duodenal mucosa is lined by a single layer of cells shaping tall villi and short crypts of Lieberkhün [1]. This single cellular layer, built with enterocytes, goblet cells, enteroendocrine cells and Paneth cells forms a barrier between the hostile luminal microenvironment and the host. In the submucosa, mucus-producing Brunner's glands are found above the sphincter of Oddi.

Enterocytes, goblet cells, enteroendocrine cells and Paneth cells derive from a progenitor stem cell, located at the fourth or fifth cell position from the base of each crypt [2]. Stem cell offsprings constantly replenish the epithelial make-up of the duodenum upwards with absorptive enterocytes, goblet cells and enteroendocrine cells and downwards, towards the base of the crypts with Paneth cells [3]. In H&E stain Paneth cells display coarse eosinophilic [1], autofluorescent [4] granules in the apical aspect of the cytoplasm. These cells reside at the base of the crypts for about 20 days before being engulfed by phagocytes [5]. Paneth cells contain immunoglobulins A and G, mRNAs for tumor necrosis factor, alpha-1-antitrypsin, secretory phospholipase A, lysozyme and 8-defensins [6, 7], peptides that keep the duodenum free from pathogenic bacteria, both in newborns and adults.

Table 1 Lysozyme expression in 53 biopsies from the duodenal bulb in patients having normal mucosa, NDM (=15), chronic active duodenitis, CAD (n=7), borderline, BL (n=3), subtotal villous atrophy, SVA (n=17), or total villous atrophy, TVA (n=11)

[a] In a single crypt
[b] In a single villous

Histology/lysozyme-positive immunoreactivity	Paneth cells in "Indian file"	MMC	Goblet cells	Surface epithelium	Lumen secretion	Paneth cells absent
NDM (n=15)	14	1[a]	7[b]	1	1	
CAD (n=7)	2	6	6		2	
BL (n=3)		3	1			1
SVA (n=17)	1	16	15	2	8	3
TVA (n=11)		11	11	2	4	2

Celiac disease is a common immune-mediated condition in the proximal small intestine often leading to mucosal atrophy; it is generated by a permanent intolerance to cereal gluten proteins in genetically predisposed individuals [8]. In most Western countries the prevalence of diagnosed CD in children is 0.5–1% [9]. In Sweden, the epidemiology of childhood celiac disease (CD) has undergone dramatic changes over the recent decade [9]. Up to the early 1980s, the incidence of CD in Swedish children was about 1⁄1000 [10]. During the mid and late 1980s, a sharp increase was observed at several pediatric clinics in this country. Today, CD is the second most common chronic disease in Swedish children with an incidence of 3% [11]. Despite numerous sensitive and specific serological markers [11], duodenal biopsy remains the gold standard for diagnosing celiac disease. Following diagnosis, a lifelong strict gluten-free diet is the treatment of choice to restore mucosal normality and thereby reverting symptoms and possible complications.

In later years much attention has been focused on the abnormal microbiota present in the duodenum in patients with celiac disease. Sanchez et al. [12] found that *bifido bacterium* diversity was higher in patients with celiac disease than in controls and that *bifido bacterium adolescentis/bifido bacterium animalis lactis* were more prevalent in patients with active celiac disease than in patients with treated celiac disease and control children. Schippa et al. [13] detected more often *Bacteroides vulgatus* and *Escherichia coli* in CD patients than in controls. Recently Forsberg et al. [14] and Ou et al. [15] found rod-shape bacteria attached to the intestinal epithelium in patients with celiac disease.

During a deliberate search for medical antibiotics, Alexander Fleming [16] discovered one of the natural defense substances against bacterial infection that he denominated lysozyme, an ancient protein whose origin goes back an estimated 400 to 600 million years [17]. Lysozyme, also known as muramidase or N-acetylmuramide glycanhydrolase, is a family of enzymes (EC 3.2.1.17) which damage bacterial cell walls by catalyzing hydrolysis of 1,4-beta-linkages between N-acetylmuramic acid and N-acetyl-D-glucosamine residues in a peptidoglycan and between N-acetyl-D-glucosamine residues in chitodextrins [18]. In humans, lysozyme is encoded by the LYZ gene [17, 18]. Lysozyme is today regarded as an innate enzyme with potent non-immunological antibacterial properties in the gastrointestinal tract (GI) [19]; in the normal gastric mucosa lysozyme is expressed in the surface epithelial cells, in the cells of the neck region of the body-fundic mucosa and in the antro-pyloric glands [20], in the goblet cells in gastric intestinal metaplasia (IM) [21] and in Barrett's esophagus [22]. Lysozyme is also expressed in the granules of normal Paneth cells found in the small intestine and right colon [23], in metaplastic Paneth cells evolving in the crypts of the left colon in patients with microscopic colitis [24] and with inflammatory bowel disease [24] (IBD) of the colon, as well as in colonic tumors [25].

Due to the increasing awareness of an abnormal duodenal microflora in celiac disease [12–15, 26] it was considered of interest to investigate the expression of the natural antibacterial enzyme lysozyme in duodenal biopsies from patients with celiac disease.

Materials and methods

Fifty-three consecutive double duodenal biopsies, from the bulb (1st portion) and from the second portion (*pars descendens*) of the duodenum, were investigated: 15 had histologically normal mucosa, 7 had chronic active duodenitis,

Table 2 Lysozyme expression in 53 biopsies from the *pars descendens duodeni* in patients having normal mucosa NDM (=15), chronic active duodenitis, CAD (n=7), borderline, BL (n=3), subtotal villous atrophy, SVA (n=17), or total villous atrophy, TVA (n=11)

Histology/lysozyme-positive immunoreactivity	Paneth cells in "Indian file"	Mucus metaplasia in crypts	Goblet cells	Surface epithelium	Lumen secretion	Paneth cells absent
NDM (n=15)	15					
CAD (n=7)	5	2	3			
BL (n=3)	2	1				
SVA (n=17)	5	12	7		2	1
TVA (n=11)	4	7	3	1	2	

Table 3 The age and the gender of patients having duodenal biopsies showing normal duodenal mucosa, NDM (=15), chronic active duodenitis, CAD (n=7), borderline, BL (n=3), subtotal villous atrophy, SVA (n=17) or total villous atrophy, TVA (n=11). Range in brackets

	Mean age (range)	Gender (F/M ratio)
NDM	3.9 years (2–7)	9:6
CAD	5.2 years (3–8)	3:4
BL	3.0 years (2–4)	2:1
SVA	5.2 years (2–7)	11:6
TVA	3.9 years (2–7)	7:4

3 were borderline, 17 had subtotal villous atrophy (SVA) and 11 had total villous atrophy (TVA).

Definitions

- *Normal duodenal mucosa* (NDM): Duodenal mucosa showing normal villous-crypt architecture (villous-crypt ratio 3:1 to 5:1) and intraepithelial lymphocytes not exceeding 25 IELs/100 epithelial cells (mean+2 SD) [27].
- *Chronic active duodenitis* (CAD): Duodenal mucosa showing in the *lamina propria* increased the number of lymphocytes, some plasma cells and neutrophils. Neutrophils could also infiltrate the villi and the crypt epithelium.
- *Borderline* (BL) or Marsh type I (infiltrative): Duodenal mucosa showing normal villous-crypt architecture and increased number of intraepithelial lymphocytes (IEL, >30 lymphocytes/100 surface enterocytes).
- S*ubtotal villous atrophy* (SVA) or Marsh type IIIB: Duodenal mucosa with still recognizable rudimentary villi having increased number of IEL.
- Total villous atrophy (TVA) or Marsh type IIIC: Duodenal mucosa with no discernible digitations having increased number of IEL.

  Cases of Marsh type II (hyperplastic) or Marsh type III A (partial villous atrophy) were not found in the present survey.
- *Mucus metaplasia in duodenal crypts (MMC):* Mucus secreting cells replacing the Paneth cells normal population.

Sections (5 μm) were pre-treated with Enzyme 1 (Leica Microsystems, Wetzlar, Germany) for 5 min, incubated for 30 min with anti-human lysozyme antiserum (Dako A 0099, DAKO, Glostrup, Denmark) on a Leica Bond MAX (Leica Microsystems, Wetzlar, Germany) diluted (1:1600) in Antibody Diluent AR 9352 ((Leica Microsystems, Wetzlar, Germany), developed in Developing kit (DS 9800, Bond Refine Polymer DAB kit, Leica Microsystems, Wetzlar, Germany) with hematoxylin–eosin (H&E).

As in previous work [21, 24, 25] the intensity of lysozyme expression was classified into negative (0), slight (+), moderate (++) or marked (+++). In cases showing regional variations in lyozyme intensity, the highest degree of lyozyme expression was recorded. Lysozyme expression in biopsies with BL, SVA and TVA was compared to that in NDM and CAD.

Statistical analysis

The Mann–Whitney test was used to compare difference between groups. Statistical significance was defined as $p<0.05$.

The Regional Ethical Committee approved the study.

Results

Biopsies from the first part of the duodenum (duodenal bulb) are presented in Tables 1 and 2 and from the 2nd part (*pars descendens duodeni*) in Table 3.

Duodenal bulb

a) *Lysozyme expression in NDM*: At low power examination sections with normal histology displayed lysozyme-positive Paneth cells arranged in "Indian file" at the base of the crypts in 14 of the 15 cases (93.3%) (Table 1 and Fig. 1). In the remaining case,

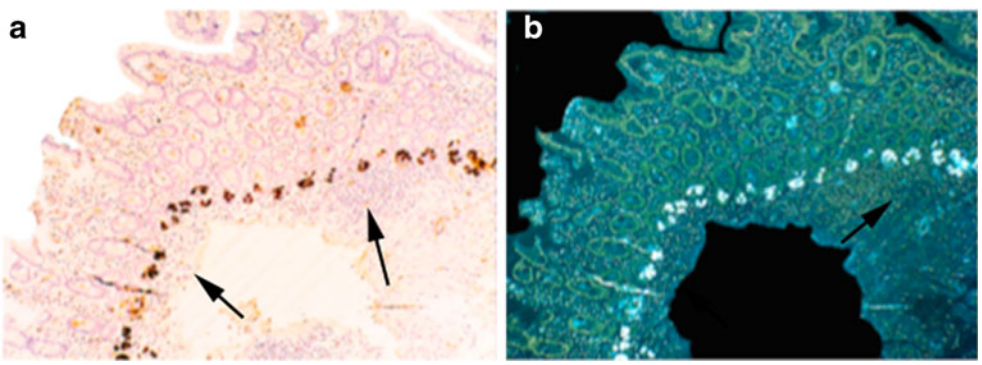

Fig. 1 **a** Normal duodenal mucosa showing Panneth cells arranged in "Indian file" at the base of the crypts at arrows (duodenum, lysozyme stain× 10). **b** The same picture using the INVERT function of a Photoshop program (Ps Adobe Photoshop CS3 extended)

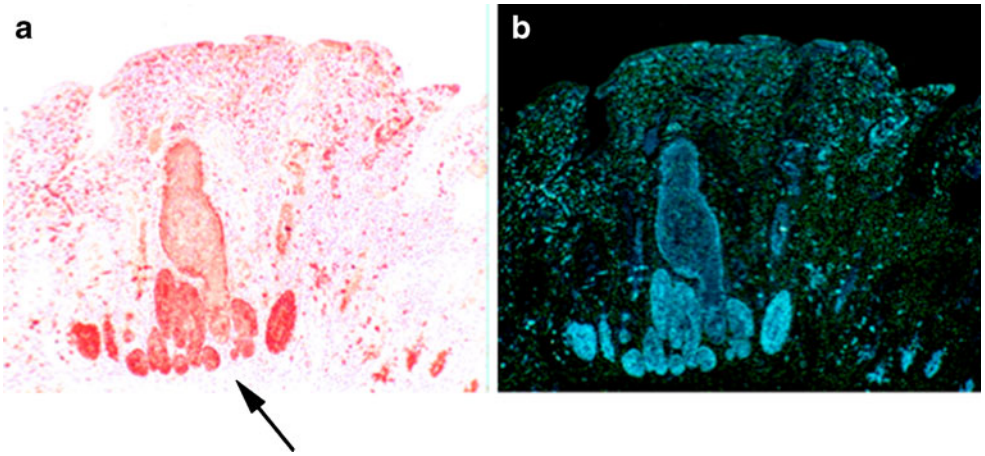

Fig. 2 **a** Chronic active duodenitis showing partial lysozyme-rich mucus metaplasia of the crypts at arrows (duodenum, lysozyme stain×20). **b** The same picture using the INVERT function

lysozyme-positive MMC was found in a single crypt intercalated between neighboring crypts with Paneth cells. At that point the "Indian file" arrangement was disrupted. Lysozyme-expressing goblet cells were found in two consecutive crypts-villi in 7 cases.

b) *Lysozyme expression in CAD*: In 71.5% (5/7) consecutive crypts exhibited lysozyme-positive MMC (Fig. 2). Lysozyme-positive goblet cells were also present in single crypts-villi in 7 cases. In the remaining 28.5% (2/7) of the CAD cases, Paneth cells were found normally arranged in "Indian file".

c) *Lysozyme expression in BL*: In 2 of the BL cases, lysozyme-positive MMC was present in consecutive crypts. In the remaining case of BL, lysozyme-positive MMC had replaced all Paneth cells in all crypts in entire sections.

d) *Lysozyme expression in SVA and TVA*: Because of similar results, these two subgroups were considered together. Of the 28 cases with SVA and TVA in Table 1, lysozyme-positive MMC were found in consecutive crypts in 96.4% (27/28) (Figs. 3 and 4). In the remaining case (3.5%) lysozyme-positive Paneth cells were normally arranged in "Indian file". Lysozyme-expressing goblet cells in crypts and villi were recorded in 92.8% (26/28) of the SVA–TVA cases (Fig. 5). Enterocytes expressed lysozyme in 14.3% or in 4 of the 28 cases (Fig. 6) and lysozyme-positive luminal secretion was found in 42.9% (12/28) of the cases (Figs. 3 and 5).

In 19.3% (6/31) of cases with BL–SVA–TVA, MMC had replaced all Paneth cells in all crypts in entire sections (Fig. 6).

In some cases with BL/SVA/TVA, MMC involved several consecutive but still recognizable crypts and in others, MMC involved relatively large areas of neighboring, sometimes amalgamated crypts (Fig. 7). In the latter modality, no discernible crypt could be recognized.

Comparison between NDM, CAD and BL/SVA/TVA

The proportion of cases with lysozyme-positive Paneth cells in "Indian file" was significantly higher in NDM and CAD than in BL/SVA/TVA ($p<0.05$). The proportion of cases with lysozyme-positive MMC in consecutive crypts was significantly higher in CAD and BL/SVA/TVA than in NDM ($p<0.05$). The proportion of cases in which lysozyme-positive MMC had replaced all Paneth cells in all crypts in entire sections was significantly higher in BL/SVA/TVA than in CAD and NDM ($p<0.05$). Finally, the

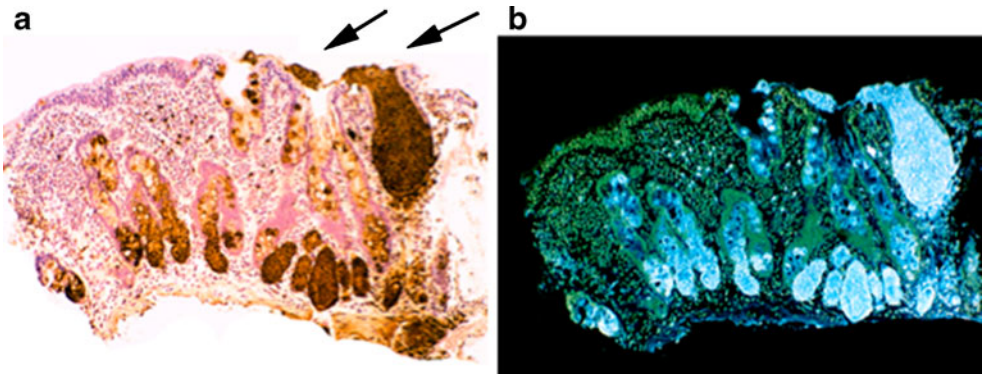

Fig. 3 **a** Total villous atrophy showing lysozyme-rich mucus metaplasia of the crypts. Note lysozyme-expressing goblet cells and lysozyme-expressing secretion on the lumen between crypts at arrows (duodenum, lysozyme stain×20). **b** The same picture using the INVERT function

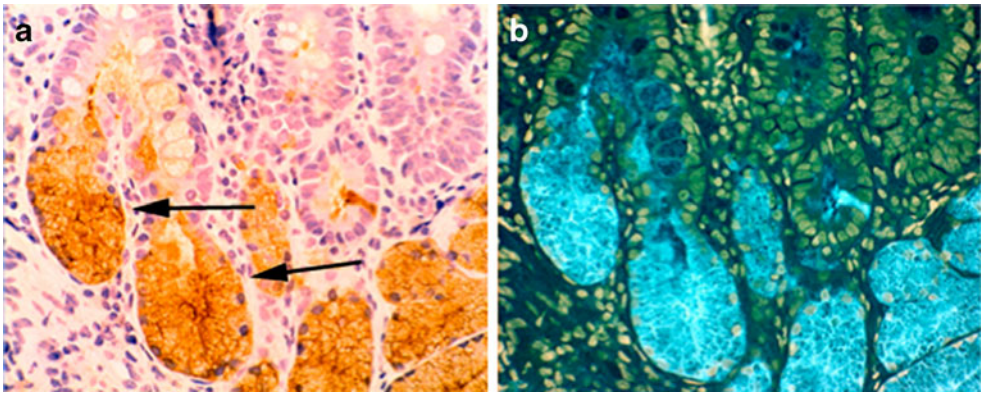

Fig. 4 **a** Detail of total villous atrophy showing lysozyme-rich mucus metaplasia of the crypts, at arrows. Note the absence of Paneth cells (duodenum, lysozyme stain×40). **b** The same picture using the INVERT function

proportion of cases with lysozyme-positive luminal secretion was significantly higher in BL/SVA/TVA than in CAD and NDM ($p<0.05$).

Pars descendens duodeni

Results condensed in Table 3 show that MMC as well as the other pathological parameters listed in Table 1 were less frequent in *pars descendens duodeni* than in the duodenal bulb. In fact, some cases with SVA and TVA showed Paneth cells in "Indian file" and MMC could not be recorded.

No apparent differences between the various aforementioned subgroups and the age and gender of patients were found (Table 3).

Discussion

Sections from the duodenal bulb challenged with anti-lysozyme showed Paneth cells arranged in "Indian file" in the majority of the NDM cases, highlighting the usual position of the normal Paneth cells along the base of the crypts [4]. In only one of the NDM cases, MMC was found in a single crypt and the usual linear arrangement of Paneth cells in "Indian file" was interrupted at that spot. In 4 cases with NDM lysozyme-expressing goblet cells were recorded in single crypts. Considering the antibacterial nature of this enzyme [16, 18, 23, 24], it would appear that even the normal duodenal mucosa might focally increase the production of lysozyme when confronted with commensal bacterial infections. This notion seems to be validated by the finding that in cases with ongoing active duodenal inflammation (CAD), lysozyme-rich MMC was found at the base of the crypts and in goblet cells. In cases with BL/SVA/TVA increased production of lysozyme was often found in several consecutive crypts with MMC, in goblet cells in several consecutive crypts and villi and in the secretion present at the luminal aspect of the mucosa.

The occurrence of MMC with increased lysozyme immune-reactivity in multiple crypts in cases with BL/

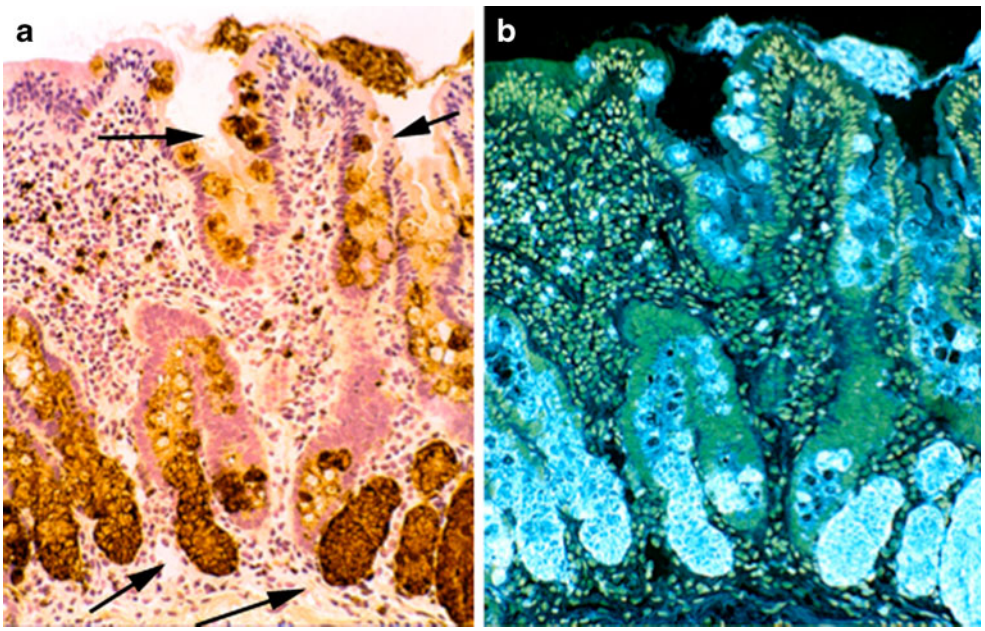

Fig. 5 **a** Another case of total villous atrophy showing lysozyme-rich mucus metaplasia of the crypts (*arrows*), in goblet cells (*arrows*) and in luminal secretion. (Duodenum, lysozyme stain×20). **b** The same picture using the INVERT function

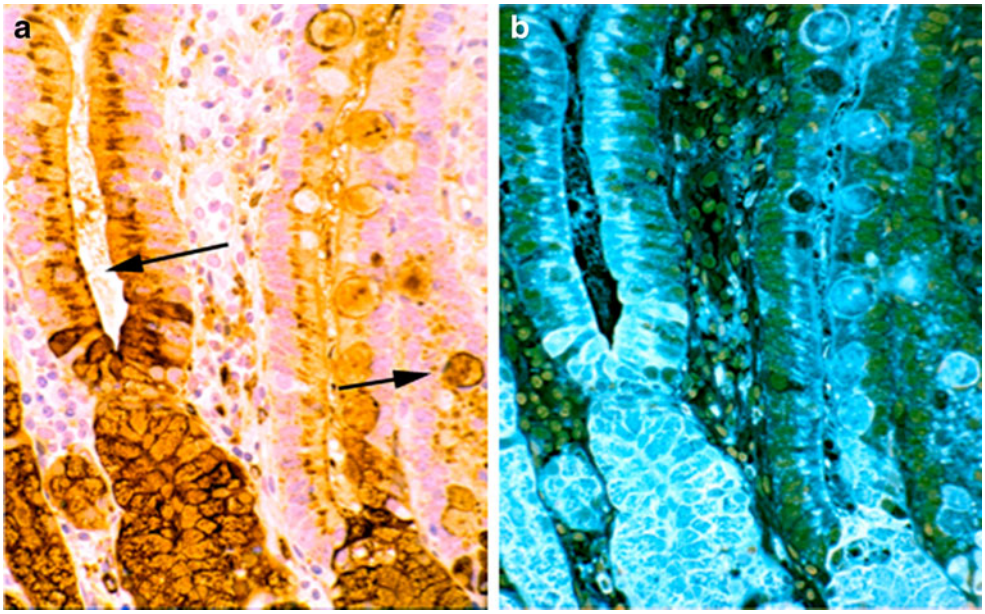

Fig. 6 **a** Detail of total villous atrophy showing lysozyme-rich mucus metaplasia of the crypts, goblet cells and enterocytes at arrows (duodenum, lysozyme stain×40). **b** The same picture using the INVERT function

SVA/TVA was unexpected. It would appear that in celiac disease, large areas of lysozyme-rich mucus cell metaplastic crypts had substituted all Paneth cells. Although the mechanism behind this conundrum remains elusive it is possible that whereas in normal individuals, the number of lysozyme-producing Paneth cells at the base of the crypts [4, 7] might be sufficient to cope with mild bacterial attacks, in celiac disease the number of lysozyme-rich Paneth cells in the crypts might be insufficient to neutralize abnormal duodenal bacteria [12–15]. Rationally, there might exist a critical limit for the number of Paneth cells that can be housed at the base of single crypts. Because to this plausible limitation, duodenal crypts would undergo mucus metaplastic transformation to increase the demands in antibacterial lysozyme required by the hostile bacterial flora. This view appears to be substantiated by the fact that Paneth cells were not present in BL/SVA/TVA cases having MMC occupying all crypts. Of note, villi overlying MMC areas retained their normal cellular differentiation with absorptive enterocytes and goblet cells, strongly suggesting that stem cell reprogramming embraced Paneth cells exclusively and no other differentiated cells in the duodenal mucosa.

Intestinal cells are constantly produced from a stem cell reservoir [28, 29] that gives rise to proliferating transient amplifying cells, which subsequently differentiate into one of the four principal cell types. Studies on mice indicate that development and differentiation in the crypts of the small intestine are under the control of at least three signaling pathways known as canonical Wnt, Notch and Indian hedgehog [30, 31]. The canonical Wnt pathway is the key regulator of proliferation of the stem cells in the crypts, its activation being essential for the maintenance of the crypt cell population [32]. Signaling pathways, including the Notch signaling pathway coordinate these differentiation processes [33]. Pharmacological inhibition through γ-secretase inhibitors or genetic inactivation of the Notch signaling pathway results in the complete loss of proliferating crypt progenitors due to their conversion into post-mitotic goblet cells [32]. The basic helix-loop-helix transcription factor *Math1* is essential for the lineage-specifying choice to adopt one of various cell-differentiating fates. *Math1* and Notch signaling is critical in intestinal homeostasis [34].

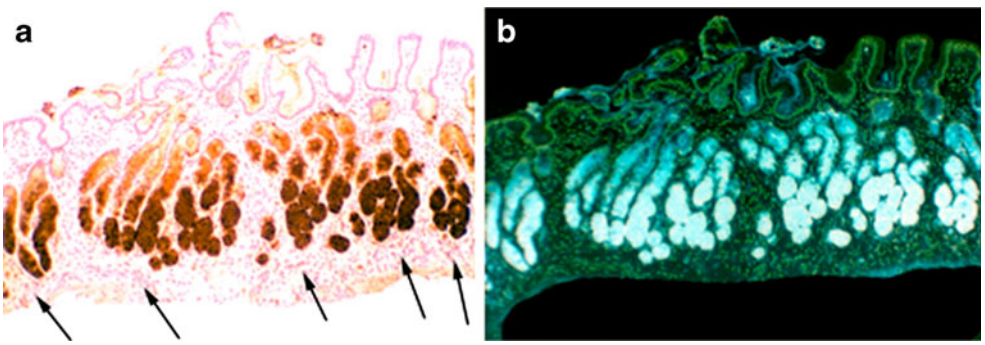

Fig. 7 **a** Left panel: Subtotal villous atrophy showing the replacement of Paneth cells by lysozyme-rich mucus metaplasia in all crypts (*arrows*). (Duodenum, lysozyme stain×20). **b** The same picture using the INVERT function

Conversion of intestinal stem cells into goblet cells upon inhibition of the Notch signaling pathway requires *Math1*. Without *Math 1*, cells remain in the progenitor stem cell pool and can only become enterocytes; in fact, the intestine of *Math 1*-deficient mice lacks Paneth, goblet and enteroendocrine cells [35]. Varnat et al. [36] showed that peroxisome proliferator receptor 8 (PPAR8) a nuclear hormone receptor in the GI tract, is expressed at the bottom of the crypts where Paneth cells normally reside. PPAR8 beta/delta partly control Paneth cell homeostasis by down-regulating the expression of the Indian hedgehog (ihh), a signal sent by Paneth cells to differentiate. The trans-amplifying progenitors are under the Wnt signal domain, whereas differentiated cells, other than Paneth cells, are present in areas where the canonical Wnt signal is inactive [36]. A family of bHLH (basic-helix-loop-helix) transcription factors and its upstream Notch signaling also plays a fundamental role in regulating the differentiation and cell type specification of intestinal epithelial cells [37]. Cdc42 (a small GTPase activated by integrins, growth factor, cytokine receptors and cadherins) is important for the terminal differentiation of progenitor cells, regulating β-catenin degradation [38]. The nuclear accumulation of β-catenin in the small intestine, mainly located in cells at the base of the crypts decreases as the cell moves toward the top of the crypts. Thus, β-catenin accumulation correlates with areas of cell proliferation whereas β-catenin degradation occurs in areas with cell differentiation [39].

From the above it might be inferred that the development and differentiation of various cell lineages is achieved by diverse molecular signals normally sent to stem cells in duodenal crypts [29]. Against this background and in light of present results we are prone to speculate that in celiac disease, stem cells might have re-programmed the normal ontogenic production of Paneth cells in the crypts, and that a new phenotype, the lysozyme-producing mucus cell was generated, resulting in the formation of consecutive lysozyme-rich glands, called MMC in this work. Lysozyme-rich MMC in celiac disease might mirror an antimicrobial adaptation of stem cells [29] to signals generated by pathogenic duodenal bacteria1 [12, 13]. Interestingly goblet cells in crypts and villi also contributed to this antimicrobial adaptation by increasing lysozyme production. The molecular mechanism(s) behind the abrogation of Paneth cells in duodenal crypts and its substitution by LPMMC in celiac disease remains to be elucidated.

The study presented may open a new window of research aimed to ascertain the molecular mechanism(s) involved in the abrogation of the Paneth cell population in duodenal crypts and its substitution by lysozyme-rich MMC in celiac disease.

In closing, it might be pertinent to quote what the Scottish bacteriologist, biologist and pharmacologist Alexander Fleming said in his Presidential address to the Royal Society of Medicine 80 years ago [16]:

> "I choose lysozyme as the subject for this address for two reasons, firstly because I have a fatherly interest in the name and, secondly, because its importance in connection with natural immunity does not seem to be generally appreciated".
> To Sir Alexander Fleming (1881–1955), in recognition

Conflict of interest statement We declare that we have no conflict of interest.

References

1. Gramlich T, Petras R (2007) Small intestine/duodenum. In: Mills SE (ed) Histology for pathologists, 3rd edn. Lippincott Williams & Wilkins, Philadelphia, pp 613–616
2. He XC, Zhang J, Tong WG, Tawfik O, Ross J, Scoville DH, Tian Q, Zeng X, He X, Wiedemann LM, Mishina Y, Li (2004) BMP signaling inhibits intestinal stem cell self-renewal through suppression of Wnt-beta-catenin signaling. Nat Genet 36:1117–1121
3. de Santa BP, van den Brink GR, Roberts DJ (2003) Development and differentiation of the intestinal epithelium. Cell Mol Life Sci 60:1322–1332, Review
4. Rubio CA, Nesi G (2003) A simple method to demonstrate normal and metaplastic Paneth cells in tissue sections. In Vivo 17:67–71
5. Ayabe T, Ashida T, Kohgo Y, Kono T (2004) The role of Paneth cells and their antimicrobial peptides in innate host defense. Trends Microbiol 12:394–398
6. Sundbom M, Elphick DA, Mahida YR, Cunliffe RN, Midtvedt T, Engstrand L, Rubio CA, Axelsson LG (2007) Alteration in human defensin-5 expression following gastric bypass surgery. J Clin Pathol 60:1029–1034
7. Di Sabatino A, Miceli E, Dhaliwal W, Biancheri P, Salerno R, Cantoro L, Vanoli A, De Vincenzi M, Blanco Cdel V, MacDonald TT, Corazza GR (2008) Distribution, proliferation, and function of Paneth cells in uncomplicated and complicated adult celiac disease. Am J Clin Pathol 130:34–42
8. Dewar DH, Ciclitira PJ (2005) Clinical features and diagnosis of celiac disease. Gastroenterology 128(Suppl 1):S19–24, Review
9. Högberg L, Stenhammar L (2009) Celiac disease: diagnosis criteria in young children. Nat Rev Gastroenterol Hepatol 6:447–448
10. Ivarsson A, Högberg L, Stenhammar L, Swedish Childhood Coeliac Disease Working Group (2010) The Swedish Childhood Coeliac Disease Working Group after 20 years: history and future. Acta Paediatr 99:1429–1431
11. Myléus A, Ivarsson A, Webb C, Danielsson L, Hernell O, Högberg L, Karlsson E, Lagerqvist C, Norström F, Rosén A, Sandström O, Stenhammar L, Stenlund H, Wall S, Carlsson A (2009) Celiac disease revealed in 3% of Swedish 12-year-olds born during an epidemic. J Pediatr Gastroenterol Nutr 49:170–176
12. Sánchez E, Donat E, Ribes-Koninckx C, Calabuig M, Sanz Y (2010) Intestinal *Bacteroides* species associated with coeliac disease. J Clin Pathol 63:1105–1111
13. Schippa S, Iebba V, Barbato M, Di Nardo G, Totino V, Checchi MP, Longhi C, Maiella G, Cucchiara S, Conte MP (2010) A distinctive 'microbial signature' in celiac pediatric patients. BMC Microbiol 10:175–179

14. Forsberg G, Fahlgren A, Hörstedt P, Hammarström S, Hernell O, Hammarström ML (2004) Presence of bacteria and innate immunity of intestinal epithelium in childhood celiac disease. Am J Gastroenterol 99:894–904
15. Ou G, Hedberg M, Hörstedt P, Baranov V, Forsberg G, Drobni M, Sandström O, Wai SN, Johansson I, Hammarström ML, Hernell O, Hammarström S (2009) Proximal small intestinal microbiota and identification of rod-shaped bacteria associated with childhood celiac disease. Am J Gastroenterol 104:3058–3067
16. Fleming A (1922) On a remarkable bacteriolytic element found in tissues and secretions. Proc Roy Soc Sec B 93:306–317
17. Yoshimura K, Toibana A, Nakahama K (1988) Human lysozyme: sequencing of a cDNA, and expression and secretion by *Saccharomyces cerevisiae*. Biochem Biophys Res Commun 150:794–801
18. Peters C, Kruse U, Pollwein R, Grzeschik K, Sippel (1989) The human lysozyme gene. Sequence organization and chromosomal localization. Eur J Bioch 182:507–512
19. Wehkamp J, Chu H, Shen B, Feathers RW, Kays RJ, Lee SK, Bevins CL (2006) Paneth cell antimicrobial peptides: topographical distribution and quantification in human gastrointestinal tissues. FEBS Lett 580:5344–5350
20. Saito H, Kasajima T, Masuda A, Imai Y, Ishikawa M (1988) Lysozyme localization in human gastric and duodenal epithelium. An immune-cytochemical study. Cell Tissue Res 251:307–313
21. Rubio CA, Befrits R (2009) Increased lysozyme expression in gastric biopsies with intestinal metaplasia and pseudopyloric metaplasia. Int J Clin Exp Med 2:248–253
22. Rubio CA, Lörinc (2011) Lysozyme is upregulated in Barrett's mucosa. Histopathology (in press)
23. Tang Q, Wang L, Tao K, Ge C, Jing Li Y, Peng JC, Geng M (2006) Expression of polymeric immunoglobulin receptor mRNA and protein in human Paneth cells: Paneth cells participate in acquired immunity. Am J Gastroenterol 101:1625–1632
24. Rubio CA (2011) Lysozyme expression in microscopic colitis. J Clin Pathol (in press)
25. Rubio CA (2003) Colorectal adenomas produce lysozyme. Anticancer Res 23:5165–5171
26. Helmerhorst E, Zamakhchari M, Schuppan D, Oppenheim F (2010) Discovery of a novel and rich source of gluten-degrading microbial enzymes in the oral cavity. PLoS One 5:13264–13267
27. Hayat M, Cairns A, Dixon MF, O'Mahony S (2002) Quantitation of intraepithelial lymphocytes in human duodenum: what is normal? J Clin Pathol 55:393–394
28. Scoville DH, Sato T, He XC, Li L (2008) Current view: intestinal stem cells and signaling. Gastroenterology 134:849–864, Review
29. Rubio CA (2011) Putative stem cells in mucosas of the esophagogastrointestinal tract. Chapter 10. In: Singh SR (ed) Stem cell, regenerative medicine and cancer. Nova Science Haupauge, NY, pp 281–310
30. Kosinski C, Stange DE, Xu C, Chan AS, Ho C, Yuen ST, Mifflin RC, Powell DW, Clevers H, Leung SY, Chen X (2010) Indian hedgehog regulates intestinal stem cell fate through epithelial–mesenchymal interactions during development. Gastroenterology 139:893–903
31. Barker N, van de Wetering M, Clevers H (2008) The intestinal stem cell. Genes Dev 22:1856–1864
32. Nakamura T, Tsuchiya K, Watanabe T (2007) Crosstalk between Wnt and Notch signaling in intestinal epithelial cell fate decision. J Gastroenterol 42:705–710
33. Klaus A, Birchmeier W (2008) Wnt signalling and its impact on development and cancer. Nat Rev Cancer 8:387–398
34. Shroyer NF, Helmrath MA, Wang VY, Antalffy B, Henning SJ, Zoghbi HY (2007) Intestine-specific ablation of *Mouse atonal homolog 1* (*Math1*) reveals a role in cellular homeostasis. Gastroenterology 132:2478–2488
35. VanDussen KL, Samuelson LC (2010) Mouse atonal homolog 1 directs intestinal progenitors to secretory cell rather than absorptive cell fate. Dev Biol 346:215–223
36. Varnat F, Heggeler BB, Grisel P, Boucard N, Corthésy-Theulaz I, Wahli W, Desvergne B (2006) PPAR beta/delta regulates Paneth cell differentiation via controlling the hedgehog signaling pathway. Gastroenterology 131:538–553
37. Tanigawa Y, Yakura R, Komiya T (2007) The bHLH transcription factor Tcf12 (ME1) mRNA is abundantly expressed in Paneth cells of mouse intestine. Gene Expr Patterns 7:709–713
38. Babbin BA, Jesaitis AJ, Ivanov AI, Kelly D, Laukoetter M, Nava P, Parkos CA, Nusrat A (2007) Formyl peptide receptor-1 activation enhances intestinal epithelial cell restitution through phosphatidylinositol 3-kinase-dependent activation of Rac1 and Cdc42. J Immunol 179:8112–8121
39. Peignon G, Durand A, Cacheux W, Ayrault O, Terris B, Laurent-Puig P, Shroyer NF, Van Seuningen I, Honjo T, Perret C, Romagnolo B (2011) Complex interplay between β-catenin signalling and Notch effectors in intestinal tumorigenesis. Gut 60:166–176

Virchows Arch (2011) 459:347–349
DOI 10.1007/s00428-011-1136-4

CASE REPORT

Gastric pseudo-signet ring cells: a potential diagnostic pitfall

Caroline Hughes · Godman Greywoode · Runjan Chetty

Received: 10 May 2011 / Revised: 12 July 2011 / Accepted: 25 July 2011 / Published online: 12 August 2011
© Springer-Verlag 2011

Introduction

Signet ring cells are characterised by a cytoplasmic inclusion or vacuole that pushes and displaces the crescent-shaped nucleus to the periphery of the cell. When the nuclei of the cells are hyperchromatic, pleomorphic and manifest mitoses, and when the cells infiltrate the lamina propria, this represents the histologic hallmark of signet ring cell carcinoma.

The review of the medical literature reveals that the occurrence of mucus-negative pseudo-signet ring cells was first described in gastrectomy specimens of Japanese patients 25 years ago [1]. The authors of this paper Rubio et al. continued to publish extensively on this topic and postulated that these "pseudo-signet cells" or "glassy cells" may be due to environmental exposures [2].

Benign epithelial signet ring cells in the stomach have also been reported previously in association with ischaemia and ulceration [3–5]. We report two cases of benign signet ring cell change in gastric biopsy specimens which we believe to be a degenerative non-neoplastic change.

Clinical histories

Case 1

A 63-year-old female had a long-standing history of dyspepsia, epigastric pain and fullness. She was on proton pump inhibitor treatment for a year and on follow-up endoscopy was found to have a small raised mucosal nodule in the gastric fundic region. This was biopsied.

Case 2

A 68-year-old female had a history of dysphagia. She was known to have had proton pump inhibitor treatment and on endoscopy was found to have a 5-mm raised gastric antral nodule which was biopsied.

Materials and methods

Both biopsies were fixed in 10% neutral buffered formalin, processed routinely and haematoxylin and eosin sections produced. Immunohistochemistry was performed on the formalin-fixed tissue for the following antibodies: CAM 5.2, AE1/3, synaptophysin, chromogranin and E-cadherin.

Results

Microscopy

Both cases showed similar microscopic appearances. There were clusters of cell aggregates superficially within the fundic mucosa simulating signet ring cell carcinoma in situ (Fig. 1). The clusters were well circumscribed and retained the configuration and architecture of adjacent normal fundic glands with occasional admixed normal parietal cells. Cytologically, the cells contained eccentric bland nuclei and cytoplasmic vacuoles that had a clear or glassy appearance (Fig. 2). In neither case did we see invasion of these cells into the lamina propria of the mucosa. These cells lined the fundic glands in a single row. This excluded the differential diagnosis of pagetoid spread of carcinoma where signet ring cells spread below the normal epithelium.

C. Hughes (✉) · G. Greywoode · R. Chetty
Department of Cellular Pathology, John Radcliffe Hospital,
Level 1, Academic Centre, Headley Way, Headington,
Oxford OX3 9DU, UK
e-mail: Caroline.Hughes@orh.nhs.uk

R. Chetty
Department of Cellular Pathology/Nuffield Department of Clinical Laboratory Sciences, Oxford Radcliffe Hospitals Trust/
Biomedical Research Centre, University of Oxford,
Oxford, UK

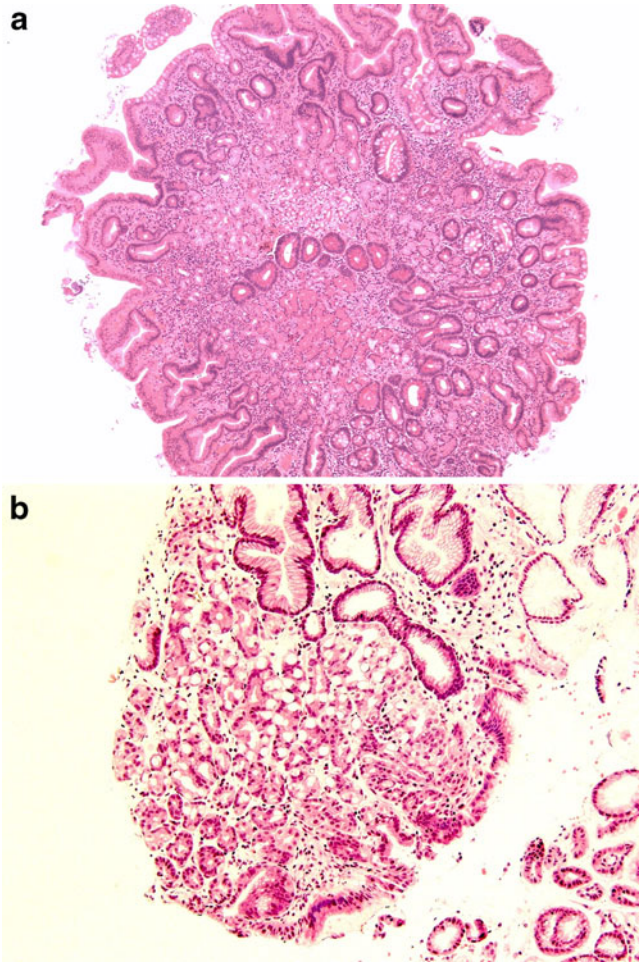

Fig. 1 **a**, **b** Low-power magnification demonstrating the clusters of signet ring cells associated with glands within the mucosa of both cases. (H&E ×200)

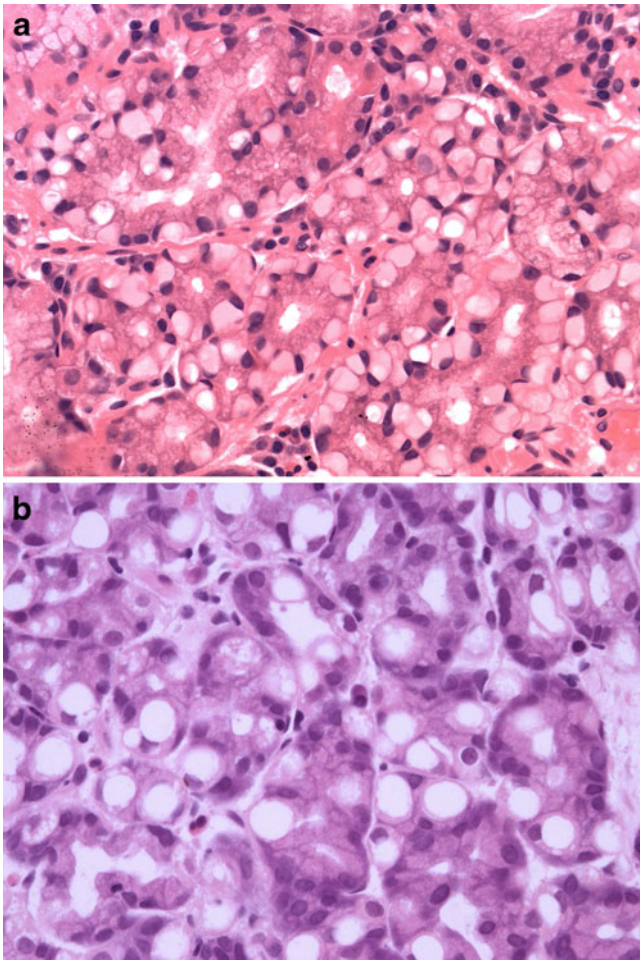

Fig. 2 **a**, **b** Under higher magnification, the cytoplasm of signet ring type cells varies from being vacuolated to pale and opaque. Adjacent cells also have a microvesicular appearance to the cytoplasm. (H&E ×400)

In both cases, the benign signet ring cell aggregates were immunohistochemically positive with antibodies to cytokeratins, but negative for neuroendocrine markers and mucin stains, apart from an apical rim of cytoplasmic mucin positivity (PAS positive and diastase resistant) in some cells reflecting the normal mucin content of the cell. On careful scrutiny of fundic glands in the vicinity of the signet ring cell aggregates, there was some degenerative vacuolation and some microvesicular change within parietal and mucous neck cells.

Surrounding gastric mucosa showed mild chronic gastritis with evidence of reactive gastropathy and established changes of long-term proton pump use. Case 1 also showed intestinal and Paneth cell metaplasia. There was no evidence of activity, *Helicobacter pylori* or intestinal metaplasia. The mucosa did not display atrophy and glands away from the signet ring cell change did not show endocrine cell hyperplasia (Fig. 3).

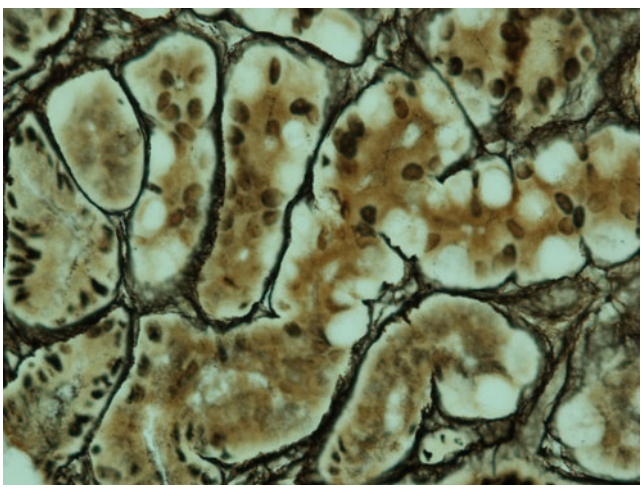

Fig. 3 Reticulin stain highlights signet ring cells confined within gland basement membranes. (Reticulin ×400)

Discussion

In both our cases showing pseudo-signet ring cell change in the stomach, the differential diagnosis included signet cell ring carcinoma (in situ as no lamina propria invasion), neuroendocrine clear cell proliferations and benign signet cell change associated with ischaemia. Signet ring cell carcinoma in situ has been described in hereditary gastric carcinoma as signet ring cell lesions within fundic glands and pagetoid spread of signet ring cells [6, 7].

Signet ring cells in this entity are positive on mucin staining and therefore signet ring cells which are negative on mucin staining can be excluded from a diagnosis of signet cell carcinoma in situ. Signet ring cells which are positive for intracytoplasmic mucin, however, are not necessarily prema-lignant, as we note that in the recently published article by Boncher et al., the benign signet ring cells in their report were positive for intracytoplasmic mucin [5]. The mucin staining in our cases showed only a narrow rim of residual cytoplasmic staining, while the vacuoles were negative.

Neuroendocrine cell hyperplasia and neuroendocrine tumours can show signet ring cell like features. This can cause confusion with signet ring cell carcinoma [8, 9]. Neuroendo-crine hyperplasia was a diagnostic consideration in both our cases particularly as neuroendocrine cell hyperplasia has been reported in cases of long-term proton pump inhibitor use [10]; however, this was excluded in our cases due to negativity of the pseudo-signet cells for neuroendocrine markers.

Of particular interest in our cases was that on careful scrutiny of adjacent fundic mucosa we noted degenerative vacuolation and microvesiculation in parietal and fundic neck cells. We hypothesise that benign pseudo-signet ring cell change may be a degenerative phenomenon. Benign pseudo-signet ring cell change as a degenerative phenom-enon has previously been reported in benign prostatic hyperplasia in the prostate [11].

In our experience, the occurrence of benign pseudo-signet ring cell aggregates is rare and can be a diagnostic pitfall that must be differentiated from signet-ring cell carcinoma in situ and neuroendocrine proliferations of the stomach. Important morphological features in these cases suggestive of the diagnosis were that the benign pseudo-signet cells were in the superficial fundic glands without lamina propria invasion and the association with adjacent fundic mucosa degenerative vacuolation.

Conflict of interest We declare that we have no conflict of interest.

References

1. Rubio CA, Kato Y, Kitagawa T, Sugano H (1986) A pitfall in the interpretation of intestinal metaplasia of the stomach. Acta Path Microbiol Immunol Scand 95:165–166
2. Rubio CA, Mandai K, Jónasson JG, King A, Nesi G, Kogan Z, Pisano R, Miller M, Owen D (2005) Gastric glassy cells: a study of 3202 gastrectomy specimens from dwellers of the Atlantic and Pacific basins. J Environ Pathol Toxicol Oncol 24:281–289
3. Mitsuhashi T, Lauwers GY, Ban S et al (2006) Post-gastric endoscopic mucosal resection surveillance biopsies: evaluation of mucosal changes and recognition of potential mimics of residual adenocarcinoma. Am J Surg Pathol 30:650–656
4. Dimet S, Lazure T, Bedossa P (2004) Signet-ring cell change in acute erosive gastropathy. Am J Surg Pathol 8:1111–1112
5. Boncher J, Bronner M, Goldblum JR, Liu X (2011) Reticulin staining clarifies florid benign signet ring cell change with mitotic activity in a penetrating gastric ulcer. Am J Surg Pathol 35:762–766
6. Carneiro F, Charlton A, Huntsman DG (2010) Hereditary diffuse gastric cancer. In: Bosman FT, Carneiro F, Hruban RH, Theise ND (eds) WHO classification of tumours of the digestive system, 4th edn. IARC, Lyon, pp 59–63
7. Barber ME, Save V, Carneiro F, Dwerryhouse S, Lao-Sirieix P, Hardwick RH, Caldas C, Fitzgerald RC (2008) Histopathological and molecular analysis of gastrectomy specimens from hereditary diffuse gastric cancer patients has implications for endoscopic surveillance of individuals at risk. J Pathol 216:286–294
8. Luk IS, Bhuta S, Lewin KJ (1997) Clear cell carcinoid tumor of stomach: a variant mimicking gastric xanthelasma. Arch Pathol Lab Med 121:1100–1103
9. Ordonez NG, Mackay B, el-Naggar A, Bannayan GA, Duncan J (1993) Clear cell carcinoid tumour of the stomach. Histopathology 22:190–193
10. Owen D, Kerr W, Sturby T, Richardson P, El-Serag H (2011) Gastric histology in children treated with proton pump inhibitors long term, with emphasis on enterochromaffin cell-like hyperplasia. Aliment Pharmacol Ther Hassall E 33:829–836
11. Bhuyan P, Mahapatra S, Pujari S, Rath J (2010) Signet-ring cell change in benign prostatic hyperplasia—a rare case report. WebmedCentral Urology 1:WMC00688

Virchows Arch (2011) 459:351–352
DOI 10.1007/s00428-011-1112-z

LETTER TO THE EDITOR

Pachydermia verrucosa…of the (very) bad kind!

Gil Patrus Pena · José de Souza Andrade-Filho

Received: 18 June 2011 / Accepted: 20 June 2011 / Published online: 6 July 2011
© Springer-Verlag 2011

To the editor,

The recent article of Cardesa et al. [1], on the polemic case of the Kaiser's cancer, raised the possibility of a hybrid verrucous carcinoma, in order to reconcile Virchow's findings in the biopsies with the fatal outcome. To testify the likelihood of this possibility, we have had a similar case recently, in the esophagus, whose multiple previous biopsies were not diagnostic, and an infiltrating well-differentiated squamous carcinoma reaching the muscular wall was identified in the esophagectomy specimen (Fig. 1).

Despite Virchow's great reputation as a pathologist, his diagnostic "imprecision," in that particular case, was attributed to his little familiarity with biopsy interpretation [2]. However, the following account of Dr. Lauren V. Ackerman's experience with the lesion that he later labeled as verrucous carcinoma illustrates how tricky this diagnosis in biopsy specimens may be:

> "Pathologists, examining microscopic sections of an exquisitely brand, benign-appearing squamous proliferation are more likely to confuse the lesion with a benign process. Indeed, this problem was the root of Dr. Ackerman's interest in this lesion. An anecdote that he related to the authors and many others during his extensive travels dealt with his early experience at the Ellis Fischel Cancer Center and a patient who had multiple biopsies of an oral cavity lesion which Dr. Ackerman had repeatedly labeled as "keratosis". Finally, in desperation the surgeon demanded that Dr. Ackerman personally examine the patient and confronted him with an obviously invasive lesion extending through the oral cavity and involving the skin of the cheek. "What kind of keratosis is that?" asked the surgeon. "The bad kind!" replied Dr. Ackerman, and not long thereafter his seminal article on verrucous carcinoma was published." [3].

Ackerman was a renowned surgical pathologist, with large experience in biopsy interpretation, and repeatedly labeled as "keratosis" a lesion that was found later to be of the "bad kind." One might wonder if he would be primarily able to discern the Kaiser's "pachydermia verrucosa" as one of such a bad kind.

More than learning about the Kaiser's disease itself, the study of a pathology case may serve to disclose the intimate nature of a pathology diagnostic task [4]. In a given case, the pathologist departs from a fragment of the reality and, through an observational act, makes an observational statement; in the second step, an interpretational statement is made through an interpretational act [5].

There is not a single, permanent rule that allows one to transit between a piece of reality, to the observational and then to interpretational statement. These are immanent planes whose connections fluctuate, with no fixed points or lines. Reality, of which we receive only a piece, continuously changes in the patient's living body; different observable aspects may gain or lose importance, as we know more or less about an extensive reality, including clinical, radiological, bacteriological, molecular, and other observations; finally, the tacit and the explicit knowledge which we use to interpret our observations incessantly move. Pathology evolves as a science, as pathologists reclassify, reorganize, redescribe, and reinterpret those pieces of reality. Diagnostic labels emerge, submerge, and reemerge from the reobservation and reinterpretation of archived reality fragments. Pathological entities represent

G. P. Pena · J. d. S. Andrade-Filho
Servico de Anatomia Patologica, Hospital Felicio Rocho,
Belo Horizonte, MG, Brazil

G. P. Pena (✉)
Rua Uberaba, 418 sala 102,
Belo Horizonte, MG 30180-080, Brazil
e-mail: gilpena@gold.com.br

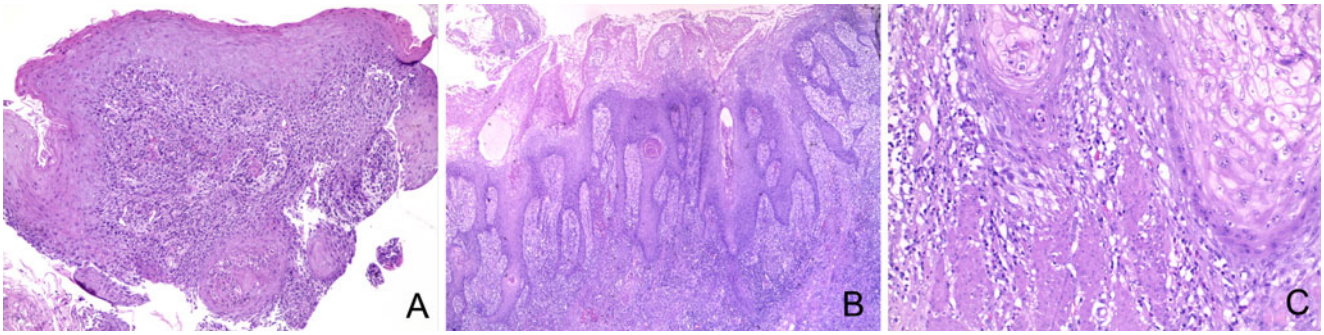

Fig. 1 A case of esophageal carcinoma, possibly similar to the Kaiser's cancer. A "jumbo" endoscopic biopsy (**a**), showing well-differentiated squamous epithelial proliferation with marked papillomatosis. Despite downward epithelial growth, bona fide stromal invasion could not be characterized. Two previous biopsies presented with similar findings. Given the endoscopic findings of a neoplastic growth, a suggestion was made of the possibility of verrucous carcinoma. In the surgical specimen, an evidently neoplastic proliferation is seen, with vegetant superficial growth (**b**) as well as deep infiltration into the muscular layer (**c**)

more or less demarcated territories in the interpretational plane. The Kaiser's real disease defied elucidation, as one could not then territorialize within the interpretative realm of either pure or hybrid verrucous carcinoma.

References

1. Cardesa A, Zidar N, Alos L, Nadal A, Gale N, Klöppel G (2011) The Kaiser's cancer revisited: was Virchow totally wrong? Virchows Arch 458:649–657
2. Wick MR, Mills SE (1990) Surgical pathology. In: Damjanov I, Linder J (eds) Anderson's pathology, 10th edn. Mosby, St. Louis, p 34
3. Mills SE, Gaffey MJ, Frierson HF Jr (2000) Tumors of the upper aerodigestive tract and ear. 3rd series, fascicle 26. Armed Forces Institute of Pathology, Washington, p 75
4. Pena GP (2010) O relato de caso como situação gnosiológica: reflexões sobre a prática diagnóstica em patologia a partir de um caso de abetalipoproteinemia. Rev Bras Educ Med. [online]. 34: 622–626. Available from: http://www.scielo.br/scielo.php?script=sci_arttext&pid=S0100-55022010000400019&lng=en&nrm=iso. ISSN 0100–5502. doi:10.1590/S0100-55022010000400019
5. Pena GP, Andrade-Filho JS (2009) How does a pathologist make a diagnosis? Arch Pathol Lab Med 133:124–132

Virchows Arch (2011) 459:353–359
DOI 10.1007/s00428-011-1134-6

ORIGINAL ARTICLE

Expression of JL1 in Burkitt lymphoma is associated with improved overall survival

Ilseon Hwang · Heounjeong Go · Yoon Kyung Jeon · Young Hyeh Ko · Dok Hyun Yoon · Cheolwon Suh · Joo Ryung Huh · Hyangsin Lee · Minchan Gil · Chan-Sik Park

Received: 20 April 2011 / Revised: 7 July 2011 / Accepted: 19 July 2011 / Published online: 4 August 2011
© Springer-Verlag 2011

Abstract JL1 is a novel molecule expressed in the surface of hematopoietic precursor cells, but not on any other mature human tissue. Accordingly, JL1 is expressed in acute lymphoblastic leukemia (ALL) cells and can be used both for specific diagnosis and as a target for treatment. However, expression of JL1 by lymphomas has not been thoroughly assessed. Burkitt lymphoma is a potentially curable aggressive lymphoma, but prognostic markers that stratify risk have not been established. We therefore assayed JL1 expression in Burkitt lymphoma patients to assess its value as a prognostic marker for this disease. Tissue microarray blocks of formalin-fixed paraffin-embedded tissue samples from patients with Burkitt lymphoma and other B-cell lymphomas, at the Asan Medical Center and Seoul National University Hospital from January 1998 to December 2008 were immunohistochemically assayed using a mouse monoclonal antibody against JL1. We found that 30.2% of Burkitt lymphoma samples, but no other lymphoma samples, were positive for JL1. JL-1 expression was significantly correlated with patient survival (P=0.022), but not with other clinical manifestations of the disease, with 91.6% of JL1-positive patients achieving complete remission in response to chemotherapy and 6.25% experiencing disease recurrence. JL1 positivity was significantly correlated with prolonged overall survival by both Kaplan–Meier survival (P=0.035) and Cox proportional hazard model (P=0.043) analysis. JL1 expression in Burkitt lymphoma was positively correlated with overall survival and better response to chemotherapy, suggesting that JL1 may be a prognostic marker for risk stratification in these patients.

Keywords JL1 · Burkitt lymphoma · Predictive factor · Prognosis · Immunohistochemistry

I. Hwang
Department of Pathology,
Keimyung University School of Medicine,
194 Dongsan-Dong, Choong-Ku,
Daegu, South Korea

H. Go · Y. K. Jeon
Department of Pathology and Tumor Immunity Medical Research Center, Seoul National University College of Medicine,
Seoul, South Korea

Y. H. Ko
Department of Pathology, Samsung Medical Center,
Sungkyunkwan University School of Medicine,
Seoul, Suwon, South Korea

D. H. Yoon · C. Suh
Department of Oncology,
University of Ulsan College of Medicine,
86 Asanbyeongwon-gil, Songpa-gu,
Seoul, South Korea

J. R. Huh · C.-S. Park (✉)
Department of Patholgy, Asan Medical Center,
University of Ulsan College of Medicine,
86 Asanbyeongwon-gil, Songpa-gu,
Seoul 138-736, South Korea
e-mail: Csikpark@amc.seoul.kr

H. Lee · M. Gil · C.-S. Park
Cell Dysfunction Research Center,
University of Ulsan College of Medicine,
86 Asanbyeongwon-gil, Songpa-gu,
Seoul, South Korea

Introduction

JL1 is a unique cell surface protein expressed exclusively in subpopulations of hematopoietic precursor cells and not in other mature human tissue [1, 2]. In the thymus, JL1 is specifically expressed in stage II double-positive (CD4+ CD8+) human cortical thymocytes [2]. In the bone marrow,

JL1 expression is restricted to CD34+ CD10+ lymphoid precursors, immature B cells, and immature cells of myelomonocytic lineages, but is not present on AC133+ CD34+ pluripotent stem cells [1]. JL1 expression is therefore observed in acute lymphoblastic leukemia (ALL) cells but not on peripheral mature lymphocytes. JL1 may serve as an excellent adjunctive marker for specific detection of leukemic cells, even in patients with scant infiltrates of leukemia cutis, as we reported previously [1–4]. Furthermore, the exclusive expression of JL1 in such cells suggests that this protein may be a promising target for specific immunotherapeutic agents in the treatment of leukemia-related diseases. For example, an anti-JL1 antibody could be covalently linked to toxins or nucleic acids, including siRNAs [5–7]. Although the expression profile of JL1 has been comprehensively investigated in various leukemias and normal tissues, its expression in lymphomas has not been thoroughly assessed.

The World Health Organization (WHO) (2008) has classified Burkitt lymphoma as an aggressive B-cell non-Hodgkin's lymphoma, characterized by a high degree of proliferation and deregulation of the *c-Myc* gene [8, 9]. This extremely aggressive biology results in fulminant presentation of the lymphoma in most patients, resulting in medical emergencies requiring immediate interventions [10]. Consequently, Burkitt lymphoma is rapidly fatal if not treated appropriately with brief, very intensive chemotherapy regimens, including CNS prophylaxis [11]. The complete chemotherapeutic response and overall survival rates of patients with Burkitt lymphoma are about 80–90% and 80%, respectively, but some patients with Burkitt lymphoma do not respond to chemotherapy [12, 13]. Furthermore, an enhanced response has been associated with an increase in treatment-related toxicity, which is especially problematic in adult patients. Recent trials of a modified chemotherapy regimen in selected low-risk patients showed a reduced incidence of toxicities but a similar efficacy compared with the standard chemotherapy regimen [14]. Therefore, prognostic markers identifying patients at low risk would be valuable in selecting appropriate treatments for individual patients. An ideal biomarker would be detectable by immunostaining during the initial phase of diagnosis. We therefore evaluated the pattern of JL1 expression in Burkitt lymphoma and assessed whether expression of JL1 in Burkitt lymphoma could assist in predicting patient's prognosis.

Materials and methods

Selection of patients

We retrospectively evaluated the medical records of 53 patients with Burkitt lymphoma (42 from the Asan Medical Center and 11 from Seoul National University Hospital), 20 with diffuse large B-cell lymphoma, 20 with follicular lymphoma, 20 with marginal zone B-cell lymphoma, and 20 with mantle cell lymphoma, who had been treated at the respective hospitals between January 1998 and December 2008. Archived paraffin blocks of tissue samples from lymph node, stomach, intestine, liver, and kidney, but not from bone marrow were retrieved, and 4-μm sections were stained with hematoxylin and eosin (H&E). All findings were again reviewed by an expert panel, consisting of two pathologists, who diagnosed patients according to the current WHO criteria based on sample morphology, immunophenotype, and cytogenetic findings, including the presence or absence of a c-Myc translocation. Biopsy specimens classified as Burkitt lymphoma showed typical morphologic features and immunophenotypes, including medium-sized tumor cells, a diffuse monotonous pattern of growth, round nuclei with finely clumped and dispersed chromatin, deeply basophilic cytoplasm, many mitotic figures, and an extremely high proliferation fraction (Ki-67 score >90%). All samples were immunohistochemically positive for the B-cell markers (CD20 and CD19) and the adjunctive markers (CD10 and Bcl6), but negative for Bcl-2, CD3, and terminal deoxytransferase.

The study protocol was approved by the Institutional Review Board (IRB) of the Asan Medical Center (no. 2009–0214), which waived the need for informed consent.

Production of tissue microarray blocks

Formalin-fixed, paraffin-embedded tissue samples were used for tissue microarray (TMA). Representative areas of each tumor were marked on each H&E-stained slide, and the corresponding areas of tissue blocks were sampled. The designated areas of each donor block were collected using a tissue cylinder punch of 3 mm diameter, and samples were transferred to a recipient block. Small tissue samples (<2 cm in greatest dimension) which could not be used for tissue microarrays, therefore, were used entirely for H&E and immunohistochemical staining.

Immunohistochemical staining

Sections (4 μm thick) from TMAs were cut from 10% (v/v) formalin buffer, embedded in paraffin, mounted onto Superfrost Plus glass slides (VWR Scientific, West Chester, PA) and incubated at 60°C for 15 min. The slides were deparaffinized in xylene, rehydrated in graded alcohol solutions, and washed in tap water. Endogenous peroxidase activity was blocked by the addition of 3% (v/v) H_2O_2. Slides were placed in a steam cooker filled with 10 mM sodium citrate buffer, pH 6.0, for antigen retrieval. After treatment with a blocking agent (Dako, Carpinteria, CA,

Table 1 Clinical manifestations of Burkitt lymphoma

Clinical manifestation	Value
Mean age, years (range)	44.3 (0–86)
Gender (M/F)	37:16
Extranodal involvement	41/53 (77.4%)
Performance status[a]	
0	4/48 (8.3%)
1	22/48 (45.8%)
2	13/48 (27.1%)
3	7/48 (14.6%)
4	2/48 (4.2%)
Presence of B symptoms[a]	8/48 (16.6%)
Ann Arbor stage	
I	12/53 (22.6%)
II	9/53 (17.0%)
III	3/53 (5.7%)
IV	29/53 (54.7%)
Bone marrow involvement[a]	14/47 (29.8%)
Refused chemotherapy	5/53 (9.4%)
Complete remission[a]	33/41 (80.5%)
Recurrence[a]	9/52 (17.3%)
Death	15/53 (28.3%)

All values are expressed as numbers (with percentages) unless otherwise indicated

[a] Manifestations including missing values, represented in denominators

USA) for 10 min to block nonspecific protein binding, samples were incubated with a mouse monoclonal anti-JL1 antibody (dilution 1:100; the kind gift of Professor Seong Hoe Park of Seoul National University) for an additional hour. The samples were incubated with a biotinylated anti-mouse antibody for 30 min, and antigen–antibody complexes were visualized using a streptavidin–horseradish peroxidase conjugate (DAKO LSAB kit; Dako, Los Angeles, CA, USA), with diaminobenzidine as the chromogen. Slides were counterstained with Meyer's hematoxylin for 3–5 min. Fetal thymic tissue (sampled at 28 weeks of gestational age) was used as a positive control, and reactive lymph nodes from patients with stomach cancer and normal bone marrow from patients with malignant lymphoma were used as negative controls.

JL1 immunopositivity was evaluated by staining intensity (0, negative; 1, weak; 2, moderate; 3, strong) and the proportions of positive cells (0, 0% positive; 1, ≤10%; 2, >10% and ≤50%; and 3, >50%). Samples were considered positive for JL1 when staining intensity was >1 (moderate-to-strong) and >50% of cells were positive.

Clinical variables of Burkitt lymphoma patients

Clinical data collected from the records of the 53 patients with Burkitt lymphoma included age, Ann Arbor stage, bone marrow findings, presence of B symptoms, performance status, date of diagnosis, treatment response, date of relapse, date of last follow-up, and cause of death. Patients

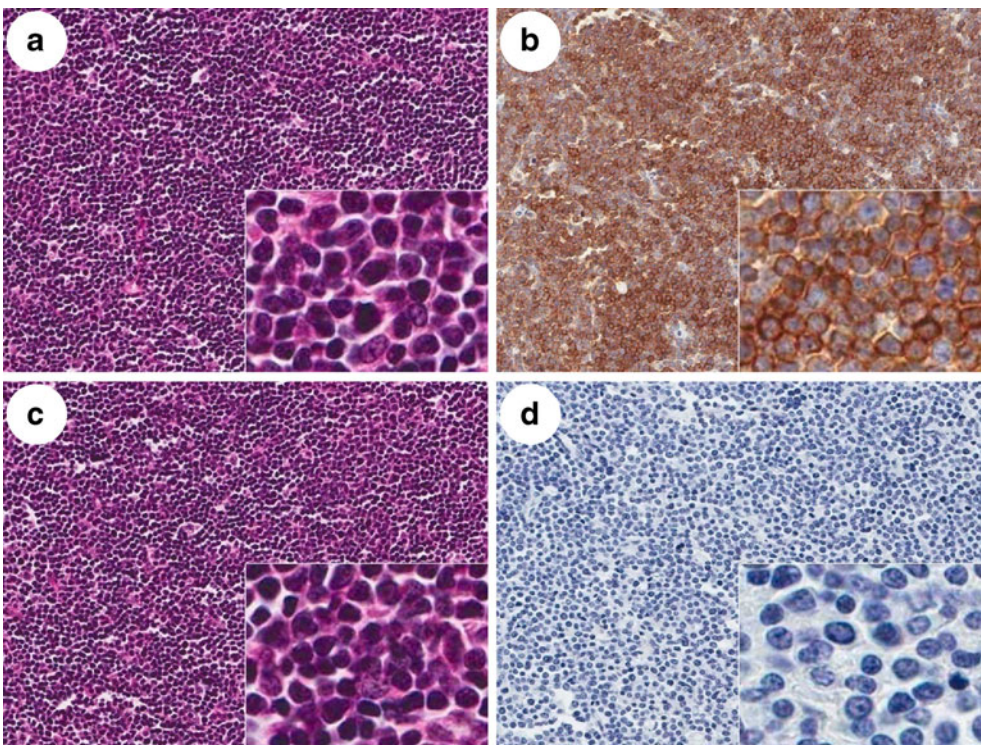

Fig. 1 Expression of JL1 in Burkitt lymphoma cells. **a**, **c** Diffuse growth pattern of Burkitt lymphoma cells. **b** Immunostaining with anti-JL1 antibody of the tissue sample in **a**, showing positivity for JL1 expression in the cell membrane. **d** Immunostaining of the sample in **c**, showing non-expression of JL1

were classified into two groups, those with Ann Arbor stage IV and those with <IV disease. Treatment response was assessed according to WHO response criteria. Complete remission (CR) was defined as no evidence of residual disease, partial response (PR) as a ≥50% reduction in tumor burden from onset of treatment, and progressive disease as a ≥25% increase in lesion size. Clinical data are summarized in Table 1. Data with missing values are marked with asterisk and the actual numbers of patients included for each analysis represented in denominators.

Statistical analysis

The PASW statistical package, version 18.0 for Windows, was used for all statistical analysis. The relationship between JL1 immunoreactivity and each clinical variable was evaluated using the χ^2 or Fisher's exact test, as appropriate. Overall survival was measured from the date of diagnosis to the date of death or the last follow-up according to the Kaplan–Meier method and the Cox regression test, and survival rates were compared using the log-rank test. P values <0.05 were considered statistically significant, and all P values correspond to two-sided significance tests.

Results

JL1 Expression in Burkitt Lymphoma

The mean age of all 53 patients with Burkitt lymphoma was 44.3 years (range, 0–86 years). Patients were divided into two age groups, those aged ≤16 and >16 years according to previous studies on Burkitt lymphoma [15, 16]. The mean age of the younger group was 8.4 years (range, 0–15 years), and the mean age of the older group was 53.7 years (range,

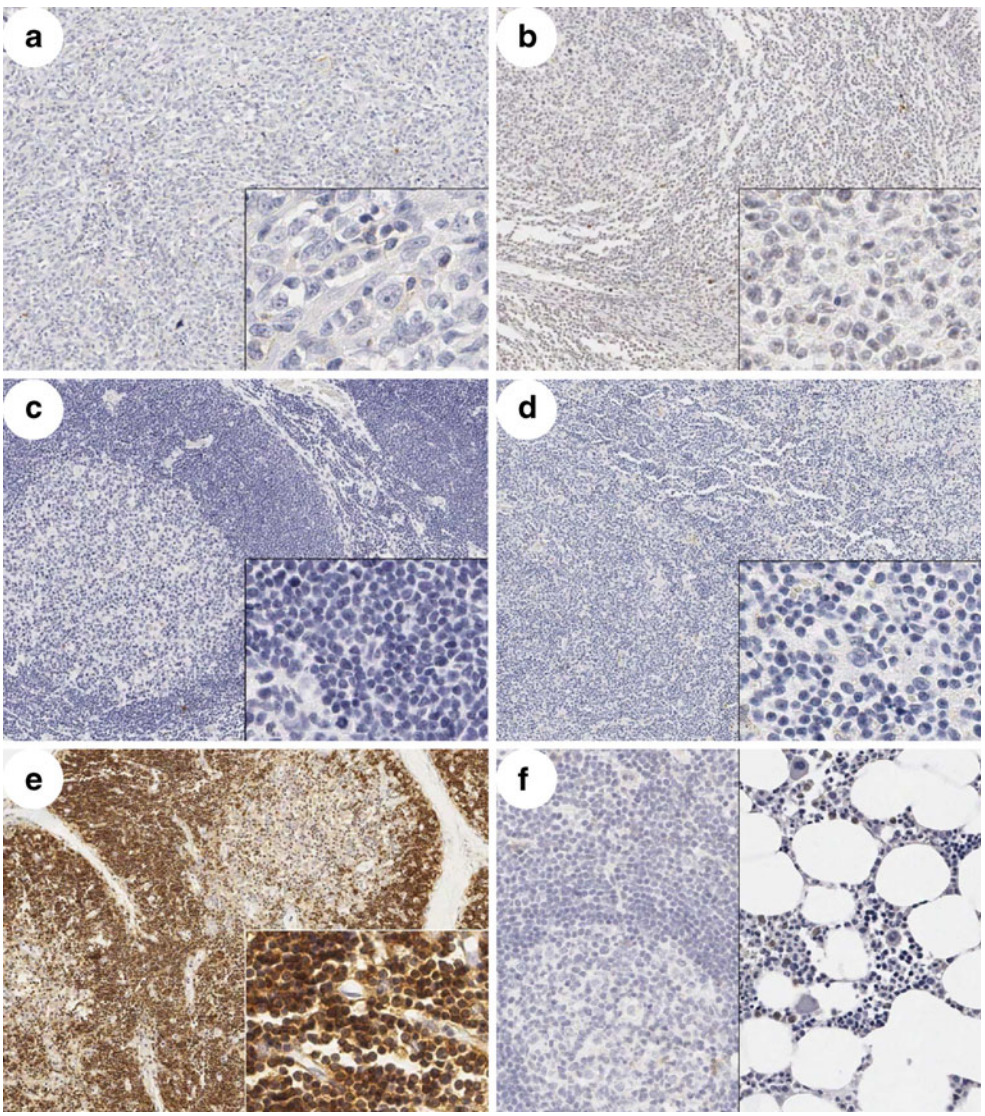

Fig. 2 Absence of JL1 expression in samples from patients with **a** diffuse large B-cell lymphoma, **b** follicular lymphoma, **c** mantle cell lymphoma, and **d** marginal zone B-cell lymphoma. Thymic cells were strongly positive for JL1 (**e**), whereas all inflammatory cells of reactive lymph nodes (*right*) and hematopoietic cells of normal bone marrow (*left*) were negative when stained with anti-JL1antibody (**f**)

17–86 years). The clinical manifestations of Burkitt lymphoma were similar in these two groups.

Of the 53 patients with Burkitt lymphoma, 16 (30.2%) were positive for JL1 immunoreactivity. Histopathologic features did not differ significantly between JL1-positive (Fig. 1a and b) and JL1-negative patients (Fig. 1c and d). JL1 expression was not observed in any patient with any other type of B-cell lymphoma, including diffuse large B-cell, mantle cell and follicular lymphoma (Fig. 2a–d). The positive control samples, thymocytes in the cortical area, were strongly positive and showed a membranous pattern (Fig. 2e), whereas the negative controls, reactive lymph nodes from patients with stomach cancer and normal bone marrow samples from patients with malignant lymphoma, were completely negative (Fig. 2f).

JL1 expression in Burkitt lymphoma was significantly correlated with overall survival rate (P=0.022), but not with any other characteristic such as age, gender, tumor site, performance status, bone marrow involvement, presence of B symptoms, or Ann Arbor stage. Although statistical significance was not achieved, 91.1% of JL1-positive patients achieved CR in response to chemotherapy and only one experienced recurrence of disease (Table 2).

Kaplan–Meier analysis showed that overall survival was significantly longer in patients with than without JL1 expression (P=0.035), but was not associated with patient age (P=0.336), bone marrow involvement (P=0.109) or tumor stage (P=0.096) (Fig. 3). Survival was significantly poorer in patients with high (3, 4) than low (0–2) performance status (P=0.004), and in patients with than without B symptoms (P=0.024). We further analyzed the three significantly associated factors with a multivariate Cox proportional hazard model. JL1 expression (hazard ratio [HR] 0.120; 95% confidence interval [CI], 0.016–0.934; P=0.043) and presence of B symptoms (HR 4.426; 95% CI, 1.451–13.504; P=0.009) were significantly correlated with overall survival, whereas performance status was not (P=0.139).

Table 2 Correlations between JL1 expression and clinical manifestations of Burkitt lymphoma

	JL1 immunoreactivity		P value
	Positive	Negative	
Age (years)			
≤16	4	7	0.716
>16	12	30	
Gender			
Male	11	26	1.000
Female	5	11	
Site			
Nodal	4	8	1.000
Extranodal	29	29	
Performance status			
0, 1, 2	14	25	0.239
3, 4	1	8	
B symptom			
No	10	32	0.197
Yes	4	4	
Ann Arbor stage			
I, II, III	7	17	1.000
IV	9	20	
Bone marrow			
No involvement	11	22	0.503
Involvement	3	11	
Response to chemotherapy			
Partial response	1	7	0.398
Complete remission	11	22	
Recurrence			
Yes	15	28	0.245
No	1	8	
Survival			
Lived	15	23	0.022
Died	1	14	

Discussion

Among the ongoing challenges in the treatment of Burkitt lymphoma are the need for refinement of diagnosis, possibly using molecular tools that may identify patients with aberrant disease; improved risk stratification, which may allow the use of lower-intensity regimens in low-risk patients and alternative therapies in patients who are unlikely to respond; and newer treatment modalities selectively targeting the underlying biological mechanisms of this very aggressive lymphoma. An aggressive regimen is essential for treatment of patients with Burkitt lymphoma. The National Comprehensive Cancer Network (NCCN) has recommended the use of CODOX-M or HyperCVAD for low-risk patients, and CODOX-M/IVAC (with or without rituximab) or HyperCVAD alternating with methotrexate plus cytarabine, with or without rituximab, for high-risk patients [11]. Although these regimens can be readily used in younger patients, their significant toxicity profiles frequently preclude their use in older patients [10]. Hematological and neurological toxicities are particularly problematic, and 40% of older patients cannot complete their entire assigned regimen. It may therefore be necessary to individualize treatment regimens for adults, using predictors of therapeutic response, with less aggressive regimens being used to treat good responders.

Although the principal prognostic factors affecting survival in patients with Burkitt lymphoma have yet to be determined, some features have been associated with poor outcomes in both adults and children; these include

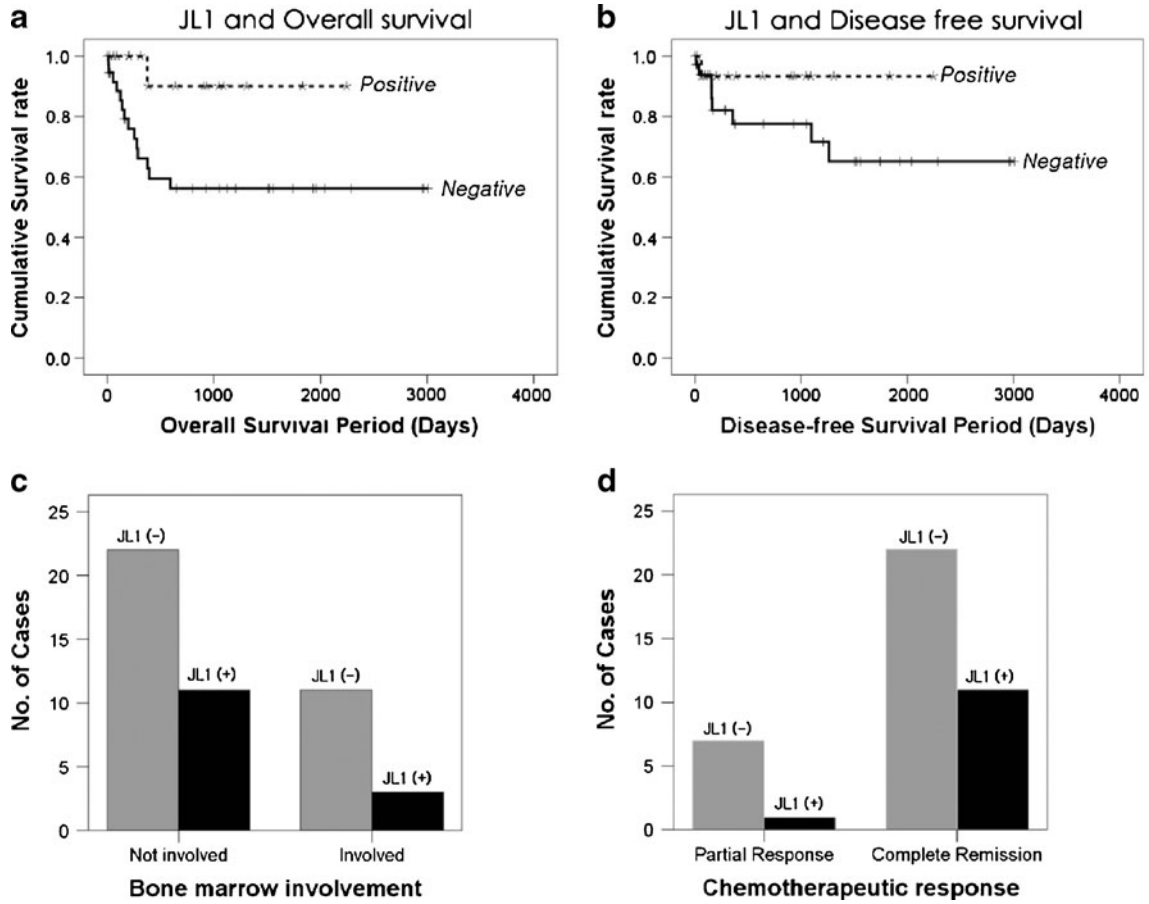

Fig. 3 Correlation of JL1 expression and clinical parameters, including survival rate. JL1 expression was significantly correlated (P=0.035) with prolonged overall survival (**a**). No JL1-positive, but some JL1-negative, patients showed tumor recurrence (**b**, disease-free survival). JL1 was not expressed in Burkitt lymphoma patients with bone marrow involvement (**c**). All patients with JL1-positive, but only some patients with JL1-negative, Burkitt lymphoma achieved complete remission in response to chemotherapy (**d**)

advanced age, advanced disease stage, poor performance status, bulky disease, high LDH concentration, and involvement of the CNS or bone marrow [16–18]. Increased expression of the apoptosis-related molecule c-flip and reduced expression of caspase-3 have been associated with resistance to chemotherapy and shorter overall survival [16, 19, 20]. We found that JL1 expression was significantly correlated with longer overall survival in patients with Burkitt lymphoma. Our raw data showed that JL1 positivity was associated with better response to chemotherapy (91.1% vs. 75.8%) and lower recurrence rate (6.2% vs. 22.2%) than JL1 negativity. These differences, however, were not statistically significant, possibly due to the small numbers of patients included in these groups. The correlations between JL1 expression and the expression of the apoptosis-related molecules c-flip and caspase-3 have yet to be determined. Risk stratification and the possibility of creating risk-adapted treatment strategies may assist in the design of appropriate therapies for individual patients. JL1, which can be assayed immunohistochemically, may be a useful marker for risk stratification of Burkitt lymphoma.

We observed JL1 expression in samples from 30.2% of our Burkitt lymphoma patients. JL1 expression has been previously reported in acute leukemia and bone marrow hematopoietic precursor cells, but not in mature human tissue or mature lymphoid neoplasms [3, 21, 22]. The discrepancies between the JL1 expression patterns observed in the present study and those of previous studies may be due to the relatively small proportion of JL1-positive Burkitt lymphomas and the relatively low numbers of Burkitt lymphoma samples tested in previous studies. In addition, JL1 is expressed in the Ramos Burkitt lymphoma cell line, but not the BJAB line (also a Burkitt lymphoma cell line), suggesting that JL-1 is expressed heterogeneously among Burkitt lymphomas [5].

The functional significance of JL1 expression in Burkitt lymphoma is unclear, principally because no molecule reacting with anti-JL1 antibody has yet been identified. Although the morphologic features of Burkitt lymphoma cells that do and do not express JL1 are similar, bone marrow involvement is more common in patients with non-JL1-expressing cells. Interestingly, JL1 was shown to

induce homotypic adhesion of immature thymocytes in vitro, a reaction mediated by interaction of LFA-1 and ICAM-1, and cytoskeletal reorganization [23]. These findings indicate that JL1 may be involved in migration or metastasis of Burkitt lymphoma, and may thus serve as a new target for specific treatment. In addition, although no specific JL1 function in lymphomagenesis has yet been described, JL1 expression per se may indicate that targeting of this molecule could be useful in individualized immunotherapy in patients with JL1-positive Burkitt lymphoma. Coupling of anti-JL1 antibodies with various toxic molecules may be effective as a form of leukemia-specific immunotherapy [1, 3, 5–7].

We found that tissue samples from 16 of 53 (30.2%) patients with Burkitt lymphoma were immunohistochemically positive for JL1, whereas samples from patients with other types of lymphoma were uniformly negative. Overall survival was longer in patients with JL1-positive than JL1-negative Burkitt lymphoma. JL1-positive Burkitt lymphoma may be defined as a specific disease subtype associated with better patient prognosis.

Acknowledgments We thank Professor Seong Hoe Park (Seoul National University, College of Medicine, Seoul, Korea) for generously providing the anti-JL1 antibody. This study was supported by a grant (no. W10-408) from the Asan Institute for Life Sciences, Seoul, and by the National Research Foundation of Korea, funded by the Korean Government (MEST) (grant no. NRF-2008-R13-023-2010-0029519).

Conflict of interest We declare that we have no conflict of interest.

References

1. Shin YK, Choi EY, Kim SH, Chung J, Chung DH, Park WS, Jung KC, Kim HS, Park S, Kim HJ, Park MH, Min CK, Kim CC, Park SH (2001) Expression of leukemia-associated antigen, JL1, in bone marrow and thymus. Am J Pathol 158:1473–1480
2. Park SH, Bae YM, Kwon HJ, Kim TJ, Kim J, Lee SJ, Lee SK (1993) JL1, a novel differentiation antigen of human cortical thymocyte. J Exp Med 178:1447–1451
3. Park YS, Park SH, Park SJ, Kim Y, Jang KT, Ko YH, Lee MW, Huh JR, Park CS (2010) Expression of JL1 is an effective adjunctive marker of leukemia cutis. Arch Pathol Lab Med 134:95–102
4. Park CS, Park SH (1999) Diagnostic usefulness of monoclonal antibody for T lymphoblastic lymphoma/acute lymphoblastic leukemia-specific JL1 antigen in paraffin embedded tissue. Korean J Pathol 33:1033–1038
5. Shin YK, Choi YL, Choi EY, Kim MK, Kook MC, Chung J, Choi YK, Kim HS, Song HG, Park SH (2003) Targeted cytotoxic effect of anti-JL1 immunotoxin against a human leukemic cell line and its clinical implications. Cancer Immunol Immunother 52:506–512
6. Suh W, Chung JK, Park SH, Kim SW (2001) Anti-JL1 antibody-conjugated poly (L-lysine) for targeted gene delivery to leukemia T cells. J Control Release 72:171–178
7. Lee YK, Kim KS, Kim JS, Baek JE, Park SI, Jeong HY, Yoon SS, Jung KC, Song HG, Park YS (2010) Leukemia-specific siRNA delivery by immunonanoplexes consisting of anti-JL1 minibody conjugated to oligo-9 Arg-peptides. Mol Cells 29:457–462
8. Delsol G (2008) The 2008 WHO lymphoma classification. Ann Pathol 28(1):S20–S24
9. Bellan C, Stefano L, de Giulia F, Rogena EA, Lorenzo L (2009) Burkitt lymphoma versus diffuse large B-cell lymphoma: a practical approach. Hematol Oncol 27:182–185
10. Sehn LH (2008) Management of Burkitt lymphoma: a continuing challenge. Oncology (Williston Park) 22(13):1519, 1522–1523
11. Aldoss IT, Weisenburger DD, Fu K, Chan WC, Vose JM, Bierman PJ, Bociek RG, Armitage JO (2008) Adult Burkitt lymphoma: advances in diagnosis and treatment. Oncology (Williston Park) 22:1508–1517
12. Perkins AS, Friedberg JW (2008) Burkitt lymphoma in adults. Hematol Am Soc Hematol Educ Program 341–348
13. Kenkre VP, Stock W (2009) Burkitt lymphoma/leukemia: improving prognosis. Clin Lymphoma Myeloma 9(Suppl 3):S231–S238
14. Lacasce A, Howard O, Lib S, Fisher D, Weng A, Neuberg D, Shipp M (2004) Modified magrath regimens for adults with Burkitt and Burkitt-like lymphomas: preserved efficacy with decreased toxicity. Leuk Lymphoma 45:761–767
15. Bellan C, Lazzi S, De Falco G, Nyongo A, Giordano A, Leoncini L (2003) Burkitt's lymphoma: new insights into molecular pathogenesis. J Clin Pathol 56:188–192
16. Valnet-Rabier MB, Challier B, Thiebault S, Angonin R, Margueritte G, Mougin C, Kantelip B, Deconinck E, Cahn JY, Fest T (2005) c-Flip protein expression in Burkitt's lymphomas is associated with a poor clinical outcome. Br J Haematol 128:767–773
17. Lozanski G, Heerema NA, Flinn IW, Smith L, Harbison J, Webb J, Moran M, Lucas M, Lin T, Hackbarth ML, Proffitt JH, Lucas D, Grever MR, Byrd JC (2004) Alemtuzumab is an effective therapy for chronic lymphocytic leukemia with p53 mutations and deletions. Blood 103:3278–3281
18. Patte C, Auperin A, Michon J, Behrendt H, Leverger G, Frappaz D, Lutz P, Coze C, Perel Y, Raphael M, Terrier-Lacombe MJ (2001) The Societe Francaise d'Oncologie Pediatrique LMB89 protocol: highly effective multiagent chemotherapy tailored to the tumor burden and initial response in 561 unselected children with B-cell lymphomas and L3. Leukemia Blood 97:3370–3379
19. Nomura Y, Yoshida S, Karube K, Takeshita M, Hirose S, Nakamura S, Yoshino T, Kikuchi M, Ohshima K (2008) Estimation of the relationship between caspase-3 expression and clinical outcome of Burkitt's and Burkitt-like lymphoma. Cancer Sci 99:1564–1569
20. Blum KA, Lozanski G, Byrd JC (2004) Adult Burkitt leukemia and lymphoma. Blood 104:3009–3020
21. Park WS, Bae YM, Chung DH, Kim TJ, Choi EY, Chung JK, Lee MC, Park SY, Park MH, Park SH (1998) A cell surface molecule, JL1: a specific target for diagnosis and treatment of leukemias. Leukemia 12:1583–1590
22. Kim TJ, Park SH (1998) Immunotherapeutic potential of JL1, a thymocyte surface protein, for leukemia. J Korean Med Sci 13:455–458
23. Lee GK, Jung KC, Park WS, Kook MC, Park CS, Sohn HW, Bae YM, Song HG, Park SH (1999) LFA-1- and ICAM-1-dependent homotypic aggregation of human thymocytes induced by JL1 engagement. Mol Cells 9:662–667

Virchows Arch (2011) 459:361–366
DOI 10.1007/s00428-011-1140-8

ORIGINAL ARTICLE

Prognostic implication of types of tumor-associated macrophages in Hodgkin lymphoma

Mona A. A. Zaki · Naoki Wada · Junichiro Ikeda · Hirohiko Shibayama · Koji Hashimoto · Tamotsu Yamagami · Yoichi Tatsumi · Machiko Tsukaguchi · Hironori Take · Mitsuru Tsudo · Eiichi Morii · Katsuyuki Aozasa

Received: 28 June 2011 / Revised: 11 August 2011 / Accepted: 15 August 2011 / Published online: 28 August 2011
© Springer-Verlag 2011

Abstract To evaluate roles of tumor-associated macrophages (TAMs) for prognosis of classical Hodgkin lymphoma (CHL). Expression of markers for TAMs, CD68, HLA-DR, CD163, HLA-DR/CD68 (M1), and CD163/CD68 (M2) was immunohistochemically examined in 82 cases with CHL. Positively stained cells were counted and correlation of number of TAMs and patients' survival time was analyzed. Number of CD163+ cells and M2 cells was significantly correlated with shorter overall survival ($P<0.05$), while it was marginally significant for CD68+ cells ($P=0.0827$). HLA-DR+cells and M1 cells showed no significant correlation with overall survival. When confined to mixed cellularity subtype, number of M1 cells was correlated with favorable prognosis ($P<0.05$), while M2 did not ($P=0.7$). Older age and male sex were unfavorable factors for prognosis. At multivariate analysis, number of CD163+ cells, M2+ cells, and age were independent factors for poor overall survival ($P=0.03$, 0.02, and 0.01, respectively). CD163+ cells and M2 cells might work to be tumor promotive in CHL. M1 cells might be tumor suppressive in mixed cellularity type.

Keywords Tumor-associated macrophages · M1 type · M2 type · Hodgkin lymphoma · Immunohistochemistry · Double staining · Prognosis

Introduction

Hodgkin lymphomas (HL) are histologically characterized by the presence of mono-(Hodgkin cells) and/or multinucleated Reed–Sternberg cells (RS cells) scattering in various amounts and kinds of inflammatory cells. Two different biologic entities are recognized within HL: nodular lymphocyte predominance (NLP) and classical HL (CHL) comprising nodular sclerosis (NS), mixed

Mona A.A. Zaki and Naoki Wada equally contributed to this study.

M. A. A. Zaki · N. Wada · J. Ikeda · E. Morii · K. Aozasa (✉)
Department of Pathology (C3),
Osaka University Graduate School of Medicine,
2-2 Yamadaoka,
Suita, Osaka 565-0871, Japan
e-mail: aozasa@molpath.med.osaka-u.ac.jp

H. Shibayama
Department of Hematology and Oncology,
Osaka University Graduate School of Medicine,
Suita, Osaka, Japan

K. Hashimoto
Department of Internal Medicine, Kansai Rosai Hospital,
Amagasaki, Hyogo, Japan

T. Yamagami
Department of Hematology, NTT West Osaka Hospital,
Osaka, Japan

Y. Tatsumi
Department of Hematology, Kinki University School of Medicine,
Osakasayama, Osaka, Japan

M. Tsukaguchi
Department of Hematology, Sakai Municipal Hospital,
Sakai, Osaka, Japan

H. Take
Department of Internal Medicine, Toyonaka Municipal Hospital,
Toyonaka, Osaka, Japan

M. Tsudo
Department of Hematology, Osaka Red Cross Hospital,
Osaka, Japan

cellularity (MC), lymphocyte-rich (LR), and lymphocyte depletion (LD) type. With the advance in the treatment for HL in the past few decades, 5-year survival rate in the favorable prognosis group reached to 98%, while that in the unfavorable group was at least 85% [1]. Assessment of stage of disease is a prerequisite for appropriate management of HL. For this, the Ann Arbor staging and the International Prognostic Factors Project on Advanced HL were established [2]. Even with advances in therapeutic modalities and accurate assessment of stage, however, prediction of outcome might be difficult in some cases of HL.

Roles of tumor-associated macrophages (TAMs) for tumor behaviors have attracted attention of researchers [3–7]. Recent study showed that estimation of amount of TAMs in lesional tissues, as revealed by immunohistochemical detection with CD68, could be used for prediction of prognosis of CHL [4]. TAMs recognize tumor-associated antigens and stimulate cytotoxic T lymphocytes to activate the anti-tumor immune responses. In contrast, some TAMs could induce immune tolerance and enhance progression and metastasis of tumors or stimulate angiogenesis and invasion into extracellular matrix [5, 6].

The most common marker used for immunohistochemical detection of TAMs is CD68, which is expressed in a wide range of monocytes/macrophages or dendritic cells. TAMs are polarized into two extreme forms, M1 and M2, which represent the major inflammatory components in many tumors. M1 TAMs secrete different types of chemokines and cytokines such as interleukin (IL)-1, IL-12, IL23, tumor necrosis factor-α (TNF-α), human leukocyte antigen (HLA)-DR, nitrogen intermediates and reactive oxygen. M1 TAMs are characterized by their ability to promote tumor regression response. On the other hand, M2 TAMs promote tumor progression and metastasis. M2 TAMs express considerable amount of CD206 (mannose receptor), CD204 (scavenger receptor A), IL-1, IL-10, CC ligand 22 (CCL22), and CD163 [7, 8].

To examine whether prognosis of patients with HL could be predicted based on the appearance of M1 or M2 TAMs, double staining with use of HLA-DR/ CD68 (M1 macrophages) and CD163/CD68 (M2 macrophages) were performed in 82 cases of CHL.

Materials and methods

Patients

During the period from November 1999 to April 2010, a total of 4,800 cases with lymphoproliferative diseases were registered with the Osaka Lymphoma Study Group (OLSG), Osaka, Japan. Histologic specimens obtained by biopsy were fixed in 10% formalin and routinely processed for paraffin embedding. Histologic sections cut at 4 μm were stained with hematoxylin and eosin and immunoperoxidase procedure (ABC method). All of the histologic sections were reviewed by one of the authors (KA), and classified according to the WHO classification. The diagnosis of malignant lymphoma was confirmed in 3,826 (79.7%) of 4,800 cases. Of these 3,826 cases, 3,508 (91.7%) were NHL and 318 (8.3%) HL. Among HL cases, 26 cases were NLP and 260 CHL, which comprised 164 cases of MC, 77 NS, 32 LR, 15 LD, and unspecified in four. Eighty-two cases of CHL, in which adequate clinical data were available, were selected for the present study. They included 52 cases of MC, 20 NS, six LR, and four LD cases. Clinical characteristics of these cases are summarized in Table 1.

Immunohistochemistry (IHC)

Monoclonal antibodies used for IHC were CD20, CD3, CD30 and CD68 (Clone: PG-M1) (Dakocytomation, Glostrup, Denmark, 1:400, 1:50, 1:50 and 1:50, respectively), HLA-DR (Medical & Biological Laboratories, Nagoya, Japan, 1:50), and CD163 (Novocastra-Leica, Wetzlar, Germany, 1:50).

Immunohistochemical double staining of HLA-DR/CD68 and CD163/ CD68 was performed using En vision™ G|2 double staining kit (Dako, Glostrup, Denmark) according to the manufacturer's instructions. The same method for antigen retrieval (Dako Pascal to heat) was employed in single and double staining. Primary antibodies HLA-DR or CD163 were labeled with brown color using DAB+and CD68 with red color by using permanent red. According to the previous study [6, 8], the average number of positively stained cells in six representative fields (0.146 mm^2) of tissue section, where the number of stained cells was the largest, was counted by the two investigators (NW and MAAZ) in a blind fashion. The number of Hodgkin–RS cells was rather similar in the fields selected and not counted. The cutoff point was set at the median number of positive cells.

Statistical analysis

Overall survival rates were calculated with the Kaplan–Meier method, and survival curves were compared by the logrank test. Multivariate analysis was performed with the Cox proportional hazard regression model.

Results

Clinical findings

Clinical findings are summarized in Table 1. Age of the patients in all CHL cases ranged from 15 to 85 (mean, 54) years with a male to female ratio of 55:27. Tumor stage was

Table 1 Clinical characteristics of 82 patients

Disease	Case no.	Age range (mean)years	Male/female	Stage (n=79)	
				I–II	III–IV
Mixed cellularity	52	16–84 (58)	17:9	27	24
Nodular sclerosis	20	17–78 (40)	13:7	12	6
Lymphocyte-rich	6	26–76 (55)	5:1	6	0
Lymphocyte-depleted	4	64–85 (74)	3:1	2	2
Total	82	15–85 (54)	55:27	47	32

evaluated in 79 cases according to the Ann Arbor staging system: 40.5% of the cases showed advanced diseases (Stages III and IV). Most patients with early stage (I and II) are treated with radiotherapy and/or combination chemotherapy, while those with advanced stage (III and IV) are treated with combination chemotherapy. The standard combination chemotherapy used with most of the patients is *ABVD* regimen (adriamycin, bleomycin, vinblastine, and dacarbazine).

Follow-up periods for survivors ranged from 8.8 to 115 (mean 47.5) months. Twenty-three (28%) patients died.

Histopathological findings

RS cells were positive for CD30 and either negatively or weakly positive for CD20 in two of 52 cases of MC, two of six cases of LR, and one of four cases of LD. Generally, M2 cells (CD163/CD68) predominated M1 cells (HLA-DR/CD68) in every subtype of CHL (Fig. 1). The number of single positive cells for HLA-DR (mean=150) was larger than that for CD163 (mean=104), and that was the smallest for CD68 (mean=72.2). The median number of TAMs was used as the cutoff value: number of TAM, clinicopathological parameters, and prognosis of patients are summarized in Table 2.

Univariate analysis

The number of CD163+ cells showed a significant correlation with shorter overall survival (P=0.03). In contrast, the number of HLA-DR+cells had no significant correlation with overall survival (P=0.6191), while CD68+ cells showed a marginal significance (P=0.0827). At double staining, the number of HLADR+/CD68+ (M1) cells showed no significant correlation with prognosis (P=0.255), while patients with a larger number of CD163+/CD68+ (M2) cells showed less favorable prognosis than those with smaller number (P<0.05) (Fig. 2).

Prognostic significance of appearance of CD68, HLA-DR, CD163, M1, or M2 TAMs was evaluated by stage. Overall survival rates in patients with low TAM (CD68, HLA-DR, CD163, M1, or M2) and high TAM group were estimated by early stage (stages I and II, 47 cases) and advanced stage (stages III and IV, 32 cases) with the

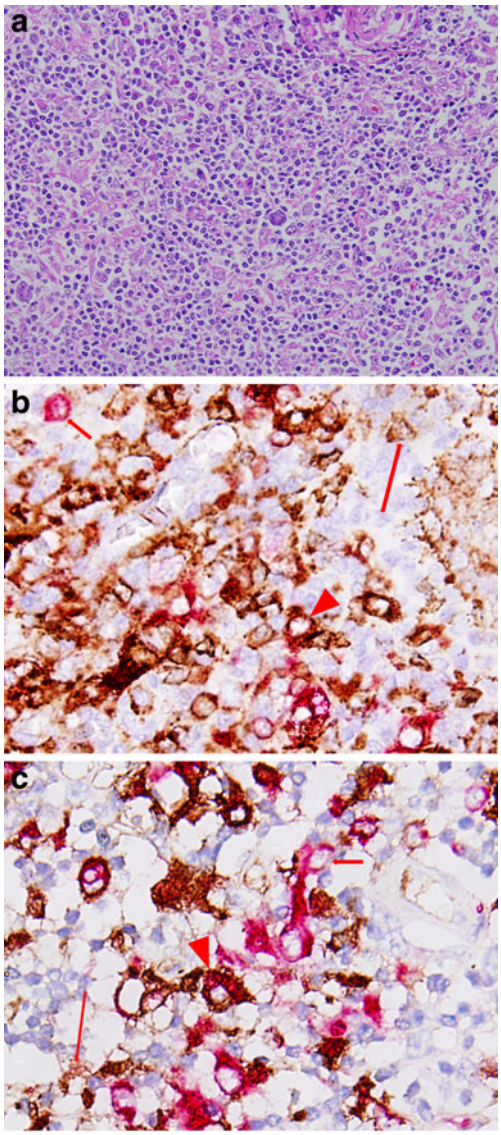

Fig. 1 Mixed cellularity subtype of classical Hodgkin lymphoma. **a** Multinucleated Reed–Sternberg cells (RS cells) are admixed with numerous inflammatory cells including macrophages, lymphocytes, eosinophils, and plasma cells. Hematoxylin and eosin stain. ×400. **b** Single positive cells for HLA-DR (brown) [*long arrow*], and CD68 (red) [*short arrow*], double positive cells for HLA-DR and CD68 (brown and red) [*arrow head*]. **c** Single positive cells for CD163 (brown) [*long arrow*] and CD68 (red) [*short arrow*], double positive cells for CD163 and CD68 (brown and red) [*arrow head*]

Table 2 Tumor-associated macrophages, clinicopathological parameters and prognosis of patients

	Cases no.	Mean of TAM* (range)	Median (Cutoff value)	Univariate analysis			Multivariate analysis
				Histological subtype			
				MC	NS	Total of all subtypes	
TAMs							
CD68	82	72.2 *(6–235)	60.3	0.5358	0.21	0.0827	0.0728
HLA-DR	82	150 *(4–797)	111.3	0.2578	0.506	0.6191	–
CD163	82	104.7* (3–427)	93.8	0.2824	0.198	0.03	0.0308
M1	82	17 *(0–101)	9.6	0.03862	0.151	0.255	–
M2	82	44.5 *(2–245)	31	0.6991	0.26	0.048	0.0258
Sex							
Male	55				P=0.0635		0.0728
Female	27						
Age			59 years				
≥59	44				P=0.0131		0.0131
<59	37						
Stage							
I–II	47				P=0.2071		–
III–IV	32						

TAM tumor-associated macrophages, *MC* mixed cellularity, *NS* nodular sclerosis, *LR* lymphocyte-rich, *LD* lymphocyte depletion

* Mean number of TAMs in six high power fields

Kaplan–Meier method, and survival curves were compared by the logrank test. Prognosis of high CD163 group was significantly worse than that of low CD163 group in early (P=0.036) but not advanced stages.

MC subtype was the major group of this study, and statistical analysis revealed significant correlation between the number of M1 cells and prognosis of patients (P<0.05), while M2 did not (P=0.6991). Patients with a larger number of M1 cells showed more favorable prognosis than those with a smaller number. In NS subtype, any significant correlation between the number of TAM and prognosis was not found. Older age and male sex were unfavorable factors for prognosis (P=0.013 and P=0.06, respectively). There was no significant correlation between stage of disease and prognosis (P=0.2).

Multivariate analysis

The number of CD163+ cells, CD163+/CD68+ (M2) cells, and age proved to be independent factors for prognosis of HL (P=0.0308, 0.0258, and 0.0131, respectively). While CD68+ cells and sex showed marginal significance (P=0.0728).

Discussion

Hodgkin lymphoma (HL) is a disease principally involving lymphoid tissues, and characterized by the presence of RS cells admixed with various amounts of reactive inflammatory cells. The incidence of HL varies according to geographical location, age, and the socioeconomic class. It comprises less than 10% of all malignant lymphomas in Japan, but is more common in Western countries (40–45%). Males predominate females in most of the countries. The incidence increases at the fourth decade of life in Japan, while showing a bimodal pattern in Western countries, with first peak at 15–35 years and second at over 55 years old. The incidence of MC type is highest in Japan, while NS is the commonest in Western countries [9, 10].

It is well known that TAMs represent a major component of inflammatory cells in many kinds of tumors such as lymphomas, melanoma, and carcinomas [3–8]. Several studies suggested the association between number of TAMs and the prognosis of patients with tumors. Dual role of TAMs, either tumor regressive (M1) or progressive (M2), is considered to be generated by their immune responses against tumors [11–13]. Expression of CD68, HLA-DR, and CD163 is commonly used for identification of TAMs, although these molecules are also expressed in other kinds of cells, i.e., CD68 in Langerhans cells and immature CD1a-positive dendritic cells, HLA-DR in peripheral lymphocytes, and CD163 in some dendritic cells. [14–16]. Then, we performed double immunohistochemical staining of HLA-DR/CD68 and CD163/ CD68 to specifically identify the M1 and M2 TAMs.

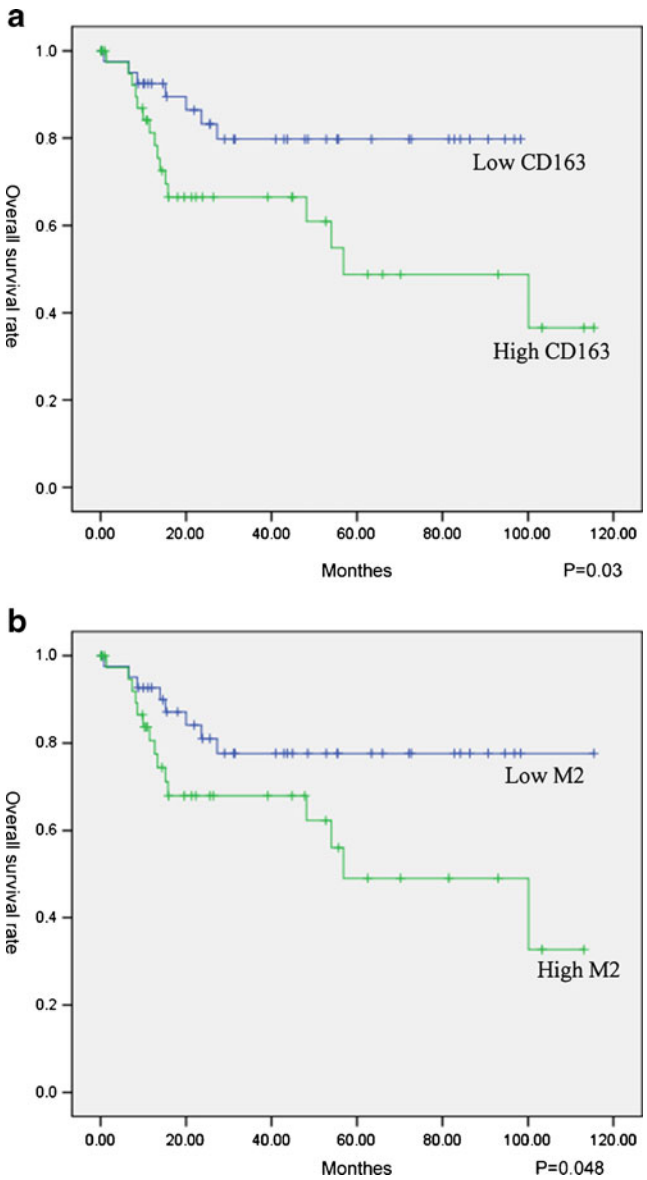

Fig. 2 **a** The overall survival rate in patients with higher number of CD163+ cells was significantly worse than that of lower number (p=0.03). **b** The overall survival rate in patients with higher number of CD163+/CD68+ cells was significantly worse than that of lower number (p<0.05)

At the single immunostaining, the number was highest for HLA-DR+cells, while lowest for CD68+ cells. The number of cells positive for CD68+ was smaller than that positive for CD163+ is in agreement with the previous studies [7, 17, 18], showing count numbers of tumor-infiltrating CD68+ macrophages were lower than those of CD163+ macrophages in HL and other malignancies such as malignant melanoma and leiomyosarcoma. At the double immunostaining, the number of M2 (CD163+/CD68+) cells was higher than that of M1 (HLA-DR+/CD68+) cells. These findings suggest that HLA-DR+cells were less labeled with CD68 than CD163, or HLA-DR might be expressed in a wider range of cells other than TAM. In some cases, CD163 expression seems to be relatively confined to CD68+ TAMs, because only a few cells were single positive for CD163+ at double staining.

A number of CD163+ cells or M2 type TAMs in the tumor tissues were associated with unfavorable prognosis of patients (P=0.03 and P=0.048 respectively). The number of CD68+ cells showed a marginal significance for prognosis in the present study (P=0.0827). These results are roughly in agreement with the recent studies. Steidl et al. [4] reported a strong association between the increased number of CD68+ cells and the poor prognosis of CHL defined by the disease-specific survival in both univariate and multivariate analyses but not by progression-free survival. They used gene expression profiling in an independent cohort of 166 cases of CHL. Kamper et al. [17] reported that the number of CD68+ or CD163+ cells correlated with the shorter event-free survival at the univariate analysis, while CD68, but not CD163, was significantly correlated with overall survival at the multivariate analysis. They constructed the tissue microarray, and then 288 cases were evaluated immunohistochemically. The slight discrepancies found between the present study, Steidl's, and Kamper et al.'s studies might be due to differences in methodologies employed, number of cases examined, or different characteristics of diseases themselves.

Multivariate analysis revealed that the number of CD163+ cells and M2 cells was an independent factor for unfavorable prognosis in CHL. In contrast, the number of HLA-DR+cells had no significant correlation with overall survival (P=0.6191). Older age proved to be an independent factor for poor prognosis of CHL (P=0.0131) at both univariate and multivariate levels. Steidl et al. [4] and Kamper et al. [17] also reported that older age correlated with the adverse prognosis. While male sex showed marginal significance for poor prognosis (P=0.06). Kamper et al. reported a significant correlation of sex with overall (P=0.05) but not with the event-free survival, but Steidl et al. reported no significant correlation with sex.

Interestingly, the number of M1+ cells but not HLA-DR+ cells was significantly correlated with favorable prognosis of patients with MC type (P=0.03), which comprised 63.4% of the current cases. This finding showed the importance of studying characteristics of CHL by each histological subtype. There have been no reports describing effects of M1 cells for prognosis of patients with CHL. Kamper et al. [17] reported the higher expression of CD68 and CD163 in TAMs of MC compered to NS subtypes.

In conclusion, the present study suggests practical implication for counting M2-TAMs, as defined CD163+ or CD163+/CD68+ cells in prediction of prognosis of patients with CHL. The number of M1-TAM correlated with prognosis of patients with MC type, suggesting further

study on prognostic roles of M1, M2-TAMs in each histological subtype of CHL.

Acknowledgements The authors thank Ms. M. Tone, T. Sawamura, M. Sugano, and E. Maeno for their technical assistance.

This work was supported by grants from the Ministry of Education, Culture, Sports, Science and Technology, Japan (#20590364, #20014010).

References

1. Fermé C, Eghbali H, Meerwaldt JH, Rieux C, Bosq J, Berger F, Girinsky T, Brice P, van't Veer MB, Walewski JA, Lederlin P, Tirelli U, Carde P, Van den Neste E, Gyan E, Monconduit M, Diviné M, Raemaekers JM, Salles G, Noordijk EM, Creemers GJ, Gabarre J, Hagenbeek A, Reman O, Blanc M, Thomas J, Vié B, Kluin-Nelemans JC, Viseu F, Baars JW, Poortmans P, Lugtenburg PJ, Carrie C, Jaubert J, Henry-Amar M (2007) Chemotherapy plus involved-field radiation in early-stage Hodgkin's disease. N Engl J Med 357:1916–1927
2. Ansell SM, Armitage JO (2006) Management of Hodgkin lymphoma. Mayo Clin Proc 81:419–426
3. Lewis CE, Pollard JW (2006) Distinct role of macrophages in different tumor microenvironments. Cancer Res 66:605–612
4. Steidl C, Lee T, Shah SP, Farinha P, Han G, Nayar T, Delaney A, Jones SJ, Iqbal J, Weisenburger DD, Bast MA, Rosenwald A, Muller-Hermelink HK, Rimsza LM, Campo E, Delabie J, Braziel RM, Cook JR, Tubbs RR, Jaffe ES, Lenz G, Connors JM, Staudt LM, Chan WC, Gascoyne RD (2010) Tumor-associated macrophages and survival in classic Hodgkin's lymphoma. N Engl J Med 362:875–885
5. Buddingh EP, Kuijjer ML, Duim RA, Bürger H, Agelopoulos K, Myklebost O, Serra M, Mertens F, Hogendoorn PC, Lankester AC, Cleton-Jansen AM (2011) Tumor-infiltrating macrophages are associated with metastasis suppression in high-grade osteosarcoma: a rationale for treatment with macrophage activating agents. Clin Cancer Res 17:2110–2119
6. Dai F, Liu L, Che G, Yu N, Pu Q, Zhang S, Ma J, Ma L, You Z (2010) The number and microlocalization of tumor-associated immune cells are associated with patient's survival time in non-small cell lung Cancer. BMC Cancer. 10: 220. Available at: http://www.biomedcentral.com/1471-2407/10/220
7. Jensen TO, Schmidt H, Møller HJ, Høyer M, Maniecki MB, Sjoegren P, Christensen IJ, Steiniche T (2009) Macrophage markers in serum and tumor have prognostic impact in American Joint Committee on Cancer stage I/II melanoma. J Clin Oncol 7:3330–3337
8. Ma J, Liu L, Che G, Yu N, Dai F, You Z. (2010) The M1 form of tumor-associated macrophages in non-small cell lung cancer is positively associated with survival time. BMC Cancer. 10:112. Available at: http://www.biomedcentral.com/1471-2407/10/112
9. Glaser SL, Hsu JL (2002) Hodgkin's disease in Asians: incidence patterns and risk factors in population-based data. Leuk Res 26:261–269
10. Aozasa K, Ueda T, Tamai M, Tsujimura T (1986) Hodgkin's disease in Osaka, Japan (1964–1985). Eur J Cancer Clin Oncol 22:1117–1119
11. Tjiu JW, Chen JS, Shun CT, Lin SJ, Liao YH, Chu CY, Tsai TF, Chiu HC, Dai YS, Inoue H, Yang PC, Kuo ML, Jee SH (2009) Tumor-associated macrophage-induced invasion and angiogenesis of human basal cell carcinoma cells by cyclooxygenase-2 induction. J Invest Dermatol 129:1016–1025
12. Lamagna C, Aurrand-Lions M, Imhof BA (2006) Dual role of macrophages in tumor growth and angiogenesis. J Leuk Biol 80:705–713
13. Al-Sarireh B, Eremin O (2004) Tumor-associated macrophages (TAMS): disordered function, immune suppression and progressive tumour growth. J R Coll Surg Edinb 5:1–16
14. Caux C, Vanbervliet B, Massacrier C, Dezutter-Dambuyant C, de Saint-Vis B, Jacquet C, Yoneda K, Imamura S, Schmitt D, Banchereau J (1996) CD34+ hematopoietic progenitors from human cord blood differentiate along two independent dendritic cell pathways in response to GM-CSF+TNF alpha. J Exp Med 184:695–706
15. Nakamura H, Saji H, Aute I, Kawasaki N, Hosaka M, Ogata A, Saijo T, Kato H (2003) Peripheral leukocytes with HLA-DR+/CD8-phenotype are associated with prognosis in patients with lung cancer. Anticancer Res 23:4149–4152
16. Maniecki MB, Møller HJ, Moestrup SK, Møller BK (2006) CD163 positive subsets of blood dendritic cells: the scavenging macrophage receptors CD163 and CD91 are coexpressed on human dendritic cells and monocytes. Immunobiology 211:407–417
17. Kamper P, Bendix K, Hamilton-Dutoit S, Honoré B, Nyengaard JR, d'Amore F (2011) Tumor-infiltrating macrophages correlate with adverse prognosis and Epstein–Barr virus status in classical Hodgkin's lymphoma. Haematologica 96:269–276
18. Lee CH, Espinosa I, Vrijaldenhoven S, Subramanian S, Montgomery KD, Zhu S et al (2008) Prognostic significance of macrophage infiltration in leiomyosarcomas. Clin Cancer Res 14:1423–1430

Virchows Arch (2011) 459:367–375
DOI 10.1007/s00428-011-1142-6

ORIGINAL ARTICLE

The role of tumor hypoxia in MUC1-positive breast carcinomas

Juliana Silva Zanetti · Danilo Fiqueredo Soave · João Paulo Oliveira-Costa · Giórgia Gobbi da Silveira · Leandra Náira Zambelli Ramalho · Sérgio Britto Garcia · Sérgio Zucoloto · Alfredo Ribeiro-Silva

Received: 18 May 2011 / Revised: 1 August 2011 / Accepted: 18 August 2011 / Published online: 3 September 2011
© Springer-Verlag 2011

Abstract Mucin 1 (MUC1) is a glycoprotein that is expressed on apical cell membranes in a variety of normal tissues. MUC1 is involved in cell signaling, inhibition of cell–cell and cell matrix adhesion, apoptosis, proliferation, and transcription. Hypoxia is an important factor that promotes cancer metastasis and stimulates angiogenesis and tumor progression. Hypoxia inducible factor 1 (HIF-1α) and carbonic anhydrase IX (CAIX) are two molecules that are involved in this process. The role of hypoxia in MUC1+ invasive ductal breast carcinomas is not well established. In this study, the expression of MUC1 was correlated with the hypoxia-associated markers HIF-1α and CAIX, as well as several immunohistochemical markers and clinicopathologic features of prognostic significance in 243 invasive ductal carcinomas. MUC1 was overexpressed in 37.0% of patients and correlated with the expression of estrogen receptor (p=0.0001), progesterone receptor (p=0.0001), HIF-1α (p=0.006), VEGF (p=0.024), and p53 (p=0.025). In breast cancer, MUC1 expression has been associated with increased degradation of inhibitor of NF-κB (IκBα), driving NF-κB to the nucleus and blocking apoptosis and promoting cell survival. We analyzed NF-κB expression in MUC1+ breast carcinoma and found a very significant relationship between these proteins (p=0.0001). Our findings indicate that MUC1 may play a role in the regulation of hormone receptors by increasing the inactivation of p53 and targeting NF-κB to the nucleus. Our data also support the notion that activation of HIF-1α in MUC1+ breast carcinomas may modulate VEGF expression, allowing a metabolic adaptation to hypoxia.

Keywords MUC1 · Breast cancer · Hypoxia · HIF-1α · NF-κB · Tissue microarray

J. S. Zanetti · D. F. Soave · J. P. Oliveira-Costa · G. G. da Silveira · L. N. Z. Ramalho · S. B. Garcia · S. Zucoloto · A. Ribeiro-Silva (✉)
Department of Pathology, Ribeirão Preto Medical School, University of São Paulo,
Avenida Bandeirantes 3900,
Ribeirão Preto, SP 14049-900, Brazil
e-mail: arsilva@fmrp.usp.br

Introduction

The majority of human cancer is the result of many genetic alterations that promote abnormal growth, including alterations in apoptotic pathways, activation of proto-oncogenes into oncogenes, inactivation of tumor suppressor genes, and several other changes [1]. The accumulation of genetic errors allows the cells to reproduce without restriction, invade local tissues, and establish distant metastasis. During cancer development and progression, the increased proliferative activity leads to tumor overgrowth and, consequently, an insufficient local supply of oxygen and nutrition [2].

Hypoxia is an important factor that promotes cancer metastasis [3] and is associated with more aggressive tumor phenotypes [4]. The microenvironment caused by hypoxia stimulates angiogenesis, extracellular matrix degradation, and tumor progression. All of the cellular responses caused by hypoxia are mediated by the hypoxia inducible factor 1 (HIF-1α) [5]. HIF-1α expression is characteristic of the early stages of carcinogenesis and has been correlated with increased intratumoral angiogenesis, cancer progression, poor patient prognosis, and chemotherapy or radiotherapy resistance [2]. Carbonic anhydrase IX (CAIX) is expressed in several kinds of cancer, but not in normal tissues, and is a major downstream target of HIF-1α. The function of CAIX is to regulate pH by the hydration of carbonic dioxide to carbonic acid, which controls the acidification of the tumor environment [5, 6].

Mucin proteins are a large family of glycoproteins expressed by many epithelial cells and their malignant counterparts [7]. Abnormal expression of mucins is related to cancer development [4]. Mucins also influence cellular growth, differentiation, transformation, adhesion, and invasion in malignant neoplasms [8]. Mucins are classified into two main classes: membrane bound, such as mucin 1 (MUC1), and secreted or gel forming, such as MUC2 [8–11].

MUC1 is expressed on the cell membrane in a variety of normal tissues where it is exclusively present on the apical surface of epithelial cells [12]. This protein is involved in cell signaling, inhibition of cell–cell and cell matrix adhesion, immunoregulation [8, 13, 14] apoptosis, proliferation, and transcription [15]. In breast cancer, MUC1 accumulates in the cytosol and is targeted to the nucleus, where it interacts with estrogen receptor α (ERα) and co-activates ERα target genes [16]. The MUC1 oncoprotein can be aberrantly overexpressed in up to 90% of human breast cancers [7, 10, 13, 17–19].

Interest has been increasing in the role of mucin members in breast cancer due to their potential role as prognostic indicators and their involvement in cancer therapy [8]. Patients with MUC1+ tumors develop both humoral and cellular immune responses against MUC1 antigens from malignant cells [14]. Both carbohydrate and peptide epitopes of MUC1 are immunogenic in humans [20]. Based on these observations, MUC1 has become a target of interest for immunotherapy of breast cancers, and several MUC1-based cancer vaccines have been developed [18].

The role of tumor hypoxia in the pathogenesis of MUC1+ tumors remains poorly understood. This study aims to evaluate the relationship between the expression of MUC1 and several tumor hypoxia-related markers in patients with breast carcinomas. In addition, several well-established prognostic factors were evaluated.

Materials and methods

Patients

The protocol used in this study conformed to the ethical guidelines of the 1975 Declaration of Helsinki and was approved by the local Ethics Committee. Two hundred forty-three (243) cases of invasive breast ductal carcinomas diagnosed between 1994 and 2004 were randomly retrieved from the files of the Department of Pathology of Ribeirão Preto School of Medicine. The following information was retrieved from the medical files: age, menopausal status, tumor size, metastasis to regional lymph nodes, recurrence, distant metastasis, death, disease-specific survival, metastasis-free survival, and disease-free survival. The selection of patients was based on the histopathologic diagnosis. For each case, all available hematoxylin and eosin (H&E) stained sections were reviewed to confirm the diagnosis of invasive ductal carcinoma and to select a representative block for immunostaining.

Cases with incomplete data and/or insufficient material were excluded from the study. The cases were graded according to the current guidelines of the Scarff–Bloom–Richardson grading system modified by Elston and Ellis [21]. None of patients had received any treatment before the biopsy procedure.

Disease-specific survival, metastasis-free survival, and disease-free survival were defined respectively as the number of months from diagnosis to the time of death due to breast cancer, the time from diagnosis until the appearance of distant metastasis, and the time from diagnosis to the occurrence of local recurrence or metastasis.

Tissue microarray (TMA)

The H&E slides were reviewed by an experienced pathologist (ARS) to delimit the most significant tumor area in each case. This region was then selected to construct a tissue microarray (TMA) paraffin block. For TMA block construction, core biopsies (1-mm diameter) were punched from the selected regions of each of the 243 donor paraffin blocks and arrayed into a new recipient paraffin block using a Manual Tissue Arrayer I (Beecher Instruments, Silver Spring, MD, USA). Three-micrometer-thick sections were cut from the TMA paraffin block using the paraffin tape-transfer system (Instrumedics, Saint Louis, MO, USA). One section was stained with H&E to confirm the presence of the tumor by light microscopy.

Immunohistochemistry

All of the tissue samples had been fixed in 4% neutral formalin and embedded in paraffin. Immunohistochemical staining was performed using the Biocare Medical Mach 4 Universal Polymer Detection (Concord, CA, USA). The protocol used has been described elsewhere [1]. The dilution and source of the primary antibodies used in this study were MUC1 (1:50, clone 695, Biocare Medical, Concord, CA, USA); HIF-1α (1:50, clone H1alfa67-sup, Abcam, Cambridge, UK), p53 (1:50, clone DO-7, Novocastra, Newcastle upon Tyne, UK), estrogen receptor (ER) (1:100 clone 6 F11, Novocastra, Newcastle upon Tyne, UK), progesterone receptor (PR) (1:100, clone 16, Novocastra, Newcastle upon Tyne, UK), Ki67 (1:100, clone MM1, Novocastra, Newcastle upon Tyne, UK), CAIX (1:100, Abcam, Cambridge, UK), VEGF (1:100, clone A-20: sc 152, Santa Cruz, Palo Alto, CA, USA), and NF-κB

(1:50, clone p65F-6: sc 8008, Santa Cruz, Palo Alto, CA, USA). The reaction was developed with diaminobenzidine (DAB) and followed by hematoxylin counterstaining.

In accordance with the literature, the immunohistochemistry study was evaluated as follows. The cases in which more than 10% of the neoplastic cells stained for Ki67 (nuclear staining) were considered highly proliferative. The cases were interpreted as ER, PR, and p53 positives if more than 10% of the neoplastic cells showed nuclear staining [9]. For HIF-1α expression, only homogenously and darkly stained nuclei were considered, and cases were considered positive when more than 1% of the neoplastic cells were stained. CAIX was considered positive when more than 1% of the neoplastic cells were stained (membrane staining) [5, 21–23]. The percentage of VEGF-positive cancer cells was assessed by two observers (ARS and LZR). Taking into account the extent of positive staining, we divided our cases into two groups: low/medium reactivity (0–69% positive cells) and high reactivity (70–100% positive cells) in accordance with Giatromanolaki et al. [6]. For NF-κB p65, we evaluated the percentage of cells that expressed the protein in each case, and then we evaluated the most frequent percentage to establish the cut-off. We noticed that the most frequent percentage was 10%, and therefore, we decided to establish our cut-off as expression in less than 10% of cells was considered negative, and expression in more than or equal to 10% was considered positive.

Normal breast samples were used as the positive control for MUC1. Cases of invasive ductal carcinoma previously known to be positive for Ki67, ER, PR, p53, HIF-1α, CAIX, and VEGF were used as positive controls. Negative controls for immunostaining were prepared by omission of the primary antibody. For MUC1, we used the same cut-off established by Sangoi et al.: score negative (0) when 0–5% of the cells were positive for MUC1; focally positive (1+) when 5–10% of the cells were positive; positive (2+) when more than 10–50% of the cells were positive; and diffusely positive (3+) when more than 50% of the cells were stained [24]. For statistical analysis, we dichotomized MUC1 as negative (0 and 1+) and positive (2+ and 3+). The slides were read by two experienced pathologists (ARS and LZR).

After immunohistochemistry reactions, the slides were scanned into high-resolution images using Aperio ScanScope XT (Aperio, Vista, CA, USA). The images were then visualized in the software Image Scope (Aperio, Vista, CA, USA).

TUNEL assay

Paraffin-embedded breast tissue sections were deparaffinized and incubated with 20 μg/mL proteinase K (Promega Corporation, Madison, WI, USA). A DeadEnd peroxidase in situ apoptosis detection kit (DeadEnd TUNEL; Promega Corporation, Madison, WI, USA) was used for transferase-mediated dUTP-biotin nick-end labeling (TUNEL) staining. In brief, the samples were treated with 3% hydrogen peroxide to quench endogenous peroxidase activity. After adding equilibration buffer, the sections were treated with terminal deoxynucleotidyl transferase and digoxigenin–dNTPs for 60 min at 37°C. The specimens were then treated with anti-digoxigenin-peroxidase for 30 min at 37°C, colorized with DAB, and counterstained with Mayer's hematoxylin. Finally, the slides were rinsed, dehydrated, and mounted. A negative control was prepared by omitting the terminal deoxynucleotidyl-transferase enzyme to control for nonspecific incorporation of nucleotides or binding of the enzyme-conjugate. The number of TUNEL-positive cells was evaluated by the percentage of nuclear-stained cells in each sample, from which mean values were obtained. The cells were considered positive when obvious brown nuclear staining was detected. Labeled inflammatory cells were not considered. All of the TUNEL cases were counted using an immersion objective (×100), and the stained cells contained dots in the perinuclear or nuclear region. The TUNEL cut-off was established in accordance with the most frequent percentages: labeling of less than 5% of cells was considered to be negative, and labeling of 5% or more cells was considered to be positive staining.

Statistical analysis

Statistical analyses and tests were performed with the commercially available PASW Statistics 17.0 software (Chicago, IL, USA). The relationships between MUC1 expression, immunohistochemical findings, and clinicopathologic features were tested with cross tables applying the χ^2 (three or more variables) or Fisher tests (two variables), and all of the tests were two-tailed. Kaplan–Meier curves using the log-rank test were used to estimate and compare disease-specific survival, disease-free survival, and metastasis-free survival. To observe the independent prognostic value of immunoexpression of MUC1, we performed a Cox proportional hazards model. A p value of <0.05 was considered significant.

Results

Clinical findings

The median age of patients ($n=243$) included in this study was 55 (range, 25–85 years); 101 patients were younger than 50 years, and 142 were older than 50 years. Eighty-seven patients were pre-menopausal, and 156 were post-menopausal. All tumors were classified as not

otherwise specified (NOS) invasive ductal carcinomas, with sizes ranging from 0.5 to 18 cm. Seventy-two patients had tumors measuring less than 2 cm, while 100 patients had tumors between 2 and 5 cm, and 71 patients had tumors larger than 5 cm. One hundred fourteen patients were lymph node negative, and 129 patients had positive lymph nodes. The tumors were classified as grade I (90 [37.0%]), grade II (116 [47.7%]), and grade III (37 [15.2%]) according to the Bloom and Richardson system modified by Elston and Ellis [21]. In accordance with the Clinical Staging System, created by the American Joint Committee on Cancer [25], 33 patients were stage I, 109 were stage II, 89 were stage III, and 12 were stage IV. Distant metastasis occurred in 71 patients, and 75 patients died. MUC1 expression did not correlate with tumor size, pathological stage, age, menstrual status, nodal status, or tumor grade. All of the clinical results are shown in Table 1.

Table 1 Relationship between MUC1 expression and clinicopathologic features of prognostic significance

	MUC1 (n=243)				p
	Negative		Positive		
	n (153)	%	n (90)	%	
Age (years)					0.511
<50	64	41.8	37	41.1	
>50	89	58.2	53	58.9	
Menstrual status					0.318
Pre-menopausal	57	37.3	30	33.3	
Post-menopausal	96	62.7	60	66.7	
Size (mm)					0.901
<20	44	28.8	28	31.1	
20–50	63	41.2	37	41.1	
>50	46	30.1	25	27.8	
Tumoral grade					0.968
I	56	36.3	34	37.8	
II	74	48.4	42	46.7	
III	23	15.0	14	15.6	
Lymph nodal status					0.424
Negative	73	47.7	41	45.6	
Positive	80	52.3	49	54.4	
Stage					0.499
I	17	11.1	16	17.8	
II	72	47.1	37	41.1	
III	56	36.6	33	36.7	
IV	08	5.2	04	4.4	

Our data did not show any significant p value for MUC1 staining according to prognostic features

The n values represent the number of MUC1 cases: negative (0 and 1+) and positive (2+ and 3+) by immunohistochemical analysis

Immunohistochemical findings

Our data showed that 90 of the 243 cases were positive for MUC1 (Fig. 1a; 37.0%) and 153 cases were negative for MUC1 (63.0%). Fifty-three cases were positive for HIF-1α (21.8%), 86 were positive for Ki67 (35.4%), 159 were positive for ER (Fig. 1c; 65.4%), 148 were positive for PR (60.9%), 64 were positive for CAIX membrane staining (Fig. 1f; 26.3%), 45 were positive for VEGF (Fig. 1d; 18.5%), and 158 were positive for p53 (65.0%). MUC1+ breast carcinomas significantly correlated with HIF-1α expression (p=0.006) and VEGF expression (p=0.024), but not with CAIX cytoplasmic staining. The expression of the tumor suppressor gene p53 and the expression of hormonal markers according to MUC1 expression were p53 (Fig. 1b; p=0.025), ER (p=0.0001), and PR (p=0.0001). MUC1+ breast carcinomas did not correlate with expression of the proliferation marker Ki67 (Fig. 1e; p=0.099). All of the immunohistochemical correlations with MUC1 expression are shown in Table 2. MUC1+ carcinomas showed a significant relationship with NF-κB immunohistochemical staining (p=0.0001).

The Fisher test results for NF-κB immunohistochemical staining (cytoplasmic and/or nuclear staining) showed a significant relationship with MUC1+ carcinomas (p=0.0001). We had 103 positive cases (42.3%) for NF-κB in which 65 patients were positive with both MUC1 and NF-κB. NF-κB expression was not observed in normal tissues.

MUC1+ carcinomas displayed significant DNA fragmentation (demonstrated by the TUNEL assay; p=0.0001). The greater the number of MUC1+ cells, the greater the degree of DNA fragmentation (Tables 3 and 4).

Discussion

This work evaluated the hypoxia effect on MUC1+ breast carcinomas. According to scientific literature, MUC1 expression can be analyzed by immunohistochemistry assay with several different "cut-offs." We followed the same cut-off used by Sangoi et al. [24]. MUC1 is a protein that may be expressed in different ways. In normal cells, MUC1 is only expressed in apical membrane. In cancer cells, MUC1 may be expressed in membrane and in cytoplasm. All of these expressions are based on semi-quantity and semi-quality analysis where the percentage of cells and their intensity is considered for the final established cut-off. So, in order to maintain a homogeneous cut off, we followed the work of Sangoi et al. [24]. Similar to these authors, we characterized MUC1 expression in zero, 1+, 2+, and 3+, and after, these results were dichotomized in positive and negative. Rakha et al. had observed that MUC1 was positive in 91% of patients, but MUC1 overexpression

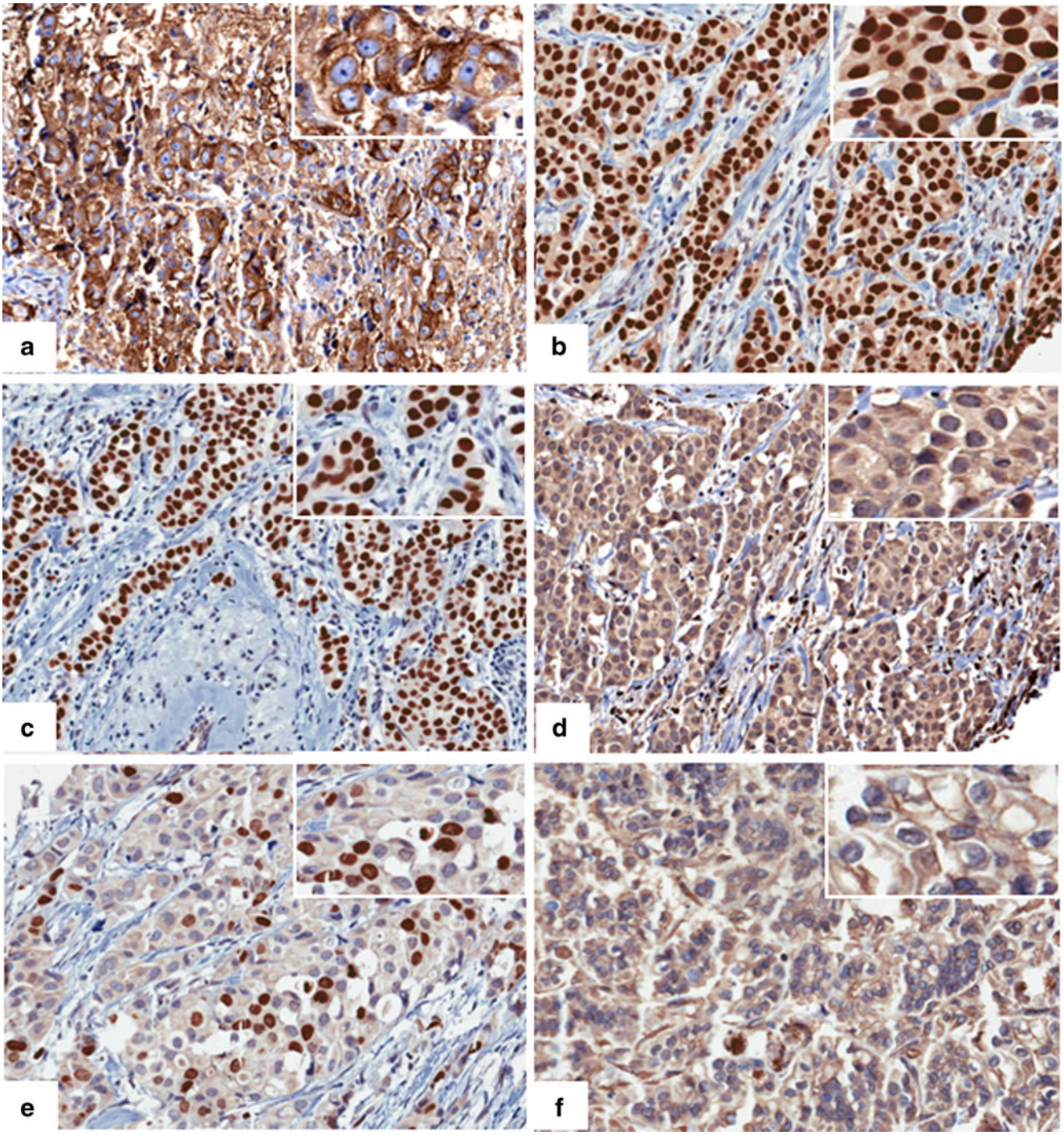

Fig. 1 Neoplastic breast cancer cells positive for (**a**) MUC1 (in detail: membrane staining), (**b**) p53 (in detail: nuclear staining), (**c**) estrogen receptor (in detail: nuclear staining), (**d**) VEGF (in detail: cytoplasmic staining), (**e**) Ki67 (in detail: nuclear staining), and (**f**) CAIX (in detail: membrane staining). Immunohistochemical reactions, magnifications ×200 and ×400 (detail)

was only 42% of them [8]. Our results are in accordance with these findings. In our work, more than 90% of the cases were positive for MUC1 (1+, 2+, and 3+), but only 37% was considered as overexpression.

MUC1 is usually present on the apical surface of secretory epithelia in normal cells and in malignant tissues, where there is an expression of this mucin in up to 90% of cases [8, 15]. This overexpression leads to the loss of cell–cell and cell–extracellular matrix adhesion and, therefore, promotes cancer metastasis [6, 13]. In the mammary gland, MUC1 is regulated by the progesterone receptor (PR) and pro-inflammatory cytokines [17]. MUC1 overexpression

Table 2 Relationship between MUC1 expression and tumor hypoxia-related markers and other immunohistochemical markers

	MUC1 (n=243)				p
	Negative		Positive		
	n (153)	%	n (90)	%	
HIF-1α					0.006
Negative	128	83.7	62	68.9	
Positive	25	16.3	28	31.1	
CAIX					0.075
Negative	118	77.1	61	67.8	
Positive	35	22.9	29	32.2	
Ki67					0.099
Negative	104	68.0	53	58.9	
Positive	49	32.0	37	41.1	
PR					0.0001
Negative	76	49.7	77	50.3	
Positive	19	21.1	71	78.9	
ER					0.0001
Negative	71	46.4	13	14.4	
Positive	82	53.6	77	85.6	
p53					0.025
Negative	61	39.9	24	26.7	
Positive	92	60.1	66	73.3	
VEGF					0.024
Negative	131	85.6	67	74.4	
Positive	22	14.4	23	25.6	
NF-κB					0.0001
Negative	115	75.2	25	27.8	
Positive	38	24.8	65	72.2	

The n values represent the dichotomization of cases by immunohistochemical analysis for MUC1

drives tumor formation primarily through its interaction with transcription factors, such as p53, estrogen receptor (ER) [15, 26] and β-catenin, or through signaling modulation [15]. MUC1 maintains effectors of growth and survival pathways, such as β-catenin and p53, as well as maintaining nuclear hormone receptors, such as ERα, in stabilized and active configurations [27].

In the present study, MUC1 was overexpressed in 37.0% of the patients, while 60.9% and 65.4% were PR and ER positives, respectively, and 65.0% were p53 positive. Our data showed a significant relationship between MUC1, hormonal receptors (ER and PR), and p53. These findings suggest that MUC1 overexpression correlates with increased inactivation of p53. Moreover, our data support a putative role for ER and PR in MUC1 regulation. These findings are in accordance with some studies in the literature that have shown a significant relationship between ER and MUC1 [8, 13]. However, in an experimental study, Zhou et al. did not find any relationship between ER and MUC1 regulation [28].

In breast cancers, MUC1 is regulated by cytokines and peptide hormones through NF-kB and STAT transcription factors [26]. In breast cancer, MUC1, similarly to NF-κB, blocks apoptosis and induces cell transformation. Many breast tumors overexpress MUC1 and have an activated NF-κB pathway, which promotes cell survival [27]. The NF-κB family is comprised of five members: RelA (p65), NF-κB1 (p50), NF-κB2 (p52), c-Rel, and RelB. The most prevalent forms are the p50 and p65 DNA binding subunits [29]. NF-κB proteins are present in the cytoplasm in association with inhibitory proteins, called inhibitors of κB (IκBs), and their degradation allows translocation of NF-κB into the nucleus where it binds to specific DNA sequences and activates the transcription of multiple genes [11, 27, 29, 30]. Due to this fact, immunohistochemistry for NF-κB shows a cytoplasmic and/or nuclear staining [29]. MUC1 expression has been associated with increased degradation of IκBα by its phosphorylation and targeting of NF-κB p65 to the nucleus (this event allow decrease NF-κB in cytoplasm and an increase this protein to nucleus), and this activation of the NF-κB pathway blocks apoptosis [27].

Table 3 The Fisher test result for MUC1 and TUNEL assay

MUC1 and TUNEL cross tabulation					
			TUNEL		Total
			Negative	Positive	
MUC1	Positive	Count	115	38	153
		% within MUC1	75.2%	24.8%	100.0%
	Negative	Count	25	65	90
		% within MUC1	27.8%	72.2%	100.0%
Total		Count	140	103	243
		% within MUC1	57.6%	42.4%	100.0%

Cross tabulation results: MUC1 and TUNEL. Negative and positive patients and respective percentages (SPSS table)

Table 4 Significant relationship between MUC1 overexpression and DNA fragmentation detected by the TUNEL assay

MUC1 carcinomas associated with DNA fragmentation

	Value	df	Asymp. Sig. (two-sided)	Exact Sig. (two-sided)	Exact Sig. (two-sided)
Pearson χ^2	52.104	1	0.0001		
Continuity correction	50.181	1	0.0001		
Likelihood ratio	53.339	1	0.0001		
Fisher's exact test				0.0001	0.0001
Linear-by-linear association	51.889	1	0.0001		
N of valid cases	243				

Fisher test between MUC and TUNEL assay: very significant *p* value (SPSS table)

Furthermore, MUC1 also contributes to the activation of NF-κB, promoting cell survival [27]. Our data showed a significant inactivation of p53 and activation of NF-kB, suggesting that apoptosis may be dysfunctional in MUC1-positive breast carcinomas. In this work, we found that a higher MUC1 expression is associated with an increase in DNA fragmentation (shown by the TUNEL assay). These results suggest that DNA damage is present when MUC1 is overexpressed, contributing to the accumulation of genetic errors in these kinds of carcinomas. Regarding NF-κB expression in MUC1-positive carcinomas, we observed that NF-κB was not expressed at a significant level in normal tissues, suggesting that a similar role can exist between NF-κB and Bcl-2 in the apoptosis pathway [31].

In addition to the link between MUC1 and apoptosis, MUC1 has also been linked to proliferation in cancer [15]. In our study, we evaluated in MUC1-positive breast carcinomas the immunoexpression of Ki67, a proliferation marker that identifies cells in G1, S, G2, and M phases of the cell cycle [32]. In this work, there was no significant correlation between MUC1 and Ki67. Previous studies have shown that the cellular appearance and location of the Ki-67 protein throughout the cell cycle is not homogeneous, and little is known of its function in cell division [33]. Possibly due to these uncertainties, we did not find significant expression of Ki67 in MUC1 positive breast carcinomas.

Hypoxia can affect the development of tumors by inhibiting proliferation and stimulating apoptotic or necrotic cell death. Under hypoxic conditions, tumor cells become more resistant to chemotherapy and show more invasiveness and a metastatic phenotype [2]. The low oxygen concentration in tumors can modulate, by inhibiting or stimulating, gene expression and affect metabolic processes [2] that increase the stability of HIF-1α [34]. HIF-1α is not detected in normal breast tissue. It is detected only in hypoxia conditions, so because of this literature data, when HIF-1α is present, even a low expression (1%) is considered significant. This fact justifies the low cut off established for HIF-1α in this work [5]. In hypoxic conditions, HIF-1α binds to the hypoxia response elements, modulating many target genes, including VEGF, inducible nitric oxide synthase (iNOS), and insulin growth factor-1 (IGF-1) [34], increasing the oxygen or allowing a metabolic adaptation to hypoxia [5]. In addition, the promoter region of the HIF-1α gene contains several NF-κB p65 binding sites [35], and this association has been found to be related to the regulation of apoptosis. Our data showed significant HIF-1α expression in MUC1+ breast carcinomas. We can correlate these results with cellular signaling for the transcription of hypoxia genes by NF-κB, which can activate HIF-1α [36]. These data are affirmed by a work that shows that an impairment in NF-κB results in the loss of HIF-1α mRNA, which reduces HIF-1α levels in response to hypoxia [37].

CAIX is important in helping to eliminate the hypoxia-generated acid load in glycolysis and, in breast cancer, its high level is associated with high grade in ductal carcinoma in situ and poor histological grade in invasive ductal carcinoma. CAIX is a major downstream target of HIF-1α [5]. In breast cancer, CAIX expression has been associated with a poor outcome. Giatromanolaki et al. have demonstrated a correlation between MUC1 and CAIX. In their study, CAIX was associated with an upregulation of MUC1 [6]. Our results showed no significant relationship between CAIX and MUC1 expression and no correlation of CAIX expression with metastasis or poor outcome in MUC1+ breast carcinomas.

MUC1 is related to VEGF expression, as demonstrated by Hattrup and Gendler [15]. In their work, cells treated with siRNA for MUC1 displayed a reduced transcription of VEGF, suggesting that MUC1 can promote angiogenesis and stromal proliferation [15]. VEGF overexpression has been observed in up to 96% of ductal carcinomas, and its overexpression is correlated with the remodeling of stromal fibroblasts of pre-malignant lesions in breast [38]. VEGF expression in breast cancer correlates with tumor growth and metastasis [15], and the expression of VEGF in breast tissue is affected by estrogen. Indeed, there is an important increase in VEGF

expression in normal breast tissue of pre-menopausal women compared to that of post-menopausal women [39]. Giatromanolaki et al. have shown that MUC1 overexpression correlates with microvessel density. They showed that there is a significant co-expression of MUC1 with VEGF and bFGF receptor in breast cancer, suggesting that the malignant transformation in MUC1+ breast carcinomas includes a simultaneous activation of both angiogenic and migration-related pathways [40].

Angiogenesis is induced by VEGF through its interaction with receptors expressed primarily on the vascular endothelial cell membrane. VEGF is upregulated by HIF-1α [34, 41]. As previously mentioned, our data showed significant HIF-1α expression in MUC1+ breast carcinomas, suggesting a possible role for MUC1 in VEGF regulation.

The findings presented in this report, combined with a detailed literature review, suggest that tumor hypoxia may be important in the pathogenesis of MUC1+ breast carcinomas. However, further studies are necessary to understand the pathways in which the key regulators of hypoxia may interact with MUC1. The present study can also contribute to future research examining the potential for MUC1 to be a putative therapeutic target for breast carcinomas.

Acknowledgements The authors wish to acknowledge the technical assistance of Deisy Mara da Silva and Laura Midori Kawasse.

Conflicts of interest We declare that we have no conflicts of interest.

References

1. Ribeiro-Silva A, Moutinho MA, Moura HB et al (2006) Expression of checkpoint kinase 2 in breast carcinomas: correlation with key regulators of tumor cell proliferation, angiogenesis, and survival. Histol Histopathol 21:373–382
2. Koda M, Kanczuga-Koda L, Sulkowska M et al (2010) Relationships between hypoxia markers and the leptin system, estrogen receptors in human primary and metastatic breast cancer: effects of preoperative chemotherapy. BMC Cancer 10:1–8
3. Sun L, Lin S, Zhao R et al (2010) The saponin monomer of dwarf lilyturf tuber, DT-13, reduces human breast cancer cell adhesion and migration during hypoxia via regulation of tissue factor. Biol Pharm Bull 33:1192–1198
4. Vordermark D (2010) Hypoxia-specific targets in cancer therapy: role of splice variants. BMC Med 12:1–3
5. Chen CL, Chu JS, Su WC (2010) Hypoxia and metabolic phenotypes during breast carcinogenesis: expression of HIF-1α, GLUT1, and CAIX. Virchows Arch 457:53–61
6. Giatromanolaki A, Koukourakis MI, Sivridis E et al (2001) Expression of hypoxia-inducible carbonic anhydrase-9 relates to angiogenic pathways and independently to poor outcome in non-small cell lung cancer. Cancer Res 61:7992–7998
7. Schumacher U, Adam E (1998) Immunohistochemical detection of the MUC1 gene product in human cancers grown in *scid* mice. J Histochem Cytochem 46:127–134
8. Rakha EA, Boyce WG, El-Rehim DA et al (2005) Expression of mucins (MUC1, MUC2, MUC3, MUC4, MUC5AC and MUC6) and their prognostic significance in human breast cancer. Mod Pathol 18:1295–1304
9. O'Connell JT, Zhi-Ming S, Ehud D et al (1998) Altered mucin expression is a field change that accompanies mucinous (colloid) breast carcinoma histogenesis. Hum Pathol 29:1517–1523
10. Raina D, Ahmad R, Joshi MD et al (2009) Direct targeting of the mucin 1 oncoprotein blocks survival and tumorigenicity of human breast carcinoma cells. Cancer Res 69:5133–5141
11. Voynow JA, Gendler SJ, Rose MC (2006) Regulation of mucin genes in chronic inflammatory airway diseases. Am J Respir Cell Mol Biol 34:661–665
12. Nassar H, Pansare V, Zhang H et al (2004) Pathogenesis of invasive micropapillary carcinoma: role of MUC1 glycoprotein. Mod Pathol 17:1045–1050
13. Abba MC, Nunez MI, Colussi AG et al (2006) GATA3 protein as a *MUC1* transcriptional regulator in breast cancer cells. Breast Cancer Res 8:R64
14. Heuser C, Ganser M, Hombach A et al (2003) An anti-MUC1-antibody–interleukin-2 fusion protein that activates resting NK cells to lysis of MUC1-positive tumour cells. Br J Cancer 89:1130–1139
15. Hattrup CL, Gendler SJ (2006) MUC1 alters oncogenic events and transcription in human breast cancer cells. Breast Cancer Res 8:R37
16. Khodarev NN, Pitroda SP, Beckett MA et al (2009) MUC1-induced transcriptional programs associated with tumorigenesis predict outcome in breast and lung cancer. Cancer Res 69:2833–2837
17. Brayman MJ, Dharmaraj N, Lagow E et al (2007) MUC1 expression is repressed by protein inhibitor of activated signal transducer and activator of transcription-y. Mol Endocrinol 21:2725–2737
18. Huyn ST, Burton JB, Sato M et al (2009) A potent, imaging adenoviral vector driven by the cancer-selective mucin-1 promoter that targets breast cancer metastasis. Clin Cancer Res 15:3126–3134
19. Yin L, Li Y, Ren J et al (2003) Human MUC1 carcinoma antigen regulates intracellular oxidant levels and the apoptotic response to oxidative stress. J Biol Chem 278:35458–3564
20. Apostolopoulos V, Mckenzie IF, Pietersz GA (1996) Breast cancer immunotherapy: current status and future prospects. Immunol Cell Biol 74:457–464
21. Fitzgibbons PL, Page DL, Weaver D et al (2000) Prognostic factors in breast cancer. College of American Pathologists Consensus Statement 1999. Arch Pathol Lab Med 124:966–978
22. Mangia A, Chiriatti A, Tommasi S et al (2009) BRCA1 expression and molecular alterations in familial breast cancer. Histol Histopathol 24:69–76
23. Rydén L, Jirstro K, Haglund M et al (2010) Epidermal growth factor receptor and vascular endothelial growth factor receptor 2 are specific biomarkers in triple-negative breast cancer. Results from a controlled randomized trial with long-term follow-up. Breast Cancer Res Treat 120:491–498
24. Sangoi AR, Higgins JP, Rouse RV et al (2009) Immunohistochemical comparison of MUC1, CA125, and Her2Neu in invasive micropapillary carcinoma of the urinary tract and typical invasive urothelial carcinoma with retraction artifact. Mod Pathol 22:660–667
25. Singletary SE, Greene FL (2003) Revision of breast cancer staging: the 6th edition of the TNM classification. Semin Surg Oncol 21:53–59
26. Lagow EL, Carson DD (2002) Synergistic stimulation of MUC1 expression in normal breast epithelia and breast cancer cells by interferon-γ and tumor necrosis factor-α. J Cell Biochem 86:759–772

27. Ahmad R, Raina D, Trivedi V et al (2007) MUC1 oncoprotein activates the IκB kinase β complex and constitutive NF-κB signalling. Nat Cell Biol 9:1419–1427
28. Zhou X, DeSouza MM, Julian J et al (1998) Estrogen receptor does not directly regulate the murine Muc-1 promoter. Mol Cell Endocrinol 143:65–78
29. Braz MM, Ramalho FS, Cardoso RL et al (2010) Slight activation of nuclear factor kappa-B is associated with increased hepatic stellate cell apoptosis in human schistosomal fibrosis. Acta Trop 113:66–71
30. Nakshatri H, Nakshatri PB, Martin DA et al (1997) Constitutive activation of NF-kB during progression of breast cancer to hormone-independent growth. Mol Cell Biol 17:3629–3639
31. Chang F, Lee JT, Navolanic PM et al (2003) Involvement of PI3K/Akt pathway in cell cycle progression, apoptosis, and neoplastic transformation: a target for cancer chemotherapy. Leukemia 17:590–603
32. Oliveira-Costa JP, Zanetti J, Oliveira LR et al (2010) Significance of topoisomerase IIIβ expression in breast ductal carcinomas: strong associations with disease-specific survival and metastasis. Hum Pathol 41:1624–1630
33. Urruticoechea A, Smith IE, Dowsett M (2005) Proliferation marker Ki-67 in early breast cancer. J Clin Oncol 23:7212–7220
34. Ban HS, Uno M, Nakamura H (2010) Suppression of hypoxia-induced HIF-1a accumulation by VEGFR inhibitors: different profiles of AAL993 versus SU5416 and KRN633. Cancer Lett 296:17–26
35. Qiao Q, Nozaki Y, Sakoe K et al (2010) NF-kB mediates aberrant activation of HIF-1 in malignant lymphoma. Exp Hemathol 38:1199–1208
36. Sharma V, Dixit D, Koul N et al (2011) Ras regulates interleukin-1β-induced HIF-1α transcriptional activity in glioblastoma. J Mol Med 89:123–136
37. Newton IP, Kenneth NS, Appleton PL et al (2010) Adenomatous polyposis coli and hypoxia-inducible factor-1α have an antagonistic connection. Mol Biol Cell 21:3630–3638
38. Raica M, Cimpeana AM, Ribatti D (2009) Angiogenesis in premalignant conditions. Eur J Cancer 45:1924–1934
39. Silva BB, Santos AR, Pires CG et al (2009) Effect of raloxifene on vascular endothelial growth factor expression in breast carcinomas of postmenopausal women. Cell Prolif 42:506–510
40. Giatromanolaki A, Koukourakis MI, Sivridis E et al (2000) Coexpression of MUC1 glycoprotein with multiple angiogenic factors in non-small cell lung cancer suggests coactivation of angiogenic and migration pathways. Clin Cancer Res 6:1917–1921
41. Bluff JE, Menakuru SR, Cross SS et al (2009) Angiogenesis is associated with the onset of hyperplasia in human ductal breast disease. Br J Cancer 101:666–672

Virchows Arch (2011) 459:377–382
DOI 10.1007/s00428-011-1144-4

ORIGINAL ARTICLE

Angiogenesis in triple-negative adenoid cystic carcinomas of the breast

Semir Vranic · Snjezana Frkovic-Grazio · Nurija Bilalovic · Zoran Gatalica

Received: 15 June 2011 / Revised: 19 August 2011 / Accepted: 22 August 2011 / Published online: 4 September 2011
© Springer-Verlag 2011

Abstract We compared microvascular density (MVD), lymph vessel density (LVD), and the expression of hypoxia pathway-associated proteins between primary triple-negative adenoid cystic carcinoma of the breast (TN-ACC) and grade-matched triple-negative breast carcinomas of no special type (TNBC). Twelve TN-ACC and 15 TNBC were investigated immunohistochemically for CD31, podoplanin (D2-40), von Hippel–Lindau protein (pVHL), and hypoxia-inducible factor-1alpha (HIF-1α) protein. All cases were lymph node negative (pN0). The study revealed a median MVD (CD31) of 34 vessels/mm^2 (mean ± SD, 41.33±6.5/mm^2) in the TN-ACC subgroup and a median of 55 microvessels (mean ± SD, 54.9±6.3/mm^2) in the TNBC subgroup. The median LVD (D2-40) was 10.5/mm^2 (mean ± SD, 11.9±1.5/mm^2) in the TN-ACC subgroup and 15.0/mm^2 (mean ± SD, 16.9± 2.5/mm^2) lymph vessels in the TNBC subgroup. The differences were not statistically significant (P=0.93, P= 0.67, respectively). pVHL was detectable in all TN-ACCs whereas two cases of TNBC had less than 5% of the positive cells. HIF-1α protein expression was significantly higher in the tumor cell population than in adjacent normal cells in both subgroups (P=0.009 for TNBC and P=0.028 for TN-ACC, respectively), but there was no significant difference between the two tumor groups. Up-regulation of the hypoxia-induced signaling is seen in both TN-ACC and grade-matched TNBC. Despite its perceived low malignant potential, TN-ACC of the breast does not differ in the number of blood and lymphatic vessels in comparison with the grade-matched TNBC. The reported biologic differences between TN-ACC and TNBC do not appear to result from neoangiogenesis.

Keywords Adenoid cystic carcinoma · Triple-negative carcinoma · Breast · Angiogenesis · Hypoxia

S. Vranic (✉) · N. Bilalovic
Department of Pathology,
Clinical Center of the University of Sarajevo,
Bolnička 25,
BA-71000 Sarajevo, Bosnia and Herzegovina
e-mail: semir.vranic@gmail.com

S. Vranic · Z. Gatalica
Department of Pathology,
Creighton University School of Medicine,
Omaha, NE, USA

S. Frkovic-Grazio
Department of Gynecological Pathology and Cytology,
University Clinical Hospital Ljubljana,
Ljubljana, Slovenia

S. Frkovic-Grazio
Department of Obstetrics and Gynecology,
University Clinical Hospital Ljubljana,
Ljubljana, Slovenia

Z. Gatalica
Caris Life Sciences,
Phoenix, AZ, USA

Introduction

Angiogenesis is one of the hallmarks of cancer [1, 2]. Tumor growth is angiogenesis dependent, and therefore, the forming of new blood vessels represents an essential step for survival in a hypoxic tumor environment [3, 4]. Additionally, the density of blood and lymphatic vessels correlates with aggressiveness and metastatic potential of breast carcinomas [5].

Many solid tumors adapt to hypoxia, defined as tissue oxygen level lower than 7% of concentration observed in normal and well-vascularized tissues [6]. The key regulator

of hypoxia-induced adaptation is hypoxia-inducible factor-1α (HIF-1α) [6]. Under normal oxygenation, HIF-1α is hydroxylated and slated for degradation via von Hippel–Lindau (VHL)-dependent ubiquitination pathway. However, under hypoxic or pseudohypoxic conditions, prolyl hydroxylase enzymes (PHD) are inhibited, and HIF-1α escapes degradation. Stable HIF-1α then translocates to the nucleus where it can heterodimerize with HIF-1β (*ARNT*) to form an active HIF transcription complex leading to expression of genes that can enhance survival in hypoxic conditions: glucose metabolism and angiogenesis, or reduce apoptosis [7]. *VHL* gene is an important regulator of HIF-1α and consequently tumor angiogenesis [8]. Its genetic alterations have been rarely seen in breast cancer [9–11].

Triple-negative, basal-like breast carcinoma represents a subtype of breast carcinoma linked to an aggressive clinical course and poor prognosis due to its high metastatic potential [12, 13]. In contrast, adenoid cystic carcinoma of the breast is a special type of triple-negative basal-like breast carcinoma associated with excellent prognosis [14–16].

The objectives of this study were to investigate microvascular density (MVD) and the hypoxia pathway proteins in triple-negative adenoid cystic carcinomas (TN-ACC) and compare the results with grade-matched triple-negative breast carcinomas of no special type (TNBC).

Materials and methods

Breast tissue samples

Formalin-fixed, paraffin-embedded tissues of 12 primary TN-ACC and 15 grade-matched TNBC were retrieved from the pathology archives of the authors' affiliated institutions. Both tumor types were graded using the Nottingham histologic grading as recommended by the 7th American Joint Committee on Cancer recommendations [17]. Both cohorts were previously characterized for various biologic characteristics and recently reported [16, 18, 19].

Immunohistochemistry

Endothelium of the tumor microvessels was highlighted using CD31 antibody (Table 1). MVD was quantified using Weidner et al. criteria [20]. Briefly, each slide was first scanned at low power to identify the areas with the highest number of blood vessels ("hot spot" areas). Three areas with the highest number of blood vessels were counted using a graticule that measured 1 mm^2.

Assessment of lymph vessel density (LVD) was performed in sections immunostained with podoplanin (D2-40, Table 1) using the same approach as in the assessment of MVD.

Table 1 Clones, dilutions, sources of antibodies, and types of tissue pretreatment used in the study

Antibody (clone)	Dilution	Source	Antigen retrieval (water bath)
CD31 (JC70A)	1:80	DakoCytomation	pH 9.0 EDTA (20 min)
Podoplanin (D2-40)	1:5	DakoCytomation	pH 9.0 EDTA (20 min)
VHL (Ig33)	1:100	LabVision	pH 6.0 citrate buffer (20 min)
HIF-1α (H1α 67)	1:1,000	AbCam	pH 6.0 citrate buffer (20 min)

pVHL was calculated as a percentage of positive tumor cells. Only membranous/cytoplasmic staining was considered specific.

For HIF-1α scoring, a median HIF-1α expression in normal/benign glands served as a cutoff point for evaluation in both subgroups. Only nuclear HIF-1α expression was considered specific [21].

Immunohistochemical assays for estrogen receptor (ER; clone 6F11, Ventana Medical Systems, Tucson, AZ; clone SP1, Lab Vision, Fremont, CA), progesterone receptor (PR; clone 16, Ventana Medical Systems; clone PgR636, Dako, Glostrup, Denmark), and Her-2/neu protein (Clone CB11, Ventana Medical Systems) were previously done and reported [16, 18]. Positive and negative controls for each marker were used according to the supplier's data sheets.

Statistical analysis

Mann–Whitney *U* test was used to compare the means of lymph vessel density and microvessel density between the subgroups. The continuous variables (CD31, D2-40, pVHL, HIF-1α) were divided into two categories according to the median values, and the associations between these variables and other clinicopathologic parameters were done using 2× 2 contingency tables and Fisher's exact test. A *P* value was set at <0.05. All statistical analyses were performed using the Statistical Package for Social Sciences software (v. 17.0; SPSS Inc., Chicago, IL).

Results

Patients' characteristics

All patients were women. The mean age of the TN-ACC patients was 59.6 years (range, 43–78 years) and 58.5 years (range, 43–76 years) for the TNBC patients.

Histopathologic and immunohistochemical characterization of TN-ACC and TNBC of the breast

Both cohorts have been previously studied for various biologic characteristics and recently reported [16, 18, 19]. Clinicopathologic characteristics of both cohorts are summarized in Table 2. Briefly, the subgroups were grade-matched triple-negative breast carcinomas (ER/PR/Her-2/neu negative), and all were lymph node negative (pNo).

Two of the TN-ACC cases had known distant metastases (to kidneys) [16, 22]. Status of the distant metastases was not known for the TNBC group.

Lymph vessel density and microvessel density in TN-ACC and TNBC of the breast

Evaluation of MVD revealed a median of 34 blood vessels/mm^2 (mean ± SD, 41.33±6.5) in the TN-ACC group and a median of 55 microvessels/mm^2 (mean ± SD, 54.9±6.3) in the TNBC group (Fig. 1a, b). The median LVD was 10.5/mm^2 (mean ± SD, 11.9±1.5) in the TN-ACC group and 15.0/mm^2 (mean ± SD, 16.9±2.5) in the TNBC group (Fig. 1c, d). The differences for both variables were not statistically significant between the groups (P=0.93 for MVD and P=0.67 for lymph vessel density, Mann–Whitney U test).

Unequivocal lymphatic or vascular invasion was not evident by either CD31 or D2-40 staining in any of the TN-ACC cases including two cases with distant metastases. In contrast, two TNBC cases exhibited unequivocal lymphatic and vascular invasion of which one had extensive peritumoral vascular invasion.

Table 2 Clinicopathologic characteristics of both cohorts

Characteristic	TN-ACC	TNBC
Tumor size		
<2 cm	3 (25%)	2 (18.2%)[a]
2–5 cm	7 (58.3%)	6 (54.5%)
>5 cm	2 (16.7%)	3 (27.3%)
Histologic grade[b]		
1	3 (25%)	2 (13.3%)
2	6 (50%)	8 (53.3%)
3	3 (25%)	5 (33.3%)
Axillary lymph nodes		
Axillary dissection	8 (66.7%)	12 (80%)
Sentinel lymph node biopsy	4 (33.3%)	3 (20%)
Type of surgery		
Mastectomy	8 (66.7%)	11 (73.3%)
Breast-conserving surgery	4 (33.3%)	4 (26.7%)

[a] Data were not available for four cases

[b] Both tumor types were graded using the Nottingham histologic grading

Cellular hypoxia pathway-associated proteins in TN-ACC and TNBC of the breast

pVHL expression was detectable in all TN-ACC cases (Fig. 2a). It was also demonstrable in the majority of the TNBC cases (Fig. 2b) with only two cases having less than 5% of the positive cells. The mean percentage of the pVHL positive cancer cells was 84% in TN-ACC and 71% in TNBC (P=0.42). Adjacent ductal epithelium retained pVHL expression in all cases when available for evaluation.

HIF-1α protein nuclear expression was rarely observed in normal breast epithelium with an average of 2% of the positive cells. In contrast, this protein was observed in all tumors with the mean percentage of positive tumor cells of 15% in TN-ACC and 17% in TNBC (Fig. 2c, d). This was statistically significant in both groups (P=0.009 for TNBC and P=0.028 for TN-ACC, respectively).

Correlation between the biologic variables and clinicopathologic parameters

HIF-1α protein expression was strongly associated with the tumor grade in the TNBC subgroup (P=0.025), while a trend towards a significant positive association was observed in the TN-ACC subgroup (P=0.08, Fisher's exact test). No other significant correlation was seen among the tested variables.

Discussion

The tumor growth and progression are directly dependent on the development of new blood vessels (angiogenesis) [3, 5]. It increases the opportunity of the tumor cells to enter the circulation and develop metastases, the most common cause of cancer-related mortality [5]. It is usually measured by microvessel density that correlates well with tumor aggressiveness [5]. Triple-negative basal-like breast carcinomas tend to have an aggressive behavior and poor outcome mainly due to their high metastatic potential [13]. This subtype is also characterized by higher microvessel density compared with the non-basal and the non-triple-negative breast carcinomas [13]. On the other hand, TN-ACC of the breast is well known to have an indolent clinical course with favorable outcome [14–16] despite molecular and gene expression profiling studies that revealed an unfavorable gene signature and molecular portrait compatible with that seen in highly aggressive triple-negative, basal-like breast carcinomas [23, 24]. Our study for the first time highlighted that the number of blood and lymphatic vessels did not differ significantly in the TN-ACC subgroup in comparison with grade-matched triple-negative breast carcinomas of no special type. These results indicate that the discrepancy in

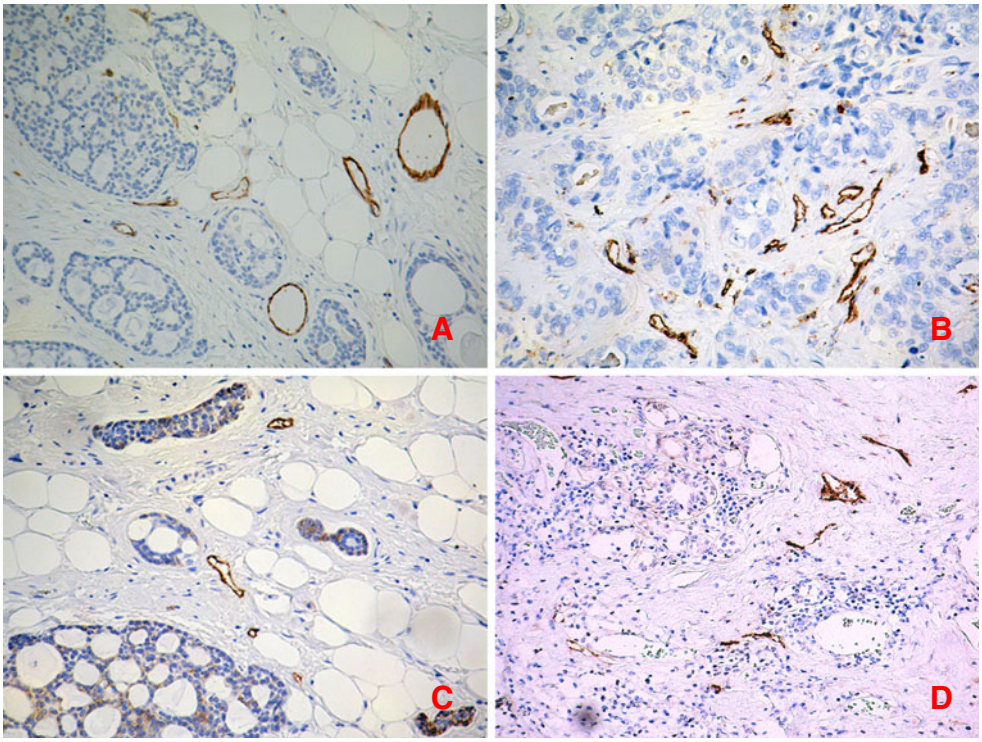

Fig. 1 Endothelium of the tumor microvessels highlighted using CD31 antibody in a case of triple-negative adenoid cystic carcinoma of the breast (**a**) and a case of triple-negative breast carcinoma (**b**); lymph vessel density measured by podoplanin (D2-40) in triple-negative adenoid cystic carcinoma (**c**) and triple-negative breast carcinoma (**d**) (×20)

clinical behavior and aggressiveness between TN-ACC and TNBC probably cannot be attributed to the blood and lymphatic vessel density.

Angiogenesis is closely regulated by cellular hypoxia [25]. Hypoxia occurs in many disease processes, and it is common in solid tumors due to the tumor outgrowing the existing vasculature [25]. Neoplasms surviving in the hypoxic environment are usually associated with aggressive behavior, increased tumor cell motility, metastasis, and poor outcome [26, 27]. Central to the hypoxic response of the

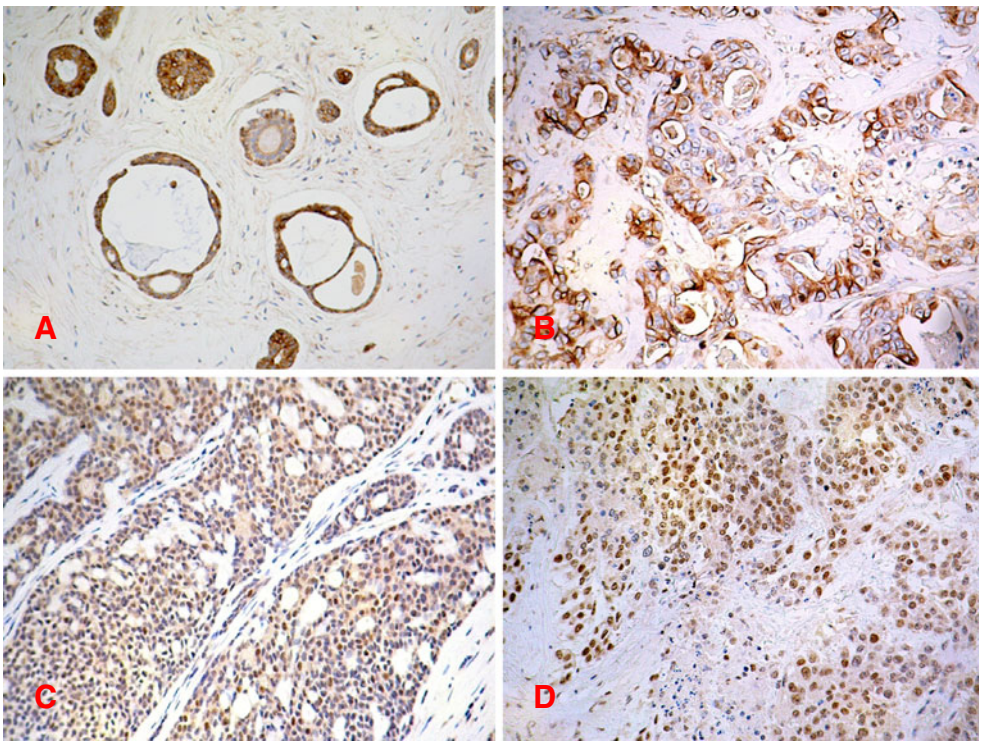

Fig. 2 pVHL was demonstrable in the majority of TN-ACCs (**a**) and triple-negative breast carcinomas (**b**); HIF-1α protein nuclear expression with moderate intensity in TN-ACC case (**c**) and triple-negative breast carcinoma (**d**) (×20)

tumor cells is the transcription factor HIF-1α [28]. Nuclear translocation of HIF-1α protein leads to the up-regulation of transcription of the genes involved in cell proliferation, angiogenesis, and glucose metabolism and is associated with tumor progression in various human tumors [7, 29]. In breast cancer, its deregulation is also associated with increased proliferation and angiogenesis, down-regulation of estrogen receptor, and shorter survival in patients with negative lymph nodes [27, 30–32]. Our study revealed that HIF-1α protein is commonly up-regulated in both TN-ACC and TNBC which is in line with the study of Rakha et al. that revealed activation of hypoxia-related proteins in TNBC [33]. Earlier studies also showed that up to 62% of all breast carcinomas are hypoxic if HIF-1α protein is used as a marker of hypoxia [6, 34]. The percentage of HIF-1α positivity in breast cancer tumor cells however varies between the studies due to the various cutoff values the investigators used [35, 36]. We observed low HIF-1α protein expression in benign/normal glands (~2%), which is in agreement with previous reports [28], and both of our tumor cohorts exhibited significantly higher percentages of positive cells. Concordant with our IHC results, we observed consistent overexpression of HIF-1α mRNA in three cases of breast ACC in various metastatic sites and overexpression of VEGFα mRNA in one case, using whole genome expression array (HumanHT-12 v4 beadChip, Illumina Inc., San Diego, CA) (Gatalica Z, unpublished observation).

Another important regulator of angiogenesis is the *VHL* gene (3p26-p25) [8]. Its product, VHL protein (pVHL), is a component of an Skp1–Cdc53–F-box (SCF)-like ubiquitin–ligase complex that targets the α-subunits of the hypoxia-inducible factor for poly ubiquitylation and proteasomal degradation [37]. Genetic alterations of the *VHL* gene have been linked to hereditary and sporadic clear cell renal cell carcinomas [38]. Earlier studies reported that *VHL* gene and pVHL are not commonly involved in breast cancer carcinogenesis [9–11]. Consistent with those studies, all TN-ACC and a majority of TNBC cases in our study retained pVHL expression. Furthermore, no 3p locus loss was observed in a series of breast ACC recently reported [39].

We conclude that up-regulation of the hypoxia-induced signaling is commonly seen in both TN-ACC and grade-matched TNBC when compared to the surrounding normal tissues. Despite its low malignant potential, TN-ACC of the breast does not differ in the number of blood and lymphatic vessels in comparison with the grade-matched TNBC.

Acknowledgments We are grateful to Ms. Mindee C. Kurtis, Creighton Medical Laboratories, Creighton University Medical Center (Omaha, NE) for excellent technical assistance.

Conflict of interest We declare that we have no conflict of interest.

References

1. Hanahan D, Weinberg RA (2011) Hallmarks of cancer: the next generation. Cell 144:646–674
2. Hanahan D, Weinberg RA (2000) The hallmarks of cancer. Cell 100:57–70
3. Folkman J (2007) Is angiogenesis an organizing principle in biology and medicine? J Pediatr Surg 42:1–11
4. Weinberg RA (2007) The biology of cancer. Garland Science, Taylor & Francis Group, LLC, New York
5. Weidner N (2004) The importance of tumor angiogenesis. Am J Clin Pathol 122:675–677
6. Lundgren K, Holm C, Landberg G (2007) Hypoxia and breast cancer: prognostic and therapeutic implications. Cell Mol Life Sci 64:3233–3247
7. Haase VH (2006) The VHL/HIF oxygen-sensing pathway and its relevance to kidney disease. Kidney Int 69:1302–1307
8. Calzada MJ (2010) Von Hippel-Lindau syndrome: molecular mechanisms of the disease. Clin Transl Oncol 12:160–165
9. Lantzsch T, Hefler L, Koelbl H, Lampe D (2002) Expression of von Hippel-Lindau gene protein in breast cancer tissue. Gynecol Oncol 84:186–187
10. Sourvinos G, Miyakis S, Liloglou TL, Field JK, Spandidos DA (2001) Von Hippel-Lindau tumour suppressor gene is not involved in sporadic human breast cancer. Tumour Biol 22:131–136
11. Corless CL, Kibel AS, Iliopoulos O, Kaelin WG Jr (1997) Immunostaining of the von Hippel-Lindau gene product in normal and neoplastic human tissues. Hum Pathol 28:459–464
12. Mohammed RA, Ellis IO, Mahmmod AM et al (2011) Lymphatic and blood vessels in basal and triple-negative breast cancers: characteristics and prognostic significance. Mod Pathol 24:774–785
13. Sabatier R, Jacquemier J, Bertucci F et al (2011) Peritumoural vascular invasion: a major determinant of triple-negative breast cancer outcome. Eur J Cancer Mar 8 doi:10.1016/j.ejca.2011.02.002
14. Khanfir K, Kallel A, Villette S et al (2011) Management of adenoid cystic carcinoma of the breast: a rare cancer network study. Int J Radiat Oncol Biol Phys (in press) May 11. doi:10.1016/j.ijrobp.2010.12.008
15. Ghabach B, Anderson WF, Curtis RE, Huycke MM, Lavigne JA, Dores GM (2010) Adenoid cystic carcinoma of the breast in the United States (1977 to 2006): a population-based cohort study. Breast Cancer Res 12:R54
16. Vranic S, Frkovic-Grazio S, Lamovec J et al (2010) Adenoid cystic carcinomas of the breast have low Topo IIα expression but frequently overexpress EGFR protein without EGFR gene amplification. Hum Pathol 41:1617–1623
17. Edge SB, Byrd DR (2010) AJCC cancer staging manual, 7th edn. Springer, Berlin
18. Zhang XT, Kang LG, Ding L, Vranic S, Gatalica Z, Wang ZY (2011) A positive feedback loop of ER-α36/EGFR promotes malignant growth of ER-negative breast cancer cells. Oncogene 30:770–780
19. Vranic S, Gurjeva O, Frkovic-Grazio S, Palazzo J, Tawfik O, Gatalica Z (2011) IMP3, a proposed novel basal phenotype marker, is commonly overexpressed in adenoid cystic carcinomas but not in apocrine carcinomas of the breast. Appl Immunohistochem Mol Morphol Mar 22 (in press) doi:10.1097/PAI.0b013e3182143399
20. Weidner N, Semple JP, Welgh WR, Folkman J (1991) Tumor angiogenesis and metastasis – correlation in invasive breast carcinoma. N Engl J Med 324:1–8
21. Yan M, Rayoo M, Takano EA, KConFab Investigators, Fox SB (2009) BRCA1 tumours correlate with a HIF-1alpha phenotype

and have a poor prognosis through modulation of hydroxylase enzyme profile expression. Br J Cancer 101:1168–1174
22. Vranic S, Bilalovic N, Lee LM, Kruslin B, Lilleberg SL, Gatalica Z (2007) PIK3CA and PTEN mutations in adenoid cystic carcinoma of the breast metastatic to kidney. Hum Pathol 38:1425–1431
23. Weigelt B, Geyer FC, Reis-Filho JS (2010) Histological types of breast cancer: How special are they? Mol Oncol 4:192–208
24. Weigelt B, Horlings HM, Kreike B et al (2008) Refinement of breast cancer classification by molecular characterization of histological special types. J Pathol 216:141–150
25. Otrock ZK, Hatoum HA, Awada AH et al (2009) Hypoxia-inducible factor in cancer angiogenesis: structure, regulation and clinical perspectives. Crit Rev Oncol Hemat 70:93–102
26. Voss MJ, Moller MF, Powe DG, Niggemann B, Zanker KS, Entschladen F (2011) Luminal and basal-like breast cancer cell show increased migration induced by hypoxia, mediated by an autocrine mechanism. BMC Cancer 11:158
27. Bos R, Zhong H, Hanrahan CF et al (2001) Levels of hypoxia-inducible factor-1 alpha during breast carcinogenesis. J Natl Cancer Inst 93:309–314
28. Kimbro KS, Simons JW (2006) Hypoxia-inducible factor-1 in human breast and prostate cancer. Endocr Relat Cancer 13:739–749
29. Carroll V, Ashcroft M (2006) Role of hypoxia-inducible factor (HIF)-1A versus HIF-2A in the regulation of HIF target genes in response to hypoxia, insulin-like growth factor-I, or loss of von Hippel-Lindau function: implications for targeting the HIF pathway. Cancer Res 66:6264–6270
30. Bos R, van Diest PJ, de Jong JS, van der Groep P, van der Valk P, van der Wall E (2005) Hypoxia-inducible factor-1alpha is associated with angiogenesis, and expression of bFGF, PDGF-BB, and EGFR in invasive breast cancer. Histopathology 46:31–36
31. Bos R, van der GP, Greijer AE et al (2003) Levels of hypoxia-inducible factor-1alpha independently predict prognosis in patients with lymph node negative breast carcinoma. Cancer 97:1573–1581
32. Ryu K, Park C, Lee Y (2011) Hypoxia-inducible factor 1 alpha represses the transcription of the estrogen receptor alpha gene in human breast cancer cells. Biochem Biophys Res Commun 407:831–836
33. Rakha EA, Elsheikh SE, Aleskandarany MA et al (2009) Triple-negative breast cancer: distinguishing between basal and nonbasal subtypes. Clin Cancer Res 15:2302–2310
34. Vleugel MM, Bos R, Buerger H et al (2004) No amplifications of hypoxia-inducible factor-1alpha gene in invasive breast cancer: a tissue microarray study. Cell Oncol 26:347–351
35. Trastour C, Benizri E, Ettore F et al (2007) HIF-1alpha and CA IX staining in invasive breast carcinomas: prognosis and treatment outcome. Int J Cancer 120:1451–1458
36. van der Groep P, Bouter A, Menko FH, van der Wall E, van Diest PJ (2008) High frequency of HIF-1alpha overexpression in BRCA1 related breast cancer. Breast Cancer Res Treat 111:475–480
37. Kaelin WG Jr (2002) Molecular basis of the VHL hereditary cancer syndrome. Nat Rev Cancer 2:673–682
38. Lin F, Shi J, Liu H et al (2008) Immunohistochemical detection of the von Hippel-Lindau gene product (pVHL) in human tissues and tumors: a useful marker for metastatic renal cell carcinoma and clear cell carcinoma of the ovary and uterus. Am J Clin Pathol 129:592–605
39. Lopez-Garcia MA, Wetterskog D, Lambros MB et al (2011) Genomic profiling of adenoid cystic carcinomas of the breast. Mod Pathol 24(suppl1):52A (meeting abstract 205)

Virchows Arch (2011) 459:383–390
DOI 10.1007/s00428-011-1143-5

ORIGINAL ARTICLE

Detection of Slit2 promoter hypermethylation in tissue and serum samples from breast cancer patients

Ga-Eon Kim · Kyung Hwa Lee · Yoo Duk Choi · Ji Shin Lee · Jae Hyuk Lee · Jong Hee Nam · Chan Choi · Min Ho Park · Jung Han Yoon

Received: 1 June 2011 / Revised: 9 August 2011 / Accepted: 21 August 2011 / Published online: 6 September 2011
© Springer-Verlag 2011

Abstract Promoter hypermethylation has been shown to be a common mechanism for inactivation of tumor suppressor genes in breast cancer. The aim of this study was to investigate the prevalence of Slit2 promoter hypermethylation in both the tumor and serum samples of breast cancer patients with ductal carcinoma in situ (DCIS) or invasive breast carcinoma (IBC). The methylation status of Slit2 was investigated in 210 tissue samples (15 breast with no pathological findings, 26 DCIS, and 169 IBC samples) and 123 corresponding serum samples (15 breast with no pathological findings, 26 DCIS, and 82 IBC samples) using methylation-specific polymerase chain reaction. Immunohistochemical staining for Slit2 was also performed using tissue microarray blocks to determine whether Slit2 promoter hypermethylation correlated with loss of Slit2 expression. Slit2 promoter hypermethylation was not detected in breast tissue and serum samples from patients with no pathological findings. DCIS or IBC showed a statistically higher frequency of Slit2 promoter hypermethylation compared to breast with no pathological findings in both the tissue and serum samples; however, there were no statistically significant differences between DCIS and IBC samples. Similar Slit2 promoter hypermethylation patterns were seen in the tissue samples and corresponding serum specimens ($p<0.001$). Slit2 promoter hypermethylation was associated with loss of Slit2 expression. These results suggest that Slit2 promoter hypermethylation appears to be responsible for functionally silencing Slit2 expression. Slit2 promoter hypermethylation may be considered as a possible serum marker for early detection of breast cancer.

Keywords Breast cancer · Slit2 · Methylation · Tissue · Serum · Biological marker

G.-E. Kim · K. H. Lee · Y. D. Choi · J. S. Lee · J. H. Lee · J. H. Nam · C. Choi
Department of Pathology,
Chonnam National University Medical School,
Gwangju, Republic of Korea

G.-E. Kim · K. H. Lee · Y. D. Choi · J. S. Lee · J. H. Lee · J. H. Nam · C. Choi · M. H. Park · J. H. Yoon
Research Institute of Medical Sciences,
Gwangju, Republic of Korea

M. H. Park · J. H. Yoon
Department of Surgery,
Chonnam National University Medical School,
Gwangju, Republic of Korea

J. S. Lee (✉)
Department of Pathology,
Chonnam National University Hwasun Hospital,
160, IIsim-ri, Hwasun-eup,
Hwasun-gun, Jeollanam-do 519-809, Republic of Korea
e-mail: jshinlee@hanmail.net

Introduction

DNA methylation is an enzyme-induced chemical modification that usually occurs in cytosine-guanine dinucleotide-rich areas (CpG islands) in the gene promoter regions. Hypermethylation of CpG islands in the gene promoter regions is generally associated with gene silencing due to the abrogation of gene transcription [1]. As promoter hypermethylation is an early event in carcinogenesis and is often present in the precursor lesions of a variety of cancers, DNA methylation could serve as a marker for the early diagnosis of cancer [2–4].

The presence of circulating tumor DNA in the blood (plasma/serum) of cancer patients has been described several years ago [5]. Circulating serum-methylated DNA

may potentially be a novel diagnostic marker for cancer. The use of methylated genes for aiding cancer diagnosis is based on the assumption that methylation at specific sites in the promoter regions of certain genes is confined to malignancy or premalignant lesions [6]. Many CpG islands have been identified to be hypermethylated in breast cancers, resulting in promoter inactivation and gene silencing [7–9]. Some studies evaluate the role of CpG island hypermethylation in tissue and blood samples as possible diagnostic markers in breast cancer patients [10–12]. In our recent studies, we have demonstrated that the quantitative detection of aberrant DNA methylation in tissue and serum samples may be a promising high-throughput approach for the diagnosis of invasive breast carcinoma (IBC) and ductal carcinoma in situ (DCIS) [13, 14]. However, 100% sensitivity could not be reached by increasing the number of genes analyzed, pointing to the fact that identification of additional genes that are selectively methylated in DCIS and IBC is necessary.

Slits are secreted proteins that regulate axon guidance, branching, and neuronal migration during development [15, 16]. The Slit gene family consists of three members, Slit1, Slit2, and Slit3. All of them are expressed in the nervous system, but Slit2 is also expressed in non-neuronal tissues such as lung, breast, kidney, and heart, suggesting innovative roles in addition to axon guidance [17]. Slits are ligands for transmembrane receptors, the Robo (roundabout) gene family [18]. Slit2 interacts with Robo1 to mediate repulsive cues in axon guidance [19], neuronal migration [20], and leukocyte chemotaxis [21].

Emerging evidence suggests that Slit2 appears to function as a novel tumor suppressor gene. Both Slit2 overexpression and Slit2-containing conditioned medium have been shown to suppress breast cancer cell growth in vitro [22]. Recently, we have demonstrated that Slit2 suppresses tumor growth in vivo by silencing Sdf1/Cxcr4 within breast epithelium [23]. Consistent with its tumor suppressor activity, Slit2 has been shown to be downregulated, primarily through DNA hypermethylation, in a number of cancer types [24–29]. There have been two studies evaluating the role of CpG island hypermethylation in breast cancer patients [22, 30]. Slit2 promoter hypermethylation was detected in 43–59% of breast cancers and, importantly, in their paired serum DNA, suggesting its potential as a noninvasive biomarker. However, these two studies have focused on invasive breast cancers. Furthermore, a relatively small numbers of cases were included in these studies.

In this study, we investigated the prevalence of Slit2 promoter hypermethylation in both the tumor and serum samples of breast cancer patients with DCIS or IBC. We also studied the expression of Slit2 protein by immunohistochemistry and compared its expression with methylation status of Slit2.

Materials and methods

Tissue and serum samples

Between March 2008 and December 2008, a group of 195 women (mean age=51 years, range 25–82 years) with breast cancer (26 DCIS and 169 IBC cases) were selected for this study. The tissue and serum samples were provided by the Chonnam National University Hwasun Hospital National Biobank of Korea, a member of the National Biobank of Korea, which is supported by the Ministry of Health, Welfare, and Family Affairs. Serum was separated from blood before surgery. A total of 5 mL blood samples were collected in EDTA-free tubes. The tubes were coagulated during approximately 1 h, after which the serum samples were centrifuged at 3,000×*g* (15 min) at 4°C, and supernatant was carefully transferred into 2-mL microtubes. Serum samples were kept at −160°C until their analysis. All samples were obtained with informed consent under the institutional review board-approved protocols. Clinicopathologic parameters evaluated in each IBC case included the patient's age at initial diagnosis, histologic type, tumor size, nodal status, Notthingham combined histologic grade, stage, hormone receptor status (estrogen receptor-α (ER-α) and progesterone receptor (PR)), and HER-2 expression (Table 1). Positivity for ER-α or PR was defined as the detection of at least 10% of invasive tumor cells showing nuclear staining. HER-2 immunostaining was considered positive when strong (3+) membranous staining was observed in at least 30% of tumor cells, whereas cases with 0 to 2+ were regarded as negative. All the IBC patients had never received any previous chemotherapy or radiotherapy. By the World Health Organization criteria [31], there were 3 low-grade DCISs, 19 intermediate-grade DCISs, and 4 high-grade DCISs. Fifteen normal breast tissue samples were taken from women with no pathological breast lesions.

Of the 210 tissue samples, 123 (comprising of 15 breasts with no pathological findings, 26 DCIS, and 82 IBC samples) had paired serum samples available for analysis.

DNA extraction, sodium bisulfite treatment, and MSP analysis

For tissue DNA extraction, one 5-μm tissue section was deparaffinized by treatment with xylene (2×, 10 min each). Using a hematoxylin–eosin-stained slide of an adjacent section as a guide, the region of interest was manually scraped off to ensure a cell population of more than 70% target cells in each preparation. The scraped tissue was extracted in 27 μl TNES (10 mM Tris, pH 8.0, 150 mM NaCl, 2 mM EDTA, 1% SDS) containing 3 μl proteinase K for 4 h at 52°C. The tissue extract was heat inactivated at

Table 1 Relationship between invasive breast carcinoma tissue samples showing Slit2 promoter hypermethylation and different clinicopathological parameters

Characteristics	Cases *N* (%)	Slit2 methylation *N* (%)	*P* value[a]
Age (years)			<0.05
≤51	98 (58.0)	40 (40.8)	
>51	71 (42.0)	43 (60.6)	
Histopathologic type			ns
Invasive ductal carcinoma, NOS	153 (90.4)	75 (49.0)	
Invasive lobular carcinoma	4 (2.4)	3 (75.0)	
Invasive micropapillary carcinoma	2 (1.2)	1 (50.0)	
Medullary carcinoma	4 (2.4)	2 (50.0)	
Mucinous carcinoma	5 (3.0)	2 (40.0)	
Metaplastic carcinoma	1 (0.6)	0 (0)	
Tumor size (cm)			ns
≤2	80 (47.3)	36 (45.0)	
2–5	81 (47.9)	43 (53.1)	
>5	8 (4.8)	4 (50.0)	
Status of nodal metastasis			ns
0	88 (52.1)	44 (50.0)	
1–3	52 (30.8)	25 (48.1)	
4–9	17 (10.1)	10 (58.8)	
≥ 10	12 (7.0)	4 (33.3)	
Histological grade[b]			ns
1	26 (15.4)	10 (38.5)	
2	72 (42.6)	36 (50.0)	
3	67 (39.6)	36 (53.7)	
Stage			
I	51 (30.2)	26 (51.0)	ns
II	87 (51.5)	43 (49.4)	
III	31 (18.3)	14 (45.2)	
Estrogen receptor-α			< 0.05
Negative	77 (45.6)	31 (40.3)	
Positive	92 (54.4)	52 (56.5)	
Progesterone receptor			ns
Negative	76 (45.0)	37 (48.7)	
Positive	93 (55.0)	46 (49.5)	
HER-2			ns
Negative	131 (77.5)	66 (50.4)	
Positive	38 (22.5)	17 (44.7)	

NOS not otherwise specified, *ns* not significant

[a]Analyzed by χ^2 test

[b]All invasive breast carcinomas except medullary carcinoma were graded by Nottingham combined histologic grade system

99°C for 7 min and clarified by centrifugation at 13,000 rpm for 30 s. The supernatant was used directly as a source of DNA. DNA from serum samples (200 μl per column) was obtained by using i-genomic Blood DNA Extraction Mini Kit (iNtRON Biotechnology Inc., Seoul, Korea) according to the manufacturer's recommendations. A final elution volume of 50 μl was obtained.

The extracted tissue and serum DNA was treated with sodium bisulfite using the EZ DNA MethylationTM Kit (Zymo Research, Orange, CA), converting all unmethylated, but not methylated, cytosine to uracil. All bisulfite-modified DNA were resuspended in 10 μl of elution buffer and stored at −20°C until subsequent methylation-specific polymerase chain reaction (MSP).

For the MSP, 2 μl sodium bisulfite-treated DNA was added to 23 μl of reaction buffer [1.25 mM dNTP, 16.6 mM $(NH_4)_2SO_4$, 67 mM Tris, pH 8.8, 6.7 mM $MgCl_2$, 10 mM β-mercaptoethanol, 0.1% DMSO, and 1.25 U of Platinum Tag (Sigma, St. Louis, MO)] containing 100 ng each of forward and reverse primers specific to the unmethylated and methylated DNA sequences. The forward and reverse primers for the methylated Slit2 sequence were 5′-GGG AGG CGG GAT TGT TTA G-3′ and 5′-CAT AAC GCG CGA AAA TAC AC-3′, respectively. The forward and

reverse primers for the unmethylated sequence were 5′-GTG GGA GGT GGG ATT GTT TA-3′and 5′-ACC TCT CCC TCA CCC TCA AC-3′, respectively. The PCR amplification protocol was as follows: at 95°C for 10 min, then denatured at 94°C for 45 s, annealing at 52°C for 45 s, extension at 72°C for 45 s for 30 cycles followed by a 5-min final extension. Primers and PCR conditions used for the MSP assay of Slit2 have been previously described [27]. For each MSP reaction, MDA-MB-231 breast cancer cell line DNA treated in vitro with SssI methyltransferase (New England Biolabs, Hertfordshire, UK) as a positive control for methylated reaction and normal lymphocyte DNA as a positive control for unmethylated reaction and water with no DNA template as a control for contamination were included. After amplification, each PCR product was electrophoresed on a 2% agarose gels, stained with ethidium bromide, and visualized under UV illumination.

Tissue microarray construction

Tissue microarray was constructed with a custom-built precision instrument (Beecher Instruments, Silver Spring, MD). Hematoxylin- and eosin-stained sections were reviewed, and the area of interest was marked on the slide. Three cores of 2.0 mm in diameter were punched out of the donor block and placed at a distance of 0.2 mm in the recipient block.

Immunohistochemical analysis of Slit2 expression

Automated immunohistochemical staining for Slit2 was performed using the Bond-max system (Leica Microsystems, Bannockburn, IL), which is able to process up to 30 slides at a time. Slides were labeled and dried for 1 h at 60° C. Slides carrying tissue sections cut from paraffin-embedded tissue microarray blocks were labeled and dried for 1 h at 60°C. These slides were then covered by Bond Universal Covertiles (Leica Microsystems) and placed into the Bond-max instrument. All subsequent steps were performed by the automated instrument according to the manufacturer's instructions (Leica Microsystems), in the following order: (1) deparaffinization of tissue on the slides with Bond Dewax Solution (Leica Microsystems) at 72°C for 30 min; (2) heat-induced epitope retrieval (antigen unmasking) with Bond Epitope Retrieval Solution 1 (Leica Microsystems) for 20 min at 100°C; (3) peroxide block placement on the slides for 5 min at ambient temperature; and (4) incubation with Slit2 (1:400 dilution, Chemicon, Temecula, CA) primary antibodies, for 15 min at ambient temperature; (5) incubation with Post Primary reagent (Leica Microsystems) for 8 min at ambient temperature, followed by washing with Bond Wash solution (Leica Microsystems) for 6 min; (6) Bond Polymer (Leica Microsystems) placement on the slides for 8 min at ambient temperature, followed by washing with Bond Wash and distilled water for 4 min; (7) color development with DAB (3,3′-diaminobenzidine tetrahydrochloride) as a chromogen for 10 min at ambient temperature; and (8) hematoxylin counterstaining for 5 min at ambient temperature, followed by mounting of the slides. For negative controls, sections were treated similarly with the exception of the primary antibody. Tissue microarrays were digitized (Aperio Technologies, Vista, CA), and cytoplasmic immunoreactivity of Slit2 expression was scored. In brief, the proportion score (the estimated percentage of cells staining positively: 0, none; 1, <1%; 2, 1–10%; 3, 10–30%; 4, 30–60%; 5, >60%) is added to the average staining intensity score (0, no staining; 1, weak; 2, intermediate; 3, strong). These values were added together to provide a single integrated score for Slit2, and the average data were used for further analysis. Tumors having a final staining score of >2 were considered as positive [23].

Statistical analysis

The χ^2 test was used for group comparison. For the statistical analysis, a two-sided p value <0.05 was considered to indicate statistical significance. Data were analyzed using the SPSS software (version 13.5 for Windows; SPSS INC., Chicago, IL).

Results

Frequency of Slit2 promoter hypermethylation in tissue and serum samples

Slit2 promoter hypermethylation was detected in 45.2% (12 of 26) of DCIS and 49.1% (83 of 169) of IBC tissue samples. No hypermethylation was detected in breasts with no pathological findings. Representative results of the MSP assay are shown in Fig. 1. The frequency of Slit2 promoter hypermethylation was found to progressively increase along the continuum from normal breast tissue to IBC tissue samples ($p<0.001$). DCIS and IBC tissue samples showed a statistically higher frequency of Slit2 promoter hypermethylation compared to that in breasts with no pathological findings ($p<0.01$ and $p<0.001$, respectively). On the contrary, methylation frequency between DCIS and IBC tissue samples was not statistically different. Although not statistically significant, the incidence of Slit2 promoter hypermethylation was higher in high nuclear grade DCIS tissue sample: 33.3% (one of three) for grade 1, 42.1% (eight of 19) for grade 2, and 75.0% (three of four) for grade 3.

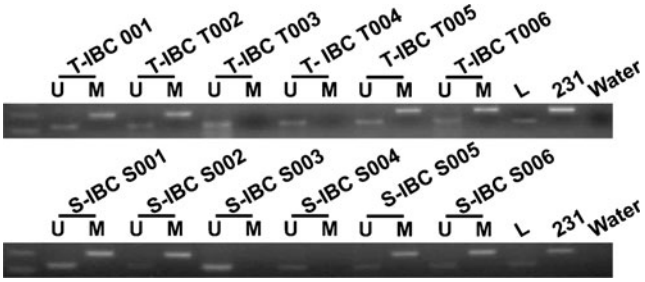

Fig. 1 Representative results of methylation-specific PCR analysis for Slit2 in tissue (*T*) and serum (*S*) samples of invasive breast carcinoma (*IBC*) patients. Lanes *U* and *M* correspond to unmethylated and methylated DNA, respectively. DNA from normal lymphocytes (*L*) and MDA-MB-231 (231) breast cancer cell lines served as positive controls for unmethylated and methylated genes, respectively. Water served as a control for contamination

We next assessed the relationship between the methylation status of Slit2 and clinicopathologic factors for IBC (Table 1). With the exception of age and ER-α, no other risk factors showed a significant association with promoter hypermethylation of Slit2. Slit2 methylation was associated with older patient age at diagnosis ($p<0.05$). Slit2 hypermethylation was more frequently associated with ER-α-positive IBC ($p<0.05$).

Next, serum DNA was analyzed for presence of methylation, using the same PCR-based methylation assay performed in tissue DNA. Of the 210 tissue samples, 123 had paired serum samples available for analysis. Slit2 promoter hypermethylation was detected in 0% (0 of 15) of breasts with no pathological findings, 38.5% (10 of 26) of DCIS, and 45.1% (37 of 82) of IBC serum samples. DCIS and IBC serum samples showed a statistically higher frequency of Slit2 promoter methylation compared to that in breasts with no pathological findings ($p<0.01$ and $p<0.001$, respectively). We found a similar pattern of Slit2 methylation changes between the serum samples and their paired tissues ($p<0.001$) (Table 2). In 47 patients, the Slit2 promoter hypermethylation was detected in both the DCIS or IBC tissue samples and in their corresponding serum samples. In 10 patients, the hypermethylated Slit2 promoter was present in tumor tissue samples but not in the paired serum samples. The Slit2 promoter hypermethylation was never detected in the serum samples if it was not present in the tumor tissue samples.

Immunohistochemical analysis of Slit2 expression

To determine whether the Slit2 promoter hypermethylation was correlated with the loss of Slit2 expression, immunohistochemical staining using an anti-Slit2 antibody was carried out in all the tissue samples that were subjected to methylation analysis in this study. With the exception of five IBC cases, immunohistochemistry results were interpretable in all the cases. Representative results of Slit2 immunohistochemistry are shown in Fig. 2. In all of the 15 breasts with no pathological findings, mammary epithelium including myoepithelial cells showed cytoplasmic immunoreactivity for Slit2. Slit2 immunoreactivity was detected in a subset of DCIS and IBC. Slit2 immunoreactivity was detected exclusively in the cytoplasm of the tumor cells, whereas the stroma was either negative or weakly positive. When DCIS and invasive carcinomas coexisted, Slit2 immunostaining in DCIS was usually equal to the staining of the corresponding invasive carcinomas. Loss of Slit2 expression (negative) in tumor cells was observed in 42.3% (11 of 26) of DCIS and 42.1% (69 of 164) of IBC tissue samples. When the Slit2 expression was compared with the methylation status of Slit2, Slit2 expression was more frequently lost in breast tissue samples displaying methylation ($p<0.01$ for DCIS and $p<0.001$ for IBC, respectively; Table 3).

Discussion

Slit2 can act as a tumor suppressor gene. Previous studies have shown that Slit2 promoter region was hypermethylated in various types of human cancers. In the present study, promoter hypermethylation of Slit2 was examined in both the tumor and serum samples of breast cancer patients with DCIS or IBC. We found that Slit2 is frequently hypermethylated in DCIS and IBC and Slit2 promoter hypermethylation correlates with loss of Slit2 expression.

The Slit family of large extracellular matrix secreted and membrane-associated glycoproteins are known to be important mediators of the repulsive cues on axons and growth cones during neural development [15, 16]. Human Slits (Slit1, Slit2, and Slit 3) are candidate ligands for the repulsive guidance receptors, the Robo gene family. Slit–Robo

Table 2 Results of Slit2 promoter hypermethylation in ductal carcinoma in situ or invasive breast carcinoma tissue samples and their corresponding serum samples

	Serum samples		*P* value[a]
	Slit2 unmethylated	Slit2 methylated	
Slit2 unmethylated in tissue samples	51	0	<0.001
Slit2 methylated in tissue samples	10	47	

[a]Analyzed by χ^2 test

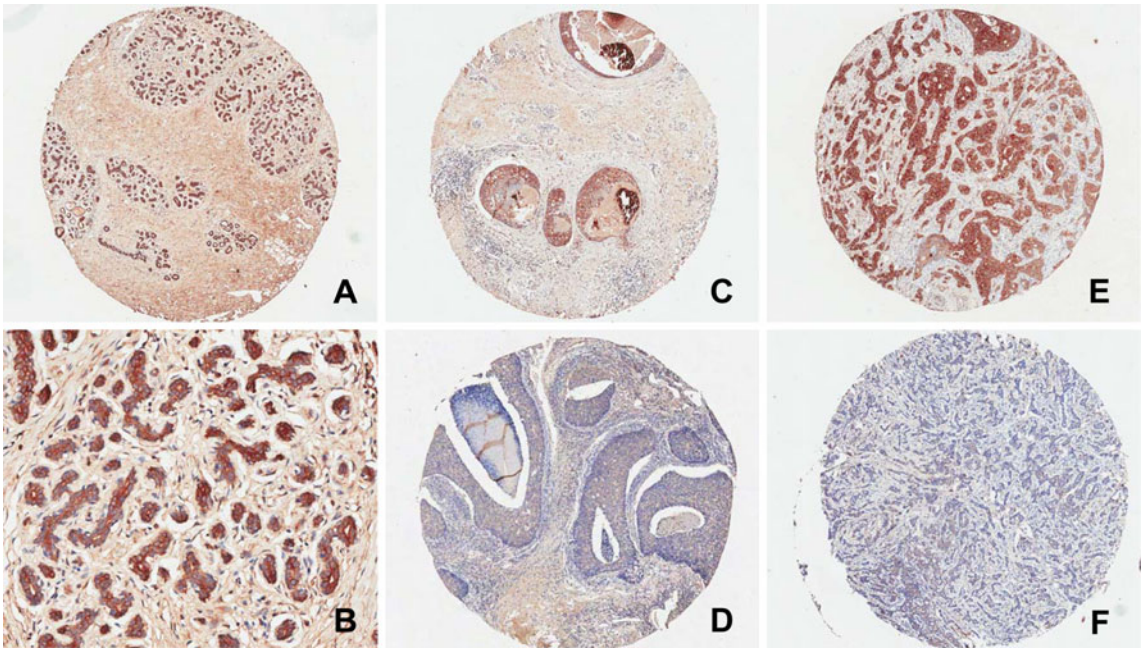

Fig. 2 Positive and negative immunohistochemical staining of Slit2 in the breast with no pathological findings, DCIS, and IBC. Breast tissue with no pathological findings tissue showed strong, diffuse cytoplasmic staining representing a positive expression of Slit2 (**a**, **b**). DCIS (**c**) and IBC (**e**) showed strong positivity in Slit2 unmethylated samples. In DCIS (**d**) and IBC (**f**) displaying methylation, loss of Slit2 expression was observed

interactions mediate the repulsive cues on axons and growth cones during neural development [18]. Slit–Robo signaling, however, is not restricted to development, and loss of these cues likely plays an important role during tumor progression [27].

Ectopic expression of Slit2 in several breast cancer cell lines suppressed growth and reduced colony formation abilities. Additionally, secreted Slit2 in conditioned medium from Slit2-transfected COS-7 cells reduced the cell number and growth of these breast cancer cell lines [22]. Recently, we have observed that loss of Slit2 in human breast carcinoma cells results in upregulation of the Sdf1 and Cxcr4 signaling axis [23]. The interaction of Sdf1 and Cxcr4 promotes cell growth, enhances tumor migration and invasion, and contributes to tumor metastasis within the tumor microenvironment [32, 33].

Accumulation of genetic and epigenetic alterations results in the development of breast carcinoma [34]. It is becoming increasingly apparent that methylation of CpG islands in promoter regions of tumor suppressor genes is a major epigenetic mechanism leading to inactivation of these genes [1]. Earlier studies have also reported a high frequency of Slit2 promoter hypermethylation in a broad spectrum of tumors including breast cancer [20, 24–30]. Dallol et al. detected hypermethylation of Slit2 in 43.4% (23/53) of invasive ductal breast carcinoma samples [22]. Sharma et al. also detected hypermethylation of Slit2 in 58.3% (21/36) of breast cancer lesions [30]. In this study, which included 169 IBC cases, we identified Slit2 promoter hypermethylation in 49.1% of IBC tissue samples.

Since breast cancer is curable if detected early, promoter hypermethylation for the detection of DCIS constitutes an approach that merits further investigation. To the best of our knowledge, there are no data available on Slit2 promoter hypermethylation in DCIS patients. In this study, Slit2 promoter hypermethylation was seen in 45.2% of DCIS

Table 3 Slit2 expression in ductal carcinoma in situ or invasive breast carcinoma tissue samples according to Slit2 promoter hypermethylation status

	Ductal carcinoma in situ			Invasive breast carcinoma[a]		
	Slit2 negative	Slit2 positive	*P* value[a]	Slit2 negative	Slit2 positive	*P* value[a]
Slit2 unmethylated	2 (14.3%)	12 (85.7%)	< 0.01	13 (15.9%)	69 (84.1%)	<0.001
Slit2 methylated	9 (75.0%)	3 (25.0%)		56 (68.3%)	26 (31.7%)	

[a] Analyzed by χ^2 test

tissue samples. Methylation frequency in DCIS and IBC tissue samples was not statistically different. These findings suggest that Slit2 promoter hypermethylation is an early event in breast carcinogenesis, and it is a good candidate for DNA methylation-based molecular diagnostic markers for DCIS. Consistent with our results, previous studies have reported the detection of promoter hypermethylation of other genes in breast tissue samples from patients with DCIS [12, 35, 36].

Previous studies have reported that Slit2 promoter hypermethylation is associated with loss of Slit2 expression [22]. In this study, we have demonstrated a significant correlation between the promoter hypermethylation of Slit2 and the data obtained from the immunohistochemical analyses. Promoter hypermethylation of Slit2 resulted in loss of Slit2 protein expression in the tissue samples displaying methylation. These data provide evidence that Slit2 promoter hypermethylation is a major mechanism involved in Slit2 gene inactivation, resulting in impaired Slit2 function during the development of breast cancer. However, DCIS or IBC without Slit hypermethylation were also negative for Slit2 expression. These observations suggested that promoter hypermethylation is not the only mechanism of silencing of Slit2 gene. Other mechanism appears to be implicated in the Slit2 gene silencing in such tumors.

Indirect diagnostic biomarkers from blood may offer the best potential for use in screening of cancer. Recently, circulating tumor DNA has been identified in the serum and plasma from patients with various cancers [5]. These circulating nucleic acids have demonstrated similar alterations in methylation as those found in primary breast cancer [12]. Identification of these methylation events in the serum and plasma samples may be a useful tool in breast cancer detection [10–12, 14]. Sharma et al. also carried out Slit2 promoter methylation analysis in 36 primary breast cancers and paired sera [30]. Promoter hypermethylation of Slit2 was seen in 58.3% of breast cancers, and complete concordance was observed. This study focused on invasive breast cancers and did not include DCIS cases. Of the 210 tissue samples used in this study, 123 had paired serum samples available for analysis. Slit2 promoter hypermethylation was detected in 0% (0 of 15) of breasts with no pathological findings, 38.5% (10 of 26) of DCIS, and 45.1% (37 of 82) of IBC serum samples. We found a similar pattern of Slit2 methylation changes between the serum samples and their paired tissues. The results of our study show that serum samples represent the hypermethylation status of tissue samples well, given the high concordance. These results are in accordance with the previous studies and strengthen the evidence that methylated serum DNA is tumor derived. Because single gene methylation has not been specific enough to be used for screening, a panel of candidate hypermethylated genes with optimal sensitivity and specificity for DCIS and IBC are necessary. Therefore, Slit2 is a good candidate for the panel of methylation markers in detection of IBC and its precursor DCIS in the serum samples.

However, our study had some important limitations; the number of patients with DCIS or no pathological breast lesions was relatively small. This study did not include benign diseases. Certain benign diseases, especially benign tumors, may also exhibit altered gene methylation [37]. Therefore, additional studies are needed to elucidate the role of Slit2 promotor hypermethylation as a tool for detection of DCIS/IBC in the serum samples.

Conflicting results have been reported about the correlation between detection of methylated genes and clinical or histopathological features. In the present study, no other risk factors showed a significant association with promoter hypermethylation of Slit2 with the exception of age and ER-α. On the contrary, Sharma et al. did not find any significant association of Slit2 promoter hypermethylation with clinicopathological features including age and ER-α status [30].

In conclusion, we have shown that Slit2 promoter hypermethylation occurred almost exclusively in IBC and its precursor DCIS. Slit2 promoter hypermethylation was associated with loss of Slit2 expression. The serum samples represented the Slit2 hypermethylation status of tissue samples well. Our results suggest that Slit2 promoter hypermethylation appears to be responsible in functionally silencing Slit2 expression. Slit2 promoter hypermethylation may be considered as a possible serum marker for early detection of breast cancer.

Acknowledgements This study was supported by a grant (CRI10056-1) from Chonnam National University Hospital Research Institute of Clinical Medicine.

We have no conflict of interests to declare.

References

1. Baylin SB (2005) DNA methylation and gene silencing in cancer. Nat Clin Pract Oncol Suppl 1:4–11
2. Brooks JD, Weinstein M, Lin X et al (1998) CG island methylation changes near the GSTP1 gene in prostatic intraepithelial neoplasia. Cancer Epidemiol Biomarkers Prev 7:531–536
3. Lamy A, Sesboue R, Bourguignon J et al (2002) Aberrant methylation of the CDKN2a/p16INK4a gene promoter region in preinvasive bronchial lesions: a prospective study in high-risk patients without invasive cancer. Int J Cancer 100:189–193
4. Kim JH, Choi YD, Lee JS et al (2010) Assessment of DNA methylation for the detection of cervical neoplasia in liquid-based cytology specimens. Gynecol Oncol 116:99–104
5. Anker P, Mulcahy H, Chen XQ et al (1999) Detection of circulating tumour DNA in the blood (plasma/serum) of cancer patients. Cancer Metastasis Rev 18:65–73
6. Duffy MJ, Napieralski R, Martens JW et al (2009) Methylated genes as new cancer biomarkers. Eur J Cancer 45:335–346

7. Wajed SA, Laird PW, DeMeester TR (2001) DNA methylation: an alternative pathway to cancer. Ann Surg 234:10–20
8. Momparler RL, Bovenzi V (2001) DNA methylation and cancer. J Cell Physiol 183:145–154
9. Lee JS, Lo PK, Fackler MJ et al (2007) A comparative study of Korean with Caucasian breast cancer reveals frequency of methylation in multiple genes correlates with breast cancer in young, ER, PR-negative breast cancer in Korean women. Cancer Biol Ther 6:1114–1120
10. Dulaimi E, Hillinck J, Ibanez de Caceres I et al (2004) Tumor suppressor gene promoter hypermethylation in serum of breast cancer patients. Clin Cancer Res 10:6189–6193
11. Hoque MO, Feng Q, Toure P et al (2006) Detection of aberrant methylation of four genes in plasma DNA for the detection of breast cancer. J Clin Oncol 24:4262–4269
12. Mirza S, Sharma G, Prasad CP et al (2007) Promoter hypermethylation of TMS1, BRCA1, ERalpha and PRB in serum and tumor DNA of invasive ductal breast carcinoma patients. Life Sci 81:280–287
13. Lee JS, Fackler MJ, Teo WW et al (2008) Quantitative promoter hypermethylation profiles of ductal carcinoma in situ in North American and Korean women: Potential applications for diagnosis. Cancer Biol Ther 7:1398–1406
14. Kim JH, Shin MH, Kweon SS et al (2010) Evaluation of promoter hypermethylation detection in serum as a diagnostic tool for breast carcinoma in Korean women. Gynecol Oncol 118:176–181
15. Yuan W, Zhou L, Chen JH et al (1999) The mouse SLIT family: secreted ligands for ROBO expressed in patterns that suggest a role in morphogenesis and axon guidance. Dev Biol 212:290–306
16. Brose K, Bland KS, Wang KH et al (1999) Slit proteins bind Robo receptors and have an evolutionarily conserved role in repulsive axon guidance. Cell 96:795–806
17. Wu JY, Feng L, Park HT et al (2001) The neuronal repellent Slit inhibits leukocyte chemotaxis induced by chemotactic factors. Nature 410:948–952
18. Stein E, Tessier-Lavigne M (2001) Hierarchical organization of guidance receptors: silencing of netrin attraction by slit through a Robo/DCC receptor complex. Science 291:1928–1938
19. Dickson BJ, Gilestro GF (2006) Regulation of commissural axon pathfinding by slit and its Robo receptors. Annu Rev Cell Dev Biol 22:651–675
20. Wu W, Wong K, Chen J et al (1999) Directional guidance of neuronal migration in the olfactory system by the protein Slit. Nature 400:331–333
21. Prasad A, Qamri Z, Wu J et al (2007) Slit-2/Robo-1 modulates the CXCL12/CXCR4-induced chemotaxis of T cells. J Leukoc Biol 82:465–476
22. Dallol A, Da Silva NF, Viacava P et al (2002) SLIT2, a human homologue of the Drosophila Slit2 gene, has tumor suppressor activity and is frequently inactivated in lung and breast cancers. Cancer Res 62:5874–5880
23. Marlow R, Strickland P, Lee JS et al (2008) SLITs suppress tumor growth in vivo by silencing Sdf1/Cxcr4 within breast epithelium. Cancer Res 68:7819–7827
24. Dallol A, Krex D, Hesson L et al (2003) Frequent epigenetic inactivation of the SLIT2 gene in gliomas. Oncogene 22:4611–4616
25. Dallol A, Morton D, Maher ER et al (2003) Latif F. SLIT2 axon guidance molecule is frequently inactivated in colorectal cancer and suppresses growth of colorectal carcinoma cells. Cancer Res 63:1054–1058
26. Astuti D, Da Silva NF, Dallol A et al (2004) SLIT2 promoter methylation analysis in neuroblastoma, Wilms' tumour and renal cell carcinoma. Br J Cancer 90:515–521
27. Narayan G, Goparaju C, Arias-Pulido H et al (2006) Promoter hypermethylation-mediated inactivation of multiple Slit–Robo pathway genes in cervical cancer progression. Mol Cancer 15:5–16
28. Dunwell TL, Dickinson RE, Stankovic T et al (2009) Frequent epigenetic inactivation of the SLIT2 gene in chronic and acute lymphocytic leukemia. Epigenetics 4:265–269
29. Jin J, You H, Yu B et al (2009) Epigenetic inactivation of SLIT2 in human hepatocellular carcinomas. Biochem Biophys Res Commun 379:86–91
30. Sharma G, Mirza S, Prasad CP et al (2007) Promoter hypermethylation of p16INK4A, p14ARF, CyclinD2 and Slit2 in serum and tumor DNA from breast cancer patients. Life Sci 80:1873–1881
31. Tavasassoli FA, Devilee P (2003) Intraductal proliferative lesions. In: Tavassoli FA et al (eds) World Heath Organization Classification of Tumours. Pathology and Genetics of Tumours of the Breast and Female Genital Organs. IARC, Lyon, pp 63–73
32. Burger JA, Kipps TJ (2006) CXCR4: a key receptor in the crosstalk between tumor cells and their microenvironment. Blood 107:1761–1767
33. Alsayed Y, Ngo H, Runnels J et al (2007) Mechanisms of regulation of CXCR4/SDF-1 (CXCL12)-dependent migration and homing in multiple myeloma. Blood 109:2708–2717
34. Baylin SB, Chen WY (2005) Aberrant gene silencing in tumor progression: implications for control of cancer. Cold Spring Harb Symp Quant Biol 70:427–433
35. Fackler MJ, McVeigh M, Evron E et al (2003) DNA methylation of RASSF1A, HIN-1, RAR-beta, Cyclin D2 and Twist in in situ and invasive lobular breast carcinoma. Int J Cancer 107:970–975
36. Lee JS (2007) GSTP1 promoter hypermethylation is an early event in breast carcinogenesis. Virchows Arch 450:637–642
37. Kim JH, Choi YD, Lee JS et al (2009) Borderline and malignant phyllodes tumors display similar promoter methylation profiles. Virchows Arch 455:469–475

Virchows Arch (2011) 459:391–398
DOI 10.1007/s00428-011-1145-3

ORIGINAL ARTICLE

Metastasis to sentinel lymph nodes in breast cancer is associated with maturation arrest of dendritic cells and poor co-localization of dendritic cells and CD8$^+$ T cells

Aaron Scott Mansfield · Paivi Heikkila · Karl von Smitten · Jukka Vakkila · Marjut Leidenius

Received: 22 June 2011 / Revised: 20 August 2011 / Accepted: 22 August 2011 / Published online: 6 September 2011
© Springer-Verlag 2011

Abstract The regional immune systems of patients with breast cancer are immunosuppressed. Dendritic cells are professional antigen-presenting cells and present cancer-associated antigens to the adaptive immune system in sentinel lymph nodes. Dendritic cells may promote, or inhibit, an adaptive immune response to specific antigens. Our aim was to assess whether dendritic cells were associated with nodal metastasis in patients with breast cancer. Sentinel lymph nodes of 47 patients with breast cancer with varying degrees of nodal disease and ten controls were evaluated using immunohistochemistry for the accumulation of dendritic cells in general (CD1a$^+$), mature dendritic cells (CD208$^+$), and plasmacytoid dendritic cells (CD123$^+$). Cytotoxic T cell and regulatory T cell accumulation were also evaluated. Sentinel lymph nodes with macrometastases demonstrated fewer mature dendritic cells than sentinel lymph nodes without metastasis (p=0.028), but not controls. There were fewer mature dendritic cells to cytotoxic T cells in sentinel lymph nodes with metastasis than those without (p=0.033). Also, there were more regulatory T cells to mature dendritic cells in sentinel lymph nodes with metastasis than those without (p=0.02). In conclusion, our study suggests that sentinel lymph nodes with metastasis have arrest of maturation of dendritic cells, fewer mature dendritic cell interactions with cytotoxic T cells, and more regulatory T cells than sentinel lymph nodes without metastasis in patients with breast cancer. These findings extend our understanding of regional immunosuppression and suggest that most regional immunosuppressive changes are associated with nodal metastasis in breast cancer.

Keywords Breast cancer · Lymph nodes · Dendritic cells · Regulatory T cells · Immunosuppression · Metastasis

Introduction

Metastasis to lymph nodes is one of the strongest predictors of survival in patients with breast cancer [1–3]. Axillary lymph node clearance has been replaced by sentinel lymph node biopsy in the appropriate clinical setting [4]. Improved selectivity in lymph node dissection has resulted in a more detailed analysis of the removed nodes, and greater attention is being paid to the immune status of these nodes.

Sentinel lymph nodes (SLN) are unique in that they represent both the sites of T cell activation and early metastasis. Dendritic cells (DCs) are professional antigen-presenting cells whose roles in tumor immunity are being elucidated. Following antigen capture in the periphery, and under the influence of stimulatory molecules, DCs mature and migrate to lymph nodes to present antigen to naive T

A. S. Mansfield · K. von Smitten · M. Leidenius
Breast Surgery Unit, Helsinki University Central Hospital, Helsinki, Finland

P. Heikkila
Department of Pathology, Helsinki University Central Hospital, Helsinki, Finland

J. Vakkila
Hematology Research Unit, Helsinki University Central Hospital, Helsinki, Finland

A. S. Mansfield (✉)
Division of Hematology, Department of Oncology, Mayo Clinic, 200 First St SW,
Rochester, MN 55905, USA
e-mail: mansfield.aaron@mayo.edu

lymphocytes to promote an inflammatory T cell response [5]. In the absence of stimulatory signals, DCs remain immature and promote antigen-specific anergy [6]. Previous studies have presented conflicting data on the accumulation of mature DC in SLN with or without metastasis in patients with breast cancer [7–10]. Plasmacytoid DCs (pDCs) are found in the peripheral blood and inflamed lymph nodes. In response to viruses, pDCs can differentiate into mature DCs and secrete interferons α and β [11]. In vitro studies suggest that pDCs promote tolerance to antigens and express indolamine 2,3-dioxygenase (IDO), a tryptophan-degrading enzyme that inhibits T cell proliferation [12, 13].

Sentinel lymph nodes (SLNs) of patients with breast cancer demonstrate evidence of immunosuppression [14]. Metastasis to SLNs has been correlated with accumulation of immunosuppressive regulatory T cells [14–16]. Furthermore, alterations in regional immunity in early-stage breast cancer have been correlated with worse disease-free survival [17]. By the time disease is clinically detectable, breast tumors have likely developed mechanisms to escape immunosurveillance. As the innate immune system would respond to breast cancer prior to the initiation of an adaptive response, we sought to evaluate innate immunity in SLNs from patients with early-stage breast cancer.

We have previously shown that accumulation of $Foxp3^+$ cells in SLNs is associated with metastasis to SLNs in breast cancer [14]. Since $Foxp3^+$ T cells interfere with DC development and function, we chose to examine DC status in SLNs. More specifically, we looked for associations between metastatic disease in SLNs and accumulation of myeloid $CD1a^+$ DC and $CD208^+$ DC, and plasmacytoid $CD123^+$ DC. CD1a is a member of the lipid antigen-presenting molecules that are expressed by various subsets of DC including Langerhans cells, lymph node interdigitating cells, and tumor-infiltrating DC [18, 19]. Thus, CD1a can be regarded as a universal marker for immature and mature forms of DC. CD208 on the other hand is a lysosomal antigen that is expressed relatively late upon DC maturation process, being therefore a rather specific marker for mature DC [20]. In this report, we show that in metastatic lymph nodes, mature $CD208^+$ DC are sparse. Since the number of intranodal $CD1a^+$ DC is similar in metastatic and non-metastatic lymph nodes, the results suggest that DC maturation is arrested in metastatic patients.

Patients, materials, and methods

We used the SLN of 47 patients with breast cancer treated at the Breast Surgery Unit of Helsinki University Hospital between 2001 and 2003. A prospectively collected database was searched to select patients without nodal metastases and patients with varying sizes of nodal metastases. These patients had either tumor-negative SLNs ($n=11$), SLNs with micrometastases ($n=16$), or SLNs with macrometastases ($n=20$) as defined by the International Union Against Cancer (UICC) TNM classification system [21]. To summarize the nodal classification system, isolated tumor cells are classified as no greater than 0.2 mm and micrometastasis as between 0.2 and 2 mm. Although not a part of the formal classification system, we use macrometastasis to refer to lesions equal to or larger than 2 mm. We had too few patients with isolated tumor cells to include in this study. The clinicopathological data are summarized in Table 1. Also SLNs from ten control patients who underwent SLN biopsy due to a false-positive core needle biopsy were examined. The control patients had premalignant conditions like lobular neoplasia in situ or atypical ductal hyperplasia, but not ductal carcinoma in situ or invasive breast cancer.

The SLNs were histologically assessed intraoperatively using serial sectioning and immunohistochemistry [22, 23]

Table 1 Patient and tumor characteristics

	Macrometastases	Micrometastases	Tumor-free
Number	20	16	11
Age[a]	59 (50–69)	66 (51–71)	54 (48–70)
Type			
Ductal	12	8	5
Lobular	9	6	3
Other	0	2	3
Tumor size[a] (mm)	16 (15–24)	16 (13–19)	17 (14–22)
Tumor stage			
T1b	2	3	1
T1c	12	10	6
T2	6	6	5
Tumor grade			
I	5	3	4
II	12	12	3
III	3	1	4
ER			
Positive	19	15	9
Negative	1	1	2
PR			
Positive	10	13	8
Negative	10	3	3
MIB-1			
Positive	10	5	5
Negative	10	11	6

There were no statistical differences between the groups

ER estrogen receptor, *PR* progesterone receptor, *MIB-1* proliferation index

[a] Median (range)

and postoperatively by review by a trained pathologist. Following intraoperative analysis, tissue samples were fixed in formalin, embedded in paraffin, and stored in a tissue bank for future retrieval.

Formalin-fixed, paraffin-embedded lymph nodes were sectioned into 3- to 4-μm slices and affixed on glass slides. Samples were heated for half an hour at 56°C, then deparaffinized in xylene, rehydrated in a graded alcohol series, and washed in water. We analyzed samples for all DCs using CD1a, cytotoxic T cells using CD8, pDCs using CD123, and mature DCs using CD208, which is also known as dendritic cell lysosomal-associated membrane protein. For antigen retrieval, samples that were to be stained for CD1a, CD8, and CD123 were microwaved for a total of 20 min in an ethylenediaminetetraacetic acid buffer. No antigen retrieval was performed for samples to be stained for CD208. Endogenous peroxidase activity was quenched in a bath of methanol and hydrogen peroxide for 30 min. Antibodies against CD1a (Novocastra, UK, NCL-CD1a-235), CD8 (Novocastra), CD123 (ATLAS Antibodies, Sweden, HPA003539), and CD208 (Immunotech SAS, France, PN IM3448) were incubated with specimens overnight at concentrations of 1:10, 1:25, 1:25, and 1:20, respectively, at 4°C. Envision Advance-Kit (Dako, Denmark) was used for the detection of CD1a and CD8. TSA Kit NEF 812 was used for the detection of CD123. ABC Kit Pk-6102 was used for the detection of CD208. Peroxidase activity was localized for all samples using a bath of 3-amino-9-ethyl carbazole and hydrogen peroxide for 15 min. Samples were counterstained with Harris hematoxylin for 30 s and mounted. Foxp3 was used to analyze regulatory T cells as we previously described [14].

Samples were reviewed for representative areas of staining. Positively stained cells in the non-metastatic regions of the SLN were quantified as the percentage of all cells in a minimum of three high-powered fields (×400 magnification) and averaged. In some cases, fewer fields were able to account for all positive staining. Non-metastatic regions were used to allow the comparison of lymphocytes between patients with and without metastasis. In SLN with metastasis, the areas of metastasis were assessed for tumor-infiltrating cytotoxic T cells. A Nikon eclipse 80i microscope was used for quantification and image acquisition.

JMP (SAS Institute Inc., USA) was used for statistical analysis and GraphPad Prism 4.03 (GraphPad Software Inc., USA) used for creation of the graphs. Some outliers were not displayed on graphs, but were reported in "Results." Basic statistics were used to analyze our grouped data. Our power to detect large effect sizes (Cohen's $d=0.8$) with an alpha of 0.05 in two-tailed tests with our total sample size of 57 was 0.842. Since the data were non-parametric, the Mann–Whitney U and Kruskal–Wallis tests were used to compare the groups based on nodal status. Tukey's multiple comparison test was used if the Kruskal–Wallis test was significant. The Spearman rank order correlation coefficient was used to determine whether there was a correlation between the stains.

Results

Dendritic cells are distributed similarly between sentinel lymph nodes with and without metastasis

$CD1a^+$, $CD123^+$, and $CD208^+$ DCs were located amongst T cells in the paracortical areas in the SLNs without metastasis and controls (Fig. 1). Morphologically, $CD1a^+$ DCs were round and macrophage-like cells, whereas $CD208^+$ cells were dendritic interdigitating cells.

In the SLNs with metastasis, we examined areas not immediately adjacent to metastases where the normal cellular architecture was preserved. In the SLNs with metastasis, DCs resided in the paracortical areas, similarly as in control and tumor-free SLNs.

Few mature $CD208^+$ dendritic cells are present in the paracortex of metastatic lymph nodes

There were significantly more $CD208^+$ DCs in SLNs without metastasis (median, 3.4%; range, 0.01–10.1%) than in SLNs with macrometastases (median, 0.1%; range, 0.05–8.09%) or SLNs in controls (median, 0.9%; range, 0.1–6.08%, $p=0.028$; Fig. 2a).

The accumulation of $CD123^+$ pDCs was similar between controls (median, 0.47%; range, 0–2.3%), tumor-free SLNs (median, 0.44%; range, 0.1–1.4%), and SLNs with metastases (median, 0.48%; range, 0–3.1%, $p=0.88$).

CD1a detects both immature and most of the mature DCs. The relative frequencies of $CD1a^+$ DCs were similar in the control SLNs (median, 10.4%; range, 6–19%), in the tumor-free SLNs (median, 11.1%; range, 0–16%), as well as in the metastatic SLNs (median, 12.7%; range, 0–20%, $p=0.25$).

Accordingly, the median proportion of mature $CD208^+$ DCs of all DCs, as measured by $CD1a^+$ cells, was significantly lower in SLNs with metastasis (median, 3.3%; range, 0.23–100%) compared with SLNs without metastasis (median, 31.1%; range, 0.47–72%, $p=0.031$; Fig. 2b).

Dendritic cell and $CD8^+$ T cell co-localization are infrequent in the paracortex of SLNs with metastasis

$CD8^+$ T cells resided in the paracortex of SLNs and their frequency was increased among the cancer patients, regardless of the presence or absence of metastasis. There were fewer $CD8^+$ T cells in control SLNs (median, 14.1%; range, 8.4–21.5%) compared with SLNs without metastasis

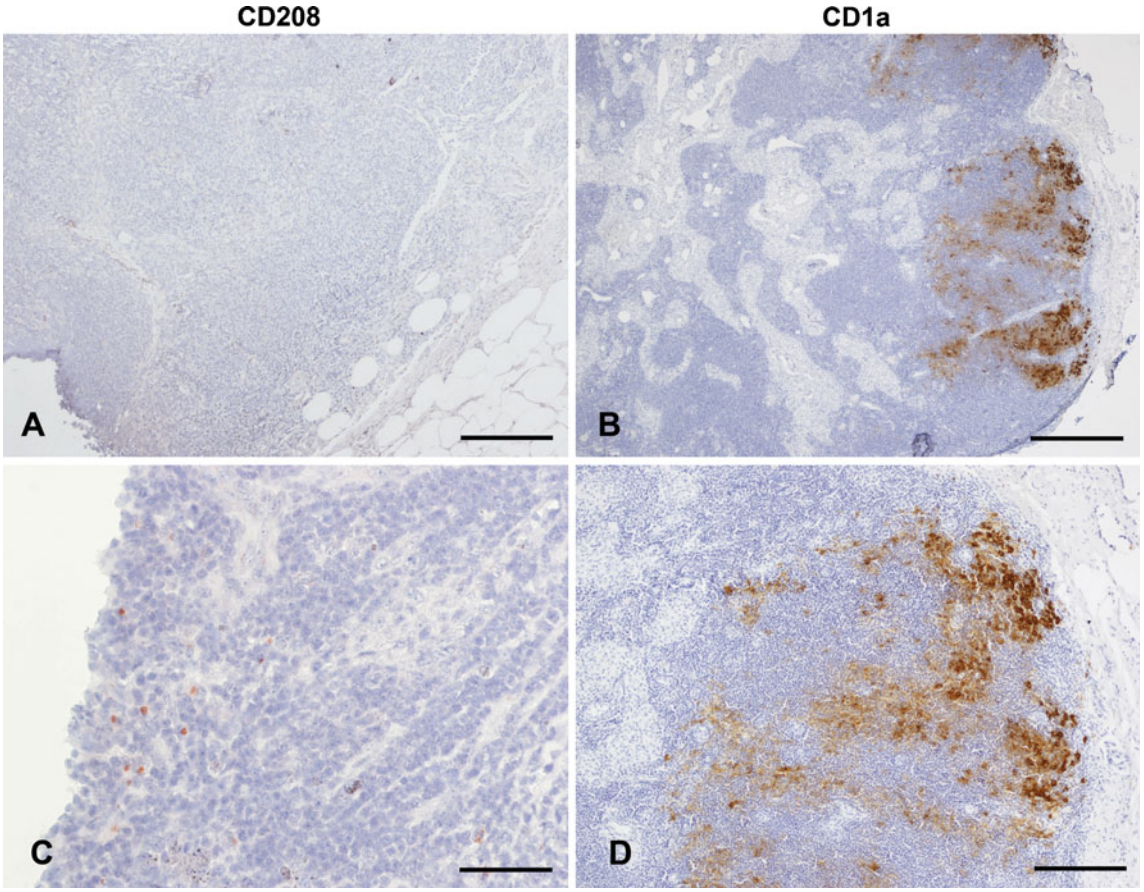

Fig. 1 Photomicrograph of dendritic cells in sentinel lymph nodes. Representative micrographs of samples stained for CD208 and CD1a are displayed *above* with low-resolution images in the *top row* and high-resolution images in the *bottom row*. The *scale bar* in the *bottom right corners* represent 200 μm for (**a**), 500 μm for (**b**), 50 μm for (**c**), and 200 μm for (**d**)

(median, 21.5%; range, 16.6–42%, p=0.005) and SLNs with metastasis (median, 24.7%; range, 5–42%, p=0.001). The difference between SLNs with or without metastasis was not significant (Fig. 3a).

The median ratio of CD208$^+$ DCs to CD8$^+$ T cells was lower in SLNs with metastasis than in those without metastasis (p=0.033). In metastatic lymph nodes, there were 1.4 (range, 0.19–53) mature DC to 100 CD8$^+$ T cells,

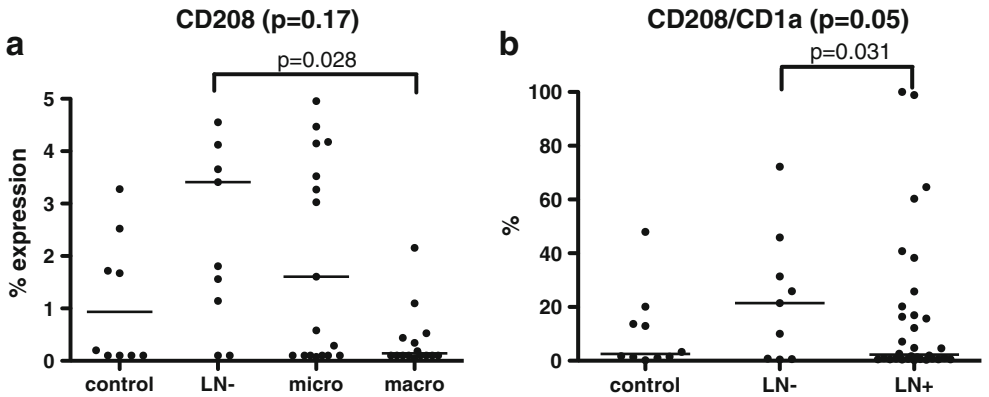

Fig. 2 Graphs of mature dendritic cell distribution by groups. These figures demonstrate the accumulation of CD208$^+$ DCs in SLNs by group. **a** Shows how SLNs with macrometastases have fewer CD208$^+$ DCs compared with SLNs without metastasis. **b** Shows how the proportion of mDCs to all DCs is lower in SLNs with metastases than those without. The *horizontal bars* among the *scatter dots* represent the median of each group. The statistical significance of each group comparison is noted in the heading. *Bars on top of the graphs* with p values represent the statistically significant intergroup comparisons

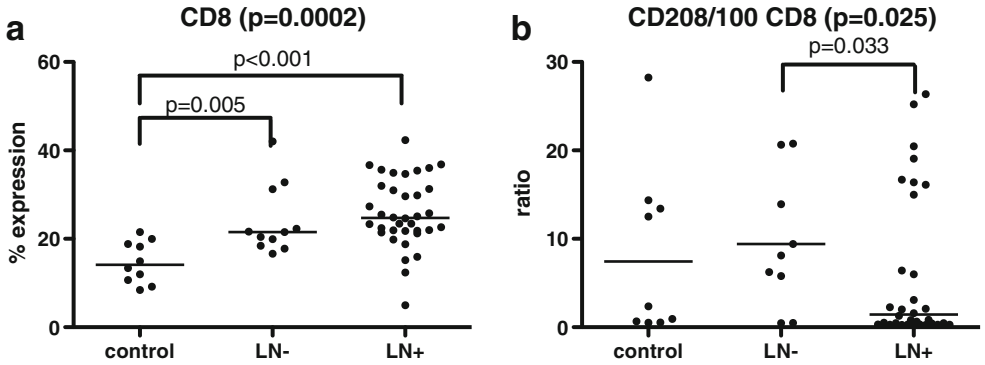

Fig. 3 Graphs of cytotoxic T cell distribution by groups. These figures demonstrate the accumulation the accumulation of $CD8^+$ T cells in SLNs by groups. **a** Shows how there were fewer $CD8^+$ T cells in control SLNs than in SLNs from patients with breast cancer. **b** Shows how SLNs with metastasis had a lower ratio of mature DC to cytotoxic T cells than SLNs without metastasis or controls. The *horizontal bars* among the *scatter dots* represent the median of each group. The statistical significance of each group comparison is noted in the heading. *Bars on top of the graphs* with *p* values represent the statistically significant intergroup comparisons

whereas in non-metastatic lymph nodes the respective ratio was 9.4 (range, 0.45–46.8) DC to 100 $CD8^+$ T cells. There were no statistically significant differences compared with the control SLNs (4 DC to 100 CD8 T cells, range, 0.5–35, $p=0.25$; Fig. 3b).

$Foxp3^+$ T cells outnumber $CD208^+$ mature dendritic cells in SLNs with metastasis

We previously reported that the accumulation of $Foxp3^+$ cells is associated with SLN metastases in breast cancer [14]. We combined the previous data (obtained from the same patients and SLNs) with the present study and calculated the median ratio of $Foxp3^+$ cells to $CD208^+$ cells in the SLNs. There was a higher ratio of $Foxp3^+$ T cells to $CD208^+$ DCs in SLNs with metastasis (median, 68.4; range, 0–464) compared with SLNs without metastasis (median, 4.4; range, 1.74–241, $p=0.02$), but there was no difference in the ratio observed in control SLNs (median, 27.1; range, 1.3–134, $p=0.14$; Fig. 4).

In our previous study, we also examined the expression of IDO. We did not observe IDO expression in paracortical areas of SLNs; rather, we found the expression of IDO in the marginal and medullar sinuses [14]. There was no difference in the ratio between IDO^+ cells to DC between control or cancer patients regardless of nodal status (data not shown).

The $Foxp3^+$-to-$CD8^+$ ratio inversely correlates with intrametastatic $CD8^+$ T cells

Since the findings described in this and in our earlier study [14] suggest that the cellular microenvironment in metastatic lymph nodes is immunosuppressed, we studied the $CD8^+$ T cell infiltrate in the SLNs with metastasis and related that to the cellular composition of the paracortical T cell area. It was observed that the ratio of $Foxp3^+$ cells to $CD8^+$ T cells in paracortical areas correlated positively with paracortical plasmacytoid dendritic $CD123^+$ cells ($r=0.554$, $p=0.014$) and inversely with intrametastatic $CD8^+$ T cell numbers ($r=-0.543$, $p=0.020$; Fig. 5). However, neither paracortical plasmacytoid $CD123^+$ cell numbers nor the ratio of $Foxp3^+$ cells to $CD8^+$ T cells was related to the metastatic status of SLNs. There were no significant correlations between mature and immature dendritic cells, or regulatory and cytotoxic T cells in SLN with or without metastasis.

Discussion

We found that there are fewer mature $CD208^+$ DCs in SLNs with macrometastasis than in SLNs without metastasis. We

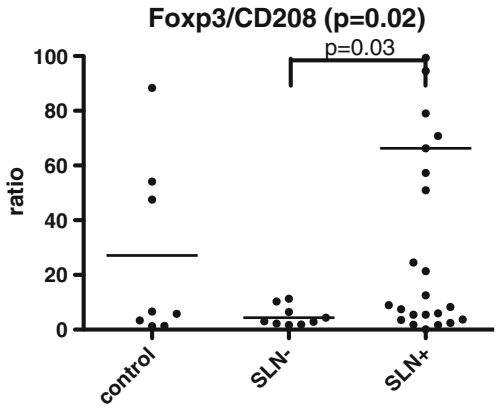

Fig. 4 Graph of ratio of regulatory T cells to mature dendritic cells by groups. This figure demonstrates how there was a higher ratio of regulatory T cells to mature dendritic cells in SLNs with metastasis compared with SLNs without metastasis and controls. The *horizontal bars* among the *scatter dots* represent the median of each group. The statistical significance of each group comparison is noted in the heading. *Bars on top of the graphs* with *p* values represent the statistically significant intergroup comparisons

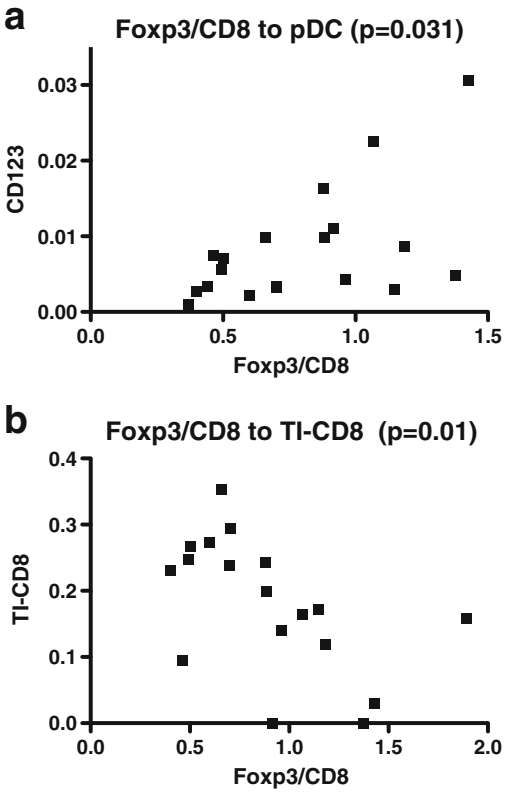

Fig. 5 Correlation of regulatory T cells to cytotoxic T cells to immature dendritic cells and tumor-infiltrating cytotoxic T cells. **a** Shows how a higher ratio of regulatory T cells to cytotoxic T cells correlates with the accumulation of immature dendritic cells in the paracortex of SLN (r=0.554, p=0.014). **b** Shows how a higher ratio of regulatory T cells to cytotoxic T cells in the paracortex of SLN inversely correlates with infiltration of nodal metastases by cytotoxic T cells (r=−0.543, p=0.02)

did not demonstrate any difference in the accumulation of $CD1a^+$ or $CD123^+$ cells between our groups. There was a relatively low ratio of mature DCs to all DCs in SLNs with metastasis compared with SLNs without metastasis and controls. These results suggest that there is arrest of dendritic cell maturation in SLNs with metastatic involvement. The observed ratio of $Foxp3^+$ T cells to $CD208^+$ DCs suggests that arrest of dendritic cell maturation may be secondary to the accumulation of Tregs, or that fewer mature dendritic cells favor the accumulation of Tregs. A recent study pointed out that most nodal interdigitating $CD208^+$ cells derive from migratory DC, and therefore it may be that the arrest in maturation does not occur in LN but in tumor tissue [24]. It is of interest that in tumor tissue, $CD208^+$ DC and $CD1a^+$ DC have distinctive localization patterns [25]. In epithelial squamous cell cancer, $CD208^+$ DCs reside within the tumor tissue and are clustered with T cells, whereas immature $CD1a^+$ DCs accumulate at epithelial sites. It would be important to study the tumor area in breast cancer patients with metastasis compared with patients without metastasis and to reveal whether the observed differences in SLN described in this paper are already evident at the tumor site.

Mature DCs present antigens to elicit an immune response. The relatively low ratio of $CD208^+$ DCs to $CD8^+$ T cells suggests that there is insufficient antigen presentation in SLNs with metastasis and likely less cytotoxicity directed toward the primary tumor, allowing tumor progression.

Similar to our results, another study demonstrated a trend toward more mature DCs, as measured by CD83, in SLNs without metastasis than SLNs with metastasis in patients with breast cancer; no difference in the accumulation of immature DCs was found between these sets of lymph nodes either [9]. Another study found that in breast cancer patients without metastatic disease, there were more mature DCs, as measured by CD208, in SLNs without metastasis compared with non-SLNs; however, there was no difference between SLNs and non-SLNs once there was nodal involvement [7]. We cannot directly compare our results to this study as we did not investigate non-SLNs. At least two studies have shown a reduction in DC numbers and maturity in SLNs compared with non-SLN in patients with melanoma [26, 27]. Another study showed that regional lymph nodes with metastasis from patients with melanoma were primarily infiltrated by immature DCs. These DCs expressed high levels of HLA-DR, suggesting that they were able to present antigens, but they lacked expression of co-stimulatory CD40 and CD86 molecules [28]. In summary, most evidence suggests that SLNs have diminished the accumulation of mature DCs in the presence of nodal metastasis and are likely immunosuppressed in both breast cancer and melanoma.

We did not find a relation of $CD123^+$ cell accumulation to nodal status in our study, but there was a positive correlation between $CD123^+$ cell accumulation and the ratio of $Foxp3^+/CD8^+$ T cells in the paracortex of SLNs. The high ratio of $Foxp3^+/CD8^+$ T cells suggest that these T cells are suppressed and do not function properly. Accordingly, fewer tumor-infiltrating $CD8^+$ T cells were seen in these patients. Infiltration of primary breast tumors by pDCs was found to be an independent adverse prognostic factor [29]. In one study of patients with melanoma, more pDCs were found in SLNs with metastasis than in tumor-free SLNs [30]. These pDCs in SLNs with metastases were found to express CD86, but not CD80 or CD83, which suggests incomplete activation and a possible tolerogenic role of these DCs. Although we did not investigate co-stimulatory markers, the correlation of pDCs with regulatory T cells suggests that pDCs are associated with immunosuppression in breast cancer.

We found greater accumulation of $CD8^+$ T cells in SLNs of patients with breast cancer than controls; however, the functional status of these cytotoxic $CD8^+$ T cells is

uncertain. The low proportion of $CD208^+$ DC of all DC and the low ratio of $CD208^+$ DC to CD8 T cells, especially in metastatic lymph nodes, suggest that the cellular microenvironment suppresses rather than stimulates T cell function. In accordance with this hypothesis, a recent study looked at the intracellular cytokine profiles of T cells from peripheral blood in women newly diagnosed with breast cancer prior to treatment. It was found that $CD4^+$ and $CD8^+$ cells produced fewer Th1 and Th2 cytokines in response to stimulation with the mitogen phorbol myristate acetate and ionomycin than healthy controls [31].

We used CD1a as a marker to quantify the majority of dendritic cells and CD208 to capture most of the mature dendritic cells. Most immature dendritic cells express CD1a and retain this expression during maturation. CD208 is expressed by mature dendritic cells, but not all mature dendritic cells. Additionally, a small portion of $CD208^+$ cells do not express CD1a [24]. Regardless, there is no single perfect marker for immature or mature dendritic cells. Our use of these markers does allow for gross quantification of the majority of dendritic cells within the lymph nodes.

In conclusion, our study suggests that there is arrest of dendritic cell maturation in sentinel lymph nodes with metastasis in breast cancer. The arrest may occur in lymph nodes or at the tumor site. Furthermore, sentinel lymph nodes with metastasis demonstrate worse co-localization of mature dendritic cells and cytotoxic T cells than sentinel lymph nodes without metastasis in patients with breast cancer. These findings extend our understanding of regional immunosuppression and suggest that most immunosuppressive changes are associated with nodal metastasis in breast cancer.

Acknowledgments The authors would like to thank Eija Heiliö for her assistance with immunohistochemistry. The Helsinki University Central Hospital Research Fund provided funding for this work.

Conflicts of interest The authors have no conflicts of interest to declare.

References

1. Mansour EG, Ravdin PM, Dressler L (1994) Prognostic factors in early breast carcinoma. Cancer 74(1 Suppl):381–400
2. Nemoto T, Vana J, Bedwani RN, Baker HW, McGregor FH, Murphy GP (1980) Management and survival of female breast cancer: results of a national survey by the American College of Surgeons. Cancer 45(12):2917–2924
3. Rosen PP, Groshen S, Saigo PE, Kinne DW, Hellman S (1989) Pathological prognostic factors in stage I (T1N0M0) and stage II (T1N1M0) breast carcinoma: a study of 644 patients with median follow-up of 18 years. J Clin Oncol 7(9):1239–1251
4. Leidenius MH, Krogerus LA, Toivonen TS, von Smitten KA (2005) Sentinel node biopsy is not sensible in breast cancer patients with large primary tumours. Eur J Surg Oncol 31(4):364–368
5. Jonuleit H, Schmitt E, Schuler G, Knop J, Enk AH (2000) Induction of interleukin 10-producing, nonproliferating CD4(+) T cells with regulatory properties by repetitive stimulation with allogeneic immature human dendritic cells. J Exp Med 192 (9):1213–1222
6. Mahnke K, Schmitt E, Bonifaz L, Enk AH, Jonuleit H (2002) Immature, but not inactive: the tolerogenic function of immature dendritic cells. Immunol Cell Biol 80(5):477–483. doi:10.1046/j.1440-1711.2002.01115.x
7. Bembenek A, Li J, Loddenkemper C, Kemmner W, Stein H, Wernecke KD, Schlag PM (2008) Presence of mature DC-$Lamp^+$ dendritic cells in sentinel and non-sentinel lymph nodes of breast cancer patients. Eur J Surg Oncol 34(5):514–518
8. Huang RR, Wen DR, Guo J, Giuliano AE, Nguyen M, Offodile R, Stern S, Turner R, Cochran AJ (2000) Selective modulation of paracortical dendritic cells and T-lymphocytes in breast cancer sentinel lymph nodes. Breast J 6(4):225–232
9. Poindexter NJ, Sahin A, Hunt KK, Grimm EA (2004) Analysis of dendritic cells in tumor-free and tumor-containing sentinel lymph nodes from patients with breast cancer. Breast Cancer Res 6(4): R408–R415
10. Treilleux I, Blay JY, Bendriss-Vermare N, Ray-Coquard I, Bachelot T, Guastalla JP, Bremond A, Goddard S, Pin JJ, Barthelemy-Dubois C, Lebecque S (2004) Dendritic cell infiltration and prognosis of early stage breast cancer. Clin Cancer Res 10(22):7466–7474
11. Lande R, Gilliet M (2010) Plasmacytoid dendritic cells: key players in the initiation and regulation of immune responses. Ann N Y Acad Sci 1183:89–103. doi:10.1111/j.1749-6632.2009.05152.x
12. Munn DH, Shafizadeh E, Attwood JT, Bondarev I, Pashine A, Mellor AL (1999) Inhibition of T cell proliferation by macrophage tryptophan catabolism. J Exp Med 189(9):1363–1372
13. Munn DH, Zhou M, Attwood JT, Bondarev I, Conway SJ, Marshall B, Brown C, Mellor AL (1998) Prevention of allogeneic fetal rejection by tryptophan catabolism. Science 281(5380):1191–1193
14. Mansfield AS, Heikkila PS, Vaara AT, von Smitten KA, Vakkila JM, Leidenius MH (2009) Simultaneous Foxp3 and IDO expression is associated with sentinel lymph node metastases in breast cancer. BMC Cancer 9:231
15. Matsuura K, Yamaguchi Y, Osaki A, Ohara M, Okita R, Emi A, Murakami S, Arihiro K (2009) FOXP3 expression of micrometastasis-positive sentinel nodes in breast cancer patients. Oncol Rep 22(5):1181–1187
16. Matsuura K, Yamaguchi Y, Ueno H, Osaki A, Arihiro K, Toge T (2006) Maturation of dendritic cells and T-cell responses in sentinel lymph nodes from patients with breast carcinoma. Cancer 106(6):1227–1236
17. Kohrt HE, Nouri N, Nowels K, Johnson D, Holmes S, Lee PP (2005) Profile of immune cells in axillary lymph nodes predicts disease-free survival in breast cancer. PLoS Med 2(9):e284
18. Caux C, Massacrier C, Vanbervliet B, Dubois B, de Saint-Vis B, Dezutter-Dambuyant C, Jacquet C, Schmitt D, Banchereau J (1997) $CD34^+$ hematopoietic progenitors from human cord blood differentiate along two independent dendritic cell pathways in response to GM-CSF+TNF alpha. Adv Exp Med Biol 417:21–25
19. Barral DC, Brenner MB (2007) CD1 antigen presentation: how it works. Nat Rev Immunol 7(12):929–941. doi:10.1038/nri2191
20. de Saint-Vis B, Vincent J, Vandenabeele S, Vanbervliet B, Pin JJ, Ait-Yahia S, Patel S, Mattei MG, Banchereau J, Zurawski S, Davoust J, Caux C, Lebecque S (1998) A novel lysosome-associated membrane glycoprotein, DC-LAMP, induced upon DC maturation, is transiently expressed in MHC class II compartment. Immunity 9(3):325–336

21. Sobin LHWC (ed) (2002) TNM classification of malignant tumors, 6th edn. Wiley, New York
22. Leidenius MH, Krogerus LA, Toivonen TS, Von Smitten KJ (2003) The feasibility of intraoperative diagnosis of sentinel lymph node metastases in breast cancer. J Surg Oncol 84(2):68–73
23. Leikola JP, Toivonen TS, Krogerus LA, von Smitten KA, Leidenius MH (2005) Rapid immunohistochemistry enhances the intraoperative diagnosis of sentinel lymph node metastases in invasive lobular breast carcinoma. Cancer 104(1):14–19
24. Angel CE, Chen CJ, Horlacher OC, Winkler S, John T, Browning J, MacGregor D, Cebon J, Dunbar PR (2009) Distinctive localization of antigen-presenting cells in human lymph nodes. Blood 113(6):1257–1267. doi:10.1182/blood-2008-06-165266
25. Liu J, Lu G, Li Z, Tang F, Liu Y, Cui G (2010) Distinct compartmental distribution of mature and immature dendritic cells in esophageal squamous cell carcinoma. Pathol Res Pract 206 (9):602–606. doi:10.1016/j.prp.2010.03.011
26. Cochran AJ, Morton DL, Stern S, Lana AM, Essner R, Wen DR (2001) Sentinel lymph nodes show profound downregulation of antigen-presenting cells of the paracortex: implications for tumor biology and treatment. Mod Pathol 14(6):604–608
27. Essner R, Kojima M (2002) Dendritic cell function in sentinel nodes. Oncology (Williston Park) 16(1 Suppl 1):27–31
28. Polak ME, Johnson P, Di Palma S, Higgins B, Hurren J, Borthwick NJ, Jager MJ, McCormick D, Cree IA (2005) Presence and maturity of dendritic cells in melanoma lymph node metastases. J Pathol 207(1):83–90
29. Polak ME, Borthwick NJ, Gabriel FG, Johnson P, Higgins B, Hurren J, McCormick D, Jager MJ, Cree IA (2007) Mechanisms of local immunosuppression in cutaneous melanoma. Br J Cancer 96 (12):1879–1887
30. Gerlini G, Urso C, Mariotti G, Di Gennaro P, Palli D, Brandani P, Salvadori A, Pimpinelli N, Reali UM, Borgognoni L (2007) Plasmacytoid dendritic cells represent a major dendritic cell subset in sentinel lymph nodes of melanoma patients and accumulate in metastatic nodes. Clin Immunol 125(2):184–193. doi:10.1016/j.clim.2007.07.018
31. Campbell MJ, Scott J, Maecker HT, Park JW, Esserman LJ (2005) Immune dysfunction and micrometastases in women with breast cancer. Breast Cancer Res Treat 91(2):163–171. doi:10.1007/s10549-004-7048-0

Virchows Arch (2011) 459:399–407
DOI 10.1007/s00428-011-1120-z

ORIGINAL ARTICLE

Specific expression of ZO-1 and *N*-cadherin in rosette structures of various tumors: possible recapitulation of neural tube formation in embryogenesis and utility as a potentially novel immunohistochemical marker of rosette formation in pulmonary neuroendocrine tumors

Kaishi Satomi · Yukio Morishita · Shingo Sakashita · Yuzuru Kondou · Shuichiroh Furuya · Yuko Minami · Masayuki Noguchi

Received: 19 March 2011 / Revised: 29 June 2011 / Accepted: 4 July 2011 / Published online: 23 July 2011
© Springer-Verlag 2011

Abstract Neuroendocrine tumors can develop in various organs. All of these tumors are designated on the basis of their morphologic characteristics evident by light microscopy, and by immunohistochemistry for antigens such as synaptophysin, chromogranin-A, and CD56/NCAM. In the present study, we attempted to demonstrate the localization of Zonula occludens-1 (ZO-1) and *N*-cadherin in rosette structures of neuroendocrine tumors using immunohistochemistry and to clarify their specific distribution in rosettes in human pulmonary neuroendocrine tumors in comparison with various types of adenocarcinoma. Among 40 neuroendocrine tumors of the lung examined, 18 cases (45%) and 22 cases (55%) were positive for ZO-1 and *N*-cadherin, respectively. In addition, we divided the cases into two types: 16 cases of Flexner-type tumor and 24 cases of Homer–Wright-type tumor. We then determined the Rosette Index (RoI; the percentage fraction of rosette structures positive for ZO-1 or *N*-cadherin among the total number of rosette structures). The Flexner-type neuroendocrine tumors showed significantly higher levels of RoI in ZO-1 than the Homer–Wright-type neuroendocrine tumors (median; 38.8% vs 0%, $p<0.001$). On the other hand, *N*-cadherin and ZO-1 were hardly detected in tubular adenocarcinomas in various organs, and their immunoreactivities differed significantly between adenocarcinoma and pulmonary neuroendocrine tumor (ZO-1, mean 0.23% vs 18%, $p<0.0001$; *N*-cadherin, mean 0% vs 33%, $p<0.0001$). In conclusion, expression of ZO-1 and *N*-cadherin may reflect the mechanisms leading to rosette formation in neuroendocrine tumors, which possibly recapitulate neural tube formation in embryogenesis and could represent a specific immunohistochemical marker for neuroendocrine carcinoma of the lung.

Keywords ZO-1 · *N*-cadherin · Neuroendocrine carcinoma · Endocrine carcinoma · Carcinoid · Lung

K. Satomi · Y. Morishita · S. Sakashita · Y. Minami · M. Noguchi (✉)
Department of Diagnostic Pathology, Graduate School of Comprehensive Human Sciences, University of Tsukuba, 1-1-1 Tennodai,
Tsukuba-shi, Ibaraki 305-8575, Japan
e-mail: nmasayuk@md.tsukuba.ac.jp

Y. Kondou · S. Furuya
Department of Pathology, Tsukuba University Hospital, 2-1-1 Amakubo,
Tsukuba-shi, Ibaraki 305-8576, Japan

Introduction

Neuroendocrine tumors of the lung are subdivided into four entities, including typical and atypical carcinoid tumors, small cell lung carcinoma (SCLC) and large cell neuroendocrine carcinoma (LCNEC) [1, 2]. Among these tumors, carcinoids are considered to be relatively indolent, whereas SCLC and LCNEC are thought to be highly aggressive [3–13].

Neuroendocrine tumors can develop in a variety of organs, including the digestive system, endocrine system, urogenital system, and soft tissues [14]. All of these tumors

are classically designated as neuroendocrine tumors on the basis of their characteristic morphological features, including organoid, trabecular, palisading, or rosette growth patterns (Fig. 1). As well as these light-microscopical morphologic characteristics, dense-core neurosecretory vesicles evident by electron microscopy are helpful for diagnosis. Recently, immunohistochemistry, particularly for synaptophysin, chromogranin-A, and CD56/NCAM, has been applied successfully to identify neuroendocrine features. Among the various morphological and immunohistochemical markers, the characteristic morphological feature of rosette formation is strongly pathognomonic, but the molecular mechanism responsible for rosette formation, or its biological significance, is still unclear.

Rosette structures are a very useful morphological marker of neuroendocrine differentiation and are divided into two types: the Flexner type and the Homer–Wright types [15] (Fig. 1). The rosette structure appears as a radial arrangement of tumor cells resembling a rose. The Flexner-type rosette is a spoke- and wheel-shaped tumor cell formation with lumina, which is frequently detected in ependymoma, retinoblastoma, and immature teratoma (Fig. 1a). The Homer–Wright rosette is a circular or spherical grouping of tumor cells around a pale, eosinophilic, central area but lacking lumina, which is typically seen in medulloblastoma and neuroblastoma (Fig. 1b).

On the other hand, embryologically, neural differentiation is characterized by development of the neural tube. Since the morphological structure of the rosette in pulmonary neuroendocrine tumors mimics that of the neural tube, we have hypothesized that rosette structures within neuroendocrine tumors recapitulate the early stage of neural tube formation.

Various proteins are known to be components of the neural tube/neural rosette structure: PAX6, nestin, Sox1, Sox2, and *N*-cadherin as constitutive proteins of neuroepithelium, or PLZF, DACH1, MMRN1, PLAGL1, NF2F1, DMTR3, LMO3, FAM70A, EVI1, ZNF312, LIX1, RSPO3, Shroom-3, and Zonula occludens-1 (ZO-1) as proteins that are associated with the development of neural tube/neural rosette structure [16–19]. Among these molecules, ZO-1 and *N*-cadherin show characteristic localization, especially in early-stage neural rosettes that develop from human embryonic stem cells [17].

N-cadherin, also known as cadherin 2, is a member of the cadherin family. *N*-cadherin is also known to be present, and to accumulate, in the adherens junctions of the apical portion of neuroepithelial cells in chick and mouse embryos [20, 21]. In human tumors, *N*-cadherin is differentially expressed in pulmonary tumors and is observed predominantly in neuroendocrine lung lesions, neuroendocrine hyperplasia, typical carcinoid tumor, atypical carcinoid tumor, SCLC and LCNEC. Neuroendocrine hyperplasia, typical carcinoid, small cell lung carcinoma, and large cell neuroendocrine carcinoma demonstrate diffuse membranous *N*-cadherin immunoreactivity, whereas atypical carcinoid exhibits strong and diffuse and membranous immunoreactivity [22].

ZO-1, also known as tight junction protein 1, is a 225-kDa tight junction-associated polypeptide [23]. It is not only concentrated at tight junctions in epithelial cells but also colocalized with the cadherin molecule in non-epithelial tissue [24]. Since ZO-1-deficient mice show a lethal embryonic phenotype, it is thought that ZO-1 plays essential roles in development [25, 26].

It is also known that expression of ZO-1 is maintained both before and after closure of the neural tube in both chick and mouse neuroepithelium [18]. In human embryonal stem cells (hESCs), the formation of neural rosettes is initiated by acquisition of cell polarity, as demonstrated in vitro by redistribution of ZO-1 in the apical membrane, being expressed evenly on the surface of undifferentiated

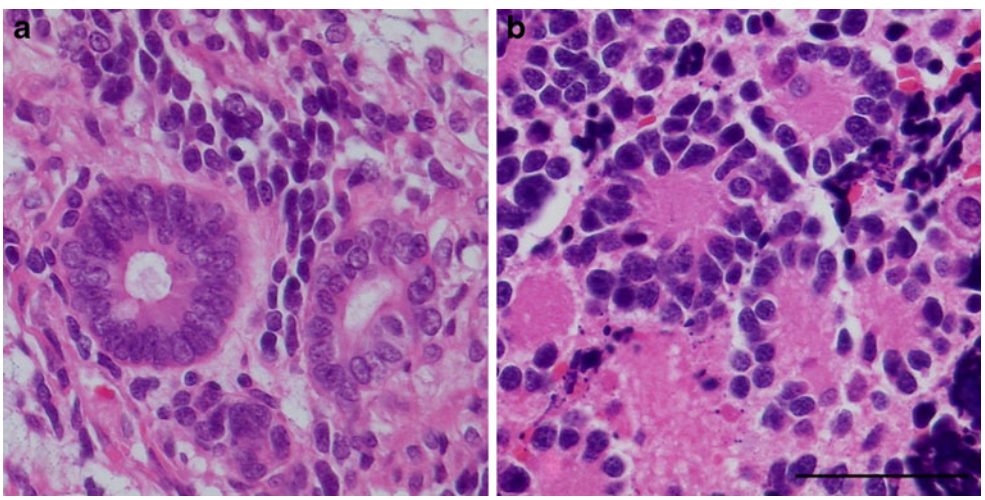

Fig. 1 Histological evaluation of tumor type with rosette structures. Rosette structures distinguished as arrangements of several polarized cells. The Flexner-type rosette in retinoblastoma contains lumina (**a**), while the Homer–Wright-type rosette in neuroblastoma does not (**b**). We defined tumors as the Flexner-type (in which rosettes with lumina are predominant) or the Homer–Wright-type (in which rosettes without lumina are predominant). Scale *bar* 50 μm

hESCs [17]. These reports indicate that ZO-1 is colocalized with *N*-cadherin and plays an important role in neurogenesis.

In the present study, we attempted to clarify the mechanisms leading to rosette formation in neuroendocrine tumors with reference to neural tube formation during embryogenesis using ZO-1 and *N*-cadherin as key proteins of neuroendocrine tumor rosette structures and demonstrated the specific distribution of the two proteins in rosettes of human pulmonary neuroendocrine tumors. Our findings suggested that ZO-1 and *N*-cadherin are useful immunohistochemical markers for clarifying the biological significance of rosette structures, as well as being a diagnostic feature of neuroendocrine tumors.

Materials and methods

Patients and tissue specimens

A total of 101 specimens that had been surgically resected at Tsukuba University Hospital (Ibaraki, Japan) between 1975 and 2009 were retrieved. Written informed consent had been obtained from the patients between 1996 and 2009. All of the cases examined were anonymized, and this study was approved by the institutional review board of the University of Tsukuba. Among these cases, 58 showed rosette formation, including two medulloblastomas, one ependymoma, three neuroblastomas, one olfactory neuroblastoma, two retinoblastomas, two immature teratomas, one mature teratoma, one pineoblastoma, one neurocytoma, one atypical carcinoid of the colon, one atypical carcinoid of the thymus, five typical carcinoids of the lung, two atypical carcinoids of the lung, 25 large cell neuroendocrine carcinomas of the lung, eight small cell carcinomas of the lung, and two large cell carcinomas of the lung. The remaining 43 cases were well-differentiated tubular adenocarcinomas, including three adenocarcinomas of the lung, ten adenocarcinomas of the stomach, ten adenocarcinomas of the colon, five adenocarcinomas of the pancreas, five adenocarcinomas of the bile duct, and ten ductal carcinomas of the breast.

Immunohistochemistry

For immunohistochemical analysis, the following antibodies were used as primary antibodies: anti-*N*-cadherin (6 G11, mouse monoclonal, Dako, Copenhagen, Denmark), anti-ZO-1 (epitope; residues 463–1109 of ZO-1, rabbit polyclonal, Zymed Laboratories, San Francisco, USA), anti-synaptophysin (27 G12, mouse monoclonal, Nichirei Bioscience, Tokyo, Japan), anti-chromogranin-A (A0430, rabbit polyclonal, Dako), and anti-CD56/NCAM (1B6, mouse monoclonal, Nichirei Bioscience).

All specimens had been previously fixed in 15% formalin and paraffin-embedded. Serial sections of the materials were cut at a thickness of 3 μm. Slides were deparaffinized in xylene and dehydrated in methanol. The EnVision® (Dako) signal enhancement system was employed for analysis of all antibodies. Heat-mediated antigen retrieval was used for visualization of *N*-cadherin, synaptophysin (pressure pan treatment, 15 min at 105°C), chromogranin-A, and CD56/NCAM (autoclave treatment, 10 min at 120°C), and an enzymatic antigen retrieval method employing Dako proteinase K Ready-to-use was adopted for ZO-1 (5 min at room temperature; Dako). Tissues were incubated with ChemMate POD Blocking Solution (Dako) for 5 min at room temperature. After blocking, the sections were incubated with the primary antibody diluted in Dako REAL Antibody Diluent (Dako) for 30 min at room temperature. Dilutions used for the primary antibodies were: *N*-cadherin and ZO-1, 1:50; chromogranin-A, 1:500; synaptophysin and CD56/NCAM, pre-diluted. Tissues were washed in TBS and incubated with ENVISION+Dual Link Polymer (Dako) for 30 min. Visualization was performed by incubation with the DAB+ Liquid System (Dako) for 5 min. After being rinsed in water, the sections were counterstained with hematoxylin and mounted. These immunohistochemical processes were performed with a histostainer (Nichirei Biosciences).

The positive controls for immunohistochemistry were liver tissue for anti-*N*-cadherin, normal bronchiole epithelium for anti-ZO-1, and pancreatic islet tissue for anti-synaptophysin, anti-chromogranin-A, and anti-CD56/NCAM.

Evaluation of rosette structure types

Rosette structures can be distinguished as arrangements of several polarized cells. In this study, we distinguished the tumor type as Flexner-type tumors (in which rosette structures with lumina are predominant and correspond to the Flexner type) or Homer–Wright-type tumors (in which rosette structures without lumina are predominant and correspond to the Homer–Wright type; Fig. 1a, b). If any individual case included both types of rosette structure, it was classified according to the predominant type present.

Evaluation of immunostaining

Immunoreactivity in the cytoplasm and/or cell membrane of neural tube-like structures in immature teratoma was classed as negative or positive for *N*-cadherin. On the other hand, immunoreactivity that was evident as apical membrane staining or dot-like positivity in the center of the structure was evaluated as ZO-1 positivity. We used the Rosette Index (RoI) for evaluating the quantity of the rosette structures expressing each of the proteins. The RoI

is defined as the percentage of positive rosette structures among the total in each tumor. We counted 100 rosette structures in each tumor. We considered specimens to be negative for ZO-1 or *N*-cadherin if the RoI score was less than 5%. All histological evaluations were judged by three pathologists (KS, SS, and YK), each of whom examined the RoI score independently without any information, and a 10% score difference was tolerated. If the evaluations differed by over 10%, the pathologists discussed the case, and a consensus diagnosis was reached.

Statistical analysis

Statistical analysis was performed with the SPSS 9.0 software package (SPSS Inc., Chicago, IL, USA). Mann–Whitney *U* test was applied for assessment of anti-ZO-1 positivity as a parameter of RoI. Fisher's exact test was performed for analysis of patient profiles. For all analyses, a significance level of $p<0.05$ was adopted.

Results

Patient background

Among the 40 neuroendocrine tumors of the lung, including five typical carcinoid tumors, two atypical carcinoid tumors, 25 large cell neuroendocrine carcinomas, and eight small cell carcinomas, the clinicopathological characteristics including gender ($p=0.230$, $p=0.180$), pathological stage ($p=0.550$, $p=0.312$), lymphatic duct invasion (Ly factor; $p=0.842$, $p=0.816$), vascular invasion (V factor; $p=0.822$, $p=0.218$), and lymph node status (N factor; $p=0.071$, $p=0.836$) did not show any significant difference between cases positive and negative for both ZO-1 and *N*-cadherin.

Neuroendocrine tumors of the lung and other tumors with rosette structures

The results of immunohistochemical staining in neuroendocrine tumors of the lung and other tumors with rosette structures (total 58 cases, described in "Materials and methods") are summarized in Table 1. Rosette structures are observed in various tumors: neuroblastoma (Fig. 2a), immature teratoma (Fig. 2b), large cell neuroendocrine carcinoma of the lung (Fig. 2c), and small cell carcinoma of the lung (Fig. 2d). Cytoplasmic and/or cell membrane staining for *N*-cadherin were evident in these tumors (Fig. 2 e–h). Among the cases positive for *N*-cadherin, 18 (49%) showed a strong diffuse (cytoplasmic and cell membrane) staining pattern, and only 19 (51%) showed a strong cell membrane staining pattern. *N*-cadherin immunoreactivity was evident not only in rosette structures but also other tumor cells. On the other hand, staining for ZO-1 was accentuated on the apical membrane of tumor cells that formed rosette structures and, at higher cell densities, was localized in the center of the rosettes (Fig. 2 j–l). There were no correlations between *N*-cadherin and ZO-1 expression ($R=0.13$, $p=0.28$) or *N*-cadherin localization (diffuse versus cell membrane) and ZO-1 expression ($p=0.43$).

The rate of *N*-cadherin positivity in most of the tumors exceeded that of ZO-1 positivity (Table 1). Comparison of immunoreactivity between *N*-cadherin and ZO-1 showed that their positivity rates were 55% versus 45% in pulmonary neuroendocrine tumors ($p=0.021$) and 83% versus 22% in other rosette-forming tumors ($p=0.03$), respectively. However, the rate of ZO-1 positivity in LCNEC of the lung tended to be higher than that of *N*-cadherin (52% vs 44%, $p=0.12$). Although the number of cases was limited, 100% of the immature teratomas examined were positive for both ZO-1 and *N*-cadherin (Table 1).

Table 1 *N*-cadherin and ZO-1 expression in all tumors with rosette structures

		No. of positive cases[b]		
	Total	*N*-cadherin	ZO-1	*p* Value
Pulmonary neuroendocrine tumors				
Typical carcinoid of the lung	5	4 (80%)	1 (20%)	0.068
Atypical carcinoid of the lung	2	1 (50%)	1 (50%)	0.66
LCNEC of the lung	25	11 (44%)	13 (52%)	0.12
Small cell carcinoma of the lung	8	5 (62.5%)	3 (37.5%)	0.043
	40	22 (55%)	18 (45%)	0.021
Other rosette-forming tumors				
Large cell carcinoma of the lung	2	2 (100%)	0 (0%)	0.16
Immature teratoma	2	2 (100%)	2 (100%)	0.18
Others[a]	14	11 (78.6%)	2 (14.3%)	0.008
	18	15 (83.3%)	4 (22.2%)	0.03

LCNEC large cell neuroendocrine carcinoma

[a] Others: ependymoma, mature teratoma, medulloblastoma, neuroblastoma, neurocytoma,olfactory neuroblastoma, pineoblastoma, retinoblastoma, and atypical carcinoid of the colon

[b] Positive cases are adopted if RoI is 5% or more

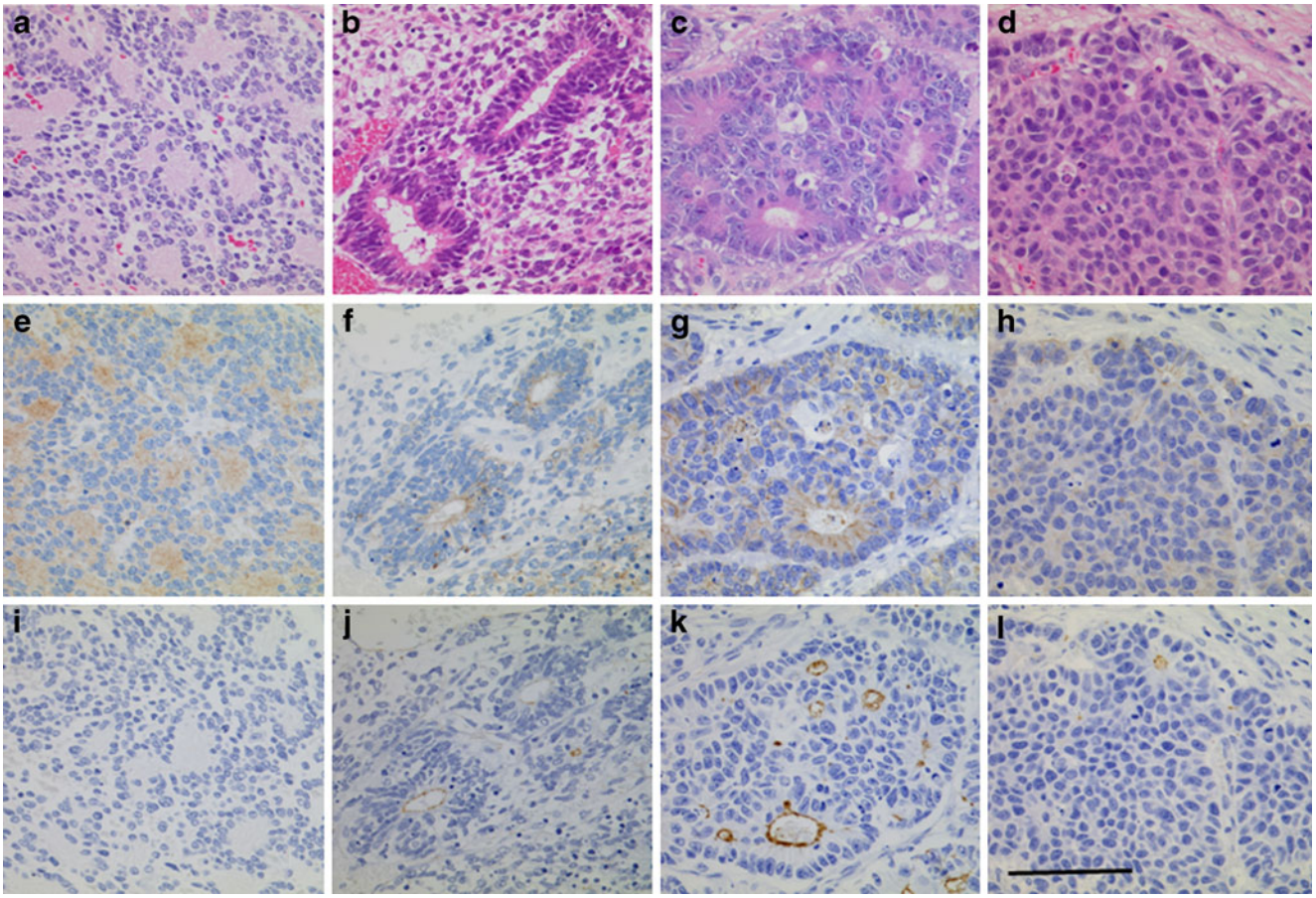

Fig. 2 Histological characterization of tumors with rosette structures. Neuroblastoma (**a**, **e**, **i**), immature teratoma (**b**, **f**, **j**), large cell neuroendocrine carcinoma of the lung (**c**, **g**, **k**), and small cell carcinoma of the lung (**d**, **h**, **l**) are shown. Immunoreactivity for *N*-cadherin (**e**, **f**, **g**, **h**) and ZO-1 (**i**, **j**, **k**, **l**) is shown. Scale *bar* is 100 μm

Histological features of rosette structures in neuroendocrine tumors

As mentioned in "Materials and methods," we found two patterns of rosette structure in neuroendocrine tumors: Flexner-type rosettes and Homer–Wright-type rosettes (Fig. 1). We divided pulmonary neuroendocrine tumors into two types: Flexner-type tumors (in which rosette structures with lumina were predominant) and Homer–Wright-type tumors (in which rosette structures without lumina were predominant). On this basis, 16 tumors were considered to be the Flexner-type and 24 were considered to be the Homer–Wright-type (Table 2). The Flexner-type tumors included one carcinoid tumor (1/7, 14.3%), 12 LCNECs (12/25, 48%), and three SCLCs (3/8, 37.5%). We then determined the RoI for both ZO-1 and *N*-cadherin. Flexner-type neuroendocrine tumors showed significantly higher values of RoI for ZO-1 than Homer–Wright-type neuroendocrine tumors (median, 38.8% vs 0%; 25th percentile, 19.3% vs 0%; 75th percentile, 55.5% vs 0%; $p<0.001$, respectively; Fig. 3). However, there were no significant differences of RoI between the two types of tumor for *N*-cadherin (median and mean, 52.2% vs 6.7% and 38.4% vs 24.6%, $p=0.387$, respectively; data not shown).

Table 2 Pathological diagnosis of Flexner-type and Homer–Wright-type pulmonary neuroendocrine tumors

Pulmonary neuroendocrine tumors	Number of tumors		
	Total	Flexner-type	Homer–Wright type
Typical carcinoid	5	0 (0%)	5 (100%)
Atypical carcinoid	2	1 (50%)	1 (50%)
LCNEC of the lung	25	12 (48%)	13 (52%)
Small cell carcinoma	8	3 (37.5%)	5 (62.5%)
	40	14 (35%)	26 (65%)

LCNEC large cell neuroendocrine carcinoma

Carcinomas with tubular structures

In order to examine the expression of ZO-1 and *N*-cadherin in tubular adenocarcinomas, in which it is sometimes difficult to discriminate rosettes from glandular structures,

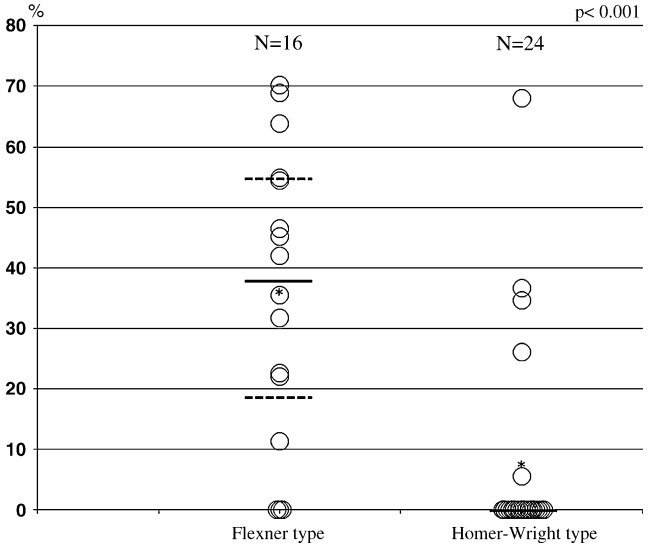

Fig. 3 ZO-1-positive rosette structures in neuroendocrine tumor of the lung (total 40 cases). Flexner-type tumors (in which rosette structures with lumina are predominant) showed significantly higher values of rosette index for ZO-1 than Homer–Wright-type tumors (in which rosette structures without lumina are predominant; $p<0.001$). *Asterisk*: mean; *solid line*: median; and *dashed line*: 25th and 75th percentiles, respectively. Statistical analysis was performed by *U* test

we assessed 43 well-differentiated tubular adenocarcinomas (described in "Materials and methods"; Fig. 4a–d). There was no positive staining for *N*-cadherin among adenocarcinomas of the lung (Fig. 4e), stomach (Fig. 4f), colon, pancreas (Fig. 4g), bile duct, and breast (Fig. 4h). All of the tubular adenocarcinomas were also negative for ZO-1 (Fig. 4 i–l), except for one ductal carcinoma of the breast (Fig. 4l, insert) in which the ductal structures were negative for other common neuroendocrine markers such as synaptophysin, chromogranin-A, and CD56/NCAM, although a few cases were positive for neuroendocrine markers (Table 3). Among ten tumors of the breast, one invasive ductal carcinoma was positive for ZO-1 and also for estrogen receptor and progesterone receptor, but negative for Her2 protein.

The immunoreactivities for both ZO-1(median and mean, 0% vs 0% and 0.23% vs 18%, $p<0.0001$) and *N*-cadherin (median and mean, 0% vs 0% and 0% vs 33% $p<0.0001$) differed significantly between adenocarcinoma and pulmonary neuroendocrine tumor.

Discussion

In this study, we demonstrated positive immunoreactivity for both *N*-cadherin and ZO-1 in neuroendocrine tumors showing rosette formation. It was of considerable interest that staining of the rosettes was similar to that of neural tube/neural rosettes in immature teratoma. These results indicated that both Flexner-type and Homer–Wright-type rosettes may mimic the neural tube in embryos, not only morphologically but also functionally. In tumors positive for ZO-1 and *N*-cadherin, ZO-1 positivity was localized in rosette structures, especially at the apical membrane of the constituent tumor cells, and the staining pattern was very rosette-specific, especially in Flexner-type tumors (Fig. 2). The correlation between ZO-1 and *N*-cadherin in Flexner-type tumors was significant ($R=0.595$, $p=0.004$). These results suggested that ZO-1 and *N*-cadherin are molecules playing a specific role in rosette morphology, not only in the neural tube but also pulmonary neuroendocrine tumor. In the early stage of neurogenesis, ZO-1 acts as a tight junction protein and regulates rosette growth to control symmetric versus asymmetric differentiation of neural stem cells. ZO-1 functions as a cross-linker between α-catenin and the actin cytoskeleton. The interaction between ZO-1 and *N*-cadherin is a key determinant of stable localization of both adherens junctions and gap junctions in the intercalated disks of rat myocytes, and expression of ZO-1 and *N*-cadherin, in relation to the so-called "cadherin switch", has also been reported in melanoma. The present study suggests that the former mechanism, regulating the turnover of stem cells, is more likely, although additional experimental studies to verify this possibility will be needed [27, 28].

There are two types of neuroendocrine markers: morphological markers such as rosette formation and palisading of the tumor cells, and immunohistochemical markers such as synaptophysin, chromogranin-A, and CD56/NCAM. These two marker types are frequently used for routine surgical diagnosis, but the relationship between them has not been studied in detail. In this study, we showed that ZO-1 and *N*-cadherin, which are specifically expressed in the neural tube, are characteristically expressed in the rosette structures of neuroendocrine tumors. Therefore, ZO-1 and *N*-cadherin are markers that are closely associated with neuroendocrine morphology and could be implicated in the formation of rosette structures.

Among the pulmonary neuroendocrine tumors, carcinoid tumor and SCLC are diagnosed on the basis of purely morphological criteria [2]. However, to diagnose LCNEC, positivity for an immunohistochemical marker (at least one among synaptophysin, chromogranin-A, and CD56/NCAM [2]) is required. These three neuroendocrine markers were considered to be useful for diagnosis of LCNEC. However, this set of immunohistochemical markers is provisional and is simply used empirically. We suggest that ZO-1 or *N*-cadherin could also be a useful marker of neuroendocrine differentiation and may be positive in cases of large cell carcinoma (LCC) with neuroendocrine morphology. LCC with neuroendocrine morphology mimics LCNEC but is negative for all three neuroendocrine markers. However, if

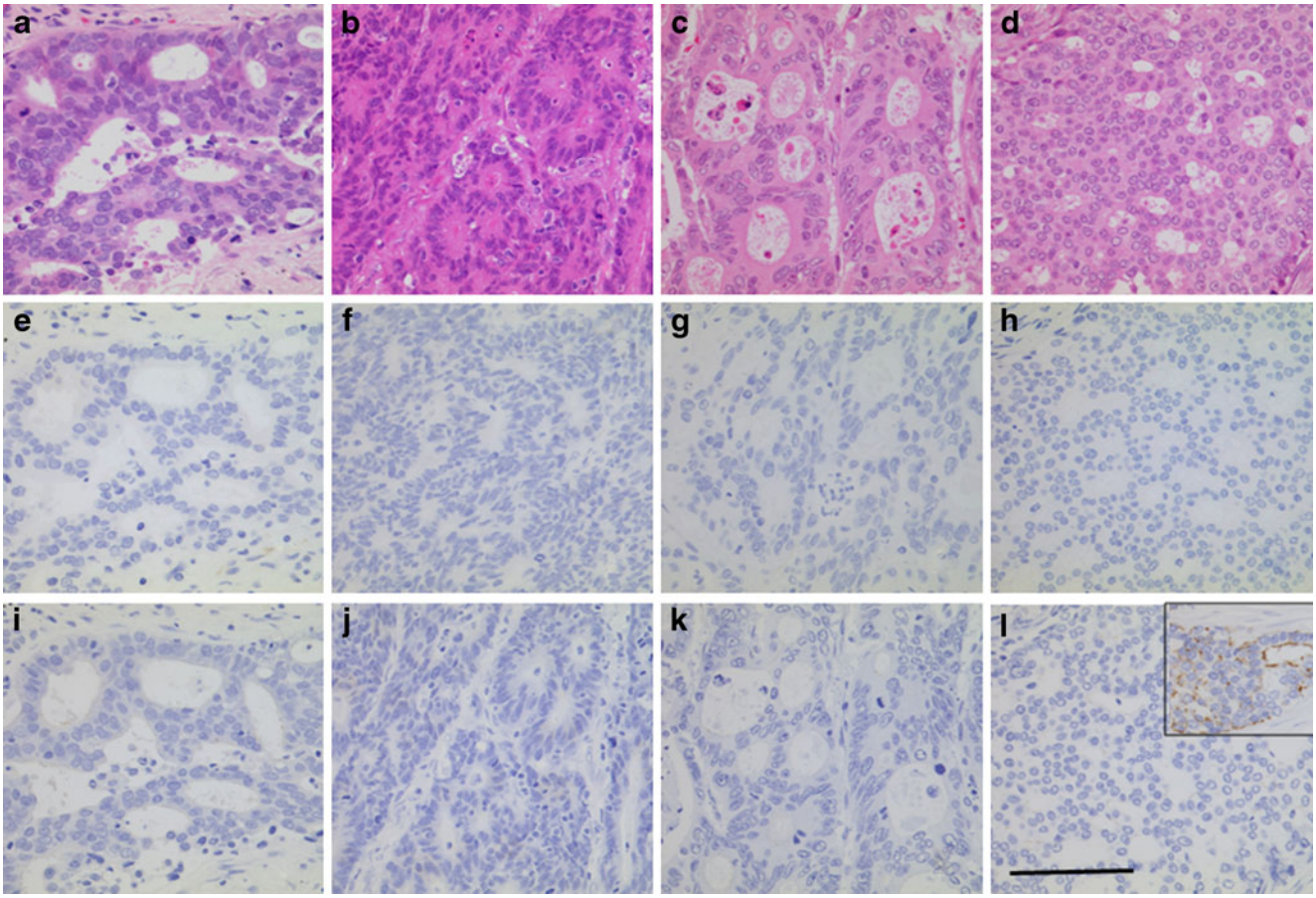

Fig. 4 Histological characterization of carcinomas with tubular structures. Lung adenocarcinoma (**a**, **e**, **i**), stomach adenocarcinoma (**b**, **f**, **j**), pancreas adenocarcinoma (**c**, **g**, **k**), and breast carcinoma (**d**, **h**, **l**) are shown. There is no immunoreactivity for *N*-cadherin (**e**, **f**, **g**, **h**) and ZO-1 (**i**, **j**, **k**, **l**). *Insert* is a ZO-1-positive area in invasive region of breast carcinoma in one of ten cases (**l**). Scale *bar* is 100 μm

positivity for ZO-1 and/or *N*-cadherin can be demonstrated, both LCNEC and LCC with neuroendocrine morphology may prove to be closely related tumors biologically and classifiable into a similar category.

SCLC and LCNEC are both high-grade neuroendocrine carcinomas of the lung. The present study demonstrated that a significantly higher proportion of SCLC cases (p= 0.043) were positive for *N*-cadherin than for ZO-1 and that more cases of typical carcinoid and atypical carcinoid (p= 0.068 and 0.66) were positive for *N*-cadherin than for ZO-1 (Table 1). Interestingly, however, the positivity rate for ZO-1 (52%) was relatively higher in LCNEC than in SCLC

Table 3 Immunohistochemical status of carcinomas with tubular structures

		No. of positive cases (%)				
	Total	Syn.	Ch-A.	CD56.	*N*-cadherin	ZO-1
Lung	3	1 (33%)	0 (0%)	0 (0%)	0 (0%)	0 (0%)
Stomach	10	2 (20%)	0 (0%)	0 (0%)	0 (0%)	0 (0%)
Colon	10	1 (10%)	0 (0%)	0 (0%)	0 (0%)	0 (0%)
Pancreas/bile duct	10	0 (0%)	0 (0%)	0 (0%)	0 (0%)	0 (0%)
Breast	10	1 (10%)	1[a] (10%)	1[a] (10%)	0 (0%)	1 (10%)

The percentage values are rounded to the nearest whole number

Syn synaptophysin, *Ch-A* chromogranin-A, *CD56* CD56/NCAM

[a] Positivity for both was recognized in an identical case and was positive for estrogen receptor and progesterone receptor, but negative for Her2 protein. This case was diagnosed as primary ductal carcinoma with neuroendocrine features since the case did not show specific neuroendocrine morphological findings and had intraductal carcinoma component

(37.5%) or carcinoid tumor (28.6%; Table 1). This difference may have been attributable to the rosette subtypes present. SCLC and carcinoid tumors frequently include Homer–Wright-type rosettes, which express ZO-1 less frequently than Flexner-type rosettes (Table 2 and Fig. 3). These results indicate that LCNEC is more closely associated with neural tube formation than is the case for SCLC and suggest that these two high-grade neuroendocrine carcinomas of the lung originate from different cells, and/or have different mechanisms of carcinogenesis.

In order to compare the immunohistochemical characteristics of rosettes and tube-like structures, we examined 43 well-differentiated tubular adenocarcinomas for their expression of ZO-1 and *N*-cadherin. Almost all cases were negative for both ZO-1 and *N*-cadherin (Fig. 4 and Table 3). This was not surprising because the tubular structures of adenocarcinoma are not rosettes and would thus be nearly negative for both proteins. The present results indicated that ZO-1 and *N*-cadherin would be very powerful immunohistochemical markers for differentiating rosettes from tubular structures in adenocarcinoma. On the other hand, it was interesting to note that one ductal carcinoma of the breast (1/43, 2.3%) expressed ZO-1 strongly in the apical area of tubular structures only in the invasive area (RoI=32.3%), the staining pattern being similar to that of Flexner-type rosettes (Fig. 4**l**, insert). However, this case was negative for other markers of neuroendocrine differentiation (synaptophysin, chromogranin-A, and CD56/NCAM). Therefore, the biological significance of ZO-1 may differ from that of other common neuroendocrine markers.

To our knowledge, this is the first report to have pointed out the similarity between rosette structures in pulmonary neuroendocrine tumors and the embryonic neural tube. Although this study is descriptive and preliminary, our findings allow us to propose a completely original concept that will undoubtedly be helpful for understanding the mechanisms leading to rosette formation in neuroendocrine tumors, recapitulating formation of the neural tube during embryogenesis. On the basis of these results, we propose that ZO-1 and *N*-cadherin are very useful immunohistochemical markers of rosettes in pulmonary neuroendocrine tumors, allowing them to be differentiated from glandular structures in adenocarcinoma, especially in small specimens. This knowledge may be of help in understanding the biological features of pulmonary neuroendocrine tumor and the essential differences between LCNEC and SCLC.

Since the number of cases examined here was limited, we did not analyze the outcome of the studied patients. Therefore, it will be necessary to confirm the outcome in a prospective study using a large cohort. A few previous studies have examined the contribution of ZO-1 to prognosis. Their findings have indicated that the level of ZO-1 messenger RNA is a valuable indicator of outcome in patients with non-small cell lung cancer and that there is no significant correlation between the level of ZO-1 immunoexpression and outcome in gastric cancer [29] [30]. On the other hand, Asamura et al. have reported that the diagnosis of LCNEC is a predictor of poor outcome [31]. It would be interesting to analyze the outcome of cases of large cell carcinoma lacking expression of synaptophysin, chromogranin-A, and CD56/NCAM, but showing ZO-1- and *N*-cadherin-positive rosette formation, which until now have not been classified as LCNEC.

In conclusion, analysis of ZO-1 and *N*-cadherin may help to clarify the mechanisms leading to rosette formation in neuroendocrine tumors, in the context of neural tube formation during embryogenesis, and may have utility in the diagnosis of pulmonary neuroendocrine tumors in differentiating rosettes from glandular structures in adenocarcinoma, especially in small specimens.

Conflict of interest statement We declare that we have no conflicts of interest.

References

1. Colby TV KM, Travis WD. Large cell neuroendocrine carcinoma:, In: Colby TV KM, Travis WD, editors (1995) Tumors of the lower respiratory tract. Armed Forces Institute of Pathology:248–257
2. Travis WD BE, Müller-Hermelink HK, Harris CC editor (2004) Pathology and Genetics of Tumours of the Lung, Pleura, Thymus and Heart. World Health Organization Classification of Tumours 10
3. Arrigoni MG, Woolner LB, Bernatz PE (1972) Atypical carcinoid tumors of the lung. J Thorac Cardiovasc Surg 64(3):413–421
4. Carretta A, Ceresoli GL, Arrigoni G, Canneto B, Reni M, Cigala C, Zannini P (2000) Diagnostic and therapeutic management of neuroendocrine lung tumors: a clinical study of 44 cases. Lung Cancer 29(3):217–225
5. Garcia-Yuste M, Matilla JM, Alvarez-Gago T, Duque JL, Heras F, Cerezal LJ, Ramos G (2000) Prognostic factors in neuroendocrine lung tumors: a Spanish Multicenter Study. Spanish Multicenter Study of Neuroendocrine Tumors of the Lung of the Spanish Society of Pneumonology and Thoracic Surgery (EMETNE-SEPAR). Ann Thorac Surg 70(1):258–263
6. Gould VE, Linnoila RI, Memoli VA, Warren WH (1983) Neuroendocrine cells and neuroendocrine neoplasms of the lung. Pathol Annu 18(Pt 1):287–330
7. Jiang SX, Kameya T, Shoji M, Dobashi Y, Shinada J, Yoshimura H (1998) Large cell neuroendocrine carcinoma of the lung: a histologic and immunohistochemical study of 22 cases. Am J Surg Pathol 22(5):526–537
8. Naranjo Gomez JM, Gomez Roman JJ Behaviour and survival of high-grade neuroendocrine carcinomas of the lung. Respir Med 104 (12):1929–1936
9. Peng WX, Sano T, Oyama T, Kawashima O, Nakajima T (2005) Large cell neuroendocrine carcinoma of the lung: a comparison with large cell carcinoma with neuroendocrine morphology and small cell carcinoma. Lung Cancer 47(2):225–233
10. Takei H, Asamura H, Maeshima A, Suzuki K, Kondo H, Niki T, Yamada T, Tsuchiya R, Matsuno Y (2002) Large cell neuroendocrine carcinoma of the lung: a clinicopathologic study of eighty-seven cases. J Thorac Cardiovasc Surg 124(2):285–292

11. Warren WH, Faber LP, Gould VE (1989) Neuroendocrine neoplasms of the lung. A clinicopathologic update. J Thorac Cardiovasc Surg 98 (3):321–332
12. Warren WH, Gould VE, Faber LP, Kittle CF, Memoli VA (1985) Neuroendocrine neoplasms of the bronchopulmonary tract. A classification of the spectrum of carcinoid to small cell carcinoma and intervening variants. J Thorac Cardiovasc Surg 89(6):819–825
13. Warren WH, Memoli VA, Gould VE (1988) Well differentiated and small cell neuroendocrine carcinomas of the lung. Two related but distinct clinicopathologic entities. Virchows Arch B Cell Pathol Incl Mol Pathol 55(5):299–310
14. Kloppel G (2007) Tumour biology and histopathology of neuroendocrine tumours. Best Pract Res Clin Endocrinol Metab 21(1):15–31
15. Wippold FJ 2nd, Perry A (2006) Neuropathology for the neuroradiologist: rosettes and pseudorosettes. AJNR Am J Neuroradiol 27(3):488–492
16. Koch P, Opitz T, Steinbeck JA, Ladewig J, Brustle O (2009) A rosette-type, self-renewing human ES cell-derived neural stem cell with potential for in vitro instruction and synaptic integration. Proc Natl Acad Sci U S A 106(9):3225–3230
17. Elkabetz Y, Panagiotakos G, Al Shamy G, Socci ND, Tabar V, Studer L (2008) Human ES cell-derived neural rosettes reveal a functionally distinct early neural stem cell stage. Genes Dev 22 (2):152–165
18. Aaku-Saraste E, Hellwig A, Huttner WB (1996) Loss of occludin and functional tight junctions, but not ZO-1, during neural tube closure–remodeling of the neuroepithelium prior to neurogenesis. Dev Biol 180(2):664–679
19. Nishimura T, Takeichi M (2008) Shroom3-mediated recruitment of Rho kinases to the apical cell junctions regulates epithelial and neuroepithelial planar remodeling. Development 135(8):1493–1502
20. Hatta K, Takeichi M (1986) Expression of N-cadherin adhesion molecules associated with early morphogenetic events in chick development. Nature 320(6061):447–449
21. Hatta K, Takagi S, Fujisawa H, Takeichi M (1987) Spatial and temporal expression pattern of N-cadherin cell adhesion molecules correlated with morphogenetic processes of chicken embryos. Dev Biol 120(1):215–227
22. Zynger DL, Dimov ND, Ho LC, Laskin WB, Yeldandi AV (2008) Differential expression of neural-cadherin in pulmonary epithelial tumours. Histopathology 52(3):348–354
23. Stevenson BR, Siliciano JD, Mooseker MS, Goodenough DA (1986) Identification of ZO-1: a high molecular weight polypeptide associated with the tight junction (zonula occludens) in a variety of epithelia. J Cell Biol 103(3):755–766
24. Itoh M, Nagafuchi A, Yonemura S, Kitani-Yasuda T, Tsukita S, Tsukita S (1993) The 220-kD protein colocalizing with cadherins in non-epithelial cells is identical to ZO-1, a tight junction-associated protein in epithelial cells: cDNA cloning and immunoelectron microscopy. J Cell Biol 121(3):491–502
25. Tsukita S, Yamazaki Y, Katsuno T, Tamura A, Tsukita S (2008) Tight junction-based epithelial microenvironment and cell proliferation. Oncogene 27(55):6930–6938
26. Katsuno T, Umeda K, Matsui T, Hata M, Tamura A, Itoh M, Takeuchi K, Fujimori T, Nabeshima Y, Noda T, Tsukita S, Tsukita S (2008) Deficiency of zonula occludens-1 causes embryonic lethal phenotype associated with defected yolk sac angiogenesis and apoptosis of embryonic cells. Mol Biol Cell 19(6):2465–2475
27. Palatinus JA, O'Quinn MP, Barker RJ, Harris BS, Jourdan J, Gourdie RG ZO-1 determines adherens and gap junction localization at intercalated disks. Am J Physiol Heart Circ Physiol 300 (2):H583-594
28. Smalley KS, Brafford P, Haass NK, Brandner JM, Brown E, Herlyn M (2005) Up-regulated expression of zonula occludens protein-1 in human melanoma associates with N-cadherin and contributes to invasion and adhesion. Am J Pathol 166(5):1541–1554
29. Wang Y, Zhou J, Zeng F, Huang Y, Zhou S, Liu X [Expression and clinical significance of ZO-1 in patients with non-small cell lung cancer]. Zhongguo Fei Ai Za Zhi 14 (2):146–150
30. Ohtani S, Terashima M, Satoh J, Soeta N, Saze Z, Kashimura S, Ohsuka F, Hoshino Y, Kogure M, Gotoh M (2009) Expression of tight-junction-associated proteins in human gastric cancer: down-regulation of claudin-4 correlates with tumor aggressiveness and survival. Gastric Cancer 12(1):43–51
31. Asamura H, Kameya T, Matsuno Y, Noguchi M, Tada H, Ishikawa Y, Yokose T, Jiang SX, Inoue T, Nakagawa K, Tajima K, Nagai K (2006) Neuroendocrine neoplasms of the lung: a prognostic spectrum. J Clin Oncol 24(1):70–76

Virchows Arch (2011) 459:409–414
DOI 10.1007/s00428-011-1138-2

ORIGINAL ARTICLE

Epithelial marker expression does not rule out a diagnosis of Ewing's sarcoma family of tumours

Isidro Machado · Samuel Navarro · Jose A. López-Guerrero · Marco Alberghini · Piero Picci · Antonio Llombart-Bosch

Received: 5 July 2011 / Revised: 10 August 2011 / Accepted: 16 August 2011 / Published online: 2 September 2011
© Springer-Verlag 2011

Abstract Epithelial marker expression has been reported in Ewing's sarcoma family of tumors (ESFT). However, cytokeratin (CK), epithelial membrane antigen (EMA), and carcino embryonic antigen (CEA) prevalence has not been assessed thoroughly in a large series of genetically confirmed ESFT. The aim of the present study is to confirm the presence of epithelial markers in a large group of ESFT tested genetically for any of their specific gene fusions and the differential diagnosis with other small round cell tumors. To establish the prevalence of epithelial markers, we then performed immunohistochemical studies with antibodies CK (AE1/AE3), CK8/18, CK34β12, EMA, E-cadherin, and CEA on 415 genetically confirmed ESFT. Immunoreactivity to cytokeratin, EMA, and CEA was present in 19.2%, 6.6%, and 20.8% of cases, respectively. There was no significant association between epithelial markers and histological subtypes, but the atypical variant of ESFT expressed these markers in a high proportion compared with the peripheral neuroectodermal tumors and the conventional variant. The present findings confirm that epithelial marker expression in ESFT, including EMA and CEA, does not rule out a diagnosis of ESFT, and the integration of clinical, radiological, histopathological, immunohistochemical, and molecular genetic findings should form the basis for the diagnosis of bone and soft tissue sarcomas, especially in tumors with atypical or unusual phenotype.

Keywords Ewing's sarcoma · Epithelial markers · Immunohistochemistry · CK · EMA · CEA

I. Machado · S. Navarro · A. Llombart-Bosch (✉)
Pathology Department, University of Valencia,
Blasco Ibañez, 16,
46015 Valencia, Spain
e-mail: antonio.llombart@uv.es

J. A. López-Guerrero
Molecular Biology Department,
Instituto Valenciano de Oncología,
Valencia, Spain

I. Machado
Pathology Department, Instituto Valenciano de Oncología,
Valencia, Spain

M. Alberghini · P. Picci
Pathology Department, Instituto Orthopedic Rizzoli,
Bologna, Italy

Introduction

Ewing's sarcoma family of tumors (ESFT) is formed by a group of small round cell tumors (SRCT) genetically defined by specific chromosomal translocations which result in a fusion of the *EWSR1* gene, mainly with a member of the ETS family of transcription factors: *FLI1* (11q24), *ERG* (21q22), *FEV* (2q33), *ETV1* (7p22), and *ETV4* (17q12) [1–6]. Other gene fusions have been described in ESFT, including *FUS/ERG*, *FUS/FEV*, *EWSR1/PATZ1*, *EWSR1/SP3*, *EWSR1/NFATc2*, *BRD4/NUT*, *CIC/DUX4* [5, 6], and *EWSR1/SMARCA5* [7]. The histopathology includes three larger categories according to their predominant morphological criteria: conventional Ewing's sarcoma (ES), peripheral neuroectodermal tumors (PNET), and atypical ES comprising all subtypes distinct from the other two types [2, 3]. ESFT appears to have the potential for differentiating toward mesenchymal, neural, and epithelial lineages. The immunohistochemical (IHC) study in a large series of ESFT previously described by Llombart-Bosch et al. [2] confirmed the diagnostic value of CD99, HNK1, Fli1, and CAV1, which together cover more than 99% of ESFT

and substantiated the mesenchymal and neural differentiation of this neoplasm [2–4].

Cytokeratin (CK) and other epithelial markers have been reported to be expressed in ESFT, confirming the tendency towards epithelial differentiation [8–18]. Particular attention must be paid to the atypical ESFT in which an epithelial differentiation may be present, especially when expressing epithelial membrane antigen (EMA) [2, 3]. In these cases, the histology might not be diagnostic, making the differential diagnosis with other SRCT more challenging [2, 3, 6, 14]. Here, the support of molecular techniques (fluorescence in situ hybridization (FISH) and/or reverse transcription polymerase chain reaction (RT-PCR)) is mandatory in order to exclude other types of SRCT.

The most relevant publications regarding epithelial immunoexpression in ESFT have been performed in relatively small series of cases [8–10, 14]; therefore, its prevalence has not been systematically assessed so far. In addition, EMA and carcino embryonic antigen (CEA) immunohistochemical expression in genetically confirmed ESFT has not yet been described.

The objective of the present study is to confirm the presence of epithelial markers in a large group of ESFT that were tested genetically for any of their specific gene fusions [1–3] and the differential diagnosis with other SRCT.

Material and methods

Formalin-fixed, paraffin-embedded blocks from 415 specimens of ESFT were retrieved from the archives of participating centers of the PROTHETS and EuroBoNeT projects, as previously described [2]. The histopathological analyses were performed on the whole tissue sections, and all tumors were histological classified as conventional, PNET, or atypical variant as described by Llombart-Bosch et al. [2]

Twenty-four tissue microarrays (TMAs) were constructed; each TMA included two representative cores for each case (1-mm diameter) as well as normal tissue controls. TMA sections, 4 μm thick, were processed for immunohistochemistry (IHC). Antigen retrieval was performed by pressure cooker boiling at 1.2 atm for 3 min in 10 mmol/L citrate buffer (pH 6.0). The labeled streptavidin–biotin method (Dako) was performed, followed by revelation with 3,3′-diaminobenzidine as conventional protocols. Tumors were immunostained using TMA at UVEG with the commercially available antibodies summarized in Table 1. Normal kidney or liver tissue served as positive controls. Negative controls consisted of the substitution of buffer for the primary antibody. The immunostaining score was classified as non-informative (scant material, artifact, tumor necrosis), negative (mild in <5%), or positive: 1+ (mild in 5–10%), 2+ (moderate in 10–50%), and 3+ (intense in >50%) mainly cytoplasmic, paranuclear, or membranous staining. All sections were evaluated independently by three pathologists (IM, SN, and ALLB), and any differences were resolved by consensus. All cases had previously been shown to be positive for the ESFT-specific translocations by RT-PCR and/or FISH (data describe elsewhere) [1, 2]. All the statistical analyses were carried out using the SPSS software (version 15.0.1, SPSS, Chicago, IL, USA).

Table 1 List of antibodies, source, and dilution

Antibodies	Source	Dilution
CK(AE1/AE3)	Dako	1/50
CK 8/18	Novocastra	1/50
CK 34β12	Novocastra	1/50
E-cadherin	Novocastra	1/20
EMA	Dako	1/200
CEA	Dako	1/50

Results

Immunohistochemical expression of epithelial markers is summarized in Table 2. All tumors positive for CK 8/18, CK 34β12, EMA, CEA, or E-cadherin were also positive for CK (AE1/AE3). Figures 1 and 2 show epithelial immunoexpression in the present series.

Table 2 Immunohistochemical expression of epithelial markers in Ewing's sarcoma family of tumors

Epithelial marker	ESFT
CK (AE1/AE3)	
Positive	76 (19.2%)
Negative	319 (80.8%)
CK8/18	
Positive	28 (12%)
Negative	207 (88%)
CK 34β12	
Positive	9 (4%)
Negative	220 (96%)
EMA	
Positive	18 (6.6%)
Negative	256 (93.4%)
CEA	
Positive	57 (20.8%)
Negative	217 (79.2%)
E-cadherin	
Positive	10 (3%)
Negative	368 (97%)

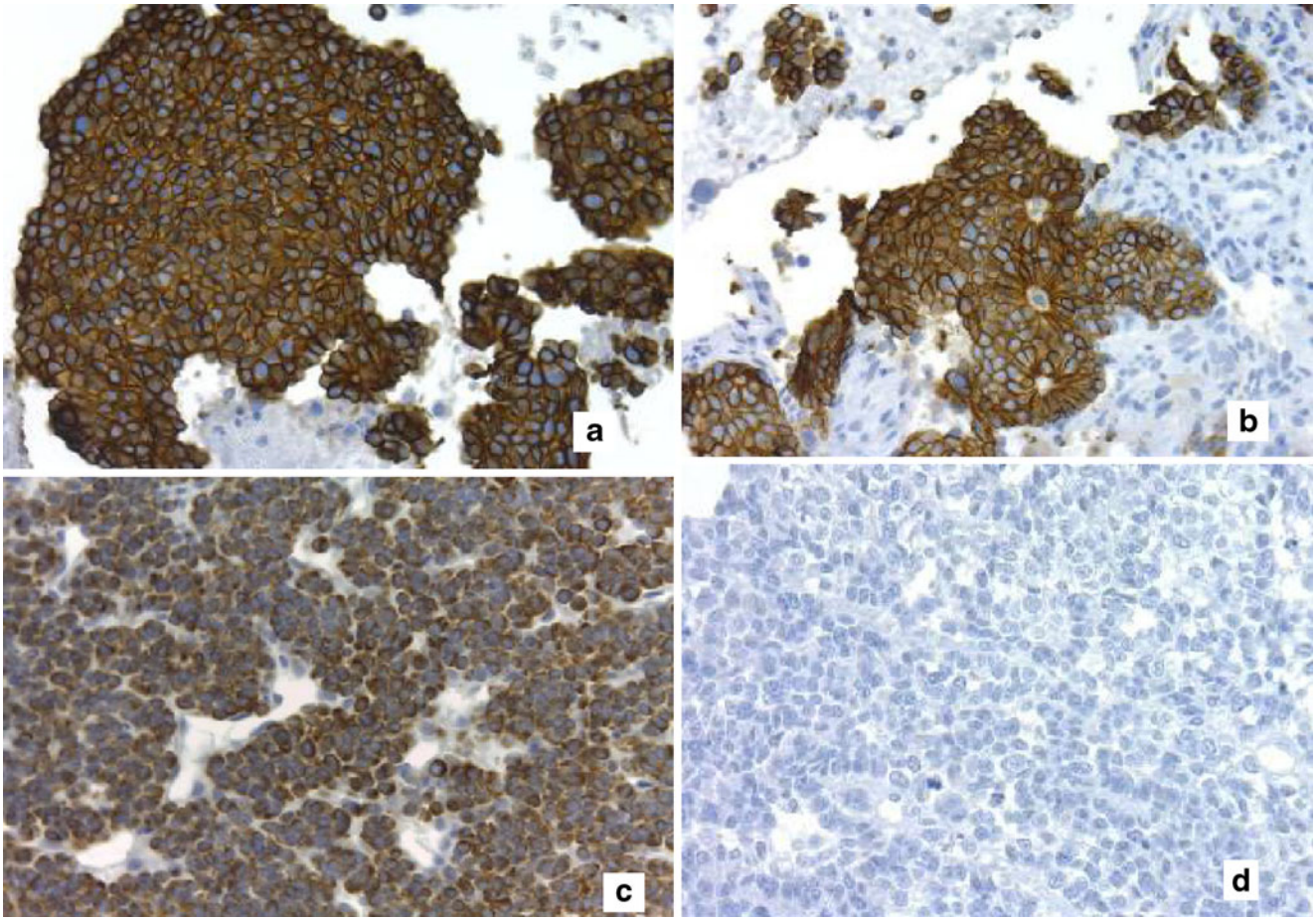

Fig. 1 **a** Strong Pan-CK (AE1/AE3) expression in atypical ESFT ×40. **b** Membranous CK immunoexpression in PNET ×40. **c** Strong cytoplasmic and membranous CEA expression in atypical ESFT ×40. **d** Negative E-cadherin immunoexpression in PNET ×40

Positive cases revealed CK (AE1/AE3), CK 8/18, CK 34β12, CEA, or EMA cytoplasmic, paranuclear/dot-like, or membranous patterns of immunoexpression. A combination of cytoplasmic and membranous staining was frequently observed. However, positive cases for E-cadherin revealed only a membranous pattern of immunoexpression.

The correlations between epithelial marker immunoexpression and the histological subtypes of ESFT are summarized in Table 3. Although the statistical analysis did not reveal significant results, except for E-cadherin expression, the atypical variant expressed a high proportion of the epithelial markers.

Discussion

Immunohistochemical studies in ESFT have demonstrated that 20–46% of these tumors express cytokeratins, suggestive of partial epithelial marker expression [8, 9, 14, 16]. This finding may be associated with intercellular junction formation in cytokeratin-positive ESFT at ultrastructural level [8, 9, 12, 16, 19]. This alteration has also been observed in several of these same cases analyzed at electron microscopy level by our group (Peydro-Olaya et al. [19]). The epithelial differentiation in ESFT was first reported by Hutter et al. in 1965, in 25 cases of primitive sarcoma of the bone (PSB), including a case of Ewing's sarcoma with the presence of squamous pearls [8, 20]. Although ESFT may reveal epithelial trends, mainly at IHC level, in the present series we did not find squamous pearls in any of the cases, leading us to suspect that the cases reported by Hutter et al. [8, 20], carried out before the molecular era, were probably PSB with multipotential capacity of differentiation and not ESFT. In 1987, Moll et al. [8, 21] communicated 11 cases of ESFT with cytokeratin 8/18 immunoexpression in 81% of tumors. Additional epithelial IHC studies with small series of ESFT were performed in subsequent years where the percentage of positivity for epithelial markers fluctuated from 50% as reported by Navarro et al. [22] to 0% as published by Dierick et al. [23] and Miettinen et al. [24]. Most of the studies were based only on the histological diagnoses, performed with or without CD99 IHC expres-

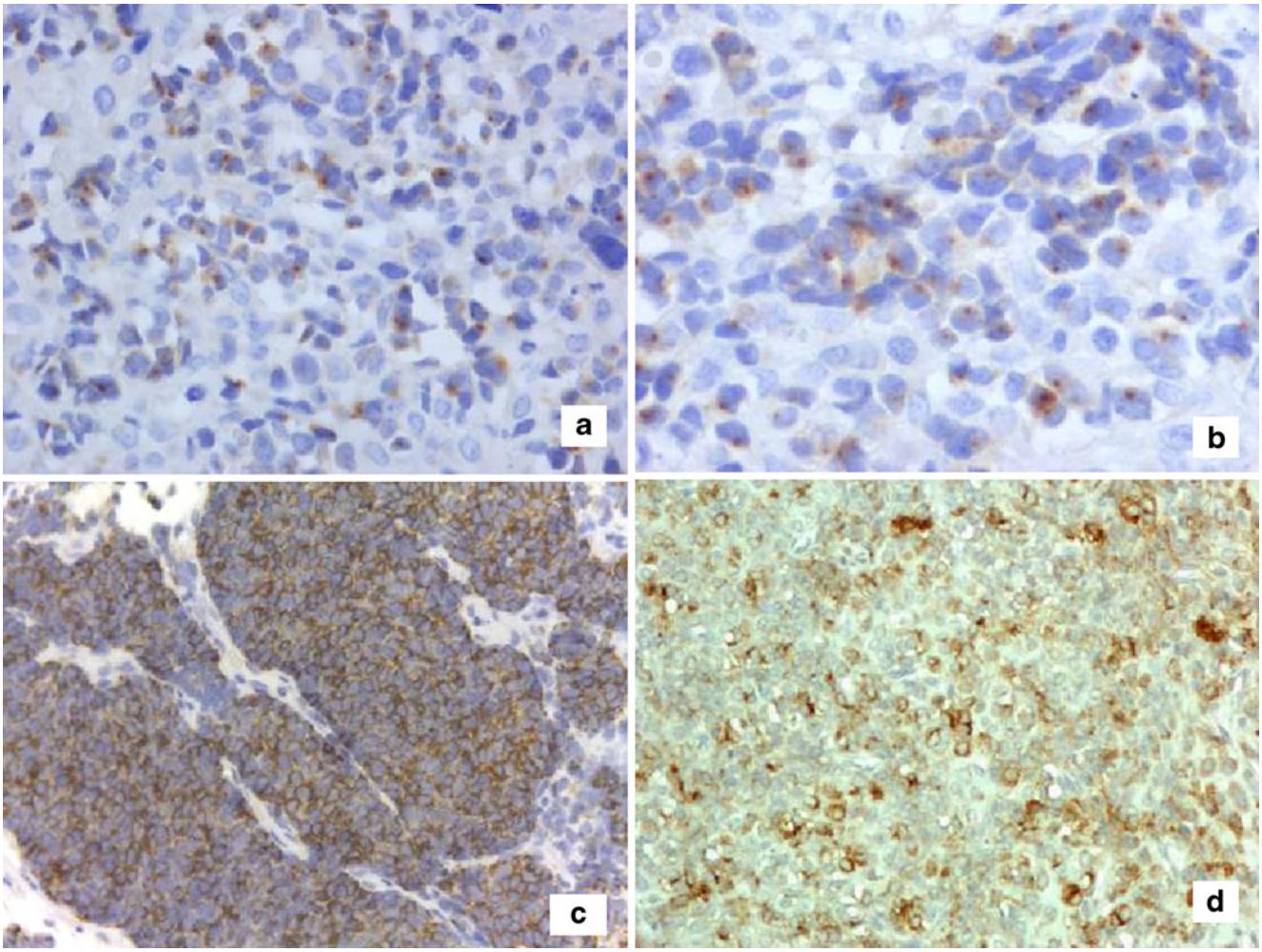

Fig. 2 **a** Moderate cytoplasmic and dot-like EMA expression in atypical ESFT ×40. **b** Dot-like (Golgi-stained) EMA expression in atypical ESFT ×100. **c** Strong cytoplasmic and membranous EMA expression in PNET ×40. **d** Moderate cytoplasmic and membranous EMA immunoexpression in conventional ESFT ×40

sion, except the studies with genetically confirmed tumors performed by Navarro et al. [22] and Hasegawa et al. [17]; therefore, the possible inclusion of other SRCT (synovial sarcomas, desmoplastic small round cell tumors, etc.) cannot be excluded in these series of tumors lacking genetic confirmation. In recent years, new studies in genetically confirmed tumor series (Table 4) have been published, providing a more accurate prevalence of epithelial markers in ESFT [8, 9, 11, 14, 16].

The majority of these studies have described CK expression in ESFT [8, 9, 11, 14, 16], and additionally, Gu M et al. [8] and Schuetz et al. [16] have also reported CAM5.2 and E-cadherin immunoexpression, respectively; however, staining for EMA, CEA, CK8/18, and 34β12 has not been described until the present series. Cytokeratin positivity was usually detected in most of these studies, including the present series, with either cytoplasmic, Golgi/perinuclear, or membranous location. The significance of demonstrating that ESFT can be positive for cytokeratin in a significant number of cases (19.2% in the present series) indicated the need to distinguish them from other SRCT that are usually positive for cytokeratins and to emphasize that epithelial marker expression in any SRCT does not rule out the possibility of ESFT [3, 8, 9, 16]. Soft tissue tumors, including synovial sarcoma, desmoplastic small round cell tumor (DSRCT), malignant rhabdoid tumor, epithelioid sarcoma, myoepithelial carcinoma, and other carcinomas including neuroendocrine carcinoma, and bone tumors, mainly small cell osteosarcoma, are the most frequent SRCT with epithelial marker expression that can mimic ESFT at clinical, histopathology, IHC, and molecular levels in pediatric or adult patients [2–4, 6–9, 14]. In these particular cases, the definitive diagnosis may require the demonstration of a specific gene fusion by RT-PCR and, particularly in tumors with *EWSR1* translocation, by FISH and CK expression (DSRCT, ESFT, and myoepithelial carcinoma) [2–4, 6].

EMA and CEA expression in ESFT has not been assessed in a large series of ESFT; only Gonin et al. [18] have

Table 3 Correlations between epithelial marker immunoexpression and the histological subtypes

Marker	Conventional	PNET	Atypical	*p*
CK				
Positive	46 (18.3%)	8 (14.5%)	22 (24.7%)	0.268
Negative	205 (81.7%)	47 (85.5%)	67 (75.3%)	
CK8/18				
Positive	15 (10%)	3 (10%)	10 (18%)	0.232
Negative	134 (90%)	29 (90%)	44 (82%)	
CK 34β12				
Positive	7 (5%)	0 (0%)	2 (4%)	0.454
Negative	138 (95%)	31 (100%)	51 (96%)	
EMA				
Positive	10 (6.1%)	2 (4.5%)	6 (9.1%)	0.595
Negative	154 (93.9%)	42 (95.5%)	60 (90.9%)	
CEA				
Positive	33 (20.1%)	9 (20.5%)	15 (22.7%)	0.906
Negative	131 (79.9%)	35 (79.5%)	51 (77.3%)	
E-cadherin				
Positive	4 (2%)	0 (0%)	6 (8%)	0.004
Negative	249 (98%)	50 (100%)	69 (92%)	

published EMA positivity in one case of ESFT with molecular confirmation located in the adrenal gland. The prevalence of EMA positivity in ESFT seems to be relatively low when compared to CK expression, as happens in the present series where 6.6% of the tumors expressed this marker. Thus, CK expression and EMA expression in SRCT do not exclude the possibility of an ESFT.

Indeed, EMA and/or CEA expression in ESFT further complicates the differential diagnosis with other SRCT located mainly in the soft tissue (poorly differentiated synovial sarcoma, malignant rhabdoid tumor, myoepithelial carcinomas, and other carcinomas including neuroendocrine tumors) and SRCT located in the bone (small cell osteosarcomas and primitive sarcoma of the bone). In these cases, molecular analyses (FISH and RT-PCR) are mandatory to determine the specific genetic alteration [2–4, 6, 18]. Nevertheless, additional immunohistochemical results in combination with molecular data can favor a specific diagnosis. Poorly differentiated synovial sarcoma is frequently indistinguishable from atypical ESFT and particularly from those expressing CK and EMA [3]. In these cases, the detection by molecular methods of *SYT* or *EWSR1* rearrangements clarifies the final diagnosis. Malignant rhabdoid tumor usually reveals loss of INI1 expression, and the *EWSR1* rearrangement in this type of tumor has not been described so far [3]. Myoepithelial carcinoma usually reveals calponin which has not been described so far in ESFT and additionally myoepithelial carcinomas can reveal S100 and GFAP in a lesser proportion, both of which are sporadically expressed in ESFT [3, 25–27]. Furthermore, molecular studies fail to detect any gene fusions associated with ESFT in myoepithelial carcinomas [3, 25–27]. Despite the fact that ESFT can reveal focal neuroendocrine immunoexpression, chromogranin-A, synaptophysin, and CD56 immunoexpression in neuroendocrine tumors is much higher when compared with ESFT [3, 28]. The findings of malignant osteoid formation support the possibility of small cell osteosarcoma in atypical bone ESFT [3]. In addition, small cell osteosarcoma can reveal desmin, not reported until now in atypical ESFT [3].

No previous studies regarding ESFT have established a correlation between the histological subtypes and CK expression [8, 9, 14, 16, 17]. In the present study, despite the lack of statistical significance, except for E-cadherin positivity, the atypical variant of ESFT more frequently expressed the epithelial markers. Therefore, special attention must be paid to the atypical ESFT because their histology might not be diagnostic and the clinical behavior more problematic. The support of molecular techniques is mandatory in order to exclude an SRCT other than ESFT. Atypical SRCT with CK, EMA, or CEA expression, soft tissue location, and the presence of trabecular, tubular, or pseudoglandular patterns complicate the differential diagnosis with atypical adamantinoma-like ESFT, soft tissue myoepithelial carcinoma, neuroendocrine metastatic carcinoma, or poorly differentiated carcinoma, even more so when considering the fact that most of myoepithelial carcinoma and some neuroendocrine carcinomas may harbor the *EWSR1* translocation [3, 25–28].

Table 4 Epithelial markers immunoexpression in genetically confirmed ESFT series

References	Number	CK	EMA	CEA	CAM5.2	CK 8/18	34β12	E-cadherin
Gu et al. [8]	50	20%	dns	dns	20%	dns	dns	dns
Collini et al. [9]	41	31.7%	dns	dns	dns	dns	dns	dns
Folpe et al. [14]	66	32%	dns	dns	dns	dns	dns	dns
Schuetz et al. [16]	30	46%	dns	dns	dns	dns	dns	0%
Present series, 2011	415	19.2%	6.6%	20.8%	dns	12%	4%	3%

dns data not shown

E-cadherin expression in the present series was very low, a fact that is concordant with a previous study published by Schuetz et al. [16], in which no E-cadherin expression was observed in any of the 30 tumors studied, suggesting that ESFT probably lose E-cadherin expression [16, 29].

In conclusion, the present IHC findings confirm that epithelial marker expression in ESFT, including EMA and CEA, does not rule out a diagnosis of ESFT. Therefore, the integration of clinical, radiological, histopathological, IHC, and molecular genetic findings should form the basis for the diagnosis of bone and soft tissue sarcomas, especially in tumors with atypical or unusual phenotype. Additionally, further studies are required to determine to what degree this epithelial immunoexpression in ESFT offers any clinical prognostic significance.

Acknowledgments This study was performed with grants from the European Union (EuroBoNeT project contract no. 018814).

Conflict of interest statement We declare that we have no conflict of interest.

References

1. Machado I, Noguera R, Pellin A et al (2009) Molecular diagnosis of Ewing sarcoma family of tumors: a comparative analysis of 560 cases with FISH and RT-PCR. Diagn Mol Pathol 18:189–199
2. Llombart-Bosch A, Machado I, Navarro S et al (2009) Histological heterogeneity of Ewing's sarcoma/PNET: an immunohistochemical analysis of 415 genetically confirmed cases with clinical support. Virchows Arch 455:397–411
3. Machado I, Noguera R, Mateos EA et al (2011) The many faces of atypical Ewing's sarcoma. A true entity mimicking sarcomas, carcinomas and lymphomas. Virchows Arch 458:281–290
4. Romeo S, Dei Tos AP (2010) Soft tissue tumors associated with EWSR1 translocation. Virchows Arch 456:219–234
5. Ordóñez JL, Osuna D, García-Domínguez DJ et al (2010) The clinical relevance of molecular genetics in soft tissue sarcomas. Adv Anat Pathol 17:162–181
6. Gamberi G, Cocchi S, Benini S et al (2011) Molecular diagnosis in Ewing family tumors: the Rizzoli experience—222 consecutive cases in four years. J Mol Diagn 13:313–324
7. Sumegi J, Nishio J, Nelson M, Frayer RW, Perry D, Bridge JA (2011) A novel t(4;22)(q31;q12) produces an EWSR1-SMARCA5 fusion in extraskeletal Ewing sarcoma/primitive neuroectodermal tumor. Mod Pathol 24:333–342
8. Gu M, Antonescu CR, Guiter G, Huvos AG, Ladanyi M, Zakowski MF (2000) Cytokeratin immunoreactivity in Ewing's sarcoma: prevalence in 50 cases confirmed by molecular diagnostic studies. Am J Surg Pathol 24:410–416
9. Collini P, Sampietro G, Bertulli R et al (2001) Cytokeratin immunoreactivity in 41 cases of ES/PNET confirmed by molecular diagnostic studies. Am J Surg Pathol 25:273–274
10. Jimenez RE, Folpe AL, Lapham RL et al (2002) Primary Ewing's sarcoma/primitive neuroectodermal tumor of the kidney: a clinicopathologic and immunohistochemical analysis of 11 cases. Am J Surg Pathol 26:320–327
11. Folpe AL, Hill CE, Parham DM, O'Shea PA, Weiss SW (2000) Immunohistochemical detection of FLI-1 protein expression: a study of 132 round cell tumors with emphasis on CD99-positive mimics of Ewing's sarcoma/primitive neuroectodermal tumor. Am J Surg Pathol 24:1657–1662
12. Srivastava A, Rosenberg AE, Selig M, Rubin BP, Nielsen GP (2005) Keratin-positive Ewing's sarcoma: an ultrastructural study of 12 cases. Int J Surg Pathol 13:43–50
13. Woestenborghs H, Debiec-Rychter M, Renard M, Demaerel P, Van Calenbergh F, Van Gool S, Sciot R (2005) Cytokeratin-positive meningeal peripheral PNET/Ewing's sarcoma of the cervical spinal cord: diagnostic value of genetic analysis. Int J Surg Pathol 13:93–97
14. Folpe AL, Goldblum JR, Rubin BP et al (2005) Morphologic and immunophenotypic diversity in Ewing family tumors: a study of 66 genetically confirmed cases. Am J Surg Pathol 29:1025–1033
15. Parham DM, Hijazi Y, Steinberg SM et al (1999) Neuroectodermal differentiation in Ewing's sarcoma family of tumors does not predict tumor behavior. Hum Pathol 30:911–918
16. Schuetz AN, Rubin BP, Goldblum JR et al (2005) Intercellular junctions in Ewing sarcoma/primitive neuroectodermal tumor: additional evidence of epithelial differentiation. Mod Pathol 18:1403–1410
17. Hasegawa SL, Davison JM, Rutten A, Fletcher JA, Fletcher CD (1998) Primary cutaneous Ewing's sarcoma: immunophenotypic and molecular cytogenetic evaluation of five cases. Am J Surg Pathol 22:310–318
18. Gonin J, Larousserie F, Dousset B et al (2011) An unusual adrenal tumor: Ewing tumor. Ann Pathol 31:28–31
19. Peydro-Olaya A, Llombart-Bosch A, Carda-Batalla C, Lopez-Guerrero JA (2003) Electron microscopy and other ancillary techniques in the diagnosis of small round cell tumors. Semin Diagn Pathol 20:25–45
20. Hutter RVP, Foote FW Jr, Francis KC, Sherman RS (1965) Primitive multipotential primary sarcoma of bone. Cancer 19:1–25
21. Moll R, Lee I, Gould VE, Berndt R, Roessner A, Franke WW (1987) Immunocytochemical analysis of Ewing's tumors. Patterns of expression of intermediate filaments and desmosomal proteins indicate cell type heterogeneity and pluripotential differentiation. Am J Pathol 127:288–304
22. Navarro S, Cavazzana AO, Llombart-Bosch A, Triche TJ (1994) Comparison of Ewing's sarcoma of bone and peripheral neuro-epithelioma. An immunocytochemical and ultrastructural analysis of two primitive neuroectodermal neoplasms. Arch Pathol Lab Med 118:608–615
23. Dierick AM, Roels H, Langlois M (1993) The immunophenotype of Ewing's sarcoma. An immunohistochemical analysis. Pathol Res Pract 189:26–32
24. Miettinen M, Lehto V-P, Virtanen I (1982) Histogenesis of Ewing's sarcoma. An evaluation of intermediate filaments and endothelial cell markers. Virchows Arch 41:277–284
25. Antonescu CR, Katabi N, Zhang L et al (2011) EWSR1-ATF1 fusion is a novel and consistent finding in hyalinizing clear-cell carcinoma of salivary gland. Genes Chromosomes Cancer 50:559–570
26. El-Kabany M, Al-Abdulghani R, Ali AE, Francis IM, Hussein SA (2011) Soft tissue high grade myoepithelial carcinoma with round cell morphology: report of a newly described entity with EWSR1 gene rearrangement. Gulf J Oncolog 1:73–77
27. Brandal P, Panagopoulos I, Bjerkehagen B, Heim S (2009) t(19;22)(q13;q12) Translocation leading to the novel fusion gene EWSR1-ZNF444 in soft tissue myoepithelial carcinoma. Genes Chromosomes Cancer 48:1051–1056
28. Malone VS, Dobin SM, Jones KA, Donner LR (2010) CD99-positive large cell neuroendocrine carcinoma with rearranged EWSR1 gene in an infant: a case of prognostically favorable tumor. Virchows Arch 457:389–395
29. Kang HG, Jenabi JM, Zhang J et al (2007) E-cadherin cell–cell adhesion in ewing tumor cells mediates suppression of anoikis through activation of the ErbB4 tyrosine kinase. Cancer Res 67:3094–3105

Virchows Arch (2011) 459:415–422
DOI 10.1007/s00428-011-1141-7

ORIGINAL ARTICLE

MTA1 expression correlates significantly with cigarette smoke in non-small cell lung cancer

Lei Xu · Xiao-yun Mao · Chui-feng Fan · Hua-chuan Zheng

Received: 21 March 2011 / Revised: 20 July 2011 / Accepted: 18 August 2011 / Published online: 3 September 2011
© Springer-Verlag 2011

Abstract Metastasis tumor antigen 1 (MTA1), a novel candidate metastasis-associated gene, is known to increase the migration and invasion of various tumor cells in vitro. Expression of MTA1 has been shown to be closely correlated with aggressiveness in a variety of human cancers including non-small cell lung cancer (NSCLC). Cigarette smoke is the most established risk for lung carcinogenesis; however, its effects on the progression of NSCLC are still unclear. In this study, we investigated MTA1 expression and analyzed its association with cigarette smoke in NSCLC by immunohistochemistry. To gain a deeper insight into the molecular mechanism underlying the relation between MTA1 and cigarette smoke, we treated the NSCLC cell lines with cigarette smoke extract (CSE). MTA1 mRNA levels and proteins were detected in NSCLC cell lines via reverse transcriptase-polymerase chain reaction (RT-PCR) and western blot analysis. Matrigel invasion assay was performed to evaluate cell invasive ability with the treatment of CSE. Immunohistochemical analysis showed MTA1 expression in NSCLC (61/96, 63.5%) was higher than that in adjacent normal lung tissues (15/96, 15.6%; $p<0.05$). Moreover, it was significantly associated with smoking history ($p<0.05$). The results of RT-PCR and western blotting showed the upregulation of MTA1 after the treatment of CSE in NSCLC cell lines. Matrigel invasion assays showed that MTA1 upregulation and cell invasion was accompanied with the treatment of CSE in the NSCLC cell lines. MTA1 expression correlated with cigarette smoke in NSCLC and suggested that it may play an important role in the smoked-related progress of NSCLC.

Keywords MTA1 · Cigarette smoke · NSCLC · Invasion

L. Xu (✉)
Department of Respiratory Medicine, The 4th Affiliated Hospital of China Medical University,
No. 4, Shangdong Road, Yuhong District,
Shenyang, Liaoning 110032, China
e-mail: xl_cmu@126.com

X.-y. Mao
Department of Breast Surgery and Surgical Oncology, Research Unit of General Surgery, The 1st Affiliated Hospital of China Medical University,
Shenyang, Liaoning 110001, China

C.-f. Fan
Department of Pathology, The 1st Affiliated Hospital and College of Basic Medical Sciences of China Medical University,
Shenyang, Liaoning 110001, China

H.-c. Zheng
Department of Biochemistry and Molecular Biology,
College of Basic Medical Sciences of China Medical University,
Shenyang, Liaoning 110001, China

Introduction

Metastasis tumor antigen 1 (MTA1), a candidate member of the metastasis-associated gene family, is a component of the nucleosome remodeling and deacetylating (NuRD) complex and has been implicated in tumor metastasis [1]. As a part of the NuRD complex, MTA1 regulates transcription of its targets by modifying the acetylation status of the target chromatin and cofactor accessibility to the target DNA [2]. Current models suggest that MTA1 regulates metastatic potential as part of the multiprotein Mi-2/nucleosome remodeling and NuRD by controlling the epithelial-to-mesenchymal transition [3, 4]. It also plays an important role in tumorigenesis and tumor aggressiveness. Overexpression of MTA1 has been shown to be closely

correlated with aggressiveness in a variety of human cancers including non-small cell lung cancer (NSCLC) [5–7]. Lung cancer ranks among the most lethal malignancies worldwide, with an incidence exceeding 1,000,000 cases per year. Mounting evidence indicates that aberrant expression/activity of epigenetic regulators of gene expression contributes significantly to lung carcinogenesis [8]. The vast majority of these neoplasms are directly attributable to cigarette smoking. Whereas the link between cigarette smoking and lung cancer risk is well established, the epigenetic mechanisms by which tobacco smoke initiates and maintains the malignant phenotype of lung cancer remain poorly understood. In the present study, we investigated MTA1 expression and analyzed its association with cigarette smoke in NSCLC.

Materials and methods

Patients and tissue samples

Tumor specimens including NSCLC tissues and paired non-tumor portion (with >5 cm distance from the primary tumor's edge) from 96 patients with NSCLC were obtained between 2009 and 2010 following surgical resection at the Fourth Affiliated Hospital of China Medical University. None of the patients had received radiotherapy, chemotherapy, or immunotherapy prior to tumor excision. Of the patients, 60 are male and 36 are female, creating a 1.67:1 ratio of male to female. Patients' ages at the time of surgery ranged from 26 to 79, with an average age of 57.9 years old. All specimens were re-evaluated for diagnosis following the World Health Organization histological classification of tumors of lung cancer in 2010 [9], and 43 squamous cell carcinomas, 48 adenocarcinomas, 4 large cell carcinomas, and 1 adenosquamous carcinomas were confirmed. The tumors were classified according to the TNM stage revised by the National Comprehensive Cancer Network (NCCN) [10]. The patients were divided into three groups based on smoke history: 25 never smokers (less than 100 cigarettes smoked in a lifetime, with or without exposure to involuntary smoking from the spouse or at workplace), 32 former smokers [smoking cessation for 2 years or more before diagnosis; average cumulative tobacco smoking, 14.8 pack-years, pack-years = (number of cigarettes smoked per day × number of years smoked)/20], and 39 current smokers (36.1 pack-years). This study was approved by the Ethical Committee of China Medical University, and the written informed consents were obtained from each patient. All samples were made anonymous, and none of the researchers conducting the experiments in the study had access to clinicopathological data.

Immunohistochemistry

Formalin-fixed and paraffin-embedded specimens were cut into 4-μm-thick sections, which were subsequently de-waxed and hydrated. Immunohistochemical staining for MTA1 (sc-17773, Santa Cruz, 1:200) was performed using UltraSensitive™ S-P kits (Maixin-Bio; People's Republic of China) according to the manufacturer's instructions and using the reagent supplied with the kit. For the negative control, phosphate-buffered saline was used in place of the primary antibodies. We adopted the German semi-quantitative scoring system in considering the staining intensity and area extent, which has been widely accepted and used in previous studies [11–13]. Every lesion was given a score according to the intensity of the staining (no staining = 0, weak staining = 1, moderate staining = 2, strong staining = 3) and the extent of stained cells (0%=0, 1–10%=1, 11–50%=2, 51–80%=3, 81–100%=4; negative means 0% area staining). The final immunoreactive score was determined by multiplying the intensity scores with the extent of positivity scores of stained cells, with the minimum score of 0 and a maximum score of 12 [11–13]. Slides were independently examined by two pathologists. However, if there was a discrepancy in individual scores, both pathologists re-evaluated together by reaching a consensus agreement before combining the individual scores. To obtained statistical results, a final score equal to or less than 1 was considered as negative, while scores of 2 or more were considered as positive.

Cell line and cell culture conditions

NSCLC cell lines including the higher metastatic BE1 cells, the lower metastatic LH7 cells, and lung adenocarcinoma A549 cells were chosen for this study and cultured in RPMI 1640 medium (Gibco, USA) supplemented with 10% fetal bovine serum (FBS) (Hyclone, USA) in a 5% CO2 humidified atmosphere at 37°C.

Preparation of cigarette smoke extract

Cigarette smoke extract (CSE) was prepared by a modification of the method of Carp and Janoff [14]. In brief, two cigarettes without filters, each containing 1.3 mg of nicotine and 15 mg of tar, were combusted with a modified syringe-driven apparatus. The smoke was bubbled through 50 ml of serum-free 1640, and the resulting suspension was adjusted to pH 7.4 with concentrated NaOH and then filtered through a 0.22-μm pore filter to remove bacteria and large particles. This medium was defined as 100% CSE. The resulting CSE was applied to cell cultures within 30 min of preparation.

MTT assay to pick up the optimal concentration of CSE

We picked the optimal concentration of CSE by the 3-(4,5-dimethylthiazol-2-yl)-2,5-diphenyltetrazoliumbromide (MTT) assay. Briefly, 2,000 cells were seeded in each well of a 96-well plate (eight repeats). Every group (n=6 in every group) was treated with varying concentrations of CSE (10%, 20%, 40%, 60%, and 100%) or fresh medium (control) for 16 h at 37°C. Then, 5 mg/ml MTT was added to each well and incubated for 4 h. The cells were lysed by adding 150 μl/well of dimethyl sulfoxide and read at 490 nm absorbance wavelength in microplate reader. The results showed that 20% is the optimal concentration of CSE.

Treatments of CSE at concentration of 20%

The cells were seeded at a density of 5×10^6 cells in 100-mm dishes containing culture medium supplemented with RPMI 1640 containing 10% FBS in a total final volume of 10 ml. Then, the cells were exposed to fresh medium (control) or to 20% concentrations of CSE for 16 h at 37°C in a humidified atmosphere containing 5% CO_2, and after exposure, the cells were washed twice with phosphate-buffered solution.

Reverse transcriptase PCR

The cell lines were treated with CSE or fresh medium (control) as previous mentioned. Total RNA was extracted with TRLZOL reagent (Invitrogen, USA), and the quality of RNA was analyzed by A260/A280 ratio and gel analysis. The reverse transcription was performed with RNA polymerase chain reaction (PCR) Kit (AMV Ver.3.0, Takara, Japan) according to the manufacturer's protocols. Primers specific to human MTA1 were forward, 5′-AGCTACGAGCAG CACAACGGGGT-3′, and reverse, 5′-CACGCTTGGTTTCC GAGGAT-3′. The PCR conditions were 94°C (3 min) and 20× 30 cycles of 94°C (30 s), 58°C (30 s), and 72°C (30 s). PCR products were electrophoresed on a 2% agarose gel, and semiquantitative evaluation of MTA1 mRNA expression levels was performed relative to expression of the house keeping genes glyceraldehyde-3-phosphate dehydrogenase (GAPDH). The primers for GAPDH were forward, 5′-CCACCCATGG CAAATTCCCATGGCA-3′, and reverse, 5′-TCTAGACGG CAGGTCAGGTCCACC-3′. The expected PCR products were 290 bp for MTA1 and 597 bp for GAPDH.

Western-blot analysis

After CSE treatments, the cells were harvested and the cell pellets were washed with ice-cold phosphate-buffered saline and then lysed in lysis buffer containing 10 mM Tris (pH 7.5), 150 mM NaCl, 10 mM ethylenediaminetetraacetic acid (EDTA), 1% sodium dodecyl sulfate (SDS), 1 mM sodium orthovanadate, and a mixture of protease inhibitors (1 mM phenylmethylsulfonyl fluoride, 1 μg/mL pepstatin A, and 2 μg/mL aprotinin). The lysates were sonicated for 10 s, centrifuged for 20 min at 20,000×g, and then stored at −70°C. Equal amounts (25 μg) of the cell lysates were resolved by 12% SDS-PAGE and transferred to polyvinylidene fluoride membranes. After blocking, blots were incubated with mouse anti-MTA1 monoclonal antibody (sc-17773, Santa Cruz, 1:250) or β-actin (Zhongshan Golden Bridge Biotechnology, 1:1000) overnight at 4°C and followed by each corresponding second antibody at room temperature for 1 h at 37°C. Then, the results were developed by ECL (Pierce Biotechnology, USA). The protein bands were then analyzed using the BioImaging System (UVP, USA). The grayscale values of the MTA1 were normalized to the values of the corresponding β-actin band to determine the expression level of the protein. The experiments were repeated at least three times independently.

Matrigel invasion assay

Cell invasive ability was examined using a 24-well Transwell with 8.0-μm pore polycarbonate membrane inserts (Corning Inc., New York, NY, USA) according to the manufacturer's protocol. The Matrigel (100 μl/ml) was applied to the upper surface of the membranes. After the treatment of CSE for 16 h, cells were seeded on the upper chamber (5×10^4 cells/well) and incubated for 24 h. The cells without treatment served as the control. Cells that had invaded the surface of the membrane were fixed with methanol and stained with hematoxylin. The cells that invaded and moved onto the lower surface of the filter membrane were counted in ten random high power fields (×400) by an inverted microscope. The experiment was repeated three times, and the data were shown in mean ± standard deviation (SD).

Statistical analysis

SPSS version 13.0 for Windows was used for all analyses. The Pearson's chi-square test was used to analyze the relationship between MTA1 expression and clinicopathological factors. One-way analysis of variance (ANOVA) was performed to compare data from the densitometry analysis of MTT, western blotting, and reverse transcriptase (RT)-PCR. Statistical significance in this study was set at $p<0.05$. The association between MTA1 expression and invasive ability of cells was assessed using the Spearman's correlation test. All reported p values are two-sided.

Results

Expression of MTA1 in NSCLC and adjacent non-neoplastic lung tissues

The results of immunohistochemistry revealed the nuclear and cytoplasm staining of the MTA1 protein in the lung cancer, whereas the adjacent normal lung tissue (including alveolar epithelial cells and bronchial epithelial cells examined) showed very weak or even no staining of epithelial cells (Fig. 1). Total positive rate of MTA1 expression in adjacent normal lung tissues was 15.6% (15/96). MTA1 expression in NSCLC (61/96, 63.5%) was higher than that in adjacent normal lung tissues ($p<0.05$). The relationship between MTA1 expression and different clinicopathological factors in NSCLC is shown in Table 1. We had three cases of micropapillary predominant adenocarcinoma and one case of solid predominant with mucin production adenocarcinoma which had MTA1-positive expression. MTA1 expression was significantly associated with smoking history, lymph node metastasis, and TNM stage ($p<0.05$), but not with age, gender, histological type, adenocarcinoma subtype, and T stage.

Effect of CSE on cell proliferation by MTT

The results of MTT demonstrated that significant cytotoxicity was evoked by CSE in A549 and LH7 with the concentration of 40%, 60%, and 100%, and it was a dose-dependent cytotoxicity, in BE1 with the concentration of 60% and 100% (Table 2). So, 20% is the optimal concentration of CSE.

Treatment of CSE upregulated MTA1 expression

Western blotting and RT-PCR results showed that MTA1 protein expression and mRNA were found quite weak in A549, and higher metastatic BE1 cells have intense MTA1 expression compared with the lower metastatic LH7 cells. To explore further the relation between MTA1 expression and cigarette smoke in NSCLC, we treated the NSCLC cell lines with CSE. The results of RT-PCR and western blotting showed the upregulation of MTA1 protein expression and mRNA after the treatment of CSE in NSCLC cell lines ($p<0.05$, Fig. 2).

Treatment of CSE increased invasive ability of NSCLC cells was dependent on MTA1

Matrigel invasion assays showed that the invasive ability of the A549, LH7, and BE1 cells was enhanced with the treatment of CSE. The A549, LH7, and BE1 cells had fewer numbers of cells which invaded onto the lower surfaces of the Transwell filters than cells treated with CSE at concentration of 20% ($p<0.05$; Fig. 3). The Spearman's correlation test revealed that the number of invasive cells was significantly positively associated with the MTA1 protein expression ($p=0.004$, correlation coefficient=0.946) and mRNA in NSCLC cells ($p=0.008$, correlation coefficient=0.927). The invasive ability of NSCLC cell lines was significantly positively associated with MTA1 expression.

Discussion

Lung cancer is the most frequently diagnosed malignancy with enormous public health implications as it is one of the

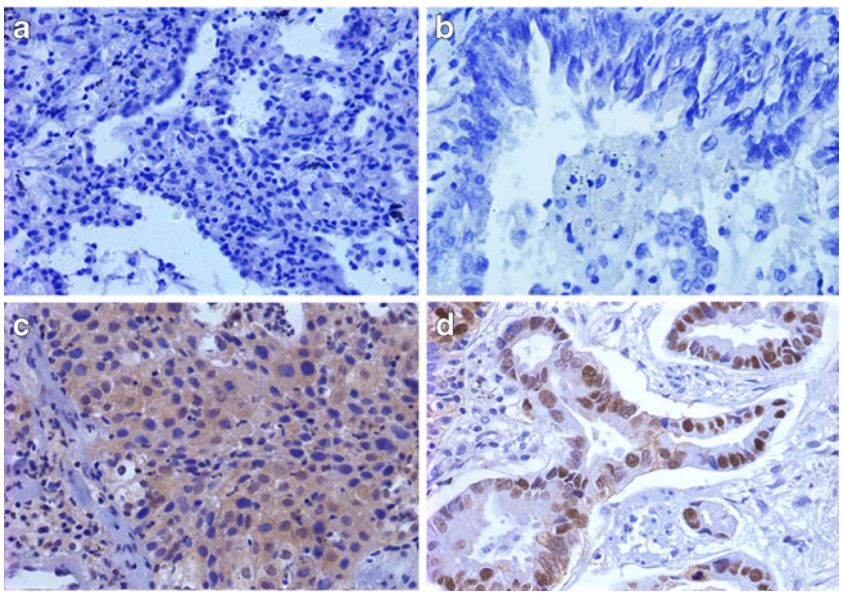

Fig. 1 The patterns of MTA1 expression were mixed nuclear/cytoplasmic staining. **a** Negative MTA1 expression in the alveolar cells. **b** Negative MTA1 expression in the bronchial epithelial cells. **c** Positive MTA1 immunostaining was seen in lung squamous cell carcinoma. **d** Positive stain of MTA1 was shown in lung adenocarcinoma. Original magnification, all ×400

Table 1 Relationship between MTA1 expression and clinicopathological factors in 96 patients with NSCLC

Variables	n=96	MTA1 expression		p value
		Negative, n=35	Positive, n=61	
Age (years)				$p>0.05$, $\chi^2=2.67$
≤55	39	18	21	
>55	57	17	40	
Gender				$p>0.05$, $\chi^2=2.88$
Male	60	18	42	
Female	36	17	19	
Histological type				$p>0.05$, $\chi^2=1.50$
Squamous cell carcinoma	43	14	29	
Adenocarcinoma	48	18	30	
Large cell carcinoma and adenosquamous carcinoma	5	3	2	
Adenocarcinoma subtype				$p>0.05$, $\chi^2=5.162$
Adenocarcinoma in situ and minimally in invasive adenocarcinoma	8	3	5	
Lepidic predominant adenocarcinoma	10	3	7	
Acinar predominant adenocarcinoma	18	10	8	
Papillary predominant adenocarcinoma	8	2	6	
Micropapillary predominant and solid predominant with mucin production adenocarcinoma	4	0	4	
TNM stage				$0.01<p<0.05$, $\chi^2=4.43$
I and II	58	26	32	
III and IV	38	9	29	
T stage				$p>0.05$, $\chi^2=0.00$
T1 and T2	71	26	45	
T3 and T4	25	9	16	
Lymph node metastasis				$0.01<p<0.05$, $\chi^2=6.50$
Yes	41	10	31	
No	55	25	30	
Smoking history				$p<0.01$, $\chi^2=9.84$
Never smokers	25	15	10	
Former smokers	32	8	24	
Current smoker	39	10	29	

leading cause of cancer-related death in the world. NSCLC is the largest histological subgroup of lung cancer [15]. The prognosis of patients with NSCLC principally correlates with tumor metastasis, which is the major cause of treatment failure in patients with NSCLC. MTA1, a novel candidate metastasis-associated gene, is known to increase the migration and invasion of various tumor cells in vitro [16–18]. In our study, we found that MTA1 expression was generally absent or focally weak in adjacent normal lung tissue by immunohistochemistry. In contrast, MTA1 expression in NSCLC (61/96, 63.5%) was significantly higher than that in adjacent normal lung tissues. Analyses of various tumor tissues have also found overexpression of MTA1 mRNA, or protein is correlated positively with the extent of tumor invasion or lymph node metastasis [7, 19–21]. Consistent with our research, its expression was

Table 2 Effects of different concentration of CSE on cell proliferation as measured by MTT method after exposure to CSE for 3 h

Group	$A_{490\ nm}$ (mean ± SD)		
	A549	LH7	BE1
Control	0.875±0.138	0.627±0.078	0.725±0.103
10%	0.823±0.097	0.609±0.095	0.720±0.189
20%	0.761±0.123	0.601±0.111	0.711±0.082
40%	0.647±0.155[a]	0.499±0.033[a]	0.645±0.063
60%	0.432±0.093[a]	0.487±0.062[a]	0.598±0.081[a]
100%	0.372±0.278[a]	0.406±0.083[a]	0.591±0.076[a]

[a] Values are statistically significant by one-way ANOVA tests ($p<0.05$)

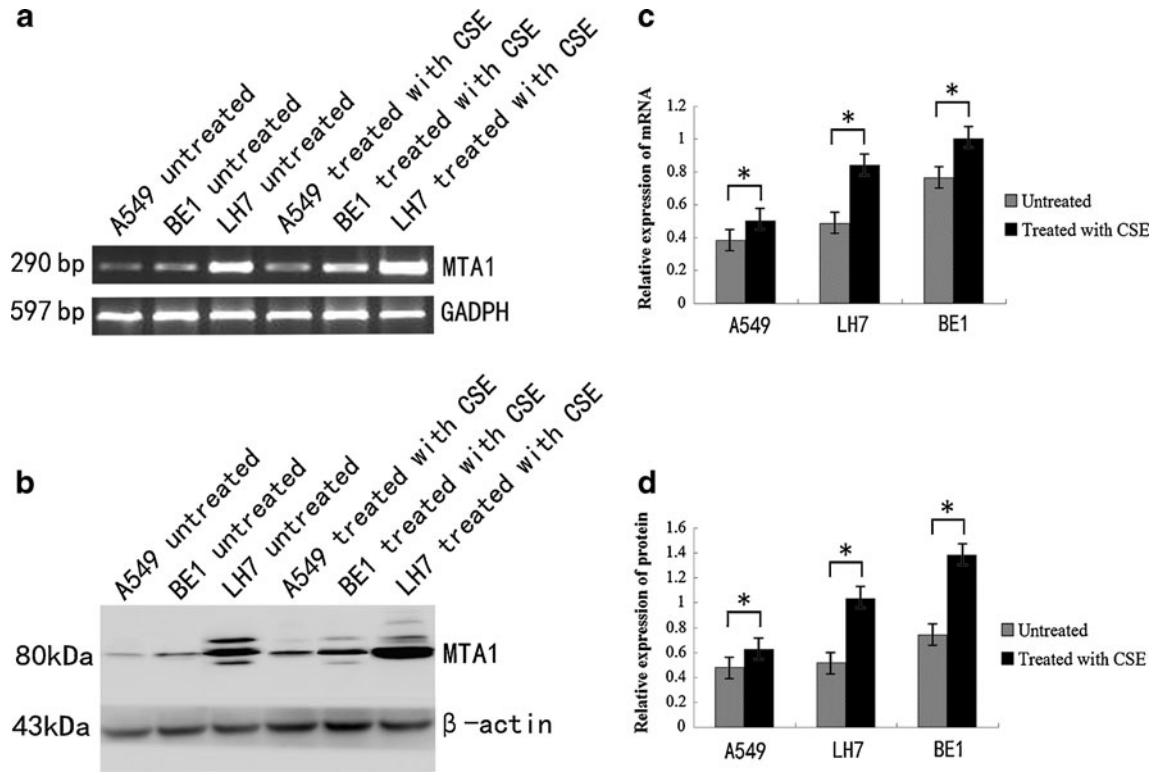

Fig. 2 Treatment of CSE in NSCLC cell lines upregulated MTA1 expression. **a** RT-PCR showed the upregulation of MTA1 mRNA after the treatment of CSE in NSCLC cell lines. **b** Western blotting showed the upregulation of MTA1 protein expression after the treatment of CSE in NSCLC cell lines. **c** MTA1 mRNA in NSCLC cell lines was statistically analyzed. **d** MTA1 protein expression in NSCLC cell lines was statistically analyzed. Data represented the mean ± SD of three independent experiments.*$p<0.05$

significantly associated with lymph node metastasis and TNM stage in NSCLC, but not with age, gender, histological subtype, tumor grade, and T stage. Micropapillary and solid adenocarcinomas are prone to early metastasis and rapid progression. We had three cases of micropapillary predominant adenocarcinoma and one case of solid predominant with mucin production adenocarcinoma which had MTA1-positive expression. Further investigation about the relation between MTA1 expression and micropapillary and solid adenocarcinomas appear to be warranted in NSCLC carcinogenesis. Patients with positive MTA1 expression had a significant metastatic phenotype. We observed a significant association between MTA1 expression and smoking history in NSCLC. No previous research reported MTA1 expression had relation with cigarette smoke. Cumulative evidence indicates that cigarette smoke

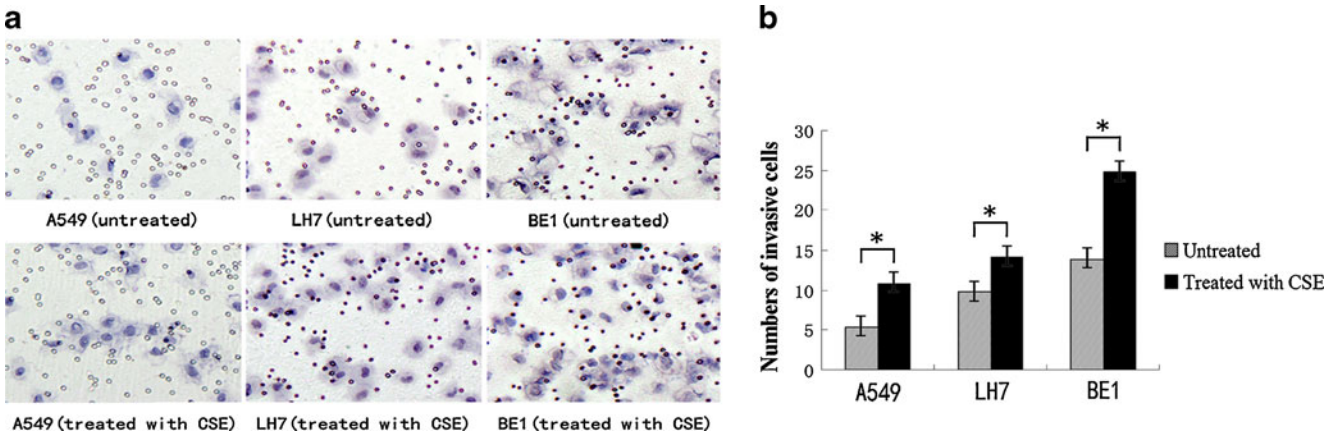

Fig. 3 Treatment of CSE increased invasive ability of NSCLC cells. **a** Matrigel invasion assay showed that the invasive ability of the A549, LH7, and BE1 cells was enhanced with the treatment of CSE. **b** Number of cells invading onto the lower surfaces of the filter was counted. Data represented the mean ± SD of three independent experiments. *Columns*, mean ($n=3$); *bar*, SD; *$p<0.05$

can promote tumor cell proliferation, survival, migration/invasion, and tumor angiogenesis and thus serves as a potent carcinogen. To date, the detailed molecular mechanisms whereby cigarette smoke enhances tumor growth and progression remain largely unknown. So, we hypothesized that cigarette smoke might affect MTA1 expression.

To gain a deeper insight into the molecular mechanism underlying the relation between MTA1 and cigarette smoke, we treated the NSCLC cell lines with CSE and further to detect MTA1 protein expression and mRNA level. First, we found that the expression of MTA1 was quite weak in A549 cells, while the higher metastatic BE1 cells expressed the maximal level of MTA1, compared with the lower metastatic LH7 cells. This pattern of MTA1 expression may indicate the invasive and metastatic malignant phenotype of NSCLC. So, it is acceptable that positive MTA1 expression stimulated cell proliferation and is more aggressive.

MTA1 is a subunit of the nuclear remodeling and NuRD complex, which is associated with chromatin remodeling and histone deacetylase activity. Acetylation is a key post-translational modification of many proteins and is responsible for the regulation of a number of critical intracellular pathways. Our results also suggest that MTA1 upregulation was accompanied with the treatment of CSE, but the mechanism of MTA1 upregulation after CSE treatment is not yet clear. Zhang et al. investigated the effects of nicotine on the expression of hypoxia-inducible factor-1 alpha (HIF-1α) and its downstream target gene, vascular endothelial growth factor (VEGF) in NSCLC cell lines A549 and H157 by western blot or ELISA. They found the increased HIF-1α and VEGF expression in NSCLC cells after the treatment of nicotine [22]. Takeuchi et al. reported that the levels of HIF-1α had been increased after the male Wistar rats were exposed to cigarette smoke for 12 weeks (CSE rats) [23]. Moon HE revealed that MTA1 has deacetylation activity on HIF-1α in vivo by immunoprecipitation and acetylation assays, and MTA1 increased the transcriptional activity of HIF-1α by stabilization of the HIF-1α protein [24]. HIF-1α is closely related to the increased metastatic potential of cancer cells with high MTA1 expression [24, 25]. MTA1 also enhanced the expression of VEGF to enhance the invasion of tumor cells, a target molecule of HIF-1α [24, 26, 27]. Yoo et al. provided evidence of a positive cross-talk between HIF-1α and MTA1, which was mediated by histone deacetylase-1 (HDAC1) recruitment, and indicated a close connection between MTA1-associated metastasis and HIF-1α-induced tumor angiogenesis [28, 29]. We thus purpose a mechanism that increased levels of MTA1 that might be involved in the tumor invasion and metastasis caused by smoke exposure and may enhance stability of HIF-1α protein by recruiting HDAC1 in the cell invasion of NSCLC cells in vitro.

In conclusion, the present study shows that, first, positive MTA1 expression in NSCLC (61/96, 63.5%) was significantly higher than that in adjacent normal lung tissues, and the protein is mainly localized to the nuclear and cytoplasm of the cancer cells; second, MTA1 expression was significantly associated with the patients' smoking history; third, MTA1 upregulation and cell invasion was accompanied with the treatment of CSE in the NSCLC cell lines; and four, smoke exposure may enhance cell invasion in vitro by upregulating the MTA1 protein expression and mRNA. These unique findings have greatly extended our current knowledge about the molecular mechanisms underlying the tumorigenic activities of cigarette smoke and provide potential targets for the development of novel anticancer therapy in the management of local and systemic diseases in tobacco-associated human lung cancer.

Conflicts of interest The authors declare that they have no conflict of interest.

References

1. Molli PR, Singh RR, Lee SW, Kumar R (2008) MTA1-mediated transcriptional repression of BRCA1 tumor suppressor gene. Oncogene 27:1971–1980
2. Ghanta KS, Pakala SB, Reddy SD, Li DQ, Nair SS, Kumar R (2010) MTA1 coregulation of transglutaminase 2 expression and function during inflammatory response. J Biol Chem 286:7132–7138
3. Zhang XY, DeSalle LM, Patel JH, Capobianco AJ, Yu D, Thomas-Tikhonenko A, McMahon SB (2005) Metastasis-associated protein 1 (MTA1) is an essential downstream effector of the c-MYC oncoprotein. Proc Natl Acad Sci USA 102:13968–13973
4. Bowen NJ, Fujita N, Kajita M, Wade PA (2004) Mi-2/NuRD: multiple complexes for many purposes. Biochim Biophys Acta 1677:52–57
5. Hofer MD, Chang MC, Hirko KA, Rubin MA, Nosé V (2009) Immunohistochemical and clinicopathological correlation of the metastasis-associated gene 1 (MTA1) expression in benign and malignant pancreatic endocrine tumors. Mod Pathol 22:933–939
6. Murakami M, Kaul R, Robertson ES (2008) MTA1 expression is linked to ovarian cancer. Cancer Biol Ther 7:1468–1470
7. Zhu X, Guo Y, Li X, Ding Y, Chen L (2010) Metastasis-associated protein 1 nuclear expression is associated with tumor progression and clinical outcome in patients with non-small cell lung cancer. J Thorac Oncol 5:1159–1166
8. Xing J, Stewart DJ, Gu J, Lu C, Spitz MR, Wu X (2008) Expression of methylation-related genes is associated with overall survival in patients with non-small cell lung cancer. Br J Cancer 98:1716–1722
9. Travis WD, Brambilla E, Noguchi M, Nicholson AG, Geisinger KR, Yatabe Y, Beer DG, Powell CA, Riely GJ, Van Schil PE, Garg K, Austin JH, Asamura H, Rusch VW, Hirsch FR, Scagliotti G, Mitsudomi T, Huber RM, Ishikawa Y, Jett J, Sanchez-Cespedes M, Sculier JP, Takahashi T, Tsuboi M, Vansteenkiste J, Wistuba I, Yang PC, Aberle D, Brambilla C, Flieder D, Franklin W, Gazdar A, Gould M, Hasleton P, Henderson D, Johnson B, Johnson D, Kerr K, Kuriyama K, Lee JS, Miller VA, Petersen I, Roggli V, Rosell R, Saijo N, Thunnissen E, Tsao M, Yankelewitz D

(2011) International association for the study of lung cancer/American thoracic society/European respiratory society international multidisciplinary classification of lung adenocarcinoma. J Thorac Oncol 6:244–285
10. Goldstraw P, Crowley J, Chansky K, Giroux DJ, Groome PA, Rami-Porta R, Postmus PE, Rusch V, Sobin L (2007) The IASLC Lung Cancer Staging Project: proposals for the revision of the TNM stage groupings in the forthcoming (7th) edition of the TNM classification of malignant tumours. J Thorac Oncol 2:706–714
11. Kok LF, Lee MY, Tyan YS, Wu TS, Cheng YW, Kung MF, Wang PH, Han CP (2010) Comparing the scoring mechanisms of p16INK4a immunohistochemistry based on independent nucleic stains and independent cytoplasmic stains in distinguishing between endocervical and endometrial adenocarcinomas in a tissue microarray study. Arch Gynecol Obstet 281:293–300
12. Koo CL, Kok LF, Lee MY, Wu TS, Cheng YW, Hsu JD, Ruan A, Chao KC, Han CP (2009) Scoring mechanisms of p16INK4a immunohistochemistry based on either independent nucleic stain or mixed cytoplasmic with nucleic expression can significantly signal to distinguish between endocervical and endometrial adenocarcinomas in a tissue microarray study. J Transl Med 7:25
13. Manne U, Myers RB, Moron C, Poczatek RB, Dillard S, Weiss H, Brown D, Srivastava S, Grizzle WE (1997) Prognostic significance of Bcl-2 expression and p53 nuclear accumulation in colorectal adenocarcinoma. Int J Cancer 74:346–358
14. Carp H, Janoff A (1978) Possible mechanisms of emphysema in smokers. In vitro suppression of serum elastase-inhibitory capacity by fresh cigarette smoke and its prevention by antioxidants. Am Rev Respir Dis 118:617–621
15. Jemal A, Siegel R, Ward E, Hao Y, Xu J, Thun MJ (2009) Cancer statistics, 2009. CA Cancer J Clin 59:225–249
16. Mahoney MG, Simpson A, Jost M, Noé M, Kari C, Pepe D, Choi YW, Uitto J, Rodeck U (2002) Metastasis-associated protein (MTA)1 enhances migration, invasion, and anchorage-independent survival of immortalized human keratinocytes. Oncogene 21:2161–2170
17. Toh Y, Oki E, Oda S, Tokunaga E, Ohno S, Maehara Y, Nicolson GL, Sugimachi K (1997) Overexpression of the MTA1 gene in gastrointestinal carcinomas. Correlation with invasion and metastasis. Int J Cancer 74:459–463
18. Hofer MD, Kuefer R, Varambally S, Li H, Ma J, Shapiro GI, Gschwend JE, Hautmann RE, Sanda MG, Giehl K, Menke A, Chinnaiyan AM, Rubin MA (2004) The role of metastasis-associated protein 1 in prostate cancer progression. Cancer Res 64:825–829
19. Toh Y, Nicolson GL (2009) The role of the MTA family and their encoded proteins in human cancers. Molecular functions and clinical implications. Clin Exp Metastasis 26:215–227
20. Sasaki H, Moriyama S, Nakashima Y, Kobayashi Y, Yukiue H, Kaji M, Fukai I, Kiriyama M, Yamakawa Y, Fujii Y (2002) Expression of the MTA1 mRNA in advanced lung cancer. Lung Cancer 35:149–154
21. Park JO, Jung CK, Sun DI, Joo YH, Kim MS (2011) Relationships between metastasis-associated protein (MTA) 1 and lymphatic metastasis in tonsil cancer. Eur Arch Otorhinolaryngol 268:1329–1334
22. Zhang Q, Tang X, Zhang ZF, Velikina R, Shi S, Le AD (2007) Nicotine induces hypoxia-inducible factor-1alpha expression in human lung cancer cells via nicotinic acetylcholine receptor-mediated signaling pathways. Clin Cancer Res 13:4686–4694
23. Takeuchi Y, Takahashi M, Fuchikami J (2008) Vulnerability of gastric mucosa to prednisolone in rats chronically exposed to cigarette smoke. J Pharmacol Sci 106:585–592
24. Moon HE, Cheon H, Chun KH, Lee SK, Kim YS, Jung BK, Park JA, Kim SH, Jeong JW, Lee MS (2006) Metastasis-associated protein 1 enhances angiogenesis by stabilization of HIF-1alpha. Oncol Rep 16:929–935
25. Miyake K, Yoshizumi T, Imura S, Sugimoto K, Batmunkh E, Kanemura H, Morine Y, Shimada M (2008) Expression of hypoxia-inducible factor-1alpha, histone deacetylase 1, and metastasis-associated protein 1 in pancreatic carcinoma. Correlation with poor prognosis with possible regulation. Pancreas 36: e1–e9
26. Sharma G, Mirza S, Parshad R, Srivastava A, Gupta SD, Pandya P, Ralhan R (2011) Clinical significance of Maspin promoter methylation and loss of its protein expression in invasive ductal breast carcinoma. Correlation with VEGF-A and MTA1 expression. Tumour Biol 32:23–32
27. Kai L, Wang J, Ivanovic M, Chung YT, Laskin WB, Schulze-Hoepfner F, Mirochnik Y, Satcher RL Jr, Levenson AS (2011) Targeting prostate cancer angiogenesis through metastasis-associated protein 1 (MTA1). Prostate 71:268–280
28. Yoo YG, Kong G, Lee MO (2006) Metastasis-associated protein 1 enhances stability of hypoxia-inducible factor-1alpha protein by recruiting histone deacetylase 1. EMBO J 25:1231–1241
29. Yoo YG, Na TY, Seo HW, Seong JK, Park CK, Shin YK, Lee MO (2008) Hepatitis B virus X protein induces the expression of MTA1 and HDAC1, which enhances hypoxia signaling in hepatocellular carcinoma cells. Oncogene 27:3405–3412

Virchows Arch (2011) 459:423–429
DOI 10.1007/s00428-011-1126-6

ORIGINAL ARTICLE

Rare histological variants in ependymomas: histopathological analysis of 13 cases

Marco Gessi · Klaus Kuchelmeister · Libero Lauriola · Torsten Pietsch

Received: 15 February 2011 / Revised: 19 April 2011 / Accepted: 20 April 2011 / Published online: 27 July 2011
© Springer-Verlag 2011

Abstract Ependymomas are rare brain tumors representing about 3% of all intra-cerebral and spinal neoplasms. The WHO classification recognizes various rare histological ependymoma variants (i.e., lipidized ependymoma, giant cell ependymoma, etc.). However, a detailed analysis of a larger series of such cases is still lacking. We analyzed 13 case of ependymoma presenting unusual histological features. The data analysis of our series and its comparison to the cases published in literature did not reveal any close association between these features and the clinical parameters (such as age or localization). Moreover, some of these features can be found combined in individual tumors, suggesting that these variants may represent a spectrum of differentiation rather than true specific entities. However, awareness on these rare histological patterns in ependymomas is necessary in the differential diagnosis with other primary or secondary brain tumors.

Keywords Ependymoma · Cartilage · Metaplasia · Cell vacuolization · Giant cells · Melanin

M. Gessi (✉) · K. Kuchelmeister · T. Pietsch
Inst. of Neuropathology, University of Bonn Medical Center,
Sigmund-Freud-Strasse 25,
53127 Bonn, Germany
e-mail: mgessimd@yahoo.com
e-mail: marco.gessi@ukb.uni-bonn.de

L. Lauriola
Dept. of Pathology, Catholic University,
Rome, Italy

Introduction

Ependymomas are rare brain tumors representing about 3% of all intra-cerebral and spinal neoplasms [11]. The WHO classification recognizes three different ependymoma subtypes based on histopathology, clinical features, and behavior: ependymoma (WHO grade II), anaplastic ependymoma (WHO grade III), and myxo-papillary ependymoma (WHO grade I) [11]. Moreover, ependymoma may also occasionally show clear cell, tanycytic, and papillary features [11]. However, the WHO classification also indicates under the term "other patterns" various other rare histological variants such as giant cell or melanotic ependymomas [11]. To date, the incidence of these rare histological patterns in ependymoma is not known [2, 16] and the current knowledge mainly derives from single case reports present in literature. In this view, a detailed analysis of a large case series is still lacking. In this report, we analyze the clinico-pathological features of a series of 13 ependymomas presenting unusual histopathological features.

Materials and methods

The cases were retrieved from the archive of the German Brain Tumor Reference Center Bonn between 1994 and 2010 (cases 1–10 and 12–13) while case #11 was contributed by the Department of Pathology, Catholic University, Rome, Italy.

Tissue sections of the cases were incubated overnight at 60°C, dewaxed in xylene, and dehydrated. Routine staining (including H&E, Reticulin, Prussian blue, Alcian blue, Alcian blue-PAS and Schmorl's stains) was performed using standard procedures. Immunohistochemical analysis with

antibodies against vimentin (Dako, Glostrup, Denmark), MAP-2 (Dako), synaptophysin (Dako), HMB45 (Dako), Melan-A (Dako), glial fibrillary acidic protein (GFAP, Dako), neurofilament protein (Dako), EMA (Dako), S100 (Dako), pan-cytokeratin (LU-5) (Bachem, Darmstadt, Germany), TTF-1 (Zymed, San Francisco, CA, USA) and KI67 antigen (MIB-1, Dako) was performed on a Ventana Immunostainer (Roche Diagnostics, Mannheim, Germany) or on a TECAN semi-automated staining system (TECAN, Crailsheim, Germany).

Results

Clinical and radiological findings

The clinical findings are reported in detail in Table 1. We identified four ependymomas with foci of cartilage, six cases showing extensive cell vacuolization, one pigmented ependymoma, and two cases with giant cell features. The overall incidence at the Reference Center Bonn is about 0.5% of all ependymomas diagnosed between 1994 and 2010. Eight cases affected the fourth ventricle region; five were spinal. The tumor size varied from 1 to 7 cm in diameter. The age of the patients ranged from 1 to 59 years and the incidence was almost equally distributed in male and female patients (M–F ratio, 0.85). Prevalence in adult patients was found for the cases with extensive vacuolization. MRI data was available in five cases but these tumors did not show specific neuroradiological features different from standard ependymomas. One case (#2) presenting bone tissue formation appeared as focally calcified in MRI scans. Data concerning the extent of surgical resection were available for six patients: the tumors in cases #2, #11, #12, and #13 were completely resected while only an incomplete resection was achieved in cases #1 and #4. Follow-up data were available in detail only for two cases. Case #11 relapsed 2 years after the first surgery without evidence of histological tumor progression. Case #5 with pigmented features recurred 3 years after the initial diagnosis, showing histological progression (increased mitotic activity, areas of necrosis and vascular proliferation) but lacking the pigmentation present in the primary lesion.

Histopathology

Case 1–4. Ependymoma with chondroid metaplasia

These cases were characterized by the presence of cartilage with or without bone formation. The cartilage tissue appeared well demarcated to the adjacent, surrounding ependymoma tissue and composed exclusively of mature cartilage without areas of myxoid degeneration and without the presence of multinucleate cells or mitoses (Fig. 1a, b).

The amount of cartilage varied consistently from small cartilage nests to a subtotal fraction of ependymal tumor tissue. Usually, large areas of dystrophic calcifications associated with cartilage were present. In three cases, the cartilage underwent transition to mature bone tissue

Table 1 Unusual histological features in ependymomas: clinico-pathological findings in 13 cases

Case	Sex	Age	Site	WHO grade	Histological features	Histochemistry	IHC
1	F	1	IV	WHO III	cart	na	GFAP+, EMA+,
2	F	2	IV	WHO III	cart-oss	na	GFAP+, EMA+
3	F	3	IV	WHO II	cart-oss	na	GFAP+, EMA+
4	F	53	IV	WHO I (sep/ep)	cart-oss	na	GFAP+, EMA na
5	M	31	IV	WHO III	pigm	PAS+, Schmorl+	HMB45−, MELAN-A−, GFAP+
6	F	40	T12	WHO II	GC	AL+, PAS−	GFAP+; EMA na
7	M	56	C4	WHO II	GC	na	GFAP+; EMA+
8	M	40	Cervical	WHO II	EV	AL-PAS−	EMA+, GFAP+
9	M	54	C5–6	WHO II	EV	AL-PAS−	EMA+, GFAP+, CK+
10	M	59	C4–5	WHO II	EV	AL-PAS−	EMA+, GFAP+
11	F	30	IV	WHO II	EV	na	EMA+, GFAP+
12	M	15	IV	WHO II	EV[a]	AL-PAS−	EMA na, GFAP+
13	F	54	III–IV	WHO II	EV[a]	AL-PAS−	EMA−, GFAP+, CK+

F female, *M* male, *III* third ventricle, *IV* fourth ventricle, *C* cervical, *T* thoracic, *cart* cartilage, *oss* ossification, *pigm* pigmented, *GC* giant cell, *sep* subependymoma, *ep* ependymoma, *EV* extensive vacuolization, *EMA* dot- and ring-like staining pattern, *AL-PAS* Alcian-PAS, *AL* Alcian blue, *CK* cytokeratins, *na* not available

[a] Due to EMA negativity in case #13 and overall cell morphology in case #12, both cases can be also interpreted as lipomatous ependymoma, but a confirmatory ultrastructural analysis could not be performed

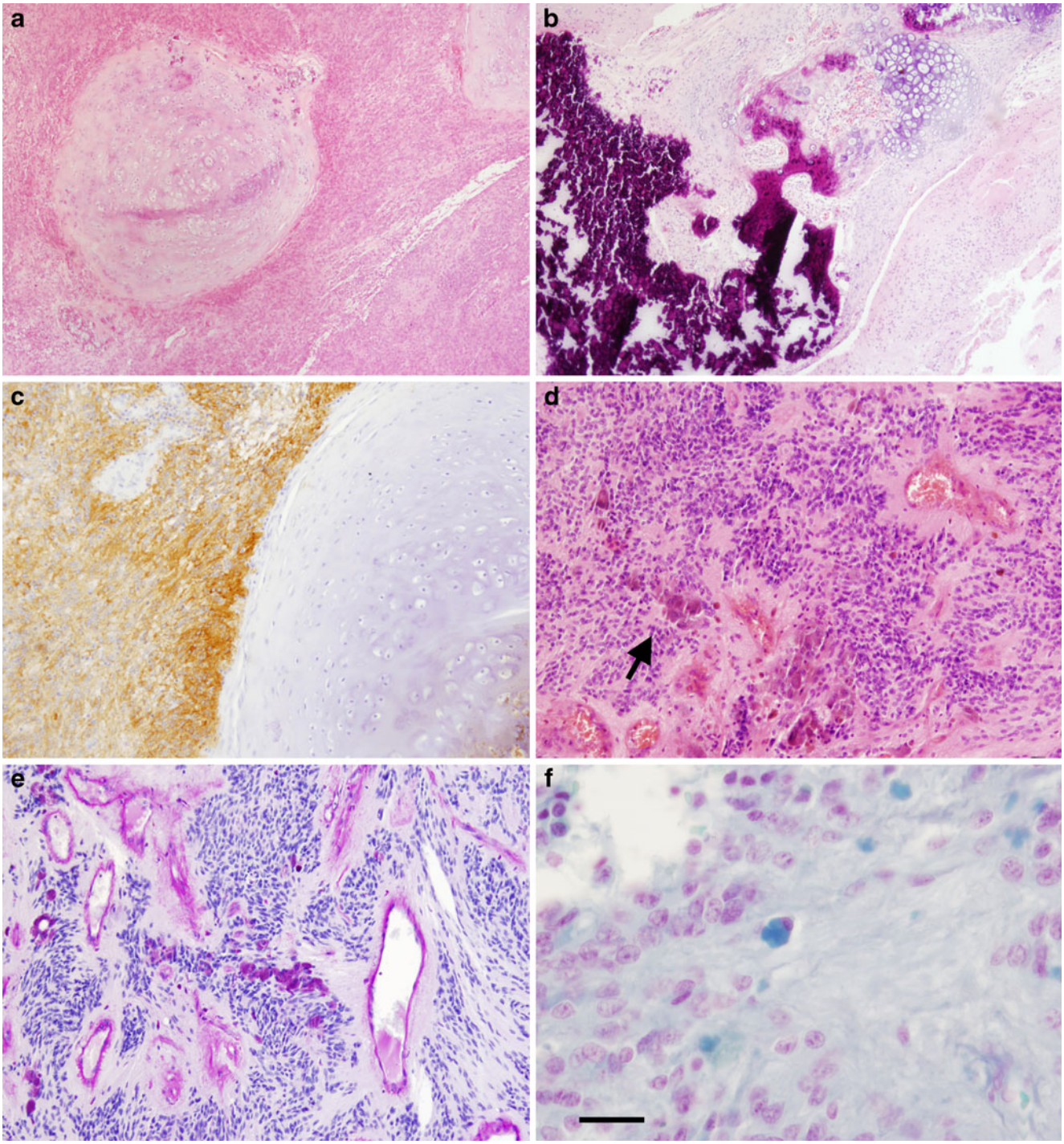

Fig. 1 Histopathological spectrum of rare variants of ependymoma: ependymoma with chondroid metaplasia and pigmented ependymoma. **a** Case #3 showing cartilage nodules within the tumor tissue. **b** In case #2, the cartilage presented mineralization and bone formation. **c** The GFAP-positive ependymoma areas were well demarcated from cartilage (case #2). **d**, **e** Pigmented ependymoma (case #5) showing deposits of neuromelanin–lipofuscin (*arrow*) which are positive with PAS staining. **f** Scattered rare cells presenting positivity with Schmorl's stain were present. **a**, **b**, **d** H&E stain; **c** GFAP; **e** PAS stain; **f** Schmorl's stain for melanin. *Scale bar*: **a**, **b** 300 μm; **c** 150 μm; **d**, **e** 100 μm; **f** 50 μm

(Fig. 1b). Cartilage and bone tissue were also encountered in a case of mixed subependymoma/ependymoma which also presented at the same time microcystic changes. All the cases showed variable immunohistochemical positivity for GFAP and MAP-2 protein in ependymoma cells (Fig. 1c). The cartilage was S100 positive. A dot-like EMA positivity

was found in the ependymoma cells of all three cases examined.

Case 5. Pigmented ependymoma (melanotic ependymoma)

The case showed classic ependymoma histology with perivascular pseudorosettes. Scattered intracellular deposits of PAS positive material, compatible with lipofuscines (Fig. 1d arrow, e), as well as scattered rare single cells showing positivity with melanin Schmorl's staining (Fig. 1f) were identified. The tumor focally showed spindle, tanycytic-like features. The proliferation activity (MIB-1) was focally elevated. The lesion also presented areas of hemorrhage with perivascular haemosiderin deposits which were positive with Prussian blue staining. Some melanin-positive cells presented immunohistochemical positivity with GFAP. The tumor cells showed focally a dot-like positivity with an EMA antibody. Immunostaining with HMB45 and Melan A antibodies, respectively, was negative in tumor tissue. The relapsing tumor showed features of anaplasia, with high mitotic rate and areas of necrosis, but lacked pigment deposits as seen in the primary lesion.

Case 6–7. Giant cell ependymoma

The cases presented areas with giant cells, showing bizarre nuclear features (Fig. 2a, b). Multinucleation in giant cells was frequently observed. Multifocally, tumor #6 showed myxoid changes with intravacuolar alcianophilic mucoid substances (Fig. 2a, c). However, the perivascular growth pattern (perivascular pseudorosettes) was always identifi-

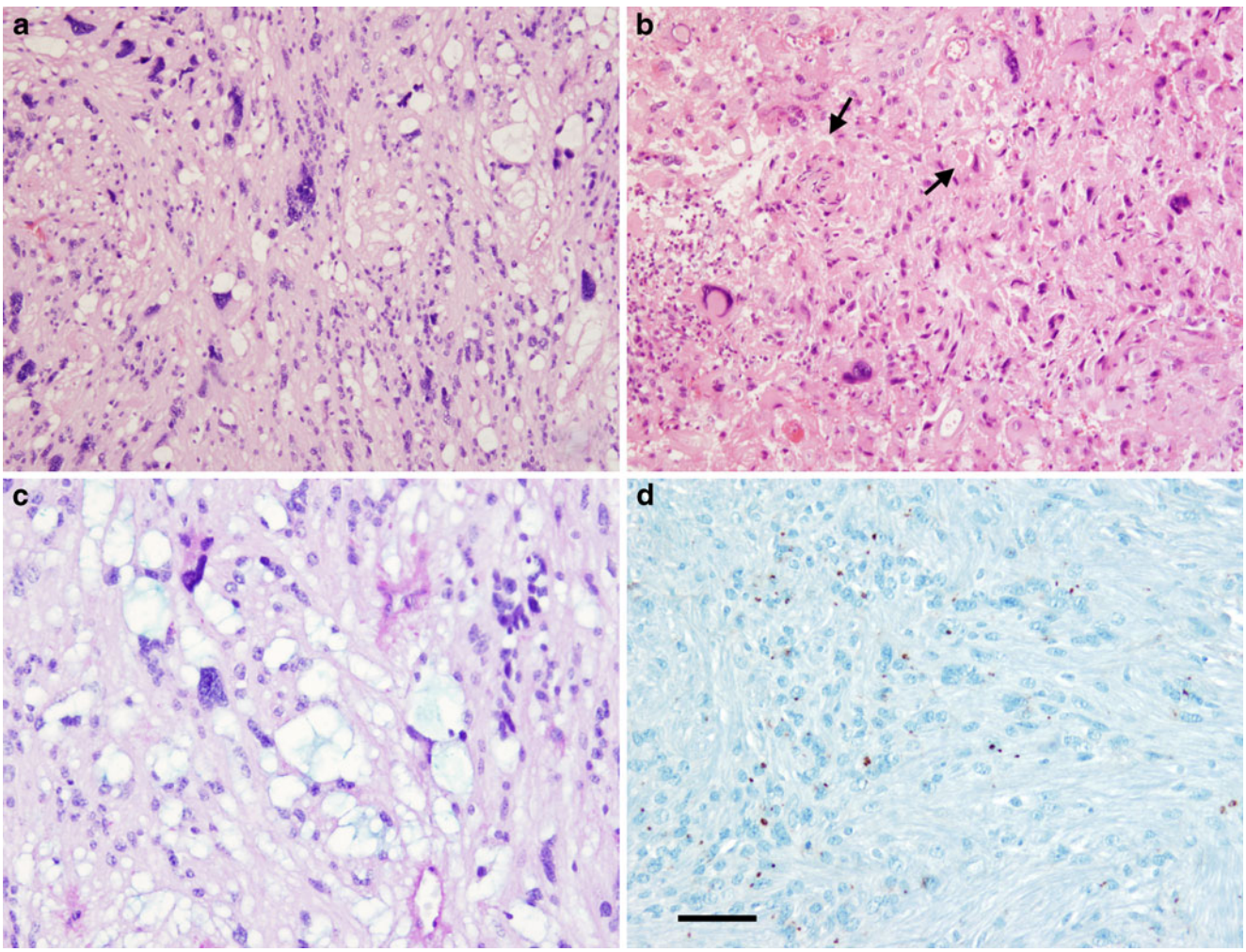

Fig. 2 Histopathological spectrum of rare variants of ependymoma: giant cell ependymoma. **a** Giant cell ependymoma with large, bizarre, and sometimes multinucleated cells (case #6). The cells also showed extensive vacuolization and cytoplasmic accumulation of alcianophilic material. **b** Case #7 was characterized by the presence of cells with rounded or spindle nuclear morphology, with elongated and sometimes fibrillary cytoplasm. Scattered giant cells with irregularly shaped nuclei and extracellular eosinophilic material aggregates resembling protein droplets (*arrows*) were seen. **c** The cells presented myxoid alcianophilic content in Alcian blue staining (case #6). **d** EMA immunostaining revealed dot-like positivity in tumor cells (case #7). **a**, **b**, H&E stain; **c** Alcian blue. *Scale bar*: **a**, **b** 100 μm; **c**, **d** 75 μm

able—also in the giant cell areas. There was no evidence of rhabdoid cells or deposits of dense PAS-positive material described in other cases of giant cell ependymoma. The mitotic activity was low. Case #7 was characterized by the presence of cells with rounded or spindle nuclear morphology, with elongated and sometimes fibrillary cytoplasm. Multifocally giant cells with irregularly shaped nuclei were seen (Fig. 2b). Moreover, scattered cells with abundant eosinophilic cytoplasm were also observed (Fig. 2b). Deposits of extracellular eosinophilic material similar to "protein droplets" (Fig. 2b, arrows) were present. Prominent myxoid changes as observed in case #6 were absent. The mitotic and proliferative activity in both tumors was low. In case #7, a dot-like immunohistochemical staining pattern with EMA antibody was seen (Fig. 2d) also in isolated giant cells.

Case 8–13. Ependymoma with extensive tumor cell vacuolization

Cells with cytoplasmatic vacuolization can be occasionally encountered in standard ependymomas, but we included in the analysis only cases in which cell vacuolization was a predominant feature of the tumoral tissue; we also excluded cases with total or partial clear cell ependymoma features [11]. Cells with signet ring-like vacuolization were encountered as scattered single cells or small groups (Fig. 3a–c). In these cells, the vacuolization of the cytoplasms varied in size and appeared as uniloculated "empty spaces" on paraffin sections. In one case, the signet ring-like cells showed very small cytoplasm and prominent picnotic nuclei (Fig. 3d). The vacuoles were negative in Alcian-PAS staining (Fig. 3e). Sometimes ependymoma cells show a large vacuole resembling adipocytes or lipoblasts, with large and often multi-lobulated vacuoles with indented pycnotic nuclei (Fig. 3c). In all cases, focal areas with classical ependymoma histology were observed. Moreover, all the cases showed variable immunohistochemical positivity for GFAP and MAP-2 protein and a strong expression of S100 protein. In the majority of cases, a ring-like EMA positivity was variably found in vacuolized cells (Fig. 3f) also focally in lipoblast-like cells. In one case, EMA staining was negative. The tumor cells expressed, to a variable extent, cytokeratins in two of four cases examined. The staining with TTF-1 antibody was negative in all the four cases investigated.

Discussion

Ependymomas are tumors that may show an unusual histopathological pattern but, although described in various case reports and short reports, their incidence is unknown [11]. Based on our study, these features occur in about 0.5% of ependymomas, anaplastic ependymoma, and myxopapillary ependymoma.

Based on the analysis of the published cases together with those of our series, the presence of cartilage occurs in the fourth ventricle area and affects pediatric as well as adult patients [1, 6, 8, 9, 12]. In our series, we also identified cartilage areas in one case of mixed ependymoma/subependymoma. In three cases in our series, the chondromatous tissue also showed bone formation. We did not find any relationship with tumor grade of ependymoma and the cartilage does not show areas of cellular atypia or malignant features. In this view, the presence of cartilage could be considered, in our opinion, a simple metaplastic change of normal mesenchymal stromal tissue present in the tumor tissue.

As expected, in this ependymoma type, the clinical behavior seems to be related to the grade of ependymoma. In one report, the presence of cartilage and bone tissue has been associated with a worse prognosis in univariate analysis [8]. In one case [1], the extensive metaplastic changes with osteoid formation as well as foci of cartilaginous differentiation were present only in a relapsing anaplastic ependymoma, which showed a very aggressive clinical behavior [1].

Only a few cases of "pigmented" ependymomas have been described [3, 14]. The nature of the pigment present in these tumors has been reported as melanin or a mixture of lipofuscin and neuromelanin. Lipofuscin is derived from the oxidation of lipids and lipoprotein sources. Neuromelanin is derived from the auto-oxidation of catecholamine precursors [3]. The distinction between these types can be obtained by electron microscopy or by special staining. In our case, we found cells with PAS-positive lipofuscin/neuromelanin and only few PAS-negative cells positive with Schmorl's staining (Fig. 1f), compatible with true melanin. The negativity with HMB45 and Melan A as well as GFAP positivity in pigmented cells suggested that these cells were no true melanocytes. Differently from other cases reported [3, 14], our case showed clinical and histological tumor progression: the tumor recurred 3 years after the initial diagnosis, also showing a histological progression but lacking the pigmentation present in the primary lesion.

The cellular polymorphism among giant cell ependymomas [4, 5, 10, 13, 18] has been attributed to degenerative changes with no worse prognosis in the absence of other anaplastic features, although other authors interpreted the giant cells as a potential sign of a more aggressive clinical behavior [10, 18]. As other rare variants, the cases show infratentorial or supratentorial localization [4, 5, 10, 13, 18]. Our cases can be added to the few descriptions of such lesions in the cervical and thoracic spinal cord [5, 18], but no information in terms of follow-up was available for these two cases. Some of the cases described, as our case #6, presented areas of extensive myxoid features, similar to that found in

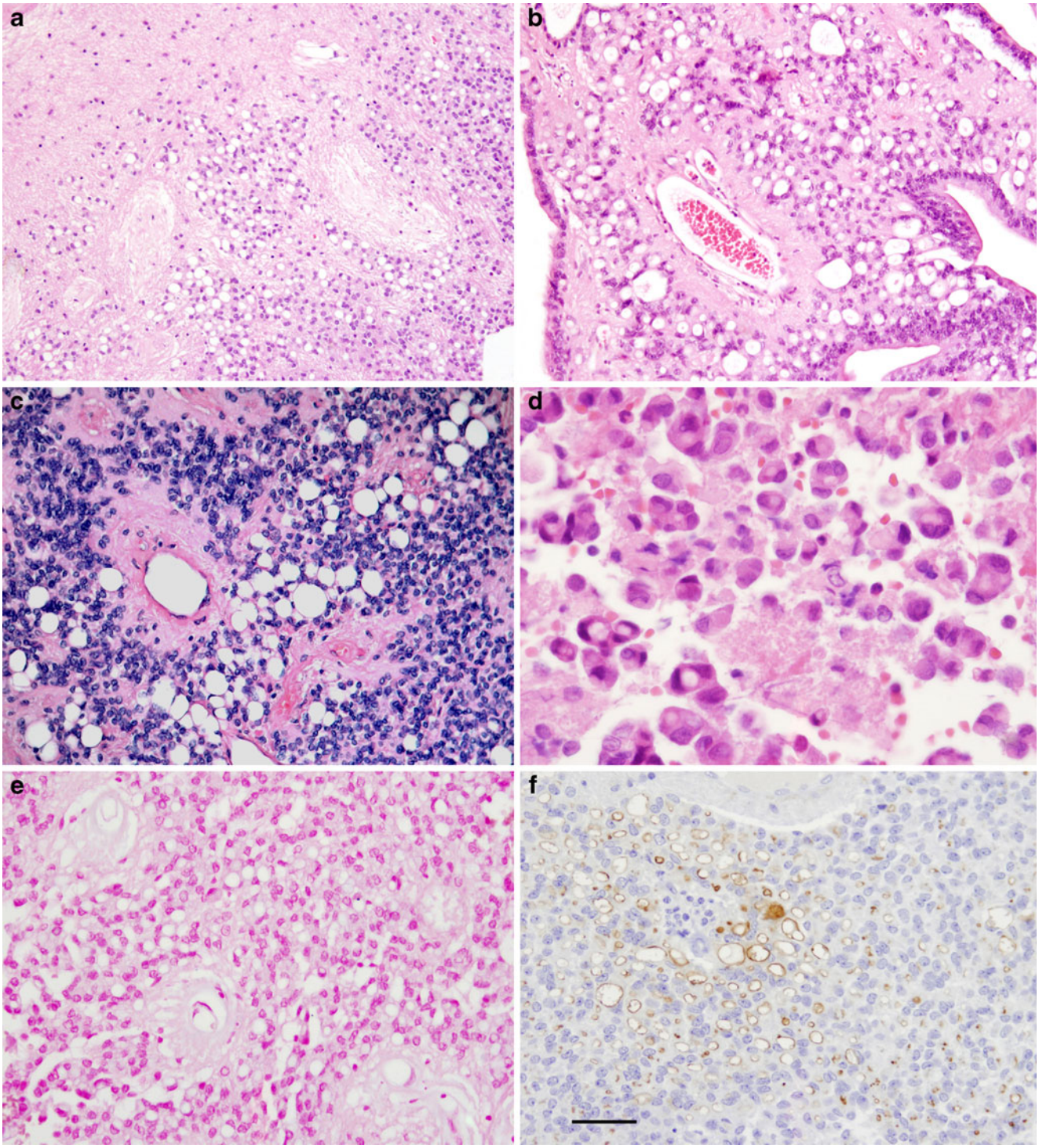

Fig. 3 Histopathological spectrum of rare variants of ependymoma: ependymoma with extensive vacuolization. The amount of tumor cell vacuolization may vary from single signet ring-like cells (**a**, **b**) to large lipoblast-like elements (**c**) (cases #13, #9, and #11, respectively). **d** Case #10 presenting small cell with hyperchromatic, epithelial-like features and signet ring appearance of cytoplasm. **e** The vacuoles did not show positivity with Alcian-PAS staining (case #9). **f** EMA in ependymoma with extensive vacuolization with ring- and dot-like staining pattern. **a**–**d** H&E stain; **e** Alcian-PAS; **f** EMA. *Scale bar*: **a** 200 μm; **b**, **c**, **e**, **f** 100 μm; **d** 50 μm

myxopapillary ependymoma. In case #7, we found extracellular deposits of eosinophilic material, similar to protein droplets which are encountered in pilocytic astrocytomas.

As in ependymoma with cartilaginous metaplasia, also in ependymoma with extensive vacuolization, the analysis of our series and of cases described in literature did not reveal

a correlation with tumor localization, age of the patient, tumor grade (WHO grade II and grade III), or clinical behavior [7, 15–17].

The eye-catching feature of cytoplasmatic cellular vacuolization, in terms of signet ring-like changes or the presence of lipoblast-like cells, has been described in "ependymomas with extensive vacuolization" or "signet ring ependymoma" and in the [7, 17] "lipomatous" ependymomas [15, 16], respectively. The presence of EMA ring-like positivity within the vacuoles in tumor cells, reported in ependymoma with extensive vacuolization but not in the lipomatous ependymoma [7, 15, 16], can be used to empirically distinguish both tumor types, but a definitive distinction can be performed only by using ultrastuctural examination and special staining on frozen sections (i.e., Oil Red O), showing the ultrastuctural features of vacuoles and their content. The archive material selected for our analysis was not suitable for electron microscopy. In ependymomas with extensive vacuolization, these vacuoles represent cytoplasmatic lumina and do not show an accumulation of intracellular lipids. The lipoblast-like morphology and the expression of GFAP and S100 protein in neoplastic cells can be observed in both tumor subtypes.

An interesting feature was the presence in two cases of cytokeratin expression. Because ependymoma cells can variably express cytokeratins [11], the combination of signet ring-like features and cytokeratins expression could be a potential misleading feature in the differential diagnosis with carcinoma metastasis. The IHC profile (S100+, Vimentin+, GFAP+) is helpful for this distinction. In our cases, the low proliferation activity in ependymomas with extensive vacuolization was also an additional diagnostic tool to recognize the exact non-metastatic nature of the lesions.

The analysis and selection process of our case series showed that different features may be combined in the same tumor and, in particular, cell vacuolization may be focally observed in "standard" ependymomas. Moreover, our data analysis combined with the other cases published revealed no specific association with clinical parameters (localization or age) or other pathological features in ependymoma. These observations suggest that these features may represent a spectrum of differentiation rather than true entity-defining features. The importance of the recognition of these patterns is more related to the differential diagnosis with other primary or secondary brain tumors (giant cell glioblastoma, melanoma, and metastasis of signet ring carcinoma) than in the identification of specific new ependymoma subgroups.

Acknowledgments Special thanks are due to Dr. A. von Bueren (Hamburg, Germany).

Conflicts of interest All the authors declare that they have no conflicts of interest.

References

1. Bannykh S, Baehring JM (2007) Images in neuro-oncology: rapid development of osseous and chondrous metaplasia in recurrent anaplastic ependymoma. J Neurooncol 81:257–258
2. Burger PC, Scheithauer BW (2007) Tumors of the central nervous system. AFIP atlas of tumor pathology, IV series. ARP, Washington, pp 145–169
3. Chan AC, Ho LC, Yip WW, Cheung FC (2003) Pigmented ependymoma with lipofuscin and neuromelanin production. Arch Pathol Lab Med 127:872–875
4. Cooper PB, Katus M, Moores L, Geyer D, Smirniotopoulos JG, Sandberg GD, Rushing EJ (2006) Rare giant cell ependymoma in an octagenarian. Case report and review of the literature. J Neurosurg 105:908–911
5. Fourney DR, Siadati A, Bruner JM, Gokaslan ZL, Rhines LD (2004) Giant cell ependymoma of the spinal cord. Case report and review of the literature. J Neurosurg 100:75–79
6. Ghosal N, Murthy G, Dadlani R, Hegde AS, Singh D (2010) Recurrent posterior fossa anaplastic ependymoma with prominent chondroid metaplasia: a case report and review of literature. Indian J Pathol Microbiol 53:787–789
7. Hirato J, Nakazato Y, Iijima M, Yokoo H, Sasaki A, Yokota M et al (1997) An unusual variant of ependymoma with extensive tumor cell vacuolization. Acta Neuropathol 93:310–316
8. Ho DM, Hsu CY, Wong TT, Chiang HA (2001) Clinicopathologic study of 81 patients with ependymomas and proposal of diagnostic criteria for anaplastic ependymoma. J Neurooncol 54:77–85
9. Jain A, Rishi A, Suri V, Garg A, Sharma MC, Sarkar C, Sharma BS (2009) Recurrent ependymoma with cartilaginous metaplasia in an adult: report of a rare case and review of literature. Clin Neuropathol 28:101–104
10. Jeon YK, Jung HW, Park SH (2004) Infratentorial giant cell ependymoma: a rare variant of ependymoma. Pathol Res Pract 200:717–725
11. Mc Lendon RE, Wiestler OD, Kros JM, Korshunov A, Ng HK (2007) Ependymoma. In: Louis DN, Ohgaki H, Wiestler OD, Cavenee WK (eds) WHO classification of tumours of the central nervous system, 4th edn. IARC, Lyon, pp 74–78
12. Mridha AR, Sharma MC, Sarkar C, Garg A, Singh MM, Suri V (2007) Anaplastic ependymoma with cartilaginous and osseous metaplasia: report of a rare case and review of literature. J Neurooncol 82:75–80
13. Pal P, Fernandes H, Ellison DW (2005) Woman aged 24 years with fourth ventricular mass. Brain Pathol 15:367–368
14. Rosenblum MK, Erlandson RA, Aleksic SN, Budzilovich GN (1990) Melanotic ependymoma and subependymoma. Am J Surg Pathol 14:729–736
15. Ruchoux MM, Kepes JJ, Dhellemmes P, Hamon M, Maurage CA, Lecomte M, Gall CM, Chilton J (1998) Lipomatous differentiation in ependymomas: a report of three cases and comparison with similar changes reported in other central nervous system neoplasms of neuroectodermal origin. Am J Surg Pathol 22:338–346
16. Sharma MC, Arora R, Lakhtakia R, Mahapatra AK, Sarkar C (2000) Ependymoma with extensive lipidization mimicking adipose tissue: a report of five cases. Pathol Oncol Res 6:136–140
17. Vajtai I, Mucsi Z, Varga Z, Bódi I (1999) Signet-ring cell ependymoma: case report with implications for pathogenesis and differential diagnosis. Pathol Res Pract 195:853–858
18. Zec N, Girolami U, Schofield DE, Scott RM, Anthony DC (1996) Giant cell ependymoma of the filum terminale. A report of two cases. Am J Surg Pathol 20:1091–1101

Virchows Arch (2011) 459:431–440
DOI 10.1007/s00428-011-1119-5

ORIGINAL ARTICLE

Expression of the ribonucleases Drosha, Dicer, and Ago2 in colorectal carcinomas

Dionysios J. Papachristou · Angeliki Korpetinou · Efstathia Giannopoulou · Anna G. Antonacopoulou · Helen Papadaki · Petros Grivas · Chrisoula D. Scopa · Haralabos P. Kalofonos

Received: 6 April 2011 / Revised: 2 June 2011 / Accepted: 30 June 2011 / Published online: 18 July 2011
© Springer-Verlag 2011

Abstract The pathogenesis of colorectal carcinoma (CRC) is a complex process that involves the recruitment of both genetic and epigenetic mechanisms. Recent studies underline the cardinal role of small, noncoding RNA molecules, called microRNAs (miRs), in the pathobiology of numerous physiological and pathological processes, including oncogenesis. MiR biogenesis and maturation is mainly regulated by the nuclear ribonuclease Drosha and the cytoplasmic ribonucleases Dicer and Ago2. In the present study, we investigated the expression and distribution of these molecules in three colon cancer cell lines and in human CRC samples. Drosha, Dicer, and Ago2 mRNA and protein expression was assessed with real-time PCR, western blotting, and immunofluorescence. Our experiments showed that Drosha, Dicer, and Ago2 were expressed in all the cell lines and in the majority of the CRC samples examined. The mRNA levels of Dicer were significantly augmented in stage III compared to stage II tumors. Our results suggest that Drosha, Dicer, and Ago2 are possibly implicated in CRC pathobiology and that Dicer might have a role in the progression of these tumors to advanced stages.

Keywords Colorectal carcinoma · Drosha · Dicer · Ago2 · MicroRNA

Introduction

Colorectal cancer (CRC) is a malignant neoplasm that originates from the epithelium of colon or rectum. It is one of the most common cancers in humans as it represents approximately 8.5% of all new malignancies and is the second most common cause of cancer-related death in the

D. J. Papachristou · A. Korpetinou · E. Giannopoulou · H. P. Kalofonos
Department of Clinical Oncology, University of Patras, School of Medicine, Patras, Greece

D. J. Papachristou
Department of Pathology, University of Pittsburgh, School of Medicine, Pittsburgh, PA, USA

D. J. Papachristou · A. Korpetinou · H. Papadaki
Department of Anatomy-Histology-Embryology, University of Patras, School of Medicine, Patras, Greece

A. G. Antonacopoulou · H. P. Kalofonos
Molecular Oncology Laboratory, Department of Medicine, Division of Oncology, University of Patras, School of Medicine, Patras, Greece

P. Grivas
Department of Internal Medicine, Division of Hematology/Oncology, University of Michigan, Comprehensive Cancer Center, Ann Arbor, MI, USA

C. D. Scopa
Department of Pathology, University of Patras, School of Medicine, Patras, Greece

H. P. Kalofonos (✉)
Division of Oncology and Clinical Oncology Laboratory, Department of Medicine, University Hospital of Patras, 26504 Rio, Greece
e-mail: kalofon@med.upatras.gr

Western world, affecting men and women equally [1]. The pathogenesis of CRC is a complex process that is tightly controlled by multiple layers of regulatory mechanisms, which entail the accumulation of both genetic and epigenetic alterations in the proliferating cells [2].

In the past few years, a gradually increasing volume of in vitro and in vivo studies has documented that a variety of physiological processes such as chromatin remodeling, genome rearrangement, developmental timing, tissue morphogenesis, and stem cell maintenance are connected with a class of small (16–29 nt), noncoding RNAs called microRNAs (miR) [3]. MiRs regulate gene expression in a cell-specific fashion either via cleavage of targeted mRNA at posttranscriptional level or via repression of translation [3, 4]. They also possess fundamental roles in a great spectrum of pathological conditions namely cardiovascular, rheumatologic, infectious, inflammatory, autoimmune, and metabolic diseases. Not surprisingly, a considerable amount of studies has demonstrated that miRNAs are also implicated in cancer development and progression [5–7]. The biogenesis of miRs is a process that incorporates a series of finely tuned molecular events [3]. The maturation of miRs is accomplished by a set of enzymes, collectively referred to as the "miR machinery." Within the nucleus, Drosha, an RNase III endonuclease, cleaves the primary miRs, giving genesis to 60–70 nt stem-loop intermediate miR precursors (pre-miRs). The exportin 5/RanGTP complex facilitates the transportation of pre-miRs from the nucleus to the cytoplasm, where they are further processed by the RNase III ribonuclease Dicer, generating the mature miR molecules. Mature miRs are then loaded upon a large multi-proteinic assembly called RNA-induced silencing complex (RISC). RISC binds to double-stranded RNA and regulates gene expression either by direct destruction of the targeted mRNA through perfect complementarity or by translational repression via partial complementarity to 3′ untranslated regions of the target mRNA [6, 8]. Major components of RISC are the argonaut proteins (Ago 1–4); among them, only Ago2 mediates miR-dependent degradation of target mRNAs in mammals.

Recent reports have provided a wealth of data documenting that deregulations of specific miRs are implicated in the pathogenesis of CRC and are associated with decreased overall survival and poor prognosis [9, 10]. Moreover, several investigators have examined the expression and the role of the constituents of the miR machinery in various epithelial tumors (e.g., carcinomas of respiratory system, breast, ovary, and prostate, pleomorphic adenomas of the salivary gland) [11–17]. Very recently Faber and colleagues have assessed the cellular levels and prognostic significance of Dicer in CRC with immunohistochemistry [18]. In the present study, we aimed to investigate the expression of Drosha, Dicer, and Ago2 in human colon cancer cell lines, as well as in a well-characterized panel of human colorectal carcinomas of all grades and stages and examined the correlation of the mRNA levels of these ribonucleases with various clinicopathologic parameters, including tumor grade, stage, and patient survival.

Materials and methods

Patients

The present study has been designed and performed according to the institutional bioethical guidelines and has been approved by the bioethical committee of the University of Patras, following the directions of the Declaration of Helsinki. The design of the study, methodological approach, and data presentation were based on the REMARK criteria, a consensus of quality guidelines about biomarker prognostic studies [19]. We performed a retrospective chart review of patients who were operated at the University Hospital of Patras, Greece, between 1990 and 2004. We selected 76 consecutive patients with formalin-fixed paraffin-embedded (FFPE) surgical specimens of primary colorectal carcinomas that were available in the tissue archive of the Pathology Department of the University Hospital of Patras, Greece. We only included patients with available clinicopathological data at the time of diagnosis. We excluded patients who received any preoperative (neoadjuvant) chemotherapy or radiotherapy. The patients' clinicopathological features are collectively presented in Table 1. Of the 76 patients, 48 (63%) were male and 28 (36%) female, aged 30–90 years (mean age 65.1 years). Twenty-three neoplasms (30%) were located in the rectum, 34 (45%) in the right colon, and 19 (25%) in the

Table 1 Patients' clinicopathological features

Number of patients	76	
Age median (range)	65 (30–90)	
Gender	Female	28 (36%)
	Male	48 (64%)
Tumor location	Rectum	23 (30%)
	Right colon	34 (45%)
	Left colon	19 (25%)
Tumor histopathological grade	WD tumor	17 (22%)
	MD tumor	54 (71%)
	PD tumor	5 (7%)
Tumor stage (AJCC/IUAC)	I	5 (7%)
	II	30 (39%)
	III	36 (47%)
	IV	5 (7%)
Follow-up median (range)	54 (3–106) months	

WD well differentiated, *MD* moderately differentiated, *PD* poorly differentiated, *AJCC/IUAC* American Joint Committee on Cancer/International Union Against Cancer

left colon. In all cases, tumor sampling included at least three tissue blocks. Twenty-seven paired normal colorectal FFPE tissue samples were also used. All slides were reexamined, and the type and grade of each tumor were reevaluated in a blinded fashion by two experienced pathologists (DJP and CDS). All the tumors of our study were staged according to the American Joint Committee on Cancer/International Union Against Cancer (AJCC/IUAC). Five neoplasms (7%) were stage I (3, T1 N0 M0; 2, T2 N0 M0), 30 (39%) stage II (T3 N0 M0), 36 (47%) stage III (15, T1–2 N1–2 M0; 21, T3 N1–2 M0) and 5 (7%) stage IV (any T any N M1). Patients were followed for a period of 3–106 months (mean=56.8 months; median=54 months, SD=23.78 months). Follow-up data were available for 74 out of the 76 patients that were included in our study.

Patients with stage II, III, and IV CRC were treated with fluoropyrimidine-based chemotherapy. Before initiation of postoperative chemotherapy, all patients were assessed by physical examination, routine blood hematological and biochemical analysis, and imaging studies (chest X-ray and abdominal computerized tomography scans).

Cell culture

DLD-1, HT-29, and Caco-2 colon cancer cell lines were purchased from the American Type Culture Collection (ATCC; Manassas, VA). DLD-1 and HT-29 cells were cultured in RPMI 1640 medium with 2 mM L-glutamine and supplemented with 10 mM HEPES, 1 mM sodium pyruvate, 4.5 g/L glucose, 1.5 g/L sodium bicarbonate, and 10% fetal bovine serum (FBS) as recommended by ATCC. Caco-2 cells were cultured in Eagle's minimum essential medium with Earle's BSS and 2 mM L-glutamine and supplemented with 1.0 mM sodium pyruvate, 0.1 mM nonessential amino acids, 1.5 g/L sodium bicarbonate, and 20% fetal bovine serum as also recommended by ATCC. Cells were cultured at 37°C, 5% CO_2, and 100% humidity.

RNA isolation and cDNA synthesis

Equal amounts of cells from each cell line were cultured in 10-cm cell culture dishes up to 80% confluency. Total RNA was extracted from cells using Absolutely RNA RT-PCR kit (Stratagene, La Jolla, USA) and from FFPE tissue samples using the Absolutely RNA FFPE kit (Stratagene) according to manufacturer's instructions. In order to avoid contamination from the adjacent nonneoplastic tissues, the following protocol was applied. Briefly, six unstained 5-μm-thick deparaffinized serial sections were obtained from each sample. Viable tumor-rich areas were selected as targets and marked on routine hematoxylin–eosin-stained sections; corresponding areas were microdissected from adjacent unstained deparaffinized sections. Tissue microdissection was performed manually with a sterile surgical blade under direct stereoscopic microscope visualization. An average of three tumor targets that did not contain nonneoplastic tissues was selected for microdissection [20]. Integrity of RNA was confirmed by visualization of ribosomal bands by EtBr-stained agarose gel (2%) electrophoresis. RNA was quantified using Nanodrop 1000 (Thermo Scientific, Wilmington, Denmark). First-strand cDNA was synthesized from cell line RNA by Superscript III First-Strand Synthesis System (Invitrogen) both from samples and Human Reference Total RNA (Stratagene). For those reactions, 1 μg of RNA and a final concentration of 3 ng/μL random hexamers (Invitrogen) were used in a total volume of 50 μL. First-strand cDNA was synthesized from a constant quantity (1.6 μg) of total RNA extracted from the tissue samples as previously described [21].

Real-time PCR

Quantification of Drosha, Dicer, and Ago2 mRNAs both from cell and tissue samples and human total reference RNA (referred to as calibrator) was performed using gene-specific primers as shown in Table 2 and SYBR Green I intercalation dye in Brilliant Sybr Green QPCR Master Mix (Stratagene) in a total volume of 25 μL. Each reaction mixture contained 50 ng of cDNA and a final primer concentration of 300 nM for *Dicer*, *Ago2*, and Alu-Sq and 100 nM for *Drosha*. The primers for *Drosha*, *Dicer*, and *Ago2* are shown in Table 2. All PCR cycling conditions included a heating step at 95°C for 10 min at the beginning of every run. Samples for *Dicer* and *Ago2* were then cycled 49 times at 95°C for 30 s, 58°C for 20 s, and 72°C for 20 s. Samples for *Drosha* were cycled 45 times at 95°C for 30 s, 60°C for 20 s, and 72°C for 20 s. Expressed Alu-Sq repeat levels were also similarly quantified, as described previously [22]. Samples were cycled 45 times at 95°C for 30 s, 58°C for 20 s, and 72°C for 20 s. In addition, a standard curve was included in each run for assay validation. Drosha, Dicer, and Ago2 mRNA levels from cell

Table 2 Primers used in quantitative PCR, the amplicon sizes and the melting temperature (Tm) of each reaction

Target	Sequence	Amplicon size (bp)	Tm (°C)
Drosha F	5′-CAAAGGCAAGACGCACAG-3′	74	59.1
Drosha R	5′-CATAGGACGACACGGCTTG-3′		59.3
Dicer F	5′-AATGCTGAAACTGCAACTGAC-3′	78	58
Dicer R	5′-TCCACAATCCACCACAATC-3′		57.6
Ago2 F	5′-CCTCCCATGTTTACAAGTCG-3′	82	58.1
Ago2 R	5′-TCTTTGTCCTGCCACAATG-3′		58.2

F forward primer, *R* reverse primer, *bp* base pairs

and tissue samples were normalized to respective calibrator and Alu-Sq levels.

Cell lysate preparation

Caco-2, DLD-1, and HT-29 cell lines were plated at 1×10^6 cells per 10-cm cell culture dishes. Incubation of cells was terminated when cultures reached 80% confluency by adding lysis buffer (25 mM HEPES pH 7.5, 150 mM NaCl, 5 mM EDTA, 1% Triton X-100, 10% glycerol, 1 mM phenylmethylsulphonylfluoride, 2 mM Na orthovanadate, and 10 mM leupeptin). After lysis, three sonication cycles of 5 s were performed. Cell debris was pelleted by centrifuging at 7,000 rpm, 4 min, at 4°C, and the supernatant was obtained. Protein concentration was determined by Bradford assay, and 200 μg of total protein were used for SDS-PAGE electrophoresis.

Immunoblotting

Cell lysate samples were reduced in Laemmli buffer with mercaptoethanol and analyzed by SDS-PAGE electrophoresis in 8% gels. Proteins were transferred to Immobilon-P (Millipore, Massachusetts, USA) PVDF membrane according to standard procedures. Membranes were blocked in 5% (*w*/*v*) nonfat dry milk in Tris-buffered saline pH 7.4 containing 0.05% Tween 20 (TBS-T) for 2 h at room temperature and then incubated with a rabbit polyclonal anti-Ago2 antibody (1 μg/mL; Abcam, Cambridge, UK), a mouse monoclonal anti-Dicer1 antibody (2 μg/mL, Abcam), a rabbit polyclonal anti-Drosha antibody (1 μg/mL, Abcam), or a mouse monoclonal anti-actin antibody (1:1,000, Chemicon, Temecula, USA) overnight, at 4°C. After three washes in TBS-T, membranes were further incubated with horseradish peroxidase-conjugated goat anti-mouse IgG (1:2,500; Upstate, Lake Placid, NY) or goat anti-rabbit IgG (1:2,500, Upstate) for 1 h at room temperature. Detection of the immunoreactive proteins was performed by chemiluminescence horseradish peroxidase substrate SuperSignal (Pierce, Rockoford, USA), according to manufacturer's instructions.

Immunofluorescence

Caco-2, DLD-1, and HT-29 cell lines were cultured in chamber slides until they reached 80% confluency (Nunc, Rochester, USA). Cells were fixed with 4% paraformaldehyde in phosphate buffer solution (PBS) for 10 min at room temperature and then rinsed three times in 5 min with PBS. Cells were incubated for 1 h in 3% bovine serum albumin solution supplemented with 10% FBS at 37°C. After the incubation with blocking solution, cells were rinsed once with PBS for 5 min and they were treated overnight at 4°C with the following antibodies: anti-Drosha polyclonal (0.1 μg/mL, 0.90 mg/mL; Abcam), anti-Dicer monoclonal (1:50, 1.00 mg/mL; Abcam), and anti-Ago-2 monoclonal antibody (1:100, 0.50 mg/mL, Abcam), diluted in blocking solution. Cells were rinsed three times in 5 min with PBS, and then an anti-mouse antibody conjugated with Alexa Fluor 594 (1:1,000; Invitrogen, Molecular Probes, Eugene, OR, USA) or an anti-rabbit antibody conjugated with Alexa Fluor 488 (1:1,000, Invitrogen, Molecular Probes) diluted in blocking solution was added for 30 min at 37°C. A fluorescent dye was used for staining the nucleus (1:10,000, Toto-3 iodide; Invitrogen, Molecular Probes). Cells were rinsed three times in 5 min with PBS and mounted on glass sides. Fluorescence was visualized using a Leica TCS LSI confocal microscope.

Histological analyses

Histological analyses were conducted on FFPE tissue samples from colorectal carcinomas and normal colonic tissues that were retrieved from the archives of the Department of Pathology of the University Hospital of Patras Medical School, Patras, Greece. For histopathological grading of the examined neoplasms, we used the "2000 version" of the World Health Organization classification of tumors [23]. Tumors were graded according to the percentage of glandular differentiation. More specifically, adenocarcinomas that displayed tubular structures in >95%, 50–95%, and 5–50% of the tumor were considered as well differentiated (grade 1), moderately differentiated (grade 2) and poorly differentiated (grade 3) neoplasms, respectively. When the glandular component occupied less than 5% of the tumor, the neoplasm was considered undifferentiated (grade 4). Grades 1 and 2 adenocarcinomas were considered low, while grades 3 and 4 adenocarcinomas were considered as high-grade neoplasms [23].

Statistical analyses

In order to compare the nonparametric variable scores between normal and neoplastic tissue as well as between carcinomas of different stage and grade, the Mann–Whitney test was employed. The strength of association among nominal variables was assessed by Kendall's τ test. Analyses for time to tumor progression (TTP) and overall survival (OS) were assessed using the Kaplan–Meier method, and different subgroups were compared using the logrank test. TTP was estimated from the date of surgery/biopsy until the date of the first documented tumor relapse. OS was defined as the time elapsed calculated from the date of the biopsy or surgery until the death because of the disease. All differences were considered statistically significant if $P<0.05$. P values were two tailed. All statistical analyses were performed using the SPSS 13.0 for Windows (version 13.0, SPSS Inc., Chicago, IL, USA).

Results

Expression of Drosha, Dicer, and Ago2 in colon cancer cell lines

Drosha, Dicer, and Ago2 mRNA and protein levels were examined in three colon cancer cell lines using quantitative RT-PCR, western blot, and immunofluorescence. We found that all the examined molecules were expressed in the three tested cell lines at both mRNA and protein level (Fig. 1a, b). At the protein level, Dicer and Ago2 were detected primarily in the cytoplasm, while Drosha localization was both cytoplasmic and nuclear (Fig. 2). Of note, the cellular levels of Dicer and Ago2 as defined by western blotting were disproportionate with their mRNA levels. In particular, even though the protein levels of Dicer in the Caco2 and DLD-1 cells were similar, the mRNA expression of Dicer was lower in DLD-1, compared to the Caco2 cells as shown in Fig. 1. With regards to Ago2, its protein levels were lower in the DLD-1 compared the Caco2 and HT-29 cells; nevertheless, its mRNA expression in DLD-1 was augmented in Caco2 in comparison to the other cells lines (Fig. 1a, b). Moreover, albeit Drosha was detected in all the examined cell lines by immunofluorescence, we failed to detect this protein with western blot assay (data not shown).

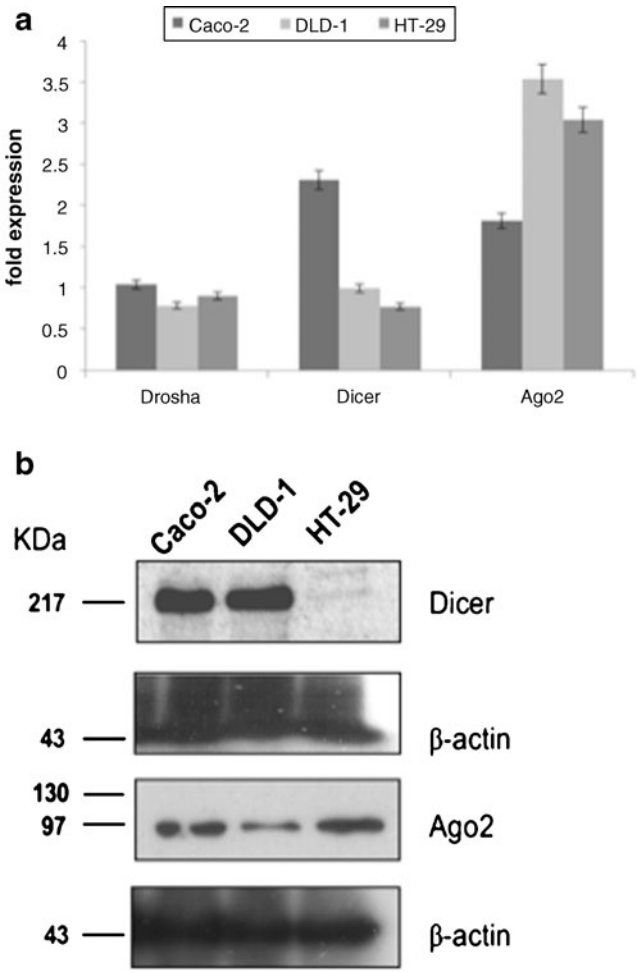

Fig. 1 **a** Relative levels of Drosha, Dicer and Ago2 mRNA expression in Caco-2, DLD-1, and HT-29 colon cancer cell lines, as defined by RT-PCR analysis. All values are relative to calibrator gene expression (mean±SD from triplicate readings). These values are representative for two independent experiments with similar results. **b** Western blotting results showing the expression of Drosha, Dicer, and Ago2 proteins in Caco-2, DLD-1, and HT-29 colon cancer cell lines

Expression of Drosha, Dicer, and Ago2 mRNA in tissue samples: Dicer mRNA levels are associated with CRC of advanced stage

Drosha mRNA was expressed in the vast majority of normal colonic epithelia [25/27 (92.6%) normal cases] and in 37/76 (48.7%) CRC cases (Table 3). Among the tumors that expressed *Drosha*, 8 (21.6%) were well, 25 (67.6%) were moderately, and 4 (10.8%) were poorly differentiated (Fig. 3a). With regard to stage, *Drosha* was not detected in stage I tumors. It was expressed in 13/31 (41.9%) stage II, 22/35 (62.8%) stage III, and 2/5 (40.0%) stage IV malignancies (Fig. 3d). Among the cases that expressed *Drosha*, 12/32 (37.5%) relapsed and 9/32 (28.1%) patients died of the disease. Among the cases that did not reveal *Drosha* mRNA expression, 15/37 (40.5%) relapsed and 12/37 (32.4%) patients died of the disease (Table 4). The mRNA levels of *Drosha* did not display significant differences between normal and neoplastic epithelia, as well as between high- and low-grade neoplasms (Mann–Whitney *U* test, $P=0.09$ and $P=0.370$, respectively). In addition, no significant association was observed between Drosha mRNA levels and tumors of different stages ($P>0.05$, for all correlations).

Dicer mRNA was expressed in both the normal and the cancerous colonic epithelium. Indeed, it was detected in 20/27 (74%) normal and in 48/76 (63.2%) neoplastic samples (Table 3). With regards to CRC histopathological grade, *Dicer* was expressed in 12/17 (70.6%) well, 33/54 (61.2%) moderately, and 3/5 (60.0%) poorly differentiated carcinomas (Fig. 3b). Regarding tumor stage, *Dicer* was expressed in 0/5 (0.0%) stage I, 13/30 (43.3%) stage II, 30/36 (83.3%) stage III, and 5/5 (100.0%) stage IV cases (Fig. 3e). The mRNA levels of Dicer did not display any significant differences between normal and malignant epithelia, as well as between high- and low-grade carcinomas ($P=0.223$ and $P=0.570$, respectively). Notably, however, *Dicer* gene expression was significantly higher in stage III as compared to stage II CRC ($P=0.032$, Fig. 3e). Among the cases that expressed Dicer mRNA, 16/40 (40.0%) progressed and in 11/40 (27.5%) cases, the patients died because of their tumor. As regards to the cases that did not display Dicer

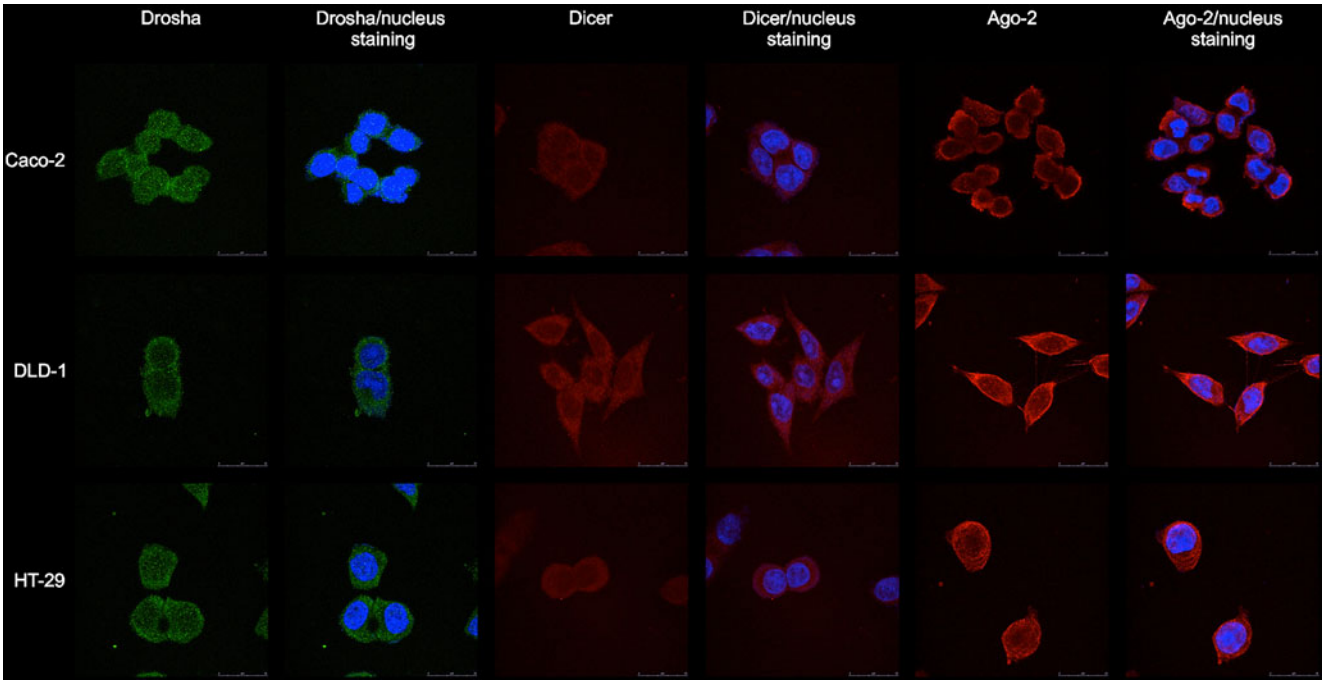

Fig. 2 Immunofluorescence analyses illustrating the expression and localization of Drosha, Dicer, and Ago2 in the three colon cancer cell lines examined. Nucleus is stained *blue*. Note that the expression of Dicer and Ago2 (*red*) is principally cytoplasmic, whereas Drosha exhibits both nuclear and cytoplasmic localization (magnification at ×40)

mRNA expression, 8/28 (28.6%) relapsed and 6/28 (21.4%) patients died because of their disease (Table 4).

Ago2 mRNA was detected in 15/27 (55.5%) normal and in 43/76 (56.6%) cancerous samples (Table 3). It was expressed in 11/17 (64.7%) well, 30/54 (55.5%) moderately, and 2/5 (40.0%) poorly differentiated carcinomas (Fig. 3c). Furthermore, *Ago2* was detected in 0/5 (0.0%), 17/30 (56.6%), 25/36 (69.4%), 1/5 (20.0%) of stage I, II, III, and IV cases, respectively (Fig. 3f). We did not observe significant differences in Ago2 mRNA levels between normal and neoplastic epithelia, as well as between high- and low-grade carcinomas (P=0.128 and P=0.370, respectively). Among the cases that expressed Ago2 mRNA, 16/39 (44.4%) relapsed, whereas in 10/39 (25.6%) cases, the patients died because of their tumor. Regarding cases that did not express *Ago2*, 7/31 (22.6%) relapsed and 6/31 (19.4%) patients died because of their disease (Table 4). Of note is that Ago2 mRNA levels tended to be elevated in stage III compared to stage II CRC (P=0.08). In addition, we did not unwrap any significant association between *Drosha*, *Dicer*, or *Ago2* expression levels and patient age and gender or tumor location and size (P>0.05 for all correlations). Finally, our statistical analyses revealed that the mRNA levels of Drosha, Dicer, and Ago2 were strongly and positively correlated to each other (Kendall's τ=0.415–0.256, P=0.0001–0.004; Fig. 3g).

Table 3 Drosha, Dicer, and Ago2 mRNA expression levels in relation to tumor grade and stage

Status	Number of cases	Drosha mRNA expression (median)	Dicer mRNA expression (median)	Ago2 mRNA expression (median)
NE	27	0.00–13.27 (3.63)	0.00–3.1 (2.02)	0.00–1.05 (0.68)
Grade				
WD	17	0.00–6.30 (2.40)	0.00–3.92 (2.24)	0.00–1.30 (0.74)
MD	54	0.00–7.69 (2.22)	0.00–3.71 (1.79)	0.00–1.20 (0.68)
PD	5	0.00–4.68 (2.34)	0.00–2.65 (1.32)	0.00–0.83 (0.42)
Stage (AJCC/IUAC)				
I	5	0.00–0.00 (0.00)	0.00–0.00 (0.00)	0.00–0.00 (0.00)
II	30	0.00–7.69 (1.98)	0.00–3.17 (1.47)	0.00–1.23 (0.68)
III	36	0.00–6.29 (2.53)	0.00–3.92 (2.24)	0.00–1.26 (0.71)
IV	5	0.00–0.00 (0.00)	0.00–4.22 (3.52)	0.00–2.9 (1.04)

NE normal epithelium, *WD* well-differentiated tumor, *MD* moderately differentiated tumor, *PD* poorly differentiated tumor

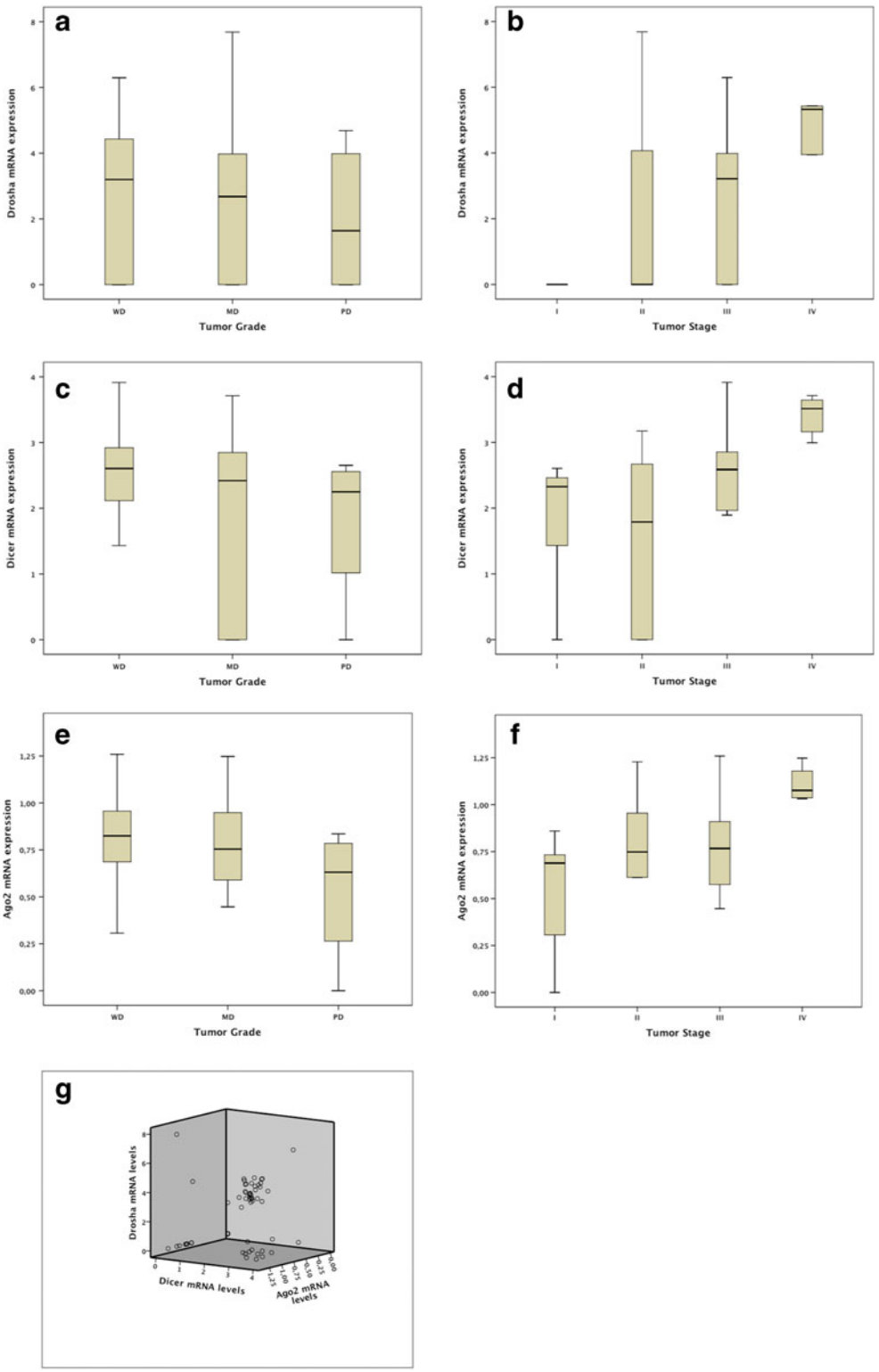

Fig. 3 Box plot graphs depicting the Drosha, Dicer, and Ago2 mRNA expression levels in comparison to tumor histopathological grade (**a**–**c**) and stage (**d**–**f**). Stage III carcinomas revealed significantly higher Dicer mRNA levels as compared to stage II neoplasms (**e**). A 3-D scatterplot showing that the association between Drosha, Dicer, and Ago2 mRNA expression levels in colorectal carcinomas is significant ($P<0.05$, for all the correlations) (**g**)

The expression levels of *Drosha*, *Dicer*, and *Ago2* are not associated with overall survival in human CRC

Univariate analysis showed that Drosha, Dicer, and Ago2 mRNA levels did not reach statistical significance as predictors of OS ($P>0.05$ for all). Moreover, no association was uncovered between the expression levels of the examined ribonucleases and TTP. Finally, patients' gender and age as well as tumor location and size had no impact on survival.

Table 4 Absolute number and percentage of patients with and without Drosha, Dicer and Ago2 mRNA expression that relapsed and died of the disease (DOD)

	mRNA expression	Relapse	DOD
Drosha	Yes	12/32 (37.5%)	9/32 (28.1%)
	No	15/37 (40.5%)	12/37 (32.4%)
Dicer	Yes	16/40 (40.0%)	11/40 (27.5%)
	No	8/28 (28.6%)	6/28 (21.4%)
Ago2	Yes	16/39 (44.4%)	10/39 (25.6%)
	No	7/31 (22.6%)	6/31 (19.4%)

Discussion

It is well documented that the discovery of miRs has added substantial information as regards to gene regulation in both health and disease. Not surprisingly, several studies have shown that various miRs, namely miR-20a, miR-21, miR-106a, miR-181b, and miR-203, are implicated in every step of colorectal carcinogenesis and appear to have prognostic and predictive value [24]. Drosha, Dicer, and Ago2 are central components of the miR-regulating network. Therefore, a gradually increasing number of studies are aiming to investigate the implication of these ribonucleases in cancer pathobiology. Herein, we sought to examine the expression of Drosha, Dicer, and Ago2 in human colorectal carcinomas and normal colonic epithelium. First, we examined whether these molecules were expressed in the three human colon cancer cell lines Caco2, DLD-1, and HT-29. At the level of mRNA, all of the tested ribonucleases were expressed in all the tested cell lines. However, we did not detect Drosha in any of the assessed cell lines by western blotting. This is not surprising, since the detection sensitivity of western blotting is lower than that of modern immunofluorescence methods that we used. In fact, confocal microscopy uncovered that Dicer and Ago2 were located primarily in the cytoplasm of the examined cells, while Drosha displayed both nuclear and cytoplasmic localization. According to our findings, the mRNA levels of Dicer and Ago2 did not completely correlate with the protein levels, suggesting the implication of posttranscriptional modifications in CRC. Collectively, our in vitro results suggested that these three crucial elements of the miR machinery are expressed in colon cancer cells and that they may play a role in colon carcinogenesis.

Triggered by these findings, we were prompted to explore the expression of *Drosha*, *Dicer*, and *Ago2* on tissue samples from human colorectal adenocarcinomas and assess their correlation with specific clinicopathological parameters. We demonstrated that the mRNA levels of these endoribonucleases were positively and highly correlated to each other, providing evidence toward an "orchestrated" function of the miR-regulating pathway in human CRC. Furthermore, we found that Drosha, Dicer, and Ago2 mRNA was expressed in both normal and neoplastic tissues. Similar to reports from breast carcinoma, we did not observe any significant differences in the mRNA levels of the examined molecules between normal and neoplastic epithelia [25], although Drosha cellular levels displayed a tendency to be augmented in normal tissues. Since the nature of our study is quantitative, differences in the mRNA expression do not prove or disprove the implication of these ribonucleases in the pathogenesis of CRC. Clearly, further studies are required in order to define the precise role of Drosha, Dicer, and Ago2 in colorectal carcinogenesis.

Previous studies have documented that Drosha directly influences the development and clinical outcome of malignancies such as ovarian and breast cancer [13, 25]. Notably, the nuclear localization of this protein is essential for its enzymatic activity. It has been recently shown that Drosha accurate localization is largely dependent upon phosphorylation at Ser300 and Ser302 residues [26]. In the present we detected Drosha in both the nucleus and the cytoplasm of the tested CRC cell lines. This finding could be possibly ascribed to dysfunction of the signal transduction pathways that regulate the phosphorylation of serine residues of this enzyme in CRC.

Dicer is the central and consequently the best studied component of the miR-processing network. In line with a very recent immunohistochemical study on CRC tissue samples, in the present study, we found that Dicer mRNA was expressed in human CRC. This is in harmony with previous publications having reported Dicer deregulation in prostate, breast, ovarian, lung, salivary gland, central nervous system, and colorectal cancers [11–18, 27–30]. Statistical analysis of our results did not reveal significant differences in the mRNA levels of Dicer between normal and transformed epithelia, as well as between adenocarcinomas of different histopathological grades and locations. In addition, no substantial associations were uncovered between Dicer expression levels and patient age or gender. Nonetheless, in the present study, we found that Dicer mRNA levels were significantly higher in stage III compared to stage II neoplasms. This is a potentially interesting finding. Indeed, according to the AJCC classification, stage II colorectal adenocarcinomas have not developed lymph node metastases, whereas stage III tumors have, meaning that they are associated with poorer prognosis [23]. Therefore, our results most probably suggest that Dicer might have a key role in the progression of this neoplasm to more aggressive forms. This is in symphony with a recent microarray-based molecular study having demonstrated that differences in the expression of miR-320, miR-498, and miR-21 are correlated with recurrence-free survival of stage II CRC patients [10]. In

a very recent publication, Faber et al. have reported that Dicer overexpression could serve as a strong predictor of poor prognosis in CRC [18]. Notably, however, in the present work, we did not unveil any significant association between Dicer mRNA levels and TTP or OS. This disagreement between the two studies could be attributed to several reasons. For instance, since *Dicer* expression is largely subjected to posttranscriptional modifications, Dicer mRNA levels as measured by PCR may not be well correlated with protein levels as detected by immunohistochemistry [31]. Moreover, our study included a relatively small number of patients with available survival data, a limitation that could also account for the aforementioned dissimilarity between the two studies. Obviously, additional multicenter studies on larger sample size are required to clarify this issue.

The mechanisms that regulate Dicer-related oncogenesis are still obscure. Chiosea et al. using microarray methodologies have shown that *Dicer* gene locus is deleted in precancerous lesions and invasive lung adenocarcinomas [11]. Human *Dicer* gene is located at the chromosomal region 14q32.13, which is altered in several types of human cancer. According to studies on neuroblastoma and breast cancer cell lines, the regulation of *Dicer* gene is controlled by alternative transcription initiation and splicing [28, 30]. It has been recently demonstrated that in ovarian cancer *Dicer* and *Drosha* genes undergo single-nucleotide mutations that may be responsible for ovarian carcinogenesis [13]. In light of these well-documented reports, we advance the hypothesis that genomic alterations, such as amplification, may account for the elevated expression of *Dicer* in the stage III CRC of our series.

As mentioned previously, Ago proteins are highly specialized small RNA-binding molecules that mediate miR and siRNA functions [32]. Since Ago2 is a vital constituent of the miR machinery, it is reasonable to hypothesize that perturbations of its expression might play a role in neoplasia. Towards this direction, a recent study on cell cultures demonstrated that ERα-negative breast cancer cells exhibit increased Ago2 mRNA and protein levels [33]. Tempted by this and other studies and based upon data from our in vitro experiments, in the present investigation, we aimed at answering the question whether Ago2 mRNA is deregulated in human colorectal tumor tissues. We found that Ago2 is expressed in both normal and neoplastic colon epithelium at mRNA level and that its expression levels had a tendency to be augmented in tumors of higher grades and stages; however, this difference did not reach statistical significance. This implies that although Ago2 is plausibly implicated in colorectal pathobiology, its role in the progression of these tumors remains subtle.

In the last part of our study, we examined whether the expression levels of *Drosha*, *Dicer*, and Ago2 were associated with patients' clinical outcome and overall survival. Results from previous studies on other types of epithelial malignancies are controversial. For instance, Merrit and colleagues have recently demonstrated that in patients with ovarian cancer, Dicer downregulation was robustly associated with adverse clinical outcome [13, 34]. Likewise, Choisea et al., applying molecular microarray-based studies, revealed decreased Dicer expression levels in invasive, advanced lung adenocarcinomas [11]. On the contrary, reports on prostate cancer proposed that augmented Dicer levels are associated with reduced survival [15]. In the present study, we did not observe any significant correlation between Dicer mRNA expression and survival, a finding that is in line with other studies on breast and gastric carcinomas [23, 35]. The reason for these differences has not been defined yet. A possible explanation could be that like miRs, the RNAi-regulating network also functions in a tumor-specific manner.

In conclusion, our study provides novel evidence that Drosha, Dicer, and Ago2 are expressed in CRC. Moreover, it stresses the possibility that Dicer mRNA expression levels can be associated with the acceleration of CRC to more advanced stages. However, further investigation on larger sample size of patients is warranted in order to illuminate the molecular mechanisms that underlie the role and function of the miR machinery components in CRC development and progression.

Conflict of interest All authors declare that they have no conflict of interest.

References

1. Potter JD (1999) Colorectal cancer: molecules and populations. J Natl Cancer Inst 91:916–932
2. Grade M, Becker H, Liersch T, Ried T, Ghadimi BM (2006) Molecular cytogenetics: genomic imbalances in colorectal cancer and their clinical impact. Cell Oncol 28:71–84
3. Carthew RW, Sontheimer EJ (2009) Origins and mechanisms of miRNAs and siRNAs. Cell 136:642–655
4. Ambros V (2009) The functions of animal microRNAs. Nature 431:343–349
5. Drakaki A, Iliopoulos D (2009) MicroRNA gene networks in oncogenesis. Curr Genomics 10:35–41
6. Gregory RI, Shiekhattar R (2005) MicroRNA biogenesis and cancer. Cancer Res 65:3509–3512
7. Croce CM (2009) Causes and consequences of microRNA dysregulation in cancer. Nat Rev Genet 10:704–714
8. Meister G, Tuschl T (2004) Mechanisms of gene silencing by double-stranded RNA. Nature 431:343–349
9. Volinia S, Calin GA, Liu CG, Ambs S, Cimmino A, Petrocca F, Visone R, Iorio M, Roldo C, Ferracin M, Prueitt RL, Yanaihara N, Lanza G, Scarpa A, Vecchione A, Negrini M, Harris CC, Croce CM (2006) A microRNA expression signature of human solid tumors defines cancer gene targets. Proc Natl Acad Sci U S A 103:2257–22561

10. Schepeler T, Reinert JT, Ostenfeld MS, Christensen LL, Silahtaroglu AN, Dyrskjøt L, Wiuf C, Sørensen FJ, Kruhøffer M, Laurberg S, Kauppinen S, Ørntoft TF, Andersen CL (2008) Diagnostic and prognostic microRNAs in stage II colon cancer. Cancer Res 68:6416–6424
11. Chiosea S, Jelezcova E, Chandran U, Luo J, Mantha G, Sobol RW, Dacic S (2007) Overexpression of Dicer in precursor lesions of lung adenocarcinoma. Cancer Res 67:2345–2350
12. Grelier G, Voirin N, Ay AS, Cox DG, Chabaud S, Treilleux I, Léon-Goddard S, Rimokh R, Mikaelian I, Venoux C, Puisieux A, Lasset C, Moyret-Lalle (2009) Prognostic value of Dicer in human breast cancers and association with the mesenchymal phenotype. Br J Cancer 101:673–683
13. Merritt WM, Lin YG, Han LY, Kamat AA, Spannuth WA, Schmandt R, Urbauer D, Pennacchio LA, Cheng JF, Nick AM, Deavers MT, Mourad-Zeidan A, Wang H, Mueller P, Lenburg ME, Gray JW, Mok S, Birrer MJ, Lopez-Berestein G, Coleman RL, Bar-Eli M, Sood AK (2008) Dicer, Drosha, and outcomes in patients with ovarian cancer. N Engl J Med 359:2641–2650
14. Flavin RJ, Smyth PC, Finn SP, Laios A, O'Toole SA, Barrett C, Ring M, Denning KM, Li J, Aherne ST, Aziz NA, Alhadi A, Sheppard BL, Loda M, Martin C, Sheils OM, O'Leary JJ (2008) Altered eIF6 and Dicer expression is associated with clinicopathological features in ovarian serous carcinoma patients. Mod Pathol 21:676–684
15. Chiosea S, Jelezcova E, Chandran U, Acquafondata M, McHale T, Sobol RW, Dhir R (2006) Up-regulation of Dicer, a component of the microRNA machinery, in prostate adenocarcinoma. Am J Pathol 169:1812–1820
16. Chiosea SI, Barnes EL, Lai SY, Egloff AM, Sargent RL, Hunt JL, Seethala RR (2008) Mucoepidermoid carcinoma of upper aerodigestive tract: clinicopathologic study of 78 cases with immunohistochemical analysis of dicer expression. Virchows Arch 452:629–635
17. Zhang X, Cairns M, Rose B, O'Brien C, Shannon K, Clark J, Gamble J, Tran N (2009) Alterations in miRNA processing and expression in pleomorphic adenomas of the salivary gland. Int J Cancer 124:2855–2863
18. Faber C, Horst D, Hlubek F, Kirchner T (2011) Overexpression of Dicer predicts poor survival in colorectal cancer. Eur J Cancer 47 (9):1414–1419
19. McShane LM, Altman DG, Sauerbrei W, Taube SE, Gion M, Clark GM (2005) REporting recommendations for tumor MARKer prognostic studies (REMARK). Nat Clin Pract Urol 2:416–422
20. Papachristou DJ, Goodman MA, Cieply K, Hunt JL, Rao UN (2006) Comparison of allelic losses in chondroblastoma and primary chondrosarcoma of bone and correlation with fluorescence in situ hybridization analysis. Hum Pathol 37:890–898
21. Antonacopoulou AG, Tsamandas AC, Petsas T, Liava A, Scopa CD, Papavassiliou AG, Kalofonos HP (2008) EGFR, HER-2 and COX-2 levels in colorectal cancer. Histopathology 53:698–706
22. Vermeulen J, De Preter K, Lefever S, Nuytens J, De Vloed F, Derveaux S, Hellemans J, Speleman VJ (2011) Measurable impact of RNA quality on gene expression results from quantitative PCR. Nucleic Acid Res 39(9):e63
23. Hamilton SR, Vogelastein B, Kude S, Riboli E, Nakamura S, Hainaut P, Rubio CA, Sobin LH, Fogt F, Winawer SJ, Goldgar DE, Jass JR (2000) Carcinoma of the colon and rectum. In: Hamilton SR, Aaltonen LA (eds) Pathology and genetics: tumors of the digestive system. IARC Press, Lyon, pp 104–119
24. Slaby O, Svoboda M, Michalek J, Vyzula R (2009) MicroRNAs in colorectal cancer: translation of molecular biology into clinical application. Mol Cancer 28:102
25. Dedes KJ, Natrajan R, Lambros MB, Geyer FC, Lopez-Garcia MA, Savage K, Jones RL, Reis-Filho JS (2010) Down-regulation of the miRNA master regulators Drosha and Dicer is associated with specific subgroups of breast cancer. Eur J Cancer 47:138–150
26. Tang X, Zhang Y, Tucker L, Ramratnam B (2010) Phosphorylation of the RNase III enzyme Drosha at Serine300 or Serine302 is required for its nuclear localization. Nucleic Acids Res 38:6610–6619
27. Potenza N, Papa U, Russo A (2009) Differential expression of Dicer and Argonaute genes during the differentiation of human neuroblastoma cells. Cell Biol Int 33:734–738
28. Potenza N, Papa U, Scaruffi P, Mosca N, Tonini GP, Russo A (2010) A novel splice variant of the human dicer gene is expressed in neuroblastoma cells. FEBS Lett 584:3452–3457
29. Faggad A, Budczies J, Tchernitsa O, Darb-Esfahani S, Sehouli J, Müller BM, Wirtz R, Chekerov R, Weichert W, Sinn B, Mucha C, Elwali NE, Schäfer R, Dietel M, Denkert C (2010) Prognostic significance of Dicer expression in ovarian cancer-link to global microRNA changes and oestrogen receptor expression. J Pathol 220:382–391
30. Irvin-Wilson CV, Chaudhuri G (2005) Alternative initiation and splicing in dicer gene expression in human breast cells. Breast Cancer Res 7:R563–569
31. Wiesen JL, Tomasi TB (2009) Dicer is regulated by cellular stresses and interferons. Mol Immunol 46:1222–1228
32. Liu J, Carmell MA, Rivas FV, Marsden CG, Thomson JM, Song JJ, Hammond SM, Joshua-Tor L, Hannon GJ (2004) Argonaute2 is the catalytic engine of mammalian RNAi. Science 305:1437–1441
33. Adams BD, Claffey KP, White BA (2009) Argonaute-2 expression is regulated by epidermal growth factor receptor and mitogen-activated protein kinase signaling and correlates with a transformed phenotype in breast cancer cells. Endocrinology 150:14–23
34. Merritt WM, Bar-Eli M, Sood AK (2010) The dicey role of Dicer: implications for RNAi therapy. Cancer Res 70:2571–2574
35. Tchernitsa O, Kasajima A, Schäfer R, Kuban RJ, Ungethüm U, Györffy B, Neumann U, Simon E, Weichert W, Ebert MP, Röcken C (2010) Systematic evaluation of the miRNA-ome and its downstream effects on mRNA expression identifies gastric cancer progression. J Pathol 222:310–319

Virchows Arch (2011) 459:441–447
DOI 10.1007/s00428-011-1128-4

ORIGINAL ARTICLE

ERG gene rearrangement status in prostate cancer detected by immunohistochemistry

Sara Moscovita Falzarano · Ming Zhou · Paula Carver · Toyonori Tsuzuki · Kelly Simmerman · Huiying He · Cristina Magi-Galluzzi

Received: 7 March 2011 / Revised: 7 April 2011 / Accepted: 20 April 2011 / Published online: 20 July 2011
© Springer-Verlag 2011

Abstract *TMPRSS2–ERG*, the most common gene fusion in prostate cancer, is associated with expression of a truncated protein product of the oncogene *ERG*. A novel anti-ERG monoclonal antibody has been recently characterized. We investigated the correlation between *ERG* rearrangement assessed by fluorescence *in situ* hybridization (FISH) and ERG expression detected by immunohistochemistry in a large cohort of patients treated with radical prostatectomy for clinically localized prostate cancer. Thirteen tissue microarrays comprising 305 tumors and a subset of 112 samples of nonneoplastic prostatic tissue were assessed for *ERG* rearrangement status by FISH and for ERG expression by immunohistochemistry. Accuracy of ERG detection by immunohistochemistry in predicting *ERG* status as assessed by FISH (criterion standard) was calculated in terms of sensitivity, specificity, positive and negative predictive values. Of 305 tumor foci, 103 (34%) showed *ERG* rearrangement by FISH. ERG was detected by immunohistochemistry in 100 (33%) cases, 99 of which were FISH positive. ERG detection by immunohistochemistry demonstrated a sensitivity and specificity of 96% and 99%, respectively, with positive and negative predictive values of 99% and 98%, respectively. None of the 112 samples of nonneoplastic prostatic tissue was rearranged by FISH or showed any ERG expression. In conclusion, ERG detection by immunohistochemistry in prostate cancer was highly predictive of *ERG* rearrangement as assessed by FISH in a large cohort of prostatectomy patients. Given the high yield and the easier task of performing immunohistochemistry vs. FISH, ERG assessment by immunohistochemistry may be useful for characterizing *ERG* status in prostate cancer.

Keywords ERG · Fluorescence *in situ* hybridization · Immunohistochemistry · Prostate cancer

S. M. Falzarano · M. Zhou · P. Carver · K. Simmerman · H. He · C. Magi-Galluzzi
Pathology and Laboratory Medicine Institute, Cleveland Clinic, Cleveland, OH, USA

M. Zhou · C. Magi-Galluzzi
Glickman Urological & Kidney Institute, Cleveland Clinic, Cleveland, OH, USA

T. Tsuzuki
Department of Pathology, Nagoya Daini Red Cross Hospital, Nagoya, Japan

S. M. Falzarano
Department of Pathology and Human Oncology, University of Siena, Siena, Italy

C. Magi-Galluzzi (✉)
Department of Anatomic Pathology, Cleveland Clinic, 9500 Euclid Avenue, L25, Cleveland, OH 44195, USA
e-mail: magic@ccf.org

Introduction

Tumor-associated molecular alterations occurring in leukemias, lymphomas, sarcomas and some epithelial tumors have been useful in defining distinct pathologic entities and may also serve as specific diagnostic and prognostic markers [1]. Several highly sensitive and specific techniques have been used for the detection of such molecular alterations. Among these, polymerase chain reaction (PCR) and fluorescence *in situ* hybridization (FISH) are the most commonly applied. However, because of their relatively high costs and need of qualified personnel, they cannot

always be easily implemented as routine tests in clinical laboratories.

Some genetic alterations result in the expression of novel, disease-specific protein products, which may represent tumor-specific targets. Antibodies directed against proteins encoded by genetic alterations are useful tools in the characterization of diagnostic subtypes of hematologic malignancies, such as acute myeloid leukemia and many lymphomas [2].

Immunohistochemistry is a routine laboratory procedure and a relatively simple, low-cost method compared to molecular techniques. However, to be effective in replacing or complementing the molecular characterization of genetic alterations, the sensitivity and specificity of the immunohistochemical test need to be assessed against the criterion standard for the detection of such alterations.

Recurrent chromosomal rearrangements leading to the fusion of the androgen receptor-regulated gene *TMPRSS2* and *ETS* transcription factors are present in about half of prostate cancers from radical prostatectomy series [3–5]. v-ets erythroblastosis virus E26 oncogene homolog (avian) (*ERG*) is the most common fusion partner and its rearrangements have been extensively investigated by FISH [3, 4], which shows deletion or translocation of its 5′end in fusion-positive cases.

TMPRSS2–ERG fusion by FISH is highly specific for prostate cancer. FISH signal patterns of *ERG* rearrangement have never been detected in nonneoplastic prostate tissue samples, including benign prostatic hyperplasia and several forms of prostate atrophy [4, 6], although detection of fusion transcripts by PCR has occasionally been reported in nonneoplastic tissue [7, 8]. Moreover, in a recent study, Scheble et al. [9] screened 54 different tumor types other than prostate cancer and found FISH signal patterns specific of *ERG* rearrangements in none of them.

The genetic alteration leads to the juxtaposition of androgen-responsive regulatory elements of *TMPRSS2* to *ERG* sequence, with consequent overexpression of the rearranged *ERG* gene [5, 10]. In the most commonly detected fusion transcripts of *TMPRSS2–ERG* positive cases, *TMPRSS2* contributes only untranslated sequences, thus resulting in the overproduction of a truncated ERG protein product, rather than a chimeric protein [5, 11]. Studies exploring the potential role of a truncated ERG protein, analogous to *ERG* rearrangement product, in prostate tumorigenesis reported controversial results, with overexpression of *ERG* being found to induce a neoplastic phenotype of prostate cells (mouse prostatic intraepithelial neoplasia) in some [11, 12], but not in others [13].

The truncated protein product of *ERG* rearrangement may be targeted as immunohistochemical surrogate for the gene fusion and may help elucidate its role in tumor development and progression, as previously hypothesized [11].

Two independent studies recently addressed the immunohistochemical detection of the fusion product by testing two different monoclonal antibodies [14, 15]. Furusato et al. [14] developed a mouse anti-ERG monoclonal antibody and found it to be highly specific in distinguishing prostate cancer foci from benign glands on whole mount sections of prostate. They also noticed a strong concordance between mRNA levels of fusion transcripts detected by branched-chain DNA signal amplification and ERG immunohistochemistry, as well as between *ERG* rearrangement detected by FISH and ERG protein expression in a smaller sample of prostate specimens (10). Park et al. [15] characterized a novel rabbit anti-ERG monoclonal antibody directed against the C-terminus of the most common gene fusion product. They found that ERG protein expression determined by immunohistochemistry with this antibody highly correlated with the *ERG* rearrangement status determined by FISH on prostate cancer tissue microarrays from two independent patient cohorts.

In this study, we aimed to provide independent confirmation of the accuracy of ERG expression detected by the rabbit anti-ERG monoclonal antibody used by Park et al. [15] in predicting *ERG* rearrangement as assessed by FISH (criterion standard) in a large cohort of patients treated with radical prostatectomy for clinically localized prostate cancer.

Materials and methods

Study population and tissue microarray construction

Two hundred and seventy-one patients treated with radical prostatectomy for clinically localized prostate cancer were included in the study. Cases were selected in part based on previous assessment of *ERG* rearrangement status by FISH, as previously reported [16, 17]. Thirteen tissue microarrays, composed of up to three representative 1.5 mm tissue cores for each tumor and one 1.5 mm core for paired nonneoplastic prostate tissue in a subset of 112 cases, were constructed from formalin-fixed paraffin-embedded radical prostatectomy blocks. Two of 13 tissue microarrays (46 patients) were from an outside institution (Nagoya Daini Red Cross Hospital, Nagoya, Japan). Concomitant separate tumors were sampled when identified, as previously described [16]. Patients' clinical data (including age and pre-operative PSA) and radical prostatectomy pathologic parameters (including Gleason score and pathologic stage), when available, were collected in an institutional board approved database.

ERG gene rearrangement assessment by FISH

A dual-color interphase break-apart FISH assay was performed on the 13 formalin-fixed paraffin-embedded tissue microarrays to assess the *ERG* gene rearrangement status, as previously described [4, 5, 16]. Briefly, two differentially labeled Bacterial artificial chromosome (BAC) FISH probes were used: the Biotin-14-dCTP labeled BAC clone RP11-24A11 (eventually conjugated to produce a red signal) for the neighboring 3′ centromeric region of the *ERG* locus and the Digoxigenin-dUTP labeled BAC clone RP11-372O17 (eventually conjugated to produce a green signal), for the neighboring 5′ telomeric region. According to this break-apart probe system, a nucleus without *ERG* rearrangement shows 2 pairs of juxtaposed red and green signals, forming yellow signals (class N, or negative for fusion); a nucleus with *ERG* rearrangement through translocation (class Esplit) shows one pair of still combined red and green signals (a yellow signal), while the other breaks into a single red and a single green signal (split signal); a nucleus with *ERG* rearrangement through deletion (class Edel) shows one yellow signal and a single red signal, while the green signal (5′ region) is lost. Any case with *ERG* signal abnormalities in >10% of the neoplastic cells was scored as positive and classified accordingly, as previously described [16]. In addition, the presence of multiple copies of the *ERG* rearrangement sequence, with or without retention of the green signal (class 2 + Esplit and 2 + Edel, respectively) was assessed in all evaluated nuclei. Tissue hybridization, washing, and fluorescence detection were performed as previously described [18].

The samples were analyzed under a 100× oil immersion objective using a Leica DM-RB fluorescence microscope equipped with appropriate filters. The corresponding hematoxylin and eosin section was available for side-by-side comparison with the FISH section. Evaluation of the slides was performed by a pathologist (SMF) and a medical technologist (KS) with experience in analyzing FISH. For each case at least 50 morphologically intact, nonoverlapping nuclei were scored. Technical difficulties included insufficient (<50 cells) or absent diagnostic material to evaluate and very weak or absent probe signals.

Evaluation of ERG protein expression by immunohistochemistry

Immunohistochemistry was performed on 4 μm sections of the 13 formalin-fixed paraffin-embedded tissue microarrays using a Discovery XT automated stainer (Ventana Medical Systems, Tucson, AZ). Antigen retrieval was performed in Tris/Borate/EDTA buffer, pH 8.0–8.5, for 8 min at 95°C, 12 min at 100°C, and then 8 min at room temperature. The slides were then incubated with an anti-ERG rabbit monoclonal antibody (1:100 dilution, clone ID: EPR3864, Catalog Number 2805-1, Epitomics, San Diego, CA) for 32 min at room temperature. A secondary antibody (OmniMap anti-Rabbit HRP; Tuscon, AZ) was applied for 16 min at room temperature. The chromogenic substrate (ChromoMap DAB, Tucson, AZ) was applied for 8 min at room temperature. Slides were counterstained with hematoxylin II. Using the vascular endothelial cells as internal positive control, the expression of ERG protein was evaluated as negative or positive in prostate glands, regardless of the intensity of staining. A tumor was judged positive if any of the evaluable cores showed a positive staining.

Statistical analysis

To compare the predicted accuracy of immunohistochemistry ERG protein detection in determining the *ERG* rearrangement status as assessed by FISH (criterion standard), sensitivity, specificity, positive and negative predictive values and 95% Confidence Intervals (CI) were calculated using the NCSS 2007 software (Kaysville, UT). Associations for ERG expression status and clinicopathologic features were also explored using the SPSS software (Chicago, IL). Equality of continuous variables was tested using the Student *t* test and that of categorical variables was tested using chi-square test.

Results

Study population

Patients' mean age at time of diagnosis was 61 years (range: 40–81). Mean pre-operative PSA was 8.3 ng/mL (range: 0.9–66.8). Prostatectomy Gleason score was 6 in 76 (28%), 7 in 161 (59%), ≥8 in 33 (12%) and indeterminate in 1 (1%) patient who received neoadjuvant androgen deprivation therapy. Pathological stage was available in 264 (97%) cases, and was pT2 in 179 (68%), pT3a in 74 (28%) and pT3b in the remaining 11 (4%) cases.

Comparison of ERG expression detected by immunohistochemistry and *ERG* status assessed by FISH

Three hundred and five tumors were evaluable for both immunohistochemistry and FISH, one for each of the 271 patients and a concomitant separate tumor focus in 34 (12%) cases. *ERG* rearrangement by FISH was found in 103 (34%) tumors. Of the FISH positive tumors, 49 (47%) were classified as Edel, 47 (46%) as Esplit, and 7 (7%) as combined Edel + Esplit. Duplication of the rearranged

sequence with deletion of the 5′ sequence was observed in 4 cases (2 + Edel) (Fig. 1).

ERG expression by immunohistochemistry was detected in 100 (33%) cases, 99 of which were FISH positive (Fig. 2). We identified one (<1%) tumor demonstrating ERG protein expression in one of the 2 informative cores without any detectable *ERG* rearrangement as assessed by FISH. Conversely, four (1%) cases with *ERG* rearrangement by FISH, two Edel and two Esplit, had no detectable ERG protein expression in any of the informative cores. The endothelial cells (positive control) were strongly positive for ERG immunohistochemistry in these cores.

The overall sensitivity and specificity of ERG protein expression by immunohistochemistry in predicting *ERG* rearrangement status were 96% (95% CI 90% to 99%) and 99% (95% CI 97% to 100%), respectively, with a positive predictive value of 99% (95% CI 94% to 100%) and a negative predictive value of 98% (95% CI 95% to 99%).

Of the 34 patients with two separate concomitant tumor foci, 24 (71%) were homogeneous for *ERG* rearrangement status (present or absent in both tumor foci), whereas 10 (29%) were heterogeneous, with one tumor focus harboring the *ERG* rearrangement and not the other. ERG protein was concordantly expressed in the *ERG* rearranged focus, whereas no expression was found in the *ERG* fusion-negative focus.

Except for 6 (2%) cases, all TMA cores of a given tumor revealed homogeneity for rearrangement status and corresponding ERG expression. In the 6 cases, 1 of the informative tumor cores showed rearrangement by FISH (5 Edel, 1 Esplit) as well as protein expression by immunohistochemistry, and the remaining cores showed no rearrangement or protein expression.

None of the 112 tissue samples of benign prostatic tissue was rearranged by FISH or showed ERG protein expression by immunohistochemistry.

No significant association was found between ERG expression and clinicopathological parameters, such as age, pre-operative PSA, Gleason score, and pathologic stage.

Discussion

Chromosomal translocations often result in the expression of either hybrid gene products with new properties or inappropriately expressed normal proteins. Monoclonal antibodies to these proteins are useful tools in the characterization of diseases, such as hematologic and mesenchymal malignancies [2, 19].

Recurrent chromosomal aberrations resulting in overexpression of *ETS* gene family members, primarily *ERG*, have been identified and characterized in prostate cancer [11]. *ERG* rearrangements mostly lead to the production of a truncated protein that can be detected by immunohistochemistry.

Two groups recently conducted a comparative evaluation of *TMPRSS2–ERG* gene fusion status and ERG oncoprotein expression by immunohistochemistry using two different anti-ERG monoclonal antibodies. Park et al. [15] compared *ERG* gene rearrangement analysis by FISH and ERG detection by immunohistochemistry using a novel rabbit anti-ERG monoclonal antibody, in a combined multi-institutional cohort consisting of 207 patient tumors. Furusato et al. [14] evaluated the expression of ERG in 261 tumors using a mouse anti-ERG monoclonal antibody: in a subset of 35 specimens the authors made the comparative analysis with *TMPRSS2–ERG* gene fusion status assessed by branched-chain DNA assay, and in a subset of 10 with *ERG* gene rearrangement assessed by FISH. Both groups found a high concordance between fusion status and ERG protein expression. They also showed that both antibodies recognize all the protein

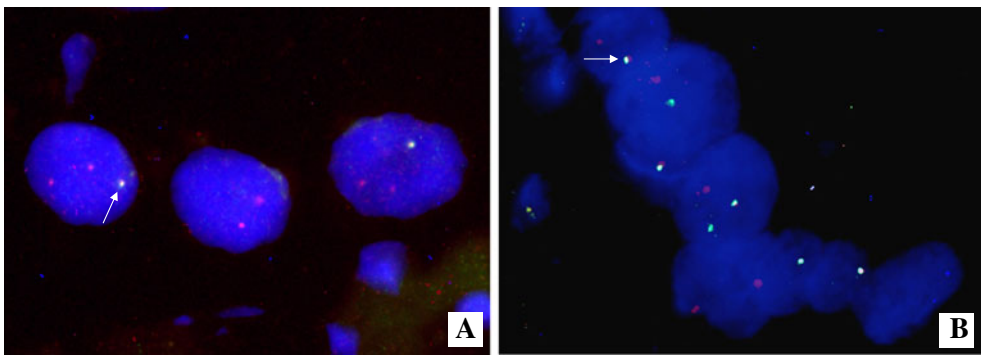

Fig. 1 *ERG* rearrangement by break-apart FISH. For the non-rearranged *ERG* locus, the set of probes appear either as juxtaposed red and green signals or a yellow spot due to the overlap between the red or green probes (arrows). The red and green signals are separated when an *ERG* gene rearrangement occurs. Loss of the green signal complementary to the 5′ telomeric region of *ERG* represents a deletion in this chromosomal region and indirectly indicates a fusion of the *TMPRSS2* and *ERG* loci (Edel). Duplication of the red signal complementary to the 3′ *ERG* region may also occur (2+Edel) **a.** Separate and distinct red and green signals indicate *ERG* rearrangement by translocation (Esplit) **b.** (**a** and **b**, ×100)

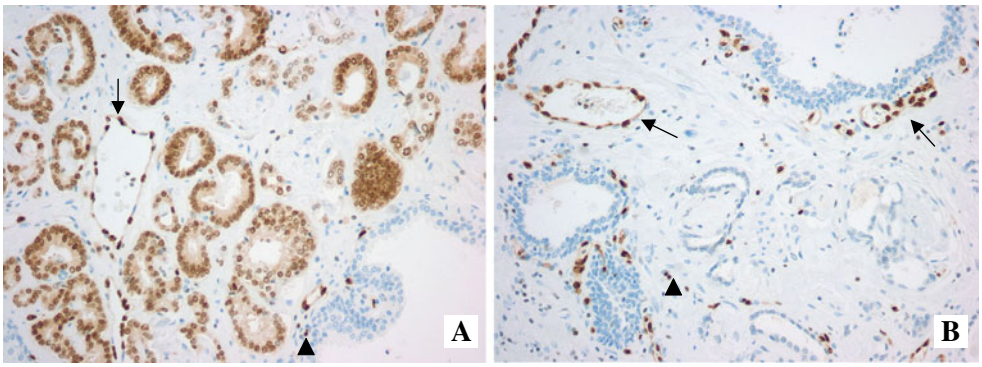

Fig. 2 Immunohistochemical detection of ERG protein expression. ERG protein expression by immunohistochemistry is detected in nuclei of prostate cancer cells (**a**). Vascular endothelial cells (arrows) and infiltrating stromal lymphocytes (arrowheads) show positive ERG expression in both ERG-positive (**a**) and ERG-negative (**b**) tumor samples (×20)

products resulting from genomic fusions of ERG protein-coding sequences and regulatory sequences of any of the known 5′ fusion partners (*TMPRSS2*, *SLC45A3* and *NDRG1*), as well as the wild type ERG [14, 15].

Similar to Park et al. [15], we found that immunohistochemical detection of ERG protein in prostate cancer using the same rabbit anti-ERG monoclonal antibody is highly predictive of *ERG* rearrangement status assessed by FISH. In our study group of 305 tumors, we found a sensitivity of 96%, which is comparable to the 95.7% reported by Park et al., whereas the specificity we found was slightly higher than the one reported by the same authors (99% vs. 96.5%). The specificity of a test depends on the number of "false positive" that the test picks up compared against the criterion standard. We found only one (1/305≤1%) case demonstrating ERG protein expression without *ERG* rearrangement by FISH (false positive), whereas Park et al. found 4 (4/207=2%) of such discordant cases. Technical reasons may in part explain this finding. Alternatively, *ERG* overexpression in prostate cancer may occur through mechanisms other than gene rearrangements detectable by the FISH break-apart system, as previously hypothesized [15]. Together with chromosomal translocations, amplification, point mutations, and activation by insertions of new regulatory sequences may be responsible for oncogenic activation of cellular genes, including the *ETS* family (reviewed by Seth et al. [20]). Although consistent amplification of *ERG* or *ETV1* in prostate cancer samples with respective transcript overexpression has not been found [5], further studies may help characterize alternative mechanisms of *ERG* overexpression.

We also observed 4 cases with *ERG* rearrangement as assessed by FISH and no expression of ERG protein (false negative). Likewise, in the study by Park et al. [15], 4 false negative cases from one of the two evaluated cohorts were reported. Besides technical issues, the inefficient transcription and/or translation of the gene fusion product may be responsible for cases with gene rearrangement by FISH which do not express detectable levels of the protein. The transcription of *TMPRSS2–ERG* fusion gene is driven by androgen signaling pathway and it is conceivable that, if the androgen pathway is defective, prostate cancer cells with *TMPRSS2–ERG* gene fusion may not express ERG protein at a level high enough to be detected by immunohistochemistry. Although Park et al. showed no difference in protein expression between *ERG* rearranged tumors harboring *SLC45A3–ERG* or *NDRG1–ERG* gene fusions and those harboring *TMPRSS2–ERG* gene fusion [15], still unknown 5′ partners might result in gene fusions without ERG protein overexpression, thus explaining some of the "false negative" cases [21, 22]. In the present study, we did not evaluate the 5′ partners of *ERG* rearranged cases.

Importantly, we also found high positive and negative predictive values (99% and 98%, respectively) of ERG protein detection by immunohistochemistry, which are comparable to those reported by Park et al. [15]. The high positive predictive value denotes the high probability that a positive ERG immuno-expression reflects the underlying presence of *ERG* rearrangement in the tumor tested; on the other hand a high negative predictive value implies a high likelihood that if prostate cancer cells do not express ERG protein as detected by immunohistochemistry, the tumor does not harbor the gene rearrangement. Those values do however depend on the overall prevalence of *ERG* rearrangement in the population under study. In our study population, 34% (103/305) of tumors showed *ERG* rearrangement by FISH. This frequency is similar to the value of 30% (134/445) found by Attard et al. [23], although lower than the value of 47% (60/128) and 40% (32/79) reported by Park et al. in their cohorts [15], or the commonly referred value of 48.5% (115/237) found by Perner et al. [4], who also assessed *ERG* gene alterations using a FISH break-apart assay. Since the incidence of *ERG* rearrangements may vary in relation to different clinicopathological characteristics, such as clinical stage [23], patient race [16], Gleason score [23] and prostate cancer zone of origin [4, 16], the distinct compositions of the prostate tumor sets surveyed in each study may in part explain these differences.

In line with prior studies [24–26], we observed interfocal heterogeneity for *ERG* rearrangement between distinct tumors within the same prostate gland. The overall

incidence of 29% reported herein was slightly lower than those reported by others (41% to 51%) [24–26]. However, the cases evaluated in this study with more than one tumor per prostate gland included patients with a predominant transition zone tumor and a secondary peripheral zone tumor [16]. Transition zone prostate cancer harbor *TMPRSS2–ERG* fusion in lower percentages of cases, as previously reported [16], which may artificially increase the number of concordantly negative tumor foci in each patient, thus resulting in a lower rate of intertumoral heterogeneity detected.

All but 6 of our cases demonstrated intrafocal homogeneity for rearrangement status and concordant ERG protein expression. Intrafocal heterogeneity for *ERG* rearrangement has been reported in literature, ranging from 1 to 3% [4, 17, 26].

Similar to Park et al., we found no significant association between ERG expression and clinicopathological parameters, such as age, pre-operative PSA, Gleason score, and pathologic stage. Furusato et al. found that although ERG expression did not correlate with most clinicopathological features, when individual tumors were considered, higher Gleason score showed significant correlation with ERG-positive immunostaining [14]. Clinicopathological variables have been previously reported to be inconsistently correlated with fusion status [3, 4, 16, 17, 23, 25]. The different compositions of patient populations may explain the controversial results in literature.

ERG protein expression in vascular endothelial cells was herein used as positive internal control for the immunostaining, as endothelial cells lining blood vessels and capillaries show positive reactivity to anti-ERG antibodies in tumors as well as in nonneoplastic tissue samples [15, 27]. Infiltrating stromal lymphocytes also expressed ERG protein, as reported previously [15]. Since *ERG* rearrangement by FISH has never been found in lymphocytes or endothelial cells of either benign or neoplastic tissue specimens, the observed positive staining is consistent with antibody detection of a wild type ERG protein, as previously hypothesized [15]. *ERG* gene has in fact been shown to be constitutively expressed in vascular endothelial cells and related to endothelial homeostasis and angiogenesis; in addition *ERG* seems to play a role in lymphocyte development and differentiation [28, 29].

A potential limitation to this study is that cases were selected in part based on previous assessment of *ERG* rearrangement by FISH [16, 17] thus not representing temporally consecutive, unselected radical prostatectomy series.

Our findings independently confirmed the high concordance of ERG protein expression by immunohistochemistry with *ERG* rearrangement by FISH in a larger cohort of cases of clinically localized prostate cancer from radical prostatectomy specimens. Although the cases were not from a single institution, both FISH and immunohistochemistry results and interpretation were reviewed by a single pathologist.

Given the specificity of *ERG* rearrangement FISH patterns for neoplastic prostate, immunostaining with the anti-ERG antibody can be utilized as a surrogate for the genetic alteration. ERG immunohistochemistry has the advantage of being easily implemented as a routine laboratory technique; it has a high yield and can be rapidly performed and simply interpreted on tissue sections by light microscopy. The internal control represented by endothelial cells and infiltrating stromal lymphocytes contributes to the straightforward interpretation of immunostaining results.

The evaluation of ERG protein expression pattern in prostate cancer by immunohistochemistry may improve the understanding of its role in prostate tumorigenesis. Additional efforts are needed to further characterize the rare prostate cancer cases with discordant results between FISH rearrangement and ERG protein expression.

Disclosure/Conflict of Interest The authors declare that they have no conflict of interests.

References

1. Rabbitts TH, Stocks MR (2003) Chromosomal translocation products engender new intracellular therapeutic technologies. Nat Med 9(4):383–386
2. Falini B, Martelli MP, Tiacci E, Ascani S, Thiede C, Pileri SA (2010) Immunohistochemical surrogates for genetic alterations of CCDN1, PML, ALK, and NPM1 genes in lymphomas and acute myeloid leukemia. Best Pract Res Clin Haematol 23 (3):417–431
3. Mehra R, Tomlins SA, Shen R, Nadeem O, Wang L, Wei JT, Pienta KJ, Ghosh D, Rubin MA, Chinnaiyan AM, Shah RB (2007) Comprehensive assessment of TMPRSS2 and ETS family gene aberrations in clinically localized prostate cancer. Mod Pathol 20(5):538–544
4. Perner S, Mosquera JM, Demichelis F, Hofer MD, Paris PL, Simko J, Collins C, Bismar TA, Chinnaiyan AM, De Marzo AM, Rubin MA (2007) TMPRSS2–ERG fusion prostate cancer: an early molecular event associated with invasion. Am J Surg Pathol 31(6):882–888
5. Tomlins SA, Rhodes DR, Perner S, Dhanasekaran SM, Mehra R, Sun XW, Varambally S, Cao X, Tchinda J, Kuefer R, Lee C, Montie JE, Shah RB, Pienta KJ, Rubin MA, Chinnaiyan AM (2005) Recurrent fusion of TMPRSS2 and ETS transcription factor genes in prostate cancer. Science 310(5748):644–648
6. Mosquera JM, Mehra R, Regan MM, Perner S, Genega EM, Bueti G, Shah RB, Gaston S, Tomlins SA, Wei JT, Kearney MC, Johnson LA, Tang JM, Chinnaiyan AM, Rubin MA, Sanda MG (2009) Prevalence of TMPRSS2–ERG fusion prostate cancer among men undergoing prostate biopsy in the United States. Clin Cancer Res 15(14):4706–4711

7. Clark J, Merson S, Jhavar S, Flohr P, Edwards S, Foster CS, Eeles R, Martin FL, Phillips DH, Crundwell M, Christmas T, Thompson A, Fisher C, Kovacs G, Cooper CS (2007) Diversity of TMPRSS2–ERG fusion transcripts in the human prostate. Oncogene 26(18):2667–2673
8. Furusato B, Gao CL, Ravindranath L, Chen Y, Cullen J, McLeod DG, Dobi A, Srivastava S, Petrovics G, Sesterhenn IA (2008) Mapping of TMPRSS2–ERG fusions in the context of multi-focal prostate cancer. Mod Pathol 21(2):67–75
9. Scheble VJ, Braun M, Beroukhim R, Mermel CH, Ruiz C, Wilbertz T, Stiedl AC, Petersen K, Reischl M, Kuefer R, Schilling D, Fend F, Kristiansen G, Meyerson M, Rubin MA, Bubendorf L, Perner S (2010) ERG rearrangement is specific to prostate cancer and does not occur in any other common tumor. Mod Pathol 23 (8):1061–1067
10. Petrovics G, Liu A, Shaheduzzaman S, Furusato B, Sun C, Chen Y, Nau M, Ravindranath L, Dobi A, Srikantan V, Sesterhenn IA, McLeod DG, Vahey M, Moul JW, Srivastava S (2005) Frequent overexpression of ETS-related gene-1 (ERG1) in prostate cancer transcriptome. Oncogene 24(23):3847–3852
11. Tomlins SA, Laxman B, Varambally S, Cao X, Yu J, Helgeson BE, Cao Q, Prensner JR, Rubin MA, Shah RB, Mehra R, Chinnaiyan AM (2008) Role of the TMPRSS2–ERG gene fusion in prostate cancer. Neoplasia 10(2):177–188
12. Klezovitch O, Risk M, Coleman I, Lucas JM, Null M, True LD, Nelson PS, Vasioukhin V (2008) A causal role for ERG in neoplastic transformation of prostate epithelium. Proc Natl Acad Sci USA 105(6):2105–2110
13. Carver BS, Tran J, Gopalan A, Chen Z, Shaikh S, Carracedo A, Alimonti A, Nardella C, Varmeh S, Scardino PT, Cordon-Cardo C, Gerald W, Pandolfi PP (2009) Aberrant ERG expression cooperates with loss of PTEN to promote cancer progression in the prostate. Nat Genet 41(5):619–624
14. Furusato B, Tan SH, Young D, Dobi A, Sun C, Mohamed AA, Thangapazham R, Chen Y, McMaster G, Sreenath T, Petrovics G, McLeod DG, Srivastava S, Sesterhenn IA (2010) ERG oncoprotein expression in prostate cancer: clonal progression of ERG-positive tumor cells and potential for ERG-based stratification. Prostate Cancer Prostatic Dis 13(3):228–237
15. Park K, Tomlins SA, Mudaliar KM, Chiu YL, Esgueva R, Mehra R, Suleman K, Varambally S, Brenner JC, MacDonald T, Srivastava A, Tewari AK, Sathyanarayana U, Nagy D, Pestano G, Kunju LP, Demichelis F, Chinnaiyan AM, Rubin MA (2010) Antibody-based detection of ERG rearrangement-positive prostate cancer. Neoplasia 12(7):590–598
16. Falzarano SM, Navas M, Simmerman K, Klein EA, Rubin MA, Zhou M, Magi-Galluzzi C (2010) ERG rearrangement is present in a subset of transition zone prostatic tumors. Mod Pathol 23 (11):1499–1506
17. Falzarano SM, Zhou M, Hernandez AV, Klein EA, Rubin MA, Magi-Galluzzi C (2011) Single focus prostate cancer: pathological features and ERG fusion status. J Urol 185(2):489–494
18. Rubin MA, Varambally S, Beroukhim R, Tomlins SA, Rhodes DR, Paris PL, Hofer MD, Storz-Schweizer M, Kuefer R, Fletcher JA, Hsi BL, Byrne JA, Pienta KJ, Collins C, Sellers WR, Chinnaiyan AM (2004) Overexpression, amplification, and androgen regulation of TPD52 in prostate cancer. Cancer Res 64 (11):3814–3822
19. Espinosa I, Lee CH, Kim MK, Rouse BT, Subramanian S, Montgomery K, Varma S, Corless CL, Heinrich MC, Smith KS, Wang Z, Rubin B, Nielsen TO, Seitz RS, Ross DT, West RB, Cleary ML, van de Rijn M (2008) A novel monoclonal antibody against DOG1 is a sensitive and specific marker for gastrointestinal stromal tumors. Am J Surg Pathol 32(2):210–218
20. Seth A, Watson DK (2005) ETS transcription factors and their emerging roles in human cancer. Eur J Cancer 41(16):2462–2478
21. Esgueva R, Perner S, LaFargue CJ, Scheble V, Stephan C, Lein M, Fritzsche FR, Dietel M, Kristiansen G, Rubin MA (2010) Prevalence of TMPRSS2–ERG and SLC45A3-ERG gene fusions in a large prostatectomy cohort. Mod Pathol 23(4):539–546
22. Pflueger D, Rickman DS, Sboner A, Perner S, LaFargue CJ, Svensson MA, Moss BJ, Kitabayashi N, Pan Y, de la Taille A, Kuefer R, Tewari AK, Demichelis F, Chee MS, Gerstein MB, Rubin MA (2009) N-myc downstream regulated gene 1 (NDRG1) is fused to ERG in prostate cancer. Neoplasia 11 (8):804–811
23. Attard G, Clark J, Ambroisine L, Fisher G, Kovacs G, Flohr P, Berney D, Foster CS, Fletcher A, Gerald WL, Moller H, Reuter V, De Bono JS, Scardino P, Cuzick J, Cooper CS (2008) Duplication of the fusion of TMPRSS2 to ERG sequences identifies fatal human prostate cancer. Oncogene 27(3):253–263
24. Mehra R, Han B, Tomlins SA, Wang L, Menon A, Wasco MJ, Shen R, Montie JE, Chinnaiyan AM, Shah RB (2007) Heterogeneity of TMPRSS2 gene rearrangements in multifocal prostate adenocarcinoma: molecular evidence for an independent group of diseases. Cancer Res 67(17):7991–7995
25. Perner S, Demichelis F, Beroukhim R, Schmidt FH, Mosquera JM, Setlur S, Tchinda J, Tomlins SA, Hofer MD, Pienta KG, Kuefer R, Vessella R, Sun XW, Meyerson M, Lee C, Sellers WR, Chinnaiyan AM, Rubin MA (2006) TMPRSS2:ERG fusion-associated deletions provide insight into the heterogeneity of prostate cancer. Cancer Res 66(17):8337–8341
26. Barry M, Perner S, Demichelis F, Rubin MA (2007) TMPRSS2–ERG fusion heterogeneity in multifocal prostate cancer: clinical and biologic implications. Urology 70(4):630–633
27. Mohamed AA, Tan SH, Mikhalkevich N, Ponniah S, Vasioukhin V, Bieberich CJ, Sesterhenn IA, Dobi A, Srivastava S, Sreenath TL (2010) Ets family protein, erg expression in developing and adult mouse tissues by a highly specific monoclonal antibody. J Cancer 1:197–208
28. Birdsey GM, Dryden NH, Amsellem V, Gebhardt F, Sahnan K, Haskard DO, Dejana E, Mason JC, Randi AM (2008) Transcription factor Erg regulates angiogenesis and endothelial apoptosis through VE-cadherin. Blood 111(7):3498–3506
29. Anderson MK, Hernandez-Hoyos G, Diamond RA, Rothenberg EV (1999) Precise developmental regulation of Ets family transcription factors during specification and commitment to the T cell lineage. Development 126(14):3131–3148

Virchows Arch (2011) 459:449–456
DOI 10.1007/s00428-011-1131-9

ORIGINAL ARTICLE

Tumor budding and dedifferentiation in gallbladder carcinoma: potential for the prognostic factors in T2 lesions

Keita Kai · Naohiko Kohya · Kenji Kitahara · Masanori Masuda · Atsushi Miyoshi · Takao Ide · Osamu Tokunaga · Kohji Miyazaki · Hirokazu Noshiro

Received: 26 April 2011 / Revised: 10 July 2011 / Accepted: 11 July 2011 / Published online: 22 July 2011
© Springer-Verlag 2011

Abstract Dedifferentiation (DD) is often encountered in gallbladder carcinoma (GBC) and poor prognosis with budding (BD) has been reported for other malignancies. However, the features of DD and BD in GBC remain unclear. The purpose of this study was to clarify the features and prognostic potential of DD and BD in GBC. A total of 80 patients with GBC (excluding intramucosal cancer) were enrolled. DD was histopathologically evaluated as tumors in which the grade of the invasive front is higher than the grade at the surface. BD was defined as an isolated single cancer cell or a cluster of fewer than five cancer cells at the invasive front. Of the 80 patients, 47 (58.8%) were positive for BD and 33 (41.2%) were positive for DD. Both BD and DD correlated significantly with disease-specific survival in univariate analysis ($P<0.0001$ and $P=0.0013$, respectively), but they were not identified as independent prognostic factors by multivariate analysis. In univariate analysis according to T stage, both BD and DD correlated significantly with survival in patients with T2 ($n=32$) tumor ($P=0.0011$ and $P=0.0018$, respectively), whereas no prognostic impact in patients with T1b ($n=8$), T3 ($n=34$), or T4 ($n=6$) tumor. Both DD and BD are frequently observed in GBC and reflect prognosis, particularly for T2 lesions. Therefore, the status of BD and DD should be taken into consideration in pathological reports on GBC.

K. Kai (✉) · M. Masuda · O. Tokunaga
Department of Pathology and Microbiology, Faculty of Medicine, Saga University,
Nabesima 5-1-1,
Saga City, Saga 849-8501, Japan
e-mail: kaikeit@cc.saga-u.ac.jp

N. Kohya · K. Kitahara · A. Miyoshi · T. Ide · K. Miyazaki · H. Noshiro
Departments of Surgery, Faculty of Medicine, Saga University, Saga, Japan

Keywords Gallbladder carcinoma · Dedifferentiation · Tumor budding

Introduction

Gallbladder cancer (GBC) is generally considered a rare malignant neoplasm, but incidences of GBC in Chile, Poland, India, and Japan are relatively high [1–3]. Under pathological examination, a well-differentiated adenocarcinoma in the mucosal layer is often observed to dedifferentiate into poorly or moderately differentiated adenocarcinoma on the invading side. However, little investigation has been undertaken into the status and prognostic impact of dedifferentiation (DD) in GBC.

Tumor budding (BD) is another morphological feature that can be seen at the invasive front in malignant neoplasms. This finding is generally accepted to indicate the presence of single tumor cells or small tumor clusters at the invasive front. The concept of BD was first established in colorectal cancer and was considered to be associated with the initial phase of tumor invasion [4, 5] and then with metastatic activity [6–8] and prognostic outcome [9–13]. The same findings have been reported for other malignancies, such as esophageal or laryngeal squamous cell carcinoma and gastric adenocarcinoma [14–18]. However, no studies appear to have described BD in GBC.

The utility of pathological assessment for BD in colorectal cancer is emphasized by the prognostic impact in submucosal invasive cancer [13]. BD is thus now considered to be a useful tool for determining treatment strategies for early colorectal cancer. From this perspective, we have interest in the BD status of GBC, especially in the tumors invading the subserosa (T2 tumor according to TNM classifications). The biological behavior of T2 tumors

in GBC can vary widely. Some cases follow a good course after surgery, while others show adverse outcomes. Thus, if BD status reflects patient prognosis, this finding would represent a useful tool for determining treatment strategies in T2 GBC.

The purpose of this study was to investigate the status, features, and prognostic impact of DD and BD in patients with GBC and to verify the usefulness of DD and BD as prognostic markers in patients with T2 lesions.

Materials and methods

Patients and staging

A total of 90 GBC patients underwent surgical treatment for primary lesions between 1989 and December 2009 at Saga University Hospital. Of these, 10 patients who had noninvasive intramucosal cancer were excluded from the study. The remaining 80 patients (24 men, 56 women) with invasive GBC were enrolled in this study. Informed consent for the use of resected tissue was obtained from all patients, and the study protocol was approved by the Ethics Committee of the Faculty of Medicine at Saga University. Mean age at the time of surgery was 68.5 years (range, 45–87 years). Clinical and histopathological staging was based on the TNM Classification of Malignant Tumors by the International Union against Cancer [19]. Eight patients (10.0%) were classified as T1b, 32 (40.0%) as T2, 34 (42.5%) as T3, and 6 (7.5%) as T4. After the histopathological study of the entire tumor, one most intensive section was selected and this paraffin block was applied for the analysis of BD and DD.

Pathological classification and evaluation of DD

Histology was separately evaluated at the surface of the tumor and at the invading side. Three categories were classified: G1, well-differentiated adenocarcinoma; G2, moderately differentiated adenocarcinoma; and G3+others, poorly differentiated adenocarcinoma and other histological types of carcinoma. DD was judged as positive when histology at the invasive front was dedifferentiated compared to surface histology (Fig. 1). Cases with the same G score at the tumor surface and at the invasive front were judged as DD-negative. No cases showed higher G score at the tumor surface than at the invasive front.

Evaluation of BD

BD was defined as an isolated single cancer cell or cluster of fewer than five cancer cells at the invasive front. After choosing one field where BD was the most intensive, a BD count was made in the field using a ×20 magnification objective lens. A field with five or more buds was judged as positive. Immunohistochemical study of cytokeratin AE1/AE3 (dilution 1:50; Dako Cytomation, Glostrup, Denmark) was performed in 77 cases for which tissues were available for the further assessment of BD, as inflammatory cells often masks small cluster of tumor cells at the invasive front of GBC (Fig. 2).

Statistical analysis

Statistical analyses were performed using JMP version 8 software (SAS Institute, Cary, NC, USA). Statistical analysis to compare the two groups was performed using Student's *t* test, the chi-square test, and Fisher's exact test, as appropriate. The agreement between BD and DD was analyzed by kappa statistic analysis. All survival analyses were performed using disease-specific survival, determined from the time of surgery to the time of cancer-related death or most recent follow-up. Postoperative survival was calculated using the Kaplan–Meier method. Differences in survival curves were compared using the log-rank test. Cox proportional hazards models were applied for multivariate analysis. A value of $P<0.05$ was considered statistically significant.

Results

Clinicopathologic features of GBC with or without BD and DD

In terms of findings at the tumor surface, 53 patients (66.3%) were classified as G1, 20 (25%) as G2, and 7 (8.8%) as G3+others (undifferentiated carcinoma, $n=1$; adenosquamous carcinoma, $n=1$; squamous cell carcinoma, $n=1$), whereas 22 patients (27.5%) were classified as G1, 29 (36.3%) as G2, and 29 (36.3%) as G3+others (undifferentiated carcinoma, $n=1$; adenosquamous carcinoma, $n=3$; squamous cell carcinoma, $n=1$; solid adenocarcinoma, $n=2$; small cell carcinoma, $n=1$) at the invasive front. Among the 80 patients, 47 (58.8%) were positive for BD and 33 (41.2%) were positive for DD (Table 1). The kappa score for concordance between DD and BD was 0.33 (standard error, 0.102; $P=0.0833$). BD was associated with T stage ($P=0.0003$), lymph node (LN) metastasis ($P<0.0001$), and histological type at the invasive front ($P<0.0001$), but was not associated with age, gender, distant metastasis, or histological type at the tumor surface. DD was associated with gender ($P=0.0295$), LN metastasis ($P<0.0001$), distant metastasis ($P=0.0005$), surface histological type at the tumor surface ($P=0.0016$), and histological type at the invasive front ($P<0.0001$), but was not associated with age or T stage.

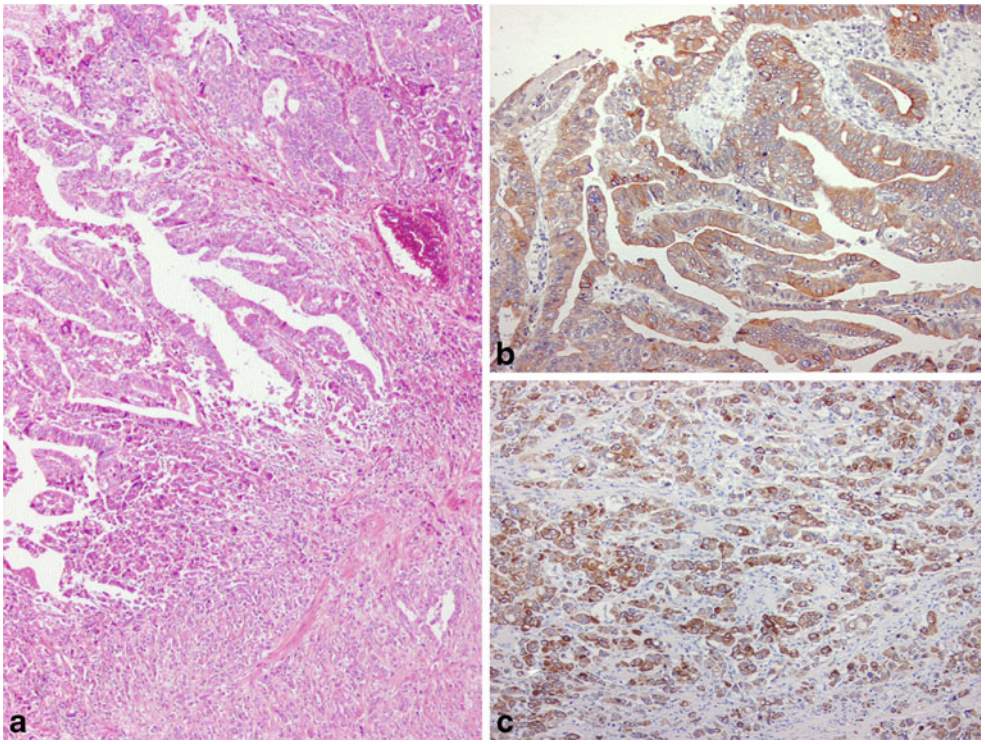

Fig. 1 A representative case of DD. **a** Well-differentiated adenocarcinoma showing DD into poorly differentiated adenocarcinoma at the subserosal layer (hematoxylin and eosin (HE), original magnification ×40). **b** Immunohistochemical staining of cytokeratin at the tumor surface. The tubular structure of the tumor was highlighted (original magnification ×100). **c** Immunohistochemical staining for cytokeratin at the invasive front of the tumor. The dedifferentiated structure of the tumor is highlighted (original magnification ×100)

Survival analysis in 80 GBC patients

Median duration of follow-up was 37.8 months (range, 8–120 months). Results of univariate and multivariate analyses with disease-specific survival in 80 GBC patients are shown in Table 2. In univariate analysis, both BD and DD correlated significantly with survival ($P<0.0001$ and $P=0.0013$, respectively). Other variables showing significant correlations with survival were T stage ($P<0.0001$), LN metastasis ($P<0.0001$), distant metastasis ($P=0.0002$), curability ($P=0.0095$), and histology at the invasive front ($P<0.0001$). Multivariate analysis of the significant variables identified from univariate analysis was performed using Cox's proportional hazards model, with only LN metastasis ($P=0.0103$) identified as an independent prognostic factor.

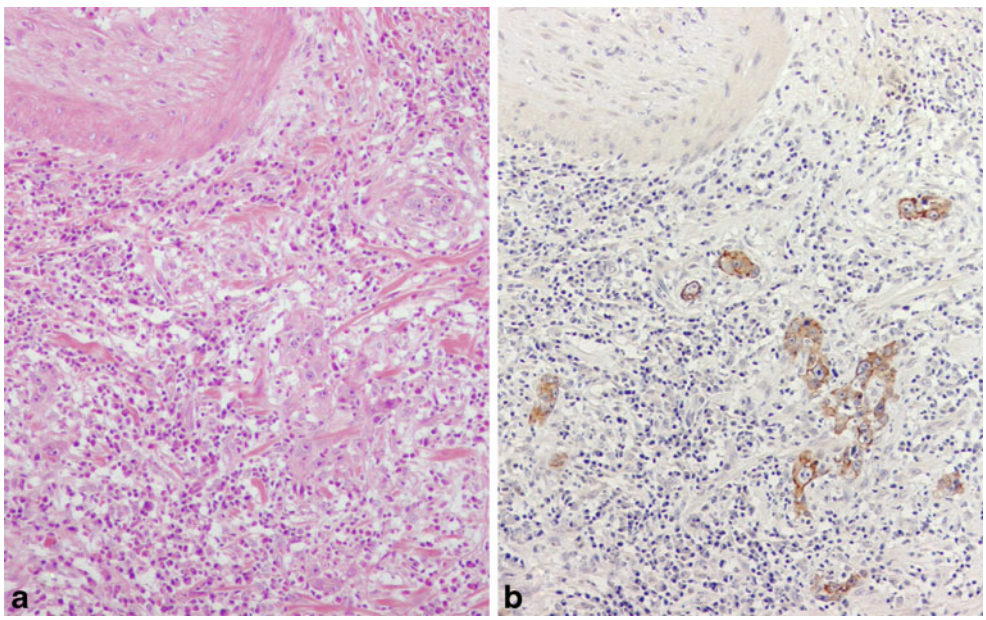

Fig. 2 A representative case of BD with inflammation. **a** The invasive front of GBC. The dense inflammation masks a small cluster of tumor cells (HE, original magnification ×100). **b** Clusters of tumor cells are highlighted by immunohistochemical staining of cytokeratin (original magnification ×100)

Table 1 Clinicopathologic features of gallbladder cancer with or without BD and DD

Characteristics	Total	No. of patients (%)			No. of patients (%)		
		BD (+)	BD (−)	*P*	DD (+)	DD (−)	*P*
No. of patients	80	47 (58.8)	33 (41.2)		38 (47.5)	42 (52.5)	
Age (mean±SD)	68.5±9.0	68.6±9.2	68.3±8.9	0.9071	69.9±8.6	67.1±9.2	0.1659
Gender				0.2999			0.0295
Male	24	12 (50.0)	12 (50.0)		7 (29.2)	17 (70.8)	
Female	56	35 (62.5)	21 (37.5)		31 (55.4)	25 (44.6)	
TMN classification							
T				0.0003			0.1411
1b	8	1 (12.5)	7 (87.5)		1 (12.5)	7 (87.5)	
2	32	14 (43.8)	18 (56.2)		15 (46.9)	17 (53.1)	
3	34	27 (79.4)	7 (20.6)		19 (55.9)	15 (44.1)	
4	6	5 (83.3)	1 (16.7)		3 (50)	3 (50)	
N				<0.0001			<0.0001
0	38	8 (36.4)	14 (63.6)		9 (23.7)	29 (76.3)	
1	42	25 (78.1)	7 (21.9)		29 (69.1)	13 (30.9)	
M				0.1937			0.0005
0	65	36 (55.4)	29 (44.6)		25 (38.5)	40 (61.5)	
1	15	11 (73.3)	4 (26.7)		13 (86.7)	2 (13.3)	
Histology at the surface				0.174			0.0016
G1	53	28 (52.8)	25 (31.2)		31 (58.5)	22 (41.5)	
G2	20	13 (65.0)	7 (35.0)		7 (35.0)	13 (65.0)	
G3+others	7	6 (85.7)	1 (14.3)		0 (0.0)	7 (100.0)	
Histology at the invasive front				<0.0001			<0.0001
G1	22	3 (13.6)	19 (86.4)		0 (0.0)	22 (100.0)	
G2	29	20 (69.0)	9 (31.0)		16 (55.2)	13 (44.8)	
G3+others	29	24 (82.8)	5 (17.2)		22 (75.9)	7 (24.1)	

BD budding, *DD* dedifferentiation

Survival according to BD and DD in each T stage

Figures 3 and 4 show the survival curves of patients with stage T2 or T3 GBC according to the status of BD or DD. In the 32 patients with a T2 tumor, 5-year survival rates for BD-positive and BD-negative patients were 49.5% and 94.1%, respectively, and those for DD-positive and DD-negative patients were 53.1% and 90.1%, respectively. BD-negative and DD-negative groups showed significantly favorable survival compared to the BD-positive (P=0.001) and DD-positive groups (P=0.0016). Further survival analyses for T2 tumor by Cox's proportional hazards model are shown in Table 3. In univariate analysis, both BD and DD correlated significantly with survival (P=0.0011 and P=0.0018, respectively). Other variables that showed significant correlations with survival were LN metastasis (P=0.016), distant metastasis (P=0.022), and histological type at the invasive front (P=0.0196). Multivariate analysis using the variables identified as significant in univariate analysis was performed but revealed no independent prognostic factors. In the 34 patients with T3 tumor, 5-year survival rates for BD-positive and BD-negative patients were 7.1% and 25.0%, respectively, while those for DD-positive and DD-negative patients were 10.4% and 11.7%, respectively. In patients with T3 tumor, no prognostic impact was associated with the status of BD (P=0.2624) or DD (P=0.8069). The T1b group (n=8) experienced no cancer-related deaths. In the T4 group (n=6), one patient was alive up to 120 months after surgery. Excluding that case, the median duration of survival for patients with T4 tumor was 5.8 months (range, 1.1–31.3 months). No significant correlations were observed in patients with T4 tumor between survival and either BD or DD (P=0.0833 and P=0.1823, respectively).

Risk of LN metastasis by BD or DD in T2 and T3 GBC patients

Table 4 shows the correlation of BD and DD with LN metastasis among T2 and T3 GBC patients. With T2 GBC, 10 patients (31.3%) had LN metastasis at the time of surgery. In those patients, BD was observed in seven patients, whereas DD was seen in eight patients. A

Table 2 Survival analysis for all patients

Characteristics		Number	Univariate analysis		Multivariate analysis	
			HR (95%CI)	*P*	HR (95%CI)	*P*
BD	Negative	33	1	<0.0001	1	0.2483
	Positive	47	6.55 (2.70–19.56)		2.02 (0.62–7.23)	
DD	Negative	42	1	0.0013	1	0.3728
	Positive	38	3.28 (1.58–7.32)		0.63 (0.24–1.77)	
Age	<69	37	1	0.0852		
	≤69	43	0.54 (0.26–1.09)			
T	T1b, T2	40	1	<0.0001	1	0.0749
	T3, T4	40	6.01 (3.09–14.53)		2.22 (0.92–5.91)	
N	N0	38	1	<0.0001	1	0.0103
	N1	42	10.39 (4.46–28.38)		4.83 (1.45–16.92)	
M	M0	65	1	0.0002	1	0.502
	M1	15	4.61 (2.14–9.56)		1.32 (0.58–3.01)	
Curability	R0	69	1	0.0095	1	0.3921
	R1, R2	11	4.18 (1.47–10.46)		1.58 (0.53–4.22)	
Adjuvant therapy	Done	13	1	0.5189		
	Not done	67	0.71 (0.28–2.16)			
Histology at the surface	G1, G2	73	1	0.138		
	G3+others	7	2.44 (0.72–6.33)			
Histology at the invasive front	G1, G2	51	1	<0.0001	1	0.2393
	G3+others	29	4.79 (2.34–10.07)		1.61 (0.73–3.70)	

HR hazard ratio, *CI* confidence interval, *R0* no pathologic residual tumor, *R1* pathologic residual tumor, *R2* macroscopic residual tumor

significant correlation with LN metastasis was observed for DD (P=0.0209), but not for BD (P=0.0623). In T2 GBC, 11 patients were both BD-positive and DD-positive and 14 patients were both BD-negative and DD-negative. Significant differences were observed in the comparison of LN metastasis between both BD-positive and DD-positive patients and any BD-negative or DD-negative patients (P=0.0396). More marked difference was observed between both BD-negative and DD-negative patients and any BD-positive or DD-positive patients (P=0.0059). In T3 GBC patients, 27 patients (79.4%) had LN metastasis, with BD in 23 patients (85.2%) and DD in 18 patients (66.7%). As with T2 patients, a significant correlation with LN metastasis was observed for DD (P=0.0282), but not for BD (P=0.1346). In T3 GBC, 16 patients were both BD-positive and DD-positive and 4 patients were both BD-negative and DD-negative. The significant differences were observed in the comparison of LN metastasis between both BD-negative and DD-negative patients and any BD-positive or DD-positive patients (P=0.0107).

Discussion

The predominant histological type in advanced GBC is moderately or poorly differentiated adenocarcinoma. However, even in those cases, a well-differentiated adenocarcinoma is often found at the surface of the tumor. The present

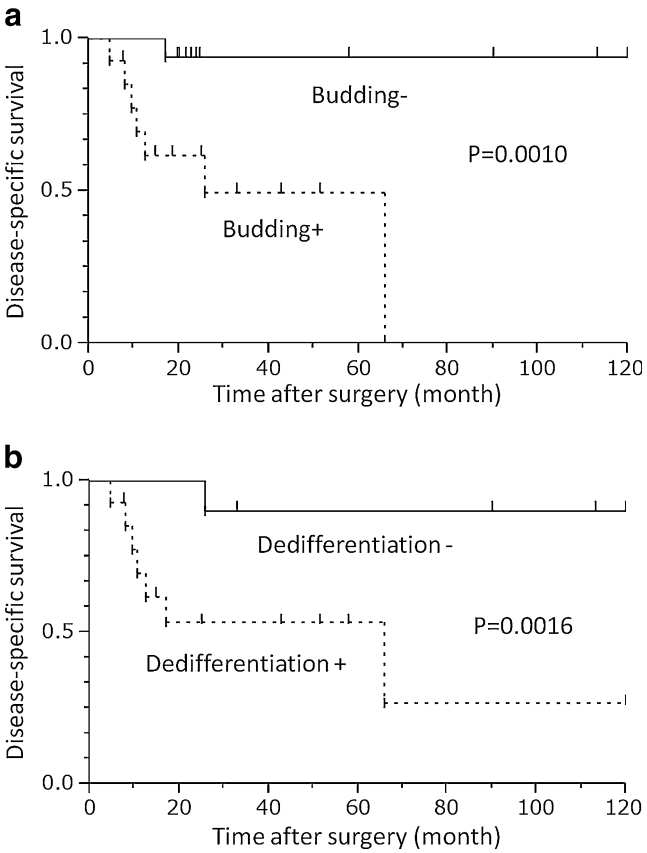

Fig. 3 Kaplan–Meier curves of patients with T2 tumor (n=32) according to the presence or absence of BD (**a**) and DD (**b**)

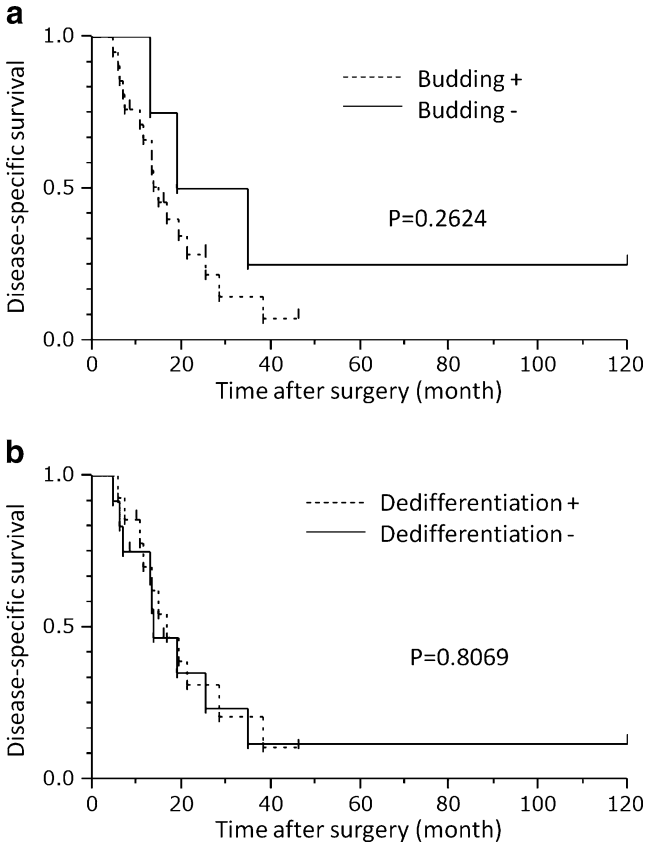

Fig. 4 Kaplan–Meier curves of patients with T3 tumor (n=34) according to the presence or absence of BD (**a**) and DD (**b**)

study revealed relatively high rates of DD (41.2%) and BD (58.8%) in GBC. In this study, to evaluate DD as objectively as possible, we defined DD as "tumors in which the grade of the invasive front is higher than the grade at the surface." Therefore, DD-negative cases of the current study contain a small number of poorly differentiated cases. On the other hand, evaluation of BD strictly followed previous reports in colorectal cancer [8, 12, 13]. Although both BD and DD are similar concepts and show some degree of overlap, BD cases without DD and DD cases that did not meet BD criteria were occasionally observed. Actually, the kappa statistic analysis revealed low concordance between DD and BD in this study (kappa score=0.33). Therefore, these two categories were analyzed individually. Interestingly, BD and DD in this study showed different characteristics. BD was significantly associated with high T stage, whereas DD was not. BD was more apparent on the invasive front at subserosal tissue or tissue beyond serosa where inflammatory reactions were usually concomitant. In cases with DD, morphological changes were usually apparent at the border of muscularis propria and subserosal layer.

Univariate analysis showed that both DD and BD correlated significantly with disease-specific survival. However, neither DD nor BD were identified as independent prognostic factors in multivariate analysis, contrasting with previous studies for colorectal or other malignant tumors reporting BD as an independent prognostic factor [11, 14–18]. Survival analysis according to T stage showed significant correlations with poor prognosis for both BD and

Table 3 Survival analysis for T2 patients

Characteristics		Number	Univariate analysis	
			HR (95%CI)	*P*
BD	Negative	18	1	0.0011
	Positive	14	16.88 (2.77–329.10)	
DD	Negative	17	1	0.0018
	Positive	15	13.90 (2.42–262.03)	
Age	<69	13	1	0.1491
	≤69	19	0.36 (0.073–1.45)	
N	N0	22	1	0.016
	N1	10	5.81 (1.40–28.79)	
M	M0	29	1	0.022
	M1	3	6.76 (1.37–28.01)	
Curability	R0	29	1	0.0943
	R1, R2	3	5.21 (0.71–27.33)	
Adjuvant therapy	Done	6	1	0.9925
	Not done	26	1.01 (0.16–19.39)	
Histology at the invasive front	G1, G2	24	1	0.0196
	G3	8	5.80 (1.36–24.79)	
Lymphatic vessels invasion	ly0	10	1	0.0742
	ly1	22	5.02 (0.87–94.74)	
Venous invasion	v0	22	1	0.2964
	v1	10	2.33 (0.44–11.22)	

There was no G3 case in surface histology

Table 4 Risk of LN metastasis by BD or DD in T2 and T3 patients

Characteristics		T2				T3			
		N(+)	N(−)	Odds ratio (95%CI)	*P* value	N(+)	N(−)	Odds ratio (95%CI)	*P* value
BD	Negative	3	15	1	0.0623	4	3	1	0.1346
	Positive	7	7	5.0 (0.99–25.34)		23	4	4.31 (0.69–27.03)	
DD	Negative	2	15	1	0.0209	9	6	1	0.0282
	Positive	8	7	8.57 (1.43–51.36)		18	1	12.0 (1.25–115.36)	
Both BD- and DD-positive		6	5	1	0.0396	15	1	1	0.0512
Any BD- or DD-negative		4	17	0.196 (0.039–0.98)		12	6	0.133 (0.014–1.26)	
Both BD- and DD-negative		1	13	1	0.0059	1	3	1	0.0107
Any BD- or DD-positive		9	9	13.0 (1.39–121.38)		26	4	19.5 (1.61–236.61)	

BD budding, *DD* dedifferentiation

DD in stage T2 GBC, but no such correlations were observed for T3 and T4 lesions. These results may be affected by differences in biological behaviors at metastatic sites, as the present study only investigated primary tumors in subjects. Actually, in 34 patients with T3 tumors in the current study, 27 patients (79.4%) had LN metastasis and 10 patients (29.4%) had distant metastasis. In six patients with a T4 tumor, five patients (83.3%) had LN metastasis and two patients (33.3%) had distant metastasis. DD correlated significantly with LN metastasis, but BD unexpectedly did not show any similar significant relationships to stage T2 or T3 GBC. In the subgroup analysis, the robustness of statistical analysis is weakened because of the reduced sample size. Although the impact of DD with LN metastasis was emphasized by combination of BD and the present results indicate the malignant potential of BD in GBC, the impacts of BD on survival and LN metastasis seem poorer in comparison to previous reports of other organs [6–18]. We speculate that the definition of BD in this study involved not only sprouting tumor cells, but also tumor clusters destroyed by host–inflammatory reactions. To clarify the biological features of BD in GBC, further clinical and basic research is required.

The optimal therapeutic strategy for GBC invading the subserosa (TNM classification, T2 tumor) remains controversial. Several arguments have been put forward justifying radical surgery, including regional lymphadenectomy with or without bile duct resection, and partial hepatectomy around the gallbladder fossa or S4a+S5 subsegmentectomy in comparison to simple cholecystectomy [20–26]. Survival benefits of radical procedures for T2 tumors over simple cholecystectomy alone have been described in several reports [23–29]. Radical lymphadenectomy is recommended because the rate of LN metastasis in T2 tumors in GBC is quite high (range, 46.1–61.9%) and radical LN dissection improves long-term survival in patients with LN metastasis [24, 27, 29]. However, some groups advocate simple cholecystectomy alone as providing long-term survival in patients with T2 tumor, and others suggest that simple cholecystectomy may be justified by a subset analysis of patients with T2 tumor according to certain pathological criteria, such as depth of subserosal invasion and horizontal tumor spread in the subserosal layer [30–33]. Thus, if a pathological investigation could discriminate patients with favorable prognosis even by limited surgery for stage T2 GBC, these patients would be freed from extended radical surgery. To make an intraoperative decision, histological examination by frozen section is necessary. Measuring the exact depth of invasion on frozen section is not always easy. The presence of inflammatory reactions means that assessment of BD on frozen section is often difficult. Conversely, assessment of DD is easily performed even on frozen examination. Although DD status shows significant correlations with both LN metastasis and prognosis, the DD cases in T2 lesion showed the rate of 11.8% (2 out of 17 cases) of LN metastasis. Therefore, the assessment of DD by frozen section would be one of the considerations for extended resection or lymphadenectomy but could not be independent information to override the need for nodal resection. Preoperative diagnosis of stage T2 GBC is not easy, irrespective of advances in medical imaging. Stage T2 GBC is thus often discovered incidentally after routine cholecystectomy. In such cases, the state of BD and DD would be one consideration along the lines of performance status, complications, and age for deciding on additional surgical treatment.

In conclusion, this is the first report on the status and features of DD and BD in GBC, in association with clinical implications. As both DD and BD are frequently observed in GBC and correlate with prognosis, particularly for T2 lesions, these factors should be taken into consideration in pathological reports on GBC.

Acknowledgements We would like to thank Mr. Fumihiro Mutoh for his contribution to the immunohistochemical study. We are also grateful to Eiko Kawasaki and Akemi Yamaguchi for their contributions to data collection. This work was supported by the Ministry of Education, Culture, Sports, Science and Technology KAKENHI Grant-in-Aid for Young Scientists (B) 21791299.

Disclosure The authors declare that they have no conflict of interest.

References

1. Miller G, Jarnagin WR (2008) Gallbladder carcinoma. Eur J Surg Oncol 34:306–312
2. Randi G, Franceschi S, La VC (2006) Gallbladder cancer worldwide: geographical distribution and risk factors. Int J Cancer 118:1591–1602
3. Kayahara M, Nagakawa T (2007) Recent trends of gallbladder cancer in Japan: an analysis of 4,770 patients. Cancer 110:572–580
4. Gabbert H, Wagner R, Moll R, Gerharz CD (1985) Tumour dedifferentiation: an important step in tumour invasion. Clin Expl Met 3:257–279
5. Prall F (2007) Tumour budding in colorectal carcinoma. Histopathology 50:151–162
6. Morodomi T, Isomoto H, Shirouzu K, Kakegawa K, Irie K, Morimatsu M (1989) An index for estimating the probability of lymph node metastasis in rectal cancers. Lymph node metastasis and the histopathology of actively invasive regions of cancer. Cancer 63:539–543
7. Okuyama T, Oya M, Ishikawa H (2002) Budding as a risk factor for lymph node metastasis in pT1 or pT2 well-differentiated colorectal adenocarcinoma. Dis Colon Rectum 45:628–634
8. Ueno H, Mochizuki H, Shinto E, Hashiguchi Y, Hase K, Talbot IC (2002) Histological indices in biopsy specimens for estimating the probability of extended local spread in rectal cancer. Cancer 94:2882–2891
9. Hase K, Shatney C, Johnson D, Trollope M, Vierra M (1993) Prognostic value of "tumour budding" in patients with colorectal cancer. Dis Colon Rectum 36:627–635
10. Ueno H, Mochizuki H, Hatsuse K, Hase K, Yamamoto T (2000) Indicators for treatment strategies of colorectal liver metastases. Ann Surg 231:59–66
11. Ueno H, Murphy J, Jass JR, Mochizuki H, Talbot IC (2002) Tumour "budding" as an index to estimate the potential of aggressiveness in rectal cancer. Histopathology 40:127–132
12. Ueno H, Price AB, Wilkinson KH, Jass JR, Mochizuki H, Talbot IC (2004) A new prognostic staging system for rectal cancer. Ann Surg 240:832–839
13. Ueno H, Mochizuki H, Hashiguchi Y et al (2004) Risk factors for an adverse outcome in early invasive colorectal carcinoma. Gastroenterology 127:385–394
14. Brown M, Sillah K, Griffiths EA et al (2010) Tumour budding and a low host inflammatory response are associated with a poor prognosis in oesophageal and gastro-oesophageal junction cancers. Histopathology 56:893–899
15. Sarioglu S, Acara C, Akman FC et al (2010) Tumor budding as a prognostic marker in laryngeal carcinoma. Pathol Res Pract 206:88–92
16. Roh MS, Lee JI, Choi PJ (2004) Tumour budding as a useful prognostic marker in esophageal squamous cell carcinoma. Dis Esophagus 17:333–337
17. Koike M, Kodera Y, Itoh Y et al (2008) Multivariate analysis of the pathologic features of esophageal squamous cell cancer: tumor budding is a significant independent prognostic factor. Ann Surg Oncol 15:1977–1982
18. Gabbert HE, Meier S, Gerharz CD, Hommel G (1992) Tumor-cell dissociation at the invasion front: a new prognostic parameter in gastric cancer patients. Int J Cancer 50:202–207
19. Sobin L, Gospodarowicz M, Wittekind C (eds) (2009) TNM classification of malignant tumors, 7th edn. Wiley, Hoboken
20. Pilgrim C, Usatoff V, Evans PM (2009) A review of the surgical strategies for the management of gallbladder carcinoma based on T stage and growth type of the tumour. Eur J Surg Oncol 35:903–907
21. Cubertafond P, Gainant A, Cucchiaro G (1994) Surgical treatment of 724 carcinomas of the gallbladder. Results of the French Surgical Association Survey. Ann Surg 219:275–280
22. Kayahara M, Nagakawa T, Nakagawara H, Kitagawa H, Ohta T (2008) Prognostic factors for gallbladder cancer in Japan. Ann Surg 248:807–814
23. Kohya N, Miyazaki K (2008) Hepatectomy of segment 4a and 5 combined with extra-hepatic bile duct resection for T2 and T3 gallbladder carcinoma. J Surg Oncol 97:498–502
24. Shimada H, Endo I, Togo S, Nakano A, Izumi T, Nakagawara G (1997) The role of lymph node dissection in the treatment of gallbladder carcinoma. Cancer 79:892–899
25. Wise PE, Shi YY, Washington MK et al (2001) Radical resection improves survival for patients with pT2 gallbladder carcinoma. Am Surg 67:1041–1047
26. Shimizu Y, Ohtsuka M, Ito H et al (2004) Should the extrahepatic bile duct be resected for locally advanced gallbladder cancer? Surgery 136:1012–1017
27. Bartlett DL, Fong Y, Fortner JG, Brennan MF, Blumgart LH (1996) Long-term results after resection for gallbladder cancer. Implications for staging and management. Ann Surg 224:639–646
28. de Aretxabala XA, Roa IS, Burgos LA, Araya JC, Villaseca MA, Silva JA (1997) Curative resection in potentially resectable tumours of the gallbladder. Eur J Surg 163:419–426
29. Shirai Y, Yoshida K, Tsukada K, Muto T, Watanabe H (1992) Radical surgery for gallbladder carcinoma. Long-term results. Ann Surg 216:565–568
30. Kohya N, Kitahara K, Miyazaki K (2010) Rational therapeutic strategy for T2 gallbladder carcinoma based on tumor spread. World J Gastroenterol 16:3567–3572
31. Wakai T, Shirai Y, Yokoyama N, Ajioka Y, Watanabe H, Hatakeyama K (2003) Depth of subserosal invasion predicts long term survival after resection in patients with T2 gallbladder carcinoma. Ann Surg Oncol 10:447–454
32. Oertli D, Herzog U, Tondelli P (1993) Primary carcinoma of the gallbladder: operative experience during a 16 year period. Eur J Surg 159:415–420
33. Sasaki R, Uesugi N, Itabashi H et al (2005) Clinicopathological study of depth of subserosal invasion in patients with pT2 gallbladder carcinoma. J Surg Oncol 92:83–88

Virchows Arch (2011) 459:457–463
DOI 10.1007/s00428-011-1137-3

CASE REPORT

Clonal trisomies 7,10 and 12, normal 3p and absence of VHL gene mutation in a clear cell tubulopapillary carcinoma of the kidney

Alexander Wolfe · Sheila M. Dobin · Petr Grossmann · Michal Michal · Ludvik R. Donner

Received: 29 March 2011 / Revised: 28 June 2011 / Accepted: 27 July 2011 / Published online: 7 August 2011
© Springer-Verlag 2011

Introduction

Papillary renal cell carcinomas represent 10–15% of carcinomas of the kidney. They are divided into two major groups, type 1 and type 2, which differ in their morphology and clinical behavior. The type 2 tumors are more aggressive. The patients present with higher stage and their survival is shorter [1]. Another type that was originally described as a benign renal angiomyoadenomatous tumor [2, 3], is a clear cell tubulopapillary renal cell carcinoma. It is a rare, biologically indolent tumor with tendency to bilaterality and multicentricity that often arises in patients with renal disease and has a predilection for patients of African ancestry [2–9]. Because this tumor is not known to recur or metastasize, its classification as a carcinoma is debatable. The tumors are surrounded by thick pseudocapsules that contain smooth muscle. They are often cystic with papillary, tubular and solid areas. Their nuclei are mildy pleomorphic with tendency to be situated towards the surface. They express cytokeratin 7 and epithelial membrane antigen (EMA), are variably positive for carbonic anhydrase 9, and are negative for CD10, α-methylacyl-CoA racemase and parvalbumin. Although several cases were studied by fluorescence in situ hybridization (FISH), no case was previously studied by cytogenetics.

A. Wolfe · S. M. Dobin · L. R. Donner (✉)
Department of Pathology, Scott and White Healthcare/The Texas A&M Health Science Center College of Medicine,
2401 South 31st Street,
Temple, TX 76508, USA
e-mail: ldonner@swmail.sw.org

P. Grossmann · M. Michal
Sikl's Department of Pathology, School of Medicine,
Charles University,
Pilsen, Czech Republic

Case report

The patient was a 66-year-old Black woman with a history of hypertension, monoclonal gammopathy and an endometrioid carcinoma of the left ovary. Bilateral salpingo-oophorectomy was performed in September 2008. Nephrologic examination performed in June 2007 resulted in finding three 1.68–2.44 cm Bosniak 3 cysts in the right kidney and a 1.6 cm Bosniak 2 cyst in the left kidney as well as multiple smaller densities throughout both kidneys. Although the renal cystic lesions remained stable, partial nephrectomy of the right kidney was performed in December 2009 and of the left kidney in April 2010. She remained clinically stable without any sign of recurrence during her last examination in May 2011.

Materials and methods

Immunohistochemistry Immunohistochemical staining was performed on formalin-fixed, paraffin-embedded sections using the EnVision +DAB System (Dako, Carpinteria, CA). Monoclonal antibodies against following antigens were used: keratin 7, EMA, RCC, α-methylacyl-CoA racemase, CD10, desmin, h caldesmon, Ki-67 (Dako) and phosphohistone H3. (Millipore, Billerica, MA). The slides to be immunostained for phosphohistone H3, Ki-67 and α-methylacyl-CoA racemase were treated by EnVision™ FLEX Target retrieval solution low pH (Dako), the remaining slides by EnVision™ FLEX Target retrieval

Table 1 PCR primers used in mutation analysis of the *VHL* gene

Gene/exon	Name	Primers (sequence 5′→3′)
VHL/exon 1	VHL e1-1	CGCGAAGACTACGGAGGT
	VHL e1-2	CTCTTCTTCAGGGCCGTA
	VHL e1-3	GAGGCAGGCGTCGAAGAG
	VHL e1-4	GCGATTGCAGAAGATGACCT
	VHL e1-5	GCCGAGGAGGAGATGGAG
	VHL e1-6	CCCGTACCTCGGTAGCTGT
	VHL e1-7	CCGTATGGCTCAACTTCGAC
	VHL e1-8	GCTTCAGACCGTGCTATCGT
VHL/exon 2	VHL e2-1	ACCGGTGTGGCTCTTTAACA
	VHL e2-2	TCCTGTACTTACCACAACAACCTT
VHL/exon 3	VHL e3-1	GCAAAGCCTCTTGTTCGTTC
	VHL e3-2	ACATTTGGGTGGTCTTCCAG
	VHL e3-3	CAGGAGACTGGACATCGTCA
	VHL e 3-4C	CCATCAAAAGCTGAGATGAAAC

solution high pH (Dako) except for slides to be immunostained for RCC. These slides were not subjected to any antigen retrieval.

Cytogenetics A total of 41 cells were examined from two cultures established with cells from fresh tissue exposed to collagenase and two cultures established from explants. The

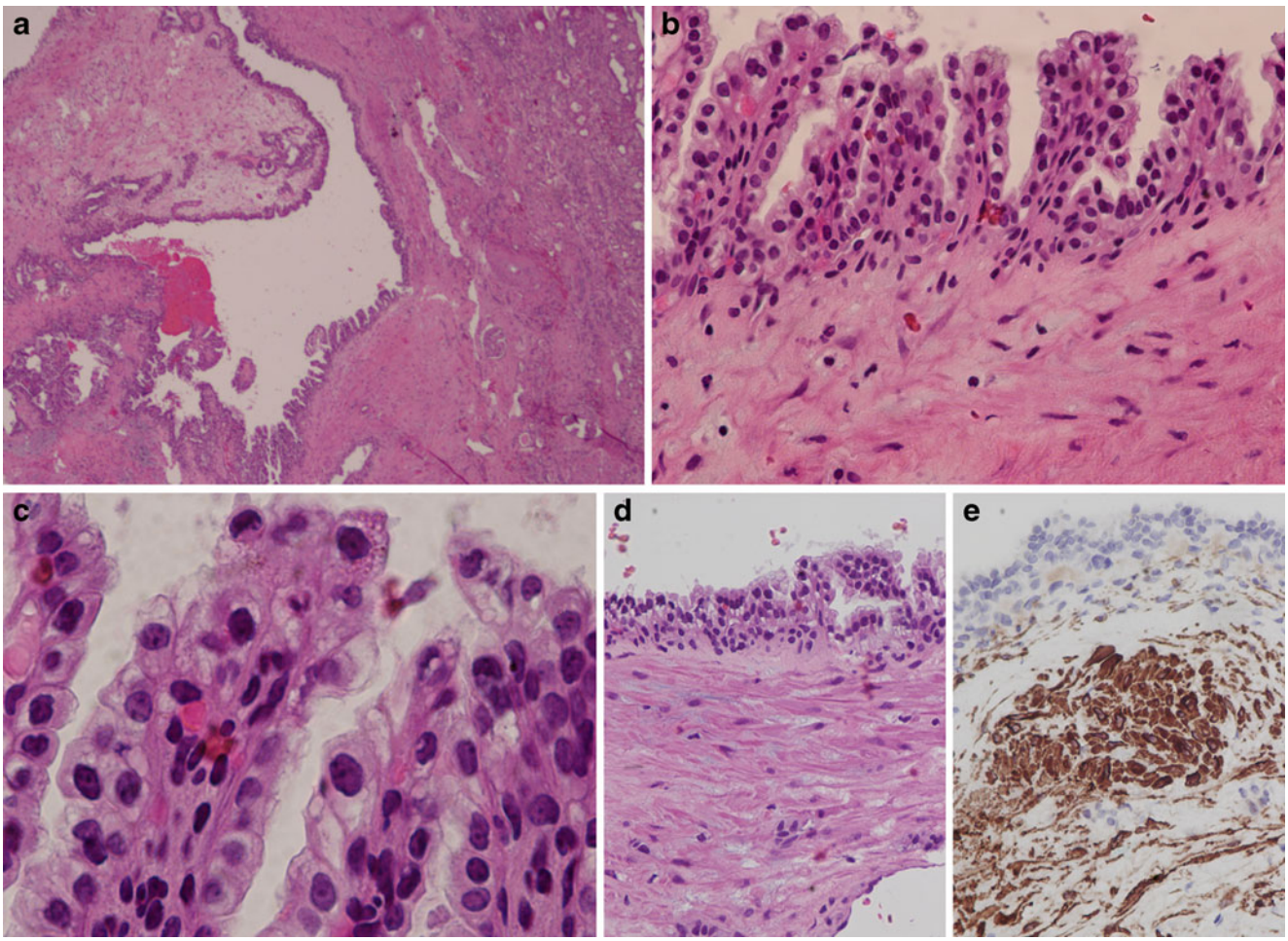

Fig. 1 Histology of the left renal tumor. Note the presence of thick pseudocapsules, cysts (**a**), papillae lined by clear epithelium (**b**, **c**), smooth muscle in the pseudocapsule (**d**) expressing h caldesmon (**e**)

floating cells were discarded and the cells adhering to the dish were harvested 13 days later. Karyograms of G-banded metaphases were prepared from all clonal and nonclonal cells.

Fluorescence in situ hybridization Aliquot of the left renal tumor cells harvested for cytogenetic study was hybridized with FITC-labeled centromere 7 probe CEP7 (Rainbow Scientific, Windsor, CT) and Spectrum Green labeled centromere 10 and 12 probes CEP10, CEP12 (Abbott Laboratories, Abbott Park, IL). The hybridization efficiency was 100%. The Spectrum Orange labeled RB1 probe (Abbott) was used as an internal control. Two hundred nuclei were analyzed in each sample.

Molecular genetics DNA was extracted from formalin-fixed, paraffin-embedded tissue by the NucleoSpin® Tissue Kit (MACHEREY-NAGEL, Duren, Germany) according to the manufacturer's protocol.

Table 2 Cytogenetic findings in tumor cells

Clonal cells	Cultures
47,XX,+7	Collagenase A
48,XX,+7,+10	Collagenase B
44,XX,−8,+10,−16,−17	Explant B
45,XX,+10,−5,−13,−20	Collagenase A
48,X,−X,+2,+10,+mar	Explant B
48,XX,+10,+12	Explant A
48,XX,+7,+12	Collagenase B
47,XX,+12	Collagenase A
47,XX,+12	Collagenase B
Nonclonal cells	
46,XX,t(3;7)(q24;q11.1)	Explant B
46,XX,t(6;21)(p10;p10)	Explant B
47,XX,+X	Collagenase A
43,XX,−5,−7,−17	Collagenase A

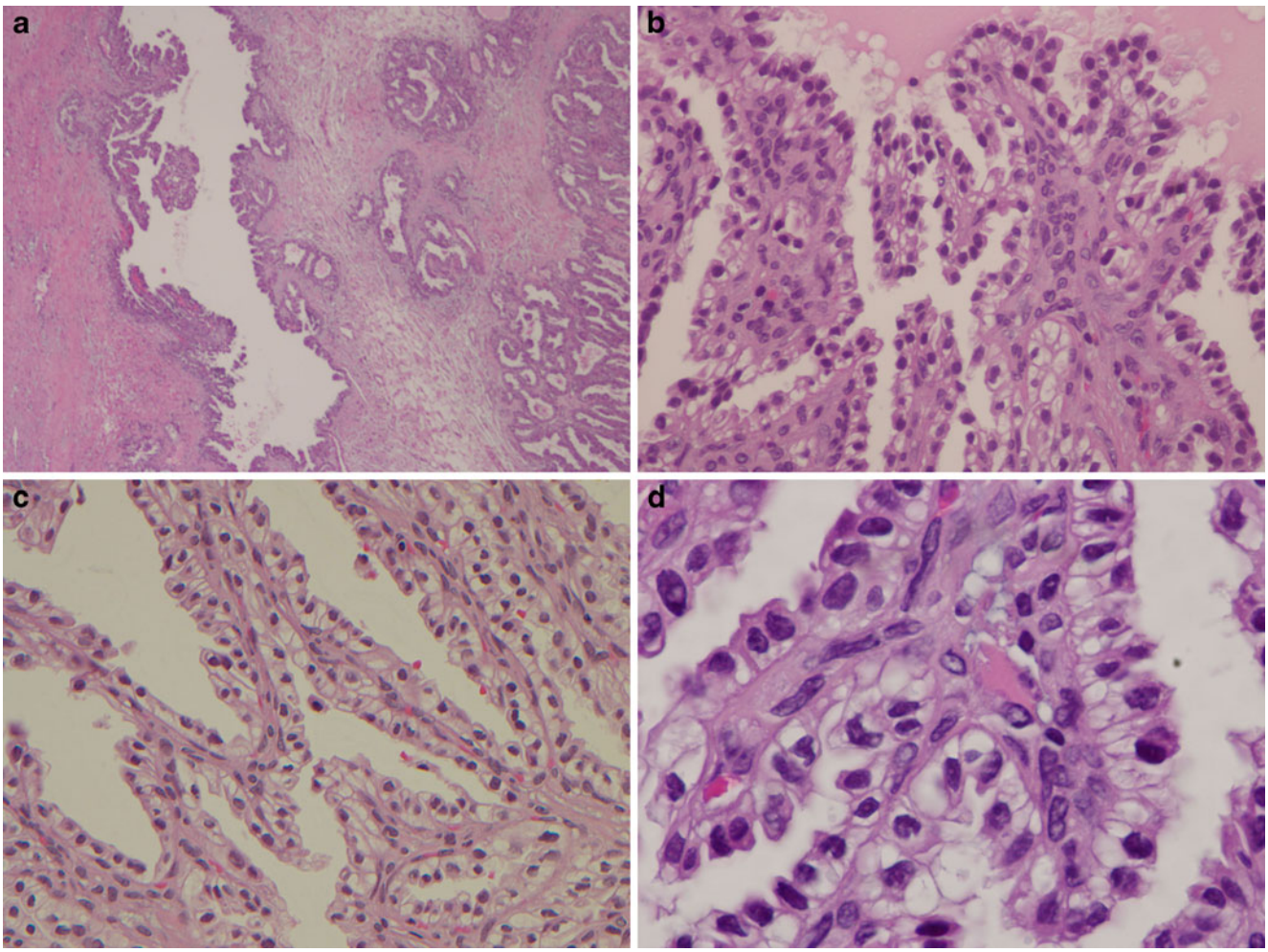

Fig. 2 Histology of the right renal tumor. Note the presence of branching tubules with papillary formations (*right part* of **a**) and the presence of delicate papillae (**c**)

Mutation analysis of exons 1, 2 and 3 of the VHL gene was performed using polymerase chain reaction (PCR) and direct sequencing. PCR was carried out using eight primers for VHL/exon 1, two primers for VHL/exon2 and four primers for VHL/exon 3 (Table 1). The amplified PCR products were purified with magnetic particles Agencourt® AmPure® (Agencourt Bioscience Corporation, A Beckman Coulter Company, Beverly, MA), sequenced using Big Dye Terminator Sequencing kit (Applied Biosystems, Foster City, CA), purified with magnetic particles Agencourt® Clean SEQ® and subsequently run on an automated sequencer ABI Prism 3130x1 (Applied Biosystems, Foster City, CA) at a constant voltage of 13.2 kV for 20 min.

Results

Pathologic study All four cystic tumors were histologically very similar. They were multiloculated, composed of several 0.1–0.9 cm cysts and were surrounded by thick fibrous pseudocapsules that often coalesced into oligocellular dense stroma. The cysts were lined by a layer of cuboidal to cylindrical epithelial cells with low grade, regular, round nuclei, medium-sized nucleoli and well-defined, mostly clear, cytoplasm that contained abundant glycogen. Mostly stubby papillary projections lined by a single layer of clear cell epithelium were present in all four tumors though they were only focal

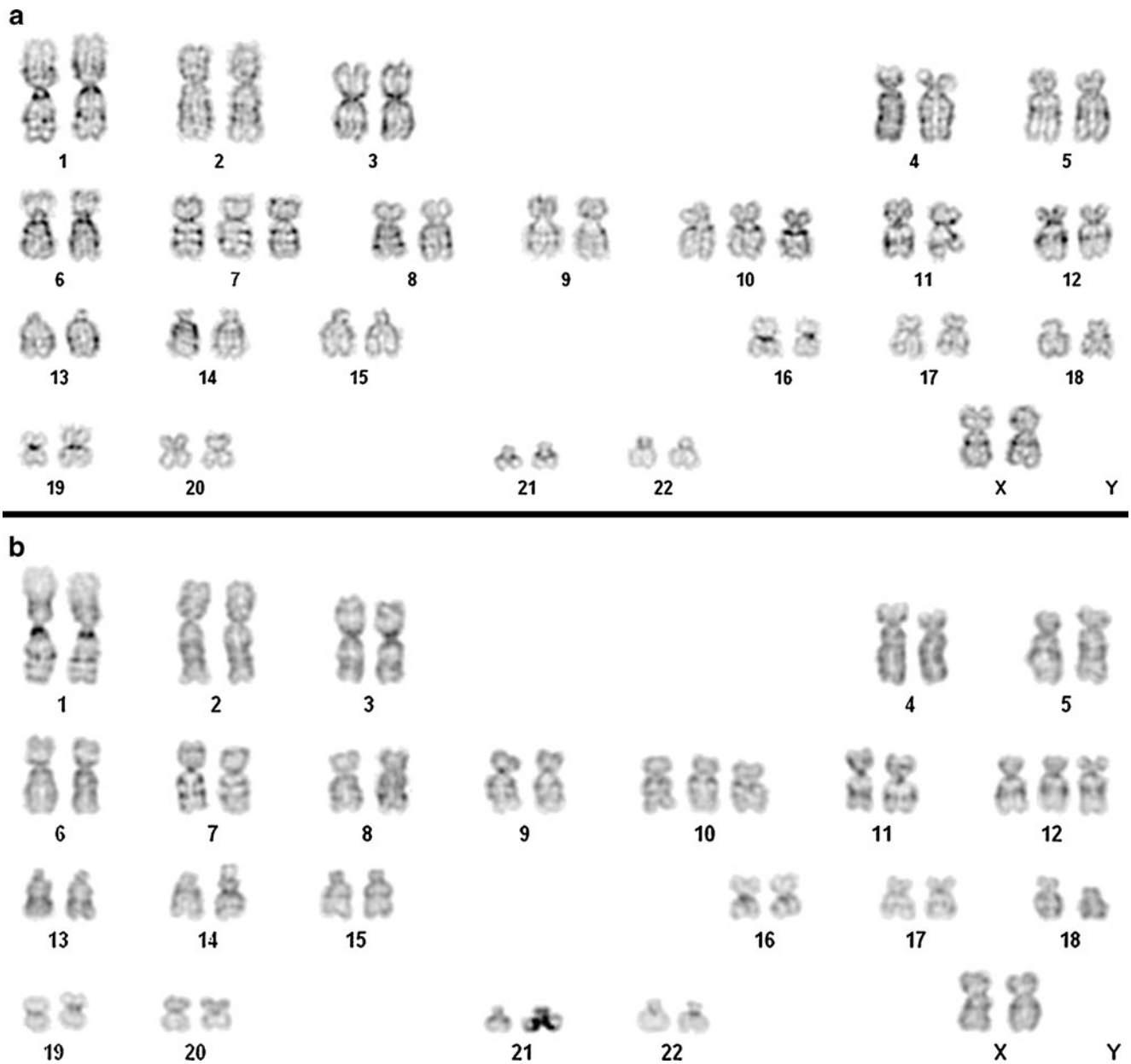

Fig. 3 Karyotypes of the left renal tumor. Note the presence of trisomies 7 and 10 (**a**), and trisomies 10 and 12 (**b**)

in the tumor of the left kidney (Fig. 1) and scanty in two tumors of the right kidney. Another right renal tumor also contained branching tubules with papillary formations and even delicate slender papillae (Fig. 2). The thick oligocellular stroma of all four tumors contained focal to abundant disorganized bundles of spindle cells with eosinophilic cytoplasm and cigar-shaped nuclei that were expressing desmin and even more h-caldesmon and were consistent with smooth muscle. The stroma of the papillae was free of any inflammatory cells. The epithelium of the three right renal and the left renal tumors was strongly positive for cytokeratin 7 and EMA and negative for RCC and α-methylacyl-CoA racemase. The CD10 was also not expressed except for a single right renal tumor where the epithelium was multifocally positive. The absence of necrosis in all four tumors was remarkable. The proliferation rate of the neoplastic epithelium was minimal—3% of epithelial cells in the left renal tumor and 0% cells in the studied right renal tumor expressed Ki-67. Likewise, no mitoses were found in the 20 high power fields of the neoplastic epithelium of both tumors, not even in sections immunostained for mitotic marker phosphohistone H3. Because these tumors are known to express cytokeratin 7 and EMA and to be negative for CD10 and α-methylacyl-Co A racemase [4], our diagnosis is supported by the immunohistochemical data. The uninvolved renal tissue contained a few obsolete glomeruli, focally hyalinized stroma and many hemosiderin deposits.

Cytogenetic study Cells with trisomy 12 and normal diploid cells were seen in both the collagenase-treated and explant cultures but cells with trisomy 7 were observed only in both collagenase-treated cultures. The karyotype of cells with the clonal abnormalities was 47, XX,+12[2]/47~48,XX,+7,+10,+12[cp6]. There were two nonclonal cells, one with t(3;7)(q24;q11.1) and the other with t(6;21)(p10;p10). The remaining cells had karyotype 46,XX (Table 2, Fig. 3).

Interphase fluorescence in situ hybridization study Trisomy 7 was seen in 8% of the cells, trisomy 10 in 7% and trisomy 12 in 6% (Fig. 4). It corresponds to 10% of cytogenetically studied cells with trisomy 12, 25% cells with trisomy 10 and 15% with trisomy 12. The FISH and the cytogenetic results were concordant.

Molecular genetics All three exons of the VHL gene were of the wild type. No mutations of the gene were present.

Discussion

Clear cell tubulopapillary renal cell carcinoma is a relatively recently described entity with characteristic morphologic features and an immunophenotype with a tendency for bilaterality (up to 20% of cases) and multicentricity (up to 15 tumors per kidney) [2–9]. There are, however, also occasional tumors with papillary areas and clear cell changes that are difficult to classify either as clear cell renal carcinomas or papillary renal carcinomas. Some of these tumors are clear cell renal cell carcinomas with focal papillary formations, while other tumors have papillary architecture with extensive (5–100%, median 10%) clear cell change but variable immunoreactivity for cytokeratin 7 and α-methylacyl-CoA racemase. These tumors are in need of further studies [10–12].

The vast majority of papillary renal cell carcinomas type 1 and type 2 are sporadic, though rare cases are hereditary. The hereditary type 1 tumors and 5–13% of sporadic ones are caused by mutations in the tyrosine kinase domain of the MET proto-oncogene at 7q31 [13], while the hereditary

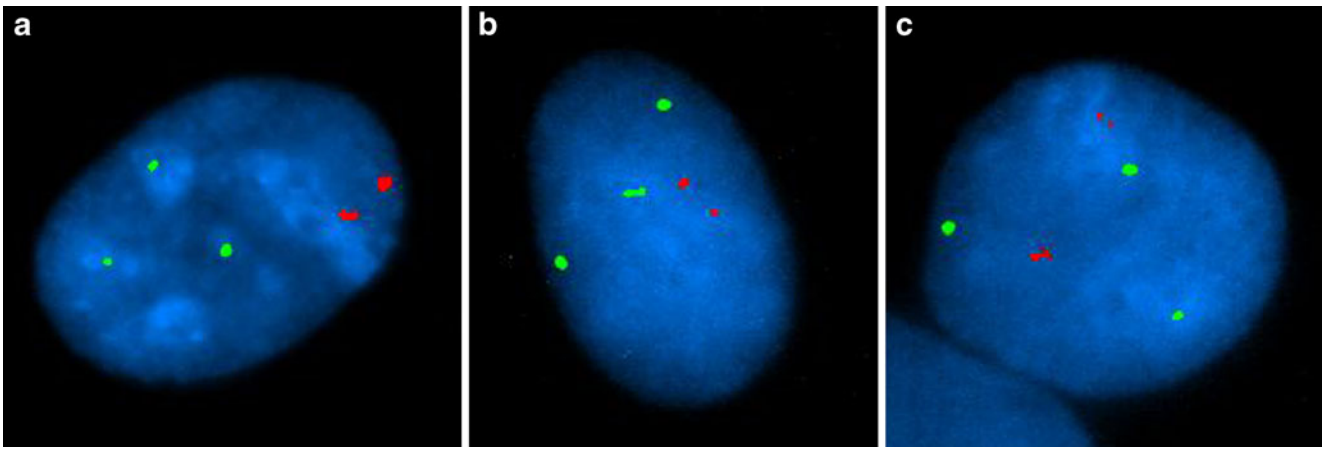

Fig. 4 Interphase FISH of the left renal tumor. Note three green signals for centromeres of chromosomes 7 (**a**), 10 (**b**) and 12 (**c**). The red signals represent the RB1 gene at 13q14

type 2 tumors are caused by mutations of the FH gene at 1q24. The FH gene codes for fumarate hydratase, a component of the Krebs cycle [14]. Chromosomal instability is a prominent feature of all three types of papillary renal cell neoplasms. It necessarily results in increased number of oncogenes and decrease of tumor suppressor genes in occasional cells, leading thus to neoplastic process [15]. A number of chromosomal gains and losses were detected in papillary renal cell carcinomas type 1 and type 2 by cytogenetics, FISH and comparative genomic hybridization. There is a considerable overlap in chromosomal gains and losses between both types of tumors. Gains of 7 and 17 and loss of Y chromosome seem to be the most common changes in type 1 tumors while losses of 1p, 3p, 21 and gains of 5q were so far observed only in type 2 tumors [16–20]. Nonetheless, cytogenetic profiles for type 1 and type 2 tumors are not distinct [21]. Molecular genetic study of multicentric papillary renal cell carcinomas revealed that almost all tumors developed independently. It is in contrast to multicentric renal cell carcinomas, clear cell type, where all tumors are genetically identical and result from intraparenchymal metastases [22].

Monoclonal gains of chromosomes 7, 10 and 12 were detected in our tumor and their presence was verified by FISH study of interphase nuclei. Trisomy 7 is frequently seen in papillary renal cell carcinomas types 1 and 2. Trisomy 12 was in a study of 13 type 1 and 13 type 2 tumors detected in four tumors of type 1 and only in two tumors of type 2 and trisomy 10 was found only in a single type 2 tumor and not in any type 1 tumors [16]. In another study, trisomy 10 was present in 6/57 papillary renal cell carcinomas. However, these tumors were not divided by subtype [19].

The increased number of cells with nonclonal abnormalities in our tumor is indicative of chromosomal instability. Our tumor was likely undergoing clonal evolution. Genetic studies of clear cell tubulopapillary renal cell carcinomas are limited. Eight tumors were studied by FISH using centromeric probes for chromosomes 3,7,17 and Y and a probe for 3p25 and one tumor also using centromeric probes for chromosomes 16 and 20. Trisomy 7 together with monosomy 17, 16 and 20 was detected in one tumor, trisomy 17 in another tumor. No other chromosomal gains or losses were found [2]. A study of 11 tumors detected trisomy 7 and 17 only in a single tumor [8]. Trisomy 17 was not seen in our tumor. In another FISH study, monosomy of chromosome 1 was detected in three tumors and monosomy of chromosomes 11 and 16 in all four tumors [23]. Finally, no trisomy of chromosomes 7 or 17 was detected by single nucleotide polymorphism arrays and the results were confirmed by FISH [9]. Several FISH studies also included analysis of the status of 3p. Losses of 3p were not found in any clear cell tubulopapillary carcinoma.

The tumor suppression gene VHL located on 3p25 is known to play a crucial role in the development of clear cell renal cell carcinomas [24, 25]. This gene was not mutated neither in our case of clear cell tubulopalliary carcinoma, nor in several previously studied tumors [3, 8, 9, 26].

Trisomy 7 and, less often, trisomy 10 were also detected in short cell cultures of normal renal tissue [27, 28]. They were attributed to aneuploid population of infiltrating T lymphocytes [29]. In one study, polysomy 7 was detected in 26 of 35 clear cell renal cell carcinomas, all nine papillary renal carcinomas and all three chromophobe renal cell carcinomas [30]. In another study, trisomy 7 was detected in 25% of renal cell carcinomas, clear cell type. Three of four of these tumors with trisomy 7 had also rearranged short arm of chromosome 3 and the VHL gene was mutated in all of them [31]. These tumors were, therefore, also genetically distinct from papillary renal cell carcinomas. Given the limitations of available data and their occasional seemingly contradictory nature, we possess so far only a hazy picture concerning the role of chromosomal gains and losses in renal tumorigenesis. Additionally, more complete studies are needed to ascertain their significance. Our study supports genetic relatedness of our tumor to papillary renal cell carcinomas and not to renal cell carcinoma, clear cell type.

Acknowledgement We declare that we have no conflict of interest and the research was supported by intramural funds of Scott & White Healthcare, Temple, Texas.

References

1. Delahunt B, Eble JN (1997) Papillary renal cell carcinoma: a clinicopathologic and immunohistochemical study of 105 tumors. Mod Pathol 10:537–544
2. Michal M, Hes O, Havlicek F (2000) Benign renal angiomyoadenomatous tumor: a previously unreported renal tumor. Ann Diagn Pathol 4:311–315
3. Michal M, Hes O, Nemcova J, Sima R, Kuroda N, Bulimbasic S, Franco M, Sakaida N, Danis D, Kazakov DV, Ohe C, Hora M (2009) Renal angiomyoadenomatous tumor: morphologic, immunohistochemical, and molecular genetic study of a distinct entity. Virchows Arch 454:89–99
4. Tickoo SK, dePeralta-Venturina MN, Harik LR, Worcester HD, Salama ME, Young AN, Moch H, Amin MB (2006) Spectrum of epithelial neoplasms in end-stage renal disease: an experience from 66 tumor-bearing kidneys with emphasis on histologic patterns distinct from those in sporadic adult renal neoplasia. Am J Surg Pathol 30:141–153
5. Gobbo S, Eble JN, Grignon DJ, Martignoni G, MacLennan GT, Shah RB, Zhang S, Brunelli M, Cheng L (2008) Clear cell papillary renal cell carcinoma: a distinct histopathologic and molecular genetic entity. Am J Surg Pathol 32:1239–1245
6. Srigley JR, Delahunt B (2009) Uncommon and recently described renal carcinomas. Mod Pathol 22:S2–S23
7. Cheng L, Zhang S, MacLennan GT, Lopez-Beltran A, Montironi R (2009) Molecular and cytogenetic insights into the pathogen-

esis, classification, differential diagnosis, and prognosis of renal epithelial neoplasms. Hum Pathol 40:10–29
8. Aydin H, Chen L, Cheng L, Vaziri S, He H, Ganapathi R, Delahunt B, Magi-Galluzzi C, Zhou M (2010) Clear cell tubulopapillary renal cell carcinoma: a study of 36 distinctive low-grade epithelial tumors of the kidney. Am J Surg Pathol 34:1608–1621
9. Rohan SM, Xiao Y, Liang Y, Dudas ME, Al-Ahmadie HA, Fine SW, Gopalan A, Reuter VE, Rosenblum MK, Russo P, Tickoo SK (2011) Clear-cell papillary renal cell carcinoma: molecular and immunohistochemical analysis with emphasis on the *von Hippel–Lindau* gene and hypoxia-inducible factor pathway-related proteins. Mod Pathol [Epub ahead of print]
10. Haudebourg J, Hoch B, Fabas T, Cardot-Leccia N, Burel-Vandenbos F, Vieillefond A, Amiel J, Michiels JF, Pedeutour F (2010) Strength of molecular cytogenetic analyses for adjusting the diagnosis of renal cell carcinomas with both clear cells and papillary features: a study of three cases. Virchows Arch 457:397–404
11. Klatte T, Said JW, Seligson DB, Rao PN, de Martino M, Shuch B, Zomorodian N, Kabbinavar FF, Belldegrun AS, Pantuck AJ (2011) Pathological, immunohistochemical and cytogenetic features of papillary renal cell carcinoma with clear cell features. J Urol 185:30–35
12. Mai KT, Faraji H, Desantis D, Robertson SJ, Belanger EC, Levac J (2010) Renal cell carcinoma with mixed features of papillary and clear cell cytomorphology: a fluorescent in situ hypridization study. Virchows Arch 456:77–84
13. Schmidt L, Junker K, Nakaigawa N, Kinjerski T, Weirich G, Miller M, Lubensky I, Neumann HP, Brauch H, Decker J, Vocke C, Brown JA, Jenkins R, Rishard S, Bergerheim U, Gerrard B, Dean M, Linehan VM, Zbar B (1999) Novel mutations of the MET proto-oncogene in papillary renal cell carcinomas. Oncogene 18:2343–2350
14. Bratslavsky G, Sudarshan S, Neckers L, Linehan WM (2007) Pseudohypoxic pathways in renal cell carcinoma. Clin Cancer Res 13:4667–4671
15. Martinez AC, van Wely KH (2010) Are aneuploidy and chromosome breakage caused by a CINgle mechanism? Cell Cycle 9(12) [Epub ahead of print]
16. Antonelli A, Tardanico R, Balzarini P, Arrighi N, Perucchini L, Zanotelli T, Cozzoli A, Zani D, Cunico SC, Simeone C (2010) Cytogenetic features, clinical significance and prognostic impact of type 1 and type 2 papillary renal cell carcinoma. Cancer Genet Cytogent 199:128–133
17. Bentz M, Bergerheim US, Li C, Joos S, Werner CA, Baudis M, Gnarra J, Merino MJ, Zbar B, Linehan WM, Lichter P (1996) Chromosome imbalances in papillary renal cell carcinoma and first cytogenetic data of familial cases analyzed by comparative genomic hybridization. Cytogenet Cell Genet 75:17–21
18. Jiang F, Richter J, Schraml P, Bubendorf L, Gasser T, Sauter G, Mihatsch MJ, Moch H (1998) Chromosomal imbalances in papillary renal cell carcinoma: genetic differences between histological subtypes. Am J Pathol 153:1467–1473
19. Klatte T, Pantuck AJ, Said JW, Seligson DB, Rao NP, LaRochelle JC, Schuch B, Zisman A, Kabbinavar FF, Belldegrun AS (2009) Cytogenetic and molecular tumor profiling for type 1 and type 2 papillary renal cell carcinoma. Clin Cancer Res 15:1162–1169
20. Sanders ME, Mick R, Tomaszewski JE, Barr FG (2002) Unique patterns of allelic imbalance distinguish type 1 from type 2 sporadic papillary renal cell carcinoma. Am J Pathol 161:997–1005
21. Gunawan B, von Heydebreck A, Fritsch T, Huber W, Ringert RH, Jakse G, Fuzesi L (2003) Cytogenetic and morphologic typing of 58 papillary renal cell carcinomas: evidence for a cytogenetic evolution of type 2 from type 1 tumors. Cancer Res 63:6200–6205
22. Jones TD, Eble JN, Wang M, MacLennan GT, Delahunt B, Brunelli M, Martingnoni G, Lopez-Beltran A, Bonsib SM, Ulbright TM, Zhang S, Nigro K, Cheng L (2005) Molecular genetic evidence for the independent origin of multifocal papillary tumors in patients with papillary renal cell carcinomas. Clin Cancer Res 11:7226–7233
23. Kuroda N, Michal M, Hes O, Taguchi T, Tominaga A, Mizobuchi K, Ohe C, Sakaida N, Uemura Y, Shuin T, Lee GH (2009) Renal angiomyoadenomatous tumor: fluorescence in situ hybridization. Pathol Int 59:689–691
24. Herman JG, Latif F, Weng Y, Lerman MI, Zbar B, Liu S, Samid D, Duan DS, Gnarra JR, Linehan WM (1994) Silencing of the VHL tumor-suppressor gene by DNA methylation in renal carcinoma. Proc Natl Acad Sci U S A 91:9700–9704
25. Clifford SC, Prowse AH, Affara NA, Buvs CH, Maher ER (1998) Inactivation of the von Hippel–Lindau (VHL) tumour suppressor gene and allelic losses at chromosome arm 3p in primary renal cell carcinoma: evidence for a VHL-independent pathway in clear cell renal tumourigenesis. Genes Chromosomes Cancer 22:200–209
26. Kuroda N, Shiotsu T, Kawada C, Shuin T, Hes O, Michal M, Ohe C, Mikami S, Pan CC (2010) Clear cell papillary renal cell carcinoma and clear cell renal cell carcinoma arising in acquired cystic disease of the kidney: an immunohistochemical and genetic study. Ann Diagn Pathol Jun 17. [Epub ahead of print]
27. Elfving P, Cigudosa JC, Lundgren R, Limon J, Mandahl N, Kristofferson U, Heim S, Mitelman F (1990) Trisomy 7, trisomy 10, and loss of the Y chromosome short-term cultures of normal kidney tissue. Cytogenet Cell Genet 53:123–125
28. Kovacs G, Brusa P (1989) Clonal chromosome aberrations in normal kidney tissue from patients with renal cell carcinoma. Cancer Genet Cytogenet 37:289–290
29. Dal Cin P, Aly MS, Delabie J, Ceuppens JL, Van Gool S, Van Damme B, Baert L, Van Poppel H, Van Den Berghe H (1992) Trisomy 7 and trisomy 10 characterize subpopulations of tumor-infiltrating lymphocytes in kidney tumors and in the surrounding kidney tissue. Proc Natl Acad Sci USA 89:9744–9748
30. Moch H, Sauter G, Gasser TC, Bubendorf L, Richter J, Presti JC Jr, Waldman FM, Mihatsch MJ (1998) EGF-r gene copy number changes in renal cell carcinoma detected by fluorescence in situ hybridization. J Pathol 184:424–429
31. Kuroda N, Tamura M, Shiotsu T, Nakamura S, Tagucni T, Tominaga A, Hes O, Michal M, Kawada C, Shuin T, Lee GH (2010) Chromosomal abnormalities of clear cell renal cell carcinoma: frequent gain of chromosome 7. Pathol Int 60:9–13

Virchows Arch (2011) 459:465–475
DOI 10.1007/s00428-011-1151-5

REVIEW AND PERSPECTIVE

Periostin expression and epithelial-mesenchymal transition in cancer: a review and an update

Laura Morra · Holger Moch

Received: 8 June 2011 / Revised: 20 September 2011 / Accepted: 26 September 2011 / Published online: 14 October 2011
© The Author(s) 2011. This article is published with open access at Springerlink.com

Abstract Periostin, also called osteoblast-specific factor 2, is a secreted cell adhesion protein, which shares a homology with the insect cell adhesion molecule fasciclin I. It has been shown to be an important regulator of bone and tooth formation and maintenance, and of cardiac development and healing. Recent studies revealed that periostin plays an important role in tumor development and is upregulated in a wide variety of cancers such as colon, pancreatic, ovarian, breast, head and neck, thyroid, and gastric cancer as well as in neuroblastoma. Periostin binding to the integrins activates the Akt/PKB- and FAK-mediated signaling pathways which lead to increased cell survival, angiogenesis, invasion, metastasis, and importantly, epithelial-mesenchymal transition of carcinoma cells. In this review we summarize recent clinicopathological studies that have investigated periostin expression in lung, kidney, prostate, liver cancer, and malignant pleural mesothelioma and discuss the role of periostin isoforms in tumorigenesis and their potential as targets for stroma-targeted anticancer therapy.

Keywords Periostin · EMT · Isoform · Stroma · Target

Background

Periostin, also termed osteoblast-specific factor 2, is a 93.3-kDa secreted protein and shares a homology with the insect cell adhesion molecule fasciclin I. It promotes integrin-dependent cell adhesion and motility and belongs to the superfamily of TGF-β-inducible proteins [1, 2]. Its N-terminal region contains a signal peptide (SP) for its secretion, and a cysteine-rich region (EMI domain) which promotes the formation of multimers in non-reducing conditions. Adjacent to the SP and the EMI domains, four internal homologous repeats (FAS domains) are located; these are homologous to the insect cell adhesion protein fasciclin I and act as ligands for the integrins [1, 2]. The C-terminal region of periostin consists of a hydrophilic domain. The N-terminal region of periostin is highly conserved, while the C-terminal region of the protein varies depending on the isoform [1, 3]. The N-terminal region regulates the cell function by binding to integrins at the plasma membrane of the cells through its FAS domains. The C-terminal region of the protein regulates the cell–matrix organization and interactions by binding extracellular matrix (ECM) proteins such as collagen I/V, fibronectin, tenascin C, acid mucopolysaccharides, such as heparin and periostin itself [4]. Periostin was shown to be able to bind the integrins αvβ3, αvβ5, and α6β4, promoting the recruitment of the epidermal growth factor receptor (EGFR) and the activation of the Akt/PKB and FAK-mediated signaling pathways. Periostin-activated signaling pathways promote cellular survival, angiogenesis, and resistance to hypoxia-induced cell death. Additionally, periostin can be upregulated in response to the stress of hypoxia in the human A549 non-small cell lung cancer cell line and in rat pulmonary arterial smooth muscle cells (PASMCs) [5, 6]. The study of Li et al. demonstrated that upregulation of periostin in PASMCs is mediated through Ras signaling [6] (Fig. 1).

The desmoplastic tumor stroma constitutes the so-called tumor microenvironment, which supports growth, invasion, and immune evasion of the tumor. It is formed by a stromal matrix in which cancer cells and the peri-tumoral stromal

L. Morra · H. Moch (✉)
Institute for Surgical Pathology, University Hospital Zurich,
Schmelzbergstrasse 12,
CH-8091 Zurich, Switzerland
e-mail: holger.moch@usz.ch

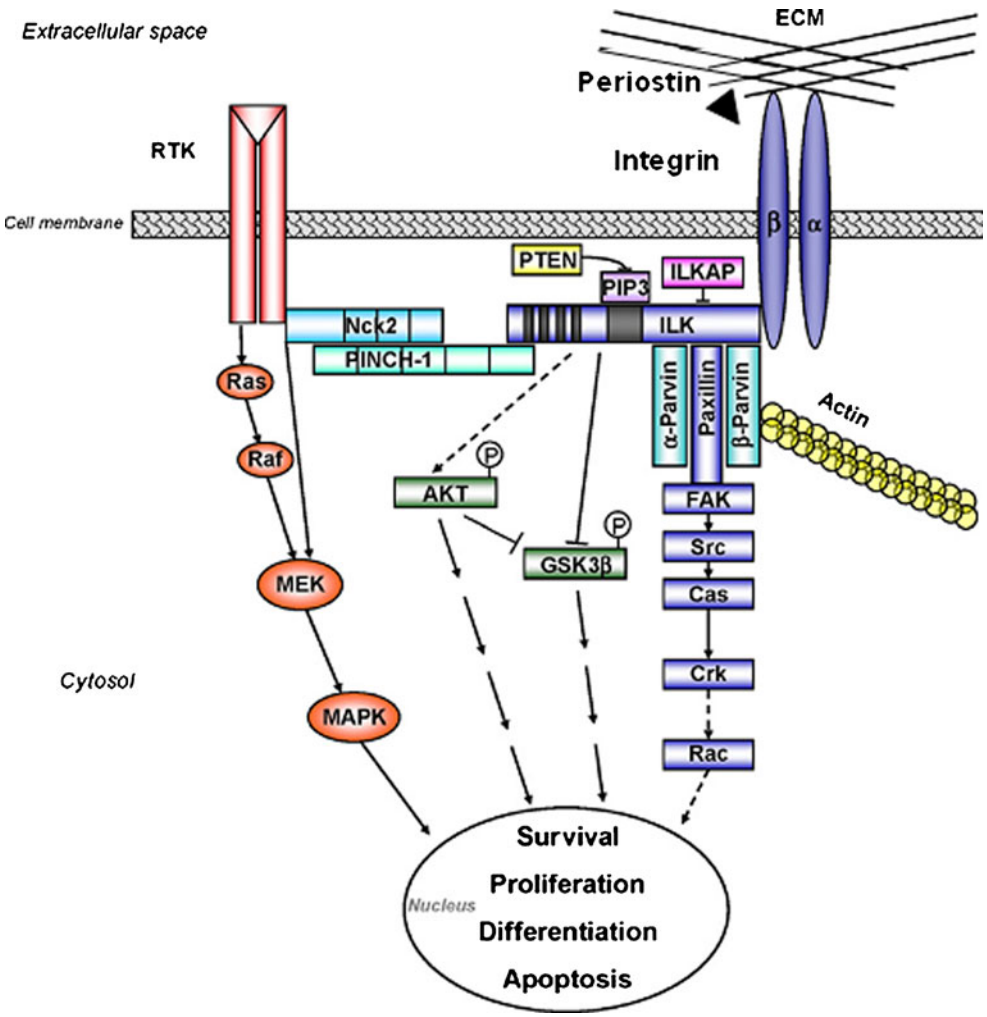

Fig. 1 Periostin-activated signaling pathways. Periostin binding to integrins initiates the crosstalk between those integrins and the receptor tyrosine kinases (RTKs), such as EGFR, at the plasma membrane. This crosstalk activates the Akt/PKB and the FAK-mediated signaling pathways. Ras signaling activates periostin under hypoxic conditions. Reprinted from [69]

cells are embedded. The tumor stromal cells consist of tumor-associated endothelial cells (TECs), cancer-associated fibroblasts (CAFs), and tumor-associated macrophages, as well as distinct sets of tumor-directed lymphocytes. All these cell types produce growth factors, angiogenic factors, and proteolytic enzymes which sustain the tumor growth and angiogenesis and degrade the ECM, enhancing the tumor cell invasion and metastasis [7]. Furthermore, an excessive production of ECM proteins such as periostin, collagen, and fibronectin may contribute to the generation of a tumor-supportive microenvironment (Fig. 2). Within this context, the matrix protein periostin (gene *POSTN*) plays an important role, regulating cell function and cell–matrix interactions.

Periostin probably exerts its pro-tumorigenic effect not only through its binding to the integrins and the consequent activation of intracellular pathways which determine an enhanced invasiveness, but also through its effect on the ECM fibrillogenesis. The C-terminal region of periostin has been shown to interact with ECM molecules by immunoprecipitation and binding assays [4, 8]. Together with those studies showing colocalization of periostin with fibronectin, collagen, and tenascin C [8], these findings suggest that periostin regulates collagen fibrillogenesis and biomechanical properties of connective tissues, forming reticular structures. Considering that alterations in the ECM components of the tumor microenvironment have a remarkable impact on the invasive and metastatic process, it is possible that periostin promotes an ECM organization that supports invasion and metastasis (Fig. 3).

Periostin protein is physiologically expressed in a wide variety of normal adult tissues and fetal tissues, such as embryonic periosteum, periodontal ligament, placenta, cardiac valves, adrenal glands, lung, thyroid, stomach, colon, vagina, ovary, testis, prostate, and breast [1, 9]. Moreover, periostin is expressed in tissues under stress conditions, such as heart under pressure or volume overload, skeletal muscle after injury, and in pulmonary aortic smooth muscle cells in response to hypoxia [6, 10, 11]. Periostin has been shown to be essential for bone and tooth formation and maintenance [2], for heart develop-

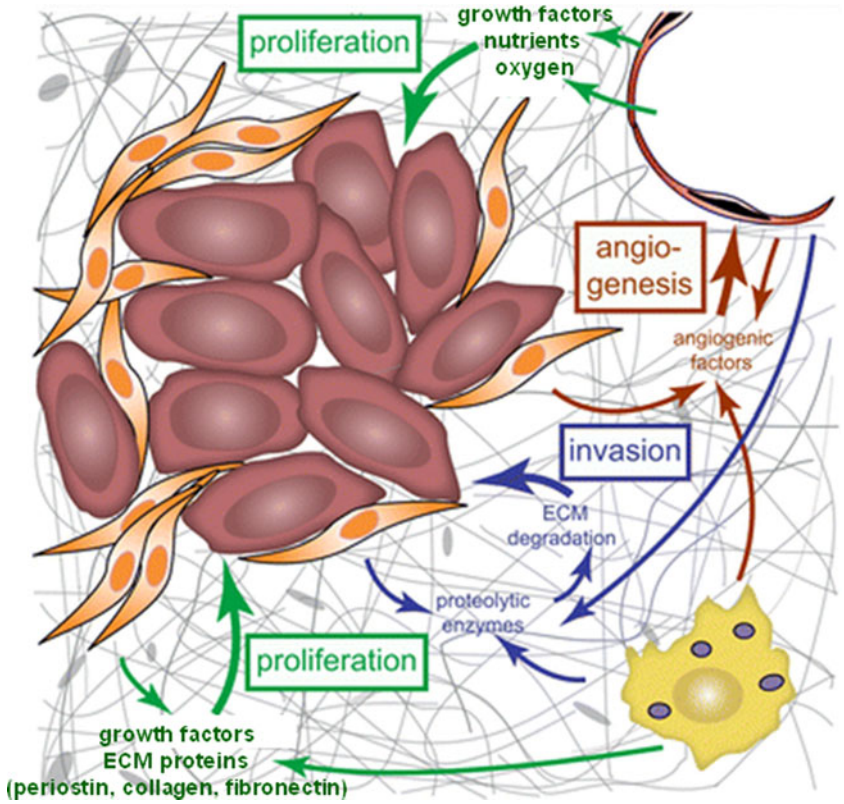

Fig. 2 Tumor microenvironment and its influence on tumor development. Tumor stromal cells, e.g., CAFs, TECs, and tumor-associated macrophages (TAMs), express growth factors sustaining tumor growth. Among these are angiogenic factors promoting angiogenesis, proteolytic enzymes catalyzing the degradation of the ECM, and ECM proteins creating a tumor supporting environment. All these factors together regulate tumor cell growth, invasion, and finally metastasis. Tumor cells are depicted in *brown*, CAFs in *orange*, TECs in *red*, and TAMs in *yellow*. Reprinted from [7]

ment, and healing after acute myocardial infarction [12]. Periostin-deficient mice have a mild phenotype characterized by alterations in periodontal ligament and craniofacial ECM [13], structural valvular anomalies [14], and reduced fibrosis after myocardial infarction [15].

Periostin upregulation has been reported for many cancer types, as non-small cell lung cancer (NSCLC), renal cell carcinoma (RCC), malignant pleural mesothelioma (MPM), and others [16–21] and is consequently defined as a tumor-enhancing factor. Only a few reports in bladder cancer and osteosarcoma have described periostin as a tumor-inhibiting factor [22, 23]. Moreover periostin upregulation has been reported also for chronic sinusitis and recent studies suggest that periostin may be part of a negative-feedback loop regulating allergic airway inflammation [24, 25]. Importantly, periostin is involved in the epithelial-mesenchymal transition (EMT) of carcinoma cells [6, 17, 19, 26, 27].

In this review, we summarize the current knowledge about the role of periostin in the process of EMT and discuss its potential as a target for anticancer therapies directed against the tumor stroma. Furthermore, we summarize current knowledge about periostin expression in the different tumor components of NSCLC, MPM, prostate cancer (PC), RCC, hepatocellular carcinoma (HCC), and bile duct carcinoma (BDC) [16, 20, 21, 28, 29] (Table 1).

Epithelial-mesenchymal transition and periostin

It is well known that the EMT process is fundamental during the embryonic development of multicellular organisms [30]. In addition to embryonic development, the EMT also participates in tumor progression. This is not unexpected, considering that analogies between the two processes (embryonic development and tumor progression) frequently occur. An increasing number of genes and signaling pathways that are involved in embryonic development are also found to be involved in tumorigenesis [31]. However there is much evidence that the EMT process is responsible for dissemination of primary tumor epithelial cells to the sites of metastasis and for the dedifferentiation program that leads to increased malignant behavior of the tumor [30] (Fig. 4).

On a morphologic basis, EMT in vitro can be recognized by the presence of spindle-shaped cells, emission of pseudopodia, and increased intercellular separation, which reflects the acquisition of a mesenchymal phenotype, increased motility, and loss of cell–cell adhesion. Furthermore, the EMT of cancer cells is characterized by an upregulation of mesenchymal proteins such as periostin, vimentin, fibronectin, and N-cadherin, accompanied by a downregulation of epithelial markers such as E-cadherin.

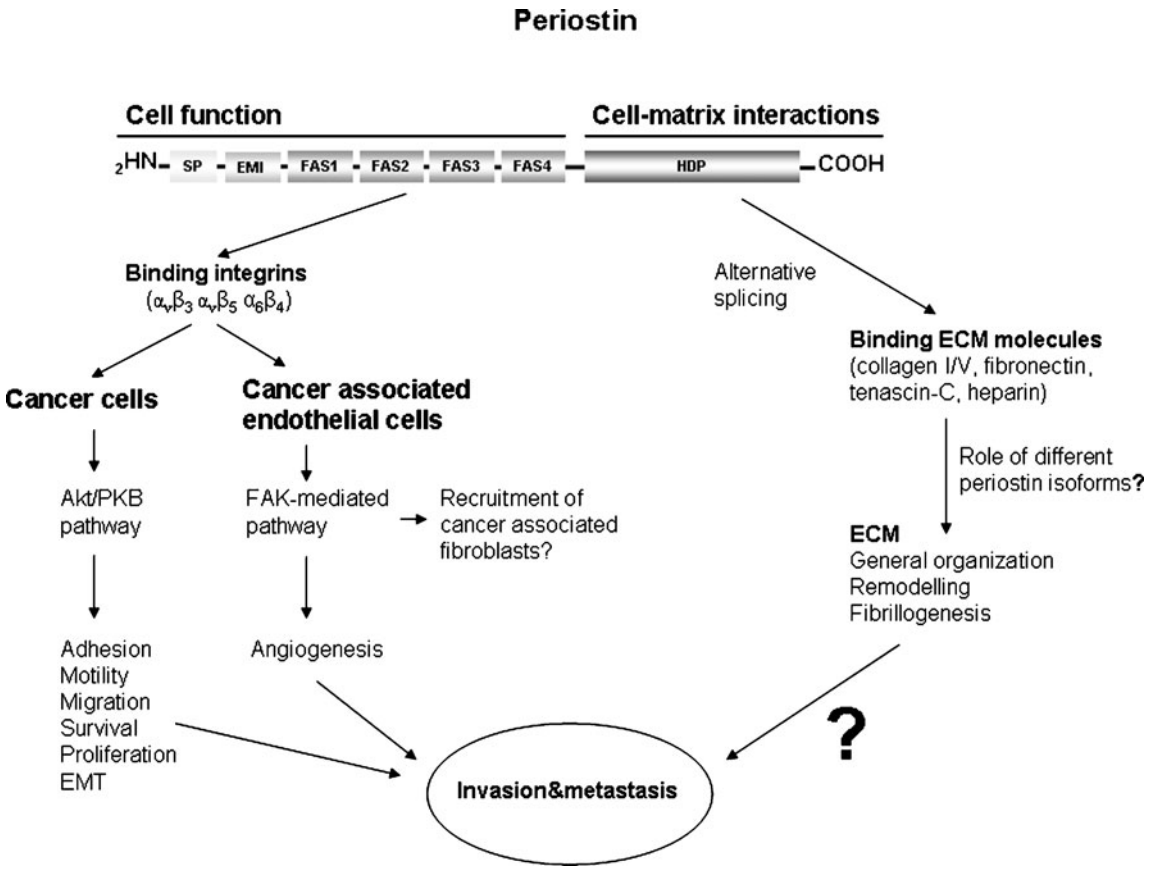

Fig. 3 The role of periostin in cancer. The N-terminal region of the protein influences cell function, while the C-terminal influences cell–matrix interactions. Through its FAS domains, periostin binds to integrins and activates the Akt/PKB and the FAK-mediated signaling pathways, leading to increased tumor invasion and metastasis. The C-terminal region of periostin binds extracellular matrix (ECM) molecules and influences the general organization of the extracellular matrix. Periostin splice isoforms differ in the C-terminal and it is still not known if they contribute differentially to ECM formation and to the global invasive and metastatic potential of the protein

On a functional basis, gain of N-cadherin expression, together with loss of E-cadherin, leads to alterations in the epithelial cell shape and motility by dissociation of intercellular adherens junctions, promoting only weak homophilic cell adhesion interactions [30, 31]. In vitro, lack of E-cadherin determines acquisition of a mesenchymal phenotype and invasive behavior, which can be reversed if E-cadherin is restored and constitutively expressed [32]. In vivo, it has been shown that E-cadherin-negative cell lines have an increased tumorigenic potential when implanted as xenografts in nude mice [30]. Clinical studies showed that E-cadherin expression is inversely correlated with high-grade cancers or with poor survival [33, 34]. On a molecular basis, E-cadherin is

Table 1 Overview of correlations found, by immunohistochemical studies on NSCLC, MPM, PC, RCC, and BDC tissue microarrays (TMAs), between epithelial and stromal periostin expression and clinicopathological parameters

Tumor type	Poor survival	Differentiation grade	Stage of disease	Reference
Non-small cell lung cancer	Stromal expression		Epithelial and stromal expression	Soltermann et al. [16]
Malignant pleural mesothelioma	Epithelial expression			Schramm et al. [20]
Prostate cancer	Stromal expression	Epithelial and stromal expression	Epithelial expression	Tischler et al. [28]
Renal cell carcinoma	Epithelial expression	Epithelial and stromal expression	Epithelial expression	Dahinden et al. [21]
Bile duct carcinoma	Epithelial expression			Riener et al. [29]

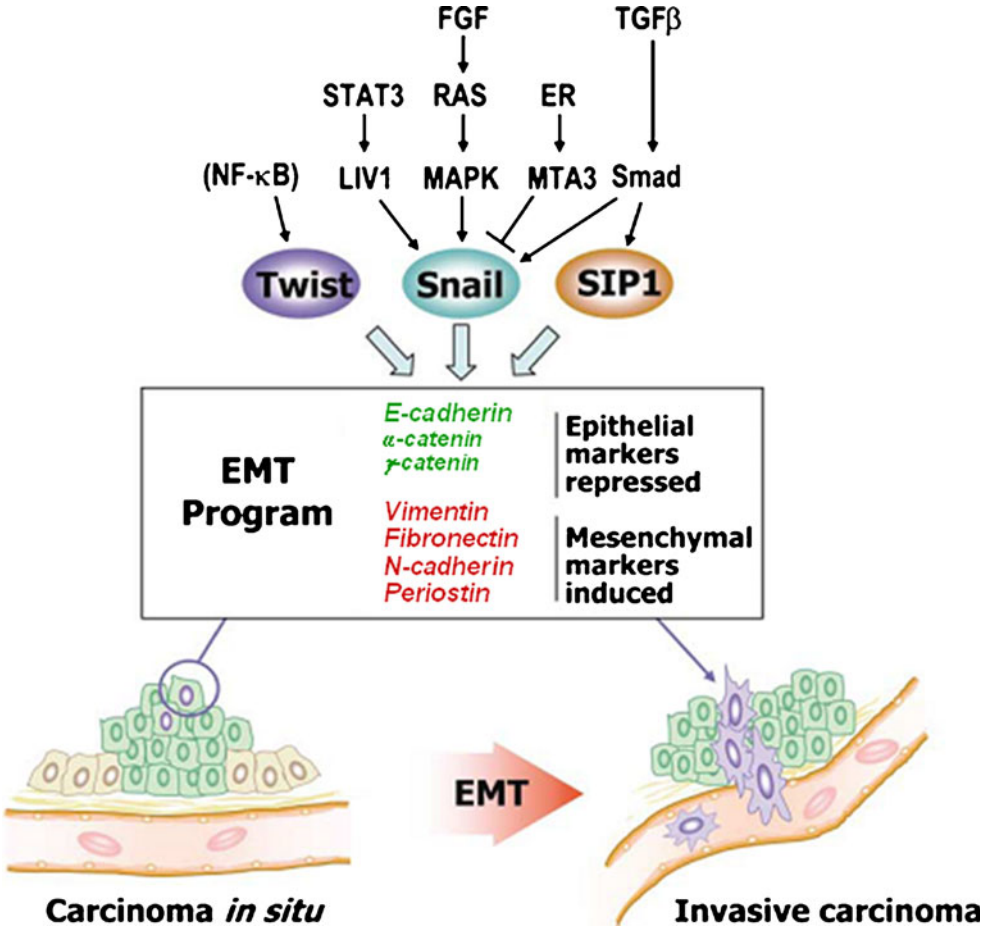

Fig. 4 Drivers and mediators of EMT. Early stage tumor cells (*green*) maintain epithelial properties similar to the neighboring normal epithelium (*brown*). The overexpression of master regulators of EMT, such as *Twist*, *Snail*, and *SIP1* in cancer cells (*shown with purple nuclei*) leads to dramatic changes in the gene expression profile and cellular behavior. Twist, Snail, and SIP1 suppress the expression of E-cadherin and trigger expression of an entire EMT transcriptional program through as yet unknown mechanisms. Reprinted from [31]

downregulated by epigenetic mechanisms, such as promoter hypermethylation and transcriptional repression. Transcriptional repressors of E-cadherin are the zinc finger proteins Snail and SIP1 and the basic helix-loop-helix transcription factor Twist, all of which have the ability to recognize and bind E boxes in the E-cadherin promoter [35–37]. Snail, SIP1, and Twist are therefore inducers of EMT and promote tumor cell invasion. Activation of several growth factor receptors, including tyrosine kinase receptors such as the hepatocyte growth factor receptor c-Met, the ErbB protein family, and the fibroblast growth factor, the insulin growth factor, and the transforming growth factor-β (TGF-β) receptors, have been found to induce EMT in vitro and in vivo [38–41]. Downstream effectors of these activated receptors belong to the Ras and the mitogen-activated protein kinase pathway, the phosphoinositide 3-kinase pathway, or to the TGF-β-SMAD pathway, which all lead to Snail expression [30, 31, 35]. Recently, the DNA binding factor LIV1 has been found to promote activation of Snail through a STAT3-dependent pathway [42] (Fig. 4).

The matrix protein periostin was shown to be not only a marker of EMT, but to be itself an inductor of this phenomenon [26, 27]. Indeed Yan et al. demonstrated that ectopic expression of periostin in tumorigenic but non-metastatic 293T cells can induce EMT and promote invasion and metastasis in vivo [26]. Upregulation of periostin was accompanied by upregulation of vimentin, fibronectin, and active MMP-9, while E-cadherin and N-cadherin expression was unaltered. Periostin signaling pathway in 293T cells seems to require interaction with αvβ5 integrin and recruitment of EGFR, as demonstrated by the fact that periostin-induced increase in cell adhesion, migration and invasion can be blocked by incubation with anti-integrin αvβ5 antibody or with tyrphostin 25, an EGFR kinase inhibitor.

Kim et al. found that periostin was able to induce EMT and an increased invasiveness in prostate cancer cell lines by downregulation of E-cadherin via Snail and increased phosphorylation of Akt [27]. Opposite effects were observed using bladder cancer cell lines, indicating that periostin regulates E-cadherin in a cell-type-dependent way. Furthermore, the C-terminal region of periostin was not sufficient for induction of EMT in prostate cancer cells, indicating that the induction of EMT is mediated by the N-terminal region of periostin.

However, examination of the expression pattern of EMT markers (such as periostin, vimentin, fibronectin, N-

cadherin, E-cadherin, and β-catenin) or members of the Akt/PKB signaling pathway allows determination of their occurrence and clinical significance in vivo. Therefore, an increasing number of immunohistochemical studies aim to characterize EMT expression profiles and their prognostic significance.

Periostin expression in different tumor types

Upregulation of periostin has been observed in many cancer types, such as neuroblastoma [43], head and neck [44], nasopharyngeal [45], thyroid [46], oral [47], breast [48], and ovarian cancer [19]. Elevated periostin levels were also detected in the serum from thymoma [49] and breast [50] cancer patients as well as in serum and pleural effusions of lung cancer patients [51, 52]. In the following, recent data on periostin expression will be described for different tumor types.

Non-small cell lung cancer

Periostin expression in normal healthy lung tissue has been observed [9] and its upregulation in cancerous lung tissue has been reported [16, 53] and associated with EMT [16]. Recently, periostin was identified in malignant pleural effusions from lung adenocarcinoma by mass spectrometric N-glycoprotein profiling [52] and its serum levels were shown to be higher compared with the normal control in NSCLC. The normal control consisted of pleural effusions from patients with cardiac disease but no neoplasia. Soltermann et al. compared the expression of EMT proteins such as periostin and vimentin, the MET protein versican, and classical desmoplasia markers such as collagen and elastin, in NSCLC by immunohistochemical analysis of tissue microarrays (TMAs). From these studies, it was derived that stromal periostin is a prognostic factor for decreased progression-free survival in NSCLC, and together with epithelial periostin, it was also significantly associated with several clinicopathological parameters such as squamous cell carcinoma histotype, higher stage, higher pT, higher pM, larger tumor size, and vessel infiltration, as well as with male gender [16]. Moreover, stromal periostin expression was significantly associated with epithelial cytoplasmic expression of vimentin and with collagen, but not with elastin, suggesting that during tumor progression the stromal fibrillogenesis in NSCLC may switch from elastin to periostin [16]. However, periostin stromal expression in NSCLC is mostly due to the intra-tumoral component, rather than to the peritumoral component of the stroma (own unpublished data). Interestingly, periostin was also correlated with the MET marker versican [16]; the expression of versican has been shown to be associated with tumor recurrence and more advanced disease in NSCLC [54].

Malignant pleural mesothelioma

MPM consists of different histotypes, including epithelioid, sarcomatoid, and biphasic. The biphasic MPM is a mixed histotype which is associated with both epithelial and mesenchymal phenotypes. The sarcomatoid and epithelioid histotypes resemble the EMT–MET transdifferentiation, being associated with the epithelial and mesenchymal differentiation state of the cell, respectively.

Schramm et al. conducted an immunohistochemical study on more than 350 MPM patients. Members of a putative MPM–EMT signaling cascade were analyzed: the EMT marker periostin, the EGFR, integrin β1, the inhibitor of Akt signaling pathway phosphatase and tensin homolog (PTEN), the integrin-linked kinase (ILK), and the two cell cycle regulators, p21 and p27. The results showed that expression of periostin in tumor cells can be considered as an independent prognostic factor for overall survival [20]. Indeed high periostin levels in tumor cells correlated with poor survival, whereas high cytoplasmic PTEN, ILK, or nuclear p21 and p27 correlated with better survival.

Interestingly, both stromal and tumor cell periostin expression was associated with the sarcomatoid histotype, indicating that periostin is associated with the mesenchymal differentiation state of the cell [20]. Contrary to periostin, high EGFR and integrin β1 expression nuclear p27 were associated with the epithelioid histotype of MPM.

Prostate cancer

A limited number of studies have investigated periostin expression in prostate cancer [9, 28, 55]. Periostin expression in normal prostate tissue has been detected by western blot analysis [9]. Tsunoda et al. detected periostin among several genes by a screening for three-dimensional culture (3DC)-associated genes. Non-malignant prostatic epithelial cells, cultured in two-dimensional culture (2DC) and 3DC, were compared with 40 PC samples and their matched non-neoplastic prostate epithelium. Candidate genes were further validated by quantitative real time (RT)-PCR. Since periostin mRNA showed the highest levels among all the genes upregulated in 3DC, its protein expression was further evaluated by immunohistochemistry (IHC). Cancer cells of early stage but not advanced stage prostate cancer had an increased periostin expression compared with normal glands [55]. Tischler et al. [28] analyzed periostin expression by IHC in more than 400 prostate tumors. Contrary to Tsunoda et al., both stromal

and epithelial periostin expression was found to be increased in advanced and metastatic tumors [28]. They also reported increased periostin expression in the tumor stroma compared with the stroma around normal prostate glands. Furthermore, they showed that stromal periostin is upregulated in high-grade prostate cancers and affirmed stromal periostin as a progression factor for prostate-specific antigen relapse-free survival.

Renal cell carcinoma

Periostin was identified as an accessible biomarker from the blood stream after ex vivo perfusion and biotinylation of surgically resected human kidney carcinoma [56]. Its tumor specificity was further confirmed by IHC. Periostin showed a prominent vascular and stromal staining pattern [56]. Interestingly, the MET protein versican and the EMT protein periostin were found to have similar stromal expression patterns in RCC [56] as well as in NSCLC [16].

A bioinformatic network modeling approach, comparing immunohistochemical stainings from TMAs of RCC patients, analyzed periostin along with several other proteins to elucidate molecular pathways influenced by the von Hippel-Lindau (*VHL*) gene and the *PTEN* gene, which are often deregulated in clear cell RCC [21]. Both epithelial and a stromal periostin staining was observed. In particular, epithelial periostin was significantly increased in high-grade and high-stage tumors and was significantly associated with poor overall survival [21]. In an estimated graphical log-linear model, periostin was also found to be positively associated with nuclear *PTEN*, phosphorylated ribosomal protein p-S6, and nuclear p21, whereas cytoplasmic *PTEN* and inactive non-phosphorylated ribosomal protein S6 correlated with a prolonged survival [21]. Recently, we identified several periostin isoforms in renal tissue by direct sequencing, one of which was found to be tumor associated [57].

Hepatocellular and bile duct carcinomas

Periostin has been found to enhance tumor progression in several gastrointestinal cancers such as colon, gastric, and pancreatic cancer [17, 58, 59]. Few studies have investigated periostin expression in human liver [18, 29, 60]. Tilman et al. analyzed periostin mRNA levels by quantitative RT-PCR in six HCC and five normal liver samples: periostin mRNA levels were increased by an average 65-fold in tumor [60]. Additionally, among various tumor types, strong periostin upregulation was mostly observed in liver and pancreatic tumors [60]. Baril et al. analyzed periostin expression by IHC in multiple tumor types including 11 HCC: liver tumors showed the highest periostin levels, together with breast, pancreatic, colon and larynx tumors. Recently, Riener et al. [29] performed the first immunohistochemical analysis on a large number of liver cancer patients (91 HCC and 116 BDC), which represented also the first report on periostin expression in BDC. Their study showed that expression of epithelial periostin was increased in higher-grade HCC and was shown to be an independent prognostic marker for poor overall survival in BDC. Periostin expression was also detected in the stroma of both HCC and BDC but did not correlate with clinicopathological parameters. Periostin expression was also analyzed in normal bile ducts, gallbladder epithelium, and hepatocytes, which showed a weak periostin cytoplasmic expression.

These immunohistochemical studies show that, depending on the cancer type, either epithelial or stromal periostin expression is associated with different tumor behavior (Table 1). One might hypothesize the existence of an autocrine/paracrine periostin loop between stromal and epithelial tumor cells and that the protein is secreted at a site where it can exert its strongest effect, namely at the interface between tumor and stroma. Furthermore, different splice variants of periostin might result in different biological effects, if they are secreted either by tumor stromal cells or by tumor epithelial cells.

Periostin isoforms and alternative splicing

Up to six different splice isoforms of periostin have been reported, four of which have been fully sequenced and annotated [3, 56] (Table 2). The isoforms of periostin are between 83 and 93 kDa in mass and differ in their C-terminal sequences, characterized by individual presence or absence of cassette exons 17–21 (UniProtKB/Swiss-Prot, March 2011); its N-terminus is conserved. Periostin isoforms were initially detected in pre-osteoblast cells, and it has been shown that the levels of osteoblast-specific differentiation markers were markedly reduced when the activity of these proteins was blocked in the mouse

Table 2 Schematic representation of the periostin cassette exons in the four known isoforms (isoforms 1–4)

Isoform	Exon						
1	1–16	17	18	19	20	21	22–23
2	1–16			19	20	21	22–23
3	1–16		18	19	20		22–23
4	1–16			19	20		22–23

Periostin splice isoforms are characterized by an individual presence or absence of cassette exons 17–21

osteoblast cell line MC3T3-E1. These results suggest that these proteins play a role in the differentiation of osteoblasts [3].

The periostin C-terminal domain probably modulates the protein function by binding to ECM molecules such as fibronectin and collagen [61]. Indeed, Norris et al. demonstrated that the C-terminal domain of periostin binds collagen I, concluding that it is involved in fibrillogenesis and influences the biomechanical properties of fibrous connective tissues [4]. On the basis of comparative studies of periostin sequences among vertebrates, Hoersch and Andrade-Navarro suggested that the C-terminal domain of periostin is able to bind the matrix proteins collagen and fibronectin, and that each isoform may exert its influence on the ECM fibrillogenesis differently [61]. Therefore, alternative splicing of periostin isoforms seems to reflect the differential modulation of the periostin function in the ECM. This hypothesis is supported by the finding that downregulation and/or loss by alternative splicing of the periostin non-spliced form, together with expression of variant I (isoform 4 in UniProtKB/Swiss-Prot database), promotes increased invasiveness in in vitro and in vivo experiments using the human bladder cancer cell line SBT991, the mouse malignant melanoma cell line B16F10, and nude mice [22, 62]. Given that periostin isoforms have a differential invasive potential, it remains to be clarified how exactly periostin isoforms modulate the ECM formation and if this periostin-isoform-modulated ECM formation has an influence on the global invasive and metastatic potential of the protein.

Alternative splicing contributes to the expansion of transcriptomic diversity. It is achieved by the interplay of several RNA-binding proteins that associate with pre-mRNA transcripts, determining an exon skipping or inclusion in the mature RNA transcript [63]. Several ubiquitous families of proteins that regulate splicing have been identified and they act in cooperation with tissue-specific regulators of splicing [64]. Warzecha et al. identified the epithelial splicing regulatory proteins 1 and 2 (ESRP1 and ESRP2) as cell-type-specific regulators of transcripts that switch splicing during the EMT [65]. Those two RNA-binding proteins promote alternative splicing events with function in cell–cell adhesion, polarity, and migration, influencing the phenotypic morphological changes that are observed in the EMT. This complex alternative splicing network reveals an important post-transcriptional aspect in addition to the changes in gene expression that underlie the EMT. In particular, it was shown that downregulation of the ESRPs leads to an increase in exon skipping events in the penultimate exons of the C-terminal transcript regions of all analyzed proteins. These events are thought to be functionally relevant because the skipped exons were in multiples of three nucleotides, allowing translation into different protein isoforms. Even though periostin was not identified among the transcripts regulated by ESRP1 and ESRP2, periostin isoforms are generated by alternative splicing in the penultimate exons of the C-terminal transcript region and the skipped exons are in multiples of three. Therefore it is possible that periostin transcripts are regulated during EMT by specific splice-regulatory proteins and that those transcripts have an influence on the morphologic and functional changes associated with the EMT.

Periostin as a target for immunotherapy

In RCC, periostin was found to be overexpressed in the subendothelial stroma of the tumor neovasculature [56]. It was suggested that periostin represents a potential target for anticancer therapies directed against the subendothelial stroma (so called “tumor vascular targeting” [66]). Indeed, the tumor neovasculature is tumor specific and discrete from normal adult tissue, except for a local and transient angiogenesis that occurs during specific processes such as tissue regeneration and inflammation [67].

Castronovo et al. found periostin to be an accessible antigen from the blood stream after ex vivo perfusion and biotinylation of surgically resected human renal carcinomas [56]. The ex vivo biotinylation of surgically resected renal carcinomas allowed a selective labeling of tumor vascular structures. Subsequent proteomic analysis of the biotinylated specimens allowed the identification of several proteins in the tumor portions, including periostin, which was the most abundant tumor-associated protein identified in RCC [56]. Validation of periostin as a tumor-associated antigen was performed by IHC and PCR. IHC showed overexpression of periostin in tumor samples, with a prominent vascular and stromal pattern of staining. PCR analysis yielded stronger periostin expression in fetal and tumor specimens [56]. These data suggested that oncofetal periostin variants might represent even more specific tumor targets.

In conclusion, upregulation in tissues and body fluids of many tumor types, accessibility from the blood stream, and correlation with malignant behavior and with poor prognosis speak in favor of the potential usefulness of periostin as a target for immunotherapy. Further, ECM proteins such as periostin, fibronectin, or tenascin C belong to a class of proteins that can be considered suitable tumor antigens for targeted delivery of therapeutic agents because of their accessibility, specificity, stability, and abundance [56, 66]. The therapeutic potential of periostin has recently been evaluated by Castronovo et al. [56] and by Kudo et al. [68], with the conclusion that stroma-targeting represents a valid option in anticancer therapy.

Conflict of interests The authors declare no conflict of interest.

Open Access This article is distributed under the terms of the Creative Commons Attribution Noncommercial License which permits any noncommercial use, distribution, and reproduction in any medium, provided the original author(s) and source are credited.

References

1. Takeshita S, Kikuno R, Tezuka K, Amann E (1993) Osteoblast-specific factor 2: cloning of a putative bone adhesion protein with homology with the insect protein fasciclin I. Biochem J 294(Pt 1):271–278
2. Horiuchi K, Amizuka N, Takeshita S, Takamatsu H, Katsuura M, Ozawa H, Toyama Y, Bonewald LF, Kudo A (1999) Identification and characterization of a novel protein, periostin, with restricted expression to periosteum and periodontal ligament and increased expression by transforming growth factor beta. J Bone Miner Res 14:1239–1249
3. Litvin J, Selim AH, Montgomery MO, Lehmann K, Rico MC, Devlin H, Bednarik DP, Safadi FF (2004) Expression and function of periostin-isoforms in bone. J Cell Biochem 92:1044–1061
4. Norris RA, Damon B, Mironov V, Kasyanov V, Ramamurthi A, Moreno-Rodriguez R, Trusk T, Potts JD, Goodwin RL, Davis J, Hoffman S, Wen X, Sugi Y, Kern CB, Mjaatvedt CH, Turner DK, Oka T, Conway SJ, Molkentin JD, Forgacs G, Markwald RR (2007) Periostin regulates collagen fibrillogenesis and the biomechanical properties of connective tissues. J Cell Biochem 101:695–711
5. Ouyang G, Liu M, Ruan K, Song G, Mao Y, Bao S (2009) Upregulated expression of periostin by hypoxia in non-small-cell lung cancer cells promotes cell survival via the Akt/PKB pathway. Cancer Lett 281:213–219
6. Li P, Oparil S, Feng W, Chen YF (2004) Hypoxia-responsive growth factors upregulate periostin and osteopontin expression via distinct signaling pathways in rat pulmonary arterial smooth muscle cells. J Appl Physiol 97:1550–1558, discussion 1549
7. Hofmeister V, Schrama D, Becker JC (2008) Anti-cancer therapies targeting the tumor stroma. Cancer Immunol Immunother 57:1–17
8. Takayama G, Arima K, Kanaji T, Toda S, Tanaka H, Shoji S, McKenzie AN, Nagai H, Hotokebuchi T, Izuhara K (2006) Periostin: a novel component of subepithelial fibrosis of bronchial asthma downstream of IL-4 and IL-13 signals. J Allergy Clin Immunol 118:98–104
9. Tai IT, Dai M, Chen LB (2005) Periostin induction in tumor cell line explants and inhibition of in vitro cell growth by anti-periostin antibodies. Carcinogenesis 26:908–915
10. Katsuragi N, Morishita R, Nakamura N, Ochiai T, Taniyama Y, Hasegawa Y, Kawashima K, Kaneda Y, Ogihara T, Sugimura K (2004) Periostin as a novel factor responsible for ventricular dilation. Circulation 110:1806–1813
11. Goetsch SC, Hawke TJ, Gallardo TD, Richardson JA, Garry DJ (2003) Transcriptional profiling and regulation of the extracellular matrix during muscle regeneration. Physiol Genomics 14:261–271
12. Conway SJ, Molkentin JD (2008) Periostin as a heterofunctional regulator of cardiac development and disease. Curr Genomics 9:548–555
13. Rios H, Koushik SV, Wang H, Wang J, Zhou HM, Lindsley A, Rogers R, Chen Z, Maeda M, Kruzynska-Frejtag A, Feng JQ, Conway SJ (2005) Periostin null mice exhibit dwarfism, incisor enamel defects, and an early-onset periodontal disease-like phenotype. Mol Cell Biol 25:11131–11144
14. Snider P, Hinton RB, Moreno-Rodriguez RA, Wang J, Rogers R, Lindsley A, Li F, Ingram DA, Menick D, Field L, Firulli AB, Molkentin JD, Markwald R, Conway SJ (2008) Periostin is required for maturation and extracellular matrix stabilization of noncardiomyocyte lineages of the heart. Circ Res 102:752–760
15. Oka T, Xu J, Kaiser RA, Melendez J, Hambleton M, Sargent MA, Lorts A, Brunskill EW, Dorn GW 2nd, Conway SJ, Aronow BJ, Robbins J, Molkentin JD (2007) Genetic manipulation of periostin expression reveals a role in cardiac hypertrophy and ventricular remodeling. Circ Res 101:313–321
16. Soltermann A, Tischler V, Arbogast S, Braun J, Probst-Hensch N, Weder W, Moch H, Kristiansen G (2008) Prognostic significance of epithelial-mesenchymal and mesenchymal-epithelial transition protein expression in non-small cell lung cancer. Clin Cancer Res 14:7430–7437
17. Bao S, Ouyang G, Bai X, Huang Z, Ma C, Liu M, Shao R, Anderson RM, Rich JN, Wang XF (2004) Periostin potently promotes metastatic growth of colon cancer by augmenting cell survival via the Akt/PKB pathway. Cancer Cell 5:329–339
18. Baril P, Gangeswaran R, Mahon PC, Caulee K, Kocher HM, Harada T, Zhu M, Kalthoff H, Crnogorac-Jurcevic T, Lemoine NR (2007) Periostin promotes invasiveness and resistance of pancreatic cancer cells to hypoxia-induced cell death: role of the beta4 integrin and the PI3k pathway. Oncogene 26:2082–2094
19. Gillan L, Matei D, Fishman DA, Gerbin CS, Karlan BY, Chang DD (2002) Periostin secreted by epithelial ovarian carcinoma is a ligand for alpha(V)beta(3) and alpha(V)beta(5) integrins and promotes cell motility. Cancer Res 62:5358–5364
20. Schramm A, Opitz I, Thies S, Seifert B, Moch H, Weder W, Soltermann A (2010) Prognostic significance of epithelial-mesenchymal transition in malignant pleural mesothelioma. Eur J Cardiothorac Surg 37:566–572
21. Dahinden C, Ingold B, Wild P, Boysen G, Luu VD, Montani M, Kristiansen G, Sulser T, Buhlmann P, Moch H, Schraml P (2010) Mining tissue microarray data to uncover combinations of biomarker expression patterns that improve intermediate staging and grading of clear cell renal cell cancer. Clin Cancer Res 16:88–98
22. Kim CJ, Yoshioka N, Tambe Y, Kushima R, Okada Y, Inoue H (2005) Periostin is down-regulated in high grade human bladder cancers and suppresses in vitro cell invasiveness and in vivo metastasis of cancer cells. Int J Cancer 117:51–58
23. Yoshioka N, Fuji S, Shimakage M, Kodama K, Hakura A, Yutsudo M, Inoue H, Nojima H (2002) Suppression of anchorage-independent growth of human cancer cell lines by the TRIF52/periostin/OSF-2 gene. Exp Cell Res 279:91–99
24. Sehra S, Yao W, Nguyen ET, Ahyi AN, Tuana FM, Ahlfeld SK, Snider P, Tepper RS, Petrache I, Conway SJ, Kaplan MH (2011) Periostin regulates goblet cell metaplasia in a model of allergic airway inflammation. J Immunol 186:4959–4966
25. Platt MP, Soler ZM, Kao SY, Metson R, Stankovic KM (2011) Topographic gene expression in the sinonasal cavity of patients with chronic sinusitis with polyps. Otolaryngology—head and neck surgery. Am Acad Otolaryngol Head Neck Surg 145:171–175
26. Yan W, Shao R (2006) Transduction of a mesenchyme-specific gene periostin into 293T cells induces cell invasive activity through epithelial-mesenchymal transformation. J Biol Chem 281:19700–19708
27. Kim CJ, Sakamoto K, Tambe Y, Inoue H (2011) Opposite regulation of epithelial-to-mesenchymal transition and cell inva-

siveness by periostin between prostate and bladder cancer cells. Int J Oncol 38:1759–1766
28. Tischler V, Fritzsche FR, Wild PJ, Stephan C, Seifert HH, Riener MO, Hermanns T, Mortezavi A, Gerhardt J, Schraml P, Jung K, Moch H, Soltermann A, Kristiansen G (2010) Periostin is up-regulated in high grade and high stage prostate cancer. BMC Cancer 10:273
29. Riener MO, Fritzsche FR, Soll C, Pestalozzi BC, Probst-Hensch N, Clavien PA, Jochum W, Soltermann A, Moch H, Kristiansen G (2010) Expression of the extracellular matrix protein periostin in liver tumours and bile duct carcinomas. Histopathology 56:600–606
30. Thiery JP (2002) Epithelial-mesenchymal transitions in tumour progression. Nat Rev Cancer 2:442–454
31. Kang Y, Massague J (2004) Epithelial-mesenchymal transitions: twist in development and metastasis. Cell 118:277–279
32. Chen WC, Obrink B (1991) Cell-cell contacts mediated by E-cadherin (uvomorulin) restrict invasive behavior of L-cells. J Cell Biol 114:319–327
33. Oka H, Shiozaki H, Kobayashi K, Inoue M, Tahara H, Kobayashi T, Takatsuka Y, Matsuyoshi N, Hirano S, Takeichi M et al (1993) Expression of E-cadherin cell adhesion molecules in human breast cancer tissues and its relationship to metastasis. Cancer Res 53:1696–1701
34. Hirohashi S (1998) Inactivation of the E-cadherin-mediated cell adhesion system in human cancers. Am J Pathol 153:333–339
35. Nieto MA (2002) The snail superfamily of zinc-finger transcription factors. Nat Rev Mol Cell Biol 3:155–166
36. Comijn J, Berx G, Vermassen P, Verschueren K, van Grunsven L, Bruyneel E, Mareel M, Huylebroeck D, van Roy F (2001) The two-handed E box binding zinc finger protein SIP1 downregulates E-cadherin and induces invasion. Mol Cell 7:1267–1278
37. Yang J, Mani SA, Donaher JL, Ramaswamy S, Itzykson RA, Come C, Savagner P, Gitelman I, Richardson A, Weinberg RA (2004) Twist, a master regulator of morphogenesis, plays an essential role in tumor metastasis. Cell 117:927–939
38. Khoury H, Dankort DL, Sadekova S, Naujokas MA, Muller WJ, Park M (2001) Distinct tyrosine autophosphorylation sites mediate induction of epithelial mesenchymal like transition by an activated ErbB-2/Neu receptor. Oncogene 20:788–799
39. Meiners S, Brinkmann V, Naundorf H, Birchmeier W (1998) Role of morphogenetic factors in metastasis of mammary carcinoma cells. Oncogene 16:9–20
40. Valles AM, Boyer B, Badet J, Tucker GC, Barritault D, Thiery JP (1990) Acidic fibroblast growth factor is a modulator of epithelial plasticity in a rat bladder carcinoma cell line. Proc Natl Acad Sci U S A 87:1124–1128
41. Morali OG, Delmas V, Moore R, Jeanney C, Thiery JP, Larue L (2001) IGF-II induces rapid beta-catenin relocation to the nucleus during epithelium to mesenchyme transition. Oncogene 20:4942–4950
42. Yamashita S, Miyagi C, Fukada T, Kagara N, Che YS, Hirano T (2004) Zinc transporter LIVI controls epithelial-mesenchymal transition in zebrafish gastrula organizer. Nature 429:298–302
43. Sasaki H, Sato Y, Kondo S, Fukai I, Kiriyama M, Yamakawa Y, Fuji Y (2002) Expression of the periostin mRNA level in neuroblastoma. J Pediatr Surg 37:1293–1297
44. Kudo Y, Ogawa I, Kitajima S, Kitagawa M, Kawai H, Gaffney PM, Miyauchi M, Takata T (2006) Periostin promotes invasion and anchorage-independent growth in the metastatic process of head and neck cancer. Cancer Res 66:6928–6935
45. Chang Y, Lee TC, Li JC, Lai TL, Chua HH, Chen CL, Doong SL, Chou CK, Sheen TS, Tsai CH (2005) Differential expression of osteoblast-specific factor 2 and polymeric immunoglobulin receptor genes in nasopharyngeal carcinoma. Head Neck 27:873–882
46. Puppin C, Fabbro D, Dima M, Di Loreto C, Puxeddu E, Filetti S, Russo D, Damante G (2008) High periostin expression correlates with aggressiveness in papillary thyroid carcinomas. J Endocrinol 197:401–408
47. Siriwardena BS, Kudo Y, Ogawa I, Kitagawa M, Kitajima S, Hatano H, Tilakaratne WM, Miyauchi M, Takata T (2006) Periostin is frequently overexpressed and enhances invasion and angiogenesis in oral cancer. Br J Cancer 95:1396–1403
48. Shao R, Bao S, Bai X, Blanchette C, Anderson RM, Dang T, Gishizky ML, Marks JR, Wang XF (2004) Acquired expression of periostin by human breast cancers promotes tumor angiogenesis through up-regulation of vascular endothelial growth factor receptor 2 expression. Mol Cell Biol 24:3992–4003
49. Sasaki H, Dai M, Auclair D, Kaji M, Fukai I, Kiriyama M, Yamakawa Y, Fujii Y, Chen LB (2001) Serum level of the periostin, a homologue of an insect cell adhesion molecule, in thymoma patients. Cancer Lett 172:37–42
50. Sasaki H, Yu CY, Dai M, Tam C, Loda M, Auclair D, Chen LB, Elias A (2003) Elevated serum periostin levels in patients with bone metastases from breast but not lung cancer. Breast Cancer Res Treat 77:245–252
51. Sasaki H, Dai M, Auclair D, Fukai I, Kiriyama M, Yamakawa Y, Fujii Y, Chen LB (2001) Serum level of the periostin, a homologue of an insect cell adhesion molecule, as a prognostic marker in nonsmall cell lung carcinomas. Cancer 92:843–848
52. Soltermann A, Ossola R, Kilgus-Hawelski S, von Eckardstein A, Suter T, Aebersold R, Moch H (2008) N-glycoprotein profiling of lung adenocarcinoma pleural effusions by shotgun proteomics. Cancer 114:124–133
53. Sasaki H, Lo KM, Chen LB, Auclair D, Nakashima Y, Moriyama S, Fukai I, Tam C, Loda M, Fujii Y (2001) Expression of periostin, homologous with an insect cell adhesion molecule, as a prognostic marker in non-small cell lung cancers. Jpn J Cancer Res 92:869–873
54. Pirinen R, Leinonen T, Bohm J, Johansson R, Ropponen K, Kumpulainen E, Kosma VM (2005) Versican in nonsmall cell lung cancer: relation to hyaluronan, clinicopathologic factors, and prognosis. Hum Pathol 36:44–50
55. Tsunoda T, Furusato B, Takashima Y, Ravulapalli S, Dobi A, Srivastava S, McLeod DG, Sesterhenn IA, Ornstein DK, Shirasawa S (2009) The increased expression of periostin during early stages of prostate cancer and advanced stages of cancer stroma. Prostate 69:1398–1403
56. Castronovo V, Waltregny D, Kischel P, Roesli C, Elia G, Rybak JN, Neri D (2006) A chemical proteomics approach for the identification of accessible antigens expressed in human kidney cancer. Mol Cell Proteomics 5:2083–2091
57. Morra L, Rechsteiner M, Casagrande S, Duc Luu V, Santimaria R, Diener PA, Sulser T, Kristiansen G, Schraml P, Moch H, Soltermann A (2011) Relevance of periostin splice variants in renal cell carcinoma. Am J Pathol 179:1513–1521
58. Li JS, Sun GW, Wei XY, Tang WH (2007) Expression of periostin and its clinicopathological relevance in gastric cancer. World J Gastroenterol 13:5261–5266
59. Ben QW, Jin XL, Liu J, Cai X, Yuan F, Yuan YZ (2011) Periostin, a matrix specific protein, is associated with proliferation and invasion of pancreatic cancer. Oncol Rep 25:709–716
60. Tilman G, Mattiussi M, Brasseur F, van Baren N, Decottignies A (2007) Human periostin gene expression in normal tissues, tumors and melanoma: evidences for periostin production by both stromal and melanoma cells. Mol Cancer 6:80
61. Hoersch S, Andrade-Navarro MA (2010) Periostin shows increased evolutionary plasticity in its alternatively spliced region. BMC Evol Biol 10:30
62. Kim CJ, Isono T, Tambe Y, Chano T, Okabe H, Okada Y, Inoue H (2008) Role of alternative splicing of periostin in human bladder carcinogenesis. Int J Oncol 32:161–169

63. Wang ET, Sandberg R, Luo S, Khrebtukova I, Zhang L, Mayr C, Kingsmore SF, Schroth GP, Burge CB (2008) Alternative isoform regulation in human tissue transcriptomes. Nature 456:470–476
64. Nilsen TW, Graveley BR (2010) Expansion of the eukaryotic proteome by alternative splicing. Nature 463:457–463
65. Warzecha CC, Jiang P, Amirikian K, Dittmar KA, Lu H, Shen S, Guo W, Xing Y, Carstens RP (2010) An ESRP-regulated splicing programme is abrogated during the epithelial-mesenchymal transition. EMBO J 29:3286–3300
66. Neri D, Bicknell R (2005) Tumour vascular targeting. Nat Rev Cancer 5:436–446
67. Bischoff J (1995) Approaches to studying cell adhesion molecules in angiogenesis. Trends Cell Biol 5:69–74
68. Kudo Y, Siriwardena BS, Hatano H, Ogawa I, Takata T (2007) Periostin: novel diagnostic and therapeutic target for cancer. Histol Histopathol 22:1167–1174
69. Hehlgans S, Haase M, Cordes N (2007) Signalling via integrins: implications for cell survival and anticancer strategies. Biochim Biophys Acta 1775:163–180

Virchows Arch (2011) 459:477–485
DOI 10.1007/s00428-011-1147-1

ORIGINAL ARTICLE

A critical analysis of three quantitative methods of assessment of hepatic steatosis in liver biopsies

Mariana Catta-Preta · Leonardo Souza Mendonca · Julio Fraulob-Aquino · Marcia Barbosa Aguila · Carlos Alberto Mandarim-de-Lacerda

Received: 21 June 2011 / Revised: 24 August 2011 / Accepted: 26 August 2011 / Published online: 8 September 2011
© Springer-Verlag 2011

Abstract The issue of adequately quantitatively evaluating hepatic steatosis is still unresolved. Therefore, we compared three methods of quantitative assessment. Two groups of mice (n=10 each) were fed standard chow (10% fat, SC group) or a high-fat diet (60% fat, HF group) for 16 weeks, and hepatic triglyceride (HT) and liver tissue were then studied. Paraplast-embedded tissues stained by hematoxylin and eosin (H-E) were compared to frozen sections stained by Oil Red-O (ORO). In addition, the volume density of steatosis (Vv[steatosis, liver]) was measured by point counting (P-C, sections H-E or ORO) or by image analysis (I-A, sections ORO). HT was significantly higher in the HF group (104% greater, P= 0.0004) than in the SC group. With P-C and H-E, Vv [steatosis, liver] was 4.80±0.90% in the SC group and 33.50±3.17% in the HF group (600% greater, P<0.0001). With P-C and ORO, Vv[steatosis, liver] was 4.86±0.89% in the SC group and 25.21±1.27% in the HF group (420% greater, P<0.0001). With I-A and ORO, Vv[steatosis, liver] was 4.17±0.85% in the SC group and 23.35±1.58% in the HF group (460% greater, P<0.0001). Correlations between Vv[steatosis, liver] and HT were strong and significant in all methods. In conclusion, all methods were appropriate and reproducible. In P-C and H-E, there is a slight overestimation of steatosis in the HF animals in comparison to frozen sections and ORO; in frozen sections, differences between P-C and I-A are insignificant.

M. Catta-Preta · L. S. Mendonca · J. Fraulob-Aquino · M. B. Aguila · C. A. Mandarim-de-Lacerda (✉)
Laboratory of Morphometry, Metabolism and Cardiovascular Diseases, Biomedical Center, State University of Rio de Janeiro, Av 28 de Setembro 87 fds, 20551-030, Rio de Janeiro, RJ, Brazil
e-mail: mandarim@uerj.br
URL: www.lmmc.uerj.br

Keywords NAFLD · Assessment of steatosis · Semi-quantitative scaling · Point counting · Image analysis · Stereology

Introduction

Non-alcoholic fatty liver disease (or NAFLD) is the most common liver disease in Western countries [1], affecting approximately 30% of the population of the USA and 75–100% of obese and morbidly obese people [2, 3]. Although initial characteristics are benign, NAFLD is the starting point of more serious diseases such as non-alcoholic steatohepatitis (or NASH), liver cirrhosis, and hepatocellular carcinoma [4].

Steatosis can take either of two forms of pathologic anatomy, depending on the size of the lipid vesicles present. These are microvesicular steatosis, where fat is stored in multiple small vesicles, and macrovesicular steatosis, where fat is stored in a single large vesicle. In microvesicular steatosis, hepatocytes appear with a cytoplasm rich in small vesicles with multiple cores [5]. Not much is known about the pathogenesis of microvesicular steatosis, but, in general, it has a worse prognosis than does macrovesicular steatosis [6].

Non-invasive assessment of hepatic steatosis is possible and should be standardized [7]; both T1-weighted dual-echo magnetic resonance (MR) imaging and one-proton MR spectroscopy have excellent diagnostic accuracy as compared to ultrasonography and computed tomography [8]. Still, a liver biopsy is used to establish or confirm the diagnosis of a particular type of liver disease, as well as for staging disease severity. Although a liver biopsy is considered the "gold standard" to assess hepatic steatosis and steatohepatitis, it is not without practical difficulties and controversies [7, 9]. Overall, a biopsy is still very useful because it provides information about the prognosis of the disease its proper clinical management [10, 11].

Semi-quantitative quantification of hepatic steatosis is considered strongly observer-dependent and poorly reproducible [9], and is known to overestimate the values of steatosis in liver biopsies and lead to misdiagnoses [12]. New automatic methods have promising diagnostic and prognostic perspectives [13]. Therefore, current standards of assessment, previously published data, and the clinical relevance of hepatic steatosis as a criteria for liver surgery and transplantation must be challenged [9].

The issue of adequately quantitatively evaluating hepatic steatosis remains unresolved. Therefore, the present study aimed to quantify steatosis and compare two methods of staining and two methods of quantitative assessment. The staining methods used were H-E on paraffin-embedded sections and Oil Red-O on frozen sections. The quantitative evaluations of steatosis used were the "point counting" and computerized "image analysis" methods.

Material and methods

Animal model

All procedures were conducted according to conventional standards for animal testing (Publication No. NIH 85-23, revised 1996). The care of the animals also followed the standards imposed by the State University of Rio de Janeiro and was approved by the local ethics committee.

In this study, two groups of ten C57BL/6 mice at 3 months of age were divided into two groups ($n=10$ for each group). One group was fed standard rodent chow containing 10% fat (standard chow or SC group) according to AIN93M (American Institute of Nutrition recommendation for laboratory rodents) [14]. Another group was fed a diet containing 60% fat (high-fat or HF group), which is a model already tested in our laboratory to induce steatosis [15, 16]. The diets were prepared specifically for this study by Pragsolucoes (www.pragsolucoes.com.br, Jau, SP, Brazil) and were given to the animals for 16 weeks. More information about the composition of the diets is shown in Table 1.

Table 1 Composition of the experimental diets

Content (g/kg)	Diets	
	SC	HF
Casein (≥85% protein)	140.0	190.0
Cornstarch	620.7	250.7
Sucrose	100.0	100.0
Soybean oil	40.0	40.0
Lard	–	320.0
Fiber	50.0	50.0
Vitamin mix[a]	10.0	10.0
Mineral mix[a]	35.0	35.0
L-Cystin	1.8	1.8
Choline	2.5	2.5
Antioxidant	0.008	0.008
Total grams	1,000	1,000
Energy content (kcal/kg)	3,573	5,404
Carbohydrates (%)	76	26
Protein (%)	14	14
Lipids (%)	10	60

HF high-fat diet, *SC* standard chow

[a] Vitamin mix and mineral mix are in accordance with the AIN-93 guidelines

Euthanasia

After 16 weeks of their respective diets, the animals were deeply anesthetized (sodium pentobarbital, 150 mg/kg), and livers were quickly removed and prepared for the different methods.

Determination of hepatic triglycerides

Several fragments of the liver of each animal were frozen at −80°C for biochemical analysis. Hepatic triglyceride levels were measured according to previously published protocol [17]. This determination was then used as a comparison with the results of quantitative histopathology. Briefly, 50 mg of frozen liver tissue was placed in the ultrasonic processor with 1 ml of isopropanol. The homogenate was centrifuged at 2,000×*g* and 5 μl of the supernatant was used with a kit for measuring triglycerides in a semi-automatic biochemical analyzer (K55; Bioclin, Belo Horizonte, MG, Brazil).

Paraplast-embedded material stained with hematoxylin and eosin (H-E)

Some fragments of the liver of each animal were instantly fixed [freshly prepared formaldehyde 4% (wt/vol) in 0.1 M phosphate buffer, pH 7.2] for 48 h at room temperature. Random fragments were dehydrated in graded alcohols of increasing concentration to absolute alcohol and were then cleared in xylene and embedded in Paraplast Plus (Sigma-Aldrich, St. Louis, MO, USA). The material was sectioned at 5 μm and then stained with H-E.

Frozen material stained with Oil Red-O (ORO)

Other fragments of the liver of each animal with volumes of approximately 1 cm^3 were embedded in Tissue-Tek OCT (Finetechnical Sakura, Tokyo, Japan) in aluminum molds, frozen quickly in liquid nitrogen, and stored at −80°C until microtomy. Frozen sections with 10-μm thickness were

obtained in a cryostat (SLEE cryostat SEM, Mainz, Germany), dried at room temperature for 60 min, fixed in 10% formaldehyde for 10 min, and then frozen and again dehydrated for 60 min. Afterward, the sections were placed in 100% propylene glycol for 3 min, stained with a solution of ORO pre-heated for 8 min at 60°C, differentiated in 85% propylene glycol for 3 min, washed in tap water for another 3 min, and mounted with glycerin.

Sampling for evaluation of steatosis

Several non-consecutive sections were obtained from each fragment in both Paraplast-embedded material and frozen material. The intensity of hepatic steatosis was studied in the histological slices as described. Thus, two sets of slices were analyzed: slices stained with H-E (Paraplast-embedded material) and slices stained with ORO (frozen material). Using these slices, two procedures to assess hepatic steatosis were made: point counting (P-C) and image analysis (I-A). With H-E-stained material, it was only possible to use P-C, but both methods were used with slices stained with ORO. For each staining method, at least ten non-consecutive random digital images were obtained per animal (BX51 microscope, ×100 planachromatic objective, DP71 camera; Olympus Co., Tokyo, Japan). The images were taken in TIFF format, at 36-bit depth, and a resolution of 1,280×1,024 pixels.

Evaluation of steatosis by point counting

Digital images were projected on a high-resolution LCD flat-panel monitor (LG Electronics, Seoul, South Korea) (Fig. 1). A test system consisting of 36 test points (P_T) was assembled on the monitor. The volume density of hepatic steatosis (Vv[steatosis, liver]) was then estimated as the ratio of the points hitting the vesicles of fat (Pp) compared to the number of test points [18]: Vv[steatosis, liver]=Pp[steatosis]/P_T. This method was performed with Paraplast-embedded material stained with H-E and with frozen sections stained with ORO.

Evaluation of steatosis by image analysis

Computer-based image analysis used the software Image Pro Plus, version 7.01 for Windows (Media Cybernetics, Silver Springs, MD, USA). The digital images (Figs. 2 and 3) were prepared for the analysis as follows [19]: (a) hepatic tissue was segmented in a pure black and white image, (b) the fat vesicles were selected and assigned to white color, (c) the remaining liver tissue was selected and assigned to black color, and (d) the percentage of area occupied by white color (steatosis) in the whole image was measured using the histogram tool.

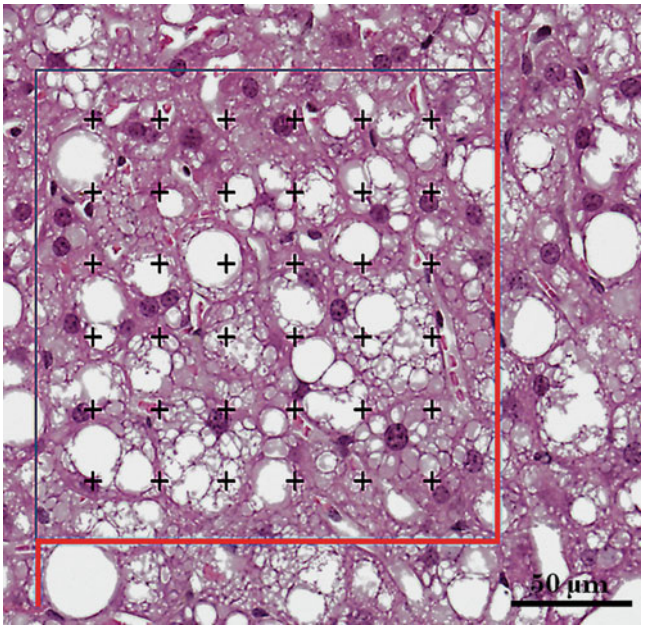

Fig. 1 Photomicrograph of the liver showing abundant macro- and microvesicular steatosis in an animal fed a high-fat diet (digital image of Paraplast-embedded material stained by hematoxylin and eosin). The volume density of steatosis was assessed by point counting after a test system containing 36 test points was superimposed on the photomicrograph (see "Materials and methods" for details)

The reproducibility and variability of the measures

Besides the evaluation made by the authors, other three different observers received basic training to assess the quantifications using the same set of images used by the authors. Therefore, the intra- and inter-observer variability and reproducibility were analyzed.

Data analysis

The normal distribution of the data was tested using the Kolmogorov–Smirnov test, and then the differences between the SC and HF groups were examined with Student's *t* test or among all groups with one-way ANOVA and post hoc Tukey's test. A P value <0.05 was considered statistically significant. In addition, a study of correlation and linear regression was performed, putting hepatic triglyceride levels on the abscissa (X axis) and Vv[steatosis, liver] on the ordinate (Y axis). The first-degree equations of the linear regressions were determined (fitted by the least squares method). The slopes of the equations were then compared (slopes test) (GraphPad Prism version 5.03 for Windows; GraphPad Software, San Diego, CA, USA). The measures obtained by the three additional observers were analyzed for the central tendency and variability. All values are given as mean ± SEM.

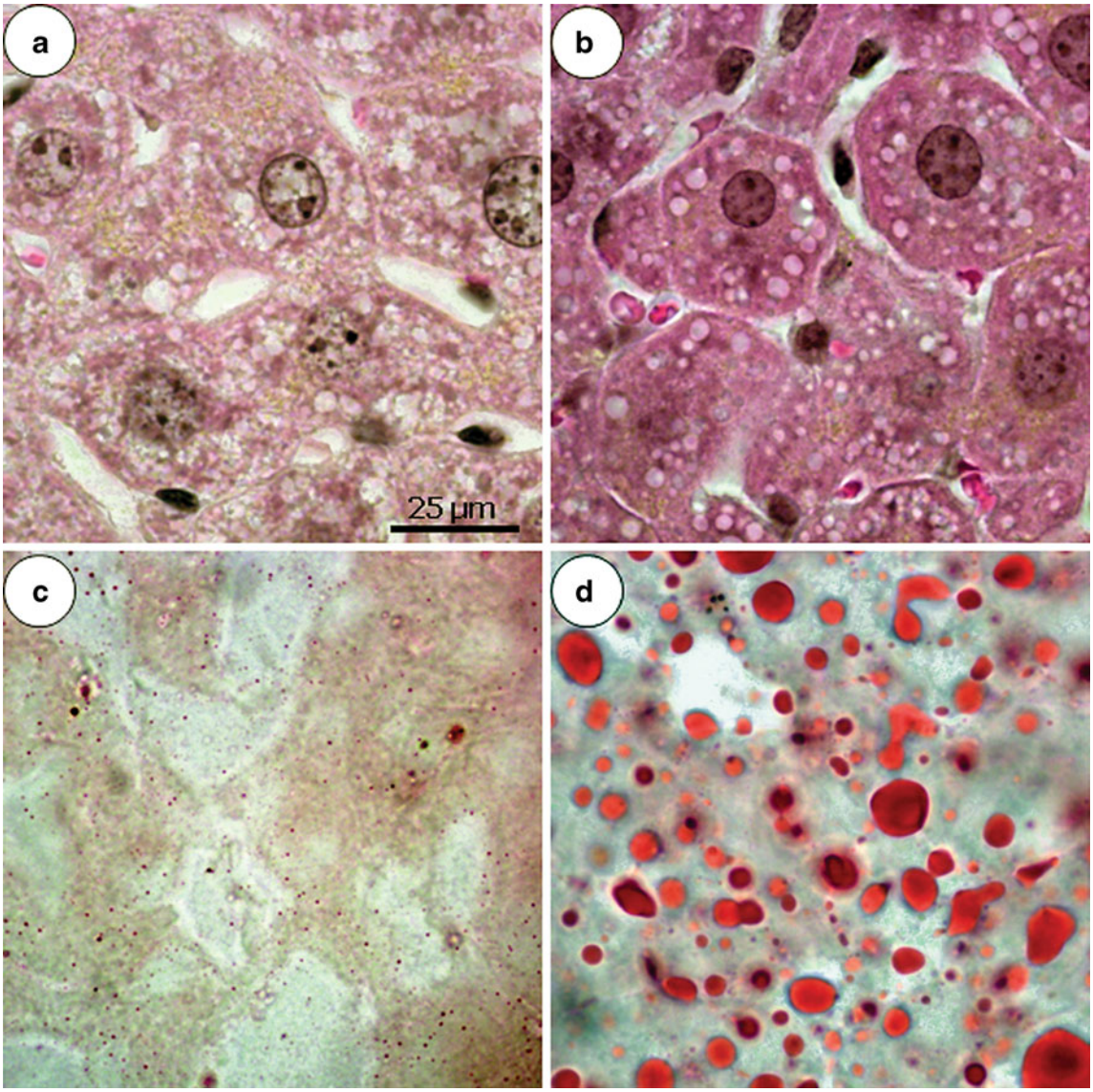

Fig. 2 Photomicrographs of liver sections (same magnification for all sections). Digital images of Paraplast-embedded material stained by hematoxylin and eosin: **a** SC group, **b** HF group. Digital images of frozen sections stained by Oil Red-O: **c** SC group, **d** HF group. Macro- and microvesicular steatosis can easily be identified in the HF group with both embedding and staining methods. However, in Paraplast-embedded material stained by hematoxylin and eosin, we observe that the intra-hepatic spaces were formerly occupied by both fat and glycogen, while in the frozen sections stained by Oil Red-O, the fat itself is stained. *HF* high-fat diet, *SC* standard chow

Results

Hepatic triglycerides

The hepatic triglyceride content was significantly higher in the HF group (104% greater, $P=0.0004$) than in the SC group (Table 2). The photomicrographs of liver tissue from the two groups show this difference clearly (Fig. 2). It was evident that the HF diet induced the formation of much more developed intra-hepatic fat vesicles than those produced by the SC diet.

Paraplast-embedded material stained with H-E

Analysis by point counting

The slides of liver tissue stained by H-E were not difficult to identify as having hepatic steatosis, but we knew beforehand that not all spaces observed correspond to regions previously occupied by fat. The results are shown in Table 2; the Vv[steatosis, liver] was 4.80±0.90% in the SC group and 33.50±3.17% in the HF group (600% greater, $P<0.0001$).

Table 2 Hepatic triglycerides (TG) and volume density of hepatic steatosis (Vv[steatosis, liver]) determined by different methods

Data analysis	Hepatic TG (mg/dl)/mg		Vv[steatosis, liver] %					
			P-C and H-E		P-C and ORO		I-A and ORO	
	SC	HF	SC	HF	SC	HF	SC	HF
Mean	2.78	5.68*	4.80	33.50*	4.86	25.21*, **	4.17	23.35*,**
SD	0.95	1.43	2.86	10.04	2.81	4.03	2.69	4.99
SEM	0.30	0.45	0.90	3.17	0.89	1.27	0.85	1.58
CV %	34	25	60	30	58	16	65	21
CE %	11	8	19	9	18	5	20	7

Significant differences are denoted by a single asterisk, when different from SC counterpart (*t* test, $P<0.05$), or by double asterisks, when different from HF group determined by P-C and H-E method (one-way ANOVA and post hoc Tukey's test, $P<0.05$)

CE coefficient of error, *CV* coefficient of variation, *H-E* hematoxylin and eosin stain, *HF* high-fat group, *I-A* image analysis method, *ORO* Oil Red-O stain, *P-C* point-counting method, *SC* standard chow group, *SD* standard deviation, *SEM* standard error of the mean

Analysis by image analysis

As stated earlier, this method of tissue preparation is not adequate for study by I-A, and so it was not performed.

Frozen material stained with ORO

Analysis by point counting

ORO staining was excellent in terms of both intensity and accuracy for identifying intra-hepatic fat vesicles. This facilitated the use of the P-C method to estimate Vv[steatosis, liver] in both groups. The results are shown in Table 2; Vv [steatosis, liver] was 4.86±0.89% in the SC group and 25.21±1.27% in the HF group (420% greater, $P<0.0001$).

Comparing Vv[steatosis, liver], as evaluated by P-C with the two staining methods, with the H-E stain, no difference was observed in the SC group, but Vv[steatosis, liver] was overestimated by 25% in the HF group in H-E sections in comparison to the ORO sections (Table 2).

Analysis by image analysis

Using the same slices that were studied by P-C, I-A was performed to assess hepatic steatosis in both the SC and HF groups. The ORO stain was essential to this analysis because of its good contrast between fat vesicles and the remaining liver tissue. The results of this analysis are detailed in Table 2; Vv[steatosis, liver] was 4.17±0.85% in the SC group and 23.35±1.58% in the HF group (460% greater, $P<0.0001$).

Using the ORO stain, no significant differences were observed in Vv[steatosis, liver] comparing the P-C and I-A methods across the same group (SC or HF). However, Vv [steatosis, liver] was overestimated by 33% in the HF group using H-E sections evaluated by P-C in comparison to I-A and ORO sections.

Linear regressions: comparison of slopes

Figure 4 shows the linear regression lines obtained for each different method. Each line represents the analysis of data obtained by a staining method and/or its assessment method. No significant difference was found comparing the slopes, and all the correlations were strong and significant. The strongest coefficient of correlation was observed with I-A and ORO ($R=0.95$, $P<0.0001$), followed by P-C and ORO ($R=0.88$, $P=0.0009$) and finally P-C and H-E ($R=0.82$, $P=0.004$).

Intra- and inter-observer variability

The results are shown in Table 3. Considering the three assessments of the Vv[steatosis, liver] obtained by the additional observers, the calculated coefficient of variation (CV) was astonishingly low for the method P-C and H-E, but it was progressively higher for the methods P-C and ORO, and I-A and ORO. In all cases, the HF group had lower CV than SC group for all methods.

Discussion

In this study, we induced hepatic steatosis to compare quantification methods. The separate measurement of hepatic triglycerides was important for characterizing the fatty livers in animals fed the HF diet to compare the observed histopathologic features of steatosis (similar to previous observations using this model) [16, 20, 21]. The HF diet causes obesity and comorbidities such as dyslipi-

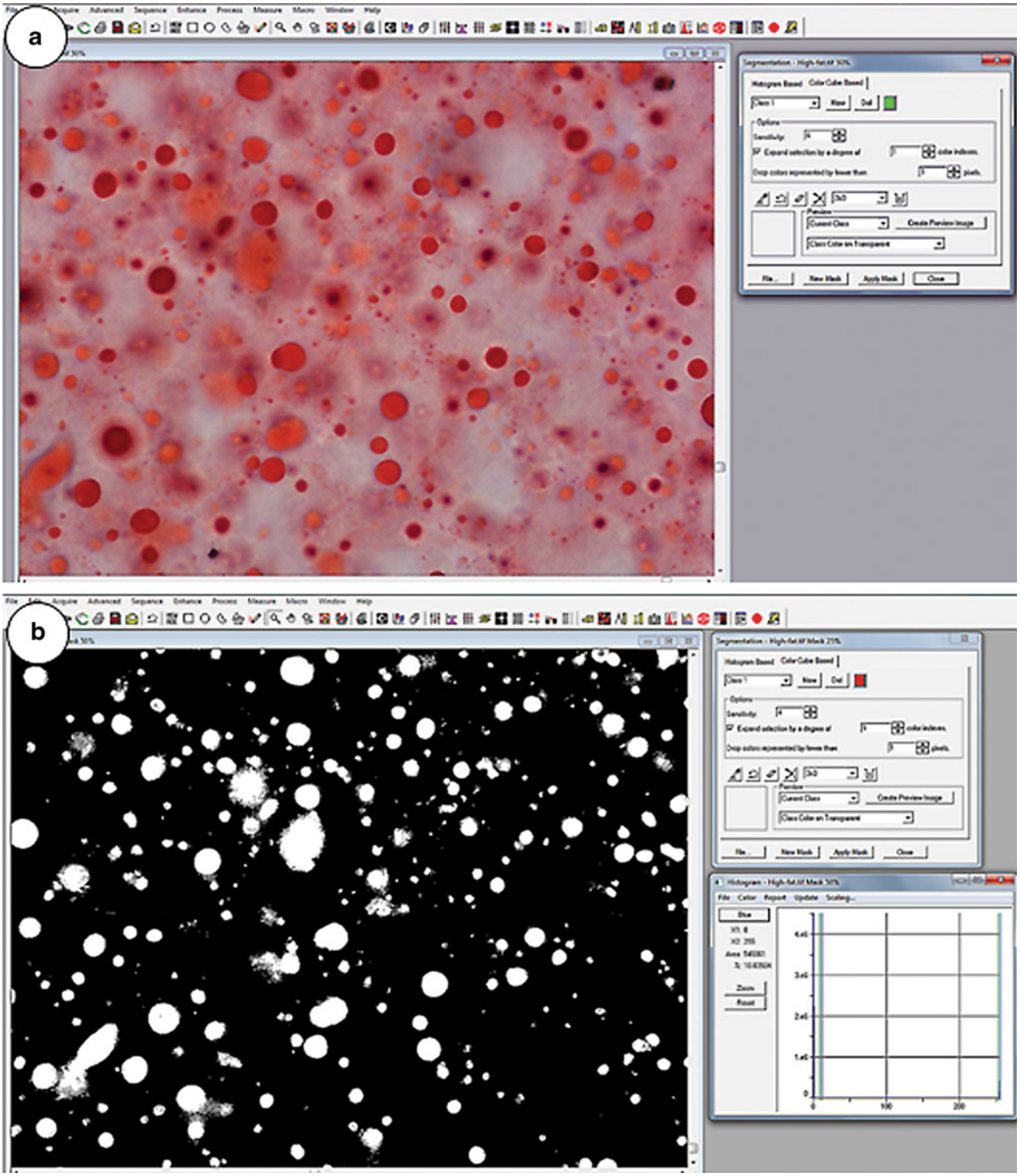

Fig. 3 The two steps of the Image Analysis method to assess hepatic steatosis (digital image of frozen section stained by Oil Red-O): **a** image taken by the software preparing the analysis; **b** after image segmentation (transformation to pure black and white image, white assigned to fat vesicles and black assigned to remaining liver tissue). The relative area fraction of "white" color was determined automatically with the histogram tool (*right bottom corner*)

demia and insulin resistance in C57BL/6 mice, and these animals showed increased liver mass and NAFLD [15]. C57BL/6 mice fed a HF diet also show hypertrophy of adipocytes, as well as hypertrophy of pancreatic islets

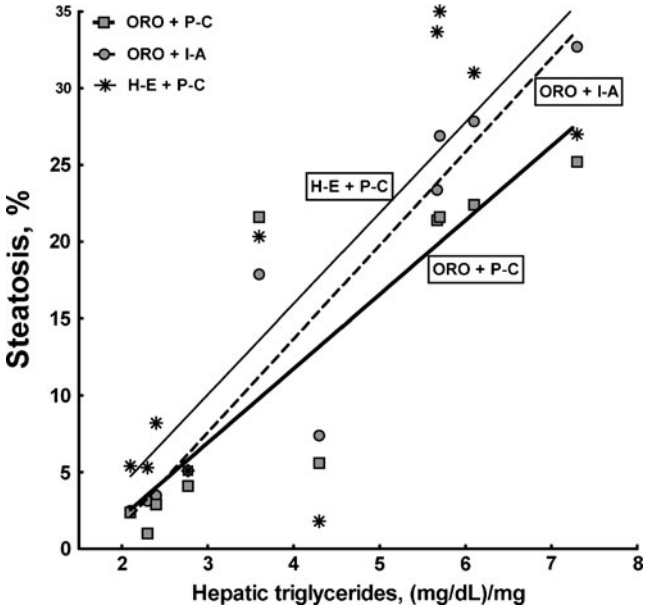

Fig. 4 Graphed linear regressions of the volume density of steatosis (*Y* axis) against hepatic triglycerides levels (*X* axis). No difference among the slopes of the lines was observed (slope test). The coefficients of correlation of these lines were as follows: I-A+ORO (R=0.95, P<0.0001); P-C+ORO (R=0.88, P=0.0009); and P-C+H-E (R=0.82, P=0.004)

concomitant with hyperinsulinemia and increased immunodensity for insulin and glucagon and reduced expression of GLUT-2 in the islets, indicating adverse morphological remodeling and impaired pancreatic tissue function [16].

The staining methods for microscopy in routine liver studies include H-E, trichrome (useful in assessing liver fibrosis), reticulin or its equivalent (for assessment of hepatic architecture), periodic acid-Schiff diastase (to evaluate glycogen, basement membrane, and vessel wall), and staining for iron [22]. One disadvantage of these staining methods is the loss of lipid droplets during processing for paraffin embedding, which, of course, compromises the evaluation of hepatic steatosis. To complicate matters, there are also spaces in the hepatocytes in places once occupied by glycogen. Thus, not all the spaces observed with H-E staining are unequivocally the remains of vesicles of steatosis [23, 24]. It is well understood that there are difficulties in detecting lipid microvesicles after paraffin embedding, and this can cause both an underestimation of the degree of fatty change and a misdiagnosis of "normal" liver that, in fact, contains high levels of microsteatosis [25]. The regular use of special stains such as ORO and Sudan III should be common to stain fat in the liver. However, these methods require frozen sections, which are not made routinely in most laboratories.

Table 3 The variability of the estimation of the volume density of hepatic steatosis (Vv[steatosis, liver]) as determined by three additional observers

Data analysis	Vv[steatosis, liver] %					
	P-C and H-E		P-C and ORO		I-A and ORO	
	SC	HF	SC	HF	SC	HF
Mean	5.0	33.6	3.3	21.3	3.1	22.3
SD	0.2	0.4	0.9	1.6	1.4	5.1
CV %	4.0	1.2	27.3	7.5	45.2	22.9

CV coefficient of variation, *H-E* hematoxylin and eosin stain, *HF* high-fat group, *I-A* image analysis method, *ORO* Oil Red-O stain, *P-C* point-counting method, *SC* standard chow group, *SD* standard deviation

The semi-quantitative evaluation of steatosis is characterized by the use of a subjective scale based on a multigrade proportional area occupied by fat in the hepatocytes or the percentage of hepatocytes in a given biopsy [26]. The histology of the liver is graded according to a number of histological factors, usually by a histopathologist, although there is little consistency in the scale used [26, 27]. Usually the scales have four or five degrees, with different boundaries between grades. For steatosis, a four-grade scale may be zero, mild, moderate, and intense; thus, empirically, we can accept that 0 means no steatosis, 1 is up 33%, 33–66% is between 1 and 2, and 3 is >66% [25]. This grading system is recommended by the American Gastroenterology Association to assess NAFLD [28]. More recently, it was proposed that hepatic steatosis should be evaluated on a five-grade scale: grade 0, no or minimal steatosis (<5%); grade 1, ≥5% but <25%; grade 2, ≥25% but <50%; grade 3, ≥50% but <75%; and grade 4, ≥75% [29].

In 2002, the National Institute of Diabetes and Digestive and Kidney Diseases of the United States sponsored the Pathology Committee of the Network of Clinical Research about NASH (NASH Clinical Research Network) to develop a scoring system for the entire spectrum of NAFLD. The system was developed and validated by nine different pathologists in the group after two double-blind trials of 32 biopsies of adults and 18 pediatric biopsies. In this scoring system, the components of steatosis, lobular inflammation, and hepatocellular ballooning are semi-quantified [30]. It was actually a modification of the existing Brunt scoring system for fibrosis, whereby a score for 1 was changed to include mild fibrosis (1b) and then dense fibrosis or perisinusoidal fibrosis (1c). Scores above 5 in this classification suggest a diagnosis of "steatohepatitis installed", while scores between 0 and 2 carry the diagnosis of "definitely not NASH" [31].

In the recent literature, there has been a demand for a more accurate and reproducible method for estimating hepatic steatosis in biopsies [32, 33]. Whatever the method used (semi-quantitative, P-C, or I-A), the problem arises from the method used to stain liver tissue. Thus, usually,

the evaluation is based on a quantitative "negative" image of fat, i.e., spaces that should have been occupied by fat that was removed during processing of the material.

The method of P-C was classically used to estimate volume densities in a series of studies [34, 35], including for hepatic steatosis [18, 36]. The method of I-A allows measurement of the area of steatosis in liver biopsy material and generates a continuous variable that facilitates statistical analysis [29]. In addition, digital quantification of steatosis can be consistently more precise and reproducible than manual assessment of steatosis in grades 1 (1% to <6%) and 2 (6% to <34%) (semi-quantitative analysis) and may prove to be especially preferable in clinical trials of pharmacotherapeutic agents [37].

Experimental studies have attempted to quantify liver fibrosis based on the number and size of lesions. A proposed scale was (−) not detected, (±) rare, (+) mild, (++) moderate, and (+++) intense [38]. Because increased steatosis has been associated with increased fibrosis, I-A may also be helpful in measuring fibrosis [39], mainly if slices are stained by picrosirius red to enhance the collagen fibers [40, 41]. The I-A is particularly important if we consider that today images are captured by digital cameras and image handling is done entirely within the computer [42].

It is very important to note that the variability of the estimate of Vv[steatosis, liver] was very low with the method "P-C and H-E", which can be an additional advantage of this method. It is natural that the variability is greater in the estimate of Vv[steatosis, liver] when there is no obvious steatosis (which was the case with the SC group). In the HF group (which had marked steatosis), the variability of the estimate of Vv[steatosis, liver] by three observers can be considered acceptable.

In conclusion, the present study compared three methods for assessing hepatic steatosis. All of the methods detected a far greater amount of steatosis in animals fed an HF diet than in animals fed a standard chow. Thus, from that standpoint, all methods were appropriate. In frozen sections stained with ORO, the small differences in the assessment of hepatic steatosis (by P-C or by I-A) were insignificant. In material embedded in Paraplast, stained with H-E, and then analyzed by P-C, there was a slight overestimation of steatosis in HF animals in comparison to frozen sections stained by ORO. Paraplast-embedded material stained by H-E, however, has the advantage of being already in use in the vast majority of routine histopathology laboratories, requiring no special attention. All three methods proved to be reproducible. Therefore, all are better than the subjective semi-quantitative scaling currently used to assess hepatic steatosis.

Acknowledgments The authors thank Thatiany Marinho and Angelica Figueiredo for their technical assistance. This research was supported by the Brazilian agencies CNPq (Conselho Nacional de Ciencia e Tecnologia, www.cnpq.br) and FAPERJ (Fundacao para o Amparo a Pesquisa do Estado do Rio de Janeiro, www.faperj.br).

Conflict of interest The authors declare that they have no conflict interest.

References

1. Erickson SK (2009) Nonalcoholic fatty liver disease. J Lipid Res 50(Suppl):S412–416
2. Browning JD, Szczepaniak LS, Dobbins R, Nuremberg P, Horton JD, Cohen JC, Grundy SM, Hobbs HH (2004) Prevalence of hepatic steatosis in an urban population in the United States: impact of ethnicity. Hepatology 40:1387–1395
3. Farrell GC, Larter CZ (2006) Nonalcoholic fatty liver disease: from steatosis to cirrhosis. Hepatology 43:S99–S112
4. Brunt EM, Tiniakos DG (2010) Histopathology of nonalcoholic fatty liver disease. World J Gastroenterol 16:5286–5296
5. Burt AD, Mutton A, Day CP (1998) Diagnosis and interpretation of steatosis and steatohepatitis. Semin Diagn Pathol 15:246–258
6. Sherlock S (1995) Alcoholic liver disease. Lancet 345:227–229
7. Tannapfel A, Denk H, Dienes H-P, Langner C, Schirmacher P, Trauner M, Flott-Rahmel B (2011) Histopathological diagnosis of non-alcoholic and alcoholic fatty liver disease. Virchows Archiv 458:511–523
8. van Werven JR, Marsman HA, Nederveen AJ, Smits NJ, ten Kate FJ, van Gulik TM, Stoker J (2010) Assessment of hepatic steatosis in patients undergoing liver resection: comparison of US, CT, T1-weighted dual-echo MR imaging, and point-resolved 1H MR spectroscopy. Radiology 256:159–168
9. El-Badry AM, Breitenstein S, Jochum W, Washington K, Paradis V, Rubbia-Brandt L, Puhan MA, Slankamenac K, Graf R, Clavien PA (2009) Assessment of hepatic steatosis by expert pathologists: the end of a gold standard. Ann Surg 250:691–697
10. Adams LA, Angulo P (2007) Role of liver biopsy and serum markers of liver fibrosis in non-alcoholic fatty liver disease. Clin Liver Dis 11:25–35, viii.
11. Contos MJ, Sanyal AJ (2002) The clinicopathologic spectrum and management of nonalcoholic fatty liver disease. Adv Anat Pathol 9:37–51
12. Franzen LE, Ekstedt M, Kechagias S, Bodin L (2005) Semiquantitative evaluation overestimates the degree of steatosis in liver biopsies: a comparison to stereological point counting. Mod Pathol 18:912–916
13. Liquori GE, Calamita G, Cascella D, Mastrodonato M, Portincasa P, Ferri D (2009) An innovative methodology for the automated morphometric and quantitative estimation of liver steatosis. Histol Histopathol 24:49–60
14. Reeves PG, Nielsen FH, Fahey GC Jr (1993) AIN-93 purified diets for laboratory rodents: final report of the American Institute of Nutrition ad hoc writing committee on the reformulation of the AIN-76A rodent diet. J Nutr 123:1939–1951
15. Fraulob JC, Ogg-Diamantino R, Fernandes-Santos C, Aguila MB, Mandarim-de-Lacerda CA (2010) A mouse model of metabolic syndrome: insulin resistance, fatty liver and non-alcoholic fatty pancreas disease (NAFPD) in C57BL/6 mice fed a high fat diet. J Clin Biochem Nutr 46:212–223
16. Souza-Mello V, Gregorio BM, Cardoso-de-Lemos FS, de Carvalho L, Aguila MB, Mandarim-de-Lacerda CA (2010) Comparative effects of telmisartan, sitagliptin and metformin alone or in combination on obesity, insulin resistance, and liver and pancreas remodelling in C57BL/6 mice fed on a very high-fat diet. Clin Sci (Lond) 119:239–250

17. Vieira VJ, Valentine RJ, Wilund KR, Woods JA (2009) Effects of diet and exercise on metabolic disturbances in high-fat diet-fed mice. Cytokine 46:339–345
18. Aguila MB, Pinheiro AR, Parente LB, Mandarim-de-Lacerda CA (2003) Dietary effect of different high-fat diet on rat liver stereology. Liver Int 23:363–370
19. Mandarim-de-Lacerda CA, Fernandes-Santos C, Aguila MB (2010) Image analysis and quantitative morphology. Methods Mol Biol 611:211–225
20. Marques CM, Motta VF, Torres TS, Aguila MB, Mandarim-de-Lacerda CA (2010) Beneficial effects of exercise training (treadmill) on insulin resistance and nonalcoholic fatty liver disease in high-fat fed C57BL/6 mice. Braz J Med Biol Res 43:467–475
21. Nascimento FA, Barbosa-da-Silva S, Fernandes-Santos C, Mandarim-de-Lacerda CA, Aguila MB (2010) Adipose tissue, liver and pancreas structural alterations in C57BL/6 mice fed high-fat-high-sucrose diet supplemented with fish oil (n−3 fatty acid rich oil). Exp Toxicol Pathol 62:17–25
22. Brunt EM (2010) Pathology of nonalcoholic fatty liver disease. Nat Rev Gastroenterol Hepatol 7:195–203
23. Ahishali E, Demir K, Ahishali B, Akyuz F, Pinarbasi B, Poturoglu S, Ibrisim D, Gulluoglu M, Ozdil S, Besisik F, Kaymakoglu S, Boztas G, Cakaloglu Y, Mungan Z, Canberk Y, Okten A (2010) Electron microscopic findings in non-alcoholic fatty liver disease: is there a difference between hepatosteatosis and steatohepatitis? J Gastroenterol Hepatol 25:619–626
24. Straub BK, Schirmacher P (2010) Pathology and biopsy assessment of non-alcoholic fatty liver disease. Dig Dis 28:197–202
25. Garcia Urena MA, Colina Ruiz-Delgado F, Moreno Gonzalez E, Jimenez Romero C, Garcia Garcia I, Loinzaz Segurola C, Gonzalez P, Gomez Sanz R (1998) Hepatic steatosis in liver transplant donors: common feature of donor population? World J Surg 22:837–844
26. Brunt EM, Janney CG, Di Bisceglie AM, Neuschwander-Tetri BA, Bacon BR (1999) Nonalcoholic steatohepatitis: a proposal for grading and staging the histological lesions. Am J Gastroenterol 94:2467–2474
27. Turlin B, Mendler MH, Moirand R, Guyader D, Guillygomarc'h A, Deugnier Y (2001) Histologic features of the liver in insulin resistance-associated iron overload. A study of 139 patients. Am J Clin Pathol 116:263–270
28. Sanyal AJ (2002) AGA technical review on nonalcoholic fatty liver disease. Gastroenterology 123:1705–1725
29. Turlin B, Ramm GA, Purdie DM, Laine F, Perrin M, Deugnier Y, Macdonald GA (2009) Assessment of hepatic steatosis: comparison of quantitative and semiquantitative methods in 108 liver biopsies. Liver Int 29:530–535
30. Kleiner DE, Brunt EM, Van Natta M, Behling C, Contos MJ, Cummings OW, Ferrell LD, Liu YC, Torbenson MS, Unalp-Arida A, Yeh M, McCullough AJ, Sanyal AJ (2005) Design and validation of a histological scoring system for nonalcoholic fatty liver disease. Hepatology 41:1313–1321
31. Wieckowska A, Feldstein AE (2008) Diagnosis of nonalcoholic fatty liver disease: invasive versus noninvasive. Semin Liver Dis 28:386–395
32. Lee JH, Kim D, Kim HJ, Lee CH, Yang JI, Kim W, Kim YJ, Yoon JH, Cho SH, Sung MW, Lee HS (2010) Hepatic steatosis index: a simple screening tool reflecting nonalcoholic fatty liver disease. Dig Liver Dis 42:503–508
33. Lee SS, Park SH, Kim HJ, Kim SY, Kim MY, Kim DY, Suh DJ, Kim KM, Bae MH, Lee JY, Lee SG, Yu ES (2010) Non-invasive assessment of hepatic steatosis: prospective comparison of the accuracy of imaging examinations. J Hepatol 52:579–585
34. Cruz-Orive LM, Weibel ER (1990) Recent stereological methods for cell biology: a brief survey. Am J Physiol 258:L148–156
35. Weibel ER (1989) Measuring through the microscope: development and evolution of stereological methods. J Microsc 155:393–403
36. Souza-Mello V, Mandarim-de-Lacerda CA, Aguila MB (2007) Hepatic structural alteration in adult programmed offspring (severe maternal protein restriction) is aggravated by post-weaning high-fat diet. Br J Nutr 98:1159–1169
37. Rawlins SR, El-Zammar O, Zinkievich JM, Newman N, Levine RA (2010) Digital quantification is more precise than traditional semiquantitation of hepatic steatosis: correlation with fibrosis in 220 treatment-naive patients with chronic hepatitis C. Dig Dis Sci 55:2049–2057
38. Nakano S, Nagasawa T, Ijiro T, Inada Y, Tamura T, Maruyama K, Kuroda J, Yamazaki Y, Kusama H, Shibata N (2008) Bezafibrate prevents hepatic stellate cell activation and fibrogenesis in a murine steatohepatitis model, and suppresses fibrogenic response induced by transforming growth factor-beta1 in a cultured stellate cell line. Hepatol Res 38:1026–1039
39. Neves RH, de Barros M, Alencar AC, Costa-Silva M, Aguila MB, Mandarim-de-Lacerda CA, Machado-Silva JR, Gomes DC (2007) Long-term feeding a high-fat diet causes histological and parasitological effects on murine schistosomiasis mansoni outcome. Exp Parasitol 115:324–332
40. DeLeve LD, Wang X, Kanel GC, Atkinson RD, McCuskey RS (2008) Prevention of hepatic fibrosis in a murine model of metabolic syndrome with nonalcoholic steatohepatitis. Am J Pathol 173:993–1001
41. Neves RH, Alencar AC, Aguila MB, Mandarim-de-Lacerda CA, Machado-Silva JR, Gomes DC (2007) Light and confocal microscopic observations of adult *Schistosoma mansoni* from mice fed on a high-fat diet. J Helminthol 81:361–368
42. Tschanz SA, Burri PH, Weibel ER (2011) A simple tool for stereological assessment of digital images: the STEPanizer. J Microsc 243(Pt 1):47–59

Virchows Arch (2011) 459:487–493
DOI 10.1007/s00428-011-1158-y

ORIGINAL ARTICLE

Molecular morphometric analysis shows relative intra-tumoural homogeneity for KRAS mutations in colorectal cancer

Liora Farber · Edna Efrati · Hela Elkin · Yehudit Peerless · Edmond Sabo · Ofer Ben-Izhak · Dov Hershkovitz

Received: 18 July 2011 / Accepted: 11 October 2011 / Published online: 21 October 2011
© Springer-Verlag 2011

Abstract KRAS mutation status has a significant role determining anti-epidermal growth factor receptor (anti-EGFR) treatment response in colon carcinoma patients. Malignant transformation is a dynamic process and therefore, it is conceivable that, at a certain point, the tumor cells' mass might be heterogeneous for particular mutations. Therefore, the fraction of tumor cells carrying a particular mutation may be more relevant for treatment than the simple determination of presence or absence of mutation. The purpose of this study is to assess whether or not KRAS mutation status is heterogeneous and, if so, to what extent in colon carcinoma samples. Deoxyribonucleic acid was extracted from formalin-fixed paraffin-embedded samples of colon carcinoma and analyzed for the presence of KRAS mutation. The relative fraction of mutated versus wild-type KRAS alleles was evaluated by real-time polymerase chain reaction. Additionally, the relative fraction of cancer cells in the tissue sample was evaluated using computer assisted morphometric analysis. Using this data, we calculated the fraction of mutation containing cells in the samples. Colon carcinoma (169 cases) were analyzed, and a KRAS mutation was found in 75 cases (44%), of which 42 were available for morphometric analysis. In 41 (97.6%) of these cases, the fraction of mutation containing tumor cells was 50% or higher, indicating the absence of significant KRAS mutation status heterogeneity. There was a strong positive correlation (R=0.66, P<0.0001) between the fraction of mutated KRAS alleles and the fraction of cancer cells in the samples. The strong positive correlation between the fraction of mutated KRAS alleles and the fraction of cancer cells in the samples indicate homogeneity of KRAS mutation status in colorectal carcinoma.

Keywords Colon carcinoma · KRAS · Intra-tumor heterogeneity · Morphometry

Farber and Efrati contributed equally to the project.

L. Farber · Y. Peerless · E. Sabo · O. Ben-Izhak · D. Hershkovitz (✉)
Institute of Pathology, Rambam Health Care Campus,
PO Box 9602, Haifa 31096, Israel
e-mail: d_hershkovitz@rambam.health.gov.il

L. Farber · Y. Peerless · O. Ben-Izhak · D. Hershkovitz
B. Rappaport Faculty of Medicine,
Technion-Israel Institute of Technology,
Haifa, Israel

E. Efrati · H. Elkin
Center for Translational Genetics,
B. Rappaport Institute for Research in the Medical Sciences,
Technion-Israel Institute of Technology,
Rambam Health Care Campus,
Haifa, Israel

E. Sabo
Legacy Heritage Clinical Research Institute,
Rambam Health Care Campus,
Haifa, Israel

Introduction

Colon carcinoma is a common malignancy with important implications for population morbidity and mortality. Colorectal cancer (CRC) is the third leading cause of cancer-related death in the Western world. Incidence rates, however, have been decreasing over the past 20 years, thanks to screening and polyp removal.

The current view held is that the majority of sporadic colorectal carcinomas originate from adenomas, through distinct histological steps characterized by increasing dyspla-

sia. Cancer development is a multistep process in which cells continuously gain deoxyribonucleic acid (DNA) aberrations. An aberration that gives the cell a survival or a growth advantage will eventually be present in a large proportion of the tumor cells. Given the dynamic nature of malignancy, it is biologically plausible that a certain moment the tumor cells will be heterogeneous for some of the aberrations gained.

The pathogenesis of colon adenocarcinoma occurs via the adenoma–carcinoma sequence. Inactivation of the adenomatous polyposis coli (APC) tumor suppressor gene occurs early on, followed by mutations of the KRAS oncogene, and later on mutations and deletions of the p53 and deleted in colorectal carcinoma (DCC) tumor suppressor genes [1]. The RAS mutation has been the focus of interest in many studies [2]. The current view is that KRAS mutation has more of a role in the initiation of tumors than in progression [3]. RAS mutation is present in only one third of colorectal carcinomas [4]. In contrast, the incidence of KRAS mutations in adenomas is reported to be up to 85% [3]. This finding also indicates the dynamic genetic nature of tumor progression.

Recent efforts for cancer treatment have focused on the development of pathway-specific medications that are directed against specific genetic alterations in the cancer cell. Anti-epidermal growth factor receptor (anti-EGFR) antibodies comprise one such pathway-specific treatment and were shown to be effective for colon carcinoma [5]. The benefit is restricted to colon carcinoma with a wild-type KRAS gene [6]. Current treatment guidelines dictate that only patients with colon carcinoma harboring wild-type KRAS will be eligible for anti-EGFR treatment [7].

Various testing modalities for KRAS mutation have been developed, direct sequence analysis and real-time polymerase chain reaction (PCR) being two common methods [8]. More than 98% of all KRAS mutations in CRC are point mutations located in adjacent codons 12 and 13. Real-time PCR based methods have a high sensitivity and the ability to identify a mutation present in less than 1% of the cells sampled [9]. This sensitivity might be of clinical relevance since, in some cases, the tissue sampled for KRAS mutation contains a small fraction of malignant cells and a large fraction of stromal and inflammatory cells. However, this increased sensitivity might pose a problem when the tumor tissue is heterogeneous with regard to KRAS mutation status. For example, a patient harboring KRAS mutation in 5% of his tumor tissue would screen positive in these sensitive tests and would therefore not be eligible for anti-EGFR treatment, even though 95% of the tumor cells might be affected by this treatment. Given the increasing evidence for intra-tumor heterogeneity, we wanted to examine the extent of this phenomenon for the KRAS gene in colon cancer.

Methods

Research population and DNA extraction

The research was conducted on DNA samples extracted from archived formalin-fixed paraffin-embedded (FFPE) tissue samples of colon carcinoma. The study was approved by the local ethics committee. An area comprised of at least 70% tumor tissue was microscopically dissected, and DNA was extracted using the QuickExtract FFPE DNA extraction kit (Epicenter, Madison, WI, USA) according to manufacturer instruction. Following treatment with RNase A (Qiagen, Hilden, Germany), DNA was purified using the DNA clean and concentrator kit (Zymo Research, Orange, CA, USA). Patients' DNA samples were evaluated for the presence of *KRAS* mutations using locked nucleic acid (LNA)-based PCR clamping method as previously described [10]. This method can detect KRAS mutations present in as little as 1% of the sample. Samples that were positive for KRAS mutation were further evaluated using quantitative real-time PCR and morphometric analysis as detailed below (Fig. 1).

Quantitative real-time PCR

To determine the fraction of mutated KRAS in the tissue sample, we designed primers specific for each of the mutations identified in KRAS as well as for the wild-type sequence (Table 1). DNA extracted from the FFPE samples was PCR-amplified using the SYBR Green JumpStart Taq ReadyMix (Sigma, St. Louis, MO, USA) on a Rotor-Gene 6000 thermocycler (Corbett Research, Sydney, Australia) using a primer pair specific for the mutation in the sample, as well as a primer pair for the corresponding wild-type sequence. Reaction conditions were 95° for 15 min, followed by 40 cycles of 95° for 10 s, 60° for 15 s, and 72° for 20 s. Each sample was analyzed in duplicate. For quantification, standard curves were obtained using serially diluted DNA amplified in the same real-time PCR run. The samples were then evaluated for the relative fraction of mutated KRAS versus wild-type copies, and F-mutation was calculated (Fig. 1). F-mutation is the fraction of cells in the sample that carry KRAS mutation. To calculate F-mutation we used the formula 2×mutated DNA/(mutated +wild-type DNA). In the numerator, the value of mutated DNA is amplified by 2 because a KRAS mutation occurs as a rule in only one of the two alleles.

Quantitaive image analysis

In order to establish the proportion of tumor versus nontumor cells, histological slides retrieved from the archives of the pathology department were immunohistochemically stained with anti-cytokeratin antibody (Lab Vision, Fremont, CA,

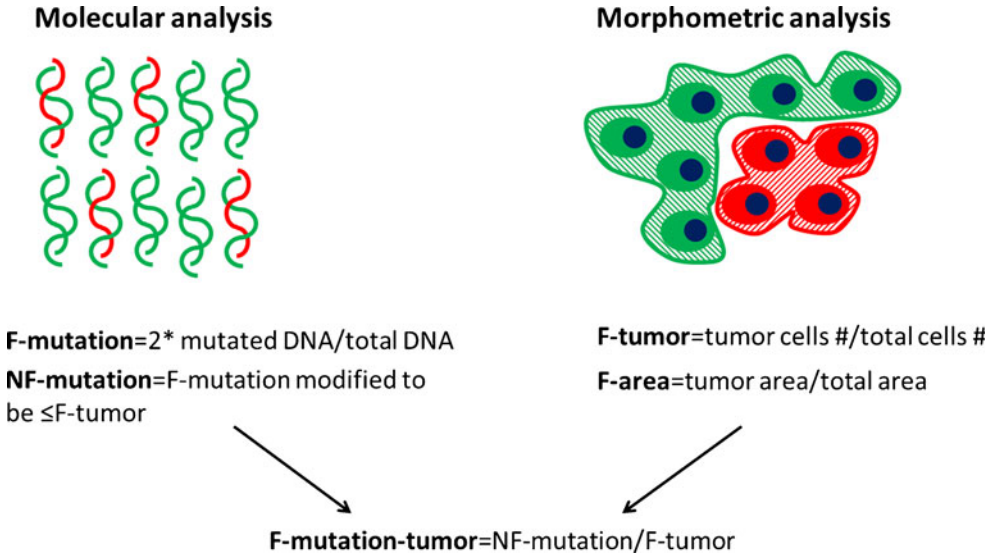

Fig. 1 Molecular analysis and morphometric analysis method. For the morphometric analysis, we measured the number and area of tumor cells (*red*) as well as the number and area of nontumor cells (*green*). In the example presented in the figure, the fraction of tumor cells (F-tumor) would be 40% (four out of ten cells). The area fraction of tumor cells (*F-area*) would be the *red-striped area* divided by the total striped area (*red* and *green*). For the molecular analysis we determined the relative amount of WT (*green*) and mutated (*red*) copies of KRAS as detailed in the text. The figure presents an example of analysis on ten cells, four of which contain a heterozygous mutation in KRAS. Using real-time PCR, we found that the amount of mutated DNA is 4 and the amount of WT DNA is 16. We then used the formula presented to calculate the fraction of mutation containing cells (F-mutation). In the example presented: 2×4/(4+16)=40%, indicating that the mutation is present in 40% of the cells. We then normalized F-mutation (NF-mutation) to be smaller or equal to F-tumor (F-mutation cannot be higher than F-tumor since non-tumor cells are not expected to harbor KRAS mutation). NF-mutation was used to calculate the fraction of tumor cells that contain a mutation (F-mutation tumor). In the example presented in the figure, 40%/40%=1, or, in other words, all the tumor cells in the samples contain KRAS mutation

USA), thus enhancing the observer's ability to visually separate between tumor cells and nontumor elements (such as stroma, vessels, and inflammation). For area measurements, stained slides were entirely scanned at a magnification of × 20 using the dotSlide 2.0 virtual microscopy system (Olympus, Germany and Japan). The digital virtual images were then loaded in an image analysis system (Image Pro Plus 6.3, MediaCybernetics, Massachusetts, USA). The total area of the tumor was segmented from other elements (stroma, lymphatic aggregates, and normal colonic crypts) and measured. For cell number counts, representative images of the tumor and other tissue elements were further captured at a magnification of × 400, and cells were counted using the Image Pro Plus program (Fig. 2). The total number of cells within each tissue element (tumor, stroma, lymphocytes, normal) was then calculated by using a mathematical extrapolation. This information was used to calculate variables F-tumor and F-area (Fig. 1).

Table 1 Primers used for quantitative real-time PCR

Primer name	Primer sequence
KRAS F	5′-GCCTGCTGAAAATGACTGAA-3′
KRAS R c.35G>C	5′-CACTCTTGCCTACGCCAG-3′
KRAS R c.35G>A	5′-CACTCTTGCCTACGCCAT-3′
KRAS R c.35G>T	5′-CACTCTTGCCTACGCCAA-3′
KRAS R c.35G>G (WT)	5′-CACTCTTGCCTACGCCAC-3′
KRAS R c.38G>A	5′-AGGCACTCTTGCCTACGT-3′
KRAS R c.38G>G (WT)	5′-AGGCACTCTTGCCTACGC-3′
KRAS R c.34G>C	5′-ACTCTTGCCTACGCCACG-3′
KRAS R c.34G>A	5′-ACTCTTGCCTACGCCACT-3′
KRAS R c.34G>T	5′-ACTCTTGCCTACGCCACA-3′
KRAS R c.34G>G (WT)	5′-ACTCTTGCCTACGCCACC-3′

Statistical methods

In order to assure a statistical power of 90% for identification of a phenotype (KRAS mutation status heterogeneity) that is present in 5% of the population, we needed a sample size of at least 32 cases with KRAS mutation. Our sample size corresponds to this requirement. The data was tested for normality using the Kolmogorov–Smirnov test. Correlation between the variables was evaluated using the Pearson's coefficient of correlation. The least squares error method was used to build a linear regression function for the relationship between the tumor area fraction and the number of tumor cells. Two-tailed *P*-values of 0.05 or less were considered to be statistically significant.

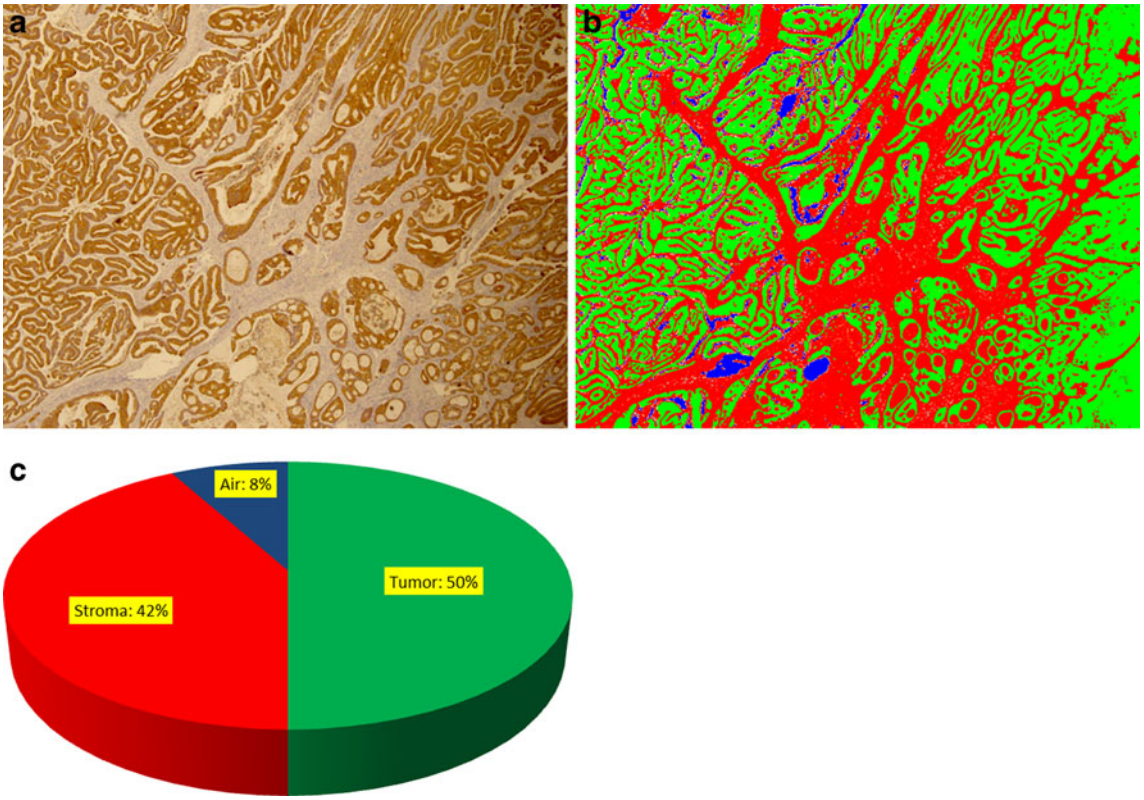

Fig. 2 Image captured of CRC sample at ×400 (**a**), Quantification of various tissue types with color labeling (**b**), Relative fractions of tumor, stroma, and air in the particular sample (**c**)

Results

Using LNA-based PCR clamping assay, DNA extracted from 169 samples of colon carcinoma was scrutinized for the presence of KRAS mutation, and 75 positive cases were identified. Of these, 42 cases were available for morphometric analysis and were analyzed for F-mutation, F-area, and F-tumor. The mean F-area was 45.46±15.18%. The range of F-area was 12.21–80.60%. The mean F-tumor was 50.65±18.06%. The range for F-tumor was 16.85–86.83%.

Real-time PCR was used to quantify KRAS mutation in the samples. In some cases, F-mutation was larger than F-tumor. In these cases, normalization was established in which F-tumor was assigned as the value for F-mutation (meaning that 100% of the tumor cells carry a mutation). This is because it is not possible for the fraction of KRAS-mutated cells (F-mutation) to exceed the fraction of tumor cells, as normal cells do not harbor KRAS mutations. For the normalized F-mutation (NF-mutation), the mean percentage of mutated DNA was 48.34±18.5% and the range was 5.05–86.83%.

The fraction of mutation-carrying tumor cells (F-mutation tumor) was defined as NF-mutation divided by F-tumor. The mean value for F-mutation tumor was 93.76± 13.90%, and the range was 29.97–100%. Of the 42 cases analyzed, the calculated fraction of mutation containing tumor cells (F-mutation tumor) was 100% or more in 27 (64.3%) cases, 50–100% in 14 (33.3%), cases and less than 50% in a single case (2.4%). This indicates that, in the vast majority of the tumors, there is no considerable heterogeneity of KRAS mutation.

There was a strong positive correlation (R=0.66, P<0.0001) between the NF-mutation and F-area (Fig. 3). F-area and F-tumor also demonstrate a strong positive correlation (R=0.78, P<0.0001; Fig. 4). Linear regression analysis was performed

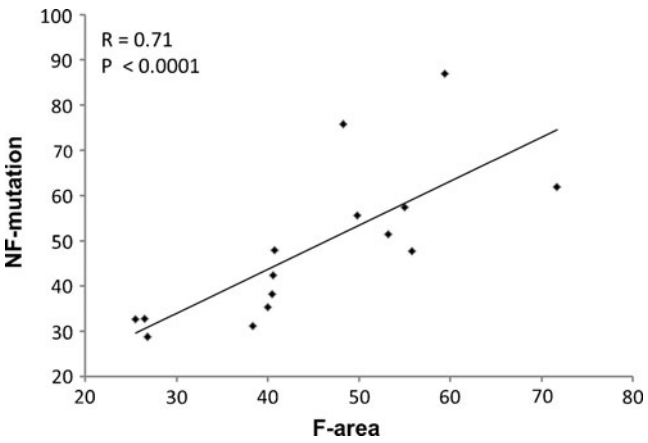

Fig. 3 Positive correlation between NF-mutation and F-area

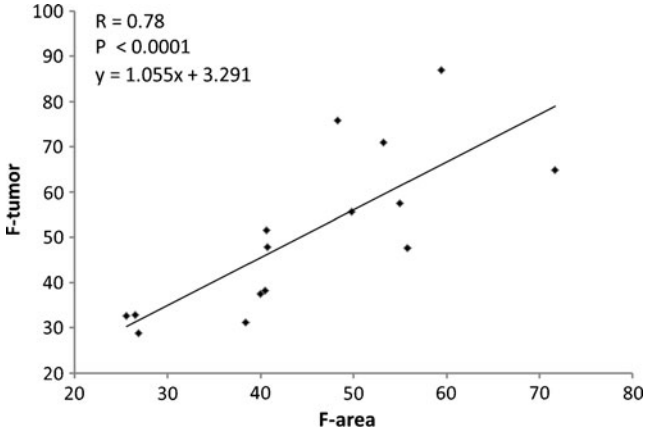

Fig. 4 Positive correlation between F-tumor and F-area

in order to obtain a predictive formula of F-tumor as a function of F-area.

Discussion

The purpose of the present study was to find out whether a KRAS mutation might be present in a minority of tumor cells within a tumor tissue samples. Our findings, including the strongly positive correlation between the NF-mutation and F-area indicates that this is not the case in colon carcinoma. This is consistent with conclusions drawn from other studies. KRAS mutation is an early event in colorectal carcinoma, which is supported by its tendency to be carried by the majority of tumor cells in a tumor tissue sample. By the time cancer is diagnosed, the mutation occurs in the majority of the tumor cells.

The concordance between KRAS mutation in a primary colorectal carcinoma and its corresponding KRAS-mutated metastasis is additional evidence of KRAS mutation homogeneity in CRC. The first adequately powered study on the subject-analyzed KRAS mutations in 305 paired samples of colorectal carcinomas and liver metastases. Of the primary tumors, 108 had KRAS mutation, and, overall, there was 96.4% concordance between these primary lesions and their KRAS-mutated metastases [11]. Similarly, Cejas et al. [12] compared KRAS mutation status in primary CRC tumors and their corresponding metastases in liver and lung. Of the 110 patients in the study, KRAS mutation was found in 37 of the primary tumors and 40 of the matching metastases, yielding a concordance rate of 94%. Interestingly, a higher percentage of KRAS mutation was found in primary tumors of patients with lung metastases, as compared with patients that had liver metastases. With a somewhat smaller sample size, Mariani et al. [13] achieved similar findings. Of 38 patients with primary CRC tumors and matched metastases, 20 patients had KRAS mutation in the primary lesion and corresponding metastasis, yielding a concordance rate of 97%.

However, there are some studies of which the results differ from those aforementioned, which might suggest heterogeneity in KRAS mutation status of colorectal carcinomas. Park et al. [14] studied various biomarkers in 75 metastatic CRC patients. Of these patients, 19 (27.5%) had KRAS mutation, but concordance between their primary tumors and metastases was only 76%. This outcome contrasts with those from many other studies and can be attributed to the small number of paired primary and metastatic site tissue samples available in this study. Another possible factor in these discrepant results is population ethnicity. This particular study utilized an Asian population, and there is not much data regarding KRAS mutation rates in this group.

An interesting case study from 2010 proposes that discordance of KRAS mutation in a primary tumor and its metastasis can result from a later switch in mutation status. In this case study, a patient with colon carcinoma and liver metastases initially responded to cetuximab but then relapsed and became resistant to treatment. KRAS mutation was not detected in the primary tumor or synchronous liver metastases, but later, two different KRAS mutations were detected in metachronous liver metastasis samples [15]. Therefore, the presence of discrepancy in KRAS mutation status between primary tumor and metastasis is consistent with, but does not necessarily indicate, heterogeneity in the primary tumor.

Discrepancy in KRAS mutation status has also been studied in primary and metastatic lung carcinoma. Cortot et al. [16] looked at 21 patients with primary nonsmall-cell lung cancer and distant metastases. Using sensitive methods, they showed concordance between primary lesion and metastasis in only three out of six patients. In a different study on KRAS mutation in primary and metastatic lung carcinoma, Monaco et al. [17] found concordance in 2 out of 11 cases, a rate of 18%. It is important to note the small sample sizes in these two studies. However, since KRAS mutation occurs later in the multistep carcinogenesis of lung carcinoma, it may be that the implications of these results are not fully applicable to KRAS in colon carcinoma, where KRAS mutation is an early event.

A recent study by Goranova et al. used a multipoint microsampling method to evaluate intratumor genetic heterogeneity in colon carcinoma [18]. Primary tumors (42) were analyzed with multipoint microsampling for subpopulations with regard to mutations in APC, TP53, and KRAS. In most of the cases, there was more than one subpopulation in each primary tumor. However, consistent with our findings, in most cases with KRAS mutation, it

was present in more than 50% of the areas sampled, and only one case showed the presence of KRAS mutation in less than 50% of the areas sampled. We believe that despite the finding of some intratumor heterogeneity in most of the samples, clinical decisions should be based on the genetic characteristics of most of the tumor cells and not some minor subpopulations. As demonstrated in our study, in colon carcinoma when KRAS mutation is present, the mutation is shared by the vast majority of the tumor cells in the sample.

This study also proposes a simple and objective method for the evaluation of tumor cell fraction in the sample. This information is important since different KRAS mutation detection methods have different analytical sensitivities, and the choice of a suitable testing modality should be based on the results of histological examination of fraction of tumor cells. Interestingly, there is considerable variability between different testing centers in the evaluation of tumor cell fraction [19]. In the present study, we described two different methods for the evaluation of tumor cell fraction. The first one is more time-consuming and involves counting the number of tumor cells in relation to the number of stromal and other cells in the sample. The other method can be carried out by calculation of the area of the tumor and nontumor tissue. This second method would be quicker, easier to perform, and it strongly correlated with the first method of computing the fraction of tumor cell number. Moreover, the linear regression statistical procedure allowed us to build a formula that allows one to predict the fraction of tumor cell numbers, using the tumor area, assessed by computerized image analysis. In other words, this statistical linear relationship between F-area and F-tumor can be utilized to calculate the value of the F-tumor, based on the more easily measured F-area. Additionally, the fraction of tumor area correlated with the genetic data from the samples, suggesting that measuring of tumor area might be a valid method for determining tumor fraction in the samples. This method should be considered as a standardized method for the evaluation of tumor cell fraction.

In conclusion, in our sample set, we did not find any significant intratumor heterogeneity for KRAS mutation. We propose the routine use of computerized image analysis as a standardized method for accurately establishing the fraction of tumor cells when assessing KRAS mutation status in colonic carcinoma samples.

References

1. Leslie A, Carey FA, Pratt NR, Steele RJ (2002) The colorectal adenoma–carcinoma sequence. Br J Surg 89(7):845–860
2. Bos JL (1989) Ras oncogenes in human cancer: a review. Cancer Res 49(17):4682–4689
3. Giaretti W, Rapallo A, Sciutto A, Macciocu B, Geido E, Hermsen MA, Postma C, Baak JP, Williams RA, Meijer GA (2000) Intratumor heterogeneity of k-ras and p53 mutations among human colorectal adenomas containing early cancer. Anal Cell Pathol 21(2):49–57
4. Al-Mulla F, Going JJ, Sowden ET, Winter A, Pickford IR, Birnie GD (1998) Heterogeneity of mutant versus wild-type Ki-ras in primary and metastatic colorectal carcinomas, and association of codon-12 valine with early mortality. J Pathol 185(2):130–138
5. Cunningham D, Humblet Y, Siena S, Khayat D, Bleiberg H, Santoro A, Bets D, Mueser M, Harstrick A, Verslype C, Chau I, Van Cutsem E (2004) Cetuximab monotherapy and cetuximab plus irinotecan in irinotecan-refractory metastatic colorectal cancer. N Engl J Med 351(4):337–345
6. Karapetis CS, Khambata-Ford S, Jonker DJ, O'Callaghan CJ, Tu D, Tebbutt NC, Simes RJ, Chalchal H, Shapiro JD, Robitaille S, Price TJ, Shepherd L, Au HJ, Langer C, Moore MJ, Zalcberg JR (2008) K-ras mutations and benefit from cetuximab in advanced colorectal cancer. N Engl J Med 359 (17):1757–1765
7. Allegra CJ, Jessup JM, Somerfield MR, Hamilton SR, Hammond EH, Hayes DF, McAllister PK, Morton RF, Schilsky RL (2009) American society of clinical oncology provisional clinical opinion: testing for KRAS gene mutations in patients with metastatic colorectal carcinoma to predict response to anti-epidermal growth factor receptor monoclonal antibody therapy. J Clin Oncol 27 (12):2091–2096
8. Wang HL, Lopategui J, Amin MB, Patterson SD (2010) KRAS mutation testing in human cancers: the pathologist's role in the era of personalized medicine. Adv Anat Pathol 17(1):23–32
9. Kotoula V, Charalambous E, Biesmans B, Malousi A, Vrettou E, Fountzilas G, Karkavelas G (2009) Targeted KRAS mutation assessment on patient tumor histologic material in real time diagnostics. PLoS One 4(11):e7746
10. Efrati E, Elkin H, Peerless Y, Sabo E, Ben-Izhak O, Hershkovitz D (2010) LNA-based PCR clamping enrichment assay for the identification of KRAS mutations. Cancer Biomark 8(2):89–94
11. Knijn N, Mekenkamp LJ, Klomp M, Vink-Borger ME, Tol J, Teerenstra S, Meijer JW, Tebar M, Riemersma S, van Krieken JH, Punt CJ, Nagtegaal ID (2011) KRAS mutation analysis: a comparison between primary tumours and matched liver metastases in 305 colorectal cancer patients. Br J Cancer 104(6):1020–1026
12. Cejas P, Lopez-Gomez M, Aguayo C, Madero R, de Castro Carpeno J, Belda-Iniesta C, Barriuso J, Moreno Garcia V, Larrauri J, Lopez R, Casado E, Gonzalez-Baron M, Feliu J (2009) KRAS mutations in primary colorectal cancer tumors and related metastases: a potential role in prediction of lung metastasis. PLoS One 4(12):e8199
13. Mariani P, Lae M, Degeorges A, Cacheux W, Lappartient E, Margogne A, Pierga JY, Girre V, Mignot L, Falcou MC, Salmon RJ, Delattre O, De Cremoux P (2010) Concordant analysis of KRAS status in primary colon carcinoma and matched metastasis. Anticancer Res 30(10):4229–4235
14. Park JH, Han SW, Oh DY, Im SA, Jeong SY, Park KJ, Kim TY, Bang YJ, Park JG (2011) Analysis of KRAS, BRAF, PTEN, IGF1R, EGFR intron 1 CA status in both primary tumors and paired metastases in determining benefit from cetuximab therapy in colon cancer. Cancer Chemother Pharmacol 68 (4):1045–1055
15. Bouchahda M, Karaboue A, Saffroy R, Innominato P, Gorden L, Guettier C, Adam R, Levi F (2010) Acquired KRAS mutations during progression of colorectal cancer metastases: possible

implications for therapy and prognosis. Cancer Chemother Pharmacol 66(3):605–609
16. Cortot AB, Italiano A, Burel-Vandenbos F, Martel-Planche G, Hainaut P (2010) KRAS mutation status in primary nonsmall cell lung cancer and matched metastases. Cancer 116(11):2682–2687
17. Monaco SE, Nikiforova MN, Cieply K, Teot LA, Khalbuss WE, Dacic S (2010) A comparison of EGFR and KRAS status in primary lung carcinoma and matched metastases. Hum Pathol 41 (1):94–102
18. Goranova TE, Ohue M, Shimoharu Y, Kato K (2011) Dynamics of cancer cell subpopulations in primary and metastatic colorectal tumors. Clin Exp Metastasis 28(5):427–435
19. Bellon E, Ligtenberg MJ, Tejpar S, Cox K, de Hertogh G, de Stricker K, Edsjo A, Gorgoulis V, Hofler G, Jung A, Kotsinas A, Laurent-Puig P, Lopez-Rios F, Hansen TP, Rouleau E, Vandenberghe P, van Krieken JJ, Dequeker E (2011) External quality assessment for KRAS testing is needed: setup of a european program and report of the first joined regional quality assessment rounds. Oncologist 16 (4):467–478

Virchows Arch (2011) 459:495–502
DOI 10.1007/s00428-011-1153-3

ORIGINAL ARTICLE

Aggressive B cell lymphomas of the gastrointestinal tract: clinicopathologic and genetic analysis

Song-Yi Choi · Seok Jin Kim · Won Seog Kim · Kihyun Kim · Young-Hyeh Ko

Received: 5 May 2011 / Revised: 31 August 2011 / Accepted: 3 October 2011 / Published online: 15 October 2011
© Springer-Verlag 2011

Abstract Aggressive B cell lymphomas of the gastrointestinal tract include Burkitt lymphoma (BL), diffuse large B cell lymphoma, and B cell lymphoma, unclassifiable, with features intermediate between DLBCL and BL. To investigate the clinical characters of DLBCL/BL of the gastrointestinal (GI) tract, 101 cases of aggressive B cell lymphoma of the GI tract were analyzed by immunohistochemistry and fluorescence in situ hybridization (FISH) using break apart probe for c-MYC gene. For cases with c-MYC rearrangement, additional FISH studies with MYC/IgH fusion probe, BCL2 break apart probe, and BCL6 break apart probe were performed. MYC rearrangement was detected in 23 of 101 cases of aggressive B cell lymphomas (22.5%). The cases with MYC rearrangement were divided into 14 BL, three DLBCL/BL, and six DLBCL. One of the three DLBCL/BL had double translocation for MYC and BCL6 gene. Clinically, DLBCL/BL of the GI tract was more akin to Burkitt lymphoma than it is to GI tract DLBCL with c-MYC rearrangement. The overall prognosis of patients with DLBCL/BL was the worst among aggressive B cell lymphomas. DLBCL/BL is uncommon category of B cell lymphoma in the GI tract with aggressive clinical course despite of intensive chemotherapy.

Keywords Gray zone lymphoma · Burkitt lymphoma · Diffuse large B cell lymphoma · Intermediate lymphoma · c-MYC

S.-Y. Choi
Department of Pathology,
Chungbuk National University Hospital,
Cheongju, South Korea

S. J. Kim · W. S. Kim · K. Kim
Division of Hematology-Oncology, Department of Medicine,
Sungkyunkwan University School of Medicine,
Seoul, Republic of Korea

Y.-H. Ko (✉)
Department of Pathology, Samsung Medical Center,
Sungkyunkwan University School of Medicine,
50 Irwon-dong, Gangnam-gu,
Seoul 135-710, Republic of Korea
e-mail: yhko310@skku.edu

Introduction

MYC gene is located in chromosome 8 and codes for a transcription factor that regulates transcription of specific target genes. Mutations, rearrangement, and translocation of this gene lead to the unregulated expression of many genes some of which are involved in cell proliferation and result in the formation of cancer [1]. Burkitt's lymphoma is a prototype of malignant lymphoma associated with c-MYC gene translocation, which is detected in 80–90% of cases by fluorescence in situ hybridization (FISH) technique. In Burkitt's lymphoma, c-MYC gene at 8q24 is involved in three translocations, most commonly with immunoglobulin (Ig) heavy chain gene at 14q32 or less frequently with Ig light chain genes at 2p12 or 22q11 [2].

c-MYC translocation is not specific for Burkitt's lymphoma and has been observed in other type of malignant lymphomas. c-MYC translocation is observed in diffuse large B cell lymphoma in 7–14% of de novo cases [3, 4]. In diffuse large B cell lymphoma, c-MYC is often translocated with non-Ig gene partners including BCL6, PAX5, etc.

In 2008, the World Health Organization (WHO) introduced a new category of B cell lymphoma, unclassifiable, with features intermediate between diffuse large B cell lymphoma (DLBCL) and Burkitt lymphoma (BL)

(DLBCL/BL). DLBCL/BL is a heterogeneous category that is not considered a distinct disease entity, but is useful in allowing the classification of cases not meeting criteria for classical BL or DLBCL [5]. The majority of the cases in this category have morphologic features between BL and DLBCL, but have immunophenotypes that are consistent with BL (CD10+, BCL6+, BCL2−, and MUM-1-) [5–7]. Some cases may have a more typical morphology of BL, but may have an atypical immunophenotype, such as strong positivity for BCL2, negativity for BCL6, or low Ki67 proliferation index [5–7].

Approximately 20–55% DLBCL/BL cases have MYC translocations [8–10], and unlike BL, the genetic features are atypical including translocation with a non-Ig gene partner, a complex karyotype [10–12], and concurrent BCL2 and/or BCL6 translocation (so-called double hit or triple hit lymphoma) [6, 9, 10]. "Double-hit" lymphoma displays aggressive behavior with high stage and shows less-responsiveness to the chemotherapy [8, 12, 13].

In gastrointestinal tract, MYC rearrangement was reported in large proportion of aggressive B cell lymphoma [14, 15]. Majority of MYC rearranged lymphomas in GI tract is Burkitt lymphoma; however, DLBCLs of GI tract also show high frequency of MYC rearrangement in 28–50% [14–17]. Since the introduction of the DLBCL/BL category to the WHO classification, the frequency and clinical features of DLBCL/BL among MYC rearranged aggressive B cell lymphoma of the GI tract have remained a matter of concern; however, there have been no studies regarding the issue. Herein, we analyzed histological, immunophenotypic, and genetic findings of 101 cases of aggressive B cell lymphoma of the GI tract to investigate the frequency and clinical features of DLBCL/BL in the GI tract.

Materials and methods

Study sample

The files of the Samsung Medical Center Pathology Department were retrospectively searched for cases diagnosed as DLBCL, DLBLC/BL, or BL between 1999 and 2009. Total 122 cases of aggressive B cell lymphoma of GI tract were found, among which 101 cases were selected because paraffin embedded tissue and clinical information were available.

Ethical approval for this retrospective study was granted by the institutional review board of the Samsung Medical Center.

The clinical information of each patient was obtained from medical records. The data included gender, age at diagnosis, primary site, international prognostic index (IPI), and survival.

Immunophenotyping

Immunohistochemical stains were performed on paraffin sections using antibodies to the following antigens: CD20, CD3, CD10, BCL2, BCL6, cyclin D1, TdT, and Ki-67 (DAKO).

Genetic analysis

Cytogenetics

Conventional G-band karyotype analysis was performed in bone marrow aspirate material using standard methods. Because bone marrow was free of tumor in a majority of cases; karyotypic analysis was successful in only four cases. The karyotype results were reported according to the 2005 International System for Human Cytogenetic Nomenclature.

Fluorescence in situ hybridization

Interphase FISH was performed using the Vysis LSI MYC Dual Color, Break Apart Rearrangement Probe for all selected cases. In the cases with MYC rearrangement, additional FISH analysis was performed using the Vysis LSI MYC Dual Color, dual translocation Probe, the Vysis LSI BCL2 Dual Color, Break Apart Rearrangement Probe, and the Vysis LSI BCL6 Dual Color, Break Apart Rearrangement Probe (Abbott Molecular, Des Plaines, IL, USA).

Statistical analyses

Overall survival was calculated from the date of diagnosis until death or date of last follow-up and was estimated using the Kaplan–Meier method. Statistical analyses were performed using SPSS V.17.0 for Windows (SPSS, Chicago, IL, USA).

Results

Histological classification of cases

Histological findings were reviewed for all cases and divided into diffuse large B cell lymphoma, prototype of Burkitt lymphoma, atypical BL, and other category. Prototype of BL consisted of monomorphic medium-sized tumor cells with round nuclei and multiple small nucleoli (Fig. 1a). Atypical BL showed medium sized tumor cells, but with greater nuclear pleomorphism than prototype of BL (Fig. 1b). DLBCL indicated conventional large cell lymphoma with vesicular nuclei and nuclear pleomorphism (Fig. 1c). Other category comprised of aggressive B cell lymphomas that were not classified either atypical BL, prototype of BL, or DLBCL.

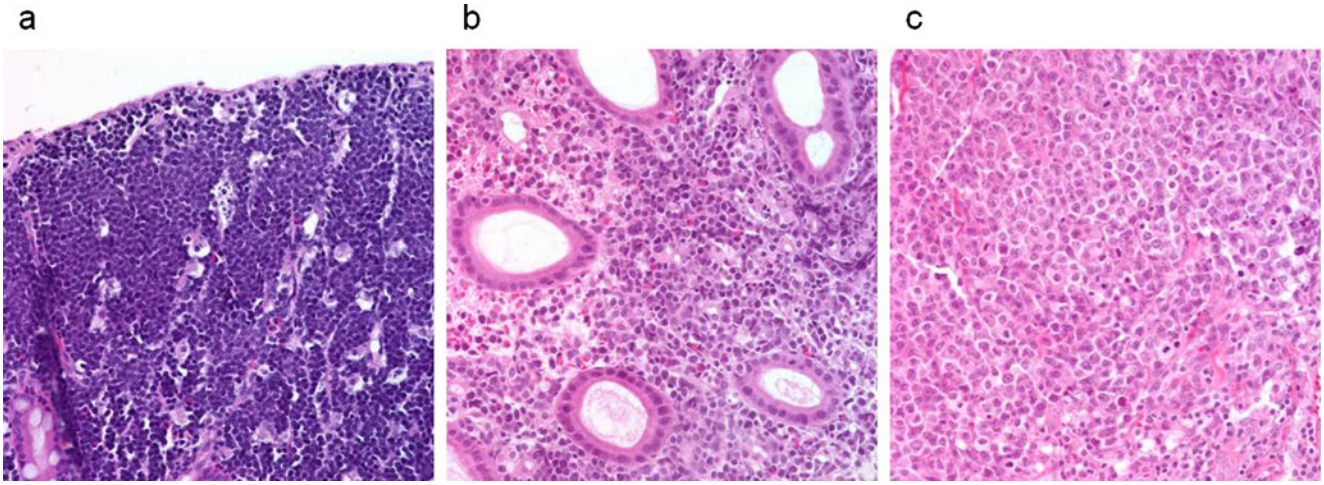

Fig. 1 Morphology of Burkitt lymphoma and diffuse large B cell lymphoma. **a** Prototype of Burkitt lymphoma (case 11). **b** Atypical Burkitt lymphoma (case 5) shows mild variation in size of tumor cells with nuclear irregularity. **c** Diffuse large B cell lymphoma (case 19) shows large tumor cells with vesicular nucleus

Table 1 Characteristics of aggressive B cell lymphoma of gastrointestinal tract with MYC rearrangement

Diagnosis	Case	Age/sex	Site	Therapy	Outcome	OS (month)	Morphology	Immunophenotype CD10/BCL2/BCL6	FISH[a] MYC/BCL2/BCL6	Karyotype (bone marrow)
BL	1	52/F	Intestine	CHOP-like	Re,DOD	7	B	+/m+/+	+(IgH)/−/−	Simple[b]
	2	42/M	Intestine	intensified	AND	27	B	+/w+/+	+(IgH)/−/−	Complex[c]
	3	34/M	Intestine	intensified	AND	41	B	+/m+/+	+(IgH)/−/−	NED
	4	85/F	Stomach	CHOP-like	DOD	1	B	+/w+/+	+(IgH)/ND/ND	ND
	5	39/M	Stomach	intensified	AND	41	AB	+/−/+	+(IgH)/−/−	ND
	6	55/F	Stomach	intensified	AND	78	B	+/−/+	+(IgH)/−/−	NED
	7	59/M	Intestine	intensified	AND	73	B	+/−/+	+(IgH)/−/−	NED
	8	46/M	Intestine	intensified	AND	60	B	+/−/+	+(IgH)/−/−	ND
	9	48/F	Stomach	CHOP-like	AND	19	B	+/w+/+	+(IgH)/−/−	NED
	10	28/M	Intestine	intensified	AND	31	B	+/−/+	+(IgH)/ND/ND	NED
	11	73/F	Intestine	intensified	DOD	2	B	+/−/+	+(BA) [d]/−/−	Simple[b]
	12	53/M	Stomach	intensified	Re,DOD	5	AB	+/−/+	+(IgH)/−/−	ND
	13	60/F	Stomach	CHOP-like	DOD	2	B	+/w+/+	+(IgH)/−/−	NED
	14	76/F	Stomach	CHOP-like	DOD	80	B	+/−/+	+(IgH)/ND/ND	ND
DLBCL/BL	15	69/M	Intestine	CHOP-like	Re,DOD	21	Mixed AB-DLBCL	+/−/+	+(BA)[d]/−/−	ND
	16	36/M	Stomach	intensified	DOD	6	Large AB	+/−/+	+(BA)[d]/−/+	Complex[c]
	17	59/M	Stomach	intensified	DOD	1	Large AB	+/−/+	+(BA)[d]/−/−	ND
DLBCL	18	33/F	Stomach	CHOP-like	AND	68	DLBCL	−/+/+	+(BA)[d]/−/−	NED
	19	78/M	Intestine	CHOP-like	DOD	76	DLBCL	−/+/+	+(BA)/[d]−/+	NED
	20	50/F	Stomach	CHOP-like	AND	43	DLBCL	−/+/+	+(BA)[d]/−/−	NED
	21	42/M	Stomach	CHOP-like	AND	144	DLBCL	−/+/+	+(BA)[d]/−/−	NED
	22	47/M	Stomach	CHOP-like	Re,DOD	31	DLBCL	−/+/−	+(BA)[d]/−/+	NED
	23	39/M	Stomach	CHOP-like	AND	124	DLBCL	−/+/+	+(BA)[d]/−/−	NED

AND Alive, no evidence of disease; *DOD* died of disease; *ND* not done; *NED* no evidence of disease; *OS* overall survival; *Re* relapsed; *B* prototype of BL; *AB* atypical BL; *W* weak; *M* moderate

[a] FISH: FISH carried out using break apart probe

[b] Simple karyotype: no or only few cytogenetic abnormalities

[c] Complex karyotype: ≥3 numerical or structural aberrations

[d] (BA): positive for MYC break apart probe and negative for MYC/IgH fusion probe

Based on the histological criteria, the cases were divided into typical BL (12 cases), atypical BL (two cases), conventional DLBCL (84 cases), and other type (three cases).

Immunohistochemical and FISH study (Table 1)

Prototype of BL and atypical BL

Majority of histological BL and atypical BL showed immunohistochemical profile of CD10+, BCL2−, and BCL6+, which was typical for BL. Ki67 labeling index was more than 99%. Six cases showed weak or moderate expression of BCL-2, which is acceptable finding for BL [2]. All these cases showed MYC gene rearrangement: MYC gene was rearranged with IgH gene in 13 cases and with Igλ light chain gene in one case. No double hit or triple hit lymphoma was observed. Karyotype performed in bone marrow showed simple karyotype in two cases (cases 1 and11) and complex karyotype in one case (case 2, 47,XY,dup(4)(q31.1q35),+7,t(8;14)(q24.1;q32)[12]/47, sl,-7,+i(7)(q10)[8]t(8;14)(q24.1;q32)t(8;22)(q24.1;q11.2)

Diffuse large B cell lymphoma

MYC rearrangement was detected in six cases of 84 DLBCL (7%). DLBCL with MYC rearrangement showed typical histological findings of DLBCL. Rearrangement was detected with MYC break apart probe, but not with MYC-IgH fusion probe. CD10 was negative. BCL2 and BCL6 were positive. Two cases had concurrent BCL6 rearrangement. No karyotype was analyzed in bone marrow sample because bone marrow was not involved by the tumor.

Other types

Three cases belonged to this category because they could not be classified into either BL or DLBCL. Case 15 displayed Burkitt lymphoma-like area characterized by monomorphic tumor cells with starry-sky pattern, which are very similar to BL; however, tumor cells were slightly larger than BL (Fig. 2a). In addition, large cell lymphoma-

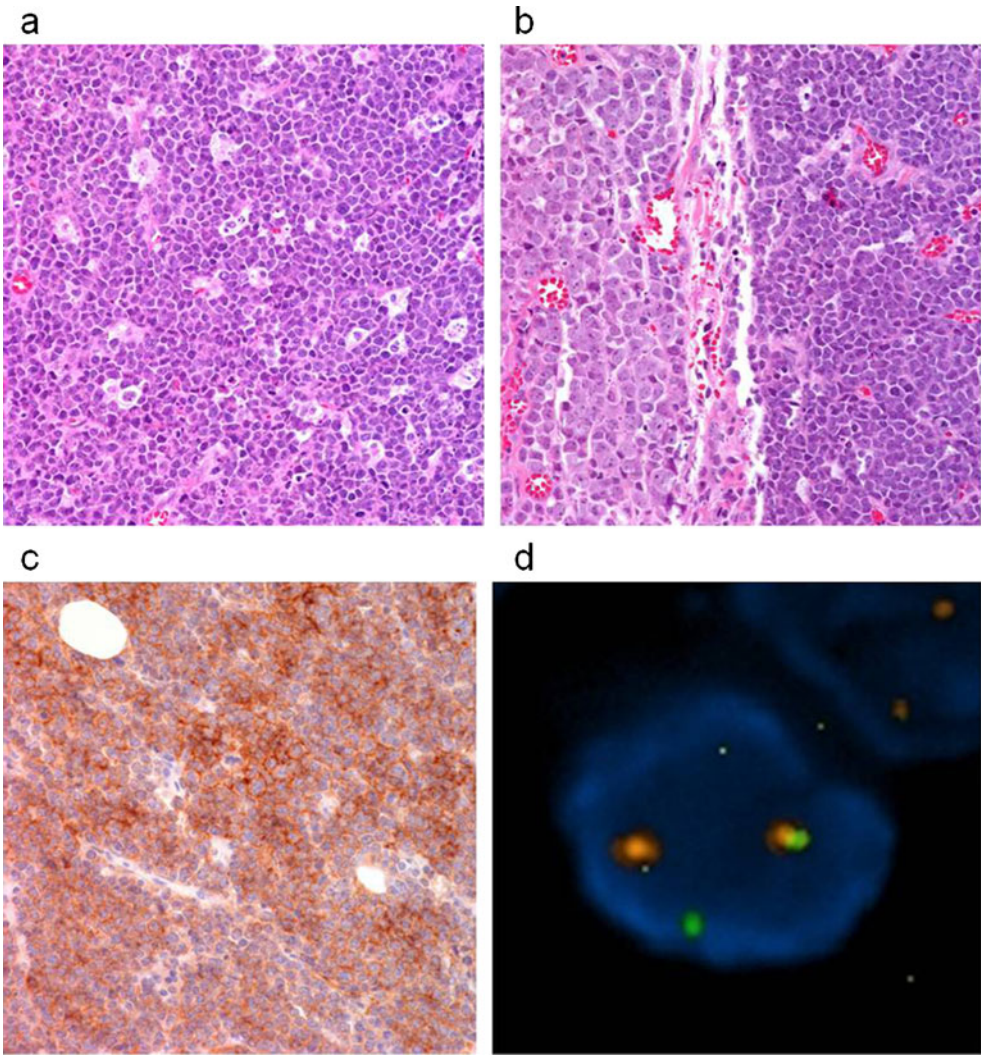

Fig. 2 B cell lymphoma, unclassifiable, with features intermediate between DLBCL and BL (case 15). **a** The tumor showed Burkitt lymphoma-like histological pattern with slightly larger tumor cells. **b** Burkitt lymphoma like area was coexisted with large cell lymphoma area. **c** Tumor cells were positive for CD10. BCL2 was negative. **d** FISH study showed positive signal for C-MYC break probe, but not for MYC/IgH fusion probe

like area coexisted in continuity with Burkitt-like area. Immunoblast-like or large centroblast-like tumor cells present (Fig. 2b). Immunophenotype of the tumor was CD10+ (Fig. 2c), BCL2−, and BCL6+. MYC translocation was detected with MYC break apart probe (Fig. 2d), but not with MYC-IgH translocation probe. Case 16 was double hit lymphoma. Histological pattern of tumor was similar to BL; however, tumor cells were more pelomorphic than typical BL (Fig. 3a). Immunophenotype of the tumor was CD10+ (Fig. 3b), BCL2−, and BCL6+. Translocation involving MYC gene and BCL-6 gene was detected with break apart probe (Fig. 3c, d). MYC/IgH fusion translocation was negative. Cytogenetic study using bone marrow aspirate revealed complex karyotype: 46 XY, add(3)(p13),add(6)(q23),+?8,−20,+2mar(Re8). Case 17 showed large tumor cells with blast-like nuclear features. Immunophenotype was CD10+, BCL2−, and BCL6+. Ki67 labeling index was more than 99%. MYC translocation was detected using MYC break apart probe, but not with MYC-IgH fusion probe. CyclinD1 and TdT were negative in three cases.

Clinical characteristics of aggressive B cell lymphomas of the GI tract with MYC rearrangement including BL, DLBCL/BL, and DLBCL

Based on the results of histological, immunohistochemical, and FISH studies, prototype of BL and atypical BL were classified as BL and three cases of other type were classified as DLBCL/BL. The clinical characteristics of the 14 BL, three DLBCL/BL, and six cases of DLBCL cases were compared and summarized in Table 2.

The DLBCL/BL cases were clinically more similar to the BL cases than to the DLBCL cases. The frequency of advanced stage (III and IV) disease was significantly higher in DLBCL/BL and BL cases than in DLBCL (DLBCL/BL, 66.7%; BL, 71.4%; DLBCL, 0%). BM involvement was common in DLBCL/BL (2/3, 50%) and BL (6/14, 43%),

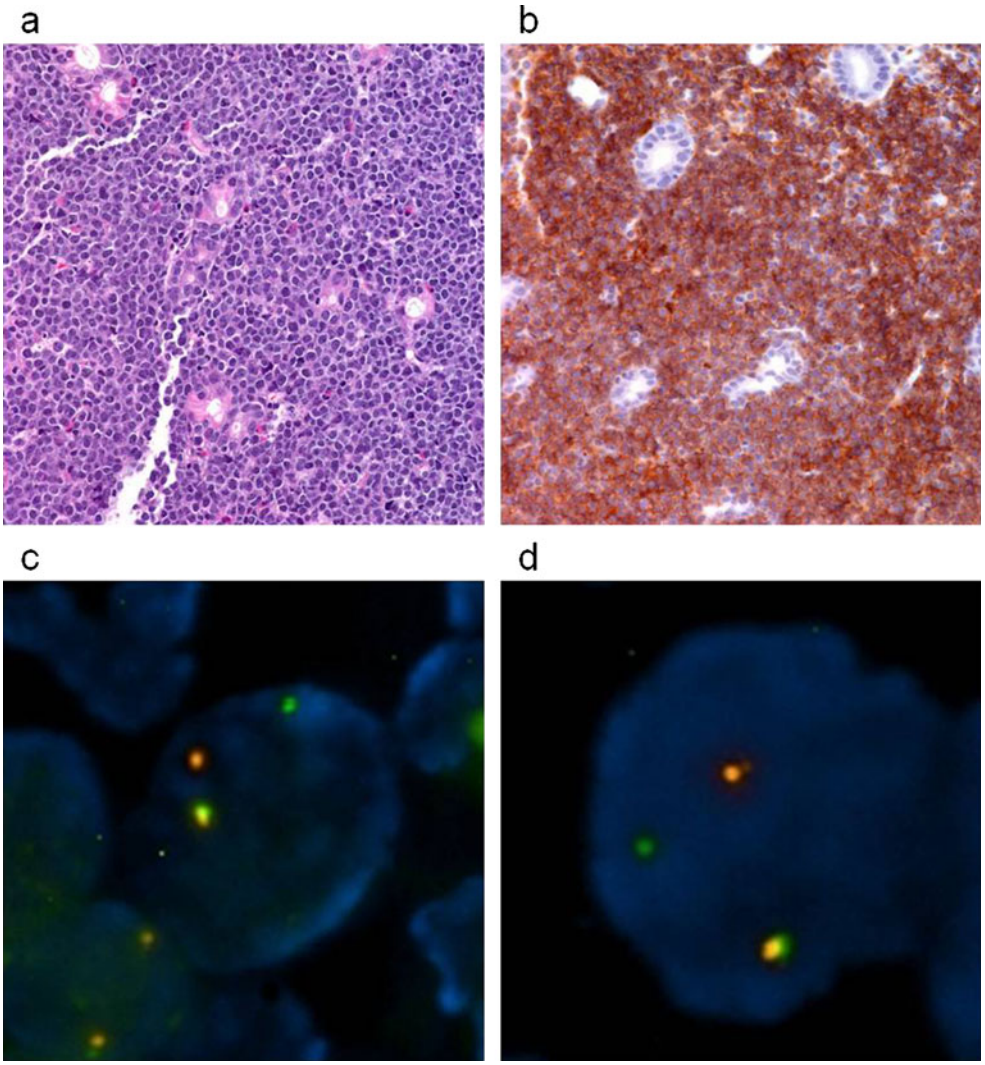

Fig. 3 B cell lymphoma, unclassifiable, with features intermediate between DLBCL and BL. Double hit lymphoma (case 16). **a** Histological pattern was similar to Burkitt lymphoma. Tumor cells were more pelomorphic than BL with nuclear irregularity. **b** Positivity for CD10. **c** FISH study showed positive signal for C-MYC break probe, but not for MYC/IgH fusion probe. **d** Positive signal for BCL6 break apart probe

Table 2 Comparison of clinical characteristics of GI tract aggressive B cell lymphoma with MYC translocation

	GI tract B cell lymphoma with MYC translocation		
	BL (n=14)	DLBCL/BL (n=3)	DLBCL (n=6)
Sex			
Female	7 (50.0%)	0 (0.0%)	2 (33.3%)
Male	7 (50.0%)	3 (100.0%)	4 (66.7%)
Age			
<60 years	11 (78.6%)	2 (66.7%)	5 (83.3%)
≥60 years	3 (21.4%)	1 (33.3%)	1 (16.7%)
Site			
Stomach	7 (50.0%)	2 (66.7%)	5 (83.3%)
Intestine	7 (50.0%)	1 (33.3%)	1 (16.7%)
Ann Arbor stage			
I or II	4 (28.6%)	1 (33.3%)	6 (100.0%)
III or IV	10 (71.4%)	2 (66.7%)	0 (0.0%)
BM involvement			
Negative	8 (57%)	1 (33.3%)	6 (100.0%)
Positive	6 (43%)	2 (66.7%)	0 (0.0%)
IPI score			
0.1. or 2	7 (50.0%)	1 (33.3%)	6 (100.0%)
3,4, or 5	7 (50.0%)	2 (66.7%)	0 (0.0%)

The statistical analysis was not able to perform because of small number of cases

but rare in MYC rearranged DLBCL (0/6, 0%). A high IPI score was present in two of three patients (66.7%) with DLBCL/BL, seven of 14 patients (50%) with BL and none of 6 (0%) with DLBCL.

Survival analysis

We analyzed the overall survivals of patients with MYC rearranged aggressive lymphomas in the GI tract including DLBCL/BL, BL, and DLBCL. For comparison, 76 cases of MYC-rearrangement negative DLBCL were included. The median follow-up was 37 months (range, 1–164 months). The survival of patients with DLBCL/BL was the worst. All three patients with DLBCL/BL in the GI tract died of disease 1, 6, and 21 months after diagnosis. The 3-year overall survival rates of patients with DLBCL/BL, BL, and MYC-positive DLBCL were 0%, 64%, and 82%, respectively (P<0.0001, log-rank test; Fig. 4).

Discussion

We investigated the clinicopathologic characteristics of MYC rearranged aggressive B cell lymphoma of the GI tract with a special interest on DLBCL/BL. DLBCL/BL can be designated when the tumor shows intermediate histological findings between BL and DLBCL. BL-like cases tend to show atypical immunophenotype for BL and MYC rearrangement with non-Ig gene partners. Large cell lymphoma-like cases tend to show typical immunophenotype for BL (CD10+, BCL2−, and BCL6+) associated with

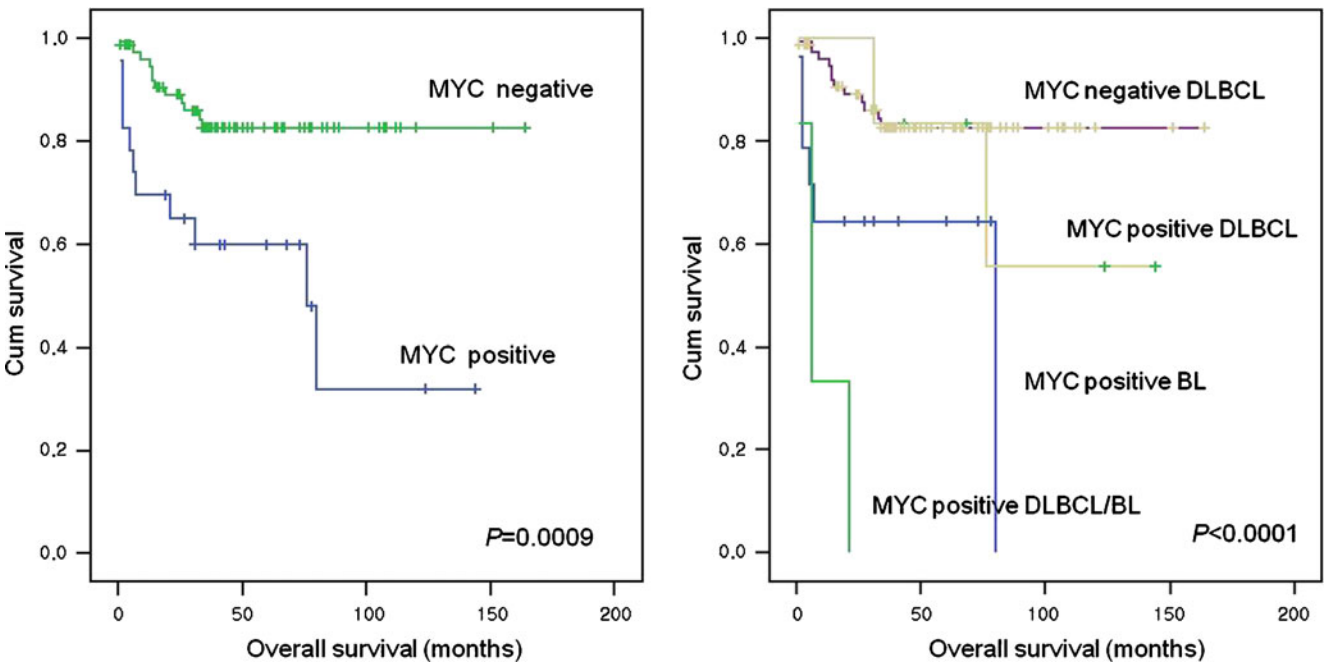

Fig. 4 Comparison of overall survival rates among DLBCL/BL, BL, and DLBCL of the gastrointestinal tract with regard to the MYC translocation and disease category. Kaplan–Meier survival curves for overall survival are plotted (log-rank test)

double hit translocation of MYC gene and BCL2 gene or BCL6 gene [5, 7]. Because the histology is similar to BL, a subset of DLBCL/BL cases may be previously diagnosed as BL or atypical BL [6].

In our series, overall histological pattern of DLBCL/BL was reminiscent of BL, however, they could not be classified as such because of histological difference including larger tumor size and nuclear irregularity. In one case, BL-like area was merged into large cell lymphoma-like area, which suggested histological transformation. DLBCL/BL is a heterogeneous category, and some of them may be transformed from low grade B cell lymphoma or large cell lymphoma. MYC rearrangement in the GI tract environment may lead to Burkitt-like morphological transformation of B cell lymphoma. One of our cases was double hit lymphoma with both MYC and BCL6 translocation. According to previous studies, approximately 3–5% of high-grade B cell lymphomas demonstrate the dual translocation genotype [4, 11], and 30–60% of the "double-hit" lymphomas fall into the DLBCL/BL category [8, 9, 11–13, 18, 19]. Conversely, there are few reports about the incidence of dual translocations in DLBCL/BL. A single study found dual MYC and BCL2 translocation in three cases (11%) out of 27 adult Burkitt-like lymphomas [8].

DLBCL/BL presents more commonly in extra-nodal sites, but no preferential site has been recognized [8, 20]. A recent study showed that six of 12 (50%) DLBCL/BL cases presented as a retroperitoneal or perirenal mass [12]. In our series, the frequency of DLBCL/BL was very low among aggressive B cell lymphoma of the GI tract. Three of 23 MYC-rearranged aggressive B cell lymphomas (13%) and three of 101 all aggressive B cell lymphoma (3%) of the GI tract were classified as DLBCL/BL.

The clinical outcomes of DLBCL/BL, especially double hit lymphoma, are very poor. Although number of cases was too few, DLBCL/BL in our series was more akin to BL than DLBCL based on their IPI scores and survival. The patients with DLBCL/BL died of their disease within a short time despite chemotherapy. Such poor outcomes for DLBCL/BL were expected because the tumors bear poor prognostic factors such as MYC rearrangement, BCL2 overexpression, and complex karyotype [10, 11].

In the gastrointestinal tract, c-MYC rearrangement is very common compared with nodal lymphoma and has been reported in 10–46% of DLBCL [14–17, 21]. The partner gene for MYC translocation was reported as IgH gene in five of seven cases in one study [21], while other studies demonstrated translocation exclusively with non-Ig gene [14, 16, 17]. Generally, MYC translocation in DLBCL has been known to be associated with high IPI score, high stage, and poor prognosis [3, 4, 22]. In contrast, MYC translocation in GI tract DLBCL was not associated with bone marrow involvement [16] or inferior overall survival compared to MYC-translocation negative DLBCL [14, 15, 17, 21].

In conclusion, DLBCL/BL is an uncommon category of B cell lymphoma in GI tract with aggressive clinical course and shorter survival despite of intensified chemotherapy. New therapeutic approach is required for treatment of DLBCL/BL patients to increase survival.

Acknowledgment This study is supported by Samsung Biomedical Research Institute grant(C-B0-202-2) and a grant of the Korea Health Care technology R&D Project, Ministry for Health & Welfare Affairs, Republic of Korea (A092255).

Conflict of interest statement We declare that we have no conflict of interest

References

1. Boxer LM, Dang CV (2001) Translocations involving c-myc and c-myc function. Oncogene 20:5595–5610
2. Leoncini L, Raphael M, Stein H, Harris NL, Jaffe ES, Kluin PM (2008) Burkitt lymphoma. In: Steven H, Swerdlow EC, Harris NL, Jaffe ES, Pileri SA, Stein H, Thiele J, Vardiman JW (eds) WHO classification of tumours of haematopoietic and lymphoid tissues, 4th edn. IARC, Lyon, pp 265–266
3. Barrans S, Crouch S, Smith A, Turner K, Owen R, Patmore R, Roman E, Jack A (2010) Rearrangement of MYC is associated with poor prognosis in patients with diffuse large B-cell lymphoma treated in the era of rituximab. J Clin Oncol 28:3360–3365
4. Niitsu N, Okamoto M, Miura I, Hirano M (2009) Clinical features and prognosis of de novo diffuse large B-cell lymphoma with t (14;18) and 8q24/c-MYC translocations. Leukemia 23:777–783
5. Kluin PM, Harris NL, Stein H, Leoncini L, Raphael M (2008) B-cell lymphoma, unclassifiable, with features intermediate between diffuse large B-cell lymphoma and Burkitt lymphoma. In: Steven H, Swerdlow EC, Harris NL, Jaffe ES, Pileri SA, Stein H, Thiele J, Vardiman JW (eds) WHO classification of tumours of haematopoietic and lymphoid tissues, 4th edn. IARC, Lyon, pp 265–266
6. Hasserjian RP, Ott G, Elenitoba-Johnson KS, Balague-Ponz O, de Jong D, de Leval L (2009) Commentary on the WHO classification of tumors of lymphoid tissues (2008): "Gray zone" lymphomas overlapping with Burkitt lymphoma or classical Hodgkin lymphoma. J Hematop. doi:10.1007/s12308-009-0039-7
7. Slack GW, Gascoyne RD (2011) MYC and aggressive B-cell lymphomas. Adv Anat Pathol 18:219–228
8. McClure RF, Remstein ED, Macon WR, Dewald GW, Habermann TM, Hoering A, Kurtin PJ (2005) Adult B-cell lymphomas with Burkitt-like morphology are phenotypically and genotypically heterogeneous with aggressive clinical behavior. Am J Surg Pathol 29:1652–1660
9. Haralambieva E, Boerma EJ, van Imhoff GW, Rosati S, Schuuring E, Muller-Hermelink HK, Kluin PM, Ott G (2005) Clinical, immunophenotypic, and genetic analysis of adult lymphomas with morphologic features of Burkitt lymphoma. Am J Surg Pathol 29:1086–1094
10. Hummel M, Bentink S, Berger H, Klapper W, Wessendorf S, Barth TF, Bernd HW, Cogliatti SB, Dierlamm J, Feller AC, Hansmann ML, Haralambieva E, Harder L, Hasenclever D, Kuhn M, Lenze D, Lichter P, Martin-Subero JI, Moller P, Muller-Hermelink HK, Ott G, Parwaresch RM, Pott C, Rosenwald A,

Rosolowski M, Schwaenen C, Sturzenhofecker B, Szczepanowski M, Trautmann H, Wacker HH, Spang R, Loeffler M, Trumper L, Stein H, Siebert R (2006) A biologic definition of Burkitt's lymphoma from transcriptional and genomic profiling. N Engl J Med 354:2419–2430

11. Johnson NA, Savage KJ, Ludkovski O, Ben-Neriah S, Woods R, Steidl C, Dyer MJ, Siebert R, Kuruvilla J, Klasa R, Connors JM, Gascoyne RD, Horsman DE (2009) Lymphomas with concurrent BCL2 and MYC translocations: the critical factors associated with survival. Blood 114:2273–2279
12. Snuderl M, Kolman OK, Chen YB, Hsu JJ, Ackerman AM, Cin PD, Ferry JA, Harris NL, Hasserjian RP, Zukerberg LR, Abramson JS, Hochberg EP, Lee H, Lee AI, Toomey CE, Sohani AR (2010) B-cell lymphomas with concurrent IGH-BCL2 and MYC rearrangements are aggressive neoplasms with clinical and pathologic features distinct from Burkitt lymphoma and diffuse large B-cell lymphoma. Am J Surg Pathol 34:327–340
13. Macpherson N, Lesack D, Klasa R, Horsman D, Connors JM, Barnett M, Gascoyne RD (1999) Small noncleaved, non-Burkitt's (Burkitt-like) lymphoma: cytogenetics predict outcome and reflect clinical presentation. J Clin Oncol 17:1558–1567
14. van Krieken JH, Raffeld M, Raghoebier S, Jaffe ES, van Ommen GJ, Kluin PM (1990) Molecular genetics of gastrointestinal non-Hodgkin's lymphomas: unusual prevalence and pattern of c-myc rearrangements in aggressive lymphomas. Blood 76:797–800
15. Van Krieken JH, Medeiros LJ, Pals ST, Raffeld M, Kluin PM (1992) Diffuse aggressive B-cell lymphomas of the gastrointestinal tract. An immunophenotypic and gene rearrangement analysis of 22 cases. Am J Clin Pathol 97:170–178
16. Raghoebier S, Kramer MH, van Krieken JH, de Jong D, Limpens J, Kluin-Nelemans JC, van Ommen GJ, Kluin PM (1991) Essential differences in oncogene involvement betweenprimary nodal and extranodal large cell lymphoma. Blood 78:2680–2685
17. Kramer MH, Hermans J, Wijburg E, Philippo K, Geelen E, van Krieken JH, de Jong D, Maartense E, Schuuring E, Kluin PM (1998) Clinical relevance of BCL2, BCL6, and MYC rearrangements in diffuse large B-cell lymphoma. Blood 92:3152–3162
18. Cogliatti SB, Novak U, Henz S, Schmid U, Moller P, Barth TF (2006) Diagnosis of Burkitt lymphoma in due time: a practical approach. Br J Haematol 134:294–301
19. Kanungo A, Medeiros LJ, Abruzzo LV, Lin P (2006) Lymphoid neoplasms associated with concurrent t(14;18) and 8q24/c-MYC translocation generally have a poor prognosis. Mod Pathol 19:25–33
20. Bellan C, Stefano L, de Giulia F, Rogena EA, Lorenzo L (2009) Burkitt lymphoma versus diffuse large B-cell lymphoma: a practical approach. Hematol Oncol 27:182–185
21. Nakamura S, Ye H, Bacon CM, Goatly A, Liu H, Kerr L, Banham AH, Streubel B, Yao T, Tsuneyoshi M, Savio A, Takeshita M, Dartigues P, Ruskoné-Fourmestraux A, Matsumoto T, Iida M, Du MQ (2008) Translocations involving the immunoglobulin heavy chain gene locus predict better survival in gastric diffuse large B-cell lymphoma. Clin Cancer Res 14:3002–3010
22. Savage KJ, Johnson NA, Ben-Neriah S, Connors JM, Sehn LH, Farinha P, Horsman DE, Gascoyne RD (2009) MYC gene rearrangements are associated with a poor prognosis in diffuse large B-cell lymphoma patients treated with R-CHOP chemotherapy. Blood 114:3533–3537

Virchows Arch (2011) 459:503–510
DOI 10.1007/s00428-011-1150-6

ORIGINAL ARTICLE

Expression of apoptosis-related proteins and its clinical implication in surgically resected gastric carcinoma

Min A Kim · Hee Eun Lee · Hye Seung Lee · Han-Kwang Yang · Woo Ho Kim

Received: 14 March 2011 / Revised: 8 August 2011 / Accepted: 10 September 2011 / Published online: 27 September 2011
© Springer-Verlag 2011

Abstract Apoptosis, via caspase cascade, is involved in tumorigenesis and progression, and thus, altered apoptosis-related protein expressions have clinical and prognostic significance. Moreover, the apoptosis pathway is highlighted due to the recent introduction of apoptosis-targeted therapy for several genes such as the X-linked inhibitor of apoptosis protein (XIAP). XIAP is the most potent direct inhibitor of caspase, and XIAP-associated factor 1 (XAF1) and secondary mitochondrial activator of caspase/direct IAP-binding protein with low PI (Smac/DIABLO) are negative regulators of XIAP. In this study, we evaluated the expression of these proteins and investigated their clinical and prognostic significance in gastric carcinomas. Immunohistochemical analysis by using the tissue array method was performed for XIAP, survivin, Bcl-2, XAF1, Smac/DIABLO, and cleaved caspase-3 proteins in 1,162 surgically resected gastric carcinoma cases. XIAP expression was related to the advanced stage. The expression of XIAP showed negative relationship with XAF1 and Smac/DIABLO expressions. In addition, XIAP expression was associated with a poor prognosis and was also proved to be an independent prognostic factor. Cleaved caspase-3 expression was related to the early stage. In addition, cleaved caspase-3 expression was associated with a favorable prognosis and was also proved to be an independent prognostic factor. The expression of XIAP showed an inverse relationship with cleaved caspase-3. In addition, the expression of XAF1 and Smac/DIABLO had a positive relationship with cleaved caspase-3. These findings are consistent with their known functions, and they may help to identify individuals best suited for apoptosis-targeted therapy as a baseline data in gastric carcinoma.

Keywords Apoptosis · X-linked inhibitor of apoptosis protein · Caspase-3 · Stomach neoplasms · Immunohistochemistry · Survival analysis

M. A. Kim · H. E. Lee · W. H. Kim (✉)
Department of Pathology, Seoul National University College of Medicine,
28 Yeongeon-dong, Jongno-gu,
Seoul 110-799, Republic of Korea
e-mail: woohokim@snu.ac.kr

H. S. Lee
Department of Pathology,
Seoul National University Bundang Hospital,
166 Gumi-ro, Bundang-gu,
Seongnam-si, Gyeonggi-do 463-707, Republic of Korea

H.-K. Yang
Department of Surgery, Seoul National University College of Medicine,
Seoul, Republic of Korea

Introduction

Apoptosis, a programmed cell death, is involved in tissue homeostasis and tumorigenesis. Morphologically, it is characterized by the condensation of chromatin, and biochemically, it is characterized by DNA fragmentation into oligonucleosome-sized fragments [1]. The caspases are involved in signaling and execution of apoptotic cell death, and caspase-3 is a major effecter caspase, which cleaves its target substrates to affect changes associated with apoptosis [1].

Caspase activity is negatively regulated by inhibitor of apoptosis proteins (IAPs), which are characterized by one or more baculovirus IAP repeat (BIR) [2]. An important function of IAPs is to bind various caspases, such as caspase-3, and to antagonize their function. They were originally identified in BIRs, where they provide a mechanism for enhancing viral propagation through inhibition of defensive apoptosis by host insect cells [2]. Mammalian IAPs include

X-linked IAP (XIAP), neuronal IAP (NIAP), cellular IAP-1 (cIAP-1), cIAP-2, testis-specific IAP (TS-IAP), survivin, BIR-containing ubiquitin-conjugating enzyme (BRUCE), and livin [3]. Among them, XIAP is the most potent direct inhibitor of caspases, whereas the other IAPs can bind but not inhibit caspase activity. XIAP significantly inhibits apoptosis induced by many trigger factors, such as serum withdrawal and etoposide exposure [3].

XIAP-associated factor 1 (XAF1) is a zinc finger-rich protein and directly associates with XIAP to antagonize XIAP-mediated caspase-3 inhibition [4]. XAF1 is able to elicit XIAP re-localization from the cytosol to the nucleus, perhaps as a means of sequestering XIAP [4]. Secondary mitochondrial activator of caspase/direct IAP-binding protein with low PI (Smac/DIABLO) is a mitochondrial protein that also promotes some form of apoptosis via its ability to eliminate IAP-mediated caspase inhibition [5]. Smac/DIABLO has been shown to exit the mitochondria and enter the cytosol during apoptosis. The mitochondrial efflux of Smac/DIABLO, in response to a variety of pro-apoptotic agents, was found to be profoundly inhibited in Bcl-2-overexpressing cells [6]. To summarize the complex interaction, capase-3 is an effecter caspase that is negatively regulated by IAPs. However, this protein–protein interaction is inhibited by XAF1 and Smac/DIBALO that are positively regulated by Bcl-2-overexpressing cells.

Bcl-2 is another anti-apoptotic protein, which is localized in intracellular membranes, mostly in the outer mitochondrial membrane, nuclear membrane, and the endoplasmic reticulum. At these sites, Bcl-2 controls ion channels, caspase status, and cytochrome c localization, and has an anti-apoptotic function [7].

Expressional changes in these apoptosis-related proteins have been investigated in various cancers such as renal cell carcinoma [8], hepatocellular carcinoma [9], colorectal carcinoma [10], non-small cell lung cancer (NSCLC) [11], and breast cancer [12], because of their important contributions during tumorigenesis. Studies have proven that IAP overexpression is generally correlated with poor prognosis [11–13]. In gastric carcinoma (GC), one or several protein expressions of survivin, caspase family, XIAP, XAF1, Smac/DIABLO, and Bcl-2 were evaluated [14–19]. However, to our knowledge, multiple protein expression, expressional correlation, and their clinical significance have not been simultaneously evaluated. Moreover, these proteins are recently highlighted due to development of the apoptosis-targeted drugs [20–23]. Therefore, studies for the altered expression of apoptosis-related proteins as a prognostic markers and predictive markers for probable targeted therapy are needed. In the present study, we evaluated the expression of apoptosis-related proteins and the relationship between the expressions of those proteins in surgically resected large-scale GC specimens. In addition, we examined correlations between the expressions of apoptosis-related proteins and clinicopathologic parameters including prognostic significance.

Materials and methods

Patients

Consecutively collected, surgically resected GC tissue specimens were obtained from 1,162 patients at Seoul National University Hospital between January 1, 1995 and December 31, 1996 [24]. Clinicopathologic parameters were evaluated by reviewing medical charts and pathologic records. The detailed patient demographic and clinicopathologic parameters are summarized in Table 1. Outcomes were determined from the date of surgery until death or December 31, 2006, which resulted in a follow-up period range from 1 to 108 months. Cases lost to follow-up and deaths caused by problems other than GC were censored during the survival analysis. No patients received preoperative therapy. This study was approved by the Institutional Review Board of Seoul National University Hospital.

Tissue array methods and immunohistochemistry

Tissue array blocks were prepared according to the method used in our previous study [24], and 21 array blocks were made. The following six apoptosis-related antibodies were selected: anti-XIAP (1:50, mouse monoclonal, BD Bioscience,

Table 1 Patients' demographic and clinicopathologic variables

Factor	Case number (%)
Sex	
Male	774 (66.6)
Female	388 (33.4)
Lauren classification	
Intestinal type	463 (39.8)
Diffuse type	632 (54.4)
Mixed type	67 (5.8)
Tumor invasion	
Early gastric carcinoma	340 (29.3)
Advanced gastric carcinoma	822 (70.7)
Lymph node metastasis	
Absent	450 (38.7)
Present	712 (61.3)
Pathologic stage (AJCC 6th edition)	
I	474 (40.8)
II	254 (21.9)
III	259 (22.3)
IV	175 (15.1)

cytoplasmic staining), survivin (1:400, rabbit polyclonal, R&D system, nuclear), Bcl-2 (1:100, mouse monoclonal, Dakocytomation, nuclear), XAF1 (1:200, rabbit polyclonal, ProSci, nuclear), Smac/DIABLO (1:2000, rabbit polyclonal, ProSci, nuclear), and cleaved caspase-3 (1:50, rabbit monoclonal, Cell Signaling, cytoplasmic and nuclear). Immunohistochemical staining was performed using a streptavidin peroxidase procedure after an antigen retrieval process by using microwave. Although there are no consensus criteria for the immunopositivity of each antibody used in this study, 10% of the tumor cells as a positive criteria gave us a good result in our previous experiments analyzing ten tumor suppressor genes [25], and 56 tumor-associated genes [24]. Therefore, immunostaining results were considered to be positive when more than 10% of the tumor cells were moderately or strongly stained.

Statistical analysis

Quantitative variables were compared using the Fisher's exact test, Pearson's chi-square test, or Pearson's relation probability test and continuous variables were compared using the Student's*t* test by analysis of variance. Survival curves were plotted using the Kaplan–Meier product-limit method and the significances of the difference between the survival curves was determined using the log–rank test. Multivariate analysis was performed using Cox proportional hazards regression modeling. All statistical tests were two-sided, and statistical significance was accepted for $P<0.05$. All analyses were performed using the SPSS version 17.0 (SPSS, Chicago, IL).

Results

Correlations between the expressions of apoptosis-related proteins and clinicopathologic parameters

Cytoplasmic XIAP expression is negative or weakly positive in normal gastric mucosa. However nuclear survivin, XAF1, and Smac/DIABLO expressions are positive in gastric mucosa. Nuclear Bcl-2 expression is negative in normal gastric mucosa. Cytoplasmic and nuclear expressions of cleaved caspase-3 are positive in normal gastric mucosa.

In the tumor tissue, IAP expression frequencies were 20.0% (221/1103 cases) for XIAP, 57.3% (617/1076 cases) for survivin and 10.0% (112/1125 cases) for Bcl-2. In contrast, the protein expression frequencies of the inhibitors of XIAP were 76.6% (804/1049 cases) for XAF1 and 13.9% (146/1050 cases) for Smac/DIABLO. Finally, the expression frequency of cleaved caspase-3 was 68.9% (730/1060 cases). Figure 1 shows the representative pictures of positive and negative cases for antibodies.

Table 2 summarizes the relationship between protein expressions and clinicopathologic parameters. XIAP expression was found to be significantly related to an intestinal type histology by Lauren classification than overall cases ($P<0.001$) and advanced stage ($P=0.002$). Survivin expression was found to be related to a higher proportion of diffuse type histology by Lauren classification, early stage and negativity of lymph node metastasis ($P=0.003$, $P<0.001$ and $P=0.017$, respectively). Bcl-2 expression was found to be associated with an intestinal type histology by Lauren classification ($P=0.005$), and XAF1 expression was found to be related to early stage ($P=0.002$), whereas Smac/DIABLO expression was found to be associated with higher proportion of a diffuse type histology than overall cases ($P<0.001$). Cleaved caspase-3 expression was found to be related to the intestinal type histology, early stage, and negativity of lymph node metastasis in this study ($P=0.014$, $P<0.001$ and $P<0.001$, respectively).

The expressions of apoptosis-related proteins and survival analysis

The mean duration of follow-up was 65.2±38.1 months after surgery. Thirteen patients (1.1%) were lost to follow-up, but this did not significantly impact the survival analyses. During the follow-up period, 480 of the 1149 patients (41.8%) died.

The overall survival rate of patients with XIAP expression, as determined by the log-rank test, was significantly lower than that of those without XIAP expression ($P=0.008$; Fig. 2a). In addition, it was found that the overall survival of patients with higher stages and XIAP-expressing tumors was significantly shorter than that of those with non-XIAP in a higher stage (stages III and IV; $P=0.011$; data not shown). Multivariate analysis was performed to determine the prognostic significance of XIAP, radical resection, and pathologic stage. pTNM stage and radical surgery were still the strongest independent prognostic factor ($P<0.001$ and $P<0.001$, respectively). However, pathologic XIAP expression was also found to be an independent indicator of prognosis (hazard ratio 1.354, $P=0.006$; Table 3).

In contrast, positivity of cleaved caspase-3 was found to be significantly associated with a favorable prognosis ($P<0.001$; Fig. 2b). We also performed the survival analysis, as determined by the log-rank test, in low (stages I and II) and high (stages III and IV) pTNM stages. As a result, we found that the overall survival rate of patients who showed cleaved caspase-3 expression was significantly higher than that of those who did not show expression in patients with low and high stages ($P<0.011$ and <0.016, respectively; data not shown). Multivariate analysis was performed to determine the relations between prognosis and cleaved caspase-3, radical resection, and pathologic stage. Cleaved caspase-3 expression independently predicted survival

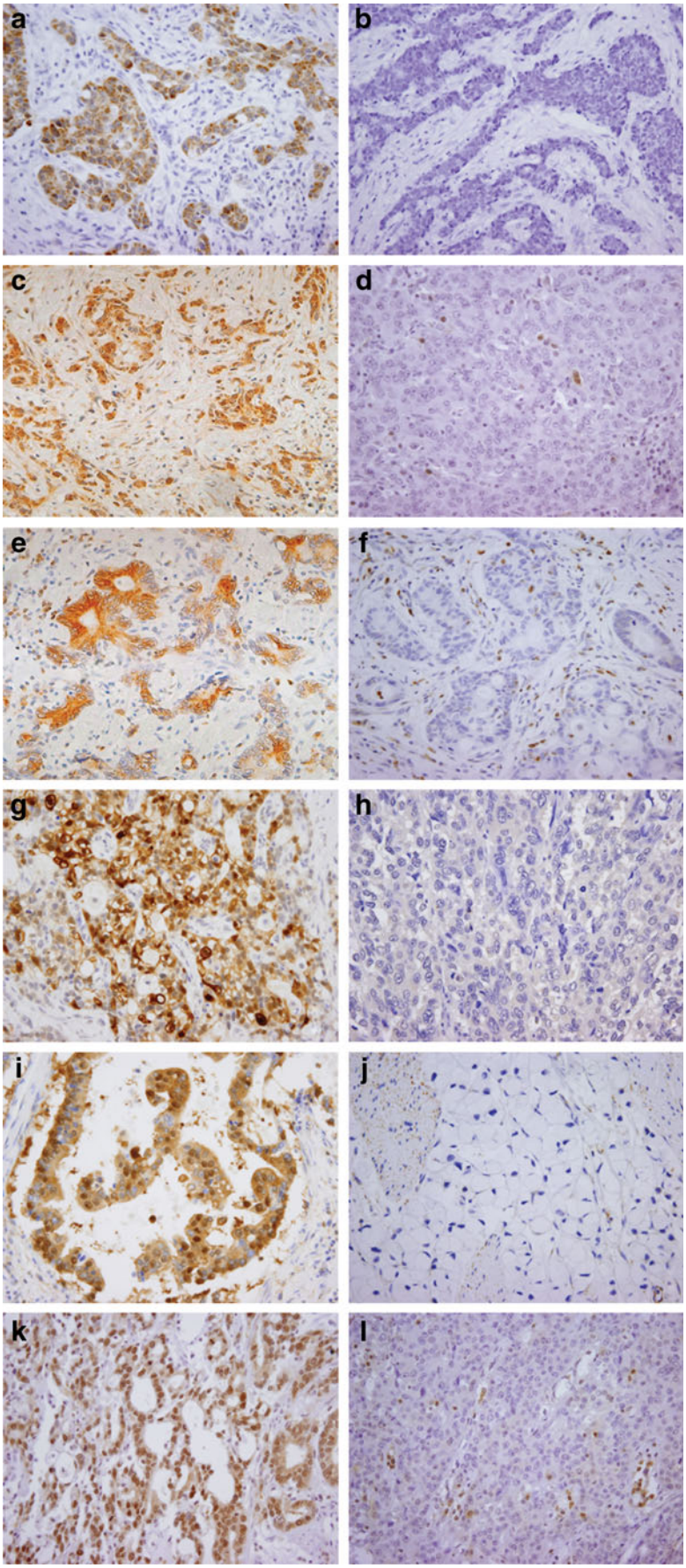

Fig. 1 Representative figure of immunohistochemical staining pattern for the apoptosis-related proteins. **a** Cytoplasmic XIAP-positive. **b** XIAP-negative. **c** Nuclear survivin-positive. **d** Survivin-negative. **e** Nuclear Bcl-2-positive. **f** Bcl-2-negative. **g** Nuclear XAF1-positive. **h** XAF1-negative. **i** Nuclear Smac/DIABLO-positive. **j** Nuclear Smac/DIABLO-negative. **k** Cytoplasmic and nuclear cleaved caspase-3-positive. **l** Cleaved caspase-3-negative. (Original magnification×400)

Table 2 Associations between the expressions of apoptosis-related proteins and clinicopathologic parameters

Positive case no./total valid case no. (%)	Lauren classification positive case no. (%)				Tumor invasion positive case no. (%)			LN metastasis positive case no. (%)		
	Intestinal	Diffuse	Mixed	*P*-value	EGC	AGC	*P*-value	Absent	Present	*P*-value
XIAP 221/1103 (20.0)	121/439 (27.6)	86/599 (14.4)	14/65 (21.5)	<0.001	42/299 (14.0)	179/804 (22.3)	0.002	75/408 (18.4)	146/695 (21.0)	N.S
Survivin 617/1076 (57.3)	224/435 (51.5)	359/578 (62.1)	34/63 (54.0)	0.003	193/281 (68.7)	424/795 (53.3)	<0.001	247/398 (62.1)	370/678 (54.6)	0.017
Bcl-2 112/1125 (10.0)	59/447 (13.2)	51/612 (8.3)	2/66 (3.0)	0.005	40/316 (12.7)	72/809 (8.9)	N.S	46/431 (10.7)	66/694 (9.5)	N.S
XAF1 804/1049 (76.6)	320/416 (76.9)	436/570 (76.5)	48/63 (76.2)	N.S	226/271 (83.4)	578/778 (74.3)	0.002	290/376 (77.1)	514/673 (76.4)	N.S
Smac/DIABLO 146/1050 (13.9)	31/420 (7.4)	107/569 (18.8)	8/61 (13.1)	<0.001	41/269 (15.2)	105/781 (13.4)	N.S	48/376 (12.8)	98/674 (14.5)	N.S
Cleaved caspase-3 730/1060 (68.9)	318/433 (73.4)	376/566 (66.4)	36/61 (59.0)	0.014	246/286 (86.0)	484/774 (62.5)	<0.001	303/386 (78.5)	427/674 (63.4)	<0.001

EGC Early gastric carcinoma, *AGC* advances gastric carcinoma, *N.S.* not significant

(hazard ratio, 0.728; $P=0.001$), although stage ($P<0.001$), and radical surgery ($P<0.001$) were still stronger predictive factors (Table 3). However, survivin, Bcl-2, XAF1, or Smac/DIABLO expressions were not found be significantly related to the outcome.

Relationships between the expressions of apoptosis-related proteins

XIAP expression was found to be negatively correlated with XAF1 and Smac/DIABLO, which have opposite function with XIAP. Furthermore, XIAP expression was found to be inversely correlated with cleaved caspase-3 expression (relation probability −0.154). In contrast, XAF1 and Smac/DIABLO expressions were found to be positively related to cleaved caspase-3 expression. However, expressions of survivin and Bcl-2 were not found to be significantly related. The results are summarized in Table 4.

Discussion

GC is one of the leading causes of cancer-related mortality especially in East Asia and South America. Several mechanisms have been suggested to explain the process of neoplastic transformation and tumor progression, but the major carcinogenic processes are largely unknown because of their complicated mechanisms. However, new diagnostic, preventive, and therapeutic developments would undoubtedly benefit from a thorough understanding of the mechanisms responsible for tumor initiation, progression, and drug responsiveness.

The proteins evaluated in the present study are known to be associated with apoptosis, and alterations in the expressional cascades of apoptosis-related proteins would be responsible for transformation and progression in various cancers. Out of the known apoptosis-related proteins, IAPs play key roles by inhibiting the functions of caspases, and of the eight known human IAP proteins, XIAP is the most potent and versatile inhibitor of caspases and apoptosis [26].

Recently, the apoptosis pathway is highlighted due to the introduction of apoptosis-targeted therapy for several genes. For example, XIAP has been suggested for targeted therapy, and preclinical and clinical trials have been conducted on AEG35156 (Aegera Therapeutics, Montreal, Quebec, Canada), and antisense oligodeoxynucleotide to XIAP [20, 21]. Preclinical data confirmed that AEG35156 down-regulated XIAP expression, enhancing cancer cell apoptosis in vitro, and demonstrated antitumor effects in multiple xenograft models as a single agent [20]. In the clinical data, AEG35156 knocked down its target and appeared very effective when combined with chemotherapy

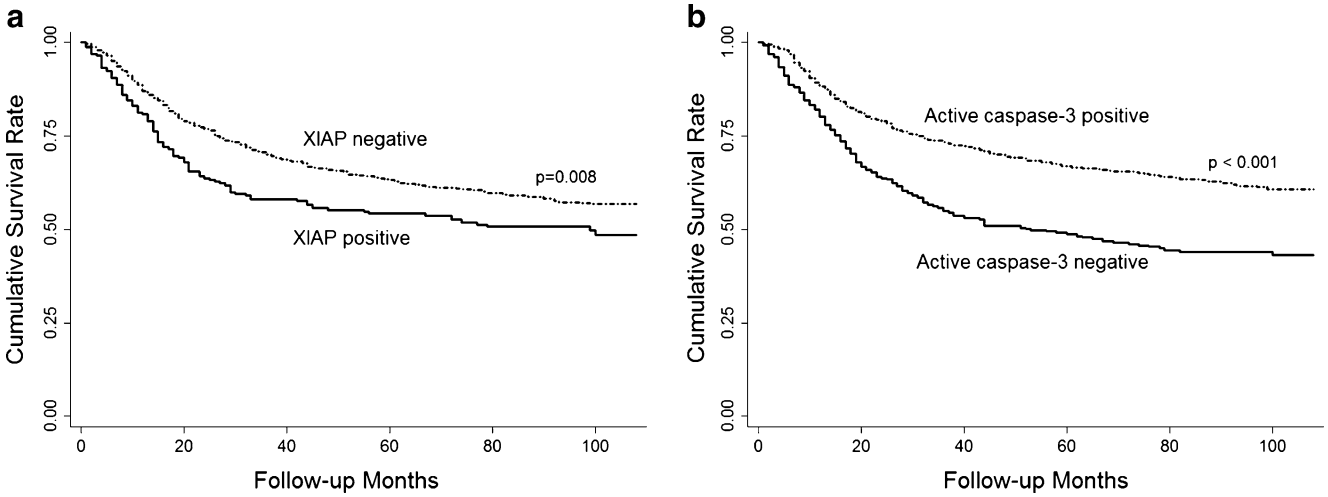

Fig. 2 Survival curves obtained using the Kaplan–Meier method by the log–rank test. **a** XIAP expression. **b** Cleaved caspase-3 expression

in patients with acute myelogenous leukemia that was refractory to a single induction regimen at the highest tested [21]. In addition, phase I and II trials have been conducted on a YM155, small molecule inhibitor of survivin, in advanced solid tumors [22, 23]. In vitro, YM155 suppresses survivin gene expression, resulting in the reduction of protein levels and functions and subsequently abrogates survivin-mediated apoptosis with no effect on other apoptotic pathways. YM155 inhibits the growth of a number of human cancer cell lines in vitro. Clinical trial shows that, in patients with advanced refractory NSCLC, YM155 monotherapy has a modest antitumor activity and is well tolerated. Owing to increasing attention on the apoptosis pathway, we evaluated the expression and clinical significance of apoptosis-related proteins including XIAP. In addition, we examined the relationships between these protein expressions.

In the present study, XIAP, cleaved caspase-3, XAF1, and Smac/DIABLO expression rates were 20.0%, 68.9%, 76.6%, and 13.9%, respectively. The expression of XIAP was found to be negatively related to the expressions of XAF1 and Smac/DIABLO which antagonize XIAP functionally. In the case of cleaved caspase-3, the expression was inversely correlated with the expression of XIAP and positively correlated with the expressions of XAF1 and Smac/DIABLO. Furthermore, the XIAP expression rates were lower in the early stage than their average expression rates. On the other hand, the expression rate of cleaved caspase-3 was higher in the early stage compared than the advanced stage. In the survival analysis, XIAP expression was found to be an independent prognostic factor of a poor outcome, whereas cleaved caspase-3 expression was found

Table 3 Multivariate analyses of predictive factors for survival (Cox proportional hazards model)

Prognostic factors	Hazard ratio (95% CI)	*P*-value
pTNM stage		<0.001
I vs. II	3.658 (2.647–5.054)	
I vs. III	7.427 (5.488–10.051)	
I vs. IV	16.135 (11.589–22.465)	
Residual tumor after surgery		<0.001
Absent vs. Present	1.776 (1.330–2.371)	
XIAP		0.006
Positive vs. negative	1.354 (1.091–1.680)	
pTNM stage		<0.001
I vs. II	3.469 (2.485–4.842)	
I vs. III	7.283 (5.340–9.935)	
I vs. IV	15.217 (10.831–21.380)	
Residual tumor after surgery		<0.001
Absent vs. present	1.700 (1.271–2.272)	
Active caspase-3		0.001
Positive vs. negative	0.728 (0.602–0.880)	

CI Confidence interval

Table 4 Pearson's relation probability of expression status between the apoptosis-related proteins in gastric carcinomas

	XIAP	Survivin	Bcl-2	XAF1	Smac/DIABLO	Cleaved caspase-3
XIAP						
Survivin	-.068*					
Bcl-2	.017	0.010				
XAF1	-.083**	0.062	−0.020			
Smac/DIABLO	-.078*	0.058	−0.041	0.050		
Cleaved caspase-3	-.154**	0.202**	0.042	0.192**	0.106**	

*P-value<0.005, **P-value<0.001

to be as an independent prognostic factor of a better outcome. This result was consistent with those of previous studies [16, 17, 27], and we demonstrated the concordant results for their function in large-scale GC cases by IHC methods. Therefore, when we consider that XIAP-expressing patients showed poor outcome, these patients are probable candidates for therapy by anti-XIAP agents. Further studies are needed to prove it.

The mechanism responsible for the regulation of XIAP expression has not been clearly elucidated up to date. Tamm et al. [28] insisted that *XIAP* mRNA levels are not correlated with its protein levels, which suggest that XIAP expression may be post-transcriptionally regulated. Loss of heterozygosity or somatic mutation of *XAF1* has not been reported in any kind of cancers. However, Byun et al. [29] showed transcriptional silencing of XAF1 by aberrant promoter methylation. Therefore, epigenetic silencing may be one of the regulation mechanisms of *XAF1*. They also proved that loss or abnormal reduction of XAF1 was inversely correlated with *p53* mutation [29]. Shibata et al. [16, 17] reported that increased XIAP to XAF1 ratio is combined with altered *XAF1* splicing in GC. They also reported that disturbed XIAP and XAF1 expression balance is an independent prognostic factor. Therefore, further studies on regulatory mechanisms are required for the expression of XIAP and XAF1.

Smac/DIABLO is released from the mitochondria together with cytochrome c during mitochondria-induced apoptosis. Furthermore, the binding of Smac/DIABLO to XIAP has been proposed to destabilize the XIAP-caspase interaction by steric hindrance and thus to disrupt the XIAP-caspase complex [30]. In contrast, XAF1 mRNA is normally expressed in the nuclei of all kinds of tissues, but the expression level is very low or undetectable. Transient overexpression of XAF1 sensitizes tumor cells to the proapoptotic events, such as serum withdrawal and etoposide exposure, and reverses the XIAP-mediated inhibition of caspase-3 activity [4]. Finally, Smac/DIABLO and XAF1 have the same net effect to XIAP, but they act in a different manner; these cascades have the same results, as the key effecter molecule of apoptosis, caspase-3. Our data also showed that the expression of XAF1 and Smac/DIABLO had the same effect on cleaved caspase-3 expression.

Survivin is one of the IAP members and thus inhibits apoptosis by suppressing the caspase cascade. However, in the study, survivin expression was found to be positively related to cleaved caspase-3 expression, which was not expected considering their function. An apparent contradiction has been reported regarding the relation between survivin and apoptosis. De Oliveira Lima et al. [31] have reported that the expressions of survivin and cleaved caspase-3 are positively related and that survivin expression is positively correlated with the apoptotic index. However, as was expected for their functional considerations, an inverse correlation was reported by Rodel et al. [32]. Further investigations are required to clarify these conflict results on larger series or using antibodies against different epitopes of this protein in various cancers.

In the present study, we found that XIAP expression was related to poor survival, whereas survivin expression was not. Of note, XIAP protein expression is an independent prognostic marker in GC, as in other cancer types [13]. These results support the concept that XIAP is one of the most potent and versatile inhibitors of caspases.

In summary, XIAP and cleaved caspase-3 expressions were found to be associated with tumor invasion and to be independent prognostic factors. Furthermore, XIAP was found to be inversely related to the expression of XAF1, Smac/DIABLO, and cleaved caspase-3, whereas cleaved caspase-3 expression was found to be positively related with the expressions of XAF1 and Smac/DIABLO. This finding is consistent with their known functions of these proteins and may help to identify individuals who are best suited for apoptosis-targeted therapy, including XIAP, as a baseline data in GC.

Acknowledgment This study was supported by grant no. 04-2008-0470 from the SNUH Research Fund.

Conflicts of Interest None

References

1. Hussein MR, Haemel AK, Wood GS (2003) Apoptosis and melanoma: molecular mechanisms. J Pathol 199:275–288. doi:10.1002/path.1300
2. Salvesen GS, Duckett CS (2002) IAP proteins: blocking the road to death's door. Nat Rev Mol Cell Biol 3:401–410. doi:10.1038/nrm830
3. Hunter AM, LaCasse EC, Korneluk RG (2007) The inhibitors of apoptosis (IAPs) as cancer targets. Apoptosis 12:1543–1568. doi:10.1007/s10495-007-0087-3
4. Liston P, Fong WG, Kelly NL et al (2001) Identification of XAF1 as an antagonist of XIAP anti-caspase activity. Nat Cell Biol 3:128–133. doi:10.1038/35055027
5. Verhagen AM, Ekert PG, Pakusch M et al (2000) Identification of DIABLO, a mammalian protein that promotes apoptosis by binding to and antagonizing IAP proteins. Cell 102:43–53. doi:10.1016/S0092-8674(00)00009-X
6. Adrain C, Creagh EM, Martin SJ (2001) Apoptosis-associated release of Smac/DIABLO from mitochondria requires active caspases and is blocked by Bcl-2. EMBO J 20:6627–6636. doi:10.1093/emboj/20.23.6627
7. Karam JA, Lotan Y, Karakiewicz PI et al (2007) Use of combined apoptosis biomarkers for prediction of bladder cancer recurrence and mortality after radical cystectomy. Lancet Oncol 8:128–136. doi:10.1016/S1470-2045(07)70002-5
8. Kempkensteffen C, Fritzsche FR, Johannsen M et al (2009) Down-regulation of the pro-apoptotic XIAP associated factor-1 (XAF1) during progression of clear-cell renal cancer. BMC Cancer 9:276. doi:10.1186/1471-2407-9-276

9. Augello C, Caruso L, Maggioni M et al (2009) Inhibitors of apoptosis proteins (IAPs) expression and their prognostic significance in hepatocellular carcinoma. BMC Cancer 9:125. doi:10.1186/1471-2407-9-125
10. Xiang G, Wen X, Wang H, Chen K, Liu H (2009) Expression of X-linked inhibitor of apoptosis protein in human colorectal cancer and its correlation with prognosis. J Surg Oncol 100:708–712. doi:10.1002/jso.21408
11. Chen P, Li J, Ge LP, Dai CH, Li XQ (2010) Prognostic value of survivin, X-linked inhibitor of apoptosis protein and second mitochondria-derived activator of caspases expression in advanced non-small-cell lung cancer patients. Respirology 15:501–509. doi:10.1111/j.1440-1843.2010.01710.x
12. Hinnis AR, Luckett JC, Walker RA (2007) Survivin is an independent predictor of short-term survival in poor prognostic breast cancer patients. Br J Cancer 96:639–645. doi:10.1038/sj.bjc.6603616
13. Ramp U, Krieg T, Caliskan E et al (2004) XIAP expression is an independent prognostic marker in clear-cell renal carcinomas. Hum Pathol 35:1022–1028. doi:10.1016/j.humpath.2004.03.011
14. Tu SP, Liston P, Cui JT et al (2009) Restoration of XAF1 expression induces apoptosis and inhibits tumor growth in gastric cancer. Int J Cancer 125:688–697. doi:10.1002/ijc.24282
15. Tong QS, Zheng LD, Wang L et al (2005) Downregulation of XIAP expression induces apoptosis and enhances chemotherapeutic sensitivity in human gastric cancer cells. Cancer Gene Ther 12:509–514. doi:10.1038/sj.cgt.7700813
16. Shibata T, Noguchi T, Takeno S et al (2008) Disturbed XIAP and XAF1 expression balance is an independent prognostic factor in gastric adenocarcinomas. Ann Surg Oncol 15:3579–3587. doi:10.1245/s10434-008-0062-4
17. Shibata T, Mahotka C, Wethkamp N et al (2007) Disturbed expression of the apoptosis regulators XIAP, XAF1, and Smac/DIABLO in gastric adenocarcinomas. Diagn Mol Pathol 16:1–8. doi:10.1097/01.pdm.0000213471.92925.51
18. Vallbohmer D, Drebber U, Schneider PM et al (2009) Survivin expression in gastric cancer: association with histomorphological response to neoadjuvant therapy and prognosis. J Surg Oncol 99:409–413. doi:10.1002/jso.21271
19. Tsamandas AC, Kardamakis D, Tsiamalos P et al (2009) The potential role of Bcl-2 expression, apoptosis and cell proliferation (Ki-67 expression) in cases of gastric carcinoma and correlation with classic prognostic factors and patient outcome. Anticancer Res 29:703–709
20. Dean E, Jodrell D, Connolly K et al (2009) Phase I trial of AEG35156 administered as a 7-day and 3-day continuous intravenous infusion in patients with advanced refractory cancer. J Clin Oncol 27:1660–1666. doi:10.1200/JCO.2008.19.5677
21. Schimmer AD, Estey EH, Borthakur G et al (2009) Phase I/II trial of AEG35156 X-linked inhibitor of apoptosis protein antisense oligonucleotide combined with idarubicin and cytarabine in patients with relapsed or primary refractory acute myeloid leukemia. J Clin Oncol 27:4741–4746. doi:10.1200/JCO.2009.21.8172
22. Giaccone G, Zatloukal P, Roubec J et al (2009) Multicenter phase II trial of YM155, a small-molecule suppressor of survivin, in patients with advanced, refractory, non-small-cell lung cancer. J Clin Oncol 27:4481–4486. doi:10.1200/JCO.2008.21.1862
23. Satoh T, Okamoto I, Miyazaki M et al (2009) Phase I study of YM155, a novel survivin suppressant, in patients with advanced solid tumors. Clin Cancer Res 15:3872–3880. doi:10.1158/1078-0432.CCR-08-1946
24. Lee HS, Cho SB, Lee HE et al (2007) Protein expression profiling and molecular classification of gastric cancer by the tissue array method. Clin Cancer Res 13:4154–4163. doi:10.1158/1078-0432.CCR-07-0173
25. Lee HS, Lee HK, Kim HS, Yang HK, Kim WH (2003) Tumour suppressor gene expression correlates with gastric cancer prognosis. J Pathol 200:39–46. doi:10.1002/path.1288
26. Eckelman BP, Salvesen GS, Scott FL (2006) Human inhibitor of apoptosis proteins: why XIAP is the black sheep of the family. EMBO Rep 7:988–994. doi:10.1038/sj.embor.7400795
27. Okada E, Murai Y, Matsui K et al (2001) Survivin expression in tumor cell nuclei is predictive of a favorable prognosis in gastric cancer patients. Cancer Lett 163:109–116. doi:10.1016/S0304-3835(00)00677-7
28. Tamm I, Kornblau SM, Segall H et al (2000) Expression and prognostic significance of IAP-family genes in human cancers and myeloid leukemias. Clin Cancer Res 6:1796–1803
29. Byun DS, Cho K, Ryu BK et al (2003) Hypermethylation of XIAP-associated factor 1, a putative tumor suppressor gene from the 17p13.2 locus, in human gastric adenocarcinomas. Cancer Res 63:7068–7075
30. Wu G, Chai J, Suber TL et al (2000) Structural basis of IAP recognition by Smac/DIABLO. Nature 408:1008–1012. doi:10.1038/35050012
31. De Oliveira LF, De Oliveira CH, Barrezueta LF et al (2009) Immunoexpression of inhibitors of apoptosis proteins and their antagonist SMAC/DIABLO in colorectal carcinoma: correlation with apoptotic index, cellular proliferation and prognosis. Oncol Rep 22:295–303. doi:10.3892/or_00000437
32. Rodel F, Hoffmann J, Grabenbauer GG et al (2002) High survivin expression is associated with reduced apoptosis in rectal cancer and may predict disease-free survival after preoperative radio-chemotherapy and surgical resection. Strahlenther Onkol 178:426–435. doi:10.1007/s00066-002-1003-y

Virchows Arch (2011) 459:511–519
DOI 10.1007/s00428-011-1152-4

ORIGINAL ARTICLE

SMAD4 protein expression and cell proliferation in colorectal adenocarcinomas

Adriana Handra-Luca · Sylviane Olschwang · Jean-François Fléjou

Received: 2 April 2011 / Revised: 28 September 2011 / Accepted: 2 October 2011 / Published online: 16 October 2011
© Springer-Verlag 2011

Abstract The TGFβ signalling pathway is a growth inhibitor system that operates in both normal and tumour cells. Alterations to components of this pathway, including SMAD4, result in resistance to growth inhibition and uncontrolled proliferation. The aim of this study was to analyse the relationships between SMAD4, a key protein in the growth-inhibiting TGFβ pathway; cell proliferation proteins Ki67, p27 and S-phase kinase-associated protein 2 (SKP2); and mismatch repair (MMR) proteins as well as prognostic indicators in colorectal adenocarcinomas. A series of 230 sporadic colorectal adenocarcinomas were studied using tissue microarrays by immunohistochemistry for SMAD4, Ki67, p27, SKP2 and MMR protein (hMLH1, hMSH2 and hMSH6) expression. Protein expression was analysed with respect to pathological prognostic criteria. Loss of SMAD4 nuclear expression (27/230, 12%) correlated with the presence of lymph node metastases, MMR protein expression and the absence of p27 in tumour cells ($p=0.04$, $p=0.08$ and $p=0.03$, respectively). A high Ki67 index did not correlate with SMAD4 expression; however, it did correlate with moderate or poor histological differentiation, SKP2 expression and aberrant or absent MMR protein expression ($p=0.02$, $p<0.01$ and $p<0.01$, respectively). In conclusion, the results of our study suggest that the loss of SMAD4, occurring in 12% of colorectal adenocarcinomas, correlated with the presence of lymph node metastases and absence of p27 expression but not with high cellular proliferation. However, high proliferation correlated with SKP2 and aberrant MMR protein expression. Although the advantage of immunohistochemistry is high throughput, our results allow only an initial evaluation, and subsequent studies, including genetic analyses, are required.

Keywords Colon · Adenocarcinoma · Pathology · Proliferation · Mismatch repair · SMAD4 · p27

Abbreviations

MMR	Mismatch repair
SKP	S-phase kinase-associated protein
TMA	Tissue microarray
TNM	Tumour node metastasis (classification)

Introduction

The TGFβ signalling pathway is a growth inhibitor system that operates in both normal and tumour cells. Conformation

A. Handra-Luca (✉)
Service d'Anatomie Pathologique, APHP Avicenne Université Paris 13/Nord Medecine, EA3406,
125 rue de Stalingrad,
93000 Bobigny, France
e-mail: adriana.handra-luca@avc.aphp.fr

S. Olschwang
Centre de Recherches en Cancérologie de Marseille INSERM UMR891,
Marseille, France

S. Olschwang
Institut Paoli-Calmettes Marseille,
Marseille, France

J.-F. Fléjou
Service d'Anatomie pathologique,
APHP Saint Antoine Université Paris 6,
Paris, France

J.-F. Fléjou
INSERM UMRS938,
Paris, France

changes within complexes containing the bone morphogenetic protein, TGFβ and ALK receptors transmit intracellular signals resulting in SMAD4 nuclear translocation, which is essential for signal transduction [1, 2]. Loss of SMAD4 expression, generally due to gene mutations [3, 4], plays a role in neoplastic transformation, both in benign conditions like digestive polyposis syndrome [5, 6] and in malignant tumours, including pancreatic and colorectal adenocarcinomas [7–11].

Mutations in components of the TGFβ/SMAD4 pathway in colorectal adenocarcinomas result in resistance to growth inhibition and uncontrolled proliferation [2]. Uncontrolled cellular proliferation is related to the expression of cyclin-dependent kinase inhibitors such as the p27 protein [8, 12–14]. The level of p27 decreases mainly by an S-phase kinase-associated protein 2 (SKP2), CDK2/cyclin A-associated protein p45 (SKP2)-dependent degradation; this degradation being responsible for cell transition from the G1 to the S phase of the cell cycle [15–17]. The aim of this study was to analyse the relationship between SMAD4 expression; cell proliferation proteins Ki67, SKP2 and p27; mismatch repair (MMR) protein expression and pathological prognostic factors in colorectal adenocarcinomas.

Methods

Patients

A total of 230 patients with sporadic colorectal adenocarcinomas, treated by surgical resection, were selected [18, 19]. The patients were retrospectively analysed for age, gender, tumour location, histological differentiation and tumour node metastasis (TNM) classification (tumour (T), lymph node metastases (N) and distant metastases (M)). We did not select patients who had multiple primary colorectal tumours, multiple malignancies, personal and/or familial histories of cancer or preoperative treatment. Since patients were followed up after surgery and treated in different centres, survival data were not fully available and therefore were not included in the analysis.

Tissue microarray

Tissue microarrays (TMA) were assembled from formalin-fixed, paraffin-embedded tissues. The haematoxylin and eosin-stained slides were retrospectively analysed, and representative tumour zones were selected for TMA construction. Three TMA slides were assembled from formalin-fixed, paraffin-embedded tissues using a 0.6-mm-diameter punch (Beecher Instruments, Woodland, CA, USA). The arrays comprised 3 tissue cores for each tumour and 36 cores for normal colon mucosa [20, 21].

Immunohistochemistry

Immunohistochemistry was performed with the following antibodies: SMAD4, Ki67, p27, SKP2, hMLH1, hMSH2 and hMSH6 (Table 1). Consecutive, 5-μm thick sections were cut, mounted on silanised slides, dried overnight at 37°C, dewaxed in xylene and rehydrated in graded alcohols. For Ki67, hMLH1, hMSH2 and hMSH6 antibodies, the slides, after peroxidase blocking with 3% peroxide in methanol for 30 min, were placed in a microwave oven in citrate buffer (pH 6.0) for 15 min at 750 W and 15 min at 150 W for antigen retrieval. All slides were processed using an automatic immunostainer (Optimax Plus 1.5, Biogenex, San Ramon, CA, USA) and the biotin–streptavidin–peroxidase technique (Supersensitive Detection Kit, Biogenex). The antibodies against Ki67, hMSH2 and hMSH6 antigens were applied for 30 min, whereas the antibody against hMLH1 was applied for 1 h. The slides were developed with aminoethylcarbazole as a chromogen and counterstained with Mayer's hemalun.

For p27 and SKP2 antibodies, antigen retrieval was performed by heating the slides in a water bath for 30 min at 98°C in 10 mmol/L citrate buffer with a pH of 6.0 (Biogenex). Endogenous peroxidase activity was blocked by incubation in 3% H_2O_2 for 15 min. After rinsing in distilled water, the slides were placed in phosphate-buffered saline (PBS) containing 0.1% Tween 20 (Amresco, Solon, OH, USA) for 5 min. The primary antibody was applied at 4°C overnight in a 1:100 dilution of PBS. The slides were washed two times for 5 min each time in PBS-Tween. Antigens were detected using LSAB+kit and 3,3′-diaminobenzidine (Dako, Carpinteria, CA, USA) as a chromogen. Slides were counterstained with haematoxylin, rinsed in tap water, dehydrated, placed in xylene and mounted. A positive control was included with each analysis. Tissue loss during processing occurred in 17 cases.

Immunohistochemical evaluation

The immunohistochemical evaluation of tumour protein expression was performed without prior knowledge of other data. Only nuclear staining was considered for all antibodies, and the percentage of positive nuclei for each tumour was calculated [22]. A core was considered negative for SMAD4 if there was no nuclear staining in the tumour cells [23, 24]. For Ki67 immunostaining, we considered two groups of tumours, either with a low or high index, by using median expression as the cutoff (median/cutoff, 52%; range, 0–95%). Negative or positive expression groups were considered for SKP2 (SKP2: median/cutoff, 0; range, 0–57%) and for p27 (cutoff, 30% [25]). A core was considered negative for hMLH1, hMSH2 or hMSH6 when no nuclear staining was observed. The mismatch repair

Table 1 Primary antibodies used for immunohistochemistry

Antibody	Clone	Company	Dilution	Staining	Control tissue
SMAD4	sc-7966	Santa Cruz Biotechnology	1:300	Nuclear	Normal colon
Ki67	MIB-1	Dako	1:100	Nuclear	Normal lymph node
$P27^{kip}$	57	BD Transduction Laboratories	1:50	Nuclear	Normal tonsil
SKP2	1G12E9	Zymed Laboratories Inc	1:100	Nuclear	Normal tonsil
hMLH1	G168-728	Pharmingen	1:70	Nuclear	Normal colon
hMSH2	FE11	Calbiochem	1:100	Nuclear	Normal colon
hMSH6	44	Becton Dickinson	1:100	Nuclear	Normal colon

function was considered altered when immunohistochemistry for at least one of the MMR proteins, hMLH1, hMSH2 or hMSH6, showed loss (absence) of expression. We did not include PCR analysis to confirm the immunohistochemical results obtained in this study, as done in previous studies [20, 26, 27].

Statistical analysis

Fisher's or chi-square test was used to analyse the association between the expression of cell proliferation proteins (considered as categorical variables after classifying according to previously reported cutoffs or using the median value of the percentage of stained tumour cells as the cutoff); tumour (T) component of TNM classification (for statistical analysis, T1 and T2 tumours were considered one group and T3 and T4 tumours, as a different group); lymph node metastases (N of the TNM classification; for the statistical analysis, N1 and N2 were considered one group and were compared with the N0 group of tumours); distant metastases (M of TNM classification); tumour histological differentiation; tumour location; patient age; as well as hMLH1, hMSH2 and hMSH6 expression in the tumour. A level of 0.05 was considered to indicate statistical significance, and all tests were two sided.

Results

Main clinicopathological characteristics of colorectal adenocarcinomas and SMAD4 protein expression

The main clinicopathological features of the 230 patients, with respect to SMAD4 tumour expression, are noted in Table 2. Most tumours were located in the distal colon (75%) and showed well or moderate histological differentiation. Lymph node metastases were observed in 55% of patients, and synchronous liver metastases in 15% of patients. Loss of nuclear SMAD4 was observed in 27 tumours (12%) (Fig. 1). Lymph node metastases were more frequently observed in patients with SMAD4-negative tumours ($p=0.04$). Tumour location, histological differentiation and T of the TNM classification did not correlate with SMAD4 expression.

Relationship between cell proliferation protein expression and SMAD4 expression in colorectal adenocarcinomas

A high Ki67 proliferation index was noted in 114 (50%) adenocarcinomas. p27 Protein expression was observed in 30 tumours (13%) and SKP2 expression in 113 tumours (49%) (Fig. 1). A high Ki67 index correlated with moderate or poor histological tumour differentiation and with SKP2 expression ($p=0.02$ and $p<0.01$, respectively) (Table 3). An inverse relationship between SKP2 and p27 expression was noted in 115 tumours: 99 SKP2-positive/p27-negative tumours and 16 SKP2-negative/p27-positive tumours. However, this relationship was not statistically significant. There was no statistically significant relationship between SMAD4 tumour expression and Ki67 or SKP2. All SMAD4-negative tumours were p27-negative as well ($p=0.03$).

Relationship between SMAD4 tumour expression, cell proliferation and mismatch repair protein expression in colorectal adenocarcinomas

The hMLH1, hMSH2 and hMSH6 proteins were expressed in 208/230 (90%) tumours. The MMR protein tumour expression correlated with low Ki67 expression ($p<0.01$) and with a loss of SMAD4 expression ($p=0.08$) (Table 4).

In tumours with MMR protein expression, SKP2 expression correlated with high Ki67 ($p=0.01$). SMAD4-negative tumours showed a tendency to harbour lymph node metastases, but this trend was not significant ($p=0.06$). In the group of 22 patients with aberrant, absent MMR protein expression, the presence of lymph node metastases correlated with SKP2 tumour expression ($p<0.01$).

Discussion

The results of our study suggest that in colorectal adenocarcinomas, the loss of SMAD4 nuclear expression,

Table 2 Main clinicopathological characteristics of the 230 patients with colorectal adenocarcinomas, according to SMAD4 tumour expression

	SMAD4 negative tumours 27 patients (12%)	SMAD4 positive tumours 203 patients (88%)	*p* value
Gender			
Female	15 (56%)	88 (43%)	0.30
Male	12 (44%)	115 (57%)	
Age (years)			
Range (median)	42–83 (61)	29–94 (64)	
Location			
Proximal	4 (15%)	53 (26%)	0.30
Distal	23 (85%)	150 (74%)	
Differentiation			
Well	16 (59%)	92 (45%)	0.22
Moderate	9 (33%)	78 (38%)	
Poor	2 (7%)	33 (16%)	
T TNM			
T1 and T2	4 (15%)	33 (19%)	1
T3 and T4	23 (85%)	170 (84%)	
N TNM			
N0	7 (26%)	96 (47%)	0.04
N1 and N2	20 (74%)	107 (53%)	
M TNM			
M0	23 (85%)	172 (85%)	1
M1	4 (15%)	31 (15%)	

TNM tumour node metastasis classification

defining a group of colorectal carcinomas with impaired TGFβ signalling, correlated with the presence of lymph node metastases. The loss of SMAD4 nuclear expression occurred in 12% of tumours, and this is in agreement with previous studies that reported SMAD4 inactivation in 2–63% of the cases. This broad range in the frequency of SMAD4 alterations could be explained by the inclusion of different histological tumour types, by different interpretations of immunostaining criteria or by tumour heterogeneity despite using the same antibody [23, 28–32]. In the present study, we investigated a 'homogeneous' group of invasive adenocarcinomas. Only SMAD4 nuclear staining was considered because current data are contradictory in terms of whether cytoplasmic staining and low staining intensity is an accurate reflection of gene status [33] or of signal transduction [32, 34–36]. Immunohistochemistry allows analysis of a large number of tumours and thus robust statistical analyses. However, immunohistochemistry is not helpful in detecting rare genetic changes or in differentiating between the presence of mutant allele combined with a loss of heterozygosity or a homozygously deleted DPC4 gene [33].

SMAD4 alterations are not observed in precancerous lesions such as adenomas [23, 37] and occur in approximately 5% of non-invasive epithelial colorectal lesions [8, 37]. When considering invasive adenocarcinomas, SMAD4 mutations are more frequent and correlate with an advanced, metastatic tumour stage [8, 23, 30, 36–38]. Additional support for this relationship could be derived from data showing significant correlations between loss of immunohistochemical SMAD4 tumour expression or loss of 18q heterozygosity and lymph node [31, 39], liver or distant metastases [23, 30, 31, 36, 39, 40]. The results of our study suggest that aggressive disease, characterized by the presence of lymph node metastases, correlated with the loss of SMAD4 nuclear expression, which is in agreement with a metastasis promoter effect observed in colon cancer models [41, 42].

An unexpected finding in our series was the lack of correlation between SMAD4 tumour expression and cell proliferation. The underlying biological processes that explain this finding observed in invasive colorectal adenocarcinomas are difficult to establish by immunohistochemistry alone; further studies on cell lines are required to elucidate this information. However, complex SMAD4 signalling interferes not only with the promotion of metastasis but also with other carcinogenic mechanisms

Fig. 1 Immunohistochemical staining for SMAD4 (**a** positive tumour, **b** negative tumour), Ki67 (**c** tumour with high expression, **d** tumour with low expression), p27 (**e** positive tumour, **f** negative tumour) and SKP2 (**g** positive tumour, **h** negative tumour) in colon adenocarcinomas (original magnification, ×100). The *arrows* point to rare stained nuclei (**d**) and *asterisks* indicate internal controls (fibroblasts or reactive lymphocytes)

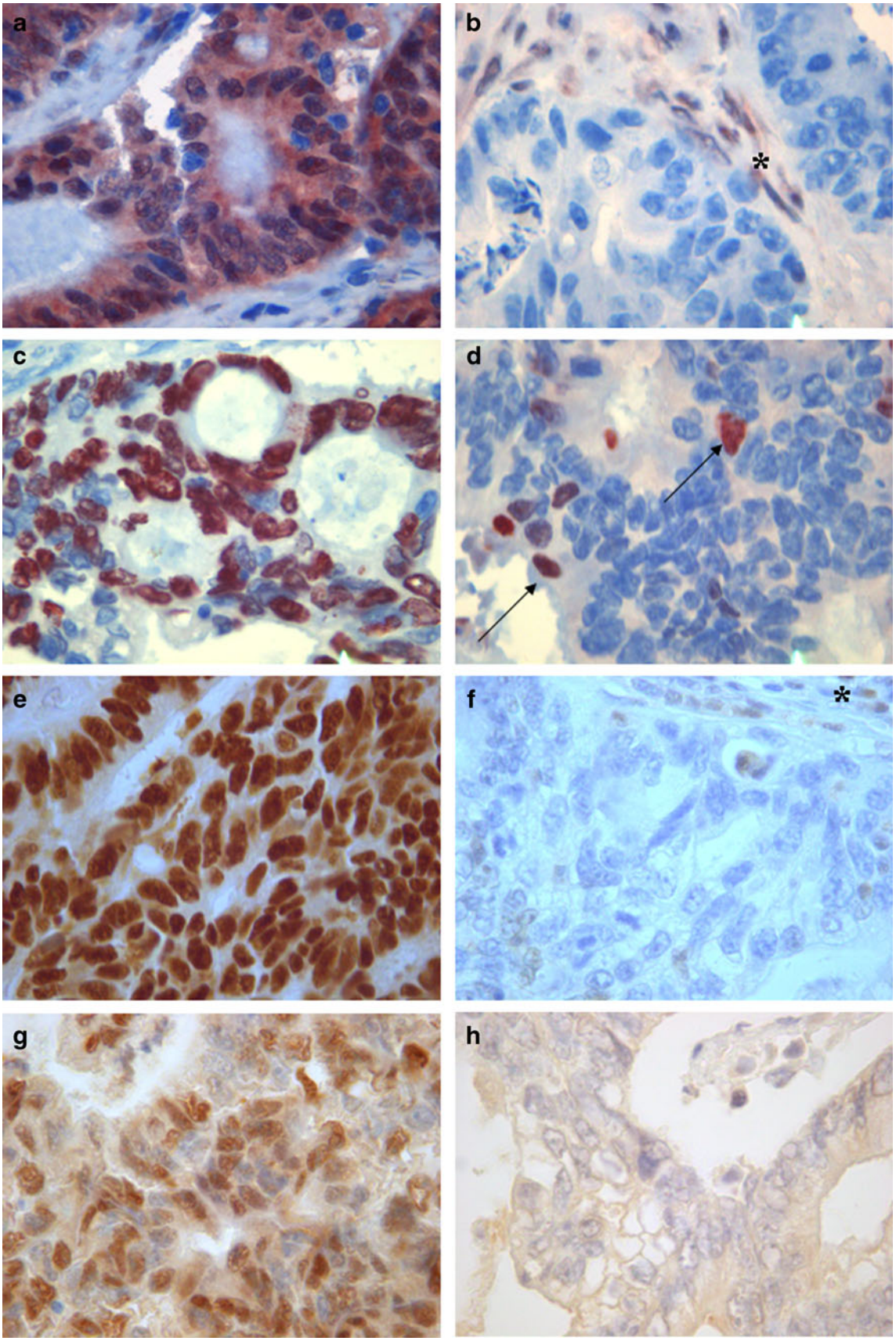
a
b
*
c
d
e
f
*
g
h

Table 3 Relationships between cell proliferation index Ki67 and cell cycle proteins SKP2 and p27 expression in colorectal adenocarcinomas

	Ki67 expression Low index	Ki67 expression High index	*p* value
SKP2 expression			<0.01
Absent	70	47	
Present	46	67	
P27 expression			0.88
Negative	101	99	
Positive	15	15	

such as apoptosis [43, 44], altered cell adhesion [45, 46], promotion of invasion [47] or angiogenesis [48], and this might explain the lack of correlation with the Ki67 index. The extent to which the TGFβ/SMAD signalling interferes with other pathways such as RAS, MAPK, PI3K or WNT and which of these pathways is dominant in mediating cell proliferation in colorectal adenocarcinomas remains difficult to establish [49]. Moreover, interference with inhibitory SMAD7 [44] and phase-specific cell cycle effect of SMAD4 signalling cannot be ruled out because assessment of tumour cell proliferation as noted by the Ki67 index allows only a global evaluation of the amount of proliferating tumour cells in the G1, S or M phases.

Interestingly, SMAD4 tumour expression correlated with the cell cycle inhibitor and G1-S phase modulator p27, a relationship that, to our knowledge, has not previously been reported [50–53]. This suggests a possible mechanism of interference of SMAD4 with cell cycle control in colorectal adenocarcinomas. This finding is not surprising since TGFβ/SMAD2/3 mediates growth inhibition by increasing levels of p27 in endometrial carcinoma cell lines [14, 54] and warrants further research on colon cancer cell lines. In agreement with reported data [55–57], p27 tumour expression did not correlate with cell proliferation in our series. Interference of p27 cell cycle inhibitor protein with promotion of apoptosis [58], tumour cell differentiation [55, 57] or p27 functioning as a tumour-suppressor gene associated with metastatic disease [15, 57–60] might explain the lack of correlation between p27 tumour expression and the Ki67 index. Similar to previously reported data [61, 62], we found an inverse relationship in the level of immunohistochemical expression between SKP2 and p27 in 43% of the tumours, although this association was not statistically significant. The role of SKP2 in tumour biology is probably more complex since the F-box protein is also required for DNA replication during the S phase. SKP2 interacts with the cyclin A-CDK2 complex [17] and probably interferes with the growth of aneuploid cell populations [63]. In agreement with previous studies [64], we found a statistically significant correlation between SKP2 tumour expression and increased cell proliferation.

Altered TGFβ signalling occurs in both microsatellite stable and unstable colorectal carcinoma phenotypes [8], results of the experimental model created by Woodford-Richens et al. [65] suggesting that SMAD4 mutations occur before tumours become aneuploid/polyploid and chromosomal instability appears, but after the divergence of microsatellite stable and unstable pathways. Loss of SMAD4 nuclear signalling is not likely to play a major role in the carcinogenesis of microsatellite unstable tumours, characterized by an alterations in MMR protein expression and function. Similar to other reported data [28, 30], we observed that loss of SMAD4 nuclear expression was infrequent and showed a tendency to relate to aberrant MMR protein expression ($p=0.08$). However, a complete lack of correlation between SMAD4 expression and presence of microsatellite instability has been reported in early onset colorectal cancer [29] and in inflammatory bowel disease-associated colorectal adenocarcinomas [52].

Table 4 SMAD4, Ki67, SKP2 and p27 proteins expression in colorectal adenocarcinomas according to the status of tumour mismatch repair proteins

	Intact MMR protein expression 208 tumours (90%)	Loss of MMR protein expression 22 tumours (10%)	*p* value
SMAD4			0.08
Negative	27 (13%)	0 (0%)	
Positive	181 (87%)	22 (100%)	
Ki67			<0.01
Low index	111 (53%)	5 (23%)	
High index	97 (46%)	17 (77%)	
SKP2			0.37
Negative	108 (52%)	9 (41%)	
Positive	100 (48%)	13 (59%)	
P27			0.18
Negative	183 (88%)	17 (77%)	
Positive	25 (12%)	5 (23%)	

MMR mismatch repair

Events other than abnormal SMAD4 signalling, such as TGFβRII mutation, could be related to abnormal TGFβ signalling in tumours lacking the MMR protein [66–68].

Interestingly, we found that cell proliferation as evaluated by the Ki67 index was significantly higher in tumours with aberrant, absent MMR protein expression. The direct relationship we observed between SKP2 tumour expression and the presence of lymph node metastases in this group of tumours suggest a role of SKP2 in tumour aggressiveness.

Although our study is in accordance with the current guidelines for tumour biomarker studies [69, 70], there are limits in regards to tumour heterogeneity and correlations with survival. In order to address the impact of tumour heterogeneity on tumour protein expression, we used established and published TMA-specific methodologies and cutoffs. Since patients were postoperatively followed up and treated in different medical centres, the survival data were incompletely available and therefore were of limited use for our study.

In conclusion, the results of this immunohistochemical study of a series of 230 colorectal adenocarcinomas suggest that the loss of SMAD4 protein expression correlates with the presence of lymph node metastases. SMAD4 was expressed in all tumours with altered MMR protein expression, and a high tumour cell proliferation correlated with altered MMR protein expression. Loss of SMAD4 expression did not correlate with cell proliferation as shown by the Ki67 index but did correlate with the absence of p27 cell cycle inhibitory protein expression. Although there was no significant relationship between the lack of p27 and SKP2 expression in our series, but only between SKP2 and Ki67, exploring the impact of cell proliferation and, in particular, that of SKP2 in colorectal adenocarcinomas tumour biology might be of clinical interest. Inhibitors of the ubiquitin-mediated proteolysis pathway might be responsible for the degradation of several proteins including SMAD4 and p27 [16, 71, 72]. Bortezomib, an inhibitor of this system, displays antitumour activity against several cancer types including colorectal adenocarcinoma [73], by targeting p27 protein likely through a SKP2-dependent process [74, 75].

Acknowledgements The authors thank the *Societé Française de Pathologie*. We are grateful to Ema Dragoescu and to Pr P Fouret, and we thank Florence Jourdan, Nicole Sebbagh and Jacques Paries.

Conflict of interest statement We declare that we have no conflict of interest.

References

1. Massague J (1998) TGF-beta signal transduction. Annu Rev Biochem 67:753–791
2. Miyazono K (2000) Positive and negative regulation of TGF-beta signalling. J Cell Sci 113:1101–1109
3. Hahn SA, Schutte M, Hoque AT et al (1996) DPC4, a candidate tumor suppressor gene at human chromosome 18q21.1. Science 271:350–353
4. Miyaki M, Kuroki T (2003) Role of Smad4 (DPC4) inactivation in human cancer. Biochem Biophys Res Commun 306:799–804
5. Friedl W, Kruse R, Uhlhaas S et al (1999) Frequent 4-bp deletion in exon 9 of the SMAD4/MADH4 gene in familial juvenile polyposis patients. Genes Chromosomes Cancer 25:403–406
6. Howe JR, Roth S, Ringold JC et al (1998) Mutations in the SMAD4/DPC4 gene in juvenile polyposis. Science 280:1086–1088
7. Blobe GC, Schiemann WP, Lodish HF (2000) Mechanisms of disease: role of transforming growth factor (beta) in human disease. N Engl J Med 342:1350–1358
8. Elliott RL, Blobe GC (2005) Role of transforming growth factor beta in human cancer. J Clin Oncol 23:2078–2093
9. Riggins GJ, Kinzler KW, Vogelstein B et al (1997) Frequency of Smad gene mutations in human cancers. Cancer Res 57:2578–2580
10. Schutte M, Hruban RH, Hedrick L et al (1996) DPC4 gene in various tumor types. Cancer Res 56:2527–25230
11. Thiagalingam S, Lengauer C, Leach FS et al (1996) Evaluation of candidate tumour suppressor genes on chromosome 18 in colorectal cancers. Nat Genet 13:343–346
12. Loda M, Cukor B, Tam SW et al (1997) Increased proteasome-dependent degradation of the cyclin-dependent kinase inhibitor p27 in aggressive colorectal carcinomas. Nat Med 3:231–234
13. Ogino S, Kawasaki T, Kirkner GJ et al (2007) Loss of nuclear p27 (CDKN1B/KIP1) in colorectal cancer is correlated with microsatellite instability and CIMP. Mod Pathol 20:15–22
14. Polyak K, Kato JT, Solomon MJ et al (1994) p27Kip1, a cyclin-Cdk inhibitor, links transforming growth factor-beta and contact inhibition to cell cycle arrest. Genes Dev 8:9–22
15. Lloyd R, Erickson LA, Jin L et al (1999) p27/kip1: a multifunctional cyclin-dependent kinase inhibitor with prognostic significance in human cancers. Am J Pathol 154:313–323
16. Hershko D, Bornstein G, Ben-Izhak O et al (2001) Inverse relation between levels of p27(kip1) and of its ubiquitin ligase subunit SKP2 in colorectal carcinomas. Cancer 91:1745–1751
17. Zhang H, Kobayashi R, Galakionov K et al (1995) p19/Skp1 and p45/SKP2 are essential elements of the cyclin A-CDK2 S phase kinase. Cell 82:915–925
18. Bosman F, Carneiro F, Hruban H, Theise N (eds) (2010) WHO classification of digestive tumours, 4th edn. IARC, Lyon
19. Edge SB, Byrd DR, Compton CC et al (eds) (2010) American Joint Committee on Cancer AJCC cancer staging manual, 7th edn. Springer, New York
20. Jourdan F, Sebbagh N, Comperat E et al (2003) Tissue microarray technology: validation in colorectal carcinoma and analysis of p53, hMLH1, and hMSH2 immunohistochemical expression. Virchows Arch 443:115–121
21. Kononen J, Bubendorf L, Kallioniemi A et al (1998) Tissue microarrays for high-throughput molecular profiling of tumour specimens. Nat Med 4:844–847
22. Handra-Luca A, Ruhin B, Lesty C et al (2006) P27, SKP2, and extra-cellular signal-related kinase signalling in human salivary gland mucoepidermoid carcinoma. Oral Oncol 42:1005–1010
23. Maitra A, Molberg K, Albores-Saavedra J et al (2000) Loss of Dpc4 expression in colonic adenocarcinomas correlates with the presence of metastatic disease. Am J Pathol 57:1105–1111
24. Maitra A, Adsay NV, Argani P et al (2003) Multicomponent analysis of the pancreatic adenocarcinoma progression model using a pancreatic intraepithelial neoplasia tissue microarray. Mod Pathol 16:902–912

25. Hoos A, Urist MJ, Stojadinovic A et al (2001) Validation of tissue microarrays for immunohistochemical profiling of cancer specimens using the example of human fibroblastic tumors. Am J Pathol 158:1245–1251
26. Rigau V, Sebbagh N, Olschwang S et al (2003) Mirosatellite instability in colorectal carcinoma. The comparison of immunohistochemistry and molecular biology suggests a role for hMSH6 immunostaining. Arch Pathol Lab Med 127:694–700
27. Lindor NM, Burgart LJ, Leontovich O et al (2002) Immunohistochemistry versus microsatellite instability testing in phenotyping colorectal tumours. J Clin Oncol 20:1043–1048
28. Montgomery E, Goggins M, Zhou S et al (2001) Nuclear localization of Dpc4 (Madh4, SMAD4) in colorectal carcinomas and relation to mismatch repair/transforming growth factor-beta receptor defects. Am J Pathol 158:537–542
29. Royce SG, Alsop K, Haydon A et al (2010) The role of SMAD4 in early onset colorectal cancer. Colorectal Dis 12:213–219
30. Salovaara R, Roth S, Loukola A et al (2002) Frequent loss of SMAD4/DPC4 protein in colorectal cancers. Gut 51:56–59
31. Xie W, Rimm DL, Lin Y et al (2003) Loss of SMAD signalling in human colorectal cancer is associated with advanced disease and poor prognosis. Cancer J 9:302–312
32. Xu WQ, Jiang XC, Yu YY et al (2007) Expression of TGF-beta1, TbetaRII and Smad4 in colorectal carcinoma. Exp Mol Pathol 82:284–291
33. Wilentz RE, Su GH, Dai JL et al (2000) Immunohistochemical labeling for Dpc4 mirrors genetic status in pancreatic adenocarcinomas. A new marker of DPC4 inactivation. Am J Pathol 156:37–43
34. Alazzouzi H, Alhopuro P, Salovaara R et al (2005) SMAD4 as a prognostic marker in colorectal cancer. Clin Cancer Res 11:2606–2611
35. Alhopuro P, Alazzouzi H, Sammalkorpi H et al (2005) SMAD4 levels and response to 5-fluorouracil in colorectal cancer. Clin Cancer Res 11:6311–6316
36. Tanaka T, Watanabe T, Kazama Y et al (2006) Chromosome 18q deletion and Smad4 protein inactivation correlate with liver metastasis: a study matched for T- and N-classification. Br J Cancer 95:1562–1567
37. Miyaki M, Iijima T, Konishi M et al (1999) Higher frequency of Smad4 gene mutation in human colorectal cancer with distant metastasis. Oncogene 20:3098–3103
38. Koyama M, Ito M, Nagai H et al (1999) Inactivation of both alleles of the DPC4/SMAD4 gene in advanced colorectal cancers: identification of seven novel somatic mutations in tumours from Japanese patients. Mutat Res 406:71–77
39. Tanaka T, Watanabe T, Kazama Y, Tanaka J et al (2008) Loss of Smad4 protein expression and 18qLOH as molecular markers indicating lymph node metastasis in colorectal cancer—a study matched for tumor depth and pathology. J Surg Oncol 97:69–73
40. Losi L, Bouzourene H, Benhattar J (2007) Loss of Smad4 expression predicts liver metastasis in human colorectal cancer. Oncol Rep 17:1095–1099
41. Xiao DS, Wen JF, Li JH et al (2006) Effect of DPC4 gene on invasion and metastasis of colorectal carcinoma cells. Acta Biochim Biophys Sin (Shanghai) 38:883–892
42. Zhang B, Halder SK, Kashikar ND et al (2010) Antimetastatic role of Smad4 signaling in colorectal cancer. Gastroenterology 138:969–980
43. Dai JL, Bansal RK, Kern SE (1999) G1 cell cycle arrest and apoptosis induction by nuclear Smad4/Dpc4: phenotypes reversed by a tumorigenic mutation. Proc Natl Acad Sci U S A 96:1427–1432
44. Halder SK, Beauchamp RD, Datta PK (2005) Smad7 induces tumorigenicity by blocking TGF-beta-induced growth inhibition and apoptosis. Exp Cell Res 307:231–246
45. Schwarte-Waldhoff I, Klein S, Blass-Kampmann S et al (1999) DPC4/SMAD4 mediated tumor suppression of colon carcinoma cells is associated with reduced urokinase expression. Oncogene 18:3152–3158
46. Volmer MW, Radacz Y, Hahn SA et al (2004) Tumour suppressor Smad4 mediates downregulation of the anti-adhesive invasion-promoting matricellular protein SPARC: landscaping activity of Smad4 as revealed by a “secretome” analysis. Proteomics 4:1324–1334
47. Reinacher-Schick A, Baldus S, Romdhana B et al (2004) Loss of Smad4 correlates with loss of the invasion suppressor E-cadherin in advanced colorectal carcinomas. J Pathol 202:412–420
48. Schwarte-Waldhoff I, Schmiegel W (2002) Smad4 transcriptional pathways and angiogenesis. Int J Gastrointest Cancer 31:47–59
49. DeVita VR, Hellman S, Rosenberg SA (eds) (2005) Cancer principles and practice of oncology, 7th edn. Lippincott Williams and Wilkins, Philadelphia
50. Biankin AV, Biankin SA, Kench JG et al (2002) Aberrant p16 (INK4A) and DPC4/Smad4 expression in intraductal papillary mucinous tumours of the pancreas is associated with invasive ductal adenocarcinoma. Gut 50:861–868
51. Hill KA, Wang KL, Stryker SJ, Gupta R, Weinrach DM, Rao MS (2004) Comparative analysis of cell adhesion molecules, cell cycle regulatory proteins, mismatch repair genes, cyclooxygenase-2, and DPC4 in carcinomas arising in inflammatory bowel disease and sporadic colon cancer. Oncol Rep 11:951–956
52. Kang YK, Kim WH, Jang JJ (2002) Expression of G1-S modulators (p53, p16, p27, cyclin D1, Rb) and Smad4/Dpc4 in intrahepatic cholangiocarcinoma. Hum Pathol 33:877–883
53. Zeng L, Rowland RG, Lele SM et al (2004) Apoptosis incidence and protein expression of p53, TGF-beta receptor II, p27Kip1, and Smad4 in benign, premalignant, and malignant human prostate. Hum Pathol 35:290–297
54. Lecanda J, Ganapathy V, D’Aquino-Ardalan C et al (2009) TGFbeta prevents proteasomal degradation of the cyclin-dependent kinase inhibitor p27kip1 for cell cycle arrest. Cell Cycle 8:742–756
55. Ciaparrone M, Yamamoto H, Yao Y et al (1998) Localization and expression of p27KIP1 in multistage colorectal carcinogenesis. Cancer Res 58:114–122
56. Palmqvist R, Stenling R, Oberg A et al (1999) Prognostic significance of p27(Kip1) expression in colorectal cancer: a clinico-pathological characterization. J Pathol 188:18–23
57. Thomas GV, Szigeti K, Murphy M et al (1998) Down-regulation of p27 is associated with development of colorectal adenocarcinoma metastases. Am J Pathol 153:681–687
58. Katayose Y, Kim M, Rakkar AN et al (1997) Promoting apoptosis: a novel activity associated with the cyclin-dependent kinase inhibitor p27. Cancer Res 57:5441–5445
59. Liu DF, Ferguson K, Cooper GS et al (1999) p27 cell-cycle inhibitor is inversely correlated with lymph node metastases in right-sided colon cancer. J Clin Lab Anal 13:291–295
60. Yao J, Eu KW, Seow-Choen F et al (2000) Down-regulation of p27 is a significant predictor of poor overall survival and may facilitate metastasis in colorectal carcinomas. Int J Cancer 89:213–216
61. Shapira M, Ben-Izhak O, Bishara B et al (2004) Alterations in the expression of the cell cycle regulatory protein cyclin kinase subunit 1 in colorectal carcinoma. Cancer 100:1615–1621
62. Shapira M, Ben-Izhak O, Linn S et al (2005) The prognostic impact of the ubiquitin ligase subunits SKP2 and Cks1 in colorectal carcinoma. Cancer 103:1336–1346
63. Nakayama K, Nagahama H, Minamishima YA et al (2000) Targeted disruption of SKP2 results in accumulation of cyclin E and p27 (Kip), polyploidy and centrosome duplication. EMBO J 19:2069–2081

64. Li JQ, Wu F, Masaki T et al (2004) Correlation of Skp2 with carcinogenesis, invasion, metastasis, and prognosis in colorectal tumors. Int J Oncol 25:87–95
65. Woodford-Richens KL, Rowan AJ, Gorman P et al (2001) SMAD4 mutations in colorectal cancer probably occur before chromosomal instability, but after divergence of the microsatellite instability pathway. Proc Natl Acad Sci U S A 98:9719–9723
66. Grady WM, Myeroff LL, Swinler SE et al (1999) Mutational inactivation of transforming growth factor beta receptor type II in microsatellite stable colon cancers. Cancer Res 59:320–324
67. Iacopetta BJ, Welch J, Soong R et al (1998) Mutation of the transforming growth factor-beta type II receptor gene in right-sided colorectal cancer: relationship to clinicopathological features and genetic alterations. J Pathol 184:390–395
68. Parsons R, Myeroff LL, Liu B et al (1995) Microsatellite instability and mutations of the transforming growth factor beta type II receptor gene in colorectal cancer. Cancer Res 55:5548–5550
69. Locker GY, Hamilton S, Harris J et al (2006) ASCO 2006 update of recommendations for the use of tumor markers in gastrointestinal cancer. J Clin Oncol 24:5313–5327
70. McShane LM, Altman DG, Sauerbrei W, Statistics Subcommittee of the NCI-EORTC Working Group on Cancer Diagnostics et al (2005) Reporting recommendations for neoplastic marker prognostic studies. J Clin Oncol 23:9067–9072
71. Moren A, Hellman U, Inada Y et al (2003) Differential ubiquitination defines the functional status of the tumor suppressor Smad4. J Biol Chem 278:33571–33582
72. Nalepa G, Rolfe M, Harper JW (2006) Drug discovery in the ubiquitin-proteasome system. Nat Rev Drug Discov 5:596–613
73. Mani A, Gelmann EP (2005) The ubiquitin-proteasome pathway and its role in cancer. J Clin Oncol 23:4776–4789
74. Boccadoro M, Morgan G, Cavenagh J (2005) Preclinical evaluation of the proteasome inhibitor bortezomib in cancer therapy. Cancer Cell Int 5:18
75. Cusack JC (2003) Rationale for the treatment of solid tumors with the proteasome inhibitor bortezomib. Cancer Treat Rev 29:21–31

Virchows Arch (2011) 459:521–527
DOI 10.1007/s00428-011-1154-2

ORIGINAL ARTICLE

JAK2-V617F-mutated myeloproliferative neoplasms reveal different allele burden within hematopoietic cell lineages: a microdissection study of bone marrow trephine biopsies

Andreas Kreft · Thomas Kindler · Erik Springer · Charles James Kirkpatrick

Received: 9 June 2011 / Revised: 26 September 2011 / Accepted: 3 October 2011 / Published online: 18 October 2011
© Springer-Verlag 2011

Abstract The JAK2-V617F mutation is prevalent in almost all patients with polycythemia vera (PV) and about half of the cases of essential thrombocythaemia (ET) and primary myelofibrosis (PMF). A different allele burden in these entities has long been noticed, but little is known about its distribution among the neoplastic hematopoietic cell lineages within the bone marrow. We conducted a microdissection study of JAK2-V617F-mutated myeloproliferative neoplasms (MPN); 10 cases each of ET, PV, and PMF, with separate analysis of the JAK2 mutation status in three hematopoietic cell lines (i.e., megakaryo-, granulo-, and erythropoiesis). Different numbers of cell lineages harboring the JAK2-V617F mutation were found, being the lowest in ET (17/30), higher in PV (24/30) and in PMF (22/30). The megakaryopoiesis was the most commonly mutated cell lineage (24/30 cases). By analyzing microdissectates we were able to demonstrate a different allele burden of the JAK2-V617F mutation in the megakaryo-, erythro-, and granulopoiesis within the bone marrow of a given case of MPN. We demonstrated differences in the number of mutated cell lineages. The different mutation status may contribute to the different phenotypes of ET, PV, and PMF.

Keywords MPN · JAK2-V617F mutation · Microdissection

A. Kreft (✉) · E. Springer · C. J. Kirkpatrick
Institut für Pathologie, Universitätsmedizin Mainz,
Langenbeckstr. 1,
55101 Mainz, Germany
e-mail: kreft@pathologie.klinik.uni-mainz.de

T. Kindler
Division of Hematology, Oncology and Pneumology,
Internal Medicine 3, Universitätsmedizin Mainz,
Langenbeckstr. 1,
55101 Mainz, Germany

Introduction

Chronic myeloproliferative neoplasms (MPNs) are disorders of the hematopoietic stem cell, which normally give rise to megakaryo-, granulo-, and/or erythropoiesis [1]. In MPNs, recurrent genetic aberrations have been identified, of which the bcr–abl translocation (Philadelphia chromosome; Ph) in chronic myeloid leukemia was described first. Recently, another gain of function mutation, the janus kinase 2 (JAK2)-V617F mutation, has been identified in patients with Ph-negative MPNs [2, 3]. This mutation leads to constitutive activation of JAK2 and phosphorylation of downstream effectors such as STATs [1]. In contrast to bcr–abl, the JAK2 mutation does not result in a distinct entity or phenotype but can be detected in the three most common Ph-negative MPNs with different frequencies; as a constant finding in polycythemia vera (PV) and in about half of the patients with essential thrombocythaemia (ET) and primary myelofibrosis (PMF), respectively [4].

In those MPNs which are mutated, the JAK2-V617F allele is not distributed equally among the neoplastic cells. Several studies revealed the coexistence of JAK2-V617F mutated and wild-type cells as well as variations in the allele burden of individual mutated cells, being either homo- or heterozygous [5–10]. Some authors therefore argue that the JAK2-V617F mutation is only a secondary event in the cascade of the clonal pathogenesis of the Ph-negative MPNs [10–12]. In addition, differences in allele burden are seen between the entities, of which ET has the lowest burden. More mutations were found in PV and the highest allele load was seen in PMF [13–16].

As the allele burden is generally calculated from peripheral granulocytes [5–12, 15, 17] or cell culture studies of hematopoietic progenitor cells [5, 14, 18], there is no immediate information about the distribution of the

JAK2-V617F alleles among the hematopoietic cell lineages within the bone marrow. As distinct hematopoietic cell lineages may harbor the mutation, a different allele burden of megakaryo-, granulo-, and erythropoiesis may contribute to the different clinical phenotypes of ET, PV, and PMF. To address this question, we performed a direct analysis of the bone marrow by microdissection of trephine biopsies.

Patients and methods

We investigated 30 consecutive diagnostic bone marrow trephine biopsies from patients with Ph-negative, JAK2-V617F-mutated MPNs in chronic phasis from the files of the Institut für Pathologie, Universitätsmedizin Mainz, Germany from 2008 to 2010. All the biopsies, seven each of PV and ET and six with PMF, were taken as part of the primary diagnostic workup, without prior chemotherapy. The diagnosis was made according to the current WHO criteria [19]. The patient's characteristics are given in Table 1.

The bone marrow trephine biopsies were fixed in glutaraldehyde–formalin for at least 8 h and subsequently decalcified in EDTA. Standard histochemical staining was performed using Giemsa, Periodic acid Schiff reaction, Turnbull's iron stain, and the naphtanol-ASD-chloresterase reaction. Grading of marrow fibrosis was performed using a three-tiered scoring system [20].

Microdissection was done to extract megakaryo-, granulo-, and erythropoiesis from the bone marrow trephine biopsies, using a P.A.L.M. laser capture microscope (P.A.L.M. Microlaser Technologies AG, Bernried, Germany). To facilitate separation, the different cell lineages were highlighted by immunohistochemistry using the DAB-method: Megakaryopoiesis with antibodies against factor VIII (MS-722-P0, LabVision, Fremont, CA, USA, pretreatment with proteinase (S3007, Dako, Glostrup, Denmark), 1:50), granulopoiesis with antibodies against myeloperoxydase (RB 335, LabVision, pretreatment with pressure cooking in buffer pH 6.1 (K8001, Dako, Glostrup, Denmark), 1:200), and erythropoiesis with antibodies against hemoglobin (Hb) (AO118, Dako, Glostrup, Denmark, no pretreatment, 1:2,000), stained each on separate slides. At least 100 megakaryocytes or 200 nucleated erythropoietic or granulopoietic cells respectively were extracted for separate molecular biological analysis (Fig. 1).

The obtained cell fractions were digested with proteinase K, followed by DNA extraction using phenol–cloroform–isoamyl alcohol and precipitated with ethanol. Semi-nested PCR was performed using primer pairs flanking the region of JAK2-V617 (forward primer: CTTTCTTTGAAGCAGCAAG TATGA, reverse primer CTGACACCTAGCTGTGATCCTG, semi-nested reverse primer AGATGCTCTGAGAAAGG CATTA) yielding PCR products of 181 nt and 131 nt, respectively. PCR was performed with the Fast Cycle PCR Mix (Qiagen, Hilden, Germany) for 35 cycles (first and nested), 5 s at 96°C, 5 s at 60°C, and 7 s at 68°C.

With all the DNA preparations used in this study, a minimum of two independent PCRs were amplified. In any PCR setup, a negative (reagents only) control and a positive (i.e., high-quality human genomic DNA) control were amplified. Finally, after ExoSAP-IT digestion (Amersham Biosciences, Freiburg, Germany), all PCR products were directly sequenced using Sanger Chemistry (Beckman-Coulter, Krefeld, Germany) and analyzed with the Beckman CEQ8000 capillary gel electrophoresis system.

Results

Histological evaluation of the evaluated bone marrow trephine biopsies revealed atypical, enlarged megakaryocytes, and most of the biopsies of PMF showed an extended granulopoiesis and in cases of PV an additional increased erythropoiesis. Marrow fibrosis was not seen in the patients with ET, but in 4/10 of the patients with PV (two grade 1 and one each for grades 2 and 3) as well as in 8/10 patients with PMF (two prefibrotic, three grade 1, three grade 2, and two grade 3). Blasts were not increased in any of the cases.

Upon microdissection the JAK2-V617F mutation was found in 70% of DNA samples derived from different cell lineages (41/60, Table 2). However, there were substantial differences between the MPN entities:

Table 1 Patient's characteristics

	ET	PV	PMF
Patients	10	10	10
Median age (range)	64 (33–83)	70 (59–80)	73 (52–89)
Gender m/w	4/6	4/6	6/4
Median WBC (range)	11,000/μl (3,900–20,700)	17,300/μl (12,100–36,400)	19,600/μl (3,800–40,500)
Median Hb (range)	14.1 g/dl (10.4–16.3)	13.3 g/dl (10.9–18.4)	10.0 g/dl (8–14.2)
Median platelet (range)	970,000/μl (693,000–1,530,000)	485,000/μl (226,000–1,39,9,000)	457,000/μl (100,000–971,000)

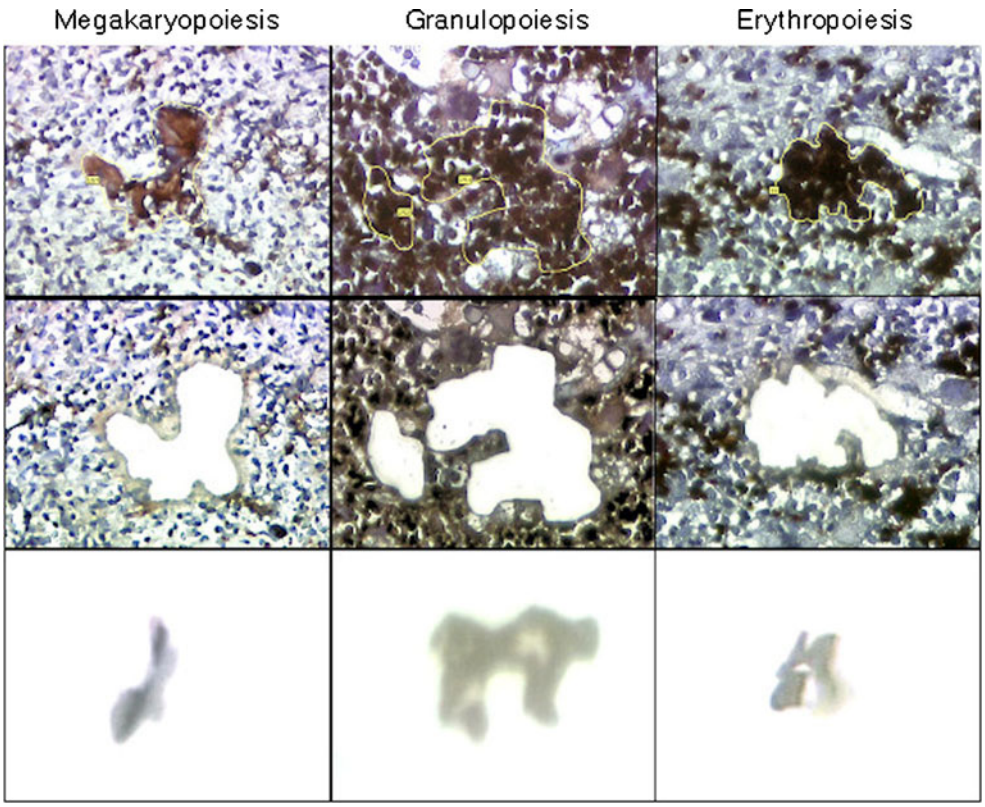

Fig. 1 Screenshots from the laser capture microscope of microdissection of the three hematopoietic cell lines highlighted by immunohistochemistry and encircled for microdissection (megakaryopoiesis: factor VIII, granulopoiesis: myeloperoxydase, and erythropoiesis: erythropoietin) revealing the areas selected for microdissection (*first line*), the slides after dissection (*second line*), and the tissue gained by microdissection in the fastening of the test tube (*third line*)

Essential thrombocythaemia: The lowest number of affected lineages was found in ET (56%), with 7/10 megakaryocytic-, 4/10 granulopoietic-, and 6/10 erythropoietic lineages harboring the mutation. Interestingly, two cases with JAK2 wild-type (wt) megakaryopoiesis had the highest platelet counts (1,530,000 and 1,099,000/μl, respectively), whereas the third case with JAK2 wt megakaryopoiesis has the lowest thrombocyte count (6,930,000/μl) The patients with the highest Hb concentration (16.3 and 15.5 g/dl) were among those who had JAK2-V617F-mutated erythropoiesis. The lowest portion of mutated cell lineages was found within the granulopoiesis. In only two of the ET patients were the JAK2-V617F mutation detected in all three hematopoietic cell lineages.

Polycythemia vera: In PV microdissectates, the JAK2-V617F mutation was detected in 80% of cell lineages investigated, including almost all erythropoietic cell lineages (9/10). As in ET, one PV patient without the mutation in megakaryocytes had the highest platelet count (767,000/μl), whereas the other patient with wild-type JAK2 revealed a rather low thrombocyte count (383,000/μl). The three granulopoietic cell lineages, which were negative for the JAK2-V617F mutation, produced average leukocyte counts in this entity (13,100; 19,700; and 20,900/μl). Seven of the 10 PV cases had all three cell lines mutated.

Primary myelofibrosis: In PMF the percentage of mutated cell lineages were about as high as in PV (73%). In half of the 10 PMF patients, the JAK2-V617F mutation was detected in all three cell lineages. The megakaryopoietic cells in 9/10 case were positive for the mutation. Lesser numbers were found in the granulopoiesis (7/10) and erythropoiesis (6/10). Interestingly one of the patients with the JAK2 wt within the erythropoiesis had the highest Hb value (14.2/μl).

Discussion

The JAK2-V617F mutation is prevalent in the majority of bcr–abl-negative MPN patients and has been shown to play a key role in neoplastic cellular proliferation. Recently, the JAK2-V617F mutation has been included as a diagnostic criterion in the WHO diagnostic system [19]. Although JAK2-V617F is an integral element of the pathophysiology of ET, PV, and PMF, these disorders are divergent in their clinical presentation and biological prognosis, ranging from an almost normal life expectancy in ET to a median survival of only 3 to 4 years in PMF [19]. Therefore, the mutational status per se does not account for the different disease phenotypes.

Microdissection study of histological slides represents a well-established method to study genetic aberrations, and

Table 2 Prevalence of JAK2-V617F mutation in megakaryo-, erythro-, and granulopoiesis of polycythemia vera, essential thrombocythaemia, and primary myelofibrosis

Entity	Patient	Megakaryopoiesis JAK2-V617F mutation	Granulopoiesis JAK2-V617F mutation	Erythropoiesis JAK2-V617F mutation
ET	1	−	−	+
	2	−	+	−
	3	−	+	+
	4	+	−	−
	5	+	−	−
	6	+	−	−
	7	+	−	+
	8	+	−	+
	9	+	+	+
	10	+	+	+
PV	1	−	−	+
	2	−	−	+
	3	+	−	−
	4	+	+	+
	5	+	+	+
	6	+	+	+
	7	+	+	+
	8	+	+	+
	9	+	+	+
	10	+	+	+
PMF	1	−	+	+
	2	+	−	−
	3	+	−	−
	4	+	−	−
	5	+	+	−
	6	+	+	+
	7	+	+	+
	8	+	+	+
	9	+	+	+
	10	+	+	+

PV polycythemia vera, *ET* essential thrombocythaemia, *PMF* primary myelofibrosis, + JAK2-V617F mutated, − wild type of JAK2

therefore this technique has been used to investigate bone marrow trephine biopsies in JAK2-V617F-mutated MPNs [21–23]. Since we used immunohistochemistry and all microdissections were performed by an experienced hematopathologist (A.K.), we can assure that all DNA samples obtained upon microdissection were of the desired cell lineage. However, as nested PCR was necessary to obtain sufficient product for sequencing, biased amplification of wild-type or mutated alleles is possible Thus we are not in a position to provide reliable data of hetero- or homozygosity of the JAK2-V617F mutation status in the analyzed cell lineages.

Due to technical reasons, the method of Sanger sequencing may be insensitive in detecting low amount gene alterations, especially if less than 15% of the investigated cells harbor the mutation [24]. Thus low amounts of mutated alleles, which were reported in a number of ET and some PV [13–16], may not be discovered by this technique. Since these values were calculated from blood samples, they were not comparable an investigation of nucleated bone marrow cells, as we performed. If there are differences in the mutation status of the three hematopoietic cell lineages, the amount of mutated alleles should be higher in the separated cell lineages compared with the average, and therefore not difficult to detect. Although we could not exclude minor mutated cell populations in our micro dissected cell fractions which were labeled as wild type of the JAK2 gene, we could report the mutation if it was prevalent a major cell fraction of the morphological homogenous cell compartment.

To investigate the clinically relevant allele burden, some authors compared the JAK2-V617F allele load in progenitor cells and mature blood cells and found different results.

The allele burden was significantly higher in peripheral blood cells, whereas the allele burden of progenitor cells more likely seems to represent the course of the disease [14, 25]. Using the microdissection technique, we found that in JAK2-V617F-mutated MPNs not all neoplastic hematopoietic cell lineages harbored the mutation. However, our methodology involved investigation of the progenitor cells as well as the later stages of maturation. Our investigation of 30 MPN patients revealed differences between disease entities and a heterogenic distribution among the hematopoietic cell lineages.

Several studies have identified the JAK2-V617F allelic burden to correlate with different disease phenotypes, being the lowest in ET, increased in PV, and being the highest in PMF [13–15, 17, 18, 26]. This corresponds well with our finding of JAK2-mutated MPNs of which 17/30 cell lineages in ET, 24/30 in PV, and 22/30 in PMF harbor the mutation. Differences between the entities were most striking between ET, of which only 2/10 cases harbors the JAK2-V617F mutation in all three hematopoietic cell lineages, and PV as well as PMF, in which mutated JAK2 was detected in all three cell lineages in 5/10 and 6/10 cases, respectively. These differences in the affected lineages may explain the different allele burden and also seem to reflect the clinical course of the diseases. As many authors have reported the coexistence of JAK2-V617F mutated and wild-type hematopoietic progenitor cells in patients with JAK2-V617F-mutated MPNs [5–10, 14, 18, 27], the maturation of those heterogeneous progenitors within the bone marrow has given rise to hematopoietic cells of different lineages, which may be either mutated in their major cell compartment or not.

Regarding megakaryopoiesis as the cell line representing the highest prevalence of the JAK2-V617F mutation (24/30), our results correspond well with data from Hussein et al. who also used the microdissection technique on bone morrow trephines and compared megakaryocytes to the rest of the bone marrow cells [21]. In contrast, other investigators have found almost equal allele burden in megakaryocytes and other bone marrow cells [23] or even a lower percentage of mutated cells within megakaryopoiesis as compared with erythro- and granulopoiesis [28], of which the latter study was not performed by microdissection but by in situ PCR. However, since atypical megakaryocytes are always present in MPNs and are the key diagnostic criterion in bone marrow histopathology [29], it seems plausible that megakaryocytes are most likely affected during the neoplastic process and carry a high allelic burden. In our samples the majority of ET, PV, and PMF were found positive for the JAK2-V617F mutation within the megakaryocytes.

In ET less than half of the investigated granulopoietic and only 6/10 of the erythropoietic cell lineages were mutated, mirroring the generally unremarkable hemoglobin level and rarely elevated leukocyte count in this entity and correspond to the low allele burden as reported from the literature [13–16]. In contrast, in PV nearly all analyzed erythropoietic cells (9/10 lineages) contained the JAK2-V617F mutation, reflecting high Hb values as the most distinct and eponymous clinical finding of this disorder. In PMF and PV, at least half of the samples show the JAK2-V617F mutation in all three lineages. This finding may indicate that an early progenitor, still able to differentiate into all three lineages, acquire the JAK2-V617F mutation. In comparison, it is possible that a more committed progenitor may be affected in ET.

Another pathogenetic concept suggests that the JAK2-V617F mutation happens as a secondary event during the neoplastic process [27, 30, 31]. Interestingly, the most acute leukemias secondary to JAK2-V617F-mutated MPNs are JAK2 wt [22, 32], indicating a higher malignant potential of clonal, JAK2 wt progenitor cells. Moreover the rather high thrombocyte counts in the only two cases of ET with JAK2 wt megakaryopoiesis may indicate a further loss of regulation and a higher proliferative potential in those megakaryocytes. Therefore, it is tempting to speculate that a first, as yet unknown, genetic hit is acquired at the hematopoietic stem cell level causing clonal expansion. As a second step, the JAK2-V617F mutation is acquired in more committed progenitor cells and defines the disease phenotype [10–12].

In PV, which as an entity almost always carries a JAK2-V617F mutation, a high allele burden was associated with some clinical features such as myelofibrosis and duration of disease [14, 33–36]. Due to our small sample size, we were not able to find a significant association of hematologic abnormalities and the mutational status of the different cell lineages. In data from the literature, ET patients carrying the JAK2-V617F mutation exhibit higher Hb levels, higher leukocyte counts, and lower platelet counts, as well as a higher risk of thrombosis [37]. In our JAK2-V617F-mutated ET group of patients, those with mutated megakaryopoiesis had a lower platelet counts, compared with the wild-type cell lineages

By analyzing the different cell lineages for the JAK2-V617F mutation, we were able to describe a different mutation status in megakaryo-, erythro-, and granulopoiesis within the bone marrow of a given case of MPN. Although we investigated only 30 patients, we were able to demonstrate some remarkable—albeit not truly distinctive—differences in the number of mutated cell lineages, being the lowest in ET and the highest in PV and PMF. The different mutation status may contribute to the different phenotypes of ET, PV, and PMF. In JAK2-V617F-mutated ET, the mutation status of the megakaryopoiesis may have some influence on the platelet count within the peripheral blood.

Conflict of interest statement The authors declare that they have no conflict of interest.

References

1. Skoda R (2007) The genetic basis of myeloproliferative disorders. Hematology 2007:1–9
2. Kralovics R, Passamonti F, Buser AS et al (2005) A gain-of-function mutation of JAK2 in myeloproliferative disorders. N Engl J Med 352:1779–1790
3. Jones AV, Kreil S, Zoi K et al (2005) Widespread occurrence of the JAK2 V617F mutation in chronic myeloproliferative disorders. Blood 106:2162–2168
4. Hussein K, Bock O, Kreipe H (2007) Histologic and molecular classification of chronic myeloproliferative disorders in the age of JAK2: persistence of old questions despite new answers. Pathol Biol 74:72–80
5. Jamieson CHM, Gotlib J, Durocher JA et al (2006) The JAK2 V617F mutation occurs in hematopoietic stem cells in polycythemia vera and predisposes toward erythroid differentiation. Proc Natl Acad Sci 103:6224–6229
6. Ishii T, Bruno E, Hoffman R et al (2006) Involvement of various hematopoietic-cell lineages by the JAK2V617F mutation in polycythemia vera. Blood 108:3128–3134
7. Pardanani A, Lasho TL, Finke C et al (2007) Extending Jak2V617F and MplW515 mutation analysis to single hematopoietic colonies and B and T lymphocytes. Stem Cells 25:2358–2362
8. Delhommeau F, Dupont S, Tonetti C et al (2007) Evidence that the JAK2 G1849T (V617F) mutation occurs in a lymphomyeloid progenitor in polycythemia vera and idiopathic myelofibrosis. Blood 109:71–77
9. Beer PA, Jones AV, Bench AJ et al (2009) Clonal diversity in the myeloproliferative neoplasms: independent origins of genetically distinct clones. Br J Haematol 144:904–908
10. Scott LM, Scott MA, Campbell PJ et al (2006) Progenitors homozygous for the V617F mutation occur in most patients with polycythemia vera, but not essential thrombocythemia. Blood 108:2435–2437
11. Jamal R, Belisle C, Lessard MC et al (2008) Evidence suggesting the presence of a stem cell clone anteceding the acquisition of the JAK2-V617F mutation. Leukemia 22:1472–1474
12. Antonioli E, Guglielmelli P, Poli G et al (2007) Polycythemia vera following autologous transplantation for AML: insights on the kinetics of JAK2V617F clonal dominance. Blood 110:4620–4621
13. Larsen TS, Pallisgaard N, Møller MB et al (2007) The JAK2 V617F allele burden in essential thrombocythemia, polycythemia vera and primary myelofibrosis—impact on disease phenotype. Eur J Haematol 79:508–515
14. Alison RM, Donna MW, Ophelia R et al (2008) Phenotypic variability within the JAK2 V617F-positive MPD: roles of progenitor cell and neutrophil allele burdens. Exp Hematol 36:1480–1486
15. Antonioli E, Guglielmelli P, Poli G et al (2008) Influence of JAK2V617F allele burden on phenotype in essential thrombocythemia. Haematologica 93:41–48
16. Alessandra C, Guido F, Elisabetta A et al (2009) JAK2V617F allele burden and thrombosis: a direct comparison in essential thrombocythemia and polycythemia vera. Exp Hematol 37:1016–1021
17. Passamonti F, Rumi E, Pietra D et al (2006) Relation between JAK2 (V617F) mutation status, granulocyte activation, and constitutive mobilization of CD34+ cells into peripheral blood in myeloproliferative disorders. Blood 107:3676–3682
18. Stein BL, Williams DM, Rogers O et al (2011) Disease burden at the progenitor level is a feature of primary myelofibrosis: a multivariable analysis of 164 JAK2 V617F-positive myeloproliferative neoplasm patients. Exp Hematol 39:95–101
19. Swerdlow SH, Campo E, Harris NL et al (ed) (2008) World Health Organization classification of tumours: pathology and genetics of tumours of the haematopoetic and lymphoid tissues. IARC, Lyon
20. Kreft A, Weiß M, Wiese B et al (2003) Chronic idiopathic myelofibrosis: prognostic impact of myelofibrosis and clinical parameters on event-free survival in 122 patients who presented in prefibrotic and fibrotic stages. Ann Hematol 82:605–611
21. Hussein K, Brakensiek K, Büsche G et al (2007) Different involvement of the megakaryocytic linage by the JAK2 V617F mutation in polycythenia vera, essential thrombocythemia and chronic idiopathic myelofibrosis. Ann Hematol 86:245–253
22. Kreft A, Springer E, Lipka DB et al (2009) Wild-type JAK2 secondary acute erythroleukemia developing after JAK2-V617F-mutated primary myelofibrosis. Acta Haematol 122:36–38
23. Kremer M, Horn T, Koch I et al (2008) Quantitation of the JAK2V617F mutation in microdissected bone marrow trephines: equal mutational load in myeloid lineages and rare involvement of lymphoid cells. Am J Surg Pathol 32(6):928–935
24. Rohlin A, Wernersson J, Engwall Y et al (2009) Parallel sequencing used in detection of mosaic mutations: comparison with four diagnostic DNA screening techniques. Hum Mutat 30:1012–1020
25. Dupont S, Masse A, James C et al (2007) The JAK2 617V>F mutation triggers erythropoietin hypersensitivity and terminal erythroid amplification in primary cells from patients with polycythemia vera. Blood 110:1013–1021
26. Hussein K, Bock O, Theophile K et al (2009) JAK2V617F allele burden discriminates essential thrombocythemia from a subset of prefibrotic-stage primary myelofibrosis. Exp Hematol 37:1186–1193
27. Lambert JR, Everington T, Linch DC et al (2009) In essential thrombocythemia, multiple JAK2-V617F clones are present in most mutant-positive patients: a new disease paradigm. Blood 114:3018–3023
28. Gattenlohner S, Serfling E, Einsele H et al (2008) Molecular insights into the morphology of myeloproliferative neoplasms using an in situ PCR assay specific for the JAK2 mutation V617F. Leukemia 23:196–199
29. Georgii A, Büsche G, Kreft A et al (1999) Histological classification and grading of bone marrow biopsies provides prognostic data at diagnosis in patients with chronic myeloproliferation. Haematologica 83(suppl 1):169–174
30. Kralovics R, Teo S-S, Li S et al (2006) Acquisition of the V617F mutation of JAK2 is a late genetic event in a subset of patients with myeloproliferative disorders. Blood 108:1377–1380
31. Nussenzveig RH, Swierczek SI, Jelinek J et al (2007) Polycythemia vera is not initiated by JAK2V617F mutation. Exp Hematol 35:32–38
32. Theocharides A, Boissinot M, Girodon F et al (2007) Leukemic blasts in transformed JAK2-V617F-positive myeloproliferative disorders are frequently negative for the JAK2-V617F mutation. Blood 110:375–379
33. Guglielmelli P, Barosi G, Pieri L et al (2009) JAK2V617F mutational status and allele burden have little influence on clinical phenotype and prognosis in patients with post-polycythemia vera and post-essential thrombocythemia myelofibrosis. Haematologica 94:144–146
34. Passamonti F, Rumi E, Pietra D et al (2010) A prospective study of 338 patients with polycythemia vera: the impact of JAK2

(V617F) allele burden and leukocytosis on fibrotic or leukemic disease transformation and vascular complications. Leukemia 24:1574–1579

35. Silver RT, Vandris K, Wang YL et al (2011) JAK2V617F allele burden in polycythemia vera correlates with grade of myelofibrosis, but is not substantially affected by therapy. Leuk Res 35:177–182
36. Vannucchi AM, Antonioli E, Guglielmelli P et al (2007) Prospective identification of high-risk polycythemia vera patients based on JAK2V617F allele burden. Leukemia 21:1952–1959
37. Vannucchi AM, Antonioli E, Guglielmelli P et al (2008) Clinical correlates of JAK2V617F presence or allele burden in myeloproliferative neoplasms: a critical reappraisal. Leukemia 22:1299–1307

Virchows Arch (2011) 459:529–538
DOI 10.1007/s00428-011-1139-1

ORIGINAL ARTICLE

In Inverted Papillomas HPV more likely represents incidental colonization than an etiological factor

Klemen Jenko · Boštjan Kocjan · Nina Zidar · Mario Poljak · Primož Strojan · Miha Žargi · Olga Blatnik · Nina Gale

Received: 15 July 2011 / Revised: 10 August 2011 / Accepted: 16 August 2011 / Published online: 9 September 2011
© Springer-Verlag 2011

Abstract Inverted papillomas (IPs) are the most frequent type of sinonasal papillomas. These benign but destructive lesions are known for their high recurrence rate, probably due to incomplete excision. Our aim was to investigate the frequency of human papillomavirus (HPV) infection in patients with IPs and in IPs associated with squamous cell carcinoma (IPsSCC) and to compare it with the frequency of HPV infections in the control group. The influence of HPV infection on the malignant alteration and recurrence rate of IPs was also evaluated. Paraffin-embedded tissue samples from 68 patients with sinonasal IPs and 5 patients with IPsSCC were analyzed in this retrospective study. The control group consisted of 47 patients who had undergone septoplasty or mucotomy of the inferior turbinate. PCR amplification with consensus primer sets was performed to detect alpha-HPVs, and direct sequencing of the PCR products with the same primers was used to determine the HPV genotypes in the samples. We detected HPV DNA in 20 (30.3%) patients with IPs, in 3 (60%) patients with IPsSCC, and in 6 (13%) patients from the control group. The frequency of HPV infection in the study group was statistically significantly higher (p=0.032) than in the control group. The presence of HPV DNA was not a statistically significant predictor of the recurrence of IPs (p=0.745) nor was it a statistically significant risk factor for associated SCC (p=0.32). Since HPV type 11 was the predominant genotype in the IPs, IPsSCC, and in the control cases, we presume that HPV infection may represent incidental colonization rather than being an important etiological factor of IPs.

Keywords Inverted papillomas · Nasal cavity and paranasal sinuses · HPV infection · PCR · Recurrences · Malignant alteration

K. Jenko · M. Žargi
Department of Otorhinolaryngology and Cervicofacial Surgery,
University Medical Center,
Ljubljana, Slovenia

K. Jenko
e-mail: klemen.jenko@yahoo.com

M. Žargi
e-mail: miha.zargi@kclj.si

B. Kocjan · M. Poljak
Faculty of Medicine, Institute of Microbiology and Immunology,
University of Ljubljana,
Ljubljana, Slovenia

B. Kocjan
e-mail: bostjan.kocjan@mf.uni-lj.si

M. Poljak
e-mail: mario.poljak@mf.uni-lj.si

N. Zidar · O. Blatnik · N. Gale (✉)
Faculty of Medicine, Institute of Pathology,
University of Ljubljana,
Korytkova 2,
1000 Ljubljana, Slovenia
e-mail: nina.gale@mf.uni-lj.si

N. Zidar
e-mail: nina.zidar@mf.uni-lj.si

O. Blatnik
e-mail: olga.blatnik@gmail.com

P. Strojan
Institute of Oncology,
Ljubljana, Slovenia
e-mail: pstrojan@onko-i.si

Introduction

A group of sinonasal papillomas, referred to collectively as Schneiderian papillomas (SPs), are derived from the ectodermal ciliated respiratory mucosa or so-called Schneiderian membrane. Hyams proposes that SPs are divided into three groups: exophytic, inverted (IPs), and cylindrical or oncocytic [1]. Each particular entity shows distinct pathomorphologic features as well as differences in location, aggressiveness, recurrence rate, and predisposition to malignant alteration [1–5]. SPs are rare benign neoplasms, representing 0.4% to 4.7% of all sinonasal tumors [6, 7]. IPs are by far the most frequent type of SPs, representing 47% to 79% of these lesions [6, 7]. IPs are characterized as benign but destructive lesions, with the highest incidence between the fifth and seventh decades [6], and they are uncommon in children [8]. Males are affected two to five times more frequently than females. The leading clinical symptom is unilateral nasal obstruction, observed in 80% to 98% of patients, followed by epistaxis, a feeling of pressure, retronasal drip, and clear rhinorrhea [6]. The typical presentation of IPs is a unilateral and unicentric polypoid lesion on the lateral wall of the nasal cavity. Histologically, IPs are characterized by invagination of the hyperplastic epithelium, ranging from squamous to ciliated columnar with goblet cells into the underlying stroma [9–13]. Recurrence rates differ significantly, ranging from 6% to 33%, and are probably due to incomplete excisions [14]. IPs may be associated with basal cell hyperplasia, epithelial atypias, and/or invasive squamous cell carcinoma (SCC). Overt malignancy may arise from the IPs or may appear as a concomitant tumor, synchronously or metachronously [15].

The etiology of IPs remains enigmatic. Several studies have proposed human papillomaviruses (HPV) infection; however, there is no convincing evidence that HPV infection is the most important etiological factor. The purpose of our case–control study was to elucidate further the putative role of HPV in a group of patients with IPs and those with IPsSCC, in comparison with a control group of patients who had undergone septoplasty or mucotomy of the compensatory hypertrophied inferior turbinate. An additional aim was to evaluate the correlation between HPV infection and the recurrence rate of IPs, as well as the correlation between of HPV infection and malignant alteration of IPs.

Material and methods

Material

Our retrospective study included 68 patients (53 males and 15 females) with sinonasal IPs and 5 patients (four males and one female) with IPsSCC. The control group included 47 patients (27 males and 20 females) who had undergone septoplasty or mucotomy of the compensatory hypertrophied inferior turbinate. All patients were treated between 1994 and 2005 at the Department of Otorhinolaryngology and Cervicofacial Surgery, University Clinical Center Ljubljana, Slovenia.

Tissue processing

Formalin-fixed, paraffin-embedded tissue specimens were handled in the Department of Pathology, Faculty of Medicine, University of Ljubljana. To avoid inter-observer variations, two pathologists (N.G. and N.Z.) reviewed all pathological slides and were in agreement with the final pathological reports.

DNA extraction and quantification

DNA was extracted from two 10-μm tissue sections of previously selected paraffin blocks of each case of IPs, IPsSCC, and normal nasal mucosa, using a QIAamp DNA FFPE Tissue Kit (Qiagen, Hilden, Germany), as suggested by the manufacturer. Bound DNA was eluted with 100 μl of buffer AE and stored at −20°C until use. The concentration of DNA was estimated by spectrophotometric analysis at 260 nm using a Biophotometer spectrophotometer (Eppendorf, Berlin, Germany).

The quality of each DNA sample was verified by real-time polymerase chain reaction (RT-PCR) amplification of a 268-bp fragment of the human beta-globin gene, as described previously [16]; for RT-PCR amplification, up to 100 ng (up to 5 μl) of each of the samples was used per 25-μl reaction. Successful amplification of the human beta-globin gene fragment indicated that the DNA sample was adequate for HPV DNA detection and that no PCR inhibitors were present.

HPV detection and genotyping

In order to detect alpha-HPVs, PCR amplification was performed on all samples using a HotStarTaq® *Plus* DNA Polymerase kit (Qiagen, Hilden, Germany) and consensus GP5+/GP6+ and CPI/CPIIg primer sets, targeting approximately 150-bp fragments of the alpha-HPV L1 gene and 188-bp fragments of the alpha-HPV E1 gene, respectively; up to 100 ng (up to 5 μl) of the extracted DNA was used for PCR in a 25-μl reaction volume. All amplifications were carried out on a Gene Amp® PCR 9700 instrument (PE Applied Biosystems, Foster City, CA) using the GP5+/GP6+ TDP3 amplification protocol [17]. All known precautions to avoid a PCR product carry-over and sample-to-sample contamination were rigorously taken, as described previously

[18–20]. The HPV genotypes present in the investigated samples were determined by direct sequencing of the GP5+/GP6+ PCR products with the same primers as those used for PCR, as described previously [21].

Statistical analyses

The Yates-corrected chi-square test was used for comparison of two large groups, namely the group of patients with IPs and those with IPsSCC, and the control group. Fisher's exact test, two-tailed, was applied for statistical analysis of smaller groups of patients. The relative risk of occurrence of SCC in IPs was calculated for the HPV DNA presence as a risk factor. Two-way contingency table analyses, available on statpages.org, were performed for all calculations.

Results

Clinical data

The mean age of males with IPs was 54 years (range, 30 to 77 years) and of females, 65 years (range, 37 to 85 years). The female patient with IPsSCC was 73 years old, and the mean age of the three males was 65 (range, 45 to 77 years). Among the IPsSCC, there were four synchronous and one metachronous tumors. In the control group, the mean age of men was 37 years (range, 20 to 70 years) and of women, 37 (range, 21 to 70 years). The most common presenting symptom in patients with IPs and IPsSCC was unilateral nasal obstruction, detected in 81% and 100% of patients, respectively. Other complaints in patients with IPs were nasal mass, discharge, pain, and otitis media, and in patients with IPsSCC, combined unilateral hearing loss and nasal discharge, headache, anosmia, diplopia, anopsia, and pain. The distribution of anatomical sites of IPs was the following: lateral nasal wall, 28 (41.1%); ethmoid sinus, 7 (10.2%); maxillary sinus, 20 (29.4%); ethmoid and maxillary sinuses, 10 (14.7%); ethmoid, maxillary, and sphenoid sinuses, 2 (2.9%); ethmoid and sphenoid sinuses and frontal recessus, 1 (1.4%). Eight patients with IPs were treated with a lateral rhinotomy, and the recurrence rate was 63% (5/8); 48 patients were treated endoscopically, and the recurrence rate was 19% (9/48). An additional 12 patients with involvement of the maxillary sinus were treated endoscopically with an adjunctive transantral approach, and none of them had a recurrence of IPs (0/12). The overall recurrence rate in patients treated for IP was 20.5% (14/68).

Histologically, IPs were characterized by invagination of ribbons of squamous epithelium into edematous fibrous stroma in 29 cases (42.6%), of ciliated columnar and/or transitional epithelium in 8 cases (11.8%), and of ciliated columnar and/or transitional epithelium and squamous epithelium in 31 cases (45.6%) (Fig. 1). The inverted epithelial areas were surrounded by an intact basement membrane, and no evidence of invasive growth was observed. Intraepithelial microcysts were characteristically present; regular mitoses were present in the lower third of epithelia. Epithelial atypias were found in three cases, in two of mild and in one case of severe degree.

All five patients with malignant alteration of IPS had squamous cell carcinoma of different grades, from II to III. In one case, a direct transition from IP to SCC was evident while in the remaining four cases, a concomitant growth of IP and invasive SCC was detected (Fig. 2). Endoscopic resection was performed in the patient with involvement of the lateral nasal wall only. He did not receive postoperative radiotherapy. The patient with the lateral nasal wall and nasopharynx involvement was treated with endoscopic resection and postoperative radiotherapy. In additional two patients with extended disease, the resection was done using an external approach with lateral rhinotomy. Both of them received postoperative radiotherapy. The fifth patient, with progression of IPsSCC to orbit and fossa pterygopalatina, was treated by radiotherapy as a definite treatment.

HPV detection

A 268-bp fragment of the beta-globin gene was amplified successfully in 107 tissue samples of 66 of 68 patients with IPs and in all 5 patients with IPsSCC, and in 46 of 47 tissue samples of the control group. Two patients with IPs and one individual of the control group with negative results of internal control amplification were therefore excluded from further study.

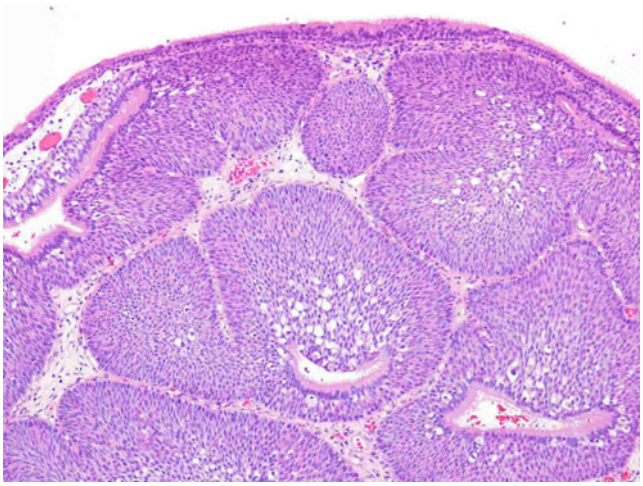

Fig. 1 Endophytic growth pattern of the metaplastic squamous epithelium arising from the surface respiratory epithelium. Epithelial inverted proliferations are characteristically infiltrated by inflammatory cells

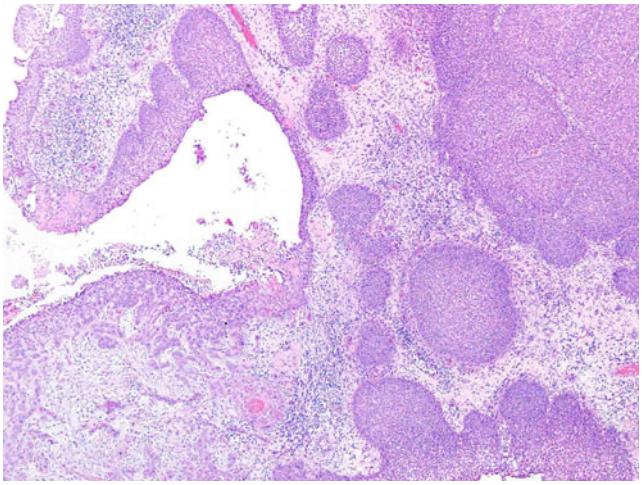

Fig. 2 Obvious transition from benign inverted papilloma to invasive squamous cell carcinoma

The results of HPV DNA detection are summarized in Table 1. Nineteen of 66 patients with IPs were positive for HPV-11 and one for HPV-6, while three of five patients with IPsSCC were positive for HPV-11. In the control group, six patients (13%) were positive for HPV, five of them for HPV-11 and one for HPV-16.

Statistical data

The presence of HPV DNA in patients with IPs and patients with IPsSCC was statistically significantly higher in comparison with the control group (chi-square=4.617 Yates corrected, p=0.032). In the group of 68 patients with IPs, recurrences were observed in 14 (20.5%) cases. Tissue samples of 66 patients were available for detection of HPV. Five of 14 (35.7%) patients with recurrent IPs were HPV DNA positive, as well as 15 (28.8%) of 52 patients without recurrent disease. The presence of HPV DNA in patients with IPs was not a statistically significant predictor of the recurrence of IPs (p=0.745; Fisher's exact test, two-tailed). The risk of associated SCC in HPV DNA-positive IPs was 3/23 (13%), and the risk of associated SCC in HPV-negative IPs was 2/48 (4%). The relative risk of the occurrence of SCC associated with HPV-positive IPs was 3.1 (95% confidence interval was 0.7–15.3).

The association of HPV-11 DNA detection as a risk factor and occurrence of IPsSCC was statistically not significant (p=0.32; Fisher's exact test, two-tailed)

Discussion

Local aggressiveness, high rate of recurrence, and malignant alteration are widely recognized characteristics of IPs, while the etiopathogenesis remains to be elucidated [6, 22, 23]. HPV infection probably plays an important but still not well defined role in their formation [7, 24, 25]. In our study, the rate of detected HPV in IPs was 29.6% (20/66). Nineteen of 20 HPV-positive IPs in our study showed HPV-11, and one showed HPV-6. These data were compared with the results of 22 published studies in which PCR was used for HPV detection [15, 22, 23, 26–44]. As summarized in Table 2, a total of 720 IPs have been analyzed in previous studies, and HPV DNA was detected in 203 (28.1%). However, HPV positivity determined in various PCR studies differed markedly, ranging from 0% to 79% (Table 2). Even more controversial meta-analysis data were published by Syrjänen, who reviewed a number of studies, in which a total of 1,041 IPs and IPsSCC were analyzed. Using various hybridization methods, HPV DNA was detected in 347 (33.3%) cases, ranging from 0% to 100% [4]. Barnes reported similar controversial results for 341 IPs, selected from 20 studies with 131 (38%, ranging from 0% to 100%) HPV-positive IPs, tested using various HPV molecular methods [7].

Taking into consideration only PCR-based studies, a number of technical factors may account for the observed striking differences in HPV prevalence rates (reviewed in [19]). PCR is extremely sensitive to false-positive results from a variety of sources, such as the interpretation of results or, more likely, from true HPV-negative specimens contaminated with HPV DNA. In order to overcome contamination problems, which in our opinion cannot be successfully eliminated solely by

Table 1 Prevalence rates of HPV DNA in patients with sinonasal inverted papillomas, patients with inverted papillomas associated with squamous cell carcinoma, and in tissue specimens of the control group

	Total number of patients	HPV negative, no. (%)	HPV positive, no. (%)	HPV genotype, no. (%)
IPs	66	46 (69.7)	20 (30.3)	HPV-11, 19 (95)
				HPV-6, 1 (5)
IPsSCC	5	2 (40)	3 (60)	HPV-11, 3 (100)
IPs and IPsSCC	71	48	23	HPV-11, 22 (96)
				HPV-6, 1 (4)
Control group	46	40 (87)	6 (13)	HPV-11, 5 (83)
				HPV-16, 1 (17)

IPs inverted papillomas, *IPsSCC* inverted papillomas associated with squamous cell carcinoma, *HPV* human papillomavirus

Table 2 Prevalence rates of HPV DNA in IPs determined by PCR

Reference (author/year of publication/no. of reference	No. of IPs	No. of IPs positive for HPV	% of HPV positivity	Type of HPV
Judd R/1991/[26]	9	0	0	0
Kashima HK/1992/[27]	29	7	24	2× HPV-6
				5× HPV-11
Furuta Y/1992/[28]	19	3	15.7	3× HPV-11
McLachlin CM 1992/[29]	15	2	13.3	2× HPV-6/11
Arndt O/1994/[30]	26	17	65.3	14× HPV-6/11
				19× HPV-16
				10× HPV-6/11 and 16
Beck JC/1995/[22]	29	17	59	11× HPV-6
				5× HPV-11
				1× HPV-18
Buchwald C/1995/[31]	52	3	6	3× HPV-6/11
MacDonald/1995/[32]	20	9	45	ND
Shen J/1996/[33]	40	17	42.5	5× HPV-6
				12× HPV-11
Bernauer/1997/[34]	20	6	30	L1 cons
Zhou Y/1997/[35]	38	30	79	30× HPV-11
				18× HPV-16
				2× HPV-18
Mirza N/2007/[15]	30	6	20	NI
Hwang CS/1998/[36]	36	3	8.3	2× HPV-11
				1× HPV-6
Kassim SK/1998/[37]	10	4	40	4× HPV-16
Wang D/1998/[38]	36	21	58.3	ND
Saegusa M/1999/[39]	28	6	35.8	6× HPV-16/18 only
				5× HPV-16
Weiner JS/1999/[40]	69	5	6.8	3× HPV-11
				2× HPV-16
Kraft M/2001/[41]	34	1	2.9	1× HPV-11
McKay SP/2005/[42]	11	2	18.1	1× HPV-11
				1× HPV-18
Hoffmann M/2006/[43]	26	3	11.5	3× HPV-6/11
Kim JY/2007/[44]	57	7	12.3	1× HPV-6/11
				1× HPV-31
				1× HPV-35/58
				2× HPV-52
				2× HPV ND
Altavilla G/2008/[23]	20	14	70	8× HPV-6/11
				1× HPV-18
				5× HPV ND
Present study	66	20	30	1× HPV-6
				19× HPV-11
Total	720	203	28.1	

IPs inverted papillomas, *HPV* human papillomavirus, *HPV cons*. HPV positive, after L1/L2 consensus primer PCR, *ND* HPV type not detected

classical anti-contamination procedures, we used a uracil-*N*-glycosylase method in our study. Additionally, in order to minimize the possibility of false-negative results due to the heterogeneity of HPV genotypes, two different PCR consensus primers, targeting different HPV genes, were applied. We are convinced that the extremely high HPV prevalence rates obtained in some studies, mainly those performed in the early 1990s, were influenced by some

false-positive results and have thus caused confusion about the etiology of IPs.

Additional factors may also generate extreme variations in HPV DNA detection in IPs [4, 7, 40]; unsuitable formalin fixation of IPs, partial investigation of IPs (variability of the presence of HPV DNA throughout the specimen), and inaccurate selection of IPs in a strictly histological sense, for example, are always possible concerns [31, 44, 45]. Controversial data of HPV DNA presence in IPs may also reflect differences in populations, as determined by Kim and co-workers when comparing Korean, North American, and European populations [44]. In trying to eliminate heterogeneity within IP specimens, we investigated a total of 107 tissue samples obtained from 66 patients with IPs and 5 patients with IPsSCC. We did not observe any differences in HPV DNA appearance in tissue specimens in a single patient. Technical specificities, such as fixation duration and length of tissue storage, may considerably affect DNA quality [25, 27]. However, our previous experience with DNA recovery from 15-year-old paraffin blocks of laryngeal papillomas is an appropriate assurance of adequate methodology [20, 46]. In addition, it is also important to ascertain that the histological characteristics of IPs are strictly considered as a specific group of SPs. In the current study, two experienced pathologists carefully reviewed all included IPs that fulfilled the required histological criteria described in the most recent WHO book on tumors of the head and neck [47].

The present study also included a comparative investigation of HPV DNA prevalence in patients with IPs and a control group: 6 (13%) of 46 persons in the control group were positive for HPV, of which 5 were positive for HPV-11 and 1 for HPV-16 (Table 1), in comparison to 29.6% of positivity in the IPs group. The presence of HPV DNA in patients with IPs was statistically significantly higher than in the control group (chi-square=4.617 Yates corrected, p=0.032). In contrast to our findings, none of 21 biopsies of healthy persons (surgery after fractures or nasoseptal deviations) was positive for HPV DNA in a study by Buchwald et al. [48]. Lawson and co-workers also reported that none of 216 sinonasal tissue samples and 91 sinonasal polyps or sinusitis specimens was related to HPV infection [25]. In addition, HPV DNA was found in only 1 of 48 nasal smears, and the authors concluded that HPV is rarely present in normal nasal mucosa [49]. In contrast, a study by Bryan found HPV-6/11 in as high as 60% (9/15) of specimens of nasopharyngeal mucosa [50]. In our study, HPV-11 was the predominant type of IPs, IPsSCC, and in specimens of non-affected nasal mucosa. It would be reasonable to suspect that HPV infection may represent incidental colonization rather than being an important etiological factor of IPs.

In view of the clinical and morphological evidence of IPs, some doubts arise as to whether HPV infection is the most decisive etiological factor, and Barnes raised the following questions: Why is the virus in IPs so site specific to the lateral wall of the nasal cavity? Why are IPs invariably unilateral? Why do IPs not appear in children who are more susceptible to viral infections than adults [7]? Bearing these doubts in mind and comparing the morphological characteristics of IPs with laryngeal papillomas and anogenital warts (condylomas), which are certainly related to HPV infection, we cannot satisfactorily answer these questions. It is therefore not surprising that there is no generally accepted view about the pathogenesis of these lesions.

Recurrences of IPs typically occur within 2–3 years after surgical therapy, although they may be delayed for many years. The type of surgery significantly influences the recurrence rate. Using limited transnasal excisions or the Caldwell–Luc procedure, recurrence rate ranged from 40% to 80% [51–53]; with the use of more radical lateral rhinotomy with medial maxillectomy, the recurrence rate fell to a range from 0% to 50% [52, 53]. In a study by Waitz, the recurrence rate after extranasal surgery was 19%, and after endonasal resections, 17% [54]. Han et al. also used a combined transantral approach for IPs located on the lateral wall of the maxillary sinus. They detected a 10% recurrence rate after an endonasal or combined endonasal and transantral approach [53]. With endoscopic medial maxillectomy, the recurrence rate according to Sukenik and Casiano was 21% [55] and 0% in a series from Tomenzoli et al. [56]. Current recurrence rates using endoscopic resections, however, vary from 0% to 44% [12, 57]. In our study, we detected recurrences in 14 of 68 (20.5%) patients within a period from 2 months up to 11 years. The recurrence rate was 63% (5/8) with lateral rhinotomy and 19% (9/48) after endonasal resections. We had no recurrences (0/12) in our patients with involvement of the maxillary sinus, treated with a combined endonasal and transantral approach.

Recurrences of IPs have also been related to HPV infection [25]. Beck et al. reported a high recurrent rate of HPV-positive IPs (13 of 15) in comparison with HPV-negative IPs (none of 10) [22]. In our study, 5 of 14 (35.7%) patients with recurrences had HPV-11-positive IPs. However, HPV DNA positivity was not a statistically significant predictor of the recurrence of IPs in our patients.

In relation to the histomorphological characteristics of IPs, the presence of epithelial atypia has also been considered to be a possible cause of recurrence of IPs but has not been proved [1, 7, 8, 58]. Only three patients in the present study showed epithelial atypia, two had mild and one, severe epithelial changes. In the two patients with recurrent IPs, HPV type 6 appeared in one with mild and in one with severe epithelial atypia and HPV positivity. The small number of patients with IPs with epithelial atypia

does not allow reliable evaluation of the relation between recurrence rate and epithelial atypia.

The malignant alteration of IPs has been widely recognized [1, 4, 8, 22, 23, 42–44, 59–65]. Of all carcinomas associated with IPs, 61% are synchronous and 39%, metachronous [66]. It has been reported that some clinical and morphological characteristics of IPs, such as bone invasion, an increased ratio between the epithelial component versus stroma, the appearance of squamous epithelial hyperplasia, increased mitotic activity, and a decrease in the number of eosinophils, were related to malignant alteration [64]. In contrast, other authors have stated that morphological criteria, such as atypia, mitotic rate, keratinization, and the time interval to recurrence or frequency of recurrence, did not reliably predict the risk of malignization of IPs [22, 51, 66, 67]. The incidence of malignant alteration of IPs in 22 published series, from 1963 to 1995, ranged from 2% to 27%. In detail, 150 (11%) of 1,350 IPs were associated with carcinoma [7]. The incidence of malignant alteration in the present study was 6.9% (5/72). This result also correlates with findings of some recent series, ranging from 6% (3/53) [68], 8.8% (3/34) [69], to 9% (8/89) [10]. So as to avoid a possible influence of different methodologies of HPV detection, we have summarized 16 studies in which PCR was used in order to try to obtain reliable information of HPV infection in IPsSCC [22, 23, 28–31, 33, 36, 38, 40, 42, 44, 70–72]. The detection rate of HPV DNA in IPsSCC (synchronous or metachronous) ranged from 0% to 100% (Table 3). High-risk HPV type 16 was the predominant type of infection in these series (13 cases), followed by HPV type 18 in six cases, HPV type 11 in four cases, HPV type 6/11 in three cases, and HPV type 16/18 in one case. Low-risk HPV type 11 was found in all three cases of IPsSCC (60%) in our study. Despite the small overall number of IPsSCC, our results are not statistically suggestive that HPV-11 infection might be involved in malignant alteration of IPs. A theory accepted worldwide suggests that malignant alteration can be assigned to the specific viral genes E6 and E7 of high-risk HPV types 16 and 18 and their respective proteins, causing cell immortalization with increased efficiency when they are expressed together [73]. On the other hand, recent studies on cervical and penile cancer have to a certain degree changed our view of HPV-11, which is generally regarded as a low-risk alpha-HPV genotype, etiologically linked only with benign epithelial tumors. Recent collabo-

Table 3 Prevalence rates of HPV DNA in squamous cell carcinomas ex inverted papillomas determined by PCR

Reference (author/year of publication/no. of reference)	No. of IPsSCC	No. of IPsSCC positive for HPV	% of HPV positivity in IPsSCC	Type of HPV
Furuta Y/1992/[28]	7	2	28.6	2× HPV-16
McLachlin CM/1992/[29]	2	1	50	1× HPV-16
Gilain L/1993/[70]	3	1	33.3	ND
Ardnt O/1994/[30]	3	3	100	3× HPV-6/11 and 16
Buchwald C/1995/[31]	5	2	40	1× HPV-6
				1× HPV-18
Beck JC/1995/[22]	10	3	25.6	1× HPV-6
				1× HPV-11
				1× HPV-16
Shen J/1996/[33]	6	1	16.6	1× HPV-16
Caruana SM/1997/[71]	4	2	50	2× HPV-16
Wang D/1998/[38]	23	16	69	ND
Hwang CS/1998/[36]	5	2	40	2× HPV-16
Weiner JS/1999/[40]	1	1	100	1× HPV-18
Buchwald C/2001/[72]	28	4	14.2	1× HPV-6/11
				1× HPV-16/18
				1× HPV-6/11 and 16
				1× HPV-18
McKay SP/2005/[42]	6	3	50	3× HPV-18
Kim JY/2007/[44]	7	0	0	–
Altavilla G/2008/[23]	1	0	0	–
Present study	5	3	60	3× HPV-11
Total	116	44	38	

IPs inverted papillomas, *IPsSCC* inverted papillomas associated with squamous cell carcinoma, *HPV* human papillomavirus, *PCR* polymerase chain reaction, *ND* HPV type not detected

rative international genotyping studies on a large number of anogenital cancers collected worldwide have identified a number of cases of cervical and penile cancer in which, using the most sensitive HPV genotyping methods, HPV-11 was identified as the only HPV genotype present in the tissue sample [74, 75]. Although the importance of this finding has not yet been clarified, it is well known that particular genomic variants of HPV-11, e.g., those containing specific amino acid substitutions in E6 ORF:I92L (nt 186) and G122E (nt 466), can impair episomal maintenance of HPV [76] and transform neonatal rat kidney epithelial cells in cell transformation assays, with an efficiency comparable to HPV-16 [77]. Consequently, McGlennen et al. proposed that these mutations in HPV-11 E6 ORF may be potentially oncogenic [77]. On the other hand, it must be taken into consideration that most of our IPs (19/20), as well as control cases (HPV 5/6), were HPV-11 positive. Definite evidence of an etiologic role of HPV in IPs and IPsSCC is thus lacking. HPV infection may represent only an incidental colonization rather than an important etiological factor in the etiopathogenesis of IPs and IPsSCC. However, we could not entirely exclude the possibility that some IPs might be HPV-11 related.

In conclusion, we found that HPV DNA presence was statistically significantly higher in patients with IPs in comparison with the control group. The presence of HPV DNA was not a statistically significant predictor of the recurrence of IPs, nor was it a statistically significant risk factor for associated SCC in IPs. Since HPV type 11 was the predominant genotype in the IPs, IPs associated with SCC and in the control group, we tend to the opinion that HPV infection may represent incidental colonization rather than being an important etiological factor of IPs. However, the possibility exists that at least some IPs might be HPV-11 induced.

Conflict of interest The authors declare that they have no conflict of interest.

References

1. Hyams VJ (1971) Papillomas of the nasal cavity and paranasal sinuses. A clinicopathological study of 315 cases. Ann Otol Rhinol Laryngol 80:192–206
2. Michaels L, Young M (1995) Histogenesis of papillomas of the nose and paranasal sinuses. Arch Pathol Lab Med 119:821–826
3. Michaels L (1996) Benign mucosal tumors of the nose and paranasal sinuses. Semin Diagn Pathol 13:113–117
4. Syrjänen KJ (2003) HPV infections in benign and malignant sinonasal lesions. J Clin Pathol 56:174–181
5. Tanvetyanon T, Qin D, Padhya T et al (2009) Survival outcomes of squamous cell carcinoma arising from sinonasal inverted papilloma: report of 6 cases with systematic review and pooled analysis. Am J Otolaryngol 30:38–43
6. Sauter A, Matharu R, Hörmann K et al (2007) Current advances in the basic research and clinical management of sinonasal inverted papilloma (review). Oncol Rep 17:495–504
7. Barnes L (2009) Diseases of the nasal cavity, paranasal sinuses and nasopharynx. In: Barnes L (ed) Surgical pathology of the head and neck. Informa Healthcare, New York, pp 343–422
8. Lawson W, Ho BT, Shaari CM, Biller HF (1995) Inverted papilloma: a report of 112 cases. Laryngoscope 105:282–288
9. Vrabec DP (1994) The inverted Schneiderian papilloma: a 25-year study. Laryngoscope 104:582–605
10. Pasquini E, Sciarretta V, Farneti G et al (2004) Inverted papilloma: report of 89 cases. Am J Otolaryngol 25:178–185
11. Mendenhall WM, Hinerman RW, Malyapa RS et al (2007) Inverted papilloma of the nasal cavity and paranasal sinuses. Am J Clin Oncol 30:560–563
12. Oikawa K, Furuta Y, Itoh T et al (2007) Clinical and pathological analysis of recurrent inverted papilloma. Ann Otol Rhinol Laryngol 116:297–303
13. Guillemaud JP, Witterick IJ (2009) Inverted papilloma of the sphenoid sinus: clinical presentation, management, and systematic review of the literature. Laryngoscope 119:2466–2471
14. Wormald PJ, Ooi E, van Hasselt CA et al (2003) Endoscopic removal of sinonasal inverted papilloma including endoscopic medial maxillectomy. Laryngoscope 113:867–873
15. Mirza S, Bradley PJ, Acharya A et al (2007) Sinonasal inverted papillomas: recurrence, and synchronous and metachronous malignancy. J Laryngol Otol 121:857–864
16. Jančar N, Kocjan BJ, Poljak M et al (2009) Distribution of humanpapillomavirus genotypes in women with cervical cancer in Slovenia. Eur J Obstet Gynecol Reprod Biol 145:184–188
17. Evans MF, Adamson CS, Simmons-Arnold L et al (2005) Touchdown General Primer (GP5+/GP6+) PCR and optimized sample DNA concentration support the sensitive detection of human papillomavirus. BMC Clin Pathol 5:10
18. Poljak M, Seme K (1996) Rapid detection and typing of human papillomaviruses by consensus polymerase chain reaction and enzyme-linked immunosorbent assay. J Virol Methods 56:231–238
19. Poljak M, Seme K, Gale N (1998) Detection of human papillomaviruses in tissue specimens. Adv Anat Pathol 5:216–234
20. Poljak M, Seme K, Gale N (2000) Rapid extraction of DNA from archival clinical specimens: our experiences. Pflug Arch Eur J Physiol 439:R42–R44
21. Kocjan BJ, Poljak M, Seme K et al (2005) Distribution of human papillomavirus genotypes in plucked eyebrow hairs from Slovenian males with genital warts. Infect Genet Evol 5:255–259
22. Beck JC, McClatchey KD, Lesperance MM et al (1995) Human papillomavirus types important in progression of inverted papilloma. Otolaryngol Head Neck Surg 113:558–563
23. Altavilla G, Staffieri A, Busatto G et al (2008) Expression of p53, p16(INK4A), pRb, p21(WAF1/CIP1), p27(KIP1), cyclin D1, Ki-67 and HPV DNA in sinonasal endophytic Schneiderian (inverted) papilloma. Acta Otolaryngol 31:1–8
24. Perez-Ordoñez B (2009) Hamartomas, papillomas and adenocarcinomas of the sinonasal tract and nasopharynx. J Clin Pathol 62:1085–1095
25. Lawson W, Schlecht NF, Brandwein-Genser M (2008) The role of the human papillomavirus in the pathogenesis of Schneiderian inverted papillomas: an analytic overview of the evidence. Head Neck Pathol 2:49–59
26. Judd R, Zaki SR, Coffield LM et al (1991) Human papillomavirus type 6 detected by the polymerase chain reaction in invasive sinonasal papillary squamous cell carcinoma. Arch Pathol Lab Med 115:1150–1153
27. Kashima HK, Kessis T, Hruban RH et al (1992) Human papillomavirus in sinonasal papillomas and squamous cell carcinoma. Laryngoscope 102:973–976

28. Furuta Y, Takasu T, Asai T et al (1992) Detection of human papillomavirus DNA in carcinomas of the nasal cavities and paranasal sinuses by polymerase chain reaction. Cancer 69:353–357
29. McLachlin CM, Kandel RA, Colgan TJ et al (1992) Prevalence of human papillomavirus in sinonasal papillomas: a study using polymerase chain reaction and in situ hybridization. Mod Pathol 5:406–409
30. Arndt O, Nottelmann K, Brock J et al (1994) Inverted papilloma and its association with human papillomavirus (HPV). A study with polymerase chain reaction (PCR). HNO 42:670–676
31. Buchwald C, Franzmann MB, Jacobsen GK et al (1995) Human papillomavirus (HPV) in sinonasal papillomas: a study of 78 cases using in situ hybridization and polymerase chain reaction. Laryngoscope 105:66–71
32. MacDonald MR, Le KT, Freeman J et al (1995) A majority of inverted sinonasal papillomas carries Epstein-Barr virus genomes. Cancer 75:2307–2312
33. Shen J, Tate JE, Crun CP et al (1996) Prevalence of human papillomavirus (HPV) in benign and malignant tumors of the upper respiratory tract. Mod Pathol 9:15–20
34. Bernauer HS, Welkoborsky HJ, Tilling A et al (1997) Inverted papillomas of the paranasal sinuses and the nasal cavity: DNA indices and HPV infection. Am J Rhinol 11:155–160
35. Zhou Y, Hu M, Li Z (1997) Human papillomavirus (HPV) and DNA test in inverted papillomas of the nasal cavities and paranasal sinuses. Zhonghua Er Bi Yan Hou Ke Za Zhi 32:345–347
36. Hwang CS, Yang HS, Hong MK (1998) Detection of human papillomavirus (HPV) in sinonasal inverted papillomas using polymerase chain reaction (PCR). Am J Rhinol 12:363–366
37. Kassim SK, Ibrahim SA, Eissa S et al (1998) Epstein-Barr virus, human papillomavirus, and flow cytometric cell cycle kinetics in nasopharyngeal carcinoma and inverted papilloma among Egyptian patients. Dis Markers 14:113–120
38. Wang D, Li Y, Sun K (1998) Nasal inverted papilloma and human papilloma virus. Lin Chuang Er Bi Yan Hou Ke Za Zhi 12:118–119
39. Saegusa M, Hashimura M, Machida D et al (1999) Down-regulation of CD44 standard and variant isoforms during the development and progression of uterine cervical tumours. J Pathol 187:173–183
40. Weiner JS, Sherris D, Kasperbauer J et al (1999) Relationship of human papillomavirus to Schneiderian papillomas. Laryngoscope 109:21–26
41. Kraft M, Simmen D, Casas R et al (2001) Significance of human papillomavirus in sinonasal papillomas. J Laryngol Otol 115:709–714
42. McKay SP, Grégoire L, Lonardo F et al (2005) Human papillomavirus (HPV) transcripts in malignant inverted papilloma are from integrated HPV DNA. Laryngoscope 115:1428–1431
43. Hoffmann M, Klose N, Gottschlich S et al (2006) Detection of human papillomavirus DNA in benign and malignant sinonasal neoplasms. Cancer Lett 239:64–70
44. Kim JY, Yoon JK, Citardi MJ et al (2007) The prevalence of human papilloma virus infection in sinonasal inverted papilloma specimens classified by histological grade. Am J Rhinol 21:664–669
45. Gaffey MJ, Frierson HF, Weiss LM et al (1996) Human papillomavirus and Epstein-Barr virus in sinonasal Schneiderian papillomas. An in situ hybridization and polymerase chain reaction study. Am J Clin Pathol 106:475–482
46. Gale N, Poljak M, Kambič V et al (1994) Laryngeal papillomatosis: molecular, histopathological, and clinical evaluation. Virchows Arch 425:291–295
47. Barnes L, Tse LLY, Hunt JL (2005) Schneiderian papillomas. WHO classification of tumours. Pathology and genetics of head and neck tumours. IARC Press, Lyon, pp 28–32
48. Buchwald C, Franzmann MB, Jacobsen GK et al (1994) Human papillomavirus and normal nasal mucosa: detection of human papillomavirus DNA in normal nasal mucosa biopsies by polymerase chain reaction and in situ hybridization. Laryngoscope 104:755–757
49. Eike A, Buchwald C, Rolighed J et al (1995) Human papillomavirus (HPV) is rarely present in normal oral and nasal mucosa. Clin Otolaryngol Allied Sci 20:171–173
50. Bryan RL, Bevan IS, Crocker J et al (1990) Detection of HPV 6 and 11 in tumours of the upper respiratory tract using the polymerase chain reaction. Clin Otolaryngol Allied Sci 15:177–180
51. Lawson W, Biller HF, Jacobson A et al (1983) The role of conservative surgery in the management of inverted papilloma. Laryngoscope 93:148–155
52. McCary SW, Gross CW, Reibel JF et al (1994) Preliminary report: endoscopic versus external surgery in the management of inverting papilloma. Laryngoscope 104:415–419
53. Han JK, Smith TL, Loehrl T et al (2001) An evolution in the management of sinonasal inverting papilloma. Laryngoscope 111:1395–1400
54. Waitz G, Wigand ME (1992) Results of endoscopic sinus surgery for the treatment of inverted papillomas. Laryngoscope 102:917–922
55. Sukenik MA, Casiano R (2000) Endoscopic medial maxillectomy for inverted papillomas of the paranasal sinuses: value of the intraoperative endoscopic examination. Laryngoscope 110:39–42
56. Tomenzoli D, Castelnuovo P, Pagella F et al (2004) Different endoscopic surgical strategies in the management of inverted papilloma of the sinonasal tract: experience with 47 patients. Laryngoscope 114:193–200
57. Cannady SB, Batra PS, Sautter NB et al (2007) New staging system for sinonasal inverted papilloma in the endoscopic era. Laryngoscope 117(7):1283–1287
58. Ridolfi RL, Lieberman PH, Erlandson RA et al (1977) Schneiderian papillomas: a clinicopathologic study of 30 cases. Am J Surg Pathol 1:43–53
59. Weissler MC, Montgomery WW, Turner PA et al (1986) Inverted papilloma. Ann Otol Rhinol Laryngol 95:215–221
60. Beck JC, McClatchey KD, Lesperance MM et al (1995) Presence of human papillomavirus predicts recurrence of inverted papilloma. Otolaryngol Head Neck Surg 113:49–55
61. Syrjänen S (2005) Human papillomavirus (HPV) in head and neck cancer. J Clin Virol 32S:S59–S66
62. Nachtigal D, Yoskovitch A, Frenkiel S (1999) Unique characteristics of malignant schneiderian papilloma. Otolaryngol Head Neck Surg 121:766–771
63. Katori H, Nozawa A, Tsukuda M (2005) Markers of malignant transformation of sinonasal inverted papilloma. Eur J Surg Oncol 31:905–911
64. Katori H, Nozawa A, Tsukuda M (2006) Increased expression of matrix metalloproteinase-2 and 9 and human papilloma virus infection are associated with malignant transformation of sinonasal inverted papilloma. J Surg Oncol 93:80–85
65. Eggers G, Eggers H, Sander N et al (2005) Histological features and malignant transformation of inverted papilloma. Eur Arch Otorhinolaryngol 262:263–268
66. Barnes L (2002) Schneiderian papillomas and nonsalivary glandular neoplasms of the head and neck. Mod Pathol 15:279–297
67. Batsakis JG, Suarez P (2001) Schneiderian papillomas and carcinomas: a review. Adv Anat Pathol 8:53–64

68. Thorp MA, Oyarzabal-Amigo MF, du Plessis JH et al (2001) Inverted papilloma: a review of 53 cases. Laryngoscope 111:1401–1405
69. Kaufman MR, Brandwein MS, Lawson W (2002) Sinonasal papillomas: clinicopathologic review of 40 patients with inverted and oncocytic schneiderian papillomas. Laryngoscope 112:1372–1377
70. Gilain L, Favre M, Planquart X et al (1993) Human papillomavirus and nasosinusal inverted papilloma. Ann Otolaryngol Chir Cervicofac 110:321–325
71. Caruana SM, Zwiebel N, Cocker R et al (1997) p53 alteration and human papilloma virus infection in paranasal sinus cancer. Cancer 79:1320–1328
72. Buchwald C, Lindeberg H, Pedersen BL et al (2001) Human papilloma virus and p53 expression in carcinomas associated with sinonasal papillomas: a Danish epidemiological study 1980–1998. Laryngoscope 111:1104–1110
73. zur Hausen H (2002) Papillomaviruses and cancer: from basic studies to clinical application. Nat Rev Cancer 2:342–350
74. Smith JS, Lindsay L, Hoots B et al (2007) Human papillomavirus type distribution in invasive cervical cancer and high-grade cervical lesions: a meta-analysis update. Int J Cancer 121:621–632
75. Li N, Franceschi S, Howell-Jones R, Snijders PJ, Clifford GM (2011) Human papillomavirus type distribution in 30,848 invasive cervical cancers worldwide: variation by geographical region, histological type and year of publication. Int J Cancer 128:927–935
76. Oh ST, Longworth MS, Laimins LA (2004) Roles of the E6 and E7 proteins in the life cycle of low-risk human papillomavirus type 11. J Virol 78:2620–2626
77. McGlennen RC, Ghai J, Ostrow RS et al (1992) Cellular transformation by a unique isolate of human papillomavirus type 11. Cancer Res 52:5872–5878

Virchows Arch (2011) 459:539–545
DOI 10.1007/s00428-011-1149-z

ORIGINAL ARTICLE

PLAG1 expression in cutaneous mixed tumors: an immunohistochemical and molecular genetic study

Atsuji Matsuyama · Masanori Hisaoka · Hiroshi Hashimoto

Received: 10 May 2011 / Revised: 11 August 2011 / Accepted: 8 September 2011 / Published online: 17 September 2011
© Springer-Verlag 2011

Abstract Cutaneous mixed tumors, also known as chondroid syringomas, are benign cutaneous adnexal tumors that exhibit remarkable histopathological similarities to pleomorphic adenoma of the salivary gland. Thus far, there is little information on the genetic profiles of cutaneous mixed tumors, although specific genetic aberrations including fusion genes involving *PLAG1* and *HMGA2* have been demonstrated in pleomorphic adenomas. In the present study, we conducted an immunohistochemical evaluation of PLAG1 and a reverse transcription–polymerase chain reaction (RT–PCR) assay to detect fusion gene transcripts associated with pleomorphic adenoma, including the CTNNB1-PLAG1, LIFR-PLAG1, CHCHD7-PLAG1, TCEA1-PLAG1, HMGA2-FHIT, HMGA2-NFIB, and HMGA2-WIF1 fusion transcripts; this was performed using formalin-fixed paraffin-embedded tumor tissue specimens of 16 cutaneous mixed tumors including one sample with an adenocarcinoma component. All 16 cutaneous mixed tumors were immunoreactive to PLAG1, which was predominantly expressed in cells with myoepithelial or chondroid differentiation accounting for >80% of cells, whereas PLAG1 expression in glandular or squamous tumor cells was restricted to <20% of cells. The carcinoma component in the mixed tumor was also positive for PLAG1. On the other hand, all eight cutaneous adnexal tumors other than the mixed tumor were negative for PLAG1. In RT–PCR analysis, no fusion gene transcripts involving *PLAG1* or *HMGA2* were identified in any of the cases. Concordant with previous studies, our results support the close relationship between cutaneous mixed tumors and pleomorphic adenomas of the salivary gland. However, the mechanism of PLAG1 expression in cutaneous mixed tumors appears to be possibly different from that of pleomorphic adenomas.

Keywords Mixed tumor · Skin · PLAG1 · Immunohistochemistry · RT–PCR · Fusion gene

A. Matsuyama (✉) · M. Hisaoka · H. Hashimoto
Department of Pathology and Oncology, School of Medicine,
University of Occupational and Environmental Health,
1-1 Iseigaoka, Yahatanishi-ku,
Kitakyushu 807-8555, Japan
e-mail: amatsu@med.uoeh-u.ac.jp

Introduction

Cutaneous mixed tumors, also known as chondroid syringomas, are benign cutaneous adnexal tumors that occur most often in the head and neck region [1]. They occur as well-circumscribed nodules usually less than 3 cm in diameter and exhibit remarkable histopathological similarities to pleomorphic adenoma of the salivary gland composed of combined ductular epithelium, myoepithelial cells, and a characteristic chondromyxoid matrix [1]. Despite detailed morphological observations, including ultrastructural examination [1–3], there is little information on the genetic profile of cutaneous mixed tumors at present.

Pleomorphic adenoma of the salivary gland has been cytogenetically demonstrated to carry specific chromosomal aberrations, most of which result in fusion genes involving *PLAG1* on 8q12 [4–10] or *HMGA2* on 12q13–15 [9–13]; these are considered to play important roles in the pathogenesis of this type of tumor. Several fusion partners, including *CTNNB1* [6, 7], *CHCHD7* [4], *LIFR* [6, 8], and *TCEA1* [4, 5] fused to *PLAG1* as well as *NFIB* [11], *FHIT* [12], and *WIF1* [13] fused to *HMGA2*, were identified by using reverse transcription (RT)–polymerase chain reaction (PCR), fluorescence in situ hybridization (FISH), or chromogenic in situ hybridization (CISH)

performed on fresh tumor tissue specimens. Some tumor-specific genetic alterations including chromosomal translocations can also be specifically identified immunohistochemically via the proteins translated from the fusion gene transcripts [14–17]. The PLAG1 protein is a nuclear oncoprotein that functions as a DNA-binding transcription factor and is overexpressed not only in pleomorphic adenoma but also in lipoblastoma [18], hepatoblastoma [19], lymphocytic leukemia [20], and pediatric gastrointestinal stromal tumors [21]. Previously, we detected the CTNNB1-PLAG1, LIFR-PLAG1, CHCHD7-PLAG1, and HMGA2-WIF1 fusion transcripts in 12 of 45 pleomorphic adenomas of the salivary glands by RT–PCR of formalin-fixed paraffin-embedded (FFPE) tumor tissue specimens [22] as well as the immunohistochemical expression of PLAG1 in all 45 tumors by using a commercially available antibody for PLAG1 [22]. These results suggest that PLAG1 overexpression is specific and constant in pleomorphic adenomas irrespective of detectable PLAG1 or HMGA2 fusion transcripts.

In the present study, we aimed to determine whether the gene rearrangements that exist in pleomorphic adenomas are present in cutaneous mixed tumors. To do so, we conducted an immunohistochemical evaluation of PLAG1 with a commercially available anti-PLAG1 antibody and RT–PCR assays to detect fusion genes involving *PLAG1* or *HMGA2* in pleomorphic adenomas, using FFPE tumor specimens of cutaneous mixed tumors of the skin.

Materials and methods

Eighteen cutaneous tumors previously diagnosed as chondroid syringomas or mixed tumors were retrieved from the files of the Department of Pathology and Oncology, School of Medicine, University of Occupational and Environmental Health, Kitakyushu, Japan; the hematoxylin-and-eosin-stained slides of each case were critically reviewed. Of the 18 cases, two lesions that had arisen in the skin of the parotid region or the eyelid were excluded because it was difficult to distinguish them from pleomorphic adenomas arising in the adjacent parotid or lacrimal glands. Thus, 16 cases were included in this study. Eight cutaneous sweat gland tumors other than the cutaneous mixed tumor, including three eccrine poromas, three hidradenomas, and two spiradenomas were also immunohistochemically examined and served as negative controls. Each case of pleomorphic adenoma of the salivary gland with the CTNNB1-PLAG1, LIFR-PLAG1, CHCHD7-PLAG1, or HMGA2-WIF1 fusion gene already detected by RT–PCR [22] served a positive control for both RT–PCR assays and immunohistochemical analyses. Only one positive control case with the HMGA2-WIF1 fusion gene was available, and each control case with CTNNB1-PLAG1, LIFR-PLAG1, or CHCHD7-PLAG1was selected randomly. No positive control tumors for other fusion gene transcripts could be obtained [22].

RNA was extracted from the FFPE tissues of the tumors, reverse transcribed in complementary DNA (cDNA), and treated with RNase H as described previously [17, 22]. The integrity of the RNA for RT–PCR was confirmed by amplification of the phosphoglycerate kinase (PGK) and porphobilinogen deaminase (PBGD) transcripts [22]. PCR was performed using forward and reverse primers designed to specifically amplify the junctional regions of the fusion genes involving *PLAG1* or *HMGA2* as follows: PLAG1-exon2R, 5′-gac cgt cac aga atg aag ca-3′; PLAG1-exon3R, 5′-gcc agt ccc att gac tct tc-3′; CHCHD7-exon1F, 5′-gtg agc cat tga cgt gtt tg-3′; CTNNB1-exon1F, 5′-gag gaa ggt ctg agg agc ag-3′; LIFR-exon1F, 5′-agc tca gaa agg gag cct ct-3′; TCEA1-exon1F, 5′-gct ttg cca aga aga tgg ac-3′; HMGA2-exon2F, 5′-cct aag aga ccc agg gga ag-3′; HMGA2-exon3F, 5′-agc aga agc cac tgg aga aa-3′; FHIT-exon9R1, 5′-ctg atc tcc aag agg cag ga-3′; FHIT-exon9R2, 5′-tga aag tag acc cgc aga gc-3′; NFIB-exon9R, 5′-ccg gta aga tgg gtg tcc ta-3′; WIF1-exon3R, 5′-gga cat tga cgg ttg gat ct-3′; WIF1-exon4R, 5′-aaa tgc tgc cac ccc atc-3′; WIF1-exon9R, 5′-att ggc att tgt tgg gtt ca-3′; and WIF1-exon10R, 5′-tta agt gaa ggc gtg tgc tg-3′ [22]. The amplification profile consisted of 40 cycles of denaturation at 94°C for 30 s, annealing at 59°C for 30 s, and elongation at 72°C for 30 s, followed by a final extension at 72°C for 10 min.

In our immunohistochemical analysis, Histofine Simple Stain MAX PO (Nichirei, Tokyo, Japan), which employs the universal immunoenzyme amino acid polymer method, was used. Specimens were incubated with the polyclonal anti-PLAG1 antibody (1:500; Sigma-Aldrich Co., St. Louis, MO, USA) for 24 h after heated antigen retrieval in 10 mM citrate buffer (pH 6.0). To examine the myoepithelial differentiation of a case of adenocarcinoma arising in a cutaneous mixed tumor, the following antibodies were used: AE1/AE3 (monoclonal, 1:200; Dako, Glostrup, Denmark), CAM5.2 (monoclonal, 1:10; BD Biosciences, Franklin Lakes, NJ, USA), alpha smooth muscle actin (SMA, 1A4, monoclonal, 1:150; Dako), muscle-specific actin (HHF35, monoclonal, 1:50; Enzo Diagnostics, New York, NY, USA), desmin (D33, monoclonal, 1:50; Dako), calponin (CALP, monoclonal, 1:100; Dako), glial fibrillary acidic protein (GFAP, 6F2, monoclonal, 1:100; Dako), and p63 (4A4, monoclonal, 1:50; Dako). Ki-67 (MIB-1, monoclonal, 1:50; Dako) and bcl2 (124, monoclonal, 1:30; Dako) were used as proliferation and apoptosis-regulating markers, respectively. For antigen retrieval, heating in 10 mmol/l citrate buffer (pH 6.0) was performed before the immunoreaction for calponin and bcl2 and in ethylenediamine tetraacetic acid solution (EDTA) (pH 9.0) for p63 and MIB-1. Protease treatment was

performed before the immunoreactions for AE1/AE3, CAM5.2, and CK7. The antigenic sites were linked using the universal immunoenzyme amino acid polymer method (Histofine Simple Stain MAX PO; Nichirei), and the reaction products were visualized by immersing the sections in 0.2 mg/ml diaminobenzidine in 0.05 mol/l Tris–HCl buffer (pH 7.6) containing 0.003% hydrogen peroxide.

Results

The clinicopathological and immunohistochemical features of the 16 cutaneous mixed tumors are summarized in Table 1.

There were 10 male and six female patients, ranging in age from 26 to 85 years (mean age, 63.5 years). Seven tumors were located in the facial skin, four in the nose, four in the scalp, and one in the back. Histologically, the tumors were composed of mixtures of myoepithelial tumor cells exhibiting spindle, sheet-like, or plasmacytoid appearances with branching glandular, keratinizing, cartilaginous components, and a chondromyxoid or hyalinized stroma (Fig. 1a–c). In one case, the tumor was composed of a benign mixed tumor component alternating with high-grade adenocarcinomatous areas in a glandular or nested growth fashion embedded in a hyalinized fibrosclerotic stroma (Fig. 2a, b) accompanied by focal ossification.

Immunohistochemically, the tumor cells in all 16 cutaneous mixed tumors exhibited nuclear immunoreactivity to PLAG1 (Fig. 1d). Among the tumor components in benign mixed tumors, more than 80% (mean, 90.3%) of spindled, plasmacytoid, or polygonal epithelioid myoepithelial cells and chondroid cells were immunoreactive to PLAG1, whereas the expression of the glandular or keratinizing squamous components was confined to less than 20% of cells (mean, 6.7%), regardless of the presence or absence of an adenocarcinoma component. Myoepithelial tumor cells were positive for bcl2 around the glandular structures, whereas glandular tumor cells were essentially negative (Fig. 3a). MIB-1-positive tumor cells were distributed in both myoepithelial and epithelial components, and limited to <1% of cells in all benign cutaneous mixed tumors (Fig. 3b). The carcinomatous component observed in one case was positive for AE1/AE3 and CAM5.2; weakly stained by S100 (Fig. 2c); and negative for SMA, HHF35, desmin, calponin, GFAP, p63, and bcl2. Most of the adenocarcinoma cells were PLAG1 positive (Fig. 2d) as well as adjacent benign myoepithelial tumor components. The MIB-1 index of the carcinoma component was 15.5%. On the other hand, all eight cutaneous sweat gland tumors other than the mixed tumor were negative for PLAG1.

In the RT–PCR analyses using FFPE tumor tissues, PGK and PBGD transcripts were successfully amplified in all 16 cutaneous mixed tumors. The RT–PCR analyses for the fusion transcripts associated with pleomorphic adenoma of the salivary gland revealed the absence of all tested fusion transcripts in all of the cutaneous mixed tumors (Fig. 4).

Table 1 Clinicopathologic features of 16 cutaneous mixed tumors

Case	Age/sex	Location	Tumor size (mm)	Proportion of each tumor component						PLAG1 expression	
				Glandular	Squamous	Spindle or stellate	Plasmacytoid	Polygonal myoepithelial	Chondromyxoid	Myoepithelial and chondroid components	Epithelial component
1	26/F	Face	3	40		20	<5	20	20	95	1
2	50/M	Face	13	10		<5	5	40	40	95	5
3	55/M	Nose	4	30	<5	20		5	40	90	5
4	57/F	Face	4	20		5	10	5	60	80	10
5	58/M	Nose	6	5	<1	5	15	5	70	90	20
6	59/F	Face	11	30	<5	<5	<5	30	30	95	1
7	61/F	Face	4	10	<5	<5	<5	20	60	80	10
8	62/M	Scalp	14	5		<5		20	70	90	1
9	66/M	Nose	9	5	5	10	10	50	20	95	1
10	66/M	Scalp	13	30		10	10	30	20	95	5
11	66/M	Scalp	9	5	5	10	10	30	40	90	5
12[a]	67/F	Scalp	67	30		<5	20	40	10	90	10
13	77/M	Back	8	30	20	<5		40	10	95	10
14	78/M	Face	8	50		20		20	10	80	1
15	83/F	Face	8	10	10	<5	20	40	20	90	10
16	85/M	Nose	7	50		<5	5	20	20	95	10

[a] Mixed tumor of the skin with an adenocarcinoma component. Proportion of each tumor component is that in benign tumor areas

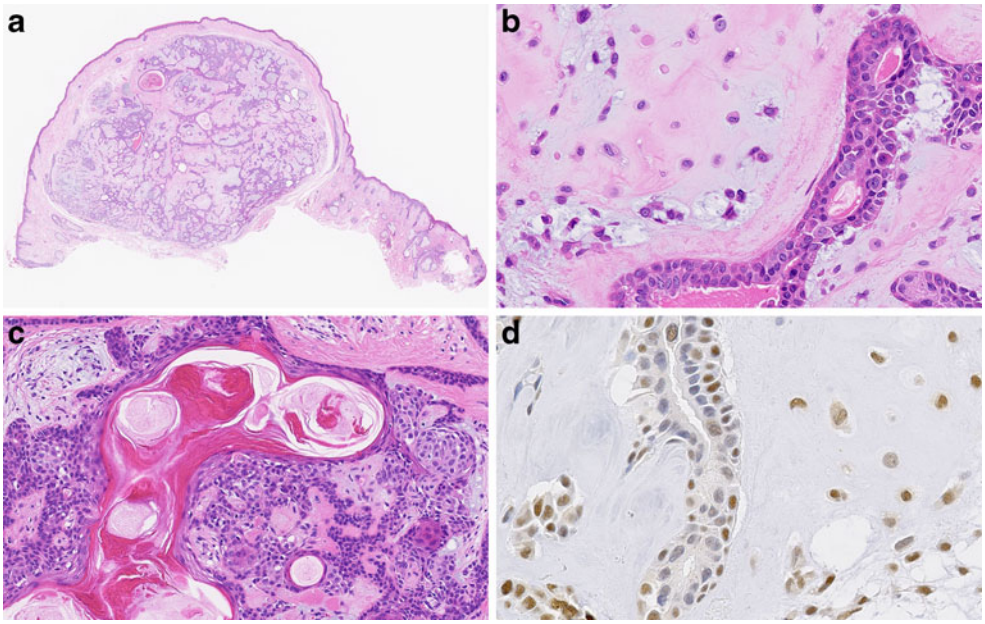

Fig. 1 **a** A cutaneous mixed tumor appearing as a well-circumscribed lesion located in the dermis containing branching epithelial cords. **b** The tumor exhibits ductal structures with an outer layer of myoepithelial cells embedded in a chondromyxoid stroma. **c** Epithelial cords exhibiting keratinization. **d** Immunohistochemical detection of PLAG1 expression in many tumor cells, predominantly cells exhibiting myoepithelial or chondroid differentiation. PLAG1-negative ductal cells can also be observed

Discussion

Based on the striking morphological overlap, cutaneous mixed tumors are considered to be the cutaneous counterpart of pleomorphic adenomas of the salivary gland. Although chromosome and gene rearrangements in pleomorphic adenomas have been extensively analyzed cytogenetically by RT–PCR, FISH, or CISH techniques mainly using fresh or frozen tumor specimens, genetic alterations in cutaneous mixed tumors have not been adequately studied. One of the reasons for this may be that frozen tumor material of cutaneous mixed tumors is not usually available because these tumors are small due to their superficial location, although larger tumors are reported

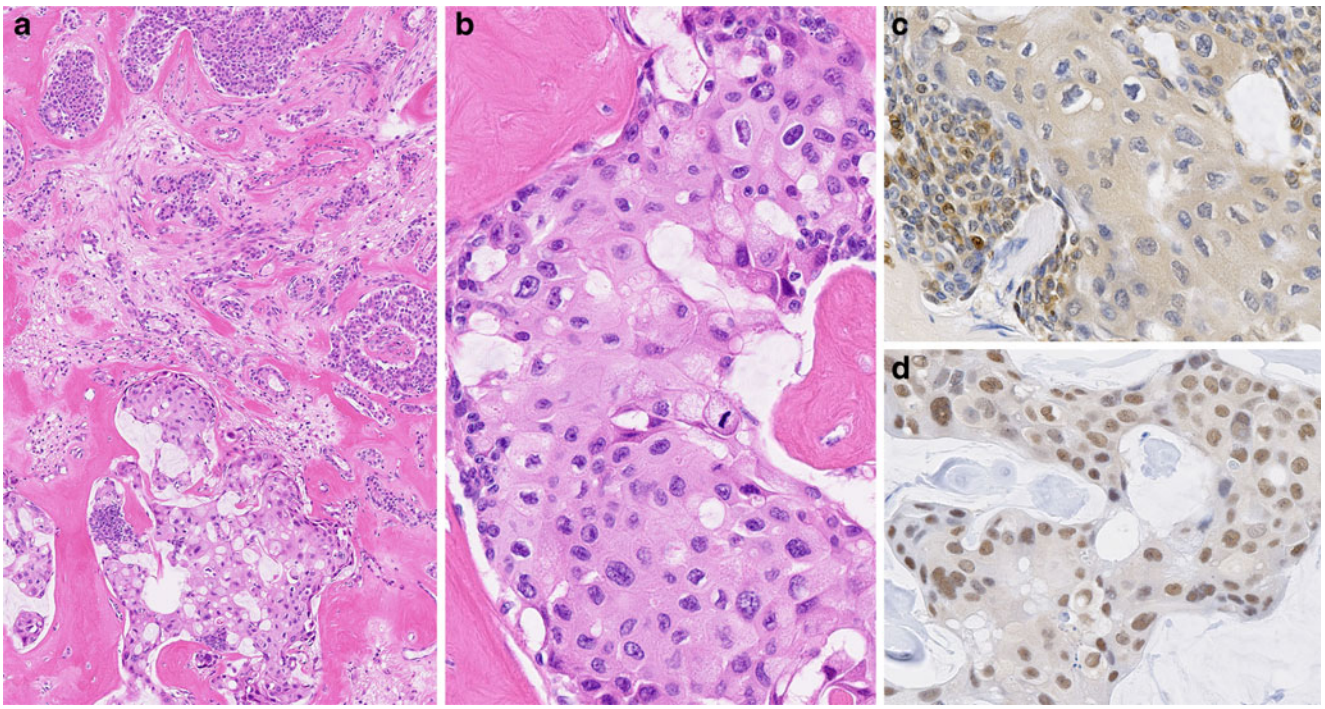

Fig. 2 Mixed tumor with an adenocarcinomatous component. **a** Benign mixed tumor (*top*) alternating with nests of the high-grade adenocarcinoma component (*bottom*) embedded in a hyalinized stroma. **b** A high-power magnification of the carcinoma component. **c** Myoepithelial tumor cells in benign cutaneous mixed tumor are positively immunoreactive to S100, whereas the carcinoma component is weakly stained. **d** Immunohistochemical detection of PLAG1 expression in the carcinoma cells

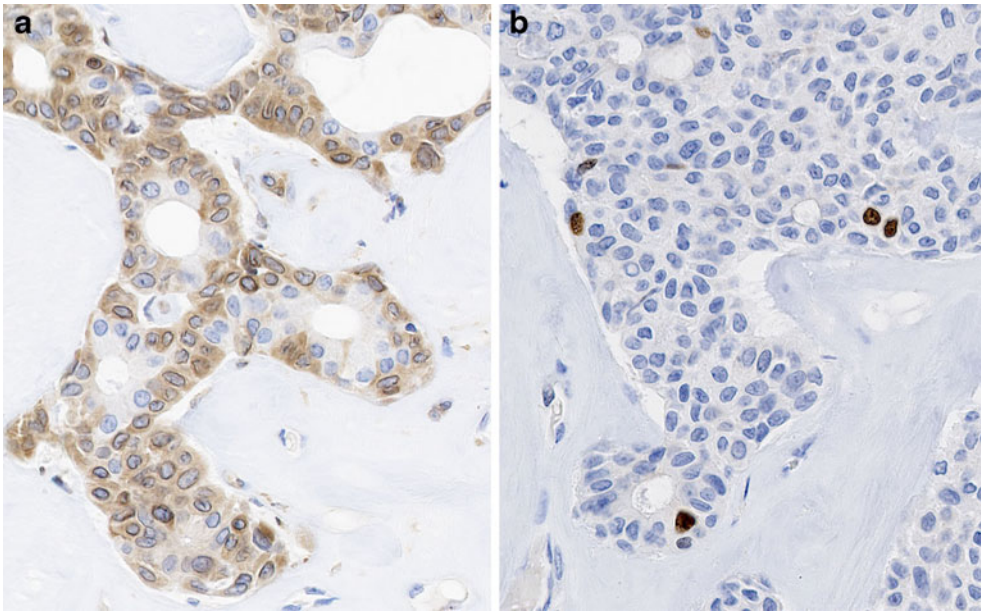

Fig. 3 **a** The myoepithelial tumor cells around the glandular structures in the cutaneous mixed tumors are immunoreactive to bcl2, whereas most glandular tumor cells are negative. **b** A small number of tumor cells containing myoepithelial and glandular cells are positive for MIB-1

[23]. Assays that can be performed on FFPE tumor specimens are needed to evaluate the genetic relationship between pleomorphic adenomas and cutaneous mixed tumors. We previously performed RT–PCR analysis to detect the *CTNNB1-PLAG1*, *LIFR-PLAG1*, *CHCHD7-PLAG1*, *TCEA1-PLAG1*, *HMGA2-FHIT*, *HMGA2-NFIB*, and *HMGA2-WIF1* fusion gene transcripts along with immunohistochemical analysis of PLAG1 on a series of FFPE tumor tissue specimens of pleomorphic adenomas of the salivary gland in order to assess possible genetic alterations. Four fusion gene transcripts including CTNNB1-PLAG1, LIFR-PLAG1, CHCHD7-PLAG1, and HMGA2-WIF1 were detected in 24% of the pleomorphic adenomas, whereas the immunohistochemical expression of PLAG1 was identified in all of the pleomorphic adenomas examined [22]. In the present study, we examined whether cutaneous mixed tumors are associated with PLAG1 by using RT–PCR and immunohistochemical methods. The results show that none of the 16 cutaneous mixed tumors possessed any of the fusion gene transcripts investigated, although all of them were immunoreactive to PLAG1. Similar to the expression patterns seen in the pleomorphic adenomas of the salivary gland [22, 24], we observed that PLAG1 was almost constantly expressed in tumor cells with myoepithelial or chondroid differentiation, whereas its expression was limited in glandular or squamous tumor cell components. The distribution of PLAG1 expression was not associated with the proliferatory or apoptosis-inhibiting signals demonstrated by immunohistochemistry for MIB-1 or bcl2. The variability of the PLAG1 expression among the tumor cell types may be due to an additional genetic event accompanied by epithelial differentiation. Another possibility may be that the suppression of the PLAG1 expression is related to the epigenetic mechanism because PLAG1 overexpression is crucial event in all mixed tumors of the skin and is probably derived from genetic aberrations. Although it seems unlikely that cutaneous mixed tumors develop via the same molecular mechanisms as those involved in pleomorphic adenomas such as *PLAG1* gene fusion, with the same frequency, PLAG1 may play an important role in the pathogenesis of both tumor types in light of its constant immunohistochemical expression. The aberrant expression of PLAG1 protein in cutaneous mixed tumors is worth noting. It may be a result of the cryptic gene aberrations as seen in a subset of pleomorphic

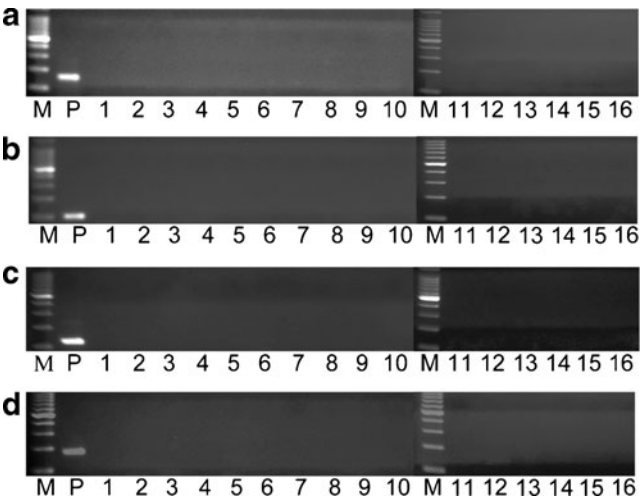

Fig. 4 The CTNBB-PLAG1 (**a**), LIFR-PLAG1 (**b**), CHCHD7-PLAG1 (**c**), and HMGA2-WIF1 (**d**) fusion transcripts were not identified by RT–PCR in any of the 16 cutaneous mixed tumors. *M* 100-bp DNA ladder. *P* positive controls (pleomorphic adenomas). *Lanes 1–16* cutaneous mixed tumors

adenomas [4, 5, 9] because PLAG1 has been demonstrated to be expressed in pleomorphic adenomas, including not only tumors with PLAG1-associated fusion genes or cryptic PLAG1 rearrangements but also tumors possessing the HMGA2-associated fusion gene [22]. Alternatively, epigenetic factors may be involved because PLAG1 has been shown to be overexpressed in chronic lymphocytic leukemia via microRNAs, including miR-181a, miR-181b, miR-107, and miR-424 [20].

Malignant transformation of cutaneous mixed tumor is an extremely rare phenomenon. In the present study, we examined a case of a cutaneous mixed tumor with an adenocarcinoma component that was morphologically diagnosed. The results indicate that adenocarcinoma cells were weakly positive for S100 and negative for SMA, HHF35, desmin, calponin, GFAP, and p63, indicating the minor residual or suppressed myoepithelial phenotype. PLAG1 was diffusely expressed in both the carcinomatous benign components; this is of great interest because PLAG1 expression in benign glandular components was limited. This phenomenon is common with carcinomas ex pleomorphic adenomas of the salivary glands [22] and suggests that the adenocarcinoma component in this case was derived from myoepithelial tumor cells in the benign mixed tumor. Moreover, a common PLAG1 alteration is considered to be an early molecular event. Additional genetic events may induce both the loss of PLAG1 expression and squamous or glandular differentiation; malignant or high-grade transformation may be the result of other additional genetic abnormalities or accumulated chromosomal aberrations as in carcinoma ex pleomorphic adenoma of the salivary gland or other types of tumors [25–27]. Alternatively, other factors might alter or suppress PLAG1 expression because PLAG1 overexpression is a crucial event in mixed tumors of the skin and is probably derived from genetic aberrations. Further investigations of additional cases are required to clarify the genetic and epigenetic backgrounds of this phenomenon in cutaneous mixed tumors.

We also examined eight cutaneous sweat gland tumors other than mixed tumors; all of them were negative for PLAG1. Although the number of the negative control cases was small, PLAG1 was specifically overexpressed in mixed tumors among the cutaneous tumors examined. The immunohistochemistry of PLAG1 may be useful for diagnosing mixed tumors exhibiting monotonous or unusual morphology such as a hyaline cell-rich type [1]. On the other hand, PLAG1 expression cannot distinguish cutaneous mixed tumors from pleomorphic adenomas of the salivary gland if the tumor arises adjacent to the major or minor salivary glands; however, it should be noted that salivary gland tumors have a higher potential for local recurrence and malignant transformation than cutaneous ones.

In conclusion, all 16 cutaneous mixed tumors examined exhibited constant immunohistochemical PLAG1 expression with a heterogeneous expression pattern among the tumor cell components as in the pleomorphic adenomas. However, no PLAG1- or HMGA2-associated fusion transcripts were detected in any of the tumors. The morphological overlap is further reinforced by the observed immunohistochemical PLAG1 expression, suggesting that cutaneous mixed tumors and pleomorphic adenomas of the salivary glands are closely related. However, the mechanism of PLAG1 overexpression in cutaneous mixed tumors may be different from that in pleomorphic adenomas.

Conflict of interest statement We declare that we have no conflict of interest.

References

1. LeBoit PE, Burg G, Weedon D, Sarasin A (eds) (2006) World Health Organization classification of tumours. Pathology and genetics of skin tumours. IARC, Lyon
2. Headington JT (1961) Mixed tumors of skin: eccrine and apocrine types. Arch Dermatol 84:989–996
3. Mambo NC (1984) Hyaline cells in a benign chondroid syringoma. Report of a case and findings by conventional and electron microscopy. Am J Dermatopathol 6:265–272
4. Asp J, Persson F, Kost-Alimova M, Stenman G (2006) CHCHD7-PLAG1 and TCEA1-PLAG1 gene fusions resulting from cryptic, intrachromosomal 8q rearrangements in pleomorphic salivary gland adenomas. Genes Chromosomes Cancer 45:820–828
5. Aström AK, Voz ML, Kas K, Roijer E, Wedell B, Mandahl N, Van de Ven W, Mark J, Stenman G (1999) Conserved mechanism of PLAG1 activation in salivary gland tumors with and without chromosome 8q12 abnormalities: identification of SII as a new fusion partner gene. Cancer Res 59:918–923
6. Martins C, Fonseca I, Roque L, Pereira T, Ribeiro C, Bullerdiek J, Soares J (2005) PLAG1 gene alterations in salivary gland pleomorphic adenoma and carcinoma ex-pleomorphic adenoma: a combined study using chromosome banding, in situ hybridization and immunocytochemistry. Mod Pathol 18:1048–1055
7. Kas K, Voz ML, Röijer E, Aström AK, Meyen E, Stenman G, Van de Ven WJ (1997) Promoter swapping between the genes for a novel zinc finger protein and beta-catenin in pleiomorphic adenomas with t(3;8)(p21;q12) translocations. Nat Genet 15:170–174
8. Voz ML, Aström AK, Kas K, Mark J, Stenman G, Van de Ven WJ (1998) The recurrent translocation t(5;8)(p13;q12) in pleomorphic adenomas results in upregulation of PLAG1 gene expression under control of the LIFR promoter. Oncogene 16:1409–1416
9. Bullerdiek J, Wobst G, Meyer-Bolte K, Chilla R, Haubrich J, Thode B, Bartnitzke S (1993) Cytogenetic subtyping of 220 salivary gland pleomorphic adenomas: correlation to occurrence, histological subtype, and in vitro cellular behavior. Cancer Genet Cytogenet 65:27–31
10. Mark J, Dahlenfors R, Wedell B (1997) Impact of the in vitro technique used on the cytogenetic patterns in pleomorphic adenomas. Cancer Genet Cytogenet 95:9–15
11. Geurts JM, Schoenmakers EF, Röijer E, Aström AK, Stenman G, van de Ven WJ (1998) Identification of NFIB as recurrent translocation partner gene of HMGIC in pleomorphic adenomas. Oncogene 16:865–872

12. Geurts JM, Schoenmakers EF, Röijer E, Stenman G, Van de Ven WJ (1997) Expression of reciprocal hybrid transcripts of HMGIC and FHIT in a pleomorphic adenoma of the parotid gland. Cancer Res 57:13–17
13. Persson F, Andrén Y, Winnes M, Wedell B, Nordkvist A, Gudnadottir G, Dahlenfors R, Sjögren H, Mark J, Stenman G (2009) High-resolution genomic profiling of adenomas and carcinomas of the salivary glands reveals amplification, rearrangement, and fusion of HMGA2. Genes Chromosomes Cancer 48:69–82
14. Llombart-Bosch A, Machado I, Navarro S, Bertoni F, Bacchini P, Alberghini M, Karzeladze A, Savelov N, Petrov S, Alvarado-Cabrero I, Mihaila D, Terrier P, Lopez-Guerrero JA, Picci P (2009) Histological heterogeneity of Ewing's sarcoma/PNET: an immunohistochemical analysis of 415 genetically confirmed cases with clinical support. Virchows Arch 455:397–411
15. Murphy AJ, Bishop K, Pereira C, Chilton-MacNeill S, Ho M, Zielenska M, Thorner PS (2008) A new molecular variant of desmoplastic small round cell tumor: significance of WT1 immunostaining in this entity. Hum Pathol 39:1763–1770
16. Argani P, Lal P, Hutchinson B, Lui MY, Reuter VE, Ladanyi M (2003) Aberrant nuclear immunoreactivity for TFE3 in neoplasms with TFE3 gene fusions: a sensitive and specific immunohistochemical assay. Am J Surg Pathol 27:750–761
17. Li XQ, Hisaoka M, Shi DR, Zhu XZ, Hashimoto H (2004) Expression of anaplastic lymphoma kinase in soft tissue tumors: an immunohistochemical and molecular study of 249 cases. Hum Pathol 35:711–721
18. Hibbard MK, Kozakewich HP, Dal Cin P, Sciot R, Tan X, Xiao S, Fletcher JA (2000) PLAG1 fusion oncogenes in lipoblastoma. Cancer Res 60:4869–4872
19. Zatkova A, Rouillard JM, Hartmann W, Lamb BJ, Kuick R, Eckart M, von Schweinitz D, Koch A, Fonatsch C, Pietsch T, Hanash SM, Wimmer K (2004) Amplification and overexpression of the IGF2 regulator PLAG1 in hepatoblastoma. Genes Chromosomes Cancer 39:126–137
20. Pallasch CP, Patz M, Park YJ, Hagist S, Eggle D, Claus R, Debey-Pascher S, Schulz A, Frenzel LP, Claasen J, Kutsch N, Krause G, Mayr C, Rosenwald A, Plass C, Schultze JL, Hallek M, Wendtner CM (2009) miRNA deregulation by epigenetic silencing disrupts suppression of the oncogene PLAG1 in chronic lymphocytic leukemia. Blood 114:3255–3264
21. Agaram NP, Laquaglia MP, Ustun B, Guo T, Wong GC, Socci ND, Maki RG, DeMatteo RP, Besmer P, Antonescu CR (2008) Molecular characterization of pediatric gastrointestinal stromal tumors. Clin Cancer Res 14:3204–3215
22. Matsuyama A, Hisaoka M, Nagao Y, Hashimoto H (2011) Aberrant PLAG1 expression in pleomorphic adenomas of salivary gland: a molecular genetic and immunohistochemical study. Virchows Arch 458:583–592
23. Kakuta M, Tsuboi R, Yamazaki M, Sakuma M, Yoshikata R, Ogawa H (1996) Giant mixed tumor of the face. J Dermatol 23:369–371
24. Debiec-Rychter M, Van Valckenborgh I, Van den Broeck C, Hagemeijer A, Van de Ven WJ, Kas K, Van Damme B, Voz ML (2001) Histologic localization of PLAG1 (pleomorphic adenoma gene 1) in pleomorphic adenoma of the salivary gland: cytogenetic evidence of common origin of phenotypically diverse cells. Lab Invest 81:1289–1297
25. Morio T, Morimitsu Y, Hisaoka M, Makishima K, Hashimoto H (2002) DNA copy number changes in carcinoma in pleomorphic adenoma of the salivary gland: a comparative genomic hybridization study. Pathol Int 52:501–507
26. Hisaoka M, Okamoto S, Morimitsu Y, Tsuji S, Hashimoto H (1998) Dermatofibrosarcoma protuberans with fibrosarcomatous areas. Molecular abnormalities of the p53 pathway in fibrosarcomatous transformation of dermatofibrosarcoma protuberans. Virchows Arch 433:323–329
27. Kiechle M, Hinrichs M, Jacobsen A, Lüttges J, Pfisterer J, Kommoss F, Arnold N (2000) Genetic imbalances in precursor lesions of endometrial cancer detected by comparative genomic hybridization. Am J Pathol 156:1827–1833

Virchows Arch (2011) 459:547–553
DOI 10.1007/s00428-011-1148-0

CASE REPORT

High-resolution genomic profiling of an adult Wilms' tumor: evidence for a pathogenesis distinct from corresponding pediatric tumors

Jenny Karlsson · Linda Holmquist Mengelbier · Peter Elfving · David Gisselsson Nord

Received: 4 July 2011 / Revised: 31 August 2011 / Accepted: 6 September 2011 / Published online: 23 September 2011
© Springer-Verlag 2011

Abstract Wilms' tumor (WT), the most common kidney tumor among children, is characterized by a triphasic morphology consisting of blastemal, epithelial, and stromal components. Adult WT is a rare malignancy displaying similar histological features. We here present the first published high-resolution genomic analysis of a mixed-type adult WT. This revealed a more pronounced genetic complexity than usually observed in children with mixed-type WT. The majority of chromosomes displayed uniparental disomies, and microdeletions were present in genes with known importance for tumor formation (*LRP1B*, *FHIT*, and *WWOX*) or organogenesis (*NEGR1* and *ZFPM2*), abnormalities not previously reported for pediatric WT. Our results indicate that adult WT is a biological entity distinct from the corresponding pediatric tumor type.

Keywords Adult Wilms' tumor · Kidney · SNP array

Introduction

Wilms' tumor (WT) is the most common renal neoplasm among children and constitutes 5–6% of all childhood cancers [1]. Adults can also be affected by WT, but this happens rarely, and there are less than 300 cases reported in the literature [2]. Adults with WT usually have more advanced disease and present with higher tumor stage compared to children [3]. In children with WT, the most common large-scale chromosomal abnormalities include loss of heterozygosity (LOH) for 1p, gain of 1q, LOH for 7p, and LOH or hemizygous deletion of 16q [4–7]. Gain of 1q and LOH 16q are both associated with poor outcome in WT patients diagnosed with favorable histology [4, 5]. In addition, gain of genetic material on chromosomes 6, 7, 8, 12, 13, and 18 are also frequently detected [8]. The genetic profile for WT in adults has not been studied in any detail, and previous studies have been largely limited to conventional chromosome-banding analysis [9–15].

Adult WTs usually affects people in their mid-20s [3, 16]; however, in this study, we describe an adult WT in a woman who received her diagnosis at 71 years of age. We have investigated the genomic profile at a high level of resolution with single nucleotide polymorphism (SNP) array, a technique enabling the detection of both copy number alterations and copy number neutral allelic imbalances, such as uniparental disomies (UPDs). The tumor displayed a complex genetic profile, highly diverse from those typically observed in pediatric WTs. This indicates that WT in adults constitutes a distinct biological entity resulting from a different mechanism of pathogenesis compared to WT in children.

Clinical history

The patient was a 71-year-old woman referred to the University Hospital in Lund, Sweden, because of a tumor in her right kidney. Standard renography showed 19% and 81% intrarenal plasma flow distribution in her right and left kidney, respectively, and imaging studies showed unspecific atrophy of the left kidney. She underwent partial

J. Karlsson (✉) · L. Holmquist Mengelbier · D. Gisselsson Nord
Department of Clinical Genetics, BMC B13,
University and Regional Laboratories, Lund University,
221 84 Lund, Sweden
e-mail: jenny.karlsson@med.lu.se

P. Elfving
Department of Urology, Skåne University Hospital,
Malmö, Sweden

resection of the right kidney with macroscopically adequate margins and remained free of recurrence by magnetic resonance imaging during the 10-year follow-up period.

Materials and methods

Histopathology and immunohistochemistry

The patient was analyzed as a part of a larger study on genomic alterations in kidney tumors, which had been approved by the regional ethics review board. Sectioning, hematoxylin–eosin staining, and immunohistochemistry of the tumor were performed according to standard protocols. All antibodies were from DAKO (Glostrup, Denmark). Cytokeratins AE1/3 (M3515), CD56 (M7340), WT1 (6 F-H2), smooth muscle actin (M0851), estrogen receptor, progesterone receptor, and p53 (M7001) were detected by mouse monoclonal antibodies, whereas S-100 (Z0311) and chromogranin A (A0430) were detected by polyclonal rabbit antibodies.

Chromosome analysis

Tumor cells were short-term cultured and analyzed with G-banding as previously described [17]. Reported adult WTs with abnormal karyotypes were found by searching for "Wilms' tumor" in patients above 18 years of age in the Mitelman Database of Chromosome Aberrations and Gene Fusions in Cancer (http://cgap.nci.nih.gov/Chromosomes/Mitelman).

SNP array analysis

Genomic DNA was extracted with the DNeasy Blood and Tissue Kit, Qiagen (Valencia, CA) and hybridized to the Illumina HumanCNV370-Duo Genotyping BeadChip, Illumina (San Diego, CA) at the SCIBLU Genomic Centre at Lund University. Data were first normalized with an algorithm in the Illumina Beadstudio software (Illumina) and then with the tQN software [18]. Genomic aberrations were detected by visual examination in the BeadStudio software and alterations including more than ten SNPs were scored as significant. Aberrations corresponding to known copy number variants (CNVs) published in the Database of Genomic variants (http://projects.tcag.ca/variation/) were excluded. Structural aberrations were annotated by the last normal SNP before and the first normal SNP after the unbalanced segment. The SNP array platform and consequently the data interpretation were based on the UCSC hg 18/NCBI build 36 sequence assembly.

Results

Histopathological features

The resection specimen from the right kidney showed an $11 \times 11 \times 5$ cm tumor located ventrally, exhibiting a predominantly solid, pale surface with focal necrotic areas. Microscopic examination revealed a well-encapsulated, triphasic tumor dominated by stromal areas with occasional smooth muscle-like features (Fig. 1a and b), intermixed with epithelial elements. The latter areas either exhibited nests or sheets of cytoplasm-rich cells (Fig. 1c) or consisted of well-differentiated tubular structures separated by loose stroma. There were occasional phyllodes-like areas showing compression of the tubular structures and subepithelial stromal condensation (Fig. 1d). The third tumor component consisted of islands of immature blastema-like cells (Fig. 1e) showing only focal positivity for cytokeratins. Approximately one third of cells in these areas were positive for CD56 (Fig. 1f). Stainings for S-100, chromogranin A, estrogen, and progesterone receptors were negative. Mitotic figures were readily observed, predominantly in the blastema-like elements (Fig. 1g). Both epithelial and blastema-like areas were positive for WT1, showing cytoplasmic staining in a majority of cells and only focal nuclear positivity (Fig. 1h). There were no anaplastic features and p53 staining was negative (not shown). Surgical margins were negative for tumor cells, and there was neither capsular invasion nor sinus invasion. No nephrogenic rests were observed in the kidney parenchyma included in the specimen. The diagnosis of a mixed-type WT was made by the primary pathologist and confirmed after review.

Genetic profile

A notable clonal variability was detected with G-banding analysis with different numerical changes in all investigated cells. Two main clones were identified: one hyperdiploid with a trisomy 3 and one near-triploid. To establish a composite karyotype, the SNP data were combined with the G-banding results (Tables 1 and 2). All chromosomes except the X-chromosome showed abnormal genomic profiles (Table 2) with trisomies for chromosomes 5, 8, 12, 15, 16, and 19 (exemplified in Fig. 2d) and tetrasomies for chromosomes 7, 17, 18, and 20 (exemplified in Fig. 2f). An isochromosome i(1)(q10) was observed in two of the G-band-stained cells (Fig. 2a), and the SNP data denoted the presence of three extra copies of the entire long arm of chromosome 1 (Fig. 2b). UPDs were present for 13 of the chromosomes (Fig. 2b–c, Table 2). We found homozygous microdeletions that did not overlap with published CNVs in chromosomes 1, 2, 3, 8, and 16 (Table 2). Three of the

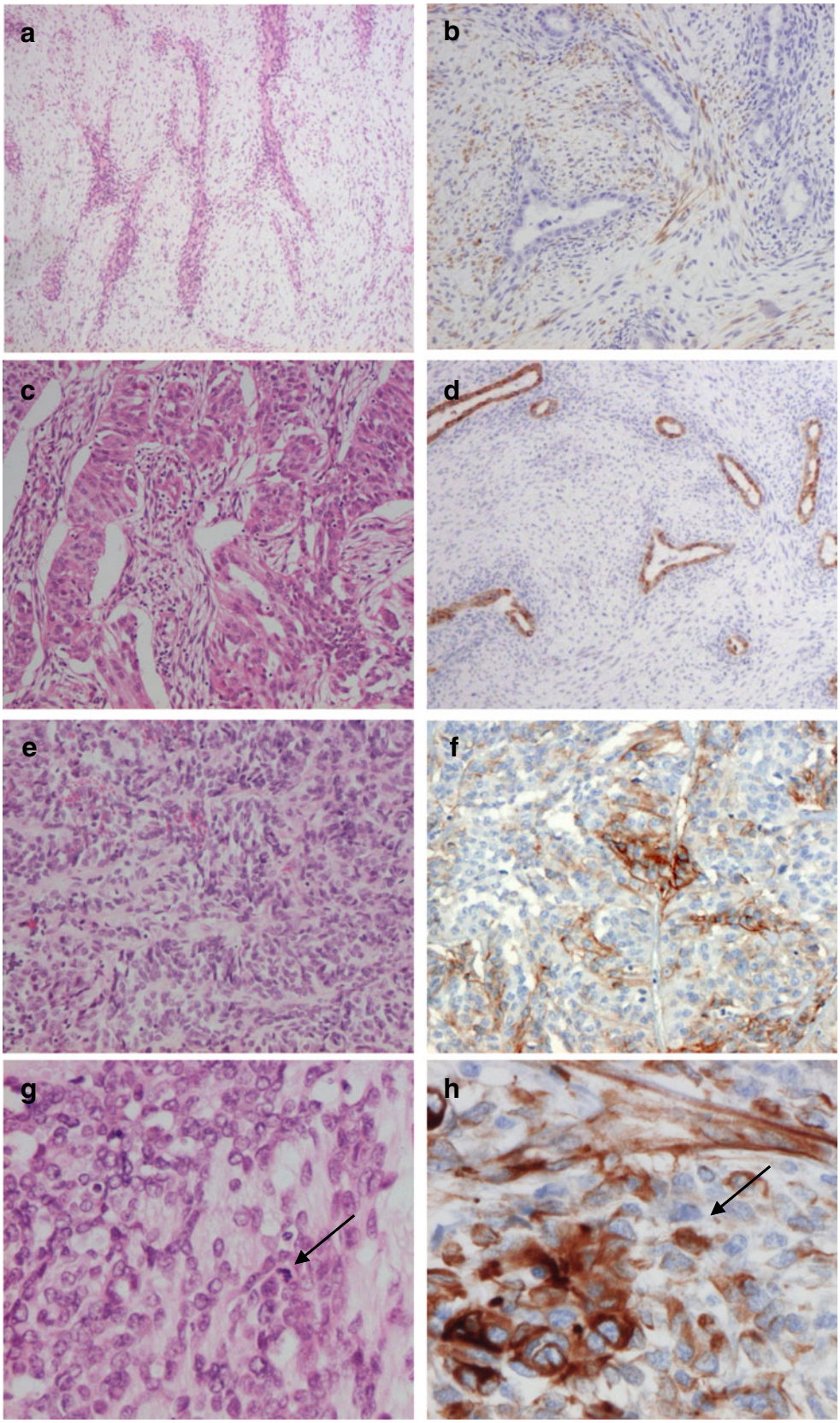

Fig. 1 Histopathology and protein expression. Stromal elements (**a**) with areas of smooth muscle differentiation positive for smooth muscle actin (**b**) were mixed with dense epithelial cord-like (**c**) areas as well as scattered cytokeratin-positive tubular structures showing subepithelial stromal condensation (**d**). The blastema-like elements typically consisted of dense islands of cells with scarce cytoplasm (**e**). These elements showed scattered mitoses (**g**, *arrow*) and regional positivity for CD56 (**f**) and WT1 (**h**), with the latter antibody typically resulting in cytoplasmic staining with only occasional staining also of the nucleus (*arrow* in **h**)

deletions were in genes located in common fragile sites: in chromosome 2, low-density lipoprotein receptor-related protein 1B (*LRP1B*) in FRA2F; in chromosome 3, fragile histidine triad protein (*FHIT*) in FRA3B (approximately

Table 1 A summary of published karyotypes in adult Wilms' tumor

Case	Karyotype	Age/Sex	Reference
1	54-57,X,-Y,+add(1)(p13),-2,+add(7)(p21),+8,+add(12)(p11),+add(12)(q14),+i(12)(p10), +add(16)(q13),+21,+3-8mar	30/M	Gillis et al. [9]
2	90,XXXX,+2,+2,+2,+2,-5,-15,-16,-17,-17,i(17)(q10)x2	20/F	Li et al. [10]
3	81-84,XX,-X-X,del(1)(q41)*2,-5,-5,+del(6)(q15),i(7)(q10)*2,-9,-9,add(11)(p11) x2,-17,-17,-18,-18,-19,-19,-20,-22,-22,3–6mar	26/F	Rubin et al. [11]
4	45,X,-Y,i(7),(q10)	37/M	Fletcher et al. [12]
5	44,Y,-X,?del(12)(p?),-13,-13,-22,-22,+3mar	55/M	Sherwood et al. [13]
6	46,XY,ins(10;1)(q26;p31p34)/50,idem,+6,+12,+12,+17	26/M	Sheng et al. [14]
7	46,XY	18/M	Tawil et al. [15]
8	61,XX,del(1)(p31p31),i(1)(q10),-2,del(2)(q22q22),-3,del(3)(p14p14),-4,-6,+7, del(8)(q23q23),-9,-10,-11,-13,-14,-15,del(16)(q23q23)del(16)(q23q24), +17,+18,+20,-21,-22/47,XX,+3	71/F	This study

25% of this deletion was part of a CNV); and in chromosome 16, WW domain-containing oxidoreductase (*WWOX*) in FRA16D. In chromosome 16, we also detected a subclone with loss of the distal part of 16q starting at 81.5 Mbp (Fig. 2e). The deletions in chromosomes 1 and 8 affected neuronal growth regulator 1 (*NEGR1*; Table 2

Table 2 Numerical and structural aberrations detected by SNP array

Chr	Number of chrs	Allelic ratio	Alteration	Start position (kbp)	End position (kbp)	Start SNP	End SNP	Size (kbp)	Genes in microdeleted region
1	2	2:0	Homozygous deletion	71850	72255	rs928615	rs10518395	405	*NEGR1*
			Gain	143540	247184	rs28736716	rs35622786	103644	
2	2	2:0	Homozygous deletion	141448	142121	rs980288	rs2890601	673	*LRP1B*
3	2	2:0	Homozygous deletion	60253	60565	rs2049847	rs1158425	312	*FHIT*
4	2	2:0							
5	3	2:1							
6	2	2:0							
7	4	2:2							
8	3	2:1	Homozygous deletion	106624	106939	rs4734875	rs1948537	316	*ZFPM2*
9	2	2:0							
10	2	2:0							
11	2	2:0							
12	3	2:1							
13	2	2:0							
14	2	2:0							
15	3	3:0							
16	3	2:1	Homozygous deletion	77089	77365	rs3419	rs7199334	276	*WWOX*
			Hemizygous deletion[a]	81508	88819	rs1991027	rs12325137	7311	
17	4	2:2							
18	4	2:2							
19	3	2:1							
20	4	2:2							
21	2	2:0							
22	2	2:0							

[a] The deletion is in a subclone

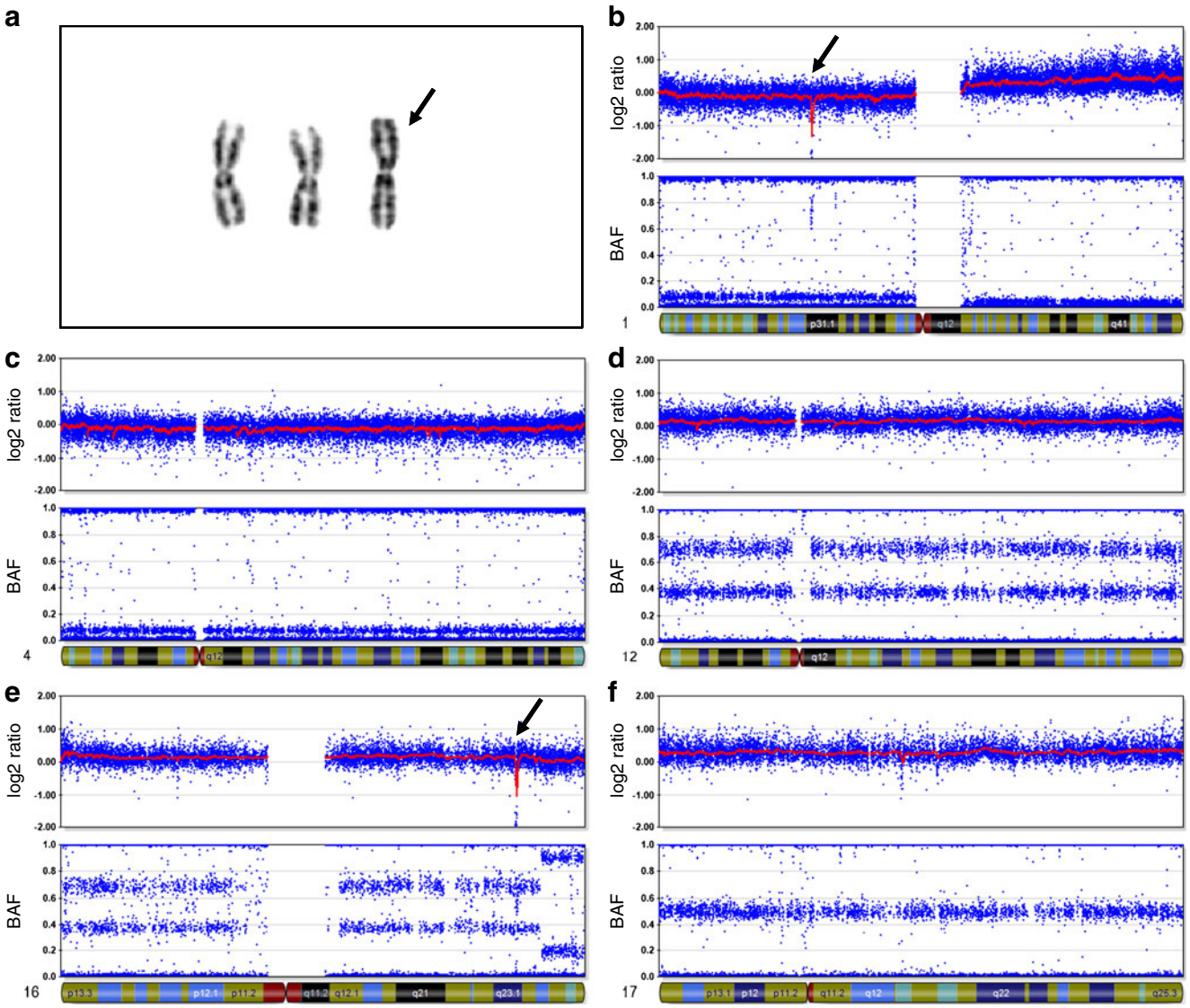

Fig. 2 G-banding and SNP-array analysis, **a** G-banding of chromosome (*chr.*) 1 with the arrow pointing at the isochromosome i(1)(q10) SNP-array profiles (**b–f**), where the log2 ratio depicts the copy number profile, which is close to 0 in diploid cells. In the B Allele Frequency (*BAF*) plots, are heterozygous SNPs positioned around 0.5 and homozygous SNPs close to 0 and 1. **b** Chr. 1 with 2 p-arms and 5 q-arms, **c** chr. 4 displays uniparental disomy , **d** trisomy 12 with the allelic ratio 2:1, **e** trisomy 16 (2:1) with a subclone with a deletion of the distal part of one q-arm starting at 81.5 Mbp, and **f** tetrasomy 17 in allelic balance (2:2). The *arrows* in **b** and **e** indicate the deletions in *NEGR1* in chr. 1 and *WWOX* in chr. 16, respectively

and Fig. 2b) and zinc finger protein multitype 2 (*ZFPM2*), respectively. All deletions included both intronic and exonic areas except for the deletion in the *WWOX* gene that was situated in an intronic area.

Discussion

Only approximately 3% of all WTs occur in adults [3]. Due to its infrequency, WT is not suspected when adults develop kidney tumors, and the proper diagnosis can be hard to determine. In this report, we describe a case of adult WT in a 71-year-old woman, a remarkably high age for a patient presenting with this tumor type. The age and sex of the present patient together with the event-free clinical course and the presence of both stromal and epithelial tumor areas could indicate the differential diagnosis of mixed epithelial and stromal tumor of the kidney (MEST), a usually benign tumor typically affecting middle aged or older women [19, 20]. However, in contrast to the findings in the present case, MEST is characterized by a positive estrogen and progesterone receptor staining and should be devoid of blastema-like elements [21]. The latter is also true for mesoblastic nephroma, another less likely differential diagnosis. The

triphasic histology, WT1 positivity, and the presence of blastema-like foci favored the diagnosis of WT in the present case. However, the histology was, to some extent, different from pediatric WTs. In particular, blastemal cells in pediatric WTs typically have a higher nuclear:cytoplasmic ratio than in the present case and are often completely cytokeratin-negative. The presence of focal cytokeratin positivity in the least differentiated cells in the present tumor could indicate that its proliferative blastema-like component was more well-differentiated than typical pediatric WT blastema. This could, in turn, have contributed to its favorable clinical outcome.

Previous studies have indicated differences in somatic genomic changes between pediatric and adult WTs. However, due to its infrequency, karyotypes have been reported for only eight tumors including this case (Table 1); one of the tumors (case 7) displayed a normal karyotype [15], while six of the cases (cases 1–3, 5, 6, and 8) displayed multiple numerical changes. The only recurrent prominent cytogenetic aberration is the finding of a 7q isochromosome, i(7)(q10) in cases 3 and 4 [11, 12], which has also been observed by FISH analysis in another not karyotyped tumor [11]. The predominant clone of the tumor analyzed here, displayed a high ploidy level with more pronounced genetic heterogeneity than usually observed in children with mixed-type histology WT, and the karyotype resembles, to some extent, the complex genetic profile often found in an anaplastic childhood WT [6], although this adult tumor had no anaplastic features. The presence of UPDs in the majority of the chromosomes detected by SNP array indicates that the ploidy level was first altered to a near-haploid level, followed by polyploidization of the tumor genome and expansion of the polyploid clone. To our knowledge, this complex sequence of events has not been described for WT in adults or children before, although some previously published chromosome-banding karyotypes of adult WTs have shown similar complex scenarios including multiple structural changes. UPDs cannot be detected with G-banding analysis, and no adult WT has been analyzed with SNP-array before. Thus it is possible that some previously analyzed tumors did encompass UPDs and had undergone similar whole genome duplication events.

Through SNP-array analysis we also detected the presence of five homozygous microdeletions. Three of the deletions are mapped to extremely large genes in common fragile sites: *LRP1B* (FRA2F), *FHIT* (FRA3B), and *WWOX* (FRA16B) [22]. In other studies, these three genes have proven to have importance for tumor formation in different cancer cell lines or in mouse models [23–25]. However, the finding should be interpreted with caution, since there is a possibility that aberrations in fragile sites are secondary to metabolic stress during clonal expansion. Two other genes were also partly deleted: *NEGR1* encodes a protein involved in neurite outgrowth [26, 27], and *ZFPM2* engaged in hematopoiesis and cardiogenesis [28]. Alterations in these genes have not been specifically reported or probed for in a WT context before, and we can only speculate on the significance of the discovered microdeletions for the development of the tumor investigated in this study.

In summary, the present study supports previous observations indicating that the genomic alterations involved in WT pathogenesis are different in older patients than in children, denoting adult WT as a biological entity distinct from the corresponding pediatric tumor type despite their largely similar histological appearance.

Acknowledgments We are grateful for the technical assistance of the Swegene Centre for Integrative Biology at Lund University (SCIBLU). We would also like to thank our grant sponsors, namely, Swedish Childhood Cancer Foundation, the Swedish Cancer Society, the Swedish Research Council, Crafoord Foundation, Gunnar Nilsson Cancer Foundation, the Royal Physiographic Society, and the Medical Faculty at Lund University.

Conflicts of Interest None

References

1. Davidoff AM (2009) Wilms' tumor. Curr Opin Pediatr 21(3):357–364. doi:PAS.0b013e31802bdd56/MOP.0b013e32832b323a
2. Terenziani M, Spreafico F, Collini P, Piva L, Perotti D, Podda M, Gandola L, Massimino M, Cereda S, Cefalo G, Luksch R, Casanova M, Ferrari A, Polastri D, Valagussa P, Fossati-Bellani F (2004) Adult Wilms' tumor: a monoinstitutional experience and a review of the literature. Cancer 101(2):289–293. doi:jcp./cncr.20387
3. Reinhard H, Aliani S, Ruebe C, Stockle M, Leuschner I, Graf N (2004) Wilms' tumor in adults: results of the society of pediatric oncology (SIOP) 93-01/society for pediatric oncology and hematology (GPOH) study. J Clin Oncol 22(22):4500–4506. doi:10.1200/JCO.2004.12.099
4. Grundy PE, Breslow NE, Li S, Perlman E, Beckwith JB, Ritchey ML, Shamberger RC, Haase GM, D'Angio GJ, Donaldson M, Coppes MJ, Malogolowkin M, Shearer P, Thomas PR, Macklis R, Tomlinson G, Huff V, Green DM (2005) Loss of heterozygosity for chromosomes 1p and 16q is an adverse prognostic factor in favorable-histology Wilms tumor: a report from the national wilms tumor study group. J Clin Oncol 23(29):7312–7321. doi:10.1200/JCO.2005.01.2799
5. Hing S, Lu YJ, Summersgill B, King-Underwood L, Nicholson J, Grundy P, Grundy R, Gessler M, Shipley J, Pritchard-Jones K (2001) Gain of 1q is associated with adverse outcome in favorable histology Wilms' tumors. Am J Pathol 158(2):393–398. doi:10.1016/S0002-9440(10)63982-X
6. Wittmann S, Zirn B, Alkassar M, Ambros P, Graf N, Gessler M (2007) Loss of 11q and 16q in Wilms tumors is associated with anaplasia, tumor recurrence, and poor prognosis. Genes Chrom Cancer 46(2):163–170. doi:jcp./gcc.20397
7. Powlesland RM, Charles AK, Malik KT, Reynolds PA, Pires S, Boavida M, Brown KW (2000) Loss of heterozygosity at 7p in Wilms' tumour development. Br J Cancer 82(2):323–329. doi:10.1054/bjoc.1999.0922

8. Kaneko Y, Homma C, Maseki N, Sakurai M, Hata J (1991) Correlation of chromosome abnormalities with histological and clinical features in Wilms' and other childhood renal tumors. Cancer Res 51(21):5937–5942
9. Gillis AJ, Oosterhuis JW, Schipper ME, Barten EJ, van Berlo R, van Gurp RJ, Abraham M, Saunders GF, Looijenga LH (1994) Origin and biology of a testicular Wilms' tumor. Genes Chrom Cancer 11(2):126–135
10. Li P, Perle MA, Scholes JV, Yang GC (2002) Wilms' tumor in adults: aspiration cytology and cytogenetics. Diagn Cytopathol 26 (2):99–103. doi:jcp./dc.10048
11. Rubin BP, Pins MR, Nielsen GP, Rosen S, Hsi BL, Fletcher JA, Renshaw AA (2000) Isochromosome 7q in adult Wilms' tumors: diagnostic and pathogenetic implications. Am J Surg Pathol 24 (12):1663–1669
12. Fletcher JA, Renshaw AA (1996) Isochromosome 7q in adult Wilms' tumor. Cancer Genet Cytogenet 86(2):168–169. doi:0165-4608(95)00172-7
13. Sherwood JB, Bard R, Bhargava M, Burns ER, Iqbal MA (1989) A human adult Wilms' tumor. Histologic, ultrastructural, and cytogenetic analysis. Cancer Genet Cytogenet 42(1):35–42. doi:0165-4608(89)90005-8
14. Sheng WW, Soukup S, Bove K, Gotwals B, Lampkin B (1990) Chromosome analysis of 31 Wilms' tumors. Cancer Res 50 (9):2786–2793
15. Tawil A, Cox JN, Roth AD, Briner J, Droz JP, Remadi S (1999) Wilms' tumor in the adult—report of a case and review of the literature. Pathol Res Pract 195(2):105–111, discussion 113–104
16. Izawa JI, Al-Omar M, Winquist E, Stitt L, Rodrigues G, Steele S, Siemens DR, Luke PP (2008) Prognostic variables in adult Wilms tumour. Can J Surg 51(4):252–256
17. Dahlen A, Debiec-Rychter M, Pedeutour F, Domanski HA, Hoglund M, Bauer HC, Rydholm A, Sciot R, Mandahl N, Mertens F (2003) Clustering of deletions on chromosome 13 in benign and low-malignant lipomatous tumors. Int J Cancer 103 (5):616–623. doi:jcp./ijc.10864
18. Staaf J, Lindgren D, Vallon-Christersson J, Isaksson A, Goransson H, Juliusson G, Rosenquist R, Hoglund M, Borg A, Ringner M (2008) Segmentation-based detection of allelic imbalance and loss-of-heterozygosity in cancer cells using whole genome SNP arrays. Genome Biol 9(9):R136. doi:10.1186/gb-2008-9-9-r136
19. Adsay NV, Eble JN, Srigley JR, Jones EC, Grignon DJ (2000) Mixed epithelial and stromal tumor of the kidney. Am J Surg Pathol 24(7):958–970
20. Michal M, Hes O, Bisceglia M, Simpson RH, Spagnolo DV, Parma A, Boudova L, Hora M, Zachoval R, Suster S (2004) Mixed epithelial and stromal tumors of the kidney. A report of 22 cases. Virchows Arch 445(4):359–367. doi:10.1007/s00428-004-1060-y
21. Turbiner J, Amin MB, Humphrey PA, Srigley JR, De Leval L, Radhakrishnan A, Oliva E (2007) Cystic nephroma and mixed epithelial and stromal tumor of kidney: a detailed clinicopathologic analysis of 34 cases and proposal for renal epithelial and stromal tumor (REST) as a unifying term. Am J Surg Pathol 31 (4):489–500. doi:10.1097/PAS.0b013e31802bdd5600000478-200704000-00001
22. Smith DI, Zhu Y, McAvoy S, Kuhn R (2006) Common fragile sites, extremely large genes, neural development and cancer. Cancer Lett 232(1):48–57. doi:10.1016/j.canlet.2005.06.049
23. Prazeres H, Torres J, Rodrigues F, Pinto M, Pastoriza MC, Gomes D, Cameselle-Teijeiro J, Vidal A, Martins TC, Sobrinho-Simoes M, Soares P (2010) Chromosomal, epigenetic and microRNA-mediated inactivation of LRP1B, a modulator of the extracellular environment of thyroid cancer cells. Oncogene. doi:10.1038/onc.2010.512
24. Zanesi N, Fidanza V, Fong LY, Mancini R, Druck T, Valtieri M, Rudiger T, McCue PA, Croce CM, Huebner K (2001) The tumor spectrum in FHIT-deficient mice. Proc Natl Acad Sci USA 98 (18):10250–10255. doi:10.1073/pnas.191345898 191345898
25. Aqeilan RI, Croce CM (2007) WWOX in biological control and tumorigenesis. J Cell Physiol 212(2):307–310. doi:10.1002/jcp.21099
26. Marg A, Sirim P, Spaltmann F, Plagge A, Kauselmann G, Buck F, Rathjen FG, Brummendorf T (1999) Neurotractin, a novel neurite outgrowth-promoting Ig-like protein that interacts with CEPU-1 and LAMP. J Cell Biol 145(4):865–876
27. Schafer M, Brauer AU, Savaskan NE, Rathjen FG, Brummendorf T (2005) Neurotractin/kilon promotes neurite outgrowth and is expressed on reactive astrocytes after entorhinal cortex lesion. Mol Cell Neurosci 29(4):580–590. doi:10.1016/j.mcn.2005.04.010
28. Jack BH, Crossley M (2010) GATA proteins work together with friend of GATA (FOG) and C-terminal binding protein (CTBP) co-regulators to control adipogenesis. J Biol Chem 285, 2010/08/14 edn. doi:M110.141317 [pii] 10.1074/jbc.M110.141317

Virchows Arch (2011) 459:555–556
DOI 10.1007/s00428-011-1146-2

ERRATUM

Erratum to: Splenomegaly, hypersplenism and peripheral blood cytopaenias in patients with classical Anderson–Fabry disease

João Paulo Oliveira · Carmen Valbuena · António Baldaia Moreira · Elsa Fonseca · Carlos Soares · Elisa Leão Teles · Stephen Waldek

Published online: 18 September 2011
© Springer-Verlag 2011

Erratum to: Virchows Arch (2008) 453:291–300
DOI 10.1007/s00428-008-0651-4

The original version of this article unfortunately contained a mistake. The reference citations in Table 5 are incorrect.

The following is the updated version of Table 5.

The online version of the original article can be found at http://dx.doi.org/10.1007/s00428-008-0651-4.

J. P. Oliveira
Department of Medical Genetics,
Faculty of Medicine,
Porto, Portugal

J. P. Oliveira · A. B. Moreira · C. Soares
Department of Nephrology, Hospital São João,
Porto, Portugal

C. Valbuena · E. Fonseca
Department of Pathology,
Faculty of Medicine and Hospital São João,
Porto, Portugal

E. L. Teles
Department of Paediatrics, Hospital São João,
Porto, Portugal

S. Waldek
Adult Inherited Metabolic Diseases, Hope Hospital,
Salford, UK

J. P. Oliveira (✉)
Serviço de Genética Médica, Faculdade de Medicina,
Universidade do Porto,
4200-319 Porto, Portugal
e-mail: jpo@med.up.pt

Table 5 Summary of previous case reports of patients with Anderson-Fabry disease and symptomatic reticuloendothelial organ involvement or thrombocytopaenia

Ref. #	Organ enlargement				Thrombocytopaenia[a]	Additional notes
	Age	L	LN	S		
[6]	22		X		45.0×10^9/l	Platelet count normalised following splenic X-ray irradiation.
[6]	18		X		72.0×10^9/l	Platelet count normalised following splenic X-ray irradiation.
[7]	32	X		X	29.8×10^9/l	
[8]	30			X		Splenomegaly later confirmed at laparotomy for appendicitis and at autopsy [3].
[9]	28		X			LNBx showing lipid deposits in macrophages.
[9]	25		X			
[4, 32]	23		X	X		Surgical mesenteric LNBx and SBx showing vacuolated cells.
[10]	18		X			LNBx showing typical lamellated Gb3 deposits in EM examination.
[11, 33]	10	X	X	X		LNBx showing histiocytes with foamy cytoplasmic appearance.

Ref. # reference number. Age in years. *LN* lymph node; *L* liver; *S* spleen

[a] Platelet count, in patients with thrombocytopaenia."*X*" manifestation present. *Bx* biopsy. *EM* electron microscopy

Virchows Arch (2011) 459:557–563
DOI 10.1007/s00428-011-1165-z

REVIEW AND PERSPECTIVES

T cell/histiocyte-rich large B-cell lymphoma: an update on its biology and classification

Thomas Tousseyn · Christiane De Wolf-Peeters

Received: 26 September 2011 / Accepted: 26 October 2011 / Published online: 12 November 2011
© Springer-Verlag 2011

Abstract T cell/histiocyte-rich large B-cell lymphoma (THRLBCL), originally considered an uncommon variant of Diffuse Large B-Cell Lymphoma (DLBCL), is recognized by the World Health Organisation as a separate clinicopathological entity since 2008. It predominantly affects middle aged men often presenting with advanced stage disease frequently involving spleen, liver and bone marrow at time of diagnosis. According to the WHO, this lymphoma is morphologically characterized by less than 10% of large neoplastic B cells in a background of abundant T cells and frequently histiocytes. Differentiating THRLBCL from other lymphoproliferative disorders such as Nodular Lymphocyte Predominant Hodgkin Lymphoma (NLPHL) and Lymphocyte-Rich classical Hodgkin lymphoma (LRcHL) is important from a clinical point of view and can be achieved in most cases, given adequate biopsy specimens, by careful morphological and immunohistochemical evaluation of both the neoplastic cells as well as the nonneoplastic stromal component. According to this WHO definition, THRLBCL is still considered a clinically heterogeneous entity, though it is noted that especially the cases containing numerous histiocytes behave aggressively and show resistance to current therapies for DLBCL. Gene expression profiling studies of THRLBCL provided evidence for a prominent role for this histiocytic component that is important for a tolerogenic host immune response in which they may assist neoplastic cells in escaping the T cell-mediated immune surveillance. Therefore, reserving the diagnosis of THRLBCL to cases containing a large proportion of histiocytes might be relevant, as modulating their activity could provide new therapeutic options.

Keywords T cell/histiocyte-rich large B-cell lymphoma (THRLBCL) · Review · Nodular Lymphocyte Predominant Hodgkin Lymphoma · Refining diagnostic criteria

T. Tousseyn · C. De Wolf-Peeters
Morphology and Molecular Pathology Section,
University Hospitals KU, Leuven,
Leuven, Belgium

T. Tousseyn (✉)
Department of Pathology,
Minderbroederstraat 12, blok Q,
3000 Leuven, Belgium
e-mail: thomas.tousseyn@uzleuven.be

Introduction

After the description by several groups of a striking infiltrate of reactive T cells in different types of B-cell lymphomas Ramsay et al. introduced in 1988 the term ‘T cell-rich B-cell lymphoma’ (TCRBCL) [1–3]. TCRBCL, occasionally misinterpreted as T cell lymphomas before the era of immunohistochemistry, has been recognized as a caveat for pathologists. A particular subgroup of these TCRBCL may mirror Nodular Lymphocyte Predominant Hodgkin Lymphoma (NLPHL), is characterized by a histiocyte-rich stroma and a poor clinical outcome [4, 5] (Fig. 1). To stress the importance of the histiocytes in these cases, our group introduced in 1992 the term ‘histiocyte-rich B-cell lymphoma’ (HRBCL) for these TCRBCL in which the background population consisted not only of small reactive T cells but mainly of reactive histiocytes [5].

In the 2001, WHO classification T cell/histiocyte-rich large B cell lymphoma (THRLBCL) was listed as a variant of diffuse large B cell lymphoma (DLBCL) and defined by the ‘presence of scattered large B cells in a background rich in T cells, together with or without histiocytes’ [6]. Within this variant of DLBCL, HRBCL was included. Of interest,

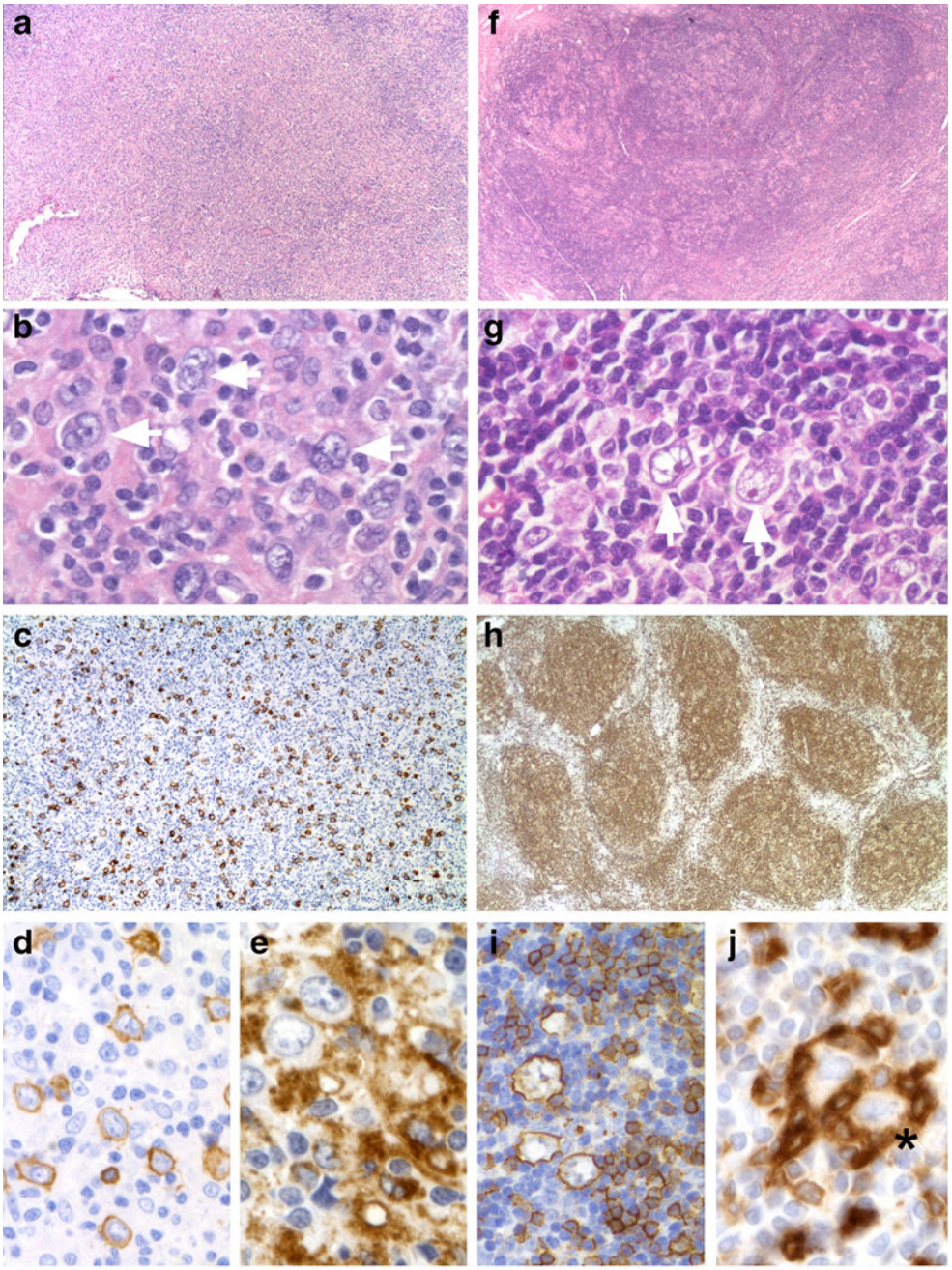

Fig. 1 Morphological and immunohistochemical characterization of THRLBCL (**a**–**e**) and NLPHL (**f**–**j**). At low magnification, H&E staining illustrates the diffuse (**a**) versus nodular (**b**) pattern of lymph node involvement in THRLBCL and NLPHL, respectively. The CD20-positive (**c**–**d**) large atypical cells (*arrow*) of THRLBCL are embedded in stroma-rich in CD68-positive histiocytes (**e**) and small T lymphocytes in the absence of small B cells. In contrast, in NLPHL (**f**–**j**), CD20-positive LP cells (*arrow* in **g**) are embedded in nodular aggregates of small B cells (**h**–**i**) and surrounded by rosettes of CD3+/CD57+ T cells (*asterisk* in **j**)

clinicopathological studies on THRLBCL according the WHO criteria, thus including cases with a variable number or no histiocytes, resulted in a heterogeneous group of lymphomas with clinical presentation varying from mild to rapidly progressive end-stage disease [7–13].

To improve our diagnostic criteria and concept of HRBCL, a thorough morphologic and immunophenotypic evaluation of 60 cases was performed and the following diagnostic criteria proposed for recognition of an entity we called 'Histiocyte-rich T cell-rich Large B-cell lymphoma' [14]: (1) a disturbed lymph node architecture due to a diffuse (or vaguely nodular) neoplastic infiltrate; (2) composed of scattered large atypical neoplastic B cells lacking the expression of CD15; representing only a minority of the overall cell population and occurring as solitary cells (or in very small clusters); and (3) a reactive background infiltrate composed of nonepithelioid histiocytes surrounding the neoplastic cells, small T cells not forming rosettes, and near absent small B cells in the neoplastic areas.

This lymphoma was finally considered as a separate clinicopathological entity in the World Health Organization (WHO) 2008 classification on lymphoid tumors. Based on a consensus expert panel, the 2001 definition on THRLBCL was adapted to cover the lymphoma we

described as 'Histiocyte-rich T cell-rich Large B-cell lymphoma', and the entity THRLBCL was characterized by 'a limited number of scattered, large, atypical B cells embedded in a background of abundant T cells and frequently histiocytes' [15]. Still, the presence of numerous histiocytes was not considered a prerequisite for the diagnosis leaving the entity diagnosed as such too heterogeneous to our opinion.

In this review, we will focus on the pitfalls of diagnosing this rare entity, provide molecular genetic evidence that supports our suggestion to reserve the diagnosis THRLBCL only for cases with a prominent histiocytic background and provide some hope for new therapeutic approaches by mediating their function.

Morphological and immunohistochemical features of THRLBCL

Morphologically, most cases of THRLBCL show a complete disruption of the normal nodal architecture. However, vague nodularity may be present. Scattered large atypical neoplastic B cells are surrounded by a prominent inflammatory background. The neoplastic B cells do not form aggregates or sheets but can vary in size and morphology and can resemble immunoblasts, Hodgkin/Reed–Sternberg-like (HRS) cells or Lymphocyte Predominant-like (LP) cells, typical of DLBCL, classical Hodgkin lymphoma, or NLPHL, respectively [12, 16]. They are embedded within clusters of bland-looking histiocytes and T cells, but T lymphocyte rosetting is typically absent.

Immunohistochemical analysis shows that the neoplastic B cells of THRLBCL mark positive for CD45, CD20 and CD79a, but lack the expression of CD5, CD15 and CD138. Only in rare cases do they express CD30. Tumor cells are typically immunopositive for Bcl6 suggesting their derivation from germinal center B cells although they are mostly CD10-negative. Bcl2 expression, a negative predictive factor in DLBCL, was shown to be positive in up to 50% of THRLBCL. Expression of other histochemical markers such as epithelial membrane antigen (EMA) is variable. The tumoral microenvironment is histochemically characterized by CD68+ histiocytes and lymphocytes with a CD3+/CD5+ profile, which may be CD4+ but most often TIA1+/CD8+ [12, 14, 17, 18].

Differential diagnosis

Even with careful examination of both the neoplastic cells as well as the nonneoplastic cells using immunohistochemistry, differentiating THRLBCL from other hematologic tumors may often remain difficult. The morphologic and immunohistochemical features distinguishing THRLBCL from NLPHL and classical Hodgkin's lymphoma (cHL) are discussed below and summarized in Table 1.

a. THRLBCL versus NLPHL

Indeed, the distinction between THRLBCL and Nodular Lymphocyte Predominant Hodgkin lymphoma (NLPHL also known as 'paragranuloma') may be difficult. Nevertheless, an important difference between both lymphomas lies in their clinical presentation and prognosis. Therefore, it is crucial to distinguish both entities as NLPHL is an indolent disorder with a favorable prognosis and does not require aggressive treatment in stark contrast to THRLBCL, especially the variant containing many histiocytes [14, 19]. At low magnification, the distinction may not be easy because although THRLBCL most often has a diffuse appearance, it might present with a nodular pattern in a large proportion of cases. Similarities in morphology and immunophenotype of the neoplastic cells further complicate the differential diagnosis. Indeed, the LP (Lymphocyte Predominant) cells or 'popcorn' cells of NLPHL and the scattered neoplastic cells of THRLBCL share many characteristics including the expression of pan-B cell markers while lacking the classic HL markers CD15 and CD30 (see Table 1) (adapted from Ref. [20]). In both THRLBCL and NLPHL, neoplastic cells display features of germinal center cells.

However, although NLPHL and THRLBCL are related in as far as their cell of origin is concerned, these lymphomas apparently differ in the host immune response they elicit and differential diagnosis on a pathological basis largely relies on characteristics of the nonneoplastic environment [21, 22]. In THRLBCL, the background stroma is composed of CD8+/TIA1+ small T cells and large numbers of nonepitheloid histiocytes surrounding the neoplastic cells, while small B cells are rare in the neoplastic areas. On the contrary, NLPHL affects the B follicle, and its stroma is composed mainly of small B lymphocytes, with CD4+/CD57+ T cells rosetting around the LP cells. Applying a follicular dendritic cell (FDC) marker, like CD21 or CD23, is helpful as FDC meshworks are partially preserved in the nodular areas containing the small bystander B cells in NLPHL. In contrast, in THRBCL typically affecting the extrafollicular compartment, these follicle mantles and FDC networks are lacking. Alternatively, to FDC stainings, IgD staining can be used to show the presence of residual IgD+ follicle mantles that favor NLPHL [23] above THRBCL. In THRLBCL, large IDO expressing dendritic cells are located in the vicinity of tumor cells and this is not observed in NLPHL. Nearly all stromal components, but not the

Table 1 Differentiating pathologic features between THRBCL and NLPHL

	THRLBCL	NLPHL
Overall architectural pattern	Diffuse (or vaguely nodular)	Nodular, pattern A (or diffuse)
FDC network (CD21+)	Absent	Disturbed
Residual IgD+ follicle mantles	Absent	Present
Large neoplastic cellss	Scarce	Scarce
Morphology	IB, HRS, LP	LP ('popcorn')
IHC profile		
LCA/CD45	+	+
CD20	+	+
CD79a	+	+
PAX5/BSAP	+	+
BOB1	+	+
OCT2	+	+
PU.1	−/+	+
CD30	−/+	−/+
CD15	−	−
Bcl-6	+/−	+
EBV	−/+	−
STAT1	−	(+)
EMA	−/+	+/−
Bystander cells	Abundant	Abundant
Small B cells (CD20+)	No to few	Abundant
Small T cells (CD3+)	Numerous	Numerous
Predominant population	CD8+	CD4+
CD4+ rosetting	No	Frequent
CD57+ rosetting	No	Frequent
Histiocytes (CD68+)	Numerous; nonepithelioid	Few; if present forming epithelioid granulomas
IDO expressing DCs	Present	Absent

THRLBCL T cell/histiocyte-rich large B-cell lymphoma, *NLPHL* Nodular Lymphocyte Predominant Hodgkin Lymphoma, *IB* immunoblastic, *HRS* Hodgkin/Reed–Sternberg, *LP* lymphocyte predominant, *IHC* immunohistochemical, *EBV* Epstein–Barr virus; *EMA* epithelial membrane antigen, *FDC* follicular dendritic cells, *DC* dendritic cells, *IDO* indoleamine 2,3-dioxygenase

neoplastic cells, in THRLBCL express STAT1, while in NLPHL STAT1 expression is confined to large dendritic cells adjacent to the T-cell rosettes and some weak expression is discerned in the popcorn cells [23].

Fan et al. described four different immunoarchitectural patterns in NLPHL, with the nodular B cell-rich form (pattern A) being the most frequent and classical form, which should be easy to distinguish from THRLBCL [24]. However, the differential diagnosis becomes more challenging when the number of T cells increases (T cell-rich nodular areas or pattern D) or when the LP cells are predominantly localized outside the B cell-rich nodules (THRLBCL-like areas or patterns C/E). From a purely morphological perspective, distinguishing NLPHL/pattern E from THRBCL is virtually impossible, especially in small biopsy specimens. It is the clinical setting of an advanced clinical stage at time of diagnosis and poor response to treatment that can suggest the diagnosis of THRBCL, while a limited stage and favorable response to treatment would favor the diagnosis of diffuse NLPHL. Since transition was suggested of a NLPHL pattern to a T cell/histiocyte-richlike or diffuse pattern [25], this was not related to a bad prognosis [26, 27]. Finally, increase in the number of atypical cells resembling the image of DLBCL does occur in both NLPHL and THRLBCL only heralding a worse prognosis in the latter [14].

b. THRLBCL versus LRcHL

At low power examination, lymphocyte-rich classical Hodgkin's lymphoma (LRcHL) can mimic THRLBCL as both entities are characterized by scarce neoplastic cells embedded in a nonneoplastic inflammatory stroma. Without additional immunohistochemical stainings, it is sometimes difficult to distinguish the large atypical cells in THRLBCL from Hodgkin/Reed–Sternberg cells typical for cHL. While the large atypical cells of THRLBCL express CD20, they lack expression of CD15 and CD30. Based on their opposite immunohistochemical profile, the

combined use of CD20 and CD15 is helpful to differentiate THRLBCL from LRcHL. Apart from differences in the neoplastic cells, careful study of the nonneoplastic background reveals differences in the composition of the nonneoplastic cells, which in LRcHL typically is composed of abundant small T cells that do form rosettes around the neoplastic cells in the absence of histiocytes [28].

Does THRLBCL occur in childhood?

However, the disease entity THRLBCL preferentially affects middle aged men, a handful of reports were made about TCRBCL (not necessarily THRLBCL) in the pediatric population where it tends to be a local disease [29, 30]. They report a striking predominance of the male gender and unique morphological characteristics of the atypical B cells (large lobulated nucleus with pale chromatin resembling LP cells) as well as absence of EBV infection. In contrast to the reports on THRLBCL in adults, only few pediatric patients presented with advanced stages, and bone marrow involvement by TCRBCL in children was never reported. The little available information on therapy and follow-up showed that the prognosis was favorable after a short intensive polychemotherapy regimen for aggressive lymphomas [30]. In our experience, THRLBCL is extremely rare, if even existing, in a pediatric population and other conditions should be ruled out first, in particular, congenital or acquired immunodeficiencies causing an aberrant immune respons or Hodgkin lymphoma.

Is THRLBCL related to EBV?

Although the association between EBV and THRBCL has not been extensively studied, EBV positivity is not a typical feature of THRLBCL and only a small portion of reported cases display in situ findings of latent EBV infection (e.g., EBER or LMP1 positivity), mostly in cases that show a morphologic resemblance to cHL [31]. Nevertheless, the consensus chapter on THRLBCL in the 2008 WHO classification advises to consider these cases within the spectrum of aggressive EBV-positive DLBCL and avoid classifying them as THRLBCL. One may wonder if some of these cases represent a type of "grey zone lymphoma" with features intermediate between cHL and THRLBCL and correspond to HL cases reported in the older literature that were associated with a poorer prognosis that showed expression of CD20 but not CD15 [32].

Molecular genetics of THRLBCL

The molecular genetic background of THRLBCL is hardly explored as the number of atypical B cells is very low. In single cell analyses of the atypical cells in THRLBCL, monoclonal immunoglobulin rearrangements have been demonstrated [33]. However, conventional PCR technique on whole tissue sections to detect clonality is limited by the number of neoplastic cells.

Cytogenetic analysis was successful in a limited number of cases only but no recurrent abnormalities have been identified yet [21, 34–36]. Comparative genomic hybridization performed on microdissected tumor cells demonstrated that chromosomal imbalances are more numerous in NLPHL as compared to those found in THRLBCL [36]. This finding strongly argues against the hypothesis that THRLBCL develops from NLPHL as tumor progression cannot coincide with a decreased number of chromosomal abnormalities. However, the atypical B cells in both lymphomas were found to share rare imbalances on chromosomes 4q and 19p suggesting a similar precursor for both disorders.

The difficulty of performing molecular genetic studies or microarray gene expression profiling in THRLBCL is that the signature of the neoplastic cells will be outnumbered by the signature of the predominant stromal reaction. Isolation of single tumor cells from the nonneoplastic background is required if one wants to investigate the gene expression profile of the neoplastic cell component but these data are largely lacking at present.

Interestingly, as gene expression profiling of several lymphoma types has shown, the profile of lymphomas is not only defined by the characteristics of the neoplastic cells but also of the stromal component or host immune response that plays a role in predicting the prognosis [37, 38]. To investigate whether the microenvironment surrounding the neoplastic cells of THRBCL could play an important role in determining the clinical outcome in THRLBCL, we investigated the functional meaning and the biological significance of this distinctive stroma by comparing the gene expression profile of whole tissue sections from THRLBCL cases (with prominent histiocytic component) with that of NLPHL [23]. Our GEP profiles of THRLBCL indicate a macrophage/histiocyte-activated status by which the tumor cells acquire several mechanisms to escape T cell-mediated immune surveillance by suppressing the proliferation and activation of effector T cells and their conversion to regulatory T cells. Similar to the data from Chetaille et al., the molecular signature we found in THRLBCL was dominated by an interferon-dependent pathway including STAT-1 [39]. Both IFN-γ as well as proteins that are upregulated in macrophages upon treatment with IFN-γ, including indoleamine 2,3-dioxygenase (IDO) and Chemokine (C–C motif) ligand 8 (CCL8), are upregulated in THRLBCL. CCL8, one of the most potent monocyte chemoattractants, may contribute to the histiocyte-rich composition of the stroma in THRLBCL while IFN-γ is

responsible for the activation of histiocytes and, in synergy with Toll-like receptor ligands, for the production of high levels of IDO by histiocytes and dendritic cells. IDO, which might be expressed by tumor cells as well, has been described to promote tumoral immune tolerance in a variety of hematopoietic malignancies [40, 41]. IDO degrades tryptophan thus lowering tryptophan concentration in the local microenvironment. Such altered microenvironment protects tumor cells from rejection by the immune system as T lymphocytes are very sensitive to tryptophan shortage. IDO thus suppresses local T cell responses and alters the conversion of effector T cells into T regulatory cells. Our findings may explain the peculiar composition of the stroma in THRLBCL as well as the bad prognosis of these patients.

Of interest, other genes found to be upregulated in THRLBCL overlapped significantly with genes found to be related to an unfavorable immune response in a subset of follicular lymphomas and genes found to be related to host inflammatory response in DLBCL [37, 38]. Our data are also in concordance with the GEP study by Monti et al. that recognized a particular subtype of DLBCL, which they indicated as DLBCL with "host inflammatory response" [42]. Cases of this subtype showed several characteristics reminiscent of THRLBCL, not only by their morphology but also by their clinical presentation and outcome.

On the contrary, the molecular signature in NLPHL identified B-cell characteristics, implying that the follicular component seen in typical NLPHL is the predominant feature. Since there was minimal overlap with the signature from the purified lymphocyte-predominant cells as reported by Brune et al., [43] we concluded that the profile was determined by the abundant background B cells and not by the scarce neoplastic cells.

Treatment

Multiple study groups compared the clinical outcome between DLBCL and THRLBCL. Some retrospective studies showed comparable outcome, while others report that THRLBCL, especially using a more restricted diagnosis (rich in histiocytes), has a worse prognosis and may, therefore, need more aggressive therapy [7, 14, 44, 45]. This dichotomy results in uncertainty about the best therapeutic approach when the diagnosis of THRLBCL is made. Nevertheless, new insights in the molecular pathogenesis of this disease will provide clues for targeted therapy with newly developed drugs adapted to the specific characteristics of the neoplastic cells or its stromal component. Mediating the host stromal response that is hallmarked by an increased expression of IFN-γ, CCL8, IDO and VSIG4, could, e.g., be done through inhibition of IDO [46].

Conclusion and perspectives

T cell/histiocyte-rich B-cell lymphoma (THRLBCL) is a relatively new entity. Morphologically differentiating THRLBCL from Nodular Lymphocyte Predominant Hodgkin Lymphoma (NLPHL) is not always easy. Since these entities have a different prognosis and require a different therapeutic approach, an initial correct histopathological diagnosis is of the utmost importance. The clue to a correct differential diagnosis lies in the careful morphologic and immunohistochemical examination of the tumor microenvironment, which defines the major difference between the two entities.

GEP studies stress the significant role of the microenvironment in THRLBCL and emphasize the crucial role of its histiocytes supporting their presence as a diagnostic hallmark in the identification of this particular lymphoma. Because of these results, we suggest to diagnose lymphoma cases as THRLBCL only if the nonneoplastic component is rich in histiocytes. However, in addition to further studies on the biological significance of the peculiar stroma characterizing THRLBCL, molecular and cytogenetic studies of isolated tumor cells are necessary to provide more insights in the pathogenesis and the more precise delineation of THRLBCL from other lymphomas.

References

1. Jaffe E et al (1984) Diffuse B cell lymphoma with T cell predominance in patients with follicular lymphoma or 'pseudo T cell lymphoma'. Lab Investig 50:27A–28A
2. Mirchandani I et al (1985) B-cell lymphomas morphologically resembling Tcell lymphomas. Cancer 56:1578–1583
3. Ramsay AD, Smith WJ, Isaacson PG (1988) T-cell-rich B-cell lymphoma. Am J Surg Pathol 12(6):433–443
4. Chittal SM et al (1991) Large B-cell lymphoma rich in T-cells and simulating Hodgkin's disease. Histopathology 19(3):211–220
5. Delabie J et al (1992) Histiocyte-rich B-cell lymphoma. A distinct clinicopathologic entity possibly related to lymphocyte predominant Hodgkin's disease, paragranuloma subtype. Am J Surg Pathol 16 (1):37–48
6. Gatter KC, Warnke R (2001) Diffuse large B-cell lymphomas. In: Jaffe ES, Harris NL, Stein H, Vardiman J (eds) World Health Organization classification of tumours. Pathology and genetics of tumours of haematopoietic and lymphoid tissues. IARC Press, Lyon, pp 171–4
7. Bouabdallah R et al (2003) T-cell/histiocyte-rich large B-cell lymphomas and classical diffuse large B-cell lymphomas have similar outcome after chemotherapy: a matched-control analysis. J Clin Oncol 21(7):1271–1277
8. De Wolf-Peeters C, Pittaluga S (1995) T-cell rich B-cell lymphoma: a morphological variant of a variety of non-Hodgkin's lymphomas or a clinicopathological entity? Histopathology 26(4):383–385
9. Greer JP et al (1995) T-cell-rich B-cell lymphomas: diagnosis and response to therapy of 44 patients. J Clin Oncol 13(7):1742–1750
10. Harris NL (1999) Hodgkin's lymphomas: classification, diagnosis, and grading. Semin Hematol 36(3):220–232
11. Krishnan J, Wallberg K, Frizzera G (1994) T-cell-rich large B-cell lymphoma. A study of 30 cases, supporting its histologic

heterogeneity and lack of clinical distinctiveness. Am J Surg Pathol 18(5):455–465
12. Lim MS et al (2002) T-cell/histiocyte-rich large B-cell lymphoma: a heterogeneous entity with derivation from germinal center B cells. Am J Surg Pathol 26(11):1458–1466
13. Rodriguez J, Pugh WC, Cabanillas F (1993) T-cell-rich B-cell lymphoma. Blood 82(5):1586–1589
14. Achten R et al (2002) T-cell/histiocyte-rich large B-cell lymphoma: a distinct clinicopathologic entity. J Clin Oncol 20 (5):1269–1277
15. Swerdlow SH, Campo E, Harris NL, Jaffe ES, Pileri SA, Stein H et al (2008) WHO classification of tumours of haematopoietic and lymphoid tissues, 4th edn. International Agency for Research on Cancer, Lyon
16. Dogan A et al (2003) Micronodular T-cell/histiocyte-rich large B-cell lymphoma of the spleen: histology, immunophenotype, and differential diagnosis. Am J Surg Pathol 27(7):903–911
17. Fraga M et al (2002) T-cell/histiocyte-rich large B-cell lymphoma is a disseminated aggressive neoplasm: differential diagnosis from Hodgkin's lymphoma. Histopathology 41(3):216–229
18. Gascoyne RD et al (1997) Prognostic significance of Bcl-2 protein expression and Bcl-2 gene rearrangement in diffuse aggressive non-Hodgkin's lymphoma. Blood 90(1):244–251
19. Diehl V et al (1999) Clinical presentation, course, and prognostic factors in lymphocyte-predominant Hodgkin's disease and lymphocyte-rich classical Hodgkin's disease: report from the European Task Force on Lymphoma Project on Lymphocyte-Predominant Hodgkin's Disease. J Clin Oncol 17(3):776–783
20. Abramson JS (2006) T-cell/histiocyte-rich B-cell lymphoma: biology, diagnosis, and management. Oncologist 11(4):384–392
21. Brauninger A et al (1999) Molecular analysis of single B cells from T-cell-rich B-cell lymphoma shows the derivation of the tumor cells from mutating germinal center B cells and exemplifies means by which immunoglobulin genes are modified in germinal center B cells. Blood 93(8):2679–2687
22. Marafioti T et al (1997) Origin of nodular lymphocyte-predominant Hodgkin's disease from a clonal expansion of highly mutated germinal-center B cells. N Engl J Med 337(7):453–458
23. Van Loo P et al (2009) T-cell/histiocyte-rich large B-cell lymphoma shows transcriptional features suggestive of a tolerogenic host immune response. Haematologica 95(3):440–448
24. Fan Z et al (2003) Characterization of variant patterns of nodular lymphocyte predominant hodgkin lymphoma with immunohistologic and clinical correlation. Am J Surg Pathol 27(10):1346–1356
25. Hansmann ML et al (1989) Nodular paragranuloma can transform into high-grade malignant lymphoma of B type. Hum Pathol 20 (12):1169–1175
26. Boudova L et al (2003) Nodular lymphocyte-predominant Hodgkin lymphoma with nodules resembling T-cell/histiocyte-rich B-cell lymphoma: differential diagnosis between nodular lymphocyte-predominant Hodgkin lymphoma and T-cell/histiocyte-rich B-cell lymphoma. Blood 102(10):3753–3758
27. Torlakovic E et al (2001) The transcription factor PU.1, necessary for B-cell development is expressed in lymphocyte predominance, but not classical Hodgkin's disease. Am J Pathol 159(5):1807–1814
28. Sanders ME et al (1988) Molecular pathways of adhesion in spontaneous rosetting of T-lymphocytes to the Hodgkin's cell line L428. Cancer Res 48(1):37–40
29. Lones MA, Cairo MS, Perkins SL (2000) T-cell-rich large B-cell lymphoma in children and adolescents: a clinicopathologic report of six cases from the Children's Cancer Group Study CCG-5961. Cancer 88(10):2378–2386
30. Tiemann M et al (2005) Proliferation rate and outcome in children with T-cell rich B-cell lymphoma: a clinicopathologic study from the NHL-BFM-study group. Leuk Lymphoma 46(9):1295–1300
31. Axdorph U et al (2002) T-cell-rich B-cell lymphoma—diagnostic and therapeutic aspects. APMIS 110(5):379–390
32. Jaffe E, Muller-Hermelink H (1999) Relationship between Hodgkin's disease and nonHodgkin's lymphomas. In: Mauch P, Armitage J, Diehl V et al (eds) Hodgkin's disease. Lippincott Raven, Philadelphia, pp 181–194
33. Osborne BM, Butler JJ, Pugh WC (1990) The value of immunophenotyping on paraffin sections in the identification of T-cell rich B-cell large-cell lymphomas: lineage confirmed by JH rearrangement. Am J Surg Pathol 14(10):933–938
34. Achten R et al (2002) Histiocyte-rich, T-cell-rich B-cell lymphoma: a distinct diffuse large B-cell lymphoma subtype showing characteristic morphologic and immunophenotypic features. Histopathology 40(1):31–45
35. Braeuninger A et al (1997) Hodgkin and Reed–Sternberg cells in lymphocyte predominant Hodgkin disease represent clonal populations of germinal center-derived tumor B cells. Proc Natl Acad Sci USA 94(17):9337–9342
36. Franke S et al (2001) Lymphocyte predominance Hodgkin disease is characterized by recurrent genomic imbalances. Blood 97 (6):1845–1853
37. Dave SS et al (2004) Prediction of survival in follicular lymphoma based on molecular features of tumor-infiltrating immune cells. N Engl J Med 351(21):2159–2169
38. Lenz G et al (2008) Stromal gene signatures in large-B-cell lymphomas. N Engl J Med 359(22):2313–2323
39. Chetaille B et al (2009) Molecular profiling of classical Hodgkin lymphoma tissues uncovers variations in the tumor microenvironment and correlations with EBV infection and outcome. Blood 113(12):2765–3775
40. Curti A et al (2009) The role of indoleamine 2,3-dioxygenase in the induction of immune tolerance: focus on hematology. Blood 113(11):2394–2401
41. Ninomiya S et al (2011) Indoleamine 2,3-dioxygenase in tumor tissue indicates prognosis in patients with diffuse large B-cell lymphoma treated with R-CHOP. Ann Hematol 90(4):409–416
42. Monti S et al (2005) Molecular profiling of diffuse large B-cell lymphoma identifies robust subtypes including one characterized by host inflammatory response. Blood 105(5):1851–1861
43. Brune V et al (2008) Origin and pathogenesis of nodular lymphocyte-predominant Hodgkin lymphoma as revealed by global gene expression analysis. J Exp Med 205(10):2251–2268
44. El Weshi A (2007) T-cell/histiocyte-rich B-cell lymphoma: clinical presentation, management and prognostic factors: report on 61 patients and review of literature. Leuk Lymphoma 48 (9):1764–1773
45. Aki H et al (2004) T-cell-rich B-cell lymphoma: a clinicopathologic study of 21 cases and comparison with 43 cases of diffuse large B-cell lymphoma. Leuk Res 28(3):229–236
46. Lob S et al (2009) Inhibitors of indoleamine-2,3-dioxygenase for cancer therapy: can we see the wood for the trees? Nat Rev Cancer 9(6):445–452

Virchows Arch (2011) 459:565–572
DOI 10.1007/s00428-011-1157-z

ORIGINAL ARTICLE

Frequency and clinical significance of placental histological lesions in an unselected population at or near term

Sangeeta Pathak · Christoph C. Lees · Gerald Hackett · Flora Jessop · Neil J. Sebire

Received: 29 June 2011 / Revised: 2 September 2011 / Accepted: 10 October 2011 / Published online: 27 October 2011
© Springer-Verlag 2011

Abstract Associations between specific placental histological abnormalities and obstetric outcomes are reported. However, most data are based either on high-risk cases or relate to case–control studies selected from those with abnormal placental histology findings, with the unavoidable biases that these approaches entail. This study reports the frequency of the several common, objective and predefined histological abnormalities of the placenta as identified by pathologists blinded to all clinical information. A total 1,153 women were recruited from an unselected population delivering at 34–43 weeks. Histological findings in common obstetric outcome groups were compared to those of the unselected population, and odds ratios and predictive values were calculated. Normal histological findings were present in 72.1% of pregnancies with normal outcomes and in 79.1%, 66.6%, 80%, and 74.8% of pregnancies affected by pre-eclampsia (PET), pregnancy-induced hypertension (PIH), gestational diabetes (GDM), and small for gestational age (SGA), respectively. Chronic placental underperfusion was seen more frequently in PIH (odds ratio (OR) 2) and SGA (OR 1.4), while villitis of unknown aetiology was observed more commonly in cases with PIH (OR 3.2). Fetal thrombotic vasculopathy was twice as common in cases with GDM whilst massive perivillous fibrin deposition was much more frequent in those with PET (OR 20.2) and SGA (OR 8.9). Chorangiomata were 13 times more common in pregnancies with PET. However, in all cases, positive predictive values were low, with the majority of cases with histological abnormalities being associated with normal outcome. At term, specific placental histological lesions are significantly more common in complicated pregnancies, but the clinical significance of such lesions in a specific case remains uncertain, since the majority will be identified from clinically uncomplicated normal pregnancies.

Keywords Placenta · Pathology · Infarct · Outcome · Risk

S. Pathak · C. C. Lees · G. Hackett
Division of Fetal-Maternal Medicine,
Rosie Maternity-Addenbrooke's Hospital,
Cambridge University Hospitals NHS Foundation Trust,
Hills Road,
Cambridge CB2 2QQ, UK

F. Jessop
Department of Pathology, Addenbrooke's Hospital,
Cambridge University Hospitals NHS Foundation Trust,
Hills Road,
Cambridge CB2 2QQ, UK

N. J. Sebire (✉)
Department of Paediatric Pathology, Camelia Botnar Laboratories,
Great Ormond Street Hospital,
Great Ormond Street,
London WC1N 3JH, UK
e-mail: SebirN@gosh.nhs.uk

Introduction

Though recommendations for placental histological examination in the UK and USA exist [1, 2], the clinical significance of many histologically detectable placental lesions remains uncertain, especially in the context of an unselected low-risk population. Most studies in this area are based on retrospective review of clinical cases from categories of abnormal histological findings or abnormal obstetric outcomes; the placentas thus submitted are by definition at increased risk of being abnormal. In addition, since most studies are retrospective, reporting pathologists have had access to the clinical information available at submission when reporting the cases, introducing a source of bias. Clinical information provided can significantly affect interpretation of placental histological features [3]. Little data exist reporting the frequency and pattern of histological lesions present in the placenta in an unselected population at or near term, with histological findings identified by pathologists entirely blinded to all clinical information.

Complications such as pre-eclampsia (PET), pregnancy-induced hypertension (PIH), gestational diabetes (GDM), and small for gestational age (SGA) are associated with prematurity and increased perinatal morbidity and mortality [4–6]. Several placental lesions have been reported in association with these complications [7–9] in selected populations, and it is apparent that no specific placental lesion is characteristic of any one particular obstetric outcome category. For example, in pre-eclampsia, spiral arteries remain 'untransformed' [10], remaining muscular due to the incomplete invasion of trophoblast, leading to high-resistance blood flow passing through these vessels and abnormal uteroplacental blood flow. Though ischaemic-type changes have been observed in the majority of severe preterm cases [8, 11], there may be subjectively normal placental histological findings even in cases of clinically severe disease at or near term [12, 13]. Features such as infarction, extensive perivillous fibrin deposition and chronic villitis are more frequent in SGA in some studies [14] but not others [15] and are well-reported in clinically normal pregnancies.

The frequency of common histological lesions present in an unselected, prospectively recruited population of placentas from deliveries at or near term with histological features reported by pathologists completely blinded to all clinical information is unknown. The aims of this study are to use this approach to determine the frequency of predefined placental histopathological abnormalities in an unselected population delivering at or near term in relation to common obstetric pregnancy outcomes and to determine the clinical significance of the interpretation of such lesions by calculating sensitivity, positive predictive values and odds ratio in relation to obstetric outcomes.

Methods

This was a prospective study performed in a large maternity unit offering care and delivery both for 'low risk' pregnancies and those requiring tertiary services. The study was approved by the Cambridgeshire ethical committee (ref. no. 07/Q0106/51), and written consent was obtained from the women taking part in the study. No attempt was made at selection by any maternal characteristics. Unselected women were recruited over a 13-month period (2007–2008). Of 1,159 women with singleton pregnancy initially recruited antenatally, 1,153 women were included who delivered at 34–43 weeks gestation and in whom the placenta was available for examination. This study includes unselected cases recruited specifically for the study purposes and is not a retrospective review of cases submitted as part of clinical practice to a histopathology department.

The placentas were placed in a labelled double bag within 20 min of delivery, which was kept in a dry, clean 1–2-l plastic container with an airtight lid and in a fridge with the temperature maintained at 4–6°C. All placentas were examined macroscopically by technicians trained specifically for this study under the direct supervision of a consultant paediatric pathologist in a specialist histopathology department. The cord was excised from the point of insertion into the chorionic plate; blood was drained from the placenta, and adherent blood clots removed from the maternal surface. All extraplacental membranes were trimmed from the chorionic plate, and the placenta was weighed on a fixed electronic scale. Details of the methods are entirely standard and are described in detail elsewhere [16, 17]. The placenta was serially sliced and examined macroscopically, and blocks were obtained from membranes, umbilical cord and the full thickness of the placental parenchyma according to standard diagnostic protocols [18]. Three standard samples were taken from the umbilical cord: maternal end, fetal end and from the centre. Three full-thickness central and one peripheral parenchymal block were taken, and one 'en face' block was taken from the maternal surface. Additional blocks were taken from any macroscopic abnormality. To avoid sampling bias, all samples that were taken were examined histologically.

Histological examination of haematoxylin and eosin-stained sections was subsequently performed by two specialist paediatric pathologists (NJS/FAJ) who classified any histological features according to previously agreed and standard criteria (Appendix 1). Pathological lesions were recorded for the purpose of this study as present' or absent'. In cases where there was presence of more than one histological lesion, each lesion was recorded. The pathologists performing the histological examinations were completely blinded to all clinical information, including gestational age, the cases being identified by study number only and reported in batches purely for the purposes of the study. Cases were reported independently by two pathologists, and any discrepancy was resolved by consensus, giving priority to the possible presence of any abnormality. Specific histological subtypes predefined in this study included no significant histological abnormality, ascending genital tract infection, chronic placental underperfusion, intervillous thrombus, villitis of unknown aetiology (VUE), fetal thrombotic vasculopathy, massive perivillous fibrin deposition, chronic histiocytic intervillositis, chorioangiosis, chorangioma and retroplacental haematoma/abruption. Brief descriptions of diagnostic criteria for these abnormalities are provided in Appendix 1 but are based on widely accepted and published standard criteria from major textbooks [18] (Fig. 1).

Histological findings of placentas from cases with normal outcome were compared with those from patients with obstetric complications: pre-eclampsia (PET), pregnancy-induced hypertension (PIH), gestational diabetes (GDM) and small for gestational age (SGA). Definitions of the common obstetric outcome groups of PET, PIH, GDM and SGA are briefly described: Pre-eclampsia was defined as blood pressure ≥140/

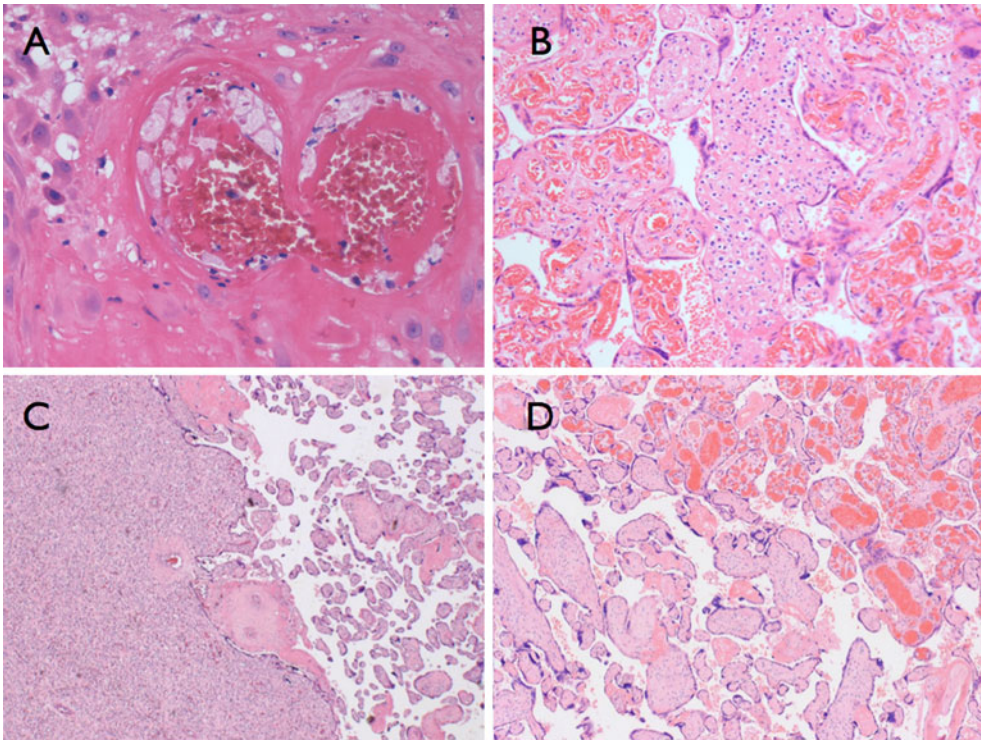

Fig. 1 Photomicrographs demonstrating placental histological lesions including **a** acute atherosis, **b** villitis of unknown aetiology, **c** chorioangioma and **d** fetal thrombotic vasculopathy. (haematoxylin and eosin)

90 on two or more occasions after 24 weeks, at least 6 h apart, with significant proteinuria of more than 300 mg/l in a 24-h collection in a previously normotensive woman [19, 20]. We also included women with ≥2+ in a urine sample in the absence of a demonstrable urinary tract infection in this group. PIH was defined as blood pressure ≥140/90 in pregnancy after 20 weeks without any evidence of proteinuria. According to WHO criteria, gestational diabetes is carbohydrate intolerance resulting in hyperglycaemia of variable severity with onset or first recognition during pregnancy. The definition applies irrespective of whether or not insulin is used for treatment or the condition persists after pregnancy. We defined the gestational diabetes according to WHO criteria: fasting blood glucose level ≥7 mmol/l or 2 h post 75 mg of oral glucose load ≥7.8 mmol/l [21]. Birth weight <10th centile for gestational age defined the SGA group. To calculate these, we used the standard UK 4-in-1 charts (girls and boys), which are the growth charts designed principally for hospital use for preterm and term babies and their follow-up [22].

Descriptive statistics were performed for each obstetric outcome category, and the frequency of each common histological diagnosis was reported (Table 1). Comparison of the significance of differences in frequencies of common histological lesions between groups was performed using chi-square test (comparison of proportions). Pearson chi-square test was used to determine significance of differences in frequencies between the groups where the number of cases was more than five, with Yates's continuity correction. $P \leq 0.05$ was considered significant. Odds ratios were calculated for histological categories in the obstetric outcome groups (disease present versus absent). Odds ratio, positive predictive value and sensitivity were calculated for histological features for obstetric outcome groups.

Results

Of the total 1,153 cases, placental histological findings were available in 1,122. Details of the obstetric outcome groups are provided in Table 1. Table 2 reports maternal, neonatal and placental characteristics of the study participants. The frequency of histological lesions in the clinical outcome groups is provided in Table 3. The majority of cases in all groups revealed no significant histological abnormality: 72.1%, 79.1%, 66.6%, 80% and 74.8%, respectively, in the normal, PET, PIH, GDM and SGA groups. There was no difference in the incidence of ascending genital tract infection between any of these obstetric outcome groups at or near term. Certain placental histological findings were more common in particular outcome groups, such as VUE and PIH, FTV and GDM, MPFD with PET and SGA, and chorangioma with PET. However, despite the increased odds

Table 1 Prevalence of common obstetric outcome cases in the study population

	1,153 cases; % (*n*)
PET	2.3 (27)
PIH	2.6 (30)
GDM	4 (46)
SGA	9.3 (107)

Table 2 Maternal and neonatal characteristics of those included in the study

Maternal characteristics	Number	Mean (range) ± SD
Age	1,153	30.9 (16–46)±5.73
GA at del (weeks)	1,153	39.5 (34–43)±1.39
% Nulliparity (*n*)	1,148	48 (551)
% Smoker (*n*)	1,150	9.2 (106)
% Caucasians (*n*)	1,143	91.4 (1,045)
% Emergency C/S (*n*)	1,153	11.4 (131)
% Induced labour (*n*)	1,153	19.6 (226)
Neonatal characteristics		
Birth wt	1,153	3,488.7 (1,180–5,120)±495
% Females (*n*)	1,153	46.5 (536)
% Males (*n*)	1,153	53.5 (617)
% Neonatal admissions (*n*)	1,153	5.7 (66)

ratios of these specific histological findings for obstetric complications, the overall sensitivity and positive predictive value for any specified histological lesions was low, with the majority of histological abnormalities being associated with normal obstetric outcome (Table 4).

Discussion

The findings of this study have demonstrated first, that in an unselected population delivering at or near term, the majority of placentas demonstrate no significant histological abnormality. Secondly, we confirm that certain histological features are more frequent in association with specific obstetric complications, but no histological feature is associated with definitive diagnosis of a clinical complication. Finally, since most pregnancies are uncomplicated, the sensitivity and positive predictive value of most histological findings for pregnancy outcome in this population is low, with the vast majority of pregnancies demonstrating any particular histological feature having a normal outcome, even when that feature is strongly associated with a complication such as PIH or pre-eclampsia. Therefore, whilst data based on highly selected groups of complicated pregnancies, in whom placentas were submitted according to indications as part of clinical care, have correctly reported a range of histological lesions in pregnancies with adverse obstetric outcomes, most—if not all—are not specific to any particular outcome group and importantly are also commonly found in normal pregnancies.

The lack of finding statistically significant differences in some placental lesions is unsurprising. For example, the incidence of histological chorioamnionitis is strongly related to the gestational age at delivery, being strongly associated with severe preterm delivery, but is not related to complications such as PIH or SGA. The frequency reported at 20–24 weeks of gestation is >80%, falling to <10% of deliveries at term [23]. We report a similar frequency of histological chorioamnionitis in this cohort of a near-term unselected population, indicating that the criteria used for classification are consistent with previous studies and therefore supporting correct interpretation. Similarly, the frequencies of clinical

Table 3 Frequency of predefined histological lesions in reference population and common obstetric outcome groups

Predefined histological features	Normal population % (*n*=935)	PET % (*n*=24)	PIH % (*n*=27)	GDM % (*n*=45)	SGA % (*n*=106)
Normal histology	71.6 (669)	79.1 (19)	66.6 (18)	80 (36)	74.8 (79)
Ascending genital tract infection	11.3 (106)	8.3 (2)	11.1 (3)	4.4 (2)	10.3 (11)
Chronic placental underperfusion	7.7 (72)	4.2 (1)	14.8 (4)	4.4 (2)	10.4 (11)
Intervillous thrombus	5 (47)	8.3 (2)	3.7 (1)	6.8 (3)	–
Villitis of unknown aetiology	3.7 (35)	–	11.1 (3)	–	3.7 (4)
Fetal thrombotic vasculopathy	1 (9)	–	–	2.2 (1)	0.9 (1)
Chorangiosis	0.9 (8)	–	–	2.2 (1)	–
Massive perivillous fibrin deposition	0.2 (2)	4.2 (1)	–	–	1.9 (2)
Chorangioma	0.3 (3)	4.2 (1)	–	–	0.9 (1)
Chronic histiocytic intervillositis	0.2 (2)	–	–	–	0.9 (1)

Total % is >100%, as some placentas had more than one histological lesion, and each histological lesion has been counted separately

Table 4 Odds ratios (95% confidence interval; OR), positive predictive values (PPV) and sensitivity for selected histological findings and outcomes in unselected pregnancies at or near term

	CPU–yes	CPU–no	OR (95% CI)	PPV	Sensitivity
PET	1	23	0.52 (0.09–3.1)	1.4%	0.042 (0.01–0.20)
Normal population	72	863			4.2%
PIH	4	23	2 (0.74–5.9)	5.3%	0.15 (0.06–0.32)
Normal population	72	863			15%
GDM	2	43	0.52 (0.09–3.09)	1.4%	0.04 (0.007–0.196)
Normal population	72	863			4.2%
SGA	11	95	1.39 (0.72–2.68)	13.3%	0.104 (0.06–0.17)
Normal population	72	863			10.4%
	VUE–yes	VUE–no			
PIH	3	24	3.21 (1.0–10.54)	7.9%	0.11 (0.04–0.27)
Normal population	35	900			11%
	FTV–yes	FTV–no			
GDM	1	44	2.34 (0.38–14.71)	10%	0.02 (0.004–0.09)
Normal population	9	926			2%
SGA	1	105	0.98 (0.159–6.064)	10%	0.01 (0.002–0.038)
Normal population	9	926			1%
	Chorangiosis–yes	Chorangiosis–no			
GDM	1	44	2.63 (0.42–16.73)	11%	0.02 (0.004–0.09)
Normal population	8	927			2%
	MPFD–yes	MPFD–no			
PET	1	23	20.28 (2.58–161.89)	33%	0.04 (0.008–0.099)
Normal population	2	933			4%
SGA	2	104	8.97 (1.57–51.39)	50%	0.02 (0.01–0.03)
Normal population	2	933			2%
	Chorangioma–yes	Chorangioma–no			
PET	1	23	13.51 (1.88–99.30)	25%	0.04 (0.008–0.116)
Normal population	3	932			4%
SGA	1	105	2.96 (0.42–20.91)	25%	0.01 (0.002–0.026)
Normal population	3	932			1%

CPU chronic placental underperfusion, *VUE* villitis of unknown aetiology, *FTV* fetal thrombotic vasculopathy, *MPFD* massive perivillous fibrin deposition, *PET* pre-eclampsia, *PIH* pregnancy-induced hypertension, *GDM* gestational diabetes mellitus, *SGA* small for gestational age

complications such as PET, PIH, SGA and GDM and histological findings, such as fetal thrombotic vasculopathy, are also broadly similar to published epidemiological data, indicating that both our population and interpretation of histological findings are consistent with expected frequencies. This supports the generalisibility of the findings in placentas from deliveries at or near term; however, these findings should not be applied to pregnancies with more severe complications resulting in preterm deliveries.

The sensitivity for most histological findings was low. It is recognized that diagnostic macroscopic and histological changes in the placenta from cases with PET and PIH may not be present even in clinically severe disease. Previous studies have reported increased frequency of abnormal histological features, such as placental infarcts, in placentas from pregnancies which are complicated by preterm PET/PIH. In the current study, the frequency of chronic placental underperfusion, VUE, MPFD and chorioangiomata were indeed greater in pregnancies with PET/PIH; however, since the incidence of PET and PIH in an unselected population is so low compared to the frequency of normal uncomplicated pregnancies, the positive predictive value of such histological features is very low. For example, even though this study has demonstrated that chorioangiomata are much commoner in cases with PET, most cases of PET will not show such lesions (low sensitivity), and the

majority of cases with chorioangiomata present will have a normal outcome (low positive predictive value).

Previously described histological features in gestational diabetes are similar to those of pre-existing diabetes mellitus; however they are usually less pronounced and reduced in frequency [24, 25]. The pathological findings of the placenta do not predict the severity of the disease or relate to the duration of the disease, [25] and in practice, any morphological changes are usually subtle and difficult to identify on routine examination. Some specific histological lesions are more frequent, for example, placentas from diabetic pregnancies show increased incidence of vascular pathological changes such as FTV and chorangiosis which we also demonstrate [18]. In the present study, both of these histological lesions were more than twice as common in pregnancies complicated with GDM compared to the normal population, but both FTV and chorangiosis have very low sensitivities for the detection of GDM and positive predictive values of 10%; on finding FTV in an unselected placenta at term, >90% of cases will not be associated with GDM or any other obstetric complication. Nevertheless, it should be recognized that, based on previous case–control study data, FTV may be associated with fetal/neonatal complications such as visceral thrombotic lesions, regardless of whether they are GDM related or not. However, since the majority of these cases will be apparently clinically uncomplicated pregnancies, as demonstrated in the present series, according to most guidelines and the practice of the majority of centres, these placentas will not be routinely examined, and hence, the presence of such lesions will remain unrecognized!

Histological lesions found in association with SGA were, as expected, primarily those of chronic placental underperfusion, VUE, MPFD, chorangioma, fetal thrombotic vasculopathy and chronic histiocytic intervillositis. SGA by our definition encompasses not only small, growth restricted babies but also those constitutionally small. These are all expected histological features based on previous case–control study data and represent changes secondary to the maternal vascular compromise leading to abnormal placental perfusion or other specific IUGR associations. Interestingly, the frequency of histological changes of chronic placental underperfusion was only slightly greater in cases with SGA compared to normals, highlighting the fact that in pregnancies delivering with mild growth restriction at term, there may be minimal morphological changes in the placental parenchyma, the sensitivity for SGA being only 10%. Conversely, similar morphological features may be commonly seen at term in pregnancies resulting in normal outcomes, with >85% of all cases with histological changes such as infarcts being included in the normal group. Previous studies considering placentas from clinically preselected outcome groups will therefore intrinsically overestimate the importance of any identified histological finding since the vast majority of pregnancies with normal outcome do not undergo placental examination. Furthermore, selecting known 'normal' cases as controls is also inappropriate because the pathologist will be biassed as to the supposed clinical significance of a histological finding if the outcome is already known.

The major strengths of this study are the prospective recruitment and collection of a large number of unselected cases near term, specifically for study purposes, with uniform methodology of placental examination and outcome definitions. A unique feature to remove any interpretative bias is that all histological examinations were performed by two independent paediatric pathologists who were blinded to all clinical details, including outcome and gestational age. All histological features were recorded in an unbiased manner for the entire population, comparison of frequencies of histological lesions across subgroups in the absence of any interpretive bias. The weaknesses of the study are that, despite of prospective recruitment of over 1,000 women, many histological abnormalities have a low incidence, and only small numbers of cases were recorded in some outcome groups. Therefore, where we have low number of cases in outcome groups, the odds ratio with wide confidence interval may not be robust. Also, these findings cannot be extrapolated to preterm cases, in which the frequency of complications and pathophysiology of disease is different. The data from this study must not therefore be used to suggest that there is no value in placental histological examination, since strong data exist from high-risk case control studies regarding association between certain placental lesions and obstetric complications. However, the data do provide contemporaneous reference data regarding the frequencies of a range of placental histological features in an unselected population delivering at or near term in the UK and highlight the important finding that simply demonstrating the presence of a placental histological 'lesion' should not necessarily be regarded as evidence of a clinically significant obstetric complication or causation, and the clinical significance of placental pathological features should not be over interpreted.

In summary, we present the frequencies of specific placental histological features in an unselected population in the late third trimester and report that whilst certain histological features are found more commonly in association with complicated pregnancies, the sensitivity and positive predictive values for these findings are generally low. The vast majority of placentas with histological abnormalities will be seen in clinically normal pregnancies, and histological examination may be normal even in the presence of clinically severe obstetric disease.

Funding The study was supported by grants from Cambridge Fetal Care and Addenbrooke's Charitable Trust.

Conflict of interest The authors declare that they have no conflict of interest.

Appendix 1

Table 5 Diagnostic criteria for predefined histological categories

Diagnosis	Diagnostic criteria
Ascending genital tract infection	Any combination of: neutrophils in the fetal membranes, accumulating at the choriodecidual junction or umbilical cord
Chronic placental underperfusion	Small, hypovascular chorionic villi with increased syncytial knots, placental infarction >1 cm (non-peripheral) and/or atherosis
Intervillous thrombus	Localised, nodular and circumscribed old or recent thrombi within the intervillous space
Villitis of unknown aetiology	Morphologically increased chronic inflammatory cells affecting groups of chorionic villi in the absence of known clinical or histological aetiological factor/organisms (such as TORCH group, enterovirus, varicella, syphilis, syphilitic spirochetosis and other bacterial and protozoal infections)
Fetal thrombotic vasculopathy	Lesions of the placenta due to occlusion of the chorionic or major fetal villous stem artery by a thrombus, causing avascular distal villi
Chorangiosis	10 or more villi with 10 or more capillaries/villous cross section in 10 or lower power microscopic fields
Massive perivillous fibrin deposition	Significant deposition of perivillous fibrin involving more than 50% of the villous parenchyma
Chorangioma	A well-circumscribed, nodular lesion composed of vascular channels, stromal cells and surrounded by trophoblasts
Chronic histiocytic intervillositis	Marked mononuclear histiocytic inflammatory cell infiltrate with associated fibrin deposition in the intervillous space without associated villitis or chorioamnionitis

References

1. Langston C, Kaplan C, Macpherson T, Manci E, Peevy K, Clark B, Murtagh C, Cox S, Glenn G (1997) Practice guideline for examination of the placenta: developed by the Placental Pathology Practice Guideline Development Task Force of the College of American Pathologists. Arch Pathol Lab Med 121:449–476
2. Hargitai B, Marton T, Cox PM (2004) Best practice no 178. Examination of the human placenta. J Clin Pathol 57:785–792
3. Khong TY, Gordijn SJ (2003) Quality of placental pathology reports. Pediatr Dev Pathol 6:54–58
4. Sibai B, Dekker G, Kupferminc M (2005) Pre-eclampsia. Lancet 365:785–799
5. Macintosh MC, Fleming KM, Bailey JA, Doyle P, Modder J, Acolet D, Golightly S, Miller A (2006) Perinatal mortality and congenital anomalies in babies of women with type 1 or type 2 diabetes in England, Wales, and Northern Ireland: population based study. BMJ 333:177
6. Garite TJ, Clark R, Thorp JA (2004) Intrauterine growth restriction increases morbidity and mortality among premature neonates. Am J Obstet Gynecol 191:481–487
7. Zhang P, Schmidt M, Cook L (2006) Maternal vasculopathy and histologic diagnosis of preeclampsia: poor correlation of histologic changes and clinical manifestation. Am J Obstet Gynecol 194:1050–1056
8. Roberts DJ, Post MD (2008) The placenta in pre-eclampsia and intrauterine growth restriction. J Clin Pathol 61:1254–1260
9. Daskalakis G, Marinopoulos S, Krielesi V, Papapanagiotou A, Papantoniou N, Mesogitis S, Antsaklis A (2008) Placental pathology in women with gestational diabetes. Acta Obstet Gynecol Scand 87:403–407
10. Brosens IA, Robertson WB, Dixon HG (1972) The role of the spiral arteries in the pathogenesis of preeclampsia. Obstet Gynecol Annu 1:177–191
11. Salafia CM, Pezzullo JC, Ghidini A, Lopez-Zeno JA, Whittington SS (1998) Clinical correlations of patterns of placental pathology in preterm pre-eclampsia. Placenta 19:67–72
12. Sebire NJ, Goldin RD, Regan L (2005) Term preeclampsia is associated with minimal histopathological placental features regardless of clinical severity. J Obstet Gynaecol 25:117–118
13. Shanklin DR, Sibai BM (1989) Ultrastructural aspects of preeclampsia. I. Placental bed and uterine boundary vessels. Am J Obstet Gynecol 161:735–741
14. Oliveira LH, Xavier CC, Lanaa M (2002) [Changes in placental morphology of small for gestational age newborns]. J Pediatr (Rio J) 78:397–402
15. Altemania M, Gonzattia R (2003) [Villitis of unknown etiology in placentas of pregnancies with hypertensive disorders and of small-for-gestational-age infants]. Rev Assoc Med Bras 49:67–71
16. Pathak S, Hook E, Hackett G, Murdoch E, Sebire NJ, Jessop F, Lees C (2010) Cord coiling, umbilical cord insertion and placental shape in an unselected cohort delivering at term: relationship with common obstetric outcomes. Placenta 31:963–968
17. Pathak S, Sebire NJ, Hook L, Hackett G, Murdoch E, Jessop F, Lees C (2011) Relationship between placental morphology and histological findings in an unselected population near term. Virchows Arch 459:11–20
18. Fox H, Sebire NJ (2007) Pathology of the Placenta. W.B. Saunders, London
19. Davey DA, Macgillivray I (1988) The classification and definition of the hypertensive disorders of pregnancy. Am J Obstet Gynecol 158:892–898
20. Brown MA, Lindheimer MD, De Swiet M, Van Assche A, Moutquin JM (2001) The classification and diagnosis of the hypertensive disorders of pregnancy: statement from the Interna-

tional Society for the Study of Hypertension in Pregnancy (ISSHP). Hypertens Pregnancy 20:IX–XIV
21. WHO (2006) World Health Organisation/International Diabetes Federation, definition and diagnosis of diabetes mellitus and intermediate hyperglycemia
22. http://Www.Healthforallchildren.Co.Uk/. Four-in-one (decimal) growth charts (birth-20 yrs). London: Child Growth Foundation 1996/1
23. Sebire NJ, Goldin RD, Regan L (2001) Histological chorioamnionitis in relation to clinical presentation at 14–40 weeks of gestation. J Obstet Gynaecol 21:242–245
24. Fox H (1969) Pathology of the placenta in maternal diabetes mellitus. Obstet Gynecol 34:792–798
25. Jones CJ, Fox H (1976) Placental changes in gestational diabetes. An ultrastructural study. Obstet Gynecol 48:274–280

Virchows Arch (2011) 459:573–580
DOI 10.1007/s00428-011-1155-1

ORIGINAL ARTICLE

Clinicopathologic features of advanced gallbladder cancer associated with adenomyomatosis

Keita Kai · Takao Ide · Masanori Masuda · Kenji Kitahara · Atsushi Miyoshi · Kohji Miyazaki · Hirokazu Noshiro · Osamu Tokunaga

Received: 13 July 2011 / Revised: 23 August 2011 / Accepted: 6 October 2011 / Published online: 26 October 2011
© Springer-Verlag 2011

Abstract Adenomyomatosis of the gallbladder has not been considered to have malignant potential, but gross features of adenomyomatosis are sometimes encountered in gallbladders resected under a diagnosis of gallbladder carcinoma. The purpose of this study was to determine the clinicopathologic features and survival rates in cases of gallbladder cancer with gross features of adenomyomatosis. The study subjects were 97 surgically treated gallbladder carcinoma patients. Only gallbladder showing typical gross features of adenomyomatosis was judged as adenomyomatosis-positive gallbladder cancer. In terms of gross findings, 25 cases (25.8%) were classified as adenomyomatosis-positive. The status of adenomyomatosis was significantly associated with the T stage (P=0.0004), lymph node (LN) metastasis (P<0.0001), distant metastasis (P=0.008), and stage (P=0.0005). In the adenomyomatosis-positive group, 16 of the 25 cases (64.0%) were classified as segmental type and 9 cases (36.0%) were classified as fundal type. No diffuse-type cases were present in this series. The status of adenomyomatosis correlated significantly with survival (P=0.0007). However, the multivariate analysis of significant variables identified from the univariate analysis identified only T stage (P=0.0178) and LN metastasis (P=0.0048) as independent prognostic factors. Subset analysis with T stage according to the status of adenomyomatosis showed no significant impact on survival. These results indicate that adenomyomatosis-positive gallbladder cancer is more often diagnosed clinically in the advanced stages. Since preceding adenomyomatosis may prevent the early detection of gallbladder cancer, the usefulness of preventive cholecystectomy in cases of asymptomatic adenomyomatosis should be considered.

Keywords Gallbladder carcinoma · Adenomyomatosis · Rokitansky–Aschoff sinuses

K. Kai (✉) · M. Masuda · O. Tokunaga
Department of Pathology and Microbiology, Faculty of Medicine, Saga University,
Nabesima 5-1-1,
Saga City, Saga 849-8501, Japan
e-mail: kaikeit@cc.saga-u.ac.jp

T. Ide · K. Kitahara · A. Miyoshi · K. Miyazaki · H. Noshiro
Department of Surgery, Faculty of Medicine, Saga University, Saga, Japan

Introduction

Adenomyomatosis of the gallbladder is defined as an epithelial proliferation and hypertrophy of the muscularis with outpouching of the mucosa into or through the thickened muscular layer, forming the so-called Rokitansky–Aschoff sinuses (RAS) [1, 2]. These histological changes are often distributed diffusely or segmentally, or are found at the fundus, and form well-known gross features categorized as diffuse-type, fundal (localized)-type, and segmental-type adenomyomatosis [1–3].

Adenomyomatosis of the gallbladder has not been considered to have malignant potential. However, several reports have suggested that gallbladder cancer may originate from adenomyomatosis [4–8] or have insisted that segmental-type adenomyomatosis shows an increased risk of progression to gallbladder cancer [3, 9]. As these previous studies were limited to investigations of excised gallbladder specimens due to gallbladder disease as well as other surgical diseases involving the gallbladder, they reported the incidence of gallbladder cancer in large numbers of cholecystectomy specimens, but the details of clinicopathologic findings that might clarify relationships between gallbladder cancer, adenomyomatosis, and

survival outcomes were not shown. The incidence of gallbladder cancer in adenomyomatosis reportedly ranged from 1% to 6.6% in all excised gallbladders with adenomyomatosis [3, 9, 10]. Despite the low incidence of incidental gallbladder cancer in adenomyomatosis, the gallbladders excised due to gallbladder cancer sometimes show gross features of adenomyomatosis.

The purpose of this study was to determine the clinicopathologic features and survival rates in cases of gallbladder cancer with gross features of adenomyomatosis.

Material and methods

Patients and staging

The study subjects were 97 consecutive gallbladder cancer patients who underwent surgical treatment between 1989 and August 2010 at Saga University Hospital under a diagnosis of gallbladder cancer or suspected gallbladder cancer as the primary lesion. Informed consent for the use of the resected tissue was obtained from all patients, and the study protocol was approved by the Ethics Committee of the Faculty of Medicine at Saga University. Clinical and histopathological staging were based on the TNM Classification of Malignant Tumors by the International Union Against Cancer [11].

Pathological evaluation of adenomyomatosis

The evaluation of adenomyomatosis was performed based on the gross features of specimens, according to a previous study [3]. The judgment of adenomyomatosis was restricted to typical gross cases of gallbladder cancer because only RAS formation is common in the gallbladder. Briefly, adenomyomatosis was classified as one of three types, as follows. The segmental type was defined as an annular stricture comprising a thickened wall dividing the gallbladder lumen into separate interconnected compartments with or without diffuse wall thickening on the fundal side. The fundal type was defined as a hemispheric elevated lesion with a central dimple located at the tip of the fundus. The diffuse type was defined as a thickened wall throughout the entire gallbladder. Even if RAS was histologically identified in the background gallbladder, cases that did not show gross features were categorized into the non-adenomyomatosis group. The predominant histological subtype of gallbladder cancer was identified based on each pathological report.

Statistical analysis

Statistical analyses were performed using the JMP version 8 software program (SAS Institute, Cary, NC, USA). The statistical analyses comparing the two groups were performed using Student's t test, the χ^2 test, and Fisher's exact test, as appropriate. All survival analyses were performed using disease-specific survival, determined from the time of surgery to the time of cancer-related death or the most recent follow-up. Postoperative survival was calculated using the Kaplan–Meier method. Differences in survival curves were compared using the log-rank test. Cox proportional hazards models were applied for the multivariate analysis. Values of $P<0.05$ were considered to be statistically significant.

Results

Clinicopathologic features of gallbladder cancer with or without adenomyomatosis

The 97 patients with surgically treated gallbladder cancer included 31 males and 66 females. Mean age at the time of surgery was 68.7 years (range, 40–87 years). According to the classification of gross findings, 25 cases (25.8%) were classified as adenomyomatosis-positive gallbladder cancer (Table 1). The absence of adenomyomatosis was significantly associated with the T stage ($P=0.0004$), lymph node (LN) metastasis ($P<0.0001$), distant metastasis ($P=0.008$), and stage ($P=0.0005$). Of the 25 patients in the adenomyomatosis-positive group with T2–T4 lesions, 21 patients showed LN metastasis (84.0%) and 11 patients displayed distant metastasis (44.0%). The presence or absence of adenomyomatosis was not associated with age and sex. Of the 97 patients with gallbladder cancer, 36 patients (37.1%) were accompanied with gallstone disease, which was not associated with adenomyomatosis.

Histologic type of adenomyomatosis in patients with gallbladder cancer

The rate of the predominant histologic type in the adenomyomatosis-positive and adenomyomatosis-negative groups is shown in Fig. 1. The details of histologic typing of adenomyomatosis-positive gallbladder cancer were as follows: well-differentiated tubular carcinoma, $n=7$ (28.0%); moderately differentiated tubular carcinoma, $n=10$ (40.0%); poorly differentiated adenocarcinoma, $n=3$ (12.0%); and other histologic type, $n=5$ (20.0%), comprising mucinous carcinoma, adenosquamous carcinoma, solid carcinoma, small cell carcinoma, and undifferentiated carcinoma spindle and giant cell type ($n=1$ each). The details of the histologic typing of adenomyomatosis-negative gallbladder cancer were as follows: papillary adenocarcinoma, $n=18$ (25.0%); well-differentiated tubular adenocarcinoma, $n=21$ (29.2%); moderately differentiated tubular carcinoma, $n=20$ (27.8%); poorly differentiated

Table 1 Clinicopathologic features of gallbladder cancer with or without adenomyomatosis

Characteristics	No. of patients (%)			*P* value
	Total	Adenomyomatosis (−)	Adenomyomatosis (+)	
No. of patients	97	72	25	
Age (mean±SD)	68.7±9.3	68.3±9.7	69.7±8.1	0.5288
Gender				0.3135
Male	31 (32.0)	25 (34.7)	6 (24.0)	
Female	66 (68.0)	47 (65.3)	19 (76.0)	
TNM classification				
T				0.0004
1a	11 (11.3)	11 (15.3)	0	
1b	8 (8.3)	8 (11.1)	0	
2	32 (33.0)	27 (37.5)	5 (20.0)	
3	39 (40.2)	21 (29.2)	18 (72.0)	
4	7 (7.2)	5 (6.9)	2 (8.0)	
N				<0.0001
0	50 (51.6)	46 (63.9)	4 (16.0)	
1	47 (48.4)	26 (36.1)	21 (84.0)	
M				0.008
0	77 (79.4)	62 (86.1)	15 (60.0)	
1	20 (20.6)	10 (13.9)	10 (40.0)	
Stage				0.0005
IA	18 (18.6)	18 (25.0)	0	
IB	22 (22.7)	20 (27.8)	2 (8.0)	
IIA	10 (10.3)	7 (9.7)	3 (12.0)	
IIB	21 (21.7)	14 (19.4)	7 (28.0)	
III	6 (6.2)	3 (4.2)	3 (12.0)	
IV	20 (20.6)	10 (13.9)	10 (40.0)	
Gallstone				0.077
Present	36 (37.1)	23 (31.9)	13 (52.0)	
Absent	61(62.9)	49 (68.1)	12 (48.0)	

adenocarcinoma, n=6 (8.3%); and other histologic type, n=7 (9.7%), comprising mucinous carcinoma (n=1), undifferentiated carcinoma (n=1), adenosquamous carcinoma (n=2), squamous cell carcinoma (n=1), signet ring cell carcinoma (n=1), and solid adenocarcinoma (n=1). A significant difference in the histologic types was seen between the adenomyomatosis-positive and adenomyomatosis-negative groups (P=0.01).

Clinicopathologic features of gallbladder cancer according to the gross type of adenomyomatosis

The clinicopathologic features of gallbladder cancer according to the gross type of adenomyomatosis are shown in Table 2. Of the 25 cases of adenomyomatosis-positive gallbladder cancer, 16 cases (64.0%) were classified as segmental-type adenomyomatosis (Fig. 2) and 9 cases (36.0%) were classified as fundal-type adenomyomatosis (Fig. 3). No diffuse-type adenomyomatosis was identified in our gallbladder cancer patient group. The segmental type includes cases showing diffuse wall thickening on the fundal side. Cancer had developed at the fundal side of segmental adenomyomatosis in 14 of the 16 cases. In the remaining two cases, the cancer had developed at the lumen of the neck side (Fig. 4). Cases suggesting gallbladder cancer that had developed from the RAS (Fig. 5) or cases of multiple cancers developing at the fundal side of segmental adenomyomatosis (Fig. 6) were included in this series. No significant differences in age, sex, or TNM classification were observed between the cases of segmental-type and fundal-type adenomyomatosis. Of the 25 cases of adenomyomatosis-positive gallbladder cancer, 13 cases (52.0%) were accompanied by gallstone disease. Although the segmental-type adenomyomatosis group showed a relatively high frequency of concomitant gallstone disease (10 out of 16 cases, 62.5%), no significant association was identified between the type of adenomyomatosis and the frequency of concomitant gallstone disease. However, a comparison between the

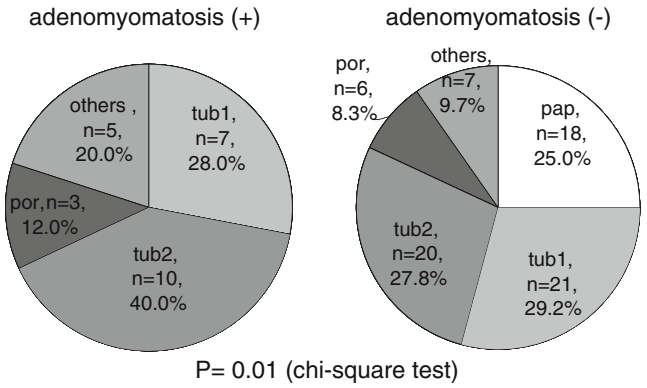

Fig. 1 The rate of predominant histologic type in adenomyomatosis-positive and adenomyomatosis-negative gallbladder cancer groups. *pap* papillary adenocarcinoma, *tub1* well-differentiated tubular carcinoma, *tub2* moderately differentiated tubular adenocarcinoma, *por* poorly differentiated adenocarcinoma. Details of others in adenomyomatosis-positive gallbladder cancer are as follows: mucinous carcinoma, $n=1$; adenosquamous carcinoma, $n=1$; solid carcinoma, $n=1$; small cell carcinoma, $n=1$; undifferentiated carcinoma spindle and giant cell type, $n=1$. Details of others in adenomyomatosis-negative gallbladder cancer are as follows: mucinous carcinoma, $n=1$; undifferentiated carcinoma, $n=1$; adenosquamous carcinoma, $n=2$; squamous cell carcinoma, $n=1$; signet ring cell carcinoma, $n=1$; solid adenocarcinoma, $n=1$

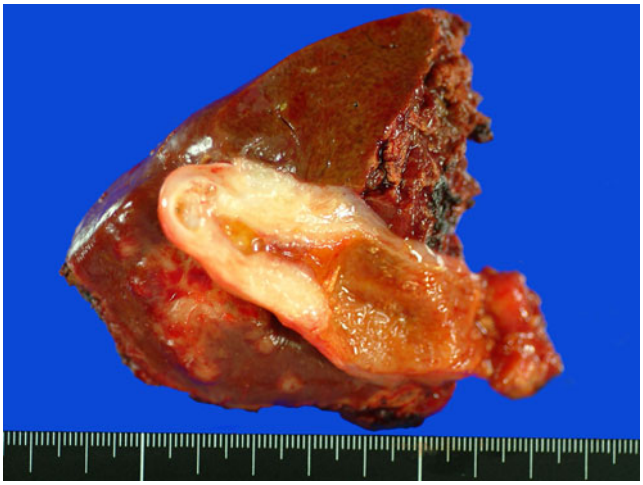

Fig. 2 A representative gross image of segmental-type adenomyomatosis-positive gallbladder cancer. Segmental type includes cases showing diffuse wall thickening on the fundal side

segmental adenomyomatosis group ($n=16$) and the other 81 gallbladder cancer cases showed a significantly higher rate of concomitant gallstones in patients with segmental adenomyomatosis ($P=0.0214$).

Table 2 Clinicopathologic features of gallbladder cancer according to the type of adenomyomatosis

Characteristics	No. of patients (%)			*P* value
	Total	Adenomyomatosis (s)	Adenomyomatosis (f)	
No. of patients	25	16 (64.0)	9 (36.0)	
Age (mean±SD)	69.7±8.1	67.5±8.9	73.6±4.3	0.0654
Gender				0.3135
Male	6 (24.0)	3 (18.8)	3 (33.3)	
Female	19 (76.0)	13 (82.3)	6 (66.7)	
TNM classification				
T				0.0929
2	5 (20.0)	4 (25.0)	1 (11.1)	
3	18 (72.0)	12 (75.0)	6 (66.7)	
4	2 (8.0)	0	2 (22.2)	
N				0.5312
0	4 (16.0)	2 (12.5)	2 (22.2)	
1	21 (84.0)	14 (87.5)	7 (77.8)	
M				0.6079
0	15 (60.0)	9 (56.3)	6 (66.7)	
1	10 (40.0)	7 (43.8)	3 (33.3)	
Stage				0.9752
IB	2 (8.0)	1 (6.3)	1 (11.1)	
IIA	3 (12.0)	2 (12.5)	1 (11.1)	
IIB	7 (28.0)	4 (25.0)	3 (33.3)	
III	3 (12.0)	2 (12.5)	1 (11.1)	
IV	10 (40.0)	7 (43.8)	3 (33.3)	
Gallstone				0.1583
Present	13 (52.0)	10 (62.5)	3 (33.3)	
Absent	12 (48.0)	6 (37.5)	6 (66.7)	

Adenomyomatosis (s) segmental type of adenomyomatosis, *Adenomyomatosis (f)* fundal type of adenomyomatosis

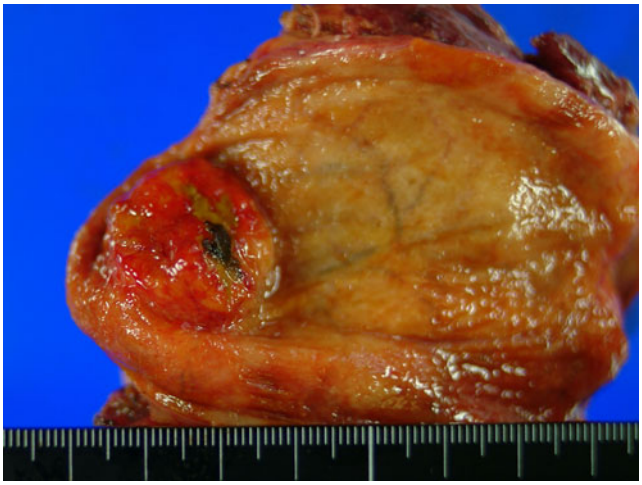

Fig. 3 A representative gross image of fundal-type adenomyomatosis-positive gallbladder cancer

Survival analysis

The median duration of follow-up was 25.3 months (range, 6–120 months). The results for disease-specific survival in the 97 gallbladder cancer patients are shown in Table 3. In the univariate analysis, the presence of adenomyomatosis correlated significantly with survival (P=0.0007). Other variables showing significant correlations with survival were sex (P=0.0426), T stage (P<0.0001), LN metastasis (P<0.0001), and distant metastasis (P<0.0001). A multivariate analysis of the significant variables identified from the univariate analysis was performed using Cox's proportional hazards model, revealing that only the T stage (P=0.0178) and LN metastasis (P=0.0048) were independent prognostic factors.

The survival curves for all 97 patients according to the status of adenomyomatosis are shown in Fig. 7. The adenomyomatosis-positive gallbladder cancer group showed a significantly worse survival (P=0.0001). This difference in survival disappeared in the subset analysis of the patients with stage T2 or T3 disease according to the status of adenomyomatosis. In the 25 gallbladder cancer patients with adenomyomatosis, no significant difference in survival was observed between those with segmental-type and fundal-type adenomyomatosis.

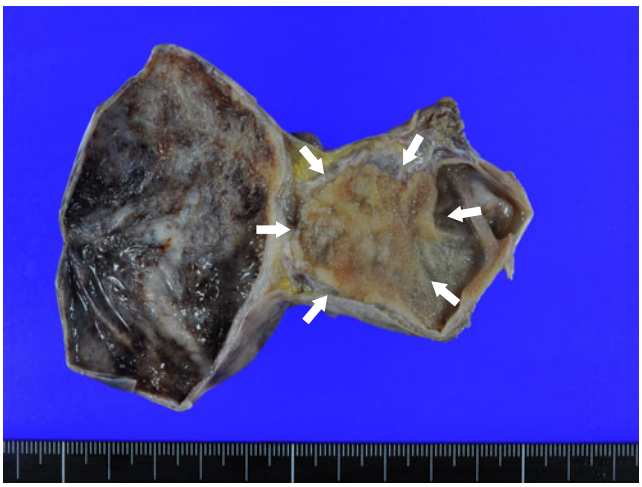

Fig. 4 A case in which the tumor (*arrows*) developed on the neck side of segmental-type adenomyomatosis

Discussion

Adenomyomatosis of the gallbladder is relatively common and usually asymptomatic, typically being discovered incidentally on abdominal imaging or on histological examination of cholecystectomy specimens taken for concomitant cholelithiasis or cholecystitis [12, 13]. Several investigators have suggested a relationship between gallbladder cancer and adenomyomatosis [3, 9]. However, carcinogenesis of the gallbladder is generally considered to correlate with the presence of gallstones rather than the presence of adenomyomatosis [10, 14]. The magnitude of risk for gallbladder cancer in patients with adenomyomatosis has not yet been clearly established.

The present study demonstrated a relatively high incidence of gross adenomyomatosis features (25.8%) in gallbladder cancer. In our university hospital, many patients with advanced gallbladder cancer have been treated, while the numbers of ordinary cholecystectomies performed have been relatively small. Therefore, there were few cases of incidentally detected gallbladder cancer during cholecystectomy in our series. Consistent with previous reports, our series contained no cases of diffuse-type adenomyomatosis [3, 9]. The survival analysis revealed a significantly worse survival of the adenomyomatosis-positive group. However, no significant differences were observed in the survival analysis of each T stage subgroup. This result indicates that adenomyomatosis-positive gallbladder cancer is often diagnosed clinically at an advanced stage.

Whether the gross appearance of adenomyomatosis really precedes carcinogenesis or if it forms as a result of cancerous invasion into the gallbladder wall still remains to be solved. We speculate that "gross appearance of adenomyomatosis precedes carcinogenesis" based on the following findings: many cases of segmental adenomyomatosis showed no sequence of cancerous tissue to the annular stricture and some cases of adenomyomatosis were identified by medical checkup before gallbladder cancer was found. If adenomyomatosis precedes carcinogenesis, the next question is whether the cancer is derived directly from the RAS or not. In our series, the RAS was consistently observed at the annular structure and/or the thickened wall of the adenomyomatosis. Although some cases suggested that carcinogenesis arose

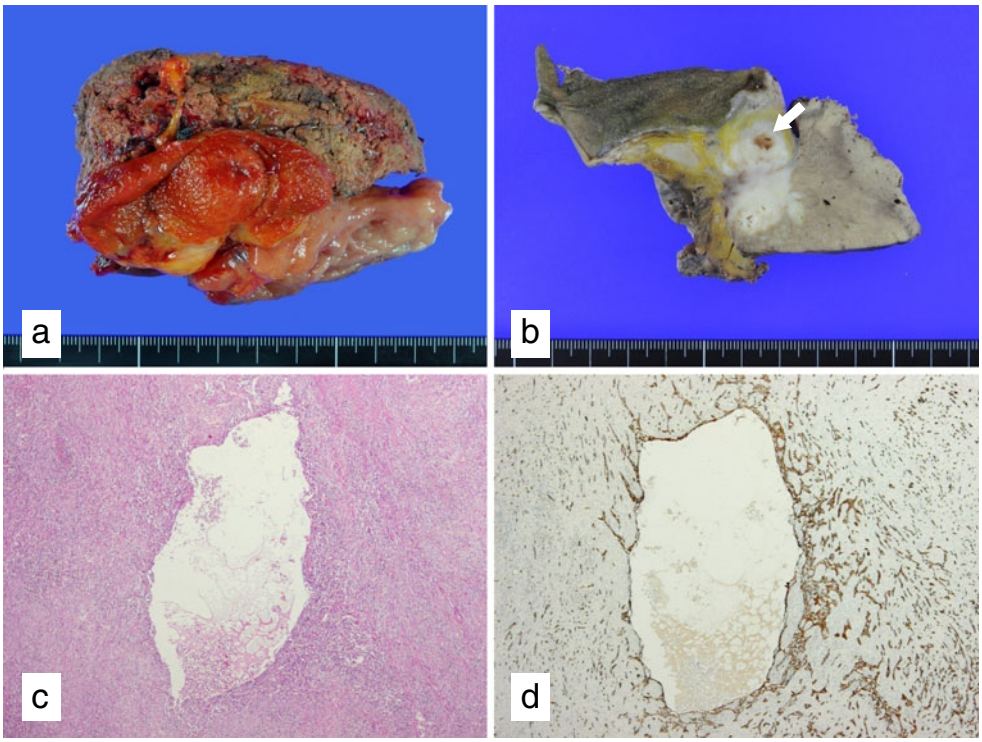

Fig. 5 Case presentation suggesting the development of gallbladder cancer from RAS. **a** Gross appearance. Fundal-type adenomyomatosis with a central dimple is defined. **b** The tumor predominantly proliferated in subserosal tissue and directly invaded into liver parenchyma, while showing no sequential connection to mucosal tissue. The dilated RAS contains bile-like material (*arrow*). **c** A RAS-like structure surrounded by spindle-shaped tumor and mesenchymal cells (original magnification, ×20). No sequential connection of mucosa and tumor was identified on histopathological examination. **d** Immunohistochemistry for cytokeratin 7. Spindle-shaped tumor cells were highlighted by cytokeratin 7. This case was finally diagnosed as undifferentiated carcinoma spindle and giant cell type (original magnification, ×20)

from the RAS, extensive cancer invasion prevented the pathological evaluation of carcinogenesis from RAS in most of the cases. To address this possibility, a study of the early stage cases specifically describing metaplasia, dysplasia, and carcinoma in the RAS would be needed. No cases of in situ or microinvasive cancer arising from RAS were found in our study population.

Gallstone disease is closely associated with carcinogenesis in gallbladder cancer [15–17] and segmental-type adenomyomatosis is frequently accompanied by gallstone disease [18]. The incidence of gallstone disease was relatively low in the present series (37.1%) compared to previous reports, but was high (62.5%) in patients with segmental-type adenomyomatosis. An elevated intraluminal pressure

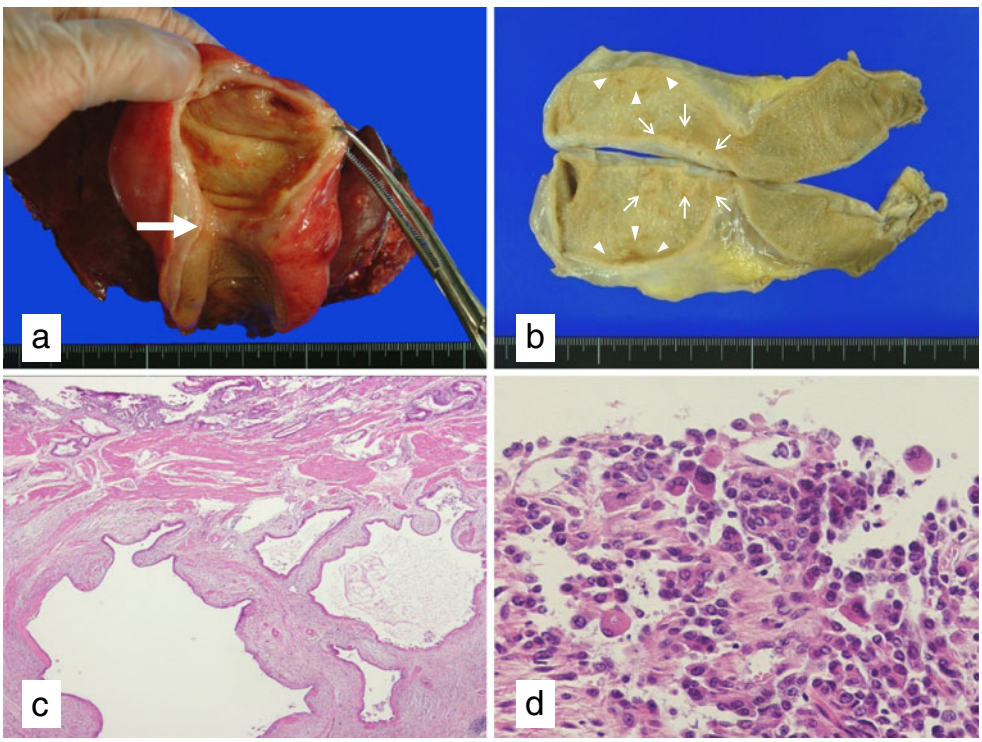

Fig. 6 Cases of multiple cancers that developed on the fundal side of segmental adenomyomatosis. **a** Gross appearance. Segmental-type adenomyomatosis with annular stricture (*arrow*) is defined. **b** Two discontinuous cancer lesions were microscopically identified in this case (*arrows* poorly differentiated carcinoma penetrating the serosa, *arrowheads* moderately differentiated tubular adenocarcinoma invading up to the muscularis propria). Although the volume of tumor was relatively small at the gallbladder, multiple metastatic nodules had already formed at the liver. **c** Many of RAS were identified at the annular structure. **d** Poorly differentiated adenocarcinoma proliferated at the mucosa and then invaded. No sequence of tumor and RAS was identified in this case (original magnification, ×200)

Table 3 Survival analysis

Characteristics		Number	Univariate analysis		Multivariate analysis	
			HR (95%CI)	*P* value	HR (95%CI)	*P* value
Adenomyomatosis	Negative	72	1	0.0007	1	0.9716
	Positive	25	3.85 (1.81–7.97)		0.98 (0.42–2.28)	
Age	<69	45	1	0.1205		
	≤69	52	0.97 (0.94–1.01)			
Gender	Male	31	1	0.0426	1	0.80
	Female	66	2.35 (1.02–6.31)		0.88 (0.33–2.60)	
T	T1, T2	51	1	<0.0001	1	0.0178
	T3, T4	46	7.56 (3.47–18.31)		3.06 (1.21–8.35)	
N	N0	50	1	<0.0001	1	0.0048
	N1	47	12.71 (5.45–34.76)		5.99 (1.72–21.80)	
M	M0	77	1	<0.0001	1	0.1335
	M1	20	7.67 (3.65–16.04)		1.87 (0.82–4.43)	

HR hazard ratio, *CI* confidence interval

and metaplasia at the fundal lumen in case of segmental adenomyomatosis is also considered to be a risk factor for gallbladder cancer [3, 9]. In fact, the present study and previous investigations have shown that gallbladder cancer arises predominantly at the fundal side of segmental-type adenomyomatosis [3, 9, 10]. No adenomyomatosis-specific molecule-based study has been reported. Mutations of the *KRAS*, *TP53*, and *CDNK2A* genes have been reported in invasive gallbladder carcinoma [14], but molecular pathways of carcinogenesis in the gallbladder have not been clearly established. Gallbladder cancer arising with fundal-type adenomyomatosis has also been reported [4, 8] and our series included nine cases of fundal-type adenomyomatosis-positive gallbladder cancer. The risk factors for fundal-type adenomyomatosis have been little investigated and remain unclear.

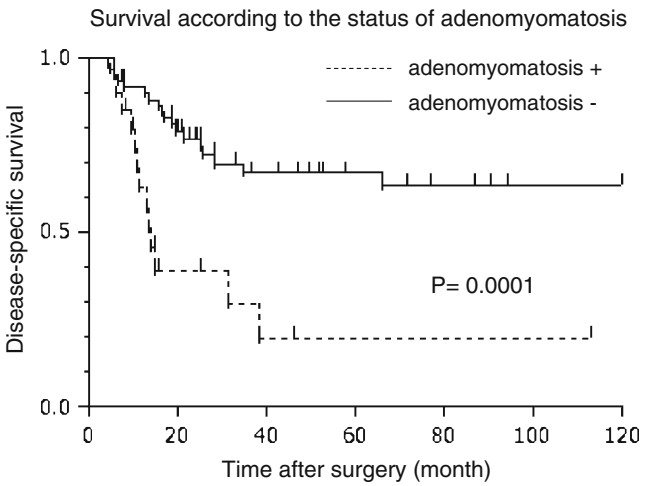

Fig. 7 Kaplan–Meier curves for all 97 patients according to the presence or absence of adenomyomatosis. The adenomyomatosis-positive gallbladder cancer group showed significantly poorer outcomes (P=0.0001)

The histological tendencies in adenomyomatosis-associated gallbladder cancer have not been investigated in previous studies. All of our present cases were stage T2 or higher, and no cases showed a predominant histologic type of papillary adenocarcinoma. Papillary-type gallbladder cancer associated with adenomyomatosis has been reported, but has been restricted to in situ or microinvasive cancer [4–8]. Adenomyomatosis-positive gallbladder cancer was also more frequently associated with the poorly differentiated histologic type compared to adenomyomatosis-negative cases. This could be explained by dedifferentiation, which is frequently observed in gallbladder cancer when the tumor invades deeper than the muscle layer [19].

In the present study, adenomyomatosis-positive gallbladder cancer was diagnosed as advanced stage cancer by several imaging modalities. The characteristics of imaging patterns in gallbladder cancer have been reported as follows: a mass replacing the gallbladder in 40–65% of cases; focal or diffuse gallbladder wall thickening in 20–30%; and an intraluminal polypoid mass in 15–25% [20–24]. If the tumor develops sufficiently to form a mass, the tumor may invade deeper than the muscle layer through the RAS. Gallbladder wall thickening by cancer invasion may be difficult to discriminate from wall thickening due to the preceding adenomyomatosis. Given these concerns, making an exact preoperative diagnosis of early stage gallbladder cancer with adenomyomatosis seems extremely difficult, as shown in our series.

Surgical intervention for patients with asymptomatic adenomyomatosis remains controversial [3, 4, 13]. Some investigators do not consider gallbladder adenomyomatosis as a premalignant lesion and believe that delaying the treatment of asymptomatic patients will not affect morbidity [13]. Others consider this condition to be a precursor of gallbladder cancer and advise regular ultrasonographic gallbladder surveillance, and suggest that cholecystectomy

should be performed when thickening or irregularity of the gallbladder wall is detected [4]. Cholecystectomy is now commonly performed by laparoscopic surgery with a low degree of surgical invasiveness. As the clinical diagnosis of early gallbladder cancer with adenomyomatosis is quite difficult, the utility of preventive cholecystectomy should, therefore, be taken into consideration for the management of asymptomatic adenomyomatosis patients.

In conclusion, the present study revealed an unexpectedly high incidence of accompanying adenomyomatosis in resected specimens of gallbladder cancer and revealed that adenomyomatosis-positive gallbladder cancer is often diagnosed clinically at an advanced stage. Gallbladder cancer shows marked geographical and ethnic variations [25–27]. Accumulation of studies from other institutions and other countries are thus required to confirm the relationship between adenomyomatosis and gallbladder cancer. If it is confirmed that many cases of actual gallbladder cancer were clinically detected in the advanced stage because of preceding adenomyomatosis, preventative cholecystectomy for asymptomatic adenomyomatosis patients might contribute to reducing the mortality caused by gallbladder cancer.

Acknowledgment This work was supported by the Ministry of Education, Culture, Sports, Science and Technology KAKENHI Grant-in-Aid for Young Scientists (B) 21791299.

Disclosure The authors declare that they have no conflict of interest.

References

1. Jutras JA, Longtin JM, Levesque HP (1960) Hyperplastic cholecystoses. AJR 83:795–827
2. Jutras JA, Levesque HP (1966) Adenomyoma and adenomyomatosis of the gallbladder. Radiol Clin North Am 4:483–500
3. Ootani T, Shirai Y, Tsukada K, Muto T (1992) Relationship between gallbladder carcinoma and the segmental type of adenomyomatosis of the gallbladder. Cancer 69:2647–2652
4. Aldridge MC, Gruffaz F, Castaing D, Bismuth H (1991) Adenomyomatosis of the gallbladder. A premalignant lesion? Surgery 109:107–110
5. Funabiki T, Matsumoto S, Tsukada N, Kimura T, Yoshizaki S, Horibe Y (1993) A patient with early gallbladder cancer derived from a Rokitanski–Aschoff sinus. Surg Today 23:350–355
6. Kawarada Y, Sanda M, Mizumoto R, Yatani R (1986) Early carcinoma of the gallbladder, noninvasive carcinoma originating in the Rokitansky–Aschoff sinus: a case report. Am J Gastroenterol 81:61–66
7. Terada T (2008) Gallbladder adenocarcinoma arising in Rokitansky–Aschoff sinus. Pathol Int 58:806–809
8. Albores-Saavedra J, Shukla D, Carrick K, Henson DE (2004) In situ and invasive adenocarcinomas of the gallbladder extending into or arising from Rokitansky–Aschoff sinuses: a clinicopathologic study of 49 cases. Am J Surg Pathol 28:621–628
9. Nabatame N, Shirai Y, Nishimura A, Yokoyama N, Wakai T, Hatakeyama K (2004) High risk of gallbladder carcinoma in elderly patients with segmental adenomyomatosis of the gallbladder. J Exp Clin Cancer Res 23:593–598
10. Albores-Saavedra J, Henson DE, Klimstra DS (2000) Tumors of the gallbladder, extrahepatic bile ducts and ampulla of Vater. In: Rosai J, Sobin LH (eds) Atlas of tumor pathology, 3rd series. Armed Forces Institute of Pathology, Washington
11. Sobin L, Gospodarowicz M, Wittekind C (2009) TNM classification of malignant tumors, 7th edn. Wiley, Hoboken
12. Fotopoulous JP, Crampton AR (1964) Adenomyomatosis of the gallbladder. Med Clin North Am 48:9–36
13. Ram MD, Midha D (1975) Adenomyomatosis of the gallbladder. Surgery 78:224–229
14. Albores-Saavedra J, Klöppel G, Adsay NV, et al (2010) Carcinomas of gallbladder and extrahepatic bile ducts. In: Bosman FT, Carneiro F, Hruban RH, Theise ND (eds) WHO classifications of tumors of the digestive system. International Agency for Research on Cancer, Lyon, pp 266–273
15. Miyazaki M, Takada T, Miyakawa S et al (2008) Risk factors for biliary tract and ampullary carcinomas and prophylactic surgery for these factors. J Hepatobiliary Pancreat Surg 15:15–24
16. Sheth S, Bedford A, Chopra S (2000) Primary gallbladder cancer: recognition of risk factors and the role of prophylactic cholecystectomy. Am J Gastroenterol 95:1402–1410
17. Hsing AW, Bai Y, Andreotti G et al (2007) Family history of gallstones and the risk of biliary tract cancer and gallstones: a population-based study in Shanghai, China. Int J Cancer 121:832–838
18. Nishimura A, Shirai Y, Hatakeyama K (2004) Segmental adenomyomatosis of the gallbladder predisposes to cholecystolithiasis. J Hepatobiliary Pancreat Surg 11:342–347
19. Kai K, Kohya N, Kitahara K et al (2011) Tumor budding and dedifferentiation in gallbladder carcinoma: potential for the prognostic factors in T2 lesions. Virchows Archive 459:449–456. doi:10.1007/s00428-011-1131-9
20. Levy AD, Murakata LA, Rohrmann CA Jr (2001) Gallbladder carcinoma: radiologic–pathologic correlation. Radiographics 21:295–314
21. Franquet T, Montes M, Ruiz de Azua Y, Jimenez FJ, Cozcolluela R (1991) Primary gallbladder carcinoma: imaging findings in 50 patients with pathologic correlation. Gastrointest Radiol 16:143–148
22. Lane J, Buck JL, Zeman RK (1989) Primary carcinoma of the gallbladder: a pictorial essay. Radiographics 9:209–228
23. Yeh HC (1979) Ultrasonography and computed tomography of carcinoma of the gallbladder. Radiology 133:167–173
24. Yum HY, Fink AH (1980) Sonographic findings in primary carcinoma of the gallbladder. Radiology 134:693–696
25. Miller G, Jarnagin WR (2008) Gallbladder carcinoma. Eur J Surg Oncol 34:306–312
26. Randi G, Franceschi S, La VC (2006) Gallbladder cancer worldwide: geographical distribution and risk factors. Int J Cancer 118:1591–1602
27. Kayahara M, Nagakawa T (2007) Recent trends of gallbladder cancer in Japan: an analysis of 4,770 patients. Cancer 110:572–580

Virchows Arch (2011) 459:581–586
DOI 10.1007/s00428-011-1167-x

ORIGINAL ARTICLE

Cyclooxygenase-2 expression in esophageal epithelium before and after photodynamic therapy for Barrett's esophagus with high-grade dysplasia or intramucosal carcinoma

Patrick Yachimski · Mari Mino-Kenudson · Margaret E. Sherwood · William P. Puricelli · Norman S. Nishioka · Gregory Y. Lauwers

Received: 12 September 2011 / Revised: 20 October 2011 / Accepted: 31 October 2011 / Published online: 13 November 2011
© Springer-Verlag 2011

Abstract Cyclooxygenase-2 expression is upregulated in Barrett's esophagus and esophageal adenocarcinoma. Photodynamic therapy using porfimer sodium can result in ablation of dysplasia and intramucosal carcinoma, eradication of Barrett's esophagus, and restitution of squamous epithelium. The aim of this study was to determine the effect of photodynamic therapy on cyclooxygenase-2 expression in esophageal epithelium. Paired pre- and post-photodynamic therapy biopsy samples from the same anatomical levels of 20 individuals who had undergone photodynamic therapy for Barrett's esophagus with high-grade dysplasia and/or intramucosal carcinoma were immunostained using a cyclooxygenase-2 monoclonal antibody. Cyclooxygenase-2 expression was graded in squamous epithelium, Barrett's esophagus, and neoplasia (if present) as follows: grade 0 (no staining), grade 1 (staining in 1–10% of cells), grade 2 (staining in 11–90% of cells), and grade 3 (staining in >90% of cells). Pre-photodynamic therapy median cyclooxygenase-2 expression was grade 2 (range 1–3) in neoplastic foci and grade 1 (range 1–3) in nondysplastic Barrett's esophagus (P=0.0009 for pairwise comparison). With the exception of a few cells staining in the basal epithelial layers, median cyclooxygenase-2 expression was graded as 0 (similar to controls) in both pre-photodynamic therapy squamous epithelium and post-photodynamic therapy neosquamous epithelium. This was significantly lower when compared to either neoplastic foci (P<0.0001) or nondysplastic Barrett's esophagus (P<0.0001) pre-photodynamic therapy. Notably, in four patients with post-photodynamic therapy recurrent neoplasia, cyclooxygenase-2 expression returned to elevated levels. Cyclooxygenase-2 expression is elevated in Barrett's esophagus with high-grade dysplasia or intramucosal carcinoma prior to photodynamic therapy. Following successful photodynamic therapy, cyclooxygenase-2 expression in neosquamous epithelium returns to a low baseline level similar to that observed in native esophageal squamous epithelium. Post-photodynamic therapy neoplastic recurrence is associated with elevated cyclooxygenase-2 expression. Prospective studies should determine whether cyclooxygenase inhibitors have a role as adjuvant therapy to prevent recurrence of Barrett's esophagus following endoscopic therapy.

Patrick Yachimski and Mari Mino-Kenudson contributed equally to this study.

P. Yachimski · W. P. Puricelli · N. S. Nishioka
Gastrointestinal Unit, Massachusetts General Hospital,
Harvard Medical School,
Boston, MA, USA

P. Yachimski · M. E. Sherwood · W. P. Puricelli · N. S. Nishioka
Wellman Center for Photomedicine,
Massachusetts General Hospital, Harvard Medical School,
Boston, MA, USA

M. Mino-Kenudson · G. Y. Lauwers
Pathology Department, Massachusetts General Hospital,
Harvard Medical School,
Boston, MA, USA

P. Yachimski (✉)
Division of Gastroenterology, Hepatology & Nutrition,
Vanderbilt University Medical Center,
1660 The Vanderbilt Clinic,
Nashville, TN 37232-5280, USA
e-mail: patrick.yachimski@vanderbilt.edu

Keywords Barrett's esophagus · Photodynamic therapy · Cyclooxygenase · High-grade dysplasia · Esophageal adenocarcinoma

Introduction

Barrett's esophagus (BE) describes the replacement of esophageal squamous epithelium by specialized columnar, i.e., intestinal-type epithelium. It is typically diagnosed in individuals with long-standing gastroesophageal reflux disease (GERD) and represents the principal risk factor for esophageal adenocarcinoma [1].

Cyclooxygenase (COX) is the rate-limiting enzyme in prostaglandin synthesis. Of the two isoforms that have been characterized, COX-2 is the inducible form, whose synthesis can be upregulated by several cytokines, growth factors, and tumor promoters. COX-2 expression is upregulated in Barrett's esophagus with and without dysplasia and in esophageal adenocarcinoma [2–4]. In Barrett's and esophageal adenocarcinoma, COX-2 expression correlates with the expression of genes involved in tumorigenesis, including the anti-apoptotic bcl-2 [5] and epithelial growth factor receptor [6]. Furthermore, the degree of COX-2 overexpression may have prognostic implications with respect to the presence of metastases and overall survival in patients with esophageal adenocarcinoma [7, 8].

Photodynamic therapy (PDT) is a drug and device modality in which neoplastic ablation is achieved by administration of a photosensitizing agent and subsequent light illumination of target tissue. Mechanisms of tissue injury include generation of reactive oxygen singlets, as well as altered prostaglandin release [9] and modifications in the microvascular environment [10]. Sustained COX-2 expression has been observed in mouse sarcoma and carcinoma cell lines following PDT, and addition of a specific COX-2 inhibitor both attenuates COX-2 expression and enhances the tumoricidal effect of PDT in an in vivo mouse model [11]. COX-2 expression is similarly upregulated following hypericin-mediated PDT of human bladder transitional cell cancer in vitro [12].

COX-2 expression in human esophageal epithelium has been characterized in Barrett's chemoprevention studies [13, 14]. Data are limited, however, regarding the effect of PDT on COX-2 expression in BE. With the hypothesis that PDT alters COX-2 expression in esophageal epithelium, the objective of this study was to characterize in vivo COX-2 expression before and after PDT for Barrett's esophagus containing high-grade dysplasia (HGD) or intramucosal carcinoma (IMC).

Methods

PDT protocol

The protocol for this retrospective review of medical records and examination of histopathologic specimens was approved by the Partners Human Research Committee.

Patients with BE containing HGD and/or IMC are candidates for PDT at our institution. The PDT protocol, employing porfimer sodium photosensitizer (Photofrin, Axcan Pharma, Mont-Saint-Hilaire, Quebec, Canada) and subsequent light delivery during upper gastrointestinal endoscopy, has been previously described [15].

Pre-treatment staging includes four-quadrant jumbo forceps biopsy at 2-cm intervals along the entire length of BE, with additional biopsies as necessary for nodular areas of mucosa. Following PDT, repeat endoscopy with biopsy is performed at months 3, 6, 9, and 12. In all cases, the histopathologic diagnoses of BE and dysplasia are determined by experienced gastrointestinal pathologists using standard criteria [16].

Gastric acid suppression via proton pump inhibitor (PPI) is prescribed for all PDT-eligible patients immediately after diagnosis of HGD/IMC and is continued indefinitely following PDT. Patients taking aspirin or nonsteroidal anti-inflammatory drugs are instructed to stop these medications prior to gastrointestinal endoscopic procedures, including upper gastrointestinal endoscopy with PDT.

Subject selection

Twenty subjects with a complete histopathologic response to PDT, defined as eradication of metaplastic BE and replacement with neosquamous epithelium, were identified in a pre-existing tissue database of patients who had undergone PDT between the years 1997 and 2007 [17]. Of those, four subjects experienced recurrence of neoplasia after the complete histopathologic response. For each of the 20 subjects, paired pre-PDT and post-PDT biopsies, and one with recurrence, if present, from matching anatomic locations were selected for immunohistochemical analysis. In addition, five esophagi from subjects without Barrett's esophagus were selected as controls.

Immunohistochemistry

Selected formalin-fixed, paraffin-embedded tissue sections from biopsies of human esophagus epithelium were immunostained using a commercially available COX-2 monoclonal antibody (Cayman Chemical, Ann Arbor, Michigan). Sections (4 μm thick) were first deparaffinized for 10 min in xylene, rehydrated to 95% alcohol and washed in phosphate-buffered saline (PBS). Heat-induced

epitope retrieval (DakoCytomation) was performed by warming the sections in a heated water bath for 30 min (99°C) and then cooling the slides slowly to room temperature under cold water and washing three times with PBS. The sections were then incubated for 20 min with 1.5% normal horse serum (Vector Laboratories) to block nonspecific binding and washed with PBS. The sections were incubated with the primary antibody (1:50 dilution) overnight in a moist chamber at 4°C, washed, incubated with biotinylated horse anti-mouse immunoglobulin G (1:200 dilution; Vector Laboratories), and washed again. The sections were then incubated with an avidin-peroxidase conjugate (Vector), washed three times with PBS, incubated with 3,3′-diaminobenzidine tetrahydrochloride (DAB reagent, Vector) for 2–9 min with frequent microscopic checking until the background staining became just barely visible, and washed. The sections were then counterstained briefly in a dilute hematoxylin stain (Gill's) and washed three times in warm water.

Sections of human colon cancer were used as a positive control for staining. For negative controls, sections were processed as discussed previously, except that the primary antibody was omitted for overnight incubation.

Immunohistochemical scoring system

COX-2 immunostained specimens were independently reviewed by two gastrointestinal pathologists (MMK and GYL). Immunostaining was scored according to a semi-quantitative scoring system: grade 0 (no staining), grade 1 (weak diffuse cytoplasmic staining with stronger staining limited in less than 10% of cells) (Fig. 1a), grade 2 (moderate to strong cytoplasmic staining in 10–90% of cells), and grade 3 (strong staining in >90% of cells) (Fig. 1b) [7].

In instances in which more than one type of epithelium was present in pre-PDT biopsies and follow-up biopsies with recurrent dysplasia, a COX-2 immunostain score was assigned to each tissue type present: BE, dysplastic BE, squamous epithelium, and basal layer of squamous epithelium. Post-PDT biopsies received two immunostain scores: squamous epithelium and basal layer of squamous epithelium.

When there was a discrepancy in immunostain scores assigned by the two pathologists, the mean of the two scores was assigned.

Statistical analysis

Univariate analysis was performed to obtain summary statistics for immunohistochemical grading, including median immunohistochemical grade by tissue type and treatment status. Immunohistochemical grade was treated as a continuous variable, and a normal distribution was not assumed. Pairwise comparison was performed using nonparametric Wilcoxon rank sum testing. All statistical analyses were performed using SAS version 9.1 software. Statistical significance was defined as a two-sided P value less than 0.05.

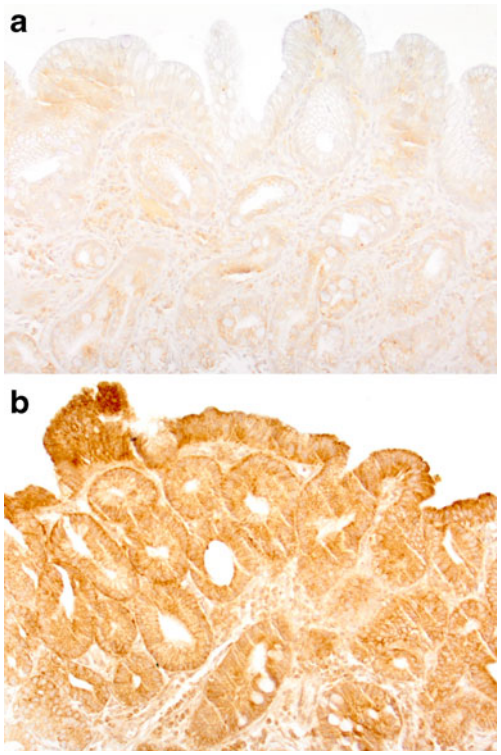

Fig. 1 **a** Nondysplastic Barrett's epithelium demonstrating grade 1 COX-2 immunostain. **b** Barrett's epithelium with HGD demonstrating grade 3 COX-2 immunostain

Results

Subject characteristics

The cohort consisted of 13 male and 7 female subjects, with a mean age of 69.7 (range 45–87) years at the time of PDT. All subjects reported prescription PPI use both at the time of initial pre-PDT endoscopy with biopsy and at post-PDT follow-up endoscopy with biopsy. Seven subjects reported use of aspirin or other nonselective or selective COX inhibitor.

Mean length of BE pre-PDT was 6.9 (range 3–13) cm. Nine subjects had evidence of IMC on pre-treatment biopsies. For the remaining 11 subjects, HGD represented the highest grade of pre-treatment dysplasia.

Pre-treatment COX-2 expression

In nine patients, pre-PDT biopsies contained squamous epithelium in addition to neoplastic BE. With the exception of the basal cell layer that showed positive staining, COX-2 expression was absent in squamous epithelium (grade 0)

(Fig. 2). The same was true for squamous epithelium in the five control cases from subjects without Barrett's esophagus.

The median COX-2 expression was grade 2 (range 1–3) in both areas of IMC and those of HGD, and grade 1 (range 1–3) in nondysplastic Barrett's. There was no discernible difference in COX-2 expression between HGD and IMC. However, COX-2 expression in IMC or HGD was higher than that in nondysplastic Barrett's (P=0.001).

The degree of pre-PDT COX-2 expression in areas of IMC or HGD was not influenced by patient age or gender. Similarly, history of reported use of a selective or nonselective COX inhibitor did not influence pre-PDT COX-2 expression.

Post-treatment COX-2 expression

Median time elapsed between pre-PDT and post-PDT biopsies was 152.5 (range 89–1,146) days. Biopsies in all 20 subjects contained neosquamous epithelium and no evidence of BE.

Similar to pre-PDT squamous epithelium, COX-2 expression in neosquamous epithelium, with the exception of the basal epithelial layer, was graded as 0 in all cases.

COX-2 expression in neosquamous epithelium post-PDT was lower than pre-PDT COX-2 expression in either dysplastic (median grade 2 vs grade 0, P<0.0001) or nondysplastic BE (median grade 1 vs grade 0, P<0.0001) (Fig. 3).

Notably, in four subjects who later went on to develop recurrent HGD post-PDT, COX-2 expression returned to elevated levels (grades 2–3) in dysplastic tissue. There was no difference in COX-2 expression in neosquamous epithelium, including the basal cell layer between subjects with recurrence and those without.

Discussion

Although the current study is limited by its small size, the results indicate that COX-2 expression in neosquamous, i.e., restored esophageal epithelium, returns to low, baseline levels following porfimer sodium PDT for Barrett's HGD or IMC irrespective of the presence or absence of recurrence during follow-up. The lack of difference in COX-2 expression of neosquamous epithelium between subjects with recurrence and those without could be explained by sampling error (buried dysplasia that was not captured by a superficial biopsy, etc.). No trends or difference was identified in COX-2 expression when comparing different grades of mucosal carcinoma, although the ability to detect difference may be limited by sample size.

Fig. 2 Positive COX-2 staining is seen in the basal cell layer; otherwise, squamous epithelium demonstrates grade 0 immunostain

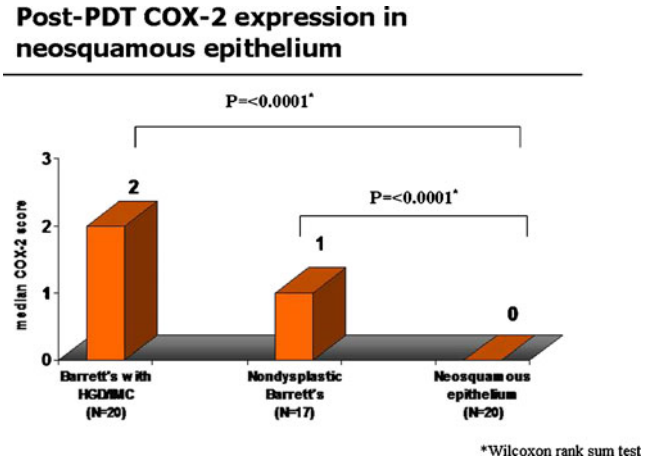

Fig. 3 *Bars* depict median COX-2 immunostain scores in Barrett's HGD/IMC prior to PDT, nondysplastic Barrett's prior to PDT, and neosquamous epithelium following PDT

This study compares COX-2 expression in BE pre-PDT with that in neosquamous epithelium (rather than persistent BE) following PDT. We believe that this comparison is relevant for consideration in the histopathologic development of BE. Current interest and attention is focused upon the concept of a pluripotent esophageal stem cell, responsible for development of esophageal squamous epithelium/neosquamous epithelium, or, in an alternate pathway, metaplastic development of BE. While the precise location of the esophageal stem cell has yet to be precisely defined, one hypothesis is that these cells are located in the esophageal gland ducts [18–20]. Genotypic and phenotypic variation, including COX-2 expression, in this squamous population may therefore have implications for progression to either remission or recurrence of BE following endoscopic eradication therapy.

Phenotypic conversion to normal epithelium, including COX-2 expression, following PDT does not necessarily imply that the epithelium is genetically normal. Persistent genetic abnormalities, including p53 mutation, can be found in nondysplastic BE despite successful PDT-mediated ablation of HGD [21]. Additional data suggest that both p53 mutation and Ki-67 overexpression are present in columnar epithelium [22] and even in squamous

islands following incomplete ablation of BE via argon plasma coagulation or multipolar electrocoagulation [23]. It has also been reported that a focus of neosquamous epithelium had p16 alterations identical to that found in surrounding Barrett's epithelium [24].

The mechanistic and molecular responses to PDT may not be stereotypical and may instead vary according to the specific photosensitizing agent [25]. To this end, molecular mechanisms of tissue injury and response to endoscopic ablation may vary according to the ablation modality. In many centers, PDT is no longer the primary endoscopic treatment option for Barrett's-associated neoplasia, having been supplanted in recent years by alternative treatment modalities, including endoscopic mucosal resection and radiofrequency ablation. The future applicability of this study's findings may therefore be limited as PDT recedes further from the endoscopic treatment armamentarium. The cellular response to endoscopic ablation therapies other than PDT, including post-treatment alteration in COX-2 expression, should be evaluated and characterized. Assessment of COX-2 expression following radiofrequency ablation might be of particular interest, given the growing use of this modality.

Our data also suggest that among patients who develop recurrent dysplastic BE following initial complete ablation with PDT, COX-2 expression returns to elevated levels. This raises the question as to whether HGD/IMC patients might benefit from adjuvant COX-2 inhibition following successful ablation therapy. Whereas the prospective Chemoprevention for Barrett's Esophagus Trial failed to demonstrate a benefit of COX-2 inhibitor therapy alone as a secondary prevention strategy for dysplastic BE patients [14], a tertiary prevention strategy of COX-2 inhibition following PDT would have theoretical benefits. Addition of COX-2 inhibition likely could benefit such a population enriched with dysplastic patients at increased cancer risk, and such an approach should be evaluated prospectively. This study did not control for pharmacologic use of COX inhibitors. Seven among the 20 patients in this cohort reported use of selective or nonselective COX inhibitors. The extent to whether nonsteroidal anti-inflammatory drugs or other COX inhibitors influence COX-2 expression following endoscopic treatment for BE could be evaluated in a controlled prospective fashion.

The present study was not designed to assess the acute in vivo response of esophageal epithelium to PDT. However, this also remains an attractive area for investigation and potential pharmacologic intervention. As previously described in an in vivo mouse sarcoma and carcinoma model, addition of a specific COX-2 inhibitor enhances the tumoricidal effect of PDT [11]. In vitro work has suggested a possible synergistic effect of aminolevulinic acid PDT and specific COX-2 inhibition on oral squamous cell cancer [26]. Combination therapy with PDT and angiogenesis inhibitors has been described in the treatment of macular degeneration [27], and some cell lines may demonstrate enhanced tumor response to PDT with the addition of bevacizumab [28, 29].

In summary, our study demonstrates elevated COX-2 expression in BE with HGD or IMC, consistent with prior published data. Following complete ablation of columnar epithelium with porfimer sodium PDT, in vivo COX-2 expression returns to baseline levels in neosquamous epithelium. Further increases in COX-2 expression can be seen in patients with recurrent dysplasia following PDT ablation. COX-2 inhibition should be investigated as a target for pharmacologic intervention as a chemopreventive strategy following endoscopic therapy.

Disclosures None of the authors has any financial disclosures or potential conflicts of interest relevant to this manuscript

References

1. Falk GW (2002) Barrett's esophagus. Gastroenterology 122:1569–1591
2. Kuramochi H, Vallbohmer D, Uchida K et al (2004) Quantitative, tissue-specific analysis of cyclooxygenase gene expression in the pathogenesis of Barrett's adenocarcinoma. J Gastrointest Surg 8:1007–1016
3. Morris CD, Armstrong GR, Bigley G et al (2001) Cyclooxygenase-2 expression in the Barrett's metaplasia–dysplasia–adenocarcinoma sequence. Am J Gastroenterol 96:990–996
4. Lagorce C, Paraf F, Vidaud D et al (2003) Cyclooxygenase-2 is expressed frequently and early in Barrett's oesophagus and associated adenocarcinoma. Histopathology 42:457–465
5. Shimizu D, Vallbohmer D, Kuramochi H et al (2006) Increasing cyclooxygenase-2 (COX-2) gene expression in the progression of Barrett's esophagus to adenocarcinoma correlates with that of bcl-2. Int J Cancer 119:765–770
6. Ly Y, Wo JM, Ray MB et al (2006) Cyclooxygenase-2 and epithelial growth factor receptor up-regulation during progression from Barrett's esophagus to adenocarcinoma. World J Gastroenterol 12:928–934
7. Buskens CJ, Van Rees BP, Sivula A et al (2002) Prognostic significance of elevated cyclooxygenase 2 gene expression in patients with adenocarcinoma of the esophagus. Gastroenterology 122:1800–1807
8. France M, Drew PA, Dodd T, Watson DI (2004) Cyclo-oxygenase-2 expression in esophageal adenocarcinoma as a determinant of clinical outcome following esophagectomy. Dis Esophagus 17:136–140
9. Henderson BW, Donovan JM (1989) Release of prostaglandin E2 from cells by photodynamic treatment in vitro. Cancer Res 49:6896–6900
10. Reed MWR, Wieman JT, Doak KW et al (1989) The microvascular effect of photodynamic therapy: evidence for a possible role of cyclooxygenase products. Photochem Photobiol 50:419–423
11. Ferrario A, von Tiehl K, Wong S et al (2002) Cyclooxygenase-2 inhibitor treatment enhances photodynamic therapy-mediated tumor response. Cancer Res 62:3956–3961
12. Hendrickx N, Volanti C, Moens U et al (2003) Up-regulation of cyclooxygenase-2 and apoptosis resistance by p38 MAPK in

hypericin-mediated photodynamic therapy of human cancer cells. J Biol Chem 52:52231–52239
13. Kaur BS, Khamnehei N, Iravani M et al (2002) Rofexocib inhibits cyclooxygenase 2 expression and activity and reduces cell proliferation in Barrett's esophagus. Gastroenterology 123:60–67
14. Heath EI, Canto MI, Piantadosi S et al (2007) Secondary chemoprevention of Barrett's esophagus with celecoxib: results of a randomized trial. J Natl Cancer Inst 99:545–557
15. Yachimski P, Puricelli W, Nishioka NS (2008) Patient predictors of esophageal stricture development following photodynamic therapy. Clin Gastroenterol Hepatol 6:302–308
16. Goldblum JR, Lauwers GY (2002) Dysplasia arising in Barrett's esophagus: diagnostic pitfalls and natural history. Semin Diagn Pathol 19:12–19
17. Mino-Kenudson M, Ban S, Ohana M et al (2007) Buried dysplasia and early adenocarcinoma arising in Barrett's esophagus after porfimer-photodynamic therapy. Am J Surg Pathol 31:403–409
18. Chang CL, Lao-Sirieix P, Save V et al (2007) Retinoic acid-induced glandular differentiation of the oesophagus. Gut 56:906–917
19. Coad RA, Woodman AC, Warner PJ et al (2005) On the histogenesis of Barrett's oesophagus and its associated squamous islands: a three-dimensional study of their morphological relationship with native oesophageal gland ducts. J Pathol 206:388–394
20. Leedham SJ, Preston SL, McDonald SA et al (2008) Individual crypt genetic heterogeneity and the origin of metaplastic glandular epithelium in human Barrett's oesophagus. Gut 57:1041–1048
21. Krishnadath KK, Wang KK, Taniguichi K et al (2000) Persistent genetic abnormalities in Barrett's esophagus after photodynamic therapy. Gastroenterology 119:624–630
22. Dvorak K, Ramsey L, Payne CM et al (2006) Abnormal expression of biomarkers in incompletely ablated Barrett's esophagus. Ann Surg 244:1031–1036
23. Garewal H, Ramsey L, Sharma P et al (1999) Biomarker studies in reversed Barrett's esophagus. Am J Gastroenterol 94:2829–2833
24. Paulson TG, Xu L, Sanchez C et al (2006) Neosquamous epithelium does not typically arise from Barrett's epithelium. Clin Cancer Res 12:1701–1706
25. Solban N, Pal SK, Alok SK et al (2006) Mechanistic investigation and implications of photodynamic therapy induction of vascular endothelial growth factor in prostate cancer. Cancer Res 66:5633–5640
26. Akita Y, Kozaki K, Nakagawa A et al (2004) Cyclooxygenase-2 is a possible target of treatment approach in conjunction with photodynamic therapy for various disorders in skin and oral cavity. Br J Dermatol 151:472–480
27. Dhalla MS, Shah GK, Blinder KJ et al (2006) Combined photodynamic therapy with verteporfin and intravitreal bevacizumab for choroidal neovascularization and age-related macular degeneration. Retina 26:988–993
28. Ferrario A, Gomer CJ (2006) Avastin enhances photodynamic therapy treatment of Kaposi's sarcoma in a mouse tumor model. J Environ Pathol Toxicol Oncol 25:251–259
29. Bhuvaneswari R, Yuen GY, Chee SK, Olivo M (2007) Hypericin-mediated photodynamic therapy in combination with Avastin (bevacizumab) improves tumor response by downregulating angiogenic proteins. Photochem Photobiol Sci 6:1275–1283

Virchows Arch (2011) 459:587–593
DOI 10.1007/s00428-011-1164-0

ORIGINAL ARTICLE

Prognostic significance of Tiam1 expression in papillary thyroid carcinoma

Chuen Hsueh · Jen-Der Lin · Chia-Fen Yang · Yu-Sun Chang · Tzu-Chieh Chao · Jui-Hung Sun · I-Chin Wu · Ngan-Ming Tseng · Shir-Hwa Ueng

Received: 9 August 2011 / Revised: 5 October 2011 / Accepted: 26 October 2011 / Published online: 11 November 2011
© Springer-Verlag 2011

Abstract T lymphoma and metastasis gene 1 (Tiam1) is a guanine nucleotide exchange factor (GNEF) that regulates the guanosine triphosphatase to facilitate the exchange of guanosine diphosphate for guanosine triphosphate. It specifically activates Rac1, a member of the Rho family of GTPases. Tiam1 is involved in cell proliferation, cytoskeletal organization, cellular adhesion, and transcriptional activation. It has been suggested that alterations in Tiam1 expression might contribute to the progression of various human cancers. The usefulness of Tiam1 expression as a prognostic marker in papillary thyroid carcinoma (PTC) has not been investigated yet. The aim of this study was to analyze the expression of Tiam1 in PTC as well as its association with the clinicopathologic features and prognostic significance. Surgical tissue samples were taken from 106 PTC patients who had been followed up for at least 9.3 years. Strong expression of Tiam1 was detected in 54% of the cases. Tiam1 expression was associated significantly with various clinicopathologic parameters, such as gender (P=0.039), tumor multicentricity (P=0.0124), histologic subtype (P=0.0427), TNM stage (P=0.0151), and distant metastases at diagnosis (P=0.0001). Survival analysis showed that the Tiam1 low-expression group had a significantly shorter overall survival time than Tiam1 high-expression group (P=0.0007). Multivariate analysis showed that Tiam1 expression was a significant and independent prognostic indicator (P=0.0090) for PTC patients. Tiam1 expression may be a novel and independent prognostic marker of PTC patients.

Keywords Tiam1 · Papillary carcinoma · Thyroid · Prognosis · Survival

C. Hsueh · S.-H. Ueng
Department of Pathology, Chang Gung Memorial Hospital, Linko, Chang Gung University College of Medicine, Kwei-Shan, Taoyuan, Taiwan

J.-D. Lin · J.-H. Sun
Department of Internal Medicine, Chang Gung Memorial Hospital, Linko, Chang Gung University College of Medicine, Kwei-Shan, Taoyuan, Taiwan

C.-F. Yang
Department of Pathology, En Chu Kong Hospital, New Taipei City, Taiwan

Y.-S. Chang · I.-C. Wu
Chang Gung Molecular Medicine Research Center and Graduate Institute of Basic Medical Sciences, Chang Gung University College of Medicine, Kwei-Shan, Taoyuan, Taiwan

T.-C. Chao
Department of Surgery, Chang Gung Memorial Hospital, Linko, Chang Gung University College of Medicine, Kwei-Shan, Taoyuan, Taiwan

N.-M. Tseng
Department of Radiation Oncology, Chang Gung Memorial Hospital, Linko, Chang Gung University College of Medicine, Kwei-Shan, Taoyuan, Taiwan

C. Hsueh (✉)
Department of Pathology, Chang Gung Memorial Hospital, 5 Fu-Hsing Street, Kwei-Shan, Taoyuan 333, Taiwan
e-mail: ch9211@adm.cgmh.org.tw

Introduction

Thyroid cancer is the most common malignancy of the endocrine system, and papillary thyroid carcinoma (PTC) is its most frequent form. The prognosis of PTC is generally favorable, yet recurrence and/or distant metastases may

develop in about 10% to 15% of the patients, with a relatively poor prognosis [1]. How to identify such patients for a more intensive therapy to improve their outcome remains difficult. Earlier investigations have shown that patient age, tumor size, extrathyroid extension, and distant metastases are independent risk factors associated with mortality of PTC [2–4]. Other potential prognostic indicators include gender, lymph node status, tumor multicentricity, completeness of resection, and histologic subtype [2–4]. Since the incidence of PTC has been increasing in the last two decades worldwide [5, 6], it becomes more important to find reliable and consistent biomarkers as predictors of aggressive behavior of PTC.

T lymphoma and metastasis gene 1 (Tiam1) was identified first in 1994 by in vitro selection for invasiveness in a murine T lymphoma cell line [7]. It is one of the GNEFs that regulate the guanosine triphosphatase (GTPases) to facilitate the exchange of guanosine diphosphate (GDP) for guanosine triphosphate (GTP). The GTPases are active when bound to GTP and inactive when bound to GDP. The best known GTPases are the members of Rho family including Rac, Cdc42, and Rho. They are involved in cell proliferation and differentiation, cytoskeletal organization, cellular adhesion, and transcriptional activation. Tiam1 catalyzes the dissociation of GDP from inactive Rac, Rho, and Cdc42 in vitro, and from inactive Rac only in vivo [8]. Activation of these proteins in turn initiates downstream pathways that promote migration and invasion, and contribute to the development of the metastatic phenotype.

A number of reports suggest that alterations in Tiam1 expression might contribute to the progression of various human cancers. The increased Tiam1 expression in a given tumor may be positively or negatively correlated with tumor aggressiveness or patient survival. For instance, a positive correlation has been found in colon, breast, prostate, hepatocellular, and nasopharyngeal carcinomas as well as esophageal squamous cell carcinoma [9–14]. A negative correlation has been detected in renal cell carcinoma (RCC) and gastric adenocarcinoma [15, 16]. As for Tiam1 expression in PTC, only two previous reports in Chinese literature have found its overexpression in PTC compared to normal and benign thyroid tissues, with the association of higher clinical stage and lymph node metastasis [17, 18]. To the best of our knowledge, there have been no studies on the potential usefulness of Tiam1 as a prognostic marker for PTC up to date. This is the first study to determine the prognostic significance of Tiam1 expression in PTC patients. We investigated the expression pattern of Tiam1 in surgical tissue specimens from 106 PTC patients by immunohistochemical staining, and correlate the results with clinicopathologic parameters and patient survival. Our aim is to assess the Tiam1 expression in PTC and its possible association with disease progression and outcome.

Materials and methods

Surgical specimens were obtained from 106 patients with PTC diagnosed after thyroid surgery at the Chang Gung Memorial Hospital (CGMH) from 1994 to 1999. Patients with no evidence of lymph node involvement at the time of surgery underwent total thyroidectomy, and patients with gross lymph node metastases underwent total thyroidectomy with regional lymphadenectomy. The patients had undergone a postoperative follow-up till the end of 2010. The follow-up period ranged from 0.2 to 15.4 years with at least 9.3 years in survival cases. All patients who had a positive postoperative whole body scan received ^{131}I ablation, with a dose of 1.1 GBq (30 mCi) in most of them. Patients with foci of ^{131}I uptake extended beyond the thyroid bed were given increased therapeutic doses at 3.7–7.4 GBq (100–200 mCi). All specimens were formalin fixed and paraffin embedded. The corresponding hematoxylin–eosin slides were retrieved from the archives of the Department of Pathology at CGMH and reviewed for confirmation of diagnosis and adequacy of the materials. The histopathologic classification of the tumor samples was based on "Pathology and Genetics of Tumours of Endocrine Organs" by the World Health Organization in 2004 [19]. The clinical stage was defined according to American Joint Committee on Cancer criteria in 2002 [20]. Recurrence and survival data were ascertained through the Tumor Registry at CGMH and chart review. This study was approved by the Institutional Review Board at the CGMH.

Immunohistochemistry

Immunohistochemical detection of Tiam1 was performed on formalin-fixed, paraffin-embedded, 5-μm-thick sections using Bond polymer refine detection system (Leica Microsystems, Germany) and Bond immunostainer (Leica Microsystems). The primary antibodies used were rabbit anti-Tiam1 monoclonal antibody (clone 236B4; Cell Signaling Technology, Danvers, MA, USA) at a dilution of 1:400. After deparaffinization, antigen retrieval was performed with Bond ER1 buffer. Sections were incubated with the primary antibody at room temperature for 60 min, followed by poly-horseradish peroxidase anti-mouse/rabbit IgG reagent to localize the primary antibody, and the complex was visualized using diaminobenzidine. The sections were then counterstained with hematoxylin, dehydrated, cleared, and mounted. Colonic adenocarcinoma was used as positive control, and only cytoplasmic staining was considered positive. The immunostained slides were evaluated by

two pathologists (CH and C-FY) independently without knowing the clinicopathologic information. A histoscore (*H* score; range=0–300) was calculated by multiplying the intensity score (0=negative; 1=weak; 2=intermediate; 3=strong; Fig. 1a–d) and the fraction score (percentage of positive tumor cells; range=0–100). If the difference between the two observers' final histoscore was >50, the particular tissue section was reevaluated at a head-to-head microscope.

Statistical analysis

We used intraclass correlation coefficient to assess the interobserver agreement and interobserver variability of the immunohistochemical scoring. A coefficient of reliability >0.74 indicates a strong agreement between observers, in between 0.6 and 0.74 indicates a good agreement, in between 0.40 and 0.59 indicates a fair agreement, and <0.4 indicates a poor agreement [21]. Correlations of Tiam1 expression levels above or below the median value of 180, with various clinicopathological parameters including age, gender, tumor size, extent of tumor, lymph node status, tumor multicentricity, histologic subtype, clinical stage, the presence or absence of locoregional recurrence, and distant metastasis at diagnosis, were performed in all PTC patients. With the help of SPSS 10.0 for Windows (SPSS Inc, Chicago, IL), statistical significance in categorical data was determined by a χ^2 test. Survival was analyzed by the Kaplan–Meier method and compared by log-rank tests. The survival analysis was based on overall survival. Survival time was calculated as the time from the beginning of diagnosis or operation to death or last follow-up for overall survival. Patients who died without local recurrence or distant metastasis were not excluded for the analysis. The variables that were statistically significant by univariate analysis were assessed by multivariate Cox regression hazards model to detect independent predictors of survival. Two-tailed *P* values of .05 or less were considered to be statistically significant.

Results

Clinicopathologic characteristics

Of 106 patients, 83 (78%) were female and 23 (22%) were male. Their median age at diagnosis was 43.5 years (range, 15–81 years). The mean duration of follow-up was 9.6 years (range, 0.2–15.4 years). Extrathyroid extension of the tumor was found in 34 patients (32%). Initial lymph node metastases were present in 12 patients (11%). Multicentric tumors were detected in 11 patients (10%). Histologically, of 106 PTCs, 84 (79%) were classical type, 18 (17%) were follicular variant, and 4 (4%) were tall cell variant. The former two were referred to as low-risk type while the tall cell variant as high-risk type. There were 63 patients at stage I disease (59%). Locoregional recurrence was noted in 12 patients (11%); it was defined as cancer tissue that recurred 6 months after surgery or other adjuvant therapy. The patients with distant metastases detected by ^{131}I whole body scan within 1 year after operation were not considered

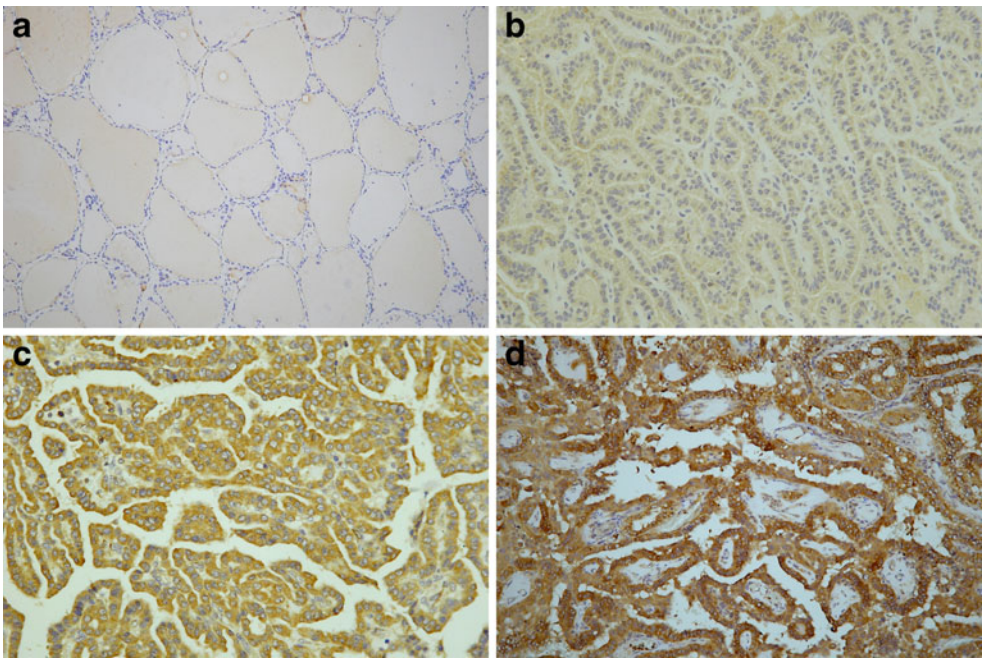

Fig. 1 Immunostaining of Tiam1 is negative in the non-neoplastic thyroid follicles (**a**) and positive in the cytoplasm of the tumor cells with either weak (**b**), intermediate (**c**), or strong (**d**) intensity, respectively

as tumor recurrence. At the time of initial surgery, 17 patients presented with distant metastases (16.0%), but 2 of them became disease free after treatment. During follow-up, four patients developed distant metastases. Tumor related death occurred in 19 of 23 patients.

Immunohistochemical study

Of 106 samples, the tumor cells showed heterogeneous cytoplasmic staining for Tiam1, whereas the nonneoplastic follicular cells showed negative or faint cytoplasmic staining generally weaker than or occasionally equal to tumor cells. The *H* scores of the tumors ranged from 10 to 300, with a median of 180. Therefore, we used an *H* score of 180 as the cutoff line to divide the patients into low-expression group (*H* score <180) and high-expression group (*H* score ≥180). The interobserver variability of the *H* score was low according to an intraclass correlation coefficient of 0.87, indicating a strong interobserver agreement.

Association between Tiam1 expression and clinicopathologic characteristics

Fifty seven (54%) of the 106 cases had high Tiam1 expression, and 49 cases (46%) had low Tiam1 expression. The association between clinicopathologic characteristics of patients and Tiam1 expression was shown in Table 1. Low Tiam1 expression was significantly correlated with male patients, tumor multicentricity, tall cell variant, TNM stage, distant metastases at diagnosis, and mortality. However, there was no correlation between Tiam1 expression and age at diagnosis, tumor size, tumor extent, lymph node status, and locoregional recurrence, respectively.

Table 1 Association between Tiam1 expression and clinicopathological characteristics in 106 patients with papillary thyroid carcinoma

	Low Tiam1 expression (n=49)	High Tiam1 expression (n=57)	P value
Age (years), range	19~75	15~81	0.1907
<45	23 (46.9%)	34 (59.6%)	
≥45	26 (53.1%)	23 (40.4%)	
Gender			0.0390[a]
Female	34 (69.4%)	49 (86.0%)	
Male	15 (30.6%)	8 (14.0%)	
Tumor size (cm)			0.2575
<2	21 (42.9%)	27 (47.4%)	
≥2 and ≤4	11 (22.4%)	18 (31.6%)	
>4	17 (34.7%)	12 (21.0%)	
Extrathyroid invasion			0.2568
No	36 (73.5%)	36 (63.2%)	
Yes	13 (26.5%)	21 (36.8%)	
Lymph node metastases			0.3717
No	43 (87.7%)	51 (89.5%)	
Yes	6 (12.3%)	6 (10.5%)	
Tumor multiplicity			0.0124[a]
No	40 (81.6%)	55 (96.5%)	
Yes	9 (18.4%)	2 (3.5%)	
Histological subtype			0.0427[a]
Low risk	45 (91.8%)	57 (100%)	
High risk	4 (8.2%)	0 (0%)	
TNM stage			0.0151[a]
Stage I	23 (46.9%)	40 (70.2%)	
Stage II~IV	26 (53.1%)	17 (29.8%)	
Locoregional recurrence			0.3717
No	42 (85.7%)	52 (91.2%)	
Yes	7 (14.3%)	5 (8.8%)	
Distant metastases at diagnosis			0.0001[a]
No	33 (67.3%)	56 (98.2%)	
Yes	16 (32.7%)	1 (1.8%)	
Mortality	15 (30.6%)	4 (7.0%)	0.0016[a]

[a]Statistically significant

Correlation of Tiam1 expression with overall survival and tumor specific survival

The expression level of Tiam1 was significantly correlated with overall survival in PTC patients (P=0.0007). Overall survival was better for patients with high expression level of Tiam1 than low expression level (Fig. 2). The 5-year overall survival in the low-expression group and high-expression group was 73% as opposed to 100%, while the 10-year overall survival was 69% as opposed to 945%.

Independent prognostic factors by multivariate analysis

Cox regression analysis showed that only age and expression level of Tiam1 were independent prognostic indicators (P=0.0001 and P=0.0090, Table 2). The parameter with the strongest independent association with worse overall survival was over 45 years of age [hazard ratio (HR)=1.103; 95% confidence interval (CI)=1.052~1.158]. Low Tiam1 expression was another independent adverse prognostic factor (HR=5.011; 95% CI=1.495~16.796). Gender, tumor size and multicentricity, histologic subtype, and locoregional recurrence showed no significant influence on survival.

Table 2 Multivariate analysis of different parameters in 106 patients with papillary thyroid carcinoma by Cox proportional hazard model

Parameter	Overall survival		
	HR	95% CI	P value
Age (years)			
<45	1.000	1.052~1.158	0.0001[a]
≥45	1.1103		
Gender			
Male	1.000	0.216~1.910	0.4259
Female	0.642		
Tumor size (cm)			
≥2	1.000	1.017~1.146	0.0642
<2	1.400		
Tumor multicentricity			
No	1.000	0.469~10.936	0.3087
Yes	2.265		
Histological type			
Low risk	1.000	0.248~4.041	0.9999
High risk	<0.001		
Locoregional recurrence			
No	1.000	0.000	0.9765
Yes	0.000		
Tiam1 expression			
High	1.000	1.495~16.796	0.0090[a]
Low	5.011		

HR hazard ratio, *CI* confidence interval

[a] Statistically significant

Discussion

The current study shows that Tiam1 is significantly overexpressed in almost all PTCs when compared to nonneoplastic thyroid tissues. High expression of Tiam1 was detected in 54% and low expression in 46% of the cases. The expression level of Tiam1 was correlated with gender, tumor multicentricity, histologic subtype, TNM stage, distant metastases at diagnosis, and mortality. Survival analysis revealed that the Tiam1 low-expression group had a significantly worse overall survival (P=0.0007) than the Tiam1 high-expression group. Multivariate analysis showed that strong Tiam1 expression was a significant and independent prognostic parameter (P=0.009) for improved survival in PTC patients. Thus, high Tiam1 expression might be a novel and independent prognostic marker for PTC patients. After independent validation, low Tiam1 expression might be used as a marker to identify high-risk patients for more aggressive treatment.

Human Tiam1 gene is located on chromosome 21q22.11, expressed in almost all adult tissues, especially at high levels in the brain and testis [22]. Tiam1 is thereby suggested to have essential roles in cell function. It has also been involved in the regulation of migration, invasion, and metastasis of tumor cells since Tiam1 increases invasion and metastasis in various human tumor cell lines including melanoma, neuroblastoma, and carcinomas of the

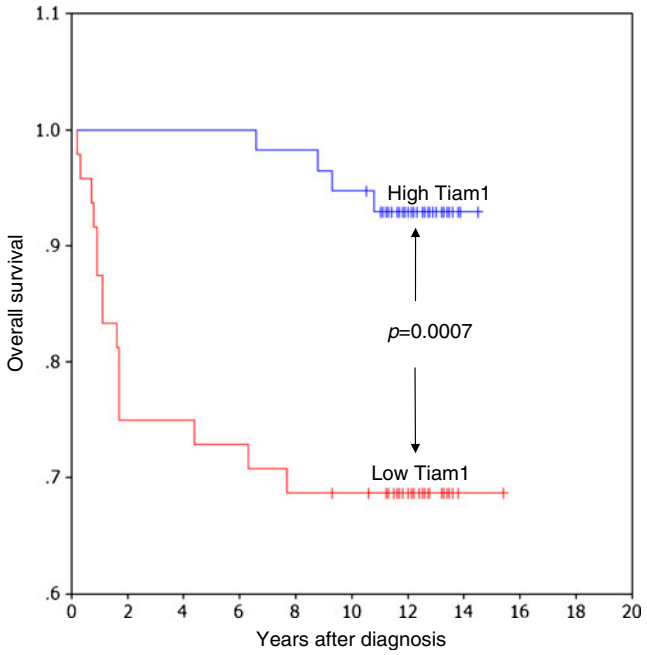

Fig. 2 Low Tiam1 expression is significantly associated with worse overall survival by Kaplan–Meier analysis (10-year survival, 69% versus 95%; P=0.0007)

breast, lung, ovary, urinary bladder, and pancreas [23]. Moreover, Tiam1 has been implicated in oncogenic transformation of cells. Previous studies have shown that N-terminal truncation of the Tiam1 protein activates its oncogenic potential in NIH3T3 cells [23], and a distinct mutation in Tiam1 in the RCC cell lines is sufficient to transform NIH3T3 cells [24]. Tiam1-deficient mice are resistant to the development of Ras-induced skin tumors [25].

Earlier investigations have demonstrated that increased Tiam1 expression is associated with aggressive behavior of the tumor and worse outcome of the patients in a number of malignant tumors such as breast, prostate, and liver cancers as well as nasopharyngeal carcinoma (NPC) and esophageal squamous cell carcinoma (ESCC). Strong Tiam1 expression correlates with higher tumor grade in breast carcinoma [10]. High Tiam1 expression level in prostate cancer correlates with disease recurrence, the presence of lymph vessel invasion, and high Gleason scores, and is an independent predictor of decreased disease-free survival [11]. Overexpression of Tiam1 in hepatocellular carcinoma significantly correlates with shorter overall survival [12]. Tiam1 protein upregulation in NPC and ESCC is significantly correlated with advanced clinical stage and poorer prognosis [13, 14]. On the other hand, Tiam1 tends to be associated with favorable prognosis in gastric adenocarcinoma [16]. Tiam1 protein has been found to be localized to intercellular adhesions in Madin–Darby canine kidney (MDCK) II epithelial cells. Overexpression of Tiam1 not only enhances cadherin-mediated cell–cell adhesion in both mesenchymal-like Ras-transformed MDCKII cells and NIH3T3 fibroblasts, but also inhibits cell migration and induces an epithelial-like morphology [26–28]. This epithelial phenotype is characterized by Rac-mediated suppression of Rho activity. Rac signaling is able to antagonize Rho activity at the GTPase level, and the reciprocal balance between Rac and Rho activity accounts for cellular morphology and migratory behavior in NIH3T3 fibroblasts [29]. In human RCC cell lines, Tiam1 expression inhibits tumor cell migration by promoting E-cadherin-mediated adhesion as well as through upregulating tissue inhibitor of metalloproteinases-1 (TIMP-1) and TIMP-2 [15]. Hence, Tiam1 appears to have a contrasting effect on cellular migration, invasion, and adhesion. Its effect could be either stimulating or inhibitory in vitro and depends on the type of cells and substrate. The inverse correlation of Tiam1 expression level with TNM stage and patient survival in PTC suggests a stronger influence of Tiam1 on cellular adhesion than on cellular migration.

In conclusion, the current study demonstrates that Tiam1 overexpression is common in PTC. Low expression of Tiam1 is associated with male patients, tumor multicentricity, tall cell variant, TNM stage, distant metastases at diagnosis, and mortality. Low Tiam1 expression is significantly correlated with worse survival of PTC patients. After further validation, Tiam1 may serve as an independent prognostic indicator to identify PTC patients in need of additional treatment. Further investigations are warranted to elucidate the role of Tiam1 in PTC.

Acknowledgments This study was supported by grants from the Ministry of Education, Taiwan, ROC (EMRPD1A0391, to CH) and the Chang Gung Medical Research Program (NMRPG376073, to J-DL).

Conflict of interest The authors declare that they have no conflict of interest.

References

1. Hay ID, Thompson GB, Grant CS, Bergstralh EJ, Dvorak CE, Gorman CA, Maurer MS, Mclver B, Mullan BP, Oberg AL, Powell CC, van Heerden JA, Goellner JR (2002) Papillary thyroid carcinoma managed at the Mayo Clinic during six decades (1940–1999): temporal trends in initial therapy and long-term outcome in 2444 consecutively treated patients. World J Surg 26:879–885
2. Hay ID, Bergstralh EJ, Goellner JR, Ebersold JR, Grant CS (1993) Predicting outcome in papillary thyroid carcinoma: development of a reliable prognostic scoring system in a cohort of 1779 patients surgically treated at one institution during 1940 through 1989. Surgery 114:1050–1057
3. DeGroot LJ, Kaplan EL, McCormick M, Straus FH (1990) Natural history, treatment, and course of papillary thyroid carcinoma. J Clin Endocrinol Metab 71:414–424
4. Shaha AR, Shah JP, Loree TR (1996) Risk group stratification and prognostic factors in papillary carcinoma of thyroid. Ann Surg Oncol 3:534–538
5. Davies L, Welch HG (2006) Increasing incidence of thyroid cancer in the United States 1973–2002. JAMA 295:2164–2167
6. Enewold L, Zhu K, Ron E, Marrogi AJ, Stojadinovic A, Peoples GE, Devesa SS (2009) Rising thyroid cancer incidence in the United States by demographic and tumor characteristics, 1980–2005. Cancer Epidemiol Biomarkers Prev 18:784–791
7. Habets GG, Scholtes EH, Zuydgeest D, van der Kammen RA, Stam JC, Berns A, Collard JG (1994) Identification of an invasion-inducing gene Tiam-1, that encodes a protein with homology to GDP-GTP exchangers for Rho-like proteins. Cell 77:537–549
8. Michiels F, Habets GG, Stam JC, van der Kammen RA, Collard JG (1995) A role for Rac in Tiam1-induced membrane ruffling and invasion. Nature 375:338–340
9. Liu L, Wu DH, Ding YQ (2005) Tiam1 gene expression and its significance in colorectal carcinoma. World J Gastroenterol 11:705–707
10. Adam L, Vadlamudi RK, McCrea P, Kumar R (2001) Tiam1 overexpression potentiates heregulin-induced lymphoid enhancer factor-1/beta-catenin nuclear signaling in breast cancer cells by modulating the intercellular stability. J Biol Chem 276:28443–28450
11. Engers R, Mueller M, Walter A, Collard JG, Willers R, Gabbert HE (2006) Prognostic relevance of Tiam1 protein expression in prostate carcinomas. Br J Cancer 95:1081–1086
12. Ding Y, Chen B, Wang S, Zhao L, Chen J, Ding Y, Chen L, Luo R (2009) Overexpression of Tiam1 in hepatocellular carcinomas predicts poor prognosis of HCC patients. Int J Cancer 124:653–658

13. Qi Y, Huang B, Yu L, Wang Q, Lan G, Zhang Q (2009) Prognostic value of Tiam1 and Rac1 overexpression in nasopharyngeal carcinoma. ORL J Otorhinolaryngol Relat Spec 71:163–171
14. Liu H, Shi G, Liu X, Wu H, Fan Q, Wang X (2011) Overexpression of Tiam1 predicts poor prognosis in patients with esophageal squamous cell carcinoma. Oncol Rep 25:841–848
15. Engers R, Springer E, Michiels F, Collard JG, Gabbert HE (2001) Rac affects invasion of human renal cell carcinomas by up-regulating tissue inhibitor of metalloproteinases (TIMP)-1 and TIMP-2 expression. J Biol Chem 276:41889–41897
16. Walch A, Seidl S, Hermannstädter C, Rauser S, Deplazes J, Langer R, von Weyhern CH, Sarbia M, Busch R, Feith M, Gillen S, Höfler H, Luber B (2008) Combined analysis of Rac1, IQGAP1, Tiam1 and E-cadherin expression in gastric cancer. Mod Pathol 21:544–552
17. Wang HX, Xiao XG, Li JH (2007) The expression of Tiam 1 in thyroid carcinoma and its clinical significance. China J Mod Med 17:2437–2440
18. Ye YH (2010) Expression of Tiam-1, Flt-4 and CXCR4 in thyroid papillary carcinomas tissues and their clinical significance. Chin J Cancer Prev Treat 17:498–500
19. LiVolsi VA, Mazzaferri EL, Schneider AB et al (2004) Papillary carcinoma. In: Delellis RA, Lloyd RV, Heitz PU, Eng C (eds) World Health Organization classification of tumors, pathology and genetics of tumors of endocrine organs. International Agency for Research on Cancer, Lyon, pp 57–66
20. Sobin LH, Wittekind C (2002) UICC: TNM classification of malignant tumours. Wiley, New York, pp 52–56
21. Kirkegaard T, Edwards J, Tovey S, McGlynn LM, Krishna SN, Mukherjee R, Tam L, Munro AF, Dunne B, Bartlett JM (2006) Observer variation in immunohistochemical analysis of protein expression, time for a change? Histopathology 48:787–794
22. Habets GG, van der Kammen RA, Stam JC, Michiels F, Collard JG (1995) Sequence of the human invasion-inducing *Tiam1* gene, its conservation in evolution and its expression in tumor cell lines of different tissue origin. Oncogene 10:1371–1376
23. van Leeuwen FN, van der Kammen RA, Habets GG, Collard JG (1995) Oncogenic activity of Tiam1 and Rac1 in NIH3T3 cells. Oncogene 11:2215–2221
24. Engers R, Zwaka TP, Gohr L, Weber A, Gerharz CD, Gabbert HE (2000) Tiam1 mutations in human renal-cell carcinomas. Int J Cancer 88:369–376
25. Malliri A, van der Kammen RA, Clark K, van der Valk M, Michiels F, Collard JG (2002) Mice deficient in the Rac activator Tiam1 are resistant to Ras-induced skin tumours. Nature 417:867–871
26. Minard ME, Kim LS, Price JE, Gallick GE (2004) The role of the guanine nucleotide exchange factor Tiam1 in cellular migration, invasion, adhesion and tumor progression. Breast Cancer Res Treat 84:21–32
27. Hordijk PL, ten Klooster JP, van der Kammen RA, Michiels F, Oomen LC, Collard JG (1997) Inhibition of invasion of epithelial cells by Tiam1-Rac signaling. Science 278:1464–1466
28. Malliri A, van Es S, Huveneers S, Collard JG (2004) The Rac exchange factor Tiam1 is required for the establishment and maintenance of cadherin-based adhesions. J Biol Chem 279:30092–30098
29. Sander EE, ten Klooster JP, van Delft S, van der Kammen RA, Collard JG (1999) Rac downregulates Rho activity: reciprocal balance between both GTPases determines cellular morphology and migratory behaviour. J Cell Biol 147:1009–1021

Virchows Arch (2011) 459:595–605
DOI 10.1007/s00428-011-1161-3

ORIGINAL ARTICLE

Intratumoural lymph vessel density is related to presence of lymph node metastases and separates encapsulated from infiltrative papillary thyroid carcinoma

C. Eloy · J. Santos · P. Soares · M. Sobrinho-Simões

Received: 13 September 2011 / Revised: 18 October 2011 / Accepted: 19 October 2011 / Published online: 12 November 2011
© Springer-Verlag 2011

Abstract Papillary thyroid carcinoma (PTC) gives frequently rise to nodal metastases via lymphatic vessels while follicular thyroid carcinoma (FTC) metastasises mainly via blood vessels to lung and bones. The follicular variant of PTC (FVPTC) encompasses the infiltrative subtype (I-FVPTC), which shares most of the features of classic PTC (CPTC), and the encapsulated subtype (E-FVPTC), which appears to be related to minimally invasive FTC. In an attempt to contribute to the understanding of the aforementioned differences, we evaluated intratumoural and peritumoural lymph vessels density (LVD), using the immunomarker D2-40 in a series of E-FVPTC, I-FVPTC, and CPTC with known *BRAF* and *RAS status*. None of the E-FVPTC cases presented extra-thyroid extension, lymph vessel invasion or nodal metastases, at variance with I-FVPTC and CPTC cases. The *BRAF* V600E mutation was detected in 8.3% of E-FVPTC, 25.0% of I-FVPTC and in 40.7% of CPTC, while *N-RAS* Q61R mutation was detected only in 10.3% of FVPTC cases. Only one case of E-FVPTC (8.3%) had intratumoural D2-40-stained vessels in contrast to their presence in 76.5% of the cases of I-FVPTC. Intratumoural LVD determined by D2-40 expression correlated with the occurrence of extra-thyroid extension, lymph vessel invasion and lymph node metastases in PTC cases. At variance with intratumoural LVD, peritumoural LVD was not associated with any clinic-pathological or molecular feature, being similar in E-FVPTC, I-FVPTC and CPTC. Our study highlights the role of intratumoural lymph vessels in PTC nodal metastisation and reinforces the importance of distinguishing E-FVPTC from I-FVPTC regarding invasiveness, metastatic pattern and molecular profile.

Keywords Papillary thyroid carcinoma · Lymphangiogenesis · D2-40 · Prognosis, lymph node metastasis

C. Eloy · M. Sobrinho-Simões
Pathology Department, Hospital de São João, Porto, Portugal

C. Eloy · P. Soares · M. Sobrinho-Simões
Pathology Department, Medical Faculty of the University of Porto, Porto, Portugal

C. Eloy · J. Santos · P. Soares · M. Sobrinho-Simões
Institute of Molecular Pathology and Immunology of the University of Porto (IPATIMUP), Porto, Portugal

C. Eloy
Dentistry Faculty of the University of Porto, Porto, Portugal

C. Eloy (✉)
Anatomic Pathology, Hospital de São João, Alameda Professor Hernani Monteiro, 4200-451 Porto, Portugal
e-mail: catarinaeloy@hotmail.com

Introduction

One of the reasons that justify the attempts to distinguish papillary thyroid carcinoma (PTC) from follicular thyroid carcinoma (FTC) relies on the different preferential routes of metastatic spread associated with these two thyroid cancer histotypes [1]. While PTC has a tendency to give rise to lymph node metastases via lymphatic vessels, FTC metastasises mainly via blood vessels to lung and bones [1–3].

Although traditionally included in the PTC group [1], the follicular variant of PTC (FVPTC) encompasses a subtype of encapsulated tumours, which tend to share

features with both classic PTC (CPTC) and FTC [4–7]. Besides the rare and aggressive multinodular subtype of FVPTC [8], cases of FVPTC may be classified according to their peripheral growth pattern in two categories: infiltrative (or poorly circumscribed) subtype (I-FVPTC) and encapsulated subtype (E-FVPTC) [4, 9]. The I-FVPTCs share most of the morphological features of CPTC, give frequently rise to lymph node metastases and disclose *BRAF* V600E mutation in 26% of the cases [4, 10], whereas the E-FVPTCs seem morphologically related to minimally invasive FTC, often disclose *RAS* mutations and *PAX8/PPARgama* rearrangements [10–12] and follow an extremely benign course in the absence of unequivocal signs of capsular or vascular invasion [13, 14]. In the presence of vascular invasion, the E-FVPTCs tend to give rise, like FTC, to blood-borne metastases [4, 9, 15].

The peculiar metastatic properties of the FVPTC subtypes are not fully understood and may be related to angiogenesis. Several groups have reported an increased expression of factors promoting the formation of new blood vessels (hemangiogenesis) in PTC in comparison with normal thyroid tissue [16, 17]; such factors are variably correlated with tumour size [17, 18], increased microvessel count using CD31 [19], increased risk of recurrence and decreased disease-free survival [18, 20].

The expression of lymphangiogenic factors (VEGF-C and VEGF-D) appears to be increased in PTC in comparison with normal thyroid tissue [16, 17, 21, 22], benign lesions [16, 17, 21, 22] and FTC [23]. The increased expression of lymphangiogenic factors in PTC is related with increased intratumoural and peritumoural lymph vessel density (LVD) [21, 22, 24]. The association between the expression of lymphangiogenic factors in PTC and the occurrence of lymph node metastases was observed by some groups [17, 22, 24–26], whereas others did not detect such association [16, 21].

In the past, the endothelial markers used to identify vessels, like factor VIII, CD31, CD34 and von Willebrand factor, highlighted both lymphatic and blood vessels [18, 19, 27–30]. The situation has changed with the finding of lymphatic vessel specific immunomarkers [31, 32], which have been used to determine the intratumoural and the peritumoural LVD in several thyroid tumour types, such as the lymphatic endothelium-specific markers D2-40 (podoplanin) [3, 21, 33, 34], LYVE-1 (lymph vessel endothelial hyaluronan receptor) [16, 33, 35] and VEGFR-3/flt-4 (VEGF receptor-3) [22, 24, 25].

The intratumoural LVD has been found to be higher in PTC than in follicular adenoma (FA) [16, 21] and higher in FVPTC than in FA or FTC [34]. Some authors reported an association amongst increased PTC intratumoural LVD and male gender [35], multifocal disease [35], invasiveness [25] and occurrence of lymph node metastases [22, 24, 25, 35], in contrast to other groups that did not find any association between PTC intratumoural LVD and the above mentioned features [16, 21].

The peritumoural LVD was similar in PTC, FTC and FA in the series of Giorgadze et al. [34], while in the series of Garcia et al. [21], FTC cases disclosed higher peritumoural LVD than PTC. There are conflicting results regarding the association between PTC peritumoural LVD and the occurrence of lymph node metastases [21, 24].

Amongst the molecular alterations associated with PTC, *BRAF* V600E mutation has been variably associated with the occurrence of vascular invasion [36, 37] and lymph node metastases [37–40], while *RAS* mutations have been related to the occurrence of vascular invasion [12] and scarcity of lymph node metastases [12].

The aim of the present study was to evaluate the intratumoural and peritumoural LVD using the immunomarker D2-40 in a series of thoroughly analysed 29 cases, encompassing 12 cases of E-FVPTC and 17 cases of I-FVPTC, and to compare the data thus obtained with those of a similarly analysed series of 32 cases of CPTC.

As ultimate goals we intended to find if there were, firstly, any relationship between the levels of intratumoural and peritumoural LVD and the three histo(sub)types of PTC, and, secondly, any relationship between the aforementioned factors (LVD and histo(sub)types) and the clinico-pathological and molecular features of the cases with a special emphasis on their nodal metastatic *status*.

Materials and methods

Tumour samples

A series of 61 PTC cases were retrieved from the Cancer Registry of the Pathology Department of Hospital São João: 29 FVPTC and 32 CPTC. Both FVPTC and CPTC groups included cases with lymph node metastases and cases without metastases and, at least, 10 years of follow-up. None of the patients died from the disease. Small tumours with 1 cm or less in diameter that were classified according to their growth pattern as FVPTC or CPTC were included in FVPTC and CPTC groups, respectively.

All samples had been fixed in formalin and embedded in paraffin. Clinical data were collected from the reports and clinical files; haematoxylin and eosin slides were retrieved from the archives and reviewed independently by two pathologists (CE and MSS), and the tumours were classified using the WHO criteria [1]. FVPTC cases were classified as E-FVPTC whenever the tumour was totally surrounded by a capsule with or without signs of focal invasion and as I-FVPTC whenever the tumours displayed an infiltrative (poorly circumscribed) growth pattern. All

CPTC cases were either totally or partially poorly circumscribed, i.e. disclosed at least one area of infiltrative growth pattern. Vascular invasion was considered to be present whenever at least one image of unequivocal venous vessel invasion was observed within the capsule or outside the tumour mass. Lymph vessel invasion was considered to be present whenever at least one image of unequivocal invasion of lymph vessel was observed regardless of being or not stained by D2-40.

Mutation screening

Genomic DNA was extracted from 10-μm sections of 55 tumours: 28 FVPTC and 27 CPTC (the remaining six cases had insufficient available material).The detection of *BRAF* (exon 15) and *N-RAS* (exon 2) gene mutations was performed as previously described [37]. Sequences of *BRAF* and *N-RAS* genes were amplified using the primer pairs previously reported [34]. PCR products were submitted to electrophoresis in agarose gel and purified by enzymatic treatment. Purified samples were sequenced on both strand, and mutated samples were re-extracted, amplified and sequenced to confirm the result.

Immunohistochemistry

Immunohistochemical staining was performed using streptavidin–biotin technique. Sections of 2-μm thickness were cut from paraffin blocks and placed on coated slides. The slides were dried, deparaffinised in Clear Rite (Richard-Allan, Thermo Scientific) and hydrated in sequential gradients of ethanol. For antigen retrieval, sections were immersed in 10 mM sodium citrate buffer, pH 6.0 and then heated for 15 min. Endogenous peroxidase was blocked with 3% hydrogen peroxidase in methanol (Panreac) for 10 min in humid chamber, and then avidin blocking and biotin blocking were performed (Lab Vision, Thermo Scientific). In order to block unspecific bounding to hydrophobic epitopes, the sections were immersed in Ultra V Block (Lab Vision, Thermo Scientific) for 10 min at room temperature. Slides were incubated overnight at 4°C with D2-40 monoclonal antibody (D2-40, Signet laboratories, Dedham, MA, USA) in a 1:25 dilution.

Then, slides were incubated with biotinylated secondary goat antibody and streptavidin–peroxidase complex (Lab Vision, Thermo Scientific) for 10 min at room temperature. The sections were developed with DAB solution (DAKO Corporation) according to the manufacturer's instructions and counterstained with haematoxylin (J.T.Baker, Deventer, Holland). Adequate positive and negative controls in tissue microarrays were used.

Assessment of lymph vessel density

D2-40 expression was considered positive whenever cytoplasmatic staining of endothelial cell of lymphatic vessels was observed. The evaluation of expression was performed by counting positive D2-40 structures with morphological features of lymphatic vessels, clearly separated from adjacent vessels and from other soft tissue components, as previously described [41]. Packed vessels were assumed as constituting a single lymphatic unit. Analysis was performed at ×200 magnification in the areas of highest vascularity (hot spots). The LVD of each case corresponds to the average obtained in counting 10 hot spot fields. The evaluation of D2-40 expression and lymph vessel counting was performed blindly in intratumoural and peritumoural areas of all FVPTC and CPTC cases except in three FVPTC cases in which the remaining non neoplastic thyroid tissue was insufficiently represented. The intratumoural lymph vessels were defined as vessels within the tumour area, whereas peritumoural lymph vessels included vessels in both the capsule and in the remaining non tumoural thyroid tissue.

Statistical analysis

The results are expressed as absolute values, percentages and/or mean ± standard deviation. The χ^2 test with Yates correction and the Students' t test (unpaired) were used in the statistic analysis. Two values were considered significantly different whenever $p<0.05$ and suggestively different when $p<0.10$.

Results

The clinico-pathological and molecular features and the LVD data on the 29 cases of FVPTC separated into E-FVPTC ($n=12$) and I-FVPTC ($n=17$) are summarised in Table 1. The respective data on the 32 cases of CPTC are summarised in Table 2.

Clinico-pathological and molecular features

The comparison of the clinico-pathological and molecular features of the PTC groups is summarised in Table 3.

FVPTC and CPTC groups differ regarding extra-thyroid extension ($p=0.045$) and lymph node metastases ($p=0.038$), which were more prevalent in CPTC. FVPTC cases tended to have more often vascular invasion ($p=0.075$), and less often lymph vessel invasion ($p=0.094$) and *BRAF* V600E mutation ($p=0.080$) than CPTC cases (Table 3).

E-FVPTC cases presented significantly less often vascular invasion ($p=0.029$) and lymph node metastases ($p=0.009$) than I-FVPTC cases (Table 3). None of the E-FVPTC cases presented extra-thyroid extension, lymph vessel invasion or lymph node metastases while in cases with infiltrative growth pattern (I-FVPTC *plus* CPTC), occurrence of extra-thyroid extension was observed in 32.7% of the cases, lymph vessel invasion was also

Table 1 Clinical, morphological and molecular features of the 29 cases of FVPTC (12 cases of E-FVPTC and 17 cases of I-FVPTC) and respective intratumoural and peritumoural LVD

Case	Gender	Age (years)	Tumour size (cm)	M	EE	LI	VI	LNM	*RAS*	*BRAF*	I-LVD	P-LVD
E-FVPTC												
1	F	32	2.0	−	−	−	+	−	−	−	0.0	8.1
2[a]	F	51	1.4	−	−	−	−	−	−	−	0.0	15.4
3	F	39	1.0	+	−	−	−	−	Q61R	−	0.6	11.5
4[a]	F	48	0.6	−	−	−	−	−	−	−	0.0	14.1
5	F	30	0.5	−	−	−	−	−	−	−	0.0	14.2
6	F	28	2.8	+	−	−	+	−	−	−	0.0	6.8
7[a]	F	34	3.5	−	−	−	−	−	−	−	0.0	9.8
8	M	61	4.0	−	−	−	+	−	−	V600E	0.0	12.7
19	M	35	3.5	−	−	−	+	−	Q61R	−	0.0	18.0
10	F	50	2.5	−	−	−	−	−	−	−	0.0	10.3
11	F	52	2.5	+	−	−	−	−	−	−	0.0	14.2
12	F	66	2.5	+	−	−	−	−	−	−	0.0	18.2
I-FVPTC												
13	F	26	1.8	+	−	−	+	−	−	V600E	0.0	11.5
14	F	36	0.5	−	−	−	−	−	−	V600E	0.5	10.1
15	F	21	0.6	−	−	−	−	−	−	−	4.8	9.7
16	F	37	0.3	−	−	−	+	−	−	−	0.0	8.6
17	F	47	3.0	−	−	−	−	−	Q61R	−	0.0	9.8
18	F	32	4.7	+	−	−	+	−	−	−	1.0	21.0
19	F	58	1.5	+	−	+	+	−	−	V600E	0.3	9.8
20	F	54	1.8	+	−	+	+	−	−	−	0.2	10.0
21	M	45	4.0	−	−	−	−	−	−	−	0.1	9.4
22	M	57	9.5	−	+	+	+	+	−	−	4.4	14.0
23	F	56	0.8	+	−	+	+	+	−	−	1.3	1.5
24	M	21	2.5	−	+	−	+	+	−	−	2.0	ND
25	F	20	1.0	+	−	−	+	+	ND	ND	6.0	21.0
26	F	49	2.2	−	−	−	+	+	−	−	3.9	15.0
27	F	43	4.0	+	+	−	+	+	−	−	0.1	ND
28	F	43	1.5	+	+	−	+	+	−	V600E	4.3	ND
29[b]	M	63	1.8	−	−	−	+	+	−	−	0.0	10.8

M male, *F* female, + presence, − absence, *M* multicentricity, *EE* extra-thyroid extension, *LI* lymph vessel invasion, *VI* vascular invasion, *LNM* lymph node metastases, *I* intratumoural, *P* peritumoural, *ND* not determined

[a] Cases without capsular invasion, [b] case with concomitant distant metastases

[b] Case with concomitant distant metastases

observed in 32.7% of the cases, and lymph node metastases were detected in 75.0% of the cases (p=0.026, p=0.014 and p=0.0006, respectively; Tables 1, 2 and 3).

The only clinico-pathological or molecular feature significantly associated with the occurrence of lymph node metastases was the presence of extra-thyroid extension (p= 0.0004; Tables 1 and 2). In cases without extra-thyroid extension, the occurrence of lymph vessel invasion was related to lymph node metastases (p=0.022).

The *BRAF* V600E mutation was detected in one case of E-FVPTC (8.3%), four cases of I-FVPTC (25.0%) and in 11 cases of CPTC (40.7%; Tables 1 and 2).

The *N-RAS* Q61R mutation was detected only in FVPTC cases (10.3%), encompassing two cases of E-FVPTC and one case of I-FVPTC (Tables 1 and 2).

D2-40 expression in intratumoural and peritumoural lymph vessels

The D2-40 expression in the endothelial cells in intratumoural location highlighted small thin-walled lymph vessels with tiny lumina located in the dependence of fibrous septa arising from the tumour capsule (Fig. 1a) or amongst tumour cells (Fig. 1b). The D2-40 positive lymph

Table 2 Clinical, morphological and molecular features of the 32 cases of CPTC and respective intratumoural and peritumoural LVD

Case	Gender	Age (years)	Tumour size (cm)	M	EE	LI	VI	LNM	*RAS*	*BRAF*	I-LVD	P-LVD
1	M	58	0.8	−	−	−	−	−	ND	ND	0.0	7.0
2	F	31	3.5	+	−	−	−	−	−	−	0.2	9.8
3	F	35	0.3	−	−	+	−	−	ND	ND	0.3	8.1
4	F	40	1.5	−	−	−	−	−	−	V600E	0.4	8.7
5	M	25	1.2	−	−	−	+	−	−	−	2.0	10.9
6	F	30	0.6	+	−	−	−	−	−	V600E	0.0	7.9
7	F	23	2.5	−	−	+	−	−	−	−	0.9	15.8
8	M	65	2.3	−	−	−	−	−	−	−	0.0	16.5
9	F	21	2.0	−	−	+	+	−	−	V600E	0.0	14.1
10	F	79	2.8	−	+	−	−	−	−	−	0.0	16.0
11	F	65	3.5	−	+	+	−	−	−	V600E	0.0	8.3
12	F	28	2.5	−	−	−	+	−	−	−	0.0	12.0
13	F	28	2.0	−	−	−	+	−	−	V600E	0.0	14.1
14	F	47	4.5	−	+	+	+	−	−	V600E	5.1	9.3
15	F	28	0.9	−	−	−	−	+	−	V600E	0.2	13.0
16	F	21	1.2	−	−	+	−	+	−	−	0.1	19.3
17	F	22	1.9	+	−	+	−	+	−	−	0.7	18.0
18	F	30	1.3	−	+	−	+	+	−	−	0.5	14.7
29	F	56	0.7	+	−	+	−	+	−	−	1.0	10.3
20	F	18	1.5	+	+	−	+	+	−	−	0.0	12.0
21	F	22	0.8	−	−	−	−	+	ND	ND	0.2	12.5
22	F	56	0.8	+	−	+	−	+	ND	ND	0.7	13.4
23	M	42	1.6	+	+	−	−	+	−	−	2.2	3.7
24	F	38	3.0	+	−	−	+	+	−	V600E	0.0	14.3
25	F	35	1.7	−	−	−	+	+	−	V600E	1.4	11.7
26[a]	M	11	6.0	+	+	+	+	+	−	−	0.4	14.3
27[a]	F	56	2.4	−	+	−	−	+	−	−	1.5	11.5
28	F	83	7.5	−	+	−	−	+	−	V600E	1.0	11.3
29	F	18	3.6	+	−	+	+	+	−	−	3.1	13.3
30	M	14	2.5	+	+	+	−	+	−	−	2.0	14.0
31	F	32	1.1	−	+	−	−	+	−	V600E	0.4	7.3
32	F	56	7.5	+	+	−	−	+	ND	ND	0.6	20.0

M male, *F* female, + presence, − absence, *M* multicentricity, *EE* extra-thyroid extension, *LI* lymph vessel invasion, *VI* vascular invasion, *LNM* lymph node metastases, *I* intratumoural, *P* peritumoural, *ND* not determined

[a] Case with concomitant distant metastases

vessels were found less often at the centre of the tumours than in the periphery, particularly at the invasive front of the infiltrative tumours.

In both FVPTC subgroups and in the CPTC group, there was, besides the subset of lymph vessels with D2-40 expression, a majority of small thin-walled, nearly collapsed, D2-40 negative capillary vessels of uncertain origin, and ectatic lymph vessels in the remaining thyroid tissue. Such D2-40 negative capillary vessels were morphologically indistinguishable from vessels with D2-40 expression (Fig. 1c, d).

D2-40 expression in the peritumoural thyroid tissue highlighted thin-walled ectatic lymph vessels (Fig. 1e) in all cases. Peritumoural lymph vessels with D2-40 expression showed, in some cases displaying infiltrative growth, neoplastic thrombi within their lumina (Fig. 1f). Neoplastic thrombi were not observed within the intratumoural thin-walled vessels without D2-40 expression.

All the blood vessels with an organised wall surrounded by a smooth muscle layer, in which the presence of vascular invasion was searched, did not disclose D2-40 expression in the endothelial cells (Fig. 1g). Neoplastic thrombi were also detected in peritumoural thick-walled vessels (Fig. 1h).

Complex networks of lymph vessels expressing D2-40 were detected in the peritumoural tissue in association with

Table 3 Clinical, morphological and molecular features of PTC cases

Features	E-FVPTC n(%)	I-FVPTC n(%)	CPTC n(%)	FVPTC vs CPTC *(p)*	E-FVPTC vs I-FVPTC *(p)*	E-FVPTC vs I-FVPTC+CPTC *(p)*
Gender				>0.999	>0.999	>0.999
Female	10 (83.3)	13 (76.5)	26 (81.3)			
Male	2 (16.7)	4 (23.5)	6 (18.7)			
Age				0.302	0.716	0.342
>45 years	6 (50.0)	7(41.2)	10 (31.3)			
≤45 years	6 (50.0)	10 (58.8)	22 (68.7)			
Tumour size				0.767	>0.999	>0.999
>1.0 cm	9 (75.0)	12 (70.6)	25 (78.1)			
≤1.0 cm	12 (25.0)	5 (29.4)	7 (21.9)			
M	4 (33.3)	8 (47.1)	12 (37.5)	0.798	0.703	0.749
EE	0 (0.0)	4 (23.5)	12 (37.5)	0.045	0.121	0.026
LI	0 (0.0)	4 (23.5)	12 (37.5)	0.094	0.059	0.014
VI	4 (33.3)	13 (76.5)	11 (34.4)	0.075	0.029	0.520
LNM	0 (0.0)	8 (47.1)	18 (56.3)	0.038	0.009	0.0006
RAS Q61R	2 (16.7)	1 (6.3)	0 (0.0)	0.236	0.355	0.117
BRAF V600E	1 (8.3)	4 (25.0)	11 (40.7)	0.080	0.560	0.147

M multicentricity, *EE* extra-thyroid extension, *LI* lymph vessel invasion, *VI* vascular invasion, *LNM* lymph node metastases

lymphoid aggregates and in perithyroidal lymph nodes with and without metastases (Fig. 1i, j).

Intratumoural LVD

In 11 out of 12 cases of E-FVPTC (91.7%), not a single intratumoural D2-40 stained vessel was observed (Table 1). Case 3 of the E-FVPTC subgroup was the only one with D2-40-positive intratumoural lymph vessels and was a *N-RAS* mutated tumour that did not show signs of extra-thyroid extension, lymph vessel invasion or vascular invasion, nor had given rise to lymph node metastases (Table 1). At variance with E-FVPTC, the majority of I-FVPTC cases (76.5%) had intratumoural D2-40 positive lymph vessels.

The mean intratumoural LVD was significantly higher in I-FVPTC (1.7±2.1) and in CPTC (0.8±1.1) than in E-FVPTC (0.05; $p=0.020$ and $p=0.030$, respectively; Fig. 2a). It was also higher in I-FVPTC than in CPTC ($p=0.049$; Fig. 2a).

The mean intratumoural LVD was significantly higher in tumours with extra-thyroid extension ($p=0.041$), lymph vessel invasion ($p=0.026$) and lymph node metastases ($p=0.008$; Table 4). In FVPTC cases, the mean intratumoural LVD was significantly higher in I-FVPTC cases with lymph node metastases ($p=0.047$) and significantly lower in E-FVPTC cases with wild-type *N-RAS* ($p=0.016$; Table 4).

Peritumoural LVD

The mean peritumoural LVD was similar in FVPTC (E-FVPTC, 12.8±3.6; I-FVPTC, 11.6±5.0, $p=0.501$) and in CPTC (12.3±3.7; $p=0.888$; Fig. 2b). In all PTC groups, the mean peritumoural LVD was significantly higher than the mean intratumoural LVD ($p<0.0001$), and it was not significantly associated with any clinico-pathological or molecular feature, namely lymph vessel invasion ($p=0.626$) or lymph node metastases ($p=0.288$).

Figure 3 highlights the most impressive differences observed between E-FVPTC and I-FVPTC+CPTC.

Discussion and conclusions

The results we have obtained show the different meaning of peritumoural and intratumoural lymph vessels. The abundance of D2-40 positive peritumoural lymph vessels was similar in the three groups of PTC (E-FVPTC, I-FVPTC and CPTC) as it had been previously reported by Giorgadze et al. [34] in their series of follicular patterned lesions. Peritumoural LVD was not related to any clinico-pathological feature, namely the occurrence of lymph vessel invasion or lymph node metastasis, thus supporting the results of Garcia et al. [21]. The mean peritumoural LVD determined by D2-40 expression was higher than intratumoural LVD as previously reported [21] and was similar in all groups of PTC cases, thus implying that such feature does not appear to be modulated by the tumour histotype.

In contrast to the abovementioned peritumoural findings, the search for intratumoural lymph vessels disclosed a clear cut difference between E-FVPTC and I-FVPTC and CPTC. D2-40 positive lymph vessels were not detected within 11 out of 12 tumours of the E-FVPTC group, a result that fits

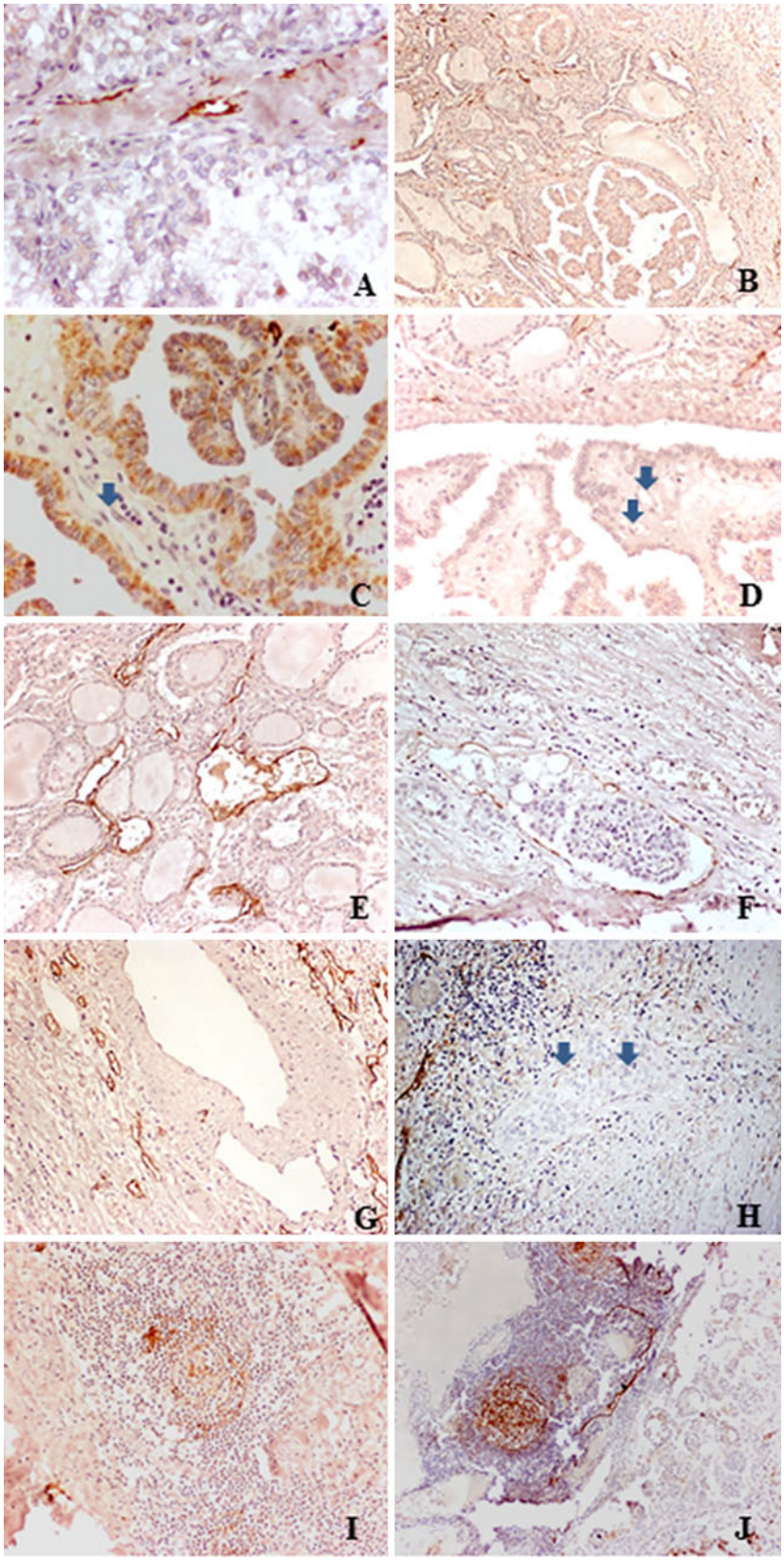

Fig. 1 D2-40 expression in the endothelial cells. **a** D2-40-positive intratumoural lymph vessels in a fibrous septum (case 14 CPTC, ×400); **b** D2-40-positive intratumoural lymph vessels between tumour cells at the invasive front (case 29 CPTC, ×100); **c** intratumoural lymph vessels D2-40 expression and thin walled vessels without D2-40 expression(*arrow*) (case 29 CPTC, ×400); **d** intratumoural thin walled vessels without D2-40 expression (*arrows*) in this area (case 29 CPTC, 200x); **e** D2-40-positive peritumoural lymph vessels (case 10 FVPTC, ×100); **f** D2-40-positive intratumoural lymph vessel with neoplastic thrombus in the lumen (case 22 FVPTC, ×200); **g** peritumoural medium sized vein without D2-40 expression surrounded by D2-40-positive small lymph vessels (case 7 FVPTC, ×200); **h** D2-40-negative peritumoural vein with neoplastic thrombus in the lumen (case 20 FVPTC, ×200); **i** complex network of D2-40-positive lymph vessels in the peritumoural tissue associated with a lymphoid aggregate (case 10 FVPTC, ×100) and **j** complex network of D2-40-positive lymph vessels in a perithyroidal lymph node with PTC metastases (case 27 CPTC, ×100)

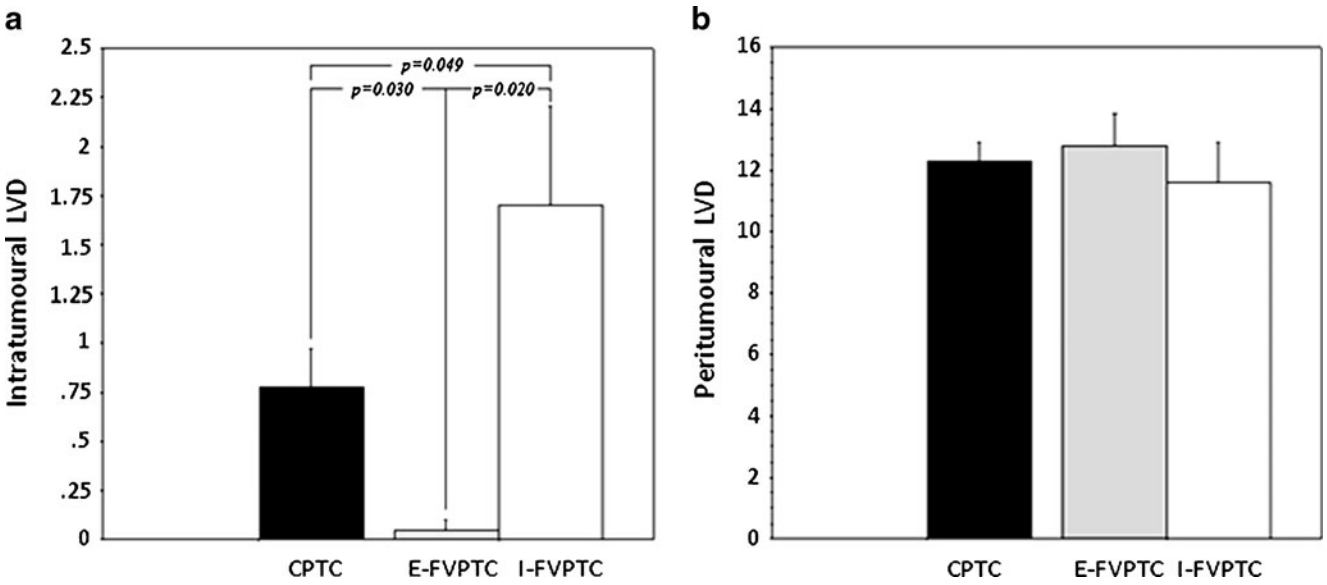

Fig. 2 Comparison between the LVD in the FVPTC group (E-FVPTC and I-FVPTC) and in the CPTC group. **a** Graphic representing the mean intratumoural LVD in the three PTC groups; **b** Graphic representing the mean peritumoural LVD in the three PTC groups

with the absence of lymph vessel invasion and lymph node metastases in E-FVPTC. A very low frequency of identifiable intratumoural lymph vessels had been reported by other groups in FA [16, 21, 34] and FTC [16, 34].

Table 4 Relationship between the intratumoural LVD and the morphological and molecular features of FVPTC (E-FVPTC and I-FVPTC) and CPTC cases

Features	E-FVPTC		I-FVPTC		CPTC		I-FVPTC+CPTC		PTC	
	Mean±SD	*p* value	Mean±SD	*p* value	Mean±SD	*p* value	Mean±SD	*p* value	Mean±SD	*p* value
M		0.170		0.930		0.616		0.696		0.560
Present	0.2±0.3		1.7±2.3		0.9±1.0		1.2±1.6		1.0±1.5	
Absent	0.0±0.0		1.7±2.1		0.7±1.2		1.0±1.6		0.8±1.4	
EE		–		0.289		0.156		0.181		0.041
Present	–		2.7±2.1		1.1±1.5		1.5±1.7		1.5±1.7	
Absent	0.1±0.2		1.4±2.1		0.6±0.8		0.9±1.5		0.7±1.3	
LI		–		0.363		0.104		0.135		0.026
Present	–		2.4±2.6		1.2±1.5		1.6±1.9		1.6±1.9	
Absent	0.1±0.2		1.4±1.9		0.5±0.7		0.6±1.3		0.6±1.2	
VI		0.506		0.715		0.192		0.078		0.052
Present	0.0±0.0		1.8±2.1		1.1±1.7		1.5±1.9		1.3±1.8	
Absent	0.1±0.2		1.4±2.3		0.6±0.7		0.7±1.0		0.6±1.0	
LNM		–		0.047		0.532		0.084		0.008
Present	–		2.8±2.2		0.9±0.9		1.5±1.6		1.5±1.6	
Absent	0.1±0.2		0.8±1.5		0.6±1.4		0.7±1.4		0.5±1.2	
RAS		0.016		0.439		–		0.468		0.404
Q61R	0.3±0.4		0.0±0.0		–		0.0		0.2±0.3	
Wild type	0.0±0.0		1.5±1.9		0.9±1.2		1.1±1.5		0.9±1.4	
BRAF		0.779		0.852		0.771		0.600		0.993
V600E	0.0		0.0		0.8±1.5		0.9±1.6		0.9±1.6	
Wild-type	0.1±0.2		1.5±1.9		0.9±1.0		1.2±1.5		0.9±1.0	

M multicentricity, *EE* extra-thyroid extension, *LI* lymph vessel invasion, *VI* vascular invasion, *LNM* lymph node metastases

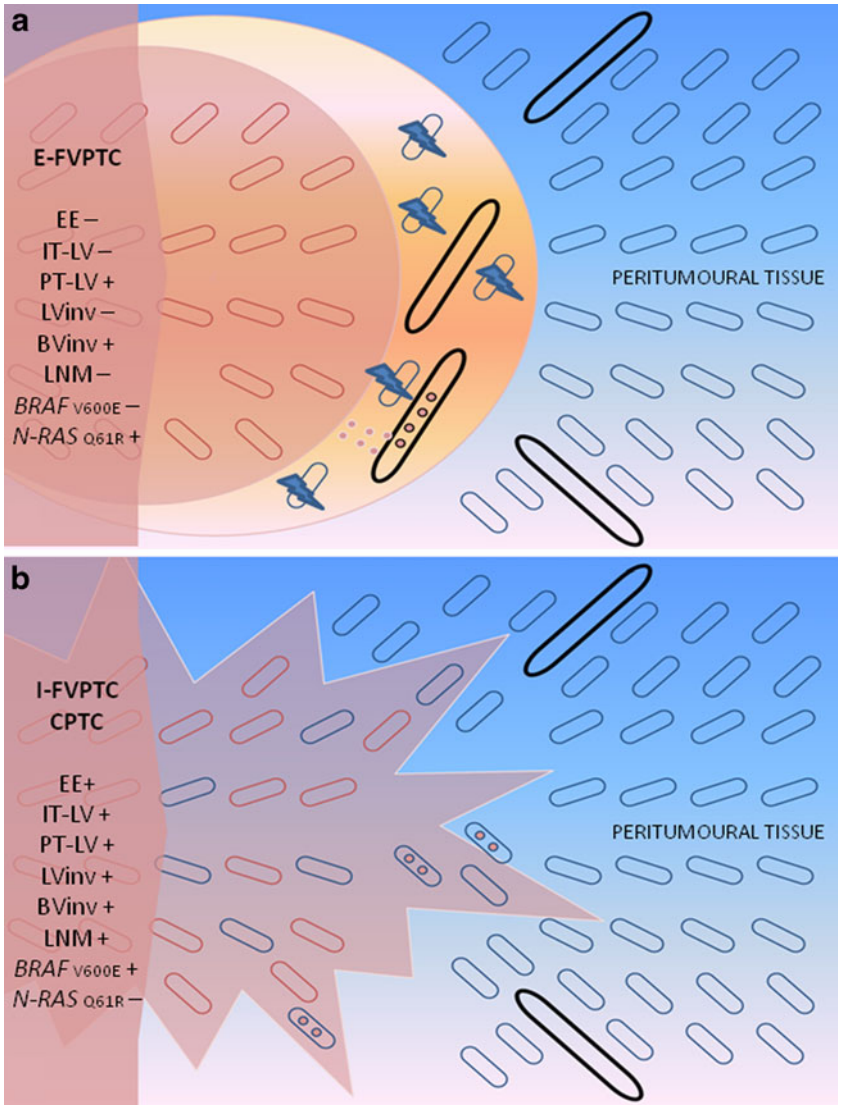

Fig. 3 Summary of the most impressive findings concerning the distinction between E-FVPTC (**a**) and I-FVPTC+CPTC (**b**) (*red vessels* D2-40-negative intratumoural thin-walled vessels; *blue vessels* D2-40 positive intratumoural and peritumoural lymph vessels; *black vessels* thick-walled veins; *blue thunder over blue vessel* collapsed D2-40-positive lymph vessel; *pink spots* neoplastic thrombi; *EE* extra-thyroid extension; *IT-LV* D2-40-positive intratumoural lymph vessels; *PT-LV* peritumoural lymph vessels; *LVinv* lymph vessel invasion; *BVinv* blood vessel invasion, *LNM* lymph node metastasis)

Together with the differences on the molecular features, i.e. the scarcity of *BRAF* V600E mutation [10] and prominence of *RAS* mutations [10], also confirmed in the present study, the rarity of extra-thyroid extension, intratumoural lymph vessels, lymph vessel invasion and lymph node metastases in E-FVPTC contributes to separate E-FVPTC from I-FVPTC and to approach the former to minimally invasive FTC [4, 9, 15]. It remains to be clarified whether the absence of intratumoural D2-40 positive lymph vessels in most E-FVPTCs, as well as in other follicular patterned tumours, reflects a low capacity of incorporation (with or without proliferation) of lymphatic vessels since the first steps of tumourigenesis, or their disappearance by collapsing mechanism (or by other mechanism) secondary to the increased intratumoural pressure, during the neoplastic development of encapsulated tumours [31].

The results we have obtained contribute also to show that I-FVPTC cases share most of the features of CPTC cases [4, 9]. In our series, this is particularly obvious regarding the poorly circumscribed peripheral growth pattern occasionally accompanied by vascular invasion and extra-thyroid extension, occurrence of *BRAF* V600E mutation, abundance of intratumoural lymphatic vessels, frequent lymph vessel invasion and frequent occurrence of lymph node metastases.

The significant association we observed between intratumoural LVD and occurrence of lymph node metastases confirms the data reported by several groups [22, 24, 25, 35] and contradicts others [16, 21]. In our series, lymph vessel invasion appears to be the second strongest factor associated with the occurrence of lymph node metastases after extra-thyroid extension. The relation between high intratumoural LVD determined by D2-40 and lymph node metastases is indirectly confirmed by the absence of nodal metastasis in E-FVPTC cases that do not have intratumoural lymphatic vessels despite the abundance of peritumoural lymph vessels.

There is not enough evidence in the literature to link mutations of oncogenes such as *BRAF* and *N-RAS* with proliferation of blood and/or lymph vessels. In the present series, the occurrence of *BRAF* mutation was not significantly associated with intratumoural LVD. The *N-RAS* mutation was detected in the only case of the E-FVPTC group with intratumoural lymph vessels, but it does not seem appropriate to draw any conclusions on the putative relationship between *N-RAS* mutation and lymphangiogenesis from just a single case.

In our series, as in others [35], all lymph vessels disclosing neoplastic thrombi in their lumina expressed D2-40, suggesting that the intratumoural D2-40 negative vessels may constitute less efficient pathways for PTC dissemination. It remains to be clarified if the D2-40 expression in such cases induced by the presence of the neoplastic thrombi or if intratumoural D2-40 vessels, mainly located at the invasive front, as observed by Hall et al. [35], is the result of the invasion of peritumoural tissues with subsequent incorporation of the originally peritumoural D2-40 positive lymph vessels in the bulk of the tumour. The latter hypothesis is favoured by the association we found between extrathyroid extension and intratumoural high LVD. In this scenario, the absence of an invasive front, as well as the presence of a well constituted capsule, could prevent the recruitment of D2-40 positive peritumoural lymph vessels and their invasion, as suggested by the nearly absence of D2-40 positive intratumoural lymph vessels in E-FVPTC of our series.

The peritumoural small sized veins, including capsular veins that presented luminal neoplastic trombi, point to unequivocal vascular invasion. Vascular invasion was observed in 26 out of 61 cases of PTC, but such invaded veins did not express D2-40 in the endothelial cells, arguing against the hypothesis that the expression of D2-40 may be induced in endothelial cells by neoplastic thrombi. The neoplastic thrombi seen in the thick-walled vessels may result from invasion of small intratumoural vessels or from the direct invasion of such thick-walled blood vessels, which present a well-developed muscle layer probably able to resist the effect of the intratumoural pressure over the capsule [31, 42]. The increment in the intratumoural interstitial pressure is thought to be partially due to the functionally impaired lymphatic system in tumours, with respect to fluid and macromolecules [43]. In our series, the number of cases with distant metastases is too low (data not shown) to allow the clarification of the role played by D2-40 positive and negative vessels in the occurrence of blood borne metastasising.

These findings highlight the role played by intratumoural lymphangiogenesis in lymph node metastisation at variance with the controversial importance of intratumoural angiogenesis in the metastatic potential of FTC and PTC [16, 18, 28–30]. While in CPTC, the most important pathway of initial dissemination appears to be via intratumoural lymph vessels, in encapsulated follicular patterned tumours, the invasion via veins of the capsule or outside the tumour is necessary to predict blood-borne metastasis [3, 44].

Summing up, intratumoural LVD determined by D2-40 expression correlates with the occurrence of extra-thyroid extension, lymph vessel invasion and lymph node metastases in PTC. Intratumoural D2-40 stained vessels are rare in E-FVPTC. At variance with intratumoural LVD, the peritumoural LVD is not associated with any clinical, morphological or molecular feature and is similar in E-FVPTC, I-FVPTC and CPTC. Our study highlights the role of intratumoural lymph vessels in PTC nodal metastisation and reinforces the importance of distinguishing E-FVPTC from I-FVPTC regarding invasiveness, metastatic pattern and molecular profile.

Acknowledgments This work was partially supported by a grant from Prof. Edward Limbert SPEND/GENZYME–Year 2007. Part of the data reported in this study were obtained in the project "Identificação de factores prognósticos e de selecção terapêutica em carcinomas diferenciados da tireoide", which is supported by Fundação Calouste Gulbenkian. IPATIMUP is an Associate Laboratory of the Portuguese Ministry of Science, Technology and Higher Education, and is partly supported by the Fundação para a Ciência e Tecnologia.

Conflict of interest The authors declare no conflict of interest.

References

1. DeLellis RA, Lloyd RV, Heitz PU, Eng C (2004) World Health Organization classification of tumors of endocrine organs. IARC, Lyon
2. Rosai J, Carcangiu ML, DeLellis RA (1992) Tumors of the thyroid gland. AFIP 3rd series. Armed Forces Institute of Pathology, Washington
3. Lin X, Zhu B, Liu Y, Silverman JF (2010) Follicular thyroid carcinoma invades venous rather than lymphatic vessels. Diag Pathol 5:8
4. Castro P, Fonseca E, Magalhaes J, Sobrinho-Simoes M (2002) Follicular, papillary, and "hybrid" carcinomas of the thyroid. Endocr Pathol 13:313–320
5. Liu J, Singh B, Tallini G, Carlson DL, Katabi N, Shaha A, Tuttle RM, Ghossein RA (2006) Follicular variant of papillary thyroid carcinoma: a clinicopathologic study of a problematic entity. Cancer 107:1255–1264
6. Sobrinho-Simões M, Preto A, Rocha AS, Castro P, Máximo V, Fonseca E, Soares P (2005) Molecular pathology of well-differentiated thyroid carcinomas. Virchows Arch 447:787–793
7. Sobrinho-Simões M, Eloy C, Lobo C, Magalhães J, Amaro T (2011) Follicular thyroid carcinoma. Mod Pathol 24:S10–S18
8. Ivanova R, Soares P, Castro P, Sobrinho-Simões M (2002) Diffuse (or multinodular) follicular variant of papillary thyroid carcinoma: a clinicopathologic and immunohistochemical analysis of ten cases of an aggressive form of differentiated thyroid carcinoma. Virchows Arch 440:418–424
9. Sobrinho-Simões M, Eloy C, Vinagre J, Soares P (2010) Molecular pathology of thyroid tumors: diagnostic and prognostic relevance. Int J Surg Pathol 18:209S–212S

10. Rivera M, Ricarte-Filho J, Knauf J, Shaha A, Tuttle RM, Fagin JA, Ghossein RA (2010) Molecular genotyping of papillary thyroid carcinoma follicular variant according to its histologic subtypes (encapsulated vs infiltrative) reveals distinct BRAF and RAS mutation patterns. Mod Pathol 23:1191–1200
11. Castro P, Rebocho AP, Soares RJ, Magalhães J, Roque L, Trovisco V, Vieira de Castro I, Cardoso de Oliveira M, Fonseca E, Soares P, Sobrinho-Simões M (2006) PAX8-PPARg rearrangement is frequently detected in the follicular variant of papillary thyroid carcinoma. J Clin Endocrinol Metab 91:213–220
12. Zhu Z, Gandhi M, Nikiforova MN, Fischer AH, Nikiforov YE (2003) Molecular profile and clinical-pathologic features of the follicular variant of papillary thyroid carcinoma. An unusual high prevalence of RAS mutations. Am J Clin Pathol 120:71–77
13. Piana S, Frasoldati A, Di Felice E, Gardini G, Tallini G, Rosai J (2010) Encapsulated well-differentiated follicular-patterned thyroid carcinomas do not play a significant role in the fatality rates from thyroid carcinoma. Am J Surg Pathol 34:868–872
14. van Heerden JA, Hay ID, Goellner JR, Salomao D, Ebersold JR, Bergstralh EJ, Grant CS (1992) Follicular thyroid carcinoma with capsular invasion alone: a nonthreatening malignancy. Surgery 112:1130–1136
15. Baloch ZW, LiVolsi VA (2001) Encapsulated follicular variant of papillary thyroid carcinoma with bone metastases. Mod Pathol 13:861–865
16. De la Torre NA, Buley I, Wass JAH, Turner HE (2006) Angiogenesis and lymphangiogenesis in thyroid proliferative lesions: relationship to type and tumour behavior. Endocr Relat Cancer 13:931–944
17. Bunone G, Vigneri P, Mariani L, Butó S, Collini P, Pilotti S, Pierotti MA, Bongarzone I (1999) Expression of angiogenesis stimulators and inhibitors in human thyroid tumours and correlation with clinical pathological features. Am J Pathol 155:1967–1976
18. Akslen LA, LiVolsi VA (2000) Increased angiogenesis in papillary thyroid carcinoma but lack of prognostic importance. Hum Pathol 31:439–442
19. Tanaka K, Sonoo H, Kurebayashi J, Nomura T, Ohkubo S, Yamamoto Y, Yamamoto S (2002) Inhibition of infiltration and angiogenesis by trombospondin-1 in papillary thyroid carcinoma. Clin Cancer Res 8:1125–1131
20. Lennard CM, Patel A, Wilson J, Reinhardt B, Tuman C, Fenton C, Blair E, Francis GL, Tuttle RM (2001) Intensity of vascular endothelial growth factor expression is associated with increased risk of recurrence and decrease-free survival in papillary thyroid cancer. Surgery 129:552–558
21. Garcia EA, Simões K, Wakamatsu A, Ressio RA, Alves VAF, Longatto-Filho A, Camargo RS (2010) lymphatic vessel density and VEGF-C expression are significantly different among benign and malignant thyroid lesions. Endocr Pathol 21:101–107
22. Yu X-M, Lo C-Y, Chan W-F, Lam K-Y, Leung P, Luk JM (2005) Increased expression of vascular endothelial growth factor C in papillary thyroid carcinoma correlates with cervical lymph node metastases. Clin Cancer Res 11:8063–8069
23. Fellmer PT, Sato K, Tanaka R, Okamoto T, Kato Y, Kobayashi M, Shibuya M, Obara T (1999) Vascular endothelial growth factor-C gene expression in papillary thyroid carcinomas. Surgery 126:1056–1061
24. Yasuoka H, Nakamura Y, Zuo H, Tang W, Takamura Y, Miyauchi A, Nakamura M, Mori I, Kakudo K (2005) VEGF-D expression and lymph vessels play an important role for lymph node metastasis in papillary thyroid carcinoma. Mod Pathol 18:1127–1133
25. Liang QC, Wei QY, Fan SQ (2006) Expression of VEGF-C and angiogenesis, and lymphangiogenesis in papillary thyroid carcinoma. Zhong Nan Xue Xue Bao Yi Xue Ban 31:414–416, 419
26. Tian X, Cong M, Zhou W, Zhu J, Lui Q (2008) Relationship between protein expression of VEGF-C, MMP-2 and lymph node metastasis in papillary thyroid cancer. J Int Med Res 36:699–703
27. Segal K, Shpitzer T, Feinmesser M, Stern Y, Feinmesser R (1996) Angiogenesis in follicular tumors of the thyroid. J Surg Oncol 63:95–98
28. Ishiwata T, Iino Y, Takei H, Oyama T, Morishita Y (1998) Tumor angiogenesis is an independent prognostic indicator in human papillary thyroid carcinoma. Oncol Rep 5:1343–1348
29. Goldberg JD, Portugal LG, Wenig BL, Ferrer K, Wu JC, Sabnani J (1997) Well-differentiated thyroid carcinomas: p53 mutation status and microvessel density. Head Neck 20:152–158
30. Dhar DK, Kubota H, Kotoh T, Tabara H, Watanabe R, Tachibana M, Kohno H, Nagasue N (1998) Tumor vascularity predicts recurrence in differentiated thyroid carcinoma. Am J Surg 176:442–447
31. Jain RK, Fenton BT (2002) Intratumoural lymphatic vessels: a case of mistaken identity or malfunction? J Natl Cancer Inst 94:417–421
32. Shayan R, Achen MG, Stacker SA (2006) Lymphatic vessels in cancer metastasis: bridging the gaps. Carcinogenesis 27:1729–1738
33. Schoppmann SF, Birner P, Stockl J, Kalt R, Ullrich R, Caucig C, Kriehuber E, Nagy K, Alitalo K, Kerjaschki D (2002) Tumour-associated macrophages express lymphatic endothelial growth factors and are related to peritumoural lynphangiogenesis. Am J Pathol 161:947–956
34. Giorgadze TA, Baloch ZW, Pasha T, Zhang PJ, LiVolsi VA (2005) Lymphatic and blood vessel density in the follicular patterned lesions of thyroid. Mod Pathol 18:1424–1431
35. Hall FT, Freeman JL, Asa SL, Jackson DG, Beasley NJ (2003) Intratumoural lymphatics and lymph node metastases in papillary thyroid carcinoma. Arch Otoryngol Head Neck Surg 129:716–719
36. Elisei R, Ugolini C, Viola D, Lupi C, Biagini A, Giannini R, Romei C, Miccoli P, Pinchera A, Basolo F (2008) BRAF(V600E) mutation and outcome of patients with papillary thyroid carcinoma: a 15-year median follow-up study. J Clin Endocrinol Metab 93:3943–3949
37. Eloy C, Santos J, Soares P, Sobrinho-Simões M (2011) The preeminence of growth pattern and invasiveness and the limited influence of *BRAF* and *RAS* mutations in the occurrence of papillary thyroid carcinoma lymph node metastases. Virchows Arch 459:265–276. doi:10.1007/s00428-011-1133-7
38. Niemeier LA, Kuffner HA, Carty S, Stewart AF, Nikiforov YE (2010) A combined molecular–pathological score to predict aggressiveness of thyroid papillary microcarcinoma. Mod Pathol Abst 578:131A
39. Kim KH, Kang DW, Kim SH, Seong IO, Kang DY (2004) Mutations of the BRAF gene in papillary thyroid carcinoma in a Korean population. Yonsei Med J 45:818–821
40. Xing M, Clarck D, Guan H, Ji M, Dackiw A, Carson KA, Kim M, Tufaro A, Ladenson P, Zeiger M, Tufano R (2009) BRAF mutation testing of thyroid fine-needle aspiration biopsy specimens for preoperative risk stratification in papillary thyroid cancer. J Clin Oncol 27:2977–2982
41. Longatto-Filho A, Pinheiro C, Pereira SMM, Etlinger D, Moreira MAR, Jubé LF, Queiroz GS, Baltazar F, Schmitt FC (2007) Lymphatic vessel density and epitelial D2-40 immunoreactivity in pre-invasive and invasive lesions of the uterine cervix. Gynecol Oncol 107:45–51
42. Lubkin SR, Jackson T (2002) Multiphase mechanics of capsule formation in tumors. J Biomech Eng 124:237–243
43. Leu AJ, Berk DA, Lymboussaki A, Alitalo K, Jain RK (2002) Absence of functional lymphatics within a murine sarcoma: a molecular and functional evaluation. Cancer Res 60:4324–4327
44. Rosai J (2011) Rosai and Ackerman's surgical pathology, 10th edn. Elsevier Mosby, London

Virchows Arch (2011) 459:607–614
DOI 10.1007/s00428-011-1156-0

ORIGINAL ARTICLE

Typing of renal tumors by morphological and immunocytochemical evaluation of fine needle aspirates

Margareta Strojan Fležar · Helena Gutnik · Jera Jeruc · Irena Srebotnik Kirbiš

Received: 8 June 2011 / Revised: 1 September 2011 / Accepted: 4 October 2011 / Published online: 4 November 2011
© Springer-Verlag 2011

Abstract Image-guided fine needle aspiration biopsy (FNAB) of renal masses can accurately evaluate malignancy. Adjunct methods are needed for accurate typing of renal cell carcinomas (RCC) and benign neoplasms. Cytopathological diagnoses of 79 routine ultrasound-guided FNAB of renal lesions were compared to consequent histological diagnosis and size of tumors. Cytology samples were sufficient for immunocytochemical subtyping in 43 cases (54.4%). The median tumor size was 2.8 cm, with 57 cases (76%) smaller than or equal to 4 cm. When a panel of immunocytochemical stainings (vimentin, CK7, CD117, P504S) was applied, accurate diagnoses were obtained in 11/12 (91.7%) of clear cell RCC (CRCC), 14/17 (82.3%) of papillary RCC (PRCC) and 5/7 (71.4%) of chromophobe RCC (ChRCC), respectively. Substantial cell pleomorphism with unusual immunostainings led to erroneous diagnosis of pheochromocytoma in CRCC with eosinophilic cytoplasm. Only 30% of CRCC were correctly diagnosed in the group without immunostaining, seven were suspicious for CRCC, and the remainder had unrepresentative material for CRCC. Cytopathological diagnoses were less accurate in oncocytomas (n=11), regardless of immunocytochemical staining. Cystic nephromas (n=2) and MEST (n=1) were overdiagnosed as suspicious and positive for PRCC, respectively, with immunocytochemical staining not assisting in correct diagnosis. RCC can be accurately typed as CRCC, PRCC or ChRCC in fine needle aspirates in a routine clinical setting if the cellular material is sufficient and a panel of antibodies is used (vimentin, CK7, P504S, CD117). The classification of oncocytomas and cystic nephromas is not reliable since atypical morphology and immunocytochemical reactions overlap with RCC.

Keywords Renal neoplasm · Fine needle aspiration biopsy · Immunocytochemistry · Small renal mass

M. Strojan Fležar (✉) · H. Gutnik · J. Jeruc · I. Srebotnik Kirbiš
Institute of Pathology, Faculty of Medicine,
University of Ljubljana,
Korytkova 2,
SI-1000 Ljubljana, Slovenia
e-mail: margareta.strojan-flezar@mf.uni-lj.si

Introduction

Many cytopathology studies have reported that image-guided fine needle aspiration biopsy (FNAB) is a useful diagnostic method for the evaluation of renal masses, with the earliest reports dating back to the 1980s [1–4]. However, urologists have considered preoperative percutaneous biopsy of renal mass only in selected cases since the majority of lesions were reliably diagnosed by imaging techniques before surgery [5]. Changes in the management of patients with renal tumors have recently led to increased interest in percutaneous biopsy, either core biopsy or FNAB. Compared to core biopsy, FNAB is less invasive for the patient with comparable diagnostic accuracy for diagnosing renal malignancy [5–7].

Preoperative morphological diagnosis is especially important in small renal masses since these lesions prove benign in a higher percentage in surgical resection tissues than in all renal masses, so surgery could be spared in cases with biopsy proven benign renal lesions [5]. Alternatively, a surgical approach may be altered (radical vs. partial nephrectomy) even though it is still mostly influenced by the size and location of the tumor. While FNAB has proved accurate for differentiating malignant from benign renal lesions, it is less reliable for subtyping renal carcinomas [7–10]. Immunohistochemistry has been shown to be helpful for accurate subtyping in core biopsies but there

are only a few reports on the use of immunocytochemistry on FNAB samples of small series of renal tumors [11–15].

In our retrospective study, we analyzed the performance of FNAB supplemented by immunocytochemical staining in more than half of the cases for preoperative diagnostic assessment of renal tumors in an everyday routine clinical setting.

Materials and method

The computer database of the Institute of Pathology, Faculty of Medicine, University of Ljubljana was searched for ultrasound (US)-guided fine needle aspiration biopsies of renal lesions with consequent histological diagnosis. Among 227 US-guided FNAB of renal lesions retrieved, 79 had histology. In 43 cases, immunocytochemical staining was performed to make the cytopathological diagnosis. Complete pathological reports, including tumor size, were available for all 79 cases in the study.

All FNAB of renal lesions were performed under US guidance by an attending radiologist according to the standard procedure, using a 22-gauge needle attached to a 10-ml syringe. Two smears were prepared on site from each cell sample and air dried. The material left in the needle and syringe was suspended in short-term storage cell medium. When cytomorphological evaluation of the Giemsa-stained direct smear suggested carcinoma, the cell suspension was used to prepare cytospins, using a Shandon cytospin 4 cytocentrifuge (Thermo Shandon Inc., Pittsburg, Pennsylvania, USA). Depending on the cellularity of the cell suspension in cases in which sufficient material was obtained by FNAB, two to six cytospins were prepared. Cytopsins were immediately fixed in Delaunay solution (ethanol: acetone 1:1 with 0.5 ml/l trichloracetic acid) and stained according to the Papanicolaou method. Immunostaining was performed in the automated immunostaining system NexES (Ventana Medical Systems Inc., Tucson, Arizona, USA). Bound primary antibodies were detected using an iView detection kit (Ventana Medical Systems Inc., Tucson, Arizona, USA). Typically, antibody panels included RCC (renal cell carcinoma) marker (PN-15, Cell Marque Corp., Rocklin, LA, USA), vimentin (clone V9, DacoCytomation, Glostrup, Denmark), CK7 (clone OV-TL 12/30, DacoCytomation, Glostrup, Denmark), P504S (α-methylacyl-CoA racemase; clone 13H4, DakoCytomation, Glostrup, Denmark), and CD 117 (C-kit; rabbit polyclonal antibody, DakoCytomation, Glostrup, Denmark). Depending on the morphological appearance of the tumor cells in Giemsa-stained direct smears and clinical data, additional antibodies were used (chromogranin, HMB45, etc.).

Original cytopathological diagnoses were compared to final histopathological diagnosis. Tumor sizes were presented as mean ± standard deviation, median and range. The size of renal tumors and accuracy of cytopathological diagnoses were compared between cases without immunocytochemical staining and cases with immunostaining by means of the nonparametric Mann–Whitney U test. A p-value of ≤ 0.05 was considered statistically significant.

Results

Size was reported on the histology in 75/79 cases and in four cases size could not be assessed (one case was a core biopsy, one case had tissues fragments only, one was terminal nephrosclerosis in total nephrectomy and one was abscedent necrotizing chronic pyelonephritis on autopsy). The median tumor size was 2.8 cm and the mean was 3.4 cm (±2.18; range from 1 cm to 13 cm) with 57 cases (76%) smaller than or equal to 4 cm.

Of the 79 US-guided FNAB, five cases (6.3%) had insufficient material for diagnosis, 17 (21.5%) were negative for malignancy, 16 (20.2%) were suspicious for carcinoma and 41 (51.9%) were diagnosed as carcinomas (Table 1). The median size of tumors with insufficient material in FNAB was 2.3 cm (mean 2.82±1.51 cm, range 1.5–4.8 cm), while the median size of the remainder was 2.8 cm (mean 3.42± 2.22 cm, range 1–13 cm). There was no statistically significant difference in size between the two sample groups ($p>0.05$).

In 43 cases (54.4%), immunocytochemical staining was performed and cytological diagnosis was rendered based on morphology and immunoreactions (Table 2). In the remaining 36 cases, (45.6%) the cytological diagnosis was the result of cytomophological evaluation only (Table 2). The median size of cases with immunocytochemical staining was 2.5 cm (mean 3.3±2.3 cm, range 1 cm to 13 cm) while the median was 2.9 cm (mean 3.5±2.0 cm, range 1.2 cm to 9.4 cm) in cases without immunocytochemical staining. There was no statistically significant difference in size between lesions with or without immunocytochemical stainings ($p<0.05$).

Table 1 Cytological classification of renal masses in fine needle aspirates

Cytology	Histology benign	Histology carcinoma	Total
Insufficient material	2	3	5 (6.3%)
Negative[a]	11	6	17 (21.5%)
Suspicious[a]	5	11	16 (20.2%)
Positive[a]	1	40	41 (51.9%)
Total	19 (24%)	60 (76%)	79 (100%)

[a] For malignancy

Table 2 Cytological diagnoses in renal masses in relation to immunostaining reactions

		FNAB without immunostaining			FNAB with immunostaining		
Histology	Number	Cytological diagnosis	Number	Total (*N*)	Cytological diagnosis	Number	Total (*N*)
Clear cell RCC	34	CRCC	7 (30.4%)	23	CRCC	11 (100%)	11
		Suspicious for CRCC	7				
		Other[a]	9				
CRCC with eosinophilic cytoplasm	1	–		–	Pheochromocytoma	1 (0%)	1
Papillary RCC	18	CRCC	1 (0%)	1	PRCC	14 (82.3%)	17
					Suspicious for PRCC	1	
					CRCC	2	
Chromophobe RCC	7	–		–	ChRCC	5 (71.4%)	7
					Suspicious for ChRCC	1	
					Carcinoma	1	
Oncocytoma	11	Oncocytoma Oncocytoma vs. ChRCC	2 (28.6%)	7	Oncocytoma	2 (50%)	4
		Oncocytoma vs. angiomyolipoma	1		Oncocytoma vs. ChRCC	2	
		Other[b]	1				
			3				
Cystic nephroma/MEST	3	–	–	–	PRCC	1	3
					Suspicious for PRCC	1	
					Suspicious for carcinoma	1	
Other benign lesions	5	Benign	4	5	–	–	–
		Atypical cells, suspicious for carcinoma	1				
Total	79			36			43

Percentage of concordant cases are reported in brackets

CRCC clear cell renal cell carcinoma, *PRCC* papillary renal cell carcinoma, *ChRCC* chromophobe renal cell carcinoma, *MEST* mixed epithelial stromal tumor

[a] Other: insufficient material (3), normal renal structures (3), cyst (2), angiomyolipoma (1)

[b] Other: insufficient material (2), normal renal structures (1)

FNABs without immunocytochemical staining

The majority of tumors (23/36 cases) without immunocytochemical staining were clear cell renal cell carcinomas (CRCC) on subsequent histology and accurate cytological diagnosis was made in seven cases (30.4%) and an additional seven cases were correctly suspicious for CRCC. In these cases, the cytomorphological features were characteristic for CRCC but cellular material was scarce, so a final positive diagnosis of carcinoma was not signed out. An incorrect cytological diagnosis of benign cystic lesion was given in two cases in which only blood and a few macrophages were found in the fluid sent for cytological examination. Another case was wrongly diagnosed as angiomyolipoma because only a few large three-dimensional moderately cellular stromal fragments were found in a blood sample. The remaining six cases contained only normal renal structures or no diagnostic cells.

One papillary RCC (PRCC) was diagnosed as CRCC, although on review, the morphology was suggestive of PRCC. However, immunostaining was unfortunately not performed.

A diagnosis of oncocytoma was made in two cases and in a further two, differential diagnoses of oncocytoma were suggested vs. chromophobe RCC (ChRCC) or angyomiolipoma.

Benign lesions were correctly diagnosed as benign in four of five cases (histological diagnoses: two simple cortical cysts, terminal nephrosclerosis, chronic and acute pyelonephritis with abscess formation). However, a few atypical cells in one case cautioned against the possibility of carcinoma; in this case, histological examination revealed a very rare benign renal tumor, namely a juxtaglomerular cell tumor.

FNAB's with immunocytochemical staining

Cytological diagnoses were more specific in 43 cases with immunoreactions. Among renal cell carcinomas, 11/12 CRCC (91.7%), 14/17 (82.3%) PRCC and 5/7 ChRCC (71.4%) were accurately typed, with 83.3% of overall correct classification for different types (Figs. 1 and 2). A further one case was correctly suspicious for PRCC and one case for ChRCC, in both cases direct Giemsa-stained smears were paucicellular and cell suspensions for cytospins were also scarce, so a limited antibody panel could be used (Table 3). One case of ChRCC was recognized as carcinoma but, similarly as above, a direct smear was scanty, with only two cytospins available for immunostaining so no typing was attempted. Two PRCC were diagnosed as CRCC on FNAB. The morphological features suggested CRCC and, in addition, CK7 and P504S were negative in one case and CK7 was only focally positive and P504S not done in the other case (Table 3).

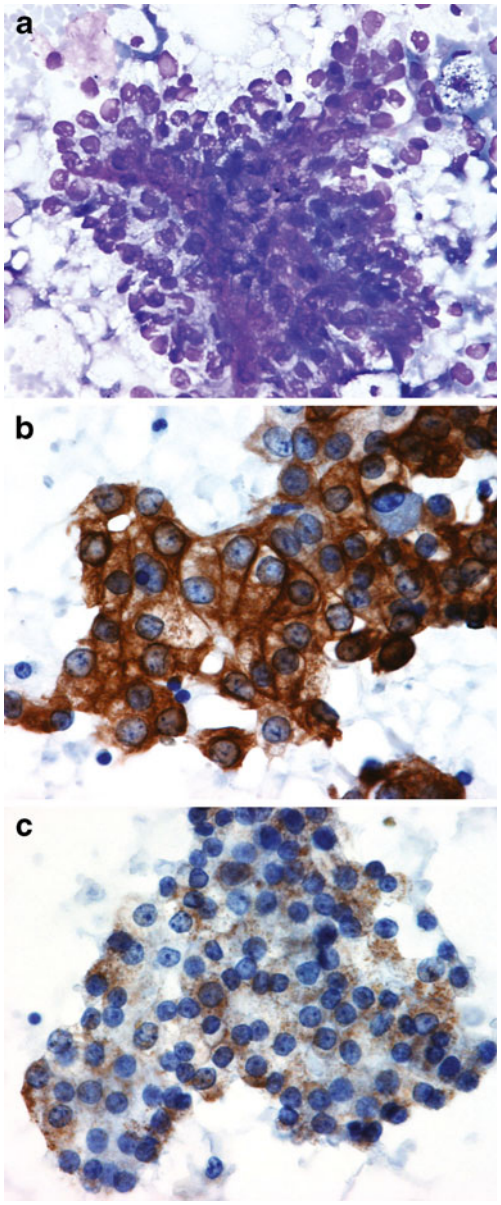

Fig. 1 Renal cell carcinoma, papillary type, in fine needle aspirate: **a** fibrovascular core with clear cells and a siderophage (×600, Giemsa), **b** cells were CK7 positive (×600) and **c** P504S positive (×600)

A histologically confirmed CRCC with predominant population of cells with eosinophilic cytoplasm (1/12 CRCC) was not recognized in a FNAB specimen and a cytological diagnosis of pheochromocytoma was signed out due to substantial cellular and nuclear pleomorphism accompanied by abundant thick eosinophilic material in the cell clusters and in the background (Fig. 3). Moderately intensive positive immunostaining for chromogranin and negative RCC marker staining led to the erroneous diagnosis (Table 3).

Among benign tumors, two oncocytomas had a specific diagnosis, both being CK7 negative; another two cases with dissociated cells and benign morphology but with CK7 diffuse and focal positivity, respectively, led to a differential

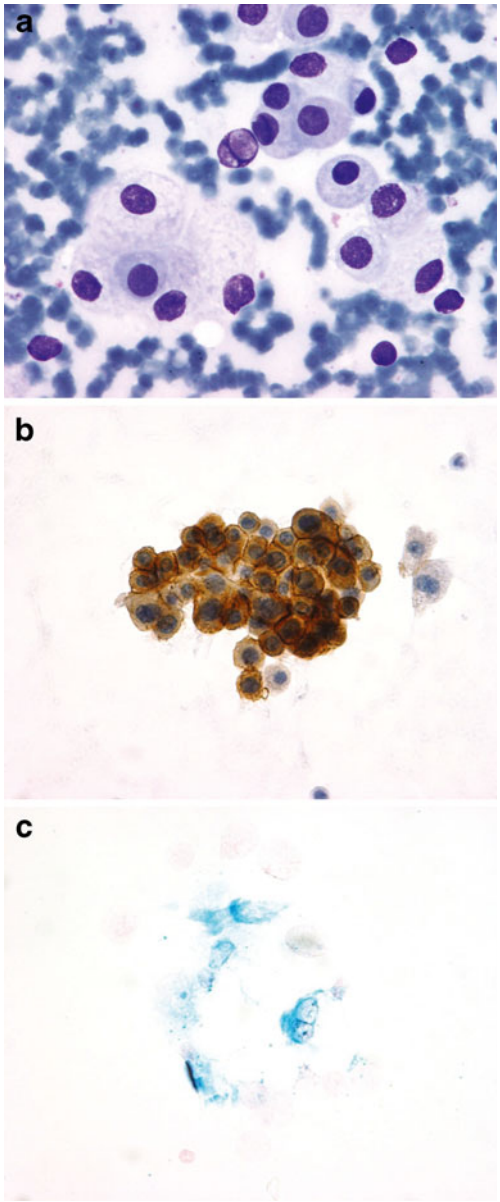

Fig. 2 Renal cell carcinoma, chromophobe type, in fine needle aspirate: **a** a small cluster and few dissociated large cells with anizonucleosis (Giemsa, ×600), **b** cells were CD117 positive (×600) and **c** positive Hale colloidal iron stain (×600)

diagnosis of oncocytoma (regarding morphology) vs. ChRCC (regarding positive CK7). All four oncocytomas were vimentin negative and CD117 positive.

Cytological diagnosis supported by immunocytochemical reactions was also incorrect in two cases of cystic nephromas and one mixed epithelial stromal tumor (MEST). All three had a similar morphology, with papillalike structures and macrophages, with cells exhibiting mild to moderate atypia. All three were vimentin positive, CK7 positive, MEST was P504S positive, while cystic nephromas were P504S negative. MEST was diagnosed as PRCC, one case of cystic nephroma was

Table 3 Immunocytochemical reactions in FNA of renal carcinomas

Histology	Number	Cytological diagnosis	Number	Immunocytochemical reactions					
				RCC	VIM	CK7	P504S	CD117	Other
Clear cell RCC	11	CRCC	11	+ (8/8)	+ (11/11)	− (8/9)	ND	− (2/2)	−HMB45 (2/2)
CRCC with eosinophilic cytoplasm	1	Pheochromocytoma	1	− (1/1)	+ (1/1)	− (1/1)	ND	ND	± CHROM (1/1)
Papillary RCC	17	PRCC	14	+ (13/13)	+ (12/12)	+ (14/14)	+ (14/14)	ND	ND
		Suspicious for PRCC	1	ND	+ (1/1)	+ (1/1)	+ (1/1)	ND	ND
		CRCC	2	+ (1/1)	+ (2/2)	± (1/2)−(1/2)	− (1/1)	ND	ND
Chromophobe RCC	7	ChRCC	5	− (3/4)	− (5/5)	+ (5/5)	ND	+ (5/5)	ND
		Suspicious for ChRCC	1	± (1/1)	− (1/1)	ND	ND	ND	ND
		Carcinoma	1	ND	− (1/1)	− (1/1)	ND	ND	ND
Total	36		36	28/36	33/36	34/36	15/36	7/36	3/36

CRCC clear cell renal cell carcinoma, *PRCC* papillary renal cell carcinoma, *ChRCC* chromophobe renal cell carcinoma, + positive, − negative, *ND* not done

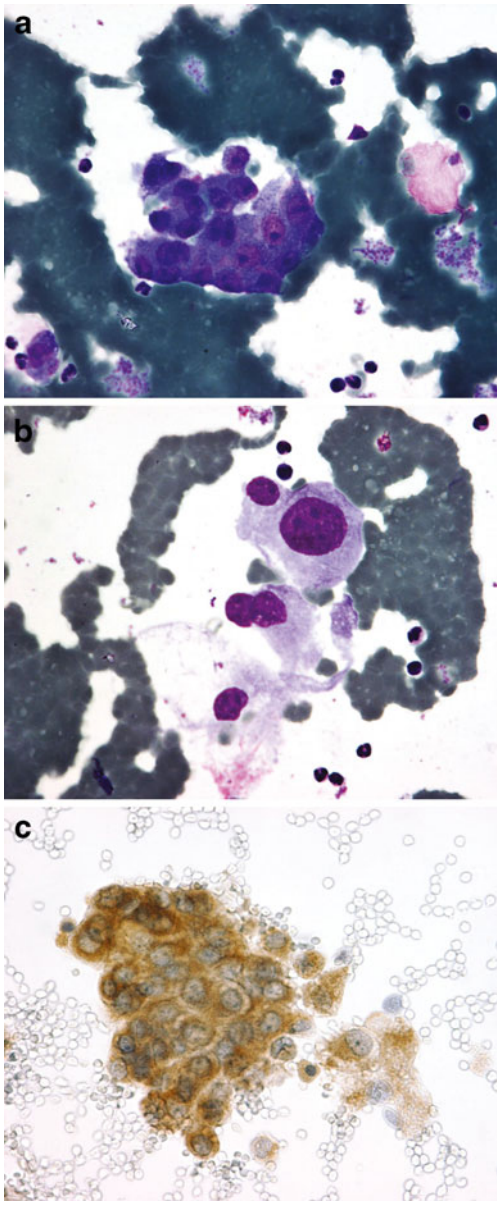

Fig. 3 Clear cell renal cell carcinoma with eosinophilic cytoplasm in fine needle aspirate: **a** thick eosinophilic material in cell cluster and in the background (Giemsa, ×400), **b** cellular and nuclear pleomorphism (Giemsa, ×600) and **c** positive chromogranin immunohistochemical staining (×600)

suspicious for PRCC and one suspicious for carcinoma, with no typing attempted.

Discussion

The diagnostic utility of FNAB has been documented and the cytomorphology of renal tumors for most different types of renal cell carcinomas has been well described and correlated to histology in recent decades [16]. FNAB is easier to perform and has lower morbidity compared to needle core biopsy but some controversy remains about its diagnostic accuracy and applicability.

Some previous reports have indicated that needle core biopsy diagnostic sensitivity is decreased and failure rate increased with smaller mass size; conversely no differences in the accuracy of cytological diagnosis were reported in an ex vivo FNAB study related to small renal masses (≤4 cm) [7, 17, 18]. Our study proved that FNAB can be successfully used in small renal masses, since the majority (76%) of our tumors were equal to or smaller than 4 cm. The overall rate of insufficient material for diagnosis was low (6.3%, Table 1) and it was not related to the size of the mass. As a general observation in cytopathology, unrepresentative samples containing only normal renal structures led to false negative diagnosis of a few CRCC (Table 2). Moreover, cytopathological diagnoses were less specific and not conclusive in cases with scanty material that did not allow additional immunocytochemical staining (Table 2).

Only seven of 23 (30.4%) of CRCC in the group with no immunocytochemical staining had a specific diagnosis, compared to 11/12 (91.7%) CRCC with an accurate diagnosis when plentiful material was obtained and adjunct methods were used. Other studies have reported good or even excellent concordance between FNAB and histological diagnosis for CRCC although their diagnoses were based only on cytomorphology [8–10]. Although the cytological characteristics of CRCC are well defined, limited cytological material with only few cell groups precluded definite diagnosis of carcinoma—as a general rule in cytology—on FNAB in seven of 23 cases in our study. In two cases of cystic CRCC, only macrophages and blood-stained fluid were obtained and led to an erroneous diagnosis of benign cystic lesion. Previous studies have cautioned that such cases should be diagnosed as non-diagnostic rather than negative [8]. Likewise, specimens containing only normal renal or fibrous tissue should probably be considered nondiagnostic as proposed for core biopsies [19]. To summarize, CRCC can be accurately diagnosed by FNAB provided that sufficient and representative material is obtained.

The morphology of PRCC has been well described in retrospective cytological studies [20–22]. However, it has been reported that PRCC is frequently misdiagnosed in FNAB samples in routine diagnostic work-up [8–10]. In contrast, we found that the majority (82.3%) of PRCC with immunocytochemical staining (VIM+, CK7+, P504S+) had accurate cytological diagnosis (Fig. 1). Only two cases were erroneously diagnosed as CRCC since CK7 staining was negative in one case and weakly positive in the other. It has been proposed that positive CK7 aids in differentiating PRCC from CRCC although about 20% of PRCC do not express CK7 and on the other hand 10–15% of CRCC exhibit CK7 positivity [23–25]. Additionally, positive

P504S staining was initially considered characteristic of PRCC but was also later reported in CRCC in up to 68.9% in one series [24, 26]. In our series, all PRCC cases with P504S staining showed a positive granular cytoplasmic reaction. We retrospectively stained spare archival cytospins of CRCC in our series and found less than 50% of cells positive in 2/5 cases (data not shown in tables) so P504S should be evaluated in further studies. After careful evaluation of morphology, therefore, a panel of markers is mandatory to obtain accurate diagnosis in PRCC [23, 24]. However, in rare cases, overlapping morphologic and immunohistochemical findings do not allow definite classification of RCC, even after histopathological examination of resection specimens [27].

The most problematic in our series was cytological diagnosis of pheochromocytoma in histologically confirmed CRCC with predominant population of cells with eosinophilic cytoplasm (Fig. 3). Pleomophic nuclei and cells with abundant thick eosinophilic material in the cell clusters and in the background, in combination with moderately intensive immunostaining for chromogranin and negative RCC marker staining led to erroneous diagnosis. The RCC marker has been reported to have high specificity for CRCC in biopsies of primary and metastatic tumors and also in FNAB specimens. However, the sensitivity was rather low so negative staining does not exclude primary RCC [13, 28]. To the best of our knowledge, there is no data available on chromogranin staining in RCC.

In specimens with morphology suggestive of ChRCC, immunocytochemical staining was performed to aid final cytopathological diagnosis [29–31]. Our five cases with a combination of negative vimentin, positive CK7 and CD117 had accurate diagnosis (Fig. 2). In contrast, an incomplete panel and unusual CK7 negative staining led to less specific diagnosis in our two cases, as reported previously [32].

Although the cytomorphology of oncocytoma has been well described and compared to chromophobe type of RCC, especially in retrospective review studies, it seems that it cannot be reliably reproduced in everyday routine diagnostic assessment [8, 16, 31]. The morphology partially overlaps with that of chromophobe type of RCC and is especially challenging in cases with more pronounced cytological atypia. Immunocytochemical staining is of limited usefulness because both neoplasms stain positive with CD117 and are negative for vimentin. Some cases of oncocytoma may be CK7 positive, too, as was also observed in our analysis. Differentiation between membrane and cytoplasmic CK7 staining is not reliable in cytological samples since the membrane covers the whole cell compared to cut cell in a tissue block [32]. Hale's colloidal iron staining was tried as proposed on a cytospin of ChRCC and showed a few positive cells; however, the majority of cells were destroyed during the procedure [16] (Fig. 3C). Spare cytospins to adapt the staining procedure for cytology are difficult to obtain so we cannot at the moment use this method in our routine work. Renshaw suggested that such borderline cytology cases could be signed out as oncocytic neoplasm, suggesting a differential diagnosis of oncocytoma and renal cell carcinoma, particularly chromophobe type [16].

Our analysis showed that cystic nephroma and MEST in FNAB presented with cytomorphology and immunocytochemical reactions very similar to papillary type of RCC. These neoplasms were consequently overdiagnosed as either suspicious or even positive for PRCC. These lesions were similarly misdiagnosed in previous reports. Moreover, some authors considered cystic nephromas undiagnosable by FNAB [4, 10].

Our study showed that FNAB can accurately classify major subtypes of RCC in a routine clinical setting independent of tumor size, when sufficient cellular material is obtained and cytomorphology is supplemented by immunocytochemical staining. However, an unusual cytomorphology or lack of experience in rare renal neoplasms accompanied by an unusual immunophenotype was prone to misdiagnosis. In our study, the method was less accurate in diagnosing oncocytomas and cystic nephromas because atypical morphology and immunocytochemical reactions overlapped with ChRCC and PRCC, respectively.

Acknowledgement This study was supported by the Slovenian Research Agency grant P3-0054.

References

1. Orell SR, Langlois SL, Marshall VR (1985) Fine needle aspiration cytology in the diagnosis of solid renal and adrenal masses. Scan J Urol Nephrol 19:211–216
2. Pilloti S, Rilke F, Alasio L, Garbagnati F (1988) The role of fine needle aspiration in assessment of renal masses. Acta Cytol 32:1–9
3. Kelley CM, Cohen MB, Raab SS (1996) Utility of fine-needle aspiration biopsy in solid renal masses. Diagn Cytopathol 14:14–19
4. Renshaw AA, Granter SR, Cibas ES (1997) Fine-needle aspiration of the adult kidney. Cancer 81:71–88
5. Laguna MP, Kümmerlin I, Rioja J, de la Rosette JJMCH (2009) Biopsy of renal mass: where are we now? Curr Opin Urol 19:447–453
6. Volpe A, Kachura JR, Geddie WR, Evans AJ, Gharajeh A, Saravanan A, Jewett MAS (2007) Techniques, safety and accuracy of sampling of renal tumors by fine needle aspiration and core biopsy. J Urol 178:379–386
7. Kümmerlin IPED, Smedts F, ten Kate FJW, Horn T et al (2009) Cytological punctures in the diagnosis of renal tumors: a study on accuracy and reproducibility. Eur Urol 55:187–198
8. Renshaw AA, Lee KR, Madge R, Granter SR (1997) Accuracy of fine needle aspiration in distinguishing subtypes of renal cell carcinoma. Acta Cytol 41:987–994

9. Masoom S, Venkataraman G, Jensen J, Flanigan RC, Wojcik EM (2009) Renal FNA-based typing of renal masses remains a useful adjunctive modality: evaluation of 31 renal masses with correlative histology. Cytopathology 20:50–55
10. Adeniran AJ, Al-Ahmadie HA, Iyengar P, Reuter V, Lin O (2010) Fine needle aspiration of renal cortical lesions in adults. Diagn Cytopathol 38:710–715
11. Volpe A, Mattar K, Finelli A et al (2008) Contemporary results of percutaneous biopsy of 100 small renal mases: a single center experience. J Urol 180:2333–2337
12. Liu J, Fanning CV (2001) Can renal oncocytomas be distinguished from renal cell carcinoma on fine-needle aspiration specimens? Cancer Cytopathol 93:390–397
13. Godken N, Mukunyadzi P, James JD, Godken M (2003) Diagnostic utility of renal cell carcinoma marker in cytopathology. Appl Immunohistochem Mol Morphol 11:116–119
14. Lim JC, Wojcik EM (2006) Fine-needle aspiration cytology of papillary renal cell carcinoma: the association with concomitant secondary malignancies. Diagn Cytopathol 34:797–800
15. Tejerina E, Gonzáles-Peramato P, Jiménez-Heffernan JA et al (2009) Cytological features of chromophobe renal cell carcinoma, classic type. Report of nine cases. Cytopathology 20:44–49
16. Renshaw AA (2002) Subclassification of renal cell neoplasms: an update for practicing pathologist. Histopathology 41:283–300
17. Schimdbauer J, Remzi M, Memarsadeghi M et al (2008) Diagnostic accuracy of computed tomography-guided percutaneous biopsy of renal masses. Eur Urol 53:1003–1012
18. Lechevallier E, Andre M, Barriol D et al (2000) Fine-needle cutaneous biopsy of renal masses with helical CT guidance. Radiology 216:506–510
19. Shannon BA, Cohen RJ, de Bruto H, Davies RJ (2008) The value of percutaneous preoperative needle core biopsy for diagnosing benign lesions among small, incidentally detected renal mass. J Urol 180:1257–1261
20. Flint A, Cookingham C (1987) Cytologic diagnosis of papillary variant of renal-cell carcinoma. Acta Cytol 31:325–329
21. Dekmezian R, Sneige N, Shabb N (1991) Papillary renal-cell carcinoma: fine-needle aspiration of 15 cases. Diagn Cytopathol 7:198–203
22. Granter SR, Perez-Atayde RAA (1998) Cytologic analysis of papillary renal cell carcinoma. Cancer Cytopathol 84:303–308
23. Skinnider BF, Amin MB (2005) An immunohistochemical approach to the differential diagnosis of renal tumors. Semin Diagn Pathol 22:51–68
24. Allory Y, Bazille C, Viellefond A et al (2008) Profiling and classification tree applied to renal epithelial tumours. Histopathol 52:158–166
25. Mertz KD, Demichelis F, Sboner A et al (2008) Association of cytokeratin 7 and 19 expression with genomic stability and favorable prognosis in clear cell renal cell cancer. Int J Cancer 123:569–576
26. Lin F, Brown RE, Shen T, Yang XY, Schuerch C (2004) Immunohistochemical detection of P504S in primary and metastatic renal cell carcinomas. Appl Immunohistochem Mol Morphol 12:153–159
27. Gobbo S, Eble JN, Maclennan GT et al (2008) Renal cell carcinomas with papillary architecture and clear cell components: the utility of immunohistochemical and cytogenetical analyses in differential diagnosis. Am J Surg Pathol 32:1780–1786
28. McGregor DK, Khurana KK, Cao C et al (2001) Diagnosing primary and metastatic renal cell carcinoma. The use of monoclonal antibody 'renal cell carcinoma marker'. Am J Surg Pathol 25:1485–1492
29. Akhtar M, Ali MA (1995) Aspiration cytology of chromophobe cell carcinoma of kidney. Diagn Cytopathol 13:287–294
30. Renshaw AA, Granter SR (1996) Fine needle aspiration of chromophobe renal cell carcinoma. Acta Cytol 40:867–873
31. Wiatrowska BA, Zakowski MF (1999) Fine needle aspiration biopsy of chromophobe renal cell carcinoma and oncocytoma. Comparison of cytomorphological features. Cancer Cytopathol 87:161–167
32. Mathers ME, Pollock AM, Marsh C, O'Donnell (2002) Cytokeratin 7: a useful adjunct in the diagnosis of chromophobe renal cell carcinoma. Histopathology 40:563–567

Virchows Arch (2011) 459:615–621
DOI 10.1007/s00428-011-1160-4

ORIGINAL ARTICLE

TLE1 is expressed in the majority of primary pleuropulmonary synovial sarcomas

Leonardo Saúl Lino-Silva · Juan Pablo Flores-Gutiérrez · Natalia Vilches-Cisneros · Hugo Ricardo Domínguez-Malagón

Received: 26 August 2011 / Revised: 4 October 2011 / Accepted: 18 October 2011 / Published online: 10 November 2011
© Springer-Verlag 2011

Abstract Pleuropulmonary synovial sarcoma (PPSS) is a rare entity, similar to synovial sarcoma of soft tissue (STSS). There are 120 published cases of PPSS, but no studies have explored the expression of TLE1. In soft tissues, it has been proven a useful marker, but in tumors of other sites, its expression has not been explored. The main objective was to study the expression and diagnostic sensitivity and specificity of TLE1 in a group of PPSS, of which the diagnosis was corroborated by fluorescence in situ hybridization confirming t(X;18) in a tissue microarray. Immunohistochemistry including TLE1, vimentin, CD99, CD56, bcl-2, AE1-AE3, EMA, CD34, CK7, CK19, calponin, and S-100 was performed on all PPSS and on 25 control cases (five carcinomas, ten mesotheliomas, and ten thoracic sarcomas). TLE1 was positive in 11 cases (73.3%); bcl-2 and vimentin in 100%; calponin and CD56 in 26.6%; CD99, CK AE1-AE3, CK19, CK7, and EMA in 80%; and S100 negative in all. The only biphasic PPSS was positive for epithelial markers only in the epithelial component. TLE1 was negative in all control cases. TLE1 is expressed in 73% of PPSS, a value inferior to that reported in STSS, but is highly specific for PPSS. TLE1 may therefore be of value in the differential diagnosis of PPSS, but should be used in a panel of antibodies.

Keywords Synovial sarcoma · Pleuropulmonary sarcomas · TLE1

This work was partially presented in the *100th Annual Meeting of the USCAP*, San Antonio, TX, 2011 poster presentation (poster no. 1776).

L. S. Lino-Silva · H. R. Domínguez-Malagón
Department of Anatomic Pathology,
Instituto Nacional de Cancerología,
México City, Mexico

J. P. Flores-Gutiérrez · N. Vilches-Cisneros
Department of Anatomic Pathology, Hospital Universitario,
Universidad Autónoma de Nuevo Leon,
Monterrey, Mexico

L. S. Lino-Silva (✉)
Avenida San Fernando No. 22, Colonia Sección XVI,
CP 14080 México City, Mexico
e-mail: saul.lino.sil@gmail.com

Introduction

Synovial sarcoma (SS) is a high-grade soft tissue tumor that occurs mainly in para-articular locations of the extremities, affecting young adults. It has well-defined histological features with monophasic and biphasic types. The SS in the pleuropulmonary region (PPSS) has histological features similar to soft tissue SS and was first described by Zeren et al. [14], but it was Essary et al. [23] who considered it a different clinicopathological entity due to the specific translocation t(X; 18)(p11,q11) that causes the fusion of SYT and SSX genes which can be detected by gene fusion analysis or evidence of break-apart test fluorescence in situ hybridization (FISH) [1]. Initially, PPSS included tumors arising not only in the pleura and lung but also those arising in the chest wall, heart, and mediastinum. When only tumors arising in the pleura and lung are considered as genuine PPSS, there are less than 100 cases published to date. Clinical symptoms include cough, chest pain, and dyspnea. On chest radiographs, PPSS typically appears as a well-delimited mass with uniform opacity, situated in the pleura or in the lung and often accompanied by an ipsilateral pleural effusion [2]. CT scan shows a well-circumscribed, heterogeneously enhanced non-calcified lesion without bone involvement. Magnetic resonance imaging provides a better demonstra-

Table 1 Clinical characteristics of pleuropulmonary synovial sarcoma

Case no.	Age (years)	Sex	Tumor site	Size (cm)	Subtype	Follow-up/outcome
1	38	M	Pleura	10	Monophasic	12 m/AWD
2	37	F	Lung	8	Monophasic	31 m/AWD
3	59	F	Lung	31	Monophasic	18 m/DOD
4	28	F	Lung	10	Monophasic	6 m/DOD
5	73	M	Pleura	1.9	Monophasic	40 m/AWD
6	32	M	Pleura	3.2	Monophasic	37 m/DOD
7	41	M	Lung	3.5	Monophasic	13 m/AWD
8	40	F	Pleura	20	Monophasic	17 m/DOD
9	22	F	Lung	12	Biphasic	12 m/AWD
10	35	M	Pleura	5	Monophasic	46 m/AWD
11	27	M	Lung	11.4	Monophasic	12 m/AWD
12	37	F	Lung	18	Monophasic	22 m/DOD
13	20	F	Lung	4.5	Monophasic	39 m/DOD
14	35	F	Pleura	4	Monophasic	13 m/DOD
15	30	M	Lung	5.2	Monophasic	12 m/AWD

Survival expressed in months (m)

DOD dead of disease, *AWD* alive with disease, *M* male, *F* female

tion of the solid and multilocular fluid-filled internal components of the lesion, with peripheral rim enhancement after the intravenous administration of a gadolinium-based contrast material [3].

The main objective of this study was to report 15 new cases of genuine PPSS seen in our institution, all with a rearrangement at the *SS18* gene (*SYT*), to describe its clinical characteristics and to determine its immunohistochemical profile, including the recently developed antibody TLE1. The other purpose was to explore the feasibility of the FISH test on a tissue microarray (TMA).

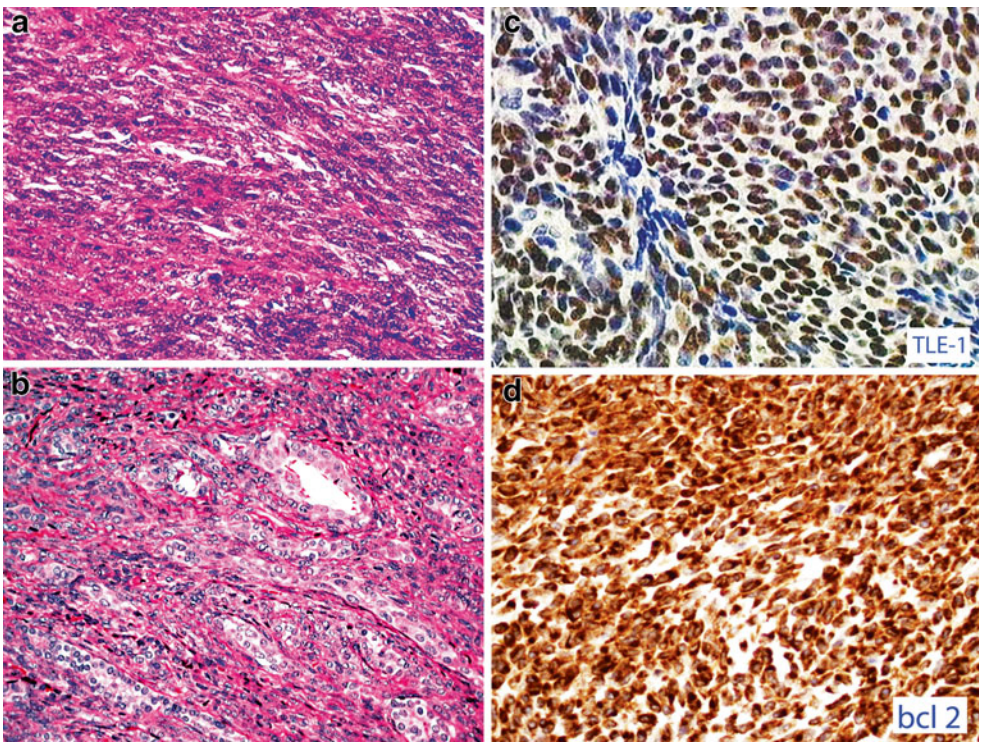

Fig. 1 **a** Monophasic PPSS showing a spindle cell neoplasm with hemangiopericytoma-like pattern and little nuclear atypia. **b** Biphasic PPSS with glandular epithelial structures adjacent to a malignant spindle cell component. **c** TLE1, diffuse and strong nuclear expression in pleuropulmonary synovial sarcoma. **d** Bcl-2 cytoplasmic expression in pleuropulmonary synovial sarcoma. **e** Tissue microarray and FISH test show at least tree fluorescent signals of chromosome X and 18 representing the X:18 translocation

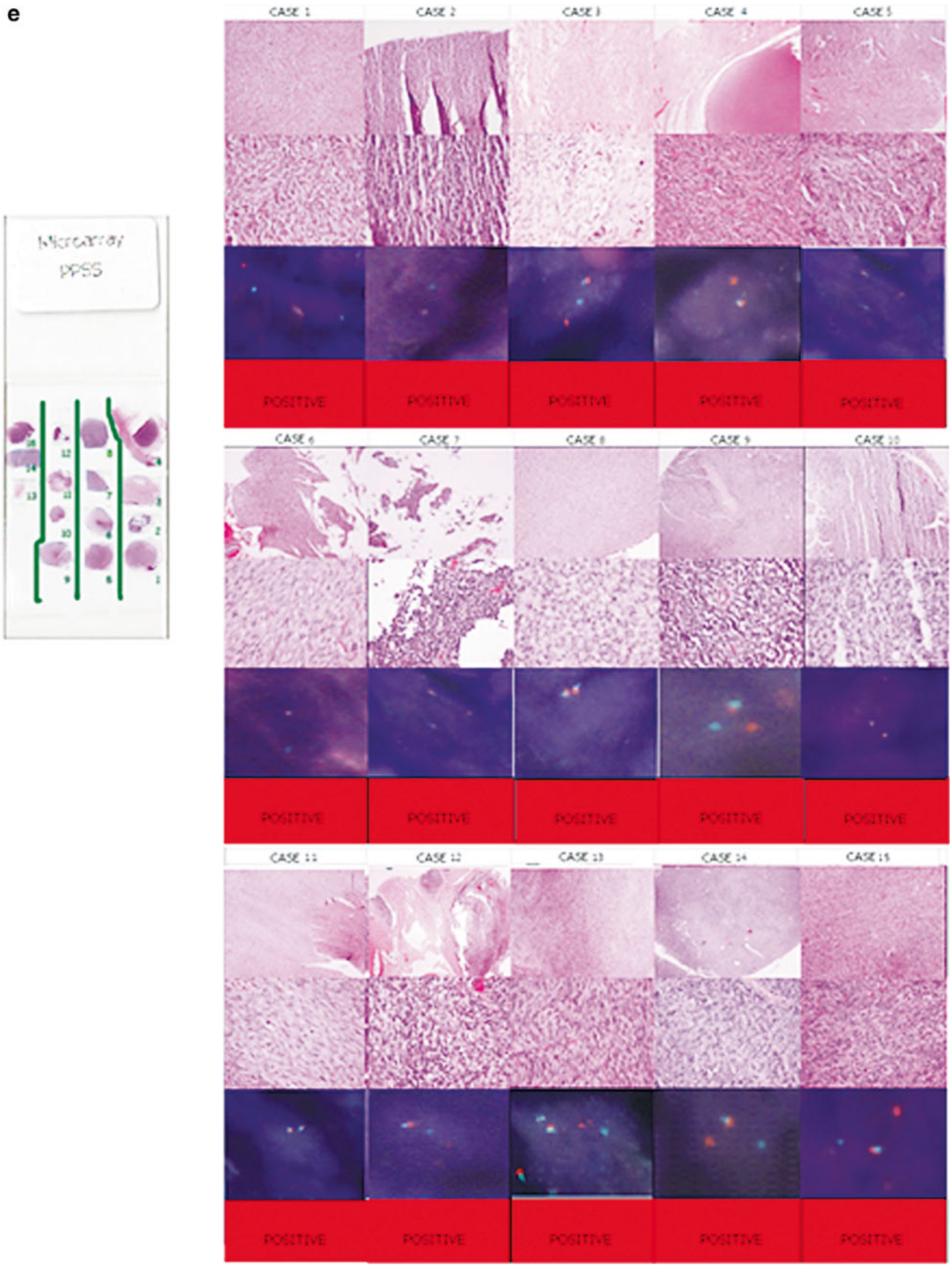

Fig. 1 (continued)

Material and methods

The cases analyzed were collected from the archives of the surgical pathology department of our institution. This study was performed in accordance with the protocols and rules of the ethics and research committee of our institution. A search over a period of 10 years (2000–2010) revealed a total of 37 cases of SS located in the lung and pleura. Of these, 17 represented metastatic SS and were excluded. Five additional cases were eliminated for lack of tissue for molecular analysis. In total, 15 cases were eligible for analysis (Table 1).

Chest radiographs, computed tomography, magnetic resonance imaging, or positron emission tomography/computed tomography studies were available for all 15 cases. Clinical information and follow-up data were obtained from patient records. All cases were biopsy specimens obtained by core needle or open incisional biopsy. Hematoxylin- and eosin-stained sections and paraffin-embedded tissue were available in all cases. Tumors were classified as monophasic or biphasic according to the World Health Organization criteria [3]. The monophasic type was composed of densely packed spindle cells arranged in short fascicles often with a hemangiopericytoid vascular pattern (Fig. 1a). Biphasic tumors contained spindle cell as well as epithelial components with malignant epithelial cells forming gland-like spaces and tubulo-papillary structures (Fig. 1b).

Histological preparations stained with hematoxylin and eosin were evaluated separately by two pathologists (HRDM and LSLS), and from each case, a representative area of 5×5 mm from the tumor was selected to construct the TMA, allowing 15 cases in a single paraffin block (Fig. 1e). As the synovial SS is a homogeneous tumor with little variability between histological fields, we took only one fragment of tissue. For biphasic tumors, we verified that both components were included, through an initial evaluation with hematoxylin and eosin prior to immunohistochemistry and molecular studies (Fig. 1e). Additionally, we used 25 control cases for immunohistochemistry for TLE1, which were evaluated in full sections. To this end, we chose pleuropulmonary or mediastinal tumors that resemble SS, including five spindle cell carcinomas, ten spindle cell mesotheliomas, six malignant fibrous histiocytomas, three malignant peripheral nerve sheath tumors, and one leiomyosarcoma.

Immunohistochemistry was performed on sections obtained from the TMA and on whole sections using commercially available antibodies according to the manufacturer's instructions, with recommended dilutions (Table 2). After deparaffinization, antigen retrieval was performed using an automated immunostainer (Ventana, Tucson, AZ) with mild Tris-based buffer (CC1, Ventana). Tissue sections were incubated with isotypic antibodies (immunoglobulins); this was followed by washing and detection with the i-View DAB kit (Ventana). For TLE1, nuclear staining was considered positive; cytoplasmic staining for all the other antibodies. Based on intensity, a three-point scale was chosen: mild, moderate, or strong. In addition, we considered the staining diffuse when >30% of neoplastic cells were positive; focal if a smaller percentage of cells stained. For each of the antibodies, we performed positive and negative controls on full histological sections using tissues recommended by the manufacturer.

Table 2 Summary of antibodies performed

Antibody	Laboratory	Clone	Dilution
Bcl-2	Dako, Carpintera CA	124	1:20
CD34	Dako, Carpintera CA	QBEnd 10	1:40
CKAE/1AE3	Dako, Carpintera CA	AE1/AE3	1:200
CK7	Dako, Carpintera CA	OV-TL 12/30	1:160
CK19	Dako, Carpintera CA	RCK108	1:50
CD99	Dako, Carpintera CA	12E7	1:80
Calponin	Dako, Carpintera CA	CALP	1:600
EMA	Dako, Carpintera CA	E29	1:100
S-100	Dako, Carpintera CA	Policolnal	1:800
TLE-1	Santa Cruz Biochemicals, Santa Cruz, CA	sc-9121	1:20
Vimentin	Dako, Carpintera CA	Vim3B4	1:400

All cases were studied by break-apart FISH on 3- to 4-μm unstained sections of the TMA using the LSI SYT dual-color break-apart probe, flanking the *SS18 [SYT]* 18q11.2 region, according to previously described standard laboratory methods [5]. The signal was developed by 10-μL Locus Specific Identifier (Vysis, Inc., Downers Grove, IL). The FISH slides were read separately by two pathologists (JPFG and NVC) at ×1,000 magnification on an Olympus BX51 fluorescence microscope equipped with appropriate filters (Olympus, Tokyo, Japan). Fluorescent signals from a minimum of 100 intact non-overlapped nuclei were counted. FISH was interpreted positive when it showed at least one red and one green split nuclear signal.

Results

Clinical data were available for all patients. There was no gender predilection: seven cases (47%) were in males and eight (53%) in females. The median age was 37 years, (range, 20–73 years). The median tumor size was 10 cm (range, 1.9–31 cm). The typical clinical presentation was a pleural or pulmonary mass associated with thoracic pain and cough.

The median follow-up was 6–46 months. Five patients died of disease (33%) and the remaining ten are alive with progressive disease not amenable for surgical treatment.

Nine of the 15 cases were localized in the lung (60%) and six in the pleura (40%). One case was a biphasic tumor and the other 14 monophasic spindle cell synovial sarcomas.

Immunohistochemical and FISH results are summarized in Table 3 and Fig. 1e. The FISH test was positive in all 15 cases (100%), showing splitting of the fluorescent signal consistent with a rearrangement involving *SYT* (Fig. 1e).

TLE1 was positive in 11 cases (73%), with strong and diffuse staining in 50% and diffuse–weak in the remaining cases (Fig. 1c) on the TMA and the full sections. All control cases were negative. This result shows 73% sensitivity and 100% specificity of TLE1 staining for PPSS.

Staining for bcl-2 protein and vimentin was positive in 100% of cases (Fig. 1d), CD56 was positive in ten cases (67%), calponin in four cases (27%), and EMA, CK AE1/AE3, CK19, CK7, and CD99 in two cases each (12%) in TMA sections, but positive in whole sections of 12 cases (80%). CD34 was focally positive in one case (7%) and S-100 negative in all cases.

Discussion

The term synovial sarcoma was coined in 1936 because the morphological features of the tumor are similar to those of the early developmental stages of joints, namely, cleft-like spaces surrounded by subsynovial spindle cells [6]. Currently, SS is regarded as a mesenchymal tumor characterized by a spindle cell component and an inconstant and variable epithelial component. In the 2002 World Health Organization Classification of Tumors of Soft Tissues and Bones, SS is classified as a malignant soft tissue tumor of uncertain differentiation [7]. Unusual locations of SS have been reported, including in the head and neck region, thorax, and internal organs such as the lung, kidney, liver, or prostate [8].

SS is characterized cytogenetically by a t(X;18)(p11.2; q11.2) translocation that results in the fusion of the *SYT* gene on chromosome 18 with the *SSX1* or *SSX2* gene on chromosome X. Epithelial and spindle cells of the biphasic type both carry the translocation [9]. The *SYT–SSX1* fusion is present in the majority of biphasic tumors, while *SYT–SSX1* and *SYT–SSX2* fusions are observed with equal frequency in tumors of the monophasic subtype. This distinctive chromosomal translocation is present in >90% of synovial sarcomas regardless of subtype, and it appears to be specific. However, there are reports of other tumors like fibrosarcoma and malignant fibrous histiocytoma that have shown the same translocation [10, 11]. It has been shown that this translocation correlates with TLE1 expression by immunohistochemistry [26]. It has also been demonstrated in mesothelioma [22], but to our knowledge, no studies have been performed by FISH for the t(X;18) in mesothelioma. Two rare fusion genes variants, *SYT–SSX4*=t(X;18)(p11;q13) and *SYTL1–SSX1*=t(X;20)(p11; q13) have been shown recently in a small proportion of cases [27–31]. Regarding the molecular analysis of t(X;18) in PPSS, in two previous studies, t(X;18) was reported in 36 of 39 patients (92%) and in 40 of 40 cases [2, 21]. We found the SYT translocation in 15 of 15 tested cases (100%); five cases were excluded because they were core needle biopsies with scant material insufficient for analysis. In our study, the FISH test was performed in a tissue microarray and showed high specificity. It is therefore a

Table 3 FISH and immunohistochemical findings

Case No.	FISH (X:18)	TLE-1	Bcl2	VIM	EMA	AE1/AE3	CK7	CK19	Calponin	CD34	CD99	S-100	CD56
1	+	++	++	+	−	−	−	−	−	−	−	−	+
2	+	++	++	+	−	−	−	−	−	−	−	−	+
3	+	++	+	+	−	−	−	−	−	−	−	−	−
4	+	+	F	+	−	−	−	−	−	−	−	−	−
5	+	++	++	+	−	−	−	−	−	−	−	−	+
6	+	−	+	+	−	−	−	−	−	−	−	−	+
7	+	−	+	+	−	−	−	−	+	−	+	−	−
8	+	+	F	+	−	−	−	−	−	−	−	−	−
9	+	−	+	++	++	++	++	++	−	−	−	−	+
10	+	++	++	+	F	−	−	−	−	−	−	−	+
11	+	−	++	+	−	−	−	−	−	−	−	−	+
12	+	+	++	++	−	−	−	−	+	−	−	−	+
13	+	+	+	+	−	−	−	−	+	F	F	−	−
14	+	+	+	F	−	+	+	+	−	−	−	−	+
15	+	+	+	+	−	−	−	−	+	−	−	−	+

− Negative; + weak positive, diffuse; ++ strong positive, diffuse; *f* focal positive

practical and reliable method to analyze several cases together, resulting in a highly cost-effective method.

Most SS display at least focal immunoreactivity for epithelial markers. Reportedly, 90% of all synovial sarcomas are cytokeratin-positive, more pronounced in the epithelial component than in the spindle component [12–14]. The more frequently expressed are CK7 (79%), CK19 (60%), and CK8/18 (45%); no other spindle cell sarcomas exhibit these cytokeratins consistently [15, 16]. Up to 30% show focal immunoreactivity for S-100 protein. CD99, the product of the *MIC2* gene, shows membranous or cytoplasmic staining in 60–70% of SS. Bcl-2 protein is diffusely positive in virtually all SS, especially in the spindle cells, but is of limited diagnostic value since many other tumors express this antigen [17]. Calponin has also been frequently found in SS; it may be useful in recognizing poorly differentiated variants since other round cell tumors are negative for this antigen [4]. CD34 is almost always negative in synovial sarcoma. The immunohistochemical profile in our series of PPSS is similar to that reported in soft tissue SS with some differences: 100% of cases were positive for vimentin and Bcl-2. CD56 was positive in 67% and calponin in 27%. However, epithelial markers and CD99 were expressed in a minority of cases studied by TMA (12%), however in whole sections were positive in 80% of cases and CD34 focally positive in one case.

A new immunohistochemical marker is Transducin Like Enhancer of Split 1 (TLE1), a protein that interacts with TLE2, glycoprotein 130, UTY, HES6, RUNX3, SIX3, and RUNX1 proteins involved in cellular proliferation. It belongs to the Groucho/TLE/Grg family of co-repressors that affect many signaling pathways. Human TLE1 operates with some critical transcription factors that regulate the survival, hematopoiesis, and differentiation of normal cells [5]. It is overexpressed when t(X;18) occurs. It was shown that TLE1 in SS causes the overexpression of Bcl-2. Experimental knockdown of TLE1 in fibroblasts and synovial cells did not affect cell proliferation or enhance the cytotoxicity of chemotherapy, which suggests that TLE1 can be a good target for selectively treating synovial sarcoma without causing damage to the host tissue. However, further studies will be needed to determine a potential therapeutic role for TLE1 [32]. In the largest series of 259 cases of molecularly confirmed synovial sarcomas using a TMA, TLE1 was reported positive in 96%, but negative in others [18–20, 24, 25]. However, in another large series using whole tissue sections, it was found positive in other sarcomas, especially malignant peripheral nerve tumors [21]. In a recent series of spindle cell mesotheliomas, Matsuyama et al. [22] described focal and weak positivity in 28 malignant mesotheliomas regardless of histologic subtype. We included in our control series ten spindle cell mesotheliomas; all were negative. We did not, however, include epithelioid or mixed subtypes.

In conclusion, the molecular, immunohistochemical, and histological features of PPSS are very similar to SS in soft tissues. They are diffusely positive for vimentin and bcl-2, focally for EMA and keratin, and negative for CD34 and S100. TLE1 expression is highly specific, but less frequent than reported in soft tissue SS. Detection of *SYT* rearrangement by FISH is a valuable diagnostic adjunct that can be effectively performed on TMA.

Conflict of interest statement We declare that we have no conflict of interest.

References

1. Aubry MC, Bridge JA, Wickert R et al (2002) Primary monophasic synovial sarcoma of the pleura: five cases confirmed by the presence of SYT–SSX fusion transcript. Am J Surg Pathol 25:776–781
2. Begueret H, Galateau-Salle F, Guillou L et al (2005) Primary intrathoracic synovial sarcoma: a clinicopathologic study of 40 t (X;18)-positive cases from the French Sarcoma Group and the Mesopath Group. Am J Surg Pathol 29:339–346
3. Fletcher CD (2002) World Health Organization classification of tumors of soft tissue and bone. IARC, Lyon
4. Fligman I, Lonardo F, Jhanwar SC et al (1996) Molecular diagnosis of synovial sarcoma and characterization of a variant SYT–SSX2 fusion transcript. Am J Pathol 147:1592–1599
5. Gaertner E, Zeren EH, Fleming MV et al (1996) Biphasic synovial sarcomas arising in the pleural cavity. A clinicopathologic study of five cases. Am J Surg Pathol 20:36–45
6. Takenaka S, Ueda T, Naka N (2008) Prognostic implication of SYT–SSX fusion type in synovial sarcoma: a multi-institutional retrospective analysis in Japan. Oncology Reports 19:467–476
7. Folpe Al, Schmidt RA, Chapman D et al (1998) Poorly differentiated synovial sarcoma: immunohistochemical distinction from primitive neuroectodermal tumors and high grade malignant peripheral nerve sheath tumors. Am J Surg Pathol 22:673–682
8. Fischer C, Montgomery E, Healey V (2003) Calponin and h-caldesmon expression in synovial sarcoma; the use of calponin in diagnosis. Histopathology 42:588–593
9. Verbeke SLJ, Fletcher CDM, Alberghini M et al (2010) A reappraisal of hemangiopericytoma of bone; analysis of cases reclassified as synovial sarcoma and solitary fibrous tumor of bone. Am J Surg Pathol 34:777–783
10. Mirzoyan M, Muslimani A, Setrakian S, Swedh M, Daw HA (2008) Primary pleuropulmonary synovial sarcoma. Clinical Lung Cancer 9:257–261
11. Olsen SH, Thomas DG, Lucas DR (2006) Cluster analysis of immunohistochemical profiles in synovial sarcoma, malignant peripheral nerve sheath tumor and Ewing's sarcoma. Mod Pathol 19:659–568
12. Guillou L, Wadden C, Kraus MD (1996) S-100 protein reactivity in synovial sarcomas—a potentially frequent diagnostic pitfall: immunohistochemical analysis of 100 cases. Appl Immunohistochem 4:167–172
13. Heuvel SE, Hoekstra HJ, Bastiaannet E (2009) The classic prognostic factors tumor stage, tumor size, and tumor grade are the strongest predictors of outcome in synovial sarcoma: no role

for SSX fusion type or ezrin expression. Appl Immunohistochem Mol Morphol 17:189–195
14. Zeren H, Morán CA, Suster S et al (1995) Primary pleuropulmonar sarcomas with features of monophasic synovial sarcoma: a clinicopathological, immunohistochemical and ultrastructural study of 25 cases. Human Pathol 26:474–480
15. Safar A, Wickert R, Nelson M et al (1998) Characterization of a variant SYT–SSX1 synovial sarcoma fusion transcript. Diag Mol Pathol 7:283–287
16. Sistla R, Tameem A, Vidyasagar VS (2010) Intraarticular synovial sarcoma. Indian J of Pathol and Microbiol 53:115–116
17. Terry J, Saito T, Subramanian S et al (2007) TLE1 as a diagnostic immunohistochemical marker of synovial sarcoma emerging from gene expression profiling studies. Am J Surg Pathol 31:240
18. Kosemehmetoglu K, Vrana JA, Folpe AL (2007) TLE1 expression is not specific for synovial sarcoma: a whole section study of 163 soft tissue and bone neoplasms. Mod Pathol 22:872–878
19. Krskova L, Sumerauer D, Stejskalova E, Kodet R (2007) A novel variant of SYT–SSX1 fusion gene in a case of spindle cell synovial sarcoma. Diagn Mol Pathol 16:179–183
20. Van de Rijn M, Barr FG, Xiong QB et al (1999) Poorly differentiated synovial sarcoma: an analysis of clinical, pathologic and molecular genetic features. Am J Surg Pathol 23:106–112
21. Ladanyi M, Antonescu CR, Leung DH (2002) Impact of SYT–SSX fusion type on the clinical behavior of synovial sarcoma: a multi-institutional retrospective study of 243 patients. Cancer Res 62:135–140
22. Matsuyama A, Hisaoka A, Iwasaki M, Iwashita M, Hishinaga S, Hashimoto H (2010) TLE1 expression in malignant mesothelioma. Virchows Arch 457:577–583
23. Essary LR, Vargas SO, Fletcher CD (2002) Primary pleuropulmonary synovial sarcoma: reappraisal of a recently described anatomic subset. Cancer 94:459–469
24. Hartel PH, Fanburg-Smith JC, Frazier AA et al (2007) Primary pulmonary and mediastinal synovial sarcoma: a clinicopathologic study of 60 cases and comparison with five prior series. Mod Pathol 20:760–769
25. Jagdis A, Rubin BP, Tubbs RR, Pacheco M, Nielsen TO (2009) Prospective evaluation of TLE1 as a diagnostic immunohistochemical marker in synovial sarcoma. Am J Surg Pathol 33:1743–1751
26. Knösel T, Heretsch S, Altendorf-Hofmann A, Richter P, Katenkamp K, Katenkamp D, Berndt A, Petersen I (2010) TLE1 is a robust diagnostic biomarker for synovial sarcomas and correlates with t(X;18): analysis of 319 cases. Eur J Cancer 46:1170–1176
27. Lee W, Han K, Charles P, Harris A, Shim S, Kim S, Meisner LF (1993) Analysis of chromosome rearrangement in synovial sarcoma cells from paraffin-embedded specimens. Am J Pathol 142:15–19
28. Mandhal N, Heim S, Arheden K et al (1998) Multiple karyotypic rearrangements, including t(X;18)(p11;q11), in a fibrosarcoma. Cancer Genet Cytogenet 30:323–327
29. Pelmus M, Guillou L, Holstein I et al (2002) Monophasic fibrous an poorly differentiated synovial sarcoma: immunohistochemical reassessment of 60 t(X:18)(SYT-SSX)-positive cases. Am J Surg Pathol 26:1434–1440
30. Suster S, Fischer C, Moran CA (1998) Expression of bcl-2 oncoprotein in benign and malignant spindle cell tumors of soft tissue, skin, serosal superfices and gastrointestinal tract. Am J Surg Pathol 22:863–872
31. Törnkvist M, Brodin B, Bartolazzi A et al (2002) A novel type of SYT/SSX fusion: methodological and biological implications. Mod Pathol 15:679–685
32. Seo SW, Lee H, Lee HI, Kim HS (2011) The role of TLE1 in synovial sarcoma. J Orthop Res 29:1131–1136

Virchows Arch (2011) 459:623–625
DOI 10.1007/s00428-011-1159-x

LETTER TO THE EDITOR

Pancreatic adenocarcinoma with multiple eosinophilic extracellular deposits consistent with noncalcified psammoma bodies

Nora I. Schneider · Thomas Bauernhofer · Helmut Schöllnast · Arthur Ott · Cord Langner

Received: 5 October 2011 / Accepted: 12 October 2011 / Published online: 30 October 2011
© Springer-Verlag 2011

Dear Editor,

Adenocarcinomas commonly show extracellular mucin deposits, which, e.g., in breast cancer, may undergo secondary degenerative changes such as calcification. Psammoma bodies representing lamellated calcifications are a common morphologic feature of papillary carcinoma of the thyroid, serous adenocarcinoma of the ovary, and meningiomas.

A 63-year-old male presented with unspecific epigastric pain and obstructive jaundice. Abdominal computed tomography revealed a mass lesion within the head of the pancreas, measuring 1.8 cm in the largest diameter, with infiltration of the duodenal wall, stricture of the distal bile duct, and dilatation of the biliary system. In addition, cancer spread to regional lymph nodes and liver was noted (Fig. 1). Endoscopy disclosed ulceration of the duodenal mucosa by penetrating tumor and multiple biopsies were obtained.

Upon histology, the tumor turned out to be a poorly differentiated ductal adenocarcinoma. The tumor infiltrated the duodenal mucosa, showed multifocal lymphatic permeation, and was characterized by multiple eosinophilic extracellular deposits that were commonly, yet not invariably surrounded by cancer cells (Fig. 2a–b). The deposits were PAS-positive (Fig. 2c) and appeared lamellated, consistent

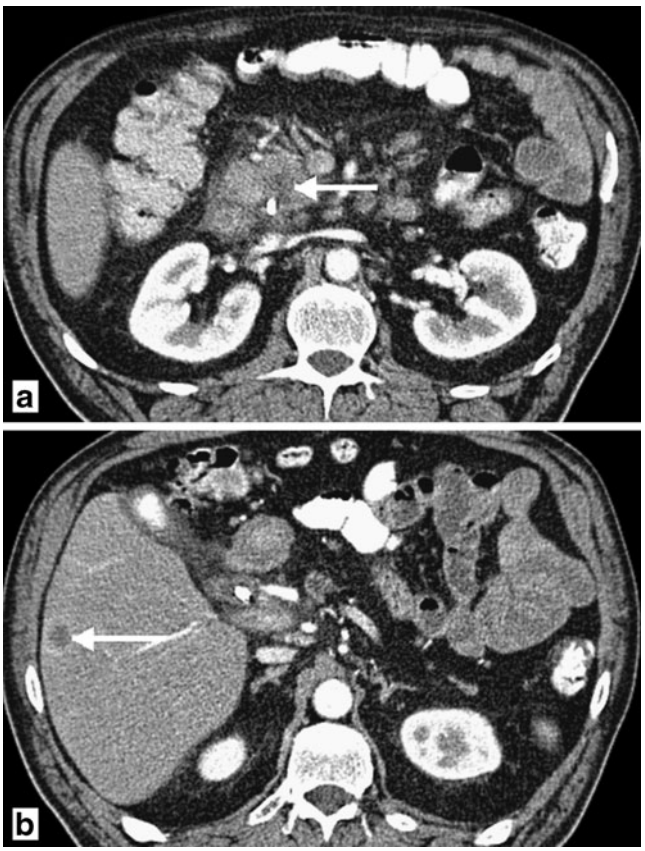

Fig. 1 Tumor lesion within the head of the pancreas, measuring 1.8 cm in the largest diameter (**a**, *arrow*) with cancer spread to regional lymph nodes and liver (**b**, *arrow*)

N. I. Schneider · A. Ott · C. Langner (✉)
Institute of Pathology, Medical University of Graz,
Auenbruggerplatz 25,
8036 Graz, Austria
e-mail: cord.langner@medunigraz.at

T. Bauernhofer
Department of Internal Medicine, Division of Oncology,
Medical University of Graz,
Graz, Austria

H. Schöllnast
Department of Radiology,
Division of General Radiological Diagnostics,
Medical University of Graz,
Graz, Austria

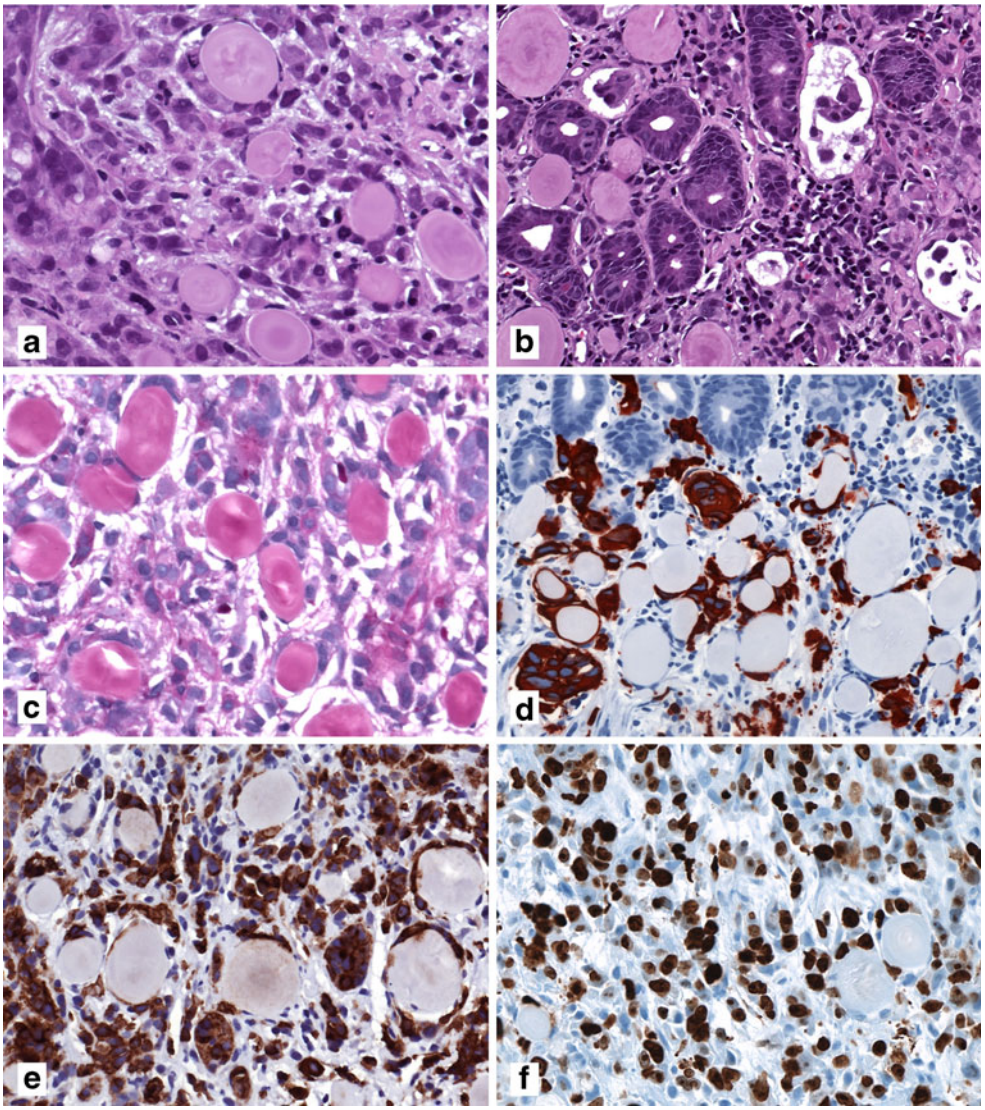

Fig. 2 Poorly differentiated ductal adenocarcinoma of the pancreatic head showing multiple lamellated eosinophilic extracellular deposits consistent with noncalcified psammoma bodies (**a**). Note tumor infiltration of the duodenal mucosa with lymph vessel invasion (**b**). PAS-stain (**c**). The neoplastic cells expressed keratin 7 (**d**) and MUC1 (**e**), proving the pancreatobiliary nature of the lesion. MIB-1 proliferation index 80% (**f**)

with noncalcified psammoma bodies. The tumor cells stained for keratin 7 (Fig. 2d) and MUC1 (Fig. 2e), while staining for keratin 20, MUC2, CDX-2, MUC5AC as well as neuroendocrine markers including synaptophysin, chromogranin A, neuron-specific enolase, NCAM/CD56, and somatostatin rendered negative results, thus proving the pancreatobiliary nature of the malignancy. The MIB-1 proliferation index was 80% (Fig. 2f). Pyrosequencing applying the PyroMark Q24 KRAS kit (Qiagen, Valencia, CA) revealed *KRAS* mutation in codon G12D.

Psammomatous calcifications are rare in gastrointestinal tract tumors. To the best of our knowledge, there are only two reports on hyaline globule or psammoma body formation in pancreatic adenocarcinoma. Kuroda et al. [1] described a 59-year-old male with anaplastic cancer showing rhabdomyoblastic differentiation and intracytoplasmatic hyaline globule-like structures. The second case, presented by Ohike et al. [2], refers to an 83-year-old female with ductal adenocarcinoma featuring multiple osteopontin-positive psammomatous calcifications within glandular lumina as well as within the tumor stroma. Our case, illustrating eosinophilic extracellular deposits consistent with noncalcified psammoma bodies, thus appears to be unique. The pathogenesis of the lamellated deposits remains elusive and intracellular precursor lesions were not identified. Similar to the so-called Liesegang rings, the deposits may have resulted from supersaturation of a colloidal solution with heavy ions that undergo intermittent episodes of chelation [3].

The lesion has to be differentiated from solid-pseudopapillary neoplasms of the pancreas and from neuroendocrine tumors that may both occasionally contain PAS-positive extracellular deposits [4, 5]. In particular, duodenal somatostatinoma has to be considered in differential diagnosis. This tumor originating from the periampullary region commonly shows psammoma body

formation within glandular structures but is characterized by immunoreactivity for somatostatin as well as for other neuroendocrine markers.

In conclusion, we present the case of a pancreatic adenocarcinoma with infiltration of the duodenal wall that was characterized by formation of multiple eosinophilic extracellular deposits consistent with noncalcified psammoma bodies. This peculiar lesion has to be differentiated from other tumors originating in this location, particularly duodenal somatostatinoma.

Disclosure statement The authors declare that no financial or other conflict of interest exist in relation to the content of the article.

References

1. Kuroda N, Iwamura S, Fujishima N et al (2007) Anaplastic carcinoma of the pancreas with rhabdoid features and hyaline globule-like structures. Med Mol Morphol 40:168–171
2. Ohike N, Sato M, Kawahara M, Ohyama S, Morohoshi T (2008) Ductal adenocarcinoma of the pancreas with psammomatous calcification: report of a case. JOP 9:335–338
3. Gilchrist HM, Wick MR, Patterson JW (2010) Liesegang rings in an apocrine hidrocystoma: a case report and review of literature. J Cutan Pathol 37:1064–1066
4. Taccagni GL, Carlucci M, Sironi M, Cantaboni A, Di Carlo V (1986) Duodenal somatostatinoma with psammoma bodies: an immunohistochemical and ultrastructural study. Am J Gastroenterol 81:33–37
5. Meriden Z, Shi C, Edil BH et al (2011) Hyaline globules in neuroendocrine and solid-pseudopapillary neoplasms of the pancreas: a clue to the diagnosis. Am J Surg Pathol 35:981–988

Virchows Arch (2011) 459 (Suppl 1):S1–S329
DOI 10.1007/s00428-011-1113-y

ABSTRACTS

Plenary Oral Free Paper Sessions

Thursday, 1 September 2011, 11.00–12.00, Hall 5bc

PL-01 Plenary Oral Free Paper Session

001

Investigation of the correlation between up-regulated ERG expression and PTEN loss with capsular penetration in prostate cancer

R. Dittamore*, R. Nagle, L. Brosch, E. Abril, C. Cortez, A. Algotar, W. Meek, K. McDaniel, E. Dexter, B. Dalkin, G. Pestano
*Roche Diagnostics, Tucson, USA

Objective: Previous studies have demonstrated the existence of ETS gene rearrangement in prostate cancers. TMPRSS2–ERG gene fusion is the most common rearrangement and the overexpression of the ERG oncogene occurred in 50% of localized and metastatic prostate cancers. Studies have identified the relationship between ERG overexpression and PTEN deletions as a critical gateway to predicting poor outcome. We hypothesized that ERG overexpression and PTEN deletions status may correlate with capsular penetration.
Method: From a cohort of 210 fully embedded prostatectomy patients, we selected cases that had capsular penetration, pT3a with a contralateral organ confined lesion. PTEN and ERG expression were compared between the penetrating lesion (CP) and the contralateral organ confined lesion (non-CP).
Results: See image

Results:

Groups	CP (N, %)	Non-CP (N, %)	Total	Odds Ratio	p-value
Pos PTEN & Neg ERG	13 (31.7)	18 (43.9)	31	Ref	
Pos PTEN & PosErg	17 (41.5)	18 (43.9)	35	1.4	0.51
Neg PTEN & Pos ERG	6 (14.6)	1 (2.44)	7	8.3	0.06
Neg PTEN & Neg ERG	5 (12.2)	4 (9.76)	9	1.7	0.47
Total	41	41			

Conclusion: Our analysis of this cohort showed an OR of 8.3, indicating that capsular penetration is 8.3 times more likely in lesions demonstrating negative PTEN expression and positive ERG over-expression. This profile was generated after comparison with lesions demonstrating a normal expression profile for PTEN and ERG (Pos PTEN and Neg ERG). We conclude that having an expression profile of PTEN loss and ERG over-expression appears to be a risk factor for capsular penetration in prostate cancer. Additional studies should be conducted in larger, prospective and retrospective biopsy studies to validate these findings.

002

EGFR gene copy number assessment from areas with highest EGFR expression predicts response to anti-EGFR therapy in colorectal cancer

A. Aalgars*, M. Lintunen, R. Ristamäki, J. Sundström
*Dept. of Oncology, Turku University Hospital, Finland

Objective: Only 40–70% of metastatic colorectal cancers (mCRC) with wild-type KRAS oncogene respond to anti-epidermal growth factor receptor (anti-EGFR) antibody treatment. EGFR amplification has been suggested as an additional marker to predict the response. However, improved methods for bringing the EGFR analysis into routine laboratory are needed.
Method: The material consisted of 80 patients with mCRC, 54 of them receiving anti-EGFR therapy. EGFR gene copy number (GCN) was analysed by automated silver in situ hybridisation (SISH). Immunohistochemical EGFR protein analysis was used to guide the SISH assessment.
Results: Clinical benefit was seen in 73% of high-EGFR (≥ 4.0) GCN patients, in comparison to 59% of KRAS WT patients. Only 20% of low-EGFR GCN patients responded to therapy. A high EGFR GCN number associated with longer progression-free survival ($p<0.0001$) and overall survival ($p=0.004$). Together with KRAS analysis, EGFR GCN identified the responsive patients to anti-EGFR therapy more accurately than either test alone. The clinical benefit rate of KRAS WT/high GCN tumours was 82%.
Conclusion: Our results demonstrate that automated EGFR SISH, in combination with KRAS mutation analysis, can be a useful and easily applicable technique in routine diagnostic practise for selecting patients for anti-EGFR therapy.

003

Different CHEK2 germline mutations are associated with distinct immunophenotypic molecular subtypes of breast cancer

P. Domagala*, D. Wokolorczyk, C. Cybulski, T. Huzarski, J. Lubinski, W. Domagala
*Dept. of Pathology, Pomeranian Medical University, Szczecin, Poland

Objective: We tested the hypothesis that distinct mutations in breast cancer (BC) susceptibility gene involved in DNA repair, i.e. CHEK2, may be associated with particular immunophenotypic molecular subtypes of this cancer.
Method: Two groups of patients (1,255 with BCs and 5,496 healthy controls) were genotyped for four CHEK2 mutations (I157T and three truncating mutations: 1100delC, IVS2+1 G>A, del5395). BCs were tested by immunohistochemistry on tissue microarrays for ER, PR, HER-2, EGFR, and CK5/6 and were assigned to appropriate subtypes of immunophenotypic molecular classification.
Results: There was a significant association between CHEK2 mutations and the immunophenotypic molecular classification (p=0.004). CHEK2-associated cancers were predominantly luminal (108/117=92.3%). CHEK2-I157T variant was associated with the luminal A subtype (p=0.01), whereas CHEK2-truncating mutations were associated with the luminal B subtype (p=0.005). Comparing the prevalence of CHEK2 mutations in BC with controls revealed that carriers of I157T variant had OR of 1.80 for luminal A subtype and carriers of truncating mutations had OR of 6.26 for luminal B subtype of BC.
Conclusion: To our knowledge, this is the first study showing that specific mutations in the same susceptibility gene are associated with different immunophenotypic molecular subtypes of BC. This association represents independent evidence supporting the biological significance of immunophenotypic molecular classification.

004

11q22.3-q25 deletions are associated with atypical carcinoids and a poor clinical outcome

E.-J. Speel*, D. Swarts, R.-J. van Suylen, A.-M. Dingemans, W. de Herder, R. de Krijger, E. Smit, F. Thunnissen, C. Seldenrijk, A. Perren
*Maastricht UMC, Pathology, The Netherlands

Objective: Lung carcinoids are neuroendocrine tumors that can be subclassified as typical (TC) or atypical (AC) carcinoids. Our aim was to identify the genetic alterations which can improve the prediction of prognosis.
Method: We investigated 34 lung carcinoids (18 TCs, 15 ACs, 1 unclassified) by arrayCGH on 3.7k genomic BAC arrays (resolution ≤1 Mb). Results were correlated with clinical patient data and long-term follow-up.
Results: When comparing ACs with TCs, our data revealed: (1) a significant difference in the average number of chromosome arms altered (9.6 versus 4.2, p=0.036), with five ACs having≥15 chromosome arms altered; (2) in ≥30% of ACs multiple gains and losses (≥1 Mb); and (3) 11q deletions in 8/15 ACs vs. 1/18 TCs (p=0.004), which was confirmed by FISH. The four critical regions of interest in ≥45% of ACs comprised 11q14.1, 11q22.1-q22.3, 11q22.3-q23.2 and 11q24.2-q25, all telomeric of MEN1 at 11q13. There was a strong association of 11q22.3-q25 loss with a poorer prognosis, alone or in combination with the absence of 9q34.11 alterations (p=0.0022 and p=0.00026, respectively).
Conclusion: A subgroup of ACs can be identified harboring 11q22.3-q25 deletions, with a significantly poorer prognosis as compared to carcinoids without these 11q deletions.

Oral Free Paper Sessions

Tuesday, 30 August 2011, 14.00–16.30, Room 206

OFP-01 Oral Free Paper Session Breast Pathology I

001

Is it rational to detect HER-2/neu gene amplification in breast cancer patients without expression of HER2 protein? Results of HER retest project

A. Ryska*
*Faculty Hospital Hradec Kralove, The Fingerland Dept., Czech Republic

Objective: HER-2/neu is in Czech Republic tested by IHC, only 3+ and 2+ cases are confirmed by ISH. No information about IHC-/ISH+tumors is available. The aim of our study was to investigate the frequency of such cases and find an economically acceptable testing algorithm.
Method: There were 617 HER2 IHC- cases collected; these were repeatedly tested in participating reference laboratories by IHC (Ventana Pathway) and ISH (Ventana Dual Colour SISH). Details on histological type, grade, size, number of examined/positive lymph nodes, hormonal receptor (ER, PR) status, and proliferative activity were recorded.
Results: A concordant result of HER2 IHC between primary and reference lab was seen in 535 (86.7%) cases.

Of 82 (13.3%) discrepant cases, 13 (2.1%) were 3+ and 69 (11.2%) were equivocal (2+); only 12 (1.9%) of these were amplified. total of 21/535 (3.4%) cases had IHC-/ISH+ phenotype. These were significantly more frequently (1) non-lobular, non-mucinous and non-papillary, (2) with loss of ER and/or PR and (3) pT2 or higher.

Conclusion: A high (96%) clinically relevant concordance between primary and reference labs was shown. The subgroup of IHC-/ISH+cases is quite small (3.4%); however, in pT2 or higher non-lobular, non-mucinous and non-papillary tumors with loss of ER and/or PR expression, their frequency reaches 11.8%.

002

Histopathologic characteristics and disease-free survival of mammary Paget disease

C. Albarracin*, A. Gullett, V. Prieto, C. Kelly, X. Duan, R. Bassett, K. Klein, E. Resetkova, D. G. Rosen, Y. Wu, N. Sneige
*UT- MD Anderson Cancer Center, Pathology, Houston, USA

Objective: Mammary Paget disease (MPD) is a rare entity with a heterogeneous presentation. We evaluated the clinicopathologic features and outcomes of a large cohort of MPD patients in our institution.

Method: Histologic, radiologic and clinical features were evaluable in 319 of 546 MPD patients.

Results: MPD patients were classified into three groups: 18 without underlying breast carcinoma (PD), 97 with DCIS (PDCIS), and 204 with IDC (PIDC). The carcinomas in MPD were more likely to be HER2-positive as compared to carcinomas in the general population. In a subset of cases, HER2 was coexpressed in Paget cells and underlying carcinoma in 71% of PIDC and 100% of PDCIS. Clinically, MPD without underlying carcinoma was not associated with recurrence (locoregional or distant) if completely excised.

Conclusion: The three major groups of MPD had different clinicopathologic characteristics and survival, suggesting that these features can be incorporated in the management of MPD.

003

FGFR1 in metastatic and primary lobular breast carcinoma. A biological rationale for new therapeutic option

E. Brunello*, M. Brunelli, A. Nottegar, E. Manfrin, S. Pedron, E. Vittoria, M. Chilosi, S. Gobbo, G. Martignoni, F. Bonetti
*University of Verona, Pathology and Diagnostic, Italy

Objective: Lobular breast carcinoma usually shows poor responsiveness to chemotherapies and often lacks targeted therapies. Since FGFR1 expression has been shown to play pivotal roles in breast cancer tumorigenesis and FGFR1 inhibitor has been recently developed, we sought to analyze the status of FGFR1 gene in lobular breast carcinoma.

Method: Twenty infiltrative lobular carcinomas where recruited and tissue microarrays were constructed (three cores for each case), 11 of which had available matched loco-regional lymph-nodal metastasis. FGFR1 gene (8p12) amplification was evaluated by cromogenic in situ hybridization (CISH) (Zytovision) analyses.

Results: Three (15%) primary lobular breast carcinomas showed FGFR1 amplification (cluster of signals), whereas in 11 (55%) any abnormality was not observed. Six cases (30%) had three cromogenic signals. Two of 11 metastasis (18%) were amplified; 2/11 (18%) were not. The seven remaining cases (64%) showed three cromogenic signals.

Conclusion: (1) A subset of lobular breast carcinoma, either primary or metastatic, shows FGFR1 amplification or gains of cromogenic signals; (2) there is heterogeneity in matched primary and metastatic carcinomas; (3) in the era of tailored therapies, patients affected by the lobular subtype of breast carcinoma with FGFR1 amplification could be approached to the new target biological therapy such as FGFR-1 inhibitor.

004

HER2 over expression: direct comparison between SP3 monoclonal antibody and polyclonal antibody with double-check assessment and FISH correlation

V. Caceres*, G. Acosta Haab, S. Sarancone, I. Frahm
*Productos Roche, Oncology, Buenos Aires, Argentina

Objective: Given that the high-impact results on subsequent patient management, accuracy, precision, and reproducibility of HER2 testing are critical, recently developed rabbit monoclonal antibodies are reported to have greater sensitivity and specificity than rabbit polyclonal antibodies. This study was aimed to confirm the reliability improvement of Her2 testing by using monoclonal antibody SP3 as an alternative to polyclonal antibody routinely used in our laboratories.

Method: Therefore, 336 primary breast carcinomas tissue paraffin blocks were analyzed using both antibodies: polyclonal anti HER2 and rabbit monoclonal clone SP3. The results were interpreted as per ASCO-CAP guidelines and scored by two independent investigators. Following current recommendations, the HER2 equivocal and discordant cases were re-tested by FISH.

Results: A total of 327 cases (97.32%) showed coincident staining (274 were scores negative, 4 equivocal and 50

positive) and 9 (2.67%) were discordant as assessed by two blinded pathologists, respectively. The non-coincident results are summarized in Table 1.

Conclusion: Although with an elevated concordance rate (97.32%), SP3 shows better definition in negative tumors (partial membrane staining is avoided). In equivocal cases, SP3 demonstrates higher sensitivity and specificity than polyclonal antibody (excellent correlation with FISH). Our results indicate that SP3 antibody provides a more robust assessment of Her2 over-expression, in line with previously published results; nevertheless, in HER2 equivocal tumors, according to ASCO-CAP guidelines, FISH assay should be performed.

SP3	Polyclonal	Number (cases)	FISH
Equivocal	Positive	2	Negative
Negative	Equivocal	4	Negative
Negative	Positive	3	Negative

005

Tumor grading performed on microarray samples: an attempt to devise an applicable scheme

L. Dalton*, D. Page
*South Austin Medical Center, Pathology, USA

Objective: The potential of many novel prognostic and predictive markers are often evaluated using miniscule samples of cancer placed in microarrays (MA). Subsequently, the results are often compared with grade whereby the assessment of a "traditional histologic grade" (THG) was based on the evaluation of the entire tumor. Sample bias becomes a concern. We have attempted to devise a grading scheme in which a microarray grade (MG) will be comparable to THG.

Method: The progression (PM) and stage 1 prognostic (1 PM) microarrays were obtained from the USA National Cancer Institute (NCI) Cancer Diagnosis Program. Subjective evaluations of multiple morphologic parameters were performed on each MA sample such as overlapping of nuclei and size of nuclei. An evaluation of the importance of each parameter was performed by a clustering algorithm.

Results: MG was significantly correlated with THG even though what was subjectively evaluated was not identical. High versus low grade discrepancies were rare (5 of 501 samples). Both THG and MG showed a significant correlation with patient outcome ($p<0.001$). Of concern was that 90 of 591 of the MA samples were deemed to be inadequate for evaluation.

Conclusion: MG can be used as an adjunct to THG. That MG is strongly correlated with THG provides added evidence of the reproducibility in the grading of breast cancer.

006

A precision-guided sequential slicing of the resected breast tissue

S. Ichihara*, S. Moritani, M. Hasegawa
*Nagoya Medical Center, Dept. of Pathology, Japan

Objective: To determine the disease extent, the resected breast tissue is usually cut into parallel sections, each measuring around 5 mm in thickness. This step has usually been performed by pathologists or pathology assistants using a trimming knife without special devices. Therefore, the quality of conventional slicing is highly dependent on the skill of the operators, often resulting in undesirable variations in thickness or flatness. This hampers the quantification of disease extent based on the number of sections containing the disease.

Method: In order to improve the reproducibility in slicing, we have designed an apparatus which can locate the trimming knife to cut equidistantly as well as hold the object during slicing. The basic element of the apparatus is a parallel row of needles, which is spaced equidistantly (e.g. 3.5 mm) and extends in a common plane. This apparatus can be used as a single row of needles or its combination. A needle protector works to keep the needles straight and prevent the operators from hurting themselves.

Results: The neighboring needles provided the space where the knife moves regularly. This device was applicable to the other organs such as the digestive tract and lungs.

Conclusion: With this device, the evaluation of disease extent is more accurate and reproducible.

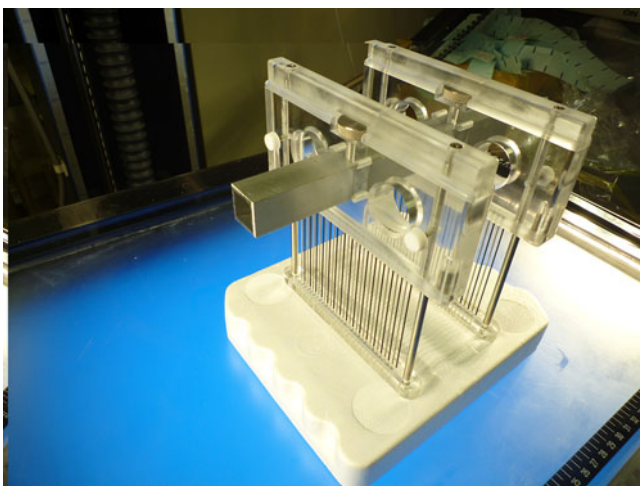

007

Ultrarapid cytokeratin immunohistochemistry for intraoperative assessment of breast cancer sentinel lymph nodes

J. Isola*, V. Manni, M. Tirkkonen, P. Kujala, L. Paljärvi, K. Lähteenmäki, C. Vasama
*University of Tampere, Institute of Biomedical Technology, Finland

Objective: The feasibility of ultrarapid immunohistochemistry (pan-CK and CK19 IHC) was studied for the intraoperative assessment of breast cancer sentinel lymph nodes.
Method: The ultrarapid IHC staining protocol consisted of acetone fixation (2 min), followed by incubations with anti-cytokeratin-HRP conjugate (3 min at +42 C), DAB chromogen (1.5 min at +42 C), and hematoxylin counterstain (10 s) using the Cytonel-Plus and Cytonel-19 kits (Jilab Inc, Tampere, Finland). The study material consisted of 249 and 60 consecutive breast cancer patients (for pan-CK and CK19, respectively). One to four sentinel nodes were studied for each patient. Routine stainings and ultrapid IHC were done on adjacent frozen sections.
Results: When compared to standard postoperative histopathology, intraoperative frozen section examination (routine stain and ultrarapid pan-CK) identified 56 of 66 metastases (including macro- and micrometastases and ITC). In a retrospective review, information provided by ultrarapid IHC was considered as crucial in 11 cases. Therefore, with the aid of ultrarapid IHC, the proportion of "late positives" was reduced roughly by half (from 21/248 to 10/248 cases in the total material). The patient material studied with ultrarapid CK19 yielded similar results.
Conclusion: We conclude that ultrarapid IHC (pan-CK or CK19) is a useful aid in the intraoperative examination of sentinel lymph nodes of breast cancer patients.

008

Distribution of molecular breast cancer subtypes among Iranian women and their correlation with clinical and histopathological parameters

M. Kadivar *, A. Joulaee, B. Fakhri, N. Mafi
*Tehran University, Dept. of Pathology, Iran

Objective: Breast cancer is a heterogeneous disease also affected by the ethnicity of the patients and which is classified into four molecular subtypes with distinct clinical behavior. Since there was not enough data on the subtypes in Iran, we carried out this study to investigate the prevalence and clinicopathologic features of each subtype among Iranian women.
Method: A total of 604 women diagnosed with breast cancer during 2003–2008 were included and these cases were categorized into four molecular subtypes using immunohistochemical stains: luminal-A, luminal-B, basal cell-like and HER2/neu. Through a retrospective analytical study, the prevalence of each subtype and its association with patient demographics and tumor characteristics (size, grade, lymph node involvement and vascular invasion) were investigated using SPSS.
Results: Luminal-A subtype accounted for 50.2%, luminal-B 24.3%, basal cell-like 16.6% and HER2/neu 8.9%. The prevalence of all subtypes increased with age except the basal cell-like which was the most prevalent in the age group$p<40$ years. Basal cell-like and HER2/neu subtypes were associated with larger tumor sizes, higher grades and more lymph node involvement ($p<0.05$); HER2/neu was also correlated with vascular invasion ($p<0.05$).
Conclusion: Luminal-A and luminal-B were more prevalent in older ages. Basal cell-like, the most aggressive subtype, was more prevalent in young women similar to that of Western countries and unlike China and Taiwan.

009

Urokinase-type plasminogen activator and plasminogen activator-inhibitor-1 related signalling pathways differ between primary breast cancers and lymph node metastases

K. Malinowsky *, C. Wolff, D. Berg, T. Schuster, A. Walch, H. Bronger, H. Mannsberger, C. Schmidt, U. Korf, H. Höfler, K.-F. Becker
*Technische Universität München, Inst. für Pathologie, Germany

Objective: The urokinase-type plasminogen activator (uPA) and its inhibitor PAI-1 support migration and invasion in cancer cells. Clinically, both factors are used to stratify node-negative breast cancer patients for chemotherapy. The aim of our study was to compare uPA- and PAI-1-associated signalling pathways in primary breast cancer tissues (PT) and lymph node metastasis (LNM).
Method: Using reverse-phase protein arrays (RPPA), we analysed formalin-fixed and paraffin-embedded tissues from 201 primary breast cancers and 52 corresponding lymph node metastases for the expression of 37 signalling proteins.
Results: PAI-1 expression correlated with the levels of FAK, PI3K, ILK, pAKT and ROCK while uPA expression was associated with the expression of ER, pERK, pp38 and Hsp27 in primary tumours. The expression of uPA correlated between PTs and LNMs while PAI-1 expression did not. The pathway correlations found in PTs did not persist in LNMs. Comparing the expression of individual

signalling molecules in PTs and LNMs, persistent correlations were revealed only for some of the molecules independent of a specific pathway.
Conclusion: Our results indicate the substantial deregulation of uPA- and PAI-1-related signalling in metastases compared to primary breast cancers and may help to explain why uPA and PAI-1 reached clinical relevance only for node-negative tumors.

Tuesday, 30 August 2011, 17.00–19.30, Room 201

OFP-02 Oral Free Paper Session Breast Pathology II

001

Should HER-2 Score 0/1+ breast cancer cases be retested by in situ hybridisation? Results of a multicenter retesting study

A. Reiner *, S. Lax, P. Regitnig, C. Kronberger, Z. Jasarevic, S. Bogner
*Donauspital Wien, Inst. für Pathologie, Austria

Objective: The variation of HER-2-immunohistochemistry (IHC) may give false-negative results. For scores 0/1+, in situ hybridization is not recommended routinely.
Method: A total of 570 breast cancers from five pathology departments scored 0/1+ by IHC (HercepTest or 4B5-antibody) were retested by HER2-Dual-SISH (BDISH) in a central laboratory. For evaluation, the CAP/ASCO guidelines were used.
Results: There were 25 cases (4.38%) amplified by BDISH but only two cases showed ratios >3.26 (6.35, 6.48). There were 17 cases (2.98%) which showed equivocal amplification. A total of 24 BDISH-amplified cases were further analyzed by IHC (4B5) and FISH (Vysis-Abbott). There were 17/24 BDISH-amplified cases (71%) which showed IHC scores 2+/3+, while 7 cases showed scores 0/1+. There were 3/13 score 2+ and 3/4 score 3+ cases amplified by FISH. Amplification by FISH also showed a low level. All score 0/1+ cases were non-amplified by FISH. Only 1/17 BDISH-equivocal amplified carcinomas was confirmed equivocal by FISH. Overall, after a multistep retesting, amplification occurred in only 17 cases (2.98%).
Conclusion: HER-2-amplification is rare in HER-2 negative breast carcinomas tested by IHC and mostly occurs at low level. Thus, HER-2 testing by routine IHC as a first step seems to be reliable. Low-level amplification seems to be diagnosed more frequently by BDISH compared to FISH.

002

Mutations of exon 1 and exon 2 of β-catenin gene in invasive breast carcinomas

L. Nakopoulou *, I. Theohari, I. Giannopoulou, C. Magkou, P. Rafailidis, K. Tzelepis, A. Nomikos, C. Papadimitriou
*Papagou, Greece

Objective: Mutations of β-catenin gene, particularly in the 3rd exon, are rare in breast cancer. The aim of our study was the identification of somatic mutations in the regulatory exons 1 and 2 of β-catenin in invasive breast carcinomas.
Method: One hundred thirty-six (136) samples were used (56 sporadic and 80 familial cases). DNA isolation from paraffin-embedded tissues and PCR were performed for the detection of mutations and real-time PCR for the measurement of β-catenin copy numbers.
Results: Point mutations in either exon were detected in 30.9% of the cases. The mutations in either exon and in exon 1 were more often detected in sporadic cases ($p=0.041$ and $p=0.031$, respectively). Patients with mutations and familial history were found to have a shorter disease-free survival ($p=0.049$). No associations were observed between gene amplification status and β-catenin expression.
Conclusion: For the first time, we report the existence of mutations in exons 1 and 2 of β-catenin gene in invasive breast cancer, which correlated with worse disease-free survival in patients with a family history. As regulatory regions, exons 1 and 2 are important for the proper transcription and translation of β-catenin, and their mutations might contribute to its abnormal expression in breast carcinomas.

003

High throughput testing of connexins in breast cancer using multilayer, multichannel fluorescence digital microscopy

I. Zsakovics *, M.A. Szasz, P. Balla, J. Kulka, T. Krenacs
*Semmelweis University, 1st Dept. of Pathology, Budapest, Hungary

Objective: Connexin (Cx) channels (gap junctions) between adjacent cells are involved in cell homeostasis and their deregulation is linked to carcinogenesis. New data suggest their stage-dependent occurrence during tumor progression.
Method: We have tested the expression of 10 out of the 21 connexin isotypes in 252 breast cancer samples of all grades included in tissue microarrays by setting up a unique technique utilizing multichannel, multilayer fluorescence digital microscopy (Pannoramic Scan, 3DHISTECH, Budapest) allowing their rapid and validated testing.
Results: In normal breast, we have confirmed the expression of Cx43 and Cx26. In addition, we found Cx32, Cx30, Cx23, Cx46, and Cx30.2 for the first time. In breast cancer, the frequency of Cx43-positive cases was significantly higher in grade 1 than in grade 2 tumors, which however, showed a relative increase again in grade 3 cancers of poor prognosis. This finding and that more than half of proliferating luminal B tumors expressed Cx43 may explain the nearly but not significant 5-year disease-free survival advantage of Cx43-positive cases. Also, we have detected Cx26, Cx32, Cx30,

Cx46, and Cx23 for the first time in 10–20% of high-grade proliferating cancers.
Conclusion: Our results suggest a biphasic, i.e. tumor-suppressive and tumor-adaptive, potential for connexins in breast cancer.

004

Epigenetic silencing in non-neoplastic epithelia identifies E-cadherin (CDH1) as a target for the chemoprevention of lobular neoplasia

H.-S. Yoon *, D.-H. Zou, D. Perez, P. Guilford, B. Humar
*University of Otago, Dunedin School of Medicine, New Zealand

Objective: Lobular breast cancer (LBC) ranges from atypical lobular hyperplasia (ALH), lobular carcinoma in situ (LCIS) and invasive lobular carcinoma (ILC). The epigenetic silencing of the E-cadherin gene (CDH1) is thought to be involved in E-cadherin downregulation and frequently observed in ILC. Here we investigate whether CDH1 promoter methylation is already present in in situ lesions and thus contributes to the initiation of ILC.
Method: We examined microdissected archived tissue from 20 LBCs by methylation-specific PCR to determine the CDH1 methylation status of lobular lesions.
Results: Nineteen of the 20 LBCs had a hypermethylated CDH1 promoter, including 13/14 ILCs and 13/13 ALHs or LCIS. Bisulphite sequencing indicated that methylation was complete within the investigated promoter fragment. Intriguingly, CDH1 methylation was likewise present in 8/8 adjacent non-neoplastic epithelia, but not in 6/6 mammary epithelia from healthy subjects. E-cadherin protein and mRNA were down-regulated in in situ lesions relative to adjacent epithelia. These results together indicate that CDH1 promoter methylation occurs in LBC prior to E-cadherin down-regulation and neoplastic formation.
Conclusion: We thus propose that epigenetic silencing represents the first of the two hits required to silence both CDH1 alleles for LBC to develop. This also suggests increased disease susceptibility, providing an explanation for the multifocal presentation of LBC.

005

The effect of prolonged formalin fixation on the immunohistochemical detection of HER2

J. Goedhals *, G. Le Roux, M. Myburg
*University of the Free State, Bloemfontein, South Africa

Objective: The human epidermal growth factor receptor 2 gene (HER2) amplification status is an important prognostic marker in breast cancer. The American Society of Clinical Oncology/College of American Pathologists guideline recommends that the specimens used for HER2 testing should be fixed for between 6 and 48 h. Many of the specimens evaluated by the Department of Anatomical Pathology, University of the Free State/NHLS, are received from other parts of the country and are in formalin for longer than 48 h. The aim of this study was therefore to evaluate the effects of prolonged formalin fixation on HER2 immunohistochemistry.
Method: Ten mastectomy specimens with positive (3+) immunohistochemistry for HER2 and sufficient residual tumour following routine processing were included in the study. Sections of tumour were submitted for processing and staining twice a week. The Ventana anti-HER2/neu (clone 4B5) rabbit monoclonal primary antibody was used.
Results: The immunohistochemistry for HER2 became negative in two cases after 39 and 46 days, respectively. The remaining eight cases remained positive after periods of between 32 and 123 days with an average of 66 days.
Conclusion: Prolonged formalin fixation does appear to result in reduced immunoreactivity for HER2. However, the periods involved should not be clinically relevant in most cases.

Sunday, 28 August 2011, 08.00–11.30, Room 207

OFP-03 Oral Free Paper Session Cardiovascular Pathology

001

Autonomic innervation of thoracic veins: morphological substrate of atrial fibrillation

I. Kholová *, A. Haaparanta, O. Jääskeläinen, R. Leinonen, T. Tolonen, T. Paavonen
*Laboratory Centre, Dept. of Pathology, Tampere, Finland

Objective: Atrial fibrillation is the commonest sustained tachyarrhythmia. Morphological substrates of atrial fibrillation were found in myocardial sleeves around thoracic veins. This study sought to examine morphologically and immunohistochemically autonomic nerve distribution in thoracic veins and vein–atrium junctions.
Method: We performed immunohistochemical staining on 48 pulmonary veins, 50 caval veins and 9 atria samples using antibodies to tyrosine hydroxylase, choline acetyltransferase and GAP-43. The morphometrical analysis was performed with a computer-assisted system (ImageJ).
Results: Adrenergic and cholinergic nerves and ganglia were often co-located. Their density varied at different compartments. The nerve structures were present both within myocardial sleeves and in surrounding fibro-fatty tissue.

Conclusion: Adrenergic and cholinergic nerves and ganglia play a role in atrial fibrilation triggers from thoracic veins. The selective targeting of either vagal or sympathetic nerves due to co-localization is impossible.

002
Ischemic heart disease in postmortem CT and CT angiography

K. Michaud *, S. Grabherr, F. Doenz, P. Mangin
*University Center of Legal Med, DUMSC, Lausanne, Switzerland

Objective: Postmortem radiology had in recent years appeared in the field of forensic medicine and is now considered by some authors as a good replacement for conventional autopsy and by others as a complementary examination. Although postmortem CT radiological imaging is very useful in demonstrating traumatic lesions, its utility is still quite limited in the cardiovascular field. This limitation could be minimized by the introduction of postmortem angiography. At the University Center of Legal Medicine of Lausanne, CT scans and postmortem multiphase CT angiography are used in cases with a suspicion of ischemic heart disease.
Method: The goal of this presentation is to demonstrate some correlations between postmortem CT, CT angiography and conventional autopsy examination in cases of ischemic heart disease.
Results: We observed that the native CT scan can show only some pathological findings as cardiac tamponade and calcifications of coronary arteries. However, postmortem angiography allows a better visualization of coronary arteries and evaluation of stenosis and occlusion as well as better imaging of soft tissue.
Conclusion: The interpretation of postmortem modern radiology is a new field for both forensic pathologists and radiologists who have to learn to read the postmortem modified images. The information obtained from both parties can help to further the understanding of CT and CT angiography in postmortem cases.

003
Inflammatory infiltration in the atrial myocardium and the left ventricle of patients with atrial fibrillation

L. Mitrofanova *, S.Y. Ho, P. Platonov
*Almazov HBE Centre, Dept. of Pathology, St. Petersburg, Russia

Objective: Inflammatory response is associated with the presence of atrial fibrillation (AF). However, it is not clear whether inflammation is confined to the atria only or the venticles are also affected.

Method: A histologic study and an immunohistochemical analysis were performed using antibodies against CD3-antigen on the autopsy specimens collected from 30 patients (age 64±12 years) in three age-matched groups: t without AF, 10 with paroxysmal AF and 10 with permanent AF. The specimens were taken from crista terminalis (CT), posterior left atrium (LA) and LV. Average CD3+ cell count/mm^2 was compared between tissue sampling locations and groups in regard to AF history.
Results: The average number of CD3+ cells/mm^2 was 7.6±4.4 at CT, 4.2±2.0 at LA and 6.3±3.2 at LV in patients without AF (ns). In paroxysmal AF, the cell count was 19.2±7.8 at CT, 14.6±5.4 at LA and 18.0±4.0 at LV (ns). In permanent AF, it was 24.4±7.8 at CT, 25.1±8.6 at LA and 17.0±7.9 at LV (ns). Cell count was higher at all locations in patients with AF compared with controls ($p<0.001$).
Conclusion: Chronic myocardial inflammation is common in patients with a history of AF and is not limited to the atria only.

004
Sudden cardiac death caused by isolated coronary vasculitis

K. Norita *, S.V. de Noronha, M.N. Sheppard
*Imperial College London, Histopathology, UK

Objective: Isolated coronary vasculitis is a rare and diagnostically challenging cause of sudden cardiac death (SCD). There are currently no large-scale series on this rare entity.
Method: This is a retrospective non-case–control observational study of ten SCD cases with isolated coronary vasculitis referred to the Cardiac Risk in the Young (CRY) unit at the Royal Brompton Hospital in a database of 1,980 cases.
Results: Five male and five female cases were observed—mean age 40.7±18.3 years and range 15–71 years. Six deaths occurred in the hospital following symptoms or cardiac arrest in the community; the remaining died at rest at home ($n=4$). The appearances ranged from aneurysms of the coronary artery to occlusive lesions mimicking atheroma to masses imitating tumour. The types of vasculitis detected were eosinophilic ($n=5$), of which two were associated with Churg–Strauss syndrome; lymphoplasmacytic vasculitis ($n=2$), one confirmed to be IgG4-related; lymphocytic vasculitis ($n=1$); idiopathic giant cell arteritis ($n=1$); and occlusive mixed vasculitis ($n=1$). The majority of cases ($n=7$) showed myocardial damage including inflammation which extended from the coronaries.
Conclusion: This study shows that isolated coronary vasculitis is a rare cause of SCD. It has a variable macroscopic and microscopic appearance that pathologists need to be aware of.

005

Correlation of histopathological findings with the application of microwave radiometry in atherosclerotic plaques in a rabbit model

G. Agrogiannis *, K. Nikolaos, A. Stofas, K. Toutouzas, A. Synetos, E. Tsiamis, M. Drakopoulou, C. Stefanadis, E. Patsouris
*National University of Athens, School of Medicine, Greece

Objective: Microwave radiometry (MR) is a method for measuring temperature from internal tissues at microwave frequencies. We investigated whether thermal heterogeneity measured by MR is correlated to histological findings in an experimental model.
Method: Twenty-four rabbits were randomized to either normal (n=12) or cholesterol-rich diet (n=12) for 6 months. Thereafter, temperature measurements of the abdominal aortas were performed noninvasively with microwave radiometry. All aortas were divided by optical coherence tomography in five segments. The temperature difference (ΔT) of each segment was assigned as the temperature of each segment minus the minimal temperature of the five segments. Histological sections were analyzed semiquantitatively according to the degree of inflammatory cell density and CD3 immunoreactivity.
Results: MR detected that the ΔT of atherosclerotic aortic segments were significantly higher compared to the ΔT of the controls (MR, 1.02±0.23°C versus 0.21±0.09°C, p<0.001; IVT, 0.19±0.03°C versus 0.01±0.01°C, p<0.001). The temperature differences measured by MR correlated with inflammatory cell density and CD3 immunoreactivity (p<0.05).
Conclusion: The results of the current study justify the clinical application of MR for the detection of inflammatory activation in atherosclerotic plaques.

006

Correlation between plaque histology and microwave radiometry for the identification of carotid 'vulnerable plaque'

G. Agrogiannis *, N. Kavantzas, A. Stofas, M. Drakopoulou, A. Synetos, K. Toutouzas, S. Christodoulos, E. Patsouris
*National University of Athens, School of Medicine, Greece

Objective: Microwave radiometry (MR) is a new non-invasive method that allows in vivo measuring of the internal temperature of tissues. This study aims to investigate in human carotid arteries whether thermal heterogeneity measured by MR is associated with histologic findings.
Method: Twenty-one patients undergoing carotid endarterectomy were preoperatively evaluated by temperature measurements with MR. During the thermographic measurements, thermal heterogeneity (ΔT) was assigned as the maximal temperature along the carotid artery minus the minimum temperature. The carotid plaques and the lesions were histologically evaluated. The subsequent association of thermographic with histologic findings was performed.
Results: Fatty plaques had higher temperature differences compared to mixed and calcified plaques (1.664±0.36°C vs 1.180±0.045°C vs 0.96±0.207°C accordingly, p<0.01). Plaques with ulcerated surface had higher temperature differences compared to plaques with irregular and regular surfaces (1.883±0.35°C vs 1.325±0.128°C vs 1.014±0.195°C accordingly, p<0.01 for all comparisons). A significantly higher ΔT was found in plaques with a thin fibrous cap (1,592±0.373°C vs 1.038±0.192°C, p<0.01) and elevated inflammatory infiltrate (1,700±0.359°C vs 1.091±0.187°C, p<0.01).
Conclusion: Increased thermal heterogeneity detected by MR in carotid atherosclerotic lesions showed good correlates with histologic findings.

Wednesday, 31 August 2011, 08.00–11.30, Room 206

OFP-04 Oral Free Paper Session Cytopathology

001

Diagnostic accuracy of Shandon PapSpin liquid-based cytology in oral dysplasia and malignancy

A. Afrogheh *, L. Majara, A. Pelser, S. L. Sellars, J. Hille, P. T. Schubert, C. A. Wright
*NHLS, Dept. of Pathology, Cape Town, South Africa

Objective: While a single "high-quality" LBC study has shown a high sensitivity and specificity in the detection of oral dysplasia and malignancy, the high cost of LBC cannot be borne by African countries. We evaluate the efficiency of an alternative technique, Shandon PapSpin LBC, in the diagnosis of oral dysplasia and malignancy.
Method: We compared the diagnostic accuracy of PapSpin with that of biopsy in 69 patients. Transepithelial cytology specimens were obtained using a Cytobrush. The cytology specimens were graded and scored using a novel oral cytologic grading and scoring system, respectively.
Results: Histological diagnosis of dysplasia or invasive SCC was made in 51 of the 69 cases. Histology confirmed the cytological diagnosis of dysplasia or malignancy in 49 of the 51 cases. The sensitivity was 96% and the specificity 100%. The best cutoff value for distinguishing reactive/mildly dysplastic lesions from high-grade/invasive SCC was determined as a cytologic score of 3, representing a sensitivity of 95% and a specificity of 96%.
Conclusion: The PapSpin in association with a transepithelial technique is a highly sensitive, specific and economical screening test in the detection of oral dysplasia and malignancy. The proposed oral cytologic grading system correlates well with histology. The novel oral cytologic scoring system shows promise as a simple,

reliable and reproducible scoring system. In addition, the liquid residual allows for immunocytochemical testing.

002

Benefits of ultrasound-guided fine needle aspiration cytology before lymph node biopsy in melanoma patients

A. Ben Lakhdar *, M. ILIE, G. Tomasic, L. Chami, C. Robert, P. Vielh
*Gustave Roussy, Pathology, Paris, France

Objective: A reliable method is needed to evaluate the lymph node status in patients with melanoma. The aim of this study was to evaluate the efficiency of fine needle aspiration cytology (FNAC) as a diagnostic tool in the interpretation of suspicious lymphadenopathy.
Method: One hundred seventy-five FNACs were performed in 142 patients with a suspicious lymph node in an open study conducted in a French melanoma regional referral centre. Cytopathological diagnosis was classified as malignant, benign, suspicious for malignancy or unsatisfactory. Sensitivity, specificity, positive and negative predictive values and positive and negative likelihood ratios were calculated.
Results: Ninety-seven of the 175 FNACs were malignant (55.4%), 62 of 175 (35.4%) were benign, 5 of 175 (2.8%) were suspicious for malignancy and 11 of 175 (6.4%) were unsatisfactory. Among the 158 FNACs in which a definitive diagnosis could be given, sensitivity was 95% and specificity was 96.61% with a positive predictive value of 97.93% and a negative predictive value of 91.93%.
Conclusion: FNAC is a rapid, safe, easy and non-expensive diagnostic technique which can be used for the initial diagnosis of metastatic lymphadenopathy in melanoma and to better discriminate between cases in which the surgical treatment of the lymph node basin should be performed and only necessitating follow-up among patients.

003

Validation of immunocytochemical stains on the Cellient™ Automated Cell Block System

B. van Hemel *, A. ten Hoor, T. Ruitenbeek, A. Suurmeijer
*UMC Groningen, Dept. of Pathology, The Netherlands

Objective: With the Cellient™ Automated Cell Block System, cytologic specimens may be transferred to a paraffin tissue block in 30 min, which allows for the rapid microscopic evaluation of tumor cells. As part of our immunocytochemical quality assurance system, we tested a large number of antibodies (38) routinely used for the classification of tumors.
Method: Cellient cell blocks of tumor cytology (FNAs or serous fluids) were selected from cases in which immunohistochemistry had also been performed on tissue sections from tumors of the same patient. We evaluated 38 different antibodies and 4 different retrieval and/or immunostaining protocols: without pretreatment but with amplifier ("Cyto"), Ultra CC1 (tris EDTA buffer; pH 8.5), Ultra CC2 (citrate buffer; pH 6.0) and Ultra CC1 mixed with Unifix®. The immunostaining results were scored positive (and semi-quantitively) or negative.
Results: All antibodies gave a positive result in at least one of the four immunostaining protocols and 20 antibodies (53%) give a positive result in all four conditions. For each antibody, optimal staining conditions were selected for implementation in daily practice.
Conclusion: The Cellient™ Automated Cell Block System creates a cell block in 30 min with low hands-on time. In our experience, immunocytochemistry is readily performed, which allows for the proper classification of tumors.

004

Cytologic, immunocytochemical and molecular study in samples of spontaneous urine: usefulness in the diagnosis of urothelial carcinoma

A. Bueno Remacha *, N. Combalia, R. Martos Calvo, A. B. Galvan, I. Costa Trachsel, J. Prats, M. Rey Ruhi, A. Gelabert Mas
*Hospital Parc Taulí, Anatomia Patologica, Sabadell, Spain

Objective: This studi aims to assess the diagnostic usefulness of cytology stained with Papanicolaou, cytokeratin 20 (CK20), p16INK4a (p16) and Vysis UroVysion® (FISH) in spontaneous urine in the follow-up of urothelial tumor.
Method: The method involved is the study of spontaneous urine in 137 consecutive patients prior to cystoscopy. ThinPrep® samples were stained with Papanicolaou, CK20, p16 and FISH (n=116). Cytological diagnosis, semiquantitative evaluation and comparison with cystoscopy and concommitant biopsy (n=50) were made.
Results: Cystoscopy was positive in 41 and negative in 96. Taking this one as the gold standard, the sensibility (S), specificity (E) and s (A) of the techniques were: cytology—S, 56% E, 92.7% A, 81.7% CK20; S, 58.5% E, 93.7% A, 83.2% p16; S, 41.4% E, 92.7% A, 77.3% FISH; S, 70.2% E, 87.3% A, 81.8%. The biopsies (n=50) showed 20 high-grade carcinoma (HGC), 16 low grade, 2 in situ carcinoma (ISC) and 12 normal. Two cases with negative cystoscopy were positive to cytology, CK20, p16 and FISH; the biopsies showed a vesical ISC and a urethral HGC.
Conclusion: The accuracy of all techniques is similar; p16 is the lowest. FISH has the major sensibility and CK20 is the most specific. A positivity of all techniques with a negative cystoscopy recommends the ruling out of a neoplasia of the urinary tract or an ISC.

005

Oral ulcerative lesions. Cytologic investigation with scraping and brushing

S. Divani *, G. Kalodimos, K. Koti, A. Konstantinou, A. Fericean
*Volos General Hospital, Dept. of Clinical Cytology, Greece

Objective: Oral ulcer is associated with multiple causes. Factors that provoke the various types of ulcers include stress, vitamin deficiencies, alcohol, hormonal changes, sudden weight loss and use of tobacco. Persistent ulcers require a formal diagnosis and further investigation including biopsy since it is well known that these may be a sign of oral cancer.
Method: We analyzed the cytological findings of 63 patients with oral ulcerative lesions. Most of the patients, 45/63 (71.4%), referred a pain or burning sensation at the site of the ulcer. The scrapings for cytological examination were taken with a cytobrush and a plastic spatula and the specimens were prepared according to the Thin Prep technique.
Results: A total of 22/63 (34.9%) painful ulcers showed bacterial infection whereas in six cases (9.5%) herpes was revealed. Trauma was the cause of ulceration in 10 patients (15.8%) and mycosis was found in 19 cases (30.1%). Squamous carcinoma was the cytological diagnosis for six (9.5%) persistent ulcers.
Conclusion: Although most mouth ulcers are caused by bacteria, fungi or viruses, oral cancer could be the diagnosis. Other ulcer causes include autoimmune diseases, chemical injuries, kidney failure, trauma, lichen planus, pemphigoid, Bechets disease, periodontal disease or drug reactions. CMV infection, wich is common in renal transplant recipients, affects the mouth in rare cases, causing ulcers.

006

Value of p16 assessment for the diagnosis of low-grade urothelial carcinoma in urinary cytology

N. Juanpere *, F. Alameda, B. Lloveras, L. Pijuan, J. Gimeno, E. Romero, J. Munne, L. Lopez, S. Serrano, J. Lloreta
*Hospital del Mar, Dept. of Pathology, Barcelona, Spain

Objective: Urinary cytology (UC) has low sensitivity in the diagnosis of low-grade urothelial (LGU) tumors. The expression of p16 in urothelial tumors is variable and it is said to be associated with a more aggressive phenotype. The aim of our study has been to assess if p16 immunohistochemistry increases the sensitivity of UC in the diagnosis of LGU carcinoma.
Method: Three consecutive UCs from 83 patients, all of whom underwent subsequent cystoscopy and biopsy, were included. p16 immunohistochemistry (mtmLabs, Heidelberg, Germany) was performed in cytology and biopsy specimens (Ventana, Roche Diagnostics, Mannheim, Germany). Cases were considered positive when they showed atypical urothelial cells with nuclear and cytoplasmic p16 expression.
Results: A total of 48/83 biopsies were LGU carcinomas. In all but one, the previous cytology was negative. The remaining 35 biopsies were benign. From these, 12 cytologies were positive and 23 negative (S, 2%; E, 65.7%; NPV, 33%; PPV, 7.7%). Regarding p16 expression in cytology, with a cutoff of three or more p16+ urothelial cells, 38 cases were positive. In 32 of these, the biopsy was also positive (S, 66.7%; E, 82.8%; NPV, 64%; PPV, 84%).
Conclusion: Immunohistochemical detection of p16 in UC is able to increase the sensitivity and specificity of cytology for the diagnosis of LGU carcinoma.

007

Expression of Epstein–Barr virus and granzyme B in cytologic smears of histiocytic necrotizing lymphadenitis

J.-Y. Kim *, J.-E. Kwon, H.-J. Kim, K.-M. Park
*Inje University, Sanggye Paik Hospital, Seoul, Republic of Korea

Objective: Histiocytic necrotizing lymphadenitis (HNL) is a nonneoplastic disease of the lymph nodes that is self-limiting in course. We tried to find out the relationship between the expression of Epstein–Barr virus (EBV), granzyme B, and other phenotypic markers and disease pathogenesis.
Method: The fine needle-aspirated (FNA) cytologic smears from 38 patients were subjected to immunohistochemical staining for granzyme B, CD3, CD4, CD8, CD20, and CD68 in addition to in situ hybridization for EBV.
Results: The mean age of 28 female and 10 male patients was 22.8 years. CD8-positive T cells were noted in 65.0% of the smears (13/20 cases), whereas CD4 and CD68 were rarely observed. Granzyme B reactivity was seen in lymphocytes, especially in apoptotic areas, and in histiocytes, with positive rates of 25.0% (9/36) and 11.1% (4/36). Most FNA smears showed immunoreactivity to both CD3 and CD20, with a predominance of CD3-positive cells. In situ hybridization for EBV was positive in 22.9% (8/35) of the cases. The immunohistochemical staining and EBV in situ hybridization results obtained in bleached FNA smears were similar to those in histologic sections.
Conclusion: Although EBV positivity and granzyme B immunoreactivity are noted in HNL, they do not appear to have any apoptosis-associated role.

008

Grading of follicular lymphoma in cytology

U. Klopcic *, J. Lavrencak, V. Kloboves Prevodnik
*Institute of Oncology, Dept. of Cytopathology, Ljubljana, Slovenia

Objective: The treatment and prognosis of follicular lymphoma (FL) depends on its grade. At present, there is no generally accepted method for the grading of FL in cytology. We attempted to set up a grading system for FL on cytology samples using flow cytometry. We tested our hypothesis that lymphoma cells larger than T lymphocytes are most likely centroblasts and that their percentage among all FL cells would reflect the grade of FL.
Method: A total of 52 cases of primary FL with cytology and histology available for the same lymph node were included in the study. The cytology samples of FL were evaluated according to the percentage of the large FL cells. Grading of FL in histological specimens was determined according to Mann and Berard method. The percentage of large FL cells in cytological specimens was compared with a histologicaly determined grade by using Mann–Whitney test.
Results: A histological examination revealed 27 low-grade (grade 1 or 2) and 25 high-grade FL (grade 3). The percentage of large FL cells in the cytological samples was significantly higher in high-grade FL than in low-grade FL (p=0.004).
Conclusion: Flow cytometry enables the reliable grading of FL on cytological samples, comparable to the grading on histological specimens.

Wednesday, 31 August 2011, 14.00–16.30, Room 201

OFP-05 Oral Free Paper Session Dermatopathology—Soft Tissue Pathology

001

Melanocytic lesions with eczematous reaction (Meyerson's phenomenon): a histopathological analysis of 64 cases

J. Pizem *, B. Luzar
*University of Ljubljana, Medical Faculty, Slovenia

Objective: Eczematous reaction in melanocytic naevi (Meyerson's phenomenon) still remains under-recognized and the spectrum of morphological features poorly defined.
Method: We analysed consecutive melanocytic lesions with eczematous reaction noted microscopically.
Results: Sixty-four melanocytic lesions with eczematous reaction, occurring in 57 patients (27 males and 30 females), most often located on the back (31 cases), included 16 common acquired naevi, 3 naevi with congenital features, 2 Spitz naevi, 29 dysplastic neavi, 6 melanomas in situ, and 8 invasive melanomas. The intensity of reaction was mild (24 cases) and moderate/severe (40 cases). Although it was the most pronounced in non-dysplastic naevi, a moderate/severe reaction was noted in 6/14 melanomas. Pagetoid growth was noted in 7/21 non-dysplastic naevi (limited to the lower half of the epidermis), 10/29 dysplastic naevi, and 14/14 melanomas. Moderate/severe cytological atypia was noted only in dysplastic naevi (14/29) and melanomas (14/14).
Conclusion: Eczematous reaction of varying intensity can involve all types of melanocytic naevi and also in situ or invasive melanomas. Although an eczematous reaction in ordinary melanocytic naevi can be associated with pagetoid growth, moderate/severe cytological atypia, very prominent pagetoid spread, and older age of the patient indicate a dysplastic naevus or melanoma.

002

Atypical Spitz nevi in Iceland 1988–2008

B. A. Agnarsson *, A. M. Jonsdottir
*University Hospital, Dept. of Pathology, Reykjavik, Iceland

Objective: In 1948 Sophie Spitz described a mostly benign melanocytic lesion in children and young people which microscopically resembled melanoma (Spitz nevus). Later, atypical Spitz nevi were described, but their status in terms of biological behaviour has been unclear. The purpose of this study was to investigate atypical Spitz nevi diagnosed in Iceland during a 20-year period and assess their biological behaviour.
Method: Patients diagnosed between 1988 and 2008 in Iceland were identified. Clinical information was obtained and a search was made through the Icelandic Cancer Registry to identify patients who either experienced a later recurrence or who received a subsequent diagnosis of melanoma (primary or metastatic).
Results: A total of 97 patients were diagnosed (M/F =1.9). The mean age at diagnosis was 29 years (range 8–64). Most lesions in women were on the lower extremity (79%) but the most lesions in males were on the trunk (29%). The surgical margin of excision was negative in 66% of cases, but a subsequent wider excision was performed in 57%. None of the patients has had any evidence of a local recurrence or a later diagnosis of melanoma.
Conclusion: None of the atypical Spitz nevi included in this study have demonstrated amalignant behaviour.

003

Comparison of various melanocytic markers for the diagnosis of melanomas

D. Nonaka *
*Christie NHS Foundation Trust, Dept. of Histopathology, Manchester, UK

Objective: Malignant melanoma can simulate a variety of benign and malignant neoplasms, and immunohistochemistry is crucial for the diagnosis, particularly in metastatic tumour.
Method: A total of 69 cases of melanomas comprised of 37 primary and 32 metastatic melanomas were stained with

Sox10, S100, MITF, TRP1, tyrosinase, Melan A and HMB-45. The histotype includes 43 epithelioid (conventional) and 26 spindle cell type (including desmoplastic subtype).

Results: Expression was seen in the following order (overall, epithelioid, spindle): 97, 95, 100% for Sox10; 91, 86, 100% for S100; 39, 53, 15% for MITF; 36, 47, 19% for TRP1; 54, 74, 19% for tyrosinase; 59, 88, 12% for Melan A; 59, 84, 19% for HMB-45. Two Sox10-negative melanomas were negative for all other markers. Three out of six S100-negative melanomas were negative for all other markers except for Sox10 expression in one case, while the other three expressed more than one amongst MITF, TRP1, tyrosinase, Melan A and HMB-45.

Conclusion: Sox10 is the most sensitive marker for melanomas, followed by S100. Spindle cell melanomas appear constantly positive for Sox10 and S100 while they express other markers only in 10–20% of cases. For S100-negative epithelioid melanomas, other markers may be expressed and should be included in panels.

004

Genital seborrheic keratoses are human papillomavirus-related lesions: a linear array genotyping test study

J. Tardío *, E. Bancalari, A. Moreno, L. Martín Fragueiro
*Hospital Universitario de Madrid, Dept. of Pathology, Fuenlabrada, Spain

Objective: The pathogenesis of seborrheic keratosis (SK) is not well known. Controversy exists about the meaning of human papillomavirus (HPV) detection in genital SKs.

Method: Thirty-nine genital SKs, 16 extragenital SKs and 9 non-SK genital lesions have been studied by polymerase chain reaction for HPV using a linear array genotyping test that detects 37 genital HPV types.

Results: Twenty-seven of the 39 genital SK specimens (69%) were positive for HPV. All patients with HPV-positive samples were between 22 and 53 years of age. Histological features could not discriminate between positive and negative lesions. Twenty-six of the 27 positive cases (96%) contained HPV6, HPV55 was detected in one lesion (4%) and, in one specimen (4%), multiple HPV types were found. HPV was detected in only 2/16 extragenital SK samples (13%) and in 0/9 non-SK genital lesions.

Conclusion: Our results support a pathogenic relationship between HPV and genital SK, with a strong predilection for HPV6, whereas its presence is rare in most of the remaining non-SK cutaneous genital lesions as well as in extragenital SKs. HPV cannot be found in a minority of genital SKs using highly sensitive techniques and, therefore, other presently unknown factors may also be implied in the pathogenesis of these lesions.

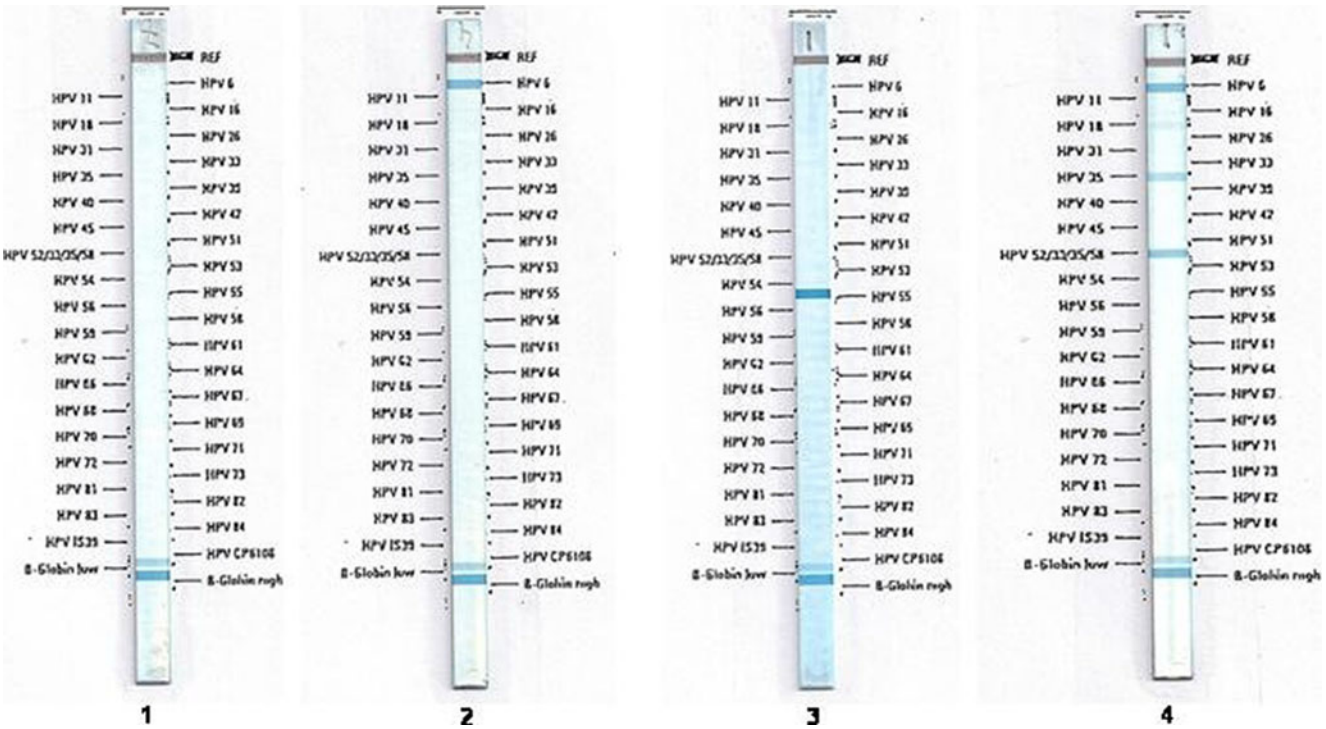

005

Expression of pS6 Ser235/236 effector of mTOR pathway may be a prognostic parameter in patients with cutaneous melanomas

J. Vinagre *, H. Pópulo, F. Azevedo, P. Soares, J. M. Lopes
*IPATIMUP, Cancer Biology, Porto, Portugal

Objective: Melanoma represents less than 5% of skin cancer, although it is responsible for the majority of skin cancer-related deaths. The mTOR pathway is involved in many biological processes and has been linked to tumour development in cutaneous melanoma.

Method: In order to evaluate whether the expression of mTOR pathway effectors in cutaneous melanoma correlates with disease-free and overall survival, follow-up data were collected from a series of cutaneous melanoma patients from Department of Dermatology and Oncology Registry of Hospital de São João, and from Roreno (Oncology Registry of North Region). Kaplan–Meier curves and univariate and multivariate analysis were performed in a cutaneous melanoma series previously studied for the expression of mTOR pathway effectors.

Results: Follow-up data were available for 79 patients (94%). Patients with tumours expressing moderate/high levels of pS6 Ser235/236 showed significantly shorter overall survival ($p=0.01$) and shorter disease-free survival ($p=0.02$) than patients with tumours with negative/low pS6 Ser235/236 expression. Univariate Cox regression analysis confirmed the significance of pS6 Ser235/236 expression level as a marker of poor survival, although this significance was not observed in the multivariate analysis.

Conclusion: Our results suggest that pS6 Ser235/236 expression may be used as a putative prognostic parameter in patients with cutaneous melanoma.

006

Accelerated cell cycle progression and connexin 43 expression correlates with recurrence potential in giant cell tumor of bone

T. Krenács *, M. Maros, P. Balla, L. Moskovszky, Z. Sapi, M.-S. Benassi, P. Picci
*Semmelweis University, 1st Dept. of Pathology, Budapest, Hungary

Objective: Giant cell tumor of bone (GCTB), an aggressive osteolytic lesion, can frequently recur but the pathobiology is obscure. Elevated cell cycle progression is generally related to tumor progression.

Method: We have tested cell cycle regulatory proteins and connexins (known to control cell cycle) in 94 primary non-recurrent and 82 recurrent GCTB using immunohistochemistry in tissue microarrays and digital microscopy.

Results: Nuclear expression of Ki67 (only B56 of three clones), the post-G1 cell cycle promoters cyclin A and cdk2 and the cdk inhibitor p21waf1 showed a statistical correlation with GCTB recurrence. G1 phase arrest (high mcm2 but low cyclin A levels) was detected in 30% primary but only in 16% recurrent cases. Pre-osteoclasts and giant cells expressed early G1(S)-phase cyclins (−D1 and -E), p21waf1, rare Ki67 and cytoplasmic p16ink4, but no post-G1-phase promoters. Cx43, Cx30, Cx46, Cx50 and Cx62 were found primarily in GCTB stromal cells where Cx46 is related to hypoxia adaptation. Cx30, Cx43 and Cx46 showed elevation in recurrent cases.

Conclusion: Increased growth fraction detected with post G1-phase markers correlates with GCTB recurrence. Cell cycle is initiated in giant cells but it is arrested in the G1 phase by p21waf1. Elevated connexin levels in recurrent cases further support the benign phenotype of GCTB.

007

Gene and protein expression of EPHRIN B3 differentiates synovial sarcomas from other mesenchymal tumor types

K. Carvalho *, F. Soares, I. Cunha
*Faculdade de Medicina da USP, Dept. of Gynecology, São Paulo, Brazil

Objective: Soft tissue tumors (STT) are grouped together because they show similarities in histological appearance, clinical presentation and/or clinical behavior. Among STT, synovial sarcoma (SS) represents a diagnostic challenge since it shows histological features similar to other spindle cell tumors. The discovery of molecular markers can help in the diagnosis and knowledge of SS biology. Our goal was to identify relevant molecular markers for diagnosis, prognosis and treatment of synovial sarcomas.

Method: Using a cDNA platform (with 4,800 genes), we looked for differentially expressed genes that discriminated SS from the diverse other types of STT (including fibromatosis, fibrosarcoma, leyomiosarcoma, liposarcoma, MPNST, GIST, and others). Gene validation was developed by Immunohistochemical (480 samples) and qRT-PCR (65 samples, using TaqMan detection system).

Results: cDNA microarray results pointed to a set of genes that discriminate synovial sarcomas from the other histological types of STT analyzed. Among these genes, ENPHRIN B3 presented higher levels in synovial sarcomas. The qRT-PCR showed synovial sarcomas

with higher transcript levels than all other STT histological types ($p<0.0001$). The immunohistochemical analysis corroborates cDNA microarray and qRT-PCR results.
Conclusion: All results indicated that ENPHRIN B3, both at protein and transcriptional levels, represents a potential diagnostic marker for synovial sarcomas.

008
Immunohistochemical expression of estrogan and progesterone receptors in cartilagenous tumors

V. Siozopoulou *, A. Batistatou, S. Kamina, N. Simou, A. Zioga, V. Malamou-Mitsi
*University Hospital of Ioannin, Dept. of Pathology and Cytology, Ioannina, Greece

Objective: It has been shown that most cartilagenous tumors (CT) express estrogen receptor-a (ERa) protein, while progesterone receptor (PR) has not yet been investigated. Our study addresses the immunohistohemical (IH) expression of ERa and PR in benign and malignant CT and correlates it with clinicopathological findings.
Method: IH staining for ERa (ERAb-11, Clone1D5, NewMarkers) and PR (PgR6-36 DAKO) was performed in 20 CT, 7 enchondromas (EC) and 13 chondrosarcomas (CS, 7 grade1 and 6 grade 2) and scored according to the Allred system.
Results: Eighty-six percent of EC expressed ERa poorly (score 3–5) and PR richly (score 7.8). Fifty-seven percent of CS grade1 were negative for ERa and PR, 29% were poorly positive for ERa (score 4.5) and intermediate for PR (score 6) and 14% were rich for ERa and PR (score 7 and 8, respectively). Fifty percent of CS grade 2 were negative for ERa and PR, 33% were poorly positive for ERa (score 3.4) and intermediate for PR (score 6) and 17% were rich for ERa and PR (score 7 and 8, respectively).
Conclusion: ERa and PR are expressed in the majority of CT, but only in about half of CS. Therefore, targeted antiestrogen therapy should be applied in selected cases.

Tuesday, 30 August 2011, 08.00–11.30, Room 206

OFP-06 Oral Free Paper Session Digestive Diseases Pathology I

001
Her-2 in carcinomas of the esophagus and its metastases

P. Birner *, B. Jesch, S. F. Schoppmann
*Medizinische Universität Wien, Inst. für Pathologie, Austria

Objective: Her-2 is a membrane-bound tyrosine kinase, and a targeted therapy has recently been shown to be beneficial for patients with advanced gastroesophageal cancer.
Method: Her-2 expression was investigated in 341 esophageal carcinomas [152 squamous cell carcinomas (SCC), 189 adenocarcinomas (AC)], 39 cases of Barrett´s mucosa, and 11 cases of squamous cell dysplasia. If present ($n=176$), lymph node and distant metastases were also investigated. Gene amplification was assessed by colorimetric in situ hybridization.
Results: Positive Her-2 status was found in 15.3% of ACs and 3.9% of SCCs. Positive Her-2-status was more common in dysplastic Barrett´s mucosas compared with nondysplastic ones ($P=0.04$). There was no correlation between Her-2 status and patients' survival. In 95.3% of ACs and 98.6% of SCCs, respectively, Her-2 status was identical in the primary tumor and lymph node metastases ($p>0.05$, sign test). A total of 86.3% of distant metastases from AC and all from SCC had identical Her-2 status compared to primary tumors.
Conclusion: Her-2 overexpression is rare in SCCs but is found in 15.3% of ACs, where amplification and overexpression seem to be early events in carcinogenesis. Although Her-2-overexpression seems to have no influence on survival, overexpressing esophageal ACs have to be considered as targets for an anti-Her-2 therapy.

002
Optical projection tomography as a diagnostic tool for colorectal polyps

M. Coats *, S. Wedden, G. Cranston, J. Farrell, L. Mitchell, J. Wilson, R. Steele, F. Carey
*University of Dundee, Clinical and Population Science, UK

Objective: Colonic polypoid cancers are the earliest detectable form of colorectal cancer (CRC) and, if completely excised, offers a potential cure. The diagnosis can be problematic due to epithelial misplacement but may be improved using 3D imaging. Optical projection tomography (OPT) is an in vitro 2D and 3D imaging technique and our aim was to explore its diagnostic potential in early CRC.
Method: This was a retrospective study of excised colonic polyps from a screening population. OPT was used to obtain qualitative diagnostic information and results were compared to standard haematoxylin and eosin (H&E)-stained sections.
Results: A total of 264 polyps were examined from 141 patients (62% male; median age 62 years). Surface morphology was easily identifiable by OPT and comparable with H&E diagnosis: tubular (27%), tubulovillous (70%) or villous (3%). Low-grade dysplasia (58%) was distinguishable from high-grade dysplasia (24%) and invasive cancer

(18%) using OPT but differentiation between the latter two was less distinct. However, OPT demonstrated additional features (e.g. surface ulceration, epithelial misplacement and vasculature patterns) that were not present on examined H&E sections.

Conclusion: OPT has identified features of colonic polyps not always present on standard 2D histopathology. It may prove useful in guiding the diagnoses of colonic polypoid cancers but requires further validation as a robust diagnostic tool.

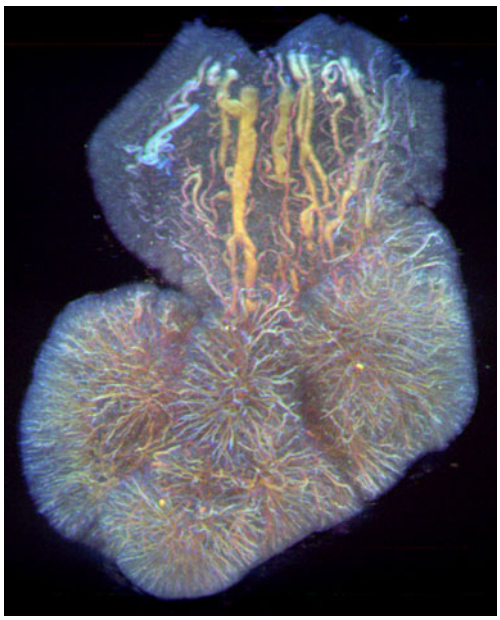

003

Expression patterns of pIGFR and assessment of pIGF-1R and MMP7 positive expression as predictive markers of chemoresistance in wild-type K-RAS metastatic colorectal carcinoma treated with panitumumab and mFOLFOX6. The PULSE Trial

M. Cuatrecasas [*], C. Horndler, J. Codony-Servat, J. C. Mendez, C. Fernandez-Martos, V. Alonso, P. Jares, M. Rubini, J. Maurel

[*]Hospital Clinic Barcelona, Dept. of Pathology, Barcelona, Spain

Objective: The active (phosphorylated) form of the insulin growth factor receptor (pIGF-1R) activates via transactivation the epidermic growth factor (EGFR). pIGF-1R is expressed in advanced colorectal carcinomas (CRC). CRC cells produce matrilysin (MMP-7), which at its time can activate IGF-1R and liberate IGF-1 by the degradation of IGFBP-3. Expression levels of p-IGF-1R may have prognostic value and influence on therapy response in patients with metastatic CRC.

Method: The aim of this prospective study is to estimate progression-free survival by using immunohistochemistry (IHC) expression in patients with wild-type K-RAS metastatic CRC treated with panitumumab and mFOLFOX6. We have studied the first 35 of 240 patients, including K-RAS codons 12–13 mutations, IHQ expression and location of pIGF-1R, and expression of MMP7, hMLH1, hMSH2, hMSH6, hPMS-2, PTEN and caveolin.

Results: Four different patterns of pIGF-1R staining were seen: (a) membrane 20%, (b) cytoplasm 20%, (c) dot-like perinuclear 80%, and (d) nuclear in 5% of patients. Although a predominant pattern was observed, several patterns often coexisted in the same tumor.

Conclusion: Our preliminary results show an increased pIGF-1R and MMP7 expression on histologically high-grade and clinically aggressive CRC. Nuclear location of pIGFR-1 occurred in highly aggressive CRC.

004

HER2/PTEN/Akt pathway deregulation in colon adenocarcinoma based on intraoperative imprint and tissue microarrays analysis

E. Falidas [*], E. Tsiambas, G. Theodoropoulos, S. Papadopoulos, A. Karameris, C. Goudeli, C. Villias, I. Bramis

[*]NIMTS Hospital, Dept. of Surgery, Athens, Greece

Objective: PTEN is a negative regulator of the signal transduction HER2neu/PI3-K/PTEN/Akt pathway. PTEN down-regulation affects the sensitivity of breast adenocarcinoma to targeted anti-HER/neu treatment (trastuzumab). We investigated the role of PTEN in colorectal adenocarcinoma (CA) and the simultaneous deregulation HER2/neu and Akt on tissue and cell substrate.

Method: Intra-operative imprints were taken from 60 patients with primary CA, followed by tissue microarrays based on the corresponding paraffin blocks (core diameter=1.5 mm). Thirty cores of colon adenomas expanded the analysis. Immunohistochemistry and chromogenic in situ hybridization (CISH) protocols were performed on tissue cores and the corresponding imprints, respectively. Protein expression levels were measured by applying a digital image analysis macro.

Results: Combined protein and gene analysis demonstrated 19/60 (31.6%) cases with HER2/neu overexpression and 9/60 (15%) with gene amplification. Simultaneous HER2 and AKT overexpression combined with PTEN down-regulation was observed in 14/60 (23.3%) cases, correlated with the neoplasm's grade (p=0.021). Multivariate analysis (carcinomas vs adenomas) demonstrated that increased PTEN expression reduces the CA risk by 77% (RR: 0.23; 95% OA: 0.12–0.42, p<0.0001).

Conclusion: The simultaneous deregulation of HER2/PTEN/AKT correlates with the differentiation in CA. PTEN expression is a major and independent prognostic factor regarding the risk of carcinogenesis in colon.

005

Increased proliferation of intestinal epithelial cells is associated with elevated frequencies of granzyme B-positive intraepithelial lymphocytes in collagenous colitis

V. Genitsch *, D. Kassahn, C. Mueller
*Universität Bern, Inst. für Pathologie, Basel, Switzerland

Objective: The aim of this study was to investigate the proliferation of intestinal epithelial cells (IEC) in collagenous colitis (CC) and ulcerative colitis (UC).
Method: We compared CC, UC and healthy control (HC) patients (n=10 each) by the expression of genes (entire tissue sections and laser capture microdissected cell populations) and immunohistochemical analysis using formalin-fixed, paraffin-embedded colonic biopsies.
Results: In CC, the proliferation rates (Ki-67) of superficial IEC were significantly elevated compared to UC (p<0.01) and HC (p<0.001). The transcription rate of KGF, KGFR and TGFα was not heightened in CC; therefore, these growth factors do not seem to be critically involved in the increased proliferation of IEC in CC. The observed proliferation could occur as a consequence of a TNFα-induced apoptosis; however, the TNFα expression in CC was comparable to HC. CXCL9 mRNA was increased in microdissected IEC in CC compared to HC (p<0.05) and could act as a chemoattractant for the elevated numbers of intraepithelial lymphocytes (IELs) in CC. The number of granzyme B-positive IELs in CC correlated with the proliferation rate of superficial IEC (r=0.8109; p=0.011).
Conclusion: The observed increased proliferation of IEC in CC compared to UC and HC might compensate for IEL-mediated cytotoxicity in CC.

006

Comparative study of immunopathological mechanisms operative in patients with collagenous colitis, ulcerative colitis and non-inflamed, normal colon

V. Genitsch *, D. Kassahn, C. Müller
*Universität Bern, Inst. für Pathologie, Basel, Switzerland

Objective: The objectives were to identify the immunopathological mechanisms that contribute to the different courses of disease in ulcerative (UC) and collagenous colitis (CC).
Method: We compared the expression of genes related to macrophages, T-lymphocytes and intestinal epithelium from CC, UC and healthy control (HC) patients (n=10 each) using formalin-fixed, paraffin-embedded colonic biopsies (entire tissue sections and laser capture microdissected cell populations).
Results: GATA3 and T-bet expression profiles do not indicate a functional polarization of T-cells into Th1+ or Th2+ cells. Furthermore, the expression of TGFβ1/3 and FoxP3 is exclusively increased in UC, suggesting a counter-regulation to inflammation through an increased accumulation of Tregs. The transcription of TSLP is reduced in CC in comparison to HC (p<0.05). In CD68+ cells, TREM1 mRNA is markedly increased only in UC (p<0.05), whereas TREM2 expression is comparably low in UC and CC. Furthermore, M2 (MRC1, IL-10) and M1 (Cxcl-9, MCP1, CCR2) macrophage markers showed either a low expression in CC or no significant differences between the three groups.
Conclusion: Our data indicate differential macrophage differentiation in UC vs. CC vs. HC; however, they could not be assigned to an M1 or M2 phenotype. The CD68+ cells in CC rather show an overall low activity, which might be due to the decreased TSLP expression in CC.

007

Intratumoral budding (ITB) predicts worse outcome in stage I–III colorectal cancer patients

E. Karamitopoulou *, A. Kondi-Pafiti, V. Kölzer, D. Karandrea, K. Gennatas, E. Patsouris, A. Lugli, I. Zlobec
*University of Athens, 1st Dept. of Pathology, Greece

Objective: Tumor budding at the invasive front (peritumoral budding; PTB) is an established prognostic parameter in colorectal cancer (CRC). However, its prognostic significance within the tumor center (intra-tumoral budding or ITB) remains unknown. Our aim was to determine the correlation of ITB with PTB and the prognostic impact of ITB in CRCs.
Method: Whole tissue sections of 215 CRCs with full clinico-pathological and follow-up information were stained with cytokeratin AE1/AE3. Presence of ITB and PTB was scored across ten HPFs. Measurements were correlated to patient and tumor characteristics.
Results: There was a strong correlation between increased ITB and PTB (p<0.0001). High-grade ITB was linked to higher tumor grade (p<0.0001), TNM-stage (p=0.0005), vascular invasion (p<0.0001) and infiltrating tumor border configuration (p=0.0019) but not to distant metastasis or KRAS mutation. In univariate analysis, high-grade ITB had a significant effect on outcome (p<0.0001), particularly in TNM I–III (p<0.0001). Stage-matched multivariable analysis in non-metastatic patients, including therapy information, confirmed the strong negative effect of ITB on prognosis (p=0.0167).
Conclusion: The independent prognostic role of ITB in non-metastatic CRCs supports its assessment in pre-operative colon cancer biopsies and its potential impact on pre- and post-operative clinical decisions.

008

Infiltrating tumor border configuration is associated with KRAS mutation and poor survival in colorectal cancer

E. Karamitopoulou *, V. Kölzer, A. Kondi-Pafiti, D. Karandrea, K. Gennatas, E. Patsouris, A. Lugli, I. Zlobec
*University of Athens, 1st Dept. of Pathology, Greece

Objective: Tumor border configuration is an established prognostic parameter in colorectal cancer (CRC). Our aim was to determine its correlation with patient clinico-pathological parameters and KRAS mutational status.
Method: Tumor border configuration was assessed by two pathologists in 215 CRCs with full clinico-pathological and follow-up information. Findings were correlated to the patient and tumor characteristics. Genomic DNA could be extracted in 196 cases and sequencing of KRAS codons 12 and 13 was performed.
Results: A total of 151 CRCs (70.2%) had infiltrating, 43 (20%) pushing and 21 (9.8%) mixed pushing/focally infiltrating margins. An infiltrating border was significantly associated with higher-grade ($p=0.0009$), TNM stage ($p<0.0001$), and lymphatic/vascular invasion ($p<0.0001$). KRAS mutations occurred in 39% of patients with infiltrating in comparison to 15.4% with pushing border ($p=0.0214$). Patients with infiltrating margins had significantly shorter survival time compared to pushing and/or mixed tumors ($p<0.0001$), independent of adjuvant therapy ($p=0.0007$). Stage III patients with pushing margins had more favourable survival time ($p=0.039$) compared with mixed or infiltrating borders (5-year overall survival: 100%, 68.6% and 23%, respectively).
Conclusion: Tumor border configuration has an independent prognostic impact, especially in stage III CRCs. The more frequent occurrence of KRAS mutations in patients with infiltrating borders suggests a possible pathogenetic link.

009

A multifactorial histopathologic prognostic score accurately classifies three groups of gastric carcinoma patients with different outcome after neoadjuvant chemotherapy followed by surgery and is superior to the current UICC staging system

R. Langer *, D. Reim, A. Novotny, C. M. zum Büschenfelde, J. Engel, H. Friess, H. Höfler, K. Becker
*Technische Universität München, Inst. für Pathologie, Germany

Objective: For gastric carcinoma treated with neoadjuvant chemotherapy (CTX) before surgery, postoperative staging classifications used for non-treated tumors may not accurately predict patients´ prognosis.
Method: We evaluated 428 gastric carcinoma specimens following a cisplatin-based CTX and examined if a multifactorial histopathologic prognostic score (PRSC) can discriminate prognostic subgroups of patients. The factors UICC ypT-category, ypN-category and histopathological tumor regression were assigned a value from 1 to 3 (ypT0-ypT2=1 point; ypT3=2 points; ypT4=3 points; ypN0=1 point; ypN1-2=2 points; ypN3=3 points; <10% residual tumor/tumorbed=1 point; 10-50% residual tumor/tumorbed=2 points; and >50% residual tumor/tumorbed=3 points) and a three-tiered PRSC based on the sum value was determined (group A: 3–4 points; group B: 5–7 points; group C: 8–9 points).
Results: The PRSC discriminated significantly different prognostic groups (group A: 76 patients; group B: 210 patients; group C: 142 patients; $p<0.001$). In multivariate analysis including UICC stage, R-status, tumor diameter, lymphatic vessel invasion, grading and Lauren´s classification, the PRSC was the only independent prognostic factor for overall survival ($p=0.001$).
Conclusion: The proposed PRSC clearly identifies three subgroups of gastric cancer patients after neoadjuvant CTX and surgery with different clinical outcomes and is superior to the current UICC staging system for estimation of prognosis.

010

C-myc genomic status in hepatocellular carcinoma and its potential role for target therapy

F. Pedica *, M. Brunelli, S. Pecori, M. Chilosi, A. Scarpa, S. Pedron, E. Vittoria, I. Cataldo, G. Martignoni, P. Capelli
*University of Verona, Pathology and Diagnostic, Italy

Objective: Hepatocellular carcinoma (HCC) is one of the leading causes of cancer-related death and an optimal therapy is lacking. The role of c-myc in HCC carcinogenesis has been well established and nowadays new drugs targeting the c-myc pathway oncogene have been developed. We sought to investigate the status of the c-myc molecule in 45 selected cases of HCC from our department archive.
Method: Forty-five formalin-fixed and paraffin-embedded hepatocellular carcinomas were examined for c-myc aberrations by break-apart FISH probes. Probes specific for the centromeric part of chromosome 8 (CEP8) and for the c-myc locus (at 8q24) were used to assess both c-myc amplification and chromosomal gain. C-myc double signals (in >90% of nuclei), gains (three signals in >10% nuclei for both probes) and amplification >3 c-myc signals in >10% of nuclei with 8p/CEP8>2 were clustered.
Results: We found three distinctive genotypic patterns: 31% showed c-myc gene amplification, 38% had gains of both c-myc and CEP8, and 31% were dysomic.

Conclusion: Our results show that c-myc is frequently involved in HCC biology. We suggest that c-myc is noteworthy to be further investigated in HCC as a potential therapeutical target and could be used to identify subsets of HCC which could benefit from anti-c-myc targeted drugs.

Wednesday, 31 August 2011, 17.00–19.30, Room 201

OFP-07 Oral Free Paper Session Digestive Diseases Pathology II

001

Early-onset and late-onset colorectal carcinoma of the left colon show different clinical, pathological and molecular features

E. Pilozzi *, G. Zardo, A. Ciolfi, E. Duranti, M. C. Giustiniani, C. Maresca, F. Allevato, M. Ferri, L. Ruco
*Ospedale Sant´Andrea, Dept. of Clinical and Molecular Medicine, Roma, Italy

Objective: About 15% develop in subjects ≤50 years (early onset). The aim of our study was to compare the clinical, pathological and molecular feature of early-onset microsatellite stable (MSS) colorectal carcinoma of the left colon (LCC<50) and late-onset MSS left colorectal carcinoma (LCC>70).
Method: A total of 22 MSS LCC <50 and 21 MSS LCC> 70 were selected. Pathological (growth pattern, grading, stage, vascular invasion, tumor-infiltrating lymphocytes) and molecular features (K-RAS mutation, BRAF mutation) were evaluated. The genome methylation status of CpG islands was investigated using Restriction Landmark Genome Scanning (RLGS).
Results: LCC <50 showed advanced stage (III or IV) and an infiltrative pattern of growth in about 60% of cases compared to 28% of LCC >70. KRAS was mutated in 38% of LCC <50 and in 19% of LCC >70. All mutations but one affected codon 12. No mutation of BRAF was identified in either groups. RLGS showed that even if the number of methylation events did not differ between the two groups, the sequences of DNA methylated in each group were different.
Conclusion: Early-onset left colorectal carcinomas show more aggressive pathological and clinical features. The different patterns in DNA methylation between the two groups suggest that they may differ in their molecular pathogenesis.

002

CDKN2A methylation is a highly unfavourable prognostic factor in colorectal cancer: a histomorphological, molecular and large-scale protein expression study

I. Zlobec *, M. Bihl, A. Foerster, A. Rufle, A. Lugli
*Universität Bern, Inst. für Pathology, Switzerland

Objective: The aim of this study was to determine the independent prognostic effect of CDKN2A (p16) methylation in colorectal cancer and to establish a protein profile of methylated cases.
Method: A total of 422 colorectal cancers were analyzed for KRAS, BRAF, microsatellite instability (MSI) and CDKN2A methylation. Tissue microarrays were investigated for a large panel (n=40) of selected markers related to Wnt, TGF-beta, and MAP/Kinase pathways, cell cycle, metastasis and angiogenesis. A total of 128 pancytokeratin-stained whole tissue sections could be evaluated for tumor budding (high-grade: >5 buds/HPF).
Results: CDKN2A methylation occurred in 16.1% of cases and was associated with right-sided tumor location, BRAF mutation, higher tumor grade (p<0.0001, all), lymph node metastasis (p=0.0018), high-level MSI (MSI-H) (p=0.0302) and poor survival (p=0.0006). A total of 16/16 MSI-H with CDKN2A methylation had high-grade budding (p=0.008). Methylation was linked to increased laminin5γ2 (p=0.019) and decreased CDX2 (p=0.0032) in MSI-H.
Conclusion: CDKN2A methylation is an adverse prognostic factor in colorectal cancers. In MSI-H cases, CDKN2A may lead to poor survival by conferring a high-grade tumor budding phenotype through the deregulation of Wnt signalling molecules laminin5γ2 and CDX2 rather than through β-catenin/E-cadherin.

003

Impact of CpG island methylator phenotype and microsatellite instability on tumor budding in colorectal cancer

I. Zlobec *, M. Bihl, V. Kölzer, A. Foerster, A. Rufle, A. Lugli
*Universität Bern, Inst. für Pathology, Switzerland

Objective: The aim of this study was to determine the association and independent prognostic effect of tumor budding in colorectal cancer with high-level CpG island methylator phenotype (CIMP), microsatellite instability (MSI), KRAS, BRAF, and 0-6-methylguanine DNA methyltransferase (MGMT).
Method: A molecular analysis for five CIMP-related promoters (CRABP1, MLH1, p16INK4a, CACNA1G, NEUROG1), MGMT, MSI, KRAS and BRAF was performed on colorectal cancers from 127 patients. Tumor budding was evaluated on pan-cytokeratin-stained whole tissue sections and classified as low- or high-grade (HG) based on receiver operating characteristic curve analysis.
Results: Tumor budding was not associated with KRAS, BRAF, CIMP, or MGMT. A combined analysis of MSI/CIMP showed that MSI [p=0.006] rather than CIMP (p=0.356) was related to tumor budding. The adverse effect of HG budding on outcome was independent of MSI [p=

0.025; HR, 2.15], KRAS [p=0.047; HR, 2.04], BRAF [p=0.018; HR, 2.37], CIMP [p=0.046; HR, 2.01], MGMT [p=0.05; HR, 1.91], and CIMP/MSI [p=0.046; HR, 2.05].
Conclusion: Although HG budding is less frequent in MSI-H cancers, its negative prognostic effect is independent of the five molecular alterations investigated. These results stress that efforts to standardize the evaluation of tumor budding should continue to be given precedence.

004
Glycoprotein-340/DMBT1 is a noble prognostic marker in colorectal cancer

H.-J. Chang *, H.-Y. Yeo, B.-C. Kim, J.-W. Park, S.-Y. Kim, K.-H. Kim, S.-S. Paeng, B.-C. Yoo, D.-Y. Kim
*National Cancer Center, Dept. of Pathology, Goyang, Republic of Korea

Objective: Glycoprotein-340 (gp-340) is one of the alternative splicing products of DMBT1 (deleted in malignant brain tumor). DMBT1 encodes a large scavenger receptor cysteine-rich protein and it was originally deleted in medulloblastoma and glioblastoma multiforme cell lines. Its functions have been suggested in tumor suppression, epithelial cell differentiation, and innate immune defense of mucosa. Previously, we detected DMBT1 in stools of colorectal cancer patients. Here, we aimed to evaluate the clinicopathologic significance of DMBT1 expression in colorectal cancer.
Method: The immunohistochemical expression of gp-340/DMBT was evaluated in 385 primary colorectal cancers by an estimation of immunoreactive scores (staining intensity × percentage of stained tumor cells), and the results were compared with the clinicopathological parameters.
Results: The mean immunoreactive score (ISs) of gp-340 was 117.26±58.71 (range, 0–285). The low expression of gp-340 (ISs≤150) was significantly related to serum CEA level, higher histologic grade, advanced stage, lymph node metastasis, and infiltrative growth. Loss of gp-340 expression (ISs≤10) was present in 16 cases (4.4%), and the loss of expression was an independent poor prognostic factor (P=0.023).
Conclusion: Gp-340/DMBT1 may play a role during disease progression of colorectal cancer and loss of gp-340 expression in primary colorectal cancer is significantly associated with poor survival.

005
Caveolin-1 and DOG1 immunoexpression in GISTs diagnosis: a comparative study on 152 cases

C. Iosif *, S. Enache, A. Georgescu, M. Comanescu, M. Stoicea, C. Ardeleanu
*INCD Victor Babes, Dept. of Pathology, Bucharest, Romania

Objective: Gastrointestinal stromal tumors (GISTs) are the most common primary mesenchymal neoplasias of the gastrointestinal tract, typically expressing CD117 and CD34. For years, several markers including caveolin-1 were tested for improving GISTs diagnosis accuracy. Recently, DOG1 immunohistochemical expression in GISTs was reported.
Method: We performed a retrospective study on formalin-fixed, paraffin-embedded samples from 152 cases of confirmed GISTs, aiming to characterize their immunohistochemical profile, including DOG1 and caveolin-1 expressions. Tissue samples were evaluated immunohistochemically for CD117, CD34, DOG1 and caveolin-1.
Results: The patients (M/F=62:90), aged 28 to 84, had spindle cell-type GISTs in 57.23% of cases, epithelioid in 31.57% and mixed pattern in 11.2% of cases. Immunohistochemically, CD117 was positive in 91.45% of GISTs, CD34 in 88.8%, DOG1 in 67.1% and caveolin-1 in 73.68% of the tumors. Of C-kit-negative GISTs, 92.3% expressed caveolin-1, 61.5% were DOG1-positive and 53.8% expressed both caveolin-1 and DOG1.
Conclusion: Our results suggest that caveolin-1 could be considered as a sensitive marker in GISTs, together with CD117, CD34 and DOG1 for diagnostic purposes. This significant expression in CD117-negative GISTs could represent an immunohistochemical alternative in establishing the diagnosis of these tumors.

006
Up-regulation of peroxiredoxin V and VI has potential as prognostic biomarkers in gastric cancer

J.-M. Kim *, Y.-S. Kim, D.-S. Lee
*Cancer Research Institute, Dept. of Pathology, Daejeon, Republic of Korea

Objective: Peroxiredoxins (Prxs) are novel peroxidases with high antioxidant efficacy associated with tumor biology in several kinds of cancer. However, few studies have investigated the expression of Prxs in human gastric cancer and its impact on disease prognosis or patient survival.
Method: We investigated the expression of all six isoforms of Prxs by Western blotting using nine gastric cancer cell lines and immunohistochemical staining in tissue microarrays containing 210 gastric cancer tissues. Additionally, we examined the correlation between the expression of Prxs and clinicopathological parameters.
Results: Several Prxs isoforms were overexpressed in gastric cancer cell lines and tissues to varying degrees; the expression of Prx I-IV was high in gastric cancer tissues, but the expression of Prx V and VI varied due to tumor parameters. The high expression of Prx I-IV was not associated with clinicopathological parameters. However, the expression of Prx V and VI were linked to large tumor size, tumor depth,

lymph node involvement, and higher TNM stage. Also, the expression tended to be correlated with a reduced 5-year survival rate. In multivariable analysis, Prx V was the only isoform associated with patient survival (high Prx V; $p=0.01$). **Conclusion:** The results of this study suggest that the expression of Prx proteins is increased in gastric cancer. The expression of Prx V and VI play important roles during gastric cancer progression and may be indicators of patient survival. Further investigations are needed to determine whether Prx V and VI could be used as biomarkers and therapeutic targets for gastric cancer.

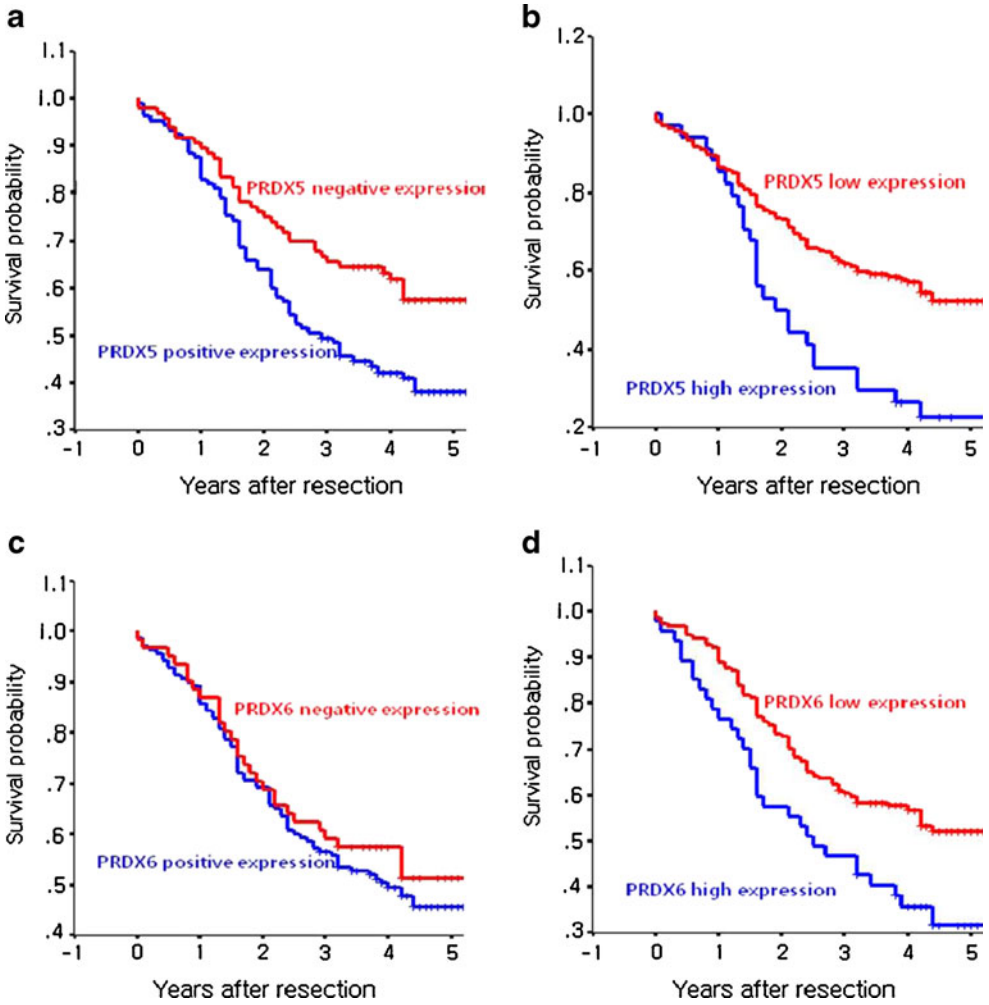

007

Characterization of the role of galectin-1 (Gal-1) in pancreatic tumors

J. Munne Collado *, N. Martinez Bosch, M. Moreno Merino, M. Iglesias Coma, L. Comerma Blesa, P. Navarro Medrano
*Hospital del Mar, Dept. of Pathology, Barcelona, Spain

Objective: Human exocrine pancreatic tumors are predominantly ductal adenocarcinomas although the cell originating the tumor—acinar, ductal or endocrine cells—is still a matter of debate. Galectin-1 is a multifunctional protein involved in both physiological and pathological functions, including tumor progression. In pancreatic cancer, Gal-1 is highly overexpressed, mainly in the stroma. Here we have used the Ela-1-myc transgenic model to know better the pathogenesis and contribution of galectin-1 in pancreatic tumor progression.

Method: We produced three types of transgenic mice by crossing Ela-1-myc transgenic mice and Gal-1 knockouts. Therefore, all mice overexpressed the oncogene c-myc under the control of the promoter elastase-1, which targets c-myc expression to pancreatic acinar cells, but they differed as to the number of alleles of galectin-1 expressed. Given these genetic modifications, mice developed pancreatic tumors that were resected and performed for histopathological analysis.

Results: Mice with lack of expression of galectin-1 presented more tumor necrosis and less angiogenic network and their adenocarcinomas showed more acinar differentiation.
Conclusion: It seems that Galectin-1 plays a role in tumor progression and would also take part in pancreatic tumor differentiation. All these data point at galectin-1 as an interesting molecular target for future therapeutic tools in pancreatic cancer.

008

Effect of COX-2 inhibitor lumiracoxib, the anti-TNF-alpha etanercept and your association on TNBS-induced colitis in Wistar rats

A.P. Ribeiro Paiotti *, C.T. Fujiyama Oshima, R. Artigiani Neto, D.A. Ribeiro, S.J. Miszputen, M. Franco
*Universidade Federal São Paulo, Dept. of Pathology, Brazil

Objective: Crohn´s disease (CD) is associated with gut barrier dysfunction. Besides the baseline barrier defect, a subgroup of patients also expresses an intestinal barrier hyperresponsiveness to nonsteroidal anti-inflammatory drugs. On the other hand, the anti-TNF treatment has brought benefits to these patients. To evaluate the effect of lumiracoxib, a selective-cyclooxygenase-2 (COX-2) inhibitor, and etanercept (ETC), a tumour necrosis factor alpha (TNF-alpha) antagonist, were studied as to their association on the 2,4,6-trinitrobenzene sulfonic acid (TNBS)-induced experimental colitis.
Method: Wistar rats (n=47) were randomized into seven groups as follows: (1) Sham: sham induced-colitis; (2) TNBS: nontreated induced colitis (50 mg/kg); (3) lumiracoxib control (6 mg/kg); (4) lumiracoxib-treated induced colitis; (5) ETC control (5 mg/kg); (6) ETC-treated induced colitis; (7) lumiracoxib-ETC-treated induced colitis.
Results: Rats from groups 2 and 4 presented statistically significant similar macroscopic and histopathological features as compared with the other groups. There was no reduction in the levels of mRNA and protein expression of COX-2 and TNF-alpha in these two groups. Rats from groups 6 and 7 presented an improvement of macroscopic and histopathological damages in the distal colon. In addition, they exhibited decreased levels of mRNA expression of COX-2 and TNF-alpha and down-regulation at the cellular level of these proteins, as well as prostaglandin E2 (PGE2).
Conclusion: In TNBS-induced colitis in rats, treatment with lumiracoxib was not able to reduce morphological damages. On the contrary, treatment with etanercept attenuated the intestinal injury and reduced inflammation in TNBS-induced colitis, producing a protective effect on the potential damage caused by lumiracoxib.

009

KRAS wild-type status in patients with metastatic colorectal cancer using cetuximab plus FOLFIRI or FOLFOX4 regimen as the second/third-line setting: in comparison with the first-line setting

J.-Y. Wang *, S.-R. Lin
*Kaohsiung Medical University, Dept. of Surgery, Taiwan

Objective: This study was prospectively conducted to compare the role of KRAS wild type in predicting the efficacy and toxicities of cetuximab combination chemotherapy as the first-line or second/third-line therapy in mCRC patients.
Method: A total of 74 mCRC patients receiving cetuximab combined with FOLFOX4 or FOLFIRI as the first-line (group A) or the second/third-line setting (group B) were enrolled in this study. Wild-type KRAS had been identified by direct sequencing. The associations between clinical response/progression-free survival (PFS)/overall survival (OS)/toxicities and cetuximab combination chemotherapy timing (first-line or second/third-line setting) were evaluated.
Results: The overall response rate (complete response plus partial response) was comparable to 63.2% for group A and 38.9% for group B, respectively (RR=0.603; 95% CI, 0.369–0.985; P=0.037). PFS showed a statistically significant longer survival of group A than group B (P=0.0027), and OS also showed a significant longer survival of group A than group B (P=0.0212).
Conclusion: This study represents the validation of a molecular predictor of KRAS wild-type status response to cetuximab combination chemotherapy for mCRC patients, whereas its predictive role is less prominent in the second/third-line setting than in the first-line setting.

Sunday, 28 August 2011, 14.00–16.30, Room 206

OFP-08 Oral Free Paper Session Endocrine Pathology–Electron Microscopy

001

Proposal for a simplified Mib1 assessment in pancreatic endocrine tumours

A. Blank *, L. Boos, I. Zlobec, P. Komminoth, A. Perren, A. M. Schmitt
*Universität Bern, Inst. für Pathologie, Switzerland

Objective: The prediction of biological behaviour in pancreatic endocrine tumours (PET) is challenging in the absence of metastases. The assessment of the proliferation index by Mib1,

which is used for grading of PET, requires counting of 2,000 cells according to ENETS guidelines. As this procedure is not feasible in clinical routine, the aim of the present study was to simplify the assessment of the proliferation index in PET.

Method: Using a tissue micro-array containing 133 primary sporadic PET, Mib1 staining was examined by counting the number of positive tumour cells per HPF (0.2 mm^2). Results were correlated with Mib1 proliferation index (2%) as well as with survival data. A ROC analysis was performed to obtain the optimal cutoff for the number of tumour cells positive for Mib1.

Results: The number of Mib1-positive tumour cells correlated significantly with the Mib1 proliferation index. ROC analysis showed a cutoff of ≤7 tumour cells/0.2 mm^2 staining with Mib1 for optimal risk stratification in the present cohort.

Conclusion: In the present study, we demonstrate a simplified method to assess the proliferation of PET by counting the number of tumour cells staining with Mib1. This method could substitute for the presently recommended proliferation index.

002

Detection of BRAF, KRAS and EGFR mutations in papillary thyroid carcinoma

N. Fakhruddin *, R. Mahfouz, R. Abdelkhalik, L. Yahya, G. Zaatari

*American University of Beirut, Medical Center, Lebanon

Objective: Papillary thyroid carcinoma (PTC) has a higher incidence in Arab countries (6%) as compared to Europe and the United States (1.5%). RET/PTC, BRAF, and Ras aberrations occur in PTC. EGFR pathway crosstalks with these factors. We aim at determining the frequency BRAF, Ras and EGFR in PTC, which may influence the extent of surgical procedures and use of tyrosine kinase inhibitors.

Method: Thyroid cancer cases were collected over 10 years. Kras and BRAF mutations were detected by StripAssay Kits. EGFR mutations will be detected using real-time PCR. BRAF V600E negative cases will be analyzed by sequencing of BRAF exons 11 and 15.

Results: Thyroid cancer presented 11% of all thyroidectomies. PTC and microcarcinoma constituted 93% and 13%, respectively; 5% had lymphnode metastases. Thyroid cancer incidence has increased by 17%. Kras mutations were not detected. BRAF mutations were present in 46% of PTC and associated with metastasis but not the low-grade variants. No correlation with tumor size or age was shown.

Conclusion: Considering the high and increasing incidence of PTC in our ethnic group and the prevalence of BRAF mutations, molecular evaluation in a bigger population and correlation with clinical profiles may influence the diagnostic, prognostic and therapeutic protocols.

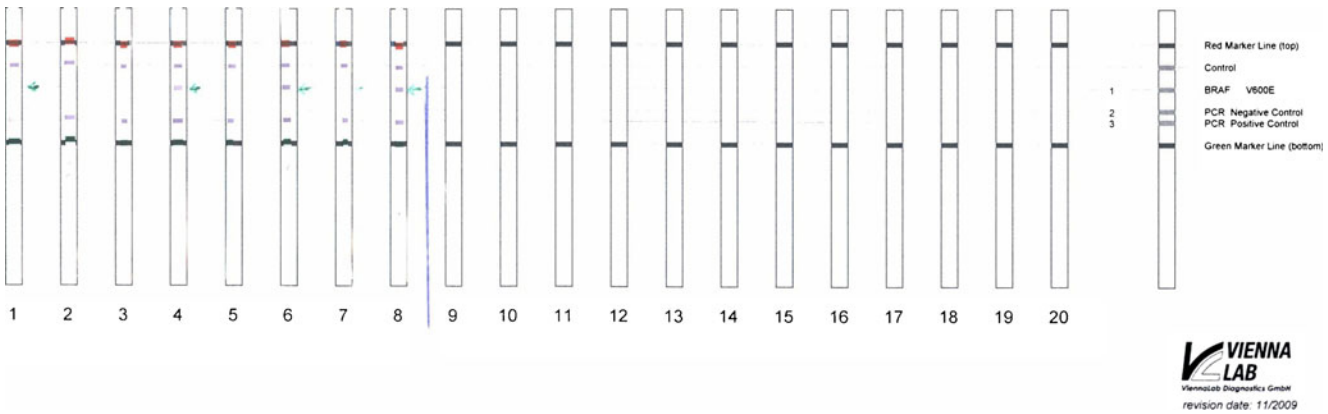

003

Loss of estrogen receptor β expression predicts poor outcome in follicular thyroid carcinoma

A. Heikkilä *, J. Hagström, P. Siironen, J. Louhimo, I. Heiskanen, H. Mäenpää, C. Haglund, J. Arola

*Haartman Institute, Dept. of Pathology, University of Helsinki, Finland

Objective: The expression of estrogen receptors (ER) has been previously demonstrated in breast, ovarian, prostate, and colon cancers with an increased α and a loss of β receptor expressions. In papillary thyroid carcinoma, ER expression is controversial; the expression of ERα is generally low and that of ERβ is high although lacking a correlation with clinicopathological features. In this study,

we examined the role of ERs in follicular thyroid adenomas (FTAs), well-differentiated follicular thyroid carcinomas (WDFTCs) and poorly differentiated follicular thyroid carcinomas (PDFTCs).
Method: The material consisted of 83 FTA, 36 WDFTC and 7 PDFTC samples from patients treated in Helsinki University Central Hospital (HUCH) between 1990 and 2009. Eight patients had died of FTC and, in addition, five patients had a metastasized disease. Tissue microarray blocks were used for the immunohistochemical analysis of ERα and ERβ.
Results: Nuclear ERβ expression was significantly lower in carcinomas than in adenomas. In FTCs and WDFTCs, ERβ was inversely correlated with poor prognosis and with MIB-1 immunoexpression. ERα expression lacked correlation with clinical or histological characteristics.
Conclusion: Loss of ERβ immunoexpression predicts a poor outcome and its measurement may be worthwhile in aggressively acting follicular thyroid carcinomas.

004

An analysis of clinicopathological factors in Japanese pancreatic neuroendocrine tumor patients according to 2010 WHO classification

A. Kasajima *, K. Ishida, F. Fujishima, F. Motoi, H. Ootsuka, Y. Nakamura, M. Watanabe, M. Unno, H. Sasano
*Tohoku University Hospital, Dept. of Pathology, Sendai, Japan

Objective: A newly revised WHO classification for pancreatic neuroendocrine tumor (PNET) published in 2010 defines histological grades exclusively based on mitotic counts and/or Ki67 labeling index. However, it remains debatable whether this classification reflects the biological behavior of non-Western PNET patients.
Method: Clinicopathological factors of 63 Japanese patients with PNETs (G1:28, G2:30, G3:5), as well as immunolocalization of somatostatin receptors (SSTRs) were evaluated and analyzed according to the criteria of WHO 2010.
Results: Results of grading determined according to WHO 2010 were significantly correlated with tumor size ($p<0.001$), nodal status ($p=0.002$), distant metastasis ($p=0.003$) and stage ($p<0.001$) of the patients. The presence of peripancreatic and vascular invasion was also significantly associated with the gradings above ($p=0.004$ and $p<0.001$, respectively). The positive immunoreactivity of SSTR1, 2A, 2B, 3 and 5 was detected in 55.6%, 81.5%, 63.0%, 42.6% and 44.4% of the cases examined, respectively, with no statistical correlation of the results with WHO 2010 grading.
Conclusion: The newly developed WHO 2010 grading of PNET was significantly associated with clinicopathological factors in Japanese patients, suggestive of its utility in Japanese PNET patients. Additionally, the presence of histologically identified peripancreatic and vascular invasion was also significantly related to the new WHO 2010 of PNET.

005

Achaete-scute-1 expression in poorly differentiated neuroendocrine carcinomas (NECs)

S. La Rosa *, A. Marando, C. Capella
*Ospedale di Circolo, Dept. of Pathology, Varese, Italy

Objective: Achaete-scute-1 (ASH1), a transcription factor involved in the differentiation of lung neuroendocrine cells, has been identified in lung NECs. Moreover, a few papers suggested its expression in non-pulmonary NECs. Our aim was to study the distribution of ASH1 in NECs of different sites to evaluate its usefulness as a diagnostic marker for lung NEC.
Method: A total of 161 NECs of the lung, skin, head and neck, gut, pancreas, prostate, urinary bladder and uterus were immunostained using two anti-ASH1 specific antibodies (pASH1, polyclonal, Abcam and mASH1, monoclonal, BDPharmigen).
Results: pASH1-immunoreactivity (IR) was observed in 87/161 (54%) NECs and mainly in those located in the lung (68%), nose (76%), gut (53.8%), bladder (61%) and prostate (70%). mASH1-IR was found in 73/155 (47%) cases: 90% of lung, 56% of nasal, 17% of gut, 45% of prostatic and 75% of bladder NECs. The sensitivity and specificity of both antibodies in detecting lung NECs were 68.2% and 44.2% for pASH1 and 90% and 50% for mASH1, respectively.
Conclusion: The two antibodies showed different sensitivity and specificity in detecting lung NECs. Since ASH1 expression was observed in several NECs of different sites, it may be suggested that it may play a role in the pathogenesis or progression of NECs.

006

Grading of neuroendocrine tumours requires high-quality assessment practice

S. M. Remes *, J. Arola, H. Helin, J. Isola, V. Tuominen
*Helsinki University Hospital, HUSLAB, Dept. of Pathology, Finland

Objective: The new WHO 2010 classification of neuroendocrine tumours (NETs) is based on grading them according to proliferation index (PI). This classification introduces Ki-67 antigen as the most important criterion for tumour-grading, influencing patients' prognosis and choice of the treatment. The purpose of this study was to evaluate the assessment practice of PI value in NETs and its influence on tumour-grading.
Method: The tumour material consists of 51 NETs from the pancreas (n=31) and ileum (n=20). The slides were stained with standard immunohistochemical protocol. The proliferation index was assessed conventionally by a microscope and with a new Internet-based image analysis software, ImmunoRatio. The evaluation guidelines for PI were based on the WHO 2010 criteria.
Results: The reproducibility of the ImmunoRatio to reanalyse the PI values and tumour grade was almost perfect compared to the conventional assessment which suffered from variation (p<0.01). The PI values and tumour grade between conventional and ImmunoRatio assessment by a qualified observer were in good agreement, confirming the validity of this software to produce standard PI values.
Conclusion: ImmunoRatio is a qualified method to analyse objectively the Ki-67 PI-based tumour grade in NETs.

007
MUC1 is detected in nuclear pseudoinclusions of papillary thyroid carcinoma

F. Renaud *, S. Aubert, P. Devos, B. Bouchindhomme, P. Pigny, C. do Cao, M. Dherbomez, F. Pattou, B. Carnaille, J.-L. Wemeau, E. Leteurtre
*Lille University Hospital, Anatomie Cytologie Pathologique, Lille Cedex, France

Objective: MUC1 is a membrane-bound mucin expressed in various human carcinomas and associated with a poor prognosis. In thyroid, MUC1 was described at the apical pole of normal follicular cells whereas it was detected in the cytoplasm of some papillary thyroid carcinoma (PTC). Our objective was to analyse the expression of MUC1 in a series of thyroid tumors with a special focus on the precise localization of the staining.
Method: We performed a detailed morphological analysis of 132 thyroid tumors (66 PTC and 66 adenomas). MUC1 immunohistochemistry was realized on tissue microarray.
Results: MUC1 expression was observed in 58% of PTC and 7% of adenomas. More precisely, MUC1 was either cytoplasmic or both cytoplasmic and apical in PTC. Interestingly, we noticed a strong expression of MUC1 inside the nuclear pseudoinclusions.
Conclusion: This study is the first to describe MUC1 inside nuclear pseudoinclusions in PTC, which are one of the most helpful criteria for the diagnosis. Some authors have previously described precise ultrastructural or immunohistochemical modifications in the nucleus of PTC tumor cells. Nevertheless, the curious morphology of the nucleus in PTC remains to be elucidated.

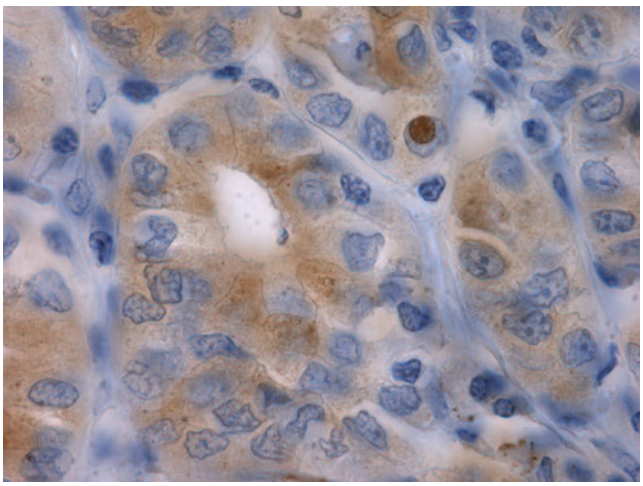

008
Immunohistochemical expression of D2DR, SST2 and SST5 receptors in prolactinomas and thyrotropinomas

D. Rotin *, L. Astafieva, B. Kadashev, O. Paklina
*NN Burdenko, Inst. of Neurosurgery, Dept. of Pathology, Moscow, Russia

Objective: The management of patients with different types of pituitary adenomas (PA) requires a multidisciplinary approach, including target therapy (dopamine agonists and somatostatin analogues). The aim of the study was to determine and evaluate D2DR, sst2 and sst5 expression in prolactinomas and thyrotropinomas.
Method: A total of 26 prolactinomas (female—10, male—16, age 16–61 years, median—32) and 13 thyrotropinomas (female—9, male—4, age 11–63 years, median—25) from the patients operated in our institute were immunostained with antibodies to prolactin, growth hormone, TSH, ACTH, FSH, LH and to receptors—dopamine D2DR and somatostatin sst2 and sst5.
Results: Strong staining of D2DR occurred in all 26 prolactinomas. The expression of sst2 and sst5 was also seen in all 26 prolactinomas but was variable (from "+" to "+++"). Thyrotropinomas expressed D2DR in nine cases (64%), sst5 in five cases (36%) and sst2 only in two cases (14%).
Conclusion: Dopamine agonists are considered to be first-line treatment of patients with prolactinomas. Nevertheless,

a differential approach to thyrotropinomas including the determination of somatostatin and dopamine receptors could be the key to target the therapy of either of these types of PA.

009

A computational model of the relations between macrophages, progenitor cells and oncocells in experimental tumorigenesis

O. El-Hassoun *, Z. Valaskova, L. Maruscakova, J. Jakubovsky, I. Hulin
*Comenius University, School of Medicine, Bratislava, Slovakia

Objective/Purpose: Cooperation with host cells is necessary for tumorigenesis. In our work, we aim to find a quantitative relation between oncocells, macrophages, and progenitor cells and to express this relation in a mathematical model.
Method: We injected fibrosarcoma cells in rats and performed peritoneal lavage every week for 4 weeks. With laser cytometry, we measured the amount of oncocells (VNT+), macrophages (CD68), and progenitor cells (CD34+). We used these numbers to calculate the parameter V (the volume of the pyramid formed by plotting the measured parameters in a 3D graph). Then, we used V to recalculate the number of oncocells (oncocell load) by an equation that requires V, macrophages, and progenitor cells. We compared the calculated values with the cytometer-measured values.
Results: We found that our mathematical model is a valid method for calculating the oncocell load in a given compartment.
Conclusion: The mathematical interpretation of cellular interactions in cancer offers prospective markers that are applicable in a quantitative description. Our mathematical model could determine whether the recruitment of macrophages is reasonable or decisive. A complex evaluation of tumorigenesis and growth by giving an adequate attention to the different levels of tumor–host interactions is a step towards redefining cancer staging and therapy.

010

Ultrastructural morphometry of hepatocytes in patients with chronic hepatitis C virus infection and prediction of malignant transformation

A. Shalaby *, S. Mansy, N. Marie, A. Abdel-Fatah, A. Helmy, E. Esmat, H. Solaiman
*University College Hospital, Dept. of Histopathology, Galway, Ireland

Objective: Hepatitis-C-virus (HCV) infection is associated with an increased incidence of hepatocellular carcinoma (HCC). The prediction of cellular turnover to HCC can decrease tumour-related mortality. We aim to assess the ultrastructural morphometry of hepatocytes and interhepatocytic spaces in relation to the stage of HCV infection and identify indicators that predict the malignant transformation to HCC.
Method: Liver specimens were harvested from 15 HCV patients and 5 patients with HCC complicating HCV who underwent partial hepatectomy. The specimens were examined by light and electron microscopy. Ultrastructural morphometry for 30 mononuclear hepatocytes was performed for each case using Soft-Imaging-System-Analysis-2.1.
Results: There was a positive correlation between intercellular spaces and the progression of the stages of HCV (R=0.776, P=0.001). HCC had a significantly smaller cell area (145.85±34.77 vs 241.78±47.77, P=0.005), cell perimeter (51.2±6.77 Vs 63.45±5.58, P=0.004), and maximum cell diameter (15.69±1.7 vs 20.65±1.39, P<0.0001) compared to HCV. HCC had a significantly greater maximum nuclear diameter (7.25±0.4 vs 6.02±0.65, P=0.007), total nuclear area (2.68±0.045 vs 1.71±0.26, P<0.001) and nucleocytoplasmic ratio (0.35±0.06 vs 0.113±0.025, P<0.0001).
Conclusion: Larger-scale studies are required to verify if these parameters in the advanced stages of HCV could be utilized to alert for malignant cellular transformation.

Sunday, 28 August 2011, 17.00–19.30, Room 206

OFP-09 Free Paper Session Gynaecological Pathology

001

Podoplanin expression in cervical squamous cell carcinoma

R. Canas Marques *, F. Silva, A. Félix
*IPOLFG, Dipt. di Anatomia Patológica, Lisbon, Portugal

Objective: Squamous cell carcinoma of the uterine cervix is the second most frequent cancer in women and has a high mortality rate. Podoplanin is a transmembrane glycoprotein that plays a role in cellular proliferation and adhesion. Previous studies have correlated this protein with tumour invasion and metastases. The aim of this study was to assess podoplanin epithelial expression in cervical squamous cell carcinoma (SCC) and correlate its expression with tumour invasion, recurrence and metastases.

Method: We selected 81 cases of SCC, 11 in situ and 70 invasive. Clinico-morphological data were reviewed. The immunohistochemistry study was done using D2-40 antibody. Statistical analysis was performed using Fisher exact test.
Results: Podoplanin (D2-40) was expressed in 90.9% (10/11) of in situ SCC cases and in 30 (42.8%) of the invasive SCC cases and this difference was statistically significant (p=0.0033). Only 15.8% (3/19) of the cases with metastases had podoplanin epithelial expression and, comparing with the non-metastatic invasive cases, this difference had statistical significance (p=0.0064). No relation was found between podoplanin expression and follow-up status, clinical stage or recurrence.
Conclusion: Loss of epithelial podoplanin expression in uterine cervical squamous cell carcinoma is associated with tumoral stromal invasion and presence of metastasis.

002

Morphology and genetics of endometrial samples in cases of early pregnancy loss

I. Kostyuchek *, A. Taits, V. Gargin, O. Polushkina, G. Tolibova, M. Kleshchov, S. Vorobev
*Ott Institute, Dept. of Pathology, St. Petersburg, Russia

Objective: The most common reason of early pregnancy loss (EPL) is chromosomal anomaly (60.0%); the second is endocrine disturbance (35.0%). To improve clinical diagnosis, it is necessary to know more about the causes of EPL.
Method: A total of 112 samples after uterine curettage in the cases of EPL were genetically, histologically and immunohistochemically examined.
Results: Chorionic tissue samples with chromosomal anomaly (n=82) had 80.5% characterized by dystrophic changes of stroma and abnormal vascular development of chorionic villi. The same changes were observed in 40.0% of chorion samples with normal karyotype (n=30). After a histological examination (71 cases), samples were divided in two groups: first—with disturbance of endometrial decidualization (n=37); second—without it (n=34). High expression of estrogen receptors (ER) in endometrial glands (U=442.0; p<0.05) and decidual tissue (U=407.0; p<0.05) was observed in the first group. The number of progesterone receptors (PR) in endometrial glands was the same in both groups (U=509.0; p=0.17). A high level of PR in decidual tissue was found in the second group (U=450.0; p<0.05).
Conclusion: The sensitivity of histological investigation as a marker of chromosomal anomaly of chorionic tissue is 0.80; the specificity is only 0.60. The histological features and expression of ER and PR in endometrial glands and decidua make it a possibility to think about endocrine abnormality in women with EPL.

003

Unilateral ovarian metastasis of gastric adenocarcinoma simulating primary ovarian yolk sac tumour

F. Nogales *, E. Stacher, O. Preda, P. Goyenaga, J. Aneiros-Fernandez, F. Moinfar, A. Nicolae
*Universidad de Granada, Dept. de Anatomia Patologica, Spain

Objective: Ovarian neoplasms with high levels of serum AFP usually correspond to primary yolk sac tumours (YST). Their unusual, heterogeneous patterns are difficult to recognize and may be misdiagnosed. We present two cases of unilateral ovarian metastasis of gastric adenocarcinoma that simulated primary ovarian YSTs.
Method: Case histories: Case 1: A 44-year-old patient with a left 20-cm ovarian mass and elevated serum AFP. Case 2: A large ovarian tumor in a 26-year-old pregnant patient. Both were apparent FIGO1 stage.
Results: Microscopically, case 1 presented a solid and glandular pattern composed by vacuolated cells with numerous hyaline globules, mimicking both the primary glandular variant of YST and clear cell carcinomas. In case 2, a polyvesicular pattern was admixed with extensive areas of adenocarcinoid and occasional foveolar-type epithelium-lined cysts. Both cases had angioinvasion and shared a similar immunophenotype with glypican3, CDX2 and SALL4 positivity, while AFP and HepPar1 expression were restricted to case 1. Subsequent image staging studies revealed primary gastric tumors in both, histologically corresponding to an AFP producing gastric clear-cell/hepatoid adenocarcinoma in case1 and a diffuse type in case 2.
Conclusion: A diagnosis of ovarian YST should not rely on immunophenotype alone when classical YST areas are absent and tumour emboli is present. Metastases of extragonadal tumors producing AFP should be considered.

004

Triage of ASC-US and LSIL cases by p16/Ki-67 dual-stain immunocytochemistry: results from the EEMAPS study

D. Schmidt *, C. Bergeron, K. J. Denton, R. Ridder
*Institut für Pathologie, Mannheim, Germany

Objective: HPV testing is frequently used for the triage of Pap cytology results categorized as ASC-US. The specificity of HPV testing, however, is negatively influenced by the HPV prevalence in younger age groups, which also prevents it from being efficiently used in cases of LSIL.
Method: The diagnostic performance of a new dual-staining approach for p16/Ki-67 in retrospectively collected cases of ASC-US or LSIL Pap cytology was studied. The sensitivity and specificity for detection of underlying high-grade CIN were compared to HPV testing. A total of 362 cases of ASC-US and 415 LSIL with corresponding QC-reviewed biopsy results and HPV test results were available. The presence of one or more dual-stained cervical epithelial cell(s) defined a positive test result.
Results: Positive dual-stained cytology results provided a sensitivity for underlying HGCIN of 92.2% (71/77) for ASC-US and 94.2% (129/137) for LSIL cases, comparable to HPV testing results. In contrast, specificity was found to be at 80.6% (ASC-US) and 68.0% (LSIL), significantly higher than the specificity rates observed for HPV testing (36.3% in ASC-US; 19.1% in LSIL cases, respectively).
Conclusion: Dual-stained cytology for p16/Ki-67 in this study showed both high sensitivity and high specificity levels for initial Pap cytology results categorized as ASC-US or LSIL. In addition to the potential for improving current ASC-US triage algorithms, this new test may for the first time provide a triage option for LSIL cytology.

005

Extragenital metastatic tumors of the ovaries—series of 118 cases

D. Vuralli Bakkaloglu *, S. Batur, S. Ilvan
*Istanbul Universitesi, Cerrahpasa Tip Fakultesi, Turkey

Objective: Ovaries, after liver and lungs, are common sites for metastasis. The gastrointestinal system and breast are the most frequent primary origins. Metastatic tumors can be diagnosed after/during or even before the primary tumor.
Method: A total of 118 cases of metastatic tumors of extragenital origin that were diagnosed at our department throughout the years 1990–2010 are included in our study. We analysed the cases according to primary tumor, age, laterality, diameter, macroscopy and time of the diagnosis.
Results: A total of 55 cases are colon, 37 are stomach, 14 are breast, 3 are lung, 2 are lymphoma, 2 are peritoneum, 1 is renal, 1 is malign pheochromocytoma, 1 is thymoma, 1 is abdominal leiomyosarcoma, and 1 is biliary in origin. The age range is 21–83, with an average of 48. A total of 72 cases are bilateral, 28 are localized on the right, 18 are on the left; 51 cases are solid, 11 are cystic, 56 are both solid and cystic. There were 53 cases found after and 37 cases before the primary tumor. In 28 cases, the primary and the metastatic tumor were defined at the same time.
Conclusion: In order to predict the prognosis and schedule the treatment, the primary origin should be known. As shown in our study, the colon and the stomach are the first sites to be searched, but the primary tumor can be at any region of the body.

006

The usefulness of p57KIP2 immunohistochemical staining and genotyping test in the diagnosis of the complete hydatidiform mole

M. T. Yacoubi *, H. Landolsi, S. Brahem, M. Gribaa, S. Hmissa
*University Hospital Sousse, Dept. of Cyto-Histopathology, Tunisia

Objective: The accurate diagnosis of complete hydatidiform mole (CHM) and its differentiation from partial hydatidiform mole (PHM) and nonmolar hydropic abortions (HA) is important for the accurate management of patients. In earlier diagnosed cases, the histological diagnosis may be difficult. The aim of this study was to compare the accuracy of p57KIP2 immunohistochemistry with that of nuclear DNA microsatellite polymorphism in identifying CHM.
Method: DNA analysis by short tandem repeat genotyping were performed in 30 cases as described below: 10 cases with negative p57KIP2 immunostaining but histologically diagnosed as 9 PHM and 1 HA, and 20 cases diagnosed as CHM by histology and confirmed by negative p57KIP2 immunostaining.
Results: In ten cases with a challenge between discordant histological and immunohistological diagnoses, microsatellite DNA genotyping analysis agreed with the results of p57KIP2 staining, confirming the diagnosis of CHM. The genotyping analysis of 20 cases of CHM with negative p57KIP2 immunostaining indicated the absence of maternal contribution and the homozygosity for a single paternal allele in concordance with the androgenetic and monospermic origin of CHM in these cases.
Conclusion: We confirmed that p57KIP2 immunohistochemistry can be used as successfully as DNA micro-

satellite genotyping for distinguishing CHM from its mimics.

007

Diagnostics of coexistent endometrial carcinoma in high-risk endometrial hyperplasia: significance of the 4c-rule and EIN for outcome prediction

A. Ørbo *, B. Moe, I. Pettersen, M. Arnes, K. Hanssen
*University of Tromsø, Research Group of Gynecologic, Tromsø, Norway

Objective: Reliable predictive methods for uterus sparing are crucial for treatment decision among women who want to preserve their fertility and for seriously ill patients for whom surgery is hazardous. Thus, prediction of myoinvasive carcinoma by objective histomorphometry and subjective diagnostics were investigated in high- risk endometrial biopsies diagnosed as D-score<0.
Method: In retrospect, 45 cases diagnosed as high-risk hyperplasia (D-score<0) of whom ten turned out to have concurrent carcinoma were investigated. Histomorhometric 4C- rule and EIN classification were used to predict the outcome of hysterectomy (cancer or not).
Results: 4C- rule assessment predicted myoinvasion with a sensitivity of 87% and a specificity of was 79%. Single nuclear parameters like perimeter and short axis differed significantly between hyperplasia and invasive carcinoma to assess the probability of myoinvasive disease ($p<0.0001$ and shortest axis $p<0.0001$). The sensitivity and specificity of the EIN classification to predict coexistent carcinoma or not was 50% and 97%, respectively.
Conclusion: 4C- rule assessment predicted myoinvasion with a sensitivity of 87% and a specificity of was 79%. Single nuclear parameters like perimeter and short axis differed significantly between hyperplasia and invasive carcinoma to assess the probability of myoinvasive disease ($p<0.0001$ and shortest axis $p<0.0001$). The sensitivity and specificity of the EIN classification to predict coexistent carcinoma or not was 50% and 97%, respectively.

008

An opportunistic screening program for cervical cancer in a rural hospital in Zambia: cyto-histological results of the first 5 years

S. Guzzetti *, D. Fenocchio, P. Giovenali, F. Sopracordevole, L. Viberti
*Ospedale Valdese—ASLTO1, S.C. di Anatomia Patologica, Turin, Italy

Objective: Since 2006, an opportunistic screening program for cervical cancer was developed in the Mtendere Mission Hospital (MMH) in Chirundu, Zambia, with the aid of the Italian NGO "Associazione Patologi Oltre Frontiera" (APOF) that built a pathology department and trained local staff in slides equipment for histology and cytology as well in Pap smear diagnoses.
Method: Pap smears were initially performed mainly on HIV-positive women already enrolled in an antiretroviral therapy program. In 2008, the MMH organized an awareness campaign aimed at the hospital's catchment population and, with the cooperation of the Italian Society of Colposcopy (SICPCV), an outpatient clinic for cervical cancer was open to manage the diagnostic and therapeutic second level.
Results: From 2006 to 2010, 7,155 Pap smears were performed. The overall positive cases (≥ASC-US or AGC) were 998 (13.9%) with a constant decrease of the overall positive ratio (23.2% in 2006 and 10.4% in 2010). The ratio of unsatisfactory cases also decreased over time (9.2% in 2006 and 5.5% in 2010). The second-level diagnostic and/or therapeutic procedures altogether performed (cervical biopsies, conizations, loop excisions and hysterectomies) were 900.
Conclusion: In low-resource settings, a screening based on Pap smear can achieve good results in reducing the incidence of cervical cancer.

Monday, 29 August 2011, 08.00–11.30, Room 204–205

OFP-10 Oral Free Paper Session Haematopathology I

001

Identification of Merkel cell polyomavirus in chronic lymphocytic leukemia cells by fluorescence in situ hybridization (FISH)

E.-J. Speel *, A. Haugg, N. Pantulu, C. Pallasch, A. Kurz, H. Kvasnicka, G. Cathomas, C. Wendtner, A. zur Hausen
*Maastricht UMC, Dept. of Pathology, The Netherlands

Objective: Merkel cell polyomavirus (MCPyV) is detected in approximately 80% of Merkel cell carcinomas (MCC). We have recently reported the presence of MCPyV in highly purified tumor cells of CLL ($n=19/70$, 27.1%) (*Blood* 2010 Sep 3), including six cases with a novel 246-bp deletion in the helicase gene of the LTAg. Our aim was to determine the physical status of MCPyV by fluorescence in situ hybridization (FISH).
Method: FISH was performed using the MCPyV genome as probe on two previously reported paraffin-embedded

MCPyV positive CLL cases (EDTA decalcified bone marrow trephines) and five MCPyV-positive MCC.
Results: FISH detected specific MCPyV DNA signals in the nuclei of MCPyV-positive CLL and MCC cells. In contrast, to particularly punctate FISH signals in MCC indicating viral integration, the CLL cases revealed especially granular signals (of different intensity and size). No signals were obtained by MCPyV FISH in control breast or colon cancer specimens.
Conclusion: The specific detection of MCPyV in CLL cells further supports our previous report of a possible involvement of MCPyV in a significant subset of CLL. The specific but rather granular nuclear FISH signals in MCPyV-positive CLL cells may point to an episomal presence of MCPyV or to an integrated virus together with transcribed RNA, which needs further study.

002

Type II enteropathy-associated T-cell lymphoma (EATL): clinico-pathological features of a rare intestinal T-cell neoplasm

S.-Y. Tan *
*Singapore General Hospital, Dept. of Pathology, Singapore

Objective: EATL is an uncommon lymphoma associated with celiac disease in western populations whereas type II EATL is more common in Asia where celiac disease is rare.
Method: Clinical and pathological data of intestinal T-cell lymphomas were reviewed and immunohistochemistry was performed, including MATK, a novel marker of type II EATL that we have identified. Where sufficient material was available, PCR for clonality was performed.
Results: Type II EATL comprises the vast majority (9/13) of primary intestinal T-cell lymphoma. As previously described, neoplastic cells are monotonous in appearance with prominent intra-epithelial lymphocytes. However, the villous architecture is preserved with atrophy only seen in mucosa directly overlying the main tumour. Despite increased intraepithelial lymphocytes, no significant villous atrophy or crypt hyperplasia is seen in mucosa away from the tumour. The immunophenotype is typically CD2+ CD3+ CD5- CD7+ TIA1+ CD56+ CD4- CD8+ EBER-. However, cases lacking CD56 and CD8 are noted and there may be increased EBV+ B-cells, which can create confusion with extranasal NK/T cell lymphoma.
Conclusion: Type II EATL is the commonest form of primary intestinal T-cell lymphoma in Asian populations. Some cases lack CD56 and CD8 expression that is typically seen but a high-level nuclear expression of MATK can help in its diagnosis.

003

Bone marrow involvement in extranodal diffuse large B-cell lymphomas arising in mucosa-associated lymphoid tissues

T. Balharek *, J. Marcinek, P. Szepe, L. Plank
*Jessenius Medical Faculty, Dept. of Pathology, Martin, Slovakia

Objective: Diffuse large B-cell lymphoma (DLBCL), not otherwise specified (NOS), is a heterogenous group of aggressive lymphomas with variable prognosis, which may arise as primary or secondary lymphoma in nodal or extranodal (EN) tissues. DLBCL may develope concordant or discordant bone marrow (BM) involvement, showing either large (blastic) or small cell component with different prognostic impact.
Method: We performed a retrospective analysis of BM involvement in pretreatment staging BM biopsies of DLBCL NOS diagnosed in mucosa-associated lymphoid tissue (MALT) localisations at our department in years 2004–2011.
Results: We identified 434 EN-DLBCL arising in MALT; 54 (12.4%) of them showed the presence of a small B-cell component in primary biopsy. Pretreatment staging BM biopsy was available in 107 cases; 95 (88.2%) had negative BM, including all 17 cases with concommitant low-grade component in primary biopsy. BM was infiltrated only in 12 (11.2%) cases of entirely pure EN-DLBCL; 11 showed small B-cell infiltrate and only 1 was blastic.
Conclusion: EN lymphomas are considered to have some unique features. EN-DLBCL represents a mixture of primary and secondary lymphomas. Their tendency to BM infiltration seems to be low. When BM is involved, the infiltrate usually shows a discordant small cell morphology, which suggests a dissemination of primary low-grade lymphoma.

004

Immunoexpression of p65 in diffuse large B-cell lymphoma (DLBCL) is not a prognostic factor in DLBCL

V. Cemerikic-Martinovic *, O. Markovic, D. Marisavljevic, N. Drndarevic, T. Martinovic
*Beo-lab, Dept. of Histopathology, Belgrade, Serbia

Objective: Aberrant nuclear factor-κB (NF-κB) activation has been implicated in the pathogenesis of lymphoma. In this study, we examined the expression of p65, NF-κB

subunit and its impact on therapy response and the survival in diffuse large B-cell lymphoma (DLBCL).

Method: Fifty-five DLBCLs treated with immunochemotherapy (R-CHOP, R-EPOCH) were evaluated with antibody against p65 using the standard immunohistochemical method.

Results: Immunoexpression of p65 manifested as cytoplasmic or as mix (cytoplasm and nuclear) staining. Cytoplasm p65 immunoexpression was found in all 55 cases. Nuclear staining was noticed in 19 (34.5%) cases. The immunoexpression of p65 did not correlate with clinical and laboratory parameters. In addition, immunoexpression of p65 was not in significant correlation with bcl-2 and Ki-67 immunoexpression (p=0.509, p=0.450, respectively). There was not a significant difference in the response to therapy in relation to the immunoexpression of p65 (p=0.270). The expression of p65 was also not associated with the shorter survival of our DLBCL patients (p=0.768).

Conclusion: These results suggest that p65 is constitutively expressed in DLBCL. According to these results, the expression of p65 is not a prognostic factor in DLBCL. As the number of cases was limited, it is necessary to confirm these results in a larger series of patients before making definitive conclusions.

005

Clinical significance of survivin immunoexpresion in nodal diffuse large B-cell lymphoma (DLBCL)

V. Cemerikic-Martinovic *, O. Markovic, D. Marisavljevic, N. Drndarevic, M. Tamara, D. Jovanovic

*Beo-lab, Dept. of Histopathology, Belgrade, Serbia

Objective: Survivin, a unique member of the inhibitor of apoptosis family, is overexpressed in some types of lymphoma. We analyzed the influence of survivin immunoexpression on the therapy response and clinical outcome of nodal DLBCL patients.

Method: We analyzed lymph node biopsy specimens obtained from 78 patients with newly diagnosed nodal DLBCL treated with CHOP or R-CHOP regimen using the standard immunohistochemical method.

Results: Survivin immunoexpression (≥35%) has been found in 52.6% patients and observed as cytoplasmic staining in 31 or mixed (cytoplasmic and nuclear) in 10 positive patients. Survivin immunoexpression was in significant correlation with Ki-67 immunoexpression. Besides the numerous clinical parameters, survivin positivity was found to be an unfavorable factor for therapy response and shorter survival. The therapy response was achieved in 81.1% survivin-positive patients and in only 43.3% survivin-negative patients (p=0.018). Patients with survivin immunoexpression had significantly better response to immunochemotherapy in comparison to chemotherapy (p=0.05). The median survival of survivin-negative patients was 79.09 months and that of survivin-negative patients was 41.47 months (p=0.004).

Conclusion: The results of this study showed that the dysregulation of survivin expression had an important role in the determination of biological features DLBCL. Survivin is a useful tool in predicting therapy response and overall survival of patients with DLBCL.

006

Splenic diffuse red pulp small B-cell Lymphoma (SDRL): a multiparametric study of 16 cases and comparative evaluation of bone marrow and splenectomy specimens

G. Kanellis *, T. Papadaki, E. Pouliou, A. Tasidou, E. Stefanoudaki, A. Anagnostopoulos, M. Ponzoni, K. Stamatopoulos

*Evangelismos Hospital, Dept. of Hematopathology, Athens, Greece

Objective: The study aims were: (1) to obtain evidence about the ontogeny of SDRL and its relationship to "classic" splenic marginal-zone lymphoma (SMZL) and (2) to assess the diagnostic value of bone marrow biopsy (BMB) histopathology in the documentation of SDRL when splenectomy specimens are unavailable.

Method: Morphological (H&E), immunohistochemical and IGH PCR/sequencing findings of 16 SDRL cases were evaluated on both spleen and BMB specimens.

Results: The morphological and detailed immunohistochemical results are listed in Tables 1 and 2. Immunogenetic analysis revealed heterogeneity regarding IGHV gene repertoire and mutational status, with a low frequency of the IGHV1-2 gene (only 1/11 cases with available data), in stark contrast to its over-representation in SMZL.

Conclusion: Our findings (1) show that BMB cannot serve as a reliable substitute of the spleen histopathology for the documentation of SDRL and its differential diagnosis from SMZL, (2) confirm the considerable immunophenotypic heterogeneity of SDRL in analogy to what has been reported for SMZL, (3) reveal immunophenotypical similarities between SDRL and SMZL, indicating their possible common origin from the various B-cell subpopulations of the normal splenic

marginal zone and (4) indicate different modes of selection of the clonogenic progenitors, as evidenced by the markedly different immunoglobulin gene repertoires between SDRL vs. SMZL.

TABLE 1: HISTOPATHOLOGICAL FINDINGS

Spleen	
Pattern of infiltration	
Diffuse	16/16 (100%)
Morphology	
Small cells	16/16 (100%)
Bone marrow biopsy	
Pattern of infiltration	
Pure intrasinusoidal	3/12 (25%)
Interstitial	7/12 (58%)
& paratrabecular	2/7(29%)
& intrasinusoidal	3/7 (43%)
& diffuse and nodular	1/7(14%)
& diffuse	1/7 (14%)
Diffuse	2/12 (17%)
Morphology	
Small lymphocytes	11/12 (92%)
Pure monocytoid population	1/12 (8%)

TABLE 2. IMMUNOHISTOCHEMICAL FINDINGS

	Spleen	Bone Marrow Biopsy
CD20,CD79a,bcl2	16/16 (100%)	12/12 (100%)
CD5	3/16 (19%)	1/9 (11%)
DBA44	15/16 (94%)	8/9 (89%)
CD27	7/12 (58%)	5/8 (63%)
TRAP	6/9 (67%)	3/5 (60%)
IgG	5/15 (33%)	2/7 (29%)
IgM	8/11 (73%)	5/7 (71%)
IgD	6/14 (43%)	3/8 (38%)

CD23, CD43, bcl6, CD10, CyclinD1 and CD3 were negative in all 16 spleen and all 12 BMB samples.

007

Monophasic splenic marginal zone lymphoma: a morphological and immunohistochemical study of six cases

G. Kanellis *, T. Papadaki, M. Fameli, I. Dousis-Anagnostopoulou, P. Foukas, E. Pouliou, T. Mavrommatis
*Evangelismos Hospital, Dept. of Hematopathology, Athens, Greece

Objective: Splenic marginal zone lymphoma (SMZL) is mainly represented by the classical form with biphasic white pulp nodules. However, the 2008 WHO classification also recognizes a minor variant of SMZL with monophasic marginal zone-like white pulp nodules. The aim of our study is to present the clinical, morphological and immunohistochemical findings of six cases of monophasic SMZL.

Method: Related details are shown in Table1.

Results: Spleen histopathology—The histology was predominantly nodular, focally confluent pattern of infiltration of the spleen due to the expansion of the white pulp (WP; WP nodules >80%) with a mild red pulp infiltration. Cytologically, the nodules are monophasic and composed almost entirely of lymphocytes with marginal-zone-like morphology. Immunohistology: CD20+, CD79α+, BCL2+, CD27+, CD35+, CD21+(x 6), IgD+(1/6), DBA.44-, Cyclin-D1-, BCL6-, CD5-, CD23-, CD43-, annexinA1-, MUM1-(x 6).

Conclusion: Our findings:

(a) Confirm and extend the 2008 WHO classification and previous reports (Papadaki et al. 2007; Dufresne et al. 2010), indicating that besides biphasic cytology for "classical" SMZL, a proportion of SMZLs may show monophasic cytology with predominately MZ-like cells in the spleen

(b) Reveal an almost "constant" immunophenotype among the monophasic cases of SMZL with MZ-like cells (CD27+, CD21+, CD35+ and DBA44-) mimicking the profile of normal splenic marginal zone B cells. This is in contrast to

"classical" biphasic SMZL which shows considerable heterogeneity regarding the expression of these markers

Table 1.

Study Group	6 patients
Ages	62-78 years old
Splenomegaly (spleen weight 750-1730gr)	6/6
Lymphocytosis	6/6 (4 with villous lymphocytes)
Anemia	4/6
Neoplastic lymphocytic infiltration of the bone marrow	6/6
Methods	
Morphology	Hematoxylin & eosin
Immunohistochemistry	CD20, CD79α, BCL2, CD27, CD35, CD21, DBA.44, CyclinD1, BCL6, CD5, CD23, CD43, IgD, Annexin A1, MUM1.

Monday, 29 August 2011, 17.00–19.30, Room 210

OFP-11 Oral Free Paper Session Haematopathology II

001

Impact of the reactive microenvironment on the bone marrow involvement of follicular lymphoma

H. Rajnai *, C. Bodor, Z. Balogh, É. Gagyi, J. Csomor, T. Krenács, E. Tóth, A. Matolcsy
*Semmelweis University, 1st Dept. of Pathology, Budapest, Hungary

Objective: Gene expression and immunohistochemical studies suggested that the immune microenvironment of follicular lymphoma (FL) plays an important role in the clinical behaviour of the disease. In 40–70% of FL cases, the bone marrow (BM) is involved at diagnosis which has been considered as a poor prognostic factor. Although lymph node (LN) and BM compartments of FL are related to the same neoplastic clone, several differences have been reported between the tumor cells within these compartments.
Method: To investigate the role of the microenvironment in the BM involvement, automated image-segmentation-based localization and quantitation were performed in whole digital slides of immunostained tissue microarrays of formalin-fixed paraffin-embedded tissue biopsies of LNs and corresponding BMs of 35 patients.
Results: We found significant differences in the microenvironment of the BM compared to the microenvironment of the matching LN. Furthermore, we observed significantly less infiltrating CD8+T-cells and CD68+ macrophages in LNs of cases involving the bone marrow.
Conclusion: Our study showed that lower grade and proliferation of the BM could be explained by the different composition of the microenvironment. On the other hand, different tumor cell growth in LN and BM may generate a different microenvironment. Our study also suggested that T lymphocytes and macrophages play a relevant role in the prevention of tumor cell propagation.

002

Utility of a new monoclonal rabbit antibody to cyclin D1, clone EP12 for subclassifying small B-cell lymphomas through immunohistochemistry

B. Spaulding *, K. Oftebro, G. Nielsen
*Dako North America, Dept. of Biomarkers, Carpinteria, USA

Objective: In this study, we report on the use of a new monoclonal rabbit antibody to cyclin D1, clone EP12, for the routine subclassification of small B-cell lymphomas and compare its performance in immunohistochemistry to monoclonal rabbit anti-cyclin D1, clone SP4.
Method: Routinely processed tissue sections from mantle cell lymphoma (MCL) and follicular cell lymphoma (FCL) tissue blocks and from normal tissue microarrays (TMAs) were procured for this study. Immunostaining was performed using monoclonal rabbit anti-cyclin D1, clone EP12 and monoclonal rabbit anti-cyclin D1 clone SP4 as a control reagent.
Results: Clone EP12 positively stained the neoplastic cells of 14/14 MCLs and 0/11 FCLs. On TMAs of normal tissue, clone EP12 identified a variety of normal tissue elements consistent with the known distribution of cyclin D1, including a subset of lymphoid, endothelial, stromal and epithelial cells. When comparing the immunostaining results of clone EP12 to SP4, the two antibodies exhibited a consistent immunoreactivity pattern, with the exception that clone SP4 weakly stained a subset of follicular lymphoma cells on 4/11 tissues that were unreactive with EP12.
Conclusion: We have demonstrated that the new monoclonal rabbit anti-cyclin D1, clone EP12, is a highly sensitive antibody with a specificity similar to clone SP4. Clone EP12 is useful for the diagnosis of small B-cell lymphoproliferative disorders.

003

A nationwide study of "in situ" follicular lymphoma in Hungary

B. Timar *, J. Csomor, H. Rajnai, T. Micsik, A. Matolcsy
*Semmelweis University, 1st Dept. of Pathology, Budapest, Hungary

Objective: Follicular lymphoma (FL) is the most common adult lymphoma in the western world. FL is usually disseminated at presentation, but several studies described and analysed the presence of "in situ" follicular lymphoma, where focal germinal centers (GC) strongly express bcl-2, whereas most of the remaining GCs show bcl-2-negative follicular hyperplasia.
Method: In our study, we did a retrospective analysis on 887 peripheral lymph node biopsies from 38 pathology departments in Hungary. We included only biopsies where the indication was lymph node enlargement suspicious of lymphoma. Excluded were the regional lymph nodes from cancer patients. We screened the cases with a panel of antibodies (bcl-2, CD3, CD20).
Results: We found that most cases were reactive, predominantly follicular hyperplasias. Only 20 cases were found where several GCs had a higher number of bcl-2-expressing cells than CD3 cells. A board of pathologists analyzed these cases. A total of 18 cases were found to be primary follicles. Two cases had follicular hyperplasia with several tangentionally cut secondary follicles at the marginal zone level.
Conclusion: In summary, we have not found any primary "in situ" FL cases in our nationwide study and concluded that "in situ" FL does not provide a relevant diagnostic problem in the everyday routine.

004

Nationwide multicentre proficiency testing for cyclin D1 immunohistochemistry: the Canadian Immunohistochemistry Quality Control (CIQC) experience

Z. W. Chen *, M. Copete, J. Garratt, D. Pilavdzic, S. Klassen, L. Manning, l. Quenneville, B. Gilks, E.E. Torlakovic
*University of Toronto, Dept. of Anatomical Pathology, Canada

Objective: Cyclin D1 immunohistochemistry (IHC) is critical to the diagnosis of mantle cell lymphoma (MCL). Anti-cyclin D1 antibodies with superior sensitivity and specificity are commercially available and excellent results with cyclin D1 IHC testing are expected. Using a multi-institutional survey of Canadian laboratories, we aim to determine the quality of cyclin D1 IHC performed nationwide.
Method: Sections of tonsil, appendix and mantle cell lymphoma were sent to 59 participating laboratories to be stained with their routine cyclin D1 protocol. The assessors scored the results as optimal, good or poor according to pre-established scoring criteria.
Results: A total of 13/59 (22%) participants had poor results in the form of insufficient staining (11) or false-positive staining (2). Insufficient staining was not related to any specific antibody of choice but rather to suboptimal protocols. Two cases of false-positive, selective staining of germinal centres were associated with a specific lot of an otherwise excellent cyclin D1 clone.
Conclusion: Cyclin D1 IHC is variable in the nationwide CIQC experience. Our results emphasize the importance of external quality assurance for the proper calibration of cyclin D1 IHC.

005

Lymphomatoid granulomatosis: a clinicopathologic study of 8 cases

A. Martinez-Peñuela *, A. Panizo, J. Pardo, I. Rodriguez, J. M. Martinez-Peñuela
*Hospital de Navarra, Dept. of Pathology, Pamplona, Spain

Objective: Lymphomatoid granulomatosis is a rare lymphoproliferative disease involving extranodal sites, predominantly the lung. Little is known about its relationship to lymphoma, and Epstein–Barr virus (EBV) infection is present in most cases.
Method: Eight cases of lymphomatoid granulomatosis were evaluated clinicopathologically. All patients were Caucasian. Two patients were immunosupressed. There were three women and five men with a median age of 56.7 years. The unique involvement of the brain was observed in two cases, another case affected only the brain stem, and five cases had only pulmonary presentation.
Results: Biopsy specimens showed nodular polymorphous mononuclear cell infiltrate, containing CD20-positive large B lymphocytes and CD3-positive small lymphocytes along with plasma cells and histiocytes. In

almost all cases, there were vascular infiltration and small areas of necrosis. All of the cases showed evidence of EBV infection by in situ hybridization. Five cases were classified as grade 1 and 3 as grade 2 based on the proportion of large B cells. As a recent study has described a lymphomatoid granulomatosis-like lesion in the context of IgG-4-related lung disease, we performed IgG4 antibody to rule out the disease. All cases were negative to IgG4. Two patients received chemotherapy and the rest were not treated apart from the surgery. All patients are alive.

Wednesday, 31 August 2011, 14.00–16.30, Room 206

OFP-12 Oral Free Paper Session Head and Neck Pathology

001

Analysis of the role of homeobox genes HOXA1 and HOXB7 in oral squamous cell carcinoma

C. Cavalcante Bitu *, M. Carrera, M. F. de Souza Setúbal Destro, S.D. da Silva, K. Gotardello Zecchin, L. P. Kowalski, E. Graner, R. Della Coletta
*University of Oulu, Dept. of Dentistry, Finland

Objective: The HOX gene family has a major role in development; however, it also appears to be dysregulated in malignancies. Our goal was to verify the role of HOXA1 and HOXB7 on tumor-associated phenotypes and whether their expressions are associated with clinicopathological features of the tumors.
Method: We overexpressed HOXA1 or HOXB7 in HaCAT cell line, inhibited their expression in the SCC-9 oral carcinoma cell line and performed immunohistochemical analysis in SCC samples.
Results: Our results show that HOXA1 and HOXB7 overexpression in HaCAT cells promotes proliferation, whereas their downregulation in SCC-9 cells decreases it. A high number of HOXA1-positive cells correlated with T and N stage, tumor cellular differentiation and proliferative potential of the tumors and also to a shorter overall survival in 5 years than patients with low positivity (p=0.026). The positivity for HOXB7 was correlated to alcohol consumption, clinical N stage, vascular infiltration and tumor proliferative potential and was also correlated to a shorter overall survival (p=0.009) and a tendency towards shorter disease-free survival (p=0.083). A positive correlation between HOXA1 and HOXB7 immunohistochemical expression was observed (rs=0.25, p<0.008).
Conclusion: In conclusion, our results suggest that the overexpression of HOXA1 and HOXB7 can contribute to tumor progression and may be important determinants of OSCC patient's prognosis.

002

Differentiated dysplasia is a frequent precursor or associated lesion in invasive squamous cell carcinoma (SCC) of the oral cavity and pharynx

M. Kurrer *, R. Arsenic
*Pathologie Institut Enge, Zürich, Switzerland

Objective: The classification of oral/pharyngeal SCC precursor lesions is controversial.
Method: We reviewed all SCC resection specimens (excluding tonsil) and all preceeding biopsies on file in our hospital (1992–2009).
Results: Five patterns of SSC precursor or associated lesions were identified: pleomorphic (similar to full-thickness laryngeal dysplasia) (21/156), basaloid (similar to anal basaloid dysplasia) (6/156), differentiated (similar to vulvar dVIN or lichenoid lesions with large cells, large nuclei, prominent eosinophilic nucleoli, abundant eosinophilic cytoplasm, prominent desmosomes, and minimal basal or suprabasal cell irregularities) (61/156), mixed (differentiating pleomorphic with superficial maturation) (44/156) as well as verrucous (open raisin-like nuclei without prominent nucleoli) (7/156). Keratinization was common but variable in differentiated, mixed differentiating and verrucous dysplasia. A total of 14/156 showed no precusor lesion. The progression of isolated differentiated dysplasia was documented in 13% (21/155) over months to years.
Conclusion: Full-thickness epithelial dysplasia is present in less than 20% of oral/pharyngeal SCC. Differentiated dysplasia is a frequent precursor/associated lesion in oral/pharyngeal SCC. Failure to recognise differentiated dysplasia results in the underdiagnosis of patients at risk for SCC. Our cases of documented progression of differentiated dysplasia call for efforts to refine the criteria for the separation of differentiated dysplasia from morphologically related lichenoid lesions.

003

EGFR expression, activating phosphorylations (Tyr-845 and Tyr-1068) and gene amplification in oral squamous cell carcinoma (SCC): a tissue-microarray study with clinical–pathologic correlations

N. S. Losito *, G. Pannone, G. Aquino, A. Santoro, P. Bufo, R. Franco, G. Botti, G. De Rosa
*Fondazione Pascale, Dept. of Surgical Pathology, Napoli, Italy

Objective: EGFR over-expression has been suggested as a prognostic marker in OSCC because of a significative correlation among its amplification status and the occurrence of metastases and poorly differentiated tumors. The aim of this work is to define the key role of EGFR in oral carcinogenesis.
Method: On prognostic tissue microarrays from 149 OSCCs, EGFR expression and its phosphorylation on Tyr-845 and Tyr-1068 were evaluated by immunohistochemistry and confirmed by Western blotting; the amplification of the polysomic status was determined by FISH.
Results: Immunohistochemically, EGFR was over-expressed in OSCCs; both pEGFR-Tyr-845 and pEGFR-Tyr-1068 were mainly distributed in high histological grades and advanced stages. By FISH, we noted a strong correlation between protein immunostaining and gene amplification. The global proportion of gene amplification in OSCCs was 14%; the amplified OSCCs were mainly distributed in high histological grade and advanced stage sub-groups. By Kaplan–Meier curves, we can generalize that survival is shorter in patients with positive pEGFR-Tyr-845 tumors and that for more advanced stages this positivity is predictive of worst response to current chemotherapy.
Conclusion: These results confirm the central role of EGFR as a biomarker and underline the potential role of phosphorylated EGFR and its pathway as a new target therapy in OSCC.

004

Myoma organotypic model: novel in vitro and in vivo applications

T. Salo *, S. Teppo, S. Nurmenniemi, C. Bitu, M. Vered, D. Dayan, P. Nyberg
*University of Oulu, Dept. of Diagnostics and Oral Medicine, Finland

Objective: Tumor microenvironment (TME) hypoxia induces angiogenesis and promotes carcinoma growth, invasion and spread. A new in vitro organotypic model (human leiomyoma tissue) (Nurmenniemi et al., *Am J Pathol*, 2009), developed for invasion studies, approximates the natural TME. We report the use of this model in the research of TME hypoxia and the advantages following its transplantation into nude mice.
Method: Conditions mimicking hypoxia were created by treating the myoma+HSC-3 tongue carcinoma cell discs with 100 μM cobalt chloride ($CoCl_2$, $n=5$) and the invasion depth was measured. In addition, myoma and collagen gel+fibroblasts (CF) discs were cultured for 7–10 days alone ($n=5$, each) or with HSC-3 cells ($n=5$, each) and then transplanted and kept for 6 weeks subcutaneously in nude mice ($n=20$).
Results: $CoCl_2$-treated myoma discs showed a 1.3-fold deeper carcinoma invasion compared to control ($p<0.00595$). The growth pattern of transplanted myoma+HSC-3 cells simulated at best the invasion pattern of the patient carcinoma whereas the cells in CF discs simulated mainly dysplasia or early invasion.
Conclusion: Hypoxia-mimetic markedly increased the carcinoma invasion in myoma. The transplants of the myoma simulated the invasive growth of tongue carcinoma in vivo unlike the classic collagen model.

005

Juvenile psamomatoid ossifing fibroma of jaw—diagnostic challenge

J. Sopta *, R. Drazic, V. Mijucic, D. Ristic, S. Raicevic
*School of Medicine Belgrade, Inst. of Pathology, Serbia

Objective: Juvenile psamomatoid ossifying fibroma (JPOF) is a controversial lesion that has been distinguished from the larger group of ossifying fibroma on the bases of the age of the patients, most common site of involvement and behavior.
Method: Thirteen cases of JPOF were diagnosed at the Institute of Pathology during the last 10 years. Patients' age, sex, localization of the lesion, duration of the disease, the quantity of bone spherules, their cellularity, the existence of hemorrhage, inflammation, and endochondral ossification in the stroma of the tumor were analyzed and correlated with the main symptoms of ten patients.
Results: All patients had swelling that lasted between 3 and 20 months (mean 10.4 months). Other clinical symptoms were facial asymmetry, eye bulb protrusion, and teeth displacement. The evolution of the tumor was longer in the mandible (12.3 months) than in maxilla (9.5 months). The main histomorphological diagnostic criterion for JPOF was psammoma-like structures. In lesions with a longer case history, the number of "psammomatoid" bodies was greater. In lesions with a shorter course of the disease, their number was lower and stromal hemorrhage and inflamma-

tion were presented. One patient had a secondary superposition of ABC.

Conclusion: The histological appearance of JPOF may be influenced by the tumor evolution. A significant correlation between the clinical course of the disease and histological parameters has been certified.

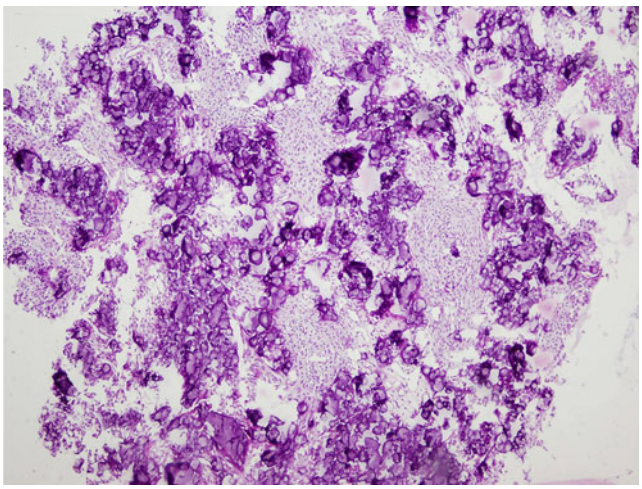

006

Chromosomal instability predicts the progression of premalignant head and neck lesions

E.-J. Speel *, E. Bergshoeff, R. Nelissen, T. Siebers, S. Fleskens, J. van der Laak, T. Merkx, R. Takes, P. Slootweg, B. Kremer
*Maastricht UMC, Dept. of Pathology, The Netherlands

Objective: A major dilemma in the management of patients with precursor lesions of the head and neck mucosa lies in deciding which lesions will progress into carcinoma. Because histopathological examination is troubled by inter-observer variability, our aim was to evaluate the value of chromosomal instability (CIN) detected by fluorescence in situ hybridization (FISH) to identify lesions at risk for progression.

Method: We examined a series of paraffin-embedded premalignant oral (n=106) and laryngeal (n=75) lesions by FISH using chromosome 1- and 7-specific centromere probes. CIN was defined as the presence of chromosome imbalances and/or polyploidization. Results were correlated with histopathological and clinical follow-up data.

Results: In both oral and laryngeal precursor lesions, the 5-year progression-free survival rate was ~90%. The outcome of routine histopathology did only predict malignant progression when comparing severe dysplasia with lower-stage precursor lesions (hyperplasia, mild and moderate dysplasia) ($p \leq 0.038$). CIN was significantly associated with a lower progression-free survival as compared with lesions without CIN ($p < 0.001$).

Conclusion: The tumorigenesis of the head and neck mucosa is associated with the development of CIN, which can reliably identify lesions at risk for malignant progression. Therefore, an intensive follow-up and/or a more aggressive treatment of lesions with CIN should be considered and, for example, examined in prospective studies.

007

Schmincke's visionary concept of lymphoepithelial tumours: historic errors and EBV and HPV pathogenesis

S. Ihrler *, P. Zengel, M. Mollenhauer
*Universität München, Inst. für Pathologie, Germany

Objective: The term 'lymphoepithelioma Schmincke–Regaud' was applied to certain pharyngeal carcinomas from the early twentieth century. However, the concept of lymphoepithelioma was subsequently discredited. The reason for this swing of opinion was unclear, and we decided to investigate it.

Method: This study maily involved an evaluation of historical literature.

Results: Schmincke in 1921 reported nasopharyngeal and tonsillar carcinomas with lymphoepithelial morphology and radiosensitivity, and he introduced the concept of lymphoepithelioma. Regaud in 1921 reported a case of carcinoma of the hypopharynx that was of conventional squamous differentiation. Capell in 1934 introduced the concept of a Schmincke-type and Regaud-type lymphoepithelioma, which added to the increasing confusion of terms. Schmincke's concept of lymphoepithelioma was initially widely accepted (Ewing, Doerr) but eventually misinterpreted because of the focus on isolated aspects of histological differentiation, localization, and pathogenesis (EBV/HPV).

Conclusion: The publication by Schmincke in 1921 of the first account of carcinoma with lymphoepithelial differentiation, the lymphoepithelioma, was clouded by confusion from the outset initially because of the misinterpretation of the case described by Regaud. Increasing confusion of terms then led to the discreditation of this concept. However, Schmincke's visionary concept of a histologically atypical, radiosensitive carcinoma of lymphoepithelial organs different from typical squamous cell carcinoma is now, 90 years later, accepted partly because of the EBV association of nasopharyngeal and HPV association of tonsillar carcinomas.

008

Expression of epidermal growth factor receptor (EGFR) does not correlate with prognosis, T and N stage in salivary gland carcinomas

I. Stárek *, A. Skálová, L. Kučerová
*Faculty Hospital, Olomouc, Czech Republic

Objective: EGFR expression in salivary carcinomas was analyzed and correlated with survival, T and N stage.
Method: EGFR immunoreaction was assessed by a histoscore 0, 1+, 2+, 3+. Disease-specific survival was calculated by Kaplan–Meier method; correlations with T and N stage were established with Fisher's exact test.
Results: A total of 60.5% of all carcinomas were EGFR+. Adenoid cystic, salivary duct, mucoepidermoid, acinic cell carcinoma and carcinoma ex pleomorphic adenoma showed immunopositivity in 65.5%, 47.8%, 83.3%, 20% and 100% of cases. Positive immunoreaction was also recorded in malignant mixed tumours (1/2), adenocarcinomas NOS (1/1), papillary–cystic adenocarcinomas (1/1), secretory (1/1) and undifferentiated carcinomas (2/2). A small cell carcinoma and cribriform cystadenocarcinoma were both EGFR-negative. The disease-specific survival in EGFR-positive carcinomas differed from that in EGFR-negative ones, but no statistic significance was recorded.
Conclusion: Salivary carcinomas show a variable EGFR reaction. Neither a prognostic significance of EGFR expression nor its correlation with and T and N stage was demonstrated. This study was supported by grant no. NS9725-4/2008, IGA, Ministry of Health, Czech Republic.

009

Clinical significance of histone deacetylase (HDAC)-4 and -6 expression in human malignant and benign thyroid lesions

S. Theocharis *, C. Giaginis, P. Alexandrou, I. Delladetsima
*University of Athens, Dept. of Forensic Medicine and Toxicology, Greece

Objective: Class II histone deacetylases (HDACs) have been associated with human tumor development and progression and HDAC inhibitors are currently being explored as anti-cancer agents in clinical trials. The present study aimed to evaluate the clinical significance of HDAC-4 and HDAC-6 protein expression in human malignant and benign thyroid lesions.
Method: HDAC-4 and HDAC-6 protein expression was assessed immunohistochemically on paraffin-embedded thyroid tissues obtained from 74 patients with benign and malignant lesions.
Results: The incidence of HDAC-6 positivity was higher in malignant compared to benign thyroid lesions (p=0.0072). Both HDAC-4 and HDAC-6 positivity showed a distinct discrimination between cases with papillary carcinoma and hyperplastic nodules (p=0.0394 and p=0.0061, respectively). HDAC-6 positivity was significantly correlated with follicular cells' proliferative capacity reflected by Ki-67 protein statement (p=0.0041). In malignant thyroid lesions, both HDAC-4 and HDAC-6 positivity were correlated with tumor size (p=0.0047 and p=0.0089, respectively). HDAC-4 positivity was associated with capsular invasion (p=0.0128). A positive relationship between HDAC-4 and HDAC-6 protein expression was also noted (Rs=0.3666, p=0.0013).
Conclusion: HDAC-4 and HDAC-6 may be associated with the malignant thyroid transformation and could be considered as useful biomarkers to improve the diagnostic scrutiny in thyroid neoplasia.

010

Clinical significance of histone deacetylase (HDAC)-1 and -2 expression in human malignant and benign thyroid lesions

S. Theocharis *, C. Giaginis, P. Alexandrou, I. Delladetsima
*University of Athens, Dept. of Forensic Medicine and Toxicology, Greece

Objective: Class I histone deacetylases (HDACs) have been associated with human tumor development and progression and HDAC inhibitors are currently being explored as anti-cancer agents in clinical trials. The present study aimed to evaluate the clinical significance of HDAC-1 and HDAC-2 protein expression in human malignant and benign thyroid lesions.
Method: HDAC-1 and HDAC-2 protein expression was assessed immunohistochemically on paraffin-embedded thyroid tissues obtained from 74 patients with benign and malignant lesions.
Results: HDAC-2 expression was higher in malignant compared to benign thyroid lesions (p=0.0010). In malignant thyroid lesions, HDAC-1 expression was correlated with tumor size (p=0.0143) and HDAC-2 expression with lymphatic (p=0.0228) and vascular invasion (p=0.0144). The cellular pattern of HDAC-1 and HDAC-2 distribution (nuclear vs nuclear and cytoplasmic) showed a distinct discrimination between malignant and benign thyroid lesions (p=0.0021 and p=0.0033, respectively). HDAC-2 expression was correlated with follicular cells' proliferative capacity reflected by Ki-67 protein statement (p=0.0192). A positive relationship between HDAC-1 and HDAC-2 protein expression was also noted (Rs=0.2967, p=0.0103).
Conclusion: HDAC-1 and HDAC-2 may be associated with the malignant thyroid transformation and could be considered as useful biomarkers and possible therapeutic targets in this type of neoplasia.

011

Clinical significance of FAK and Src expression in mobile tongue squamous cell carcinoma (SCC)

S. Theocharis *, J. Klijanienko, C. Giaginis, P. Alexandrou, P. Fragkou, X. Sastre-Garau
*University of Athens, Dept. of Forensic Medicine, Greece

Objective: Focal adhesion kinase (FAK) and Src have been implicated in human tumor development and progression. The present study aimed to evaluate the clinical significance of FAK and Src proteins' expression in patients with mobile tongue squamous cell carcinoma (SCC).
Method: FAK and Src protein expression was assessed immunohistochemically on tumoral samples obtained from 48 mobile tongue SCC patients and was studied in relation with clinicopathological parameters and patients' overall and disease-free survival.
Results: Increased FAK and Src protein immunoexpression was noted in well-differentiated tumors compared to poorly differentiated ones (p=0.0455 and p=0.0301, respectively). FAK and Src protein expression did not correlate with the other clinicopathological parameters examined. Mobile tongue SCC patients with high Src expression presented a longer overall and disease-free survival (log-rank test, p=0.0145 and p=0.0388, respectively). Nevertheless, in multivariate analysis, only the depth of invasion was proved to be an independent prognostic factor in overall and disease-free patients' survival (Cox regression, p=0.0313 and p=0.0481, respectively).
Conclusion: The present study supported evidence, for the first time, regarding the possible FAK and Src proteins' implication in mobile tongue SCC.

Tuesday, 30 August 2011, 17.00–19.30, Room 206

OFP-13 Oral Free Paper Session IT in Pathology—History of Pathology

001
Histopathological identification of Muisca´s mummy in Boyacá, Colombia

B. Bernal *, G. H. de la Medicina Grupo de Salud Publica
*Universidad de Zaragoza, Dept. de Inmunologia, Spain

Objective: Artificial mummification of human corpses in America was common to most Andean pre-Hispanic societies to which the Muiscas belonged. We characterized bio-anthropologically and paleopathologically the first Muisca mummy in Boyacá, Colombia. The mummy was a guy with evidence of pre-Hispanic tuberculosis, a knowledge that was made due to the multidisciplinary approach.
Method: A modified Ruffer technique was used for the histo-pathological identification. Tissues were taken of the lung pleura, muscle, skin, and hair. These were labeled and placed in a mixture of ethyl alcohol at 96% and 48%, water, and buffered formaldehyde at 5%, where they were kept for a week. We were verifying their state of hydration.
Results: Macroscopic changes were not seen on the first day. On the seventh day, a state of hydration was evidenced similar to the tissue set in formaldehyde. Then, samples were set in formaldehyde at 10% for 1 day and the routine process was done. Crosscuts were stained with hematoxylin and eosin to be observed with conventional light microscopy.
Conclusion: The histopathological samples showed denatured extracellular matrix without evidence of epithelium. Just one sample taken from the thoracic cavity could be identified as pleura in the presence of collagen and a simple flat epithelium of discontinuous coating.

002
Integrating the WebMicroscope into undergraduate medicine: a realistic experiment

L. Helle *, P. Kronqvist
*University of Turku, Centre for Learning Research, Finland

Objective: The objective of the instructional experiment was to boost skills in microscopic pathology through the use of the WebMicroscope with an emphasis on the knowledge of normal cells and tissues. The purpose of this study was to evaluate the experiment.
Method: The measures implemented were as follow: (1) Web-based materials to review normal cell and tissue, (2) Web-based "entrance exam", (3) digitized slides with abnormal features indicated by graphics and text and normal areas for comparison, and (4) three virtual quizzes taken in class for self-diagnostic purposes. The design was pretest–posttest with historical controls. The pretest was taken approximately 1 week after the "entrance exam" and the posttest 1 week before the exam in microscopy. The participants were third-year medical students (20+57).

Results: The preliminary results indicated that, as expected, the experimental group drastically outperformed the historical controls (by 45%) on the pretest. However, on the posttest, the historical controls outperformed the experimental group (by 31%).
Conclusion: Boosting the entrance level skills clearly does not boost the final skills. The key to success may lie in making the students externally accountable for their learning throughout training.

003
Pathology in numbers: extracting functional states from microscopic still images

G. Kayser *, K. Kayser
*Universitätsklinik Freiburg, Inst. für Pathologie, Germany

Objective: Tissue-based diagnosis remains the gold standard for disease classification, especially in oncology, and represents the basis for therapy in modern medicine. Formalin-fixed, paraffin-embedded tissue, which pathologists deal with in daily routine diagnostics, represents only a snapshot in the development of a disease. Thus, histology has not been regarded to as an investigation with functional disease information. Is this true?
Method: Biochemical reactions are subject to theorems of thermodynamics. Since all living cells rely on biochemical reactions, they and the resulting networks can be considered as a more or less organized and structured system deemed to obey general thermodynamic theorems, too. Therefore, we applied the principles of thermodynamics onto histological image analysis in the form of syntactic structure analysis and entropy calculations.
Results: In our experiences, the entropy states of tissues can reliably describe the functional states of different diseases. In several studies, we were able to show that syntactic structural analysis in tissue-based diagnostics can add important information to the development of malignancies. Herein we present the concept of applied thermodynamics in histology, a numerical description of functional states of histological sections.
Conclusion: The concept of structural entropy can add significant biological information to a broad spectrum of diseases, especially malignancies.

004
WebMicroscope as a computer-based system for the practical examination of dental students in oral pathology

J. Szymas *, M. Lundin, J. Lundin
*University of Mecial Sciences, Dept. of Clinical Pathology, Poznan, Poland

Objective: Before our experiment, virtual microscopy had not been used in an examination setting. In order to be able to implement this system, we needed to find a solution of a difficult technical issue: providing a secure access to local teaching resources from a teaching laboratory through a general Internet access without any noise or interruptions.
Method: We decided to use two servers (Poznan, Poland and Helsinki, Finland) and technology of a secure browser for viewing digitized histological slide and answering multiple choice questions at the same time. An on-line practical examination was evaluated based on students' results as well as a questionnaire.
Results: During the last 5 years, an overall 92% concordance rate has been achieved. These results were independent from the number of slides used during the practicals. All students felt that the quality of digitized slides was superior and rating 9.5 on a 1–10 scale. No technical disturbances have occurred so far.
Conclusion: Evaluations of our examination system have provided us with a number of insights into the quality and effectiveness of digitized slides as a tool for learning and assessment. Current technologies are feasible for examination through broadband Internet.

Thursday, 1 September 2011, 08.00–10.45, Room 201

OFP-5 Oral Free Paper Session Molecular Pathology

001
Expression of eIF3a in gall bladder carcinomas

J. Haybaeck *, A. Mashta, R. Spilka, C. Lackner, P. Obrist
*Medizinische Universität Graz, Inst. für Pathologie, Austria

Objective: Gall bladder carcinoma (GBC) is the most common biliary tract cancer, usually diagnosed at advanced stages, with a 5-year survival rate<10%. eIF3a is the largest subunit of eukaryotic translation initiation complex eIF3, which regulates a subset of mRNAs involved in cell cycle regulation. eIF3a is up-regulated in many cancers and its suppression leads to the inhibition of tumour cell proliferation in vitro.
Method: We investigated the expression of eIF3a in GBC in order to discover and describe new prognostic GBC markers. eIF3a expression was determined by immunohistochemistry on paraffin-embedded tissue of 74 GBC patients. eIF3a expression was compared to survival data. The mRNA and protein expression levels of eIF3a were analysed in three GBC cell lines by immunocytochemistry, western blotting and quantitative real-time PCR.
Results: Higher intensity scores of GBC display a lower 5-year survival rate when compared to GBC with lower intensity. The expression of eIF3a mRNA levels in all cancer cell lines tested was approximately twofold higher than in controls.

Conclusion: The over-expression of eIF3a in GBC is an indicator of a more aggressive GBC type with a lower 5-year survival rate. GBC cell lines provide a model for studying the mechanistic role of eIF3a in GBC progression.

002

Intra-tumor KRAS mutation heterogeneity in colorectal carcinoma: a molecular morphometric study

D. Hershkovitz *, L. Farber, H. Elkin, Y. Peerless, E. Sabo, O. Ben-Izhak, E. Efrati
*Rambam Health Care Campus, Dept. of Pathology, Haifa, Israel

Objective: Malignant transformation is a dynamic process and, therefore, it is plausible that at a certain point the tumor cell mass will be heterogeneous for particular mutations. This might be clinically relevant since KRAS mutation status has a role in the treatment decisions for colon carcinoma patients. In the present study, we assessed the degree of KRAS mutation status heterogeneity in colon carcinoma using molecular and morphometric methods.
Method: DNA was extracted from FFPE colorectal carcinoma samples, and the relative fraction of wild-type versus mutated KRAS was evaluated by real-time PCR. Additionally, we used image analysis to calculate the fraction of tumor cells within the samples. The values from both tests were combined to calculate the fraction of tumor cells harboring a mutation.
Results: The data from the molecular and morphometric analysis showed a high correlation. Of the 42 cases with the KRAS mutation analyzed, the mutation was carried in less than 50% of the tumor cells in a single case, indicating the absence of significant KRAS mutation status heterogeneity in colon carcinoma.
Conclusion: Colon carcinoma showed little heterogeneity with regard to KRAS mutation status. We also found out that our morphometric analysis could be used as a standardized method for the evaluation of tumor cell fraction within samples.

003

Large-scale expression analysis of the histone methyltransferase, putative oncoprotein MMSET, in human cancers

E. Santoni-Rugiu *, H. Hudlebusch, J. Skotte, B. L. Petersen, E. Ralfkiaer, K. Helin
*Rigshospitalet Copenhagen, Dept. of Pathology, Denmark

Objective: The transcription regulator histone methyltransferase (MMSET) is overexpressed in a subgroup of multiple myelomas with t(4;14)(p16;q32) and poor prognosis. We assessed MMSET involvement in other human cancers.
Method: We developed mAbs and immunostained tissue microarrays (TMAs) containing 3,774 different tumor samples and 904 corresponding normal tissues. The selected expression patterns were validated on independent TMAs specific for bladder cancer (n=1,293), colon cancer (n=1,206), and neuroblastoma (n=164) coupled to clinico-pathological data. mRNA/protein levels were monitored during cell lines' proliferation/differentiation by qPCR and immunoblotting. A lentiviral gene-silencing system and shRNA constructs were used for MMSET knockdown.
Results: As opposed to normal counterparts, multiple cancer types including GI tract, urinary bladder, female genitals, skin, and lung overexpressed MMSET. The expression correlated with bladder cancer aggressiveness but was more pronounced in early stages of colon carcinogenesis. In neuroblastomas, high MMSET levels correlated with poor survival, unfavorable Shimada histology, N-MYC amplification, and metastatic disease, whereas chemotherapy induced neuroblastoma differentiation and MMSET downregulation. Primitive neuroblast-rich embryonic or teratomatous structures, but not more differentiated derivatives, overexpressed MMSET, too. Accordingly, the differentiation of neuroblastoma or normal neural progenitor cell lines caused significant MMSET-downregulation. MMSET–RNA knockdown revealed that MMSET is a requirement for cell proliferation.
Conclusion: MMSET might affect the development/proliferation/differentiation of several cancer types and qualify as a prognostic marker and potential therapeutic target.

004

KRAS mutation detection in endoscopic biopsies of colorectal carcinoma: validity for response to anti-EGFR therapy

L. Carvalho *, A. Alarcão, P. Couceiro, M. Reis Silva, M.J. D'Aguiar, L. Teixeira, T. Ferreira, V. Sousa
*Amadora, Portugal

Objective: Colorectal carcinoma, with high frequency and being the leading cause of cancer-related deaths worlwide, also exhibits KRAS mutations (30–40%) associated with poor response to anti-EGFR therapies. Downstream signalling pathway KRAS-MAPK of EGFR needs to be overtaken to get tyrosine-kinase antibodies clinical response. The aim of this piece of work was to show the sequencing results of KRAS mutations search in very small pieces of adenocarcinoma obtained by endoscopy.
Method: Seventeen formalin-fixed paraffin-embedded endoscopic biopsies of colorectal carcinoma were reviewed by pathologists after clinical demanding, to tumour frag-

ment selection in haematoxylin-eosin stains, as representative areas for mutational analysis of KRAS—codons 12 and 13. DNA extraction was performed for polymerase chain reaction (PCR) and codons 12 and 13 were studied by direct sequencing.
Results: In the 17 samples, 8/17 were KRAS wild-type, 5/17 showed KRAS point mutation in codon 12 and 4/17 were reported as undetermined for KRAS mutation-insufficient obtained DNA.
Conclusion: The search of KRAS somatic mutations entered recently in routine practice for the treatment of metastatic colorectal adenocarcinoma with cetuximab and small biopsies being chosen for this purpose as the only archival material available of the primary tumour, preventing other invasive procedures and saving health costs.

005

Uterine cellular leiomyoma with high proliferative index versus leiomyosarcoma: analyses of allelic imbalance

G. Frank *, A. Shikeeva, T. Kekeeva, L. Zavalishina, Y. Andreeva
*Hertsen's Research Oncological Institute, Dept. of Pathology, Moscow, Russia

Objective: Uterine leiomyosarcoma (ULMS) is a rare and highly malignant smooth muscle tumor. Differential diagnosis between uterine cellular leiomyoma with high proliferative index (ULM) and ULMS is currently one of the basic problems in pathology. We investigated allelic imbalance (AI) and discovered genetic differences between ULM and ULMS.
Method: Microsatellite analysis was evaluated by PCR using seven polymorphic markers for chromosomal regions 10q22.1 (D10S1146, D10S218), 10q26.13 (D10S1213), 10p13 (D10S24), 9p21.3 (D9S942), 3p14.3 (D3S1295) and 18q22.3 (D18S390) in 24 patients with ULMS. A total of 39 patients with ULM were used as control.
Results: Our results demonstrated the high frequency of AI in ULMS samples (average frequency was 40%). The comparative analysis between groups of patients with ULMS and ULM showed higher frequencies of genetic changes for ULMS. The specificity and sensitivity of the system comprising LOH markers scored 97% and 95%, respectively.
Conclusion: This research showed a big difference in the AI analysis of ULMS compared to ULM. This approach may be helpful for an accurate distinction between ULMS and ULM. However, this diagnostic system requires an increase in the number of molecular markers. Altogether these data indicate that AI analysis can be successfully used for the improvement in differential diagnosis of uterine smooth muscle tumors.

006

Analysis of PI3K/AKT and MAPK pathways in lung cancer: application of HRM analysis and pyrosequencing

A. Saetta *, J. Vardaki, S. Sakellariou, I. Chatziandreou, P. Tsioli, E. Trigka, A. Tserga, E. Palliou,
P. Korkolopoulou, P. Eustratios
*Athens, Greece

Objective: This study aims to provide a mutational analysis of genes involved in MAPK and PI3K signaling cascades and their correlation with clinicopathological characteristics of non-small cell lung cancer (NSCLC) patients.
Method: We examined 97 cases of NSCLC, for mutations in exons 18, 19, 20, 21 of EGFR gene, in codons 12 and 13 of K-RAS gene, in exon 15 of B-RAF gene and in exon 20 of PIK3CA gene, by high-resolution melting analysis, sequencing or pyro-sequencing. Laser capture microdissection (LCM) was performed in 50 biopsies for the isolation of tumor cells. p-AKT, p-mTOR and p-p70S6K expression levels were assessed by immunohistochemistry in 13 cases with available tissue.
Results: EGFR mutations were observed in 11.3% of the cases, K-RAS mutations in 15.5%, and B-RAF mutations in 5.2% and 7.2% in PIK3CA gene. No mutations were detected in squamous carcinomas. In most cases, >10% of tumor cells were positive for p-AKT, p-mTOR and p-p70S6K.
Conclusion: Currently, NSCLC patients are stratified according to their EGFR status for individualized therapy (EGFR TKIs). The presence of mutations in K-RAS, B-RAF and PIK3CA genes suggests their possible role as potential targets for novel therapeutic approaches as well as biomarkers for the efficiency of targeted therapies.

007

The effect of neutral-buffered formalin fixation on DNA preservation in paraffin-embedded tissue

A.-N. Seo *, Y.-K. Bae, S.-Y. Kwon, H.-R. Jung, J.-Y. Park
*Kyungpook National University, School of Medicine, Daegu, Republic of Korea

Objective: The preservation of optimized DNA and its extraction from formalin-fixed, paraffin-embedded (FFPE) tissues are important issues. It was doubted that the 10% neutral-buffered formalin is indeed an ideal fixation solution for DNA preservation over the non-buffered formalin as conventionally recommended. In this study, the relationship between the efficiency of DNA extraction from FFPE tissue and buffered formalin was evaluated.
Method: Four different types of formalin solution were prepared, then several tissues that are routinely processed

paraffin-embedding protocols were fixed in four separate groups, but the other conditions were the same. DNA was extracted using a QIAmp DNA minikit (QIAGEN), and the quality of DNA was analyzed using a NanoDrop ND-1000 spectrophotometer (Theromo) and an Agilent 2100 bio-analyzer DNA 1000 kit in four FFPE-fixed types of solution within a 7-day average storage periods, and then experiments were repeated after 3 and 9 months.

Results: The purity of absorbance ratio and quality revealed no remarkable differences between the four types of fixation solution.

Conclusion: The study findings demonstrate that DNA preservation is quite unaffected by neutral buffer where there is a short manufacturing period of formalin and adequate formalin fixation time before embedding in paraffin.

008

BRAF and GNAQ mutation cellular effects in mTOR pathway activation in human cells (BRAF mutational status is a candidate biomarker for response to mTOR inhibitors therapy)

J. Vinagre [*], H. Pópulo, A. Faustino, S. Tavares, J. M. Lopes, P. Soares
[*]IPATIMUP, Cancer Biology, Porto, Portugal

Objective: Melanoma can occur in the skin and in the eye. Somatic mutations in BRAF and GNAQ gene have been described as key genetic alterations that contribute to cutaneous and uveal melanoma development, respectively. We have previously observed the differential activation of the MAPK and AKT/mTOR signalling pathways in cutaneous and uveal melanoma harbouring these mutations (Populo et al., 2011).

Method: HEK293 cells were transfected with BRAFWT, BRAFV600E, GNAQWT, GNAQQ209P and GNAQQ209L vectors. The expression of ERK1/2 and several mTOR pathway effectors was evaluated by western blot, along with BrdU (proliferation) and TUNEL (apoptosis) assays. Cutaneous and uveal melanoma cell lines displaying different BRAF and GNAQ mutational status were treated with the mTOR inhibitor RAD001.

Results: A significant increase in the level of pmTOR Ser2448 and pS6 Ser235/236 proteins was observed only in cells transfected with BRAF vectors. RAD001 treatment inhibited the phosphorylation of mTOR, S6 and 4EBP1 in all the cell lines tested but G361 cell line, which harbours a BRAF mutation, was the most sensitive cell line to RAD001.

Conclusion: Our results indicate that BRAF or GNAQ activation shows distinct intracellular signalling properties. BRAF mutational status can be a possible biomarker for the effectiveness of mTOR inhibitors therapy.

009

KRAS mutation analysis on low percentage of tumor cells: The importance of standardization and quality assurance

H. van Krieken[*], J. Dijkstra, F. Shieh, G. Hoefler, S. Richman, D. Heidemann, J. Diebold, E. Rouleau, E. Boers, G. Miltenberger, M. Ligtenberg, S. Tejpar, J. Lawrence
[*]Radboud University Nijmegen, The Netherlands

Objective: KRAS mutation analysis is a prerequisite for treating colorectal cancer patients with EGFR targeting therapies: in case the tumor has wild-type KRAS effect of the treatment can be expected in most of the patients, but in case there is an activating mutation the treatment is actually detrimental. Several reliable test methods are available when there is sufficient tumor tissue, but there are indications that at least some of the tests are not reliable when the tumor cell content of a tissue is low (<30%), which is the case in up to 20% of the samples. To determine the reliability of several commonly used KRAS mutation tests at low levels of tumor cells.

Method: DNA samples and artificial tissues (AS) with known percentage of KRAS mutated cells were distributed over 10 laboratories throughout Europe, each with ample experience with KRAS mutation analysis and having passed the European Society of Pathology quality assurance program. The laboratories were selected such that the 4 most commonly used tests systems were represented twice. Distributed samples contained 0, 5, 10 or 15% tumor cells. All laboratories were blinded to the content of the samples. Test methods included Sanger sequencing, pyrosequencing, high resolution melting (HRM) and ARMS-PCR with the light cycler and the ABI system as read out.

Results: There were significant differences in the interlaboratory reliability of the used test methods. Only the ARMSPCR and HRM had a high enough concordance rate for all samples combined. Taking all samples together ARMS PCR had the greatest reliability. There was only one test failure using DNA and 4 using the AS, indicating that DNA extraction methods are important and need optimizing. Few false positive results were found, one using DNA and HRM, 3 using the AS, 2 with HRM, one using ARMS PCR on the ABI. Important differences became clear after breaking down the results to tumor percentages: All but one laboratory, using Sanger sequencing, correctly identified all mutations in DNA samples with 15% and with 10% tumor

cells. Three laboratories, using Sanger sequencing, ARMSPCR, Pyrosequencing, missed each one mutation in DNA samples with 15% tumor cells, but the number of missed mutations was higher in case of AS with 10%: up to 33% in one laboratory using Sanger sequencing. In case of 5% tumor cells, either distributed as DNA or as AS the majorirty of laboratories missed mutations, and there was only one laboratory using HRM identified all mutations when 2.5% tumor cells were present.
Conclusion: Tumor samples with 15% tumor cells can be correctly analysed using different test methods, but at lower percentages, 2.5, 5 and 10%, only ARMS-PCR and HRM detect almost all mutations. Using HRM however results in a few false positives which is of more concern than false negatives. Combining all results ARMS PCR was the method resulting highest correct interlaboratory agreement. These data underline the importance of standardization of test methods and quality assurance, especially when the percentage of tumor cells is lower than 15%.

Thursday, 1 September 2011, 08.00–10.45, Room 207

OFP-15 Oral Free Paper Session Nephropathology

001

Renal retinol reabsorption is essential in tubular damage and regeneration

J. H. Bräsen *, V. Maus, P. Böckmann, D. Dragun, F. C. Luft, A. Linkermann, U. Kunzendorf,
T. Willnow
*Universitätsklinikum Kiel, Inst. für Pathologie, Germany

Objective: For the determination of the influence of reabsorbed retinoids on the regeneration of renal tubular epithelial cells following ischemia–reperfusion, we used complete retinol binding protein (RBP) knockout and cre-Lox Megalin knockout as well as wild-type mice.
Method: Renal ischemia was induced by arterial occlusion followed by reperfusion on all animals of the three groups. Analysis of renal pathology was performed at day 2 and 7, respectively. The parameters included damage scoring, cell typing (macrophages, B/T-cells), proliferation/apoptosis (Ki-67, cleaved caspase-3) as well as staining for Megalin, RBP, TGF-beta and FoxP3.
Results: At day 7, RBP knockout mice showed significanty aggravated histological damage scores compared to controls correlating with impaired renal function and less proliferating and apoptotic cells. Interstitial CD3-positive T cells were significantly reduced in RBP knockouts at day 2 compared to controls, further reduced at day 7, whereas in controls T cells increased towards day 7. Regulatory T-cells were reduced in RBP knockouts at all timepoints compared to controls. Megalin knockouts revealed a reduced but still detectable Megalin expression and showed alterations lying between wild-type and RBP knockouts.
Conclusion: Reabsorbed retinoids obviously play a relevant role in renal tubular pathology and regeneration following ischemia–reperfusion injury and might be therapeutically useful.

002

Histopathological findings and analysis of the oxidative and nitrosative stress in lung and kidney tissue from Pandemic 2009 Influenza A (H1N1) infection

R. Granados *, P. Fernández Segoviano, N. Nin, J. Lorente, C. Sánchez Rodríguez, L.S. Ver, L. Soto, J. Hidalgo, J. Ortín, A. Esteban
*Hospital Universitario Getafe, Dept. of Pathology, Spain

Objective: H1N1 infection may elicit severe respiratory dysfunction and acute kidney injury (AKI) leading to death. Most of the pathogenic events, such as the specific cell target for the infection, have not been elucidated. We present the histopathological findings, the involvement of oxidative stress, and the localization of viral particles in lung and kidney epithelial cells from nine fatal cases.
Method: Postmortem lung and/or kidney tissue was obtained from nine PCR-diagnosed H1N1 patients. Histological analysis, including double-immunofluorescence for aquaporin 1, CD10, cytokeratin 7, CD34, oxidized dihydroethydium (DHE), NO synthase (iNOS), nitrotyrosine (NT), and human influenza nucleoprotein (NP), was performed. Confocal microscopic analysis was used for localizing viral particles.
Results: Diffuse alveolar damage was seen in all cases and viral NP inside type 1 pneumocytes was found in three of six lung samples. Kidneys from the two patients with AKI had acute tubular necrosis (ATN) in distal tubules. These cases selectively showed viral NP immunoreactivity in distal tubule and parietal Bowman's capsule epithelium. Increased DHE, iNOS and NT parallel the histological findings.
Conclusion: Fatal H1N1 viral infection causes pulmonary distress and AKI with ATN, courses with prolonged oxidative stress and replicated virus in distal tubules, Bowman´s capsule epithelial cells, and alveolar type 1 pneumocytes.

003

Thrombotic microangiopathy and increased nitrosative and oxidative stress in an animal model of induced sepsis

R. Granados *, L. El Bouayadi, N. Nin, A. Ferruelo, C. Sanchez Rodriguez, Y. Rojas, P. Cardinal, A. Esteban, M. De Paula, J.-A. Lorente
*Hospital Universitario Getafe, Dept. of Pathology, Spain

Objective: Renal dysfunction in severely ill septic patients correlates with a very high mortality. Since the physiopathological events of this complication are not fully understood, animal model studies are of great interest.
Method: An experimental (n=16) intravenous 1.5×109 UFC/ml *E. coli* solution or control (n=9) sterile saline was injected in pigs. Vital signs and renal blood flow was monitorized. Twenty-four morphological criteria were semiquantitatively analyzed for glomerular, tubulointerstitial, and vascular damage. The expression of inducible nitric oxide synthase (iNOS) and nitrotyrosine (NT) by western blot, and of cytokines IL-6 and TNF by RT-PCR, was measured in the renal cortex.
Results: All animals receiving bacteria developed signs of clinical sepsis. From these, 62.5% showed glomerular thrombotic microangiopathy, mostly diffuse and global. Rare foci of mesangiolysis and acute tubular necrosis were seen. Control animals showed normal morphology. Significant elevation of iNOS and NT protein, and increased gene expression of IL-6, iNOS and TNF, was seen in septic animals.
Conclusion: Our sepsis-induced animal model reproduces the hemodynamic compromise and renal failure of septic patients. Increased oxidative and nitrosative activity and elevated inflammatory mediators are seen in renal cortex. The development of thrombotic microangiopathy is most probably the result of an increased thrombogenic effect of damaged glomerular endothelium.

004

Transgelin upregulation in renal fibrosis

F. Karagianni *, K. Kypreou, N. Prakoura, P. Politis, V. Kaltezioti, S. Psarras, S. Pagakis, D. Goumenos, A. Charonis
*BRFAA, Histology Laboratory, Athens, Greece

Objective: Renal fibrosis, a hallmark of chronic kidney disease, is poorly understood at the molecular level. The objective of our studies is to better understand the mechanisms/molecules involved in renal fibrosis.
Method: A proteomic analysis of renal tissue from the ureteric obstruction-induced fibrosis in rodents was used to identify novel fibrosis-related macromolecules; among them, transgelin was further studied. Western blotting, real-time PCR and immunohistochemistry/immunofluorescence were used to confirm proteomic findings and identify the cell type responsible for transgelin upregulation and the cellular compartment involved. Furthermore, biopsy material from patients with renal diseases was used to assess transgelin expression.
Results: Transgelin transcripts and protein were upregulated. At early stages, the interstitial compartment was expressing transgelin, mainly cells surrounding glomeruli. Transgelin-expressing cells were fibroblast-like, based on their morphology, with an extensive co-distribution with α-SMA and lack of co-distribution with endothelial and immune system markers, exhibiting both cytoplasmic and nuclear staining. At later stages, epithelial cells of the parietal layer of Bowman's capsule and cells inside the glomerulus exhibited expression. In the cases of membranous nephropathy, IgA nephropathy and focal segmental glomerulosclerosis, transgelin was expressed in glomeruli and periglomerular fibroblast-like cells.
Conclusion: Transgelin is upregulated in fibrotic renal diseases and could be used as a novel marker for renal fibrosis.

005

Renal lesions aggravation are prevented by low doses of sitagliptin in a rat model of type 2 diabetes

C. Mega *, H. Vala, J. Oliveira, R. Fernandes, F. Mascarenhas-Melo, B. Parada, R. Pinto, F. Teixeira, F. Reis, E. Teixeira de Lemos
*University of Coimbra, Lab. of Pharm. & Exp. Therapeutic, Portugal

Objective: Diabetic nephropathy is a major microvascular complication of diabetes and progression to end-stage renal disease. Thus, the ability of antidiabetic drugs to ameliorate renal disease is as important as their capability to control glucose. While the glucose-lowering effects of incretin-dipeptidyl peptidase-IV (DPP-4) are well known, the effects on the kidney remain to be elucidated. This study aimed to evaluate the effects of a 6-week treatment with low-dose sitagliptin in renal dysfunction in ZDF rats, an animal model of type 2 diabetes.
Method: Diabetic ZDF male rats (20 weeks old) were treated with vehicle or sitagliptin (10 mg/kg BW/day) during 6 weeks (n=8 each). Specimens of kidney were stained with haematoxylin–eosin and periodic-acid–Schiff and examined by light microscopy. Damage was assessed by evaluating glomerular and tubulointerstitial lesions (interstitial fibrosis/tubular atrophy—IFTA). A semiquantitative rating for each slide, from 0 (absent) to 3 (severe and extensive damage), was assigned to each component. Vascular lesions were scored from 0 to 2.
Results: Renal morphology in ZDF rats was associated with mesangial expansion and extensive sclerosis. Sitagliptin prevented the glomerular and vascular lesions and IFTA in diabetic ZDF rats.
Conclusion: The obtained results suggest that sitagliptin could provide an additional therapeutic benefit in diabetes-associated nephropathy.

006

Classification of the histopathological changes in Macedonian patients with IGA nephropathy according to Oxford classification and its prognostic significance (single-centre experience)

G. Petrusevska *, L. Grcevska, S. Kostadinova, M. Bogdanovska, V. Nikolov, M. Polenakovic
*Medical Faculty Skopje, Inst. of Pathology, Macedonia

Objective: Four pathological variables—mesangial hypercellularity score, segmental glomerulosclerosis, endocapillary hypercelullarity and tubular atrophy/interstitial fibrosis—were recommended by the Oxford clasiffication to be taken into account for predicting the outcome in IgA nephropathy. In this study, we correlated these variables with the outcome of the disease in 40 adult patients with IgA nephropathy.
Method: We used standard histological and immunofluorescent procedures on renal biopsies for the diagnosis of IgAN. Standard HE, PAS, Trichrome Goldner and Silver-methenamine–Jones were used to determine four variables as 0/1. The clinical data were obtained from the out-patient files of the patients. The whole follow-up period was 3–27 years.
Results: The average survival of the whole group was 10.8 ±7.47 years. Mesangial hypercelullarity was confirmed to be associated with the renal outcome, as well as glomerular sclerosis, endocapillary hypercellularity and tubular atrophy/interstitial fibrosis. An analysis of the patients with a severe form of the disease (nephrotic syndrome) showed that the survival of the patients was associated only with the degree of the tubulointerstitial changes. In the group of patients with mild clinical form, the predictive value of segmental glomerulosclerosis on renal survival was found.
Conclusion: This study included 40 patients with polymorphic clinical features, and the four histological variables proposed by the Oxford Classification were important for the outcome of the disease.

007

Chronic calcineurin inhibitor-induced nephrotoxicity in kidney transplant recipients: histological markers not so specific

M. Rabant *, R. Snanoudj, V. Royal, C. Girardin, E. Morelon, C. Legendre, L.-H. Noël
*Hôpital Necker, Dept. of Nephrology, Paris, France

Objective: The specificity of chronic histological lesions induced by calcineurin inhibitors (CNI) is often questioned, but few studies have directly compared long-term lesions in renal transplant patients who received this treatment and those who did not.
Method: We conducted a retrospective study of 141 kidney transplant recipients treated with (n=48) or without (n=93) cyclosporine (CsA) to compare the histological lesions observed at 3-month, 24-month and 10-year protocol biopsies.
Results: All of the chronic elementary lesions (glomerulosclerosis, interstitial fibrosis, tubular atrophy, arteriolar hyalinosis (ah), fibrointimal thickening) progressed in frequency and severity in both groups, although significantly more in the CsA group. The 10-year biopsy results showed that 92% of patients in the CsA-treated group and 65% in the control group had ah lesions. When we focused on muscular arteriolar hyaline deposits more specific to cyclosporine arteriolopathy, we observed these lesions in 68% of CsA patients and 28% of patients who had never received cyclosporine. CsA was not the sole factor involved in the development of arteriolar hyalinosis and was independently associated with an increased risk of graft loss.
Conclusion: In summary, we observed that histological lesions commonly attributed to cyclosporine nephrotoxicity were not sufficiently specific to definitively ascertain CNI nephrotoxicity diagnosis.

008

A mild form of Alport syndrome: hereditary nephropathy in the absence of extra-renal features

H.-S. Yoon *, M. Eccles
*University of Otago, Dunedin School of Medicine, New Zealand

Objective: Mutations in the type IV collagen gene, COL4A5, are associated with Alport syndrome (AS), characterized by glomerulonephropathy and end-stage renal failure (ESRF), characteristic ophthalmic signs and high-tone sensorineural deafness. Approximately 600 mutations of COL4A5 have been identified, including alterations in the non-collagenous NC1 domain.
Method: We performed linkage analysis and sequencing to identify the mutation in a New Zealand family with Alport syndrome and late-onset renal failure without hearing loss or eye abnormalities.
Results: We report a novel Cys1638Tyr alteration in the NC1 domain of COL4A5, identified in a moderately large family, eight of whom were confirmed by renal biopsy to have nephropathy. Only three of eight mutant males progressed to ESRF. The remaining five mutant males exhibit either chronic renal disease at ages 36, 46 and 72 or as yet show no renal disease at ages 39 and 39. Extra-renal manifestations were absent from all family members carrying the mutation.
Conclusion: This subsitutional mutation is the first reported to affect the tenth of 12 cysteine residues in the NC1 domain and is compared with other mutations involving the NC1 domain reported previously. We also

review mild forms of AS and discuss the relationship between AS and benign familial nephropathy.

Tuesday, 30 August 2011, 17.00–19.30, Room 207

OFP-16 Oral Free Paper Session Neuropathology—Ophthalmic Pathology

001

High-grade gliomas express higher levels of IDH1 mRNA which could be a factor to account for the greater aggressiveness of these tumors

M. E. Couce *, M. L. Sampol, M. Brell, A. Felpete, R. Guevara de Bonis, J. Ibañez
*Hospital University Son Espases, Pathology, Palma de Mallorca, Spain

Objective: Gliomas are the most common type of primary brain tumors. Somatic point mutations in the isocitrate dehydrogenase 1 gene (IDH1) are frequent in gliomas, particularly in low grades. Those gliomas with the mutation carry a better prognosis.
Method: In order to characterize these tumors further, we investigated the mRNA expression of IDH1 and the presence or absence of the G395A mutation in 32 gliomas. We pursued this study by analyzing en block resection specimens.
Results: We found no differences in mRNA expression between the central and peripheral regions of these tumors. However, we identified a significantly higher expression of IDH1 mRNA in high-grade gliomas when compared with low-grade ones. Our series show a lesser incidence of mutation in high-grade gliomas, in agreement with previously published data, with comparative findings between distant areas.
Conclusion: This study shows that those gliomas with IDH1 WT are associated with a higher expression of IDH1 mRNA independently of the tumor area. This could in turn lead to an increase in enzyme activity and more presence of NADPH which is needed for cellular growth. The greater reducing power in these cells could account for the greater aggressiveness of these gliomas.

002

The deposition of iron in globus pallidus of the human brain and its relation with glycoconjugates deposition

L. Maruscakova*, M. Kopani, O. El-Hassoun, J. Jakubovsky, I. Hulin
*Comenius University, Dept. of Pathology, Bratislava, Slovakia

Objective: Iron deposits were described in different areas of the brain; however, the causes and outcomes of such deposits are still unknown. Our aim is to investigate the relation between iron deposits and acid glycoconjugates found in brain tissue.
Method: Postmortem samples of globus pallidus were taken from patients with no iron metabolism disorders nor a neurodegenerative disease. Histological sections were prepared and stained with haematoxylin and eosine, Perl's method for Fe(III) detection and Alcian blue for acidic glycoconjugates (pH 2.5) and evaluated using light microscopy.
Results: We detected granular iron deposits around glial cells and blood vessels that colocalize to glycoconjugates accumulation.
Conclusion: There is a possible relation between iron deposits and glycoconjugates. It is known that the iron in plasma binds to transferrin and is released in lower pH: (1) We suppose that the acidic glycoconjugates can cause lower pH and the releasing of iron into the brain tissue; (2) We assume that glycoconjugates accumulate with age, cause lower pH and create iron aggregates; (3) Simultaneously, glycoconjugates might operate like regulators and protectors as they can form complexes with Fe and protect tissues from the production of free radicals by the iron.

003

Histopathological effects of low-level laser therapy (LLLT) on rat sciatic nerve regeneration

M. Mashhoudi *, F. Moayer, M. Tajziehchi, M.H. Heidari
*Tehran, Iran

Method: Twelve Wistar adult male rats (250–300 g) were divided into two groups randomly. All rats have undergone surgery in aseptic condition and a lesion was induced on their right sciatic nerve under general anesthesia. Immediately after inducing lesion in the test group, nerve was irradiated directly with 2 J energy at 100 mW power for 40 s. The experimental group was irradiated with 4 J energy at 200 mW power for 40 s during 21 days across the skin surface and one rat was chosen randomly from each group on the end of the 1st, 3rd, 5th, 7th, 14th, and 21st days after surgery and was sacrificed.
Results: Intense reduction of hemorrhages and increase in blood supply were shown after laser irradiation. There was a profound increase in the number of Schwann cells in the e group. In the c group, large numbers of inflammatory cells were shown in contrast with the e group in which these decreased to the least amount. Inflammation and chromatolysis of perikaryon were few in comparison to the c group. In the laser group, the degeneration process was postponed and Walerian degeneration was decreased. Axonal density in the treated group was greater than in the control group. The nerve sheath diameter in the lesion region was greater than that of the c group on the 21st day.

004

Pathology of brain metastases from unknown primary carcinoma

D. Rotin *, A. Golanov, L. Shishkina, L. DeLeon, O. Potapova
*NN Burdenko Neurosurgery Inst., Dept. of Pathology, Moscow, Russia

Objective: Brain metastases are known to be the most frequent malignant tumors of the central nervous system. There are some locations of primary cancer affecting the brain with metastases. Nevertheless, in 15–20%, primary cancer is undetected on the moment of neurosurgical operation. Our aim was to determine the primary locations of tumors in cases of metastatic brain carcinomas.
Method: Among 789 patients with brain metastases of different carcinomas operated in our institution, 122 had an unknown primary source (15.5%). We performed IHC in all cases with the wide panel of antibodies including cytokeratins, TTF-1, CDx2, GCDFP-15, etc. A detailed follow-up of these patients including autopsy data in some cases were also investigated.
Results: We found that the most frequent primary form was lung carcinoma—59 cases (48, 4%), followed by colorectal—23 (18.9%), renal cell carcinoma—12 (9.8%) and breast—5 cases (4.1%). There were rare locations of primary carcinoma in single cases, such as pancreas, cervix, thyroid and salivary gland (all in a single case).
Conclusion: The determination of primary site of cancer in brain metastases is important and a necessary problem. Colliding with brain metastases from unknown primary locations, physicians have to remember about lung, colorectal and renal cell carcinoma firstly, meaning, the possibility of some other rare locations.

005

Ependymomas—series of 121 cases

D. Vuralli Bakkaloglu *, B. Oz
*Istanbul Universitesi, Cerrahpasa Tip Fakultesi, Turkey

Objective: Ependymomas are slow-growing tumors of glial origin that occur at any site along the ventricular system. They account for 3–9% of all neuroepithelial tumors. To predict the clinical behaviour of this less common tumor, we analysed the data of the patients with ependymoma.
Method: A total of 121 cases of ependymomas diagnosed at our department throughout the years 2000–2011 are included in our study. We reviewed the cases according to age, sex, histologic subtype, WHO grades, location, cellularity, pleomorphizm, mitosis rate, vascular endothelial proliferation, necrosis, immunoreactivity for GFAP, Kİ-67, EMA and P53.
Results: The patients' age range is 0–70 with an average of 32 years. Female/male ratio is 61/60. Ten cases are WHO Gr 1-myxopapillary variant, 78 cases are Gr 2; 9 tanycytic, 6 clear cell, 2 cellular, 1 papillary, 1 melanocytic, 59 classic, 33 cases are Gr 3–1 atypic, 32 anaplastic variant, 3 of which transformed to glioblastoma-Gr 4. GFAP is always positive, Kİ-67 range is 0–65%, EMA is positive in 1/3, partially positive in almost half of the cases, P53's range is 0–50%.
Conclusion: Cellularity, pleomorphism, mitosis rate, vascular endothelial proliferation, necrosis, Kİ-67, P53 scores are helpful in predicting the prognosis. EMA, not as sensitive as GFAP, may have an important role in differential diagnosis of ependymomas.

007

Extracranial metastasis of meningioma: a case report

M. Vozmitel *, T. Nabebina, Y. Bogdaev, A. Dubrovskij
*National Cancer Centre, Minsk, Belarus

Objective: Although extremely rare benign meningiomas may metastasize, the previous existence of a cranial neoplasm, the non-contiguous site of metastasis and the close histological resemblance point towards the metastatic nature of extracranial lesion.
Method: A 67-year-old woman appealed to the hospital because of backache. Computer tomography demonstrated lesions with expansile radiolucency at her scapula and pelvis. Metastasis from occult primary tumor was suspected.
Results: The pelvic mass was biopsied and histologically it was characterized by spindle cells proliferation with focal storiform/whorling pattern. The whorls were typified by epithelioid cells with indistinct borders and ovoid nuclei containing intranuclear vacuoles. Tumor cells demonstrated Vim, panCK and EMA-positivity, whilst GFAP demonstrated S100-negativity. Having known that the patient had had a craniotomy 18 years before due to intracranial benign meningioma, we reviewed the original slides and found out the histological identity of both lesions. The diagnosis of metastatic meningioma was proved.
Conclusion: The real problem in a case such as ours is how to interpret so microscopically an unusual bone lesion. If a pathologist has not been told that the patient was treated for meningioma previously, he might never have considered the diagnosis of meningioma at all.

008

A clear cell renal carcinoma causing resistance to VEGF inhibitors in an age-related macular degeneration (AMD)?

J. Vinagre *, M. Falcão, C. Eloy, P. Soares, J.M. Lopes
*IPATIMUP, Dept. of Cancer Biology, Porto, Portugal

Objective: AMD refers to a common eye disease associated with aging that increasingly affects the macula. We report a previously healthy 72-year-old male with choroidal neovascularisation secondary to AMD with a poor response to intravitreal VEGF inhibitors (bevacizumab and ranibizumab). The patient was evaluated systemically for unspecific abdominal pain that disclosed the presence of a sporadic clear cell renal carcinoma. Following tumour excision, the patient's condition improved without further anti-VEGF treatment. Six months after the tumour excision, his ocular condition was stable. There is no evidence of tumour recurrence.
Method: Molecular characterization of the VHL gene and immunohistochemistry staining for HIF-1α and downstream proteins (VEGF, GLUT-1 and AC) were done in the clear cell renal carcinoma.
Results: An analysis of VHL gene in the tumour revealed the presence of a deletion. Immunostaining of the tumour area when compared to the normal tissue area presented a strong nuclear expression of HIF-1α as well as an increase of VEGF, GLUT-1 and AC expression.
Conclusion: Due to the nature of the renal carcinoma (presenting a VHL mutation), we believe that the patient's lack of response to the treatment for AMD with anti-VEGF therapy was mostly due to the angiogenic-released factors from the tumour.

Monday, 29 August 2011, 08.00–11.30, Room 210

OFP-17 Oral Free Paper Session Paediatric Pathology

001

Higher viral frequency in bronchoalveolar lavage of children with chronic lower respiratory disorders

F. Calabrese *, F. Lunardi, S. Bugin, D. Snijders, E. Perissinotto, M. Valente, A. Barbato
*University of Padua, Italy

Objective: The role of infectious agents in children with recurrent/chronic lower respiratory disorders is not clear, whereas it is well known, in particular for viral infections, in acute respiratory diseases. The purpose of this study was to evaluate the frequency of infections, in particular viral infections, in children with recurrent/chronic lower respiratory disorders and to correlate their presence with the immunological pattern of bronchoalveolar lavage (BAL).
Method: BAL was performed in 80 children affected by recurrent/chronic lower respiratory disorders. Immunophenotype including proinflammatory mediators such as eosinophil cationic protein (ECP), interleukin 8 (IL-8), tumour necrosis factor α (TNF) and respiratory viral genomes were investigated in all BALs.
Results: Viral genomes were detected in 50/80 (62.5%) children. Rhinovirus was the principal virus detected (26/50, 52%). A higher percentage of neutrophils and increased IL-8 expression were detected in virus-positive than virus-negative children. ECP values resulted to be significantly higher in children with rhinovirus than in those with other viruses.
Conclusion: Respiratory viruses, especially rhinovirus, seem to play an important role in children with recurrent/chronic lower respiratory disorders and to be associated with changes in BAL immunophenotype. Further studies are needed to confirm the persistence of viruses in these patients and to identify eventual therapeutic strategies.

002

Genotype–phenotype correlations in hepatic mitochondrial diseases

L. Galmiche *, A.-S. Lebre, F. Lacaille, M. Girard, J.-C. Fournet, P. de Lonlay, A. Rotig, V. Verkarre
*Necker Hospital, Dept. of Pathology, Paris, France

Objective: Mitochondrial diseases (MD) are respiratory chain defects. They are clinically and genetically heterogeneous and may be linked to defects of mitochondrial or nuclear DNA. However, a causal gene is identified in only 20% of them. Hepatic pediatric MD are usually very severe. Some of them are due to mitochondrial DNA (mtDNA) depletion (decreased amount of mitochondrial DNA).
Method: We retrospectively studied the liver biopsies of seven children with liver MD and determined the genetic defect.
Results: Four patients with mtDNA depletion had cytolysis, cholestasis or liver failure. Liver biopsy was performed at 6.5 years of age. Two of them had mutations of DGUOK and severe histologic lesions (clarifications, giant cell hepatitis, necrosis, microvacuolar steatosis, iron histiocytic overload). A patient was mutated for PEO1 and had mild steatosis and necrosis. Liver biopsy was normal in a POLG mutated patient. Three patients had no mtDNA depletion (MT-CYB and MT-ATP6 mutations or mtDNA deletion). They presented with cholestasis or cytolysis. Liver biopsy at 3.8 years showed large clarifications or mild lobular necrosis.

Conclusion: Histological abnormalities are earlier noticed during mtDNA depletion. Patients mutated with DGUOK seem to have a distinct and more severe histological presentation. However, genotype–phenotype correlations remain delicate considering the heterogeneity and the scarcity of MD.

003

Correlation of cancer stem cell marker, CD133, with clinicopathological parameters in pediatric solid tumours: a study using tissue microarray

M. Mehrazma *, Z. Madjd, E. Kalantari, M. Panahi, A. Hendi
*Ali-Asghar Children Hospital, Dept. of Pathology and Laboratory Medicine, Tehran, Iran

Objective: Based on cancer stem cell concept model, a small population of cells with unique self-renewal properties and malignant potential exists in solid tumors. Recent evidences indicate that CD133, a kind of transmembrane protein, can be used as a universal marker of tissue stem/progenitor cells as well as cancer stem cells. This study was carried out to investigate the expression and clinical significance of stem cell marker CD133 in a series of pediatric solid tumours.
Method: Immunohistochemical staining was performed on paraffin blocks prepared with tissue microarray to detect the expression of CD133 in 32 patients with Wilm's tumour, 18 with neuroblastoma, 30 lymphoma and 21 other solid tumors. The association between the expression of CD133 and tumour type and other properties were analyzed.
Results: The expression rates of CD133 in Wilm's tumour, neuroblastoma and lymphoma were 44%, 39% and 24%, respectively. The expression of CD133 in neuroblastoma patients with unfavorable histology was significantly higher than that in patients with a favorable histology (p-value =0.011). Moreover, this positive rate was significantly higher in younger children (p-value=0.025). No significant association was found between CD133 expression and tumour parameters in other pediatric tumours.
Conclusion: CD133 can be an important indicator for prognosis of neuroblastoma; therefore, this molecule may play a role as a potential clinical marker in younger children suffering from neuroblastoma.

004

Annulate lamellae is rarely detected in pediatric tumors: an ultrastructural study of 55 pediatric neoplasms

B. Ngan *
*Hospital for Sick Children, Pediatric Laboratory Medicine, Toronto, Canada

Objective: Cyto-organelle annulate lamella (AL) comprises arrays of stacked membrane cisternae. It contains membrane proteins from nuclear pore complexes. Its assembly and disassemby coincides with the dissolution of the nuclear envelope in the mitosis of normal cells.
Method: Electron microscopic analysis was performed in 55 pediatric tumors that were collected over the past 3 years in our hospital. The cyto-organelles of tumor cells were examined. Tumor diagnoses were made by multimodality analyses that included histopathology, appropriate immunohistochemistry, molecular analyses, cytogenetic analyses by FISH and electron microscopy. All tumor tissues were obtained fresh and fixed in glutaldehyde.
Results: Amongst the 55 pediatric tumors, there were 13 sarcomas, 7 fibroblastic/myofibroblasstic tumors, 7 lymphohistiocytic neoplasms, 5 endocrine tumors, 3 H&N carcinomas, 2 vascular, 2 germ cell-sex cord-stromal tumors, 2 PMNST, 2 solid pseudopapillary tumor of pancreas (SPPTP); one each of paraganglioma, hepatoblastoma, Wilms, granular cell, chondroblastic/osteoblstoma, rhabdoid, secretory carcinoma breast and PECOMA. AL was detected only in four tumors. These were one of two SPPTP, dysgerminoma, nasal adenocarcinoma and neuroendocrine carcinoma.
Conclusion: AL is infrequently found in pediatric neoplasms. It is present in diverse tumor types. Its rare occurence is similar to reports of adult neoplasms with SPPTP being more frequent.

005

Immunohistochemical analysis of Bcl-2 expression in Wilm's tumor

G. Basta-Jovanovic *, S. Radojevic, D. Brasanac, S. Djuricic, M. Jovanovic, L. Bogdanovic, I. Baralic, S. Glumac
*School of Medicine, Inst. of Pathology, Belgrade, Serbia

Objective: Different proteins–regulators of apoptosis, such as Bcl-2, BclX, and Bax, have influence on the rate of apoptosis in various tumors. The aim of our study was to

investigate Bcl-2 protein overexpression in Wilms tumor, to compare it with the expression in normal renal tissue as well as to see if there is a correlation between Bcl-2 overexpression in Wilms tumor with tumor stage, histological type and prognostic group.

Method: A total of 30 cases of Wilms tumor and 5 samples of normal kidney tissue were studied using streptavidin–biotin complex technique. Bcl-2 expression levels were semi-quantitatively scored.

Results: The overexpression of Bcl-2 was observed in the majority of cases (72.1%), more often in the blastemal than in the epithelial component of Wilms tumor: 64.2% and 18.6%, respectively ($p<0.05$). There was a statistically significant relationship between Bcl-2 overexpression and tumor stage ($p<0.05$). Bcl-2 was found to be less frequent in high-risk tumors than in tumors with good prognosis but without statistical significance ($p>0.05$). Overexpression of Bcl-2 was detected significantly more often in cases of WT with diffuse anaplasia compared to the other histological types ($p<0.05$).

Conclusion: Our results suggest that the overexpression of Bcl-2 may be associated with an unfavorable prognosis of Wilm's tumor.

006

Extraosseous Ewing's sarcoma with foci of neuroblastoma-like differentiation

H. Sartelet *, V. Kokta, K. Vali, M. Beaunoyer, P. Teira
*CHU Sainte Justine, Dept. of Pathology, Montreal, Canada

Objective: Peripheral primitive neuroectodermal tumor (pPNET)/Ewing's sarcoma and neuroblastoma are distinct tumors belonging to the group of undifferentiated solid pediatric tumors. Final diagnosis is based on histology, immunohistochemistry, cytogenetics, and molecular biology findings.

Method: We report a case of a 14-year-old girl who presented with an asymptomatic mobile right lower quadrant mass diagnosed on ultrasound examination. At surgery, a mobile retroperitoneal mass with a short mesentery, originating at the iliac bifurcation, was removed in its entirety and measured 9×6.5×5 cm.

Results: Histological evaluation revealed a largely undifferentiated malignant small cell tumor with multiple microscopic foci of neuropil containing maturing neuroblasts. Immunohistochemical studies revealed two distinct components: the first, consisting of sheets of undifferentiated cells was CD99+ and CD56-, whereas the second, the multiple foci of neuropil and maturing neuroblasts was CD99- and CD56+. FISH revealed the presence of EWSR1 (22q12) translocation in 92% of the malignant cells. MYCN was not amplified. The tests for t(11;22)(EWS/FLI1) and t(21;22)(EWS/ERG) performed by RT-PCR were negative.

Conclusion: Therefore, the final diagnosis corresponds to an extraosseous Ewing sarcoma with foci of neuroblastoma-like differentiation. This is the first case in which neuroblastoma-like differentiation has been noted in PNET/Ewing sarcoma without prior chemotherapy.

007

VEGF and Flt-1 expression levels in placentas from diabetic pregnancies

A. Shchegolev *, E. Dubova, K. Pavlov, M. Nagovitsyna, R. Esayan, O. Tkacheva, M. Shestakova, G. Sukhikh
*V.I. Kulakov Scientific Center, Dept. of Pathology, Moscow, Russia

Objective: Placental anomalies, particularly chorionic villi vascular structure disturbances, play an important role in diabetes mellitus pathogenesis in pregnant subjects.

Method: To evaluate the patterns of VEGF and Flt-1 (VEGFR2) expression in placentas from diabetic pregnancies, we examined 29 term placentas from a pregnant subject with type 1 diabetes (D1) ($n=12$) and gestational diabetes (GD) ($n=17$) (the first and the secnd group) and 6 term placentas from normal pregnancy (control group). We performed morphological and immunohistochemical (with VEGF and Flt-1 antibodies) analyses of all placentas.

Results: In both D1 and GD groups we revealed elevated VEGF expression levels, particularly in the endothelial cells and syncytiotrophobast of terminal villi, than in control group. The levels of VEGF expression in D1 were higher than those in GD. The levels of VEGF expression in the stem villi endothelial cells were higher in diabetic groups than in control group but were equal among D1 and GD. Flt-1 expression levels in endothelial cells of the terminal and stem villi were much higher in diabetic groups than in the control group. In turn, Flt-1 expression levels in D1 group were higher than in GD group.

Conclusion: The revealed features reflect moderate preplacental hypoxia, associated with hyperglycemia. These changes were much prominent in the case of D1.

008

Gastroschisis: a retrospective study of 34 cases focused on the anomalies of the developmental intestinal wall

N. Toran-Fuentes *, J.C. Ferreres, M. Garrido, J.L. Peiró, I. Strohecker, S. Ramón y Cajal
*H. U. Vall d´Hebron, Dept. of Pediatric Pathology, Barcelona, Spain

Objective: Gastroschisis is a congenital anterior abdominal wall defect with herniation of the abdominal contents (liver, stomach, small intestine, colon, ovaries) into the amniotic sac. Vascular and molecular mechanisms have been hypothesized as a cause of gastroschisis. Gastroschisis is characterized by a severe gastrointestinal dismotility in newborns.
Method: A total of 34 cases have been studied: 13 specimens from autopsy material and 21 intestinal biopsies from neonates and infants with gastroschisis. Immunohistochemistry techniques were used to determine the development of all the components of the abdominal wall: myenteric plexus (S-100 protein), ganglion cells (NSE), interstitial cells of Cajal (c-kit) and the musculature (smooth muscle actin).
Results: The absence or hypoplasia of interstitial cells of Cajal (40%), reduction of the neural crest cells and enteric neurons (13%), and immature differentiation of smooth muscle cell (2%) supports an associated defect in neuromuscular development induced by amniotic fluid that is restricted to the eviscerated intestine. The remaining cases have no histological lesions.
Conclusion: Our pathologist reports have been definitive to decide the termination of pregnancy between 34 and 35 weeks to reduce the time of exposure to the amniotic fluid. Histological findings can establish the post-surgical behaviour of the patients.

009

Fetal akinesia sequence: fetopathological study of 17 cases

M. T. Yacoubi *, A. Bdioui, N. Ben Jamaa, S. Miladi, S. Hmissa, C. Fallet Bianco
*University Hospital Sousse, Dept. of Cyto-Histopathology, Tunisia

Objective: Fetal akinesia sequence (FAS) covers a large spectrum of developmental abnormalities due to a lack of intrauterine fetal movement, sharing heterogeneous etiologies. The aim of this study is to evaluate the role of neuropathological examination in order determine the cause of fetal akinesia.
Method: A total of 17 fetuses with akinesia were studied in the Department of Pathology between 1997 and 2003. Complete fetopathological study with neuropathological examination was performed.
Results: The mother's age ranged between 22 and 31 year. Fetuses are aged between 19 to 41 weeks with a sex ratio of 1.5. The karyotype was normal in ten cases. Akinesia was found in more than one case in three families. The lack or decrease of intra-uterine fetal movements was found in all cases. Isolate arthrogryposis was seen in four cases, with amyotrophy in four cases, facial dysmorphy in nine cases and multiple pterygium in one case. Neurogenic origin was detected in 14 cases with a decrease of apoptotic neurons in the spine. Myogenic involvment was found only in one case.
Conclusion: Brain, spine and muscle should be examined in context of FAS. The understanding of various pathogenetic processes involved in the emergence of FAS should be improved in order to propose better information and genetic counseling to parents.

Thursday, 1 September 2011, 08.00–10.45, Room 204–205

OFP-18 Oral Free Paper Session Pulmonary Pathology—Thymus Pathology

001

Feasibility of molecular analysis in endobronchial ultrasound-guided transbronchial aspiration using liquid-based preparation

C. Delattre *, C. Descarpentries, B. Bouchindhomme, C. Fournier, F. Escande, M.-C. Copin
*CHRU Lille, Inst. of Pathology, France

Objective: The purpose of this report was to investigate the feasibility of epidermal growth factor receptor (EGFR) and KRAS molecular analysis in endobronchial ultrasound-guided transbronchial needle aspiration (EBUS-TBNA) sample on a daily practice.
Method: We included patients with an EBUS-TBNA positive for adenocarcinoma or non-small cell carcinoma. Specimens were collected on a liquid-based preparation and proceeded on paraffin-embedded cell blocks after ThinPrep procedure. Molecular analysis was performed by a SnaP-

shot assay for EGFR and by pyrosequencing for KRAS on suitable samples (> 5% of tumor cells).
Results: The molecular analysis was feasible in 48 (89%) samples carried out on 54 patients selected. Six cytological specimens could not be tested (insufficient DNA after extraction: $n=5$, absence of tumor cell after standard tumor typing procedure: $n=1$). Molecular analysis showed KRAS and EGFR mutations in tumor samples from 12 and 3 patients, respectively.
Conclusion: KRAS and EGFR gene analysis has a good yield on EBUS-TBNA specimens and can be easily performed routinely on the remaining paraffin-embedded sample after a standard diagnostic procedure using a liquid-based preparation.

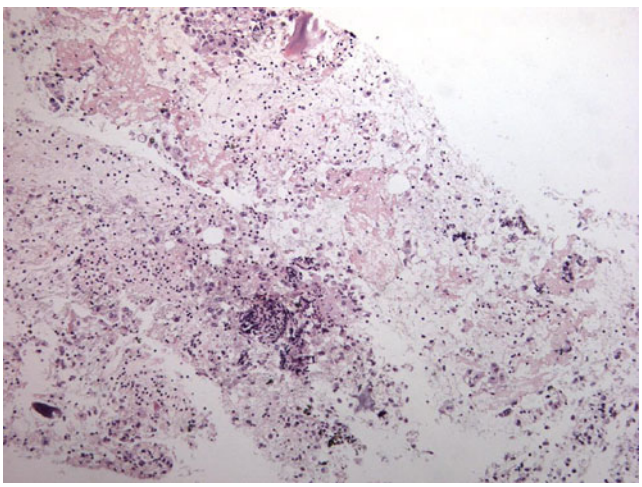

002

Interobserver variability in the application of the novel IASLC/ATS/ERS classification of lung adenocarcinoma

W. Weichert *, A. Warth, A. Stenzinger, A.-C. von Brünneck, B. Goeppert, I. Petersen, P. Schnabel
* Medizinische Universität Heidelberg, Inst. für Pathologie, Germany

Objective: Recently, an international consensus classification for adenocarcinomas of the lung has been published. The cornerstone of this new classification is the quantification of different growth patterns. However, it is largely unknown how reproducible this classification can be done in the routine diagnostic setting.
Method: We selected 100 constitutive cases of lung adenocarcinoma resection specimen from our archives. All tumors were classified independently by three experienced pulmonary pathologists and by two pathologists in training.
Results: An average of four tumour-bearing slides was available for analysis per case. The most frequent predominant pattern was acinar (42%), followed by solid (34%), lepidic (17%), micropapillary (4%) and papillary (3%). In most cases, a mixed subtype was evident; pure growth patterns were rare (8%). The κ-values for the denomination of a predominant pattern revealed a substantial agreement for pulmonary pathologists (0.58–0.72) but only fair agreement for pathologists in training (0.22–0.37). Agreement was highest for the solid pattern, followed by lepidic and acinar growth. Interobserver variability was considerably reduced in a second evaluation round after the initiation of a training session.
Conclusion: Our data imply that the novel classification of adenocarcinomas of the lung is applicable with acceptable interobserver variability when done by pulmonary pathologists.

003

Heterogeneity of large cell carcinoma of the lung: an immunophenotypic and miRNA-based analysis

M. Barbareschi *, C. Cantaloni, V. Del Vescovo, A. Cavazza, R. Carella, G. Rossi, G. Pelosi,
M. Papotti, M. A. Denti
*S. Chiara Hospital, Dep. of Pathology, Trento, Italy

Objective: Large cell carcinoma (LCC) of the lung is heterogeneous and may be of a different cell lineage.
Method: We analyzed 56 surgically resected lung tumors, classified as LCC on the basis of pure morphological grounds, using a panel of immunophenotypic markers (TTF-1, citokeratin 7, napsin A; SQCC, p63, cytokeratin 5, desmocollin 3 and Δnp63) and the quantitative analysis of miR-205 (mi-R sample score method, mRSS).
Results: Based on immunoprofiles, 19 (34%) cases were re-classified as adenocarcinomas (ADC), 14 (25%) as squamous cell carcinomas (SQCC), and 23 (41%) cases were unclassifiable. According to the mRSS, 36 cases were classified as ADC and 20 as SQCC. Of the 23 cases unclassifiable on the basis of the immunoprofiles, 18 were classified as ADC and 5 as SQCC according to mRSS.

Conclusion: Our data show that an extended panel of immunohistochemical markers can be re-classified around 60% of LCC as ADC or SQCC. However, a relevant percentage of LCC may escape convincing immunohistochemical classification, and mRSS could be used for further typing, but its clinical relevance needs further confirmation. This study has been partially supported by grants of the Provincia Autonoma di Trento and of the Fondazione Cassa di Risparmio di Trento e Rovereto.

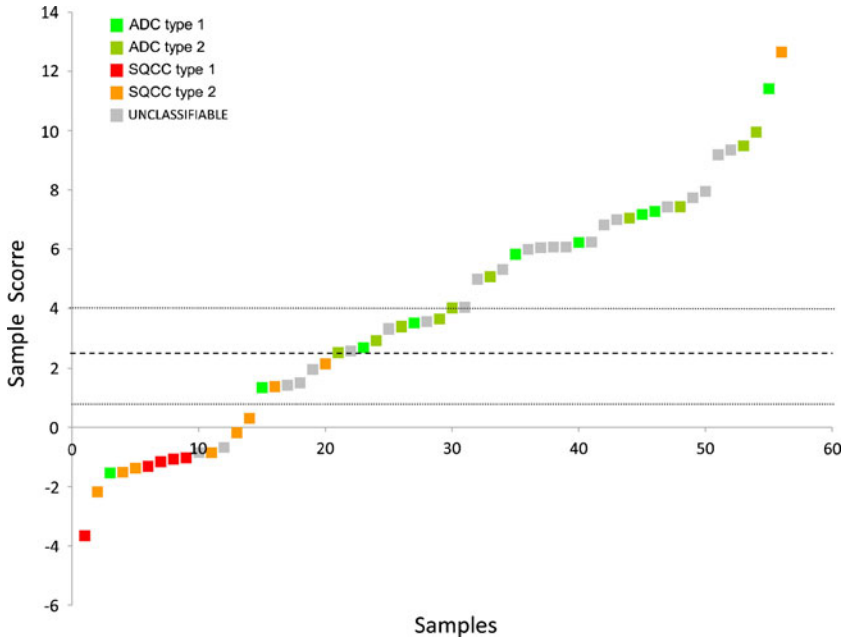

004

Factors influencing long-term survival in patients with malignant pleural mesothelioma: a study of 182 cases from the Mesonat register and the French National Mesothelioma Surveillance Program

M. Paciencia *, N. Le Stang, C. Drougard, F. Galateau-Sallé
*University Hospital, Dept. of Pathology, Caen, France

Objective: Malignant pleural mesothelioma (MPM) is a tumor with a median survival time of 12 months. However, some patients survive for more than 3 years. The aim was to identify the factors influencing the long-term survival in patients with MPM.

Method: Between 1998 and 2006, 182 cases were collected from the French National Mesothelioma Surveillance Program. We evaluated the prognostic impact of the epidemiological characteristics, clinical manifestations, histology subtype, and expression of p53 and p16. Moreover, inflammation, necrosis, angiogenesis and nuclear pleomorphism were analyzed in 57 patients who survived more than 3 years and 53 patients who died before 3 years. Kaplan–Meier method, log-rank test, and Cox model were used in the statistical analysis.

Results: Univariate analysis identified younger age, weight loss, epithelioid subtype, female gender, no dyspnea, no asthenia, expression of p16 and no overexpression of p53 as prognostic factors, which was confirmed in multivariate analysis, except for clinical and epidemiological factors. The patients with the longest survival showed high levels of CD8+ tumor-infiltrating lymphocytes, increased angiogenesis, inconspicuous necrosis and bland cytology.

Conclusion: Loss of p16 and overexpression of p53 are interesting prognostic factors since they can be easily diagnosed by immunoreactivity. The stimulation of CD8+ lymphocytes can be a potential therapeutic strategy to improve the outcome.

005

Thymic myoid cells could protect lymphocytes in thymic medulla from apoptosis in vivo: a preliminary immunohistochemical study

I. Varga *, V. Sisovsky, V. Jablonska-Mestanova, S. Polak, M. Adamkov
*Comenius University, Faculty of Medicine, Bratislava, Slovakia

Objective: Thymic myoid cells correspond to a rare cell population localized in the thymic medulla. They possess

the antigenic characteristics of skeletal muscle fibers. Their exact biological role remains unclear, but they are involved into the pathogenesis of myasthenia gravis. We analyzed a correlation between the number of myoid cells and the expression of anti-apoptotic protein Bcl-2 in lymphocytes in human thymuses.

Method: The study was conducted on 30 specimens of children thymuses, which were removed due to surgery for different cardiac malformations. The sections were stained for the expression of desmin and α-actin (markers of myoid cells) and the expression of anti-apoptotic Bcl-2 protein.

Results: Thymic myoid cells had a spindle-like shape and were located in the medullary region. Bcl-2-positive lymphocytes were located mostly in thymic medulla, but they were found also occasionally in thymic cortex. In thymuses with a higher number of myoid cells, we found a higher expression of anti-apoptotic Bcl-2 oncoprotein in lymphocytes.

Conclusion: In our study, we observed that lymphocytes express a higher level of anti-apoptotic protein Bcl-2 in case of the presence of a higher number of myoid cells. Our preliminary results show that myoid cells can protect lymphocytes from apoptosis. This study was supported by grant 1/0902/11-VEGA MSSR.

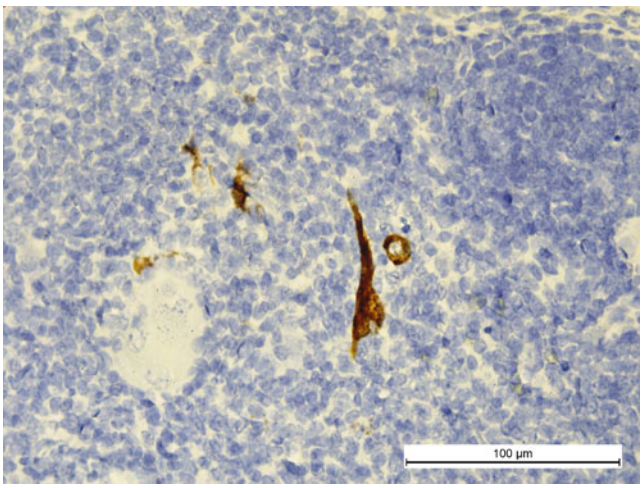

006

Pathomorphology of the thymus in post-mortem examinations in Paediatric Pathology Department

L. Volkova *, V. Bondarev
*Kursk State Med. University, Dept. of Pathological Anatomy, Russia

Objective: The actual problem of paediatric pathology is post-mortem morphological diagnosis of thymus disorders for the verification of congenital or acquired immunodeficiency. The aim of this study was the evaluation of the incidence of variants of thymus pathology in the structure of paediatric mortality in Kursk and associations with immunodeficiency (ID).

Method: H&E/Van Geison methods were employed; in some cases, immunohistochemistry was used; the diagnostics of ID was based on a retrospective analysis of clinicopathological features in 63 paediatric autopsy examinations.

Results: The main variants of post-mortem diagnosis were the following: (1) accidental involution (AI) of thymus of different degrees (1–2—"starry sky", 3—inversion of cortex and medulla, 4–5—atrophy of thymus); (2) thymus hyperplasia (TH); (3) thymus dysplasia and hypoplasia—histopathologic manifestation of the congenital ID. A high incidence of AI and THIt—potential morphological features of acquired ID— was revealed; the cases were analysed to determine the interrelations with ID.

Conclusion: (1) AI of the 4–5 degree is the morphological equivalent of acquired ID; (2) AI of the 3 degree can be considered as ID after an analysis of the clinicopathological features; (3) TH is a heterogeneous group of conditions; the interpretation of the associations of TH with ID can be given after an analysis of the possible etiopathogenetic factors.

007

Analysis of angiogenic factors and COX-2 expression in cartilaginous tumors: clinical and histological correlation

E. Amstalden *, F. Cintra
*UNICAMP, Dept. of Pathology, Campinas, Brazil

Objective: Histological grades in chondrosarcomas (CSs) are standard for predicting tumor outcome. Distinction between enchondromas (ECs) and grade 1 CS is often difficult. Angiogenesis induced by the neoplasm could assist in this task. Angiogenesis can be measured by VEGF and CD34 expression. This work aims to study the role of angiogenesis and COX-2 expression in cartilaginous tumors correlating with prognosis. Proangiogenic factors can be induced by COX-2.

Method: A total of 21 ECs and 58 conventional CSs were evaluated regarding clinical and histopathologic findings, angiogenesis markers (VEGF; CD34) and COX-2 expression. For VEGF and COX-2 analysis, a score was adopted based on the proportion of stained tumor cells (0=no stained cells; 1+= <10%; 2+= 10% to 50%; 3+=>50%). Microvessel density (MVD) measurement was made by Chalkley method through CD34 using a minimum of five "hot spot" areas in ×10 objective.

Results: Poor outcome was associated with higher grades CSs; CS developing in flat bone; CD34 over-expression (>5.9 vessels/5 HPFs). CD34-MVD was higher in flat bones. Immunolabeling for COX-2 and VEGF was not helpful in distinguishing between these tumors.

Conclusion: CD34-MVD may help to predict the outcome and improve the understanding of CSs pathogenesis. No

variable proved useful in distinguishing low-grade CSs from ECs. FAPESP-09/51473-0.

008
Bronchiolar–pulmonary diseases and lung cancer histological typing

L. Carvalho *
*Amadora, Portugal

Objective: Current discussion runs from the clinical value of tobacco non-tumoral lung diseases as concommitantly induced upper and lower airways together with parenchime diseases. In a randomized series of 44 surgical specimens of lung cancer, six or more samples were selected in surrounding parenchime to register pulmonary alterations of non-smoking and smoking patients.
Method: Normal lung/discrete centrilobular emphysema was registered in five non-smokers lung of adenocarcinomas and one male epidermoid carcinoma (EC); BALT hyperplasia with Mucinous BAC (female), granulomatous bronchiolitis with adenocarcinoma (male) and constrictive/lymphocytic bronchiolitis and BALT hyperplasia around a solid adenocarcinoma (male).
Results: The 36 smokers adenocarcinomas, 14 ec and other histological types: 3 lcnec; 2 adenosquamous carcinoma; 2 sarcomatoid-pleomorphic carcinoma; lcc and sclc combined with adenocarcinoma, had monotonous morphological parenchyma alterations, encompassing 28 emphysema, 17 DIP, 14 constrictive bronchiolitis, 12 NSIP-like pattern, 7 respiratory bronchiolitis and 7 BALT hyperplasia.
Conclusion: Anna-Luise Katzenstein proposed the smokers' lung disease may be dependent on individual genetic susceptibility to have elastic net destructive emphysema (neutrophils?), fibroblastic response/TGF-β at membranous bronchioles towards NSIP-like fibrosis and constrictive bronchiolitis as centrilobular lesions and finally, immunologic answer/macrophages colony forming with DIP and respiratory bronchiolitis. These conclusions come from 10/12 cases of NSIP-like together with constrictive bronchiolitis and 6/12 with isolated emphysema.

Sunday, 28 August 2011, 14.00–16.30, Room 207

OFP-19 Oral Free Paper Session Uropathology I

001
Molecular prognostic signature in clear cell renal carcinoma

M. Brunelli *, S. Gobbo, D. Segala, V. Ficarra, G. Novara, G. Martignoni
*University of Verona, Pathology and Diagnostic, Italy

Objective: We investigated the correlation between loss of chromosome 9p, 14q and gains 5q and the SSIGN score in clear cell renal carcinoma.
Method: We selected 388 patients affected by clear cell renal carcinoma with outcomes. The SSIGN score was: low (0–2); intermediate (5–6) and high risk (≥10) groups. We performed a FISH analysis using probes mapping on chromosome 9p, 14q and 5q.
Results: A total of 19% of patients showed loss of 9p and 23% loss of 14q, 21% gains of 5q. There were 178 patients who showed a 0–2, 154 a 5–6 and 152 a >10 SSIGN score. A total of 180 patients were pT1-2 and 200 pT3-4. Loss of 9p was detected in 60% of patients with >10, in 20% with 5–6, and 5% in patients with 0–2 SSIGN score. Loss of chromosome 9p/14q resulted related to local extension and lymph nodal metastases. Patients with tumors demonstrating loss of 9p/14q showed a median cancer-specific survival of 16 months whereas patients with tumors without loss displayed a median cancer-specific survival of 101 months (long rank test, $p=0.01$). Gains of 5q showed a better outcome.
Conclusion: Loss of 9p, 14q and 5q may represent a molecular prognostic signature in patients affected by clear cell renal cell carcinoma.

002
Cyclin D1 amplification and protein overexpression independently predict survival in metastasizing bladder cancer

A. Fleischmann *, D. Rotzer, R. Seiler, G. N. Thalmann
*Universität Bern, Inst. für Pathologie, Switzerland

Objective: The frequency and prognostic impact of cyclin D1 gene (CCND1) amplification and protein overexpression in metastasizing bladder cancers are unknown.
Method: One hundred fifty lymph node positive patients with urothelial bladder cancer underwent cystectomy and lymphadenectomy. Tissue microarrays were constructed with four tumor samples per patient, two each from the primary tumor and from metastases. CCND1 was evaluated by fluorescence in situ hybridisation (FISH) and the protein by immunohistochemistry.
Results: CCND1 amplification was similar in primary tumors (18%) and metastases (21%) and highly homogeneous in both tumor components (kappa: 0.8 and 0.9). Cyclin D1 expression was significantly higher in amplified compared to non-amplified cancers ($p<0.001$); however, among the 25% of tumors with highest cyclin D1 expression, only half were amplified. CCND1 amplification in primary tumors and cyclin D1 overexpression in metastases were independent predictors of early death ($p<0.02$ each). Survival of patients treated

additionally with cis-platin could not be stratified by cyclin D1 status.

Conclusion: CCND1 amplification is an important but not the only mechanism for cyclin D1 overexpression in bladder cancer. Cyclin D1 status adds independent prognostic information; however, this information is lost after chemotherapy, suggesting that cyclin D1 is also a predictive marker.

003

Tracing the metabolic profile of prostate cancer progression

N. Gomes *, J. R. Vizcaíno, D. Esteves, C. Lopes, F. Baltazar
*Rio Tinto, Portugal

Objective: One of the most common properties of cancer cells is a metabolic change into high glycolysis and lipogenesis to satisfy the increased demand for energy for autonomous growth. Despite its implication in virtually all malignant cells, the role of altered cellular metabolism as an essential factor in prostate malignancy has been largely ignored. In this work, we aimed to study ten key metabolic proteins involved in lipid and glycolytic metabolism in benign prostate, PIN lesions and prostate cancer to give an insight into the metabolic adaptations in prostate cancer progression. Also, we aimed to correlate the expression of these metabolic proteins with known aggressiveness marker proteins such as CD44, CD147 and MDR1.

Method: Prostate samples were obtained from 114 patients with prostate carcinoma. Areas representing carcinoma, normal prostate and PIN lesions were selected and immunohistochemistry was performed. Data were stored and analyzed using the SPSS statistical software.

Results: We observed an overexpression of proteins involved in both glycolysis and lipogenesis in prostate cancer and already in the precursor lesions. Also, we noted that some of these proteins are associated with the poor prognosis protein markers studied.

Conclusion: It seems that prostate cancer cells combine the overexpression of both glycolysis and lipogenesis proteins. Assessment of metabolic alterations is important and it appears to be indicative of prostate cancer progression.

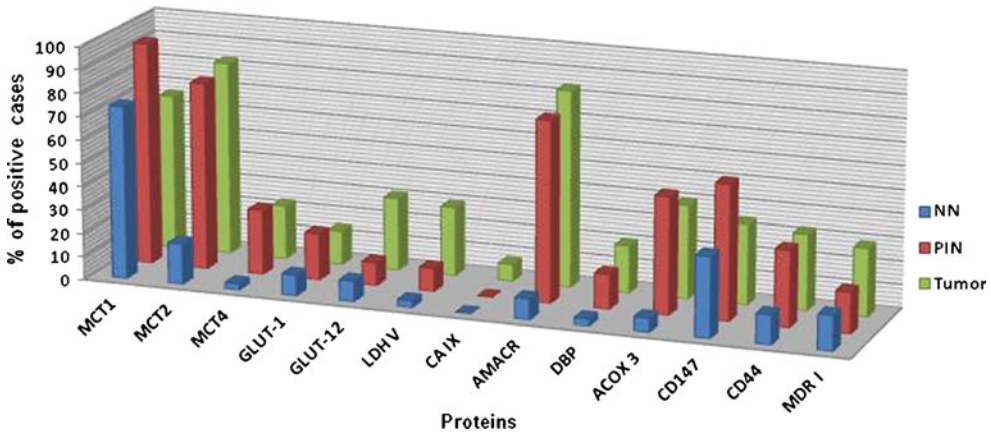

004

Margin status of the vas deferens in radical prostatectomy specimens. Relevance or waste of time?

R. Grobholz *, M. Saar, J. Kamradt, L. Trojan, C. Sauer
*Kantonsspital Aarau, Pathologisches Institut, Switzerland

Objective: Examination of the margin status of radical prostatectomy specimens is of interest but the examination of the vas deferens margin is not generally recommended.

Method: A total of 2,701 consecutive prostatectomy specimens in 1995–2009 (Mannheim, $n=1{,}932$) and 2007–2009 (Homburg, $n=769$) were reviewed for tumor infiltration of the vas deferens margin and were correlated with clinico-pathological data.

Results: In 41/2,701 cases (1.5%), a positive margin of the vas deferens was detected. In 12 cases, even a bilateral infiltration was present. All tumors were locally advanced [pT3a ($n=1$), pT3b ($n=34$), pT4 ($n=6$)]; 15 (37%) had lymph node metastases. The Gleason scores ranged from 7 to 9. Preoperative PSA was between 3.1 and 127 ng/ml (mean 28.02 ng/ml). In all cases with seminal vesicle infiltration (40/41), the positive margin of the vas deferens was on the same side. In 11/15 patients (73%) with pN1 status lymph node metastases, seminal vesicle infiltration and positive margin of vas deferens were seen on the same

side. In 16 cases (39%), infiltration of the vas deferens was the only positive margin of the whole specimen.
Conclusion: A positive margin of the vas deferens is an infrequent finding but in 39% the only positive margin. A histological evaluation of the vas deferens margin seems therefore reasonable.

005
Her 2/neu gene and VEGF in bladder cancer in Egypt: relationship to schistosomiasis

O. Hammam *, A. Abel Hadi, I. Abdel Aziz, O. Mahmoud, M. Zahran, A. Alkholy, M. Akl, M. Wishahi
*Theodor Bilharz Research Institute, Dept. of Pathology, Giza, Egypt

Objective: To assess Her2/neu protein and gene and soluble VEGF in some urinary bladder lesions in Egyptian patients.
Method: Her 2/neu protein and gene were detected using IHC and FISH techniques and serum level of VEGF by Eliza were detected in 35 patients with chronic cystitis without or with schistosomiasis. A total of 135 were schistosomal-associated malignant patients and 50 of non-schistosomal-associated urothelialcarcinoma carcinoma. There were 20 normal controls.
Results: Her 2/neu protein overexpressed in a malignant group was recompared to control and chronic schistosomal cystitis groups ($p<0.01$), higher in urothelial carcinoma group 72.2% compared to SCC 40% with $p<0.01$ and in high than low grade tumor with $p<0.01$. Her 2/neu gene amplification was 33.35% in SCC and 58.2% in urothelial carcinoma, higher in high than low grade tumor with $p<0.01$, also higher in invasive tumors than non-invasive tumors ($p<0.01$). The serum VEGF positive rates for SCC, urothelial carcinoma, chronic cystitis and normal controls were 94.7%, 89%, 22.9%, and 5%, respectively.
Conclusion: Our study showed that 78.9% of invasive urothelial bladder carcinomas present with a Her 2/neu amplification which had been assessed by a standardized IHC using FISH in the ambiguous cases. Association between increased VEGF levels with high grade and tumor invasion in bladder cancer patients indicates that VEGF may play a role in the invasion and metastasis of cancer and may serve as an indicator of tumor progression and future recurrence.

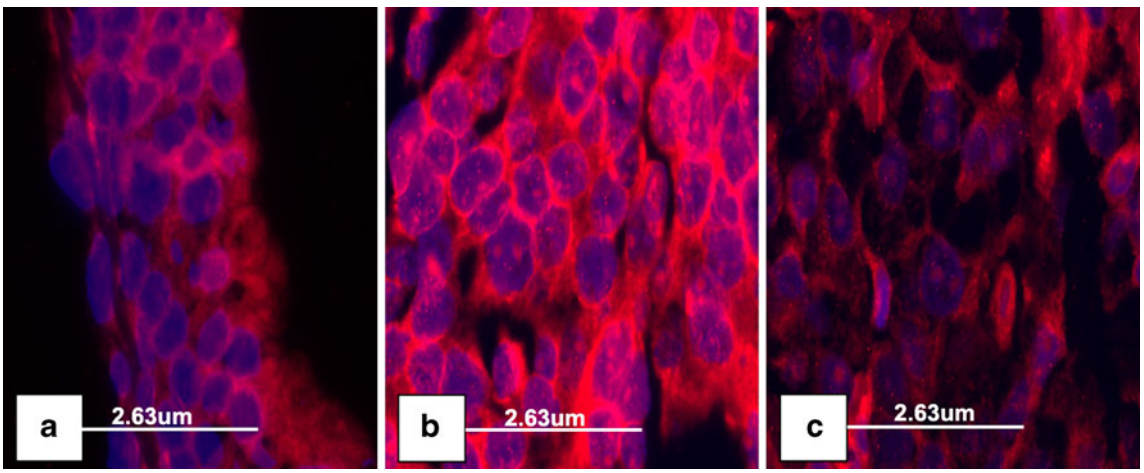

006
Quantification of extraprostatic extension in prostate cancer: different parameters correlated to biochemical recurrence after radical prostatectomy

C. Hulsbergen-van de Kaa *, B.A.M.H. van Veggel, I.M. van Oort, J.A. Witjes, L.A.L.M. Kiemeney
*Radboud UNMC, Dept. of Pathology, Nijmegen, The Netherlands

Objective: Different methods to substage extraprostatic extension (EPE) were correlated to biochemical recurrence (BCR) after radical prostatectomy (RP).
Method: A total of 157 consecutive RP specimens with EPE were completely embedded. A total of 23 patients with adjuvant therapy or detectable postoperative PSA levels were excluded, leaving 134 patients for BCR analysis. Data were analyzed using Kaplan–Meier survival and Cox regression analyses.
Results: In univariable analysis, maximal radial distance (RD) was associated with BCR, as continuous ($P=0.006$) and dichotomous ($P=0.002$) parameter. In multivariable analysis, independent predictors of BCR were preoperative PSA ($P=0.006$), Gleason score ($P=0.001$), positive surgical margins ($P=0.005$), maximal RD dichotomized at 0.6 mm (=one high-power field (HPF); HR 3.4; 95% CI 1.48-7.85;

P=0.004), total RD (P=0.009) and EPE quantification according to Epstein (P=0.002), and to Wheeler (P=0.004). The 5-year risk of BCR was 20% (95% CI, 0.65–0.94) in patients with RD≤0.6 mm and 47% (95% CI, 0.41–0.65) with RD>0.6 mm. The restriction of focal EPE in no more than two slides (Epstein and Wheeler) gave no better results.
Conclusion: Maximal RD dichotomized at one HPF is an objective method to subdivide EPE and a strong, independent predictor for BCR after RP. Its use is recommended for substaging pT3a in future TNM classifications.

007

Long-term outcome and neuroendocrine differentiation in conservatively treated prostate cancers

S. Jeetle *, Z.H. Yang, E. Stankiewicz, G. Fisher, J. Cuzick, D. Berney
*Barts Cancer Institute, LA63 Molecular Oncology, London, UK

Objective: Differentiation of prostate carcinoma (PC) to a neuroendocrine phenotype is thought to be associated with a poorer prognosis but there is controversy whether it is an independent prognostic marker. We wished to determine whether chromogranin-A (CG), as a marker of neuroendocrine differentiation, was a biomarker of outcome in a cohort of conservatively treated prostate cancers with long-term follow-up.
Method: A total of 806 patients with clinically localized PC treated by non-curative means diagnosed from 1991 to1996 with a contemporary assessment of Gleason score and serum PSA were available. The end-point was death from PC. CG immunohistochemistry was performed and expression measured semi-quantitatively on tissue micro-arrays (2,483 cores).
Results: CG expression correlated positively with Gleason score (p<0.001, χ^2=28.35) and it was a significant predictor of cause-specific survival (hazard ratio [HR] 1.61, 95% CI 1.152.27, P=0.008) on univariate analysis. In multivariate analysis, there was no significant association with cause-specific survival over and above Gleason score and PSA.
Conclusion: Neuroendocrine differentiation is a poor prognostic factor, predicting death from PC, but it shows no significance on multivariate analysis. We suggest that apart from the identification of the small cell variant, which may require systemic chemotherapy, it need not be assessed in routine practice.

008

Coexpression of FGFR1 and NCAM in RCC

J. Markovic-Lipkovski *, C. Müller, A. Vuksanovic, C. Tulic, M. Djokic, S. Cirovic, D. Dundjerovic,
S. Tatic, G. Müller
*University of Belgrade, Faculty of Medicine, Serbia

Objective: Neural cell adhesion molecule (NCAM) is important for cell migration and it could be expressed on renal cell carcinoma (RCC). Fibroblast growth factor receptor (FGFR1-4) is critical for cell growth and differentiation and could be overexpressed in RCC. Since the interaction between FGFR1 and NCAM is closely related, this study evaluated the expression of FGFR1 and NCAM in RCC.
Method: A total of 35 RCC samples (18 clear cell, 9 pappilary, 6 chromophobe, 2 sarcomatoid) were analyzed by immunohistochemistry and double immunofluorescent staining. Antibodies which recognize different NCAM isoforms were applied. By RT-PCR, different NCAM (120, 140, 180) were detected using specific primers.
Results: Renal cancer cells slightly varied in expression on different NCAM molecules. More than half of the analyzed cases coexpressed FGFR1 and NCAM 180. The coexpression of FGFR1 and NCAM was detected in clear cell, pappilary, sarcomatoid, and only one case of chromophobe RCC. The number of cancer cells which coexpressed FGFR1 and NCAM seems to correlate with tumor malignancy according to tumor grading and staging. However, 20% of cases were negative for both markers and 20% were negative either for NCAM or for FGFR1. All tested samples for RT-PCR showed predominantly NCAM 140, although 120 and 180 were present in a lesser extent.
Conclusion: The coexpression of FGFR1 and NCAM may be relevant for tumor growth and malignancy in renal cell carcinomas.

009

The expression of cell-surface Glycoprotein CD44 in lesions of prostate gland

V. D. Samaras *, C. Barbatis, P. Lazari, O. Pantzartzi, H. Gakiopoulou, S. Theocharis, H. Poulias,
A.C. Lazaris
*Red Cross and Athanasaki Hospital, Athens, Greece

Objective: CD44 is a cell surface glycoprotein involved in cell adhesion/migration and a putative stem cell marker. We studied the expression of CD44 in prostatic adenocarcinoma (PCa), high-grade prostatic intraepithelial neoplasia (HGPIN) and nodular adenomatous hyperplasia (NH) as there are conflicting data in the international literature, and the stem cell in prostatic carcinogenesis is still elusive.
Method: CD44 was immunohistochemicaly detected in 55 areas from 45 cases of radical prostatectomy specimens with organ-confined PCa. All sections were included: HGPIN, PCa and NH. Positive staining was defined as 1+ (<10% of epithelial cells), 2+ (10-50%), or 3+ (>50%). The correlation of immunopositivity with Gleason score and TNM stage was investigated.

Results: CD44 was strongly expressed (score 3+) in 55.6%, 35.6% and 31.1% of areas with NH, HGPIN and PCa, respectively. The expression levels of CD44 was stronger in NH compared to PCa and HGPIN ($p=0.002$ and $p=0.007$, respectively). No significant difference was detected between HGPIN and PCa areas ($p=0.075$). Gleason score and TNM stage were not significantly associated with the distribution of PCa CD44 expression.
Conclusion: HGPIN and PCa show a reduced expression of CD44 and the exact role of this phenomenon in prostatic carcinogenesis needs further investigation.

Sunday, 28 August 2011, 17.00–19.30, Room 207

OFP-20 Oral Free Paper Session Uropathology II

001

CD8 in the differential diagnosis of renal tumors

V. D. Samaras *, C. Barbatis, E. Nikolopoulos, C. Poullou, M. Kefala, A. Tsikou-Papafragou, H. Poulias
*Red Cross and Athanasaki Hospital, Athens, Greece

Objective: Renal tumors constitute a heterogeneous group of neoplasms with different histopathological features and prognostic implications. Cytokeratins have been utilized for differential diagnosis and subtyping. CD8 is a transmembrane glycoprotein expressed primarily by thymocytes and cytotoxic/suppressor T cells and labels native cytokeratin 15 (CK15). This is a preliminary study of CD8 expression in renal tumors given that this molecule has not been studied in these neoplasms so far.
Method: We immunohistochemically assessed 24 clear cell renal cell carcinomas (ccRCCs), 6 papillary renal cell carcinomas (pRCCs), 3 chromophobe renal cell carcinomas (chRCCs) and 3 oncocytomas.
Results: Diffuse, strong, membranous CD8 expression was observed in all chRCCs and in two out of three oncocytomas. Statistical analysis showed that CD8 was significantly overexpressed in chRCCs and oncocytomas compared to ccRCCs and pRCCs ($p<0.001$). Only two ccRCCs and one pRCC were diffusely positive for this marker and the majority of these tumors demonstrated either focal positivity (14 cases) or they were negative for CD8 (13 cases).
Conclusion: Although low molecular weight cytokeratins are believed to be expressed in all of the abovementioned renal tumors, CK15 (identified by means of CD8 immunolabeling) seems to be principally expressed in chRCCs and oncocytomas. This marker could be useful in the diagnosis of distal nephron renal neoplasms.

002

Immunohistochemical study of cytokeratines 7 and 19 in prostatic neoplasia

A. Tanoglidi *, H. Moyrtzoukos, C. Bouropoulos, N. Ferakis, N. Nikolaou, H. Poulias, C. Barbatis
*Red Cross and Athanasaki Hospital, Dept. of Pathology, Athens, Greece

Objective: The aim of this study was to assess the expression of both CKs in prostates with adenocarcinoma (PCa) and their probable relationship to the evolution of the disease and diagnostic uselfulness.
Method: Six sites were selected from each of ten prostatectomy specimens with organ- confined PCa including normal ducts and acini/90, adenomatous hyperplasia (AH) 25, proliferative microacini (PMA) 27, PIN3 28 and PCa 32. The distribution patterns of CK7 and CK19 were assessed in basal and luminal cells and an arbitrary semiquantitative method was applied only for luminal positive epithelium.
Results: Basal/luminal cells of normal ducts are CK7+/CK19+, but luminal acinar cells are CK7-/CK19- with occasional CK19+. Luminal CK7+ cells were observed in AH (58%), PIN3 (84%) and PMA (95%). A total of 75% of PCa lack CK7 and scattered positive cells (<10%) were seen only in eight cases. CK19 luminal positivity characterises AH (96%) particularly in areas of cellular tufting, PIN3 (96%) with diffuse or focal expression and PCa (84%) but with reduced intensity.
Conclusion: The gradual increase of CK7+ luminal cells in AH and PIN3 supports the theory that PIN3 initiates from ductal epithelium. The extensive luminal cell overexpression of both CKs in prostates with PCa indicates an increased pool of transient multiplying cells during prostatic neoplasia.

003

Intraductal carcinoma in prostate biopsies: diagnosis and prognostic impact

T. van der Kwast *, N. Al-Daoud, J. Thoms, M. Milosevic, R. Bristow
*University Health Network, Dept. of Pathology, Toronto, Canada

Objective: Intraductal carcinoma of the prostate has long been regarded as the intraductal spread of prostatic

adenocarcinoma. Its presence in radical prostatectomy specimens is regarded as an indicator of unfavourable disease. We investigated the prognostic significance of the presence of intraductal carcinoma in prostate biopsies prior to radiotherapy.

Method: HE-stained needle biopsies of 119 men with intermediate-risk prostate cancer were examined for the presence of intraductal carcinoma by two pathologists (TvdK, NAD). Univariate analysis only revealed PSA as a prognosticator. Kaplan–Meier analysis was performed with intraductal carcinoma as dichotomous variable. Biochemical recurrence after radiotherapy was the outcome parameter.

Results: Intraductal carcinoma was identified in 19% of the prostate biopsies based on the presence of demarcated rounded contours of ducts filled with neoplastic cells and the presence of basal cells at the peripheral rim (Fig. 1). Intraductal carcinoma was a strong independent prognosticator for early (< 36 months) biochemical recurrence (HR 8.9, CI95% 1.6–48.8, p=0.015).

Conclusion: Intraductal carcinoma can easily be identified in prostate needle biopsies. Its presence is a strong independent prognosticator for early biochemical failure after radiotherapy. If confirmed in additional studies, intraductal carcinoma should routinely be reported in prostate biopsies.

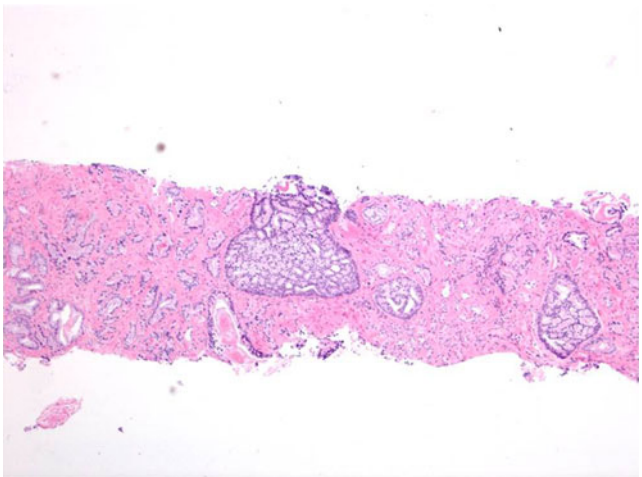

005

PCA3 mRNA expression in isolated HGPIN compared with cancer associated HGPIN

I. de Torres *, M.T. Quiles, M.A. Arbós, C. Blazquez, A. Doll, J. Reventos, J. Morote

*Hospital Vall d´ Hebron, Dept. of Pathology, Barcelona, Spain

Objective: PCA3 is a new marker highly specific in relation to the PSA gene in post-prostate massage urine that is useful in ruling out prostatic carcinoma after a negative prostate biopsy. Recent data suggest a lower efficacy of PCA3 score in men with HGPIN in previous biopsy. The aim of this study was to determine the differences in PCA3 gene expresión between isolated and cancer-associated HGPIN (I-HGPIN vs CA-HGPIN).

Method: Total mRNA was isolated and amplified from laser-assisted microdissected foci of benign prostatic tissue (BT), prostatic carcinoma (PC) and AC-HGPIN from 15 radical prostatectomy frozen specimens and I-HGPIN from 13 radical cistoprostatectomy parafin-embedded blocks of patients with bladder cancer. PCA3 mRNA levels were measured by real-time qPCR. The results were analysed with Friedman and post-hoc Dunn's multiple comparison tests.

Results: PCA3 mRNA expresion was detected in 80% of BT, 86.7% of AC-HGPIN and 92.9% of PC. Qualitative PCA3 mRNA expresión was detected in 61.5% of I-HGPIN samples. PCA3 mean quantitative expresión was 20.7-fold increased (p=0.0002) in AC-HGPIN and PC related to BT.

Conclusion: PCA3 mRBNA expression is significantly increased in CA-HGPIN lesions as well as qualitatively expressed in I-HGPIN lesions supporting that a specific threshold of PCA3 should be established in those patients.

006

PAX8 and AMACR reliably distinguish Xp11.2 translocation renal cell carcinoma from alveolar soft part sarcoma and renal epithelioid angiomyolipoma/PEComa

A. Laury *

*Brigham & Women´s Hospital, Dept. of Pathology, Boston, USA

Objective: Xp11.2 translocation renal cell carcinoma (tRCC), alveolar soft part sarcoma (ASPS), and renal epithelioid angiomyolipoma/PEComa (eAML) have overlapping morphologic features and can be difficult to distinguish especially when presenting as a metastasis. tRCC and ASPS are known to contain TFE3 gene rearrangements, leading to an overexpression of the TFE3 protein. Recently, TFE3 expression has also been reported in a subset of PEComas. The goal of this study was to determine if a panel of immunostains, including PAX8 and PAX2, can discriminate tRCC from ASPS and eAML.

Method: Six of each tumor were immunostained for PAX8, PAX2, TFE3, AMACR, and RCC antigen. PAX8, PAX2, and TFE3 were evaluated for nuclear staining, whereas cytoplasmic/membranous staining was considered positive for AMACR and RCC.
Results: All tRCCs were positive for PAX8; two were positive for RCC. In contrast, only three tRCCs were weakly positive for PAX2. All ASPSs and eAMLs were completely negative for PAX8 and PAX2. AMACR was diffusely positive in all tRCCs, but only one ASPS and no eAMLs. TFE3 was diffusely positive in all ASPSs and five tRCCs, and none of the eAMLs.
Conclusion: Strong and diffuse immunoreactivity for PAX8 and AMACR reliably distinguishes tRCC from ASPS and renal eAML.

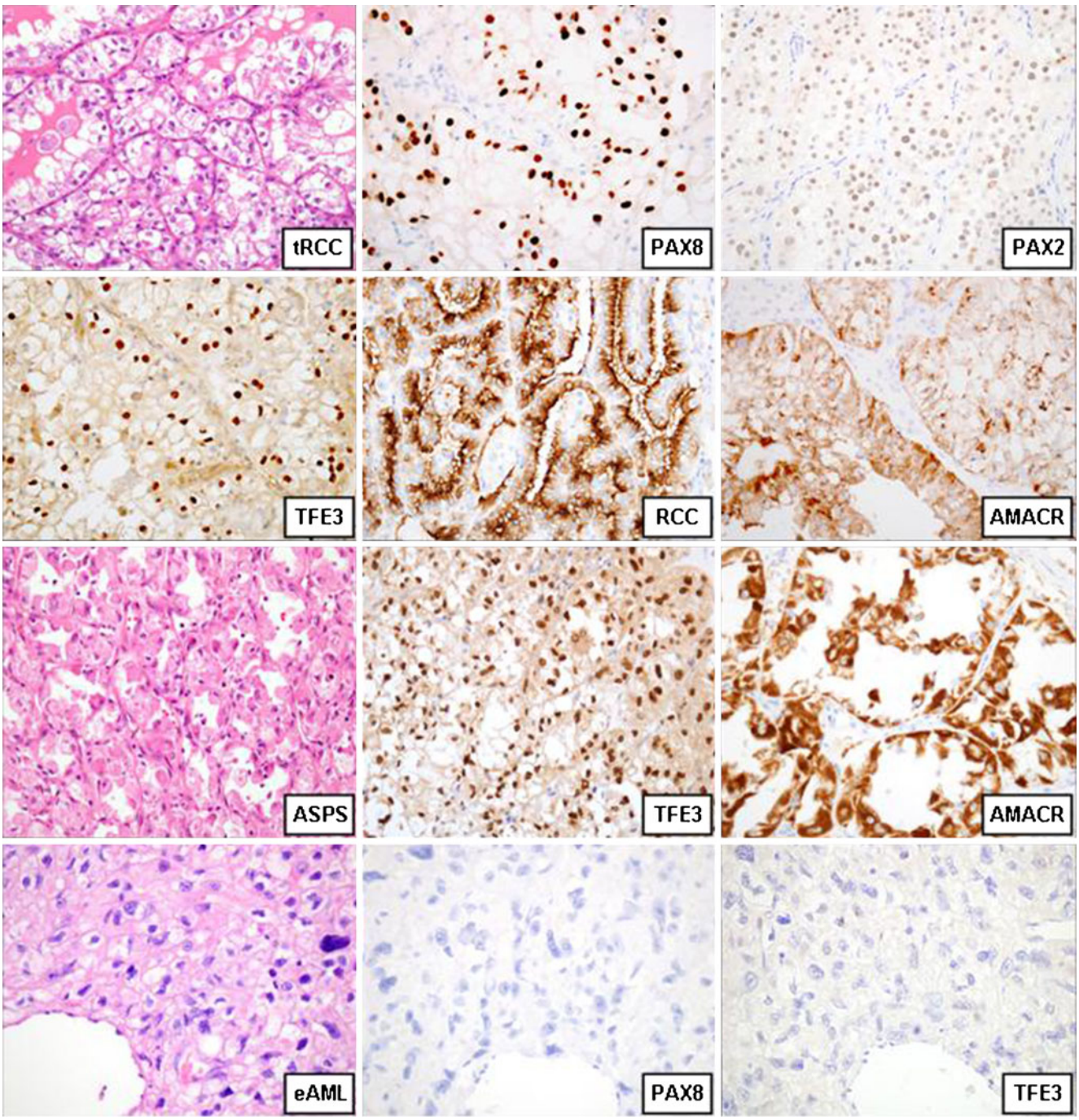

007

Modified UroVysion FISH scoring criteria increase the urothelial carcinoma detection rate in case of equivocal urinary cytology

E.-J. Speel *, C. Huysentruyt, M. Baldewijns, A. Ruland, R. Tonk, P. Vervoort, K. Smits, C. van de Beek
*Maastricht UMC, The Netherlands

Objective: UroVysion is a four-target fluorescence in situ hybridisation (FISH) technique to detect urothelial carcinoma (UC) in urinary cytology. The aim of this retrospective study is to investigate the UC detection rate of a modified UroVysion test in patients with equivocal urinary cytology. The modification comprised the addition of a cytological pre-screening technique and different evaluation criteria.
Method: A thin-layer slide was prepared of the residual urine sample of 82 patients with equivocal urinary cytology, pre-stained and pre-screened to confirm the presence of atypical urothelial cells. The same slide was used for the UroVysion test and scored according to different evaluation criteria. Results were compared with the outcome of cystoscopic and histologic findings.
Results: UroVysion detected 68% of the UCs when the manufacturer's evaluation criteria were applied. In case of altered evaluation criteria, the sensitivity increased to 81% when at least one copy number change of a probe target was considered as a positive test. The specificity only decreased from 84% to 82%.
Conclusion: Our data suggest that the sensitivity of the UroVysion test can be increased with the addition of a cytological pre-screening technique prior to the UroVysion test and a modification of the UroVysion evaluation criteria.

008

Intra- and periprostatic lymphatic vessels and their role in the propagation prostatic adenocarcinomas

P. Stoemmer *, P. Torres Galea
*Forschungslabor Pathologie, Gemeinschaftspraxis Pathologie, Augsburg, Germany

Objective: The zonal architecture of the prostate was rediscoverd by McNeal (1968); the intra- and periprostatic distribution in normal and neoplastic prostate is largely unknown in spite of their oncological importance.
Method: A total of 20 FFPE prostates (each 40–50 blocks) were stained with lymphatic vessel marker D2-40 (DCS Hamburg, Germany), strictly oriented and analysed for localisation, direction and diameter of lymphatic vessels.
Results: The density of intraprostatic lymphatic vessels is low. The lymphatic vessels of the transition zone are small, oriented parallel to the urethra and drain to the lymphatics of the prostatic apex and (perhaps less) to the mural lymphatics of the bladder: they do not connect to central and peripheral lymphatics. Central zone shows in its apical part paraurethrally oriented vessels, and in the basal parts radially oriented lymphatic vessels, draining into the radial-oriented lymph vessels of the peripheral zone. In the outer, subcapsular muscle coat of the prostate, the lymphatic vessels show a circumferential orientation, draining the lymph to the large network of vertically oriented lymphatic vessels in the vicinity of seminal vesicles and pelvis.
Conclusion: Various patterns of intraprostatic tumour propagation and the importance of lymphangiosis carcinomatosa near the seminal vesicle and the invasion of apex prostatae are deduced by localisation and connections of the lymphatic vessels.

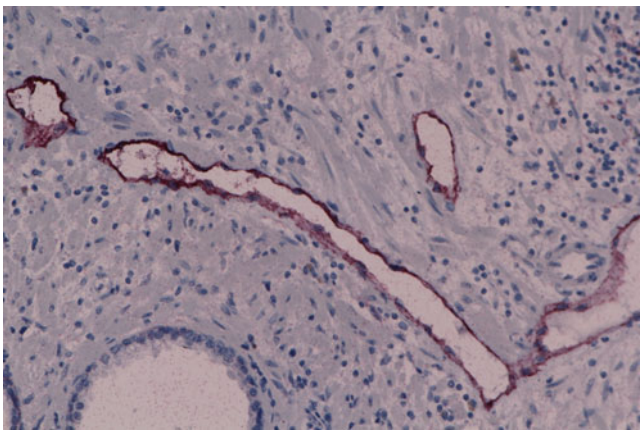

Poster Sessions

Sunday, 28 August 2011, 09.30–10.30 and 16.30–17.00, Hall 5

PS-01 Poster Session Breast Pathology

001

Clinical impact of Her-2 assessment in minor morphological subtypes of breast carcinoma by ASCO/CAP guidelines

E. Brunello *, M. Brunelli, A. Nottegar, E. Manfrin, S. Pedron, E. Vittoria, M. Chilosi, S. Gobbo,
G. Martignoni, F. Bonetti
*University of Verona, Pathology and Diagnostic, Italy

Objective: Minor morphological subtypes (non-ductal, non-lobular) breast carcinomas represent around 10–15% of cases. To address the paucity of information concerning HER-2 amplification for minor subtypes according to new ASCO/CAP cutoffs, we studied a series of non-ductal non-lobular breast cancer.
Method: There were 41 cases of minor subtype of breast carcinoma: six medullary, two adenoid cystic, five apocrine,

five signet ring, five mucinous, five tubular, three small cell, ten papillary were studied. We evaluated HER-2/neu status by comparing the original FDA and new ASCO/CAP scoring systems. HER-2 immunoexpression was analyzed by using Hercept Test and in cases (2+) we assessed the Her-2/neu status by FISH.
Results: All tubular, mucinous, squamous, medullary, papillary, adenoid cystic did show a negative Her-2 value at both IHC (0–1+) and FISH (−) levels using both FDA and ASCO/CAP cutoffs. Signet ring, apocrine and small cell carcinomas showed a discordance between cutoffs with a heterogeneous selection to therapy.
Conclusion: The Her-2 assessment in minor (non-ducta, non-lobular) subtypes of breast carcinoma by ASCO/CAP guidelines does not overall change the rate of patients candidated to trastuzumab therapy. A better selection of this cohort of patients to targeted therapy resides in new cutoffs or probably in other correlated biological characters.

002

Ki-67 labeling index by molecular subtype of breast cancer

A. Abolins *, I. Strumfa, I. Melbarde-Gorkusa, G. Trofimovics, E. Miklasevics, J. Gardovskis
*Hereditary Cancer Institute, Dept. of Pathology, Riga, Latvia

Objective: Ki-67 protein is used as proliferating cell marker. In breast cancer (BC), despite the large number of publications, there is still a lack of publications characterising Ki-67 expression.
Method: Consecutive BC cases were identified by archival search, examined by BC protocol, fixed and processed routinely. The expression of Ki67 was routinely assessed by immunohistochemistry (IHC) with monoclonal MIB1 antibody. Molecular subtype (luminal A, luminal B, HER2 positive or triple negative) was determined using estrogen and progesterone receptor, HER2 expression data by IHC as well.
Results: A total of 381 cases of female invasive BC were identified (2008–2010). The distribution of molecular subtypes was as follows: luminal A constituted 69.3% [95% confidence interval 64.4–73.7], luminal B 4.7% [3.0–7.3], HER2 positive 9.7% [7.1–13.1] and triple negative—16.3% [12.6–20.3] of all cases. The mean Ki-67 labelling index in luminal A group was 15.9% [14.1–17.7], luminal B—20.6% [12.0–29.2], HER2 positive—41.6% [33.6–49.6] and triple negative—58% [50.8–65.2].
Conclusion: (1) Ki67 labelling index correlates with breast cancer molecular subtype. (2) Triple negative and HER2 positive breast cancers show statistically significantly higher Ki67 labelling index than luminal subtypes.

003

Comparative analysis of cytokeratin 5/6 expressing breast cancer by histology and molecular subtype

A. Abolins *, I. Strumfa, I. Melbarde-Gorkusa, G. Trofimovics, E. Miklasevics, J. Gardovskis
*Hereditary Cancer Institute, Dept. of Pathology, Riga, Latvia

Objective: Breast cancer (BC) is morphologically, molecularly and prognostically heterogeneous group of tumours. The expression of basal markers as cytokeratin 5/6(CK5/6) has been associated with worse prognosis than luminal subtypes. However, controversial data exist.
Method: Archive search was employed to identify consecutive invasive BC cases. By IHC, molecular subtype (luminal A, luminal B, HER2 positive or triple negative) and CK5/6 expression was determined. Diffuse strong cytoplasmic CK5/6 expression was considered positive.
Results: Among the identified 158 BC cases, 23 cases (15.9%) expressed CK5/6. The patients were female with a mean age of 59.7 years. In CK5/6+ group, ductal BC constituted 69.6%, including 81.2% G3 tumours; lobular BC constituted 17.4%, medullary BC 8.7%, but undifferentiated BC was one case (4.3%). The CK5/6+ positive BC were classified as luminal A subtype in 47.8%, luminal B 0%, HER-2 positive 8.7% and triple negative 43.5% of cases. Among triple negative BC, CK5/6+ was present in 43.4% [25.6–63.1], but in other molecular subtypes it was 10.7% [6.3–17.3].
Conclusion: (1) Majority of CK5/6+ tumours were invasive poorly differentiated ductal cancer. (2) The CK5/6 expression is significantly more frequent in triple negative breast cancer.

004

Dermatofibrosarcoma protuberans of the breast following remote flap coverage for old trauma

S. Amr *, A. Joudeh
*King Fahad Specialist Hospital, Pathology and Laboratory, Dammam, Saudi Arabia

Objective: Dermatofibrosarcoma protuberans (DFSP) is an uncommon locally aggressive low-grade malignant soft tissue tumor with a high recurrence rate. It is quite rare to have this tumor involving the skin of the breast. We report herein a case of DFSP of the breast with a review.
Method: Case report: A 47-year-old Saudi Arabian female who had a history of flap coverage for an old trauma 23 years earlier presented with a painless lesion in the skin of the left breast at the site of the scar of the earlier surgery. Computerized tomography showed a nodular thickening of the skin of the breast. Tru cut biopsy of the lesion followed

by simple mastectomy with local flap coverage was performed.
Results: Tru cut biopsy showed a fibromyxoid lesion with many spindle cells and rare mitoses. The mastectomy specimen showed a protruding lobulated nodular skin lesion measuring 11×10 cm. Sectioning showed a homogenous white rubbery tumor involving the dermis and the subcutaneous fat. Histologically, it showed spindly cells with a storiform pattern and infiltrative edges, encasing skin appendages. The tumor cells stained positively for CD34.
Conclusion: About 12 cases of DFSP of the skin of the breast had been reported in the literature. This is an additional case that occured at the site of the scar of skin flap for the treatment of an old trauma.

005

Pleomorphic malignant fibrous histiocytoma-like sarcoma of the breast with intracytoplasmic hyaline globules

S. Amr *, A. Joudeh
*King Fahad Specialist Hospital, Pathology and Laboratory, Dammam, Saudi Arabia

Objective: The so-called malignant fibrous histiocytoma (MFH) of the breast with pleomorphic features is a very rare tumor. It can occur de novo, in association with cystosarcoma phyllodes or post-radiotherapy for carcinoma of the breast. We report a rare case without history of radiotherapy or associated phyllodes tumor which exhibited peculiar intracytoplasmic hyaline globules that was positive for alpha 1 antitrypsin by immunohistochemistry.
Method: Case report: A 54-year-old post-menopausal single Saudi Arab female presented with a huge fungating left breast mass with ulceration of the skin of several months' duration. Palliative mastectomy was done following a core breast biopsy. Axillary lymphadenectomy was done.
Results: A huge fungating breast mass measuring 17×14×7 cm was seen with extension to the skin and associated ulceration. Fleshy tumor nodules beneath the skin and within the parenchyma were present. Histologically, there were large pleomorphic cells with bizarre or multilobated nuclei and many atypical mitoses seen. Many tumor cells show intracytoplasmic eosinophilic hyaline globules of variable sizes. Tumor cells were positive for immunohistochemical stains for vimentin, CD68 and alpha 1 antitrypsin. The later stained the globules as well. Stains for cytokeratins were negative.
Conclusion: This is an unusual breast sarcoma with intracytoplasmic eosinophilic globules. Such globules had been recorded only once in a case of post-radiation sarcoma of the breast.

006

Chromosome 17 centromere duplication is associated with poor prognosis in patients with invasive breast carcinomas exhibiting normal TOP2A status

Y.-K. Bae *, A. Kim, S.-H. Kang, S.-J. Lee, M.-K. Kim, S.-Y. Kwon, H.-R. Jung, J.-Y. Park
*Yeungnam University, Dept. of Pathology, Daegu, Republic of Korea

Objective: Although topoisomerase II alpha encoded by TOP2A gene is known as a major target of anthracyclines, analysis for the benefit of anthracyclines in patients with TOP2A alteration (either amplification or deletion) or TOP2A protein expression has given conflicting results so far, and there is a paucity of literature on the association of chromosome 17 centromere (CEP17) duplication with survival. The aim of this study was to investigate the prognostic significance of TOP2A alterations and CEP17 duplication in patients with invasive breast cancers.
Method: We performed single-color silver-enhanced in situ hybridization (SISH) assay for CEP17 and TOP2A on 594 invasive breast cancer samples.
Results: Amplification of TOP2A was observed in 49 (8.6%) cases and deletion of TOP2A in 63 (11.1%) of 569 informative cases. A total of 457 (80.3%) cases had normal TOP2A status. TOP2A alteration was significantly associated with a high histological grade, ER negativity, PR negativity and HER2 overexpression. Duplication of CEP17 was observed in 190 (33.4%) cases and associated with a high histological grade and HER2 overexpression. In univariate analysis, TOP2A status did not predict either overall survival or disease-free survival (DFS) in patients who received anthracycline-based chemotherapy. Duplication of CEP17 was associated with a worse DFS in patients with tumors exhibiting normal TOP2A status. In multivariate analyses, CEP17 duplication was independently predictive of poor DFS. However, its prognostic significance was lost in patients with tumors exhibiting TOP2A alterations.
Conclusion: In conclusion, this study suggests that CEP17 duplication could be a prognostic biomarker in patients with invasive breast cancers exhibiting normal TOP2A status.

007

Are simultaneous foci morphologically and clinically different in multiple breast carcinoma?

M. Boros *, C. Marian, D. Soanca, M. D. Podeanu, S. Stolnicu
*Targu Mures, Romania

Objective: The purpose of our study was to determine the incidence of multiple breast carcinoma (2007–2009) and to

investigate the pathological and clinical differences between unifocal (UF) and multiple breast cancer.
Method: A total of 91 patients with multifocal breast cancer were compared in a retrospective study with 327 patients with unifocal tumors, correlating tumor size with lymph node metastasis. The reports of every patient were reviewed.
Results: A total of 91 (21.77%) of 418 patients had multiple breast cancer, and of these 67 women (73.62%) had axillary node involvement compared with 58.71% with unifocal tumors (p=0.01). The most frequent histologic type in both groups was infiltrating ductal carcinoma (69.23% in MF/MC vs 70.03% in UF). The histologic type of multiple invasive tumor was different in 12.08% of cases. A total of 46.15% of MF/MC cases were grade III, compared with only 33.02% of UF ones. The microscopic grade was different in nine cases (9.89%). Among them, in five cases (55.55%), the secondary foci were grade III.
Conclusion: Incidence of multiple breast carcinomas in Targu Mures is similar to that reported internationally. Since tumours foci with favourable histological type or microscopic grade were observed in association with tumor foci of more agressive morphology and higher grade, it is mandatory to report every tumor focus.

008

Detection of maspin and mammaglobin transcripts as circulating tumor cell markers in peripheral blood samples from breast cancer patients

G. Burkadze *, Z. Avaliani, I. Kureli, G. Turashvili, M. Gudadze
*Tbilisi State Med. University, Dept. of Pathological Anatomy, Georgian

Objective: Detection of circulating tumor cells (CTC) in peripheral blood may serve as a prognostic marker in breast cancer patients.
Method: We examined peripheral blood samples from 75 breast cancer patients and 15 healthy controls. Patient group consisted of 30 lymph node negative patients, 30 lymph node positive patients and 15 patients with distant metastases. Reverse-transcriptase polymerase chain reaction (RT-PCR) was used for the detection of maspin and mammaglobin mRNA as CTC markers.
Results: Neither maspin nor mammaglobin transcripts were detected in lymph node negative patients and healthy controls. Both transcripts were detected in one lymph node positive patient and seven patients with distant metastasis. Only mammaglobin transcript was detected in one lymph node positive patient and one patient with distant metastasis. All patients with CTCs were HER2-/ER-/PR-, except for one patient with HER2+/ER-/PR- tumour at M1 stage. Both mammaglobin positive patients were HER2+/ER-/PR-.
Conclusion: CTCs are more likely to be detected in patients with HER2-/ER-/PR- carcinoma. This may be useful for evaluation of prognostic and predictive factors in breast cancer patients. This study was supported by the research grant from the Georgia National Science Foundation #GNSF/ST08/6-461.

009

Paget Disease of the nipple associated with carcinoma in situ or without underlying carcinoma: clinical and pathological review of 31 cases

M. Cambão *, A. Afonso, N. Maia, P. Lopes, C. Silva, C. Leal
*Portuguese Oncology Institute, Dept. of Pathology, Porto, Portugal

Objective: Nipple's Paget disease (PD) is a rare manifestation of breast carcinoma (1–2%), associated with erosive/eczematous lesions but with heterogeneous clinicoradiological presentation. Most cases have underlying high-grade carcinoma HER2+. This study evaluated the clinicopathological features of in situ carcinoma associated with PD and compared pTis with pTis DCIS/LCIS cases.
Method: A total of 31 PD cases staged as in situ carcinoma, diagnosed between 1990 and 2010, were retrieved from our files. Clinicopathological review and immunohistochemical study (hormonal receptors; HER2) were performed.
Results: Two groups were observed: PD associated with ductal carcinoma in situ (PD-DCIS, n=28) and PD with skin involvement alone (PD-S, n=3). Most (26/28) PD-DCIS presented as nipple lesions. Abnormal radiological findings were found in 7/15. All cases had nipple ducts involvement and 6/28 had >4 cm. High nuclear grade was found in 26/28; 24/28 were HER2+ and 6/28 estrogen receptor+. The 3 PD-S cases showed Paget cells with similar features. One of them had a single cutaneous recurrence 10 years after conservative surgery.
Conclusion: Morphologic features of PD are similar in PD-DCIS and PD-S. DCIS associated with PD shows a more homogeneous morphology and HER2-expression than those described for invasive carcinoma. Isolated skin involvement of PD reinforces the possible skin origin in some cases.

010

Lymph node staging in breast cancer: comparative study between total vs partial sampling of the lymph nodes

F. Climent *, N. Villena, A. Petit, M. T. Soler, I. Alarcón, E. Benito, A. Garcia Tejedor, A. López Ojeda, E. Condom
*L´Hospitalet de Llobregat, Spain

Objective: The axillary lymph node (ALN) staging (pN) is one of the most important prognostic factors in breast cancer. According to CAP 2009, sampling of LN must be adequate to detect macrometastasis. They also recommend slicing thinly each node at 2 mm. Our aim was to compare the LN staging when we performed total or partial sampling.
Method: We performed total sampling of the ALN for 1 year. Each node was thinly sliced at 2 mm, and all slices were submitted for microscopic examination. One H&E level was examined. The pathology report included the number of metastasic LN (macrometastasis, micrometastasis and isolated tumor cells), the size of the biggest metastasis and the pN staging. These parameters were studied first in an unselected slice and second, after examining the whole LN. Finally, we compared the results between the two methods.
Results: We prospectively analyzed 142 ALN dissections. The median number of LN was 19.7. The LN staging was concordant and discordant in 121 (85%) and 21 (15%) cases, respectively. We detected an increase in the number of metastasic LN in this 21 discordant cases and we detected an increase in the LN staging in 13 (62%) out of 21 cases.
Conclusion: In our study, the total sampling of the ALN showed an increase of the LN staging in 9% of the cases.

011

BRCA 1 Protein expression in human breast cancer

M. V. Comanescu *, C. Ardeleanu, C. Iosif
*Voctor Babes Institute, Dept. of Pathology, Craiova, Romania

Objective: BRCA1 gene mutations are responsible for 40–50% of hereditary breast tumors. BRCA1 gene is the first described in association with susceptibility to breast cancer. Tumors occurring in carriers of BRCA1 germ mutation have many common phenotypic, immunohistochemical and clinical features. The aim of this study was to identify the BRCA 1 protein expression and possible correlation with the histologic and immunophenotypic properties.
Method: We interpreted as positive reactions for BRCA1 nuclear and/or cytoplasmic staining in over 10% of tumor cells. The presence of only nuclear staining was not identified in this study. The presence of a weak staining of the stroma was considered background.
Results: Our study included 354 patients with invasive carcinomas with a mean age of 57.39 years old. Detailed histologic review was performed on all cases. We also identified different immunohistochemical patterns wich were correlated to the BRCA1 expression. The reaction for BRCA1 was identified in the in situ component, as well as in the invasive one. In positive cases, we identified the presence of BRCA1 staining at both nuclear and cytoplasmic in 28.57% cases. Exclusively cytoplasmic staining was recorded in 19.04% of cases.
Conclusion: The identification of BRCA1 together with clinicopathological data is important as it has an impact on therapeutic recommendations.

012

Effects of high corn oil and olive oil diets on clinical and histopathological features and on p21Ha-Ras expression in dimethylbenz(*a*)anthracene (DMBA)-induced rat mammary carcinomas

I. Costa *, M. Solanas, R. Moral, M. C. Ruiz de Villa, R. Escrich, F. J. Andreu, E. Escrich
*UDIAT-CSUPT, Dept. of Pathology, Sabadell, Spain

Objective: Dietary lipids influence breast cancer. We investigated the clinical and histopathological (HP) effects, and on p21HaRas expression, of two high-fat diets on DMBA-induced mammary carcinogenesis.
Method: Three groups of 20 Sprague–Dawley rats each had: low-fat (LFCO), high-fat corn oil (HFCOP), and high fat extravirgin olive oil (HFOOP), given 5 mg DMBA at 53 days. Analysis of latency time (LT), tumour incidence (TI) and total and rat tumour yield (TTY, RTY), of seven HP parameters and of rat mammary carcinomas grading method. Immunohistochemistry (antip21HaRas) evaluated with NOESISVISILOG5.1.
Results: HighCO diet reduced LT (77.3±32.1) and increased TI (90%), TTY (95) and RTY (3.5). HFOOP displayed similar LT (102.3±47.4), higher TI (80%) and lower TTY (69) and RTY (2.5) than LFCO (102.5± 42.3;70%;72 and 3). LFCO adenocarcinomas exhibited lower histological grade (72.5% grade1) and profile than HFCOP (59.3% grade1) and were similar to HFOOP (64.2% grade1). No differences in p21Ha-Ras expression among dietary groups but a significant p21HaRas decreasing expressions as grade increased were noted (grade 1, 56.69% positive; grade 3, 43.1%), except in HFOOP.
Conclusion: Dietary lipids influence the clinical and morphological characteristics of experimental mammary carcinogenesis, without altering p21HaRas expression, which could be affected by the malignancy of tumours, probably through a posttranslational event.

013

Breast cancer in women under 40 years of age: an audit of 142 cases from an anticancer hospital in Greece

H. Trihia *, P. Tziakou, D. Condylis, I. Lekka, I. Iakovidou, P. Dadioti-Arapantoni
*Metaxa Cancer Hospital, Piraeus, Greece

Objective: Breast cancer in young women is reported to be more aggressive compared to older breast cancer patients.
Method: Our study included 45 patients aged 26–35 ('very young') and 97 patients aged 36–40 ('less young') for the period 2000–2010.
Results: The most frequent tumour grade was grade III (55.5% vs 67%) followed by grade II (35.5% vs 24.7%) and grade I (2.2% vs 5.1%). The most common histological tumour type was invasive ductal carcinoma (71.1% vs 76.2%). Most of the tumours were T1 (33.3% vs 43.2%) and T2 (40% vs 43%) and less T3 (11.1% vs 7.2%). The nodal status was N0 (22.2% vs 29.8%), N1 (17.7% vs 30.9%), N2 (13.3% vs 18.5%) and N3 (4.4% vs 4.1%). There were tumour emboli in mean 43.3%. The molecular subtype distribution was luminal A (46.6% vs 43.2%), tripple negative (24.4% vs 19.5%) and Her-2+(20% vs 19.5%).
Conclusion: There were no particular differences between the two age groups. Young women were more likely to have endocrine-responsive tumours, most often of a higher grade, with tumour emboli and of ductal type.

014

Metaplastic breast carcinoma with chondroid differentiation in a 45-year-old woman

C. Dias *, F.E. Costa, D. Esteves, I. Leal, C. Lopes, P. Farrajota
*Porto, Portugal

Objective: Metaplastic carcinomas account for less than 1% of invasive mammary carcinomas and are characterized by an admixture of adenocarcinoma with dominant areas of spindle cell, scamous, and/or mesenchymal differentiation.
Method: We report the case of a 45-year-old woman who noticed a lump in her right breast.
Results: Patient's personal and family histories contained nothing of significance. Physical examination revealed a firm mass of about 2 cm and mammography unveiled a focal asymmetric density, in the lateral-upper quadrant of the right breast. The diagnostis by core biopsy was: metaplastic carcinoma with chondroid differentiation. The specimen obtained by conserving surgery showed a lesion of 2.3 cm with solid and cystic areas containing glistening-white and myxoid tissues. Histological examination showed co-existing malignant epithelial components (intraductal carcinoma comedo type and invasive ductal carcinoma) and mesenchymal malignant components (condrosarcoma and undifferentiated sarcoma). Immunohistochemical study showed that the tumor cells had the characteristics of epithelial cells and mesenchymal cells and were positive for basal cell markers, negative for p53 and negative for estrogen receptor, progesterone receptor and Her2.
Conclusion: Metaplastic breast carcinoma is an aggressive breast cancer subtype that is unlikely to respond to conventional hormone therapy and anti-Her2 therapies. Nevertheless, it frequently over-expresses EGFR and, thus, may respond to EGFR inhibitors.

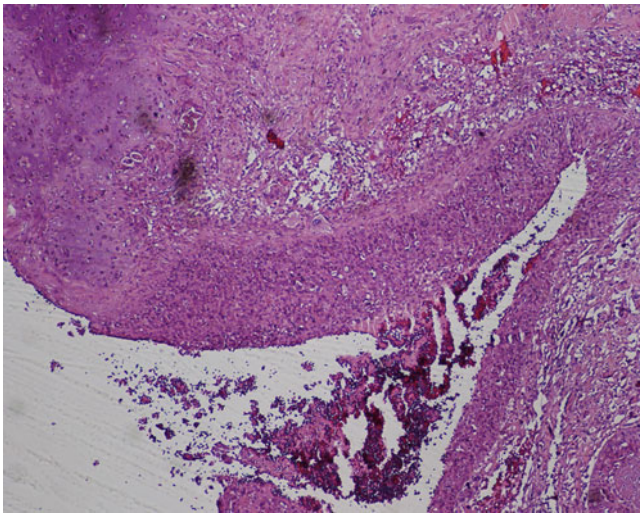

015

Validation by multiplex ligation-dependent probe amplification (MLPA) of UK NEQAS ICC & ISH breast cancer cell-lines for use in HER2 external quality assessment: a feasibility study

A. Dodson *, C. Moelans, P. van Diest, K. Miller, M. Ibrahim
*Royal Liverpool Hospital, Dept. of Cellular Pathology, UK

Objective: MLPA may be used to determine relative gene dosage; it has begun to be used in clinical diagnostics to establish HER2 gene amplification status in breast cancer. We examined the feasibility of using breast HER2 EQA cell-lines, previously characterised by immunocytochemistry (ICC) and in situ hybridisation (ISH), for EQA of HER2 gene status testing by MLPA.
Method: Formalin-fixed paraffin-embedded samples of four breast cancer cell lines (see Table) were sectioned on to slides. Samples from each cell line were individually isolated, DNA extracted and MLPA for HER2 gene amplification performed. The results were compared with protein and gene expression levels obtained by ICC and fluorescent ISH (FISH) on samples from the same batch that was used for MLPA.
Results: There was good concordance between all methodologies. All reported SK-BR-3 as positive/amplified, and MDA-MB-175 and MDA-MB-231 as negative/non-amplified. MDA-MB-453 was reported as equivocal by ICC and varyingly as borderline: non-amplified, borderline: amplified or amplified by different UK NEQAS reference centres by FISH; it was amplified by MLPA.

Conclusion: The cell lines used in EQA of HER2 ICC and ISH could also be used in MLPA. MLPA verified results obtained by ICC and ISH, and may also provide more accurate testing compared to FISH in equivocal (ICC 2+) cases.

Cell line	Protein expression by ICC	Gene amplification		
		Copy number by FISH	Ratio by FISH	Copy number by MLPA
SK-BR-3	3+	9.45-15.30	3.18-4.89	7.30
MDA-MB-453	2+	4.18-5.68	1.87-2.49	2.48
MDA-MB-175	1+	2.35-3.05	1.06-1.34	1.07
MDA-MB-231	0	1.85-2.37	0.90-1.25	1.15

016

Identification of the stroma of normal breast tissue and in breast cancer based on analysis of recombination of cellular microenvironment around vegetative nerve component of communication systems

A. Dorosevich *, S. Abrosimov
*Smolensk Institute of Pathology, Russia

Objective: Association of structural changes in epithelium and stroma of breast cancer (BC) may become markers of cancer.
Method: A total of 20 samples of normal breast tissue (NBT) and 30 samples intraductal infiltrating BC were morphometricaly studied. Absolute values of stroma cells were counted around vegetative nerve terminals (VNTs), which were revealed by treatment with paraformaldehyde and acetylcholiniodyde. Statistical analysis of frequencies of recombination around VNTs was done. The decision rule was worked out based on A. Vald's algorithm.
Results: Heterogeneity of similar cellular populations around adrenergic (AVNTs) and cholinergic (CVNTs) was found. Supposed decision algorithm admitted to make a true identification of BC stromal component in 85%, based on cells around AVNTs, and in 90% around CVNTs. Mistakes of second kind (overdiagnosis)—in 10% and 0% cases. In analysis of NBT true decisions were made in 90% around AVNTs, and in 86.6% around CVNTs were mistakes of the first kind (hypodiagnosis)—in 3.3% and 6.7% cases.

017

An unusual case of metaplastic breast carcinoma in association with heterotophic ossification of tuberculous sequela in axillary lymph nodes

N. Dursun *, C. Kelten, M. Zengin, E.R. Bozkurt
*1st Education and Research H, Dept. of Pathology, Istanbul, Turkey

Objective: Metaplastic breast carcinoma is a heterogenous group of neoplasms generally characterized by admixture of ductal adenocarcinoma with dominant areas of squamous, spindle cell, and/or mesenchymal differantiation. Heterotopic ossification of tuberculosis sequela is a rare condition today.
Method: A 67-year-old woman presented to our hospital with 1 year history of left breast mass and hard palpable multiple axillary nodes.
Results: Modified radical mastectomy and axillary dissection was performed. At the gross examination there were subareolar hemorraghic, cystic 5.5 cm mass and 16 axillary lymph nodes extracted. Histopathologicaly examination showed pure epithelial metaplastic carcinoma composed with squamous and ductal carcinoma. Mature bone formation was seen at 12 axillary lymph nodes; the rest of the four were reactive. The detailed clinical history was taken and the patient told that she had been treated for tuberculosis lymphadenitis 38 years ago, and after infection the hard lymph nodes persisted. The lymph nodes with heterotopic ossification were accepted as tuberculosis lymhadenitis sequela.
Conclusion: Metaplastic carcinomas can be seen mixed epithelial/mesenchymal. The lymph node metastasis of metaplastic carcinoma is extremely rare and but can be occur. The heterotopic ossification in lymph nodes of tuberculosis sequela is extremely rare nowadays. The rare and unexpectable conditions must be interrogated such as our case.

018

Assessment of Aurora-A kinase expression in breast cancer for early diagnosis

I. Ferchichi *, S. Sassi, A. Baccar, R. Marrakchi, J.Y. Cremet, C. PRrigent, K. Benromdhane,
A. El-Gaaied Ben Ammar
*Tunis, Tunisia

Objective: Breast cancer is the most common type of cancer in women, it's a hormone related tumor with various grade and stage presentations. The oncoprotein Aurora-A plays a crucial role during mitosis. Some studies were performed to assess the expression rate of Aurora-A protein and to reveal its role in breast cancer.
Method: We investigate the expression and localization of Aurora-A protein kinase in relation with tumor emergence and progression in breast cancer. Aurora-A status was evaluated in 107 patients with confirmed breast cancer using immunohistochemistry.
Results: The experimental findings showed that high expression of this protein was correlated with nuclear grade, expression of progesterone receptor and nodal status. The experimental results showed also that the localization of this kinase shift from cytoplasm in nonmalignant adjacent tissue to both cytoplasmic and nuclear compartment in tumoral tissue, suggesting an oncogenic role of the nuclear accumulation. We have additionally detected the overexpression of this protein in nonmalignant adjacent

tissue; cells with healthy appearance could begin early to overexpress this protein before the malignant processing is histopathologically observable.
Conclusion: The expression of the Aurora-A kinase in nonmalignant tissue may represent an earlier diagnosis tool for breast cancer.

019
GATA3 expression increases in hormone-dependent infiltrating ductal carcinoma progression

P. L. Fernandez *, J. Calvo, R. Bermudo, L. Sanchez Cid, M. Marín, L. Gelabert, M. Muñoz,
T. Thomson
*Hospital Clinic of Barcelona, Dept. of Pathology, Spain

Objective: GATA3 is a zinc-finger type transcription factor with an important role in breast development and luminal epithelial differentiation, having a tight relationship with estrogen receptors (ER) expression. In a previous microarray study, we observed a surprising upregulation of GATA3 expression in node-positive ductal infiltrating carcinomas with respect to node-negative ones. Our objectives were to determine the expression of GATA3 at the mRNA and protein levels in the progression of breast carcinomas and its possible clinicopathological implications.
Method: qRT-PCR and inmunohistochemical analyses for GATA3 expression were performed in normal breast (n=9), ductal in situ carcinoma (n=6), node-negative (n=32) and node-positive infiltrating ductal carcinomas (IDC) (n=96) and both lymph node (n=89) and distant metastases (n=16). Microdissection was performed in selected cases.
Results: GATA3 immunohistochemical expression correlated with ER positivity and with lower tumour grade. Both qRT-PCR and immunohistochemistry demonstrated significant overexpression of GATA3 in node-positive tumours when compared to node-negative ones in ER-positive cases, and this upregulation was maintained in lymph node and distant metastases.
Conclusion: GATA3 expression, although correlating with ER expression and luminal differentiation, might have a role in the progression of breast IDC towards an aggressive phenotype and in regional and distant metastases development, which seems to contradict its proposed antioncogenic capacity.

020
PI3K/Akt pathway alterations as a mechanism of resistance to trastuzumab in breast cancer

M. S. Fernández García *, I. Centeno Ramos, C. García Pravia, M. Balbín Felechosa, M. F. Fresno Forcelledo
*Hospital Central de Asturias, Dept. de Anatomía Patológica, Oviedo, Spain

Objective: There is a significant percentage of patients with metastatic breast cancer and HER2 receptor overexpression that do not respond to trastuzumab-directed therapy. Several mechanisms that explain the resistance to trastuzumab therapy have been reported. The aim of this paper is to study the alterations of one of the HER2 signalling pathways related to trastuzumab response in breast cancer.
Method: The study comprised 57 cases of metastatic breast carcinoma with HER2 overexpression (HercepTest 3+) or gene amplification (FISH). All patients were treated with trastuzumab. The assessment of PTEN expression was based on staining intensity and percentage of stained cells. We also determined the molecular alterations in PIK3CA.
Results: Our series showed a statistically significant association between a positive expression of PTEN and a better treatment response rate (p=0.003), longer time-to-progression (p=0.014) and better overall survival from treatment onset with trastuzumab (p=0.008). The presence of PIK3CA mutations was associated with lower overall survival (p=0.031).
Conclusion: Our study showed that PTEN expression and PIK3CA mutations could be considered as both prognostic and predictive biomarkers in trastuzumab-treated breast cancer.

021
Giant pseudoangiomatous stromal hyperplasia of the breast in an 18-year-old woman

H. Fuentes Vaamonde *, M.T. Gonzalez Serrano, M. Medina Perez, Y.O. Rangel Mendoza, J. Salvatierra Cuenca, D. Benito Lopez, M.T. Caro Cuenca
*HURS, Dept. of Pathology, Cordoba, Spain

Objective: Tumoral pseudoangiomatous stromal hyperplasia (PASH) of the breast is a rare benign proliferation of mesenchymal cells with a characteristic appearance of anastomosing channels imitating vessels.
Method: An 18-year-old woman presented with a history of a rapidly growing mass in the right breast, with skin ulceration. Ultrasonography showed a homogeneous and circumscribed mass. Core-biopsy and later mastectomy were carried out.
Results: The surgical specimen measured 38×27×18cm and weighted 5,005 g. The tumoral mass measured 35 cm in biggest dimension. Margins were well defined. Microscopically, epithelial lobular and ductal structures were separated by mesenchymal tissue, which contained empty irregular anastomosing spaces in a dense collagenous stroma, without fatty tissue, imitating vascular channels. The cells lining these spaces were CD34 positive and CD31 negative.
Conclusion: PASH is a benign, localised, mesenchymal proliferative lesion with possible hormonal aetiology. Characterised by the presence of slit-like spaces in dense collagenous stroma, Tthe spaces are lined by benign spindle cells with myofibroblastic differentiation. It has an excellent

prognosis. Local surgical excision with appropriate margins is the recommended treatment. Well-differentiated angiosarcoma is the most important differential diagnosis.

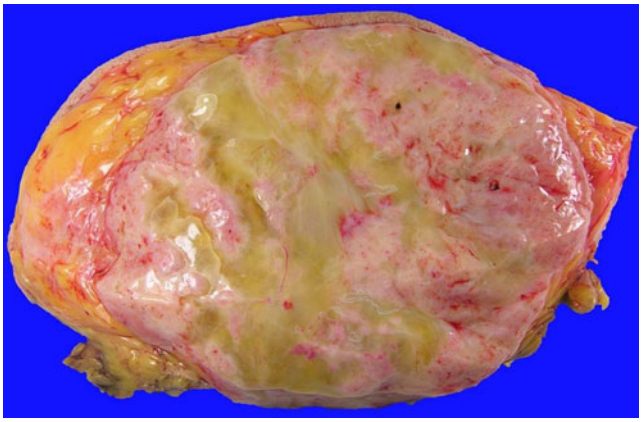

022

Reproducibility study of biomarkers in routine clinical use in breast cancer patients in Sweden

V. Gaspar *, M. Fernö
*Helsingborg, Sweden

Objective: In breast cancer patients biomarkers are used to decide which patients should be offered systemic adjuvant therapy. Hence, it is of great importance that the different pathology laboratories produce equivalent results.
Method: Slides from tissue micro-arrays with cores of 2 mm from 16 primary invasive breast cancer cases were sent to 28 laboratories in Sweden, all of which performed biomarker analysis at a daily basis. The laboratories performed immunohistochemistry for estrogen- and progesterone receptor, Ki67 and HER2 protein and in situ hybridization for the HER2 gene using their routine analysis.
Results: Results of the estrogen and progesterone receptors showed overall agreement of 98% and 84% and kappa of 0.96 and 0.69, respectively. Test of Ki67 resulted in overall agreement of 87% and kappa of 0.74. For HER2 protein staining overall agreement was 96% and kappa 0.91. In situ hybridization of HER2 showed an overall agreement of 87% and kappa of 0.72, including a category with equivocal results.
Conclusion: Biomarker analysis in Sweden is well reproducible assuring uniform basis for decision of adjuvant treatment among Swedish breast cancer patients.

023

Expression of claudins in breast cancer: high or low, what to expect?

R. Gerhard *, S. Ricardo, J. F. Cameselle-Teijeiro, F. Schmitt, J. Paredes
*IPATIMUP, Dept. of Pathology, Porto, Portugal

Objective: The claudin-low subtype is a group of breast carcinomas presenting mesenchymal and stem cell features with low expression of claudins (CLDNs)-3, -4, -7 and E-cadherin. However, several authors described that the high expression of CLDNs is also associated with aggressive clinical and biological behaviour. Our aim was to assess the expression pattern of CLDNs in invasive breast carcinomas.
Method: Immunohistochemical technique was performed to analyze the expression of CLDN-1, -3, -4 and −7 in 466 invasive breast carcinomas.
Results: We found a significant correlation between the high levels of expression of CLDN-3 and CLDN-4 and high tumour size, high histological grade and lymph node metastasis. Moreover, we found a significant correlation between CLDN-3/CLDN-4 positivity and ER negative tumours and the expression of the basal markers CK5 and P-cadherin. A total of 67.8% of the triple negative tumours have shown a high expression of CLDN-3 and/or CLDN-4, which was also significantly associated with poor patient survival.
Conclusion: We were able to detect a group of breast carcinomas with high expression of CLDN-3 and CLDN-4 that was associated with worse clinical–pathological findings and poor patient survival. CLDN-3 and CLDN-4 may have a putative role as important biomarkers in breast cancer.

024

Immunohistochemical expression of claudins in metaplastic breast cancer

R. Gerhard *, S. Ricardo, A. Albergaria, M. Gomes, A.R. Silva, A.F. Logulo, J. Paredes, F. Schmitt
*IPATIMUP, Dept. of Pathology, Porto, Portugal

Objective: The claudin-low subtype is a group of breast carcinomas with low expression of claudins (CLDNs)-3, -4, and -7. Around one third of claudin-low tumors were histologically characterized as metaplastic breast carcinoma (MBC). We intended to analyze the expression of CLDN-1, -3, -4 and -7 in a series of MBC.
Method: Sections from 13 cases of MBC were immunostained for CLDN-1, -3, -4 and 7. The expression of CLDNs was analyzed in the different components of the tumors.
Results: Weak membrane immunostaining of the epithelial neoplastic cells for CLDN-1, -3, -4 and -7 was present in 53.8%, 30.8%, 53.8% and 15.4% cases of MBC, respectively. Cytoplasmic immunostaining was observed only for CLDN-4 and occurred in eight cases (61.5%) of the 13 MBC. This pattern of staining was also found in the spindle cells in three cases. Aberrant nuclear CLDN-4 expression

was present in eight cases and was found in the different metaplastic components.

Conclusion: Our series of MBC showed a low expression of CLDNs: the membrane immunostaining of the epithelial neoplastic cells for CLDN-1, -3, -4 and -7 was weak. Cytoplasmic CLDN-4 was present in the epithelial and spindle cells and aberrantly expressed in the nuclei of the epithelial and mesenchymal cells of MBC.

025

Expression of proteins involved in epithelial–mesenchymal transition in phylloides tumors of the breast

C. Geronatsiou *, D. Koumoundourou, I. Lilis, H. Papadaki, V. Zolota
*University Hospital of Patras, Dept. of Pathology, Greece

Objective: Phylloides tumor is a prototype biphasic fibroepithelial neoplasm. Epithelial–mesenchymal transition (EMT) is a procedure that endows tumor cells with migratory and invasive properties during which cells downregulate E-cadherin expression, translocate β-catenin in the nucleus and express proteins characteristic of mesenchymal phenotype such as N-cadherin.

Method: Paraffin-embedded sections derived from 33 phylloides tumors were used (18 benign, 7 borderline and 8 malignant) and the expression of E-cadherin, N-cadherin and β-catenin, both in epithelial and stromal cells, was accessed using immunohistochemistry.

Results: The expression of E-cadherin in the epithelium was strongly correlated with tumor type ($p<0.001$), showing decreased expression in the malignant tumors, and with β-catenin epithelial expression ($p=0.043$). The perinuclear localization of β-catenin in stromal cells was significantly increased in malignant tumors ($p=0.024$). The expression of N-cadherin in stromal and epithelial cells showed a strong association with each other ($p=0.026$).

Conclusion: EMT is a procedure that seems to play a major role in tumor progression in phylloides tumors. The mesenchymal-epithelial interaction in these tumors is very challenging and plenty of molecules can be investigated to further elucidate this significant step of tumorigenesis.

026

Expression rate of human epithelial growth factor 2 in fine needle aspiration and permanent specimens of breast cancer

M. Halimi *, A. Agbali, A. Dastranj, E. Ouladsahebmadarek
*University of Medical Science, Dept. of Pathology, Tabriz, Iran

Objective: The possibility of determining HER-2/Neu (human epithelial growth factor 2) status not only on histologic samples but also on cytologic specimens obtained by fine needle aspiration (FNA) may lead the clinicians to a better treatment approach. This study aimed at determining the concordance of HER-2/Neu presence rate by immunohistochemical assessments in FNA samples and histologic sections.

Method: In this study, FNA samples, as well as their corresponding histologic sections of 90 cases with breast cancer were evaluated. The immunohistochemistry was employed for determining the HER-2/Neu amplification for both methods.

Results: Ninety specimens of women with breast cancer were assessed. The concordance rate was 70% between the two methods. The agreement was statistically significant between the two methods, as well (kappa=0.51, $p<0.001$).

Conclusion: HER-2/neu gene amplification can be reliably estimated by immunohistochemistry on breast cancer FNAs and a good correlation has been found between this and results from the corresponding histological sections.

027

Overexpression of MOESIN in stromal compartment as a new unfavourable prognostic factor in breast cancer patients

A. Halon *, P. Donizy, L. Halon, R. Matkowski
*Wroclaw Medical University, Dept. of Pathomorphology, Poland

Objective: MOESIN (membrane-organizing extension spike protein) as a membrane-cytoskeleton crosslinker in actin-enriched cellular structures such as microvilli and ruffles controls cell morphology, polarity and motility. MOESIN overexpression in cancer cells is correlated with tumour aggressive phenotype and unfavourable prognosis in breast cancer (BC) patients.

Method: Immunohistochemistry for MOESIN was performed on 311 paraffin-embedded specimens from patients with BC. Four-step (0–3) scales, taking into account intensity of colour reaction and percentage of the stained tissue area or blood vessels—SS (stromal score) and BVS (blood vessels score)—were used.

Results: MOESIN expression in stromal compartment was common: (1) stroma: SS 0 (8/311; 2.6%), SS 1 (279/311; 89.7%), SS 2 (24/311; 7.7%); SS 3 (0); (2) tumour blood vessels: BVS 0 (4/311; 1.3%), BVS 1 (246/311; 79.1%), BVS 2 (61/311; 19.6%), BVS 3 (0). Elevated SS and BVS were strongly associated with shorter disease free survival (DFS). In multivariate analysis: (1) low stromal expression of MOESIN was an independent favourable

prognostic factor and (2) high MOESIN reactivity in stromal compartment was strongly associated with shorter DFS.
Conclusion: Evaluation of MOESIN expression in stromal compartment (apart from tumour cells) in BC patients can serve as a new promising immunohistochemical prognostic marker.

028

Impact of stromal RhoA and RhoB immunoreactivity on survival in breast cancer patients

A. Halon *, P. Donizy, R. Matkowski
*Wroclaw Medical University, Dept. of Pathomorphology, Poland

Objective: RhoA and RhoB are major regulators of signal transduction pathways and play a crucial role in regulation of cellular motility and polarity. The main mechanism of their functions includes remodeling of actin cytoskeleton via variety of signaling cascades, which influence on actin polymerization, dynamic of microtubules and actomyosin complex contractility.
Method: Immunohistochemistry for RhoA and RhoB was performed on 311 paraffin-embedded specimens from patients with BC. Four-step scales (0–3), taking into account intensity of colour reaction and percentage of the stained tissue area or blood vessels—SS (stromal score) and BVS (blood vessels score)—were used.
Results: All cases demonstrated stromal and vascular expression of both markers. High RhoA and RhoB BVS strongly correlated with poor prognosis. No relationship between SS and patients survival was observed in monovariate analysis. Multivariate analysis showed that overexpression of RhoB in the stromal compartment in lymph node negative BC patients was an unfavorable prognostic factor while stromal overexpression of RhoA was associated with favorable prognosis.
Conclusion: RhoA and RhoB were found to have a significant impact on the natural history of breast cancer, affecting cytobiochemical dynamics and remodeling tumor cells, tumor blood vessels and stromal cells.

029

Pathologic, cytologic and immunohistochemical study of 26 cases of breast hamartoma: a forgotten entity

M. Herbert *, S. Mendlovic, A. Sperber, J. Sandbank
*Asaf Harofeh Medical Center, Dept. of Pathology, Zerifin, Israel

Objective: In this study, we investigate the pathological, cytological and immunohistochemical features of breast hamartoma in order to obtain a detailed profile of this somewhat uncommon lesion.
Method: This study presents a pathological, immunohistochemical and cytological analysis of 26 cases of breast hamartomas. Ten cases of fibrocystic breast changes were used as a control group. The immunohistochemical panel included estrogen (ER) and progesterone (PR) receptors, c-erbB2 protein, p53, and Ki67.
Results: The patients ranged in age from 23 to 78 years (mean 43 years). Three patients had two hamartomas in the same breast. Tumors ranged in diameter from 18 to 59 mm. Typical macroscopic, microscopic and cytologic features were noted. Immunohistochemical studies showed ER and PR receptor positivity in epithelial cells as well as in the stromal cells in all 26 cases. No c-erbB-2 protein was observed. Ki67 showed 2% positivity in epithelial cells and p53 expression was not observed.
Conclusion: The immunohistochemistry of hamartoma is generally similar to that of fibrocystic breast tissue.

030

HER2 ICC Web-based interpretive scheme: a pilot study by the UK National External Quality Assessment Scheme for Immunocytochemistry and In Situ Hybridisation (UK NEQAS ICC & ISH)

M. Ibrahim *, A. Dodson, T. O´Grady, S. Parry, K. Miller, C. Doolan, B. Jasani
*UK NEQAS ICC & ISH, University College London, Dept. of Pathology, UK

Objective: HER2 immunocytochemistry (ICC) is used, by most laboratories, as the front-line predictive testing method to establish HER2 protein levels in breast cancer patients. Therefore, expertise in the correct interpretation of HER2 ICC is crucial. The UK NEQAS ICC & ISH has in collaboration with Slidepath introduced a web-based HER2 ICC interpretive module to assess the viability of using high quality images as a teaching tool for individual scientists and pathologists to help improve the accuracy of HER2 ICC interpretation.
Method: Over 561 UK NEQAS ICC & ISH participants were invited from 54 countries to view and interpret whole scanned digitised images 5 previously reported HER2 ICC cases, selected by an expert panel. Each case also included an H&E slide and participants were also provided with the HER2 FISH gene amplification status once they had submitted their HER2 ICC score.
Results: Data from the first interpretive assessment will be shown, along with a user survey results to illustrate the viability of a web based system as an aid to scientists and pathologists engaged in interpretive HER ICC assessment.

Conclusion: The aim of the pilot study is one of education, with the key objective to promote improvement in the quality of diagnostic HER2 ICC interpretation.

031

Audit of breast biomarkers markers, HER2.ER & PR in the UK: an update by the UK National External Quality Assessment Scheme for Immunocytochemistry and In Situ Hybridisation (UK NEQAS ICC & ISH)

M. Ibrahim *, K. Herriott, S. Parry, K. Miller
*UK NEQAS ICC & ISH, University College London, Dept. of Pathology, UK

Objective: Between 2007 and 2008, UK HER2 positivity rate was on average 15% (range 9–35%). Since 2008, a Web-based breast biomarker database has been established, allowing users to input HER2 IHC/ISH and ER and PR results.
Method: Individual laboratories are requested to input their HER2 IHC/ISH, ER and PR ICC results directly into a secure web database.
Results: The current UK HER2 positivity rate remains at 15%. Individual ER and PR data show the average positive rates to be 82.3% and 68.7%, respectively. The UK audit showed the following breast biomarker status (1) ER+/PR-/HER2+ (60.5%) (2) ER-/PR-/HER2- (12.3%) (3) ER+/PR-/HER2- (11.0%) (4) ER+/PR+/HER2+ (6.2%) (5) ER-/PR-/HER2+ (5.1%) (6) ER+/PR-/HER2+ (3.1%) (7) ER-/PR+/HER2- (1.3%) and (8) ER-/PR+/HER2+ (0.4%).
Conclusion: The audit database has provided individual UK laboratory and overall UK breast biomarker status. In some cases the audit has led to laboratories re-testing their cases. The data also provides insight into whether such cases of ER-/PR+/HER2- (1.3%) and ER-/PR+/HER2+ (0.4%) are genuine or due to other pre-analytical or analytical phases as indicated by previously published studies.

032

Immunocytochemical staining of breast biomarkers HER2, ER and PR; potential pitfalls of false positive/negative staining: findings of the UK NEQAS ICC & ISH

M. Ibrahim *, S. Parry, K. Miller
*UK NEQAS ICC & ISH, University College London, Dept. of Pathology, UK

Objective: Breast HER2, ER and PR are routinely used in diagnostic immunohistochemistry. Many laboratories use commercially available standardised HER2 IHC kits, however, few laboratories use a 'standardised kit' for ER & PR, with a 'home-brew' method being the method of choice. This study highlights the results obtained from UK NEQAS HER2 ICC, ER & PR assessments.
Method: Unstained HER2 cell lines and ER/PR tissue sections are distributed on a quarterly basis for participants to stain and, return for assessment by a panel of expert assessors.
Results: HER2 ICC pass rates continue to improve, with participants using a standardised HER2 ICC kit showing a pass rate of 81% compared to 43% for those using a 'home-brew' method. With ER the for poor performance is mainly due to false negative staining of mid expressing ER tumours. In contrast, poor performance PR assessments tend to be due to false positive staining of PR negative tumours. This was principally observed with the rabbit monoclonal SP2 antibody, whose usage by NEQAS participants has decreased from 11% (2006) to 1% (2011).
Conclusion: There is still more scope for improvement in breast biomarker immunocytochemistry, with laboratories encouraged to validate their methodologies and include proper control material to gauge the sensitivity and specificity of the ICC methods.

033

Single detection kit, double antibody cocktail (D2-40/p63) protocol for identification of lymphatic vascular invasion in breast tissues containing extensive intraductal/-lobular tumour growth

I. Ivanov *, S. Popovska, T. Betova, T. Dineva
*MU-Pleven, General and Clinical Pathology, Bulgaria

Objective: When accessed on D2-40 stained slides, lymphatic vascular invasion may present interpretation difficulty, especially in breast tissues containing extensive intaductal/-lobular tumour growth because of the positivity observed in both lymphatic endothelial cells (LECs) and myoepithelial cells (MECs). The available multiple stain detection kits are time and resource consuming. The aim of this study was to develop an antibody cocktail (D2-40/p63), single detection kit protocol for identification of lymphatic vascular invasion in breast tissues.
Method: Formalin-fixed, paraffin embedded tissues from 130 breast cancer patients were examined. Immunostaining was analysed in corresponding fields of consecutive tissue slides, stained according to standard protocols with D2-40, p63 and D2-40/p63 cocktail, single detection kit.
Results: When stained with D2-40/p63 cocktail, lymphatic vessels demonstrated "continuous" intermediate to strong cytoplasm staining (LEC reactivity for D2-40), readily distinguishable from the "bead-like" staining observed in MEC of distorted duct lobular units (weak to missing cytoplasm D2-40 staining, strong p63 nuclear staining). The suggested antibody cocktail proved to be more effective than D2-40 alone in the identification of lymphatic

vascular invasion in cases containing extensive intraductal/-lobular tumour growth.
Conclusion: The suggested staining protocol enabled an effective interpretation of the nature of tumour cell harbouring D2-40 positive structures in all studied cases.

034

Breast carcinoma with neuroendocrine differentiation: clinicopathological features in five cases

C. Kelten *, Z. Gücin, S. Baykal Koca, G. Erdem Huq, E. Pasaoglu, C. Leblebici, N. Dursun, D. Can Trabulus, K. Behzatoglu, E.R. Bozkurt
*The Ministry of Health, 0st Education and Research Hospital, Istanbul, Turkey

Objective: Primary breast carcinomas with neuroendocrine differentiation are rare tumors. This tumor has controversial results in terms of its prognosis and treatment approaches.
Method: Five neuroendocrine breast carcinoma cases immunohistochemically positive for synaptophysin and/or chromogranin in more than 50% of tumor cells were evaluated in terms of their clinicopathological and immunohistochemical features. None of the cases had tumor focus in non-mammary sites.
Results: All patients were women and aged from 40 to 81 years. In all cases, tumors were unilateral with a diameter ranging from 1.5 to 3.5 cm. Two of five cases showed multifocality. All tumors were evaluated as nuclear and histological grades 2. Tumors were classified as solid cohesive in 2, solid papillary in 1, cellular mucinous in 1 and invasive ductal carcinoma with psammomatous features in 1. All tumors included solid or cribriform type in situ ductal carcinomas with or no necrosis. All tumors showed strongly and widely distributed estrogen and progesterone receptors positivity. None of the tumors displayed Her 2/neu overexpression. Lymphovascular invasion and axillary lymph node metastasis were not determined in any cases.
Conclusion: It should be kept in mind that neuroendocrine differentiation can appear in several histological patterns such as mucinous differentiation, papillary/micropapillary formation, solid-nested growth. Therefore, any breast tumor with this morphology should search carefully for neuroendocrine markers.

035

Expression of Tenascin-C in correlation with Sox2, Nanog, BMI1 and Oct4 expression in breast cancer

E. Klieser *, S. Swierczynski, N. Arnold, B. Allinger-Scharinger, O. Dietze, C. Hauser-Kronberger
*Paracelsus Universität Salzburg, Inst. für Pathologie, Austria

Objective: Tenascin-C (TNC) is a glycoprotein in the extracellular matrix which reappears in the condition of wound healing and some neoplasms such as breast cancer. Therefore, we investigated the connection between TNC and transcription factors and proteins which are involved in the self-renewal in cancer stem cells.
Method: Paraffin sections from 120 breast cancer patients were used for automated immunohistochemistry (IHC) with two different antibodies targeting TNC. Postive paraffin sections for one or both TNC- antibodies were screened for Ki67, Nanog, Oct4 and Sox2 and BMI1. IHC positive breast cancer cell lines were stained on cell slides with Ki67, Nanog, Oct4, Sox2 and BMI1. The expressions of TNC, Nanog, Oct4, Sox2 and BMI1 of these breast cancer cell lines were also analyzed in rt-PCR.
Results: A total of 50 paraffin sections were positive for one or both TNC antibodies as well as for Nanog, Oct4, Sox2 or BMI1. The rt-PCR experiments with TNC positive breast cancer cell lines presented also a high expression rate of Nanog, Oct4, Sox2 and BMI1.
Conclusion: These results reveal a correlation between Tenascin C and Nanog, Oct4, Sox2 and BMI1 which are involved in self-renewal of cancer stem cells.

036

Angiogenesis-associated parameters in metastatic breast carcinoma: correlation with the MAPK and Akt pathways, proliferation and apoptosis

H. Kourea *, M. Bobos, V. Tzelepi, A. Kominea, C. Scopa
*University of Patras Hospital, Dept. of Pathology, Greece

Objective: Vascular endothelial growth factors A (VEGFA) and C (VEGFC) and their receptors VEGFR1, VEGFR2 and VEGFR3 are expressed in neoplastic cells. The aim of our study was to investigate for relations between factors of angiogenesis, the MAPK and Akt pathways and parameters of cell proliferation and survival in metastatic breast carcinoma (MBC).
Method: Tissue microarrays consisting of duplicate, 1.5-mm cores from 72 MBCs were immunostained for VEGFA, VEGFC, VEGFR1, VEGFR2 VEGFR3 phospho-p44/42MAPK, phospho-Akt1/2/3, phospho-S6 ribosomal protein, bcl-2 and Ki-67. The immunoreactivity was assessed by H score, except for Ki-67 where the percentage of positivity was recorded. Pearson correlations between parameters were calculated by SPSS 16.0.
Results: VEGFA was correlated with bcl-2 (p=0.001, R= 0.402), VEGFC with Ki-67 (p=0.001, R0.386) and VEGFR1 (p=0.017, R0.280), VEGFR1 with VEGFR3 ($p<$ 0.001, R0.416) and phospho-S6 protein with VEGFR1 (p= 0.002, R0.361), VEGFR3 (p=0.002, R0.360) phospho-Akt (p=0.01, R0.301), phospho-p44/42MAPK ($p<$0.001, R 0.506) and Ki-67 (p=0.021, R0.274).

Conclusion: In MBC, VEGFA is associated with the antiapoptotic bcl-2, while VEGFC is associated with proliferation, possibly through an autonomous autocrine pathway involving VEGFR1, VEGFR3 and the downstream of Akt phospho-S6 protein.

037

Quantitative morphometry by image analysis of invasive ductal carcinoma

A. Kudaybergenova *, S. Kalantary, D. Matzko
*RSCRST, Dept. of Immunohistochemistry, St. Petersburg, Russia

Objective: We analyze a total number of tumor cells in invasive ductal breast carcinoma and normal ductal epithelium to establish absolute quantity tumor cells per square millimeter of histological slide.
Method: Morphometric analysis was performed using the Pannoramic Viewer software (3DHistech, Budapest) on the hematoxilin and eosin stained breast cancer tissue specimens from Baku Oncology Hospital during the 2001–2005. The study included 46 patients diagnosed with breast carcinoma and 14 cases with normal ductal epithelium behind carcinoma. For each case we analyzed the total number of tumor cell in1 mm^2; nuclear area and nuclear perimeter of these parameters were assessed by use of Statistica 6.0. Morphometric analysis yielded statistically significant differences among tumor cells and normal epithelium.
Results: Mean tumor cells in 1 mm^2 of histology slide was 4,180±251 cells, median—3,976 cells. In normal duct wall cell, the density was 2,859±456 per mm^2. Average tumor cell nuclear area was 39.11±1.09 mkm^2, with median 40.17 mkm^2 and normal ductal epithelial cell has nuclear area 45.74±1.69 mkm^2, median 44.15 mkm^2.
Conclusion: By quantitative morphometric analysis of breast cancer, the total tumor cell per mm^2 was established and main nuclear characteristic paving the way for automatic computerized image recognition for invasive ductal carcinoma.

038

A randomized multi-site method comparison and inter-laboratory reproducibility study confirm the safety and effectiveness of INFORM HER2 Dual ISH for determining HER2 gene status in invasive breast carcinoma

I. Loftin *, A. McElhinny, R. Miller, C. Garcia, I. Bai, J. Ranger-Moore, J. Ostrem, M. Padilla, T. Grogan
*Tucson, USA

Objective: Amplification and/or HER2 overexpression is associated with poor clinical outcome for patients with invasive breast carcinoma. Determination of HER2 status dictates eligibility of patients for trastuzumab (Herceptin) therapy, which can improve prognosis. FISH testing has been the gold standard for determining HER2 gene status. Here we validated the INFORM HER2 Dual ISH assay as an alternative to FISH. The assay is fully automated and is scored using light microscopy providing morphological context.
Method: A total of five sites were used to compare Her2 Dual ISH results with FISH (Vysis PathVysion) from 510 invasive breast carcinoma specimens. In addition, six cases were evaluated over five runs for inter-site, inter-reader, inter-run and intra-run reproducibility at three sites. All assay steps were fully automated on a BenchMark XT automated slide stainer, using silver metallographic and red colorimetric detections for Dual ISH.
Results: The positive and negative agreement rates with FISH results (95% CI) were 96% (92.6–97.9) and 92.3% (88.6–94.8), respectively. The HER2 Dual ISH assay also was highly reproducible in determining HER2/Chr17 ratio across sites, days, readers and runs.
Conclusion: The INFORM HER2 Dual ISH assay is reproducible and concordant with the manual FISH assay in determining HER2 status in invasive breast carcinoma.

039

Expression of Y-box binding protein-1 in invasive breast cancer is correlated with a more aggressive phenotype

S. Melissaris *, I. Vamvakaris, I. Giannopoulou, I. Theohari, K. Tzelepis, A. Nomikos, L. Nakopoulou
*University of Athens, Medical School, Greece

Objective: Y-box binding protein-1 (YB1) belongs to the cold shock superfamily and functions as a transcription-translator factor and also as a cell-cycle regulator. YB1 is overxpressed in a variety of tumors such as pediatric glioblastoma and breast cancer. Our aim was to evaluate the expression of YB1 protein in invasive breast cancer in relation to the clinicopathological parameters, hormone receptors status, c-erbB2, VEGF-C, VEGF-D and patients' survival.
Method: Immunohistochemistry was performed on paraffin sections from 235 patients with invasive breast cancer. For the statistical analysis, Pearson's chi-square test and Kaplan–Meier were used.
Results: Cytoplasmic YB1 expression was found in 38.7% of the cases and nuclear in 40%, respectively. Inverse correlation resulted between cytoplasmic YB1 and ER and PR ($p=0.007$ and $p=0.043$). Positive correlation resulted between nuclear YB1 and (a) the triple negative subtype of cancer ($p=0.013$), (b) histological grade ($p=0.045$) and (c) VEGF-C and VEGF-D ($p=0.012$ and $p=0.02$).
Conclusion: YB1 was found to be correlated with an aggressive phenotype. The correlation between YB1 and

lymphangiogenesis factors VEGF-C and VEGF-D in breast cancer was first described in our study. The association with triple negative subtype of cancer could constitute an indication for a future targeted therapy.

040

Transcriptional factors NF-kB and STAT3 are overexpressed in invasive ductal breast carcinomas and triple negative subgroup

D. Meseure *, K. Drak Alsibai, M. Trassard, F. Lerebours, R. Lidereau, I. Bieche
*Hopital Rene Huguenin, Dept. de Pathologie, Saint Cloud, France

Objective: Invasive duct carcinomas (IDC) are often associated with constitutive activation of transcription factors (TF). Recent studies suggest that interactions between activated NF-kB and STAT3 control both tumor-microenvironment dialogue and anti-apoptotic, pro-proliferative and immune response gene expression by neoplastic cells.
Method: By using RT-PCR in a series of 40 IDC, we quantified mRNA expression levels of NF-kB, STAT3, toll-like receptors (TLRs), cytokines, growth factors, (vi) hypoxia and EMT genes. Immunohistochemistry (IHC) and a retrospective RNA series of well-characterized IDC were used to confirm results and establish statistical correlations.
Results: RT-PCR revealed high mRNA levels of (1) NF-kB and STAT3, (2) genes activating NF-kB and STAT3: IL-1, IL-6, IL-8, IL-10, IL-23, TNF, IFN, TLR-8, TLR-9 and EGFR, (3) HIF1 and GLUT1 and (4) TWIST1, FOXC2, ZEB2, VIM, CDH1, ACTA2. Both stromal and neoplastic cells expressed these two TF. High positive correlations were observed between (1) NF-kB1 and STAT3 at mRNA and protein levels ($p<0.05$), (2) EGFR, TLR-9, NF-kB1, STAT3, HIF1 and GLUT1 mRNA ($p<10\text{-}7$), (3) NF-kB1, STAT3, HIF1 mRNA and EMT ($p<10\text{-}6$).
Conclusion: NF-kB and STAT3 are overexpressed in IDC and TNC. Targeting these key regulators should provide new opportunities for personalized therapy.

041

Molecular intra-operative assessment of sentinel lymph node in breast cancer: a report about routine use

M. Peoch *, C. Boutheille, P. Seffert, A. Kaddhage
*CHU de Saint Etienne, Dept. de Pathologie, France

Objective: Sentinel lymph node (SLN) biopsy is widely used as a staging procedure in early breast cancer. Conventional procedures for intra-operative assessment have a low sensitivity and lead to second surgeries when the SLN is metastatic during postoperative histology. The one-step nucleic acid amplification (OSNA) method was developed to accurately detect metastases ($\geq$ 0.2 mm) by rapid amplification of cytokeratin 19 mRNA. The use of OSNA during intra-operative clinical routine use was evaluated.
Method: A total of 197 patients were registered for OSNA routine use. A central 1-mm slice was assigned to histological examination and the other two parts of the node were completely analysed by OSNA.
Results: Both OSNA and histology detected 25 patients with metastasis. There were 17 patients found to be positive exclusively by OSNA. The positivity rate was evaluated to be 21.3%. Axillary clearance was performed during the same surgical session as the SLN biopsy. In our hands, the median time of analysis was 37 min for two SLNs from the reception of the SLN in the pathology laboratory to the result.
Conclusion: OSNA is a rapid and accurate tool for intra-operative assessment of SLN status and could reduce the need for second surgery.

042

A case of diffuse idiopathic breast neuroendocrine (NE) cell hyperplasia with NE-DCIS

K. Miura *, T. Moriki
*Hamamatsu University, School of Medicine, Japan

Objective: Neuroendocrine ductal carcinomas in situ (NE-DCIS) are about 7% in all DCIS and seen in elderly women. Bloody nipple discharge is a main clinical symptom and the prognosis is fairly good as compared to non-NE DCIS. Chromogranin-reactive neuroendocrine cells are rarely found in normal breast and their hyperplasia is not known to date. We report a case of a 72-year-old postmenopausal woman with two NE-DCIS, which are 5 and 3 mm in the maximum diameter seen in the background of diffuse idiopathic breast neuroendocrine cell hyperplasia (DIBNCH).
Method: For detecting neuroendocrine differentiation, we used neuroendocrine markers such as synaptophysin, chromogranin A, CD56, somatostatin receptor type2 (SSTR2) in immunostaining.
Results: More than half tumor cells of two intraductal carcinoma showed neuroendocrine markers although their distribution is random amongst nodules i.e. few cells were positive in one nodule and many cells were positive in others. Among NE markers, CD56 or SSTR2-ractive cells were more widely distributed as compared to synaptophysin or chromogranin A-positive cells. Moreover, CD56-positive cells were disseminated among nontumoral ductal cells, showing scattered single cells, small nodules, or linear distribution.

Conclusion: DIBNECH is a generalized proliferation of breast neuroendocrine cells and extend to form a clonal mass of NE-DCIS. DIBNECH may be a precursor lesion of breast carcinoid tumors.

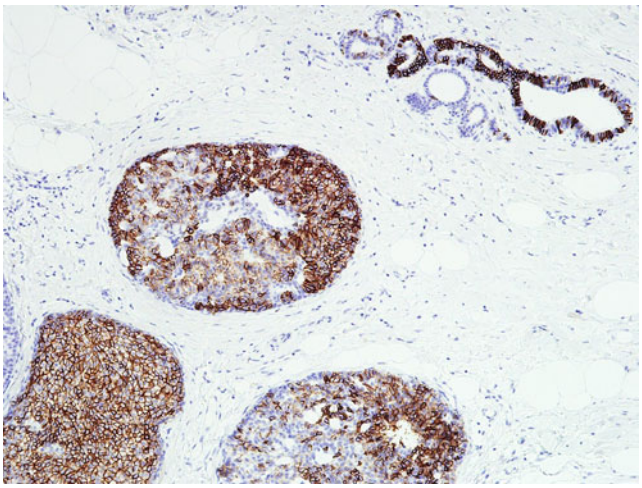

043

The expression of cyclin D1 is related to a favorable phenotype in invasive breast carcinoma

L. Nakopoulou *, K. Tzelepsis, I. Theohari, S. Melissaris, I. Giannopoulou, I. Vamvakaris, P. Rafailidis
*Papagou, Greece

Objective: Cyclin D1 is an important cell cycle regulator and has been characterized as a poor prognostic marker in various types of cancer. Our aim is to investigate the expression of cyclin D1 in invasive breast cancer in relation to clinicopathological parameters, patient's survival as well as conventional and novel biological markers such as hormonal receptors, markers of cell proliferation, apoptosis and signaling molecules.
Method: Immunohistochemistry (avidin–biotin–peroxidase complex) was performed on 4-μm-thick formalin-fixed paraffin sections obtained from 364 patients. Univariate statistical analysis was performed.
Results: Cyclin D1 was detected in the nucleus of cancer cells in 303/364 cases (83.24%). A positive correlation was found with ER ($p \leq 0.001$), Wnt-1 ($p=0.029$). Cyclin D1 was negatively related to nuclear grade ($p=0.010$), tumor size ($p=0.006$), p53 ($p=0.013$) and Topo-IIα ($p=0.007$). Patients with positive cyclin D1 expression displayed a longer overall survival ($p=0.019$).
Conclusion: Cyclin D1 seems to have a multifunctional role in different carcinomas. Our results support this notion based on the relation with a less aggressive phenotype and longer survival time. On the other hand, it seems to be involved in signaling pathways through its collaboration with Wnt-1 and GSK-3β.

044

Triple positive (androgen receptor+, estrogen receptor+ and HER2+) breast cancers

M. Orsaria *, S. Khelifa, F. Tavassoli
*S. Maria della Misericordia, Dept. of Pathology, Udine, Italy

Objective: Androgen receptors (AR) are positive in 70% to 90% of invasive breast cancers (IBCs). However, little is known about the impact of AR positivity in ER and HER2 amplified (ER+/HER2 +) cancers. Notably, despite expanded therapeutic options, ER+/HER2+ IBCs manifest aggressive behavior and resistance to Herceptin. For these reasons we decided to evaluate AR status in our ER+/HER2+ IBCs.
Method: Archival core biopsies of IBCs performed from 01/2005 to 12/2009 were reviewed. Out of 2,600 IBCs, 84 (3%) were ER+/HER2+. Paraffin blocks were available for study in 74 cases; AR immunostains were performed on all.
Results: Patients' mean age was 56.48 with 33 (44.6%) premenopausal and 41 (55.4%) postmenopausal. Out of the 74 IBCs, 70 (94.6%) were ductal including one mucinous, and 4 (5.4%) were lobular. AR was positive in all 74 (100%) cases regardless of tumor size, nuclear grade, and lymph node status. These qualify as a subset of luminal B intrinsic type IBCs.
Conclusion: The high frequency of AR co-expression in all ER+/HER2+ IBCs suggests the potential utility of anti-androgens in the management of these patients particularly when there is contraindication and/or resistance to Herceptin. A potential cross-talk between the AR and ErbB2 signaling pathways in ER+ IBCs warrants further investigation.

045

A concordance study between automated and manual HER2 FISH testing

A. O´Grady *, E. Daly, E. Kay
*Beaumont Hospital, RCSI Education/Research Centre, Dublin, Ireland

Objective: Despite FISH assays being labour intensive and technically challenging they continue to remain the gold standard laboratory assay for HER2 assessment. Currently, FISH is performed manually and can be subject to operator variation and a lack of standardization. Fully automated staining addresses a number of challenges associated with HER2 FISH testing. This study comprised a randomized and blinded concordance assessment between the automated Leica HER2 FISH System and the manual Kreatech Poseidon ERBB2 probe on 100 breast cancer cases pre-characterized for protein and/or gene amplification status.

Method: The manual test was performed following current laboratory practice. The automated test was performed using the default protocol provided by the manufacturer. Each case was enumerated within the same tumour location by marking a suitable area for scoring on the H&E, enabling true concordance to be assessed.
Results: A 3X3 concordance between the devices was calculated and a 99% agreement was described, demonstrating excellent concordance between the devices.
Conclusion: The significantly reduced labour time and excellent reliability shown by the automated device provides a genuine alternative to manual HER2 FISH testing.

046

Malignant phyllodes tumor of the breast with osteosarcomatous differentiation

E. E. Pala *, U. Kucuk, U. Bayol, D. Etit, F. Gunduz, S. Yucel, S. Cumurcu, S. Selcuk
*Tepecik Training and Research, Dept. of Pathology, Izmir, Turkey

Objective: Phyllodes tumors are rare biphasic lesions that account for less than 1% of all breast neoplasms. Histologically malignant phyllodes tumors may show considerable morphologic heterogenity such as liposarcomatous, fibrosarcomatous, rhabdomyosarcomatous, chondrosarcomatous or osteosarcomatous differentiation. Osteosarcomatous differentiation of a malign phyllodes tumor of the breast is extremely rare.
Results: A 63-year-old female was admitted with a painless, mobile mass in her right breast. Physical and radiological examination revealed a 7-cm mass in the upper outer and middle quadrants of the breast. The axillary lymph nodes were not palpable. A quadranectomy with free margins was performed without axillary dissection. Grossly the tumor was well-circumscribed, firm to hard solid mass 7 cm in diameter. Microscopically, the tumor was biphasic with benign compressed peripheral cleft-like epithelial and malignant sarcomatous component with osteogenic differentiation. Based on morphologic and immunohistochemical insignia, the case was diagnosed as 'malignant phyllodes tumor of the breast with osteosarcomatous differentiation'. After total surgical exicision of the tumor, as there was no evidence of local or distant metastasis, no adjuvant therapy, but close clinical follow-up was recommended at the tumor board. The tumor locally recurred in the breast within 10 months and treated by simple mastectomy.
Conclusion: The case was presented because of its rarity and problem of management.

047

Hypoxia inducing factor 1a (HIF-1a) expression in invasive breast cancer: correlation with tumor clinicopathological parameters

H. Papatheodorou *, M. Leotsinidis, H. Kalofonos, C. Scopa, J. Varakis, H. Papadaki
*University of Patras, School of Medicine, Patras, Greece

Objective: Hypoxia inducible factor-1α (HIF-1α) is a key regulator of hypoxia, a common feature of breast cancer that influences tumor behavior and therapeutic outcome.
Method: We investigated HIF-1a immunohistochemical expression in 96 paraffin-embedded breast cancer tissue samples and its correlation with tumor clinicopathological parameters and patient survival.
Results: Cytoplasmic and nuclear HIF-1a expression in cancer cells was identified in 98% and 85.5% of the cases, respectively, while normal breast tissue was negative. Nuclear and cytoplasmic HIF-1a expression were negatively correlated with estrogen ($r=-0.262$, $p=0.012$) and progesterone receptors ($r=-0.221$, $p=0.033$), respectively. They were also negatively correlated with Ki67 expression ($r=-0.313$, $p=0.002$ and $r=-0.219$, $p=0.032$ respectively). We also noticed a significant negative correlation between nuclear HIF-1a expression and histologic grade ($r=-0.23$, $p=0.025$).
Conclusion: Our findings confirm that HIF-1a seems to be involved in human breast carcinogenesis but further studies are needed to determine the exact role of HIF-1a in invasive breast cancer.

048

The usefulness of cell-block material for the evaluation of HER2 receptor status in breast carcinoma

W. Rezner *, A. Radowicz-Chil, J. Kopczynski, M. Ostrowski, M. Karwicka, J. Sygut
*Holycross Cancer Centre, Dept. of Neoplasm Pathology, Kielce, Poland

Objective: There is growing evidence of high usefulness of cell-block (CB) material for HER2 evaluation in breast carcinoma. We examined the concordance of HER2 assessments performed on CB and tissue section (TS) material.
Method: We compared the results of routine HER2 immunostaining in 40 patients where satisfactory CB material and subsequent TS's from primary/metastatic breast carcinoma were available. We also repeated HER2 immunostaining of the CB material and assessed its results (independently by two pathologists who than discussed consensus in discordant cases).
Results: In 11/40 of routinely assessed cases either CB or TS material revealed equivocal result (2+). Out of the remaining 29 cases 28 showed correlation between CB and

TS for positive or negative results (96%). After the reassessment of repeatedly immunostained CB material we excluded one case with unsatisfactory material, and changed HER2 status in 9 cases (4 into equivocal and 5 from equivocal into negative) so that equivocal results were observed in 8/39 cases and correlation for positive/negative HER-2 status was observed in the remaining 31 cases (100%).

Conclusion: Either routinely or retrospectively evaluated CB immunostaining for HER-2 revealed very high correlation for positive or negative receptor status with immunohistochemical assessment of tissue sections.

049

Synchronous bilateral breast cancer: clinical, morphological and epigenetic characteristics

I. Rodriguez Perez *, L. Blanco, D. Guerrero, A. Calvo, J.J. Illarramendi, N. Pérez Janices, A. Córdoba

*C. Hospitalario de Navarra, Sº de Anatomia Patologica, Pamplona, Spain

Objective: Synchronous bilateral breast cancer (SBBC) is rare and represents less than 2% of breast tumors. There is not consensus about the independent nature of two different tumors or if this simultaneous presence is due to metastasis of one of them.

Method: We studied 18 patients with invasive SBBC and we compared the clinical, pathological, immunohistochemical, and epigenetic characteristics of both tumors. Methylation status of RASSF1A, RASSF2A, ADAMTS-8, TSP-1, and IGSF-4 genes were analyzed by methylation specific-PCR, in both tumors of each patient.

Results: The morphology of both tumors was different in 6 out of 17 cases. 62.5% of the contralateral tumors showed different histological grade. 64.7% of cases were ductal carcinoma in both locations. 84% of the bilateral tumors shared the same phenotype, and 10 cases were luminal A. The results of methylation analysis are displayed in Table 1.

Conclusion: SBBC remains a controversial entity. We discuss whether this is a spread breast-to-breast or two independent tumors. To our data, the independent nature of these tumors cannot be clearly explained by the difference in histopathological and IHC features or epigenetic results.

Gene	Methylation (%), right breast	Methylation (%), left breast	Coincidence (%) between results at both locations
RASSF1A	70.6	58.8	62.5
RASSF2A	0	0	100
ADAMTS-8	23.1	46.2	70
TSP-1	40	31.3	69.2
IGSF-4	12.5	5.9	81.3

050

Calretinin expression in different molecular subtypes of ER and PR negative breast carcinomas

F. Sessa *, D. Micello, E. Dainese, N. Sahnane, A. Marando, C. Riva, C. Capella

*University of Insubria, Dept. of Human Morphology, Dept. of Pathology, Varese, Italy

Objective: Several observations have shown calretinin expression in breast carcinomas (BCs). Our aim was to investigate the frequency of the calretinin expression in a series of ER and PR negative BCs of different molecular subtypes.

Method: A total of 206 consecutive cases of ER/PR negative BCs were classified in three molecular subtypes: basal-like (ER, PR, HER2 negative, positive with at least one these markers: CK5, CK14, EGFR), HER2+ (ER/PR negative, HER2+) and null type (NT) (ER, PR, HER2 negative). The extent and intensity of immunohistochemical calretinin expression were scored semiquantitatively by a combined score of 0–3+.

Results: Calretinin staining showed both cytoplasmatic and nuclear reactivity and was found in 53.7% of our series. The basal-like was the most frequent BC subtype (53.3%); 38.3% BCs were HER2+ and 8.2% NT. Calretinin was found in 73.0% of the basal-like carcinomas with strong positivity (2.3 +) in 41% of NT and in 29.3% of HER2+ subtypes ($p<10–7$). There was a significant positive correlation of calretinin and CK5 ($p<10–7$), CK14 ($p<10–5$), EGFR ($p=0.04$). No relationship between the calretinin and the overall as well as disease-free survival was found.

Conclusion: The frequent expression of calretinin in basal-like BCs could be a pitfall in metastatic pleural disease.

051

CD44 expression in ER and PR negative ductal breast carcinomas

F. Sessa *, A. Marando, D. Micello, N. Sahnane, A.M. Chiaravalli, C. Riva, C. Capella

*University of Insubria, Dept. of Human Morphology, Dept. of Pathology, Varese, Italy

Objective: CD44 is a type I transmembrane glycoprotein receptor that binds the extracellular hyaluronan. There is evidence for the CD44 role in the progression of many cancers as well as for its expression in cancer initiating cells (CIS). We investigated the CD44 expression in ER/PR negative BCs.

Method: We immunohistochemically investigated the expression of CD44, p53, CK5 and Ki-67 in 198 BCs encompassing 126 TN BCs and 72 HER2 positive BCs, surgical removed from 1995 to 2000.

Results: CD44 expression was detected in 82.9% of TN BCs and in 58.6% of HER2 BCs. CD44+ BCs had higher expression of Ki-67 (59.8 versus 47.4 of positive cells) and

of p53 (50.2% versus 35.0%) than CD44 negative tumors. CK5 was found in 94 out 126 TN BCs; of these 89.1% were CD44+. Among the investigated parameters (grade, age, survival, pT, pN) only a younger age was statistically correlated with CD44 expression (57 years versus 64 years).
Conclusion: ER/PR negative BCs expressing CD44 are associated with markers related to a more aggressive phenotype: high proliferative index, p53 expression, basal phenotype and younger age. A high number of CIS CD44+ in these BCs may explain the early and frequent relapse of the disease.

052

Assessment of a new monoclonal rabbit antibody to estrogen receptor alpha, clone EP1 for determination of hormone receptor status on routine tissue specimens

B. Spaulding *, T. Phillips, K. Oftebro, K. Wakamiya
*Dako North America, Dept. of Biomarkers, Carpinteria, USA

Objective: The use of high-quality antibodies to estrogen receptor alpha (ERα) plays an important role in the accurate determination of hormone receptor status using analytically and clinically validated assays. In this study we evaluated the performance characteristics of a new monoclonal rabbit antibody to ERα, clone EP1.
Method: Formalin-fixed, paraffin-embedded (FFPE) tissue microarrays sections of normal and breast carcinoma tissue were used for this study. Immunohistochemistry (IHC) was performed using a new monoclonal rabbit anti-ERα, clone EP1 and monoclonal rabbit anti-ERα, clone SP1 for comparison. Tissue pretreatment and IHC staining was performed using Dako reagent and instrumentation platforms. The percentage of positively stained tumor cell nuclei was recorded and specimens were considered positive if at least 1% of tumor nuclei stained positively.
Results: On normal tissue, EP1 demonstrated nuclear positivity only in tissue types known to express ERα. When comparing clone EP1 to SP1 on a series of breast carcinomas, EP1 was found to be highly concordant with SP1.
Conclusion: Monoclonal rabbit anti-ERα, clone EP1 is a sensitive and specific antibody for demonstration of estrogen receptor in FFPE tissues. In comparison testing for determination of hormone receptor status on breast carcinomas specimens, clone EP1 produces results which are highly concordant with clone SP1.

		SP1		
		Positive	Negative	Total
EP1	Positive	20	1	21
	Negative	0	21	21
	Total	20	22	42
Kappa = 0.924 (95% CI = 0.863-0.984)				
Pos. Agr. = 100%		Neg. Agr. = 95.5%		Overall Agr. = 97.6%

053

Diagnostic problems in a small-size multifocal apocrine well-differentiated infiltrating breast carcinoma developing in a complex sclerosing lesion and apocrine adenosis

S. Stolnicu *, C. Marian, D. Soanca, M. Boros, D. M. Podeanu
*University of Medicine, Dept. of Pathology, Targu Mures, Romania

Objective: A 50-year-old patient was referred to the Department of Radiology for an annual screening mammogram.
Method: A non-palpable right breast lesion located in the superior-exterior quadrant was suggested by the presence of radio-opaque microcalcifications.
Results: On light microscopy, two adjacent different suspicious lesions were identified that were both associated with apocrine adenosis, radial scar and proliferative fibrocystic disease. The two areas of 8 respectively 10 mm diameter consisted of multiple ducts involved by low grade ductal carcinoma in situ (DCIS) of apocrine type but also distorted (by large amount of hyaline) and compressed small clusters or tubules of apocrine cells with low grade nuclei and large amount of eosinophilic granular cytoplasm. However these clusters lack myoepithelial cells on both microscopic and immunohistochemical examinations and consecutively were interpreted as infiltrating areas of well differentiated apocrine carcinoma.
Conclusion: In this case, where small sized multifocal low grade infiltrating apocrine carcinoma developed on a background of apocrine adenosis and complex sclerosing lesion the role of immunohistochemistry is mandatory to establish the absence of myoepithelial cells (completely negative for CD 10, Actin and p63). Also, low grade infiltrating apocrine carcinoma may develop from low grade apocrine DCIS since both lesions have same morphological and immunohistochemical profile.

054

Ki67 expression in triple negative and luminal A breast cancer

Y. Sullu *, G. G. Demirag, N. Ozen
*University of Ondokuz Mayis, Dept. of Pathology, Samsun, Turkey

Objective: Breast cancer expressing high levels of Ki67, a nuclear marker of cell proliferation are associated with worse prognosis. Triple negative tumors are often poorly differantiated with a higher proliferation index. Luminal A group comprises about two third of all breast cancers and is dominant subtype. Luminal A tumors have low Ki 67 index

and a favorable prognosis but prognosis and response to chemotherapy of luminal A tumors are highly variable. We investigated the expression of Ki67 by immunohistochemistry in triple negative and non-triple negative invasive ductal carcinoma that luminal A subgroup made up the majority of this group.
Method: The expression levels of Ki67 was measured by immunohistochemistry in 34 triple negative and 37 non-triple negative (29 luminal A, 5 luminal B and 3 HER2) invasive ductal carcinoma. For Ki 67 expression, a cut-off of 15% was used.
Results: We found a significantly higher proliferation index in triple negative tumors compared non-triple negative tumors (p=0.004). Expression levels of Ki 67 was high in 31 of 34 cases (91%) in triple negative group, 17 of 29 cases (%59) in luminal A group.
Conclusion: A part of luminal A tumors can be have high proliferative index so that this possibility should be consider in the treatment.

055

Breast cancer: extranuclear/intracytoplasmic expression of hormonal receptors

P. Dadioti-Arapantoni *, C. Valavanis, T. Garvessea, A. Simoulis, O. Tzaida, H. Trihia, G. Vecchini,
I. Iakovidou, I. Lekka
*HRG Greece S.A., Athens, Greece

Objective: Hormonal receptors have been established over the years as prognostic and predictive factors in breast cancer. ER and PR status is immunohistochemically detected and all the evaluation systems are based on nuclear positivity. The aim of this study is to assess the incidence of extranuclear/intracytoplasmic ER and PR expression and its significance.
Method: A total of 231 invasive breast carcinomas were evaluated immunohistochemically for ER and PR nuclear and extranuclear/cytoplasmic expression.
Results: Our evaluation revealed 76% and 70% of the tumors with nuclear ER and PgR immunoreactivity respectively. ER and PgR cytoplasmic expression was found in 6% and 15% of the carcinomas respectively, while only 3% displayed cytoplasmic expression for both markers. A total of 42.8% of ER and 38.7% of PgR cytoplasmic-expressed tumors were Grade III.
Conclusion: Recent studies suggest that ER participates in extranuclear signalling via the ER-Src-PELP1-PI3K-ILK1 pathway leading to increased cell motility/invasion. In addition intracytoplasmic localization of ER has been observed in tamoxifen-resistant breast cancer cell lines and abrogation of this resistance through ER nuclear relocalization. Thus, the assessement of hormone receptors subcellular localization might provide information of important clinical significance and putative therapeutic intervention.

056

Assessement of HER2/TopoIIa genes status as prognostic/predictive markers in high-risk breast cancer patients treated with dose-dense sequential adjuvant chemotherapy

C. Valavanis *, O. Tzaida, M. Bobos, A. Batistatou, V. Kotoula, A. Bourli, I. Papaspyrou, H. Kourea,
K. Pavlaki, P. Arapantoni-Dadioti
*Metaxa Cancer Hospital, Dept. of Pathology, Piraeus, Greece

Objective: Antracyclines and taxanes are drugs used in the treatment of high-risk breast cancer patients. The role of HER2/TopoIIa genes status as prognostic/predictive markers in the setting of dose-dense sequential adjuvant chemotherapy is not well defined. The purpose of this study is to assess the prognostic/predictive value of HER2/TopoIIa gene amplification and protein overexpression in this treatment setting.
Method: Tissue samples were obtained from 354 high-risk breast cancer patients randomized to be treated with dose-dense sequential adjuvant chemotherapy with epirubicin and CMF with or without paclitaxel. HER2/TopoIIa were assessed by immunohistochemistry and chromogenic in situ hybridization.
Results: A total of 17.5% displayed HER2 positivity, among them 96% showed HER2 amplification. As for TopoIIa, 62% classified positive, only 9% of them showed TopoIIa amplification. 64% of the HER2-positive tumors were also TopoIIa-positive assessed immunohistochemically, while only 21% of HER2-amplified tumors displayed TopoIIa amplification. No association of HER2/TopoIIa gene amplification or IHC-positivity with OS or DFS was found, except an increased risk for progression in HER2-positive patients. No benefit from paclitaxel treatment was detected for HER2/TopoIIa positive tumors.
Conclusion: HER2 and TopoIIa gene amplification or protein overexpression do not appear to be predictive for response to paclitaxel in high-risk breast cancer patients.

057

Adenoid cystic carcinoma of the breast: presentation of three cases

O. Tzaida *, I. Iakovidou, C. Valavanis, I. Kapetanidis, D. Karagianni, G. Giannakopoulos-Stanc,
P. Arapantoni-Dadioti
*Metaxa Cancer Hospital, Dept. of Pathology, Piraeus, Greece

Objective: Adenoid cystic carcinoma (ACC) is a rare special type of breast carcinoma analogous to salivary-gland ACC. It is characterized as a neoplasm with a basal/myoepithelial component, negative for hormonal receptors and c-erb-B2. Despite its relation to basal-like and tipple-negative breast carcinomas, breast ACC displays an excellent prognosis. Three cases of breast ACC, diagnosed during the last 10 years among 3,200 consecutive mastectomies, are presented.
Method: Three postmenopausal females over 55 years old, one of them underwent radical modified and two partial mastectomy plus radiotherapy for T1 tumors (1.5, 1.4 and 2 cm, respectively). Neither recurrences nor deaths were identified.
Results: A distinct cylindromatous pattern with PAS-diastase positive basal membrane material in a glandular, cribriform or solid pattern was detected. Differentiation varied from Grade I to III. Immunohistochemically two types of neoplastic cells were revealed: a luminal (CK7, CK18: +) and a dominant basal/myoepithelial one (CK 5/6, CK14, p63, actin, calponin:+). ER, PR and c-erb-B2 were negative in all cases.
Conclusion: Breast ACC is a very uncommon mammary neoplasm (0.09% of our lab breast carcinomas) histologically similar to other sites' counterparts. Prognosis is very good so recognition of this rare malignancy as a separate entity is important.

058

BRCA mutation screening in Bulgarian breast cancer patients

A. Vlahova *, R. Dodova, A. Mitkova, D. Dacheva, M. Caulevska, T. Dikov, S. Valev, M. Taushanova, C. Timcheva, V. Mitev, R. Kaneva, S. Christova
*Alexandrovska University Hosp., Dept. of Pathology, Sofia, Bulgaria

Objective: Studies of different populations worldwide demonstrate that germ line mutation in BRCA1/2 breast cancer (BC) susceptible genes account for the majority of hereditary breast and ovarian cancers.
Method: We performed mutation screening by direct sequencing of 100 Bulgarian BC patients referral for BRCA genetic testing according to the BCLC criteria.
Results: Totally, 18 BRCA mutation carriers were found. The common BRCA1 mutation 5382insC was observed in ten patients, five of which demonstrated triple negative breast cancer (TNBC) subtype. The observed mutations in the BRCA2 gene were all pathogenic alterations described in other European populations (6174delT, 1950delAGTT, 1906delCT, 2636delCCTTT and Thr1915Met). The predominant histological type found in 12 patients among the BRCA mutation carriers was invasive ductal carcinoma. Two of the index cases developed bilateral breast cancer while seven of them had both breast and ovarian cancer.
Conclusion: The frequency of the BRCA mutations in the studied cohort of BC patients (18%) was similar to that found in other populations. It has been known that Ashkenazi Jews 5382insC and 6174delT founder mutations are spread all over Central and Eastern Europe. Our results suggest that 5382insC might be also the most frequent mutation (10%) among BC patients in Bulgaria.

059

Primary diffuse large B-cell lymphoma of the breast

G. Volanska *, A. Abolins, I. Strumfa, S. Nikulsins, M. Abolina, J. Gardovskis, E. Miklasevics
*Riga Stradins University, Dept. of Pathology, Latvia

Objective: The non-Hodgkin lymphomas (NHL) comprise diverse haematologic malignant tumours arising in lymphatic nodes and extranodally. The breast is a rare location of NHL development. Primary breast lymphoma accounts for 0.05–0.53% of all malignant diseases of the breast and 2.2% of extranodal malignant lymphomas. Here we present two cases of primary diffuse large B cell lymphoma of the breast.
Method: NHL patients were identified by archive search among consecutive breast cancer cases. The clinical history, laboratory and radiologic data were reevaluated. The formalin-fixed, paraplast-embedded tissues were investigated by routine stains and immunohistochemistry (IHC).
Results: There were 2 NHL patients (86-year-old male; 66-year-old female) among 431 (0.46%) breast cancer cases. The largest tumour diameter was 20 and 3.7 cm. In both cases, the tumour had anaplastic morphology. By IHC, the neoplastic cells expressed CD45 and CD20. No expression of CD3, cytokeratins AE1/AE3 and mammoglobin was present. Proliferation fraction (by Ki-67) was high in both cases, reaching 70% and 83%.
Conclusion: Considering large anaplastic breast tumour, lymphoma should be included in the differential diagnosis in order to offer appropriate treatment. In our series, breast lymphoma is rare and represented by high-grade B-cell NHL.

060

Relationships between EGFR expression and mitotic rate or cytologic atypia in the phyllodes tumors

H.-K. Yoon *, Y.-H. Jung
*Pusan Paik Hospital, Dept. of Pathology, Busan, Republic of Korea

Objective: For the subclassification of phyllodes tumor (PT), the most reliable but problematic parameter is a mitotic count. In WHO classification, ≥10/10 HPF is required for malignant PT, but the other authors suggested ≥5/10 HPF. The utility of various markers for the subclassification of PT was still controversial.
Method: Immunohistochemical stains for smooth muscle actin (SMA), CD34, CD10, c-kit and EGFR were done in 46 PT cases. The expression of each marker was analyzed according to the classifications, cytologic atypia and degree of mitotic rate.
Results: A significant difference of EGFR expression between benign, borderline, and malignant PTs was noted, but there were no significant differences of SMA, CD34, CD 10 and C-kit expressions. A significant difference of EGFR expression was found according to absence or presence of cytologic atypia (p=0.0122), but there were no significant differences of other markers. There was a significant difference of EGFR-expression (p=0.0338) between the PTs showing 0~4 and ≥5/10HPF, but no significant difference between the PTs showing 0~9 and ≥10/10HPF (p=0.0794).
Conclusion: EGFR expression might be useful for the discrimination of malignant PT and is more common in PTs showing ≥5 mitotic count/10HPF and conspicuous cytologic atypia.

061

Incidence and histological subtypes of triple-negative breast cancer

C. Marian *, M. Boros, M. D. Podeanu, S. Stolnicu
*University County Hospital, Dept. of Pathology, Targu Mures, Romania

Objective: Triple-negative breast tumors represent a challenging group since recently published papers demonstrated an aggressive clinical course (related to the lack of effective targeted therapy) and different morphology. The aim of this study is to reveal the incidence and heterogeneous morphologic properties of triple-negative breast cancers, defined by the absence of the estrogen receptor (ER), progesterone receptor (PR) and human epidermal growth factor receptor 2 (HER2).
Method: We selected 20 cases of triple-negative breast cancers (4.91%) from 407 breast cancer patients diagnosed in our department (2009–2011).
Results: The triple negative patients (all women) were younger (mean age of 57.5 years). Of these, 11 cases presented axillary lymph nodes metastases and 6 were multifocal. A total of 13 cases were grade III ductal invasive carcinomas, while 3 were apocrine carcinomas, 2 medulary carcinomas, 1 mixed ductal-lobular carcinoma and 1 metaplastic carcinoma with osteoid differentiation; only 5 cases were associated with pushing borders, geographic necrosis and peritumoral inflammatory infiltrate.
Conclusion: Triple-negative carcinomas were described as a homogenous group of tumours, with well established criteria. We found that this group does not represent more than 5% of all breast carcinomas if correct criteria to define are applied and encompasses a wide range of subtypes with varying prognosis.

062

Evaluation of angiogenesis in adenoid cystic carcinoma of the breast

S. Vranic *, S. Frkovic-Grazio, N. Bilalovic, Z. Gatalica
*University of Sarajevo, Clinical Center, Bosnia and Herzegovina

Objective: The aim of this study was to explore microvascular density (MVD) and the expression of hypoxia pathway-associated proteins in ACC and compare them with a control group of stage-matched triple-negative breast carcinomas (TNBC).
Method: Twelve ACC of the breast and 15 TNBC were investigated immunohistochemically for CD34, podoplanin (D2.40), VHL protein, and HIF-1α protein.
Results: The mean lymphatic and MVD per square millimeters was 14 and 4, respectively, in the ACC subgroup and 18 and 6, respectively, in the TNBC subgroup (P=0.93, P=0.67, respectively). VHL protein was expressed in all 12 ACCs (100%) whereas 2 cases of TNBC (13%) had less than 5% of the positive. HIF-1α expression was significantly higher in the tumor cells in comparison with adjacent normal/benign cells in both subgroups (P=0.009 for TNBC and P=0.028 for ACC,

respectively). The mean percentage of HIF-1α positive tumor cells was 15% in ACC vs. 17% in TNBC (P=0.87). **Conclusion:** Up-regulation of the hypoxia induced signaling is seen in both ACC and TNBC when compared to the surrounding normal tissues. Despite its low malignant potential, ACC of the breast does not differ in the number of blood and lymphatic vessels in comparison with the stage-matched TNBC.

063

The extracellular matrix protein Tenascin-C promotes proliferation in breast cancer

S. Swierczynski [*], E. Klieser, S. Bastelberger, O. Dietze, C. Hauser-Kronberger

[*]Paracelsus Universität Salzburg, Inst. für Pathologie, Austria

Objective: The extra cellular matrix molecule Tenascin-C (TNC) is highly expressed during tissue repair, wound healing and pathological conditions such as cancer. Therefore we investigated the connection between TNC and cell proliferation in paraffin embedded breast cancer tissue. The linkage between EGFR and TNC expression was observed.

Methods: Paraffin sections from breast cancer patients, were used for automated immunohistochemistry (IHC) with antibodies targeting TNC and Ki67. The EGFR positive cell lines MDA-MB231 and SUM-159PT showed a increased TNC expression in RT-PCR after addition of EGF. The therapy agent IressaTM (GefitinibTM) was tested on MDA-MB231 and showed at 1 μM concentration inhibitory effects on the TNC expression. All cell lines were screened for TNC and Hh expression with IHC and RT-PCR. Migration assays were made with the TNC positive cell line MDA-MB231.

Results: The cell line MDA-MB231 showed a very good response for increasing and decreasing TNC with the therapeutic agent IressaTM. TNC showed in patient samples and cell culture assays an association with cell proliferation.

Conclusion: Our findings show the growth-promoting properties of Tenascin C in breast cancer.

064

Impact of phenothypic profile on survival in triple negative breast cancer

M. V. Comanescu [*], C. Ardeleanu

[*]Voctor Babes Institute, Dept. of Pathology, Craiova, Romania

Objective: Although considerable interest has been shown towards TNBC, there is still need of new therapeutic agents, as these tumors posses an aggressive phenotype and poor prognosis.

Method: Our retrospective study included 37 cases of TNBC with the necessary clinical and rates of follow-up data, our primary outcome of interest being the correlation between overall survival and clinicopathological and immunohistochemical profiles.

Results: The collected data included patients', tumours' and treatments' characteristics. Eight cases had long survival rates of almost 20 years. We also included in our study a dataset of invasive breast cancer non-TN, to compare the differences in profiles. Besides a detailed histological review, different combinations of immunohistochemical were used in order to study both tumoral and stomal components.

Conclusion: The lack of expression of hormone receptors and ERBB2 confers limited therapeutic options; the only viable strategy for women with TNBC being, at present, adjuvant chemotherapy. The identification of changes in the tumoral and stromal components and the interpretation of the interrelation with survival rates could provide a useful help in the future guiding of targeted therapy.

Sunday, 28 August 2011, 09.30–10.30 and 16.30–17.00, Hall 5

PS-02 Poster Session Dermatopathology

001

Immunohistochemical study of protein P53 in Egyptian psoriasis

M. El Shaer [*]

[*]National Research Centre, Dept. of Pathology, Cairo, Egypt

Objective: The histopathologic changes characteristic of psoriasis might be related to an abnormality in the apoptotic pathway.
Aim of the work: The aim of this study is to evaluate the possible role of protein P53 in the pathogenesis of psoriasis through a case control study as it could be one of the targets of psoriasis therapy.
Method: This study included 30 patients of different clinical variants of psoriasis and 25 controls with normal skin biopsies. All patients were subjected to complete history taking, clinical examination including psoriasis area and severity index (PASI) score and skin biopsies, all patients stopped topical or systemic medication 4 weeks prior to biopsies. Five-millimeter incisional biopsy specimens were taken from the 30 patients and from each biopsy one stained with hematoxylin and eosin to confirm the diagnosis, the other to be prepared for immunohistochemical detection using mouse monoclonal antibody (Do7) against P53 protein, results were compared with 25 control.
Results: Psoriatic plaques revealed P53 nuclear staining detected in 13 out of the 30 patients (43.3%), and 17 (56.7%) showed negative immunoreactivity in keratinocytes.
Conclusion: From these results it can be concluded that apoptosis plays a role in the pathogenesis of psoriasis and this may be mediated through the abnormal expression of apoptosis regulating proteins P53.

003

The comparison of basal cell carcinoma's immunohistochemical characteristic in old and young persons and in patients with another malignancy

R. Kleina *, I. Truksane, A. Dabuzinskiene, J. Kisis
*Riga Stradins University, Pathology Center, Latvia

Objective: BCC is associated with Basex-Dupre-Christol, nevoid BCC and Rombo syndromes. Rare are described associations of BCC with carcinomas of other organs (J. Kaae; M. Karagos etc.) The aim of this research was to find out the immunohistochemical differences in the BCC of old and young persons and in patients with another malignancy.
Method: We have evaluated 18 old and 10 young patients with BCC and 6 persons with BCC and cancer of non-skin location and control group with CD3, CD20, CD68, CD 117, Ki-67, MMP-9, inhibin expression inside and around. Results were analyzed with SPSS-14.
Results: A total of 39% of BCC were located on head, 22%—back with average size 1, 55±0.45 cm. The age of elderly was 69.9±2.6, but of young persons 34, 25± 1.91 years. Proliferation index in center of BCC was 13.8%, in periphery 68.3% (p=0.02) but in derma 5.2%. CD68, CD3, CD117, CD20 positive cells and inhibin and MMP-9 substances were expressed mainly around the tumor. Another cancer was in breast, urinary bladder and bronchus. Six, 1%, cases of BCC recurred.
Conclusion: Mast cells, B, T lymphocytes, CD68 and MMP9 around tumor possibly slacken the progression of BCC and were similar in all three groups. Younger persons with BCC need thorough clinical examination of internal organs.

004

Breslows thickness of cutaneous melanoma in Iceland 1980–2009

H. Stefánsson *, B. Sigurgeirsson, L. Tryggvadóttir, J.H. Ólafsson, E. Mooney, E. Ólafsdóttir,
J.G. Jónasson
*University of Iceland, Faculty of Medicine, Reykjavík, Iceland

Objective: Cutaneous melanoma incidence has increased dramatically in Iceland in the last decades. This study aims at analysing the changes in Breslows thickness of melanomas in this period.
Method: Altogether 854 cases of melanoma were diagnosed in the country in the 30 year period 1980–2009 according to the Icelandic Cancer Registry. They were stratified according to gender, age (<50, ≥50), year of diagnosis (three 10-year periods) and Breslows thickness (≤1.0, 1.01–2.0, 2.01–4.0 and >4.0 mm).
Results: The median Breslows thickness declined in males and females, respectively, from 2.15 and 1.0 mm in 1980–1989 to 0.9 and 0.6 mm in 2000–2009. When stratified by gender and age, the incidence of thin (≤ 1.0 mm) melanomas increased dramatically in all subgroups, while the intermediate (1.01–2.0 and 2.01–4) tumours only increased in older men (≥50).
Conclusion: The Breslows thickness of cutaneous melanomas has declined markedly and the dramatic increase in melanoma incidence is mainly due to an inflation in the subgroup of thinner tumours. Women have significantly thinner tumours than males. In older men tumours of intermediate thickness are increasing. This might indicate that women are more alert and future melanoma educational campaigns in Iceland should be more focused on men, particularly older men.

005

Algorithmic approach of cutaneous metastases of unknown origin

S. Zurac *, C. Popp, R. Andrei, T. Tebeica, C. Zaharia, G. Maria, L. Nichita, C. Socoliuc, F. Staniceanu, V. Chitu, C. Giurcaneanu
*Colentina University Hospital, Dept. of Pathology, Bucharest, Romania

Objective: Cutaneous metastases are sometimes the first sign of neoplastic disease, requiring a rapid and precise diagnosis in order to establish the appropriate management of the patient.
Method: We analyze 87 cases of cutaneous metastases diagnosed in our department between 2003 and 2011. In all cases, the primary was established based on morphological and immunohistochemical (IHC) features of the tumors, clinical data supporting the histopathological findings. IHC markers used in diagnostic processes were analyzed in respect of cost/effectiveness.
Results: Most of the metastases were carcinomas (most frequent originating in breast, lung and colon), melanomas and lymphomas. Few cases were renal clear cell carcinomas, urothelial carcinomas, gastric and pancreatic neuroendocrine carcinomas and isolated cases of metastatic Ewing sarcoma, peripheral neuroendocrine tumor and epithelioid sarcoma. Morphology was highly suggestive of origin site in most of the cases; most helpful special stains were PAS (glycogen and/or mucin accumulations) and reticulin stain (Gomori) (highlights tumor structures). IHC establishes the tumor type in poorly differentiated tumors and offers informations about origin.
Conclusion: Based on the frequency of metastases and the histopathologic data, we establish an algorithm to facilitate rapid and economical identification of tumor origin: morphology analysis, histochemical findings and three IHC panels including either tumor type or specific organ markers.

006

Allelic imbalance detection in the Notch1, Presenilin1 and Presenilin2 genes expression at patients with Kaposi's sarcoma

A.-M. Catrina Ene *, A. Chitu, E. Ionica, M. Costache, M. Sajin, O. Simionescu
*University of Bucharest, Dep. of Biochemistry, Romania

Objective: Microsatellite markers are useful tools for molecular genetic analysis of allelic imbalance detection in cancer. Microsatellites are short sequence tandem repeats (STRs), usually dinucleotide repeats of CA. They are valuable as DNA markers because of their high polymorphism.
Method: In the current study, we examined the DNAs that were isolated from seven Kaposi's sarcoma tumors for allelic imbalance on chromosome 9q, 14q and 1q by using PCR amplification of microsatellite markers. The presence of MSI and LOH at 12 loci [chromosome 9q (D9S158, D9S905, D9S1826, D9S1838- Notch1), 14q (D14S1028, D14S77, D14S1004, D14S43- Presenilin1), 1q (D1S504, D1S2616, D1S1644, D1S479- Presenilin2)] was evaluated.
Results: Our results revealed a moderate frequency of LOH/MSI in the microsatellite markers analyzed. Among the seven Kaposi's sarcoma cases, 5/7 showed genome instability (LOH and/or MSI) at one or more loci on the 9q, 14q and 1q chromosomes. Frequently, LOH were identified at loci D1S504, D1S479, D9S1826 and D14S43. MSI were detected at loci D1S479, D9S1838, D9S905 and D14S1028.
Conclusion: Our results provide the evidence of LOH/MSI at one or more loci on the chromosomes 9q (Notch1), 14q (Presenilin1) and 1q (Presenilin2) in KS. These microsatellites could be used as DNA markers to study the mutation profile of these genes.

007

Angiomatosis of soft tissue

M. Costache *, O. Simionescu, E. Albu, M. Sajin, D. Costache, A.M. Catrina
*Bucharest, Romania

Objective: Angiomatosis is a rare condition characterized by a diffuse proliferation of blood vessels affecting a large contiguous area of the body (usually lower extremities). The tumour is composed of adipose tissue infiltrating skeletal muscles, intermixed with blood vessels.
Case report: A 30-year-old man, I. P., had 16 years history of painless, solitary nodule on the right leg.
Method: After surgical excision the lesion was 85/70/20 mm, brown colour with yellow and white areas. Tissue specimens were fixed in 10% buffered formalin, routinely processed and embedded in paraffin, sectioned at 3 μm, then stained routinely using hematoxylin–eosin and then examined by light microscopy.
Results: The blood vessels were infiltrative in adipose tissue and skeletal muscle; combinations of different types and sizes of vessels were particularly evident (veins with irregular walls, cavernous vascular spaces and capillaries).
Conclusion: Angiomatosis of soft tissue was described by Rao and Weiss in 1992. The reported lesion was located at lower extremities, as most cases of angiomatosis, and was a long-standing lesion. However, due to the heterogeneous nature of the lesion, diagnosis may be difficult on small specimens.

008

The benefit of immunochemistry in the diagnostic of malignant melanoma

S. Dumitriu *, A. Dumitriu, R. N. Dumitriu
*UMF Iasi, Dept. of Pathology, Romania

Objective: The aim of this study is to investigate the expression of p53 and Ki67 in benign as well as in malignant cutaneous melanocytic lesions.
Method: Four specimens of benign melanocytic tumours and 19 of malignant melanocytic tumours have been stained for the p53 protein and Ki67 antigen.
Results: We found that the expression of p53 in cutaneous melanocytic lesions is associated with the invasive stage of the tumour development. The expression of Ki67 was different between benign amd malignant lesions.
Conclusion: The immunostainining for p53 and Ki67 could help us to diferentiate benign from malignant melanocytic lesions.

009
Sebaceous carcinoma of the eyelid

S. Dumitriu *, D. Radulescu, C. Costea, S. Stolnicu, L. Chelaru, D. Butcovan, A. Dumitriu
*UMF Iasi, Dept. of Pathology, Romania

Objective: Sebaceous carcinoma is a rare cutaneous malignancy that is most frequently found in the eyelids. The aim of this study is to present features, sites of origin, location, histopathologic findings and mortality.
Method: The median age was 69 years with 57% female. Initial clinical diagnosis was sebaceous carcinoma (30%), blefaroconjunctivitis (45%), basal cell carcinoma (15%) and squamos cell carcinoma (10%).
Results: Pathologically 52% presented intraepitelial involvement, 32% arose from the meibonion glands. Metastasis developed in 10% of the cases and death from metastasis in 3%.
Conclusion: Despite the fact that the clinical features of sebaceous carcinoma have been reported widely the diagnoses was suspected initially in only 27% of patients. It is hoped that the modern therapeutic approaches will result in fewer cases of recurrence and metastasis.

010
Dermatofibrosarcoma protuberans

S. Dumitriu *, D. Radulescu, S. Stolnicu, L. Chelaru, C. Costea, C. Ungureanu, C. Zamfir, A. Dumitriu
*UMF Iasi, Dept. of Pathology, Romania

Objective: Dermatofibrosarcoma protuberans is an uncommon skin tumour characterized by progressive growth and a propensity for local recurrence.
Method: We describe the clinicopathological features of five cases of dermatofibrosarcoma protuberans. A total of 89% of the cases underwent surgical excision without previous biopsy.
Results: The recurence rate was 38.3% and the median period free of disease was 22.5 months.
Conclusion: Dermatofibrosarcoma protuberans has a locally high recurence rate that has been associated with inadequate surgical margins. Most recurrences appear in the first year that it is very important to have a long-term follow-up of these patients.

011
Significance of vascular endothelial growth factor expression in skin melanoma

R. Gajanin *, V. Gajanin, Z. Krivokuca, L. Tadic-Latinovic, B. Zrnic
*Clinical Centre Banjaluka, Dept. of Pathology, Banja Luka, Bosnia and Herzegovina

Objective: Melanoma is a heterogeneous disease of skin and mucous membranes. The aim of the research is to determine the level of VEGF expression in skin melanoma in different body regions and in different primary stages of the disease.
Method: The research was conducted on bioptic materials of skin in 39 patients. On excision-made materials a routine histological preparation was done and the following parameters were determined: histological type, alteration thickness, Clark level, pTNM stage, alteration width, thickness and level of VEGF expression.
Results: Analysis confirmed that 61.54% of skin melanoma showed a high VEGF expression. Nodular and acral lentiginous melanomas showed more frequently a high level of VEGF expression, while superficial spreading melanoma showed a lower level of VEGF expression ($p=0.032$, $p<0.05$). A higher level of expression was present in thicker melanomas ($p=0.011$, $p<0.05$). The width of the lesion did not have an influence on the level of VEGF expression in melanoma (U =142.000, 0.273).
Conclusion: Melanomas show a higher level of VEGF expression. Nodular and acral lentiginous types of melanoma show a high level of VEGF expression, while a superficially spreading melanoma shows a lower level of VEGF expression. Melanomas in higher-stage disease show a higher level of VEGF expression.

012

Lobular breast carcinoma metastasis to a superficial plexiform schwannoma as the first evidence of an occult breast cancer

B. Gazic *, J. Pizem
*Institute of Oncology, Dept. of Pathology, Ljubljana, Slovenia

Objective: Tumour-to-tumour metastasis is a rare phenomenon, in which one, benign or malignant, tumour is involved by metastatic deposits from another. Only seven cases of metastases to schwannoma have so far been reported in the English literature (in a single case to a subcutaneous schwannoma).
Results: A 70-year-old woman without history of cancer presented with several skin nodules that she had noted for 6 months. Histological examination of an excised nodule showed a plexiform schwannoma containing a population (comprising about 20% of the lesion) of fairly uniform epithelioid cells, mitoses and focally small mucin vacuoles in the cytoplasm. The epithelioid cells were cytokeratin positive, S100 protein, E-cadherin and CD31 negative and expressed estrogen and progesterone receptors. Morphological and immunophenotypical features were consistent with metastasis of lobular breast carcinoma in plexiform schwannoma. Further investigations revealed bilateral metastasis of carcinoma in the axillary lymph nodes, expressing estrogen and progesterone receptors, while mammography showed no convincing tumour lesion in either breast. Complete remission was achieved 2 months after starting hormonal treatment with an aromatase inhibitor.
Conclusion: Differential diagnosis of schwannoma with epithelioid cells includes malignant transformation of schwannoma, metastasis of a carcinoma or melanoma to schwannoma, epithelioid schwannoma and schwannoma with glandular or pseudo glandular elements.

013

Primary cutaneous nodular amyloidosis of the face: A challenge diagnostic

M. T. Gonzalez Serrano *, I. Ruiz Molina, E. Solis Garcia
*Hospital Reina Sofia, Dept. of Pathology, Cordoba, Spain

Objective: Primary cutaneous nodular amiloidosis (PCNA) is the least common form of primary cutaneous amiloidosis. We present a rare case of PCNA in a young man who developed an asyntomatic nodular growth on the left side of his nose many months ago. There were no other similar nodules seen on rest of his body.
Method: A punch biopsy was done with clinical diagnosis of an anexial tumor.
Results: Biopsy of the nodule confirmed dense nodular deposits of an amorphous mass involving the upper and lower dermis. These deposit stained with Congo red showed apple-green birefringence using polarized light. Also, a chronic inflammatory infiltrate with plasma cells and giant-cell reaction were present. Further baseline investigations were done to exclude systemic involvement.
Conclusion: PCNA refers to amyloid deposition confined to the skin without systemic involvement. Lichenoid and macular amiloidosis are the most common, with deposition of amyloid in the papillary dermis. It is thought to occur as a result of deposition of amyloid L protein, produced locally by plasma cells. Light chains may be kappa or lambda, or both. The cause of PCNA is unknown.

014

Mycosis fungoides simulating epidermotropic CD8(+) cutaneous T cell lymphoma

Ö. Gököz *, A. Üner, G. Erkin, A. Ayhan
*Hacettepe University, Dept. of Pathology, Ankara, Turkey

Objective: A 22-year-old man complained of red scaly papules for 3 years and had the diagnosis of pitriasis rosea. Later, he developed widespread erythematous papules, xerotic patches and plaques.
Method: Punch biopsies with several months' intervals taken from extremities and trunk were examined histopathologically. Immunohistochemistry and TCR gene rearrangement studies were performed.
Results: First biopsies revealed atypical lymphoid infiltration in the dermis with epidermotropism. Lymphoid cells were CD8 (+) and CD7 loss were present. Molecular studies demonstrated rearrangement of gamma chain. Clinicopathological diagnosis was mycosis fungoides (MF). The patient was given erythromycin, deltacortin and nbUVB. The biopsy taken upon the emergence of a new lesion with the clinical diagnosis of pitriasis lichenoides and MF showed epidermal necrosis, CD2, CD3, CD8 and Granzyme B positive medium to large pleomorphic lymphocytic infiltration invading the vascular and adnexal structures. CD4, CD7, CD79a, CD30, CD5, CD15 and EBNA were negative. The findings were consistent with primary cutaneous aggressive epidermotropic CD8(+) cytotoxic T cell lymphoma. PUVA therapy was given and no new lesions were seen after 3 years.
Conclusion: Pitriasis lichenoides like MF is rarely seen mostly in young patients. The presented case is an unusual variant of MF with cytotoxic phenotype simulating primary

cutaneous aggressive epidermotropic CD8(+) cytotoxic T cell lymphoma.

015

Differential diagnosis in the spectrum of proliferating trichilemmal cyst to trichilemmal carcinoma by the occasion of two rare cases

C. Hadjileontis *, D. Kakoulidis, N. Nicoloudis, A. Kafanas
*Serres General Hospital, Dept. of Pathology, Greece

Objective: Proliferating trichilemmal cysts (PTC) are usually solitary tumors, most often occurring on the scalp, as a result of repeated rupture and re-epithelialization of trichilemmal cysts. Their malignant counterparts (MPTC) usually overlap PTC, both clinically and histologically, they furthermore have the potential of metastasizing. Trichilemmal carcinoma on the other hand, is considered by most authors to be a distinctive lesion that has to be differentiated from other common malignancies of the skin.
Method: We present two cases of MPTC affecting males aged 56 and 68 years old, respectively, wwere clinically misdiagnosed as benign cysts. The first one was not send for histological examination and presented with local recurrence and cervical lymph note metastasis, five years after its surgical excision. The second one that was histologically examined, was lined by a fibrous layer that was infiltrated by tumor cells, its surgical margins however were free of tumor cells.
Results: The clue figures that distinguish these three, rare, overlapping entities are the differentiation of their cells, their nuclear atypia and mitotic activity, as well as the presence of stromal invasion. By the case of this presentation we discuss problems that may arise in differential diagnosis and may affect the patient's outcome and prognosis.

016

Prediction of merkel cell polyomavirus infection in merkel cell carcinoma based on morphological characteristics

T. Iwasaki *, S. Kuwamoto, M. Kato, I. Murakami, M. Matushita, Y. Horie, O. Yamamoto, K. Hayashi
*Tottori University, Dept. of Molecular Pathology, Yonago, Japan

Objective: Merkel cell polyomavirus (MCPyV) is integrated in approximately 80% Merkel cell carcinomas (MCCs). MCPyV-positive MCCs show less metastatic tendency and better prognosis. Recently, we demonstrated statistically significant morphological differences in tumor cells between MCPyV-positive and -negative MCC. We aimed to assess the usefulness of our histological criteria differentiating MCPyV-positive and -negative MCCs given below: (1) MCPyV-negative MCC showed nuclear polymorphism with rich cytoplasm (2) and occurred with squamous cell carcinoma (SqCC).
Method: Six observers challenged estimations (five-point confidence scale) of MCPyV infection in MCCs, using H&E staining before IHC and PCR.
Results: We found concordant results in 41/43 (96%) cases for CM2B4 IHC staining. The CK20 immunoreactivity was significantly less in MCPyV-negative MCCs ($p = 0.029$). The mean accuracy, sensitivity, specificity, and AUC value of observers were 83%, 85%, 77%, and 0.89, respectively.
Conclusion: Using our histological criteria, pathologists can predict MCPyV infection using H&E staining, especially when the tumor occurs with SqCC or shows typical MCPyV-negative morphology. Observers can accurately estimate MCPyV-negative MCCs with worse prognosis. Thus, our assessments of diagnostic performance of H&E in MCCs with MCPyV infection have clinical importance.

017

Multiple cutaneous metastases: A rare and late sequelae of lacrimal gland adenoid cystic carcinoma

J. Jedrych *, A. Galan
*Yale University, Dept. of Pathology, New Haven, CT, USA

Objective: Adenoid cystic carcinoma (ACC) is an uncommon cutaneous neoplasm with over sixty primary cases reported in the literature. Metastatic ACC to the skin is even less frequent with nine previously published cases. Only one case of metastatic lacrimal gland ACC has been reported.
Method: We report a case of a 62-year-old male, who developed multiple cutaneous metastases to the scalp and back from lacrimal gland ACC 21 years after the initial diagnosis and treatment with right orbit exenteration. Initially, in the absence of previous clinical history, the cutaneous lesions were thought to be primary ACC of the skin.
Results: Histologically, the metastatic lesions were poorly circumscribed dermal and subcutaneous nodules, composed of islands of basaloid epithelial cells with ducts and cribriform pattern, mucinous stroma and prominent perineural invasion. Morphologically, the cutaneous tumors were similar to the primary ACC. The cutaneous metastases were preceded by lung and other visceral metastases. Of interest, the patient also developed chronic lymphocytic leukemia.

Conclusion: This report illustrates the importance of judicious clinico-pathologic correlation and raises awareness regarding prolonged latency of cutaneous metastases in patients with ACC, which may herald disease progression and poor prognosis.

018

Coccygeal polypoid eccrine nevus a rare amartomatous polypoid lesion of the skin

P. Katafygiotis *, A. Tsega, G. Anastasiadis, E. Boltetsou, A. Skopelitou, K. Asvesti
*Hospital of Athens, Dept. of Pathology, Greece

Objective: Eccrine nevus is considered a rare amartomatous polypoid lesion of the skin most commonly noted by the dermatologist due to localized hyperhidrosis. Until now three cases have been published under this nomenclature.
Method: We present the case of a 4.5-year-old girl with coccygeal polypoid eccrine nevus. The parents had noted the lesion, a few months earlier, because the child complained for pain when she went to sit. On clinical examination a polypoid flesh-colored lesion of 0.5 cm in diameter, on the midline of the coccyx, was noticed.
Results: Gross examination revealed a flesh colored-skin polyp measuring 0.5 cm. Microscopically, the lesion had an acanthotic and hyperkeratotic epidermis. In the center of the lesion, collections of proliferating normal eccrine glands and ducts were noticed. Blood vessels were congested and dilated. Immunohistochemical studies revealed eccrine glands positive for S-100 protein.
Conclusion: Eccrine nevi are benign lesions occurring equally in males and females. Their predilection site is the upper extremities. The coccygeal polypoid eccrine nevus has to be distinguished histologically from the common skin tag and the lumbosacral lipoma, a rare congenital anomaly found in the sacral area.

019

Cutaneous reactions associated with anti-TNF-a therapy

C. Kouvidou *, C. Vourlakou, M. Kopaka, M. A. Lianou, G. Anastasiadis, D. Rontogianni
*Evangelismos Hospital, Dept. of Pathology, Athens, Greece

Objective: TNF-a inhibitors have been proved to be very effective in the treatment of various immune mediated rheumatological, gastroenterological and dermatological diseases but they may develop cutaneous reactions.
Purpose: This study aims to describe the different histological skin lesions seen in eight patients treated with TNF-a inhibitors.
Method: Five of the patients were treated for Crohn's disease, two of them for rheumatoid arthritis and the last one for ulcerative colitis. The patients showed erythematous or pruritic rash on trunk and/or flexural areas of the extremities. The eruption began from 4 to 9 months after initiating TNF-a inhibitor.
Results: The histology showed the following reactions: eczema (1), lichenoid (1), psoriasiform (2) leukocytoclastic vasculitis (2), lupus erythematosus (1) and erythema nodosum (1). The patients have no personal or family history of dermatological diseases. Topical therapy resulted in partial or total remission in five patients, while in the remaining three after the discontinuation of the anti-TNF agent.
Conclusion: Dermatologists must be aware of these potential adverse effects and pathologists should be familiar with these cutaneous reactions. It has been suggested that the cross-regulation between TNF-a and INF may play a role in the pathogenesis of this reaction.

020

Discrimination of malignant melanomas from dysplastic nevi based on elevated cell cycle progression

T. Krenács *, G. Kiszner, I. Nemeth, E. Varga, I. Korom
*Semmelweis University, 1st Dept. of Pathology, Budapest, Hungary

Objective: Distinction of malignant from benign melanocytic tumors in borderline dysplastic lesions can be a great diagnostic challenge. Dysregulation of cell replication and elevated cell cycle progression are related to malignant phenotype.
Method: We studied proteins of cell cycle regulation in 350 tissue microarray samples of 49 primary melanomas, 16 metastases, 48 atypical nevi and 5 common nevi with immunohistochemistry using digital microscopy.
Results: Most cell cycle promoters including Ki67, mcm2, mcm6, cdk2, cyclin D1, -E and -A, geminin and topoisomerase IIα were more frequent in primary melanomas than in dysplastic nevi. Topoisomerase IIα, cyclin A and geminin of the post-G1 phase were missing in atypical nevi as opposed to melanomas. In primary melanomas, cyclin A, cyclin E and geminin expression significantly correlated with tumor thickness, Clark's level, mitotic rate and ulceration. Furthermore, geminin was significantly more frequent in metastatic than in primary melanomas.

Conclusion: Our results suggest that melanocytes in benign nevi including those of dysplastic phenotype are in a state of cellular senescence and do not activate their cell cycle regulation machinery. In contrast, most melanomas can pass through post-G1 phase and complete the cycle. Therefore, detection of cyclin A, geminin and topoisomerase IIα are potential discriminators of malignant melanoma phenotype.

021

Malignant mixed tumour of skin: a case report

W. Majdoub *, S. Sassi, M. M. Hamdane, S. Ben Slama, L. Charfi, R. Doghri, R. Sellami-Dhouib,
K. Mrad, N. Ben Hamida, K. Ben Rhomdhane
*Military Hospital, Tunis, Tunisia

Objective: Malignant mixed tumour (MMT), also called malignant chondroid syringoma, is an exceedingly rare cutaneous adnexal carcinoma. It occurs within the dermis or superficial subcutis and is composed of both epithelial and mesenchymal components.
Method: We report a case of a 47-year-old woman who presented with a 50×50-mm lesion on her left arm. This had been present for approximately 2 years and was slowly increasing in size recently.
Results: There was no history of trauma and the patient was otherwise asymptomatic. Biopsy favored a malignant adnexal tumour. A wide local excision with lymph node excision was performed. Pathology revealed a MMT with negative margins. She is closely followed and remains disease-free at 4 years postoperatively.
Conclusion: MMT shows no distinctive clinical appearance and share clinical characteristics with a wide range of benign and malignant tumors. Subsequently, clinical diagnosis is often very difficult. MMT proliferates in an invasive and destructive fashion, with a high rate of local recurrence and metastases in regional lymph nodes, lung and bone. The treatment of choice is wide local excision. There seems to be a survival advantage for patients receiving adjuvant radiation therapy.

022

Detection of Merkel cell polyomavirus in autopsy cases by PCR and immunohistochemistry

M. Matsushita *, H. Higaki, T. Iwasaki, S. Yashima, S. Kuwamoto, M. Kato, I. Murakami, Y. Horie,
Y. Kitamura
*Yonago, Japan

Objective: Merkel cell polyomavirus (MCPyV) is a novel polyomavirus that shows a strong association with Merkel cell carcinoma. MCPyV is also detected in many normal human tissues such as skin. However, it is not fully elucidated where it is present.
Method: We examined 41 autopsy cases using PCR and immunohistochemistry with MCPyV-large T antigen antibody (CM2B4).
Results: PCR revealed MCPyV-DNA in non-neoplastic samples: total autopsy cases, 29/41 (71%); adult 29/39 (74%), infants 0/2 (0%); men, 24/28 (86%); women, 5/13 (38%) (p=0.004); total human tissues, 66/572 (12%); skin, 8/15 (53%); adrenal gland, 9/33 (27%), and 16 organs (4~25%). Range of real- time PCR was 0.00026-0.22. MCPyV-DNA was detected in an ectopic pancreas of jejunum polyp among 22 benign or malignant tumors. Prevalence of MCPyV-DNA in skin is higher than other 17 organs. In immunohistochemistry using MCPyV-large T antigen antibody (CM2B4), nuclear or cytoplasmic immunoreactivity was shown in many kinds of normal cells such as lymphocytes, endothels, schwann cells, smooth muscles of vessels, thyroid follicle cells, squamous cells, glomerular epithelia and etc, which considered as latently infected cells.
Conclusion: Immunohistochemical distribution data of MCPyV-LT antigen in human tissues were not necessarily corresponded to PCR data. To identify latently infected cells accurately, developing better methods is needed.

023

Demodex mites in facial skin biopsies

M. Melachrinou *, M. Gkermpesi, C. Geronatsiou, H. Kourea
*University of Patras, Dept. of Pathology, Greece

Objective: Rosacea is a common dermatosis and the facial skin is the predominant site of involvement. Several reports have proposed that Demodex plays a pathogenic role in rosacea. The aim of this study was to examine the presence and the number of Demodex mites in facial skin of patients with rosacea and other skin lesions.
Method: The prevalence of Demodex mites was studied in facial skin biopsies of 60 patients [mean age 55.7/31 females] with histologically confirmed rosacea as study group and in 131 patients [mean age 52.3/67 females] with different types of skin lesions [DLE, seborrheic dermatitis, melanocytic nevi, seborrheic keratosis, actinic keratosis, BCC, SCC] as control group.
Results: The mite prevalence in the rosacea group (51.66%) was significantly higher than in the control group (25.85%). Demodex mites were found on all facial sites. Females were more frequently infested (51.67%) than males (48.33%). The mean mite count in the rosacea group was significantly higher than that in controls.

Conclusion: Our findings suggest that Demodex mites may represent a cofactor in the inflammatory reaction seen in rosacea.

024

Clinicopathological characterization of MCPyV-positive and -negative Merkel cell carcinomas

H. Mori *, S. Kuwamoto, M. Matushita, T. Iwasaki, M. Kato, I. Murakami, Y. Horie, O. Yamamoto, K. Hayashi
*Tottori University, Dept. of Dermatology, Yonago, Japan

Objective: Merkel cell polyomavirus (MCPyV) is a new polyomavirus that is monoclonally integrated into genomes of approximately ~80% of human Merkel cell carcinomas (MCCs). Clinicopathological differences between MCPyV-positive and –negative MCCs have not been well known. Some researchers reported that MCPyV-positive MCCs show less metastatic tendency and better prognosis. We analyzed the clinicopathological characteristics of MCPyV-positive and –negative MCCs, in which we recently demonstrated association of MCPyV infection with statistically significant morphological differences (*Hum Pathol* 2011).
Method: We investigated clinical data such as stage, metastasis and outcome, and examined the immunohistochemical expressions of cell cycle-related genes in 20 cases of MCPyV-positive and 6 cases of MCPyV-negative MCCs, which were reported. Mutation of p53 will be also analyzed.
Results: MCPyV-positive MCCs with round nuclei and lower N/C ratio showed better prognosis and significantly higher expression of Rb and less p53 expression, while MCPyV-negative MCCs with polymorphic nuclei and abundant cytoplasm showed worse prognosis. No significant differences were found in expression of p63, Mdm2, p14 or MIB-1 index. We will also present data on mutation analyses of p53.
Conclusion: MCPyV-negative MCCs have worse prognosis and develop likely through different tumorigenesis from MCPyV-positive MCCs. Therefore, assessment of MCPyV infection in MCCs is very important.

025

Melanocytic lesions of the milk-line

A.-A. Nicolau *, M. Achie, A. Mitroi, A. Chisoi, I. Poinareanu, A. Iliesiu, G. Baltatescu, M. Enciu, S. Vamesu
*Clinical Emergency Hospital, Dept. of Pathology, Constanta, Romania

Objective: Melanocytic nevi at certain anatomical sites can have a histological picture misleading to the diagnosis of atypical nevus or even malignant melanoma. Therefore, it is very important to recognize these lesions in order to differentiate them from "true" dysplastic nevi or malignant melanomas. These anatomical regions are the head and neck, especially the ear, the milk line (axilla, breast, umbilicus and groin), acral regions (palms and soles, knee, dorsum of the foot) and flexural sites.
Method: This paper includes 138 pigmentary nevi, and the following parameters were analyzed: asymmetry, nested and dychoesive pattern, intraepidermal melanocytes, absence of dermal maturation, melanocytic atypia, dermal desmoplasia and lymphocytic infiltrate.
Results: Of the 138 tumors located on the "milk-line", 13 of them are malignant. The rest microscopically have features that are difficult to distinguish from melanoma. Breast nevi exhibited significantly more atypical features than nevi from other sites. In particular, breast nevi with intraepidermal melanocytes, melanocytic atypia, and dermal desmoplasia were significantly more numerous. The atypical features we found in the milk-line nevi do not correspond to any unusual behavior.
Conclusion: A special attention should be accorded to these types of lesions because they have atypical microscopic features that may be misdiagnosed as melanomas and have a benign clinical course.

026

Cutaneous lymphoid hyperplasia in association with Leishmania Infection

D. Sakiz *, Z.S. Kahraman, N. Polat, F. Kabukcuoglu, A. Yeşilada Karasoy
*Sisli Etfal Education Hospital, Dept. of Pathology, Istanbul, Turkey

Objective: Cutaneous lymphoid hyperplasia (CLH) or pseudolymphoma is a reactive lymphoid proliferation. CLH can mimick lymphoma, both at clinical and histopathological levels. The identification of an etiological agent, prolonged follow up, immunophenotypical studies and molecular analysis allow the differential diagnosis. Cutaneous leishmaniasis (CL) is an infectious disease caused by Leishmania.
Method: A 20-year-old man presented with a 12-month history of hypertrophic, infiltrated plaque lesion with irregular border on his left arm. The clinical history showed the patient had hot water accident on the same location 5 years ago. The lesion had appeared on the burn scar tissue. An excisional biopsy of the lesion was performed.
Results: Histopathological examination of the specimen revealed ulceration of the epidermis and diffuse dermal

infiltrate of lymphocytes, plasmocytes and histiocytes and reactive germinal centers. Amastigotes were detected within the histiocytes with hematoxylin and eosin but not with Giemsa stain. Germinal centers were formed of B lymphocytes that were polyclonal with kappa and lambda, and surrounded by a population of CD3+T lymphocytes. There was not any recurrence in 1-year follow-up of the patient.

Conclusion: CLH has often been described in association with a variety of cutaneos infections. Antigens are suspected from the development of the CLH. In the present case, development of leishmania cutis with CLH on the burned skin is considered interesting.

027

Granulomatous slack skin in childhood with an unusual localization

E. Sener *, H. Bilen, E. Demirci, M. Atasoy, N. Akdeniz, N. Gürsan

*Erzurum Bolge Egitim Hastanesi, Patoloji Bolumu, Turkey

Granulomatous slack skin (GSS) is a rare cutaneous disorder that is a clinical form of cutaneous T-cell lymphoma closely related to mycosis fungoides. Occurrence in children is extremely rare, but has been reported. It is characterized by slowly progressive indurated plaques that evolve into erythematous pendulous skin folds, predominantly in the flexural areas. The inguinal and axillary folds are most often affected, in long-standing disease, other skin areas can also be involved. Unusual sites of involvement include the back, hands and eyelids. The disease usually occurs in young patients and clearly predominates in males. We reported a 17-year-old Turkish girl who presented with painless slack skin masses on extensoral area of the left lower limb. The histopathological evaluation of the biopsy specimen from the atrophic erythematous slack skin supported the diagnosis of GSS. To the best of our knowledge GSS has not been previously described in extensoral areas of the body. Because of its rarity we want to present our GSS patient with an unusual localisation.

028

Neutrophil-poor Sweet's syndrome: report of two cases

E. Sener *, H. Bilen, M. Calik, N. Akdeniz, M. Atasoy, N. Gursan

*Erzurum Bolge Egitim Hastanesi, Patoloji Bolumu, Turkey

Objective: Sweet's syndrome, also called acute febrile neutrophilic dermatosis, is characterized by fever, neutrophilia, erythematous and painful skin lesions, which show dense and diffuse neutrophilic infiltrate in the superficial dermis and papillary dermal edema, and rapid response to therapy with corticosteroids.

Method: We observed two patients with Sweet's syndrome who had painful papulonodular erythematous lesions located mainly on the upper extremities, face and neck asymmetrically, neutrophilia in blood count, increased ESR, fever, and response rapidly to corticosteroid treatment. Skin biopsies from fully developed erythematous lesions revealed very few neutrophils. We confirmed neutrophils by staining MPO (miyeloperoxidase).

Results: There has been very little published recently on neutrophil-poor Sweet's syndrome. Because of this reason we reported two patients with neutrophil-poor histology Sweet's syndrome.

029

Viral-associated trychodysplasia secondary to antineoplastic treatment in a patient with lymphoblastic leukemia

J. Suárez Peñaranda *, Gonzal.-V. Daniel, C. Aliste Santos, D. Sánchez Aguilar

*Fundación IDICHUS, Santiago de Compostela, Coruna, Spain

Objective: Viral-associated trychodysplasia (VAT) is a recently described cutaneous eruption with distinctive histopathological features. Clinically, it is characterized by follicular papules, mainly in the face, with variable degrees of alopecia. Primarily described in transplant recipients, it is being increasingly recognized in patients receiving chemotherapy for leukemia or lymphoma.

Results: A 5-year-old boy with the diagnosis of lymphoblastic leukemia under treatment with methotrexate and mercaptopurine for the last 6 months presented with an acneiform eruption for the last 2.5 months. Lesions were initially located on his face, but later they were also present in his neck, arms and thighs. They consisted of multiple, persistent hyperkeratotic follicular papules. Secondary alopecia was noted in the eyebrows. Biopsy showed large follicles distended by abnormal bulbar cells that contained numerous abnormally large trichohyaline granules. The bulb lacked an apparent hair papilla and no hair shafts were present in any of the large anagen. Treatment with emollients was unsuccessful but the condition resolved spontaneously after completing chemotherapy.

Conclusion: VAT is an unusual condition that may develop in patients under chemotherapy for leukemia and lymphoma. Probably, it is under-recognized and being aware of clinical and histopathological features may avoid unnecessary procedures or treatments.

030

Primary cutaneous aggressive epidermotropic CD8+ T-cell lymphoma: case report

J. Suárez-Peñaranda *, C. Aliste Santos, J.A. Diaz Arias, A. Bendana López, B. Vieites
*Fundación IDICHUS, Santiago de Compostela, Coruna, Spain

Objective: Primary cutaneous aggressive epidermotropic CD8+ T-cell lymphoma (PCAETCL) is an uncommon form of cutaneous T-cell lymphoma characterized by generalized patches, plaques, papulo-nodular lesions and tumors. Tumor cells express CD3, CD8, CD7, CD45RA, βF1 and cytotoxic markers. An aggressive course with visceral involvement and poor prognosis is common.
Results: A 36-year-old woman presented with generalized cutaneous tumoral lesions for the last 2 years. They ranged from 2 to 10 cm in diameter and some showed superficial ulceration. Peripheral lymph nodes were not enlarged and bone marrow was not infiltrated by the neoplasm. Histopathological examination showed a dense lymphoid infiltrate throughout the entire dermis, reaching the subcutaneous tissue. Epidermotropism was conspicuous. Neoplastic lymphocytes were medium to large with moderate pleomorphism and many mitotic figures. Immunohistochemical study showed expression of CD3, CD8, CD7, CD45RA, CD2, TIA-1 and granzyme B, while CD4 and CD20 were negative. Treatment with three different chemotherapic regimens was ineffective and the patient died due to tumor progression and infectious complications.
Conclusion: The presence of an epidermotropic CD8+ skin lymphoma should lead to exclude PCAETCL. Clinical features are essential to distinguish it from the CD8+ variant of mycosis fungoides that runs an indolent chronic course.

031

Identification of t(17;22)(q22;q13) (COL1A1/PDGFB) in dermatofibrosarcoma protuberans by fluorescence in situ hybridization in paraffin-embedded tissue microarrays: clinical and histopathological correlation in 40 cases

A. Sáez *, S. Segura, R. Salgado, A. Toll, G. Martín-Ezquerra, M. Yébenes, F. Solé, C. Barranco, B. Espinet, R. M. Pujol
*UDIAT Centre Diagnòstic, Dept. of Pathology, Sabadell, Barcelona, Spain

Objective: Dermatofibrosarcoma protuberans (DFSP) is genetically characterized by the translocation t(17;22)(q22;q13) resulting in PDGFB/COL1A1 fusion gene. Additionally, PDGFB receptor is activated offering the possibility to use imatinib mesylate (Glivec®, Novartis) as a therapeutic alternative in clinically advanced cases. Fluorescence in situ hybridization (FISH) with specific probes allows a rapid detection of this gene. The objective of the study is to analyze the presence of the translocation t(17;22)(q22;q13) by FISH in paraffin-embedded tissue microarrays (TMA) of cases diagnosed as DFSP and dermatofibromas (DF).
Method: Two TMA including 40 DFSP and 20 DF were evaluated. FISH analyses were performed using a dual-color dual-fusion non-commercial probe. Clinical and histopathological features were systematically evaluated and association with FISH results was explored.
Results: Twenty-nine DFSP and 16 DF could be successfully evaluated. Twenty-five (86%) DFSP samples were positive for the translocation, which was not present in any DF samples. Two of the negative DFSP corresponded to more undifferentiated tumors, whereas one case exhibited overlap features with DF (this case was finally considered a deeper and more cellular variant of DF).
Conclusion: The COL1A1/PDGFB fusion gene is present in most of DFSP. The detection the translocation may be an additional diagnostic tool in DFSP showing non-conclusive histological features.

032

Cutaneous lymphadenoma: a case report with evidence of pilosebaceous differentiation

M. Tsamouri *, C. Poullou, S. Kalantzakis, C. Barbatis
*Hellenic Red Cross Hospital, Dept. of Pathology, Athens, Greece

Objective: Cutaneous lymphadenoma is an uncommon tumour with distinctive unique histological features with adnexal differentiation, probably pilosebaceous. We report a new case of lymphadenoma in a 49-year-old man with a 0.8-cm postauricular cutaneous nodule with review of the literature.

Method: Formalin-fixed tissue was examined with a panel of 15 antibodies for differential diagnosis and clues to the histogenesis.
Results: The entire tumour was intradermal arranged in organoid pilar-like structures composed of basaloid cells with focal peripheral palisading embedded in dense fibrous tissue. The characteristic feature was the infiltration of most epithelial islands by a heterogeneous mononuclear cell infiltrate mainly of T- lymphocytes mixed with some B-lymphocytes, scattered S-100 dendritic cells and "Hodgkin"-like cells expressing keratins, CD30, EMA, CEA and Vim. The peripheral basal cells lacked EMA and CEA but focally expressed bcl2 and diffusely CK5/6. Ki67≤5%. A diagnosis of cutaneous lymphadenoma was made.
Conclusion: Cutaneous lymphadenoma is a rare tumour with adnexal, probably pilosebaceous, differentiation as it is indicated in our case. It requires differantiation from desmoplastic trichoblastoma, basal cell carcinoma and malignant lymphoepithelial tumor. Complete excision is curative. The pathogenesis of the inflammatory response remains unexplained.

033

Primary cutaneous apocrine carcinoma of sweat glands: a rare case report

T. Vasilakaki [*], E. Skafida, X. Grammatoglou, E. Arkoumani, E. Moustou, E. Delliou
[*]Tzaneion Hospital, Dept. of Pathology, Piraeus, Greece

Objective: Primary cutaneous apocrine gland carcinoma is a very rare malignant neoplasm. Most of these neoplasms are indolent and slowly developing but some are rapidly progressive and extremely aggresive. The treatment of choice is wide local excision with clear margins with or without lymph node dissection.
Method: We report a case of a 67-year-old man who came to our hospital with an ulcerated nodule in the right axilla measuring 1 × 0.8 cm. Bilateral breast examination, skin examination and complete lymph node survey were unremarkable. Ultrasound examination and mammogram revealed no significant lesions. The nodule was excised.
Results: Histological evaluation showed features of an apocrine gland carcinoma arising in area of high apocrine gland density. The tumor tissue invaded the papillary and reticular dermis, ulcerated the epidermis without extension to the subcutaneous tissue. The immunohistochemical study showed that the tumor cells were positive for Ker7, EMA and E Cadherin and negative for CEA, S100p and PSA. No estrogen or progesterone receptors were detected, making the diagnosis of male breast cancer metastatic to axilla unlikely.
Conclusion: Primary apocrine carcinoma of sweat glands is a very rare tumour and there are no guidelines for the treatment of recurrent or metastatic disease.

034

Familial multiple cutaneous and uterine leiomyomatosis (Reed's syndrome) as a marker of agressive renal cancer: two family case reports

S. Vazquez Navarrete [*], E. Vázquez, D. Lagama, J. Peña, M. Jaramillo
[*]Hospital Linea de la Concepcion, Spain

Objective: The autosomal dominant genetic disorder associated with multiple cutaneous leiomyomas and uterine leiomyomas is called familial hereditary leiomiyomatosis (Reed's syndrome). It has been localized to a gene of chromosome 1q42.3-43. This gene encodes fumarate hydratase and acts as tumor suppressor in this familial disorder. Up to 14% of patients with the mutation may also have renal cell carcinoma.
Method: We present two families with multiple cutaneous and uterine leiomyomas, which were sent to the genetics department for studying. In the first family, in addition with the leiomyomas, a daughter of the second generation had an early death of a renal cell carcinoma. The second family had the association of cutaneous and uterine leiomyomas and no renal carcinoma has been detected until now.
Results: As a result of the knowledge and detection of the syndrome, the members of the families at risk have a genetic testing and genetic counselling. Abdominopelvic CAT for early detection and prevention of renal cancer were performed.
Conclusion: The renal cancer in families with Reed´s syndrome is of unusual subtypes which can present with metastasic disease and associate high mortality. It is imperative to screen individuals with multiple cutaneous leiomyomas and gene mutation for renal cancer (abdominal CAT) as early detection can improve the outcome of the illness.

035

Histopathological and immunohistochemical study from 67 Brazilian patients clinically suggesting early Mycosis Fungoides

T. Yamashita [*], M.E. Marques, S. Marques
[*]Universidade Estadual Paulista, Curitiba, Brazil

Objective: Mycosis fungoides (MF) is the most common subtype of cutaneous T-cell lymphoma characterized by neoplastic skin-homing CD4+ T cells. Accurate diagnosis of early MF is difficult because of the varied clinical and histological patterns that may mimic other benign conditions.
Method: Data from 67 patients with patch lesions that seemed classical early MF were retrieved from the Department of Pathology at "Universidade Estadual Paulista "(Brazil). The male/female ratio was 2.6:1, mean age=62.1. The diagnosis was confirmed by correlation with clinical features, histopathology and immunohistochemistry technique.

Results: Out of 67 patients analysed, 17 (25.5%) had the diagnosis of early MF characterized by disproportionate epidermotropism, Pautrier's microabscesses, some degree of lymphocyte atypia, 76% epidermal hyperplasia and 88% papillary dermal fibrosis. In three (4.5%) patients the diagnosis of MF did not have all the main histopathological criteria but was also supported by CD2+, CD3+, CD4+, CD5+ and reduction of expression of CD8 and CD7; 15 (22.5%) cases remain suspicious for MF and 32 (47.5%) were ruled out as nonspecific dermatitis.
Conclusion: Indeed more than 47% were false positive for MF considering only the clinical aspects. Although immunohistochemistry may help, the majority of the diagnosis of early MF still rests upon clinical features and histopathological findings.

036

Vasculitis in Sweet syndrome: a clinicopathologic study of 47 cases

A. Zehani *, J. Chelly, A. Mebazaa, H. Nfoussi, H. Azzouz, K. Bellil, N. Kchir, S. Haouet, A. Ben Osman, M. Zitouna
*Tunis, Tunisia

Objective: Sweet syndrome, first described by Sweet in 1964, is a disease characterized by painful, erythematous nodules and plaques of rapid onset accompanied by fever and neutrophilia. It is histologically categorized as a neutrophilic dermatosis. The clinicopathologic features are so characteristic as to have elicited diagnostic criteria for the disease.
Method: Forty-seven cases of Sweet syndrome, diagnosed between 1994 and 2010, were reviewed retrospectively, noting the prevalence of vasculitis.
Results: The patient population consisted of 36 females and 11 males. The mean age was 47 years with extremes ranging from 28 to 74 years. In the majority of patients, lesions involved the upper extremity or the head and neck area. Most patients described a uniform eruption of multiple lesions. All biopsy specimens demonstrated a dermal infiltrate composed predominantly of neutrophils. The prevalence of vasculitis was 17% (eight cases).
Conclusion: Vasculitis is not a primary, immune-mediated process in Sweet syndrome but occurs secondary to noxious products released from neutrophils. It does not exclude a diagnosis of Sweet syndrome.

037

Shulman's Disease: Retrospective study of 8 cases

A. Zehani *, H. Azzouz, I. Chelly, H. Nfoussi, K. Bellil, S. Nechi, D. Ben Ghachem, H. Jemel, S. Haouet, N. Kchir, M. Zitouna
*Tunis, Tunisia

Objective: Eosinophilic fasciitis or Shulman's disease is a rare condition of unknown etiology and a poorly understood pathogenesis. It is a scleroderma-like syndrome that was first described in 1974 by Shulman. It is characterized by thickened fascia. Involvement of the dermis may occur during the progression of the disease.
Method: We report a retrospective case series of eight patients with Shulman's disease, noting the clinical and pathological characteristics.
Results: The patient population consisted of six females and two males. The mean age was 52 years with extremes ranging from 20 to 75 years. Swelling and tenderness of extremities were the major presenting symptoms. A biopsy was performed in all cases. Pathological examination showed normal epidermis. The dermis is often sclerotic with inflammatory infiltrate composed of lymphocytes, eosinophils, plasma cells, and histiocytes. Beneath the dermis, the fascia was thickened with occasionally inflammatory polymorphic infiltrate with varying numbers of eosinophils.
Conclusion: Histopathologic differential diagnosis should rule out parasite reaction and sclerodermiform diseases. These findings are similar and sometimes indistinguishable, particularly in superficial biopsies and in cases where no clinical information is provided to the pathologist. Thus, a deep biopsy to include muscle is ideal.

038

Spitz tumor in pediatric and adult population: clinical, dermoscopic, in vivo confocal microscopic and histopathologic study

S. Zurac *, D. Boda, A. Diaconeasa, R. Andrei, T. Tiberiu, C. Caruntu, R. Mustata, F. Staniceanu,
V. Chitu, C. Solovan
*Colentina University Hospital, Dept. of Pathology, Bucharest, Romania

Objective: Spitz tumor (ST) is an intriguing melanocytic lesion with incomplete deciphered biology (worrisome morphology, unspecific immunohistochemical phenotype, potential aggressive clinical behavior).
Method: We evaluated 23 cases of ST arising in pediatric and adult population. Morphologic characteristics were evaluated in both groups in correlation with ST variant (ST, ST of uncertain malignant potential—STUMP, combined ST). In vivo confocal microscopy was performed in four pediatric ST. The statistical level of significance was $P < 0.05$.
Results: Combined STs were more frequent in children and STUMP was more frequent in adulthood. Thinning of the epidermis was present in one case in each group; ulceration,

even unsignificant, was higher in pediatric group; no significant differences were noted in respect of pleomorfism, lateral intraepidermal extension or mitoses. Pagetoid ascension of the tumor cells was significantly more frequent in pediatric group (72.72% vs 30.76%, P= 0.04), especially in combined ST. Dermoscopy was unspecific. Confocal microscopy was performed in two cases of ST, one STUMP and one combined ST; the appearance was similar, highly suggestive of ST without features specific for a ST variant.
Conclusion: Morphologic appearance in ST (either classic, atypical or combined) is more worrisome in pediatric population. In vivo confocal microscopy suggests ST but cannot discern between ST variants.

039

Differential diagnosis in dermatofibrosarcoma protuberans and dermatofibroma: how difficult can it be?

S. Zurac *, R. Andrei, T. Tebeica, F. Staniceanu, A. Bastian, A. Stoica, A. Bunea, L. Sticlaru,
C. Lazaroiu, L. Petrica, V. Chitu
*Colentina University Hospital, Dept. of Pathology, Bucharest, Romania

Objective: Dermatofibrosarcoma protuberans (DFSP) and dermatofibroma (DF) are relatively frequent mesenchymal cutaneous tumors with characteristic morphology; however, differential diagnosis can be challenging, especially in special variants of DFs (cellular, deep penetrating, etc.).
Method: We evaluated 149 DFs and 16 DFSPs diagnosed in our department between 2009 and 2010. We analyzed the morphologic features (cellularity, pleomorphism, mitotic index and subcutaneous honeycomb pattern of growth) and expression of immunohistochemical (IHC) markers (CD34, tenascin, stromelisine 3, SMA, S100 protein) in both groups. The statistical level of significance was $P<0.05$.
Results: All DFSPs presented moderate/high cellularity, mild/moderate pleomorphism, low mitotic index and honeycomb pattern of adipose invasion in at least 2/3 of deep areas. DFs revealed mostly low cellularity (80.54%), mild/moderate pleomorphism in all but two cases (98.65%), similar mitotic index and honeycomb pattern of growth in subcutaneous fat focally present (31 cases, 20.80%). Focal positivity for SMA or S100 protein was present in both groups. All DFSPs were positive for CD34 (except fibrosarcomatous areas—four cases) but all DFs were negative. Tenascin and stromelisine 3 were differently expressed in DF and DFSP groups.
Conclusion: Morphologic appearance and IHC phenotype offer sufficient data to differentiate between DF and DFSP, irrespective of morphologic variant but variations within the tumor impose extensive sampling.

Sunday, 28 August 2011, 09.30–10.30 and 16.30–17.00, Hall 5

PS-03 Poster Session Haematopathology

001

The role of autophagy in multiple myeloma

A. Brunner *, S. Thangavadivel, R. Greil, K. Jöhrer
*Institute of Pathology, MUI, Innsbruck, Austria

Objective: Autophagy is a mechanism enabling cells to gain energy in a microenvironment deprived of nutrition and oxygen. In cancer cells, the precise role of autophagy is controversial. It has been suggested to act as tumor suppressor and enhancer, respectively. In multiple myeloma, no in vivo data are currently available. One of the key molecules in the regulation of autophagy is Beclin 1. In order to delineate a possible role of autophagy in myeloma survival and progression, we investigated the expression of Beclin 1 in multiple myeloma.
Method: Bone marrow specimens of patients with multiple myeloma were stained using a monoclonal antibody against Beclin 1. The extent of Beclin 1 expression was assessed as percentage of positive cells compared to the plasma cell infiltration highlighted by plasma cell specific antibodies.
Results: About half of the specimens showed cytoplasmic Beclin 1 expression with an average of 20% Beclin 1 positive plasma cells. Beclin 1 was mostly positive in small interstitial foci of plasma cells, while rarely larger sheets of plasma cell infiltrate were positive for Beclin 1.
Conclusion: Our results suggest a possible role of Beclin 1 in multiple myeloma. Further investigations will define its prognostic and therapeutic relevance.

002

Detection and tissue distribution of homeodomain interacting protein kinase 2 in mucosa-associated lymphatic tissue and in extranodal B cell lymphoma

M. Marino *, E. Gallo, C. Rinaldo, R. Martucci, E. Pescarmona, S. Soddu
*Reg. Elena Nat. Cancer Institute, Dept. of Pathology, Rome, Italy

Objective: Homeodomain interacting protein kinase 2 (HIPK2) is a serine/threonine kinase regulating gene expression by transcription factor phosphorylation and contributing to the regulation of diverse pathways, such as p53 activation. P53 in lymphomas is often wild type (wt), thus allowing to study HIPK2 activity in different TP53 gene status.
Method: We investigated HIPK2 distribution in normal mucosa-associated lymphatic tissue (MALT), in 24 MALT lymphomas and in 9 extranodal diffuse large B cell lymphomas (DLBL) with a monoclonal antibody to HIPK2,

a mouse IgM developed by one of us (SS), applied to formalin-fixed paraffin-embedded material.
Results: In normal lymphoid tissue, HIPK2 was detected in the nuclei of follicular, marginal and mantle cells as small nuclear bodies. In MALT lymphomas, four different HIPK2 expression patterns were observed: (1) small or (2) medium-sized intranuclear bodies, (3) cytoplasmic granules, (4) no reactivity at all. In DLBL, HIPK2 has been found in the nucleus in small- or medium-sized bodies (seven cases) and in the cytoplasm in two cases.
Conclusion: Our preliminary data demonstrated the detectability of HIPK2 in extranodal lymphatic tissue and in related lymphomas, and its heterogeneous reactivity pattern. Lymphomas represent a good model to study the contribution to lymphomagenesis of novel mechanisms, such as HIPK2 loss/inactivation.

003

β-Catenin activity contributes to tumor cell survival and proliferation in NPM-ALK+anaplastic large cell lymphoma (ALCL)

G. Rassidakis *, M. Karanikou, E. Drakos, L. J. Medeiros, P. Georgoulis, T. Vassilakopoulos,
P. Panayiotidis, E. Patsouris
*University of Athens, 1st Dept. of Pathology, Greece

Objective: ALCL is an aggressive T-cell non Hodgkin lymphoma frequently associated with the t(2;5)(p23;q35), resulting in the overexpression of NPM-ALK, which is capable of activating multiple oncogenic pathways. The aim of this study was to investigate the potential role of β-catenin pathway in NPM-ALK+ALCL oncogenesis.
Method: Four NPM-ALK+ALCL cell lines and control cells (Jurkat) were used for transfection experiments and pharmacologic studies. Cell viability and growth were assessed using trypan blue exclusion and MTS assays, respectively. Protein levels were analyzed by Western blot. Immunohistochemistry performed on a tissue microarray was utilized to assess β-catenin expression in ALCL patient samples.
Results: High β-catenin levels were detected by Western blot in all ALCL cell lines tested. Inhibition of β-catenin activity by quercetin resulted in a concentration-dependent decrease in cell viability and proliferation that was linked to cyclin D3 and Bcl-2 downregulation. In addition, inhibition of ALK activity led to decreased β-catenin expression. However, transfection of Jurkat cells with an active NPM-ALK plasmid did not further increase β-catenin levels. Immunohistochemistry showed variable expression and activation of β-catenin in ALCL tumor samples.
Conclusion: β-Catenin contributes to cell survival and proliferation of NPM-ALK+ALCL, providing a novel target for investigational therapy.

004

The role of AKT signaling pathway in plasma cell myeloma progression

P. Babal *, A. Janegova, P. Janega, L. Feketeova, Z. Cierna, E. Klincova
*Comenius University, Dept. of Pathology, Bratislava, Slovakia

Objective: Plasma cell myeloma (PcM) constitutes one of the most common hematological malignancies in adults. Better understanding of PcM biology could contribute to a more accurate therapy. Deregulations of AKT signaling pathway are intensively studied in modern cancer research. Activation of AKT affects the key processes of tumor progression: cell proliferation, apoptosis and angiogenesis.
Method: A total of 35 PcM FFPE bone marrow samples were evaluated by immunohistochemistry for expression of p-AKT and its effector molecules—mTOR, NFkB, cyclin D1 (cell proliferation), HIF1α, carbonic anhydrase IX, VEGF (angiogenesis), APAF, cleaved caspase 3, Bcl-2 (apoptosis).
Results: Activated AKT showed positivity in 95% (n= 33) of PcM samples. Only VEGF angiogenesis marker was expressed. HIF1α, CAIX and all proliferation markers were completely negative. Positivity of anti-apoptotic Bcl-2 and pro-apoptotic APAF protein was found in all PcM. No expression of apoptosis executing enzyme caspase 3 was observed.
Conclusion: The high expression rate (95%) of p-AKT points its important role in PcM. Tumor progression through AKT activation is probably due to the anti-apoptotic effect and blockage of apoptosis executing cascade APAF—caspase 9—caspase 3. The results indicate a possible benefit of AKT inhibitors in PcM therapy. This project was supported by GUK 199/2010.

005

Angioimmunoblastic T- cell lymphoma expressing cyclin-D1: report of a case

C. Cacchi *, B. Märkl, H. Arnholdt, W. Klapper
*Klinikum Augsburg, Inst. für Pathologie, Germany

Objective: Angioimmunoblastic T-cell lymphoma (AILT) is a very uncommon, aggressive neoplasm accounting 1–2% of all non-Hodgkin lymphomas, usually occurring in middle-elderly ages.
Method: A laterocervical lymphnode biopsy of an 89-year-old female patient was performed in our oncology department. Formalin-fixed paraffin-embedded blocks were stained with routine haematoxylin and eosin and two representative blocks were selected for immunohistochemical examination and for fluorescence in-situ hybridization (FISH).

Results: The lymph node biopsy showed an important reduction of B-cell zones. The architecture was subverted by a T-cell population (CD3+) showing sometimes a blastic-like differentiation. The majority of these cells stained with CD4, and a minority of them was CD8+. Double-stained immunohistochemistry for cyclin-D1/CD79a, cyclin-D1/CD3 and EBER/CD3 indicated that the B cell population was cyclin D1 negative but EBV positive, and a population of CD3+ cyclinD1 expressing T cell. Moreover was detected (CD23+ Ki-M4p+) a meshwork of follicular dendritic cells. No translocation t(11;14) was discovered.
Conclusion: Cyclin D1 expression is observed in many types of B-cell lymphomas (BCLs). Patients carrying AILT are prone to develop BCLs. Our case demonstrated, as recently published, that the source of cyclin D1 is represented by the malignant T cells independent of cyclin D1 translocations in these lymphomas.

006

CD5 is an unfavorable prognostic factor in diffuse large B-cell lymphoma (DLBCL) patients treated with immunochemotherapy

V. Cemerikic-Martinovic *, N. Drndarevic, D. Jovanovic, T. Martinovic, O. Markovic, D. Marisavljevic
*Beo-lab, Dept. of Histopathology, Belgrade, Serbia

Objective: CD5+ DLBCL is a clinically distinct subgroup of DLBCL that is associated with poor prognosis.
Method: In this study, we have analyzed the immunoexpression of CD5 in a group of 55 DLBCL patients treated with immunochemotherapy. The diagnosis of DLBCL was made according to the WHO classification. The expression of CD5 has been evaluated semiquantitavely as a percentage of tumor cells.
Results: Immunoexpression of CD5 has been found in ten (18.2%) patients. The expression of CD5 ranged from 30% to 100% tumor cells. Patients with CD5+ DLBCL were more closely associated with many aggressive clinical features or parameters than CD5- DLBCL: namely, the immunoexpression of CD5 was in significant correlation with advanced clinical stage (III, IV) (p=0.023), performance status (p=0.036) and presence of extranodal localization (p=0.047). The overall International Prognostic Index score was thus significantly higher for the patients with CD5+ DLBCL than for those with CD5- DLBCL (p=0.016). Immunoexpression of CD5 was found to be unfavorable factor for therapy response (p=0.026). In addition, the patients with CD5 expression had significantly the shorter survival than CD5+ shorter survival (67.1 vs 30.2 months) (p=0.012).
Conclusion: These results confirmed that CD5+ DLBCL constitute an unfavorable prognostic subgroup of DLBCL in patients treated by immunochemotherapy.

007

Primary intestinal lymphomas: review of 16 cases

L. Comerma Blesa *, M. Garcia Garcia, M. Iglesias Coma, J. Munné Collado, B. Bellosillo Paricio,
M. Baró Tomas, C. Lezana Alsina, F. Garcia Pallarols, B. Sanchez Gonzalez, S. Serrano Figueras
*Hospital del Mar, Dept. of Pathology, Barcelona, Spain

Objective: Primary intestinal lymphoma (PIL) is rare, comprising 15–20% of gastrointestinal lymphomas, and represents a heterogeneous entity regarding localization and subclassification from an anatomopathological point of view.
Method: We searched for PIL in our center during 2000–2010, diagnosed following WHO 2008 criteria, with paraffin-embedded material available. Cases with diffuse large B-cell lymphoma (DLBCL) were subclassified into germinal center B-cell like (GCB) and non-GCB or activated type, according to Hans' algorithm.
Results: We analysed 16 cases, 10 males and 6 females (mean age 63.5 years). Occlusion was the most common form of presentation. A total of 13 cases were diagnosed as DLBCL (8 non-GCB/5 GCB) primarily located in the colon (8/13), while 3 were T-cell lymphomas located in the small bowel. There were 11 patients who underwent surgery (6 with combined adjuvant chemotherapy), while 5 were treated with polychemotherapy alone. Treatment response was complete in nine patients, partial in two and with disease progression in three cases.
Conclusion: In our study, the most common type of PIL is the DLBCL of activated type located in the colon, presenting as intestinal occlusion. T-cell PILs are usually of the enteropatic type, located in the small bowel. Treatment frequently involves combining surgery with chemotherapy.

008

Primary mucosa associated lymphoid tissue lymphoma of the cecum: presentation of a very rare case

C. Hadjileontis *, E. Papadopoulou, C. Manatakis, A. Kafanas
*Serres General Hospital, Dept. of Pathology, Greece

Objective: Gastrointestinal tract is the most common site of extranodal lymphomas and accounts for 30–45% of all extranodal cases. Stomach is the most commonly involved organ followed by small intestine, colon and esophagus. Primary colorectal lymphomas are particularly rare and contribute to 0.2% of all colorectal malignancies. Clinical presentation depends upon the site of involvement. The clinical features of primary colorectal non-Hodgkin's lymphoma have no specificity. Ulcer and bossing are the two major morphologic manifestations of endoscopy.

Method: This is a case of a female patient presenting as bright red bleed per rectum, who was found to have a cecal mass, clinically diagnosed as carcinoma. The histological examination performed after left hemicolectomy revealed that the mass was due to the development of extranodal marginal zone B-cell, mucosa-associated lymphoid tissue lymphoma (MALT). No other organs were radiologically found to be involved and the bone marrow biopsy was negative for malignant infiltration.
Results: Diagnosis may be challenging, but a solitary extranodal plasmacytoma and low differentiated multiple myeloma must be excluded in such cases, especially when plasmatocytic differentiation of MALT type cells is extensive. The patient has had no recurrence a year postoperatively and remains without any chemotherapy.

009

Primary extranodal follicular lymphoma (PEFL): a morphological, immunohistochemical and genotypical study of nine cases

G. Kanellis *, T. Papadaki, L. Marinos, M. Fameli, K. Dimosthenous, G. Morphopoulos, I. Doundas,
N. Stavroyianni, E. Pouliou, E. Economaki
*Evangelismos Hospital, Dept. of Hematopathology, Athens, Greece

Objective: The aim of our study was to analyze the morphological, immunophenotypical, genotypical and clinical data of nine patients with PEFL.
Method: Nine PEFL cases, stage EI, were included in the study (5 M/4 F; age, 44–87). Sites of initial presentation: GI tract (x3), eye (x4), testis (x1), salivary gland (x1). Morphology: H&E Immunohistochemistry [CD20, CD79a, bcl-2, bcl-6, CD10, CD21, CD23, CD5, CD138, CIg (κ, λ, γ, μ, α), PAX-5, MUM-1, Cyclin D1, MIB-1, CD3, CD4, CD8]; PCR for clonal IGH rearrangements and BCL-2/IGH chimeric gene.
Results: Results are summarized in Table 1.
Conclusion: Our findings are in accordance with recent data concerning PEFL and confirm: (a) early disease stage at presentation, (b) morphological similarity to primary nodal FL, (c) phenotypic heterogeneity concerning the expression of CD10 and BCL-2 protein, and (d) genotypic heterogeneity concerning the presence of the BCL-2/IGH chimeric gene. The indolent prognosis of PEFL suggests the need for: (1) multiparametric diagnostic approach for the confirmation of the diagnosis and its differential diagnosis from other benign or malignant mimickers and (2) thorough staging in order to document the primary extranodal nature of the disease. Finally, the distinctive features of PEFL allude to a particular genetic profile with a tendency to present at extranodal sites and an indolent clinical course.

Table1.

MORHOLOGY	CASES
• "Classical" Follicular Lymphoma	6/9
• Floral variant	2/9
• Diffuse	1/9
GRADE (WHO,2008)	
• 1-2	6/9
• 3A	2/9
• 3B	1/9
IMMUNOPHENOTYPE	
• CD20,CD79a,PAX-5,SIg/CIg +	9/9
• bcl-6+, bcl-2+, CD10+	4/9
• bcl-6+ bcl-2-/+ CD10-	3/9
• bcl-6+ bcl-2- CD10+	2/9
GENOTYPIC FINDINGS	
• clonal IGH gene rearrangements	6/7
• IGH/BCL2 translocation	1/7

010

An unusual case of biphenotypic, bigenotypic mature lymphoma

T. Koletsa *, V. Kotoula, G. Karayannopoulou, G. Karkavelas, I. Kostopoulos
*Aristotle University Thessaloniki, Medical School, Greece

Objective: Immunophenotyping and genotyping is usually helpful in defining the cell lineage of peripheral lymphomas. However, lineage may occasionally remain doubtful.
Method: A 78-year-old female patient presented with hypogammaglobulinemia, general lymphadenopathy, splenomegaly and skin lesions. Lymph node and skin biopsies were sent for histologic examination. Immunohistochemistry and PCR analysis for IGH-TCR rearrangements were performed.
Results: Histologic examination revealed a complete effacement of lymph node architecture by diffuse infiltrates of lymphoma cells. Neoplastic cells were medium-sized or large with irregular nuclei and prominent one or more nucleoli. Immunophenotypically, these were CD45RO, CD3, CD5, CD4, CD20, BCL2 and MUM1 positive. A small number of lymphomatous cells were also BCL6, CD10, CD8, CD30 and CD7 positive, whereas immunostains for CD45RA, CD34, Tdt, CD56, CD23, CD15 were negative. Unexpectedly, focal positivity for CD79a and PAX5 was observed. PAX5 was expressed in CD79a positive, as well as in few CD45RO positive cells, as revealed by double staining. PCR analysis showed IGH, TCRB and TCRG monoclonal rearrangements. Histologic examination of the skin biopsy revealed infiltration by the same lymphoma cells.
Conclusion: PAX5 detection on lymphoid malignancies cannot be definitively considered as lineage specific. Prognostic or predictive significance of biphenotypic/bigenotypic lymphomas remains to be defined.

011

Subcutaneous panniculitis-like T-cell lymphoma: a rare pediatric case

L. Leça *, L.P. Afonso
*Portuguese Oncology Institute of Porto Francisco Gentil, EPE, Portugal

Objective: Subcutaneous panniculitis-like T-cell lymphoma (SPTCL) is a distinct category of cytotoxic T-cell lymphoma which preferentially infiltrates subcutaneous tissue and sometimes mimics a panniculitic inflammatory process. Described initially in 1991, it represents less than 1% of all non-Hodgkin lymphomas and is common in young adults, being extremely rare in children.
Method: Our case report describes a female child, 23 months of age, with multiple subcutaneous non-painful nodules localized on face, thighs and buttocks, associated with malaise and fever. CT scan revealed multiple areas of nodular densification of the subcutaneous tissue, predominantly on the pelvic region and face. She was submitted to excisional biopsy of one of the lesions, in which histological examination revealed SPTCL. Currently, the patient is under a chemotherapy scheme, with partial regression of the lesions.
Conclusion: SPTCL is a rare lymphoma which poses differential diagnostic problems with benign panniculitis. Rare cases affecting children have been reported in the literature, most of them occurring in females, mainly involving facial areas, in association with severe systemic symptoms and with involvement of blood marrow. It is fundamental to recognize the clinical and pathological features of this entity to avoid a late and/or incorrect diagnosis.

012

An 8-year epidemiological survey of HIV associated high grade B cell and classical Hodgkin lymphomas at Tygerberg Hospital, Western Cape, South Africa: 2003–2010

D. Maartens *, A. Abayomi, J. Bezuidenhout, G. Sissolak, P. de Witt
*NHLS/Tygerberg Hospital, Dept. of Anatomical Pathology, Parow, South Africa

Objective: The South African HIV epidemic is regarded as hyper-endemic: 5.7 million people (11.9%) out of 48 million are estimated positive. The Western Cape region has 5.3–10.7% HIV prevalence. This study describes the epidemiological aspects of high-grade B cell lymphomas and classical Hodgkin lymphomas in HIV-infected individuals diagnosed at Tygerberg Hospital (TBH), one of two tertiary/referral hospitals serving the Western and Eastern Cape.
Method: All diffuse large B cell (DLBCL), classical Hodgkin (cHL), plasmablastic (PBL) and Burkitt/atypical Burkitt (BL/aBL) lymphomas (n=652) extracted from the histopathology archives were retrospectively reviewed using WHO 2008 criteria. HIV serology, age, gender and *Mycobacterium tuberculosis* infection at lymphoma presentation were documented.
Results: HIV status was known in 317/652 cases: 40% were HIV positive with breakdown: cHL—13.4%; DLBCL/PBL—67.7% and BL/aBL—18.9%. In the DLBCL/cHL/PBL group, M:F=1:1, but BL/aBL, M:F=1:2.4. Mean age for HIV associated DLBCL, cHL and BL/aBL was 37.7, 35.1 and 28.9 years, respectively. *Mycobacterium tuberculosis* co-testing of 53 HIV positive DLBCL and cHL showed co-positivity in 26.4%.
Conclusion: A steady increase in HIV lymphomas is noted. Some characteristics of this lymphoma group are similar to existing literature, whilst some features differ.

013

Angiomatous hamartoma in an inguinal lymph node

W. Majdoub *, S. Sassi, L. Charfi, R. Doghri, M.M. Hamdane, K. Mrad, I. Abbes, R. Sellami-Dhouib, H. Arbi, K. Ben Rhomdhane
*Military Hospital, Tunis, Tunisia

Objective: Angiomyomatous hamartoma (AH) is a rare primary vascular tumor with a predisposition for the inguinal lymph nodes. We report a new case of AH of the inguinal lymph node and discuss the clinicopathological features and differential diagnosis of this rare lymph node lesion.
Method: A 49-year-old woman with no past medical history who presented with inguinal left mass with no significant edema was noted throughout the affected extremity.
Results: The mass measuring 3.5 cm in great axis was resected. The resected specimen showed irregularly distributed thick-walled vessels in the hilum, extending into the medulla and focally into the cortex of the node and associated with smooth muscle cells splaying into sclerotic stroma. These findings are compatible with an AH. The smooth muscle cells were positive for smooth muscle actin and negative for HMB45.
Conclusion: Although rare, this pathologic entity should be considered in the differential diagnosis of primary vascular tumors of the lymph node.

014

Immunoexpression of SKP2, CUL1 and P21CIP in B-cell lymphomas

M. Melachrinou *, C. Sirinian, A. Symeonidis, N. Giannakoulas, E. Vlotinou
*University of Patras, Dept. of Pathology, Greece

Objective: Several proteins involved in the ubiquitin-dependent proteolysis of p21 are upregulated in a variety of tumours. Skp2, the substrate recognition factor of SCF (Skp1-Cul1-Skp2) E3 ubiquitin ligase complex is oncogenic and frequently upregulated in cancers. We examined the expression of Skp2, Cul1 and p21 in B-cell lymphomas and their association with proliferation index (PI) and clinical parameters.
Method: A total of 130 B-cell lymphomas [aggressive: 66 DLBCLs, 13 MCLs/indolent: 9 FLs {3 Gr 1, 6 Gr 2}, 20 MZLs, 22 SLLs] were immunostained for Skp2, Cul1, p21 and MIB1. Clinical parameters were available for 101 cases (61 aggressive, 40 indolent).
Results: Skp2, Cul1, p21 and MIB1 expressions were significantly higher in aggressive lymphomas. Skp2 was correlated with Cul1 and p21, as well as PI with Skp2 and Cul1 in aggressive tumours. High levels of Skp2 and increased PI were associated with shorter DFS in aggressive lymphomas. In addition, high levels of Cul1 were associated with BM involvement in aggressive and with bulky disease in indolent lymphomas.
Conclusion: Our findings did not reveal an active p21 proteolysis mediated by SCF (Skp2) complex. High levels of p21 in aggressive lymphomas may suggest an oncogenic role, whereas the correlation of Skp2 with DFS supports its prognostic role.

015

B-cell lymphoma with focal interfollicular distribution and hyaline vascular follicle centers simulating a Castleman disease (HVCD): a misdiagnosing new entity

D. Meseure *, C. Soussain, M. Trassard, K. Drak Alsibai, C. Le Ray, J.M. Guinebretiere, C. Copie, P. Gaulard
*Hopital Rene Huguenin, Dept. de Pathologie, Saint Cloud, France

Objective: HVCD diagnosis needs exclusion of B-cell lymphomas (BCLs). Conversely, BCLs may simulate HVCD and lead to a misdiagnosis. We report a new case of HVCD-like BCL with a surprisingly spontaneously regressive evolution.
Method: A 75-year old female presented with superficial lymphadenopathies. A surgical axillary lymph node excision and a bone marrow biopsy were performed.
Results: Lymph node architecture was slighty desorganized with proeminent reactive lesions and follicles showing Castleman-like features. Lymph node was predominantly composed of CD3+ CD5+T lymphocytes. The CD20+ CD79a+CD10+ Bcl6+ B lymphocytes with a centrocytic morphology were restricted to few cells within follicules and small interfollicular foci. Genetic and molecular analysis revealed a B-cell clone with t(14;18) translocation (PCR) and BCL2 rearrangements in the interfollicular areas with only few splits within follicles. Bone marrow biopsy showed paratrabecular nodules composed of centrocytes. Surprisingly, polyadenopathies regressed without therapy. One year later, superficial lymphadenopathies were disclosed with a final diagnosis of FL with predominant T reactive cell population.
Conclusion: BCLs simulate reactive lesions with an HVCD pattern and may contribute to potential diagnostic pitfalls. Analysis of extrafollicular areas and bone marrow by IHC and PCR/FISH is useful to support a final diagnosis of BCL.

016

Extranodal NK/T-cell lymphoma, nasal type: a case report

A. Perez Rodriguez *, M. T. Mosquera Martínez
*Hospital da Costa, Dept. of Pathology, Burela, Spain

Objective: Extranodal NK/T-cell lymphoma is a predominantly extranodal lymphoma with a characteristic histologic pattern, with cytotoxic phenotype and associated with Epstein–Barr virus infection.
Method: We present the case of a 30-year-old female with an ethmoidal mass and orbital cellulitis. Resection of the lesion is performed, and an intraoperatory diagnosis was asked for. Pathological examination reveals a dense lymphomatous infiltrate made of medium-sized cells with folded nuclei, inconspicuous nuclei, accompanied by an admixture of inflammatory cells. Immunohistochemical stains were performed in order to make a differential diagnosis.
Results: The neoplastic cells immunophenotype were CD3+, CD2+, CD56+, EBV+. The proliferation index was very high (90%).
Conclusion: In a tertiary hospital, the diagnosis of a extranodal NK/T- cell lymphoma is a challenge. The histological characteristics of these kinds of lesions, especially in an intraoperative consultantion, may mimic an inflammatory process.

017

Rare involvement of central nervous system (CNS) in typical chronic lymphocytic leukemia (CLL): report of a case and literature review

G. Rassidakis *, C. Sepsa, M.-C. Kyrtsonis, V. Bartzi, G. Georgiou, P. Panayiotidis, E. Patsouris
*University of Athens, 1st Dept. of Pathology, Greece

Objective: Clinical involvement of the central nervous system (CNS) in CLL has been rarely reported. An unusual case of CNS infiltration by typical CLL is presented and

clinicopathologic features as well as treatment options of this complication are discussed.
Method: Morphologic examination, immunohistochemistry, and molecular analysis of B-cell receptor by PCR were performed on brain biopsy specimens. Cerebrospinal fluid (CSF) was analyzed by immunocytochemistry, flow cytometry and PCR techniques.
Results: A 70-year-old male presented with confusion, dizziness, weakness and cognitive dysfunction 3 years after the initial diagnosis of typical B-CLL. MRI of the head revealed multiple lesions in occipital and parietal lobes bilaterally, as in the temporal lobe. Subsequent stereotactic brain biopsy showed perivascular and focal infiltration by typical B-CLL cells expressing CD20, CD79a, CD5, and CD23. Proliferation index was very low. In addition, neoplastic B-CLL cells were present in CSF, as shown by morphology, immunocytochemistry, flow cytometry and PCR. The patient was initially treated with intrathecal administration of methotrexate and dexamethazone. His clinical status was temporarily improved but a few days later he relapsed and received additional cranial radiation.
Conclusion: Infiltration of CNS in CLL represents a rare complication of the disease and only a few well-documented cases have been reported to date.

018

HIV-associated Castleman's disease with HHV8+ and lymph node Kaposi sarcoma

S. Vazquez Navarrete *, J. Peña, D. Lagama, T. Pérez, R. González
*Hospit. Linea de la Concepcion, Spain

Objective: Multicentric Castleman´s disease (MCD) is a rare lymphoproliferative disorder that includes the classic hyaline-vascular type and the plasma cell type which is related in some cases to human herpes virus 8 (HHV8) and AIDS. A 50-year-old patient presented with fever (39º), peripheral lymphadenopathy, splenomegaly and loss of weight. At the hospital, infection of HIV was detected. As a result of presumptive diagnosis of HIV-associated lymphoma, a cervical lymph node biopsy was performed.
Method: Two 1-cm lymph nodes were processed for H/E and immunohistochemistry.
Results: Lymph nodes with reactive follicles with hyaline vascular changes and infiltration of plasmablast with light chain lambda restrictions. The interfollicular area showed a markedly high increase of polyclonal plasmocytes with kappa predominance. In some foci inside the lymph nodes there was spindle cell neoplasia HHV8 +, consistent with Kaposi´s sarcoma. Immunohistochemistry for HHV8/LNA was positive. The patient was treated with chemotherapy (CHOP), antiretrovirals and Valganciclovir and currently had ended 8 cycles with complete remission.
Conclusion: The HHV8 has pathogenic role in the new plasmablastic variant of MCD-HIV related. It is a marker for other neoplasms including Kaposi´s sarcoma follicular dendritic cells tumor which are of prognostic and therapeutic relevance.

019

Localized amyloidosis of sternum as the manifestation of multiple myeloma

G. Volanska *, I. Strumfa, I. Ozola Zalite, J. Gardovskis, E. Miklasevics, A. Vanags
*Riga Stradins University, Dept. of Pathology, Latvia

Objective: Amyloidoses are heterogenous group of diseases characterized by extracellular fibrillar protein deposits in the organs and tissues. It can be systemic or localized. We report a case of localized amyloidosis of sternum caused by multiple myeloma.
Method: The analysis of clinical history as well as computer tomography (CT) was performed. The formalin fixed, paraplast- embedded tissues were investigated by routine stains and immunohistochemistry (IHC).
Results: Sixty-six-year-old man presented at hospital with pain and swelling of sternum. The CT imaging of the chest revealed a mass lesion involving manubrium sterni. Sternal osteochondroma was suspected and resection of manubrium was performed. The haematoxylin-eosin staining revealed pale eosinophilic acellular substance with perifocal infiltration of plasmocytes and multinuclear giant cells. The Congo red staining under polarized light showed an apple green birefringence. By IHC for immunoglobulin light chains, monoclonality of plasma cells was established justifying the diagnosis of multiple myeloma.
Conclusion: Localized amyloidosis can be the first manifestation of multiple myeloma. Every case of localized amyloidosis, especially of skeletal system, must be evaluated in this aspect.

020

Primary lymphoma of the liver: A case report

A. Zizi-Sermpetzoglou *, V. Savvaidou, E. Moustou, G. Lepeniotis, S. Kokkoris
*Tzaneio General Hospital, Pireaus, Greece

Objective: Primary hepatic non-Hodgkin's lymphomas are rare entities. They occur over a wide age range from 7 to 78 years and have been reported mainly in male patients. The usual clinical manifestations are pain, hepatomegaly, palpable mass, jaundice, pleural effusion and thrombocyto-

penia. Most tumors were found to be solitary or multiple masses, while others showed diffuse infiltration.
Method: We present a case of a 68-year-old man who was admitted to our hospital due to abdomen swelling and jaundice. The patient had presented similar symptoms three years before and was given the diagnosis of liver cirrhosis. On physical examination the abdomen was non-tender with moderate ascites. Laboratory studies showed mildly elevated hepatic enzymes. The viral markers were positive for anti-HbsAb, antiHBcAb and negative for HBsAg, HCV. Tumor marker Ca19,9 reached 147.28 U/ml while CEA, AFP were normal. Abdominal Computed Tomography (CT) revealed multiple hypodense lesions in both lobes of the liver, splenomegaly and ascetic fluid with hemorrhagic component. There was no sign of lymphadenopathy.
Results: Liver biopsy examination confirmed a diagnosis of non-Hodgkin's diffuse large B-cell lymphoma. No metastasis was detected in the thoracic cavity, bone marrow and spinal fluid. In our case, however, the patient died soon after the initialization of the treatment with systemic chemotherapy.
Conclusion: Primary hepatic lymphoma is an uncommon malignancy and its manifestation as chronic active hepatitis, granulomatous cholangitis or anaplastic carcinoma makes it difficult to diagnose. Its appearance especially in a needle biopsy specimen may be difficult to interpret but recognition is important as the prognosis is favorable.

021

Plasmacytoid dendritic cell component does not differ in benign tonsils and lymph nodes with progressive transformation of germinal centres

Z. W. Chen *, A. Porwit, D. J. Bailey, E.E. Torlakovic
*Toronto, Canada

Objective: The progressive transformation of germinal centres (PTGC) is a reactive process of unknown etiology. Rare cases of PTGC with features of hyaline-vascular Castleman disease (PTGC-HVCD) have been reported. Plasmacytoid dendritic cells (pDC) are known to be increased in HVCD, but their distribution in PTGC has not been described. We aim to determine differences in numbers and distribution of pDCs in PTGC, PTGC-HVCD and tonsils with reactive follicular hyperplasia (RFH).
Methods: Immunohistochemistry for CD123, a pDC marker, was performed on six benign tonsils, four lymph nodes with PTGC and one lymph node with PTGC-HVCD. In each case, CD123+ cells were counted per 0.55 mm^2 high-power field (HPF) in ten HPFs with the largest concentrations of CD123+ cells.
Results: pDCs were localized to interfollicular areas in all cases. CD123+ cells ranged 37–143/HPF (mean 84.4) in PTGC and 45-143/HPF (mean 95.5) in tonsils with no significant difference in means. However, PTGC-HVCD contained significantly higher pDCs (145–268/HPF, mean 185.6) than all other cases ($p<0.01$, Student's t-test).
Conclusion: Numbers of pDCs do not differ in PTGC and RFH. Interestingly, the number of pDCs is significantly increased in PTGC-HVCD, suggesting that PTGC-HVCD may be a distinct biologic entity more closely related to HVCD than PTCG.

022

Primary mediastinal (thymic) diffuse large B-cell lymphoma demonstrates immunophenotypic heterogeneity of MUM1-positive T-cell subset

Z. W. Chen *, A. Porwit, D. J. Bailey, E.E. Torlakovic
*Toronto, Canada

Objective: Primary mediastinal (thymic) diffuse large B-cell lymphoma (PMBL) has a unique transcriptional signature and shares certain features with classical Hodgkin lymphoma (CHL). MUM1-positive T-cells are commonly found in CHL, but have not been studied in PMBL. We aim to determine the presence and number of MUM1-positive T-cells in PMBL.
Methods: Dual-colour immunohistochemistry for MUM1 and CD3 was performed on formalin-fixed, paraffin-embedded sections of 12 PMBL biopsy cases. The number of cells with coexpression of MUM1 and CD3 were expressed as a percentage of all CD3+ cells as determined by a manual cell count.
Results: MUM1+/CD3+ cells ranged from 0% to 27% of all CD3+ cells in all cases. There were 2/12 cases (17%) with greater than 10% MUM1+/CD3+ cells and 8/12 cases (67%) with 3% or less MUM1+/CD3+ cells.
Conclusion: MUM1+/CD3+ T-cells are present in variable numbers in a background population of inflammatory CD3 cells and may account for up to 27% of all T-cells in PMBL. These results indicate that there is immunophenotypic heterogeneity of T-cell subsets in PMBL. Further categorization of these subsets is needed to achieve a better understanding of the biology of PMBL.

023

The prognostic implication of programmed death-1-positive tumor-infiltrating lymphocytes in diffuse large B-cell lymphoma

Y.-S. Ko *, W.-Y. Kim, W.-S. Kim
*Konkuk University, Medical Center, Seoul, Republic of Korea

Objective: Programmed death-1 (PD-1), a protein that is physiologically expressed by germinal center-associated helper T cells, has an inhibitory function on T-cell activity.

Method: We examined 63 DLBCL cases and numerically quantified the amount of PD-1-positive helper T cells in a representative tumor area after immunohistochemical staining using a monoclonal antibody against PD-1. The PD-1-positive cells were counted in three different high-power fields (HPF) at ×400 magnification.
Results: Patients were divided into two groups, i.e. the group with a high number of PD-1-positive cells >20/HPF (n=33) and the group with a low number of PD-1-positive cells ≤20/HPF (n=30). The group with a high number of PD-1-positive tumor-infiltrating lymphocytes showed decreased OS, although not statistically significant (p=0.073). The increased number of PD-1-positive cells was more common in patients with advanced clinical stage and high IPI score (p=0.025 and p=0.026, respectively). The number of extranodal sites were also somewhat correlated with the status of PD-1 staining (p=0.071). However the level of PD-1-positive cells was not associated with patient age, serum LDH level and PS.
Conclusion: A high content of PD-1 positive cells might be associated with an unfavorable outcome of DLBCL patients.

024

Expression of Jun B and Jun D proteins in diffuse large B-cell lymphomas

A. Ntoulia *, A. Papoudou-Bai, M. Kateri, A. Batistatou, V. Malamou-Mitsi, P. Kanavaros, M. Bai
*University Hospital of Ioannin, Dept. of Pathology, Ioannina, Greece

Objective: The Jun family includes c-Jun, JunB and JunD that are components of the AP-1 transcription factor complex involved in cell proliferation and apoptosis.
Method: The immunohistochemical expression of Ph-c-Jun, Jun B and Jun D proteins was studied in 130 cases of DLBCL in relation to the proliferation profile.
Results: The expression of Ph-c-Jun, Jun B and Jun D was found in 67%, 97% and 97% of cases, respectively. The expression of Jun B was positively associated with Ki-67, cyclin A, B1, D2 and E, MUM1 and non-GC phenotype and negatively with CD10. Moreover, Jun D expression was positively associated with Ki-67, cyclin E and Bcl-6. Analysis of the differences in mean values between the two proliferation clusters by T-tests showed higher expression levels of the following variables in the high expression cluster: Ki-67, cyclin A, B1, D3 and E, bcl6, Jun B and Jun D (all p<0.042).
Conclusion: The association between Jun B and Jun D and high proliferation cluster in DLBCL suggests that increased Jun B and Jun D expression may be involved in their pathogenesis by favoring tumor cell proliferation.

Sunday, 28 August 2011, 09.30–10.30 and 16.30–17.00, Hall 5

PS-04 Poster Session Head & Neck Pathology

001

MYC aberrations and EBV infection are major role players in the pathogenesis of HIV-related plasmablastic lymphomas of the oral cavity

S. Boy *, M. van Heerden, C. Babb, P. Willem, W. van Heerden
*University of Pretoria, Dept. of Oral Pathology, South Africa

Objective: We present common cytogenetics features in the largest cohort of plasmablastic lymphoma (PBL) of the oral cavity to date.
Method: All cases were evaluated for a break in the IGH, MYC and BCL6 genes and positive cases were evaluated for translocation partners using LSI IgH, Myc and BCL6 dual colour break apart rearrangement probes, LSI IgH/Myc:CEP 8 tri-colour, IgH/CCND1 and IGH/BCL2 dual colour dual fusion translocation probes.
Results: Forty-five patients, mostly HIV positive, were included. Ninety-eight percent of PBL's were EBV positive on in situ hybridisation. MYC gene rearrangements were the most common genetic aberration (63%) with the IGH locus as a partner in 51% of cases. Additional complex genetic aberrations were frequent. Rearrangements of both IGH alleles were detected in 16% of cases with t(14;18) and t(11;14), respectively, involved in conjunction with a t(8;14) in two cases. Aneuploidy was observed for the BCL6 gene in 31% and CCND1 gene in 42% of cases.
Conclusion: EBV infection and MYC rearrangement are the most important events in the pathogenesis of oral cavity PBL in HIV patients. In view of treatment modalities that may be more efficient in these patients, it is critical to genetically characterise PBL at initial diagnosis.

002

Oropharynx cancer: evaluation of clinical outcome according to HPV status and radiotherapy technique

E. Bragantini *, S. Girlando, V. Vanoni, A. Bolner, F. Valduga, R. Carella, M. Barbareschi, M. Silvestrini, C. Grandi, P. Dalla Palma
*S. Chiara Hospital, Dept. of Pathology, Trento, Italy

Objective: Analyze correlation between HPV status, radiotherapy (RT) and outcome in oropharyngeal cancer (OC).

Method: A total of 62 patients with OC underwent three different RT treatment: 3D-planned simplified conventional three-field (3D-S), 3D advanced conformal (3D-A) and IMRT with simultaneous integrated boost (SIB). In 33 pts (48.4%) RT was combined with concommitant chemotherapy. HPV status was analyzed by p16-immunohistochemistry (CINtec® Histology V-Kit) and molecular biology.
Results: There were 27 patients (43.5%) were p16-positive and 34 were p16-negative (44.3%) 1 not informative. Molecular biology found 29 pts HPV positive (46.8%), 29 HPV negative (46.8%) 4 not informative. DFS at 3 years for p16-positive pts was 76.2% and p16-negative pts was 58.4% (p=0.03). OS at 3 years was 68.2% and 44.1%, respectively (p=0.002). In the p16-positive group, no statistically significant differences were found for the three different RT techniques for DFS at 3 years while for p16-negative patients, DFS for 3D-S, 3D-A and IMRT was 30%, 63% and 87% (p=0.05). DFS at 3 years for the HPV-positive and negative group was 74.5% and 56%, respectively (p=0.04).
Conclusion: p16 is an efficient predictive biomarker, comparable to HPV molecular analysis. IMRT with SIB seems to be more appropriate for HPV/p16-negative patients.

003

Morphological study of decalcified tooth after experimental transplantation in Beagle dogs

L. Carvalho *, L. Teixeira, M.J. D'Aguiar, M.F.R. Botelho, E.V.P. Carrilho, M.M. Ferreira
*Amadora, Portugal

Objective: Mandibular teeth of three Beagle dogs were submitted to surgical manipulation in order to mimic lost and re-implantation of autologous teeth. Surgical procedure was repeated at two different times: tooth bed prepared for immediate re-implantation and tooth bed preparation 7 days before transplantation. The animals were sacrificed and a morphological study applied at 9 weeks after each manipulation.
Method: The manipulated mandibles were formalin-fixed for 24 h and submitted to decalcification in TBD-1 (rapid decalcifier) for 5 days, then cut and prepared in routine procedure for paraffin embed and haematoxylin–eosin observation after sequential sections of 5 μm, to search pulp and root canal and by immunohistochemistry, the epithelial Mallassez remnants.
Results: There were no morphological differences between the two groups of studied teeth but the first group—earlier re-implantation—showed larger areas of root resorption together with higher number of odontoclasts. The second group showed re-establishment of the periodontal ligament.
Conclusion: The repair of the inflammatory response after the surgical manipulations was similar with the maintenance of the periodontal ligament, but bone-like resorption and lower areas of mesenchymal tissue were heterogeneous in the two groups with a higher significance in the second group.

004

p16 expression and human papillomavirus (HPV) prevalence in oral squamous cell carcinoma: a Brazilian population-based study

H. Neiva de Castro *, K.G. Andrada de Oliveira, A.B. Soares, V.C. de Araújo, F. Passador-Santos
*FAESF, Dept. of Pathology, Floriano, Brazil

Objective: HPV infection is reported to be prevalent within the Brazilian population. It has been shown that HPV, especially type 16, may play an important role as a promoter of carcinogenesis in a subset of oral squamous cell carcinoma (OSCC). Nevertheless, HPV prevalence in OSCC is controversial among different studies. Several studies have shown that immunohistochemical expression of the cell cycle protein p16 can be used as a convenient marker for evaluating HPV in OSCC. The aim of this study was to investigate HPV prevalence in OSCC.
Method: A total of 383 paraffin-embedded SCCs were selected. p16 (CINtec®) immunohistochemical expression was preliminarily investigated in 42 cases using tissue microarray. Samples were graded as focal or diffuse and weak or strong. Cases graded as diffuse/strong were considered positive for HPV.
Results: Eleven cases were positive for p16 protein. Among them two were diffuse/strong, three were diffuse/weak, four were focal/strong and two were focal/weak.
Conclusion: Our preliminary results indicate that the incidence of HPV is low in OSCC in the population studied. Additional molecular studies are necessary to support these results.

005

Activated leukocyte cell adhesion molecule (ALCAM/CD166) expression is frequent in salivary gland tumors—potential therapy target?

T. S. Clauditz *, A. Gontarewicz, A. Münscher, R. Knecht, C. Bokemeyer, G. Sauter, W. Wilczak
*UKE Hamburg-Eppendorf, Inst. für Pathologie, Hamburg, Germany

Objective: Activated leukocyte cell adhesion molecule (ALCAM, CD166) has been found in tumor entities like prostate, breast and squamous cell cancer, which suggests that ALCAM might be a potential therapy target. The aim of this study was a comprehensive analysis of ALCAM expression in salivary gland tumors.
Method: A tissue microarray (TMA) was constructed from 994 carcinomas and 205 adenomas of the salivary glands. Slides were analyzed by immunohistochemistry (IHC) for ALCAM (CD166) expression in 15 carcinoma/adenoma entities.
Results: ALCAM cytoplasmatic and/or membranous expression was found in all analyzed carcinomas: mucoepidermoid carcinomas (65.7%), acinic cell adenocarcinomas (68.3%), adenoid cystic carcinomas (68.4%), adenocarcinomas NOS (64.8%), epithelial-myoepithelial carcinomas (88%), polymorphous low-grade adenocarcinomas (83.3%), basal cell adenocarcinomas (95.7%), myoepithelial carcinomas (57.9%), cystadenocarcinomas (69.2%), salivary duct carcinomas (81.8%), and oncocytic carcinomas (81.8%). Furthermore, basal cell adenomas (93.2%) as well as Warthin tumors (79.1%), pleomorphic adenomas (100%) and myoepitheliomas (70%) were also found positive. No association between ALCAM expression and tumor grade in mucoepidermoid carcinomas was seen.
Conclusion: ALCAM cytoplasmatic and/or membranous immunostaining was frequently found in salivary gland tumors. This suggests that, if anti-ALCAM therapies turned out to be successful, salivary gland cancers may be good candidates for such new treatment options.

006

Expression of insulin-like growth factor II mRNA-binding protein 3 (IMP3) in head and neck squamous cell carcinoma (HNSCC)—potentials as a predictive marker?

T. S. Clauditz *, A. Gontarewicz, C.-J. Wang, A. Münscher, M. Blessmann, R. Knecht, C. Bokemeyer, G. Sauter, W. Wilczak
*UKE Hamburg-Eppendorf, Inst. für Pathologie, Hamburg, Germany

Objective: Insulin-like growth factor II mRNA-binding protein 3 (IMP3) was found to be overexpressed in various cancer types but rarely in normal tissue, suggesting its possible role in carcinogenesis. Analysis of IMP3 expression in head and neck squamous cell carcinomas (HNSCC) are rare so that we evaluated it using tissue microarray method.
Method: Immunohistochemical analysis of IMP3 was done on samples from over 400 patients. The expression was measured semiquantitatively, subsequently divided into four categories (negative, weak, medium or strong) and correlated with several available clinicopathologic parameters.
Results: Strong IMP3 expression was observed in patients with all tumor stages (pT1-4) and nodal stages (pN0-3) also showing a significant statistical correlation ($p=0.0005$ and $p=0.0304$, respectively). No further correlations were found. Separate analysis according to tumor localization (oral cavity, oropharyngeal and laryngeal) showed a significant correlation of positive IMP3 expression and overall survival ($p=0.04$) only in patients with tumors of the oral cavity. Multivariate analysis showed IMP3 as an independent predictive marker for oral squamous cell carcinoma (OSCC).
Conclusion: A significant correlation between positive IMP3 expression and overall survival of patients with oral squamous cell carcinomas was found. Therefore, IMP3 expression might be used as an independent prognostic factor in OSCC.

007

Mucin-rich salivary duct carcinoma of minor salivary gland with stromal osteoclast-like giant cells: a case report

F. E. Costa *, C. Dias, P. Farrajota, A. Duarte, C. Lopes
*Menarini Diagnosticos Lda., Paço de Arcos, Portugal

Objective: Salivary duct carcinoma (SDC) is an uncommon high-grade malignant neoplasm arising predominantly in major salivary glands. It is frequently compared to ductal carcinoma of the breast due to their great resemblance, both architecturally and cytologically. SDC with osteoclast-like giant cell tumor (GCT) is rare although it has already been reported in minor salivary glands. Furthermore, mucin-rich SDC of minor salivary gland with osteoclast-like giant cell (OGC) stromal reaction intermingled in the carcinomatous pattern is exceedingly rare.
Method: We report a case of a 51-year-old man diagnosed with a left retromolar oral neoplasia.
Results: The tumor showed mucin-rich SDC containing stromal OGC. We found the characteristic cystic nodules of tumor cells with a conspicuous central area of comedonecrosis, as well as smaller solid nodules between the cystic ones. There were mucinous areas within the tumoral mass. Surprisingly, we also found OGC scattered within the stroma. OGC were immunorreactive with CD68 and were CAM5.2 negative.
Conclusion: OGC have already been described in a wide range of extra-osseous malignancies. However, this is a rare case of mucin-rich SDC in which the OGC component, too,

arises in a pattern similar to the one found in breast duct carcinoma with OGC.

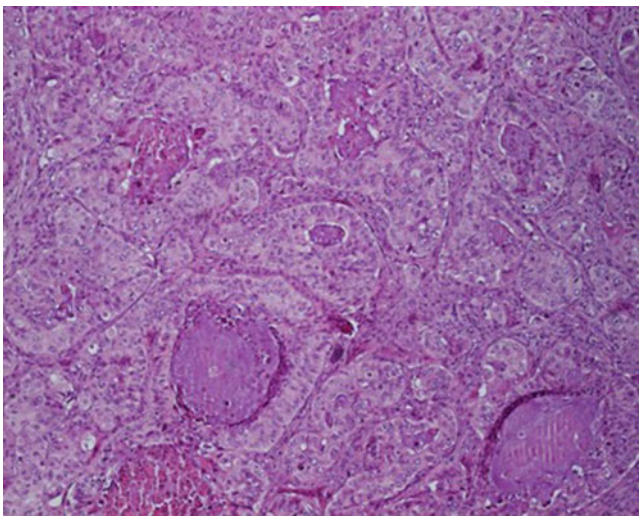

008

Synchronous papillary and squamous carcinoma occuring in a thyroglossal duct cyst: a case report

E. Demiralay *, N, Can, Ö. Yalçin, T. Çiftçi, S. Altaner
*Baskent University, Dept. of Pathology, Istanbul, Turkey

Objective: Carcinomas evolving from thyroglossal duct cyst are uncommon. Ninety-four percent of thyroglossal duct carcinomas are of thyroid origin, with most being papillary in nature, and 6% are of squamous cell origin. According to our knowledge, only two cases of mixed papillary and squamous cell carcinoma of a thyroglossal duct cyst have been reported up to date. Herein, we report a new case diagnosed as mixed papillary and squamous carcinoma arising in thyroglossal duct cyst.
Method: A 67-year-old female patient presented with a neck mass that had been present for 5 years. Cervical CT showed a mass lesion containing calcification which invaded the surrounding tissue throughout the midline and right part of the neck. Excisional biopsy was performed to the patient.
Results: The histological examination showed mixed squamous and papillary carcinoma. Immunohistochemically, while TTF1, cytokeratin 19, galectin-3 and mesothelial cell antibody were positive in papillary carcinoma, squamous cell carcinoma exhibited positivity with p63. There was no primary tumor in thyroid or anywhere.
Conclusion: Malignancy within a thyroglossal duct cyst is very rare but should be considered in the differential diagnosis of a midline neck mass. Immunohistochemical studies and radiological examination can be useful in this regard.

009

Histological features of primary parotid cancers: a 10-year report from Surrey, West Sussex and Hampshire (SWSH) Network, UK

S. Di Palma *, T. Gutierrez, R. Mathew, D. Walker, L. Pitkin, S. Whitaker, M. Bailey
*Royal Surrey County Hospital, Dept. of Histopathology, Guildford, UK

Objective: Malignant parotid tumours are uncommon representing <5% of all head and neck cancers. In the ageing population of the SWSH network, we have observed an increasing frequency. Their accurate histological classification is controversial, but we have noted that when a pathologist with a special interest in salivary gland pathology is involved, like in our network, the distribution of histological subtypes may differ from that of the literature. The aims of our study are to (a) explore the reasons behind our increased incidence of malignant parotid tumours and (b) analyse our distribution of histological subtypes compared with that of the literature.
Method: The files of the histopathology department at the Royal Surrey County Hospital (RSCH) which include material submitted from the SWSH network have been reviewed for all malignant primary parotid tumours occurring over a 10-year period.
Results: The total cases are 105, with an increased number every year. The histological subtypes are: 27% adenoid cystic, 21% carcinoma ex PA, 16% acinic, 15% invasive ductal, 15% mucoepidermoid and 4% myoepithelial carcinomas.
Conclusion: Whilst the increased incidence of parotid carcinomas may be related to both ageing population, our distribution of histological subtypes may be the result of a specialist assessment by a pathologist with an interest in salivary gland pathology.

010

Features predicting metastasis in cutaneous squamous cell carcinoma of the head and neck: a 10-year review of cases in the South East of England

S. Di Palma *, R. Mathew, D. Walker, T. Gutierrez, L. Pitkin, S. Whitaker, R. Sudderick, M. Dandford
*Royal Surrey County Hospital, Dept. of Histopathology, Guildford, UK

Objective: In the UK, the incidence of skin squamous cell carcinoma (sSCC) is rising and proportionally so is the number of their cervical and parotid lymph nodes metastases. The association between primary sSCC and metastasis may not be obvious to the reporting pathologist as most of sSCC behave as low risk cancer. The aim of this study was to compare the clinicopathological features of 72 patients with metastatic sSCC.

Method: A retrospective histological review and follow-up of primary and metastatic sSCC treated at a Regional Head and Neck Cancer Centre over the last 10 years was performed.
Results: 72 patients. M: F 5:1, median age 80 years (range 41–99) Primary location: ear (35%), scalp (22%) fronto-temporal (17%). 89%(n=48/54) were moderately or poorly differentiated. 79% had thickness >4 mm (n=23/29) and 30%(n=9/30) showed either lymphovascular or perineural infiltration. Margins were <5 mm in 94%(n=45/48) of patients, of which only 38%(n=17/45) received further excisions. 81% of patients treated for cervical nodes (63%) and parotid (57%) metastases.
Conclusion: The histopathological features associated with subsequent metastases were poor differentiation, increased thickness, lymphovascular and perineural invasion and narrow excision margins. These features need to be recorded to identify patients at high risk of metastasis and requiring closer preventative management.

011

Ossifying fibroma: a case report of special interest with two different metachronous neoplasms

E. Diakatou *, G. Liadakis, A. Kostopoulou, E. Kirodimou, T. Choreutaki
*GNA G. Gennimatas, Dept. of Pathology, Athens, Greece

Objective: Ossifying fibroma (OF) is a rare entity of the jaw which commonly occurs in the second to fourth decade. We present a case of a young male patient with two different metachronous neoplasms, one occurring in the maxilla and the other in the mandible.
Method: A 26-year-old male patient presented to our hospital with complaints of a gradually increasing swelling and disfiguration of the right mandible. Imaging studies revealed a well-demarcated mass; partial excision of the mandible was performed and the diagnosis confirmed OF After a 2-year period, the patient presented with a complaint of discomfort in the left maxilla. The X-ray and computed tomography results revealed a tumor mass and excision was performed. Histology showed a fibroosseous neoplasm with morphological and immohistochemical characteristics (Vimentin +, S-100 protein +, EMA -, CKAE1/AE3 -, SMA -, Desmin -, CD34 -) of OF with cementum-like deposits (cementifying fibroma).
Results: OF shows a predilection for the mandible (70–90%) and probably originates from a stem cell of the periodontal ligament that produces bone and cementum in a variably cellular fibrous stroma.
Conclusion: OF should not be confused with fibromas and/or osseous dysplasia, which do not constitute neoplasia and are rather reactive and proliferative conditions with non-circumscribed merging borders.

012

Human papilloma virus in early upper aerodigestive tract squamous cell carcinoma (SCC): a clinicopathologic study of 35 cases

M. C. Etxezarraga *, E. Fuertes, N. Liaño, G. Cancho, M. Zufiaurre, J. Bilbao, M. Ramirez, C. Ereño
*Hospital de Basurto, Dept. de Anatomía Patológica, Bilbao, Spain

Objective: HPV is a known agent in the pathogenesis of some squamous cell carcinomas (SCC) in the upper aerodigestive tract (UADT). Koilocytic atypia and p16INK4A (p16) immunostaining are good markers of virus infection. Our aim is to evaluate both markers in the initial stage of the disease and to define their prognostic value in terms of survival.
Method: In situ and pT1a SCCs cases of the UADT have been retrieved from Basurto and San Eloy Hospitals between 1997 and 2007. The cases were retrospectively re-evaluated for koilocytosis and immunostained with p16. Positive cases were analysed for HPV (PCR and sequencing). Clinical and follow-up data were retrieved from clinical files. Kaplan–Meier test was performed.
Results: Twenty-nine in situ and 6 pT1a SCCs were studied. Males predominated (30/5), average of 56 years. The case distributions were: larynx-hypopharynx (18), oral cavity (9), tongue base (4) and nasal cavity (4). Eigthteen (51%) p16-positive, 16 (88%) being HPV-positive. Fifteen were genotyped (93%), 12 (75%) HPV16-positive. Nine cases had other genotypes co-infection. Koilocytosis was detected in the vocal cords in five of the six HPV-positive cases. Fifty-three months was the average follow-up. Three patients suffered from a second primary metachronous tumour. Overall 5-year-survival was 99% in the HPV-positive group and 66% in the HPV-negative group, but it did not reach statistical significance.
Conclusion: Diverse HPV genotypes are present in a high proportion of early SCCs of the UADTs. Koilocytosis and p16 were closely related with HPV infection. Although not statistically significant, a longer survival in HPV-positive early tumours was observed.

013

HPV-associated papillary squamous cell carcinoma (SCC) of the larynx and hypopharynx: a clinicopathologic study of 16 cases

M. C. Etxezarraga *, E. Fuertes, N. Liaño, J. Velasco, R. Ruiz, J. Bilbao, M. Ramirez, C. Ereño
*Hospital de Basurto, Dept. de Anatomía Patológica, Bilbao, Spain

Objective: Papillary squamous cell carcinoma (PSCC) is a rare subtype of squamous cell carcinoma in the upper aerodigestive tract. Its pathogenesis remains unclear and its

diagnosis challenging. Our aim in this study is to analyse the relationship between this distinct neoplasm and the HPV status.
Method: All squamous cell carcinomas with at least 70% of papillary architecture retrieved between 1995 and 2007 in the Hospitals of Basurto and San Eloy, Basque Country, Spain, were retrospectively reviewed. The analysis included classic histopathologic criteria, immunohistochemistry for p16, and HPV detection by PCR, in situ hybridization, and DNA-sequencing. Kaplan–Meier test was performed for analysis of survival.
Results: Sixteen cases met the histological criteria of PSCC. Males predominated in the series (13 M/3 F) with an average age of 61 years (range, 38–79). Epiglottis (seven cases), vocal cords (five cases), and pyriform sinus (three cases) were the tumour site distribution. Location was not specified in one case. Surgical specimens were obtained in 11 cases (pT1, 3; pT2, 2; pT3, 6; pN0, 9; pN+, 2) and resection biopsies in 5. Papillary finger-like pattern of growth was observed in 13 cases (3 in situ and 10 invasive) and broad base pattern in 3. p16 immunostaining was seen in five cases (31%), two of them (40%) being positive for HPV-16 genotyping. Average follow-up was 71 months. Survival for HPV-16 associated cases was 66.6% after 52 months.
Conclusion: Genuine PSCCs are rare neoplasms that show a strong relationship with HPV-16. p16 immunohistochemistry is a reliable marker for HPV infection.

014

Associations of Rsf-1 overexpression with poor therapeutic response and worse survival in patients with nasopharyngeal carcinoma

H.-Y. Huang *, H.-C. Tai, C.-F. Li
*Chang Gung Memorial Hospital, Dept. of Pathology, Kaohsiung, Taiwan

Objective: Dysregulated chromatin remodeling often leads to gene silencing in cells, thereby implicating tumor development and progression. As a subunit of remodeling and spacing factor (RSF) complex, Rsf-1, a novel nuclear protein with histone chaperon function, mediates ATPase-dependent chromatin remodeling and confers a tumor aggressiveness in common carcinomas. However, the expression of Rsf-1 has never been reported in nasopharyngeal carcinoma (NPC).
Method: Rsf-1 immunoexpression was retrospectively assessed for biopsies of 108 consecutive NPC patients without initial distant metastasis and treated with consistent guidelines. The results were correlated with the clinicopathological features, therapeutic response, local recurrence-free survival (LRFS), distant metastasis-free survival (DMFS), and diseases-specific survival (DSS).
Results: Present in 49 cases (45%), Rsf-1 overexpression was associated with N2, 3 status (p=0.016), AJCC stage3, 4 (p=0.004), and incomplete therapeutic response (p=0.041). In multivariate analyses, Rsf-1 overexpression not only emerged as the sole independent adverse prognosticator for LFRS (p=0.0002, risk ratio [RR]=5.287) but also remained independently predictive of worse DMFS (p=0.0011, RR=3.185) and DDS (p<0.0001, RR=4.442), along with T3, 4 (p=0.0454) and N2, 3 (p=0.0319), respectively.
Conclusion: Rsf-1 overexpression is common and associated with adverse prognosticators and incomplete therapeutic response, which confers tumor aggressiveness through chromatin remodeling and represent a potential prognostic biomarker in NPC.

015

Human developing minor salivary glands: expression of mucins according to the morphogenesis stages

R. Ianez *, T. Teshima, C. Coutinho-Camillo, M. Buim, F. Soares, S. Lourenço
*Hospital A.C. Camargo. Dept. de Anatomia Patologica, São Paulo, Brazil

Objective: Formation of salivary glands involves proliferation of epithelial cells from stomatodeum into the underlying ectomesenchyme, culminating in a complex network of ducts and acinar bulbs. Mucins participation during this process is obscure, but they appear to contribute to luminal space formation and maturation. Our aim was to investigate mucins expression patterns and their relationship with morphogenesis of human salivary glands.
Method: Specimens of developing human salivary glands obtained from foetuses ranging from 4 to 24 weeks of gestation and fully developed salivary glands were studied for mucin immunohistochemistry—MUC1, 2, 3, 4, 5 AC and 5B, 6 and 16. Expression patterns were analysed qualitatively, according to the development stage of the salivary glands analysed.
Results: Mucins 1, 3, 4, 5B and 16 were detected during salivary gland development, being stronger in all ductal segments by the final phases of branching morphogenesis, and in mature glands. Acinar cells were negative for most mucins, including MUC1 in mature salivary glands. Mucins 2, 5 AC and 6 were negative.
Conclusion: Mucins MUC1, 3, 4, 5B and 16 showed relevant expression in developing human salivary glands and in mature glands, suggesting important roles in maturation and maintenance of the ductal network.

016

Case report: fasciitis ossificans of the larynx

E. Javadirad *, A. Almasi
*Medical School, Dept. of Pathology, Kermanshah, Iran

We describe a rare case of laryngeal fasciitis ossificans. A 58-year-old man presented with hoarseness and a nodule was found in the larynx. Excisional biopsy was performed, and follow-up laryngoscopy showed the complete resolution of this reactive lesion, and normal laryngeal function. The 0.6-cm-diameter nodule was well circumscribed and, histologically, the lesion was composed of uniform woven bone trabeculae with rimming of osteoblasts and cellular stroma. At the periphery, uniform spindle cells actively proliferated in edematous stroma. Spindle cells were immunoreactive for vimentin and α-smooth muscle actin, suggesting myofibroblastic differentiation. Fasciitis ossificans is histologically identical to myositis ossificans but tends to present no zonation phenomenon. Fasciitis ossificans is a rare form of heterotopic bone formation, commonly presenting with signs of local inflammation or pain. This patient's successful outcome suggests that conservative resection may be both diagnostic and curative.

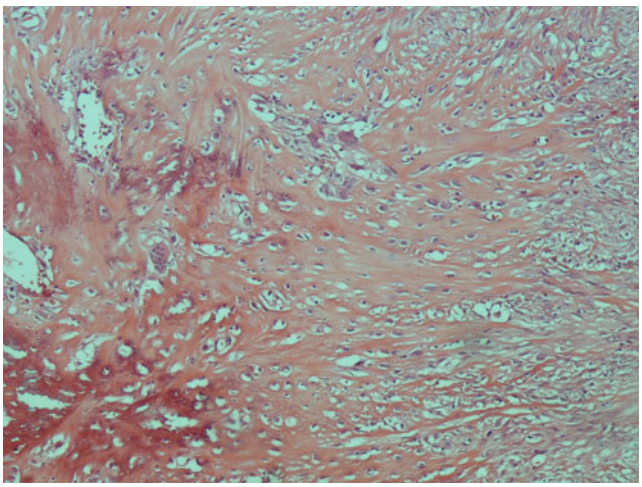

017

Anaplastic carcinoma of ectopic thyroid tissue in submandibular lymph node: report of a rare case

G. Kalodimos *, A.-M. Feritsean, S. Divani, C. Skoulakis, S. Kafki, K. Koti, E. Alexopoulou
*General Hospital of Volos, Dept. of Pathology, Greece

Objective: Development of carcinoma in ectopic thyroid tissue is a relatively frequent finding. Usually it is of the papillary type, while anaplastic/undifferentiated thyroid carcinoma (ATC) is rarely encountered.
Method: A 71-year-old Caucasian male presented with a right-sided lateral neck mass of long-standing duration, rapidly increasing in size over the last 2 months. CT scan and MRI showed a lesion close to the right submandibular gland. The thyroid was normal. FNA biopsy indicated malignancy.
Results: The excised specimen was a brownish mass with a thin capsule, almost solid on cut surface, with yellowish and haemorrhagic foci. Two lymph nodes 0.4 and 0.8 cm tissue were located peripherally. Microscopical examination revealed a highly malignant neoplasm showing immunopositivity for pancytokeratin, cytokeratin7, p53 and TTF-1. Thyroid follicles were found at the periphery of the neoplasm and in the lymph nodes. All of the above supported the diagnosis of ATC. The patient recovered well after surgery and subsequently received radiation and chemotherapy. He died 10 months after the diagnosis of distant lung metastases.
Conclusion: Our case is reported because of its rarity and literature is reviewed. Besides, we would like to stress on the fact that every neck mass should raise the suspicion of neoplastic change in ectopic thyroid tissue.

018

Comparative cytological and histopathological examination of papillary thyroid carcinoma

V. Katic *, A. Petrovic, T. Aggelopoulou, M. Milentijevic, D. Stefanovic, I. Mitic
*Policlinic of Nis, Dept. of Pathology, Serbia

Objective: Fine-needle aspiration cytology (FNAC) of the thyroid is non-invasive, cost-effective screening procedure that is valuable for distinguishing neoplastic from non-neoplastic "cold" nodules. The aim of this study was to determine the diagnosis accuracy of FNACs performed in our institutions by correlating FNAC results with histopathologic results.
Method: A total of 42 aspiration cytology specimens of papillary thyroid carcinoma, followed by thyreoidectomy, were included in this study, and the results were compared with their histological diagnoses.
Results: Rich cellular smears, anastomosing papillary fragments, small discrete cytoplasmic vacuoles and small spherical deposits of dense inspissated colloid or psammoma bodies, are importand characteristics of papillary thyroid carcinoma. However, crucial in its cytologic recognition were nuclear abnormalities with, almost pathognomonic, the following finding for papillary carcinoma: bigger nuclei with folds and grooves and with intranuclear cytoplasmic inclusions and small nucleoli. The sensitivity and specificity of thyroid FNAC for detecting papillary carcinoma were 96.2% and 94.4%.
Conclusion: Despite its limitation, thyroid FNAC remains the most-cost effective, first-line diagnostic technique.

019

Basaloid squamous carcinoma of the tongue

E. Koniaris*, A. Apostolaki, N. Arnogiannaki, M. Gazalidou, S. Tsitsiou, N. Koufopoulos, M. Sofopoulos, A. Vacarciuc
*Athens, Greece

Objective: Basaloid squamous cell carcinoma (BSCC) is an aggressive variant of squamous cell carcinoma. They account for less than 1% of all SCC of the tongue and the floor of the mouth. These tumors occur in men in the seventh decades. The tumor usually is localized in the base of the tongue and supraglottic larynx. Causative factors remain unclear, but it has been linked to tobacco, alcohol and HPV infection.
Method: We report a case of a 35-year-old woman who presented to our hospital with a 3.2-cm slightly elevated and ulcerated tumor in the right side of the tongue.
Results: Histological examination showed a solid tumor island which exhibit peripheral palisading of the neoplastic cells, focally surrounded by a thick basement membrane and admixed areas with obvious squamous differentiation. The squamous component showed mainly individual keratinization. Immunohistochemistry revealed positivity in 32βE12.
Conclusion: We should include in our differential diagnosis adenoid cystic carcinoma of the minor salivary glands which exhibits diffuse cytoplasmic vimentin expression. Merkel cell carcinoma exhibits NSE positivity. Also peripheral ameloblastoma pose diagnostic difficulites and many of them in the past have been published as basal cell carcinoma.

020

Markers for nodal metastasis in laryngeal squamous cell carcinoma

R. Kulagin *, P. Semyon, U. Anas
*Kazan Medical University, Russia

Objective: This study aims to identify markers that are relevant as predictors of lymph node metastasis in laryngeal squamous cell cancer. The aim of the present study was to investigate the prognostic significance over expression of p53 protein, cyclin D1, CD34, CD44v6, markers of cellular proliferation (Ki-67 and PCNA).
Method: Primary tumors for analyses were obtained from 90 patients. All patients were treated between the years 1992 and 2004. The expression of p53 was analyzed with monoclonal DO7 antibody, cyclin D1 (clone DCS-6), CD34 (clone QBEnd), CD44v6 (clone VFF-7), proliferate activity with Ki-67 (clone MIB-1) and PCNA (clone PC10).
Results: The value of PCNA index in patients with metastasis is significantly higher than those in patients without metastasis ($p<0.05$). Lymph node metastasis was correlated with the loss of expression of CD44v6 ($p<0.001$) in primary tumors. No significant correlations were found between positive p53, cyclin D1, Ki-67 and CD34 immunostaining and N+.
Conclusion: The present study suggests that the loss of expression of CD44v6 and high level of PCNA index may play a role in metastasis in larynx cancer and could be used as a prognostic factor.

021

Giant cell tumor of the larynx

A. Kurt *, S. A. Özmen, A. Ertas
*Bölge Egitim ve Arastirma Hastepek, Dept. of Pathology, Erzurum, Turkey

Giant cell tumors (GCT) are benign tumors generally found in the long bones. Very rarely, they can occur in the larynx and may present with dysphonia, dysphagia, or dyspnea. This lesion is a true neoplasm, presumably of the fibrohistiocytic series. Histologically, it closely resembles the more familiar true giant cell tumor of long bone. The laryngeal giant cell tumors appear, to date, to be non-metastasizing lesions; it is possible that they may recur locally if incompletely excised (although this remains to be demonstrated). A 71-year-old nonsmoking male patient had dysphonia for 4 months. Four biopsy materials, of which the biggest one was 4 mm in length, excised from the left vocal cord were examined. The tumoral mass which was composed of multinucleated giant cells like osteoclasts in the cellular and vascular stroma was seen. The lesion was stained with vimentin, CD 68 and smooth muscle actin pozitive. The findigs were characteristic of giant cell tumor of bone. On microscopic examination, numerous multinucleated osteoclast-like giant cells, within cellular and vascular stroma containing plump, oval mononuclear cells with nuclei similar to giant cells; expansile and infiltrative growth; freguent mitotic figures; often secondary cystic degeneration, reactive bone formation; no cytologic atypia. Rich wascularized stroma with extravased erythrocytes and lakes filled with blood were also noted.

022

Mucosal large cell neuroendocine carcinoma (M-LCNEC) of the head and neck regions in Japanese: a new clinico-pathologic entity

K. Kusafuka *, M. Abe, Y. Iida, T. Onitsuka, T. Nakajima
*Shizuoka Cancer Center, Dept. of Pathology, Sunto, Japan

Objective: Large cell neuroendocrine carcinoma (LCNEC) is well known as a subtype of lung cancer. Our objective is to establish mucosal LCNEC (M-LCNEC) as a new entity in the head and neck regions.
Method: We re-estimated 814 surgically resected specimens of the primary mucosal carcinoma in the head and neck regions during 2002–2009. The immunostainings for neuroendocrine (NE) markers such as CD56,

chromogranin-A and synaptophysin were performed. In the cases which were positive for>two NE markers, we re-diagnosed as "M-LCNEC".
Results: Only eight cases (0.98%) were re-diagnosed as M-LCNEC. All cases were male and the subjecs' mean age was 64.6 years old. Three cases occurred in the oropharynx, four cases in the larynx and one case in hypopharynx. Only one case showed dead of disease. Histologically, M-LCNEC showed the organoid pattern growth of large basaloid cells, in which were sometimes seen the central necrosis, rosette formation, peripheral palisading, high mitotic figures. Immunohistochemically, M-LCNEC indicated to be positive for two or three NE markers.
Conclusion: We propose that M-LCNEC can occur in the head and neck regions and is a new clinicopathological entity.

023

Should elective neck dissection be performed following radiation therapy in patients undergoing salvage total laryngectomy?

L. Leider Trejo *
*Sourasky Medical Center, Dept. of Pathology, Tel Aviv, Israel

Objective: The common treatment of patients with recurrent laryngeal SCC, after primary radiation or chemoradiation therapy is partial or total laryngectomy and neck dissection (ND). ND is usually performed even in the absence of positive neck nodes (clinically N0). ND in this population is associated with additional surgical complications and significant morbidity. There are no data on the risk of occult neck metastases after primary radiotherapy to the larynx alone or after radiation to the larynx and neck.
Method: Records of patients underwent salvage total laryngectomy with neck ND reviewed. Patients were previously treated with primary radiation/chemoradiation for laryngeal SCC. All were clinically and radiological N0. Risk of occult neck metastases and complications was assessed in patients after radiation therapy to the larynx, with or without neck sparing.
Results: A total of 34 patients were included. Average age, 61±12 years. Average time to recurrence: 18±13 months. Nine patients had bilateral ND; hence, 43 necks were assessed. There were 4/21 non-irradiated necks (19%) which were positive for nodal metastasis; 2/22 (9%) in the irradiated neck patients were positive ($p=0.4$). No ND-related morbidity was observed.
Conclusion: Although neck irradiation is associated with 10% decrease in the risk of nodal metastases relative to non-irradiated necks, this change in nodal status is not statistically significant to justify yet the abandonment of ND in this population.

024

Alveolar rhabdomyosarcoma of the tongue in a child: a case report

W. Majdoub *, S. Sassi, M.M. Hamdane, L. Charfi, K. Mrad, F. Khanchel, R. Doghri, N. Ben Hamida, S. Jlidi, K. Ben Rhomdhane
*Military Hospital, Tunis, Tunisia

Objective: Rhabdomyosarcoma (RMS) is the most common soft tissue sarcoma occurring in children. It involves rarely the tongue. Few cases are reported, and most of them are of the embryonal type. To the best of our knowledge, this is the second report.
Method: An 8-month-old boy presented with a 6-cm swelling and ulcerated mass at the base of the tongue.
Results: Radiological investigations showed a well-demarcated vascular lesion of the tongue, suggesting a lingual angioma. The mass had gradually enlarged despite a corticotherapy. A total surgical excision was performed. Histological examination revealed an ulcerated lingual mucosa infiltrated by spindle-shaped cell proliferation with abundant mucoid intercellular material. Rhabdomyoblasts were rarely seen. Immunohistochemical staining showed a strong positivity for desmin and myogenin. Therefore, pathological findings were consistent with an alveolar RMS. He received two courses of chemotherapy. Two months later, he died from severe hypoglycemia and ionic disorders.
Conclusion: RMS of the tongue is a rare malignant tumour clinically indistinguishable from a variety of benign neoplasm more frequent on this site. Therefore, it should be considered in the differential diagnosis of tongue masses and a biopsy should be performed.

025

Structural peculiarities of the fetal salivary glands in cases of complicated pregnancy

S. Morozov *
*Lugansk State Medical University, Dept. of Therapeutic, Surgical and Pediatric, Ukraine

Objective: Studies showed the importance of salivary gland function in maintaining a healthy oral environment. It is known that properties of saliva and its components may result in periodontal status and be responsible for the experience of caries. A role of the intrauterine development in structural peculiarities of the human salivary glands needs to be investigated. The aim of the present study was

to examine the morphology of fetal parotid and submandibular glands in cases of pregnancy complicated with toxemia of pregnancy.
Method: Parotid and submandibular glands of 20 human fetuses in 18–22 weeks of gestation were examined after spontaneous abortions in pregnancies complicated by toxemia of pregnancy. Salivary glands id 15 human fetuses with the same gestational age in cases of induced abortions die to social and psychological reasons were included in group of comparison. Histological slides stained with hematoxylin and eosin were studied stereologically to find out main structural components volume fractions.
Results: Results have shown the delay of acini and intralobulae ducts differentiation, decreased quantity if submandibular glands demilunes. Dystrophic changes of parenchymal elements of large salivary glands were also determined. Stereometric investigation revealed a reduction of parenchymatous elements volume fraction, decreased vascularity and decline of parenchyma/stroma index.
Conclusion: The above results verify structural impairments in intrauterine development of salivary glands in cases of complicated pregnancy. These alterations may stimulate functional abnormalities in salivary glands activities and contribute to oral pathology at children's and later age.

026

Microsatellite instability: does it play a role in young laryngeal carcinoma patients?

A. Nadal *, L. Conde, S. Moyano, I. Vilaseca, M. Moragas, A. Cardesa
*Hospital Clínic, Dept. de Anatomia Patològica, Barcelona, Spain

Objective: Squamous cell carcinoma of the larynx is a malignant neoplasm usually affecting males over 50 with alcohol and tobacco consumption history. The aim of the present study is to determine if the early development of carcinoma in young patients could be explained by an alternative pathway such as microsatellite instability (MSI) or if it follows the classical tumor suppressor pathway characterized by loss of heterozygosity.
Method: Microsatellite instability, loss of heterozygosity (LOH), and multiple mismatch repair (MMR), p16, p53 and p63 protein expression were analyzed in a series of 18 young laryngeal cancer patients.
Results: Fifty-three percent of cases presented LOH in at least one of the markers tested. Only 11% of the cases showed microsatellite instability to below. All cases retained MMR protein expression. p53, p16 and p63 expression profile was consistent with tumor suppressor pathway pattern.
Conclusion: Laryngeal carcinoma in young patients develops through the classical tumor suppressor pathway. Both immunohistochemical and molecular methods render the same results in the detection of MSI.

027

Cervical thymus

D. Nonaka *
*Christie NHS Foundation Trust, Dept. of Histopathology, Manchester, UK

Objective: The thymus and parathyroids arise from a common primordium of third/fourth pharyngeal pouch. The occurrence of cervical thymus is believed to be rare.
Method: A total of 831 cases (700 and 131 for thyroid and parathyroid diseases) were studied and histologic features were examined. CD205 (thymic epithelial marker) and p63 immunostains were applied in ambiguous cases.
Results: Thymus was seen in 10% (8.4% of thyroid surgeries and 19% of parathyroid surgeries). Present in central compartment dissection for papillary carcinoma was 29% of thymus from thyroid surgery. Thymus and parathyroid formed a single nodular configuration in 62%. Five thymus were hypercellular, with two showing follicular hyperplasia and associated with SLE and Graves disease; 33 regular; and 46 fatty. Six of 46 fatty thymus showed a few thin epithelial cords confirmed by immunostaining. Hassall's corpuscle was seen in 55 thymus; 12 spindle morphology; 2 cystic change; 3 duct formation with ciliated epithelial cells.
Conclusion: Central compartment neck dissection often contains thymus, and this may be mistaken as a lymph node, and thymic epithelial nests and Hassall's corpuscles may be interpreted as metastatic papillary carcinoma and psammoma-bodies. Awareness of cervical thymus would prevent this diagnostic pitfall. Cervical thymus may be subject to a variety of conditions which occur in mediastinal thymus.

028

A unique location for malignant melanoma: case report

I. H. Ozbudak *, S. Toru, M. Turhan, G. Ozbilim
*Akdeniz University, School of Medicine, Antalya, Turkey

Objective: Malignant melanoma developing on the ear should be considered a unique disease. Because the ear is thin-skinned and it has several anatomic subdivisions and

multiple areas of lymphatic drainage, any correlation for malignant melanoma between the ear and other locations may not be significant regarding the biological behavior and certain clinical criteria.
Method: A 70-year-old woman was referred to the hospital with a 1-year history of worsening deafness in her right ear. Otoscopy showed a smooth mass blocking the right ear canal. PET-CT confirmed a hyper metabolic soft-tissue lesion eroding through the lateral wall of the mastoid bone. Hypermetabolic right retropharyngeal lymph nodes were also detected. The patient underwent biopsy.
Results: Histopathological findings were consistent with malignant melanoma.
Conclusion: Although rare, malignant melanoma of the external ear canal is especially dangerous because detection is delayed due to its hidden location and they have very poor prognosis if the thickness of the tumor is more than 4 mm. We presented the case due to the rare incidence in this location and a review of literature was done for differential diagnosis.

029

Correlation of increased numbers of tumor-infiltrating T regulatory cells with well-differentiated oral squamous cell carcinoma (SCC)

F. Passador-Santos *, V. Montalli, A. Borges, E. Martinez, D. Rodrigues, V. Araujo, M. Napimoga
*São Leopoldo Mandic Institute, Dept. of Pathology, Valinhos, Brazil

Objective: Evidence from cancer patients suggests that increased T regulatory lymphocyte (Treg) activity may be associated with poor immune responses to tumor antigens and contribute to immune dysfunction. Since there is controversial data about the physiological role of the Treg in the tumor microenvironment, we analyzed whether there is a difference in the inflammatory cell's influx among tumors of different grades in patients with oral squamous cell carcinoma (OSCC).
Method: A total of 18 healthy subjects and 42 patients with OSCC were selected. Tumors were histologically graded as: well, moderately and poorly differentiated. A tissue microarray was employed to perform immunohistochemistry for CD8, FOXP3, CD19 and IL-10.
Results: Significant statistical increases ($p<0.05$) were observed in the number of FOXP3+ cells, CD8+ cells and IL-10 expression in the well-differentiated tumors in comparison to healthy and the poorly differentiated tumors. No difference was observed regarding the number of CD19+ cells among the three different grades.
Conclusion: The difference in the tumor grade is important for Treg cells recruitment in patients with OSCC, underlining the fact that the immune system is deregulated as a consequence of the disease.

030

Expression of apoptosis regulatory proteins p53, bcl-2 and bax in recurrent aphthous ulceration

D. Ribeiro *, J.F. Rodrigues, C. Oshima, S. Ihara, M. Franco
*Federal University Sao Paulo, Dept. of Biosciences, Santos, Brazil

Objective: Recurrent aphthous ulceration (RAU) is considered to be a chronic inflammatory disease of unknown pathogenesis. Apoptosis may represent an important event in the control of inflammation. The aim of this study was to investigate apoptosis process in RAU by means of immunohistochemistry.
Method: We studied the expression and location of p53, bcl-2 and bax in ulcerated lesions clinically diagnosed as RAU ($n=12$) and to compare it with that of oral clinically normal mucosa ($n=6$) and of other inflammatory chronic disease such as oral fibrous inflammatory hyperplasia (FIH; $n=18$).
Results: Statistically significant differences ($p<0.05$) were noticed to RAU when compared to normal mucosa. Bcl-2 and bax did not show remarkable differences between groups.
Conclusion: Taken together, the data suggest that RAU induces apoptosis as a result of p53 upregulation. This protein might be related with the aetiopathogenesis of the ulcerated oral lesions.

031

Oxidative DNA damage is a preliminary step during rat tongue carcinogenesis induced by 4-nitroquinoline 1-oxide

D. Ribeiro *, J. Noguti, S. Miranda, C. Oshima
*Federal University Sao Paulo, Dept. of Biosciences, Santos, Brazil

Objective: The aim of this study was to investigate oxidative DNA damage during 4-nitroquinoline 1-oxide (4NQO)-induced rat tongue carcinogenesis.
Method: For this purpose, male Wistar rats were distributed into three groups of ten animals each and treated with 50 ppm 4NQO solution through their drinking water for 4, 12, and 20 weeks. Ten animals were used as negative

control. The alkaline Comet assay modified with lesion-specific enzymes was used to detect single and double strand breaks, labile sites (SBs), and oxidised purines and pyrimidines.
Results: Although no histopathological abnormalities were induced in the epithelium after 4 weeks of carcinogen exposure, oxidative DNA damage was detected in the 'normal' oral epithelium. In pre-neoplastic lesions and squamous cell carcinomas induced after 12 and 20 weeks following carcinogen exposure, respectively, oxidative DNA damage was also increased ($p<0.05$) when compared to negative control.
Conclusion: In conclusion, our results suggest that oxidative DNA damage is an early event during multistep carcinogenesis assay induced by 4NQO. This kind of approach should be considered for persons with high risk of oral cancer, such as smokers or alcohol consumers.

032

Hsp70 and Hsp27 expression during medium-term oral carcinogenesis assay induced by 4-nitroquinoline 1-oxide

D. Ribeiro *, J. Noguti, A. C. Fracalossi, C. Oshima, M. Franco
*Federal University Sao Paulo, Dept. of Biosciences, Santos, Brazil

Objective: The aim of this study was to investigate Hsp 27 and Hsp 70 expression during 4-nitroquinoline 1-oxide (4NQO)-induced rat tongue carcinogenesis.
Method: For this purpose, male Wistar rats were distributed into three groups of ten animals each and treated with 50 ppm 4NQO solution through their drinking water for 4, 12, and 20 weeks. Ten animals were used as negative control.
Results: Although no histopathological abnormalities were induced in the epithelium after 4 weeks of carcinogen exposure, Hsp 27 and Hsp 70 were expresssed in the 'normal' oral epithelium. In pre-neoplastic lesions at 12 weeks following carcinogen exposure, the levels of Hsp 70 were increased ($p<0.05$) when compared to negative control. In Squamous cell carcinomas induced after 20 weeks of 4NQO, Hsp27 ans Hsp70 were expressed in some tumor cells, but no statistically significant differences ($p>0.05$) were noticed when compared to other groups.
Conclusion: Our results support the idea that expression of Hsp 70 plays a crucial role during carcinogenesis being closely related to neoplastic conversion of the oral mucosa cells.

033

A case report: leiomyosarcoma of the larynx with a recurrence

S. Rjabceva *, M. Vozmitel
*Belarusian Medical Academy, Dept. of Pathology, Minsk, Belarus

Objective: Leiomyosarcomas originate in the smooth muscles of the cutaneous and subcutaneous tissues, the lower gastrointestinal/genitourinary tract, and the vascular walls, but leiomyosarcoma of the larynx is an extremely rare neoplasm.
Method: We studied the case of laryngeal leiomyosarcoma in a 35-year-old woman. The tumor was removed surgically. Paraffin-embedded tissue was stained with hematoxylin–eosin. We used immunohistochemical markers such as smooth muscle actin (SMA), desmin, CD99 and S100.
Results: In 2008, a large polypoid mass of the larynx was detected by fiberoptic laryngoscopy, but the large size of the tumor prevented us from identifying its site of origin. The biopsy specimen showed mucosal ulceration and a submucosal tumor mass. After 2 months, the patient underwent total laryngectomy. Histopathologically, the tumor consisted of spindle-shaped cells with cigar-shaped, blunt-ended nuclei and eosinophilic cytoplasm with perinuclear vacuoles. The tumor cells formed a prominent interlacing bundles and fascicles. The small foci of necrosis were found. Mitotic activity was moderate. Immunohistochemical examination showed strong SMA and desmin positivity. CD99 and S100 actin were negative. After 2 years, tumor recurrence in the neck was detected. This recurrence was removed surgically and the patient was disease-free upon follow-up examination at 11 months.
Conclusion: Primary leiomyosarcoma of the larynx, although rare, should be diagnosed.

034

Unusual metastasis of renal cell carcinoma: a case report and review of the literature

J. Sandbank *, M. Herbert, P. Liokumovich, M. Hirsh
*Assaf Harofeh Medical Center, Dept. of Pathology, Zerifin, Israel

Objective: A primary tumor of the kidney metastasizing into the tonsil is very unusual and only anecdotal cases have been reported.
Method: We report here on an 82-year-old female with metastasis in the right tonsil that occurred 6 years following tumor nephrectomy. In addition, a review of the relevant literature was conducted.

Results: An exhaustive literature review covering the period from 1970 onwards disclosed 176 metastatic tumors in tonsils, and only nine cases were of renal origin.
Conclusion: The presence of metastases of renal cell carcinoma can be found even years following the initial curative treatment of the primary tumor, although rarely in the region of the head and neck. They can often be mistaken for benign tumors.

035

Expression analysis of proteins Cox-2, Akt, NF-κB, in head and neck squamous cell carcinoma (SCC) cells treated with Celecoxib

D. Santos Pinto *, A. Abrahão, A. Del Vecchio
*University of Sao Paulo, School of Dentistry, Brazil

Objective: Several genetic alterations are associated with the pathogenesis of squamous cell carcinoma (SCC). Some of these changes affect proteins belonging to the AKT signaling pathway. This work aims to study the expression of pAkt, NF-κB, and COX-2 involved in the AKT signaling pathway in squamous cell carcinoma lines in order to verify possible changes in translation of these molecules.
Method: Four SCC cell lines were divided into four groups: (1) untreated control group, (2) cells treated with Celecoxib, (3) cells stimulated with EGF and treated with Celecoxib, and (4) cells stimulated with EGF. Cell proliferation was monitored by cell viability test. Analysis of expression and interaction of proteins is accomplished using Western blotting. The intracellular location of proteins was verified by immunofluorescence and apoptosis by TUNEL.
Results: Treated cells show a slight reduction in pAKT and NF-κB expression, but COX2 expression was not changed. The control group of four cell lines tested for pAKT antibody showed nuclear staining. As for the treated group, this pattern was only maintained for the SCC4 and SCC9. Cell lines SCC15 and SCC25 presented both cytoplasmic and nuclear staining.
Conclusion: Since Celecoxib reduces AKT expression, its use in as an adjuvant therapeutic may be considered in future SCC therapy.

036

The increased p16 expression in recurrence of salivary gland pleomorphic adenoma

L. Soares *, A. Souza, F. Santos, A. Altemani, A. Soares, V. Araújo
*Floriano, Brazil

Objective: Pleomorphic adenoma (PA) is the most common salivary gland tumor. Although classified as benign, it has a tendency to recur—recurrent pleomorphic adenoma (RPA), as well as the ability to undergo malignant transformation. The aim of the present study was to investigate the participation of p16 in PA and RPA.
Method: A total of 5 cases of PA and 24 cases of RPA were analyzed for p16 expression, using immunohistochemical techniques via tissue microarray. A grading system based on reactivity percentage was assigned on a scale from 0 to 3. Less than 10% cell reactivity rendered a 0; 10–25% cell reactivity rendered a 1; 25–50% cell reactivity rendered a 2; and reactivity greater than 50% rendered a 3.
Results: When comparing non-recurrent with recurrent tumors, p16 reactivity was stronger in RPA than that observed in PA. In PA, the majority of the cases showed negative or low expression while in RPA the majority of the cases demonstrated strong expression.
Conclusion: This research may suggest that p16 play a role in PA recurrence. However, further investigation is required to verify the real function of this protein in RPA.

037

Low-level laser irradiation of oral squamous cell carcinoma (SCC9 and SCC25) and oral dysplasia (HaCat) derived cell lines

S. Sousa *, M. Szabo, F. Giudice, F. Sperandio
*University of São Paulo, Dept. of Oral Pathology, Brazil

Objective: Laser phototherapy of cell lines reveal different results varying from stimulation to inhibition of proliferation. The cell types, as well as the parameters of the employed laser irradiation influence these results. This study aimed to evaluate the in vitro proliferation of SCC9 and SCC25 and HaCat cell lines after laser irradiation.
Method: The irradiation was performed with both red and infra-red light, with corresponding wavelengths of 660 and 780 nm, respectively. The power was set in 40 mW and the energy densities were 2, 3 and 6 J/cm^2. A single irradiation was performed and cell proliferation was assessed in 12, 24, 48 and 72 h.
Results: Results showed differences among the groups in all periods. HaCat showed increased cell proliferation for both wavelengths. Infra-red laser at 6 J/cm2 increased cell proliferation at 72 h in SCC9 cells. Interesting results were found with the SCC25 cells, which

demonstrated higher proliferation rate when irradiated with red laser at all energy densities, and inhibition of proliferation when irradiated at 2 and 3 J/cm^2 with infrared laser light.
Conclusion: Low-level laser irradiation as performed in this study was able to modify the growing rates of squamous cell carcinoma and dysplastic cells in vitro; however, different rates were found.

038

Immunochemical tools for the differential diagnosis of basaloid squamous carcinoma of the larynx

M. Tsopanomichalou *, M. Kefala, A. Drougou, D. Lefantzis, C. Barbatis
*Hellenic Red Cross Hospital, Dept. of Pathology, Athens, Greece

Objective: Basaloid squamous cell carcinoma (BSCC) is an uncommon aggressive variant of squamous cell carcinoma (SCC) with predilection for the head and neck, but other sites have also been reported. Diagnosis of BSCC currently relies mainly on histological criteria, with a variable immunohistochemical profile, with emphasis on altered adhesion molecules expression.
Method: We studied 20 laryngectomy specimens diagnosed with BSCC since 2003 and compared them with an equal number of SCCs, all collected at the Hellenic Red Cross Hospital. Formalin-fixed sections were immunohistochemically stained for the adhesion molecules E-cadherin, beta-catenin and Ber-EP4, using the Autostainer BondMax (Leica). Data were collected and compared with the SPSS 17.0 statistical software.
Results: BerEP4 is expressed only in BSSCs, either diffusely or focally. All cases, but two, did not show nuclear β-catenin, despite abnormal E-cadherin expression, with a tendency to reduction of the later.
Conclusion: The distinction of BSCC and SCC is crucial for the prognosis of laryngeal cancer and the use of immunohistochemistry is vital for the characterisation of these entities. The antibody Ber EP4 has proven a useful marker for differential diagnosis of BSCC.

039

Histopathological features of tumor-negative lymph nodes from oral cancer patients without metastatic disease

M. Vered *, G. Schiby, I. Bello, D. Dayan, A. Rytkönen, T. Salo
*Tel Aviv University, Dept. of Oral Pathology, Israel

Objective: For the assessment of morphological changes potentially associated with priming of the lymph nodes (LNs) for metastases, tumor-negative (Tn)-LNs from neck dissections of patients with oral carcinoma without microscopic evidence for metastases (neck negative, neck-ve) were compared histopathologically with Tn-LNs from patients with metastatic disease (neck positive, neck+ve).
Method: The largest three LNs, levels I-V, were examined from each neck. LNs from neck-ve, [120 mobile tongue cancer (MTC), 143 other oral sites (OOS)] were investigated among other parameters for capsule width, degree of dilatation of the sub-capsular and medullary sinuses, number of lobes and cortical reactive follicles, and compared with Tn-LNs, neck+ve (160 MTC, 50 OOS).
Results: The number of lobes in MTC-LNs was lower than that in OOS-LNs ($p=0.02$), irrespective of the metastatic status of the neck. The mean number of reactive follicles, their relative percent and mean number per lobe were significantly lower in Tn-LNs, neck+ve in MTC compared to OOS ($p<0.05$). Increased capsule width was associated with a lower degree of dilatation of both sub-capsular and medullary sinuses ($p<0.05$).
Conclusion: Histopathological changes were found in LNs of neck-ve patients. Changes were, in part, site-specific, and probably represent defective functionality of the LNs, especially in MTC.

040

Rare pediatric tumor—melanotic neuroectodermal tumor of infancy: report of two cases

M. Vozmitel *, S. Rjabceva, A. Dubrovskij, M. Taisija
*National Cancer Centre, Minsk, Belarus

Objective: We report here two cases of melanotic neuroectodermal tumor of infancy (MNTI), which were diagnosed at our center among 2,000 annual pediatric cases for a period of 15 years.
Method: The patients were 7- and 2-month-old boys with mandibular tumors. Tumors were surgically removed.
Results: Histological slides in every case revealed a biphasic tumor embedded in a densely fibrous stroma. For both tumors, two populations of cells were typified: epithelioid and small round blue. First tumor was characterized by prevalence of epithelioid cells with moderate amount of pale pink cytoplasm and

plentiful melanin pigment granules forming glandular/tubular structures, whereas small round blue cells arranged in the nested/alveolar growth patterns represented the principal component of the second tumor. The diagnosis of melanotic neuroectodermal tumor of infancy was proved in every case. Children are free of disease for 13 years (1st case) and 1 month (2nd case).

Conclusion: Due to the variability of cell populations and melanin contents, the MNTI has the ability to simulate a broad range of neoplasm, including neuroblastoma, Ewing sarcoma, peripheral primitive neuroectodermal tumor, rhabdomyosarcoma, lymphoma, teratoma and melanoma. Therefore, MNTI needs to be kept in mind for it not to be misinterpreted as malignant tumor.

041

Olfactory neuroblastoma: clinico-pathological study of seven cases

M. T. Yacoubi *, W. Jomaa, A. Bedoui, S. Hmissa
*University Hospital Sousse, Dept. of Cyto-Histopathology, Tunisia

Objective: Olfactory neuroblastoma is a specific type of malignant neuroectodermal tumor thought to have origin from the neuroepithelial elements in the olfactory membrane. It is a rare tumor counting about 1.2% of all malignant sinonasal tumors, and occurring at any age without sex or race predilection.

Method: We reviewed seven cases of olfactory neuroblastoma diagnosed in the period between1986 and 2006, in our department. Data were collected from clinical files and pathologic reports. Histologic grading was established using Hayms system.

Results: The median age of our patients was 36 years. Symptoms were mostly nasal obstruction and epistaxis. Ophthalmologic and neurologic symptoms were seen in patients with local extension. Two tumors were grade I, three were grade II, one was grade III and one was grade IV. Immunohistochemistry was performed in all cases Six patients had a surgical treatment. Four of them had adjuvant radiotherapy. One patient had a locally advanced tumor and could not have a curative treatment.

Conclusion: In this study we reviewed the clinical and pathological features of olfactory neuroblastoma, and we discussed the differential diagnoses.

Sunday, 28 August 2011, 09.30–10.30 and 16.30–17.00, Hall 5

PS-05 Poster Session Paediatric, Perinatal Pathology

001

On current histopathological classification of vascular anomalies

J. Kobos *, P. Przewratil, E. Andrzejewska
*Medical University of Lodz, Dept. of Developmental Pathology, Poland

Objective: ISSVA classification of vascular anomalies divides them into vascular tumors and vascular malformations. It is based on their biology and clinical prognosis and is widely accepted.

Method: Records of 65 patients aged 1–15 years (mean 5.6) operated on vascular anomalies were reviewed. The initial histopathological diagnosis included: 47 capillary hemangiomas, 5 "lymphatic hemangiomas", 6 "cavernous hemangiomas", 3 "mixed hemangiomas" 3 "vascular malformations" and 1 "hemangiolipoma". Specimens of excised lesions were stained with hematoxyline and eosine and then Glut-1 (Glucose transporter 1) immunostaing was performed. All results were verified under ISSVA classification.

Results: Out of 47 capillary hemangiomas 38 turned out to be pyogenic granulomas and only 9 germine capillary infantile hemangiomas with Glut-1 positive reaction. All 5 tumors initialy diagnosed as "lymphatic hemangiomas" occured to be lymphatic malformations. Of 6 "cavernous hemangiomas" 5 emerged to be venous malformations and 1 lymphatic malformation. Among 3 "mixed hemangiomas" 2 were juvenile hemangiomas (Glut-1 positive) and 1 angiolipoma. Among 4 "vascular malformations" 2 were venous and 2 arterio-venous.

Conclusion: Apropriete histopathological diagnosis of vascular anomalies under ISSVA classification involves the consideration of histological picture along with medical history and clinical appearance. Glut-1 immunostaining should be the standard procedure in histopathological examination of vascular anomalies.

002

Comparison of the larynx-associated lymphoid tissue in the false vocal cords and subglottis in pediatric autopsies

D.T.R.S. Abate *, R.C. Rossi e Silva, J.G. Pacheco Olegario, A.K. Marques Salge, L.C. Peres,
E.C. da Cunha Castro, V. d. Paula Antunes Teixeira
*UFTM, Dept. of Biological Science, Uberaba, Brazil

Objective: To compare the distribution of cellular phenotypes of the lymphoid follicles (LF) in the false vocal cords (FVC) to the ones in the subglottic region in pediatric autopsy using morphometric techniques and immunohistochemistry, relating this distribution to the age and different causes of death.
Method: 60 Larynges of newborns and children autopsied in the period from 1993 to 2003 were collected. The fragments were prepared in order to perform histochemical and immunohistochemical techniques.
Results: The morphological analysis showed cases that presented LF only in FVC (35%), LF only in subglottic region (20%), lack of LF in FVC (30%) and lymphoid aggregates, which did not characterize an LF (15%). The cases of LF in subglottic were significantly younger compared to the ones that presented FL in the FVC (p= 0.017). The LF in the subglottic region was bigger than the LF in the FVC (p=0.020).
Conclusion: The cells that make up the LF in the FVC in newborns and children younger than one year have functional characteristics similar to LF cells in the subglottic region, suggesting that there are similarities with LALT.

003

Atypical congenital mesoblastic nephroma: A case report

H. Akgun *, M.T. Ozgun, M. Basbug
*Erciyes University, Medical Faculty, Kayseri, Turkey

Objective: Congenital mesoblastic nephroma (CMN) accounts for only 3% of renal tumors in children. CMN has two subtypes. The classic form is characterized by spindle cells and blurred borders to the renal parenchyma, rare mitoses and absence of necrosis. Atypical or cellular form is characterized by high mitotic index, hypercellularity, atypical growth pattern with necrosis, hemorrhage, and invasion of adjacent structures other than connective tissue.
Method: Ultrasonography at 22 weeks of gestation of a 27-year-old multigravid woman revealed large left renal mass. Because fetal death occurred at 32 weeks of gestation, induction of labor was performed.
Results: Histopathological examination from the autopsy revealed a mesoblastic renal tumor composed of intersecting fascicles of spindle cells interdigitating with renal glomeruli and tubules. The tumor was shown to be a cellular mesoblastic nephroma with mitotic figures more than 5 per 10 high power fields. Areas of coagulative necrosis and hemorrhage were also observed.
Conclusion: Antenatal ultrasounds allow the detection of renal tumors, especially renal mesoblastic nephromas, but only the pathological analysis of the surgical specimen can confirm this diagnosis postnatally. When a fetal intra-abdominal solid tumor is found, the differential diagnosis of fetal abdominal solid tumor includes CMN, Wilms' tumor of the kidney and congenital adrenal neuroblastoma.

004

Meckel–Gruber syndrome: two case reports

I. Amat *, A. Gregorio, M. Francisco, J. Martinez Medel, A. Cordoba, I. Rodriguez, M. Mercado, E. Orbara
*Hospital de Navarra, Dept. of Pathology, Pamplona, Spain

Objective: Meckel–Gruber syndrome is a rare and lethal autosomal recessive condition characterized by the triad of occipital encephalocele, large polycystic kidneys and polydactyly. Associated abnormalities are other CNS malformations and ductal plate malformation of the liver.
Method: We present the pathologic findings of two consecutive brother's autopsies of 15 and 21 weeks of gestation respectively. Their parents are a 35-year-old man without past medical history and a 32-year-old woman who had had three previous pregnancies; the first two were term pregnancies and the third one a stillborn suffering from lamellar icthyosis. The fourth pregnancy spontaneously finished. During last pregnancy, ultrasonographic findings were encephalocele and severe oligohydrammnios. He died 2 weeks later.
Results: The first autopsy revealed omphalocele, bilateral cystic dysplasia of the kidneys, diffuse portal fibrosis and occipital encephalocele without associated osseous defect. In the second autopsy, herniation of cerebellum and distended fourth ventricle through a widened posterior fontanelle and cystic renal dysplasia were the most striking findings.
Conclusion: Meckel–Gruber syndrome is a lethal disorder characterized by gross and histological features. Autopsy findings provide valuable information that can be used for obstetric management and to evaluate the recurrence risk in future pregnancies.

005

Malignant ectomesenchymoma: report of two pediatric cases

S. Boudjemaa *, N. Leboulanger, S. Fasola, M. Lenoir, A. Coulomb
*Hopital Armand Trousseau, Dept. of Pathology, Paris, France

Objective: Malignant ectomesenchymoma (MEM) is a rare soft tissue neoplasm of early childhood, without specific cytogenetic anomalies, presumed to derive from migratory neural clefts tissue. It's mainly consists in rhabdomyosarcoma with varying neural components.
Method: The two patients 12 and 17 months aged boys presented with a dorsoabdominal mass and a macroglossia revealed by respiratory distress.
Results: Case 1: A neuroblastoma was diagnosed on bone marrow aspiration. Resected specimen after chemotherapy consisted in a small round blue cell tumor which expressed both muscular and neural markers, than allowing the diagnosis of MEM. The child recurred and died 13 months later. Case 2: At imagery, there was a base of tongue tissular mass, which exhibited morphology and immunoprofile of embryonal rhabdomyosarcoma on biopsy. The resected specimen had a ganglioneuroblastomatous morphology. The double differentiation was retrospectively found on initial biopsy. The child is disease-free.
Conclusion: The small number of reported cases may be due to a lack of awarness of this condition, as the variable degree of admixture of neural and mesenchymal components makes difficult diagnosis on the basis of limited material. The powerful ancillary techniques available today may help in a fuller characterization of these rare tumors.

006

Multifocal mucinous bronchioloalveolar carcinoma (BAC) of incidental finding in a 12-year-old girl

A. Coulomb [*], S. Boudjemaa, M. Antoine, M. Larroquet, N. Nathan, H. Ducou Le Pointe
[*]Hopital Armand Trousseau, Dept. de Pathologie, Paris, France

Objective: BAC is an indolent non-invasive tumor with lepidic spread replacement of the bronchioloalveolar epithelium by tumor cells. In children, BAC can occur in association with type 1 congenital airway malformation (CPAM), thought to be a precursor lesion. KRAS and EGFR mutations may play an important role in its pathogenesis.
Method: A 12-year-old asymptomatic girl presented bilateral pulmonary nodules on routine chest X-rays used to screen for pulmonary tuberculosis in her school.
Results: TDM showed multiples disseminated alveolar nodules arround small airways, without CPAM. A TDM-guided fine needle biopsy was performed and showed a lepidic mucinous lesion suggesting mucinous metaplasia, adenomatosis or BAC. Surgical biopsy was advocated after multidisciplinary concertation for pathologic diagnosis and ancillary techniques. The 2-cm resected nodules exhibited BAC morphology. Tumor cells expressed CK7 and CK-20 but not TTF1 and Alk-1. KRAS and EGFR mutations were not identified. ALK and P53 status is ongoing. In the absence of effective chemotherapy and due to the unresecability of these multiple bilateral lesions, the child is closely followed up.
Conclusion: Despite the long-standing recognition of this entity, there is no established treatment paradigm for patients with multifocal BAC. Therapeutic challenges need to be clarified.

007

VEGF expression patterns in pregnant women with different degrees of obesity

E. Dubova [*], M. Bayramova, E. Borovkova, I. Makarov, K. Pavlov, A. Shchegolev
[*]V.I. Kulakov Scientific Center, Dept. of Pathology, Moscow, Russia

Objective: Obesity could be seen in 12–28% of pregnant women with no evidence to decreasing.
Method: To investigate VEGF expression in placentas from women with obesity we divided all pregnant into the groups: the first group (n=60), the second (n=28) and the third (n=12) according to the body mass index (BMI) and degree of obesity. The control group includes 21 women with normal BMI and physiologic pregnancy. All of the placentas were on term.
Results: We revealed a decrease of villous syncytiotrophoblastic VEGF expression by 6.4% in the placentas from the first and the second group and by 25.1% from the third group. VEGF expression level in the stem villi EC was negative-correlated with the degree of obesity. In contrast, VEGF expression level in the terminal villi EC was higher in the first and second group than in the third. Stem and terminal villi mesenchimal cells VEGF expression level was higher than in control group. Maximal level of expression was observed in the stem villi vessels smooth muscular cells in placentas from the second and the third group.
Conclusion: The VEGF expression patterns revealed reflect preplacental hypoxia caused by obesity and altered maternal–fetal circulation.

008

Morphological features of hearts in fetus hypoxic cardiopathy

T. Fedorina *, A. Rudi, A. Makarova
*Samara State Medical University, Russia

Objective: In the structure of newborns and infants death fatal cardiac arrhythmia takes a definite place. Analyzing all clinical and pathogenetic variants of the cardiovascular system maladaptation syndrome, hypoxic injuries with chronic placental insufficiency seems to be most prominent cause of heart changes, which can explain the mechanism of death.
Method: Morphologically 467 hearts of fetuses were investigated, dead from antenatal and intranatal hypoxia and intrauterine infection. Separate weighing of the heart chambers using electronic scales, morphometric study of the heart chambers and isolated myocardial cells were performed.
Results: In 341 cases, chronic placental insufficiency in different forms of compensation was detected; in 384 cases inflammatory placental changes were revealed. Morphologic study of the heart revealed hypertrophy of right and left ventricular, myxomatosis leaflets of heart valves, myocardial edema of the stroma, extensive hemorrhage and stasis in the vessels of microcirculation as the most frequent symptoms of the heart changes. Isolated myocardial cells also show hypertrophy of ventricular cardiomyocyties, mostly in right chamber.
Conclusion: In the presence of decompensated placental insufficiency and inflammatory changes antenatal fetal hypoxia manifests increased load on the heart and serves as a starting point for myocardial hypertrophy and subsequent changes of fetal cardiac activity.

009

Rosai–Dorfman disease with neurological involvement: report of a case

M. S. Fernández García *, N. Fuentes Martinez, B. Vivanco Allende, A. de Juan Alvarez,
L. Mantecón Fernández, M.F. Fresno Forcelledo
*Hospital Central de Asturias, Dept. de Anatomía Patológica, Oviedo, Spain

Objective: Rosai–Dorfman disease is an infrequent process that affects predominantly cervical lymph nodes in young patients. However, in 43% of cases there may be extranodal involvement, including nervous system involvement, wich manifests as firm nodules associated with the dura. The most frequent sites are the spinal cord and, intracranially, the basal regions and the cranial convexity, although the latter is less common.
Method: We report a 12-year-old girl with symptoms of paraparesis. A spinal injury at T10–T12 was detected upon initial examination. Subsequently, during the extension study, multiple foci were found: T5–T6, frontal pole, cerebellopontine angle and bilateral and symmetrical lesions on both wrists. The patient underwent partial excision of the intracranial lesion and was treated with corticosteroids.
Results: The microscopic study revealed a significant fibrotic reaction involving large groups of histiocyte-like cells associated with an inflammatory cell population. The histiocytes had vesicular nuclei with wide vacuolated cytoplasm and showed cytoplasmic inclusions of lymphocytes and other inflammatory cells. Immunohistochemically, these histiocytes were positive for CD68 and S100 protein.
Conclusion: It has been reported that the evolution of the Rosai–Dorfman disease is chronic. In our case, the patient had a torpid evolution, and she died after 5 months.

010

CD44s isoform expression in Wilm's tumor cases in Latvia

I. Franckevica *, R. Kleina
*Children's Clinical University, Dept. of Pathology, Riga, Latvia

Objective: CD44 is transmembrane glycoproteins. They may be used as prognostic markers in some human malignancies. CD44s, CD44v5, CD44v10 shows membranous immunostaining of blastemal and epithelial components of Wilm's tumor (WT). Increased blastemal expression CD44v5 in pretreated WT correlated with prognosis (Ghanem MA, 2002). Study purpose was to examine the expression of CD44s in WT cases in Latvia.
Method: Nine cases of primary tumor were analyzed. Immunohistochemical investigation was made with CD44s (clone DF 1485 DakoCytomation) antibody. We counted CD44s cells in each histological component of WT and expressed in percentage.
Results: In average of cases CD44s presence: WT epithelial-type: stromal component—29.84%, epithelial component—4.2%, blastemal component—0.39%. WT blastemal-type: stromal component—13.38%, epithelial component—reaction negative, blastemal component—8.07%. WT mixed type: stromal component—34.21%, epithelial component—11.89%, blastemal component—5.27% WT regressive type: stromal component—15.82%, epithelial component—9.84%, blastemal component—1.9%. Correlations between the amount of CD44s cells (%), WT histological types and histological risk were determined using Pearson's parametric correlation analysis.

Conclusion: (1) CD44s expression is higher in Wilm`s tumors which are composed predominantly of blastemal component. (2) There is proved positive correlation between CD44s expression in blastemal component and histological risk of tumors.

011

Macroscopic features of the hearts of fetuses and infants with intrauterine growth retardation in gestational age 27–35 weeks

V. Gargin *, V. Markovskiy, M. Myroshnychenko, I. Kostuchek, A. Simacheva
*Kharkiv National Medical University, Dept. of Pathomorphology, Ukraine

Objective: Cardiovascular system plays important role in the adaptation of children with IUGR to extra-uterine life.
Method: During the autopsy of the fetus or newborn in gestation of 27–35 weeks heart mass (HM) and wall thickness of right and left ventricles (TRV, TLV) in children with symmetric (sIUGR) and asymmetrical (as IUGR) types were measured .
Results: When measuring the HMt found significant decrease in children with IUGR (at sIUGR HM—8.52± 0.787 g, at asIUGR—6.88±0.147 g) as compared with the CG (11.17±0.561 g). In addition, more pronounced significant decrease in HM in children with asIUGR as compared with sIUGR. In children with sIUGR was found the decrease of TRV (0.319±0.005 sm) and TLV (0.331± 0.007 sm) as compared with the CG (TRV—0.368±0.008 sm, TLV—0.375±0.014 sm). In children with asIUGR was found the decrease of TRV (0.279±0.006 sm) and TLV (0.264±0.017 sm) as compared with the CG (TRV—0.368± 0.008 sm, TLV—0.375±0.014 sm). The TRV and TLV in children with asIUGR were more decrease then in children with sIUGR
Conclusion: Fetuses and newborns with IUGR had a reduction of HM, TRV and TLV.

012

Pathomorphology of immune system of fetus and children of early age from HIV-infection of mothers

I. Sorokina *, S. Sergey
*Kharkiv National Medical University, Dept. of Pathomorphology, Ukraine

Objective: The purpose of the study is devoted to the study of morpho-functional features of thymus, spleen and mesenteryal lymphatic node on early stages and in the postnatal period of ontogenesis under influencing of HIV-infection of mothers.
Method: Thymus, spleen and mesenteryal lymphatic node of 90 fetus and children from HIV-infection of mothers were included in the study. Histological, immunohistochemical, morphometric, statistical Student's *t*-test methods were used.
Results: It is set that if the infectioning of fetus happened to 7th weeks of embryogenesis, when thymus was not yet formed, in this connection there was violation of his normal structure with development of simple dysplasia. In the case of penetration of HIV-infection in the organism of fetus after 11–12 week of embryogenesis, when thymus was already formed and if the antigen loading was very large, the compensative reactions of the immune system of fetus were quickly exhausted and dysplasia developed with atrophy of thymus. At the infectioning of fetus after 11–12 week of embryogenesis, when thymus was already formed and antigen stimulation was low, as the adaptation reactions there was gyperplasia of organ.
Conclusion: It is well-proven that HIV-infection of mothers is instrumental in violation of morphogenesis of organs of the immune system of fetus (ripening and embryonisation of lymphoid and epithelial cellular population) predetermining their disfunction.

013

Intra-amniotic inflammation can influence late abortion and preterm labor

A. Kolobov *, A. Merkulova, V. Zinserling
*St. Petersburg, Russia

Objective: Preterm delivery influence perinatal morbidity and mortality worldwide. Intrauterine infection is frequent cause of spontaneous preterm labor and delivery. Recent data indicate that intra-amniotic inflammation is also a risk factor for impending preterm delivery, and morbidity of the newborns and infants.
Method: A morphological analysis of 12,371 placentas and fetal membranes during routine examination was made.
Results: A total of 706 cases (5.71%) of late abortion or preterm labor were studied. Spontaneous late abortion—31 cases, medical late abortion—8 cases, spontaneous preterm labor—526 cases, preterm labor with caesarean section—141 cases. Intra-amniotic inflammation (chorioamnionitis) was present in 80.65% cases of spontaneous late abortion, 62.5% cases medical late abortion, 58.6% cases spontaneous preterm labor and 51.5% cases with caesarean section.
Conclusion: Thus, intra-amniotic infection with histological documented chorioamnionitis is significant factor in development of late abortion and preterm labor.

014

A study of congenital and pathological causes of intrauterine fetal death in the region of Thrace using polymerase chain reaction and immunohistochemistry

M. Lambropoulou *, I. Grammatikpoulou, E. Chatzaki, E. Tsonou, A. Christopoulou, A. Popovidou, E. Kontomanolis, A. Pouliakas, A. Getsopoulou, N. Papadopoulos
*Democritus University Thrace, Dept. of Histology-Embryology, Alexandroupolis, Greece

Objective: Several factors are implicated in intrauterine fetal death. In the present study we investigated the aetiopathogenesis of intrauterine fetal death in the region of Thrace.
Method: A total of 259 aborted fetuses were categorized in five groups based on clinical data. Group (1) contagious factors (n=259), (2) hydrops fetalis (n=11), (3) neural cord dysplasias (n=14), (4) placental inflammations (n=109), (5) other reasons causing congenital abnormalities (n=41). Histological investigation was performed using PCR and immunohistochemistry in representative tissues according to the category.
Results: (1) PCR amplification for CMV, mycoplasma and chlamydia indicated two positive cases for CMV, one for mycoplasma and none for chlamydia. (2) PCR amplification for B-19 (a causing factor of hydrops fetalis) indicated one positive case. (3) Immunohistochemical staining for Sonic Hedgehog which participates in the signal pathway that designates the post-interior axis of the body indicated the diffused expression of the protein in the respective neural tissues. (4) Immunohistochemical expression of TNF-a (inflammation), Caspase 8 and 9 and M30 (apoptotic markers) indicated the degree of inflammation and apoptosis (5) Congenital abnormalities have been observed in 15.83 of all cases.
Conclusion: As more and more miscarriages are observed, the several possible causes of fetal death should be considered and further elucidated.

015

Role of placental examination in fetal death: a retrospective study of 101 cases

P. Luís *, A. Henriqueta, A. Alves, A. Costa-Silva
*CHLN—Hospital Santa Maria, Dept. of Pathology, Lsboa, Portugal

Objective: Intrauterine fetal death is often an unpredictable and unexplained event. Fetal autopsies are performed to clarify the cause of death, and the complete workup usually includes placental examination. The aim of this study is to evaluate placental causes of death.
Method: Retrospective review of 101 autopsy reports of singleton fetuses, without congenital anomalies, and their matched placentas (between 22 and 41 weeks gestation).
Results: The median gestational age at diagnosis of fetal death was 31 weeks. There were 30 cases (29.7%) grouped according to intermediate fetal death (IFD) at 22–27 weeks and 71 (70.3%) according to late fetal death (stillbirth) at 28–41 weeks. A direct cause or major contributor to fetal death was found in 69 placentas (68.3%). Etiologies were grouped according to maternal vascular supply abnormalities (MVSA) (37 cases/36.6%), fetal vascular supply abnormalities (5 cases/5%) and inflammatory lesions (IL) (27 cases/26.7%). The major relevant conditions associated with IFD were the MVSA, while in stillbirth the most frequent were the IL. In 31.7% of the cases the placental findings were not sufficient to explain the fetal death.
Conclusion: Pathological analysis of the placenta is essential in a complete fetal autopsy and can play an important role in reduction of the unexplained fetal death/stillbirth rate.

016

Case report of neurysm of umbilical cord artery in otherwise healthy fetus

J. Marcinek *, P. Slávik, M. Kalman, T. Balhárek, P. Szépe, L. Plank
*Jessenius Faculty of Medicine, Dept. of Pathology, Martin, Slovakia

Objective: Aneurysm of umbilical cord artery is a rare congenital malformation of umbilical cord with up to ten published cases. We present a case report of intrauterine asphyxia of child with this abnormality, without other congenital malformations.
Method: A 27-year-old pregnant woman without preceding complications was hospitalised at 33 weeks of gestation because of absence of fetal movents. Death fetus of male gender was delivered, which lenght and weight were appropriate for gestational age.
Results: Section showed signs of intrauterine asphyxia (subpleural, subepicardial and thymic petechial bleedings) and maceration, without any congenital malformations. Umbilical cord showed three vessels and two false knots (2×1.5 and 1 cm in size, respectively) with aneurysm of umbilical artery and intraluminal thrombus in larger knot. This vessel was accompanied by one normal umbilical artery, one vein and several small vitelline vessels. In placenta we found regressive changes and several infarctions.
Conclusion: Aneurysm of umbilical cord artery is rare; it is accompanied by high morbidity and mortality, in most cases with fetal chromosomal aberrations (mainly trisomy

18) and congenital malformations. Prenatal diagnostic of this abnormality is important for early abortion of malformated fetus or preterminal birth of healthy child because of increased risk of intrauterine asfyxion.

017

P 53 and vascular endothelial growth factor (VEGF) expression and their correlation in Langerhans cell histiocytosis (LCH)

M. Mehrazma *, F. Mahjoob, K. Arjmandi Rafsanjani, A. Lahouti
*Ali-Asghar Children Hospital, Dept. of Pathology and Laboratory Medicine, Teheran, Iran

Objective: The etiology of LCH, a disease characterized by uncontrolled proliferation of Langerhans cells, is still not well known. We studied p53 expression and also a main pro-angiogenic factor, VEGF, to determine whether they play a role in the pathogenesis of LCH and their correlation with each other.
Method: The study was performed on 21 children with LCH (11 boys and 10 girls), median age 26 months with single lesion (8) or multisystem disease (13). Immunohistochemical staining for s100 and CD1a was performed for definite diagnosis. The slides were stained for p53 and VEGF and semiquantitavely evaluated using a grading system from 0 to 5 for p53 and 0 to 2 for VEGF.
Results: in single-lesion tumors, p53 and VEGF were negative in six and positive in two patients. In multisystem lesions p53 and VEGF were positive in six and ten patients and negative in seven and three cases, respectively. There was no correlation between p 53 expression and clinical manifestation (p value=0.44) but this correlation for VEGF had significance (p value=0.02). There was also no correlation between p 53 and VEGF expression (p value=0.44).
Conclusion: Increased expression of VEGF plays a role in dissemination of disease. We could not show any relation between clinical findings and p53 expression and also with VEGF overproduction.

018

Congenital granular cell epulis: a case report

E. E. Pala *, G. Orgun Sonmez, U. Bayol, T. Gurbuz
*Tepecik Training and Research, Dept. of Pathology, Izmir, Turkey

Objective: Congenital granular cell epulis (CGCE) is a rare benign soft tissue tumor of newborns and its characteristic location is the labial aspect of the dental ridge, with a predilection for the upper jaw. The origin of CGCE is unclear. We present a case of a female newborn with a CGCE which is treated successfully with surgical excision.
Results: An otherwise healthy 1-day-old female patient was referred to the pediatric surgery department immediately after birth because of a mass at her left alveolar arc. It was completely excised. Grossly, surgical material was white colored, firm and approximately 1 cm in diameter. Microscopically, the tumor was mainly composed of nests of polygonal cells, with large, clear and granular cytoplasm and it was located just beneath the normal oral squamous epithelium and highly vascularized. Within the tumor few odontogenic remnants were also present. Tumor cells were PAS, D-PAS, S100 negative, and vimentin, NSE positive. Diagnosis was "granular cell epulis". The baby is healty with no evidence of residual or recurrent mass with a succesful total surgical excision of the tumor.
Conclusion: The case is presented to remind such a rare entity of the newborn.

019

Congenital pulmonary lymphangiectasis: case report

E. E. Pala *, U. Bayol, O. Turelik, A. Sayan, A. Arikan
*Tepecik Training and Research, Dept. of Pathology, Izmir, Turkey

Objective: Congenital pulmonary lymphangiectasis (CPL) is a very rare, developmental disease of the lung, characterized by abnormal dilatation of pulmonary lymphatics. It has previously been reported to have a very poor prognosis but recent reports have suggested improved outcomes. CPL is usually associated with congenital heart diseases.
Method: A female infant was born at 39 weeks of gestation by spontaneus delivery. At 5 days postnatal, the patient was referred to the hospital because of respiratory distress. Transthoracic echocardiography revealed a large ventricular septal defect and thorax computed tomography showed a 4×2.5-cm cystic lesion at the apical segment of the right lung.
Results: Histologic examination of the segmentectomy showed diffuse and marked dilatation of the lymphatic channels in the subpleural and septal areas. The channels were lined with flattened endothelium. The findings confirmed a primary form of CPL.
Conclusion: CPL has an agressive course. In the literature, most CPL cases are diagnosed at the autopsy section, but our case is well after surgery. The aim of this report is to mention the details of our case, differential diagnosis, treatment and prognosis.

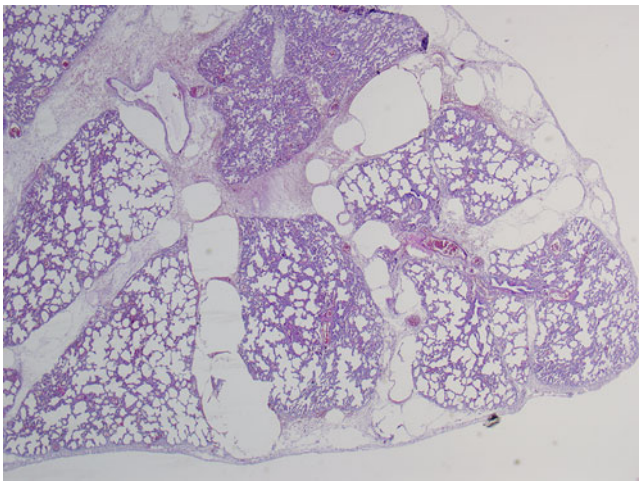

020

Post-mortem diagnosis of mitochondrial disorders in children: autopsy standards and useful auxiliary techniques

M. Pronicki *, T. Szymanska-Debinska, A. Karkucinska-Wieckowska, J. Szczepanowska, J. Sykut-Cegielska
*Children´s Memorial Health Institute, Dept. of Pathology, Warsaw, Poland

Objective: Mitochondrial disorders (MD) affecting 1/5,000 live born children are characterized by extremely varied, usually multiorgan symptoms emerging at any age from perinatal period up to adulthood. It may be assumed that many children die undiagnosed, so mitochondrial respiratory dysfunction should be invoked as a potential cause of unexpected/unclear child death.
Method: The aim of the study is to assess the usefulness of selected diagnostic methods in post mortem diagnosis of MD in pediatric clinical practice. Authors tested selected laboratory diagnostic tools in 60 consecutive pediatric autopsies.
Results: Frozen tissue samples from muscle, heart and liver should be collected during autopsy for further (histochemical, proteomic, molecular) investigation. Histological and histochemical methods used in neuromuscular pathology may be implemented up to 24 h after death. Blue Native electrophoresis and in gel activity of respiratory chain (RC) complexes as well as assessment of the level of individual subunits of mitochondrial RC with the use of Total OXPHOS Human WB Antibody Cocktail may be performed post-mortem with readable results.
Conclusion: Thorough neuropathologic examination of the brain and spinal cord is mandatory. Frozen tissue material is of great value for subsequent aimed molecular investigation.

021

An unusual molecular presentation of an alveolar rhabdomyosarcoma

H. Sartelet *, S. Hazourli, S. Cournoyer, C. Nyalendo, M. Roy-Tourangeau, P. Teira, R. Fetni
*CHU Sainte Justine, Dept. of Pathology, Montreal, Canada

Objective: Rhabdomyosarcoma is the most common sarcoma in children. Alveolar rhabdomyosarcoma (ARMS) is the second most common subtype of rhabdomyosarcoma and it is associated with poor prognosis. ARMS is characterized by cytogenetic abnormalities which are t(2;13)(q35;q14) and t(1;13)(p36;q14) resulting respectively in PAX3-FOXO1 or PAX7-FOXO1 fusion gene.
Method: We present a case of a tumour of the latissimus dorsi in a 7-year-old girl. We investigate this tumour by immunohistochemical study, comparative genomic hybridization (CGH), RT-PCR and FISH.
Results: The tumour was composed of poorly differentiated round cells that show central loss of cellular cohesion and formation of "alveolar" spaces. It expressed desmin and myogenin. RT-PCR did not detect ARMS characteristic fusions. By CGH arrays, we detected the amplification of PAX7 and of FOXO1. FISH with commercial fusion probes was negative but confirmed the amplification of FOXO1 and PAX7. By FISH, we demonstrated that an insertion of FOXO1 in PAX7 associated with a gene fusion followed by amplification as double minutes was a plausible mechanism for its genetic abnormality.
Conclusion: Our results suggest a complex rearrangement leading to a negative molecular and FISH result with fusion probes in an ARMS, demonstrating the utility of CGH arrays in molecular diagnostic of ARMS.

022

Placental morphometry in very low birth weight infants with hemorrhagic disorders

A. Shchegolev *, K. Pavlov, E. Dubova, M. Nagovitsyna, L. Alieva
*V.I. Kulakov Scientific Center, Dept. of Pathology, Moscow, Russia

Objective: Tha broad specter of neonatal pathology is complicated by the hemorrhagic disorders (HD). These disorders are associated with high risk of neonatal mortality particularly in preterm infants with moderately low (MLBW) and very low birth weight (VLBW).
Method: To determine the role of placenta in these disorders we performed morphological analysis of nine placentas from preterm VLBW with HD and 11 placentas from preterm VLBW without HD. Gestation age varied from 28 to 33 weeks. We performed

histological and morphometric and immunohistochemical investigation.
Results: In both groups the predominant type of villi was immature intermediate. On morphometry we revealed that mean intervillous space area was lesser in VLBW with HD. Mean villous area and mean single villus perimeter were higher in VLBW with HD group. On CD34 stained specimens we revealer that mean villi capillary count was equal in both groups, but mean single capillary cross-section area and mean single villus syncytiotrophoblast area were higher in VLBW with HD group.
Conclusion: The morphometric patterns revealed reflect branching angiogenesis predominance in placentas from VLBW with HD. Increased syncytiotrophoblast area could be the sign of altered placental expression of haemostatic system components.

023

Small bowel vascular malformation in children: case report

L. Spasevska *, V. Janevska, B. Dukova, G. Petrusevska, P. Petrovski, V. Cvetanovska, V. Janevski, N. Jankulovski
*Institute of Pathology, Skopje, Macedonia

Objective: Small bowel vascular malformations are an uncommon cause of gastrointestinal bleeding in childhood.
Method: We report a case of an 8-year-old boy with a history of recurrent painless melaena for the past 2 months. Laboratory investigations showed iron deficiency anemia. Colonoscopy and upper endoscopy showed no pathological lesions but capsule endoscopy showed dilated vessels in the distal ileum with normal overlying mucosa. CT angiography confirmed the presence of multiple tortuous veins and arteries over a long segment. A diagnosis of vascular malformation was made and a surgical resection of 40-cm-long segment of distal ileum was performed.
Results: Macroscopically the surgical specimen revealed multiple oval dark-red false polyps with segmental skip distribution. Microscopic examination showed thin-walled large caliber (0.68 cm) veins associated with thick-walled artery (0.78 cm in width) without aneurysmal change that were extending into the submucosal core of a fold and penetrated into the muscular layer with segmental skip distribution. Van Gieson elastic staining showed thick and tortuous internal elastic membranes.
Conclusion: In the classification system for arteriovenous malformations used by Moore et al., type II lesions usually are found in the stomach or small bowel and are congenital lesions so that they tend to occur in younger patients as in our case.

024

Role of open lung biopsy in children aged 0 to 10 years: review of 91 cases

N. Toran-Fuentes *, A. Navarro, J.C. Ferreres, M. Garrido, A. Moreno, M. Aizpurua, R. Palhua, N. Carmona, S. Ramón y Cajal
*H. U. Vall d´Hebron, Dept. of Pediatric Pathology, Barcelona, Spain

Objective: Lung wedge biopsy is nowadays the standard procedure for a therapeutic approach of children with persistent respiratory symptoms associated with interstitial lung disease.
Method: Between 2000 and 2010 we reviewed lung wedge biopsies of children with respiratory symptoms from the files of HUVH. Lobectomy, segmental resection, focal lesions or transbronchial biopsies were not included.
Results: Lung biopsy of 91 cases (46 boys, 45 girls) aged 0 to 10 were studied for diagnosis. Results were grouped into three categories: (1) disorders of infancy 28.40%, including diffuse developmental disorders 7.95%, idiopathic interstitial pneumonia 18.18% and surfactant dysfunction 1.13%; (2) disorders not specific to infancy 62.5%, composed of pathologies of the normal host 39.77%, disorders related to systemic disease 3.40%, disorders of the immunocompromised host 5.68% and other disorders masquerading as interstitial lung disease 13.63%, including arterial hypertensive vasculopathy, congestive vasculopathy and lymphatic disorders; (3) unclassified 9.09%, with normal histological biopsies 5.68% and inadequate material available 3.40%.
Conclusion: The correct diagnosis of diffuse lung diseases is essential to decide the appropriate clinical management in children. According to our experience, open lung biopsy is a safe procedure in these entities and has a high diagnostic yield in 91% of our cases.

025

Achondroplasia type of ostechondrodysplasia: case report

S. Toru *, I.H. Ozbudak, K. Karaali, I. Mendilcioglu, T. Gelen
*Akdeniz Medical School, Dept. of Pathology, Antalya, Turkey

Objective: The osteochondrodysplasia is a heterogeneous group of disorders which are commonly hereditary and characterized by an abnormal growth and remodeling of cartilage and bone. Of these, heterozygous achondroplasia is the most common nonlethal skeletal dysplasia which is characterized by a quantitative decrease in enchondral

ossification in the growth plate of bones. The distinctive clinical radiological features usually allow a precise diagnosis.

Results: Herein, we presented a 20-week male fetus with achondroplasia. It was diagnosed in intrauterine ultrasonography by short extremities and medical termination was performed by the permission of parents. Radiography revealed short extremities with bowing. Macroscopically, rhizomelic extremities, frontal boosing and dysplastic ears were found. On microscopic examination, decreasing of ossification in growth plate of bone was determined.

Conclusion: Although achondroplasia is the most common nonlethal type osteochondrodisplasia, it is a very rare entity. Achondroplasia is inherited in an autosomal dominant manner. Over 80% of individuals with achondroplasia have parents with normal stature and have achondroplasia as the result of a de novo gene mutation. It can be diagnosed by characteristic clinical and radiographic findings mostly but in individuals with atypical findings, molecular genetic testing can be used to detect a mutation in the FGFR3 gene.

026

Ultrastructural changes of the placenta with meconium-stained amniotic fluid

H. K. Türköz *, Z. Yurdakul, S. Solakoglu
*Medical Faculty of Marmara, Dept. of Pathology, Istanbul, Turkey

Objective: Meconium-stained amniotic fluid (MSAF) in term healthy pregnancies without accompanying clinical or histological evidence of hypoxia related to chronic intrauterine hypoxia.

Method: The study group was composed of mothers (n=4) and their term, appropriate for gestational age (AGA) newborns with MSAF but without meconium aspiration syndrome. The control group consisted of mothers (n=4) and their term AGA babies. Placental ultrastructural changes were examined by transmission electron microscopy (TEM).

Results: TEM investigation in the study group revealed changes which may be attributed to hypoxia in the study group.

Conclusion: Ultrastructural changes in placentas with meconium staining show that newborns with MSAF are exposed to hypoxia even if no significant clinical or histological signs were observed.

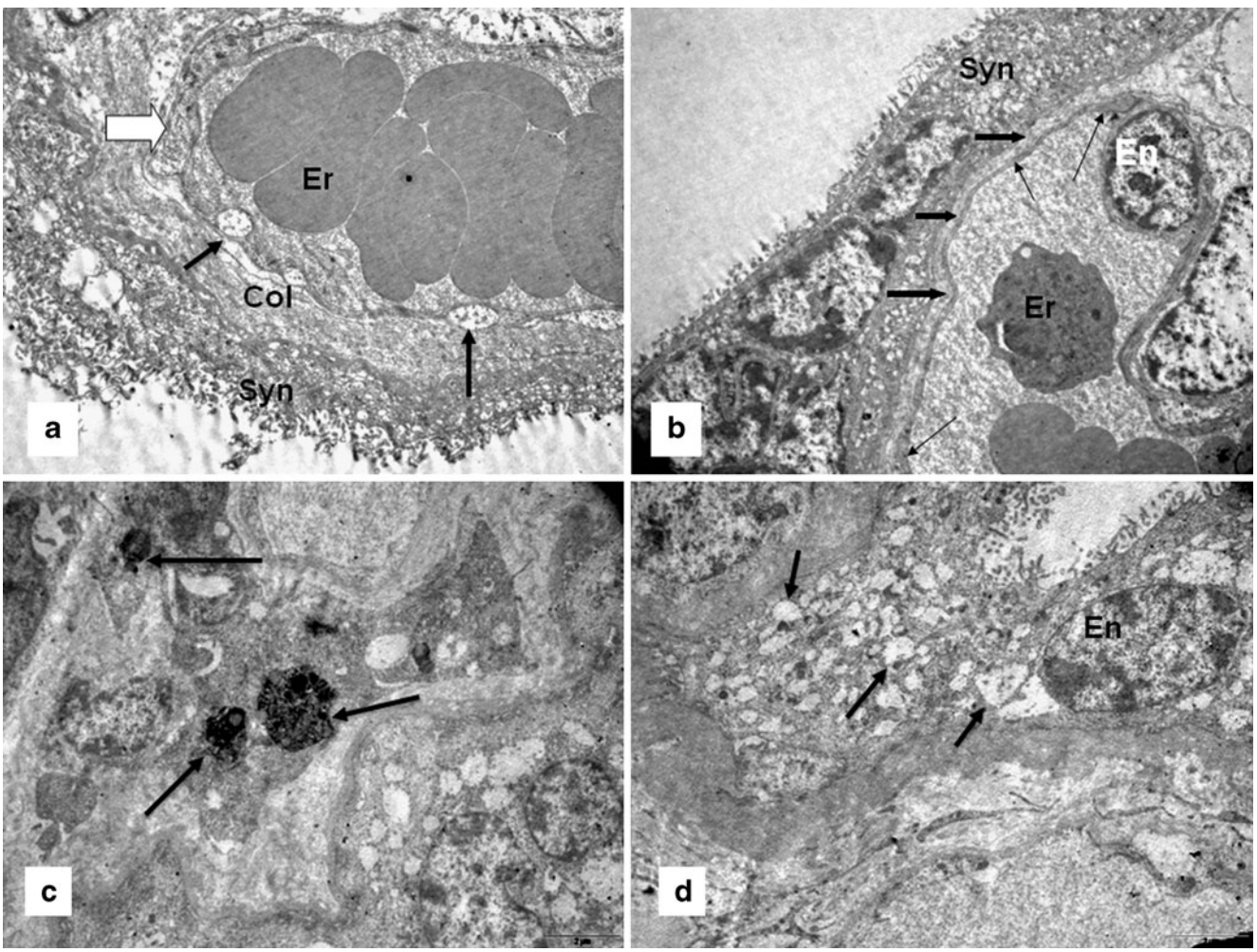

027

Prenatal diagnosis of congenital mesoblastic nephroma: a case report

M. T. Yacoubi *, S. Ben Abdelkrim, N. Ben Jamaa, S. Nouri Marchaoui, S. Hmissa
*University Hospital Sousse, Dept. of Cyto-Histopathology, Tunisia

Objective: Mesoblastic nephroma is a rare congenital tumor first described by Bolande in 1967. Prenatal ultrasound allows the detection of this tumor, but only the pathological analysis of the surgical specimen can confirm this diagnosis postnatally.
Method: We report the prenatal discoverage of a mesoblastic nephroma at 28 weeks in a context of severe polyhydramnios detected by ultrasonography, measuring 6 cm in diameter and developed in the left kidney. Intrauterine death occurred 1 week later; the parents refused the necropsy and the physician removed the mass by a mini-autopsy.
Results: Histological and immunohistochemical findings are consistent with the diagnosis of mesoblastic nephroma.
Conclusion: We discuss here the clinicopathological characteristics and the histogenesis of this rare tumor.

028

Amniotic band syndrome (ABS): a fetopathological study of 7 cases

M. T. Yacoubi *, N. Beizig, N. Ben Jamaa, S. Marchaoui-Nouri, S. Korbi, S. Ben Abdelkrim, S.H. Hmissa
*University Hospital Sousse, Dept. of Cyto-Histopathology, Tunisia

Objective: Amniotic band syndrome, also called congenital constriction band syndrome, includes intrauterine amputations, syndactylies, fetal compression deformities and constriction rings associated with disruption of the amniotic membrane. It is a sporadic and an uncommon congenital fetal abnormality with multiple disruption and disabling manifestations encountered in three of four cases.
Method: Our population consists of seven fetuses examined in the Department of Pathology of Sousse (Tunisia) according to the standard protocol.
Results: Maternal ages range between 17 and 27 years. Consanguinity is found in one case and there was no similar cases reported in the family. The gestational ages of fetuses range from 17 to 34 weeks. The defects caused by ABS where schematically divided into two groups: four cases involving the major visceral organs (head, nervous system, trunk), the second group is of member defects (amputations, syndactylies, deformations and constriction rings) in all cases. Placentas were abnormal in all cases (inflammation, short cord and/or single umbilical artery).
Conclusion: Our study allowed us to discuss about diagnostic criteria, differential diagnoses and the pathogenesis of the ABS Because the ABS is a sporadic disorder and sometimes curable, it is necessary to propose an appropriate genetic counseling and an accurate diagnosis for newborn with multiple defects so in order to suggest the management properly.

029

Renal tubular dysgenesis: a rare cause fetal anamnios

M. T. Yacoubi *, S. Ben Abdelkrim, S. Nouri Marchaoui, S. Miladi, S. Hmissa
*University Hospital Sousse, Dept. of Cyto-Histopathology, Tunisia

Objective: Renal tubular dysgenesis (RTD) is characterized by paucity or absence of proximal renal tubules, leading to anamnios. We report a new case in a fetus.
Method: A 23-year-old woman was diagnosed with anamnios at 20 weeks of pregnancy by ultrasonographic examination. Fetal autopsy was performed subsequently to intrauterine fetal death. That was her first pregnancy and a history of second-degree consanguinity was found.
Results: The fetal external examination showed hypotrophic fetus with Potter sequence. Radiographies showed skull ossification defect. Visceral dissection revealed pulmonary hypoplasia and small kidneys with normal cut surface. Microscopically, the corticomedullary differentiation was preserved, rows of immature nephron at the edges were seen as well as thickening of the arterial vessels' walls, and the number of proximal tubules was manifestly reduced. Thus, the diagnosis of RTD was made.
Conclusion: RTD is a rare autosomal recessive disease, leading to anamnios. The etiopathogenesis is controversial. It is genetically heterogeneous and linked to mutations in the genes that encode components of the renin-angiotensin system. Poor calvarial ossification, resulting in wide cranial sutures and large fontanels, is an additional feature of the disease. In conclusion, an early, persistent and isolated hydramnios requires a histological and immunohistochemical investigation of the kidneys to rule out RTD.

030

Juvenile hyaline fibromatosis: a case report and review of the literature

M. T. Yacoubi *, W. Jomaa, S. Ben Abdelkrim, A. Ben Abdelkader, S. Aloui, A. Anjorin, M. Mokni
*University Hospital Sousse, Dept. of Cyto-Histopathology, Tunisia

Objective: Juvenile hyaline fibromatosis (JHF) is a rare disease with autosomal recessive inheritance that occurs mainly in childhood and is characterized by the deposition of amorphous hyaline material in the skin and other organs. There are approximately 70 cases reported in the literature.
Method: We describe the case of a 2-year-old girl, issued from a consanguineous marriage, who presented with a slow-growing occipital swelling that had developed at 14 months. The physical examination showed a retard in neuro-psico-motor development, lips and gingival hypertrophy, hypertelorism, and two left parietal nodules.
Results: Histopathologic study demonstrated the presence of hyaline material, confirming the diagnosis of juvenile hyaline fibromatosis.
Conclusion: JHF is a very rare genetic disease. The diagnosis should be considered when a young patient presents with multiple maculopapular skin lesions, gingival hypertrophy and joint contracture. Early diagnosis and surgical intervention may be the best strategy for managing this rare disease.

Sunday, 28 August 2011, 09.30–10.30 and 16.30–17.00, Hall 5

PS-06 Poster Session Pulmonary Pathology

001

Clinical significance of epidermal growth factor receptors in non-small cell lung cancer and a prognostic role for HER2 gene copy number in female patients

S. Al-Saad [*], K. Al-Shibli, T. Donnem, S. Andersen, R. Bremnes, L.-T. Busund
[*]Tromsø, Norway

Objective: To compare the efficacy of silver in situ hybridization (SISH) and immunohistochemistry (IHC) in detecting HER2 alterations and to investigate the prevalence and prognostic significance of Erb family members in non-small cell lung cancer (NSCLC).
Method: A total of 335 patients with NSCLC were immunohistochemically tested for protein expression of all Erb family members and results were compared with gene copy number by SISH.
Results: In univariate analyses, high HER2 gene copy number was a highly significant negative prognostic indicator for disease-specific survival in women (p= 0.005). In the multivariate analysis, high HER2 gene copy number in tumor epithelial cells (p=0.03) was an independent prognostic factor for disease-specific survival in female patients.
Conclusion: IHC does not consistently identify patients likely to have a poor prognosis, whereas SISH provides superior prognostic information for female patients with NSCLC. High HER2 gene copy number in tumor epithelial cells is an independent predictor of inferior survival in female patients with primary NSCLC.

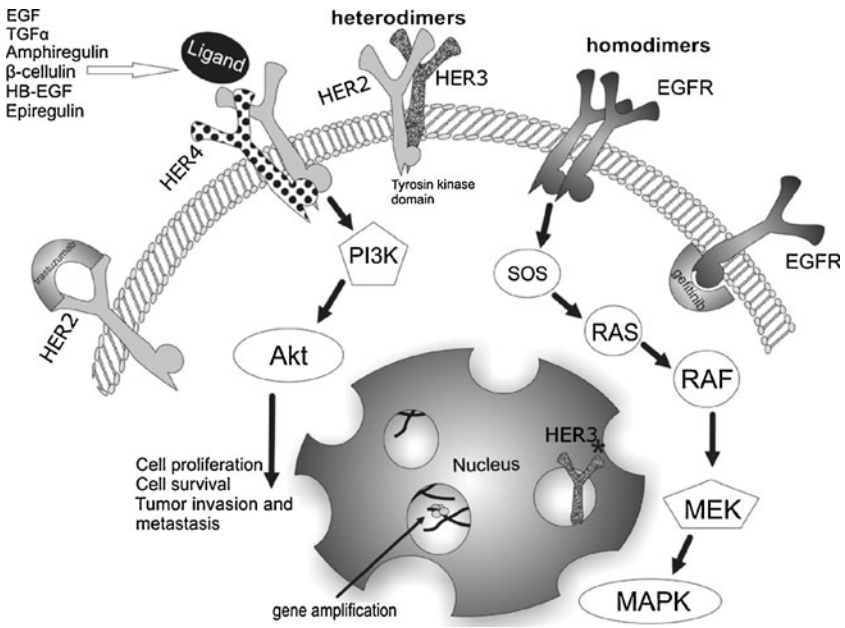

002

End-stage lung diseases with pulmonary hypertension have increased levels of tissue resident endothelial progenitor cells

F. Calabrese *, F. Lunardi, M. Schiavon, G. Fadini, C. Agostini, M. Loy, G. Marulli, F. Rea
*University of Padua, Italy

Objective: Diffuse lung diseases favour the development of vascular remodelling and pulmonary hypertension (PH). Endothelial progenitor cells (EPCs) seem to be involved in vascular remodelling. The aim of the study was to evaluate circulating and resident EPCs in end-stage lung diseases, correlating their presence with pulmonary arterial pressure (PAP).
Method: A total of 19 patients with different end-stage diseases (idiopathic PH-IPH, idiopathic lung fibrosis-IPF, chronic obstructive pulmonary disease-COPD) with and without PH were included in the study. Six non-implanted donor lungs represented normal controls. EPCs, cells co-expressing CD34 and Flk-1, were measured in blood sampled at the time of transplant from the pulmonary arteries and veins by flow cytometry and in lung sections by confocal microscopy.
Results: Tissue-resident EPC levels were significantly different according to lung disease type (p=0.001). A higher EPC number was detected in IPH and IPF with high PAP (p=0.03 for both) compared with COPD and controls. IPF patients with low PAP and the controls showed a similar number of EPCs. There was a direct correlation between tissue EPCs and PAP. No difference in circulating EPC levels among groups of patients and controls were found.
Conclusion: Tissue-resident EPCs are increased in lung diseases with high PAP. EPCs may contribute to vascular remodelling in end-stage pulmonary disease.

003

Evaluation of vessel remodelling in patients with Combined pulmonary fibrosis emphysema (CPFE) and idiopathic pulmonary fibrosis (IPF)

F. Calabrese *, N. Nannini, F. Lunardi, E. Balestro, E. Rossi, G. Marulli, M. Loy, F. Rea
*University of Padua, Italy

Objective: Combined pulmonary fibrosis and emphysema (CPFE), a syndrome with distinct clinical/radiological characteristics, has an increased risk of pulmonary hypertension (PH); little is known about its morphological and molecular substrates. The aim of our study was to evaluate the arterial remodelling and expression of transforming growth factor (TGF)-β in the lungs of patients with CPFE compared to idiopathic pulmonary fibrosis (IPF) without PH.
Method: The study was performed on lung samples of seven CPFE patients (mean age 59±6 year), 15 IPF patients (mean age 53±10 year) and five donors (mean age 30±10 year) as normal control group. In all cases morphometry was used to measure arterial intimal, medial, and total thickening and immunohistochemical expression of TGF-β was quantified in macrophages and alveolar cells.
Results: Intimal and total thickening were significantly higher in CPFE than IPF (p=0.004 and p=0.03, respectively). A trend of increased alveolar TGF-β expression was detected in CPFE compared to IPF (p=0.07). As expected, arterial remodelling and TGF-β expression were increased in IPF (both p=0.001) and CPFE (p=0.004 and p=0.003, respectively) compared to controls.
Conclusion: In conclusion, our study demonstrated that lungs with CPFE display significant arterial remodelling which may represent pathological substrate for the increased frequency of PH in the disease.

004

Survivin expression as a prognostic marker and therapeutic target in malignant pleural mesothelioma

A. Coer *, J. Hmelajk, I. Kern
*University of Primorska, Colllege of Health Care, Izola, Slovenia

Objective: Survivin expression is limited to embryonic and malignant cells. This makes survivin one of the most specific tumour markers and an important anticancer therapeutic target. The aim of our study was to define the effects of survivin expression on survival of MPM patients and to evaluate whether survivin inhibition affects chemosensitivity of MPM cells in vitro.
Method: Survivin expression, apoptotic (AI) and proliferation index (PI) were analysed in MPM specimens from diagnostic biopsies of 101 MPM patients. The inhibition of survivin expression was evaluated in vitro with posttranscriptional survivin silencing using siRNA molecules.
Results: Survivin expression was confirmed in all analysed tumour samples; median expression was 67.3% survivin positive tumour cell nuclei. Survival analysis showed that histological type, PI and age at diagnosis had significant effects on patient survival. Posttranscriptional survivin silencing using siRNA molecules caused more than 60% decrease in survivin mRNA expression and statistically significant mesothelioma cell survival reduction.
Conclusion: Our study did not confirm a prognostic role of survivin expression in MPM; its ubiquitous presence in MPM tissue samples underlines its potential role as a therapeutic target. In vitro experiments showed that

survivin inhibition successfully decreases mesothelioma cell survival and increases their sensitivity to cisplatin.

006

Pulmonary fibrosis in alveolar proteinosis: metals and mechanisms

R. Harley *
*AFIP, Pulmonary and Mediastinal Path, Washington, DC, USA

Objective: Pulmonary alveolar proteinosis (PAP) is considered the ultimate example of an alveolar filling process with little interstitial reaction or fibrosis. Cases with severe fibrosis occasionally occur after considerable time and multiple lung lavages. A subset of cases with fibrosis is caused by exposure to fine silica or metals such as aluminum. Recent cases of PAP caused by indium inhalation have included many with fibrosis.
Method: Cases of PAP of various causes were reviewed. Etiologies were separated into (1) idiopathic, (2) known GMCSF deficiency, (3) other monocyte depletion (leukemia, chemotherapy), (4) inhalation, and (5) congenital. Fibrosis was graded in cases from each category. Cause of fibrosis was assigned to (a) infection, (b) interstitial fibrogenic particles, (c) cholesterol ester crystals, and (d) others.
Results: Fibrosis in most cases of longstanding PAP is usually attributable to infection, cholesterol crystals, or a combination. Fibrosis in cases caused by metallic particles is usually secondary to cholesterol crystals but interstitial particles may play a role. Fine silica PAP in humans includes reaction to coarser particles. Fibrosis is secondary to particles cholesterol crystals contributing.
Conclusion: Causes of PAP are multifactorial. Fibrosis may occur secondary to infection and cholesterol ester crystals. Interstitial particles contribute in cases resulting from dust inhalation.

007

The presence of circulating tumor cells in chronic obstructive pulmonary disease patients is a rare cellular event

M. Ilie *, V. Hofman, E. Selva, O. Bordone, E. Long, V. Sellam, C. Bonnetaud, C. H. Marquette, P. Hofman
*CHU de Nice, Hôpital Pasteur, Laboratoire de Pathologie, France

Objective: Migration of circulating tumor cells (CTC) in the blood stream is certainly an early event occurring during lung carcinogenesis. The chronic obstructive pulmonary disease (COPD) is associated with a higher incidence of lung cancer in smoker patients and might be a preneoplastic condition for the development of non-small cell lung carcinoma (NSCLC). The purpose of this study was to look for the presence of CTC in a cohort of smoker patients having a COPD.
Method: The presence of CTC was searched in 67 COPD patients, using both the CellSearch (CS) and the isolation by size of epithelial tumor (ISET) cells methods. Results were compared to the detection of CTC in a group of 32 NSCLC patients.
Results: There were 5/67 (7%) COPD patients who had CTC (mean=4; range, 2–8 CTC) detected by CS and/or ISET methods. A total of 18/32 (56%) of lung cancer patients showed CTC (mean=18, range, 2–86). No CTC were detected in healthy individuals.
Conclusion: The detection of CTC using the CS and/or the ISET methods is a rare biological event in COPD patients. In this regard the potentiality of the CS and the ISET methods as tools for detecting early blood biomarkers of lung carcinogenesis is challenging.

008

Asbestos- and histology-related microRNAs in lung cancer

P. Nymark *, M. Guled, I. Borze, A. Faisal, L. Lahti, K. Salmenkivi, E. Kettunen, S. Anttila, S. Knuutila
*Finnish Institute of Occup. Health, Dept. of Health and Work Ability, Helsinki, Finland

Objective: Lung cancer has the highest cancer-related mortality in the world and asbestos-related lung cancer is one of the leading occupational cancers. Identifying molecular correlates of clinicopathological features in lung cancer has long been a topic of research interest.
Method: miRNA profiling was performed on 26 tumour and corresponding normal lung tissue samples from highly asbestos-exposed and non-exposed patients and on 8 control samples. Data analyses on miRNA expression, as well as integration with previously obtained mRNA and aCGH data, were performed using Chipster and a custom-developed method, respectively.
Results: Several known and new lung cancer-associated miRNAs and target genes with inverse correlation were discovered. A few DNA copy number alterations (e.g. gain at 12p13.31) were correlated with the deregulated miRNAs. Thirteen novel asbestos-related miRNAs (e.g. over-expression of miR-148b, Let-7 d, Let-7e and miR-96 and under-expression of miR-202) and inversely correlated target genes (e.g. GADD45A, FOSB, NCALD, CACNA2D2, MTSS1, EPB41L3) were identified. Furthermore, over-expression of the well known squamous cell carcinoma-associated miR-205 was linked to down-regulation of the DOK4 gene. Also, miR-27a over-

expression appeared to be associated with adenocarcinoma histology.
Conclusion: The miRNAs/genes presented here may represent interesting targets for further investigation and could eventually have potential diagnostic implications.

009

Peroxiredoxins and tropomyosins as plasma biomarkers for lung cancer and asbestos exposure

A. Rostila *, K. Vuopala, T. Toljamo, T. Nyman, I. Lindström, A. Puustinen, S. Anttila
*HUSLAB/FIOH, Dept. of Pathology, Helsinki, Finland

Objective: Lung cancer is the deadliest cancer worldwide much due to difficulties in early diagnosis. Tobacco smoking and asbestos exposure are well-known risk factors for lung cancer with well-known genetic aberrations. Their effects on plasma proteome during disease process are, however, lacking.
Method: Patients with clinical lung cancer and asbestosis, and healthy volunteers were matched for age, smoking history, and gender, and divided into four groups: lung cancer, asbestosis, lung cancer with asbestos exposure, and non-symptomatic smokers. Plasma proteins were resolved by 2-DE, detected with Image Master Software, and in-gel digested with trypsin. Resulting peptides were analysed with nanoLC-MS/MS, and identified with Mascot search engine. Expression differences were validated by immunoblotting.
Results: Most of the proteins found were abundant, glycosylated inflammatory plasma proteins. Immunological validation confirmed the overexpression of peroxiredoxin 2 and tropomyosins 3 and 4 in asbestos-exposed individuals and the downregulation of TPM3 and TPM4 in lung cancer patients. Upregulation of PRX1 was observed in both groups for lung cancer.
Conclusion: Peroxiredoxins and tropomyosins are proteins with known alterations in malignant tumours. The observed changes of plasma protein expression can enhance our understanding of cellular responses to tobacco smoking and asbestos exposure, and of the process in lung carcinogenesis.

010

Round robin test to assess the reproducibility of an epidermal growth factor receptor immunohistochemical scoring system for the therapeutically relevant classification of non-small cell lung cancer into tumors with high and low expression

J. Rüschoff *, K. Kerr, R. Büttner, Wło. T. Olszewski, V. A. Alves, H. J. Grote, P. Middel, E. Thunnissen, A. von Heydebreck, I. Celik, S. Störkel
*Pathologie Nordhessen, Diagnostische Pathologie, Kassel, Germany

Objective: High tumor epidermal growth factor receptor (EGFR) expression (an immunohistochemistry, IHC, score of ≥200 on a scale of 0–300) was shown to be associated with activity of chemotherapy-plus-cetuximab in patients with advanced non-small cell lung cancer (NSCLC). This round robin test (RRT) evaluated the interobserver reproducibility of EGFR IHC scoring.
Method: A feasibility study was undertaken that identified factors impacting on reproducibility. Subsequently, in a reference laboratory, serial sections of a NSCLC tissue microarray (TMA) were stained using the DAKO EGFR pharmDX™ kit/autostainer. An EGFR IHC score was calculated for tumors based on membrane staining intensity and frequency. After training, ten pathologists independently evaluated EGFR expression for 30 TMA cores. Interobserver agreement was calculated.
Results: The RRT showed a high interobserver agreement in EGFR IHC scoring, with an overall concordance rate of 91% and mean kappa coefficient of 0.81. Tumors with a reference score clearly below/above the cutoff (<150/≥250) were categorized with a mean concordance rate of 98%. Samples with a reference score around the cut-off (≥150–<250) showed a mean concordance rate of 74%.
Conclusion: The RRT demonstrated that after appropriate training, this method allowed a reproducible assessment of EGFR staining with respect to clinically relevant categories.

011

Are cytology samples optimal for EGFR mutation analysis for medical oncology clinics and do they measure up?

H. Sekhon *, M. Gomes, C. Souza, K. Amjadi, S. Sundaresan, S. Laurie
*Ottawa Hospital, Dept. of Pathology, Canada

Objective: Fine-needle aspirate (FNA) is useful initial diagnostic modality for yielding focal lung and metastatic lesions. A few studies have reported the feasibility using FNA samples for EGFR mutation analysis and have compared with the resected lesions but the utility of FNA samples in a routine oncological clinical setting is lacking.
Method: A total of 139 cases (79 FNA and 60 surgical) were tested for EGFR. Cell block adequacy was categorized based upon the number of tumour cells as follows: 0=0–10, 1=11–50, 2=51–100, 3=101–200 and 4 = >200 cells. All samples of adenocarcinoma cases were tested for EGFR exon 19 deletion and exon 21 L858R mutations.
Results: There were 90% of FNA specimens which had DNA amplification compared to 83% biopsy specimens. There were 16.4% of FNA cases which were positive for EGFR mutation while 15% of surgical cases were positive.

Collectively EGFR mutation was present in 16% of male and 15% of female patients while exon 19 deletion accounted for 7.2% and exon 21 L858R mutation for 8.6% of all cases.
Conclusion: FNA samples are optimal to deliver optimal amount of tumour sample for EGFR mutation analysis that is comparable to more invasive specimens.

012

Standardized handling of biopsies and cytology specimens for the diagnosis of non-small cell lung cancer (NSCLC) recommendations of an international working group

B. G. Skov *, F. Laenger, H. H. Popper, G. Rossi, F. Lopez-Rios, L. Bubendorf
*Bispebjerg University Hospital, Dept. of Pathology, Copenhagen, Denmark

Objective: Treatment of lung cancer is based on exact histotyping and molecular typing. A growing number of tests have to be performed on sparse biopsy material. Making the best use of the available tissue has become a major challenge. We report on a standard procedure for the most important diagnostic tests on small biopsies and cytology.
Method: Research of the literature and comparison of practice in centers of lung pathology in 5 countries.
Results: Supplementing conventional histotyping made on H&E and mucin stain, a minimum set of antibodies (TTF1 and p63/Ck5/6) is recommended. Testing for EGFR mutations and EML4-ALK translocations is considered the current minimum scope of molecular analysis. For EGFR testing no technical gold standard exists. FISH analysis remains the gold standard for EML4-ALK although promising immunohistochemical antibodies are coming up. Cytological specimens should be prepared as smears and a cell blocks should be prepared and handled according to the procedure for biopsies. A procedure for a specific sequence of cutting and handling the tissue block is recommended.
Conclusion: By consistently observing a simple procedure of block handling and applying quality approved and clinically relevant molecular testing, the sparse biopsy material can be optimally used making additional biopsies for molecular testing unnecessary.

013

EphA4 expression in lung cancer: an immunohistochemical study

S: Theocharis *, N. Tsoukalas, C. Giaginis, P. Alexandrou, I. Sfiniadakis, N. Kavantzas, E. Patsouris
*University of Athens, Dept. of Forensic Medicine and Toxicology, Greece

Objective: Ephrin receptors (Ephs) are frequently overexpressed in a wide variety of human malignant tumors, being associated with tumor growth, invasion, metastasis and angiogenesis. The present study aimed to evaluate EphA4 expression in lung cancer.
Method: Using tissue microarray technology, 101 paraffin-embedded tissue samples of histologically confirmed primary lung cancer cases were cored, re-embedded to the final recipient block and used for EphA4 protein immunohistochemical expression.
Results: EphA4 positivity was noted in 36 out of 101 (36%) cases. EphA4 staining intensity was classified as mild in 11 (31%), moderate in 23 (64%) and intense in 2 (5%) out of 36 positive cases. Increased EphA4 positivity and moderate/intense EphA4 staining intensity were noted in adenocarcinoma and squamous cell lung carcinoma cases compared to large cell and neuroendocrine carcinoma ones ($p=0.0049$ and $p=0.0170$, respectively). EphA4 positivity and staining intensity were associated with the presence of lymph node metastases ($p=0.0349$ and $p=0.0404$, respectively). EphA4 staining intensity was also correlated with tumor histopathological stage ($p=0.0145$). No association of EphA4 positivity nor staining intensity were noted with tumor histopathological grade, size and organ metastasis.
Conclusion: The current study supports evidence for possible EphA4 participation in lung cancer biological behavior, implying also its potent role as a therapeutic target.

014

Expression of peroxisome proliferator activated receptor-gamma (PPAR-γ) in human non-small cell lung carcinoma: correlation with clinicopathological parameters, proliferation and apoptosis-related molecules and patients' survival

S. Theocharis *, C. Giaginis, E. Politi, P. Alexandrou, J. Sfiniadakis, M. Maztourani
*University of Athens, Dept. of Forensic Medicine, Greece

Objective: Peroxisome proliferator-activated receptor-γ (PPAR-γ) has been implicated in tumor development and progression, being associated with cell differentiation, growth and apoptosis. The present study aimed to evaluate the clinical significance of PPAR-γ expression in non-small cell lung carcinoma (NSCLC).
Method: PPAR-γ expression was assessed immunohistochemically in tumoral samples obtained from 67 NSCLC patients and was statistically analyzed with clinicopathological parameters, proliferation and apoptosis related molecules and patients' survival.

Results: Positive PPAR-γ expression was prominent in 30 out of 67 (45%) NSCLC cases. PPAR-γ positivity was more frequently observed in squamous cell lung carcinoma cases compared to lung adenocarcinoma ones (p=0.048). PPAR-γ positivity was significantly associated with bcl-2 positivity (p=0.016) and borderline with c-myc positivity (p=0.052), whereas no associations were noted with histopathological grade of differentiation, TNM stage, Ki-67, p53, bax proteins' expression and patients' survival. In the squamous cell carcinoma cases, PPAR-γ positivity was associated with tumor size (p=0.038), while in adenocarcinoma with histopathological grade of differentiation (p=0.026).
Conclusion: The present study supported evidence for PPAR-γ participation in the biological mechanisms underlying the carcinogenic evolution in the lung, suggesting also the potential utility of its ligands as cell cycle modulators in future therapeutic approaches.

015

Metastatic endobronchial malignant melanoma

P. Bagci *, H. Gucer, S. Ozkaya, U. Sahin, N. Dursun
*Rize University, School of Medicine, Turkey

Objective: Endobronchial metastases from extrapulmonary tumors are very rare. Kidney, colon and breast carcinomas are the most common primaries of endobronchial metastasis. In the English literature there are few case reports that mentions metastatic melanoma in this region.
Method: A 53-year-old male with coughing, sputum expectoration and chest pain had undergone endobronchial exam and a hemorrhagic mass obstructing the right middle and lower lobar bronchus was found.
Results: On microscopic examination the tumor was an usual malignant melanoma and the diagnosis was supported with positive S100 and HMB-45 immunostains. An interview with the patient showed the primary oral malignant melanoma in the maxillary gingiva that has been treated for 3 years.
Conclusion: Endobronchial metastases from extrapulmonary tumors such as malignant melanoma are very rare. Even though it is easy to diagnose an usual melanoma even in an unusual region like this, without given history, it is not always easy to report it for practising pathologists.

016

Expression of endothelial markers in pulmonary epithelioid hemangioendothelioma

M. Bialas *, B. Papla
*Jagiellonian University, Dept. of Pathology, Cracow, Poland

Objective: Epithelioid hemangioendothelioma (EH) is a very rare neoplasm. The aim of the study was to identify the immunohistochemical profile of tumor cells in lung EH using antibodies marking endothelial cells of blood and lymphatic vessels to determine the cell line from which these tumors originate.
Method: The authors collected unique material consisting of eight cases of lung EH and examined it using immunohistochemical methods with three antibodies: CD-31, CD105 (both marking vascular endothelial cells) and D2-40 (marking lymphatic endothelial cells).
Results: In all cases, the cytoplasm of tumor cells showed strong and widespread expression of CD-31. Reaction to CD-105 antigen gave a positive result mainly in the cytoplasm of tumor cells located at the periphery of tumors, especially in highly cellular neoplasms containing spindle cells. Areas of hyalinisation and calcification were negative in both CD-31 and CD-105. Reaction to D2-40 antigen in most cases was negative. The presence of a few capillary vessels with positive endothelial cells was revealed in two cases at the periphery of the tumor—it cannot be excluded that some of them were residual lung parenchyma. Only in one case of a highly cellular tumor a small portion of spindle cells showed a positive reaction to D2-40.
Conclusion: We confirmed the origin of EH mainly from vascular endothelial cells.

017

Applying the new classification of pulmonary adenocarcinoma (*J Thorac Oncol* 2011;6:244–285) over a series of 47 cases. The difficulty of recognizing tumor invasion: usefulness of basement membrane collagen IV

M. L. Cabanas *, B. Gonzalez, A. B. Larque, J. M. Gimferrer, T. Ribalta, J. Ramirez
*Hospital Clínic Barcelona, Dept. of Pathology, Spain

Objective: The new classification of lung adenocarcinoma, particularly formerly called bronchioloalveolar carcinoma (BAC), depends mainly on the presence of invasion. This concept is usually subject to argument, therefore hindering the use of this new classification.
Method: A total of 61 cases of BAC from our department, from 2000 to 2010, were reviewed. Only 47 cases provided adequate material for this study. After H&E revision, tumors were classified as either atypical adenomatous hyperplasia (AAH), adenocarcinoma in situ (AIS), minimally invasive adenocarcinoma (MIA), lepidic predominant adenocarcinoma (LPA) or other invasive adenocarcinoma (OIA). Immunostains for basement membrane collagen IV were done in all cases.

Results: Of the 47 cases, 7 were originally classified as BAC and 40 as mixed type adenocarcinoma. After reclassification, there were 21 OIA, 15 LPA, 10 MIA and 1 AAH. Of the 7 BAC, 2 are now considered invasive adenocarcinomas. Of the 40 remaining cases, 6 are now MIA, 14 are LPA and 20 are OIA. 31 of the 47 tumors showed unequivocal negativity for the collagenIV stain in invasive areas; the remaining cases were inconclusive.
Conclusion: According to the new criteria, we had no AIS in our series, making this tumor unusually infrequent. The collagenIV immunostain is useful but not infallible for determining invasion.

018

Lung cancer on biopsies as morphology–molecular art: immunohistochemical panel and proposed adenocarcinoma classification clarification

L. Carvalho *
*Amadora, Portugal

Objective: WHO 2004 classification clarifies the patterns on biopsies supporting immunohistochemistry (IHC) and actual/future personalized therapy (as cytology–cell block).
Method: Adenocarcinoma patterns, isolated/together and large cell carcinoma particular histological types are recognized: LCNEC—TTF1, ChromA, CD56; basaloid carcinoma—CK5.6, TTF1, CK7; lymphoepithelioma-like carcinoma—CK5.6, CK7, TTF1; clear cell carcinoma—CK5.6 negative; rhabdoid phenotype carcinoma—CK7, TTF1, CK5.6, as homogeneous in specimens. Also epidermoid carcinoma subtypes (CK5.6) and adenosquamous carcinoma (CK7, TTF1, CK5.6) are recognized. sarcomatoid carcinoma (EMT) is the only epithelial malignant tumour with fusiform and/or giant cells (isolated discoesed large cells) with ADC or SQC—pleomorphic carcinoma, even without IHC. carcinoid (simply) and small cell carcinoma, also combined—CK7, CK5.6 raises no controversies.
Results: Mucinous pulmonary adenocarcinomas new group gathers mucinous multifocal BAC to be reported as multifocal mucinous adenocarcinoma and distinguishable from other mucinous gandular ADC including intestinal type adenocarcinoma (CK20, CDX2, MUC2). The non-mucinous BAC type II pneumocytes and Clara cells has to stand as BAC (lepidic from the earliest reports)/pattern.
Conclusion: The JTO February 2011 Table 2 becomes clearer—clinicians, pathologists, residents—abolishing: NSCLC, counterparts, poorly … NSCLC, morphologic, favour. MIA and AIS cases stand for numbers and IHC 2/3 Abs simultaneously should be applied.

019

Bronchiolitis as the core of pulmonary pathology: how to classify?

L. Carvalho *
*Amadora, Portugal

Objective: Bronchiolitis encompass clinical perspective of pulmonologists, radiologists, pathologists and thoracic surgeons as it is the common dealing in pulmonary diseases. Dramatic dyspnoea and minimal imagiological lesions challenge therapy and diagnosis.
Method: A clinical and pathological interpretative classification of bronchiolitis goes beyond morphology till clinical settings and therapy preview: (1) specific bronchiolitis—with a morphological marker: acute (granulocytes); constrictive (collagen); obliterans (inflammatory myofibroblastic polyp); diffuse panbronchiolitis (interstitial macrophages); respiratory (pigmented macrophages, lymphocytes, collagen); eosinophilic (eosinophils); follicular (lymphoid follicles); granulomatous (granulomata); diffuse aspiration (giant cells, macrophages); dust airway disease mineral/non-mineral (silicates/nylon); (2) non-specific bronchiolitis without specific morphological marker: acute and chronic (lymphocytes/granulocytes); chronic (collagen, lymphocytes).
Results: The microanatomy of bronchioles between larger/upper airways and alveoli, simple at microscopy, has distinct segments: membranous bronchiole (smooth muscle cell), terminal bronchiole (fibroblast), respiratory bronchiole/alveolar duct (type II pneumocytes and Clara cells), where pulmonary embriogenic synergism endoderm/mesoderm joins with superimposing of systemic diseases, upper and lower pulmonary associated diseases.
Conclusion: This TRU—terminal respiratory unit—is then where a particular set of bronchial-pulmonary carcinomas develops in the EMT—epithelial mesenchimal transition concept/stem cells. Anti-inflammatory therapy and personalized therapy for lung cancer and prevention becomes imperative mainly using mTOR inhibitors and B and T cells and macrophages blockers.

020

Thymomas WHO 2004 classification applicability

L. Carvalho *, P. Calvinho, D. Oliveira, V. Sousa, J. Bernardo, M. Antunes
*Amadora, Portugal

Objective: Thymomas classifications aim clinical and pathological understanding. The authors reviewed the clinical files of ressected thymomas with the goal of

defining which histological classification correlates with prognosis.
Method: Thymectomy of 81 patients, average age of 57, 42% males along 15 years, 38% asymptomatic, 23% had Myastenia Gravis and 16% with symptomatic triad (cough, dyspnoea and thoracic pain); two hospital deaths occurred due to heart failure. In stages I, II, III, IVA and IVB of the Masaoka classification were respectively, 52%, 37%, 0%, 1% and 10% cases; thymoma, atypical thymoma and thymic carcinoma of the Suster–Moran classification were respectively 40.7%, 45.7% and 13.5%. In the Müller-Hetmerlink/WHO 2004 classification A, AB, B1, B2, B3 and thymic carcinoma were respectively 12.3%, 35.8%, 30.9%, 14.9%, 3.7% and 2.5%.
Results: The follow-up was complete with an average time of 95.5.+63.0 months with a mortality of 14 patients (17.3%). Only 8.6% patients underwent chemotherapy while 19.7% were submitted to radiotherapy. None of the patients in Masaoka I stage underwent adjuvant therapy regardless of the other classifications.
Conclusion: This is a small series with the bias of therapeutic decision towards the Masaoka Classification, where WHO 2004 criteria based in histogenesis, maintain applicability suitable to molecular studies.

021

TTF1 negative solid pattern in lung adenocarcinomas may reflect morphogenesis

L. Carvalho *, A. Alarcão, P. Couceiro, M. Reis Silva, M. J. D'Aguiar, L. Teixeira, T. Ferreira, V. Sousa
*Amadora, Portugal

Objective: Lung adenocarcinomas are classified according to histological subtypes/patterns. Thyroid transcription factor-1 (TTF-1) is a tissue-specific transcriptional factor important in differentiation and morphogenesis of lung/thyroid/brain and was applied to classify pulmonary adenocarcinomas and also to evaluate its expression in the reported patterns.
Method: In a series of 44 lung adenocarcinoma there were: 41 acinar, 5 papillary, 13 micropapillary, 14 solid, 25 bronchiolo-alveolar (BAC) and 3 mucinous patterns. Applied immunohistochemistry panel was: TTF1, CK7 and Ki67.
Results: TTF1 expression was higher in adenocarcinomas/normal lung (p=0.0009). Expression was greater in acinar (p=0.0014), BAC (p<0.0001) and micropapillary patterns (p=0.0019) than in normal parenchime. Mucinous pattern had lower expression/normal lung (p=0.02). There were no differences between normal lung and papillary (p=0.5074) and solid patterns (p=0.5659); 6/14 cases of solid pattern were TTF1 negative and expressed CK7 while Ki67 expression was higher in this TTF1 negative group when compared to the TTF1 positive (p=0.0015).
Conclusion: Decreased expression of TTF1 in some patterns identifies a small number of cases developing from pure CK7 positive cells (bronchial?). Solid pattern show lower nuclear expression of TTF1 and combined with higher expression of Ki67 in TTF1 negative cases may reflect different morphogenesis and more aggressive biological behaviour.

022

Comparison of epidermal growth factor receptor mutations between primary and corresponding brain metastatic tumors in pulmonary adenocarcinoma

H.-K. Chen *, L.-Y. Shiu, Y.-P. Lo, C.-C. Huang
*Chang Gung Memorial Hospital, Dept. of Pathology, Kaohsiung City, Taiwan

Objective: Lung adenocarcinoma is the leading cause of cancer deaths worldwide. Epidermal growth factor receptor (EGFR) has been known to be the predictor of response to EGFR-targeted therapy in lung adenocarcinomas. Brain metastasis is identified in a large proportion of patients and significant molecular changes may occur during the metastatic process.
Method: We compared the status of EGFR mutation between the primary lung adenocarcinoma and brain metastatic lesions from 1991 to 2010. Macrodissection or microdissection was performed before DNA extraction for polymerase chain reaction amplification, followed by direct sequencing.
Results: Forty patients were included. Five of 20 (25%) patients with EGFR mutation-positive primary lung tumors had lost the mutations in metastases. For 19 patients who were EGFR mutation positive in the metastatic tumors, 4 (21%) were negative in the primary tumors. Among the 14 patients with EGFR mutation in both primary and metastatic tumors, 4 cases displayed different mutation types. The overall discordant rate was 33% (13 of 40 cases).
Conclusion: EGFR status of primary lung adenocarcinomas may not predict the status in the corresponding brain metastases. Analysis of EGFR mutations in the primary lung tumor would be inadequate for planning the use of EGFR-targeted therapy for advanced lung adenocarcinoma.

023

Small cell carcinoma of the lungs masked by pulmonary tuberculosis

S. Dumitriu *, A. Dumitriu, M. Chetrone, D. Miron, V. Ionita, I. Fulga, C. Georgescu
*UMF Iasi, Dept. of Pathology, Romania

Objective: Small cell carcinoma occurs both in the major bronchi and in the periphery of the lung. There is no known preinvasive phase or carcinoma in situ. They are the most aggressive of lung tumors, metastasize widely, and are virtually incurable by surgical means.
Method: We present the case of a 54-year-old female taking antituberculosis drugs for active pulmonary tuberculosis who was admitted to our hospital requiring further examination of a pulmonary mass in the left upper lobe.
Results: It was performed a transbronchial lung biopsy of the pulmonary mass and diagnosed small cell carcinoma. The autopsy confirmed the histopathological diagnosis.
Conclusion: This report describes a rare case of small cell carcinoma appearing during treatment for active pulmonary tuberculosis.

024

Primary choriocarcinoma of the lung arising from adenocarcinoma with divergent differentiation: a case report and literature review

M. Endo *, J.-I. Akahira, R. Chiba
*Sendai Kousei Hospital, Dept. of Pathology, Japan

Objective: Primary choriocarcinoma of the lung is an extremely rare tumour, and with coexistence of adenocarciona is furthermore considered to be rarer condition.
Method: An autopsy examination for a 45-year-old male who died due to respiratory failure with multiple tumours in both lungs is described. A review of the literature of primary choriocarcinoma is also reported.
Results: Main lesion arising from upper lobe of left lung showing remarkably hemorrhagic tumour coexisting whitish components, up to 10 cm in diameter, with multiple metastases extended in both whole lungs. Microscopically, mononucleated trophoblastic cells and with multinucleated syncytiotropoblastic cells were observed in hemorrhagic area, while sheets polygonal cells with slight mucin admixed with a few trophoblastic cells were existing predominantly in whitish components. Immunohistochemically, tropoblastic cells were strongly positive for human chorionic gonadotropin (HCG) and negative for surfactant apo-protein A (SPA) and thyroid-transcription factor 1 (TTF-1). While polygonal cells were positive for TTF-1 and partially positive for SPA, negative for HCG, indicating that the cells were adenocarcinoma originated from lung. Metastases of coriocarcinoma also into liver, kidneys pancreas, while adenocarcinoma into mediastinal lymph nodes. No tumour in retroperitoneum and testis.
Conclusion: Choriocarcinoma with coexistence another carcinoma of the lung were reported only five literature. Present case could be suggesting a pathway of divergent differentiation from extragonadal carcinoma to choriocarcinoma.

025

Correlation between phospho-BRCA1 expression and clinicopathological factors, including the occurrence of brain metastases in patients with non-small cell lung cancer

M. Gachechiladze *, I. Überall, G. Burkadze, J. Škarda
*Palacky University, Dept. of Molecular Pathology, Olomouc, Czech Republic

Objective: BRCA1 (Breast cancer1) is one of the potential molecular markers for non-small-cell lung cancer (NSCLC) patients. BRCA1 plays a central role in DNA damage response (DDR) and undergoes specific phosphorylation at ser1524 by ATM/ATR in response to various kinds of genotoxic stress.
Method: We performed BRCA1 immunohistochemistry on several tissue microarrays (TMAs) of 104 early (I, II) and advanced (III, IV) stage NSCLCs, using p1524 antibody against phosptorylated form of BRCA1 protein at ser1524 (Abcam). Patients with III and IV stage disease were treated by adjuvant cisplatin-based chemotherapy. Staining results were correlated with overall survival (OS), disease free survival (DFS) and with the occurrence of brain metastases.
Results: BRCA1 p1524 positivity was significantly correlated with longer OS and DFS in stage I and II patients ($p<0.013$), whilst OS and DFS was shorter in p1524 positive stage III and IV patients ($p=0.015$). No significant correlation was found with the occurrence of brain metastases.
Conclusion: According to our study results BRCA1 phosphorylaton, at least in ser1524, differently determines the fate of early and advanced NSCLC as well as the response to chemotherapy, but the underlying mechanisms are not completely understood. Detection of phosphorylated forms of BRCA1 might serve as useful prognostic and predictive marker for patients with NSCLC.

026

Talc-associated lung damage by chronic injection drug use on evidence of forensic autopsies

L. Grinberg *, A. Nevolin
*Ural State Medical Academy, Dept. of athology, Yekaterinburg, Russia

Objective: A widespread chronic injection drug use (CIDU) has been registered in Russia over the last 10–15 years. It is accompanied by rising mortality from acute poisoning with opiates (heroin). Moreover, there are no reliable morphological criteria of CIDU. However, it is known that drugs can be injected together with talc—containing additions which cause granulomatous changes in the lungs to the extent of emphysema development.
Method: The study includes 100 autopsy cases of persons with CIDU who died of acute poisoning with opiates in 2007–2009. Lung tissue specimens stained with haematoxylin and eosin were investigated in transmitted and polarized light.
Results: In 93 cases talc containing anisotropous crystals in lungs was revealed. In 17 cases there were giant cell granulomas in interstitium around talc crystals. Crystals were revealed in lumen of alveolar septum and in vascular walls. The size of the crystals varied within 5–20 μm. Their number varied from 5–10 to 1–2 per high power field with ×400 amplification.
Conclusion: Thus, the presence of talc containing anisotropous crystals in lungs is a reliable and highly sensitive (93%) morphological CIDU marker in current conditions in Russia (Sverdlosk region). The clinical significance of this morphological phenomenon calls for further investigation.

027

Lung placental transmogrification syndrome with bullous lung emphysema and spontaneous pneumothorax

L. Grinberg *, A. Filatova
*Ural State Medical Academy, Dept. of Pathology, Yekaterinburg, Russia

Objective: Lung placental transmogrification syndrome (LPTS) is the term denoting a specific morphological picture characterized by formation in lung parenchyma of placenta-like papillary structures that, in terms of their minute structure, are similar to placenta in early stages of pregnancy. The roots of this phenomenon are not clear but the majority of authors link it with bullous emphysema, recurrent spontaneous pneumothorax (SP) or hamartoma of lung.
Method: A total of 250 SP cases were investigated using video-thoracoscopic lung resections. Traditional morphological analysis of resectates was conducted, in a number of cases accompanied with immunohistochemical analysis.
Results: Placental transmogrification syndrome was revealed in 14 cases (5.6%) that, in terms of age and sex composion or primary/secondary SP correlation, did not differ reliably from the group of 236 cases without LPTS. Significant differences ($p<0.05$) were revealed based on predominance of recurrent pneumothorax (64.3% and 40.7%). However, the major difference is the predominance of bullous emphysema—100% with LPTS and 62.7% in the comparison group.
Conclusion: Therefore, placental transmogrification syndrome in lung resectates of patients with spontaneous pneumothorax was revealed in 5.6%. Presumably, it has a pathogenetic link with bullous lung emphysema.

028

Topoisomerase IIα expression and gene amplification in small cell lung carcinoma

I. Kern *, M. Kovacevic, T. Cufer
*University Clinic Golnik, Dept. of Pathology, Slovenia

Objective: Small cell lung carcinoma (SCLC) is very sensitive to chemotherapy. Topoisomerase IIα (TOP2A) has important role in DNA replication. Cytostatic drugs used to treat SCLC work by blocking the enzyme. The aim of this study was to determine the TOP2A expression and gene amplification in SCLC.
Method: We performed analysis of 29 bronchial biopsies samples diagnosed as SCLC. Immunohistochemical staining (monoclonal antibody clone 3F6) was evaluated semiquantitatively by determing the intensity of reaction in tumor nuclei (negative, weak, marked). Dual silver in situ hybridization was performed for gene amplification analysis. Signals were counted in 40 preserved nuclei to detect a ratio between TOP2A gene copy numbers and CEP 17, while polisomy was considered when at least 40% cells with at least four copies of TOP2A gene were observed.
Results: All 29 samples showed positive immunohistochemical nuclear reaction for TOP2A (16 weak, 13 marked). Four samples showed polisomy, while ratio TOP2A/CEP 17 value was 1.08–1.56. Most samples showed trisomy (22 of 29), while normosomy was detected in three samples.
Conclusion: This study revealed that, although the majority of the samples expressed TOP2A positive immunohistochemical nuclear staining, it is not possible to correlate it with neither polisomy nor amplification of TOP2A gene.

029

Aberrant DNA methylation of specific genes in lung cancer: is it associated with clinicopathologic features?

M. Kontic *, J. Stojsic, H. Nelson, S. Ognjanovic, D. Jovanovic
*Pulmonology Clinic, Dept. of Oncology, Belgrade, Serbia

Objective: Aim of this study was to track possible relationships between clinicopathologic features of non-small cell lung cancer patients and DNA methylation in multiple genes. We also examined quantitative methylation patterns using pyrosequencing in tumor, matching normal lung tissue and blood of patients with NSCLC.
Method: Primary tumor samples (n=65), corresponding nonmalignant lung tissues (n=65) and blood samples (n=51) were obtained from NSCLC patients. Hypermethylation status was quantified at multiple CpG sites in multiple genes- SOX1, RASSF1A, HOXA9, CDH13, MGMT, ESR1 and DAPK by pyrosequencing.
Results: Tumor hypermethylation was more frequently for adenocarcinoma at CDH13 and ESR1. A higher proportion of SSC tumors were hypermethylated at HOXA9 and SOX1 compared to other types of NSCLC. Patients with stage four more likely had hypermethylation at MGMT and patients with hypermethylation at HOX9 more likely had stage two and three tumors. Gender was associated with hypermethylation at CDH13 with females being more likely to have hypermethylated tumors. Methylation in tumors was significantly higher then in normal lung for SOX1, DAPK, RASSF1A, HOXA9 and CDH13. Tumor samples had significantly higher methylation than blood samples for all genes except DAPK.
Conclusion: Our results show that elevated methylation levels observed in genes SOX1, RASSF1A, HOXA9, CDH13, MGMT, ESR1 and DAPK were associated with some clinicopathologic features of patients. These methylation changes were cancer-specific.

030

Pulmonary hyaline membrane aspects in the forensic practice

M.-M. Koumpanaki *, A. Enache , F. Chatzinikolaou, E. Zegelidou, E. Kalyva
*Theageneion Cancer Hospital, Dept. of Pathology, Thessaloniki, Greece

Objective: We studied the preconditions and the traumatic and pathological history in 1,090 cases of sudden death at IML Timisoara in which the microscopic exam made by the usual HE coloration highlighted hyaline membrane formation at the pulmonary level.
Method: We present three characteristic cases: a newborn whose mother had gestational toxemia complicated with HELLP syndrome, a 33-year-old who died from acute bronchopneumonic inflammatory process complicated with hyaline membrane disease and a 46-year-old who presented a cranio-cerebral lesion with cranial fractures, meningial lesion, bronchopneumonia and formation of alveolar hyaline membrane.
Results: The analysis of the microscopic investigations revealed an association between the infectious processes with a silent evolution (pneumonias, bronchopneumonias, leptomeningitis) and the formation of HM on the alveoli. Considering the characteristical lack of severe symptoms we can classify the situations in which we encountered pulmonary hyaline into three groups: perinatal period associated death, sudden death in an adult with silent infectious pathology and deaths in which trauma is associated with secondary infectious processes.
Conclusion: In sudden death cases in which infectious type changes appear, the main life-threatening condition is the pulmonary hyaline membrane deposits with an important role in the genesis of the respiratory distress syndrome.

031

Capillarotoxic interstitial pneumonia with acute leptomeningitis: a case report

M.M. Koumpanaki *, A. Enache, F. Chatzinikolaou, E. Zegelidoy, P. Voultsos, E. Kalyva, H. Florou
*Theageneion Cancer Hospital, Dept. of Pathology, Thessaloniki, Greece

Objective: We analysed the nonviolent deaths in which we found acute meningitis and/or leptomeningitis associated with pluriorganic inflammatory processes.
Method: Between 2007 and 2009 at IML Timisoara 19 cases had the established cause of death as meningitis among 11 men and 8 women with ages between 34 and 79.
Results: We present the case of KHI, a 38-year-old woman with flu-like symptoms for 10 days before death at home. During the autopsy we observed 19 tegumentary lesions on the thorax and limbs, cerebelous parenchymatous hematoma, acute leptomeningitis, discrete cardiomegaly with left ventricular hypertrophy, myocardial fibrosis, aortic atheroma, hepatic and renal dystrophy, moderate spleenomegaly, left ovarian cyst, visceral edema and stasis, obesity. The microscopic examination revealed vascularite lesions also observed elsewhere. In conclusion the death was the result of a hypertoxic viral infection associated with meningitis and interstitial pneumonia (with multiple organ influence) in which the severeness of the vasculite-like vascular lesions simulated the appearance of bruising.
Conclusion: The study shows that, in cases of sudden death, meningitis may occur in the evolution of a viral infection with a clinical aspect which can hide the true severity of the condition having a quick fatal evolution. Observing bruising may sometimes require a microscopic examination for differentiating the vascular lesions in viral infections.

032

Benign mediastinal cysts: a retrospective study of 44 cases

M. Mlika *, R. Hamrouni, A. Ayadi-Kaddour, E. Braham, O. Ismail, F. El-Mezni
*Tunis, Tunisia

Objective: Benign mediastinal cysts account for 18% to 20% of the mediastinal tumors. They are divided in congenital, acquired cysts and cysts of non-consensual origin.
Method: We report a retrospective study of 44 benign mediastinal cysts diagnosed over a 15-year period (1993–2008).
Results: The 44 cases were divided in 12 bronchogenic cysts (27%), 7 lymphangiomas (16%), 9 thymic cysts (21%), 1 cradiothoracic cyst (2%), and 15 pleural-pericardiac cyst (34%). A predominance of men was observed with 25 men. The mean age was 42 years with an average range from 5 to 80 years. All of the patients were symptomatic. The most frequent symptom consisted in chest pain (85%). The most frequent tumors were located in the anterior mediastinum. The diagnosis was based on histologic study in all cases. The treatment consisted in all cases in total surgical resection via thoracotomy or thoracoscopy. No patient presented post-operative complications after a follow-up period varying from 3 months to 5 years.
Conclusion: Benign mediastinal cysts are rare tumors. Their treatment is based on surgical resection and the final diagnosis remains based on histologic study.

033

Pleuropulmonary blastoma type II: case report

I. H. Ozbudak *, V. Hazar, G. Arslan, M. Melikoglu, G. Ozbilim
*Akdeniz University, School of Medicine, Antalya, Turkey

Objective: Pleuropulmonary blastoma (PPB) is a rare pulmonary dysontogenetic tumor usually observed in childhood under the age of 6 years. It has poor prognosis with three different subtypes: cystic (type I), combined cystic and solid (type II) and solid (type III). It is composed of primitive blastema and a malignant mesenchymal stroma.
Method: A 21-month-old girl was admitted to a hospital with complaints of fever, cough and dyspnea. Computerized tomography revealed extrapulmonary mass in the right hemithorax, 7.5×7×7 cm in size, containing both solid and cystic components. The patient underwent biopsy.
Results: Microscopically, solid parts and small cystic spaces lined by low cuboidal bronchiolar epithelium were seen. Under cyst epithelium and in solid part of tumor, blastomatous cells and Desmin-positive rhabdomyoblasts were demonstrated within the myxoid stroma. Final diagnosis was PPB type II. The patient had received three cycles adjuvant chemotherapy including vincristin+adriamycin alternating actinomycin D+ifosfamide (VAI) and complete resection of tumor was done after 3 months. She is still under chemotherapy and complete remission. At the end of chemotherapy, local radiotherapy will be discussed.
Conclusion: Although on pathological aspect it is well-described, pathogenesis and therapeutic management still remain controversial. Unresectable tumors should be treated with neoadjuvant chemotherapy to reduce in resectable size.

034

Multiple pulmonary meningioma: possibly metastases from intracranial meningioma

I. H. Ozbudak *, G. Ozbilim, O. Ozbudak, G. Arslan
*Akdeniz University, School of Medicine, Antalya, Turkey

Objective: Meningioma is one of the most frequent tumors of central nervous system. Most of them are benign and are cured by surgical removal. Although local recurrence may occur, extracranial metastasis is rare. Lung is the most frequent site for metastasis.
Method: A 36-year-old woman was admitted to the hospital with complaints of cough and dyspnea. Computerized tomography revealed multiple, pleural-based, well-circumscribed, mostly calcified nodular masses in both lungs. The patient underwent left upper lobe wedge biopsy.
Results: Grossly, multiple lesions were detected and all of them had well-defined borders, whitish color and firm consistency. Microscopic examination revealed spindle meningothelial cells arranged in fascicules with massive psammoma bodies infiltrating the lung. Tumor cells were immune positive with EMA, vimentin, progesterone receptor and S-100. Histopathologic findings were consistent with meningioma. After pathology report, the patient was evaluated for intracranial meningioma. Magnetic resonance imagining showed a calcified, lobulated lesion located superior to tentorium cerebelli which is suspicious for calcified meningioma. She rejected to have cranial surgery.
Conclusion: Metastatic meningioma of lung may be a diagnostic challenge under the circumstances of unknown primary site of tumor as in the present case. Also, primary pulmonary meningioma or primary mesenchymal lung lesions can cause confusion during the diagnosis.

035

The occurrence of rheumatoid nodules and chondroid hamartoma in same patient: case report

I. H. Ozbudak *, G.A. Ocak, G. Arslan, A. Erdogan, G. Ozbilim
*Akdeniz University, School of Medicine, Antalya, Turkey

Objective: Multiple well-circumscribed pulmonary nodules larger than 2 cm are suggestive of metastatic neoplasm. Non-malignant diseases must also be considered if the nodule has changed only slightly in size and/or number during a long period of time.
Method: A 65-year-old woman was referred to our hospital for evaluation of multiple lung nodules which had been growing slowly but also showed cavitations. She had diagnosis of rheumatoid arthritis and she was treated for lung involvement with tumor necrosis factor (TNF) for the last 3 months. To exclude a possible malignancy, the patient underwent wedge biopsy of the left upper and lower lobes.
Results: One of the nodules in the left upper lobe was diagnosed as chondroid hamartoma. The rest of the nodules were consistent with rheumatoid nodules which had the morphology of necrotizing granulomas.
Conclusion: Although the clinical parameters were suggestive of rheumatoid nodules, histological examination was done to exclude malignancy and we found an additional benign lesion. The case is presented and discussed here in order to improve diagnosis and management of pulmonary nodules.

036

Integration of molecular analysis into routine care of patients with lung adenocarcinoma for directing personalized therapies

M. Paciencia *, N. Le Stang, S. Lecot-Cotigny, F. Galateau-Sallé
*University Hospital Caen, Dept. of Pathology, France

Objective: Molecular classification is a major issue in lung cancer treatment. French National Cancer Institute has recently advocated to routinely use molecular diagnostic tests in adenocarcinomas in order to improve the efficacy of targeted therapy and response to treatment.
Method: A total of 93 lung adenocarcinomas, validated according to the WHO classification, were analyzed for EGFR, KRAS, BRAF mutations and ALK FISH translocation from November 2010 to April 2011.
Results: EGFR, KRAS and BRAF mutations were respectively found in 9 (10%), 17 (18%), 0 (0) and 4 (4%) ALK translocations. One KRAS mutation was observed in a patient with ALK rearrangement. ALK translocations were associated with heavy smoker (100%), male gender (100%), older age (73 vs 62, $p<0.005$), acinar and/or papillary histological types (50%). EGFR mutations were associated with male gender (56%), no or light smokers (67%), acinar and/or papillary histological types (53%). KRAS mutations were associated with heavy smoker (87%), male gender (76%), acinar and/or papillary histological types (56%).
Conclusion: We showed that ALK translocations can be found in a different population and that co-mutations including ALK translocation exist. Unlike current algorithms, our results emphasize the need to process all biomarkers, in order to optimize personalized treatment.

037

MicroRNA expression is a potential predictor of progression and survival in lung cancer

F. J. Pardo *, K. Valencia, E. Bandrés, C. García Franco, F. Queipo, M. Ponz, F. Lecanda
*University of Navarra, Dept. of Pathology, Pamplona, Spain

Objective: miRNA expression is frequently disregulated in cancer with exciting potential as novel biomarkers and therapeutic targets. The purpose of this study was to define the expression pattern of miRNAs for prediction risk of distance-progression in lung cancer stage I–II.
Method: RNA was extracted from 28 FFPE specimens with early stages (I and II) non-small cell lung cancer (adenocarcinoma) patients who underwent potentially curative resection and no post-surgical treatment until relapse. miRNA expression profile was analyzed using TaqMan Low Density Array (TLDA) Human MicroRNA Panel v.2. miRNA expression data obtained by TLDA were normalized using RNU48 selected by Normfinder integrated in StatMiner. Hierarchical cluster analysis was performed by clustering method using Euclidean distance for similarity measuring. Validation of selected miRNAs was performed by using individual TaqMan MicroRNA Assays.
Results: Comparing the two groups (no progression vs progression) miRNA profiles, we identified the upregulation of hsa-miRNA-17 family in patients that has progressed as compared to those without progression. This family includes hsa-miR-17, hsa-miR-20b, hsa-miR-19b and hsa-miR-106a.
Conclusion: miRNA profile in FFPE early lung cancer tissues identified the upregulation of miR-17 family as potential predictor of progression disease.

038

Bleomycin and paraquat-mediated pulmonary fibrosis is IL-17 independent

E.R. Parra *, A. Fabro, M. Rangel, W. Teodoro, H. Popper, V.L. Capelozzi
*Faculdade de Medicina da USP, Dept. of Pathology, São Paulo, Brazil

Objective: Better characterization of the immunological mechanisms of pulmonary fibrosis is needed to identify new therapeutic modalities for these diseases. The aim of the current study was to characterize the mechanisms of

pulmonary fibrosis and to determine whether IL-17A plays an important regulatory role.
Method: Distinct animal models were used, including Balb-Bleomycin (BLM), Balb-Paraquat, C57-BLM and C57-KO-IL17-BLM induced pulmonary fibrosis to evaluate the fibrosis and the IL-17 role. We used the picrosirius-polarization method, weigert's resorcin-fuchsin histochemistry, immunohistochemistry, and morphometric analysis to evaluate the amounts of collagen and elastic fibers and the transforming grow factor-β (TGF-β) expression.
Results: We report here that BLM-mediated fibrosis is IL-17 independent, as IL17−/− mice developed similar amount of fibrosis when compared to control mice. In marked contrast, BLM-induced pulmonary fibrosis revealed increase of collagen fibers in all four groups (Fig 1). We found that only Balb-BLM and Balb-Paraquat presented increase of elastic fibers. A positive correlation was found between elastic and collagen fibers in Balb-BLM animals, as well as in Balb-BLM and Balb-Paraquat. In addition, we found a direct correlation between TGF and collagen in C57-KO-IL17-BLM.
Conclusion: Bleomycin and paraquat-mediated fibrosis is IL-17 independent. However, more studies are necessary to validate the regulatory role of IL-17 on pulmonary fibrosis process.

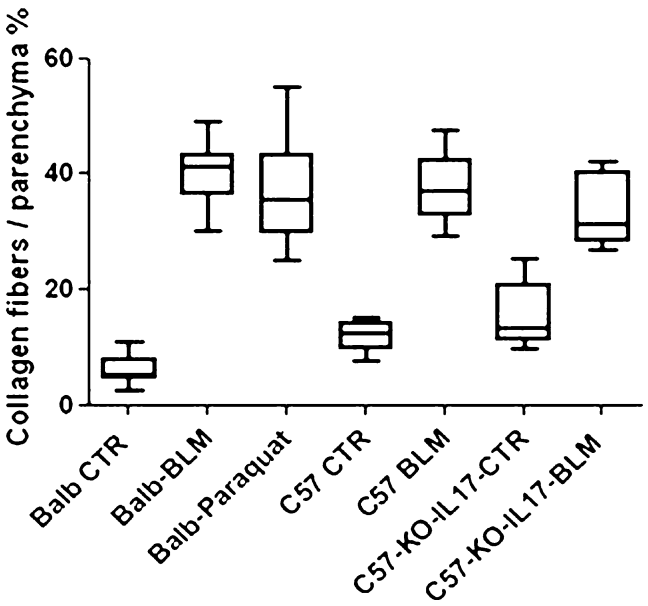

Fig. 1: Mice lungs slides were stained by Picrosirius red and viewed under polarized microscope (20×). When compared to controls all the 4 groups presented a significative increase on the amount of collagen fibers. For the groups Balb-BLM, Balb-paraquat and C57-BLM, p=0.0001; for the C57-KO-IL17-BLM group, p=0.0003.

039

Correlation between pulmonary anatomopathologic analysis and clinical manifestations in patients with pulmonary thromboembolism

E.R. Parra *, A. D. Pinto Ruppert, A. de Matos Soeiro, V.L. Capelozzi
*Faculdade de Medicina da USP, Dept. of Pathology, São Paulo, Brazil

Objective: The aim of this study was describe and associated demographic and etiologic data, anatomic pathological findings and in-vivo manifestations (acute respiratory failure [ARF], hemodynamic instability [HI] or sudden death) from autopsy reports of pulmonary thromboembolism (PTE) patients.
Method: We reviewed 291 autopsies of patients whose cause of death was PTE. The following data were obtained: age, sex, clinical in vivo manifestations, post-mortem pathological patterns and main associated underlying diseases.
Results: The median age was 64 years among 127 men and 164 women. The pulmonary histopathological changes were categorized in: diffuse alveolar damage (DAD), pulmonary edema (PE), alveolar hemorrhage (AH) and lympho/plasmacytic interstitial pneumonia (LPIP). The most prevalent pulmonary finding was PE (26.8%). Chronic obstructive pulmonary disease was positively correlated to LPIP (p=0.04). Linking in vivo manifestations to pulmonary changes were found significative relations between: ARF and PTE (OR=2.99; p=0.01); ARF and AH (OR=2.70; p=0.04); ARF and DAD (OR=8.79; p=0.03); HI and HA (OR=3.38, p=0.01) and HI and DAD (OR=11.43; p=0.02).
Conclusion: The understanding of pulmonary physiopathological mechanism involved with each PTE-associated disease can improve diagnosis in order to offer prompt treatment and reduce mortality. Financial support: FAPESP, CNPq.

040

Increase alpha-smooth muscle actin, telomerase, interleukin-4 and endothelin-1 expression in progressive pulmonary fibrosis of systemic sclerosis (SSc)

E.R. Parra *, L. Oliveira e Silva, M. Rangel, V. L. Capelozzi
*Faculdade de Medicina da USP, Dept. of Pathology, São Paulo, Brazil

Objective: Systemic sclerosis (SSc) is a multisystem connective tissue disorder characterized by excessive accumulation of extracellular matrix, resulting in progressive fibrosis and dysfunction of a number of organs. In this regards many studies suggest that several cytokines and growth factors have been implicated in the SSc.
Method: Lung specimens were obtained from 30 patients with SSc. Immunohistochemical staining for alpha-smooth muscle actin (α-SMA), anti-interleukin (IL)-4, anti-IL-13, anti-basic fibroblast growth factor (bFGF), anti-

transforming grow factor beta (TGF-β), anti-telomerase and anti-endothelin-1 (ET-1) was analyzed in alveolar septal interstitium. Score of fibrosis was determined by high-resolution computed tomography (HRCT) analysis. Pulmonary function test was also analyzed (Figure 1A).

Results: The HRCT scores divided the patients in two groups: patients with minimal and several fibrosis. The patients with several fibrosis showed statistical increased significance of α-SMA, IL-4, telomerase and ET-1 when compared with minimal fibrosis patients (Figure 1B). The high score of HRCT was negative associated with DCO (r=−0.601, p=0.01). Multivariate analysis including the immunomarkers, revealed a negative association between α-SMA and VC (r=−0.577, p=0.03) and DCO (r=−0.601, p=0.01). ET-1 had a negative association with FEV1 (r=0.436, p=0.03). α-SMA had a significant positive association with telomerase (r=0.650, p=0.001) and ET-1 (r=0. 506, p=0.01).

Conclusion: We observed an increased telomerase+expression and a continuous stimulus of IL4, ET-1 and α-SMA in several pulmonary fibrosis when compared with minimal fibrosis. These evidences suggest an active proliferation and a continuous remodeling process in the pulmonary parenchyma from patients' whit early to late stage. Financial support: FAPESP CNPq.

Objective: The aim of this preliminary study was to evaluate lymphatic vessels in pulmonary patients with systemic sclerosis comparing with normal lung tissue (NLT) and with the extension of pulmonary fibrosis obtained from high-resolution computed tomography (HRCT) score.

Method: Lung specimens were obtained from 23 females patients (47±8.9 year) with SSc. NLT were obtained from five individuals who died suddenly of non-pulmonary causes. Immunohistochemistry and histomorphometry were used to evaluate the amount of lymphatic (D2-40) expression and the percent of area occupied by these lymphatics in lung specimens. The pulmonary SSc compromising was evaluated by HRCT score. Pulmonary function tests were also considered.

Results: The density of lymphatic vessels was markedly reduced in SSc when compared with NLT group. The lymphatic area was minor in SSc than in NLT group (Figure 1A). The patients with minimal and severe fibrosis HRCT score showed similar amount of lymphatic density. The patients with several fibrosis showed increased area occupied by lymphatic than minimal fibrosis patients, (Figure 1B). The increased of

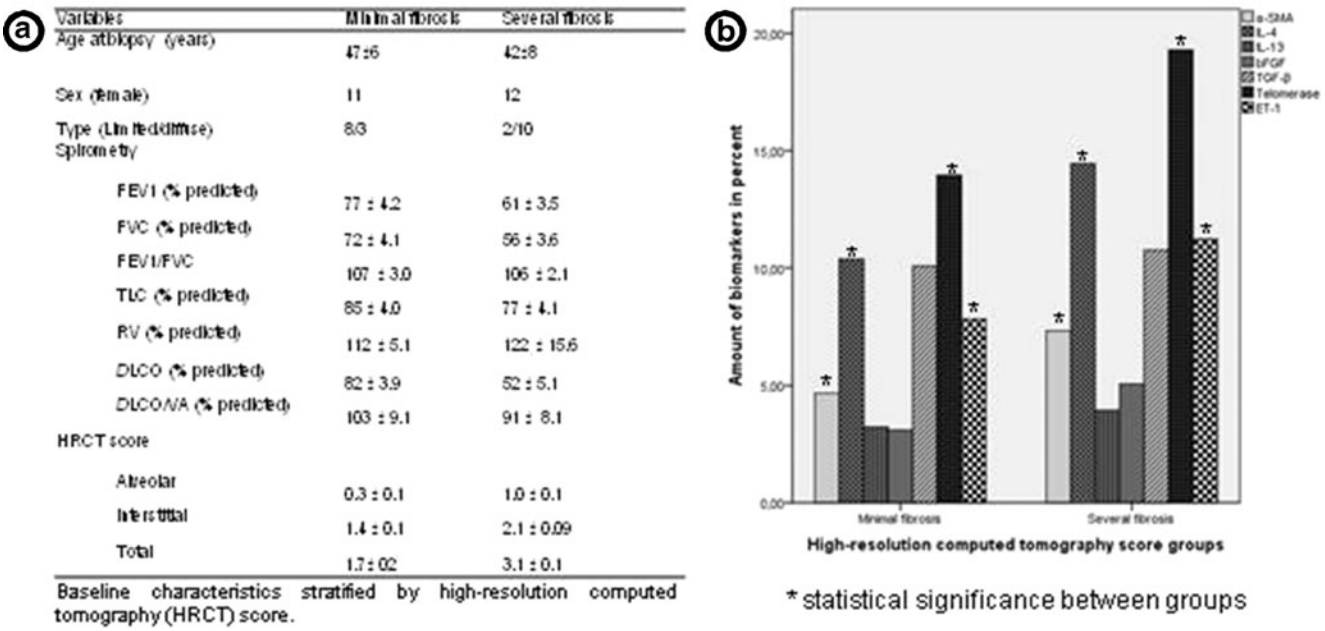

Variables	Minimal fibrosis	Several fibrosis
Age at biopsy (years)	47±6	42±8
Sex (female)	11	12
Type (Limited/diffuse)	8/3	2/10
Spirometry		
FEV1 (% predicted)	77 ± 4.2	61 ± 3.5
FVC (% predicted)	72 ± 4.1	56 ± 3.6
FEV1/FVC	107 ± 3.0	106 ± 2.1
TLC (% predicted)	85 ± 4.0	77 ± 4.1
RV (% predicted)	112 ± 5.1	122 ± 15.6
DLCO (% predicted)	82 ± 3.9	52 ± 5.1
DLCO/VA (% predicted)	103 ± 9.1	91 ± 8.1
HRCT score		
Alveolar	0.3 ± 0.1	1.0 ± 0.1
Interstitial	1.4 ± 0.1	2.1 ± 0.09
Total	1.7 ± 02	3.1 ± 0.1

Baseline characteristics stratified by high-resolution computed tomography (HRCT) score.

041

Rarefaction of lymphatic vasculature in parenchymal pulmonary remodeling of systemic sclerosis (SSc) patients

E.R. Parra *, N.B. Rigoldi Colomb, A.D. Pinto Ruppert, V. L. Capelozzi

*Faculdade de Medicina da USP, Dept. of Pathology, São Paulo, Brazil

lymphatic area occupied had a negative association with VC (r=−0.633, p=0.008), FVC (r=−0.406, p=0.04) and DCO (r=−0.610, p=0.01).

Conclusion: In conclusion, our data show that the lymphatic system is markedly affected in pulmonary SSc and this rarefaction of lymphatic vasculature is correlated with the degree of pulmonary fibrosis and

pulmonary function test. The role in the evolution and in the clinical manifestations of the lymphatics is probably very important and futures studies are necessaries. Financial support: FAPESP, CNPq.

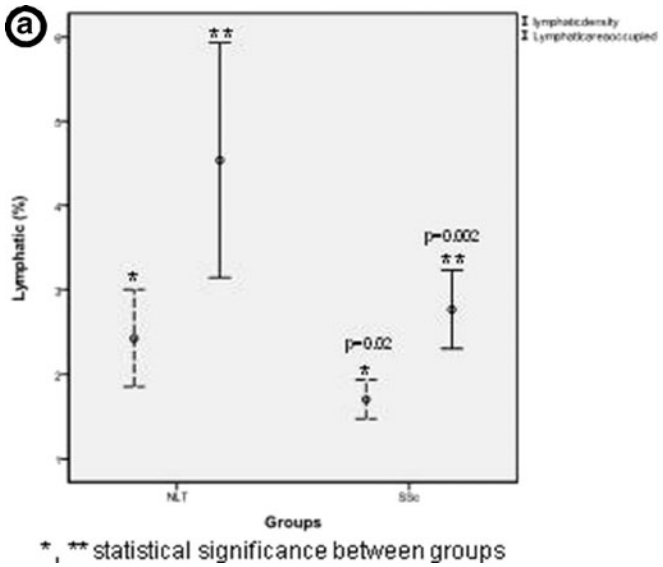

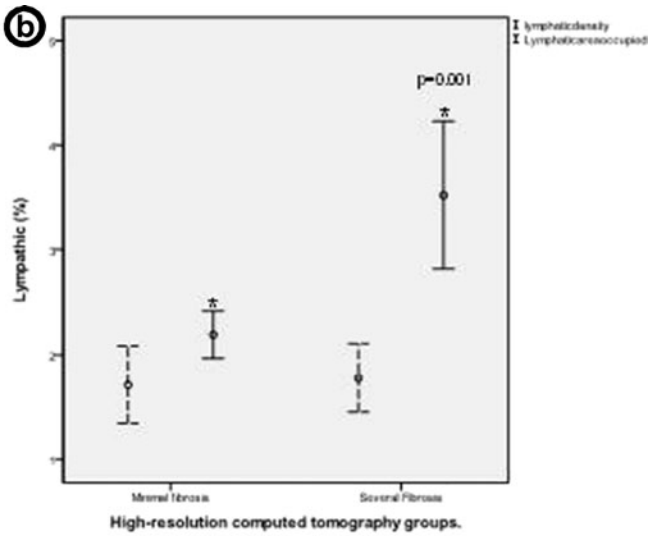

042

Lymphangiogenesis in small cell lung carcinomas: new insights in prognosis

V. Siozopoulou *, A. Batistatou, G. Hardavella, D. Stefanou
*University Hospital of Ioannina, Dept. of Pathology and Cytology, Greece

Objective: Lymphangiogenesis in tumors is involved in lymphatic metastasis. The expression and prognostic impact of D2-40 and LYVE-1 (lymphatic endothelial markers) in small cell lung carcinoma (SCLC) remain vague. We investigated the intratumoral lymphatic microvessel density (ILMVD), the presence of lymphatic invasion (LI) in SCLC and correlated them with clinical parameters.
Method: Immunohistochemical staining for D2-40 and LYVE-1 in 55 SCLC histological samples. ILMVD and LI were assessed and correlated with clinical data.
Results: D2-40 and LYVE-1 were expressed in all specimens while LI was present in 59.6%. ILMVD D2-40&LYVE-1 were associated with stage at diagnosis (p=0.017 and p=0.03, respectively) and LI (p=0.00 and p=0.02, respectively). ILMVD D2-40 was particularly associated with certain target organs for metastasis (liver: p=0.007, adrenals: p=0.002, brain: p=0.007). LI was associated with stage (p=0.00) and all target organs for metastasis (p<0.05).
Conclusion: D2-40, LYVE-1 and LI were highly expressed in SCLC and independently associated with poor patient outcome thus, presenting as potent prognostic factors at the time of diagnosis. In particular, D2-40 seems to associate with certain target organs for metastasis, presenting new prognostic insights. Defining patients' subgroups with poorer prognosis at the time of diagnosis could reinforce the development and application of new targeted therapeutic strategies.

043

Lymphangiogenesis in chronic obstructive pulmonary disease

V. Siozopoulou *, A. Batistatou, G. Hardavella, D. Stefanou
*University Hospital of Ioannina, Dept. of Pathology and Cytology, Greece

Objective: Lymphangiogenesis has been reported to be driven by mediators (e.g. hyaluronic acid) and inflammatory cells (e.g. activated CD11b+macrophages), both commonly observed in chronic obstructive pulmonary desease (COPD). We hypothesized that lymphangiogenesis is part of COPD pathogenesis. In our study we investigated the lymphangiogenetic status in COPD, measuring the lymphatic microvessel density (LMVD) and correlating it with clinical and laboratory parameters.
Method: Lung surgical specimens from 20 smokers [20 COPD-smokers (30% stage 2 GOLD) and 20 non-COPD smokers] with mean age 62.6 years (range 38–82) were immunohistochemically stained for D2-40 and LYVE-1, two selective lymphatic endothelial markers. Calculation of LMVD was performed and correlation with clinical and spirometric data followed.

Results: D2-40 and LYVE-1 were expressed in all specimens, with higher LMVD expression in COPD-smokers (p= 0.00). D2-40 and LYVE-1 LMVD were associated with the presence of COPD ($x2$=20, p<0.001) and disease severity (GOLD classification) (p<0.001).
Conclusion: D2-40 and LYVE-1 were highly expressed in COPD specimens in comparison with samples from non-COPD smokers and associated with clinical and spirometric data. Our results report for the first time the presence of newly formed lymphatic vessels in COPD, thus providing a novel insight in the pathogenesis of COPD including lymphangiogenesis.

044

Epidermal growth factor receptor mutations in different histological types of non-small cell lung carcinoma in Bulgarian patients

Y. Slavova *, S. Bichev, D. Marinova, I. Kremenski
*UHPD, Dept. of Pathology, Sofia, Bulgaria

Objective: Some epidermal growth factor receptor (EGFR) mutations in non-small cell lung carcinoma (NSCLC) correlate with positive response to treatment with tyrosine kinase inhibitors (TKI).
Method: Tissue specimens from 387 patients with NSCLC in III and IV stage were analyzed. DNA was extracted from paraffin embedded tissues and analyzed for TKI activating mutations in EGFR gene by (1) high-resolution melting technology and subsequent sequencing of aberrant profiles—73 patients, or (2) quantitative polymerase chain reaction based on Scorpions technology-314 patients.
Results: From all examined patients (n=387, me$n$=265, wome$n$=122), 35 (9.04%) were positive for TKI activating mutations of EGFR: me$n$=10, 3.8%; wome$n$=25, 20.5%. From 172 squamous cell carcinomas 8 were positive—4.65%. From 179 adenocarcinomas 24 were positive—13.4%. From other types of NSCLCs, one adenosquamous carcinoma was positive. From the positive patients—never smokers were 16 (45.7%), ex-smokers—12 (34.3%), smokers—7 (20%). Most positive patients were with grade 2 tumors (15, 42.9%). There were 24 patients with deletions in 19th exon, 10 patients with L858R point mutation in 21st exon, 1 patient with L861T point mutation in 21st exon.
Conclusion: The TKI activating mutations of EGFR are more frequent in women, in adenocarcinomas, in never smokers.

045

Immunohistochemical detection of estrogen receptor in lung carcinomas using monoclonal antibodies to estrogen receptor alpha

B. Spaulding *, K. Oftebro, T. Phillips, P. McArthur, G. Pace
*Dako North America, Dept. of Biomarkers, Carpinteria, USA

Objective: Estrogen receptor alpha (ERα) expression has been reported in non-small cell lung carcinoma (NSCLC), which is an important consideration in the differential diagnosis of lung versus metastatic breast cancer. However, variable positivity rates of ERα expression in NSCLC have been reported. In this study we evaluated ERα expression in NSCLC using three anti-ERα antibodies in IHC protocols which were benchmarked for sensitivity against the clinically validated ER/PR pharmDx™ Kit.
Method: Formalin-fixed, paraffin-embedded (FFPE) specimens from NSCLC and breast carcinoma tissue blocks were immunostained using monoclonal anti-ERα clones 6F11, SP1, and 1D5. The IHC protocol for each clone was optimized to the sensitivity of the Dako ER/PR pharmDx Kit. The percent of tumor cells with positively staining nuclei was recorded and specimens were considered ER positive if ≥1% of tumor nuclei were immunoreactive.
Results: ERα expression was demonstrated in up to 19% of the NSCLCs tested. The difference in the positivity rates in NSCLCs for the different clones and accompanying detection methods ranged from 15% for SP1 to 19% for clones 6F11 and 1D5.
Conclusion: In this study we demonstrated that ERα expression can be detected in lung carcinoma using highly sensitive detection systems, irrespective of the monoclonal antibody used.

046

Pulmonary involvement of collagen vascular disease and rheumatoid arthritis: hints and pitfalls

E. Stacher *, F. Fuerst, S. Kielhauser, W. Graninger, H. Popper
*Graz, Austria

Objective: Pulmonary involvement of collagen vascular diseases (CVD) and rheumatoid arthritis (RA) may ultimately lead to fibrosis and pulmonary hypertension. It sometimes precedes the onset of the underlying disease. The histomorphological appearance is heterogeneous, commonly with mixed patterns of interstitial pneumonias. The aim of our study is to correlate clinical and laboratory findings with a histological diagnosis suggestive of a pulmonary involvement.
Method: A total of 67 cases of pulmonary biopsies with histologically suspected involvement lacking clinical information at diagnosis were compared retrospectively with clinicolaboratory data. Re-evaluation of the slides focused on features such as fibrosis, inflammatory infiltration, alveolar hemorrhage, vasculitis, vascular changes consistent with pulmonary hypertension, granulomas, patterns of interstitial pneumonia.
Results: The prevalent feature observed was a mixture of different interstitial pneumonias combined with lymphocytic cell infiltrations with or without epithelial destruction. A total of 14 cases proved to be having pulmonary involve-

ment of an underlying CVD (preceding clinical presentation in five cases) and 26 due to RA (preceding in nine cases).
Conclusion: Pathologists should be aware of the variety of histological findings encountered in pulmonary involvement of CVD/RA with some strongly indicative features. Clinicians should carefully evaluate the pathologic report, because it may help earlier detection and treatment of the underlying disease.

047

Diagnostic value of brush biopsy in suspected bronchial carcinoma and correlation with biopsy in lung lesions

I. Stojanovic *
*University Clinical Center Nis, Dept. of Pathology, Serbia

Objective: Lung cancer is on of the most frequent malignancies. It is usually fatal and often affects middle age and old age group. Cytological examination of the cells and tissue biopsy play key role in its diagnosis. The objective of the study was to evaluate the efficacy of bronchial brushing cytology and its correlation with the biopsy.
Method: A total of 60 patients with bronchial carcinoma were studied by bronchial brushing and bronchial biopsy. In 30 patients, cancer was diagnosed by biopsy and brushing. In 30 patients, biopsy was negative, but brushing was positive, and cancer was diagnosed. The commonest tumors were squamous cell carcinoma and small cell carcinoma.
Results: Brush biopsy was positive in 69%, and 58% patients had positive biopsy. When the methods of examination were combined, the diagnosis could be established in 90% of the patients. Those methods increase the diagnostic sensitivity in lung tumors.
Conclusion: It is concluded from this study that brush cytology provided quick results as compared to bronchial biopsy. If cytology reveals atypical cells then biopsy for confirmation and clinical correlation is necessary.

048

Flow cytometric assessment of TNFa in alveolar macrophages using multiparametric analysis in patients with bronchial and interstitial lung diseases

E. Stránská *, P. Manďáková, M. Vašáková, R. Matěj
*University Hospital Motol, UPMM, Praha, Czech Republic

Objective: Alveolar macrophages (AMs) contribute to the pathogenesis of different lung diseases by producing proinflammatory cytokines. We examined the expression of tumor necrosis factor alpha (TNFa) in samples of bronchoalveolar lavage fluid (BALF) in two groups: patients with predominantly bronchial and interstitial lung diseases.
Method: TNFa production was assessed in BALF obtained from 43 patients: 13 with predominantly bronchial and 30 with interstitial lung diseases. Flow cytomeric detection of AMs was simplified by using multiparametric analysis, combination of optical parameters and expression of CD14 and CD45. Along with the percentage of TNFa production, the ratio of median fluorescence intensity (MFI) of AMs stained with anti-TNFa antibody and isotype control was calculated.
Results: Mean TNFa production in the patients with bronchial diseases was 18.75%, MFI ratio 3.18 and in the group of patients suffered by interstitial lung diseases 26.75% and MFI ratio 5.83.
Conclusion: Primary data indicate higher TNFa production in patients with interstitial lung diseases comparing to the group with diseases predominantly affecting bronchial structures. However, more data and detailed stratification within the groups of patients are needed for deeper statistical analysis of TNFa production importance in different lung diseases. Supported by IGA MZ NS/10423-3, Research project VZ FNM 00000064203.

049

Prognostic value of immunohistochemical expression of VEGF, MMP-9 and EGFR in lung adenocarcinoma

L. Tadic Latinovic *, Z. Eri, S. Knezevic Usaj, M. Panjkovic
*Clinical Centar Banja Luka, Dept. of Pathology, Bosnia and Herzegovina

Objective: Angiogenesis of tumor tissue represents key step for tumor growth, processes of invasion and metastasing. The aims of this study were to determine the prognostic value of VEGF, MMP-9 and EGFR in operable lung adenocarcinomas.
Method: In this study, 107 patients with operable lung adenocarcinoma were examined and follow-up informations for 5 years were included. Expressions of VEGF, EGFR and MMP-9 have been determined in specimens taken from material after surgical resection. No adjuvant therapy was given prior surgery. We investigated immunohistochemical expression of VEGF MMP-9 and EGFR in paraffin- embedded tissue specimens. VEGF and MMP-9 expression in tumor cells were assessed by: percentage of stained area, intensity staining and final score (product of area and intensity). EGFR expression in tumor cells was assessed by intensity of membranous positivity and percentage of stained cells.
Results: Log rank analysis showed significant association with poor survival by higher disease stage ($p=0.022$), high EGFR expression in tumor cells ($p=0.0056$) and high MMP-9 expression in tumor cells ($p=0.0002$). VEGF expression in tumor cells was not prognostic factor for survival time ($p=0.114$).
Conclusion: Important prognostic factor for lung adenocarcinomas is pathological stage and new biomarkers could be useful for the evaluation of the prognostic value in lung adenocarcinoma.

050

Endobronchial metastasis of renal cell carcinoma: case report

S. Toru *, I.H. Ozbudak, O. Ozbudak, A. Sarper, G. Ozbilim
*Akdeniz Medical School, Dept. of Pathology, Antalya, Turkey

Objective: Endobronchial metastasis (EBM) from non-pulmonary carcinoma is uncommon. The incidence is 2–5% in autopsy series. The most common extrathoracic malignancies associated with EBM are breast, renal and colorectal carcinomas.
Results: Herein we report a 65-year-old woman who had undergone a left nephrectomy 6 years ago, admitted to the hospital with a 2-month history of dispnea and hemoptysis. Computed tomography of the thorax revealed multiple mass in the left lung, enlarged hiler and mediastinal lymph nodes. Bronchoscope demonstrated an endobronchial tumor occluding the entrance to the left upper bronchus. Under general anesthesia, most of the tumor was removed. In light microscopy clear cell malign epithelial tumor was seen. Tumor cells are uniform ovoid with a clear cytoplasm and abundant vascular structures scattered within the tumor. Tumor cells are diffusely positive with CK 18, Vimentin, CD 10 and negative with CK7 and TTF-1. This case is reported as endobronchial metastasis of renal cell carcinoma.
Conclusion: Although pulmonary metastases from extrapulmonary malignancies are common, endobronchial invasion has been reported rarely. Since bronchoscopic examination is not performed routinely to all patients presenting with pulmonary metastasis and CT is not always able to demonstrate luminal lesions. So it is possible that EBM is underdiagnosed.

051

Angiogenesis of lung squamous cell carcinoma, depending of localization in bronchial tree

L. Vuckovic *, E. Zvrko, T. Nenezic
*Clinical Center of Montenegro, Dept. of Pathology, Pogorica, Montenegro

Objective: Squamous carcinoma of the lung is one of the most frequent malignant tumours. The most important factor that influences prognosis is stage of disease. Also, patients in the same stage have different survival period, so we have to continue with investigation of new prognostic factors.
Method: We investigated density of blood vessels (angiogenesis) in squamous carcinoma, according to localization in bronchial tree. We analyzed 120 patients in stages: I, II and IIIa. All patients were divided in groups, according to localization in right or left lung, and according to part of bronchial tree where carcinoma rised (principal, lobar, segmental or peripheral branches of bronchial tree).
Results: Statistical analysis showed that there was not statistical significance in number of blood vessels in groups of patients with carcinoma of left or right lung. There was statistical significance in density of blood vessels depending of localization in bronchial tree. The highest density of blood vessels was in carcinomas from principal bronchus, and the lowest density was from peripheral parts of lung.
Conclusion: Angiogenesis is important part of cancerogenesis, which influences prognosis. We can suggest that localization of carcinoma in bronchial tree has influence on process of angiogenesis.

052

Expression of cadherins in advanced non-small cell lung cancer: its relation with brain metastasis

J.-Y. Yoo *
*St. Vincent Hospital, Dept. of Pathology, Suwon, Republic of Korea

Objective: Non-small cell lung cancer (NSCLC) comprises 75–85% of all lung cancer, and approximately 25% of patients with NSCLC will develop brain metastasis. It is still unclear that which patient will develop this complication. Metastasis is closely associated with cellular properties, including cell-to-cell adhesion. Cadherins are a multifamily of transmembranous, cell-cell adhesion molecules and selectively bind to an identical molecule in a neighboring cell. The objectives of this study were to investigate the role of cadherins in the brain metastasis.
Method: Advanced NSCLCs (n=71) with (n=40) and without (n=31) brain metastasis were analyzed for E-cadherin, N-cadherin and H-cadherin by immunohistochemistry.
Results: E-cadherin was expressed in 68 samples (96%): 38/40 (95%) with and 30/31 (97%) without brain metastasis, N-cadherin in 17 tumors (24%): 11/40 (28%) with and 6/31 (19%) without brain metastasis, and H-cadherin in 57 samples (80%): 37/40 (93%) with and 20/31 (65%) without brain metastasis. No association was established among the expressions of E-cadherin, N-cadherin and H-cadherin. Brain metastasis was significantly correlated with H-cadherin expression (p=0.004).
Conclusion: H-cadherin may play a role in the development of brain metastasis in patients with advanced NSCLC and maybe a useful marker for identifying patients who are at high risk for brain metastasis.

053

Prognostic discriminants of carbonic anhydrase isoforms IX and XII in non-small cell lung cancer (NSCLC)

M. Ilie *
*CHU de Nice, Hôpital Pasteur, Laboratoire de Pathologie, France

We recently demonstrated that high CAIX expression was correlated with poor outcome and high CAXII expression was associated to better survival in NSCLC. Although CAIX and CAXII are regulated by hypoxia, we further analysed their intriguing role in tumour progression by assessing the impact on survival of both proteins in the same population of NSCLC.
Method: TMA-immunohistochemistry analysis was used to study CAIX and CAXII expression in 552 resectable NSCLC. Immunohistochemical data were correlated with clinicopathological variables and patients outcome.
Results: Low expression was present in 388/552 tumours (70%). High CAIX with low CAXII expression was noted in 60/552 (11%) cases. High CAXII with low CAIX expression was present in 87/552 (16%). 17 tumours (3%) co-expressed both proteins. CAIX and CAXII expression sub-groups correlated to smoking status (P=0.013), tumour type (P<0.0001), and tumour grade (P=0.011). In univariate and multivariate analyses, high CAIX and low CAXII expression predicted poor cumulated rate of relapse (CIR) (P<0.0001) and overall survival (OS) (P<0.0001).
Conclusion: CAIX and CAXII expression allowed the stratification of patients into groups with different CIR and OS rates. High CAIX and low CAXII expression was associated with an aggressive phenotype. Altogether, these results call for taking into consideration the CA isoform profile for effective anti-cancer treatments.

Monday, 29 August 2011, 09.30–10.30 and 16.30–17.00, Hall 5

PS-07 Poster Session Cytopathology

001

An audit of diagnostic rates of EBUS-TBNAs over a 2-year period: the Beaumont experience

C. Beggan *, C. Schilling, D. Royston
*Carrickmacross, Ireland

Objective: Endobronchial ultrasound-guided transbronchial needle aspiration (EBUS-TBNA) is a minimally invasive procedure, utilised for the diagnosis and staging of cases of pulmonary malignancy. We aim to examine the diagnostic yield of this investigation over 2 years.
Method: All cases of EBUS-TBNA over 2 years were examined for: adequacy, diagnostic rates, diagnoses, previous bronchoscopy and attendance by laboratory staff.
Results: 2009: 70% were adequate. Of these, 60% were malignant, 4% suspicious and 36% negative. Malignant diagnoses included NSCLC (26%), adenocarcinoma (27%), squamous cell carcinoma (17%), small cell carcinoma (20%) and metastatic carcinoma (10%) 2010: 74% were adequate. Of these, 50% were malignant, 3% suspicious and 47% negative. Malignant diagnoses included NSLC (8%), adenocarcinoma (41%), squamous cell carcinoma (23%) and metastatic carcinoma (10%). We also compared adequacy depending on whether laboratory staff were present at the procedure. We found that the adequacy rates were improved by lab staff attendance from 61–91% and 71–81%.
Conclusion: EBUS-TBNA is a new minimally invasive procedure introduced in our hospital in 2009 to assist in the diagnosis and staging of pulmonary malignancies. The likelihood of obtaining an adequate specimen was improved by the attendance of laboratory staff at the time of the procedure. We recommend that all EBUS-TBNA procedures are attended by laboratory staff to improve diagnostic yields.

002

Fine-needle biopsy of suspicious parathyroid lesions

R. Ivanova *, R. Kovacheva, A. Shinkov
*University Hospital of Endocrinology, Lab. of Pathomorphology, Sofia, Bulgaria

Objective: In the clinical practice parathyroid lesions are rarely investigated by ultrasound-guided fine needle biopsy and cytology. The aim of this study was to analyze the diagnostic accuracy of fine-needle cytology of suspicious parathyroid lesions.
Method: For a period of 5 years, 50 patients with clinical data for hyperparathyroidism or incidentally found extra-thyroid lesions (44 male, 6 female, mean age 53.3± 14.6 years) were selected for fine-needle biopsy under echographic control. A cyto-histological correlation was done in 16 cases.
Results: The analysis of cytological diagnosis found: a positive diagnosis in 7 cases (14%), suspicious for parathyroid lesion in 30 (60%), negative (lymph node) in 1 (2%) and unsatisfactory in 12 cases (24%). Most of the cytological smears showed small cellularity of single or small groups of epithelial cells with naked nuclei, round shaped and with stippled chromatin, absence of colloid and numerous blood cells. Only in one case was there a marked cellularity, numerous dissociated cells and clusters of cells with characterictic nuclei features and pleomorphism. The histological verification showed the presence of parathyroid adenoma in 15 cases and parathyroid carcinoma in 1 case.
Conclusion: The cytological diagnosis of parathyroid lesions is difficult, mainly for the scant cellularity of the smears. The recognition of the typical cytomorphological features might improve the accuracy of the cytological diagnosis of parathyroid lesions.

003

The analysis of fine needle aspiration cytology in children and adolescence: a 10-year experience in a single institution

E.-J. Jang *, A.-N. Seo, Y.-K. Bae, S.-Y. Kwon, H.-R. Jung, J.-Y. Park
*Kyungpook National University, Dept. of Pathology, Daegu, Republic of Korea

Objective: The purpose of this study was to determine the disease distribution in children and adolescence by FNA.
Method: The authors have reviewed cases of FNA in patients under 20 years old during the 10-year period from 1999 to 2009. The authors reviewed following biopsy.
Results: Out of total 909 cases, 405 cases were boys and 504 cases were girls. The mean age was 14.6 years. According to the diagnosis of FNA, 90.9% of cases were benign, 2% were atypical, 2.6% were malignant disease and 4.5% were inadequate specimens. The most common disease was benign reactive lymphoid hyperplasia, followed by nodular hyperplasia of thyroid, necrotizing lymphadenitis and chronic granulomatous inflammation. In 183 cases, excisional biopsy was performed and the diagnostic accuracy was 85% and sensitivity and specificity were 60% and 97%.
Conclusion: We reviewed 909 cases of FNA. The most common sites were lymph node and thyroid. The most common disease in lymph node and thyroid was benign reactive lymphoid hyperplasia and nodular hyperplasia. Compared to adult, malignant disease was occupied at a very low proportion. Most of the diseases was a benign lesion with high specificity. It is a good screening test for benign lesion reducing unnecessary tissue biopsy in children and adolescence.

004

Study of p16/Ki67 on cervical cytology

I. Marquina *, C. Cabezón, I. Esteban, A. Navarro, S. Salinas, E. Ruiz, P. Domínguez
*Infanta Sofía Hospital, Dept. de Anatomía Patológica, San Sebastián de Los Reyes, Spain

Objective: Association between p16 overexpression in cervical dysplasia and transforming activity of E7 oncoprotein of high-risk human papilloma virus (HPV) has been demonstrated. Therefore, p16 overexpression can be regarded as a substitute marker of the E7-mediated inactivation of the tumor-suppressor function of the retinoblastoma protein (pRb). Functional inactivation of pRb produces genetic instability and malignant transformation in cells with capability of DNA replication. In normal physiological conditions, the expression of a protein with tumour-supressive function and the expression of a proliferation marker exclude each other, so immunocitochemistry can be used to detect coexpression of p16 and Ki67 in cells with deregulated cell cycle in cervical cytology specimens, unrelated to morphological parameters. The presence of one or more double-immunoreactive cells may be used as an indicator of underlying CIN.
Method: We present a descriptive study of 195 cases of cervical cytology (ThinPrep®) with immunocytochemical study of p16/Ki67 (CINtec® PLUS), detection of HPV and cervical biopsy.
Conclusion: Coexpression of p16 and Ki67 could be used to detect cervical lesions that might progress to higher grade lesions or to malignant transformation. Further studies are needed to provide more information.

005

The poor man's cell block

F. Mayall *
*Musgrove Park Hospital, Dept. of Histopathology, Taunton, UK

Objective: We describe a simple method for making cell blocks from fine needle aspiration cytology specimens that we refer to as 'The Poor Man's Cell Block.'
Method: Figure 1 demonstrates the main steps in the preparation of a vapour fixed cell block: (a) The fine needle aspiration material is expelled to form a blob; (b) The universal container is left inverted for at least 6 h to allow the material to fix in vapour from a bung of formalin soaked tissue paper; (c) The material is now solid; (d) The lid is flooded with a small amount of formalin so as to help gently break the 'limpet' suction; (e) The solid cell block can be picked up, being careful not to let it dry out; (f) The specimen should be wrapped in tissue paper for processing; (g) H&E section showing the low-power appearances and high-power detail (metastatic breast carcinoma); (h) Low-power appearances and high-power detail of a cytokeratin 7 immunostain showing that the cells are densely distributed in the cell block.
Results: This method is simple and requires no special reagents or equipment. It produces high-quality cell blocks.
Conclusion: The full method has been published: *J Clin Pathol* 2010;63:837–838. doi:10.1136/jcp.2010.078410.

006

Gelatin foam cell blocks made from cytology fluid specimens

F. Mayall *
*Musgrove Park Hospital, Dept. of Histopathology, Taunton, UK

Objective: We describe a simple method of preparing cell blocks from fluids submitted for cytology using croutons of gelatin foam surgical dressing material.

Method: The method is set out in Figure 1. 1A: Residual cytology fluid sample after material has been taken for smear preparation. 1B: The sample is centrifuged and the supernatant is removed. 1 C: Small blocks of gelatin foam are cut from a sheet of dressing material. 1D: Foam absorbs the fluid to form a solid sample. 1E: The solid cell block is wrapped in tissue paper for processing. 1 F: An H&E section; the wall of the gelatin bubbles are deeply eosinophilic. 1 G: High power H&E detail, together with TTF1 nuclear staining and CK7 cytoplasmic staining of adenocarcinoma cells.

Results: This method is quicker than the agar method that we previously used and yields less variable results.

Conclusion: The full method has been published: *J Clin Pathol*. doi:10.1136/jcp.2010.088542

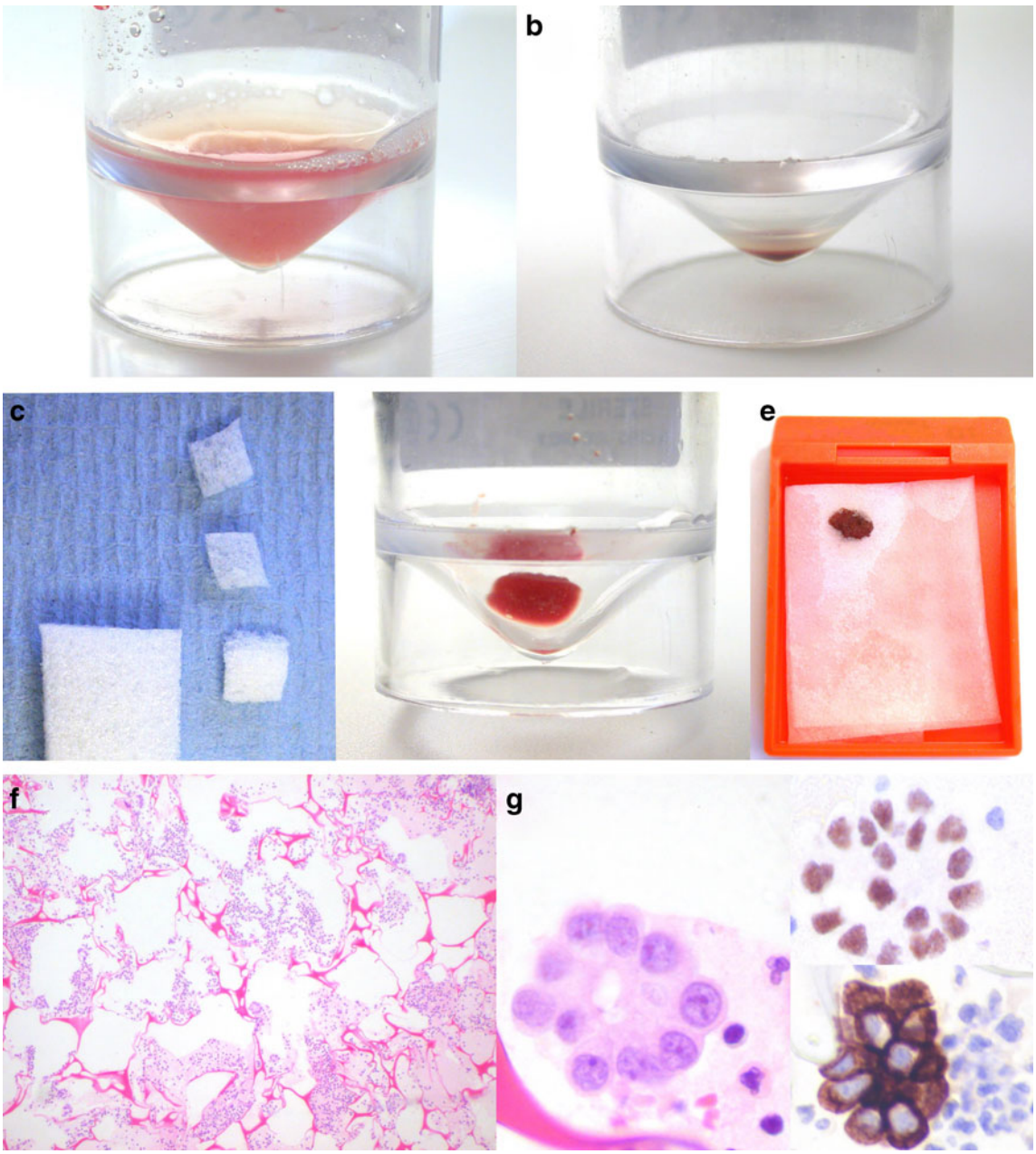

007

FNAB results of solid thyroid nodules: an institutional experience

E. E. Pala *, U. Bayol, O. Akman, C. Akdeniz, I. Gokcol Erdogan
*Tepecik Training and Research, Dept. of Pathology, Izmir, Turkey

Objective: Though overall results of the fine needle aspiration biopsy (FNAB) of solid thyroid nodules are satisfactory, the ones representing the gray zone lesions such as neoplasms, adenomas and reactive hyperplasias have always been problematic. Especially in rutine practice to avoid overdiagnosis, new, reproducible classifications are recommended.
Method: As an institude still prefering the conventional reporting systems, we have reviewed our data of the thyroid FNABs. We have chosen the histologically confirmed 139 cases with initial diagnosis of malignant, suspicious for malignancy and neoplasia on FNAB of solid thyroid masses for the study.
Results: A total of 13 of 17 malignant FNABs were carcinomas; 2 of them were adenomas, 1 adenomatous hyperplasia and 1 thyroiditis. There were 30 of the 86 suspicious cytologies represented that were carcinomas, while were 18 adenomas, 23 hyperplasias, 14 thyroiditis and one follicular neoplasia. Nine of 31 cytologic neoplasias were carcinomas on histology, 14 adenomas, 4 hyperplasias and 4 thyroiditis. Only one histologically malignant case was misdiagnosed as benign cytologically in our data.
Conclusion: Our instutitional experience of thyroid FNAB seems quite reliable with a high diagnostic accuracy.

008

Pleural effusion cytology in a girl with mediastinal mass: case report

L. Tadic Latinovic *, Z. Eri, M. Panjkovic, S. Knezevic Usaj, M. Stanetic
*Clinical Centar Banja Luka, Dept. of Pathology, Bosnia and Herzegovina

Objective: This study describes the case of a 24-year-old female who had 1.5 months history of fever, night sweats, cough and dyspnea. Physical examination was negative: no lymphadenopathy or hepatomegaly was found. Radiographs of the chest showed bilateral pleural effusion and large mediastinal mass. CT scan of the chest revealed a heterogeneous mass measuring 7×6 cm in the upper and middle mediastinum.
Method: For pleural effusion, direct smear was performed using the conventional staining with Giemsa dye. Cytologically in pleural effusion smear is found a mixed population of lymphocytes neutrophils, eosinophils and large atypical mononuclear and multinuclear cells consistent with Reed–Sternberg cells. Surgical specimen of mediastinal mass was evaluated on formalin fixed, paraffin embedded and HE stained slices. Histologyc finding was tumor tissue composed of frequent lacunar cells and diagnostic RS cells. Background infiltrate was admixture of small lymphocytes, eosinophils, neutrophils, plasma cells and macrophages. The classic RS cells had a characteristic immunophenotype CD 15+ and CD30+. Lympoid tissue was divided with marked collagen bands into circumscribed nodules.
Results: Biopsy of the mediastinal mass revealed Hodgkin's disease—nodular sclerosis type.
Conclusion: Hodgkin's disease—nodular sclerosis type—is more likely to occur in young women and involves mediastinum and cervical lymph nodes more frequently.

009

Leiomyosarcoma of vena cava diagnosed by EUS-guided FNA cytology

T. Labiano *
*University Clinic of Navarra, Dept. of Pathology, Pamplona, Spain

Leiomyosarcoma of inferior vena cava (LIVC) is an extremely rare malignancy with poor prognosis. Generally diagnosis is made after surgical resection. We describe a case of a 51-year-old woman admitted to the hospital with 2 months history of abdominal pain with a progressive increase of the abdominal perimeter. The patient developed asthenia, edema of lower limbs, mild dyspnea and weight gain. An abdominal ultrasound and angio-CT demonstrated a solid, heterogeneous, and vascularized intraluminal mass, dependent on the wall of the inferior vena cava. The mass extended from the right atrium to the level of the renal veins. EUS-FNA was performed with needles of 25-gauge with onsite cytopathologist to assess specimen adequacy. Air-dried smears were evaluated at the endoscopic room. The rest of the slides were alcohol fixed and Papanicolau stained. A cellblock was obtained. The tumor was made of groups or fascicles of atypical cells with basophilic cytoplasm and hyperchromatic, elongated nuclei with blunt "cigar-shaped" ends. Necrosis and occasional mitotic figures were found. Tumor showed intense cytoplasmic immunoreactivity with muscle-specific actin, smooth muscle myosin, and caldesmon. FLI-1 and CD-31 were negative. This case stresses the usefulness of EUS-guided FNA cytology for the non-invasive and accurate.

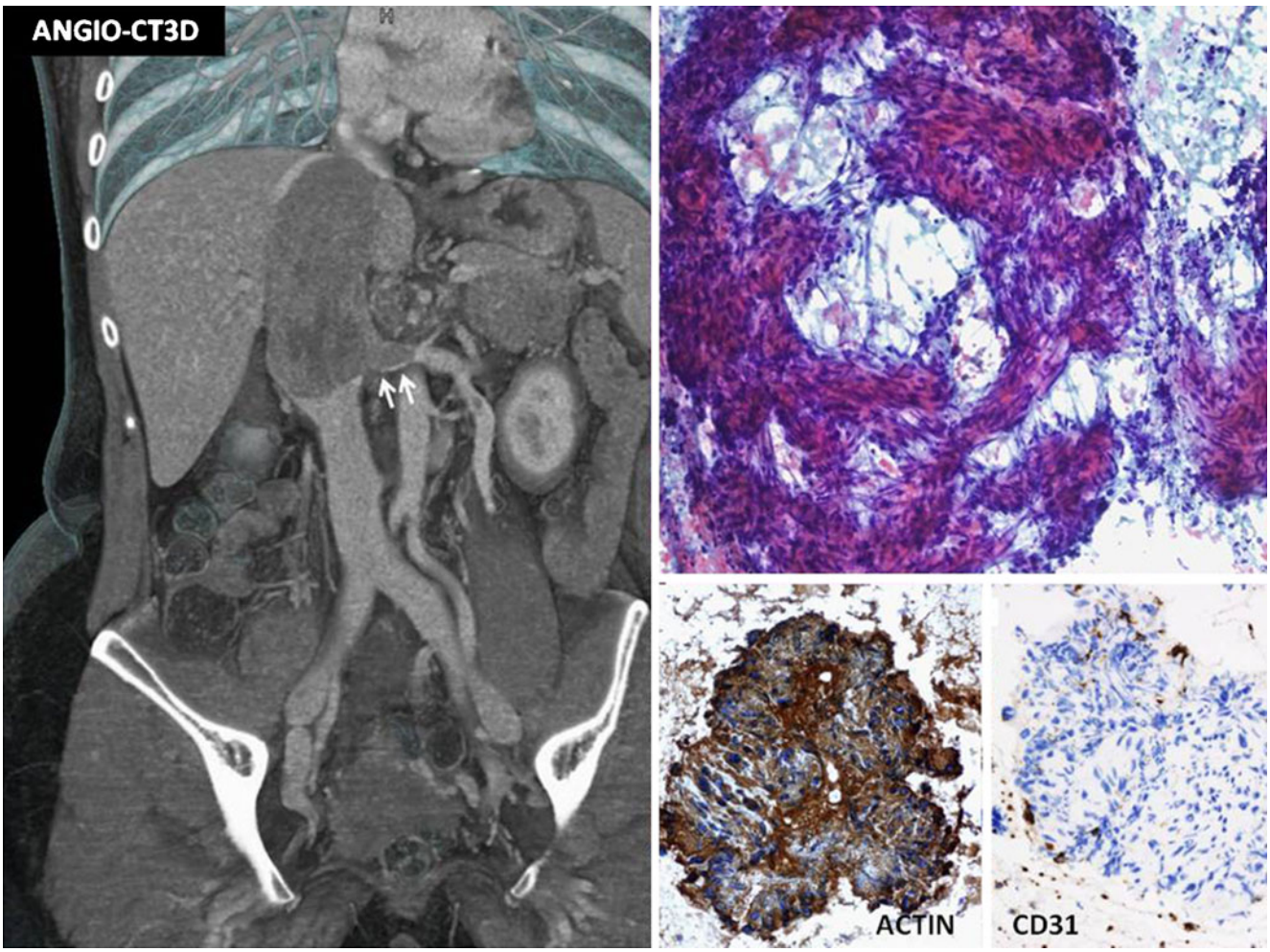

Monday, 29 August 2011, 09.30–10.30 and 16.30–17.00, Hall 5

PS-08 Poster Session Digestive Diseases Pathology

001

Morphological and immunophenotypic esophageal mucosa characterization in children with eosinophilic esophagitis: what contribution to the differential diagnosis with gastroesophageal reflux disease?

A. Alves *, A.M. Palha, M. Matos, A. I. Lopes
*Hospital de Santa Maria, CHLN, Dept. of Pathology, Lisbon, Portugal

Objective: Eosinophilic esophagitis (EE) is an emerging entity, not always easy to distinguish from gastroesophageal reflux disease (GERD). Rising interest has been given to the identification of markers that enable differential diagnosis. This study aims to provide a morphological and immunohistochemical analysis of esophageal mucosa and assessment of their contribution to the differential diagnosis between EE and GERD in children.

Method: A retrospective study of biopsies from the distal esophageal mucosa: 25 children: 10—EE, 10—GERD and 5—control group (CG). Hematoxylin–eosin, Van Gieson, PAD and immunohistochemistry for tryptase and PGR-2 (eosinophil major basic protein-MBP). Characterization of the distribution and number of eosinophils and mast cells. Evaluation of subepithelial fibrosis.

Results: EE: greater number of intraepithelial eosinophils and mast cells than in GERD; higher density of eosinophils (eight) and eosinophilic microabscesses (four) in the epithelial surface with adjacent loose squamous cells; extracellular deposits of MBP (not observed in GERD). CG: Intraepithelial eosinophils and mast cells were not observed. Elongation of the papillae is more prominent in GERD. Intense subepithelial fibrosis in EE (four) and GERD (one), absent in CG.

Conclusion: The characterization of the pattern of cellular distribution, number of mast cells, MBP and assessment of subepithelial fibrosis may contribute to the differential diagnosis between GERD and EE.

002

Reticulin staining plus Ki67 is a useful combination to confirm histological difficult diagnosis in well differentiated hepatocellular carcinoma HCC

B. Bernal *, M.J. Morandeira
*Universidad de Zaragoza, Dept. de Inmunologia, Spain

Objective: Diagnosis of a well-differentiated hepatocellular carcinoma (HCC) is difficult for young pathologists, particularly in small biopsies and aspiration cytology. The use of reticulin staining has been very helpful to define HCC against other nodules. Abnormal patterns of reticulin staining with reduced trabeculae or under three layers of thick make the diagnosis more complex. Markers such as Ki67 are helpful when used in combination with that stain.
Method: We studied the characteristics of the native liver tumor and tumor recurrence in 12 transplanted patients at the Hospital Clinico Universitario de Zaragoza in a group of 393 liver transplants. We compared in those cases the reticulin pattern, the Ki67 expression and clinical and pathological features.
Results: There were six cases of cancer, cirrhosis and histologically confirmed relapse. Relapses occurred between 219 days and 3,367 days, had a high score in Ki67 similar to primary tumor, and reticulin staining was low or absent in four of the six recurrences.
Conclusion: The study of reticulin staining and Ki67 is a useful combination to confirm the histological diagnosis of a well-differentiated HCC.

003

Gross types of hepatocellular carcinoma are closely related with the effect of arterial embolization, tumor differentiation, glucose uptake and vascular endothelial growth factor expression

K. Furuya *, K. Kito, T. Maeda, T. Kikuchi, Y. Ishimaru, S. Nakamura, H. Miki
*Ehime Prefectural Hospital, Dept. of Pathology, Matsuyama, Japan

Objective: This study aims to demonstrate the relation of gross types of hepatocellular carcinoma (HCC) with the effect of transcatheterial arterial embolization (TAE), [18 F]-fluorodeoxyglucose (FDG) uptake, tumor differentiation, and vascular endothelial growth factor (VEGF) expression.
Method: We enrolled 189 patients with HCC who are treated by hepatic resection from 2003 to 2011. Of these patients, 85 underwent TAE and 104 did not undergo TAE. The patients without TAE were examined by PET/CT. The gross types of HCC were categorized into type 1 (replacing-growth), type 2 (nodular), type 3 (confluent multinodular), and type 4 (massive). We subdivided the nodular type cases into type 2a (macro-subnodular) and type 2b (micro-subnodular: subnodules, ≤6 mm). Since HCC often presents as multiple clones of proliferating nodules, we estimated the dedifferentiation (DD) degree of each clone on the basis of three microscopic findings and added the two highest scores to obtain the DD score.
Results: All parameters including the effect of TAE, DD-score, FDG uptake, and VEGF staining grade by immunohistochemistry in type 2a cases had significantly lower values than those of type 2b and type 3 cases (P=0.001 ~ 0.004).
Conclusion: The proposed gross type categorization of HCC could be useful in daily clinical practice because of its significant relation with TAE efficacy and PET/CT data.

004

BRE score in breast cancer, Gleason score in prostate cancer and tumor budding score in colorectal cancer?

E. Karamitopoulou *, A. Kondi-Pafiti, V. Kölzer, D. Karandrea, K. Gennatas, E. Patsouris, I. Zlobec, A. Lugli
*University of Athens, 1st Dept. of Pathology, Greece

Objective: Tumor budding is linked to adverse prognosis in colorectal cancer (CRC). Our aim was to assess the reproducibility of buds measurement by evaluating 10 high-power fields (HPFs) at the invasive front and to confirm the prognostic value of buds in our setting of CRCs.
Method: Whole tissue sections of 215 CRCs with full clinico-pathological and follow-up information were stained with cytokeratin AE1/AE3. Presence of buds was scored across 10 HPFs at the invasive front by two pathologists and the measurements were correlated to the patient and tumor characteristics.
Results: Inter-observer agreement was excellent (p< 0.0001). Low-, moderate- and high-grade budding were defined as an average of <5 buds (n=78), 5–19 buds (n= 108) and ≥20 buds (n=29) per 10 HPFs, respectively. High-grade budding was associated to a higher tumor grade (p<0.0001), higher TNM-stage (p=0.0003), vascular invasion (p<0.0001), infiltrating tumor border configuration (p<0.0001) and reduced survival (p<0.0001). Multivariable analysis confirmed its independent prognostic effect (p=0.007) when adjusting for TNM-stage and adjuvant therapy.
Conclusion: Using 10 HPFs for evaluating tumor budding has independent prognostic value and shows excellent inter-observer agreement. Like the BRE and Gleason scores in breast and prostate cancers, respectively, tumor budding could be a basis for a prognostic score in CRC.

005

Tumour budding score based on 10 high-power fields (HPFs) is a reliable basis for a standardized scoring system in colorectal cancer

V. Koelzer *, M. Horcic, L. Terraciano, I. Zlobec, A. Lugli
*Universität Bern, Inst. für Pathologie, Switzerland

Objective: Tumour budding is recognized by the Union Internationale Contre le Cancer (UICC) as an additional prognostic factor in colorectal cancer (CRC) but remains unreported in daily diagnostic work due to the absence of a standardized scoring method. This study aims to assess the most reliable and reproducible scoring systems for tumour budding in CRC.
Method: Tumour budding on pancytokeratin-stained whole tissue sections from 105 pT3-4/pN0 patients was scored by two observers using 5 methods: Hase (none-minimal/moderate-severe), Nakamura (none/mild/moderate/severe), Ueno (densest region; 20x; cut-off 10 buds), densest 1 high-power field (1HPF) and 10 densest HPFs (10HPFs).
Results: Agreement was fair for Nakamura (k=0.31) and Hase (k=0.32) and moderate for Ueno (k=0.49). 1HPF and 10HPFs led to strong correlations (r=0.83; r=0.82; p<0.0001) and moderate agreement (ICC: 0.53; 0.46). Only 1HPF and 10HPFs had significant prognostic effects using both observers' scores in multivariate analysis (1HPF: p=0.0017 and p=0.0007; 10HPFs: p< 0.0001 and p=0.0067).
Conclusion: A tumour budding score based on 10HPFs is a promising alternative for assessing this feature; it is reproducible, accounts for heterogeneity and maintains the adverse effect on outcome. Large, multi-centric interobserver studies are necessary to validate this proposed method before tumour budding can be implemented into daily routine.

006

Hirschsprung's disease: role of rectal suction biopsy: data on 216 specimens

M. Z. Rahman *, J. Hannan, S. Islam
*Chittagong Medical College, Dept. of Pathology, Bangladesh

Objective: The diagnosis of Hirschsprung's disease (HD) is dependent on the histological study of rectal ganglion cells, and an open rectal biopsy was the mainstay that required general anaesthesia (GA) and carried risk of postoperative rectal bleeding. Suction rectal biopsy later gained wide acceptance and became the choice as there is no requirement of GA and virtual absence of any complications.
Method: A retrospective review of the histological findings of 216 rectal suction biopsies studied from 2005 to 2009.
Results: There were 143 male and 73 female children. A total of 196 (90.7%) children were within 1 year of age. Among 216 rectal suction biopsies 181 (83.80%) were aganglionic, 27 (12.5%) were ganglionic and 8 (3.7%) were inadequate. Majority of the patients were of less than 1 year of age (94.47%).
Conclusion: The rectal suction biopsy is a bedside procedure, safe, cheap and time-saving. There is a high degree of accuracy, simplicity and absence of complications.

007

Predictive factors of positive circumferential resection margin after radiochemotherapy for rectal cancer: The French randomized trial ACCORD12/0405 PRODIGE 2

A. Rullier *, S. Gourgou-Bourgade, F. Bibeau, C. Chassagne, C. Hennequin, P.-L. Etienne, A. Leroux, J. Berylle, T. Conroy, J.-P. Gepard
*CHU Bordeaux, Dept. of Pathology, France

Objective: Circumferential resection margin (CRM) appears as a new powerful prognostic factor of survival after surgery for rectal cancer. We aimed to evaluate predictive factors of positive CRM following preoperative radiochemotherapy in a French trial.
Method: Patients with rectal cancer were randomized in long course preoperative radiotherapy 45 Gy plus capecitabine versus 50 Gy plus capecitabine and oxaliplatin. Mesorectal excision was performed 6 weeks after treatment. Impact of clinical, pathological and surgical variables on positive CRM (≤ 1 mm) were analysed by multivariate analysis.
Results: Of 587 patients randomized, CRM was recorded in 390 cases and was positive in 8% (30/390). Patients with 50 Gy plus capecitabine and oxaliplatin had a 6% rate of positive CRM while those treated by 45 Gy plus capecitabine had a 10% rate (p=0.128). Independent factors of positive CRM were patients treated by abdominoperineal resection (OR=3.24; p=0.004), tumors with vascular invasion (OR=2.78; p=0.026) and poor histological response (Dworak 0-2) (OR=9.01; p=0.003).
Conclusion: Intensification of neoadjuvant radiochemotherapy trends to decrease the risk of positive CRM after surgery for rectal cancer. Significant predictive factors of positive CRM are related to type of surgery, especially abdominoperineal excision, and poor histological factors.

008

p16INK4a gene product and other cell cycle regulators in metaplasia, dysplasia and adenocarcinoma of Barrett esophagus

P. Stoemmer *, P. Torres-Galea
*Forschungslabor Pathologie, Gemeinschaftspraxis Pathologie, Augsburg, Germany

Objective: p16INK4 is together with p21 and p53 a tumorsuppressor protein playing an important role in cell cycle. The variety of neoplastic and non-neoplastic types of epithelia and their architecture in Barrett esophagus may be associated with it.
Method: Twenty FFPE biopsies of specialized (colonic) Barrett, 20 cases with metaplastic gastric foveolar/cardiac epithelium, and 10 cases of Barrett adenocarcinomas were analysed for the expression and distribution of gene products of p16INK4A, p21, p53.
Results: Non-neoplastic Barrett: Strong expression of p16INK4a in regenerative hyperplastic squamous epithelium. No expression in foveolar cells of esophageal gastric heterotopia. Intestinal-metaplastic cardiaglands show moderate nuclear and cytoplasmic expression. Dysplasia and neoplasia in Barrett: Low p16INK4a positivity in colon-type specialized epithelium of low-grade dysplasia. Moderate positivity in high-grade dysplasia. Most cases indeterminate for dysplasia are p16 negative. Barrett adenocarcinoma: Two patterns of p16INK4a expression in invasive Barrett adenocarcinomas: well-differentiated papillary and tubuloglandular cancers are highly positive and cancers of macroglandular or diffuse pattern or signet-cell-type show negative or low expression.
Conclusion: Transcriptional silencing of the p16 promoter by hypermethylation and augmented concentration of p53 (mutant, inactivated) is an early event in Barrett carcinogenesis, resulting in reduced production of p16INK4a-protein in dysplasia and good differentiated carcinomas. Undifferentiated carcinoma cells of diffuse and signet cell-type lose p16-expression.

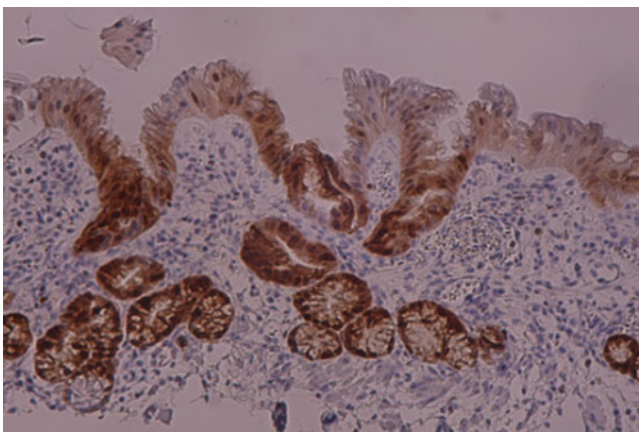

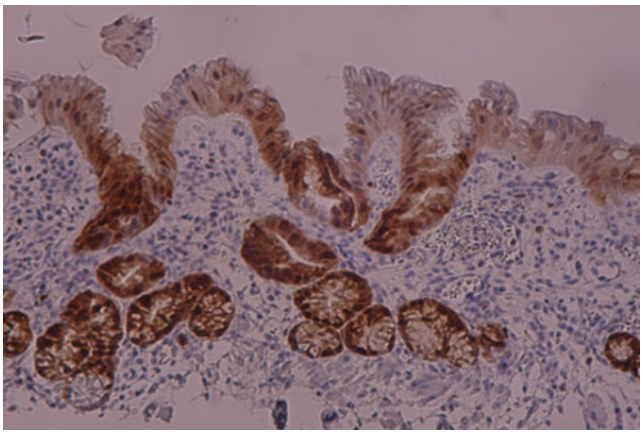

009

Prognostic significance of CD138 immunoexpression in human hepatocellular carcinoma

D. Tiniakos *, M. Paleologou, M. Karanikolas, E. Fatourou, E. Felekouras, E. Antoniou, J. Delladetsima
*University of Athens, Lab. of Histology-Embryology, Greece

Objective: CD138 is a syndecan (transmembrane heparan sulphate proteoglycan) that regulates cell-cell and cell-matrix interactions. CD138 is predominantly expressed in epithelial cells and plasmacytes. CD138 is up-regulated in some carcinomas and down-regulated in others. Limited data is available regarding hepatocellular carcinoma (HCC). We aimed to assess CD138 immunoexpression in human HCC in correlation with clinico-pathological parameters and patient survival.
Method: Immunohistochemistry for CD138 was applied on 58 samples of HCC from 45 patients (mean age 67.6 years, M/F ratio 2.75/1) followed up for 3–92 months (mean 27.6 months). The extent of CD138-specific membranous and cytoplasmic immunostaining was semiquantitavely evaluated.
Results: CD138 membranous immunoexpression was detected in all HCC, while additional cytoplasmic immunostain was seen in 50%. CD138-membranous immunostaining was inversely correlated with tumour grade (p= 0.005) and was absent from intravascular tumour emboli that showed only cytoplasmic CD138 expression. There was no correlation of CD138 immunoexpression with other clinico-pathological parameters. Cox backward stepwise regression analysis showed that increased CD138 cytoplasmic immunostaining was independently associated with decreased overall survival (p=0.049, RR 6.703, 95% CI 1.008–44.582).
Conclusion: Loss of membranous CD138 in HCC appears to be related to tumour dedifferentiation. Increased cyto-

plasmic CD138 immunoexpression may serve as marker of poor prognosis in HCC.

010

Comprehensive morphologic and molecular characterization of murine models of hepatocarcinogenesis and correlation with human hepatocellular tumors

A. Weber *, Y. Böge, L. Frick, F. Böhm, H. Schulze-Bergkamen, M. Heikenwälder
*Universität Zürich, Inst. für Chirug. Pathologie, Switzerland

Objective: We aim to characterize different mouse models by recapitulating different chemically and inflammation-induced etiologies of human hepatocarcinogenesis in order to define which model(s) reflect(s) which aspects of human hepatocarcinogenesis.
Method: In the respective models studied, mice developed hepatocellular carcinoma (HCC) due to: diethylnitrosamine (DEN) treatment; over-expression of lymphotoxin alpha and beta (LT mice); deletion of the anti-apoptotic protein Mcl1 (Mcl-1Dhep mice); transgenic c-myc proto-oncogene, or deletion of TAK1 and NEMO (TAK1LPC-KO). HCC were studied and categorized by immuno-phenotyping, aCGH, gene expression profiling, and Western blot analysis.
Results: Morphology, immuno-phenotype, and genetic changes in HCC were rather uniform in HCC of DEN-treatment and transgenic c-myc mice, but more heterogenous in the other models. Gene expression analyses revealed a mostly homogenous pattern in HCC due to DEN-treatment and transgenic c-myc, respectively, indicating highly proliferative, poorly differentiated tumors, whereas other models revealed heterogenous patterns including low proliferative, highly differentiated tumors.
Conclusion: HCC of the different murine models have different morphologies, immuno-phenotypes, chromosomal alterations and gene expression profiles, allowing to classifiy murine HCC. Hepatocarcinogenesis in LT mice and Mcl-1Dhep mice is closest to human hepatocarcinogenesis. Comparison with human HCC allows us to identify appropriate molecular targets and mouse models for therapeutic approaches to subtypes of human HCC.

011

To investigate the effect of oral administration with L-arginine, L-NAME and allopurinol in experimental intestinal ischemia/reperfusion (I/R)

G. Agrogiannis *, E. Margaritis, A. Yanni, P. Korkolopoulou, I. Doulamis, E. Patsouris, D. Perrea
*National University of Athens, School of Medicine, Greece

Objective: This study aims to investigate the effect of oral administration with L-arginine, L-NAME and allopurinol in experimental intestinal ischemia/reperfusion (I/R).
Method: One hundred twenty-eight Wistar rats were randomly separated into four groups and subjected to occlusion of superior mesenteric artery for 60 min. Control group did not receive any substance; L-Arg group received per os L-arginine (800 mg/kg), L-NAME group, L-NAME (50 mg/kg) and Allo group, allopurinol (100 mg/kg) in three equal doses. Each group was divided into four subgroups which underwent different durations of reperfusion time (0, 1, 8 and 24 h, respectively). Blood samples were collected and histological examination was performed. Serum nitric oxide (NO) and catalase, intestinal tissue myeloperoxidase (MPO), inducible nitric oxide synthase (iNOS) and nitrotyrosine (NT) were determined.
Results: Allo group exhibited the mildest histological lesions in contrast to L-NAME group which exerted the most severe. MPO was decreased significantly in Allo and L-Arg groups during reperfusion with allopurinol administration. Serum NO and catalase increased in L-NAME group after 24 h. Tissue iNOS activity and NT concentration were the highest in L-Arg group and the lowest in Allo group during the time of reperfusion.
Conclusion: Oral administration with allopurinol exerts strong protective effect on intestinal tissue suffering from I/R better than L-arginine.

012

Gastric schwannoma presented with anemia

G. Agrogiannis *, I. Kostakis, A. Vaiopoulos, N. Kavantzas, G. Kouraklis, E. Patsouris
*National University of Athens, School of Medicine, Greece

Objective: Schwannoma is a rare benign tumor of Schwann cells. In gastrointestinal tract, it is usually found in the stomach, corresponding to 0.2% of gastric tumors and 4% of benign gastric neoplasms. The cases of malignant schwannomas are rare. It is usually asymptomatic, whereas presentation with bleeding, obstruction or palpable mass is rare.
Method: A 49-year-old female presented iron deficiency anemia. Gastroscopy and abdominal CT scan showed a round submucosal tumor in the pylorus of stomach. She underwent wedge resection of the lesion.
Results: The histological examination revealed the presence of a medium-sized submucosal tumor of mesenchymal origin, which was benign (absence of nuclear atypia and high cellularity, mitoses<2/50 HPF) and encapsulated. In immunohistochemical examination of the specimen set the

diagnosis of schwannoma. Stains for c-kit, CD34, desmin and SMA were negative, whereas stains for S100, vimentin and Leu7 were positive.

Conclusion: Schwannomas have a very similar histological image with GISTs, which are more frequent than schannomas, in the hematoxylin and eosin stain. Only the use of the appropriate stains (c-kit, S100, etc.) can set the definitive diagnosis.

013

Evaluation of patients diagnosed with colorectal adenocarcinoma at single-institution in Turkey between 2004 and 2010 with respect to microsatellite instability

F. Aker *, S. Ozkara, B. Sari
*HNTRH, Dept. of Pathology, Istanbul, Turkey

Objective: Hereditary nonpoliposis colorectal cancer (HNPCC) exhibits a high rate of MSI. The comparative studies involving stage and other prognostic parameters demonstrate a better prognosis in the presence of MSI versus colon cancers without MSI.

Method: Our study included 608 cases diagnosed with colorectal adenocarcinoma in our laboratory between 2004 and 2010. The cases were re-evaluated with respect to criteria defined for MSI taking into consideration age, anatomic localization, and histopathologic criteria Immunohistochemical study was performed in appropriate blocks for using MLH-1, MSH-2, MSH-6, and PMS-2.

Results: The specimens were re-evaluated with respect to the histological criteria defined for MSI. Anti-MLH-1, anti-MSH-2, anti-MSH-6, and anti-PMS-2 antibodies were applied to the paraffin blocks of 27 cases which carried the morphological criteria suggestive of DNA repair mutation and having a high Mspath score defined by Jenkins et al. Immunohistochemical study with MLH-1, MSH-2, MSH-6, and PMS-2 for the analysis of mistmach repair was refined using the cases with higher Mspath scores.

Conclusion: In this study, we reviewed the clinical and histopathologic features of 608 cases with colorectal adenocarcinoma diagnosed in our laboratory between 2004 and 2010 and assessed pathologic features in terms of MSI. The results were discussed in view of the literature.

014

Relationship between transforming growth factor-β1 expression and clinicopathological factors in Her2-negative gastric cancers

J. Ananiev *
M. Gulubova, I. Manolova, A. Julianov
*Medical Faculty, Trakia Univer, General and Clinical Pathology, Stara Zagora, Bulgaria

Objective: Gastric cancer is still the most prevalent neoplasia in many countries. Therefore, besides the clinicopathological factors known to be prognostic markers, new independent parameters are being investigated. This study was to investigate the expression of transforming growth factor—β1 (TGF-β1) in HER2/neu negative gastric carcinomas and explore the correlations the clinicopathological characteristics and prognosis of gastric carcinoma.

Method: Specimens from 42 patients who underwent curative resection of gastric cancer were examined for the presence of HER2/neu and TGF-β1 by immunohistochemistry. The correlation between expression of the proteins and patient clinicopathological parameters was evaluated and the prognostic significance of TGF-β1 expression was assessed.

Results: All of the investigated specimens demonstrated HER2/neu-negative status. TGF-β1 protein analyses exhibited predominantly cytoplasmic and membranous immunostaining. After analysis we found that 80% of intestinal gastric cancer specimens have TGF-β1 expression, while in the diffuse type they are 43% (χ^2=4.16; p=0.041). In the final we examined whether TGF-β1 expression were correlated with prognosis. We found that median survival period was 37.03 months (range from 19.8 to 54.3 months) and the patients with TGF-β1 expression had worse prognosis after surgical therapy compared to those without expression of TGF-β1 (p=0.04).

Conclusion: We have shown that TGF-β1 expression in gastric tumour tissue with HER2/neu-negative status is of prognostic relevance in gastric cancer.

015

Morphological characteristics of HER2/neu-amplified gastric carcinomas

M. Bamba *, S. Takemura, K. Fukuda, M. Masuyama, T. Shigematsu, H. Sugihara
*Saiseikai Shiga Hospital, Dept. of Pathology, Ritto, Japan

Objective: Evaluation of HER2/neu amplification and overexpression are not easy because of their intratumoral heterogeneities that are more frequent in gastric carcinomas than in breast carcinomas. In this study, using gastric carcinomas that showed HER2/neu-amplification at least in part, we immunohistochemically analyzed heterogeneities in HER2/neu expression.

Method: This study was based on the analysis of 72 surgically resected gastric carcinoma cases. First, fluorescence in situ hybridization (FISH) was performed in all 77 lesions. Then, H&E and immunohistochemical stainings with the monoclonal antibodies MUC5AC, MUC6, CD10, MUC2, CDX2, HER2/neu and p53 were carried out in the HER2/neu-amplified cancers.

Results: Twelve out of 62 informative cancers were HER2/neu-amplified (19.4%). HER2/neu overexpression was homogeneous in four cancers, heterogeneous in seven cancers and negative in 1 cancer. Seven, five and none of the cancers were differentiated type, mixed differentiated and undifferentiated type and undifferentiated type, respectively. p53 overexpression was diffuse in eight cancers, focal in one cancer and negative in three cancers. Phenotype was intestinal in five cancers, mixed gastric and intestinal in six cancers and null in one cancer.
Conclusion: HER2/neu-amplified gastric carcinomas often showed heterogeneous overexpression for HER2/neu (58.3%) and diffuse overexpression for p53 (66.7%) and did not show pure gastric phenotype or undifferentiated type in the present study.

016

Low-level instability of microsatellite DNA in sporadic colorectal cancers

M. Bialas *, A. Klimkowska, K. Okon, R. Tomaszewska
*Jagiellonian University, Dept. of Pathology, Cracow, Poland

Objective: Microsatellite-unstable tumors can be divided into two distinct phenotypes: MSI- high (MSI-H) and MSI-low (MSI-L). The clinicopathological features of MSI-L cancers are not well defined and its significance remains controversial. However, recent studies support that MSI-L tumors may form a separate entity differing from both MSI-H and MSS ones.
Method: A total of 163 cases of colorectal cancers were assessed for MSI status. Three groups—MSS (n=133), MSI-L (n=15), MSI-H (n=15)—were compared with respect to clinical data, stage, histology, and immunoexpression of MLH1, MSH2, MSH6 and P53.
Results: In comparison to MSS cancers, the MSI-L had larger tumor size, mucinous histology and weak expression of MSH6. Statistically greater number of MSI-L tumors showed LOH for P53 and almost all of them were left-sided contrasting with MSI-H and MSS tumors. More frequent metastases and higher TNM stage as compared with MSI-H tumors indicates for worse pathologic behavior of MSI-L tumors.
Conclusion: The MSI-L category exhibits some different features, which distinguish them not only from MSI-H group but also from MSS tumors. These features may suggest that they are a third distinct group of colorectal cancers.

017

Genotyping of KRAS mutations in Bulgarian patients with colorectal cancer

S. Bichev *, I. Kremensky, A. Savov, S. Hristova
*National Genetic Laboratory, Univeristy Hospital of, Sofia, Bulgaria

Objective: Colorectal cancer (CRC) affects approximately 150,000 people each year. In the past 10 years, numerous biological agents for inhibition of EGF receptor have been developed. Nowadays, it is known that positive response of such inhibitors could be expected if KRAS oncogene is wild type.
Method: A group of 180 patients with CRC were analyzed: 111 of tumors were localized in rectum-sigma, the rest 69 were from colon regions. DNA was extracted from paraffin embedded tissues. All samples were screened by qPCR based on scorpions technology. This allows us to detect 7 somatic mutations in 12th and 13th codons of KRAS gene.
Results: We have found mutations in 46% of our patients; the rest 54% were assessed as wild type. The most common mutations were Gly13Asp, Gly12Val and Gly12Asp. A total of 98% of wild-type samples were adenocarcinomas (mainly of G2 grade); 1 tumor was of mucinous type. A total of 71.43% of KRAS wild-type cases were in IVth stage.
Conclusion: Our data shows KRAS mutated status in 46% of investigated samples which is in concordance with previous publications. Considering the high frequency of KRAS mutations in CRCs, it is mandatory to perform mutational analysis in order to establish better treatment for the patients.

018

Retrospective HER2 testing in gastric cancer biopsy specimens

K. Bjelkenkrantz *, A. Edsjö
*Lab. of Medicine Skåne, Dept of Pathology, Malmö, Sweden

Objective: Anti-Her2-treatment in advanced adenocarcinoma of the stomach and lower esophagus is a new treatment possibility. Only 20% of cancers that are HER2-positive are eligible. HER2 testing can show heterogeneity in the same cancer which makes it important to follow proven standardized procedures in testing (Rüschoff J et al., *Virchows Arch* (2010) 457:299–307.) To prepare for the starting of clinical testing we tried out the methodology on archival material.
Method: A search in the LIS system showed 225 adenocarcinoma cases diagnosed in biopsies between 2005 and 2009. In 59 cases, no diagnostic cancer growth was found and in a few instances the SNOMED coding had been faulty. Three cases could not be finished due to technical difficulties.

Results: There were 28 cases which showed amplification and an additional three cases showed immunostaining 3+ without amplification. In all 31 positive/162—19.1%.
Conclusion: Our experiences with 59 "too small specimens" show that biopsies should be large to allow for reliable testing. We suggest regional testing for these rare cancers.

019

Mutation analysis of KRAS and BRAF on endoscopic biopsy samples of colorectal varcinoma is highly concordant with resection specimens

J.E. Boers*, L. Krol, N. ´t Hart, N. Methorst, A. Knol, C. Prinsen
*Isala, Dept. of Pathology, Zwolle, The Netherlands

Objective: KRAS testing is mandatory if anti-EGFR therapy is considered in patients with metastatic colorectal cancer (CRC). In addition, BRAF mutations seem to be an important negative predictive factor for treatment response. The aim of this study is to establish the concordance of KRAS and BRAF mutational status in paired biopsy and resection specimens of the primary tumor using several analytic methods.
Method: In 126 unselected CRC patients KRAS codon 12/13 and BRAF V600E mutational status was assessed: high resolution melting (HRM); direct sequencing (DS) of the HRM PCR product; Therascreen KRAS assay (DxS, U.K.) and BRAF Pyrosequencing (Therascreen BRAF Pyro Kit, Qiagen, NL) were employed; both assays claim to require less tumor cells in comparison with DS.
Results: In resection specimens, 40 carcinomas were found to be mutated in all three detection methods; concordance with biopsy specimens was 99.2% (HRM), 98.4% (DS) and 97.4% (DxS). BRAF was mutated in 23 (HRM, DS) or 24 (Pyro) resection specimens. Concordance in biopsies was 99.2% (HRM) and 98.4% (DS, Pyro). BRAF V600E and KRAS mutations were mutually exclusive, with incidences of 19% and 33.9%, respectively.
Conclusion: KRAS and BRAF mutational status of endoscopic biopsies and resection specimens of CRC showed a >95% concordance. Endoscopic biopsies can be confidently used for molecular analysis.

020

Intestinal thesaurismosis related to docosahexaenoic acid intake in two siblings with hereditary juvenile polyposis

J. A. Bombi *, B. González, C. Duran, J. M. Turro, C. Llebaria, A. Martinez
*Hospital Clinic Barcelona, Dept. of Pathology, Spain

Objective: Docosahexaenoic acid has been used to prevent malignant transformation in colonic polypomatosis. We report here, two cases of hereditary juvenile polyposis receiving high dosis of docosahexaenoic acid (DHA) leading to intestinal thesaurismosis.
Method: Two 10-year-old siblings diagnosed of hereditary juvenile polyposis recieved a high dose of DHA as dietary supplement following their mother criteria without medical advice. In the follow-up, periodical endoscopies with polypoid resections were performed.
Results: The endoscopic polypectomy specimens were macroscopically brown-coloured mimicking colonic melanosis. Histologically the polyp showed hamartomatous architecture with otherwise typical features of hereditary juvenile polyposis. More interestingly, a dense dark brown intramacrophagic pigment was observed in the mucosa. The deposit was PAS positive but negative for Perls and Orcein stains. Electron microscopy analysis of new biopsies revealed intracytoplasmatic vacuolation in macrophages similar to the deposits of DHA described in mice models.
Conclusion: To our knowledge this is the first human report of DHA thesaurismosis in humans. We have presented the clinical, histological, histochemical and ultrastructural features of this rare condition.

021

Stem cell marker cancer testis antigen (CT 45) expression in colorectal cancer: an immunohistochemical study of 704 patients

J. H. Bräsen *, F. Gieseler, B. Sipos, W. Klapper, H. Kalthoff, W. von Schönfels, G. Klöppel,
C. Schafmayer, R. Lucius, H. Heidebrecht, C. Schrader
*Universitätsklinikum Kiel, Inst. für Pathologie, Germany

Objective: A subset of colorectal cancer derived from stem cells. Cancer testis antigen (CT45) is expressed in immature gonocytes, spermatogonia and also in germ cell tumors. There are only limited data about CT 45 expression in colorectal cancer and no data if the expression in tumor cells has an influence on the clinical course of the disease.
Method: We investigated immunohistochemically embedded tissue from 704 patients with a monoclonal antibody against CT 45 (Ki-A10). The percentage of CT45 expressing cells was quantified according to the following classification: negative, 0% to 25%, 25% to 50%, 50% to 75% and more than 75% positive tumor cells.
Results: The majority of cases were negative (n=633). A total of 71 tumor specimens were CT45 positive. The Kaplan–Meier analysis revealed no significant difference (p=0.11) in the clinical outcome of CT 45 positive and negative cases.
Conclusion: Cancer testis antigen (CT 45) is expressed in a subset of colorectal cancer. The CT 45 expression is no

prognostic factor for the clinical outcome of the disease, but it might have clinical implication for therapy decision of stem cell derived cancer.

022

Primary gastric squamous cell carcinoma in combination with intramucosal adenocarcinoma 48 years following Billroth II surgery: a case report

C. Cacchi *, B. Märkl, C. Haas, G. Jechart, M. Anthuber, H. Arnholdt
*Klinikum Augsburg, Inst. für Pathologie Germany

Objective: Squamous and adenosquamous carcinoma (SCC) of the stomach are rare tumors with unclear pathogeneses. An association between SCC and intestinal-type adenocarcinoma in gastric stump, to date, has not been reported.
Method: Tissue both from biopsy and surgical specimen were formalin fixed, processed and stained with haematoxilin and eosin, Giemsa and periodic acid Schiff. Immunohistochemistry was performed for CK5-6 and p63. For comparison of the different tumor samples, a short tandem repeat (STR) polymorphism analysis was performed.
Results: Herein we describe a report of a male 79-year-old patient with SCC and synchronous intramucosal adenocarcinoma, both of which arose 48 years after a Billroth II (BII) resection for benign stomach ulceration. The patient also exhibited gastritis polyposa cystica (GCP) in the surrounding gastric mucosa.
Conclusion: GCP condition is thought to be a risk factor for the development of gastric adenocarcinoma, even though the results of different experimental models are contradictory. Regardless of the stage, these tumors have always occurred long after the primary surgical intervention. The carcinogenesis of SCC is unclear. Squamous metaplasia of adenocarcinoma, however, seems unlikely.

023

The role of adenomatous polyposis coli protein in prevention of colorectal carcinoma in the APC+/APC1638N mouse model

Z. Cierna *, Z. Adamcikova, V. Zajac, L. Wachsmannova, V. Stevurkova, K. Hainova, V. Holec,
P. Janega, A. Janegova, E. Klincova, P. Babal
*Comenius University, Dept. of Pathology, Bratislava, Slovakia

Objective: Familial adenomatous polyposis (FAP) is an autosomal dominant disease characterised by the presence of hudreds to thousands of benign adenomatous polyps in the large intestine. FAP is a precancerous state leading without therapy inevitably to the development of colorectal carcinoma. Patients with FAP have germline mutations in the adenomatous polyposis coli (APC) gene.
Method: The study included 19 mice: 10 transgenic mice with a germline mutation in APC gene and 9 mice without this mutation. The mice were divided into experimental group treated by oral administration of bacteria *Escherichia coli* expressing the APC gene and control group without therapy. The whole gastrointestinal tract was investigated macroscopically, microscopically and immunohistochemically with the use of polyclonal rabbit antibody against APC protein.
Results: All trangenic mice (n=4) without therapy developed adenomatous polyps in the gastrointestinal tract. Transgenic mice (n=6) treated by oral administration of bacteria expressing the APC gene, developed polyps in 33.3% of cases (n=2). The remaining four mice (66.7%) were without polyp development.
Conclusion: Administration of APC gene expressing bacteria to transgenic mice with mutation in the APC gene leads to reduction in the number of mice developing polyps in gastrointestinal tract. Supported by VEGA 2/5025/27, 2/0081/08 and APVV-0404-07.

024

Gastric carcinoma with rhabdoid features: case report

M.V. Comanescu *, D. Terzea, C. Iosif, C. Ardeleanu
*Victor Babes Institute, Dept. of Pathology, Craiova, Romania

Objective: Gastrointestinal tumors with rhabdoid features are extremely rare (0.1–0.2% of all gastric carcinomas).
Method: The patient, a 61-year-old man, presented in the emergency room with severe GI bleeding, abdominal pain and weight loss, but no mass at palpation. As the bleeding was profuse, emergency laparotomy was performed and a large mass was detected, involving the lesser curvature of the stomach and the pancreas, with invasion to the coeliac trunk.
Results: The initial histopathological report was of malignant fibrous histiocytoma and immunohistochemical evaluation was recommended and the case was sent in consultation to our institute. The histopathologic exam revealed the presence of a massive malignant neoplasia, highly pleomorphic, with spindle and ovoid cells. Immunohistochemistry showed reactivity for vimentin, epithelial membrane antigen and carcinoembryonic antigen, cytokeratin-7 cytokeratin-19, cytokeratin 34BE12. No immunoreactivity was observed for S100, CD117, CDX2, MUC2 and calretinin. Mesothelin and desmin were focally positive. About 35% of cells were Ki67 positive. On the basis of morphological and immunohistochemical findings

a diagnosis of gastric carcinoma with rhabdoid features was issued.

Conclusion: In conclusion, this case is presented to emphasize the importance of recognizing this rare, but highly aggressive entity of the gastrointestinal system.

025

Coexistence of gastric cancer and multiple small gastrointestinal stromal tumors: report of a unique case and review of the literature

H. Trihia *, A. Manousopoulou, D. Condylis, I. Kasselakis, P. Tziakou, P. Dadioti-Arapantoni, I. Lekka
*Metaxa Cancer Hospital, Piraeus, Greece

Objective: The synchronous occurrence of tumours of different histotypes in the same organ has been reported more frequently in the literature. The simultaneous development of adenocarcinoma and gastric stromal tumour (GIST) has been documented rarely. We present a case of a 79-year-old male patient who underwent surgery for an advanced gastric carcinoma, where multiple subserosal nodules of GIST were incidentally discovered during the work-up of the gastrectomy specimen.

Method: A 79-year-old male was diagnosed with a proximal gastric adenocarcinoma and underwent a total gastrectomy. Subsequent examination revealed an 8.5 cm ulcerated mass along the lesser curvature. Three firm neighbouring nodules of 0.3, 0.5 and 0.7 cm were incidentally identified in the subserosa of the gastric wall, while searching for lymph nodes in the greater curvature, uniformly positive for CD117, consistent with small, 'low risk' GISTs.

Results: GISTs range from small 'low risk' tumours to sarcomas. Small GISTs are found incidentally during unrelated surgery or autopsy. Multiple GISTs are extremely rare and usually associated with hereditary diseases.

Conclusion: In any case of GI neoplasm the surgeon and pathologist should be alert to perform a thorough investigation. Our case could provide further awareness and insight into the entity of concurrent tumours.

026

A rare case of chronic intestinal pseudo-obstruction in the context of a paraneoplastic neurological syndrome

N. De La Ossa Merlano *, E. Castellà, R. López-Martos, J. Alvaro-Parra, I. Ojanguren
*HUGTiP, Dept. of Pathology, Badalona, Spain

Objective: Paraneoplastic neurological syndromes (PNSs) are a group of rare disorders caused by autoimmune reactions triggered by cancer. They occur in less than 0.01% of cancer patients. Chronic intestinal pseudo-obstruction may be the first manifestation of small cell lung carcinoma (SMLC) and its morphologic substrate is an inflammatory neuropathy involving the gastrointestinal tract. We describe an autopsy case in which this association took place.

Method: The patient was a 73-year-old male with chronic constipation, dysphagia, anti-Hu paraneoplastic syndrome, and suspected of pulmonary malignancy. He showed severe intestinal distension and faecal peritonitis secondary to intestinal obstruction leading to death. An autopsy was performed. Formalin-fixed, paraffin-embedded tissue sections were studied using haematoxylin-eosin stain and immunohistochemistry techniques.

Results: At autopsy, a mediastinal parahilar mass and severe gastrointestinal distension with faecal peritonitis was identified. On microscopic examination, a dense inflammatory infiltrate with many plasma cells was destroying the gastrointestinal plexuses. These findings were better demonstrated with immunohistochemistry for S-100 and neuron-specific enolase. A SCLC was present in the left pulmonary hilum.

Conclusion: This case highlights the importance of autopsy to confirm the relationship between inflammatory visceral paraneoplastic neuropathy and SCLC.

027

The overexpression of caveolin-1 in esophageal squamous cell carcinoma: correlation with tumor differentiation and lymph node metastasis

V. Delektorskaya *, G. Chemeris
*N.N. Blokhin Russian Cancer Research Center, Dept. of Pathology, Moscow, Russia

Objective: Caveolin-1 (CAV1) is main structural protein of caveolae membrane related to regulation of signal transduction, cell migration and metastasis. The role and expression patterns of CAV1 vary in different cancer types. In this study, we investigated the CAV1 protein expression in esophageal carcinomas.

Method: CAV1 expression was examined by immunohistochemical analysis in 52 esophageal squamous cell carcinomas (ESCC), 12 adenocarcinomas of the esophagus and in a normal esophageal epithelium. Statistical analysis was performed to correlate the CAV1 expression with clinicopathological findings and prognosis.

Results: Immunostaining for CAV1 was positive in 22 (42.3%) of 52 ESCC and 0 of 12 adenocarcinomas. The CAV1 expression was significantly higher in ESCC primary tumors compared with the corresponding normal tissues. The protein overexpression was more often seen in well/moderately differentiated than in poorly differentiated

ESCCs. CAV1 protein overexpression correlates with tumor histological differentiation (p=0.020), distant lymph node metastasis (p=0.027) and shorter survival (p=0.039). Immunostaining for CAV1 did not differ according to age, depth of invasion or pathologic TNM stage.

Conclusion: CAV1 is differentially expressed in ESCCs and adenocarcinomas of the esophagus. Our data suggest the involvement of CAV1 in differentiation and lymphatic metastasis in ESCCs. The CAV1 overexpression could be a potentially useful prognostic marker in ESCC.

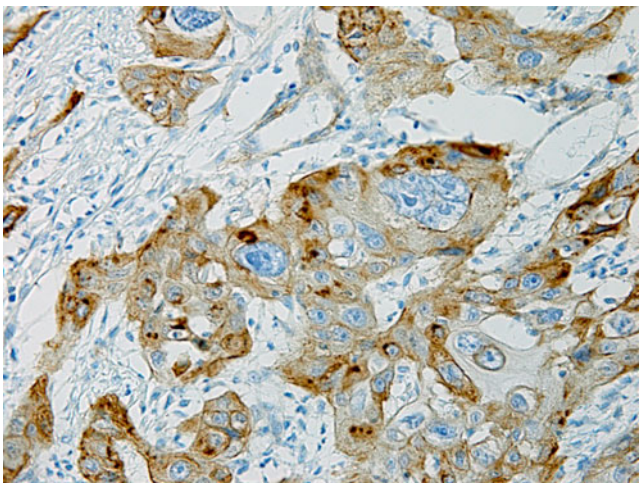

028

Clinical significance of E-cadherin and beta-catenin expression in esophageal squamous cell carcinoma

V. Delektorskaya *, G. Chemeris, A. Grigorchuk, P. Kononez, B. Polozky

*N.N. Blokhin Russian Cancer Research Center, Dept. of Pathology, Moscow, Russia

Objective: Altered expression of cell adhesion molecules has been reported to be associated with tumor progression and metastasis. The aim of the current study was to evaluate the protein expression pattern of E-cadherin and beta-catenin in esophageal squamous cell carcinomas (ESCC) and to determine the relationship between tumor characteristics and survival.

Method: The expression of E-cadherin and beta-catenin was studied in 72 primary ESCCs using immunohistochemical staining. Correlation with clinical characteristics was evaluated by multivariate analysis.

Results: The normal membranous pattern of E-cadherin expression was observed in 45.8% (33/72) of ESCCs and the protein level was negative correlated with increased TNM stage (p=0.037), lymph node metastasis (p=0.018) and poor survival (p=0.0001). Beta-catenin protein expression in the cytoplasm of tumor cells was increased in 84.7% (61/72) of cases and correlated only with poor survival (p=0.005). Cox proportional hazards regression analysis showed that E-cadherin and beta-catenin have a strong prognostic value (p=0.0022 and p=0.0103, respectively). Clinical stage and abnormal expression of E-cadherin-beta-catenin complex were independent prognostic factors throughout the multivariate analysis.

Conclusion: The close correlation with poor survival suggests that abnormal expression of the E-cadherin-beta-catenin complex may be a useful prognostic marker in ESCC patients.

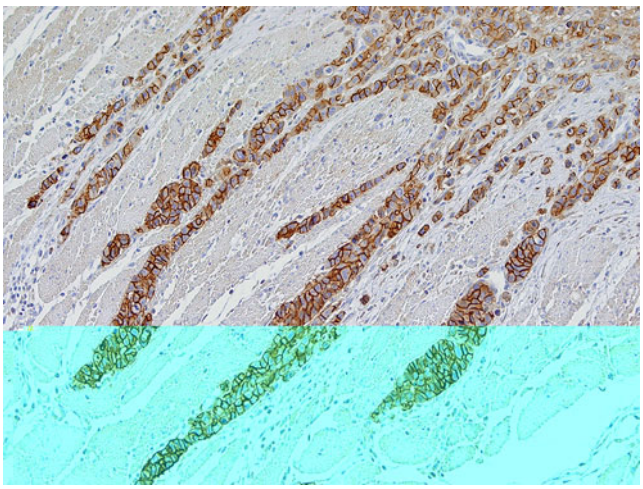

029

Indeterminate colitis irritable bowel syndrome: a potential association

M. Demonakou *, M. Choutzoumi, N. Anifantis, K. Kandilaris, N. Pantelaros, C. Pilichos, C. Barbatzas

*Sismanogleio Hospital, Athens, Greece

Objective: The etiological diagnosis of colitis is not always feasible. Therefore, the term indeterminate colitis (IC) is still in use, while information regarding the histological findings of irritable bowel syndrome (IBS) is lacking.

Method: We studied the clinical, endoscopical and histological findings of 152 patients with IC, employing Rome III criteria to discover those suffering from IBS.

Results: A total of 36/152 (24%) patients with IC suffered from IBS [11 male, 25 female (F/M):2/1] with an average age of 62 years old (41–91). There were 31% of them (21/68) evaluated on an outpatient basis, while 18% (15/84) were hospitalized. Their most frequent complaint was diarrhea (27%). Endoscopy in 47% of them was unremarkable, in 46% evidence of inflammation was found and in 7% polyps. Histology revealed distorted architecture, cryptitis, inflammatory infiltrate with increased number of eosinophils and edema in 67%, 94%, 64% and 94% of the cases, respectively. Diffuse edema could be highlighted in 52% of the cases.

Conclusion: A total of 24% of the patients with IC suffered from IBS. In the majority of cases with IC and IBS, edema, cryptitis and an increased number of eosinophils comprised the histological hallmarks. Our findings confirm that IC is associated with different entities, including IBS.

030

Metaplastic and serrated polyps of the large intestine: an epidemiological, morphological and immunophenotypical study

M. Demonakou *, A. Kalogirou, E. Pyleris, K. Kandilaris, C. Kaprilian, S. Zougri, M. Chorti
*Sismanogleio Hospital, Athens, Greece

Objective: We searched for epidemiological, morphological and immunophenotypical differences among metaplastic (MP) and serrated polyps.
Method: MP from 193 patients [134 male patients (M), 59 female patients (F), M/F ratio: 2.27] with an average age of 60 years old (age range 19–92) were studied with respect to architectural distortion, cellular atypia, eosinophilia, proliferation by Ki 67 and expression of cytokeratins CK7 and CK20 (ENVISION/DAKO).
Results: There were 18 sessile serrated adenomas diagnosed (9.3%) (18/193). No differences were found between serrated and metaplastic polyps with respect to age, gender and dimensions. The majority of MP was located in the distal large intestine in both sexes, while the majority of serrated adenomas was located in the rectosigmoid in men (51%) and the proximal colon in women (66%). At least one morphological lesion was identified in 27.5% of MP (53/193), while a perturbed expression of cytokeratins either CK7 or CK20 and abnormal proliferation were identified in 78.3% and 80% of MP respectively.
Conclusion: MP consists of a heterogeneous group. The study of their immunophenotype will assist in the description of novel subtypes, so that the variants with malignant potential could be more efficiently established.

031

Celiac disease in Meckel's diverticulum

Z. Dolenc-Strazar *, A. Cerar, M. Volavsek
*University of Ljubljana, Faculty of Medicine, Slovenia

Objective: Meckel's diverticulum is a common congenital anomaly of the small bowel, present in 2% of population, representing remnants of the omphaloenteric duct. Celiac disease, enteropathy resulting from immune reaction to gluten, a protein present in some cereals, causes impaired absorption and digestion of nutrients. Symptoms include frequent diarrhoea and weight loss. We report a rare case of celiac disease in Meckel's diverticulum in a patient without previous symptoms of celiac disease.
Conclusion: Between 50% and 60% of patients with gluten sensitivity may be asymptomatic or latent. It is important to diagnose these cases soon enough to introduce the diet and thus prevent the possibility of enteropathy-associated lymphoma.

032

Criteria for morphological diagnosis of pancreatic cystic tumors

E. Dubova *, A. Shchegolev, O. Mishnev, K. Pavlov
*V.I. Kulakov Scientific Center, Dept. of Pathology, Moscow, Russia

Objective: Determine morphological criteria of cystic pancreatic lesions differential diagnostic.
Method: We investigated 25 serous cystic tumors (SCT), 30 mucinous cystic tumors (MCT), 20 intraductal papillary-cystic neoplasms (IPMN), 21 solid-pseudopapillary tumor (SPPT), 8 neuro-endocrine tumors (NET) with cystic degeneration, 5 ductal adenocarcinoma (DA) with cystic changes and 80 postnecrotic cysts (PNC).
Results: Honeycomb-like tumor cut surface is typically for SCT, mucous contents for MCT, blood-filled cysts for SPPT. SCTs characterized by a presence of cuboidal clear cells with round basophilic nuclei and PAS-positive granules. In MCTs and IPMNs one can see mucinous cells, but MCTs have ovarian-like stroma. Its cells express estrogen and progesterone receptors. Mucinous epithelial cell and interconnections between cysts and pancreatic ducts are typical for IPMN. A presence of dysplastic/atypic cells points on borderline tumors and carcinomas. Degenerative cystic changes could be prominent in SPPT, NET and DA. Solid part of SPPT and NET is very alike, so immunohistochemistry should be performed. NET expressing neuroendocrin markers. SPPT cells expressing vimentin, α-AT, α-ACT, NSE—in cytoplasm and E-cadherin, β-catenin, cyclin-D1—in nuclei. DA cells expressing CEA, CA19-9, MUC1, panCK, DuPan2. PNC wall was composed of fibrous tissue with inflammation.
Conclusion: Final verification of pancreatic cystic lesions can be made only after complex morphological study.

033

Immunohistochemical study of 17 cases of GIST

S. Dumitriu *, D. Radulescu, S. Stolnicu, L. Chelaru, C. Zamfir, D. Butcovan, E. Morosanu, A. Dumitriu
*UMF Iasi, Dept. of Pathology, Romania

Objective: The aim of this study is to identify the prognostic factors influencing tumour recurrence and survival.

Method: A total of 17 patients with primary gastric GIST (CD117 positive) who underwent curative resection. Immunohistochemical exppresion of CD117, CD34 and Ki-67 were studied. We also studied the relationship between survival rate and Ki-67 index.
Results: Expression of CD117 was seen in 92% of cases and CD34 in 44%. There was a strong correlation between tumour size and the mitotic index, larger tumour having higher mitotic index. **Conclusion:** Ki-67 index is a good prognostic indicator for gastrointestinal stromal tumour and is related to disease specific overall survival rate.

034

KRAS and BRAF mutation status in Turkish colorectal cancers

S. Erdamar *, C. Ozkurt, A. Dirican
*Cerrahpasa Medical College, Dept. of Pathology, Istanbul, Turkey

Objective: Since metastatic colorectal cancer (mCRC) cases with no kras mutation have benefit from Anti-EGFR treatment Kras mutation status is important mCRC cases. We aimed to analyse the frequency and subtype of Kras and Braf mutation, their correlations with other clinicopathologic parameters in Turkish mCRC patients.
Method: We analysed 202 mCRC cases for KRAS mutational status of codon 12 and 13 of the KRAS by using Real-time PCR based assay using DxS Therascreen kit. TibMolbiol kit for Braf V600E mutation was used in Real-time PCR. The correlations with Kras and Braf mutation status and clinicopathological parameters was analysed statistically
Results: M/F: 1.56 and mean age, 60.64. Kras mutation was found in 42.1% of cases. The most common mutation types were 12ASP (33.3%), 12VAL (26.3%), 13ASP (17.5%). Kras mutation in mucinous carcinomas (mostly 13ASP) was higher than in adenocarcinomas. The frequency of Braf mutation was 7.1%. Tumors in transvers colon did have neither Kras nor Braf mutation. There was not significant correlation between kras mutation and pT, LN metastases, PNI. Only two Braf mutant cases showed 13ASP mutation.
Conclusion: The frequency and type of Kras and Braf mutations in Turkey showed similarity with the other studies. More detailed studies questioning correlation Kras mutation and histologic subtypes are necessary.

035

Diagnostic value of urease test, touch biopsy and biopsy in *Helicobacter pylori* infection of stomach

A. Fakhrjou *, S. Shriati, M. H. Soumi, E. Fattahi, M. Gojazadeh
*Tabriz University, Dept. of Medical Pathology, Iran

Objective: This study aims at evaluating the diagnostic value of rapid urease test (RUT), touch cytology (TC) and biopsy in *Helicobacter pylori* infection of stomach.
Method: In a cross-sectional analytic–descriptive setting, 60 patients candidate for upper gastrointestinal endoscopy were recruited during a 12-month period. Fifty-one patients enrolled. Three biopsy samples were obtained from gastric antrum, each one used for one test. The infection status for each patient was established by a concordance of two test results.
Results: Fifty-one patients, 29 females and 22 males with a mean age of 40.10±12.54 (18–72) years were studied. The definite infection was determined in 41 (80.4%) patients. RUT, TC and histopathological examination were indicative of infection in 82.4%, 82.4% and 76.5% of the cases, respectively. Sensitivity, specificity and accuracy of RUT, TC and pathology were 92.7%, 60% and 66.75; 100%, 90% and 98%; and 95.1%, 100% and 96.1%, respectively. There was medium to high concordance between 3 tests with the final findings (kappa=0.548, 0.935 and 0.884, respectively, $P<0.05$).
Conclusion: Based on our results, TC was the most sensitive and pathology was the most specific test for diagnosis of infection with HP. The specificity of RUT was apparently low in this study.

036

Evaluation of P53 gene mutation and abnormal P53 protein accumulation in colon adenocarcinoma by Immunohistochemistry method

A. Fakhrjou *, K. Saffari, S. Shadravan
*Tabriz University, Dept. of Medical Pathology, Iran

Objective: Colorectal adenocarcinoma is accompanied with different alterations at the genetic level of the cell. Among them, are mutations of P53 gene. The purpose of this study is the survey on positive cases of colorectal adenocancinoma, for P53 protein by the immunohistochemistry procedure.
Method: One hundred paraffin blocks with diagnosed as stage3 colorectal well differentiated adenocarcinoma were collected. In every specimens nucleus staining in more than 10% of cells was regarded as positive results. In all positive cases, with segregation the sexes, and in two groups patients over and under 50 years defined and compared with the statistic method (chi square).
Results: The positive staining for protein P53was in 60 patients (60%). Between two sexes, there was not any significant statistic difference. The P53 positive rate in female patients over 50 years were clearly more than the male patients over 50 years,100% and 73.1% respectively (p value=0.03). This rate, also, in patients over 50 years in

both male and female were significantly higher than patient below 50 year.
Conclusion: According to this study, between two sexes, from pointview of P53 positive rate, there was not any significant difference (however, in over 50 years age group, this rate was more in female). More studies are suggested in future with more and newer specimens and also applying additional parameters like feeding diets, and men and women's hormone situation.

037

Combined c-myc and pAKT activation in colon adenocarcinoma based on tissue microarray analysis

E. Falidas *, E. Tsiambas, G. Theodoropoulos, S. Papadopoulos, A. Karameris, C. Goudeli, C. Villias, I. Bramis
*NIMTS Hospital, Dept. of Surgery, Athens, Greece

Objective: Oncogenes' aberrant expression—via point mutations or amplification—happens frequently during colon carcinogenesis. We investigate the role of simultaneous c-myc and AKT overexpression in colorectal adenocarcinoma (CA) and its clinical impact.
Method: Based on a tissue microarray system, 60 (n=60) cores derived from corresponding paraffin blocks of patients with primary CA were transferred to the final array (core diameter=1.5 mm). Thirty cores of colon adenomas (n=30) were also used for expanding the analysis. Immunohistochemistry protocols were performed. Protein expression levels were measured by applying a digital image analysis macro.
Results: According to combined protein analysis, 27/60 (45%) cases demonstrated pAKT overexpression (moderate to high staining intensity levels), whereas 37/60 (61.1%) over-expressed c-myc. Simultaneous c-myc/pAKT over-expression was observed in 21/60 (35%) cases (kappa=0.82), correlated to the stage of the tumors (p=0.02). Additionally, AKT overall expression was strongly associated with the grade of them (p=0.001). Adenomas analysis showed moderate or low levels of expression regarding c-myc/pAKT.
Conclusion: Simultaneous deregulation of c-myc/AKT genes correlates with stage in CA. AKT overexpression correlates with a progressive dedifferentiation of the neoplasm. Based on this significance, regulation of those genes via mi RNAs is a challenging step in targeted therapeutic strategies in CA.

038

Extrahepatic hepatocellular carcinoma: a case report with genetic confirmation about its origin

F. Felipo *, B. Eizaguirre, P. Sanz, C. del Agua, L. Calera, R. Pazo
*Hospital Royo Villanova, Dept. of Pathology, Zaragoza, Spain

Objective: Extrahepatic hepatocellular carcinoma (EHC) is an extremely rare neoplasm although previously reported already in the literature. To our knowledge, this is the first case reported with genetic signature about its origin.
Method: A 30-year-old man with a history of epigastric pain showed a 13-cm retroperitoneal mass not involving adjacent organs. No other lesions were found. Laparotomy was performed and histologic, immunohistochemical and molecular studies were done.
Results: Histologic sections showed a neoplasm with trabecular pattern of growth with characteristics of hepatocellular differentiation. Immunohistochemicaly, neoplastic cells were positive for CK7, CK8, CK19, TTF-1 (cytoplasmic) and Hep-Par 1. Diagnosis was concordant with hepatocellular carcinoma, but the patient was treated with chemoterapy for germinal tumour, without therapeutic response. Theros Cancer Type® (molecular test of Grupo Ferrer for diagnostic of unknown origin tumours) confirmed with 96% of probability that it was a hepatocellular carcinoma, and second line chemotherapy with doxorrubicine and sorafenib has been started currently.
Conclusion: EHC arises from ectopic liver rests that are present rarely inside abdominal cavity, retroperitoneum or thorax. Histologic and immunohistochemical studies are usually enough to confirm the diagnosis, but in problematic cases analysis of genetic signature of the tumour may confirm the hepatocellular nature of the neoplasm.

039

Comparison of the 6th and 7th UICC TNM staging for gastric carcinomas in Romanian patients

S. Gurzu *, I. Halmaciu, L. Boc, I. Jung
*University of Medicine, Dept. of Pathology, Targu-Mures, Romania

Objective: The aim of our study was to compare the 6th and 7th AJCC/UICC staging systems in order to reveal the benefits of the newest interverntion.
Method: A total of 134 patients who undergo surgical interventions between 2008 and 2010 were enrolled in the study. They were staged using the 6th and 7th systems.
Results: According to 6th edition, 5.24% of patients were diagnosed in pT1 stage, 38.8% in pT2, 44.77 in pT3, respectively, 11.19 in pT4. In the 7th edition the number of pT2 stages significantly decreased to 6.71% and pT4 increased to 55.97% (p<0.0001). A total of 46.26% of patients presented metastases in more than six nodes, only 21.65% being diagnosed without node metastases. A significant difference between the two staging systems

regarded the grouping staging. About 15% of patients with stage IV were downstaged in stage III due to regrouping of stages II and III.
Conclusion: The new staging system of gastric carcinomas reveals that the invasion of adjacent structures, metastases in more than six lymph nodes and distant metastases remain the main factors which show an unfavorable outcome of these tumors. These parameters may explain the increasing number of gastric cancer death although its incidence is declining. This study was supported by PD 504/2010 and POSDRU/89/1.5/S/60782 projects.

040

Molecular profile of colerectal cancer: is it indeed necessary?

S. Gurzu *, I. Jung, E. Toth, Z. Szentirmay
*University of Medicine, Dept. of Pathology, Targu-Mures, Romania

Objective: The aim of our study was to analyze the importance of some molecular markers in the prognosis of these cancers.
Method: s300 CRC surgical specimens were statistically and immunohistochemically (IHC) evaluated. MSI (microsatellite instability) status was analyzed in 52 cases. We used following markers: CD8, HER-2, p53, Ki67, bcl-2, MLH-1, CEA.
Results: From the 52 cases, 9 were MSI. MLH-1 was negative and the number of tumor inflitrated lymphocytes stained with CD8 was higher in all the 9 MSI cases and 20% of tumors located on the proximal colon. CEA and Ki67 were not correlated to survival or other classical prognostic factors (node metastases, angiolymphatic invasion). HER-2 expression was correlated to lymph node metastases and bcl-2 was negative in most of CRC from advanced stages. 65% of the patients with lymph node metastases and the profile p53+/bcl-2-/HER-2+/MSS presented recurrences.
Conclusion: Based on molecular profile, CRC may be subdivided in some prognostic groups, the best prognosis showing the MSI/p53-/bcl-2+/HER-2- and the worst MSS/p53+/bcl-2±/HER-2+ cases. These subdivision may be the basis for targeted therapy in node negative CRC. This study was supported by PD 504/2010 and POSDRU/89/1.5/S/60782 projects.

041

Decreased proliferative activity of the rectal cancer tumour cells induced by therapeutic radiation

A. Halon *, J. Szelachowska P. Dziegiel, R. Tarkowski, M. Bebenek, A. Wojnar, J. Kornafel,
R. Matkowski
*Wroclaw Medical University, Dept. of Pathomorphology, Poland

Objective: The study aimed at evaluation in clinical conditions effects of radiotherapy on expression of Mini-chromosome Maintenance Protein 3 [MCM3] and Ki-67 antigen in rectal cancer.
Method: Material for the studies originated from 21 patients with rectal cancer at the II or III stage of clinical advancement (cTNM). The patients were treated using preoperative radiotherapy at the dose of 25 Gy in 5 fractions. Material for immunohistochemical studies was sampled twice: during rectoscopic examination before start of the treatment and during operation at 1 to 4 days after completion of radiotherapy.
Results: The material sampled after radiotherapy has manifested a tendency to decreased proliferative activity: the decrease in proportion of cells manifesting expression of MCM 3 was significant ($p=0.022$), while in the case of Ki-67 expression the difference approached statistical significance ($p=0.096$). Moreover the strongly positive correlation was detected between levels of Ki-67 and MCM3 in the material sampled before ($r=0.77$; $p<0.0001$) and after radiotherapy ($r=0.77$; $p<0.0001$).
Conclusion: This unequivocally points to a decrease in proliferative activity of the rectal cancer cells after radiotherapy. The result indicates that MCM3 may represent a potentially better proliferation marker than Ki 67 in this type of investigations.

042

Study the value of TNF Alpha mRNA and protein expression in patients with cirrhotic liver disease and hepatocellular carcinoma

O. Hammam *, A. Abdel Hadi, M. Zahran, O. Mahmoud, A. Anas
*Theodor Bilharz Research Institute, Dept. of Pathology, Giza, Egypt

Objective: To assess the role of hepatic expression of TNF alpha as early predictors of advancement of chronic hepatitis C, this can provide insight into the mechanisms by which HCV induces HCC.
Method: There were 100 patients enrolled: 36 with chronic hepatitis C (CHC)[16 not associated and 20 associated with cirrhosis] and 64 with hepatocellular carcinoma. Five controls. Messenger (m) RNA TNF alpha, protein expression and serum TNF alpha receptor II in hepatic tissue were measured using in situ hybridization, IHC and Eliza techiques, respectively.
Results: Over-expression of TNF alpha-mRNA and TNF alpha protein were found in the HCC compared to control

group ($p<0.01$) and CHC associated ($p<0.05$), or not associated ($p<0.01$) with cirrhosis group and increased in high grade compared to low grade HCC. sTNF-RII showed a statistical significant increase ($P<0.01$) in all diseased groups compared to the control group ($p<0.01$). It also showed a significant statistical increase in CHC with cirrhosis and HCC patients when compared to CHC without cirrhosis group ($P<0.01$) and also between HCC and CHC with cirrhosis patients ($P<0.01$).

Conclusion: The expression of TNF alpha could be used as a biological prognostic marker of hepatocellular carcinoma.

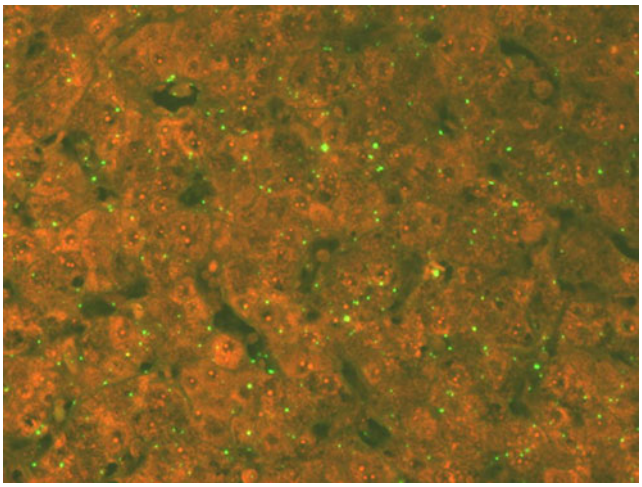

043

Collagenous colitis: clinicopathological study of 33 Japanese cases

S. Haraoka *, K. Ikeda, A. Iwashita, I. Iwashita
*Fukuoka University, Chikushi Hospital, Chikushino, Japan

Objective: Collagenous colitis is a clinicopathological entity characterized by chronic watery diarrhea and subluminal deposits of a collagen beneath the surface epithelium of large intestine. The aim of this study was to clarify the clinicopathological characteristics of collagenous colitis in Japanese patients.

Method: We analyzed clinical and pathological findings of 33 cases (mean 73.9 years old, male/female=8:25). A total of 142 biopsy specimens were obtained. Histopathologic features were analyzed by scoring method concerning four compartments of the mucosa: subepithelial collagen layer, surface epithelium, crypts, and lamina propria.

Results: According to the available information, all 21 patients were administered lansoprazole (18 cases) and NSAIDs (3 cases). Microscopically, the overall mean thickness of the subepithelial collagen band (CB) was 31.3±15.2 μm. There was no significant difference in the mean thickness of CB between the proximal colon (30.6± 13.9 μm) and distal colorectum (35.6±15.2 μm). Detachment of the surface epithelium was observed in all cases. Inflammatory cell infiltration in the lamina propria and neutrophilic infiltration in the surface epithelium were usually mild. The histopathologic abnormalities were independent of CB thickening.

Conclusion: In Japanese patients with persistent watery diarrhea and administration of lansoprazole, multiple biopsies should be performed to diagnose collagenous colitis definitely, even if endoscopic appearances are normal.

044

Diagnostic algorithm in primary malignant tumors of the liver

V. Herlea *, C. Pechianu, C. Stroescu, E. Stoica-Mustafa, A. C. Iorgescu, M. G. Hortopan, S. O. Dima, C. Vasilescu, M. Ionescu, M. Sajin, I. Popescu
*Fundeni Clinical Institute, Dept. of Pathology, Bucharest, Romania

Objective: This study proposes to analyze histopatological and immunohistochemical markers in an 82-patients lot with primary malignant tumor of liver.

Method: In order to evaluate the importance of immunohistochemistry in diagnosis of primary malignant liver tumors, we analyzed the following markers: pCEA, CK7, CK8/18, CK19, CK20, MUC1, MUC2, MUC5, Vimentine, SMA, HepPar1, CA125, NSE, Chromogranine, HMW, Keratin, CD 34, and for prognostic markers we use p53, VEGF, ki67, Bcl-2.

Results: Hepatocellular carcinoma CK 7 expression was positive in 13.04%; and CK 19 in 46.66% pCEA was positive in 64.7% cases and intensity of stain is correlated with differentiation grade: I/II grade tumours presented high-intensity positivity, and III–IV grade were weak positive. CK 8/18 show positivity for 84.84% cases. VEGF show cytoplasmic positivity in tumoral cells in 95.74% cases. Cholangiocarcinoma CK19 show positivity in 65.21% cases; CK20 was positive in 15.38% cases. Controversial results we obtain in CK7 with 45.83% positivity pCEA was positive in 75% patients. VEGF show cytoplasmatic positivity in 95.23%.

Conclusion: Combined panel CK 7, 8, 18, 17, 19 and pCEA could be useful to distinguish between various malignant tumors of liver.

045

Immonohistochemical study of MUC17 expression in human pancreatic cancer

M. Higashi *, S. Kitamoto, S. Yokoyama, K. Tabata, S. Yonezawa
*Kagoshima University, Graduate School of Medicine, Japan

Objective: Human MUC17 glycoprotein is a membrane-associated mucin that is mainly expressed in the digestive tract. Regarding to cancer pathogensis with MUC17, it has been suggested that MUC17 expression is correlate with malignancy.
Method: In the present study, we examined the expression of MUC17 by immunohistochemical analysis in invasive ductal adenocarcinomas from 67 patients. MUC17 was detected by rabbit anti-MUC17 polyclonal antibody. The results of the immunohistochemical stainings were evaluated by the percentage of positively stained carcinoma cells, which was graded as follows: -, under 5% of carcinoma cells stained; +, more than 5% under 50% of carcinoma cells stained; ++, 50% or more than carcinoma cells stained.
Results: MUC17 was expressed in neither normal epithelium nor acinar cells, excepting islet cells. The positive cases (percentages) were as follows: (-), 32 cases (48%); (+), 17 cases (26%); (++), 17 cases (26%). The positive rate in papillary adenocarcinoma is higher than that in tubular adenocarcinoma. Poorly differentiated adenocarcinoma is negative for MUC17. The survival rate of R1 patients with MUC17 expression was significantly worse than that of MUC17 negative.
Conclusion: MUC17 is a predictive factor of invasive ductal carcinoma of the pancreas.

046

Granulocytic sarcomas of the gastrointestinal tract: clinicopathologic study of the three surgically resected cases

K. Ikeda *, A. Iwashita, S. Haraoka, A. Ota, H. Tanabe, K. Oshige, T. Kanemitsu, I. Iwashita
*Fukuoka University, Chikushi Hospital, Chikushino Fukuoka, Japan

Objective: Granulocytic sarcoma (GS) is a tumor composed of immature cells of granulocytic series. Gastrointestinal GS is rare and is associated with poor prognosis. We investigated the clinicopathologic features of three surgically resected cases of gastrointestinal GS.
Method: We reviewed the clinical and pathological files of the Department Pathology Fukuoka University Chikushi Hospital and the related hospital. Routine hematoxylin-eosin-stained slides, naphthol-ASD-chloroacetate (NASD) stain and immunohistochemical stain were performed using formalin-fixed, paraffin-embedded tissue sections.
Results: All three patients were males. The median age was 50.7 years (range 36–66). The patients had a previous history of acute myeloid leukemia (AML) (two cases) and myelodysplastic syndrome (MDS) (one case). Two protruded tumors were located in the ileum and preoperatively diagnosed as malignant lymphoma. A patient with sigmoid colon adenocarcinoma was finally diagnosed as GS after the operation. The histologic features consist of a diffuse proliferation of atypical mononuclear cells admixed with maturing granulocytes and eosinophils. NASD stain was positive in all cases. The tumor cells are immunohistochemically positive for myeloperoxydase and lysozyme.
Conclusion: GS is rare and is associated with poor prognosis. A pathologist must consider GS in diagnosing the gastrointestinal tumors so that patients can get early and proper treatment.

047

Intestinal submucosal lipomas: review of cases in a 10-year period

V. Janevska *, l. Spasevska, V. Janevski, N. Jankulovski, B. Dukova, S. Komina
*Institute of Pathology, Skopje, Macedonia

Objective: Gastrointestinal tract is an uncommon localization of lipomas, but if present they are 90% submucosal and 10% subserosal. Intestinal submucosal lipomas are the most common benign nonepithelial intestinal tumors usually found incidentally. Rarely, they may cause obstruction, ulceration, perforation, intussusceptions, prolapse and massive hemorrhage. They are presented as polypoid lesions either sessile or pedunculated. We analyzed 20 cases of intestinal submucosal lipomas in a 10-year period and evaluated the age and sex distribution, location and association with other findings.
Method: We used archive pathohistologic reports and slides of intestinal submucosal lipomas diagnosed at the Institute of pathology, Medical faculty, Skopje in 10-year period (2000–2010).
Results: Forty percent of patients were in 7th decade, 30% in 8th decade and 30% in their fifties. The male/female ratio was 1:1. Colonic sumbucosal lipomas were found in 60% of cases, duodenal in 30% and jejunal in 10%. Forty percents of them were diagnosed in association with carcinomas, 20% with polypoid adenomas, 30% caused inflammation and ulcerations and 10% intussusception.
Conclusion: Colon and duodenum are the most frequent locations of intestinal submucosal lipomas. They are rare tumors occurring in 7th and 8th decade, usually found incidentally in association with carcinomas and polypod adenomas.

048

Difference in expression of VEGF-A, VEGFR-1, VEGFR-2 and microvessel density in colorectal cancer with liver metastasis

E.-H. Jeong *, J.-Y. Na, J.-H. Nam, J.-H. Lee
*CNUH, Dept. of Pathology, Gwangju, Republic of Korea

Objective: Colorectal cancer (CRC) is one of the most common malignant neoplasms and is a leading cause of mortality worldwide. Metastasis to the liver is a frequent event in patients with CRC. An essential step in the metastatic cascade is angiogenesis.
Method: This study included 45 patients who underwent a partial colectomy with hepatic resection for CRC with hepatic metastases. Immunohistochemistry was performed using vascular endothelial growth factor (VEGF)-A, VEGF receptor (VEGFR)-1, VEGFR-2, and CD34 antibodies to examine the relationship between CRC with liver metastases and angiogenesis.
Results: CRC showed significantly stronger expression of VEGF-A, VEGFR-1, and VEGFR-2 than liver metastases ($p<0.05$). Microvessel density was also higher in CRC than in liver metastases ($p<0.05$).
Conclusion: Compared with previous studies, we found a higher expression of VEGF-A, VEGFR-1, VEGFR-2, and microvessel density in CRC than in liver metastases, which could be ascribed to a difference in vessel distribution and blood supply in each organ. Given its profuse blood supply and distinct cell populations, the liver might provide a rich milieu for tumor cell growth with less expression of angiogenesis-inducing agents.

049

Colitis cystica profunda in a patient with Crohn's disease on long-term biological therapy

J. Jeruc *
*University of Ljubljana, Faculty of Medicine, Slovenia

Objective: Colitis cystica profunda (CCP) is an uncommon condition characterized by benign, mucus-filled cystic lesions within the submucosa or muscularis propria.
Results: Case report. A 30-year-old man with a history of Crohn's disease treated by biological medications underwent the ileocoecal resection. The resected specimen included the terminal ileum showing some erosions and ulcerations, while the wall of coecum was thickened, firm and sprinkled with numerous filiform polyps. Histologically, terminal ileum showed signs of active Crohn's disease and deep fissure extending from the appendix. In the coecum there were multiple cystic and glandular structures extending into submucosa and deep into muscularis propria. They were lined mostly by columnar epithelium, focally showing active inflammation and reactive atypia. Some cysts showed extensive mucine secretion mimicking mucinous adenocarcinoma. However, extensive sampling revealed no evidence of dysplasia or desmoplasia, which warranted the diagnosis of CCP.
Conclusion: In idiopathic inflammatory bowel disease, the CCP probably occurs as a result of misplacement and entrapment of regenerating glands in the submucosa during the process of reepithelialisation and healing of ulcers. Pathologists should be aware of misinterpreting this entity as a mucinous adenocarcinoma, especially as patients with chronic inflammatory bowel disease are at increased risk of developing dysplasia and carcinomas, particularly mucinous type.

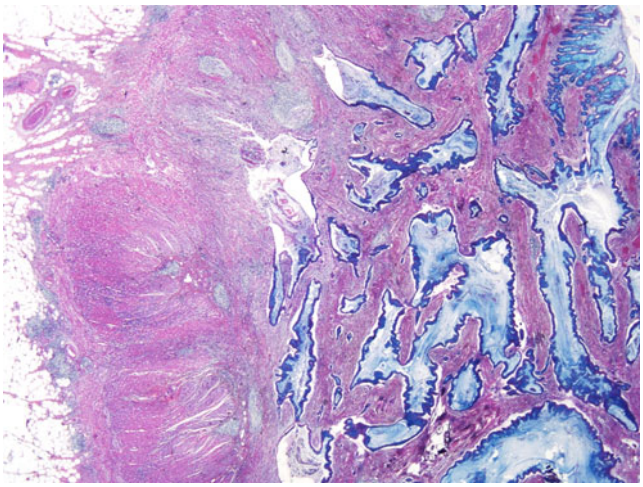

050

Synchronous gastrointerestinal stromal tumor and a well-differentiated neuroendocrine carcinoma in ileocaecal region: a case report

M.H. Karabulut *, G. Kir, M. Segmen Yilmaz, C.S. Topal, F. Gursoy Zerenler, G. Bas
*Umraniye Ea Hospital, Dept. of Pathology, Istanbul, Turkey

Objective: Gastrointestinal stromal tumors (GIST) and neuroendocrine tumors (NET) are relatively rare neoplasms of the gastrointestinal system's mesenchymal and neuroendocrine parts. It is obviously a very uncommon clinical presentation of these two tumors seen in a synchronous fashion.
Results: Case report: Herein, we report an 84-year-old male patient operated on because of an acute abdomen/ileus. Pathologic evaluation of the right hemicolectomy specimen revealed a very advanced, large-conglomerated mass of GIST invading entire ileal, caecal and right colon's mesenteric area with an intramucosal and obstructing invasion at the ascending colon. In addition, a small well-differentiated non-functioning neuroendocrine carcinoma, located in the caecum was found coincidentally. Unfortunately, the patient had expired at the early postoperative period due to cardiopulmonary failure.
Conclusion: Co-existence of the epithelial tumors and neuroendocrine neoplasms in the gastrointestinal tract is somewhat a well-known entity. But, synchrone GIST and

NET is a very rare presentation with a exceedingly few reports in the literature, and yet, we were unable to find similar combination of a concommitant ileocaecal GIST and caecal NET.

051

Ciliated foregut cyst of the gall bladder: report of a case [with literature review]

P. Katafygiotis *, A. Tsega, A. Skopelitou
*Hospital of Athens, Dept. of Pathology, Athens, Greece

Objective: Cystic lesions of the gall bladder are extremely rare. We present a 76-year-old Caucasian woman with a previous history of breast cancer, who was referred to our hospital with severe epigastralgia.
Method: Ultrasound results revealed several gallstones and a cystic lesion on the serosa of the body of the gall bladder, measuring 1.6 cm. Malignant potential could not be ruled out given the previous history of breast cancer and a laparoscopic cholecystectomy was carried out.
Results: On gross examination a cystic mass measuring 1.6×1.2×1 cm was found, filled with gelatinous whitish material. Its inner surface was smooth. No communication with the lumen of the gall bladder was found. On microscopic examination, the cystic wall was lined by ciliated, pseudostratified columnar epithelium, surrounded by thin bundles of smooth muscle. Microscopic examination of the gall bladder revealed chronic cholecystitis with cholelithiasis, along with extensive pyloric and intestinal metaplasia of the epithelium. Low-grade dysplasia was also noticed in several glands showing intestinal metaplasia.
Conclusion: Ciliated foregut cyst of the gall bladder is considered a congenital cyst. Similar cysts have been found in the liver. Although in such cases the risk of neoplasia is low, multiple sections should be performed to rule out malignancy.

052

Forgotten organs for metastases

V. Katic *, J. Gligorijevic, M. Krstic, Z. Radovanovic, A. Radovanovic, K. Katic
*Policlinic of Nis, Dept. of Pathology, Serbia

Objective: The ability to migrate and invade into surrounding tissues, blood, and lymphatic vessels is one of the marks of cancer, but underlying mechanisms controlling cell invasiveness remain poorly understood.
Method: We analyzed the histological parameters and immunohistochemical expression in ten metastatic tumors of the unusual localizations. For immunohistochemical study, the following antibodies were used: thyroglobulin, Ki-67, cytokeratin (high molecular weight), chorionic gonadotropin (hCG), vimentin, CA125, chromogranin A, S100, Melan A, MUC2, 5AC, MUC6 and both estrogen and progesterone receptors.
Results: Sudden cardiac death, 40 days after removal of the original hyroid carcinoma. Intramyocardial tumour nodules of the right atrium and ventricular septum were macroscopically seen. Abdominal granullar cell ovarian metastasis found after 23 years from its diagnosis and surgical therapy. Splenic subcapsular metastasis of the ovarian cystadenocarcinoma was surgically removed after 4 years of therapies. A 17 year-old boy had colorectal ressection, induced by "sigmoid colon carcinoma". Both histological and immunohistochemical examination has discovered testicular choriocarcinoma metastasis. Gastroduodenal and small intestinal mucosa (five cases) was infiltrated with melanoma of the eye and skin. Colon mucosa was infiltrated with renal hypernephroma (one case). Gastric signet ring cell carcinoma has given metastasis in the right breast (one case).
Conclusion: The pathways of invasion are most frequently well known, but sometimes the pathways of invasion, as the time of invasion, often are not predictable.

053

Tumor in tumor: not just a gastric adenocarcinoma with concommitant adrenal myelolipoma

C. Kouvidou *, D. Violidaki, E. Ronne, M. Chantziara, I. Chrysovergis, D. Rontogianni
*Evangelismos Hospital, Dept. of Pathology, Athens, Greece

Objective: Myelolipomas though benign are also uncommon. Few cases of myelolipomas occuring within adrenocortical adenomas or simultaneous with carcinomas have been reported. To the best of our knowledge a case of gastric adenocarcinoma metastatic to an adrenal myelolipoma has not been previously reported.
Method: An 85-year-old woman presented at our hospital with severe anaemia and gastroscopy, which indicated a gastric adenocarcinoma. Computed tomography of the abdomen revealed a 4.5-cm mass in the left adrenal gland suspicious for metastasis. The patient underwent a gastrectomy and left adrenalectomy.
Results: The histology showed a poorly cohesive gastric adenocarcinoma (WHO 2010), consisting of deeply eosinophilic and few signet ring cells. The histology of the adrenal mass showed mature adipose tissue and normal hematopoietic cells consistent with the diagnosis of myelolipoma. A careful microscopic examination revealed scattered carcinoma cells of both morphologies within the myepolipoma. The positive immunohistochemical staining

with keratin AE1/AE3 and PAS positive staining indicated their malignant nature.
Conclusion: The adrenal gland is a common site of metastasis mainly from lung and breast. The metastasis of a carcinoma to an adrenal tumor is unusual and only one case of oesophageal adenocarcinoma with metastasis to adrenocortical adenoma has been reported.

054

Appendiceal carcinoid tumour in a patient with Crohn's disease

C. Kouvidou *, A. Nikolaidis, G. Nakos, M. Chantziara, M. Konstantinou, D. Rontogianni
*Evangelismos Hospital, Dept. of Pathology, Athens, Greece

Objective: There is an increased risk of colon cancer in patients with Crohn's disease. The coexistence of other intestinal neoplasms including carcinoid tumours in these patients has also been reported.
Method: Case presentation: We report a case of a 19-year-old man with a history of Crohn's disease who had undergone ileocolic resection for refractory symptoms.
Results: The pathology showed transmural inflammation and ulceration consistent with the diagnosis of Crohn's disease. A 4-mm carcinoid tumour was found incidentally in his appendix, without serosa or fat invasion. The appendix was uninvolved of Crohn's disease and showed mild inflammation but the patient was on immunomodulator therapy. The patient did not have any sign of carcinoid syndrome.
Conclusion: Patients with Crohn's disease may be at increased risk of developing a carcinoid tumour. It has been reported that the endocrine cells of the intestine can be hyperstimulated by inflammation, leading to hyperplasia and neoplasia. Recent study suggests that its development may be secontary to distant proinflammatory mediators rather than a local inflammatory effect from adjacent Crohn's disease.

055

Prognosis of Hirschsprung's disease allied disorder (had): the value of ganglia/nerve fibers ratio

D. Kovac *, I. Gasparovic, M. Persic, I. Slavic, H. Nikolic, N. Jonjic
*Clinical Hospital Centre, Dept. of Pathology, Rijeka, Croatia

Objective: In HAD lack of ganglia and increased and abnormal proliferation of mucosal nerve fibers are found to cause congenital dismotility problems of the GIT. The aim of our study was to determine a possible connection between ganglia/nerve fibers ratio and clinical outcome in HAD, predicting possible recovery of patients even before treatment.
Method: We followed the recovery of 15 treated patients and compared their clinical outcome with histopathological findings of ganglia and nerve fibers. Sections of full-thickness bowel specimens, obtained from our patients with HAD, were stained with antibodies against neurofilament protein (NF), marking ganglia, and S-100, marking the nerve fibers.
Results: Seven out of eight patients undergoing surgery were found to have low ganglia/nerve fiber ratio while five out of seven patients not showing the need for surgery had higher ganglia/nerve fibers ratio. Among the ones with low ratio and undergoing surgery, the two out of three who manifested during the first week after birth were found to have a poorer outcome. Others mostly recuperated well.
Conclusion: We propose that the ganglia/nerve fibers ratio can be used to predict the need for invasive procedures in patients diagnosed with HAD, as well as, matched with the age symptoms arose, the clinical outcome and long term prognosis.

056

Diagnosis and prognostic evaluation of gastrointestinal stromal tumors

D. Kovac *, I. Gasparovic
*Clinical Hospital Centre, Dept. of Pathology, Rijeka, Croatia

Objective: Gastrointestinal stromal tumors (GISTs) are the most common mesenchymal malignancies of the gut. Even though recently identified as a distinct clinical and histopathologic entity, GISTs need precise evaluation of its malignant potential and clinical outcome for each patient.
Method: Retrospective analysis of 66 GIST patients diagnosed and treated in our institution.
Results: Sixty-six patients were diagnosed with GIST from 1997 to 2008. Majority of our patients were female (59.09%). Median age of all patients was 65 years with female age group older than male. Most GISTs were found in stomach (43.9%) and jejunum (24.2%) with all other sites under 10% of cases. Assessment of the malignant potential was made in all cases and we found that majority of cases were in low malignancy group (48.5%), followed by high malignancy group (39.4%). Only 3 patients (4.5%) presented metastatic disease at primary diagnosis, and we had 6 patients with reccurences with primary sites in stomach (1), jejunum (2), omentum majoris (1) and retroperitoneum (2). There are 5 patients currently on imatinib therapy. All five have a registered partial response.

The longest exposure to treatment of a patient is at 3 years. Therapy is well tolerated.

Conclusion: Established prognostic parametes are number of mitoses, largest diameter and localisation. Recent investigation in tumourogenesis of GIST showed that cytogenetic alterations also have influence in prognosis. As presented, results of our data analysis do not completely follow the established patterns of GIST presentation. Estimation should be complemented with molecular and cytogenetic analysis for survival prognosis.

057

Secondary sclerosing cholangitis occurring in patients after treatment in intensive care units: a new entity

U. Krause *, S. Hippe, V. Lippert, M. Plauth, J. Knolle
*Städtisches Klinikum Dessau, Germany

Objective: Secondary sclerosing cholangitis is caused by a variety of different factors. A new entity of secondary sclerosing cholangitis occurring after treatment in intensive care units (SSC-ICU) has been described recently. SSC-ICU seems to be a disease with unique pathological patterns.

Method: We analysed six single cases, focusing on morphological clues. Furthermore, we reviewed the literature.

Results: The most characteristic pattern of SSC-ICU is the so-called "cast". "Casts" are partial or complete occlusions of intra- and extrahepatic bile ducts with tenacious, dark-green or blackish material. Applying histological methods, one can detect bile pigment, fibrin, erythrocytes and sparse inflammatory cells in this material. However, it is very difficult to make the definitive diagnosis in liver biopsy without clinical data and without the detection of inspissated bile.

Conclusion: SSC-ICU is a new entity with characteristic pathological patterns. It is useful to know these morphologic clues to rule out other forms of secondary sclerosing cholangitis and to allow an optimal therapy.

058

p27/Kip1 and Ki-67 as prognostic factors of gastrointestinal stromal tumor (GIST)

V. Kravtsov *, O. Zayratyants, H. Shirin
*Meir Medical Center, Dept. of Pathology, Kfar-Saba, Israel

Objective: GIST is a most common mesenchymal tumor of the gastrointestinal tract. Tumor size and mitotic activity are characteristically associated with the malignant potential and prognosis of GIST. However, since neither small tumor size nor low mitotic activity can rule out malignancy, additional factors that may predict malignant behavior have been suggested.

Method: Serial sections were evaluated by immunohistochemistry after staining with antibodies against p27/Kip1 and Ki-67 in surgical material obtained from 36 patients with GIST. p27kip1 staining intensity and the percentage of positive cells, and percentage of Ki-67 positive cells were investigated for association with the malignancy risk, pathological features, overall survival, and disease-free survival.

Results: The expression of p27kip1 did not depend on that of other markers, the sizes of a tumor, its histological type, and affinity to this or that risk group. There was a statistically significant difference in the expression of Ki-67 in the groups of low (1.7%) and high (10.3%) risks.

Conclusion: The p27kip1 was not associated with malignancy of GISTs and did not serve, as a predictor of survival. The Ki-67 may used for differentiation between the groups of low and high risks, as a predictor of survival.

059

Enterobius vermicularis: a controversial cause of appendicitis

A. Kurt *, I. Çalik, E. Ö. Sener
*Bölge Egitim ve Arastirma Hastane, Dept. of Pathology, Erzurum, Turkey

Enterobius vermucularis is a cosmopolitan parasite of human residing in the lumen of the caecum and appendix. In this study, parasites were seen in appendectomy materials. These nematodes have a worldwide distribution. During the 24-month period between January 2009 and January 2011, 1842 appendiceal specimens were investigated in Erzurum Regional Research and Education Hospital, Turkey. A total of 36 were infected with *E. vermicularis* (2%). Specimens from 27 of the 36 appendices with *E. vermicularis* showed no histological evidence of acute inflammation. It is concluded that parasites in the appendix may produce symptoms which resemble acute appendicitis, but parasitic infection rarely causes adute appendicitis. At some appendices multiple *E. multilocularis* were seen. *E. vermicularis* has lateral alae with easily visible organs. Affected appendices typically show a marked transmural eosinophilic and neutrophilic infiltrate. Both adult worms and larvae may be found in the crypts. When we measured the lenght of the appendices, the average was 6.93 cm in 452 cases versus 6.85 cm in cases infected with *E. vermicularis*. Could the shortness of the appendices be effective in the frequency of the residence of parasites? The mean age of the patients was 24.

060

Autotaxin expression is correlated with prognosis of hepatocellular carcinoma

M. Lambropoulou *, I. Memet, G. Tripsianis, A. Tsaroucha, G. Kolios, V. Aidinis, A. Kiziridou, N. Papadopoulos, T.-E. Deftereou, K. Simopoulos, E. Chatzaki
*Democritus University Thrace, Dept. of Histology-Embryology, Alexandroupolis, Greece

Objective: Hepatocellular carcinoma (HCC) is one of the most common and aggressive malignancies. Autotaxin (ATX), or nucleotide pyrophosphatase/phosphodiesterase 2 (NPP2), is an exo-enzyme originally identified as a tumor cell autocrine motility factor. ATX is unique among the NPPs in that it primarily functions as a lysophospholipase D, converting lysophosphatidylcholine into the lipid mediator lysophosphatidic acid (LPA). ATX has been shown to be involved in many cancers. In this report we investigate the expression of ATX and its correlation with HCC prognosis and patient survival.
Method: ATX expression was evaluated in 28 liver biopsies obtained from patients undergoing resections for HCC using immunohistochemistry. In parallel, ATX expression was examined in ten normal liver tissues (archival material). Statistical analysis related ATX expression levels with clinicopathological and demographic characteristics and survival.
Results: Results showed a positive correlation between ATX overexpression and grade (G2–G3), hepatitis, increased AFP levels and cirrhosis. All nonmalignant biopsies were negative. Furthermore, patients with high ATX expression levels showed lower survival rate in a 25-month period as revealed by the Kaplan–Meier method.
Conclusion: Our results showed that ATX overexpression is associated with poor prognosis in HCC and indicated a diagnostic potential of this protein. Its role in the carcinogenetic process awaits further elucidation.

061

Correlations between angiogenesis, clinicopathological factors and prognosis in gastric carcinoma

E. Lazar *, S. Taban, A. Dema, D. Lazar, M. Cornianu, A. Muresan, C. Lazureanu, A. Faur, M. Grigoras
*University of Medicine, Dept. of Pathology, Timisoara, Romania

Objective: Vascular endothelial growth factor (VEGF) has a potent angiogenic activity and cyclooxygenase-2 (COX-2) supports angiogenesis by regulated production of angiogenic factors, including VEGF. Our purpose was to examine the expression of VEGF combined with COX-2 and CD34, their correlation with clinicopathological factors, and their prognostic significance in gastric carcinoma.
Method: Specimens from 61 consecutive patients with gastric carcinoma were immunohistochemically investigated for COX-2 and VEGF expression. Tumor microvessel density (MVD) was assessed using CD34 immunostaining. Correlations between the expression of VEGF, COX-2, CD34, clinicopathological factors and prognosis were studied.
Results: COX-2 and VEGF were (+) in 57.4% and 65.6% of the patients, significantly higher vs. normal gastric mucosa (4.9% and 6.5%; $p<0.001$). Positive correlation was found between VEGF and COX-2 and between VEGF and CD34. The VEGF(-) carcinomas were COX-2(+) only for 19% of the cases. The VEGF(+) carcinomas have associated COX-2 immunoreactivity in 77.5% of the cases. VEGF expression was significantly correlated only with depth of invasion ($p=0.010817$). Patients with VEGF(+) showed lower 5-year survival rates vs. VEGF(-) (12.5% vs.23.8%; $p=0.027983$).
Conclusion: In our study, VEGF expression correlates with angiogenesis and tumor progression, representing a strong prognostic indicator in patients with gastric carcinoma.

062

Correlation between cyclooxygenase-2 (COX-2) immunohistochemical expression and microvessel density in gastric carcinoma

E. Lazar *, S. Taban, A. Dema, D. Lazar, M. Cornianu, A. Muresan, C. Lazureanu, A. Faur, R. Cornea
*University of Medicine, Dept. of Pathology, Timisoara, Romania

Objective: Despite the decrease in incidence, gastric cancer remains the second leading cause of cancer-related death worldwide. Our study investigates the expression and clinicopathological significance of cyclooxygenase-2 (COX-2) and microvessel density (MVD) in gastric carcinogenesis, assessing their roles in the invasion and prognosis of gastric cancer.
Method: Using LSAB immunohistochemistry, COX-2 and CD34 expressions were examined in 61 gastric carcinomas. MVD was counted and the relationship between the biological behaviors and prognosis was analyzed.
Results: The expression of COX-2 in gastric carcinomas (57.4%) was significantly higher vs. in normal peritumoral mucosa (4.9%, $p<0.001$). The overexpression of COX-2 is significantly correlated with the presence of metastasis, depth of invasion and pTNM stage, but without influencing the prognosis. MVD in gastric carcinomas was significantly higher vs. in the normal mucosa (38.7±8 vs 12.5±5, $p<0.001$). MVD was related to Lauren classification, tumor

grade (p=0.0413) and the presence of distant metastasis (p =0.02791). MVD in COX-2-positive carcinomas (39.4±5) was markedly higher vs. COX-2-negative tumors (31.5±2), indicating a positive correlation between COX-2 expression and MVD.

Conclusion: Our study shows an intense angiogenic activity in the positive COX-2 carcinomas. COX-2 expression, via inducing angiogenesis, may play an important role in gastric carcinogenesis.

063

Endoscopic diagnosis of gastritis correlates poorly with histology

H. Leadbetter *
*Clifton Cottage Farm, Horley, UK

Objective: Previous studies have shown variable rates of concordance between the endoscopic and histological diagnosis of gastritis. Our aim was to determine the rate of agreement between endoscopic and histological diagnoses in patients undergoing endoscopy in a general hospital setting.

Method: We performed a retrospective audit of patients who had gastric biopsy at upper gastrointestinal endoscopy. Biopsies of polyp or neoplasm were excluded. The patients' details, endoscopic appearances and pathological diagnoses were compared. The histological slides were reviewed if there was any ambiguity.

Results: In total there were 400 cases, mean age 65.2 years. In 136 (34%) cases there was disagreement between the endoscopic diagnosis and histological diagnosis. In 56 there was normal endoscopy but abnormal histology, while in 80 gastritis was diagnosed endoscopically but histology was normal. The kappa statistic for this level of agreement is 0.31. There was no statistical association between the rate of discordance and the presence of *Helicobacter*, chemical gastritis, intestinal metaplasia, or any of the indications for endoscopy.

Conclusion: There was a significant discordance between the histological and endoscopic diagnoses of gastritis. We conclude that, in routine endoscopy practice, biopsy is required to make a confident diagnosis of inflammation in the gastric mucosa.

064

Two rare examples of coexistence of multiple malignancies in patients with gastrointestinal stromal tumours

L. Leça *, M. Afonso
*Portuguese Oncology Institute, EPE, Dept. of Pathology, Portugal

Objective: Almost one third of gastrointestinal stromal tumours (GISTs) are discovered incidentally during investigative/therapeutic procedures for unrelated diseases. In this regard, GISTs may coexist with different types of cancer, either synchronously or metachronously. Although the frequency of this association has not been sufficiently analyzed, it varies between 4.5% and 33% in the recent series published in the literature. The major types of GIST-associated cancers are of gastrointestinal (47%), prostatic (9%), breast (7%), hemato-lymphopoietic (7%), renal (6%), pulmonary (5%), female genital tract (5%) and neuroendocrine (3%) origins. Almost 6% of cases can be associated with more than one neoplasia.

Method: CASE REPORTS: Case 1: Man, 69 years old, with duodenal GIST, colorectal adenocarcinoma and hepatocelular carcinoma. Case 2: Man, 82 years old, with gastric GIST, gastric adenocarcinoma, intramucosal colorectal adenocarcinoma, lung carcinoma and urothelial carcinoma of the bladder.

Conclusion: The occurrence of other malignancies in patients with GISTs is unusual and only a few numbers of cases (6%) are associated with multiple neoplasias, being the most common ones breast, colorectal and prostate carcinomas and lymphomas/leukaemias. We herein report two rare examples of coexistence of multiple neoplasias in GIST patients. To our best knowledge, none of them have ever been described in the literature.

065

Undifferentiated (anaplastic) carcinoma of the pancreas with osteoclast-like giant cells

M.-A. Lianou *, M.-E. Kopaka, I. Chrysovergis, I. Gioti, M. Chantziara, M. Konstantinou, C. Kouvidou
*Athens, Greece

Objective: Undifferentiated carcinoma of the pancreas with osteoclast-like giant cells constitutes a rare aggressive tumor (less than 1% of all pancreatic malignancies).

Method: A 61-year-old woman presented to our hospital with episodes of epigastic pain and weight loss of 4.5 kg. Personal history involved type 2 diabetes mellitus. Radiological control revealead a 4-cm mass in the head of the pancreas and Whipple's procedure was performed.

Results: The histological examination showed an undifferentiated carcinoma of the pancreas consisting of areas with ductal adenocarcinoma with mucin production and areas with osteoclast-like giant cells with extensive calcification and production of immature cartilage and osteoid. PanIN I-II, perineural and vascular infiltrations were noted. The carcinoma invaded the submucosa of the duodenum, the wall of the gall bladder and a small part of the liver that was sent as frozen biopsy. The immunohistochemistry was

positive for CK7, CK17, CEA polyclonal, vimentin, CD68. A loss of expression of CEA monoclonal and SMAD-4 was found. Nine months after chemotherapy, the tumor relapsed, followed by generalised carcinomatosis in the abdominal and pelvic region.

Conclusion: Generally, the prognosis of undifferentiated carcinoma of the pancreas with osteoclast-like giant cells is very poor. A number of authors have favored an epithelial origin whereas others suggested a histiocyte/macrophage lineage of the osteoclast-like giant cells.

066

Metastatic malignant melanoma of the small bowel

M.-A. Lianou *, M. Kopaka, P. Kara, D. Violidaki, E. Ronne, G. Nakos, C. Kouvidou
*Athens, Greece

Objective: Primary melanoma is extremely rare. Malignant cutaneous, ocular, oral and anal melanoma show an unusual predilection to metastasize to the small intestine.

Method: An 85-year-old male, with a known case of malignant melanoma of the scalp, first presented 10 years ago, was admitted to our hospital with anorexia, weight loss, and diffuse abdominal pain due to bowel obstruction. The ultrasound revealed a large mass of 16 cm. in the jejunum.

Results: Microscopically, the tumor consisted of epithelioid and partly spindle cells with prominent eosinophilic nucleoli. Mitotic figures were numerous with extensive necrosis and small amount of melanin. The tumor was mainly submucosal with ulceration of the jejunal mucosa and lymph node involvement. Immunohistochemical staining was positive for HMB-45, Melan-A and S-100.

Conclusion: Metastatic melanomas of the small bowel are generally asymptomatic in the early stages, so frequent control of the intestine is mandatory. The prognosis of the metastatic melanomas is poor and the surgical removal of the intestinal metastases is the treatment of choice.

067

Gastrointestinal involvement in chronic granulomatous disease and Crohn's disease: a distinctive histopathological pattern?

P. Luís *, M. Pinto, A. Alves, A. Palha, J. Marques, S. Silva, A. Rute, A. Lopes
*CHLN—Hospital Santa Maria, Dept. of Pathology, Lisboa, Portugal

Objective: Recently, emphasis has been given to the identification of distinctive histopathological patterns in Crohn's disease (CD) and chronic granulomatous disease (CGD). Objectives: Comparative study of the gastrointestinal's mucosal involvement in children with CGD and CD; identification of histopathologic distinctive elements.

Method: Descriptive analysis of endoscopic (first evaluation) and histological findings in four children with CGD with GI symptoms and four children with CD; CD68 immunohistochemical analysis.

Results: CGD: mean age (MA) at diagnosis 34.8 months, CD: MA at diagnosis 9.1 years. The endoscopic findings were similar in both groups. Histologically, in the colon, CGD showed an inflammatory infiltrate by mono/polymorphonuclear (4), granulomas (3) focal cryptitis (3) and focal architectural distortion (2); CD demonstrated an inflammatory infiltrate of mononuclear and polymorphonuclear (4), cryptitis (4), crypt abscesses (3), ulceration (3) and granulomas (3). Despite the presence of pigmented histiocytes in both groups, the highest density in the deep part of the mucosa was observed only in CGD(4). Ileal (CD-2, CGD-1) and gastroduodenal (CD-4, CGD-4) histopathology was identical in both groups.

Conclusion: Despite the results of preliminary nature, which require further confirmation, characterization of histiocytic infiltrate and its topographic pattern is likely to be a distinctive histological finding, suggesting early diagnosis of CGD.

068

A rare benign gastric tumour

W. Majdoub *, R. Sellami-Dhouib, I. Abbes, R. Doghri, M. Driss, S. Sassi, K. Mrad, H. Ben Amor, R. Ben Ghorbel, K. Ben Rhomdhane
*Military Hospital, Tunis, Tunisia

Objective: Most mesenchymal tumors of the stomach are gastrointestinal stromal tumors (GIST). A rare group of non-GISTs include myxoïd mesenchymal neoplasms, among them plexiform fibromyxoma. It is a very rare tumour and is apparently specific to stomach occurring in the antrum and pyloric region.

Method: We report a case of a 34-year-old woman presented with a complaint of epigastralgia of 3 years' duration associated with gastroesophageal reflux.

Results: Ultrasonography revealed a gall bladder lithiasis. Computed tomography and gastroendoscopy showed a gastric submucosal tumor. Laboratory data showed no abnormalities. Partial gastrectomy and cholecystectomy was performed. Macroscopic examination of the surgical specimen revealed a 5x3cm mass of the gastric wall covered by a normal mucosa on the surface. On the cut surface a yellowish to white myxoïd tumor was seen without necrosis. After histopathological and immnohistochemical studies the diagnosis of plexiform fibromyxoma

was established. Microscopic examination of the gall bladder revealed a chronic cholecystitis. The patient has been doing well 3 months after surgery without complaints.
Conclusion: Plexiform fibromyxoma is not included in the differential diagnosis of gastric menchymal tumors because of its rarity. Surgical removal usually involves resection of the antrum. Prognosis is good and there is no tendency to recurrence.

069

Malacoplakia and colonic adenoma: a rare association

K. Manoloudaki *, E. Skafida, E. Arkoumani, A. Chatzitolios, D. Zisis
*Tzaneion Hospital, Pireus, Greece

Objective: Colonic malacoplakia is rare and frequently associated with other diseases like neoplastic or infiammatory disorders, immunodefect syndromes or drugs abuse. Association of malacoplakia with colonic adenoma is extremely rare. Up to date only four (4) cases including our case have been reported from 1974.
Method: We report a case of a 61-year-old female who presented in our hospital with intermittent abdominal pain and stool disorders. She had not any clinical background of inflammatory diseases; she was not under immunodepressive therapy. Clinical and laboratory investigations were performed with normal results. Colonoscopy revealed a polypoid lesion measuring 1 cm in the rectum. A polypectomy was performed at the time.
Results: A histopathological study of the polyp showed a low-grade dysplastic tubulovillous adenoma with typical foci of malacoplakia in the lamina propria consisting of histiocyting aggregate containing easinophilic granules and Michaelis–Gutman bodies (PAS positive, diastase resistant and Von-Kossa positing staining).
Conclusion: We reviewed 150 colonic adenomas to verify if the association of malacoplakia and colonic adenomas is more common than usally expected. No other case was found. Our observation confirmed the rarity of this association.

070

A case of metastatic gastro-duodenal melanoma with unknown site of primary origin

S. Mavropoulou *, Z. Tatsiou, D. Papadopoulou, D. Hatzibougias, P. Mavropoulos
*Xanthi General Hospital, Dept. of Pathology, Greece

Objective: Malignant melanoma (MM) metastasizing to gastrointestinal tract is detected clinically in only 2% of cases and primary focus remains occult in 2.2% of cases.
Method: We report the case of a 67-year-old female patient with unremarkable clinical history, who presented due to epigastric pain of 2 months' duration. An upper gastrointestinal endoscopy revealed multiple darkly pigmented nodular mucosal lessions in the stomach and duodenum and biopsies were taken.
Results: Microscopic examination revealed highly pleomorphic, ovoid or spindle tumor cells with melanocytic granules in the cytoplasm, present in the lamina propria of the stomach and duodenum. Overlying epithelium was unremarkable. Immunohistochemistry was positive for HMB45, Melan A and S100 protein. Accordingly, the diagnosis of metastatic MM to the stomach and duodenum was made. On clinical exploration, an obvious primary focus was not detected. Bone scintigraphy and CT-scan of the abdomen and chest showed metastatic liver, lung and bone disease. Palliative chemotherapy was not possible and the patient died 1 month later.
Conclusion: In conclusion we present an interesting case of extensive metastatic MM with unknown primary focus presented only with epigastric pain. MM is a diagnosis that should be taken into account when evaluating any gastric or duodenal mass lesions with atypical histological features.

071

Exocrine–endocrine modulation in common gastric carcinomas

L. Memeo *, V. Canzonieri, L. Del Col, C. Colarossi, T. Perin, E. Aiello, R. Sigon, R. Cannizzaro,
D. Massi,
*Mediterranean Institute of Oncology, Dept. of Experimental Oncology, Viagrande, Italy

Objective: Gastric cancers are divided into two main categories: exocrine type (carcinomas) and endocrine type (carcinoid tumors and endocrine cell carcinomas). The presence of endocrine tumor cells has been described in about 15–70% of gastric carcinomas.
Method: To evaluate the prognostic implications of endocrine differentiation in gastric carcinomas, 103 cases of adenocarcinomas and undifferentiated carcinomas were studied. Endocrine markers (chromogranin and synaptophysin) were evaluated and the analysis was extended to exocrine markers of gastric type (MUC5AC, MUC6) and of intestinal type (MUC2, CD10, villin). In carcinomas with endocrine differentiation, differentiated endocrine markers of gastric type (gastrin, somatostatin) and intestinal type (GIP, GLP-1) were also evaluated.
Results: Immunohistochemical analysis revealed that 66 tumors (64.1%) were positive for at least one generic endocrine marker. The prognosis of gastric carcinomas with endocrine differentiation was tendentially worse than that of

conventional carcinomas considering relapse rate and mortality. Patients (n=14) with >20% tumor cells positive for chromogranin A and/or synaptophysin were significantly associated to a poorer prognosis than patients with none (n=37) or minimal positivity (n=52) for these markers, even when stage-matched analysis was performed. Gastric carcinomas with exocrine gastric phenotype (n=16) significantly correlated with poorer outcome than carcinomas with exocrine (n=22) or mixed/gastrointestinal (n=64) phenotypes. Our data suggest that expression of endocrine markers of gastric type (n=26) may be considered a negative prognostic factor when compared to endocrine intestinal (n=21) or mixed/gastrointestinal (n=5) stomach carcinomas.

Conclusion: Endocrine differentiation of gastric carcinoma is a significant prognostic marker with a cut-off value of >20% positive cells.

072

Thrombomodulin and proinflammatory cytokines in patients with peptic ulcer disease and gastric cancer infected with *Helicobacter pylori*

M. Molaei *, M. Haghazali, R. Mashayekhi, H. Zojaji, M. A. Pourhoseingholi, T. Shooshtarizadeh, D. Mirsattari, M. R. Zali
*RCGLD, Tehran, Iran

Objective: *Helicobacter pylori* infects more than half of the global population. It is suggested to be related with gastritis, peptic ulcer disease and gastric cancer.

Method: Patients were divided into three groups of PUD, cancer and control (normal endoscopy) according to the results of endoscopy. The serum levels of interleukins 1, 6, 8 and 10 and thrombomodulin was determined using ELISA technique. *H. pylori* infection was diagnosed by histological examination.

Results: One hundred eleven patients were included in the study; 30 as PUD group, 30 as gastric cancer group and 51 as controls. There was no significant difference between the means of IL-1 and IL-10 levels among the three groups (P=0.744 and 0.383, respectively). IL-6, IL-8 and thrombomodulin levels were found to be statically different among the three groups (P-value<0.05). The level of IL-6, IL-8 and thrombomodulin in cancer group was significantly higher than PUD and control groups (P-value<0.05).

Conclusion: There is a significant association between H. pylori infection and serum IL-6, IL-8 and thrombomodulin but such relation is not present between H. pylori and IL-1 and IL-10. Immunity response (IL-6, IL-8 and thrombomodulin) is more severe in cancer patient than PUD.

073

Characterization of small, transitional hepatocytes in human liver

P. Nagy *, K. Dezső, S. Paku
*Semmelweis University, 1st Dept. of Pathology, Budapest, Hungary

Objective: Progenitor cell (mostly called as oval cell) driven regeneration is a well documented, often observed process in rodent liver. However, the details of this reaction are still enigmatic in human. It has recently become generally accepted that certain forms of ductular reactions correspond to oval cell proliferation. There are scarce data about the differentiation of ductular cells into hepatocytes.

Method: We have observed “small” hepatocytes in five liver biopsies, which might be transitional cells between progenitor cells and mature hepatocytes. They were characterized by immunohistochemistry.

Results: Transitional cells are similar to hepatocytes, but they are smaller. They remain components of ductular structures in fulminant liver failure specimens, but their field-like diffuse distribution was observed in two other cases (drug related liver damage). CK 7 staining fades in small hepatocytes, but they start to express HNF-4, CD10 and CYP enzymes.

Conclusion: Transitional, small hepatocytes can occasionally be observed in human livers, supporting the role of progenitor cells in pathological reactions. Their scarcity may be explained by their short lifetime. Collection and characterization of these rare cases may help us to understand their role in liver pathology.

074

Initial presentation of CML as granulocytic sarcoma within an incidental colon polyp

A. Neto *, G. Oroszi, N. Shafi, M. Rose, B. Kenney
*VA Healthcare System, Dept. of Pathology, West Haven, USA

Objective: Granulocytic sarcoma (GS) is an accumulation of malignant myeloid precursor cells in an extramedullary site. GS occurs in patients with acute myelogenous leukemia (AML), and less commonly in those with myelodysplastic syndrome (MDS) or chronic myelogenous leukemia (CML).

Method: A 55-year-old man underwent colonoscopy for hematochezia. A polyp was seen at 20 cm and biopsied. H&E and immunohistochemical staining, as well as cytogenetic studies for t(9;22), were diagnostic of granulocytic sarcoma. Three weeks later, bone marrow biopsy (BMB) was performed. Cytogenetic studies for t(9;22) were positive, and additional immunostaining supported a diagnosis of CML.

Results: The patient was treated, with good hematologic response. Multiple follow-up colonoscopies have shown benign polyps and no evidence of recurrent myeloid proliferation. Follow-up BMBs were negative. Because GS is considered equivalent to blast crisis in CML, the patient is currently awaiting a bone marrow transplant.
Conclusion: GS presenting as a colonic polyp is rare, and misdiagnosis is frequent. The pathologist needs to be aware of this entity, as it may precede or occur concurrently with AML or blast crisis CML. GS can be easily misdiagnosed in this site. Careful morphologic and immunohistochemical evaluation for evidence of myeloid differentiation is required to avoid this important error.

075

FISH analysis of p16, p53, MYC genes abnormalities in pancreatic ductal adenocarcinoma

O. Paklina *, G. Setdikova, M. Ryzhova, D. Rotin, R. Izrailov
*FMBA, Dept. of Pathology, Moscow, Russia

Objective: The aim of our study was investigation of the presence of deletions in p16 и p53 genes, and MYC amplification in PDA in correlation with low-grade and high-grade PDA.
Method: Thirty cases of PDA and seven cases of control pancreatic tissue were included in the study. FISH was performed on 4-μm thick sections of formalin-fixed paraffin-embedded (FFPE) tumors. To validate loci 9p21/p16, 17p13/tp53, 8q24/MYC locus specific identifier (LSI) DNA probes«Vysis», Abbott Inc. were used).
Results: FISH analysis of PDA revealed that most tumors had deletion of loci of interest or tested loci. Deletion of p16 gene was found in 40% (12/30) cases while deletion of p53 gene was found in 56, 7% (17/30). In 58, 3% of cases there were tumors of grade 2. In 13.3% (4/30) monosomy of 9p21 chromosome was seen. There were no statistically significant correlation between clinical and morphological data and the aberrations we found out. MYC amplification was occurred only in high-grade PDA cases (grade 3) and accounted 6.7% (2/30).
Conclusion: Deletion of both p16 and p53 genes are characteristically features of PDA. Amplification of MYC oncogene occurred only in high-grade (grade 3) patterns of PDA.

076

Perivascular epithelioid cell tumor of the ileum presenting as diverticulitis

E.E. Pala *, S. Unluoglu, U. Bayol, N. Sen Korkmaz, B. Ozenen, F. Ipekci
*Tepecik Training and Research, Dept. of Pathology, Izmir, Turkey

Objective: Perivascular epithelioid cell tumors (PEComas) are a group of rare mesenchymal neoplasms. Gastrointestinal PEComas are exceptionally rare, there being only a few case reports in the literature involving the colon and small intestine. Nearly all PEComas show immunoreactivity for both melanocytic (HMB-45 and/or melan-A) and smooth muscle (actin and/or desmin) markers.
Results: A 36-year-old male was admitted to the hospital with acute abdomen. At laparatomy, a nodular mass protruding from the ileum which clinically simulated a diverticulitis was noticed. Gross examination of the specimen revealed a 2×1.5×1-cm secondarily ulcerated solid, nodular, gray white tumor mass in the ileal wall. Histologically the tumor cells were composed of nests of round-polygonal epithelioid cells with abundant clear to slightly eosinophylic granular cytoplasm and round vesicular nuclei. The nests were seperated by thin fibrovascular septa. Necrosis and low mitotic activity was noticed in the tumor. Immunohistochemically, tumor cells were positive for SMA, HMB45 and MELAN A and negative for CD10, RCC, CD45, CD117, CD34, EMA, DESMIN. Diagnosis was PEComa of the ileum.
Conclusion: We report the case of ileal PEComa to remind the unusual presentation (diverticulitis) of these tumors, besides rarity and diagnostic difficulties.

077

A rare case of anorectal melanoma

C. Popp *, S. Zurac, G. Maria, C. Zaharia, R. Andrei, G. Mirea, F. Stăniceanu, A. Croitoru
*Colentina University Hospital, Dept. of Pathology, Bucuresti, Romania

Objective: Anorectal melanoma (ARM) is an uncommon (less than 1% of anorectal tumors and approximately 0.4–1.6% of all melanoma localizations) and aggressive tumor. Only 500 isolated cases have been reported up to now. There is no staging system for ARM due to the scarcity of data regarding the prognosis of this lesion.
Method: We report a rare case of anorectal melanoma in a 62-year-old male who presented with a history of diarrhea, tenesmus and rectal bleeding.
Results: During colonoscopy, a biopsy was performed, histopathologically diagnosed as malignant melanoma. He received interferon for 3 months in high doses and was referred to surgery for resection. A preoperative ultrasound revealed a left liver lobe mass. An abdominoperineal amputation with the resection of the left liver lobe was performed. Examination revealed a 9/4 cm solid tumor just 0.2 cm above the anal verge, and several enlarged perirectal and inguinal nodes. The ulcerated tumor consisted of strands and nests of medium/large epithelioid and spindle-

shaped cells, some with brown intracytoplasmatic pigment, invasive in the anal musculature. Metastases were present in the liver, omentum and 19 regional lymph nodes.
Conclusion: Pathological and clinical surveillance of these rare tumors is important in attempt of establishing a staging system for treatment and prognosis.

078

Transition from epithelial-type to mesenchymal-type expression of β-catenin and E-cadherin in colorectal carcinoma

A. Radowicz-Chil *, W. Rezner, M. Ostrowski, J. Kopczyński, J. Sygut
*Holycross Cancer Centre, Dept. of Neoplasm Pathology, Kielce, Poland

Objective: Carcinomatous progression is often related to switch in epithelial-like phenotype with membranous β-catenin and E-cadherin to mesenchymal-like phenotype marked by nuclear translocation of β-catenin and gradual loss of E-cadherin. This, among other markers of the process, is believed to facilitate discohesion, motility and invasion. We investigated the phenomenon in our material.
Method: We reviewed our institution records of all total colorectal carcinoma excisions in the last six years and by exclusion we chose 36 cases of well differentiated carcinomas with angioinvasion, nodal metastases and without preoperative radio/chemotherapy. We assessed tumor architecture in HE and broad-spectrum cytokeratin stained slides to select sites containing invasive front with single or small groups of cells and inner, well-differentiated portion of the tumor. In those sites we evaluated the expression of β-catenin categorized as membranous or cytoplasmic/nuclear and E-cadherin categorized as membranous or cytoplasmic/none.
Results: In all cases well-differentiated sites demonstrated membranous expression of both β-catenin and E-cadherin. Cytoplasmic/nuclear expression of β-catenin at the invasive front was detected in 24/36 cases and none or cytoplasmic expression of E-cadherin in 33/36 cases.
Conclusion: Concordantly with other research groups, we demonstrated epithelial to mesenchymal immunophenotype transition at the invasive front in majority of our cases.

079

Amphicrine tumor of the liver

I. Rodriguez Perez *, A. Martinez Penuela Marco, A. Panizo Santos, J. M. Martinez Penuela Virseda
*C. Hospitalario de Navarra, Sº de Anatomia Patologica, Pamplona, Spain

Objective: Amphicrine tumors are extremely rare and they are defined by evidence of glandular and neuroendocrine differentiation in the same cell.
Method: A 45-year-old man presented with abdominal pain and diarrhea. Endoscopy revealed a gastric ulcer and ultrasonography a 6-cm mass in the liver. Laboratory tests showed high levels of gastrin. A clinical diagnosis of Zollinger–Ellison syndrome was done. An endoscopic ultrasound examination and magnetic resonance were performed without abnormalities. With the clinical diagnosis of liver metastasis from neuroendocrine carcinoma of unknown origin, the patient was brought to surgery.
Results: The tumor consisted of sheets of cells separated by fibrous septae. There was a monomorphic population of cells. Surprinsingly there were many intracytoplasmic vacuoles, imparting a signet-ring-like appearance, which showed positivity for epithelial membran antigen and alcian blue. The tumor cells were positive of chromogranin, synaptophysin, CD56, gastrin, and cytokeratin 19. By electron microscopy we found some cells with variable numbers of dense-core membrane-bound granules of neurosecretory type and exocrine granules of mucin type.
Conclusion: To our knowledge, this is the second reported case of amphicrine tumor primarly ocurring in the liver. Initially it was suspected to be a metastasis from gastrinoma; however, the exhaustive examination showed no tumor in another location.

080

Co-occurring gastric amyloidosis and *Helicobacter pylori*-associated gastritis presenting with massive upper gastrointestinal hemorrhage

D. Sakonlaya *, K. Kuntanpreeda
*Thammasat University, Dept. of Pathology, Pathumthani, Thailand

Objective: Gastrointestinal (GI) involvement by primary systemic amyloidosis is rare, comprising of 8% of all cases and only 1% is symptomatic. Patients with gastric amyloidosis may present with upper GI bleeding, nausea/vomiting, and weight loss. Herein we reported a case of multiple myeloma with co-occurring gastric amyloidosis and *Helicobacter pylori*-associated gastritis presenting with massive upper GI bleeding.
Method: Case report of gastric amyloidosis with endoscopic and histological studies.
Results: A 86-year-old Thai male with underlying multiple myeloma and hepatitis B viral cirrhosis had passed black watery stool for 3 days with palpitation and fainting. No hematemesis, nausea/vomiting or abdominal pain were complained. Physical examination revealed hypotension and mild pallor without signs of chronic liver disease

except mild jaundice. Abdomen was soft, with no palpable mass. Rectal examination revealed melena. Esophagogastroduodenoscopy revealed diffuse severe gastroduodenitis with a superficial gastric ulcer. Biopsy of antrum showed a mild degree of chronic active gastritis associated with *H. pylori*. In addition, extracellular deposition of Congo-red-positive eosinophilic material in lamina propria and muscularis mucosae was observed. Gastric amyloidosis was diagnosed. Twenty-five days after admission, the patient died of cardiac failure with sepsis.
Conclusion: A case of gastric amyloidosis with *H. pylori*-gastritis was reported.

081

Prognostic significance of expression of Her-2, P53, Ki-67 ve Cyclin-D1 in carcinomas of the esophagus

E. Sener *, N. Gursan, H. Balta, S. Sipal, Z. Turan, A. Yilmaz
*Erzurum Bolge Egitim Hastanesi, Patoloji Bolumu, Turkey

Objective: This study aims to investigate the correlation between of expression of Her-2, P53, Ki- 67 ve cyclin-D1 and prognostic factors in patients with esophageal squamous cell carcinoma (ESCC).
Method: Primary tumors from 67 patients with ESCC were immunohistochemically studied for the expression of Her-2, cyclin D1, p53, Ki-67 labeling index (LI). Between vascular tumor invasion, lymph nodes metastases and tumor size and the expression of Her-2, Ki-67 labeling index (LI), cyclin D1, p53 was examined.
Results: The mean Ki-67 LI was 55 ± 94.9% (range, 15.1–6.1%). P53 expression was detected in 55 of the carcinomas (82%) and cyclin D1 expression was detected in 48 (71.6%). Her-2 expression was detected in two of the carcinomas (2.98%). Lower Ki-67 LI, p53 and cyclin D1 expression were detected in lymph nodes metastases and vascular tumor invasion—negative group compared with positive group (P=0, 00044, P=0.00042, P=0.0033, respectively).
Conclusion: Ki-67 LI and p53 expression, cyclin D1 expression may be used as prognostic factors for patients with esophageal carcinoma. However, the results of the current study do not support Her-2 expression as a prognostic factor.

082

Diffuse microscopic venous malformation of the stomach in a child

Z. Stojsic *, R. Stevanovic, D. Bacetic, V. Perisic
*University of Belgrade, Schoolf of Medicine, Inst. of Pathology, Serbia

Objective: Vascular anomalies are an uncommon cause of gastrointestinal bleeding in children. We present a rare case of venous malformation of the stomach as a source of recurrent episodes of massive hematemesis in an 18-month-old girl.
Method: The whole stomach was sampled for histological analysis. Sections were stained with hematoxylin–eosin and double histochemical–immunohistochemical staining with Weigert's resorcin fuchsin method for elastic tissue fibres and the streptavidin–biotin technique with the αSMA antibody.
Results: Prior to lifesaving gastrectomy, endoscopy demonstrated only erosive haemorrhagic gastritis that was confirmed in endoscopic biopsy. Gross examination of the resected stomach disclosed only diffuse mucosal haemorrhage. In 20 out of 28 sections of the gastric corpus there was a widespread distribution of large, markedly ectatic, non-tortuous and thin-walled veins in the submucosa. Some portions of mucosal lamina propria contained dilated venules and capillaries. The whole mucosa showed acute erosive gastritis. Arteries were not affected. There was frequent absence of muscular layer of the ectatic veins and, instead, small amount of elastic fibers lined by endothelium.
Conclusion: We presented a case of diffuse microscopic ectatic venous malformation of the stomach that was somewhat dissimilar to well-known angiodysplasia, lacking endoscopic and macroscopic visibility and vessels tortuosity, as a histological feature.

083

The immunohistochemical expression of MUC1 as a prognostic factor in gastric carcinoma

S. Taban *, D. Lazar, A. Dema, M. Cornianu, E. Lazar, M. Grigoras
*University of Medicine, Dept. of Pathology, Timisoara, Romania

Objective: To investigate the relationship between MUC1, MUC2 and MUC5AC expressions and clinicopathological factors in gastric carcinomas with regard to prognosis and survival.
Method: From 256 patients with gastric cancer, there were 61 selected patiens with available follow-up data (median survival time of 14.4 months, ranging from 1 to 68 months). We performed immunohistochemical reactions for MUC 1 (Ab-5), MUC2 (Ab-2) and MUC5AC (Ab-1).
Results: MUC1 was detected in 41 cases (67.2%), MUC2 in 25 cases (40%) and MUC5AC in 43 cases (70.5%). Our results showed a higher positivity of MUC1 immunoreactions in patiens with age over 61 (P=0.057). Patients with MUC1 positive carcinomas

survived significantly less than patients with MUC1 negative carcinomas (12.2% vs. 25% P=0.0047). Patients with MUC1 positive carcinomas were about two times more likely to die than those with MUC1 negative carcinomas (P=0.008). MUC2 was correlated with mucinous adenocarcinomas (87.5%, P=0.052). The data obtained are not suggestive for a relationship between survival rates and the immunohistochemical expressions of MUC2 and MUC5AC.

Conclusion: In our study, the immunohistochemical expression of MUC1 represents an important prognostic factor. The data obtained confirms the hypothesis according to which the heterogeneous expression of mucines and the "de novo" synthesis of non-gastric mucines correspond to advanced stages of gastric cancer.

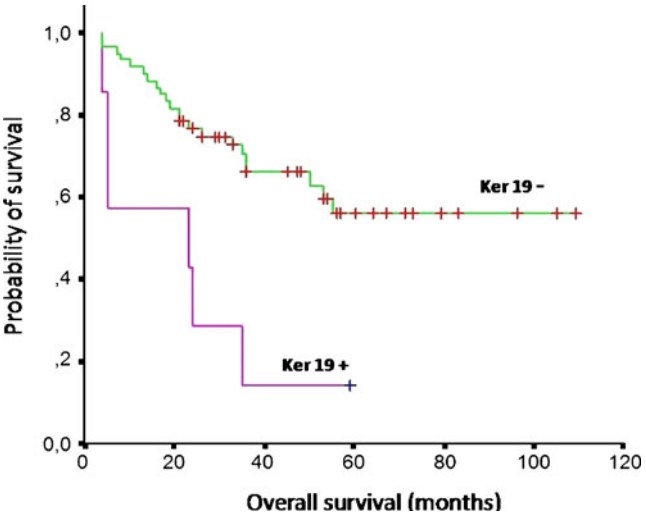

084

Keratin 19 immunophenotype is an independent predictor of survival in human hepatocellular carcinoma

D. Tiniakos *, E. Fatourou, J. Delladetsima, M. Paleologou, D. Karandrea, E. Antoniou, E. Felekouras, J. Koskinas
*University of Athens, Laboratory of Histology-Embryology, Greece

Objective: Keratin 19 (K19), a marker of hepatic progenitor cells, has been correlated with tumour recurrence and decreased overall survival mainly in Asian hepatocellular carcinoma (HCC) patients. In contrast, recent data from American post-transplant HCC patients show no prognostic significance for K19. We aimed to assess for the first time K19 expression in HCC of Greek patients in correlation with clinico-pathological parameters and survival.

Method: Immunohistochemistry for K19 was performed in 89 HCC (grade I 10, II 36, III 31, IV 11, TNM stage I 24, II 15, III 32, IV 6, aetiology HBV 35, HCV 26, alcohol 9, other 14) from 89 patients (mean age 67.11 years, 76.5% male) with mean follow-up 39.6±25.3 months. K19 immunoexpression was considered positive if >5% tumour cells were stained.

Results: K19 was positive in 9/89 (10.1%) HCCs. K19 expression tended to correlate with vascular invasion (p =0.054) but not with other clinico-pathological parameters (age, sex, tumour size, grade and stage). Cox-regression analysis revealed that K19 positivity was independently associated with increased recurrence rate (P<0.001, OR 6.022, 95% CI 2.296–15.79) and decreased overall survival (p=0.017, OR 3.845, 95% CI 1.269–11.648).

Conclusion: K19 is an independent predictor of tumour recurrence and poor overall survival in Greek HCC patients.

085

KIT mutation testing in a small intestinal gastrointestinal stromal tumor coexisting with its mimic mesentric fibromatosis

V. Tzioufa-Assimakopoulou *, V. Kotoula, G. Petrakis
*Aristotle University of Greece, Dept. of Pathology, Thessaloniki, Greece

Objective: We present a case of a 64-year-old man with synchronous development of low risk small intestinal gastrointestinal stromal tumor (GIST) and mesenteric fibromatosis (MF), a known mimic of GIST. GIST are reported to develop synchronously or metachronously with other tumors, occasionally raising diagnostic problems at the histological and immunohistochemical level. KIT gene mutations occurring in 80–85% of GIST usually help in the differentiation.

Method: We conducted a thorough histological and immunohistochemical study of both lesions. DNA was extracted from paraffin sections from these lesions and was tested for integrity. Mutation analysis was performed with cycle sequencing followed by capillary electrophoresis for KIT exons 9 and 11 with intron spanning primers.

Results: GIST immunophenotype was CD117+, CD34+, SMA+, S100+, desmin-, CD56-, b-catenin-. MF immunophenotype was CD117-, CD34-, SMA-, b-catenin+. Mutation analysis was successful only for the GIST lesion and revealed a heterozygous A>G transition in c.1484 (exon 9) resulting in the amino acid substitution p.N486S in the corresponding protein.

Conclusion: The distinction between GIST and possible mimics, as well as the identification of KIT exon 9 mutations are important for clinical decision making since high doses of imatinib should be scheduled in such cases.

086

Prevalence of gastrointestinal polyps detected by endoscopic screening

H. K. Türköz *, F.D. Kaymakçi, Ç.A. Çelikel
*Medical Faculty of Marmara, Dept. of Pathology, Istanbul, Turkey

Objective: Polypoid lesions in the gastrointestinal system are frequent lesions which may have adenomatoid/premalignant changes. We studied histology and endoscopic features of gastrointestinal polyps.
Method: A total of 3,210 pathology reports of esophagogastroduodenoscopy and colonoscopy procedures in Medical Faculty of the University of Marmara from March 2009 and March 2011 were searched for the diagnosis of gastrontestinal polyps.
Results: The number of gastrointestinal polyps was 286. A total of 8% of the polyps were localised in stomach (n=23), 2.5 percent (n=7) in small intestine and 89.5 percent (n=256) were in the colon and rectum. Prevalance of adenomatous polyps was 188 (65.7%). None of the polyps in the stomach was adenomatous. Adenomatous polyps were localised in colon and rectum (n=185, 98.5%) and ileum (n=3, 0.5%). Most of the polyps in stomach were fundic gland polyps (n=13), while the rest were hyperplastic polyps (n=10).
Conclusion: Adenomatous polyps are more frequently localised in the distal gastrointestinal system. The high ratio of fundic gland polyps in stomach is probably because of the widespread use of proton pump inhibitors.

087

ADAM9, ADAM10 and ADAM17 expression in gastritis and normal gastric mucosa

C. Uzun *, N. Erin, S. Türker, G.Ö. Elpek, B. Yildirim
*Akdeniz University, Dept. of Pathology, Antalya, Turkey

Objective: The ADAMs are membrane-anchored cell surface glycoprotein's that play important roles in inflammation. The purpose of this study was to evaluate whether the expression of three members of the ADAMs family (ADAM9, ADAM10 and ADAM17) is different among normal and inflammated gastric mucosa.
Method: Gastrectomy specimens of 32 patients were included in the study. Cases were divided in three groups. G1: normal mucosa (n=6), G2: gastritis (n=11) and G3: gastric ulcer (n=15). Serial sections were stained with ADAM9, ADAM10 and ADAM17 by immunohistochemistry. Anova and Tukey–Kramer multiple comparison tests were performed.
Results: In all cases ADAM10 expression was negative in surface epithelium, except in one case with gastritis (G2). Glandular expression was more frequent in G2($p<0.05$). Both ADAM9 and ADAM17 expression by surface epithelium were frequently detected in G1 and in G3 when compared to gastritis (G2) ($p<0.05$). In G2, glandular staining with either ADAM9 or ADAM17 was more diffuse and stronger than other groups ($p<0.05$).
Conclusion: Our results suggest that the expression of ADAM9, ADAM10 and ADAM17 might be altered by inflammation. However the decreased expression of these two glycoproteins in surface epithelium in cases with gastritis, necessitate further studies to better characterize the net effect of ADAM9 and ADAM17 in surface epithelium of the inflamed gastric mucosa.

088

Three cases of gastric adenocarcinoma with choriocarcinomatous component

C. Uzun *, F. Çelik, G.Ö. Elpek, M.T. Gelen
*Akdeniz University, Dept. of Pathology, Antalya, Turkey

Objective: Gastric adenocarcinoma with choriocarcinomatous component (GACC) is an extremely rare and highly malignant tumor with uncertain pathogenesis. Herein is described three cases of GACC with both HER-2 expression and gene amplification within the choriocarcinomatous elements.
Results: The first patient was a 50-year-old man who was admitted to the hospital with weight loss, vomiting and epigastric pain. The second case was a 42-year-old man complaining from abdominal pain. Finally, the third case was a 62-year-old woman with a 2-month history of dizziness and vomiting. In all cases, both endoscopic and radiographic imaging revealed a haemorrhagic and necrotic tumor in the stomach. Histological examination of the tumors revealed two components. In all cases while choriocarcinomatous component displayed a strong positive immunohistochemical staining for beta-subunit of human chorionic gonadotropin, areas of adenocarcinoma expressed CK7 and CEA. The assessment of HER-2 expression demonstrated that together with adenocarcinoma trophoblastic cells display strong positivity. At further investigation by FISH amplification, trophoblastic cells demonstrated a gain of chromosome 17 which is among the most common genetic change in gastric adenocarcinomas.

Conclusion: Our findings suggest that GACC genetically possesses the characteristic of both adenarcinoma and choricarcinoma and supports the theory that the choriocarcinomatous component of GACC arises from a dedifferentiation of an adenocarcinoma.

089

Immunohistochemical expression of cyclooxygenase-2 in colorectal carcinoma and its correlation with clinicopathological features

T. Vasilakaki *, E. Skafida, D. Zisis, E. Arkoumani, E. Moustou, X. Grammatoglou
*Tzaneion Hospital, Dept. of Pathology, Piraeus, Greece

Objective: Epidemiological studies have shown that the cyclooxygenase-2(cox-2) protein may be involved in colorectal carcinogenesis but whether its expression is a prognostic factor for colorectal cancer is controversial. The aim of this study was to investigate the expression of cox-2 in colorectal cancer and to correlate it with clinicopathological parameters.
Method: Immunohistochemical staining for cox-2 was carried out on a paraffin-embedded tissue section, 4 μm in thickness, from specimens of 90 patients who underwent surgery for colorectal cancer. Data about sex, age, size and location of the tumour, grade, necrosis, depth of invasion, status of lymph nodes, vascular invasion and Astler–Coller stage were obtained from all patients. The staining degree was evaluated as weak, moderate and strong. Cox-2 expression was classified in three groups corresponding to the percentage of positive carcinoma cells: (≤25%, >25%–≤50%, >50%).
Results: Tumour cells showed positive staining for cox-2 in 74 cases (82%). Cox-2 was expressed heterogeneously in the cytoplasm and the degree of staining was moderate to strong. Also cox-2 was expressed in many inflammatory interstitial cells around the tumour tissue. There was no relationship between the levels of intensity and extent of cox-2 staining and all of parameters ($p>0.05$).
Conclusion: This study suggests that cox-2 does not appear to be a reliable prognostic factor in colorectal carcinomas.

090

Metaplasia of the gastric mucosa as a criterion of evaluation of the chronic atrophic gastritis

S. Vernygorodskyi *
*VNMU, Dept. of Pathology, Vinnitsa, Ukraine

Objective: The spreading of the gastric mucosa metaplasia in pre-tumour and neoplastic processes remains uninvestigated.
Method: In the 4-year period between January 2005 and December 2009, a total of 1,165 upper gastrointestinal endoscopies with gastric biopsy were carried out at Vinnitsa Pathoanatomical Regional Bureau. In each case, haematoxylin and eosin, high-iron diaimine, alcian blue (pH 2.5 and 1.0)/periodic acid Schiff stained sections.
Results: Two main types of atrophy can be recognized: one characterized by the loss of glands, accompanied by fibrosis or fibromuscular proliferation in the lamina propria, and one characterized by the replacement of the native glands with metaplastic glands. The atrophy due to extending of intestinal metaplasia was classified into four types: 0. Indefinite for atrophy—atrophy associated with metaplasia. Metaplastic changes restricted to the foveolar segment of the gastric glands are not considered as atrophy because they do not completely replace a native gastric gland (should be reported as foveolar-restricted (i.e. partial) intestinal metaplasia). 1. Mild atrophy with intestinal metaplasia. A few native oxyntic glands are replaced by intestinalized glands. 2. Moderate antral atrophy, but, in some cases, metaplastic glands may be closely packed with a minimal amount of interglandular connective tissue (depth of the metaplasia expansion up to neck parts). 3. Severe metaplastic atrophy of the gastric mucosa (extensive intestinalization—depth of the metaplasia expansion up to lamina propria and muscularis).
Conclusion: The association between metaplasia and atrophy of the gastric mucosa was studied on the basis of biopsies of the gastric mucosa. The grades of atrophy degrees depending on the depth of the metaplasia expansion were proposed.

091

Extraintestinal presentation of Whipple disease complicated by secondary amyloidosis: a case report and review of literature

M. Vidal Borrego *, R. Orellana, A. Bueno, Ó. Pinzón, M. R. Bella, A. Casalots, E. Sanfeliu, L. Palacio, M. Rey
*Hospital Parc Taulí, Pathology, Sabadell, Spain

Objective: Whipple's disease (WD) is a rare systemic infectious disease, caused by *Tropheryma whipplei*, involving gastrointestinal tract. Classically, WD manifests with fever, diarrhea and polyarthralgias, although other forms of presentation have been described. The diagnosis is established by clinical and histological findings.

Method: The patient was 70 years old with 8-month history of abdominal pain, toxic syndrome and anemia. CT scan showed mesenteric and retroperitoneal lymphadenopathies. The lymph node was excised, suspecting a lymphoproliferative disease.
Results: Histologically, the lymph node showed distention of sinuses with foamy histiocytes, lipid vacuoles, sarcoid-like granulomas and thickened vessels. These histiocytes showed intracytoplasmic positivity for PAS, PAS-diastase and Warthin–Starry stain and were negative for mycobacterium's stain. Vessels showed Congo Red-positive material and amyloid AA protein positivity. Diagnosis was WD involving lymph node with secondary amyloidosis. Duodenal biopsy was performed with the same result. Despite antibiotic therapy, the patient underwent multisystemic failure and was exitus.
Conclusion: The diagnosis of WD is not difficult when is clinically suspected. It has been reported in about 1,000–1,500 cases in which 15% exhibit non-classic manisfestations. The presence of lymphadenopathy is not uncommon but the association of amyloidosis is very rare (only six cases were reported). WD is misdiagnosed in cases with unusual presentations and the differential diagnosis must include other entities.

092

Her2 status investigation by IHC and FISH in primary and metastatic gastric adenocarcinomas

E. Vrettou *, M. Bobos, V. Tzioufa, G. Petrakis, G. Raptou, A. Polyzou
*Aristotle University Thessaloniki, Medical School, Dept. of Pathology, Greece

Objective: Recent studies showed the predictive value of HER2 in gastric carcinomas. The aim of our study was to investigate HER2 status in primary and metastatic gastric adenocarcinomas by IHC and FISH.
Method: TMAs from 84 primary and 47 paired nodal metastases of gastric adenocarcinoma cases were created. HER2 status was investigated by IHC, mRNA and FISH according to established criteria.
Results: HER2 amplification was observed more frequently in well-differentiated tumors ($p=0.006$). A total of 13/82 (15.9%) of primary and 6/39 (15.4%) of metastatic tumors expressed HER2 protein, while gene amplification was observed in 21.4% (18/84) and 23.8% (10/42) of primary and metastatic sites, respectively. A total of 8/13 HER2 IHC positive cases and 8/68 HER2 negative IHC cases were FISH HER2 positive ($p<0.001$). In primary tumors, HER2 was amplified in 4/39 cases with negative HER2 (0, 1) and 4/29 with HER2 2+. 5/6 HER2 positive metastatic and 5/31 HER2 negative cases were FISH HER2 positive ($p=0.001$).
Conclusion: Our findings concur with the literature. The observation that FISH assay can detect tumors with negative IHC implies that combining these two techniques will probably add new patients who will benefit from targeted therapy.

093

Clinicopathological significance of metallothionein-1 and -2 expressions in hepatocellular carcinoma

E. Yu *, Y. Park
*UUMC Asan Medical Center, Dept. of Pathology, Seoul, Republic of Korea

Objective: Metallothioneins (MTs), a group of intracellular metal binding proteins, are involved in diverse cellular functions. The aims of the present study are to evaluate the relationship between the expressions of MT-1 and MT-2 in hepatocelluar carcinoma (HCC) and clinicopathological parameters of HCC and to determine the role of MT-1 and MT-2 expressions as prognostic markers in HCC.
Method: Expressions of MT-1 and MT-2 were evaluated immunohistochermically in 854 surgically respected specimens of HCC with nonneoplastic liver tissue using the tissue microarray method.
Results: Expressions of MT-1 and MT-2 were decreased in HCC compared with non-cancerous liver, and significantly correlated with tumor size ($p<0.01$), lymphatic invasion ($p<0.01$), Glisson capsule invasion ($p<0.01$), hepatitis ($p<0.01$), cirrhosis ($p<0.01$), and serum AFP ($p<0.05$). The percentage of MT-1 and MT-2-positive cells was significantly inversely correlated with histological grade ($p<0.01$). Nuclear expression without cytoplasmic expression was mainly observed in grade 3 or 4 HCC.
Conclusion: The relationship between the expressions of MT-1 and MT-2 and various poor prognostic factors may suggest a role of MTs as a prognostic marker of HCC.

094

Serrated polyps of the appendix: do they differ from their colorectal counterparts?

Y. Yuyucu Karabulut *, B. Savas, A. Ensari, N. Kursun
*Ankara University, Medical School, Dept. of Pathology, Turkey

Objective: The family of serrated polyps (SPs) comprising sessile serrated adenoma/polyps (SSA/Ps), traditional serrated adenomas (TSAs), and hyperplastic polyps

(HPs) are most commonly found in the colorectum while it is possible to see appendix localization where morphologic parameters may differ from their colorectal counterparts. We therefore, decided to review the serrated polyps of the appendix in the largest series reported so far.

Method: Among a total of 960 appendix specimens 71 SPs were found. All morphologic parameters and demographic features were compared using a two-tailed Mann–Whitney *U* test and Fisher exact test where appropriate.

Results: Of the 71 cases 2 were TSAs, 33 were SSA/Ps and 36 were HPs. There were 32 men and 39 women with a mean age of 48.5 years. Histological examination revealed that 35 SSA/Ps showed basal dilatation (n=33) and serration (n=33), T/L-shaped crypts (n=33), and ectopic crypts (n=24) with a significantly higher frequency compared to HPs (p=0.001). Eleven of the SSA/Ps had dysplastic features compared to the four HPs showing dysplasia (p=0.001).

Conclusion: Morphologic parameters such as basal crypt dilatation, basal serration, T/L-shaped crypts and, to a lesser extend ectopic crypts, seem to be the most discriminatory criteria for SAA/Ps of the appendix.

095

Expression of nuclear PTEN and cdx2 in gastric carcinoma: correlation with clinicopathologic features and prognosis

A. Zizi-Sermpetzoglou *, V. Savvaidou, E. Moustou, E. Arkoumani, N. Tepelenis
*Tzaneio General Hospital, Pireaus, Greece

Objective: Gastric cancer is the second leading cause of cancer mortality in the world. The aim of this study was to determine the value of a combined analysis of Cdx2 and nuclear PTEN expression in distinguishing histological types and prognosis of gastric cancer.

Method: We studied immunohistochemically 88 primary human gastric carcinomas from which 35 were diffuse type and 53 were intestinal type. Cdx2 and nuclear PTEN were performed on paraffin embedded section.

Results: In the diffuse type of gastric carcinomas 10/35 (29.5%) showed immunoreactivity for cdx2, while in the intestinal type the immunoreactivity was noted in 30/53 (56.6%) carcinomas. Expression of Cdx2 was significantly higher in intestinal type carcinomas that in diffuse type (p=0.029). There was clearly negative correlation between Cdx2 and nuclear PTEN expression and lymph nodes metastasis (p=0.048). The patients with Cdx2-positive and nuclear PTEN-positive expression show higher survival rate than those with Cdx2-negative (p=0.001) or nuclear PTEN-negative expression (p= 0.002). Multivariate analysis revealed that the expression of Cdx2 was independent prognostic indicator (p=0, 0012).

Conclusion: This study suggests that combined analysis of Cdx2 and nuclear PTEN has significant value in distinguishing histological types and in predicting the prognosis of gastric carcinoma.

096

Duodenal ulcer disease

A. Zubritsky *
*Moscow, Russia

Objective: The goal of this sudy was to determine the incidence of duodenal ulcer disease (DUD) on postmortem material obtained at Taldom Hospital.

Method: The method invloved was comprehensive analysis of 830 postmortem examinations of adults.

Results: We revealed 13 cases (7 men, 6 women) of DUD that had been the primary cause of death. The ulcers were chronic and in the exacerbation phase (11 cases); in two cases these were acute, a fact which had been confirmed histologically, with most common localization being the bulb of duodenum (13 cases), and the largest ulcer reached a size of 6×3 cm. The immediate cause of death was peritonitis (seven cases) and acute posthemorrhagic anaemia (six cases). In five cases, there was an observed discrepancy between clinical and postmortem diagnoses of underlying disease. The reasons for discrepancies in diagnoses were short length of stay in the hospital and severity of patient, violation of principle of making clinical diagnosis, underestimation of clinical data and misinterpretation of data obtained during operation. In one case, a patient needed an emergency surgery for health reasons.

Conclusion: The DUD as a primary cause of death amounted to 1.57% at our general somatic hospital over 15 years. In 5 (38%) cases out of 13, a discrepancy of diagnoses of the underlying disease was found and requires the provision of significant measures aimed at improving therapeutic and diagnostic work in health care setting.

097

Relationships of Cx26 with regulators of apoptosis, P53 and Bak in colorectal adenocarcinomas

A. Wincewicz *
*Bialystok, Poland

Connexin 26 (Cx26)—a representative protein of gap junctions of intercellular communication (GJIC)—was recently announced to be a factor of good prognosis in Cx-26 positive colorectal cancers versus Cx-26 negative ones. However, there is a great disagreement among various studies on the relation between Cx-26 and P53 as they were positively or negatively associated with each other. Cx-26, P53 and Bak were labelled with immunohistochemistry in 103 colorectal adenocarcinomas. There was mainly aberrant cytoplasmic expression instead of membranous one of Cx-26 pointing at disruption of intercellular ties. P53 was of nuclear expression and Bak was found in the cytoplasm. Cx-26 did not correlate with P53 (r=0.966, p=0.004). In node-negative tumours, P53 tended to positive correlation with Cx26 (r=0.262, p=0.076), while in node-positive cancers there was tendency toward negative linkage between Cx26 and P53 (r=-0.203, p=0.134). Cx-26 positively correlated with Bak in all studied colorectal tumours (r=0.375, p=0.041) and a few selected clinical and pathological groups. However, Bak failed to correlate with Cx-26 in separate subgroups of superficially invasive cancers, G3 tumours, male patients, younger than 60 years old individuals and mucinous adenocarcinomas. There was a great variability of relation between Cx-26 and P53 under the level of statistical significance. Despite that, Cx-26 probably exerts a potent suicidal impact on colorectal cancer cells on the pathway of Bak-mediated apoptosis regardless of relationship between Cx26 and P53.

098

Association between two rare tumors: extragastrointestinal stromal tumor and small intestine neuroendocrine tumor

A. C. Iorgescu *
*Fundeni Clinical Institute, Dept. of Pathology, Bucharest, Romania

Neuroendocrine tumors (NET) of the digestive tract are rare neoplasms with a low incidence (approximately 1/100,000/year) and have their origin in the APUD system. Their association with other epithelial tumors is estimated around 10%, but the association with gastrointestinal stromal tumors (GIST) is much rare. GISTs arise in the interstitial cell of Cajal or related stem cells however those arising as primary tumors outside gastrointestinal tract are being called extragastrointestinal stromal tumors (EGIST). We report a case of a 55-years-old male who was diagnosed in 2005 with a small intestine NET and in 2007 with liver and peritoneum EGIST based on immunohistochemical stains (CD117, SMA, CD34, Chromogranin, Synaptophysin, NSE, Ki67 and S-100). Recurrence occurred in May 2010 in the small intestine and peritoneum and the immunohistochemical stains suggested a poorly differentiated neuroendocrine carcinoma. This is a rare case of small intestine NET associated with multiple sites EGIST. A correct diagnosis allowed an efficient treatment and improved the patient's prognostic. The expression of c-kit protein is typical for GIST but lately the studies have shown that we can find it also in some NET. This could guide us to the carcinogenesis of these rare tumors and new targeted therapies.

099

Morphological, immunohistochemical and molecular characterization of intraductal papillary neoplasms (IPNs) of the bile duct

A. M. Schlitter *, D. Born, M.-O. Riener, J. T. Siveke, A. Perren, I. Esposito
*Technische Universität München, Inst. für Pathologie, Germany

Objective: The aim of this study was a detailed morphological classification and molecular analysis of intraductal papillary neoplasms (IPN) of the bile duct based on a European cohort.
Method: Thirty-three IPN patients were included into the cohort. Conventional histomorphological analysis and immunohistochemistry for mucin core proteins (MUC1, MUC2, MUC5AC), developmental markers (Cdx2, Pdx1, β-catenin) and protein products of tumor-suppressor genes (p53, Smad4) and molecular analyses of the k-ras gene were performed.
Results: Most IPNs were located in the extrahepatic bile duct (70%). Subtyping was done according to classification of IPMN in the pancreas in three different types: pancreatobiliary type including oncocytic type (45%), intestinal type (21%) and gastric type (9%). Twenty-four percent presented a mixed phenotype. Whereas pancreatobiliary type was prevalent in intrahepatic locations (87%), all four subtypes including a large number of mixed variants were observed in extrahepatic IPNs. The majority of IPNs were associated with an invasive carcinoma (55%). K-ras mutations were detected in 24% of microscopically dissected IPN.

Conclusion: IPNs are mostly detected in advanced stages in association with invasive carcinoma. Classification of subtypes revealed a high number of cases with mixed epithelial differentiation. Different distribution of subtypes between intra- and extrahepatic location points to a different pathogenesis of biliary IPN.

100

Serrated polyps of the colorectum: Histopathological evaluation of 89 cases and assessment of agreement between pathologists

C. Emna *, M. Samira, D. Amel, B. Douha, K. Houda, C.-D. Samia
* Tunis, Tunesia

Objective: Colorectal serrated polyps represent a heterogeneous group including hyperplasic polyps (HP), sessile serrated adenoma (SSA), traditional serrated adenomas (TSA), and mixed polyps (MP). The accurate diagnosis may be difficult using currently available histopathological criteria.
Method: Eighty nine cases diagnosed as serrated colorectal polyps were reviewed microscopically and the lesions were renamed according to the usual terminology.
Results: The mean nomber of polyps per coloscopy was 3 and their average size was 6mm (2-70mm). The diagnosis of serrated polyp was confirmed in 76 cases; the remaining cases correspond to normal mucosa, conventional adenoma or solitary rectal ulcer. Among these 76 cases, 57 were HP (75%), 5 TSA (6.6%), 1 MP (1.3%), and 6 SSA (7.9%), 3 of which displayed low grade dysplasia. The diagnosis was difficult and incertain in 7 cases (7.3%). High grade dysplasia was found in 2 cases (1TSA, 1SSA). Two patients had a synchronous colic adenocarcinoma. One patient had a hyperplasic polyposis. The overall reproductibility of the pathological diagnosis was mediocre (Kappa=0.351).
Conclusion: The study emphasizes diagnostic difficulties among pathologists especially with the recently described SSA and the need of educational interventions to improve classification of serrated polyps. It allows discussing the relevance of establishing a new category of incertain diagnosis.

101

Mucinous-type neoplasm following an usual appendectomy - what could it be?

G.-D. Buzete *
*Brasov, Romania

Ranging from mucoceles to adenocarcinomas together with multifaceted neuroendocrine tumors, neoplasms of the appendix may represent a challenge for everyday practice. We present a case of a 46 year old male with clinical symptoms of appendicitis. The appendectomy was performed without any complication; periappendicular adhesion of great omentum was described. Resection specimen consisted of a 5.5 cm long vermiform appendix with a indefinite yellowish lesion on the cut surface (after 10% neutral buffered formalin 24 hour fixation). Several paraffin embedded cross sections were examined after haematoxylin and eosin staining. For the final diagnosis both histochemical and immunohistochemical (neuroendocrine markers, CK, EMA, CEA, CA 19-9) techniques were used. Unequal thickness of the wall consists of a diffuse cell proliferation with islands, gland-like structures and trabeculae of both goblet and columnar cells. Pools of mucin dissociate the layers of the wall. Mild nuclear pleomorphism and mitotic activity are present. Examination of the serosa reveals fibrinopurulent reaction. In order to have a correct diagnosis for a mucinous type appendiceal neoplasm, one should not forget that gross description, carefully orientation, accurate slide observation together with histochemical and immunohistochemical methods are very important steps in identifying and signing out the precise entity.

Monday, 29 August 2011, 09.30–10.30 and 16.30–17.00, Hall 5

PS-09 Poster Session Electron Microscopy

001

Electron microscopy features of solid pseudopapillary pancreatic tumors

E. Dubova *, M. Nagovitsyna, B. Vtyurin, I. Chekmareva, A. Shchegolev
*V.I. Kulakov Scientific Center, Dept. of Pathology, Moscow, Russia

Objective: Solid–pseudopapillary pancreatic tumors (SPPT) are rare pancreatic lesions observed in 1–2% of all tumors of exocrine pancreas and in 5% of all cystic pancreatic tumors.
Method: We examined surgical pancreatic specimens from 19 patients with SPPT (14 females at age from 15 to 67 years and 1 male at age 61 year) and performed histological and electron microscopy investigation.

Results: On electron microscopy we revealed two cell types: the first was represented by the cells with prominent ovoid nuclei, normal mitochondria and short fragments of endoplasmic reticulum. These cells mainly formed pseudopapillary structures around the vessels. The second type of cells was extensively polymorphous. Their nuclei were segmented and segments were connected by the short bridges (coffee bean-like nuclei). Most of the mitochondria in these cells were large with light matrix, broken crests and lipofuscine granules.
Conclusion: The electron microscopy characteristic of SPPT cell confirms that most of them are of epithelial origin.

002

Detection of Luse bodies in sclerosing adenosis of breast: an ultrastructural study

O. Popova *, M. Mnikhovich, A. Shechter, S. Bogomazova, M. Ternov
*1st Moscow State Medical University, Inst. of Molecular Medicine, Russia

Objective: In view of new discoveries that can be useful for the understanding of tumor morphogenesis, a comparative ultrastructural investigation of stromal changes in sclerosing adenosis and duct carcinoma of breast, with particular inspection of matricial organization, was performed.
Method: Six biopsies from the focuses of breast duct carcinoma associated with a prominent desmoplasia and five cases of sclerosing adenosis were examined by standard transmission electron microscopic method.
Results: Myofibroblast hyperplasia and hyperelastosis with predominance of immature elastine were the conspicuous features of stromal reaction in all carcinoma cases. Among the periductal cells participating in matrix formation in sclerosing adenosis it was identified numerous active fibroblasts and resting fibroblasts whereas myofibroblasts were relatively rarely observed. In contast to carcinoma, the collagenous reaction was much more prominent than the elastic response and characterized by the presence of specific collagenous forms. In most samples of sclerosing adenosis, fibrous long-spaced collagen with periodicity of 90–120 nm known as Luse bodies was revealed. The identified long-spaced collagen was associated with the rich content of proteoglycans.
Conclusion: The Luse bodies were previously never described in sclerosing adenosis. This finding, in addition to other extracellular alterations, strengthens the concept that stromal reaction in benign and invasive tumors can involve different mechanisms of matrix turnover.

Monday, 29 August 2011, 09.30–10.30 and 16.30–17.00, Hall 5

PS-10 Poster Session Ophthalmic Pathology

001

The role of retinal pigment epithelium cells in amyloidogenesis of senile local eye amyloidosis with age-related macular degeneration

V. Ermilov *, O. Makhonina
*Volgograd State Medical University, Dept. of Forensic Medicine, Russia

Objective: Age-related macular degeneration (AMD), a blinding disorder that compromises central vision, is characterized by the accumulation of extracellular deposits, termed drusen, between the retinal pigmented epithelium (RPE) and the choroid. Ocular amyloidosis is closely connected with clinical medicine. The appearence of amyloid in eye tissues is related with development of some gerontoophthalmological diseases. They make it possible to see in a new light the problem of eye amyloidosis, as well as its place among different forms of amyloloidosis known to us as of now.
Method: With the help of selective methods of revealing amyloid and by performing electron microscopy, we investigated 111 enucleated eyes of people over 50 years of age. We found morphologic sings of AMD.
Results: Amyloid was found in 47 eyes. In the eyes with amyloidosis, morphologic changes in the form of drusen combined with changes in the RPE cells prevailed. They were seen in the decreasing number of RPE cells and their nuclei. Ultrastructural investigation showed that amyloid fibrillae are localized on the inner collagen surface of Bruch's membrane in the subretinal space.
Conclusion: The close contact amyloid fibrillae with damaged pigment cells and their presence in the invagination of the cytolemma of these cells make it possible to suggest their participation in the amyloidogenesis.

002

Macrophotography for exact topographic delimitation of affected areas in Mohs surgery for periocular tumors

L. Alfaro *, R. Martinez-Belda, L. Gomez
*Valencia, Spain

Objective: Periocular tumors need complete excision to avoid recurrences. Mohs surgery with introperative evaluation of surgical margins is a good choice in the treatment of these lesions. This technique requires a good communication between pathologists and oculoplastics to assess exact areas with tumor remnants.

Method: We have used macrophotography to handle specimens of Mohs surgery. An initial picture is taken in the operating room before resection and drawings indicate to the pathologist the location when different fragments are excised. New pictures are taken from the fragments before cryostate sections and when margins are affected the pictures are used to transmit to the oculoplastic the exact topographic position of the affected areas. A Panasonic Lumix-TZ7 camera with ×3 macro zoom allowed us to obtain full details from even the smallest fragments.
Results: Fifty-five cases were studied since 2007; forty-one were basocelular carcinomas, six squamous carcinomas, two sebaceous carcinomas, and a single case of basosquamous carcinoma, mucoepidermoid carcinoma and MALT lymphoma. Three cases showed no tumor rests. The number of fragments received as amplification of the initial resection with affected margins was variable with an average of 2.72 and a maximum of 18.
Conclusion: Macrophotography is an excellent complement for the exact delimitation of affected areas in Mohs surgery.

003
Oncocytoma (oxyphil adenoma) of the lacrymal caruncle

N. Arnogiannaki *, M. Sofopoulos, A. Apostolaki, M. Gazalidou, E. Koniaris, N. Koufopoulos, A. Vacarciuc
*St. Savvas Anticancer Hospital, Dept. of Surgical Pathology, Athens, Greece

Objective: Ocular oxyphile adenomas (oncocytomas) are rare benign tumors found usually in the lacrymal caruncle, lacrymal gland, lacrymal sac, accessory conjunctival lacrymal glands and lid apocrine glands. They account for 3–8% of all caruncular lesions. They present as small (2–5 mm) slowly growing, indolent, reddish masses sometimes cystic and are often clinically misdiagnosed as conjuctival cysts, hemangiomas, melanocytic nevi or pyogenic granulomas. There is an increased prevalence in elderly females. These tumors are usually asymptomatic and are removed for aesthetic reasons.
Method: We report a case of a 77-year-old man who presented to our hospital with a 5-mm indolent but irritating red nodule situated on inner corner of his left eye. There was no history of trauma or eye surgery. Surgical excision was made and the specimen was sent to our laboratory.
Results: Histopathologic examination demonstrated large, uniform, polygonal cells with small round nuclei, abundant eosinophylic granular cytoplasm arranged mostly in solid areas. Tubule-like formations are also observed. Mitotic figures were absent.
Conclusion: The diagnosis was oxyphyl adenoma (oncocytoma) of the lacrymal caruncle excised with clear margins, thus no further treatment is needed. Therefore, in elderly with a caruncle mass, the differential diagnosis should include oncocytoma.

004
Sebaceous gland carcinoma of the eyelid with comedocarcinoma features

N. Arnogiannaki *, M. Sofopoulos, M. Gazalidou, N. Koufopoulos, S. Tsitsiou, V. Anagnostopoulou, L. Pappa
*St. Savvas Anticancer Hospital, Dept. of Surgical Pathology, Athens, Greece

Objective: Sebaceous gland carcinoma of the eyelid is an aggressive malignancy that derives either from Zeiss or meibomian glands. Although it is uncommon, it accounts for 1% to 6% of all eyelid malignancies with a significant tendency of local recurrence (9–36%) and lymph node metastasis (14–25%). The causes remain unclear but it has been linked with Muir–Torre syndrome.
Method: A 75-year-old woman presented in our hospital with a whitish mass on her upper right eyelid. She reported two previous operations on the same eyelid and a history of colorectal and breast cancer. Excision was performed.
Results: Histological examination revealed a tumor consisted of large lobules of cells, without pallisading and with prominent central foci of necrosis forming a comedocarcinoma pattern. These lobules were separated by a fibrovascular stroma infiltrated with leukocytes. Tumor cells displayed low to moderate sebaceous differentiation with either foamy or vacuolated cytoplasm and large nuclei with prominent nucleoli. Scattered mitosis was present. Immunohistochemistry did not reveal metastatic breast carcinoma.
Conclusion: The diagnosis was sebaceous gland carcinoma with commedocarcinoma pattern. Therefore this case must be kept under surveillance for lymph node metastases and local recurrence. Considering this patient's history an evaluation of Muir–Torre syndrome and family screening are advisable.

005
Orbito-cranial adenoid cystic carcinoma with high-grade transformation: a case report

M. T. Gonzalez Serrano *, H. Fuentes Vaamonde, R. Ortega Salas, Y. O. Rangel Mendoza, M. T. Caro Cuenca, C. M. Villar Pastor, J. Salvatierra Cuenca, M. Medina Perez
*Hospital Reina Sofia, Dept. of Pathology, Cordoba, Spain

Objective: Primary neoplasms from lacrimal gland are uncommon being adenoid cystic carcinoma (ACC) the most frecuent malignant tumor. ACC with high-grade transformation (ACC-HGT) is an aggressive variant with high propensity to metastasize.
Method: A 41-year-old woman presented with facial pain and headache for 2 months. Image studies revealed a lession with orbital destruction, extension into the skull base, sphenoidal–cavernous sinuses, across the midline. Subtotal surgical removal with post-operative irradiation was perfomed. Dorsal (D3–D6) metastases were diagnosed 8 months post-surgery.
Results: First sample showed cribiform and tubular patterns with histochemical-immunohistochemical tipycal features of ACC and areas of confluent solid nests with comedonecrosis, desmoplastic areas with lost of S100, p53 overexpression and high Ki 67 index. In the second sample high-grade tumor was the predominant component.
Conclusion: ACC of the lacrimal gland is rare and metastases are uncommon. The conventional ACC component was graded (I, II, III). Recently, the high-grade component was defined as a pleomorphic area with comedonecrosis, focal loss of myoepithelial cells and mitotic activity greater than the conventional ACC component. In this case, the unusual extension with bilateral involvement and early metastases can be explained by the aggressive behaviour of ACC-HGT and justify the clinicopathologic importance of recognize this entity.

Monday, 29 August 2011, 09.30–10.30 and 16.30–17.00, Hall 5

PS-11 Poster Session Soft Tissue Pathology

001

Diagnostic and prospective therapeutic value of selected rhabdomyosarcoma markers

P. Babal *, A. Janegova, M. Leitnerova, P. Janega, L. Feketeova, E. Klinciva, D. Sejnova, D. Ilencikova, Z. Cierna, L. Plank
*Comenius University, Dept. of Pathology, Bratislava, Slovakia

Objective: Rhabdomyosarcomas embryonal (eRMS) and alveolar (aRMS) constitute most common pediatric soft tissue sarcomas. The wide range of differential diagnostic possibilities shows the need for more specific and sensitive markers. Low survival rates of high risk RMS patients require new prospective therapeutic targets.
Method: FFPE samples of 15 RMS (12-eRMS, 3-aRMS) and non-RMS soft tissue tumors were evaluated by immunohistochemistry for myogenin, MyoD1, VEGF, EGFR, COX-2, p-Akt and p-mTOR expression. The presence of PAX3/7-FKHR forming translocations, myogenin, MyoD1, gamma subunit of fetal acetylcholine receptor (AChR) and K-RAS mutational state were determined by RT-PCR.
Results: A total of 10/12 eRMS and 3/3 aRMS showed expression of myogenin, MyoD1 and gamma AChR. Non-RMS tumors were negative. Translocations were only found in aRMS. EGFR expression was characteristic for eRMS, without the presence of activating K-RAS mutation. VEGF showed intense positivity in all samples. p-AKT and p-mTOR showed overlapping expressions in 86.7% RMS. COX-2 demonstrated weak positivity in most of the samples.
Conclusion: Myogenin, MyoD1 and the fetal AChR are specific and sensitive diagnostic markers of RMS. RMS subtypes are identifiable by PAX3/7-FKHR detection and probably EGFR expression. VEGF, EGFR, COX-2 and Akt-mTOR pathway directed therapy could be prospective in RMS. Supported by CPD-NMT, 26240220052.

002

Soft-tissue tumors and Ebstein–Barr virus (EBV) in grafted-kidney patients

J. C. Goldberg *, M. Real, J. Petroni, L. Leon, G. Hillchenbach, D. Casadei
*Instituto de Nefrologia, Buenos Aires, Argentina

Objective: EBV implicated in different malignancies (skin cancers, lymphomas and Kaposi sarcomas) after solid organ transplantation EBV-associated smooth muscle tumors (EBV-SMT) are rare.
Method: Among 1,500 grafted-kidney patients, three developed EBV-SMT. Case 1: 51-year-old female, with EBV-SMT (generalized). Case 2: 46-year-old woman diagnosis of breast phylodes sarcoma, reviewed diagnosis: EBV-SMT was done. Case 3: /23-year-old man, severe abdominal pain, on laparoscopy; two tumor-like nodules were excised from gut, suspection of TBC. EBV-SMT was microscopic diagnosis.
Results: Progressive weight loss in all three patients, chronic cough in patient 1; chest X-ray showed multiple pulmonary lesions; on CT-scan paravertebral lesions. Transthoracic biopsy showed the proliferation of spindle cells with mixed cellularity. Spindle eosinophilic cells intermingled with fascicles resembling smooth muscle, and mononuclear inflamatory cells and capillary evoked myofibroblastic tumor. No mitosis, mild nuclear atypia. Negative immunohistochemestry: CD21, CD34, CD99, EMA, cytokeratin, S100, CD117. Alpha-smooth muscle actin diffusely positive, EVB-LMP negative. In situ hybridization showed EBV in the nuclei. EBV-SMT was established.

Conclusion: Smooth muscle tumors in immunocompromised are EBV associated, without immunosuppression are negative. Primary target cell of EBV are B lymphocytes; studies demonstrate that EBV is capable of infecting smooth muscle through cellular receptor for EBV CD21. Possible mechanisms of EBV related tumor genesis is integration of EBV-DNA within ALK locus in tumor cells. ALK gene rearrangement and expression are associated with inflammatory myofibroblastic tumors, anaplastic large cell lymphomas. Clonally of multifocal EBV-SMT using southern blot showed multiple tumors constituting independent primary lesions

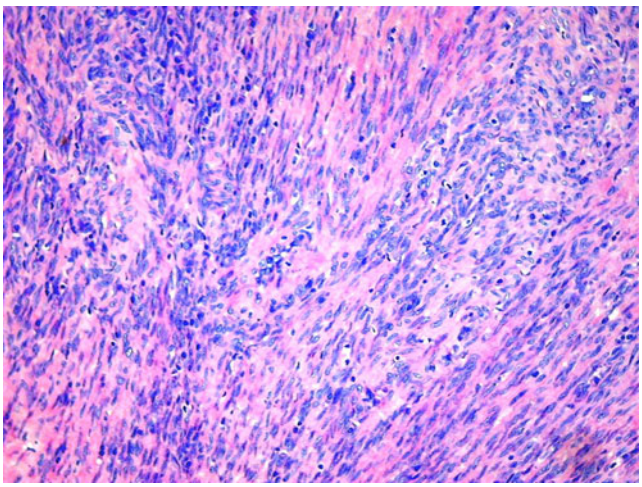

003

Spinal chordoma: our experience in 53 cases

J. Sopta *, M. Skender, V. Mijucic, S. Raicevic, D. Ristic, V. Lalosevic, J. Bokun
*School of Medicine Belgrade, Inst. of Pathology, Serbia

Objective: Chordoma is a primary malignant tumor of spine, believed to arise from notochord remnants. The aim of this study was to analyze the clinico-pathological findings, oncological and functional outcome of the patients with surgically treated chordoma.

Method: From 1995 to 2010, 53 patients with chordoma were diagnosed and surgically treated. All biopsies were stained by HE, Vimentin, CK AE1/AE3, S-100 protein, EMA, Ki 67.

Results: The extent of the lesion was defined according to Weinstein–Boriani–Biagini system. Frankel classification was used to define the level of neurological lesion. The biopsy material was analyzed for cell type, cell pleomorphism, presence of necrosis, bleeding, mixoid transformations, and hyaline cartilage. The results of treatment have been divided into chordomas of the spine above the sacrum, sacral and cranial localization. The follow-up of the patients lasted up to 65 months; the presence of rest/relapse of the tumor was being determined as well as the origins of metastasis.

Conclusion: The localization of the lesion and the type of surgical resection are the most important parameters influencing the clinical course of the disease. Tumors with prominent cell pleomorphism and higher Ki67 expression have fast relapse. En bloc resection, even the marginal one, is the therapeutic method of choice.

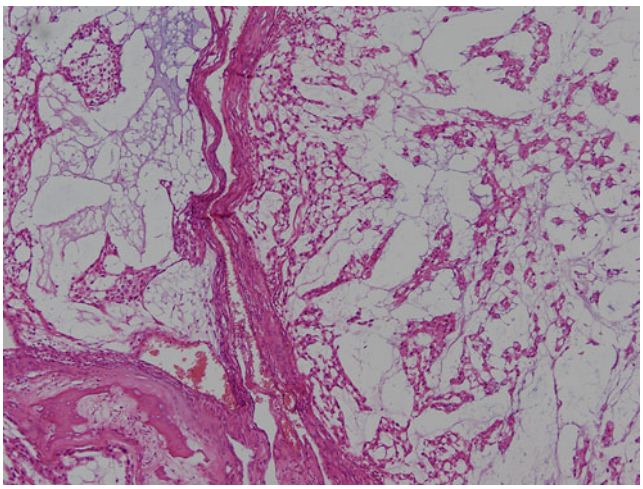

004

Dedifferentiated chondrosarcoma of soft tissue: a case report

F. Abbasi *, J. Pourghasem, A. Mohamadi, A. Esmaili
*Imam Khomeini Hospital, Pathology, Urmia, Iran

Objective: Chondrosarcoma of soft tissue is a rare neoplasm and mostly occurred in adults. Two different variants are described: mesenchymal and myxoid. The cardinal presentation is local soft tissue mass with gradual enlargement and increasing pain. There may or may not be calcification, and in uncalcified tumors the diagnosis may not even be considered by the radiologist.

Method: We represent a 52-year-old man who was admitted with enlarging, painful gluteal mass. CT scan showed a well-defined soft tissue mass without any relation to the bone.

Results: Microscopic examination of the slides taken from the tumor revealed histologic features of dedifferentiated chondrosarcoma composed of a low-grade chondrosarcoma and an angiosarcoma component. The pictures taken from the specimen shows the features of this rare tumor.

Conclusion: In dedifferentiated chondrosarcoma, the poorly differentiated component composed usually of rhabdomyosarcoma, fibrosarcoma, osteosarcoma, or pleomorphic sarcoma. However, in this case the poorly differentiated sarcoma was angiosarcoma which was confirmed by positivity for VonWillebrand factor.

005

Epithelioid hemangioendothelioma of the rib

E. Alcaraz Mateos *, J. Tudela Pallares, C. Pérez Jiménez, M. Martínez Fernández, A. Chaves Benito
*Hospital Morales Meseguer, Dept. de Anatomia Patologica, Murcia, Spain

Objective: Epithelioid hemangioendothelioma (EHE) is an uncommon, well-differentiated vascular tumor of borderline malignancy. EHE of the bone are extremely rare. A case of a young man with EHE of the rib is presented.
Method: A 36-year-old man presented with 1-year history of paresthesias and mild weakness of the lower extremities. CT scan of the dorsal spine showed an osteolytic lesion involving rib, lamina and vertebral body of D3 and D4. After two unsatisfactory FNAC, an open biopsy was performed.
Results: Histologically, a proliferation of epithelioid cells arranged in nests and anastomosing vascular channels was seen. The cells had wide eosinophilic cytoplasm with moderate pleomorphism and frecuent inconspicuous nucleoli. Mitotic activity was low (1–2 mitosis/HPF). Immunohistochemically, tumor cells were positive for CD31, CD34, weakly for actin, and focally for cytokeratin AE1/AE3. Histopathologic and immunohistochemical findings were consistent with EHE. The patient underwent resection of the mass. At 4 years of follow-up, the patient is alive and free of recurrence.
Conclusion: EHE is a rare vascular tumor which occurs in soft tissue and solid organs such as lung, liver and bone. The latter mainly affects lower extremities, and rib involvement is extremely rare. EHE is considered a low-grade tumor, biologically between hemangioma and angiosarcoma. Differential diagnosis in bone include metastatic carcinoma, epithelioid sarcoma, adamantinoma, and chondrosarcoma.

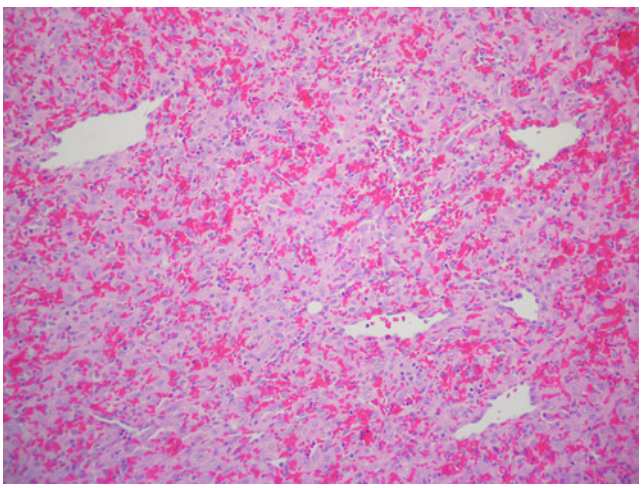

006

Lipoma of the colon clinically mimicking malignant tumor

B. Andrejic *, M. Djolai, D. Ivanov
*Novi Sad, Serbia

Objective: Lipoma is a benign tumor of adipose tissue, the most common tumor of soft tissues in human. In our paper, we report a case of lipoma in the wall of the sigmoid colon.
Method: Polypoid tumor of the colon was endoscopically detected, and it clinically appeared to be malignant. The tumor was laparoscopically removed and referred to routine pathohistological examination.
Results: After repeated colonoscopies in female patient (64 years) with abdominal pain and occult blood in the stool, established diagnose was polypus of the sigmoid colon, with changes in the mucosal intestinal epithelium suspected to be malignant. Cross-sections of the tumor revealed grey to yellow, homogenous structure. Pathohistological findings in tumor showed polypoid structure located into submucosa. Tumor was encapsulated and composed only of mature adipocytes without cellular atypia, cowered with intestinal type of mucosa. Histological image was typical of lipoma. Crypt and surface epithelium were mildly hyperplastic, without dysplastic changes.
Conclusion: Lipomas and malignant tumors of gastrointestinal system, clinically, may have similar symptoms and signs, and even radiography and endoscopy can not always give precise preoperative diagnostics. Pathohistological examination provides clear insight into nature of the tumor and provides estimation of behaviour.

007

Clinic and histopathologic features of granular cell tumor (Abrikossoff): case report

M. Aschie*, A.-A. Nicolau, A. F. Mitroi, I. Poinareanu, A. Chsoi, A. Iliesiu, G. Blatatescu, M. Enciu, P.D. Corici, I. Aschie
*Ovidius University Constanta, Faculty of Medicine, Romania

Objective: Granular cell tumor is a benign neural tumor characterized by the presence of large cells with pink granular cytoplasm. First was described by Abrikossoff as a muscular tumor, then the neural origin was demonstrated by immunohistochemical stains. Some authors consider this tumor more of an inflammatory lesion than a true neoplasm.
Method: This paper presents the case of a 70-year-old woman with multiple abdominal surgery history that accuses pain in the right side of the abdominal cavity. The

clinic and imagistic investigations reveal an abdominal mass. After extraction, the tumor is submitted to macroscopic and microscopic investigation by usual and special stains.

Results: This nodular tumor is ulcerated and present in the centre is a textile material. Microscopic examination shows foreign body granulomatous inflammation (textile material in centre, specific giant cells, macrophages, lymphocytes) and a neoplastic proliferation of large granular cell with mostly small nuclei. Immunohistochemical stains (CD68, Neuron Specific Enolase, S100 protein and vimentin) establishes the diagnosis of granular cell tumor with foreign body granulomatous inflammation.

Conclusion: The particularity of this case consists of the association between granular cell tumor and foreign body granulomatous inflammation and the atypical localization of the tumor in this case.

008

Primary subcutaneous extraskeletal osteosarcoma: case report and review of the literature

A. Betts *, E. Borg, S. Aquilina, N. Refalo
*Mater Dei Hospital, Dept. of Pathology, Msida, Malta

Objective: Extraskeletal osteosarcoma is a very rare tumour and less than 300 cases have been reported in the literature. Most of these cases are deep-seated and primary subcutaneous osteosarcomas form only a very small minority of reported cases.

Method: We present the case of a 43-year-old female who had a painless calcified subcutaneous nodule excised from her left leg. Microscopy revealed an osteosarcoma which had no connection with the underlying bone. There were no other bone or soft tissue masses anywhere else. The literature was searched for cases of primary subcutaneous extraskeletal osteosarcomas and the data obtained was tabulated.

Results: Subcutaneous osteosarcoma is very rare; however, many case reports and series do not distinguish between deep-seated and more superficial tumours. Thus, the real incidence of superficial primary extraskeletal osteosarcoma is unknown. It is not clear whether superficial subcutaneous tumours are behaviourally different from the more deep-seated tumours; however, the literature revealed a significant local recurrence and distant metastasis rate.

Conclusion: Primary subcutaneous osteosarcoma is a high-grade malignancy. The primary treatment modality is surgical and wide surgical excision with wide tumour-free surgical margins appears to be the single most important prognostic factor.

009

Myxoid liposarcoma (MLS): morphological changes induced by radiotherapy

M. Caldas *, M. Afonso
*I. Português de Oncologia, Serviço de Anatomia Patológica, Porto, Portugal

Objective: Myxoid liposarcoma (MLS) is the second most common type of liposarcoma. It represents a morphological spectrum, from purely myxoid to hypercellular/round cell morphology (RCMLS). Traditionally, it is more frequent in the lower limbs and in young adults and it is characterized by multiple local relapses, extra-pulmonary metastases and a global survival rate of 40%(RCMLS) to 90%(purely myxoid lesions). MLS is a highly radiosensitive neoplasm and thus radiotherapy may be used in neoadjuvant setting since it promotes resectability and decreases tumour size. We herein describe the morphological changes induced by radiotherapy.

Method: Case Reports: Case 1—A 49-year-old male with a 20×6.8-cm mass on the right lower leg, histologically consistent with MLS. Case 2: A 44-year-old male with a 16×5-cm mass on the right lower leg, histologically consistent with RCMLS. Both lesions were considered unresectable and treated with neoadjuvant-radiotherapy followed by limb-sparing surgery. Histological examination revealed, in both cases, fibrosis, hyalinization, lipogenic maturation, hypertrophy of medium-sized arterioles, preserved capillary network and microscopic foci of residual neoplasia.

Conclusion: Contrary to other liposarcomas, MLS is highly radiosensitive and therefore, neoadjuvant-radiotherapy may be indicated. Morphological changes induced by radiation are similar in both ends of its spectrum and their recognition required to evaluate the response rate to therapy.

010

FGFR2 represents a molecular marker that discriminate desmoid-type fibromatosis from fibrosarcomas

K. Carvalho *, F. Soares, I. Cunha
*Faculdade de Medicina da USP, Dept. of Gynecology, São Paulo, Brazil

Objective: Fibroblastic tumors represent a group of tumors that include benign tumors to high-grade sarcomas. Between these two extremes, desmoid-type fibromatosis (DTF) are clonal tumors with fibroblastic proliferation and local aggressiveness but without metastatic potential. The aim of this study was to determine differential gene expression profile and define molecules able of discriminating among desmoid-type fibromatosis (DTF) and fibrosarcoma (FS).

Method: Using a cDNA platform representing 4,608 genes, we sought for gene that could discriminate desmoid-type fibromatosis (19 samples) from fibrosarcomas (04 samples). Validation was done in 124 samples (112 DTF and 12 FS) by immunohistochemistry and 25 samples by quantitative real-time PCR (QRT-PCR).
Results: cDNA microarray results pointed a set of genes that discriminate DTF from fibrosarcomas. Among differential expressed genes selected for validation, FGFR2 (fibroblast growth factor receptor 2) was able to separate precisely DTF from fibrosarcomas. QRT-PCR and Immunohistochemical results corroborate with cDNA data with DTF showing higher expression levels of FGFR2 than fibrosarcomas. Mathematical analysis showed significant statistical values of differential expression between these two groups (p=0.0081).
Conclusion: Our results pointed FGFR2 transcript and protein levels as a potential discriminator between these fibroblastic tumors.

011

Differential gene expression of IL1β and KLK13 separate desmoid-type fibromatosis from benign mesenchymal tumors

K. Carvalho*, I. Cunha, R. Rocha, F. Soares
*Faculdade de Medicina da USP, Dept. of Gynecology, São Paulo, Brazil

Objective: Desmoid-type fibromatosis (DTF) are clonal tumors with fibroblastic proliferation and local aggressiveness but without metastatic potential. Thus, these tumors present an intermediate behavior, presenting benign and malignant characteristics. This work presents two molecular markers capable of discriminate DTF from benign mesenchymal tumors.
Method: Using a cDNA platform representing 4,608 genes, we sought for genes that discriminate DTF (16 samples) from benign mesenchymal tumors (including leyomioma, neurofibroma and others). Validation of differential expression was done in 63 samples by quantitative real-time PCR (QRT-PCR) using TaqMan detection system.
Results: cDNA microarray results pointed a set of genes that discriminate DTF from the other histological types of STT analyzed. Among differential expressed genes identified in our analysis, IL1β (Interleukin-1 beta) and KLK13 (kallikrein-13) precisely discriminated DTF from the benign samples. QRT-PCR confirmed that DTF have lower IL1β (p=0.0027) and KLK13 (p=0.001) transcript levels than all other benign tumors.
Conclusion: Our results showed that KLK13 and IL1B could precisely discriminate DTF from benign mesenchymal tumors, representing two important molecular markers. However, the role of these molecules deserves further studies in these tumor groups.

012

Myoid tumours in HIV-infected patients: diagnostic challenges

J. Deonarain*, P. Ramdial, Y. Sing
*National Health Laboratory, Dept. of Anatomical Pathology, Durban, South Africa

Objective: The classification of AIDS associated myoid-tumours (AIDS-MTs) has been plagued by ill-defined and inconsistent diagnostic criteria. The myoid immunophenotype has been inconsistently documented. This study reappraises the morphologic and immunophenotypic features of extra-uterine AIDS-MTs and the clinical profile of afflicted patients.
Method: This study employs a 5-year retrospective review of extra-uterine AIDS-MTs with reappraisal and categorisation according to current available diagnostic criteria.
Results: A total of 27 AIDS-MTs were identified. Categorisation according to EBV early RNA in situ hybridisation revealed 70.4% EBV-positive-MTs and 29.6% EBV-negative-MTs. EBV-positive MTs comprised 12/19 EBV-positive-smooth muscle tumours (SMTs) [leiomyomas (6), smooth muscle tumour of uncertain malignant potential (1), leiomyosarcomas (5)] and 7/19 EBV-positive myopericytomas [(benign (5), malignant (2)]. Tumours classified as malignant demonstrated hypercellularity, pleomorphism, increased mitoses and necrosis. Sites of tumours: EBV-positive SMTs: paraspinal (2), round ligament (1), right adrenal (1), breast (1), skin (2), palate (1), orbit (2). EBV-positive myopericytomas: skin (2), paraspinal (2), cavernous sinus (1), posterior nasal space (1), periampullary (1). EBV-negative SMTs: dermis/subcutis (8), bladder (1).
Conclusion: The spectrum of AIDS-MTs does not demonstrate subtype determined behaviour. Heightened awareness of the expanded spectrum will improve diagnosis and facilitate distinction from histopathological mimickers in specific anatomic locations.

013

Immunohistochemical and molecular study of synovial sarcoma: a case report

K. Diamantopoulou*, C. Eftychiadis, F. Danglis, I. Famelos, E. Kavoura, D. Karras, H. Mahera
*KAT General Hospital Athens, Dept. of Pathology, Greece

Objective: Synovial sarcoma (SS) is a rare aggressive soft tissue sarcoma of the extremities and is characterized by a specific chromosomal translocation t(X;18)(p11;q11), yield-

ing a fusion protein SYT-SSX1 or SYT-SSX2. The accurate morphological, immunohistochemical and molecular diagnosis of SS appears to be crucial in prognosis and control of local reccurence.

Method: A 43-year-old woman presented with a painless deep soft tissue tumor of the left leg adjacent to Achille's tendon sheath. On MRI a compact mass, measuring 3.8×2.3 cm, reminiscent of a schwannoma, was revealed. The tumor was totally excised. Formalin-fixed and paraffin-embedded tissue was examined using H-E, immunohistochemistry with Vimentin, CD99(MIC2), BCL2, CK7, CK19, CK8, CK18, CK14, EMA, CAM5.2, AE1/AE3, Caldesmon, p53, Ki-67 (DAKO) and FISH for SYT-SSX1/2 fusion.

Results: Morphologically, a biphasic malignant mesenchymal neoplasm with spindle and epithelioid cell component was observed. Spindle cells were Vimentin(+), glandular-type epithelioid cells were CKs(+) and both cell types exhibited diffuse immunopositivity for CD99, BCL2 and EMA. FISH demonstrated the characteristic SYT-SSX1/2 fusion of synovial sarcoma, biphasic type.

Conclusion: Apart from the already identified prognostic factors, such as age, size, surgical margins, histologic subtype, the specific SYT-SSX fusion transcript seems to offer a possible candidate for immunotherapy or pharmacological targeted therapy.

014

Large angiomyolipomatous hamartoma of the inguinal lymph node: a case report

T. Dzombeta *, M. Francina, K. Matkovic, I. Markovic, Z. Jukic, B. Kruslin

*University of Zagreb, School of Medicine, Dept. of Pathology, Croatia

Objective: Angiomyolipomatous hamartoma is a variant of angiomyomatous hamartoma (AMH), a rare nodal vascular tumor, identified as a distinct entity by Chan et al in 1992. To date, less than 20 cases have been described, mostly involving inguinal lymph nodes.

Results: A 52-year-old male was surgically treated due to a painful, fast-growing tumor in his left groin, which was, according to surgical report, deeply infiltrating the surrounding tissue. Grossly, the tumor measured 9 cm in diameter and contained two lymph nodes with yellowish-brown cut-surface, which appeared to be almost completely replaced with adipose tissue. Microscopically, nodal parenchyma was actually mostly replaced with bundles of smooth muscle cells, fibrous tissue and lobules of mature adipocytes. Only a few atrophic lymphatic follicles were maintained. The presence of smooth muscle cells and endothelial cells was confirmed immunohistochemically by SMA, desmin and CD 31. Hilus contained numerous thick-walled vessels extending to medulla. Pleomorphism, mitoses and necrosis were absent.

Conclusion: Considering there have not been any reported recurrences of AMH, it probably has benign behaviour and extensive resection may not be needed. Nevertheless, we believe recognition of AMH is important in differential diagnosis of other pathological conditions that may affect lymph nodes.

015

Epithelioid angiosarcoma of bone: a rare event in the daily practice

A. C. Fiandesio *, C. Villanueva Sanchez, Y. Pérez González, T. Meizoso Latova, J. Mayor Jerez, F. Alijo Serrano, C. Diego Hernández, M. J. Mestre De Juan, L. Coertés Lambea

*Hospital General Mostoles, Dept. of Surgical Pathology, Madrid, Spain

Objective: Angiosarcomas are infrequent and aggressive soft tissue neoplasms that arise from endothelial cells; they represent <1% of primary malignant bone tumors. Epithelioid angiosarcoma is a rare histologic variant with poor prognosis.

Method: A 63-year-old man with pain and multiple osteolytic lesions by PET and gammagraphy in the right ischium. We received multiple fresh fragments of cortical and intramedular bone. They were processed and embedded in paraffin.

Results: Morphology corresponds to a malignant proliferation of epithelioid cells occupying the intratrabecular space, they form cords and nests, have pleomorphic nuclei with prominent nucleoli, few mitosis without necrosis and immunohistochemistry techniques are positive for CD31, CD34, and negative for S-100 protein and CD45. Tumour cells also express EMA and cytokeratins.

Conclusion: Differential diagnosis includes a wide range of entities comprising from epithelioid hemangioendothelioma to metastatic carcinoma. Clinical significance of this diagnosis is because of the different treatment, patient outcome and prognosis. We emphasized basic and fundamental role of immunohistochemistry and morphology.

016

Malignant glomus tumor of thigh: a rare tumor of soft tissue

G. A. Gokhan Ocak *, I.E. Gurer, I.H. Ozbudak, B. Unal, A.T. Aydin

*Akdeniz University, Medical School, Antalya, Turkey

Objective: Malignant glomus tumors are rare soft tissue tumors with a 40% of metastatic rate. Diagnosis is based on clinical as well as histologic criteria and supported by immunohistochemistry. Tumor cells express SMA, type 4 collagen and caldesmon. CD34 immunopositivity is also been reported as a rare finding.
Method: Sections taken from tumor tissue were fixed with formaldehyde, embedded in paraffin, sliced 5 μm in thickness and stained with H&E. Additionally, SMA, Caldesmon, S-100, type 4 collagen, and CD34 were performed immunohistochemically.
Results: Our case is a 73-year-old man admitted to our hospital with a mass of his left thigh. The tumor was deeply seated and 9 cm in its greatest diameter. Microscopically, it consist of mostly small, uniform and rounded perivascular cells located around blood vessels. Nuclear pleomorphism is noticed focally. Mitosis and necrosis were absent. Immunohistochemically, the tumor cells were positive with SMA, type 4 collagen, caldesmon and CD34 whereas immunonegative with S-100. Our diagnosis was glomangiosarcoma in consequence of its deep location and size greater than 2 cm.
Conclusion: We presented this case due to the rarity of this tumor with unusual CD34 immunopositivity.

017

Multicentric liposarcoma: an unusual, primary presentation form of common liposarcoma with different therapeutic approach. Report of a case

C. Hadjileontis *, N. Nicolaidis, G. Harisis, E. Angelidou, A. Kafanas
*Serres General Hospital, Dept. of Pathology, Greece

Objective: Multicentric liposarcoma is an unusual presentation of common liposarcoma, in which several independent liposarcomas occur simultaneously, or at different time points. It may be difficult to establish a precise diagnosis because of the problems differentiating between recurrence or metastasis of a single liposarcoma and multicentric primary lesions.
Method: We report the case of a 65-year-old male, presenting with abdominal swelling for 2 months, who underwent surgery due to multiple masses at the mesentery, a major one measuring 6.5×4×3 cm and several smaller ones 2–4 cm in maximum diameter, as revealed by computed tomography. Frozen sections examined during surgery showed that the main tumour was of a high grade, pleomorphic liposarcoma, while histological examination performed after surgery on the smaller tumours, revealed well differentiated, low grade liposarcomas, indicating towards independent foci of evolution, rather than metastatic ones. The prevailing figures from all specimens were those of round or spindle cell lipoblasts, exhibiting increasing density from low to high grade foci, and were admixed with multiple types of atypical lipoblasts at the bigger mass. No areas of myxoid differentiation that consist the commonest histological subtype of the malignancy were found.
Results: The patient is under radiotherapy for a month, with no signs of relapse.

018

Case report: Kaposiform hemangioendothelioma of the skull in a 3-year-old boy

E. Javadirad *, S.H. Madani, A. Faramarzi
*Medical School, Dept. o Pathology, Kermanshah, Iran

Kaposiform hemangioendothelioma (KHE) appears as a single lesion at birth or early infancy in an equal sex ratio. It is a rare aggressive vascular proliferation that has been recognized as a separate entity from other childhood vascular neoplasms. A 3-year-old Iranian boy with a rapidly enlarging mass in his skull was present here. Physical examination revealed a dark red, firm mass measuring 5×4.5 cm in the posterior aspect of skull. No association with Kasabach–Merritt syndrome (KMS) was observed despite its size. Histologically, KHE is composed of infiltrating nodules with slitlike or crescentic vessels that are poorly canalized and lined by spindled endothelium cells. Immunohistochemically, both spindle and epithelioid cells were immunoreactive for CD34 and CD31, while negative for EMA, cytokeratin or S100 protein. α-SMA were detected in pericytes surrounding spindle cells. Recurrence occurred 2 months after the first operation. Wide resection was performed at second operation and the patient was still alive during the 1-year follow-up period.

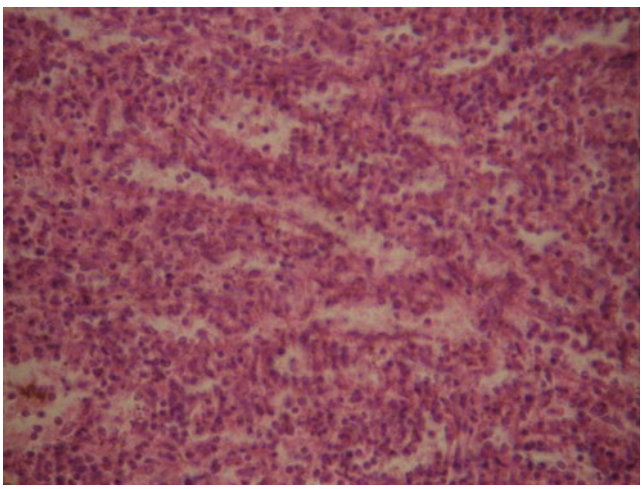

019

Renal osteodystrophy with giant tumours in a patient with end-stage kidneys

M. Kalman *, P. Szépe, J. Marcinek, T. Balhárek, L. Plank
*University Hospital Martin, Dept. of Pathology, Slovakia

Objective: Brown tumours are focal bone lesions caused by increased osteoclastic activity and fibroblastic proliferation encountered in hyperparathyroidism. The incidence of skeletal Brown tumors in patients with renal failure ranges from 1.5% to 13%. They occur as single or multiple lesions and usually affect the mandible, ribs, pelvis and femur but can be found in any bone.

Method: A 51-year-old hemodialysis patient had a progressive tumorous process of calvaria, which resulted to inoperabile state. The patient refused any intervention in the past. After several years, he was admitted to a hospital for recurrent bleeding from oral cavity. Fever, malaise, left-sided plegia, irregular breathing and heart failure developed during hospitalization. The patient died after an unsuccessful cardio-pulmonary resuscitation. Clinicians indicated autopsy to elucidate tumorous process.

Results: At autopsy, a diffuse tumorous process was found which involved the frontal bone, left maxillar sinus and mandible. Other masses were situated in thoracic vertebra and ribs also with osteolytic focuses. Additional findings included hyperplastic parathyroid glands, end-stage kidneys and cor bovinum with right-sided dilatation. A histologic examination of the skeletal masses confirms a diagnosis of osteitis fibrosa cystica associated with renal failure.

Conclusion: The case is noteworthy for its extreme presentation of renal osteodystrophy in a patient with end-stage renal failure.

020

Epithelioid malignant peripheral nerve sheath tumor: report of four cases

G. Karkavelas, G. Petrakis *, E. Beretouli, D. Gerasimidou, P. Hytiroglou
*Aristotle University of Greece, Dept. of Pathology, Thessaloniki, Greece

Objective: Epithelioid malignant peripheral nerve sheath tumors (EMPNSTs) raise difficult differential diagnostic problems from various sarcomas, carcinomas and melanoma. We report four cases of EMPNST with clinical correlation and extensive immunohistochemical assessment.

Method: The immunohistochemical panel included S-100 protein, CD57, NSE, neurofilament protein, PGP9.5, GFAP, vimentin, various keratins, EMA, SMA, desmin, CD34, HMB45 and collagen IV, in all cases, as well as additional stains, as deemed appropriate in each case.

Results: Two patients were male and two female. One patient had neurofibromatosis-1. Age ranged from 27 to 43 years. The tumors were located in the neck (n=2), right arm and left cerebellopontine angle. Origin from a nerve was found in two tumors; these exhibited alternating regions of high and low cellularity and a myxoid background. There was significant heterogeneity in immunophenotype; however, all tumors were positive for S-100 protein and at least two additional neural markers. Focal positivity for epithelial markers was seen in three cases. No positivity for desmin, HMB45, or CD117 was found.

Conclusion: An immunohistochemical panel including a variety of neural markers is essential for the diagnosis of EMPNST. Epithelial markers may also be expressed in these tumors. Nerve origin is very useful information in support of this diagnosis.

021

Extraskeletal mesenchymal chondrosarcoma: case report

E. Kimiloglu Sahan *, A. Akyildiz Igdem, F. A. Ahlatci, N. Erdoğan
*Taksim´s Research and Education, Dept. of Pathology, Istanbul, Turkey

Objective: Extraskeletal chondrosarcoma is a rare malignant tumor with different biological behaviours. Only 1% of tumors occur in extraskeletal location. Mesenchymal chondrosarcoma is a variant of chondrosarcoma, resembling primitive cartilaginous mesenchyme and arising in an extraskeletal location in half of the reported cases.

Method: A 62-year-old man presented with a 4×3×3-cm diameter mass in the proximal phalanx of his first finger of right foot. The curettage of the mass was sent to the pathology department. The histopathological diagnosis was mesenchymal tumor with myxoid areas.

Results: By the help of immunohistochemical markers, the diagnosis was extraskeletal mesenchymal chondrosarcoma.

Conclusion: Extraskeletal mesenchymal chondrosarcoma is a rare soft tissue tumor that shares imaging findings with other skeletal and soft tissue tumors.

022

Retroperitoneal dedifferentiated liposarcoma: a clinico-pathological study of six cases

W. Majdoub *, R. Sellami-Dhouib, R. Doghri, M. Driss, I. Abbes, S. Sassi, K. Mrad, L. Charfi, K. Ben Rhomdhane
*Military Hospital, Tunis, Tunisia

Objective: Well-differentiated liposarcoma (WDL) is the most common primary malignant neoplasm arising from the retroperitoneal cavity. Occasionally, and especially in the retroperitoneum, WDL can exhibit a sudden transition to a nonlipogenic sarcoma, known as dedifferentiated liposarcoma (DDL).
Method: We report six cases of retroperitoneal DDL diagnosed in the pathology department of Salah Azaïz institute from 1995 to 2010.
Results: Ages ranged from 41 years to 64 years with a median of 52 years. The sex ratio was about 1. The revealing symptoms were abdominal painful mass and ascites. Tumor size ranged from 9 to cm 52 cm. The treatment consisted in surgical removal in all cases. One patient died 2 days after surgery in the context of ionic disorders. Two patients were followed for less than 2 years Clinical outcome was unfavourable with local recurrence in two cases. Time to recurence was 14 months and 2 years. Surgical resection of the local recurrence was performed in the two cases.
Conclusion: Our data demonstrate the high recurrence rate after surgery and prompt the investigation of new combined-modality treatment approaches. The main problem is the rarity of the disease and the difficulty of prospective randomized trials.

023

Nodal metastasis of sarcoma, the debut of an osseous angiosarcoma

I. Marquina *, A. Fuertes, F. Felipo, C. del Agua
*Infanta Sofía Hospital, Dept. de Anatomía Patológica, San Sebastián de Los Reyes, Spain

Objective: Angiosarcomas represent less than 1% of malignant bone tumours. They affect long tubular bones and axial skeleton and commonly present as painful lytic lesions.
Method: A 34-year-old man with previous lumbar melanoma undergoes axillary lymphadenectomy with three metastasis of melanoma and one metastasis of high-grade pleomorphic sarcoma, positive for vimentin and actin and negative for Melan A, HMB45 and CD34. A primary sarcoma is not found in TC scan, and he is treated with radiotherapy. Four months after, a new TC scan shows bilateral lung nodes, vertebral and pelvic osteolytic lesions and a femoral mass. He suffers a pathological femur fracture.
Results: Microscopic study shows tumoral infiltration of femoral head and joint with similar histological and immunohistochemical features that the node metastasis of sarcoma. Dr. de Álava confirms that it is an epithelioid angiosarcoma with solid pattern of growth, probably primary of femoral head.
Conclusion: In the reviewed literature, the incidence of lymph node metastasis of sarcomas ranges between 2.6% and 9%, with just one case of angiosarcoma debuting as nodal metastasis. Although sarcomas rarely metastasize via lymphatic, some histological subtypes, such as epithelioid sarcoma rhabdomyosarcoma, clear cell sarcoma and angiosarcoma have shown to have a stronger predilection for lymph node metastasis.

024

Diagnosis and surgical treatment of tumors of the knee

L. Pashkevich *, T. Mohammad, S. Martinyuk
*BRSPCTO, Dept. of Pathology, Minsk, Belarus

Objective: Over 25 years in the Belarus Republic Scientific and Practical center for Traumatology and Orthopaedics have received surgical treatment of 609 patients with tumors and tumor-like lesions of the knee.
Method: We have analyzed the case histories, radiographs, the results of CT scan and MRI studies of these patients. Of these, 84 (13.8%) patients were diagnosed with primary malignant tumors, 145 (23.8%)—benign and 308 (50.6%)—tumor-like lesion.
Results: Analysis of a large clinical material by using modern radiation techniques (CT scan, MRI, scintigraphy, ultrasound, etc.), morphological studies (histochemical, immunohistochemical) allowed to develop an algorithm for the differential diagnosis. Comparison of clinical and radiological patterns with the results of pathomorphological study allowed to identify the earliest differential diagnostic criteria in each nosological form, and initial signs of malignant transformation of benign tumors and to determine the indications for more rational methods of treatment depending on the clinical course, the structure and the prevalence of various forms of neoplasms.
Conclusion: The findings have led to significantly reduce the number of diagnostic errors in the preoperative period. The so-called open biopsy with momentary removal of the pathological focus, without opening it, can only be made with clearly benign tumors.

025

An unusual peritoneal adenomatoid tumor with atypical features

K. Shelekhova *, G.I. Gafton, D.E. Matsko
*Petrov's Institute of Oncology, St. Petersburg, Russia

Objective: Adenomatoid tumors are benign neoplasms of mesothelial origin that usually have genital location. The occurrence of these tumors in extragenital location is extremely rare.

Method: We present a case of an unusual peritoneal neoplasm with morphology of infracted adenomatoid tumor and diffuse nuclear pleomorphism.
Results: A 47-year-old woman presented with an encapsulated pedunculated mass, 11×9 cm in size, attached to the hepatoduodenal ligament. The cut surface showed gray-tan spongy tissue with foci of hemorrhage. The tumor displayed combination of adenoid, angiomatoid and cystic patterns. Tumor cells had round to polygonal morphology with abundant cytoplasm and oval nuclei with small nucleoli. Many of the cells showed large cytoplasmic vacuoles. Immunohistochemistry revealed AE1/AE3, CK5/6, calretinin, mesothelin expression in the tumor cells. CD31, CEA, MOC31, CD34, CK7, CK20 were negative. Along with the typical features of adenomatoid tumor, there were areas of necrosis with hemorrhage surrounded by granulation tissue. Occasional cells with pleomorphic nuclei were noted but the mitotic index was low (Ki-67 stained about 3–5% of nuclei). The patient is alive without signs of disease 9 months after the surgery. The differential diagnosis and biological potential of the tumor is discussed.
Conclusion: This case is unique because of clinicopathological peculiarities.

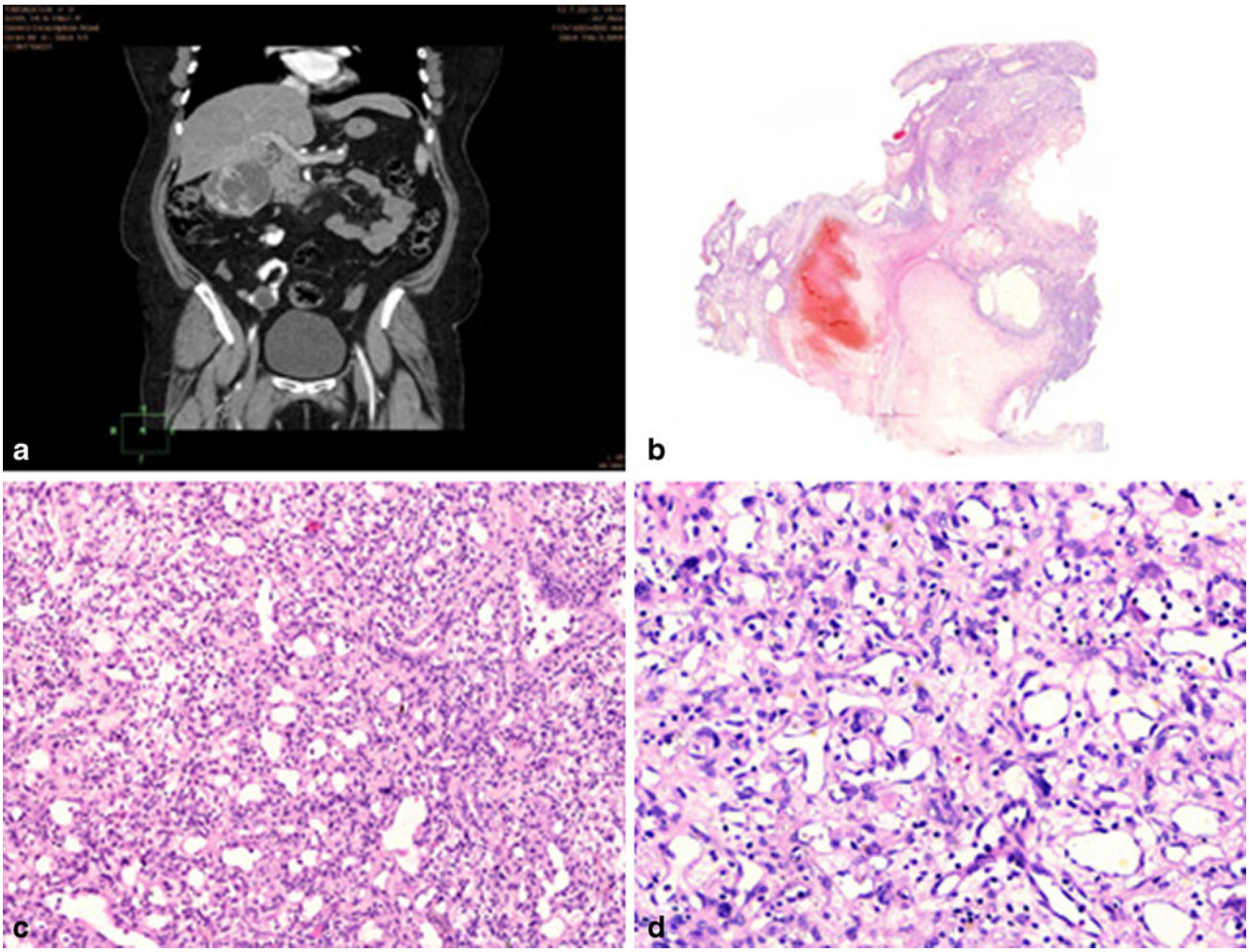

026

Malignant melanoma: cutaneous metastasis frequency and survival rate

C. Tamas *, C. Stanescu, D. Turliuc, L. Popa, C. Morosanu, D. Radulescu
*University of Medicine, Dept. of Plastic Surgery, Iasi, Romania

Objective: We studied the variation in locoregional metastasis frequency and the relation between clinical form and survival in malignant melanoma (MM).
Method: We used the Kaplan–Meier susvival curves and Cox proportional hazrds model to calculate the survival rate for 263 patients with MM, operated between 2000 and 2010.

Results: Half of the patients (51%) developed limbs MM. Patients with nodular melanoma (98) had a higher risk for cutaneous metastasis (61.22%) than the rest and a low survival rate (36.73%). There is a relation beween the number of metastatic lymph nodes and the survival rate. This rate decreases with 13.64% if more than four lymph nodes are involved: from 16 months, in a single affected lymph node, to 10 months for more than four.
Conclusion: The presence of cutaneous metastasis in MM is associated to a very low survival rate. The patients with stage I MM had the longest survival period. In the third stage, the survival rate depends on the number of the metastatic lymph nodes (57.14% IIIA; 43.50% IIIB; 12.50% IIIC). In a small number of cases (4%) the metastatic tumor was the first sign of MM.

027
Malignant melanoma: tumor lymph nodes as first clinical sign

C. Tamas *
*University of Medicine, Dept. of Plastic Surgery, Iasi, Romania

Objective: Malignant melanoma (MM), known as a very aggressive cancer, can be revealed by tumor lymph nodes.
Method: We report 11 cases (six females, five males) operated between 2002 and 2010. We excised lymph nodes with various location (five cervical, four inguinal, two both inguinal and axillar). Histological diagnoses: MM metastasis. Clinical examination discovered dark tumors on the skin in nine cases: scalp—three patients; left ear—one patient; shoulder—one patient; sacral region—one patient; thigh—one patient; foot—two patients. One male, age 75, developed a supraclavicular acromic melanoma; for one patient, we needed MNR to diagnose a brain primary tumor.
Results: Three of the patients (females, age 19–35) related recent dark tumors with temporal, deltoid or sacral location (evolution: 6–12 weeks). The male with acromic melanoma first noticed a big edema of the left lower limb, and then the spraclavicular red tumor (history: 4 weeks). Six patients described pre-existing nevus with a long history of local trauma or bleeding. We performed the excision of the skin tumors in nine cases; the acromic melanoma invaded the pleural domus, so the patient refused the surgery.
Conclusion: Small, dark nevus hidden on the scalp back in the web spaces or red spots with rapid growth should never be ignored.

028
Intimal sarcoma of the left atrium with retroperitoneal metastasis

J. Pardal *
*Hospital São João, Dept. of Pathology, Braga, Portugal

Objective: Primary cardiac sarcomas are rare tumors of mesenchymal cells. Intimal sarcoma (IS), an extremely rare tumor, occurs in large vessels with intraluminal growth. Cardiac IS usually arises in the left atrium. IS is considered to originate from subendothelial intimal mesenchymal cells.
Method: A 73-year-old woman presented dyspnea and fatigue. The clinical/imagiological study disclosed a left atrium wall mass. The histological and immunohistochemical (IHC) characteristics of the tumour supported the diagnosis of high-grade sarcoma with some features of endothelial differentiation.
Results: Two years later, she presented an intestinal occlusion due to a large retroperitoneal mass. Histological examination of the specimen revealed a sarcoma with histological/IHC features similar to the primary cardiac tumor. FISH analysis disclosed MDM2 and CDK4 amplification and IHC expression of MDM2, CDK4 and HMGA2, both in primary cardiac and retroperitoneal tumor cells, consistent with the diagnosis of IS. The patient died 4 months after the retroperitoneal metastasis and no autopsy was performed.
Conclusion: IS biology remains largely unknown and the prognosis is poor. Some reports describe frequent 12q13-14 region amplifications and gains, and mdm2 expression, supporting the role mdm2/p53 pathway in IS pathogenesis. Our case highlights the diagnostic importance of mdm2/cdk4 amplification/expression in an extremely rare case of primary cardiac IS with retroperitoneal metastasis.

029
Diagnosis difficulties in a case of desmoplastic small round cell tumor

O. M. Constantinescu *
*Bucharest, Romania

Objective: A desmoplastic small round cell tumor (DSRCT) is a rare, aggressive mesenchymal neoplasm with an extremely poor prognosis. Tumor cells co-express epithelial, mesenchymal and neuronal markers and are thought to originate from a mesothelial or submesothelial progenitor cell with the potential to undergo multilineage differentiation. Because of this, DSCRT is also called “mesothelioblastoma”.
Method: The present report reveals a case of a 25-year-old female patient, hospitalized in Fundeni Clinical Institute for peritoneal carcinomatosis. She underwent total hysterectomy with bilateral anexectomy, pelvic peritonectomy and omentectomy. Gross pathological examination of a surgical specimen revealed multiple white-gray nodules with a

microscopical appearance of a mesenchymal malignant tumor with round-oval shaped cells, hypercromatic and oval nuclei with many atypical mitoses, arranged in microtrabecular, alveolar and solid pattern. To establish a histopathological diagnosis, were performed immunohistochemical stains such as: VIM, Desmin, MNF 116, EMA, Chromogranin A, Synaptophysin, Melan A, Leu 7, CK8, Ki 67.
Results: Here we present an unusual case report of such a rare tumor developed in a female patient—tumor affecting mainly young male adults. In our case, the tumour has a less aggressive behavior; the patient is currently in a satisfactory condition, without further recurrence.

030
Splenic angiosarcoma: a case report
A. Nistor *
*Emergency University Hospital, Dept. of Anatomic Pathology, Bucharest, Romania

Objective: A rare and very aggressive malignant tumor, with a high metastatic rate and usually lethal. Incidence: 0.14–0.25 cases/1 million people/year. Mainly in adults over 40 years of age.
Methods: A 59-year-old woman with pain in the left hipocondrum, mainly at physical effort, without any signs of peritoneal irritation. Abdominal CT exam: enlarged spleen with large heterogenous masses and postcontrast liquid zones.
Method: Splee*n*=19/12/9 cm, with an intact capsule, large hemorrhagic areas with blood lakes and cystic spaces on the cut surface. The sections were parrafin-embedded and stained with hematoxylin–eosine.
Results: Microscopical typical for angiosarcoma: closely packed vascular channels with honeycomb-like pattern and hyaline cores lined by atypical endothelial cells, with hypercromatic and polymorphous nuclei, protruding in the lumen of the vascular channels. Presented areas of hemorrhage and necrosis. Immunohistochemistry: positive for Cd 31, CD34, Ki67; negative for fVIII.
Conclusion: The tumour has a very poor prognosis. Expression of endothelial markers suggests that it may originate from the lining cells of the spleen.

Monday, 29 August 2011, 09.30–10.30 and 16.30–17.00, Hall 5

PS-12 Poster Session Other Topics

001
The use of digital pathology for frozen section interpretation
J. Ay *
*Aperio, Vista, USA

Objective: Digital pathology is a useful tool for the interpretation of frozen sections especially for hospitals without a pathologist. Traditionally, in this case, a pathologist travels to the hospital where the surgery takes place, waits until the tissue is delivered, prepares the frozen sections and interprets the results at the microscope. A diagnosis is then made often influence the further course of the surgery. The travel time, waiting and processing of the frozen tissue is time-consuming, and can seriously delay a diagnosis.
Method: Digital pathology can be used as adjuvant and cost-effective tool for frozen sections as the example with sentinel lymph nodes in breast cancer shows. Once the surgeon cut the tissue and the further processing for the frozen sections is done, the slides can be scanned and managed in Aperio's Spectrum software. The remote consulting pathologist has immediate access to the frozen section for remote viewing and interpretation through the spectrum.
Results: It allows the remote pathologist also to compare the frozen section with intraoperative imprint cytology on the sentinel lymph nodes.
Conclusion: Therefore, digital pathology improves the efficiency of workflow significantly for the pathologist.

002
Implementation of the PAXgene tissue system in routine pathology
M. Kap *, R. Winther, S. Gundisch, C. Viertler, D. Groelz, W. Oosterhuis, K. Zatloukal, K.-F. Becker, U. Oelmueller, P. Riegman
*Erasmus MC, Dept. of Pathology, Rotterdam, The Netherlands

Objective: Within the EU FP7 project SPIDIA, the PAXgene Tissue System® (PAXgene) is being evaluated. After PAXgene fixation paraffin-embedded samples with histological aspects comparable with formalin-fixed tissue and molecular features comparable to fast frozen tissue samples are obtained. The PAXgene archive could provide biomedical research and molecular diagnostics with standardized, more versatile derivatives.
Method: To assess the performance of PAXgene in routine pathology, human tissue specimens were collected and divided into equal parts for fixation either with formalin or PAXgene. Sections of the obtained paraffin-embedded tissue were cut and stained. The performance of PAXgene fixed tissue in immunohistochemical and ISH assays was also assessed relative to the corresponding formalin-fixed tissues.
Results: Morphology was well preserved and some antigens in PAXgene fixed and paraffin embedded sections were detectable without the need for antigen retrieval. Comparable results were obtained with ISH and histochemical stains.

Conclusion: These results lead the way towards the implementation of PAXgene fixation in cases where both histological and molecular assays are needed for diagnosis. During this step-by-step implementation, pathologists get a chance to familiarize with the morphology and molecular advantages. Furthermore, the forthcoming PAXgene paraffin archive can be tested for stability of bio-molecules in time.

003

Fluorescent digital microscopy: multilayer, multichannel scanning for accurate analysis of small fluorescent signals including FISH

T. Krenács *, I. Zsakovics
*Semmelweis University, 1st Dept. of Pathology, Budapest, Hungary

Objective: Fluorescent-labeled samples particularly those generating small signals such as genomic fluorescent in situ hybridization (FISH) must be studied within a short time to avoid false negative results due to signal fading.
Method: In this work, the potential of fluorescent digital microscopy is demonstrated for the testing of HER2 FISH signals and connexin plaques of similar size in breast cancer samples.
Results: Fluorescent signals are randomly placed throughout the whole section thickness; thus, some remain hidden from single focus microphotography. These signals can only be revealed with confidence by scanning several focus planes (multilayer) throughout the sample for proper quantification of gene/chromosome gain such as that of HER2 in breast cancer, or signal positions to prove gene translocation such as that of t (9;22) resulting in the BCR-ABL gene fusion in chronic myeloid leukemia. Multichannel application allows more than one signal to be tested within the same sample. By combining fluorescence digital microcopy, TMA technology and project-based digital data management, validated high-throughput studies can be performed even for small and/or low intensity objects.
Conclusion: Such study on connexin cell–cell communication channels could be done in breast cancer with unprecedented precision and convenience, where permanent datasets allow the review of results for quality control.

005

Factors influencing the decline of clinical autopsy versus forensic autopsy rates in Kosovo

S. Manxhuka-Kerliu *, A. Gerxhaliu, I. Kerliu, M. Hoxha, S. Baca, F. Ahmeti, L. Kerliu, A. Podrimaj, S. Loxha, L. Shahini, G. Gashi
*University of Prishtina, Faculty of Medicine, Albania

Objective: Although autopsy rate has dramatically declined, it remains one of the most reliable methods to validate clinical diagnoses.
Method: The aim of this study was to analyze factors influencing decline of the autopsy rates in Kosovo. The clinical and forensic autopsy rates have been analyzed over a 12-year period.
Results: The highest clinical autopsy rate was 45.11% on 1998, declining to 2.77% on 2009. Younger patients, neonates, tended to have a higher clinical autopsy rate (95.31%) than adults (4.68%). Forensic autopsies have been increased from 2002 (1.38%) to 2009 (17.80%). There have been increased clinical autopsy cases due to the suspicion of medical malpractice performed at the Department of Forensic. During the 2 years (2008–2009), the most frequent causes of death according to the histopathology examination were: disseminated intravascular coagulation and acute myocardial infarction (18.8%).
Conclusion: Given the changes made in terms of autopsy regulations, they now require the family's consent in order to perform the autopsy. This regulation did not exist previously in Kosovo, resulting in a drastic influenced in this observed decline. Also, under traditional Islamic and Orthodox teachings, autopsies may be seen as a violation of human dignity and bodily integrity with spiritual implications.

006

DNA fragmentation-driven tumor cell degradation induced by modulated electro-hyperthermia

N. Meggyesházi *, G. Andócs, L. Balogh, T. Krenács
*Semmelweis University, 1st Dept. of Pathology, Budapest, Hungary

Objective: Electromagnetic field generated by capacitive coupled, modulated radiofrequency (RF) (electro-hyperthermia—mEHT) can mediate a non-invasive, low-energy density intervention in tissues through selective enrichment within the tumor without passing through cell membranes.
Method: HT29 colon–rectal cancer xenografted to the femoral region of Balb/c (nu/nu) mice was treated with a single shot mEHT for 30 min. At 0, 1, 4, 8, 14, 24, 48, 72, 120, 168, and 216 h, post-treatment samples of three mice in each group were tested using histomorphology, immunohistochemistry and DNA fragmentation (TUNEL) assay and analyzed with digital microscopy.
Results: Modulated EHT treatment resulted in a selective and progressive destruction starting from the tumor centre. Caspase-3 positive inflammatory and tumor cells occurred exclusively at the periphery of the treated tumors between 4 and 14 h. In the tumor centre, dying cells showed nuclear shrinking, apoptotic bodies and elevated TUNEL reaction

culminating at 48 h to confirm programmed cell death as the major damage pathway. The massive myeloperoxide positive leukocyte infiltration ring with apoptotic pattern accompanied by an external necrotic margin with a climax at 72 h possibly also contributed to the tumor elimination.

Conclusion: Programmed cell death was proved to be the main mechanism of electro-hyperthermia related tumor degradation accompanied by acute inflammatory cell induced necrosis.

008

Accuracy of frozen section IN Urmia University of Medical Sciences

F. Abbasi *, Z. Yekta, A. Aryan
*Imam Khomeini Hospital, Dept. of Pathology, Urmia, Iran

Objective: Background: Intraoperative consultation by frozen section is a high-risk procedure with important consequences. Therefore, it is critical to determine the efficiency of frozen section performance periodically. This study was performed to determine the accuracy of frozen section in Urmia University of Medical Sciences.

Method: We compared the results of 200 consecutive cases of frozen section with their final permanent section diagnoses in teaching hospitals of Urmia University of Medical Sciences during March 2001 to March 2008.

Results: A total of 155 neoplastic and 45 nonneoplastic specimens were studied. The overall accuracy of frozen section was 96.5%. In the diagnosis of neoplastic lesions, sensitivity, specificity, positive and negative predictive Vvalues and accuracy were 93.1%, 97.7%, 96%, 95% and 95.9%, respectively.

Conclusion: The results showed that, in Urmia University of Medical Sciences, interpretation of FS was done with high accuracy and is valuable to help surgeon to plan the best management of the operation.

009

Histopathological findings after vitamin E (tocopherol-α) administration in a rat model of non-alcoholic fatty liver disease (NAFLD)

G. Agrogiannis *, I. Doulamis, I. Tzanetakou, A. Pantopoulou, D. Perrea, N. Kavantzas, E. Patsouris
*National University of Athens, School of Medicine, Greece

Objective: The aim of this study is to examine the effect of a water-soluble variant of vitamin E (tocopherol-α) on non-alcoholic fatty liver disease (NAFLD) development and progression caused by a diet high in saturated fat in adult Wistar rats.

Method: A total of 22 adult male Wistar rats were allocated into three groups. Group A (control group, $n=6$) received a standard chow diet for 24 weeks. Group B ($n=7$) and group C ($n=9$) received standard chow enriched with 2% cholesterol (Ch) for 14 weeks and for the remaining 10 weeks their diet was enriched with 2% Ch and 40% lard fat. Group C, moreover, received water-soluble vitamin E (4.2 IU/day) during the last 10 weeks. At the end of the study, the animals were euthanized and tissues were taken for histopathologic analysis of liver.

Results: High-dose Vitamin E treatment reduced fat deposition and maintained liver architecture in the liver in group C compared to group B.

Conclusion: Vitamin C exerts a hepatoprotective role even in the presence of a high-fat atherogenic diet in a rat model. Vitamin E supplementation may aid in the prevention or treatment of NAFLD associated with a high-fat diet.

010

DNA ploidy as an independent predictor of survival in stage IV colorectal cancer (CRC)

G. Agrogiannis *, N. Kavantzas, I. Xynos, S. Tsaousi, A. Lazaris, N. Tsavaris, E. Patsouris
*National University of Athens, School of Medicine, Greece

Objective: This study explores the prognostic significance of DNA ploidy assessed by image analysis in the context of additional established prognostic factors in a patient cohort with stage IV CRC.

Method: A total of 541 patients with histologically proven metastatic CRC (UICC stage IV) were analysed and ploidy score (DNA Index) was tested for its potential relationship to survival.

Results: Mean survival time was recorded at 12.8 months. Patients with ploidy scores of 2.2–3.6 or >3.6 had 2.94 and 4.98 times higher probability of death, respectively, as compared to those patients with ploidy score <2.2; patients with CRP >15 mg/dl had 2.52 higher risk of death and patients with CRP 5–15 mg/dl had 1.72 times higher risk of death than patients with CR*P*<5 mg/dl.

Conclusion: Patients with stage IV CRC and low ploidy score, not elevated or low CRP levels, absent or mild anemia and no hypoalbuminemia may benefit more from palliative chemotherapy.

011

IGF-1 expression after platelet-rich plasma administration in ruptured tendon

G. Agrogiannis *, N. Kavantzas, D. Lyras, I. Kostakis, A. Vaiopoulos, I. Doulamis, E. Patsouris
*National University of Athens, School of Medicine, Greece

Objective: This study aims to determine whether or not a single application of platelet-rich plasma (PRP) in a ruptured tendon alters the expression of IGF-I in the early phase of healing in an animal wound model.
Method: We performed an Achilles tendon rupture model on 48 New Zealand white rabbits by transecting the tendon transversely and then injecting 0.5 mL of PRP into the tendon mass on one side and injecting saline on the contralateral control side. Six animals (12 limbs) were killed from each group at 1, 2, 3, and 4 weeks postoperatively. After the animals were killed, six paraffin sections were made from each Achilles tendon, three of which were stained with hematoxylin and eosin and subjected to microscopic examination and three of which were immunostained with an anti-IGF-I primary antibody. Density of brown diaminobenzidine (DAB) staining was evaluated to quantitatively analyze the results.
Results: IGF-I was localized in the epitenon and the endotenon, with an overexpression in the epitenon in the PRP group by the fourth week in comparison with the controls. Furthermore, the tendons treated with PRP healed more rapidly.
Conclusion: Based on these findings, PRP could be useful to surgeons treating a ruptured tendon.

012

Effect of *N*-acetylcysteine and sesame oil on liver histopathology and cardiovascular disease risk in middle-aged hypercholesterolemic mice

G. Agrogiannis [*], L.-M. Korou, N. Kavantzas, C. Koros, A. Pantopoulou, E. Patsouris, D. Perrea
[*]National University of Athens, School of Medicine, Greece

Objective: The purpose of the study was to investigate the action of *N*-acetylcysteine (NAC) and sesame oil in the lipidemic status and liver architecture of diet-induced hypercholesterolemic middle-aged mice.
Method: A total of 34 male middle-aged mice C57/bl6 were assigned to six groups: control group, group receiving test diet supplemented with 2% cholesterol and 0.5% cholic acid for 8 weeks, group receiving the test diet with NAC supplementation (230 mg/kg p.o.), group receiving test diet enriched with 10% sesame oil, group receiving control diet with NAC supplementation and group fed control diet enriched with sesame oil.
Results: NAC co-administration improved the diet induced disturbed lipid profile and led to a significant decrease of serum lipid peroxidation and alkaline phosphatase (ALP) levels, whereas both NAC and sesame oil restored nitric oxide bioavailability. Concerning liver histology, the lesions observed in NAC treated group were less severe than those seen in the other cholesterol-fed groups.
Conclusion: NAC co-administration enhanced antioxidant capacity and ameliorated serum lipid status and hepatic due to high cholesterol feeding. These findings suggest a beneficial role of NAC in dietary hypercholesterolemia.

013

Autopsies in two decades: what has changed?

A. Alves [*], P. Luís, I. Alves, C. Ferreira
[*]Hospital de Santa Maria, CHLN, Dept. of Pathology, Lisbon, Portugal

Objective: The autopsy still has an important role in medicine. The goal of this study was to analyse the autopsies performed at the HSM in the years 2009–2010 and compare with the results observed in 1998.
Method: Data collection was performed from autopsy reports of 1998, 2009 and 2010 and analysed using Epi Info®. The assessment of major diseases and causes of death was based on macroscopic autopsy findings. Excluded from the study: autopsies limited to the brain and under 1 year of age.
Results: We analysed 269 autopsy records from 2009/2010 and 307 from 1998. The rate of autopsies performed was 5.5% (2009/2010) and 11.4% (1998). The mean age was 66.8 years and the duration of hospitalization 10.7 days, (higher values than in 1998). The main pathologies and/or causes of death determined in 2009/2010 were similar to 1998: pneumonia, myocardial infarction (MI), pulmonary emboli (PE), cancer and stroke. In 2009/2010 the sensitivity of clinical diagnosis to determine the cause of death was 49.5% and for some major diseases was (1998–2009/2010): MI 40.7–47.5%; infectious diseases 69.2–38.0%; neoplasms 29.6–86.2%.
Conclusion: Despite improved diagnostic methods, the sensitivity of clinical diagnosis to determine the cause of death is low, justifying the autopsy's importance.

014

Tissue section preparation by microwave energy and comparison with routin method

S. Amoueian [*], A. Attaranzadeh
[*]Mashhad University of Medicine, Dept. of Pathology, Iran

Objective: Microwave energy is produced from electricity energy via a magnetron which is discovered about 60 years ago and, according to its several capabilities, is used in most industries. One of them is laboratory utility, especially in pathology laboratory. Histoprocessing in pathology laboratory takes time for about 24 h and diagnosis is delayed by one working day. For reducing time in diagnosis and decreasing hospital and insurance costs, and introduc-

ing an applicable way, the aim of this study is microwave oven usage in optimal tissue processing.
Method: In this study, each level of processing was done separately and finally all the levels were combined; then, results were verified.
Results: According to details of tissue processing, total time for all levels was 70 min, which enables the evaluation of slides at the same day of admission and sampling. For final judgment, 60 sample pairs were processed in routine and microwave way. Then, after a single blind comparison, the quality results of all slides including tissue clearing, preservation of tissue structure, quality and clearness of nuclei and cytoplasm, optimal staining and in overall, ability of diagnosis were satisfactory in both ways and in all 60 pairs of tissue. Distinction between them was impossible and in many of them microwave processing slides were more.
Conclusion: Total time for all levels was 70 min, which enable the evaluation of slides at the same day of admission and sampling. Specific stainings were done by this method, too.

015

Patients's perspective in disease-oriented biobanking activity: the Trentino Biobank project experience

M. Barbareschi*, S. Fasanella, S. Giuliani, C. Cantaloni, M. Macilotti,
*S. Chiara Hospital, Dept. of Pathology, Trento, Italy

Objective: Trust between donors, biobank managers and researchers is essential in biobanking. Informed consent (IC) is a standard requirement and its formulation in biobanking activity is a matter of debate. We describe our experience in daily contact with patients focusing on how they answer the questions of the IC.
Method: Since 2009 we run a disease-oriented public biobank, and submitted our broad IC to 554 potential donors of left-over tissues in a general hospital. Our IC includes a description of the project, donor rights and eight questions (see www.tissuebank.it).
Results: All patients agreed to donate their biomaterials; 0.3% denied to provide biomaterials to private companies for industrial research, 27.5% patients did not want to be recontacted by the biobank in case of unexpected findings; 19% patients did not allow sharing clinical and genetical data with relatives. Most patients felt that the complex consent module was unnecessary.
Conclusion: All patients understood the importance of biobanking and were highly compliant, underscoring the importance of trust as the fundamental element in biobanking. Broad IC was not a constraining element in their decision to donate biospecimens. Helping patients make this decision requires transparent terminology together with the ability to listen and respecting the patient's right to self-determination.

016

IgG4-related sclerosing disease with lymphadenopathy and thymus enlargement: a case report

M. Bobrov *, I. Kazantseva, S. Lishchuk, L. Gurevich, S. Terpigorev
*Moscow, Russia

Objective: IgG4-related disease is a system condition, characterized by IgG4-positive plasma cell and T-lymphocytic infiltration of different organs and tissues with development of tumor-like sclerosing and inflammatory changes simulating true, including malignant, tumors. The condition is often associated with flebitis obliterans.
Method: We report a case of generalized lymphadenopathy clinically diagnosed as malignant lymphoma in a 59-year-old woman. The patient died of bilateral pneumonia. Histological and immunohistochemical examination of autopsy material was performed.
Results: A tumor-like lesion of thymus was revealed. Histologically, massive infiltration of polyclonal IgG4-positive plasma cells of lymphatic nodules, thymus and spleen was observed. Moreover, there were lymphoplasmocytic infiltration with increased amount of IgG4-positive plasma cells with progressive sclerosis and flebitis obliterans in pancreas, parapancreatic adipose tissue, liver, kidneys, epicardium, thyroid gland, hypophysis, skin and other organs.
Conclusion: We evaluated this case as IgG4-related sclerosing disease, manifested with lymphadenopathy and thymus enlargement. The cases of IgG4-related sclerosing disease with thymus involvement are very rare. We found only one description of tumor-like thymus enlargement with plasma cell infiltration, flebitis obliterans, thymic tissue atrophy and progressive fibrosis in available sources.

017

Are mesangial cells reactive to nitrofurantoin when associated with an oxidative stress?

C. L. Zamfir *, F.E. Zugun, R.O. Temneanu, L. Tocan, E. Cojocaru, C. Gales
*University of Medicine, Dept. of Histology, Iasi, Romania

Objective: There is numerous data on renal tolerance to nitrofurantoin in generally, but only a small account about mesangial cells involvement in a direct assessment of

nitrofurantoin renal effects. Mesangial cells, due to their particular disposal, can influence the glomerular architecture and capillary stability. The use of an experimental animal model offers the possibility to estimate the effects of a long term nitrofurantoin administration and a coexistent oxidative stress on mesangial cells.

Method: Morphometrical assay of mesangial cell number, diameter and morphology was performed in a microscopic scanning analysis (observer Z1 microscope), using three groups of Wistar rats for 60 days: a control group versus a group exposed to nitrofurantoin 150 mg/kg bw/day, versus a group exposed concommitently to the same dose of nitrofurantoin and intermitent light (as an oxidative stress trigger). Prelevated renal samples were specifically treated, microscopically examined and scanned.

Results: Morphometric evaluation of mesangial cells parameters did not sustain any relevant and consistent differences between cells from all three examined groups. The renal status was not disturbed.

Conclusion: There were no detected effects of nitrofurantoin prolonged administration and associate oxidative stress on mesangial cells.

018

Erdheim–Chester disease: report of a case with retroperitoneal involvement

F. E. Costa *, M. França, C. Dias, D. Esteves, C. Peixoto, C. Lopes
*Menarini Diagnosticos Lda., Paço De Arcos, Portugal

Objective: Erdheim-Chester disease (ECD) is a rare non-Langerhans'cell, non-familial, systemic histiocytosis. It was first described in 1930 by William Chester and Jakob Erdheim as "lipid granulomatosis". It generally occurs in adults and demonstrates a slight male predominance. The disease, denoted by a characteristic radiologic and histological pattern, predominantly affects the major long bones of the extremities. Extraskeletal lesions which include the kidney, retroperitoneum, heart, lung and central nervous system occur in more than 50% of cases.

Method: We report a case of a 58-year-old man with a medical history of diabetes mellitus and peripheric arteriopathy.

Results: Computed tomography of the abdomen, pelvis and lower members was performed for angiographic evaluation. Incidentally, diffuse infiltration of the retroperitoneum with bilateral perirenal densification ("hairy kidney" appearance) was observed. The scan also revealed the ECD characteristic appearance of bilateral, symmetric osteosclerosis of the femora. Retroperitoneal tissue biopsy was made. Histology of the retroperitoneal lesion showed fibro-adipose tissue with steatonecrosis and an infiltrate of histiocytic cells. Immunohistochemically, these cells were CD68 positive and S100 negative, confirming the monocyte/macrophage lineage.

Conclusion: Although the histological features of ECD are typical, they are not diagnostic. The diagnosis is based on the remarkable imagiologic findings confirmed histopathologically.

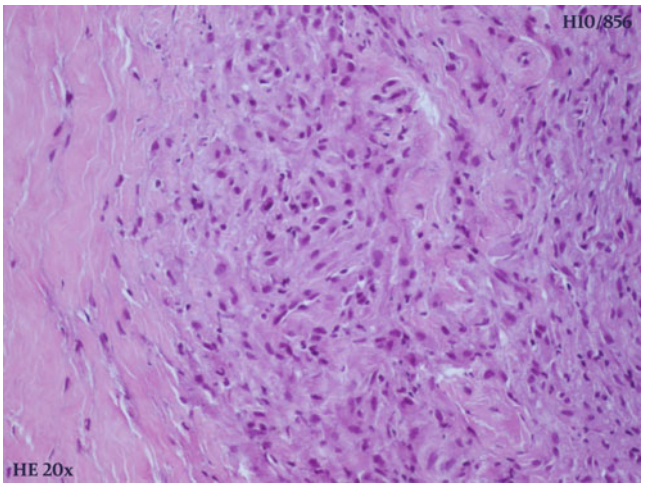

019

Intra-abdominal desmoplastic small round cell umor: a case report

Á. Hens Perez *, A. Calvo, M. J. Añon, M. Balbuena, A. Ortiz, M. Vazquez, M. Mosteiro
*Servicio Andaluz de Salud/UCA, Dept. of Pathology, Puerto Real, Spain

Objective: Desmoplastic small-round-cell tumor is a rare and highly aggressive malignancy that frequently occurs as multiple masses in the abdomen of children and young population, with distinctive histologic and immunohistochemical features.

Method: A surgical specimen of 17-year-old man with a 7-cm umbilical mass.

Results: The histological studies showed islets containing small round cells surrounded by abundant desmoplastic stroma and the typical immunophenotype of intraabdominal round cell desmoplastic tumor. Multiple peritoneal and disseminated metastatic nodes developed in the illness course, and the patient died four and half years later.

Conclusion: The median survival of this aggressive disease is about 17 months. Our patient was still alive for more than 4 years, probably caused by the tumour location debut.

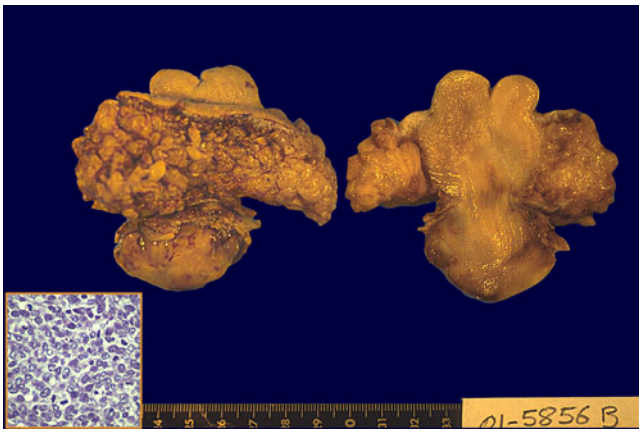

020

Case report: littoral cell angioma—a morphologic and immunohistochemical study

E. Javadirad *, M. Emami Aleagha, S. Shariat Torbaghan
*Medical School, Dept. of Pathology, Kermanshah, Iran

Littoral cell angioma is a splenic vascular tumor of splenic sinus lining cells that is considered benign in general. This report describes a case of littoral cell angioma with no malignant histological features. The lesion is composed of anastomosing vascular channels resembling splenic sinus; they are lined by endothelial cells which show mitotic activity very rare. Immunohistochemically, the tumor cells were positive for both endothelial (Factor VIII-AG, CD34) and histiocytic markers (KP1 or CD68). The morphologic and immunohistochemical findings in this tumor confirm the presence of dual (endothelial/histiocytic) characteristics of the reticuloendothelial cells lining the splenic sinus, justifying the term littoral cell angioma.

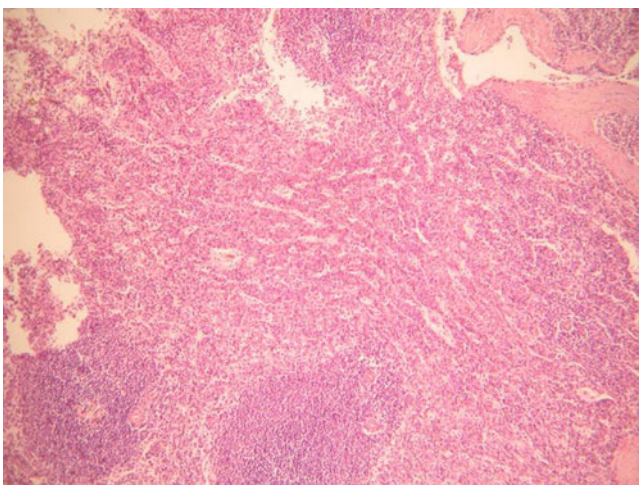

021

Coexistence of papillary urothelial carcinoma and mantle blastoid lymphoma of cervical lymph nodes: a case report

G. Kalodimos*, A.-M. Feritsean, K. Koti, A. Vardouli
*General Hospital of Volos, Dept. of Pathology, Greece

Objective: Detection of a second malignancy during the investigation of patients with bladder carcinoma is not uncommon. However, the coexistence of urothelial carcinoma with mantle blastoid lymphoma has not yet been reported.
Method: A 79-year-old Caucasian male presented with gross haematuria. Cystoscopy revealed a papillary tumour 2.5×2×1 cm in the right lateral bladder wall. CT scan of the lower and upper abdomen was normal, but further clinical investigation showed a 2-cm left cervical mass.
Results: The bladder neoplasm was an infiltrating papillary urothelial carcinoma, limited to the lamina propria. Infusions with BCG were started. FNA biopsy of the cervical mass was indicative of lymphoid malignancy. Histopathologic examination showed diffuse infiltration of lymph nodes and extranodal tissue by non-Hodgkin lymphoma, which was immunohistochemically classified as mantle blastoid lymphoma. The peripheral blood as well as other sites was not involved. The course was extremely aggressive and the patient died shortly after diagnosis.
Conclusion: According to the literature, our case is the first one reporting the coexistence of this highly malignant rare lymphoid neoplasm with bladder carcinoma.

022

Epidermal growth factor receptor and tenascin-C may mutually contribute to the recurrence potential of giant cell tumor of bone

P. Balla *, M. Maros, L. Moskovsky, P. Picci, M. Benassi, T. Krenács
*Semmelweis University, 1st Dept. of Pathology, Budapest, Hungary

Objective: The benign but potentially malignant giant cell tumor of bone (GCTB) consists of neoplastic stromal, monocytic and osteoclast type giant cells. Histopathological features cannot predict the clinical progression of GCTB. Independent data links epidermal growth factor receptor (EGFR) and tenascin-C to GCTB progression.
Method: Since tenascin-C contains EGF-like repeats we tested the correlations of EGFR and tenascin-C expression in 201 GCTB cases included into tissue microarrays using immunohistochemistry and fluorescent in situ hybridization (FISH) combined with digital microscopy (Pannoramic, 3DHISTECH, Budapest, Hungary).

Results: EGFR expression restricted to neoplastic stromal cells and that of tenascin-C were found to correlate with GCTB recurrence. EGFR signaling was primarily mediated through the MAPK pathway and less by the lipid kinase (Akt) signaling. The number of osteoclasts was significantly higher with lower mean size in EGFR positive than negative cases. There was no EGFR gene amplification or activating mutation behind elevated EGFR levels. In cell culture EGF with MCSF supported osteoclastogenesis as much as MCSF with RANKL, and EGF increased stromal cell proliferation. EGFR and tenascin-C expression almost significantly correlated with each other suggesting their functional interactions.
Conclusion: In conclusion, EGFR and tenascin-C expression is associated with GCTB progression partly through direct interactions which can help predicting recurrence potential.

023

Podoplanin expression is enhanced in fibroblast-like synoviocytes of the enlarged periprosthetic synovial lining layer in suggested metal hypersensitivity

A. Lübke *, M.M. Morlock, W. Rüther, M. Amling, J. Zustin
*UKE Hamburg-Eppendorf, Inst. für Pathologie, Germany

Objective: Enlarged fluid-filled bursae and necrotizing granulomas were reported in cases with suggested hypersensitivity reaction to metal following metal-on-metal hip resurfacing arthroplasty. Microscopically, viable areas of the periprosthetic synovial membrane displayed a proliferative desquamative synovitis along with variable amount of lymphocytes and scattered macrophages. While podoplanin expression was demonstrated in fibroblast-like synoviocytes in rheumatoid arthritis, we wished to investigate the expression of D2-40 in the proliferative desquamative synovitis in retrieved hip resurfacing arthroplasty.
Method: Podoplanin expression in human synovial tissue from ten rheumatoid arthritis patients, ten osteoarthritis patients and five cases with suggested hypersensitivity reaction following hip resurfacing arthroplasty was assessed by immunohistochemistry (D2-40).
Results: Podoplanin was highly expressed in the fibroblast-like synoviocytes throughout the synovial lining layer preferentially in rheumatoid arthritis and proliferative desquamative synovitis. The D2-40-positive fibroblast-like synoviocytes displayed characteristic tubular projections. The synovial macrophages showed negative reaction against D2-40.
Conclusion: In metal hypersensitivity reaction after implantation of metal prosthesis, the enlargement of the synovial lining cell layer was characteristically associated with proliferation of D2-40 positive fibroblast-like synoviocytes.

024

Evaluation of the morphometrical changes, VEGFR-1 and VEGFR-2 expression in the vascular structures within the third-order villi in normal and pre-eclampsia-associated pregnancies

C. M. Mihu *, S. Susman, D. Rus Ciuca, D. Mihu
*University of Medicine, Dept. of Histology, Cluj, Romania

Objective: During the fetal period the processes of angiogenesis are essential for the normal development of the placenta. In our study we sought to evaluate the changes of the third-order villi vascular structures in both normal and pre-eclampsia-associated pregnancies.
Method: The placentas were collected from 22 patients with normal pregnancies and 11 patients with pre-eclampsia. Each fragment FFPE section (5 μm) was measured morphometrically by evaluating the thickness of the vessels walls within the third-order villi. The expression of VEGFR was shown through immunohistochemistry (Sigma-Aldrich, with dilutions of 1:200 for VEGFR-1 and 1:100 for VEGFR-2, respectively).
Results: We detected a marked difference regarding the vessel wall thickness, which was increased in patients with pre-eclampsia compared to those with normal pregnancies. Immunohistochemical analysis revealed that VEGFR-1 was present in the syncitiotrophoblast and the endothelium, with a marked increase in patients with pre-eclampsia. VEGFR-2 was detected only at the endothelium level.
Conclusion: In pre-eclampsia, changes in the vascular structures (the thickness of the vessel walls) directly affect the level of resistance of the placental vessels. VEGFR-1 and VEGFR-2 are expressed differently, with an increase in expression in the case of VEGFR-1

025

Association of results of measurement of microbilogical laboratory to final outcome of the disease in patients with acute pancreatis: assessing the prognostic value

S. Patiakas *, C. Charalampous, K. Panagiotellis, M. Tsigaridaki, G. Liapas
*General Hospital of Kastoria, Microbiological Laboratory, Greece

Objective: This aims to study the reliability and sensitivity, simple, cheap and readily available laboratory tests

requested by the introduction of a patient with acute pancreatitis as prognostic indicators.
Method: We studied 46 cases of nondiabetic patients who were hospitalized with acute pancreatitis in hospital criteria Ranson>3.
Results: The blood glucose was the only statistically significant: value>150 mg/dl in the introduction, had the highest sensitivity (81.1%), good positive predictive value (73%) and even better negative predictive value (86.4%). In contrast, the hematocrit value (> 45% for men and>40% for women) to introduce and/or maintain it at constant levels during the first 24 h had a sensitivity and negative predictive value similar to the criteria in Ranson, but the specificity and positive predictive value was lower. Finally, elevated WBC (> 15,000/mm^3) and low prices Ca (<8 mg/dl) showed no statistical significance and increased price of urea (> 25 mg/dl) had the highest specificity (89.2%) but statistically significant predictive value, positive or negative, the final outcome.
Conclusion: Blood glucose at admission of patients with acute pancreatitis is a very important test for the prognosis, cheap and available, which should never be omitted, since patients with normal serum glucose (<150 mg/dl) is not at all likely to develop severe complications of pancreatitis and necrosis of the liver.

026

The evaluation of radiographically based diagnoses compared with autopsy data

C. Petri *, H. Kiaer, M. Hardt-Madsen, I. Andersen
*Tisvildeleje, Denmark

Objective: Autopsies provide the ultimate identification of diseases. The present pilot study focuses on the reliability of diagnoses based on radiographic data.
Method: Post-mortem examinations were performed on 142 patients deceased at Svendborg Hospital, Denmark, in 2010. Only 106 of these could be included in the comparative study.
Results: The male/female ratio was 1:2. Three quarters of the patients were gerontological; the rest were younger. The radiological examinations consisted of 189, performed in 106 patients. The quality of the radiological records, here defined as the extent to which they were in agreement with post-mortem pathological findings, was determined to be equivalent in 60 patients (57%). Total discrepancy was found in 25 patients (24%), while partial discrepancy was registered in 21 patients (20%). A total of 36 patients (25.35%) were unsuited for standardized comparison.
Conclusion: The fact that nearly half of the diagnoses in the study were at least partially incorrect must have had consequences for the treatment regimens designed for the patients involved. The most immediately obvious means of calibrating and refining radiographic diagnostics would be a systematic, ongoing comparison of indirect radiographic and clinical evaluations with direct pathological observations on a far larger scale than the present autopsy rate.

027

Primary peritoneal serous carcinoma with lymphatic metastases: a case report

S. Rjabceva *, I. Bokhan, I. Grinchik, M. Vozmitel
*Belarusian Medical Academy, Dept. of Pathology, Minsk, Belarus

Objective: Primary peritoneal serous carcinoma (PPSC) or extraovarian primary peritoneal carcinoma (EOPPC) is a rare malignant epithelial tumor of the peritoneum.
Method: We studied the case of PPSC in an 87-year-old woman. The woman died from heart failure. A lot of small and large nodules of peritoneum were found by autopsy. Lymph nodes were palpable. Paraffin-embedded tissue was stained with hematoxylin–eosin. We used immunohistochemical markers such as mesotelin, cytokeratin 5/6, cytokeratin (AE1/AE3) and calretinin.
Results: A size of tumor nodules was from 0.2 to 15 cm. Histopathologically, the tumor mimics a serous ovarian adenocarcinoma, but the ovaries were all normal in size and gross appearance. In some areas, the tumor arranged in clusters and in small nests separated by desmoplastic tissue. In other areas, a cystic growth pattern with intracystic tufting, and small aggregations of papillary clusters with psammoma bodies were present. The tumor cells were polyhedral with indistinct cell borders and granular eosinophilic cytoplasm with low- or moderate-grade cytological features. The tumor cells were detected in lymphatic nodule of abdomen. Immunohistochemically, the tumor showed cytokeratin (AE1/AE3) positivity. Mesotelin, cytokeratin 5/6 and calretinin were negative.
Conclusion: The morphological features of PPSC are very similar to a serous ovarian adenocarcinoma; therefore, primary ovarian cancer should be excluded.

028

Postmortem evaluation of the intraocular pressure in the diagnosis of death coming time

M. Samoylov *, Z. Sokolova, E. Kildyushov
*Russian Academy of Sciences, Central Clinical Hospital, Dept. of Pathology, Moscow, Russia

Objective: One of the most important issues of forensic medicine has been and remains the determination of the time of death. The fall of intraocular pressure (IOP) is considered to be the permanent postmortem change, which allows us to use it in determining the death time.
Method: Evaluations of the IOP in 65 corpses of persons, of mature age and of both sexes, who suddenly died were carried out. Tonometry was performed in position on the back. Environment temperature was 20±3°C. The measurements were performed every 30 min; thus, 22,680 measurements were taken in all.
Results: Postmortal IOP dynamic has been studied and the impact of a number of endogenous and exogenous factors (blood alcohol content, sex, age, rate of dying) has been examined. The methodology of IOP evaluation in the early postmortem period was created and the possibility of postmortem IOP measures using a diagnostic criterion for death coming time determination in the early postmortem period was established. The mathematical model describing the process has been developed.
Conclusion: The regularity of IOP postmortem changes was established. The device for IOP measuring was created. The measurement of IOP is a helpful diagnostic criterion for the death time determination in the early postmortem period.

029

Epithelial–mesenchymal transition in cancer of unknown primary

V. Siozopoulou *, A. Goussia, A. Stoyianni, G. Pentheroudakis, I. Nesseris, P. Oikonomou, A. Papoudou-Bai, N. Pavlidis, V. Malamou-Mitsi
*University Hospital of Ioannina, Dept. of Pathology and Cytology, Greece

Objective: Epithelial to mesenchymal transition (EMT) has been associated with advanced stage and poor outcome of patients with several solid tumors, but not in cancer of unknown primary (CUP).
Method: In TMAs from 100 CUP, we studied the immunohistochemical expression of E-Cadherin, N-Cadherin, Vimentin and Snail. EMT phenotype was defined as loss of E-Cadherin expression, expression of any of N-Cadherin, Vimentin, with concommitant expression of Snail, as assessed by the percentage of stained tumor cells.
Results: Histological diagnosis was adenocarcinoma, squamous cell carcinoma and undifferentiated carcinoma. The clinicopathologic subgroups were visceral, axillary nodal, peritoneal carcinomatosis and nodal disease. Therapy consisted of platinum-based combination regimens in 55%. The median progression-free survival (PFS) and overall survival (OS) were 7 and 12 months, respectively. EMT phenotype was seen in eight cases (8.1%) and was associated with poor OS (EMT- median OS 13 months vs EMT+median OS 8 months, logrank $p=0.023$). EMT+ phenotype was correlated with male gender, high grade and presence of visceral metastases ($p<0.05$). Other factors of poor survival were performance status >2 and non-platinum therapy ($p<0.05$).
Conclusion: EMT is infrequently seen in CUP; however, it carries significant adverse impact on patient's outcome, probably through increased tumor anaplasia and visceral dissemination.

030

Calcium sulphate bone graft substitute disadvantages: experimental study

P. D. Sirbu *, T. Petreus, D. Radulescu, S. Stolnicu, R. Asaftei, V. Poroch, P. Botez
*Gr.T.Popa UMF Iasi, Dept. of Orthopaedics Traumatology, Romania

Objective: Many different synthetic calcium-based bone graft substitutes (BGS) are currently available for clinical use. The aim of this study is to reveal the quality of integration regarding calcium sulphate (Osteoset Wright) osteoconductive bone graft substitute.
Method: The authors have performed an in vivo study on two groups of six rabbits (one test and one control) with induced bone defect in distal femoral epiphysis (a 4-mm transepiphyseal canal, parallel to the articular line). The bone defect in the test group was filled with calcium sulphate Osteoset pellets. Test group was healed by itself. Rabbits were sacrificed at 2 months after bone graft implantation. Serial sections were stained by hematoxylin-eosin, van Gieson and checked for ALP/TRACP expression by a special Takara Ltd. kit
Results: At 2 months after calcium sulphate bone graft implantation, we have observed a partial resorption of the bone substitute, with the presence of new synthesized bone with ALP-positive osteoblasts at the migrating growth pole. However, we have remarked a poor density of the material at 2 months post-implantation, with important fragmentation at the implantation place
Conclusion: Osteoset pellets must be reserved to cavity defects with small contact area with fluid, thus avoiding the BGS to dissolve too fast.

031

Unusual humeral osteosarcoma: case report

P. D. Sirbu *, W. Friedl, D. Radulescu, T. Petreus, S. Stolnicu, R. Asaftei, P. Botez
*Gr.T.Popa UMF Iasi, Dept. of Orthopaedics Traumatology, Romania

Objective: Salvage of the limb for patients with malignant tumor of the humerus continues to represent a challenge from both oncological and reconstructive standpoint.
Method: A 24-year-old female showed a pathological fracture of the left humerus at the joint of the middle and upper third of the diaphysis. Bone biopsy showed a fibroblastic osteosarcoma with vascular compound. Surveillance MRI after 8 weeks of chemotherapy showed an important tumor progression without involving axillar nerves and vessels. At this moment, she was operated by performing resection of the entire humerus and reconstruction with a Mutars total humeral modular replacement prosthesis. Tumor necrosis determined at the time of tumor resection and at repeated anatomo-pathological examination was an important prognostic factor for the improved survival rate. After 4 weeks of immobilization she started an intensive rehabilitation program and she continues the cyclic chemotherapy.
Results: Even if it was only 4 months from surgery, the patient regained a good elbow function and acceptable function of the shoulder. We may also consider the emotional acceptance from the patient as satisfactory.
Conclusion: The authors concluded that preoperative counseling and focused treatment followed by early rehabilitation led to a high level of postoperative emotional acceptance from the patient.

032

Pathomorphology of the paravertebral muscles in the idiopathic scoliosis process

J. Szarek *, I.M. Kowalski, T. Kotwicki, I. Babińska, W. Kiebzak
*University of Warmia and Mazur, Olsztyn, Poland

Objective: Incorrect posture caused by idiopathic scoliosis (IS) brings about lesions in paravertebral muscles on the concave and convex side of the spine. A comparison of those lesions is the aim of this study.
Method: The research was carried out on seven boys and seven girls aged between 11 and 18. The patients underwent surgery treatment for IS II° and III°. During this surgery, transverse and longitudinal samples of the paravertebral muscles were collected for analyses. Microtome sections were stained with haematoxylin and eosin, pursuant to the HBFP method and PAS according to McManus (indications of Pearse and Szarek et al.). Apoptosis was determined by the TUNEL method.
Results: Among the regressive lesions, necrosis of muscle fibres was observed more frequently on the convex site and atrophy on the concave site. Quite frequently, necrosis was accompanied by signs of regeneration. The index of apoptotic cells was particularly high on the convex site of the spine. A higher intensity of progressive lesions was observed in the muscles on the convex site of the spine and of regressive changes on the concave site.
Conclusion: Pathomorphological pattern proves the high differentiation of morphological lesions and their etiopathogenesis in the paravertebral muscles during the course of IS.

033

Ultrasonography of insertion tendinosis of shoulder

J. Vojtassak *, V. Sisovsky, J. Vojtassak sen, V. Vojtassakova
*Orthopaedic Practice, Bratislava, Slovakia

Objective: Insertion tendinosis of shoulder (ITS) represents a heterogeneous group of degenerative disease (focal necrosis, fibrinous exudate, fibrocartilaginous metaplasia and calcific metaplasia). Neoangiogenesis is an important pathological element of ITS. ITS is characterized by a feeling of pain in shoulder (PFS). ITS can be objectively examined by high-frequency ultrasonography (US) in early stage and can predict appropriate therapy. We detect in our study pathologic changes of ITS in PFS by US.
Method: A total of 223 patients with PFS were examined quantitatively by US for ITS. US was performed to detect pathology in supraspinatus tendon (ST).
Results: Disarray of echotexture and fusiform thickening of ST were found in 77 (35%) patients. Hyperechoic micro- and macro-calcification spots with posterior acoustic shadowing of ST were found in 72 (32%) patients. Partial tendon tear were found in 54 (24%) patients. Neoangiogenesis detected by power Doppler techniques of ST were found in 20 (9%) patients.
Conclusion: US findings of ITS represented by PFS are most common with fibrinous exudate with tendon disarray. Second common findings were calcific metaplasia. Third were focal necrosis with partial tears and at last were neoangiogenesis proved by power Doppler. US examination of ITS is a valuable, effective and non-invasive method suitable for biomedical research and medical practice.

034

Prognostic significance of angiogenesis in gastric cancer

F. Vukmirovic *
*Podgorica, Montenegro

Objective: We investigate the relationship between the angiogenesis and clinicopathologic features related to prognosis in gastric cancer patients.
Method: To assess tumor angiogenesis, microvascular density (MVD) was analyzed immunohistochemically in 83 primary gastric cancers. Any single brown-stained cell with Factor VIII that indicates an endothelial cell was

counted as a single vessel. Vessels were counted in four regions with the highest vascular density, at ×200 magnification, and the average number of microvessels was recorded.
Results: The microvascular density for 83 tumor specimen ranged from 17.5 to 51.5 with a mean MVD of 33.17±7.95. Mean microvascular density was chosen as the cut-off point; 38 patients were categorized as of low MVD and 45 patients as of high MVD. There was no significant relationship between angiogenesis and age, sex, and histological type of gastric cancer. A significant correlation was found between the angiogenesis in early and advanced gastric cancer and between gastric cancer with and without regional lymph node metastasis. Multivariate survival analysis showed that stage of dissease and angiogenesis were independent prognostic factors.
Conclusion: Angiogenesis is one of the most important prognostic factors for gastric cancer patients, and therapeutic inhibition of angiogenesis may advance poor prognosis of gastric cancer patients.

035

Role of pathologic study in the assessment of the primary site of metastatic adenocarcinoma

M.T. Yacoubi [*], S. Ben Abdelkrim, A. Ben Abdelkader, S. Hmissa
[*]University Hospital Sousse, Dept. of Cyto-Histopathology, Tunisia

Objective: Pathologists are frequently asked to determine the primary site of metastatic carcinomas of unknown origin. The purpose of this study is to estimate the degree of concordance between pathologic results and clinical/other paraclinical investigations in the orientation towards the primary site of metastatic adenocarcinomas.
Method: We studied 80 metastatic adenocarcinomas of unknown origin diagnosed between 1993 and 2003 in our department. Adenocarcinoma counts 58.3% of all metastatic malignancies of unknown origin during this period. Immunohistochemical study was performed using two or more antibodies as: CK7, CK20, TTF1, ACE, PSA, vimentin, estrogen, progesterone and EMA.
Results: The liver was the most common metastatic site followed by the lung. No primary was determined by the pathologist in 44 cases, 34 of which remained of unknown primary despite further appropriate specialized tests. The primary site suggested by the pathologist was confirmed by the clinician in 17 cases: 2 cases by histologic features only and 15 by immunohistochemistry. In the 19 remaining cases, the pathologist suggested several origins but none of them was confirmed by further investigations.
Conclusion: Conventional morphologic features are not discriminative enough. Immunohistochemistry is of precious interest in approaching metastatic adenocarcinomas of unknown primary site.

Tuesday, 30 August 2011, 09.30–10.30 and 16.30–17.00, Hall 5

PS-13 Poster Session Endocrine Pathology

001

Follicular variant of papillary thyroid carcinoma: does immunohistochemistry have a place in the diagnosis and prognosis of this variant?

A. C. Nechifor Boila [*], A. Borda, G. Sassolas, Z. Hafdi-Nejjari, F. Borson-Chazot, N. Berger, M. Decaussin-Petrucci
[*]University of Medicine and Pharmacy, Dept. of Pathology, Targu-Mures, Romania

Objective: Diagnosis of follicular variant of papillary thyroid carcinoma (FVPTC) can be difficult. We aimed to reevaluate established antibodies (HBME-1, Galectin-3, Cytokeratin-19) and to test the expression of newly proposed ones (CD56, p63) as diagnostic and prognostic tools of FVPTC.
Method: We performed an immunohistochemical analysis on a tissue micro-array of 72 cases of FVPTC. Clinico-pathologic data and follow-up were also obtained.
Results: HBME1 was the most sensitive marker, staining 62/72 (86.1%) cases. Galectin-3, Cytokeratin-19 and p63 were positive in 29.2%, 15.3% and 1.4% cases, respectively. CD56, a marker whose expression is reduced in thyroid carcinoma, was negative in 70.8% cases. When the panel HBME1+, Cytokeratin-19+ and CD56- was applied, a sensitivity of 93.1% was obtained. Follow-up was available for 49 patients (median, 4 years). Only three patients presented distant metastasis and/or persistent disease at the last evaluation. Interestingly, in these three cases Galectin-3 stained strongly positive.
Conclusion: HBME1 remains the most sensitive marker in the diagnosis of FVPTC. Moreover, the combined use of HBME1, Cytokeratin-19 and CD56 seems very useful and increases the sensitivity. Our results showed also a potential role of Galectin-3 as marker of aggressiveness in FVPTC.

002

Gastroenteropancreatic neuroendocrine tumors diagnosed at single-institution analysis in Turkey between 2004 and 2010

F. Aker *, S. Ozkara, C. Canbey, G. Gumrukcu
*HNTRH, Dept. of Pathology, Clinical Pathology, Istanbul, Turkey

Objective: Gastroenteropancreatic neuroendocrine tumors (GEP-NET) account for about 2% of all gastrointestinal tract tumors. This study was designed to re-evaluate GEP-NET cases based on the 2010 classification criteria, whose diagnoses were made in our pathology laboratory between 2004 and 2010.
Method: The histopathologic findings of 68 consecutive cases (95 specimens) with GEP-NET were re-evaluated in terms of localization, size, cellular features, necrosis, mitosis, perineural invasion, and lymphatic invasion. The patients were re-assessed according to the WHO 2010 criteria. Differentiation grades were determined. Clinical information regarding therapy and follow-up was available in 28 patients.
Results: All the cases had positive staining with at least one neuroendocrine marker. The sources of 89 specimens included in the analysis were as follows: 31 endoscopic biopsies (34.85%), 13 tru-cut/incisional biopsies (14.61%), 6 mucosectomy (6.7%), 5 appendectomy (5.61%), 18 resections (20.23%), and 12 fine needle aspiration biopsies (FNAB) mostly from the liver (13.49%). Of 28 cases whose clinical follow-up was available, 10 died, 12 were under clinical follow-up without any treatment following excision, and 6 were receiving oncological treatment.
Conclusion: This study summarizes the clinical and histopathological findings of patients with GEP-NET and provides insight into our understanding and clinical experience.

003

Angiogenesis in adrenal gland pheochromocytomas

M. Bialas *, K. Okon, G. Dyduch, M. Buziak, A. Hubalewska-Dydejczuk, A. Bulanda
*Jagiellonian University, Dept. of Pathology, Cracow, Poland

Objective: The histological picture of adrenal gland pheochromocytomas does not always allow to exclude or to confirm their malignant nature. The aim of this study was to assess the impact angiogenesis may have on the clinical course of adrenal pheochromocytomas.
Method: The aim of the study was to determine the intensity of expression of growth factors (VEGF A, C and D) in 50 pheochromocytomas and to compare the amount of blood vessels in central and peripheral areas of the tumors.
Results: Among the growth factors, VEGF A had the strongest expression, while the expression of VEGF C and D was significantly lower. The average number of vessels counted in peripheral areas of studied tumors was lower than in their central parts. Pheochromocytomas with a PASS indicator greater than 4 have a smaller average number of blood vessels than tumors with a PASS indicator below 4.
Conclusion: 1. The intensity of angiogenesis in the central parts of pheochromocytomas is greater than in the periphery, which may be related to the stimulating effects of ischemia in the central areas. 2. Pheochromocytomas with PASS indicators greater than 4 have a smaller average number of vessels in both central and peripheral areas of the tumor, which may indicate that the clinical malignancy of these tumors is not related to the extent of angiogenesis.

004

Immunohistochemical profile of adrenocortical cells, proliferative lesions and tumors of the adrenal cortex

M. Bialas *, G. Dyduch, A. Sińczk-Kuta, W. Szczepański, A. Bulanda, D. Adamek
*Jagiellonian University, Dept. of Pathology, Cracow, Poland

Objective: Advances in imaging techniques led to a significant increase in detection of proliferative lesions and tumors in the adrenal glands. The aim of the study was to identify the immunohistochemical profile of adrenocortical cells using a panel of 15 antibodies and to compare it with the immunohistochemical profile of adrenocortical cancers, adenomas and hyperplasia.
Method: Immunohistochemistry was performed in 68 cases, including 30 adenomas, 30 hyperplasias and 8 adrenocortical carcinomas using a panel of 15 antibodies: synaptophysin, chromogranin, melan A, HMB-45, S-100, calretinin, inhibin, vimentin, p-53, CK, CK7, CK20, EMA, HER-2 and Ki-67.
Conclusion:

1. Adrenocortical origin of the lesion can be confirmed by using a panel of four antibodies: melan A, calretinin, chromogranin, CK. The first two should be positive and the others negative.
2. Adrenocortical carcinoma cells express the same markers as adenomas, but the reaction is weaker and is present in a smaller percentage of cells than in adenomas.
3. The cells of the adrenal cortex, proliferative lesions and tumors derived from cortex do not express epithelial markers.

4. Synaptophysin expression was present in 10–80% of cells in adenomas, but there was no chromogranin expression; therefore, these two markers can be used to differentiate lesions of cortical and medullary origin.

005

Oncocytic (Hürthle cell) change in solid cell nests of the human thyroid gland

J. Cameselle-Teijeiro *, R. Ferreira, N. Caramés, I. Abdulkader, V. Máximo, P. Soares, M. Sobrinho-Simões
*Fundación IDICHUS, Santiago de Compostela, Coruna, Spain

Objective: Solid cell nests (SCNs) are remnants of the ultimobranchial body that are normally present in the human thyroid gland. SCNs are composed of solid and/or cystic structures of main cells admixed with a minor proportion of C cells. Although their biological meaning is unknown, main cells of SCNs harbor some properties of a stem cell phenotype and have been implicated in the histogenesis of some thyroid neoplasms.
Method: We studied the pathological, immunohistochemical, and molecular findings of a case of SCNs.
Results: A case of oncocytic SCNs was incidentally found in the thyroid gland of a 70-year-old man. About 80% of the main cells lining microcystic structures and solid nests showed abundant granular eosinophilic (oncocytic) cytoplasm strongly positive for mitochondrial "immunomarkers" such as porins, GRIM-19 and proteins of SDHB and SDHA genes. Positivity for carcinoembryonic antigen, p63, galectin-3, and HBME-1 with negativity for thyroglobulin, thyroperoxidase, vimentin and α-fetoprotein were also found. An inverse correlation was found between oncocytic metaplasia and p63 expression. Neither germinal mutation of GRIM-19, a gene encoding a mitochondrial complex I protein and involved in some oncocytic cell tumors, nor somatic BRAF mutation, were found.
Conclusion: We are reporting the first case of oncocytic SCNs. Grant PS09/02050-FEDER from ISCIII (Ministry of Science and Innovation), Spain.

006

Primary synovial sarcoma of the thyroid gland: a diagnostic challenge

M. Decaussin-Petrucci *, A. Nechifor-Boila, N. Berger, A. Borda
*Université Lyon, Dept. de Pathologie, Pierre Benite, France

Objective: Synovial sarcoma (SS) is a soft tissue neoplasm that generally occurs in the extremities of young patients. However, it can also occur in the head and neck region. To the best of our knowledge, only two cases of primary SS of the thyroid have previously been reported in the literature.
Method: A 21-year-old male presented with a rapidly growing nodule in the right thyroid lobe.
Results: Total thyroidectomy was performed and the macroscopic examination revealed a 48-mm, whitish, well-circumscribed tumour. The tumour showed a biphasic growth pattern, with a predominant spindle cell component. The spindle cells had a sparse cytoplasm, with large, pale nuclei, and high mitotic index. Immunohistochemistry revealed intense BCL2 and CD99 positivity of both epithelial and spindle cell components, while TTF1 and thyroglobulin were negative. A molecular genetic study identified the presence of SYT-SSX fusion gene transcript, and confirmed the diagnosis of SS. The patient was treated with adjuvant chemo- and radiotherapy. Unfortunately, 9 months after the initial diagnosis, a lung metastasis was found.
Conclusion: Primary SS of the thyroid is an extremely rare entity with aggressive outcome. The molecular genetic study is helpful to confirm the diagnosis.

007

Comparison of proliferative activity in parathyroid glands in primary and secondary hyperparathyroidism

E. Demiralay *, G. Altaca, B. Demirhan
*Baskent University, Dept. of Pathology, Istanbul, Turkey

Objective: Parathyroid gland hyperplasia is diffuse or nodular in secondary hyperparathyroidism (sHPT). Whether the nodular growth starts from the beginning or is a transformation of diffusely growing gland into nodular hyperplasia parallel to the severity of the disease is unknown. The disease might be unresponsive to medical treatment when nodular hyperplasia develops. This study is aimed to differentiate the characteristics of the parathyroid glands with and without nodular hyperplasia in sHPT and to investigate, if any, similarity between the nodular hyperplastic glands of sHPT and parathyroid adenomas of primary hyperparathyroidism.
Method: Hyperplasia types and parathyroid cell types and the expression of proliferating cell nuclear antigen (PCNA) and Ki-67 in parathyroid tissue were investigated histopathologically and immunohistochemically in 94 parathyroid glands of 41 patients with hyperparathyroidism
Results: A total of 63 glands showed nodular hyperplasia and 16 diffuse hyperplasia in sHPT. Chief cells predominated in the total series. Immunohistochemically, Ki-67 expressions were similar in adenomas and sHPTs. The median ratio of PCNA LI (labelling index) was 30/10³ cells in nodular hyperplasia, 16/10³ cells in diffuse hyperplasia and 30/10³ cells in adenomas ($p>0.05$).

Conclusion: These findings suggest that parathyroid adenoma and nodular hyperplasia have histopathologically and immunohistochemically similar characteristics, suggesting that both have aggressive cell proliferation.

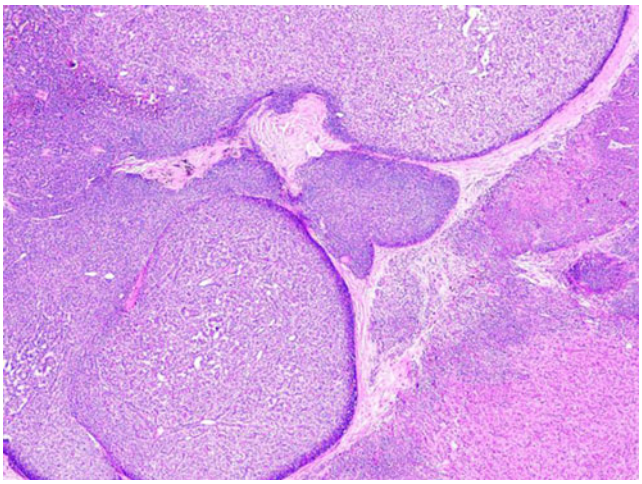

008

Relation of carbonic anhydrase IX and vascularization and its influence on biological behavior of medullary thyroid carcinoma

L. Feketeova *, M. Ondrikova, P. Janega, F. Gabalec, A. Ryska, S. Pastorekova, P. Babal
*Comenius University, Dept. of Pathology, Bratislava, Slovakia

Objective: Medullary thyroid carcinoma (MTC) is a malignant tumor derived from C cells. Therapy-resistant metastases often occur in this tumor. Carbonic anhydrase IX (CA IX) is a marker of unfavorable prognosis in breast, lung or renal cell carcinomas. Its prognostic value in MTC has not yet been established. The aim of this study was to evaluate the relation between expression of CA IX and PECAM-1 (CD 31) in MTC and its influence on tumor behavior.
Method: Archival surgical MTC specimens were immunohistochemically stained with monoclonal antibody against CA IX and CD 31. Positivity was detected by diaminobenzidine and quantified by morphometry. Relation between CA IX and CD 31 was evaluated.
Results: CA IX protein expression was found in all samples. A relation between stronger CA IX positivity and lesser vascularization was observed, and vice versa.
Conclusion: CA IX expression in MTC showed a reversed relation with vascularization of the tumor. Analysis of clinical data showed a positive correlation between patients with stronger CA IX expression, lower level of tumor vascularization and an unfavorable prognosis. This project was supported by GUK 136/2011.

009

Amyloid goiter in a patient with familial Mediterranean fever

G.A. Gokhan Ocak *, I.E. Gurer, I.H. Ozbudak, A. Ucar, H. S. Toru, C. Arici
*Akdeniz University, Medical School, Antalya, Turkey

Objective: Amyloid deposition within the thyroid gland is a relatively common phenomenon. It might be seen in medullary thyroid carcinoma, systemic secondary amyloidosis and less frequently, primary amyloidosis. To date, rare case of amyloid goitre secondary to amyloidosis associated with familial Mediterranean fever (FMF) has been reported.
Method: Sections taken from thyroid gland were fixed with formaldehyde, embedded in paraffin, sliced to 5 μm in thickness and stained with H&E. Additionally, cyrstal violet was performed histochemically.
Results: A 41-year-old female who has FMF for 5 years and has chronic renal failure for 3 years. She was recently admitted to our hospital with a neck mass. On clinical evaluation, nodular enlargement was detected in her thyroid gland and she underwent right thyroid lobectomy. On pathologic examination, gland parencyhma was extensively infiltrated by an eosinophilic amorphous material consistent with amyloid. Foreign body giant cell response and adipose tissue metaplasia were concommitant findings. Our diagnosis was amyloid goitre.
Conclusion: In countries with a high prevalence of FMF, secondary amyloidosis of the thyroid gland should be kept in mind in long-standing FMF patients.

010

Analysis of the number of p63 and calcitonin positive cells and Ki-67 proliferative index at different stages of human fetal thyroid development

M. Guimaraes *
*Hospital Sao Joao, Dept. of Pathology, Porto, Portugal

Objective: This study attempts to find if there is any relationship between the occurrence of calcitonin (CT) and p63 positive cells and the levels of Ki-67 proliferative index during the human fetal thyroid development.
Method: We studied immunohistochemically thyroglobulin (TG), thyroid transcription factor-1 (TTF-1), CT, p63 and Ki-67 of 28 well-preserved thyroid from autopsied fetuses, ranging from 12th to 37th week of gestation (WG) retrieved from the archives of our department.
Results: TG and TTF-1 were diffusely expressed in the follicular cells of every case. CT positive cells were observed in 18 cases, in the axis of one (7) or both lobes (11) from the 14th WG on. Nine of the 28 cases and 7 out of 9 cases with CT positive cells had admixed p63 positive cells which were detected either isolated, or in groups or in

a single case forming a solid cell nest. The p63 positive cells co-localized with C cells in all but one case. Ki-67 decreased from 12th to 37th WG with an increment in the 20-21st WG that should be confirmed in a larger series.
Conclusion: No correlation was found between the number of p63 and CT positive cells and Ki-67.

011

Hormonally defined pancreatic and duodenal neuroendocrine tumors differ in their transcription factor signatures: expression of ISL1, PDX1, NGN3 and CDX2

G. Hermann *, B. Konukiewitz, A. Schmitt, A. Perren, G. Kloeppel
*Assaf Harofeh Medical Center, Dept. of Pathology, Kfar Haoranim, Israel

Objective: We recently identified the transcription factor (TF) ISL1 as a marker for well-differentiated pancreatic neuroendocrine tumors (P-NETs). Expression of four TFs, ISL1, PDX1, NGN3 and CDX2, that mainly govern development and differentiation of pancreas and duodenum, were studied in hormonally defined P-NETs and duodenal (D-)NETs.
Method: Thirty-six P-NETs and 14 D-NETs were immunostained with antibodies against the four pancreatic hormones, gastrin, serotonin, calcitonin, ISL1, PDX1, NGN3 and CDX2. TF expression was correlated with the tumor's hormonal profile.
Results: Insulin-positive NETs expressed ISL1(10/10) and PDX1(9/10). Glucagon-positive tumors expressed ISL1(7/7) and mostly negative for other TFs. Gastrin-positive NETs, duodenal or pancreatic, expressed PDX1(17/18), ISL1(14/18) and NGN3(14/18). CDX2 was mainly found in gastrin-positive P-NETs (5/8) and rarely in D-NETs (1/10). Somatostatin-positive NETs, duodenal or pancreatic, expressed ISL1(9/9), PDX1(3/9) and NGN3(3/9). The remaining tumors labeled for ISL1 in addition to NGN3. No association of TF patterns with grade, size, location, metastases and functionality.
Conclusion: There is a correlation between TF patterns and certain hormonally defined P-NETs and D-NETs, suggesting an origin from embryologically determined precursor cells. These TF signatures alone do not distinguish P-NETs from D-NETs.

012

Role of TGF-Beta1 pathway in progression of thyroid cancer

K. Ivanov *, J. Ananiev, E. Onal, I. Rachkov, J. Gerenova, M. Gulubova
*Trakia University, Medical Faculty, Dept. of General and Clinical Pathology, Stara Zagora, Bulgaria

Objective: TGF-beta is well known for its potent growth inhibitory effect, mainly observed in cells of epithelial origin. The loss of TGF-beta-sensitivity, i.e. loss of growth inhibitory pathway, has been suggested to take part in cell transformation. This study evaluates the expression of factors TGF-beta1, TGF-beta RII, Smad4 and Smad7 in cases of thyroid cancer and their possible correlation with classic prognostic markers and patient survival.
Method: We investigate tissue localization of TGF-beta1, TGF-beta RII, Smad4 and Smad7 protein expression in thyroid cancer in 45 patients. Immunohistochemical staining was performed using avidin–biotin–peroxidase complex technique.
Results: TGF-beta1 expression was weak to missing in 71.1% of the samples and strong in 28.9%. TGF-beta RII expression was weak to missing in 28.2% of the samples and strong in 17.8% of them. Smad4 was observed in tumor epithelium as weak immune reaction (75.6%) and strong in the other 24.4%. Smad4 nuclear expression was missing in 91.1% of the samples. The patients' survival was shorter in the cases with higher TGF-beta1 expression in the tumor cytoplasm ($p=0.02$) and with existing Smad4 expression in the tumor nucleus ($p=0.03$).
Conclusion: TGF-beta1 expression and Smad4 expression have an impact on the progression of thyroid cancer.

013

Expression of MDM2 in papillary thyroid carcinoma and its correlation with prognostic factors

M. Jalali Nadoushan *, A. Davati, K. Allahyari
*Shahed University, Dept. of Pathology, Tehran, Iran

Objective: Different biological markers used for the determination of prognosis of papillary thyroid cancer. MDM2 is one of these markers. The purpose of this study was determination of the frequency of MDM2 expression in papillary thyroid cancer and its correlation with some prognostic factors.
Method: This study was a cross-sectional study with descriptive analytic aspects. This study was performed on 73 samples from patients with papillary thyroid cancer who came in Mostafa Khomeini Hospital in Tehran-Iran (2005-2008). MDM2 expression was assessed by immunohistochemical method. The data were analyzed with SPSS software 11.5 and analyzed with chi-square and Mann–Whitney tests.
Results: The patients' age was 41.85+16.65 years. A total of 31/5% of samples were positive for MDM2. 21.6% had lymph nodes involvement. The median size of the patients' tumor was 3.86 +2.38. There was not any significant relationship between MDM2 expression and the gender but there is a significantl direct relationship between MDM2 expression and lymph nodes involvement and tumor size ($P<0.05$).
Conclusion: It seems that overexpression of MDM2 increases metastasis to lymph nodes.

014

Expression of somatostatin receptor subtypes in human non-medullary thyroid tumors

G. Karayannopoulou *, T. Koletsa, E.T. Janson, K. Pazaitou-Panayiotou, M. Stridsberg, V. Kotoula, G. Karkavelas
*Aristotle University Thessaloniki, Medical School, Dept. of Pathology, Greece

Objective: Thyroid carcinoma (TC) is the most frequent endocrine cancer. Recently, it has been shown that somatostatin and its analogues affect the cell growth of human thyroid carcinoma cell lines. In this study the pattern of SSTR expression in non-medullary TC was examined.
Method: Archival samples from 49 patients with TC were selected. On TMA construction, cores from both TCs and their corresponding non-neoplastic thyroid tissue (NNTT) were included. Immunohistochemistry was performed using antibodies for SSTR1–SSTR5.
Results: All cases were positive for SSTR2 and SSTR3. SSTRs expression was observed chiefly in the cytoplasm of neoplastic cells. Membranous localization was observed mainly for SSTR2 (81%) and SSTR5 (56.3%). SSTR1 was expressed in all non-PTC cases in contrast to PTCs ($x2$, $p=0.034$). Diffuse cytoplasmic SSTR2 expression appeared more often in tumors sized >10 mm ($x2$, $p=0.03$). No correlation was found between the SSTR1-5 expression in TCs and NNTTs.
Conclusion: SSTR2 was the most frequently detected subtype. Although different studies have reported membranous localization of SSTR in various neoplasms, in our study SSTR expression is mainly cytoplasmic. These findings may be worthy considering in studies investigating the clinical value of somatostatin analogues in specific subsets of TCs.

015

Diagnostic utility of HBME1 and Galectin-3 in the differentiation among follicular lesions of the thyroid gland

M. L. Lai *, E. Tamponi, G. Senes, G. Faa
*Cagliari, Italy

Objective: Immunohistochemistry is frequently applied in the differential diagnosis of follicular patterned thyroid nodules. We tested the expression of HBME1 and Galectin-3, actually considered markers of malignancy, in a cohort of thyroid nodules previously classified as "indeterminate" at FNC, in order to verify their role in the interpretation of these lesions and their application in cytological diagnosis.
Method: A total of 500 follicular-patterned thyroid nodules —188 follicular adenomas, 244 cases of PTCs-follicular-variant (FVPTCs) and 68 follicular carcinomas were selected from our histological cases and tested for HBME1 and Galectin-3 immunoreactivity. Expression was graded as diffuse (>50% of neoplastic cells), focal (50-10%), and negative (<10%).
Results: A total of 86% and 89% of FVPTCs showed reactivity for HBME1 and Galectin-3, respectively. A total of 57.8% of follicular carcinomas were positive for HBME1, 50% for Galectin-3. Both HBME1 and Galectin-3 were expressed in 20% of follicular adenomas.
Conclusion: Our data confirm the high specificity of both markers in identification of FVPTCs; however, the percentage of Galectin-3 expression, in our study, was lower than previously reported. Unfortunately, the specificity of HBME1 and Galectin-3 does not appear useful in differential diagnosis among follicular neoplasms.

016

Tumefactive postmenopausal gonadotroph cell hyperplasia

O. Moshkin *, B. W. Scheithauer, E. Horvath, M. Jentoft, P. C. Collins, L. V. Syro, K. Kovacs
*PRHC, Dept. of Laboratory Medicine, Peterborough, Canada

Objective: Pituitary hyperplasia is proliferation of one cell type responding to stimulation. Gonadotroph cell hyperplasia is rare, occurring in animal castration, human primary hypogonadism (Turner/Klinefelter syndromes), gonadectomy in cancer patients, and castrate human males. Despite enhanced postmenopausal FSH/LH production, the pituitary remains small and lacks "gonadal deficiency" or "castration cells." Postmenopausal gonadotroph cell hyperplasia is typically autopsy-based.
Method: Clinical case: A 49-year-old woman with daily "hot flashes" ceased menses 1 year prior. Blood tests: FSH >400 mIU/ml (maximal postmenopausal level—114 mIU/ml), LH 110 mIU/ml (maximal postmenopausal level—58 mIU/ml), estradiol 20 pg/ml (normal postmenopausal level <40 pg/ml), prolactin normal. MRI: symmetric pituitary enlargement without chiasmal compression; a diagnosis of adenoma was rendered. Immunostains and EM were performed.
Results: Transsphenoidal biopsy revealed gonadotroph cell hyperplasia, the gonadal deficiency cells being numerous, scattered, enlarged and vacuolated due to markedly dilated rough endoplasmic reticulum. Immunostains for other hormones were normal. MIB-1 labeling was absent.
Conclusion: Tumefactive gonadotroph cell hyperplasia is unreported in postmenopausal females. The postmenopausal pituitary is normal in size and lacks "gonadal deficiency cells". Such cells are nearly limited to females and males

with primary hypogonadism. In conclusion, postmenopausal patients with symmetric pituitary enlargement should not be operated.

017

Mechanical aspects of folliculogenesis in the thyroid gland

R. Moskalenko *, A. Romanyuk, A. Logvyn
*Sumy State University, Dept. of Pathomorfology, Ukraine

Objective: The aim of this study is to research the mechanism of folliculogenesis in the thyroid gland under the influence of heavy metals salts.
Method: The research of the intraluminal pressure influence of the colloids on folliculogenesis was conducted on 40 white rats. To break the thyroid morphofunctional state of equilibrium, the experimental rats received a combination of heavy metals salts (increased amount of zinc, copper, iron, manganese, lead, chromium). Morphofunctional state of thyroid gland was studied using histological, histochemical, mathematical, and morphometric methods.
Results: As a result of the influence of combinations of heavy metals salts on the follicular apparatus, thyroid hypoactivity developed, which manifested in accumulating colloid and changing its tinctorial, physical and chemical properties, reducing the height of follicular epithelium, follicles increase in diameter, which also reflected the increasing tension in the wall of the follicle.
Conclusion: Thus, the results allow one to conclude that there is a significant role of intrafollicular colloidal pressure in the process of folliculogenesis. The difference between peripheral and central folliculogenesis occurs because of different amounts of intrafollicular pressure, which again are derived from a different functional activity of the follicular epithelium.

018

Poorly differentiated and angioinvasive thyroid follicular carcinoma in a 20-year-old male with xeroderma pigmentosum: report of a case

A. C. Nechifor Boila *, L. Depaepe, B. Balme, J.-C. Lifante, A. Borda, M. Decaussin-Petrucci
*University of Medicine and Pharmacy, Dept. of Pathology, Targu-Mures, Romania

Objective: Thyroid carcinoma in young patients is a rare condition, especially the poorly differentiated type. Xeroderma pigmentosum (XP) is an inherited disease caused by molecular defects in the nucleotide excision repair (NER) genes, which plays a critical role in the repair of DNA damage resulting from ultraviolet radiation.
Method: Case report: A 20-year-old patient with XP underwent a total thyroidectomy for two thyroid nodules of 6 and 18 mm in diameter.
Results: Histologically, the first tumor corresponded to a follicular variant of papillary thyroid carcinoma. The latter one presented a solid, trabecular growth pattern, with only a few micro-follicular areas. The nuclei did not show features of papillary carcinoma. A high mitotic activity was present, but no area of necrosis was seen. At periphery, the tumor was surrounded by a thick, irregular capsule, with evidence of minimally capsular invasion, as well as vascular invasion. Based on these settings, the diagnosis was angioinvasive thyroid follicular carcinoma with a 50% contingent of poorly differentiated carcinoma.
Conclusion: The association of these two rare diseases suggests that molecular defects in NER genes might predispose patients with XP to aggressive forms of thyroid cancer, among other types of malignancies.

019

Dendritic cells and anti-tumor immunity in the development of thyroid cancer

E. Onal *, J. Ananiev, K. Ivanova, I. Rachkov, J. Gerenova, M. Gulubova
*Trakia University, Medical Faculty, Dept. of General and Clinical Pathology, Stara Zagora, Bulgaria

Objective: Dendritic cells (DCs) play a major role in initiating the antitumor immune response. Although the clinical significance of tumor-infiltrating DCs (TIDCs) has been investigated in a variety of human cancers, we have analyzed the maturation-specific significance of TIDCs in the prognosis of patients with thyroid cancers.
Method: We evaluated 36 patients with thyroid carcinomas for the presence of TIDCs using immunohistochemistry with an anti-CD1a antibody for immature DCs and an anti-CD83 antibody for mature DCs.
Results: We found tumor infiltration with CD1a- and CD83-positive DCs in all of the cases. In all thyroid tumors, the number of CD1a-positive immature DCs prevailed over the number of CD83-positive mature DCs in tumor stroma and in the tumor border. The number of CD1a- and CD83-positive TIDCs in tumor border was inversely correlated with advanced tumor stage ($p=0.025$ and $p=0.014$, respectively). Also, the high infiltrate on CD1a-positive DCs in tumor border was found in 59.3% of patients in I and II clinical stages ($\chi 2=6.279$; $p=0.012$).
Conclusion: The specific distribution of DCs suggests a possible contribution to growth regulation of thyroid neoplasms. Our results suggest that infiltration with DCs may

be of great importance in initiating the primary anti-tumor immune response.

020

Determining levels of CA 19-9 in patients with type 2 diabetes mellitus: do patients with type 2 diabetes mellitus have increased likelihood for pancreas cancer development in relation to the general population

S. Patiakas *, M. Palaiologou, S. Sarafidis, O. Lazaridou, C. Charalampous
*General Hospital of Kastoria, Microbiological Laboratory, Greece

Objective: This study aims to determine the levels of CA 19-9 in patients with diabetes mellitus (DM) type 2.
Method: We studied the values of CA 19-9 in 52 patients with type 2 diabetes, and the results were compared with controls, 64 healthy subjects. Preceded the recording, both glycosylated hemoglobin and glucose in diabetes mellitus, while the control group who had glucose values>110 mg/dl were excluded.
Results: Patients with diabetes (average blood glucose and glycated hemoglobin 171 mg/dl and 8.3, respectively) showed a clear increase in the price of CA 19-9 (mean 23.1 ±16.3 U/ml), compared with controls (mean CA 19-9 13.6 ±7.1 U/ml). Indeed a statistically significant correlation between glycated hemoglobin values and levels of CA 19-9 was recorded (r=0.384, p<0.001).
Conclusion: It is enforced, therefore, that the above theory that relates the coexistence of diabetes with the disruption of exocrine pancreatic cells increased the risk of developing pancreatic Ca and the production of CA 19-9. Additionally, it is understood that the exploration potential of pancreatic cancer should be given special attention on diabetes mellitus patients and those of CA 19-9.

021

Metastatic disease in thyroid: the experience of two reference centers

A. Polónia *, C. Eloy, T. Amaro
*IPO-Porto, Dipt. di Anatomia Patológica, Rio Tinto, Portugal

Objective: While uncommon in clinical practice, up to 25% of autopsied patients with disseminated malignancies have metastases in the thyroid gland. Metastases in the thyroid are associated to poor prognosis and occur frequently in previously existent thyroid nodules.
Method: We retrospectively studied 29 cases of metastatic disease in the thyroid retrieved from the files of the Portuguese Institute of Oncology-Porto and São João Hospital.
Results: Fine-needle aspiration cytology (FNAC) was the initial diagnostic procedure (75.8%). The metastases were more frequent in females and in patients older than 40 years. The primary tumor site was identified in all but three cases, breast being the most common (31.0%), followed by kidney (13.8%) and esophagus (13.8%). The most common histological type was ductal carcinoma of the breast (31.0%), squamous cell carcinoma of the esophagus, of the lung and of uncertain origin (27.6%) and renal cell carcinoma (13.8%). In four cases, the metastasis preceded the diagnosis of the primary tumour. The time from diagnosis of the primary tumour to metastasis to the thyroid gland was less than 12 months in 35.0% of the cases.
Conclusion: In our series, the mean time survival after the occurrence of a metastasis in the thyroid is higher in patients submitted to thyroidectomy.

022

Metastasis of Merkel cell carcinoma in the thyroid

A. Polónia *, C. Eloy, T. Amaro
*IPO-Porto, Dipt. di Anatomia Patológica, Rio Tinto, Portugal

Objective: Merkel cell carcinoma (MCC) is a rare primary cutaneous neoplasm with neuroendocrine differentiation. Metastases to thyroid are rarely observed and almost always correlate with poor prognosis. In patients with a known history of malignancy, it is important to include metastases in the differential diagnosis.
Method: A 56-year-old female, followed for MCC in the leg since 2006, presented with a multinodular goiter. The patient underwent fine-needle aspiration of the largest nodule, and a diagnosis of colloid nodule was made. The histological examination of the nodule showed an encapsulated tumour with a solid pattern of growth. The cells were monotonous with scant cytoplasm and nuclear molding.
Results: The immunohistochemistry study disclosed a perinuclear dot-like staining expression in tumor cells for Cam5.2 and CK20 and diffuse expression for chromogranin A and synaptophysin. Expression for CK7, TTF-1, thyroglobulin and calcitonin was absent in the tumour cells. The patient is alive without any signs of disease after 11 months of follow-up.
Conclusion: Metastases morphologically resemble the primary tumour but it may also display architecture and cytomorphology similar to some primary thyroid neoplasms. An immunohistochemical panel is helpful to separate metastatic from primary neoplasms. We report the

first case documented by histology of MCC metastasis to the thyroid.

023

An unusual association: pancreatic intraductal papillary mucinous neoplasm and pancreatic endocrine tumor

C. Popp *, T. Tebeică, S. Zurac, R. Andrei, E. Grămadă, F. Stăniceanu
*Colentina University Hospital, Dept. of Pathology, Bucuresti, Romania

Objective: The synchronous presence of pancreatic endocrine tumors (PETs) has rarely been described among patients with intraductal papillary mucinous neoplasms (IPMNs).
Method: We describe a rare case with combined IPMN and PET diagnosed based on histology and immunohistochemistry studies. Additionally, a review of the existing literature describing patients with concommitant IPMN and PET was conducted.
Results: A 77-year-old female presented with recurrent abdominal pain and body weight loss. The preoperative CT scan highlighted a cystic lesion of the pancreas body and the patient underwent distal pancreatectomy. Macroscopical examination revealed an 11-mm cystic cavity in close relationship to an 8-mm solid mass located in the adjacent pancreatic parenchima. On light microscopy, the cystic mass was an IPMN with low grade epithelial dysplasia and the solid lesion proved to be a well differentiated PET. Four other reports described this association among 14 patients, in most cases the preoperative diagnosis comprising only one type of pathology.
Conclusion: Whether the association of IPMN and PET is real or by chance is intriguing as both are rare tumors and only few reports and hypotheses are available so far. Nevertheless, this possible association should be always kept in mind due to the low rate of accurate preoperative diagnostic.

024

NM23-H1 and COX-2 in papillary carcinoma of the thyroid gland

B. Sarcevic *, M. Mikovic Perisa
*University Hospital for Tumours, Dept. of Pathology, Zagreb, Croatia

Objective: Papillary carcinoma of thyroid gland is an epithelial tumor with an excellent prognosis. There is a small group of patients who present a tumor with more aggressive behavior what also exist in the group of the patients with papillary microcarcinoma.
Method: A series of 136 papillary carcinoma from 2000-2007 were analyzed using standard immunohistochemical staining (IHS) procedures for nm23-H1 and COX-2. From the total number of patients, 58 were with papillary microcarcinoma. Results of IHS were graded with index of IHS into four categories: negative, slight, moderate and strong.
Results: The majority of tumours were positive on nm23-H1 and COX-2, and that in tumours with a COX-2 expression the reaction of nm23-H1 is also positive ($P<0.001$). The nm23-H1 is significantly positive in the classical and follicular variant of papillary carcinoma, whereas COX-2 is significantly positive in the follicular variant. However, COX-2 expression in papillary microcarcinoma is related with metastases to regional lymphnodes ($P=0.017$).
Conclusion: The results imply that most papillary tumours of aggressive type are COX-2 positive and nm23-H1 negative. Also, the findings suggested that the nm23-H1 and COX-2 may be good marker that can isolate papillary microcarcinoma with the aggressive behavior.

025

The prognostic role of forkhead transcription factor FOXP3 expression in papillary thyroid cancer

C. Ugolini *, A. Proietti, R. Elisei, F. Basolo
*AOUP, Dept. of Laboratory Medicine, Pisa, Italy

Objective: The forkhead transcription factor FOXP3 is important in function of regulatory T cell (Treg). FOXP3 expression has been recently demonstrated in tumor cells and in microenvironment of different tumors. The correlation between papillary thyroid cancer (PTC) and lymphocytic infiltration is strong, even if not completely understood. Our study tries to verify the prognostic impact of FOXP3 expression in a series of PTC with follow-up.
Method: A total of 105 PTCs with a medium follow-up of 15 years were analyzed by immunohistochemistry for FOXP3. The expression was evaluated in epithelial tumor cells and in collateral lymphocytes. For all patients, clinicopathological features were considered.
Results: A total of 45 out of 105 (43%) PTCs analyzed expressed FOXP3. In neoplastic cells FOXP3 staining was cytoplasmatic. Significative correlations were found between FOXP3 expression and the presence of extrathyroid tumor invasion ($p=0.04$) and distant metastasis ($p=0.04$). Moreover, the expression of FOXP3 was correlated with radioiodine resistance ($p=0.0005$). A total of 29 (28%) out of 105 specimens stained for FOXP3 resulted positive in lymphocytes and 76 (72%) negative. No significance was observed among FOXP3 lymphocyte expression and all clinico-pathological features.

Conclusion: We suggest that FOXP3 could be taken in consideration as a prognostic marker and probably could be applied also in preoperative examination.

026

Evaluation of CD56, HMBE1, Galectin-3 and CK19 expression status in neoplastic and non-neoplastic thyroid diseases

I. Iakovidou *, C. Valavanis, G. Giannakopoulos-Stanc, C. Loutraris, I. Ieronimaki, G. Vecchini, P. Arapantoni-Dadioti
*Metaxa Cancer Hospital, Dept. of Pathology, Piraeus, Greece

Objective: We assesssed the diagnostic value of protein expression using antibodies against HMBE1, Galectin-3, CK19 and CD56 in normal thyroid epithelium, follicular thyroid lesions, follicular and papillary neoplasms. Our aim was to disclose the diagnostic value of these markers in distinguishing papillary carcinoma including follicular variant and follicular lesions and neoplasms.
Method: A total of 252 cases were studied (22 cases of multiple thyroid diseases). Neoplastic cases included 5 follicular adenomas, 146 carcinomas (18 follicular, 121 papillary, 3 anaplastic, 4 medullary, 1 not otherwise specified). A total of 96 cases of non-neoplastic thyroid diseases were included. Five cases of follicular neoplasm of uncertain malignant potential and 11 cases of metastatic papillary carcinoma were also studied.
Results: Patterns and intensity of immunoreactivity were scored. A strong positive expression of HMBE1, Galectin-3 and CK19 in a 100% of papillary carcinomas and negative expression to CD56 in 85.83% was observed. All the follicular neoplasms displayed positive CD56 expression and negative HMBE1 expression.
Conclusion: HMBE1 and CD56 are useful markers in differential diagnosis between papillary and follicular thyroid carcinoma. Our results are in concordance with those of the Canadian team (Demellawy et al., 2008). We noted the extra-ordinary positive CD56 immunoreactivity of metastatic and high-grade papillary carcinomas.

027

The characteristic of the ACTH-secreting extrapituitary neuroendocrine tumors

I. Voronkova *, A.M. Lapshina, L.E. Gurevich, A.Y. Abrosimov, E.I. Marova, L.Y. Rozhinskaya
*Endocrinology Research Center, Moscow, Russia

Objective: Last year, there was an observed increase in the reported incidence of neuroendocrine tumors (NETs), including NETs accompanied by hypercorticism. That is why the morphological characteristics of these NET interest to us.
Method: In the study were included 29 patients with ACTH -secreting NET (ectopic ACTH syndrome). A total of 24 NETs were located in the lungs: 11 atypical and 8 typical carcinoids, 5 small cell carcinoma; 5 in the thymus: 1 atypical and 2 typical carcinoids, 2 small cell carcinoma; 1 kidney carcinoid and 1 well-differentiated neuroendocrine carcinoma of appendix. Immunohistochemical study was performed on ACTH-ectopic tumors with antibodies to ACTH, corticotropin-releasing hormone (CRH), GH, prolactin, SSTR 1-5 and D2R.
Results: Immunohistochemical study showed that the cause of hypercorticism has been production of ACTH in 19 cases, CRH in 3 and ACTH+CRH in 7 cases. Polyhormonal activity was found in 13 cases. The most frequent combination was ACTH+GH+prolactin (five cases). From the 26 cases, only two showed no expression SSTR 1-5 subtypes. The expression of D2R was found in eight cases. Co-expression of SSTR and D2R was detected in eight cases.
Conclusion: In our study, we demonstrated that the NEO associated with hypercorticism may have different localization, differentiation's degree, hormonal activity and expression SSTR 1-5 and D2R.

028

Papillary carcinoma of thyroid and adrenal carcinoma in a patient with a RET S649L mutation

F. Barreto *
*Hospital de São João, Dept. of Pathology, Vila Nova de Gaia, Portugal

Missense germline mutations of the RET proto-oncogene are associated with multiple endocrine neoplasia type 2 (MEN 2) and familial medullary thyroid carcinoma (FMTC). Case report: We describe a case of a 46-year-old Caucasian male that was submitted to total thyroidectomy and left adrenalectomy for tumours in both organs: histopathology disclosed papillary carcinoma of the thyroid and adrenal carcinoma. Whole sectioning of the remaining thyroid disclosed morphologic and immunohistochemical evidence of C cell hyperplasia. Staging procedures did not disclose other alterations and laboratory work-up was within normal range, including calcitonin levels. The patient carries a rare germline mutation in the transmembrane domain of the RET proto-oncogene (exon 11, codon 649, TCGSer_TTGLeu). Thyroid papillary carcinoma and adrenal carcinoma have not been frequently described in the setting of MEN2. S649L mutation is histologically characterized by C cell hyperplasia, low penetrance of

medullary thyroid carcinoma (MTC) with low agressive potential. Germline testing of RET can be used to distinguish cases of sporadic from hereditary C cell hyperplasia/FMTC and distinct RET mutations may suggest a predilection for a particular phenotype and clinical course. It is also important to test additional family members for the same mutation and provide genetic counseling.

029

Primary thyroid paraganglioma: a case report with fine needle aspiration cytology, histology and immunohistochemical features

E. Tamponi *, G. Faa, G. Senes, G. Pinna, M.L. Lai
*Cagliari, Italy

Objective: Primary thyroid paraganglioma (PTPG) is a rare tumor and causes fine-needle aspiration cytology (FNAC) diagnostic difficulties. Only four cytological cases of PTPG were reported in the literature; two of them had "unsatisfactory" results.
Method: FNAC of a right lonely 30-mm large, solid, thyroid nodule, cold on scan, was performed in a 45-year-old euthyroid male affected by thyroiditis. On the bases of FNAC results, the patient underwent thyroidectomy and the thyroid was sent for histology.
Results: FNAC showed rare solid nests of cells with mild cytologic atypia allowing the diagnosis of "indeterminated follicular lesion". Histology showed a neoplasm composed of sheets and solid nests of cells, negative at immunohystochemistry for thyroglobulin, calcitonin, TTF1 and positive for chromogranin, synaptophysin, NSE; S-100 was focally expressed. On the bases of these findings the final diagnosis of PTPG was made.
Conclusion: This is the first case of PTPG in thyroiditis reported in the literature. As in the other two diagnostic cases described at FNAC, no morphological specific change was present and cytological diagnosis resulted very difficult. Our data suggest that immunohistochemistry is mandatory for the citolological and histological diagnosis of PTPG.

030

Pheocromocytoma, contralateral suprarenal medullary hyperplasia and retroperitoneal neuroblastoma in a 27-year-old man

C. Dias *
*Porto, Portugal

One third of patients with pheochromocytomas and paragangliomas are carriers of germline mutations. There are several disorders associated with familial pheochromocytoma and paraganglioma, these include: multiple endocrine neoplasia type 2, von Hippel-Lindau syndrome, neurofibromatosis type 1 and familial paraganglioma. We report the case of a 27-year-old man with hypertension. His father had a bilateral pheocromocytoma 10 years ago and his test for genetic mutation of RET was negative. The patient's blood and urinary tests revealed high levels of catecholamines. Computed tomography demonstrated a left suprarenal mass, a large retroperitoneal mass and a posterior mediastinic mass. Suprarenals' and retroperitoneal masse´s histology and immunohistochemical study revealed: a pheocromocytoma on the left suprarenal, medullary hyperplasia on the right suprarenal and a neuroblastoma in the retroperitoneal mass. Neuroblastoma is a common malignancy among children, but rarely does it occur in adults. The occurrence of pheocromocytoma and neuroblastoma separated in the same patient is also very rare. These facts, the family history and the age of onset, suggest a familial syndrome. The patient is being tested for genetic mutations, and the surgery of mediastinic mass is scheduled.

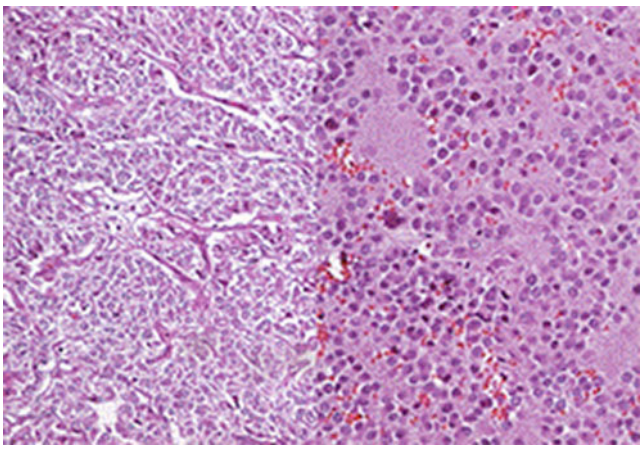

031

Diagnostic difficulties in pancreatic neuroendocrine tumors

V. Herlea *, C. Pechianu, E. Stoica-Mustafa, A. Iorgescu, D. Moldovan, S.O. Dima, V. Tomulescu,
I. Popescu
*Fundeni Clinical Institute, Dept. of Pathology, Bucharest, Romania

Objective: Pancreatic neuroendocrine neoplasms represent a group of rare tumours with predominantly neuroendocrine differentiation. They have an incidence of 1–1.5/100,000 and can be either functional or non-functional.
Method: We have studied 32 patients with neuroendocrine pancreatic neoplasms admitted, diagnosed and treated in Fundeni Clinical Institute in the last 5 years. Immunohistochemical tests (Syn, Chromo, NSE, Ki67, insulin, somatostatin) were performed and based on their results an accurate diagnosis was possible.

Results: A total of 15 patients were males and 17 were females with ages between 24 and 71, with an average of 49.2 years. The tumor's diameter ranged between 0.4 and 14 cm. The primary tumor site was in the pancreatic head for 16 cases, pancreatic head and tail 1 case, pancreatic body 1 case, pancreatic body and tail 6 cases, and pancreatic tail 9 cases. Using WHO Classification 2010, we have found 18 neuroendocrine tumors from which 7 are non-functional and 14 were neuroendocrine carcinoma. The tumors were assessed immunohistochemically with several markers and a correlation between their expression and several tumor-related factors (age, sex, location, size, grade, stage) was investigated.
Conclusion:

1. Immunohistochemistry is crucial in order to improve the pathological diagnostic in pancreatic neuroendocrine tumors.
2. WHO Classification 2010 represents a step forward involving immunohistochemistry.

Tuesday, 30 August 2011, 09.30–10.30 and 16.30–17.00, Hall 5

PS-14 Poster Session Gynaecological Pathology

001
Predicting the Pap test by a formula

R. Bontekoe *, D. Kester, M. Boon
*Bontekoe Research, Leiden, The Netherlands

Objective: Fully automatic generation of mathematical models is a novel branch in computer science; a model can be envisioned as a long formula. We have developed a model to be applied to the medical history of a woman, with the aim to predict the outcome of the next Pap test.
Method: From the Leiden Cytological and Pathological Laboratory (LCPL) archive of one million records we have selected 1,100 women who, on average, underwent five tests. Data such as the woman's age, previous Pap tests, various inflammations, and at least two HPV tests are exploited by the model generation software. The outcomes are compared with the actual values, after which the model is adjusted.
Results: The best model is selected and applied to predict the next Pap test outcome of a different group of women. Again these are compared to the actual outcomes. From such comparisons we are confident that the model is able to indicate risks of developing cervical cancer for any woman.
Conclusion: The next Pap test outcome can be predicted, to a certain extent, by entering a woman's medical history into a formula generated by our evolutionary software.

002
Immunohistochemical (IHC) characteristics and gene polymorphism of ER, VEGF, MMP9 in women with MASS syndrome

T. Demura *, E. Kogan, M. Kesova, N. Kan, A. Donnikov, G. Sukhikh
*RCOGO, Dept. of Anatomic Pathology, Moscow, Russia

Objective: The aim of the study was to investigate IHC characteristics and ER, VEGF, MMP9 gene polymorphism in uterine scars after cesarean section in women with MASS syndrome.
Method: A total of 90 pregnant women with uterine scar were recruited in the study (age from 18 to 40 years). They were divided into two groups: with MASS syndrome and without (45 vs. 45). IHC detection of ER, VEGF, and MMP9 was performed on paraffin sections with antibodies to ER alpha and beta (Lab Vision). Molecular–genetic analysis was made using fluorescent hybridization probes and melting curve analysis to detect gene polymorphisms.
Results: Uterine scar showed signs of connective tissue disorganization: mucoid and fibrinoid changes. IHC analyses revealed a very low expression of ER alpha in both groups, whereas ER beta and MMP9 were rather high in the group with MASS syndrome. Molecular analysis showed gene polymorphism of ER, VEGF, and MMP9 in patients with MASS syndrome.
Conclusion: The obtained results show that MASS syndrome is characterized by connective tissue disorganization and higher ER beta expression in the uterine scar. ER alpha may show low expression due to down regulation under progesterone. MASS syndrome may be genetically determined disorder as these patients show ER alpha and beta genes polymorphism. ER beta decrease may predict uterine scar dehiscence in women with MASS syndrome.

003
Endometrial receptivity: morphological and molecular features (tight junctions remodeling)

E. Kogan *, T. Demura, Z. Aroyan, V. Smolnikova
*RSOGP, Dept. of Anatomic Pathology, Moscow, Russia

Objective: Endometrial receptivity is based on inner uterine layer remodeling and on cell–cell contacts in particular. Claudins are known to be the main tight junction constituents, controlling the apical membrane. The goal of the study was to evaluate claudins in the endometrium in the period of implantation window.
Method: The study was performed on endometrial samples obtained in the implantation window period from 30 women involved in IVF programs (25–37 years) with tubal factor of infertility. Samples were divided according to the

IVF outcome (did get pregnant and did not) with the following morphological and immunohistochemical analyzes (antibodies to claudin 3 and 5).
Results: Patients with negative IVF outcome showed an inadequate endometrial transformation and a low number of mature pinopodes (≤ 20% in surface epithelium) than in the other group (≥ 50%). The analyses of tight junctions revealed claudins 3 and 5 to be low in the apical membrane in the group with negative IVF outcome (3 and 5–≤0.5 score) and to be rather high in the group with positive IVF outcome (3 4.5, 5 3.5 score).
Conclusion: The obtained results suggest tight junctions to play a crucial role in implantation as the structural components of apical membrane which have to go through a series of events resulting in mature pinopodes development.

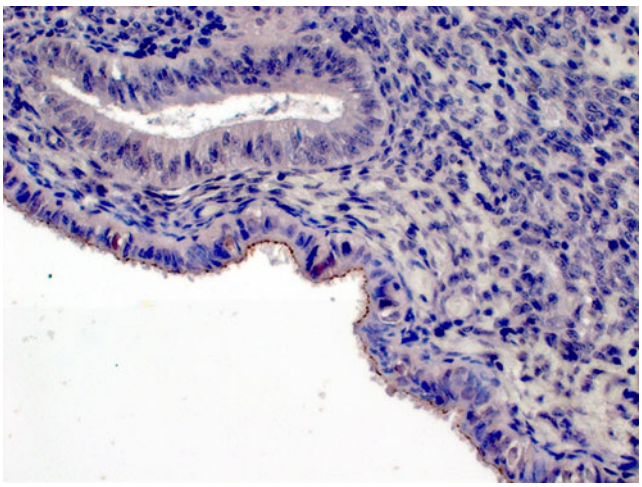

004

Cervical intraepithelial neoplasia (CIN) progression

E. Kogan *, T. Demura, N. Faizullina, L. Ezhova
*RSOGP, Dept. of Anatomic Pathology, Moscow, Russia

Objective: The goal of the study was to investigate morphological and molecular CIN progression predictors.
Method: Surgical and biopsy material was used from 33 patients with HPV infection and different morphology: flat condyloma (11), CIN1 (10), CIN2 (10), CIN3 (13) and microinvasive cervical cancer (8). Morphological analysis, chromogen in situ hybridization (CISH) with HPV DNA 16 and 18 and immunohistochemical analyses was performed on serial paraffin sections with antibodies to Ki-67, COX-2, p16 (ink4a).
Results: High-grade CIN was shown to lack viral DNA in basal epithelial layer, while p16 (INK4a) and COX-2 were preserved. Basal keratinocytes were not involved at the stages of flat condiloma and CIN 1-3. In microinvasive cervical carcinoma basal keratinocytes were replaced by tumor cells Ki-67 and COX-2 positive.
Conclusion: HPV carcinogenic effect via cell genes and proteins while the virus itself is no more important. Thus, Ki-67 and COX-2 are of the essence for establishing the stage of disease progression. Expression of Ki-67 and COX-2 in basal keratinocytes may be recommended as markers of micro-invasion in difficult diagnostic cases.

005

Malaria and its relationship with cervical carcinoma. Results from an ongoing epidemiological study at Mulago Hospital in Kampala, Uganda

M. Odida *, R. Schmauz
*Makerere University, Dept. of Pathology, Kampala, Uganda

Objective: The role of malaria in the pathogenesis of cervical carcinoma has been suggested by results of a previous ecological study from Uganda.
Method: To assess the role of malaria in cervical carcinoma, antibody assays were done on sera collected from a case–control study of 316 cervical carcinoma cases and 314 control women which was conducted between September 2004 and December 2006, in Kampala, Uganda. Antibody titres greater than eight were taken as indicators of previous severe attacks. Odds ratios (OR) and 95% confidence intervals (CI) were estimated using logistic regression for all cervical carcinomas and the two subtypes of squamous cell carcinoma and adenocarcinoma, adjusting for HIV status and age possible confounders.
Results: High malaria antibody titres was associated statistically significantly with increased OR (1.8, 95% CI 1.3-2.7). When the analysis was done for the two subtypes, the OR was statistically significantly increased for squamous cell carcinomas (OR 1.8, 95% CI 1.2-2.7) and not for adenocarcinomas (OR 2.0, 95% CI 0.9-4.4).
Conclusion: Severe malaria is a possible cofactor for cervical carcinoma risk in tropical areas, especially for the squamous subtypes. Further work is in progress to assess the impact of malaria on humoral responses to HPV and other infections on cervical carcinoma risk.

006

Abnormal Pap smears: a clinicopathological and demographic data of 139 cases

M. Z. Rahman *, U. Banik, S. R. Aktar Siddiqui
*Chittagong Medical College, Dept. of Pathology, Bangladesh

Objective: In order to counsel women and to organize a public health system for cervical cancer screening by Pap smear examination, it is imperative to know the pattern of

premalignant and malignant lesions. This study observed a clinicopathological and demographical analysis for establishing the pattern of epithelial cell abnormality in Pap smear.
Method: A total of 1,699 patients underwent Pap smear examination. The prevalence of epithelial cell abnormality in Pap smear was calculated in proportions/percentages. Specimen adequacy and reporting was assessed according to the revised Bethesda system
Results: Among the 1,699 Pap smears, 139 (8.18%) revealed epithelial cell abnormality. A total of 26 smears revealed high-grade lesions and malignancy, most of which were found to be in the 30–39 and ≥45 age group of women. A total of 75 (53.96%) women were in the 20–44 age group and 64 (46.04%) were in ≥45 age group. A bimodal age distribution was detected in the epithelial cell abnormality with the bulk being diagnosed in the patients aged 45 or above. Overall, one third of the patients with an abnormal Pap smear result showed a healthy cervix in per vaginal examination.
Conclusion: A raised prevalence of epithelial cell abnormality reflects the lack of awareness about cervical cancer screening. Women aged 45 or above harbor the bulk of the premalignant and malignant lesions in Pap smear, signifying that these women are the under-users of cytological screening.

007

HPV-mRNA detection in patients with HPV infections

M. C. Antonio Rongioletti *, F. Papa, M.B. Majolini, C. Vaccarella, I. Simonelli, M.C. Giustiniani, V. Mazzucchi, R. Mari, P. Pasqualetti, A. Fabiano, G.M. Liumbruno
*San Giovanni Calibita Hospital, Dept. of Clinical Pathology, Rome, Italy

Objective: HPV is associated with almost all cervical cancerous lesions. To date, HPV-DNA testing is recommended, but data from previous studies suggest that HPV mRNA testing may distinguish clinically relevant from irrelevant high-risk HPV infections.
Method: A total of 131 samples were tested by conventional Pap smear and cervical biopsy, HPV-DNA test and typing, E6/E7-mRNA expression from HPV types 16, 18, 31, 33, 45. K-statistic value was used in order to identify possible significant associations.
Results: Cervical biopsy: negative (NEG): 23 (17.5%); low-grade squamous intraepithelial lesion (LSIL): 82 (62.6%); high-grade squamous intraepithelial lesion (HSIL): 26 (19.9%). A total of 88/131 samples (67.2%) were positive to the HPV-DNA test and 46/131 (35.1%) to the HPV-mRNA test. The HPV-DNA test was positive in 64.7% of NEG, 55% of LSIL and 73.9% of HSIL; the E6/E7-mRNA test was positive in 29.4% of NEG, 30.0% of LSIL and 60.9% of HSIL. In a subgroup of 23 of these patients with negative results to the biopsy and Pap smear, four (17%) were positive to the mRNA test and have developed following cervical lesion.
Conclusion: The mRNA test might be a promising option for improving diagnosis and management of negative and LSIL patients with persistent or progressive HPV infections.

008

Expression of oncoproteins and tumour suppressor genes in non-molar hydrophic abortions, partial and complete hydatidiform moles

M. T. Yacoubi *, H. Landolsi, N. Missaoui, S. Brahem, S. Hmissa
*University Hospital Sousse, Dept. of Cyto-Histopathology, Tunisia

Objective: Hydatidiform moles (HM) are characterized by an abnormal proliferating trophoblastic tissue and carry a potential of malignant transformation. Similar to other human cancers, malignant transformation in gestational trophoblastic tumours is likely a multistep process and involves multiple genetic alterations including activation of oncogenes and inactivation of tumour suppressor genes.
Method: We investigate the expression of bcl-2 and mdm-2 oncoproteins and p53, p21 and Rb tumour suppressor genes in non-molar hydropic abortions (HA), partial HM (PHM) and complete HM (CHM). This expression was determined immunohistochemically by specific antibodies for these proteins on formalin-fixed paraffin sections of 38 HA, 49 PHM and 133 CHM.
Results: Positive staining for bcl-2 and mdm-2 oncoproteins and of p21 was significantly higher in CHM and PHM than in HA ($p<0.05$) but there was no significant difference for the expression of these proteins between CHM and PHM. The expression of p53 and Rb was significantly higher in CHM than PHM and HA ($p<0.05$).
Conclusion: Altered expression of oncoproteins and tumour suppressor genes may be important in the pathogenesis of HM. A possible role of the over-expression of p53 and Rb in CHM is an attempt to modulate the excessive proliferative activity in trophoblastic cells.

009

The accuracy of intraoperative aspiration cytology in the diagnosis of ovarian tumors

F. Abbasi *, S. Naji, Z. Yekta, H. Ayatollahi, B. Khalifezadeh
*Imam Khomeini Hospital, Dept. of Pathology, Urmia, Iran

Objective: The objective of this study was to determine the accuracy of cytology in the intraoperative diagnosis of ovarian tumors and to compare it with frozen section (FS) and permanent section.

Method: We compared the accuracy of intraoperative cytology (IOC) with FS in 105 cases of ovarian tumors received in Urmia Imam Khomeini and Shahid Motahari hospitals during March 2007 to March 2008.
Results: The sensitivity of both techniques of FS and IOC was 93.1%. The specificity of FS and IOC were 98.7% and 94.7%, respectively. The positive predictive value of FS was 96.4% and of IOC 87.1%. The negative predictive value of both methods was 97.4%. The accuracy of FS and IOC was 97.1% and 94.3%, respectively. The area under receiver operating characteristic (ROC) curve was 0.959 for FS and 0.939 for IOC.
Conclusion: These results showed that IOC can be performed for intraoperative diagnosis of ovarian tumors as an alternative to FS; however, a combination of these two techniques is more reliable.

010

Neurogenic cyst of the ovary: an uncommon form of monodermal teratoma

L. Alfaro *, J. Lluna, M. Roca, F. Sevilla, M. Hernandez
*Valencia, Spain

Objective: Teratomas integrated by a predominant or exclusive component of ectodermal or endodermal tissue are known as monodermal teratomas.
Method: A 10-year-old girl presented with an ovarian cyst with a diameter of 16 cm, which rossly showed a smooth grayish surface. Abundant clear translucent liquid filled the cyst, with a thin wall of 2–5 mm. Tiny excrescences emerged in the internal surface. Conventional sections were submitted for H/E staining and posteriorly immunohistochemical analysis was performed.
Results: Mature glial elements and choroid plexus tissue were the unique components of the cyst. No immature neuroectodermal or ependimal areas were seen. A scanty stripe of ovarian cortical stroma with primordial follicles was limited to a few regions of the cyst. Absence of atypical cells and infiltrative growth, with minimal mitotic activity pointed to a benign lesion. S100and enolase expression was common along the different areas and ki67 showed a proliferative index lower than 2% keratin-stained choroid plexus cells.
Conclusion: Very few cases of this kind of monodermal teratomas have been described. Of special interest is that despite of their benign nature they can reach a considerable size and develop in young girls. As in our case, thin wall may require extensive sampling to identify ovarian stromal rests and assure neurogenic components.

011

Immunohistochemical correlations between p16, p53 and L1 human papillomavirus capsid protein expression in cervical intraepithelial lesions

C. Amalinei *, R. Balan, S. Giusca, D. Ciobanu, C. Grigoriu, I.-D. Caruntu
*University of Medicine, Dept. of Histology, Iasi, Romania

Objective: As an attempt to clarify the role of cell cycle regulators in the progression of squamous intraepithelial lesions (SILs), the aims of our study were to characterize the immunostaining pattern of p16 and p53 and their relationship with the histologic grade of precursor lesions of cervical carcinoma and to evaluate the association between the immunohistochemical expression of these two proteins and L1 HPV (human papillomavirus) capsid protein.
Method: The study involved 24 patients with a diagnosis of LSIL (low-grade squamous intraepithelial lesion) and 16 patients with HSIL (high-grade squamous intraepithelial lesion) (cervical intraepithelial neoplasia, CIN2=6 cases and CIN3=10 cases). The conventional smears were evaluated for the immunoexpression of L1 HPV capsid protein and the subsequent biopsies for the immunoexpression of p16 and p53.
Results: The L1 HPV capsid protein was expressed in 45.83% of LSILs and 25% of HSILs. p16 was positive in 66.66% of LSILs, 83.33% of CIN2 and 100% of CIN3. p53 expression was detected in 54.16% of LSILs and in 50% of HSILs.
Conclusion: The correlative analysis of p16 status and L1 HPV capsid protein expression can be useful in the assessment of progression risk of SILs, p53 being only a qualitative biomarker.

012

Latent presentation of rectal endometriosis mimicking rectal adenocarcinoma

J. Attard *, A. Attard, J. Psaila, J. DeGaetano
*Xaghra, Gozo, Malta

Objective: Endometriosis of the gastrointestinal tract occurs in up to 37% of patients with pelvic endometriosis with a predilection for the rectosigmoid colon. We describe a case of endometriosis of the rectum in which an initial diagnosis of “Probable adenocarcinoma” was made.
Method: Our case is that of a 54-year-old woman who presented with bleeding per rectum. Her past history was remarkable for total abdominal hysterectomy. Colonoscopy showed an ulcerated anterior rectal lesion. Radiology

showed a mass invading through the rectal wall. The biopsy showed an atypical glandular proliferation and a diagnosis of "Probably adenocarcinoma" was made and the patient was given neoadjuvant chemoradiotherapy followed by an anterior resection.
Results: Anterior resection specimen showed a white, firm, ill-defined mass involving all layers of the rectum and microscopically features of endometriosis. Immunohistochemistry showed that the glands were ER and CK7 positive and the CK20 and CEA negative. Immunohistochemistry was repeated on the original biopsy which showed the same immunoprofile.
Conclusion: This case represents a rare presentation of endometriosis of the rectum mimicking adenocarcinoma, clinically, histologically and radiologically. Endometriosis must always come to mind in women with unusual glands in the colorectum. Immunohistochemistry is crucial for a correct diagnosis to be made.

013

Immunohistochemical assessment of epidermal growth factor receptor (EGFR) in relationship with human papillomavirus (HPV) L1 capsid protein in cervical squamous intraepithelial lesions

R. Balan *, C. Amalinei, S. Giusca, V. Gheorghita, D. Ciobanu, I. D. Caruntu
*University of Medicine, Dept. of Morphological Sciences, Iasi, Romania

Objective: We analyzed the immunohistochemical pattern of epidermal growth factor receptor (EGFR) in cervical squamous intraepithelial lesions (SILs) in correlation with L1 HPV capsid protein in order to determine the relationship between EGFR expression and the infection status of human papillomavirus (HPV).
Method: The study included 40 cases, 24 LSIL (low grade SIL) (CIN1, cervical intraepithelial neoplasia) and 16 HSIL (high grade SIL) (six cases of CIN2 and ten cases of CIN3). The immunoexpression of L1 HPV protein was assessed on conventional cervico-vaginal smears and EGFR was immunohistochemically evaluated on the corresponding cervical biopsies.
Results: The HPV L1 capsid protein was expressed in 45.83% of LSIL and 25% of HSIL. EGFR was overexpressed in 62.4% of HSIL (58.4% CIN2 and 41.6% CIN3) and 37.6% LSIL.
Conclusion: The immunoexpression of L1 HPV has clinical application in the progression assessment of the cervical precancerous lesions without a correlation to the grade of the cervical SIL. EGFR is expressed by all proliferating squamous epithelial cells, thus corresponding with the grade of SIL. The evaluation of EGFR status, correlated with L1 HPV protein expression, can provide useful data of progression risk of cervical squamous intraepithelial lesions.

014

The impact of P-gp/topoisomerase I and P-gp/HER2 immunophenotypes on ovarian carcinoma features

J. Bar *, K. Szczudło, P. Nowak, A. Lis-Nawara, L. Noga, J. Rabczyński, M. Jeleń
*Medical University, Wroclaw, Poland

Objective: Up to now, several biological parameters might be considered as prognostic and predictive factors in ovarian carcinomas. So, we evaluated the immunohistochemical expression of P-gp, topoisomeras I (topo I) and HER2 and its correlation with variables of ovarian carcinomas.
Method: P-gp, topo I and HER2 expression was analyzed on 132 malignant ovarian tumors using immunohistochemistry (IHC). The immunoexpression of HER2 was confirmed by fluorescence in situ hybridization (FISH) analysis.
Results: Expression of P-gp, topo I and HER2 was observed in 38.4%, 51.6%, 63.7% ovarian carcinomas respectively. Comparison studies between the FISH assays for HER2 and the corresponding IHC showed 89% concordance. P-gp was associated with serous ovarian carcinomas ($p=0.02$) and with well/moderately differentiated tumors ($p=0.03$). The differences between P-gp expression and FIGO stage were on statistical borderline ($p=0.07$). Positive correlation between P-gp and topo I expression in ovarian carcinomas was revealed ($p=0.005$). The P-gp/topo I- positive immunophenotype was associated with serous ovarian carcinomas ($p=0.01$) and well/moderately differentiated tumors ($p=0.01$). The P-gp/HER2-positive cases show trend towards higher occurrence in III/IV than I/II FIGO stages ($p=0.07$).
Conclusion: This study revealed that individual pathological features of ovarian cancers are associated with activation of P-gp/topo I or P-gp/HER2 immunophenotypes.

015

Primary malignant nerve sheath tumor of the uterine cervix: a case report and literature review

N. Basheska *, S. Veljanovska
*Clinic of Radioth. and Oncology, Dept. of Histopathology, Skopje, Macedonia

Objective: Primary malignant nerve sheath tumor (MNST) of the uterine cervix is an extremely rare neoplasm. We

report another case of this uncommon tumor and review all previously documented cases.
Method: The repeated curettements in a 57-year-old woman with a history of prolonged vaginal bleeding revealed polypoid fragments of a sarcomatous neoplasm. In August 1997, total abdominal hysterectomy with bilateral salpingo-oophorectomy was performed. Postoperatively, the patient received six courses of chemotherapy. Twenty-three months later, a local vaginal and left parametrial recurrence appeared and persisted for months despite the external radiotherapy and chemotherapy implemented. Fifty-seven months following the surgery, the patient died from lung metastases.
Results: The cervix was enlarged, markedly distorted by 5.5×2.5×2.5-cm neoplasm involving predominantly the upper lip. Microscopically, the tumor had a variable sarcomatous appearance, suggestive of a MNST. Immunohistochemical examination demonstrated that many of the tumor cells reacted only with S-100 and vimentin.
Conclusion: Only nine cases of MNST at this location have been reported presenting as polypoid masses measuring from 1.2 to 6 cm, occurring in patients ranging in age from 22 to 73 years. This additional case suggests that primary MNST of the uterine cervix appear to have clinical and pathological features similar to MNST at other locations.

016

Sarcomatoid squamous cell carcinoma of the uterine cervix: an HPV-related tumor with epithelial origin

L. Bejan *, S. Stolnicu
*Emergency County Hospital, Dept. of Pathology, Targu Mures, Romania

Objective: Sarcomatoid squamous cell carcinoma (SSCS) is a well-documented entity elsewhere but occurs rarely in the female genital tract with only 20 reported cases in the uterine cervix.
Method: We present a SSCS in which a diagnostic immunophenotype excluded other malignant tumors.
Results: A 72-year-old woman had abnormal vaginal bleeding and a cervical mass which was treated by radical hysterectomy. Macroscopically, the cervix revealed a 4-cm soft, irregular, polypoid tumor. Histologically, the tumor had minor areas of poorly differentiated classic keratinizing squamous component which was overgrown by a well-delineated, secondary extensive and heterogeneous growth of spindle or round cell sarcomatoid elements. Immunohistochemically, both had a similar phenotype which was positive for CAM5.2, AE1/AE3, CK5/6, p63 and p16, suggesting a squamous identity. Actin and H-caldesmon were negative in both components but vimentin was positive only in the sarcomatoid component. PCR demonstrated the presence of HPV16.
Conclusion: The positivity of the sarcoma-like component for epithelial markers and p16 favours a common epithelial squamous origin of both components of the lesion and an association with HPV- infection. Since the tumor has a biphasic pattern, immunohistochemistry must be performed to exclude other malignant tumors that may have different treatment and prognosis.

017

MSI and mucinous differentiation in uterine endometrioid carcinoma

I. Busmanis *, I. Chew
*Singapore General Hospital, Dept. of Pathology, Singapore

Objective: In addition to morphologic correlates described in cases of endometrioid carcinoma (EC) in patients with HNPCC, a feature in colonic MSI malignancies is mucinous differentiation. This study was aimed to examine if the presence of mucinous differentiation in EC affords any predictive value of likelihood of MSI positivity and also to determine if any clinico-morphologic features characterise this particular group. No patients in this series were known to have Lynch syndrome.
Method: A total of 11 cases were extracted from SGH files of nine hysterectomy and two curettage specimens and immunohistochemistry performed for four mismatch repair proteins (MMRP). Nuclear reactivity was accorded a positive result.
Results: Median age was 57 years old. Four cases showed normal expression of MMRP. Seven cases showed abnormal expression as follows: 3 cases; MSH2+/MSH6+ and MLH1-/PMS2—2 cases; MSH2+/MSH6- and MLH1+/PMS2- 2 cases; MSH2+/MSH6- and MLH1+/PMS2+. Of six cases, one tumour was isthmic; five tumours were stage Ia and one stage Ib. Two of each were grades I, II, and III.
Conclusion: A total of 7/11 (63%) cases of EC with mucinous differentiation were MSI+, a higher incidence than reported for conventional EC. No specific correlation was seen with high grade, isthmic location or lymphocytic reaction, as described in HNPCC.

018

miRNA expression and neoplastic transformation in the uterine cervix

P. Castillo *, C. Svanholm-Barrie, M. del Pino, I. Alonso, V. Fusté, J. Gaber, D. H. Persing, J. Ordi
*Hospital Clínic Barcelona, Dept. of Pathology, Spain

Objective: To determine the micro RNA expression in normal uterine cervix (NUC) and carcinomas of the uterine

cervix (CUC) and to identify specific profiles of expression that might be used as biomarkers of progression.
Method: There were 28 CUC and 25 NUC analyzed. Total RNA was prepared using TRIzol® and RecoverAll. MiRNA and small RNA reference gene expression were analyzed using RT-PCR assays. As endogenous references small RNAs (RNU44+U47+RNU48) were used. Data were analyzed according to Kolomogorov–Smirnov and Mann–Whitney test.
Results: There was always an overlap between the expressions in normal vs. tumor samples. The miRNAs overexpressed in cervical carcinoma were miR-1246, miR-1290, miR-1308, miR-142-3p miR-1826, miR-200c, miR-205, miR-21, miR483-5p, miR491-3p miR-720, miR-765 and miR-31, but only miR-205, miR-200c and miR-1290 reached statistical significance. miR-205 was up-regulated in squamous cell carcinomas but downregulated in adenocarcinomas. Six genes, CDKN2A, MKI67, TOP2A, MMP9, BIRC5 and MCM5 were overexpressed in CUC, in line with the miRNA overexpression.
Conclusion: miRNAs are differently expressed in neoplastic and normal cervix, and this correlates with the expression of certain oncoproteins possibly controlled by those miRNAs.

019

Malignant melanoma metastatic to the endometrium: report of two cases

L. Chira * C.C. Santos, I. Timar, K. Szabo, S. Stolnicu, F. F. Nogales
*Emergency Country Hospital, Dept. of Pathology, Targu Mures, Romania

Objective: Malignant melanoma is rarely a primary tumor in the female genital tract. In the uterine corpus, it develops only as a metastasis from various sites (less than 15 cases reported to date). We present two cases of metastases of malignant melanoma of the skin to the endometrium.
Method: Two 56- and 67-year-old patients were admitted for abnormal vaginal bleeding. In both of them, curettage was followed by total hysterectomy. Clinical history revealed that they had been previously diagnosed with malignant melanoma of the skin 1 and 3 years ago, respectively.
Results: On microscopy, nests or cords of atypical epithelioid cells, with intracytoplasmic melanin pigment were detected adjacent to atrophic endometrial glands. Cells were positive for S-100 protein, Melan A, Thyrosinase, Vimentin and HMB-45. On the hysterectomy specimen, in the uterine cavity, there were 3- and 1-mm diameter well-circumscribed nodules of atypical spindle cells with intracytoplasmatic melanin pigment. Infiltration occurred preferently along the endometrial and endocervical surfaces and that myometrial invasion was only small.
Conclusion: If atypical bleeding takes place in postmenopausal patients with a diagnosis of malignant melanoma of the skin, endometrial metastases should be excluded. The prognosis of the patients is very poor; both patients are alive with clinical disease.

020

Significance of perinecrotic expression of CA9 and Glut-1 in endometrial carcinoma

K.-U. Choi *, M.-G. Pak, J.-H. Lee, D.-H. Shin, M.-Y. Sol
*Pusan National University, Dept. of Pathology, Yangsan, Republic of Korea

Objective: Tumor hypoxia has been known to be associated with aggressive phenotypes and tumor resistance to therapy. Several tens of genes are induced by tumor cells to suvive in a microenvironment of hypoxia. The aim of this study was to evaluate the prognostic value of CA9 and Glut-1 that are major factors of hypoxia-induced pathway in endometrial carcinoma.
Method: Archival tissue was retrieved from 144 patients and expression of CA9 and Glut-1 were analyzed using immunohistochemistry.
Results: A significantly increased expression of two markers was found at the perinecrotic area of tumor cells. A trend to worse disease-free survival was noted with increased perinecrotic expression of CA9 and Glut-1. Particularly, perinecrotic co-expression of CA9 and Glut-1 was prognostic. Positive correlation was not observed between CA9 and Glut-1.
Conclusion: Perinecrotic expressions of CA9 and Glut-1 are important prognostic factors in endometrial carcinoma. More aggressive treatment may be necessary to improve the outcome of patients showing these patterns.

021

CD44 expression in glandular lesions and adenocarcinoma of the uterine cervix

N.V. Danilova *, Y.Y. Andreeva, P.G. Malkov, L.E. Zavalishina, G.A. Frank
*Moscow State University, Medical Faculty, Russia

Objective: CD44 is an adhesion molecule, which binds hyaluronic acid and participates in a number of cell-cell interactions. CD44 postulated to play a role in process of tumor invasion and metastases. To clarify the possible role of CD44 in progression of uterine cervical adenocarcinomas this investigation was carried out.

Method: There were 43 cases studied, including benign glandular lesions (10), dysplastic lesions/adenocarcinoma in situ (AIS) (16) and invasive adenocarcinoma (IA) (17). All cases were reviewed by three pathologists to obtain a consensus diagnosis. Immunohistochemical staining for CD44 (clone DF1485) was performed on 4-μm sections of formalin-fixed, paraffin-embedded specimens.
Results: In 85% cases of benign, 93% dysplastic lesions and 90% AIS moderate and strong membrane expression observed. There was not any statistical difference in the groups considered. However, significantly decreased expression was observed in 92% cases of IA. Simultaneously, a strong expression in stromal component was observed around IA and in sites of microinvasion. Thus, redistribution of CD44 from cells to stroma was observed in sites of invasion.
Conclusion: The results suggest that CD44 is associated with invasive features of cervical adenocarcinoma and may be valuable marker of stromal invasion.

022

Omental pregnancy: a rare ectopic pregnancy

S. Dumitriu *, A. Dumitriu, M. Chetrone, D. Miron, V. Ionita, I. Fulga, C. Georgescu
*UMF Iasi, Pathology, Romania

Objective: Omental pregnancy is a rare entity. The diagnostic is difficult and still continues to challenge the clinicians.
Method: We present the case of a 49-year-old female who presented to the hospital with abdominal pain for a few years.
Results: The repeat laparascopy showed omental and peritoneal ectopic decidua. Histopathological examination confirmed it to be an intraabdominal pregnancy.
Conclusion: We conclude that an abdominal pregnancy, though rare, has a seven times higher mortality than non-abdominal pregnancies.

023

Four cases of simplex (differentiated) variant of vulvar intraepithelial neoplasia

N. Dursun *, C. Leblebici, M. Zengin, F. Gunver, E. R. Bozkurt
*1st Education and Research Hospital, Dept. of Pathology, Istanbul, Turkey

Objective: Simplex (differentiated) variant of vulvar intraepithelial neoplasia (VIN) (carcinoma in situ, simplex type) is relatively an infrequent form of VIN. The diagnosis of simplex variant of vulvar intraepithelial neoplasia (SVIN) is difficult and there is conflicting data in the literature if SVIN is a precursour of vulvar squamous cell carcinoma (VSCC).
Method: There were 344 biopsies of vulva evaluated for VIN and VSCC. There were 15 cases of VIN and 8 cases of VSCC analyzed for SVIN.
Results: Four cases had SVIN. The mean age of the patients was 80 (versus 69 for ordinary VSCC). Three of the cases were adjacent to keratinizing VSCC; one was seperate. Two were with early carcinoma; two were widely invasive. All the cases had thickened epidermis. There was parakeratosis. The keratinocytes had dense eosinophilic cytoplasm atypical nuclei at the basal layer, but the superficial keratinocytes were without atypia. Laminin were made to the carcinomas with early invasion.
Conclusion: Despite the data in the literature, all of our SVIN cases were accompanying VSCC. This showed that the detailed examination of the adjacent epithelium in VSCC patients can increase the incidence of SVIN. Futhermore, it is important to emphasize the diagnosis of SVIN and early dermal invasion by neoplastic cells has difficulties.

024

Ovarian cellular fibroma with deposition of hyaline globules: a case report

D. Esteves *, P. Farrajota, C. R. Dias, F. E. Costa
*Hospital de Santo Antonio, Dept. de Anatomia Patologica, Porto, Portugal

This case report is of a patient years of age, with cellular ovarian fibroma containing hyaline globules, this being an unusual association, rarly described in articles. The cellular fibroma is characterized by bland nuclei, three or fewer mitotic figures per 10 high-power fiels and immuohistochemically the tumor was vimentin, CD56, calretinin postive with smooth muscle actin being only focally positive. The neoplastic cells formed densely cellular areas which alternated with a hypocellular, reticular-pattern like areas, associated with clusters of hyaline globules, these being periodic acid-Shift and mucicarmne positive and Alcan blue negative. The hyaline globules were not an insignificant finding, but rather an eye-catching sign, ranging from 3 to 20 um, intra- and extracelllarly. In more compact areas, between the spiral cells, we also observed cells with a signet-ring appearence. The differential diagnoses from Krukenberg tumor and Yolk sac tumor is discussed.

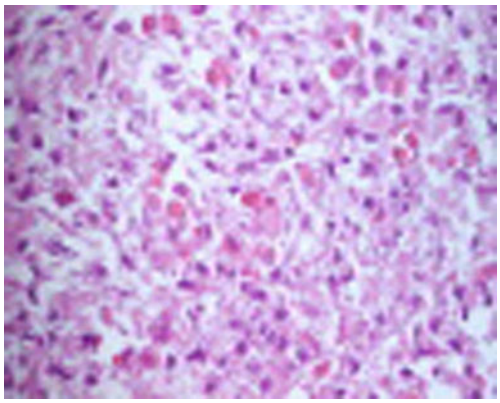

025

Diagnostic value of protein KI67 (MIB-1) staining in abnormal pap smears of postmenopausal women

A. Fakhrjou *, A. Bonakdari, S. Shadravan, M. Sayahemelli, A. Dastrangetabrizi
*Tabriz University, Dept. of Medical Pathology, Iran

Objective: The aim of this study was to determine the diagnostic value of protein Ki67 staining in abnormal pap smears of postmenopausal women.
Method: In a case–control setting, pap smears obtained before and after estrogen treatment of 75 postmenopausal women (cases) with an atypical pap smear and in the 75 normal pap smears of postmenopausal women (controls) were restained with the monoclonal antibody Ki-67 (MIB-1). This study was performed in Iran/Tabriz Imam Reza hospital during a 12-month period. The frequency of Ki-67+ cells the diagnostic value were compared between the two groups.
Results: Seventy-five patients and 75 normal women with the mean age of 60.4±4.5 (54–71) and 59.9±4.3 (58–77) years were enrolled on the study as the cases and controls, respectively (p=0.504). The mean age of marriage were 21.0±4.6 and 21.1±4.7 years, respectively (p=0.930). The two groups were matched for the smoking (6.7% and 2.7%), cervical cancer (2.7% and 1.3%), sexually transmitted disease (28% and 17.3%) and taking oral contraceptive pills (42.7% and 37.3%). There was one (2.7%) Ki-67+specimen in the control group, with no Ki-67+ specimen in the cases (p=0.500). Accordingly, the specificity and positive predictive value of this marker was 99.3% and 100%, respectively, in discriminating between normal and abnormal pap smears.
Conclusion: Based on our results, an abnormal pap smear in postmenopausal women with Ki-67- cells indicates a nonmalignant condition. However, a Ki-67+ specimen is not always a sign of malignancy.

026

Bilateral well-differentiated Sertoli cell tumor and serous cystadenoma in a patient with androgen insensitivity syndrome: a case report

I. Fernández Vega *, C. García Pravia, V. Blanco Lorenzo, B. Vivanco Allende, F. Fresno Forcelledo
*Asturias Central University Hospital, Dept. of Pathology Service, Oviedo, Spain

Objective: Late diagnosis of androgen insensitivity syndrome associated to bilateral large well-differentiated Sertoli cell tumor is unusual.
Method: A 78-year-old phenotypic woman was suffering an orthopnea and irritative cough for 1 year. The patient had a history of primary amenorrhea. CT images incidentally revealed two large right and left abdominal masses, one of them solid and the other with a cystic component. Other CT image findings were absent uterus, short and blind end vagina.
Results: Due to a suspected Morris syndrome, a laparotomy was performed. The left side abdominal mass had a size of 20 × 19 cm and weighted 2.7 kg. The size of the right side tumor's solid part was 4.5 × 4 cm, and the cyst component tumor was 8.5 × 6 cm. Both solid lesions had a uniform tubular pattern of polygonal cells with granular and clear cytoplasm. Cystic structure was composed of a fibrous wall lined by an epithelium without atypia. The immunophenotype of the lesions was typical. Serum tumor markers were negative. The cytogenetic study revealed a 46 XY karyotype. The pathological diagnosis was a well-differentiated Sertoli cell tumor with serous cyst.
Conclusion: We report a rare case of late diagnosis of androgen insensitivity syndrome associated to bilateral Sertoli tumor with a unilateral cystic component.

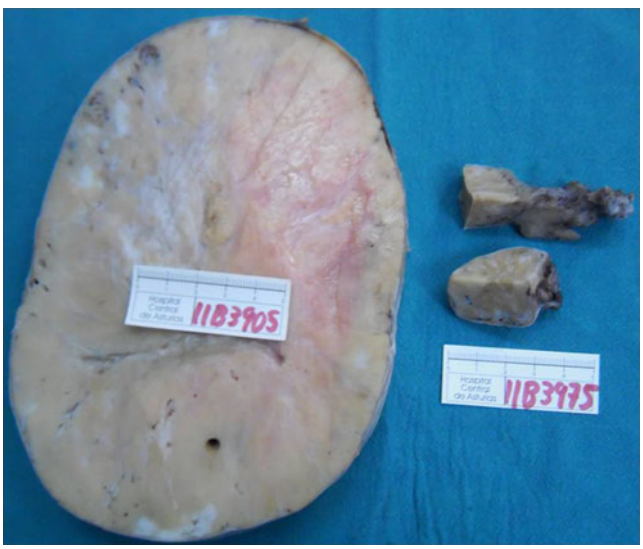

027

Clear cell adenocarcinoma of the cervix: a clinico-pathological study

M. M. Hamdane *, R. Sallami Dhouib, K. Mrad, S. Sassi, M. Driss, I. Abess, L. Charfi, R. Ben Ghorbel, K. Ben Romdhane
*Salah Azaiez Institute, Dept. of Pathology, Ariana, Tunisia

Objective: Cervical clear cell adenocarcinoma (CCCA) is defined histologically as an adenocarcinoma that is a composed mainly of clear or hobnail cells arranged in solid, tubulocystic and/or papillary patterns.
Method: A retrospective study of 17 cases of CCAC, diagnosed in the histopathology's department of the Salah Azaiez institue, between 1993 and 2010.
Results: There were 17 women with a mean age of 58 years. All of them presented with a breakthrough bleeding. In all cases, physical examination revealed an ulcerative budding cervical tumor. All patients underwent biopsies. Histological examination showed a carcinomatous proliferation arranged in glandular (82%), papillary (47%), solid (35%) and/or trabecular (23%) patterns. The tumor cells were usually pleomorphic with abundant clear cytoplasm and atypical nuclei. Hobnail cells were found in 58.8% of cases. Abdominopelvic ultrasound excludes another gynecologic primary in all cases. Ten women underwent a Radical hysterectomy with lymphadenectomy, often preceded by radiotheray.
Conclusion: Although well known because of its association with exposure to diethylstilbestrol in young women, the peak frequency of CCCA is actually in the postmenopausal group. Histologically, this tumor is similar to clear cell adenocarcinoma of the ovary and the endometrium. Therefore, the possibility of secondary involvement of the cervix from another gynecologic primary must be excluded.

028

Primary neuroendocrine differentiated mucinous adenocarcinoma of the vulva

M. M. Hamdane *, S. Sassi, K. Mrad, F. Khanchel, W. Majdoub, L. Charfi, R. Doghri, N. Ben Hamida, I. Abbes, K. Ben Romdhane
*Salah Azaiez Institute, Dept. of Pathology, Ariana, Tunisia

Objective: Primary mucinous adenocarcinoma of the vulva (PMAV) is a rare cancer which is characterized by aggressiveness.
Method: We report a new case of primary vulvar mucinous adenocarcinoma.
Results: A 72-year-old women presented a vulvar nodule. Physical examination, revealed a mobile, indurate, ulcerated nodule on the left labium minus. A local excision of the vulvar was performed. On gross examination, the vulvar specimen was a multinodular lesion with a glistening appearance and soft consistency. Microscopic examination showed a carcinoma infiltrating the dermis within an abundant mucoïd material. It was composed of irregular cords and clusters of small, round tumor cells with eosinophilic or vacuolised cytoplasm and poorly atypical nuclear with small nucleoli. Immunohistochemical stains revealed that the tumor cells were positive for estrogen receptors, progesterone receptors, chromogranin, synaptophysin, carcino-embryonnal antigen and focally positive for the cytokeratin 7 and EGFR. They were negative for the cytokeratin 20 and GCDFP-15. No extra-vulvar primary was found. The diagnosis of a PMVA was made. The patient underwent a radical vulvectomy.
Conclusion: Because of its rarity, little is known about PMAV. Histologically, there is nothing to distinguish this tumor from another mucinous adenocarcinoma. Therefore, the possibility of secondary involvement, especially from a cervical or a digestive primary must be excluded.

029

Expression of Sox2 in cervical cancer

C. Hauser-Kronberger *, N. Arnold, S. Swierczynski, E. Klieser, C. Zuchna, O. Dietze
*Hospital Salzburg PMU, Inst. für Pathologie, Austria

Objective: Sox2—the SRY (sex determining region Y)-box 2 transcription factor, as the key trigger in maintaining pluripotency and the self renewal capacity of embryonic stem cells, has shown to be up regulated in several cancer types. Aim of this morphological study was to demonstrate Sox2 expression in cervical dysplasia and cancer and its correlation with potent stem cell markers, prognosis and p16.
Method: Formalin-fixed paraffin embedded (FFPE) tissue from 25 squamous cervical cancer and 20 high-grade CIN were immunostained using an automated staining platform (Dako, DN). Antibodies were used detecting Sox2, Nanog, Oct4, the oncogene (BMI1), CD133 and p16. Additionally the HPV-positive cervical cancer cell line Caski was evaluated for the expression of Sox2.
Results: Sox2 expression seems to be associated with high-grade dysplasia and cervical cancer and HPV (p16-positivity). Sox2+ cervical cancer seem to be poorly differentiated, revealing a stem cell-like phenotype of these tumors. The results of the immunohistochemical experiments for Sox2 positive cervical cancer and high grade CIN showed also protein-expression of Oct4, CD133 and BMI1.
Conclusion: These results reveal a correlation between Sox2 and the tumor-initiating cell (TIC) relevant proteins (Nanog, Oct4, BMI1) in cervical cancer.

030

Epithelioid trophoblastic tumor: report of a case

Á. Hens Perez *, M.J. Añon, M.I. Moreno, G. Muñoz
*Servicio Andaluz de Salud/UCA, Dept. of Pathology, Puerto Real, Spain

Objective: Epithelioid trophoblastic tumor (ETT) is a rare form of trophoblastic disease characterized by the growth of intermediate trophoblast cells with features that made it distinct from placental-site trophoblastic tumor and choriocarcinoma.
Method: A case of a 46-year-old female with an abdominal mass is reported. Prehysterectomy clinical diagnosis was leiomyosarcoma. The diagnosis of gestational trophoblastic disease was not suspected.
Results: Grossly, there was a solid uterine mass with necrosis on cut sections. Histologic features include a growth pattern of monomorphic, epithelioid cells forming nests and solid masses within a hyaline matrix and extensive necrosis with a geographic configuration. Immunohistochemically, there was diffuse positive for cytokeratin, cytokeratin 18, CD10 and p63.
Conclusion: Expression of p63 and cytokeratins is important to recognize the trophoblastic nature of this neoplasm and to be able to distinguish it from other neoplastic forms of gestational trophoblastic disease.

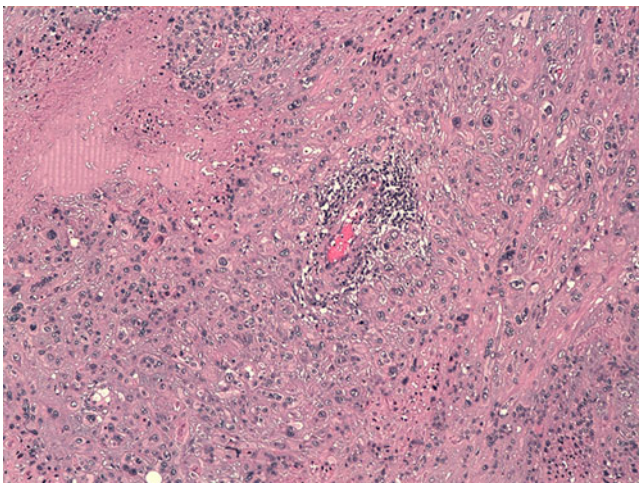

031

Validation of a new method for high sensitivity detection and genotyping of human papillomaviruses without the need of DNA extraction

E. Herráez *, B. Espigares, E. Lara, R. García-del Moral, A. Olmo
*Máster Diagnóstica, Research and Development, Granada, Spain

Objective: Several HPV detection methods are available on the market. However, enhanced methods with faster performance, higher sensitivity and specificity are still required. HPV Direct Flow CHIP is a CE-IVD system for automatic HPV screening and identification of 36 genotypes by direct PCR and reverse dot blot hybridization. Both fresh and paraffin embedded clinical samples are analyzed directly, without previous DNA extraction. This system allows full sample processing in less than 2 hours.
Method: There were 2,000 cervical samples tested by HPV Direct Flow CHIP without DNA purification.
Results: The test yielded a comparable reproducibility, sensitivity and specificity when assayed with paired unprocessed and purified-DNA samples. Analytical sensitivity was 1-10 copies of viral genome equivalents (NIBSC standards). HPV positivity for normal, ASCUS, LSIL and HSIL clinical samples was 33%, 82%, 89% and 100% respectively. Clinical sensitivity for HSIL or worse (≥CIN2) was 100% ($p<0.001$). Clinical specificity for<HSIL (<CIN2), was 62.6% ($p<0.001$).
Conclusion: HPV Direct Flow CHIP is an automated, fast, sensitive and reliable test for simultaneous HPV screening and genotyping, starting from non-processed clinical samples. This platform may offer a highly sensitive and cost-effective alternative to cytological PAP test for cervical cancer screening.

032

Lobular endocervical glandular hyperplasia associated with STK11 mutation: report of a case of Peutz–Jeghers syndrome

A. Hirasawa *, T. Akahane, T. Tsuruta, K. Banno, N. Susumu, K. Sugano, D. Aoki
*Keio University, School of Medicine, Dept. of Obstetics and Gynaecology, Tokyo, Japan

Objective: Peutz–Jeghers syndrome (PJS) has been frequently associated with adenoma malignum, a subtype of cervical adenocarcinoma. Lobular endocervical glandular hyperplasia (LEGH) has recently been proposed to be a possible precursor of adenoma malignum. It has been reported that many cases previously diagnosed as adenoma malignum now would be diagnosed as LEGH. However, only a few reports have focused on a possible link between LEGH and glandular tumor of the uterine cervix associated with PJS. Herein, we report a case of LEGH found in a PJS patient positive for STK11 mutation.
Method: The patient was a 42-year-old woman with a diagnosis of PJS during childhood. She noticed her 7-year-old son to have a similar pigmentation of the lips, the oral cavity, and the fingers to hers, raising her concern that the son might have PJS like her. She

brought him to our outpatient genetic counseling clinic. After obtaining her informed consent, mutation analysis of STK11 gene was performed in the present mother, and deletion was identified in the exon.
Results: We gave explanation during genetic counseling that the mother should be screened for cervical lesions for surveillance purposes, and thus she visited our gynecological department. At her first visit, gynecological examination revealed excessive watery vaginal discharge and pathological examination of the surgical specimen revealed the presence of LEGH, but there was no evidence of adenoma malignum.
Conclusion: In women with PJS, not only periodic observation of the intestinal tract but also surveillance of the uterine cervix are essential, keeping in mind the presence of cervical LEGH and adenoma malignum.

033

Diffuse adenomatoid tumour of uterus: a case report and its pathological features

M. Ikonomi *, S. Kadare, S. Celiku
*Universitary Hospital Centre, Dept. of Pathologic Anat, Tirana, Albania

Objective: Adenomatoid tumor is a rare benign, usually small lesion. It is often accompanied by smooth muscle proliferation and is known as leiomyoadenomatoid tumour.
Method: We report an unusual case of diffuse adenomatoid tumour. Pathologic examination of the hysterectomy specimen was done and microscopic slides were coloured for H-E, and immunohistochemical stain for and AE1/AE3, EMA, SMA, Ki67.
Results: Pathologic examination showed a diffuse mass which replaced most of the myometrum in the entire corpus uteri. Microscopic examination revealed the presence of tubular structures, clear vacuolated cells, with a bland appearance, separated in an infiltrative fashion by smoth muscle cells. In the mass there were areas of necrosis. The differential diagnosis was with a malignant neoplasm because of irregular pseudoinfiltration with cuboidal cells, the presence of necrotic areas of infarction, and the presence of glandular structures in the hypertrophic smooth muscle bundles that mimicked an infiltrating carcinoma for a leiomyoma of myometrium. Immunohistochemistry revealed positivity for AE1/AE3, EMA and SMA in the muscular component.
Conclusion: The purpose of reporting this case is not only for reporting a rare lesion but also for such tumors can pose diagnostic difficulties which may lead to more aggressive therapy if not correctly interpreted.

034

The ovaries in cadmium toxicity: experimental study

S. Jancic *, M. Ilic, D. Jovanovic, D. Peric, N. Jancic, G. Rancic, M. Knezevic
*University of Kragujevac, Medical Faculty, Serbia

Objective: Carcinogenic effects of cadmium on lungs, testicles and prostate are well-known, but there have been insufficient reports about the effect of cadmium on ovaries. The aim of this study was to estimate ovarian changes in rats chronically exposed to cadmium (Cd).
Method: The study was carried out on female Wistar rats (n=22, age=35-37 day, body mass 120-140 g), divided in control (n=11) and experimental group (n=11). The rats of the experimental group were treated with 15 mg/kg Cd dissolved (as $CdCl_2$) in drinking water. The animals were sacrificed three months later. Histological, histochemical and immunohistochemical (cytokeratin AE1/AE3 and Ki 67) studies of ovaries were performed.
Results: Changes without neoplastic nature like decrease in ovary's volume, reduction in the rate of follicular development and numerous corpora lutea formation were found in the vicinity of preneoplastic changes: papillomatous epithelial hyperplasia and inclusion cysts, microglandular formations with dysplasia and seromucinous microcystic formation.
Conclusion: Cadmium is a potent carcinogen capable to induce the wide spectrum of preneoplastic lesions in the ovaries and disturb the structure and function of ovaries.

035

Prediction of recurrence after treatment for high-grade cervical intraepithelial lesions: the role of endocervical margins

D. Jasar *, K. Kubelka-Sabit, V. Filipovski
*Clinical Hospital Sistina, Dept. of Diagnostic Laboratories, Skopje, Macedonia

Objective: The aim of the current study was to evaluate the endocervical resection margins as prognostic marker linked to recurrent intraepithelial neoplasia, following ultrascision-knife conization for high-grade intraepithelial lesions (HSIL).
Method: In a retrospective study, 312 women with HSIL were included (mean age 32.8 years, range 17-57). Ninety-six patients were diagnosed as CIN II (31%), 140 as CIN III (45%) and the remaining 76 with CIS (24%). Ultrascision knife technique was performed in all

patients, in a period from 2003-2009. During the follow-up period (12 to 84 months, mean 46), the results of the follow-up biopsies and PAP-smears were accessible in 136 patients only.

Results: From a total of 136 patients, 52 (38%) had clear endocervical margins, while in 84 (62%), endocervical margins were involved. Recurrences were observed in 13/23 in the CIN II group (56%, $p>0.05$), 38/79 (48%, $p=0.03$) in the CIN III group and 26/39 (66%, $p=0.02$) in the CIS group.

Conclusion: Extensive endocervical cone margin involvement after conization for HSIL is a strong predictor for recurrent disease. Therefore, the type of HSIL area of involved endocervical margins should be evaluated in order to plan further management.

036

Diagnostic value of proliferatin index including MIB1 and argyrophilic nucleolar organizer regions proteins in uterine smooth muscle tumors

E. Javadirad *, S.H. Madani, M. Rahbar, S. Khazaei
*Medical School, Dept. of Pathology, Kermanshah, Iran

Objective: Uterine smooth muscle tumors are the most common human neoplasm. They are divided clinically as benign and malignant but there is another group of lesions which is difficult to place in these two categories, so-called smooth muscle tumors of uncertain malignant potential (STUMP) and differentiation of these tumors on the basis of H&E staining is impossible. The goal of this study was finding of distinguishing objective biomarkers and a survey of proliferation markers comparing these three groups of tumors.

Method: Twenty-one cases in each group of above mentioned tumors were selected randomly (63 cases in total) from pathobiology laboratories and studied by using immunohistochemistry (IHC) staining for Ki-67 expression and special Argyrophilic Nucleolar Organizing Regions (AgNOR) staining method.

Results: Ki-67 was expressed in 63.15% of leiomyosarcomas (LMS), 4.76% of STUMPs and 0% of leiomyoma group. Ki-67 expression between LMS and STUMP, and also between LMS and leiomyoma were significantly different ($P<0.0001$). Mean AgNOR dots were 2.55±0.03, 2.55, 0.66.4.04, and 8.12±0.13 in leiomyoma, STUMP and leiomyosarcoma, respectively. Significant differences between the three groups were observed ($P<0.0001$).

Conclusion: AgNOR and Ki-67(MIB1) proliferation markers expression between LMS and STUMP were significantly different. Due to difficulty in differentiation LMS from STUMP, finding objective biomarkers is useful and practical. For this purpose, the present study recommends Ki-67 and AgNOR staining which are reliable, simple and rapid methods.

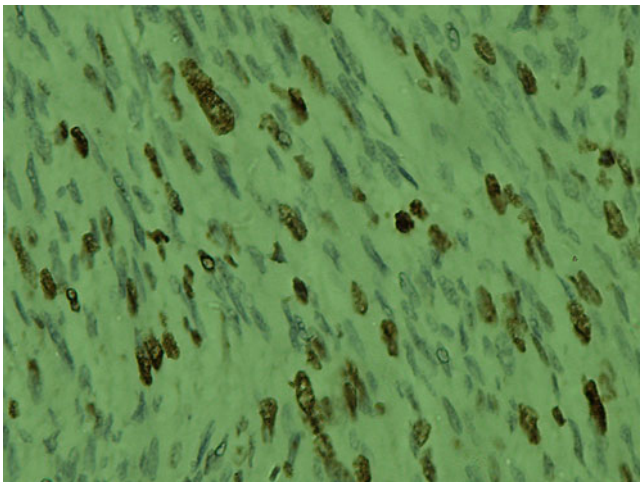

037

Mesothelial cyst of the round ligament: case report and short review of the current literature

P. Katafygiotis *, A. Nomikos, P. Patsaouras, M. Dilalakis, S. Chranioti
*Hospital of Athens, Dept. of Pathology, Greece

Objective: The round ligament extends from the uterus, through the inguinal canal, and ends in the region of the mons pubis and labia major. We present a case of a mesothelial cyst of the round ligament of a 35 year-old woman who developed left lower quadrant pain.

Method: Surgical excision of a cyst of the left round ligament. The gross examination of the resection specimen revealed a cyst measured 1.8 cm. The cyst was lined with a single layer of flattened or cuboidal cells that have the characteristic appearance of mesothelial cells. The cells were positive for the immunohistochemical marker calretinin.

Results: The diagnosis of mesothelial cyst of round ligament was given.

Conclusion: A mesothelial cyst of the round ligament is a rare developmental disorder and occurs mainly in women in their late third or fourth decades. Clinically, it is frequently misdiagnosed as one of commoner diseases such as an inguinal hernia, femoral hernia, lipoma, and lymphadenopathy upon physical examination. Furthermore, a mesothelial cyst of the extraperitoneal round ligament should be included in the differential diagnosis of an inguinal mass in female patients. In the absence of symptoms or of a progressive increase in size,

surgical removal of a cyst of the round ligament is not mandatory.

038

Merkel cell carcinoma metastatic to uterine regional lymph nodes with an unknown primary site: Report of a case

P. Katafygiotis *, E. Minaidou, A. Polymeris, E. Papaspirou
*Hospital of Athens, Dept. of Pathology, Greece

Objective: In this report, we refer the rare case of a woman with a primary uterine carcinoma coexisting with a metastatic Merkel cell carcinoma [MCC] in the uterine regional lymph nodes, with an unknown primary site.
Method: A 54-year old postmenopausal woman presented with menorhagia. Endometrial sampling showed an endometrioid adenocarcinoma grade I. Subsequent hysterectomy revealed the same type of carcinoma. From 25 excised regional lymph nodes, five out of six from the right side of the uterus were infiltrated by small uniform neoplastic cells. The architectural pattern of the tumor was uniform, arranged in solid sheetlike growth, whereas the neoplastic cells had clear nuclei with dispersed chromatin and little cytoplasm. Tumor cells stained positive for cytokeratin 20, chromogranin, synaptophysin, whereas LCA, Bcl-2, CD3, CD20, CK7, Vimentin, CD99, CK5/6, TTF1 and HMB-45 were completely negative.
Results: The diagnosis was consistent with a metastatic MCC. The primary origin of this malignancy remained undetermined since clinically the patient had no skin lesions.
Conclusion: The appropriate therapeutic approach is debatable but the prognosis is considered analogous to stage IV "distant metastatic disease" according to the new AJCC MCC staging system (AJCC Cancer Staging Manual, 2009).

039

Spherule-like cellular stroma in clear cell carcinoma of the ovary: its utility in frozen section diagnosis

N. Kato *, J. Higuchi, S. Ogata, T. Motoyama
*Yamagata University, Dept. of Pathology, Japan

Objective: In ovarian clear cell carcinomas (CCCs), the stroma often shows hyaluronan-rich spherule-like appearance without stromal cells. The aim of this study is to evaluate if this spherule-like acellular stroma is helpful for frozen section diagnosis of CCCs, especially when they show papillary architecture that can be confused with serous tumors. The mechanism of how spherule-like acellular stroma is formed is also analyzed.
Method: Frozen sections of 40 CCCs and 30 serous tumors (22 malignant and 8 borderline) were reviewed. HAC-2, a CCC cell line, was cultured in vitro and examined cytochemically and ultrastructurally.
Results: Spherule-like acellular stroma was found in 18 of 19 CCCs with predominant papillary architecture, including ten CCCs that were incorrectly diagnosed as serous tumors intraoperatively. In contrast, the stroma of serous tumors was irregular in shape and usually contained stromal cells or vessels. By suspension culture, cell aggregates of HAC-2 first expressed hyaluronan at the cell-cell borders then formed hyaluronan-laden spherule-like spaces, which should be derived from the intercellular spaces.
Conclusion: Spherule-like acellular stroma is useful for differential diagnosis between CCCs and serous tumors in frozen sections. Intercellular spaces where tumor-derived hyaluronan accumulates are a potent resource of spherule-like acellular stroma.

040

PTEN positive and PTEN negative endometrial adenocarcinomas (EAC)

E. Kogan *, T. Demura, N. Faizullina, B. Bantish
*RSOGP, Dept. of Anatomic Pathology, Moscow, Russia

Objective: The aim of our study is to investigate PTEN positive and PTEN negative EAC.
Method: The study was performed on biopsy samples and surgical material of endometrium from 101 patients (aged 27–72 years) with morphologically proved simple endometrial hyperplasia (EH) without atypia (25), complex EH without (25) and with atypia (18), EIN (18) and EAC (20). Control group consisted of endometrial samples taken from healthy women before IUD placing (20). Immunohistochemical analyzes was performed on endometrial samples using primary antibodies to PTEN (Dako Cytomation, 1:100), Ki-67 (Dako Cytomation, 1:200) and claudins 3 and 5 (Lab Vision, ready-to-use).
Results: Two types of EAC were observed: PTEN positive (8) and PTEN negative (12). PTEN and membrane localization of claudins is gradually decreased in the sequence of carcinogenesis—from normal endometrium to EH without and with atypia, and is almost absent in EIN and EAC.
Conclusion: The obtained results may indicate differences in EACs origin. Patients with PTEN negative

endometrium might be at a higher risk for EIN and EAC development.

041

Epithelium hyperplasia foci without and with atypia in adenomyosis

E. Kogan *, N. Nizyaeva, T. Demura, L. Ezhova, A. Unanyan
*RSOGP, Dept. of Anatomic Pathology, Moscow, Russia

Objective: The aim of this study was to investigate morpho- and immuno-phenotypes in adenomyosis foci epithelium (Ep).
Method: The study was performed on surgical material of excised uteri from 70 patients of the age 35–78 with adenomyosis and with combination of adenomyosis. Immunohistochemical study was performed on serial paraffin slides. Monoclonal and polyclonal antibodies to ApoCas, Ki-67, MMP-2, MMP-9, TIMP-1, COX-2, E-cadherine, EGFR, VEGF, Claudin -3 (Cl) and Cl-5 were used as primary antibodies.
Results: We found five variants of Ep in adenomyotic foci: (1) Ep as an endometrial proliferation phase, (2) Ep as endometrial secretion one, (3) hyperplasic Ep without atypia, (4) atypical hyperplasic Ep (AHP) and (5) Ep with atrophy. Immunophenotype of AHP differs from other variants by high expression oncomarckers such as Ki-67, EGFR, COX-2, VEGF, MMP-2, MMP-9, TIMP-1, and is characterized by disturbance in localization of Cl-3, Cl-5. They were found in both Ep cell membrane and cytoplasm. These markers were similar in EA.
Conclusion: Hyperplastic Ep with atypia in adenomyotic foci may give origin to carcinoma of the uterine corpus.

042

Expression of Akt, m-TOR and MAPK in endometrial carcinoma

H. Kourea *, M. Nikolaou, V. Tzelepi, H. Kalofonos, G. Decavalas, C. Scopa
*University of Patras Hospital, Dept. Pathology, Greece

Objective: The MAPK and Akt/mTOR pathways are frequently activated in various tumor types but data on endometrial cancer are limited. The purpose of this study is to investigate the clinical significance of the expression of activated, phosphorylated MAPK, Akt and mTOR in endometrial carcinoma.
Method: Endometrial carcinomas operated in our institution from 1995-2010 were reviewed. On 118 cases with available tissue blocks, clinical data were recorded and immunohistochemistry for phospho-p44/42MAPK (Thr202/Tyr204), phospho-Akt (Ser473) and phospho-mTOR (Ser 2448) was performed. Non-neoplastic endometrium was seen adjacent to tumor in 60 cases. The immunoreactivity was assessed by H score in neoplastic and non-neoplastic tissue. Statistical analysis was performed using SPSS 16.0.
Results: Expression of phospho-Akt was seen only in tumor. The expression of phospho-p44/42MAPK was higher in tumor compared to non-neoplastic endometrium ($p<0.001$) but phospho-mTOR expression was higher in non-neoplastic endometrium than in tumor ($p=0.001$). Expression of phospho-Akt was correlated with phospho-p44/42MAPK ($p=0.002$, $r=0.309$). Expression of the markers was not associated with stage, grade and survival. Stage and grade were associated with survival.
Conclusion: Akt and MAPK pathways appear activated in endometrial carcinoma. Further research is necessary to clarify whether these proteins could be used as targets in the management of selected endometrial carcinomas.

043

Microscopic lesions in uterine tube in endometrium carcinoma: how effective is the macroscopic sampling techniques? And are these lesions having an effect on prognosis?

O. Kulaç *, A. Usubütün
*Hacettepe University, Faculty of Medicine, Ankara, Turkey

Objective: The finding of tubal lesions in patients who carry BRCA mutations and the marked correlation between endometriosis and endometrioid/clear cell ovarian carcinomas, fallopian tubes attracted attention and started to examine extensively. We applied a longitudinal sampling method including the fimbria, representing a wider area of the tube, instead of "ring-shaped" classical sampling. With this method we detected more microscopic tubal lesions. To evaluate this observation a retrospective study was conducted.
Method: Endometrioid type endometrial carcinoma cases without visible macroscopic tubal lesions were randomly selected. Longitudinally sampled 100 cases and classically sampled 100 cases were chosen for the study.
Results: No lesion was detected in classically-sampled cases. However, in longitudinally-sampled cases, we found four cases with tubal lesions. All were located in fimbria except one. In two cases tubal tumors were invasive. In all cases, tubal and primary tumors were morphologically similar. Two cases also had endometriosis foci. All tubal lesions were contiguous with non-neoplastic tubal epithelium.
Conclusion: For endometrial carcinoma cases, by longitudinal sampling more lesions may appear in fallopian

tubes. Tube may be a potential primary source for endometrioid lesions. However, prognostic value of existence of incidental microscopic invasive tubal tumor awaits further investigation.

044

Two cases of Peutz–Jeghers syndrome with sex cord stromal tumor with annular tubules and minimal deviation adenocarcinoma of cervix caused by somatic mutation of STK11 gene

S.-Y. Kwon *, H.-R. Jung, J.-Y. Park, Y.-K. Bae
*Keimyung University, Dept. of Pathology, Daegu, Republic of Korea

Objective: Peutz–Jeghers syndrome (PJS) is a rare autosomal dominant inherited disorder which is characterized by the development of hamartomatous polyps in the gastrointestinal tract and mucocutaneous pigmentation on the lips and oral mucosa. The patients with PJS have an increased risk of developing intestinal malignancies and other malignancies in pancreas, liver, lung, and breast and gynecologic malignancies. Many malingnancies with PJS are reported a mutation of tumor suppressor gene, STK11/LKB1 gene, which is located on chromosome 19p13. We report herein two cases of PJS with minimal deviation adenocarcinoma of cervix.
Method: Case 1 is a 36-year-old woman with symptom of hypermonorrhea. Also, she had cystically dilated both ovaries diagnosed with sex cord tumor with annular tubules (SCTATs) and mucinous cystadenoma and metastatic carcinoma from the cervix. Case 2 is a 35-year-old woman with symptom of watery vaginal discharge. The ovaries of case 2 were diagnosed with sex cord tumor with annular tubules (SCTATs).
Results: Grossly, the cervix from both of cases showed markedly enlargement involved by tumor. Microscopically, well-differentiated atypical glands were infiltrating into the entire myometrium. By DNA sequencing analysis, case 1 was identified a frame shift mutation of codon 132(TGC to CGC) in exon 3 of STK11/LKB1 gene. Case 1 had represented more aggressive clinical course and expired 1 year later of operation.
Conclusion: In general, the somatic mutation of STK11/LKB1 gene has reported to the poor prognosis of malignancies.

045

Replication protein A in ovarian adenocarcinomas: correlation with MCM-2, MCM-5 and prognostic significance

G. Levidou *, K. Ventouri, A. Nonni, H. Gakiopoulou, A. Bamias, P. Fragkou, E.-A. Trigka, M.A. Dimopoulos, E. Patsouris, P. Korkolopoulou
*University of Athens, Dept. of Pathology, Greece

Objective: Replication protein (RP) A is a ssDNA-binding protein required for the initiation of DNA replication and the stabilization of ssDNA. Collaboration with several molecules, i.e. MCM2-7 complex has been suggested to be imperative for the accomplishment of its multifaceted role.
Method: In this study, we investigated the immunohistochemical expression of RPA2 subunit in correlation with MCM-2 and -5 and assessed its prognostic significance in 76 patients with ovarian adenocarcinomas (OC).
Results: RPA2 protein expression was observed in all cases, whereas the distribution of staining intensity varied from weak to strong. RPA2 expression was correlated with tumour stage ($p=0.0053$) and the presence of residual disease ($p=0.0001$). Moreover, RPA2 immunoexpression was positively correlated with MCM-2 ($p=0.0001$) and MCM-5 ($p<0.0001$) expression. In multivariate survival analysis RPA2 expression emerged as an independent predictor of adverse outcome ($p<0.0001$) along with tumour histological grade. RPA2 remained an independent predictor of survival ($p=0.0036$) even after adjustment for MCM-2 and MCM-5 expression.
Conclusion: Our results further support the interrelation of RPA2 protein with MCM-2 and -5 in OCs. Moreover, RPA2 protein may have an important role in ovarian tumourigenesis, and may serve as a useful independent molecular marker for stratifying patients with OC in terms of prognosis.

046

Squamous cell carcinoma arising in an ovarian mature cystic teratoma: a case report

W. Majdoub *, F. Bougrine, N. Majdoub, I. Msakni, B. Laabidi, M. Hamdane, F. Khanchel, L. Messoudi, A. Bouziani, R. Rachdi
*Military Hospital, Tunis, Tunisia

Objective: Malignant transformation in a mature cystic teratoma (MCT) of the ovary is rare. The most common malignancy is squamous cell carcinoma (SCC), which accounts for about 75% of malignant transformations.
Method: We report a case of 57-year-old woman gravida 5, para3, who presented with a 2-month history of metrorrhagia, anorexia and weight loss.
Results: Physical examination revealed a palpable and painless mass of the hypogastric region. Ultrasonography showed a well-outlined mass of the right adnexa. Laboratory tests showed a high rate of CA 125 antigen. Exploratory laparotomy was performed and revealed a twisted right cystic ovary. A hysterectomy with bilateral adnexectomy was performed. Grossly, the cystic mass measured 16 cm in diameter. It contained hair and yellowish fluid. The cyst wall thickness was thin in most areas, but a region measuring 4 cm in the greatest dimension was also seen. Histopathologic

examination revealed mature cystic teratoma with malignant transformation to an invasive keratinizing SCC. Subsequently, she received adjuvant chemotherapy. Clinical outcome was favourable two years after.
Conclusion: MCT is a common and benign ovarian neoplasm but there are evidences for some factors as risk factors for malignancy. Clinicians as well as pathologists should keep this rare type of tumor in mind.

047

Ovarian gynandroblastoma: a case report

W. Majdoub *, F. Bougrine, N. Majdoub, I. Msakni, B. Laabidi, M. Hamdane, F. Khanchel, M. Basly, A. Bouziani, R. Rachdi
*Military Hospital, Tunis, Tunisia

Objective: Gynandroblastoma is a very rare sex-cord stromal neoplasm containing both a granulosa cell and a Sertoli–Leydig cell tumor. It occurs generally in young women but may be encountered in a wide age range.
Method: We report a case of a 36-year-old woman gravida 3 para2 presented with a 3-year history of amenorrhea.
Results: Physical examination revealed clinical signs of hyperandrogenism. On pelvic examination, a firm mass of 6 cm was filling the pelvis. Laboratory data showed markedly raised serum concentrations of testosterone. Transabdominal ultrasound and computed tomography scan of the pelvis and abdomen showed a bulky right ovary, but no other abnormalities. An ovarian source of androgens was suspected and surgery was arranged. Exploratory laparotomy was performed and the right adnexa were excised. Histopathological examination revealed tubules of Sertoli cells admixed with rounded islands of granulosa cells growing in a microfollicular pattern. Hyperandrogenaemia normalized post-operatively. Clinical outcome is favourable 1 year after surgery.
Conclusion: We have to consider this rare tumour in the differential diagnosis of hyperandrogenism. This tumour has a good prognosis and almost all tumours are benign at presentation. The treatment is surgical based on a salpingo-oophorectomy.

048

Intavenous leiomyomatosis of the uterus: is it a life threatening disease?

K. Manoloudaki *, E. Skafida, E. Arkoumani, A. Georgiakakis, E. Liarmakopoulos, P. Lampropoulos
*Tzaneion Hospital, Pireus, Greece

Objective: Intravenous leiomyomatosis is a rare neoplasm in which gross nodule of benign smooth muscle tissue grow in the veins of myometrium or extend into uterine and extrauterine veins (about ten of these cases in the vena cava and heart). The exact etiology is unclear.
Method: We report a case of intravenous leiomyomatosis in a 40-year-old woman who presented with pelvic pain. A clinical and US investigation revealed a pelvic mass. Hysterectomy with bilateral salpingo-oophorectomy was performed.
Results: Gross examination disclosed enlargement of uterus by some worm-like extensions into the uterine veins of a broad ligament and right adnexa. Histologically, a benign smooth muscle tumour/leiomyoma was revealed.
Conclusion: Despite the intravascular location the prognosis in most cases is good. Generally, 70% of patients can be cured by hysterectomy and excision of any extrauterine tumour is technically feasible; 30% have recurrence of the disease. In a small percentage of patients, the disease may be fatal because of extension into the hepatic veins, the heart and even the lung. According to these, a careful pathology examination and a regular follow-up are recommended.

049

A rare case of uterine tumor resembling ovarian sex cord tumor

S. Mavropoulou *, Z. Tatsiou, I. Amplianitis, N. Bontis
*Xanthi General Hospital, Dept. of Pathology, Greece

Objective: Uterine tumors resembling ovarian sex cord tumors (UTROSCTs) are extremely rare tumors which were first described by Clement and Scully in 1976.
Method: We report the case of a 70-year-old woman who presented with postmenopausal bleeding. On examination she was found to have a polypoid tumor protruding from cervix. Tumor removal and diagnostic curettage were performed.
Results: Histological examination revealed an atrophic endometrial polyp with four well-circumscribed nodules, consisting of endometrial stroma and epithelial-like structures with cells growing in cords, nests, or form tubules, cuboidal to columnar with scanty amphophilic or pale cytoplasm. No significant cellular atypia or mitotic activity was noted. Immunohistochemistry was positive for CD10 and inhibin, and negative for smooth muscle actin, desmin and epithelial membrane antigen. Accordingly, the diagnosis of UTROSCT type I was made. The patient is in regular follow-up without any further treatment and 15 months later has no signs of recurrence.
Conclusion: In conclusion we report an extremely rare case of an UTROSCT type I, arising in an endometrial polyp. Although these neoplasms are considered as having an uncertain, but probably low likelihood of recurrence, in rare

cases metastasis occurred. Subsequently, a long term follow-up is mandatory to fully understand the behaviour of these unusual tumors.

050

Extranuclear steroid-initiated signaling by progestin and mifepristone: concentration-dependent inhibition of Ishikawa cell proliferation and induction of apoptosis

B. T. Moe *, A. Ørbo, G. Sager, A.B. Vereide
*University Hospital N-Norway, Dept. of Pathology, Tromsø, Norway

Objective: Previous studies suggest that at least 60% of patients with endometrial hyperplasia respond to progestin therapy. In the present study, Ishikawa cells (endometrial adenocarcinoma) were used to mimic the in vivo situation. A pharmacological analysis of the effects of progestins/antiprogestins to determine their sensitivity and their order of potency was conducted.
Method: Progesterone, levonorgestrel, medroxyprogesterone acetate and mifepristone were added to Ishikawa cell cultures. Cell cycle analysis, annexin V-FITC binding, DNA fragmentation and detection of mitochondrial transmembrane potential were performed with a flow cytometer equipped with an argon-ion laser (488 nm).
Results: Different progestins exhibited differing potencies for inhibition of cell growth: Levonorgestrel (IC50=3.9± 0.4 μM)>medroxyprogesterone acetate (IC50=30.4± 3.4 μM)>progesterone (IC50=60.3±6.2 μM). Surprisingly, the progesterone inhibitor, mifepristone (0.2–23 μM), did not antagonize the antiproliferative effect of progesterone but had a progesterone-mimicking effect with an IC50 value of 19.0±1.7 μM.
Conclusion: The pharmacological concentrations of both progestins/antiprogestins lead to cell cycle retardation and induction of apoptosis. In combination, mifepristone caused an additive effect rather than antagonizing the action of progesterone. The present results also suggest that progesterone and mifepristone, in high concentrations, interact with non-classical molecular targets and that the antiproliferative effect is conveyed by signals having an extranuclear initiation.

051

High prevalence of human papillomavirus genotypes 16, 31 and 58 in uterine cervical lesions of patients from Madrid (Spain)

E. Moro Rodriguez *, B. García Espinosa, E. Álvarez Fernández
*Universidad Rey Juan Carlos, Dept. of Histology and Anatomical Pathology, Madrid, Spain

Objective: Human papillomavirus (HPV) genotype distribution and co-infection occurrence were studied in uterine cervical specimens from Madrid (Spain).
Method: A total of 539 abnormal specimens were studied: 20 benign (B) specimens, 353 low-grade squamous intraepithelial lesions (LSIL), 159 high-grade squamous intraepithelial lesions (HSIL) and 7 invasive cervical carcinomas (ICC). HPV genotyping was performed using PCR and tube array hybridization.
Results: We detected 31 different HPV types: 15 carcinogenic high-risk, 3 probably carcinogenic high-risk, 11 carcinogenic low-risk and 3 indeterminate carcinogenic risk. The most frequent HPV genotypes found in all specimens were HPV16 (25.2%), 31 (10.32%) and 58 (7.77%). HPV 18 was only detected in 4.82% of total specimens. Co-infections were found in 0% of B, 31.72% of LSIL, 19.49% of in HSIL and 0% of ICC. The highest percentage of HR/PHR HPVs was found in those specimens with HSIL (91.96%).
Conclusion: The high prevalence of HPVs 31 and 58 and the low prevalence of HPV18 suggest the limited effectiveness of HPV vaccination in Madrid. These results reinforce the necessity of epidemiological studies to know the HPV type prevalence in each geographic area and regional variation in the distribution of certain HPV types, and this should be taken into account in the future production of vaccines.

052

Evaluation of pathologic findings in patients with endometriosis and adenomyosis compared with clinical and sonographic findings in Javahery Hospital from September 2005 to September 2010

R. Mozaffari Kermani *, S. Eslampour
*Javaheri Hospital, Dept. of Pathology, Tehran, Iran

Objective: Endometriosis and adenomyosis are two main gynecological disorders leading to abdominal pain, dysfunctional uterine bleeding, and infertility. The pathological findings are differed according to the age and hormonal status of patients. This study was conducted to evaluate the pathological and clinical and also the sonographic characteristics of patients with endometriosis and adenomyosis and their association.
Method: In this cross-sectional descriptive–analytical study, the clinical data of 155 in-patients who suffered from endometriosis and adenomyosis in Javahery hospital in Tehran were analyzed with respect to the pathological, sonographic, and clinical characteristics of patients.
Results: The most cervical findings included nonspecific and cystic chronic cervicitis that was seen in 30.5% and 21.2%, respectively. The leading four types of endometrial findings were autolyzed endometrium (18.1%), endometrium in proliferative phase (16.7%), atrophic endometrium

([10.6%), and disordered proliferative endometrium (7.4%). The leading types of myometrial findings were intramural leiomyomas (32.1%), concommitant intramural and submucosal leiomyoma (20.6%]), and adenomyosis (17.8%). The most ovarian findings were simple follicular cyst (44%). The most clinical findings in patients were dysfunctional uterine bleeding (57.2%) and abdominal pain (38.5%). There was a statistically significant association between the clinical symptoms and the pathological findings of endometrium, myometrium, cervix, and ovaries ($P>0.05$). Also, there was a statistically significant association between sonographic and pathological findings of endometrium, myometrium, cervix, and ovaries ($P>0.05$).

Conclusion: We should strengthen the screening program of endometriosis and adenomyosis according to clinical findings, and pay more attention to prevention and control of other gynecological reproductive organ lesions at the same time.

053

Granulocytic sarcoma of the uterine cervix: a case report

M. Mrcela *, M. Pajtler, M. Milojkovic
*University Hospital Osijek, Dept. of Pathology, Croatia

Objective: Granulocytic sarcoma (GS) is an unusual manifestation of acute myeloid leukemia (AML). Localized granulocytic sarcoma of the uterine cervix as a primary manifestation, preceding peripheral blood and bone marrow evidences of acute myeloic leukemia is very rare. Diagnosis of localized GS is difficult and is often confused with other neoplastic conditions.

Method: We report a case of GS of the uterine cervix in a 46-year-old woman. Involvement of the cervix was the first manifestation of AML. The patient underwent colposcopy which was suspicious for malignancy. Colposcopically directed biopsy and cervical smear were taken.

Results: Cervical cytology smear stained with Papanicolaou stain contained numerous clusters of malignant cells that had monotonous appearance, with ovoid nuclei with coarse chromatin pattern and scanty cytoplasm. Cervical biopsy demonstrated diffuse infiltration of cervical tissue with uniform undifferentiated blastic tumor cells that were immunohistochemically stained positive for LCA, CD68, CD43, MPO, lysozyme and partly for CD117 but were negative for CD20, CD3, CD4, CD7, CD8, CD45RO, CD 56, CD34, that was consistant with granulocytic sarcoma. Soon after the diagnosis, the disease progressed to AML and despite of aggressive chemotherapy the patient died 6 months later.

Conclusion: Granulocytic sarcoma of the cervix in its localized form is a rare entity. Awareness of this entity, supported with immunohistochemical findings, leads to correct diagnosis but the poor prognosis still remains.

054

Number of lymph nodes in endometrial cancer staging: what is the reality?

B. Muezzinoglu *, A. Corakci
*Kocaeli University, Dept. of Pathology, Turkey

Objective: The impact of lymphadenectomy on the prognosis of endometrioid carcinoma (ECa) has been demonstrated. However, there is no consensus with regard to the adequacy of lymph node (LN) number. Various studies and protocols require different number of lymph node (15–35) for defining adequacy.

Method: In this study, we aimed to see the number of LN obtained in surgical staging material in a single institute performed by two surgeons in 5 years. We retrospectively rewieved the pathology report of 119 consecutive ECa surgically staged at our instution from 1/1/2006 to 31/12/2010. The surgeons were two gynecologic oncologists with multiple years of experience.

Results: The diagnoses include 101 Type I ECa, 18 Type II ECa. The total number of pelvic LN per patient ranged from 0 to 32 (median 14.77). Although left pelvic LN (median 7.95) were more than right LN (median 7.02), the difference was insignificant ($p=0.071$). The number of paraaortic LN ranged from 0 to 11 (mean 3.68).

Conclusion: Greater than 30% of patients in this study had >20 LN resected. The majority of cases that had lower number of LN were obese type I ECa. Surgical management of uterine cancer needs to be standardized and extensive LN dissection should be performed when clinically feasible.

055

What is the pathologic characteristics of endometrial cancer in women 70 years of age and older?

B. Muezzinoglu *, S. Corak, A. Corakci
*Kocaeli University, Dept. of Pathology, Turkey

Objective: Endometrioid carcinoma (EC) is the most common gynecologic cancer. The incidence of different types of EC is known to increase with age.

Method: We aimed in this study to analyze the histopathologic characteristics of EC in elder patients. All cases of EC diagnosed at our center between January 2006 and December 2010 were retrieved and the information from the pathology reports at the time of surgery was recorded.

Results: There were 177 cases of EC which have undergone surgery in this period. Thirty-seven cases (2.9%) were >70 at the time of surgery, age range 71–88, mean 76.2. There were 28 type I (24.3%) and 9 type II tumors (75.7%) in elder patients. The rate was 12.1% and 87.9% in patients younger than 70 years. Histologic grade was slightly higher in elder patients (p=0.667). In terms of clinical stage the elder patients had significantly more agressive tumor than the younger patients (p=0.017).
Conclusion: EC >70 years is not uncommon. One fourth of old age EC were type II. There was no significant difference in histologic type and grade of tumors when old age group is concerned. Hovever, the EC in >70 years of age group had higher clinical stage than in patients of younger age group.

056

Does image compression significantly influence the quantitative angiogenesis analysis of ovarian neoplasms?

J. Nicolosi *, A. Yoshida, L. Sarian, C. Silva, L. Andrade, S. Derchain, J. Vassallo, A. Schenka
*State University of Campinas, Dept. of Anathomic Pathology, Poços de Caldas, Brazil

Objective: Our main goal was to investigate the impact of digital image format/compression on manual and semiautomatic quantification of angiogenesis in ovarian epithelial neoplasms.
Method: There were 405 digital images obtained from ovarian tumours which were equally divided into five groups: images captured in TIFF, low compression and high compression JPEG formats, as well as low and high compression JPEG images converted from the TIFF files. Microvessel density (MVD) counts and CD34+ endothelial areas manually and semiautomatically determined from TIFF images were compared to those from the other four groups.
Results: Mostly, the correlations between TIFF and JPEG images were very high (intraclass correlation coefficients greater than 0.8), specially for low compression JPEG images obtained by capture, regardless of the variable considered. The only exception consisted in the use of high compression JPEG files for semiautomatic MVD counts, which resulted in intraclass correlation coefficients of lesser than 0.7. Nonetheless, even then, interconversion between TIFF and JPEG values could be successfully achieved using prediction models established by linear regression.
Conclusion: Image compression does not seem to significantly compromise the accuracy of angiogenesis quantitation in ovarian epithelial tumors, although low compression JPEG images should always be preferred over high compression ones.

057

Leiomyomatosis peritonealis disseminata in preeclamptic pregnant women

E.E. Pala *, G.H. Pala, U. Bayol, F. S. Pehlivan
*Tepecik Training and Research Center, Dept. of Pathology, Izmir, Turkey

Objective: Leiomyomatosis peritonealis disseminata (LPD) is characterized by multiple peritoneal nodules of varying sizes on the omentum and peritoneal surfaces, grossly mimicking disseminated carcinoma, lymphoma, tuberculosis and desmoid tumors. The lesion usually occurs in women of childbearing age. The possible causes could be divided into hormonal, subperitoneal mesenchymal stem cells, metaplasia, genetic or iatrogenic.
Method: We describe a 25-year-old preeclamptic pregnant woman. She was urgently taken to the cesarean section. Multiple nodules were seen on the surface of the omentum and peritoneum, especially the pelvic, uterine, salpinx, and bladder. Partial omentectomy was done.
Results: Histopathological examination revealed small nodules consisting whorls of desidualized spindle cells. Immunohistochemical study also supports the diagnosis.
Conclusion: The clinical course of LPD is asymptomatic. The disease is usually detected unexpectedly at the time of a cesarean section or laparotomy. So this entity should be considered in the differential diagnosis of multiple peritoneal nodules especially in women of reproductive age.

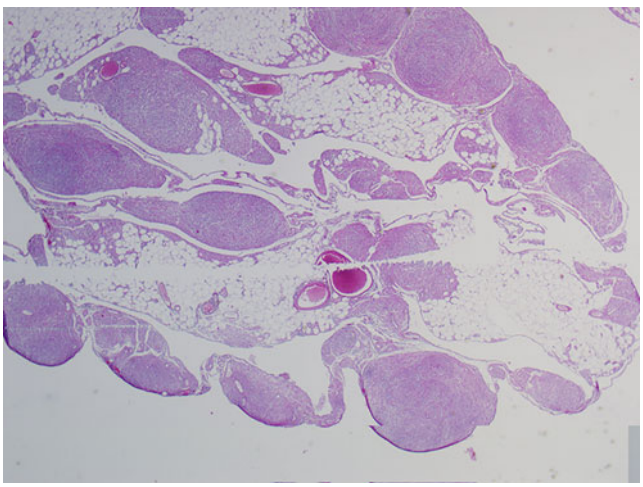

058

Study utility measurement of cancer indicators in dedection of malignancy in women after menopause

S. Patiakas *, K. Rousos, M. Tsigaridaki, S. Sarafidis, M. Palaiologou, C. Charalampous

*General Hospital of Kastoria, Microbiological Laboratory, Greece

Objective: This study aims to evaluate the predictive value of tumor markers in detecting situations of gynecological malignancy in women after menopause.

Method: We studied 106 cases of healthy women (aged 52 to 83 years), without any evidence of malignancy postmenopausal, regarding the tumor markers AFP, CEA, Ca-125, Ca 19-9 and Ca 15-3.

Results: Increased value of CEA showed 24 patients (24.5%), of whom 20 (28.6%) were>65 years and 4 (11.1%) <65. Increased price AFP showed 8 patients (7.5%), all>65 years. Also, increased value Ca-125 showed 16 patients (17%) of whom 12 (rate 17.1%) were>65 years and 4 (11.1%) <65. Finally, an increase of Ca 15-3 in the index occurred in 24 women (22.6%), of which 22 (31.4%) were>65 years and 2 (11.1%) <65, while a high price Ca 19-9 was recorded in 14 women (13.2%) which was also all>65 years.

Conclusion: It turns out therefore that the usefulness of measurement of tumor markers in cases of postmenopausal women is small, since the sensitivity is considerably limited. Indeed, it appears that the false rise in prices of tumor markers, mainly the index CEA, followed index Ca 15-3, related breast cancer, and the ratio Ca-125 related cancer ovarian most frequent forms of gynecological cancers.

059

Loss of E-cadherin and β-catenin may indicate EMT (epithelial–mesenchymal transition) in cervical lesions: correlation with p16 INK4a and high risk HPV expression

P. Ravazoula *, G. Michail, D. Koumoundourou, M. Gembersi

*University Hospital of Patras, Dept. of Pathology, Greece

Objective: Transcriptional silencing is the predominant mechanism of p16INK4a and E- cadherin gene inactivation in malignant epithelial lesions. B-catenin is connected with E-cadherin and alteration of Cadherin-catenin complexes has a major role in EMT. HPV virus is involved in cervical lesions. The purpose of our study was the assessment of E-Cadherin and B-catenin in cervical lesions and the investigation of their correlation with each other, with p16INK4a and HPV expression.

Method: There were 60 specimens of cervical lesions used (8 CIN I, 13 CIN II, 26 CIN III, and 13 invasive carcinomas. The expression of all molecules was studied by immunohistochemistry using anti-E-cadherin, anti-β-catenin, anti- p16 and anti-HPVantibody (against proteins of HPV types 1, 6, 11, 16, 18 and 31). The statistical analysis was implemented using SPSS13 for windows.

Results: The expression of β-catenin was strongly correlated with E-cadherin's immunostaining ($p=0.027$). Correlation between HPV immunolabeling and positive β-catenin immunostaining approached borderline ($p=0.065$). A significant correlation emerged between β-catenin and HPV expression in invasive carcinomas, while a reverse association was found between HPV and E-cadherin.

Conclusion: E-cadherin and β-catenin seem to correlate with HPV expression in cervical lesions though their exact role in tumor progression needs to be further elucidated.

060

Determination of the origin of complete hydatidiform moles by analysing polymorphic DNA regions

V. Repiska *, D. Bohmer, I. Shawkatova, V. Sisovsky, L. Danihel

*Comenius University Bratislava, Faculty of Medicine, Dept. Medical Biology, Slovakia

Objective: Choriocarcinoma is a rare, extremely malignant type of epithelial tumuor arising from the trophoblast. A complete hydatidiform mole is the most common precursor to choriocarcinoma. There are two types of complete moles: heterozygous and homozygous, while the heterozygous moles carry an increased predisposition to transformation to choriocarcinoma. Polymerase chain reaction (PCR) analysis of polymorphic DNA regions enables to distinguish the two forms thus providing a usefull tool in determining the relative risk of choriocarcinoma in patients with complete hydatidiform moles.

Method: Using PCR amplification and agarose gel electrophoresis the highly polymorphic DNA variable number tandem repeat (VNTR) regions (ApoB, Col2A, MCT118) and human leukocyte antigens (HLA) regions (DRB1 and DQB1) in trophoblast epithelial cells from a total of ten human biopsy tissue specimens with choriocarcinoma were analyzed.

Results: There were nine out of ten samples found to be of heterozygous origin; only one choriocarcinoma sample was of homozygous origin.

Conclusion: We have proved that both, VNTR and/or HLA analysis by the means of PCR amplification are precise and reliable procedures suitable for the differential diagnosis of complete hydatidiform moles. Both methods provided sufficient information to determine the genetic origin of

molar tissue; however, the VNTR method is more easy to perform and less expensive.

061

Clinical, colposcopic and pathological characteristics of cervical and vaginal high-grade lesions negative for HPV by Hybrid Capture 2

L. Rodriguez Carunchio *, M. del Pino, I. Alonso, P. Castillo, A. Torné, A. Rodriguez, J. Ordi
*Hospital Clínic Barcelona, Dept. of Pathology, Spain

Objective: Less than 5% of women with cervical high-grade squamous intraepithelial lesions (HG-SIL) show a negative Hybrid Capture 2 (HC2) result. We analyzed the HPV genotypes by PCR, and the clinical and pathological differential characteristics of these patients.
Method: There were 646 women with a histological diagnosis of HG-SIL and a simultaneous HC2 test identified. Patients with a negative HC2 result were selected. HPV was typed in the biopsy specimen in all by PCR, and p16INK4a immunostaining was performed. The clinical and pathological characteristics of these women were compared with a control group of HG-SIL with positive HC2 result.
Results: There were 20 women (3.1%) with HG-SIL who had a negative HC2. All biopsies were positive for p16INK4. PCR analysis detected HPV types included in HC2 test in 55% of the cases. False negative HC2 tests increased with age ($p=0.002$) and were more frequent in patients with non satisfactory colposcopy or small sized lesions ($p<0.001$).
Conclusion: A negative HC2 test is an infrequent event in women with HG-SIL. Common HPV types are identified in over half of the cases. Older women and patients with small lesions or non satisfactory colposcopy have a higher rate of HC2 negative results.

062

The tumor supressor gene designated PTEN and proliferation markers (KI-67, P53 AND PCNA) as evaluating elements for the malignancy potential in atypical endometrial hyperplasia

M. Sajin *, M. Costache
*University Hospital, Dept. of Pathology, Bucharest, Romania

Objective: Atypical endometrial hyperplasia (increase in gland/stroma ratio, disorder number and shape of the glands like modifications of the glandular epithelium: exhibits loss of nuclear polarity, stratification, etc) is a lesion associated with the uterine leiomyomas. The study was realized at the Universitary Emergency Hospital Bucharest, Romania on 681 endometrium biopsies taken in the period 2006–2010 from women with ages between 45 and 55.
Method: Hematoxylin–eosin-stained slides of endometrial formalin-fixed, paraffin-embedded tissue has emphasized in 171 cases the simple hyperplasia (SH), in 262 cases the complex hyperplasia (CH), in 68 cases the simple atypical hyperplasia (SAH) and in 190 cases the complex atypical hyperplasia (CAH). We performed the indirect tristadial ABC method of IHC for three antibodies: PTEN, Ki-67, P53 and PCNA on formalin-fixed embedded tissue taken by biopsies from 122 cases (22 SH, 13 CH, 87 SAH and CAH).
Results: PTEN was focal positive for SAH, diffuse for CAH and for some cases of SH and CH. Ki-67 and PCNA were also very frequent in group SAH and CAH.
Conclusion: PTEN, Ki-67, P53 and PCNA take part in the process of endometrial carcinogenesis following probably molecular pathways and determine the malignity potential of atypical hyperplasia of endometrium.

063

Angiomyofibroblastoma of the vulva

J. Salvatierra *, H. Fuentes Vaamonde, Y.O. Rangel Mendoza, M.T. Gonzalez Serrano, M.E. Sanchez Frias, M. d. Mar Moreno Rodriguez, M. Medina Perez
*Hospital Reina Sofia, Dept. de Anatomia Patologica, Cordoba, Spain

Objective: Angiomyofibroblastoma is a rare, benign mesenchymal neoplasm of the lower female genital tract of middle-age women. It is a well-circumscribed tumor characterized by alternating hypocellular and hypercellular areas with abundant thin-walled blood vessels.
Method: A 45-year-old woman had a right labia major mass and pain for several months without any other symptoms or signs.
Results: The resected specimen contained a subcutaneous solid and soft tumor of 6.5×5.5×5 cm, well-circumscribed, and non-encapsulated with a pinkish-gray cut-surface. It was microscopically characterized by numerous, thin-walled capillary-like vascular channels and plasmacytoid cells around blood vessels. No mitotic or atypical cells were seen. The stroma was edematous and mixoid. Immunohistochemistry results indicate that the tumor cells were

positive for estrogen and progesterone receptors and negative for cytokeratine, desmin, CD34, S-100 protein and actin.

Conclusion: It is important to recognize this entity because of its benign behaviour unlike other mesenchymal tumors of the vulva, which have an aggressive behaviour and in order to avoid any potential therapeutic implications.

064

Morphological evaluation of the endometrium in infertility

M. Samoylov *, V. Bessmertnaya, K. Serebrennikova, O. Mishnev
*Russian Academy of Sciences, Central Clinical Hospital, Moscow, Russia

Objective: Comprehensive morphological evaluation of the endometrium in infertility may open new ways to obtain implantation window adequacy and improve results of the assisted reproductive technologies (ART) treatment.

Method: Curettages and Pipelle biopsies mid-luteal phase endometrium from 92 women with infertility asked for ART treatment were obtained. Routine histological examination, scanning electron microscopy, immunohistochemical determination of estrogens (alpha and beta) and progesterone receptors, Ki67, P27, cyclin E expression were performed.

Results: Immunohistochemical parameters in groups with different infertility factor correlated with endometrial pathology spectrum: luteal phase defect, simple focal endometrial hyperplasia, endometrial polyps, chronic plasmacytic endometritis. Discordance of the steroid reception and proliferative processes in the presence of the normal serum hormones levels, peculiarities of the nuclear and cytoplasmic expression of P27 and cyclin E reflecting cell cycle activity—did not correspond to the normal window of implantation. Imperfection of the pinopodes development in infertility was also established.

Conclusion: Morphological and immunohistochemical description of endometrium is significant indicator for prosperous in vitro fertilization and embryo transfer. ART programs treatment results in our clinic confirm that endometrial immunohistochemical and ultrastructural characteristics should be taken into account. This makes it possible to personify the therapeutic approach as well as to improve the endometrial answer to the induction of ovulation.

065

Umbilical endometriosis: a case report

E. Sener *, R. Aktimur, F. Erdogan, S. Sipal
*Erzurum Bolge Egitim Hastanesi, Patoloji Bolumu, Turkey

Objective: Endometriosis is a condition in which endometrial stroma and glands are found outside of the uterine cavity. Although it is most commonly confined to the pelvis, it can present extra-pelvic sites like abdominal viscera, abdominal wall, extremities, lungs, and brain. The umbilicus is one of the less common sites for the localization of ectopic endometrium.

Method: A 41-year-old multigravida woman had a 4-month history of umbilical mass and cylic pain. She had no cyclic bleeding and she had no pelvic surgery. Physical examination revealed a 3×4-cm, tender, irreducible umbilical hernia with dark skin discoloration. Microscopic examination of the specimen revealed an admixture of benign endometrial glands and stroma consistent with endometriosis.

Results: Umbilical endometriosis may simulate an umbilical hernia on physical examination. Clinical diagnosis is difficult, and umbilical endometriosis can be easily confused with other conditions such as benign and malignant tumours.

066

Mullerian adenosarcoma of the uterus: a case report

E. Sener *, S. Sipal, B. Gundogdu, H. Balta
*Erzurum Bolge Egitim Hastanesi, Patoloji Bolumu, Turkey

Objective: Adenosarcoma is a rarely observed variant of mixed mesodermal tumour of the uterus, consisting of benign glandular elements and malignant stromal component.

Method: This is a case report of a 33-year-old woman who initially presented with abnormal vaginal bleeding and a mass protruding through the cervical canal of which was biopsied.

Results: Haematoxylen and eosin (H&E) stained slides were examined. Histologically, it had glandular and stromal elements. At low-power examination, the glands were widely seperated by the abundant stromal companent and the glands were lined by benign-appearing endometrioid cells that were columnar and pseudostratified. Most of the glands were cystic and some of the glands had leaf-like configuration. The stromal cells were strongly positive for estrogen receptor and exhibited a low Ki-67 proliferating index.

Conclusion: Adenosarcoma must be differentiated from other mullerian tumors, mainly carcinosarcoma and endometrial stromal sarcoma.

067

Progesterone receptor in normal endometrium and in I and II type of endometrial carcinoma

V. Sisovsky *, M. Palkovic, J. Porubsky, L. Danihel
*Comenius University Bratislava, Faculty of Medicine, Dept. of Pathology, Slovakia

Objective: Progesterone receptor (PR), 98 kDa protein, a member of the steroid receptor superfamily of transcription factors; together with progesterone plays a central coordinate role in regulating reproductive events associated with the establishment and maintenance of pregnancy (ovulation, uterine and mammary gland development), and neurobehavioral expression associated with sexual responsiveness.

Method: Archived formalin-fixed and paraffin-embedded human biopsy hysterectomy and curettage tissue specimens with normal proliferative endometrium (PE), endometrioid (EC) grade G1 and G3 and clear cell (CCC) subset of endometrial carcinoma were evaluated by immunohistochemistry, by light microscope semiquantitatively, for the PR expression in nuclei of endometrial epithelial cells.

Results: The PR expression was high in PE, but it was gradually going down with the grade of EC (type I—less aggressive). In CCC (type II—aggressive) the expression of PR was not found.

Conclusion: There is high expression of PR in PE. Malignant changes of endometrium are accompanied by a decrease in PR expression. EC (type I) express PR, whereas CCC (type II) is negative. The quantity of PR is indirectly proportioned to the grade of EC. PR evaluation by immunohistochemistry could be the relevant component usable in biomedical research as well as in clinical practice. Supported by the grant 2007/28-UK-05 MZ SR.

068

Pro-apoptotic B-cell lymphocytic leukemia/lymphoma oncoprotein 2-associated X protein expression changes in neoplastic endometrium

V. Sisovsky *, M. Palkovic, V. Repiska, L. Masak, M. Kopani, I. Hudecova, N. Gasparovicova, J. Porubsky, L. Danihel
*Comenius University Bratislava, Faculty of Medicine, Dept. of Pathology, Slovakia

Objective: B-cell lymphocytic leukemia/lymphoma oncoprotein 2 (BCL-2) -associated X protein (BAX) pro-apoptotic partner, 21 kDa, belongs to BCL-2 protein family. Protein BAX is in the outer mitochondrial membrane of cells also. Bax gene overexpression accelerates programmed cell death. The study evaluates a relationship between the morphological appearance of normal endometrium and of endometrial carcinoma (ECa), and the degree of Bax expression.

Method: A total of 42 archived formalin-fixed and paraffin-embedded human biopsy hysterectomy and curettage tissue specimens with normal proliferative endometrium (PE), endometrioid (EC) grade G1 and G3 and serous (SC) subset of ECa were evaluated by immunohistochemistry, by light microscope semiquantitatively, for the Bax expression (BAX) in cytoplasm of endometrial epithelial cells.

Results: The Bax expression (BAX) was low in PE, but it was gradually going up with the grade of EC (less aggressive phenotype). In SC (aggressive phenotype) the expression of Bax (BAX) was the highest.

Conclusion: Neoplastic endometrial changes are accompanied by an increase in Bax expression. The highest expression of Bax is related to the aggressive type of ECa. Evaluation of BAX by immunohistochemistry could be relevant component which may be useful in biomedical research as well as in clinical practice. Supported by the grant 2007/28-UK-05 MZ SR.

069

Ki-67, c-met, e-cadherin, beta-catenin expression in eutopic and ectopic endometrium in adenomyosis

M. Solomahina *, I. Voloschuk
*Sechenov First MSMU, Dept. of Anatomic Pathology, Moscow, Russia

Objective: The aim of the study was to investigate Ki-67, c-met, e-cadherin, beta-catenin expression in eutopic and ectopic endometrium in adenomyosis.

Method: The study was performed on excised uteri from 69 patients in proliferative phase: 51—with adenomyosis, 18—control group. IHC was made with Ki-67, c-met, e-cadherin, beta-catenin antibodies.

Results: Patients with adenomyosis showed higher ki-67 in eutopic than ectopic endometrium, c-met was higher in glandular epithelium than in stroma and e-cadherin and beta catenin expression was growing higher with the depth of ectopic foci.

Conclusion: Decreased ki-67 expression in ectopic than eutopic endometrium may be due to the fact that material was taken in proliferative phase. C-met increase may indicate epithelial migration, triggering basal endometrium

invasion in myometrium. E-cadherin and beta-catenin expression show stability of cell adhesion in adenomyotic foci and indicates similarity of ectopic and basal layer endometrium.

070

DNA mismatch repair proteins immunohistochemistry in young women with endometrial cancer

M. Sotiropoulou *, P. Markoulis, E. Minaidou, V. Pavlou, Z. Voulgaris
*Alexandra Hospital, Dept. of Histopathology, Athens, Greece

Objective: The endometrium is the commonest site of extraintestinal malignancy in Lynch Syndrome. Endometrial carcinoma in young women is rare. Aim of this study was the estimation of related to DNA Mismatch Repair (DNA-MMR) proteins in women younger than 40 years with endometrial carcinoma.

Method: Immunohistochemistry was performed using MLH1, MSH2 and MSH6 in tissue of 31 endometrial cancers in patients ≤40 years. All slides reviewed for histological parameters (type, grade).

Results: The patients' age was 27-40 years (mean age 36). Endometrial carcinomas were predominantly endometrioid type (29/31) and most low grade (Figo grade I-II, 69%), one clear cell and one undifferentiated. A significant number of patients had synchronous ovarian carcinoma (5/31, 16%). Loss of expression of at least one protein showed 16/31 cases (48.4%) and most common MLH1 and MSH2 (38.7% and 35.4%, respectively). The loss of MSH6 expression in two cases (6.5%) coexisted with MSH2 loss.

Conclusion: Most endometrial carcinomas in young women are of endometrioid histology, well to moderately differentiated. A significant proportion of these tumors showed loss of DNA-MMR by immunohistochemistry. In young patients with endometrial cancer immunohistochemistry can select patients to refer for genotyping analysis.

071

Non-tumoral placental lesions: statistical study 2008–2010 at the University Emergency Hospital Bucharest

M. V. Stanculescu *, M. Sajin, G. Bruma
*Bucharest, Romania

Objective: The non-tumoral placental lesions can be separated into inflammatory, vascular and development disorders of the membranes, umbilical cord and placenta. All of them may have severe effects on the fetus, especially neurologic disability. The aim for this comunication is to report a clinical-morphological study effectuated on a retrospective lot of 474 cases of term placentas analysed in 2008–2010 at the University Emergency Hospital Bucharest.

Method: After the macroscopic examination, the fragments from placenta, umbilical cord and membranes were fixed in 10% formaldehyde solution, paraffin-embedded, cut and stained with hematoxiylin–eosin and Van Gieson.

Results: In our study, from all 474 of term placentas, we found chorioamnionitis 115 cases (acute 36, chronic 79), at the umbilical cord: funisitis 7 cases, vascular lesions 13 cases, hematomas 4 cases, thrombotic vessels 115 cases and at the placenta: villitis 16 cases (acute 12, chronic 4), infarct 91 cases (recent 79, old 12), hematomas 162 cases, placenta previa 4 cases, accreta 8 cases and increta 4 cases. The patients were between 17 and 40 years old.

Conclusion: Placental lesions require an important attention from both clinician and pathologist. Their identification may predict recurrence risk or suggest options for prevention or therapy.

072

Human papillomavirus infections in a Romanian ambulatory gynecological ward

C. Stefanescu *, C. Voinea, P. I. Calistru
*CDT, Dept. of Gynecology, Bucharest, Romania

Objective: Human papillomavirus (HPV) high-risk (HR) types are the causal factor for premalignant dysplasia and cervical cancer. Taking into account the heterogeneity of HPV types across and within populations this study aims to assess the HPV frequency in Romanian women.

Method: We identified 21 different types of HR HPV, from 117 women at the Medical Centre in Bucharest, aged 16-59, included into a retrospective 22-month study, positive for the virus analyzed by LINEAR ARRAY HPV® assay.

Results: These women were infected by a single or multiple HPV types. HR types were found in 85.5% of women and the ten most frequent genotypes in order of decreasing frequency were 16, 53, 18, 52, 31, 73, 58, 66, 33, 45. Differences in frequency of HR HPV types were found for presence of cervical lesions in our study: HR-types 53 in ASCUS and L-SIL; HR-types 16, 18 in H-SIL, ASCH. Differences in frequency were found also for different HPV species and women age.

Conclusion: Compared with studies from other countries, our data indicated differences in frequency of HR-HPV type infection, an association of HR-types HPV 16, 18, 53, 31, 33, 51, 52, 58, 66 and cervical lesions, and a trend for distinct distribution of HPV types by age.

073

Primary signet ring cell adenocarcinoma of the cervix developing from intestinal-type adenocarcinoma with a positive response to irradiation

S. Stolnicu *, K. Szabo, D. Chifu, R. Nicolau, F. F. Nogales
*University of Medicine, Dept. of Pathology, Targu Mures, Romania

Objective: Signet ring cell adenocarcinoma of the cervix is usually of metastatic origin. However, in rare cases, it can develop as a primary, with only 12 cases reported to date.
Method: We present the case of a 41-year-old patient diagnosed 3 years before on a cervical biopsy of a mixed CIN III and in situ adenocarcinoma of the cervix intestinal type that was excised by a cone biopsy.
Results: Cytologic follow-up for a period of 3 years revealed no abnormal cells. She eventually presented with a polypoid mass protruding through the external cervical os. The biopsy showed a solid proliferation of characteristic signet ring cells that were positivity for CK 7, CEA, p16, focally for CK 20, negative for CA125, Vimentin, ER, PR (supporting a cervical immunophenotype). The patient underwent radiotherapy followed by surgery. A remaining 35-mm tumor was located in the cervical wall and had a polypoid appearance. Microscopically, dissecting pools of mucin devoid of tumor cells were seen infiltrating the cervical wall.
Conclusion: This is the first documented case demonstrating a precursor lesion of intestinal type adenocarcinoma for a primary signet ring carcinoma of the cervix. This case also demonstrates the positive actinic response in this adenocarcinoma of intestinal type.

074

Primary high-grade serous carcinoma of the fallopian tube with a mixed microcystic and signet-ring cell morphology

S. Stolnicu *, L. Bejan, D. Radulescu, F. F. Nogales
*University of Medicine, Dept. of Pathology, Targu Mures, Romania

Objective: Serous carcinoma with mixed microcystic pattern and signet-ring cells (*Int J Gynecol Pathol*, 2001; 20:323) is very unusual in the ovary. To date, only 12 cases of this type of primary serous ovarian carcinoma have been published, but this is the first case with an origin in the tubal fimbriae.
Method: A 72-year-old woman, without a known family history of ovarian or breast cancer, presented left adnexal tumor and ascites. Laparatomy revealed multiple metastases involving the omentum, pelvic peritoneum, left pelvic lymph nodes, gall bladder and large bowel serosa.
Results: Left fallopian tube fimbriae contained a 10-mm tumor with predominant microcystic growth pattern with many in situ foci. Some of these cells were of signet ring appearance with intracytoplasmic mucin. Other areas, especially in the metastases, were of papillary type with psammoma bodies and high nuclear grade. The tumor cells were positive for CA125, CK7, WT1, p53, ER/PR but proved negative for CK20, CDX2, GCDFP-15 and mammaglobin.
Conclusion: These aspects revealed an exceedingly rare example of a mullerian high grade serous carcinoma of the fallopian tube exhibiting an unusual pattern, suggestive of metastasis. Immunohistochemistry and morphology supported the finding of a precursor intraepithelial lesion in the fimbriae and excluded gastrointestinal and breast primaries.

075

Pre-screening and pre-vaccination prevalence of cervical abnormal smears in Romania

K. E. Szabo *
*Emergency County Hospital, Dept. of Pathology, Targu Mures, Romania

The aim of this study was to evaluate the prevalence of different types of cervical cytological abnormalities for a period of 4 years (2006–2009) before the initiation of a national screening and a vaccination programme in Romania. A total of 10,248 patients coming from ten private medical centers from different geographical regions of Romania have been included in the study and the smears sampled and stained using Papanicolau method have been classified according to the Bethesda system. The prevalence of cervical abnormalities was 8.47% and the prevalence of type ASC-US, ASC-H, LSIL, HSIL, AGC, SCC lesions, in situ adenocarcinoma and invasive adenocarcinoma

represented 2.84%, 4.86%, 0.32%, 1.08%, 0.06%, 0.02%, 0.03% and 0%. ASC lesions represented 709 (6.91%) of the total number of abnormal cytology examinations. The prevalence of abnormal smears is increased in Romania, similar to other European countries, which indicates the necessity of starting a national and regional screening programme. The purpose of centralization and release of data regarding the precursor lesions is to compare them with the ones of other European countries in order to generate new European policies of public health.

076

An unusual lesion of the clitoris: benign granular cell tumor

S. Taban *, A. Dema, M. Cornianu, E. Lazar, R. Cornea
*University of Medicine, Dept. of Pathology, Timisoara, Romania

Objective: Granular cell tumor involving the clitoris is extremely rare and only a few cases are reported in the literature. We present the case of a young patient with a nodular tumor of the clitoris.
Method: The 35-year-old patient presented with a slow-enlarging mass of the clitoris. The tumor was subcutaneous and nodular (2.3 cm on average). Multiple histological sections were stained for HE and immunohistochemically for S100 protein, vimentin, CD68, smooth muscle actin and desmin.
Results: The tumor cells exhibit an infiltrative pattern of grow, intense granular cytoplasm, small hypercromatic nuclei and less than two mitoses per 10 high power fields. The cytoplasmic granules were periodic acid schiff (PAS) positive. Immunohistochemical staining revealed a strong cytoplasmic expression of S100 and CD68, suggesting a diagnosis of granular cell tumor. The patient had no recurrence at 6 months' follow-up.
Conclusion: The granular cell tumor of the clitoris should be considered in the differential diagnosis of clitoral masses.

077

Transitional cell carcinoma of the ovary: a case report

O. Tzaida *, C. Valavanis, G. Giannakopoulos-Stanc, O. Ignatova, G. Vecchini, P. Arapantoni-Dadioti
*Metaxa Cancer Hospital, Dept. of Pathology, Piraeus, Greece

Objective: Transitional cell tumors of the ovary, characterized by transitional (urothelial-type) epithelial component, are uncommon neoplasms, among which the transitional cell carcinoma (TCC) is a challenging rarity. A case of advanced stage ovarian TCC with emphasis in the diagnostic dilemmas and a brief literature review is presented.
Method: A 63-year-old, heavily smoking woman presented with abdominal symptoms (pain, swelling) persisting for the last 3 months. Pelvic ECHO/CT demonstrated bilateral tumor masses measuring 5 and 4 cm, respectively, accompanied by ascites, secondary intestinal and omentum localizations and suspicious liver metastasis without urinary bladder involvement. Despite the combined multi-drug administration, the patient died 4 months after the diagnosis.
Results: All the tumors were composed of malignant high-grade transitional type nests and multilayered papillae resembling malignant urothelial neoplasm with minor elements of common serous carcinoma, foci of necrosis and stromal invasion. An obvious benign or borderline Brenner tumor element was not apparent. In the differential diagnosis metastatic urothelial, undifferentiated and serous ovarian CA was included. Immunohistochemical analysis confirmed the primary ovarian origin revealing CKAE1-AE3, CK7, CA-125, WT1, EMA, p53 positive reaction, while CK20, uroplakin-3, p63, and EGFR were negative.

078

Immunohistochemical profile and DNA ploidy of endometrial carcinoma

Z. Vernerova *, P. Libalova, D. Pintérova, K. Tikovsky, B. Svoboda
*3rd Faculty of Medicine, Dept. of Pathology, Praque, Czech Republic

Objective: Two different clinicopathological subtypes are recognised in endometrial carcinoma (ECA) the oestrogen-related (type I, endometrioid) and the non-oestrogen related (type II, non-endometrioid). To determine better the group of high-risk patients many alternative factors are tested as prognostic indicators.
Method: There were 79 ECA studied. DNA ploidy was evaluated from preoperative biopsy and postoperative specimens. Paraffin sections were used for immunohistochemistry.
Results: The average age at diagnosis was 66 years; 16% (12) of them had non-endometroid carcinoma (serous, clear cell, etc.); there were 21% of grade 1, 41% of grade

2, and 37% of grade 3 tumors. The proportion of DNA aneuploid tumors was 17% (13/79). There was a concordance 96% in evaluation of DNA ploidy from preoperative vs. postoperative samples and the same result, 96%, was obtained for comparison of fresh/frozen vs. paraffin-embedded tissue samples in our series. Non-endometroid carcinomas showed significantly higher p53 expression, whereas both ER and PR including E-cadherin and β-catenin were more often positive in endomerioid tumors.
Conclusion: Our results indicate that the differences in immunohistochemical profiles of ECA when correlate with DNA ploidy and histological grade could help in predicting biologic behavior and planning treatment in these patients.
Supported by Ministry of Health of Czech Republic (project IGAMZCR NS9975-4/2008).

079

In situ PCR detection of HPV16 and 18 in cervical carcinoma using an automated staining system

H. Wang *, S. Thakur, S. Mysore, S. Guddu, A.R. Poongothai, K.L. Kalra
*BioGenex Laboratories, Cell Pathology, Fremont, USA

Objective: Molecular examination of HPV DNA is the gold standard for detection of HPV. In this study, we demonstrated in situ PCR (ISP) detection of HPV16 and 18 using of fully automated staining system.
Method: A total of 30 cervical carcinoma samples were tested. Primers were designed to amplify the E6 region of HPV16 and 18. Fluorescein-labeled dUTPs were incorporated during PCR amplification, and subsequently amplicons were detected with anti-fluorescein antibody. HPV16 and 18 CISH were performed using oligo probes. A fully automated staining system Xmatrx® was used.
Results: The sensitivity of this detection was found to be as low as one to two copies of HPV16 using SiHa cell lines. All the 30 cervical carcinoma samples were detected positive for HPV16 and 18 by ISP, while 22/30 were found to be positive for HPV16, and 21/30 positive for HPV18 by CISH respectively. There was no HPV16 detected from breast, colon carcinoma and control cervical tissues.
Conclusion: ISP detection of HPV is found to be more sensitive compared to CISH. Fully automated ISP offers rapid and sensitive method for histological localization of HPV. This may be useful for the early screening of HPV infection in cervical scrapings and cervical intraepithelial neoplasia.

080

Validation of ProEx C as a biomarker for premalignant and malignant lesions of the cervix

H. Wang *, P. Terinate, Y. Gao, M. Wei, A.R. Poognothai, K. L. Kalra
*BioGenex Laboratories, Dept. of Cell Pathology, Fremont, USA

Objective: Cervical cancer is the second most common cancer among women worldwide. Many studies have confirmed a strong correlation between p16 over-expression and cervical cancer. A newer biomarker ProEx C has been implicated as a useful marker for cervical cancer.
Method: Total of 28 cases of cervical carcinoma samples were included. All tissue samples were examined for expression of ProEx C, p16 and Ki67. In addition, cervical ThinPrep samples were also tested. Fully automated Xmatrx™ system was used for the staining.
Results: Overexpression of ProEx C was found in all 28 cases of cervical carcinoma tissues. Upregulated expression of p16 was observed in all 28 cases. The p16 staining was limited within those cancerous cells. Simultaneous double staining for ProEx C/p16 demonstrated that over 90% of cancer cells co-expressed these two biomarkers. ProEx C and p16 double positive cells were also observed on ThinPrep slides from those cases with high grade and cervical cancer.
Conclusion: (1) ProEx C is a sensitive proliferation biomarker for the diagnosis of cancer. (2) Combination of ProEx C and p16 may increase the sensitivity and specificity in cervical cancer detection. (3) ProEx C and p16 double staining may be useful for cervical cytology.

081

Mesonephric adenocarcinoma of the uterine corpus: report of three cases

Y. Wani *, K. Notohara, M. Fujibayashi
*Kurashiki Central Hospital, Dept. of Pathology, Japan

Objective: Mesonephric adenocarcinoma (MA) is a rare tumor arising in the uterine cervix, often associated with mesonephric remnants or hyperplasia. MA of the corpus is vanishingly rare, and its presence is controversial, mainly attributable to the absence of mesonephric elements. We documents three corpus cases of MA.
Method: HE slides from three cases were reviewed and all cases were stained with CD10, calretinin, estrogen receptor

(ER), progesterone receptor (PR) and androgen receptor (AR).

Results: All patients were post-menopausal women (73, 79 and 59 years). The two tumors were identified at the further examination of multiple lung nodules and the rest were due to genital bleeding. The maximum sizes of the tumors were 10, 5.6 and 8 cm, respectively. All tumors were exclusively confined to the myometrium, focally exposed to the endometrium without exophytic mass or endometrial hyperplasia. Microscopically, all tumors contained coalescent small tubules with eosinophilic materials in the lumen. Vast majority of the tumor was the glandular elements with pseudostratified, hyperchromatic nuclei, which seemingly resembled with endometrioid or serous adenocarcinoma. No mesonephric remnants or hyperplasia identified. The immunohistochemical results showed CD10;3/3, Calretinin;2/3, ER;0/3, PR;0/3, AR;1/3.

Conclusion: MA of uterine corpus showed the morphological and immunohistochemical resemblance to the cervical counterparts except the absence of the mesonephric remnants or hyperplasia.

082

Screening for NLRP7 mutations in Tunisian patients with recurrent and sporadic hydatidiform moles

M. T. Yacoubi *, H. Landolsi, C. Rittore, M. Gribaa, S. Hmissa, I. Touitou

*University Hospital Sousse, Dept. of Cyto-Histopathology, Tunisia

Objective: Hydatidiform mole (HM) is commonly non-recurrent. Familial recurrent hydatidiform moles (FRHM) are a rare recessive condition associated with homozygous mutations in human NLRP7 gene. Our objective was to look for the presence of NLRP7 mutation in women with recurrent (RHM) and non-recurrent HM.

Method: NLRP7 mutations were screened by direct DNA sequencing of all exons of NLRP7 gene in: one family with FRHM, one patient with sporadic RHM and 38 patients with sporadic HM.

Results: For the family with RHM, we found a homozygous stop codon, c.1708 G>T (p.E570X), in two symptomatic sisters and in a third sister who presented with a spontaneous non-molar abortion. No mutation was found in the sporadic case of RHM. In the sporadic cases of HM, five patients were heterozygous for four missense mutations: two novel mutations, c.544 G>A (p.Val182Met) in one patient and c.1480 G>A (p.Asp494Thr) in two patients and two already reported mutations, c.1532A>G (p.Lys511Arg) and c.2156 C>T (p.Ala719Val). These variants were lacking in 170 unrelated controls.

Conclusion: As homozygous NLRP7 mutations are thought to be associated with a failure status as the occurrence of recurrent HM, the heterozygous state could be a risk factor for non recurrent mole.

083

A rare case of microfollicular thyroid carcinoma arising in struma ovarii (SO)

M. T. Yacoubi *, N. Beizig, S. Ben Abdelkrim, N. Labaied, S. Hmissa, W. Stita, L. Jaidene, M. Mokni

*University Hospital Sousse, Dept. of Cyto-Histopathology, Tunisia

Objective: Struma ovarii (SO) is a monodermal teratoma in which thyroid tissue is the predominant component. It is usually unilateral. The malignant transformation counts about 0, 1 to 0, 3% of all ovarian teratoma, consisting of a papillary carcinoma, but rarely a follicular carcinoma is seen.

Method: A 54-year-old female presented with pelvic and abdominal pain, fever and vomiting. Physical examination revealed a mobile abdominopelvic mass. The ultrasonography showed a right adnexal mass measuring 14 cm with solid and cystic components. A total abdominal hysterectomy with bilateral adnexectomy and an appendicectomy was performed. Gross examination showed a right ovary entirely occupied by a well-defined multinodular mass measuring 16×11×8.5 cm. The cut surface showed multiple cavities filled by a visquous yellow fluid associated with solid whitish areas. Microscopically, the right ovary was completely replaced by an infiltrative malignant neoplasm, composed by microfollicles filled by colloid. The follicular lining cells had typical vesicular nuclei.

Results: This tumor was classified as a follicular carcinoma arising in a SO, staged Ia according to FIGO.

Conclusion: Due to the paucity of cases published, it is difficult to predict the natural progression of this disease, its management and the long-term prognosis.

084

Müllerian adenosarcoma with sarcomatous overgrowth of the ovary: case report and review of the literature

O. Yapicier *, F. Gucer, S. S. Ramadan, G. L. Keeney

*Anadolu Medical Center, Dept. of Pathology, Kocaeli, Turkey

Objective: Müllerian adenosarcoma is a rare neoplasm that can arise in both uterine and extrauterine locations. We report a patient presented with right ovarian tumor diagnosed as Müllerian adenosarcoma with sarcomatous overgrowth.
Method: A 50-year-old female patient was presented with abdominal pain and right sided ovarian mass to our Gynaecology Department. After frozen section examination, she underwent comprehensive surgical staging without residual tumor in the abdomen.
Results: Macroscopically the tumor is yellow in color, lobulated, has some necrotic areas and minor component of papillary structures. Microscopic examination shows a tumor composed of glandular and stromal elements. The glandular component has the appearance of endometrioid glands. These glands are somewhat dilated and in areas resembling the glands seen in phylloides tumor of the breast. High-power magnification shows mild cytologic atypia and occasional mitotic figures. There are areas where the stromal component is increased with no interspaced glands. The stroma in these foci demonstrates marked cytologic atypia. After surgery, the patient received six cycles of platin-based chemotherapy including cisplatin and adriamycin. After 4 years of follow up, the patient is disease-free.
Conclusion: Ovarian adenosarcomas have a worse prognosis than uterine adenosarcomas presumably because of the greater ease of peritoneal spread. However, complete surgical resection followed by platin-based chemotherapy seems to be of clinical significance.

085

Clinicopathological significance of BCL-2 and BAX proteins expression in primary ovarian carcinomas

S. Yigit *, L. Demir, F. Kusku Cabuk, O. Tarhan, H. Ellidokuz, Ç. Erten, I. Somali
*Dept. of Pathology, Izmir, Turkey

Objective: Background/aim: Recent studies have focused on the role of the genes regulating the balance between proliferation and apoptosis in primary ovarian carcinoma. Our aim was to detect the immunohistochemical expression of the the apoptosis-related proteins Bcl-2 and Bax.
Method: Immunohistochemical Bcl-2 and Bax expression results were re-evaluated in 83 primary ovarian carcinomas according to the staining intensity 1 to 3 and percentage staining cytoplasms 0 to 3. The results were charted with FIGO staging, prognosis and platinium sensitivity.
Results: The Bcl-2 and Bax protein expression was detected in 28.9% and in 69.8%, respectively. Neither Bcl-2 nor Bax alone was correlated to histological type and histological grade. Bcl-2 was significantly low in the advanced stages (FIGO III- IV) compared to the earlier stages (FIGO I-II), (p=0.005). Low Bcl-2/low Bax expression was statistically significant of shorter median overall survival compared to low Bcl-2/high Bax expression in advanced stage (29.6 months vs 48.7 months p=0.05). Therefore, the Bax expression was higher in platinium sensitive group (p=0.04).
Conclusion: The results support that the combined evaluation of Bax and Bcl-2 may provide additional prognostic prediction especially in stage III–IV patients.

086

The value of p16INK4a protein expression in cervical epithelium to assess the risk of cancer development

L. Zakhartseva *, K. Pekur, V. Kropelnytskyi, E. Manzhura, L. Pak
*Kyiv City Oncology Hospital, Dept. of Pathology, Ukraine

Objective: Early detection of cervical neoplasia with a high risk of cancer progression allow adequate treatment of patients and improve survival. Besides histological examination of lesion and HR-HPV-infection detection, one of the most important methods is an immunohistochemical evaluation of protein p16ink4a. P16ink4a protein expression may help in assessing the risk of developing cervical carcinoma.
Method: There were 41 patients aged 18–58 years who were treated at the Kiev City Oncology Center. Histological and immunohistochemical examination was performed on biopsy and cervical conization material. For immunohistochemical evaluation of protein p16INK4a test system CINtec ® Histology kit (mtm laboratories AG, Germany) was used, which is based on the mouse monoclonal antibody (clone E6H4) against the human protein p16INK4a, visualization system EnVision+(DAKO). All of the patients were observed dynamically.
Results: Of the 41 examined patients with cytological diagnosis of CIN, there were 31 identified cases with the expression of p16INK4a (75%). In eight cases (19.5%), there was a revealed expression in CIN1-2 and further progression to CIN3 was observed in two of them (25%). In 15 patients with expression of p16INK4a (48%), relapses were observerd. In four cases (12.9%), high-grade CGIN was developed. There were

four revealed cases of p16INK4a expression in HPV-negative patients.
Conclusion: P16INK4a protein expression is a reliable marker for risk assessment of invasive cervical carcinoma.

087
Intravenous leiomyoadenomyosis of the uterus: a case presentation

F. Zerenler *, G. Kir, M.S. Yilmaz, C.S. Topal, M.H. Karabulut
*Umraniye Education Research Hospital, Dept. of Pathology, Istanbul, Turkey

Objective: Leiomyomatosis has many histomorphologic variants. Our report describes a case of intravenous leiomyoadenomyosis of the uterus which we did not find any article about this variant in the English literature.
Results: The patient, a 46-year-old woman, has complaints of hypermenorrhea and dysmenorrhea for 5 years. Ultrasonography showed 105×70-mm-sized uterus with heterogeneous texture and there is a 32×26-mm-sized nodular image at corpus uteri. Total hysterectomy and left oophorectomy were performed. At gross examination, the myometrium was 4 cm in thickness and showed a 3.5-cm-diameter myomatous nodule with intravascular vermiculous components. Histologically, adenomyosis component was observed in the leiomyom and also in the intravenous leiomyomatosis components.
Conclusion: In this report, we presented a rare variant of intravenous leiomyomatosis with adenomyosis component which may be important for the histopathologic differential diagnosis.

088
Dermatofibrosarcoma protuberans of the pube–vulva

A. Zizi-Sermpetzoglou *, V. Savvaidou, S. Fournogerakis, E. Moustou, N. Tepelenis, N. Vlachakos
*Tzaneio General Hospital, Pireaus, Greece

Objective: Dermatofibrosarcoma protuberans (DFSP) is a rare cutaneous tumor of low/intermediate malignant potential. In rare cases, the female genital system is involved.
Method: A 66-year-old woman presented to our hospital complaining of long-standing painless nodules in the area of pube–vulva. On physical examination, there was a diffuse area of erythematous induration measuring 8×5 cm. Within this area, there are smaller nodules. The patient was offered vertical excision with the reconstruction of the area. On gross examination three nodules of various sizes were found located on the skin of the specimen. The nodules were hard in consistency with light brown color. Two more multilobutated nodules were found in the adipose tissue.
Results: The histological diagnosis showed a tumor. The neoplasm was composed of proliferative neoplastic spindle cells arranged in a storiform pattern. The immunohistochemical study showed diffuse and stronge positivity for CD34 and Vimentin, while SMA, CD117 and S100p. were negative. The final diagnosis was dermatofibrosarcoma protuberans.
Conclusion: DFSP of the pube-vulva is an uncommon low-grade malignancy involving the skin and subcutaneous adipose tissue. The treatment for DFSP has been wide local excision (WLE), but due to microscopic projections of the tumor, it leads to incomplete excision in 20-49% of the cases.

089
Angioleiomyoma of the uterus: a case report and review of the literature

A. Zizi-Sermpetzoglou *, E. Moustou, N. Tepelenis, J. Kaniaris, E. Arkoumani, V. Savvaidou
*Tzaneio General Hospital, Pireaus, Greece

Objective: Angioleiomyoma is an uncommon type of leiomyomas of the uterus that originates from smooth muscle cells and contains thick-walled vessels. Only a few cases of uterine angioleiomyomas have been reported.
Method: We present a case of a 45-year-old premenopausal woman who presented with a 5-month history of lower abdominal pain and abnormal uterine bleeding. On physical examination an enlarged, irregular uterus was found. Pelvic ultrasound disclosed uterine enlargement and multiple leiomyomas. A total hysterectomy and bilateral salpingo-oophorectomy was performed. On gross examination the uterus was lobulated. The cut surface showed many intramural and subserosal tumors. One of them with a great dimension of 6.5 cm was white-yellow in color and exhibited hemorrhage.
Results: On microscopic examination the tumor with a dimension of 6.5 cm was composed of interlacing smooth muscle bundles intermingled with abundant thick-walled vessels. The vascular and spindle cell component was immunoreactive with Vimentin and SMA. The final histopathologic diagnosis was angioleiomyoma. All the other tumors were leiomyomas.
Conclusion: Angioleiomyoma is a benign neoplasm. It develops usually between the fourth and sixth decade. Pain is the dominant clinical feature. It is a well-circumscribed neoplasm that contains at least foci of typical spindled smooth muscle cells. Surgical excision is the treatment of choice.

090

Immunohistochemical expression of matrix metalloproteinases MMP-2, MMP-9 and MMP-11 in epithelial ovarian tumors

V. Zolota *, E. Vlotinou, D. Koumoundourou, M. Melachrinou, C. Kalofonos
*University of Patras, Mecical School, Greece

Objective: Matrix metalloproteinases (MMPs) are enzymes implicated in the degradation and invasion of extracellular matrix and the acquisition of a malignant phenotype
Method: Tissue samples from 60 patients with ovarian epithelial (49 serous and 11 mucinous) neoplasms (45 infiltrating and 15 borderline) were explored by immunohistochemistry using monoclonal antibodies against MMP-2, MMP-9 and MMP-11. Immunostaining results were scored by using the HSCORE.
Results: The epithelial as well as stromal expression of MMP-2, MMP-9, and MMP-11 were stronger in ovarian tumors than in ovarian benign tumor tissue ($P<0.01$). A strong correlation was emerged between the elevated expression of all three markers ($P<0.01$). MMP-11 expression was significantly increased in mucinous neoplasms compared with serous ones ($P<0.05$). There was a trend for epithelial expression of MMP-2 and MMP-9 to be higher in serous infiltrating versus borderline tumors. Also, the percentage of cases showing triple, elevated, diffuse expression of all three MMPs was higher in the subgroup of serous infiltrating compared with the subgroup of borderline tumors.
Conclusion: Our results suggest that MMP-11 is frequently overexpressed in mucinous ovarian tumors and may therefore contribute to mucinous ovarian tumor development. Enhanced expression of MMP-2 and MMP-9 may lead to increased infiltration capacity of serous ovarian tumors.

091

Female adnexal tumors of probable Wolffian origin: problem of a rare entity

E.A. Hicham *, M. Fadwa
*Laboratoire My Driss, Casablanca, Morocco

Objective: Female adnexal tumors of probable Wolffian origin (FATWOs) were defined in 1973 by Kariminejad and Scully. There rare tumors arising in the broad ligament from the remnants of the mesonephric duct wich is considered to have a low malignant potential. Although this tumor diagnosis is based on exclusion of other possibilities, these tumors do not otherwise closely resemble any neoplasm arising from either a Mullerian duct derivate or the surface of the ovary epithelium. The presenting symptoms, malignant potential, and metastatic activity of these rare tumors are very variable.
Method: We report a case of FATWOs disease. A 40-year-old woman who presented with a painful pelvic mass underwent a laparotomy with tumor resection. The ovary and unterus were free from any disease. Pathology findings confirmed a FATWO based on morphology and immunochemistry.
Results: Surgical approach was the mainstay of treatment and, in some cases, radiation therapy with or without chemotherapy was administered. Their prognosis does not correlate with their clinical presentation or their cytology. However, the presence of capsular invasion and especially a high number of mitoses are elements justifying caution regarding their prognosis.
Conclusion: FATWOs represent a rare entity of uncertain prognosis. Diagnosis must exclude ovarian neoplasm.

092

Successful treatment of endometrial hyperplasia by the levonorgestrel impregnated intrauterine system coincides with down-regulated progesterone receptor A and B

A. Ørbo *, M. Arnes, I. Pettersen, K. Larsen, K. Hanssen, B. Moe
*University of Tromsø, Research Group of Gynecologic, Tromsø, Norway

Objective: A retrospective population-based observational study was undertaken to investigate whether regression of endometrial hyperplasia observed after 3 months of treatment with levonorgestrel impregnated intrauterine system device (LNG-IUS) was sustained after 6 months. Also to investigate whether these effects were still occurring synchronously with extinguished expression of progesterone receptors and increased apoptosis.
Method: In 41 patients with endometrial hyperplasia histopathological treatment response was investigated by light microscopy comparing LNG-IUS ($n=25$) and oral medroxyprogesterone ($n=16$). Expression of PR-A, PR-B, ER-alfa, ER-beta, Bcl-2, BAX, Caspase-3 and MT (metallothionein) investigated by immunohistochemistry, results evaluated by semi-quantitative H-score.
Results: All LNG-IUS-treated patients had therapy response after 6 months. PR-A and PR-B in glands were almost extinguished for IUD users compared to the oral group. Estrogen receptors were also reduced. Co-existent changes in apoptosis were differently modulated in glands and stroma in the two treatment groups. Bcl-2 was different in glands and stroma in responders and non-responders to oral therapy.
Conclusion: The study confirms that LNG-IUS can be safely used for 6 months as treatment for hyperplasia. The clinical effect is accompanied by almost extinguished PR-receptors in glands coinciding with modulation of apoptosis. The results strongly indicate that progestins activate non-classical initiated signaling pathways.

093

Villous tree morphometry in diabetic pregnancies

K. Pavlov *
*V.I. Kulakov Scientific Center, Dept. of Pathology, Moscow, Russia

Objective: Diabetes mellitus is associated with some maternal and fetal complications and elevated maternal and fetal morbidity and mortality.
Method: This study aims to perform a comparative analysis of placentas from pregnant with gestational diabetes (GD) and type 1 diabetes (D1). It consists of 29 term placentas from pregnant with D1 and GD (the 1st and the 2nd group) and 6 term placentas from normal pregnancy (control group). We performed morphological, immunohistochemical and morphometrical analysis of all placentas.
Results: In both D1 and GD group we revealed patterns of branching angiogenesis and moderate-to-low degree of villous edema. We revealed decreasing of intervillous space relative area both in D1 and GD groups. Mean sizes of the terminal and mature intermediate villi as well as villous area and perimeter were also decreased in diabetic groups. In CD34 stained specimens we revealed increasing capillary amount in D1 and GD and decreasing of the area and perimeter of a single capillary in this groups. Overall capillary area and perimeter of a single villus were decreased in both GD and D1, but the degree of villous vascularisation was lesser in D1 and GD then in control group.
Conclusion: Revealed features reflect moderate preplacental hypoxia, associated with hyperglycemia.

094

Myxoma at ovary

A. Kurt *, S.A. Özmen, M. Demir
*Bölge Egitim ve Arastirma Hastane, Dept. of Pathology, Erzurum, Turkey

Myxomas are the part of the rarely seen benign tumors of soft tissue. In this study, a case of ovarian myxoma in a 14-year-old menarchal girl is reported. This paper details the gross and microscopic pathology and immunocytochemical profile of this rare tumor. A dark gray-coloured smooth surfaced mass at her right ovary was excisied. The cross-section was regulary bordered and contained areas which were filled with soft viscous, gelatin-like material. Its size was 10×8.5×6.5 cm and its weight was 396 g. There were solid dirty white coloured areas and partly bloody areas in some places. The diameter of the tumor was 10×8.5×6.5 cm. Histopathologically, in the loose myxomatous stroma under the fibrous capsula, a tumoral mass was seen which is composed of cells generally spindle in type but sometimes star-shaped. Cellular atypi, mitosis and necrosis were not seen; there was bleeding. Histochemically, it was stained positive with Alcian blue and musin. Immunohistochemically vimentin, smooth muscle actin were focally pozitive, desmin, CD 34 were negative. In this instance, histomorphologically, histochemically and with immunohistochemical findings "ovarian myxoma" was diagnosed. Ovarian myxomas recently have been reported as new, distinct pathologic entities that show a myxoid, moderately cellular proliferation of spindle and stellate cells interspersed with areas of fibrosis, hemorrhage, and delicate vascular spaces.

Tuesday, 30 August 2011, 09.30–10.30 and 16.30–17.00, Hall 5

PS-15 Poster Session Nephropathology

001

Incidental renal tumors: a forensic study

C. Amalinei *, C. Grigoriu, L. Knieling, R. Balan, D. Ciobanu, I.-D. Caruntu
*University of Medicine, Dept. of Histology, Iasi, Romania

Objective: Renal tumors or tumorlike conditions may be incidentally found in forensic autopsies. We report 13 cases of such conditions, renomedullary interstitial cell tumors ($n=11$), angiomyolipoma ($n=1$), and endometriosis ($n=1$) respectively, diagnosed during 1 year in our institute.
Method: After gross inspection and serial sectioning of both kidneys, suspicious samples were processed for routine staining, Masson trichrome and selected immunohistochemical markers.
Results: The renomedullar interstitial cell tumors presented as small nodules situated in the midportion of the medullary pyramids; the angiomyolipoma presented as a small subcapsular yellowish tumor and the endometriosis presented as a brown-reddish small tumorlike condition. Microscopy disclosed small, stellate, or polygonal cells in a loose stromal background, with entrapped peripherical tubules, in the renomedullary interstitial cell tumors. In angiomyolipoma, an admixture of vessels showing hyalinized wall, smooth muscle, fat, and perivascular epithelioid cells, exhibiting pleomorphism, hyperchromatic bizarre nuclei, multinucleation, and HMB-45 immunopositivity were identified. The renal endometriosis was composed of endometrial glands (exhibiting PR positivity and CD10 immunonegativity), stroma, hemosiderin-laden macrophages, and smooth muscle.

Conclusion: Incidental renal tumors or tumorlike conditions in adults are of particular interest in forensic practice, as they are a subject pertinent to the themes of histogenesis and malignancy differential diagnosis.

002

Expression of progenitor markers in correlation with NCAM in human fetal kidney

S. Cirovic*, J. Markovic-Lipkovski, G. Müller, S. Tatic, D. Dundjerovic, N. Radunovic, C. Müller
*University of Belgrade, Faculty of Medicine, Serbia

Objective: Structures of adult kidney arise from interactions between metanephric mesenchyme and ureteric bud. The neural cell adhesion molecule (NCAM) is widely expressed during development. Coexpression of NCAM and other progenitor markers in fetal tissue was investigated in this study.
Method: Human fetal kidney tissue on different stages of gestation was analyzed using double immunofluorescent staining of NCAM and stem cell markers TRA-1-60, CD24, CD133, CD34, as well as PSA-NCAM, FGFR1 and Ki67. RT-PCR was used to evaluate NCAM isoforms.
Results: RT-PCR shows presence of 120, 140, and 180 kDa isoforms. Mesenchymal cells around ureteric bud were NCAM+PSA/NCAM- and without any coexpression with all tested markers. FGFR1+NCAM- mesenchyme cells were found in this area; single cells CD133+NCAM- and CD34+NCAM- were also found here. TRA-1-60, CD24 and CD133 stain uretetic bud. PSA/NCAM+NCAM+, Ki67+NCAM+, CD24+NCAM+was detected in cap mesenchyme, pretubular aggregates, renal vesicle, comma and S-shaped body. In these areas NCAM coexpression with TRA-1-60, CD34, CD133 and FGFR1 was not detected.
Conclusion: Different coexpression of NCAM with CD24, CD133, and TRA-1-60 suggests that more than one type of renal stem cells exist. PSA-NCAM is important for early development of the nephron. Interestingly, only restricted number of cells coexpressed FGFR1 and NCAM.

003

Correlation between cytokines and renal fibrosis in hypertensive pregnant rats (SHR) subjected to physical training

D.T.R.S. Abate*, L.G. de Almeida Oliveira, O. Barbosa Neto, J.R. Machado, V.J. Dias da Silva, A.C. Guimarães Faleiros, M.A. Reis
*UFTM, Dept. of Biological Science, Uberaba, Brazil

Objective: The development of renal injury occurs due to a multifactorial, dynamic process involving the participation of inflammatory cells that produce mediators. We were analyze the effects of physical training by swimming in relation to hemodynamic and morphological changes in the kidney of pregnant chronic hypertensive rats (SHR) and your control group (WKY).
Method: There were 12 pregnant rats divided into two groups: trained hypertensive (HT) or normotensive (NT). In the end of training, mean arterial pressure (MAP) was analyzed, and a fragment of kidney was stained with picrossirius and quantification of the percentage of tubulointerstitial fibrosis (%F) and that of cytokines (IL-10, TGF-β and TNF-α) was made.
Results: There was a significant positive correlation between TGF-β and renal fibrosis ($p<0.001$) and a negative correlation between IL-10 and renal fibrosis and between TNF-α and renal fibrosis in SHRs subjected to physical training.
Conclusion: The mechanism by which hypertension can damage the kidney is not yet fully defined; exercise training attenuated the blood pressure levels, however, it did not prevent kidney damage caused by hypertension and due to organic changes present during pregnancy.
CNPq, FAPEMIG.

004

Challenges in the treatment of late antibody mediated rejection (AMR): the controversial role of bortezomib (BZ)

H. Gakiopoulou*, E. Theodoropoulou, G. Vlachopanos, A. Iniotaki, J. Boletis, G. Zavvos, E. Patsouris
*National University of Athens, First Department of Pathology, Greece

Objective: BZ has been considered to represent a promising drug with anti-humoral activity. We present two patients with AMR who were treated with BZ.
Method: The two patients underwent a renal biopsy 2 and 3 years after transplantation due to a slight deterioration of renal function accompanied by proteinuria in the second one. A diagnosis of AMR according to Banff 1997/2009 updates was made. Following the biopsy, both patients were treated with BZ. PRAs (Panel Reactive Antibodies) were measured before and after every treatment.
Results: After treatment, renal function of both patients returned near the pre-biopsy levels and proteinuria of the second patient decreased significantly. The first patient showed no decrease of the titers of donor specific antibodies (DSAs) and interestingly, a second and later a third DSA appeared. The second patient showed a transient decrease of DSA titers which, however, subsequently increased with a concurrent increase in proteinuria and stable renal function. A second renal transplant biopsy was then performed which demonstrated morphologic evidence of acute and chronic

tissue injury with diffuse C4d staining and a 15% increase of interstitial fibrosis and tubular atrophy.
Conclusion: The efficacy of BZ in the management of AMR does not seem to overcome the known therapeutic limitations regarding long-lived antibody levels (further than 1-year post-transplant).

005

Renal transplant IgA nephropathy: report of ten cases

H. Gakiopoulou*, E. Theodoropoulou, A. Stofas, M. Lelouda, E. Chaviaras, G. Vlachopanos, J. Boletis, G. Zavvos, E. Patsouris
*National University of Athens, 1st Dept. of Pathology, Greece

Objective: IgA nephropathy in renal transplants represents in most cases recurrence of the primary disease and less commonly de novo disease. We present ten cases of renal transplant IgA nephropathy in relation to clinicopathological parameters.
Method: Ten renal transplant biopsies were investigated by means of light microscopy using conventional histochemical and immunohistochemical stains and under immunofluorescence microscopy by which a diagnosis of IgA nephropathy was made.
Results: Mean time from renal transplantation to IgA nephropathy detection was 47.33 months. The primary disease was unknown in seven patients. All developed glomerular hematuria which was the main indication for biopsy in six patients. In one, the main indication was the sudden onset of proteinuria while in two it was the deterioration of renal function. The latter demonstrated focal segmental glomerular necrosis reminiscent of the lesions described in the native renal biopsy. In two cases with stable renal function, the presence of interstitial inflammation and mild tubulitis created a differential diagnostic problem with subclinical borderline acute rejection.
Conclusion: Immunofluorescence in renal transplant biopsies reveals cases of IgA nephropathy in several patients with unknown primary disease. Although in most cases the presence of IgA deposits does not seem to influence renal function, a proportion of patients does exhibit renal dysfunction related to IgA nephropathy and possibly to the severity of the disease in the native kidneys.

006

Goodpasture's syndrome with concommitant immune complex mixed membranous and mesangiocapillary proliferative glomerulonephritis

V. Jurcic*, A. Vizjak, A. Aleš, J. Jeruc, J. Wieslander, D. Ferluga
*University of Ljubljana, Medical Faculty, Slovenia

Objective: Concurrence of Goodpasture´s (GP) syndrome with proliferative glomerulonephritis has only rarely been described.
Method: Kidney biopsies were processed for light, immunofluorescence and electron microscopy according to standard techniques. Anti-glomerular basement (GBM) antibodies were detected by immunofluorescence, standard anti-GBM enzyme-linked immunosorbent assay (ELISA) and anti-GBM ELISA for IgG subclasses.
Results: In addition to extracapillary crescents, glomeruli showed diffuse mesangial and segmental endocapillary proliferation. Linear IgG immunofluorescence along the GBM and distal tubular BM was accompanied by fine granular IgG deposits along the GBM. Deposits were subepithelial and mesangial. Rebiopsy revealed also segmental lobulated pattern with mesangial interposition, double contours of GBM and subendothelial deposits. Standard ELISA was negative. ELISA for IgG subclasses revealed low value of IgG4 antibodies against NC1 domain of alpha 3 chain of type IV collagen, which corresponds to GP antigen.
Conclusion: We describe unusual GP syndrome with concommitant immune complex mixed membranous and proliferative glomerulonephritis with a histologic pattern of mesangial, endocapillary and, in rebiopsy, also mesangiocapillary proliferation, in addition to extracapillary proliferation. The clinical picture was characterized by a recurrent but non-progressive course, nephrotic syndrome, normal renal function and low values of anti-GBM antibodies, identified only by more sensitive non-commercial ELISA technique.

007

Renal cell carcinoma with papillary growth: clinicopathologic immunohistochemical profiling: analysis of 9 cases and review of the literature

F. Khanchel *, R. Dhouib, R. Doghri, S. Sassi, M. Driss, K. Mrad, I. Abbes, D. Kacem, K. Ben Romdhane
*Salah Azaiz, Dept. of Pathology, Tunis, Tunisia

Objective: Renal cell carcinoma (RCC) is a heterogenous group of tumor with distinct histologic features, molecular characteristics and clinical outcome. RCC with papillary growth include papillary carcinoma and others varieties containing papillary component. Recently, described entity not in WHO classification of renal cell carcinoma can be discussed.
Method: We analyzed cases of of RCC with papillary component registered in the Department of Pathology Salah Azaïz Institut from 1992 to 2010.
Results: Nine cases were registered. The histological spectrum included: papillary RCC (22%), Xp11.2 translocation-associated RCC (33%), mucinous tubular spindle cell carcinoma (22%) and a clear RCC with papillary growth component (22%). The patient's ages ranged from 10 to 76 years. The ratio of males to females was 0.5. Renal

tumor size ranged from 1.2 to 17 cm. Two patients presented with papillary RCC; one had characteristic type 2 morphology and the second had type 1 morphology. Three cases of Xp11.2 translocation associated RCC are seen in young patients. The tumors lacked cytokeratin expression and were confirmed by nuclear reactivity to TFE3 protein. Two cases showed typical morphological features of mucinous tubular spindle cell.
Conclusion: The large heterogenous group of RCC with papillary growth contain morphological and molecular distinct tumor with different prognosis. Increased awareness and a high index of suspicion are key of the correct recognition of these entities.

008

Epitheliod angiomyolipoma of the kidney: a case report and review of the literature

C. Kouvidou*, M. Lianou, M. Kopaka, P. Kara, I. Gioti, D. Rontogianni
*Evangelismos Hospital, Dept. of Pathology, Athens, Greece

Objective: Epithelioid angiomyolipoma is a rare recently identified variant of renal angiomyolipoma. It may occur in patients with or without tuberous sclerosis and may potentially be malignant.
Method: Case presentation: We report a 70-year-old woman who presented at our hospital with pain. The ultrasound and the CT scan revealed a 16-cm mass of mixed heterogeneity in the right kidney suspicious for renal cell carcinoma. The patient underwent a right radical nephrectomy. She had no history of tuberous sclerosis.
Results: The histology revealed a neoplasm that composed of epithelioid and spindle cells with densely eosinophilic or clear cytoplasm, occasional blood vessels and isolated adipocytes. Areas of necrosis and degeneration of the tumor were present. The immunohistochemical staining was strongly positive for Melan-A, HMB-45, MFT, CD117, focally positive for actin, S100, ER, PGR and negative for RCC, CD10, CK7, EMA, Vimentin and TFE-3 indicating the diagnosis of epithelioid angiomyolipoma. Extrarenal extension was found but no renal vein involvement. There was no recurrence and metastases after 1-year follow up.
Conclusion: Epithelioid angiomyolipoma is a rare tumor with a potentially aggressive behavior; therefore, long-term post-operative follow-up is mandatory.

009

Reduction of podocytes number in primary nephrotic syndrome in children

T. Liatkouskaya*, I. Sakharau, E. Cherstvy, A. Sukalo, V. Savosh, N. Tur
*Belarussian Medical University, Dept. of Pathology, Minsk, Belarus

Objective: Proteinuria in primary nephrotic syndrome (PNS) is due to development of structural and functional defects in the glomerular–filtration barrier. The present study was designed to investigate the quantitative changes of cells and capillaries in kidney glomeruli in children with PNS.
Method: Kidney biopsy specimens were obtained from 31 children with PNS and 30 children with isolated hematuria. The sections were stained with WT1 antibody to reveal podocytes. Images of five glomeruli from each section were analyzed. The following indices were calculated: podocyte density (podocyte number per 10,000 sq mkm), other cells density and capillary density (similarly), podocyte number per capillary.
Results: Of the 33 children with PNS, 22 children had minimal changes (MC) at histology, 4 children had mesangial proliferation (MP), 5 children had focal segmental glomerular sclerosis (FSGS). In the hematuria group, 4, 23 and 3, respectively. Podocyte density was significantly decreased in NS group compared with hematuria group. Podocyte density was also decreased in each of histological variants. Podocyte density and capillary density in NS group decreased in direction MC>MP>FSGS showing positive correlation. In hematuria group, no differences in morphometric indices between histological variants were found.
Conclusion: The number of podocytes and capillaries in kidney glomeruli is decreased in primary NS.

010

Progression of renal disease in the Zucker Diabetic Fatty rat: an experimental model of type 2 diabetes

C. Mega*, H. Vala, J. Oliveira, R. Fernandes, F. Mascarenhas-Melo, B. Parada, R. Pinto, F. Teixeira, F. Reis, E. Teixeira de Lemos
*University of Coimbra, Lab. of Pharmacology and Exp. Therapeutic, Portugal

Objective: The Zucker Diabetic Fatty (ZDF-fa/fa) rat is one of the most attractive models for the study of type 2 diabetes. Characterization of hydronephrosis in this model may provide useful insights into the mechanism of diabetic nephropathy progression. This study aimed to identify and characterize the evolution of hydronephrosis in Zucker Diabetic fatty (ZDF) rat.
Method: Male diabetic obese ZDF (fa/fa) rats were sacrificed at 8, 14, 20 and 26 weeks of age and compared with their lean counterparts ZDF (+/+) with de same age. Kidney slices stained with hematoxylin-eosin and periodic acid-Schiff were evaluated. A semiquantitative rating was assigned for hydronephrosis and scored from 0 (normal) to 3 (severe), based on conformational aspects of the papilla and calyx and cortex compression.

Results: A marked progression in the severity of hydronephrosis was observed. All end-disease state rats, 26 weeks of age, showed hydronephrosis, which was more severe and precocious in the diabetic rats (scoring 2, 3) in comparison to lean controls (scoring 1). No relevant cortical atrophy was found.
Conclusion: Hydronephrosis evolution in the ZDF rats is age-related and aggravated by diabetes but doesn't hinder morphological evaluation and, thus, might represents a feasible model for the preclinical study of therapeutic interventions in diabetic nephropathy.

011

Muckle–Wells syndrome and renal amyloidosis: a case report

C. L. Menendez*, E. García, M. de la Torre, S. González, D. Rodríguez, M. Poch, V. Venta, C. Murias, B. Corrales, E. Fuente, J. Palacio
*Hospital de Cabueñes, Dept. of Pathology, Gijon, Spain

Objective: Muckle-Wells syndrome (MWS) is a rare autosomal dominant disease that belongs to a group of hereditary febrile syndromes characterized by recurrent and self-limited episodes of fever, urticaria, arthralgia and conjunctivitis since childhood. Amyloidosis is the main complication. It is associated with mutations in the NLRP3 gene which codifies cryopyrin, a protein responsible for regulating the production of certain proinflamatory cytokines like interleukin-1.
Method: The patient is a 25-year-old man with occasional high fever, abdominal cramps, arthralgia and rare skin rashes. His liver and spleen were enlarged, also some lymph nodes. No personal or familiar relevant diseases. Main Lab. tests: GGT: 57; virus and ANA, negative.
Results: A renal biopsy showed focal amyloid AA in glomerular mesangia. A liver biopsy had minimal steatosis, discrete periportal inflammatory activity, sinusoidal ectasia and no amyloid. In order to discard an autoinflamatory disease, a mutational analysis of related genes was performed and a mutation of the CIAS1 gen, subtype p.Lys-173-Glu, heterocigotic in exon 3 was found. This rare variant (not described previously) correlated with his clinical history and was consistent with MWS.
Conclusion: It is essential to think of these heritable autoinflamatory diseases and perform genetic studies since new effective therapies and genetic counselling can be done.

012

The pathological evaluation of non-neoplastic kidney disorder in tumor nephrectomy specimen

F. Noroozinia*, F. Abbasi, R. Porali, H. Behnamfard
*Imam Khomeini Hospital, Dept. of Pathology, Urmia, Iran

Objective: Renal cell carcinoma consists of 1–3% of all visceral malignancies and 85% of all adult kidney malignancies. Nephrectomy is the treatment of choice for renal tumors. The accurate pathologic evaluation of the non-neoplastic renal parenchyma in nephrectomy specimens is important for subsequent management.
Method: The patients with renal cell carcinoma who underwent surgery between 2000 and 2009 at our department were studied. Paraffin-embedded blocks were retrieved from hospital archive, stained by H&E and PAS staining. Microscopic examination was performed on non-tumoral portions as far from the tumor as possible.
Results: A total of 29% of cases were normal. The most frequent pathologic findings were vascular sclerosis with parenchymal scarring and pyelonephritis. Other findings include focal and diffuse mesengial hypercellularity, FSGN, MPGN, and MGN. Frequent findings were parenchymal scarring and vascular change in clear cell type 36% and papillary 41%—normal in chromophobe 53.8%. Although there is not any statistical relation between the gender of a patient and pathologic finding, there was a statistical relation between age and pathologic finding. Vascular sclerosis with parenchymal scarring and glomerular disease increased before 55 years of age and chronic pyelonephritis after 55 years age.
Conclusion: We advise PAS and H&E staining of non-neoplastic area in all of the tumor nephrectomy specimens.

013

Glomerular lesions associated with lymphoid malignancies

M. Otani*, H. Hayashi, S. Hiraiwa, S. Yoshida, Y. Ueda, H. Serizawa
*Tokyo Medical University, Hachioji Medical Center, Japan

Objective: Glomerular lesion associated with malignancy is well established. Especially, hematopoietic neoplasia is famous for its cause. We encountered some cases of renal lesions accompanied with lymphoid malignancies and discuss their pathogenesis.
Method: The specimens of five cases were obtained from renal biopsy or autopsy. Each case was diagnosed as lymphoid malignancy accompanied with renal lesions by clinically or pathologically. The obtained specimens were stained with conventional HE, PAS, PASM and MT stains. Some cases were followed by immunohistochemical, immunofluorescent and electron microscopical examinations.
Results: Three cases were induced by B-cell lymphomas, and other cases were T-cell type. The ratio of gender is 3:2 (male/female) and the average of the patients' age was 74.4 years old (64 to 88). The glomerular lesions showed glomerulonephritis (GN), such as MN, membranoproliferative glomerulonephritis (MPGN), focal segmental glomerulosclerosis (FSGS) and ANCA-related GN. In one case,

the lymphoma cells invaded into glomeruli directly from surroundings.

Conclusion: Glomerular lesions may complicate nearly all forms of lymphoid malignancies. It is reported that the frequency is less than 2% of the patient population. The pathogenesis of glomerular lesions in the setting of lymphomatous process is probably diverse and our cases suggest antibody-mediated, lymphokine-mediated or directly invaded nephrotoxicity might play a role.

014

Activity as well as level of neprilysin (CD10) is decreased in renal cell carcinoma

T. Ipekci*, I. H. Ozbudak, N. Erin, B. Akkaya, M. Baykara
*Akdeniz University, School of Medicine, Antalya, Turkey

Objective: Neprilysin (CD10) is a peptidase involved in the hydrolysis of inflammatory neuropeptides. Decreased neprilysin activity was associated with tumor progression and poor prognosis. Herein, we studied the changes in neprilysin activity as well as the pattern of immunostaining in renal cell carcinoma (RCC).

Method: The extent and pattern of CD10 staining was evaluated in 60 RCC and adjacent uninvolved renal tissue. CD10 staining intensity (SI) and percentage of stained cells (PP) were assessed using scales. Overall immunoreactivity of CD10 was evaluated by immunoreactivity score (IRS) (IRS=SI × PP). Neprilysin activity was measured in freshly frozen tissues using a flourometric technique.

Results: Neprilysin activity was significantly lower in tumor tissue compared to neighboring renal tissue regardless of tumor type. No staining was found in tumor tissue of 40 cases; however, all the neighboring uninvolved kidney tissue was intensely stained. The degree of loss of neprilysin staining in tumor tissue also correlated with the stage of the disease such that staining was significantly lower in patients with metastatic disease or with T3a tumors.

Conclusion: Neprilysin activity as well as immunostaining was markedly decreased in RCC. These results demonstrate that loss of neprilysin activity might have a role in tumorigenesis and aggressiveness of RCC.

015

The glomerular mitotic activity in cases of lupus nephritis

L. Pashkevich*, V. Savosh, T. Letkovskaja, E. Cherstvoj, I. Kazyra, A. Sukalo, N. Tur
*BRSPCTO, Dept. of Pathology, Minsk, Belarus

Objective: The purpose of our study was to reveal possible relationships between number of glomerular dividing cells and lupus nephritis (LN) activity.

Method: We used renal biopsy specimens obtained from ten patients with LN from the Republic Center of Pediatric Nephrology, Minsk, Belarus. Proliferation activity was examined by immunohistochemistry using antibodies to protein Ki-67.

Results: To characterize the protean renal manifestations of SLE, we used the classification of the International Society of Nephrology (2004). The class IVof LN was described in nine of ten cases. The activity index was generally high and varied from 6 to 14. We found out the morphology of class III only in one patient (activity index was 4). The analysis of quantitative assessment of dividing cell showed a statistically significant (p=0.00813) positive correlation between the number of Ki-67-positive glomerular cells and activity index of LN. A highly significant correlation was also evident between the mitotic activity of glomerular cells and the active immunologic manifestations such as anemia, visceral and skin lesions etc. (p=0.026).

Conclusion: The increased number of Ki-67-possitive glomerular cells in cases with active LN suggests the mitotic activity index as a possible factor of severe clinical course.

016

Clinicopathological analysis of kidney diseases in adults: a report based on the databases from 7 nephropathological centers in Poland

A. Perkowska-Ptasinska*, A. Bartczak, A. Halon, K. Okon, J. Kowalewska, A. Marszalek, A. Korolczuk, M. Danilewicz, M. Wagrowska-Danilewicz
*Warsaw Medical University, Inst. of Transplantation, Poland

Objective: We aimed at establishing the distribution of biopsy-based kidney disease recognitions among patients with different types of clinical syndromes.

Method: We analyzed 1,882 cases collected in seven nephropathological centers in Poland in years 2009–2010.

Results: The three leading recognitions in the whole group studied encompassed: IgA nephropathy (IgA-N) (19%), FSGS (17%) and membranous GN (MGN) (11%). In the group comprising patients between 18-40 years of age the most prevalent diagnoses were: IgA-N (25%), FSGS (14%) and lupus nephropathy (LN) (14%), whereas among those older than 60 years of age there was a domination of MGN (18%), FSGS (17%) and amyloidosis (13%). In the nephrotic patients' group there was a prevalence of FSGS (19%), MGN (17%) and minimal change disease (13%), whereas among those who presented with nonnephrotic proteinuria the leading diagnoses encompassed: IgA-N (28%), FSGS (16%) and LN (10%). The nephritic syndrome was most commonly associated with IgA-N (26%), crescentic GN (15%) and FSGS (9%). Among those patients who had kidney biopsy at the time of profound renal insufficiency (CKD stages 4 and 5)

dominating recognitions were: crescentic GN (21%), IgA-N (13%) and FSGS (9%).
Conclusion: The above data puts a new light on the epidemiology of kidney diseases in Poland.

017

Histologic findings in protocol biopsies on 1 and 6 months in kidney transplant recipients in R. Macedonia

G. Petrusevska*, G. Spasovski, J. Masin-Spasovska, B. Dimova, M. Bogdanovska, S. Kostadinova, R. Jovanovic, B. Dukova
*Medical Faculty Skopje, Inst. of Pathology, Macedonia

Objective: We analyzed main histopathological changes in the protocol biopsies from the grafts with stable renal function taken at one and six months using Banff Classification. We used immunohistochemical stainings for TGFb, Ki67 and in situ hybridization for the detection of apoptosis.
Method: A total of 28 paired biopsy specimens from allografted kidneys performed at 1 and 6 months were analysed on standard histological sections stained with HE, PAS, Trichrome-Goldner and Silvermethenamine-Jones. Biopsies were considered adequate when they contained more than seven glomeruli and at least one artery. Additional immunohistochemical stainings for TGFb and Ki67 by LSAB immunoperoxidase were done, as well as ApoPtag in situ hybridization for the detection of apoptosis.
Results: Histopathological diagnosis included six specimens with normal findings. Borderline changes were found in 10/28 in the 1- and 6-month biopsies. Signs of acute rejection were found in 13/28 and 12/28 cases at 1- and 6-months biopsy, respectively. There was a significant increase of CAN in the second allograft biopsy after 6 months. Immunohistochemical analysis showed an increased proliferative index in all of the biopsies and significant apoptotic activity in the cases with CAN.
Conclusion: Changes in the cell proliferation and apoptosis might influence in the development of CAN as well as they might have a role in the pathogenesis of the chronic alograft changes.

018

Amyloidosis due to fibrinogen A α-chain: first case report in Latin America

M. Reis*, J. Machado, D. Abate, F. Oliveira, V. Laterza, W. Rodrigues, A. C. Faleiros, R. Correa
*University Triangulo Mineiro, ICBN, Uberaba, Brazil

Objective: Amyloidosis by fibrinogen A α-chain-AFib is one of the most common types of hereditary renal amyloidosis in Europe. However, in Latin America, no one case was previously reported.
Method: Renal biopsy—case report
Results: Clinical history: Brazilian female patient, 52 years old, previously healthy, normal blood pressure, presenting no symptoms. In the last 7 months, she had been showing proteinuria (3.71 g/24 h), without hematuria. Serum proteins: 5.89 g/dl and serum albumin: 3.78 g/dl. The renal biopsy was performed. Light microscopy: only in the glomerular compartment, there were congofilic deposits ("apple-green" birefringence under polarized light) which replaced the mesangial matrix and capillaries. These deposits were strong immunoreactivity for fibrinogen global in all glomeruli and negative for IgA, IgG, IgM, C1q, C3, kappa and lambda. In electron microscopy, there were organized deposits which replaced the normal matrix and present in capillary walls, specially in the subendothelial spaces. Diagnosis: amyloidosis by fibrinogen Aα-chain-AFib.
Conclusion: The patient presented proteinuria, and the histological appearance is amyloidosis due to fibrinogen A alfa-chain, with isolated glomerular involvement. It is one of the most prevalent types of hereditary renal amyloidosis. So renal amyloidosis should be routinely included in the differential diagnosis of renal failure and especially in proteinuria/nephrotic syndrome patients and specially attention of hereditary amyloidosis, such as AFib. CNPq, Fapemig, Funepu, UFTM.

019

The clinicopathologic significance of endothelial tubuloreticular inclusions in glomerular diseases

K.-S. Suh*, C.-J. Lee
*Chungnam National University, Dept. of Pathology, Daejeon, Republic of Korea

Objective: The presence of tubuloreticular inclusions (TRIs) in endothelial cells (ECs) always evokes suspicion of their association with viral infections or autoimmune diseases. However, other underlying diseases can be associated with TRI expression. Since identification of the underlying disease is of primary consideration for management of glomerulonephritis (GN), it is important to clarify the clinical significance of TRI expression.
Method: We studied 104 renal biopsy cases having TRI. We investigated their clinicopathological profiles and focused on potential connections with underlying diseases.
Results: Among 104 renal biopsy cases, 62 cases (59.6%) were associated with lupus nephritis (LN) and 19 cases (18.3%) were associated with a viral infection (HBV 13, HCV 3, and HIV 3 cases). Other underlying disease groups and their number of associated cases included idiopathic MGN (7), IgA nephropathy (7), ANCA-associated glomer-

ulopathy (1), and others (8). Among seven MGN cases and seven IgA nephropathy cases, one MGN case and two IgA nephropathy cases exhibited a decrease in the serum C3 level with no evidence of SLE.
Conclusion: TRIs were identified in idiopathic MGN and other glomerular diseases, including IgA nephropathy and ANCA-associated glomerulopathy. A diagnosis of LN should be considered because TRIs associated with a full-house immunofluorescence pattern are usually found in LN.

020
Cystic renal tumour in young females

J.-C. Tille *, S. Sid´ Amar, J. Hauser, M.-F. Pelte
*University Hospital Geneva, Dept. of Clinical Pathology, Switzerland

Objective: Cystic nephroma is a rare benign cystic stromal and epithelial tumour of the kidney occuring most often in young women.
Method: Case report
Results: A 29-year-old obese woman was hospitalised for fever associated with sensibility of the right hypochondrium. Abdominal CT scan showed a right renal mass. A nephrectomy was performed and macroscopally the kidney was involved by a cystic tumor of 17 cm, well-demarcated, multiloculary, with cysts varying between 0.5 and 4.5 cm in diameter separated by thin septas. Histologically, these cysts were lined by a single layer of flattened to low-cuboidal epithelium with a hobnail feature. Tumoral cells had an eosinophilic cytoplasm with an oval nucleus containing fine granulary chromatine with small nucleoli. No mitoses were found. At immunohistochemistry the epithelial cells were positive for cytokeratines 7 and 19 and the stromal cells were positive for estrogen and progesterone receptors.
Conclusion: Cystic nephroma is a mixed epithelio-stromal cystic benign tumour occurring frequently in young females. This entity could be confused with the mixed epithelial and stromal tumour of the kidney observed in older women. Recent molecular analyses indicate that both entities could represent a spectrum of the same lesion called by some authors "renal epithelial and stromal tumour".

021
Crescent or full moon, pauci-immune crescentic nephritis

M. Unlu*, D. Ates, S. Kiremitci, Y. Ozluk, B. H. Ozdemir, I. I. Gonul, B. Akkaya, D. Orhan, G. Gonlusen, D. Baydar, S. Sarioglu
*Dokuz Eylul Universty, Medical School, Izmir, Turkey

Objective: Pauci-immune glomerulonephritis (PGN) is characterized by extracapillary proliferation (ECP) in glomeruli. The number and size of the crescents are variable between different cases. This study aims to determine prognostic value of range of extracapillary lesions in PGN.
Method: There were 126 cases of PGN identified from nine institutions. Clinical information and follow-up from patients were obtained. Histopathological features of biopsies were reviewed. Number, type (cellular, fibrocellular, fibrous) and the grade of ECP were taken into consideration. ECP was graded from I to III (ECP-I: crescent occupying <50% of Bowman's space (BS); ECP-II: occupying ≤50% BS without full obliteration; ECP-III: complete BS obliteration).
Results: Mean follow-up was 614.14+740.95 days. A total of 36 cases (28.6%) ended up in permanent dialysis. Univariate analysis showed a significant association between high serum creatinine in the follow-up and the presence of ECP-III lesions involving >50% glomeruli in biopsy (p=0.01). Levels of tubular atrophy, interstitial fibrosis and inflammation were the other significant variables (each p<0.05).
Conclusion: The presence of full moon (ECP-III) crescents in a large quantity (>50%) of glomeruli in PGN predicts unfavorable prognosis. We believe that this feature must be added to pathology reports, which can be one of the useful adjuncts for guiding appropriate treatment.

022
Synchronous renal cell carcinoma and urothelial carcinoma of the renal pelvis in the left kidney

S. Vazquez Navarrete *, J. Peña, D. Lagama, P. Pérez
*Hospital Linea de la Concepcion, Spain

Objective: Synchronous renal cell cancer and urothelial cancer in the same kidney are rare (0´14% of all renal cell tumors). Renal cell tumors are 1% of all adult´s tumors while urothelial carcinoma has an incidence of 7% in the population.
Method: An 88-year-old woman was admitted to the hospital complaining for hematuria and a computerized tomographic scan (CAT) showed a left renal mass. As a result, a nephrectomy was performed.
Results: The left kidney was removed and in the upper pole an 8-cm, solid, brown and round tumor with some necrotic areas. The adjacent renal pelvis contained a separate, soft, whitish tumor (3 cm) with smooth surface. Syncronous association of cromofobe renal cell carcinoma Furhman grade 2, spreading through the renal capsule. From that main tumor sharply demarcated and with no transitional area between these two tumors was a urothelial high-grade (III) papillary and solid carcinoma. The ureteral surgical margin was free of neoplasia. The cromofobe renal cell carcinoma was positive for CK 7, and negative for CK 20, vimentine and CD10. The urothelial pelvic carcinoma was CK 7 and CK20 positive.
Conclusion: The simultaneous occurrence of renal cell carcinoma and papillary urothelial carcinoma in the renal

pelvis does not have a worse prognosis than either of the cancers alone. They are best managed with radical surgery.

023

Cryoglobulinemic glomerulonephritis in patient with Sjögren's syndrome associated with rheumatoid arthritis and systemic lupus erythematosus: case report

M. Wagrowska-Danilewicz *, M. Danilewicz, Z. Gozdzik
*Medical University of Lodz, Dept. of Nephropathology, Poland

Objective: Sjögren's syndrome is a chronic inflammatory disease characterized by lymphocyte-mediated infiltration of exocrine glands, especially lacrimal and salivary glands. It may be a primary disorder or associated with other connective tissue diseases.
Method: We present a 48-year-old female with a 7-year history of Sjögren's syndrome associated with rheumatoid arthritis and systemic lupus erythematosus. She was admitted to the nephrology department due to anemia, thrombocytopenia, nephrotic syndrome, hematuria, and renal insufficiency. Serologic work-up was positive for RF, SSA, SSB, and ds-DNA and negative for c-ANCA, and p-ANCA.
Results: The patient underwent a kidney biopsy which showed membrano-proliferative glomerulonephritis with granular staining for C3 in mesangium and along glomerular capillary walls. The patient was treated with hemodialysis, steroids, and cyclophosphamide with improvement in renal function. One year later the patient was admitted to the hospital due to proteinuria and renal failure. The second biopsy revealed cryoglobulinemic glomerulonephritis with a large number of monocytes/macrophages in glomeruli, hyaline thrombi and abundant PAS-positive material within glomerular capillaries. Electron microscopy study showed organized microtubular deposits in subendothelial space and in the glomerular capillary lumens.
Conclusion: The presented case shows that kidney biopsy should be considered in the clinical evaluation of kidney dysfunction in a patient with Sjögren's syndrome.

024

Fibrillary glomerulonephritis in a patent with type 2 diabetes mellitus: case report

M. Wagrowska-Danilewicz *, M. Danilewicz, K. Wroblewski, M. Sodolska, D. Moczulski
*Medical University of Lodz, Dept. of Nephropathology, Poland

Objective: Chronic kidney disease in patients with diabetes is rarely confirmed by renal biopsy. We present a case of a 74-year-old woman treated for 10 years for diabetes type 2 and hypertension. She was admitted to the clinic due to progressive decrease in the renal function and malaise. Despite the good control of blood pressure and glycemia there was an increase in serum creatinine level up to 192 μmol/l with a decrease in GFR-MDRD to 22 ml/min/1.73 m^2. A urinalysis showed the presence of proteinuria and hematuria.
Method: In the absence of diabetic retinopathy and an unclear reason for the renal failure, renal biopsy was performed.
Results: The renal tissue contained six globally sclerosed glomeruli and six glomeruli with mesangial matrix expansion, diffuse capillary walls thickening and mild segmental hypercellularity. Congo red staining was negative. In tubulointerstitial compartment focal fibrosis, tubular atrophy and lymphocytic infiltrates were seen. Immunofluorescence revealed week IgG, C3, kappa and lambda light chains staining in mesangial areas and focally along the capillary loops. Electron microscopy evaluation revealed linear, non-branching, randomly arranged fibrils resembling those of amyloid, but approximately twice as thick. Fibrillary deposits were found in the subepithelial space, subendothelial space, mesangium, and within the glomerular basement membrane.
Conclusion: The presented case shows that the renal biopsy should be performed in patients with diabetes type 2 presenting atypical symptoms.

025

Can gamma/delta T cells mediate acute interstitial nephritis?

T. Wiech *, M. Werner, M. J. Mihatsch, P. Fisch
*Universitätsklinik Freiburg, Inst. für Pathologie, Germany

Objective: This study is an investigation of a possible role of T cells expressing the gamma/delta T-cell receptor (TCR) in acute interstitial nephritis (AIN).
Method: Biopsies with AIN (n=5) were assessed for TCR alpha/beta and gamma/delta protein expression by immunohistochemistry. Positive cells were counted in 10 high power fields (HPF). Spectratyping of the TCR gamma- and delta-chain genes was performed using RNA isolated from frozen sections on the one case with increased numbers of gamma/delta T cells. Additionally, clonality of the TCR gamma gene was analyzed.
Results: Compared to four other patients, one case of AIN, likely associated with *Yersinia enterocolitica* infection, had an increased number of intraepithelial (average 2.6 vs. 0.025 cells per HPF) and interstitial (4.1 vs. 1.1 per HPF) gamma/delta T cells. Spectratyping revealed a clonally restricted expression of Vdelta1 and Vgamma5 while TCR gamma clonality analysis showed a polyclonal pattern. Quantification of intraepithelial (2.5 vs. 3.5 per HPF) and interstitial (27.6 vs. 36.8 per HPF) alpha/beta T cells did not show major differences.
Conclusion: The predominance of intraepithelial gamma/delta T cells suggests a pathogenic role in the AIN of this

patient. We plan to investigate more cases in order to examine if this may be a recurrent finding in infection related AIN.

026

The significance of OTUB1 expression in mesangial cells in vitro and in vivo

Z. Zhang *, Y. Zhang, R. Hu, H. Wu, M. Guo
*Fudan University, Shanghai Medical College, People's Republic of China

Objective: OTUB1 is a member of ovarian-tumor-domain-containing proteases family. It has been reported that OTUB1 is expressed in kidney tissue. But its concrete cellular location and function in the kidney remains unclear. Decorin is an important factor for antagonizing glomerulonephritides, and its degradation is mediated by ubiquitination. This study is to investigate the role of OTUB1 expression in mesangial cells and its relationship with decorin during glomerulonephritis.
Method: OTUB1 and decorin expression were detected by quantitative real-time PCR and Western blot with stimulation of IL-1β and Anti Thy1 Serum (ATS) in cultured rat mesangial cells. OTUB1 upregulation was confirmed by immunohistochemistry staining in 55 human kidney biopsies with varied common glomerulonephritides. Immunoprecipitation assay was performed to investigate the interaction between OTUB1 and decorin.
Results: OTUB1 mRNA and protein were constitutively expressed in mesangial cells and was upregulated with stimulation of IL-1β and ATS. OTUB1 overexpression was observed in the mesangium of glomeruli during glomerulonephritides. The immunoprecipitation assay demonstrated that OTUB1 interacts with decorin and enhances the degradation of decorin.
Conclusion: These data show that the inflammatory injury mediates OTUB1 upregulation in mesangial cell, which may attribute the promoting effect of OTUB1 on glomerulinephritides through the decrease of DCN level.

027

Structure of glomerulopathies in nephorology clinic (analysis of biopsies)—decade 1999–2008

V. Sipovskiy *
*St-Petersburg Medical State University, Nephrology Research Institute, Russia

Objective: An analysis of the glomerulopathies for the period 1999–2008 was performed.
Method: The study has been performed by the analysis of renal biopsies which were carried out in 1999–2008. We investigated the relationships between glomerulopaties during the corresponding periods. The groups of primary glomerulopaties (PGP), secondary glomerulopaties (SGP), glomerulonephritis with hereditary and metabolic pathology (GNHM), vascular nephropathy (VN), tubulointerstitial nephropathy (TN), nephropathy under different pathologies were distingiushed. PGP were subdivided on membranoproliferative glomerulonephritis (MPGN), focal segmental glomerulosclerosis (FSGS), membranous nephropathy (MN), minimal change disease (MCD), crescentic glomerulonephritis (CGN), acute diffuse proliferative glomerulonephritis (ADPGN), mesangial proliferative glomerulonephritis (MGN: non-IgA- and IgA-nephropathy). Systemic lupus erythematosus (SLE), amyloidosis, and vasculitis were selected in the SGP.
Results: Decreasing PGP and increasing SGP values were revealed. The ratio of diseases into PGP has changed due to the increase of IgA—nephropathy, MCD, and MN. Secondary glomerulopaties showed the changes in the ratio of nosological groups. So for 10 years the percentage of the deseases into the group was changed due to increasing the number of vasculitis and reducing the patients with amyloidosis and SLE.
Conclusion: Our results suggest reliable dynamics of nosological types into the groups which generally corresponds to the dates of other authors.

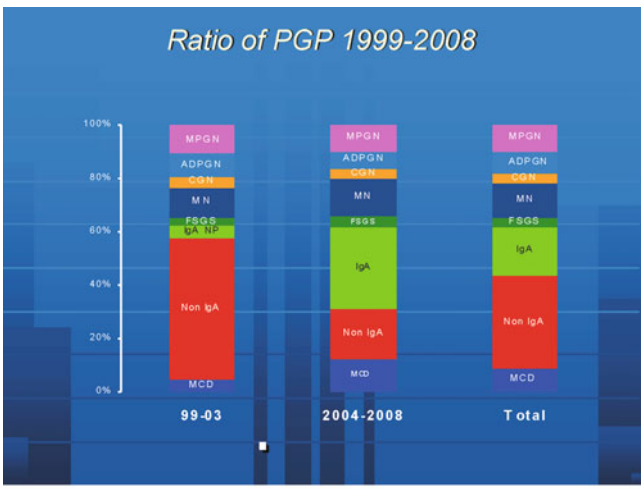

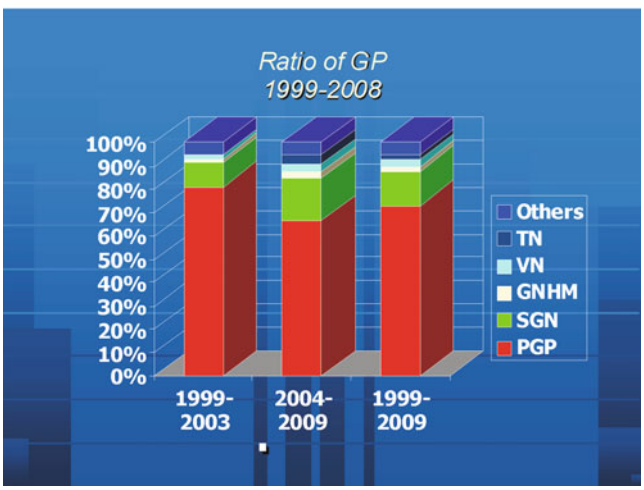

028

Increase of lymphocytes and TGF-β influence the renal impairment in hypertensive pregnant rats (SHR)

J. Machado *
*UFTM, Dept. of Immunology, Uberaba, Brazil

Objective: The hypertension (HAS) can lead to glomerulosclerosis and renal tubulointerstitial fibrosis. The inflammatory process and yours mediators has been investigated with target of kidney damage in the HAS. We check the expression of inflammatory cells and cytokines in conditions of normotension and hypertension in pregnant rats.
Method: There were 12 pregnant rats divided into two groups: sedentary hypertensive (SHR) or normotensive (WKY). To check the heart rate (HR), mean arterial pressure (MAP), and the correlation of body weight and kidney weigh, analyze of cytokines TGF-β and T lymphocytes (CD3) by immunohistochemistry and percentual quantification of tubulointerstitial fibrosis.
Results: The MAP in SHR was higher ($p=0.015$) and the HR also ($p=0.288$). The SHR shower higher cells CD3 positive ($p<0.001$), greatest expressions of TGF-β ($p<0.001$) and%Fibrosis significant highest ($p<0.001$).
Conclusion: The SHR had higher renal impairment with increased fibrosis. This can be justified by the increase of inflammatory cells and pro-fibrotic cytokines.

029

Morphological and immunohistochemical analysis of kidney in pregnant rats spontaneously hypertensive (SHR) subjected to physical training

D.T.R.S. Abate*
*UFTM, Dept. of Biological Science, Uberaba, Brazil

Objective: The development of renal injury occurs due to a multifactorial, dynamic process involving the participation of inflammatory cells that produce mediators. We were analyze the effects of physical training by swimming in relation to hemodynamic and morphological changes in the kidney of pregnant chronic hypertensive rats (SHR) and your control group (WKY).
Method: There were 24 pregnant rats divided into four groups: sedentary hypertensive (HS) or normotensive (NS) and trained hypertensive (HT) or normotensive (NT). In the end of training was analyze mean arterial pressure (MAP), and a fragment of kidney was stained with picrossirius and was made quantification of the area of mesangial matrix (MM) and of tufo glomeruli (TG), and the percentage of tubulointerstitial fibrosis (%F) and the of cytokines.
Results: Rats that underwent physical training had lower values of MAP ($p=0.015$). The HT showed a lower area of MM ($p=0.018$); however, there was higher %F ($p<0.001$) and expression of TGF-β ($p<0.001$), of TNF-α ($p<0.001$) and of IL-10 ($p<0.001$).
Conclusions: The exercise training attenuated the blood pressure, however, did not prevent kidney damage caused by hypertension. We believe that physical training done have been inadequate to their physiological conditions, justifying the findings of more renal damage in animals trained.

Tuesday, 30 August 2011, 09.30–10.30 and 16.30–17.00, Hall 5

PS-16 Poster Session Neuropathology

001

Angiocentric glioma: case report and literature review

H. Baldaia*, L. Castro, S. Carpenter, A. Fernandes, M. J. Gil da Costa, J. Silva, J. Pereira, M. Bastos
*Hospital de S João, Dept. of Pathology, Porto, Portugal

Objective: Angiocentric glioma is a rare central nervous system (CNS) neoplasm.
Method: We describe the case of a 22-month-old girl with a 10-cm angiocentric glioma located in the right temporal lobe and review the 40 published cases.
Results: The main morphologic feature of this tumour was the angiocentric arrangement of monomorphic bipolar tumour cells showing expression of vimentin, GFAP, variable expression of S100 protein and a "dot-like" cytoplasmic immunollabeling for EMA. The age at diagnosis was between 2 and 70 years, with no gender predisposition. The clinical presentation was mainly intractable epilepsy. The lesion was located supratentorially, particularly in the temporal lobe (33%). Duration of follow-up was between 1 month and 13 years. Of the 37 patients with follow-up, one had a recurrence as an anaplastic astrocytoma and eventually died of the disease. The remaining patients with seizure history were either seizure-free or experienced only rare seizures.
Conclusion: We herein describe an angiocentric glioma with the earliest age at diagnosis reported so far and review the literature with emphasis on the histological and immunohistochemical aspects, as well as differential diagnosis.

002

Reversible dementia due to intra-vascular lymphoma of the central nervous system

L. Bleggi-Torres*, P.J. Leite, S. Leite, M. Teixeira Machado, E. Coutinho Nunes, R. Pasquini
*Universidade Federal do Paraná, Dept. de Patologia Médica, Curititba, Brazil

Objective: The main causes of dementia include degenerative, vascular, metabolic and infective disorders; tumors rarely present with memory disturbance. The authors present a case of dementia due to intra-vascular lymphoma.
Method: The case was of a76-year-old female patient with hypertension and diabetes mellitus since 2007. In August 2010 she started with a rapidly progressive cognitive impairment with memory loss, speech dysfunction and functional abnormalities. She also developed abdominal pain, global dysphasia, ataxia and loss of consciousness. ESR=105 mm, CRP=30 mg/L. CSF with protein 73, leucocytes: 6.2; glucoses 78, erythrocytes 13.1. Thorax and abdominal CTScan normal. Brain NMR with small infarcts. A brain biopsy was performed.
Results: HE sections showed recent infarct and brain vessels containing several large abnormal lymphoid cells and mitosis. Immunohistochemistry positive for LCA, CD20 and Ki67 index of up to 80%. The final diagnosis of intra-vascular large B cell lymphoma with areas of haemorrhagic infarction was made.
Conclusion: Dementia due to intra-vascular lymphoma is an uncommon but well established entity; most cases reported in the literature are large B cell lymphomas; the present patient received chemotherapy with improvement of cognitive functions remaining alive and well 10 months after the initial diagnosis.

003

nNOS expression at brain regions of animals after Bburn injury and affect of ACE inhibitor, captopril

E. Demiralay*, Y. Sağlam, E. N. Özdamar, A. Ö. Şehirli, G. Şener, E. Sağlam
*Baskent University, Dept. of Pathology, Istanbul, Turkey

Objective: This study aimed to investigate the role of endogenous neuronal nitric oxide synthatase (nNOS) on brain injury in the early phase of burn injury and the effect of angiotensin II converting-enzyme (ACE) inhibitor captopril on it.
Method: Spraque Dawley rats (200–300 g) were exposed to 900 C (burn) or 250 C (control) water bath for 10 s. ACE group was treated with i.p. 1 mg/kg captopril immediately after burn injury. nNOS is studied in brain areas by immunohistochemistry.
Results: There was no difference between cerebellar and hypothalamic areas nNOS expression of all groups. nNOS activity increased in frontal cortex, striatum, midbrain in the burn group compared to control. At frontal cortex, nNOS expression significantly decreased after ACE inhibitor treatment ($p<0.05$). The striatal nNOS of ACE group significantly increased when compared to control group ($p=0.001$). At midbrain of animals, nNOS decreased in ACE group. The

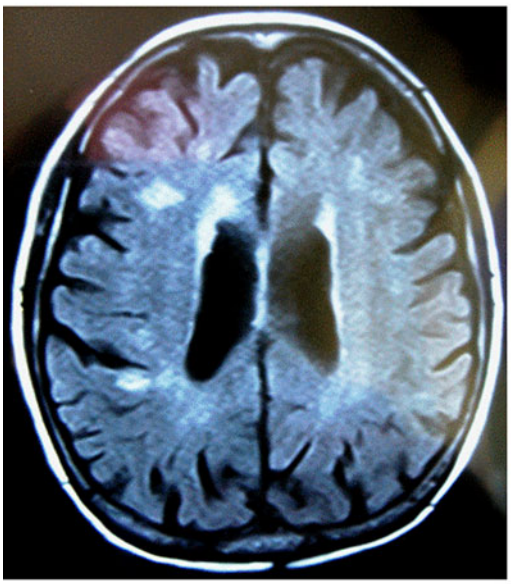

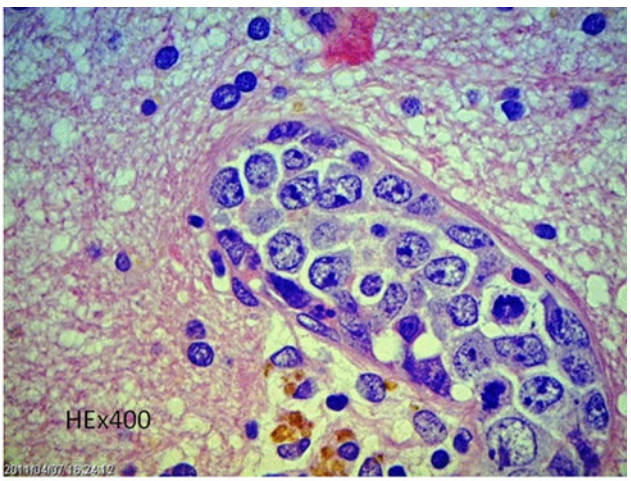

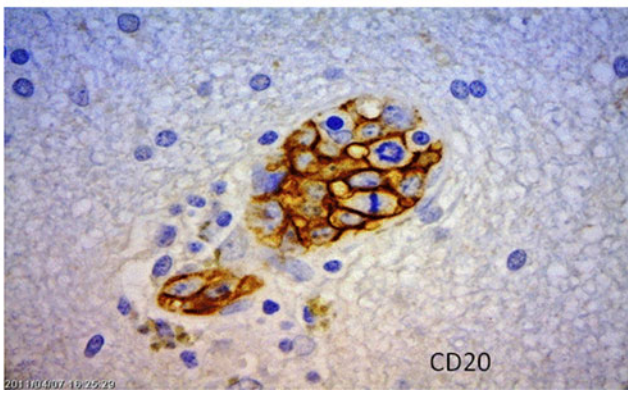

hippocampal nNOS did not change after burn injury and significantly increased after ACE inhibitor therapy ($p<0.05$).
Conclusion: Brain damage occurs after systemic thermal injury. Our data showed that the pathophysiological events following burn injury appear to be related to an acute inflammatory reaction which is modulated by nNOS in frontal cortex, striatum, midbrain and captopril treatment positively affected nNOS in the frontal cortex and midbrain.

004
Pacemaker cells in the arachnoideal villi

E. Egyed-Zsigmond *
*University of Medicine, Dept. of Morphology, Targu Mures, Romania

Objective: Interstitial cells of Cajal (ICC) are pacemaker cells. They have special properties that make them unique in their ability to generate and propagate slow waves in gastrointestinal muscles. Ultra structural observations revealed that certain types of ICC are intercalated between nerves and smooth muscle cells and indicate that they may act as a route for neurotransmission. We presumed that the filtration through the arachnoideal villi had an active component such as to anchor the contraction of the villi. We also presumed that the ICC might possess such ability.
Method: Analysis by immunohistochemical staining for Desmin, S100, Citokeratin, Vimentin, SMA, CD34, CD117 arachnoideal villous structure of 25 pathological processed cases.
Results: We got positivity for Desmin, S100, citokeratin, vimentin and CD117.
Conclusion: The presence of C-kit (CD117) positive cells in 70% of cases demonstrate by immunohistochemical staining that the ICC are structural elements of the arahnoideal villi.

005
Gliosarcoma with multiple cauda equina roots metastases

Y. Gorbacheva*, K. Paltseva, G. Evzikov, O. Egorov, A. Timoshenkov, L. Shishkina
*1st Moscow Medical University, Dept. of Pathology, Krasnogorsk, Russia

We report a rare case of gliosarcoma metastases arising in the spinal roots of a 28-year-old man. The patient was undergone surgical removal of the temporooccipital tumor 16 months ago (first surgery). MRI revealed a multiple small masses of cauda equina roots and patient was operated again (second surgery). On light microscopy the brain tumor showed biphasic pattern and the spinal roots masses formed from large, round undifferentiated cells with eosinophilic cytoplasm and peripheral located nucleus. The immunohistochemistry evidenced the heterogeneous (glial and mesenchymal) immunoprofile of brain neoplastic cells: S100 +, GFAP+areas and vimentin+ areas, and glial immunoprofile of spinal roots metastases. Tumor cells were negative for EMA, BerEp4, desmin.
Conclusion: Thus, the immunohistochemistry showed the gliosarcoma glial sources of cauda equina roots metastases.

006
Angiocentric glioma: a rare paediatric tumour associated with epilepsy

W. Grajkowska*, P. Daszkiewicz, M. Roszkowski, J. Peregud-Pogorzelski, E. Matyja
*Children´s Memorial Health Institute, Dept. of Pathology, Warsaw, Poland

Objective: Angiocentric glioma is a low-grade tumour in children with a longstanding epilepsy and distinct clinico-pathological features. Typical for angiocentric glioma is the presence of spindle-shaped cells, radially oriented around cortical blood vessels.
Method: The authors report two cases of angiocentric gliomas. A 15-year-old girl with chronic and intractable partial epilepsy underwent surgery for cystic tumour located in the right temporal lobe. A 14-year-old boy with intractable seizures revealed an extensive cortical lesion within the left parieto-occipital area on imaging studies. Craniotomy was performed with total excision.
Results: In both cases histopathology revealed tumours composed of elongated cells forming rosette-like pattern around blood vessels, as well as schwannoma-like areas. The neoplastic cells displayed immunoreactivity for GFAP, S-100, vimentin and EMA. The diagnosis of angiocentric gliomas was established. The patients were discharged home in a good condition with no seizure recurrence.
Conclusion: Appropriate diagnosis is important for adequate and successful treatment.

007
Devious pathology imitating brain tumour—adult polyglucosan body disease

A. Halon *, E. Iwaneczko
*Wroclaw Medical University, Dept. of Pathomorphology, Poland

Objective: Adult polyglucosan body disease (APBD) is a rare, progressive neurologic disorder characterized by the presence of intra-axonal polyglucosan bodies (PBs) in the central and peripheral nervous system. Patients usually present in the fifth or sixth decade of life with upper and lower motor neuron involvement, neurogenic bladder and dementia. APBD may represent a neuropathological hall-

mark of the adult form of glycogenosis type IV of the central nervous system caused by a deficiency of glycogen branching enzyme (α-1,4 glucan 6-transglucosylase).
Method: We analysed a case of an 81-year-old man who presented focal neurological symptoms. The patient was operated because of intracranial tumour suggestive of oligodendroglioma in CT.
Results: Neuropathological examination of removed tumour mass did not reveal any neoplastic tissue. The main microscopic abnormality was massive accumulation of round, acellular, PAS-positive PBs in the cortex and white matter of the whole specimen. PBs were observed in the processes of neurons, astrocytes and microglia cells most frequently around the vessels and diffusely beneath the pia.
Conclusion: This case of APBD presents dissonance between radiological and morphological examinations. There is no efficient method of its prevention or therapy. Applied in this case was neurosurgery as symptomatic treatment. Triheptanoin pharmacotherapy is under investigation.

008

Long-term mildronate neuroprotective effects in a rat model of Parkinson's disease

S. Isajevs *, D. Svirina, J. Pupure, J. Rumaks, S. Svirskis, Z. Dzirkale, B. Jansone, V. Z. Klusa
*Riga, Latvia

Objective: The aim of the present study was to evaluate mildronate [3-(2,2,2-trimethylhydrazinium) influence on inflammatory, neuroregenerative, as well as GABAergic and cholinergic pathways by analyzing glutamate decarboxylase 65/67 (GAD65/67), acetylcholinesterase (Achase), c-jun/AP-1, IL-1β, GAP-43 and Ki-67 expression in the brain striatum of animal model of Parkinson disease (PD).
Method: PD was modeled by 6-OHDA intrastriatal injection in rats. Mildronate was administered at doses 10, 20 and 50 mg/kg for 2 weeks intraperitoneally prior to 6-OHDA injection. The expression of markers was assessed immunohistochemically.
Results: The obtained results showed that 6-OHDA caused an increase in GAD65/67, IL-1β and c-jun/AP-1 expression in rat striatum. However, 6-OHDA decreased the numbers of Achase positive fibers. Mildronate at dose 50 mg/kg decreased GAD65/67, IL-1β and c-jun/AP-1 expression. In addition, mildronate increased the numbers of Achase nerve fibers.
Conclusion: Neuroprotective effects of mildronate involve antiinflammatory, GABAergic and cholinergic pathways. These data indicate mildronate's long-term effects as well as usefulness of its administration for the protection/delay of the progression of PD. Acknowledgement. ESF project Nr.2009/0217/1DP/1.1.1.2.0/09/APIA/VIAA/031.

009

Pure alexia of a Japanese pathologist: a case report

Y. Kimula *
*Osaka, Japan

Objective: A Japanese pathologist became pure alexia. A 62-year-old man, pathologist, had hypertension for 3 years without therapy. He had a 3-cm-diameter sized hemorrhage in the parietal lobe of the left cerebrum, left angular gyrus.
Method: He could not read the Japanese characters, namely katakana and hiragana. He had lost to read English alphabet and numbers. However, he can read Chinese characters. He can also read the Devanagari characters, which he had learned at his 50 years old for 7 years.
Results: Since he had memories of pictures of microscope in his right hemisphere of the brain, he could set pathological diagnosis to the patients through the light microscope. He did not show aphasia or paralysis. The first week of the disease he complained double vision and right homonymous hemianopsia, which disappeared after 2 weeks.
Conclusion: He felt the distress of kinesthetic, position, and spatial senses for a few months. He has got his memories of Japanese characters, English alphabets, and numbers after 4 years of rehabilitation therapy.

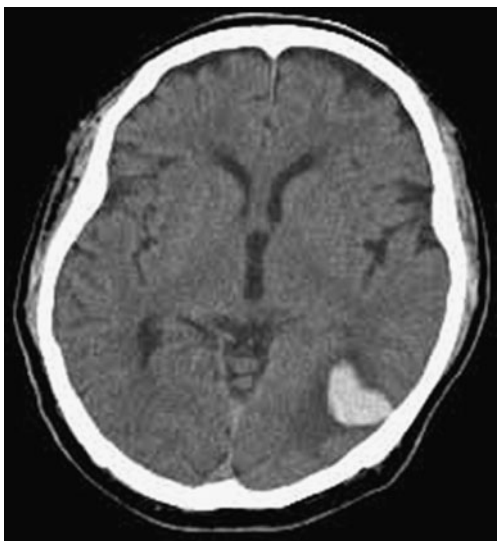

010

Benign epithelioid schwannoma of the pharynx: report of two cases

S. Mavropoulou *, Z. Tatsiou, A. Marinou, S. Papaemmanouil, G. Kougioumtzidis
*Xanthi General Hospital, Dept. of Pathology, Greece

Objective: Benign schwannoma has various morphologic patterns. Although an epithelioid variant of malignant schwannoma is well recognized, a benign counterpart has not yet been defined and may pose a challenge in histopathologic diagnosis.
Method: In the current study, we describe two cases of benign epithelioid schwannoma found in the pharynx of a 42-years-old man and a 48-years-old woman. The lesions were 3 and 1.5 cm in diameter and well circumscribed.
Results: On histological examination the tumors were composed of epithelioid or elongated cells with eosinophilic or amphiphilic cytoplasm, densely or loosely arranged in cords and nests, low mitotic activity and no evidence of nuclear pleomorphism or necrosis. Immunohistochemically, the neoplastic cells expressed S-100 protein with proliferation marker ki67 5%, whereas they were negative for cytokeratines, HMB45, SMA, desmin, CD68, LCA, CD117, CD99 and chromogranin. The patients nine months later have no symptoms of recurrence.
Conclusion: In conclusion, we report two exceedingly rare cases of benign epithelioid schwannoma of the pharynx, whose recognition is important because it may be misinterpreted as a malignant neuroectodermal, mesenchymal, epithelioid, or melanocytic tumor. The benign nature of the lesions was evident by a constellation of features, including sharp circumscription, bland morphology, low mitotic activity and a benign clinical course.

011

Diffusion tensor and dynamic susceptibility contrast MRI for the assessment of high-grade gliomas

A. Ntoulia *, A. Goussia, A. Zikou, G. Alexiou, P. Kosta, E. Lampri, L. Astrakas, S. Voulgaris, A. Kyritsis, M. Argyropoulou, V. Malamou-Mitsi
*University Hospital of Ioannina, Dept. of Pathology, Greece

Objective: The non-invasive assessment of glioma's proliferation is important for treatment planning, monitoring therapy response, biopsy guidance and estimation of prognosis. We investigated prospectively the correlation between diffusion tensor (DTI), dynamic susceptibility contrast (DSC) perfusion MRI metrics and Ki-67 index in high-grade gliomas.
Method: Twenty patients (ten males, ten females; mean age: 49.5 years) were operated on for glioma. DTI and DSC MRI were performed prior to surgical excision. Lesion/normal ratios were calculated for the apparent diffusion coefficient (ADC), fractional anisotropy (FA), relative cerebral blood volume (rCBV), cerebral blood flow (rCBF) and mean transit time (rMTT) ratio. In the excised tumor specimens, Ki-67 (MIB1) expression was evaluated immunohistochemically.
Results: The histological diagnosis was glioblastoma (n=17), anaplastic astrocytoma (n=2) and anaplastic oligoastrocytoma (n=1). A statistical correlation was observed between Ki-67 and ADC (r=-0.527, p=0.017), FA (r=0.565, p=0.0095), rCBV (r=0.646, p=0.043), rMTT (r=0.671, p=0.033) ratio. Karnofsky Performance Score over 80, near total resection and age under 60 years were associated with a better outcome, though the difference was not statistically significant. No correlation was found between ADC, FA, rCBV, rCBF, rMTT and the overall survival.
Conclusion: ADC, FA, rCBVand rMTT tumor/normal tissue ratios may represent indicators of glioma's proliferation.

012

Cerebellar meningioangiomatosis: radiologically mimicking a high-grade glial tumor

E.E. Pala *, U. Bayol, R. Beyhan, O. Binatli, D. Oncel
*Tepecik Training and Research Institute, Dept. of Pathology, Izmir, Turkey

Objective: Meningioangiomatosis (MA) is a rare, non-neoplastic probably hamartomatous condition, characterized by intracortical proliferation of meningothelial cells, capillary sized vessels and fibroblasts. It occurs sporadically and in patients with neurofibromatosis type 2. Cases typically present with seizures but may also be asymptomatic
Method: A 24-year-old man had a 15-year history of seizures. He presented with ataxia, gait and speech disturbance and left arm motor seizures. Computed tomography showed a cerebellar 5.5×2.5-cm heterogeneous density lesion with hemorrhage and edema. Postcontrast magnetic resonance imaging scans revealed the same lesion with peripheral bandlike contrast enhancement. Also a parietal meningiom and hamartomatous lesions in the basal ganglia were observed. The cerebellar lesion was totally resected.
Results: Histopathologic examination of the specimen showed thickened meninges with proliferation of uniform capillary-like blood vessels, perivascular cuffs of meningothelial cells and spindle shaped fibroblast in the underlying cortex. Necrosis and mitoses were absent.
Conclusion: The diagnosis was MA. After surgery he had medically intractable seizures. We report the case because

of unexpected clinical course, cerebellar localization and radiological features.

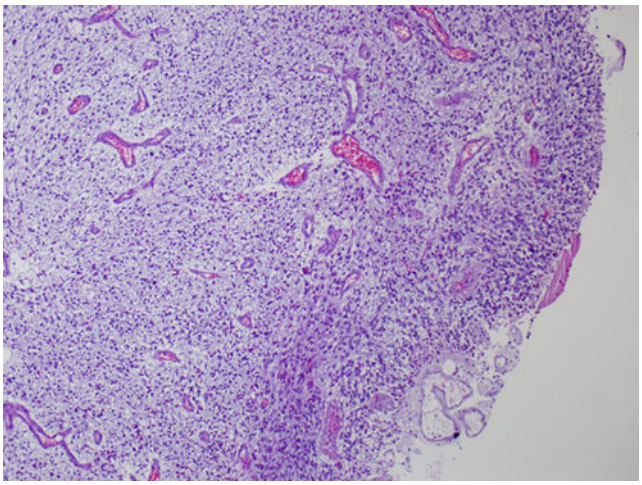

013

Long-term effects of sodium valproate in amylasis levels in the blood serum

S. Patiakas*, K. Panagiotellis, M. Palaiologou, C. Charalampous, U. Tsiatsiou
*General Hospital of Kastoria, Microbiological Laboratory, Greece

Objective: This is a study on the levels of amylase in serum of patients receiving valproic acid therapy and aims to investigate the potential risk of acute pancreatitis, which may involve the long-term use of medication. Recall that valproic acid, a drug commonly given to abstractions, automation, partial and generalized tonic–clonic seizures, was referred to in the literature in that it is a very common cause of acute pancreatitis.
Method: Our material consisted of serum samples from 58 patients. Normal values were on the serum amylase 20-70 UI/L, and valproic acid is 50-100 mg/ml.
Results: Of the total patients, only four (6.9%) had elevated amylase of serum. In three cases it was very small; however, in one case, it was found to co-exist with moderate amylasimia (265 UI/L) and a small increase in liver function. Finally, no patient experienced pancreatitis.
Conclusion: It is established that the therapeutic dose of medication does not cause amylasemia which is likely to cause pancreatitis; however, a slight increase of amylase in blood serum of these patients is not rare. Therefore, it is incumbent on epileptic patients regular laboratory testing, the levels of the drug, and amylase (and sometimes indicators of liver function) to avoid unpleasant complications.

014

Recurrent behaviour in spindle cell oncocytoma of the adenohypophysis

T. Ribalta *, D. Martínez, M. Sanchez, V. Fusté, A. Palacin
*Hospital Clinic Barcelona, Dept. of Anatomical Pathology, Spain

Objective: The spindle cell oncocytoma of the adenohypophysis (SCO) is a rare, primary, non-endocrine neoplasm of the adult recently codified by the WHO Classification of Tumours of the CNS, which clinically mimics a non-functioning macroadenoma. A derivation from adenohypophyseal folliculostellate cells has been suggested. Microscopically, the tumour is composed of interlacing bundles of spindle and epithelioid cells with eosinophilic and finely granular cytoplasm due to accumulation of mitochondria. The differential diagnosis includes pituitary adenoma, meningioma, schwannoma, and pituicytoma. Immunohistochemical examination is essential for the correct diagnosis. The treatment is surgical resection and the clinical course is usually benign. However, because of the rarity, the etiopathogenesis and natural history of these tumours have not been fully characterized yet.
Method: We present two patients (male, 41, 69) with a SCO, which showed several recurrences starting 8 months after surgery.
Results: Histological and immunohistochemical features were typical in both cases and remained unaltered at recurrences except for a slight increased MIB-1LI in the recurrent tumours. One patient died after a second recurrence three years after diagnosis, and the other is currently alive with tumour 21 months after diagnosis.
Conclusion: Our cases illustrate that pathologically typical SCO may show early-onset multiple recurrences without increasing atypical features. More experience with these tumours is required to understand the spectrum of behaviours of this rare neoplasm.

015

Spinal epidural angiolipoma in adult

M. Skender Gazibara *, E. Manojlovic Gacic, T. Gazibara, S. Raicevic, D. Grujicic
*University of Belgrade, School of Medicine, Serbia

Objective: Spinal epidural angiolipomas (SEA) are uncommon clinico-pathological entitity. They comprise varying proportions of mature fat and angiomatose elements.
Method: In the period 2005–2010, we have diagnosed five adults with angiolipoma. These patients have undergone neurosurgical intervention due to lower limb weakness, feet tingling and gait impairment. Surgically removed tissue was

routinely processed and stained by standard haematoxylin-eosine and van Gieson elastic method. For an immunohistochemical analysis, the following markers were applied: desmine, alpha-smooth muscle actine and CD34.
Results: Out of five patients diagnosed with angiolipoma, three were females aged 51 to 56 and two were male patients aged 70 and 81. In all cases tumor was located in the thoracic region, yet in different levels (from Th3 to Th11) causing compression of the spinal cord. Grossly, surgically removed tissue was of fairly soft consistency, colored yellowish-brown. Histologically, they were characterized by mature adipose tissue associated with numerous blood vessels of different types that ranged from capillaries to thick-walled vessels with smooth muscle layer proliferation. In some of them foci of recent hemorrhage were present.
Conclusion: Our case series of five patients clustered in a short time interval is of great importance for further investigation of such rare entities.

016

Spindle cell oncocytoma of the adenohypophysis: a case report

D. Violidaki *, E. Ronne, D. Papantoniou, T. Argyrakos, C. Magkou, D. Rontogianni
*Evangelismos General Hospital, Dept. of Pathology, Athens, Greece

Objective: Since its first description in 2002, spindle cell oncocytoma of the adenohypophysis numbers 14 cases. Our case recapitulates the basic characteristics already described, exhibiting however some unique features.
Method: Our 73-year-old female patient presented with peripheral visual loss. Cranial MRI revealed a solid 2–cm intrasellar tumor, considered to be a non-functioning macrodenoma and transsphenoidal resection followed.
Results: Histology demonstrated a predominantly spindle cell neoplasm with eosinophilic and focally granular cytoplasm. Mitotic activity and necrosis were absent. The entities that entered the differential diagnosis were meningioma, schwannoma, spindle cell oncocytoma of the adenohyphosis, pituicytoma, granular cell tumor of the neurohypophysis, oncocytic pituitary adenoma. The neoplasm was assessed with a broad panel of antibodies to conclude to the characteristic but not specific immunoprofile of the spindle cell oncocytoma of the adenohypophysis: vimentin, EMA, S100, galectin-3, TTF-1, and GFAP. Keratins, synaptophysin, pituitary hormones, thyroglobulin, neurofilaments and CD68 were negative. The nuclear expression of Ki67 was 2%, but all the tumor cells exhibited also membranous staining.
Conclusion: Spindle cell oncocytoma of the adenohypophysis is a rare entity with postulated origin from the folliculostellate cells. Although the morphologic and immunohistochemical criteria are well described, supplementary data determining its biologic behaviour are necessary.

017

Focal cortical dysplasias of brain: composition and geometry of the extracellular matrix—an immunohistochemical study

J. Zamecnik *, L. Vargová, M. Cicanic, A. Homola, P. Krsek, P. Marusic, E. Sykova
*Charles University Prague, Dept. of Pathology and Moleular Medicine, Czech Republic

Objective: Changes in the geometry and composition of the extracellular space (ECS) may influence the epileptogenesis in the focal cortical dysplasias (FCD).
Method: The tissue ECS geometry (i.e. the geometrical factor "tortuosity" reflecting various ECS diffusion barriers) were studied in cortical samples of 55 patients surgically treated for epilepsy, including 20 patients with FCD type I and of 6 patients with FCD type II by the real time iontophoretic method. The samples were consequently subject to immunohistochemical analysis of the composition of extracellular matrix (ECM) and GFAP.
Results: In both FCD type I and FCD type II, the tortuosity of the ECS was significantly increased. Although no significant changes in ECM composition were noted in FCD type I (when compared to controls), we observed increase in GFAP+glial processes in both FCD types and pathological accumulation of some ECM molecules (i.e. tenascins and chondroitin sulphate) in the ECS of FCD type II.
Conclusion: The ECS of FCD has increased tortuosity reflecting the increase of diffusion barriers in the ECS. We propose that disturbed extrasynaptic transmission through the ECS of such cortex represents another factor contributing to the epileptogenicity of FCD. Supported by IGA MZCR NS9915-4 and MZOFNM2005.

018

Histological and immunohistochemical evaluation of rat sciatic nerve regeneration after application of collagen–polyvinyl alcohol scaffold

O. Zarnescu *, A. Mihai, E. Utoiu, L. Moldovan, I. P. Florescu
*Bucharest University, Dept. of Histology, Romania

Objective: It has been demonstrated that severe nerve injuries require surgical repair and need a scaffold to promote the regeneration of the injured peripheral nerve. A variety of biomaterials, including synthetic and natural

biomaterials have attempted to be employed to bridge nerve defects. In this study we evaluated rat sciatic nerve regeneration using a biodegradable nerve guides composed of natural polymer collagen (COL) and water-soluble synthetic polymer, polyvinyl alcohol (PVA) in a ratio of 1:1.
Method: A 1-cm segment of the sciatic nerve was removed and replaced by biodegradable nerve guide. Proximal and distal stumps were secured into the ends of a nerve scaffold. After 12 weeks, the COL-PVA tube and the regenerating nerves were harvested and processed for histology. Penetration and proliferation of Schwann cells into the conduit was evaluated by S-100 immunohistochemistry.
Results: The histological results demonstrated that the COL-PVA conduits were capable of leading the damaged axons and Schwann cell through the injured area.
Conclusion: The results from the in vivo study suggest that COL-PVA biomaterial could facilitate re-innervations of damaged sciatic nerve and might offer a potential treatment modality to peripheral nerve injuries. This work was supported by Project Regenes, No. 42-137/2008.

019

Langerhans cell histiocytsis of the cranial vault

A. Zehani *, H. Azzouz, I. Chelly, H. Nfoussi, K. Bellil, S. Nechi, D. Ben Ghachem, H. Jemel, S. Haouet, N. Kchir, M. Zitouna
*Tunis, Tunisia

Objective: Langerhans cell histiocytosis (LCH), previously known as histiocytosis X, is a rare disorder characterized by clonal proliferation and excess accumulation of pathologic Langerhans cells causing local or systemic effects. Bone is the most common organ involved. The most frequent sites of the bony lesions are the skull, femur, mandible, pelvis and spine.
Method: Six cases of cranial LCH, diagnosed between 1999 and 2010, were reviewed retrospectively, noting the clinical and pathological characteristics.
Results: The patient population consisted of four males and two females. The mean age was 11 years with extreme ranging from 3 to 27 years. Bone pain was the major presenting symptom. Imaging features showed an osteolytic lesion of the cranial vault. Surgery was performed in all cases. Pathological examination revealed an infiltrate composed of Langerhans cells, macrophages, lymphocytes, plasma cells and a variable fraction of eosinophils. The nuclei of Langerhans cells are typically slightly eccentric, ovoid, reniform or convoluted with and inconspicuous nucleoli. The cytoplasm is large and eosinophilic. Immunohistochemically, Langerhans cells consistently express S-100 protein and CD1a.
Conclusion: Clinical presentation and behaviour are heterogeneous and can range from a solitary lytic bone lesion with a favourable course to a fatal disseminated leukaemia-like form, with a wide spectrum of intermediate clinical presentations between these two extremes.

020

Pituitary blastoma: confirmation of an entity

B. Scheithauer *, E. Horvath, T. Abel, C. Deal, Y. Robitaille, R. Osamura, K. Kovacs
*Mayo Clinic, Dept. of Neuropathology, Rochester, USA

Objective: Pituitary blastoma is a rare, recently described neonatal pituitary tumor exhibiting Rathke epithelium as well as undifferentiated, secretory and folliculostellate cells (Scheithauer et al., *Acta Neuropathol* 116: 657, 2008). Its components reflect pituitary development.
Method: We report two additional cases in a 9-month-old male and a 13-month-old female patient. MRI scans in both showed large, invasive sellar/suprasellar masses. Endocrine testing demonstrated elevated, nonsuppressible plasma ACTH levels in the male and no hyperfunction in the female. Diabetes insipidus was lacking. Both patients received chemotherapy (temozolomide). Subtotal resections were achieved; one tumor was re-excised upon recurrence.
Results: Histologically, the tumors featured islands of secretory cells in association with small cells and Rathke epithelium-forming large glands; one featured primitive, spindle cell stroma. Cell proliferation was noted (3 and 16 mitoses/10 hpf; MIB-1 indices of 50% and 60%). The immunophenotype of both tumors included synaptophysin, chromogranin, keratins and primarily ACTH. Germ cell markers were negative. The ultrastructure of one tumor showed three cell types including small, primitive, glycogen-rich cells ("blastema"), folliculostellate cells with follicle formation, and corticotrophic cells (150–400 nm secretory granules, perinuclear intermediate filament bundles).
Conclusion: Our findings confirm the diagnosis of pituitary blastoma, align it with blastomas of other organs, and suggest that specific genetic abnormalities underlie its genesis.

Tuesday, 30 August 2011, 09.30—10.30 and 16.30–17.00, Hall 5

PS-17 Poster Session Uropathology

001

Histopathology of urinary bladder biopsy: a data on 151 specimens

M. Z. Rahman *, S. Islam, M. M. Hoque, M. S. Uddin Ahamed
*Chittagong Medical College, Dept. of Pathology, Bangladesh

Objective: Urinary bladder (UB) cancer ranks the 9th most common cancer worldwide of all urinary tract cancers. Approximately 90% of the epithelial tumors are transitional cell carcinoma (TCC). The distribution of histologic types varies in different populations. This study observed the histopathological features of UB biopsy, pointing out the pitfalls of diagnosis.
Method: A total 151 specimens of UB biopsies from 2005 to 2009 were studied. TCCs were graded as low- and high-grade tumours. Pathological staging was also done according to the TNM system.
Results: Among 151 specimens, 126 (83.44%) revealed malignant. 124 (98.42%) of them were TCC, 1 (0.79%) squamous cell carcinoma and 1 (0.79%) metastatic adenocarcinoma. Male to female ratio is 11.4:1 in TCC patients. Mean age was 60.63 years and highest incidence 36 (29.03%) was in 50-59 years age group. 37.1% were low grade and 62.9% were high grade tumors. 82 (66.13%) of the TCC specimen were adequate and 45 (54.88%) of them were in stage pT1, 28 (34.15%) in stage pT2, 06(7.32%) in stage pT3 and 3(3.67%) in stage pT4. 91.9% of the invasive tumors were in the age group above 50 years. 36 (66.6%) of 54 high grade tumor were invasive (stage pT2-4). 33.87% cases were found inadequate revealing absence of muscular layer.
Conclusion: Incidence of bladder cancer is increasing. Its early diagnosis with proper grading and staging may reduce the morbidity and mortality from bladder cancer, but it needs special care while taking biopsy specimen to reduce the rate of inadequacy.

002

Differential changes in ADAM proteins in renal cell carcinoma

B. Akkaya *, N. Erin, B. Akkaya, T. Ipekci, I.H. Ozbudak, M. Baykara
*Akdeniz University, Dept. of Pathology, Antalya, Turkey

Objective: ADAMs are a family of metalloproteases. Increasedn expression of ADAM9, ADAM10, ADAM17 was associated with tumor progression. We studied the changes in the alpha-secretase activity as well as immunostaining intensity of these ADAMs in RenalCellCarcinoma (RCC).
Method: Alpha-secretase activity was determined flourometrically in freshly frozen RCC and neighboring kidney tissue of 60 patients. ADAMs staining intensity (SI) and percentage of stained cells (PP) were assessed using scales. Overall immunoreactivity of ADAMs was evaluated by immunoreactivity score (IRS) (IRS=SI × PP).
Results: Alpha-secretase activity as well as ADAM9 immunostaining was significantly lowers (more than 50%) in tumor compared to the neighboring tissue regardless of tumor type. ADAM17 immunoreactivity, however, were lower in early disease compared to advanced carcinoma in papillary type but not clear cell carcinoma. Surprisingly, decreased expression of ADAM17 in advanced carcinoma of clear cell was observed. ADAM10 levels were significantly lower in all types compared to neighboring tissue and there was no difference between early and advanced disease.
Conclusion: The aberrant (cytoplasmic) expression of all ADAMs however was observed in tumor. Aberrant expression of ADAM17 may promote tumor progression in papillary cell type. Further studies are needed to evaluate possible anti-tumoral effects of alpha-secretase activity.

003

Quantification of extraprostatic perineural spread and its prognostic value in pT3a pN0 M0 R0 prostate cancer patients

K. Aumayr*, M. Breitegger, P. Mazal, A. Koller, M. Marberger, M. Susani, A. Haitel
*Medizinische Universität Wien, Inst. für Klinische Pathologie, Austria

Objective: The prognostic relevance of the amount of extraprostatic cancer spread in nerves in prostate cancer patients is not well established.
Method: There were 88 patients included in our study with pT3a pN0 M0 R0 prostate cancer treated with retropubic prostatectomy. A total of 87 of them showed perineural invasion; 54 were confined to the prostate; 33 showed cancer spread in extraprostatic nerves, which was quantified by counting each transverse section of nerves infiltrated by cancer in totally embedded specimen. Biochemical relapse was established by serum PSA levels of≥0.2 ng/mL as well as PSA≥0.4 ng/mL and higher according to the EAU guidelines.
Results: Extraprostatic but not intraprostatic perineural infiltration was significantly more often found in tumors of higher Gleason score. Intraprostatic number of infiltrated nerves (NIN) correlated with extraprostatic NIN. There was no association between extraprostatic or intraprostatic NIN and Gleason score, lymphatic, or blood vessel invasion. Extraprostatic neural infiltration in<10 nerves extended relapse free survival in univariate analysis for PSA 0.2 ng/mL and 0.4 ng/mL (p=0.002, p<0.000001, respectively) and remained significant in multivariate analysis for PSA 0.4 ng/mL (p=0.039).
Conclusion: A high amount of extraprostatic NIN correlates with tumor progression and seems to be an independent prognostic parameter.

004

Researching the correlation between surfactant protein-A and surfactant protein-D expression in high-grade prostatic intraepithelial neoplasia

C. I. Bassorgun*, I.H. Ozbudak, Meryem I.E. Karanis, O. Kankavi, M.A. Ciftcioglu, M. Baykara
*Akdeniz University, Dept. of Pathology, Antalya, Turkey

Objective: Prostatic adenocarcinoma is the most common cancer in males. High-grade prostatic intraepithelial neoplasia (PIN) is the earliest accepted stage in prostatic carcinogenesis. PIN is the abnormal proliferation within the prostatic ducts, ductules, and large acini of premalignant foci of cellular dysplasia and carcinoma in situ without stromal invasion. Surfactant proteins were first determined in lung tissue and thought to be lung-specific for many years. As a result of studies performed up to date, surfactant proteins were also shown in joint synovial fluid, gastric and colonic mucosa, periton, pleura, liver, kidney, pancreas, urinary and male–female genital tract.
Method: In this study, we searched about surfactant proteins-A (SP-A) and surfactant proteins-D (SP-D) expression in prostatic tissue and high grade prostatic intraepithelial neoplasia. In this study, 35 radical prostatectomy materials were evaluated; SP-A and SP-D were applied immunohistochemically on non-tumoral prostatic tissue and high grade prostatic intraepithelial neoplasia.
Results: As the results were evaluated; SP-A and SP-D expressions were both seen in non-tumoral tissue and high-grade prostatic intraepithelial neoplasia.
Conclusion: In high-grade prostatic intraepithelial neoplasia areas, increased SP-A and SP-D expression was detected.

005

A case of synchronous bilateral testicular seminoma

G. Benkhedda *, A. Lamouti
*Blida, Algeria

Objective: Testiculary cancer generally affects young men. It represents between 1% and 2% of male neoplasms and 3.5% of urological tumors in general. Bilateral testis tumors are rare and the majority of cases are classic seminoma presenting metachronously.
Method: We report a case of a 34-year-old man with a remote surgical history of orchiopexy for bilateral undescended testicles.
Results: Macroscopy: Both testes were enlarged with solid masses measuring 72×51 mm in diameter on the right side and 9.6×7 mm on the left side. The cut surface of the tumors are fleschy and lobulated and varies in color from cream to tan to pink. Small areas of hemorrhage have seen. Microscopy: The tumors were composed of monotonous sheets of uniform round cells with rather clear cytoplasm and centrally located round nuclei. The fibrous stroma shows lymphocytic infiltrate.
Conclusion: Patients with synchronous bilateral testicular germ cell tumors might gererally fare well, as they often present with early-stage disease. Treatment is no different for patients with bilateral germ cell tumors for patients with unilateral germ cell tumors. However, a special consideration is warranted for patients with bilateral masses because of the psychological and endocrine sequelae of surgical castration.

006

Focal partial and complete prostatic atrophy: a detailed morphologic study on presence of chronic inflammation and aberrant immunohistochemical expression

A. Billis*, A.C.S. Piaza, L. Meirelles, L.L.L. Freitas, J.F.L. Bonfitto, L.B.E. Costa
*University of Campinas, School of Medicine, Brazil

Objective: It is controversial whether chronic inflammation is a cause or a secondary phenomenon in atrophy.
Method: The frequency and concommitance of partial and complete atrophy, presence of chronic inflammation and the aberrant immunohistochemistry of the secretory compartment in both subtypes (using 34betaE12, p63, PSA, PAP, androgen receptor, CK8, CK18, Cam 5.2, CK5, CK14, c-myc, and c-met) was studied on 120 needle prostatic biopsies.
Results: Complete atrophy was present in 118/120(98.3%) biopsies; partial atrophy in 69/120 (58.1%) biopsies, and in 67/120 (55.8%) biopsies both lesions were found. Aberrant expression was present only in complete atrophy and probably is the expression of an intermediary cell phenotype. In 32/120 (26.6%) biopsies partial atrophy merged with complete atrophy in the same focus as well as in the same gland which is highlighted by the aberrant phenotypic expression. Chronic inflammation was seen only in complete atrophy.
Conclusion: Partial atrophy and complete atrophy are frequently found in the same biopsy. The mergence of these two lesions seems to favor that partial atrophy precedes complete atrophy. The absence of inflammation in partial atrophy as well as in areas of mergence between the lesions favors the idea that chronic inflammation may be a secondary phenomenon.

007

Infiltrative urothelial carcinoma discovered by diffuse in situ carcinoma involving the prostatic ducts: a clinical and pathological diagnostic challenge

A. Borda *, A. Dema, A. Loghin, M. Decaussin-Petrucci, K. Branzaniuc, N. Berger
*University of Medicine and Pharmacy, Tirgu Mures, Romania

Objective: Intraductal urothelial carcinoma (UC) is an unusual finding on prostatic biopsy (PB) and may be confused with prostatic adenocarcinoma.
Method: A 62-year-old patient was treated for 3 months for a subacute prostatitis without success. Subsequently, a PB was performed. It showed an involvement of the peripheral prostatic ducts (PDs) by a very atypical multilayered epithelium. On immunohistochemistry, the tumoral cells were PSA and P504S negative and CK7-CK20 positive. The basal cell layer of the PDs was preserved and expressed p63. Therefore, a diagnosis of intraductal UC was made.
Results: The cystoscopy showed diffuse superficial bladder lesions with positive cytology. On cystoprostatectomy, a 2-cm pT2 infiltrating UC was found, accompanied by diffuse CIS, involving the bladder, the urethra and the PDs. No invasive component was found in the prostate.
Conclusion: Involvement of the PDs by the UC of the bladder is the result of direct extension from the underlying urethra. Usually, the centrally located PDs are more often concerned than the peripheral ones. It was the case of our patient in whom UC was detected by PB of the peripheral zone and represented a serious diagnostic challenge. The prognosis of bladder UC is not modified by in situ PDs involvement.

008

TGF-β: expression in chromophobe renal cell carcinoma and oncocytoma

S. Cesarec*, A. Demirovic, Z. Demirovic, T. Dzombeta, M. Bezjak, D. Tomas, B. Kruslin
*Zagreb, Croatia

Objective: The most important and challenging differential diagnosis of chromophobe renal cell carcinoma (CRCC) is renal oncocytoma (RO). Recent research has shown differences in the presence and thickness of tumor-surrounding capsule between CRCC and RO. Our aim was to investigate and compare TGF-β expression in CRCC and RO in order to assess its potential role in capsule formation.
Method: We investigated 16 CRCCs and 18 RO for the immunohistochemical expression of TGF-β. Expression was analyzed in the tumor, the capsule and surrounding renal parenchyma. Reaction was grouped by intensity, quantity and type, as follows: intensity—absent/weak, medium, strong; quantity—<10% of cells, 10-50% of cells, >50% of cells; type—membranous, mixed, cytoplasmic.
Results: The intensity of TGF-β was weaker in CRCC than the one observed in RO ($p<0.05$),. It was predominantly membranous ($p<0.001$), unlike RO, which exhibited a predominantly cytoplasmic reaction. The intensity and quantity of TGF-β expression in tumor capsule and surrounding renal parenchymsa did not show any difference between CRCC and RO ($p>0.05$).
Conclusion: The process of capsule formation remains an enigma in the investigation of CRCC and RO. There are some differences in TGF-β expression pattern between CRCC and RO which can be used to distinguish them.

009

Primary versus solitary secondary carcinoma of the kidney: presentation of a very rare case and differential diagnosis considerations

H. Trihia*, M. Parcharidou, P. Tziakou, D. Petsis, P. Dadioti-Arapantoni
*Metaxa Cancer Hospital, Piraeus, Greece

Objective: Kidney metastases from thyroid cancer are rare. Less than 20 cases have been documented in the literature, of both follicular and papillary type. All of these tumours have demonstrated immunoreactivity with thyroglobulin and/or TTF1 and confirmation of a neoplasm in the thyroid.
Method: We describe a case of a solitary renal tumour in a 70-year-old woman with a history of partial thyroidectomy 30 years ago. She underwent right nephrectomy. The differential diagnosis included thyroid papillary carcinoma follicular variant and primary thyroid-like follicular carcinoma of the kidney.
Results: Metastatic tumours are of great significance since they may represent the only symptom of an undiscovered malignancy. Thyroid-like follicular renal cell carcinoma represents a unique histologic subtype of renal cell carcinoma of low malignant potential. Accurate diagnosis is possible after a metastasis from a primary thyroid carcinoma is ruled out both immunohistochemically and clinically.
Conclusion: Our case may offer more insight into the recently described entity of this primary tumour of the kidney as it shared common histological features, although assumed to be metastatic, due to TTF1 positivity. Its primary importance is to distinguish it from metastastic thyroid carcinoma as it carries completely different prognostic and therapeutic implications.

010

Neuroendocrine dedifferentiation of a prostate adenocarcinoma after hormonal treatment

A. Dema *, S. Taban, A. Borda, C. Lazureanu, M. Cornianu, A. Muresan, D. Herman, D. Onet, D. Popovici, S. Dema
*University of Medicine, Dept. of Pathology, Timisoara, Romania

Objective: The concept of neuroendocrine (NE) differentiation in prostate carcinoma has two major aspects: prostate tumors with primary NE differentiation and NE differentiation occurred during hormonal therapy for prostate adenocarcinoma, with the extreme case of tumor dedifferentiation into a NE hormone resistant carcinoma with poor prognosis and rapidly fatal evolution.
Method: The patient, 62 years old, with a history of poorly differentiated prostate adenocarcinoma, hormonally treated with the decrease and then constant maintenance of serum PSA level to 0.01 ng/ml, was admitted in the hospital 8 years after prostate tumor diagnosis and 3 years after ceasing of hormone therapy, with multiple bone and liver metastases.
Results: The serum levels of CgA, NSE, CEA, CA19.9 and serotonin were elevated. The histopathological examination of the fine needle biopsy fragment from a liver metastatic lesion revealed high-grade neuroendocrine carcinoma, small cell type. Despite the prompt chemotherapy, the disease has progressed, with the occurrence of brain metastases and the patient's death 6 months after the detection of the metastatic disease.
Conclusion: The present case confirms the diagnostic difficulties of metastatic undifferentiated small cells tumors, and on the other hand, draws attention to the possibility of NE dedifferentiation as a result of hormone deprivation in patients with prostate cancer.

011

Expression of basal cell markers in prostate carcinomas

A. Dema *, D. Herman, C. Lazureanu, E. Lazar, M. Cornianu, S. Costi, F. Miclea, D. Anderco, A. Faur, A. Loghin
*University of Medicine, Dept. of Pathology, Timisoara, Romania

Objective: The expanding use of serum prostate-specific antigen (PSA) determination has resulted in a consistent increase in the number of prostate core needle biopsies (NB) with difficult lesions that often require further IHC investigations. The most used reactions to elucidate these lesions are those that identify basal cells and P504S/AMACR.
Method: There were investigated 100 specimens of prostate carcinoma with High Molecular Weigh Cytokeratin (HMWCK) and p63. The expression of basal cell markers was evaluated in the carcinomatous cells.
Results: In 4% of the investigated prostate adenocarcinomas positive reaction for one or both basal cell markers was identified in tumor cells: one case of poorly differentiated prostate adenocarcinoma showed rare p63-positive tumor cells nuclei, in the absence of reactivity for HMWCK in that area. In other three cases, we noticed HMWCK reactivity in the tumor cells with focal distribution, as follows: a prostate adenosquamous carcinoma that expressed also p63 in squamous areas' cells, a foamy gland carcinoma and an intraductal contingent of prostate adenocarcinoma.
Conclusion: Basal cell markers were expressed in a small percentage of prostate adenocarcinomas. Awareness of aberrant basal cells markers reactivity is essential for the correct classification of prostate lesions and for avoiding diagnostic errors.

012

Unusual patterns of high-grade prostatic intraepithelial neoplasia: morphological and immunohistochemical aspects

A. Dema *, S. Taban, C. Lazureanu, E. Lazar, A. Borda, A. Muresan, D. Anderco, A. Loghin,
R. Cornea, L. Daminescu
*University of Medicine, Dept. of Pathology, Timisoara, Romania

Objective: High-grade prostatic intraepithelial neoplasia (HGPIN) is the most likely precursor of prostate adenocarcinoma. There are described four basic architectural patterns, plus several architectural and cytological variants, some recently characterized. This paper presents three HGPIN lesions with particular morphology.
Method: The three patients were aged between and 67 and 74 years. Immunohistochemical (IHC) investigation was performed with anti-p63, anti-HMWCK, PSA and AMACR antibodies.
Results: All three HGPIN lesions were associated with invasive carcinoma. The first case showed a gland with flat HGPIN, AMACR-positive, in combination with a luminal contingent of foamy AMACR-negative cells. The second case presented on TUR material, a single HGPIN focus with inverted pattern associated with tufting subtype. The third case revealed a particular aspect: foamy histiocytes and spotty calcifications in the apical portion of some HGPIN micropapillae.

Conclusion: All three HGPIN lesions were associated with invasive carcinoma. The first case showed a gland with flat HGPIN, AMACR-positive, in combination with a luminal contingent of foamy AMACR-negative cells. The second case presented on TUR material, a single HGPIN focus with inverted pattern associated with tufting subtype. The third case revealed a particular aspect: foamy histiocytes and spotty calcifications in the apical portion of some HGPIN micropapillae.

013

Mucinous adenocarcinoma of the urinary bladder

S. Dumitriu *, A. Dumitriu, M. Chetrone, D. Miron, V. Ionita, I. Fulga, C. Georgescu
*UMF Iasi, Dept. of Pathology, Romania

Objective: Mucinous adenocarcinoma of the urinary bladder occurs more commonly in males than in females and affects adults within a peak incidence in the sixth decade of life.
Method: We present a case of a 73-year-old female who presented to the hospital with haematuria, dysuria and mucosuria.
Results: Grossly, the tumour was exofitic, ulcerating and exhibited a gelatinous appearance. Histologically, the tumour showed abundant mucin with tumour cells floating within the mucin.
Conclusion: We present this case for the rarity of this form of adenocarcinoma.

014

Lesion that mimic prostate carcinoma: the role of high molecular weight cytokeratin in differential diagnosis with a well-differentiated adenocarcinoma: case report

M. Enciu *, M. Aschie, A.-A. Nicolau, A. Chisoi, I. Poinareanu, A. Iliesiu, A. F. Mitroi, G. Baltatescu, F. Voinea
*Emergency County Hospital, Dept. of Pathology, Constanta, Romania

Objective: Prostate adenocarcinoma is the most common malignant disease of prostate and is the second leading cause of cancer mortality in men. A major problem diagnosis is differentiating adenocarcinoma of the large number of atypical glandular proliferations that mimics prostate adenocarcinoma.
Method: We present the case of a 73-year-old male admitted in the Second Surgery Department of Emergency County Hospital, Constanta, with intense dysuria and incomplete retention of urine.
Results: Pathologic examination of the transurethral resection specimen can not exclude a well differentiated adenocarcinoma and require immunohistochemical techniques—CK HMW to confirm the diagnosis. To evaluate the immunohistochemistry results we compared this case with two cases of benign and malignant lesions of prostate. This technique showed the presence of basal cells in lesion suspected for malignancy which demonstrates the benign nature of lesion. In case of malignant lesion the basal cells were absent.
Conclusion: In conclusion, high molecular weight cytokeratin is extremely useful in the differential diagnosis between a benign lesion that mimics prostate carcinoma avoiding a false positive diagnosis.

015

MMP-2 and MMP-9 in lymph node positive bladder cancer

A. Fleischmann *, R. Seiler, G. N. Thalmann
*Universität Bern, Inst. für Pathologie, Switzerland

Objective: Matrix metalloproteinases (MMP), particularly MMP-2 and MMP-9, participate in tumor progression of various cancers. Their significance in urothelial bladder cancer (UBC) is unclear. Expression analysis of MMP-2 and MMP-9 in normal urothelium, tumor centre, invasion front and lymph node metastases might help to elucidate their relevance in UBC.
Method: One hundred fifty nodal positive UBC patients underwent cystectomy and lymphadenectomy. MMP expression (H-score) was determined in a tissue-microarray and correlated with tumor characteristics (stage; number, total diameter and extranodal extension of metastases) and survival.
Results: Expression significantly increased from normal urothelium over primary tumors to metastases in MMP-9 (median scores: 20, 50, 65; $p<0.005$) but not in MMP-2 (median scores: 5, 22, 10; $p<0.005$). Expression in the tumour centre and at the invasion front was not different in both MMP. No association between MMP expression and histopathological tumour characteristics were identified. There was a non-significant trend for better outcome of primary tumors with high MMP-2 expression.
Conclusion: MMP-2 and MMP-9 expression in UBC was not increased at the invasion front suggesting an infiltration strategy independent of MMP-2 and MMP-9 activity. Larger series are needed to detect a potential significant survival benefit in cancers with high MMP-2 expression.

016

Neuroendocrine differentiation is significantly more frequent in lymph node metastases than in corresponding primary prostate cancers

A. Fleischmann *, C. Rocha, I. Zlobek, G. N. Thalmann
*Universität Bern, Inst. für Pathologie, Switzerland

Objective: Neuroendocrine serum markers in prostate cancer have recently attracted considerable attention for their ability to predict tumor progression and monitor disease. However, little is known about distribution of neuroendocrine tumor cells in the various Gleason patterns (GP) and in metastases.
Method: A tissue-microarray was constructed from 119 hormone-naïve lymph node positive, surgically treated prostate cancers containing tissues from all GP present in every primary tumor and corresponding lymph node metastases. Extent of neuroendocrine differentiation (chromogranin A) was correlated with different tumor features and survival.
Results: Chromogranin A showed progressive and significant increase in expression from normal glands to primary tumor to lymph node metastases (0.4%, 1%, 2.6%; $p<0.001$). The trends for higher chromogranin A expression in higher GP, more and larger metastases in chromogranin A positive metastases and poor survival in chromogranin A positive primary tumors were not significant ($p>0.05$).
Conclusion: Neuroendocrine differentiation is more frequent in nodal metastases than in matched primary prostate cancer. This suggests a correlation of high neuroendocrine serum markers with metastatic disease what might be the pathophysiological basis for the reported survival prediction according to elevated neuroendocrine serum markers. To better understand the prognostic relevance of neuroendocrine differentiation in prostate cancer tissue larger populations should be evaluated.

017

Paratesticular endometriosis in a man with a prolonged hormonal therapy for prostatic carcinoma

M. Fukunaga *
*Jikei University Daisan Hospital, Dept. of Pathology, Tokyo, Japan

Objective: A very rare case of paratesticular endometriosis in a 69-year-old male with prostatic carcinoma, who had a history of 9-year hormonal therapy, is presented.
Results: The lesion was a monolocular cyst, 5.2×3.1×.3.0 cm in size, containing bloody serous fluid in the left paratestis. Microscopically, the cyst was partly lined by a single layer of cytologically bland cuboidal or columnar cells. A small number of glands were scattered in the underling stoma composed of closely packed small round or ovoid cells resembling endometrial stromal cells, and abundant c arterioles. Hemosiderin-laden histiocytes were observed. The lesion was indistinguishable from endometrium. Immunohistochemically, the lining cells of the cyst and glands were positive for CAM5.2, vimentin and carletinin and were negative for CD10, estrogen- and progesterone-receptors, indicating mesothelial profiles. The stromal cells expressed vimentin, estrogen- and progesterone-receptors and CD10. The findings indicated stromal endometriosis associated with the tunica vaginalis. Among six other reported males with genitourinary endometriosis, five had been treated with estrogens for carcinoma of the prostate.
Conclusion: A history of estrogen therapy for prostatic carcinoma should suggest the possibility of endometriosis. Mullerian or endometrioitc metaplasia under the influence of estrogen may be the mechanism of this lesion.

018

Histopathological, histochemical and clinical examination of malakoplakia: case report

L. Golubovic*, S. Zivkovic, I. Golubovic, G. Lilic, I. Dimkovski
*Clinical Center Nis, Dept. of Hematology, Serbia

Objective: Malakoplakia ("soft plaque") is rare chronic granulomatous condition, that can affect any organ, but the urinary bladder is the most frequently affected organ. Having in the mind that the histological analysis is the only method providing a positive diagnosis and the possibility of healing with a simple medical treatment of the malakoplakia, we report this case.
Method: A 74-year-old male presented in Urology hospital with complaints dysuria, nocturia and haematuria, associated with suprapubic pain. He also suffered from diabetes mellitus and hipertension. Multiple biopsies of the involved arieas of the urinary bladder were taken with biopsy forceps and fixed in formaldehyde solution. Paraffin sections were stained with HE, PAS and Koss' techniques.
Results: On clinical examination he was pale. Laboratory investigations showed hemoglobin of 7 mg/dl. Midstream urin showed numerous red blood cells and numerous leucocytes. Cystoscopic, ultrasound and CT imaging appearances were non-specific, simulating those of neoplasms. Histopathology has revealed hyperplastic, reactive, bladder mucosa, infiltrated with sheets of histiocytes and rare lymphocytes; histiocytes had the abundant granular PAS+cytoplasm. In addition, Von Koss' stain showed laminated mineralized concretions known as Michaelis-Gutmann bodies, both within the mactrophages and between cells, representing the pathognomonic histologic finding of the Malakoplakia.
Conclusion: Definitive diagnosis of Malakoplakia is histopathological, essential for appropriate conservatrive management. The genesis of malakoplakic lesion is still uncertain.

019

Primary paraganglioma of urinary bladder: a case report

M. T. Gonzalez Serrano *, J. Salvatierra, M. E. Sanchez Frias, H. Fuentes Vaamonde, Y. O. Rangel Mendoza, M. T. Caro Cuenca, R. Ortega Salas, M. Medina Perez
*Hospital Reina Sofia, Dept. of Pathology, Cordoba, Spain

Objective: Urinary bladder paraganglioma represents 0.06% of all bladder tumors and 6% of extra-adrenal pheochromocytomas. Usually develops in young adult women. Because its low incidence rate is rarely encountered, and the prognosis is not well established.
Method: We described a case of a 26-year-old man with hematuria and disuria, without any symptons suggesting an endocrine active paraganglioma. Ultrasonography revealed a solid, hypervascularized mass with heterogeneous enhancemet, arising from the left lateral wall of the bladder, confirmed by cistoscopy. The patient underwent transurethral resection.
Results: Histologically, the tumor cells were rounded with granular cytoplasm and ovoid nuclei, arranged in a nested pattern, separated by a prominent vascular network with infiltration of muscle leyer. Immunohistochemistry were positive for chromogranin, NSE, S-100 protein and synaptophysin.
Conclusion: Urinary bladder paraganglioma may be misdiagnosed when characteristic symptoms are absent, and should be considered as a differential diagnosis. Because the prognosis of urinary bladder paraganglioma is similar to adrenal pheochromocytoma the treatment modalities include transurethral resection and cystectomy (partial or total), although laparoscopic partial cystectomy may be the first treatment of choice.

020

Comparison of prostate immunohistochemical characteristics and serum PSA level in prostate diseases

J. Grygorieva*, S. Gychka
*Clinical Hospital “Feofania”, Dept. of Pathology, Kiev, Ukraine

Objective: Serum prostatespecific antigen (PSA) level is not always correlate with clinical data in prostate diseases. So, the aim of our investigation was to describe the mechanism of serum PSA level rising and to compare it to expression of PSA, p63 protein and AMACR in prostate tissue.
Method: The comparison of serum PSA level, morphological and immunohistochemical characteristics (expression of PSA, p63 protein and AMACR) were made in Clinical hospital "Feofania" Prostate biopsy tissues samples with benign nodular hyperplasia (BNH) (44 patients), prostatic intraepithelial neoplasia (PIN) (28 patients) and prostate cancer (97 patients) were investigated.
Results: Serum PSA level rose with glandular hyperplasia, acinar epithelium proliferation, microvessel density, presence of inflamation. Expression of PSA in prostate tissue correlated with serum PSA level in all cases. Expression of p63 protein in all cases of BNH and PIN was positive, in all cases of cancer—negative. Expression of AMACR was strongly positive in all cases of prostate cancer and moderately positive in one case of PIN.
Conclusion: There is a necessity of taking into consideration morphological and immunohistochemical characteristics during interpretation of clinical data and selection of therapeutic approach.

021

WWOX expression in prostatic adenocarcinoma

G. Güner*, G. Guler, K. Huebner, D. Ertoy Baydar
*Hacettepe University, Faculty of Medicine, Ankara, Turkey

Objective: WWOX is known as a tumor suppressor gene. Belonging to a family involved in sex hormone metabolism, it is expressed in most human tissues, especially those that are sex-hormone related. Loss of WWOX is reported in many human cancers. We studied immunohistochemical expression of WWOX in prostate cancer.
Method: Tissue microarrays of prostatic adenocarcinoma were constructed from randomly selected 71 radical prostatectomies. Each case was re-evaluated for histomorphologic prognostic variables. Clinical data was obtained from hospital records. In addition, 5-μm sections were prepared from microarrays and stained immunohistochemically with primary anti-wwox antibody. Tumors were evaluated visually for staining intensity and extent.
Results: A total of 64 cases were eligible for the assessment of staining. Wwox expression was common in prostatic carcinoma, only 3 out of 64 were negative. There were 22 cases which expressed wwox strongly. Strong wwox expression correlated significantly with Gleason score (GS) (p= 0.008). Lower-score tumors showed intense-diffuse wwox positivity more commonly (55% for GS=6, 26% for GS≥7). There was no statistical association between wwox and other variables (PSA, pT, surgical margins, tumor volume).
Conclusion: Complete loss of wwox expression is rare in prostatic adenocarcinoma. Strong wwox staining is more frequent in better differentiated tumors. Thus, loss of wwox may be an indicator of aggressive disease in prostate malignancy.

022

The role of caspase 3 and cyclin D1 in bladder cancer associated or not associated with schistosomiasis

O. Hammam *, A. Abdel Hadi, M. Akl, H. Al-Gansoury
*Theodor Bilharz Research Institute, Dept. of Pathology, Giza, Egypt

Objective: We investigated expression of caspase-3 and cyclin D1 in bladder tissue to evaluate their role on the tumorgenesis and progression in bladder cancer (associated with schistosomiasis or not associated).
Method: Immunohistochemical method was used to determine the expression of caspase-3 and cyclin D1 in 45 cases of bladder cancer (30 TCC and 15 SCC), 10 control and 10 bilharzial cystitis.
Results: Caspase 3 was present in 90% of control cases, 80% in benign conditions and 48% of bladder cancer which was significantly lower than that in control ($P<0.001$) and was decreased in SCC compared to TCC cases $P<0.05$, it decrease in bilharzial compared to non bilharzial cancer $P<0.01$. Caspase-3 expression level was correlated with the grades of TCC ($P<0.01$) and with clinical stages ($P<0.05$). The overall expression of cyclin-D1 in malignant conditions was 50.6% and was not expressed in control cases and was expressed in 10% in bilharzial cystitis. Expression of cyclin-D1 was more significant in low-grade and superficial than in high-grade and invasive tumors.
Conclusion: Caspase 3 and cyclin-D1 expression in bladder tissue can be of help in detection of bladder cancer and can be used more effectively in combination with other tumor markers.

023

Characteristics of prostate cancer in the western part of Romania

D. Herman*, S. Costi, S. Taban, C. Lazureanu, I. Herman, R. Bardan, V. Dumitrascu, D. Grecu
*County Hospital Timisoara, Dept. of Pathology, Romania

Objective: Prostate cancer is the most common noncutaneous cancer among men. Despite the widespread use of PSA testing in our country, the disease is still diagnosed in an advanced stage.
Method: All prostate pathological material, obtained by core needle biopsy, transurethral resection and radical prostatectomy, provided by our urology department during the last 3 years (2008–2010) was reviewed.
Results: A total of 455 patients out of 1,554 with histologically evaluated prostatic tissue were diagnosed with prostate cancer, with a mean age of 70.58 years and a PSA level between 1.25 and 4,300 ng/ml. Regarding the tumour grade, 64.8% were moderately differentiated (Gleason score 5–7), a significant part (30.7%) was poorly differentiated, just a few were well differentiated. Analyzing the correlation of the Gleason score between biopsy and prostatectomy, we found a perfect match in 62.5% cases; for the remaining cases the Gleason score was underestimated in biopsies by 1-2 points. The grading of the prostatectomies revealed that almost all were Gleason score 6-7, whereas the staging pointed out that half of them were organ confined, mostly bilateral (pT2c), the others presenting extracapsular invasion (pT3).
Conclusion: We have to improve the investigation tools in order to diagnose prostate cancer at an earlier stage, in terms of age and stage of disease.

024

The importance of pathological report in echo-guided transrectal prostate needle biopsy in prostate cancer

M. Hortopan *, V. Herlea, M. Mihai, C. Pechianu, S. Voinea, S. T. Patrascoiu, C. Vrabie, M. Chitescu, I. Sinescu
*Fundeni Clinical Institute, Dept. of Pathology, Bucharest, Romania

Objective: Histopathology examination is considered the essential element in diagnostic confirmation of prostate cancer and it has a decisive role in the following therapeutic attitude.
Method: Group A: There were 83 patients with clinical changes of the prostate suggestive for cancer with PSA 4-15 ng/ml. Group B: There were 63 patients without clinical changes suggestive for cancer, with modified PSA: 51 patients with PSA 4-10 ng/ml and 12 patients with PSA above 10 ng/ml.
Results: In group A 70 patients presented a sonograph image suggestive for prostate cancer, but only 51 of them were histological confirmed. In group B, among the patients with PSA levels from 4 to 10 ng/ml, the ecography was suggestive in 20 cases, but only in 6 of them were histologically confirmed. As regards to the other 12 pts with a PSA>10 ng/ml, eight exhibit changes at the TRUS, four of them being confirmed by the pathologist.
Conclusion: The echo-guided prostate needle biopsy and histological examination are routine procedures in the urologic practice and have a decisive role in the diagnosis, staging and prognosis evaluation of the prostate cancer.

025

Plasmocytoid urothelial carcinoma: a case report and short review of the literature

P. Katafygiotis *, L. Abou-Asabeh, S. Karalis, A. Nomikos, S. Chranioti
*Hospital of Athens, Dept. of Pathology, Greece

Objective: This study aims to present a case of a plasmacytoid urothelial carcinoma.
Method: A 76-year-old man was presented with hematuria. The cystoscopy revealed multiple exophytic masses which were sampled and fixed under formalin buffer. We found a sheetlike pattern of mainly single neoplastic cells with plasmocytoid features. The neoplastic cells were three to five times larger than normal lymphocytes, had an abundant eosinophilic cytoplasm

rarely vacuolated, displaying an eccentrically located nucleus with inconspicuous nucleoli and increased mitotic rate. The tumor had a second histological profile of high-grade urothelial carcinoma without an "in situ" component. Immunohistochemically tumor cells were strongly positive for CK7, CK20, AE1/AE3 but negative for CD138 and LCA.
Results: The diagnosis of plasmacytoid urothelial carcinoma was given.
Conclusion: Plasmocytoid urothelial carcinoma is a rare subtype of urothelial carcinoma first described by Sahin et al and Zukerberg et al in 1991. Less than 40 cases have been mentioned in the literature. The histological characteristic of this subtype of urothelial carcinoma is the morphological profile of the neoplastic cells which resemble plasma cells.

026

Sertoliform cystadenoma of the Rete test's: case report

E. Kimiloglu Sahan [*], A. Akyildiz Igdem, K. Elvin
[*]Taksim´s Research and Education, Dept. of Pathology, Istanbul, Turkey

Objective: Sertoliform cystadenoma of the rete testis is a benign tumor of the Rete testis and it is a rare entity. It was first reported by Jones et al. in 1997.
Method: A 47-year-old man presented with a mass of rete testis. Orchiectomy was performed. The microscopical diagnosis was adenomatoid tumor in another pathology laboratory. The patient asked for a consultation of the preperations to our pathology department because he had another mass of 4–5 mm in diameter in his other testis.
Results: Because of its localization and the low Ki-67 proliferation index, the negativity of immunohistochemical markers for sex cord tumors, the positivity of epithelial markers. The case was diagnosed as sertoliform cystadenoma of the rete testis.
Conclusion: We present the case because of its rareness.

027

Primitive neuroectodermal tumor of kidney: case report

E. Kimiloglu Sahan [*], A. Akyildiz Igdem, I. Ozaydin, N. Erdogan
[*]Taksim´s Research and Education, Dept. of Pathology, Istanbul, Turkey

Objective: Primitive neuroectodermal tumor of kidney is a malignant small round cell tumor that exhibits neuroepithelial differentiation and occurs most commonly in bone and soft tissues of children and young adults. It was first reported by Stout in 1918.
Method: A 29-year-old man presented with abdominal pain. Computed tomography showed a mass at the mid pole of right kidney. He was operated. The specimen was sent to our department. The microscopic diagnosis of the nephrectomy specimen was malignant small round cell tumor.
Results: By the help of immunohistochemistry the diagnosis was primitive neuroectodermal tumor.
Conclusion: We report the case because of its rareness in kidney and the possibility of this tumor should be put in mind in the young adults also.

028

Mixed germ cell tumour with polyembryoma of the testis: a case report

E. Koniaris[*], M. Sevastiadou, N. Arnogiannaki, A. Apostolaki, M. Gazalidou, V. Anagnostopoulou, H. Kostara
[*]Athens, Greece

Objective: Testicular mixed germ cell tumors (MGCT) is a disease predominantly of young men, representing approximately 2% of all male malignancies. Testicular MGCTs may be divided in two categories on the basis of whether they are composed of a single histologic pattern or more. Polyembryoma is an exceptionally rare gonadal neoplasm, but may be present also as a component in a mixed germ cell tumour.
Method: In our hospital a 41-year-old male presented with a testicular tumor. The patient underwent orchectomy. Macroscopically the tumor measured 4.8 cm and showed solid and cystic areas with hemorrhage and necrosis.
Results: Histologic examination showed features characteristics of immature teratoma, embryonal carcinoma and a prominent component of polyembryoma. The tumor cells were arranged in necklace-like fashion. Foci of polyembryoma had a prominent loose myxomatous mesenchyme in the background upon which the embryoid bodies were set.
Conclusion: Polyembryoma is an extremely rare component of the gonadal MGCTs and perhaps the most photogenic of all. Its foundamental unit, the embryoid body, is a miniature yolk sac and amniotic cavity. This enigmatic and picturesque entity virtually never occurs in pure form but consists as a component of MGCTs.

029

Villous adenocarcinoma in urethra and anterior vagina: report of a case and review of the literature

H. Kourea [*], H. Papaioannou, E. Fokaefs, C. Scopa
[*]University of Patras, Dept. of Pathology, Greece

Objective: Villous neoplasms of urethra and vagina are extremely rare. We present a case of villous adenocarcinoma arising from villous adenoma involving both urethra and anterior vagina and review the literature.
Method: A 49-year old woman complains of recurrent urinary tract infections over the past 6 months. MRI shows a 4x3-cm abscess-like lesion in the anterior vaginal wall, involving the urethra and draining in its lumen. The diagnosis of urethral diverticulum is rendered and transurethral resection of the lesion follows.
Results: Villous adenoma, intestinal-type, with foci of adenocarcinoma in situ, are noted adjacent to the urothelium. Within the fibromuscular stroma of the tissue fragments, rounded or angulated glandular structures are observed raising the suspicion of infiltrating adenocarcinoma. Imaging studies, colonoscopy, and colposcopy 1 month prior to operation are unremarkable. On resection, intestinal type adenocarcinoma infiltrates the tissue between urethra and vagina. Foci of villous adenoma and in situ adenocarcinoma are observed on the vaginal mucosa. The tumor was positive for CK20, CDX2 and CEA but also for CK7, unlike colonic carcinomas.
Conclusion: We describe the fourth case of intestinal type adenocarcinoma arising from villous adenoma in the periurethral area raising the issue of urethral or vaginal origin and discuss the histogenesis.

030

Mixed epithelial and stromal tumor of the kidney: report of a case and review of the literature

H. Kourea*, I. Bota, M. Mavraidis, E. Fokaefs, C. Scopa
*University of Patras, Dept. of Pathology, Greece

Objective: Mixed epithelial and stromal tumor of the kidney (MEST) is a relatively rare, recently recognized neoplasm, presenting primarily in perimenopausal women. We present a case and review the literature.
Method: A 69-year-old woman presents with renal colic. On imaging studies, in the upper pole of the right kidney and protruding in the perirenal fat, a hypoechoic lesion (ultrasound), with hypodense, non-homogeneous uptake (C/T) and peripheral calcifications is noted. A right nephrectomy is performed.
Results: A circumscribed, 4.2×3.7×3-cm, solid and cystic, tan-yellow mass is observed, protruding in the renal pelvis and perirenal fat. Histologically, a biphasic tumor, consisting of macrocysts, microcysts and tubules separated by a variably cellular and hyalinized stroma is noted. The epithelial cells are flattened, cuboidal, at times hobnail, clear or eosiniphilic, without atypia. The stroma close to the cysts is reminiscent of ovarian-type stroma, with subepithelial condensation and foci of "luteinization". Acute and chronic inflammation with hemorrhage, hemosiderin deposits and prominent calcifications are seen. The epithelium expresses CK8/18 and vimentin and the stroma SMA, MSA, vimentin, ER and PR.
Conclusion: MEST is considered as the renal counterpart of mixed epithelial stromal neoplasms of the hepatobiliary apparatus. This benign entity is amenable to nephron-sparing resection.

031

Estrogen receptor expression, its prognostic value and its relation with other biomolecular markers in prostate cancer patients

T. Liatkouskaya*, V. Zakharava,, M. Puchinskaya, E. Cherstvoy, L. Pashkevich, O. Sukonko, A. Rolevich, I. Masanskiy, L. Sagalchik, M. Ivanovskaya, V. Savosh
*Belarussian Medical University, Dept. of Pathology, Minsk, Belarus

Objective: It has been shown that estrogens play a role both in normal prostate functioning and in pathogenesis of its diseases.
Method: Expression of ERα, androgen receptors (AR), Ki-67, chromograninA, p53, Bax in surgical material after radical prostatectomy y 68 PCa patients was studied using immunostaining.
Results: ER expression in epithelial cells (ER-E) was revealed in 48.5% of cases, in stroma (ER-S)—89.7%. Statistically reliable medium correlations were found between ER-E, ER-S, overall ER expression (ER-T) and other biomolecular markers: direct correlations with Ki-67, chromograninA, p53 and inverse correlations with Bax, AR. Kaplan–Meier analysis did not reveal reliable impact of ER expression upon the incidence of unfavorable outcomes of Pca. However, in case of combination of such unfavorable prognostic factors, as decreased AR expression, Bax and large number of chromogranin A-positive cells in PCa with enhanced ER-T expression statistically reliable evidence of poorer prognosis was obtained in comparison with cases where only one of the abovementioned factors was present.
Conclusion: ER expression is not of independent prognostic value in PCa patients, but simultaneous presence of enhanced ER expression and decreased AR expression, Bax and large number of chromograninA-positive cells in PCa is associated with reliably poorer prognosis.

032

Dysadherin expression in prostatic adenocarcinoma and adjacent benign prostatic tissue

R. Limani*, Z. Marušic, L. Gashi Luci, M. Ulamec, D. Tomas, B. Krušlin
*Clinical Center of Kosovo, Faculty of Medicine, Pristina, Serbia

Objective: Dysadherin is a recently described cancer associated cell membrane glycoprotein, which has anti cell-cell adhesion function. Its expression has not been studied in prostate tissue. We assessed immunohistochemical expression of dysadherin in formalin-fixed and paraffin-embedded radical prostatectomy specimens of prostatic adenocarcinoma and correlated it with the expression in adjacent high grade prostatic intraepithelial neoplasia (HGPIN) and benign prostatic tissue.
Method: There were 52 prostate tissue samples included. Positive staining of lymphocytes is used as an internal control. The percentage of positive epithelial cells, the staining pattern and intensity are evaluated. Staining was graded as 0, if no cells were stained, 1+ if less than 50% of cells were stained and 2+if more than 50% of cells were stained. Intensity was graded as weak, moderate and strong.
Results: Aberrant nuclear and cytoplasmic staining patterns of dysadherin were observed. There was no statistical difference in the intensity of nuclear expression of dysadherin in benign prostatic tissue, HGPIN and prostatic adenocarcinoma. Cytoplasmic expression was stronger in prostatic adenocarcinoma and HGPIN compared to adjacent benign prostatic tissue ($p<0.001$).
Conclusion: This is the first report of dysadherin expression in prostate tissue. Our study results suggest an association between cytoplasmic dysadherin expression and prostatic adenocarcinoma.

033

Early micropapillary prostatic ductal adenocarcinoma mimicking nephrogenic adenoma

A. Loghin *, A. Dema, S. Taban, O. Preda, A. Borda
*University of Medicine and Pharmacy, Tirgu Mures, Romania

Objective: Prostatic ductal adenocarcinoma (PDAC) accounts for 1% of prostate cancers. Most commonly it is discovered in advanced stages with large cribriform and/or papillary growth pattern.
Method: We report the case of a 79-year-old patient who underwent transurethral resection for prostatic hyperplasia. In one fragment we noticed a small exofitic papillary proliferation composed of fine fibrovascular cores lined by simple cuboidal epithelium that sometimes becomes pseudostratified. In addition, small tubules were present in the underlying stroma. The cells lining these structures were small, with round, regular, hyperchromatic nuclei. Small nucleoli were present only in the infiltrative component. A diagnosis of nephrogenic adenoma (NA) was considered. To confirm it, an immunohistochemical study was performed.
Results: Surprisingly, the cells of this proliferation strongly expressed P504S and PSA. They were negative for PAX2, CK7, 34βE12 and p63. Based on this immunohistochemical profile and the papillary morphology a diagnosis of early micropapillary PDAC was made.
Conclusion: Due to their similar growth pattern, differentiation of PDAC and NA can sometimes be difficult, particularly in small/early lesions arising in prostatic urethra and bearing a benign appearance. In these cases, the immunohistochemical profile is an important clue to the diagnosis.

034

Small cell carcinoma of the urinary bladder: case report

A. Loghin*, C. Marian, E. Fulop, K. Branzaniuc, A. Borda
*University of Medicine and Pharmacy, Tirgu Mures, Romania

Objective: Small cell carcinoma (SCC) of the urinary bladder is a rare and aggressive cancer, with early metastases and poor prognosis.
Method: We report the case of a 74-year-old patient who underwent transurethral resection for a macroscopic haematuria. Histological examination showed nests and sheets of small or intermediate cells separated by a delicate fibrovascular stroma. This proliferation infiltrated the bladder wall up to the muscle layer. Tumor cells had uniformly small, round-to-oval nuclei, scant cytoplasm and frequent mitoses. The overlying bladder mucosa was intact, without in situ, papillary or invasive urothelial carcinoma. As differential diagnosis involves metastatic SCC from other sites, high-grade urothelial carcinoma and lymphoma, an immunohistochemical study was performed.
Results: Tumor cells expressed chromogranin-A, synaptophysin, NSE, and were negative for CK7, CK20, TTF1 and also for LCA, CD3 and CD20. The computerized tomography scan did not reveal any other tumor. Based on the cytological aspect, the immunohistochemical profile, and the clinical examination, a diagnosis of SCC of the bladder was made.
Conclusion: Due to its aggressiveness, the recognition of the primary SCC of the bladder has important prognostic and therapeutic implications. Microscopy can be challenging and must be supported by immunohistochemistry and clinical investigations.

035

CD10 and CD26 activity and expression in renal tumours

J. I. López *, L. Blanco, I. Pérez, B. Sanz, J. Gil, A. Varona, J. Irazusta, L. Andrés, A. Gaafar, G. Larrinaga
*Hospital de Cruces, Dept. of Anatomic Pathology, Barakaldo, Spain

Objective: CD10 and CD26 are ectopeptidases that play a key role in the control of cell growth and differentiation. The aim of this study is to delineate the profile of activity and expression of CD10 and CD26 in clear cell (CCRCC) and chromophobe (ChRCC) renal cell carcinomas and in renal oncocytomas (RO).
Method: CD10 and CD26 activity and mRNA expression have been investigated in a series of 75 CCRCC, 10 ChRCC and 8 RO. Conventional immunohistochemistry, fluorimetric quantitative assays (expressed in units of peptidase per milligram of protein), and mRNA analysis (given in relative units of expression with TBP, PPLA, ACTB, and SDHA as genes of reference) were performed.
Results: Males predominated in the series (37 M/8 F) with an average age of 62.5 years (range, 37–78). Tumor grade in the CCRCC group was G2, 23 cases (51.1%); G3, 15 cases (33.3%); and G4, 7 cases (15.6%). Stage was pT1, 23 cases (51.1%); pT2, 5 cases (11.1%); pT3, 17 cases (37.6%). CD10 and CD26 immunostaining was positive in CCRCC and negative in ChRCC and RO. The activity of both peptidases was significantly decreased in tumor vs non-tumor tissue in CCRCC ($p<0.001$), ChRCC ($p<0.001$) and RO ($p<0.001$). However, the expression of both was significantly decreased only in ChRCC ($p<0.05$).
Conclusion: CD10 and CD26 are strongly down-regulated in CCRCC, ChRCC and RO. These results support the role of both peptidases in the malignant transformation of renal tubules and suggest its potential use in routine practice as diagnostic and prognostic tools.

036

Cystinyl–aminopeptidase activity in renal cell carcinomas

J. I. López*, J. Gil, L. Andrés, A. Gaafar, B. Sanz, I. Pérez, L. Blanco, G. Larrinaga
*Hospital de Cruces, Dept. of Anatomic Pathology, Barakaldo, Spain

Objective: The involvement of peptidases in the oncogenesis of several tumours has been investigated in recent years. Kidney is one of the major tissues known to express cystinyl-aminopeptidase (CAP), but little is known about its precise role in renal neoplasia
Method: Soluble and membrane-bound CAP activities have been prospectively analysed in 64 renal cell carcinomas.
Results: The average age of patients was 62 years (range 37–79), with a clear male predominance (50 M/14 F). The series included 50 clear cell renal cell carcinomas (CCRCC), 6 papillary renal cell carcinomas (PRCC) and 8 chromophobe renal cell carcinomas (ChRCC). Tumour diameters oscillated between 2.5 and 14 cm (average 7.1 cm). Grade distribution was G2: 32 cases, G3: 22 cases and G4: 10 cases. Staging was 15 pT1a, 17 pT1b, 7 pT2, 12 pT3a and 13 pT3b. The tumour vs. non-tumour CAP ratio was significantly decreased in CCRCCs ($p<0.001$), in PRCCs ($p<0.001$), and in ChRCCs ($p<0.001$). After stratification by stage and grade within the CCRCC group, pT3 category had significant higher levels of membrane-bound CAP activity than pT1 one ($p<0.05$), and high grade cases (G3/4) had a significant higher soluble CAP activity than low grade ones (G2) ($p<0.01$).
Conclusion: Membrane-bound and soluble CAP activity is decreased in renal cell carcinomas when compared with non-tumour renal tissues. Membrane-bound CAP activity is higher in pT3 than in pT1 CCRCC cases. Soluble CAP activity is higher in G3/4 than in G2 CCRCC cases. These data may open additional possibilities in the prognostic evaluation of renal cell carcinomas.

037

Aspartyl aminopeptidase (AspAP), neutral aminopeptidase (APN) and neutral endopeptidase (NEP) predict survival in clear cell renal cell carcinoma

J.I. López*, L. Andrés, B. Sanz, I. Pérez, A. Gaafar, L. Blanco, J. Gil, G. Larrinaga
*Hospital de Cruces, Dept. of Anatomic Pathology, Barakaldo, Spain

Objective: Several authors have demonstrated the implication of peptidases in diverse carcinogenetic processes, but the role of these enzymes in renal tumours still remains unclear. The aim of this study is to evaluate the activity profile of a broad spectrum of peptidases in a consecutive series of clear cell renal cell carcinomas (CCRCC) and correlate these results with survival.
Method: A total of 80 CCRCCs were prospectively collected to analyze the activity, measured by fluorimetric methods, of a series of 11 peptidases (APN, NEP, DPP-IV, CAP, APA, APB, Asp-AP, PEP, PG-1, ACE, ACE-2).
Results: Males predominated in the series (64 M/16 F) with an average age of 62.3 years. Tumour grade distribution was G1:3, G2:38, G3:28, G4:11 and Staging pT1a:17, pT1b:24, pT2:11, pT3a:16, pT3b:11, pT4:1. Average follow-up was 64.7 months and the overall mortality rate reached 27.5%. Log-rank test (Kaplan–Meier) showed two populations with different 5-year survival in Asp-AP (aspartyl-aminopeptidase) ($p=0.037$) and APN (neutral aminopeptidase, CD13) ($p=0.049$) activities when the cut-off was made at 5,000 units of peptidase per milligram of protein. Cox regression analysis showed that survival was related to APN ($p=0.026$) and NEP (neutral endopeptidase, CD10) ($p=0.045$) values.
Conclusion: The activity of Asp-AP, APN (CD13) and NEP (CD10) peptidases measured by simple fluorimetric methods distinguishes two populations with different survival in CCRCCs. This new finding could be used as a potential additional tool when defining the prognosis of these patients.

038

Interfocal and intrafocal ERG expression in prostate cancer

C. Magi-Galluzzi*, S.M. Falzarano, H. He, P. Carver, M. Zhou
*Cleveland Clinic, Dept. of Anatomic Pathology, USA

Objective: ERG heterogeneity has been documented in prostate cancer (PCA). We investigated ERG protein expression in distinct PCA foci and extensive tumors from radical prostatectomies (RP).
Method: A single pathologist reviewed and mapped 547 RP; 46 were selected for this study: 33 with 2 separate cancer foci (bifocal-PCA) and 13 with cancer involving almost the entire gland (extensive-PCA). A representative section of each distinct focus and two far apart sections of extensive-PCA were stained with p63/ERG cocktail. ERG presence or absence and intrafocal heterogeneity (>10% of ERG-negative tumor cells within a positive tumor section) were assessed.
Results: Of the 46 patients, 65% had at least one ERG positive tumor focus. When individual tumors were considered, 57% of 66 distinct foci from bifocal-PCA were ERG-positive. In 29 (88%) patients both tumor foci were concordantly positive or negative. Of 13 extensive PCA, 85% showed concordant expression of ERG in separate sections. Intrafocal heterogeneity was observed in 6/38 bifocal-PCA and in 5/9 extensive-PCA. In two cases, negative areas of otherwise positive PCA were located in the transition zone.
Conclusion: Although interfocal and intrafocal heterogeneity exists, ERG expression would not qualify as a good marker of clonality given the high concordance between different tumor foci in the same prostate.

039

Primary epididymal leiomyosarcome: an unusal cause of scrotal mass

W. Majdoub *, F. Bougrine, M. Hamdane, I. Msakni, F. Khanchel, R. Khiari, B. Laabidi, A. Bouziani, N. Ben Raies
*Military Hospital, Tunis, Tunisia

Objective: Primary epididymal leiomyosarcoma is exceedingly rare with only 17 cases reported in literature.
Method: Herein, we report an additional case in a 73-year-old man and describe its clinicopathological features.
Results: Our patient presented with a 6-month history of hard indolent mass in his left testis which had enlarged during the past 2 months. Physical examination showed a 6-cm hard mass confined to the left epididymis. Ultrasonography showed a hypoechoic lesion. Serum tumor markers were negative. The patient underwent a radical left inguinal orchidectomy. Macroscopic examination of the surgical specimen showed that the epididymis was entirely occupied by a 6-cm well-defined mass. Histologically, the tumor was composed of slender and slightly plump smooth muscle cells that were arranged in interlacing fascicles. Many cells showed marked nuclear pleomorphism and mitoses. Focal areas of necrosis were noted. Immunohistochemically, tumor cells showed positive staining for smooth muscle actin. Computed tomography did not reveal additional masses elsewhere. Adjuvant radiotherapy was not performed because the patient refused. Clinical outcome was favourable four years after.
Conclusion: Primary epididymal leiomyosarcoma is uncommon, raising diagnostic difficulties. Its prognosis is usually favourable. Local recurrence and/or distant metastasis have been reported. Long-term follow-up is therefore mandatory for these patients.

040

A case of advanced bladder cancer in a young neurological female patient

S. Mavropoulou *, Z. Tatsiou, I. Galanos, P. Nasos
*Xanthi General Hospital, Dept. of Pathology, Greece

Objective: Urothelial carcinoma of the urinary bladder is typically a disease of older individuals wheras young patients exhibit unique pathologic and molecular features and a more indolent behaviour.
Method: We present the case of a 30-year-old woman who presented in our hospital due to macroscopic hematuria. She had a clinical history of meningomyelocele, neurogenic bladder and intermittent urethral catheterization for 10 years and a recent urinary infection. Cystoscopy showed a solid bladder tumor and a transurethral biopsy was performed.
Results: Histological examination revealed a high-grade urothelial carcinoma which invaded deeply the muscle layer of the bladder wall. The tumor cells exhibited marked nuclear pleomorphism, often bizarre giant cells, occasionally 'signet ring' cells and small cells. The mitosis, often atypical, were abundant. A staging MRI-scan of the abdomen showed swelling of the bladder wall with infiltration of the pericystic fat and large bowel. The patient received palliative radiation therapy and died 34 days after the diagnosis.
Conclusion: In conclusion, although urothelial carcinoma in young adults is usually associated with low grade and low stage disease, it should be kept in mind to accurately evaluate young neurological patients, follow them up regularly and not to rule out the possibility of an advanced disease.

041

Cyclooxygenase-2 as a possible predictive marker for bladder carcinoma

M. Moussa *, Z. Omran
*Theodor Bilharz Research Institue, Dept. of Pathology, Giza, Egypt

Objective: The aim of the current study was to elucidate the possible involvement of COX-2 in human bladder carcinoma by examining its expression on different lesions of tissue biopsies and urine cytology samples.
Method: A total of 65 patients were included in the study. They represented seven control cases; pure chronic cystitis (n=12); premalignant lesions (18) in the form of squamous metaplasia (n=8) or urothelial dysplasia (n=10) as well as transitional cell carcinoma (n=18), and squamous cell carcinoma (n=10).
Results: The study revealed positive COX-2 expression on the urothelial and inflammatory cells of cystoscopic biopsies from all cases of pure chronic cystitis, squamous metaplasia and SqCC compared to 42.8% and 71.4% of normal controls respectively. The score of urothelial COX-2 expression was sequentially up-regulated from normal to chronic cystitis ($p<0.05$) to malignant changes ($p<0.05$). In TCC, COX-2 was over-expressed on both urothelial and inflammatory cells in advanced tumors. Urine cytology samples were positive for COX-2 in a comparable manner to that observed in cystoscopic biopsies.
Conclusion: COX-2 was involved in both inflammatory bladder lesions and bladder carcinoma. Positive urothelial cell expression in both cystoscopic biopsies and urine cytology samples was valuable as a predictive marker for bladder carcinoma. However, positivity of inflammatory cells has no prognostic indication of disease progression.

042

Is Epstein criteria predictive for the insignificant prostate cancer in Turkish population?

B. Muezzinoglu *, H. Yilmaz, O. Dillioglugil
*Kocaeli University, Dept. of Pathology, Turkey

Objective: Contemporary Epstein criteria represent the most widely used scheme for clinically insignificant prostate cancer (PCa). The criteria consist of PSA density <0.15, Gleason score ≤6, fewer than three biopsies with prostate cancer and up to 50% of cancer involvement in any core.
Method: We aimed to determine the percentage of pathologically confirmed unfavorable prostate cancer among patients of a single instutition in Turkey, who met the contemporary Epstein criteria for clinically insignificant PCa. The adverse pathological characteristics were defined as Gleason Score (GS) ≥7 and/or non-organ confined disease. The study consisted of 259 men who underwent radical prostatectomy (RPS) between 2002 and 2008 at a single academic institute. Of these men, 26 (10%) fulfilled the criteria.
Results: Among 26 men, 8 had (30.7%) GS 7 on RP specimen. Extraprostatic extension was detected in four cases. There was no case with seminal vesicle involvement and lymph node metastasis. On follow-up of 19 patients, there was no evidence or biochemical recurrence (mean follow up 36.6 months).
Conclusion: Our results showed that when the Epstein criteria applied in our patients for prediction of clinically insignificant PCa, a significant proportion of the patients might have unfavourable pathologic features. This emphasizes the need for future studies for addition of novel markers for improving the predictive accuracy of existing criteria.

043

Glandular yolk sac tumours developing from high grade transitional cell carcinomas of the renal pelvis and bladder

A. Nicolae*, A. Dema, P.L. Fernandez Ruiz, M. Iacob, P. Goyenaga, O. Preda, F. Nogales
*Universidad de Granada, Dept. de Anatomia Patologica, Spain

Objective: The glandular variant of yolk sac tumour (YST) is difficult to recognize when associated with somatic tumours. Embryonal tumour differentiation from urothelial neoplasms is uncommon. We present for the first time, the association of two high grade urothelial carcinomas (HGUC) with extensive areas of glandular YST.
Method: Case histories: Case 1, a male, 47, with a testicular germ cell tumour, chemotherapy-treated 17 years ago, had a lumbar mass and high levels of serum β-hCG. CT scan showed a renal mass infiltrating the psoas with lung and vertebral metastases. Case 2, a female, 81, presented an invasive bladder tumour with haematuria and elevated AFP.
Results: Microscopically, both cases showed areas of HGUC admixed with glandular/papillary YST structures lined by AFP, Glypican3, CDX-2 and SALL4 positive columnar vacuolated cells. Scattered hCG positive syncytiotrophoblasts were present in case 1. Focal HepPar1 positive hepatoid cells were identified in case 2.
Conclusion: The distinctive vacuolated epithelium with a characteristic immunophenotype discriminates glandular YST from other primary or secondary malignant glandular proliferations of the urinary tract. Further pluripotential-type differentiations (trophoblastic/hepatoid) were also found. The association of HGUCs with YST and hepatoid/trophoblastic areas is unique and its pathogenesis could be related to the pluripotent malignant stem cells present in the somatic tumour.

044

Mice: an animal model for bladder cancer

C. Vasconcelos-Nóbrega*, R. Arantes-Rodrigues, H. Vala, A. Colaço, L. Santos, L.F. Palomino, C. Lopes, P.A. Oliveira
*Escola Sup. Agrária de Viseu, Dzerv, Portugal

Objective: Bladder cancer is a common malignancy and an important cause of morbidity and mortality in western world. Animal models are the centre of experimental researches aiming to elucidate our knowledge about carcinogenesis, its treatment and prevention. Mice have a lower urinary tract comparable to humans.
Method: A total of 22 ICR male mice were randomized into two groups (I and II). Group I was the negative control drinking tap water, and group II received *N*-butyl-N-(4-hydroxybutyl) nitrosamine (BBN) in drinking water during 12 weeks. Euthanasia was executed 1 week after BBN exposition.
Results: All animals from group I exhibited normal urothelium. In group II, 100% of animals exhibited histological changes. 62.79% were preneoplastic lesions (simple hyperplasia, nodular hyperplasia, dysplasia) and 37.21% were neoplastic lesions (carcinoma in situ, invasive carcinoma, epidermoid metaplasia).
Conclusion: Experimental urinary bladder tumours are useful models for the study of urinary bladder carcinogenesis and for the evaluation of new therapeutic strategies. In mice, chemically induced bladder cancer is nearly always of the invasive type and the incidence of spontaneous tumours is very rare. The similarity between human's and mice's bladder cancer allows the investigation of several aspects that can't be studied under clinical conditions, such as pharmacokinetics and toxicity.

045

Meloxicam inhibits the progression of mice urothelial lesions chemically induced

R. Arantes-Rodrigues [*], A. Videira-Henriques, V. Ribeiro, R. Pinto-Leite, C. Vasconcelos-Nóbrega, H. Vala, C. Lopes, A. Colaço, P. A. Oliveira
[*]Escola Sup Agrária de Viseu, DZERV, Viseu, Portugal

Objective: Meloxicam, an anti-inflammatory drug, is a cyclooxygenase-2 inhibitor that has been used in cancer research. The goal of this work was to evaluate the effects of meloxicam on mouse urothelial lesions chemically induced.
Method: During 12 weeks, ICR male mice received *N*-butyl-N-(4-hydroxybutyl)nitrosamine (BBN) in drinking water, after meloxicam was administered by intraperitoneal route (20 mg/kg), 5 days a week, during six consecutively weeks. At the end of treatment, mice only exposed to BBN and mice exposed to BBN and treated with meloxicam, were sacrificed and their urinary bladders were collected.
Results: Urinary bladders from control groups revealed no changes. The incidence of urothelial lesions on mice exposed to BBN and not treated was: simple hyperplasia 80%, nodular hyperplasia 40%, dysplasia 90%, carcinoma in situ 10%, papillary neoplasms of low malignant potential 10%, low-grade papillary tumour 20%, high-grade papillary tumour 30% and invasive carcinoma 20%. On the other hand, mice treated with meloxicam showed: simple hyperplasia 77.8%, nodular hyperplasia 44.4% and dysplasia100%.
Conclusion: According to our results in mice treated with meloxicam we just observed preneoplastic lesions, in mice not treated with meloxicam we identified all the spectrum of urothelial neoplastic lesions. It appears that meloxicam prevented the progression of urothelial lesions.

046

Sex differences in bladder cancer chemoprevention by green tea

A. Videira-Henriques [*], S. Ferreira, I. Almeida, R. Arantes-Rodrigues, C. Vasconcelos-Nóbrega, H. Vala, A. Colaço, P. A. Oliveira
[*]Escola Sup Agrária de Viseu, DZERV, Viseu, Portugal

Objective: In bladder cancer prevention studies, it is important to investigate how both sexes respond to different agents. The purpose of this experiment was to evaluate the protective effect of green tea consumption in bladder cancer induced by *N*-butyl-*N*-(4-hydroxybutyl)nitrosamine (BBN) in Mus musculus of both sexes.
Method: There were 21 male and 20 female mice randomly assigned into three groups (I-Green tea+BBN, II-BBN and III-Green tea) in both sexes. The green tea was prepared daily at a concentration of 0.5% during 20 weeks and BBN was administrated by gavage in mean doses of 7.25 mg/mouse for week, through 10 weeks. After 20 weeks, animals were sacrificed and all bladders were collected for histological study.
Results: In males, the group that showed a higher incidence of lesions was BBN+Green tea group. In females, the BBN group was the one with more histological lesions. A higher incidence of inflammatory infiltrate was observed in group exposed to BBN, followed the BBN+green tea group, and finally green tea group. These observations were consistent for both sexes.
Conclusion: We can conclude that green tea has a potential prevention effect of bladder cancer in females. The histological alterations were probably due to the influence of green tea in the metabolism acceleration of females and the protective effect of estrogens.

047

Polypoid endometriosis of the urinary bladder: a case report

A. Ozagari[*], D. Sakiz, F. Kabukcuoglu, G. Eken, O. Tanriverdi
[*]Sisli Etfal Teaching Hospital, Dept. of Pathology, Istanbul, Turkey

Objective: The urinary tract is not usually involved by endometriosis. When it is involved, the bladder is the most

common site, with a prevalence of 1–15% in women with endometriosis. Endometriosis can occur in several forms. Bladder endometriosis is usually of deeply infiltrating type. Less frequently, endometriosis can grow through the mucosa and produce a polypoid mass.
Method: We present a case of polypoid endometriosis of the bladder in a 49-year-old woman.
Results: The patient presented with dysuria and hematuria. At cystoscopy a polypoid mass, 1.5×0.8 cm in dimension, was found near the left ureteral orifice. The patient had a transurethral resection. Microscopic examination showed a polypoid lesion covered by normal urothelium. The lesion was composed of irregularly shaped glands lined by endometrial epithelium in an edematous and vascularized stroma. Some glands surrounded by thin rims of endometriotic stroma. The features suggestive of low grade mullerian adenosarcoma such as periglandular stromal hypercellularity, stromal atypia, and intraglandular stromal papillae were not identified.
Conclusion: Polypoid endometriosis is a rare manifestation of endometriosis that can be confused with a neoplasm either clinically or histologically. Awareness of the lesion and attention to its typical histological features should facilitate its distinction from neoplastic lesions.

048

Morphological and clinical spectrum of adult-onset Xp11.2 translocations/TFE3 gene fusions renal cell carcinoma (RCC): a series of 73 cases

A. Panizo *, I. de Torres, A. Martinez-Peñuela, F.J. Queipo, J.J. Sola, J. Pardo
*Hospital de Navarra, Dept. of Pathology, Pamplona, Spain

Objective: RCC associated with Xp11.2 translocations are rare tumors reported in adults.
Method: We identified 73 TFE3 RCC in adults (>20 yrs.). Morphology, IHC, and clinical data were assessed.
Results: Patients' sex: 50 M/23 F (mean age 55 yrs). Mean tumor size: 7.4 cm; right kidney: 41, and left: 32. TNM at diagnosis: pT1 (n=22), pT2 (n=12), pT3 (n=36), pT4 (n=3), pN+(n=13), and pM+(n=24). Five morphological patterns were found: solid/tubular, alveolar, pseudopapillary, true papillary, and multicystic. Tumors were composed of clear (41%), eosinophilic (14%) or mixed cells (45%). Fuhrman grade: 2 (15%), 3 (66%), and 4 (19%). IHC study: 100% strongly expressed TFE3, CD10, and P504s. Two cases contained ASPL/TFE3 gene fusion. Follow-up for 61 cases (median 25 months; range 2-208): 11 patients alive without disease, 28 patients alive with metastasis, and 21 died of the disease. Distant metastases were: lung (35), retroperitoneum (29), bone (24), liver (23), mediastinum (20), CNS (8).
Conclusion: TFE3 RCCs occur in adults, and exhibited heterogeneous morphology. We recommend evaluating the TFE3 IHC expression in adult renal tumors with multiple morphologies or unclassified RCC. Overall, adult TFE3 RCCs were frequently associated with an advanced stage, distant metastasis at presentation and an aggressive clinical course.

049

Real value of complete histologic sampling of prostate needle biopsy specimens

F. J. Pardo*, A. Panizo, F. Queipo, A. Martinez Peñuela, R. Carias, T. Laviano, J. J. Sola
*University of Navarra, Dept. of Pathology, Pamplona, Spain

Objective: The aim of this study was to evaluate what constitutes adequate sampling of prostate transperineal biopsies to improve the accuracy of diagnosis.
Method: This study was of 300 consecutively identified prostate transperineal biopsies. Average patient age was 57 years. For all cases, two blocks with at least six cores in each were paraffin- embedded. Three levels from each block were reviewed for the presence of adenocarcinoma and Gleason pattern. Slides were stained with H&E and doubtful cases were studied by immunohistochemistry with antibodies anti racemase, p63 and 34βE12.
Results: Of 300 PTB samples evaluated, 61 (20.3%) contained prostate cancer, 6 cases were diagnosed as ASAP and 5 cases more had high-grade PIN areas. Minimal cancer involving less than 5% of sampled tissue was found in 11 (3.6%) patients. In 57 cases diagnostic carcinoma was present on all 3 levels (93.4%), on 2 levels in 3 specimens (4.9%), and on 1 level in 1 case (1.6%). Immunohistochemistry was helpful for diagnosis in 9 (3%) cases.
Conclusion: We conclude that 94% of the cases of prostatic carcinoma may be diagnosed by the study of only one level per tissue core; however, biopsies routinely sampled at three levels minimize the misdiagnosed cases.

050

The experimental model of obstructive acute pyelonephritis induced non-clostridial infection

D. Pasechnik*, M. Kogan, J. Naboka, H. Ibishev, Z. Gazaev, I. Gudima
*Rostov Regional Hospital, Dept. of Pathology, Rostov on Don, Russia

Objective: It is known that the main agents of acute pyelonephritis (AP) are the family Enterobacteriaceae, dominated by *E. coli*. The role of non- clostridial bacteria in the development of AP has not been studied.

Method: Obstructive AP was experimentally caused in New Zealand rabbits. Group I (11 rabbits) was infected with anaerobic bacteria (*Peptostreptococcus* sp.), group II (eight rabbits) was infected with *E. coli*, and group III (eight rabbits) was subjected to a mixed infection. At 3, 7, 14, and 21 days after infection, we carried out a bacteriological and morphological study of urine and tissues of the left and right kidneys.
Results: In groups I and II we obtained a classic morphological pattern of acute pyelonephritis. At 3 days after the mono-infection with Peptostreptococcus sp. and E. coli, we observed purulent inflammation in the renal sinus, septic phlebitis, papillary necrosis. At 7 days, there were kidney infarctions and the first signs of immune reaction. In the group with a mixed infection, the hemorrhagic and necrotic changes dominate over the inflammatory reaction. The bacteriological study confirms the results of the morphological study.
Conclusion: Thus, we experimentally showed, for the first time, that non-clostridial bacteria in the form of mono-infection or as part of a mixed infection are able to cause acute pyelonephritis.

051

The origin of fibrous capsule (pseudocapsule) in renal cell carcinoma

D. Pasechnik *
*Rostov Regional Hospital 2, pathology, Rostov On Don, Russia

Objective: The formation of fibrous capsule (FC) around the cancer is frequently observed with the development of renal cell carcinoma (RCC).
Method: We studied 320 cases (144 males and 176 females, aged 29–79 years), who received nephrectomy of RCC. There were 25 cases RCC (clear RCC—19, papillary RCC, types 1–4, chromophobe RCC—2) stained with monoclonal antibodies (DAKO, Novocastra) against Pan-cytokeratin, vimentin, α smooth muscle actin (SMA), collagen I, IV, fibronectin, tenascin-C, TGF- ß1.
Results: The development of FC is observed at early stages of RCC growth. FC thickness was 1 to 3 mm, uneven. The interstitial nephritis around FC was presented in 72% of cases. FC was composed of collagen I, IV fibers, myofibroblast-like SMA- and vimentin-positive cells. Cancer cells did not express SMA, (TGF)-ß1. Tenascin C, fibronectin were located at the periphery of a tumor occasionally adjoined FC. The tubular epithelial cells in the tissue surrounding the FC stained positively for (TGF)-ß1, vimentin and SMA.
Conclusion: The FC was formed by host kidney cells, not by RCC cells. The fibrogenesis in the capsule of the RCC could be connected with myofibroblasts. The FC formation may result from interaction between tumor and host kidney and epithelial-mesenchymal transition of tubular cells.

052

Citogenetic diagnosing of bladder urothelial carcinoma using fluorescent in situ hybridization

S. Petrov*, K. Malkhasyan, R. Khasanov
*Kazan Cancer Center, Pathology, Russia

Objective: Patients with bladder cancer are still requiring close follow up with frequent cystoscopies. This study aims at assessing the FISH analysis, as a procedure capable to highlight hidden features of tumor and help to individualize treatment tactics.
Method: The bladder washings of 50 primary bladder cancer patients were taken prior to TURB and analysed with commercial FISH assay UroVysion®.
Results: All patients were divided into groups according to maximum stage and grade of the tumor. The sensitivity of the method was 81.5%, 91.7% and 100% for the Ta, T1 and T2 stage groups, respectively. For the G1, G2 and G3 groups the sensitivity was 70%, 100% and 100%, respectively. In addition, the rate of detecting genetically abnormal cells was significantly higher in the T2 stage compared to the Ta and combined Ta+T1 group, as well as in the G3 group compared to the G1 and G2 groups. The mean signal number from each chromosome was insignificantly increasing with the stage and grade of tumor. The detection of <40% of genetically abnormal cells was predicting the absence of muscle invasion and the G3 tumor with more then 90% reliability.
Conclusion: The FISH method is a highly sensitive in early bladder cancer detection and is able to predict the morphological character of the tumor even before surgery.

053

Morphological germ cell particularities in simple and complex testicular embryonal carcinoma

I. Poinareanu*, M. Aschie, A. F. Mitroi, A. Chisoi, A. Iliesiu, A. A. Nicolau, M. Enciu, G. I. Baltatescu, A. M. Cretu, S. Vamesu, V. Tode
*Ovidius University Constanta, Faculty of Medicine, Romania

Objective: The incidence of testicular germ tumors presents a remarkable geographical range. Researches regarding the causes of appearance of testicular germ tumors were guided by their beginning assumptions since intrauterine life and consist differentiate abnormal fetal primordial germ cell populations. Embryonic carcinoma is the most undifferentiated testicular tumor malignant, composed of large cells, with different architectural aspects.
Method: It should be noted that embryonic carcinoma metastases can differentiate to seminoma, coriocarcinoma or teratoma in over 8% of cases. Immunohistochemistry, tumor cells of embryonic carcinomas express PLAP in 85–95% of cases, focal expression and less marked than in

seminomas. There are expressed epithelial markers: citokeratins, or antitrypsin, LEU7, vimentin, LDH and ferritine.
Results: Retrospective and prospective study was examinated in techniques of immunohistochemistry and morphometric in histopathological diagnosis of certainty in ambiguous cases, the establishment of a full morphological diagnostic protocol embryonic testicular carcinoma.
Conclusion: Testicular embryonal carcinoma is a malignant germ tumor that can develop in several forms. Due to cell variability and degrees of complexity of testicular tumors composed embryonic carcinoma lesions gives a prognosis testicular germinal tumor. Linking aspects with histopathological variables and with the morphometric immunohistochemical results we achieve a complete histologic diagnosis protocol of complex embryonic testicular carcinoma.

054

Renal solitary fibrous tumor: case report

G. Resul *, M. Aschie, J. Stanisici
*Constanta, Romania

Objective: Renal mesenchimal tumors represent up to 10% of the renal tumors, the most frequents been the angiomyolipoma and the sarcoma. The renal solitary fibrous tumor (SFT) is a rare entity.
Method: We report a case of a 43-year-old man presenting at the hospital with an incidental echographical finding of a right renal tumor 12 cm in diameter. A total right nephrectomy was made.
Results: The histopathological exam showed a spindle cells neoplasm with moderate atypical nuclei. The cells are disposed in a storiform way or having a "patternless" aspect in a collagenous stroma. It is associated with a hemangiopericytoma type of vascularisation. It was counted as five mitoses/10 high power fields. Immunohistochemistry showed reactivity for vimentine, Bcl2 and CD99. Immunohistochemical stains for CD34, HMB45, KL1 and EMA were negative. The proliferation index Ki67 was 40%.
Conclusion: Renal localisations of SFT are rares. The CD34 is positive in the quasitotality of benign SFT cases but it can be negative in 5% of malignant forms. The negativity of CD34 should not exclude the diagnosis of SFT and it can represent an aggravation factor.

055

Mixed epithelial and stromal tumour of the kidney with malignant transformation

R. Santi*, A. Franchi, M. Paglierani, M. Pepi, D. Villari, G. Nicita, G. Nesi
*University of Florence, Dept. of Pathology, Italy

Objective: Mixed epithelial and stromal tumour (MEST) of the kidney is a rare neoplasm, more frequently encountered in middle-aged women. Although the majority of MESTs behave in a benign fashion, both sarcomatous and carcinomatous transformations have been observed. Multilocular cystic renal cell carcinoma, angiomyolipoma with epithelial cysts and synovial sarcoma of the kidney should be considered in the differential diagnosis.
Method: A 71-year-old woman underwent surgery for a huge cystic mass in the left kidney.
Results: Grossly, the mass measured 20 cm in the greatest diameter and was composed of firm areas merged with multiple cysts filled with serous, focally haemorrhagic fluid. On light microscopy, the epithelial component showed medium-sized to large cysts lined by flat or cuboidal cells. The stromal component consisted of markedly cellular fascicles of spindle cells and displayed numerous mitoses. By immunohistochemistry, oestrogen and progesterone receptors were detected in the nuclei of the stromal cells. Interphase fluorescent in situ hybridization (FISH) analysis for the t (X;18) translocation excluded synovial sarcoma.
Conclusion: Even though malignant transformation has been reported in few cases of MEST, its occurrence suggests extensive sampling and careful examination of this controversial neoplasm of the kidney.

056

Trends in grade and stage over time in a population-based study of bladder cancer in Northern New England

A. Schned *, P. Lenz, L. Moore, A. Johnson, D. Silverman, M. Schwenn, K. Kelsey, D. Baris, M. Karagas
*Dartmouth-Hitchcock Medical Centre, Dept. of Pathology, Lebanon, USA

Objective: Previous studies in urogenital cancers suggest a possible migration toward lower stage and grade in tumors at the time of diagnosis. Studies in bladder cancer, however, are limited and results vary. We investigated these trends in a population-based case–control cohort of urothelial bladder cancer cases from 1998 to 2004 in three states in northern New England.
Method: There were 1.091 newly diagnosed bladder cancer cases from New Hampshire, Maine, and Vermont from 2001 to 2004, divided into equal time spans of two years each, compared for stage and grade at diagnosis to 327 previously studied cases from New Hampshire from 1998 to 2000. A single review pathologist classified all tumors in both studies.
Results: Over time, we found an increase in% of papillary urothelial tumors of low malignant potential and a decrease of low-grade papillary urothelial carcinomas (*p*-trend

0.009). Among high-grade papillary urothelial carcinomas, the percent of non-invasive tumors rose from 35.1% to 48.1% (*p*-trend 0.02).
Conclusion: The distribution of tumor stage and grade, as well as the observed trends, were similar across all three states, suggesting similar histological, behavioral, and epidemiological characteristics. The results appear to parallel trends in grade and stage identified in other urogenital cancers over time.

057
Expression of Jun activation domain-binding protein 1 in urothelial carcinoma of the upper urinary tract

M.-T. Sung *, H.-Y. Huang
*Chang Gung Memorial Hospital, Dept. of Pathology, Kaohsiung, Taiwan

Objective: Jun activation domain-binding protein 1 (Jab 1), a coactivator of transcription factor, promoted cell proliferation through the ubiquitin/proteasome pathway and its overexpression was reported in some neoplasia. To elucidate the significance of Jab 1 in urothelial carcinoma of the upper urinary tract, the expression of Jab 1 and its relationship between tumor progression were investigated.
Method: We undertook the analysis of m-RNA expression of Jab 1 in paired tumor and normal tissue by semiquantitative reverse transcription polymerase chain reaction (RT-PCR) in 33 patients of urothelial carcinoma of the upper urinary tract, including both renal and ureteral tumors, and explored the correlation between Jab 1 expression and tumor aggressiveness.
Results: Urothelial carcinomas were shown overexpression of Jab 1 in 52% (17/33) cases. The incidence of Jab 1 overexpression in patients harboring invasive cancers is 68% (13/19), higher than those with non-invasive tumors (28%, 4/14). A significant correlation between high Jab1 expression and both advanced tumor stage and high tumor grade was found.
Conclusion: Our data suggest Jab 1 may play a significant role in tumor progression in urothelial carcinoma of the upper urinary tract.

058
Neuroendocrine carcinoma of the urinary bladder: presentation of four cases

O. Tzaida*, G. Giannakopoulos-Stanc, C. Valavanis, I. Iakovidou, O. Batsi, D. Karagianni,
P. Arapantoni-Dadioti
*Metaxa Cancer Hospital, Dept. of Pathology, Piraeus, Greece

Objective: Neuroendocrine carcinoma of the urothelium (NCU) is an extremely rare malignancy (less than 1% of bladder cancer) that mimics pulmonary counterparts. Molecular data indicates that both urothelial and small cell carcinoma originate from the same stem cell in the urothelium.
Method: Four cases of NCU, concerning three men (65, 70, 71 years old) and one woman (68 years old) diagnosed two in biopsy material and two in radical cystectomy during the last 5 years. CT revealed urinary bladder as the only tumor localization. Adjuvant cytotoxic chemotherapy was administered to the patients, two of whom died in less than 1 year.
Results: A pure neuroendocrine carcinoma with small and large cells was detected in two cases. The other two cases displayed coexistence of small cell carcinoma with conventional urothelial carcinoma. Three cases were classified as pT2 and one pT3. Immunohistochemically neuroendocrine markers (NSE, Chromogranin, Synapthophysin, Leu-7, NCAM) were positive.
Conclusion: Neuroendocrine carcinoma of the urothelium is a very rare and aggressive malignancy. The diagnosis can be made by the typical morphologic and immunophenotypic features. The primary urinary origin must be documented by exclusion of metastasis of other possible sites in accordance with laboratory and clinical findings.

059
Synchronous renal collecting duct carcinoma and renal cell carcinoma: a case report

I. Iakovidou *, G. Giannakopoulos-Stanc, P. Tziakou, M. Parcharidou, M. Vrontaki, C. Valavanis
*Metaxa Cancer Hospital, Dept. of Pathology, Piraeus, Greece

Objective: Synchronous occurrence of renal collecting duct carcinoma (CDC) and a renal cell carcinoma (RCC) clear cell type is extremely rare. CDC represent 0.4-2% of all renal carcinomas.
Method: A man, 53 years old, was admitted for hematuria. Routine laboratory tests were normal except for increased urea and creatinine. MRI revealed heterogeneous echoic 10-cm mass in the inferior pole of the kidney with invasion of the medullary area and beyond renal capsule. Nephrectomy was carried out. Our patient died in postoperative period with multiple metastases.
Results: Histopathological examination of the specimen showed a conventional RCC, clear cell type, Fuhrman nuclear grade 3, and a CDC. The CDC was composed of

pleomorphic high-grade malignant cells, with eosinophilic cytoplasm. Atypical mitotic figures, desmoplasia and inflammatory reaction were present. We noted presence of necrosis and invasion of renal vein. Immunohistochemical study demonstrated HMWCK, CK7, EMA positivity, vimentin and RCC negativity in CDC, with a typical immunophenotype of RCC.
Conclusion: CDC is highly aggressive carcinoma, originating in the medullary collecting duct (mesonephric structure). Microsatellite analysis displayed LOH in 1q32.1-32.2 in 60%. Radical nephrectomy, chemotherapy, immunotherapy or local radiotherapy appear to have a limited role on prognosis of this disease.

060

AMACR polymorphic variant rs3195676 and prostate cancer aggressiveness in Bulgarian patients

A. Vlahova*, T. Dikov, S. Christova, D. Kachakova, A. Mitkova, M. Genadieva, E. Popov, C. Slavov, V. Mitev, R. Kaneva
*Alexandrovska University Hospital, Dept. of Pathology, Sofia, Bulgaria

Objective: Expression of the α-methylacyl-CoA racemase (AMACR) gene involved in fatty acids metabolism has been established as a sensitive and specific biomarker for the diagnosis of prostate cancer (PC). Several studies have found that polymorphisms in AMACR, especially rs3195676 (Met9Val), alter the risk for PC.
Method: The case–control study of the polymorphic variant rs3195676 was performed using blood DNA samples from 188 PC cases and 163 controls. The PC patients underwent biopsy with histology and IHC (AMACR, p63, HMWC and Ki67) for diagnosis and grading.
Results: The polymorphic variant did not show association with increased PC risk after comparison of all samples and controls. In terms of the aggressiveness of the disease, the genotype C/C (OR=0.18, p=0.05) and C allele (OR=0.55, p=0.055) demonstrated association with reduced risk for development of PC with high Gleason score and metastasis and the results are close to statistical significance.
Conclusion: The case control studies of different cohorts including either familial or sporadic PC cases suggest that rs3195676 in AMACR is associated with PC. This is the first study that finds correlation between this polymorphism and the aggressive form of PC. Results need to be confirmed in larger cohort of Bulgarian patients.

061

Juxtaglomerular cell tumor as a rare cause of hypertension: report of a case

M. Volavsek *, Z. Ovcak
*University of Ljubljana, Faculty of Medicine, Slovenia

Objective: Juxtaglomerular cell tumor is a rare usually benign renal neoplasm arising from juxtaglomerular apparatus. We report a case of a 24-year old woman with severe hypertension (up to 180/110 mmHg) from age 15 and ultrasonographically detected tumor of the left kidney.
Method: Repeated fine needle aspiration cytology of the tumor revealed features of "neoplasm, most likely malignant epithelial". Partial nephrectomy of a cystic and haemorrhagic incapsulated tumor measuring 2 cm in greatest diameter was performed.
Results: Histologically, the tumor was composed of solid sheets/nests of polygonal cells with round to oval nuclei and abundant eosinophilic cytoplasm interspersed with mastocytes. Low power view disclosed a hemangiopericytic vascular pattern. Immunohistochemically, tumor cells were vimentin+and CD34+. Negative were: EMA, different CKs, CD10, RCC, HHF-35, SMA, desmin, CD117, S-100, CD31, synaptophysin, chromogranin. Although renin antibody was unavailable, diagnostic rhomboid cytoplasmic renin protogranules were found by elecron microscopy.
Conclusion: Juxtaglomerular cell tumor is relatively rarely encountered in everyday urological pathology practice. Mostly benign, exceptionally malignant and even nonfunctional cases were described. Clinical and patological diagnosis of this "reversible" cause of severe hypertension in young adults is challenging and electron microscopy, although unusual in tumor pathology, is of diagnostic importance.

062

Perivascular epithelioid cell tumour (PEComa) of the ureter: a diagnostic challenge

S. Yerly *, J. Renard, S.-N. Tran, C. Iselin, M.-F. Pelte
*Universitätsklinik Genf, Inst. für Klinische Pathologie, Switzerland

Objective: PEComas are unusual and recently described mesenchymal tumours composed of HMB-45-positive epithelioid cells. Thought to derive from perivascular cells like angiomyolipoma, lymphangioleiomyomatosis or clear cell "sugar" tumour, they arise most commonly at visceral, retroperitoneal, and abdominopelvic sites. This is the first case of ureteral PEComa.

Method: A left ureteral mass, located very close to the kidney and responsible for hydronephrosis, is discovered in a 33-year-old man. Ureteropyeloscopy with sampling is performed. Cytological examination shows benign urothelial cells. Histological analysis reveals an atypical clear cell proliferation. No immunohistochemistry is done and an infiltrating renal clear cell carcinoma is diagnosed. A nephro-ureterectomy is decided.
Results: A circumscribed parietal ureteral tumour is found. Histologically, a proliferation of atypical clear and/or epithelioid cells around an elaborate fibrovascular network is seen. Some of the tumour cells display dark-brown melanin pigment and show HMB-45-positive immunostaining. The combination of cytomorphology, evidence of melanin pigmentation and distinctive immunohistochemistry favour a diagnosis of PEComa.
Conclusion: The rarity and polymorphic appearance of PEComa may account for difficulties in considering the diagnosis, especially when located in an unusual anatomical site. However, awareness of this unusual entity and its distinctive immunohistochemical profile invariably leads to a correct diagnosis.

063

Morphological differential diagnosis of hyperplasic, atrophic and precancerous lesion of the prostate

V. Zakharava *, T. Liatkouskaya, E. Cherstvoy, I. Masanskiy, L. Sagalchik, M. Ivanovskaya
*Belarus State Medical University, Dept. of Pathology, Minsk, Belarus

Objective: Postatrophic hyperplasia (PAH) and proliferative inflammatory atrophy (PIA) of the prostate demonstrate common biological and morphological features with precancerous lesions. Our aim was to study immunomorphological peculiarities of PAH and PIA.
Method: Immunostaining and image analysis were used for assessment of cytological atypia, degree of basal cells (BC) loss, expression of AMACR, cyclinD1, topoIIa and TGFβ.
Results: In the PAH/PIA group the BC layer was fragmented in 77% of cases, but the median of BC loss (6%/0%) did not differ from benign prostatic hyperplasia (BPH). Nuclei and nucleoli parameters, frequency of cases (83%/67%) and cells (14%/13%) with nucleoli≥1 μm in the PAH/PIA group did not differ from same in precancerous lesion. No reliable difference was found between the area of AMACR expression in cases of PAH/PIA (2.5%/0.7%) and those of BPH (1.2%). However, in the PAH/PIA group the area of cyclinD1 expression (28%/31%) and frequency of topoIIa-positive cells (0/0.3%) was higher and the area of TGFβ expression (4%/2%) was lower than in BPH and did not differ from precancerous lesions ($p<0.001$).
Conclusion: PAH and PIA occupy intermediate position between BPH and PCa. By their cytological properties and expression of cell cycle markers and TGFβ they are closer to precancerous lesions.

064

Primary adenocarcinoma of the seminal vesicles: a phantom tumor

A. Zizi-Sermpetzoglou*, E. Moustou, V. Savvaidou, E. Arkoumani, N. Tepelenis, K. Stamatiou
*Tzaneio General Hospital, Pireaus, Greece

Objective: Primary adenocarcinoma of the seminal vesicles (ASV) is a very rare neoplasm with less than 50 histologically confirmed cases reported in the literature. The diagnosis is generally difficult and it is based on a combination of morphologic, immunohistochemical, and clinical findings, including radiologic examination. We present a case of primary ASV found upon investigation of inguinal lymphadenopathy.
Method: A 46-year-old man presented with bilateral inguinal lymphadenopathy and lymphedema. A pair of palpable, painless left sub-clavicle lymph nodes was also found. The patient had a normal, painless rectal digital examination. Biopsy of lymph nodes revealed a malignant neoplasm showing histologic and immunohistochemical characteristics of a non-mucin producing, low differentiated carcinoma. TRUS of the prostate revealed an inhomogeneous transitional zone, but failed to identify any focal lesion. On cystoscopy, the bladder neck was edematous while the remaining bladder mucosa was normal.
Results: Biopsy specimens from both bladder neck, prostate and seminal vesicles revealed an anaplastic non-mucin producing, low differentiated carcinoma positively stained for Ca-125, CK7, CKL, CKH and negatively for PSA, PSAP and CK20. A diagnosis of ASV was proposed in accordance with the World Health Organization (WHO) classification criteria. The patient underwent aggressive chemotherapy. Despite the initial response he died 6 months later.
Conclusion: A definitive diagnosis of ASV is generally difficult and multiple biopsies are needed in order to determine whether or not the tumor is primary to the seminal vesicles. The prognosis of these tumours is extremely poor, as they are often extensive when diagnosed.

065

Prediction of response to BCG treatment in non-muscle invasive bladder cancer patients through interleukin-6 and -10 ratio

R. Santi *, T. Cai, R. Bartoletti, G. Nesi
*University of Florence, Dept. of Pathology, Italy

Objective: Non-muscle invasive bladder cancer (NMIBC) patients who fail BCG therapy show a poor prognosis even when treated with salvage cystectomy.
Method: A group of 121 consecutive urological outpatients (72 affected with NMIBC and 49 controls) were selected. Urine samples for dipstick analysis and interleukin analysis were collected before TUR and subsequent 6 weekly BCG instillations. IL-6 and IL-10 concentrations were determined by solid phase ELISA Quantikine immunoassay. Patients with NMIBC were stratified according to IL-6/IL-10: Group A ≤0.09 and Group B >0.10.
Results: At enrolment, IL-6/IL-10 was not statistically different in patients and controls. Out of the 72 patients with NMIBC, 38 (52.7%) showed IL-6/IL-10 ≤0.09 (Group A) while 34 (47.3%) >0.10 (Group B). A significant difference between IL-6/IL-10 and status at follow-up was found ($p=0.006$). The Kaplan–Meier curves demonstrated that group B patients had a significantly better probability to be recurrence-free than Group A patients ($p=0.0002$). On multivariate analysis, IL-6/IL-10 ($p<0.003$) and the number of lesions ($p<0.001$) were identified as independent predictors of BCG response.
Conclusion: This prospective study highlights the feasible role of IL-6/IL-10 value in predicting recurrence after BCG therapy in NMIBC.

066

Dedection and morphological profile of early stages bladder carcinoma: preliminary study

I.A. Plesea *, P. Tomescu, M.A. Enache, O.P. Dragoescu, A. Panus, F.C. Popescu, S.D. Enache
*University of Medicine Craiova, Dept. of Pathology, Romania

Objective: The authors made a preliminary morphological evaluation of bladder carcinomas in early stages of evolution-ESBT (T0, Ta, T1).
Method: The studied material consisted of 22 cases of urothelial bladder carcinoma, detected by white light cystoscopy (WLC) and fluorescent cystoscopy (photodynamic diagnosis—PDD). Tissue samples were stained with HE and immunomarked for androgen receptor (AR). The assessed parameters were: tumor number, dimensions, grading and staging, and quantitative scores for AR intensity expression (ARI) and AR density expression (ARD).
Results: All cases had more than one tumoral area and in 1/3 of them PDD revealed at least one more tumoral area/case, as compared with WLC. Mean tumoral Ø was 1.82 cm (STDEV 0.48) and was not clearly related neither with tumor grade nor with tumor stage. G2 grade (G1/G2/G3—7/13/2 cases) and T1 stage (T0/Ta/T1—0/4/18 cases) dominated. ARI and ARD were inversely related (ie, while ARD increased ARI decreased) and both decreased with tumor grade.
Conclusion: The studied ESBT were multiple tumors, with significant dimensions and expressed AR but whose intensity and density decreased with tumor grade. Their detection was clearly improved by PDD.

067

Adenocarcinoma on needle prostatic biopsies: does reactive stroma predict biochemical-free survival in patients following radical prostatectomy?

A. Billis *, L. Meirelles, L.L.L. Freitas, A.S. Polidoro, H.A. Fernandes, M.M. Padilha, L.A. Magna, L.O. Reis, U. Ferreira
*University of Campinas, School of Medicine, Brazil

Objective: Only two studies in the literature has shown that carcinoma with intense reactive stroma (RS) on needle prostatic biopsies predicts time to biochemical recurrence (TBCR) in patients after radical prostatectomy (RP).
Method: Reactive stroma was graded as 0 (no RS), 1 (slight), 2 (moderate), and 3 (intense). The final grading was considered in the core with the most extensive carcinoma (index core).
Results: From a total of 266 needle prostatic biopsies, 143 (53.8%), 55 (20.7%), 54 (20.3%), and 14 (5.3%) showed no (grade 0), slight (grade 1), moderate (grade 2), and intense (grade 3) RS, respectively. Biopsies with RS (desmoplasia) were significantly associated with clinical stage T2, higher preoperative PSA, more extensive tumors in biopsy and RP, and pathologic stage>T2. Only grade 3 RS was significantly associated with TBCR and a significant predictor of TBCR on univariate analysis but not on multivariate analysis.
Conclusion: Biopsies with desmoplasia are significantly associated with several clinicopathological adverse findings; however, only grade 3 RS significantly predicts TBCR following RP on univariate analysis but not on multivariate analysis. Another limitation of RS as predictor of TBCR is the small percentage (5.3%) of biopsies showing grade 3 RS.

068

The significance of proliferative inflammatory atrophy for prostatic carcinogenesis

S. Taban *, C. Lazurean, D. Herman, D. Anderco, M. Botoca, A. Muresan, C. Moldovan, A. Dema
*University of Medicine, Dept. of Pathology, Timisoara, Romania

Objective: Focal prostatic atrophy, which is frequently associated with chronic inflammation, seems to be a highly proliferative lesion. We examined proliferative inflammato-

ry atrophy (PIA) for the expression of p53 and proliferative activity.
Method: We examined 67 consecutive needle biopsies and radical prostatectomy with associated PIA lesions (38 cases of benign hyperplasia and 29 malignant lesions). Immunohistochemical stainings were performed using p53 (DO-7), MIB-1, PSA and 34betaE12. Normal epithelium, foci of atrophic cells, high-grade prostatic intraepithelial neoplasia (HGPIN) and prostatic carcinoma (PC) were scored for p53 and KI-67.
Results: The mean Ki-67 LI in the secretory layer was higher in PIA lesions (5.4%) vs. normal epithelium (0.4%) ($P<0.001$). The proportions of KI-67 positive nuclei were significantly higher in HGPIN (11.7%) and PC (12.9% $P<0.001$). p53 protein positivity was noted in nine cases of PC (31%). We observed p53 nuclear staining in 0.8% of basal cells in normal prostate acini, a value significantly lower than 3.2% and 1.1% of basal and luminal epithelial p53 positive cells of PIA lesions.
Conclusion: Our results revealed p53 immunostaining in the luminal epithelial cells in PIA lesions. Increased cell proliferation demonstrates the hyperproliferative status of PIA and the possible direct relationship with prostate carcinogenesis.

Wednesday, 31 August 2011, 09.30–10.30 and 16.30–17.00, Hall 5

PS-18 Poster Session Cardiovascular Pathology

001
Ischemia detection in acute coronary syndrome

L. Kakturskiy *, A. Philippov
*Research Institute of Moscow, Dept. of Human Morphology, Russia

Objective: The basis of an acute coronary syndrome (ACS) is an ischemia of the myocardium which is diagnosed by clinical and morphological methods.
Method: Autopsy material from 84 cases of ACS has been examined (62 males, 22 females, 48-67 years). Macro- and microscopic tests on myocardial ischemia were used including NBT-macrotest. In 23 cases morpho-functional comparisons with vital ECG data have been carried out.
Results: The damaged vulnerable atherosclerotic plaques have been found in all cases as a trigger of ACS. As a sign of myocardial ischemia sarcomere hyperrelaxation has been found by polarizing microscopy. Wavy deformation of muscular fibers as well as microcirculatory disorders were permanently seen. NBT-test revealed focuses of myocardial ischemia in the left ventricle wall and in interventricular septum. By comparing the ECG with NBT-test it was apparent that in early ischemia without Q-wave NBT-test was constantly positive.
Conclusion: Morphological basis of ACS is a myocardial ischemia provoced by rupture of vulnerable atherosclerotic plaques. Ischemia is detected on morphological signs. NBT test allows to reveal a myocardium ischemia in an early stage without a Q-wave.

002
The importance of expert cardiac pathology for the investigation of sudden cardiac death: results from a fast track cardiac pathology service in the UK

S. de Noronha *, K. Ohta-Ogo, E. Behr, M. Papadakis, W. Banya, J. Wells, S. Sharma, M. Sheppard
*NHLI, Imperial College London, Dept. of Histopathology, UK

Objective: We report an innovative fast track cardiac pathology service for victims of sudden cardiac death (SCD) in the UK.
Method: A prospective non-case control study of SCD. Data analysis period was 2007–2009.
Results: There were 720 SCD cases referred, the majority of whom were young males (66%, 2:1), median age 31 years. The main cardiac pathological diagnoses were normal heart ($n=320$) (indicating possible channelopathy), cardiomyopathy ($n=205$) and coronary artery pathology ($n=71$). The most common cardiomyopathies were: idiopathic LVH ($n=54$), HCM ($n=42$), ARVC ($n=29$) and obesity related cardiomyopathy ($n=29$). A cardiac histopathological diagnosis was provided by referring pathologists in a sample of 158/200 consecutive cases of SCD where 40% ($\kappa=0.49$) differed from the final diagnosis by MNS. Referring pathologists were more inclined to diagnose pathology rather than designate the heart as normal, attributing isolated fatty infiltration of the right ventricle to ARVC and left ventricular hypertrophy in absence of myocyte disarray to HCM.
Conclusion: This large prospective study highlights the importance of inherited cardiac disease as indicated by at least 75% of our cases. It also highlights disparity in diagnoses between pathologists. We provide a prompt cardiac pathology diagnostic service nationwide that facilitates the referral of families to specialist inherited cardiac disease clinics.

003

Physical training triggered a decrease of heart fibrosis

D.T.R.S. Abate *, M.M. Mauad Cintra, J.R. Machado, O. Barbosa Neto, V.J. ´Dias da Silva, L. Rocha, M.A. dos Reis
*UFTM, Dept. of Biological Science, Uberaba, Brazil

Objective: The aim of this study was to morphologically analyze the heart of spontaneously hypertensive rats submitted to physical training or not. There were 12 spontaneously hypertensive rats (SHR) and 12 Wistar–Kyoto (WKY) normotensive rats used.
Method: The experimental groups were divided in: (1) hypertensive sedentary group (HS) (n=6); (2) hypertensive trained group (HT) (n=6); (3) normotensive sedentary group (NS) (n=6); (4) normotensive trained group (NT) (n=6). After the end of the swimming protocol period, the animals were first anesthetized for blood pressure measurement. At the end of the experiments, the rats were induced to euthanasia and the hearts used for the study were removed. The analysis of the left ventricular fibrosis, the slides were stained with picrossirius and were visualized under polarized light. Images were captured by a conventional microspore and analyzed by KS 300 (KONTRON- ZEISS).
Results: When the average blood pressure (ABP) and the heart frequency (HF) were compared with the physical training, it was verified that the physical activity—swimming—decreased the ABP and the HF. The heart fibrosis percentage was significantly higher in the sedentary groups, as compared to the trained groups (p<0.001).
Conclusion: The swimming physical training triggered a decrease of heart fibrosis. CNPq, FAPEMIG, CAPES.

004

The morphological heterogeneity of vimentin positive interstitial cells of myocardium

C. M. Ardeleanu *, A. Georgescu, F. Filipoiu, S. Enache, M. Comanescu, M. Ceausu, M. Stoicea,
F. Staniceanu
*Roche Romania S.r.l., Dept. of Oncology, Bucharest, Romania

Objective: Fibroblasts are the most numerous interstitial cells of myocardium. Aim: To evaluate the interstitial Vimentin positive spindle cells in fetal and adult myocardium.
Method: We analysed paraffin embedded autopsy myocardium samples from 10 fetuses and 10 adults (ischemic or not). Immunohistochemistry: Vimentin (V9, Dako), DDR2 (H-108, Santa Cruz, CA) and alpha-Smooth Muscle Actin (1A4, Dako). Visualisation: Dako EnVision.
Results: The spindle-shaped cell population positive for Vimentin had variable plump or slender nuclei differently sized, more numerous in the fetal myocardium. The cytoplasm stained for Vimentin presented bipolar processes, some with rich ramifications, oriented along the capillaries, interconnected with others, or extended around the myocytes. In fetal and normal adult myocardium, 28.13% and 24.60% of the spindle shaped cells expressed alpha-SMA mostly in the capillary walls. In the ischemic myocardium 69.56% of spindle cells expressed alpha-SMA, suggesting their myofibroblastic nature. The fetal subepicardial myocardium expressed also DDR2, while the adult ischemic myocardium expressed it diffusely.
Conclusion: We concluded that the interstitial spindle-shaped cells of the myocardium are heterogeneous in shape and processes; this is suggesting for different functions. Acknowledgement. Work supported by CNCSIS Grant 1388/2008, Bucharest.

005

Performance of routine C4d and C3d immunostaining on protocol endomyocardial biopsies (EMBs) in a prospective and unselected cohort of heart transplant patients

P. Bruneval *, A. Loupy, A. Cazes, J.-P. Duong Van Huyen
*Hopital Europeen Georges Pompidou, Dept. de Pathologie, Paris, France

Objective: In heart transplants, subclinical forms of antibody mediated rejection (AMR) are increasingly recognized in protocol EMBs as an emerging cause of late transplant failure. The clinical relevance of systematic C4d/C3d evaluation in unselected protocol EMBs remains to be determined.
Method: This prospective study included all the protocol EMBs (n=260 in 100 patients) performed in our institution for 1 year from October 1st 2009 to September 30th 2010.
Results: The prevalence of positive C4d was 3.1%. 38/260 EMBs (14.6%) showed histological evidence of microvascular inflammation (MI+) in which 8.3% were positive for C4d and 55.6% for C3d staining, respectively (sensitivity for C4d vs C3d: p<0.01). Among the biopsies with evidence of microvascular inflammation (MI+), 42.2% did not show any C4d or C3d deposition. Finally, the prevalence of positive DSA in the MI+group without C4d/C3d deposition was 73.3% as compared to 77.3% in the MI+-C4d/C3d-positive group.
Conclusion: C4d staining has a high specificity but very low sensitivity in clinically stable patients. C3d has a significantly higher sensitivity than C4d alone to predict concommitant microvascular inflammation. Importantly, microvascular inflammation, even without C4d/C3d deposition is associated with circulating DSA. These data suggest that C4d/C3d positivity may not be sufficient for the diagnosis of AMR, excluding patients from this specific diagnosis.

006

Isolated thoracic aortitis: a novel member of IgG4-related disease? Clinicopathological study of 11 cases

J. Laco *, I. Steiner, T. Holubec, J. Dominik, Z. Holubcova, J. Vojacek
*University Hospital Fingerland, Dept. of Pathology, Hradec Kralove, Czech Republic

Objective: Isolated thoracic aortitis (ITA) is diagnosed in a variable proportion of patients operated on for aneurysm of ascending aorta. However, the etiopathogenesis of ITA remains unclear.
Method: Using immunohistochemistry, we studied 11 cases of ITA in order to determine the role of IgG4-mediated immune responses in its pathogenesis.
Results: The series included nine females and two males aged 52–79 years. All patients developed aortic incompetence due to aneurysm of ascending aorta. The microscopic findings included the presence of lymphoplasmacellular infiltrate of varied intensity involving the adventitia and media of aorta and fibrosis. This inflammation was associated with severe medial elastic fiber defects. Obliterative phlebitis of the vasa vasorum was absent. Immunohistochemically, the inflammatory infiltrate comprised T- and B-lymphocytes as well as plasma cells. The plasma cell population was polyclonal with a predominance of IgG-producing cells. In all the cases, IgG4-producing plasma cells were detected. In five cases, the count exceeded 20 cells per 1 high power field. The IgG4/IgG ratio ranged from 0.07 to 0.98 (median 0.55).
Conclusion: Our results suggest that a subset of ITA may represent aortic manifestation of IgG4-related disease.

007

Intimal sarcoma of the aorta: an uncommon cause of sudden back pain and upper limb ischemia

S. Medina Román *, L. Naranjo Hans, J.F. Pérez Ochoa, E. Castellà, I. Ojanguren
*HUGTiP, Dept. of Pathology, Badalona, Spain

Objective: Sarcomas of great vessels are uncommon agressive neoplasms. One of the most useful classifications divides them into mural and luminal. The latter arise predominantly from the intima and show the poorest outcome. We present an autopsy case of this entity.
Method: A 46-year-old woman consulted for sudden back pain and developed acute right upper limb ischemia at emergency room. Imaging techniques revealed brachiocephalic trunk stenosis and bilateral adrenal masses. The patient underwent a myocardial infarction and died. Autopsy examination was performed and formaline-fixed, parafin tissue sections were studied using haematoxilin-eosin stains and immunohistochemistry techniques.
Results: Multiple intraluminal polyps were identified in the brachiocephalic trunk, aortic valve and root of the aorta. A bilateral adrenal mass (5 cm each) and a right foream subcutaneous tumor (3.5 cm) were found. Microscopically, these lesions showed atypical spindle-shaped cells arranged in a storiform pattern with focal myxoid, epithelioid areas and hihg number of mitotic figures. Tumour cells were positive for vimentine and immunoreactive for actin. The subendothelial growth pattern was demonstrated by the expression of CD31 on luminal surfaces.
Conclusion: Definitive diagnosis of intimal sarcoma of the aorta is usually achieved by autopsy and shoul be entertained when dealing with vascular lesions.

008

Left ventricular fibrillar collagenous matrix remodelling in chronic ischemia

D. Pangonyte *, J. Palubinskiene, D. Kazlauskaite, L. Utkiene, V. Buneviciene, L. Peciulyte, D. Baltusnikas
*Lithuanian University of Health, Clinic of Pathology, Kaunas, Lithuania

Objective: The aim of the study was to evaluate peculiarities of human myocardial interstitial collagen matrix remodelling in the left ventricular myocardium due to chronic ischemia.
Method: Hearts of suddenly deceased males who died suddenly out-of-hospital (within 6 h of the onset of the terminal event) due to the first acute (n=51) and repeated (n=35) event of ischemic heart disease (IHD) were studied. The control group consisted of males (n=26) of similar age who succumbed to external causes. Collagen was stained with picro-sirius red, computerised image analysis system was applied for histomorphometry.
Results: Interstitial collagen percentage volume, perimeter and the number of separate foci of fibres per field of left ventricular myocardium in the pre-infarction IHD group was greater than in the controls (by 31%, 26% and 19%, respectively, $p<0.05$). The induced collagen matrix remodelling process progresses during the post-infarction phase: collagen percentage volume of left ventricular myocardium was higher by 40%, matrix perimeter by 39%, and number of fibres per field by 32% in the post-infarction IHD group as compared with the same indices of pre-infarction IHD group ($p<0.05$).
Conclusion: Remodelling of left ventricular myocardium interstitial collagen network is induced due to chronic myocardial ischemia (before the first myocardial infarction) and progresses after the myocardial infarction.

009

Comparative study on levels of homocystein and LP(A)-lipoproteinis among patients with positive history of cerebrovascular accident and the general population

S. Patiakas *, M. Palaiologou, S. Sarafidis, M. Tsigaridaki, C. Charalampous, K. Rousos
*General Hospital of Kastoria, Microbiological Laboratory, Greece

Objective: To record the levels of homocysteine and LP (A), lipoprotein A, in patients with previous history of cerebrovascular accident (stroke) (CVA) and to correlate with those in the general population.
Method: We studied 36 patients (group A), who suffered in the recent past (<1 year) a CVA. All identified levels of homocysteine in an immunoenzymic analyst, and Lp (a) lipoprotein in biochemical analyzer, while our results were compared with 90 healthy subjects (group B).
Results: In group B we had the following results: (a) increase only of homocysteine: 24 person-rate of 26.7%, (b) an increase of only Lp (a): 36 people—40%, and finally (c) simultaneous growth of both homocysteine and Lp (a): 16 person-rate 17; 8%, In contrast, in group A, the corresponding results were as follows: (a) increase only of homocysteine: 14 person-rate 38.9%, (b) an increase of only Lp (a): 19 person-rate of 52.8%, and finally (c) simultaneous growth of both homocysteine and Lp (a): 8 people—22.3%.
Conclusion: It appears, therefore, that in the general population there is a very large proportion with increased Lp (a) primarily, but also hyperhomocystinemia or even elevated levels of both, and a comparative study has demonstrated that in patients with a history of CVA found even higher (statistically significant) increase.

010

Primary malignant peripheral nerve sheath tumor of the heart: a case report

S. Rjabceva *, M. Vozmitel
*Belarusian Medical Academy, Dept. of Pathology, Minsk, Belarus

Objective: Malignant peripheral nerve sheath tumor (MPNT) is an unusual sarcoma of the heart. The aim of this study is to describe the histopathological and immunohistochemical features of this tumor.
Method: We studied the case of a 48-year-old man with MPNT of the heart. We used immunohistochemical markers such as CD99, bcl-2, SMA, vimentin, WT1, D2-40, S100.
Results: A tumor size was 21x17x12 cm. Histologically, the tumor showed a fascicular growth with abrupt transition between cellular and more myxoid areas. In the cellular areas the parallel orientation of the cells was found. The spindled cells of tumor had oval nuclei with or without wavy configuration. Focally, it was detected the "epithelioid"-looking tumor cells with more round nuclei. The foci of necrosis and hemorrhages, a striking perivascular hyalinization were found, but mitotic activity was low. Immunohistochemical examination showed focal vimentin positivity. CD99, bcl-2, WT1 and smooth muscle actin were completely negative. The staining S100 protein was focal and limited to a small number of cells. However, the more the cells stained positive for D2-40.
Conclusion: Although the tumor cells revealed vimentin and D2-40 positivity, our diagnosis of the tumor was MPNT.

011

Myocardial fibrosis in the patients having heart failure with reduced and preserved ejection fraction

N. Solomakhina *, O. Popova, L. Gundarova, V. Warshavsky
*1st Moscow State Medical University, Russia

Objective: Myocardial fibrosis plays a key role in heart failure both with reduced ejection fraction (HFREF) and preserved ejection fraction (HFPEF). The purpose of the study is to compare patterns of myocardial fibrosis and collagen types I and III in HFREF and HFPEF.
Method: There were 11 myocardium autopsies of patients who had ischemic etiology and acutely decompensated heart failure investigated: HFREF (six) or HFPEF (five). The intensity of immunohistochemical staining of collagen-I and III was estimated in paraffin sections semiquantitatively according to the 5-scale number. Collagen fractions in myocardium were classified as peremysial, endomysial and perivascular.
Results: Content of endomysial collagen was significantly higher in HFPEF than in HFREF group (1.6 vs.0.5; $p(U)=0.034$). Differences in perimysial collagen fractions were insignificant. Content of interstitial fibrosis, presented as combination of endomysial and perimysial fractions, was higher in HFPEF (3.2 vs. 1.67, $p(U)=0.047$). Ratio of interstitial collagen to perivascular collagen was increased in HFPEF compared to HFREF. It was found significantly more prevalence of collagen III in HFPEF than in HFREF in endomisyal, perimisyal and perivascular fractions. It was not found differences of collagen I between the fractions.
Conclusion: Significantly increased prevalence of type III collagen in all fibrosis fractions in HFPEF myocardium supports the hypotheses of different matrix remodeling in HFREF and HFPEF.

012

Metastasis of malignant skin melanoma in heart and pericardium: a case report

E. Stefanovic *, D. Nezic, L. Lausevic Vuk, P. Otasevic
*Dedinje Cardiovascular Institute, Dept. of Pathology, Belgrade, Serbia

Objective: Skin melanoma is one of the most malignant tumors in the human. After the liver, heart is the frequent place for the metastasis of this tumor. Melanoma metastases are often clinically expressed as pericardial effusion. Cases of acute cardiac tamponade, even sudden deth in these patients have been described.
Method: Female patient admitted to the hospital due to the fatigue, weakness, dyspnea and tachycardia with operated melanoma of the right lower leg 6 years before (nodular type, by Klark IV, tickness by Breslow 10 mm).
Results: Echocardiographic examination revealed large circular pericardial effusion and oval tumor formation, size 85×35 mm attached to the parietal pericardium. Histopathological finding showed that tumor tissue consist of atypical melanocytes with low mitotic activity. Tumor cells were not pigmented, immunohistohemic reaction with antibodies aganst S-100 protein was positive.
Conclusion: Although melanoma is malignant tumor with high malignancy potential, sporadic cases of succesfull surgical tumor resection from the heart cavities, with long survival time and good quality of life have been described. We can conclude that, in some cases especially in younger patients, surgical resection of the tumor could be the therapy of choice for the patients.

013

Atrial myxoma with fibrosiderotic (GAMNA-GANDY) nodule: case report

S. Toru *, I.H. Ozbudak, O. Erbasan, G. Ozbilim
*Akdeniz Medical School, Dept. of Pathology, Antalya, Turkey

Objective: In autopsy series the incidence of primary cardiac tumors ranges from 0.02 to 2.8 and they are predominantly in benign nature (75%). Of these, atrial myxomas are the most common type.
Results: A 75-year-old man was admitted to hospital with chest pain and dyspnea on effort. He has hypertension, smoking history and coronary artery disease. During the examination, transthoracic echocardiography revealed an impaired left ventricule ejection fraction and a mass in the left atrium which was attached to the interatrial septum and measured as 20×21 mm. The patient was underwent surgical resection. Macroscopically, the tumor was well-circumscribed, firm and 3.5×3×2 cm in size. Histologically, tumor is composed of stellate and globular myxoma cells embedded within an abundant acid mucopolysaccharide ground substance. Peculiar vessel-like structures, hemorrhage, mononuclear inflammation, fibrotic nodules with pigments (Gamna-Gandy nodules) are seen. Immunohistochemically; gland-like areas are positive with S-100 and kalretinin, stromal-inflammatory cells are positive with vimentin. Whole tumor is negative with pan-cytokeratin and smooth muscle actin. This case is reported as left atrial myxoma with Gamna-Gandy nodules.
Conclusion: Gamna-Gandy nodules probably are organization and scarring of small perivasculer hemorrhage, ischemia, because of this mechanism the probable clinic presentation myxomas with Gamna-Gandy nodules with embolic processes.

014

Primary cardiac chondroma: a rare case presenting with acute pulmonary edema

C. Zioga *, V. Tzioufa-Assimakopoulou, E. Nenopoulou, Y. Chatzizisis, K. Koskinas, V. Kamperidis, K. Anastasiadis
*Aristotle University of Greece, Dept. of Pathology, Thessaloniki, Greece

Objective: A 62-year-old man was referred to our hospital with 3-day onset of exertional dyspnea and chest pain.
Method: The electrocardiogram showed ST segment depression in the anterior leads. Biochemical tests were within normal limits. Shortly after admission, the patient developed acute pulmonary edema. Transthoracic echocardiogram demonstrated a heterogeneous mass with predominant echodensity and regions with cystic appearance, within the left atrium. The patient was urgently referred for tumor excision. The mass was arising from the left atrial wall through a narrow stalk adjacent to the posterior mitral valve annulus and did not invade the myocardium.
Results: Macroscopically the mass was smooth, multilobulated, predominantly solid, and measured 6.1×3.9 cm. Histological examination showed pure benign hyaline chondroid tissue with regions of cystic degeneration and absence of cytologic atypia, abnormal mitotic figures, sarcomatous, or myxoid regions. The diagnosis was primary cardiac chondroma. Postoperative clinical evaluation and imaging testing excluded potential extracardiac tumors with chondroid differentiation, such as teratoma. The patient had an uneventful postoperative course at 6-month follow-up.
Conclusion: Primary cardiac tumors are rare entities, with a prevalence ranging between 0.001% and 0.25%. Cardiac chondroma is an extremely rare primary cardiac tumor, with only 2 cases previously reported to our knowledge. We report a new case.

015

Interruption of the aortic arch: an autopsy study of 27 cases

J. L. Vasiljevic *, R. Stevanovic, B. Lekic
*Medical School of Belgrade, Dept. of Pathology, Serbia

Objective: During the period 1965–2010, 42.922 autopsies were performed, including 2,098 cases of congenital heart diseases (4.9%), with 27 cases (1.3%) of interruption of aortic arch (IAA).
Method: Modified Rokitanski technique was used, with aim to investigate: (1) various types (2) associated cardiac and extracardiac anomalies,(3) causes of death.
Results: IAA was found in 23 and atresia of AoA in 4 cases. The left AoA was interrupted 22 times, atretic in 4 cases, and only in one cese we found interruption of the right AoA (type C, distal to the right common carotid artery)). There were 18 cases of type B, 4 cases of type A, and all cases with atresia (fibrous cord), were distal to the left subclavian artery (type A?). Assiciated cardiac anomalies were present in 26 cases: PDA in all, ASD in 8, VSD in 21, bicuspid Ao valve in 3, AVSD in 1, and C-TGA in 2 cases. Associated extracardiac anomalies were found: urinary tract-7x, anomalous pulmonary lobulation-5X, polysplenia-4x, digestive tract-3x, meningocoele-1x.
Conclusion: Our findings are consistent with the majority of large series of IAA cases. As none of autopsied cases was operated, the causes of death were related to heart failure or cardio-respiratory insufficiency. IAA has poor chance for survival if not operated or treated with Prostaglandin.

Wednesday, 31 August 2011, 09.30–10.30 and 16.30–17.00, Hall 5

PS-19 Poster Session History of Pathology

001

Coimbra—University History and The Museum of Pathology

L. Carvalho *, A. Lopes, F. Gomes, L. Teixeira, M.J. D'Aguiar, P. Couceiro
*Amadora, Portugal

Objective: Coimbra University dates from 1290, when First Dinasty King D Dinis—The Poet—raised the University of Coimbra, occupying the Moorish Palace. Catholic Priests were Professors of Law, Philosophy and Humanistics. Medicine and Pharmacy/Chemistry quite developed at the same time. Coimbra, Bologna and Oxford are considered the oldest Universities in Europe.
Method: The Anatomical Pathology Museum of the Faculty of Medicine—University of Coimbra started in 19th century and saw the huge gathering of samples after 28 of May 1956 when Professor Renato Trincão (1920–1996), Pathologist, was Director of the Institute of Anatomical Pathology (till 1990), installed at the building of the Faculty of Medicine—Portugal was under a corporative political system (António Salazar).
Results: The Mmuseum runs an area of 500 m^2 occupied by XIII expositors, keeping around 1,000 cases formalin fixed, air dried, wax models, books and photographs. Visits are constantly required by Secondary School Teachers of Biology, Faculties of Sciences and Artists also ask for sightseeing.

Wednesday, 31 August 2011, 09.30–10.30 and 16.30–17.00, Hall 5

PS-20 Poster Session Infectious Diseases Pathology

001

A rabbit model for primary and lifelong persistent Epstein–Barr virus infection

K. Hayashi *, K. Takashima, K. Okuno, K. Kanai, K. Kato, S. Sano, H. Sugihara, M. Kato, I. Murakami, K. Nagata
*Tottori University, Dept. of Molecular Pathology, Yonago, Japan

Objective: EBV infects most humans by adulthood, who become lifelong carriers of EBV. Certain adolescents with primary EBV-infection develop infectious mononucleosis. EBV–infection is associated with various diseases, neoplasms and hematological disorders. The detailed mechanism of primary and persistent EBV-infection in humans has remained unsolved. Here, we present the rabbit model of primary and persistent infection.
Method: EBV from B95-8 was administered in male Japanese White rabbits which were sequentially imaged by ultrasonography or CT, and examined for EBV-DNA quantity and anti-EBV antibodies in blood. Five primary EBV-infected rabbits were followed up for life and examined by autopsy.
Results: Six of seven rabbits inoculated intravenously with EBV demonstrated transient splenomegaly, increased anti-EBV-VCA titers and/or EBV-DNA in blood. On 14th day, EBER1-positive lymphocytes expressing LMP1, EBNA2, or ZEBRA infiltrated in splenectomized white pulps from two EBV-infected rabbits. These included B or T lymphocytes and oligoclonal pattern was shown by EBV clonality analysis. Two of five EBV-infected rabbits demonstrated lifetime EBV-infection with EBV-DNA detection in blood, and died on day 1,522 or 1,400. Autopsy revealed infiltration of EBER1- and/or LMP1-positive lymphocytes accompanied with mild hemophagocytosis in spleens or lymph nodes.
Conclusion: This lifetime persistent EBV-infected rabbit model may be useful for studying human EBV-infection mechanism.

002

CD68+ cells in human placenta with herpes virus infection

A. Kolobov *, V. Karev, N. Khubulava, V. Zinserling, D. Niauri
*St. Petersburg, Russia

Objective: The infectious pathology contributes in development of placenta insufficiency. Herpes virus infection may be primary or due to reactivation during pregnancy of a latent infection. The aim of present study was to reveal the expression CD68 in different parts of human placentas in infections caused by viruses of herpes family (a simple herpes—HSV and cytomegalovirus—CMV).
Method: Ten placentas from women with herpes virus infection, with a HSV—five cases, with a CMV—three cases, a combination of two viruses—two cases has been studied. As control, 16 placentas were taken without infectious lesions. Immunohistochemically on the paraffin sections of placentas were revealed expression of CD68, HSV-1, HSV-2 and CMV.
Results: In all placentas with herpes virus infection were found enlarged cells with basophilic intranuclear inclusions, located primarily in cytotrophoblast. Lymphocytic infiltration located in stroma of villi. The focal expression of CD68 was noted in 13.07±0.83% cases (in control—2.02±0.60%).
Conclusion: Thus, in placentas with herpes infection, typical histological changes and expression of CD68 are noted to be increased.

003

Expression of CD14 in human placenta with HIV infection

A. Kolobov *, V. Karev, N. Khubulava, V. Zinserling, D. Niauri
*St. Petersburg, Russia

Objective: Human immunodeficiency virus type 1 (HIV-1) to infect human cells has to counteract a number of cellular receptors. Placental transmission of HIV-1 has been described but is incompletely understood. The transmission rate from mother to child is about 4.5%. Placental cytokines and chemokines influence HIV replication in trophoblast. The decidual CD14+ cells constitute potential targets of HIV-1 infection.
Method: There were 12 placentas from women with HIV-1 infection; as control—16 placentas without HIV infection. Immunohistochemically on the paraffin sections expression CD14 and p24 was revealed in placentas.
Results: In 60% placentas with HIV-1 infection was present p24 antigen. The focal expression of CD14 was found in 10.04±1.37% cases (in control—3.21±0.43%).
Conclusion: Thus, in placentas with HIV-1 infection, p24 can be revealed in majority of cases and increased expression of CD14 is noted.

004

Cryptococcosis in patients with HIV in AIDS stage

A. M. Konstantinova *, V.A. Zinserling, N.V. Vassilieva
*St. Petersburg State University, Medical Department, Russia

Objective: Nowadays infection caused by cryptococci (C) is important for HIV-patients in AIDS stage.
Method: There were 23 autopsies of HIV-infected patients with C. analyzed in the Botkin Infectious Hospital in St. Petersburg between January 1990 and January 2010. Different histological stains and morphometric analysis were used.
Results: Twelve patients were male and eight were female; the median age was 36.3 years. CD 4+ cell median level was 51 c./μl. In 19 cases cryptococcosis was generalized infection with involvement of 4.6 organs per patient. Colocalisation of C and caseous necrosis due tuberculosis at the same site in lung and C and herpes simplex virus in meninges were noted. In damaged organs different types of inflammatory reactions were present. There were no relations between them and host's immune status or treatment. High virulent C strains cause formation of large cysts with numerous roundish agents. Low virulence strains cause granulomatous reactions with deformated fungi. In untreated patients, the capsule thickness and cell diameter of C is larger in lung then in meninges. After antifungal treatment, these parameters are higher in meninges than in lungs. The thickest capsule is in meninges of HAART treated patients.

005

Systemic fungal infection implications in atherosclerosis in autopsied patients

J. Machado *, L. Silveira, L. Oliveira, A.P. Espindula, M. Reis, C. Cavellani, V. Teixeira, M. Ferraz
*UFTM, Dept. of Immunology, Uberaba, Brazil

Objective: The infectious process can stimulate the process of fibrosis between infections by microorganisms. This study aims to describe the occurrence of systemic fungal infection in autopsied patients, to relate atherosclerosis and systemic fungal infection, and to quantify the collagen fibers in the aorta of patients with systemic fungal infections.
Method: It was conducted a retrospective study with a control group matched by age, identifying patients who had systemic fungal infection, analyzing aortas macroscopically and microscopically.
Results: It was found that 7% of patients were with systemic fungal infection, 56% for *Candida albicans*, 25% of *Cryptococcus* sp, 11% of *Pneumocystis jiroveci*, 4% of *Histoplasma capsulatum*, and 4% of *Paracoccidioides brasiliensis*. Macroscopic analysis of the group with systemic fungal infection showed that 66% had mild

atherosclerosis, 17% moderate and 17% severe. In the control group, there were 47% mild, 43% moderate and 10% severe ($p>0.05$). The amount of collagen in the group of patients with systemic fungal infection was significantly higher than in the control group of patients ($p<0.001$).

006

Imbalance between pro-inflammatory and anti-inflammatory cytokines increase cardiac injury in experimental Chagas' disease

J. Machado *, M. Silva, C. Borges, L. Castellano, M. Reis, J. lazo, V. Rodrigues, D. Rogrigues
*UFTM, Dept. of Immunology, Uberaba, Brazil

Objective: Chagas' disease is caused by a *T. cruzi* infection, and Colombian strain has high tropism for cardiac tissue. Cytokines and nitric oxide are key mediators in intracellular infections.
Method: In this study we evaluated BALB-c, C57Bl/6 and C56Bl/6 iNOS-/- mice; 5 mice from each group were inoculed with Colombian strain and evaluated in 15th day and 5 mice were evaluated in 90th day of the experimental infection. We analyzed the presence of T. cruzi nests, inflammatory infiltrate and fibrosis in cardiac tissue and cytokine production by Spleen cells culture.
Results: C57Bl/6 showed a significantly higher number of nests in the acute phase than BALB-c mice and significantly lower amount than C57Bl/6 iNOS-/-. C57Bl/6 showed significantly higher cardiac infiltrate than the BALB-c in the chronic phase of the infection. Fibrosis and IFN-γ levels were significantly higher in BALB-c. IL-10 was significantly higher in both the acute phase and chronic phase in C57Bl/6 mice compared to BALB-c.
Conclusion: There were greater cardiac injuries in BALB-c compared to C57Bl/6. This is probably a result of an imbalance between pro-inflammatory and anti-inflammatory cytokines. The absence of nitric oxide appears not to directly influence the development of experimental heart injuries.

007

Bone marrow of patients with acquired immunodeficiency syndrome

J. Machado *, N. Dias, A.P. Espindula, C. Cavellani, M. Reis, V. Teixeira, M. Ferraz
*UFTM, Dept. of Immunology, Uberaba, Brazil

Objective: Bone marrow abnormalities are frequently observed in individuals with AIDS at all stages of the disease. Analyze the morphometric method through the thickness of the trabecular bone in AIDS patients autopsied.
Method: A total of 72 samples collected from the upper third of the external were analyzed . Patients were grouped: with AIDS ($n=36$) and without AIDS ($n=36$). The fragments were performed the hematoxylin and eosin and performed using the program KS 300 (Kontron–Zeiss).
Results: Patients with AIDS showed a significant reduction in the thickness of trabecular bone compared to those without AIDS ($p=<0.001$). Among AIDS patients, women showed a significant reduction in trabecular thickness compared to men ($p=0.004$) and non-whites a significant reduction of trabecular bone thickness when compared to whites ($p<0.001$).
Conclusion: AIDS causes decrease a thickness of the trabecular bone in both genders and color, and this decrease is more pronounced in women and in patients considered non-whites. These findings may reflect a physiological response to antigen stimulation of the virus. However, many of these anomalies are directly related to HIV replication in the bone marrow, considered a reservoir of the virus.

008

Pseudomembranous colitis (PMC) epidemic in the autopsy room

T. Micsik *, B. Timar, L. Fonyad, B. Csernus, G. Princz, J. Csomor
*Semmelweis University, 1st Dept. of Pathology Budapest, Hungary

Objective: Pseudomembranous colitis (PMC) is a severe complication of long-lasting antibiotic treatment, when normal bacteria are eradicated and Clostridium Difficile (CD) can overgrow causing severe, life-threatening, but usually treatable diarrhoea. Recent data showed that the 027 ribotype CD, a more agressive and toxin overproducing strain has swept through America and Europe causing severe cases with eleveted mortality rate.
Method: In our Central Hospital for Infectious Diseases we realized in 2011 the accumulation (20% of all deaths) of fatal PMCs affecting the whole large bowel. We collected all clinical, microbiological and autopsy data to characterize this epidemic.
Results: We recognized the traits of this new strain in our hospital's autopsy cases. Only a part of these patients had severe predisposing illnesses (eg. heamatologic tumors) while the others acquired the disease outward the hospitals and without earlier antibiotic treatment. Characteristic clinical finding was that these patients were primarily treated with vancomycin but later they had an early and fatal relapse.
Conclusion: We could demonstrate that the 027 ribotype CD-strain has reached our hospitals causing a kind of PMC epidemic. Important is to emphasize that 027 CD-strain caused fatal infections not only with nosocomial/antibiosis or oncologic background but also in elderly and otherwise healthy outward patients.

009

Detection of sexually transmitted infection and human papillomavirus in negative cytology bymultiplex-PCR

S.-M. Noh *, N.-H. Cho
*Seoul, Republic of Korea

Objective: The aim of this study was to determine the prevalence of human papillomavirus (HPV) and 15 species that cause sexually transmitted infections (STIs) in negative cytology. In addition, we compared the diagnostic performance of multiplex polymerase chain reaction (PCR) with widely available techniques used to detect HPV.
Method: We recruited 235 women of reproductive age who had negative cytology findings in a liquid-based cervical smear. STIs were identified by multiplex PCR, and HPV genotypes by multiplex PCR, hybrid capture 2, and DNA microaray; discordant results were analyzed by direct sequencing.
Results: Approximately 96.6% of patients with negative cytology results were positive for pathogens that cause STIs. The pathogens most frequently detected were Gardnerella vaginalis, Ureaplasma urealyticum. The incidence of HPV in negative cytology was 23.3%. Low-risk HPV infection was significantly correlated with *Chalmaydia trachomatis*, and high-risk HPV infection was significantly correlated with group B streptococcus. The analytical sensitivities of the multiplex PCR and DNA microarray were higher than 80%, and the analytical specificity was nearly 100% for all tests.
Conclusion: Multiplex PCR yielded results that most of patients with negative cytology were positive for pathogens that cause STIs and were more similar to that of DNA microarray than that of hybrid capture 2 in terms of analytical sensitivity and prediction value of HPV infection.

010

Relationship of angiogenesis, tryptase- and chymase-positive mast cells with fungal proliferation in oral paracoccidioidomycosis

F.A. Oliveira *, J. Silva, D. Teixeira, M. Pereira, E. Duarte, E. Vencio
*Federal University of Goiás, IPTSP, Goiânia, Brazil

Objective: The aim of this study was to correlate the densities of mast cells and vessels with fungal proliferation in oral paracoccidioidomycosis.
Method: Eleven cases of chronic disease were selected. Hematoxylin/eosin staining was used for histological evaluation, Grocott staining was employed for fungal quantification and immunohistochemistry was used for quantification of mast cells (anti-mast cell chymase and tryptase) and vessels (anti-CD 34). The densities were measured in 32 fields viewed at ×40 magnification and analyzed with the AxionVision 3.1-Zeiss software. Pearson's (r) coefficient test was used.
Results: Irregularities, hyperplasia, ulceration and microabscesses of the mucosa were seen. In some cases, the granulomas were well formed. No difference was observed between the densities of chymase- and tryptase-positive mast cells (26.5 ± 21.7 vs. $28.8\pm26.1/mm^2$, $p>0.05$). The density of vessels was $87.7\pm37.9/mm^2$. Positive, but not statistically significant, correlation was found between the densities of *P. brasiliensis* and mast cell chymase ($r=0.47$ $p=0.13$), tryptase ($r=0.22$ $p=0.49$) and vessels ($r=0.57$ $p=0.06$).
Conclusion: Angiogenesis and mast cells are associated with increased fungal proliferation in oral paracoccidioidomycosis, which indicates that these cells may contribute with an immunosuppressive function in the pathogenesis of the disease. Furthermore, the fungus may possibly participate in the induction of angiogenesis through still unknown mechanisms.

011

Spinal infections

S.-S. Paeng *, W.-G. Liu, S.-H. Lee
*Seoul Chungdam Wooridul Hospital, Dept. of Pathology, Republic of Korea

Objective: The clinical features of spondylodiscitis, either tuberculous or non-tuberculous, are similar. And differential diagnosis between preoperative- existing spondylodiscitis and severe degenerative dics changes are difficult. Identifying causative pathogens is important for appropriate treatment for spinal infections.
Method: We retrospectively reviewed the medical records and pathologic slides of 200 patients who had diagnosed spondylodiscitis at our hospital from May 2005 to December 2010. We analyzed gender, age, erythrocyte sedimentation rate (ESR) and C-reactive protein (CRP) value, glucose level, AFB staining, ordinary culture and sensitivity results, polymerase chain reaction (PCR) for tuberculosis, and MRI findings.
Results: Among 200 patients, we identified pathogens in 101 patients. Most infections were caused by Gram-positive methicilin-resistant *Staphylococcus aureus* (31 cases) and tuberculosis (31 cases). ESR level was elevated in 143 cases (over 20 mm/h), CRP level was elevated in 121 cases (over 4 mg/L). Most cases had positive MRI findings. Postoperative infections cases were seventy-seven.
Conclusion: Early diagnosis and prompt treatment for spinal infections are important for successful nonsurgical treatment of spondylodiscitis and prevention of complications. In early infection period, netrophils infiltration with necrosis is most important finding to differentiate from severe intervertebral disc degenerative changes.

012

Pathological and clinical aspects in HIV-TB coinfections

G. Resul *, M. Aschie, S. Rugina, S. Halichidis, I. Serban
*Constanta, Romania

Objective: The incidence of tuberculosis (TB) is more than eight times higher in HIV positive than in HIV negative population. The cases with HIV-TB coinfection is characterized by multiple clinical forms, multidrug resistance at tuberculostatic therapy and unfavorable clinical course.
Method: This is a retrospective study of the necropsy cases of HIV-TB coinfection. The macro- and microscopical analysis of the tissue fragment sampled from the organs with pathological changes was performed after tissue processing and the using of routine and special stains. The assessment of correlations between the pathological reports and the clinical manifestations of these patients was made.
Results: The pulmonary and extrapulmonary forms of TB were observed in all the cases. The extrapulmonary TB was represented mainly by the lymph nodes, splenic, renal and hepatic localizations. The clinical manifestations depend on multiple localizations of TB lesions and are variable depending on level of CD4 lymhocytes.
Conclusion: TB is the most common cause of death among AIDS patients worldwide. Extra-pulmonary TB is more likely as CD4 count declines with atypical clinical manifestations. The pathological aspects are specific for TB disease.

013

HHV8 expression in lymph node biopsies of HIV positive patients

J. Thiart *, J. Goedhals, G. Le Roux, M. Myburg, C.A. Beukes
*University of the Free State, Dept. of Anatomical Pathology, Bloemfontein, South Africa

Objective: Three histological patterns of HIV lymphadenitis (A, B and C) have been described which correspond to clinical stages of acute, chronic and burnout. The Plasma cell variant of Castleman disease (PC-CD) has in common with pattern B and C of HIV lymphadenitis, involuted follicles with hyaline germinal centers and vascular proliferation. HHV8- associated multicentric Castleman disease (MCD) occurs in immunosuppressed individuals, especially HIV-positive patients, and is now thought to be a distinct entity with risk of progression to HHV8-positive plasmablastic lymphoma. The aim of our study was to assess the incidence of HHV8-associated MCD and the incidence of HHV8 expression in HIV lymphadenopathy.
Method: Stains for HHV8 were performed on 95 lymph node biopsies received in our department from 2004 to April 2011 of patients known to be HIV positive.
Results: A total of 78 nodes were negative and 17 stained positive for HHV8. A total of 15 of the positive nodes fitted the criteria for HHV8 associated MCD. Four were associated with Kaposi sarcoma. Two nodes showed focal interfollicular staining and will be discussed further.
Conclusion: A very high index of suspicion is necessary to diagnose HHV8 associated MCD, as features are non-specific and show overlap with HIV lymphadenopathy patterns B and C.

Wednesday, 31 August 2011, 09.30–10.30 and 16.30–17.00, Hall 5

PS-21 Poster Session IT in Pathology

001

The utility of multispectral imaging to improve the visualization of pathology images

P. Bautista *, N. Hashimoto, Y. Yagi
*Boston, USA

Objective: The application of multispectral imaging to image analysis in pathology has been actively investigated in recent years. In this study we utilized multispectral information to enhance hematoxylin and eosin (H&E) stained tissue structures, which are generally differentiated using special stains.
Method: Two independent experiments were done: (1) the differentiation of collagen fibers and (2) the enhancement of eosinophils. Multispectral images corresponding to regions of interests were captured using the multispectral microscope system in the laboratory. To improve the visualization of collagen fiber spectral enhancement combined with linear transformation of the spectral transmittance was applied. To enhance the presence of eosinophils, spectral feature extracted from the application principal component analysis (PCA) is used to enhance the presence of eosinophils.
Results: Liver tissue slides and gastrointestinal tract biopsies were considered in our experiment. The application of the spectral enhancement and transformation of spectral transmittance resulted to clearer distinctions between collagen fiber and smooth muscles in liver images. Moreover, using spectral features improves the detection of eosinophils.
Conclusion: Stained tissue structures have unique spectral response. These unique spectral attributes are better captured with multispectral imaging. Utilizing multispectral imaging would improve the visualization of tissue structures and thereby the accuracy of a diagnosis.

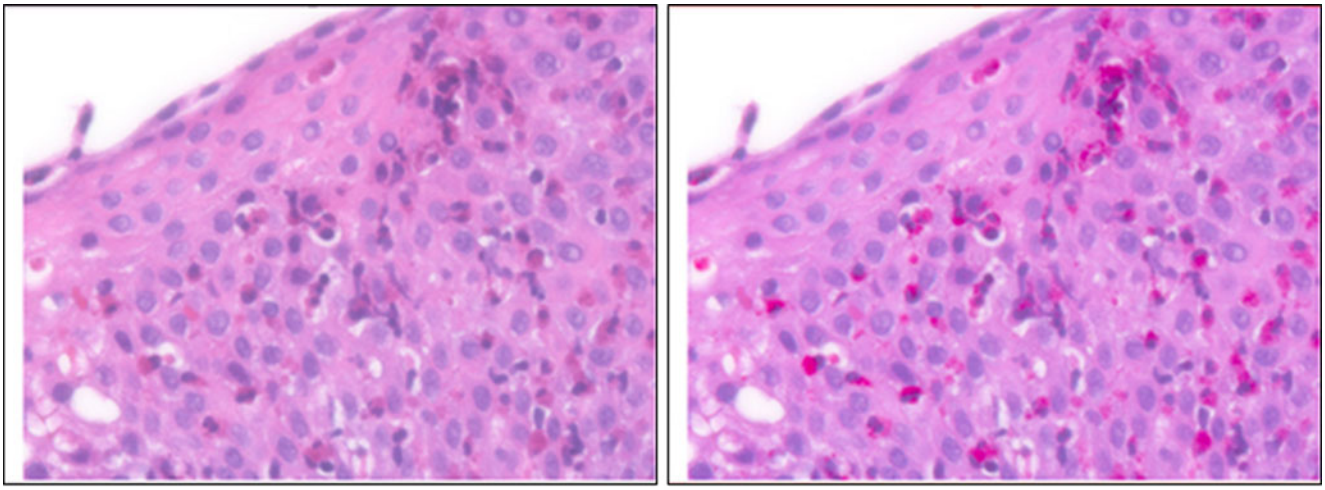

003

Digital pathology for improved patient care

O. Eichhorrn *
*Aperio, Vista, USA

Objective: Digital pathology is a great technology which brings important benefits to pathologists, hospitals, and reference labs. Like any new technology, the key is knowing how to implement it. What value does it bring to me? How do I start? How does it integrate into my workflow? How do I validate it? This talk will answer these questions.
Results: Aperio and its partners have installed over 400 systems at 230 hospitals worldwide. Aperio's vision is to help hospitals and healthcare organizations improve patient care by providing comprehensive solutions for digital pathology including whole slide scanning, image viewing, management, and analysis. Aperio's Discover Your Path program is integral to realizing this vision by generating a customer-specific staged adoption roadmap. Using a guided, personalized assessment, Discover Your Path enables each healthcare institution to objectively rank applications by near-term value, yielding a customized implementation path and timing plan.
Conclusion: Digital pathology can best be leveraged today by value-added patient care activities which vary by institution, and Discover Your Path identifies these in rank order.

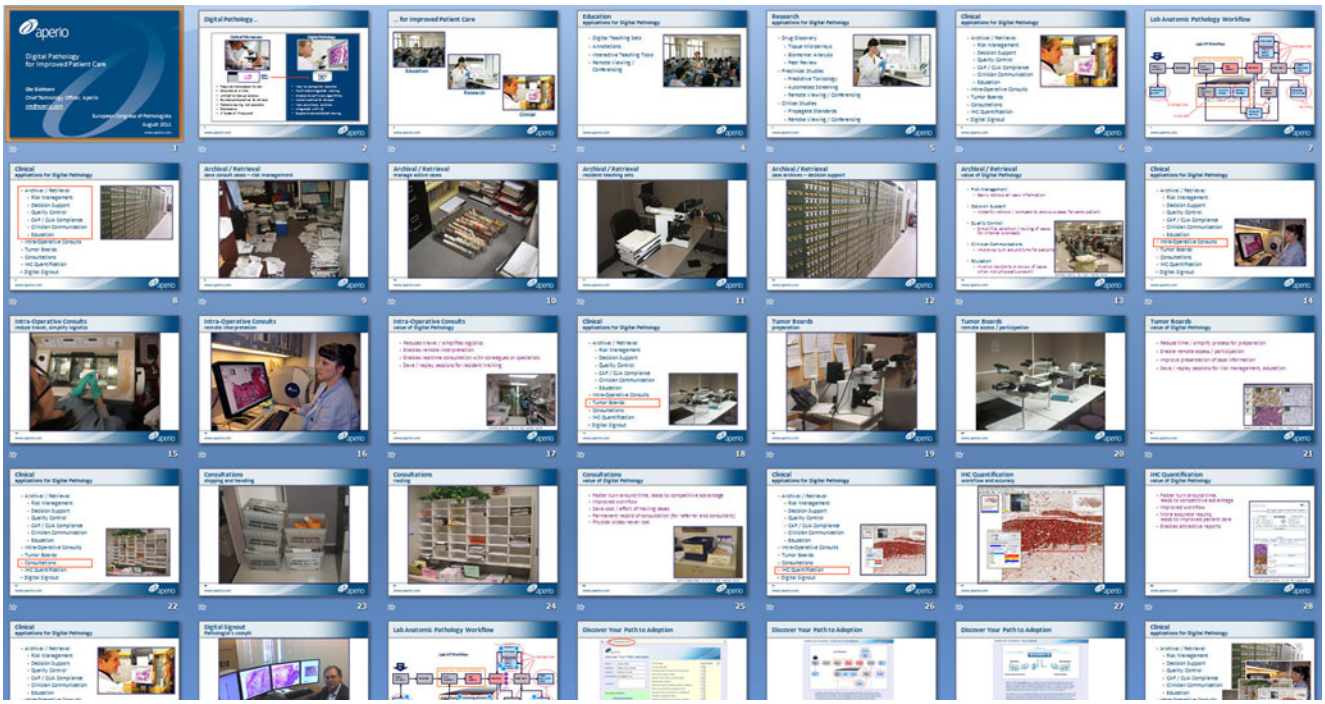

004

Digital pathology in the cloud

O. Eichhorrn *
*Aperio, Vista, USA

Objective: Digital pathology is making its way from academic medical centers and research institutions into reference labs and hospitals, and is being used today in a variety of specific clinical applications where it provides value. One of the best uses has been to facilitate consultations, internally within pathology groups, and externally between groups, either for informal consultations or for formal secondary interpretations.

Results: For these applications the capability to share information quickly and securely over wide-area networks "in the cloud" is essential. In this presentation we'll discuss some of the concepts behind digital pathology and wide-area networks, and talk about specific considerations for security and performance. We'll then walk through some real-world examples of Digital Pathology in the Cloud.

Conclusion: We will conclude by sharing an actual pathology case with everyone in attendance!

005

Digital microscopy in histopathology teaching, continuous education and teleconsultation

L. Fónyad *, B. Molnár, A. Matolcsy
*Semmelweis University, 1st. Dept. of Pathology, Budapest, Hungary

Objective: In recent years, numerous papers have been published concerning the reliability of digital slides (DS) in routine surgical patholgy practice. Many "pros" and "cons" were recognised in terms of routine application of DS. Undoubtedly, beside the technical aspects there's been criticisms of user friendliness and acceptance of DS. The

2011/2012 academic year may finally give us answers for some of these subjective questions, as the residents entering into pathology program at Semmelweis University in 2011 had used DS exclusively during their gradual training.

Method: In the past 4 years our digital histopathology classroom has served about 1,200 students and around 2,000 h of practice. It is equipped with 40 PCs with 1,000 Mbps broadband intranet connection. We use approximately 200 DS. An external server with 24-h access to DS is also available. We have collected user experience data from this period of gradual training and also conducted a survey among the new pathology fellows to evaluate their acceptance of DS.

Conclusion: DS are more suitable for education than optical slides. Digital microscopy is more acceptable to pathology residents who used DS in gradual training.

006

Encoding pathology diagnosis with SNOMED CT: feasibility of migration from SNOMED II to SNOMED CT

M. Garcia Rojo *, A. Laurinavicius, V. Punys, S. Gehring
*Hospital General de Ciudad Real, Dept. of Pathology, Spain

Objective: Pathology information systems have been using SNOMED II for many years, and in most cases, they are in a migration process to SNOMED CT. COST Action IC0604 (EURO-TELEPATH) has considered terminology normalization one of its strategic objectives.

Method: Legacy (mainly SNOMED II) morphological diagnosis consisted of 2,320 concepts that were extracted from the iSoft Patwin pathology information system into a MS Access database. Most (70%) of the concepts were manually encoded using CliniClue Xplorer with SNOMED CT 2011-01-31 International Release.

Results: Only 1,076 (44%) of the legacy concepts could be represented using SNOMED CT morphological abnormality sub-hirearchy. An additional 48% of the total concepts could be coded, mainly using the disorder hierarchy, e.g. Rosacea (1,104 concepts), or "finding" hierarchy, e.g. World Health Organization (WHO) grade I (in 71 concepts). Post-coordination (using more that one SNOMED CT concept) was needed to represent 469 (19%) of the local terms.

Conclusion: The morphological abnormality sub-hierarchy of SNOMED CT need to be significantly extended and improved to because useful for pathologists. A consensus is needed to encode pathology reports with the adequate hierarchies and concepts. This will make more feasible the implementation of pathology structured reports and virtual slides efficient management.

007

New paradigms of decision support of surgical pathology via integration of digital microscopy and distant consultation in routine reporting: Hungarian experiences

P. Gombas *, B. Molnar, I. Szucs, J. Kulka
*Szent-Borbala County Hospital, Division of Pathology, Tatabánya, Hungary

Objective: Routine workflow has been changed using digital microscopy in surgical pathology routine. Increase of information requires new ways of decision support. Textual data contents, gross image archives and digital histology enable new paradigms locally and globally.

Method: In the routine practice of large hospital pathology department 80–150 cases will be reported using 100–500 slides. Interesting, rare, uncertain and educational cases will be scanned (Mirax Scan) than uploaded on slide server. Complex institutional database as clinical data, other diagnostic modalities, pathology past history, slide/smear archive and teleconsultation connection will be analyzed in integrated unity locally and remotely.

Results: Speed, accuracy, prognostic power of reporting are altered by new forms of decision support. 1. Standardized digital measurement data will be incorporated in reports. 2. Gross image and past digital slide case archive provide fast evaluation of morphological case history. 3. Outside observers perform external quality control ruinously. 4. Off line/on line remote consultations are performed in daily practice. 4. Hospital information system enables complete case history analyzing. Teaching subdivisions and decision-making boards obtain indexed case databases with all required information.

Conclusion: In our experiences, traditional workflow of surgical pathology has been converted in the integrated digital histology laboratory by using new information technology tools.

008

Usefulness of radio frequency identification (RFID)-based system to improve the tissue samples traceability and security in biobanking: experience of a single institution (CHU Nice, France).

M. Ilie *, O. Bordone, E. Selva, V. Hofman, V. Gavric-Tanga, E. Pedrazzi, C. Lagardére, P. Mayer,
J. Mouroux, C. Chabannon, P. Hofman
*CHU de Nice, Hôpital Pasteur, Laboratoire de Pathologie, France

Objective: The hospital at Nice Sophia University (France) launched a pilot program using a custom-built RFID-based system in order to develop a more efficient, accurate and secure way to identify biospecimens within the biobank and to track them as they moved from the pathology laboratory to the biobank. The purpose of the project was to evaluate the benefits of the RFID technology in biobanking field.
Method: A total of 80 patients having surgery for lung cancer were included in this study. For recording, the system included handheld RFID readers which are equipped with wireless LAN radios and are used by hospital personnel for checking inventories of cryotubes. Other components included a fixed compact RFID station, which provided identification of RFID-enabled cryogenic tubes in racks.
Results: A tota of 160 tissue samples were included in this pilot study. This system allowed one to control the time of cold ischemia, the storage in the pathology laboratory, and in the biobank. Informations were present on the RFID tag and maintained at low temperatures.
Conclusion: RFID technology has advantages in comparison with other tracing technologies, including the lack of a line-of-sight requirement, the ability of tags to withstand harsh environments, and the ability to track items in real time.

009

The CQPath program: improving routine immunohistochemistry by use of references and total quality management

M. Kap [*], E. de Bruyn
[*]Erasmus MC, Dept. of Pathology, Rotterdam, The Netherlands

Objective: Besides being the most used tool for differential diagnosis, immunohistochemistry (IHC) is also used to determine prognosis or treatment susceptibility. It is therefore important that daily IHC results are of optimal quality. Ring trials, however, show disturbing inter laboratory variation in IHC outcome, leading to miss-treatment of patients.
Method: Within our department the CQPath program was developed. By using digital images as reference for all IHC stainings, technicians are able to score the quality of IHC slides. These scores are linked to all analytical parameters. By saving all scores in a database, the IHC process can not only be monitored in time, but it can also be improved immediately when needed.
Results: At our department we managed to reduce the error rate with 20% by joining the Nordiqc ring trials plus another 7% by daily monitoring with CQPath. Software development is ongoing to provide algorithms to determine cause of errors and the subsequent actions needed to improve IHC protocols.
Conclusion: The reference images can be found online at www.cqpath.com. The total quality management software will become available soon. We believe inter laboratory variation will decrease and patient care and cost efficiency will improve when CQPath references and TQM are used.

011

Automated digital morphometry of high contrast tissue elements using color filtering

T. Mezei [*], L. Denes, J. Jung, I. Egyed-Zs.
[*]UMPh Targu Mures, Dept. of Pathology, Romania

Objective: In pathology, tissue analysis by means of digital morphometry became a widely used quantification method of various tissue parameters. Digital morphometry delivers precise and highly reproducible results in mathematical format. The purpose of our study was to develop an accessible method to perform morphometry on specific tissue elements.
Method: We used three different types of tissue samples and staining procedures: non-hodgkin lymphoma (CD34 marker, immunohistochemistry, DAB), liver fibrosis (trichrome stain) and skeletal muscle (hematoxylin-eosin). For image analysis we used ImageJ software and its macro language.
Results: We developed an algorithm that fits generic morphometry demands. The method is based on HSB color filtering. Using this method one is able to quantify the proportion of DAB positive tissue area (using immunohistochemistry); it enables determination of fibrosis (using trichrome stain) and striated muscle fiber diameter and distribution (using HE).
Conclusion: We conclude that the use of ImageJ and automatic color segmentation is a reliable and accessible way of performing various morphometric measurements and tasks. In addition, we are confident that the accessibility of this method will extend its future applications to other areas of pathology and histology.

012

Automated image analysis for diagnostic and predictive histopathology

T. Micsik *, L. Krecsak, G. Kiszler, D. Szabo, T. Krenacs, L. Ficsor, B. Molnar
*Semmelweis University, 1st Dept. of Pathology Budapest, Hungary

Objective: Targeted therapy requires determination of related biomarkers which directly influence therapy decisions. Accuracy of testing can be improved via digital microscopy. 3DHISTECH's (Budapest, Hungary) offers dedicated software tools for unbiased, semi-automated scoring of nuclear and cell membrane signals generated by immunohistochemistry.
Method: We have tested the NuclearQuant software for estrogen (clone 6 F11) and progesterone (clone 1A6) receptor detection, and the MembraneQuant software for HER2 (clone 4B5) analysis in 100 breast cancers by comparing pathologists' routine evaluation with the digital analysis. Slides were digitized and thresholds selected to cover all positivity ranges. Both applications scored and classified each cell into various positivity-classes and a field score was given per annotation.
Results: We found excellent agreement both with nuclear (Quadratic weighted κ=0.981, Quick-index: 0-8) and with membranous (quadratic weighted κ=0.946, range 0 to +++) staining between the results of the digital and semiquantitative evaluations. Furthermore, permanent annotations and measurement data are also offered for quality assurance.
Conclusion: In conclusion, we successfully validated the NuclearQuant and MembraneQuant applications as reliable tools for unbiased evaluation of target therapy related immunostaining signals to support the efficiency of predictive pathology and the related therapy. Flexible adjustment also allows these applications to test any other biomarkers.

013

Are we ready for routine digital sign-out?

B. Molnar *, L. Fonyad, T. Krenacs, T. Micsik, T. Virag, V. Varga
*3DHISTECH Ltd., Budapest, Hungary

Objective: Slide scanners with digital microscopy software solutions became available since the early 2000s. They are used today in limited diagnostic, education and research applications. For routine H/E specimen sign out still the glass slides and microscopy is the primary choice.
Method: Comparison of optical and digital pathology workflow in an academic setting with 500 slides/day load. Development and evaluation of necessery new generation slide scanner, server and digital pathology workstation (DPW) tools including optimised microscope controll functions.
Results: Evaluation and sign-out time on glass slides were shorter first than on the digital slides. The new scanner scanned (20 s/cm^2 speed) directly to the server. The new digital pathology workstation including a microscope X/Y/Z movement compartment supported the parellel opening, viewing and evaluation of the respective slides as efficient as at the glass slide based work after optimisation.
Conclusion: The new generation of digital slide scanners with the increased scanning speed opened the way to whole laboratory digitalisation. The server and DPW applications with a microscope control unit can contribute to the routine sign-out of the digital slides as efficient as the traditional optical one.

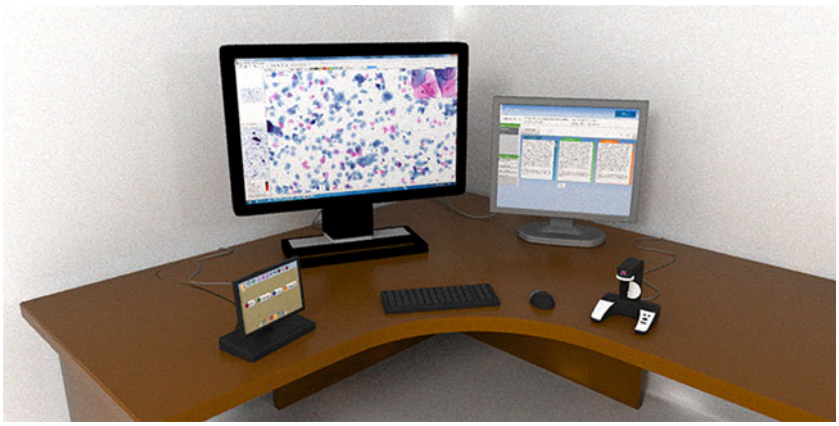

014

An IT software system for using experience in veterinary pathological anatomy

H. Vala *, P. Tomé
*CI&DETS, Polytechnic Institute of Viseu, Portugal

Objective: Veterinary anatomical pathology is a medical specialty similar to human anatomical pathology, which aims to obtain a final pathological diagnosis, applying criteria based mostly in the knowledge of the gross and histological lesions. The main difficulties in veterinary pathological diagnosis are related to the various animal species a pathologist has to deal with, the use of exhaustive classifications of different types, the costs, the subjectivity and the urgency in issuing the report. So, the urgent need to compile all available information to obtain a diagnosis, in a short period of time, is the constant challenge placed to the professional experts in the area concerned.
Method: The authors propose a framework and a software system (which uses experience) that can be useful for diagnosis purposes. The framework is based on the analysis of the bibliography of the domain. The software system applies case-based reasoning for retrieving past solved cases and suggest the solution to the veterinarian professional.
Results: The software system was already tested in a set of 921 and revealed that 69.6% of cases could be adapted, indicating a high level of similarity.
Conclusion: Both proposals can be useful tools in helping to make a better diagnosis.

015

Histopathologic patterns of nervous system tumors based on computer vision methods and whole slide imaging (WSI)

S. Walkowski *, J. Szymas
*Poznan, Poland

Objective: Making an automatic diagnosis based on virtual slides, which are normally viewed by pathologists, is a big challenge. Determining whether a case belongs to a single class, representing a specific disease, could be the first step in the diagnosing process. In this work we focus on WHO Classification of Tumours of the Central Nervous System. We try to design a method which allows to automatically distinguish virtual slides which contain histopathologic patterns characteristic for glioblastoma–pseudopalisading necrosis and discriminate cases with neurinoma (schwannoma), which contain similar structures–palisading (Verocay bodies).
Method: Our method is based on creating a pattern with a set of features which can describe pseudopalisading necrosis and distinguish it from palisades. These parameters are initially used in image segmentation to extract nuclei on the slide, find necrosis areas and locate regions with high density and specific mutual arrangement of nuclei. Structural analysis of boundaries formed by these regions is done for final classification.
Results: Described method is tested on a set of over a dozen virtual slides, captured using robotic Microscope Axioplan 2e (ZEISS) with objective Planapo 20x/0.75, equipped with Camera Axiocam HRc (ZEISS). The scanning process produced 1300x1030 tiles, with 15% overlap, which were stitched into single images.

016

Manual generation of virtual slides: a simplistic alternative for small biopsies

L. Alfaro *, M. Roca
*Valencia, Spain

Objective: Digital pathology has progressed greatly in the last years and has brought fascinating new advances. One of them is virtual microscopy giving the chance to study cases on computer screens from whole slide images simulating traditional view on a microscope. Generation of virtual slides was done with sophisticated scanners. The main obstacle for this technology is its high cost.
Method: We have design a simplistic alternative in the generation of virtual slides for small and needle biopsies. We took pictures in a microscope with a conventional camera with a magnification of ×20 that allows covering full width of prostate, breast, kidney, liver and corneal biopsies. Pictures were taken with an overlap of 20–30%. When the full biopsy was recorded, all pictures were stitched with a specific software: Microsoft Image Composite Editor.
Results: Stitched pictures were exported into a big plain jpg file and from it transformed into the pyramidal structure of images habitually used for virtual microscopy. These files are accessible from web servers and have full quality for diagnosis
Conclusion: The manual generation of virtual slides is a feasible option for small biopsies. Bigger specimens require increasing the number of pictures taken with the camera and convert the process in long and tedious

017

Morphological analysis of atherosclerosis in aorta and carotid autopsies of pacients

J. Machado *, V. Monteiro, L. Oliveira, A.P. Espindula, P. Ferraz, L. Ramalho, C. Cavellani, M. Reis, V. Teixeira, M. Ferraz
*UFTM, Dept. of Immunology, Uberaba, Brazil

Objective: The development of lipid deposits causes the increase of collagen. This study aims to compare the morphological characteristics of carotid and aorta by evaluating the amount of collagen and elastic fibers of tunica media.
Method: Sixty fragments of carotid arteries and 30 of aortas were made with the staining for elastic fibers and collagen. The morphometry was performed to quantify the elastic and collagen fibers of the media of the carotid artery and aorta.
Results: It was observed that in females the amount of collagen and elastic fibers in the aorta and carotid are higher than in males. In the measurement of fibers was observed among non-elderly had more collagen and elastic fibers than the elderly group. By correlating the amount of collagen and elastic fibers with age was observed that with increasing age there is a decrease of collagen and elastic fibers in the carotid artery and aorta.
Conclusion: With age there is a reduction of collagen and elastic fibers, but age is an important risk factor for arterial stiffening and risk factor for cardiovascular disease. The stiffening of arteries with advancing age and with exposure to risk factors involves predominantly the aorta and carotid arteries.

018

Data ware and software of the support recognition system when diagnosting oncopathology

R. Moskalenko *, A. Dovbysh, A. Romanyuk
*Sumy State University, Dept. of Pathomorphology, Ukraine

Objective: The aim of the study is the development of the method of express-control of morphological changes in tumors with the help of recognition of their histograms that were got in the process of histological microscopy.
Method: The Sumy State University Laboratory of Intellectual Systems developed an informational extreme method that was put to the basis of the investigation.
Results: The novelty of the investigation lies in the optimization of spatial–temporal parameters of functioning of the recognition system through special transformation in the process of studying of "a priori" indistinct division of attribute space to classes of recognition into distinct division that provides creation of correct rules (according to the educational matrix). Under these conditions the optimization of functioning parameters is done on every stage of education by means of possible changes in search of global maximum of informational criterion of functional effectiveness of the recognition system in admitted region of its function and simultaneous update of optimal image containers.
Conclusion: The developed means of informational extreme method of data ware and software of the system of recognition of non-stationary images–histograms are going to be used for the solution of the task of high-authentic and operative recognition of histograms of cell of organs and tissues in oncopathology.

019

Automated evaluation of the Ki-67 LI in whole slide images: the antibody factor

J. Slodkowska *, T. Markiewicz, B. Grala, K. Pleskacz, P. Murawski, W. Kozlowski
*Military Institute of Medicine, Dept. of Pathomorphology, Warsaw, Poland

Objective: Immunohistochemistry (ihc) has an expanding role in the diagnosis and management of tumours. Some brain tumours are graded according to the cellular pleomorphism and Ki-67 Labeling Index (KI-67 LI). The ihc procedure and manual measurement can profoundly affect the immunoquantitation results. The digital whole slide images (WSIs) can be distributed electronically for a remote automated evaluation of ihc stains expression. We determined whether remote automated quantitation of Ki-67 LI in WSIs differed in various ihc staining protocols.
Method: There were 76 WSIs created (Aperio ScanScope CS) from the glass slides of oligodendrogliomas and meningiomas immunostained for Ki-67 antigen: 1/manually—with MIB-1 antibody, and 2/with FLEX Ki-67 Antigen Clone MIB-1 RTU with Autostainer (Dako). Aperio's Image Scope software provided functionality for a remote viewing of WSI. KI-67 LI were determined in 20 HPF (x40) of the highest labelling, 3 times by 2 pathologists with CAMI software.
Results: The statistical analysis of the Ki-67 LI results was based on the Kolmogorov-Smirnov Test and Wald-Wolfowitz Levene'a. The obtained preliminary results do not allow to present any statistical significant differences between two types of ihc staining procedures.
Conclusion: The study has been partly supported by the Dako (Denmark) and the COST Action IC0604.

020

Virtual slide microscopy: the Romanian experience

T. Mezei *, Z. Pavai, E. Horvath, L. Chira, A. Borda, J. Jung, I. Egyed-Zs.
*UMPh Targu Mures, Dept. of Pathology, Romania

Objective: The development of virtual slide acquisition technologies lead to the introduction of high throughput

digital slide scanners into everyday pathology work and education. Our purpose was to present our 2 years' experience with a digital slide scanner system and to briefly present its related activities over this period.

Method: The period of the study extends from July 2008 to March 2011. The scanning instrument is a Zeiss MiraxScan digital slide scanner attached to a Fujitsu-Siemens Celsius Workstation. The scanned specimens consisted of standard sized glass specimen mounts.

Results: The digital slides serve the following purposes: morphometric studies, teaching, documentation and consultation. The fields of medicine that mostly took advantage of this new opportunity includes: pathology, anatomy, histology, molecular biology, physiology. In the mentioned period of time a total number of 4,750 slides were scanned. All slides are currently archived untill full capacity is reached.

Conclusion: The use of digital slides has been successfully introduced into our Pathology Department serving many research and teaching activities. We conclude that its introduction was necessary to further improve the research and teaching environment of our university. Nevertheless, we intend to extend its potential towards teleconsultation by creating a telepathology workstation to be included in the EURO-TELEPATH network.

021

Functionality of digital microscopes – what is useful?

N. Zerbe *, G. Kayser, K. Kayser, J. Szymas, P. Hufnagel
*Berlin, Germany

Objective: A wide range of digital microscopes and virtual microscopy applications have been developed and used in education and research within the last decade. We analyzed their main concepts, features and drawbacks for identifying perspectives in functionality and tissue-based diagnosis.

Results: We presented several key features that should be available within the next generation digital microscopes. Especially, CAN and CAD have a high potential since they add an additional benefit for pathologists compared to conventional microscopy. Supplementary diagnosis quality, reproducibility and speed will be improved.

Conclusion: Currently available digital microscopes come with a wide range of basic features. However, for routine purposes several useful extensions should be added. In the daily diagnostic process the first and foremost requirement for digital microscopy is the instantaneous feedback while navigating through the tissue. Seamless integration into pathology and laboratory information systems (PLIS, AP-LIS) and DICOM-conform connectivity to PACS systems are widely accepted as important components for virtual microscopy. Image analysis (IA) on whole slide images is rapidly developing. Although several vendors currently adding image analysis capabilities to digital microscopes, most of them are proprietary and highly specialized. Therefore, it is necessary to define standardized interfaces for digital microscopes for extending their IA capabilities. Digital microscopes should be able to integrate services like image analysis, data mining and statistics, provided as web based services. High level extensions to digital microscopes are computer assisted navigation (CAN) and computer aided diagnosis (CAD). CAN enables comfortable navigation and interaction within or between whole slide images for several contexts such as tracing a relevant area through serial sections. These areas can be automatically linked across different slides or stains by maintaining the relative position. CAD techniques such as decision support and content based image retrieval (CBIR) show an emerging development activity and are already available for specific research contexts. For daily use they have to be integrated in user-friendly GUIs.

022

Demands on scanner developments based on technical and human tests

P. Hufnagel *, Th. Schrader, G. Rojo, A. Laurinavicius, G. Kayser
*Berlin, Germany

The number of commercially available slide scanners is increasing from year to year. More or less all systems are under permanent development. With respect to limited time and technical knowledge it is a problem for pathologists to check which scanner is appropriate for their concrete application. On the other hand it is a problem for the vendors to understand the different evaluation results of image quality, speed and handling by several pathologists. The 1st European Scanner Contest in 2010 offered the possibility to initiate a dialogue between vendors and pathologists based on series of identical specimens. In the quality test 3 diagnostic relevant regions of 10 different specimens scanned with 7 different scanners have been compared. The regions had a size of 1000x1000 pixels and were viewed on calibrated monitors of identical type. About 30 pathologists ranked the quality of the images using a special developed computer program. In the mass test series of nearly identical sets of 30 specimens had to be scanned with the aim of maximal scanning speed and amount of slide in focus.We found several differences in quality and speed between the scanners, which took part in the contest. So it was possible to find the fastest scanner and the scanner with overall best image quality. Nevertheless we found also that the evaluation of the quality was different

between pathologists. This experience corresponds to the different microscope settings preferred by pathologist as well as to differences in the staining practice of pathology laboratories. Another reason was the different anticipation of the pathologist, which mostly corresponded to the intended application field of virtual microscopy: education, TMA analysis, second opinion, etc.Pathologists and vendors are talking sometimes at cross-purposes. It is necessary to define a specific set of features, which is independent of the individual perception but reflects the demands of pathologists. Such parameters should support the fair comparison of different scanners for concrete applications or application fields. An example is the focus corrected speed, which was introduced on the 1st ESC.

Wednesday, 31 August 2011, 09.30–10.30 and 16.30–17.00, Hall 5

PS-22 Poster Session Molecular Pathology

001

Loss of epigenetic silencing in genomic repeat elements provides a cancer biomarker

J. Costa *, P. Lizardi, S. Szpakowski
*Yale School of Medicine, Dept. of Pathology, New Haven, USA

Objective: Close to 50% of the human genome harbors repetitive sequences (REs) derived from mobile DNA elements. In normal cells these sequences are tightly regulated by epigenetic silencing. In cancer cells, REs are demethylated with potential loss of silencing. Numerous reports of transcriptional activation of retrotransposons in human cancer exist but their role in the pathogenesis of cancer remains unclear.
Method: We use a method for the study of relative genomic DNA methylation that lends itself to analysis of he methylated sequences either by sequencing or by array methodology. For the arrays, probes were designed to map as closely as possible to every CpG island in the human genome. Including a replicated subset the number of probes/array was 377,000.
Results: We measured DNA methylation in 37 SCCs of the oral cavity, non-tumoral adjacent tissues and ten normal oral mucosa samples. Among the 257,599 REs probed, 5% to 8% showed disease related alterations. These alterations could be used as efficient classifiers distinguishing tumor tissue from "field effect" from normal epithelial cells.
Conclusion: The methylation status of specific repeat elements can be used as a marker for cancer and a metric of instability and cellular stress that constitutes a potential marker for cancer risk.

002

Euphorbia tirucalli as a possible cofactor in inducing EBV-driven malignant transformation

G. De Falco*, S. Mannucci, A. Carugi, A. Luzzi, A. Gozzetti, L. Leoncini, C.A. Van den Bosch
*University of Siena, Dept. of Human Pathology and Oncology, Italy

Objective: We aimed at determining if exposure to *Euphorbia tirucalli*, a plant known to possess EBV-activating substances, has a similar geographical distribution to endemic Burkitt's Lymphoma, and has been shown to activate EBV from its latent form inside B-lymphocytes, may contribute to lymphomagenesis. *E. tirucalli* extracts can also induce chromosomal abnormalities when added to EBV-infected cord blood B lymphocytes, 10% of which represent MYC translocation.
Method: Cord blood-derived cell lines were treated with plant extracts, the expression of EBV-coded proteins was checked, to assess EBV reactivation. Finally, the occurrence of chromosomal translocations was investigated by FISH.
Results: Cells treated with *E. tirucalli* showed a modulation of EBV latency genes, as increasing doses of *E. tirucalli* determined the expression of Zebra and LMP1, an enhanced expression of the EBV early antigen EAD, and upregulation of EBNA1 and EBNA2. Interestingly, though no chromosomal translocations for c-MYC were detected, treatment induced polysomies for MYC, and a consequent up-regulation of c-MYC expression was also observed, which might be in accordance with the induction of Burkitt lymphoma. In addition, treatment with plant extracts determined BCL-2 over-expression.
Conclusion: Our preliminary results suggest that *E. tirucalli* is able to reinduce EBV activation and determine c-MYC altered expression, which may thus contribute to the genesis of BL.

003

MicroRNA-induced DNA methyltransferase upregulation leads to aberrant hypermethylation in HIV-positive aggressive B-cell lymphomas

G. De Falco *, A. Luzzi, F. Morettini, V. Pinnacchio, A. Onnis, C. Bellan, L. Leoncini
*University of Siena, Dept. of Human Pathology and Oncology, Italy

Objective: HIV-induced immune activation of B-cells is thought to contribute to the increased frequency of B-cell malignancies observed in HIV-infected individuals. The HIV-encoded Tat protein is thought to participate in B-cell abnormalities observed in vivo. Tat increases the expression of interleukins 6 (IL6), which in turn

promotes B-cell stimulation, and may upregulate the expression of methyltransferases (DNMTs), resulting in abnormal patterns of DNA methylation, which is frequent in cancer. In particular, DNMT1 is considered a maintenance DNA methyltransferase, whereas DNMT3a and DNMT3b are generally regarded as de novo DNA methyltransferases.
Method: Primary tumors of HIV-positive and HIV-negative DLBCL and BL were tested for their expression of DNMTs by qRT-PCR. The expression of specific microRNAs predicted to have them as targets was then investigated. The in vivo results were further confirmed in Tat-transfected human cell lines.
Results: DNMTs were found upregulated both in HIV-positive primary tumors and in Tat-transfected cell lines. In accordance, we observed specific downregulation of microRNAs targeting DNMTs only in HIV-positive tumors and Tat-transfected cell lines. Upregulation of DNMTs induced by microRNAs seems to rely on Tat-induced IL6 expression.
Conclusion: Dysregulation of DNA methyltransferases induced by HIV may result in the aberrant methylation of important tumor suppressor and cell cycle regulatory genes, eventually initiating or enhancing neoplastic growth.

004
Specificity and sensitivity of immunohistochemistry for detecting EGFR mutations in lung cancer cells

P. Fouret *, M. Ilie, S. Roux, M. Alifano, V. Hofman, F. Leroy-Ladurie, I. Rouquette, P. Validire, F. Vaylet, P. Hofman
*Pitié-Salpêtrière APHP, Dept. de Pathologie, Paris, France

Objective: We evaluated the sensitivity and specificity of immunohistochemistry with antibodies that were raised against peptides matching EGFR mutant sequences to identify EGFR mutations in 65 smokers and 68 non-smokers with lung adenocarcinoma.
Method: Immunohistochemistry was performed with monoclonal antibodies against peptides matching E746_A750del or L858R mutations. Negativity (no or faint staining in<10% tumour cells) was ascertained by two investigators. Exons 19 and 21 were sequenced in both sense and antisense directions from two independent amplifications.
Results: Thirty-one and 25 mutations were detected in exon 19 and 21, respectively. Mutations were more frequent in never smokers compared to smokers (P=0.006). By immunohistochemistry, 10 and 5 cases were positive for exon 19 and exon 21 mutation, respectively. Two of ten cases immunoreactive with exon 19 mutation antibody were wild type for exon 19 by sequencing. Among 123 negative cases with exon 19 mutation antibody, 23 were mutated in exon 19. One of five cases immunoreactive with exon 21 mutation antibody was wild type for exon 21 by sequencing. Among 128 negative cases with exon 21 mutation antibody, seventeen were mutated in exon 21 by sequencing. **Conclusion:** In our hands, immunohistochemistry with currently available 'mutation-specific' antibodies has indeed a high specificity (>98%), but lack sensitivity.

005
Impact of delayed fixation on protein profiles in clinical tissue samples

S. Gündisch *, S.M. Hauck, H. Sarioglu, C. Viertler, M. Kap, C. Schott, P. Riegman, K. Zatloukal, K.-F. Becker
*Med. Universität München, Inst. für Pathologie, Germany

Objective: The European consortium SPIDIA (www.spidia.eu) systematically addresses the impact of pre-analytical factors on the molecular portrait of clinical tissue samples. In this study we focussed on potential changes of the proteome under ischemic conditions.
Method: Homogeneous human liver samples were collected in the operating theatre under different ischemic conditions and cryopreserved. Biological replicates were analyzed using one-dimensional gel electrophoresis followed by liquid chromatography-tandem mass spectrometry (LC-MS/MS). Validation studies were performed by reverse phase protein array (RPPA) and Western blot.
Results: The LC-MS/MS results indicate that only a small percentage of proteins was significantly differentially regulated among the different ischemia time points. Interestingly, we found that Cytokeratin 18 was upregulated after 360 min of ischemia, while in contrast GAPDH expression was found to be very stable. Analysis by RPPA and Western blot confirmed these data. Importantly, we found a high patient-to-patient variability with regard to protein expression.
Conclusion: Since we could not detect a consistent global trend towards up- or downregulation of the proteome upon ischemia, we conclude that the proteome seems to be more stable than expected in clinical tissue samples. However, the observed high patient-to-patient variability might be a major hurdle in future protein biomarker discovery programs.

006
Identification of cells with cancer stem cell phenotype in rhabdomyosarcoma

M. Hermanova *, I. Zambo, J. Sana, J. Skoda, J. Neradil, P. Chlapek, P. Mudry, A. Vasikova, K. Zitterbart, J. Sterba, R. Veselska
*St. Anne University Hospital, 1st Dept Pathological Anatomy, Brno, Czech Republic

Objective: Co-expression of nestin and CD133 is considered to be a cancer stem cell marker in different tumors. Our study analyzed their expression in rhabdomyosarcomas and rhabdomyosarcoma-derived cell lines.
Method: The expression of CD133 and nestin was examined in ten rhabdomyosarcoma tissue samples, and in five rhabdomyosarcoma cell lines using immunohistochemistry, immunofluorescence, and immunoblotting. Flow cytometry was employed to measure changes in CD133 expression in rhabdomyosarcoma cells during cultivation.
Results: CD133 and nestin were detected in all ten tumor tissue samples and five cell lines with variable frequency of CD133+, nestin+, and CD133+/nestin+cells in individual samples. Immunoblotting subsequently confirmed the expression of CD133 and nestin in all examined cell lines. An increasing expression of CD133 was observed in relation to the cultivation. All derived cell lines expressed genes required for maintaining stem cell state (Oct3/4 and nucleostemin) in addition to CD133 and nestin. Additionally, the ability to self-renew was confirmed in vitro using single cell colony forming assay.
Conclusion: Our results represent the first evidence of CD133 expression in rhabdomyosarcoma tissue and in rhabdomyosarcoma cell lines. In addition, the co-expression of CD133 and nestin suggests a possible presence of cancer cells with a stem-like phenotype in these tumors.

007

Improvement of the "pre-analytical" phase control in a molecular pathology laboratory using radio frequency identification (RFID)-based system: experience of a single institution (CHU Nice, France)

M. Ilie *, O. Bordonne, E. Selva, V. Hofman, V.G. Tanga, E. Pedrazzi, C. Lagardére, P. Mayer,
J. Mouroux, C. Chabannon, P. Hofman
*CHU de Nice, Hôpital Pasteur, Human Tissue Biobank, France

Objective: The upstream control of the steps present between resection of tumor samples and molecular analysis has proved to be crucial since the quality of biospecimen determines the reliability of the molecular biology results. The purpose of this study was to evaluate the benefits of the RFID technology in the traceability and security of non fixed specimens from the surgical room until the pathology laboratory.
Method: In the operating room, the specimens were placed in plastic bags identified with passive high-frequency RFID tags. The cryotubes moved to the pathology laboratory via a pneumatic tube, a process that takes less than a minute. After gross macroscopy selection the samples located in cryotubes were frozen in nitrogen. The tubes were scanned into the database via a system fixed compact RFID station.
Results: For each surgical specimen, time between the departure from the operating room until the frozen procedure was accurately measured and recorded (mean= 19 min; range, 10–32 min).
Conclusion: One benefit of this RFID system is that it enables the hospital to know when specimen tubes are moved form one location to another, thereby helping the facility to keep track of them and to reduce the time of cold ischemia.

008

The analysis of the gene expression pattern by the appropriateness of specimen collection site with microarray experiments

J.-H. Kim *, C. Choi, J.-S. Lee
*Jeju National University, Medical School, Republic of Korea

Objective: The tumor tissues that are collected in the biobank may contain variable amounts of non-neoplastic tissue. Until now, there has been a lack of consensus on the criterion of percentage of tumor component in collected tumor. The purpose of this experiment is to suggest the criterion.
Method: A total of 22 samples (20 tumor samples and two normal samples) were obtained from two cases of colon cancer. Illumina Human HT-12 expression 48K BeadChip arrays were used. We performed unsupervised hierarchical clustering with variable criteria of tumor component in tumor tissues (10%, 30%, and 50%). The numbers of genes differentially expressed by at least twofold and fivefold between normal and tumor tissues were calculated.
Results: Cancer and normal groups were accurately separated on a dendogram, even when 10% of the tumor component was included. According to the decreased percentage of tumor component in the tumor tissue, the number of differentially expressed genes diminished.
Conclusion: The criterion of percentage of tumor component in tumor tissue cannot be determined because of tissue heterogeneity and intratumoral heterogeneity. Recording the percentage of tumor and various non-neoplastic tissues by histopathological examination prior to storage is crucial in laboratories and biobank.

009

Loss of beta2-microglobulin protein expression is correlated with lack of distant metastasis and favourable clinical outcome in mismatch repair-deficient colorectal cancer

V. Koelzer *, D. Kassahn, D. Baumhoer, K. Baker, I. Zlobec
*Universität Bern, Inst. für Pathologie, Switzerland

Objective: We investigated the effect of beta-2-microglobulin (B2M) protein expression on clinical outcome in mismatch repair (MMR)-deficient and -proficient colorectal cancer patients and correlated our findings to specific populations of tumour-infiltrating lymphocytes.
Method: Using tissue microarrays, 98 MMR-deficient and 310 MMR-proficient colorectal cancers were immunostained for B2M, CD3, CD16, CD163, CD20, CD4, CD45RO, CD56, CD68, CD8, FoxP3, GranzymeB, iNOS, mast cell tryptase, MUM1, PD1 and TIA-1. A second cohort of 737 patients was used to validate the prognostic findings.
Results: Loss of B2M expression was more frequent in MMR-deficient (19/98; 19.4%) compared to MMR-proficient (22/310; 7.1%) tumours ($p<0.001$). In MMR-deficient cases, B2M loss was linked to mucinous histology ($p<0.001$), higher tumour grade ($p=0.019$), absence of local recurrence ($p=0.034$) and, in both cohorts, showed a trend towards a more favourable outcome ($p=0.124$; $p=0.12$). All 19 (100%) MMR-deficient cases with B2M loss were non-metastatic ($p=0.048$). B2M positivity correlated with CD3+, CD8+, GranzymeB+and TIA-1+ tumour-infiltrating lymphocytes, irrespective of MMR status.
Conclusion: The absence of distant metastasis and the favourable prognostic effect associated with B2M loss is confined to MMR-deficient tumours. This supports the hypothesis that B2M loss in MMR-deficient carcinomas plays a role restricted to local tumour progression.

010

A new technology for simultaneous preservation of biomolecules and morphology in tissues

C. Viertler *, D. Groelz, K. Kashofer, S. Gündisch, P. Riegman, R. Winther, R. Wyrich, M. Kruhoffer, K.-F. Becker, U. Oelmüller, K. Zatloukal
*Medizinische Universität Graz, Inst. für Pathologie, Austria

Objective: Upcoming molecular diagnostics and emerging omics-technologies increased the need for a new tissue preservation technique that enables combined histopathological diagnostics and molecular analyses from one tissue sample. Therefore, we tested a novel stabilisation technology (PAXgene Tissue System), developed using a high-throughput screening approach.
Method: Corresponding samples from different human (non-)malignant tissues were either snap-frozen, fixed in buffered formaldehyde or with PAXgene Tissue. In a comparative study morphology, antigenicity and different biomolecules were investigated with a focus on nucleic acids preservation.
Results: PAXgene-fixed and paraffin-embedded (PFPE) samples showed outstanding RNA preservation and strong correlation of multiple mRNA and microRNA profiles with snap-frozen samples as revealed by qPCR and microarray analysis. DNA isolated from PFPE was of similar high molecular mass and well suited for long-range and multiplex PCR as well as for different sequencing techniques. Proteins showed the same electrophoretic mobility compared to cryo-preserved samples and good preservation of phosphorylation levels.
Conclusion: The versatility of the PAXgene tissue system opens new opportunities for combined morphological and molecular analyses in a series of applications scenarios e. g. clinical trials, biomarker discovery or molecular analyses of lesions where a collection of snap-frozen material is impossible for logistic, medical or ethical reasons.

011

Intratumoral heterogeneity of KRAS and BRAF mutations in primary colorectal cancer and corresponding metastases

I. Zlobec *, M. Bihl, A. Foerster, A. Rufle, A. Lugli
*Universität Bern, Inst. für Pathology, Switzerland

Objective: Mutation analysis of KRAS is recommended for metastatic colorectal cancer to identify patients suitable for anti-EGFR based therapies. Here, we test the hypothesis that tissue sampling plays a role in the incorrect assignment of wild-type and mutated gene status in metastatic colorectal cancers.
Method: Mutation analysis for KRAS (codons 12 and 13) and BRAF (codon V600E) was performed on 48 primary colorectal cancers and 32 matched metastases. Tumor from the most represented block was sampled five times each. In total 804 tissue spots were evaluable for KRAS and BRAF.
Results: In primary and metastatic tumors, KRAS mutation occurred in 37.5% and 31.3%. Frequency of intratumoral heterogeneity was 12.5% at both sites and percent-concordance was 81% [$k=0.56$ (95% CI: 0.25-0.87)]. BRAF mutation occurred in 8.3% primary and 6.3% metastatic tumors. Heterogeneity was observed in three primary tumors (6.3%) only. All 804 spots were mutually exclusive for mutation in KRAS and BRAF.
Conclusion: Although heterogeneity for KRAS and BRAF occurs in a small number of samples, it may nonetheless lead to incorrect assignment of wild-type or mutated gene status in more than 10% of tumors. This finding could have important clinical implications for patients considered for anti-EGFR-based therapies.

012

Pyrosequencing in combination with locked nucleic acid-mediated PCR-clamping increases the sensitivity of the detection of KITD816V mutations in systemic mastocytosis

S. Berezowska *, E. Born, A. Schindler, H.-P. Horny, A. Jung, K. Sotlar
*Med. Universität München, Inst. für Pathologie, Germany

Objective: KITD816V is a WHO diagnostic criterion for systemic mastocytosis (SM) and usually confined to neoplastic mast cells. They may comprise <5% of all nucleated bone marrow cells, requiring highly sensitive KITD816V detection methods. We investigated the diagnostic utility of pyrosequencing and locked nucleic acid (LNA)-mediated PCR-clamping.
Method: Pyrosequencing was compared with melting point analysis (MPA) using dilution series of WT and mutated (HMC-1 cells) DNA and DNA from FFPE bone marrow biopsies of 30 patients with KITD816V-positive SM and 22 controls. DNA was amplified by single and nested PCR both conventionally and by LNA-mediated PCR-clamping, favouring amplification of mutated alleles.
Results: Dilution series revealed comparable sensitivities of both methods (<10% of mutated alleles) using conventionally amplified DNA, with 100-fold increase by using LNA-mediated PCR-clamping. Pyrosequencing identified KITD816V mutations in 43% (13/30) of conventionally amplified DNA, in 87% (26/30) after LNA-PCR, and in all 30 cases after LNA-nested PCR, without false-positive results. Corresponding results of MPA were 50%, 87% and 100%.
Conclusion: Pyrosequencing of total DNA amplified by LNA-mediated PCR-clamping significantly increased the sensitivity in detection of KITD816V in mastocytosis, equally sensitive as in-house "gold standard" of MPA, and may be used for the assessment of known mutations in minor cell populations.

013

Correlation between polymorphisms at promoter region of the NOS3 gene and prostate cancer in Serbian population

G. Brajuskovic *, A. Brankovic, D. Savic Pavicevic, J. Mircetic, S. Cerovic, S. Tomovic, I. Vukovic, V. Vukotic, S. Romac
*Faculty of Biology, Belgrade, Serbia

Objective: Prostate cancer (PC) is the most common malignant disease in men in the Western Hemisphere. The NOS3 has a role in vascular development, regulation of the vascular tone and tumor growth in PC. In previous studies, the -786 T>C polymorphism was found to be the most important promoter alteration of the NOS3 gene that may affect the PC progression. The purpose of this study was to evaluate 786 T>C, -764A>G, -714 G>T, -690 C>T and -649 G>A polymorphisms in the promoter region of NOS3 gene as genetic indicators of the relative risk of the PC occurrence in Serbian population.
Method: In this study, we characterized these polymorphisms by PCR amplification, followed by capillary electrophoresis sequencing in the peripheral blood samples from 50 patients with PC, 50 benign hyperplasia patients and 50 individuals over 40 years of age who showed no clinical signs of any prostatic disease, that were used as controls.
Results: Three of the analyzed polymorphisms (-764A>G, -714 G>T and -649 G>A) were not detected during this study. It is interesting to observe that when the -786 T>C polymorphism was present, -690 C>T polymorphism was also found.
Conclusion: This study demonstrates no association between the -786 T>C polymorphism in the promoter of the NOS3 gene and the development of PC.

014

Analysis of five single nucleotide polymorphisms at locus 8q24 associated with prostate cancer in Serbian population

G. Brajuskovic *, J. Mircetic, D. Savic Pavicevic, S. Cerovic, S. Tomovic, N. Jeremic, I. Vukovic, V. Vukotic, S. Romac
*Faculty of Biology, Belgrade, Serbia

Objective: Prostate cancer (PC) is the most prevalent type of cancer in males, comprising about 29% of all malignant tumors. Primarily, several single nucleotide polymorphisms (SNPs) in 8q24 locus have been associated with the risk of developing PC. We analyzed five of these in Serbian population: rs1447295, rs6983267, rs4242382, rs7017300 and rs7837688.
Method: Analyses were done on 100 peripheral blood samples from 50 individuals diagnosed with PC and from 50 individuals diagnosed with benign prostatic hyperplasia that were used as a control group. The work proceeded through PCR amplification of five regions surrounding SNPs, restriction fragment length polymorphism (RFLP) analysis. The differences in genotype frequencies between case and control subjects were tested using a chi-square test with 1° of freedom.
Results: We found that in case of four SNPs (rs1447295, rs4242382, rs7017300 and rs7837688) out of five analyzed, association ($p<0.05$) with PC existed in Serbian population. We also found that patients with PC having genotypes associated with the disease have the same average Gleason score as those with “dominant” genotypes; in the case of serum PSA levels, there was no difference between these patients either.
Conclusion: Finally, the possibility of a haplotype carrying these four SNPs associated with PC is strongly suggested.

015

Detection of EGFR mutations in archival lung cancer samples by pyrosequencing

S. Cappia *, A. Cuccurullo, D. Giachino, L. Righi, E. Bacillo, C. De Risi, G. Rovere, S. Novello, M. Papotti
*San Luigi Hospital, Orbassano, Italy

Objective: Epidermal growth factor receptor (EGFR) mutation detection is often based on lung cancer archival biopsies or cytological specimens. Pyrosequencing is a sensitive method to detect mutation presence and frequency even in DNA partially fragmented cases. The objective of the study was to assess the performance of pyrosequencing in EGFR mutation detection.
Method: There were 202 selected lung adenocarcinomas tested (72 surgical specimens, 56 biopsies, 74 cytological samples, including 9 smears and 65 cell blocks). In microdissected paraffin sections and smears, exon 18-19-21 mutations were screened using EGFR-TKI response (sensitivity) kit (Diatech), real-time-PCR (RotorGene, Qiagen) and pyrosequencing (PyroMarkQ96, Biotage).
Results: Real-time-PCR and melting analyses showed abundant and specific amplification of each exon, irrespective of fixative and sample types. Pyrosequencing revealed 43/202 (21.3%) mutated samples [31 exon 19 in-frame deletions (72%) and 12 exon 21 point mutations (25.6% L858R and 2.4% L861Q)], with a respective frequency of 25.8% and 66.7% in surgical samples; 32.3% and 8.3% in biopsies; 41.9% and 8.3% in cell blocks; 0% and 16.7% in smears.
Conclusion: Mutation frequencies are similar to those reported in the literature, with no marked differences among the various sample types. Pyrosequencing combined with microdissection and real-time-PCR appears a valuable method for molecular tests in different archival specimens.

016

KRAS mutations in lung adenocarcinomas may be relevant in histological patterns, EGFR mutational status and male smokers

L. Carvalho *, A. Alarcão, P. Couceiro, M. Reis Silva, M. J. D'Aguiar, L. Teixeira, T. Ferreira, V. Sousa
*Amadora, Portugal

Objective: Lung adenocarcinomas may show different patterns/subtypes and as EGFR and KRAS mutations rationalize personalized therapy, mutations were searched in all different patterns: acinar, papillary, micropapillary, solid and mucin producing, after immunohistochemistry characterization.
Method: KRAS and EGFR mutations in 31 lung resected adenocarcinomas were studied by polymerase chain reaction (PCR), fragment analysis and direct sequencing.
Results: There were 5/31 cases with KRAS point mutations, 3 of them G12V and 2 of them G12C; 26 cases were Wt. In KRAS mutated cases, four had no EGFR mutations and one case exhibited exon 21 EGFR point mutation in two patterns (BAC and Acinar) of the same mixed type adenocarcinoma. No statistical relevance was found between exon 2 KRAS status and age (for WT and mutated) (p=0.401). KRAS mutation was more frequent in male (p=0.000) and in smokers (p=0.014).
Conclusion: EGFR mutations and KRAS mutations have been described as mutually exclusive but in this small series one case had KRAS and EGFR mutations simultaneously. Although EGFR and KRAS mutations are generally mutually exclusive, they can coexist and clinical, therapeutic and prognostic issues concerning male smoking patients become relevant as may direct personalized therapy.

017

ALK gene rearrangment in EGFR and KRAS positive lung adenocarcinomas

L. Carvalho *, M.R. Silva, A. Alarcão, P. Couceiro, D. Oliveira, V. Sousa, M. J. D´Aguiar, L. Teixeira
*Amadora, Portugal

Objective: Lung cancer is still the leading cause-related of death worldwide and adenocarcinomas harbour genetic changes to be further classified into clinical relevant molecular subsets. Tumors sensitive to epidermal growth factor receptor (EGFR) tyrosine kinase inhibitors often contain somatic mutations in the tyrosine domain of EGFR. While other tumors exhibit somatic mutations in KRAS which display primary resistance to those drugs. Another mutation is anaplastic large cell kinase gene (ALK) that is rearranged in approximately 5% of lung adenocarcinomas, indicates ALK inhibitors to be prescribed when EGFR and KRAS are wildtype.
Method: We tested 19 lung adenocarcinomas for ALK rearrangments by fluorescent in-situ hybridization (FISH) and immunohistochemistry (IHC), 14 cases harboured EGFR mutations and 5 KRAS mutations.
Results: Both techniques independently identified negative cases 17/19 (89%), except for one positive FISH and IHC case 1/19 (5%), with ALK rearranged gene (50 year old women). One FISH case was inconclusive.
Conclusion: Our findings in this subset population of EGFR and KRAS mutation positive adenocarcinomas of 5% ALK rearrangement suggests that with the emergence of moleculary-targeted therapies, it is reasonable to assume that all adenocarcinomas should be screened for ALK rearrangments, by dual testing IHC and FISH, to ensure accurate diagnosis.

018

Deregulation of mir-126 and mir-126* in primary lung tumors and lymph node metastasis

L. Carvalho *, M.R. Silva, S. Romano, P. Santos, L. Teixeira, M.J.D´Aguiar
*Amadora, Portugal

Objective: MicroRNAs are a family of small-non coding RNAs that negatively regulate gene expression at post-transcriptional level. Hsa-miR-126 was reported as down-regulated in lung cancer samples compared to non-cancerous lung tissue. This data support that low expression of hsa-miR-126 is associated with cancerous growth and progression. Information is lacking regarding their involvement in metastatic potential and differential expression in adenocarcinoma and squamous carcinoma of the lung.
Method: Representative areas of thirty seven FFPE samples of matched adjacent lung parenchyma, primary tumour and lymph node metastasis. Cells were were isolated by laser microdissection and, after RNA extraction, the two microRNAs were quantified by RT-qPCR and levels compared in between.
Results: Both miR-126 and miR-126* were found to be down-regulated in primary tumor cells comparatively to matched normal tissue (p-value<0.001). In non-metastatic tumors miR-126 and miR-126* expression was lower in squamous carcinoma (p-value=0.037 and p-value=0.035).
Conclusion: These results suggest that these microRNAs act as tumor suppressors but are not directly involved in the metastatic process. In addition, their expression seems to relate to the histology in non-metastatic tumors and might therefore be useful for their characterization and prognosis establishment.

019

Lung adenocarcinomas subtyping is not relevant for EGFR mutations, gene copy number and protein expression

L. Carvalho *, A. Alarcão, P. Couceiro, M. Reis Silva, M.J. D´Aguiar, L. Teixeira, T. Ferreira, V. Sousa
*Amadora, Portugal

Objective: Lung adenocarcinomas simple/mixed type show various (till six) patterns whose clinical relevance must be tested. A series of 44 resected adenocarcinomas were studied with c-erbB1 (clone 31 G7), EGFR gene copy number by FISH and EGFR exons 19 and 21 sequenced.
Method: Being mixed type Adenocarcinomas, the following patterns were characterized in at least two sections: 41 acinar, 5 papillary, 13 micropapillary, 14 solid, 25 with non-mucinous bronchiolo-alveolar (BAC) and 3 mucinous.
Results: EGFR higher expression in solid pattern was relevant and lower in BAC pattern. EGFR mutational status was present in 8/31 cases with exon 21 point mutations and in 10/31 cases exon 19 deletions; 4 cases had coexisting exon 21 and exon 19 mutations. Concordance between FISH results ad each mutation type (exon 21 and 19) was considered fair (k=0.3702 and k=0.3841). The concordance between mutations and immunohistochemistry expression and between FISH and IHC was not relevant (k=0.2556 and k=0.2635).
Conclusion: EGFR mutations are frequent and reflect their importance in lung adenocarcinomas pathogenesis. There is rough concordance with high gene copy number and in less extent with protein expression. Mutations were generally present in all the patterns of the same adenocarcinoma meaning that biopsies are prone to evaluation of EGFR mutational status.

020

EphrinA5 represses colon cancer cell proliferation and migration by negatively regulating EGFR stability

J.-L. Chang *, T.-H. Wang, J.-Y. Ho, H.-C. Wu, K.-T. Liu, T.-C. Chen
*Taoyuan Armed Forces General Hospital, Dept. of Pathology and Laboratory Medicine, Taiwan

Objective: Colon cancer is one of the most common human cancers worldwide. EphrinA5 is suggested to play a putative tumor suppressor role in a variety of human cancers, however little is known about its downstream regulatory mechanism in colon cancer. This study addressed the association between ephrinA5 and colon carcinogenesis and progression.
Method: We examined ephrinA5 and epidermal growth factor receptor (EGFR) expression profiles in colon cancer and normal tissues using immunohistochemistry in a 96-spot tissue microarray. Gain and loss-of-function experiments were performed on human colon cancer cell lines SW480 and WiDr to determine the biological effects of ephrinA5 in colon cancer cell proliferation, survival, and migration.
Results: EphrinA5 mRNA and protein levels were significantly reduced in colon cancer compared to normal colon tissue specimens. EphrinA5 expression was also negatively associated with tumor differentiation and clinical stages. In colon cancer cell line models, ephrinA5 exerted a negative regulatory effect on EGFR by promoting c-Cbl-mediated EGFR ubquitinylation and degradation. Nonetheless, there was no transcriptional regulation of ephrinA5 to EGFR expression in colon cancer cells. Furthermore, ephrinA5 suppressed EGFR, and thus reduced colon cancer cell proliferation, migration, and chemotherapeutic resistance.
Conclusion: EphrinA5 inhibited colon carcinogenesis and tumor progression by promoting c-Cbl-mediated EGFR

degradation. These results shed light on developing strategies of EGFR targeting and therapeutic efficiency.

021

European external quality assessment for the improvement of KRAS testing

E. Dequeker *, E. Bellon, M. Ligtenberg, G. de Hertogh, K. de Stricker, A. Edsjö, P. Laurent-Puig, J.C. Machado, E. Rouleau, J. van Krieken
*Katholieke Universiteit Leuven, Centre for Human Genetics, Belgium

Objective: KRAS mutational status in tumor cells has become an important determinant for the successful application of epidermal growth factor receptor targeting therapy in patients with colorectal cancer. In an effort to ensure optimal, uniform and reliable community based KRAS testing throughout Europe, a KRAS External Quality Assessment (EQA) scheme was set up.
Method: In total 76 laboratories from 14 different European countries participated and were divided among 6 regional schemes. For each scheme, one regional scheme organizer prepared and distributed the samples. The samples were centrally validated by a reference laboratory and included unstained sections of 10 invasive colorectal carcinomas with known KRAS genotype.
Results: From the 76 participating laboratories, 50 reported all 10 genotypes correctly (66%). The average genotyping score for the KRAS EQA scheme is 9.5/10.0 (95%). There is an overall improvement in the score of laboratories that participated also in the KRAS EQA scheme of last year. Mistakes were made both in laboratories using commercial and "in-house" validated assays. In addition, we analyzed tumor percentage analysis and written reports for educational purposes.
Conclusion: This EQA scheme is a useful tool to provide information about the performance of a given laboratory compared to others and to stimulate the optimalisation of lab procedures.

022

A national quality assurance system for HER2 testing in gastric cancer: results and experiences

A. Edsjö*, R. Palmqvist, A. Wanders, A. Olsson, G. Elmberger, A. Kolaric, S. Ignatova, M. Wolving, K. Bjelkenkrantz
*Limhamn, Sweden

Objective: Reliable assessment of HER2 overexpression and amplification in gastric biopsy specimens has become important with the introduction of anti-HER2 therapy as a treatment option for gastric cancer. Valuable experience has been gained from breast carcinoma diagnostics but differences exist in terms of staining pattern, heterogeneity and sample size. Additionally, the low and uneven volumes of incoming cases call for collaboration between the laboratories involved.
Method: In a meeting on Januari 23rd 2011 a national collaboration was initiated with three main components: 1. A quality assessment scheme with ten virtual slides of stained biopsies and ten punch biopsies from surgical specimens. 2. Continuous web based monitoring of testing results from routine diagnostics. 3. Follow-up meetings to discuss results and methodological challenges.
Results: The work with the send-out and collection of results from routine diagnostics is currently ongoing. Results from the quality assessment scheme and updated figures from HER2 status assessments will be presented.

023

Role of transforming growth factor-Beta 1 in progression and clinical outcome of colorectal cancer

M. Gulubova *, J. Ananiev, E. Alexandrova, L. Miteva, I. Manolova
*Trakia University, Medical Falculty, Dept. of General and Clinical Pathology, Stara Zagora, Bulgaria

Objective: Transforming growth factor-b 1 (TGF-b1) is a multifunctional cytokine that regulates many cellular processes. The -509 C>T polymorphism in the promoter region of TGFb1 has been associated with TGF-b1 serum level. We assessed the expression of TGF-b1 in tumor, normal mucosa and plasma in colorectal cancer (CRC) patients and investigated the relationship of -509 C>T polymorphism with TGF-b1 levels, CRC susceptibility, and the survival.
Method: TGF-b1 expression was assessed by immunohistochemistry in 205 CRC patients. TGF-b1 tissue and serum levels were measured by ELISA. Genotyping for the -509 C>T polymorphism of the TGFb1 was performed by RFLP—PCR assay.
Results: A total of 44.9% out of 205 tumors were immunostained for TGF-β1. TGF-b1 tissue levels were higher in tumor than in normal mucosa ($p<0.001$). The high TGF-β1 serum levels were associated with -509/TT genotype ($p=0.028$). There were no significant differences in genotype distribution and allele frequencies of -509 C>T polymorphism between patients and controls. However, the frequency of TT genotype among CRC patients (8%) was lower compared to healthy controls (19%, $p=0.054$). Patients with -509/TT genotype had a poorer 5-year survival than patients with the CC genotype had ($p=0.019$).
Conclusion: Our results suggest that -509 C>T polymorphism of TGFb1 may have a role in the development of CRC.

024

Organic anion transporting polypeptides 1A2, 1B1 and 1B3 are widely expressed in gastrointestinal and pancreatic cancers

V. Kounnis *
*University of Ioannina, Cancer Biobank Center, Greece

Objective: Organic anion-transporting polypeptides (OATPs) are cell membrane influx pumps which support the sodium-independed uptake of various endogenous and xenobiotic compounds. The presence of specific OATPs in the cancer cell, classifies these polypeptides as potential target candidates for novel cancer therapeutics. (I. Sainis et al., *Mar Drugs* 8, 629, 2010).
Method: The expression of OATPs 1A2, 1B1, and 1B3 was investigated in human colon (n=30), gastric (n=10) and pancreatic cancer (n=12) and in normal liver tissue by immunohistochemistry with the following antibodies: polyclonal rabbit SSV anti-OATP1A2, monoclonal mouse ESL anti-OATP1B1 and monoclonal mouse MDQ anti-OATP1B1/1B3.
Results: The immunohistochemical study revealed that OATP1A2 and 1B1 was expressed in all studied cases of colon adenocarcinoma while1B3 (using the mMDQ antibody which recognizes an epitope shared also by 1B1) was expressed in 27/30 samples. All studied cases of pancreatic adenocarcinoma showed abundant expression of the three transporters while for gastric adenocarcinoma, only OATP1B3 presented to be expressed. Liver tissue returned positive membranous stain for both 1B1 and 1B3 polypeptides. Interestingly in positive cases, almost all cancer cells were stained positive.
Conclusion: OATPs 1A2, 1B1 and 1B3 are differentially expressed in GI tract cancers. We suggest that further investigation of OATPs and other influx pumps in gastrointestinal cancers is warranted in the perspective of development of novel OATP-targeted cancer therapies.

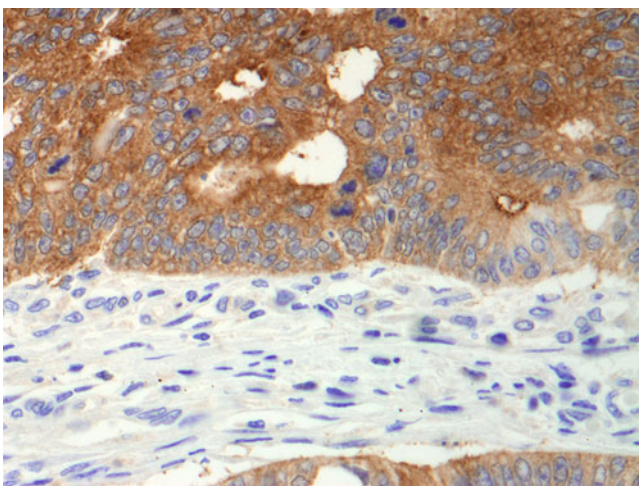

025

The analytic performance of an investigational PCR assay for the detection of KRAS mutations (codons 12/13 and 61) in formalin-fixed paraffin-embedded tissue samples of colorectal carcinoma

J. Lawrence *, J. Cao, M. Velez, C. Hoeppner, S. Lee, V. Brophy, S. Soviero
*Roche Molecular Systems, Medical and Scientific Affairs, Pleasanton, USA

Objective: KRAS mutation testing is mandatory before prescribing anti-EGFR antibodies, creating a need for well-validated assays.
Method: We describe a melting curve analysis-based investigational assay (cobas® KRAS Mutation Test), which detects 19 mutations in codons 12, 13 and 61. Analytical sensitivity was determined using DNA blends from cell lines, plasmid or FFPET specimens. The cobas® test was compared to Sanger sequencing using a panel of 188 CRC samples. Discordant results were resolved using 454 sequencing.
Results: The cobas® test detected KRAS mutations at 5% mutation using an input of 100 ng/specimen. The test showed positive percent agreement (PPA) with Sanger for codon 12/13 of 97.5% (79/81), and negative percent agreement (NPA) of 94.4% (101/107). For codon 61, PPA was 85.7% (6/7) and NPA was 99.4% (180/181). All 10 discordant samples gave 454 results consistent with the cobas® results. When the same panel of 188 tumors was retested with a different reagent lot of the cobas® test, the test results were concordant with the first lot in 186/188 (98.9%) samples.
Conclusion: The cobas® test (1) detects KRAS mutations in codons 12, 13 and 61 at 5% mutation level, (2) is highly reproducible, and (3) is more sensitive and specific than Sanger.

026

Comparison of molecular testing methods for the detection of BRAF V600E mutations in formalin-fixed paraffin-embedded tissue (FFPET) samples of malignant melanoma

F. Lopez Rios *, B. Angulo, B. Gomez, D. Mair, R. Martinez, F. Shieh, J. Vaks, R. Langland, H.J. Lawrence, D. Gonzales de Castro
*Hospital Universitario Madrid, Laboratorio de Dianas, Spain

Objective: The optimal method for detecting BRAF mutations in clinical practice is unknown.
Method: We tested 97 FFPET specimens with an investigational PCR assay (cobas® 4800 BRAF V600 Mutation

Test), ABI BRAF Mutation Reagent Analysis, and Sanger sequencing. Positive (PPA) and negative (NPA) percent agreements were determined; discordant results were resolved using 454 sequencing. 24 DNA blends were tested at 5% mutation.

Results: Invalid results were observed in 9/97 with Sanger, 7/97 with ABI, and 4/194 with cobas®. Repeatability between sites using the cobas® test was 96.8%. PPA for V600E mutation for cobas® vs. Sanger was 96.9%; NPA 98.2%. For cobas® vs. ABI, PPA was 67.3%; NPA 85.4%. For 16 cobas® negative/ABI positive samples, 454 detected 12 WT, 3 V600E2, and 1 V600K. For 6 cobas® positive/ABI negative samples, 4 were V600E and 2 V600K. Hit rates for 5% mutation blends was 100% for cobas®, 33% for Sanger, and 20.9% for ABI. Turn-around times (TAT) were ~5 days for Sanger, ~2 days for ABI and ~1 day for cobas®.

Conclusion: The cobas® Test was highly reproducible and had (1) the lowest invalid rate, (2) greater sensitivity than either Sanger of ABI, (3) higher specificity than ABI, and (4) the most rapid TAT.

027

Molecular subgroups of benign meningioma with different biochemical aggressiveness

J. M. Morales Tatay *, E. Serna García, A. Gonzalez Segura, J. M. Gonzalez Darder, R. Gil Benso, J. M. Cerdá Nicolás, C. Ginés López, D. Monleón Salvado
*Universitat de València, Facultat de Medicina, Valencia, Spain

Objective: Sometimes, meningiomas with benign histological diagnosis tend to recur. Better classification of meningiomas will improve clinical decisions in these tumors. We obtained metabolic and gene expression profiles on 30 benign and 10 atypical meningiomas.

Method: Tumor samples were obtained at the Clinic Hospital of Valencia and categorized by WHO classification. Karyotypic analyses were performed according to ISCN (1995). The GeneChip Human Genome U133 plus2.0 Array was used for gene expression analysis. Metabolic profiling of the samples was performed on frozen tissue by Nuclear Magnetic Resonance.

Results: For most of the metabolites, the values for benign meningioma with chromosomal instabilities were closer to atypical meningioma than to chromosomally normal benign meningioma. Most of the metabolic changes observed in benign meningioma with chromosomal instabilities reflect higher tumor metabolism. Gene expression profiling shows main differences in genes involved in the regulation of transcription.

Conclusion: The metabolic and gene expression profiles allow us detecting biochemical aggressiveness in otherwise benign tumors. The methodology used in this study may also open new possibilities in the diagnosis of meningioma.

028

Prognostic and predictive significance of the bcl -2/IgH translocation in malignant follicular lymphomas

M. Neagu *, C. Ardeleanu
*National Institute of Pathology, Bucuresti, Romania

Objective: In Europe follicular lymphomas constitute up to 30% of non-Hodgkin lymphomas. The aim of our study was to analyze the cytogenetical aberrations in malignant follicular lymphomas, in order to identify the prognostic and predictive value of bcl2-2/IgH translocation in these malignancies.

Method: We conducted a study on 79 patients with follicular lymphomas. The study was carried out on tissue samples selected from the "Victor Babes" National Institute of Pathology files. These samples were formalin-fixed paraffin embedded-tissues. The t(14;18) translocation, realized by the bcl 2/IgH rearrangement, supposedly occurs in almost all follicular lymphomas (FL) can be detected by FISH methods. We employed the PathVysion LSI IGH Spectrum Green/LSI bcl2 Spectrum Orange (VYSIS) kit.

Results: Twenty-two cases were selected for FISH analysis, five cases were excluded because of the processing artifacts, ten of the 17 cases without artifacts (58.8%) presented t(14:18) translocation: two cases of FL grade 1-2, two cases of FL grade 1, six cases of FL grade 3. In 66.6% of cases with t(14;18) translocation, the immunohistochemical reaction for bcl 2 protein was positive.

Conclusion: Bcl2 t(14;18) translocation plays an important role in the pathogenesis of follicular lymphoma, and is an important tool in the diagnosis and treatment.

029

Caspase 9 gene expression increased in lung chemical carcinogenesis contrasting with normal type V collagen and VEGF isoforms gene expression

E.R. Parra *, P.Y. Corrêa, R.A. Alveno, C.B. Faustino, J. de Morais, W.R. Teodoro, V.L. Capelozzi
*Faculdade de Medicina da USP, Dept. of Pathology, São Paulo, Brazil

Objective: Recently, we demonstrated an association between decreases in collagen V and apoptosis in human and mouse lung chemical carcinogenesis, but the mechanisms

involved still remains uncertain (Parra et al 2010; Souza et al 2010). Remodeling of the tumoral microenvironment was evaluated in a model of chemical carcinogenesis in the mouse lung.
Method: Ultrastructural analysis, tridimensional reconstruction and mRNA gene expression were used to evaluate the amount, structure and genic expression of collagen V, vascular endothelial growth factor (VEFG) isoforms (120.164, 168) and caspase-9 in two groups of male Balb/c mice: a) animals that received two intraperitoneal doses of 3 g/kg urethane carcinogen (n=15); and b) animals submitted to a sham procedure (n=4). Both groups were sacrificed after 120 days.
Results: The lung tumors present an adenoid pattern with loose stroma composed by reduced collagen fibers. Tridimensional reconstruction showed normal spatial organization of the fibers, normal synthesis in cellular cultures and normal gene expression of type V collagen and VEFG isoforms. An important significant higher caspase-9 expression was observed in tumoral areas when compared with control group.
Conclusion: The results suggest that chemical lung carcinogenesis does not induce type V collagen and VEFG issoforms genes damage but increased the expression of caspase-9 gene. The decrease observed of this collagen in the tumoral parenchyma probably is caused by active destruction of the fibers after their synthesis and in this context the activation of caspase-9 probably is not sufficient to stop the growth neoplastic cells. Financial support: FAPESP, CNPq.

030

Alterations of cell cycle regulators in conventional renal-cell carcinomas after the Chernobyl accident: comparison with Spanish cases

A. Romanenko *, A. Vozianov, A. Llombart-Bosch
*Institute of Urology, Dept. of Pathology, Kiev, Ukraine

Objective: During the 24-year period subsequent to the Chernobyl accident, the morbidity of malignant renal tumors in Ukraine has increased from 4.7 to 10.8 per 100,000 of the total population. Conventional (clear-cell) is the most common subtype, accounting for 75% of all renal cell carcinomas (RCCs).
Method: There is hypothesized evidence that chronic long-term, low-dose ionising radiation effects cell cycle regulatory molecules and influences renal-cell carcinogenesis. The aim of our study was to assess, by immunohistochemistry on tissue microarray sections, p53, mdm2, p21WAF/CIP1, cyclin D1, cyclin G, p16INK4a, p14ARF and Ki-67 protein expression in 97 conventional renal cell carcinomas (cRCCs) and 36 peritumoral kidney tissue from Ukrainian patients, with different degrees of radiation exposure after the Chernobyl accident, in comparison with 37 tumors and 18 peritumoral kidney tissues from Spanish patients.
Results: Strong significant differences between the Ukrainian and Spanish groups were found in the elevated levels of mdm2, p21WAF1/CIP1, cyclin D1, cyclin G and especially p14ARF expression, however, no relationships with tumor nuclear grade was observed.
Conclusion: Our findings suggest that chronic long-term, low-dose IR exposure leads to activation and alteration of both p53/mdm2/p21 WAF1/CIP1 protein expression and p16INK4a/p14ARF locus proteins which could lead to disruption and loss of cell cycle checkpoints and, thereby, to enhanced tumor progression and aggressiveness.

031

Promoter methylation analysis in breast cancer patients: clinicopathological associations

A. Saetta *, A. Tserga, G. Levidou, N. Michalopoulos, G. Zografos, P. Korkolopoulou, E. Patsouris
*Athens, Greece

Objective: Aberrant promoter methylation leads to tumor suppressor gene inactivation. Our aim is to study the involvement of promoter methylation of 8 genes in breast tumorigenesis in association with clinicopathological characteristics.
Method: DNA was extracted from 49 fresh tumor specimens. The analysis was carried out by the bisulfite method followed by MSP-PCR, High Resolution Melting Analysis (HRM) or pyrosequencing.
Results: High frequency of promoter methylation was found in APC (50%), DCR1 (40.4%), DAPK1 (37.5) and RASSF1 (33.3%) whereas low methylation in MGMT (10.2%), GSTP1 (6.25%) and PTEN (2%). MGMT methylation was observed in elder patients (p=0.0149), whereas GTSP1 methylation seemed to be more frequent in younger patients (p=0.0890). GSTP1 methylation was adversely correlated with tumor histological grade (p=0.053). Tumors with advanced T-category showed higher frequency of RASSF1 and DAPK1 methylation (p=0.033 and p=0.078). There was a trend for a positive correlation between higher percentage of total methylation status and N-category (p=0.0874).
Conclusion: The detected high level of methylation in APC, DCR1, DAPK1 and RASSF1 genes may imply their importance for breast tumorigenesis. GSTP1 methylation constitutes possibly an early event in breast tumorigenesis whereas RASSF1 and DAPK methylation are observed in later stages.

032

MGMT methylation analysis of human gliomas: comparative study using different techniques

A. Saetta *, G. Maravelis, P. Tsioli, S. Sakellariou, Z. Liakouli, P. Korkolopoulou, E. Patsouris
*Athens, Greece

Objective: Gliomas are the most common brain tumors (80% of astrocytomas). Methylation of the MGMT promoter is an epigenetic phenomenon playing an important role to the optimal choice of targeted therapy, such as alkylating agents. Our aim is to compare three different methods of MGMT promoter methylation assessment, regarding their sensitivity and accuracy.
Method: There were 25 brain samples analyzed for MGMT promoter methylation by MSP (methylation-specific PCR) confirmed by sequencing, MS-HRMA (methylation-sensitive high resolution melting analysis) and pyrosequencing. A different number of CpG regions was examined with each method. We tested 8 CpGs with MSP, 16 CpGs with MS-HRMA and 10 CpGs with Pyrosequencing.
Results: MGMT promoter methylation was identified using MSP in 14 out of 19 samples. MS-HRMA revealed 12 positive out of 22 cases. Pyrosequencing showed a high percentage of methylation in 4 cases, medium methylation in 3 and low in 12 out of a total of 19 samples.
Conclusion: A difference of accuracy between the different methods was observed. In brief, we propose the use of MSP as a method complementary to HRM. The most accurate method seems to be pyrosequencing which is the only one providing quantitative results, although their significance for treatment decisions remains to be determined.

033

Metabolic subgroups in high-grade glioma show correlation to angiogenesis pathways

E. Serna García *, P. Doñate Macian, J.M. Morales Tatay, A. Gonzalez Segura, J.M. Gonzalez Darder, J.M. Cerda Nicolas, C. Lopez Gines, D. Monleon Salvado
*Universitat de València, Facultat de Medicina, Valencia, Spain

Objective: The metabolic consequences of different angiogenesis gene expression profiles in gliomas are still unknown. Gene expression profiling of different metabolic phenotypes of high grade glioma may provide new information for better management of this disease. We show high grade glioma NMR molecular profiles correlated with gene expression profiles of 30 high-grade glioma biopsies.
Method: Forty samples of human glioma tissue (23 GBM and 7 AA) were obtained and characterized at the Clinic Hospital of Valencia. The GeneChip Human Gene 1.0 ST Array was used for gene expression analysis. Metabolic profiling of the samples was performed on frozen tissue by nuclear magnetic resonance.
Results: Metabolic profiling revealed two major subgroups within samples with histopathological diagnosis of GBM. The phospholipids pattern, the glycolytic ratio and the glutamine/glutamate metabolic are the major differences between subgroups. Microarrays gene expression analysis revealed more than 300 probesets significantly different between these metabolic subgroups.
Conclusion: There is a correlation between genes involved in angiogenesis and metabolic profiles. This correlation involves metabolites closely related to higher glycolytic rate, to proliferation and to hypoxia.

034

A novel germline SDHB mutation in a GIST patient without associated paraganglioma or pheochromocytoma

J. Vinagre *, R. Celestino, A. Gouveia, J. Lima, A. Faustino, P. Soares, J. M. Lopes
*IPATIMUP; ICBAS; FMUP, Porto, Portugal

Objective: Gastrointestinal stromal tumors (GISTs) are the most common mesenchymal neoplasms of the gastrointestinal tract. The gain-of-function mutations of the KIT or PDGFRA genes represent the most prevalent molecular alterations in GISTs. In Carney–Stratakis dyad, patients develop multifocal GISTs and multicentric paragangliomas (PGLs) and they present germline mutations of the succinate dehydrogenase subunits B (SDHB), C (SDHC) and D (SDHD). We report a 26 year-old man presented a spindle cell intermediate risk GIST with absence of KIT/PDGFRA/BRAF gene mutations.
Method: Molecular characterization KIT/PDGFRA/BRAF genes; immunohistochemistry for proteins SDHA and SDHB; MLPA for SDHB.
Results: Molecular analysis disclosed absence of KIT/PDGFRA/BRAF gene mutations and a germline mutation of the SDHB (c.T282A). GIST tumor revealed loss of the wild-type allele of SDHB gene and complete loss of SDHB expression by immunochemistry. The same germline mutation in SDHB was present in the patient's mother; however the mother does not show signs of GIST and/or PGL.
Conclusion: The studied GIST has a novel SDHB germline mutation without KIT/PDGFR/BRAF mutations. The absence of PGL in our patient as well as the absence of GIST and/or PGL in the carrier mother raises the possibility that our patient may represent an incomplete phenotype of the Carney–Stratakis syndrome or a distinct entity.

035

UKNEQAS external quality assessment pilot schemes for molecular genetic analysis of EGFR and KRAS

Z. Deans *, N. Bilbe, P. Taniere, C. Clark, M. Ibrahim, A. Dodson, I. Cree, K. Miller, A. Abbs, R. Butler
*UKNEQAS for Molecular Genetics; Inst. of Human Genetics; Center for Life, Newcastle-upon-Tyne, UK

Objective: Since 2010 UKNEQAS has provided pilot external quality assessment schemes (EQAs) for molecular analysis of EGFR in non-small cell lung cancer and KRAS in metastatic colorectal cancer in collaboration between UKNEQAS for Molecular Genetics and UKNEQAS for Immunocytochemistry and In Situ Hybridisation. The joint EQA scheme reflects cross-discipline testing in this area.
Method: For each scheme three clinical scenarios and FFPE tumour sections were distributed. Participants tested for EGFR or KRAS gene changes according to normal procedures and issued interpretative clinical reports in their usual format. Results were assessed for genotyping accuracy, interpretation and clerical accuracy.
Results: There were 27 laboratories which participated in the first EGFR EQA run; six laboratories (22%) reported incorrect genotypes including false positives, false negatives and sample swap errors. The KRAS EQA detected genotyping errors in 10% of 43 laboratories. A p.Gly12Asp KRAS paraffin-embedded cell line was successfully used as EQA material with 97.5% of participants detecting the mutation. Interpretation errors were identified in both schemes. General report content was variable, often with unclear patient identifiers, ambiguous mutation nomenclature, lacking testing details or test sensitivity.
Conclusion: The genotyping errors and variability in reporting format highlights the critical requirement for EQA in this molecular discipline and the development of best practice guidelines.

036

Aberrant expression of MicroRNA-146a and MicroRNA-218 in cervical cancer

H. Wang *, P. Terinate, Y. Gao, K. L. Kalra
*BioGenex Laboratories, Dept. of Cell Pathology, Fremont, USA

Objective: MicroRNAs (miRNAs) are small noncoding RNAs with regulatory functions as tumor suppressors and oncogenes. Increasing evidence indicates that a substantial number of miRNAs are aberrantly expressed in various forms of cancer. However, information about miRNAs in cervical cancer is limited.
Method: Cervical cancer TMA samples (BioGenex TS-4215) were used in this study, probes for miRNA-146a and miRNA 218 were labeled with 5'-fluorescein. The probes were in situ hybridized and followed by poly-HRP detection. Fully automated Xmatrx system was used for the experiments.
Results: Among the 33 cervical cancer TMA samples, up-regulated expression of miRNA-146a in cancer cells was observed in 22 tissue samples (22/33, 66.7%). There were 11 cervical cancer samples that exhibited basal level expression. Only 8 out of 33 cervical cancer samples demonstrated elevated levels of miRNA-218 (8/33, 24.2%), 19/33 (58%) showed basal level expression, and 6/33 samples (18%) displayed lower expression level.
Conclusion: miRNA-146a expression is up-regulated in certain cervical cancer samples. This may be used as a biomarker for the molecular diagnosis of cervical cancer. However, in certain samples of cervical cancers, miRNA-218 displayed down-regulation. The significance of miRNA-146a up-regulation and clinical prognosis need further determination.

037

Detection of Merkel cell polyomavirus in neuroendocrine carcinomas: a pilot study

C.-C. Huang *, C.-M. Chen
*Chang Gung Memorial Hospital, Dept. of Pathology, Kaohsiung, Taiwan

Objective: Merkel cell carcinoma (MCC) is the eponym for primary cutaneous neuroendocrine carcinoma (NEC). Merkel cell polyomavirus has been identified to be clonally integrated in the genome of the majority of MCC. However, the status of MCC in NECs of other organs was rarely studied.
Method: There were 5 MCCs of skin and 19 NECs/small cell carcinomas of various organs retrieved from the pathology archives. Detection of Merkel cell polyomavirus by LT1 and LT3 PCR was performed.
Results: The cases included five NECs/small cell carcinomas of lung, three of liver, two of mediastinum, one of breast, one of uterus, one of stomach, one of rectum, three of lymph node metastasis and two of bone metastasis. Merkel cell polyomavirus DNA was identified in all the 5 cases of MCC and in none of the 19 specimens of NECs of other organs.
Conclusion: The prevalence of Merkel cell polyomavirus in MCC was high in this study, which agreed with the previous reports. NECs of other organs seem to be unrelated to MCC by the study with limited cases. A large-scaled study would be helpful to explore the preva-

lence of Merkel cell polyomavirus in NECs of various organs.

Wednesday, 31 August 2011, 09.30–10.30 and 16.30–17.00, Hall 5

PS-23 Poster Session Thymus and Mediastinal Pathology

001

Evaluation of VEGF pathway in thymic epithelial tumours

F. Calabrese *, N. Nannini, F. Lunardi, F. Di Chiara, G. Marulli, F. Rea
*University of Padua, Italy

Objective: It is difficult to predict thymic tumour behaviour on the basis of the morphology alone. Neoangiogenesis, an essential event for tumour development and progression, is regulated by different angiogenic factors: vascular endothelial growth factor (VEGF) and its receptors (R1, R2, R3) represent the primary involved pathway. Tissue evaluation of VEGF pathway has been reported in anecdotic reports. The aim of the study was tissue evaluation of VEGF pathway in different types of thymic epithelial tumours.
Method: The study was performed on 60 patients (mean age 53±13 yrs, 47 thymic epithelial neoplasia, 10 thymic hyperplasia and 3 residual thymic tissue). VEGF and its receptors were investigated in all thymic samples by immunohistochemistry using semi-quantitative analysis.
Results: VEGF pathway was positive in all thymic epithelial tumours while it was negative in residual thymic tissues and positive in the few epithelial cells of thymic hyperplasia. A significant higher VEGF and its receptors R1 and R3 expression was detected in the group of more aggressive thymic tumours (type B3 and thymic carcinoma) compared to the other thymomas (all $p<0.05$).
Conclusion: A strong VEGF pathway expression could have a role in the development/invasiveness of more aggressive thymic epithelial tumours. Antiangiogenic agents might be considered potential targeted therapy in more aggressive tumours.

002

Ectopic mediastinal parathyroid adenoma: a potential diagnostic pitfall

L. Bejan *, A. Nechifor-Boila, D. Milutin, A. Borda
*Emergency County Hospital, Dept. of Pathology, Targu Mures, Romania

Objective: Ectopic parathyroid adenoma is an uncommon entity occurring in the mediastinum. Mostly it appears in the antero-superior mediastinum in the vicinity or within the thymus gland. They may be non-functioning or associated with primary hyperparathyroidism.
Method: A 68-year-old woman suffering from nephrolithiasis and high blood presure presented with dry cough, mild dyspnoea, weight loss and asthenia. CT scan reveals a 4.5-cm cystic lesion in the postero-superior mediastinum suspicious for a hydatic cyst. The patient underwent surgery.
Results: On gross examination, the mediastinal mass was cystic. Microscopy revealed a sclerotic wall with calcification and ossification, and within the wall there were islands of polygonal tumor cells transversed by fibrovascular septa. The tumor cells were uniform, with dark round nuclei and a moderate amount of clear, lightly eosinophilic and oxyphilic cytoplasm. Mitotic figures were absent. An immunohistochemical study was performed for the differential diagnosis. The tumor was positive for Chromogranin, PTH and CAM 5.2.
Conclusion: The lack of frank invasion and the lack of cellular atypia and mitoses, in this immunophenotypical context plead for a diagnosis of ectopic parathyroid adenoma.

003

The thymic microscopic structure of the infant's thymuses with congenital heart defects

I. Varga *, V. Sisovsky, V. Jablonska-Mestanova, S. Polak, M. Adamkov
*Comenius University, Faculty of Medicine, Bratislava, Slovakia

Objective: The development of the thymus and heart are closely related while in both, the neural crest cells play an important role. The study evaluates an association between the congenital heart defects, and the structure of thymic Hassall´s bodies.
Method: A total of 36 archived formalin-fixed and paraffin-embedded human biopsy thymectomy (for cardiovascular malformations) tissue specimens from infants were evaluated by conventional histological stains, by light microscope, for the thymic Hassall´s bodies structure.
Results: There were the considerable variations in size as well as in quantity of Hassall´s bodies. In most cases, the Hassall´s bodies were large with the heterogeneous amorphous material enclosed in cystic dilatations. In thymuses of infants with ventricular septal defect, atrioventricular septal defect and tetralogy of Fallot, the huge Hassall´s bodies with the cystic dilatation filled up with cell detritus were found. Small-sized Hassall´s bodies corresponding with infant age in cases with pulmonary valve atresia, atrial septal defect and in some cases of transposition of great arteries were observed.
Conclusion: We assume that the changes of microenvironment of the thymic medulla are associated with disrupted

migration of the neural crest cells which are essential in the normogenesis of both heart and thymus. Supported by the Grant 1/0902/11-VEGA MSSR.

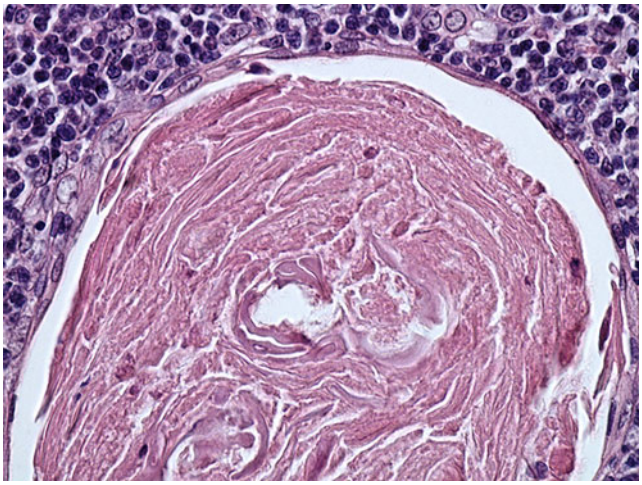

004

Pathohistological characteristic of mediastinal cyst

F. Vukmirovic *
*Podgorica, Montenegro

Objective: Mediastinal cysts are rare pathological entity and they consist 10% to 15% of radiological detected masses of this region. However, though rare, histopathologic changes differentiate such a diverse group of entities with different clinical significance. Also, cystic degeneration of solid tumors in this localisation are not rare.

Method: In our study we include 163 patients which were operated due to radiologicaly detected mediastinal tumor mass in ten year period of time (1992–2003). We analyzed the histopathological types of these lesions.

Results: From 163 diagnosed mediastinal masses we found 29 cystic formations (17.8%). We documented 14 (48.3%) mesothelial and 15 (51.7%) non-mesothelial cysts. Bronchogenic (5 cases or 33.3%) and dermoid (4 cases or 26.7%) cysts were the most frequent of non-mesothelial cysts, thymic cysts we found in 3 (20%) patients while parathyroid cysts had only 1 (6.7%) patient. Cystic tumors were diagnosed in 3 (20%) cases of non-mesothelial cysts, from which 2 (13.3%) cavernose lymphangiomas and 1 (6.7%) cystic schwannoma.

Conclusion: Though rare changes, mediastinal cysts are very diverse group of pathological changes. In our study all of these changes were benign. We have to emphasize that some mediastinal tumors can have cystic apperance.

005

Correlation of leukocyte antigens HLA phenotypes, markers of CD differentiation and concentration of cytokines with various types of locally advanced thymomas

G. Mylovydova *, O. Klimova, V. Boyko, A. Bozhkov, S. Sushkov, L. Drozdova, T. Kordon
*Institute of Gen. and Urg. Surgery, Laboratory of Pathomorphology, Kharkiv, Ukraine

Objective: The diagnostic importance of specific immunophysiological markers associated with various types of locally advanced thymomas in myasthenia was studied.

Method: Immunocytochemistry, immunofluorescence (CD16, CD19) methods, immune-enzyme analysis (concentration of IL-4, IL-8, γ-IFN, prostaglandin Å2, organ-specific antibodies), serologic method for HLA-DR antigens typing were used.

Results: HLA-DR1 and LA-DR5 phenotypes have been frequently revealed at lymphoid thymomas (LT); HLA-DR3, LA-DR7—at lymphoepithelial (LET); HLA-DR1, HLA-DR3—at epithelial (ET). HLA-DR5, HLA-DR52 phenotypes were associated with granulomatous thymoma (GT). In LT patients CD4+ T-helpers and CD16+ are significantly increased, CD8+ is lowered. The significant double increase of CD19+, CD16+; IL-4 and prostaglandin Å2 augmentation; augmentation of organ-specific antibodies to liver tissue to 0.050±0.003 Å units, γ-IFN sharp decrease were revealed in patients with LET. The decrease of IL-2, IL-4, IL-6 was detected in GT. IL-8 concentration was substantially increased in ET and GT.

Conclusion: Various types of locally advanced thymomas are associated with various phenotypes of class II histocompatibility antigens and formed on the background of specific changes of CD-markers expression, interleukins and interferon production that allows to carry out differential diagnostics of thymomas and to choose the treatment approach including thymus excision, prognostic of disease course.